

Iulian Vasile Antoniac  
*Editor*

# Handbook of Bioceramics and Biocomposites

---

# Handbook of Bioceramics and Biocomposites



---

Iulian Vasile Antoniac  
Editor

# Handbook of Bioceramics and Biocomposites

With 367 Figures and 80 Tables

 Springer Reference

*Editor*

Iulian Vasile Antoniac  
University Politehnica of Bucharest  
Bucharest, Romania

ISBN 978-3-319-12459-9                      ISBN 978-3-319-12460-5 (eBook)  
ISBN 978-3-319-12461-2 (print and electronic bundle)  
DOI 10.1007/978-3-319-12460-5

Library of Congress Control Number: 2016933676

© Springer International Publishing Switzerland 2016

This work is subject to copyright. All rights are reserved by the Publisher, whether the whole or part of the material is concerned, specifically the rights of translation, reprinting, reuse of illustrations, recitation, broadcasting, reproduction on microfilms or in any other physical way, and transmission or information storage and retrieval, electronic adaptation, computer software, or by similar or dissimilar methodology now known or hereafter developed.

The use of general descriptive names, registered names, trademarks, service marks, etc. in this publication does not imply, even in the absence of a specific statement, that such names are exempt from the relevant protective laws and regulations and therefore free for general use.

The publisher, the authors and the editors are safe to assume that the advice and information in this book are believed to be true and accurate at the date of publication. Neither the publisher nor the authors or the editors give a warranty, express or implied, with respect to the material contained herein or for any errors or omissions that may have been made.

Printed on acid-free paper

This Springer imprint is published by SpringerNature  
The registered company is Springer International Publishing AG Switzerland

*Dedicated to the memory of  
Professor Raquel LeGeros and  
Professor Daniel Bunea*



---

## Foreword

This 44-chapter *Handbook of Bioceramics and Biocomposites* edited by Prof. Iulian Antoniac of the University of Bucharest provides a comprehensive view of one of the best investigated classes of biomaterials in research and practice, namely bioceramics and related biocomposites.

In his logical approach to this theme, Prof. Antoniac uses a tripartite division, beginning with the “History and Materials Fundamentals” in which 15 chapters cover terrain from the early developments via different bioceramic classes to an exciting variety of composites, for example with polymers, graphene, or natural biopolymers, such as collagen. The fact that the first two chapters, which are on the history and development of bioceramics and bioactive glasses, are authored by the two “fathers” of these fields, Profs. Guy Daculsi and Larry Hench, respectively, puts the standard of the entire handbook on elevated ground. Nevertheless, the choice of the remaining authors is ample proof that the Editor was determined to make no compromises with respect to the knowledge, experience, and standing of all those chosen to be contributors.

The middle part, “Materials Engineering and Biological Interactions,” is naturally sub-divided into 6 chapters which address biomimetic strategies and process engineering of these biomaterials, followed by a set of 6 chapters with a life science emphasis. In the latter, surface engineering techniques and themes quintessential to interactions with living systems, including protein interactions as well as engineering approaches to reduce microorganism adhesion, are discussed. In addition, testing systems *in vitro* and *in vivo* as well as bioceramic strategies for tissue engineering especially of the musculoskeletal system have an important focus.

The third and final part, “Clinical Performance in Bioresorbable and Load-Bearing Applications,” is a state-of-the-art resumé of what bioceramics and biocomposites have so far achieved in patient care. It is fitting that in this sub-divided part, the field of orthopedics should lead the way, followed by dentistry, and then completed with other applications, including carriers for medication and implants for cranioplasty or the orbital region.

Professor Antoniac has succeeded in compiling a comprehensive handbook which will undoubtedly become a standard reference work on the theme of bioceramics and biocomposites. The all-embracing nature of the approach he has



adopted has been highly effective in spanning the traditional fields of development in these biomaterial classes as well as their novel modifications, which hold promise for a wide range of clinical applications in the future. He and his truly international author team have to be congratulated on this invaluable contribution to the biomaterial literature.

C. James Kirkpatrick M.D., Ph.D., D.Sc., F.R.C.Path.  
Emeritus Professor of Pathology  
Johannes Gutenberg University  
Mainz, Germany

---

## Preface

Information related to different aspects about bioceramics and biocomposites science together with their accompanying technology and applications in medical practice is scattered in the relevant literature.

In providing this *Handbook of Bioceramics and Biocomposites*, the editor believes that the latter stage has been reached in many parts of these investigated classes of biomaterials in research and practice. Also, many medical applications based on the bioceramics and composites are in clinical use for a long time and researchers have been studying their performance in order to offer potential solutions for their improvement.

In approaching his task, the Editor has tried to bring together into one source book all the information that is available about bioceramics and related biocomposites in terms of material fundamentals, materials engineering, biological interactions, and clinical performance in various medical applications, from orthopedics and dentistry to carriers for medication and implants for cranioplasty or the orbital region.

In order to do this, I asked for the help of many colleagues worldwide to be contributors to this handbook. Another important fact was that the contributors have different backgrounds, from materials science to biology or clinicians in different medical specializations.

The topic of bioceramics and related biocomposites has attracted many researchers of other fields to make contributions, at the same time helping traditional ceramic science and technology in its transition to work at multidisciplinary research frontiers. Having a synergic effect with the rapid developments of related areas, e.g., tissue engineering, nanotechnology, drug delivery, smart materials, and structures, bioceramics and related biocomposites has become a frontier field of research leading to many technological breakthroughs.

As a result, *Handbook of Bioceramics and Biocomposites* has expanded to three main parts. They cover the following topics:

The first part, “History and Materials Fundamentals,” sub-divided into 15 chapters addresses history and development, fundamental properties, and presentation of the main bioceramics, like alumina, zirconia, calcium phosphates, hydroxyapatite, and carbonate apatite, and a large variety of related composites, from ceramic-polymer to grapheme-ceramic. “In order to move forward we must look back.” Based on this consideration and as a sign of respect for the pioneers that opened this

field, the first two chapters of this handbook are dedicated to the history and development of bioceramics and bioactive glasses. Authored by two pioneers of bioceramics and related biocomposites, these chapters demand higher and elevated standards for all contributors of the handbook. Other chapters of this part present the fundamental properties and different aspects about the major bioceramics, like alumina, zirconia, calcium phosphates, hydroxyapatite, and carbonate apatite, and a large variety of related composites, from ceramic-polymer to grapheme-ceramic.

The second part, “Materials Engineering and Biological Interactions,” covers two important aspects: biomimetic strategies, and surface engineering and interactions with living cells. Six chapters are dedicated to biomimetic strategies and present essential requirements and manufacturing and evaluation aspects for different bioceramics and related composites used for tissue engineering and regeneration. The last six chapters of this part are dedicated to surface engineering and interactions with living cells, and describe processing technologies, characterization, and biocompatibility evaluation of different bioceramic coatings and biocomposites.

The last part, “Clinical Performance in Bioresorbable and Load-Bearing Applications,” provides a generous view on the clinical performance of various medical applications which comprise 17 chapters. The field of orthopedics and dentistry lead the way. Many clinicians have contributed to these parts describing the performance of various implants based on their clinical experience or retrieval analysis. The last chapters of this part describe other applications, including carriers for medication and implants for cranioplasty or the orbital region. This part is very important because the dedicated chapters are written mainly by clinicians, who could appreciate better the performance of various bioceramics and related biocomposites. Until the end, the clinical applications of the new bioceramics or related biocomposites must be the main target of the researchers who work in this field, and collaborative activities with clinicians are very useful and important.

It is hoped that the handbook will be used and useful, not perfect but a valuable contribution to the bioceramics and related biocomposites field that I believe is evolving sufficiently to deserve such a publication. The handbook can also serve as the basis of instructional course lectures for audiences ranging from advanced undergraduate students to post-graduates in materials science and engineering and biomedical engineering.

I wish readers to find the *Handbook of Bioceramics and Biocomposites* informative and useful in their endeavors.

March 2016  
Bucharest, Romania

Iulian Vasile Antoniac

---

# Contents

## Volume 1

<b>Part I History and Materials Fundamentals</b> .....	<b>1</b>
<b>1 History of Development and Use of the Bioceramics and Biocomposites</b> .....	<b>3</b>
Guy Daculsi	
<b>2 Bioactive Glass Bone Grafts: History and Clinical Applications</b> .....	<b>23</b>
Larry L. Hench	
<b>3 Fundamental Properties of Bioceramics and Biocomposites</b> .....	<b>35</b>
Maria Grazia Raucci, Daniela Giugliano, and Luigi Ambrosio	
<b>4 Bioinert Ceramics: Zirconia and Alumina</b> .....	<b>59</b>
Corrado Piconi and Alessandro Alan Porporati	
<b>5 Calcium Phosphates</b> .....	<b>91</b>
Sergey V. Dorozhkin	
<b>6 Hydroxyapatite: From Nanocrystals to Hybrid Nanocomposites for Regenerative Medicine</b> .....	<b>119</b>
Anna Tampieri, Michele Iafisco, Simone Sprio, Andrea Ruffini, Silvia Panseri, Monica Montesi, Alessio Adamiano, and Monica Sandri	
<b>7 Cationic and Anionic Substitutions in Hydroxyapatite</b> .....	<b>145</b>
Ilaria Cacciotti	
<b>8 Carbonate Apatite Bone Replacement</b> .....	<b>213</b>
Kunio Ishikawa	
<b>9 Natural and Synthetic Polymers for Designing Composite Materials</b> .....	<b>233</b>
Bogdan C. Simionescu and Daniela Ivanov	

<b>10</b>	<b>Ceramic-Polymer Composites for Biomedical Applications</b> . . . . .	287
	Toshiki Miyazaki, Masakazu Kawashita, and Chikara Ohtsuki	
<b>11</b>	<b>Collagen–Bioceramic Smart Composites</b> . . . . .	301
	Iulian Vasile Antoniac, Madalina Georgiana Albu, Aurora Antoniac, Laura Cristina Rusu, and Mihaela Violeta Ghica	
<b>12</b>	<b>Bioactive Glass-Biopolymer Composites for Applications in Tissue Engineering</b> . . . . .	325
	Yaping Ding, Marina T. Souza, Wei Li, Dirk W. Schubert, Aldo R. Boccaccini, and Judith A. Roether	
<b>13</b>	<b>Resin-Based Dental Composite Materials</b> . . . . .	357
	Hanadi Y. Marghalani	
<b>14</b>	<b>Composite Hybrid Membrane Materials for Artificial Organs</b> . . .	407
	Stefan Ioan Voicu and Marius Sandru	
<b>15</b>	<b>Graphene-Bioceramic Composites</b> . . . . .	431
	Xingyi Xie and Marta Cerruti	
	<b>Part II Materials Engineering and Biological Interactions: Biomimetic Strategies</b> . . . . .	<b>469</b>
<b>16</b>	<b>Essential Requirements for Resorbable Bioceramic Development: Research, Manufacturing, and Preclinical Studies</b> . . . . .	471
	Guy Daculsi, Eric Aguado, and Thomas Miramond	
<b>17</b>	<b>Biomimetic Strategies to Engineer Mineralized Human Tissues</b> . . . . .	503
	Sandra Pina, Joaquim Miguel Oliveira, and Rui L. Reis	
<b>18</b>	<b>Biomimetics and Marine Materials in Drug Delivery and Tissue Engineering</b> . . . . .	521
	Andy H. Choi, Sophie Cazalbou, and Besim Ben-Nissan	
<b>19</b>	<b>Silicate-Based Bioactive Composites for Tissue Regeneration</b> . . . .	545
	Y.L. Zhou, Z.G. Huan, and J. Chang	
<b>20</b>	<b>Biomimetic Customized Composite Scaffolds and Translational Models for the Bone Regenerative Medicine Using CAD-CAM Technology</b> . . . . .	585
	Isidoro Giorgio Lesci, Leonardo Ciocca, and Norberto Roveri	
<b>21</b>	<b>In Vitro and In Vivo Evaluation of Composite Scaffolds for Bone Tissue Engineering</b> . . . . .	615
	Svetlana Schussler, Khadidiatou Guiro, and Treena Livingston Arinze	

**Volume 2**

**Part III Materials Engineering and Biological Interactions: Surface Engineering and Interactions with Living Cells . . . . . 637**

**22 Processing Technologies for Bioceramic Based Composites . . . . . 639**  
Ipek Akin and Gultekin Goller

**23 Glass-Ceramics: Fundamental Aspects Regarding the Interaction with Proteins . . . . . 667**  
C. Gruian, E. Vanea, H.-J. Steinhoff, and Simion Simon

**24 Bioceramic Coatings for Metallic Implants . . . . . 703**  
Alina Vladescu, Maria A. Surmeneva, Cosmin M. Cotrut, Roman A. Surmenev, and Iulian Vasile Antoniac

**25 Sol-gel Nanocoatings of Bioceramics . . . . . 735**  
B. Ben-Nissan, A.H. Choi, I.J. Macha, and S. Cazalbou

**26 Biomaterial Functionalized Surfaces for Reducing Bacterial Adhesion and Infection . . . . . 757**  
Maria G. Katsikogianni, David J. Wood, and Yannis F. Missirlis

**27 Biocomposites used in Orthopedic Applications: Trends in Biocompatibility Assays . . . . . 785**  
Martin J. Stoddart and Mauro Alini

**Part IV Clinical Performance in Bioresorbable and Load-Bearing Applications: Orthopedics . . . . . 819**

**28 Perspective and Trends on Bioceramics in Joint Replacement . . . 821**  
Corrado Piconi and Giulio Maccauro

**29 Evolution of Cementation Techniques and Bone Cements in Hip Arthroplasty . . . . . 859**  
Marius Niculescu, Bogdan Lucian Solomon, George Viscopoleanu, and Iulian Vasile Antoniac

**30 Retrieval Analysis of Hip Prostheses . . . . . 901**  
Iulian Vasile Antoniac, Florin Miculescu, Dan Laptoiu, Aurora Antoniac, Marius Niculescu, and Dan Grecu

**31 Clinical Limitations of the Biodegradable Implants Used in Arthroscopy . . . . . 935**  
Rodica Marinescu and Iulian Vasile Antoniac

**32 Bioceramics and Biocomposites in Spine Surgery . . . . . 967**  
Gianluca Vadalà, Fabrizio Russo, Luca Ambrosio, and Vincenzo Denaro

<b>Part V Clinical Performance in Bioresorbable and Load-Bearing Applications: Dentistry</b> .....	<b>989</b>
<b>33 Biofilm Formation on Implants and Prosthetic Dental Materials</b> .....	991
Lia Rimondini, Andrea Cochis, Elena Varoni, Barbara Azzimonti, and Antonio Carrassi	
<b>34 Guided Bone Regeneration for Dental Implants</b> .....	1029
Mishel Weshler and Iulian Vasile Antoniac	
<b>35 Performance of Dental Composites in Restorative Dentistry</b> .....	1075
Diana Dudea, Camelia Alb, Bogdan Culic, and Florin Alb	
<b>36 Clinical Evaluation of Disilicate and Zirconium in Dentistry</b> .....	1115
Domenico Baldi, Jacopo Colombo, and Uli Hauschild	
<b>37 Ceramic Veneers in Dental Esthetic Treatments</b> .....	1129
Dan Pătroi, Teodor Trăistaru, and Sergiu-Alexandru Rădulescu	
<b>38 Alveolar Augmentation Using Different Bone Substitutes</b> .....	1159
Cena Dimova, Biljana Evrosimovska, Katerina Zlatanovska, and Julija Zarkova	
<b>39 CAD-CAM Processing for All Ceramic Dental Restorations</b> .....	1201
Alexandru Eugen Petre	
<b>40 Failure Analysis of Dental Prosthesis</b> .....	1217
Florin Miculescu, Lucian Toma Ciocan, Marian Miculescu, Andrei Berbecaru, Josep Oliva, and Raluca Monica Comăneanu	
<b>Part VI Clinical Performance in Bioresorbable and Load-Bearing Applications: Other Applications</b> .....	<b>1247</b>
<b>41 Bioceramics and Composites for Orbital Implants: Current Trends and Clinical Performance</b> .....	1249
Francesco Baino	
<b>42 Current Implants Used in Cranioplasty</b> .....	1275
Dumitru Mohan, Aurel Mohan, Iulian Vasile Antoniac, and Alexandru Vlad Ciurea	
<b>43 Marine Biomaterials as Drug Delivery System for Osteoporosis and Bone Tissue Regeneration</b> .....	1309
Joshua Chou and Jia Hao	
<b>44 Antibacterial Potential of Nanobioceramics Used as Drug Carriers</b> .....	1333
T.S. Sampath Kumar and K. Madhumathi	
<b>Index</b> .....	<b>1375</b>

---

## About the Editor



### **Iulian Vasile Antoniac**

Faculty Materials Science and Engineering  
University Politehnica of Bucharest  
Bucharest, Romania

Professor Dr. habil. Iulian Vasile Antoniac is a materials science engineer working in the field of biomaterials and medical devices. Professor Antoniac is the past World President of the International Society for Ceramics in Medicine (ISCM) and past President of the Romanian Society for Biomaterials (SRB).

He completed his Ph.D. in Materials Science and Engineering from University Politehnica of Bucharest (UPB), Romania, in 1998. After several specializations in laboratories of Switzerland, Portugal, France, and the USA on surface analysis, composite materials, implant design, and biomaterials characterizations, his scientific interest spans from the synthesis and characterization of biomaterials and interactions with living tissues, retrieval implant analysis, biodegradable magnesium alloys, ceramic coatings on metallic biomaterials, to the new ceramic composites and scaffolds based on nanostructured and biologically inspired biomaterials for bone regeneration. He received in 2013 his post-doctoral degree in Materials Science and Engineering from UPB, completed his habilitation in 2015 (habilitation thesis was on “orthopedic biomaterials”), and now is the leader of Biomaterials Group from Faculty of Materials Science and Engineering, University Politehnica of Bucharest, Romania.

His professional and scientific activity comprises more than 200 international journal papers and conference proceedings, 7 research monographs, and over 10 patents in the areas of biomaterials and their clinical applications that received many international awards at the International Exhibition of Inventions. He was the recipient of the Daniel Bunea Award of the Romanian Society for Biomaterials in 2005 and the Excellence Award of the Romanian Society for Biomaterials in 2012, top individual awards offered by this professional organization. He also acts as a member of the international editorial board and reviewer for many journals and conferences on biomaterials and bioceramics.





---

## Contributors

**Alessio Adamiano** Institute of Science and Technology for Ceramics (ISTEC), National Research Council (CNR), Faenza, Italy

**Eric Aguado** ONIRIS, National Veterinary School of Nantes, Nantes, France

**Ipek Akin** Istanbul Technical University, Department of Metallurgical and Materials Engineering, Maslak, Istanbul, Turkey

**Camelia Alb** Department of Prosthetic Dentistry and Dental Materials, University of Medicine and Pharmacy “Iuliu Hatieganu”, Cluj–Napoca, Romania

**Florin Alb** Department of Periodontology, University of Medicine and Pharmacy “Iuliu Hatieganu”, Cluj–Napoca, Romania

**Madalina Georgiana Albu** INCDTP – Division of Leather and Footwear Research Institute, Bucharest, Romania

**Mauro Alini** AO Research Institute Davos, Davos Platz, Switzerland

**Luca Ambrosio** Department of Orthopaedic and Trauma Surgery, Campus Bio-Medico University of Rome, Rome, Italy

**Luigi Ambrosio** Department of Chemical Sciences and Materials Technology, National Research Council of Italy, Rome, Italy

**Aurora Antoniac** Faculty of Materials Science and Engineering, University Politehnica of Bucharest, Bucharest, Romania

**Iulian Vasile Antoniac** University Politehnica of Bucharest, Bucharest, Romania

**Treena Livingston Arinzeh** Department of Biomedical Engineering, New Jersey Institute of Technology, Newark, NJ, USA

**Barbara Azzimonti** Dipartimento di Scienze della Salute, Università del Piemonte Orientale, Novara, Italy

**Francesco Baino** Institute of Materials Physics and Engineering, Applied Science and Technology Department, Politecnico di Torino, Torino, Italy

**Domenico Baldi** Department of Fixed Prosthodontics, University of Genova, Genova, Italy

**Besim Ben-Nissan** School of Chemistry and Forensic Science, Faculty of Science, University of Technology Sydney, Ultimo, NSW, Australia

**Andrei Berbecaru** Faculty of Materials Science and Engineering, University Politehnica of Bucharest, Bucharest, Romania

**Aldo R. Boccaccini** Institute of Biomaterials, University of Erlangen-Nuremberg, Erlangen, Germany

**Ilaria Cacciotti** Engineering Department, University of Rome “Niccolò Cusano”, Rome, Italy

Italian Interuniversity Consortium on Materials Science and Technology (INSTM), Rome, Italy

**Antonio Carrassi** Dipartimento di Scienze Biomediche, Chirurgiche ed Odontoiatriche, Università degli Studi di Milano, Milan, Italy

**Sophie Cazalbou** CIRIMAT Carnot Institute, CNRS-INPT-UPS, Faculty of Pharmacie, University of Toulouse, Toulouse, France

**Marta Cerruti** Department of Mining and Materials Engineering, McGill University, Montreal, QC, Canada

**J. Chang** State Key Laboratory of High Performance Ceramics and Superfine Microstructure, Shanghai Institute of Ceramics, Chinese Academy of Sciences, Shanghai, China

**Andy H. Choi** School of Chemistry and Forensic Science, Faculty of Science, University of Technology Sydney, Ultimo, NSW, Australia

**Joshua Chou** Advanced Tissue Regeneration and Drug Delivery Group, University of Technology Sydney, Sydney, NSW, Australia

**Lucian Toma Ciocan** Dental Medicine Faculty, “Carol Davila” University of Medicine and Pharmacy from Bucharest, Bucharest, Romania

**Leonardo Ciocca** Department of Biomedical and Neuromotor Sciences, University of Bologna, Bologna, Italy

**Alexandru Vlad Ciurea** University of Medicine and Pharmacy “Carol Davila” Bucharest, Bucharest, Romania

**Andrea Cochis** Dipartimento di Scienze della Salute, Università del Piemonte Orientale, Novara, Italy

Dipartimento di Scienze Biomediche, Chirurgiche ed Odontoiatriche, Università degli Studi di Milano, Milan, Italy

**Jacopo Colombo** Department of Fixed Prosthodontics, University of Genova, Genova, Italy

**Raluca Monica Comăneanu** Faculty of Dental Medicine, Titu Maiorescu University, Bucharest, Romania

**Cosmin M. Cotrut** Materials Science and Engineering Faculty, University Politehnica of Bucharest, Bucharest, Romania

**Bogdan Culic** Department of Prosthetic Dentistry and Dental Materials, University of Medicine and Pharmacy “Iuliu Hatieganu”, Cluj–Napoca, Romania

**Guy Daculsi** Dental Faculty, Laboratory for Osteoarticular and Dental Tissue Engineering, INSERM U791, Nantes University, Nantes, France

**Vincenzo Denaro** Department of Orthopaedic and Trauma Surgery, Campus Bio-Medico University of Rome, Rome, Italy

**Cena Dimova** Faculty of Medical Sciences, Dental Medicine, Macedonia FYR, University “Goce Delcev” – Stip, Stip, FYR Macedonia

**Yaping Ding** Institute of Polymer Materials, University of Erlangen-Nuremberg, Erlangen, Germany

**Sergey V. Dorozhkin** Moscow, Russia

**Diana Dudea** Department of Prosthetic Dentistry and Dental Materials, University of Medicine and Pharmacy “Iuliu Hatieganu”, Cluj–Napoca, Romania

**Biljana Evrosimovska** Faculty of Dentistry, Macedonia, FYR, University “Sts. Cyril and Methody” Skopje, Skopje, FYR Macedonia

**Mihaela Violeta Ghica** Faculty of Pharmacy, University of Medicine and Pharmacy “Carol Davila” Bucharest, Bucharest, Romania

**Daniela Giugliano** Institute of Polymers, Composites and Biomaterials (IPCB), National Research Council of Italy (CNR), Naples, Italy

**Gultekin Goller** Istanbul Technical University, Department of Metallurgical and Materials Engineering, Maslak, Istanbul, Turkey

**Dan Grecu** Department of Orthopaedics, University of Medicine and Pharmacy Craiova, Craiova, Romania

**Cristina Gruian** Faculty of Physics and Institute of Interdisciplinary Research in Bio Nano-Sciences, Babes-Bolyai University, Cluj–Napoca, Romania

**Khadidiatou Guiro** Department of Biomedical Engineering, New Jersey Institute of Technology, Newark, NJ, USA

**Jia Hao** Oral Implantology and Regenerative Dental Medicine, Tokyo Medical and Dental University, Tokyo, Japan

**Uli Hauschild** Department of Fixed Prosthodontics, University of Genova, Genova, Italy

**Larry L. Hench** Department of Biomedical Engineering, Florida Institute of Technology, Melbourne, FL, USA

**Z. G. Huan** State Key Laboratory of High Performance Ceramics and Superfine Microstructure, Shanghai Institute of Ceramics, Chinese Academy of Sciences, Shanghai, China

**Michele Iafisco** Institute of Science and Technology for Ceramics (ISTEC), National Research Council (CNR), Faenza, Italy

**Kunio Ishikawa** Department of Biomaterials, Faculty of Dental Science, Kyushu University, Fukuoka, Japan

**Daniela Ivanov** “Petru Poni” Institute of Macromolecular Chemistry, Iasi, Romania

**Maria G. Katsikogianni** Laboratory of Biomechanics and Biomedical Engineering, Department of Mechanical Engineering and Aeronautics, University of Patras, Rion, Patras, Greece

Biomaterials and Tissue Engineering Group, School of Dentistry, University of Leeds, Leeds, UK

Advanced Materials Engineering, Faculty of Engineering and Informatics, University of Bradford, Bradford, UK

**Masakazu Kawashita** Graduate School of Biomedical Engineering, Tohoku University, Sendai, Japan

**Dan Laptoiu** Department of Orthopaedics and Trauma I, Colentina Clinical Hospital, Bucharest, Romania

**Isidoro Giorgio Lesci** Department of Chemistry “G. Ciamician”, University of Bologna, Bologna, Italy

**Wei Li** Institute of Biomaterials, University of Erlangen-Nuremberg, Erlangen, Germany

**Giulio Maccauro** Medicine and Surgery Department, Clinical Orthopedics and Traumatology Institute, Catholic University, Rome, Italy

**I. J. Macha** School of Chemistry and Forensic Science, Faculty of Science, University of Technology Sydney, Ultimo, NSW, Australia

**K. Madhumathi** Department of Metallurgical and Materials Engineering, Indian Institute of Technology Madras, Chennai, Tamil Nadu, India

**Hanadi Y. Marghalani** Operative Dentistry Department, King Abdulaziz University, Jeddah, Saudi Arabia

**Rodica Marinescu** Carol Davila University of Medicine, Bucharest, Romania

**Florin Miculescu** Faculty of Materials Science and Engineering, University Politehnica of Bucharest, Bucharest, Romania

**Marian Miculescu** Faculty of Materials Science and Engineering, University Politehnica of Bucharest, Bucharest, Romania

**Thomas Miramond** Laboratory for Osteoarticular and Dental Tissue Engineering, INSERM U791, Nantes University, Nantes, France

**Yannis F. Missirlis** Laboratory of Biomechanics and Biomedical Engineering, Department of Mechanical Engineering and Aeronautics, University of Patras, Rion, Patras, Greece

**Toshiki Miyazaki** Graduate School of Life Science and Systems Engineering, Kyushu Institute of Technology, Kitakyushu-shi, Fukuoka, Japan

**Aurel Mohan** University of Oradea, Oradea, Romania

**Dumitru Mohan** University of Oradea, Oradea, Romania

**Monica Montesi** Institute of Science and Technology for Ceramics (ISTEC), National Research Council (CNR), Faenza, Italy

**Marius Niculescu** Department of Orthopaedics and Trauma I, Colentina Clinical Hospital, Bucharest, Romania

Faculty of Medicine, Titu Maiorescu University, Bucharest, Romania

**Chikara Ohtsuki** Graduate School of Engineering, Nagoya University, Nagoya, Aichi Prefecture, Japan

**Josep Oliva** Clinica Oliva Dental, Barcelona, Spain

**Joaquim Miguel Oliveira** 3B's Research Group – Biomaterials, Biodegradables and Biomimetics, University of Minho, Headquarters of the European Institute of Excellence on Tissue Engineering and Regenerative Medicine, Taipas/Guimarães, Portugal

ICVS/3B's – PT Government Associate Laboratory, Braga/Guimarães, Portugal

**Dan Pătroi** UMF Carol Davila, Department of Fixed prosthodontics and Occlusology, Bucharest, Romania

**Silvia Panseri** Institute of Science and Technology for Ceramics (ISTEC), National Research Council (CNR), Faenza, Italy

**Alexandru Eugen Petre** Department of Prosthodontics, Discipline of Fixed Prosthodontics and Dental Occlusion, University of Medicine and Pharmacy "Carol Davila", Bucharest, Romania

**Corrado Piconi** Medicine and Surgery Department, Clinical Orthopedics and Traumatology Institute, Catholic University, Rome, Italy

**Sandra Pina** 3B's Research Group – Biomaterials, Biodegradables and Biomimetics, University of Minho, Headquarters of the European Institute of Excellence on Tissue Engineering and Regenerative Medicine, Taipas/Guimarães, Portugal  
ICVS/3B's – PT Government Associate Laboratory, Braga/Guimarães, Portugal

**Alessandro Alan Porporati** Medical Products Division, CeramTec GmbH, Plochingen, Germany

**Sergiu-Alexandru Rădulescu** UMF Carol Davila, Department of Fixed prosthodontics and Occlusology, Bucharest, Romania

**Maria Grazia Raucci** Institute of Polymers, Composites and Biomaterials (IPCB), National Research Council of Italy (CNR), Naples, Italy

**Rui L. Reis** 3B's Research Group – Biomaterials, Biodegradables and Biomimetics, University of Minho, Headquarters of the European Institute of Excellence on Tissue Engineering and Regenerative Medicine, Taipas/Guimarães, Portugal  
ICVS/3B's – PT Government Associate Laboratory, Braga/Guimarães, Portugal

**Lia Rimondini** Dipartimento di Scienze della Salute, Università del Piemonte Orientale, Novara, Italy

**Judith A. Roether** Institute of Polymer Materials, University of Erlangen-Nuremberg, Erlangen, Germany

**Norberto Roveri** Department of Chemistry "G. Ciamician", University of Bologna, Bologna, Italy

**Andrea Ruffini** Institute of Science and Technology for Ceramics (ISTEC), National Research Council (CNR), Faenza, Italy

**Fabrizio Russo** Department of Orthopaedic and Trauma Surgery, Campus Bio-Medico University of Rome, Rome, Italy

**Laura Cristina Rusu** University of Medicine and Pharmacy "Victor Babes" Timisoara, Timisoara, Romania

**T. S. Sampath Kumar** Department of Metallurgical and Materials Engineering, Indian Institute of Technology Madras, Chennai, Tamil Nadu, India

**Monica Sandri** Institute of Science and Technology for Ceramics (ISTEC), National Research Council (CNR), Faenza, Italy

**Marius Sandru** Department of Polymer Particles and Surface Chemistry, Sector Biotechnology and Nanomedicine, SINTEF Materials and Chemistry, Trondheim, Norway

**Dirk W. Schubert** Institute of Polymer Materials, University of Erlangen-Nuremberg, Erlangen, Germany

**Svetlana Schussler** Department of Biomedical Engineering, New Jersey Institute of Technology, Newark, NJ, USA

**Bogdan C. Simionescu** Department of Natural and Synthetic Polymers, “Gheorghe Asachi” Technical University, Iași, Romania

“Petru Poni” Institute of Macromolecular Chemistry, Iasi, Romania

**Simion Simon** Faculty of Physics and Institute of Interdisciplinary Research in Bio Nano-Sciences, Babes-Bolyai University, Cluj-Napoca, Romania

**Bogdan Lucian Solomon** Royal Adelaide Hospital, Department of Orthopaedics and Trauma, Centre for Orthopaedic and Trauma Research and Discipline of Orthopaedics and Trauma, The University of Adelaide, Adelaide, SA, Australia

**Marina T. Souza** Department of Materials Engineering, Federal University of São Carlos, São Carlos, SP, Brazil

**Simone Sprio** Institute of Science and Technology for Ceramics (ISTEC), National Research Council (CNR), Faenza, Italy

**Heinz-Jürgen Steinhoff** Department of Physics, University of Osnabruk, Osnabruk, Germany

**Martin J. Stoddart** AO Research Institute Davos, Davos Platz, Switzerland

**Roman A. Surmenev** Department of Experimental Physics, Tomsk Polytechnic University, Tomsk, Russia

**Maria A. Surmeneva** Department of Experimental Physics, Tomsk Polytechnic University, Tomsk, Russia

**Anna Tampieri** Institute of Science and Technology for Ceramics (ISTEC), National Research Council (CNR), Faenza, Italy

**Teodor Trăistaru** UMF Carol Davila, Department of Fixed prosthodontics and Occlusology, Bucharest, Romania

**Gianluca Vadalà** Department of Orthopaedic and Trauma Surgery, Campus Bio-Medico University of Rome, Rome, Italy

**Emilia Vanea** Faculty of Physics and Institute of Interdisciplinary Research in Bio Nano-Sciences, Babes-Bolyai University, Cluj-Napoca, Romania

**Elena Varoni** Dipartimento di Scienze Biomediche, Chirurgiche ed Odontoiatriche, Università degli Studi di Milano, Milan, Italy

**George Viscopoleanu** Department of Orthopaedic Surgery, “Foisor” Orthopaedic Hospital, Bucharest, Romania

**Alina Vladescu** National Institute for Optoelectronics, Magurele, Romania

**Stefan Ioan Voicu** Faculty of Applied Chemistry and Materials Sciences, University Politehnica of Bucharest, Bucharest, Romania

**Mishel Weshler** Laniado Hospital, Netanya, Israel



---

**David J. Wood** Biomaterials and Tissue Engineering Group, School of Dentistry, University of Leeds, Leeds, UK

**Xingyi Xie** College of Polymer Science and Engineering, Sichuan University, Chengdu, Sichuan, China

**Julija Zarkova** Faculty of Medical Sciences, Dental Medicine, Macedonia FYR, University “Goce Delcev” – Stip, Stip, FYR Macedonia

**Y. L. Zhou** State Key Laboratory of High Performance Ceramics and Superfine Microstructure, Shanghai Institute of Ceramics, Chinese Academy of Sciences, Shanghai, China

**Katerina Zlatanovska** Faculty of Medical Sciences, Dental Medicine, Macedonia FYR, University “Goce Delcev” – Stip, Stip, FYR Macedonia

---

**Part I**

**History and Materials Fundamentals**

---

# History of Development and Use of the Bioceramics and Biocomposites

# 1

Guy Daculsi

## Contents

Fabrication and Properties .....	7
Introduction of Macroporosity and Microporosity .....	10
Physicochemical Properties .....	12
Mechanical Properties .....	14
Bioactivity and Osteogenic Properties .....	14
The Challenge of Bioactive Bioceramics in Bone Regenerative Medicine .....	16
CaP Bioceramic Composites .....	16
Conclusion .....	17
References .....	18

---

## Abstract

Bioceramics is a relatively new field; it did not exist until the beginning of 1970, when these materials were shown to restore osteoarticular and dental functions, as well as act as a replacement material for autografts and allograft bone reconstructions. Bioceramics used to replace, repair, or reconstruct human body parts or complex living tissues have differences in their chemical nature, properties, and applications, such as the use of alumina for hip prosthesis versus CaP bioceramics for bone regeneration. Alumina is classified as an inert bioceramic, while CaP bioceramics are considered bioactive biomaterials, able to be absorbed or bond directly with bone. This review concentrates on the development and use of bioceramics and biocomposites and is limited to CaP bioceramics. Bioactive bioceramics are recommended for use as an alternative or additive to autogenous bone for various procedures: orthopedic and dental applications, scaffolds for tissue engineering, vectors for gene therapy, and as a drug delivery system.

---

G. Daculsi (✉)

Dental Faculty, Laboratory for Osteoarticular and Dental Tissue Engineering, INSERM U791,

Nantes University, Nantes, France

e-mail: [guy.daculsi@univ-nantes.fr](mailto:guy.daculsi@univ-nantes.fr)

© Springer International Publishing Switzerland 2016

I.V. Antoniac (ed.), *Handbook of Bioceramics and Biocomposites*,

DOI 10.1007/978-3-319-12460-5\_2

3

There are two physical properties of bioceramics that are considered important for optimal biological performance, which includes bioceramic-cell interactions, bioceramic resorption, the bioceramic-tissue interface, and new bone formation. These fundamental properties are interconnecting macroporosity and appropriate microporosity. CaP bioceramics are a recent development in bone surgery that act as a replacement for auto- and allografts, which have been engineered less than 100 years from the first medical applications and less than 30 years from the initial manufacturing of medical devices and experiments with bone regeneration. Bioactive bioceramics have largely contributed to this revolution in medicine. Numerous innovations in this field are now appearing; it is the beginning of bioceramics and not the “has-been medical device.”

---

**Keywords**

Bioceramics • Calcium phosphate • Physicochemical properties • Biological properties

Bioceramics is a relatively new field; it did not exist until the beginning of 1970, when these materials were shown to restore osteoarticular and dental functions, as well as act as a replacement material for autografts and allograft bone reconstructions. Since the turn of the millennium, numerous synthetic bone graft materials have become available as alternatives to autogenous bone for the purposes of repair, substitution, and augmentation. Included in these synthetic biomaterials are special glass ceramics that are described as bioactive glasses and calcium phosphates (CaPs, i.e., calcium hydroxyapatite; HA; tricalcium phosphate, TCP; and biphasic calcium phosphate, BCP). A review [1] has provided an amalgamation of the important historical information about CaP bioceramics. Albee, in 1920, reported the first successful application of a CaP reagent for the repair of a bone defect in a human patient. More than 50 years later, both the clinical use of a TCP preparation in surgically created periodontal defects in animals and the use of dense HA as an immediate replacement for tooth roots were reported. In the early 1980s, synthetic HA and  $\beta$ -TCP became commercially available as substitute bone materials for dental and medical applications [2]. Despite the abundance of literature, books, marketed products, and clinical data, there are still many myths, errors, and critical analyses of results concerning the ability to regenerate or rebuild bone tissue in humans.

To address these issues, it is first necessary to recall some definitions:

The first definition of “biomaterials” that specifically mentioned “bioceramics” was provided in 1983 by the National Institutes for Health during a conference on the clinical applications of biomaterials in the USA [3]: “*A biomaterial is any substance, other than a drug, or combination of substances, synthetic or natural origin, which can be used for any period of time, as a whole or as a part of a system which treats, augments, or replaces any tissue, organ, or function of the body.*”

In 1986, David Williams and the European Society for Biomaterials [4] significantly simplified the definition of a biomaterial to “*a non-viable material used in a medical device intended to interact with [a] biological system.*”

In addition to these general definitions, it was necessary to differentiate between the different types of bioceramics. Bioceramics used to replace, repair, or reconstruct human body parts, or complex living tissues have differences in their chemical nature, properties, and applications, such as the use of alumina for hip prosthesis versus CaP bioceramics for bone regeneration. Alumina is classified as an inert bioceramic, while CaP bioceramics are considered bioactive biomaterials, able to be absorbed or bond directly with bone.

This review concentrates on the development and use of bioceramics and biocomposites and is limited to CaP bioceramics. The history from 1770 to 1950 of CaP was recently published [5]. Furthermore, there is already a sizable literature about non-resorbable, bio-inert bioceramics such as alumina or zirconia [6].

There are two pioneers that largely contributed to the use of apatites for biological procedures: Gérard Montel from France who received his PhD in Paris in 1956 [7] and Racquel LeGeros who received hers in 1967 in New York [8]. A symposium of the CNRS “Centre National de La Recherche Scientifique” on biological apatites established the basis of the physical chemistry and crystallography of biological apatites [9]. Elliott [10] confirmed the specificity of biological apatites.

These important contributions, in addition to the knowledge about calcium orthophosphate from mineralogy, are the basis for biomineralization during the 16–18 and the subsequent development of CaP bioceramics. In 1988, the first International Bioceramic Symposium was initiated by H. Oonishi in Osaka, and the first volume of Bioceramics was published [11]. This was the origin of the International Society for Ceramics in Medicine, with whom numerous pioneers and past presidents are associated (Besim Ben Nissam, Mario Barbosa, Williams Bonfields, Ian Clarke, Guy Daculsi, Paul Ducheyne, Larry Hench, Kunio Ishikawa, Sabri Kayali, Sukyoung Kim, Tadashi Kokubo, Racquel LeGeros, Panjian Li, Antonio Moroni, Takashi Nakamura, Hajime Ohgushi, Hironobu Oonishi, Marcello Prado, Laurent Sedel, Yli Urpo, Xingdong Zhang, Iulian Antoniac, etc.). The society organizes annual meetings for bioceramics around the world. Twenty-six symposia have been organized; the last one was Bioceramics 26 and took place in Barcelona (Maria Pau Ginebra). The focus of these symposia has evolved over the years, from classic bio-inert bioceramics to resorbable bioceramics and the introduction of scaffolds, composites, and biotechnologies applied to CaP bioceramics.

The abbreviations for various CaPs are presented in Table 1.

Interestingly, the use of calcium orthophosphate for clinical applications (e.g., bone grafting) largely preceded all of the previous studies on CaP synthesis and characterization, the biological crystals, and the analysis of their specificity.

In 1920, Albee reported the first successful use of a CaP reagent for the repair of a bone defect in human [12]. Then, largely through the separate efforts of Jarcho, de Groot, Aoki, and LeGeros [13–17], synthetic HA and  $\beta$ -TCP became commercially available as bone substitution materials for dental and medical applications. From these initial studies on bioceramics, a controversy developed concerning the resorption and clinical efficiency of these materials from the preclinical and first clinical reports. This controversy stemmed from the initial characterization of deficiency; often only the Ca:P ratio was considered, and a complete crystallographic analysis was not

**Table 1** Various calcium phosphates

Abbreviation	Explanation
CaP	Any calcium orthophosphate
MCPM	Monocalcium phosphate monohydrate $\text{Ca}(\text{H}_2\text{PO}_4)_2 \cdot \text{H}_2\text{O}$
MCPA	Monocalcium phosphate anhydrous $\text{Ca}(\text{H}_2\text{PO}_4)_2$
OCP	Octacalcium phosphate $\text{Ca}_8\text{H}_2(\text{PO}_4)_2 \cdot 5\text{H}_2\text{O}$
DCPD	Dicalcium phosphate dihydrate, $\text{CaHPO}_4 \cdot 2\text{H}_2\text{O}$ , named also brushite
DCPA	Dicalcium phosphate anhydrous, $\text{CaHPO}_4$ , named also monetite
TetCP	Tetracalcium phosphate, $\text{Ca}_4(\text{PO}_4)_2\text{O}$
$\beta$ -TCP	Beta tricalcium phosphate $\text{Ca}_3(\text{PO}_4)_2$
Mg-whitlockite	$\beta$ -TCP like with structural $\text{HPO}_4^{2-}$ and $\text{Mg}^{2+}$ ions
ACP	Amorphous calcium phosphate that gives no X-rays diffraction peak pattern
ACa,Mg,CO <sub>3</sub> P	As above but with $\text{Mg}^{2+}$ , $\text{CO}_3^{2-}$ (and $\text{HCO}_3^-$ ) ions contain
OHap, or HA	Hydroxyapatite $\text{Ca}_{10}(\text{HPO}_4)_6(\text{OH})_2$

performed. Crystallographic analyses are essential to identify the ionic content of the materials, such as carbonates, magnesium, and other substitutions, which can strongly influence their resorption, interaction with cells, and biocompatibility.

More than 50 years after Albee's report, the clinical use of a TCP preparation in surgically created periodontal defects in animals was reported by Nery et al. [18], and the use of dense HA as immediate root replacements for teeth was reported by Denissen [19]. Characterization of the deficiency was also reported for mixtures of HA and TCP. The term BCP was first used by Ellinger et al. [20] to describe the bioceramic previously known as TCP by Nery et al. in 1975 [21]; in 1986, it was shown by LeGeros to consist of a mixture of 80 % HA and 20 %  $\beta$ -TCP using X-ray diffraction [17].

The first basic studies performed on BCP that varied the HA: $\beta$ -TCP ratios were reported by LeGeros et al. [22–24]. These studies demonstrated that the bioactivity of these ceramics could be controlled by manipulating the HA: $\beta$ -TCP ratios. Subsequent studies on BCP [25–29] led to a significant increase in the manufacture and use of commercial BCP bioceramics as bone substitution materials for dental and orthopedic applications [30–38], providing various shapes for blocks and various particles sizes for granules (Fig. 1).

The development of CaP bioceramics and other related biomaterials for bone grafts necessitated control of the processes of biomaterial resorption and bone formation at the expense of the biomaterial. Synthetic bone graft materials are now available as alternatives to autogenous bone for repair, substitution, or augmentation. The first patent on HA ceramics was made by Jarcho in 1978 [39] and will be one of the first commercial products used in human "Calcite™." The commercial CaP bioceramic products that are currently available are listed on Table 2.

The main attractive feature of bioactive bioceramics such as HA,  $\beta$ -TCP, BCP, and substituted, non-stoichiometric HA is their ability to form a strong direct bond with the host bone, resulting in a strong interface compared to bio-inert or biotolerant materials that form a fibrous interface [38, 40–44]. The dynamic interface formed



**Fig. 1** Various shapes of CaP bioceramics

between the bioactive material and host bone is believed to result from a sequence of events involving interactions with the cells, i.e., formation of carbonate HA (CHA; similar to bone mineral) through dissolution/precipitation processes [23, 42, 43, 45, 46].

Commercial CaP bioceramics are sold in Europe, the USA, Brazil, Japan, Korea, Taiwan, and China as bone graft or bone substitute materials for orthopedic and dental applications under various trademarks (Table 2). Bioactive bioceramics are recommended for use as an alternative or additive to autogenous bone for various procedures: orthopedic and dental applications, scaffolds for tissue engineering, vectors for gene therapy, and as a drug delivery system. These commercial bioceramics are available as blocks, particulates (granules), and custom-designed shapes, such as wedges for tibial opening osteotomies, cones for spine and knee applications, and as an insert for vertebral cage fusions. Additionally, they are also available in a particulate form for injectable moldable materials that can be combined with polymers (natural or synthetic) [47].

---

## Fabrication and Properties

There are numerous studies describing the production of CaP bioceramics [48–52]. Apatite is considered calcium deficient when the Ca:P ratio is lower than the stoichiometric value of 1.67 for pure calcium hydroxyapatite,  $\text{Ca}_{10}(\text{PO}_4)_6(\text{OH})_2$ . Calcium-deficient apatites (CDAs) may be represented by the formula  $\text{Ca}_{10-x}\text{M}_x(\text{PO}_4)_{6-y}(\text{HPO}_4)_y(\text{OH})_2$ , where M represents other ions (e.g., sodium or magnesium) that can be substituted for the calcium (Ca) ions. Calcium deficiency in apatites depends on the synthesis conditions (precipitation or hydrolysis methods), reaction pH, and temperature [38, 42, 53, 54].

**Table 2** Commercially available products

Calcium orthophosphate	Trade name and producer
HA	Cementek (Teknimed, France)
	Osteogen (Impladent, NY, USA)
	Actifuse (ApaTech, UK)
	Apaceram (Pentax, Japan)
	ApaPore (ApaTech, UK)
	Bioroc (Depuy-Bioland, France)
	Bonefil (Pentax, Japan)
	BoneMedik (MetaBiomed, China)
	Bonetite (Pentax, Japan)
	Boneceram (Sumitomo Osaka Cement, Japan)
	BoneSource (Stryker Orthopaedics, NJ, USA)
	Calcitite (Zimmer, IN, USA)
	Cerapatite (Ceraver, France)
	HAP91 (JHS Biomaterials, Brazil)
	Neobone (Toshiba Ceramics, Japan)
Ostegraf (Ceramed, CO, USA)	
Ostim (Heraeus Kulzer, Germany)	
Synatite (SBM, France)	
Bovine bone apatite (unsintered)	BioOss (Geitslich, Switzerland)
	Laddec (Ost-Developpement, France)
	Lubbock (Ost-Developpement, France)
	Oxbone (Bioland biomateriaux, France)
	Tutoplast (IOP, CA, USA)
Bovine bone apatite (sintered)	BonAP
	Cerabone (aap Implantate, Germany)
	Endobon (Merck, Germany)
	Osteograf (Ceramed, CO, USA)
	PepGen P-15 (Dentsply Friadent, Germany)
$\beta$ -TCP	Bioresorb (Sybron Implant Solutions, Germany)
	Biosorb (SBM S.A., France)
	Calciresorb (Ceraver, France)
	Cerasorb (Curasan, Germany)
	Ceros (Thommen Medical, Switzerland)
	ChronOS (Synthes, PA, USA)
	Conduit (DePuy Spine, USA)
	Granulado (Keramit, Spain)
	JAX (Smith and Nephew Orthopaedics, USA)
	Osferion (Olympus Terumo Biomaterials, Japan)
	OsSatura TCP (Integra Orthobiologics, CA, USA)
	Syncera (Oscotec, Korea)
Vitoss (Orthovita, PA, USA)	

*(continued)*



**Table 2** (continued)

Calcium orthophosphate	Trade name and producer
BCP (HA + $\beta$ -TCP)	4Bone (MIS, Israel)
	Atlantik (MedicalBiomat, France)
	BCP Bicalphos (Medtronic, MN, USA)
	Biosel (Depuy Bioland, France)
	BonePlus (Mega'Gen, Korea)
	BoneSave (Stryker Orthopaedics, NJ, USA)
	BonitMatrix (Dot, Germany)
	Calciresorb (Ceraver, France)
	CellCeram (Scaffdex, Finland)
	Ceraform (Teknimed, France)
	Ceratite (NGK Spark Plug, Japan)
	Cross-Bone (Biotech International, France)
	Eliz (Kyeron, The Netherlands)
	Eurocer (FH Orthopedics, France)
	Graftys BCP (Graftys, France)
	Hatric (Arthrex, Naples, FL, USA)
	Indost (Polystom, Russia)
	Kainos (Signus, Germany)
	MBCP, MBCP+ (Biomatlante, France)
	OptiMX (Exactech, USA)
	OsSatura BCP (Integra Orthobiologics, CA, USA)
	OssGen (OssGen Inc, Korea)
	Osteosynt (Einco, Brazil)
	SBS (Expanscience, France)
Sinbone HT (Purzer, Taiwan)	
TCH (Kasios, France)	
Triosite (Zimmer, IN, USA)	
Tribone (Stryker, Europe)	
XPand (XPand Bioetch, The Netherlands)	
BCP (HA + $\alpha$ -TCP)	Skelite (Millennium Biologix, ON, Canada)
FA + BCP (HA + $\beta$ -TCP)	FtAP (Polystom, Russia)
Carbonateapatite	Healos (Orquest, CA, USA)
Coralline HA	Interpore (Interpore, CA, USA)
	ProOsteon (Interpore, CA, USA)

Currently, the precipitation of HA,  $\beta$ -TCP, and formation of HA/TCP mixtures (BCP) are performed using CDA. CDA is obtained by precipitation under various pH and temperature conditions: the lower the pH, the higher the temperature required for the precipitation of apatite [38, 42]. For example, CDA can be produced by precipitation at 80–100 °C at low pH (pH 4–6). At lower temperatures and lower pH, non-apatitic CaPs, e.g., dicalcium phosphate dihydrate (DCPD;  $\text{CaHPO}_4 \cdot 2\text{H}_2\text{O}$ ) or octacalcium phosphate (OCP;  $\text{Ca}_8\text{H}_2(\text{PO}_4)_6 \cdot 5\text{H}_2\text{O}$ ), are obtained [42].

Another method of CDA preparation is hydrolysis of non-apatitic CaPs, including amorphous CaP,  $\text{Ca}_x(\text{PO}_4)_y$ ; DCPD; dicalcium phosphate anhydrous,  $\text{CaHPO}_4$ ; OCP; and  $\beta$ -TCP,  $\text{Ca}_3(\text{PO}_4)_2$  [38, 42, 54–56]. During hydrolysis of DCPD in NaOH solutions, the calcium deficiency of the unsintered apatite and the subsequent HA: $\beta$ -TCP ratio of the BCP produced after sintering can be controlled by two variables: the concentration of the NaOH solution and the ratio of the weight of the DCPD to the volume of the NaOH solution [54].

After creation of the raw powder, all of the processes used to manufacture bioceramics require high temperatures, in excess of 1000°. Under this condition, there is thermal decomposition of CDA, HA, and other CaP compounds that can affect their chemical nature, biological properties (dissolution), mechanical properties (grain boundaries and lattice defects), and biocompatibility (e.g., CaO content) [57].

## Introduction of Macroporosity and Microporosity

In 1971, Klawitter and Hulbert [58] demonstrated the importance of porosity for bone graft substitutions. Porous ceramics are potentially attractive because of their large interconnecting pore structure, which facilitates bone ingrowth, cell colonization, and new vascularization. There are numerous publications that describe the processes for creation of porous bioceramics and how to determine the optimal pore size. Indeed, from these studies, we now know that the ideal pore size for tissue growth is 300–600  $\mu\text{m}$  [59]. Other studies have demonstrated that with the same porous structure,  $\beta$ -TCP generally degrades more rapidly than ceramics made of HA [60]. To understand the macroporosity of the coral skeleton that was used, the aragonite or calcite were thermally decomposed into CaPs in the presence of an alkaline phosphate solution. Other methods to elucidate the macroporosity include release with hydrogen peroxide, the release of oxygen during heating involving a macropore, and, more classically, the use of a porogen (naphthalene, polyethylene, camphor, poly(methyl methacrylate), polyurethane, sugar, starch, etc.). After mixing the porogen with the powder, or a template with a slurry, during heating, the organic phase is volatilized or oxidized, leaving calibrated spaces behind.

During the first 10 years of bioceramic development, studies focused on the chemical nature (HA or TCP) and macroporosity of the materials. Indeed, the biological properties of the bioceramic – degradation-dissolution, absorption, and biological interactions (with the fluid, cells, and tissues) – depend on the micro- (microscale) and macrostructure (macropores, particle size, and blocks) of the material.

There are two physical properties of bioceramics that are considered important for optimal biological performance, which includes bioceramic-cell interactions, bioceramic resorption, the bioceramic-tissue interface, and new bone formation. These fundamental properties are interconnecting macroporosity and appropriate microporosity [38, 61, 62]. Macroporosity is introduced into the CaP ceramic through incorporation of volatile materials (e.g., naphthalene, hydrogen peroxide,

**Fig. 2** Macroporosity in CaP bioceramics (biphasic calcium phosphate MBCP)

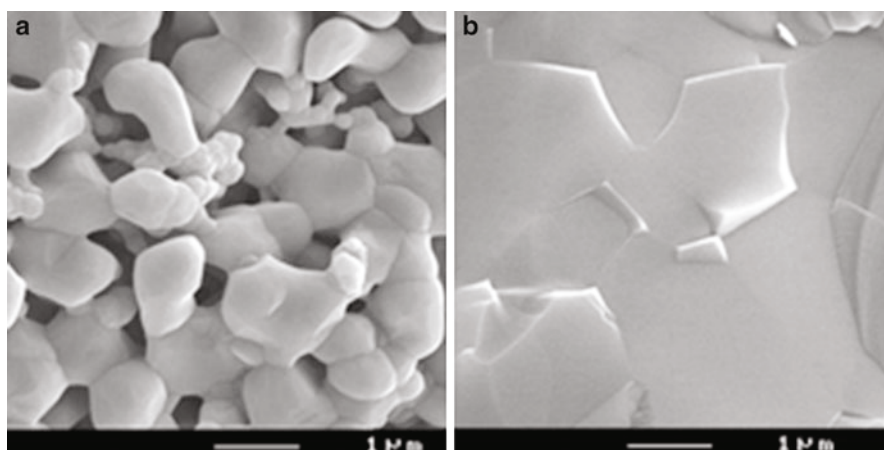
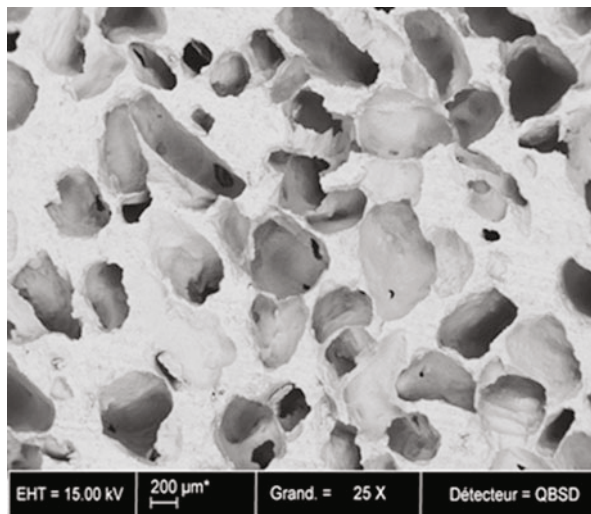


**Fig. 3** BCP sintered at 1050 °C (a) and 1200 °C (b)

or other porogens [polymers, sugar, starch, etc.], heating at temperatures that induce sublimation or calcination (80–500 °C), and subsequent sintering at higher temperatures [14, 61] (Fig. 2). Microporosity is a consequence of the temperature and duration of sintering: the higher the temperature, the lower the microporosity and the lower the specific surface area (Fig. 3a, b). From our own experience, it appears that micropores enhance the diffusion and permeability of the bioceramic, increasing the interconnections of the macropores.

Only a few publications have investigated the importance of microporosity; however, some of the previous studies appear to show that the osteoinductive

properties of bioactive ceramics are due to their micropore content [63]. Other reports demonstrated that the higher osteogenic properties in bony sites with equivalent macroporosity have a higher content of micropores [64, 65].

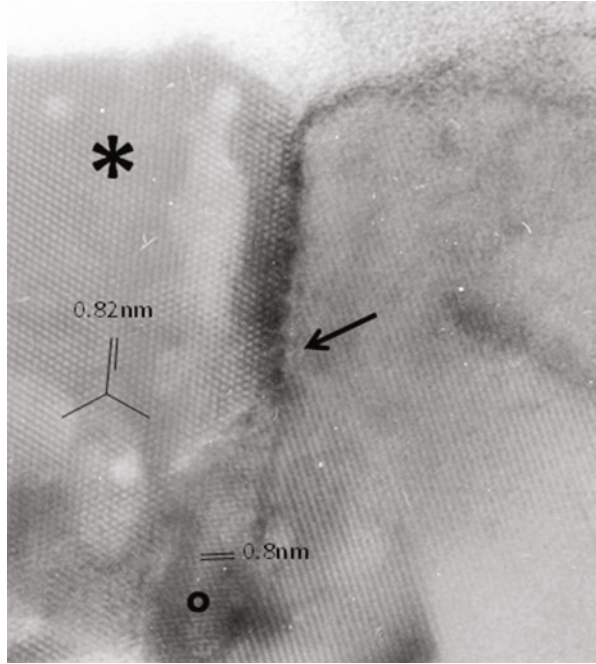
Analysis of the currently available commercial CaP bioceramics revealed that most materials have a porosity of 70 %, although large differences can be observed among the registered bioceramics. The total porosity (macroporosity plus microporosity) of these products is reported to be approximately 70 % of the bioceramic volume. However, the ratios of macroporosity and microporosity are often different, with the percent microporosity varying from 3 % to 25 %. Low percent microporosity and low surface area can result in lower bioactivity and lower dissolution properties.

## Physicochemical Properties

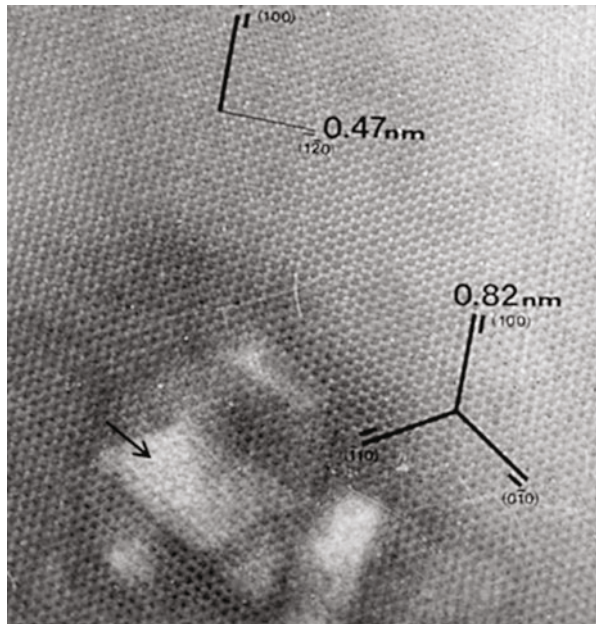
Because  $\beta$ -TCP has a higher solubility than HA [66], the extent of dissolution of bioceramics with comparable macroporosity and particle size will depend on the HA: $\beta$ -TCP content: increased HA leads to less dissolution. Dissolution is also affected by the method of synthesis and sintering of the material. The specific surface area, microporosity, mechanical properties, and method of particle release can influence the degradation-dissolution and absorption properties of the bioceramic by the surrounding cells and tissue. This phenomenon may be caused by processing variables (sintering time and temperature) that could affect the total macroporosity and microporosity: the greater the macroporosity and microporosity, the greater the extent of dissolution. *In vivo*, dissolution of bioceramics is accompanied by a decrease in crystal size and increase in macroporosity and microporosity.

While the influences of crystal size, microporosity, and pore content on bioceramic properties have been studied, few papers have focused on the atomic and nanoscale structures of these materials. Crystal defects, grain boundaries, and lattice defects have largely only been studied in minerals, metals, and ceramics [6]. Biomineralization has been investigated using high-resolution transmission electron microscopy (TEM) [67, 68]. In 1991 [69], one report revealed the different kinds of lattice defects in CaP ceramics at the unit cell level (Fig. 4). The authors found that the ultrastructural properties depended on the sintering temperature. Numerous lattice defects, including atomic vacancies, dislocations, and two types of grain boundaries, were described. In another study, a new type of three-dimensional lattice defect was observed at the nanoscale level in an HA bioceramic sintered at low temperature (900 °C). This defect involved intrinsic nanopores within the material (Fig. 5). The defects in the nanostructure of bioceramic crystals have an important role in the dissolution process and demonstrate that all bioceramics are soluble (both HA and TCP), in contrast to claims about the non-resorbability of HA often reported in the literature. The extent of bioceramic dissolution depends on the number of defects [70] and cell mediation (Fig. 6). Based on these data, the notion that HA bioceramics are “non-resorbable” should be revisited and revised.

**Fig. 4** High-resolution transmission electron microscopy of HA(\*) and TCP phase (°), with grain boundaries (arrow) associating the two phases in BCP at the molecular level



**Fig. 5** Unit cell and 3-D lattice defects involving nanoporosity in low-temperature sintered HA bioceramic



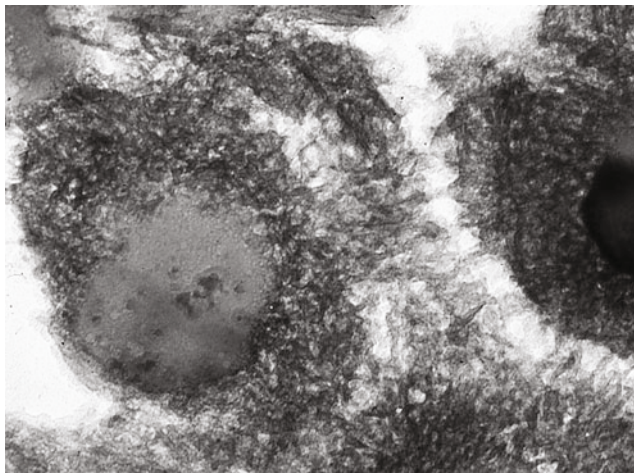


**Fig. 6** Macrophages biological dissolution of HA bioceramic crystal (Calcitite™), phagolysosome containing HA crystals with dissolution areas (*arrow*)

## Mechanical Properties

The pore size and percent macroporosity of BCP ceramics are believed to affect their mechanical properties [70]. The preparation method was also found to have a significant influence on the compressive strength of the material. The compressive strength reported for bioactive bioceramics varies from 0.5 to 12 MPa. However, the mechanical properties by themselves are not the best criteria for predicting the efficacy of bone ingrowth. For example, BCP with high mechanical properties and low microporosity (resulting from high sintering temperatures) can exhibit reduced bioresorption and bioactivity. However, the initial mechanical properties can increase  $2\text{--}3 \times$  ( $2\text{--}6$  MPa) a few weeks after implantation due to the physicochemical events of dissolution and biological precipitation into the micropores [29, 71].

## Bioactivity and Osteogenic Properties

Bioactivity is the ability of a material to form CHA on its surface *in vitro* [40, 72] or *in vivo* [5, 73–75]. Osteoinductivity is the ability of a material to induce bone formation *de novo* or ectopically (in non-bone-forming sites). CaP bioceramics do not usually display osteoinductive properties. However, several reports have shown osteoinductive properties in some CaP bioceramics, such as coralline HA (derived from coral), BCP [76–78], and TCP [79, 80]. Reddi [81] hypothesized that these apparent osteoinductive properties are the ability of particular ceramics to concentrate bone growth factors circulating in the biological fluids; these growth factors can then induce bone formation. Ripamonti [76] and Kuboki [77] independently postulated that the geometry of the material is a critical parameter in bone formation. Others have

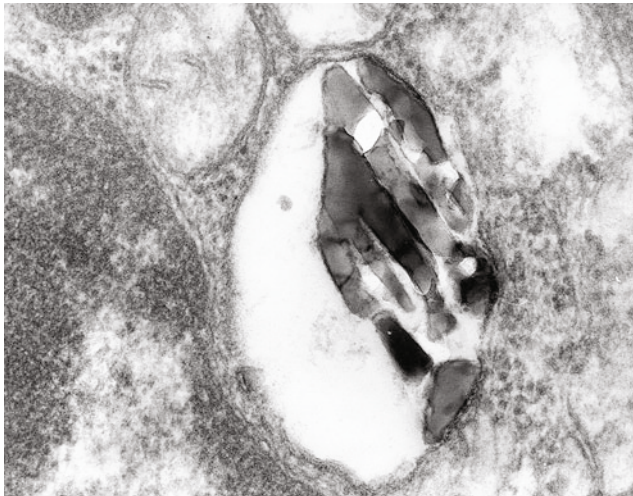


**Fig. 7** Biological apatite precipitation (*arrow*) on residual calcium phosphate crystals after implantation. (high-resolution transmission microscopy)

speculated that low oxygen tension in the central region of the implants might provoke dedifferentiation of pericytes from blood microvessels into osteoblasts [82]. It has been also suggested that the nanostructured rough surface or the surface charge of implants might cause asymmetrical division of stem cells into osteoblasts [79].

The surface microstructure appears to be a common property of biomaterials that can induce ectopic bone formation. Recent studies have indicated the critical role of micropores during ceramic-induced osteogenesis. For example, it was reported that bone formation occurred in the muscle of dogs inside porous CaP ceramics that displayed surface microporosity; however, osteogenesis was not observed inside macroporous ceramics with a dense surface [80]. It was also reported that metal implants coated with a microporous layer of OCP could induce ectopic bone formation in the muscle of goats, while a smooth layer of carbonated apatite on porous metal implants was not able to induce osteogenesis [83]. In all of the previous experiments, ectopic bone formation occurred inside macroporous ceramic blocks. Therefore, ceramic properties such as composition, geometry, porosity, size, and microstructure are critical parameters for bone formation.

The main explanations for the osteoinductive properties of CaP bioceramics appear to be the formation of microcrystals with Ca:P ratios similar to those of bone apatite crystals observed after implantation, interaction with the biological fluids and cells, and the combined effects of integration of non-collagenic proteins involved in cell adhesion, stem cell differentiation in an osteogenic line, and biomineralization. Using high-resolution TEM, it was demonstrated that the formation of these bone apatite-like microcrystals (Fig. 7) that appeared after implantation of CaP (HA, TCP, and BCP) were nonspecific, i.e., not related to the implantation site (osseous or non-osseous sites), subject of implantation, or type of CaP bioceramic [24, 37].

## The Challenge of Bioactive Bioceramics in Bone Regenerative Medicine

Tissue engineering for bone regeneration involves the seeding of osteogenic cells (e.g., mesenchymal stem cells, MSCs) onto the appropriate scaffolds and subsequent implantation of the seeded scaffolds into the bone defect. Bone marrow-derived MSCs are multipotent cells that are capable of differentiating into, at a minimum, osteoblasts, chondrocytes, adipocytes, tenocytes, and myoblasts [84–89]. MSCs can be isolated from a small volume of bone marrow and cultured because of their proliferative capacity; they maintain their functionality after expansion in culture and cryopreservation [87]. Therefore, MSCs are a readily available and abundant source of cells for tissue engineering applications. Bioactive CaP ceramics, in combination with cells and tissue engineering derivatives, are the new challenge in bone regeneration.

---

### CaP Bioceramic Composites

There are numerous clinical situations where materials are needed to restore and regenerate bone, and the best material for this process is an autologous bone graft. However, there are numerous limitations with autologous bone grafts that have described in the literature [90–92]. The ideal synthetic biomaterial should be injectable and moldable, set in the defect, and favor bone apposition and growth while being degraded by body fluids and cells. Ultimately, the material should be replaced by mature bone tissue within a healing period of weeks [7]. Composite biomaterials for bone repair have been developed in the last 30 years. A composite material is composed of at least two or more phases: a continuous phase (the matrix consisting of polymers) and a dispersed phase (consisting of granules, fibers, etc.). There should be an interaction between the two phases, with a specific interface that plays an important role in the mechanical performance, environmental stability, handling, rheological properties, and biological performance of the material [93].

In an effort to make generic CaP bioceramics more biomimetic to bone, as well as support new minimally invasive surgical techniques, multiphasic biomaterials were developed that associated inorganic solid state chemistry (CaP bioceramics) with inorganic polymers (hydrogel and polymers of synthetic or natural origin) to replace and regenerate bone tissue in osseous or dental defects, or for resorbable osteosynthesis; some of these association of bioceramic and polymers are presented in Table 3. This multidisciplinary research involves solid state chemistry with CaP bioceramics, organic chemistry with synthetic polymers, and biochemistry with polymers of natural origin. Several composites have been created using collagen, fibrin, silk, or various synthetic polymers (polysaccharides, polycaprolactone, poloxamer, poly(ethylene glycol), etc.) [94–97].

In a composite biomaterial, the putty associates the various bioactive properties of the bioceramic and provides numerous advantages for the handling, surgical indication, and kinetics of bone regeneration. For resorbable osteosynthesis, essentially the polyesters (PLA and GLA, and derivatives, copolymers) were used in



**Table 3** Example of some composites on the European or US market

HA/collagen	Bioimplant (Connectbiopharm, Russia)
	Bonject (Koken, Japan)
	CollapAn (Intermedapatite, Russia)
	HAPCOL (Polystom, Russia)
	LitAr (LitbicAr, Russia)
HA/sodium alginate	Bialgin (Biomed, Russia)
HA/Poly-L-lactic acid	SuperFIXSORB30 (Takiron, Japan)
TCP/PLLA, PLA	Bilock (Biocomposite, USA)
	Bioscrew (Conmed, USA)
BCP/PLDLLA	Osteotwin (Biomatlante, France)
HA/polyethylene	HAPEX (Gyrus, TN, USA)
HA/CaSO <sub>4</sub>	Hapset (LifeCore, MIN, USA)
Algae-derived HA	Algipore (Dentsply Friadent, Germany)
BCP/collagen	Collagraft (Zimmer, IN, USA)
	Matribone (Biom'Up, France)
BCP/fibrin	TricOS (Baxter BioScience, France)
BCP/silicon	FlexHA (Xomed, FL, USA)
HA Si/poloxamer	Actifuse Apattech-Baxter
BCP/polysaccharide	Inn'Os (Biomatlante, France)

combination with a mineral content. Numerous resorbable osteosynthesis, plaque, nails, screws, spine cages, etc. were used other the world through the pioneering efforts of Michel Vert particularly [98].

## Conclusion

CaP bioceramics are a recent development in bone surgery that act as a replacement for auto- and allografts, which have been engineered less than 100 years from the first medical applications and less than 30 years from the initial manufacturing of medical devices and experiments with bone regeneration. In 2014 during an ESB meeting in Liverpool, Larry Hench reported four points in the history of healthcare revolutions:

1. Prevention of loss of life (1850–1950; clean water, antiseptics, antibiotics, immunization, and sterilization)
2. Replacement of tissues (1950–present; antiseptics, antibiotics, sterilization, and biomaterials)
3. Regeneration of tissues (1980–present; tissue engineering and in situ gene activation)
4. Prevention of tissue loss (2000–present)

Bioactive bioceramics have largely contributed to this revolution in medicine. Numerous innovations in this field are now appearing; it is the beginning of bioceramics and not the “has-been medical device.”

## References

1. Daculsi G, Jegoux F, Layrolle P (2010) The micro macroporous biphasic calcium phosphate concept for bone reconstruction and tissue engineering. In: *Advanced biomaterials*. Wiley, New York, pp 101–141
2. de Groot K (ed) (1983) *Ceramics of calcium phosphate: preparation and properties*. In: *Bioceramics of calcium phosphate*. CRC Press, Boca Raton, pp 100–114
3. Galletti PM, Boretos JW (1983) Report on the consensus development conference on clinical applications of biomaterials, November 1983. *J Biomed Mater Res* 17(3):539–555
4. Williams DF (1987) *Definitions in biomaterials: proceedings of a consensus conference of the European Society for Biomaterials*, Chester, England, March 3–5, 1986, vol 4. Elsevier, Amsterdam
5. Dorozhkin SV (2013) A detailed history of calcium orthophosphates from 1770s till 1950. *Mater Sci Eng C* 33(6):3085–3110
6. Carter CB, Norton MG (2007) *Ceramic materials. Science and engineering*. Springer, New York, p 716
7. Montel GR (1958) *Contribution a l'étude des mecanismes de synthese de la fluorapatite*. Masson et Cie, Paris
8. LeGeros R (1967) *Crystallographic studies on the carbonate substitution in the apatite structure*. New York University, New York
9. CNRS (ed) (1974) *Physico-Chimie et Cristallographie des apatites d'Intérêt Biologique*, vol 230, *Colloques Internationaux CNRS*. Editions du Centre National de la Recherche Scientifique, Paris
10. Elliott J (1964) *The crystallographic structure of dental enamel and related apatites*. University of London, London
11. Oonishi H, Aoki H, Sawai K (eds) (1989) *Bioceramics*, vol 1. Ishiyaku-Euro America, Tokyo/St. Louis
12. Albee F (1920) Studies in bone growth: triple calcium phosphate as a stimulus to osteogenesis. *Ann Surg* 71:32–36
13. Jarcho M (1981) Calcium phosphate ceramics as hard tissue prosthetics. *Clin Orthop* 157:259–278
14. DeGroot K (ed) (1983) *Ceramics of calcium phosphate : preparation and properties*. In: *Bioceramics of calcium phosphates*. CRC Press, Boca Raton, pp 100–114
15. Metsger DS, Driskell T, Paulsrud J (1982) Tricalcium phosphate ceramic – a resorbable bone implant: review and current status. *J Am Dent Assoc* 105(6):1035–1038
16. Akao M, Aoki H, Kato K (1981) Mechanical properties of sintered hydroxyapatite for prosthetic applications. *J Mater Sci* 16(3):809–812
17. LeGeros RZ (1988) Calcium phosphate materials in restorative dentistry. *Adv Dent Res* 2:164–183
18. Nery EB, Lynch KL, Hirthe WM, Mueller KH (1975) Bioceramic implants in surgically produced infrabony defects. *J Periodontol* 63:729–735
19. Denissen HW (1979) PhD thesis, Vrije Universiteit, Amsterdam
20. Ellinger RF, Nery EB, Lynch KL (1986) Histological assessment of periodontal osseous defects following implantation of hydroxyapatite and biphasic calcium phosphate ceramics: a case report. *Int J Periodontics Restorative Dent* 3:223
21. Nery EB, Lynch KL, Hirthe WM, Mueller KH (1975) Bioceramic implants in surgically produced infrabony defects. *J Periodontol* 63:729–735
22. LeGeros RZ, Nery E, Daculsi G, Lynch K, Kerebel B (1988). In vivo transformation of biphasic calcium phosphate of varying b-TCP/HA ratios: ultrastructural characterization. *Third World Biomaterials Congress* (abstract no. 35)
23. LeGeros RZ, Daculsi G (1990) In vivo transformation of biphasic calcium phosphate ceramics: ultrastructural and physicochemical characterization. In: Yamamuro N, Hench L, Wilson J (eds) *Handbook of bioactive ceramics*, vol 2. CRC Press, Boca Raton, p 1728

24. Daculsi G, LeGeros RZ, Nery E, Lynch K, Kerebel B (1989) Transformation of biphasic calcium phosphate ceramics: ultrastructural and physico-chemical characterization. *J Biomed Mater Res* 23:883–894
25. Nery EB, LeGeros RZ, Lynch KL, Kalbfleisch J (1992) Tissue response to biphasic calcium phosphate ceramic with different ratios of HA/ $\beta$ -TCP in periodontal osseous defects. *J Periodontol* 63:729–735
26. Daculsi G, Passuti N (1990) Effect of macroporosity for osseous substitution of calcium phosphate ceramic. *Biomaterials* 11:86–87
27. Daculsi G, Passuti N, Martin S, Deudon C, LeGeros RZ (1990) Macroporous calcium phosphate ceramic for long bone surgery in human and dogs. *J Biomed Mater Res* 24(379):39
28. Daculsi G, Bagot D'arc M, Corlieu P, Gersdorff M (1992) Macroporous biphasic calcium phosphate efficiency in mastoid cavity obliteration. *Ann Otol Rhinol Laryngol* 101:669–674
29. Trecant M, Delecrin J, Royer J, Goyenvallée E, Daculsi G (1994) Mechanical changes in macroporous calcium phosphate ceramics after implantation in bone. *Clin Mater* 15:233–240
30. Gouin F, Delecrin J, Passuti N, Touchais S, Poirier P, Bainvel JV (1995) Comblement osseux par céramique phosphocalcique biphasee macroporeuse : a propos de 23 cas. *Rev Chir Orthop* 81:59–65
31. Ransford AO, Morley T, Edgar MA, Webb P, Passuti N, Chopin D, Morin C, Michel F, Garin C, Pries D (1998) Synthetic porous ceramic compared with autograft in scoliosis surgery. A prospective, randomized study of 341 patients. *J Bone Joint Surg Br* 80(1):13–18
32. Cavagna R, Daculsi G, Bouler J-M (1999) Macroporous biphasic calcium phosphate: a prospective study of 106 cases in lumbar spine fusion. *J Long Term Eff Med Implants* 9:403–412
33. Soares EJC, Franca VP, Wykrota L, Stumpf S (1998) Clinical evaluation of a new bio ceramic ophthalmic implant. In: LeGeros RZ, LeGeros JP (eds) *Bioceramics 11*. World Scientific, Singapore, pp 633–636
34. Wykrota LL, Garrido CA, Wykrota FHI (1998) Clinical evaluation of biphasic calcium phosphate ceramic use in orthopaedic lesions. In: LeGeros RZ, LeGeros JP (eds) *Bioceramics 11*. World Scientific, Singapore, pp 641–644
35. Malard O, Guicheux J, Bouler JM, Gauthier O, Beauvillain de Montreuil C, Aguado E, Pilet P, LeGeros R, Daculsi G (2005) Calcium phosphate scaffold and bone marrow for bone reconstruction in irradiated area : a dog study. *Bone* 36:323–330
36. Daculsi G (1998) Biphasic calcium phosphate concept applied to artificial bone, implant coating and injectable bone substitute. *Biomaterials* 19:1473–1478
37. Daculsi G, Laboux O, Malard O, Weiss P (2003) Current state of the art of biphasic calcium phosphate bioceramics. *J Mater Sci Mater Med* 14(3):195–200
38. LeGeros RZ, Lin S, Rohanizadeh R, Mijares D, LeGeros JP (2003) Biphasic calcium phosphates: preparation and properties. *J Mater Sci Mater Med* 14:201–210
39. Jarcho M (1978) Hydroxylapatite ceramic. US Patent 1978, N(4,097,935)
40. Hench LL, Splinter RJ, Allen WC, Greelee TK (1978) Bonding mechanisms at the interface of ceramic prosthetic materials. *J Biomed Mater Res* 2:117–141
41. Hench LL (1994) *Bioceramics: from concept to clinic*. *J Am Ceram Soc* 74:1487–1510
42. LeGeros RZ (1991) Calcium phosphates in oral biology and medicine. *Monographs in oral sciences*, vol 15. Myers H (ed), S. Karger, Basel
43. LeGeros RZ, Daculsi G, Orly I, LeGeros JP (1991) Substrate surface dissolution and interfacial biological mineralization. In: Davies JED (ed) *The bone biomaterial interface*. University of Toronto Press, Toronto, pp 76–88
44. Osborne J, Newsely H (1980) The material science of calcium phosphate ceramic. *Biomaterials* 1:108–111
45. Heughebaert M, LeGeros RZ, Gineste M, Guilhem A (1988) Hydroxyapatite (HA) ceramics implanted in non-bone forming sites: physico-chemical characterization. *J Biomed Mater Res* 22:257–268

46. Daculsi G, LeGeros RZ, Heugheart M, Barbieux I (1990) Formation of carbonate apatite crystals after implantation of calcium phosphate ceramics. *Calcif Tissue Int* 46:20–27
47. Daculsi G, LeGeros R (2008) Tricalciumphosphate/hydroxyapatite biphasic calcium phosphate (BCP) bioceramics. In: Kokubo T (ed) *Bioceramics and their clinical applications*. Woodhead Publishing, Cambridge, UK, pp 395–424
48. Best S (1990) Characterization, sintering and mechanical behaviour of hydroxyapatite ceramics. PhD thesis, University of London
49. Raemdonck W, Ducheyne P, De MP (1984) Calcium phosphate ceramics. In: Ducheyne P, Hastings GW (eds) *Metal and ceramic biomaterials, vol II, Strength and surface*. CRC Press, Boca Raton, pp 143–166
50. Ducheyne P, Lemons JE (eds) (1988) *Bioceramics: material characteristics versus in vivo behaviour, vol 523*. Ann NY Acad Sc, New York
51. Yamamuro T, Hench LL, Wilson J (eds) (1990) *CRC handbook of bioactive ceramics, vol II, Calcium phosphate and hydroxylapatite ceramics*. CRC press, Boca Raton
52. Aoki H (1991) Science and medical applications of hydroxyapatite, vol 50. Japan Association of Apatite Sciences (JAAS), Takayama Press Centre Co, Tokyo, pp 27–30
53. Daculsi G (2006) Biphasic calcium phosphate granules concept for injectable and mouldable bone substitute. *Adv Sci Technol* 49:9–13
54. Boulter JM, LeGeros RZ, Daculsi G (2000) Biphasic calcium phosphates: influence of three synthesis parameters on the HA/ $\beta$ -TCP ratio. *J Biomed Mater Res* 51:680–684
55. Daculsi G, Khairoun I, LeGeros RZ, Moreau F, Pilet P, Bourges X, Weiss P, Gauthier O (2006) Bone ingrowth at the expense of a novel macroporous calcium phosphate cement. *Key Eng Mater* 330–332:811–814
56. LeGeros RZ, Zheng R, Kijkowska R, Fan D, LeGeros JP (1994) Variations in composition and crystallinity of ‘hydroxyapatite (HA)’ preparations. In: Horowitz E, Parr JE (eds) *Characterization and performance of calcium phosphate coatings for implants, vol 1198*, American Society for Testing Materials STP. ASTM, Philadelphia, pp 43–53
57. Welch JH, Gutt W (1961) High temperature studies of the system calcium oxide-phosphorus pentoxide. *J Chem Soc*:4442–4444
58. Klawitter JJ, Hulbert SF (1971) Application of porous ceramics for the attachment of load bearing internal orthopaedic applications. *J Biomed Mater Res* 2:161–229
59. Ito K, Ooi Y (1990) Osteogenic activity of synthetic hydroxylapatite with controlled texture- on the relationship of osteogenic quantity with sintering temperature and pore size. In: Yamamuro T, Hench LL, Wilson J (eds) *CRC handbook of bioactive ceramics, vol II, Calcium phosphate and hydroxylapatite ceramics*. CRC Press, Boca Raton, pp 39–44
60. Klein CPAT, Patka P, Hollander W (1990) A comparison between hydroxylapatite and  $\beta$ -whitlockite macroporous ceramics implanted in dog femurs. In: Yamamuro T, Hench LL, Wilson J (eds) *CRC handbook of bioactive ceramics, vol II, Calcium phosphate and hydroxylapatite ceramics*. CRC Press, Boca Raton, pp 53–60
61. LeGeros RZ (2002) Properties of osteoconductive biomaterials: calcium phosphates. *Clin Orthop Relat Res* 395:81
62. Bohne W, Pouezet JA, Peru L, Daculsi G (1993) Heating of calcium phosphate crystals: morphological consequences and biological implications. *Cells Mater* 3:377–382
63. Chan O, Coathup MJ, Nesbitt A, Ho CY, Hing KA, Buckland T, Campion C, Blunn GW (2012) The effects of microporosity on osteoinduction of calcium phosphate bone graft substitute. *Acta Biomater* 8(7):2788–2794
64. Malmström J, Adolfsson E, Arvidsson A, Thomsen P (2007) Bone response inside free-form fabricated macroporous hydroxyapatite scaffolds with and without an open microporosity. *Clin Implant Dent Relat Res* 9(2):79–88
65. Hing KA, Annaz B, Saeed S, Revell PA, Buckland T (2005) Microporosity enhances bioactivity of synthetic bone graft substitutes. *J Mater Sci Mater Med* 16(5):46–75

66. LeGeros RZ (1993) Biodegradation and bioresorption of calcium phosphate ceramics. *Clin Mater* 14:65–88
67. Kerebel B, Daculsi G, Verbaere A (1976) Ultrastructural and crystallographic study of biological apatites. *J Ultrastruct Res* 57:266–275
68. Daculsi G, Pouezat JA, Peru L, Maugars Y, Legeros RZ (1991). In: Bonucci E (ed) Ectopic calcifications in mineralization in biological systems. CRC Press Boca Raton. 32 p
69. Daculsi G, LeGeros RZ, LeGeros J, Mitre D (1991) Lattice defects in calcium phosphate ceramics: high resolution TEM ultrastructural study. *J Biomed Mater Res App Biomat* 2:147–152
70. Daculsi G, LeGeros R, Mitre D (1989) Crystal dissolution of biological and ceramic apatites. *Calcif Tissue Int* 45:95–103
71. Bouler JM, Trécant M, Delécrin J, Royer J, Passuti N, Daculsi G (1996) Macroporous biphasic calcium phosphate ceramics : influence of five synthesis parameters on compressive strength. *J Biomed Mater Res* 32:603–609
72. LeGeros RZ (1993) Biodegradation and bioresorption of calcium phosphate ceramics. *Clin Mater* 14:65–88
73. Basle MF, Chappard D, Grizon F, Filmon R, Delecrin J, Daculsi G, Rebel A (1993) Osteoclastic resorption of CaP biomaterials implanted in rabbit bone. *Calcif Tissue Int* 53:348–356
74. Gauthier O, Bouler J-M, Aguado E, Pilet P, Daculsi G (1998) Macroporous biphasic calcium phosphate ceramics: influence of macropore diameter and macroporosity percentage on bone ingrowth. *Biomaterials* 19(1–3):133–139
75. Kokubo T, Takadama H (2006) How useful is SBF in predicting in vivo bone bioactivity? *Biomaterials* 27(15):2907–2915
76. Ripamonti U (1991) The morphogenesis of bone in replicas of porous hydroxyapatite obtained by conversion of calcium carbonate exoskeletons of coral. *J Bone Joint Surg Am* 73:692–703
77. Kuboki Y, Takita H, Kobayashi D (1998) BMP-induced osteogenesis on the surface of hydroxyapatite with geometrically feasible and nonfeasible structures: topology of osteogenesis. *J Biomed Mater Res* 39:190–199
78. Le Nihouannen D, Daculsi G, Saffarzadeh A, Gauthier O, Delplace S, Pilet P, Layrolle P (2005) Ectopic bone formation by microporous calcium phosphate ceramic particles in sheep muscles. *Bone* 36(6):1086–1093
79. Habibovic P, Yuan H, van der Valk CM, Meijer G, van Blitterswijk CA, De Groot K (2005) Microenvironment as essential element for osteoinduction by biomaterials. *Biomaterials* 26:3565–3575
80. Yuan H, Kurashina K, Joost de Bruijn D, Li Y, de Groot K, Zhang X (1999) A preliminary study of osteoinduction of two kinds of calcium phosphate bioceramics. *Biomaterials* 20:1799–1806
81. Reddi AH (2000) Morphogenesis and tissue engineering of bone and cartilage: inductive signals, stem cells and biomimetic biomaterials. *Tissue Eng* 6:351–359
82. Diaz-Flores L, Gutierrez R, Lopez-Alonso A, Gonzalez R, Varela H (1992) Pericytes as a supplementary source of osteoblasts in periosteal osteogenesis. *Clin Orthop Relat Res* 000 (275):280–286
83. Barrere F, van der Valk CM, Dalmeijer RA, Meijer G, van Blitterswijk CA, de Groot K, Layrolle P (2003) Osteogenicity of octacalcium phosphate coatings applied on porous titanium. *J Biomed Mater Res* 66A:779
84. Pittenger MF, Mackay AM, Beck SC, Jaiswal RK, Douglas R, Mosca JD, Moorman MA, Simonetti DW, Craig S, Marshak DR (1999) Multilineage potential of adult human mesenchymal stem cells. *Science* 284:143–147
85. Caplan AI, Fink DJ, Goto T, Linton AE, Young RG, Wakitani S, Goldberg V, Haynesworth SE (1993) In: Wetzel JD (ed) Mesenchymal stem cells for tissue repair. The anterior cruciate ligament: current and future concepts. Raven, New York, pp 405–417
86. Jaiswal N, Haynesworth SE, Caplan AI, Bruder SP (1997) Osteogenic differentiation of purified culture-expanded human mesenchymal stem cells in vitro. *J Cell Biochem* 64:295–312

87. Bruder SP, Jaiswal N, Haynesworth SE (1997) Growth kinetics, self-renewal, and the osteogenic potential of purified human mesenchymal stem cells during extensive subcultivation and following cryopreservation. *J Cell Biochem* 64:278–294
88. Kadiyala S, Jaiswal N, Bruder SP (1997) Culture-expanded, bone marrow-derived mesenchymal stem cells can regenerate a critical-sized segmental bone defect. *Tissue Eng* 3:173–185
89. Livingston AT, Peter S, Archambault M, Van Den Bos C, Gordon S, Kraus K, Smith A, Kadiyala S (2003) Allogeneic mesenchymal stem cells regenerate bone in a critical-sized canine segmental defect. *J Bone Joint Surg Am* 85-A:1927–1935
90. Heary RF, Schlenk RP, Sacchieri TA, Barone D, Brotea C (2002) Persistent iliac crest donor site pain: independent outcome assessment. *Neurosurgery* 50:510–516
91. Silber JS, Anderson DG, DaVner SD, Brislin BT, Leland JM, Hilibrand AS, Vaccaro AR, Albert TJ (2003) Donor site morbidity after anterior iliac crest bone harvest for single-level anterior cervical discectomy and fusion. *Spine* 28:134–139
92. Tomford WW (2000) Bone allografts: past, present and future. *Cell Tissue Bank* 1(2):105–109
93. De Santis R, Guarino V, Ambrosio L (2009) Composite biomaterials for bone repair. In: Planell JA, Best SM, Lacroix D (eds) *Bone repair biomaterials*, Woodhead publishing in biomaterials. CRC Press, Boca Raton, pp 252–270
94. Turczyn R, Weiss P, Lapkowski M, Daculsi G (2000) In situ self hardening bioactive composite for bone and dental surgery. *J Biomater Sci Polym Ed* 11(2):217–223
95. Włodarski KH, Włodarski PK, Galus R (2008) Bioactive composites for bone regeneration. Review. *Ortop Traumatol Rehabil* 10(3):201–210
96. Mouriño V, Cattalini JP, Roether JA, Dubey P, Roy I, Boccaccini AR (2013) Composite polymer-bioceramic scaffolds with drug delivery capability for bone tissue engineering. *Expert Opin Drug Deliv* 10(10):1353–1365
97. Rezwani K, Chen QZ, Blaker JJ, Boccaccini AR (2006) Biodegradable and bioactive porous polymer/inorganic composite scaffolds for bone tissue engineering. *Biomaterials* 27(18):3413–3431
98. Suming L, Michel V (1999) Biodegradable polymers: polyesters. In: Mathiowitz E (ed) *Encyclopedia of controlled drug delivery*. Wiley, New York, pp 71–93

---

# Bioactive Glass Bone Grafts: History and Clinical Applications

# 2

Larry L. Hench

## Contents

History of Bioactive Glasses .....	24
Bioactive Bone Grafts: Regeneration of Tissues .....	26
Bioactive Glass Bone Grafts: Genetic Control of Tissue Regeneration .....	26
Bioactive Glass Bone Grafts: Clinical Applications .....	28
Implications for the Future .....	32
References .....	32

---

## Abstract

The second generation of biomaterials concept, based upon a unique composition range of calcium, sodium phosphosilicate (CSPS) glasses, and glass-ceramics, involved bonding of the implant material to the bone. It is essential to recognize that no man-made material can respond to changing physiological loads or biochemical stimuli, as do living tissues. This compromise limits the lifetime of all man-made body parts. Recognizing this fundamental limitation also signals that we have reached a limit to current medical practice that emphasizes replacement of tissues. For the twenty-first century, it is critical to emphasize a more biologically based method of repair-regeneration of tissues. Third-generation bioactive materials with controlled release of biochemical stimuli provide the starting point for this shift toward a more biologically based approach to repair of diseased or damaged tissues, e.g., regeneration of tissues. Bioactive glass bone grafts are based upon this concept of in situ regeneration of bone with structure, architecture, and mechanical strength equivalent to normal cortical and cancellous bone. We need to remember that only a little more than 40 years ago, the

---

Larry L. Hench: deceased

L.L. Hench (✉)

Department of Biomedical Engineering, Florida Institute of Technology, Melbourne, FL, USA  
e-mail: [larryhench@embarqmail.com](mailto:larryhench@embarqmail.com); [larry.hench001@gmail.com](mailto:larry.hench001@gmail.com)

concept of a material that would not be rejected by living tissues also seemed impossible. This is now a clinical reality that has benefited tens of millions of people and should stimulate new concepts in the years ahead.

### Keywords

Bioactive glasses • Bone grafts • Tissue regeneration • Regenerative medicine

## History of Bioactive Glasses

In 1969 a second generation of biomaterials was discovered for use in repairing and replacing diseased or damaged parts of the body [1–5]. This new concept, based upon a unique composition range of calcium, sodium phosphosilicate (CSPS) glasses, and glass-ceramics, involved bonding of the implant material to the bone. Such materials were called bioactive. Table 1 summarizes the composition of bioactive glasses and glass-ceramics and their level of bioactivity. The glasses with highest levels of bioactivity, class A, bond to both bone and soft connective tissues by means of osteostimulation and osteoconduction. Slower bonding materials, class B bioactivity, bond only to bone by a process of osteoconduction. Discussions of classes of bioactivity are presented in other reviews.

Bioactive materials elicit a controlled action and reaction in the physiological environment. The mechanism of bonding of bioactive glasses (composed of  $\text{Na}_2\text{O}$ - $\text{CaO}$ - $\text{P}_2\text{O}_5$ - $\text{SiO}_2$ ) to living tissue, published in 1971 [3], involves 11 reaction steps [4]. As illustrated in Fig. 1, the first five steps occur on the surface of 45S5 Bioglass. The reactions begin by rapid ion exchange of  $\text{Na}^+$  with  $\text{H}^+$  and  $\text{H}_3\text{O}^+$  from the surrounding physiological solutions in contact with the surface of the bioactive glass. The ion exchange is followed by a polycondensation reaction of a very large concentration of surface silanols ( $\text{Si-OH HO-Si}$ ) to create a very high surface area silica ( $\text{SiO}_2$ ) gel, which provides a large number of surface reactive sites for heterogeneous

**Table 1** Composition and properties of bioactive glasses and glass-ceramics used clinically for medical and dental applications

Composition (wt%)	45S5 Bioglass (NovaBone)	S53P4 (AbminDent1)	A/W glass-ceramic (cerabone)
$\text{Na}_2\text{O}$	24.5	23	0
$\text{CaO}$	24.5	20	44.7
$\text{CaF}_2$	0	0	0.5
$\text{MgO}$	0	0	4.6
$\text{P}_2\text{O}_5$	6	4	16.2
$\text{SiO}_2$	45	53	34
Phases	Glass	Glass	Apatite Beta-wollastonite Glass
Class of bioactivity	A*	A	B



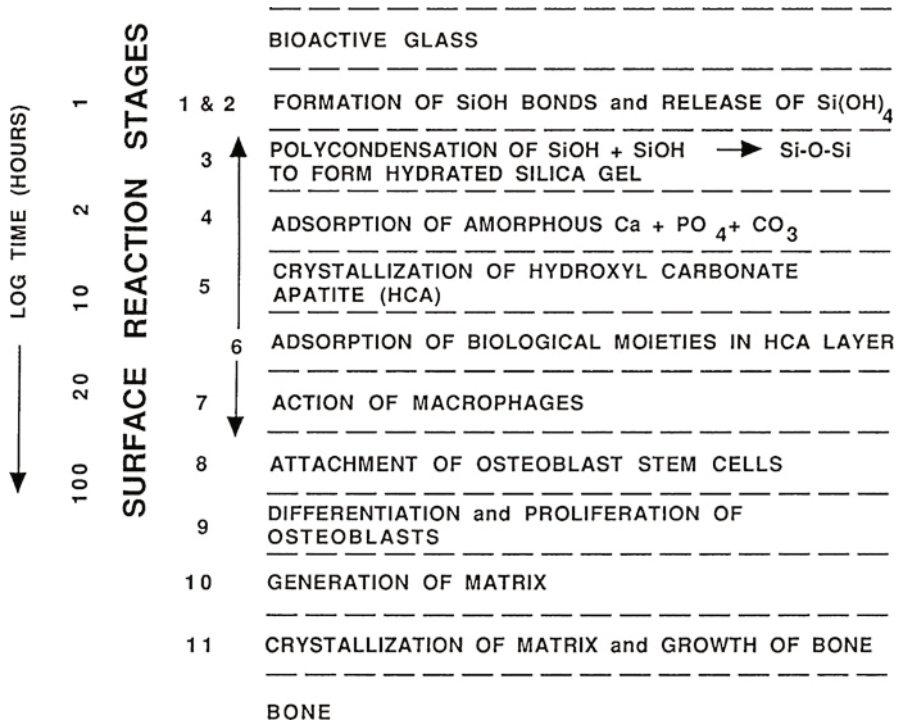


**Fig. 1** Sequence and rates of reaction stages to grow new bone at the interface with 45S5 bioactive glass

nucleation and crystallization of a biologically reactive hydroxyl-carbonate apatite (HCA) layer equivalent to the inorganic mineral phase of bone.

The growing HCA layer on the surface of the material is an ideal environment for six cellular reaction stages, shown in sequence in Fig. 1. The cellular mechanisms include colonization by osteoblast stem cells (stage 8) followed by proliferation (stage 9) and differentiation (stages 10 and 11) of the cells to form new bone that has a mechanically strong bond to the implant surface. The sequence of cellular stages only occurs on the bioactive glass surface if the preceding five stages of surface reactions have progressed rapidly, within minutes to hours, as indicated by the logarithmic time scale in Fig. 1. If the surface reacts too slowly, the cellular stages are delayed and the material bonds only slowly to bone via osteoconduction along the interface of the material and host bone.

By the mid-1980s bioactive materials had reached clinical use in numerous orthopedic and dental applications [4]. Synthetic hydroxyapatite (HA) ceramics had begun to be routinely used as porous implants, powders, and coatings on metallic prostheses to provide bioactive fixation [5, 6]. The presence of sparingly soluble HA coatings led to a tissue response (termed *osteoconduction*) where bone grew along the coating and formed a mechanically strong interface [5, 6]. Bioactive glasses and

glass-ceramics, based upon the original 45S5 Bioglass<sup>®</sup> formulation [3], were being used as middle ear prostheses to restore the ossicular chain and treat conductive hearing loss and as endosseous ridge maintenance implants to preserve the alveolar ridge from the bone resorption that follows tooth extraction [7]. The mechanically strong and tough bioactive A/W glass-ceramic, developed at Kyoto University, was used for replacement of vertebrae in patients with spinal tumors [8]. In 1998 a centennial feature article of the American Ceramic Society documented the rapid growth of clinical use of first- and second-generation bioceramics [4].

---

## Bioactive Bone Grafts: Regeneration of Tissues

The clinical success of first-generation, bio-inert, and second-generation bioactive and resorbable implants has met many of the medical needs of a rapidly aging population. However, survivability analyses of most prostheses [7, 9] show that a third to half of medical devices fail within 15–25 years. Failures require patients to have revision surgery that is costly to the patients and to society and comprises a significant contribution to the rapidly rising costs of healthcare. Thirty years of research has had relatively small effects on failure rates of medical devices made from first- and second-generation biomaterials [7].

For decades the approach to healthcare has been based upon trial and error experiments that require use of many animals and large numbers of human clinical trials. This approach needs to be replaced with a more affordable and more reliable alternative for the younger, 40–70 years old, patients. Improvements of either first- or second-generation biomaterials are limited in part because “All man-made biomaterials used for repair or restoration of the body represents a compromise” [1, 4].

It is essential to recognize that no man-made material can respond to changing physiological loads or biochemical stimuli, as do living tissues. This compromise limits the lifetime of all man-made body parts. Recognizing this fundamental limitation also signals that we have reached a limit to current medical practice that emphasizes *replacement of tissues*. For the twenty-first century, it is critical to emphasize a more biologically based method of *repair-regeneration of tissues*.

Third-generation bioactive materials with controlled release of biochemical stimuli provide the starting point for this shift toward a more biologically based approach to repair of diseased or damaged tissues, e.g., regeneration of tissues [10]. Bioactive glass bone grafts are based upon this concept of in situ regeneration of bone with structure, architecture, and mechanical strength equivalent to normal cortical and cancellous bone.

---

## Bioactive Glass Bone Grafts: Genetic Control of Tissue Regeneration

Third-generation biomaterials, such as bioactive glass particulates of 45S5 Bioglass, are designed to stimulate specific cellular responses at the level of molecular biology [10]. During the first decade of the twenty-first century, the concepts of bioactive

materials and resorbable materials converged; third-generation bioactive glasses and hierarchical porous foams are being designed to activate genes that stimulate regeneration of living tissues.

The key design principle of such third-generation materials is to control the rate of release of specific ionic stimuli that activate or regulate the function of genes in progenitor cells.

*In Situ Tissue Regeneration.* This approach involves the use of biomaterials in the form of powders, solutions, or doped micro- or nanoparticles to stimulate local tissue repair [11, 12]. Certain formulations of bioactive materials release chemicals in the form of ionic dissolution products at controlled rates that activate the cells in contact with the stimuli. The cells produce additional growth factors that in turn stimulate multiple generations of growing cells to self-assemble into the required tissues in situ, along the biochemical and biomechanical gradients that are present.

The advantage offered by regenerative medicine is genetic control of the tissue repair process. The result is equivalent to repaired natural tissue in that the new structure is living and adaptable to the physiological environment.

There is growing evidence to support the hypothesis governing design of third-generation biomaterials, i.e., generation of specific cell responses to controlled release of biochemical stimuli. For example, when a particulate of bioactive glass is used to fill a bone defect, there is rapid regeneration of bone that matches the architecture and mechanical properties of bone in the site of repair. Both osteoconduction and osteoproduction [13] occur as a consequence of rapid reactions on a bioactive glass surface [4]. The surface reactions release critical concentrations of soluble Si, Ca, P, and Na ions that give rise to both intracellular and extracellular responses at the interface of the glass with its cellular environment. Attachment and synchronized proliferation and differentiation of osteoblasts rapidly occur on the surface of bioactive materials [14].

Osteoprogenitor cells capable of forming new bone colonize the surface of highly bioactive materials. Slow release of soluble ions from the material stimulates cell division and production of growth factors and extracellular matrix proteins. Mineralization of the matrix follows and the mature osteoblast phenotype, encased in a collagen-HCA matrix (osteocytes), is the final product both in vitro and in vivo [13–24].

Numerous studies have established that there is genetic control of the cellular response to the most reactive of the bioactive glasses (45S5 Bioglass). Seven families of genes are upregulated when primary human osteoblasts are exposed to the ionic dissolution products of bioactive glasses [17–24]. The gene expression occurs within 48 h and includes enhanced expression by more than twofold of the families of genes listed in Table 2. See Xynos et al. for a listing of the genes and the extent of their upregulation [17].

The upregulated genes encode nuclear transcription factors and cell cycle regulators. Potent growth factors, especially insulin-like growth factor II (IGF-II), were increased by 3.2-fold along with IGF binding proteins and proteases that cleave IGF-II from their binding proteins. Similar bioactive induction of the transcription of at least five extracellular matrix components (2–3.7-fold) and their secretion and

**Table 2** Families of genes upregulated or activated by ionic dissolution products from bioactive glass

1.	Transcription factors and cell cycle regulators	2 to 5 fold
2.	Signal transduction molecules	2 to 6 fold
3.	Proteins in DNA synthesis, repair, recombination	2 to 3 fold
4.	Growth factors and cytokines	2–3.2-fold
5.	Cell surface antigens and receptors	2 to 7 fold
6.	Extracellular matrix components	2–3.7-fold
7.	Apoptosis regulators	1.6–4.5-fold

self-organization into a mineralized matrix is responsible for the rapid formation and growth of bone nodules and differentiation of the mature osteocyte phenotype [14–16, 24].

Studies have confirmed the results of the early Xynos et.al. findings and extended the generality to include several types of precursor cells and differing sources of biologically active Ca and Si ionic stimuli [14–17]. Bone biology and gene array analyses of five different *in vitro* models using four different sources of inorganic ions provide the experimental evidence for a genetic theory of osteogenic stimulation [17–25].

All experiments showed enhanced proliferation and differentiation of osteoblasts toward a mature, mineralizing phenotype without the presence of any added bone growth proteins, such as bone morphogenetic proteins (BMPs). Shifts in osteoblast cell cycles were observed as early as 6 h for most experiments, with elimination (by apoptosis) of cells incapable of differentiation [14]. The remaining cells exhibited enhanced synthesis and mitosis. The cells quickly committed to generation of extracellular matrix (ECM) proteins and mineralization of the matrix.

Gene array analyses showed early upregulation or activation of seven families of genes (Table 2) that favored both proliferation and differentiation of the mature osteoblast phenotypes, including: transcription factors and cell cycle regulators (six with increases of two- to fivefold); apoptosis regulators (three at 1.6–4.5-fold increase); DNA synthesis, repair, and recombination (four at two- to threefold); growth factors (four at two- to threefold) including IGF-1I and VEG F; cell surface antigens and receptors (four at two- to sevenfold, especially CD44); signal transduction molecules (three at two- to sixfold); and ECM compounds (five at 2–3.7-fold).

---

## Bioactive Glass Bone Grafts: Clinical Applications

Figure 2 summarizes the time line for development of clinical products of bioactive glass from the date of the first discovery of 45S5 Bioglass in November 1969. The first products approved by FDA in the mid-1980s were bulk implants cast from molten 45S5 Bioglass: the MEP (middle ear prostheses) for replacement of diseased or damaged or missing ossicles and the ERMI (endosseous ridge maintenance

1969	Discovery of bone bonding to 45S5 Bioglass at University of Florida
1971	First peer reviewed publications of bonding of bone to bioactive glasses and glass-ceramics [1–3]
1972	Bonding of Bioglass bone segments and coated femoral stems in monkeys
1975	Bioglass dental implants bonded in baboon jaws
1981	Discovery of soft connective tissue bonding to 45S5 Bioglass
1981	Toxicology and biocompatibility studies (20 <i>in vitro</i> and <i>in vivo</i> ) published to establish safety for FDA clearance of Bioglass products
1985	First medical product (Bioglass Ossicular Reconstruction Prosthesis) (MEP) cleared by FDA via the 510(k) process
1987	Discovery of osteoproduction (osteostimulation) in use of Bioglass particulate in repair of periodontal defects
1988	Bioglass Endosseous Ridge Maintenance Implant (ERMI) cleared by FDA via the 510 (k) process
1993	Bioglass particulate for use in bone grafting to restore bone loss from periodontal disease in infrabony defects (Perioglas) cleared by FDA via the 510 (k) process
1995	Perioglas obtained CE Mark in Europe
1996	Use of Perioglas for bone grafts in tooth extraction sites and alveolar ridge augmentation cleared by FDA via the 510 (k) process
1999	European use of 45S5 particulate for orthopedic bone grafting (NovaBone)
2000	FDA clearance for use of NovaBone in general orthopedic bone grafting in non-load bearing sites
2000	Quantitative comparison of rate of trabecular bone formation in presence of Bioglass granules versus synthetic HA and A/W glass-ceramic
2000	Analysis of use of 45S5 Bioglass ionic dissolution products to control osteoblast cell cycles
2001	Gene expression profiling of 45S5 Bioglass ionic dissolution products to enhance osteogenesis
2004	FDA clearance of 45S5 particulate for use in dentinal hypersensitivity treatment (NovaMin)
2011	Acquisition of NovaMin technology by Glaxo-Smith-Kline and world launch of Sensodyne Repair and Protect toothpaste for prevention of dentinal hypersensitivity and gingivitis

**Fig. 2** Chronology of science and clinical product development of 45S5 Bioglass

implant) for replacement of the roots of teeth for patients wearing dentures. The clinical results of the second-generation bulk 45S5 implants were outstanding with >90 % success over extended time periods.

While the second-generation Bioglass<sup>®</sup> materials performed admirably in replacing diseased or missing hard tissue, the discoveries that Bioglass<sup>®</sup> could positively affect osteoblasts and, in fact, “stimulate” them to produce more bone tissue earlier than other synthetic biomaterials led to the concept of “osteoproduction” and “osteostimulation” [13]. In order to take advantage of this property, and of the need to regenerate diseased or missing tissues, the development of third-generation Bioglass<sup>®</sup> products focused on using particles rather than monolithic shapes [2].

The first NovaBone<sup>®</sup> particulate material cleared for sale in the USA was PerioGlas<sup>®</sup>, which was cleared via the 510(k) process in December 1993 [2].

In 1995, PerioGlas<sup>®</sup> obtained a CE mark and marketing of the product began in Europe.

The initial indication for the product was to restore bone loss resulting from periodontal disease in infrabony defects. In 1996, additional indications for use were cleared by FDA, including use in tooth extraction sites and for alveolar ridge augmentation [2].

The first paper to describe potential use of 45S5 Bioglass<sup>®</sup> particulate in repair of periodontal defects was published in 1987 by Dr. June Wilson and Professor Sam Low, Department of Periodontology, and colleagues at the University of Florida [13]. A detailed study of the monkey model and clinical results was documented many years ago and published in previous papers [2, 4].

Over its nearly 20-year clinical history, PerioGlas<sup>®</sup> has demonstrated excellent clinical results with virtually no adverse reactions to the product. Numerous clinical studies have demonstrated the efficacy of the product in multiple uses [2]. To date, PerioGlas<sup>®</sup> is sold in over 35 countries, and the manufacturer estimates that the product has been used in more than one million surgeries (Data on file at NovaBone Corporation, Alachua, Florida, USA).

Building on the successes of PerioGlas<sup>®</sup> in the market, a Bioglass<sup>®</sup> particulate for orthopedic bone grafting was introduced into the European market in 1999, under the trade name NovaBone<sup>®</sup> [2]. The product was cleared for general orthopedic bone grafting in non-load-bearing sites in February 2000. The material 45S5 Bioglass is now widely used in many types of orthopedic and dental applications as shown in Table 3.

The osteoblast cell culture results reviewed above correlate with clinical results using the same bioactive material, 45S5 Bioglass [2, 25, 26]. An especially important finding is clinical equivalence of results from synthetic bioactive glass bone grafts of the composition 45S5 to use of autogenous grafts in the same clinical applications. Clinical studies that compare the success of autogenous bone grafts versus grafts of the gene-activating glasses show equivalent rates of bone regeneration and fewer side effects with the bioactive glasses [25, 26].

For example, iliac crest autograft is currently the gold standard for spinal fusion. However, there are disadvantages of an autogenous graft including increased blood loss, increased operative time, second-site morbidity, and pain.

A comparative study of bioactive glass (45S5 Bioglass) versus iliac crest autograft for spinal fusion in adolescent idiopathic scoliosis (AIS) has been reported for a group of 88 consecutive patients [26]. Forty patients received iliac crest autograft, and 48 received Bioglass synthetic bone graft (NovaBone particulate) with a minimum of 2-year follow-up.

The results showed fewer infections (2 % vs. 5 %) and fewer mechanical failures (2 % vs. 7.5 %) in the Bioglass group. Loss of correction of the main thoracic curve was also less for the Bioglass group (11 % vs. 15.5 %).

The conclusions for this retrospective study were:

1. Bioglass is as effective as iliac crest graft to achieve fusion and maintain correction in AIS.

**Table 3** Medical and dental products based upon 45S5 Bioglass

Orthopedics
Trauma
Long bone fracture (acute and/or comminuted); alone and with internal fixation
Femoral nonunion repair
Tibial plateau fracture
Arthroplasty
Filler around implants (acetabular reconstruction)
Impaction grafting
General
Filling of bone after cyst/tumor removal
Spine fusion
Interbody fusion (cervical, thoracolumbar, lumbar)
Posterolateral fusion
Adolescent idiopathic scoliosis
Cranial-facial
Cranioplasty
Facial reconstruction
General oral/dental defects
Extraction sites
Ridge augmentation
Sinus elevation
Cystectomies
Osteotomies
Periodontal repair
Dental-maxillofacial-ENT
Toothpaste and treatments for dentinal hypersensitivity
Pulp capping
Sinus obliteration
Repair of orbital floor fracture
Endosseous ridge maintenance implants
Middle ear ossicular replacements (DoueK MED)

2. Fewer complications were seen in the bioactive glass group of patients.
3. The morbidity of iliac crest harvesting can be avoided by use of bioactive glass in spinal fusion.

These are important conclusions for the twenty-first-century challenge of affordable healthcare for the aged. Elimination of need for second-site (iliac crest) surgery in elderly patients that require spinal fusion or other reasons for a bone graft means less exposure to anesthesia and potential for infection. Use of the synthetic bone graft of bioactive glass also avoids pain and healing of the second site.

An extensive range of medical and dental clinical applications of third-generation bioactive glasses, marketed as NovaBone and PerioGlas, has evolved over the last

two decades, as summarized in Table 3. Clinical success is excellent for these applications, as discussed by Gaisser and Hench in Chapter 11 in *Introduction to Bioceramics*, 2nd edition [25].

---

## Implications for the Future

A genetic basis for development of a third generation of biomaterials provides the scientific foundation for molecular design of bioactive materials for in situ tissue regeneration and repair, preferably using minimally invasive surgery. There are significant economic and humanistic advantages to each of these new approaches that may aid in solving the problems of care for an aging population. It should be feasible to design a new generation of gene-activating biomaterials tailored for specific patients and disease states. New, predictive analytical methods are becoming available that can aid in developing such innovative approaches to affordable healthcare. These noninvasive analysis methods can be developed to make it possible for patients to be diagnosed and prescribed specific treatments based upon molecular biological data from their own cells rather than have to rely upon statistical trial and error prescriptions. Perhaps of even more importance is the possibility that bioactive stimuli can be used to activate genes in a preventative treatment to maintain the health of tissues as they age. Only a few years ago this concept would have seemed impossible. We need to remember that only a little more than 40 years ago the concept of a material that would not be rejected by living tissues also seemed impossible. This is now a clinical reality that has benefited tens of millions of people and should stimulate new concepts in the years ahead.

---

## References

1. Hench LL (1991) Bioceramics: from concept to clinic. *J Am Ceram Soc* 74:1487–1510
2. Hench LL, Wilson J, Greenspan DC (2004) Bioglass: a short history and bibliography. *J Aust Ceram Soc* 40:1–42
3. Hench LL, Splinter RJ, Allen WC, Greenlee TK Jr (1971) Bonding mechanisms at the interface of ceramic prosthetic materials. *J Biomed Mater Res* 2(1):117–141
4. Hench LL (1998) Bioceramics. *J Am Ceram Soc* 81(7):1705–1728
5. Yamamuro T, Hench LL, Wilson J (eds) (1990) CRC handbook of bioactive ceramics, vol 2: Calcium phosphate and hydroxylapatite ceramics, CRC Press, Boca Raton, Florida
6. Klein CPAT, Wolke JGC, deGroot K (1993) Stability of Calcium Phosphate Ceramics and Plasma Sprayed Coating. In: Hench LL, Wilson J (eds) *An introduction to bioceramics*. World Scientific, London, p 199
7. Hench LL, Wilson J (eds) (1996) Clinical performance of skeletal prostheses. Chapman and Hall, London, pp 214–236 and 255–270
8. Yamamuro T (1996) A/W Glass-Ceramic: Clinical Applications. In: Hench LL, Wilson J (eds) *An introduction to bioceramics*. World Scientific, London, p 89–105
9. Wroblewski BM, Fleming PA, Siney PD (1999) Charnley low-frictional torque arthroplasty of the hip. 20-to-30 year results. *J Bone Joint Surg Br* 81(3):427–430
10. Hench LL, Polak JM (2002) Third-generation biomedical materials. *Science* 295:1014–1017



11. Jones JR (2012) Review of bioactive glass: from Hench to hybrids. *Acta Biomater.* doi:10.1016/j.actbio.2012.08.023
12. Hench LL, Jones JR, Fenn MB (2012) *New materials and technologies for healthcare.* Imperial College Press, London
13. Wilson J, Low SB (1992) Bioactive ceramics for periodontal treatment: comparative studies. *J Appl Biomater* 3:123–169
14. Xynos ID, Hukkanen MVJ, Batten JJ, Buttery ID, Hench LL, Polak JM (2000) Bioglass 45S5 stimulates osteoblast turnover and enhances bone formation *In vitro*: implications and applications for bone tissue engineering. *Calcif Tissue Int* 67(4):321–329
15. Hench LL, Xynos ID, Buttery LD, Polak JM (2000) Bioactive materials to control cell cycle. *J Mater Res Innov* 3:313–323
16. Xynos ID, Edgar AJ, Buttery DKL, Hench LL, Polak JM (2000) Ionic products of bioactive glass dissolution increase proliferation of human osteoblasts and induce insulin-like growth factor II mRNA expression and protein synthesis. *Biochem Biophys Res Commun* 276:461–465
17. Xynos ID, Edgar AJ, Buttery DKL, Hench LL, Polak JM (2001) Gene-expression profiling of human osteoblasts following treatment with the ionic products of bioglass (R) 45S5 dissolution. *J Biomed Mater Res* 55:151–157
18. Bielby RC, Christodoulou IS, Pryce RS, Radford WJP, Hench LL, Polak JM (2004) Time- and concentration-dependent effects of dissolution products of 58S sol-gel bioactive glass on proliferation and differentiation of murine and human osteoblasts. *Tissue Eng* 10:1018–1026
19. Bielby RC, Pryce RS, Hench LL, Polak JM (2005) Enhanced derivation of osteogenic cells from murine embryonic stem cells after treatment with ionic dissolution products of 58S bioactive sol-gel glass. *Tissue Eng* 11:479–488
20. Christodoulou I, Buttery LDK, Saravanapavan P, Tai GP, Hench LL, Polak JM (2005) Dose- and time-dependent effect of bioactive gel-glass ionic-dissolution products on human fetal osteoblast-specific gene expression. *J Biomed Mater Res B Appl Biomater* 74B:529–537
21. Christodoulou I, Buttery LDK, Saravanapavan P, Tai GP, Hench LL, Polak JM (2005) Characterization of human foetal osteoblasts by microarray analysis following stimulation with 58S bioactive gel-glass ionic dissolution products. *J Biomed Mater Res B Appl Biomater* 77B:431–446
22. Gough JE, Jones JR, Hench LL (2004) Nodule formation and mineralisation of human primary osteoblasts cultured on a porous bioactive glass scaffold. *Biomaterials* 25:2039–2046
23. Hench LL (2003) Glass and genes: the 2001 W. E. S. Turner memorial lecture. *Glass Technol* 44:1–10
24. Jones JR, Tsigkou O, Coates EE, Stevens MM, Polak JM, Hench LL (2007) Extracellular matrix formation and mineralization of on a phosphate-free porous bioactive glass scaffold using primary human osteoblast (HOB) cells. *Biomaterials* 28:1653–1663
25. Hench LL (ed) (2013) *Introduction to bioceramics*, 2nd edn. Imperial College Press, London
26. Ilharborde B, Morel E, Fitoussi F, Presedo A, Souchet P, Pennecot G, Mazda K (2008) Bioactive glass as a bone substitute for spinal fusion in adolescent idiopathic scoliosis: a comparative study with iliac crest autograft. *J Pediatr Orthop* 28:347–351

Maria Grazia Raucci, Daniela Giugliano, and Luigi Ambrosio

## Contents

Introduction .....	36
Bioceramics .....	37
Physicochemical Properties of Bioceramics .....	38
Porosity Properties of Bioceramic Scaffolds .....	41
Biological Properties of Bioceramics .....	43
Mechanical Properties of Bioceramics .....	45
Biocomposites .....	46
Sol–Gel Approach to Prepare Biocomposite Materials .....	47
Types of Reinforcements Used for Biocomposites .....	49
Biological and Mechanical Properties of Biocomposites .....	52
Incorporation of Biomolecules .....	53
Conclusions .....	54
References .....	54

## Abstract

Several varieties of ceramics, such as bioglass-type glasses, sintered hydroxyapatite, and glass-ceramic A–W, exhibit specific biological affinity, i.e., direct bonding to surrounding bone, when implanted in bony defects. These bone-bonding ceramics are called bioactive ceramics and are utilized as important bone substitutes in the medical field. However, there is a limitation to their clinical applications because of their inappropriate mechanical properties. Natural

M.G. Raucci (✉) • D. Giugliano

Institute of Polymers, Composites and Biomaterials (IPCB), National Research Council of Italy (CNR), Naples, Italy

e-mail: [mariagrazia.raucci@cnr.it](mailto:mariagrazia.raucci@cnr.it); [daniela.giugliano@unina.it](mailto:daniela.giugliano@unina.it)

L. Ambrosio

Department of Chemical Sciences and Materials Technology, National Research Council of Italy, Rome, Italy

e-mail: [luigi.ambrosio@cnr.it](mailto:luigi.ambrosio@cnr.it)

bone takes a kind of organic–inorganic composite, where apatite nanocrystals are precipitated on collagen fibers. Therefore, problems with the bioactive ceramics can be solved by material design based on the bioactive composites. In this chapter, an overview of fundamental properties of ceramics and biocomposite materials for biomedical application was reported.

---

**Keywords**

Bone tissue • Bioceramics • Biocomposites • Biomimetic materials • Biocompatibility • Bioactivity • Osteoconductive • Hydroxyapatite • Porosity • Scaffolds • Mechanical properties

---

**Introduction**

Native bone tissue possesses a nanocomposite structure, mainly composed of nonstoichiometric hydroxyapatite (HA;  $\text{Ca}_{10}(\text{PO}_4)_6(\text{OH})_2$ ) and collagen fiber matrix, that provides appropriate physical and biological properties, especially mechanical support and protection for the vertebrate skeleton. However, bone needs to be repaired or regenerated upon damage. The demand in the surgical market is highlighted by the fact that there are approximately four million operations involving bone grafting or bone substitutes performed around the world annually [1]. Currently, different types of bone grafts and bone graft substitutes, such as autografts, allografts, and alloplastic or synthetic bone grafts, are used for surgical treatments [2, 3]. Autografts compose approximately 58 % of the bone substitutes, whereas allografts constitute approximately 34 % [2]. As autografts have all the properties necessary for new bone growth, they are considered the gold standard for bone repair. However, the disadvantages of autografts include limited availability, donor site morbidity, and risk of disease transmission from donor to recipient [3]. Therefore, allografts are attractive alternatives to autografts; however, they are not usually osteoinductive or osteogenic, they have risks of an immunological reaction or disease transmission, and they have insufficient mechanical properties for load-bearing bone applications. Therefore, there is a great demand for synthetic grafts for fracture repair, and there is also scope to improve existing graft materials. Therefore, it gives rise to an abundant demand for safe and effective materials for use in tissue regeneration [4]. Biomaterials in the form of implants (sutures, bone plates, joint replacements, ligaments, vascular grafts, heart valves, intraocular lenses, dental implants, etc.) and medical devices (pacemakers, biosensors, artificial hearts, blood tubes, etc.) are widely used to replace and/or restore the function of traumatized or degenerated tissues or organs, to assist in healing, to improve function, to correct abnormalities, and thus to improve the quality of life of the patients. The world market for biomaterials is estimated to be around \$12 billion per year, with an average global growth of between 7 % and 12 % per annum. Biomaterials are expected to perform in our body's internal environment, which is very aggressive. For example, the pH of body fluids in various tissues varies in the range from 1 to 9. During daily activities, bones are subjected to a stress of approximately 4 MPa,

whereas the tendons and ligaments experience peak stresses in the range 40–80 MPa. The mean load on a hip joint is up to three times the body weight (3000 N), and the peak load during jumping can be as high as ten times body weight. More importantly, these stresses are repetitive and fluctuating depending on the activities such as standing, sitting, jogging, stretching, and climbing [5]. In the early days, all kinds of natural materials such as wood, glue, and rubber and tissues from living forms and manufactured materials such as iron, gold, zinc, and glass were used as biomaterials based on trial and error. The host responses to these materials were extremely varied. Some materials were tolerated by the body, whereas others were not. Under certain conditions (characteristics of the host tissues and surgical procedure), some materials were tolerated by the body, whereas the same materials were rejected in another situation. Over the last 30 years, considerable progress has been made in understanding the interactions between the tissues and the materials. Researchers have coined the words “biomaterial” and “biocompatibility” [6] to indicate the biological performance of materials. Materials that are biocompatible are called biomaterials, and the biocompatibility is a descriptive term which indicates the ability of a material to perform with an appropriate host response, in a specific application [6]. In simple terms, it implies compatibility or harmony of the biomaterial with the living systems. Therefore, structural compatibility refers to the mechanical properties of the implant material, such as elastic modulus (or  $E$ , Young’s modulus) and strength, implant design (stiffness, which is a product of elastic modulus,  $E$  and second moment of area,  $I$ ), and optimal load transmission (minimum interfacial strain mismatch) at the implant/tissue interface. Optimal interaction between biomaterial and host is reached when both the surface and structural compatibilities are met. Clinical experience clearly indicates that not all off-the-shelf materials (commonly used engineering materials) are suitable for biomedical applications. The various materials used in biomedical applications may be grouped into (a) metals, (b) ceramics, (c) polymers, and (d) composites made from various combinations of (a), (b), and (c).

This chapter is intended to provide an overview of bioceramics and organic–inorganic composites obtained by sol–gel technology used in the biomedical field.

---

## Bioceramics

No material implanted in an organism is absolutely bioinert – each one stimulates a reaction in living tissue. The selection and improvement of biomaterials are a long process of trial and error which, according to contemporary research, is defined by four basic types of reaction between the material and the living organic tissue with which it is in contact [7]. There is not a sharp distinction between the various types of materials: they may be biotoxic, bioinert, bioactive, or bioresorbable to various degrees. Among inorganic substances, the only bioactive and bioresorbable materials are ceramics. A bioactive ceramics occupy an intermediate position between bioinert and bioresorbable [8]. A material can be designated as bioactive when it stimulates a specific biological reaction at the material–tissue interface, occurring with the formation of biochemical bonds between the living tissue and the material.

The formation of such bonds with the surface of hydroxyapatite ceramics was first observed in the late 1960s [9]. The distinction between a bioactive and bioresorbable ceramics might be associated with only a structural factor: a nonporous hydroxyapatite ceramics behave as a bioinert material and is retained in an organism for at least 5–7 years without change, while a highly porous ceramics of the same composition can be resorbed in a time of the order of 1 year.

Several varieties of ceramics have been found to exhibit bone-bonding performance. They are called bioactive ceramics, meaning that they can elicit biological activity. Bioglass-type glasses in the system  $\text{Na}_2\text{O}-\text{CaO}-\text{SiO}_2-\text{P}_2\text{O}_5$  [10], sintered hydroxyapatite ( $\text{Ca}_{10}(\text{PO}_4)_6(\text{OH})_2$ ) [11], and glass-ceramic A–W are known to be bioactive ceramics. In the glass-ceramic A–W, oxyfluorapatite ( $\text{Ca}_{10}(\text{PO}_4)_6(\text{O},\text{F}_2)$ ) and  $\beta$ -wollastonite ( $\text{CaO} \cdot \text{SiO}_2$ ) crystals are dispersed in a  $\text{MgO}-\text{CaO}-\text{SiO}_2$  glassy matrix. Most bioactive ceramics bond to bone through a low crystalline apatite layer formed on their surfaces in the body environment, created by a chemical reaction with body fluid. The apatite formation in vivo can be also observed in simulated body fluid (SBF;  $\text{Na}^+$  142.0,  $\text{K}^+$  5.0,  $\text{Mg}^{2+}$  1.5,  $\text{Ca}^{2+}$  2.5,  $\text{Cl}^-$  147.8,  $\text{HCO}_3^-$  4.2,  $\text{HPO}_4^{2-}$  1.0, and  $\text{SO}_4^{2-}$  0.5 mol/m<sup>3</sup>) with a similar concentration to inorganic ions as human blood plasma [12]. In order to construct fundamental knowledge on novel bioactive materials design, apatite formation behavior on materials with different surface structures has been investigated in SBF by using metal oxide hydrogels and self-assembled monolayers (SAMs). Based on these results, several surface functional groups, such as Si–OH, Ti–OH, Zr–OH, Ta–OH, COOH, and  $\text{SO}_3\text{H}$  [13], are found to be effective for triggering the heterogeneous nucleation of the apatite. In addition to surface functional groups, apatite formation is governed not only by the functional groups but also several other factors, such as ion release enhancing the apatite nucleation from the materials, and by a spatial gap constructed on the material surfaces [14].

## Physicochemical Properties of Bioceramics

Ceramics include a large class of nonmetallic materials whose chemical compositions, bond types, and properties vary over a very wide range. Therefore, it was logical to search among ceramics for bioactive and bioresorbable as well as bioinert materials. Bioceramics are more biocompatible with an organism than other implanted materials; have less effect on the immune system; have a broader range of biochemical, mechanical, and other properties; and can be adapted to a wider range of functional possibilities and lifetime requirements in the organism.

A characteristic feature of the reaction of a material with a biosystem is the defining role of its structure. Therefore, ceramics (which can be distinguished as a class of materials in which structure is the basic physical parameter which determines service properties) by their nature are optimally suited for use in biosystems and additionally offer a wide range of possibilities to vary properties under such conditions. Thanks to these two factors, the use of bioceramics in surgery is substantially more effective than that of other implanted materials.

*Bioinert Ceramics.* The term bioinert refers to any material that once placed in the human body has minimal interaction with its surrounding tissue; examples of these are stainless steel, titanium, alumina, partially stabilized zirconia, and ultrahigh molecular weight polyethylene. Generally, a fibrous capsule might form around bioinert implants; hence, its biofunctionality relies on tissue integration through the implant. Many of the more “traditional” ceramics have been used for bioceramic applications. Alumina and zirconia, for example, have been used as inert materials for a range of applications from the 1960s. Their high hardness, low friction coefficient, and excellent corrosion resistance offer a very low wear rate at the articulating surfaces in orthopedic applications. Microstructures are controlled to inhibit static fatigue and slow crack growth while the ceramic is under load. Alumina is currently used for orthopedic and dental implants. It has been utilized in wear bearing environments such as the total hip arthroplasties (THA) as the femoral head generating reductions in wear particles from ultrahigh molecular weight polyethylene (UHMWPE). Other applications for alumina encompass porous coatings for femoral stems, porous alumina spacers (specifically in revision surgery), and in the past as polycrystalline and single crystal forms in dental applications as tooth implants [15].

*Bioactive and Resorbable Ceramics.* A very typical case in surgical practice is the healing of bone defects which are formed in the operational removal of cysts, tumors, and genetic defects. For this purpose a bioactive ceramics able to reliably integrate with bone and maintain its strength over a long period of time is required, or else a resorbable which gradually disappears and is replaced with healthy bone. Porous granules and powders of bioactive and resorbable ceramics are very often used to fill bone defects. This is possible because of the bonding of dispersed ceramic material in the wound with blood fibrin and thrombin and after some time also with collagen fibers and elements of newly formed bone tissue, resulting in the creation of a so-called bone–ceramic complex with adequate strength. The formation of such a complex is observed also when bone defects are filled with porous granules of a bioinert ceramics. However, the use of resorbable ceramics is particularly effective, thanks to the eventually complete replacement of this complex with whole bone [16]. Bioactive and resorbable ceramics are used in all types of bone reconstruction, in particular for the fabrication of implants which densely fuse with bone (e.g., in skull restorations after operations or trauma), tooth-root implants, biological tooth fillings, cure of diseases of the periodontia (tissue around teeth), maxillofacial reconstruction, grafting and stabilizing skull bone, joint reconstruction, for the endoprosthesis of hearing aids, cosmetic eye prostheses, etc. Resorbable ceramics also aid in the restoration of tendons, ligaments, small blood vessels, and nerve fibers. Hydroxyapatite (HA) enters into the composition of bioactive and bioresorbable ceramics or substances close to it in composition which form HA crystals by the reaction with the organism at the implant–biomedium interface.

Synthetic HA ( $\text{Ca}_{10}(\text{PO}_4)_6(\text{OH})_2$ ) is a complete chemical and crystallochemical analogue of bone mineral. Synthetic and natural HA differ only in structure. In bone, HA is present in the form of microcrystalline platelets with the approximate dimensions  $(1.5\text{--}3.5) \times (5.0\text{--}10.0) \times (40.0\text{--}50.0)$  nm. The strongest cortical bone is a

composite material consisting of HA crystals (70 mass %) bonded with collagen fibers (30 mass %) [17]. Collagen is fibrous albumin composed of three peptide chains, each of which is twisted into a left-rotated spiral, intertwined to form a right-rotated spiral. For every turn of the triple spiral, there are ten turns of each individual chain. Various forms of synthetic HA (from highly dispersed powder to nonporous ceramics) do not exactly reproduce the structure of the natural HA crystals of bone but nevertheless are included in the metabolic processes of a living organism and reprocessed by the organism at a rate which depends on the structure, chemical composition, and specific surface area of the HA. The compound  $\beta$ -tricalcium phosphate (TCP)  $\text{Ca}_3(\text{PO}_4)_2$  is also a bioactive and resorbable ceramic material and, to a lesser degree, so are other calcium phosphates. All calcium phosphates convert to HA in the internal media of the organism.

Certain calcium phosphate glass-crystalline materials and glasses which, like HA ceramics, are able to develop strong biochemical bonds with adjacent bone tissue, thanks to the formation of HA microcrystals on their surfaces upon reaction with the physiological fluid, are also considered as bioactive ceramics. Glass-crystalline materials may be considered as in essence ceramics with high concentrations of glass phase, while bioactive glasses are materials which contain small amounts of crystalline phase, or nuclei, formed by selective chemical solution and (or) annealing [18].

The basis for such a generalization is the property which all of these materials have in common – bioactivity. This signifies that in a biological medium, after a certain period of time, a biologically active layer consisting of microcrystals of hydroxyapatite plus a small amount of carbonate groups – hydroxycarbonate apatite (HCA) – forms on their surfaces.

These crystals are structurally and chemically identical to the mineral component of bone and form strong chemical bonds with adjacent bone tissue.

Most current bioceramic research utilizes this solution to measure the bioactivity of an artificial material by examining apatite-forming ability on its surface in *simulated body fluids* (SBF). This synthetic body fluid is highly supersaturated in calcium and phosphate in respect to apatite under even normal conditions. Therefore, if a material has a functional group effective for the apatite nucleation on its surface, it can form the apatite spontaneously [14]. It is widely accepted that the essential requirement for an artificial material to bond to living bone is the formation of bonelike apatite layer on its surface. Formation of the bonelike apatite layer on the bioactive materials can be produced in a SBF with ion concentrations almost equal to those of the human blood plasma. Osteoblasts have been shown to proliferate and differentiate on this apatite layer (Fig. 1).

The mechanism of formation of a direct chemical bond between dense HA ceramics and bone can be described as follows: a cellular bone matrix composed of differentiated osteoblasts appears on the surface of the ceramics, which forms a 3–5 mm thick amorphous zone of increased electron density with a higher concentration of phosphate ions and calcium.

Following this collagen bundles appear which connect the amorphous zone and bone cells. Next, crystals of bone mineral form in the amorphous zone. As this zone matures, the bonding region shrinks to 0.05–0.2 mm. As a result, the living bone is

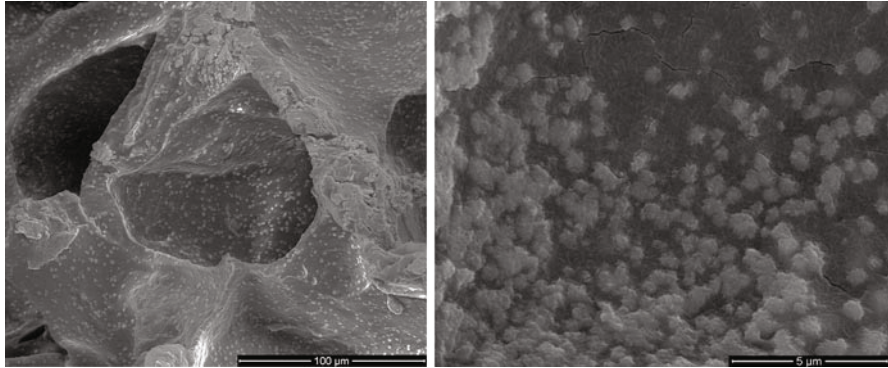


**Fig. 1** Biomineralized scaffold of polycaprolactone/hydroxyapatite (*PCL/HA*) after treatment in simulated body fluid (7 days) at different magnification

joined to the implant by a thin epitaxially bonded layer [19]. Transmission electron microscopic analysis of the crystal structure of the bone–HA interface indicates that there is practically complete epitaxial reproduction by the growing crystals of bone–HA of the orientation of apatite crystals on the implant surface.

The mechanism of formation of HCA crystals on the surface of bioceramics with a glass phase is similar and also includes several steps [20]: formation of an amorphous silica gel, partially dissolved by the organism via exchange of alkaline cations of the glass with protons of the biomedium; condensation and repolymerization of the silicate layer surface impoverished in alkaline and alkaline-earth cations; migration of  $\text{Ca}^{2+}$  and  $\text{PO}_4^{3-}$  ions to the surface through the silicate layer; adsorption of calcium and phosphate ions from the biomedium with formation, on the silicate layer surface, of an amorphous film enriched in calcium phosphate; and crystallization of the calcium phosphate film with the participation of  $\text{OH}^-$  and  $\text{CO}_3^{2-}$  ions to form HCA microcrystals.

The parameters of this process (bioactivity characteristics) are determined basically by the chemical, not the phase, composition of the material (ratio of glass and crystalline phases), although the phase and structural states strongly affect the strength and other properties.

The strength properties of bioactive ceramics are substantially lower than those of bioinert. Highest strength is found in nonporous HA and in the glass-ceramic Cerabone A–W, but the bend strength and crack resistance of these materials are five to seven times lower than that of high-strength  $\text{ZrO}_2$  ceramics. By synthesizing bioactive ceramic–biopolymer composites, it is possible to somewhat increase tensile strength and impact toughness and at the same time decrease Young's modulus, bringing the elasticity of the biomaterial close to that of bone.

### **Porosity Properties of Bioceramic Scaffolds**

In spite of the serious mechanical limitations, bioceramics of calcium orthophosphates are available in various physical forms: powders, particles, granules



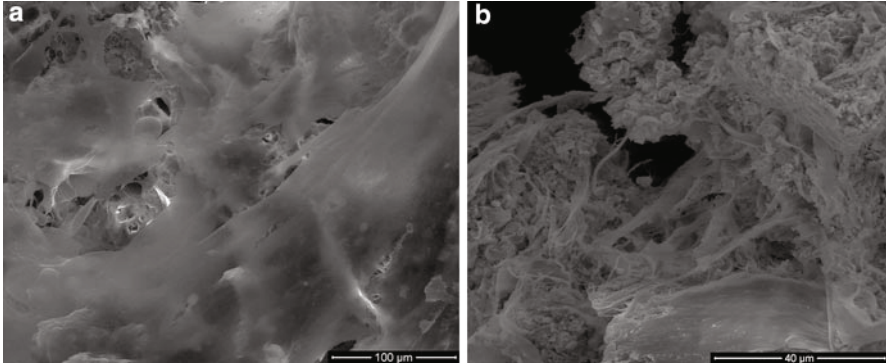


**Fig. 2** (a) Scaffold material based on PCL/HA colonized by human mesenchymal stem cells after 14 days cell culture; (b) hMSC as bridge between wall pores

(or granulates [21]), dense blocks, porous scaffolds, injectable formulations, self-setting cements, implant coatings, and composite component of different origin (natural, biological, or synthetic). Furthermore, custom-designed shapes like wedges for tibial opening osteotomy, cones for spine and knee, and inserts for vertebral cage fusion are also available [22]. Surface area of porous bodies and scaffolds is much higher, which guarantees good mechanical fixation in addition to providing sites on the surface that allow chemical bonding between the bioceramics and bones [19]. Furthermore, pore sizes are directly related to bone formation, since they provide surface and space for cell adhesion and bone ingrowth. On the other hand, pore interconnection provides the way for cell distribution and migration, as well as it allows an efficient *in vivo* blood vessel formation suitable for sustaining bone tissue neoformation and possibly remodeling. Namely, porous HA bioceramics can be colonized by bone tissues [23]. Therefore, interconnecting macroporosity (pore size  $>100\ \mu\text{m}$ ) [24], which is defined by its capacity to be colonized by cells, is intentionally introduced in solid bioceramics (Fig. 2).

Macroporosity is usually formed due to release of various volatile materials, and, for that reason, incorporation of pore creating additives (porogens) is the most popular technique to create macroporosity. The porogens are crystals or particles of either volatile (they evolve gases at elevated temperatures) or soluble substances, such as paraffin, NaCl,  $\text{NaHCO}_3$ , gelatin, poly(methyl methacrylate), or even hydrogen peroxide [25]. Obviously, the ideal porogen should be nontoxic and be removed at ambient temperature, thereby allowing the ceramic/porogen mixture to be injected directly into a defect site and allowing the scaffold to fit the defect [24]. Sintering particles, preferably spheres of equal size, is a similar way to generate porous three-dimensional (3D) bioceramics of calcium orthophosphates. However, the pores resulting from this method are often irregular in size and shape and not fully interconnected with one another. A wetting solution, such as polyvinyl alcohol, is usually used to aid compaction, which is achieved by pressing the particles into cylinders at approximately 200 MPa [26].

Several other techniques, such as replication of polymer foams by impregnation, dual-phase mixing technique, freeze casting, stereolithography, and foaming of gel-casting suspensions, have been applied to fabricate porous calcium orthophosphate bioceramics [27].

In vivo response of calcium orthophosphate bioceramics of different porosity was investigated, and hardly any effect of macropore dimensions (150, 260, 510, and 1220  $\mu\text{m}$ ) was observed [28]. In another study, a greater differentiation of mesenchymal stem cells was observed when cultured on 200  $\mu\text{m}$  pore size HA scaffolds when compared to those on 500  $\mu\text{m}$  pore size HA [29]. The latter finding was attributed to the fact that the higher pore volume in 500  $\mu\text{m}$  macropore scaffolds might contribute to the lack of cell confluency leading to the cells proliferating before beginning differentiation. Besides, the authors hypothesized that bioceramics having a less than optimal pore dimensions induced quiescence in differentiated osteoblasts due to reduced cell confluency.

Already in 1979, Holmes suggested that the optimal pore range was 200–400  $\mu\text{m}$  with the average human osteon size of  $\sim 223$   $\mu\text{m}$  [30], while in 1997 Tsuruga and coworkers suggested that the optimal pore size of bioceramics that supported ectopic bone formation was 300–400  $\mu\text{m}$  [31]. Therefore, there is no need to create calcium orthophosphate bioceramics with very big pores; however, the pores must be interconnected [24]. Interconnectivity governs a depth of cells or tissue penetration into the porous bioceramics, as well as it allows development of blood vessels required for new bone nourishing and wastes removal [32]. Meanwhile, the presence of microporosity provides both a greater surface area for protein adsorption and increased ionic solubility.

Studies showed that increasing of both the specific surface area and pore volume of bioceramics might greatly accelerate the process of biological apatite deposition and, therefore, enhance the bone-forming bioactivity. More importantly, the precise control over the porosity, pore sizes, and internal pore architecture of bioceramics on different length scales is essential for understanding of the structure–bioactivity relationship and the rational design of better bone-forming biomaterials.

## Biological Properties of Bioceramics

The most important differences between bioactive bioceramics and all other implanted materials are inclusion in the metabolic processes of the organism, adaptation of either surface or the entire material to the biomedium, integration of a bioactive implant with bone tissues at the molecular level, or complete replacement of resorbable material by healthy bone tissues. All of the enumerated processes are related to the effect of an organism on the implant. Nevertheless, another aspect of implantation is also important – the effect of the implant on the organism. For example, using of bone implants from corpses or animals, even after they have been treated in various ways, provokes a substantially negative immune reactions in the organism, which substantially limits the use of such implants. In this connection, it is useful to dwell on the biological properties of bioceramic implants, particularly

those of calcium orthophosphates, which in the course of time may be resorbed completely [33].

It has been accepted that no foreign material placed within a living body is completely compatible. The only substances that conform completely are those manufactured by the body itself (autogenous) and any other substance that is recognized as foreign initiates some types of reactions (host–tissue response). The reactions occurring at the biomaterial/tissue interfaces lead to time-dependent changes in the surface characteristics of the implanted biomaterials and the tissues at the interface [34]. In order to develop new products, it is desirable to understand the *in vivo* host responses. Like any other species, biomaterials and bioceramics react chemically with their environment, and, ideally, they should not induce any change or provoke undesired reaction in the neighboring or distant tissues.

Generally, both bioactivity and bioresorbability phenomena are fine examples of chemical reactivity and calcium orthophosphates (both non-substituted and ion-substituted ones) fall into these two categories of bioceramics [35]. A bioactive material will dissolve slightly but promote formation of a surface layer of biological apatite before interfacing directly with the tissue at the atomic level which results in the formation of a direct chemical bond with bone. Such an implant will provide a good stabilization for materials that are subject to mechanical loading. A bioresorbable material will dissolve and allow a newly formed tissue to grow into any surface irregularities but may not necessarily interface directly with the material. Consequently, the functions of bioresorbable materials are to participate in the dynamic processes of formation and reabsorption that take place in bone tissues; so bioresorbable materials are used as scaffolds or filling spaces allowing tissue infiltration and substitution.

A distinction between the bioactive and bioresorbable bioceramics might be associated with a structural factor only. For example, bioceramics made from nonporous, dense, and highly crystalline HA behave as a bioinert (but a bioactive) material and are retained in an organism for at least 5–7 years without changes, while a highly porous bioceramics of the same composition can be resorbed approximately within a year.

Before recently, it was generally considered that, alone, any type of synthetic bioceramics possessed neither osteogenic nor osteoinductive properties and demonstrated minimal immediate structural support. When attached to the healthy bones, osteoid is produced directly onto the surfaces of bioceramics in the absence of a soft tissue interface. Consequently, the osteoid mineralizes, and the resulting new bone undergoes remodeling. However, several reports have already shown some osteoinductive properties of certain types of calcium orthophosphate bioceramics [36]. Although in certain *in vivo* experiments an inflammatory reaction was observed after implantation of calcium orthophosphate bioceramics [37], the general conclusion on using calcium orthophosphates with Ca/P ionic ratio within 1.0–1.7 is that all types of implants (bioceramics of various porosities and structures, powders, or granules) are not only nontoxic but also induce neither inflammatory nor foreign-body reactions. An intermediate layer of fibrous tissue between the implants and bones has never been detected. Furthermore, calcium orthophosphate implants display the ability to directly bond to bones [33].

When a bioceramic implant is fixed in the human body, a space filled with biofluids exists next to the implant surface. With time, proteins will be adsorbed at the bioceramic surface that will give rise to osteoinduction by proliferation of cells and their differentiation toward bone cells, revascularization, and eventual gap closing. Ideally, a strong bond will be formed between the implant and surrounding tissues. Osteoblasts cultured on HA bioceramics are generally reported to be completely flattened, and its cytoplasmic edge is difficult to distinguish from the HA surfaces after 2 h incubation [38]. Osteoblasts cultured on porous HA bioceramics appeared to exhibit a higher adhesion, an enhanced differentiation, and suppressed proliferation rates when compared to nonporous controls. Furthermore, formation of distinct resorption pits on HA [39] and  $\beta$ -TCP [40] surfaces in the presence of osteoclasts was observed. A surface roughness of calcium orthophosphate bioceramics was reported to strongly influence the activation of mononuclear precursors to mature osteoclasts [39]. Mesenchymal stem cells are one of the most attractive cell lines for application as bone grafts. Early investigations by Okumura et al. indicated an adhesion, proliferation, and differentiation, which ultimately became new bone and integrated with porous HA bioceramics [41]. Recently, Unger et al. showed a sustained coculture of endothelial cells and osteoblasts on HA scaffolds for up to 6 weeks [42]. Furthermore, a release of factors by endothelial and osteoblast cells in coculture supported proliferation and differentiation was suggested to ultimately result in microcapillary-like vessel formation and supported a neo-tissue growth within the scaffold [42].

## Mechanical Properties of Bioceramics

In the body, the mechanical properties of natural bone change with their biological location because the crystallinity, porosity, and composition of bone adjust to the biological and biomechanical environment. The properties of synthetic calcium phosphates vary significantly with their crystallinity, grain size, porosity, and composition (e.g., calcium deficiency) as well. In general, the mechanical properties of synthetic calcium phosphates decrease significantly with increasing amorphous phase, microporosity, and grain size. High crystallinity, low porosity, and small grain size tend to give higher stiffness, compressive and tensile strengths, and greater fracture toughness. It has been reported that the flexural strength and fracture toughness of dense HA are much lower in a dry condition than in a wet condition [43]. Moreover, by comparing the properties of HA and related calcium phosphates with those of cortical bone, it was found that bone has a reasonably good compressive strength though it is lower than that of HA. But bone has a significantly higher fracture toughness than HA. The mechanical properties are even lower for porous HA structures [43]. The high tensile strength and fracture toughness of bone are attributed to the tough and flexible collagen fibers reinforced by HA crystals. Hence, calcium phosphates alone cannot be used for load-bearing scaffolds despite their good biocompatibility and osteoconductivity.

## Biocomposites

Even bioactive ceramics cannot substitute in load-bearing portions of bone, because their fracture toughness is lower and their Young's modulus is higher than those of human cortical bone. In addition, these ceramics are difficult to form into the desired shapes during implantation. Novel bioactive bone substitutes with high flexibility and high machinability are desired in the medical field. Natural bone takes a kind of organic–inorganic composite, where apatite nanocrystals are precipitated on collagen fibers. Therefore the organic–inorganic composites inspired by the bone structure are expected to solve these problems. In fact, the development of composite scaffold materials is attractive as advantageous properties of two or more types of materials can be combined to suit better the mechanical and physiological demands of the host tissue. For instance, natural and synthetic polymers such as collagen, polylactic acid (PLA), polyglycolic acid (PGA), copolymers from the grafting of PLA and PGA (PLGA), or polycaprolactone (PCL) showed suitable properties for the application in tissue engineering [44]. By taking advantage of the formability of polymers and including controlled volume fractions of a bioactive ceramic phase, mechanical reinforcement of the fabricated scaffold can be achieved [45]. At the same time, the poor bioactivity of most polymers can be counteracted. Probably the most important driving force behind the development of polymer/bioceramic composite scaffolds for bone tissue engineering is the need for conferring bioactive behavior to the polymer matrix, which is achieved by the bioactive inclusions or coatings. The degree of bioactivity is adjustable by the volume fraction, size, shape, and arrangement of fillers [47]. It has been shown that increased volume fraction and higher surface-area-to-volume ratio of fillers favor higher bioactivity; hence, in some applications the incorporation of fibers instead of particles is favored [46]. Addition of bioactive phases to bioresorbable polymers can also alter the polymer degradation behavior, by allowing rapid exchange of protons in water for alkali in the glass or ceramic. This mechanism is suggested to provide a pH-buffering effect at the polymer surface, modifying the acidic polymer degradation. In related research, it has been reported that polymer composites filled with HA particles hydrolyzed homogeneously due to water penetrating the interfacial regions [47]. Ideally, the degradation and resorption kinetics of composite scaffolds are designed to allow cells to proliferate and secrete their own extracellular matrix, while the scaffolds gradually vanish, leaving space for new cell and tissue growth. The physical support provided by the 3D scaffold should be maintained until the engineered tissue has sufficient mechanical integrity to support itself.

Recently, composite materials comprising a bioactive phase within a biodegradable polymer matrix have been developed. In particular, the challenging idea to design *tissue-inspired composite materials* moves toward the synthesis of ceramic–polymer composites which show advantages over either pure ceramic or polymer [48, 49], resulting in a superior material for the specific application. Traditionally, calcium phosphate-based ceramics have proved to be attractive materials for biological applications. Among these bioceramics, particular attention has been given to hydroxyapatite  $\text{Ca}_{10}(\text{PO}_4)_6(\text{OH})_2$  whose atomic calcium to phosphorus (Ca/P) ratio is 1.67.

In recent years, design studies of scaffold composite materials were performed to successfully reproduce the microenvironment required to support and nurture the molecular interactions which occur within tissues, between cells, and within the mineralized extracellular matrix (ECM). It is well known that scaffold architecture plays a crucial role in initial cell attachment and subsequent migration into and through the matrix and in mass transfer of nutrients and metabolites, providing sufficient space for development and later remodeling of the organized tissue [50].

An adequate definition of the morphological features (i.e., pore size) is strongly required to assure cell adhesion, molecular transport, vascularization, and osteogenesis. For instance, small pores (with diameters of few microns) favor hypoxic conditions and induce osteochondral formation before osteogenesis occurs [51]. In contrast, scaffold architectures with larger pores (several 100  $\mu$  in size) rapidly induce a well-vascularized network and lead to direct osteogenesis [51].

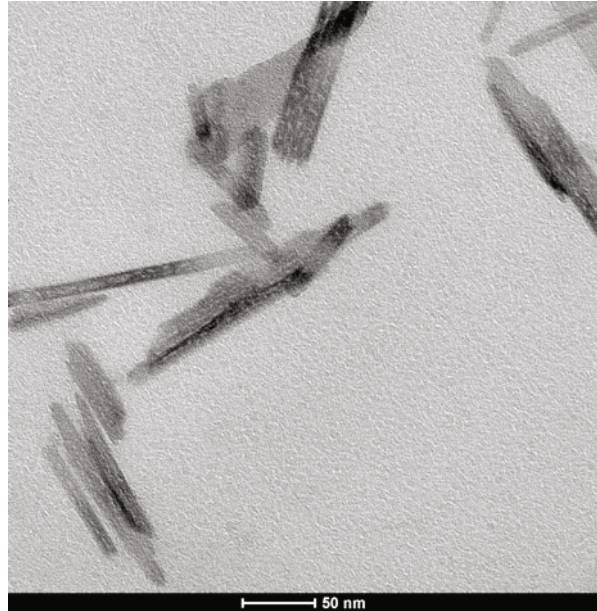
There are numerous ways to synthesize HA. Widely used processes include aqueous colloidal precipitation, sol–gel, solid-state, and mechanochemical methods. These may be synthesized at room temperature and provide the ability to control directly the particle and grain sizes [48]. In comparison with traditional strategies involving physical mixing of HA, they assure a more controlled and fine distribution of crystallites of compounds into polymer matrices. This provides an improved mechanical response in terms of strength, stiffness, toughness, and fatigue resistance to reach the complete mechanical compatibility [46].

### **Sol–Gel Approach to Prepare Biocomposite Materials**

A sol–gel method enables the powder less processing of glasses, ceramics, and thin films or fibers directly from solution. Precursors are mixed at the molecular level, and variously shaped materials may be formed at much lower temperatures than it is possible by traditional methods of preparation. One of the major advantages of sol–gel processing is the possibility to synthesize hybrid organic–inorganic materials. Combination of inorganic and organic networks facilitates the design of new engineering materials with exciting properties for a wide range of applications.

The organic–inorganic hybrid materials may be prepared in various ways. The simplest one relies on dissolution of organic molecules in a liquid sol–gel [52]. The other way uses the impregnation of a porous gel in the organic solution. In the third type, the inorganic precursor either already has an organic group or reactions occur in a liquid solution to form chemical bonds in the hybrid gel. The sol–gel process itself leads to formation of gels from mixtures of liquid reagents (sols) at room temperatures. It involves several steps: the evolution of inorganic networks, formation of colloidal suspension (sol), and gelation of the sol to form a network in a continuous liquid phase (gel). During the “aging” step (after gelation and before drying), the sol–gel-derived material expulses the liquid phase (solvent which can be water or alcohol) in the process called syneresis. Drying of the obtained gels, even at room temperature, produces glass-like materials called xerogels (i.e., xeros). The process generates a porous material, where the pore size depends on such factors as

**Fig. 3** Hydroxyapatite nanocrystals (HA) synthesized by sol-gel technology



time and temperature of the hydrolysis and the kind of catalyst used. The diameter of the pores is directly related to the shrinkage of the “wet” gels. During the drying process, the gel volume decreases even several times (which is the main reason of cracking).

In particular, the sol-gel process for preparing HA usually can produce fine-grained microstructure containing a mixture of nano-to-submicron crystals (Fig. 3). These crystals can be better accepted by the host tissue. The sol-gel product is characterized by nanosize dimension of the primary particles. This small domain is a very important parameter for improvement of the contact reaction and the stability at the artificial/natural bone interface. Moreover, the high reactivity of the sol-gel powder allows a reduction of processing temperature and any degradation phenomena occurring during sintering [53]. Moreover, the low temperature of process allows to introduce bioactive molecules (i.e., growth factors, peptides, dendrimer, antibiotics) sensible to high temperature [54]. The major limitation of the sol-gel technique application is linked to the possible hydrolysis of phosphates and the high cost of the raw materials. On the other hand, most of the sol-gel processes require a strict pH control, vigorous agitation, and a long time for hydrolysis. These problems were solved by using a non-alkoxide-based sol-gel approach where the calcium and phosphate precursors are calcium nitrate tetrahydrate and phosphorous pentoxide, respectively [53]. More importantly, gel formation is achieved without the need for any refluxing steps. In this case, the  $P_2O_5$  reacts with alcohol to form  $P(O)(OR)_3$  oxyalkoxide with the liberation of water, which in turn partially hydrolyzes the oxyalkoxide precursors. The presence of phosphorus hydroxyl alkoxide is not sufficient in itself to form a gel, indicating the important role of  $Ca(NO_3)_2 \cdot 4H_2O$ . It may be speculated that  $Ca(NO_3)_2 \cdot 4H_2O$  probably results in the

generation of alkoxy-nitrate salts which participate in a polymerization reaction with the partially hydrolyzed phosphate precursors, the polymerization reaction thereby resulting in the gel. For the synthesis of the organic–inorganic composite material PCL/HA, the polymer may be added during the production of inorganic phase in order to allow the chemical interactions between the components [55, 56]. Molecular-level mixing of calcium and phosphorous precursors with the polymer chains derived from the sol–gel process resulted in composites having enhanced dispersion and exhibiting good interaction between the inorganic phase and the polymer matrix. Several studies have demonstrated by FTIR and AFM analyses the presence of hydrogen bond in the composite materials synthesized by sol–gel method [56]. Moreover, the presence of HA particles in the composite material beneficially offsets the acidic release from the polymer through the alkaline calcium phosphate and mitigates erosion problems associated with the release of acidic degradation products. *In vivo* and *in vitro* measurements of pH in bone chambers have shown that the pH drop is 0.2 units near the eroding polyesters [57]. Furthermore, it is possible to evaluate a homogeneous distribution of n-HA crystals with 10–30 nm as diameter and 40–50 nm as length obtained by sol-gel process. A homogeneous distribution of nanoscale hydroxyapatite particles in the polymeric matrix allows an increase of bioactive potential of materials. Many investigations of nanophase materials to date have illustrated their potential for bone repair. For example, increased osteoblast adhesion on nano-grained materials in comparison to conventional (micron grained) materials has been reported [58]. Osteoblast proliferation *in vitro* and long-term functions were also enhanced on ceramics with grain or fiber sizes <100 nm [10]. In addition to osteoblast responses, modified osteoclast behavior has also been documented on nanophase ceramics, and *in vivo* studies have demonstrated increased new bone formation on metals coated with n-HA compared to conventional apatite.

## Types of Reinforcements Used for Biocomposites

The reinforcements used for biomedical composites are of two types: fibers and particulates that are harder and stronger than the matrix and hence reinforce the composites. Properties of biomedical composites are strongly affected by a number of factors [46], such as:

1. Reinforcement shape, size, and size distribution
2. Reinforcement properties and volume percentage
3. Bioactivity of the reinforcement (or the matrix)
4. Matrix properties (molecular weight, grain size, etc.)
5. Distribution of the reinforcement in the matrix
6. Reinforcement–matrix interfacial state

Among these factors, properties of constituent materials are major influencing factors. However, factors such as composite architecture (the reinforcement percentage, distribution and orientation, etc.) and reinforcement–matrix bonding condition



also play important roles. By carefully controlling these factors, the mechanical and biological performance of bioactive composites can be tailored so as to meet various clinical requirements. Brief discussions of major factors for bioactive particle-filled polymers are given in this section.

The physical characteristics (shape, size, size distribution, etc.) of the reinforcement are very important in determining mechanical properties of a composite. In the idealized situation for mathematical modeling of the mechanical behavior of a particulate composite, the reinforcement is normally assumed to have a spherical shape. In reality, bioactive, reinforcing particles may have an irregular, platy, or acicular shape. HA particles in commercially available, spray-dried powders can have an irregular shape, which are composed of tightly bonded HA crystallites. This type of irregular shape is preferred to the spherical shape, as the molten polymer can penetrate into troughs on the particle surface during high temperature composite processing and thus form mechanical interlock with the particle at the ambient or body temperature, whereas the smooth surface of spherical particles does not provide such a locking mechanism and thus in the absence of chemical bonding between the polymer and the particle will debond from the polymer when a tensile stress is applied. When particles of calcium phosphates produced via the precipitation method are directly used for the composites, the nanometer size particles generally have the acicular shape. In such a situation, the aspect ratio (i.e., the width-to-length ratio) of the particles is an important parameter, and the orientation of acicular particles should be considered.

Using the conventional processing technology to produce bioactive composites, the average size of bioactive particles (primary particles) normally ranges from several micrometers to tens of micrometers. Fine ceramic particles tend to combine together to form strongly bonded aggregates which may further unite to produce even larger structures, commonly termed “agglomerates.” To form high-quality and high-performance ceramic–polymer composites, the particle agglomerates or aggregates must be broken down during composite processing into primary particles (i.e., the smallest particulate pieces of the minor component existing in as-fabricated or as-received ceramic powder) which are sufficiently dispersed in the polymer matrix. Dispersing particles from the condensed state to the intermediate state may not be sufficient as the particle contacting points will provide crack initiation sites or act to enhance crack propagation thus causing premature failure of the composite when the composite is under mechanical stresses. Ideally, particles present in the composite should be in a dispersed state, as shown in Fig. 4.

The hard bioceramic particles in composites not only provide the reinforcement but also render the composite bioactive when there is a sufficient amount of the particles in the composite. For achieving the reinforcing effect, factors such as the size, shape, and mechanical properties of the particles need to be considered. For example, Young’s modulus values of bulk HA, bioglass, and glass-ceramic A–W are 80–120 GPa [59], 30–35 GPa, and 118 GPa [60], respectively. If a high bioactivity level is desired for achieving a strong bond between the composite implant and the host tissue within a short period, bioceramics exhibiting high degrees of bioactivity

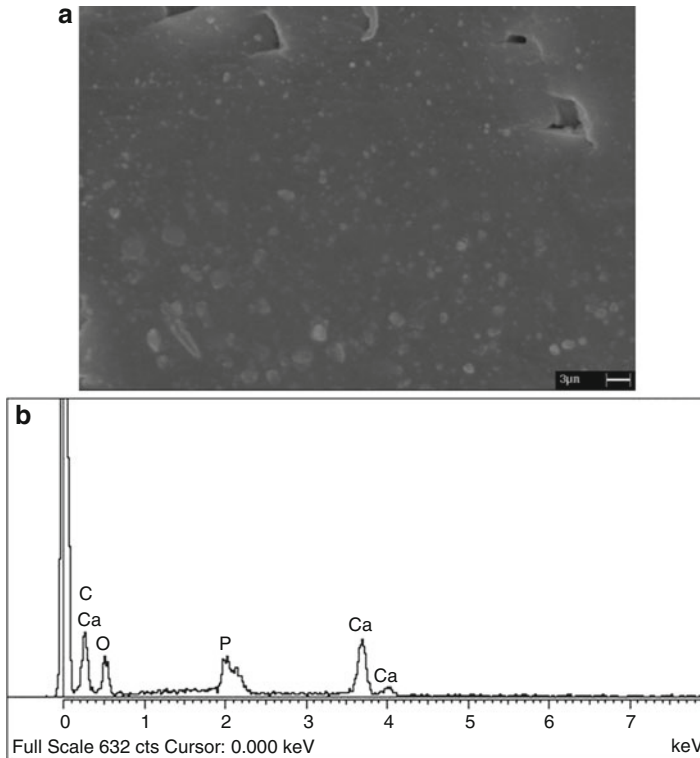


**Fig. 4** (a) SEM image: distribution of hydroxyapatite nanoparticles in polymeric matrix PCL/HA; (b) EDS analysis performed on ceramic particles, atomic ratio Ca/P 1.65

such as bioglass can be selected for the composite. Different bioceramics have their own characteristics, and the judicious selection of a particular bioceramic for the composite is based on the clinical requirement, the composite production route, and sometimes the cost involved.

When selecting a polymer among different grades of the polymer for the matrix of a composite, attention needs to be paid to its average molecular weight, which can affect various characteristics of the polymer including melting/crystallization behavior, viscosity at processing temperatures, mechanical properties, and degradation behavior if the polymer is biodegradable. It is obvious that the polymer of the highest average molecular weight among different grades should be used for tissue substituting composites as strength and stiffness comparable to those of the tissue are required of the composite. However, compromises on the selection may have to be made with regard to processability of the polymer, and hence, the composite as, among many practical concerns, too high a viscosity at the elevated processing temperature will not yield a defect-free, thermally non-degraded composite.

## Biological and Mechanical Properties of Biocomposites

Ceramic–polymer composites are widely studied alongside their application in bone/tissue regeneration because of the excellent combination of bioactivity and osteoconductivity of the ceramics and the flexibility and shape controllability of the polymers. For example, HA and TCP powders were mechanically mixed with different polymers, such as poly(glycolic acid), PCL, and their copolymers, and their biomedical applications were studied [61]. The addition of bioactive ceramic particles, fibers, or whiskers to polymers improves not only the biological properties but also the mechanical properties of polymeric scaffolds [62]. The mechanical properties of the nanocomposites play a significant role in bone tissue engineering.

Laurencin's group developed a nanocomposite using PLGA microspheres as a matrix and amorphous calcium phosphate nanoparticles as a reinforcement phase to optimize the structure of the sintered microsphere matrix with various microsphere diameters. They studied the osteoconductivity of the optimal structure with respect to human osteoblasts [62]. The cell studies demonstrated that the primary cultured human cells proliferated through the pores of the matrix and also continued to express their osteoblast phenotype. The compressive modulus of 64.7 MPa was obtained by heating the microspheres at 4 °C for 90 min, with a high polymer–ceramic ratio [62]. This modulus is within the range of trabecular bone. Since bone is composed of HA and collagen, many attempts have been made to introduce nano-HA (n-HA) particles into a polymer matrix to improve the mechanical as well as biological properties of the scaffolds and mimic the synthetic structure of bone [62, 63]. Sharifi et al. developed a new biodegradable nanocomposite based on poly(hexamethylene-carbonate-fumarate) and n-HA [64]. The storage modulus of the nanocomposite increased with increasing n-HA content due to the enhanced interaction between HA particles and poly(hexamethylene-carbonate fumarate) at their interface. The cell proliferation of the poly(hexamethylene-carbonate-fumarate)–HA composites was significantly increased by the addition of n-HA particles into the composites. Therefore, this composite scaffold can be used for bone tissue engineering applications. Raucci et al. developed a composite consisting of HA and PCL through the mediation of a surfactant oleic acid, where the HA nanoparticles were uniformly dispersed within the PCL matrix [65]. The composites showed significant improvement of osteoblastic cell proliferation and osteogenic differentiation of human mesenchymal stem cells (hMSC) compared with the conventional nanocomposites. This nanocomposite may be useful in bone tissue regeneration. Cui et al. investigated the in vitro and in vivo biodegradation of a biomimetic bone scaffold composite, n-HA/collagen/PLA, which can be used for bone tissue engineering [66]. The compressive strengths increased with increasing PLA content in the composites and reached the lower limit (1 MPa) of natural cancellous bone. The elastic modulus was at the maximum value of 47.3 MPa in the case of 10 % PLA-containing composites, which is comparable with the compressive modulus of trabecular bone (50 MPa). Within a week, osteoblasts adhered, spread, and proliferated throughout the pores of the scaffold composite materials. In vivo, a rabbit segmental defect model was used to evaluate these nanocomposites. It was observed

that the segmental defect was integrated 12 weeks after surgery, and the implanted composite was partially substituted by new bone tissue. This composite scaffold was shown to be a promising material for bone tissue engineering.

The bioactivity and mechanical properties of the nanocomposite scaffolds depend on the shape and size of HA particles on the nanocomposites. Roohani-Esfahani et al. prepared a nanocomposite biphasic calcium phosphate scaffold by coating a nanocomposite layer consisting of HA nanoparticles and PCL and found that the compressive strength of the HA nanoparticle composite-coated scaffolds was  $2.1 \pm 0.17$  MPa, which was significantly higher than that of pure HA/ $\beta$ -TCP ( $0.1 \pm 0.05$  MPa) and micron HA composite-coated scaffolds ( $0.29 \pm 0.07$  MPa) [67]. The use of nanoparticles instead of the micron-sized particles resulted in enhancement of the interfacial bonding between the nanosized particles and the polymer matrix, due to a higher surface area and better wettability. It can also be concluded that the needle-shape particles had significant capability to increase mechanical properties of PCL compared with rod and spherical shapes. These needle-shaped scaffolds also showed the strongest osteoblast differentiation profile compared with other groups, suggesting their potential application in bone tissue regeneration. Composites containing collagen and calcium phosphate have received much more attention because they mimic the basic composition of bone. Cunniffe et al. developed a novel collagen–n-HA nanocomposite scaffold via suspension and immersion methods [68]. The composite scaffolds produced by the suspension method were up to 18 times stiffer than the collagen ( $5.50 \pm 1.70$  vs.  $0.30 \pm 0.09$  kPa). The *in vitro* analysis suggested that there was no significant difference in cell number observed in the case of nanocomposites prepared by the suspension method as compared with the collagen control. The collagen–n-HA nanocomposite scaffold exhibited higher mechanical properties and the same high biological activity as the collagen control scaffold, demonstrating its potential as a bone graft substitute in orthopedic regenerative medicine. Barbani et al. synthesized gelatin/HA nanocomposite-based porous scaffolds using freeze-drying [69]. The elastic modulus of the nanocomposites was very close to natural bone. Biological tests showed good adhesion and proliferation of human MSCs. Luo et al. prepared a HA–gelatin nanocomposite using a coprecipitation method in the presence of aminosilane as a chemical linker to facilitate the binding and solidification of the HA–gelatin nanocomposite [70]. This nanocomposite exhibited a compressive strength of 133 MPa and showed a good biocompatibility based on cell adhesion, proliferation, alkaline phosphate synthesis, and mineralization studies.

## Incorporation of Biomolecules

The possibility of incorporating growth factors into composites formed by biodegradable polymers and bioactive glasses or HA inclusions has started to be explored [71].

Integrins, laminin, and RGD proteins were shown to be essential for cell attachment to materials surfaces [72]. The immobilization of these proteins should not only

promote cell adhesion and proliferation but also increase wettability of hydrophobic polymers such as PDLA. To control protein adhesion and release kinetics, different protein immobilization routes can be used as demonstrated for polymer surfaces [73] and ceramic surfaces [74]. Certain growth factors were shown in *in vivo* studies to be osteoinductive. Possible growth factors include bone morphogenetic proteins, transforming growth factor beta, VEGF, and insulin-like growth factor [75]. Immobilizing these growth factors on the scaffold surface might significantly shorten the bone healing process and reduce patient recovery time.

The incorporation of biomolecules does not allow extreme temperature ranges ( $>70\text{ }^{\circ}\text{C}$ ) or extremely aggressive chemical conditions during processing, being a challenge to the scaffold fabrication process. To achieve this aim, a sol–gel processing might be a strategy to incorporate biomolecules during scaffold fabrication [54]. To the authors' knowledge, however, sol–gel-derived bioactive organic–inorganic hybrids have not yet been formed into highly interconnected porous structures, which is essential for application of these composites as scaffolds.

---

## Conclusions

Bone tissue engineering has emerged as a new area of regenerative medicine, and biomaterials have an essential function concerning cell adhesion, spreading, proliferation, differentiation, and tissue formation in three dimensions. Material design based on organic–inorganic composites not only improves weak points in ceramic biomaterials but also provides various biological functions such as drug delivery and tissue regeneration.

From the materials science perspective, the present challenge in tissue engineering is to design and fabricate reproducible bioactive and bioresorbable 3D scaffolds of tailored porosity and pore structure, which are able to maintain their structure and integrity for predictable times, even under load-bearing conditions.

To improve the osteoconductive and osteoinductive material properties, the incorporation of biomolecules such as growth factors with the aim to accelerate local bone healing is promising and currently under extensive research. Incorporating biomolecules during scaffold processing however is not simple as biomolecules are sensitive to elevated temperatures and extreme chemical conditions. This aim is achieved by using a sol–gel route that also allows a good dispersion of ceramic particles in biocomposites allowing to enhance the fundamental properties of materials.

---

## References

1. Brydone AS, Meek D, Maclaine S (2010) Bone grafting, orthopaedic biomaterials, and the clinical need for bone engineering. *Proc Inst Mech Eng H* 224:1329–1343

2. James R, Deng M, Laurencin C, Kumbar S (2011) Nanocomposites and bone regeneration. *Front Mater Sci* 5:342–357
3. Duan B, Wang M, Zhou WY, Cheung WL, Li ZY, Lu WW (2010) Three-dimensional nanocomposite scaffolds fabricated via selective laser sintering for bone tissue engineering. *Acta Biomater* 6:4495–4505
4. Scholz MS, Blanchfield JP, Bloom LD et al (2011) The use of composite materials in modern orthopaedic medicine and prosthetic devices: a review. *Compos Sci Technol* 71:1791–1803
5. Black J (1992) Biological performance of materials fundamentals of biocompatibility. Marcel Dekker, New York
6. Williams DF (1998) Consensus and definitions in biomaterials. In: de Putter C, de Lange K, de Groot K, Lee AJC (eds) *Advances in biomaterials*. Elsevier, Amsterdam, pp 11–16
7. Hench LL (1998) Bioceramics. *Am Ceram Soc* 81:1705–1727
8. Hench LL, Wilson J (1993) *An introduction to ceramics*. World Scientific, London
9. Hench LL, Splinter RJ et al (1971) Bonding mechanisms at the interface of ceramic prosthetic materials. *J Biomed Mater Res* 2:117–141
10. Hench LL (1991) Bioceramics; from concept to clinic. *J Am Ceram Soc* 74:1487–1510
11. Jarcho M, Bolen CH, Thomas MB, Bobick J, Kay JF, Doremus RH (1976) Hydroxyapatite synthesis and characterization in dense polycrystalline forms. *J Mater Sci* 11:2027–2035
12. Cho SB, Nakanishi K, Kokubo T et al (1995) Dependence of apatite formation on silica gel on its structure: effect of heat treatment. *J Am Ceram Soc* 78:1769–1774
13. Kawai T, Ohtsuki C, Kamitakahara M et al (2004) Coating of apatite layer on polyamide films containing sulfonic groups by biomimetic process. *Biomaterials* 25:4529–4534
14. Sugino A, Tsuru K, Hayakawa S et al (2009) Induced deposition of bone-like hydroxyapatite on thermally oxidized titanium substrates using a spatial gap in a solution that mimics a body fluid. *J Ceram Soc Jpn* 117:515–520
15. Boretos JW (1987) Advances in bioceramics. *Adv Ceram Mater* 2:15–24
16. Hench LL, Splinter RJ, Allen WC, Greenlee TK (1972) Bonding mechanisms at the interface of ceramic prosthetic materials. *J Biomed Mater Res Symp* 2:117–141
17. Hulbert SF, Bokros JC, Hench LL, Wilson J, Heimke G (1997) Ceramics in clinical applications, past, present and future. In: Vincenzini P (ed) *Ceramics in clinical applications*. Elsevier, Amsterdam, pp 3–27
18. Sola A, Bellucci D, Raucci MG, Zeppetelli S, Ambrosio L, Cannillo V (2011) Heat treatment of  $\text{Na}_2\text{O}-\text{CaO}-\text{P}_2\text{O}_5-\text{SiO}_2$  bioactive glasses: densification processes and post-sintering bioactivity. *J Biomed Mater Res A* 100A:305–322
19. Van Blitterswijk CA, Grote JJ, Kuypers W et al (1985) Bioreactions at the tissue-hydroxyapatite interface. *Biomaterials* 6:243–251
20. Kokubo T (1990) Surface chemistry of bioactive glass-ceramics. *J Non-Cryst Solids* 120:138–151
21. Sanchez-Sálcedo S, Arcos D, Vallet-Regi M (2008) Upgrading calcium phosphate scaffolds for tissue engineering applications. *Key Eng Mater* 377:19–42
22. Daculsi G, Jegoux F, Layrolle P (2009) The micro macroporous biphasic calcium phosphate concept for bone reconstruction and tissue engineering. In: Basu B, Katti DS, Kumar A (eds) *Advanced biomaterials: fundamentals, processing and applications*. John Wiley & Sons, Inc., Hoboken, NJ, p 768
23. Jones AC, Arns CH, Sheppard AP, Hutmacher DW, Milthorpe BK, Knackstedt MA (2007) Assessment of bone ingrowth into porous biomaterials using MICRO-CT. *Biomaterials* 28:2491–2504
24. Mastrogiacomo M, Scaglione S, Martinetti R, Dolcini L, Beltrame F, Cancedda R et al (2006) Role of scaffold internal structure on in vivo bone formation in macroporous calcium phosphate bioceramics. *Biomaterials* 27:3230–3237
25. Zhang HG, Zhu Q (2007) Preparation of porous hydroxyapatite with interconnected pore architecture. *J Mater Sci Mater Med* 18:1825–1829

26. Ota Y, Kasuga T, Abe Y (1997) Preparation and compressive strength behaviour of porous ceramics with  $\beta$ - $\text{Ca}_3(\text{PO}_3)_2$  fiber skeletons. *J Am Ceram Soc* 80:225–231
27. Potoczek M, Zima A, Paszkiewicz Z, Słószarczyk A (2009) Manufacturing of highly porous calcium phosphate bioceramics via gel-casting using agarose. *Ceram Int* 35:2249–2254
28. von Doernberg MC, von Rechenberg B, Bohner M et al (2006) In vivo behavior of calcium phosphate scaffolds with four different pore sizes. *Biomaterials* 27:5186–5198
29. Mygind T, Stiehler M, Baatrup A et al (2007) Mesenchymal stem cell in growth and differentiation on coralline hydroxyapatite scaffolds. *Biomaterials* 28:1036–1047
30. Holmes RE (1979) Bone regeneration within a coralline hydroxyapatite implant. *Plast Reconstr Surg* 63:626–633
31. Tsuruga E, Takita H, Wakisaka Y, Kuboki Y (1997) Pore size of porous hydroxyapatite as the cell-substratum controls BMP-induced osteogenesis. *J Biochem* 121:317–324
32. Hing K, Annaz B, Saeed S, Revell P, Buckland T (2005) Microporosity enhances bioactivity of synthetic bone graft substitutes. *J Mater Sci Mater Med* 16:467–475
33. Dubok VA (2000) Bioceramics – yesterday, today, tomorrow. *Powder Metall Met Ceram* 39:381–394
34. Ducheyne P, Qiu Q (1999) Bioactive ceramics: the effect of surface reactivity on bone formation and bone cell function. *Biomaterials* 20:2287–2303
35. Ohtsuki C, Kamitakahara M, Miyazaki T (2009) Bioactive ceramic-based materials with designed reactivity for bone tissue regeneration. *J R Soc Interface* 6:S349–S360
36. le Nihouannen D, Daculsi G, Saffarzadeh A et al (2005) Ectopic bone formation by microporous calcium phosphate ceramic particles in sheep muscles. *Bone* 36:1086–1093
37. Nagase M, Baker DG, Schumacher HR (1988) Prolonged inflammatory reactions induced by artificial ceramics in the rat pouch model. *J Rheumatol* 15:1334–1338
38. Malik MA, Puleo DA, Bizios R, Doremus RH (1992) Osteoblasts on hydroxyapatite, alumina and bone surfaces in vitro: morphology during the first 2 h of attachment. *Biomaterials* 13:123–128
39. Gomi K, Lowenberg B, Shapiro G, Davies JE (1992) Resorption of sintered synthetic hydroxyapatite by osteoclasts in vitro. *Biomaterials* 20:91–96
40. Okuda T, Ioku K, Yonezawa I et al (2007) The effect of the microstructure of  $\beta$ -tricalcium phosphate on the metabolism of subsequently formed bone tissue. *Biomaterials* 28:2612–2621
41. Okumura M, Ohgushi H, Tamai S (1990) Bonding osteogenesis in coralline hydroxyapatite combined with bone marrow cells. *Biomaterials* 12:28–37
42. Unger RE, Sartoris A, Peters K et al (2007) Tissue like self-assembly in cocultures of endothelial cells and osteoblasts and the formation of microcapillary like structures on three-dimensional porous biomaterials. *Biomaterials* 28:3965–3976
43. de Groot K, Lein CPAT, Wolke JGC, de Blik-Hogervost JMA (1990) Chemistry of calcium phosphate bioceramics. In: Yamamuro T, Hench LL, Wilson J (eds) *Handbook of bioactive ceramics*. CRC Press, Boca Raton, pp 3–16
44. Chiu JB, Liu C, Hsiao BS, Chu H, Hadjiargyrou M (2007) Functionalization of poly(L-lactide) nanofibrous scaffolds with bioactive collagen molecules. *J Biomed Mater Res A* 83A:1117–1127
45. Boccaccini AR, Maquet V (2003) Bioresorbable and bioactive polymer/bioglass(R) composites with tailored pore structure for tissue engineering applications. *Compos Sci Technol* 63:2417–2429
46. Wang M (2003) Developing bioactive composite materials for tissue replacement. *Biomaterials* 24:2133–2151
47. Shikunami Y, Okuno M (2001) Bioresorbable devices made of forged composites of hydroxyapatite (HA) particles and poly-lactide (PLLA). Part II: practical properties of miniscrews and miniplates. *Biomaterials* 22:3197–3211
48. Basile MA, Gomez D' Ayala G, Laurienzo P, Malinconico M, Della Ragione F, Oliva A (2012) Development of innovative biopolymers and related composites for bone tissue regeneration: study of their interaction with human osteoprogenitor cells. *J Appl Biomater Funct Mater* 10:210–214

49. Catauro M, Raucci MG, De Marco D, Ambrosio L (2006) Release kinetics of ampicillin, characterization and bioactivity of TiO<sub>2</sub>/PCL hybrid materials synthesized by sol–gel processing. *J Biomed Mater Res* 77A:340–350
50. Ng AM, Tan KK, Phang MY et al (2008) Differential osteogenic activity of osteoprogenitor cells on HA and TCP/HA scaffold of tissue engineered bone. *J Biomed Mater Res* 85A:301–312
51. Karande TS, Ong JL, Agrawal CM (2004) Diffusion in musculoskeletal tissue engineering scaffolds: design issues related to porosity, permeability, architecture, and nutrient mixing. *Ann Biomed Eng* 32:1728–1743
52. Raucci MG, D'Antò V, Guarino V, Zeppetelli S, Ambrosio L (2010) Biocompatibility and osteoconductivity studies on hydroxyapatite-polymer composite scaffolds prepared by chemical synthesis. *J Appl Biomater Biomech* 8:123
53. Linhart W, Peters F, Lehmann W et al (2001) Biologically and chemically optimized composites of carbonated apatite and polyglycolide as bone substitution materials. *J Biomed Mater Res* 54:166–171
54. Raucci MG, Alvarez-Perez MA, Meikle S, Ambrosio L, Santin M (2014) Poly(epsilon-Lysine) dendrons tethered with phosphoserine increase mesenchymal stem cell differentiation potential of calcium phosphate gels. *Tissue Eng A* 20:474–485
55. Dessì M, Raucci MG, Zeppetelli S, Ambrosio L (2012) Design of injectable organic–inorganic hybrid for bone tissue repair. *J Biomed Mater Res A* 100:2063–2070
56. Raucci MG, Guarino V, Ambrosio L (2010) Hybrid composite scaffolds prepared by sol–gel method for bone regeneration. *Compos Sci Technol* 70:1861–1868
57. Liu H, Webster TJ (2007) Nanomedicine for implants: a review of studies and necessary experimental tools. *Biomaterials* 28:354–369
58. Kokubo T (1998) Apatite formation on surfaces of ceramics, metals and polymers in body environment. *Acta Mater* 46:2519–2527
59. Lü X, Zheng B, Tang X, Zhao L, Lu J, Zhang Z, Zhang J, Cui W (2011) In vitro biomechanical and biocompatible evaluation of natural hydroxyapatite/chitosan composite for bone repair. *J Appl Biomater Biomech* 9:11–18
60. Mobasherpour I, Soulati Heshajin M, Kazemzadeh A, Zakeri M (2007) Synthesis of nanocrystalline hydroxyapatite by using precipitation method. *J Alloys Compd* 430:330–333
61. Ronca A, Ambrosio L, Grijpma DW (2012) Design of porous three-dimensional PDLLA/nano-hap composite scaffolds using stereolithography. *J Appl Biomater Funct Mater* 10:249–258
62. Khan YM, Katti DS, Laurencin CT (2004) Novel polymer-synthesized ceramic composite-based system for bone repair: an in vitro evaluation. *J Biomed Mater Res A* 69:728–737
63. Raucci MG, Alvarez-Perez MA, Demitri C, Sannino A, Ambrosio L (2012) Proliferation and osteoblastic differentiation of hMSCs on cellulose-based hydrogels. *J Appl Biomater Funct Mater* 10:302–307
64. Sharifi S, Kamali M, Mohtaram NK et al (2011) Preparation, mechanical properties, and in vitro biocompatibility of novel nanocomposites based on polyhexamethylene carbonate fumarate and nanohydroxyapatite. *Polym Adv Technol* 22:605–611
65. Raucci MG, D'Antò V, Guarino V, Sardella E, Zeppetelli S, Favia P, Ambrosio L (2010) Biomimetic porous composite scaffolds prepared by chemical synthesis for bone tissue regeneration. *Acta Biomater* 6:4090–4099
66. Liao SS, Cui FZ (2004) In vitro and in vivo degradation of mineralized collagen-based composite scaffold: nanohydroxyapatite/collagen/poly(L-lactide). *Tissue Eng* 10:73–80
67. Roohani-Esfahani SI, Nouri-Khorasani S, Lu ZF, Appleyard R, Zreiqat H (2010) The influence hydroxyapatite nanoparticle shape and size on the properties of biphasic calcium phosphate scaffolds coated with hydroxyapatite–PCL composites. *Biomaterials* 31:5498–5509
68. Cunniffe GM, Dickson GR, Partap S, Stanton KT, O'Brien FJ (2010) Development and characterisation of a collagen nano-hydroxyapatite composite scaffold for bone tissue engineering. *J Mater Sci Mater Med* 21:2293–2298



69. Barbani N, Guerra GD, Cristallini C et al (2012) Hydroxyapatite/gelatin/gellan sponges as nanocomposite scaffolds for bone reconstruction. *J Mater Sci Mater Med* 23:51–61
70. Luo TJM, Ko CC, Chiu CK, Llyod J, Huh U (2010) Aminosilane as an effective binder for hydroxyapatite–gelatin nanocomposites. *J Sol–Gel Sci Technol* 53:459–465
71. Anselme K (2000) Osteoblast adhesion on biomaterials. *Biomaterials* 21:667–681
72. Kang IK, Kwon BK, Lee JH, Lee HB (1993) Immobilization of proteins on poly(methyl methacrylate) films. *Biomaterials* 14:787–792
73. Williams RA, Blanch HW (1994) Covalent immobilization of protein monolayers for biosensor applications. *Biosens Bioelectron* 9:159–167
74. Heule M, Rezwan K, Cavalli L, Gauckler LJ (2003) A miniaturized enzyme reactor based on hierarchically shaped porous ceramic microstruts. *Adv Mater* 15:1191–1194
75. Jansen JA, Vehof JWM, Ruhe PQ et al (2005) Growth factor-loaded scaffolds for bone engineering. *J Control Release* 101:127–136

Corrado Piconi and Alessandro Alan Porporati

## Contents

Introduction .....	60
Alumina .....	61
Alumina: Physical Properties .....	62
Alumina: Mechanical Properties .....	63
Alumina Stability .....	66
Zirconia .....	67
Zirconia Physical Properties .....	68
Zirconia Mechanical Properties .....	70
Zirconia Stability .....	71
Zirconia Radioactivity .....	72
Alumina–Zirconia Composites .....	73
Zirconia-Toughened Alumina .....	74
Alumina-Toughened Zirconia .....	78
Biocompatibility of Bioinert Ceramics .....	80
In vitro Tests .....	81
In vivo Tests .....	81
Carcinogenicity .....	81
Reaction to Ceramic Wear Debris .....	83
Processing of Bioinert Ceramics for Joint Replacements .....	85
Summary .....	87
References .....	87

---

C. Piconi (✉)

Medicine and Surgery Department, Clinical Orthopedics and Traumatology Institute, Catholic University, Rome, Italy

e-mail: [corpico@libero.it](mailto:corpico@libero.it)

A.A. Porporati

Medical Products Division, CeramTec GmbH, Plochingen, Germany

e-mail: [a.porporati@ceramtec.de](mailto:a.porporati@ceramtec.de)

---

**Abstract**

Alumina and zirconia are used as biomaterials since long. The use of alumina, especially, as a dental implant and porous bone substitute was reported in the first half of the 1960s.

Both these ceramics exhibit a high chemical inertness, which is the reason for their high biological safety even at the higher specific surfaces. Due to their hardness being higher than the other metal alloys, alumina and zirconia found their main application as biomaterials in the articular surfaces of joint replacements. Today, the use of zirconia ball heads has practically ceased in hip arthroplasty. Zirconia ceramics are used mostly in dentistry, while in orthopedics are still in use in some niche products. In association with alumina, zirconia is used in the ceramic composites that are presently the reference bioinert ceramic for clinical applications. This chapter is an overview of the development of bioinert ceramics, as well as of their physical and mechanical properties. The behavior of the present composite bioinert ceramics is also described in detail, and a review is given of the studies carried out to assess the biological safety of alumina and zirconia. Finally, the flow sheet of a possible production process for the manufacture of bioinert ceramic components is outlined.

---

**Introduction**

At the end of the 1960s, arthroplasty was becoming a well-accepted procedure in orthopedics, thanks to the introduction devices making use of a metal-on-metal (MoM) and metal-on-polyethylene (MoP) bearings. The medium term follow-ups nevertheless were showing the relevance of the reactions to wear debris in the cascade of events leading to osteolysis and to aseptic loosening of implants. There was the need of low-wear bearings, and Dr. Pierre Boutin, a surgeon with practice in Pau, a town in southern France, started to investigate the feasibility of an all-ceramic bearing making use of high purity alumina. It is likely that Boutin focused his attention on alumina on the basis of the good clinical results obtained by the alumina dental implants developed by Sandhaus in Switzerland and by Driskell in the USA in the same period [1]. Alumina was by that time the most advanced ceramic material, thanks to the availability of high alumina powder Degussit Al23 in the market that allowed to overcome many limitations of the former ceramic precursors. While it is likely that these pioneers selected alumina for its inertness in the biological environment, this concept has been abandoned since a long while because it is known that whatever material once implanted elicits a host reaction. Nevertheless, the concept of “bioinert” ceramics is still used to distinguish alumina and zirconia from the so-called bioactive or bioreactive materials, and in this way it is also used in the title of this chapter.

Zirconia was introduced as a biomaterial during the second half of the 1980s [2]. The mechanical properties of zirconia allowed overcoming some limitation in design of alumina ceramic devices. Moreover, the better mechanical properties of zirconia led to consider the ceramic components made out this material (essentially

ball heads for Total Hip Replacements) more forgiving about mechanical stresses than the corresponding alumina ones. Unfortunately, the Yttria-stabilized Tetragonal Zirconia Polycrystals (Y-TZP) – i.e., the zirconia ceramic largely used as a biomaterial – is a metastable material whose processing has several criticalities. This led to a number of failures and to the practical abandonment of zirconia in orthopedics around the year 2000, and to a review of the requirements specified in international standards for load bearing ceramics for clinical applications. While the use of zirconia in orthopedics was stopped, there was a growing interest in dentistry where presently this material is used for the production of dental implants, as well for CAD-CAM production of bridges, crowns, and in structures of dentures [3].

So far, alumina and zirconia are used in a synergistic way in alumina-zirconia composites, which are the standard load-bearing bioceramics in hip arthroplasty. “Bioinert” ceramic composites are showing mechanical and wear behavior that allowed designing of a number of innovative medical devices during the last years and other ones to come in the future (see Chap. 28, “► [Perspective and Trends on Bioceramics in Joint Replacement](#),” this Handbook).

---

## Alumina

Alumina (Aluminum oxide –  $\text{Al}_2\text{O}_3$ ) is one of the biomaterials with longer clinical use. Alumina has about 45 years of clinical record in orthopedics where it is still in use as “pure” alumina either as a component of high-performances ceramic composites. The material characteristics improved through the years thanks to the improvements introduced in raw materials (ceramic precursors) and in ceramic processing. Alumina is so widely accepted in orthopedics that even in scientific journals the use of the term “ceramic” without any other specification is indicating alumina, a wording that seems to ignore that a number of other ceramics are today in clinical use. However, in this chapter, we will follow the current use, then “ceramic” will mean “alumina”, if not differently specified.

The German Patent by M. Rock, issued in 1933, contains the first mention of alumina as a material for the construction of “artificial spare parts . . . for humans and animal bodies” [4]. It was uneventful, and the real use of alumina in medical device took place during the 1960s in dental implants thanks to Sandhaus and Driskell [1]. In the same years, Sir John Charnley demonstrated the advantages of “low friction arthroplasty” of the hip over former devices. It was in this atmosphere that Dr. Pierre Boutin with the help of one of his patients, who was a top manager of a CGE France factory that was nearby the Boutin’s practice in Pau, developed the first alumina-on-alumina bearing in total hip arthroplasty. In this device, both the stem and the cup were cemented into the host bone, while the ball head was fixed on a cylindrical trunnion at the extremity of the stem by epoxy glue, a solution that was source of a number of early failures in the first series and was soon abandoned.

Besides Boutin, several other researchers in Germany, Japan, and in the USA were investigating the biomedical applications of alumina during the same years. In Germany, Langer in Keramed, Heimke in Friedrichsfeld, Dörre in Feldmühle, and

Maier in Rosenthal were working in a wide research program funded by the Ministry of Research to develop alumina clinical implants.

In Japan, Oonishi and Kawahara developed alumina devices in close cooperation with Kyocera engineers. Especially relevant are the development of alumina knee replacements (see Chap. 28, “► [Perspective and Trends on Bioceramics in Joint Replacement](#)”) and the use of alumina single crystal hip replacement stems implanted after resection of bone tumors. In the USA, Smith, Hulbert, Driskell, and Ducheyne were investigating the potential of alumina in replacing segmental bone defects and in dental implants [5].

The German research program was aimed to develop hip replacements designed to achieve cementless fixation in the host bone, i.e., by a screw-like profile of the cup. The clinical use of these early large and heavy monolithic devices allowed surgeons and engineers to assess the clinical advantages of alumina-on-alumina bearings in terms of wear reduction and absence of particle-induced osteolysis. Poor outcomes were due to the component design or to failures in the cementation. Nevertheless, in younger patients with good bone quality – in which good primary stability in the cortical bone was achieved – several positive clinical results had been reported [6, 7].

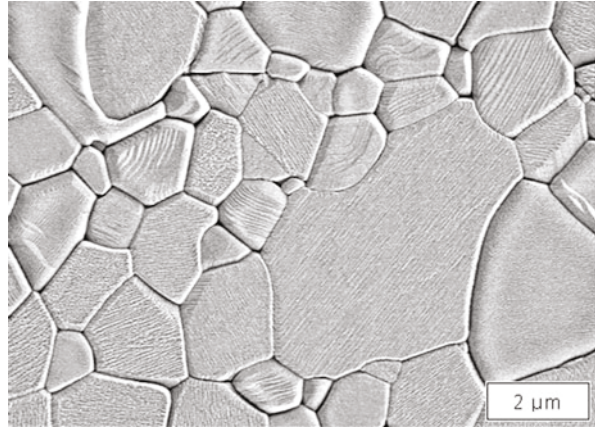
## Alumina: Physical Properties

Alumina (Aluminum oxide,  $\text{Al}_2\text{O}_3$ ) applications as a biomaterial are based on the microstructural properties of this oxide that may occur in many metastable phases, which irreversibly transform into alpha-alumina if heated above 1200 °C. Alpha-alumina is a close packed hexagonal arrangement of oxygen ions that constitute a very high thermodynamically stable phase. Alpha-alumina (also known as corundum, or emery if containing impurities), that is, the material selected for biomedical application, is well known in nature as being the matrix of several gemstones, e.g., ruby red in color for the presence of chromium, or sapphire, blue in color due to both titanium and iron.

The alumina molecule contains strong ionic and covalent chemical bonds between  $\text{Al}^{3+}$  and  $\text{O}^{2-}$  ions that are the origin of the high melting point, hardness, and resistance to the attack of strong inorganic acids of this material. In other words, alpha-alumina is aluminum metal in its highest oxidative state with high chemical and physical stability: namely, it also has a marked resistance to the attack of strong inorganic acids, like e.g., orthophosphoric or hydrofluoric acid. The low electric and thermal conductivity and the high melting point are also due to the energy of the ionic-covalent bonds in the solid.

In the lattice of alpha-alumina, each aluminum cation  $\text{Al}^{3+}$  is surrounded by oxygen anions  $\text{O}^{2-}$  forming two regular triangles on both sides, twisted by 180° and lying on parallel planes. The surface layer of  $\text{O}^{2-}$  anions allow the chemisorption on the surface of  $\text{OH}^+$  groups, then the bonding of water molecules or proteins. In other words, the surface has high wettability, e.g., higher of several metallic alloys.

**Fig. 1** Microstructure of the monolithic alumina BIOLOX<sup>®</sup> forte (Courtesy CeramTec GmbH, Plochingen, Germany)



Surface wettability along with high hardness (2000–2200 GPa) makes alpha-alumina the ideal material in industrial wear applications (e.g., ruby ball bearings) as well as for the components of the bearings for arthroprostheses joints, whose surface, thanks to the high hardness of alpha-alumina, is extremely resistant to scratching. On the other hand, the high hardness that characterizes this material results in complex and costly machining (Fig. 1).

The extremely smooth surface finish achievable by diamond polishing (typical values:  $R_a = 0.02 \mu\text{m}$ ,  $R_t = 0.5 \mu\text{m}$ ), the hardness, and the wettability of alpha-alumina are the reasons of the low wear of the joint replacement bearings making use of alumina components.

A further physical property to be controlled to achieve the best clinical outcomes in alumina bioceramics is the residual porosity of the products. The porosity fraction influences the mechanical properties as explained in the following but especially the open porosity fraction has to be controlled. Namely, liquids and gases can penetrate the ceramic by open porosity, and then it is mandatory to avoid open porosity in alumina devices to be used in the human body.

## Alumina: Mechanical Properties

Alumina, as most ceramics, has moderate tensile and bending resistance and a brittle fracture behavior. Unlike in metals, there is no yielding at the tip of cracks in alumina to dissipate stress. The unavoidable presence of surface defects, notches, and internal flaws increases locally the stress concentration. Especially tensile stresses stimulate the growth of the size of defects, until they become real cracks, and the ceramic fractures. The brittle fracture behavior of alumina (its low toughness) is the main limit in designing alumina components. In addition, because the population of defects in ceramics components has a large scatter in size and in location (see Table 1), the relationships between stress distribution, failure probability, and strength in ceramics need to be discussed on a statistical basis [8].

**Table 1** Physical properties of alpha-alumina

Property	Units	Value
Crystallography	–	Hexagonal
Lattice parameter a	nm	0,476
Lattice parameter c	nm	1,299
Melting point	K	2310
Density (theoretical)	g/cm <sup>3</sup>	3,986
Thermal expansion coeff.	–	6,5
Thermal conductivity (298 K, >99.9%TD)	W/m K	30
Specific heat (298 K)	J/Kg K	8–10 10 <sup>-4</sup>

**Table 2** Defects in ceramics and their origin

Defect type	Defect size	Origin
Delamination	1–100 µm	Powder consolidation. Sintering cycle. Uncontrolled shrinkage
Organic inclusion	0.1–5 µm	Powder (batch) contamination
Inorganic inclusion	0.01–1 µm	Powder (batch) contamination
Surface defects after green machining	0.01–0.05 µm	Binder selection, batch preparation
Porosity due to powder aggregation	0.03–1 µm	Binder selection, batch preparation Powder consolidation
Residual porosity	0.001–1 µm	Powder consolidation, incomplete sintering
Large grains	Depending on microstructure	Powder selection. Batch preparation. Sintering cycle
Surface defects after hard machining	0.001–0.5 µm	Grinding tools selection. Machining parameters
Inhomogeneous grain size	0.0005–1 µm	Powder selection. Batch preparation. Sintering cycle

Alumina is an ionic-covalent solid that does not yield under load as metal and alloys do. The strong chemical bonds in alumina are the roots of several of its behaviors, e.g., the low electric and thermal conductivity, the high melting point that makes it practically impossible to shape alumina by casting, and high hardness that characterizes this material which makes its machining complex and costly.

Ceramics used in joint replacements are polycrystals obtained by the consolidation of powders. Their structure contains a number of “defects” (See Table 2) that may develop their size under stress without any apparent strain at macroscopic level until they reach a critical size, giving origin to the real crack eventually that leads to the catastrophic fracture of the piece. An evident difference between ceramic and metals is that ceramics do not show plastic deformation or yielding before fracture. In other words, ceramic under stress accumulate elastic energy with negligible strain. The energy stored in the material will be

released suddenly would its level overcome a given threshold, originating the fracture of the ceramic part. The defects – especially the ones that are long and thin in shape – are “sensitive” to tensile stresses, which stimulate their growth (the defective surfaces are “thrown apart”) while compressive loads result safer because they tend to “close” the defect.

This behavior can be controlled by the selection of a proper high-purity raw material, by the reduction of the grain size (meaning smaller grain boundaries) and an increase in density (meaning less porosity, less flaws) either by the introduction of toughening mechanism (e.g., by the transformation of selected phase in the material). Nevertheless, although the tensile (bending) strength of several ceramics could exceed the one of many metallic alloys, these materials show fracture energies lower than the metal ones, a fact that has to be carefully taken into account in the design of ceramic components.

One can assume that a ceramic piece will break as a chain: a chain fails if a single link fails. In the same way, ceramic fails if a single “defect” grows under stress until failure. It is noted that the distribution of defects in the structure of a ceramic is not casual, but depends on the overall production process. The design of ceramics must then be made by a probabilistic approach, taking into account the probability that above a given stress level, a single defect can develop its size and grow leading the piece to failure. This is made by applying the theory developed by W. Weibull [9]. Briefly, he developed a mathematical model which is today incorporated in the ISO standard 20501 [10] that allows to determine the probability that a given number of ceramic parts obtained by a given production process can survive until a given stress threshold. This is obtained by the mathematical processing of a set of fracture stress measured on a series of samples identical in shape and volume. The results are the Weibull characteristic strength,  $\sigma_0$ , and the Weibull modulus,  $m$ . They are representing respectively the stress threshold for the survival of 37 % of the samples and the variability of the fracture stress among the samples. The higher the  $m$ , the lower the variability in strength and the reliability of the production process of the material.

As a biomaterial, alumina ceramic has undergone deep improvements in mechanical properties during 40 years of clinical use as described in Chap. 28, “► [Perspective and Trends on Bioceramics in Joint Replacement](#)” of this Handbook. The improvements in the selection of raw materials used as precursors and in sintering process resulted in marked reduction in grain size and in the increase in density, close to the theoretical one [11]. The microstructural improvements gave remarkable increase in bending strength (from less than 400 MPa to more than 630 MPa in pure alumina components – see Table 3). However, only the introduction in clinics of the alumina composite allowed overcoming the limits of alumina in terms of mechanical properties. The toughness and bending strength of the most used alumina composite BIOLOX<sup>®</sup> *delta* (CeramTec GmbH, Plochingen, Germany) are more than twice the former market leader BIOLOX<sup>®</sup> *forte* (CeramTec GmbH, Plochingen, Germany), which is a monolithic alumina.



**Table 3** Mechanical properties of medical grade alumina and alumina composites

Property	Units	Alumina (1970s)	BIOLOX <sup>®</sup> (since 1974)	BIOLOX <sup>®</sup> forte (since 1995)	BIOLOX <sup>®</sup> <i>delta</i>	Ceramys <sup>®</sup> ATZ
Al <sub>2</sub> O <sub>3</sub> content	Vol %	99.1–99.6	99.7	>99.8	80	20
ZrO <sub>2</sub> Content	Vol %	–	–	–	17	80
Density	g/cm <sup>3</sup>	3.90–3.95	3,95	3.97	4,37	5.51
Average grain size Al <sub>2</sub> O <sub>3</sub>	μm	≤4.5	4	1.75	0.56	0.4
Young modulus	GPa	380	410	407	358	–
Hardness	GPa	17.7	20 (HV1)	20 (HV1)	19 (HV1)	15 (HV20)
Flexural strength	MPa	>300	400	631	1384	1039
Fracture toughness	MPa m <sup>1/2</sup>	3.5	4	4.5	6.5	7.4

## Alumina Stability

The long-term stability of alumina in the body environment is one of the cornerstones of its selection as a biomaterial. Strength degradation may occur in alumina due to permeation of liquids through open porosity, which in this way can interact with the microstructural defects (flaws) that are intrinsic to ceramics microstructure, as discussed above. High density and zero open porosity are characteristics relevant for the reliability of alumina components to be used in joint replacements.

The defects in the microstructure of the material have a size (subcritical size) that does not influence the mechanical properties. Nevertheless, depending on several variables (e.g., chemical species concentration, environment, temperature, and stress level) they can grow at a very low speed reaching a critical size, leading the piece to failure. This behavior is known as Subcritical Crack Growth (SCG).

Especially in the late 1970s, SCG was a relevant problem in some alumina devices used in joint replacements, because of the impurity of alkali, calcium and silicon oxides contained in precursors.

Strength degradation can take place for calcium segregation at grain boundaries, as well as for CaO interactions with the aqueous environment. Silica limits densification and promotes grain growth during sintering, decreasing the material strength. Alkalis (e.g., NaO) may segregate at grain boundaries and their dissolution in physiologic liquids may lead to accelerated fatigue fracture [5]. Although the incidence of this problem was not the same for all the materials manufactured at that time, the control of the strength degradation due to chemical impurities in alumina was achieved only after the release of the standard ISO 6474 in 1980 that specified the minimum purity requirements of alumina for clinical implants.

## Zirconia

The metal zirconium is known from very ancient times: the name is a derivation of the Arabic *Zargon*, (golden in color), which derives in turn from the Persian *Zar* (Gold) and *Gun* (Color). Zirconium gemstones are cited in the St. John Apocalypse among the ones forming the walls of the Heavenly Jerusalem. Zirconia, the metal dioxide ( $ZrO_2$ ), was identified in 1789 by German chemist Martin Heinrich Klaproth, and was used for a long time as pigment for ceramics.

The development of zirconia (zirconium dioxide:  $ZrO_2$ ) ceramics as a biomaterial started in the mid-1980s, to manufacture ball heads for total hip replacements able to overcome the mechanical limits of the alumina ceramics produced on that time. The early developments were oriented toward Magnesia-Partially Stabilized Zirconia (MgPSZ), in which tetragonal phase is present as small acicular precipitates within large cubic grains ( $\varnothing 40 \div 50 \mu m$ ) forming the matrix. As this feature may negatively influence the wear properties of the polyethylene used in the acetabular components that are coupled to zirconia ball heads in total hip replacements, most of the developments were focused on Yttria-stabilized Tetragonal Zirconia Polycrystal (Y-TZP), a ceramic formed almost completely by submicron-sized grains, which become a standard material for clinical applications (Fig. 2) [2]. In addition, it is noted that the tetragonal acicular phase is nucleated within cubic zirconia grain during aging steps on cooling, maintaining precisely controlled time/temperature conditions. This implies a tough process control that may not be compatible with mass production requirements.

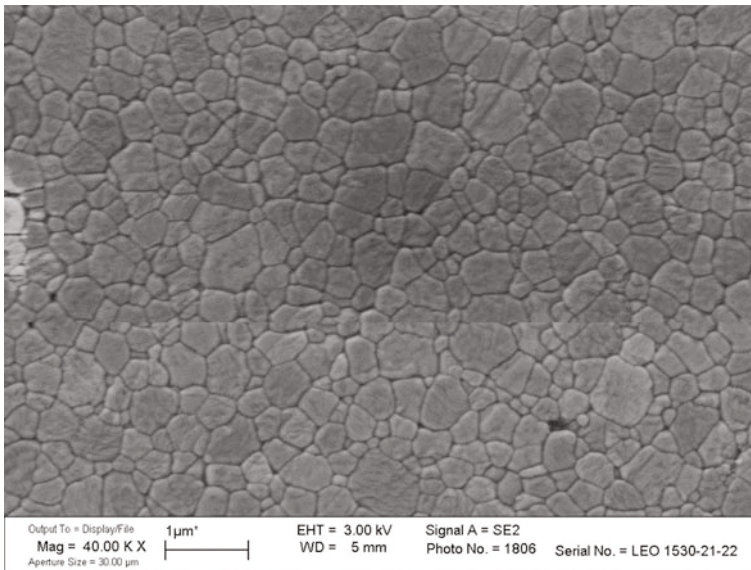


**Fig. 2** Microstructure of Y-TZP (Cortesy Dr. L.Pilloni, ENEA, Italy)

The use of zirconia in hip joint arthroplasty is now almost abandoned, since the worldwide recall that affected the product that was the leader of the market in 2000. So far, Y-ZTP ceramics are used especially in dentistry as blanks for CAD-CAM machining of crowns, bridging either structures for full partial dentures, as well as dental implants and abutments for titanium fixtures [1]. In orthopedics, Y-TZP is used only in the femoral components of two total knee replacements models. Readers are addressed to Chap. 28, “► [Perspective and Trends on Bioceramics in Joint Replacement](#),” this Handbook, for further details.

## Zirconia Physical Properties

Zirconia (Zirconium dioxide,  $ZrO_2$ ) is an allotropic oxide, i.e., with the same chemical formula it may occur in three crystal structures – monoclinic, tetragonal, and cubic – depending on temperature. Its crystal lattice is monoclinic up to 1170 °C when it shifts to tetragonal, a crystal shape which is maintained up to 2370 °C. At this temperature the tetragonal lattice shifts into cubic, and it maintains this form up to melting (2680 °C). The changes in crystal structure of zirconia are reversible and are associated to changes in volume and shape of the crystal cells. On cooling, the change in volume of unconstrained crystals in the cubic-tetragonal transition is about 2.5 %, while it is about 4 % in the tetragonal-monoclinic phase transition. Especially the  $t \rightarrow m$  transformation that takes place at a temperature in the range 1000–1200 °C on cooling is of technological interest (Table 4).

In a polycrystal the strain generated by the lattice expansion and by the shear strain due to the change in shape of the tetragonal cell implies an increase of stress on the neighboring, untransformed grains. At a macroscopic level, this can shatter sintered products of pure zirconium dioxide. For these reasons, pure unstabilized Zirconium dioxide was used mainly either as a refractory or as a pigment until 1929, when the stabilization of cubic phase to room temperature was demonstrated by

**Table 4** Physical properties of zirconia. Data on alumina reported for comparison

Material		Zirconia			Alumina
		Monoclinic	Hexagonal	Cubic	Hexagonal
Crystallography	–	Monoclinic	Hexagonal	Cubic	Hexagonal
Lattice parameter a	nm	0.5156	0.5094	0.5124	0.476
Lattice parameter b	nm	0.5191	0.5177	–	–
Lattice parameter c	nm	0.5304	–	–	1.299
Density (theoretical)	$g/cm^3$	5.83	6.1	6.06	3.98
Melting point	K	2790			2310
Thermal expansion coeff.	–	5–10			6.5
Thermal conductivity (298 K) (>99.9 %TD)	W/m K	2.5			30

Ruff et al. [12]. Cubic zirconia is still used as an abrasive in jewelry to replace diamonds thanks to its lower cost and high refractive index.

Engineering applications of zirconia ceramics were made possible by the discovery of the stabilization of the tetragonal phase to room temperature. This ceramic that was composed of zirconia in cubic and tetragonal phase was named Partially Stabilized Zirconia (PSZ) by its discoverers [13] because the low concentration of the stabilizing oxide does not allow the full stabilization of the cubic phase. PSZ was obtained using calcium oxide as stabilizer, but successively either magnesium oxide (magnesia, MgO) or yttrium oxide (yttria,  $Y_2O_3$ ) was used for this role. The real breakthrough in zirconia came in 1975 with the publication in Nature of the paper “Ceramic Steel?” by Garvie et al. [14]. They reported an observation of increased toughness due to the transformation of the tetragonal phase into monoclinic phase in MgO-stabilized PSZ (Mg-PSZ). This transformation performs as an effective dissipative mechanism for fracture energy. It takes place in a “martensitic” way as in some steels, hence the title of the paper. The phase transition (i) is not associated with transport of matter (it is diffusionless); (ii) is athermal, because it takes place at a temperature range and not at a given temperature; and (iii) involves a change in shape of the crystal lattice. Shortly after Rieth et al. [15] and Gupta et al. [16] showed successfully that a zirconia ceramic would be almost completely formed by tetragonal grains at room temperature, using Yttrium Oxide (Yttria –  $Y_2O_3$ ) as stabilizer of the tetragonal phase was made feasible. These ceramic materials, that were called Yttria-Tetragonal Zirconia Polycrystal (Y-TZP), contained 2–3 mol% yttria ( $Y_2O_3$ ). Y-TZP is almost completely constituted by tetragonal grains some hundreds of nanometers in size (0.3–0.5  $\mu\text{m}$ ). Cubic zirconia as well as monoclinic grains can be present as minor phases. It is noted that a number of oxides have been studied as stabilizers for zirconia (CaO, MgO,  $Y_2O_3$ ,  $CeO_2$ ,  $Er_2O_3$ ,  $Eu_2O_3$ ,  $Gd_2O_3$ ,  $Sc_2O_3$ ,  $La_2O_3$ , and  $Yb_2O_3$ ). In zirconia applied in biomedical applications, studies were focused on materials stabilized by CaO, MgO, and CeO but the ceramic that was developed industrially for the production of a medical devices was the one stabilized by  $Y_2O_3$  [17].

The tetragonal grains have the ability to transform into monoclinic; the transformation implies some 4 % volume expansion in free grains. This is the origin of the toughness of the material, e.g., of its ability to dissipate fracture energy. When the constraint exerted on the grains is relieved, i.e., by a crack advancing in the material, the grains next to the crack tip shift into monoclinic phase. The neighboring grains then experience some strain to accommodate both the change in volume of the transformed grain and the shear strain due to the change in shape of the crystal cells. These microstructural changes take place at the expense of the elastic stresses that lead to the advancement of the crack. At a macroscopic level, this results in the increase of toughness of the material. It is noted that, besides the energy dissipated in the phase transformation as described, the crack has to also overcome the compressive stress field due to the volume expansion of the grains to advance further.

There are several very accurate reviews of the models proposed to explain the mechanisms of transformation toughening in zirconia ceramics, [18–20] which the reader can refer for details.

Briefly, the model proposed by Lange [18] explains the transformation in terms of change in total free energy ( $\Delta G_{t-m}$ ). This model describes the change in free energy as the sum of three quantities: (i) change in chemical free energy ( $\Delta G_c$ ), (ii) strain energy, due to the expansion of the transformed particles ( $\Delta G_{SE}$ ), and (iii) change in surface energy depending on the shape change of the particle and on microcracking, e.g.,:

$$\Delta G_{t-m} = \Delta G_c + \Delta G_{SE} + \Delta G_s$$

While the change in chemical free energy ( $\Delta G_c$ ) depends on temperature and chemical composition, the strain energy change  $\Delta G_{SE}$  ( $>0$ ) depends on stiffness of the matrix and on the residual stress due to processing that is unavoidable in a sintered polycrystal due to the mismatch of thermal expansion coefficients of the two phases. The third term ( $\Delta G_s$ ) represents the change in free energy due to the change in the surface of grains during phase transition, as well as the formation of new surface due to microcracking. As remarked by Lughì and Sergo [17], the contribution to the free energy change of this term becomes relevant only when the size of the grains is in the order of magnitude of some tens of nanometers or so, because it is a function of the square of the crystal size, while the other two terms scale with its cube.

In a summary, the energy dissipated in the transformation and then the contribution of the phase transformation to mechanical properties depends on three main features of the material:

- The concentration of the stabilizing oxide (Yttria)
- The constraint exerted by the matrix onto grains
- The size and shape of grains and their homogeneous distribution

The equilibrium among these characteristics should be carefully tuned, to maintain the tetragonal phase in Y-TZP in a metastable state, optimizing in this way the contribution of the transformation to the mechanical properties of the material. The grains size should be fine and evenly distributed to avoid the increase of energy required for the transformation, and to decrease the size of grain boundaries. Yttria concentration too should be tuned, to maximize the fraction of tetragonal phase retained at room temperature and on its “transformability.” The residual stresses in the matrix generated on cooling by the differences in shrinkage in the crystal lattice and the stiffness of the material are also giving a marked contribution to the energy threshold occurring to the tetragonal grains to transform into monoclinic. Care is to be given to maintain the structure of Y-TZP in a metastable state: it has been demonstrated experimentally that there is a decrease in bending strength when the material is overstabilized.

## Zirconia Mechanical Properties

The transformation toughening mechanism described in the former part of this chapter results in the remarkable mechanical behavior of zirconia (Table 5). Zirconia

**Table 5** Mechanical properties of zirconia. Data on alumina behavior reported for comparison

Property	Units	Y-TZP	Mg-PSZ	Alumina (1970s)	HIP Alumina
Al <sub>2</sub> O <sub>3</sub> content	Vol %	–	–	99.1–99.6	>99.8
Density	g/cm <sup>3</sup>	6	5,5	3.90–3.95	3,97
Average grain size	µm	0,3–0,5	40–70	≤4.5	1,75
Flexural strength	MPa	900–1200	400–650	>300	650
Young modulus	GPa	210	210	380	400
Fracture toughness	MPa m <sup>1/2</sup>	7–9	8–11	3,5	4,5
Hardness	GPa	12,5	12,5	18	20–21

is an ionic ceramic polycrystal, then there is not the plastic strain before fracture characteristic of metals and of metallic alloys that is the dissipative mechanism for fracture energy in these materials.

Although zirconia has a high fracture strength, toughness is lower than in metals, although twice the one of high-density alpha-alumina (9–12 MPa m<sup>1/2</sup> Vs. 4–6 MPa m<sup>1/2</sup>). Y-TZP bending strength is above 900 MPa (4-point bending), than in the order of the one of several alloys, while the elastic modulus of zirconia – about 200 GPa, similar to the modulus of Titanium alloys – is a feature that makes easy to design metal to ceramic connections because this minimizes microstrains under load.

Besides bending strength and toughness, the hardness and thermal conductivity of zirconia are the behavior of zirconia especially relevant for its use in structural application in dentistry. Zirconia has a very low thermal conductivity (e.g., about one-tenth of alumina) and this has to be taken into account during hard machining of zirconia components by grinding because the thermal spikes that may arise would trigger the progressive degradation (LTD) of the mechanical properties of the material. This can happen also in total hip replacements bearing surfaces in case of starved lubrication. This behavior, along with the hardness of zirconia, which is lower than that of alumina (12–13 GPa Vs. 20–21 GPa) and sensitive to scratching, has discouraged the use of zirconia in ceramic-on-ceramic THR bearings.

As a conclusive remark on zirconia, it is worthwhile to underline that the behavior of this material strongly depends on the selection of the ceramic precursors and on their tailoring for the consolidation process during the batch preparation step, on the machining and surface finish of the componenets, all characteristics peculiar to each ceramic manufacturer. Overall, end users must keep in mind that zirconia is a metastable material whose behavior depends not only on the processing conditions but also on the environmental conditions that the components will experience during their lifetime.

## Zirconia Stability

It is an established behavior that the metastable tetragonal phase in Y-TZP ceramics can spontaneously transform into monoclinic. The discovery of this behavior – termed “aging”, hydrothermal transformation, or Low Temperature Degradation (LTD) – is due to Kobayashi et al. [21] who observed the degradation in the

mechanical properties with the progress of transformation. In the following of this chapter we use the three terms indifferently.

LTD is characterized by several well-assessed features: (i) the transformation starts at the surface of the material and progresses into it; (ii) the monoclinic transition of the tetragonal grains in the surface results in a surface uplift; (iii) the stresses lead to grain pull-out and surface cracking; (iv) the transformation penetrates into the material, enhancing the extent of the process; (v) as the cracks extension progresses, one can observe the decrease of the material density and the reduction in strength and toughness of the ceramic.

There is experimental evidence that LTD can take place also at room temperature in a humid environment. However, it is enhanced at temperatures above 100 °C under saturated steam.

Due to its mechanical relevance, aging in zirconia ceramics has been investigated since the first attempts to use this ceramic as a biomaterial [2]. Nevertheless, none of the models developed so far give a comprehensive representation of this behavior [17].

The models more debated were proposed by Sato et al. [22], Yoshimura et al. [23], and more recently by Chevalier et al. [24]. Sato's and Yoshimura's models are based on the local reaction interaction of preferential sites in the material surface with water molecules. The first model [22] is based on the reaction between water and Zr-O-Zr bridges at the grain boundaries, resulting in the formation of Zr-OH bonds. Following this model, this is leading to the change in the conditions for the stabilization of the tetragonal phase at room temperature, triggering the transformation into monoclinic and the cascade of events of LTD. Also, the Yoshimura model [23] takes into account the formation of Zr-OH bonds, which give origin to stress fields in the crystal lattice. Once higher than a given threshold, the transformation starts leading to material degradation with its progress. The model proposed by Chevalier [24] is based on the filling by  $O^{2-}$  ions of the oxygen vacancies due to the presence of the trivalent Yttrium in the  $ZrO_2$  lattice.

LTD is especially evident on Y-TZP, while other zirconia (Mg-PSZ, Ce-TZP) are not affected by this problem. In contrast, the mechanical behavior of both these zirconia are largely surpassed by the Y-TZP ones, a fact that makes the latter ceramic the one preferred for clinical use, formerly in orthopedics and now in dentistry.

The rate of strength degradation can be controlled acting on several parameters: high density, small and uniform grain size, creation of a spatial gradient of yttria concentration and introduction of grains within the matrix of Alumina that can delay the onset of the transformation. All the above parameters are controlled by the manufacturing process and by the physicochemical behavior of the precursors selected for the production of the ceramic. Then LTD is peculiar to each Y-TZP material and of each manufacturing process.

## Zirconia Radioactivity

The issue of radioactivity of zirconia used in medical devices was raised during the second half of the 1980s after the sudden increase in the level of attention of

the general public to the presence of radionuclides in the environment. This happened after two severe accidents in nuclear power plants (Three Miles Island, Chernobyl) that occurred at that time. In fact, zirconia ores are associated to  $^{238}\text{U}$ ,  $^{232}\text{Th}$ , and to their decay products in concentrations depending on the source. The presence of radionuclides in low-purity, low-cost zirconia, e.g., sands used in smelting works or in refractories – is monitored by the public health authorities since long. The production of the chemical used in the preparation of the high-purity ceramic precursors of zirconia enacts the effective separation of radioactive contaminants from the powders. However, the use of zirconia in medical devices imply to characterize this feature, and a significant number of studies was published during the first half of 1990s during the setup of the standard ISO 13356 concerning zirconia for clinical implants [2]. It has been demonstrated that separation technologies used in the purification of nuclear wastes [25] allows to obtain chemicals suitable for the production of high-purity zirconia precursors with specific gamma activity lower than the one of human body, i.e., less than 50 Bq/kg [1]. It is noted that some bioceramics used in dentistry since a long while have specific activity far higher than the one of zirconia, e.g., feldspathic porcelains due to the natural abundance of 40 K in Potassium.

---

## Alumina–Zirconia Composites

The addition of alumina to zirconia, forming an alumina–zirconia composite ( $\text{Al}_2\text{O}_3\text{--ZrO}_2$ ) lowers significantly the zirconia transformation kinetics. For this reason, the two phase alumina–zirconia material has been marketed for orthopedic applications after zirconia material was abandoned. The explanation of the retardation of phase transformation kinetics afforded by only minor alumina concentration when zirconia is the major phase is not satisfying yet. Such ceramic composite materials are commonly defined as Alumina-Toughened Zirconia (ATZ) ceramics. Instead, alumina containing small amount of zirconia, commonly referred as zirconia-toughened alumina (ZTA) or alternatively named alumina matrix composite (AMC), is also exceptionally resistant to hydrothermal aging. Moreover, because of topological reasons, the slower aging kinetics is perhaps clearer in these materials, where alumina is the major phase. In fact, its presence in the zirconia phase, finely distributed into the material and consequently the zirconia grains, isolated by the stiff zirconia matrix, the percolative pathway risk is reduced and consequently degradation cannot continue deep into the material. As a consequence, the ZTA doesn't increase in roughness as the monoclinic zirconia increases after hydrothermal treatment. Furthermore, the transformation is hindered by stiff predominant alumina matrix.

However, besides the hydrothermal aging problems, the two design approaches put in evidence the basic material strategy adopted by the material scientists: the high-fracture toughness may be the leading feature in an ATZ, whereas hardness may be the main feature in a ZTA. The ZTA material had achieved in the last decade the



predominance, because of highly suitable properties for couple bearing application in THA, but perhaps, also because of the fear of mostly zirconia-based materials.

In following, these two types of material design approaches will be discussed.

## Zirconia-Toughened Alumina

The basic concept of a Zirconia-Toughened Alumina (ZTA) material is to keep or improve the alumina properties as hardness, stiffness, and thermal conductivity, which made successful for more than 40 years its use as implantable ceramic in THA and at the same time, by using zirconia as reinforcing element, to substantially increase the material fracture toughness and strength by exploiting its tetragonal to monoclinic phase transformation as described in section “[Zirconia Physical Properties](#)” of this chapter for monolithic zirconia components. The enhancement of mechanical properties is aimed to increase the reliability of alumina THA components but also to allow a higher degree of freedom in the design of THA components. The ability of zirconia phase transformation ( $t\text{-ZrO}_2 \rightarrow m\text{-ZrO}_2$ ) in ZTA ceramics is an indispensable prerequisite for their excellent mechanical properties and the degree of stabilization of the zirconia tetragonal phase at body temperature is essential for the desired toughening mechanism.  $\text{Y}_2\text{O}_3$  is the most widely used tetragonal zirconia chemical stabilizer, whose microstructure and grain size contribute to tetragonal zirconia phase stabilization. However, stabilization must be achieved such that no material degradation will occur in body environment, i.e., in aqueous liquid (synovia), which is known to potentially trigger phase transformation at the surface of ceramic components as elucidated in section “[► Zirconia Stability](#)”.

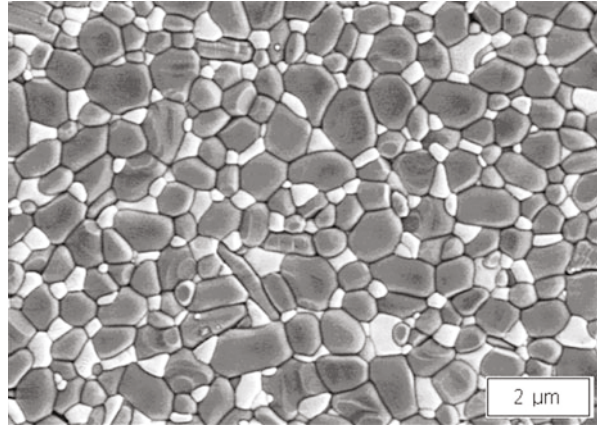
### Structure of Zirconia-Toughened Alumina

The Zirconia-Toughened Alumina is basically a 2-phase alumina matrix ceramic composite consisting of fine homogeneously dispersed zirconia grains. The zirconia volume content needs to be precisely balanced to obtain the optimum resistance against crack extension while assuring an optimal chemical stability. In this way, it may be possible to increase fracture toughness and strength of the material to the levels equal to and in some cases above those seen in monolithic zirconia.

The most successful representative of this demanding type of material in arthroplasty, is the ZTA marketed under the brand name of BIOLOX<sup>®</sup> *delta* (ISO 6474–2) manufactured by CeramTec Medical Products Division in Plochingen, Germany. BIOLOX<sup>®</sup> *delta* THA components are clinically used for more than 10 years and have been implanted in over 3.5 million cases. This material is today considered the ceramic golden standard in THA.

BIOLOX<sup>®</sup> *delta* consists of finely grained (with an average  $\text{Al}_2\text{O}_3$  diameter of about 0.5–0.6  $\mu\text{m}$ ) high-purity alumina matrix, which is very similar to the well-known monolithic alumina material BIOLOX<sup>®</sup> *forte* (ISO 6474). Common to other composite materials, its basic physical properties such as stiffness, hardness, thermal conductivity, etc. are mainly predetermined from the dominating phase. Fracture toughness and strength are increased with the addition of reinforcing elements to the

**Fig. 3** SEM image of the microstructure of the ZTA composite ceramic BIOLOX<sup>®</sup> *delta* (Courtesy CeramTec GmbH, Plochingen, Germany). The gray grains represent the alumina matrix, the white grains the zirconia phase and the elongated grains consist of reinforcing strontium hexaaluminate (SHA) platelets



microstructure. The best compromise between the mechanical properties and the chemical stability is achieved for this material by incorporating about 17 Vol.% of zirconia in the alumina matrix. Such zirconia content would be slightly higher of percolation pathway threshold limit of 16 Vol.% [24]; nevertheless, Pecharromás et al. [25] have analyzed the threshold limit for hydrothermal stability of zirconia in alumina matrix composites by steam sterilization and revealed that a relevant aging level for such material is given at 18–22 % volume content of zirconia.

As further reinforcing element, strontia (SrO) is added to the composition; this additive reacts with alumina during the sintering stage to grow in situ elongated strontium hexaaluminate (SHA) crystals with a magnetopumbite structure. These SHA platelet-shaped grains are homogeneously dispersed in the ceramic composite microstructure and provide an additional barrier to crack propagation. Indeed, their task is to deflect any subcritical cracks created during the lifetime of the ceramic. The maximum platelets length is of about 5  $\mu\text{m}$  with an aspect ratio of 5–10. Figure 3 shows the microstructure of BIOLOX<sup>®</sup> *delta*, where the gray grains represent the alumina matrix and the white grains the zirconia phase. In addition, the elongated grains consist of reinforcing SHA platelets.

These two well-known reinforcing effects in material science, transformation toughening and crack deflection, give BIOLOX<sup>®</sup> *delta* a unique strength and toughness, so far unattained by any other ceramic material extensively used in a structural application in the human body.

Additionally, stabilizing elements are also added to the reinforcing elements of the material. A minor amount of chromia ( $\text{Cr}_2\text{O}_3$ ), which is completely soluble in the alumina matrix, donates to the material its pink color; and yttria ( $\text{Y}_2\text{O}_3$ ), which is soluble in the finely distributed zirconia phase, supports the stabilization of the zirconia tetragonal phase. Its concentration has been optimized in order to obtain the maximum resistance to crack propagation, while keeping an optimal chemical stability.

However, as noted in section “► Zirconia”, the best performance is achieved by properly triggering the tetragonal zirconia transformation by means of [24]:

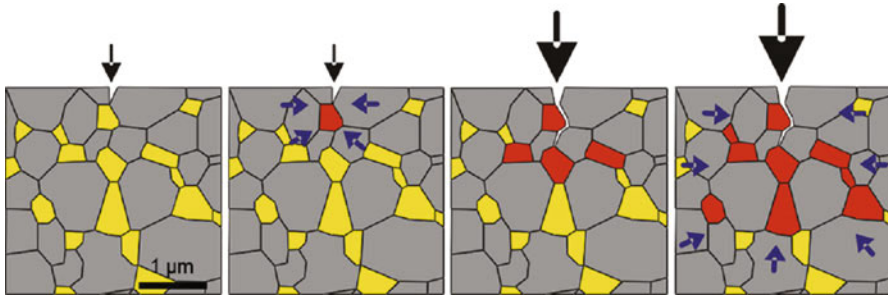


**Fig. 4** Reinforcing mechanism in BIOLOX<sup>®</sup> *delta* at crack initiation and propagation. *Yellow* particles represent tetragonal zirconia. Color change to *red* indicates monoclinic phase transformation. *Arrows* show the region of compressive stresses due to phase transformation (Courtesy CeramTec GmbH, Plochingen, Germany)

- The size, shape, and distribution of zirconia particles
- The addition of yttria
- The amount of stiff surrounding alumina matrix
- The internal and external stresses

It is a matter of fact that the above concurring factors make the design of a ZTA composite particularly difficult; higher tetragonal zirconia stabilization as a consequence, for example, of a too high yttria concentration would lead to the suppression of zirconia phase transformation annihilating almost all the improvements of ZTA. On the other hand, poor zirconia stabilization caused, for example, by zirconia uncontrolled grain growth due to a noncorrect sintering would destabilize the tetragonal phase enhancing the low-temperature degradation susceptibility. Nevertheless, in the later case, the mechanical properties might be outstanding, but the material could be unreliable leading to catastrophic consequences due to LTD affecting the product that was leader of the Y-TZP for THA market in the year 2000.

Figure 4 represents a realistic part of the microstructure. The gray particles refer to the alumina matrix and yellow to the tetragonal zirconia. The zirconia  $t \rightarrow m$  transformation is indicated by the change to red color. In the case of severe overloading, crack initiation and crack extension will occur. High tensile stresses in the vicinity of the crack tip will trigger the phase transformation of the zirconia particles. The accompanied volume expansion leads to the formation of compressive stresses which will stop the crack extension.

### **Mechanical Properties of Zirconia-Toughened Alumina**

The necessary requirements of a ZTA for a use in THA are expressed by the standard for composite materials ISO 6474–2. BIOLOX<sup>®</sup> *delta* as representative of material category fulfill the ISO requirements as shown in Table 6 (see also Table 3).

The excellent properties of the material BIOLOX<sup>®</sup> *delta* support advantageous properties of the final product, namely, ceramic hard-hard bearings for hip

**Table 6** Comparison of regular BIOLOX<sup>®</sup>delta mechanical properties with the ISO 6474–2 requirements

Property	Units	ISO 6474-2	BIOLOX <sup>®</sup> delta
Al <sub>2</sub> O <sub>3</sub> content	Vol %	–	81.6
ZrO <sub>2</sub> content	Vol %	–	17
Density	g/cm <sup>3</sup>	–	4,37
Average grain size Al <sub>2</sub> O <sub>3</sub>	µm	≤1.5	0.56
Average grain size ZrO <sub>2</sub>	µm	≤0.6	0.3
Flexural strength	MPa	≥1000	1384
Young modulus	GPa	≥320	358
Fracture toughness	MPa m <sup>1/2</sup>	≥4	6,5
Hardness (HV1)	GPa	≥16	19

**Table 7** Comparison of strength and burst load of BIOLOX<sup>®</sup>forte and BIOLOX<sup>®</sup>delta

Parameter	Test/design	Unit	BIOLOX <sup>®</sup> forte	BIOLOX <sup>®</sup> delta	Ratio delta/forte
Strength	4-point bending	MPa	620	1400	2.3
Burst load	28–12/14 L	kN	54	85	1.6
Burst load	36–12/14 M	kN	110	131	1.2

arthroplasty. Indeed, in general, the performance of any hip replacement system depends on the intrinsic material properties, the design and manufacturing quality of the whole device, the external load and the particular environment, and finally the quality of mounting and installation. The use of high-performance materials inevitably promotes the performance of a hip replacement system – however, the latter factors may be even more decisive for the success of a system, and for this reason, they were also taken into account in the ISO 6474–2. These complex correlations must be necessarily evaluated by design analysis, modeling, simulations, risk analysis, and many other tools. In order to eliminate any influences of design features most of the material testing is performed using 4-point bending bars. The burst load of the components is significantly increased as shown in Table 7 [11].

All burst loads are far above the required value of 46 kN and the maximum in vivo load at worst-case conditions of approximately 10 kN.

Kuntz et al. [11] obtained the data of the burst tests given in Table 7 from ball heads with identical geometry, titanium alloy test taper, and the same test setup. In this way, they showed that the advantage of BIOLOX<sup>®</sup>delta ball heads in the burst load came only from the higher strength of the material in comparison to the monolithic alumina BIOLOX<sup>®</sup>forte. However, although the strength of BIOLOX<sup>®</sup>delta resulted to be more than twice the strength of BIOLOX<sup>®</sup>forte, the ratio of the burst strength values was lower. The authors justified the result with the ductile deformation of the titanium alloy taper during the burst test which steadily increases the contact area of the conical bore of the ceramic ball head and the metal taper. However, generally speaking, the burst load of identical ball heads is always higher when a high-strength material is used.

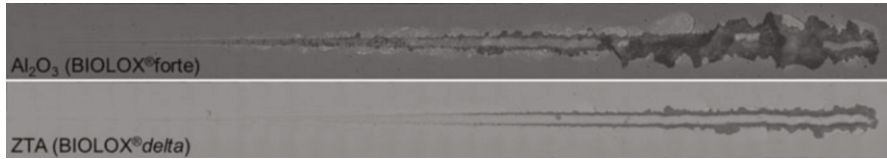


**Fig. 5** Typical scratches on BIOLOX<sup>®</sup>forte and BIOLOX<sup>®</sup>delta performed according to the standard EN 1071–3:2005. The zirconia phase transformation in BIOLOX<sup>®</sup>delta enhances the ceramic scratch resistance avoiding the extensive grain pull-out shown by the monolithic alumina

It is also of particular interest to see that the burst strength resulted to be higher for the larger ball head size. As a consequence, a clear benefit of high-performance material is also the possibility to apply a challenging design, such as components with lower wall thickness, which would be otherwise unaffordable. We need to remember that a high-performance material always increases the safety margin of the component. As result, according to the Australian Orthopaedic Association National Joint Replacement Register (AOA 2014), the fracture rate of ceramic components, with the adoption of the alumina composites, decreased drastically, making the breakage an extremely rare occurrence (i.e., 0.17/10'000 procedures for ZTA, where alumina shows 6.48 fractures for 10'000 procedures).

The wear behavior of the ZTA material is also interesting; Clarke et al. [27] showed that there is no statistical difference between ZTA and alumina BIOLOX<sup>®</sup>forte wear couples, but under off-normal conditions as in the microseparation tests, the ceramic composite material BIOLOX<sup>®</sup>delta wear couple showed significantly lower wear rate. Such behavior is justified by the phase transformation toughening acting in the ZTA material as clarified by Piconi et al. [28] with the scratch resistance measurements performed according to standard EN 1071–3:2005. Figure 5 shows a scratch comparison between BIOLOX<sup>®</sup>forte and BIOLOX<sup>®</sup>delta.

## Alumina-Toughened Zirconia

Begand et al. [29] presented during 2004 a new alumina-toughened material (ATZ) for THA. A commercial material was developed and manufactured by Mathys Orthopädie GmbH (Mörsdorf, Germany) and was introduced in the international market in 2010. Similarly to the ZTA solution presented by CeramTec GmbH a couple of years earlier, Mathys tried with its ATZ ceramic composite – marketed with the brand name Ceramys<sup>®</sup> – to combine the advantages of the two monolithic materials, Al<sub>2</sub>O<sub>3</sub> and ZrO<sub>2</sub> with the aim to avoid the disadvantages. The material and the components' properties seem to be remarkable and in some cases better than the ZTA alternative, as specified by Mathys. Nevertheless, the ATZ material has up to date not achieved the broad use of its competitor; in about 4 years Mathys declared 30,000 components sold worldwide in the market. The reason might be researched first of all in the fear of zirconia, that still exist in the THA field, and on the other

hand Mathys being a prosthetic company with whole THA implants in its portfolio, making difficult to sell its ceramic bearing solution to other prosthetic companies. Moreover, the price pressure in THA field might also be a possible explanation, with alumina being a much cheaper raw material than zirconia.

### Structure of Alumina-Toughened Zirconia

The ATZ Ceramys<sup>®</sup> consists of 80 w.% of zirconia and 20 w.% of alumina. More in detail, Schneider et al. [30] describe the ATZ Ceramys<sup>®</sup> as formed by 61 % tetragonal zirconia, 17 % cubic zirconia, approx. 1 % monoclinic zirconia, and alpha-alumina as the balance. The tetragonal zirconia phase is stabilized with 3 mol.% of yttria as for the standard monolithic zirconia (3Y-TZP). The alumina grains are finely dispersed in the zirconia matrix and the average grain size diameter approach is 0.4  $\mu\text{m}$ , both for  $\text{ZrO}_2$  and  $\text{Al}_2\text{O}_3$ . Indeed, on the paper, ATZ may appear of relatively simple design, nevertheless as pointed out previously, the properties of these special materials depend significantly on the production steps and conditions which are different for all single manufacturers.

### Mechanical Properties of Alumina-Toughened Zirconia

Ceramys<sup>®</sup> properties are summarized in Table 8. According to Oberbach et al. [31] the biaxial flexural strength (acc. to norm ISO 6474) surpassed the 1200 MPa with a Weibull modulus of 18. The burst strength performed on hip joint heads with a diameter of 28 mm with 12/14 L and 12/14 M necks and titanium alloy tapers achieved values [32] comparable to that showed by ZTA material in Table 7. The pin-on-disk wear test with ATZ/ATZ couplings using serum as fluid test medium showed to be comparable to  $\text{Al}_2\text{O}_3/\text{Al}_2\text{O}_3$  couplings (i.e., 0.152 and 0.157  $\text{mm}^3$  of weight loss, for ATZ and  $\text{Al}_2\text{O}_3$ , respectively) [32]. Instead, similarly with the ZTA case [27], the ATZ material showed a net improvement among  $\text{Al}_2\text{O}_3$  under adverse in vivo-like loading conditions (i.e., microseparation) using the hip simulator, where ATZ/ATZ outperformed the  $\text{Al}_2\text{O}_3/\text{Al}_2\text{O}_3$  couple bearing with a wear rate of 0.06  $\text{mm}^3/\text{million cycles}$  compared with the 0.74  $\text{mm}^3/\text{million cycles}$  of monolithic alumina alternative [33].

**Table 8** Mathys ATZ Ceramys<sup>®</sup> mechanical properties

Property	Units	Ceramys <sup>®</sup> ATZ
$\text{Al}_2\text{O}_3$ content	Vol %	20
$\text{ZrO}_2$ content	Vol %	80
Density	$\text{g}/\text{cm}^3$	5,51
Average grain size $\text{Al}_2\text{O}_3$	$\mu\text{m}$	0.40
Average grain size $\text{ZrO}_2$	$\mu\text{m}$	0.40
Flexural strength	MPa	>1200
Young modulus	GPa	n.s.
Fracture toughness	$\text{MPa m}^{1/2}$	7.4
Hardness (HV20)	GPa	15

### Stability of Alumina–Zirconia Composites

The resistance to environmental degradation in an alumina–zirconia composite (BIOLOX<sup>®</sup> delta) has been discussed in depth by Chevalier et al. [34]. The results show that even if an increase of monoclinic content is expected after long aging duration *in vivo*, the impact of the transformation is far from being the same that of monolithic zirconia, due to the absence of percolative phenomena in this material, as described in section “[Structure of Zirconia-Toughened Alumina.](#)” After accelerated hydrothermal treatment, the composite does not show large surface uplifts, as it is the case for 3Y-TZP, and increase in surface roughness is not detectable. Also, the mechanical behavior remains unaffected.

As stated at the beginning of the chapter, the delay in the onset of the low temperature degradation of the zirconia phase in zirconia-rich alumina–zirconia composites was not elucidated yet. Also for this reason, Ceramys<sup>®</sup> ATZ composite ceramic was extensively tested in adverse aging conditions. However, the presence of 3 mol.% yttria stabilization as that one usually used in monolithic zirconia materials may put in evidence the wish of the designer of the material to slightly overstabilize the zirconia phase, in order to avoid the occurrence of low temperature degradation, limiting on the other hand the mechanical performances. The presence of a zirconia cubic phase and very low monoclinic zirconia content in pristine conditions [30] is a consequence of the above assertion. Thus, the material exhibits a much slower overall aging kinetics in comparison with the 3Y-TZP. Nevertheless, because of the presence of the percolation mechanism, the zirconia composite seem to show a significant roughness (i.e., Ra) increase as the monoclinic phase volume content increases during the hydrothermal exposure [30]. However, the remarkable mechanical properties with the controlled zirconia t → m transformation kinetics might make of ATZ material an appealing alternative in THA.

---

### Biocompatibility of Bioinert Ceramics

The biological safety of alumina and zirconia are well established since a long time. The high oxidative status gives high chemical inertia to both ceramics, especially to alumina which is frequently taken as a negative reference in biocompatibility tests of candidate biomaterials.

Tests on alumina, zirconia, and alumina–zirconia composites were performed varying a number of different test parameters. The first remark to be made is that the materials tested were different both in physical forms (powders or dense ceramics) and in chemical and physical characteristics (e.g., reactive surface, chemical composition, impurity content, etc.). Further remarks are concerning test conditions: the *in vitro* assays were performed using extracts in various media, either in direct or indirect contact, while the cell lines used (e.g., macrophages, lymphocytes, fibroblasts, and osteoblasts) were stable from primary cultures. Similar consideration can be made on the *in vivo* tests that had been

performed in several sites of implantation in different animal models, to analyze adverse reactions in soft tissue and/or bone, as well as systemic toxicity. Comprehensive reviews are reported in [2, 5, 35].

### **In vitro Tests**

In testing materials *in vitro*, the specific surface (i.e., surface for a given volume or mass of the material) was found to be a relevant parameter, because particulate can develop some square meters per gram of reactive surface. For the same reason, the size of the particulate is a relevant parameter in these tests, because a given mass of particulate develops a higher surface as the particle size decrease. Similar consideration can be made in tests performed on porous materials.

The concentration of powders resulted relevant for cellular response. Dose-dependent cytotoxicity was observed on human lymphocytes stimulated with phytohemagglutinine in presence of partially stabilized zirconia and alumina powders as well as on fibroblasts cocultured with ceramic extracts. The concentration of ceramic powders has been reported as relevant to cellular apoptosis, e.g., in macrophages by Catelas et al. [36]. Kranz et al. [37], while challenging corundum particles to murine macrophages also observed cytotoxic reactions depending on the particle size, the more cytotoxic being the nanometric ones because of their very high specific surface (Table 9).

### **In vivo Tests**

The tissue reactions to injection of alumina or zirconia particles are much lower than after injection of metal or polyethylene particles, also at high specific surface of the material under test, e.g., after injection of alumina particles, the fibrosis observed after injection of polymeric or metallic particles was absent [38, 39]. Implants of either alumina or zirconia in bone performed in nonloaded sites show that bone comes into contact with the ceramic without fibrous interposition [35, 38].

Absence of acute systemic adverse tissue reactions to ceramics were also reported after subcutis, intramuscular or intraperitoneal, and intra-articular injection of alumina and zirconia powders in rats and/or mice, as well as by implants made into the paraspinal muscles of rabbits, rats, or in rabbit's bone (Table 10).

### **Carcinogenicity**

In 40 years of clinical use of alumina and zirconia, only one author discussed the possible link between soft tissue sarcoma and the presence of alumina ceramic bearing in a hip implant [40]. During the following years, the issue of carcinogenesis induced by ceramics has been raised especially for zirconia, due to the



**Table 9** Summary of the tests in vitro performed on bioinert ceramics and composites

First author	Publication year	Material tested	Physical form	Cell type
Harms	1979	Alumina	Powder	Macrophages Lymphocytes
Pizzoferrato	1982	Alumina	Ceramic	HeLa Fibroblasts 3 T3
Bukat	1990	Alumina & Zirconia	Ceramic	Fibroblasts 3 T3
Greco	1993	Alumina & Zirconia	Powder	Human lymphocytes
Ito	1993	Zirconia	Wear debris	L929
Li	1993	Alumina & Zirconia	Powder & ceramic	Human oral fibroblasts
Dion	1994	Alumina & Zirconia	Powder	HUVEC Fibroblasts 3 T3
Harmand	1995	Alumina & Zirconia	Powder	Fibroblasts 3 T3
Catelas	1998	Alumina & Zirconia	Powder	Macrophages J774
Mebouta	2000	Alumina & Zirconia	Powder	Human Monocytes
Torricelli	2001	Alumina & Zirconia	Powder	Osteoblasts
Lohman	2002	Alumina & Zirconia	Powder	Osteoblasts MG63
Karlsson	2003	Alumina	Nanoporous ceramic	Primary osteoblasts
Gutwein	2004	Alumina	Nanoporous ceramic	Osteoblasts CRL11372
Yagil- Kelmer	2004	Alumina	Powder	Human monocytes U937
Carinci	2004	Zirconia	Ceramic discs	Osteoblasts MG63
Hao	2005	Zirconia	Ceramic discs	Human fetal osteoblasts
Baechle	2007	Zirconia	Ceramic discs	Osteoblast-like CAL72
Sollazzo	2008	Zirconia	Colloidal coating	Osteoblasts MG63
Kranz	2009	Alumina	Powder	Macrophages RAW264.7
Att	2009	Zirconia	Ceramic discs	Primary osteoblasts
Kohal	2009	Zirconia & ATZ	Ceramic discs	Primary human osteoblasts
Maccauro	2009	ZTA	Ceramic discs	Fibroblasts C3H10T $\frac{1}{2}$
Roualdes	2010	ZTA	Ceramic discs	Primary human fibroblasts
Cho	2014	Zirconia	Ceramic discs	Osteoblast-like MC3T3-E1

**Table 10** Summary of in vivo biocompatibility studies on bioinert ceramics

First author	Publication year	Material tested	Physical form	Animal model	Implant site
Helmer	1969	zirconia	Pellets	Monkey	Femur
Hulbert	1972	Alumina & Zirconia	Discs, tubes Dense & porous	Rabbit	Paraspinal muscle
Griss	1973	Alumina	Slurry	Swiss mice	Subcutis, Knee joint
Harms	1979	Alumina	Powder	Mice	Intraperitoneal, intramuscular
Garvie	1984	Zirconia	Ceramic bars	Rabbit	Paraspinal muscle
Wagner	1986	Alumina & Zirconia	Pins	Rat	Femur
Christel	1988	Alumina & Zirconia	Pins	Rat	Paraspinal muscle
Christel	1989	Alumina & Zirconia	Pins	Rabbit	Femur
Maccauro	1992	Zirconia	Powder	Mice	Intraperitoneal
Specchia	1995	Zirconia	Pins	Rabbit	Femur
Warashina	2003	Alumina & Zirconia	Powder	Rat	Calvaria
Scarano	2003	Zirconia	Screws	Rabbit	Tibia
Sennerby	2005	Zirconia	Screws	Rabbit	Tibia, femur
Graci	2011	Alumina & Zirconia	Low-cohesion Ceramic	Rabbit	Knee joint
Marques	2013	Zirconia	Screws	Rabbit	Tibia

presence of radioactive contaminants, as discussed in section “[Zirconia Mechanical Properties](#)” of this chapter. Covacci et al. [41] investigated the possible mutagenic and oncogenic effects of a zirconia ceramic (Y-TZP) sintered from high purity powders. The results obtained showed that Y-TZP ceramic does not elicit either mutagenic or transforming effect on mouse embryo-derived fibroblasts  $C_3H_{10}T\frac{1}{2}$ , confirming the suitability of Y-TZP for application in medical devices. Maccauro et al. [42], who also challenged  $C_3H_{10}T\frac{1}{2}$  with alumina–zirconia composite ceramic samples, has reported the absence of cellular DNA damage, mutagenicity, and carcinogenicity as well.

## Reaction to Ceramic Wear Debris

Because alumina, zirconia, and their composites are used mainly in hip replacement bearings (see Chap. 28, “[► Perspective and Trends on Bioceramics in Joint Replacement](#)” in this Handbook), the biocompatibility of their wear debris was accurately characterized. Wear debris trigger a cascade of biological reactions that can eventually result in osteolysis – i.e., the loss of the mineral part of the

bone – and eventually in the aseptic loosening of the implants, making mandatory a revision surgery. Due to the economic and social relevance, researchers studied this pathology since a long time. Since 1977, Willert and Semlitsch [43] observed granulomas associated with necrosis and fibrosis due to particles accumulating in periarticular tissues that can migrate by the blood stream giving rise to systemic reactions. This was also reported by Schmalzried and Callaghan [44] who identified an “effective joint space” where the wear debris dispersed in the fluid surrounding the joint can be transported due to the pressure gradients generated by the motion of the articular joint during the patient’s daily activity. Because ceramic joint replacement bearing is especially suited for active patients, like e.g., the younger ones with longer life expectations, the long-term effects of ceramic wear debris becomes more and more relevant.

It is acknowledged that local and systemic reactions to ceramic wear debris are reduced in comparison to the ones observed in presence of metal and polyethylene (UHMWPE) debris.

Alumina wear debris has been found less active than UHMWPE debris in promoting the differentiation of osteoclasts, especially in the low concentration typical of the low wear of alumina bearings [45]. These findings are well corresponding to the ones reported by Fisher et al. [46] who demonstrated the negligible biological activity of ceramic-on-ceramic wear debris in comparison with standard polyethylene (60×) and to cross-linked polyethylene (13×).

The migration of wear debris to peripheral organs implies a high vascularization of the periprosthetic membrane that contains the debris. This feature is depending on inflammatory tissue response related to the cytotoxicity of the particles and to the release of humoral factors after phagocytosis by macrophages. A specific aspect of the tissue reaction to ceramic debris is the formation of fibrous tissue poor in vessels in absence of contaminations from metals or polymers.

Membrane surrounding ceramic debris was observed by Maccauro et al. [47], as formerly did Lerouge et al. [48] who reported that foreign body cells are typically associated to polyethylene, PMMA, and large metal particles, but rarely to ceramics. The absence of vessels in the periprosthetic tissue surrounding alumina particles in alumina-alumina joints led De Santis et al. [49] to hypothesize that ceramic debris did not migrate from the production site. Graci et al. [50] observed membrane poor in vessels surrounding ceramic debris. This finding was not depending on the nature of the ceramic tested (alumina either zirconia Y-TZP), nor on the release time of the material. Namely, periprosthetic tissue membrane surrounding ceramic debris was poor in vessels either if powders were massively inserted directly into the joint, either if debris are progressively released for a long time, by means of an original testing method developed by these Authors.

All these findings are explaining the absence of local systemic toxicity of ceramic debris in the long term, and the positive outcomes reported in the long-term follow-ups of several series of implants with ceramic-on-ceramic either ceramic-on-polyethylene bearings (see Chap. 28, “► [Perspective and Trends on Bioceramics in Joint Replacemen](#),” this Handbook).

## Processing of Bioinert Ceramics for Joint Replacements

The bioceramics used in joint replacements are belonging to the wide class of materials known as hi-tech ceramics (advanced ceramics, fine ceramics), that are obtained by precursors in form of powders obtained through the synthesis of high purity chemicals. Many synthesis processes are in use, based on solid state reactions, on gas–solid reactions, or on wet routes, e.g., coprecipitation from salt solutions, or sol-gel processes.

Precursors are formed by crystallites having size ranging from 0.01 to 0.1  $\mu\text{m}$  that are forming small particles (grains, or domains) 0.1–1  $\mu\text{m}$  in size. Grains may be packed together forming bigger agglomerates 10–100  $\mu\text{m}$  in size. Chemical, crystallographic, morphologic and bulk characteristics of powders are relevant in ceramic processing and are depending on the process used for their preparation.

Grain size is the parameter most frequently reported to characterize a powder, for its strong influence on the microstructure of the final product. A relevant parameter linked to grain size is the specific surface area that gives a rough indication of the reactivity of the powder: current values for ceramic precursors are in the order of some square meters per gram. Also the flowability of the powder is relevant for processing, as it indicates its suitability to free flow in feeding and filling the dyes used for powder consolidation, without forming coarse agglomerates.

Some of the additives that determine the characteristics of the ceramic are introduced in the powder during its synthesis, like e.g., yttria  $\text{Y}_2\text{O}_3$  in Y-TZP, or magnesia  $\text{MgO}$  in PSZ precursors.

The precursors' main characteristics are:

- High specific surface, in the order of some tens square meters per gram, a feature that makes them very reactive
- Uniformity of crystallite size
- Homogeneous chemical composition
- Flowability, e.g., the ability of the powder to flow freely, without formation of agglomerates or voids during the powder consolidation
- Ultralow content of impurities

A general flow sheet of the process used to transform the precursors in a solid body can be summarized in four main steps:

1. Batch preparation: the precursors are blended with a suitable mix of process additives depending on the consolidation route and on the desired final behavior of the product. Magnesia ( $\text{MgO}$ ) is a sintering aid commonly used to limit grain growth in alpha-alumina. Binders and lubricants are also added to the powders for dye pressing in the compaction process used in shaping the product. The ceramic composition with a consistence of slurry is then eventually milled to homogenize the composition and narrow the particle size distribution. The blend is then treated by spray drying to obtain the feedstock (e.g., in form of granules) to be used in the next step of the process.

2. **Compaction:** the feedstock (e.g., ready-to-press powders) is shaped in simple geometry (e.g., a cylinder of adequate size) by dye pressing. The product of this step (the greens) is then machined to near-net-shape. An alternative route is the near-net shaping by injection molding, a process for obtaining more complex geometries but that implies an high content of plasticizers (waxes) in the batch to achieve the necessary flowability and the proper filling of the mold. Typical density of the greens at the end of this step is about 50 % of the Theoretical Density (or 50 %TD).
3. **Consolidation.** The greens reach the reference density by sintering. This process involves minimization of the surface energy through a high- temperature thermal treatment, resulting in a solid body. In the first phase of a sintering cycle, binders are evacuated via the open porosity then porosity is evacuated from the body, leaving a polycrystalline solid with a density nearing 100 % T.D. (Typical densities of ceramic head and inlays are 99.5 %T.D. or more). The process is carried out in a furnace where the green body is fired to temperatures about 2/3 of the melting temperature of the oxide. The sintering aids introduced into the feedstock allow enhancing transport phenomena and limit grain growth

The sintering process usually is carried out in two steps. The first step (presintering) consists in heating the green body to intermediate temperature to evacuate the organic additives. As a result, the green body shrinks reaching final density some 70–80 % TD. Presintered ball heads or inlays may then be obtained by mechanical tooling, which is currently made using numerical control machines

Machined parts are then inserted in a high-temperature furnace (some 1500 °C) where in an appropriate time/temperature sequence they reach the final density (e.g., > 99.9 %TD). Sintering is usually performed in oxidizing atmosphere in gas-heated kilns but continuous (tunnel) furnaces are also in use for high volume production. In these furnaces, the green bodies are loaded on trays that are transported across a tunnel which is heated at different temperatures: time-temperature sequence depends on the trays' speed.

In both cases, final density is achieved by HIP (Hot Isostatic Pressing) treatment in high pressure batch furnaces. HIP consists in a high temperature plus high pressure treatment (e.g., 1100 °C, 1000 Bar). HIP is a relevant innovation introduced in bioceramics processing to obtain ceramics with density near to the theoretical one. Because the densification takes place at relatively low temperature, the deleterious grain growth that takes place when the process is made at higher temperature is avoided. In addition, HIP treatment allows minimizing the residual stresses within ceramic pieces thus further improving the strength and reliability of products.

4. **Machining and finishing.** The classic process to obtain ceramic heads or inlays is based on the machining of green cylinders obtained by bidirectional dye pressing of ready-to-press powders. As by this process a big volume of valuable materials is wasted, some producers use the alternative cold isostatic pressing method. After cooling, the spherical surface is polished to the desired grade, the inner cone is ground to the expected tolerance (Table 11), identification marks made by laser, and the lot is sent to final controls prior to be released to market.

**Table 11** Typical values of finish of a THR ceramic ball head

Part	Characteristic	Value [ $\mu\text{m}$ ]
Spherical surface	Deviation from sphericity	<0.1
	Deviation from nominal diameter	<0.5
	Roughness Ra	<0.02
	Roughness Rmax	<0.05
Inner taper	Deviation from straightness	0.5–0.75
	Deviation from roundness	<0.1
	Roughness Ra	0.5

A further route consists in sintering balls of the desired diameter and then machining the conical bore in the balls by ultrasonic drilling. The process may be performed either before or after HIP processing, depending on the manufacturer. This method allows ceramic manufacturers a great flexibility in production, as ball diameters are standard, while each THR manufacturer has its specification for the taper, which can then be machined on demand.

---

## Summary

The development of oxide ceramic as biomaterials was started more than 40 years ago. So far, we can note how imaginative were the pioneers who selected alumina first, then zirconia for the construction of medical devices. The biological safety and the functional biocompatibility of both the oxides have been proven since a long time, as well as their excellent wear behavior. Especially alumina has demonstrated significant advantages over other materials used in the bearings of total hip replacement. In the same way, zirconia after its practical abandonment in orthopedics on the turn of the century, has gained a new field of application in dentistry. So far, the synergistic action of alumina and zirconia is exploited in the contemporary submicron-grained ceramic composites that replaced the “pure” oxide ceramics. The behavior of composites and the innovative design of ceramic devices outclass the former generation of ceramic oxides and makes their introduction in clinics feasible as well.

---

## References

1. Piconi C, Condò SG, Kosmac T (2014) Alumina- and zirconia-based ceramics for load bearing applications. In: Shen JZ, Kosmac T (eds) *Advanced ceramics for dentistry*, 1st edn. Butterworth-Heinemann, Waltham, pp 220–253
2. Piconi C, Maccauro G (1999) Zirconia as a ceramic biomaterial. *Biomaterials* 20:1–25
3. Piconi C, Rimondini L, Cerroni L (2008) *La zirconia in odontoiatria*. Elsevier, Milano
4. Rock M (1933) *Künstliche Ersatzteile für das Innere und Aussere des menschliche und tierische Körpers*, German Patent DRP 583.589
5. Piconi C (2011) Alumina. In: Ducheyne P, Healey KE, Hutmacher DW, Grainger DW, Kirkpatrick CJ (eds) *Comprehensive biomaterials*, vol 1. Elsevier, Amsterdam, pp 73–94

6. Petzatos GE, Papadopoulos PP, Papavasiliou KA, Hatzokos IG, Agathangelidis FG, Christodoulou AG (2010) Primary cementless total hip arthroplasty with an alumina ceramic-on-ceramic bearing: results after a minimum of twenty years of follow-up. *J Bone Joint Surg Am* 92:639–644
7. Sedel L (2004) Thirty year experience with all ceramic bearings. In: Lazennec J-Y, Dietrich M (eds) *Bioceramics in joint arthroplasty*. Steinkopff, Darmstadt, pp 17–20
8. Munz D, Fett T (1999) *Ceramics. Material properties, failure behavior, materials selection*. Springer, Berlin, pp 9–18
9. Weibull W (1951) A statistical distribution function of wide applicability. *J Appl Mech* 18:293–297
10. International Standards Organization-Technical Committee ISO/TC 206 (2003) “Fine Ceramics”. Fine Ceramics (advanced ceramics, advanced technical ceramics) – Weibull statistics for strength data. ISO 20501:2003
11. Kuntz M, Masson B, Pandorf T (2009) Current state of the art of ceramic composite material BIOLOX delta. In: Mendes G, Lago B (eds) *Strength of materials*. Nova Science, Hauppauge, pp 133–158
12. Ruff O, Ebert F, Stephen E (1929) Contributions to the ceramics of highly refractory materials: II, System Zirconia-Lime. *Z Anorg Allg Chem* 180:215–224
13. Garvie RC, Nicholson PS (1972) Structure and thermodynamical properties of partially stabilized zirconia in the CaO-ZrO<sub>2</sub> system. *J Am Ceram Soc* 55:152–157
14. Garvie RC, Hannink RHJ, Pascoe RT (1975) Ceramic steel? *Nature* 258:703–704
15. Rieth PH, Reed JS, Naumann AW (1976) Fabrication and flexural strength of ultra-fine grained yttria-stabilised zirconia. *Bull Am Ceram Soc* 55:717
16. Gupta TK, Bechtold JH, Kuznickie RC, Cadoff LH, Rossing BR (1978) Stabilization of tetragonal phase in polycrystalline zirconia. *J Mater Sci* 13:1464
17. Lugh V, Sergio V (2010) Low temperature degradation -aging- of zirconia: a critical review of the relevant aspects in dentistry. *Dent Mater* 26:807–820
18. Lange FF (1982) Transformation toughening – part 1–4. *J Mater Sci* 17:225–263
19. Becher PF, Francis Rose LR (1994) Toughening mechanisms in ceramic systems. In: Swain MV (ed) *Structure and properties of ceramics*, vol 11, Materials science and technology. VCH, Weinheim, pp 409–461
20. Hannink RHJ, Kelly PM, Muddle BC (2000) Transformation toughening in zirconia-containing ceramics. *J Am Ceram Soc* 83:461–487
21. Kobayashi K, Kuwajima H, Masaki T (1981) Phase change and mechanical properties of ZrO<sub>2</sub>-Y<sub>2</sub>O<sub>3</sub> solid electrolyte after aging. *Solid State Ion* 3–4:461–487
22. Sato T, Shimada M (1985) Transformation of yttria-doped tetragonal ZrO<sub>2</sub> polycrystals by annealing in water. *J Am Ceram Soc* 68:356–359
23. Yoshimura M, Noma T, Kawabata K, Somiya S (1987) Role of H<sub>2</sub>O on the degradation process of Y-TZP. *J Mater Sci Lett* 6:465
24. Chevalier J, Gremillard L, Virkar AV, Clarke DR (2009) The tetragonal–monoclinic transformation in zirconia: lessons learned and future trends. *J Am Ceram Soc* 92:1901–1920
25. Piconi C, Casarci M (2000) Purification of chemicals for the production of biomedical grade YTZP ceramics. In: Rammlair D, Mederer J, Oberthur RB, Petinghaus H (eds) *Applied mineralogy*. Balkema, Rotterdam, pp 205–207
26. Pecharrómán C, Bartolomé JF, Requena J et al (2003) Percolative mechanisms of aging in zirconia-containing ceramics for medical applications. *Adv Mater* 15:507–511
27. Clarke IC, Pezzotti G, Green DD, Shirasu H, Donaldson T (2005) Severe simulation test for run-in wear of all-alumina compared to alumina composite THR. In: D’Antonio J, Dietrich M (eds) *Bioceramics and alternative bearings in joint arthroplasty*. Steinkopff, Darmstadt, pp 11–20
28. Piconi C, Porporati AA, Streicher RM (2015) Ceramics in THR bearings: behavior in off-normal conditions. *Key Eng Mater* 631:1–7

29. Begand S, Oberbach T, Glien W (2005) ATZ A new material with a high potential in joint replacement. *Key Eng Mater* 284–286:983–986
30. Schneider J, Begand S, Kriegel R, Kaps C, Glien W, Oberbach T (2008) Low temperature aging of alumina toughened zirconia. *J Am Ceram Soc* 91:3613–3618
31. Oberbach T, Begand S, Glien W (2007) In-vitro wear of different ceramic couplings. *Key Eng Mater* 330–332:1231–1234
32. Oberbach T, Ortmann C, Begand S, Glien W (2009) Investigations of an alumina ceramic with zirconia gradient for the application as load bearing implant for joint prostheses. *Key Eng Mater* 309–311:1247–1250
33. Al-Hajjar M, Jennings LM, Begand S, Oberbach T, Delfosse D, Fisher J (2013) Wear of novel ceramic-on-ceramic bearings under adverse and clinically relevant hip simulator conditions. *J Biomed Mater Res B Appl Biomater* 101:1456–1462
34. Chevalier J, Grandjean S, Kuntz N, Pezzotti G (2009) On the kinetics and impact of tetragonal to monoclinic transformation in an alumina/zirconia composite for arthroplasty applications. *Biomaterials* 30:5279–5282
35. Piconi C, Maccauro G, Muratori E, Brach del Prever E (2003) Alumina and zirconia ceramics in joint replacements: a review. *J Appl Biomater Biomech* 1:19–32
36. Catelas I, Petit A, Zukor DJ, Marchand R, Yahia LH, Huk OL (1999) Induction of macrophage apoptosis by ceramic and polyethylene particles in vitro. *Biomaterials* 20:625–630
37. Kranz I, Gonzalez JB, Dorfel I et al (2009) Biological response to micron- and nanometer-sized particles known as potential wear products from artificial hip joints: part II: reaction of murine macrophages to corundum particles of different size distribution. *J Biomed Mater Res* 89-A:390–401
38. Christel P (1992) Biocompatibility of surgical-grade dense polycrystalline alumina. *Clin Orthop* 282:10–18
39. Warashina H, Sakano S, Kitamura S et al (2003) Biological reaction to alumina, zirconia, titanium and polyethylene particles implanted into murine calvaria. *Biomaterials* 24:3655–3661
40. Ryu RK, Bovill EG, Skinner HB et al (1987) Soft tissue sarcoma associated with aluminum oxide ceramic total hip arthroplasty. *Clin Orthop* 216:207–212
41. Covacci V, Bruzzese N, Maccauro G et al (1999) In vitro evaluation of the mutagenic and carcinogenic power of high purity zirconia ceramic. *Biomaterials* 20:371–376
42. Maccauro G, Bianchino G, Sangiorgi S et al (2009) Development of a new zirconia-toughened alumina: promising mechanical properties and absence of in vitro carcinogenicity. *Int J Immunopathol Pharmacol* 22:773–779
43. Willert HG, Semlitsch M (1977) Reactions of the articular capsule to wear products of artificial joint prostheses. *J Biomed Mater Res* 11:157–164
44. Schmalzried TP, Callaghan JJ (1999) Current concepts review: wear in total hip and knee replacements. *J Bone Joint Surg Am* 81-A:115–136
45. Granchi D, Amato I, Battistelli L, Ciapetti G et al (2005) Molecular basis of osteoclastogenesis induced by osteoblasts exposed to wear particles. *Biomaterials* 26:2371–2379
46. Fisher J, Jin Z, Tipper J et al (2006) Tribology of alternative bearings. *Clin Orthop* 453:25–34
47. Maccauro G, Piconi C, Muratori F, De Santis V, Burger W (2003) Tissue reactions to wear debris: clinical cases vs. animal model. In: Zippel M, Dietrich M (eds) *Bioceramics in joint arthroplasty*. Steinkopff, Darmstadt, pp 81–88
48. Lerouge S, Yahia L'H, Huk O et al (1995) Wear debris and inflammatory response in tissues around failed alumina ceramic-on-ceramic hip prostheses. In: Wilson J, Hench LL, Greenspan D (eds) *Bioceramics* 8. Elsevier, New York, pp 145–150
49. De Santis E, Maccauro G, Proietti L et al (2001) Histologic and ultrastructural analysis of alumina wear debris. *Key Eng Mater* 192–195:995–998
50. Graci G, Spinelli MS, Del Bravo V et al (2011) An original method for the evaluation of in-vivo controlled release of ceramic materials. *Int J Immunopathol Pharmacol* 24(S2):107–112



Sergey V. Dorozhkin

## Contents

Introduction .....	92
Geological and Biological Occurrences .....	93
The Members of Calcium Orthophosphate Family .....	96
MCPM .....	99
MCPA (or MCP) .....	101
DCPD .....	102
DCPA (or DCP) .....	103
OCP .....	103
$\beta$ -TCP .....	104
$\alpha$ -TCP .....	105
ACP .....	106
CDHA (or Ca-def HA) .....	108
HA (or HAp or OHAp) .....	110
FA (or FAp) .....	111
OA (or OAp or OXA) .....	112
TTCP (or TetCP) .....	113
Biphasic, Triphasic, and Multiphasic Calcium Orthophosphate Formulations .....	114
Ion-Substituted Calcium Orthophosphates .....	115
Summary .....	116
References .....	116

## Abstract

The present chapter is intended to point the readers' attention to the important subject of calcium orthophosphates. They are of the special significance for the human beings because they represent the inorganic part of major normal (bones, teeth, and antlers) and pathological (i.e., those appearing due to various diseases) calcified tissues of mammals. Therefore, the majority of the artificially prepared

---

S. V. Dorozhkin (✉)  
 Moscow, Russia  
 e-mail: [sedorozhkin@yandex.ru](mailto:sedorozhkin@yandex.ru)

calcium orthophosphates of high purity appear to be well tolerated by human tissues *in vivo* and possess the excellent biocompatibility, osteoconductivity, and bioresorbability. These biomedical properties of calcium orthophosphates are widely used to construct bone grafts. In addition, natural calcium orthophosphates are the major source of phosphorus, which are used to produce agricultural fertilizers, detergents, and various phosphorus-containing chemicals. Thus, there is a great significance of calcium orthophosphates for the humankind, and, here, an overview on the current knowledge on this subject is provided.

---

**Keywords**

Calcium orthophosphates • Hydroxyapatite • Fluorapatite • Occurrence • Properties • Applications

---

**Introduction**

Due to the abundance in nature (as phosphate ores) and presence in living organisms (as bones, teeth, deer antlers, and the majority of various pathological calcifications), calcium orthophosphates are the inorganic compounds of a special interest for human being. They were discovered in 1769 and have been investigated since then [1]. According to the databases of scientific literature (Web of Knowledge, Scopus, Medline, etc.), the total amount of currently available publications on the subject exceeds 40,000 with the annual increase for, at least, 2000 papers. This is a clear confirmation of the importance.

Briefly, by definition, all calcium orthophosphates consist of three major chemical elements: calcium (oxidation state +2), phosphorus (oxidation state +5), and oxygen (reduction state -2), as a part of the orthophosphate anions. These three chemical elements are present in abundance on the surface of our planet: oxygen is the most widespread chemical element of the earth's surface (~47 mass %), calcium occupies the fifth place (~3.3–3.4 mass %), and phosphorus (~0.08–0.12 mass %) is among the first 20 of the chemical elements most widespread on our planet. In addition, the chemical composition of many calcium orthophosphates includes hydrogen, as an acidic orthophosphate anion (e.g.,  $\text{HPO}_4^{2-}$  or  $\text{H}_2\text{PO}_4^-$ ), hydroxide (e.g.,  $\text{Ca}_{10}(\text{PO}_4)_6(\text{OH})_2$ ), and/or incorporated water (e.g.,  $\text{CaHPO}_4 \cdot 2\text{H}_2\text{O}$ ). Regarding their chemical composition, diverse combinations of CaO and  $\text{P}_2\text{O}_5$  oxides (both in the presence of water and without it) provide a large variety of calcium phosphates, which are differentiated by the type of the phosphate anion, namely, ortho- ( $\text{PO}_4^{3-}$ ), meta- ( $\text{PO}_3^-$ ), pyro- ( $\text{P}_2\text{O}_7^{4-}$ ), and poly- ( $(\text{PO}_3)_n^{n-}$ ) phosphates are known. Furthermore, in the case of multi-charged anions (valid for orthophosphates and pyrophosphates), the calcium phosphates are also differentiated by the number of hydrogen ions attached to the anion. Examples include mono- ( $\text{Ca}(\text{H}_2\text{PO}_4)_2$ ), di- ( $\text{CaHPO}_4$ ), tri- ( $\text{Ca}_3(\text{PO}_4)_2$ ), and tetra- ( $\text{Ca}_2\text{P}_2\text{O}_7$ ) calcium phosphates. Here, one must stress that prefixes “mono,” “di,” “tri,” and “tetra” are related to the amount of hydrogen ions replaced by calcium [2]. However, to narrow the subject, calcium orthophosphates will be considered and discussed only. Their names, the standard abbreviations, chemical formulae, and solubility values are listed in

Table 1 [3, 4]. Since all of them belong to calcium *orthophosphates*, strictly speaking, all abbreviations in Table 1 are incorrect; however, they have been extensively used in literature for decades, and, to avoid any confusions, there is no need to modify them.

In general, the atomic arrangement of all calcium orthophosphates is built up around a network of orthophosphate ( $\text{PO}_4$ ) groups, which stabilize the entire structure. Therefore, the majority of calcium orthophosphates are sparingly soluble in water (Table 1); however, all of them are easily soluble in acids but insoluble in alkaline solutions. In addition, all chemically pure calcium orthophosphates are colorless transparent crystals of moderate hardness, but, as powders, they are of white color. Nevertheless, natural minerals of calcium orthophosphates are always colored due the presence of impurities and dopants, such as ions of Fe, Mn, and rare earth elements. Biologically formed calcium orthophosphates are the major component of all mammalian calcified tissues [5], while the geologically formed ones are the major raw material to produce phosphorus-containing agricultural fertilizers, chemicals, and detergents [6].

---

## Geological and Biological Occurrences

Geologically, natural calcium orthophosphates are found in different regions mostly as deposits of apatites, mainly as ion-substituted FA (igneous rocks), and phosphorites (sedimentary rocks) [7]. In addition, natural ion-substituted CDHA was also found, but it is a very rare mineral. Some types of sedimentary rocks can be formed by weathering of igneous rocks into smaller particles. Other types of sedimentary rocks can be composed of minerals precipitated from the dissolution products of igneous rocks or minerals produced by biomineralization (Fig. 1) [8]. Thus, due to a sedimentary origin, both a general appearance and a chemical composition of natural phosphorites vary a lot. It is a common practice to consider francolite (or carbonate-hydroxyfluorapatite regarded as its synonym) as the basic phosphorite mineral [7]. A cryptocrystalline (almost amorphous) variety of francolite (partly of a biological origin) is called collophane (synonyms: collophanit, collophanita, collophanite, grodnolite, kollophan). It occurs in natural phosphorites predominantly as fossil bones and phosphatized microbial pseudomorphs: phosphatic crusts of chasmolithic biofilms (or microstromatolites) and globular clusters with intra-particle porosities. Natural phosphorites (therefore, francolite and collophane as well) occur in various forms, such as nodules, crystals, or masses. Occasionally, other types of natural calcium orthophosphates are found as minerals, for example, clinohydroxylapatite, staffelite (synonyms: staffelit, staffelita) belonging to carbonate-rich fluorapatites (chemical formula:  $\text{Ca}_5[(\text{F},\text{O})(\text{PO}_4,\text{CO}_3)_3]$ ) and DCPD. Furthermore, calcium orthophosphates were found in meteoric stones. The world deposits of natural calcium orthophosphates are estimated to exceed 150 billion tons; from which approximately 85 % belong to phosphorites, and the remaining ~15 % belong to apatites.

As minor constituents ( $\leq 5\%$ ), natural calcium orthophosphates (both apatites and phosphorites) occur in many geological environments. Concentrations sufficient for economic use ( $> 15\%$ ) are also available. Namely, the largest world deposits of natural

**Table 1** Existing calcium orthophosphates and their major properties [3, 4]

Ca/P molar ratio	Compound	Formula	Solubility at 25 °C, $-\log(K_s)$	Solubility at 25 °C, g/L	pH stability range in aqueous solutions at 25 °C
0.5	Monocalcium phosphate monohydrate (MCPM)	$\text{Ca}(\text{H}_2\text{PO}_4)_2 \cdot \text{H}_2\text{O}$	1.14	~18	0.0–2.0
0.5	Monocalcium phosphate anhydrous (MCPA or MCP)	$\text{Ca}(\text{H}_2\text{PO}_4)_2$	1.14	~17	c
1.0	Dicalcium phosphate dihydrate (DCPD), mineral brushite	$\text{CaHPO}_4 \cdot 2\text{H}_2\text{O}$	6.59	~0.088	2.0–6.0
1.0	Dicalcium phosphate anhydrous (DCPA or DCP), mineral monetite	$\text{CaHPO}_4$	6.90	~0.048	c
1.33	Octacalcium phosphate (OCP)	$\text{Ca}_8(\text{HPO}_4)_2(\text{PO}_4)_4 \cdot 5\text{H}_2\text{O}$	96.6	~0.0081	5.5–7.0
1.5	$\alpha$ -Tricalcium phosphate ( $\alpha$ -TCP)	$\alpha\text{-Ca}_3(\text{PO}_4)_2$	25.5	~0.0025	a
1.5	$\beta$ -Tricalcium phosphate ( $\beta$ -TCP)	$\beta\text{-Ca}_3(\text{PO}_4)_2$	28.9	~0.0005	a
1.2–2.2	Amorphous calcium phosphates (ACPs)	$\text{Ca}_x\text{H}_y(\text{PO}_4)_z \cdot n\text{H}_2\text{O}$ , $n = 3–4.5$ ; 15–20 % $\text{H}_2\text{O}$	b	b	~5–12 <sup>d</sup>
1.5–1.67	Calcium-deficient hydroxyapatite (CDHA or Ca-def HA) <sup>e</sup>	$\text{Ca}_{10-x}(\text{HPO}_4)_x(\text{PO}_4)_{6-x}(\text{OH})_{2-x}$ ( $0 < x < 1$ )	~85	~0.0094	6.5–9.5
1.67	Hydroxyapatite (HA, HAp, or OHAp)	$\text{Ca}_{10}(\text{PO}_4)_6(\text{OH})_2$	116.8	~0.0003	9.5–12
1.67	Fluorapatite (FA or FAp)	$\text{Ca}_{10}(\text{PO}_4)_6\text{F}_2$	120.0	~0.0002	7–12
1.67	Oxyapatite (OA, OAp, or OXA) <sup>f</sup> , mineral voelckerite	$\text{Ca}_{10}(\text{PO}_4)_6\text{O}$	~69	~0.087	a
2.0	Tetracalcium phosphate (TTCP or TetCP), mineral hilgenstockite	$\text{Ca}_4(\text{PO}_4)_2\text{O}$	38–44	~0.0007	a

<sup>a</sup>These compounds cannot be precipitated from aqueous solutions

<sup>b</sup>Cannot be measured precisely. The comparative extent of dissolution in acidic buffer is:  $\text{ACP} \gg \alpha\text{-TCP} \gg \beta\text{-TCP} > \text{CDHA} \gg \text{HA} > \text{FA}$

<sup>c</sup>Stable at temperatures above 100 °C

<sup>d</sup>Always metastable

<sup>e</sup>Occasionally, it is called “precipitated HA (PHA)”

<sup>f</sup>Existence of OA remains questionable

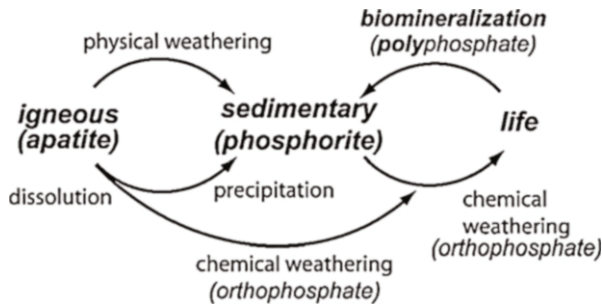


**Fig. 1** Simplified schematic of the phosphorus cycle from apatitic igneous rock to phosphorite sedimentary rock through chemical or physical weathering. Life forms accumulate soluble phosphorus species and can produce apatite through biomineralization (Reprinted from Ref. [8] with permission)

apatites are located in Russia (the Khibiny and Kovdor massifs, Kola peninsula), Brazil, and Zambia, while the largest world deposits of natural phosphorites are located in Morocco, Russia, Kazakhstan, the USA (Florida, Tennessee), China, and Australia [6, 7]. In addition, they are found at the seabed and ocean floor. The majority of natural calcium orthophosphates occur as small polycrystalline structures (spherulitic clusters). Larger crystals are rare. They usually have the crystal structure of apatites (hexagonal system, space group  $P6_3/m$ ). Giant crystals including “a solid but irregular mass of green crystalline apatite, 15 f. long and 9 f. wide” [9] and a single euhedral crystal from the Aetna mine measuring  $2.1 \times 1.2$  m with an estimated weight of 6 t [10] were found. None of them is a pure compound; they always contain dopants of other elements. For example, ions of calcium might be partially replaced by Sr, Ba, Mg, Mn, K, Na, and Fe; ions of orthophosphate may be partly replaced by  $\text{AsO}_4^{3-}$ ,  $\text{CO}_3^{2-}$ , and  $\text{VO}_4^{3-}$ ; ions of hydroxide, chloride, bromide, carbonate, and oxide may to a certain extent substitute fluoride in the crystal lattice of natural apatites. Furthermore, organic radicals have been found in natural apatites. In principle, the crystal structure of apatites can incorporate half the periodic chart in its atomic arrangement. In medicine, this property might be used as an antidote for heavy metal intoxication. Ease of atomic substitution for apatite leaves this mineral open to a wide array of compositions. The substitutions in apatites are usually in trace concentrations, but for certain dopants, large concentrations and even complete solid solutions exist (e.g.,  $\text{F}^-$  and  $\text{OH}^-$ ). To make things even more complicated, some ions in the crystal structure may be missing, leaving the crystallographic defects, which leads to formation of nonstoichiometric compounds, such as CDHA. Figure 2 shows examples of polycrystalline and single-crystalline samples of natural FA.

Manufacturing of elementary phosphorus (white and red), phosphoric acids, various phosphorus-containing chemicals, agricultural fertilizers (namely, superphosphate, ammonium orthophosphates), and detergents (principally sodium tripolyphosphate) are the major industrial applications of natural calcium orthophosphates. The annual consumption of a phosphate rock has approached ~150 million tons, and about 95 % of this production is utilized in the fertilizer industry [11].

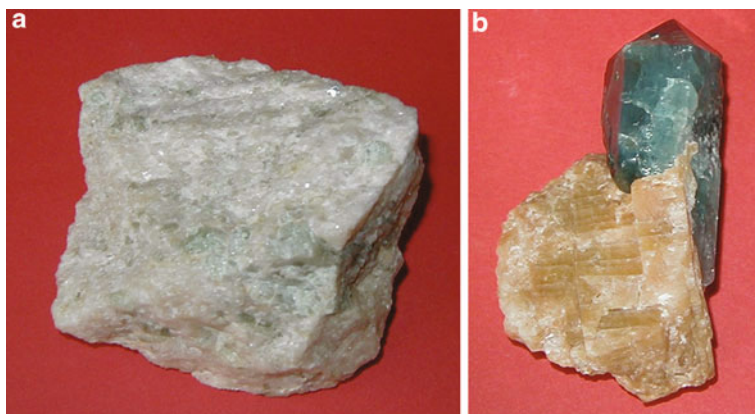


**Fig. 2** Polycrystalline (a) and single-crystalline (b) FA of a geological origin. The single crystal has a *gray-green* color due to incorporated ions of transition metals

In biological systems, many organisms, ranging from bacteria and isolated cells to invertebrates and vertebrates, synthesize calcium orthophosphates [8]. Formation of calcium orthophosphates in primitive organisms is believed to enable the storage and regulation of essential elements such as calcium, phosphorus, and, possibly, magnesium. The morphology of precipitates in these organisms (small intracellular nodules of ACP often located in mitochondria) complies with the necessities for rapid mobilization and intracellular control of the concentration of these elements. In vertebrates, calcium orthophosphates occur as the principal inorganic constituent of normal (bones, teeth, fish enameloid, deer antlers, and some species of shells) and pathological (dental and urinary calculus and stones, atherosclerotic lesions, etc.) calcifications [5]. Except for small portions of the inner ear, all hard tissue of the human body is formed of calcium orthophosphates. Structurally, they occur mainly in the form of poorly crystalline, nonstoichiometric, Ca-deficient, Na-, Mg-, and carbonate-containing HA. It is often called “biological apatite” (which might be abbreviated as BAp), bioapatite, or dahllite.

The main constituents of human bones are calcium orthophosphates (~60–70 wt%), collagen (~20–30 wt%), and water (up to 10 wt%) [12]. Detailed information on the chemical composition of the most important human normal calcified tissues is comprised in Table 2. One should note that the values mentioned in Table 2 are approximate; the main constituents can vary by a percent or more.

---

## The Members of Calcium Orthophosphate Family

In the ternary aqueous system  $\text{Ca}(\text{OH})_2 - \text{H}_3\text{PO}_4 - \text{H}_2\text{O}$  (or  $\text{CaO} - \text{P}_2\text{O}_5 - \text{H}_2\text{O}$ ) [13], there are twelve known non-ion-substituted calcium orthophosphates with the Ca/P molar ratio ranging between 0.5 and 2.0 (Table 1). An anhydrous phase diagram  $\text{CaO} - \text{P}_2\text{O}_5$  at temperatures within 200–2200 °C is shown in Fig. 3 [14]. Table 3 comprises crystallographic data of the existing calcium orthophosphates [2]. The

**Table 2** Comparative composition and structural parameters of inorganic phases of adult human calcified tissues. Due to the considerable variation found in biological samples, typical values are given in these cases [12]

Composition, wt%	Enamel	Dentine	Cementum	Bone	HA
Calcium <sup>a</sup>	36.5	35.1	~35	34.8	39.6
Phosphorus (as P) <sup>a</sup>	17.7	16.9	~16	15.2	18.5
Ca/P (molar ratio) <sup>a</sup>	1.63	1.61	~1.65	1.71	1.67
Sodium <sup>a</sup>	0.5	0.6	<sup>c</sup>	0.9	–
Magnesium <sup>a</sup>	0.44	1.23	0.5–0.9	0.72	–
Potassium <sup>a</sup>	0.08	0.05	<sup>c</sup>	0.03	–
Carbonate (as CO <sub>3</sub> <sup>2-</sup> ) <sup>c</sup>	3.5	5.6	<sup>c</sup>	7.4	–
Fluoride <sup>a</sup>	0.01	0.06	up to 0.9	0.03	–
Chloride <sup>a</sup>	0.30	0.01	<sup>c</sup>	0.13	–
Pyrophosphate (as P <sub>2</sub> O <sub>7</sub> <sup>4-</sup> ) <sup>b</sup>	0.022	0.10	<sup>c</sup>	0.07	–
Total inorganic <sup>b</sup>	97	70	60	65	100
Total organic <sup>b</sup>	1.5	20	25	25	–
Water <sup>b</sup>	1.5	10	15	10	–
<b>Crystallographic properties: Lattice parameters (<math>\pm 0.003 \text{ \AA}</math>)</b>					
<i>a</i> -axis, $\text{\AA}$	9.441	9.421	<sup>c</sup>	9.41	9.430
<i>c</i> -axis, $\text{\AA}$	6.880	6.887	<sup>c</sup>	6.89	6.891
Crystallinity index (HA = 100)	70–75	33–37	~30	33–37	100
Typical crystal sizes (nm)	100 $\mu\text{m} \times 50 \times 50$	35 $\times 25 \times 4$	<sup>c</sup>	50 $\times 25 \times 4$	200–600
Ignition products (800 °C)	$\beta$ -TCP + HA	$\beta$ -TCP+ HA	$\beta$ -TCP+ HA	HA + CaO	HA
Elastic modulus (GPa)	80	23.8 $\pm$ 3.7	15.0 $\pm$ 3.6	0.34–13.8	10
Tensile strength (MPa)	10	100	<sup>c</sup>	150	100

<sup>a</sup>Ashed samples<sup>b</sup>Unashed samples<sup>c</sup>Numerical values were not found in the literature, but they should be similar to those for dentine

most important parameters of calcium orthophosphates are the ionic Ca/P ratio, basicity/acidity, and solubility. All these parameters strongly correlate with the solution pH. The lower the Ca/P molar ratio is, the more acidic and water-soluble the calcium orthophosphate is. One can see that the solubility ranges from high values for acidic compounds, such as MCPM, to very low values for basic compounds, such as apatites, which allow calcium orthophosphates to be dissolved and

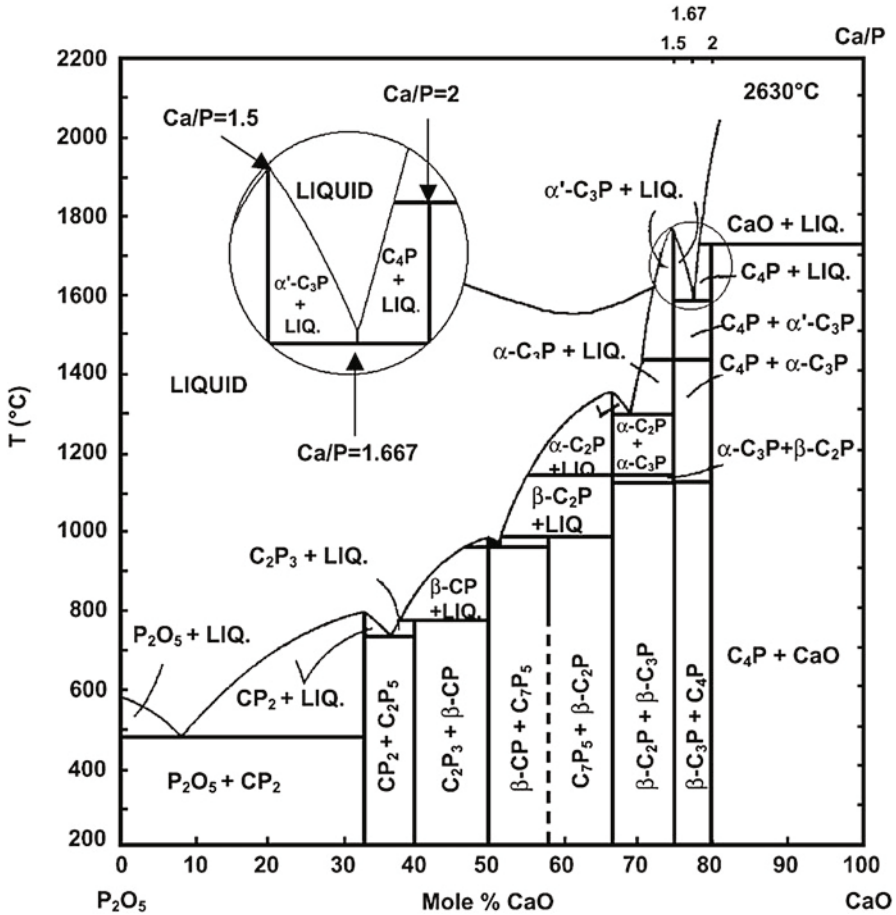


**Fig. 3** Phase diagram of the system CaO–P<sub>2</sub>O<sub>5</sub> (C = CaO, P = P<sub>2</sub>O<sub>5</sub>) at elevated temperatures. Here: C<sub>7</sub>P<sub>5</sub> means 7CaO·5P<sub>2</sub>O<sub>5</sub>; other abbreviations should be written out in the same manner (Reprinted from Ref. [14] with permission)

transported from one place to another and precipitated, when necessary. Regarding applications, some of them might be used in the food industry, and, according to the European classification of food additives, calcium orthophosphates of food grade quality are known as E341 additive.

Due to the triprotic equilibrium that exists within orthophosphate-containing solutions, variations in pH alter the relative concentrations of the four polymorphs of orthophosphoric acid (Fig. 4) [15], and thus, both the chemical composition (Fig. 5) [16] and the amount of the calcium orthophosphates are formed by a direct precipitation. The solubility isotherms of different calcium orthophosphates are shown in Fig. 6 [2, 13]. A brief description of all known calcium orthophosphates (Table 1) is given below.



**Table 3** Crystallographic data of calcium orthophosphates [2]

Compound	Space group	Unit cell parameters	Z <sup>a</sup>	Density, g cm <sup>-3</sup>
MCPM	Triclinic $P\bar{1}$	$a = 5.6261(5), b = 11.889(2), c = 6.4731(8)$ Å, $\alpha = 98.633(6)^\circ, \beta = 118.262(6)^\circ, \gamma = 83.344(6)^\circ$	2	2.23
MCPA	Triclinic $P\bar{1}$	$a = 7.5577(5), b = 8.2531(6), c = 5.5504(3)$ Å, $\alpha = 109.87(1)^\circ, \beta = 93.68(1)^\circ, \gamma = 109.15(1)^\circ$	2	2.58
DCPD	Monoclinic $Ia$	$a = 5.812(2), b = 15.180(3), c = 6.239(2)$ Å, $\beta = 116.42(3)^\circ$	4	2.32
DCPA	Triclinic $P\bar{1}$	$a = 6.910(1), b = 6.627(2), c = 6.998(2)$ Å, $\alpha = 96.34(2)^\circ, \beta = 103.82(2)^\circ, \gamma = 88.33(2)^\circ$	4	2.89
OCP	Triclinic $P\bar{1}$	$a = 19.692(4), b = 9.523(2), c = 6.835(2)$ Å, $\alpha = 90.15(2)^\circ, \beta = 92.54(2)^\circ, \gamma = 108.65(1)^\circ$	1	2.61
$\alpha$ -TCP	Monoclinic $P2_1/a$	$a = 12.887(2), b = 27.280(4), c = 15.219(2)$ Å, $\beta = 126.20(1)^\circ$	24	2.86
$\beta$ -TCP	Rhombohedral $R\bar{3}cH$	$a = b = 10.4183(5), c = 37.3464(23)$ Å, $\gamma = 120^\circ$	21 <sup>b</sup>	3.08
HA	Monoclinic $P2_1/b$ or hexagonal $P6_3/m$	$a = 9.84214(8), b = 2a, c = 6.8814(7)$ Å, $\gamma = 120^\circ$ (monoclinic) $a = b = 9.4302(5), c = 6.8911(2)$ Å, $\gamma = 120^\circ$ (hexagonal)	4 2	3.16
FA	Hexagonal $P6_3/m$	$a = b = 9.367, c = 6.884$ Å, $\gamma = 120^\circ$	2	3.20
OA	Hexagonal $P\bar{6}$	$a = b = 9.432, c = 6.881$ Å, $\alpha = 90.3^\circ, \beta = 90.0^\circ, \gamma = 119.9^\circ$	1	~3.2
TTCP	Monoclinic $P2_1$	$a = 7.023(1), b = 11.986(4), c = 9.473(2)$ Å, $\beta = 90.90(1)^\circ$	4	3.05

<sup>a</sup>Number of formula units per unit cell<sup>b</sup>Per hexagonal unit cell

## MCPM

Monocalcium phosphate monohydrate ( $\text{Ca}(\text{H}_2\text{PO}_4)_2 \cdot \text{H}_2\text{O}$ ; the IUPAC name is calcium dihydrogen orthophosphate monohydrate) is both the most acidic and water-soluble calcium orthophosphate. Although acidic calcium orthophosphates in general were known by 1795 as “superphosphate of lime” [17], their differentiation started in 1800s.

MCPM crystallizes from aqueous solutions containing dissolved ions of  $\text{H}_2\text{PO}_4^-$  and  $\text{Ca}^{2+}$  at the Ca/P ratio ~0.5 and solution pH below ~2.0. Besides, MCPM might be precipitated from aqueous solutions containing organic solvents. At temperatures above ~100 °C, MCPM releases a molecule of water and transforms into MCPA, but at temperatures  $\geq 500$  °C, MCPA further transforms into  $\text{Ca}(\text{PO}_3)_2$  [2, 3].

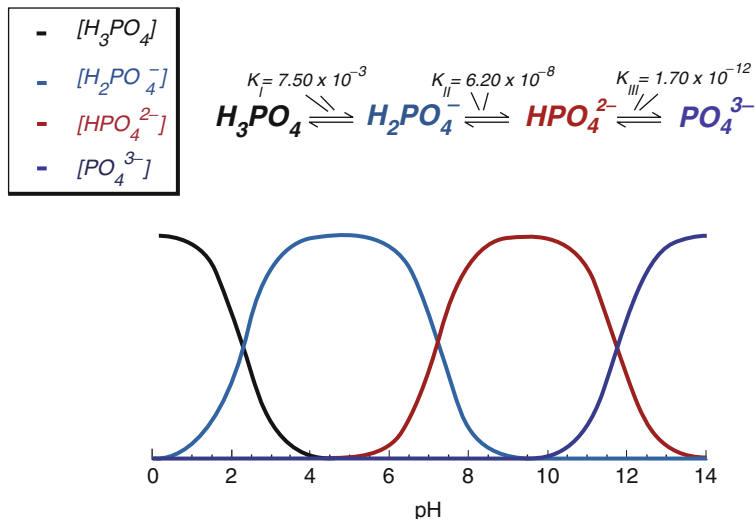


**Fig. 4** pH variation of ionic concentrations in triprotic equilibrium for phosphoric acid solutions (Reprinted from Ref. [15] with permission)

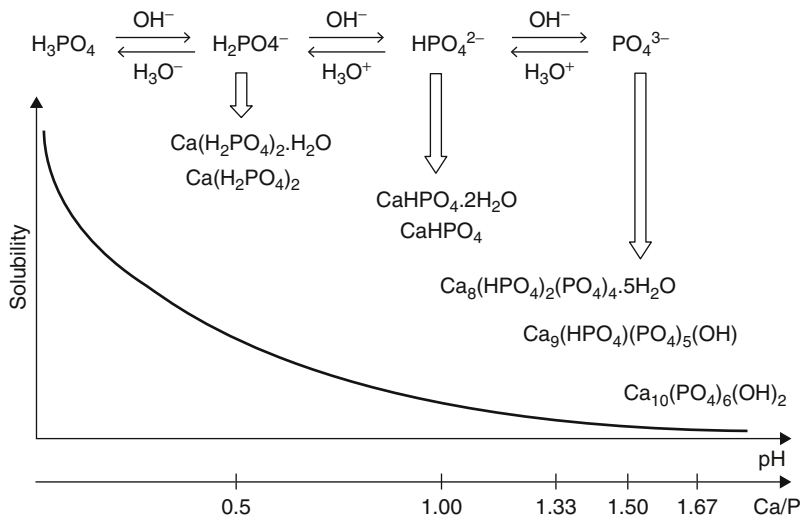


**Fig. 5** Various calcium orthophosphates obtained by neutralizing of orthophosphoric acid. Ca/P are reported in the figure. The solubility of calcium orthophosphates in water decreases drastically from *left* to *right*, HA being the most insoluble and stable phase (Reprinted from Ref. [15] with permission)

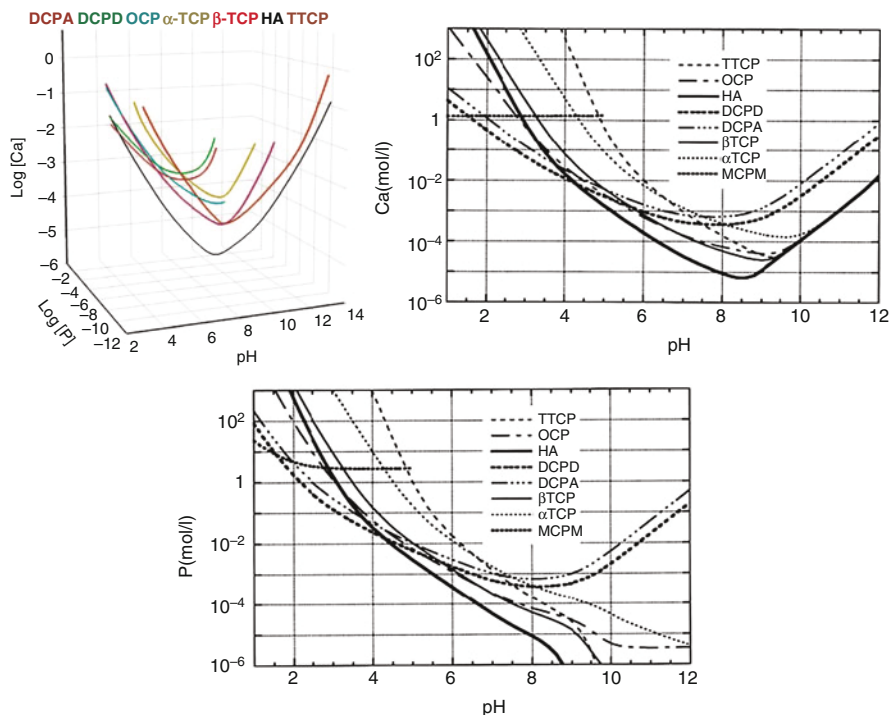


**Fig. 6** *Top*: a 3D version of the classical solubility phase diagrams for the ternary system  $\text{Ca}(\text{OH})_2\text{-H}_3\text{PO}_4\text{-H}_2\text{O}$ . *Middle and bottom*: solubility phase diagrams in two-dimensional graphs, showing two logarithms of the concentrations of (a) calcium and (b) orthophosphate ions as a function of the pH in solutions saturated with various salts

Due to high acidity and solubility, MCPM is never found in biological calcifications. Moreover, pure MCPM is not biocompatible with bones. However, in medicine, MCPM is used as a component of several self-hardening calcium orthophosphate formulations. In addition, MCPM is used as a nutrient, acidulant, and mineral supplement for dry baking powders, food, feed, and some beverages. Coupled with  $\text{NaHCO}_3$ , MCPM is used as a leavening agent for both dry baking powders and bakery dough. MCPM might be added to salt-curing preserves, pickled, and marinated foods. In addition, MCPM might be added to toothpastes and chewing gums. Besides, MCPM might be added to ceramics and glasses, while agriculture is the main consumer of a technical grade MCPM, where it is used as a fertilizer, triple superphosphate [3, 4].

### MCPA (or MCP)

Monocalcium phosphate anhydrous ( $\text{Ca}(\text{H}_2\text{PO}_4)_2$ ; the IUPAC name is calcium dihydrogen orthophosphate anhydrous) is the anhydrous form of MCPM. Although

MCPM has been known since 1807, MCPA was differentiated as “tetrahydrogen calcium phosphate,  $H_4Ca(PO_4)_2$ ” by 1879 [1]. It crystallizes under the same conditions as MCPM but at temperatures above  $\sim 100$  °C (e.g., from concentrated hot mother liquors during fertilizer production). In addition, MCPA might be prepared from MCPM by dehydration. Furthermore, it might be also prepared at ambient temperatures by crystallization in water-restricted or nonaqueous systems. Like MCPM, MCPA never appears in calcified tissues and is not biocompatible due to its acidity. There is no current application of MCPA in medicine. Due to the similarity with MCPM, in many cases, MCPA might be used instead of MCPM; however, highly hygroscopic properties of MCPA reduce its commercial applications [3, 4].

## DCPD

Dicalcium phosphate dihydrate ( $CaHPO_4 \cdot 2H_2O$ ; the IUPAC name is calcium hydrogen orthophosphate dihydrate; the mineral brushite) has been known since, at least, 1804 [17]. As a mineral, brushite was first discovered in phosphatic guano from Avis Island (Caribbean) in 1865 and named to honor an American mineralogist Prof. George Jarvis Brush (1831–1912), Yale University, New Haven, Connecticut, USA [18].

DCPD can be easily crystallized from aqueous solutions containing dissolved ions of  $HPO_4^{2-}$  and  $Ca^{2+}$  at the Ca/P ratio  $\sim 1$  and solution pH within  $\sim 2.0 < pH < 6.5$ . Other preparation techniques such as neutralization of  $H_3PO_4$  and/or MCPM solutions by CaO,  $CaCO_3$ , or more basic calcium orthophosphates ( $\alpha$ - or  $\beta$ -TCP, CDHA, HA, TTCP) are also known. Interestingly, that precipitation of DCPD by mixing a  $Ca(OH)_2$  suspension and a  $H_3PO_4$  solution in the equimolar quantities was found to occur in five stages, being HA the first precipitated phase. DCPD transforms into DCPA at temperatures above  $\sim 80$  °C, and this transformation is accompanied by  $\sim 11$  % decrease in volume and structural changes. The value for  $\Delta_r G^0$  for  $DCPD \rightarrow DCPA$  transformation is  $-1.032$  kJ/mol. Briefly, DCPD crystals consist of  $CaPO_4$  chains arranged parallel to each other, while lattice water molecules are interlayered between them [2].

DCPD is of biological importance because it is often found in pathological calcifications (dental calculi, crystalluria, chondrocalcinosis, and urinary stones) and some carious lesions. It was proposed as an intermediate in both bone mineralization and dissolution of enamel in acids (dental erosion). In medicine, DCPD is used in self-setting calcium orthophosphate formulations and as an intermediate for tooth remineralization. DCPD is added to toothpaste both for caries protection (in this case, it is often coupled with F-containing compounds such as NaF and/or  $Na_2PO_3F$ ) and as a gentle polishing agent. Other applications include a flame retardant; a slow release fertilizer, used in glass production; as well as calcium supplement in food, feed, and cereals. In the food industry, it serves as a texturizer, bakery improver, and water retention additive. In the dairy industry, DCPD is used as a mineral supplement. In addition, plate-like crystals of

DCPD might be used as a nontoxic, anticorrosive, and passivating pigment for some ground coat paints [3, 4].

### DCPA (or DCP)

Dicalcium phosphate anhydrous ( $\text{CaHPO}_4$ ; the IUPAC name is calcium hydrogen orthophosphate anhydrate; the mineral monetite) is the anhydrous form of DCPD. Although DCPD has been known since, at least, 1804, DCPA was differentiated as “monohydrogen calcium orthophosphate,  $\text{HCaPO}_4$ ” by 1879 [1]. As a mineral, monetite was first described in 1882 in rock phosphate deposits from the Moneta (now Monito) Island (archipelago of Puerto Rico), which contains a notable occurrence [19].

Due to the absence of water inclusions, DCPA is less soluble than DCPD (Table 1). Like DCPD, DCPA can be crystallized from aqueous solutions containing Ca/P ratio  $\sim 1$  at solution pH within  $\sim 2.0 < \text{pH} < \sim 6.5$  but at temperatures  $\geq 90^\circ\text{C}$ . In addition, DCPA might be prepared by dehydration of DCPD. Furthermore, it might be also prepared at ambient temperatures in water-restricted or nonaqueous systems, such as gels, ethanol, as well as in the oil-in-water and water-in-oil systems. DCPA is physically stable and resisted hydration even when dispersed in water for over 7 months in the temperature range of  $4\text{--}50^\circ\text{C}$ . A calcium-deficient DCPA was also prepared. It might be sintered at  $\sim 300^\circ\text{C}$ . Unlike DCPD, DCPA occurs in neither normal nor pathological calcifications. It is used in self-setting calcium orthophosphate formulations. Besides, DCPA might be implanted as bioceramics. Other applications include using as a polishing agent, a source of calcium and phosphate in nutritional supplements (e.g., in prepared breakfast cereals, enriched flour, and noodle products), a tableting aid, and a toothpaste component. In addition, it is used as a dough conditioner in the food industry [3, 4].

### OCP

Octacalcium phosphate ( $\text{Ca}_8(\text{HPO}_4)_2(\text{PO}_4)_4 \cdot 5\text{H}_2\text{O}$ ; the IUPAC name is tetracalcium hydrogen orthophosphate diorthophosphate pentahydrate; another name is octacalcium bis(hydrogenphosphate) tetrakis(phosphate) pentahydrate) is often found as an unstable transient intermediate during the precipitation of the thermodynamically more stable calcium orthophosphates (e.g., CDHA) in aqueous solutions. To the best of my findings [1], OCP has been known since, at least, 1843, when Percy published a paper [20], in which he described formation of “a new hydrated phosphate of lime” with a chemical formula  $2\text{CaO} + \text{PO}_5 + 6\text{H}_2\text{O}$ , in which “1 equiv. water being basic and 5 constitutional.”

The preparation techniques of OCP are available in literature. Briefly, to prepare OCP, Ca- and  $\text{PO}_4$ -containing chemicals must be mixed to get the supersaturated aqueous solutions with the Ca/P ratio equal to 1.33. However, OCP might be nonstoichiometric and be either Ca-deficient (Ca/P = 1.26) or include excessive

calcium (up to  $\text{Ca/P} = 1.48$ ) in the structure. Furthermore, a partially hydrolyzed form of OCP with  $\text{Ca/P}$  molar ratio of 1.37 might be prepared [21]. The full hydrolysis of OCP into CDHA occurs within  $\sim 6$  h. Ion-substituted OCP might be prepared as well. Crystals of OCP are typically small, extremely platy, and almost invariably twinned.

The triclinic structure of OCP displays apatitic layers (with atomic arrangements of calcium and orthophosphate ions similar to those of HA) separated by hydrated layers (with atomic arrangements of calcium and orthophosphate ions similar to those in DCPD). A similarity in crystal structure between OCP and HA is one reason that the epitaxial growth of these phases is observed. It is generally assumed that, in solutions, the hydrated layer of the (100) face is the layer most likely exposed to solution. The water content of OCP crystals is about 20 % that of DCPD, and this is partly responsible for its lower solubility [2, 21, 22].

OCP is of a great biological importance because it is one of the stable components of human dental and urinary calculi. OCP was first proposed by W. E. Brown to participate as the initial phase in enamel mineral formation and bone formation through subsequent precipitation and stepwise hydrolysis of OCP [22]. It plays an important role in formation of apatitic biominerals *in vivo*. A “central OCP inclusion” (also known as “central dark line”) is seen by transmission electron microscopy in many biological apatites and in synthetically precipitated CDHA. Although OCP has not been observed in vascular calcifications, it has been strongly suggested as a precursor phase to biological apatite found in natural and prosthetic heart valves. In surgery, OCP is used for implantation into bone defects. For the comprehensive information on OCP, the readers are referred to other reviews [21, 22].

## $\beta$ -TCP

$\beta$ -Tricalcium phosphate ( $\beta\text{-Ca}_3(\text{PO}_4)_2$ ; the IUPAC name is tricalcium diorthophosphate beta; other names are calcium orthophosphate tribasic beta or tricalcium bis(orthophosphate) beta) is one of the polymorphs of TCP. Although calcium orthophosphates with the composition close to that of TCP, CDHA, and HA were known in 1770s [1],  $\alpha$ - and  $\beta$ - polymorphs of TCP were differentiated only by 1932 [23].

$\beta$ -TCP cannot be precipitated from aqueous solutions. It is a high-temperature phase, which can be prepared at temperatures above  $\sim 800$  °C by thermal decomposition of CDHA or by solid-state interaction of acidic calcium orthophosphates, e.g., DCPA, with a base, e.g., CaO. In all cases, the chemicals must be mixed in the proportions to get the  $\text{Ca/P}$  ratio equal to 1.50. However,  $\beta$ -TCP can also be prepared at relatively low temperatures ( $\sim 150$  °C) by precipitation in water-free mediums, such as ethylene glycol. Apart from the chemical preparation routes, ion-substituted  $\beta$ -TCP can be prepared by calcining of bones: such type of calcium orthophosphates is occasionally called “bone ash.” At temperatures above  $\sim 1125$  °C,  $\beta$ -TCP is transformed into a high-temperature phase  $\alpha$ -TCP. Being the stable phase at room

temperature,  $\beta$ -TCP is less soluble in water than  $\alpha$ -TCP (Table 1). Both ion-substituted and organically modified forms of  $\beta$ -TCP can be synthesized, as well.

Pure  $\beta$ -TCP never occurs in biological calcifications. Only the Mg-substituted form ( $\beta$ -TCMP –  $\beta$ -tricalcium magnesium phosphate,  $\beta$ -(Ca, Mg)<sub>3</sub>(PO<sub>4</sub>)<sub>2</sub>) is found, which is often called whitlockite to honor Mr. Herbert Percy Whitlock (1868–1948), an American mineralogist, the curator of the American Museum of Natural History, New York City, New York, USA [24]. Since  $\beta$ -TCMP is less soluble than  $\beta$ -TCP, it is formed instead of  $\beta$ -TCP in dental calculi and urinary stones, dentinal caries, salivary stones, arthritic cartilage, as well as in some soft-tissue deposits. However, it has not been observed in enamel, dentine, or bone. In medicine,  $\beta$ -TCP is used in the self-setting calcium orthophosphate formulations and other types of bone grafts. Dental applications of  $\beta$ -TCP are also known. For example,  $\beta$ -TCP is added to some brands of toothpaste as a gentle polishing agent. Multivitamin complexes with calcium orthophosphate are widely available in the market, and  $\beta$ -TCP is used as the calcium phosphate there. In addition,  $\beta$ -TCP serves as a texturizer, bakery improver, and anti-clumping agent for dry powdered food (flour, milk powder, dried cream, cocoa powder). Besides,  $\beta$ -TCP is added as a dietary or mineral supplement to food and feed. Occasionally,  $\beta$ -TCP might be used as inert filler in pelleted drugs. Other applications comprise porcelains; pottery; enamel, used as a component for mordants and ackey; as well as a polymer stabilizer.  $\beta$ -TCP of a technical grade (as either calcined natural phosphorites or bone dust) is used as a slow release fertilizer for acidic soils [3, 4].

## $\alpha$ -TCP

$\alpha$ -Tricalcium phosphate ( $\alpha$ -Ca<sub>3</sub>(PO<sub>4</sub>)<sub>2</sub>); the IUPAC name is tricalcium diorthophosphate alpha; other names are calcium orthophosphate tribasic alpha or tricalcium bis(orthophosphate) alpha) is another polymorph of TCP, which was differentiated by 1932 [23].  $\alpha$ -TCP is also a high-temperature phase; therefore, it cannot be precipitated from aqueous solutions either. Thus,  $\alpha$ -TCP is usually prepared by the same techniques as  $\beta$ -TCP (see the previous section), but, since the  $\beta$ -TCP  $\rightarrow$   $\alpha$ -TCP transition temperature is  $\sim$ 1125 °C, calcining is performed at temperatures above  $\sim$ 1200 °C. Consequently,  $\alpha$ -TCP is often considered as a high-temperature polymorph of  $\beta$ -TCP. However, data are available that  $\alpha$ -TCP might be prepared at lower temperatures. Namely, at the turn of the millennium, the previously forgotten data that the presence of silicates stabilized  $\alpha$ -TCP at temperatures of 800–1000 °C were rediscovered again. Furthermore, sometimes,  $\alpha$ -TCP might be prepared at even lower temperatures ( $\sim$ 700 °C) by a thermal decomposition of low-temperature ACPs [25].

Although  $\alpha$ -TCP and  $\beta$ -TCP have exactly the same chemical composition, they differ by the crystal structure (Table 3) and solubility (Table 1). In the absence of humidity, both polymorphs of TCP are stable at room temperatures; however, according to a density functional study, stability of  $\beta$ -TCP crystal lattice exceeds that of  $\alpha$ -TCP. Therefore, of them,  $\alpha$ -TCP is more reactive in aqueous systems, has a

higher specific energy, and in aqueous solutions it can be hydrolyzed to CDHA. Milling increased the  $\alpha$ -TCP reactivity even more. Although,  $\alpha$ -TCP never occurs in biological calcifications, in medicine, it is used as a component of self-setting calcium orthophosphate formulations. On the other hand, the chemically pure  $\alpha$ -TCP has received not much interest in the biomedical field. The disadvantage for using  $\alpha$ -TCP is its quick resorption rate (faster than formation of a new bone), which limits its application in this area. However, the silicon stabilized  $\alpha$ -TCP (more precisely as a biphasic composite with HA) has been commercialized as a starting material to produce bioresorbable porous ceramic scaffolds to be used as artificial bone grafts. Upon implantation,  $\alpha$ -TCP tends to convert to CDHA, which drastically reduces further degradation rate. Similar to  $\beta$ -TCP,  $\alpha$ -TCP of a technical grade might be used as slow release fertilizer for acidic soils.

To conclude, one should briefly mention on an existence of  $\alpha$ -TCP polymorph, which was discovered in 1959. However, this TCP polymorph lacks of any practical interest because it only exists at temperatures between  $\sim 1450$  °C and its melting point ( $\sim 1756$  °C). It reverts to  $\alpha$ -TCP polymorph by cooling below the transition temperature [2].

## ACP

Amorphous calcium phosphates (ACPs) represent a special class of calcium orthophosphate salts, having variable chemical but rather identical glass-like physical properties, in which there are neither translational nor orientational long-range orders of the atomic positions. To the best of my findings [1], ACP was first prepared in 1845 [26]. Nevertheless, until recently [27], ACP has often been considered as an individual calcium orthophosphate with a variable chemical composition, while, in reality, ACP is just an amorphous state of other calcium orthophosphates. Therefore, in principle, all compounds mentioned in Table 1 might be somehow fabricated in an amorphous state, but, currently, only few of them (e.g., an amorphous TCP) are known [27]. Thus, strictly speaking, ACP should be excluded from Table 1. Furthermore, since ACPs do not have the definite chemical composition, the IUPAC nomenclature is not applicable to describe them.

Depending on the production temperatures, all types of ACP are divided into two major groups: low-temperature ACPs (prepared in solutions, usually aqueous ones) and high-temperature ACPs [27]. Low-temperature ACPs (described by the chemical formula  $\text{Ca}_x\text{H}_y(\text{PO}_4)_z \cdot n\text{H}_2\text{O}$ ,  $n = 3\text{--}4.5$ ; 15–20 %  $\text{H}_2\text{O}$ ) are often encountered as a transient precursor phase during precipitation of other calcium orthophosphates in aqueous systems. Usually, an ACP is the first phase precipitated from supersaturated solutions (the higher supersaturation, the better) prepared by rapid mixing of solutions containing ions of calcium and orthophosphate [2, 27]. Such ACP precipitates usually look like spherical particles with diameters in the range 200–1200 Å without a definite structure. Generally, the ACP particles are smaller if prepared under conditions of high supersaturation and/or high pH, while for a given pH, higher temperatures give larger particles. The freshly precipitated ACPs contain



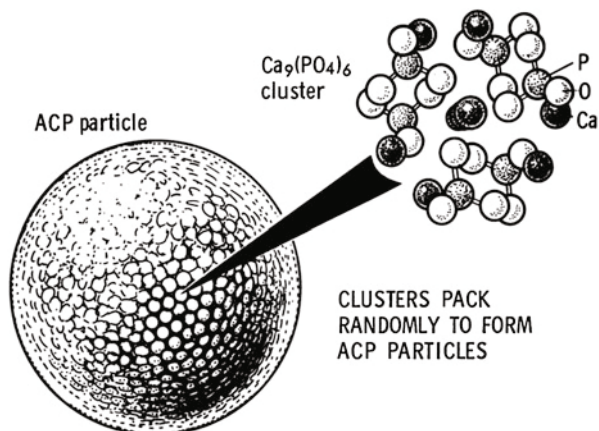
10–20 % by weight of tightly bound water, which is removed by vacuum drying at elevated temperature [28]. The amorphization degree of ACPs increases with the concentration increasing of Ca- and PO<sub>4</sub>-containing solutions, as well as at a high solution pH and a low crystallization temperature. A continuous gentle agitation of as precipitated ACPs in the mother solution, especially at elevated temperatures, results in a slow recrystallization and formation of better crystalline calcium orthophosphates, such as CDHA [2]. In addition, other production techniques of ACPs are known [27].

The lifetime of ACPs in aqueous solutions was reported to be a function of the presence of additive molecules and ions, pH, ionic strength, and temperature. Thus, ACPs may persist for appreciable periods and retain the amorphous state under some specific experimental conditions. The chemical composition of ACPs strongly depends on the solution pH and the concentrations of mixing solutions. For example, ACPs with Ca/P ratios in the range of 1.18 (precipitated at solution pH = 6.6) to 1.53 (precipitated at solution pH = 11.7) and even to 2.5 [2, 3] were described. It should be noted that unsubstituted ACPs are unstable in aqueous solutions, and even when stored dry they tend to transform into more crystalline calcium orthophosphates, such as poorly crystalline CDHA. The presence of poly(ethylene glycol), ions of pyrophosphate, carbonate, and/or magnesium in solutions during the crystallization promotes formation of ACPs and slows down their further transformation, while the presence of fluoride has the opposite effect [2, 12]. In general, low-temperature ACPs heated to ~550 °C (so that all volatiles have already escaped) remain amorphous, but further heating above ~650 °C causes their transformation into crystalline calcium orthophosphates, such as  $\alpha$ - or  $\beta$ -TCP, HA, and mixtures thereof, depending on the Ca/P ratio of the ACP heated.

High-temperature ACPs might be prepared using high energy processing at elevated temperatures [27]. This method is based on a rapid quenching of melted calcium orthophosphates occurring, e.g., during plasma spraying of HA. A plasma jet, possessing very high temperatures (~5000 °C to ~20,000 °C), partly decomposes HA. That results in formation of a complicated mixture of products, some of which would be ACPs. Obviously, all types of high-temperature ACPs are definitively anhydrous contrary to the precipitated ACPs. Unfortunately, no adequate chemical formula is available to describe the high-temperature ACPs.

In general, as all amorphous compounds are characterized by a lack of long-range order, it is problematic to discuss the structure of ACPs (they are X-ray amorphous). Concerning a short-range order (SRO) in ACPs, it exists, just due to the nature of chemical bonds. Unfortunately, in many cases, the SRO in ACPs is uncertain either, because it depends on many variables, such as Ca/P ratio, preparation conditions, storage, admixtures, etc. Infrared spectra of ACPs show broad featureless phosphate absorption bands. Electron microscopy of freshly precipitated ACPs usually shows featureless nearly spherical particles with diameters in the range of 20–200 nm. However, there is a questionable opinion that ACPs might have an apatitic structure but with a crystal size so small, that they are X-ray amorphous. This is supported by X-ray absorption spectroscopic data (EXAFS) on biogenic and synthetic samples. On the other hand, it was proposed that the basic structural unit of the

**Fig. 7** A model of ACP structure (Reprinted from Ref. [28] with permission)



precipitated ACPs is a 9.5 Å diameter, roughly spherical cluster of ions with the composition of  $\text{Ca}_9(\text{PO}_4)_6$  (Fig. 7) [2, 28]. These clusters were found experimentally as first nuclei during the crystallization of CDHA, and a model was developed to describe the crystallization of HA as a stepwise assembly of these units. Biologically, ion-substituted ACPs (always containing ions of Na, Mg, carbonate, and pyrophosphate) are found in soft-tissue pathological calcifications (e.g., heart valve calcifications of uremic patients).

In medicine, ACPs are used in self-setting calcium orthophosphate formulations. Bioactive composites of ACPs with polymers have properties suitable for use in dentistry and surgery [27]. Due to a reasonable solubility and physiological pH of aqueous solutions, ACPs appeared to be consumable by some microorganisms, and, due to this reason, it might be added as a mineral supplement to culture media. Non-biomedical applications of ACPs comprise their use as a component for mordants and ackey. In the food industry, ACPs are used for syrup clearing. Occasionally, they might be used as inert filler in pelleted drugs. In addition, ACPs are used in glass and pottery production and as a raw material for production of some organic phosphates. To get further details on ACPs, the readers are referred to special reviews [27, 29].

### CDHA (or Ca-def HA)

Calcium-deficient hydroxyapatite ( $\text{Ca}_{10-x}(\text{HPO}_4)_x(\text{PO}_4)_{6-x}(\text{OH})_{2-x}$  ( $0 < x < 1$ )) became known since the earliest experiments on establishing the chemical composition of bones performed in 1770s [1]. However, the initial appropriate term “subphosphate of lime” appeared by 1819 [30]. Other chemical formulae such as  $\text{Ca}_{10-x}(\text{HPO}_4)_{2x}(\text{PO}_4)_{6-2x}(\text{OH})_2$  ( $0 < x < 2$ ),  $\text{Ca}_{10-x-y}(\text{HPO}_4)_x(\text{PO}_4)_{6-x}(\text{OH})_{2-x-2y}$  ( $0 < x < 2$  and  $y < x/2$ ),  $\text{Ca}_{10-x}(\text{HPO}_4)_x(\text{PO}_4)_{6-x}(\text{OH})_{2-x}(\text{H}_2\text{O})_x$  ( $0 < x < 1$ ),  $\text{Ca}_{9-x}(\text{HPO}_4)_{1+2x}(\text{PO}_4)_{5-2x}(\text{OH})$ , etc. were also proposed to describe its variable composition [2, 3]. As seen from these formulae, Ca deficiency is always coupled with both OH deficiency and protonation of some  $\text{PO}_4$  groups with simultaneous

formation of the ionic vacancies in the crystal structure. In addition, CDHA often contains tightly bound water molecules, which might occupy some of these ionic vacancies. For example, there is an approach describing a lack of the hydroxide vacancies in CDHA: to perform the necessary charge compensation of the missing  $\text{Ca}^{2+}$  ions, a portion of  $\text{OH}^-$  anions is substituted by neutral water molecules. This water is removed by vacuum drying at elevated temperature. Concerning possible vacancies of orthophosphate ions, nothing is known about their presence in CDHA. It is just considered that a portion of  $\text{PO}_4^{3-}$  ions is either protonated (as  $\text{HPO}_4^{2-}$ ) or substituted by other ions (e.g.,  $\text{CO}_3^{2-}$ ). Since CDHA does not have any definite chemical composition, the IUPAC nomenclature is not applicable to describe it.

CDHA can be easily prepared by simultaneous addition of Ca- and  $\text{PO}_4$ -containing solutions in the proportions to get Ca/P ratio within 1.50–1.67 into boiling water followed by boiling the suspension for several hours (an aging stage). That is why, in literature, it might be called as “precipitated HA.” Besides, it might be prepared by hydrolysis of  $\alpha$ -TCP. Other preparation techniques of CDHA are known as well. During aging, initially precipitated ACPs are restructured and transformed into CDHA. Therefore, there are many similarities in the structure, properties, and application between the precipitated in alkaline solutions ( $\text{pH} > 8$ ) ACPs and CDHA. Some data indicated on a presence of intermediate phases during further hydrolysis of CDHA to a more stable HA-like phase. In general, CDHA crystals are poorly crystalline and of submicron dimensions. They have a very large specific surface area, typically 25–100  $\text{m}^2/\text{g}$ . On heating above  $\sim 700^\circ\text{C}$ , CDHA with  $\text{Ca/P} = 1.5$  converts to  $\beta$ -TCP and that with  $1.5 < \text{Ca/P} < 1.67$  converts into a biphasic composite of HA and  $\beta$ -TCP. A solid-state transformation mechanism of CDHA into HA +  $\beta$ -TCP biocomposite was proposed [31].

The variability in Ca/P molar ratio of CDHA has been explained through different models: surface adsorption, lattice substitution, and intercrystalline mixtures of HA and OCP [32]. Due to a lack of stoichiometry, CDHA is usually doped by other ions. The doping extent depends on the counterions of the chemicals used for CDHA preparation. Direct determinations of the CDHA structures are still missing, and the unit cell parameters remain uncertain. However, unlike that in ACPs, a long-range order exists in CDHA.

As a first approximation, CDHA may be considered as HA with some ions missing (ionic vacancies). The more amount of Ca is deficient, the more disorder, imperfections, and vacancies are in the CDHA structure. Furthermore, a direct correlation between the Ca deficiency and the mechanical properties of the crystals was found: calcium deficiency leads to an 80 % reduction in the hardness and elastic modulus and at least a 75 % reduction in toughness in plate-shaped HA crystals. Theoretical investigations of the defect formation mechanism relevant to nonstoichiometry in CDHA are available elsewhere [33].

Unsubstituted CDHA (i.e., that containing ions of  $\text{Ca}^{2+}$ ,  $\text{PO}_4^{3-}$ ,  $\text{HPO}_4^{2-}$ , and  $\text{OH}^-$  only) does not exist in biological systems. However, the ion-substituted CDHA:  $\text{Na}^+$ ,  $\text{K}^+$ ,  $\text{Mg}^{2+}$ , and  $\text{Sr}^{2+}$  for  $\text{Ca}^{2+}$ ;  $\text{CO}_3^{2-}$  for  $\text{PO}_4^{3-}$  or  $\text{HPO}_4^{2-}$ ;  $\text{F}^-$ ,  $\text{Cl}^-$ , and  $\text{CO}_3^{2-}$  for  $\text{OH}^-$ , plus some water forms biological apatite – the main inorganic

part of animal and human normal and pathological calcifications [2]. Therefore, CDHA is a very promising compound for industrial manufacturing of artificial bone substitutes, including drug delivery applications. Non-biomedical applications of CDHA are similar to those of ACP and HA. Interestingly, that CDHA was found to possess a catalytic activity to produce biogasoline [3].

## HA (or HAp or OHAp)

Hydroxyapatite ( $\text{Ca}_5(\text{PO}_4)_3(\text{OH})$ ) but is usually written as  $\text{Ca}_{10}(\text{PO}_4)_6(\text{OH})_2$  to denote that the crystal unit cell comprises two molecules; the IUPAC name is pentacalcium hydroxide tris(orthophosphate) is the second most stable and least soluble calcium orthophosphate after FA. Apatites were recognized as calcium phosphates by, at least, 1789 [1]. Here, it is worth noting that *hydroxylapatite* would be a more accurate abbreviation expansion of HA (perhaps, *hydroxideapatite* would be even better because it relates to calcium hydroxide) while by both the medical and material communities, HA is usually expanded as *hydroxyapatite*.

Chemically pure HA crystallizes in the monoclinic space group  $P2_1/b$ . However, at temperatures above  $\sim 250$  °C, there is a monoclinic to hexagonal phase transition in HA (space group  $P6_3/m$ ) [2, 3]. The detailed description of the HA structure was first reported in 1964 [34], and its interpretation in terms of aggregation of  $\text{Ca}_9(\text{PO}_4)_6$  clusters, the so-called Posner's clusters, has been widely used since publication of the article by Posner and Betts [28]. In hexagonal HA, the hydroxide ions are more disordered within each row, when compared with the monoclinic form, pointing either upward or downward in the structure. This induces strains that are compensated for by substitutions or ion vacancies. Some impurities, like partial substitution of hydroxide by fluoride or chloride, stabilize the hexagonal structure of HA at ambient temperature. Due to this reason, hexagonal HA is seldom the stoichiometric phase, and very rare single crystals of natural HA always exhibit the hexagonal space group.

Several techniques might be utilized for HA preparation; they can be divided into solid-state reactions and wet methods, which include precipitation, hydrothermal synthesis, and hydrolysis of other calcium orthophosphates. However, in all cases, Ca- and  $\text{PO}_4$ -containing chemicals must be mixed to get the Ca/P ratio strictly equal to 1.67. Nevertheless, even under the ideal stoichiometric conditions, the precipitates are generally nonstoichiometric, suggesting intermediate formation of precursor phases, such as ACP and CDHA. Usually unsintered HA is poorly crystalline and often nonstoichiometric, resembling the aforementioned CDHA. However, well crystalline HA can be prepared from an aqueous solution. HA with the Ca/P ratio  $> 1.67$  (Ca-rich HA) might be prepared. The detailed information on HA synthesis is available elsewhere [35].

Pure HA never occurs in biological systems. However, due to the chemical similarities to the bone and teeth mineral (Table 2), HA is widely used as coatings on orthopedic (e.g., hip joint prosthesis) and dental implants [36, 37]. HA bioceramics are very popular as well. Due to a great similarity to biological apatite,

over a long time HA has been used in liquid chromatography of nucleic acids, proteins, and other biological compounds and for drug delivery purposes. Also, HA is added to some brands of toothpaste as a gentle polishing agent instead of calcium carbonate. Non-biomedical applications of HA include its use as an environmentally friendly filler for elastomers, a sorbent of poisonous chemical elements and a carrier for various catalysts. Furthermore, HA by itself might act as a catalyst for formaldehyde combustion at room temperature [3].

## FA (or FAp)

Fluorapatite ( $\text{Ca}_5(\text{PO}_4)_3\text{F}$ ) but is usually written as  $\text{Ca}_{10}(\text{PO}_4)_6\text{F}_2$  to denote that the crystal unit cell comprises two molecules; the IUPAC name is pentacalcium fluoride tris(orthophosphate) is the only ion-substituted calcium orthophosphate, considered in this chapter. Since the presence of 2.5 % of fluorides in natural apatites was established by 1798 [38], this date might be accepted as the earliest hearing of FA.

FA is the hardest (5 according to the Mohs' scale of mineral hardness), most stable, and least soluble compound among all calcium orthophosphates (Table 1). Perhaps, such "extreme" properties of FA are related to the specific position of  $\text{F}^-$  ions in the center of Ca(2) triangles of the crystal structure [2]. Due to its properties, FA is the only calcium orthophosphate that naturally forms large deposits suitable for the commercial use [6] (see also Fig. 2). Preparation techniques of the chemically pure FA are similar to the aforementioned ones for HA, but the synthesis must be performed in the presence of the necessary amount of  $\text{F}^-$  ions (usually, NaF or  $\text{NH}_4\text{F}$  is added). Under some special crystallization conditions (e.g., in the presence of gelatin or citric acid), FA might form unusual dumbbell-like fractal morphology that finally is closed to spheres (Fig. 8) [39]. In addition, FA is the only calcium orthophosphate, which melts without decomposition (the melting point is  $\sim 1650^\circ\text{C}$ ); therefore, big (up to 30 cm long and, for shorter lengths, up to 1.9 cm wide) single FA crystals might be grown from FA melts. Similar to that for HA (see section "CDHA (or Ca-def HA)"), an existence of  $\text{CaF}_2$ -deficient FA was also detected but for the crystals grown from the FA melt only. In addition, FA with an excess of  $\text{CaF}_2$  was prepared. The crystal structure of FA for the first time was studied in 1930 and is well described elsewhere [2].

FA easily forms solid solutions with HA with any desired F/OH molar ratio. Such compounds are called fluorhydroxyapatites (FHA) or hydroxyfluorapatites (HFA) and described with a chemical formula  $\text{Ca}_{10}(\text{PO}_4)_6(\text{OH})_{2-x}\text{F}_x$ , where  $0 < x < 2$ . If the F/OH ratio is either uncertain or not important, the chemical formula of FHA and HFA is often written as  $\text{Ca}_{10}(\text{PO}_4)_6(\text{F},\text{OH})_2$ . The lattice parameters, crystal structure, solubility, and other properties of FHA and HFA lay in between of those for the chemically pure FA and HA. Namely, the substitution of F for OH results in a contraction in the *a*-axis with no significant change in the *c*-axis dimensions and greater resolution of the IR absorption spectra.

Similar to pure HA, pure FA never occurs in biological systems. Obviously, a lack of the necessary amount of toxic fluorides (the acute toxic dose of fluoride is

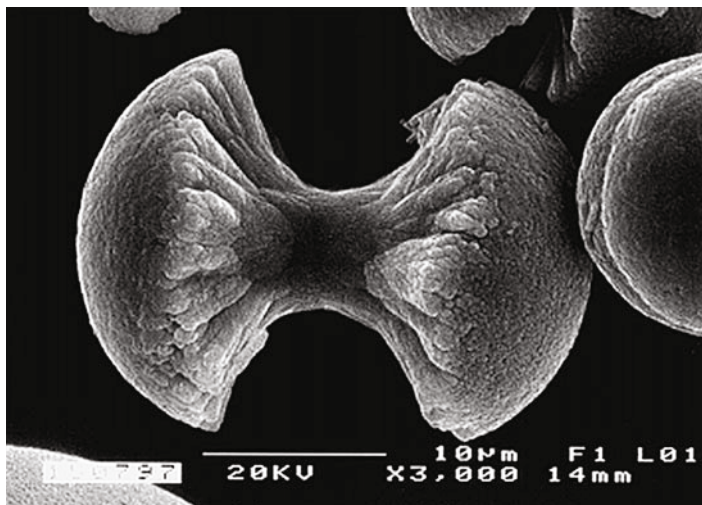


**Fig. 8** A biomimetically grown aggregate of FA that was crystallized in a gelatin matrix. Its shape can be explained and simulated by a fractal growth mechanism. Scale bar: 10  $\mu\text{m}$  (Reprinted from Ref. [39] with permission)

$\sim 5$  mg/kg of body weight) in living organisms is the main reason of this fact (pure FA contains 3.7 % mass. F). Enameloid of shark teeth [5, 12] and some exoskeletons of mollusks seem to be the only exclusions because they contain substantial amounts of fluoride, presented there as ion-substituted, nonstoichiometric FHA or HFA. Among all normal calcified tissues of humans, the highest concentration of fluorides is found in dentine and cementum, while the lowest – in dental enamel (Table 2). Nevertheless, one should stress that the amount of fluorides on the very surface of dental enamel might be substantially increased by using fluoride-containing toothpastes and mouthwashes. However, in no case, the total amount of fluorides is enough to form FA.

Contrary to the initial expectations, chemically pure FA is not used for grafting purposes. Presumably, this is due to the lowest solubility, good chemical stability of FA, and toxicity of high amounts of fluorides. However, attempts to test FA-containing formulations, ion-substituted FA, FHA, and porous FA bioceramics are kept performing. Non-biomedical applications of FA include fluorescent light tubes, laser materials (in both cases dopants are necessary), as well as catalysts [3].

### OA (or OAp or OXA)

Oxyapatite ( $\text{Ca}_{10}(\text{PO}_4)_6\text{O}$ ; the IUPAC name is decacalcium oxide hexakis(phosphate), mineral voelckerite) is the least stable and, therefore, the least known calcium orthophosphate, which, probably, does not exist at all. Nevertheless, a name “voelckerite” was introduced in 1912 by A.F. Rogers (1887–1957) for a hypothetical

mineral with the chemical composition of  $3\text{Ca}_3(\text{PO}_4)_2 + \text{CaO}$  [40], to honor an English agricultural chemist John Christopher Augustus Voelcker (1822–1884), who, in 1883, first showed an apparent halogen deficiency in some natural apatites [41]. Therefore, 1883 might be accepted as the earliest hearing of OA.

To the best of my findings, pure OA has never been prepared; therefore, its properties are not well established. Furthermore, still there are serious doubts that pure OA can exist. However, a mixture (or a solid solution?) of OA and HA (oxy-HA) might be prepared by a partial dehydroxylation of HA at temperatures exceeding  $\sim 900^\circ\text{C}$  (e.g., during plasma spray of HA) only in the absence of water vapor [42]. It also might be crystallized in glass-ceramics. OA is very unstable and has no stability field in aqueous conditions. Namely, data are available, that oxy-HA containing less than 25 % HA (i.e., almost OA) during further dehydration decomposes to a mixture of  $\alpha$ -TCP and TTCP. In addition, OA is very reactive and transforms to HA in contact with water vapor [42]. Computer modeling techniques have been employed to qualitatively and quantitatively investigate the dehydration of HA to OA. OA has the hexagonal space group symmetry  $P\bar{6}$  (174) of cesanite type, while the space group symmetry for partially dehydrated HA was found to change from hexagonal  $P63/m$  to triclinic  $P\bar{1}$  when more than *ca.* 35 % of the structurally bound water had been removed. On the *c*-axis, pure OA should have a divalent ion  $\text{O}^{2-}$  coupled with a vacancy instead of two neighboring monovalent  $\text{OH}^-$  ions.

Due to the aforementioned problems with OA preparation, it cannot be found in biological systems. In addition, no information on the biomedical applications of OA is available either. Plasma-sprayed coatings of calcium orthophosphates, in which OA might be present as an admixture phase, seem to be the only exception [37].

## TTCP (or TetCP)

Tetracalcium phosphate or tetracalcium diorthophosphate monoxide ( $\text{Ca}_4(\text{PO}_4)_2\text{O}$ ; the IUPAC name is tetracalcium oxide bis(orthophosphate); the mineral hilgenstockite) is the most basic calcium orthophosphate; however, its solubility in water is higher than that of HA (Table 1). TTCP has been known since 1883, while the mineral hilgenstockite was named to honor a German metallurgist Gustav Hilgenstock (1844–1913), who first discovered it in Thomas slag from blast furnaces [43]. Its major industrial importance stems from the fact that it is formed by the reactions between orthophosphates and lime in the manufacture of iron, and through these reactions, TTCP has a significant role in controlling the properties of the metal.

TTCP cannot be precipitated from aqueous solutions. It can be prepared only under the anhydrous conditions by solid-state reactions at temperatures above  $\sim 1300^\circ\text{C}$ , e.g., by heating homogenized equimolar quantities of DCPA and  $\text{CaCO}_3$  in dry air or in a flow of dry nitrogen [2, 44]. These reactions should be carried out in a dry atmosphere, in vacuum, or with rapid cooling (to prevent uptake of water and formation of HA). Easily DCPA might be replaced by ammonium orthophosphates, while calcium carbonate might be replaced by calcium acetate; however, in all cases,

Ca/P ratio must be equal to 2.00. Furthermore, TTCP often appears as an unwanted by-product in plasma-sprayed HA coatings, where it is formed as a result of the thermal decomposition of HA to a mixture of high-temperature phases of  $\alpha$ -TCP, TTCP, and CaO. TTCP is metastable: in both wet environment and aqueous solutions, it slowly hydrolyzes to HA and calcium hydroxide. Consequently, TTCP is never found in biological calcifications. In medicine, TTCP is widely used for preparation of various self-setting calcium orthophosphate formulations; however, to the best of my knowledge, there is no commercial bone-substituting product consisting solely of TTCP [2, 44].

To conclude the description of the individual calcium orthophosphates, one should mention on an interesting opinion [22], that all calcium orthophosphates listed in Table 1 might be classified into three major structural types. They comprise: (i) the apatite type,  $\text{Ca}_{10}(\text{PO}_4)_6\text{X}_2$ , which includes HA, FA, OA, CDHA, OCP, and TTCP; (ii) the glaserite type, named after the mineral glaserite,  $\text{K}_3\text{Na}(\text{SO}_4)_2$ , which includes all polymorphs of TCP, and, perhaps, ACP; and (iii) the Ca- $\text{PO}_4$  sheet-containing compounds, which include DCPD, DCPA, MCPM, and MCPA. According to the authors, a closer examination of the structures revealed that all available calcium orthophosphates could be included into distorted glaserite-type structures but with varying degrees of distortion [22].

## Biphasic, Triphasic, and Multiphasic Calcium Orthophosphate Formulations

Calcium orthophosphates might form biphasic, triphasic, and multiphasic (polyphasic) formulations, in which the individual components cannot be separated from each other. Presumably, the individual phases of such compositions are homogeneously “mixed” at a far submicron level ( $<0.1 \mu\text{m}$ ) and strongly integrated with each other. Nevertheless, the presence of all individual phases is easily seen by X-ray diffraction technique [31].

The usual way to prepare multiphasic formulations consists of sintering nonstoichiometric compounds, such as ACP and CDHA, at temperatures above  $\sim 700^\circ\text{C}$ . Furthermore, a thermal decomposition of the stoichiometric calcium orthophosphates at temperatures above  $\sim 1300^\circ\text{C}$  might be used as well; however, this approach often results in formation of complicated mixtures of various products including admixtures of CaO, calcium pyrophosphates, etc. [31]. Namely, transformation of HA into polyphasic calcium orthophosphates by annealing in a vacuum occurs as this: the outer part of HA is transformed into  $\alpha$ -TCP and TTCP, while the  $\alpha$ -TCP phase of the surface further transforms into CaO. Besides, in the boundary phase, HA is transformed into TTCP.

Historically, Nery and Lynch with coworkers first used the term biphasic calcium phosphate (BCP) in 1986 to describe a bioceramic that consisted of a mixture of HA and  $\beta$ -TCP [45]. Currently, only biphasic and triphasic calcium orthophosphate formulations are known; perhaps, more complicated formulations will be manufactured in the future. Furthermore, nowadays, multiphasic and/or polyphasic



compositions consisting of high-temperature phases of calcium orthophosphates, such as  $\alpha$ -TCP,  $\beta$ -TCP, HA, and, perhaps, high-temperature ACP, OA, and TTCP, are known only. No precise information on multiphasic compositions, containing MCPM, MCPA, DCPD, DCPA, low-temperature ACP, OCP, and CDHA has been found in literature [31]. Perhaps, such formulations will be produced in the future.

All BCP formulations might be subdivided into two major groups: those consisting of calcium orthophosphates having either the same (e.g.,  $\alpha$ -TCP and  $\beta$ -TCP) or different (e.g.,  $\beta$ -TCP and HA) molar Ca/P ratios. Among all known BCP formulations, BCP consisting of HA and  $\beta$ -TCP is both the most known and the best investigated. In 1986, LeGeros in USA and Daculsi in France initiated the basic studies on preparation of this type of BCP and its *in vitro* properties. This material is soluble and gradually dissolves in the body, seeding new bone formation as it releases calcium and orthophosphate ions into the biological medium. Presently, commercial BCP products of different or similar HA/ $\beta$ -TCP ratios are manufactured in many parts of the world as bone-graft or bone substitute materials for orthopedic and dental applications under various trademarks and several manufacturers. A similar combination of  $\alpha$ -TCP with HA forms BCP as well [31].

Recently, the concept of BCP has been extended by preparation and characterization of biphasic TCP (BTCP), consisting of  $\alpha$ -TCP and  $\beta$ -TCP phases. It is usually prepared by heating ACP precursors, in which the  $\alpha$ -TCP/ $\beta$ -TCP ratio can be controlled by aging time and pH value during synthesis of the amorphous precursor. Furthermore, triphasic formulations, consisting of HA,  $\alpha$ -TCP and  $\beta$ -TCP or HA,  $\alpha$ -TCP, and TTCP, have been prepared [31].

It is important to recognize that the major biomedical properties (such as bioactivity, bioresorbability, osteoconductivity, and osteoinductivity) of the multiphasic formulations might be adjusted by changing the ratios among the phases. When compared to both  $\alpha$ - and  $\beta$ -TCP, HA is a more stable phase under the physiological conditions, as it has a lower solubility (Table 1) and, thus, slower resorption kinetics. Therefore, due to a higher biodegradability of the  $\alpha$ - or  $\beta$ -TCP component, the reactivity of BCP increases with the TCP/HA ratio increasing. Thus, *in vivo* bioresorbability of BCP can be adjusted through the phase composition. Similar conclusions are also valid for both the biphasic TCP (in which  $\alpha$ -TCP is a more soluble phase) and the triphasic (HA,  $\alpha$ -TCP, and  $\beta$ -TCP) formulations. Further details on this subject might be found in a topical review [31].

## **Ion-Substituted Calcium Orthophosphates**

Finally, one should very briefly mention on the existence of carbonateapatite, chlorapatite, as well as on a great number of calcium orthophosphates with various ionic substitutions [46, 47]. In principle, any ion in calcium orthophosphates might be substituted by other ion(s). Usually, the ion-substituted calcium orthophosphates are of a nonstoichiometric nature with just a partial ionic substitution, and there are too many of them to be described here. Currently, this is a hot investigation topic; therefore, the readers are referred to the special literature [46, 47].

## Summary

The present chapter is intended to point the readers' attention to the important subject of calcium orthophosphates. They are of the special significance for the human beings because they represent the inorganic part of major normal (bones, teeth, and antlers) and pathological (i.e., those appearing due to various diseases) calcified tissues of mammals. Therefore, the majority of the artificially prepared calcium orthophosphates of high purity appear to be well tolerated by human tissues *in vivo* and possess the excellent biocompatibility, osteoconductivity, and bioresorbability. These biomedical properties of calcium orthophosphates are widely used to construct bone grafts. In addition, natural calcium orthophosphates are the major source of phosphorus, which are used to produce agricultural fertilizers, detergents, and various phosphorus-containing chemicals. Thus, there is a great significance of calcium orthophosphates for the humankind, and, here, an overview on the current knowledge on this subject is provided.

---

## References

1. Dorozhkin SV (2013) A detailed history of calcium orthophosphates from 1770s till 1950. *Mater Sci Eng C* 33:3085–3110
2. Elliott JC (1994) Structure and chemistry of the apatites and other calcium orthophosphates, vol 18, *Studies in inorganic chemistry*. Elsevier, Amsterdam, 389 pp
3. Dorozhkin SV (2011) Calcium orthophosphates: occurrence, properties, biomineralization, pathological calcification and biomimetic applications. *Biomatter* 1:121–164
4. Dorozhkin SV (2012) Calcium orthophosphates: applications in nature, biology, and medicine. Pan Stanford, Singapore, 854 pp
5. Lowenstam HA, Weiner S (1989) *On biomineralization*. Oxford University Press, New York, 324 pp
6. McConnell D (1973) Apatite: its crystal chemistry, mineralogy, utilization, and geologic and biologic occurrences, vol 5, *Applied mineralogy*. Springer, Vienna/New York, 111 pp
7. Cook PJ, Shergold JH, Davidson DF (eds) (2005) *Phosphate deposits of the world: phosphate rock resources, vol 2*. Cambridge University Press, Cambridge, MA, 600 pp
8. Omelon SJ, Grynpas MD (2008) Relationships between polyphosphate chemistry, biochemistry and apatite biomineralization. *Chem Rev* 108:4694–4715
9. Hogarth DD (1974) The discovery of apatite on the Lievre River, Quebec. *Mineral Rec* 5:178–182
10. van Velthuizen J (1992) Giant fluorapatite crystals: a question of locality. *Mineral Rec* 23:459–463
11. Abouzeid AZM (2007) Upgrading of phosphate ores – a review. *Powder Handl Process* 19:92–109
12. Daculsi G, Bouler JM, LeGeros RZ (1997) Adaptive crystal formation in normal and pathological calcifications in synthetic calcium phosphate and related biomaterials. *Int Rev Cytol* 172:129–191
13. Martin RI, Brown PW (1997) Phase equilibria among acid calcium phosphates. *J Am Ceram Soc* 80:1263–1266
14. Kreidler ER, Hummel FA (1967) Phase relationships in the system SrO-P<sub>2</sub>O<sub>5</sub> and the influence of water vapor on the formation of Sr<sub>4</sub>P<sub>2</sub>O<sub>9</sub>. *Inorg Chem* 6:884–891

15. Lynn AK, Bonfield W (2005) A novel method for the simultaneous, titrant-free control of pH and calcium phosphate mass yield. *Acc Chem Res* 38:202–207
16. León B, Jansen JJ (eds) (2009) *Thin calcium phosphate coatings for medical implants*. Springer, New York, 326 pp
17. Fourcroy AF (1804) A general system of chemical knowledge; and its application to the phenomena of nature and art. In eleven volumes. Translated from the original French by William Nicholson. vol III. Printed for Cadell and Davies, Strand; Longman and Rees, G. and J. Robinson, and J. Walker, Paternoster-row; Vernor and Hood, Poultry; Clarke and sons, Portugal-street; Cuthell and Martin, and Ogilvy and son, Holborn; and S. Bagster, Strand. London, 472 pp
18. Moore GE (1865) On brushite, a new mineral occurring in phosphatic guano. *Am J Sci* 39:43–44
19. Shepard CU (1882) On two new minerals, monetite and monite, with a notice of pyroclasilite. *Am J Sci* 23:400–405
20. Percy J (1843) Notice of a new hydrated phosphate of lime. *Mem Proc Chem Soc* 2:222–223
21. Suzuki O (2010) Octacalcium phosphate: osteoconductivity and crystal chemistry. *Acta Biomater* 6:3379–3387
22. Chow LC, Eanes ED (eds) (2001) Octacalcium phosphate, vol 18, Monographs in oral science. Karger, Basel, 167 pp
23. Bredig MA, Franck HH, Fülnder H (1932) Beiträge zur Kenntnis der Kalk-Phosphorsäure-Verbindungen. II. *Z Elektrochem Angew P* 38:158–164
24. Frondel C (1941) Whitlockite: a new calcium phosphate,  $\text{Ca}_3(\text{PO}_4)_2$ . *Am Mineral* 26:145–152
25. Kanazawa T, Umegaki T, Uchiyama N (1982) Thermal crystallisation of amorphous calcium phosphate to  $\alpha$ -tricalcium phosphate. *J Chem Tech Biotechnol* 32:399–406
26. Jones HB (1845) Contributions to the chemistry of the urine. On the variations in the alkaline and earthy phosphates in the healthy state, and on the alkalescence of the urine from fixed alkalies. *Phil Trans R Soc Lond* 135:335–349
27. Dorozhkin SV (2012) Amorphous calcium orthophosphates: nature, chemistry and biomedical applications. *Int J Mater Chem* 2:19–46
28. Posner AS, Betts F (1975) Synthetic amorphous calcium phosphate and its relation to bone mineral structure. *Acc Chem Res* 8:273–281
29. Combes C, Rey C (2010) Amorphous calcium phosphates: synthesis, properties and uses in biomaterials. *Acta Biomater* 6:3362–3378
30. Bache F (1819) A system of chemistry for the use of students of medicine. Printed and published for the author. William Fry, Printer, Philadelphia, 624 pp
31. Dorozhkin SV (2012) Biphasic, triphasic and multiphasic calcium orthophosphates. *Acta Biomater* 8:963–977
32. Rodríguez-Lorenzo L (2005) Studies on calcium deficient apatites structure by means of MAS-NMR spectroscopy. *J Mater Sci Mater Med* 16:393–398
33. Matsunaga K (2008) Theoretical investigation of the defect formation mechanism relevant to nonstoichiometry in hydroxyapatite. *Phys Rev B* 77:104106 (14 pp)
34. Kay MI, Young RA, Posner AS (1964) Crystal structure of hydroxyapatite. *Nature* 204:1050–1052
35. Sadat-Shojai M, Khorasani MT, Dinpanah-Khoshdargi E, Jamshidi A (2013) Synthesis methods for nanosized hydroxyapatite with diverse structures. *Acta Biomater* 9:7591–7621
36. Suchanek W, Yoshimura M (1998) Processing and properties of hydroxyapatite-based biomaterials for use as hard tissue replacement implants. *J Mater Res* 13:94–117
37. Dorozhkin SV (2012) Calcium orthophosphate coatings, films and layers. *Prog Biomater* 1:1–40
38. Encyclopaedia; or, a dictionary of arts, sciences, and miscellaneous literature; Constructed on a Plan, by which the different sciences and arts are digested into the Form of distinct treatises or systems, comprihending the history, theory, and practice, of each, According to the Latest Discoveries and Improvements; and full explanations given of the various detached parts of

- knowledge, where relating to Natural and Artificial Objects, or to Matters Ecclesiastical, Civil, Military, Commercial, & c. Including Elucidations of the most important Topics relative to Religion, Morals, Manners, and the Oeconomy of Life. Together with A Description of all the Countries, Cities, principle Mountains, Seas, Rivers, &c. throughout the World; A General History, *Ancient and Modern*, of the different Empires, Kingdoms, and States; and An Account of the Lives of the most Eminent Persons in every Nation, from the earliest ages down to the present times. The first American edition, in 18 volumes, greatly improved. Vol. XIV. PAS – PLA Philadelphia: printed by Thomas Dobson, at the Stone-house, N<sup>o</sup> 41, South second-street. 1798, 797 pp
39. Busch S, Dolhaine H, Duchesne A, Heinz S, Hochrein O, Laeri F, Podebrad O, Vietze U, Weiland T, Kniep R (1999) Biomimetic morphogenesis of fluorapatite-gelatin composites: fractal growth, the question of intrinsic electric fields, core/shell assemblies, hollow spheres and reorganization of denatured collagen. *Eur J Inorg Chem* 1999:1643–1653
  40. Rogers AF (1912) Dahllite (podolite) from Tonopah, Nevada: voelckerite, a new basic calcium phosphate; remarks on the chemical composition of apatite and phosphate rock. *Am J Sci Ser* 4 33:475–482
  41. Voelcker JA (1883) Die chemische Zusammensetzung des Apatits nach eigenen vollständigen Analysen. *Ber Dtsch Chem Ges* 16:2460–2464
  42. Gross KA, Berndt CC, Dinnebier R, Stephens P (1998) Oxyapatite in hydroxyapatite coatings. *J Mater Sci Mater Med* 33:3985–3991
  43. Hilgenstock G (1883) Eine neue Verbindung von P<sub>2</sub>O<sub>5</sub> und CaO. *Stahl Eisen* 3:498
  44. Moseke C, Gbureck U (2010) Tetracalcium phosphate: synthesis, properties and biomedical applications. *Acta Biomater* 6:3815–3823
  45. Ellinger RF, Nery EB, Lynch KL (1986) Histological assessment of periodontal osseous defects following implantation of hydroxyapatite and biphasic calcium phosphate ceramics: a case report. *Int J Periodont Restor Dent* 3:22–33
  46. Kannan S, Goetz-Neunhoeffler F, Neubauer J, Ferreira JMF (2008) Ionic substitutions in biphasic hydroxyapatite and β-tricalcium phosphate mixtures: structural analysis by Rietveld refinement. *J Am Ceram Soc* 91:1–12
  47. Boanini E, Gazzano M, Bigi A (2010) Ionic substitutions in calcium phosphates synthesized at low temperature. *Acta Biomater* 6:1882–1894

---

# Hydroxyapatite: From Nanocrystals to Hybrid Nanocomposites for Regenerative Medicine

# 6

Anna Tampieri, Michele Iafisco, Simone Sprio, Andrea Ruffini, Silvia Panseri, Monica Montesi, Alessio Adamiano, and Monica Sandri

## Contents

Introduction .....	120
Hydroxyapatite Nanocrystals .....	121
Hydroxyapatite in Biological Systems .....	121
Synthesis of Hydroxyapatite Nanocrystals .....	123
Ionic-Substituted Biomimetic Hydroxyapatite .....	127
Hydroxyapatite as Superparamagnetic Phase .....	130
Hybrid Nanocomposite .....	132
3D Hierarchically Organized Ceramics by Biomorphic Transformation .....	137
Summary .....	140
References .....	141

---

## Abstract

Scientific research on bone and osteochondral tissue regeneration is increasingly becoming the most promising response to a number of disabling pathologies with huge impact on the progressively growing and aging world population. The biomimicry of scaffolds with the target tissue is now universally considered to be a key requirement to properly instruct cells toward the restoration of specific physiological functioning. In this respect, this chapter presents an overview of recent findings on hydroxyapatite, biomimetic materials, and devices addressed to bone and osteochondral tissue regeneration. Particular focus is given to the novel biomimetic hydroxyapatite phases, including the newly discovered

---

A. Tampieri (✉) • M. Iafisco • S. Sprio • A. Ruffini • S. Panseri • M. Montesi • A. Adamiano • M. Sandri  
Institute of Science and Technology for Ceramics (ISTEC), National Research Council (CNR), Faenza, Italy  
e-mail: [anna.tampieri@istec.cnr.it](mailto:anna.tampieri@istec.cnr.it); [michele.iafisco@istec.cnr.it](mailto:michele.iafisco@istec.cnr.it); [simone.sprio@istec.cnr.it](mailto:simone.sprio@istec.cnr.it); [andrea.ruffini@istec.cnr.it](mailto:andrea.ruffini@istec.cnr.it); [silvia.panseri@istec.cnr.it](mailto:silvia.panseri@istec.cnr.it); [monica.montesi@istec.cnr.it](mailto:monica.montesi@istec.cnr.it); [alessio.adamiano@istec.cnr.it](mailto:alessio.adamiano@istec.cnr.it); [monica.sandri@istec.cnr.it](mailto:monica.sandri@istec.cnr.it)

superparamagnetic hydroxyapatite nanoparticles and to the biomineralization process to develop bioinspired hybrid inorganic–polymeric porous scaffolds even endowed with magnetic features. Finally, the technology to transform ligneous sources into hierarchically organized biomorphic hydroxyapatite-based porous scaffolds that may provide novel and more effective solutions to assist the regeneration of long segmental bones was described.

---

**Keywords**

Hydroxyapatite • Nanocrystals • Regenerative medicine • Biomimetics • Bone scaffold • Osteochondral scaffold • Ion-substituted hydroxyapatite • Hybrid nanocomposites • Superparamagnetism • Biomorphic transformation • Bone regeneration

---

**Introduction**

In the last decades, the development of biomaterials for bone grafting has continuously progressed and bio-devices with improved performances have been designed and manufactured. The increasing information acquired in the last years about the biological processes and mechanisms yielding the formation and structural rearrangement (remodeling) of new bone tissue has provided a consciousness of the importance of physical–chemical and structural biomimicry that bone implants should possess in order to trigger tissue regeneration.

Connective tissues can be regenerated only in the presence of scaffolds able to direct cell activity toward suitable phenotypes and to chemically and structurally assist the regeneration process [1]. In the case of hard tissues such as bone, this requires the synthesis of three-dimensional (3D) constructs that are able to exchange chemical signals promoting osteogenesis and can then be progressively resorbed during the formation and remodeling of new tissue [2]. Moreover, particularly when the regeneration of extensive portions of bone is involved, morphological and mechanical biomimetics is also strictly required, in order to allow cell colonization and the formation of a proper vascularization network. In addition, the healing of load-bearing bones also needs scaffolds with complex and organized morphology, so as to provide improved biomechanical behavior and to allow proper mechanotransduction of the mechanical stimuli down to the cell level.

For this reason, biomaterial designs have moved from dense, bioinert implants to new bioactive implants that contain active phases such as biomimetic calcium phosphate phases and porous, osteoconducting structures that have the ability to host human cells. Therefore, inert dense or microporous implants have now evolved into macroporous scaffolds designed to sustain and assist extensive cell colonization and anchorage to the existing bone, finally leading to osteointegration and progressive resorption, which allows the new bone to replace the scaffold and restore full functionality.

Therefore, the design and development of 3D scaffolds that can reproduce the structure and complex morphology of human organs/tissues is still a challenge because of limitations in currently available manufacturing technologies, and

research scientists are focusing on the unique characteristics and properties of natural structures and processes, using these as new sources of inspiration in the development of innovative devices.

**Hydroxyapatite (HA)** is recognized as the ideal material to be developed into scaffolds for bone repair, since it is the main inorganic component of bone and can easily induce cell adhesion and proliferation. Upon recognition of the true nature of the inorganic bone, i.e., a multi-substituted, poorly crystalline HA, and of the relevant function of the various ions contained in the apatite structure, biomaterial synthesis became focused on reproducing the complex chemical composition of bone. In the attempt to find a balance between composition, structure, porosity, and mechanical strength, material scientists developed many different approaches to create structures with open and interconnected pores by allowing the formation of complex structures by using natural templates.

This chapter is divided into several sections, each dealing with specific approaches (spanning from biomimetic and magnetic HA to biohybrid composites) to the regeneration of mineralized connective tissues, such as bone and osteocartilaginous regions, and concludes with the recently developed hierarchically organized scaffolds that are obtained by wood transformation.

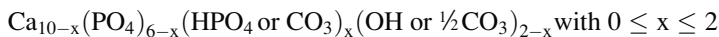
---

## Hydroxyapatite Nanocrystals

### Hydroxyapatite in Biological Systems

In biological systems, calcium phosphates are the major inorganic constituents of both normal calcifications, such as bones, teeth, fish enameloid, deer antlers, and some species of shells, and pathological calcifications, such as dental and urinary calculus and stones and atherosclerotic lesions [3]. With the exception of small portions of the inner ear, human hard tissues are composed principally of calcium phosphates. With the exception of enamel, which has a high degree of crystallinity, they are poorly crystalline carbonate-substituted nanosized apatites. In contrast to  $[\text{HA}, \text{Ca}_{10}(\text{PO}_4)_6(\text{OH})_2]$ , which is the stoichiometric apatitic phase that is the most stable and least soluble calcium phosphate at physiological conditions, nanocrystalline apatites are nonstoichiometric (Ca/P ratio less than 1.67) and calcium (and OH)-deficient and may incorporate substituted ions in the crystal lattice ( $\text{Na}^+$ ,  $\text{Mg}^{2+}$ ,  $\text{K}^+$ ,  $\text{Sr}^{2+}$ ,  $\text{Zn}^{2+}$ , etc.) [4]. The calcium and hydroxide deficiencies are responsible for the higher solubility exhibited by these nanocrystalline apatites compared with HA. They are also able to mature when submitted to humid environments; as a result, “mature” bone crystals in vertebrates are less soluble and reactive than embryonic (young) bone mineral crystals [5].

From a chemical point of view, the composition of nanocrystalline apatites differs significantly from that of HA. The global chemical composition of biological apatites (or their synthetic analogues) has been a somewhat controversial topic in recent decades but can generally be described as



Very immature nanocrystals, however, may depart from this generic formula. This formula underlines the presence of vacancies in both Ca and OH sites. For example, Legros et al. [6] analyzed various cortical bone samples, suggesting the following relatively homogeneous composition, which reveals a high vacancy content:



Minor substitutions are also found in biological apatites that involve monovalent cations (especially  $\text{Na}^+$  and  $\text{K}^+$ ). In this case, charge compensation mechanisms must be taken into account.

Recent advances in the characterization of apatite nanocrystals have been achieved through the use of spectroscopic techniques and, in particular, through Fourier transform infrared (FTIR) spectroscopy. The FTIR method is useful in characterizing the local chemical environment of phosphate, carbonate, and hydroxide ions as well as water molecules in such systems. Detailed analyses of the phosphate groups by FTIR have allowed additional bands to be identified in nanocrystalline apatites, which cannot be attributed to phosphate groups in a regular apatitic environment [7]. Rey has referred to these chemical environments as “non-apatitic” environments [8].

Taking into account all the above data, nanocrystalline apatites (whether biological or their synthetic analogues prepared under close-to-physiological conditions) may thus most probably be described as the association of an apatitic core (often nonstoichiometric) and a structured by fragile surface hydrated layer containing water molecules and rather labile ions (e.g.,  $\text{Ca}^{2+}$ ,  $\text{HPO}_4^{2-}$ ,  $\text{CO}_3^{2-}$ , etc.) [9] occupying non-apatitic crystallographic sites (although in the case of biomimetic apatites, the layer is directly exposed on the surface and not included in a “sandwich-like” structure between two “apatitic” layers).

The presence of this hydrated surface layer [10] is thought to be responsible for most of the properties of biomimetic apatites and, in particular, their high surface reactivity in relation to surrounding fluids (which is probably directly linked to a high mobility of ionic species contained within this layer) may explain, from a physical–chemical viewpoint, the role of bone mineral in homeostasis in vivo. This layer indeed contains labile ions that can potentially be exchanged by other ions from the surrounding solution or by small molecules, which may be exploited for couplings with proteins or drugs. It is interesting to remark that the typical non-apatitic features mentioned above tend to progressively disappear during the aging of the nanocrystals in solution [11]. This process is referred to as “maturation” and has been related to the progressive growth of apatite domains at the expense of the surface hydrated layer [11].

This maturation process is thought to be linked to the metastability of such poorly crystallized nonstoichiometric apatites, which steadily evolve in solution toward stoichiometry and better crystallinity [11]. This evolution can be, for example, witnessed by the decrease of the amount of non-apatitic  $\text{HPO}_4^{2-}$  ions upon aging



or else by the decreased potentialities to undergo ion exchanges [11]. One illustration of such effects can be given, for example, by the decreased exchangeability of  $\text{HPO}_4^{2-}$  by  $\text{CO}_3^{2-}$  observed on carbonated apatites matured for incremented amounts of time. Additionally, beside this compositional evolution, some structural and microstructural features also tend to evolve such as the mean crystallite size that increases upon maturation. The control of synthesis parameters such as pH, temperature, or maturation time can thus enable one to tailor the physical–chemical properties of biomimetic apatites [9] and, in particular, their surface reactivity, so to mimic, for example, mature bone mineral or else newly formed bone apatite.

## Synthesis of Hydroxyapatite Nanocrystals

Synthetic HA exhibits excellent biological properties such as biocompatibility, bioactivity, lack of toxicity, absence of inflammatory and immune responses, and relatively high bioresorbability. The preparation of synthetic HA with dimensions, morphology and chemical characteristics similar to those found in biological tissue can significantly enhance their bioactive features [3]. In the recent years, many different strategies have been employed in the preparation of synthetic nanosized HA crystals, with the most common method being stoichiometric titration of calcium hydroxide slurry with phosphoric acid up to neutrality.

However, the preparation of biomimetic nanocrystalline HA can still be considered a scientific and technological challenge [4]. As explained previously, biological apatites are known for their high defect content, which is caused in part by a relatively high percentage of impurities, all of which affect the lattice parameters, crystal morphology, crystallinity, solubility, and the thermal stability of the material.

Using as main criteria the control of structure and morphology, the HA crystallization methods can be rationally divided into high- and low-temperature approaches. The synthesis at high temperature usually involves the homogenization of precursor compounds, including  $\text{Ca}_3(\text{PO}_4)_2$  and  $\text{Ca}(\text{OH})_2$ , and their annealing at about 1000 °C. The advantage is the possibility to set the final stoichiometry of the mixture, whereas the main downsides are the long processing times and high annealing temperatures. In general, when using this method, the Ca/P ratio is a fundamental parameter; in fact, if the initial molar ratio of Ca/P is not well configured to 1.67, other calcium phosphate phases are bound to appear such as  $\alpha$ - or  $\beta$ -tricalcium phosphate (TCP) when the Ca/P value is lower than the stoichiometric ratio and CaO when the Ca/P value is higher. The  $\alpha$ -TCP phase is normally formed at temperatures around 1200 °C, whereas the  $\beta$ -TCP phase is formed at lower temperatures, up to 900 °C. In addition to the high levels of energy consumption, another major downside of high-temperature methods is the difficulty to prepare uniform nanosized crystals [12], especially due to grains coarsening at high temperatures.

On the other hand, the synthetic methods at low temperature offer the advantage to produce nanosized (and hydrated) crystals, but one disadvantage may be in some cases the presence of transient and metastable phases in the final product.

To investigate the effect of temperature on the chemical–physical features of nanosized apatite, Sakhno et al. have characterized two apatites synthesized at 40 °C and 95 °C [10]. The apatite synthesized at low temperature displayed platelet-like morphology and was constituted by a crystalline core coated by an amorphous-like surface layer of 1–2 nm. Increasing the temperature of synthesis, the platelet morphology was retained but the apatite nanoparticles exhibited a higher degree of crystallinity (evaluated by X-ray diffraction (XRD)). High-resolution transmission electron microscopy (HR-TEM) observations revealed that, in this case, the crystalline order was extended up to the particles surfaces, exhibiting clearly the planes (010), (100), and (001). Infrared spectroscopy was used to investigate the surface hydration of both materials, in terms of adsorbed H<sub>2</sub>O molecules and surface hydroxyl groups, as well as the Lewis acidity of surface cations, by removing the adsorbed water and adsorbing the molecular probe CO [10]. For both features, strong similarities between amorphous and crystalline surfaces were found. However, interestingly the apatite synthesized at 95 °C having a more crystalline surface appeared able to physisorb multilayers of water in a larger extent than the less crystallized samples.

The disadvantage of synthetic methods involving low temperature is the possible crystallization of transient phases. To explain why these extraneous phases can be crystallized, the calcium phosphate solubility diagram (at 37 °C and ionic strength 0.1 M) published by Johnsson and Nancollas can be considered [13]. According to this diagram, the calcium phosphate phases decrease their solubility with the increase of pH. At pH above 4.0, HA is the most stable phase followed by TCP and OCP, whereas at pH values lower than 4.0, the dicalcium phosphate dihydrate (DCPD) or brushite phase is more stable than HA. On the other hand, the solubility diagram calculated by solid titration published in 2009 by Pan and Darvell considers that DCPD is not the most stable phase below pH 4.2, since calcium-deficient HA is less soluble [14]. This fact is due to the metastability of DCPD, which nucleates more easily than HA at low pH. This discrepancy highlights the importance of kinetic factors when defining the pH domains in which the calcium phosphate phase can be crystallized.

The use of organic compounds as templates for the generation of inorganic structures and materials with nanosized dimensions is another interesting strategy that has received increasing attention over the last decade. For instance, the role of citrate molecular ions in controlling and stabilizing the size of bone apatite nanocrystals can be a biologically inspired lesson from nature, which can be developed into an advanced strategy to control nanomaterial fabrication. To this regard, Delgado-Lopez and coworkers recently proposed a novel protocol to obtain bioinspired citrate-covered nanocrystalline apatite [15]. This method basically consists in the thermal decomplexing of metastable calcium/citrate/phosphate solutions. Briefly, two solutions (1:1 v/v) of (i) 0.1 M CaCl<sub>2</sub> + 0.4 M Na<sub>3</sub>(Cit) and (ii) 0.12 M Na<sub>2</sub>HPO<sub>4</sub> + x mM Na<sub>2</sub>CO<sub>3</sub> (x = 0 or 100) were mixed at 4 °C, and then the temperature is raised up to 80 °C. This temperature increase causes the precipitation of apatite nanocrystals, which are then matured (up to 96 h) in the same solution at 80 °C. Citrate anions were used as a calcium complexing agent to prepare

homogeneous metastable solutions in order to avoid the instantaneous calcium carbonate or calcium phosphate precipitation. Indeed the activity of the Ca–citrate complex ( $[\text{Ca}(\text{Cit})^-]$ ) decreases at increasing temperature (Fig. 1a). The destabilization of this complex provides a gradual release of  $\text{Ca}^{2+}$  ions into the solution, which in the presence of phosphate groups causes the formation of  $[\text{CaPO}_4]^-$  and  $[\text{CaHPO}_4]^0$ , repeatedly proposed as growth units for HA [16]. The size, crystallinity, and composition of the nanoparticles can be tailored by the maturation time as well as the concentration of sodium carbonate in the mother solution. Figure 1b shows TEM images of nanocrystalline apatites corresponding to different maturation times, i.e., 5 min and 96 h, respectively. At low maturation times (5 min), poorly crystalline 100 nm-mean length nanocrystalline apatites with low carbonation degree (1.5 % w/w, mainly as B-type substitutions, i.e., carbonate replacing phosphate groups) and covered by citrate (5.9 % w/w) were obtained. Interestingly, this citrate content is close to that recently measured on bone apatite [17]. On increasing the aging time up to 96 h, the mean length and the citrate content progressively decrease while the nanoparticles become better crystallized (Fig. 1b). In addition, the presence of carbonate ions in the solution favors their incorporation in the crystal lattice up to 3.1 % (in both A and B positions) giving rise also to shorter and more isometric nanoparticles [15]. It was also reported that citrate plays the dual role of driving a growth pathway via an amorphous precursor and controlling the size of nanocrystals by the nonclassical-oriented aggregation mechanism. Citrate–apatite nanoparticles displayed excellent compatibility properties in cell biological systems, and it was demonstrated that they can be used as pH-responsive delivery system of doxorubicin inside cells.

To sum up, parameters such as pH, ionic strength, temperature, aging (maturation) time, Ca/P molar ratios, and supersaturation are very important, and they have to be considered for the control of the formation of apatites. The effects of these synthesis and post-synthesis parameters on the physical–chemical characteristics of precipitated biomimetic nanocrystalline apatites have been recently overviewed [18]. The pH significantly affects the precipitation of apatite as it influences the amount of free  $\text{OH}^-$  groups and the balance of phosphate species. A shift to low pH decreases the concentration of free  $\text{OH}^-$  groups and shifts the balance of phosphate species from  $\text{PO}_4^{3-}$  to  $\text{HPO}_4^{2-}$  to  $\text{H}_2\text{PO}_4^-$  to  $\text{H}_3\text{PO}_4$  [19] (the species found in physiological conditions being only  $\text{HPO}_4^{2-}$  and  $\text{H}_2\text{PO}_4^-$ , forming an acid–basic couple of  $\text{pK}_a \sim 7.2$ ). At low pH the phosphate groups are highly protonated, and the precipitation is less favored. Moreover, the pH can shift the surface charge of the interacting particles by changing the distribution of proton and hydroxyl groups at the interface. Although  $\text{H}_3\text{O}^+$  and  $\text{OH}^-$  are usually considered as charge-determining ions in the case of apatite particles, other ions can modify the surface charge, and in particular, in calcium-containing solutions,  $\text{Ca}^{2+}$  ions may bind to the negatively charged apatite surface at  $\text{pH} > \text{IEP}$  (isoelectric point), leaving the surface neutral rather than negative. The opposite effect can take place in phosphate-rich solutions when binding of  $\text{HPO}_4^{2-}$  species at  $\text{pH} < \text{IEP}$  may result in a negatively charged apatite particle surface rather than the positive [19].

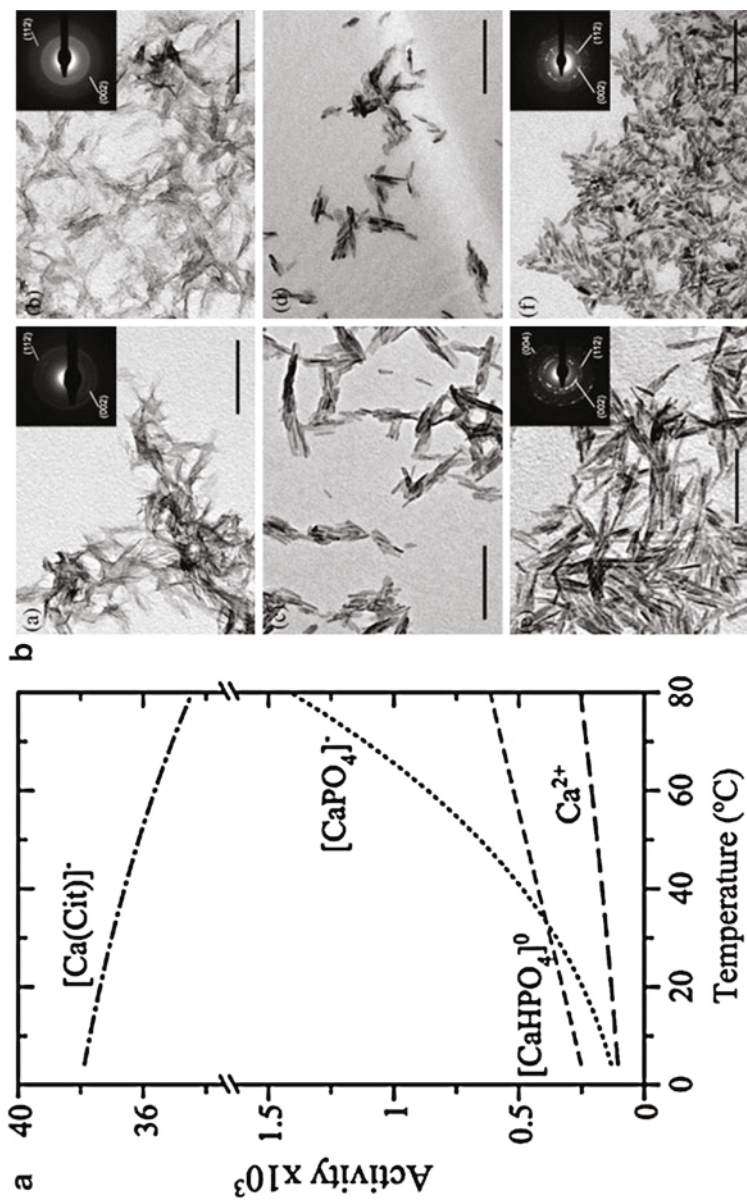


**Fig. 1** (a) Calculated activities, as a function of the temperature, of the main ionic and neutral species of the mother solution (pH 8.5) for the preparation of citrate-apatite nanoparticles by the thermal-decomplexing batch method. Note: Cit = C<sub>6</sub>H<sub>5</sub>O<sub>7</sub>. (b) TEM micrographs of citrate-apatites crystallized after 5 min (a), 2 h (c), and 96 h (e) and citrate-carbonate-apatites crystallized after 5 min (b), 2 h (d), and 96 h (f). Insets show the selected area electron diffraction (SAED) pattern collected for each sample. The scale bars are 200 nm

## Ionic-Substituted Biomimetic Hydroxyapatite

In general as described above, the shape, size, and specific surface area of HA nanocrystals appear to be very sensitive to both the reaction temperature and the reactant addition rate. HA-based materials with different stoichiometry and morphology have been prepared, with the effects of varying powder synthesis conditions on these features and on crystallinity investigated and discussed in recent studies [3, 4].

The effects of varying a number of factors have also been studied, including the concentration of the reagents, the reaction temperature and time, initial pH, aging time, and the atmosphere within the reaction vessel [20]. In order to optimize the specific biomedical applications of synthetic HA, the physical–chemical features that need to be modified are dimensions, porosity, morphology, and surface properties [15]. However, biomimetic apatites should also have a significant foreign ion content in the crystal lattice, composed of carbonate, strontium, magnesium, and silicon (Table 1) [21]. Due to its high flexible structure, apatite can host monovalent, divalent, and even trivalent cations, as well as simple monovalent anions or oxo-anions.

Ionic substitution has been proposed as a method of improving not only the biomimetic features of apatite but also the biological performance of apatite-based materials [21]. As a result, attempts have been made to synthesize HA that contains carbonate as a raw material for the manufacture of biomaterials [22]. Carbonate can substitute for  $\text{PO}_4^{3-}$  (B-type substitution) or for  $\text{OH}^-$  (A-type substitution). A and B carbonated apatites can be distinguished by their different lattice constants and by the different positions of the carbonate infrared absorption bands. In biological apatites,  $\text{CO}_3^{2-}$  substitutes mainly for  $\text{PO}_4^{3-}$  in B-type apatite [23]. Charge compensation by a  $\text{Ca}^{2+}$  vacancy, together with an H atom that bonds to a neighboring  $\text{PO}_4^{3-}$ , has been established to be the most stable arrangement [23]. Carbonate inhibits apatite crystal growth, and its incorporation usually results in poorly crystalline structures with increased solubility [19].

Recently, Iafisco et al. [24] reported a new methodology for the precipitation of carbonate-substituted apatite nanoparticles, based on the vapor diffusion sitting drop

**Table 1** Indicative ion content in human bone mineral

Ion	(mol %)	(wt %)
$\text{Ca}^{2+}$	8.7	34.8
$\text{PO}_4^{3-}$	4.9	46.6
$\text{Na}^+$	0.4	0.9
$\text{K}^+$	0.01	0.03
$\text{Mg}^{2+}$	0.2–0.5	0.5–1.3
$\text{CO}_3^{2-}$	0.5–1.3	3–8
$\text{F}^-$	0.02	0.03
$\text{SiO}_4^{4-}$	0.15–0.30	1.4–2.7
$\text{Cl}^-$	0.04	0.13
$\text{Ba}^{2+}$	Trace	Trace
$\text{Sr}^{2+}$	Trace	Trace

micromethod. The method was developed using an innovative device called the “crystallization mushroom” [25]. The advantages that this crystallization mushroom offers over other crystallization devices are reduced consumption of reagents during the crystallization process, as the volume of micro-droplets is around 40  $\mu\text{L}$ , and high reproducibility because of the possibility of running 12 batches of crystals for each experiment. This setup may therefore be suitable for the evaluation of the interactions and/or co-crystallization of apatite with small amounts of proteins, polymers, or drugs for studies in the fields of biomineralization and biomaterials. Using this approach, it has been found that mixtures containing 50 mM Ca  $(\text{CH}_3\text{COO})_2$  and 30 mM  $(\text{NH}_4)_2\text{HPO}_4$  in micro-droplets and 3 mL of a 40 mM  $\text{NH}_4\text{HCO}_3$  solution in the gas generation chamber are the optimal concentrations for the precipitation of carbonate–HA nanocrystals after 7 days of reaction. The nanocrystals were produced by solvent-mediated phase transformation of octacalcium phosphate (OCP) to apatite, with OCP most probably acting as a temporal template for the heterogeneous nucleation of apatite nuclei. The obtained crystals displayed nano-metric dimensions, carbonate ions in the crystal lattice, platelike morphology, and a low degree of crystallinity, closely resembling the inorganic phase of bones. Nassif et al. [26] also prepared carbonate–apatite by the vapor diffusion method. They used mixed solutions of  $\text{CaCl}_2$ – $\text{NaH}_2\text{PO}_4$  in the volume range of milliliters (macromethod) and either a  $\text{NH}_4\text{OH}$  and  $\text{NaHCO}_3$  solution or solid  $(\text{NH}_4)_2\text{CO}_3$  to generate the gas phase, which led, respectively, to the precipitation of B- or A-type carbonate–apatite phases. They concluded that the closest similarity between synthetic and natural apatite was obtained using an aqueous carbonate precursor; this is in accordance with the results obtained in the work of Iafisco et al. [24].

Divalent ions that replace calcium (such as magnesium and strontium) are particularly active during the first stages of the regenerative and remodeling processes [27]. In particular, magnesium is associated with the first stages of the bone formation and enhances skeletal metabolism and bone growth. Like carbonate, magnesium decreases with increasing calcification and with the aging of the bone [28]. In synthetic HA, the controlled substitution of calcium ions with magnesium increases the chemical–physical mimesis of the mineral bone. In fact, magnesium increases the kinetics of HA nucleation on collagen and retards its crystallization, affecting the size and shape of mineral nuclei. The incorporation of  $\text{Mg}^{2+}$  into the HA structure induces a disordered state on the HA surface where ions are continuously exchanged from the outer hydrated layer to the well-crystallized apatite lattice. Moreover, the replacement of calcium by magnesium in surface crystal sites increases the number of molecular layers of coordinated water [29]; all of these phenomena favor protein adsorption and the adhesion of cells to the scaffold. The increase of osteogenic activity in the presence of magnesium-substituted HA was shown in *in vivo* studies: a greater osteoconductivity over time and higher material resorption, compared to stoichiometric HA, were detected in granulated Mg–HA powders that were implanted in a rabbit’s femur [30]. Additionally, studies of osteoblast gene expression profiles from Mg–HA grafts revealed a higher expression of specific markers of osteoblast

differentiation and bone formation, which are associated with a lower osteoclastogenic potential.

Strontium is also considered to be a relevant trace ion that enhances osteogenesis while reducing bone resorption; this effect provides enhanced collagen synthesis and improved physical stabilization of the new bone matrix, as shown in *in vitro* and *in vivo* studies [31]. Due to its potential as an anti-osteoporotic agent, the incorporation of strontium ions into the HA lattice has been practiced in recent years [32], and increasing effort is being dedicated to the development of strontium-containing bone cements [33].

Like strontium, silicon is an essential trace element for the formation and stabilization of bones and connective tissues. Aqueous silicon in the form of orthosilicic acid ( $\text{Si}(\text{OH})_4$ ) has been shown to enhance osteoblast proliferation, differentiation, and collagen production and to have dose-dependent effects on osteoclast cells under *in vitro* conditions. The synthesis of silicon-substituted HA was performed, showing that silicon yields tetrahedral distortion and disorder at the hydroxyl site of the HA lattice, which can potentially decrease the stability of the apatite structure and enhance apatite solubility and bioavailability of silicon [34]. An increase of the osteoblast activity induced by silicon was also detected *in vivo* [35], where the migration of Ca, P, and Si ions to the bone–HA interface, consequent to apatite dissolution, accelerated the precipitation of biological apatite and induced bone apposition at the surface of the ceramic. Metal ions such as zinc, copper, iron, and manganese are also essential factors that enhance the functions of enzymes involved in the synthesis of the constituents of the bone matrix.

To achieve a synergistic effect, the synthesis of a multi-substituted HA phase is obtained in biomimetic conditions by carrying out the nucleation of the apatite phase in simulated body fluid (SBF) that has been enriched with biomimetic ions at 37 °C. This procedure mimics the physiological conditions of bone formation and allows synthetic HA to incorporate various ions ( $\text{Na}^+$ ,  $\text{K}^+$ ,  $\text{HPO}_4^{2-}$ ,  $\text{Mg}^{2+}$ ,  $\text{SiO}_4^{4-}$ ,  $\text{Sr}^{2+}$ ,  $\text{CO}_3^{2-}$ ), which are present in the physiological environment [36]. In particular, co-substitution with carbonate favored higher bioavailability of osteogenic chemical agents, thus increasing solubility in physiological conditions [36] and yielding improved *in vitro* results compared to silicon-free carbonated HA [37].

Biomimetic HA powders can be synthesized and used as granules to fill bone defects of limited size. However, the lack of specific morphology and mechanical stability of granulated bio-devices does not enable regeneration of extended bone parts; in this case the implantation of a 3D porous scaffold is required, with characteristics of bioactivity and osteoconductivity associated to biomechanical performance suitable for the specific implant site. More specifically, scaffolds have to provide the space for new bone formation and the necessary support for cells to proliferate and maintain their differential function. Moreover, they should exhibit suitable architectures for inducing the formation and maturation of well-organized tissue. Osteoconductivity ensures physical and mechanical integration with the surrounding bone, which in turn prevents micro-movements and the possibility of early mechanical loading *in vivo*; this process can be facilitated by the use of bioactive scaffolds that permit osteoclastic resorption.

Porosity in bone scaffolds is essential because it allows the transmission of changes in hydrodynamic pressure, thus activating mechanotransduction processes. It has been reported that around 80 % of total porosity is the critical point for ensuring both pore interconnectivity and sufficient mechanical properties of scaffolds. Pore volume and size, both at the macroscopic and the microscopic level, are significant properties of a scaffold for bone regeneration. Although no precise measurements can be provided for optimal void volumes and pore sizes due to the wide range of bone features in different anatomical districts, some general indications can be provided. Firstly, there is general consensus on the key effect of high porosity and large pores for the activation and enhancement of bone ingrowth and osteointegration of the implant after surgery. However, the extent of the porosity and the pore size should be associated with mechanical properties suitable for the specific implant site. The minimum pore size for cell colonization and substantial bone ingrowth was reported as 100  $\mu\text{m}$ , whereas smaller pores can result in the growth of un-mineralized osteoid tissue or fibrous tissue. However, there is wide consensus that the mean pore size should be approximately 300  $\mu\text{m}$  to achieve better osteogenesis, as this size provides improved vascularization and oxygenation. Macroscopic porosity (i.e., several hundreds of  $\mu\text{m}$ ) should also be interconnected with channel-like microporosity that enables fluid exchange throughout the whole scaffold, thus providing a supply of nutrients and the elimination of metabolic waste products.

Besides these general guidelines, the pore size of bone scaffolds should be designed with consideration of the features of the specific bone tissue to be repaired. In this respect, cortical bone is characterized by reduced porosity and activity and higher compression strength, compared to spongy bone, which exhibits a complex pore organization that allows physical stability and resistance against complex biomechanical stimuli. Hence, the design of bone scaffolds in a graded form allows for the reproduction of both parts of bone [38] that may improve the scaffold performance, thus enabling application in long-bone regeneration. The architecture of the scaffold is relevant since the bone ingrowth is guided by the scaffold voids and may be interrupted by lack of pore interconnection, thus creating spatially discontinuous ingrowth with the formation of bone islands throughout the whole scaffold. The formation of new bone in the inner part of the scaffold is a key feature for ensuring optimal osteointegration and reduced physical mismatch at the bone–scaffold interface.

## Hydroxyapatite as Superparamagnetic Phase

Recent research has highlighted the possibility of creating a new bioactive superparamagnetic apatite phase, paving the way for newly conceived applications in different fields, ranging from regenerative medicine to advanced anticancer therapies [39]. In fact, the major limitations of the scaffolds for bone regeneration that are currently available on the market are related to difficulties in controlling cell differentiation and angiogenesis processes and in obtaining stable scaffold



implantation in the pathological site. Extensive angiogenesis is a fundamental requirement for the complete morphological and biological maturation of the tissue, especially in the case of dimensionally critical defects.

Conventional scaffolds are still used to mimic growth factor production and delivery; however, recently the idea of utilizing magnetic scaffolds for greater additional control of the angiogenic process *in vivo* has been proposed [40]. These scaffolds can be manipulated *in situ* by means of external magnetic fields to attract angiogenic and other bioactive factors, which are in turn linked to magnetic nano-carriers. In fact, in the presence of external magnetic fields, the scaffold is magnetized, resulting in two distinct effects: cell activation in the proximity of the scaffold and driving of bone and vascular growth factors into the scaffold, through the attraction of magnetic nano-carriers linked to the active molecules and injected *in situ*. The resulting magnetic scaffold can be imagined as a fixed “station,” whose magnetization can be switched on and off by an external magnetic field. It thus provides long-term aid, supports tissue engineering, and provides a unique opportunity to adapt the regenerative response to the personal needs of the patient.

Magnetic materials most commonly used for biomedical applications are mainly based on superparamagnetic iron oxide nanoparticles (SPION), consisting in mixtures of magnetite, maghemite, and hematite, which have been demonstrated successfully both *in vitro* and *in vivo*. SPION can be synthesized with different morphologies, chemical compositions, and magnetic properties, but some limitations still exist including low magnetic moment and low cargo capacity. Additionally, although the American Food and Drug Administration (FDA) approved SPION for human *in vivo* use, several concerns about their cytotoxicity are emerging. In fact, their extensive use over a long period of time can lead to the accumulation of high quantity of iron in soft tissues and organs such as liver and kidney, causing an imbalance in their homeostasis and cytotoxic and inflammatory effects.

To overcome the limitations of SPION, new forms of biocompatible superparamagnetic nanoparticles with good magnetic moment, high drug loading, and lower iron content are thus strongly required. To this low crystallinity biomimetic HA has been prepared by substituting calcium with  $\text{Fe}^{2+}$  and  $\text{Fe}^{3+}$  ions at specific crystal sites [39]. In particular, it was demonstrated that in controlled conditions, the simultaneous addition of  $\text{Fe}^{2+}$  and  $\text{Fe}^{3+}$  species during HA synthesis carried out by neutralization leads to FeHA with a  $(\text{Fe} + \text{Ca})/\text{P}$  ratio of 1.68. This corresponds to the theoretical ratio calculated and minimizes the formation of magnetite as a secondary phase ( $<1$  wt %). X-ray diffraction (XRD) and computer simulations demonstrated that both  $\text{Fe}^{2+}$  and  $\text{Fe}^{3+}$  occupy different calcium positions in the HA lattice. The generation of two different structural domains or sub-lattices in the FeHA structure can be taken as the source of the superparamagnetism, as also revealed by magnetic investigations [39]. Additionally, the resulting material displayed effective hyperthermia properties: an increase of  $40^\circ\text{C}$  in 60 s has been detected under an alternate magnetic field of 30 mT at a frequency  $\nu = 293$  Hz [39]. Taking into account the above, new anticancer therapies can be developed by exploiting the high hyperthermia effect exhibited by the new FeHA phase. The bioactivity and bioresorbability of the new FeHA may allow the currently used

magnetite to be replaced by minimally invasive therapies based on local heating. Moreover, FeHA nanoparticles can function either as a killing agent by selective internalization by tumor cells or as carriers of antitumor drugs, linked to FeHA by thermolabile ligands: through the application of external magnetic fields, the hyperthermia will release the drug only at the specific site, thus reducing systemic side effects.

In addition magnetic cell targeting provides a very promising tool in medicine for a wide range of applications as cell manipulation and cell therapy. In order to efficiently and safely target the cells, the magnetic nanoparticles must not negatively affect cell behavior. Through a co-incubation of cells with magnetic nanoparticles, the particles are generally internalized by the spontaneous endocytosis pathway or phagocytosis. FeHA nanoparticles have shown a great potential in magnetic cell labeling to guide mesenchymal stem cells to the target site offering exciting new opportunities for effectively treating several diseases.

---

## Hybrid Nanocomposite

Despite the continuous progress in material science and technology to develop bone scaffolds with complex structures, conventional approaches are still far from developing inorganic matrices that really mimic natural tissues. In the last decade, increasing efforts were dedicated to creating fabrication methods that could reproduce biological processes thus generating complex devices with features similar to natural materials. Also, the use of natural polymers for the fabrication of bio-devices is gradually being increased. Natural polymers have the advantage of biocompatibility and biodegradability because they are the structural components of living tissues (i.e., collagen and glycosaminoglycans). In spite of the intrinsically low mechanical strength of their components, biological structures exhibit outstanding physical and mechanical properties, such as high resistance, lightness, and the ability to continuously adapt to constantly changing external stimuli; the establishment of these properties is due to the complexity and hierarchical organization of the natural structures (e.g., shells, plants, exoskeletons) from the nano- to the macroscale. The complex arrangement of nanosized organic and inorganic elements is obtained due to information exchanged at the molecular level between the organic structure, which acts as a template, and the inorganic phases that heterogeneously nucleate on it [41].

In particular, the hard tissues in mammals are generated by a biomineralization process [42], which is a complex ensemble of concomitant phenomena, driving the development of complex biologic structures, associating highly organized protein/carbohydrate matrices which function as templates for the nucleation and organization at the nanoscale of inorganic nanostructured phases where collagen-based components self-assemble and organize, thus acting as templates for the heterogeneous nucleation of ion-substituted apatites by mediation of chemical, physical, morphological, and structural control mechanisms. Such process is able to induce chemical–physical and structural complexity not achievable by any conventional

manufacturing processes as well as outstanding properties including the capacity to intelligently respond to the environmental stimuli, also including the ability of self-renewal and self-regeneration upon limited damages.

The exposed functional groups of collagen in specific regions, represented and delimited by insoluble macromolecules, act as sites of heterogeneous nucleation for the mineral phase upon precipitation of the ions present in the surrounding ECM (e.g.,  $\text{Ca}^{2+}$ ,  $\text{PO}_4^{3-}$ ,  $\text{Na}^+$ ,  $\text{K}^+$ ,  $\text{Mg}^{2+}$ ). The apatite nuclei subsequently grow under the physical constraints of the complex macromolecular organic structures and assume specific morphologies and crystal orientations, which result in the exposure of crystal planes that specifically enable the adhesion of proteins that promote focal adhesions. The structural organization of the newly formed bone proceeds from the nanometer to the macroscopic scale, where the mineral phase exhibits a complex architecture that is strictly dependent on the combination of the various phenomena that are described above [43].

Due to the large amount of information relating to the complexity of these constructs, as well as the reduced size of their elemental components, it is not possible to build a similar structure with conventional manufacturing methods. In this respect, over the past decade, the establishment of assembling processes guided by control mechanisms similar to those existing in nature is increasingly being viewed as a feasible way of creating bio-devices with smart multifunctionality. In the early 2000s, a new concept for bone scaffolding was developed, involving a biologically inspired fabrication process with the purpose of obtaining 3D constructs that strongly mimic the chemical–physical, morphological, and structural features of hard human tissues [44]. By this process, type I collagen fibrils, dispersed in quasi-physiological aqueous solutions containing ions involved in bone formation, are assembled and organized by pH variation, thus yielding hybrid fibrous mineralized constructs that mimic the composition and structure of the newly formed bone (Fig. 2, left).

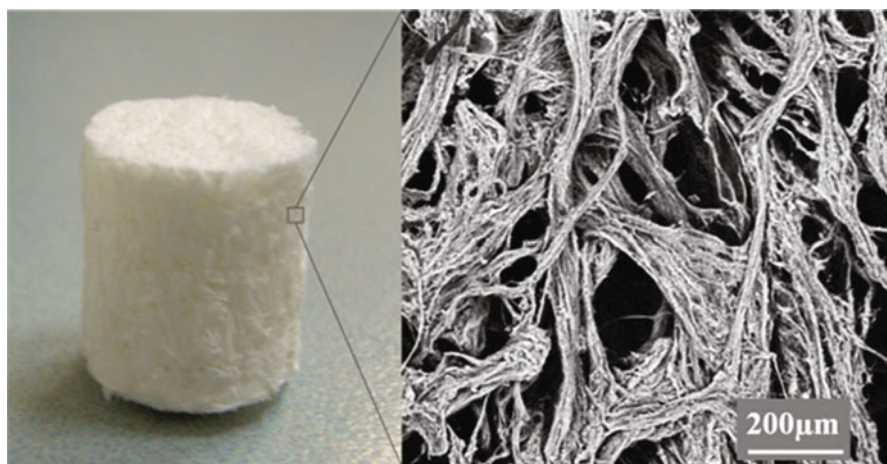


**Fig. 2** Bone scaffold made of collagen–HA obtained by bioinspired mineralization process (*left*, macroscopic view; *right*, microscopic detail)

These scaffolds exhibit biomimetic chemical–physical features (i.e., a collagen fibrous matrix) formed by the spontaneous assembling and hierarchical organization of nano-fibrils that are embedded in the nano-nuclei of biomimetic apatite (HA/collagen), the heterogeneous nucleation of which took place in specific sites corresponding to the periodic gaps of the collagen bands [45]. The devices that were obtained exhibited very high open surface and macroscopic porosity that could easily be tailored by different approaches (Fig. 2, right). The soft nature of the bioinspired hybrid HA/collagen composite allows for specific pore sizes and orientations during the synthesis process through the use of chemical cross-linking or freeze-casting/freeze-drying processes [43]. The controlled cross-linking enables the improvement of the physical stability of the scaffold against early enzymatic resorption as well as the tailoring of the pore size. In turn, pore size affects the local oxygen tension and this can influence cell differentiation; hence, a reduced pore size can promote cell differentiation in chondrocytes rather than osteoblasts.

This is of particular interest in the view of developing scaffolds for the regeneration of multifunctional tissues, such as the osteochondral or periodontal regions. Moreover, the bioinspired synthesis process allows for the control of the mineralization extent (i.e., the amount of mineral phase heterogeneously nucleated onto the collagen fibers), which can range from zero to bone-mimicking composition (i.e.,  $\approx 70\%$ ). Hence, graded hybrid composites were developed, which mimic the composition and structure of the subchondral bone and mineralized cartilage [46]. Mineral-free layers, enriched with hyaluronic acid, were also produced to mimic the cartilaginous region: processes of controlled freeze-drying allowed for the suitable orientation of the fibers of the cartilage-like layer into a columnar-like structure, converging toward the external surface into horizontal flat ribbons, thus resembling the morphology of the lamina splendens.

The morphological and compositional gradients exhibited by the multilayered osteochondral scaffold offer spatially defined environmental cues that are able to guide specific cell differentiation and fast tissue regeneration [47]. This shows the importance of biomimicry in the design of scaffolds for tissue regeneration [36]. Moreover, the possibility of controlling the processes of scaffold formation by soft chemistry offers high flexibility of production and functionalization. In this respect, due to the highly exposed surface area and the presence of many different active surface sites (e.g.,  $-\text{COO}^-$  and  $-\text{NH}_2$  groups), bioinspired hybrid composites offer the possibility to associate suitable signaling molecules to improve the biological response in terms of the amount and quality of the newly formed tissue. Relevant bio-triggers can be proteins or short peptide epitopes; for bone regeneration, the most commonly used peptide for surface modification is Arg–Gly–Asp (RGD), which is a signaling domain derived from fibronectin and laminin. Moreover, the high surface activity of natural polymers allows the possibility of biomimetic composite scaffolds with improved mechanical properties (i.e., strength, elasticity, stiffness) by association of collagen with other natural sources that are able to mediate bioinspired mineralization processes. The potential to tailor the features of multifunctional hybrid scaffolds will pave the way to the development of scaffolds with wider applications in the field of regenerative medicine. For instance, with reference to

dental tissue, the alveolar bone and cementum form upon processes of assembling and mineralization similar to those involved in the formation of bones and their main cells follow similar behavior. Dental pulp and dentinal tissue are collagen-based constructs where the degree of assembling, mineralization, and organization progressively increases from the pulp to the predentin and the dentin, therein reaching a very high mineralization extent, organized in micron-sized tubules. The application of controlled processes of casting/drying, which are able to yield channel-like morphologies, may enable the future development of scaffolds for dental regeneration, which would be a breakthrough in medicine with huge socioeconomic impacts.

The development of scaffolds with magnetic properties, as described above, may represent a new approach opening new options that cannot be adequately addressed by other methods currently in use. In particular, superparamagnetic devices can be remotely activated/deactivated by external magnetic fields; magnetic activation may open the way to novel regenerative scaffolds with multiple functions. For instance, magnetic stimulation can enhance cell activity to produce new healthy and organized tissues, as suggested by recent literature [48]; hence, new personalized approaches could be established by development of new therapies designed to favor tissue regeneration in specific clinical cases. Another possible application is the use of weak local magnetic fields as signals to recall and drive specific biochemical cues with magnetic marking. Indeed, mimicking endogenous growth factor production and delivery is still to be solved with conventional scaffolds. Recently the idea of utilizing magnetic scaffolds for an additional control of angiogenesis process *in vivo* was proposed [49]. Such scaffolds can be manipulated *in situ* by opportunely measured application of magnetic stimuli to attract or deliver angiogenic and other bioactive factors, in turn linked to magnetic nano-carriers, so to provide long-living assistance to tissue neoformation and organization.

Magnetic forces can also aid to improve the fixation of scaffolds in the implant site; a superparamagnetic implant can be stabilized by external magnetic bandages; this can help to minimize the use of external fixating media and possibly reduce the hospitalization time and the patient's pain.

In view of the establishment of these new intriguing applications, the selection of suitable superparamagnetic media to be incorporated in the bone scaffolds is nowadays limited to iron oxides (see also previous section); however, the recent development of a novel, bioactive, apatite phase with intrinsic superparamagnetic properties [39] suggests that biomimetic scaffolds with intrinsic superparamagnetic properties may be produced, with potentially no risks nor harmful effects due to incorporation of harmful nanoparticles in the human tissues. Recently, upon suitable modification of the *in-lab* biomineralization process, defined amounts of di- and trivalent iron ions were incorporated in the apatite lattice during heterogeneous nucleation on self-assembling collagen fibers, giving rise to hybrid biomimetic composites mineralized with superparamagnetic FeHA nuclei and endowed with superparamagnetic properties, minimizing the formation of potentially cytotoxic magnetic phases such as magnetite or other iron oxide phases (Fig. 3) [50]. Magnetic composites were prepared at different temperatures, and the effect of this parameter on the reaction yield in terms of mineralization degree, morphology, degradation,

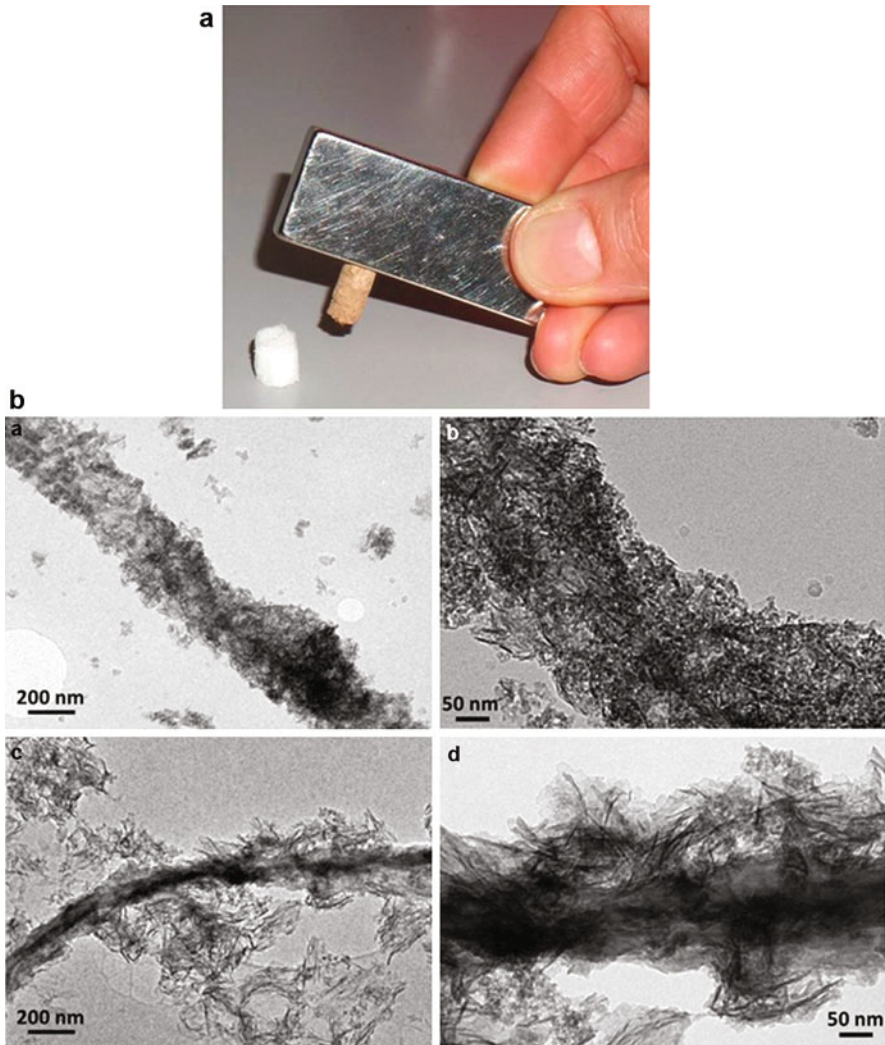


**Fig. 3** (a) Photograph of magnetic FeHA/Coll (*brownish scaffold* attached to the magnet) and nonmagnetic HA/Coll (*white scaffold*) scaffolds. (b) TEM images representative of the assembly of FeHA nanoparticles nucleated on the collagen fibers at different temperatures (i.e., (a) and (b) at 25 °C and (c) and (d) at 40 °C)

and magnetization was investigated [50]. The influence of scaffold properties on cells was evaluated by seeding human osteoblast-like cells on magnetic and nonmagnetic materials, and differences in terms of viability, adhesion, and proliferation were studied. The synthesis temperature affects mainly the chemical–physical features of the mineral phase of the composites influencing the degradation, the microstructure, and the magnetization values of the entire scaffold and its biological

performance. *In vitro* investigations indicated that the biocompatibility of the materials and the magnetization of the superparamagnetic scaffolds, induced by applying an external static magnetic field, have an activation effect on osteoblast cells controlling the bone growth and improving the whole regenerative process. These positive results will stimulate further *in vitro* and *in vivo* investigations on the potential application of these bioinspired magnetic scaffolds to trigger and direct osteogenesis and to repair large bone defects through a magnetic remote control tuning the regenerative process. Moreover, growth factors and/or other key biomolecules linked to magnetic carriers could be selectively attracted toward and within the hybrid scaffold when magnetized. The magnetic behavior of the FeHA directly nucleated on the collagen can also allow scaffold labeling to be visualized *in vivo* by magnetic resonance imaging (MRI).

Besides, the flexibility of the synthesis process allowed to tailor the extent of mineralization of the superparamagnetic hybrid composites; consequently, 3D hybrid constructs with features mimicking different mineralized and non-mineralized tissues could be synthesized and merged into morphologically/compositionally and magnetically graded composites able to mimic multifunctional anatomical regions.

---

### **3D Hierarchically Organized Ceramics by Biomorphic Transformation**

The new concept of fabrication based on the reproduction of biological processes may pave the way to a new generation of smart devices with multiple functionalities. However, the low mechanical properties of the hybrid tissue-mimicking devices that are described in the previous section, as a result of their soft nature, pose some limitations in their use. In particular, the regeneration of segmental long bones is still an unmet clinical need. Presently, the healing of load-bearing bone segments still relies on bioinert dense implants based on alumina, titanium, etc., due to the inability of the current manufacturing technologies to form mechanically strong porous inorganic structures with a hierarchical pore organization and complex morphological details in the submicron scale.

A paradigmatic change in ceramic processing and engineering is needed thus greatly expanding the existing tools enabling the development of massive and porous ceramic bodies with designed smart functions. The idea is to surpass the existing approach in ceramic development, based on powder synthesis, forming, and thermal consolidation (sintering), by developing new “one-step synthesis/consolidation processes” to obtain new 3D ceramics with properties and functions not achievable with the current manufacturing approach. This is particularly relevant when the ceramic phases with desired functional properties have low thermodynamic stability such as complex atomic composition and nanosize, so that the existing ceramic process, particularly sintering, destroys the labile phase increasing its stability but deleting its smart functional properties. Particularly, the sintering process, which is fundamental to consolidate ceramic bodies, hampers the

maintenance of ceramic phases characterized by nonstoichiometric composition, nanosize, and low crystallinity. These features, reflecting low thermodynamic stability, are very often the source of functions that cannot be expressed by a sintered, stable ceramic phase. The new processes developed in the project will be based on the transformation of complex, hierarchically organized structures obtained by the pyrolysis of natural sources (e.g., woods, plants, exoskeletons) or 3D-printed templates into ceramic phases exhibiting designed chemical composition and 3D organization into massive bodies with complex morphology, hierarchical structure, and, at the same time, optimized mechanical performance. This will greatly expand the perspective of material science toward the conception of smart approaches to generate new nature-inspired products that are gaining ever-raising interest as the next frontier in material production responding to the challenges of the next decades. Using this new approach, it will be possible to fabricate scaffolds able to actively respond to the complex biomechanical loads and activate the mechanotransduction processes, yielding formation and remodeling of new functional bone. The outstanding mechanical performances of bones are mostly due to their complex structure, hierarchically organized from the nano- to the macroscale and to the interactions taking place across all levels of organization. For this reason, scaffolds endowed with bone-like composition and similar structural complexity should assist long-bone regeneration; however, the conventional manufacturing methods do not produce inorganic, mechanically resistant scaffolds with the required bioactivity and hierarchical pore organization. The expression of chemical biomimesis in scaffolds for long-bone regeneration is made difficult by the reduced mechanical strength of HA-based materials. Several solutions based on composite materials have been studied, making use of strong bioinert or bioactive phases [51] that were dispersed in a calcium–phosphate matrix. However, the limitation in the achievement of hierarchically organized structures still remains.

To address this problem, the attention of scientists has been dedicated to investigating and reproducing complex morphologies that exist in nature, particularly among ligneous structures that strongly resemble bones in their morphology, structural organization, and mechanical performances. Like bone, wood can be regarded as a cellular material at the scale of hundred micrometers to centimeters. At the cell level, the mechanical properties are governed by the diameter and shape of the cell cross section, as well as by the thickness of the cell wall. In particular, the ratio of cell-wall thickness to cell diameter is directly related to the apparent density of wood, which in turn is a determining factor for the performance of lightweight structures. The unique hierarchical architecture of the cellular microstructure gives wood a remarkable combination of high strength, stiffness, and toughness at low density. The alternation of fiber bundles and channel-like porous areas makes the wood an elective material to be used as a template in the preparation of a new bone substitute that is characterized by a biomimetic hierarchical structure.

The transformation of wood into inorganic, hierarchically organized materials (e.g., oxide ceramics such as  $\text{Al}_2\text{O}_3$ ,  $\text{ZrO}_2$ ,  $\text{TiO}_2$ ,  $\text{MnO}$  and non-oxide ceramics such as  $\text{SiC}$ ,  $\text{TiC}$ ,  $\text{ZrC}$ ) was the subject of investigation in the late 1990s [52, 53]. This approach was addressed to the synthesis of hierarchically organized bone scaffolds



made of SiC [54], which have the advantage of offering very high fracture strength and bio-tolerated surfaces. More recently, these kinds of biomorphic transformations were also used to manufacture hierarchically organized scaffolds made of HA [55]. The complexity of the apatite phase, in comparison with oxides, carbides, and nitrides, required the settling of a multistep transformation route, where the native wood was sequentially transformed into pure carbon, calcium carbide, calcium oxide, calcium carbonate, and finally hydroxyapatite. Due to their bone-mimicking composition, microstructure, and hierarchical organization, these newly conceived bioceramics promise to offer enhanced osteogenesis, integration, and biomechanical behavior when implanted in vivo.

Woods such as rattan and sipo have strong morphological similarities to spongy and cortical bones, respectively. Rattan is characterized by channel-like pores (simulating the haversian system in bone), interconnected with a network of smaller channels (such as the Volkmann system) [55]. Sipo is a tougher, denser wood that has a microporosity that can promote cell adhesion and anchorage. The multistep transformation process (Fig. 4) allowed precise control of the phase composition,

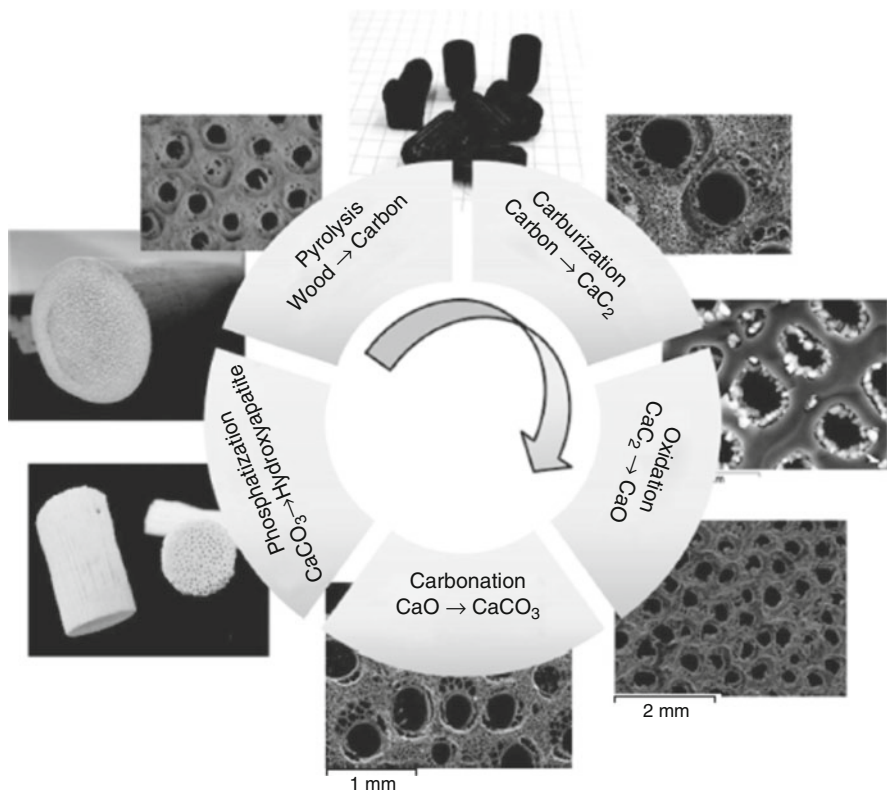


**Fig. 4** Scheme illustrating the multistep transformation process of natural wood into biomorphic HA scaffold

crystallinity, and microstructure, since the different reactions occurred between a gas and the solid template, where calcium, oxygen, carbonate, and phosphate ions were progressively added while building the HA molecules. The control of the kinetic reaction throughout the different steps of the transformation process enabled precise control of the scaffold composition, microstructure, and bioactivity [56].

Importantly, the maintenance of the original wood microstructure allowed scaffolds to exhibit mechanical strengths comparable to those of spongy bone (~4 MPa) when measured along the channel direction, even in the absence of thermal consolidation treatments. The bioactivity of the rattan-derived HA scaffolds was assessed by *in vitro* investigation of MG63 osteoblast-like cells' adhesion and morphology in contact with the scaffold, revealing a nearly complete covering of the scaffold surface after only 7 days and a good morphology of the attached cells, which were well distributed on the scaffold trabeculae. The cells appeared to interact closely with the scaffold surface, which is evidence of good material biocompatibility.

The implantation of rattan-derived scaffolds in critical defects created in the femoral distal epiphysis of skeletally mature, adult, disease-free, New Zealand white rabbits confirmed the *in vivo* bioactivity and osteoconductivity after 1-month follow-up. Extensive bone formation inside the scaffold channels with a regular architectural pattern was detected, without any inflammatory or toxic reaction against the scaffolds nor connective capsules or bone gaps.

The establishment of biomorphic transformations that are able to transform woods into biomimetic bone scaffolds can provide solutions for long-bone regeneration and can be designed in a custom-made fashion. The association of a mechanically resistant cortical-like shell and a highly biomimetic spongelike core may enable the substitution of segmental bone parts. Selected wood structures could reproduce different bone portions that are characterized by different porosities and pore distributions, as occurring in cortical and spongy bones. Such structures can enable complete regeneration of bones, in particular long bones, provided that (i) the core exhibits a structure with bone-like composition and is highly permeable to cells and physiological fluids to allow cell colonization and proliferation as well as extensive angiogenesis and (ii) the external shell exhibits porosity sufficient for cell anchorage and mechanical strength that is able to withstand biomechanical stimuli, so as to load the scaffold soon after implantation. Such devices may enable the establishment of a biological chamber that encloses a suitable environment that is conditioned to promote and enhance bone formation and remodeling. The implant will function as an *in vivo* bioreactor, thus facing an unsolved clinical problem related to the vanishing of the regenerative process at distances far from the bone-implant interface.

---

## Summary

With the continuous advances in material science and nanotechnology, great progress has been made in the development of biomedical devices for bone regeneration. However, some serious limitations still exist that are related to the development

of bio-devices mimicking the structure and composition of biological tissues with high complexity and load-bearing properties, such as extended bone and osteochondral parts or segmental bones. For this reason, in the absence of well-established regenerative devices for such applications, the related clinical needs remain unmet and their socioeconomic impact is large and continuously increasing due to the progressive aging of the population and the new lifestyles that expose younger people to serious injuries and traumas. The recent advances in materials science offer many possibilities for solving these concerns in the coming decades; the new fabrication approaches that draw inspiration from nature and from the multitude of outstanding biological structures and phenomena will enable a new generation of smart and multifunctional devices. Moreover, the recent discovery of superparamagnetism in bioactive Fe-substituted apatite will pave the way for new biomedical devices endowed with a number of smart functionalities that can be switched on and off by exposure to magnetic fields. Bioinspiration and remote activation are thus two new concepts that will allow material science and knowledge of biomaterials to progress well beyond the current state of the art and will give an outstanding contribution to the biomedical field. The preliminary steps that have already been taken in this direction are very promising, and, although the development of bioinspired materials is still in its infancy, it is rapidly becoming a priority for the development of new smart materials. It is expected that, in the years to come, a number of unmet clinical needs will benefit from a new generation of biologically inspired smart devices.

---

## References

1. Amini AR, Laurencin CT, Nukavarapu SP (2012) Bone tissue engineering: recent advances and challenges. *Crit Rev Biomed Eng* 40(5):363–408.
2. Sprio S, Ruffini A, Valentini F, D'Alessandro T, Sandri M, Panseri S, Tampieri A (2010) Biomimesis and biomorphic transformations: new concepts applied to bone regeneration. *J Biotechnol* 156(4):347–355
3. Roveri N, Palazzo B, Iafisco M (2008) The role of biomimetism in developing nanostructured inorganic matrices for drug delivery. *Expert Opin Drug Deliv* 5(8):861–877
4. Dorozhkin SV (2010) Nanosized and nanocrystalline calcium orthophosphates. *Acta Biomater* 6(3):715–734
5. Rey C, Combes C, Drouet C, Lebugle A, Sfihi H, Barroug A (2007) Nanocrystalline apatites in biological systems: characterisation, structure and properties. *Materialwiss Werkstofftech* 38 (12):996–1002
6. Legros R, Balmain N, Bonel G (1987) Age-related changes in mineral of rat and bovine cortical bone. *Calcif Tissue Int* 41(3):137–144
7. Rey C (1990) Calcium phosphate biomaterials and bone mineral. Differences in composition, structures and properties. *Biomaterials* 11:13–15
8. Rey C, Combes C, Drouet C, Sfihi H, Barroug A (2007) Physico-chemical properties of nanocrystalline apatites: implications for biominerals and biomaterials. *Mater Sci Eng C Biomim Supramol Syst* 27(2):198–205
9. Drouet C, Bosc F, Banu M, Largeot C, Combes C, Dechambre G, Estournes C, Raimbeaux G, Rey C (2009) Nanocrystalline apatites: from powders to biomaterials. *Powder Technol* 190 (1–2):118–122

10. Sakhno Y, Bertinetti L, Iafisco M, Tampieri A, Roveri N, Martra G (2010) Surface hydration and cationic sites of nanohydroxyapatites with amorphous or crystalline surfaces: a comparative study. *J Phys Chem C* 114(39):16640–16648
11. Cazalbou S, Combes C, Eichert D, Rey C, Glimcher MJ (2004) Poorly crystalline apatites: evolution and maturation in vitro and in vivo. *J Bone Miner Metab* 22(4):310–317
12. Uskoković V, Uskoković DP (2011) Nanosized hydroxyapatite and other calcium phosphates: chemistry of formation and application as drug and gene delivery agents. *J Biomed Mater Res B Appl Biomater* 96B(1):152–191
13. Johnsson MS-A, Nancollas GH (1992) The role of brushite and octacalcium phosphate in apatite formation. *Crit Rev Oral Biol Med* 3(1):61–82
14. Pan HB, Darvell BW (2008) Calcium phosphate solubility: the need for re-evaluation. *Cryst Growth Des* 9(2):639–645
15. Delgado-López JM, Iafisco M, Rodríguez I, Tampieri A, Prat M, Gómez-Morales J (2012) Crystallization of bioinspired citrate-functionalized nanoapatite with tailored carbonate content. *Acta Biomater* 8(9):3491–3499
16. Lazić S (1995) Microcrystalline hydroxyapatite formation from alkaline solutions. *J Cryst Growth* 147(1–2):147–154
17. Hu Y-Y, Rawal A, Schmidt-Rohr K (2010) Strongly bound citrate stabilizes the apatite nanocrystals in bone. In: Proceedings of the National Academy of Sciences <http://www.pnas.org/content/107/52/22425.full>
18. Vandecandelaere N, Rey C, Drouet C (2012) Biomimetic apatite-based biomaterials: on the critical impact of synthesis and post-synthesis parameters. *J Mater Sci Mater Med* 23(11):2593–2606
19. Wang L, Nancollas GH (2008) Calcium orthophosphates: crystallization and dissolution. *Chem Rev* 108(11):4628–4669
20. Koutsopoulos S (2002) Synthesis and characterization of hydroxyapatite crystals: a review study on the analytical methods. *J Biomed Mater Res* 62(4):600–612
21. Boanini E, Gazzano M, Bigi A (2010) Ionic substitutions in calcium phosphates synthesized at low temperature. *Acta Biomater* 6(6):1882–1894
22. Padilla S, Izquierdo-Barba I, Vallet-Regí M (2008) High specific surface area in nanometric carbonated hydroxyapatite. *Chem Mater* 20(19):5942–5944
23. Zapanta-Legeros R (1965) Effect of carbonate on the lattice parameters of apatite. *Nature* 206(4982):403–404
24. Iafisco M, Morales JG, Hernandez-Hernandez MA, Garcia-Ruiz JM, Roveri N (2010) Biomimetic carbonate-hydroxyapatite nanocrystals prepared by vapor diffusion. *Adv Eng Mater* 12(7):6
25. Gomez-Morales J, Delgado-López JM, Iafisco M, Hernández-Hernández MA, Prat M (2011) Amino acidic control of calcium phosphate precipitation by using the vapor diffusion method in microdroplets. *Cryst Growth Des* 11(11):4802–4809
26. Nassif N, Martineau F, Syzgantseva O, Gobeaux F, Willinger M, Coradin T, Cassaignon S, Azaïs T, Giraud-Guille MM (2010) In vivo inspired conditions to synthesize biomimetic hydroxyapatite. *Chem Mater* 22(12):3653–3663
27. Bigi A, Cojazzi G, Panzavolta S, Ripamonti A, Roveri N, Romanello M, Noris Suarez K, Moro L (1997) Chemical and structural characterization of the mineral phase from cortical and trabecular bone. *J Inorg Biochem* 68(1):45–51
28. Bigi A, Foresti E, Gregorini R, Ripamonti A, Roveri N, Shah J (1992) The role of magnesium on the structure of biological apatites. *Calcif Tissue Int* 50(5):439–444
29. Bertinetti L, Tampieri A, Landi E, Martra G, Coluccia S (2006) Punctual investigation of surface sites of HA and magnesium-HA. *J Eur Ceram Soc* 26(6):987–991
30. Landi E, Logroscino G, Proietti L, Tampieri A, Sandri M, Sprio S (2008) Biomimetic Mg-substituted hydroxyapatite: from synthesis to in vivo behaviour. *J Mater Sci Mater Med* 19(1):239–247
31. Dahl SG, Allain P, Marie PJ, Mauras Y, Boivin G, Ammann P, Tsouderos Y, Delmas PD, Christiansen C (2001) Incorporation and distribution of strontium in bone. *Bone* 28(4):446–453

32. Landi E, Tampieri A, Celotti G, Sprio S, Sandri M, Logroscino G (2007) Sr-substituted hydroxyapatites for osteoporotic bone replacement. *Acta Biomater* 3(6):961–969
33. Tadier S, Bareille R, Siadous R, Marsan O, Charvillat C, Cazalbou S, Amédée J, Rey C, Combes C (2012) Strontium-loaded mineral bone cements as sustained release systems: compositions, release properties, and effects on human osteoprogenitor cells. *J Biomed Mater Res B Appl Biomater* 100B(2):378–390
34. Vallet-Regi M, Arcos D (2005) Silicon substituted hydroxyapatites. A method to upgrade calcium phosphate based implants. *J Mater Chem* 15(15):1509–1516
35. Porter AE, Patel N, Skepper JN, Best SM, Bonfield W (2003) Comparison of in vivo dissolution processes in hydroxyapatite and silicon-substituted hydroxyapatite bioceramics. *Biomaterials* 24(25):4609–4620
36. Sprio S, Tampieri A, Landi E, Sandri M, Martorana S, Celotti G, Logroscino G (2008) Physico-chemical properties and solubility behaviour of multi-substituted hydroxyapatite powders containing silicon. *Mater Sci Eng C* 28(1):179–187
37. Landi E, Uggeri J, Sprio S, Tampieri A, Guizzardi S (2010) Human osteoblast behavior on as-synthesized SiO<sub>4</sub> and B-CO<sub>3</sub> co-substituted apatite. *J Biomed Mater Res A* 94A(1):59–70
38. Tampieri A, Celotti G, Sprio S, Delcogliano A, Franzese S (2001) Porosity-graded hydroxyapatite ceramics to replace natural bone. *Biomaterials* 22(11):1365–1370
39. Tampieri A, D'Alessandro T, Sandri M, Sprio S, Landi E, Bertinetti L, Panseri S, Pepponi G, Goettlicher J, Bañobre-López M, Rivas J (2012) Intrinsic magnetism and hyperthermia in bioactive Fe-doped hydroxyapatite. *Acta Biomater* 8(2):843–851
40. Guo C, Kaufman LJ (2007) Flow and magnetic field induced collagen alignment. *Biomaterials* 28(6):1105–1114
41. Fratzl P, Weinkamer R (2007) Nature's hierarchical materials. *Prog Mater Sci* 52(8):1263–1334
42. Weiner S (2008) Biomineralization: a structural perspective. *J Struct Biol* 163(3):229–234
43. Tampieri A, Sprio S, Sandri M, Valentini F (2011) Mimicking natural bio-mineralization processes: a new tool for osteochondral scaffold development. *Trends Biotechnol* 29(10):526–535
44. Tampieri A, Celotti G, Landi E, Sandri M, Roveri N, Falini G (2003) Biologically inspired synthesis of bone-like composite: self-assembled collagen fibers/hydroxyapatite nanocrystals. *J Biomed Mater Res Part A* 67(2):618–625
45. Sprio S, Sandri M, Panseri S, Cunha C, Tampieri A (2012) Hybrid scaffolds for tissue regeneration: chemotaxis and physical confinement as sources of biomimesis. *J Nanomater* 2012:1
46. Tampieri A, Sandri M, Landi E, Pressato D, Francioli S, Quarto R, Martin I (2008) Design of graded biomimetic osteochondral composite scaffolds. *Biomaterials* 29(26):3539–3546
47. Kon E, Delcogliano M, Filardo G, Fini M, Giavaresi G, Francioli S, Martin I, Pressato D, Arcangeli E, Quarto R, Sandri M, Marcacci M (2010) Orderly osteochondral regeneration in a sheep model using a novel nano-composite multilayered biomaterial. *J Orthop Res* 28(1):116–124
48. Dini L, Abbro L (2005) Bioeffects of moderate-intensity static magnetic fields on cell cultures. *Micron* 36(3):195–217
49. Bock N, Riminucci A, Dionigi C, Russo A, Tampieri A, Landi E, Goranov VA, Marcacci M, Dediu V (2010) A novel route in bone tissue engineering: magnetic biomimetic scaffolds. *Acta Biomater* 6(3):786–796
50. Tampieri A, Iafisco M, Sandri M, Panseri S, Cunha C, Sprio S, Savini E, Uhlarz M, Herrmannsdörfer T (2014) Magnetic bioinspired hybrid nanostructured collagen–hydroxyapatite scaffolds supporting cell proliferation and tuning regenerative process. *ACS Appl Mater Interfaces* 6(18):15697–15707
51. Sprio S, Tampieri A, Celotti G, Landi E (2009) Development of hydroxyapatite/calcium silicate composites addressed to the design of load-bearing bone scaffolds. *J Mech Behav Biomed Mater* 2(2):147–155

52. Rambo CR, Sieber H (2005) Novel synthetic route to biomorphic Al<sub>2</sub>O<sub>3</sub> ceramics. *Adv Mater* 17(8):1088–1091
53. Rambo CR, Cao J, Rusina O, Sieber H (2005) Manufacturing of biomorphic (Si, Ti, Zr)-carbide ceramics by sol–gel processing. *Carbon* 43(6):1174–1183
54. de Arellano-López AR, Martínez-Fernández J, González P, Domínguez C, Fernández-Quero V, Singh M (2004) Biomorphous SiC: a new engineering ceramic material. *Int J Appl Ceram Technol* 1(1):56–67
55. Tampieri A, Sprio S, Ruffini A, Celotti G, Lesci IG, Roveri N (2009) From wood to bone: multi-step process to convert wood hierarchical structures into biomimetic hydroxyapatite scaffolds for bone tissue engineering. *J Mater Chem* 19(28):4973–4980
56. Ruffini A, Sprio S, Tampieri A (2013) Study of the hydrothermal transformation of wood-derived calcium carbonate into 3D hierarchically organized hydroxyapatite. *Chem Eng J* 217:150–158

# Cationic and Anionic Substitutions in Hydroxyapatite

# 7

Ilaria Cacciotti

## Contents

Introduction .....	146
Biological Apatites .....	148
Hydroxyapatite Structure .....	149
Synthetic Substituted Hydroxyapatites .....	151
Cationic Vicarious Ions Substitutions .....	152
Anionic Vicarious Ions Substitutions .....	173
Summary .....	185
References .....	188

## Abstract

Hydroxyapatite (HAp,  $\text{Ca}_{10}(\text{PO}_4)_6(\text{OH})_2$ , Ca/P = 1.67) is widely employed in biomedical sector, particularly in dentistry and orthopedics, due to its chemical similarity to the mineral component of hard tissue.

However, the biological apatite, whose bone and tooth mineral phases are composed, remarkably differs from stoichiometric HAp, being Ca deficient (Ca/P < 1.67), composed of small crystals and characterized by poor crystallinity and relatively high solubility. Furthermore, it consists in carbonated apatite characterized by the presence of various amounts of vicarious ions, either incorporated within the apatite lattice or just adsorbed on the crystal surface, including anionic (e.g.,  $\text{F}^-$ ,  $\text{Cl}^-$ ,  $\text{SiO}_4^{4-}$ , and  $\text{CO}_3^{2-}$ ) and/or cationic substitutions (e.g.,  $\text{Na}^+$ ,  $\text{Mg}^{2+}$ ,  $\text{K}^+$ ,  $\text{Sr}^{2+}$ ,  $\text{Zn}^{2+}$ ,  $\text{Ba}^{2+}$ ,  $\text{Al}^{3+}$ ).

Thus, the synthesis of hydroxyapatites partially substituted by these elements has attracted a lot of interest, in order to mimic and resemble the chemical

I. Cacciotti (✉)

Engineering Department, University of Rome “Niccolò Cusano”, Rome, Italy

Italian Interuniversity Consortium on Materials Science and Technology (INSTM), Rome, Italy

e-mail: [ilaria.cacciotti@unicusano.it](mailto:ilaria.cacciotti@unicusano.it)

composition of the bone mineral component. In fact, the ability to exchange ions in apatite structure allows to design, develop, and characterize new and better calcium phosphates for certain specific applications.

This manuscript provides an overview about the majority of the investigated substitutions within the hydroxyapatite lattice, evidencing the influence of the different vicarious ions on the physical, microstructural, mechanical, and biological properties of the obtained HAp. In detail, after an introduction about the biological apatites and the stoichiometric hydroxyapatite structure, this chapter reports the synthesis and features of anionic and cationic substituted hydroxyapatites with an outline of the most important findings. Finally, the last session presents some considerations, concluding remarks, and future developments.

### Keywords

Biological apatite, substituted hydroxyapatite • Anionic ions • Cationic ions • Magnesium • Strontium • Zinc • Silver • Carbonate • Fluoride • Chloride • Silicate • Biological role • Microstructure • Mechanical properties • In vitro bioactivity • Antimicrobial properties • Cytotoxicity • Bone cell response

## Introduction

Calcium phosphates, particularly hydroxyapatite (HAp,  $\text{Ca}_{10}(\text{PO}_4)_6(\text{OH})_2$ , Ca/P 1.67), present a wide range of applications, especially in dentistry and orthopedics, as dental fillers, coatings for titanium dental implants, and bone substitutes for bone reconstruction and regeneration, due to their chemical similarity to the mineral component of hard tissue.

However, the mineral phase of the bone and teeth is erroneously assimilated to stoichiometric hydroxyapatite [1–3]. Indeed, biological apatites remarkably differ from stoichiometric HAp, being Ca deficient (Ca/P < 1.67), composed of small crystals (50 nm × 25 nm with an average thickness of about 4 nm for bone crystals [4]) and characterized by poor crystallinity and relatively high solubility, due to the low degree of crystallinity and the small crystal sizes. Moreover, they consist in carbonated apatites, characterized by the presence of various amounts of vicarious ions, either incorporated within the apatite lattice or just adsorbed on the crystal surface, including anionic (e.g.,  $\text{F}^-$ ,  $\text{Cl}^-$ ,  $\text{SiO}_4^{4-}$ , and  $\text{CO}_3^{2-}$ ) and/or cationic substitutions (e.g.,  $\text{Na}^+$ ,  $\text{Mg}^{2+}$ ,  $\text{K}^+$ ,  $\text{Sr}^{2+}$ ,  $\text{Zn}^{2+}$ ,  $\text{Ba}^{2+}$ ,  $\text{Al}^{3+}$ ) [3, 5, 6]. In fact, calcium phosphates nucleation and growth in biological systems occur in an environment rich in ions, influencing both the crystallization kinetics and thermodynamics and, consequently, their stability [7].

As reported in Table 1, the mineral phases of the bone, enamel, and dentin show slightly different ionic compositions and lattice parameters [3, 8–14].

The current trend is, therefore, to obtain calcium phosphate bioceramics partially substituted by these elements in order to mimic the chemical composition of the bone mineral component, allowing the ability to exchange ions in apatite structure to design, develop, and characterize new and better calcium phosphates for certain specific applications.



**Table 1** Chemical composition and lattice parameters of the mineral component of the bone, enamel and dentine, compared to stoichiometric HAp [3, 8–14]

Element	Bone	Enamel	Dentine	Stoichiometric HAp
<b>Calcium (Ca)</b>	34.80–36.6 wt%	36.50–37.60 wt%	40.30 wt%	39.60 wt%
<b>Phosphorous (P)</b>	15.20–17.10 wt%	17.70–18.30 wt%	18.60 wt%	18.50 wt%
<b>Carbonate (CO<sub>3</sub>)</b>	4.80–7.40 wt%	3.00–3.50 wt%	4.80 wt%	
<b>Sodium (Na)</b>	0.90–1.00 wt%	0.50–0.70 wt%	0.10 wt%	
<b>Potassium (K)</b>	0.03–0.07 wt%	0.05–0.08 wt%	0.07 wt%	
<b>Magnesium (Mg)</b>	0.60–0.72 wt%	0.20–0.44 wt%	1.10 wt%	
<b>Strontium (Sr)</b>	0.00–0.05 wt%	0.03 wt%	0.04 wt%	
<b>Zinc (Zn)</b>	0.00–39.00 ppm	263 ppm	173 ppm	
<b>Barium (Ba)</b>		125 ppm	129 ppm	
<b>Iron (Fe)</b>		118 ppm	93 ppm	
<b>Aluminum (Al)</b>		86 ppm	69 ppm	
<b>Silver (Ag)</b>		0.60 pm	2 ppm	
<b>Cobalt (Co)</b>	0–0.025 ppm	0.10 ppm	1 ppm	
<b>Manganese (Mn)</b>	0–0.17 ppm	0.60 ppm	0.60 ppm	
<b>Gold (Au)</b>		0.10 ppm	0.07 ppm	
<b>Antimony (Sb)</b>		1.00 ppm	0.70 ppm	
<b>Chlorine (Cl)</b>	0.10–0.13 wt%	0.30–0.40 wt%	0.27 wt%	
<b>Fluorine (F)</b>	0.03–0.10 wt%	0.01 wt%	0.07 wt%	
<b>Silicon (Si)</b>	0–500 pm			
<b>Chromium (Cr)</b>	0.00–0.33 ppm	1.00 ppm	2.00 ppm	
<b>Bromide (Br)</b>		34 ppm	114 ppm	
<b>Pyrophosphate (P<sub>2</sub>O<sub>7</sub>)</b>	0.07	0.022	0.10	
<b>Lattice parameters</b>				
<b>a-Axis</b>	9.410/9.49	9.441	9.421	9.430/9.432/ 9.422
<b>c-Axis</b>	6.890/6.880	6.882/6.880	6.887	6.891/6.881/ 6.880

In fact, hydroxyapatite crystal structure can accommodate substitutions by various other ions for the Ca<sup>2+</sup>, PO<sub>4</sub><sup>3-</sup>, and OH<sup>-</sup> groups [15], these ionic substitutions affecting the HAp lattice parameters, crystal morphology, crystallinity, solubility, and thermal stability. In particular, the vicarious ion incorporation within apatite lattice influences the apatite dissolution rate, remarkably enhancing the proliferation of human osteoblast-like cells in vitro and consequently encouraging osseointegration.

To resemble the mineral component of the bone, various substitutions, both cationic (substituting for the calcium) and anionic (substituting for the phosphate or hydroxyl groups), have been tried and tested, with consequent modifications of the chemical, physical, and biological properties, as demonstrated in in vitro and in vivo tests.

On the basis of the considerations given above, this chapter reports a review about the majority of the attempted substitutions within the hydroxyapatite lattice, including both anionic and cationic ions. In order to achieve this purpose, the manuscript is organized into four sections: in the first section, a brief introduction about the chemical composition of biological apatites is reported; in the second section, the structure of stoichiometric hydroxyapatite is shortly described; in the third section, an overview about the synthesis processes and the chemical, physical, microstructural, and biological properties of cationic and anionic substituted hydroxyapatites is reported; and in the fourth section, final considerations and remarks are summarized.

## Biological Apatites

Biological apatite is an inorganic calcium phosphate salt in apatite form and is the main inorganic component of biological hard tissues such as bones and teeth of vertebrates, being distributed in the organic constituents with certain sequence and direction [16].

As already evidenced, the biological apatite consists in a calcium phosphate characterized by the presence of several vicarious ions within the apatite lattice in the  $\text{Ca}^{2+}$ ,  $\text{PO}_4^{3-}$ , and  $\text{OH}^-$  sites, presenting its lattice several crystallographic sites where many different elements with different ionic charges can be accommodated, substituting the three main components (Fig. 1) [15].

In fact, to indicate the chemical composition of bioapatite, several crystallochemical formulas have been proposed, such as  $\text{M}_{10}(\text{XO}_4)_6\text{Y}_2$  (M: Ca, Sr, Ba, Pb, etc.; X: P, As, Si, etc.; Y: various anions, e.g.,  $\text{OH}^-$ ,  $\text{F}^-$ ,  $\text{Cl}^-$ , or other groups) [3],  $(\text{Ca}, \text{Na}, \text{Mg}, \text{K}, \text{Sr}, \text{Pb})_{10}(\text{PO}_4, \text{CO}_3, \text{SO}_4)_6(\text{OH}, \text{F}, \text{Cl}, \text{CO}_3)_2$  [17], and  $\text{Ca}_{8.3}\square_{1.7}(\text{PO}_4)_{4.3}(\text{HPO}_4 \text{ and } \text{CO}_3)_{1.7}(\text{OH} \text{ and } 0.5\text{CO}_3)_{0.3}\square_{1.7}$  (where  $\square$  is a vacancy) [6].

In particular, these vicarious ions are subdivided in minor groups and elements (e.g.,  $\text{CO}_3^{2-}$ ,  $\text{HPO}_4^{2-}$ ,  $\text{Na}^+$ ,  $\text{Mg}^{2+}$ ) and in trace elements (e.g.,  $\text{Sr}^{2+}$ ,  $\text{K}^+$ ,  $\text{Cl}^-$ , and  $\text{F}^-$ ), among which some at ppm level [17]. They play pivotal roles in numerous biochemical reactions strictly related to the bone metabolism.

It has to be taken into account that the chemical composition of apatite in the bone can be varied (Table 1) [18], and, furthermore, it can change with age, as investigated by Handschin and Stern [19].

The identified vicarious ions in bone and tooth apatites are  $\text{F}^-$ ,  $\text{Cl}^-$ ,  $\text{Na}^+$ ,  $\text{K}^+$ ,  $\text{Fe}^{2+}$ ,  $\text{Zn}^{2+}$ ,  $\text{Sr}^{2+}$ ,  $\text{Mg}^{2+}$ , citrate, and carbonate, in different weight percentages due to structural limits that determine their maximum content within the crystal structure. As expected, these impurities in biological apatite of bones and teeth introduce significant stresses into the crystal structure, making it less stable and more reactive.

In particular, the two main vicarious ions are carbonate and magnesium that are present in high concentrations in the bone and dentin, leading to their higher solubility and lower crystallinity (smaller crystal size) with respect to the enamel, characterized by lower  $\text{CO}_3^{2-}$  and  $\text{Mg}^{2+}$  amounts (Table 1).

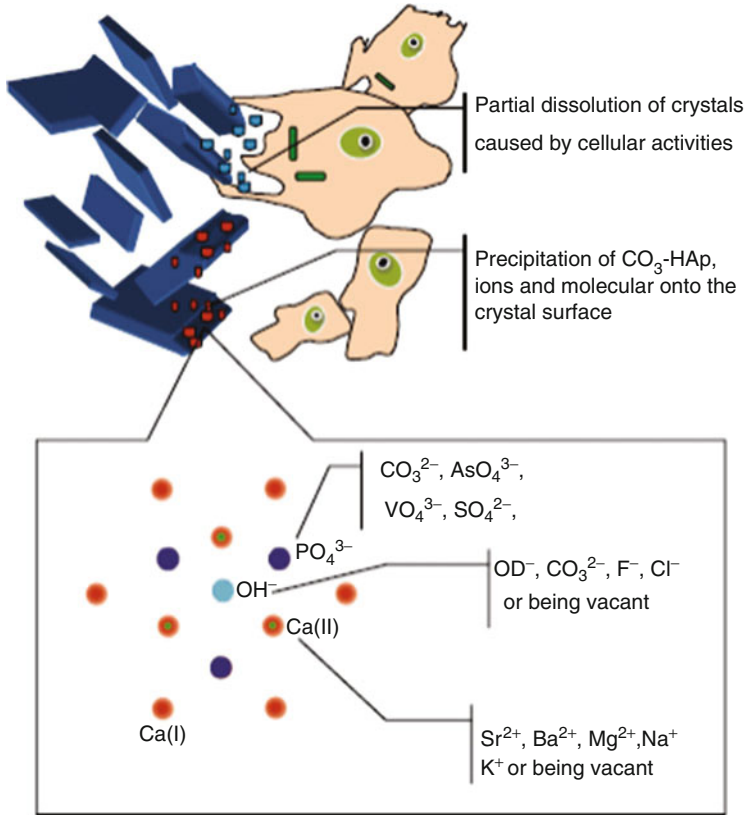


**Fig. 1** Schematic drawing of partial dissolution/precipitation of biological apatites in vivo and ionic substitutions in the crystal of HAp (Reproduced from Ref. [15] with permission)

The particular behavior of biological apatites has to be ascribed to their hallmarks, such as very small crystals, consequently high solubility, low crystallinity, nonstoichiometric composition, inner crystalline disorder, and the presence of foreign ions in the crystal lattice (Fig. 2) [20].

Biological apatites have been used as bone substitutes in oral implantology, periodontology, oral and maxillofacial surgery, and orthopedics [21, 22], being involved in the CaPs dissolution and precipitation processes, as well as the absorption and formation of bones, dentine, and cementum in vivo [23].

## Hydroxyapatite Structure

Two different crystal forms have been reported for HAp: (a) hexagonal with the lattice parameters  $a = b = 9.432 \text{ \AA}$ ,  $c = 6.881 \text{ \AA}$ , and  $\gamma = 120^\circ$  [24], and (b) monoclinic with the lattice parameters  $a = 9.421 \text{ \AA}$ ,  $b = 2a$ ,  $c = 6.881 \text{ \AA}$ ,

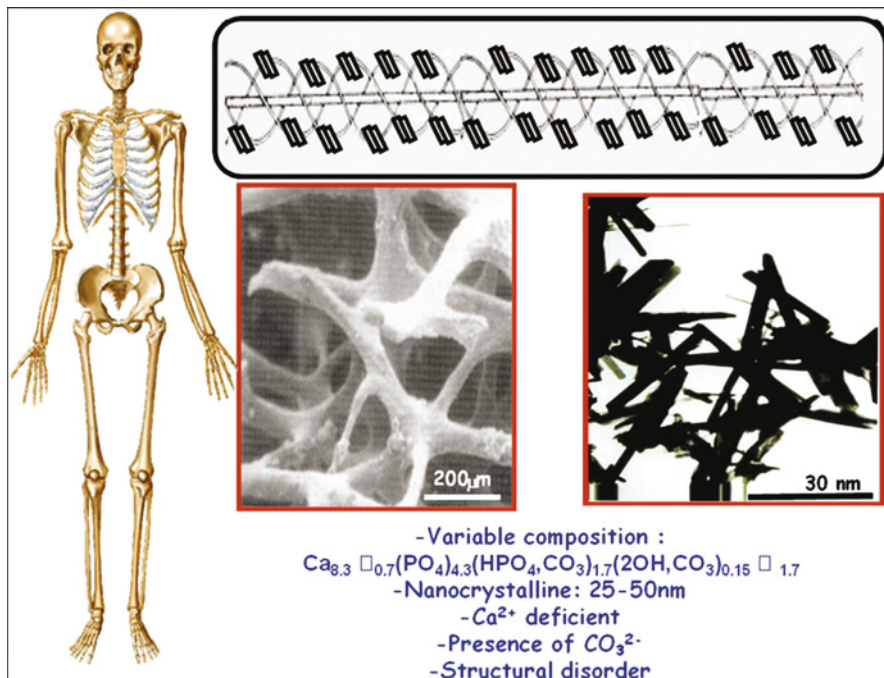


**Fig. 2** *Top*: Schematic drawing of carbonated HAp nanocrystals reinforcing the triple helix of collagen. *Middle*: Scanning electron microscopy (SEM) micrograph of cancellous bone and transmission electron microscopy (TEM) image of carbonated HAp nanocrystals. *Bottom*: Main features of biological apatites (Reproduced from Ref. [20] with permission)

and  $\gamma = 120^\circ$  [25]. These two forms share the same elements, with a stoichiometric Ca/P ratio of 1.67, mainly differing for the orientation of hydroxyl groups. In detail, in the case of hexagonal HAp, two adjacent hydroxyl groups point at the reverse direction, whereas in the case of monoclinic HAp, hydroxyl groups have the same direction in the same column and an opposite direction among columns [26].

In the case of hexagonal structure with the space group P63/m and two formula units per cell (each with 44 atoms and a Ca/P ratio of 1.67), it is possible to identify four different types of crystallographic positions in the apatite unit cell [27, 28] and two sites for calcium ions, i.e., Ca(I) and Ca(II): Ca(I) is called as the columnar Ca, and Ca(II) the screw axis Ca (Fig. 3a [29]). The screw axis Ca makes the calcium triangle and then the calcium tunnel, where the OH<sup>-</sup> ions locate (Fig. 3b, c [30, 31]). Based on this structural configuration, the OH<sup>-</sup> ions can be easily substituted by F<sup>-</sup> ions, and, in the case of tooth enamel, the OH<sup>-</sup> ions are easily released by acid attack with consequent tooth decay.

Concerning the coordination and local atomic structures, four Ca<sup>2+</sup> per unit cell (Ca(I)) are in columns parallel to the *c*-axis (Fig. 3d [31]) and are surrounded by nine oxygen atoms belonging to six PO<sub>4</sub><sup>3-</sup> tetrahedra. In detail, Ca(I) site is coordinated to six oxygen ions of the PO<sub>4</sub><sup>3-</sup> groups at the first nearest neighboring (NN) sites,

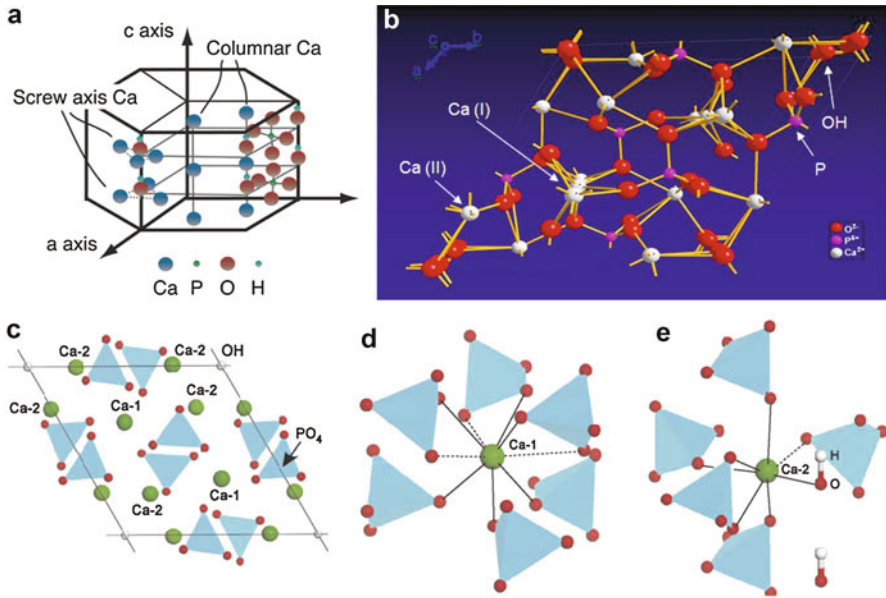


**Fig. 3** Hydroxyapatite crystal structure: (a) columnar Ca site (Ca(I)) and the screw axis Ca (Ca(II)); (b) calcium triangle and tunnel; (c) hydroxyapatite lattice viewed along the *c*-axis; (d and e) coordination and local atomic structures around Ca(I) site (d) and Ca(II) site (e) in perfect HAp (the first NN oxygen ions are linked to Ca by solid lines, while the second NN oxygen ions are linked by dashed lines) (Adapted from Ref. [29] (a), [30] (b), [31] (c-e) with permission)

whereas further three oxygen ions are located at the second NN sites. Furthermore, six Ca<sup>2+</sup> per unit cell (Ca(II)) are seven-coordinated with five PO<sub>4</sub><sup>3-</sup> groups and the hydroxide ion (Fig. 3e [31]), forming two equilateral triangles along the *c*-axis at  $z = 1/4$  and  $3/4$  (i.e., anion channel), commonly occupied by two monovalent anions (e.g., OH<sup>-</sup>, F<sup>-</sup>, Cl<sup>-</sup>) but, in some cases, also by bivalent CO<sub>3</sub><sup>2-</sup>, per unit cell. Specifically, for Ca(II) site, six oxygen ions of the PO<sub>4</sub><sup>3-</sup> groups are located at the first NN sites (belonging one of these oxygen ions to the OH<sup>-</sup> group), while a further one oxygen ion is placed at the second NN site [31]. The structure is completed by six PO<sub>4</sub><sup>3-</sup> anions, where each P atom is coordinated to four oxygen atoms.

## Synthetic Substituted Hydroxyapatites

As well known, hydroxyapatite lattice allows to accept compositional variations in its three sublattices, being able to host vicarious ions for the Ca<sup>2+</sup>, PO<sub>4</sub><sup>3-</sup>, and OH<sup>-</sup> groups [15, 32].

In fact, it has been reported that hydroxyapatite can accommodate almost half of the elements of the periodic system within its lattice [33], due to high flexibility of its structure. Specifically, cationic substitutions occur in the sites normally occupied by

$\text{Ca}^{2+}$ , including both bivalent (e.g.,  $\text{Sr}^{2+}$ ,  $\text{Ba}^{2+}$ ,  $\text{Mg}^{2+}$ , etc.) and monovalent cations (e.g.,  $\text{Na}^+$ ,  $\text{K}^+$ , etc.).

Anionic substitutions can either occur in the phosphate or hydroxyl positions. For example,  $\text{F}^-$  and  $\text{Cl}^-$  ions substitute for  $\text{OH}^-$ ;  $\text{CO}_3^{2-}$  can substitute for both  $\text{PO}_4^{3-}$  and  $\text{OH}^-$ ; P could be also substituted by C, As, V, S, etc.; and hydroxyl groups may be also replaced by left vacant [32].

As expected, the incorporation of vicarious ions within the HAp lattice causes structural changes, affecting the crystal structure, the crystallinity, the surface charge, the solubility, and other fundamental properties, leading to important changes in its biological performance. In fact, the presence of foreign ions has shown to play significant effects on thermal stability, solubility, osteoclastic and osteoblastic response in vitro, and degradation and bone regeneration in vivo, also in very small amounts.

Regarding the modification of the HAp surface structure and electrical charge by ionic substitutions, it has to be considered that in the case of difference in valency of the vicarious ions, a charge imbalance is necessary in order to respect the neutrality. The neutrality can be maintained either by the formation of supplementary vacancies [34] or by the occurrence of simultaneous substitutions of cations and anions without the formation of any vacancy or loss of charge balance [35, 36]. Thus, imbalances in the charges of the substituting ion can cause disorder within the HAp crystal structure, with consequent remarkable influence on its properties and biological performances.

Taking into account that, on the basis of the biomimetic approach, a biomaterial should resemble as closely as possible the host tissue, in terms of both architecture and chemical compositions, the optimal calcium phosphate for biomedical application should consist of apatite characterized by nonstoichiometric composition, small dimensions, low crystallinity, and the presence of vicarious ions. Thus, significant research has been carried out on substituted apatites.

## Cationic Vicarious Ions Substitutions

Vicarious cations are able to replace  $\text{Ca}^{2+}$  ions, causing a lattice alteration, in terms of contraction or expansion of the lattice parameters, on the basis of the vicarious ion diameter. Even if it is expected that bigger cations modify cell volume, leading to a lattice expansion accompanied by higher values of  $a$ -axis parameter, this does not always occur, such as in the case of monovalent cation substitution for bivalent cations. In fact, in the case of substitutions with bivalent ions (e.g.,  $\text{Mg}^{2+}$ ,  $\text{Zn}^{2+}$ ,  $\text{Sr}^{2+}$ ), no charge imbalance occurs within the apatite lattice, whereas in the case of substitutions with monovalent ions (e.g.,  $\text{Na}^+$  and  $\text{K}^+$ ), a charge imbalance is necessary in order to respect the neutrality. As already evidenced, in order to maintain the neutrality, either the formation of supplementary vacancies [34] or the occurrence of simultaneous substitutions of cations and anions without the formation of any vacancy or loss of charge balance has been observed [36].

Moreover, the accommodation of substituting cations either in the site Ca(I) or in the site Ca(II) within the apatite lattice is strongly correlated to their ionic radius [37]: a cation with a larger radius than  $\text{Ca}^{2+}$  one tends to occupy site (II), site Ca (II) being bigger in volume than site Ca(I) [38]. Furthermore, the anion presence in the channel also influences the cation distribution between the two sites Ca(I) and Ca (II), due to the ions' charge and the strength of the corresponding bonds.

The synthesis of substituted hydroxyapatite is usually carried out following the typical processes employed for that of the undoped material, such as precipitation and titration [39], sol-gel process, hydrothermal method, mechanochemical method, etc.

## Magnesium Substitution

### Biological Role of Magnesium

Among substituting cations, magnesium is widely studied, being the fourth most abundant cation in the human body. In fact,  $\text{Mg}^{2+}$  vicarious ions are typically present in a content of 0.44 wt%, 1.23 wt%, and 0.73 wt% in the natural enamel, dentin, and bone, respectively [9]. However, their amount is around 10 mol% (2 wt%) in the cartilage and bone tissue during the osteogenesis initial phases, tending to disappear in the mature tissue [40]. The progressive lowering of  $\text{Mg}^{2+}$  concentration, which is very high in the apatite phase at the beginning of remodeling, during the calcification process, is a clear sign of its involvement in the bone remodeling process [40].

Magnesium is believed to play a role in the formation of dental caries, urinary calculi, and bone deposition and mineralization [41], directly stimulating osteoblast proliferation [42]. It has been demonstrated that magnesium deficiency is directly correlated with osteoporosis, negatively influencing all skeletal metabolism stages, with consequent inhibition of bone growth, decreased osteoblastic and osteoclastic activities, osteopenia, and bone fragility [43, 44].

### Synthesis of Mg-Substituted HAP

Mg-substituted hydroxyapatites (Mg-HAPs) have been synthesized with a magnesium concentration up to 10 mol% [42, 45, 46], by precipitation method [45–61] (at room temperature [51, 55, 58, 59], in a temperature range of 40–60 °C [45, 46, 50, 52, 54] or at ~100 °C [53]), by sol-gel process [62–64], by a combination of melting and extrusion routes with the use of a melted 99.9 % pure Mg ingot [65], by surfactant-assisted microwave synthesis [66], by wet mixing [67], and by mechanochemical-hydrothermal route [42].

Even if it had been reported that maximum Mg substitution is just 1 wt% in order to retain the desired stoichiometry and phase purity using a precipitation route [40, 48], Bigi et al. [68] produced hydroxyapatite substituted with 7.5 wt% magnesium.

### Influence of $\text{Mg}^{2+}$ Substitution on Chemical, Physical, and Microstructural Properties of HAP

Regarding the precise collocation of  $\text{Mg}^{2+}$  ions within apatite lattice and the influence on the reticular parameters, different and discordant considerations have been reported.

It was demonstrated by Rietveld structure refinements, on the ground of the different metal–oxygen interactions and the different geometries of the two distinct metal sites in the apatite structure, that magnesium is essentially accommodated in Ca(II) site, as corroborated by multinucleated solid-state nuclear magnetic resonance (NMR) and X-ray absorption spectroscopy investigations [51].

On the other hand, Ren et al. [53] identified Ca(I) site in the HAp lattice as the energetically favored site for Mg substitution, on the basis of a computational study using *ab initio* generalized gradient approximation density functional theory. Their conclusion was supported by Tampieri et al. [50] who proved that the Ca(I) position is preferential for Mg substitution.

Concerning the reticular parameters, they are remarkably modified by  $\text{Mg}^{2+}$  incorporation which leads to a strong distortion of the HAp lattice. It has been reported that  $\text{Mg}^{2+}$  introduction within apatite lattice causes a reduction in the *c*-axis dimension [40, 48, 51, 54, 59, 69], due to the remarkably smaller  $\text{Mg}^{2+}$  radius (0.069 nm) than  $\text{Ca}^{2+}$  radius (0.099 nm) [69], whereas, according to Ren et al. [53], both reticular parameters, *a* and *c*, decrease with Mg amount, and, according to Farzadi et al. [55], a slight increase of lattice parameter *a* has been recorded in the case of Mg-HAp.

These discrepancies can be explained by strong dependency of the lattice parameters on the preparation method: different methodologies for the HAp synthesis could result in different hydration levels and further other defects.

Additionally,  $\text{Mg}^{2+}$  presence within HAp lattice sensibly affects its crystallization and thermal stability, inhibiting apatite crystallization, reducing crystal size, destabilizing the hydroxyapatite structure, and enhancing the solubility [40, 48, 51, 68], due to the lattice distortion as a substitution consequence. The inhibitory effect on crystallization and improved solubility result in a reduction of the thermal stability and in the promotion of the thermal conversion into Mg-substituted  $\beta$ -tricalcium phosphate ( $\beta\text{-Ca}_{3-x}\text{Mg}_x(\text{PO}_4)_2$ ) [47, 54, 61]. Besides, the incorporation of  $\text{Mg}^{2+}$  stabilizes the  $\beta$ -TCP phase, increasing its transition temperature to  $\alpha$ -TCP above 1125 °C [54, 70]. Thus, biphasic calcium phosphates (BCP) are usually produced, and the obtained materials are considered promising substitutes for bone replacement [71].

It has been also demonstrated that Mg presence strongly influences the HAp surface hydration state, retaining Mg-HAp more water at their surface than pure HAp, at the level of  $\text{H}_2\text{O}$  both coordinated to cations and adsorbed in the form of multilayers, as demonstrated by means of near-infrared (NIR) and medium-infrared (MIR) spectroscopic data [58].

Furthermore, the lattice modification obviously influences material sinterability. In particular, Cacciotti et al. [54] investigated the sintering behavior of Mg-HAps with different Mg amounts (i.e., 0.6–2.4 wt%), evidencing a displacement of their maximum sintering rate temperatures to higher values compared to pure HAp. Moreover, a higher total shrinkage was recovered and lower final densities were obtained, due to a more relevant residual porosity, whose amount increased with the Mg content.

Concerning the mechanical properties, Mg incorporation significantly decrements compressive strength and microhardness up to a Mg content of 1.8 wt%



[67] and causes an increment of the fracture toughness with Mg amount up to 0.6 wt%, content very close to the magnesium concentration in the natural bone mineral component. These experimental evidences were ascribed to the decremented average grain size, the increased microporosity, and the formation of a weak intergranular boundary [61, 67].

Thus, the monitoring of  $Mg^{2+}$  amount incorporation results in tailored crystallinity, solubility, and morphology of the synthesized nanocrystals [42].

### **Influence of $Mg^{2+}$ Substitution on Biological Properties of HAp**

The introduction of magnesium ions into HAp structure has shown to exercise a positive biological effect and to improve the osseointegrational properties of the material [72], due to the material enhanced solubility and biodegradability in physiological fluids as a consequence of the lattice modification [42, 45, 50, 68].

Comparing the effects of various cationic substitutions of HAp in *in vitro* tests, Mg-HAp showed the highest ion release into the culture medium and the highest relative cell density, together with Zn-HAp, even if the most cell apoptosis was also recorded on Mg-HAp, despite the good cell viability [73].

Landi et al. [45] obtained a hydroxyapatite similar to biological apatite in terms of composition, morphology, and crystallinity, using a Mg amount of 5.7 mol% with respect to Ca. No genotoxicity, carcinogenicity, and cytotoxicity were revealed in *in vivo* tests. Moreover, implanting Mg-HAp granules into New Zealand white rabbits, it was verified there was no *in vivo* skin irritation–sensitization and the granules resorption was enhanced with respect to pure HAp, due to the higher Mg-HAp solubility [45].

Besides, improved biocompatibility was found in the case of Mg-HAp coatings deposited on titanium substrates by electrolytic deposition [74], due to their smaller crystal size and larger specific surface, particularly at high Mg concentration (i.e., 2 wt%).

## **Strontium Substitution**

### **Biological Role of Strontium**

Strontium is a microelement present in the mineral phase of the bone and particularly in the high metabolic turnover regions [75, 76]. It is well known that this element plays a relevant role in the mineralization of bone tissue and dental caries [77], being able to induce the bone tissue formation and the inhibition of its resorption, even in small amounts.

In fact, strontium is considered as one of the most effective substances for the relief of bone pains and for bone cancer [76, 78] and osteoporosis [79] treatments, being able to exercise dual effects of stimulating osteoblast differentiation and inhibiting osteoclast activity and bone resorption [80].

For these reasons, strontium in the form of strontium ranelate has been widely used as an osteoporosis treatment, allowing *in vitro* to increase the osteoblast proliferation and activity and to decrease the osteoclast differentiation

[81–84]. Accordingly, *in vivo* studies have shown that strontium ranelate is able to promote bone formation and limit/inhibit bone resorption [82, 85].

Furthermore, strontium has demonstrated to own antibacterial properties. For example, the antibacterial activity of glass-ionomer cements was primarily ascribed to the Sr presence [86], even if Brauer et al. stated that the antibacterial action of strontium is really very poor and that its antibacterial potential in the tooth decay treatment can be improved by the combination with fluoride [87].

### Synthesis of Sr-Substituted HAp

Many works report on the substitution of  $\text{Sr}^{2+}$  ions for  $\text{Ca}^{2+}$  ions within the hydroxyapatite structure [88–91], taking into account that  $\text{Ca}^{2+}$  ion may be completely replaced with  $\text{Sr}^{2+}$  due to their similar properties and atomic radii.

Strontium-doped hydroxyapatite (Sr-HAp), with Sr concentration up to 50 mol%, has been synthesized by sol–gel process [64, 92, 93], precipitation [49, 88, 94–97], and hydrothermal method [98]. For the production of Sr-HAp coatings, micro-arc treatment [99], pulsed laser deposition [100], laser ablation [101], and biomimetic synthesis [102–104] have been employed.

### Influence of $\text{Sr}^{2+}$ Substitution on Chemical, Physical, and Microstructural Properties of HAp

Even if many authors suggested that Ca(II) site is the preferred site for strontium substitution [93, 95, 96, 105, 106], on the basis of precise structural refinements [88], it has been demonstrated that Sr atoms occupy both Ca(I) and Ca(II) sites of the apatite lattice, being favored the substitution at Ca(II) site for high doping concentrations and, on the contrary, the substitution at Ca(I) site for low doping concentrations (1.0–3.5 at%) [88, 107]. In fact, for high Sr content, the occupancy of site Ca(II) is preferential, due to the higher Sr ionic radius (0.113 nm) [88].

Moreover, as expected, the presence of  $\text{Sr}^{2+}$  into HAp crystal structure influences the lattice parameters and strongly affects crystal size and crystallinity. Indeed, both the *a*-axis and the *c*-axis linearly increase with Sr amount [88, 93–95, 108–111], and low amounts of Sr substitution lead to decreased crystal size and crystallinity, whereas at higher levels, these effects are contained [88, 95].

However, in the case of low Sr amounts (e.g., 0.3 mol% and 1.5 mol%), the presence of strontium does not influence the thermal decomposition and the crystalline phases of hydroxyapatite, obtaining comparable X-ray diffraction (XRD) patterns [96], whereas for higher strontium contents (e.g., 4 mol%), after calcination at 900 °C, the formation of additional  $\beta$ -TCP is detected, increasing its intensity with Sr amount (up to 8 mol%) [94].

Mardziah et al. [92] and Kavitha et al. [108] reported that Sr incorporation seems to stabilize the HAp phase at high temperatures. For instance, Sr-HAp powders with a Sr doping concentration of 2 mol% started to decompose with the formation of  $\beta$ -TCP as secondary phase after calcination at 900 °C, whereas  $\beta$ -TCP phase appeared in undoped powders at lower temperatures (below 800 °C) [92]. Moreover, higher Sr concentrations (up to 15 mol%) further stabilized the HAp phase, avoiding the decomposition at high temperatures and the  $\beta$ -TCP phase formation [92].

This experimental evidence could be justified with the lattice rearrangement due to larger Sr atoms with consequent relieving of the internal strains which might delay the primary particle growth and phase transformation during calcination [92, 108]. In fact, the TCP formation during thermal treatments is ascribed to the hydroxyl group decomposition in HAp.

It has also been proved that Sr incorporation influences the HAp mechanical performances: Sr-HAp (Sr content of 1.15 mol%) porous materials presented compressive strength of  $4.52 \pm 1.40$  MPa, which is within the range of the natural bone [97]. Accordingly, Kim et al. [94] demonstrated a slight increase in Vickers hardness from 5.2 to 5.5 GPa for Sr-HAp (Sr content of 8 mol%) with respect to pure HAp.

### **Influence of Sr<sup>2+</sup> Substitution on Biological Properties of HAp**

The presence of strontium ions within the hydroxyapatite lattice has shown to improve its biocompatibility and bioactivity, promoting osseointegration process, also due to the increased solubility [110–114], as a consequence of the crystal structure destabilization due to the larger Sr ionic radius [112].

Many researchers reported that Sr-HAp promotes osteoblast proliferation, enhancing ALP activity, collagen type I production and osteocalcin presence [100, 111, 115], and that it is able to reduce the number and activity of osteoclasts with respect to undoped HAp [100].

On the ground of in vitro investigation carried out using osteoblast-like MG63 cells and human osteoclasts [109], it has been concluded that the bone cell behavior is Sr<sup>2+</sup> ion dose-dependent: Sr amounts in the range 3–7 at% strongly stimulate osteoblast activity and differentiation and 1 at% of Sr doping results sufficient to inhibit osteoclast proliferation.

Lin et al. underlined that Sr-HAp with Sr content of 3.22 mol% showed the best proliferation, osteogenic differentiation, and angiogenic factor expression of human osteoblast-like MG63 cells [98]. Dos Santos Tavares et al. investigated different contents of Sr (0.5–5.0 %at) and evidenced that the analyzed amounts did not influence dehydrogenase activity, membrane integrity, or DNA content [116]. Moreover, Chung and Long [99] stated that coatings with a Sr concentration higher than 38.90 at% remarkably inhibit RAW264.7 osteoclast differentiation.

As a further demonstration of beneficial biological activity of strontium, an increased bonding strength in the case of Sr-HAp-based bone cement with respect to the traditional PMMA-based bone cement ( $3.36 \pm 1.84$  MPa vs  $1.23 \pm 0.73$  MPa) was revealed, observing new bone on the Sr-HAp cement surface and, on the contrary, a fibrous tissue encapsulating the PMMA cement [115].

Furthermore, many antimicrobial studies have been also performed, demonstrating the antibacterial activity of sol–gel–supercritical fluid drying method (SCFD)-derived Sr-HAp against *Escherichia coli* (*E. coli*), *Staphylococcus aureus* (*S. aureus*), and *Lactobacillus* [117] and the bactericidal effect of microwave method-derived Sr-HAp towards *E. coli* and *S. aureus* [118].

On the basis of all the collected results, it is possible to conclude that Sr-HAps can be considered as promising systems for the treatment of defects within osteoporotic bone, even if in vivo trials are obviously mandatory for a real clinical application.

## Zinc Substitution

### Biological Role of Zinc

Zinc is an essential microelement present in the active centers of more than 300 enzymes involved in the bone metabolism. It is able to increase enzyme activity and DNA synthesis [119] and also displays antibacterial activity, following the same mechanism of copper ions.

Zinc can be found in all biological tissues, being mostly present in the bone [120]. This cation plays pivotal roles in numerous biological functions, e.g., enzymatic activity, nucleic acid metabolism, protein synthesis, preservation of the structures and functions of the membranes and hormonal activity, and the normal growth and development of the skeletal system. Indeed, its deficiency is associated with a decrease in bone density [121], this ion being able to inhibit osteoclast differentiation and to promote osteoblast activity [122].

Some experiments with zinc sulfate were carried out in order to investigate and comprehend the underlying mechanism. On the basis of these studies, it has been shown that in the presence of zinc, alkaline phosphatase (ALP) levels increase. Additionally, the bone metabolism stimulation by Zn has been also demonstrated by *in vivo* experiments with zinc sulfate [123].

Concerning the *in vitro* action on osteoclasts, Kishi and Yamaguchi [124] reported that Zn hinders the osteoclast-like cell formation, while Moonga and Dempster [122] evidenced the strong inhibitory action of Zn on the osteoclastic bone resorption *in vitro* for zinc amounts as low as 10–14 M. Many studies have been performed in order to better and more deeply understand the mechanisms responsible for these inhibitory effects [125–127].

Owing to the key effect of  $\text{Zn}^{2+}$  cations in several metabolic processes, Zn incorporation within apatite lattice has been widely studied.

### Synthesis of Zn-Substituted HAp

Zinc-substituted hydroxyapatite (Zn-HAp) has been produced by precipitation [49, 128–138] (at room temperature [128–130, 134] or in the temperature range of 60–90 °C [131–133, 138]), ion exchange [139], hydrothermal technique at 200 °C [140], and sol–gel process [63, 141–143].

It was verified that  $\text{Zn}^{2+}$  substitution within HAp lattice is more difficult by hydrothermal method than by precipitation and that the progressive Zn substitution in HAp leads from Zn-substituted apatite to an amorphous apatite-like phase for high Zn concentrations [133].

### Influence of $\text{Zn}^{2+}$ Substitution on Chemical, Physical, and Microstructural Properties of HAp

Significant amounts of Zn can be incorporated within HAp lattice [133, 134], the substitution limit being 15 mol% according to [133] and 25 mol% according to [134].

However, there is no clear evidence of the maximum level of Zn substitution within apatite lattice. Generally, considering the level of zinc substitution, it has to be considered that the used nominal amount does not always correspond to the actual one [140]. For instance, starting from a nominal Zn concentration of 5 wt%, Zn-HAp powder with an actual Zn amount of 0.7 wt% was obtained, on the basis of energy-dispersive spectroscopy (EDS) data [136].

Moreover, Li et al. [140] observed that the synthesis conditions strongly affect the amount of Zn incorporated into HAp structure. In particular, it is influenced by the kind of base used to maintain constant the synthesis pH. In fact, synthesizing Zn-HAp starting from an aqueous solutions of calcium nitrate, zinc nitrate, and ammonium phosphate and using ammonia to maintain constant the pH, the actual substitution content of zinc was less than half that expected, whereas using sodium hydroxide to monitor the pH, the actual Zn amount was remarkably higher.

Analogously and consequently, the used base also affects the crystallinity degree, resulting in higher use of NaOH [140], the crystallinity being also influenced by the Zn dopant amount.

Regarding the effect of zinc substitution on the HAp lattice structure, there are many conflicting reports [136, 137, 144].

By combining experimental and spectroscopic results with density functional theory calculations, Tang et al. [131] demonstrated that substitution in the Ca (II) position is more energetically favored, in agreement with several reports [131, 145–151], even if this has not been experimentally verified yet. It has been also suggested that Zn substitution is favored for Ca(II) site at the HAp (0001) surface [149]. Furthermore some authors affirmed that Zn is octahedrally coordinated [145, 149], whereas Tang et al. [131] stated that it is tetrahedrally coordinated, in good agreement with Matsunaga [146].

Concerning the lattice parameters, the lattice parameter  $c$  of Zn-HAp progressively decreases with Zn content [133], owing to the difference in ionic radius between  $\text{Zn}^{2+}$  (0.074 nm) and  $\text{Ca}^{2+}$  (0.099 nm). On the other hand, the lattice parameter  $a$  tends to decrease with Zn content up to 10 mol% Zn, while this parameter begins to increase for Zn higher concentrations [138, 140, 144].

As already underlined, Zn plays an inhibiting effect on HAp crystallization and favors the  $\beta$ -TCP phase, acting in the same manner as magnesium [134, 152]. The thermal stability as well as the crystallinity of the apatite decrease significantly with increasing Zn concentration.

Some XRD studies evidenced that there was the formation of  $\alpha$ -zinc tricalcium phosphate phase after calcination at 1050 °C, in the case of Zn amount higher than 0.13 wt% [137].

In the case of very high Zn content, i.e., 20 mol% (12.39 wt%), the obtained hydroxyapatite was not stoichiometric, as demonstrated by X-ray fluorescence (XRF), and some impurity phases were detected by XRD, mainly CaO, even if scanning electron and transmission microscopies did not evidence the presence of zinc or zinc-containing compound onto the surface of the apatite crystals [144].

### **Influence of Zn<sup>2+</sup> Substitution on Biological Properties of HAp**

The biological properties of Zn-HAp have not been deeply and appropriately investigated yet.

However, it has been reported that small amounts of Zn ions within HAp lattice are actively involved in cell growth and differentiation, even if the underlying mechanism has not been clearly understood and explained yet. The presence of Zn within the apatite lattice is able to enhance its biological responsiveness [136], directly promoting osteoblastic proliferation and inhibiting the bone resorption by osteoclasts.

In fact, Zn-HAps with Zn ion amounts less than 1.2 wt% present effective bioactivity and antibacterial properties [128, 129, 153–157]. In detail, Ito et al. demonstrated an increase in osteoblast response, with enhanced mouse osteoblast-like cell proliferation in vitro, for Zn amounts up to 1.2 wt%, whereas for higher Zn contents, cytotoxicity was revealed [129].

The inhibitory action of Zn-HAps on the growth of bacteria and fungi, including *E. coli*, *S. aureus*, *Candida albicans* (*C. albicans*), and *Streptococcus mutans* (*S. mutans*), was also demonstrated [141, 142, 153, 158], a zinc content more than 1000 ppm being necessary to exhibit an antimicrobial effect.

Considering these outstanding properties, Zn-HAps were used as coatings of dental implants in order to promote tooth remineralization, allowing to reduce bacterial adherence and the tartar development, having verified their efficiency to inhibit the growth of the three most common oral pathogens, i.e., *Aggregatibacter actinomycetemcomitans*, *Fusobacterium nucleatum*, and *S. mutans* [159].

Moreover, Zn-HAps were used as carriers for the controlled release of ciprofloxacin, which exhibits antibacterial activity against *S. aureus* and *Pseudomonas aeruginosa* (*P. aeruginosa*), the most common pathogens causing bone and joint diseases. It was demonstrated that the ciprofloxacin release by the hydroxyapatite takes place in connection with the zinc ion release, increasing the antibacterial activity with the drug concentration and the number of used Zn<sup>2+</sup> ions [160]. Furthermore, the ciprofloxacin release from Zn-HAp is higher than that released from the undoped HAp. Thus Zn HAp based coatings can be seen as a rising solution in the treatment of bone tissue infections, allowing for the shortening and increasing of the efficiency of the therapy and for the reduction of the ciprofloxacin dose with consequent limitation of the resistant strain formation.

On the basis of the carried out studies, it is possible to conclude that Zn-HAp can be considered a promising material for potential applications in the repair of osteoporotic bone, combining antibacterial effects, osteoconductivity, and the capability of inhibiting osteoclast activity.

## **Silver Substitution**

### **Biological Role of Silver**

Silver (Ag) owns biocompatibility, high thermal stability, and nontoxicity towards human cells at low concentrations [161, 162].

It plays beneficial effects in the case of burn wound treatment [163]; shows strong antibacterial properties [164] against both gram-positive and gram-negative bacteria, viruses, and fungi [165, 166]; and is widely used to limit the microorganism growth in several fields, including medicine (e.g., orthopedic field, dentistry, urology (for urinary tract infections and catheters), dermatology (for the treatment of flash burns, etc.) [167–170]).

Among all the antibacterial metals, silver presents the highest efficiency at concentrations as low as 35 ppb (concentration at which there is no toxic effect on mammalian cells [171, 172]), and microorganisms are not able to develop immunity towards this metal.

The action mechanism of silver on microbial cells has not completely understood and explained yet, but it depends on its form [173]. In the case of silver ions, this action is mainly based on the ions' interaction with thiol groups (SH) of proteins, leading to the formation of S-Ag bonding [174]. In this manner, proteins located in the cell membrane and within the cytoplasm are inactivated. Simultaneously, several modifications take place in the bacteria cells, such as dysfunction of the respiratory chain and of membrane pumps, cell membrane shrinkage, and leaking out of cell contents, due to the denaturing action of silver ions [173, 175]. Furthermore,  $\text{Ag}^+$  ions are also able to interact with DNA molecules with consequent loss of capacity to replicate [173] and to promote the production of reactive oxygen species (ROS) which can irreversibly damage bacteria causing the death [176, 177] (Fig. 4a).

On the other hand, considering silver nanoparticles, the induction of the ROS formation is considered as the main mechanism of action: the interaction between ROS and the cell wall and cell membrane of bacteria leads to their depressurization

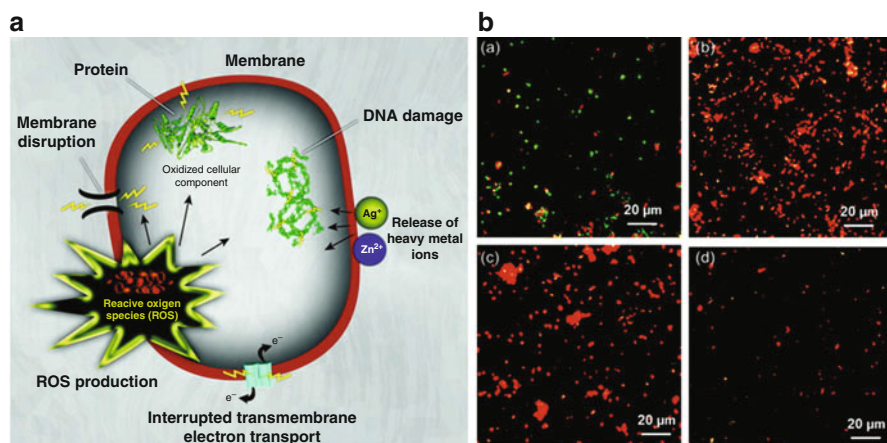


**Fig. 4** (a) Mechanisms of toxicity of nanoparticles (NPs) and metallic ions (e.g., silver and zinc) against bacteria; (b) live/dead confocal images of bacteria after 24 h of culture: (a) HAp; (b) HAp/2Ag; (c) HAp/4Ag; (d) HAp/6Ag (dead bacteria appear red, live bacteria appear green) (Adapted from Refs. [15], [208] with permission)

and to an increased permeability, with consequent leaking out of cell content and, thus, cell death [178–180].

The higher activity of  $\text{Ag}^+$  against  $\text{G}^-$  (e.g., *E. coli*) with respect to  $\text{G}^+$  bacteria (e.g., *S. aureus*) [173, 175] can be ascribed to the peptidoglycan layer of gram-positive bacteria which may protect the bacterial cell from the invasion of  $\text{Ag}^+$  ions.

### Synthesis of Ag-Substituted HAp

Silver-substituted hydroxyapatites (Ag-HAps) have been synthesized using different amounts of silver in the range 0.1–10.0 wt%, following several methods: (i) precipitation route [161, 181, 182], starting either from salt precursors [183–191] or acids as well as bases and oxides [192]; (ii) sol–gel process [141, 162, 193–196]; (iii) ion exchange between pure hydroxyapatite and a silver salt solution [161, 185, 197–199]; (iv) ultrasonic spray pyrolysis (USSP) [200]; (v) microwave method [161, 201]; (vi) combustion synthesis [202]; and (vii) co-sputtering process [203].

The synthesized materials can be submitted to either drying in an oven or freeze-drying, obtaining powders with different crystallinity degrees and specific surface areas and, consequently, different efficiencies of the antibacterial activity.

### Influence of $\text{Ag}^+$ Substitution on Chemical, Physical, and Microstructural Properties of HAp

It has been reported that precipitated powders are composed of needlelike nanometric particles with a length of 60–70 nm and a width of 15–20 nm [161, 192].

By FT-IR and XRD analyses, it was demonstrated that  $\text{Ag}^+$  ions substitute for  $\text{Ca}^{2+}$  ions within the apatite lattice [141, 161, 181, 186, 187, 189, 199, 204–206]. Indeed, the effective  $\text{Ag}^+$  incorporation within apatite lattice was testified by the identification of CaO, whose formation was ascribed to the oxidation of the free  $\text{Ca}^{2+}$  ions, available in consequence of  $\text{Ag}^+$  substitution for  $\text{Ca}^{2+}$  within apatite lattice, during the thermal treatments [141]. Yang et al. reported the formation of silver orthophosphate [199], and Sygnatowicz et al. [162] detected silver phosphate phases and metallic silver, whose presence was also identified by Diaz et al. [196] who synthesized Ag-HAp by a colloidal chemical route and a subsequent treatment in  $\text{H}_2/\text{Ar}$  atmosphere at 350 °C with consequent reduction of the  $\text{Ag}^+$  cations to elemental silver.

In particular, it has been reported that  $\text{Ag}^+$  ions substitution takes place for  $\text{Ca}^{2+}$  preferentially in Ca(I) site of HAp, leading to an increase in the lattice parameters [161, 187, 189, 192, 206], due to the bigger  $\text{Ag}^+$  ionic radius (0.128 nm vs 0.099 nm).

Furthermore, Ag incorporation causes both an increased solubility and a decremented thermal stability of the produced apatite [161, 182, 192]. For example, Ag-HAps characterized by Ag contents less than 4 at% were stable up to 700 °C, whereas thermal decomposition was revealed at low temperatures for higher Ag contents [161]. Moreover, an increased hydrophilicity was evidenced by the measurements of reduced contact angles, due to the substitution of  $\text{Ag}^+$  for  $\text{Ca}^{2+}$  with consequent charge imbalance [193].



### Influence of Ag<sup>+</sup> Substitution on Biological Properties of HAp

Concerning the biological responsiveness of Ag-HAps, it is fundamental to identify the optimal silver amount and the proper conditions of synthesis and successive drying and heat treatments in order to obtain a perfect balance and compromise between the effective antimicrobial activity and cytotoxicity.

In fact, powders with different crystallinity degrees and specific surface areas consequently show different efficiencies of their antibacterial activity. It is well known that the rate and extent of ion release from the HAp strongly depend on its specific surface area, finer crystals exhibiting faster and higher release. For example, freeze-drying allows to obtain smaller crystals with enhanced antibacterial activity [183], whereas a slower Ag<sup>+</sup> ion release and a prolonged antibacterial activity were detected in the case of powders synthesized by USSP [200].

It has been verified that Ag-HAps show antibacterial action towards bacteria, viruses, and fungi, playing a more efficient bactericidal role on gram-negative bacteria rather than gram-positive bacteria, owing to the different structures of their cell walls [181, 186, 193, 205]. Moreover, Ag-calcium phosphates have shown an antimicrobial activity comparable to that of an antibiotic treatment [204].

In particular, it was demonstrated that the addition of 100 ppm Ag<sup>+</sup> ions to sol-gel precursor-calcined HAp coatings on Ti-6Al-4 V supports was able to inhibit the *S. mutans* growth, and the Ag<sup>+</sup> ion addition up to 10,000 ppm induced an apparent inhibition zone [141]. Chen et al. performed an in vitro bacterial adhesion test, observing a significantly lower number of *Staphylococcus epidermidis* (*S. epidermidis*) and *S. aureus* on Ag-HAp (2.05 ± 0.55 wt% Ag) surface than on titanium (Ti) and HAp surfaces [203].

Furthermore, it has been demonstrated that a silver content of 0.2 wt% in Ag-HAp effectively inhibits the growth of *Klebsiella pneumoniae* (*K. pneumoniae*) and *Candida krusei* (*C. krusei*), whereas a silver content of 0.5 wt% is necessary against *E. coli* and *B. subtilis* [201] and a silver content of 1 wt% against *S. aureus* and *S. epidermidis* [207].

The efficacy of the Ag-HAp coatings on titanium substrates against *P. aeruginosa* adhesion and colonization was investigated and demonstrated by live/dead fluorescence staining [208] (Fig. 4b). From the comparison between the acquired confocal images (green and red indicate live and dead bacteria, respectively), it is evident that after 24 h of exposure, large number of live bacteria was observed on pure HAp coatings (Fig. 4b, a), whereas on 2 wt% Ag HAp (HAp/2Ag) coatings, the majority of single or colonized bacteria was found dead (Fig. 4b, b). In the case of 4 wt% Ag-doped HAp (HAp/4Ag) samples, fewer adhered bacteria were found and the detected ones were predominantly dead (Fig. 4b, c). Finally very few single or colonized bacteria adhered on the 6 wt% Ag-doped HAp (HAp/6Ag) coatings, and among them, live bacteria were very limited (Fig. 4b, d)

Two possible underlying mechanisms for the antibacterial action of Ag-HAp have been proposed [178–180, 183, 209, 210]: (i) the direct interaction between the bacterial cell membrane and silver ions due to an attraction of the microorganisms towards the surface of the hydroxyapatite by electrostatic forces and (ii) the bactericidal activity of the slowly released silver ions from the hydroxyapatite [181,

209]. In both cases, cell death occurs as a consequence of remarkable and significant morphological changes, as supported by AFM investigation [161].

Moreover, it has to be taken into account that excessive silver content within hydroxyapatite may be toxic, not only towards microorganisms but also towards mammalian tissues, and may lead to the inhibition of their growth and development and to their death in the case of too high  $\text{Ag}^+$  amounts [190, 207, 208], toxic silver concentrations being in the range 1–3  $\mu\text{g}/\text{ml}$  [191]. Thus, it is fundamental to select the silver doping amount in order to effectively kill microorganisms, without adversely influencing the mammalian tissue condition.

For example, Chen et al. did not reveal significant difference in terms of in vitro cytotoxicity between pure HAp and Ag-HAp, for Ag doping amounts of  $2.05 \pm 0.55$  wt% Ag [203].

Additionally, in vitro toxicity studies on human osteoblasts [207, 208, 211, 212], human stem cells [190], and mouse fibroblasts [213] were carried out. On the basis of in vitro studies on human stem cells, it was possible to conclude that HAp containing 0.3 wt% Ag does not play negative action on cell growth up to 7 days of culture, whereas 0.7 wt% Ag slightly inhibits their growth and 8.3 wt% Ag plays a remarkable cytotoxic effect, specifically in the case of human stem cells [190]. Concerning the in vitro experiments on human osteoblasts, Ag amounts of 2 wt% and 4 wt% represent a good balance and compromise between effective antimicrobial and cytotoxic activity [208, 211] (Fig. 4), while Ag content of 6 wt% significantly inhibits osteoblast growth, sometimes causing their death [208].

Finally, some in vitro studies were carried out for evaluating the potential application of Ag-HAps for bone repair, evidencing a comparable behavior between Ag-doped (Ag content of 1 wt%) and Ag-undoped HAps in terms of osteoblast precursor cell proliferation and differentiation and demonstrating that Ag incorporation does not induce a reduction in osteoconductivity [193].

## Potassium and Sodium Substitutions

### Biological Role of Potassium and Sodium

Potassium (K) is able to influence the biomineralization process [214] and the apatite mineral nucleation process [215].

Sodium (Na) is present as an abundant trace element in the natural bone and tooth mineral and is involved in cell adhesion and in bone metabolism and resorption process [216, 217].

### Synthesis of K-Substituted HAp and Na-Substituted HAp

Potassium-substituted hydroxyapatites (K-HAps) have been prepared by soaking HAp in potassium carbonate and potassium chloride solutions up to 8 weeks, obtaining  $\text{K}^+$  substitution for  $\text{Ca}^{2+}$  in 2 weeks [218], and by molten salt synthesis [219].

Sodium-substituted hydroxyapatites (Na-HAps) have been mainly synthesized by low-temperature processes with the formation of single-phase apatite [34, 38,

220]. Additionally, Kannan et al. [221] prepared sodium-substituted biphasic mixtures of various HA/ $\beta$ -TCP ratios through precipitation at 90 °C.

### **Influence of K<sup>+</sup> and Na<sup>+</sup> Substitutions on Chemical, Physical, and Microstructural Properties of HAp**

It has been reported that K<sup>+</sup> ions can be incorporated within apatite lattice without inducing significant changes in the structural parameters [218, 222, 223]. However, Kannan et al. [223] revealed a contraction in the *a*-axis and irregular changes in the *c*-axis in the case of K-HAps. These experimental evidences were ascribed to the formation of vacancies in the channel, as a consequence of the substitution of a monovalent cation (i.e., K<sup>+</sup>) for a bivalent cation (i.e., Ca<sup>2+</sup>), leading to a decrease of the channel diameter and, thus, of the *a*-axis parameter.

Even if it would be expected that site Ca(II) is favored for the K<sup>+</sup> occupation, due to the bigger K<sup>+</sup> ionic radius (i.e., 0.133 nm), the reverse was experimentally revealed [222]: 83 % of the K atoms were located in site (I) and 17 % in site (II).

More interestingly, potassium incorporation within apatite lattice can improve its thermal stability until 1300 °C [223], allowing treatments at very high temperatures without HAp decomposition, in order to produce structures for biomedical applications, such as porous and/or granulated materials for bone surgery.

Finally, Weissmueller et al. [219] observed that bovine serum albumin (BSA) adsorption decreased with higher K<sup>+</sup> content in the obtained spheroidal K-HAps, influencing the ionic substitutions within the apatite lattice the protein adsorption properties.

Concerning Na-HAp, it has been demonstrated that Ca(II) site of the apatite lattice represents the preferential and more favored site for Na<sup>+</sup> substitution [38]. A slight increase in the *c*-axis parameter and consequent increment in cell volume were detected with respect to pure HAp, even if no significant modifications of the crystal structure are commonly induced. It has been proved that Na<sup>+</sup> ions can be substituted for Ca<sup>2+</sup> ions into the apatite structure with supplementary vacancies [34, 38, 220, 224] or, more frequently, with Ca sites co-substituted by other anions and cations.

Furthermore, Na<sup>+</sup> incorporation within HAp lattice leads to increased thermal stability and delays the allotropic transformation of  $\beta$ -TCP to  $\alpha$ -TCP until 1200 °C [221].

## **Titanium Substitution**

### **Biological Role of Titanium**

Titanium dioxide (TiO<sub>2</sub>) has attracted a lot of attention, due to its photocatalytic properties [225, 226], being possible to exploit its photooxidative activity on organic materials, including proteins and lipids, and due to Ti(IV) antibacterial properties.

### **Synthesis of Ti-Substituted HAp**

Titanium-substituted HAp (Ti-HAp) particles with varied amounts of Ti<sup>4+</sup> ions (e.g., 0.8 and 1.6 wt% [227]) have been prepared by coprecipitation method [227–231] and by sol–gel process [64].

### **Influence of Ti<sup>4+</sup> Substitution on Chemical, Physical, and Microstructural Properties of HAp**

By Rietveld refinement analysis, it was demonstrated that Ti incorporation within apatite lattice induces a proportional increase in both *a*-axis and *c*-axis with Ti amount.

This result is in disagreement with the hypothesis that Ti<sup>4+</sup> substitutes for Ca<sup>2+</sup>, since a decrease in the unit cell parameter would be expected, due to the smaller Ti<sup>4+</sup> ionic radius (i.e., 0.0605 nm) compared to Ca<sup>2+</sup> ionic radius. In fact, Wakamura [229] proved that Ti<sup>4+</sup> in hydroxyapatite forms divalent cations, i.e., [Ti(OH)<sub>2</sub>]<sup>2+</sup> and [TiHPO<sub>4</sub>]<sup>2+</sup>, which replace calcium cations.

Furthermore, Ti incorporation into apatite structure inhibits grain growth, decreasing the grain size with Ti concentration.

### **Influence of Ti<sup>4+</sup> Substitution on Biological Properties of HAp**

Wakamura et al. [228] investigated the bactericidal action of Ti-HAp and demonstrated its photocatalytic activity for decomposing acetaldehyde and albumin under ultraviolet (UV) irradiation. Moreover, Kandori et al. [231] reported that heat-treated Ti-HAp particles with a Ti molar ratio of 0.10–0.15 are appropriate for decomposing pathogenic proteins in a blood-purified therapy under UV irradiation.

## **Manganese Substitution**

### **Biological Role of Manganese**

Manganese (Mn) affects bone remodeling and Mn deficit causes a reduction in organic matrix synthesis and delays endochondral osteogenesis [232].

Moreover, it is well known that divalent manganese ion (i.e., Mn<sup>2+</sup>) is involved in the activation of integrins, a family of receptors which mediate cellular interactions with extracellular matrix and cell-surface ligands. It has been demonstrated that Mn<sup>2+</sup> ions are able to increase the ligand affinity of integrin, thus promoting cell adhesion [233, 234].

### **Synthesis of Mn-Substituted HAp**

Hydroxyapatites substituted with small Mn amounts (Mn-HAps) (Mn amount up to 2 wt%) have been usually obtained by precipitation from aqueous solutions [232–236].

### **Influence of Mn<sup>2+</sup> Substitution on Chemical, Physical, and Microstructural Properties of HAp**

As expected, Mn<sup>2+</sup> substitutes for Ca<sup>2+</sup> in HAp lattice [236]. Consequently, Mn<sup>2+</sup> strongly influences the apatite thermal stability, favoring the complete transformation of HAp in β-TCP after thermal treatment at 1100 °C [237]. The lattice parameters of the obtained β-TCP decrease with increasing Mn<sup>2+</sup> content. Furthermore, Mn<sup>2+</sup> ion incorporation within apatite lattice affects the bioactivity of the produced material, reducing/inhibiting the apatite layer deposition in simulated body fluid (SBF) solution [103, 232, 234].

### **Influence of Mn<sup>2+</sup> Substitution on Biological Properties of HAP**

Li et al. [236] performed in vitro tests with osteoblasts on Mn-substituted hydroxyapatites, demonstrating no cytotoxicity, on the basis of extraction assay results.

Mn-HAP coatings deposited on titanium supports exhibited a remarkably beneficial effect on bone cells, and it has been proved that a relatively high Mn<sup>2+</sup> doping concentration promotes the osteocalcin production, resulting in higher than that produced in the case of Sr-HAP [103]. Similarly, Mn-doped carbonated hydroxyapatite coatings on Ti substrates were able to support human osteoblast differentiation, proliferation and metabolism activation [238].

## **Iron Substitution**

### **Biological Role of Iron**

Torell [239] carried out experiments with iron salt-based coatings on hamsters' teeth and evidenced that iron ions, even in small amounts, tend to precipitate on the enamel surface as thin acid-resistant coatings, containing gels and crystals of hydrous iron oxides, when they are into the mouth. It has been also reported that iron compounds are able to promote the nucleation of apatites, adsorbing salivary calcium and phosphate ions, and, thus, to favor the replacement of minerals, which have been dissolved during the acid phases of the caries process.

Moreover, the well-known magnetic properties of iron allow its use in several biomedical applications.

### **Synthesis of Fe-Substituted HAP**

Fe<sup>2+</sup>-substituted HAPs (Fe-HAPs) have been commonly produced by coprecipitation in an aqueous solution with different concentrations of Fe<sup>2+</sup> [236, 240–242]. Pon-On et al. [243] and Kandori et al. [244] synthesized Fe<sup>3+</sup>-substituted HAPs by microwave process and coprecipitation, respectively.

### **Influence of Fe<sup>2+</sup>/Fe<sup>3+</sup> Substitution on Chemical, Physical, and Microstructural Properties of HAP**

As expected, the presence of Fe<sup>2+</sup> ions, with a smaller radius (0.0835 nm) compared to that of Ca<sup>2+</sup>, affects the lattice parameters, decreasing the *c*-axis and increasing the *a*-axis [241].

Additionally, to maintain the charge balance, the vacancies of Ca positions in the lattice increased with the increase of Fe concentration (Ca<sub>10-x</sub>Fe<sub>x</sub>(PO<sub>4</sub>)<sub>6</sub>(OH)<sub>2-x</sub>□<sub>x</sub>, where □ is a vacancy and *x* = Fe amount) [236]. An elongation of the mean particle length was observed in the case of Fe<sup>3+</sup>-HAP compared to pure HAP [244].

Moreover, the presence of iron decreases the crystallinity and results in superparamagnetic character with 10 % and 50 % of Fe<sup>2+</sup> concentration and a weak ferromagnetic character with 30 % Fe<sup>2+</sup> concentration [241].

### **Influence of Fe<sup>2+</sup>/Fe<sup>3+</sup> Substitution on Biological Properties of HAP**

The biocompatibility of Fe<sup>2+</sup>-substituted HAP powders has been demonstrated by Wu et al. [240] and by Li et al. [236] through in vitro tests with osteoblasts.

Furthermore, Fe<sup>3+</sup>-HAp showed better and greater adsorption behavior towards bovine serum albumin (BSA), i.e., a 2.7-fold increase compared to pure HAp [244]. This experimental evidence was ascribed to both the morphological differences between Fe<sup>3+</sup>-HAp and pure HAp and the production of surface hydroxo ions (e.g., Fe(OH)<sup>2+</sup> or Fe(OH)<sup>2-</sup>), necessary to induce a hydrogen bond between the Fe-HAp and BSA molecules. In fact, mean particle length and surface hydrophilicity are pivotal factors for BSA adsorption [244].

Due to their magnetic properties, affected by several factors, including microstructure, anisotropy, and orientation, iron-doped HAp can be exploited for biomedical applications, such as drug targeting and bioseparation, including cell sorting [245].

For example, Fe-HAp can find applications as a heating mediator in hyperthermia therapy for cancer [245] and have also been tested in vivo by injecting a mixture of mixed Fe-HAp particles with phosphate buffer solution (PBS) around a cancer. A significant reduction in tumor volume was revealed in a 2-week observation period, after injection of Fe-HAp and treatment inside the magnetic field to achieve hyperthermia [246].

## Lanthanides Substitution

### Biological Role of Lanthanides

As well known, lanthanides are characterized by high bioactivity and ability to substitute calcium ions in structured molecules [9, 247, 248]. Owing to their narrow emission bands and long emission lifetime, lanthanides have been widely employed as contrast agents for magnetic resonance imaging and as luminescent probes for biosensors in several in vivo imaging applications [247, 248].

Among the rare-earth elements belonging to lanthanide family, cerium and europium are present in the human body, being able to accumulate, from the environment, in small amounts in the bones and liver [249]. However, up to date, their biological role has not been systematically investigated yet and is not clearly known, even if some studies have evidenced that cerium salts may stimulate metabolism [249].

Cerium shows a behavior comparable to that of calcium in organisms, being characterized by similar electronegativity and ionic radius (0.107 nm and 0.099 nm for Ce<sup>3+</sup> and Ca<sup>2+</sup>, respectively); thus, Ce<sup>3+</sup> ions can substitute for Ca<sup>2+</sup> ions. It can accumulate in small amounts in bones and Ce-containing compounds can stimulate the metabolism in organisms. Furthermore, it has been highlighted that Ce<sup>3+</sup> cations possess antibacterial properties [250].

In recent studies focalized on the biological properties of the cerium oxide (CeO<sub>2</sub>), it has been demonstrated that CeO<sub>2</sub> is able to induce angiogenesis through its direct effect on the oxygen modulation in intracellular environments [251] and to act on human monocytes [252], due to its ability to scavenge ROS. Additionally, its antibacterial activity against strains of *E. coli*, *B. subtilis*, *Salmonella typhimurium* (*S. typhimurium*), and *Enterococcus faecalis* (*E. faecalis*) was investigated [253, 254].

Another important rare-earth element for biomedical applications is samarium (Sm) that can be considered a good candidate for different radiation therapies used for cancer treatments [255–257].

Furthermore,  $^{153}\text{Sm}$  emits  $\beta$  rays with a small tissue penetration (0.8 mm), being more than 99 % of  $^{153}\text{Sm}$  bound to the hydroxyapatite in vivo [258].

### Synthesis of Ln-Substituted HAp

Five different lanthanide dopings in HAp (Ln-HAp) have been attempted, using light rare-earth ions ( $\text{Ln}^{3+}$ ) (i.e., lanthanum ( $\text{La}^{3+}$ ), cerium ( $\text{Ce}^{3+}$ ), praseodymium ( $\text{Pr}^{3+}$ ), neodymium ( $\text{Nd}^{3+}$ ), and samarium ( $\text{Sm}^{3+}$ )) with various Ln/(Ln + Ca) atomic ratios up to 0.15 [259].

Very recently,  $\text{La}^{3+}$ -,  $\text{Sm}^{3+}$ -,  $\text{Gd}^{3+}$ -,  $\text{Ho}^{3+}$ -,  $\text{Yb}^{3+}$ -, and  $\text{Lu}^{3+}$ -substituted HAp have been also obtained by ion exchange [260].

Cerium-substituted hydroxyapatites (Ce-HAp) have been synthesized by precipitation (Ce concentration, 5–20 at%) [261], by hydrothermal method with Ce content up to 10 wt% [262], by sol–gel–supercritical fluid drying (SCFD) method [263], and by sol–gel process (Ce concentration, 0.5–2.0 at%) [264].

Europium-substituted hydroxyapatites (Eu-HAp) can be obtained with a maximum Eu/(Eu + Ca) ratio of about 2 at% [265–268] in an alcoholic solution at physiological temperature [266, 267, 269] or in aqueous solutions [265, 270, 271].

Yttrium-doped hydroxyapatites (Y-HAp) have been synthesized by precipitation [72, 135] and hydrothermal treatment process [272, 273], and Ergun et al. [135] identified a solubility limit of yttrium in HAp greater than 7 mol%.

Samarium-substituted hydroxyapatites (Sm-HAp,  $\text{Ca}_{10-x}\text{Sm}_x(\text{PO}_4)_6(\text{OH})_2$ ,  $x = 0.01\text{--}0.1$ ) have been prepared by coprecipitation [248].

### Influence of $\text{Ln}^{3+}$ Substitutions on Chemical, Physical, and Microstructural Properties of HAp

The copresence of Ln-HAp and  $\text{LnPO}_4$  was observed for all the produced Ln-HAp systems at Ln atomic ratios  $>0.01\text{--}0.03$  [259].

The effective luminescent properties of Ln-doped HAp can be considered a sign of the occurred ionic substitution of  $\text{Ln}^{3+}$  ions into the apatite lattice. In fact, an absence of luminescence was observed when the lanthanide ions were only adsorbed on the surface, whereas Ln-HAp became luminescent after heating at 800 °C, due to the ion diffusion into the apatite lattice [274].

In particular,  $\text{Ce}^{3+}$  incorporation within the hydroxyapatite lattice induces the decrease of the crystal size to about 20 nm, a slight increase of lattice parameter  $c$ , the inhibition of the material crystallinity, and the morphological modification from rod-shaped HAp to needle-shaped Ce-HAp [261, 264].

Concerning Y-HAp, it has been evidenced that Y enhances the apatite mechanical properties with respect to pure HAp [72].

In the case of Sm-HAp, small variations of lattice constants and crystallite size were observed with increasing Sm amount, and a little influence on the particle morphology was evidenced [248].

### Influence of Ln<sup>3+</sup> Substitutions on Biological Properties of HAp

The obtained powders exhibited exceptional luminescence properties, and, thus, they could be employed for biological fluorescence labeling, their fluorescence being characterized by narrow emission bandwidths on the basis of the considered lanthanide ions (Ln<sup>3+</sup>), high photochemical stability, and long fluorescence lifetimes (up to several milliseconds) [265, 268].

Regarding Ce-HAps, Lin et al. [263] studied the antibacterial activity of these powders against *E. coli*, *S. aureus*, and *Lactobacillus* bacterial strains, revealing that the greater the Ce substitution degree for Ca, the higher the antibacterial capacity. Moreover, the good biocompatibility and osteoblastic cell responsiveness were assessed by in vitro tests on porous Ce-HAp coatings deposited on commercially pure titanium by micro-arc oxidation in an electrolytic solution containing calcium acetate,  $\beta$ -glycerol phosphate disodium salt pentahydrate ( $\beta$ -GP), and cerium nitrate [275].

In the case of Eu-HAps, their antibacterial activity was investigated against *S. aureus*, *E. coli*, *P. aeruginosa*, and *E. faecalis*, demonstrating their antibacterial action towards all the considered strains, except *E. coli*, even in the presence of low Eu<sup>3+</sup> amounts [271]. Furthermore, among the investigated Eu-HAps (Ca<sub>10-x</sub>Eu<sub>x</sub>(PO<sub>4</sub>)<sub>6</sub>(OH)<sub>2</sub>, 0 ≤ x<sub>Eu</sub> ≤ 0.2.), that with the highest Eu<sup>3+</sup> amount (i.e., 0.2) also exhibited fungicidal activity against *C. albicans*.

Concerning the Y-HAps, Liu et al. investigated their biological properties, highlighting an acceleration of the human periodontal fibroblast growth and a restriction of oral bacterial growth [273]. Moreover, Y<sup>3+</sup> ions had showed to be able to promote Saos-2 cell proliferation by methylthiazolyldiphenyl-tetrazolium (MTT) assay [276]. Accordingly, Webster et al. concluded that Y induces a greater osteoblast adhesion on bulk HAp doped with Y (up to 7 mol%) with respect to pure HAp [72]. For the displayed promising properties, Sato et al. proposed the application of Y-HAp for orthopedic applications, preparing Y-HAp-based coatings on titanium substrates by IonTite™ multistep processing and investigating their biological responsiveness [272]. They stated that the Y-HAp based coatings were characterized by a better osteoblast adhesion and promoted more calcium deposition by osteoblasts.

As far as Sm-HAps are concerned, their antibacterial properties have been demonstrated by tests against *E. faecalis* ATCC 29212 bacteria, observing that their inhibition increased with Sm content [248]. In addition, recent studies reported the use of <sup>153</sup>Sm-hydroxyapatite particles as radiation synovectomy agents for the treatment of chronic synovitis [277–279], especially knee synovitis [277, 278]. Moreover, <sup>153</sup>Sm-hydroxyapatite particles have to be considered as the best candidates for radiation synovectomy due to its shorter half-life and the lower extra-articular leakage of <sup>153</sup>Sm-hydroxyapatite [278].

Finally, a composite Eu-HAp/Ag powder was obtained by impregnating Eu-HAp with Ag<sup>+</sup> ions, which were subsequently reduced, in order to be used as an antimicrobial agent and fluorescent material for biodetection, due to its optical and bioactive properties [270].



## Gallium Substitution

### Biological Role of Gallium

Gallium presents several interesting biological properties and has shown efficacy in the treatment of many types of disorders [280].

$\text{Ga}^{3+}$  ions may replace  $\text{Fe}^{3+}$  ions in a wide range of metabolic reactions, owing to their similarity in terms of ionic radius, electronegativity, and coordination number. Moreover, its antibacterial activity is ascribed to the exchange of iron ions in protein metabolism [281, 282].

Exploiting its characteristics, gallium is commonly used in several applications and as a diagnostic and therapeutic agent in metabolic disorders of soft and hard tissues [280]. Particularly, gallium ions are clinically effective against bone resorption and for the treatment of osteoporosis and cancer-related hypercalcemias, being able to induce osteoblasts proliferation, promote bone formation, inhibit bone resorption, and thus reduce Ca concentration in plasma. These ions, usually in the form of their nitrate, increase the calcium and phosphorus content of the bone and have direct noncytotoxic effects on osteoclasts, decreasing acid secretion by osteoclasts and, thus, bone resorption [283]. Accordingly,  $\text{Ga}^{3+}$  ions are able to be easily and readily incorporated into the hydroxyapatite matrix protecting it from resorption and improving biomechanical properties of the skeletal system [283].

In addition, gallium ions exhibit immunomodulatory, antiproliferative, and anti-mitotic activities, and, therefore, they may be employed for the treatment of certain types of cancer [280].

### Synthesis of Ga-Substituted HAp

The synthesis of gallium-doped HAp (Ga-HAp) has been carried out by precipitation starting from gallium nitrate and sodium gallate solutions in order to obtain a dopant content up to 11.0 wt% [284].

### Influence of $\text{Ga}^{3+}$ Substitution on the Properties of HAp

It has been evidenced that  $\text{Ga}^{3+}$  does not substitute for  $\text{Ca}^{2+}$  as a result of heterovalent substitution, and, thus, no distortions in the apatite lattice occur.

The biological properties of the produced Ga-HAp have not been investigated yet. However, Ga-HAp could be used as orthopedic biomaterial for local applications aimed at stimulating bone growth.

## Copper Substitution

### Biological Role of Copper

Copper is an element involved in many metabolic processes, making it an essential micronutrient of almost all living organisms and presenting antibacterial properties, as testified by its antique use for the sterilization of drinking water and chest wounds [285].

The mechanism of the copper antibacterial activity has not been fully understood yet, but it should be ascribed to the Cu ability to form strong bonds with thiolic, imidazole, amine, and carboxylic groups of proteins, causing structural changes and increases in permeability and, hence, membrane transport dysfunction and cell death [153]. In addition, copper ions are able to damage the DNA and RNA, with consequent inhibition of the bacteria reproduction and/or their death [286], forming bonds with amine and amide groups, as well as with the disulfide bridges of bacteria proteins and enzymes.

The antibacterial properties of copper are also exploited by macrophages in order to improve their ability to inactivate microorganisms through the oxygen burst, on the basis of copper concentration [287]. Accordingly, copper deficiency decreases neutrophil and macrophage in vitro bactericidal activity [288]. However, several microorganisms, including *Mycobacterium tuberculosis* (*M. tuberculosis*), *S. aureus*, and *Salmonella enterica* (*S. enterica*), have developed protection mechanisms towards copper toxic effect in order to be able to survive the macrophage action [289–291].

It was proved that copper ions do not inhibit the multiplication of *S. aureus* bacteria, being *S. aureus* gram-positive bacteria, but they cause selective changes in cell membrane permeability of *Saccharomyces cerevisiae* (*S. cerevisiae*) yeasts, without changes in the vacuole membrane permeability [155], in contrast to other divalent metal cations (e.g., Zn, Co, Ni, Mn, Fe, and Sn).

In all cases, it has to be also taken into account that high concentrations of copper ions may have toxic effects, because of their ability to generate ROS.

### Synthesis of Cu-Substituted HAP

Copper-substituted hydroxyapatites (Cu-HAPs,  $\text{Ca}_{10-x}\text{Cu}_x(\text{PO}_4)_6(\text{OH})_2$  ( $x = 0.05\text{--}2.0$ )) have been synthesized by coprecipitation, using copper nitrate ( $\text{Cu}(\text{NO}_3)_2$ ) [292] or copper oxide (CuO) [153].

### Influence of $\text{Cu}^{2+}$ Substitution on Chemical, Physical, and Microstructural Properties of HAP

It has been reported that Cu ions substitute Ca sites in the HAP, with consequent decrement of both lattice parameters  $a$  and  $c$  increasing doping amounts, since dopant Cu ions are smaller than Ca ions [153]. The presence of copper ions within apatite lattice also reduces crystallinity [153].

### Influence of $\text{Cu}^{2+}$ Substitution on Biological Properties of HAP

The efficient antibacterial action of Cu-HAP against *E. coli* bacteria and *C. albicans* fungi has been demonstrated, presenting a stronger antimycotic activity compared to Zn-HAPs [153].

In the case of Cu-HAPs, it is very important to take into account the cytotoxic properties of copper against both bacteria and osteoblasts [153], having observed this effect in the case of hydroxyapatites with a  $\text{Cu}^{2+}$  content of 0.66 wt%.

## Cobalt Substitution

### Biological Role of Cobalt

Cobalt is an essential element for the correct performance of the human body, being a component of vitamin B12, necessary for the regulation of the red blood cell production, DNA synthesis in cells, and the myelin sheath formation in order to protect neurons and neurotransmitters [293]. For these reasons,  $\text{Co}^{2+}$  ions have been used as antibacterial and antiviral agents in various organic complexes [294, 295].

### Synthesis of Co-Substituted HAp

Cobalt-substituted hydroxyapatites (Co-HAps) have been synthesized by the hydrothermal method, obtaining hydroxyapatites containing 5–15 wt% of  $\text{Co}^{2+}$  [296], and by wet method, obtaining powders with a  $\text{Co}^{2+}$  content between 0.46 wt% and 3.79 wt% [297].

### Influence of $\text{Co}^{2+}$ Substitution on Chemical, Physical, and Microstructural Properties of HAp

Analyzing the obtained structure, it was noted that the actual  $\text{Co}^{2+}$  ion concentrations within the apatite lattice were lower than the nominal ones, due to differences in the constant bonding and chemical affinity of the ions  $\text{Co}^{2+}$  and  $\text{Ca}^{2+}$  [297].

Mabilleau et al. [298] evidenced that the presence of  $\text{Co}^{2+}$  and other metal ions, such as  $\text{Cr}^{3+}$  and  $\text{Ni}^{2+}$ , increases HAp crystal size and crystallinity, reducing its lattice parameter  $c$ .

### Influence of $\text{Co}^{2+}$ Substitution on Biological Properties of HAp

Antibacterial tests were carried out against *S. aureus*, *Micrococcus luteus* (*M. luteus*), *P. aeruginosa*, and *Shigella flexneri* (*S. flexneri*), evidencing that this action remarkably increased with  $\text{Co}^{2+}$  content, except for *P. aeruginosa* [297]. Moreover, the obtained materials were not toxic on the basis of hemolysis assay, and, thus, they can be employed for biomedical applications as biomaterials with additional antibacterial properties.

## Anionic Vicarious Ions Substitutions

Even if monovalent anions (e.g.,  $\text{F}^-$ ,  $\text{Cl}^-$ ) are able to substitute  $\text{OH}^-$  groups in the anion channel without charge imbalance, bivalent anions (e.g.,  $\text{HPO}_4^{2-}$ ,  $\text{CO}_3^{2-}$ ,  $\text{SO}_4^{2-}$ ,  $\text{SeO}_3^{2-}$ ,  $\text{SeO}_4^{2-}$ ) can substitute the trivalent phosphate group, balancing the charge by the formation of both hydroxide and calcium vacancies. In the case of tetravalent anion (e.g.,  $\text{SiO}_4^{4-}$ ) incorporation within the lattice, the negative charge is compensated by hydroxide vacancies.

## Carbonate Substitution

### Biological Role of Carbonate

As already evidenced, carbonate ions ( $\text{CO}_3^{2-}$ ) are the major substituent in biological apatites and are present in a content of 4–8 wt% [3, 9, 299–302].

It is important to underline that even if carbonates should belong to disordered domains of the apatite crystals, their locations are not precisely determined [303]. However, now it is generally accepted that carbonates mainly replace phosphates in biological apatite [304]. In fact,  $\text{CO}_3^{2-}$  group can substitute at two sites in the apatite lattice, i.e., the hydroxyl ion position and the phosphate ion position, leading to A-type and B-type carbonated apatites, respectively, and a platelet morphology that interfaces very efficiently with collagen fibrils [305]. The B-type substitution is the preferential carbonate substitution identified in the bone of the majority of species with the A/B ratio typically in the range 0.7–0.9 [306], even if the A/B ratio in the bone is influenced by its maturation [307].

B-type carbonated apatites are characterized by the following features: a decrease in *a*-axial length accompanied by an increase in *c*-axial length, changes in crystallite size and in the amount of crystallographic microstrains, optical birefringence and mechanical reinforcement of the bone [308], and incremented solubility [19, 309], due to the Ca– $\text{CO}_3$  bonds which are weaker than the Ca– $\text{PO}_4$  bonds. The higher solubility of bone apatite than that of tooth enamel can be ascribed to the smaller crystallite size and also higher carbonate concentration (Table 1).

### Synthesis of C-Substituted HAp

Carbonate-substituted hydroxyapatites (C-HAps) have been synthesized by several processing routes, such as coprecipitation [38, 308, 310–312], emulsion methods [313, 314], sol–gel synthesis [315], mechanochemical method [316], mechanochemical–hydrothermal synthesis [317], microwave precipitation [318], sitting drop vapor diffusion micro-method [319], and soaking in carbon dioxide ( $\text{CO}_2$ )-saturated solution [320].

Sodium hydrogen carbonate ( $\text{NaHCO}_3$ ) [308, 310], diammonium carbonate ( $(\text{NH}_4)_2\text{CO}_3$ ) [38, 312], calcium carbonate ( $\text{CaCO}_3$ ) [316], or a carbon dioxide ( $\text{CO}_2$ )-saturated solution [320] can be used as a carbonate source.

Nowadays, it is well known that apatites with low crystallinity, calcium deficiency, and carbonate content can be obtained, easily entering the carbonate in different apatite lattice structures by various techniques. On the contrary, a strict control of the synthesis conditions is needed to avoid carbonate inclusion, in order to produce stoichiometric apatites, particularly in the case of air low-temperature synthesis processes which imply absorption of atmospheric  $\text{CO}_2$  on the produced powders. However, hydroxyapatites with carbonate contents equivalent to bone  $\text{CO}_3^{2-}$  contents are difficult to synthesize in the laboratory, and the actual carbonate content is always different from the fraction of carbonates in the natural bone [321–323]. The wet route has been identified as the most adequate synthesis

methodology, allowing to force the carbonate ion substitution into the apatite lattice without introducing monovalent cations as the charge compensation mechanism [321].

### **Influence of $\text{CO}_3^{2-}$ Substitution on Chemical, Physical, and Microstructural Properties of HAp**

Racquel LeGeros started the work on the characterization of C-HAps for biomedical applications in the 1960s [305]. Since then, C-HAp has become the most extensively studied synthetic substituted HAp, with carbonate being the most abundant substitution in bone mineral [321–323].

As already evidenced, there are two types of carbonate substitution proposed in the literature with related charge compensation mechanisms, influencing both of them the material crystallographic lattice parameters: the substitution of  $\text{CO}_3^{2-}$  for  $\text{OH}^-$  (A type) and  $\text{CO}_3^{2-}$  for  $\text{PO}_4^{3-}$  (B type) [324]. A combined AB-type substitution (two carbonate ions replacing one phosphate group and one hydroxyl group, respectively) has been also identified.

The deficit in the negative charge caused by the replacement of  $\text{PO}_4^{3-}$  by  $\text{CO}_3^{2-}$  can be compensated through two mechanisms: (a) the loss of a positive charge, for example, the  $\text{Ca}^{2+}$  removal from the lattice, and (b) the replacement of a monovalent ion, typically sodium, for calcium, the ionic radii of  $\text{Ca}^{2+}$  (i.e., 0.099 nm) and  $\text{Na}^+$  (i.e., 0.098 nm) ions being quite similar [310].

On the basis of different investigations (i.e., X-ray diffraction (XRD), neutron diffraction, Fourier transform infrared spectroscopy (FT-IR), electron spin resonance spectroscopy (ESR), thermal decomposition, and nuclear magnetic resonance (NMR)), it was possible to determine that  $\text{CO}_3^{2-}$  ion incorporation within the HAp lattice leads to the preferential formation of B-type [38, 220, 224], even if Barralet et al. [310] reported that it depends on the carbonate amount:  $\text{CO}_3^{2-}$  ions are located in the A site for low carbonate contents (<4 wt%) and mainly in the B site for higher amounts.

However, the precise  $\text{CO}_3^{2-}$  disposition in the channel and its planar orientation with respect to the *c*-axis for A-type C-HAp was not clearly identified. For B-type C-HAp, there was no agreement among the studies on  $\text{CO}_3^{2-}$  substitution with respect to the original  $\text{PO}_4^{3-}$  configuration.

Substitution configurations of AB type and corresponding locations of  $\text{CO}_3^{2-}$  are further more complicated [325, 326].

Many conflicting considerations can be found in the literature. Ren et al. [327] demonstrated, using ab initio quantum mechanical calculations, that the most energetically stable substitution is AB type, followed by A type, and then B type, as corroborated by Fleet et al. [328], using XRD and FT-IR analyses.

According to the studies carried out by Peroos et al. [329], using computer modeling, A type, with two hydroxy groups replaced by one carbonate group, is energetically favored, followed by AB type, with both a phosphate group and a hydroxyl group replaced by two carbonate groups. On the other hand, considering B-type substitution, if a phosphate group is replaced by both a carbonate group and another hydroxyl group, it is energetically neutral, whereas if the replacement of the

phosphate group by a carbonate group is charge compensated by the substitution of  $K^+$  or  $Na^+$  ion for  $Ca^{2+}$  ion, the resulting B type is energetically favorable.

Moreover, it has been reported that the kind of carbonate substitution strictly depends on the followed synthesis process.

In detail, A-type carbonated HAp is commonly obtained by ion exchange either in reaction at high temperatures in a  $CO_2$  atmosphere (e.g., solid-state reactions at  $1000\text{ }^\circ\text{C}$  [330]) or soaking in a solution saturated with  $CO_2$  [320].

On the other hand, low-temperature (e.g., up to  $100\text{ }^\circ\text{C}$  [9]) synthesis routes allow obtaining B-type carbonated hydroxyapatites (with carbonates in phosphate positions) [9], even if the incorporated amount is still usually lower than the bone mineral component one. Indeed, B-type carbonated HAp can be synthesized by precipitation from solutions containing calcium, phosphate, and carbonate ions, often with the presence of either sodium or ammonia forming a co-substitution in order to maintain charge neutrality [323, 331].

The production of AB-type carbonated HAp usually involves a complex precipitation reaction with the co-substitution of either ammonium or sodium ions [332]. However Gibson and Bonfield reported a synthesis of mixed AB-type carbonated HAp, with carbonate content comparable to that of the natural bone mineral, without any co-substitution, leading to enhanced crystallite size and improved sintering behavior, mechanical properties, and biological responsiveness [333].

LeGeros [334] demonstrated that the HAp crystal lattice parameters are influenced by both the amount and the type of carbonate substitution, as supported by El Feki et al. [220]. In B-type substituted HAp, a decrease in the  $a$ -axis and an increase in the  $c$ -axis lattice dimensions are recorded, since a smaller planar carbonate ion replaces a larger, tetrahedral phosphate ion. Moreover this substitution leads to a decrease in the symmetry and in the stability of the apatite structure [335]. In the A-type substituted HAp, an increase in the  $a$ -axis lattice dimension, accompanied by a decrease of parameter  $c$ , is detected, since a larger carbonate ion substitutes for a linear smaller hydroxyl ion.

The  $CO_3^{2-}$  incorporation strongly decreases the HAp thermal stability, promoting apatite decomposition at temperatures as low as  $700\text{ }^\circ\text{C}$  [336], but it improves the sintering behavior, decreasing the temperature required to produce high strength, dense ceramics [308], and the mechanical properties with respect to pure HAp.

In fact, on the basis of the allocation, carbonate ions can influence the sinterability of hydroxyapatite. Specifically, A-type C-HAps are characterized by higher sintering temperatures [337] and B-type C-HAps by decreased sintering temperatures.

Furthermore, the substitution of carbonates within HAp lattice causes modifications of the apatite crystal morphology [310, 338], changing from a platelike to a needlelike, to a spheroidal morphology with carbonate amount [310].

Finally, many authors demonstrated a decremented crystallinity and an enhanced solubility in the case of B-type carbonated HAp in both in vitro and in vivo tests [306, 311, 339, 340].

### **Influence of $\text{CO}_3^{2-}$ Substitution on Biological Properties of HAp**

Carbonate ions play a pivotal role in bone metabolism, and for this reason, there is a relevant interest towards the use of carbonate-substituted apatites, particularly for bone graft applications.

$\text{CO}_3^{2-}$  ion substitution has been shown to increase the material bioactivity, due to its greater solubility [340–343], and to improve bone apposition rates with respect to pure HAp.

A higher degree of osteoconductivity was revealed for carbonated apatites with respect to pure hydroxyapatite, due to enhanced dissolution rate and improved solubility [341].

In *in vitro* studies carried out by Spence et al., an increased collagen production by human osteoblast cells was evidenced on the carbonated HAp compared to undoped HAp [341]. In fact, it is well known that the secretion of type I collagen strongly depends on extracellular calcium concentrations that resulted remarkably higher in cell culture medium containing carbonated HAp.

### **Fluoride Substitution**

#### **Biological Role of Fluoride**

Fluoride is essential in the diet and is necessary for normal skeletal and dental growth [344].

It has been recently reported that  $\text{F}^-$  ions might stimulate extracellular matrix formation *in vitro* and enhance bone union *in vivo*, promoting osteoblastic activities in terms of cell proliferation and differentiation [345].

Indeed, fluoride ions are able to directly act on bone cells, inducing bone formation. For example, it was demonstrated that NaF action can enhance *in vitro* proliferation and alkaline phosphatase activity of bone cells and can promote bone formation in embryonic calvaria at concentrations that stimulate bone formation *in vivo* [346, 347].

Moreover fluoride is considered as an important therapeutic agent in the osteoporosis treatment [348] and has been widely and successfully employed for this application [349–354].

#### **Synthesis of F-Substituted HAp**

Fluoride-substituted HAp (F-HAp,  $\text{Ca}_{10}(\text{PO}_4)_6(\text{OH},\text{F})_2$ ,  $\text{Ca}_{10}(\text{PO}_4)_6\text{OH}_{2-x}\text{F}_x$ ,  $x = 0-2$ ) have been synthesized by several wet techniques: (i) direct precipitation [48, 355–362]; (ii) sol-gel process [363, 364] starting from calcium nitrate and triethylphosphite in an ethanol-water-based solution; (iii) surfactant-assisted preparation [365]; (iv) soaking of hydroxyapatite in NaF solution [366]; (v) hydrolysis of tetracalcium phosphate (TTCP;  $\text{Ca}_4(\text{PO}_4)_2\text{O}$ ) in the presence of KF [367]; (vi) solution combustion method [368]; (vii) mechanochemical methods [369–372], consisting in a solid-state reaction between HAp and a source of fluorine ( $\text{CaF}_2$  [369, 370, 372] and  $\text{MgF}_2$  [370]); and (viii) fluoridation of bioapatite (BAP) isolated from bovine bone through an alkaline hydrothermal process, followed by calcination at 700 °C, using either HF or NaF [373].

## Influence of F<sup>-</sup> Substitution on Chemical, Physical, and Microstructural Properties of HAp

Many researchers analyzed the influence of F<sup>-</sup> incorporation within apatite lattice on the physicochemical properties of hydroxyapatite, such as crystallinity, lattice parameters, thermal stability, solubility, and corrosion resistance [48, 345, 374–378].

The incorporation of F<sup>-</sup> ions within the apatite lattice easily and readily occurs, even at room temperature or at body temperature [379], substituting for OH<sup>-</sup> groups in the so-called anion channel.

Fluoride anions are able to fit best into the channel site at  $z = 1/4$  and  $3/4$  in the center of the Ca(II) triangles [380], leading to a contraction of the unit cell along the  $a$ -axis direction, due to the smaller F<sup>-</sup> radius (0.119 nm) than that of a hydroxide anion (0.153 nm) [48, 360, 362, 381–384]. By contrast, the  $c$ -axis parameter increases with fluoride substitution, due to the greater crystal size [48, 382].

It has been demonstrated that the incorporation of F<sup>-</sup> ions within the HAp lattice causes improved thermal stability [356, 358, 361, 382, 384], the highest thermal stability being achieved for  $x$  greater than 0.4 in the formula  $\text{Ca}_{10}(\text{PO}_4)_6(\text{OH})_{2-x}\text{F}_x$  [358]. Additionally it leads to enhanced crystallinity [382, 385, 386] with consequent less solubility [356, 385–387].

Kim et al. investigated the effect of fluoride ions on the mechanical properties and on the inhibition of HAp decomposition, revealing that the substitution of F<sup>-</sup> for OH<sup>-</sup> is able to suppress HAp decomposition and to provide higher mechanical properties (flexural strength  $\sim 170$  MPa and Vickers hardness  $\sim 7$  GPa) [370], in agreement with other reports [361, 388].

Besides, it has been demonstrated that the presence of fluoride ions affects HAp sintering behavior, in function of F<sup>-</sup> amounts. For instance, equivalent amounts of fluoride and hydroxide ions ( $x = 1$  in  $(\text{Ca}_{10}(\text{PO}_4)_6(\text{OH})_x\text{F}_{2-x})$ ) greatly reduce the sintering temperature [361, 389, 390].

## Influence of F<sup>-</sup> Substitution on Biological Properties of HAp

F-HAp is considered as alternative potential candidate for bone repair due to its low solubility, good biocompatibility, and high thermal and chemical stability [374].

The incorporation of F<sup>-</sup> ions makes the apatite less soluble in acidic solutions and more resistant to corrosion in the body fluids, being characterized by an increment of the thermal stability and of the crystallinity with F<sup>-</sup> content. Thus, the solubility and the biological responsiveness can be tailored by modifying the F<sup>-</sup> amount.

F-HAp higher stability in biological environments with respect to pure HAp constitutes a positive factor for future prospective application (e.g., bone drug delivery system, coatings on dental and orthopedic implants, etc.). In particular, it has been demonstrated that F-HAp implants showed not only much longer resorption time than undoped calcium phosphates but also good bone tissue integration [377]. In fact, F<sup>-</sup> content strongly influences cell behavior and responsiveness: a high F<sup>-</sup> amount produces a low surface potential, which favors cell attachment, but leads to lower solubility and, thus, to a reduction in Ca<sup>2+</sup> release that could inhibit cell proliferation [387].



Furthermore, F-HAps promote new mineralization of incipient lesions and prevent, reduce, and control dental caries [48]. However, two serious health problems have been associated with high concentrations of fluoride in groundwater, namely, dental fluorosis and bone fluorosis. These pathologies can evolve into a more severe illness such as osteosclerosis or exostosis [375, 376]. Thus, it is necessary to tailor the  $F^-$  content in F-HAp to optimize the implant bioactivity and to properly control the amount of fluoride ions released from F-HAp [378].

Many studies corroborate F-HAp cytocompatibility, evidencing increased ALP levels, the osteocalcin presence [391–393], and remarkable stimulating effect on cell proliferation and differentiation activities [392].

Furthermore, F-HAp coatings showed an antibacterial action in experiments with *S. aureus*, *E. coli*, and *Porphyromonas gingivalis* (*P. gingivalis*) [394].

## Chloride Substitution

### Biological Role of Chloride

Chloride ( $Cl^-$ ) ion does not easily and readily substitute for  $OH^-$  in bone and tooth apatite, due to its larger ionic size (0.167 nm), even if this anion is present in the blood plasma in an amount of tenths of wt%. However, chloride anion is very important in the bone resorption process and organic matrix digestion, activating osteoclasts and, thus, promoting osteoclastic secretion of acid hydrolases, due to its ability to develop an acidic environment on the bone surface [380].

### Synthesis of Cl-Substituted HAp

Chloride-substituted hydroxyapatites (Cl-HAps,  $Ca_{10}(PO_4)_6(OH)_{2-x}(Cl)_x$ ,  $x = 0.2-2.0$ ) have been synthesized by several methodologies, including the mechanochemical process [395], the aqueous precipitation method with ammonium chloride ( $NH_4Cl$ ) as a source of chlorine [396–398], in a  $Cl^-$  range 0.64–6.42 wt%, and the solution combustion method [368].

### Influence of $Cl^-$ Substitution on Chemical, Physical, and Microstructural Properties of HAp

Kannan et al. [396, 397] highlighted that  $Cl^-$  substitution for  $OH^-$  in calcium-deficient apatites promotes the formation of biphasic mixtures HAp/TCP after thermal treatment, the HAp/TCP proportions depending on both chloride amount and the deficiency of calcium in the used precursors [396, 397].

The  $Cl^-$  incorporation within apatite lattice strongly influences the calculated unit cell parameters  $a$  and  $c$  and the unit cell volume, observing their increment with  $Cl^-$  contents [368, 396].

Moreover, chloride presence allows to remarkably increase HAp thermal stability, with thermal decomposition occurring above 1200 °C [396, 397], and the mechanical properties [397].

Additionally, Cho et al. [398] carried out solubility tests in deionized water, underlining that the dissolution amounts of the HAp elements increase with the  $Cl^-$  doping content, directly influencing the bioactivity. Finally, it was demonstrated

by calculation through an *ab initio* method that the total system energy rises with chloride amount, suggesting that Cl-HAp is energetically less stable with respect to pure HAp [398].

### **Influence of Cl<sup>-</sup> Substitution on Biological Properties of HAp**

Taking into account that chlorine content in the natural bone is up to 0.13 wt%, pure chlorapatite (Cl content of 6.8 wt%) cannot be considered for biomedical applications, since the total substitution of chloride ions for the hydroxyl groups causes an enhancement of the local environment acidity, leading to rapid solubilization of alkaline salts. For these reasons, the synthesis of partially chloride-substituted HAp is commonly performed and their biological performances are investigated.

Cho et al. [398] observed enhanced osteoconductivity in the case of Cl-HAp with low Cl amounts, within 4 weeks of implantation in calvarial defects of New Zealand white rabbits, due to its higher bioactivity, as demonstrated through *in vitro* tests in simulated body fluid (SBF).

Thus, Cl-HAp can be considered a promising material for potential applications in bone tissue engineering due to its remarkably improved bioactivity and osteoconductivity with respect to pure HAp [398].

## **Sulfate Substitution**

### **Biological Role of Sulfur and Sulfate**

Among the anions, inorganic sulfate is the fourth most abundant anion in human plasma and has shown to play a pivotal role in all mammalian cells for cell growth, cell matrix synthesis, and maintenance of cell membranes [399].

Sulfur and sulfates are considered as biological cements, being involved in building and rebuilding skin cells, hair, nails, and cartilage and protecting cartilage from osteoarthritis. They have been also employed for therapeutic treatment of hypercalcemia [400].

### **Synthesis of S-Substituted HAp**

Limited studies have been conducted on the substitution of sulfate ions within hydroxyapatite.

Sulfate ion-substituted hydroxyapatites (S-HAps,  $\text{Ca}_{10-x}(\text{PO}_4)_{6-x}(\text{SO}_4)_x(\text{OH})_{2-x}$ ,  $x = 0.05\text{--}0.5$ ) have been synthesized via a microwave-assisted ion exchange process, using anhydrous sodium sulfate ( $\text{Na}_2\text{SO}_4$ ) as  $\text{SO}_4^{2-}$  source [401].

### **Influence of $\text{SO}_4^{2-}$ Substitution on Chemical, Physical, and Microstructural Properties of HAp**

It has been reported that  $\text{SO}_4^{2-}$  ions substitute for  $\text{PO}_4^{3-}$  ions within the apatite lattice. The incorporation of  $\text{SO}_4^{2-}$  into apatite structure leads to increased structural disorder and, thus, decreased crystallinity, as confirmed by XRD and FT-IR spectroscopy [401].

The crystal size of S-HAp tends to decrement with  $\text{SO}_4^{2-}$  amounts, decreasing from 92 nm for  $x = 0.05$  to 40 nm for  $x = 0.5$ . However, increased lattice

parameters  $a$  and  $c$  and cell volume are detected, being ascribed to the larger sulfate ionic radius than the phosphate one (0.258 nm vs 0.238 nm) [401].

## Selenium Oxyanion Substitution

### Biological Role of Selenium

Selenium is an element fundamental for the appropriate development of the human body, protecting against oxidative stress and carcinogenesis and presenting antibacterial properties [402, 403], even if it was considered a highly toxic agent [404, 405]. Indeed, it is a component of selenoproteins and of the glutathione peroxidase enzyme, responsible for the protection of cell membranes against harmful factors [405]. It is well known that selenium plays a pivotal role in protein functions, and it is involved in the induction of cancer cell apoptosis [406]. Monteil-Rivera et al. [407] underlined that selenate ( $\text{SeO}_4^{2-}$ ) and selenite ( $\text{SeO}_3^{2-}$ ) oxyanions exert their cancer chemopreventive action by direct oxidation of thiol-containing cellular substrates, making it more efficient anticarcinogenic agents than selenomethionine or selenomethylselenocysteine with a lack of oxidation capability.

Furthermore, the selenium antibacterial action is mainly associated with oxidative stress, resulting in damage to the bacteria cell walls [403, 408–410].

Therefore, on the basis of these considerations, selenium compounds have been employed for the production of multifunctional biomaterials in order to provide the anticarcinogenic functions [411].

### Synthesis of Se-Substituted HAp

Selenium oxyanion-substituted hydroxyapatites (Se-HAps) have been synthesized by a coprecipitation method [406, 412, 413] with a Se/P molar ratio up to 1.1.

The adsorption of selenite and selenate on the HAp crystal surface has been also studied [407, 414, 415]. Monteil-Rivera et al. [407] established that selenate and selenite are not exclusively located at the HAp surface but are diffused slightly in a thickness of a few nanometers and that selenate anions were much less adsorbed than selenite [414].

### Influence of $\text{SeO}_4^{2-}/\text{SeO}_3^{2-}$ Substitution on Chemical, Physical, and Microstructural Properties of HAp

For both selenate ( $\text{SeO}_4^{2-}$ ) and selenite ( $\text{SeO}_3^{2-}$ ) substitutions for phosphate, a positively charged vacancy is formed and is compensated by simultaneous decalcification and dehydroxylation [412].

Regarding the influence on the reticular parameter, both  $a$  and  $c$  parameters are marginally influenced by selenate ion introduction, presenting  $\text{SeO}_4^{2-}$  ion the same structure of  $\text{PO}_4^{3-}$  group (i.e., tetrahedral), even if slightly larger (0.249 nm vs 0.238 nm in diameter) [412]. However, according to Kolmas et al. [412], the selenate ion incorporation within apatite lattice, up to  $x = 0.8$ , results in a slight increase in parameter  $a$ , whereas no significant changes are detected for lower levels, and the change in parameter  $c$  is not significant.

On the other hand, selenite ion introduction leads to a significant extension of the *a*-axis, while the *c*-axis remains unmodified. In fact, selenite substitution plays a significant effect on parameter *a* of cell, despite its dimensions (0.239 nm), very close to that of the phosphate ion (0.238 nm), due to the completely different spatial structure (i.e., flat trigonal pyramid geometry).

Concerning the crystallinity, contradictory results have been reported: Kolmas et al. [412] affirmed that selenite or selenate ion incorporation does not significantly influence the crystallinity, while Ma et al. [413] observed a decrease in crystallinity with increasing Se/P molar ratios.

### **Influence of $\text{SeO}_4^{2-}$ / $\text{SeO}_3^{2-}$ Substitution on Biological Properties of HAP**

On the basis of strong anticarcinogenic properties of selenium [406, 407], already described and discussed, Se-HAPs could serve as scaffolds not only for the growth of new bone tissue but also for the inhibition of the tumor cell growth and proliferation, presenting potential applications for treating bone cancers to reduce the recurrence probability.

For instance, coatings based on  $\text{SeO}_3^{2-}$ -doped carbonated hydroxyapatite were deposited on titanium substrates by pulsed laser deposition (PLD) technique, and their biological responsiveness was investigated, in terms of both cytotoxicity and antibacterial activity [403]. No cytotoxicity was recorded for Se concentrations up to 0.6 at%, and the obtained Se-HAP coatings were able to support the adhesion and proliferation of the MC3T3-E1 preosteoblasts. The obtained coatings also exhibited antibacterial activity against *S. aureus* and *P. aeruginosa*, even at very low Se concentrations (i.e., 0.6 wt%).

On the other hand, in another work, it was reported that selenate ion-doped HAPs were not toxic, whereas selenite ion-doped HAPs with the highest selenite concentration ( $x = 1.17$ ) was toxic in Spirotox and Microtox<sup>®</sup> tests [412].

## **Silicate Substitution**

### **Biological Role of Silicon**

Silicon is an essential trace element involved in metabolic processes correlated with bone and connective tissues, playing pivotal roles on the biomineralization process, the osteoblast differentiation and proliferation, the osteoblast collagen synthesis, the remodeling process, and the osteoclast development and resorption activities [416, 417].

The first studies about the influence of Si on bone metabolism and growth were carried out by *Carlisle* [14, 418, 419]. *Carlisle* demonstrated that Si is localized in active calcification sites in young mouse and rat bone and that a silicon-deficient diet causes a retarded growth and development, carrying out experiments on chicks submitted to two different diets, one Si deficient and one Si supplemented [418].

In order to investigate the silicon effect on bone cells, several studies were carried out with orthosilicic acid. In detail, it was demonstrated, using MG63 cells [420] and human osteoblasts [421], that orthosilicic acid is able to promote collagen type I synthesis and to enhance osteoblast differentiation, when Si amounts match the

physiological levels (10–20  $\mu\text{M}$ ) [420] and for higher concentrations (i.e., 50  $\mu\text{M}$ ) [421].

### Synthesis of Si-Substituted HAp

Silicate ( $\text{SiO}_4^{4-}$ )-substituted hydroxyapatites (Si-HAps,  $\text{Ca}_{10}(\text{PO}_4)_{6-x}(\text{SiO}_4)_x(\text{OH})_{2-x}$ ,  $x \sim 0.05\text{--}1.38$ ) have been synthesized by sol–gel process [422, 423], hydrothermal method [424–428], solid-state reaction methods [429–433], wet precipitation methods [71, 342, 388, 434–463], using different Si-containing precursors, such as calcium silicates ( $\text{CaSiO}_3$ ,  $\text{Ca}_2\text{SiO}_4$ ) [426], tetraethyl orthosilicate ( $\text{Si}(\text{OC}_2\text{H}_5)_4$ ) [422, 423, 425, 464], silicon acetate ( $\text{Si}(\text{OCOCH}_3)_4$ ) [436–438, 442], and silicon oxide ( $\text{SiO}_2$ ) [430].

Moreover, Si-HAps have been also produced by spark plasma sintering [465, 466].

### Influence of $\text{SiO}_4^{4-}$ Substitution on Chemical, Physical, and Microstructural Properties of HAp

It has been reported that HAp lattice can accommodate a limited Si amount, identifying 5 wt% as maximum level to be incorporated [446, 467] and 1 wt% as the minimum level necessary to provide significant biological improvements.

On the basis of structural analysis findings,  $\text{SiO}_4^{4-}$  ions substitute for the  $\text{PO}_4^{3-}$  ions within apatite structure, even if it is not clear whether the phosphorus replacement by silicon is complete or partial. Moreover, it is not possible to rule out that the silicon species remain independent phases, since it has been only verified the Si presence within the produced Si-HAps, but not its chemical nature. However, solid-state NMR spectroscopy analysis was performed on HAp containing 4.6 wt% of Si, in order to localize the  $\text{SiO}_4^{4-}$  moieties and to investigate their environment. It resulted that only a fraction of the Si atoms was incorporated within the apatite lattice in the form of  $\text{SiO}_4^{4-}$  ion, whereas a large amount of silicate units is located outside the HAp structure, corresponding to silica gel units [446].

Besides, the replacement of  $\text{PO}_4^{3-}$  ions by  $\text{SiO}_4^{4-}$  ions being a non-isoelectronic substitution, many possible mechanisms for charge compensation have been proposed, including oxygen or anionic vacancies [434] and Ca and/or H excess. Even if the creation of anionic vacancies at  $\text{OH}^-$  sites in the lattice is considered the most probable one [434, 468, 469], the predominant charge compensation mechanism strongly depends on the thermodynamic conditions during the material synthesis.

Moreover,  $\text{PO}_4^{3-}$  groups being preferentially located at HAp surface [470], their replacement by  $\text{SiO}_4^{4-}$  ions should lead to a surface charge decrement, generating a more electronegative surface, as verified through zeta potential measurements [450].

Regarding the unit cell parameters, a slight increment of the reticular constants  $a$  and  $c$  has been typically detected, due to the larger  $\text{Si}^{4+}$  ionic radius (0.42 Å) with respect to that of  $\text{P}^{5+}$  (0.35 Å) [71, 435]. However, although  $\text{Si}^{4+}$  ionic radius is bigger than that of  $\text{P}^{5+}$ , the  $\text{P}=\text{O}$  and  $\text{P}-\text{O}$  bonds (0.155 nm) are shorter than the  $\text{Si}-\text{O}$  bonds (0.161 nm), and hence the radius of the  $-\text{PO}_4$  tetrahedra is effectively smaller than that of the  $\text{SiO}_4$  tetrahedra [471]. In fact, some authors reported a small

decrement of the reticular parameter  $a$  and an increase of the  $c$  value for Si content of 0.4–1.5 wt% [71, 427, 434, 436, 438, 471].

The silicate incorporation also affects the thermal stability, as expected. Palard et al. [442] produced Si-HAPs with silicate content up to 4 mol% (~11 wt%). They concluded that single-phase Si-HAP can be obtained after thermal treatment above 700 °C in the case of low Si amounts (i.e.,  $0 < x < 1$ ), whereas for  $x > 1$ , the produced powders were composed of both HAP and  $\alpha$ -TCP, after calcination at 700 °C. On the other hand, for  $x = 4$ , the acquired XRD pattern revealed very low crystallinity, even after thermal treatment, and, consequently, the formation of a glassy phase from polycondensation of the  $\text{Si}(\text{OH})_4$  was hypothesized.

It has also reported that  $\text{SiO}_4^{4-}$  incorporation within HAP lattice inhibits the material grain growth, as demonstrated by investigation at scanning electron microscopy (SEM) [437], leading to a finer microstructure and, thus, increased material solubility [472]. This reduction in crystallite size is also supported and confirmed by XRD results [425, 439].

Concerning the sintering behavior, Si substitution generally tends to decrease the HAP sinterability, higher sintering temperatures being necessary to achieve the same level of sintered density with respect to pure HAP [71, 389, 435, 473].

### **Influence of $\text{SiO}_4^{4-}$ Substitution on Biological Properties of HAP**

In many reports, an increased bioactivity of Si-doped HAP with respect to pure HAP has been reported [342, 423, 425, 430, 434, 443, 453, 472, 474–477], highlighting that Si is able to promote in vitro osteoblast-like cell activity [434].

In vitro tests with human osteoblasts were performed by Balamurugan et al. [423] on Si-HAPs with different Si contents (i.e., 1, 3 and 5 mol%), selecting Si amount of 3 mol% as the optimal one. In fact, even if the Si amount of 5 mol% promotes rapid bone mineralization, this content may result in fast material dissolution and, thus, decreased crystallite size, which may be detrimental for cell attachment for prolonged time periods.

Enhanced cell proliferation and early formation of mineral nodules were observed on Si-HAP coatings deposited by plasma spraying [449] and electrospraying [478].

Analogously, improved rate and amount of in vivo bone apposition on Si-HAP were experimentally verified and supported through quantitative histological analysis and confocal fluorescence observation [453]. Hing et al. [447] carried out in vivo tests in a rabbit model, comparing porous HAP and Si-HAP scaffolds. They revealed a more advanced cellular infiltration and organization, neovascularization, and new bone penetration after just 1 week in the case of Si-HAP.

Furthermore, Botelho et al. [476] and Lehmann et al. [460] suggested an enhanced osteoclastic resorption activity on the Si-substituted material, as suggested by the presence of larger and more numerous resorption lacunae (Fig. 5) [460]. Interestingly, large lacunae ( $D \geq 61 \mu\text{m}$ ) were only found on Si-HAP, indicative of a more efficient differentiation process and/or a longer-lasting resorption activity by osteoclasts differentiated on Si-HAP.

However, Bohner [477] emphasized that, up to date, the improved biological performance of Si-substituted calcium phosphates (Si-CaPs) has not been clearly and

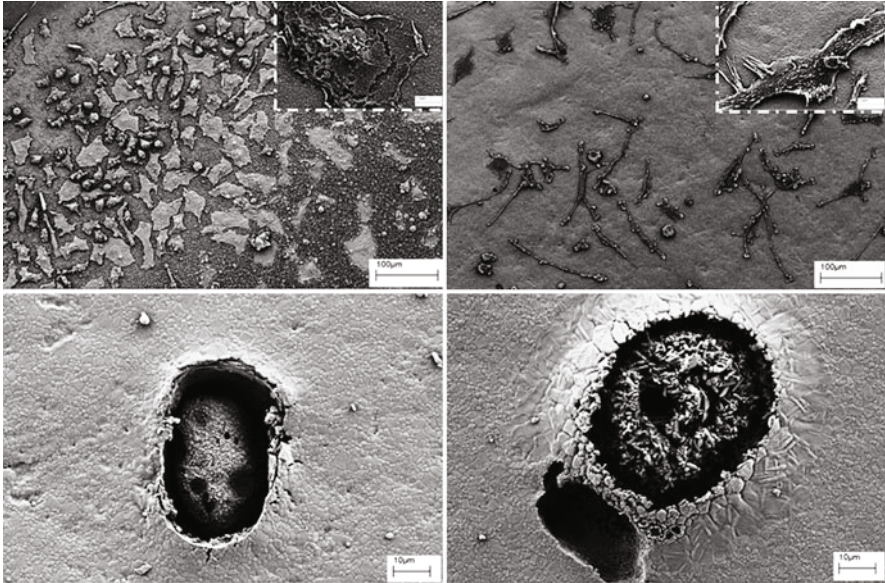


**Fig. 5** SEM micrographs of HAp (*left side*) and Si-HAp (*right side*) dense disks, after 21 days of human monocyte culture (*upper panels*) and after cell removal (*lower panels*) to see resorption pits. Magnifications: upper panels 500 $\times$  (insets, 5000 $\times$ ); lower panels 3000 $\times$  (Reproduced from Ref. [460] with permission)

experimentally correlated to either Si release or to the detected chemico-physical modifications of CaPs, induced by Si incorporation, such as superficial chemistry, topography, and microstructure. In fact, for example, the enhanced biological responsiveness could be justified with the increased number of defects, in particular around the grain boundaries, that are considered the starting point of *in vivo* dissolution [453].

## Summary

On the basis of all the collected papers, it is evident that there is a continuous, growing, and expanding attention towards ionic substitutions within the apatite lattice in order to improve their chemical, physical, and mostly biological properties.

It has to be pointed out that a deeper and more detailed investigation is necessary and strongly recommended in order to clearly comprehend the underlying mechanisms associated with the improved biological responsiveness.

In fact, up to date, no one published work about ionic substitutions within HAp lattice has certainly demonstrated the superior biological behavior of the substituted HAp and has clearly correlated their enhanced biological responsiveness to the vicarious ion/s present within the apatite lattice, as also and already underlined by Bohner [477], Boanini et al. [479], and Camaioni et al. [480].

Regardless of the conclusions reported in many papers, it is not currently clear if and how dopant ions positively affect the biological responsiveness of substituted HAp. Furthermore it is possible to hypothesize and suggest not only an ion active effect but also a passive effect ascribed to the ion-induced material modifications, in terms of surface chemistry and topography, morphology, crystallinity, microstructure, and resorbability.

Therefore, there is an urgent demand of experimental tests finalized to identify with certainty the real functional role of the dopant groups and the induced structural, morphological, and chemical alterations. It would be also fundamental and pivotal to investigate the actual functional role of all active groups present in native tissue, in order to properly select the kinds and the amounts of ions to be substituted for the three main functional groups of HAp. Additionally more efforts should be addressed to acquire a deep and complete knowledge and comprehension of the specific ion roles in cellular regulation and cell–cell signaling in both healthy and diseased tissues [481] (Fig. 6).

In fact, it is well established that the bone regeneration rate depends on several factors such as porosity, composition, solubility, and the presence of certain elements that, released during the resorption of the ceramic material, facilitate the bone regeneration carried out by the osteoblasts.

Thus the study of ionic substitutions in calcium phosphates would allow to better comprehend the improved biological properties not only of the produced materials but also of the biomineralization processes.

These substituted materials can be also seen not only as promising bone substitutes but also as drug delivery systems for the controlled-localized delivery, since the ions released during bone substitute resorption could be considered as drugs for bone disease treatment, being able to stimulate the expression of several osteoblastic cell genes [482, 483], to induce angiogenesis *in vitro* and *in vivo* [484], and to exercise possible antibacterial [485] and inflammatory [486] actions, as evidenced in the case of ionic dissolution products from 45S5 Bioglass<sup>®</sup> (e.g., Si, Ca, P, Na) and from other silicate-based glasses [487–491]. Thus it is very important to properly select both the ion doping amount, taking into account its therapeutic level and its release rate, and the ion kinds.

Moreover, few manuscripts have been focalized on the *in vitro* and/or to *in vivo* tests of substituted HAp. In most cases, the biological response promotion is only hypothesized and not experimentally verified.

Recently some efforts have been devoted to the synthesis of co- and/or multi-substituted HAp, aimed at obtaining a chemical composition which better resembles that of biological apatites. The produced systems include the co-substitution of zinc/silver [209], silver/strontium [211], carbonate/strontium [492], carbonate/magnesium [454, 493], carbonate/sodium [494], carbonate/silicate [495], yttrium/silicon [496], zinc/silicate [497], zinc/copper [498], strontium/cerium [499], magnesium/strontium [500], magnesium/silver [501], and carbonate/silicate/magnesium [454].



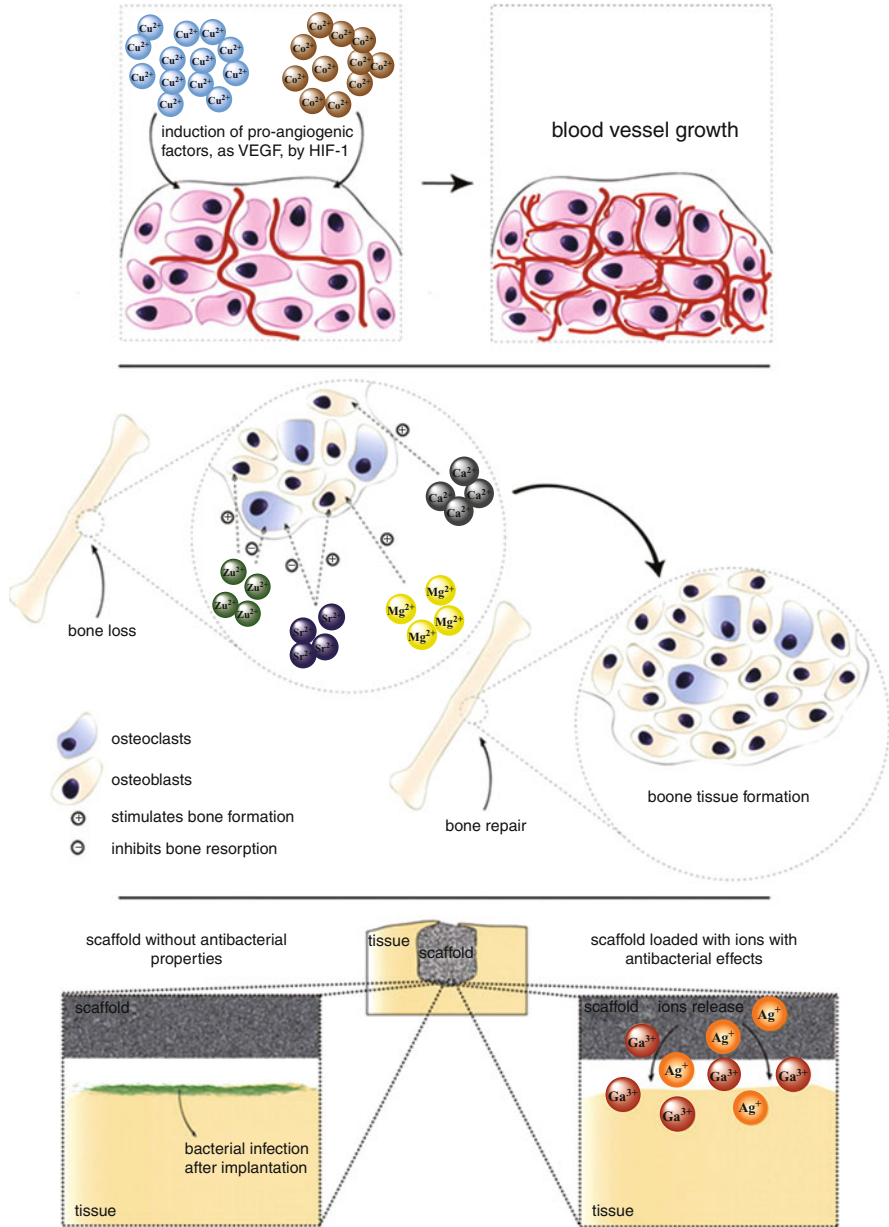


**Fig. 6** Most common specific targets of relevant metallic ions in their role of therapeutic agents (Reproduced from Ref. [479] with permission)

However, the co-substitution of multiple (more than two) ions has not deeply and systematically attempted and investigated, and thus, it can be considered as a promising research field to be still and further explored and expanded [502, 480].

---

## References

1. Kay MI, Young RA, Posner AS (1964) Crystal structure of hydroxyapatite. *Nature* 204:1050–1052
2. Dorozhkin SV (2009) Calcium orthophosphates in nature, biology and medicine. *Materials* 2:399–498
3. Elliott JC (1994) Structure and chemistry of the apatites and other calcium orthophosphates. Elsevier, Amsterdam
4. Weiner S, Wagner HD (1988) The material bone: structure–mechanical function relations. *Annu Rev Mater Sci* 28:271–298
5. Driessens F, Verbeeck R (1990) *Biomaterials*. CRC Press, Boca Raton
6. Cazalbou S, Combes C, Eichert D, Rey C (2004) Adaptive physico-chemistry of bio-related calcium phosphates. *J Mater Chem* 14:2148–2153
7. Wang L, Nancollas GH (2008) Calcium orthophosphates: crystallization and dissolution. *Chem Rev* 108:4628–4669
8. LeGeros RZ (2008) Calcium phosphate-based osteoinductive materials. *Chem Rev* 108:4742–4753
9. LeGeros RZ (1991) Calcium phosphates in oral biology and medicine. Karger, Basel
10. Daculsi G, Bouler JM, LeGeros RZ (1997) Adaptive crystal formation in normal and pathological calcifications in synthetic calcium phosphate and related biomaterials. *Int Rev Cytol* 172:129–191
11. McConnell D (1973) Apatite. Its crystal chemistry, mineralogy, utilization, and geologic and biologic occurrences. Springer, Wien
12. Li X, Sogo Y, Ito A, Mutsuzaki H, Ochiai N, Kobayashi T, Nakamura S, Yamashita K, LeGeros RZ (2009) The optimum zinc content in set calcium phosphate cement for promoting bone formation in vivo. *Mater Sci Eng C* 29:969–975
13. Garcia F, Ortega A, Domingo JL, Corbella J (2001) Accumulation of metals in autopsy tissues of subjects living in Tarragona County, Spain. *J Environ Sci Health* 36:1767–1786
14. Carlisle EM (1970) Silicon: a possible factor in bone calcification. *Science* 167:279–280
15. Liu Q, Huang S, Matinlinna JP, Chen Z, Pan H (2013) Insight into biological apatite: physiochemical properties and preparation approaches. *BioMed Res Int* 2013:929748 (13 pages)
16. Wenk HR, Heidelbach F (1999) Crystal alignment of carbonated apatite in bone and calcified tendon: results from quantitative texture analysis. *Bone* 24(4):361–369
17. Skinner HCW (2005) *Biomaterials*. Mineral Mag 69:621–641
18. Dorozhkin SV, Epple M (2002) Biological and medical significance of calcium phosphates. *Angew Chem Int Ed* 41:3130–3146
19. Handschin RG, Stern WB (1995) X-ray diffraction studies on the lattice perfection of human bone apatite (Crista Iliaca). *Bone* 16:355S–363S
20. Salinas AJ, Esbrit P, Vallet-Regí M (2013) A tissue engineering approach based on the use of bioceramics for bone repair. *Biomater Sci* 1:40–51
21. Cannizzaro G, Felice P, Leone M, Viola P, Esposito M (2009) Early loading of implants in the atrophic posterior maxilla: lateral sinus lift with autogenous bone and Bio-Oss versus crestal mini sinus lift and 8-mm hydroxyapatite-coated implants. A randomised controlled clinical trial. *Eur J Oral Implantol* 2(1):25–38

22. Stavropoulos A, Karring T (2010) Guided tissue regeneration combined with a deproteinized bovine bone mineral (Bio-Oss) in the treatment of intrabony periodontal defects: 6-year results from a randomized-controlled clinical trial. *J Clin Periodontol* 37(2):200–210
23. Horvath AL (2006) Solubility of structurally complicated materials: II. Bone *J Phys Chem Ref Data* 35(4):1653–1668
24. Posner AS, Perloff A, Diorio AF (1958) Refinement of the hydroxyapatite structure. *Acta Crystallogr* 11(4):308–309
25. Elliott JC, Mackie PE, Young RA (1973) Monoclinic hydroxyapatite. *Science* 180(4090):1055–1057
26. Ma GB, Liu XY (2009) Hydroxyapatite: hexagonal or monoclinic? *Cryst Growth Des* 9(7):2991–2994
27. Wopenka B, Pasteris JD (2005) A mineralogical perspective on the apatite in bone. *Mater Sci Eng C* 25:131–143
28. Pasteris JD, Wopenka B, Valsami-Jones E (2008) Bone and tooth mineralization: why apatite? *Elements* 4:97–104
29. Uddin MH, Matsumoto T, Okazaki M, Nakahira A, Sohmura T (2010) Biomimetic fabrication of apatite related biomaterials. In: Mukherjee A (ed) *Biomimetics learning from nature*. InTech, Rijeka, pp 289–303
30. Rivera-Muñoz EM (2011) Hydroxyapatite-based materials: synthesis and characterization. In: Fazel R (ed) *Biomedical engineering-frontiers and challenges*. InTech, Rijeka, pp 75–98
31. Matsunaga K, Murata H, Shitara K (2010) Theoretical calculations of the thermodynamic stability of ionic substitutions in hydroxyapatite under an aqueous solution environment. *J Phys Condens Matter* 22(38):384210
32. Vallet-Regí M (2008) *Biomimetic nanoceramics in clinical use from materials to applications*. Royal Society of Chemistry, Cambridge, UK
33. Hughes JM, Rakovan J (2002) The crystal structure of apatite,  $\text{Ca}_5(\text{PO}_4)_3(\text{F}, \text{OH}, \text{Cl})$ . In: Kohn MJ, Rakovan J, Hughes JM (eds) *Phosphates: geochemical, geobiological and material importance, reviews in mineralogy and geochemistry*, vol 48. Mineralogical Society of America, Washington, pp 1–12
34. El Feki H, Ben Salah A, Daoud A, Lamure A, Lacabanne C (2000) Studies by thermally stimulated current (TSC) of hydroxyl and fluoro-carbonated apatites containing sodium ions. *J Phys Condens Matter* 12:8331–8343
35. de Maeyer EAP, Verbeeck RMH (1993) Possible substitution mechanisms for sodium and carbonate in calciumhydroxyapatite. *Bull Soc Chim Belg* 102:601–609
36. de Maeyer EAP, Verbeeck RMH, Naessens DE (1993) Effect of heating on the constitution of  $\text{Na}^+$  and  $\text{CO}_3^{2-}$  containing apatites obtained by hydrolysis of monetite. *Inorg Chem* 33:5999–6006
37. Nounah A, Lacout J, Savariault JM (1992) Localization of cadmium in cadmium-containing hydroxy- and fluorapatite. *J Alloys Compd* 188:141–146
38. El Feki H, Savariault JM, Ben Salah A (1999) Structure refinements by the Rietveld method of partially substituted hydroxyapatite:  $\text{Ca}_9\text{Na}_{0.5}(\text{PO}_4)_{4.5}(\text{CO}_3)_{1.5}(\text{OH})_2$ . *J Alloys Compd* 287:114–120
39. Bianco A, Cacciotti I, Lombardi M, Montanaro L, Gusmano G (2007) Thermal stability and sintering behaviour of hydroxyapatite nanopowders. *J Therm Anal Calorim* 88:237–243
40. Bigi A, Foresti B, Gregoriani R, Ripamonti A, Roveri N, Shah JS (1992) The role of magnesium on the structure of biological apatites. *Calcif Tissue Int* 50:439–444
41. Lilley K, Gbureck U, Knowles J, Farrar D, Barralet J (2005) Cement from magnesium substituted hydroxyapatite. *J Mater Sci Mater Med* 16(5):455–460
42. Suchanek WL, Byrappa K, Shuk P, Riman RE, Janas VF, TenHuisen KS (2004) Preparation of magnesium-substituted hydroxyapatite powders by the mechanochemical-hydrothermal method. *Biomaterials* 25:4647–4657
43. Percival M (1999) Bone health & osteoporosis. *Appl Nutr Sci Rep* 5(4):1–5

44. Rude RK, Gruber HE (2004) Magnesium deficiency and osteoporosis: animal and human observations. *J Nutr Biochem* 15(12):710–716
45. Landi E, Logroscino G, Proietti L, Tampieri A, Sandri M, Sprio S (2008) Biomimetic Mg-substituted hydroxyapatite: from synthesis to in vivo behaviour. *J Mater Sci Mater Med* 19:239–247
46. Stipnice L, Salma-Ancane K, Borodajenko N, Sokolova M, Jakovlevs D, Berzina-Cimdina L (2014) Characterization of Mg-substituted hydroxyapatite synthesized by wet chemical method. *Ceram Int* 40(2):3261–3267
47. Sader MS, Moreira EL, Moraes VCA, Araújo JC, LeGeros RZ, Soares GA (2009) Rietveld refinement of sintered magnesium substituted calcium apatite. *Key Eng Mater* 396–398:277–280
48. Bertoni E, Bigi A, Cojazzi G, Gandolfi M, Panzavolta S, Roveri N (1998) Nanocrystals of magnesium and fluoride substituted hydroxyapatite. *J Inorg Biochem* 72:29–35
49. Cox SC, Jamshidi P, Grover LM, Mallick KK (2014) Preparation and characterisation of nanophase Sr, Mg, and Zn substituted hydroxyapatite by aqueous precipitation. *Mater Sci Eng C Mater Biol Appl* 35:106–114
50. Tampieri A, Celotti G, Landi E, Sandri M (2004) Magnesium doped hydroxyapatite: synthesis and characterization. *Key Eng Mater* 264–268:2051–2054
51. Laurencin D, Almora-Barrios N, de Leeuw NH, Gervais C, Bonhomme C, Mauri F, Chrzanowski W, Knowle JC, Newport RJ, Wong A, Gan Z, Smith ME (2011) Magnesium incorporation into hydroxyapatite. *Biomaterials* 32(7):1826–1837
52. Kannan S, Lemos IAF, Rocha JHG, Ferreira JMF (2005) Synthesis and characterization of magnesium substituted biphasic mixtures of controlled hydroxyapatite/ $\beta$ -tricalcium phosphate ratios. *J Solid State Chem* 178:3190–3196
53. Ren F, Leng Y, Xin R, Ge X (2010) Synthesis, characterization and ab initio simulation of magnesium-substituted hydroxyapatite. *Acta Biomater* 6(7):2787–2796
54. Cacciotti I, Bianco A, Lombardi M, Montanaro L (2009) Mg-substituted hydroxyapatite nanopowders: synthesis, thermal stability and sintering behavior. *J Eur Ceram Soc* 29:2969–2978
55. Farzadi A, Bakhshi F, Solati-Hashjin M, Asadi-Eydivand M, Azuanabu Osman N (2014) Magnesium incorporated hydroxyapatite: synthesis and structural properties characterization. *Ceram Int* 40:6021–6029
56. Yasukawa A, Ouchi S, Kandori K, Ishikawa T (1996) Preparation and characterization of magnesium-calcium hydroxyapatites. *J Mater Chem* 6:1401–1405
57. Bertinetti L, Tampieri A, Landi E, Martra G, Coluccia S (2006) Punctual investigation of surface sites of HA and magnesium-HA. *J Eur Ceram Soc* 26:987–991
58. Bertinetti L, Drouet C, Combes C, Rey C, Tampieri A, Coluccia S, Martra G (2009) Surface characteristics of nanocrystalline apatites: effect of Mg surface enrichment on morphology, surface hydration species, and cationic environments. *Langmuir* 25:5647–5654
59. Bigi A, Falini G, Foresti E, Gazzano M, Ripamonti A, Roveri N (1996) Rietveld structure refinements of calcium hydroxylapatite containing magnesium. *Acta Crystallogr B* 52:87–92
60. Lijuan X, Liyun J, Lixin J, Chengdong X (2013) Synthesis of Mg-substituted hydroxyapatite nanopowders: effect of two different magnesium sources. *Mater Lett* 106:246–249
61. Fadeev IV, Shvorneva LI, Barinov SM, Orlovskii VP (2003) Synthesis and structure of magnesium-substituted hydroxyapatite. *Inorg Mater* 39:947–950
62. Gozalian A, Behnamghader A, Daliri M, Moshkforoush A (2011) Synthesis and thermal behavior of Mg-doped calcium phosphate nanopowders via the sol–gel method. *Sci Iran F* 18:1614–1622
63. Kalita SJ, Bhatt HA (2007) Nanocrystalline hydroxyapatite doped with magnesium and zinc: synthesis and characterization. *Mater Sci Eng C* 27:837–848
64. Qaisar SA, Bilton M, Wallace R, Brydson R, Brown AP, Ward M, Milne SJ (2010) Sol–gel synthesis and TEM-EDX characterisation of hydroxyapatite nanoscale powders modified by Mg, Sr or Ti. *J Geophys Res* 241:012042

65. Khanra AK, Jung HC, Yu SH, Hong KS, Shin KS (2010) Microstructure and mechanical properties of Mg–HAP composites. *Bull Mater Sci* 33:43–47
66. Mishra VK, Bhattacharjee BN, Parkash O, Kumar D, Rai SB (2014) Mg-doped hydroxyapatite nanoplates for biomedical applications: a surfactant assisted microwave synthesis and spectroscopic investigations. *J Alloys Compd* 614:283–288
67. Zyman Z, Tkachenko M, Epple M, Polyakow M, Naboka M (2006) Magnesium-substituted hydroxyapatite ceramics. *Mater Werkst* 37:474–477
68. Bigi A, Falini G, Foresti E, Gazzano M, Ripamonti A, Roveri N (1993) Magnesium influence on hydroxyapatite crystallization. *J Inorg Biochem* 49(1):69–78
69. Mayer L, Schlam R, Featherstone JDB (1997) Magnesium-containing carbonate apatites. *J Inorg Biochem* 66:1–6
70. Cacciotti I, Bianco A (2011) High thermally stable Mg-substituted tricalcium phosphate by precipitation. *Ceram Int* 37:127–137
71. Kim SR, Lee JH, Kim YT, Riu DH, Jung SJ, Lee YJ, Chung SC, Kim YH (2003) Synthesis of Si, Mg substituted hydroxyapatites and their sintering behaviours. *Biomaterials* 24:1389–1398
72. Webster TJ, Ergun C, Doremus RH, Bizios R (2002) Hydroxylapatite with substituted magnesium, zinc, cadmium, and yttrium. II. Mechanisms of osteoblast adhesion. *J Biomed Mater Res* 59(2):312–317
73. de Lima IR, Alves GG, Soriano CA, Campaneli AP, Gasparoto TH, Ramos ES, de Sena LA, Rossi AM, Granjeiro JM (2011) Understanding the impact of divalent cation substitution on hydroxyapatite: an in vitro multiparametric study on biocompatibility. *J Biomed Mater Res A* 98A(3):351–358
74. Jiao MJ, Wang XX (2009) Electrolytic deposition of magnesium-substituted hydroxyapatite crystals on titanium substrate. *Mater Lett* 63:2286–2289
75. Blake GM, Zivanovic MA, McEwan AJ, Ackery DM (1986) SR-89 therapy – strontium kinetics in disseminated carcinoma of the prostate. *Eur J Nucl Med* 12(9):447–454
76. Dahl SG, Allain P, Marie PJ, Mauras Y, Boivin G, Ammann P, Tsouderos Y, Delmas PD, Christiansen C (2001) Incorporation and distribution of strontium in bone. *Bone* 28(4):446–453
77. Naddari T, Hamdi B, Savariault JM, El Feki H, Ben Salah A (2003) Substitution mechanism of alkali metals for strontium in strontium hydroxyapatite. *Mater Res Bull* 38(2):221–230
78. Robinson RG, Spicer JA, Preston DF, Wegst AV, Martin NL (1987) Treatment of metastatic bone pain with strontium-89. *Int J Rad Appl Instrum* 14(3):219–222
79. Canalis E, Hott M, Deloffre P, Tsouderos Y, Marie PJ (1996) The divalent strontium salt S12911 enhances bone cell replication and bone formation in vitro. *Bone* 18:517–523
80. Bonnelye E, Chabadel A, Saltel F, Jurdic P (2008) Dual effect of strontium ranelate: stimulation of osteoblast differentiation and inhibition of osteoclast formation and resorption in vitro. *Bone* 42:129–138
81. Caverzasio J (2008) Strontium ranelate promotes osteoblastic cell replication through at least two different mechanisms. *Bone* 42(6):1131–1136
82. Reginster JY (2002) Strontium ranelate in osteoporosis. *Curr Pharm Des* 8(21):1907–1916
83. Peng SL, Zhou GQ, Luk KDK, Cheung KMC, Li ZY, Lam WM, Zhou ZJ, Lu WW (2009) Strontium promotes osteogenic differentiation of mesenchymal stem cells through the Ras/MAPK signaling pathway. *Cell Physiol Biochem* 23(1–3):165–174
84. Hurtel-Lemaire AS, Mentaverri R, Caudrillier A, Courmarie F, Wattel A, Kamel S, Terwilliger EF, Brown EM, Brazier M (2009) The calcium-sensing receptor is involved in strontium ranelate-induced osteoclast apoptosis: new insights into the associated signaling pathways. *J Biol Chem* 284(1):575–584
85. Buehler J, Chappuis P, Saffar JL, Tsouderos Y, Vignery A (2001) Strontium ranelate inhibits bone resorption while maintaining bone formation in alveolar bone in monkeys (*Macaca fascicularis*). *Bone* 29(2):176–179
86. Guida A, Towler MR, Wall JG, Hill RG, Eramo S (2003) Preliminary work on the antibacterial effect of strontium in glass ionomer cements. *J Mater Sci Lett* 22(20):1401–1403

87. Brauer DS, Karpukhina N, Kedia G, Bhat A, Law RV, Radecka I, Hill RG (2012) Bactericidal strontium-releasing injectable bone cements based on bioactive glasses. *J R Soc Interface* 10 (78):1–8
88. Bigi A, Boanini E, Capuccini C, Gazzano M (2007) Strontium-substituted hydroxyapatite nanocrystals. *Inorg Chim Acta* 360(3):1009–1116
89. Okayama S, Akao M, Nakamura S, Shin Y, Higashikata M, Aoki H (1991) The mechanical properties and solubility of strontium-substituted hydroxyapatite. *Biomed Mater Eng* 1 (1):11–17
90. Li ZH, Wu JM, Huang SJ, Guan J, Zhang XZ (2010) Strontium hydroxyapatite synthesis, characterization, and cell cytotoxicity. *Adv Mater Res* 160–162:117–122
91. Liu W, Wang T, Shen Y, Pan H, Peng S, Lu WW (2013) Strontium incorporated coralline hydroxyapatite for engineering bone. *ISRN Biomater* 2013:649163 (11 pages)
92. Mardziah CM, Sopyan I, Ramesh S (2009) Strontium-doped hydroxyapatite nanopowder via sol–gel method: effect of strontium concentration and calcination temperature on phase behavior. *Trends Biomater Artif Organs* 23:105–113
93. Renaudin G, Jallot E, Nedelec JM (2009) Effect of strontium substitution on the composition and microstructure of sol–gel derived calcium phosphates. *J Sol-Gel Sci Technol* 51:287–294
94. Kim HW, Koh YH, Kong YM, Kang JG, Kim HE (2004) Strontium substituted calcium phosphate biphasic ceramics obtained by a powder precipitation method. *J Mater Sci Mater Med* 15:1129–1134
95. O'Donnell MD, Fredholm Y, de Rouffignac A, Hill RG (2008) Structural analysis of a series of strontium-substituted apatites. *Acta Biomater* 4:1455–1464
96. Li ZY, Lam WM, Yang C, Xu B, Ni GX, Abbah SA, Cheung KMC, Luk KDK, Lu WW (2007) Chemical composition, crystal size and lattice structural changes after incorporation of strontium into biomimetic apatite. *Biomaterials* 28:1452–1460
97. Landi E, Tampieri A, Celotti G, Sprio S, Sandri M, Logroscino G (2007) Sr-substituted hydroxyapatites for osteoporotic bone replacement. *Acta Biomater* 3:961–969
98. Lin K, Liu P, Wei L, Zou Z, Zhang W, Qian Y, Shen Y, Chang J (2013) Strontium substituted hydroxyapatite porous microspheres: surfactant-free hydrothermal synthesis, enhanced biological response and sustained drug release. *Chem Eng J* 222:49–59
99. Chung CJ, Long HY (2011) Systematic strontium substitution in hydroxyapatite coatings on titanium via micro-arc treatment and their osteoblast/osteoclast responses. *Acta Biomater* 7:4081–4087
100. Capuccini C, Torricelli P, Sima F, Boanini E, Ristoscu C, Bracci B, Socol G, Fini M, Mihailescu IN, Bigi A (2008) Strontium-substituted hydroxyapatite coatings synthesized by pulsed-laser deposition: in vitro osteoblast and osteoclast response. *Acta Biomater* 4:1885–1893
101. Pereiro I, Rodriguez-Valencia C, Serra C, Solla EL, Serra J, González P (2012) Pulsed laser deposition of strontium-substituted hydroxyapatite coatings. *Appl Surf Sci* 258 (23):9192–9197
102. Oliveira AL, Reis RL, Li P (2007) Strontium-substituted apatite coating grown on Ti6Al4V substrate through biomimetic synthesis. *J Biomed Mater Res* 83B:258–265
103. Bracci B, Torricelli P, Panzavolta S, Boanini E, Giardino R, Bigi A (2009) Effect of  $Mg^{2+}$ ,  $Sr^{2+}$  and  $Mn^{2+}$  on the chemico-physical and in vitro biological properties of calcium phosphate biomimetic coatings. *J Inorg Biochem* 103:1666–1674
104. Pan HB, Li ZY, Wang T, Lam WM, Wong CT, Darvell BW, Luk KDK, Hu Y, Lu WW (2009) Nucleation of strontium-substituted apatite. *Cryst Growth Des* 9(8):3342–3345
105. Zhu K, Yanagisawa K, Shimanouchi R, Onda A, Kajiyoshi K (2006) Preferential occupancy of metal ions in the hydroxyapatite solid solutions synthesized by hydrothermal method. *J Eur Ceram Soc* 26(4–5):509–513
106. Bigi A, Falini G, Gazzano M, Roveri N, Tedesco E (1998) Structural refinements of strontium substituted hydroxylapatites. *Mater Sci Forum* 278–281:814–819

107. Terra J, Dourado ER, Eon JG, Ellis DE, Gonzalez G, Rossi AM (2009) The structure of strontium-doped hydroxyapatite: an experimental and theoretical study. *Phys Chem Chem Phys* 11:568–577
108. Kavitha M, Subramanian R, Narayanan R, Udhayabanu V (2014) Solution combustion synthesis and characterization of strontium substituted hydroxyapatite nanocrystals. *Powder Technol* 253:129–137
109. Capuccini C, Torricelli P, Boanini E, Gazzano M, Giardino R, Bigi A (2009) Interaction of Sr-doped hydroxyapatite nanocrystals with osteoclast and osteoblast-like cells. *J Biomed Mater Res* 89A:594–600
110. Christoffersen J, Christoffersen MR, Kolthoff N, Barenholdt O (1997) Effects of strontium ions on growth and dissolution of hydroxyapatite and on bone mineral detection. *Bone* 20(1):47–57
111. Boanini E, Torricelli P, Fini M, Bigi A (2011) Osteopenic bone cell response to strontium-substituted hydroxyapatite. *J Mater Sci Mater Med* 22(9):2079–2088
112. Pan HB, Li ZY, Lam WM, Wong JC, Darvell BW, Luk KDK, Lu WW (2009) Solubility of strontium-substituted apatite by solid titration. *Acta Biomater* 5(5):1678–1685
113. Zhang W, Shen Y, Pan H, Lin K, Liu X, Darvell BW, Lu WW, Chang J, Deng L, Wang D, Huang W (2011) Effects of strontium in modified biomaterials. *Acta Biomater* 7(2):800–808
114. Verberckmoes SC, Behets GJ, Oste L, Bervoets AR, Lamberts LV, Drakopoulos M, Somogyi A, Cool P, Dorrine W, De Broe ME, D'Haese PC (2004) Effects of strontium on the physicochemical characteristics of hydroxyapatite. *Calcif Tissue Int* 75(5):405–415
115. Ni GX, Chiu KY, Lu WW, Wang Y, Zhang YG, Hao LB, Li ZY, Lam WM, Lu SB, Luk KDK (2006) Strontium-containing hydroxyapatite bioactive bone cement in revision hip arthroplasty. *Biomaterials* 27(24):4348–4355
116. dos Santos Tavares D, Resende CX, Quitan MP, De Oliveira Castro L, Granjeiro JM, De Almeida Soares G (2011) Incorporation of strontium up to 5 mol% to hydroxyapatite did not affect its cytocompatibility. *Mater Res* 14(4):456–460
117. Lin Y, Yang Z, Cheng J, Wang L (2008) Synthesis, characterization and antibacterial property of strontium half and totally substituted hydroxyapatite nanoparticles. *J Wuhan Univ Technol Mater Sci Educ* 23(4):475–479
118. Ravi ND, Balu R, Sampath Kumar TS (2012) Strontium-substituted calcium deficient hydroxyapatite nanoparticles: synthesis, characterization and antibacterial properties. *J Amer Ceram Soc* 95(9):2700–2708
119. Yamaguchi M, Yamaguchi R (1986) Action of zinc on bone metabolism in rats – increases in alkaline-phosphatase activity and DNA content. *Biochem Pharmacol* 35(5):773–777
120. Barrea RA, Pérez CA, Ramos AY, Sánchez HJ, Grenón M (2003) Distribution and incorporation of zinc in biological calcium phosphates. *X-Ray Spectrom* 32:387–395
121. Yamaguchi M (1998) Role of zinc in bone formation and bone resorption. *J Trace Elem Exp Med* 11:119–135
122. Moonga BS, Dempster DW (1995) Zinc is a potent inhibitor of osteoclastic bone-resorption in vitro. *J Bone Miner Res* 10:453–457
123. Yamaguchi M, Oishi H, Suketa Y (1987) Stimulatory effect of zinc on bone-formation in tissue-culture. *Biochem Pharmacol* 36(22):4007–4012
124. Kishi S, Yamaguchi M (1994) Inhibitory effect of zinc-compounds on osteoclast-like cell-formation in mouse marrow cultures. *Biochem Pharmacol* 48(6):1225–1230
125. Yamaguchi M, Uchiyama S (2004) Receptor activator of NF- $\kappa$ B ligand-stimulated osteoclastogenesis in mouse marrow culture is suppressed by zinc in vitro. *Int J Mol Med* 14(1):81–85
126. Yamaguchi M, Goto M, Uchiyama S, Nakagawa T (2008) Effect of zinc on gene expression in osteoblastic MC3T3-E1 cells: enhancement of Runx2, OPG, and regucalcin mRNA expressions. *Mol Cell Biochem* 312(1–2):157–166
127. Khadeer MA, Sahu SN, Bai G, Abdulla S, Gupta A (2005) Expression of the zinc transporter ZIP1 in osteoclasts. *Bone* 37(3):296–304

128. Sogo Y, Sakurai T, Onuma K, Ito A (2002) The most appropriate (Ca + Zn)/P molar ratio to minimize the zinc content of ZnTCP/HAP ceramic used in the promotion of bone formation. *J Biomed Mater Res* 62(3):457–463
129. Ito A, Ojima K, Naito H, Ichinose N, Tateishi T (2000) Preparation, solubility, and cytocompatibility of zinc-releasing calcium phosphate ceramics. *J Biomed Mater Res* 50:178–183
130. Ito A, Kawamura H, Otsuka M, Ikeuchi M, Ohgushi H, Ishikawa K, Onuma K, Kanzaki N, Sogo Y, Ichinose N (2002) Zinc-releasing calcium phosphate for stimulating bone formation. *Mater Sci Eng C* 22:21–25
131. Tang YZ, Chappell HF, Dove MT, Reeder RJ, Lee YJ (2009) Zinc incorporation into hydroxylapatite. *Biomaterials* 30:2864–2872
132. Fujii E, Ohkubo M, Tsuru K, Hayakawa S, Osaka A, Kawabata K, Bonhomme C, Babonneau F (2006) Selective protein adsorption property and characterization of nano-crystalline zinc-containing hydroxyapatite. *Acta Biomater* 2:69–74
133. Miyaji F, Kono Y, Suyama Y (2005) Formation and structure of zinc-substituted calcium hydroxyapatite. *Mater Res Bull* 40:209–220
134. Bigi A, Foresti E, Gandolfi M, Gazzano M, Roveri N (1995) Inhibiting effect of zinc on hydroxylapatite crystallization. *J Inorg Biochem* 58:49–58
135. Ergun C, Webster TJ, Bizios R, Doremus RH (2002) Hydroxylapatite with substituted magnesium, zinc, cadmium, and yttrium. I. Structure and microstructure. *J Biomed Mater Res* 59(2):305–311
136. Webster TJ, Massa-Schlueter EA, Smith JL, Slamovich EB (2004) Osteoblast response to hydroxyapatite doped with divalent and trivalent cations. *Biomaterials* 25:2111–2121
137. Sogo Y, Ito A, Fukasawa K, Sakurai T, Ichinose N (2004) Zinc containing hydroxyapatite ceramics to promote osteoblastic cell activity. *Mater Sci Technol* 20(9):1079–1083
138. Kumar GS, Thamizhavel A, Yokogawa Y, Kalkura SN, Girija EK (2012) Synthesis, characterization and in vitro studies of zinc and carbonate co-substituted nano-hydroxyapatite for biomedical applications. *Mater Chem Phys* 134:1127–1135
139. Hayakawa S, Ando K, Tsuru K, Osaka A, Fujii E, Kawabata K, Bonhomme C, Babonneau F (2007) Structural characterization and protein adsorption property of hydroxyapatite particles modified with zinc ions. *J Am Ceram Soc* 90(2):565–569
140. Li M, Xiao X, Liu R, Chen C, Huang L (2008) Structural characterization of zinc-substituted hydroxyapatite prepared by hydrothermal method. *J Mater Sci Mater Med* 19:797–803
141. Chung RJ, Hsieh MF, Huang CW, Perng LH, Wen HW, Chin TS (2006) Antimicrobial effects and human gingival biocompatibility of hydroxyapatite sol–gel coatings. *J Biomed Mater Res B* 76B:169–178
142. Velard F, Laurent-Maquin D, Braux J, Guillaume C, Bouthors S, Jallot E, Nedelec JM, Belaouaj A, Laquerriere P (2010) The effect of zinc on hydroxyapatite-mediated activation of human polymorphonuclear neutrophils and bone implant-associated acute inflammation. *Biomaterials* 31(8):2001–2009
143. Grandjean-Laquerriere A, Laquerriere P, Jallot E, Nedelec JM, Guenounou M, Laurent-Maquin D, Phillips TM (2006) Influence of the zinc concentration of sol–gel derived zinc substituted hydroxyapatite on cytokine production by human monocytes in vitro. *Biomaterials* 27(17):3195–3200
144. Ren F, Xin R, Ge X, Leng Y (2009) Characterization and structural analysis of zinc substituted hydroxyapatites. *Acta Biomater* 5:3141–3149
145. Terra J, Jiang M, Ellis DE (2002) Characterization of electronic structure and bonding in hydroxyapatite: Zn substitution for Ca. *Philos Mag A* 82:2357–2377
146. Matsunaga K (2008) First-principles study of substitutional magnesium and zinc in hydroxyapatite and octacalcium phosphate. *J Chem Phys* 128(24):245101
147. Chappell H, Shepherd D, Best S (2009) Zinc substituted hydroxyapatite—a comparison of modeling and experimental data. *Key Eng Mater* 396–398:729–732



148. Tamm T, Peld M (2006) Computational study of cation substitutions in apatites. *J Solid State Chem* 179:1581–1587
149. Ma X, Ellis DE (2008) Initial stages of hydration and Zn substitution/occupation on hydroxyapatite (0001) surfaces. *Biomaterials* 29(3):257–265
150. Matos M, Terra J, Ellis DE (2010) Mechanism of Zn stabilization in hydroxyapatite and hydrated (001) surfaces of hydroxyapatite. *J Phys Condes Matter* 22(14):145502 (7 pages)
151. Yin X, Calderin L, Stott MJ, Sayer M (2002) Density functional study of structural, electronic and vibrational properties of Mg- and Zn-doped tricalcium phosphate biomaterials. *Biomaterials* 23(20):4155–4163
152. Kanzaki N, Onuma K, Treboux G, Tsutsumi S, Ito A (2000) Inhibitory effect of magnesium and zinc on crystallization kinetics of hydroxyapatite (0 0 0 1) face. *J Phys Chem B* 104:4189–4194
153. Stanic V, Dimitrijevic S, Antic-Stankovic J, Mitric M, Jokic B, Plecas IB, Raicevic S (2010) Synthesis, characterization and antimicrobial activity of copper and zinc-doped hydroxyapatite nanopowders. *Appl Surf Sci* 256(20):6083–6089
154. Ohsumi Y, Kitamoto K, Anraku Y (1988) Changes induced in the permeability barrier of the yeast plasma membrane by cupric ion. *J Bacteriol* 170(6):2676–2682
155. Wang X, Ito A, Sogo Y, Li X, Oyane A (2010) Zinc-containing apatite layers on external fixation rods promoting cell activity. *Acta Biomater* 6(3):962–968
156. Yamada Y, Ito A, Kojima H, Sakane M, Miyakawa S, Uemura T, LeGeros RZ (2008) Inhibitory effect of  $Zn^{2+}$  in zinc-containing  $\beta$ -tricalcium phosphate on resorbing activity of mature osteoclasts. *J Biomed Mater Res A* 84(2):344–352
157. Kawamura H, Ito A, Miyakawa S, Layrolle P, Ojima K, Ichinose N, Tateishi T (2000) Stimulatory effect of zinc-releasing calcium phosphate implant on bone formation in rabbit femora. *J Biomed Mater Res* 50(2):184–190
158. Thian ES, Konishi T, Kawanobe Y, Lim PN, Choong C, Ho B, Aizawa M (2013) Zinc-substituted hydroxyapatite: a biomaterial with enhanced, bioactivity and antibacterial properties. *J Mater Sci Mater Med* 24(2):437–445
159. Chen X, Tang QL, Zhu YJ, Zhu CL, Feng XP (2012) Synthesis and antibacterial property of zinc loaded hydroxyapatite nanorods. *Mater Lett* 89:233–235
160. Venkatasubbu GD, Ramasamy S, Ramakrishnan V, Kumar J (2011) Nanocrystalline hydroxyapatite and zinc doped hydroxyapatite as carrier material for controlled delivery of ciprofloxacin. *3Biotech* 1(3):173–186
161. Rameshbabu N, Kumar TSS, Prabhakar TG, Sastry VS, Murty K, Rao KP (2007) Antibacterial nanosized silver substituted hydroxyapatite: synthesis and characterization. *J Biomed Mater Res A* 80A:581–591
162. Sygnatowicz M, Keyshar K, Tiwari A (2010) Antimicrobial properties of silver-doped hydroxyapatite nano-powders and thin films. *JOM* 62(7):65–70
163. George N, Faoagali J, Muller M (1997) Silvazine (TM) (silver sulfadiazine and chlorhexidine) activity against 200 clinical isolates. *Burns* 23(6):493–495
164. Klasen HJ (2000) A historical review of the use of silver in the treatment of burns. I. Early uses. *Burns* 26(2):117–130
165. Lara HH, Garza-Trevino EN, Ixtapan-Turrent L, Singh DK (2011) Silver nanoparticles are broad-spectrum bactericidal and virucidal compounds. *J Nanobiotechnol* 9:30–38
166. Wright JB, Lam K, Hansen D, Burrell RE (1999) Efficacy of topical silver against fungal burn wound pathogens. *Am J Infect Control* 27(4):344–350
167. Simchi A, Tamjid E, Pishbin F, Boccaccini AR (2011) Recent progress in inorganic and composite coatings with bactericidal capability for orthopaedic applications. *Nanomed Nanotechnol Biol Med* 7(1):22–39
168. Darouiche RO, Raad II, Heard SO et al (1999) A comparison of two antimicrobial-impregnated central venous catheters. *N Engl J Med* 340(1):1–8
169. Benn TM, Westerhoff P (2008) Nanoparticle silver released into water from commercially available sock fabrics. *Environ Sci Technol* 42(11):4133–4139

170. Jain P, Pradeep T (2005) Potential of silver nanoparticle-coated polyurethane foam as an antibacterial water filter. *Biotechnol Bioeng* 90(1):59–63
171. Hardes J, Ahrens H, Gebert C, Streitburger A, Buerger H, Erren M, Günsel A, Wedemeyer C, Saxler G, Winkelmann W, Gosheger G (2007) Lack of toxicological side-effects in silver-coated megaprotheses in humans. *Biomaterials* 28(18):2869–2875
172. Gosheger G, Hardes J, Ahrens H, Streitburger A, Buerger H, Erren M, Günsel A, Kemper FH, Winkelmann W, Von Eiff C (2004) Silver-coated megaendoprostheses in a rabbit model – an analysis of the infection rate and toxicological side effects. *Biomaterials* 25(24):5547–5556
173. Feng QL, Wu J, Chen GQ, Cui FZ, Kim TN, Kim JO (2000) A mechanistic study of the antibacterial effect of silver ions on *Escherichia coli* and *Staphylococcus aureus*. *J Biomed Mater Res* 52(4):662–668
174. Liao SY, Read DC, Pugh WJ, Furr JR, Russell AD (1997) Interaction of silver nitrate with readily identifiable groups: relationship to the antibacterial action of silver ions. *Lett Appl Microbiol* 25(4):279–283
175. Jung WK, Koo HC, Kim KW, Shin S, Kim SH, Park YH (2008) Antibacterial activity and mechanism of action of the silver ion in *Staphylococcus aureus* and *Escherichia coli*. *Appl Environ Microbiol* 74(7):2171–2178
176. Hajipour MJ, Fromm KM, Ashkarran AA, Jimenez de Aberasturi D, de Larramendi IR, Rojo T, Serpooshan V, Parak WJ, Mahmoudi M (2013) Erratum: antibacterial properties of silver nanoparticles. *Trends Biotechnol* 31(1):61–62
177. Gordon O, Slenters TV, Brunetto PS, Villaruz AE, Sturdevant DE, Otto M, Landmann R, Fromm KM (2010) Silver coordination polymers for prevention of implant infection: thiol interaction, impact on respiratory chain enzymes, and hydroxyl radical induction. *Antimicrob Agents Chemother* 54(10):4208–4218
178. Kora AJ, Arunachalam J (2011) Assessment of antibacterial activity of silver nanoparticles on *Pseudomonas aeruginosa* and its mechanism of action. *World J Microbiol Biotechnol* 27(5):1209–1216
179. Kim JS, Kuk E, Yu KN, Kim JH, Park SJ, Lee HJ, Kim SH, Park YK, Park YH, Hwang CY, Kim YK, Lee YS, Jeong DH, Cho MH (2007) Antimicrobial effects of silver nanoparticles. *Nanomed Nanotechnol Biol Med* 3(1):95–101
180. Sondi I, Salopek-Sondi B (2004) Silver nanoparticles as antimicrobial agent: a case study on *E. coli* as a model for Gram-negative bacteria. *J Colloid Interface Sci* 275(1):177–182
181. Kim TN, Feng QL, Kim JO, Wu J, Wang H, Chen GQ, Cui FZ (1998) Antimicrobial effects of metal ions ( $\text{Ag}^+$ ,  $\text{Cu}^{2+}$ ,  $\text{Zn}^{2+}$ ) in hydroxyapatite. *J Mater Sci Mater Med* 9:129–134
182. Chen Y, Zheng X, Xie Y, Ji H, Ding C, Li H, Dai K (2010) Silver release from silver-containing hydroxyapatite coatings. *Surf Coat Technol* 205:1892–1896
183. Oh KS, Kim KJ, Jeong YK, Choa YH (2003) Effect of fabrication processes on the antimicrobial properties of silver doped nano-sized HAp. *Key Eng Mater* 240–242:583–586
184. Su BH, Xiong ZX (2007) Preparation of antibacterial ceramics with silver-carrying nano-hydroxyapatite. *Key Eng Mater* 336–338:1563–1566
185. Shi CL, Ren I, Xiong ZX (2005) Preparation and effectiveness of antibacterial hydroxyapatite powder containing silver. *Key Eng Mater* 280–283:1529–1532
186. Ciobanu CS, Massuyeau F, Constantin LV, Predoi D (2011) Structural and physical properties of antibacterial Ag-doped nano-hydroxyapatite synthesized at 100 °C. *Nanoscale Res Lett* 6:613–620
187. Ciobanu CS, Iconaru SL, Le Coustumer P, Constantin LV, Predoi D (2012) Antibacterial activity of silver-doped hydroxyapatite nanoparticles against gram-positive and gram-negative bacteria. *Nanoscale Res Lett* 7:324–332
188. Ciobanu CS, Iconaru SL, Chifriuc MC, Costescu A, le Coustumer P, Predoi D (2013) Synthesis and antimicrobial activity of silver-doped hydroxyapatite nanoparticles. *Biomed Res Intern* 2013:916218 (10 pages)
189. Ciobanu CS, Iconaru SL, Pasuk I, Vasile BS, Lupu AR, Hermenean A, Dinischiotu A, Predoi D (2013) Structural properties of silver doped hydroxyapatite and their biocompatibility. *Mater Sci Eng C* 33:1395–1402

190. Thian ES, Lim PN, Shi Z, Tay BY, Neoh KJ (2012) Silver-doped apatite as a bioactive and an antimicrobial bone material. *Key Eng Mater* 493–494:27–30
191. Peetsch A, Greulich C, Braun D, Stroetges C, Rehage H, Siebers B, Koller M, Epple M (2013) Silver-doped calcium phosphate nanoparticles: synthesis, characterization, and toxic effects toward mammalian and prokaryotic cells. *Colloid Surf B Biointerfaces* 102:724–729
192. Stanic V, Janackovic D, Dimitrijevic S, Tanaskovic SB, Mitric M, Pavlovic MS, Krstic A, Jovanovic D, Raicevic S (2011) Synthesis of antimicrobial monophase silver-doped hydroxyapatite nanopowders for bone tissue engineering. *Appl Surf Sci* 257:4510–4518
193. Chen W, Oh S, Ong AP, Oh N, Liu Y, Courtney HS, Appleford M, Ong JL (2007) Antibacterial and osteogenic properties hydroxyapatite coatings produced using of silver-containing a sol gel process. *J Biomed Mater Res A* 82A(4):899–906
194. Chung RJ, Hsieh MF, Huang KC, Perng LH, Chou FI, Chin TS (2005) Anti-microbial hydroxyapatite particles synthesized by a sol-gel route. *J Sol-Gel Sci Technol* 33(2):229–239
195. Iconaru SL, Chapon P, le Coustumer P, Predoi D (2014) Antimicrobial activity of thin solid films of silver doped hydroxyapatite prepared by sol-gel method. *Scientific World Journal* 2014:165351 (8 pages)
196. Díaz M, Barba F, Miranda M, Guitián F, Torrecillas R, Moya JS (2009) Synthesis and antimicrobial activity of a silver-hydroxyapatite nanocomposite. *J Nanomater* 2009:1–6
197. Feng QL, Kim TN, Wu J, Park ES, Kim JO, Lim DY, Cui FZ (1998) Antibacterial effects of Ag-HAP thin films on alumina substrates. *Thin Solid Films* 335(1–2):214–219
198. Honda M, Kawanobe Y, Ishii K, Konishi T, Mizumoto M, Kanzawa N, Matsumoto M, Aizawa M (2013) In vitro and in vivo antimicrobial properties of silver-containing hydroxyapatite prepared via ultrasonic spray pyrolysis route. *Mater Sci Eng C* 33(8):5008–5018
199. Yang L, Ning X, Xiao Q, Chen K, Zhou H (2007) Development and characterization of porous silver-incorporated hydroxyapatite ceramic for separation and elimination of microorganisms. *J Biomed Mater Res* 81B:50–56
200. Oh KS, Kim KJ, Jeong YK, Park EK, Kim SY, Kwon JH, Ryoo HM, Shin HI (2004) Cytotoxicity and antimicrobial effect of Ag doped hydroxyapatite. *Key Eng Mater* 264–268:2107–2110
201. Costescu A, Ciobanu CS, Iconaru SL, Ghita RV, Chifiriuc CM, Marutescu LG, Predoi D (2013) Fabrication, characterization and antimicrobial activity, evaluation of low silver concentrations in silver-doped hydroxyapatite nanoparticles. *J Nanomater* 2013:194854 (9 pages)
202. Narayanan R, Singh V, Kwon TY, Kim KH (2009) Combustion synthesis of hydroxyapatite and hydroxyapatite (silver) powders. *Key Eng Mater* 396–398:411–419
203. Chen W, Liu Y, Courtney HS, Bettenga M, Agrawal CM, Bumgardner JD, Ong JL (2006) In vitro anti-bacterial and biological properties of magnetron co-sputtered silver-containing hydroxyapatite coating. *Biomaterials* 27:5512–5517
204. Ewald A, Hösel D, Patel S, Grover LM, Barralet JE, Gbureck U (2011) Silver-doped calcium phosphate cements with antimicrobial activity. *Acta Biomater* 7:4064–4070
205. Ciobanu CS, Andronescu E, Vasile BS, Valsangiacom CM, Ghita RV, Predoi D (2010) Synthesis and antimicrobial activity of silver-doped hydroxyapatite nanoparticles. *Optoelectron Adv Mater* 4:1515–1519
206. Badrou L, Sadel A, Zahir M, Kimakh L, El Hajbi A (1998) Synthesis and physical and chemical characterization of  $\text{Ca}_{10-x}\text{Ag}_x(\text{PO}_4)_6(\text{OH})_{(2-x)}\text{square}(x)$  apatites. *Ann Chim Sci Mater* 23:61–64
207. Choi JW, Cho HM, Kwak EK, Kwon TG, Ryoo HM, Jeong YK, Oh KS, Shin HI (2004) Effect of Ag-doped hydroxyapatite as a bone filler for inflamed bone defects. *Key Eng Mater* 254–256:47–50
208. Roy M, Fielding GA, Beyenal H, Bandyopadhyay A, Bose S (2012) Mechanical, in vitro antimicrobial, and biological properties of plasma-sprayed silver-doped hydroxyapatite coating. *Appl Mater Interfaces* 4(3):1341–1349
209. Samani S, Hossainipour SM, Tamizifar M, Rezaie HR (2013) In vitro antibacterial evaluation of sol-gel-derived Zn-, Ag-, and (Zn + Ag)-doped hydroxyapatite coatings against methicillin-resistant *Staphylococcus aureus*. *J Biomed Mater Res A* 101(1):222–230

210. Guo C, Li X, Dong Y (2011) Preparation and characterization of silver/hydroxyapatite nanoparticles. *Adv Mater Res* 311–313:1746–1750
211. Fielding GA, Roy M, Bandyopadhyay A, Bose S (2012) Antibacterial and biological characteristics of silver containing and strontium doped plasma sprayed hydroxyapatite coatings. *Acta Biomater* 8(8):3144–3152
212. Brajendra S, Dubey AK, Kumar S, Saha N, Basu B, Gupta R (2011) In vitro biocompatibility and antimicrobial activity of wet chemically prepared  $\text{Ca}_{10-x}\text{Ag}_x(\text{PO}_4)_6(\text{OH})_2$  ( $0.0 \leq x \leq 0.5$ ) hydroxyapatites. *Mater Sci Eng C* 31(7):1320–1329
213. Lee IS, Whang CN, Oh KS, Park JC, Lee KY, Lee GH, Chung SM, Sung XD (2006) Formation of silver incorporated calcium phosphate film for medical applications. *Nucl Inst Methods Phys Res B* 242(1–2):45–47
214. Wiesmann HP, Plate U, Zierold K, Hohling HJ (1998) Potassium is involved in apatite biomineralization. *J Dent Res* 77:1654–1657
215. Hohling HJ, Mishima H, Kozawa Y, Daimon T, Barckhaus RH, Richte KD (1991) Microprobe analyses of the potassium calcium distribution relationship in preentin. *Scan Microsc Int* 5:247–253
216. Itoh R, Suyama Y (1996) Sodium excretion in relation to calcium and hydroxyproline excretion in a healthy Japanese population. *Am J Clin Nutr* 63:735–740
217. Ginty F, Flynn A, Cashman KD (1998) The effect of dietary sodium intake on biochemical markers of bone metabolism in young women. *Br J Nutr* 79:343–350
218. Nordström EG, Karlsson KH (1992) Chemical characterization of a potassium hydroxyapatite prepared by soaking in potassium chloride and carbonate solutions. *Biomed Mater Eng* 2:185–189
219. Weissmueller NT, Schiffter HA, Pollard AJ, Tas AC (2014) Molten salt synthesis of potassium-containing hydroxyapatite microparticles used as protein substrate. *Mater Lett* 128:421–424
220. El Feki H, Savariault JM, Salah AB, Jemal M (2000) Sodium and carbonate distribution in substituted calcium hydroxyapatite. *Solid State Sci* 2:577–586
221. Kannan S, Ventura JMG, Lemos AF, Barba A, Ferreira JMF (2008) Effect of sodium addition on the preparation of hydroxyapatites and biphasic ceramics. *Ceram Int* 34:7–13
222. El Feki H, Naddari T, Savariault JM, Ben Salah A (2000) Localization of potassium in substituted lead hydroxyapatite:  $\text{Pb}_{9,30}\text{K}_{0,60}(\text{PO}_4)_6(\text{OH})_{1,20}$  by X-ray diffraction. *Solid State Sci* 2:725–733
223. Kannan S, Ventura JMG, Ferreira JMF (2007) Synthesis and thermal stability of potassium substituted hydroxyapatites and hydroxyapatite/ $\beta$ -tricalciumphosphate mixtures. *Ceram Int* 33:1489–1494
224. Wilson RM, Elliott JC, Dowker SEP, Smith RI (2004) Rietveld structure refinement of precipitated carbonate apatite using neutron diffraction data. *Biomaterials* 25:2205–2213
225. Carp O, Huisman CL, Reller A (2004) Photoinduced reactivity of titanium dioxide. *Prog Solid State Chem* 32(1–2):33–177
226. Nakata K, Fujishima A (2013)  $\text{TiO}_2$  photocatalysis: design and applications. *J Photochem Photobiol C* 13(3):169–189
227. Huang J, Best SM, Bonfield W, Buckland TOM (2010) Development and characterization of titanium-containing hydroxyapatite for medical applications. *Acta Biomater* 6:241–249
228. Wakamura M, Hashimoto K, Watanabe T (2003) Photocatalysis by calcium hydroxyapatite modified with Ti(IV): albumin decomposition and bactericidal effect. *Langmuir* 19:3428–3431
229. Wakamura M (2005) Photocatalysis by calcium hydroxyapatite modified by Ti (IV). *Fujitsu Sci Tech J* 41(2):181–190
230. Hu A, Li M, Chang C, Mao D (2007) Preparation and characterization of a titanium-substituted hydroxyapatite photocatalyst. *J Mol Catal A Chem* 267(1–2):79–85
231. Kandori K, Oketani M, Wakamura M (2013) Effects of Ti(IV) substitution on protein adsorption behaviors of calcium hydroxyapatite particles. *Colloid Surf B Biointerfaces* 101:68–73

232. Medvecký L, Štulajterova R, Parilak L, Trpčevska J, D`urišin J, Barinov SM (2006) Influence of manganese on stability and particle growth of hydroxyapatite in simulated body fluid. *Colloids Surf A* 281:221–229
233. Armulik A, Svineng G, Wennerberg K, Fässler R, Johansson S (2000) Expression of integrin subunit beta1B in integrin beta1-deficient GD25 cells does not interfere with alphaVbeta3 functions. *Exp Cell Res* 254(1):55–63
234. Mayer I, Jacobsohn O, Niazov T, Werckmann J, Iliescu M, Richard-Plouet M, Burghaus O, Reinen D (2003) Manganese in precipitated hydroxyapatites. *Eur J Inorg Chem* 7:1445–1451
235. Mayer I, Cuisinier FJG, Gdalya S, Popov I (2008) TEM study of the morphology of Mn<sup>2+</sup>-doped calcium hydroxyapatite and β-tricalcium phosphate. *J Inorg Biochem* 102(2):311–317
236. Li Y, Nam CT, Ooi CP (2009) Iron(III) and manganese(II) substituted hydroxyapatite nanoparticles: characterization and cytotoxicity analysis. *J Phys Conf Ser* 187(1):012024
237. Mayer I, Cuisinier FJG, Popov I, Schleich Y, Gdalya S, Burghaus O, Reinen D (2006) Phase relations between β-tricalcium phosphate and hydroxyapatite with manganese(II): structural and spectroscopic properties. *Eur J Inorg Chem* 7:1460–1465
238. Bigi A, Bracci B, Cuisinier F, Elkaim R, Fini M, Mayer I, Mihailescu IN, Socol G, Sturba L, Torricelli P (2005) Human osteoblast response to pulsed laser deposited calcium phosphate coatings. *Biomaterials* 26:2381–2389
239. Torell P (1988) Iron and dental caries. *Swed Dent J* 12:113–124
240. Wu HC, Wang TW, Sun JS, Wang WH, Lin FH (2007) A novel biomagnetic nanoparticle based on hydroxyapatite. *Nanotechnology* 18:165601
241. Zuo KH, Zeng YP, Jiang D (2012) Synthesis and magnetic property of irons-doped hydroxyapatite. *J Nanosci Nanotechnol* 12:7096–7100
242. Rau JV, Cacciotti I, De Bonis A, Fosca M, Komlev VS, Latini A, Santagata A, Teghil R (2014) Fe-doped hydroxyapatite coatings for orthopaedic and dental implant applications. *Appl Surf Sci* 307:301–305
243. Pon-On W, Meejoo S, Tang M (2007) Incorporation of iron into nano hydroxyapatite particles synthesized by the microwave process. *Int J Nanosci* 6:9–16
244. Kandori K, Toshima S, Wakamura M, Fukusumi M, Morisada Y (2010) Effects of modification of calcium hydroxyapatites by trivalent metal ions on the protein adsorption behavior. *J Phys Chem B* 114:2399–2404
245. Ito A, Shinkai M, Honda H, Kobayashi T (2005) Medical application of functionalized magnetic nanoparticles. *J Biosci Bioeng* 100:1–11
246. Hou CH, Hou SM, Hsueh YS, Lin J, Wu HC, Lin FH (2009) The in vivo performance of biomagnetic hydroxyapatite nanoparticles in cancer hyperthermia therapy. *Biomaterials* 30:3956–3960
247. Coelho J, Hussain NS, Gomes PS, Garcia MP, Lopes MA, Fernandes MH, Santos JD (2013) Development and characterization of lanthanides doped hydroxyapatite composites for bone tissue application. In: Nandyala SH, Santos JD (eds) *Current trends on glass and ceramic materials*. Bentham Science Publishers, Sharjah, pp 87–115
248. Ciobanu CS, Popa CL, Predoi D (2014) Sm:HAp nanopowders present antibacterial activity against *Enterococcus faecalis*. *J Nanomater* 2014:780686 (9 pages)
249. (2009) Toxicological review of cerium oxide and cerium compounds. US Environmental Protection Agency, Washington, DC. <http://www.epa.gov/iris/>
250. Yingguang L, Zhuoru Y, Jiang C (2007) Preparation, characterization and antibacterial property of cerium substituted hydroxyapatite nanoparticles. *J Rare Earths* 25:452–456
251. Das S, Singh S, Dowding JM, Oommen S, Kumar A, Sayle TX, Saraf S, Patra CR, Vlahakis NE, Sayle DC, Self WT, Seal S (2012) The induction of angiogenesis by cerium dioxide nanoparticles through the modulation of oxygen in intracellular environments. *Biomaterials* 33(31):7746–7755
252. Lord MS, Tsoi B, Gunawan C, Teoh WY, Amal R, Whitelock JM (2013) Anti-angiogenic activity of heparin functionalized cerium oxide nanoparticles. *Biomaterials* 34(34):8808–8818

253. Kuang Y, He X, Zhang Z, Li Y, Zhang H, Ma Y, Wu Z, Chai Z (2010) Comparison study on the antibacterial activity of nano-or bulk-cerium oxide. *J Nanosci Nanotechnol* 11 (5):4103–4108
254. Pelletier DA, Suresh AK, Holton GA, McKeown CK, Wang W, Gu B, Mortensen NP, Allison DP, Joy DC, Allison MR, Brown SD, Phelps TJ, Doktycz MJ (2010) Effects of engineered cerium oxide nanoparticles on bacterial growth and viability. *Appl Environ Microbiol* 76 (24):7981–7989
255. Han YJ, Loo SCJ, Phung NT, Boey F, Ma J (2008) Controlled size and morphology of EDTMP-doped hydroxyapatite nanoparticles as model for <sup>153</sup>Samarium-EDTMP doping. *J Mater Sci Mater Med* 19(9):2993–3003
256. Turner JH, Claringbold PG, Hetherington EL, Sorby P, Martindale AA (1989) A phase I study of samarium-153 ethylenediaminetetramethylene phosphonate therapy for disseminated skeletal metastases. *J Clin Oncol* 7(12):1926–1931
257. Turner JH, Claringbold PG (1991) A phase II study of treatment of painful multifocal skeletal metastases with single and repeated dose samarium-153 ethylenediaminetetramethylene phosphonate. *Eur J Cancer* 27(9):1084–1086
258. Chinol M, Vallabhajosula S, Goldsmith SJ, Klein MJ, Deutsch KF, Chinen LK, Brodack JW, Deutsch EA, Watson BA, Tofe AJ (1993) Chemistry and biological behavior of samarium-153 and rhenium-186-labeled hydroxyapatite particles: potential radiopharmaceuticals for radiation synovectomy. *J Nucl Med* 34(9):1536–1542
259. Yasukawa A, Gotoh K, Tanaka H, Kandori K (2012) Preparation and structure of calcium hydroxyapatite substituted with light rare earth ions. *Colloids Surf A* 393:53–59
260. Cawthray JF, Louise Creagh A, Haynes CA, Orvig C (2015) Ion exchange in hydroxyapatite with lanthanides. *Inorg Chem* 54(4):1440–1445
261. Sun LJ, Guo DG, Zhao WA, Wang LY, Xu KW (2014) Influences of reaction parameters and Ce contents on structure and properties of nano-scale Ce-HA powders. *J Mater Sci Technol* 30 (8):776–781
262. Feng Z, Liao Y, Ye M (2005) Synthesis and structure of cerium-substituted hydroxyapatite. *J Mater Sci Mater Med* 16(5):417–421
263. Lin Y, Yang Z, Cheng J (2007) Preparation, characterization and antibacterial property of cerium-substituted hydroxyapatite nanoparticles. *J Rare Earths* 25(4):452–456
264. Kaygili O, Dorozhkin SV, Keser S (2014) Synthesis and characterization of Ce-substituted hydroxyapatite by the sol–gel method. *Mater Sci Eng C* 42:78–82
265. Padilla Mondejar S, Kovtun A, Epple M (2007) Lanthanide-doped calcium phosphate nanoparticles with high internal crystallinity and with a shell of DNA as fluorescent probes in cell experiments. *J Mater Chem* 17:4153–4159
266. Doat A, Fanjul M, Pelle F, Hollande E, Lebugle A (2003) Europium-doped bioapatite: a new photostable biological probe, internalizable by human cells. *Biomaterials* 24:3365–3371
267. Doat A, Pelle F, Gardant N, Lebugle A (2004) Synthesis of luminescent bioapatite nanoparticles for utilization as a biological probe. *J Solid State Chem* 177:1179–1187
268. Lebugle A, Pelle F, Charvillat C, Rousselot I, Chane-Ching JY (2006) Colloidal and monocrystalline Ln<sup>3+</sup> doped apatite calcium phosphate as biocompatible fluorescent probes. *Chem Commun* 6:606–608
269. Oviedo MJ, Contreras O, Vazquez-Duhalt R, Carbajal-Arizaga CG, Hirata GA, McKittrick J (2012) Photoluminescence of europium-activated hydroxyapatite nanoparticles in body fluids. *Sci Adv Mater* 4:558–562
270. Wiglusz RJ, Kedziora A, Lukowiak A, Doroszkiewicz W, Streck W (2012) Hydroxyapatites and Europium(III) doped hydroxyapatites as a carrier of silver nanoparticles and their antimicrobial activity. *J Biomed Nanotechnol* 8(4):605–612
271. Iconaru SL, Motelica-Heino M, Predoi D (2013) Study on europium-doped hydroxyapatite nanoparticles by fourier transform infrared spectroscopy and their antimicrobial properties. *J Spectrosc* 2013:284285 (10 pages)

272. Sato M, Sambito MA, Aslani A, Kalkhoran NM, Slamovich EB, Webster TJ (2006) Increased osteoblast functions on undoped and yttrium-doped nanocrystalline hydroxyapatite coatings on titanium. *Biomaterials* 27:2358–2369
273. Liu Y, Zhou RJ, Mo AC, Chen ZQ, Wu HK (2007) Synthesis and characterization of yttrium/hydroxyapatite nanoparticles. *Key Eng Mater* 330–332:295–298
274. Mayer I, Layani JD, Givan A, Gaft M, Blan P (1999) La ions in precipitated hydroxyapatites. *J Inorg Biochem* 73:221–226
275. Huang Y, Wang Y, Ning C, Nan K, Han Y (2008) Preparation and properties of a cerium-containing hydroxyapatite coating on commercially pure titanium by micro-arc oxidation. *Rare Metals* 27(3):257–260
276. Toker SM, Tezcaner A, Evis Z (2011) Microstructure, microhardness, and biocompatibility characteristics of yttrium hydroxyapatite doped with fluoride. *J Biomed Mater Res Part B Appl Biomater* 96B(2):207–217
277. dos Santos MF, Furtado RNV, Konai MS, Castiglioni MLV, Marchetti RR, Natour J (2009) Effectiveness of radiation synovectomy with samarium-153 particulate hydroxyapatite in rheumatoid arthritis patients with knee synovitis: a controlled randomized double-blind trial. *Clinics* 64(12):1187–1193
278. O'Duffy EK, Oliver FJ, Chatters SJ, Walker H, Lloyd DC, Edwards JC, Ell PJ (1999) Chromosomal analysis of peripheral lymphocytes of patients before and after radiation synovectomy with samarium-153 particulate hydroxyapatite. *Rheumatology* 38(4):316–320
279. O'Duffy EK, Clunie GPR, Lui D, Edwards JCW, Ell J (1999) Double blind glucocorticoid controlled trial of samarium-153 particulate hydroxyapatite radiation synovectomy for chronic knee synovitis. *Ann Rheum Dis* 58(9):554–558
280. Bernstein LR (1998) Mechanisms of therapeutic activity for gallium. *Pharmacol Rev* 50(4):665–682
281. Franchini M, Lusvardi G, Malavasi G, Menabue L (2012) Gallium-containing phosphosilicate glasses: synthesis and in vitro bioactivity. *Mater Sci Eng C* 32(6):1401–1406
282. Valappil SP, Ready D, Abou Neel EA, Pickup DM, O'Dell LA, Chrzanowski W, Pratten J, Newport RJ, Smith ME, Wilson M, Knowles JC (2009) Controlled delivery of antimicrobial gallium ions from phosphate-based glasses. *Acta Biomater* 5(4):1198–1210
283. Melnikov P, Malzac A, Coelho MB (2008) Gallium and bone pathology. *Acta Ortop Bras* 16:54–57
284. Melnikov P, Teixeira AR, Malzac A, Coelho MDB (2009) Gallium-containing hydroxyapatite for potential use in orthopedics. *Mater Chem Phys* 117(1):86–90
285. Dollwet H, Sorenson J (1985) Historic uses of copper compounds in medicine. *Trace Elem Med* 2(2):80–87
286. Yang H, Zhang L, Xu KW (2009) Effect of storing on the microstructure of Ag/Cu/HA powder. *Ceram Intern* 35(4):1595–1601
287. White C, Lee J, Kambe T, Fritsche K, Petris MJ (2009) A role for the ATP7A copper-transporting ATPase in macrophage bactericidal activity. *J Biol Chem* 284(49):33949–33956
288. Li Y, Ho J, Ooi CP (2010) Antibacterial efficacy and cytotoxicity studies of copper (II) and titanium (IV) substituted hydroxyapatite nanoparticles. *Mater Sci Eng C* 30(8):1137–1144
289. Osman D, Waldron KJ, Denton H, Taylor CM, Grant AJ, Mastroeni P, Robinson NJ, Cavet JS (2010) Copper homeostasis in *Salmonella* is atypical and copper-CueP is a major periplasmic metal complex. *J Biol Chem* 285(33):25259–25268
290. Soutourina O, Dubrac S, Poupel O, Msadek T, Martin-Verstraete I (2010) The pleiotropic CymR regulator of *Staphylococcus aureus* plays an important role in virulence and stress response. *PLoS Pathog* 6(5), e1000894
291. Babu U, Failla ML (1990) Respiratory burst and candidacidal activity of peritoneal macrophages are impaired in copper-deficient rats. *J Nutr* 120(12):1692–1699
292. Shanmugam S, Gopal B (2014) Copper substituted hydroxyapatite and fluorapatite: synthesis, characterization and antimicrobial properties. *Ceram Intern Part A* 40(10):15655–15662

293. Daou S, El Chemaly A, Christofilopoulos P, Bernard L, Hoffmeyer P, Demaurex N (2011) The potential role of cobalt ions released from metal prosthesis on the inhibition of Hv1 proton channels and the decrease in *Staphylococcus epidermidis* killing by human neutrophils. *Biomaterials* 32(7):1769–1777
294. Tank KP, Chudasama KS, Thaker VS, Joshi MJ (2013) Cobalt-doped nanohydroxyapatite: synthesis, characterization, antimicrobial and hemolytic studies. *J Nanopart Res* 15:1644–1655
295. Singh K, Kumar Y, Puri P, Sharma C, Aneja KR (2012) Thermal, spectral, fluorescence, and antimicrobial studies of cobalt, nickel, copper, and zinc complexes derived from 4-[(5-bromothiophen-2-ylmethylene)-amino]-3-mercapto-6-methyl-5-oxo-[1,2,4]triazine. *Internat J Inorg Chem* 2012:873232 (9 pages)
296. Ignjatović N, Ajduković Z, Savić V, Najman S, Mihailović D, Vasiljević P, Stojanović Z, Uskoković V, Uskoković D (2013) Nanoparticles of cobalt-substituted hydroxyapatite in regeneration of mandibular osteoporotic bones. *J Mater Sci Mater Med* 24(2):343–354
297. Stănila A, Braicu C, Stănila S, Pop RM (2011) Antibacterial activity of copper and cobalt amino acids complexes. *Notulae Botanicae Horti Agrobotanici Cluj-Napoca* 39(2):124–129
298. Mabilletau G, Filmon R, Petrov PK, Baslé MF, Sabokbar A, Chappard D (2010) Cobalt, chromium and nickel affect hydroxyapatite crystal growth in vitro. *Acta Biomater* 6:1555–1560
299. Montel G, Bonel G, Heughebaert JC, Trombe JC, Rey C (1981) New concepts in the composition, crystallization and growth of the mineral component of calcified tissues. *J Cryst Growth* 53(1):74–99
300. Bigi A, Cojazzi G, Panzavolta S, Ripamonti A, Roveri N, Romanello M, Suarez KN, Moro L (1997) Chemical and structural characterization of the mineral phase from cortical and trabecular bone. *J Inorg Biochem* 68(1):45–51
301. Amjad Z (1997) Calcium phosphates in biological and industrial systems. Kluwer, Boston
302. Lafon JP, Champion E, Bernache-Assollant D (2008) Processing of AB-type carbonated hydroxyapatite  $\text{Ca}_{10-x}(\text{PO}_4)_{(6-x)}(\text{CO}_3)_x(\text{OH})_{(2-x-2y)}(\text{CO}_3)_y$  ceramics with controlled composition. *J Eur Ceram Soc* 28:139–147
303. Rey C, Collins B, Goehl T, Dickson IR, Glimcher MJ (1989) The carbonate environment in bone mineral: a resolution-enhanced Fourier Transform Infrared Spectroscopy study. *Calcif Tissue Int* 45:157–164
304. Elliott JC (2002) Calcium phosphate biominerals. In: Kohn MJ, Rakovan J, Hughes JM (eds) *Phosphates: geochemical, geobiological and material importance, reviews in mineralogy and geochemistry*, vol 48. Mineralogical Society of America, Washington, pp 427–454
305. LeGeros RZ (1965) Effect of carbonate on the lattice parameters of apatite. *Nature* 206:403–404
306. Landi E, Celotti G, Logroscino G, Tampieri A (2003) Carbonated hydroxyapatite as bone substitute. *J Eur Ceram Soc* 23(15):2931–2937
307. Rey C, Renugopalakrishnan V, Collins B, Glimcher M (1991) Fourier transform infrared spectroscopic study of the carbonate ions in bone mineral during aging. *Calcif Tissue Int* 49:251–258
308. Merry JC, Gibson IR, Best SM, Bonfield W (1998) Synthesis and characterization of carbonate hydroxyapatite. *J Mater Sci Mater Med* 9:779–783
309. Rogers KD, Daniels P (2002) An X-ray diffraction study of the effects of heat treatment on bone mineral microstructure. *Biomaterials* 23:2577–2585
310. Barralet J, Best S, Bonfield W (1998) Carbonate substitution in precipitated hydroxyapatite: an investigation into the effects of reaction temperature and bicarbonate ion concentration. *J Biomed Mater Res* 41:79–86
311. Murugan R, Ramakrishna S (2006) Production of ultra-fine bioresorbable carbonated hydroxyapatite. *Acta Biomater* 2:201–206
312. Ślósarczyk A, Paszkiewicz Z, Zima A (2010) The effect of phosphate source on the sintering of carbonate substituted hydroxyapatite. *Ceram Inter* 36:577–582



313. Koumoulidis GC, Katsoulidis AP, Ladavos AK, Pomonis PJ, Trapalis CC, Sdoukos AT, Vaimakis TC (2003) Preparation of hydroxyapatite via microemulsion route. *J Colloid Interface Sci* 259:254–260
314. Zhou WY, Wang M, Cheung WL, Guo BC, Jia DM (2008) Synthesis of carbonated hydroxyapatite nanospheres through nanoemulsion. *J Mater Sci Mater Med* 19(1):103–110
315. Fathi MH, Hanifi A, Mortazavi V (2008) Preparation and bioactivity evaluation of bone-like hydroxyapatite nanopowder. *J Mater Process Technol* 202:536–542
316. Lala S, Brahmachari S, Das PK, Das D, Kar T, Pradhan SK (2014) Biocompatible nanocrystalline natural bonelike carbonated hydroxyapatite synthesized by mechanical alloying in a record minimum time. *Mater Sci Eng C* 42:647–656
317. Suchanek WL, Shuk P, Byrappa K, Riman RE, TenHuisen KS, Janas VF (2002) Mechanochemical–hydrothermal synthesis of carbonated apatite powders at room temperature. *Biomaterials* 23:699–710
318. Zou Z, Lin K, Chen L, Chang J (2012) Ultrafast synthesis and characterization of carbonated hydroxyapatite nanopowders via sonochemistry-assisted microwave process. *Ultrason Sonochem* 19:1174–1179
319. Iafisco M, Morales JG, Hernández-Hernández MA, García-Ruiz JM, Roveri N (2010) Biomimetic carbonate–hydroxyapatite nanocrystals prepared by vapor diffusion. *Adv Eng Mater* 12: B218–B223
320. Nordström EG, Karlsson KH (1990) Carbonate-doped hydroxyapatite. *J Mater Sci Mater Med* 1:182–184
321. Rodriguez-Lorenzo LM, Vallet-Regí M (2000) Controlled crystallization of calcium phosphate apatites. *Chem Mater* 12(8):2460–2465
322. Vallet-Regí M, Gonzalez-Calbet JM (2004) Calcium phosphates as substitution of bone tissues. *Prog Solid State Chem* 32:1–31
323. Doi Y, Shibutani T, Moriwaki Y, Kajimoto T, Iwayama YJ (1998) Sintered carbonate apatites as bioresorbable bone substitutes. *J Biomed Mater Res* 39(4):603–610
324. Elliot JC, Bond G, Tombe JC (1980) Space group and lattice constants of  $\text{Ca}_{10}(\text{PO}_4)_6\text{CO}_3$ . *J Appl Crystallogr* 13:618–621
325. Fleet ME, Liu X (2004) Location of type B carbonate ion in type A–B carbonate apatite synthesized at high pressure. *J Solid State Chem* 177:3174–3182
326. Fleet ME, Liu X (2007) Coupled substitution of type A and B carbonates in sodium-bearing apatite. *Biomaterials* 28:916–926
327. Ren F, Luc X, Leng Y (2013) Ab initio simulation on the crystal structure and elastic properties of carbonated apatite. *J Mech Behav Biomed Mater* 26:59–67
328. Fleet ME, Liu X, King PL (2004) Accommodation of the carbonate ion in apatite: an FTIR and X-ray structure study of crystals synthesized at 2–4 GPa. *Am Mineral* 89:1422–1432
329. Peroos S, Du Z, de Leeuw NH (2006) A computer modeling study of the uptake, structure and distribution of carbonate defects in hydroxyapatite. *Biomaterials* 27:2150–2161
330. Ito A, Maekawa K, Tsutsumi S, Ikazaki F, Tateishi T (1997) Solubility product of OH-carbonated hydroxyapatite. *J Biomed Mater Res* 36(4):522–528
331. Vignoles M, Bonel G, Holcomb D, Young R (1988) Influence of preparation conditions on the composition of type B carbonated hydroxyapatite and on the localization of the carbonate ions. *Calcif Tissue Int* 43(1):33–40
332. Driessens FCM, Verbeeck RMH, Heijligers HJM (1983) Some physical properties of Na- and  $\text{CO}_3$ -containing apatites synthesized at high temperatures. *Inorg Chim Acta* 80:19–23
333. Gibson IR, Bonfield W (2002) Novel synthesis and characterization of an AB-type carbonate-substituted hydroxyapatite. *J Biomed Mater Res* 59(4):697–708
334. LeGeros RZ (1981) Apatites in biological systems. *Prog Cryst Growth Charact Mater* 4 (1–2):1–45
335. Chiranjeevirao SV, Voegel JC, Frank RM (1983) A method of preparation and characterization of carbonate-apatites. *Inorg Chim Acta* 78:43–46

336. Barralet J, Knowles JC, Best S, Bonfield W (2002) Thermal decomposition of synthesised carbonate hydroxyapatite. *J Mater Sci Mater Med* 13(6):529–533
337. Landi E, Tampieri A, Celotti G, Sprio S (2000) Densification behavior and mechanisms of synthetic hydroxyapatite. *J Eur Ceram Soc* 20:2377–2387
338. Liao S, Watari F, Xu G, Ngiam M, Ramakrishna S, Chan CK (2007) Morphological effects of variant carbonates in biomimetic hydroxyapatite. *Mater Lett* 61(17):3624–3628
339. LeGeros RZ, Trautz OR, LeGeros RZ, Klein L, Shirra WP (1967) Apatite crystallites: effect of carbonate on morphology. *Science* 155(3768):1409–1411
340. Porter A, Patel N, Brooks R, Best SM, Rushton N, Bonfield W (2005) Effect of carbonate-substitution on the ultrastructural characteristics of hydroxyapatite implants. *J Mater Sci Mater Med* 16(13):899–907
341. Spence G, Patel N, Brooks R, Rushton N (2009) Carbonate substituted hydroxyapatite: resorption by osteoclasts modifies the osteoblastic response. *J Biomed Mater Res A* 90A(1):217–224
342. Patel N, Best SM, Bonfield W, Gibson IR, Hing KA, Damien E, Revell PA (2002) A comparative study on the in vivo behavior of hydroxyapatite and silicon substituted hydroxyapatite granules. *J Mater Sci Mater Med* 13:1199–1206
343. Doi Y, Shibutani T, Moriwake Y, Kajimoto T, Iwayama Y (1997) Sintered carbonate apatites as bioresorbable bone substitutes. *J Biomed Mater Res* 39:603–610
344. Mertz W (1981) The essential trace-elements. *Science* 213(4514):1332–1338
345. Harrison J, Melville AJ, Forsythe JS, Muddle BC, Trounson AO, Gross KA (2004) Sintered hydroxyfluorapatites – IV: the effect of fluoride substitutions upon colonisation of hydroxyapatites by mouse embryonic stem cells. *Biomaterials* 25:4977–4986
346. Farley JR, Wergedal JE, Baylink DJ (1983) Fluoride directly stimulates proliferation and alkaline-phosphatase activity of bone-forming cells. *Science* 222(4621):330–332
347. Chavassieux P, Boivin G, Serre CM, Meunier PJ (1993) Fluoride increases rat osteoblast function and population after in vivo administration but not after in vitro exposure. *Bone* 14(5):721–725
348. Pak CY, Sakhaee K, Zerwekh JE, Parcel C, Peterson R, Johnson K (1989) Safe and effective treatment of osteoporosis with intermittent slow release sodium fluoride: augmentation of vertebral bone mass and inhibition of fractures. *J Clin Endocrinol Metab* 68:150–159
349. Cass RM, Croft JD, Perkins P, Nye W, Waterhou C, Terry R (1966) New bone formation in osteoporosis following treatment with sodium fluoride. *Arch Intern Med* 118(2):111–116
350. Farley SMG, Wergedal JE, Smith LC, Lundy MW, Farley JR, Baylink DJ (1987) Fluoride therapy for osteoporosis: characterization of the skeletal response by serial measurements of serum alkaline-phosphatase activity. *Metabolism* 36(3):211–218
351. Briancon D, Meunier PJ (1981) Treatment of osteoporosis with fluoride, calcium, and vitamin-D. *Orthop Clin North Am* 12(3):629–648
352. Riggs BL, Hodgson SF, Hoffman DL, Kelly PJ, Johnson KA, Taves D (1980) Treatment of primary osteoporosis with fluoride and calcium: clinical tolerance and fracture occurrence. *J Am Med Assoc* 243(5):446–449
353. Boivin G, Chapuy MC, Baud CA, Meunier PJ (1988) Fluoride content in human iliac bone: results in controls, patients with fluorosis and osteoporotic patients treated with fluoride. *J Bone Miner Res* 3(5):497–502
354. Guanabens N, Farrerons J, Perez-Edo L, Monagal A, Renau A, Carbonell J, Roca M, Torra M, Pavese M (2000) Cyclical etidronate versus sodium fluoride in established postmenopausal osteoporosis: a randomized 3 year trial. *Bone* 27(1):123–128
355. Roche KJ, Stanton KT (2014) Measurement of fluoride substitution in precipitated fluorhydroxyapatite nanoparticles. *J Fluor Chem* 161:102–109
356. Chen Y, Miao X (2005) Thermal and chemical stability of fluorohydroxyapatite ceramics with different fluorine contents. *Biomaterials* 26:1205–1210
357. Qu H, Wei M (2005) Synthesis and characterization of fluorine-containing hydroxyapatite by a pH-cycling method. *J Mater Sci Mater Med* 16:129–133

358. Rodriguez-Lorenzo LM, Hart JN, Gross KA (2003) Influence of fluorine in the synthesis of apatites. Synthesis of solid solutions of hydroxy-fluorapatite. *Biomaterials* 24:3777–3785
359. Manjubala I, Sivakumar M, Najma Nikkath S (2001) Synthesis and characterisation of hydroxy/fluoroapatite solid solution. *Mater Sci* 36:5481–5486
360. Wei M, Evans JH, Bostrom T, Grondahl L (2003) Synthesis and characterization of hydroxyapatite, fluoride-substituted hydroxyapatite and fluorapatite. *J Mater Sci Mater Med* 14 (4):311–320
361. Bianco A, Cacciotti I, Lombardi M, Montanaro L, Bemporad E, Sebastiani M (2010) F-substituted hydroxyapatite nanopowders: thermal stability, sintering behaviour and mechanical properties. *Ceram Int* 36(1):313–322
362. Jha LJ, Best SM, Knowles JC, Rehman I, Santos JD, Bonfield W (1997) Preparation and characterization of fluoride-substituted apatites. *J Mater Sci Mater Med* 8(4):185–191
363. Tredwin CJ, Young AM, Georgiou G, Shin SH, Kim HW, Knowles JC (2013) Hydroxyapatite, fluor-hydroxyapatite and fluorapatite produced via the sol–gel method. Optimisation, characterisation and rheology. *Dent Mater* 29:166–173
364. Cavalli M, Gnappi G, Montenero A, Bersani D, Lottici PP, Kaciulis S, Mattogno G, Fini M (2001) Hydroxy- and fluorapatite films on Ti alloy substrates: sol–gel preparation and characterization. *J Mater Sci* 36(13):3253–3260
365. Zhang HG, Zhu Q (2005) Surfactant-assisted preparation of fluoride-substituted hydroxyapatite nanorods. *Mater Lett* 59:3054–3058
366. Rodriguez-Lorenzo LM, Gross KA (2003) Encapsulation of apatite particles for improvement in bone regeneration. *J Mater Sci Mater Med* 14:939–943
367. Kurmaev EZ, Matsuya S, Shin S, Watanabe M, Eguchi R, Ishiwata Y, Takeuchi T, Iwami M (2002) Observation of fluorapatite formation under hydrolysis of tetracalcium phosphate in the presence of KF by means of soft X-ray emission and adsorption spectroscopy. *J Mater Sci Mater Med* 13(1):33–36
368. Zhao J, Dong X, Bian M, Zhao J, Zhang Y, Sun Y, Chen JH, Wang XH (2014) Solution combustion method for synthesis of nanostructured hydroxyapatite, fluorapatite and chlorapatite. *Appl Surf Sci* 314:1026–1033
369. Zhang HG, Zhu Q, Xie ZH (2005) Mechanochemical–hydrothermal synthesis and characterization of fluoridated hydroxyapatite. *Mater Res Bull* 40:1326–1334
370. Kim SJ, Bang HG, Song JH, Park SY (2009) Effect of fluoride additive on the mechanical properties of hydroxyapatite/alumina composites. *Ceram Int* 35:1647–1650
371. Fathi MH, Zahrani EM (2009) Fabrication and characterization of fluoridated hydroxyapatite nanopowders via mechanical alloying. *J Alloys Comp* 475:408–414
372. Wu CC, Huang ST, Tseng TW, Rao QL, Lin HC (2010) FT-IR and XRD investigations on sintered fluoridated hydroxyapatite composites. *J Mol Struct* 979:72–76
373. Murugan R, Sampath Kumar TS, Panduranga Rao K (2002) Fluorinated bovine hydroxyapatite: preparation and characterization. *Mater Lett* 57(2):429–433
374. Okazaki M, Miake Y, Tohda H, Yanagisawa T, Matsumoto T, Takahashi J (1999) Functionally graded fluoridated apatites. *Biomaterials* 20:1421–1426
375. Lau KW, Kesson K, Libanati CR, Baylink DJ (1998) Osteogenic actions of fluoride: its therapeutic use for established osteoporosis. In: Whitfield JF, Morley P (eds) *Anabolic treatments for osteoporosis*. CRC Press, Boca Raton, pp 207–250
376. Badillo-Almaraz VE, Armando Flores J, Arriola H, López FA, Ruiz-Ramirez L (2007) Elimination of fluoride ions in water for human consumption using hydroxyapatite as an adsorbent. *J Radioanal Nucl Chem* 271(3):741–744
377. Komlev VS, Barinov SM, Girardin E, Oscarsson S, Rosengren A, Rustichelli F, Orlovskii VP (2003) Porous spherical hydroxyapatite and fluorhydroxyapatite granules: processing and characterization. *Sci Technol Adv Mater* 4(6):503–508
378. Qu H, Wei M (2006) The effect of fluoride contents in fluoridated hydroxyapatite on osteoblast behaviour. *Acta Biomater* 2:113–119

379. Freeman JJ, Wopenka B, Silva MJ, Pasteris JD (2001) Raman spectroscopic detection of changes in bioapatite in mouse femora as a function of age and in vitro fluoride treatment. *Calcif Tissue Int* 68:156–162
380. Hughes JM, Cameron M, Crowle KD (1989) Structural variations in natural F, OH, and Cl apatites. *Am Mineral* 74:870–876
381. Moreno EC, Kresak M, Zahradni RT (1974) Fluoridated hydroxyapatite solubility and caries formation. *Nature* 247:64–65
382. Rodriguez-Lorenzo LM, Hart JN, Gross KA (2003) Structural and chemical analysis of well-crystallized hydroxyfluorapatites. *J Phys Chem B* 107(33):8316–8320
383. Kannan S, Rebelo A, Ferreira JMF (2006) Novel synthesis and structural characterization of fluorine and chlorine co-substituted hydroxyapatites. *J Inorg Biochem* 100 (10):1692–1697
384. Eslami H, Solati-Hashjin M, Tahriri M (2009) The comparison of powder characteristics and physicochemical, mechanical and biological properties between nanostructure ceramics of hydroxyapatite and fluoridated hydroxyapatite. *Mater Sci Eng C Biomim Supramol Syst* 29:1387–1398
385. LeGeros RZ, Kijkowska R, Jia W, LeGeros JP (1988) Fluoride-cation interactions in the formation and stability of apatites. *J Fluor Chem* 41(64):53–64
386. Bhadang KA, Gross KA (2004) Influence of fluorapatite on the properties of thermally sprayed hydroxyapatite coatings. *Biomaterials* 25(20):4935–4945
387. Cheng K, Weng WJ, Wang HM, Zhang S (2005) In vitro behavior of osteoblast-like cells on fluoridated hydroxyapatite coatings. *Biomaterials* 26(32):6288–6295
388. Bianco A, Cacciotti I, Lombardi M, Montanaro L, Sebastiani M, Bemporad E (2009) Pure and substituted hydroxyapatite nanopowders by precipitation. In: Acerno D, D'Amore A, Caputo D, Cioffi R (eds) *Special topics on materials science and technology-an Italian panorama*. BRILL Publisher, Leiden/Boston, pp 65–74
389. Champion E (2013) Sintering of calcium phosphate bioceramics. *Acta Biomater* 9:5855–5875
390. Senamaud N, Bernache-Assollant D, Champion E, Heughebaert M, Rey C (1997) Calcination and sintering of hydroxyfluorapatite powders. *Solid State Ion* 101–103:1357–1362
391. Montanaro L, Arciola CR, Campoccia D, Cervellati M (2002) In vitro effects on MG63 osteoblast-like cells following contact with two roughness-differing fluorohydroxyapatite-coated titanium alloys. *Biomaterials* 23(17):3651–3659
392. Wang YS, Zhang S, Zeng XT, Ma LL, Khor KA, Qian M (2008) Initial attachment of osteoblastic cells onto sol-gel derived fluoridated hydroxyapatite coatings. *J Biomed Mater Res A* 84A(3):769–776
393. Kim HW, Kim HE, Knowles JC (2004) Fluor-hydroxyapatite sol-gel coating on titanium substrate for hard tissue implants. *Biomaterials* 25(17):3351–3358
394. Ge X, Leng Y, Bao CY, Xu SL, Wang RK, Ren FZ (2010) Antibacterial coatings of fluoridated hydroxyapatite for percutaneous implants. *J Biomed Mater Res A* 95A(2):588–599
395. Fahami A, Nasiri-Tabrizi B, Ebrahimi-Kahrizsangi R (2013) Mechano-synthesis and characterization of chlorapatite nanopowders. *Mater Lett* 110:117–121
396. Kannan S, Rocha JHG, Ferreira JMF (2006) Synthesis of hydroxy-chlorapatites solid solutions. *Mater Lett* 60:864–868
397. Kannan S, Rebelo A, Lemos AF, Barba A, Ferreira JMF (2007) Synthesis and mechanical behavior of chlorapatite and chlorapatite/TCP composites. *J Eur Ceram Soc* 27:2287–2294
398. Cho JS, Yoo DS, Chung YC, Rhee SH (2014) Enhanced bioactivity and osteoconductivity of hydroxyapatite through chloride substitution. *J Biomed Mater Res A* 102(2):455–469
399. Markovich D (2001) Physiological roles and regulation of mammalian sulfate transporters. *Physiol Rev* 81(4):1499–1533
400. Evans RA, Lawrence PJ, Thanakrishnan G, Hills E, Wong SY, Dunstan CR (1986) Immobilization hypercalcaemia due to low bone formation and responding to intravenous sodium sulphate. *Postgrad Med J* 62(727):395–398

401. Alshemary AZ, Goh YF, Akram M, Razali IR, Kadir MRA, Hussain R (2013) Microwave assisted synthesis of nano sized sulfate doped hydroxyapatite. *Mater Res Bull* 48 (6):2106–2110
402. Tran PL, Hammond AA, Mosley T, Cortez J, Gray T, Colmer-Hamood JA, Shashtri M, Spallholz JE, Hamood AN, Reid TW (2009) Organoselenium coating on cellulose inhibits the formation of biofilms by *Pseudomonas aeruginosa* and *Staphylococcus aureus*. *Appl Environ Microbiol* 75(11):3586–3592
403. Rodríguez-Valencia C, López-Álvarez M, Cochón-Cores B, Pereiro I, Serra J, González P (2013) Novel selenium doped hydroxyapatite coatings for biomedical applications. *J Biomed Mater Res A* 101(3):853–861
404. Holben DH, Smith AM (1999) The diverse role of selenium within selenoproteins: a review. *J Am Diet Assoc* 99(7):836–843
405. Rayman MP (2000) The importance of selenium to human health. *Lancet* 356(9225):233–241
406. Wang Y, Ma J, Zhou L, Chen J, Liu Y, Qiu Z, Zhang S (2012) Dual functional selenium-substituted hydroxyapatite. *Interface Focus* 2:378–386
407. Monteil-Rivera F, Masset S, Dumonceau J, Fedoroff M, Jeanjean J (1999) Sorption of selenite ions on hydroxyapatite. *J Mater Sci Mater Med* 18:1143–1145
408. Tran PA, Webster TJ (2011) Selenium nanoparticles inhibit *Staphylococcus aureus* growth. *Int J Nanomedicine* 6:1553–1558
409. Tran PA, Webster TJ (2013) Antimicrobial selenium nanoparticle coatings on polymeric medical devices. *Nanotechnology* 24(15):155101
410. Dutta RK, Nenavathu BP, Talukdar S (2014) Anomalous antibacterial activity and dye degradation by selenium doped ZnO nanoparticles. *Colloids and Surf B: Biointerfaces* 114:218–224
411. Chen YC, Sosnoski DM, Gandhi UH, Novinger LJ, Prabhu KS, Mastro AM (2009) Selenium modifies the osteoblast inflammatory stress response to bone metastatic breast cancer. *Carcinogenesis* 30(11):1941–1948
412. Kolmas J, Oledzka E, Sobczak M, Nałęcz-Jawecki G (2014) Nanocrystalline hydroxyapatite doped with selenium oxyanions: a new material for potential biomedical applications. *Mater Sci Eng C* 39:134–142
413. Ma J, Wang Y, Zhou L, Zhang S (2013) Preparation and characterization of selenium substituted hydroxyapatite. *Mater Sci Eng C* 33(1):440–445
414. Monteil-Rivera F, Fedoroff M, Jeanjean J, Minel L, Barthes MG, Dumonceau J (2000) Sorption of selenite  $\text{SeO}_3^{2-}$  on hydroxyapatite: an exchange process. *J Colloid Interface Sci* 221:291–300
415. Duc M, Lefevre G, Fedoroff M, Jeanjean J, Rouchaud JC, Monteil-Rivera F, Dumonceau J, Milonjic S (2003) Sorption of selenium anionic species on apatites and iron oxides from aqueous solutions. *J Environ Radioact* 70:61–72
416. Carlisle EM (1981) Silicon: a requirement in bone formation independent of vitamin D1. *Calcif Tissue Int* 33:27–34
417. Schwarz K (1978) Significance and function of silicon in warm blooded animals-review and outlook. In: Bendz G, Lindqvist I (eds) *Biochemistry of silicon and related problems*. Plenum Press, New York, pp 207–230
418. Carlisle EM (1972) Silicon an essential element for the chick. *Science* 178:619–621
419. Carlisle EM (1982) The nutritional essentiality of silicon. *Nutr Rev* 40:193–198
420. Reffitt DM, Ogston N, Jugdaohsingh R, Cheung HFJ, Evans BAJ, Thompson RPH, Powell JJ, Hampson GN (2003) Orthosilicic acid stimulates collagen type 1 synthesis and osteoblastic differentiation in human osteoblast-like cells in vitro. *Bone* 32(2):127–135
421. Arumugam MQ, Ireland DC, Brooks RA, Rushton N, Bonfield W (2003) Orthosilicic acid increases collagen type I mRNA expression in human bone-derived osteoblasts in vitro. *Key Eng Mater* 254–256:869–872
422. Ruys AJ (1993) Silicon-doped hydroxyapatite. *J Aust Ceram Soc* 29:71–79

423. Balamurugan A, Rebelo AHS, Lemos AF, Rocha JHG, Ventura JMG, Ferreira JMF (2008) Suitability evaluation of sol–gel derived Si-substituted hydroxyapatite for dental and maxillofacial applications through in vitro osteoblasts response. *Dent Mater* 24:1374–1380
424. Tanizawa Y, Suzuki T (1994) X-ray photoelectron spectroscopy study of silicate-containing apatite. *Phosphorus Res Bull* 4:83–88
425. Aminian A, Solati-Hashjin M, Samadikuchaksaraei A, Bakhshi F, Gorjipour F, Farzadi A, Moztarzadeh F, Schmücker M (2011) Synthesis of silicon-substituted hydroxyapatite by a hydrothermal method with two different phosphorous sources. *Ceram Int* 37(4):1219–1229
426. Zhang N, Liu W, Zhu H, Chen L, Lin K, Chang J (2014) Tailoring Si-substitution level of Si-hydroxyapatite nanowires via regulating Si-content of calcium silicates as hydrothermal precursors. *Ceram Int B* 40(7):11239–11243
427. Tang XL, Xiao XF, Liu RF (2005) Structural characterization of silicon-substituted hydroxyapatite synthesized by a hydrothermal method. *Mater Lett* 59:3841–3846
428. Kim YH, Song H, Riu DH, Kim SR, Kim HJ, Moon JH (2005) Preparation of porous Si incorporated hydroxyapatite. *Curr Appl Phys* 5:538–541
429. Boyer L, Carpena J, Lacou JL (1997) Synthesis of phosphate-silicate apatites at atmospheric pressure. *J Solid State Ionics* 95:121–129
430. Hahn BD, Lee JM, Park DS, Choi JJ, Ryu J, Yoon WH, Lee BK, Shin DS, Kim HE (2010) Aerosol deposition of silicon-substituted hydroxyapatite coatings for biomedical applications. *Thin Solid Films* 518:2194–2199
431. Arcos D, Rodríguez-Carvajal J, Vallet-Regí M (2004) The effect of the silicon incorporation on the hydroxylapatite structure. A neutron diffraction study. *Solid State Sci* 6:987–994
432. Tian T, Jiang D, Zhang J, Lin Q (2008) Synthesis of Si-substituted hydroxyapatite by a wet mechanochemical method. *Mater Sci Eng C* 28:57–63
433. Chaikina M, Bulina N, Ishchenko A, Prosanov I (2014) Mechanochemical synthesis of  $\text{SiO}_4^{4-}$ -substituted hydroxyapatite, part I – kinetics of interaction between the components. *Eur J Inorg Chem* 28:4803–4809
434. Gibson IR, Best SM, Bonfield W (1999) Chemical characterization of silicon substituted hydroxyapatite. *J Biomed Mater Res* 44(4):422–428
435. Bianco A, Cacciotti I, Lombardi M, Montanaro L (2009) Si-substituted hydroxyapatite nanopowders: synthesis, thermal stability and sinterability. *Mater Res Bull* 44:345–354
436. Marques PAAP, Magalhães MCF, Correia RN, Vallet-Regí M (2001) Synthesis and characterization of silicon-substituted hydroxyapatite. *Key Eng Mater* 192–195:247–250
437. Bang LT, Ishikawa K, Othman R (2011) Effect of silicon and heat-treatment temperature on the morphology and mechanical properties of silicon-substituted hydroxyapatite. *Ceram Int* 37:3637–3642
438. Leventouri T, Bunaciu CE, Perdikatsis V (2003) Neutron powder diffraction studies of silicon-substituted hydroxyapatite. *Biomaterials* 24:4205–4211
439. Arcos D, Rodríguez-Carvajal J, Vallet-Regí M (2004) Silicon incorporation in hydroxylapatite obtained by controlled crystallization. *Chem Mater* 16(11):2300–2308
440. Best S, Bonfield W, Gi R, Jha LJ, Da Silva Santos JD (2001) Silicon-substituted apatites and process for the preparation thereof. US Patent 6312468 B1, 6 Nov 2001
441. Putlayev V, Veresov A, Pulkin M, Soïn A, Kuznetsov V (2006) Silicon-substituted hydroxyapatite ceramics (Si-HAp): densification and grain growth through the prism of sintering theories. *Mater Sci Eng Technol* 37:416–421
442. Palard M, Champion E, Foucaud S (2008) Synthesis of silicated hydroxyapatite  $\text{Ca}_{10}(\text{PO}_4)_6\text{x}(\text{SiO}_4)_\text{x}(\text{OH})_{2\text{x}}$ . *J Solid State Chem* 181:1950–1960
443. Balas F, Pérez-Pariente J, Vallet-Regí M (2003) In vitro bioactivity of silicon substituted hydroxyapatites. *J Biomed Mater Res A* 66(2):364–375
444. Bakunova N, Fomin A, Fadeeva I, Barinov S, Shvorneva L (2007) Silicon-containing hydroxylapatite nanopowders. *Russ J Inorg Chem* 52:1492–1497
445. Plokhikh NV, Soïn AV, Kuznetsov AV, Veresov AG, Putlayev VI, Tretyakov YD (2004) Synthesis of silicon-substituted hydroxyapatite. *Mendelev Commun* 14:178–179

446. Gasquères G, Bonhomme C, Maquet J, Babonneau F, Hayakawa S, Kanaya T, Osaka A (2008) Revisiting silicate substituted hydroxyapatite by solid-state NMR. *Magn Reson Chem* 46:342–346
447. Hing KA, Revell PA, Smith N, Buckland T (2006) Effect of silicon level on rate, quality and progression of bone healing within silicate-substituted porous hydroxyapatite scaffolds. *Biomaterials* 27:5014–5026
448. Gomes S, Renaudin G, Mesbah A, Jallot E, Bonhomme C, Babonneau F, Nedelec JM (2010) Thorough analysis of silicon substitution in biphasic calcium phosphate bioceramics: a multi-technique study. *Acta Biomater* 6:3264–3274
449. Tang Q, Brooks R, Rushton N, Best S (2010) Production and characterization of HA and SiHA coatings. *J Mater Sci Mater Med* 21:173–181
450. Botelho CM, Lopes MA, Gibson IR, Best SM, Santos JD (2002) Structural analysis of Si-substituted hydroxyapatite: zeta potential and X-ray photoelectron spectroscopy. *J Mater Sci Mater Med* 13(12):1123–1127
451. Guth K, Champion C, Buckland T, Hing KA (2010) Effect of silicate-substitution on attachment and early development of human osteoblast-like cells seeded on microporous hydroxyapatite discs. *Adv Eng Mater* 12(1–2):B26–B36
452. Guth K, Champion C, Buckland T, Hing KA (2011) Effects of serum protein on ionic exchange between culture medium and microporous hydroxyapatite and silicate-substituted hydroxyapatite. *J Mater Sci Mater Med* 22:2155–2164
453. Porter AE, Patel N, Skepper JN, Best SM, Bonfield W (2003) Comparison of in vivo dissolution processes in hydroxyapatite and silicon-substituted hydroxyapatite bioceramics. *Biomaterials* 24:4609–4620
454. Sprio S, Tampieri A, Landi E, Sandri M, Martorana S, Celotti G, Logroscino G (2008) Physicochemical properties and solubility behaviour of multi-substituted hydroxyapatite powders containing silicon. *Mater Sci Eng C* 28:179–187
455. Lehmann G, Palmero P, Cacciotti I, Pecci R, Campagnolo L, Bedini R, Siracusa G, Bianco A, Camaioni A, Montanaro L (2010) Design, production and biocompatibility of nanostructured porous HAp and Si-HAp ceramics as three-dimensional scaffolds for stem cell culture and differentiation. *Ceram Silikáty* 54:90–96
456. Vandiver J, Dean D, Patel N, Botelho C, Best SM, Santos JD, Lopes MA, Bonfield W, Ortiz C (2006) Silicon addition to hydroxyapatite increases nanoscale electrostatic, van der Waals, and adhesive interactions. *J Biomed Mater Res A* 78(2):352–363
457. Panteix PJ, Béchade E, Julien I, Abélard P, Bernache-Assollant D (2008) Influence of anionic vacancies on the ionic conductivity of silicated rare earth apatites. *Mater Res Bull* 43:1223–1231
458. Porter AE, Patel N, Skepper JN, Best SM, Bonfield W (2004) Effect of sintered silicate substituted hydroxyapatite on remodelling processes at the bone-implant interface. *Biomaterials* 25:3303–3314
459. Dorozhkin SV (2008) A novel, environmentally friendly process for the fabrication of calcium phosphate bioceramics. *Inorg Mater* 44:207–210
460. Lehmann G, Cacciotti I, Palmero P, Montanaro L, Bianco A, Campagnolo L, Camaioni A (2012) Differentiation of osteoblast and osteoclast precursors on pure and silicon-substituted synthesized hydroxyapatites. *Biomed Mater* 7:055001 (13pp)
461. Marchat D, Zymelka M, Coelho C, Gremillard L, Joly-Pottuz L, Babonneau F, Esnouf C, Chevalier J, Bernache-Assollant D (2013) Accurate characterization of pure silicon-substituted hydroxyapatite powders synthesized by a new precipitation route. *Acta Biomater* 9:6992–7004
462. Rau JV, Fosca M, Cacciotti I, Laureti S, Bianco A, Teghil R (2013) Nanostructured Si-substituted hydroxyapatite coatings for biomedical applications. *Thin Solid Films* 543:167–170
463. Rau JV, Cacciotti I, Laureti S, Fosca M, Varvaro G, Latini A (2014) Bioactive, nanostructured Si-substituted hydroxyapatite coatings on titanium prepared by pulsed laser deposition. *J Biomed Mater Res B*. doi:10.1002/jbm.b.33344

464. Kim SR, Riu DH, Lee YJ, Kim YH (2002) Synthesis and characterization of silicon substituted hydroxyapatite. *Key Eng Mater* 218–220:85–88
465. Xu JL, Khor KA (2007) Chemical analysis of silica doped hydroxyapatite biomaterials consolidated by a spark plasma sintering method. *J Inorg Biochem* 101:187–195
466. Xu JL, Khor KA, Lu YW, Chen WN, Kumar R (2008) Osteoblast interactions with various hydroxyapatite based biomaterials consolidated using a spark plasma sintering technique. *J Biomed Mater Res B App Biomater* 84:224–230
467. Vallet-Regí M, Arcos D (2005) Silicon substituted hydroxyapatites. A method to upgrade calcium phosphate based implants. *J Mater Chem* 15:1509–1516
468. Qiu ZY, Li G, Zhang YQ, Liu J, Hu W, Ma J, Zhang SM (2012) Fine structure analysis and sintering properties of Si-doped hydroxyapatite. *Biomed Mater* 7:045009 (11pp)
469. Gibson IR, Huang KA, Best SM, Bonfield W (1999) Enhanced in vitro cell activity and surface apatite layer formation on novel silicon-substituted hydroxyapatites. In: Ohgushi H, Hastings GW, Yoshikawa T (eds) *Proceedings of the 12th international symposium on ceramics*. World Scientific Publishing, London, pp 191–194
470. van Raemdonck W, Ducheyne P (1984) *Metal and ceramic biomaterials*. CRC Press, Boca Raton, pp 143–146
471. Porter AE, Best SM, Bonfield W (2004) Ultrastructural comparison of hydroxyapatite and silicon-substituted hydroxyapatite for biomedical applications. *J Biomed Mater Res* 68 (1):133–141
472. Pietak AM, Reid JW, Stott MJ, Sayer M (2007) Silicon substitution in the calcium phosphate bioceramics. *Biomaterials* 28:4023–4032
473. Gibson IR, Hing KA, Revell PA, Santos JD, Best SM, Bonfield W (2002) Enhanced in vivo response to silicate-substituted hydroxyapatite. *Key Eng Mater* 218–220:203–206
474. Porter AE, Botelho CM, Lopes MA, Santos JD, Best SM, Bonfield W (2004) Ultrastructural comparison of dissolution and apatite precipitation on hydroxyapatite and silicon-substituted hydroxyapatite in vitro and in vivo. *J Biomed Mater Res* 69A:670–679
475. Botelho CM, Brooks RA, Spence G, McFarlane I, Lopes MA, Best SM, Santos JD, Rushton N, Bonfield W (2006) Differentiation of mononuclear precursors into osteoclasts on the surface of Si-substituted hydroxyapatite. *J Biomed Mater Res* 78A:709–720
476. Botelho CM, Brooks RA, Best SM, Lopes MA, Santos JD, Rushton N, Bonfield W (2006) Human osteoblast response to silicon-substituted hydroxyapatite. *J Biomed Mater Res* 79A:723–730
477. Bohner M (2009) Silicon-substituted calcium phosphates—a critical view. *Biomaterials* 30:6403–6406
478. Thian ES, Ahmad Z, Huang J, Edirisinghe MJ, Jayasinghe SN, Ireland DC, Brooks RA, Rushton N, Bonfield W, Best SM (2008) The role of electrosprayed apatite nanocrystals in guiding osteoblast behaviour. *Biomaterials* 29(12):1833–1843
479. Boanini E, Gazzano M, Bigi A (2010) Ionic substitutions in calcium phosphates synthesized at low temperature. *Acta Biomater* 6:1882–1894
480. Camaioni A, Cacciotti I, Campagnolo L, Bianco A (2015) Silicon substituted hydroxyapatite for biomedical applications. In: Mucalo M (ed) *Hydroxyapatite for biomedical applications*. Woodhead Publishing Elsevier Limited Edition, Oxford, pp 343–373
481. Mourão V, Cattalini JB, Boccaccini AR (2012) Metallic ions as therapeutic agents in tissue engineering scaffolds: an overview of their biological applications and strategies for new developments. *J Royal Soc Interface* 9(68):401–419
482. Xynos ID, Edgar AJ, Buttery LDK, Hench LL, Polak JM (2001) Gene-expression profiling of human osteoblasts following treatment with the ionic products of Bioglass® 45S5 dissolution. *J Biomed Mater Res* 55:151–157
483. Hench LL (2009) Genetic design of bioactive glass. *J Eur Ceram Soc* 29:1257–1265
484. Gorustovich AA, Roether JA, Boccaccini AR (2010) Effect of bioactive glasses on angiogenesis: a review of in vitro and in vivo evidences. *Tissue Eng B Rev* 16:199–207



485. Gorriti MF, Porto López JM, Boccaccini AR, Audisio C, Gorustovich AA (2009) In vitro study of the antibacterial activity of bioactive glass-ceramic scaffolds. *Adv Eng Mater* 11:B67–B70
486. Day RM, Boccaccini AR (2005) Effect of particulate bioactive glasses on human macrophages and monocytes in vitro. *J Biomed Mater Res A* 73A:73–79
487. Cacciotti I, Lombardi M, Bianco A, Ravaglioli A, Montanaro L (2012) Sol–gel derived 45S5 bioglass: synthesis, microstructural evolution and thermal behaviour. *J Mater Sci Mater Med* 23(8):1849–1866
488. Lombardi M, Cacciotti I, Bianco A, Montanaro L (2015) RKKP bioactive glass-ceramic material via an aqueous sol–gel process. *Ceram Int* 41(3):3371–3380
489. Cacciotti I, Lehmann G, Camaioni A, Bianco A (2013) AP40 bioactive glass ceramic by sol–gel synthesis: in vitro dissolution and cell-mediated bioresorption. *Key Eng Mater* 541:41–50
490. Ledda M, De Bonis A, Bertani FR, Cacciotti I, Teghil R, Lolli MG, Ravaglioli A, Lisi A, Rau JV (2015) Interdisciplinary approach to cell-biomaterial interactions: biocompatibility and cell friendly characteristics of RKKP glass-ceramic coatings on titanium. *Biomed Mater* 10(3):035005
491. Lombardi M, Gremillard L, Chevalier J, Lefebvre L, Cacciotti I, Bianco A, Montanaro L (2013) A comparative study between melt-derived and sol–gel synthesized 45S5 bioactive glasses. *Key Eng Mater* 541:15–30
492. Landi E, Sprio S, Sandri M, Celotti G, Tampieri A (2008) Development of Sr and CO<sub>3</sub> co-substituted hydroxyapatites for biomedical applications. *Acta Biomater* 4(3):656–663
493. Landi E, Tampieri A, Mattioli-Belmonte M, Celotti G, Sandri M, Gigante A, Fava P, Biagini G (2006) Biomimetic Mg- and Mg, CO<sub>3</sub>-substituted hydroxyapatites: synthesis characterization and in vitro behaviour. *J Eur Ceram Soc* 26(13):2593–2601
494. Zyman ZZ, Tkachenko MV (2013) Sodium-carbonate co-substituted hydroxyapatite ceramics. *Process Appl Ceram* 7(4):153–157
495. Landi E, Uggeri J, Sprio S, Tampieri A, Guizzardi S (2010) Human osteoblast behavior on as-synthesized SiO<sub>4</sub> and B-CO<sub>3</sub> co-substituted apatite. *J Biomed Mater Res A* 94A(1):59–70
496. Stephen JA, Skakle JMS, Gibson IR (2007) Synthesis of novel high silicate-substituted hydroxyapatite by co-substitution mechanisms. *Key Eng Mater* 330–332:87–90
497. Friederichs RJ, Chappell HF, Shepherd DV, Best SM (2015) Synthesis, characterization and modelling of zinc and silicate co-substituted hydroxyapatite. *J R Soc Interface* 12:20150190
498. Huang Y, Zhang X, Mao H, Li T, Zhao R, Yan Y, Pang Z (2015) Osteoblastic cell responses and antibacterial efficacy of Cu/Zn co-substituted hydroxyapatite coatings on pure titanium using electrodeposition method. *RSC Adv* 5:17076–17086
499. Gopi D, Ramya S, Rajeswari D, Karthikeyan P, Kavitha L (2014) Strontium, cerium co-substituted hydroxyapatite nanoparticles: synthesis, characterization, antibacterial activity towards prokaryotic strains and in vitro studies. *Colloids Surf A* 451:172–180
500. Aina V, Lusvardi G, Annaz B, Gibson IR, Imrie FE, Malavasi G, Menabue L, Cerrato G, Martra G (2012) Magnesium- and strontium-co-substituted hydroxyapatite: the effects of doped-ions on the structure and chemico-physical properties. *J Mater Sci Mater Med* 23(12):2867–2879
501. Gopi D, Shinyjoy E, Kavitha L (2014) Synthesis and spectral characterization of silver/magnesium co-substituted hydroxyapatite for biomedical applications. *Spectrochim Acta A Mol Biomol Spectrosc* 127:286–291
502. Shepherd JH, Shepherd DV, Best SM (2012) Substituted hydroxyapatites for bone repair. *J Mater Sci Mater Med* 23:2335–2347

Kunio Ishikawa

## Contents

Introduction .....	214
Hydroxyapatite .....	216
Compositional Transformation Reaction Based on Dissolution-Precipitation Reaction Using a Precursor .....	219
Precursors and Solutions for Carbonate Apatite Block Fabrication Based on Dissolution-Precipitation Reaction .....	221
Calcium Carbonate, CaCO <sub>3</sub> .....	221
Calcium Phosphates .....	223
Calcium Sulfate .....	225
Cells' Response to Carbonate Apatite .....	226
Tissue Response to Carbonate Apatite .....	229
Summary .....	231
References .....	231

## Abstract

Although bone apatite is the carbonate apatite which contains 6–9 mass% carbonate in its apatite structure, sintered hydroxyapatite free from carbonate has been used as artificial bone substitutes since carbonate apatite cannot be sintered due to the thermal decomposition at high temperature required for sintering. We have proposed a two-step fabrication method for fabrication of carbonate apatite block. First step is the fabrication of a precursor block such as calcium carbonate and tricalcium phosphate. Then the precursor block is immersed in solution in which missing elements for the fabrication of carbonate apatite is supplied to the precursor from the solution. Based on the dissolution-precipitation reaction, the composition of the precursor is transformed to carbonate apatite, the inorganic

---

K. Ishikawa (✉)

Department of Biomaterials, Faculty of Dental Science, Kyushu University, Fukuoka, Japan  
e-mail: [ishikawa@dent.kyushu-u.ac.jp](mailto:ishikawa@dent.kyushu-u.ac.jp)

component of the bone. Carbonate apatite thus fabricated was found to upregulate osteoblastic cells' differentiation process. Osteoclasts resorbed carbonate apatite whereas no resorption pits were observed in the case of sintered hydroxyapatite. As a result, carbonate apatite showed much higher osteoconductivity than sintered hydroxyapatite. Furthermore, carbonate apatite is replaced to the bone when implanted in the bone defect, whereas sintered hydroxyapatite remained in the bone defect keeping its original shape. Therefore, carbonate apatite fabricated based on dissolution-precipitation reaction using a precursor is thought to be one of an ideal bone replacements for the next generation.

### Keywords

Carbonate apatite • Bone apatite • Calcium carbonate • Tricalcium phosphate • Calcium sulfate • Dissolution-precipitation reaction • Precursor • Bone replacement • Bone remodeling • Osteoblasts • Osteoclasts

## Introduction

13.8 billion years ago, Big Bang happened. 4.6 billion years ago, our planet, the Earth, was born in the Milky Way. Then, 4.3 billion years ago, life began from a prokaryote. Multicellular organism appeared 0.9–1 billion years ago after the appearance of a eukaryote that was 1.5 billion years ago. 500 million years ago, the ozone layer appeared. This allows movement of plants and animals from sea to land since the ozone layer prevent ultraviolet rays that did not allow plants and animals to survive. The primates appeared just 65 million years ago, and human being appeared on the Earth only several million years ago.

The first vertebrate that landed on land is believed to be *Eusthenopteron*. For landing on Earth, elemental supply and gravity were the keys. Table 1 summarizes top ten elements that are used for the construction of the human body, Earth surface,

**Table 1** Top ten elements contained in the human body, Earth surface, and seawater and the order of human body elements in each surface and seawater elements

Human body	Earth surface	Seawater	Order of human body element in	
			Earth surface	Seawater
Hydrogen	Oxygen	Hydrogen	3	1
Oxygen	Silicate	Oxygen	1	2
Carbon	Hydrogen	Sodium		9
Nitrogen	Aluminum	Chlorine	5	10
Sodium	Sodium	Magnesium	6	3
Calcium	Calcium	Sulfur		8
Phosphorus	Iron	Potassium		
Sulfur	Magnesium	Calcium		6
Potassium	Potassium	Carbon	9	7
Chlorine	Titanium	Nitrogen		4

and seawater [1]. Five out of ten elements of the human body are the same with top ten elements included in the Earth surface. In contrast, nine out of ten elements of the human body are the same with top ten elements of the sea ocean. This difference is taken as one of the proofs that life began not from the land but from the ocean. In other words, life was created from ocean using the elements contained in the ocean. One exception of the similarity of top ten elements of sea, ocean, and human body is the 7th element of human body which is phosphorous. Phosphorous is not included in the top ten elements of seawater. Concentration of phosphorous in seawater is as low as  $1.3 \mu\text{mol/L}$ . In fact, higher concentration of phosphorous in the sea results in red tide. On the other hand, magnesium that is the 5th element of seawater is not included in the top ten elements of human body. However, magnesium is the 11th element of human body. In the other words, phosphorous is the only exception of the similarity of elements of human body and seawater.

Phosphorous is known to play important roles in energy metabolism, the process of generating energy or adenosine triphosphate (ATP). Sea animal can take phosphate from the sea even though its concentration is low. However, vertebrates living on the land need to store the phosphorous in the body. And vertebrate chose the bone as its storage organ. As a result, composition of vertebrate became apatite that is one of the calcium phosphates even though an invertebrate chose calcium carbonate ( $\text{CaCO}_3$ ) as its bone composition.

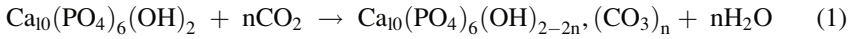
Table 2 summarizes the example of the composition of human adult. Calcium, phosphate, and carbonate are the component of hard tissue such as the bone if components wherein content is less than 1 mass% are excluded from the composition [1–3]. And crystal structural studies demonstrated that inorganic component of hard tissues are carbonate apatite ( $\text{CO}_3\text{Ap}$ ;  $\text{Ca}_{10-a}(\text{PO}_4)_{6-b}(\text{CO}_3)_c(\text{OH})_{2-d}$ ).

Two types of carbonate apatite are known based on the site of  $\text{CO}_3^{2-}$  substitution. In the general formula of apatite,  $\text{M}_{10}(\text{ZO}_4)_6\text{X}_2$ , the site of X and  $\text{ZO}_4$  is called A site and B site, respectively [2, 3]. Therefore, carbonate apatite in which  $\text{CO}_3^{2-}$  substitute for X site is called type A carbonate apatite, whereas carbonate apatite in which  $\text{CO}_3^{2-}$  substitute for  $\text{ZO}_4$  site is called type B carbonate apatite.

**Table 2** Hard tissue components of the human adult

	Enamel	Dentine	Bone
$\text{Ca}^{2+}$	36.5	35.1	34.8
$\text{PO}_4$ as P	17.7	16.9	15.2
Ca/P molar ratio	1.63	1.61	1.71
$\text{Na}^+$	0.5	0.6	0.9
$\text{Mg}^{2+}$	0.44	1.23	0.72
$\text{K}^+$	0.08	0.05	0.03
$\text{CO}_3^{2-}$	3.5	5.6	7.4
$\text{F}^-$	0.01	0.06	0.03
$\text{Cl}^-$	0.30	0.01	0.13
$\text{P}_2\text{O}_7^{4-}$	0.022	0.10	0.07
Total Inorganic	97.0	70.0	65.0
Absorbed $\text{H}_2\text{O}$	1.5	10.0	10.0

In general, high-temperature synthesis is applicable for the preparation of type A carbonate apatite,  $\text{Ca}_{10}(\text{PO}_4)_6\text{CO}_3$ , in which  $\text{CO}_3$  is substituted for the OH site. It was first prepared by the reaction between  $\text{Ca}_3(\text{PO}_4)_2$  and  $\text{CaCO}_3$  at  $900^\circ\text{C}$  in dry  $\text{CO}_2$  even though the reaction is very incomplete [4]. Type A carbonate apatite was also prepared by heating hydroxyapatite in dry  $\text{CO}_2$  at  $800\text{--}1000^\circ\text{C}$  as shown in Eq. 1 [5]:



On the other hand, low-temperature synthesis is applicable for the preparation of type B carbonate apatite,  $\text{Ca}_{10}(\text{PO}_4)_{6-a}(\text{CO}_3)_{3/2a}(\text{OH})_2$ , in which  $\text{CO}_3$  is substituted for the  $\text{PO}_4$  site. Type B carbonate apatite can be prepared easily by precipitating apatites or hydrolyzing amorphous calcium phosphate, octacalcium phosphate, or dicalcium phosphate in the presence of  $\text{CO}_3^{2-}$  or  $\text{HCO}_3^-$  ions. For example, type B carbonate apatite can be prepared by adding Ca acetate solution into  $\text{NH}_4\text{H}_2\text{PO}_4$  solution containing  $(\text{NH}_4)_2\text{CO}_3$  at pH of 7.3–8.0 and  $40\text{--}80^\circ\text{C}$  [6]. In general, crystallinity of carbonate apatite is known to decrease with  $\text{CO}_3$  content and increase with temperature [7].

---

## Hydroxyapatite

As stated above, bone apatite is carbonate apatite and carbonate apatite powder can be prepared easily, for example, by wet chemical method. However, powder including carbonate apatite powder results in crystalline inflammatory response when implanted. Therefore, carbonate apatite powder cannot be used as bone substitute. In general, sintering is employed to fabricate block or granular in ceramics. Unfortunately, carbonate apatite decomposed to other calcium phosphates at high temperature required for sintering process due to the presence of carbonate in its crystal structure. In the 1970s and later, hydroxyapatite (HAp:  $\text{Ca}_{10}(\text{PO}_4)_6(\text{OH})_2$ ) was found to be able to be sintered and shows excellent tissue response and osteoconductivity, the property of materials that bond to the bone without having fibrous tissue between the materials and the bone [8–10]. Sintered hydroxyapatite was the breakthrough for the reconstruction of bone defect since there were no osteoconductive materials before the development of sintered hydroxyapatite.

However, there was a clear difference between the bone and sintered hydroxyapatite. Autograft, the bone taken from patient's own body, is replaced to the bone, whereas sintered hydroxyapatite stayed in the body without being replaced to the bone. Bone tissue plays not only mechanical roles but also biological role including blood formation. Obviously, sintered hydroxyapatite cannot produce blood. Mechanism of the replacement of autograft to new bone is explained by bone remodeling process as shown in Fig. 1. In short, old bone is resorbed by osteoclasts and new bone is formed by the osteoblasts. Based on this bone remodeling process, the baby became adult keeping the basic skeletal structure. Also, orthodontic treatment became possible based on the bone remodeling process. Figure 2 shows the typical

**Fig. 1** Illustration of bone remodeling process. Bone remodeling is done based on the resorption of old bone by osteoclasts and new bone formation by osteoblasts

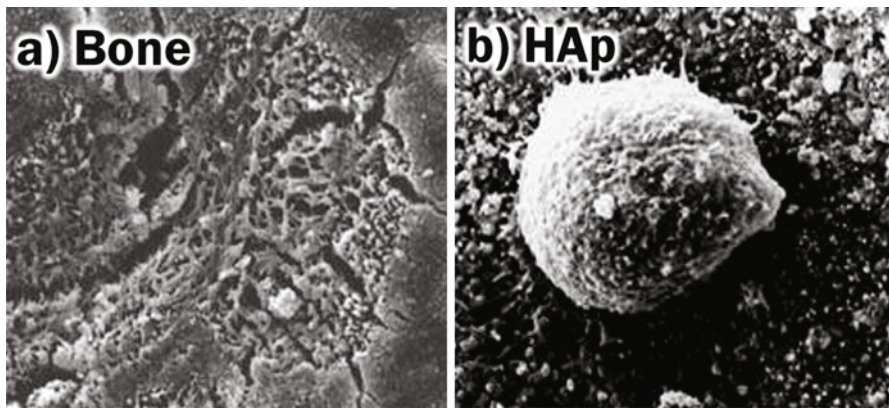
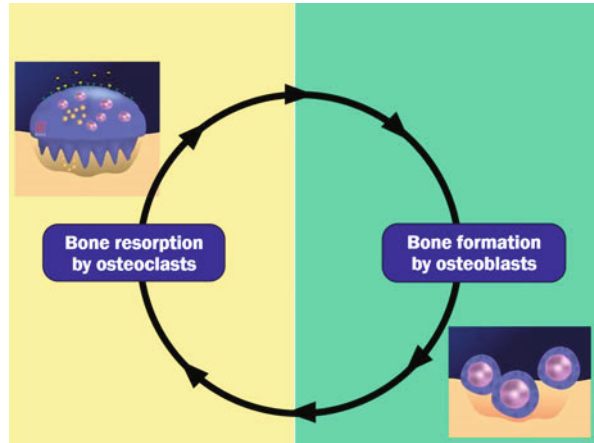


**Fig. 2** Typical scanning electron microscopic image of osteoclasts when incubated on the surface of (a) the bone and (b) sintered hydroxyapatite

SEM pictures when osteoclasts were incubated on the surface of the bone and sintered hydroxyapatite disk. In the case of the bone, resorption pits were formed on its surface. In contrast, no resorption pits were formed on the surface of sintered hydroxyapatite. It is apparent that sintered hydroxyapatite would not be replaced to new bone since it is not resorbed by osteoclasts and it is not dissolved chemically in the body fluid.

Figure 3 illustrates of the function of osteoclasts. Osteoclasts attach on the surface of the bone and sintered hydroxyapatite by organizing the so-called clear zone which is rich in actin and integrin. Inside the clear zone, ruffled border which is bone-resorbing apparatus is organized. Ruffled border secretes collagenase and hydrochloric acid to resorb bone. Howship's lacuna is formed as a result of bone resorption by osteoclasts. In the case of artificial bone substitute such as sintered hydroxyapatite, solubility in weak acidic condition is the key since it

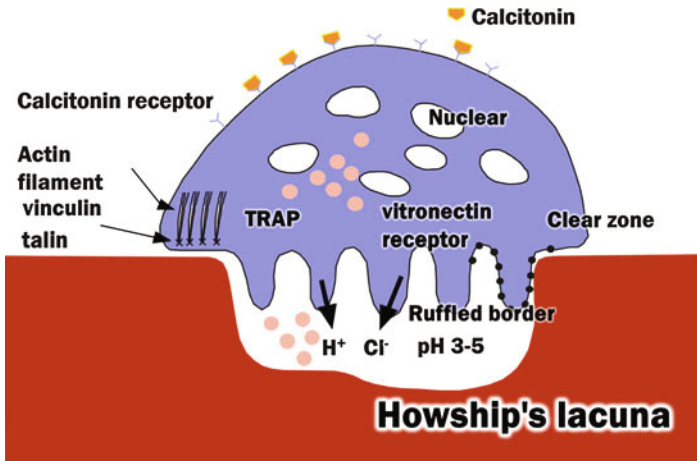


Fig. 3 Illustration of the function of osteoclasts

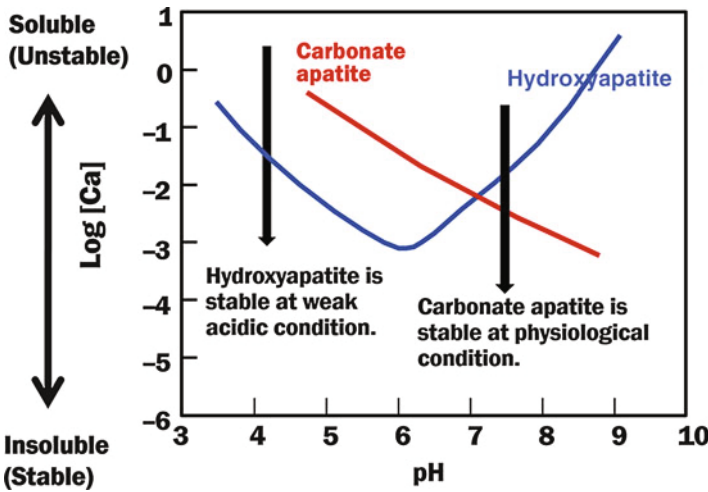


Fig. 4 Phase diagram of the solubility of hydroxyapatite and carbonate apatite as a function of pH. Solubility is expressed as the Ca concentration

does not contain collagen. Figure 4 shows the phase diagram of the solubility of hydroxyapatite and carbonate apatite as a function of pH using Ca concentration as an index of solubility. At physiological pH region or pH 7.4, carbonate apatite is the more stable phase thermodynamically than hydroxyapatite. This is the reason why not hydroxyapatite but carbonate apatite is the composition of bone apatite. If this tendency is the same with the weak acidic condition of Howship's lacuna fabricated by osteoclasts, hydroxyapatite should show higher solubility than carbonate apatite or bone apatite, and hydroxyapatite should be resorbed by

osteoclasts. However, at weak acidic pH region fabricated by osteoclasts, hydroxyapatite is stable or less soluble than carbonate apatite. And thus, carbonate apatite can be resorbed by osteoclasts, whereas hydroxyapatite cannot be resorbed by osteoclasts. In other words, hydroxyapatite can replace only the limited function of bone apatite due to the difference in solubility in acidic region.

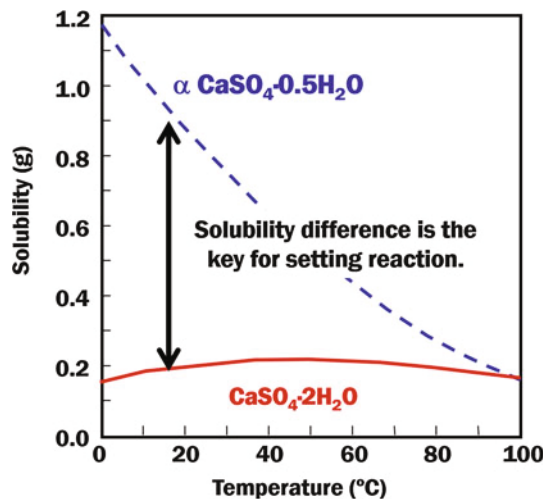
### Compositional Transformation Reaction Based on Dissolution-Precipitation Reaction Using a Precursor

Bone apatite is the carbonate apatite. Also, sintered hydroxyapatite currently used in clinics as bone substitute would not be replaced to the bone since sintered hydroxyapatite is not resorbed by osteoclasts. Therefore, carbonate apatite is thought to be superior to sintered hydroxyapatite as bone substitutes. On the other hand, sintered hydroxyapatite was fabricated in the 1970s since carbonate apatite cannot be sintered due to the thermal decomposition at high temperature required for sintering. Therefore, carbonate apatite block fabrication should be done in the other method.

One of the methods to fabricate ceramics block is a compositional transformation reaction based on dissolution-precipitation reaction. In this method, difference in thermodynamical stability is used for compositional transformation. In other words, components of a precursor or metastable phase will be dissolved partially in the solution followed by precipitation of the component of the precursor phase to form final product using also the components in the liquid.

One of the well-known dissolution-precipitation reactions is the setting reaction of gypsum. Figure 5 shows the solubility of calcium sulfate hemihydrate

**Fig. 5** Solubility of calcium sulfate hemihydrate and dihydrate as a function of temperature





( $\text{CaSO}_4 \cdot 0.5\text{H}_2\text{O}$ ) and calcium sulfate dihydrate ( $\text{CaSO}_4 \cdot 2\text{H}_2\text{O}$ ) as a function of temperature [11]. As shown, the solubility of calcium sulfate hemihydrate is larger than that of calcium sulfate dihydrate at room temperature. For example, the solubility of calcium sulfate hemihydrate and calcium sulfate dihydrate at 20 °C is 0.9 g and 0.2 g, respectively. And this difference in thermodynamical stability or the solubility is the key for the compositional transformation based on dissolution-precipitation reaction. When calcium sulfate hemihydrate is mixed with water, dissolution reaction would occur. In other words, 0.9 g of calcium sulfate hemihydrate is dissolved in 100 mL water since the solubility of calcium sulfate hemihydrate is 0.9 g (Eq. 2). The calcium sulfate hemihydrate mixed solution should contain  $\text{Ca}^{2+}$  and  $\text{SO}_4^{2-}$  equivalent to 0.2 g calcium sulfate hemihydrate. If there is no other phase that could be equivalent to the solution, the solution is saturated with respect to calcium sulfate hemihydrate and no further reaction would occur. However, there is calcium sulfate dihydrate phase and the phase is also equivalent to the solution. Furthermore, the solution is supersaturated with respect to calcium sulfate dihydrate since the solubility of calcium sulfate dihydrate is 0.2 g. Therefore,  $\text{Ca}^{2+}$  and  $\text{SO}_4^{2-}$  dissolved in the solution would be precipitated as calcium sulfate dihydrate as shown in Eq. 3. Precipitation of the  $\text{Ca}^{2+}$  and  $\text{SO}_4^{2-}$  as  $\text{CaSO}_4 \cdot 2\text{H}_2\text{O}$  makes the solution undersaturated with respect to  $\text{CaSO}_4 \cdot 0.5\text{H}_2\text{O}$  leading to the further dissolution of  $\text{CaSO}_4 \cdot 0.5\text{H}_2\text{O}$ . And dissolution of  $\text{CaSO}_4 \cdot 0.5\text{H}_2\text{O}$  makes the solution supersaturated with respect to  $\text{CaSO}_4 \cdot 2\text{H}_2\text{O}$  leading to the further precipitation of  $\text{CaSO}_4 \cdot 2\text{H}_2\text{O}$ . As a continuous dissolution-precipitation reaction,  $\text{CaSO}_4 \cdot 0.5\text{H}_2\text{O}$  transforms to  $\text{CaSO}_4 \cdot 2\text{H}_2\text{O}$ . In the case of gypsum, precipitated  $\text{CaSO}_4 \cdot 0.5\text{H}_2\text{O}$  interlock each other to set as shown in Fig. 6.

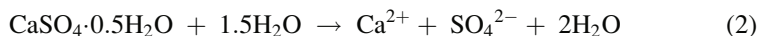
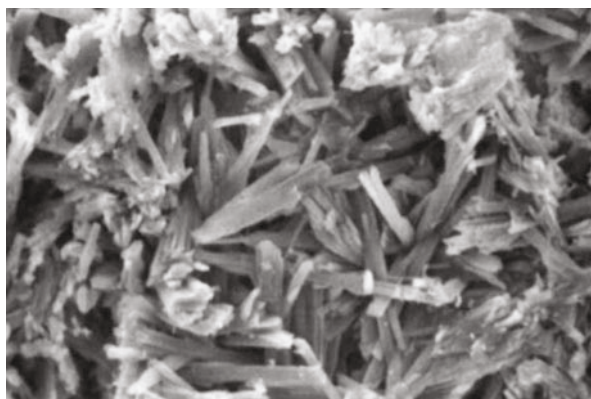


**Fig. 6** Typical scanning electron microscopic image of set gypsum



## **Precursors and Solutions for Carbonate Apatite Block Fabrication Based on Dissolution-Precipitation Reaction**

Since bone apatite is the carbonate apatite, carbonate apatite should be the most stable phase thermodynamically at least at physiological condition. Therefore, carbonate apatite block should be fabricated based on dissolution-precipitation reaction using a suitable precursor [12–19].

The precursor should contain at least one component of the carbonate apatite since the solution needs to be supersaturated with respect to the carbonate apatite based on the dissolution of the precursor. The precursor should show moderate solubility in the solution. If the solubility is too high, precipitation would not catch up with the dissolution, and thus not carbonate apatite block but carbonate apatite powder will be fabricated.

There are many precursors for the fabrication of carbonate apatite including calcium carbonate, calcium phosphates, and phosphate compound such as zinc phosphate [12–19]. There are advantage and disadvantage based on the chemical and physical properties of the precursors. Therefore, suitable precursor should be chosen based on the requirement of the procedure of carbonate apatite fabrication.

Obviously, solution is the other key for the fabrication of carbonate apatite. Composition of the carbonate apatite not supplied by the precursor should be supplied from the solution. Also, pH of the solution is an important factor to determine the degree of supersaturation of the solution with respect to carbonate apatite.

### **Calcium Carbonate, $\text{CaCO}_3$**

Calcium carbonate is one of the ideal precursors for the fabrication of  $\text{CO}_3\text{Ap}$  since it has both calcium and carbonate. Calcium carbonate can be prepared by exposing  $\text{Ca}(\text{OH})_2$  compact to carbon dioxide [12, 13, 20–22]. Advantage of the use of calcium carbonate as precursor for carbonate apatite block fabrication is its capability to fabricate carbonate apatite with relatively higher mechanical strength. This may be due, at least in part, to the incorporation of phosphate into calcium carbonate block for the fabrication of carbonate apatite block. Obviously, precursor needs to get other element from the solution or lose some elements for the fabrication of carbonate apatite since the composition of the precursor and carbonate apatite is different. In the case of calcium carbonate, phosphate ion will be taken from the solution and some carbonate will be released from the calcium carbonate. Overall reaction results in the increase in mechanical strength of carbonate apatite. In the other words, mechanical strength of carbonate apatite is higher than calcium carbonate.

Disadvantage of the use of calcium carbonate as a precursor is its relatively low stability at high temperature. There is no need to use high temperature for the fabrication of carbonate apatite block or granular. However, high temperature is

required for the fabrication of porous carbonate apatite using a porogen since porogen needs to burn out at high temperature. Calcium carbonate decomposes to calcium oxide 620 °C and 920 °C under stream of N<sub>2</sub> and CO<sub>2</sub>, respectively. Therefore, burning out temperature should be regulated carefully for the fabrication of porous carbonate apatite using porogen containing CaCO<sub>3</sub>.

Compositional transformation of CaCO<sub>3</sub> to carbonate apatite can be stated basically as Eqs. 4 and 5. The solubility of CaCO<sub>3</sub> is only 0.15 mmol/L and supplies Ca<sup>2+</sup> and CO<sub>3</sub><sup>2-</sup> into the solution as shown in Eq. 4. Of course, the solution would reach in equilibrium when the solution contains no other ions. However, when the solution contains phosphate ion, the solution would be supersaturated with respect to carbonate apatite. Thus, Ca<sup>2+</sup>, PO<sub>4</sub><sup>3-</sup>, and CO<sub>3</sub><sup>2-</sup> are precipitated on the surface of CaCO<sub>3</sub> as carbonate apatite (Eq. 5):

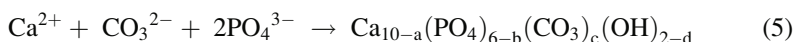
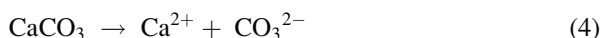
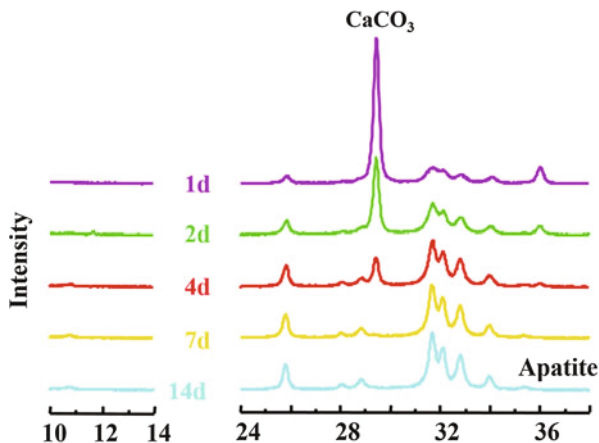
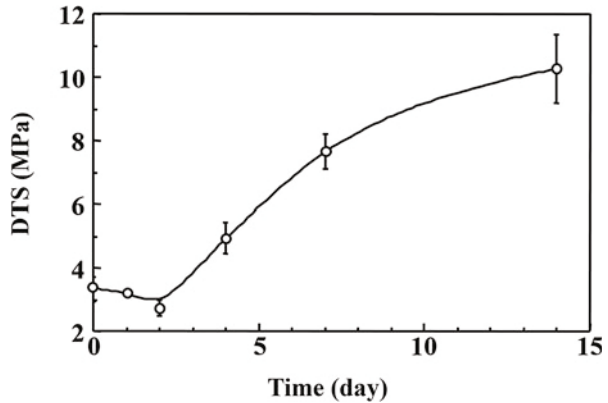


Figure 7 shows the XRD pattern of CaCO<sub>3</sub> block when immersed in 60 °C 1 mol/L Na<sub>2</sub>HPO<sub>4</sub> solution. As shown, CaCO<sub>3</sub> block transformed to carbonate apatite block gradually when immersed in 60 °C 1 mol/L Na<sub>2</sub>HPO<sub>4</sub> solution. Figure 8 summarizes the change of mechanical strength in terms of diametral tensile strength (DTS). As shown DTS value of the CaCO<sub>3</sub> block was approximately 3 MPa. The DTS value increased gradually to reach approximately 10 MPa when the composition of CaCO<sub>3</sub> block was fully converted to carbonate apatite. As described previously, this is a result of uptake of phosphate, and this increase in the mechanical strength is an advantage of use of calcium carbonate as a precursor of carbonate apatite fabrication.

**Fig. 7** Compositional change of calcium carbonate block treated with diammonium hydrogen phosphate at 60 °C



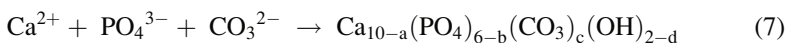
**Fig. 8** Time course of the diametral tensile strength value of the calcium carbonate block when immersed in phosphate salt solution as a function of immersion time



## Calcium Phosphates

As the name represent, calcium phosphates contain both calcium and phosphate. Therefore, solution used for the transformation from calcium phosphate needs to contain carbonate. Various calcium phosphates can be used as the precursor of carbonate apatite fabrication. Among calcium phosphates,  $\alpha$ -tricalcium phosphate ( $\alpha$ -TCP:  $\alpha$ - $\text{Ca}_3(\text{PO}_4)_2$ ) is one of the suitable precursors for the fabrication of carbonate apatite since it has suitable solubility. In fact,  $\alpha$ -TCP has been used as components of apatite cements [23]. Also, stability at high temperature should be addressed. Stability at higher temperature is useful when porogen or other materials need to be burned out during the fabrication of porous precursor.

For example, carbonate apatite foam can be fabricated from tricalcium phosphate precursor as shown in Eqs. 6 and 7.



Dissolution of tricalcium phosphate results in the release of  $\text{Ca}^{2+}$  and  $\text{PO}_4^{3-}$  into the solution as shown in Eq. 6. Note that the solution is already supersaturated with respect to hydroxyapatite. Actually, this is the initial part of the setting reaction of apatite cement [24]. When the solution contains  $\text{CO}_3^{2-}$ , the solution is supersaturated with respect to carbonate apatite. Thus,  $\text{Ca}^{2+}$ ,  $\text{PO}_4^{3-}$ , and  $\text{CO}_3^{2-}$  are precipitated on the surface of tricalcium phosphate as carbonate apatite (Eq. 7).

Figure 9 shows the sequence of  $\alpha$ -TCP fabrication of  $\alpha$ -TCP foam [17]. First, polyurethane foam used as a template is immersed in tricalcium phosphate slurry. This allows adhesion of calcium phosphate powder on the surface of polyurethane strut. Then, calcium phosphate powder adhered polyurethane foam will be heated to burn out polyurethane and sinter calcium phosphate. Structure of the  $\alpha$ -TCP foam thus fabricated is similar to cancellous bone. When  $\alpha$ -TCP foam was

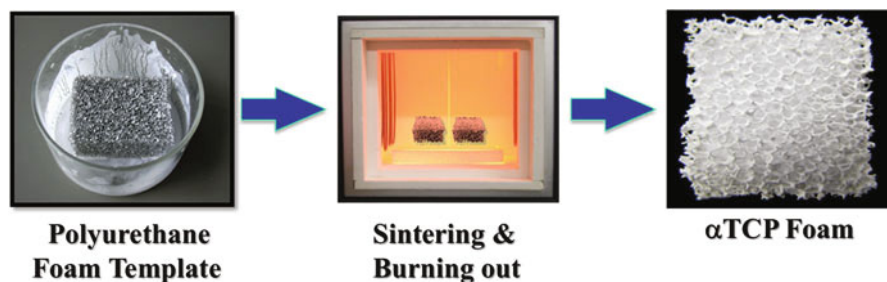


**Fig. 9** Procedure for the fabrication of  $\alpha$ -tricalcium phosphate foam

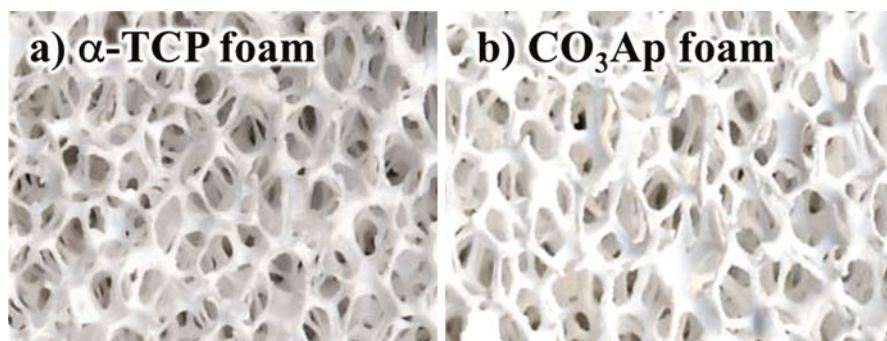


**Fig. 10** Photographs of  $\alpha$ -tricalcium phosphate foam and carbonate apatite foam

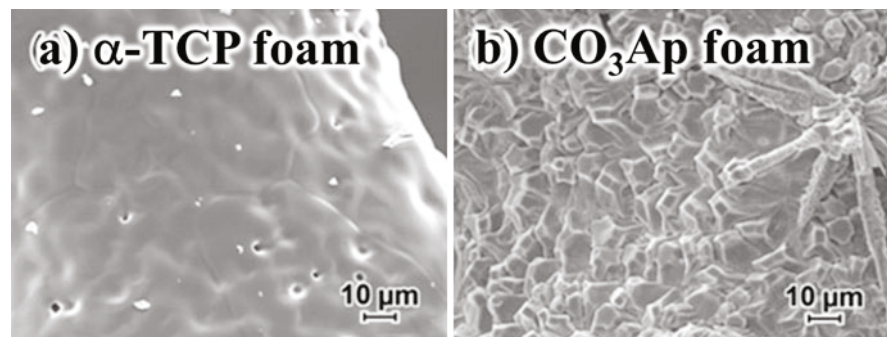


**Fig. 11** Typical scanning electron microscopic images of  $\alpha$ -tricalcium phosphate foam and carbonate apatite foam

immersed in  $(\text{NH}_4)_2\text{HCO}_3$  solution, composition of the  $\alpha$ -TCP foam transformed to carbonate apatite based on dissolution-precipitation reaction keeping its macroscopic fully interconnected porous structure as shown in Fig. 10. Although macroscopic structure is the same before and after compositional transformation based on dissolution-precipitation reaction, microstructure is different as shown in Fig. 11.

Surface of the  $\alpha$ -TCP foam is smooth which is typical for sintered ceramics. In contrast, small precipitated crystals can be seen after compositional transformation reaction. Also, the morphology of the precipitated crystals was different based on the presence and absence of  $(\text{NH}_4)_2\text{HCO}_3$  in the solution and the concentration of  $(\text{NH}_4)_2\text{HCO}_3$ .

Contents of carbonate in carbonate apatite increased with  $(\text{NH}_4)_2\text{HCO}_3$  concentration. In other words, carbonate contents in carbonate apatite can be regulated by changing the concentration of  $(\text{NH}_4)_2\text{HCO}_3$ .

## Calcium Sulfate

Calcium sulfate or gypsum has self-setting ability. Therefore, precursor with desired structure can be made much easier using calcium sulfate. In contrast to calcium carbonate and calcium phosphates that contain two components for the fabrication of carbonate apatite, calcium sulfate contains only one component, calcium, for the fabrication of carbonate apatite. Therefore, both phosphate and carbonate need to be supplied from the solution during the dissolution-precipitation reaction [19]. Calcium sulfate when dissolved releases  $\text{Ca}^{2+}$  and  $\text{SO}_4^{2-}$  into the solution as shown in Eq. 8. Although carbonate apatite  $\text{SO}_4^{2-}$  is released into the solution, only  $\text{Ca}^{2+}$  will be incorporated in the final product. When the solution contains only  $\text{PO}_4^{3-}$ , the solution would be supersaturated with respect to hydroxyapatite, and thus  $\text{Ca}^{2+}$  and  $\text{PO}_4^{3-}$  in the solution would be precipitated as hydroxyapatite as shown in Eq. 9. When the solution contains both  $\text{PO}_4^{3-}$  and  $\text{CO}_3^{2-}$ , the solution would be supersaturated with respect to carbonate apatite, and thus  $\text{Ca}^{2+}$ ,  $\text{PO}_4^{3-}$ , and  $\text{CO}_3^{2-}$  in the solution would be precipitated as carbonate apatite as shown in Eq.10:

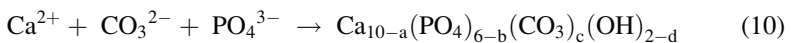
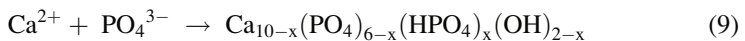
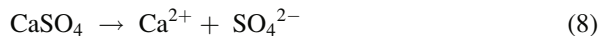
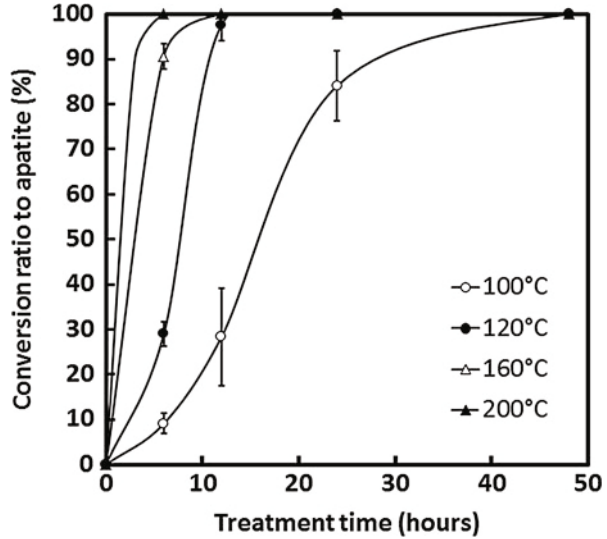


Figure 12 presents the conversion ratio of set gypsum to carbonate apatite as a function of treatment time at different treatment temperatures. Conversion ratio increased with treatment temperature.

Figure 13 presents the carbonate contents in carbonate apatite fabricated using gypsum as a precursor at different treatment temperature. As shown, carbonate contents decreased with increased treatment temperature. In other words, carbonate contents in carbonate apatite can be regulated by temperature.

It should be noted that three-dimensional (3D) gypsum structure can be fabricated using 3D printer. And the same hydroxyapatite or carbonate apatite structure can be fabricated by compositional transformation reaction by just immersing set gypsum in the solution.

**Fig. 12** Conversion ratio of gypsum to apatite as a function of time



**Fig. 13** The carbonate content of set gypsum treated at different temperatures for 48 h

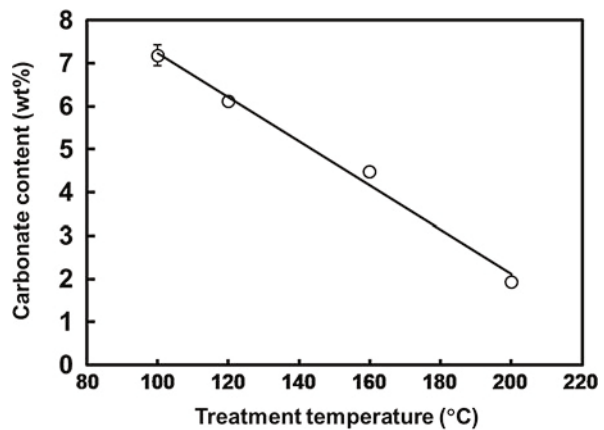
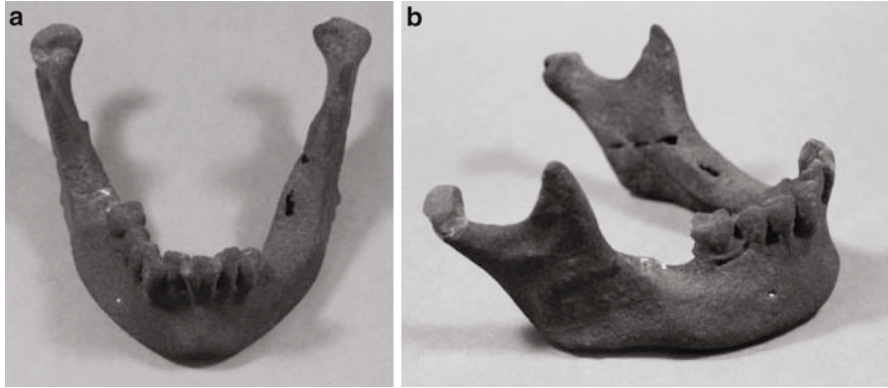


Figure 14 presents the hydroxyapatite bone substitute block fabricated using 3D gypsum printer. Therefore, order-made bone substitute is fabricated and the bone substitute can be placed at the bone defect. Also, CT image can be modified on the computer. For example, introduction of pore can be done to accelerate the bone penetration.

## Cells' Response to Carbonate Apatite

Bone remodeling is done by osteoclasts and osteoblasts as shown in Fig. 1. Therefore, osteoblastic response to carbonate apatite is one of the keys for the replacement of carbonate apatite to the bone. Of course, osteoblastic cells'



**Fig. 14** Three-dimensional printing model of mandible treated in ammonium phosphate solution at 80°C for 24 h. (a) Frontal view and (b) lateral view

response to carbonate apatite could be an indicator of osteoconductivity of carbonate apatite.

Nagai et al. evaluated effects of carbonate apatite and sintered hydroxyapatite on initial cell attachment, proliferation, and osteoblastic differentiation using human bone marrow cells (hBMCs) [25].

No difference was observed for initial cell attachment between carbonate apatite and sintered hydroxyapatite. The number of cells on carbonate apatite was less than that on sintered hydroxyapatite until day 7, after which the number of cells was similar. Clear difference was observed for the differentiation process. Type I collagen, alkaline phosphatase, osteopontin, and osteocalcin were used as makers of early-stage, mid-stage, and late-stage differentiation, respectively. As shown in Fig. 15, relative gene expression level of hBMCs for all differentiation markers, type I collagen, alkaline phosphatase, osteopontin, and osteocalcin, was higher when hBMCs were incubated on carbonate apatite than that on hydroxyapatite although the difference of gene expression between carbonate apatite and hydroxyapatite decreases with time. In other words, carbonate apatite upregulates differentiation of osteoblastic cells. This indicates higher osteoconductivity of carbonate apatite than hydroxyapatite.

Osteoclastic resorption is the other activity of cells for the bone remodeling. Figure 16 presents typical SEM pictures when osteoclastic cells were incubated on the surface of hydroxyapatite and carbonate apatite. As already described previously, the bone was resorbed by osteoclast, whereas sintered hydroxyapatite was not resorbed by osteoclasts. Carbonate apatite fabricated by compositional transformation based on dissolution-precipitation reaction of precursor showed similar behavior with the bone and resorbed by osteoclasts even though the formed pits were smaller when compared to the bone.

Therefore, carbonate apatite is similar to the bone at least for cell level.



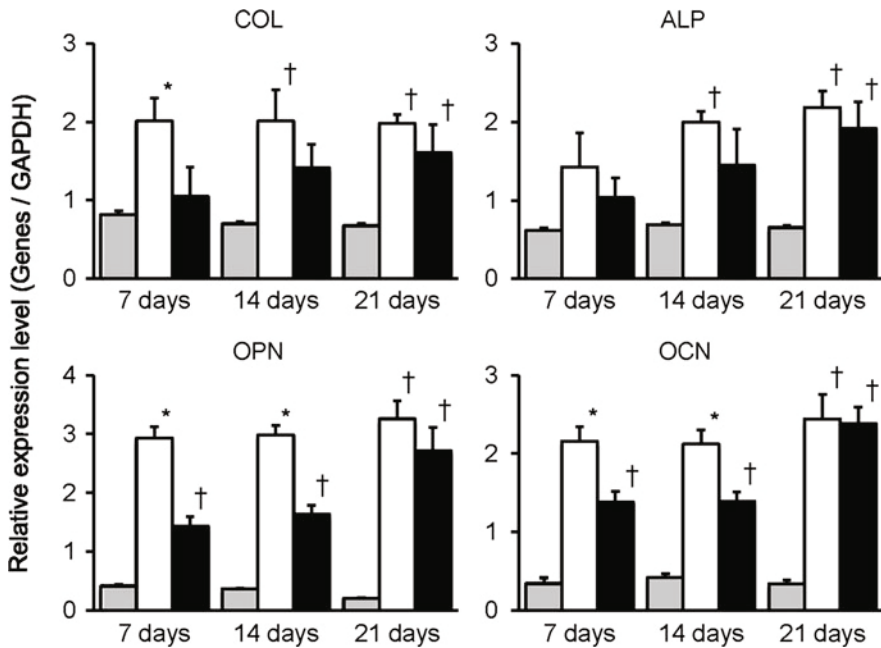


**Fig. 15** Relative mRNA expression levels normalized to GAPDH level. The mRNA expressions of osteoblastic markers, such as ALP, COL, OPN, and OCN, in the cells on the carbonate apatite disk (*white*), sintered hydroxyapatite disk (*black*), and tissue culture plate (*gray*), were assessed using RT-PCR

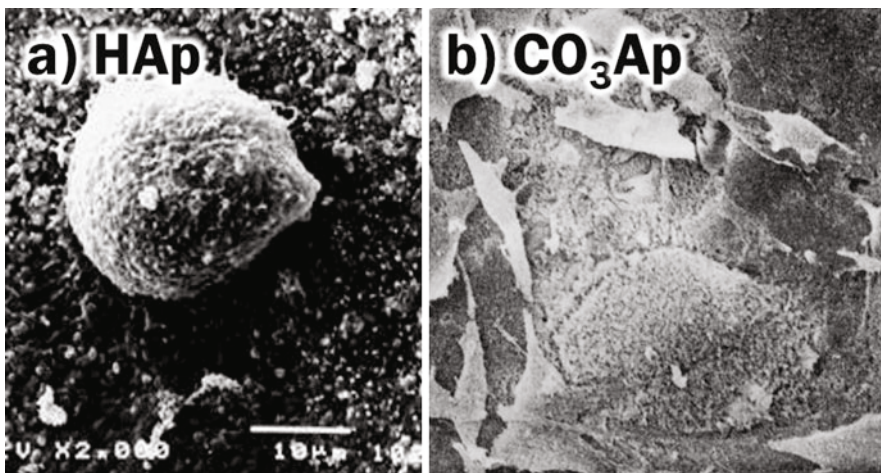
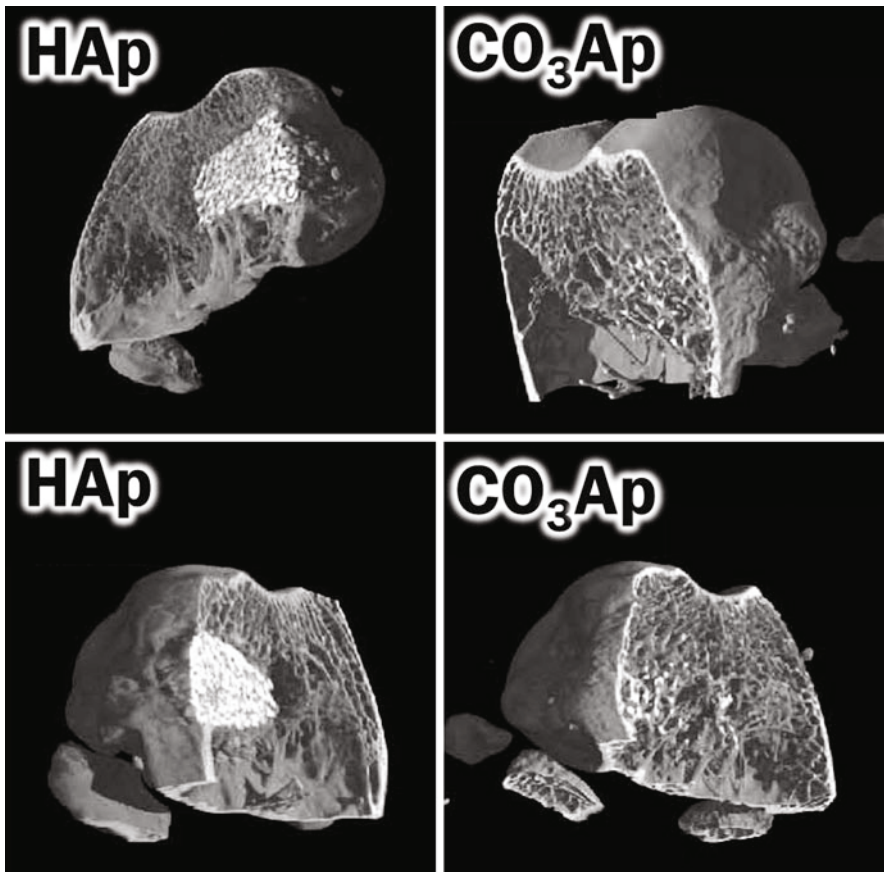


**Fig. 16** Typical scanning electron microscopic image of osteoclasts when incubated on the surface of (a) sintered hydroxyapatite and (b) carbonate apatite (Pictures of (a) are taken from Fig. 2)

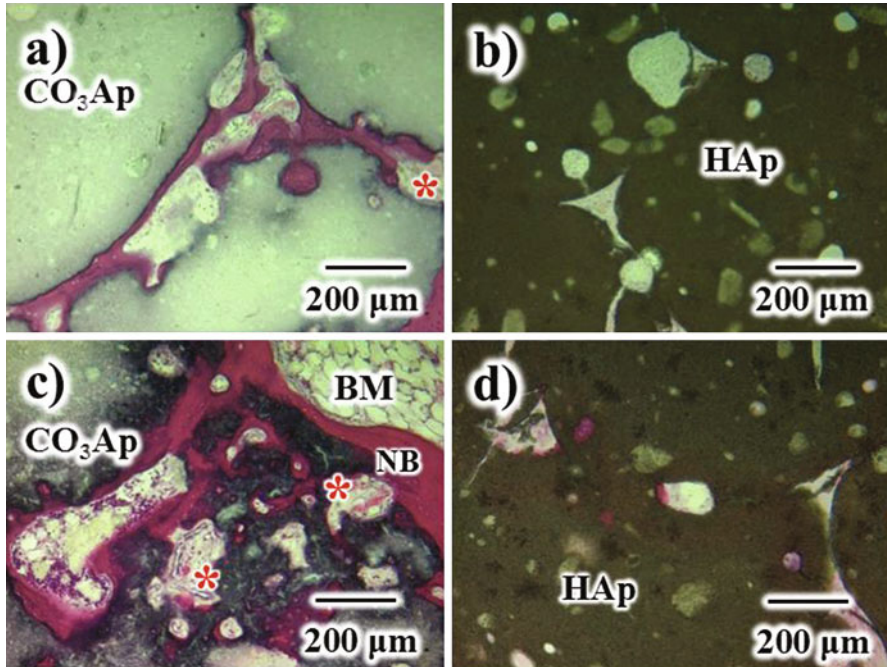
## Tissue Response to Carbonate Apatite

Figure 17 summarizes the  $\mu$ CT images of rat femur bone defect of rabbits 18 months after reconstructed with carbonate apatite granular and sintered hydroxyapatite granular [26]. As shown, sintered hydroxyapatite granular remains at the bone defect without being replaced to the bone. In contrast, carbonate apatite granular is replaced to the bone completely at this stage. This clear difference is in consistent with the previous cell study using osteoclasts. Sintered hydroxyapatite granular was not replaced to the bone since sintered hydroxyapatite is not resorbed by osteoclasts. On the other hand, carbonate apatite granular was replaced to the bone since osteoclasts are resorbed by osteoclasts.

Figure 18 summarizes the histological pictures when bone defect of rabbit femur was reconstructed with porous carbonate apatite (a) (c) and porous sintered



**Fig. 17** The  $\mu$ CT images of rabbit bone femur bone defect 18 months after reconstructed with hydroxyapatite granular and carbonate apatite granular



**Fig. 18** Histological sections stained with hematoxylin and eosin (HE staining) of rabbit femur bone defect reconstructed with (a and c) porous carbonate apatite and (b and d) porous sintered hydroxyapatite (a and b) one and (c and d) three months after implantation

hydroxyapatite fabricated using the same polyurethane foam (b) (d) [27]. In the case of porous carbonate apatite, the bone was clearly seen inside the pore as early as 1 month after implantation (Fig. 18a). Also, blood capillary formation was observed inside the pore of carbonate apatite. It should be noted that pore was larger than that of original porous carbonate apatite. This indicates that resorption of carbonate apatite also occurred at this stage. In contrast, no bone penetration was observed inside the pore of porous sintered hydroxyapatite 1 month after implantation (Fig. 18b).

Three months after implantation, pore of the porous carbonate apatite became larger when compared with that after 1 month (Fig. 18c). Again, this indicates further resorption of carbonate apatite by osteoclasts. Also, the amount of newly formed bone was larger at this stage when compared to one month. In the case of porous hydroxyapatite, small amount of the bone was formed at this stage (Fig. 18d). Obviously, the amount of newly formed bone was much smaller when compared to porous carbonate apatite.

Comparison of tissue response to porous carbonate apatite and porous sintered hydroxyapatite also in consistent to the cell study. In other words, carbonate apatite upregulates differentiation of osteoblastic cells. Therefore, higher osteoconductivity was observed in the case of carbonate apatite. Carbonate apatite is resorbed by

osteoclast, whereas sintered hydroxyapatite is not resorbed by osteoclastic cells. Therefore, carbonate apatite is replaced to the bone, whereas sintered hydroxyapatite remains as it is, and thus, sintered hydroxyapatite is not replaced to the bone.

---

## Summary

Although carbonate apatite decomposes at higher temperature required for sintering process, carbonate apatite block was found to be fabricated by compositional transformation based on dissolution-precipitation reaction using suitable precursors. Carbonate apatite thus fabricated upregulates differentiation of osteoblast and resorbed by osteoclasts. As a result of cell response to carbonate apatite, carbonate apatite shows higher osteoconductivity than sintered hydroxyapatite and would be replaced to the bone. Carbonate apatite seems to be one of the promising artificial bone replacements. Although carbonate apatite is similar to bone apatite than sintered hydroxyapatite, current carbonate apatite is not the same with bone apatite. Further studies are awaiting for the carbonate apatite as well as new artificial bone replacement which is more close to bone apatite based on the findings of carbonate apatite studies.

---

## References

1. Ishikawa K, Matsuya S, Miyamoto Y, Kawate K (2003) Bioceramics. In: Mai YW, Teoh SH (eds) Comprehensive structural integrity, vol 9, Bioengineering. Elsevier, San Diego, pp 169–214
2. LeGeros RZ (1991) Calcium phosphates in oral biology and medicine. Karger, New York
3. LeGeros RZ, Ben-Nissan B (2014) Introduction to synthetic and biological apatites. In: Ben-Nissan B (ed) Advances in calcium phosphate biomaterials. Springer, New York, pp 1–18
4. Elliot JC (1994) Structure and chemistry of the apatites and other calcium orthophosphates. Elsevier, Amsterdam
5. Ito A, Maekawa K, Tsutsumi S, Ikazaki F, Tateishi T (1997) Solubility product of OH-carbonated hydroxyapatite. *J Biomed Mater Res* 36:522–528
6. Okazaki M, Moriwaki Y, Aoba T, Doi Y, Takahashi J (1981) Solubility behavior of CO<sub>3</sub> apatites in relation to crystallinity. *Caries Res* 15:477–483
7. Ishikawa K, Ishikawa Y, Kuwayama N (1991) Preparation of carbonate-bearing hydroxyapatites and their sintering properties. *Chem Exp* 6(7):463–466
8. Aoki H, Kato K, Ogiso M (1971) Studies on the application of apatite to dental materials. *J Dent Eng* 18:86–89
9. Jarcho M (1980) Calcium phosphate ceramics as hard tissue prosthetics. *Clin Orthop Relat Res* 157:259–278
10. de Groot K (1983) Bioceramics of calcium phosphates. CRC Press, Boca Raton
11. Sekiya M (1964) Gypsum. Gihodo, Tokyo
12. Ishikawa K (2010) Bone substitute fabrication based on dissolution-precipitation reaction. *Materials* 3:1138–1155
13. Ishikawa K, Matsuya S, Lin X, Zhang L, Yuasa T, Miyamoto Y (2010) Fabrication of low crystalline B-type carbonate apatite block from low crystalline calcite block. *J Ceram Soc Jpn* 118(5):341–344

14. Suzuki Y, Matsuya S, Udoh K, Nakagawa M, Tsukiyama Y, Koyano K, Ishikawa K (2005) Fabrication of hydroxyapatite block from gypsum block based on  $(\text{NH}_4)_2\text{HPO}_4$  treatment. *Dent Mater J* 24(4):515–521
15. Lowmunkong R, Sohmura T, Takahashi J, Suzuki Y, Matsuya S, Ishikawa K (2007) Transformation of 3DP gypsum model to HA by treating in ammonium phosphate solution. *J Biomed Mater Res Part B Appl Biomater* 80B:386–393
16. Lowmunkong R, Sohmura T, Suzuki Y, Matsuya S, Ishikawa K (2009) Fabrication of freeform bone-filling calcium phosphate ceramics by gypsum 3D printing method. *J Biomed Mater Res B Appl Biomater* 90(2):531–539
17. Wakae H, Takeuchi A, Udoh K, Matsuya S, Munar M, LeGeros RZ, Nakasima A, Ishikawa K (2008) Fabrication of macroporous carbonate apatite foam by hydrothermal conversion of  $\alpha$ -tricalcium phosphate in carbonate solutions. *J Biomed Mater Res A* 87(4):957–963
18. Maruta M, Matsuya S, Nakamura S, Ishikawa K (2011) Fabrication of low-crystalline carbonate apatite foam bone replacement based on phase transformation of calcite foam. *Dent Mater J* 30(1):14–20
19. Nomura S, Tsuru K, Matsuya S, Takahashi I, Ishikawa K (2014) Fabrication of carbonate apatite block from set gypsum based on dissolution-precipitation reaction in phosphate-carbonate mixed solution. *Dent Mater J* 33(2):166–172
20. Lee Y, Hahm YM, Matsuya S, Nakagawa M, Ishikawa K (2007) Development of macropores in calcium carbonate body using novel carbonation method of calcium hydroxide/sodium chloride composite. *J Mater Sci* 42:5728–5735
21. Lee Y, Hahm YM, Matsuya S, Nakagawa M, Ishikawa K (2007) Characterization of macroporous carbonate-substituted hydroxyapatite bodies prepared in different phosphate solutions. *J Mater Sci* 42:7843–7849
22. Otsu A, Tsuru K, Maruta M, Munar ML, Matsuya S, Ishikawa K (2012) Fabrication of microporous calcite block from calcium hydroxide compact under carbon dioxide atmosphere at high temperature. *Dent Mater J* 31(4):593–600
23. Monma H, Kanazawa T (1976) The hydration of  $\alpha$ -tricalcium phosphate. *Yogyo Kyokai-Shi* 84:209–213
24. Ishikawa K (2008) Calcium phosphate cement. In: Kokubo T (ed) *Handbook of bioceramics and their application*. CRC Press, Boca Raton, pp 464–484
25. Nagai H, Fujioka-Kobayashi M, Fujisawa K, Ohe G, Takamaru N, Hara K, Uchida D, Tamatani T, Ishikawa K, Miyamoto Y (2015) Effects of low crystalline carbonate apatite on proliferation and osteoblastic differentiation of human bone marrow cells. *J Mater Sci Mater Med* 26(2):99–107
26. To be submitted
27. Nguyen XTT, Maruta M, Tsuru K, Matsuya S, Ishikawa K (submitted) Fabrication and histological study of ant colony type carbonate apatite foam. *Biomaterials*

---

# Natural and Synthetic Polymers for Designing Composite Materials

# 9

Bogdan C. Simionescu and Daniela Ivanov

## Contents

Introduction .....	235
Biomaterials for Medical Applications .....	235
Polymer Biocomposites for Medical Applications .....	239
Natural and Synthetic Biomedical Polymers .....	249
Natural Polymers .....	250
Synthetic Polymers .....	259
Fabrication of Polymer Biocomposites .....	271
Conventional Fabrication Techniques .....	273
Solution-Based Techniques .....	276
Advanced Fabrication Techniques .....	280
Summary .....	283
References .....	284

---

## Abstract

Since the 1920s when Hermann Staudinger pioneered theories on “macromolecules,” covering both natural and synthetic polymers, this concept captured the imagination of chemists to design a wide range of molecular architectures of polymeric materials with fascinating and innovative applications. Polymers were first used in medicine as biomaterials in the 1950s for cornea replacement and as blood vessel replacement. Polymeric biomaterials offer a large diversity as matrix

---

B.C. Simionescu (✉)

Department of Natural and Synthetic Polymers, “Gheorghe Asachi” Technical University, Iași, Romania

“Petru Poni” Institute of Macromolecular Chemistry, Iasi, Romania  
e-mail: [bcsimion@icmpp.ro](mailto:bcsimion@icmpp.ro)

D. Ivanov (✉)

“Petru Poni” Institute of Macromolecular Chemistry, Iasi, Romania  
e-mail: [dani@icmpp.ro](mailto:dani@icmpp.ro)

and inclusion materials in the development of biocompatible biostable, biodegradable, or bioresorbable polymeric biocomposite materials for tissue engineering and regenerative medicine applications. Natural polymers are considered as the first biodegradable biomaterials used in biomedical applications. Synthetic biostable polymers of the first generation of biomaterials were selected to provide mechanical support and minimize the host response of the related biomaterials. Biodegradable polymers have been utilized to develop biocompatible biomaterials with tuned degradability and certain structure–function relationship. The last generation of biomaterials for medical applications aims the design from biomimetic to bioinspired synthetic composite materials and systems with dynamic behavior and controlled properties, capable of inducing biological responses that mimic natural structures and processes, based on supramolecular self-assembled and smart polymer approach. Biocomposite polymer materials can be fabricated utilizing different techniques, the selection of the most appropriate being influenced by the desired application, the particularity of the type of filler (particles and fibers of different dimensions, laminae, or voids), and matrix (natural polymers, thermoplastic or thermosetting synthetic polymers), at different scale length.

#### Keywords

Natural polymers • Biostable synthetic polymers • Biodegradable synthetic polymers • Thermoplastic polymers • Thermosetting polymers • Biocomposite materials • Biomedical polymers • Biomacromolecules • Supramolecular polymers • Self-healing polymeric composites • Biomimetic materials • Bioinspired materials • Biomimetic biomaterials • Tissue replacement • Tissue regeneration

#### Abbreviations

Bis-GMA	2,2-Bis[p-(2'-hydroxy-3'-methacryloxypropoxy)phenylene]propane
CS	Chondroitin sulfate
EBPADMA	Ethoxylated bisphenol A dimethacrylate
ECM	Extracellular matrix
GAGs	Glycosaminoglycans
HA	Hyaluronic acid
HAp	Hydroxyapatite
HDPE	High-density polyethylene
LCST	Lower critical solution temperature
MMA	Methyl methacrylate
PA	Polyanhydride
PCL	Poly( $\epsilon$ -caprolactone)
PDLLA	Poly(D,L-lactic acid)
PE	Polyethylenes
PEEK	Poly(ether-ether-ketone)
PEG PEO	Polyethylene glycol
PET	Polyethylene terephthalate

---

PGA	Poly(glycolic) acid
PHA	Polyhydroxyalkanoates
PLA	Poly(lactic) acid
PLGA	Poly(lactic-co-glycolic) acid
PLLA	Poly(L-lactic acid)
PMMA	Poly(methyl methacrylate)
PNIPAM	Poly( <i>N</i> -isopropylacrylamide)
PP	Polypropylenes
PPF	Poly(propylene fumarate)
PTFE	Polytetrafluoroethylene
PTMC	Poly(trimethylene carbonate)
PU	Polyurethanes
TEGDMA	Triethylene glycol dimethacrylate
UDMA	1,6-Bis(methacryloxy-2-ethoxycarbonylamino)-2,4,4-trimethylhexane
UHMWPE	Ultrahigh molecular weight polyethylene

---

## Introduction

### Biomaterials for Medical Applications

Biomaterials for biomedical and healthcare applications are considered the natural or man-made materials other than food or drugs which are used as therapeutic or diagnostic systems, proposed to regenerate, repair, support, and replace the defect of hard or soft living tissues while in intimate contact with them [1]. The development and implementation of a wide range of novel biomaterials represent a dynamic and iterative process that involves the creation of increasingly safer, physiologically appropriate, reliable, and inexpensive replacements and devices for dysfunctional, damaged, or diseased tissues or simply for aesthetic reasons.

According to the types of host-tissue response, the development of biomaterials can be divided into four generations (Fig. 1) [2, 3]. Biomaterials of **the first generation** were selected to provide an acceptable combination of physical properties to match those of the *replaced* tissue, with nearly *bioinert* or *biostable* behavior, exhibiting no or minimal immune response, causing no foreign body reactions and preventing biological rejection. Bioinert biomaterials as medical implants and devices such prosthesis have been utilized throughout history. The early civilizations utilized sutures, prosthesis, and implants to replace damaged tissues and to provide structural support. The modern era of medical implants might be traced back to an observation in the late 1940s that the PMMA plastic shards accidentally implanted in pilot's eyes might be appropriate for implant lenses for cataractous eye. In the 1950s internal ocular lenses were innovated, the hip implant developed, the vascular graft invented, kidney dialysis revolutionized, and the ball and cage heart valve invented, all in an era before principles for medical materials were established. Classical metals and their alloys as well as nondegradable polymeric implants were typically



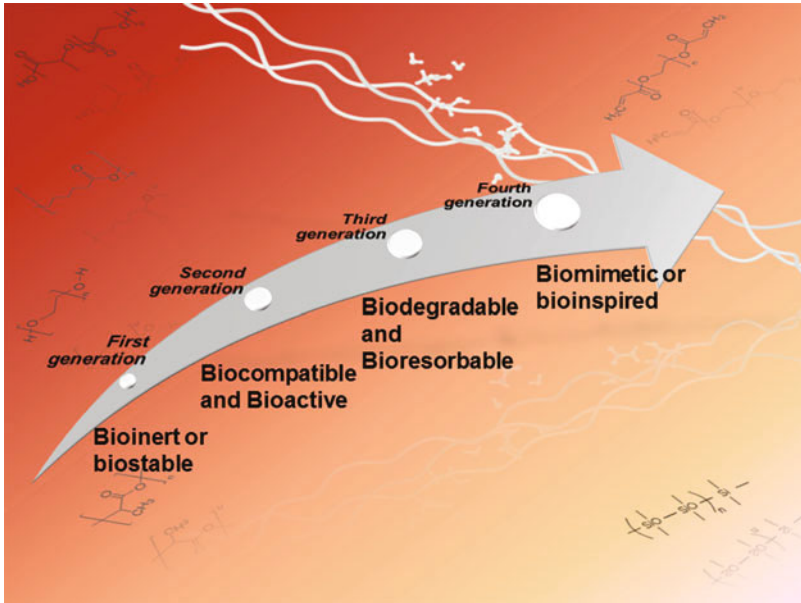


**Fig. 1** Development of biomaterials timeline

considered bioinert biomaterials that in the case of permanent implants ultimately failed. Biostable biomaterials are still used nowadays for the replacement of the tissues that cannot be regenerated due to their large losses or for the patients with less effective self-healing ability of the damaged tissues. In the second half of the twentieth century, biomaterials concept began to shift from mainly bioinert toward the development of *biocompatible* materials. From this perspective, biomaterials and their degradation by-products should not initiate a host response once implanted; biomaterials have to fulfill a number of prerequisites before they can be used in biomedical applications. *Biocompatible* and *bioactive* biomaterials represented **the second generation of biomaterials** with the aim to encourage bonding to the host tissue and enhance their integration by promoting specific responses from the host sites and stimulating the new tissue growth. Bioactive ceramics such as hydroxyapatite, some calcium phosphates, and bioactive glasses as well as their related composite materials were found to bond directly with living tissues when implanted and were extensively used to induce specific biological activity and achieve a better integration of implants. Another strategy consisted in designing implants with porous coatings and structures, hence facilitating native tissue ingrowth and achieving a stable three-dimensional interlocking with the surrounding tissue. A large number of these biomaterials still represent the state of the art of commercial products clinically used. Biomaterials research of **the third generation** is marked by a high degree of multidisciplinary and interdisciplinarity, such as materials science, chemistry and chemical engineering, biology and molecular biology, physics and biophysics, biomechanics and mechanical engineering, and nanotechnology.

As a consequence of an increase in understanding, emphasis shifted from *replacement* of tissues to *regeneration* of tissues and from a materials-and-mechanics approach to biological-based tissue-activated repair. The concept of biomaterials expanded to *biodegradable* and *bioresorbable* biomaterials with tunable degradation and resorption rate, initially incorporated into the surrounding tissue, which are time-dependently completely replaced, ideally with the same rate, by new growth tissue. The **fourth generation of biomaterials** developing nowadays is represented by the biologically inspired *biomimetic* and *smart* biomaterials and systems that mimic the natural extracellular environment and one or more functions found in nature, providing new solutions to treat diseases, support tissue regeneration, and rebuild body parts. New concepts are inspired by common design principles used by living organisms to develop heterogeneous structures with outstanding properties by combination under mild synthesis conditions of soft and hard components from a fairly limited selection, held together by association of strong and weak bonds into biological composites with hierarchical structures, at multiple length scales (nano – *nanocomposites*, micro, meso, and macro), able to adapt, remodel, and self-heal rather than far more elaborate homogeneous man-made composites with sophisticated chemical composition and architectures [4]. Biomimicry is related to inspiration by natural materials and functions and not to bioduplication [5, 6]. Biomimetic approaches can be achieved either mimicking natural structures all the way down to the molecular hierarchical organization level based on biological autonomous *self-assembly* complex structures by multiple inter- and intermolecular noncovalent interactions or using concepts from nature but designing synthetic *smart biomaterials* using conventional processing methods [7]. The central aim of supramacromolecular *self-assembly* is to design and construct ordered and dynamic structures in varying architectures, size scales and complexities, etc., with high responsivity to stimuli, environmental adaptation, and self-repair capacity, using synthetic and natural polymer building blocks. *Smart biomaterials* have been designed to interact with the surrounding cells and tissues consequent biological actions and actively participate in the regeneration of the damaged tissue, to respond and react to stimuli from its environment, and to promote modulated drug release and the inherent capacity of the body to heal and self-repair. Not only smart biomaterials need to be developed, but also *smart designs* of biomaterials systems which suppose smart strategies for tissue regeneration and drug delivery. *Biomimetic self-healing biomaterials* exhibit the ability to repair themselves and to recover functionality using the resources inherently available to them, offering a new route toward safer, longer-lasting products and components. The repair process may be autonomic or externally assisted; in both cases the recovery is triggered by damage to the material, and the chemical repair process depends on the type of involved healing mechanism (polymerization, entanglement, reversible cross-linking, etc.) [8].

The introduction of biomaterials in the biomedical field started with the use of conventional metals, ceramics, and synthetic polymers that were adapted for several clinical needs.

**Metals** and their alloys have been used for medical applications for long time because of their high wear resistance, strength and ductility, and ease manufacturing

of products with various and complex shapes. In addition, the good electrical conductivity of metals favors their use for neuromuscular stimulation devices. Metallic biomaterials are used almost exclusively for load-bearing applications and other biomedical applications of metallic biomaterials including cardiovascular and neurosurgical devices. Properties of metal materials depend on the processing method and purity of the metal, and only a relatively small number of metals are used currently in biomedical applications, primarily because of concerns over metal corrosion and biocompatibility. Sherman vanadium steel was the first metallic alloy designed for biomedical applications. Novel metallic biomaterials currently gaining increasing attention, such as bioresorbable Mg alloys and porous shape memory materials with anticorrosion ability, increased biocompatibility and low diffusion of metal ions. The inherent durability of metal implants may require multiple surgical procedures to insert, rectify, and ultimately remove the implanted structure. Moreover, metal implants do not directly bond to bone tissue, and often their ultimate fate is to be encapsulated by fibrous tissue that leads to aseptic loosening of the prosthesis.

**Ceramics** generally possess good biocompatibility compared to metals, along with resistance to corrosion and compression. Ceramics can be nonabsorbable or relatively inert (e.g., alumina, zirconia, silicone nitrides, and carbons), bioactive and surface reactive or semi-inert (e.g., certain glass ceramics and dense hydroxyapatite), and biodegradable and resorbable or noninert (e.g., aluminum calcium phosphate, hydroxyapatite, and tricalcium phosphate). The drawbacks include brittleness, low fracture strength, high density, low mechanical reliability, and lack of resilience.

**Polymers** consist in high molar mass chains or macromolecules composed of a large number of same or different repeating units known as *monomers*; the number of repeating units in a polymer represents the degree of polymerization. Polymer can have different chemical structure and properties and on the basis of these properties can be classified in different ways: based on source (natural, semisynthetic, and synthetic polymers); by chemical composition (organic and inorganic); based on constitutive monomer units (homopolymers and copolymers); by chain architecture (linear, branched, cross-linked polymers); by chain conformation (sequence of bonds and torsion angles) and configuration (stereoisomerism and tacticity); based on molecular forces (covalent bonds and noncovalent interactions); by morphology (amorphous, semicrystalline, and crystalline); based on polymerization reaction type (polyaddition, polycondensation, and metathesis polymerization); by thermal properties (elastomers, thermoplastics and thermosets); based on degradation and stability (chemical, biological, mechanical, thermal, photo degradation); by applications; etc. *Biomedical polymers* represent the largest class of materials routinely used in clinical applications because of their diversity and versatility, ranging from surgical sutures to drug-eluting devices to implants, at a reasonable cost. The chemical composition flexibility of polymers provides them with their unique physical, chemical, and biological properties, including manufacturability and eventually second processability characteristics. Although great progress has been made in the synthesis of new polymers, no single polymer can meet all the requirements, especially their low mechanical strength that cannot withstand the stresses required

in many biomedical applications. This is the reason for the design of multicomponent polymer system strategies, elaborated to obtain innovative multifunctional polymeric biomaterials. Natural polymer–synthetic polymer biomaterials present ideally suited structure properties: while the biopolymer can provide hierarchical organization or favorable interactions for biological applications, the synthetic polymer component can provide responsive behavior, enhanced structural integrity, and economic feasibility. *Self-assembly* polymer chemistry including the assembly of synthetic building blocks (including macrocycles, dendrimers, and organic–inorganic compounds, polyrotaxanes, organic–inorganic compounds), biomacromolecules (polypeptides and DNA), and especially supramolecular polymers and dynamic polymers contributed to the development of biomimetic and bioinspired materials that mimic complex and hierarchical ordered architectures found in natural models [9, 10].

The development of different types of copolymers, polymer blends, interpenetrating polymer networks, and especially polymer composites is some of different methods of significant interests, since these modifications could lead to a new range of biomaterials with desired properties.

## **Polymer Biocomposites for Medical Applications**

A single component material – metals, ceramics, or polymers – may not always provide all the required properties for a particular application, but combining one of this component with one or more other components with differing physical and chemical properties, it is possible to design composite materials with new set of unprecedented properties or with state-of-the-art properties compared to those of the individual components. Composites represent engineered materials consisting of two or more distinct components, on a scale larger than atomic size scale, with significantly different physical or chemical properties, complementary to each other. The term “component” will be preferred for composites instead of “phase” that was well defined earlier in colloid chemistry and thermodynamics [11]. In the composite materials, one heterogeneous secondary component (inclusion) is dispersed in a continuous primary component (matrix) in a continuous or discontinuous form, often exhibiting hierarchical organizations. Between matrix and secondary component, there is an interface between of the components, each component being independent but not isolated. Biomedical composites are composite materials whose constituents should be biocompatible; hence, in designing biomedical composites and predicting their performance, several issues must be considered regarding the biological response [12]. Composites differ from homogeneous materials in that considerable control can be exerted over the larger scale structure and hence over the desired properties.

Biocomposite materials depend very much upon structure and are anisotropic and multifunctional in nature and allow modulation not only of the physical or mechanical properties but also of the cellular response. Most tissues are polymeric biocomposites with sophisticated microstructure of an intimate combination of

inorganic materials, organic materials, and cells, exhibiting remarkable properties, made up of constituents whose amount, distribution, morphology, hierarchical structure, and derived properties determine the final behavior of the tissue or organ. Such natural biological composite materials are extracellular matrix, bones, teeth, cartilage, tendons, ligaments, skin, etc., while natural foams include the lung and cancellous bone. Natural composites have been stimulating the advance of biomimetic composites with improved properties that could enable the regeneration of tissues and organs.

*Smart composite biomaterials* that combine the properties of different biomaterials can target the entire range from hard tissue to soft tissue applications. Internal modulation of their behavior mainly involves biomimetic modification of chemical, physical, and biological properties that ultimately exhibit smart actions, fitting the biomimetic approach by chemistry modulation. External modulation is characteristic to smart biomaterials with controlled and sustainable drug delivering potential. The design of smart biomaterials as scaffolds for tissue engineering is based on multifunctionality and responsiveness in conjunction with shape memory properties and considers the multiple delivery of biofactors in a controllable manner, based on modulation of internal chemistry and external therapeutic molecules [13].

The properties of composites are influenced by the structure and properties of the matrix; the properties of the secondary component or inclusion; the ratio of secondary component to the matrix (secondary component volume fraction); the shape, geometry, and orientation (random or preferred orientation) of the secondary component in the composite; and the performance of interface nature between constituents. Composites are a subclass of anisotropic materials that are classified as orthotropic, with different properties in three mutually perpendicular directions. The ability to design anisotropic properties into a composite material is one of the most important advantages, most of the body tissues presenting anisotropic properties.

### **Primary Component or the Matrix**

The primary component is the matrix, which is a metal, ceramic, or polymer, and the related composites can be metal matrix composites, ceramic matrix composites, and polymer composites, respectively. The matrix performs several critical functions, including maintaining the secondary component in the proper orientation and spacing, protecting them from the environment and transferring the applied load to the secondary component, redistributing the stress. In biomedical applications, the criteria for selecting the materials to act as matrix are challenging; the materials must be biocompatible, not induce immune responses, be nontoxic and eliminated at a predetermined pattern. On the other hand, the biocomposites must possess appropriate chemical and mechanical properties and be suitable for processing techniques, sterilization, and long shelf life.

Polymer matrix composites represent the first types of biocomposites developed for medical application. The principal advantages of polymers as matrix over ceramic matrix or metal matrix are low cost, easy processability, good chemical resistance, and low specific gravity. Both natural polymers and synthetic polymers have been extensively investigated as matrix component.

*Biostable or nondegradable* polymers were used as biomaterials in early tissue engineering research in applications requiring excellent mechanical and corrosion resistance, such as UHMWPE for orthopedic application; PMMA for bone cements, dental composites, and intraocular lenses; and later PET, PU, and PTFE for vascular prosthesis, polysulfone, PEEK, etc.

Natural polymers can be considered as the first *biodegradable* biomaterials, possessing the great advantage of biological recognition, because of the presence of receptor-binding ligands inside their chemical structure. Synthetic polymers may overcome the problems related to purification, immunogenicity, and pathogen transmission of some natural polymers and may also provide a greater reproducibility and control over the material properties. The biodegradability of most resorbable synthetic biocomposites is conferred by commonly aliphatic polyesters, such as PGA, PLA, PLGA, PCL, poly(trimethylene carbonate), PU, poly(esteramide), poly(orthoesters), PA, poly(anhydride-co-imide), cross-linked PA, poly(propylene fumarate), poly(pseudo amino acids), poly(alkyl cyanoacrylates), polyphosphazenes, or polyphosphoesters. They have been widely utilized owing to their biocompatibility, controllable biodegradation, and metabolization to natural degradation products by nonenzymatic hydrolysis of ester bonds that are eliminated by natural metabolic pathways. The incorporation of inorganic phases in biodegradable polymers can alter the polymer degradation behavior because of a pH buffering effect by altering the autocatalytic effect of the acidic end groups resulting from hydrolysis of the polymer chains. Degradation rates can be controlled by varying molecular weight, alteration in enantiomers, and copolymerization. Moreover, polymers have been of interest because of the versatility and flexibility that they offer for producing well-defined highly porous scaffolds with different geometries and structures to meet the needs of specific tissue engineering applications.

*Hydrogel matrix composites* have been also designed for soft and hard tissue applications. Injectable biocomposite such as bone cements can be advantageous because it allows for easy manipulation and minimally invasive procedures by surgeons to reduce complications and to improve patient comfort. Moreover, injectable formulations provide the ability to take the shape of the cavity in which they are placed and can thus fill irregular defects. *Supramolecular composite* material is an organized, complex entity that is created from the molecular self-assembly of two or more chemical species held together by intermolecular forces, and though the field is in its infancy, a predictive tool will be generated.

## Secondary Component or the Inclusion

The properties of composites are influenced by the nature, geometry, concentration, distribution, and orientation of the inclusions. The solid inclusions may consist of polymers, ceramics, and glasses but can also consist of voids, filled with air or liquid (Fig. 2).

The principal **solid inclusion** shape categories at different length scales are the particles, with approximately same dimensions in all directions, characteristic to particulate composites; the fibers, with length dimension much greater than its cross

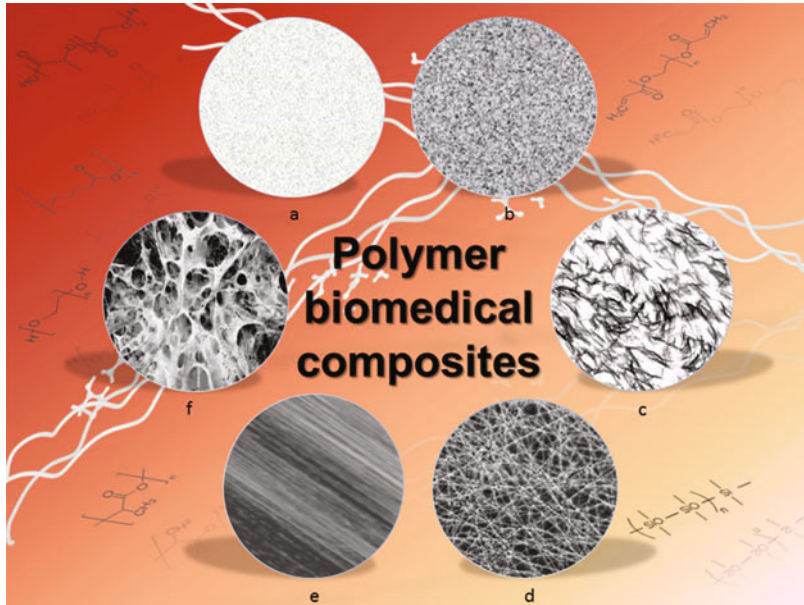


**Fig. 2** Polymer biomedical composites based on natural and synthetic polymers (in background): (a) nanocomposites; (b) micro- and macroscale particulate composites; (c) random short-fiber composites; (d) random long-fiber composites; (e) oriented long-fiber composites; (f) porous composites

section, found in fibrous composites; and platelet or lamina, characteristic to laminae of oriented fiber composites. The solid inclusions are also referred as reinforcement or filler. The orientation and distribution of inclusions in man-made composites represent the key of effective stress transfer from the surrounding matrix in particular directions and can be random or preferred.

**Particulate** inclusions may be spherical, ellipsoidal, polyhedral, or irregular. The shape of the particles is important in creating a stiff isotropic composite. Platelet inclusions are the most effective, followed by fibers, and the less effective geometry is the spherical particle. Even if the spherical particles are perfectly rigid, their stiffening effect at low concentrations is modest, while when the inclusions are more compliant than the matrix, spherical particles reduce the stiffness the less and platelet reduces it the most. **Fibers** are more effective in achieving a stiff, strong composite than particles, and the degree of anisotropy in fibrous composites is of great importance. Composites containing unidirectional fiber are very strong in the longitudinal direction, but weaker than the matrix alone when loaded transversely; for the composites that require stiffness and strength in all directions, the fibers should be oriented randomly. Micromechanics dictates that a certain volume fraction of inclusion is needed to achieve an appreciable stiffening effect; high concentrations of inclusion (high volume fraction) have a greater reinforcing effect than low concentrations.

The main inclusion materials that have been used in biomedical composites are ceramic particles, glass fibers and particles, and carbon fibers and polymer fibers that, depending upon the applications, have been either inert or absorbable.

Different **ceramic materials** have been used to reinforce biomedical composites, and because they are relatively weak and brittle materials, the preferred form has usually been particulate. These materials have included various calcium phosphates, aluminum- and zinc-based phosphates, glass and glass–ceramics, and bone mineral. **Hydroxyapatite and tricalcium phosphates** are used in orthopedics and dentistry, alone or in combination with other substances, or also as coating of metal implants, being commonly referred as bioactive ceramics because of their ability to elicit a specific biological response, promoting osseointegration. **Bioactive glasses** are added to polymeric matrices to form structural composites for their high strength-to-weight ratio; good dimensional stability; good resistance to heat, cold, moisture, and corrosion; facile fabrication; and relatively low cost. Glasses have been used with acrylic resins for dentistry applications. **Barium sulfate** ( $\text{BaSO}_4$ ) may be added to biocomposites as powder for X-ray image contrast. As an alternative method to adding radiopaque powder, metallic wires (markers) may also be used. **Carbon fibers** are a lightweight, flexible, high-strength, and high-tensile modulus being produced by the pyrolysis of organic precursor fibers. Carbon fibers have been coupled with UHMWPE, epoxy resins, polysulfone, or PEEK, and some carbon fiber composites are already in the market.

**Polymer fibers** are not comparable to carbon fibers in strength or stiffness when used to reinforce other polymers, with the possible exceptions of aromatic polyamide (aramid) or UHMWPE fibers, and high-strength, high-modulus polyethylene fiber composites are commercially available. The idea of replacement of the mineral secondary component in polymer composites resulted in creation of new types of composite materials, the **polymer–polymer composites** with natural fibers or synthetic fibrous components as reinforcement, as well as the **single-polymer** composites – also termed as one-polymer composites, homocomposites, self-reinforced composites, one-phase composites, homogeneous composites, or all-polymer composites [11]. For *polymer–polymer* and *the single-polymer composites*, the matrix and inclusion are given by different polymers, whereas in single-polymer composites they consist of the same polymer or of polymers belonging to the same type; in both composites the matrix is always isotropic compared with traditional ones. Normal tendons and ligaments are natural composite consisting of parallel strands of collagen fibers interwoven with proteoglycan components. Single-polymer composites similar to traditional composites have characteristics (stiffness, strength) of the filler different from those of the matrix. The single-polymer composites with amorphous matrix and amorphous fillers are less relevant than those with semicrystalline structure, and decreasing molecular mass is usually associated with enhanced crystallinity. Molecular entanglements in single-polymer composites may serve for improved adhesion and thus for stress transfer between the matrix and filler via the interface. They are of further interest because of avoiding the matrix-reinforcement adhesion problem, no dispersion problem, preparation, and complete regeneration; their basic disadvantage is the very narrow processing window. For example, PGA,



PLA, and PLGA have been widely used as resorbable bone fixation devices or suture materials; the mechanical properties of these materials can be enhanced by self-reinforcing processes, where the polymer matrix is reinforced by oriented fibers of the same material.

**Laminated composites** are assemblies of layers of fibrous composite materials consisting of layers or plies bonded together that can differ in relative fiber orientation and volume fraction to achieve the desired degree of anisotropy. Layers of different materials may also be used. Examples include polymer–polymer and glass–polymer laminates, and ionic polymer (e.g., sulfonated tetrafluoroethylene)–metal composite is among the new generation of smart biomaterials with significant potential for medical applications.

**Porous biocomposites** have a high ratio of surface area to volume, and the presence of voids in porous composites reduces the stiffness and influences the toughness of the material that is both acceptable and desirable in biomedical applications such porous implants or implant coatings. Trabecular bone is an example of a natural cellular composite, and the presence or absence of orientation of trabeculae affects both its stiffness and strength. For instance, for trabecular bone of unspecified orientation, the stiffness is proportional to the cube of the density and the strength as the square of the density, while for bone with oriented trabeculae, both stiffness and strength in the trabecular direction are proportional to the density. Ingrowth of tissue into implant pores is not always desirable, e.g., sponge (polyvinyl alcohol based) implants used in soft tissue augmentation surgery. Numerous metals and alloys, ceramics, and natural and synthetic polymers can be textured or rendered porous using a large variety of techniques [14]. Biomedical applications of porous biocomposites include porous biomedical devices and prostheses; scaffolds for in vitro cell culture and in vivo hard tissue-induced regeneration; and macro-, micro-, and nano-particulate foams for drug delivery, diagnostic, and sensing. Porous materials used in soft tissue applications include PU, polyamide and polyesters used in percutaneous devices, braided PP for artificial ligaments, collagen for artificial skin, or cellulose and fibrin for blood vessel replacements. Important parameters to consider while designing a porous scaffold are average pore size, pore size distribution, pore volume, pore interconnectivity, pore shape, pore throat size, and pore wall roughness. Particularly surface characteristics such as roughness, topography, and chemistry play a key role in specific cell responses such as attachment, migration, proliferation, and differentiation.

**Nanocomposites.** Recent advances in the development of **nanostuctured biocomposite materials** for medical applications have been possible due to the development of novel processing and characterization techniques. Nanocomposites are materials with at least one dimension of one component less than 100 nm and the components mixed at a nanometer scale. Decreasing the size of the inclusions results in increasing ratio of surface area to volume, and the role of interface becomes more and more important that leads to more homogeneous materials. The natural tendency to reduce this enormous surface represents the driving force for a strong aggregation tendency of the nanofiller, and if their dispersion and nanofiber orientation in matrix can be controlled, it will give rise to special characteristics including the quantum

size effect, the macro-quantum tunnel effect, and surface and interface effects. Nanocomposites may exhibit excellent physical and mechanical properties and induce nanostructured surface topographies of immense interest to biomedical applications as tissue engineering, implants, and controlled drug delivery multifunctional systems capable of imparting extra functionalities of therapy such as targeting and imaging. Bone is a natural nanocomposite in which inclusions of HAp nanocrystals are embedded in a collagen matrix. Excellent mechanical properties of bone can be traced back to its hierarchical structure and organization provided through the inorganic and organic phases at the nanoscale. Moreover, the addition of HAp or bioactive glass nanoparticles significantly improved the hydrophilicity and protein adsorption and induced a nanotopography suitable for enhanced cell growth. Biomimetic nanocomposites for osteochondral repair are also considered, in addition to natural polymers, e.g., collagen, synthetic polymers such as PLGA, poly(diols-co-citrate), and PCL.

The list of nanofillers investigated for biomedical use includes nanoparticles, nanofibers, nanotubes, nanowires, and any other nanoscaled materials or devices, and materials include silica nanoparticles, nanoclays such as montmorillonite, cellulose, titania, carbon nanotubes, oligomeric silsesquioxane, etc. [15]. Nanoparticle clusters formed by assemblies of nanoparticles, such as magnetic nanoparticles, gold nanoparticles, and quantum dots, have gained considerable attention owing to their unusual and distinct characteristics originating from the collective individual properties of the constituting nanoparticles, wide applications in disease diagnosis, imaging, and delivery of drugs and genes. **Carbon nanotubes**, with diameters of 10 nm (multiwalled nanotubes) or 1 nm (single-walled nanotubes) and lengths equal to 1000–2000 times their diameter, exhibiting many unique physical, mechanical, and chemical properties have stimulated increased interest for biomedical composite applications. Carbon nanotubes have shown great promise as sensors and in biomedical imaging since very early in their development, due to both their intrinsic properties and attachment of imaging and diagnostic small or large molecules onto their surface. Despite their interesting properties, negative sides have reported showing that nonfunctionalized nanotubes present cytotoxicity. Chemical functionalizations either covalently via chemical modification or non-covalently by adsorption of molecules onto the nanotube surface make carbon nanotubes compatible with the biological environment. However, the fabrication technique of carbon nanotubes may also play important roles in their future biomedical applications bringing opportunities for the future of cancer diagnosis and therapy, nanotube-based vaccines, and gene therapeutics and tissue engineering. **Silver and gold nanoparticles** represent another example of nanoparticles used in polymer composites due to their proven antimicrobial properties. Antimicrobial polymer composites are usually based on polymer matrix loaded with antimicrobial nanoparticles. The antimicrobial efficiency of silver, copper, and titanium nanoparticles is confirmed; however, silver is superior when compared to other metals. Recent study showed that incorporation of silver nanoparticles in nanocomposite films can render strong bactericidal properties against various Gram-positive and Gram-negative bacteria. **Iron oxide superparamagnetic nanoparticles and quantum dots** have been used to track the

biodistribution of cells. **Magnetic nanocomposites** are suitable thermoseeds for cancer treatment by hyperthermia that offer a wide range of possibilities for diagnosis and therapy. These nanoparticles may be conjugated with therapeutic agents and heat the surrounding tissue under the action of alternating magnetic fields, enabling hyperthermia of cancer as an effective adjunct to chemotherapy regimens. Moreover, the recent discovery of superparamagnetism in bioactive Fe-substituted apatite will open new opportunities for biomedical devices endowed with a number of smart functionalities that can be switched on and off by exposure to magnetic fields.

**Core-shell nanoscale structures** are also novel nanomaterials for use in tissue engineering. Usually the core of such particles can be composed of silica, silver, iron, etc., and the shell is made of the bioactive component such as HA or calcium phosphates. Such multicomponent composite systems impart multifunctionality to the biocomposites and represent interesting emerging biomaterials that can have a huge impact in the field of tissue engineering and drug delivery systems.

**Nanostructured biomaterials have been processed** either using top-down methods, which involve the fabrication of nanostructured materials out of conventional bulk materials, or bottom-up methods, which involve self-assembly of small-scale components into large-scale functional constructs, e.g., electrospinning nanofibers of natural polymers and synthetic polymers; these materials can be used to imitate the topography and architecture observed in human tissues.

**Nanocomposite hydrogels** [16]. Hydrogels due to their porous and highly hydrated polymer network structure are potential candidates as biomaterials as they can be designed to mimic the physical, chemical, electrical, and biological properties of most biological tissues. A primary limitation of hydrogels to their widespread applications consists in their poor mechanical properties. Advances in polymer chemistry, fabrication technologies, and biomolecular and tissue engineering have pushed the limit for designing composite hydrogels with customized functionality for various biomedical applications. Another approach to reinforce polymeric hydrogels includes multiple functionalities focused on incorporating nanoparticles within the hydrogel network to obtain nanocomposites with superior properties and tailored functionality, biomimetic replicating the nature of biological tissues. Nanoparticles can be simply entrapped in hydrogels, prepared inside the hydrogels or used as functionalized cross-linkers of polymer chains. A wide range of nanoparticles, such as carbon-based, polymeric, ceramic, and metallic nanomaterials, can be integrated within the hydrogel networks to obtain nanocomposite hydrogels. Polymeric nanoparticles include dendrimers, hyperbranched polymers, liposomes, polymeric micelles, nanogels, and core-shell polymeric particles. Dendrimer hydrogels consist of dendritic and globular macromolecules with hydrophobic inner structure and hydrophilic exterior groups, structure that enables the entrapment of hydrophobic therapeutic agents and their subsequent controlled release, which solves some of the existing problems of conventional hydrogels made from hydrophilic linear polymer. Most of inorganic nanoparticles consist of minerals that are already present in the body and are necessary for the normal functioning of human tissues, such as nano-HAp, synthetic silicate nanoparticles, bioactive

glasses, silica, calcium phosphate, glass ceramic, etc. Various types of metallic nanoparticles utilized to obtain nanocomposite hydrogels for biomedical applications include gold, silver, and other noble metal nanoparticles, whereas metal-oxide nanoparticles include iron oxides, titania, alumina, and zirconia, extensively used as imaging agents, drug delivery systems, conductive scaffolds, etc. Moreover, inorganic, organic, or biological nanoparticles embedded in hydrogels allow the obtaining of biomaterials capable of responding to a variety of stimuli.

## Interface

Interface, interphase, or mesophase is an important part of composites, of whose structure, properties, and adhesion strength are directly related to the performance of composites. Experiments have proved that the region between two components – primary and secondary component, respectively – is an interfacial layer with certain considerable thickness (the tertiary component of composite materials) and the contacting of the two components can bring about many of interface effects, which results in different structure and properties of the interface layer.

Interface is critical to controlling composite properties because of the interactions between matrix and inclusion materials, the overall properties of composites and every single component being not simple, and matrix and surface layer of inclusion mutually influencing and restricting each other. The interactions consist of three interrelated levels: physical interactions (such as hydrogen bonds, van der Waals, or electrostatic interactions), chemical bonding (including surface chemical composition, surface functional groups, and surface reactivity), and mechanical coupling or micromechanical interlocking (e.g., polymer chain entanglement or crystallinity).

Interface plays a decisive role on fracture toughness and reaction of composites in aqueous and corrosive environment such as body fluids. The properties of polymer composite materials are greatly determined by the soakage property between the secondary component and the matrix. For polymeric matrix composites, the structure of polymer layer on the interface is different from the polymer itself and can be affected during fabrication process. In general, good wettability can lead to high interface bond strength by decreasing the surface energy. In the cases of full infiltration, only the bond strength produced by physical adsorption can be even greater than the adhesive cohesion itself; if soakage is not efficient, it will leave gaps in the interface, which represents a source of stress concentration, hence deteriorating the material properties [17].

In order to explain the adhesion mechanism at interface and the roles played by the two phases in the two phases of composites (one phase in solution or melt status that contacts a solid phase), some theories have been developed including infiltration adsorption theory, chemical bond theory, diffusion theory, electron electrostatic theory, weak boundary layer theory and mechanical link theory, deformation layer theory, and preferential absorption layer theory. Each of these theories can only describe a particular aspect of interfacial adhesion, none of them being able to fully explain the nature of phenomenon and all the process.

Polymer composites are susceptible to damage in the form of cracks induced by chemical, physical, and mechanical fatigue, which form deep within the structure. Once cracks have formed within polymeric materials, the integrity of the composite structure is significantly compromised leading to mechanical degradation. Damage mechanism of composites is studied from the matrix, inclusions, and interface perspective under the load and medium influence, the understanding of the damage mechanism at the interface being at great importance. In the study of interface damage mechanism, there are many theoretical damage mechanisms, including the propagation of a single matrix crack accompanied by inclusion fracture and pullout, the formation of multiple matrix cracks in the absence of inclusion failure, and the formation of shear bands parallel to the loading axis.

The concept of self-healing composites has been developed, the main goal being achieved by *extrinsic* (or discontinuous) and *intrinsic* (or continuous) approach as one healing system may be nonautonomous under certain circumstances and autonomous under other conditions. An *extrinsic self-healing* approach refers to all systems in which the healing agent is included in the system as an isolated separate phase, including all container-based approaches such as capsules, fibers, and nanocarriers. The main disadvantage of this concept is the limitations with respect to repeated healing at previously damaged and healed sites. Soft spherical inclusions have been designed intentionally in polymer composites as crack stoppers to enhance the toughness such as in *self-healing polymeric composites* with the ability to repair and restore lost damage using resources inherently available to the system [18, 19]. *Intrinsic self-healing polymers* are materials capable of repairing the damage via a temporary increase in mobility leading to a reflow of the material in the damaged area, based on specific molecular structures and performance of the polymers. The dynamic nature of noncovalent interactions confer the supramolecular polymers a wide range of unique properties, such as reversibility and responsiveness to one or more stimuli, and consequently the ability of self-healing and adaptation. The strength of these interactions depend on intrinsic factors, such as the molecular weight of polymers, charge density, polarity, crystalline or amorphous nature of the switch phase, and external factors like moisture, temperature, the pH of the solvent, ionic strength, light, or the presence of electric and magnetic fields.

Composite materials with a polymer matrix absorb water when placed in a hydrated environment such as the bodily milieu, and moisture acts as a plasticizer of the matrix and shifts the glass transition temperature toward lower values, hence a reduction in stiffness and an increase in mechanical damping. Moreover, moisture absorption by polymer constituents also causes swelling that can be beneficial in some applications as dental composites since it compensates some of the shrinkage polymerization. The wetting property of polymer surface is related to its structure and composition, and modifying the surface tension can improve the wettability. On the other hand, when water adsorbed on the surface of certain ceramic composites infiltrates into the interface, it causes damage of the interface bonding by triggering chemical reactions among water, inclusion, and polymer matrix, resulting in damage of composites. In composites where the inclusion material is poorly compatible with the matrix, some modifiers can be added to the interface, such as coupling agents, in

order to improve the compatibility and adhesion of inclusions to the matrix by generating a new interface with improved properties. Another method to enhance interface bonding consists in surface treatment of inorganic materials such as for inorganic inclusion and organic polymer matrix composites that are in essence two types of nonmiscible materials.

---

## Natural and Synthetic Biomedical Polymers

Polymer properties mainly depend on their molecular-mass distribution, average molecular weight, and crystallinity, which can be controlled during synthesis of the polymer; processing method and condition is a major determinant of the properties and functions of the polymeric product. Functional polymers are special class of polymers where the polymer chains contain one or more reactive groups attached at the chain end or to the backbone. In biomedical applications, functional polymers are used as building blocks to design complex structures such as nanoparticles, bioconjugates, biocompatible surfaces, scaffolds, hydrogels, etc.

Polymers for biomedical applications need to meet certain requirements and regulations in order to be safely used inside the human body; therefore, the understanding of the different degradation processes that may occur inside the human body due to blood, tissue, or biofilm interactions is very important. Biostable or physiologically bioinert polymeric materials present stability both to hydrolytic or oxidative exposure in body environment, and also to sterilization conditions (traditional techniques used including steam, dry heat, ethylene oxide, ionizing radiation, chemicals, precipitation); they are long-term use in artificial organs or in medical devices. Biodegradable polymeric materials have temporary purpose in the body and then are degraded to small molecular compounds with tuned degradation rate that can be metabolized and/or excreted; most are used as surgical sutures and scaffolds in tissue engineering or controlled drug release [20].

The **degradation mechanisms** of polymers used in medical applications consist in chemical degradation – hydrolysis, oxidation, and enzymatic and physical degradation; the kinetics of each process differs, and the key factors are the structure of the material and the surrounding environment. The main factors that influence the rate of degradation are the chemical structure, pH, and water uptake. Polymers containing ester or amide linkages are more likely to hydrolyze or oxidize, while polyether-type polymers are more stable, showing minimal degradation during long-term exposure to the human body environment. The adsorbed water by polymer material acts as a plasticizer, altering the physical properties of the material, and may also swell the polymer, initiating the degradation of the polymer through hydrolysis. Among the most important parameters for monitoring degradation, molecular weight, mechanical properties, or monomer release can be mentioned [21, 22].

Natural polymers could provide some properties such as biocompatibility, biodegradability, low toxicity, and cell signaling, whereas synthetic polymers provide other particular features such as mechanical and physical properties and chemical and thermal stability. The organized structure of natural polymers compared with

synthetic polymers accounts the specific characteristics such as improved cell viability and tissue ingrowth. On the other hand, synthetic polymers can be easier processed into different shapes with various microstructures in comparison with natural polymers due to their sensitivity to processing conditions such as temperature and pH, IR or UV radiations, water, etc. Common polymers for medical composites, their applications, and several related commercial products are presented in Table 1. Moreover, many types of shape memory composite biomaterials can be tailored to respond to electric, magnetic, or electromagnetic fields, and it is expected that the new generation of smart biomaterials will actively promote new functional tissue regeneration and generate self-assembly of supramolecular architectures in cellular levels.

## Natural Polymers

Natural polymers exhibit a large diversity of unique complex structures and different physiological functions and may offer a variety of potential in biomedical applications due to their various properties, the most important being biocompatibility and biodegradability. Moreover, natural polymers possess many functional groups available for further chemical and enzymatic modification or conjugation with other molecules, which allows an enormous variety of biomaterials with tailorable structure and properties to be obtained. The design of composite materials by combining the advantages of different natural polymers, eventually with synthetic polymers or bioceramics, may constitute a useful approach to mimic the natural extracellular matrix (ECM) and to design biocomposite with superior mechanical and biological properties [23, 24].

Although most of these natural polymers are obtained from vegetal and mammalian sources or from worms and spiders, there are a large number of microorganisms capable of synthesizing many biopolymers. Moreover, important marine sources are fish, invertebrates, mammals, reptiles, fungi, corals, and algae; fish skin is a rich source of marine collagen, algae are a rich source for several polysaccharides, and marine crustacean shells are a rich source of alginate and chitin. In addition, proteins obtained from the blue mussels have recently been considered for use as alternatives to conventional acrylate-based adhesives [25].

## Proteins

Proteins as components of natural tissues represented an attractive biomaterial for biomedical applications. Structural proteins such a collagen, elastin, elastin-like peptides, silks, and fibrin are used as sutures, as haemostatic, in tissue engineering, and as drug delivery agents. Structural proteins are fibrous proteins characterized by long-range ordered molecular secondary structures that promote self-assembly, the formation of structural hierarchy, and thus materials-related functional roles in nature such as components of connective tissue. Proteins are able to interact favorably with cells through specific recognition domains present in their structure.

**Table 1** Common polymers for medical composites, applications, and several related commercial products

Polymer	Biomedical applications	Commercial product/ manufacturer
<i>Natural polymers</i>		
<b>Collagen</b>	Hemostatic sealant; wound healing, skin and bone graft substitute	Integra <sup>®</sup> , Helistat <sup>®</sup> /Integra LifeSciences; FloSeal <sup>®</sup> /Baxter; Collagraft <sup>®</sup> /Angiotech Pharmaceuticals; AlloDerm <sup>®</sup> /LifeCell; Promogran <sup>®</sup> /Johnson & Johnson; Biobrane <sup>®</sup> /Smith & Nephew; OrCel <sup>®</sup> /Ortec International
<b>Hyaluronic acid (HA)</b>	Wound healing; regeneration of the trachea, articular cartilage, nasal cartilage, respiratory epithelium, vasculature, and nerve tissue	HYAFF <sup>®</sup> /Fidia Farmaceutici; SYNVISCO ONE <sup>®</sup> /Genzyme; ORTHOVISC <sup>®</sup> /Johnson & Johnson
<b>Chitosan</b>	Wound dressing, dentistry	HemCon <sup>®</sup> dressings/HemCon Medical Technologies
<b>Alginate</b>	Wound healing dressings	AlgiDERM <sup>®</sup> /Bard Medical Division; Algisite <sup>®</sup> /Smith & Nephew; Hyperion Advanced Alginate Dressing <sup>®</sup> /Hyperion Medical; Kaltostat <sup>®</sup> /ConvaTec; Tegaderm <sup>®</sup> /3 M Health Care; Kalginat <sup>®</sup> /DeRoyal; CURASORB <sup>®</sup> /Kendall; Maxorb <sup>®</sup> /Medline
<i>Biostable synthetic polymers</i>		
<b>Polyethylene (PE, UHMWPE)</b>	Orthopedic and dental bone cement; tubing for drains and catheters; hard tissue ceramic composites; prosthetic joints; acetabular liners or knee inserts	Dyneema <sup>®</sup> /DSM; Force Fiber <sup>®</sup> /Teleflex Medical OEM; ALTRX <sup>™</sup> , MARATHON <sup>®</sup> -PINNACLE <sup>®</sup> Acetabular Cup System/DePuy; Cenator <sup>™</sup> acetabular cup/Corin Group PLC
<b>Polypropylene (PP)</b>	Nondegradable sutures; hernia repair	UNIFY <sup>®</sup> Polypropylene/AD Surgical; TECOPRO <sup>™</sup> MT/Ensinger Industries Inc; Propylux <sup>®</sup> HS/Westlake Plastics Co
<b>Polytetrafluoroethylene (PTFE)</b>	Bone plates; cardiovascular applications; nondegradable membranes, fine sutures	CYTOPLAST <sup>®</sup> Non-Resorb/Osteogenics Biomedical Inc; Gore-Tex <sup>®</sup> Periodontal Material and Augmentation Material, GORE-TEX <sup>®</sup> Stretch Vascular Graft/W. L. Gore & Associates; Rapidax <sup>™</sup> /Vascutek, Terumo Co; TEXOLON <sup>®</sup> /Technetics Group

*(continued)*



**Table 1** (continued)

Polymer	Biomedical applications	Commercial product/ manufacturer
<b>Poly(acrylic acid) (PAA)</b> <b>Poly(methyl methacrylate) (PMMA)</b> <b>Bis-GMA</b>	Bone cement for bone or dental restoration; glass-ionomer cement used in dental restoration	Quixfil, Esthet-X/Dentsply DeTrey; Filtek Supreme, Z250/3 M ESPE; FillMagic/Vigodent SA Ind.; TE-Econom, Tetric Ceram HB/Ivoclar Vivadent; AlloDerm <sup>®</sup> /LifeCell Inc; Cortoss <sup>™</sup> /Orthovita, Inc; BioCranium <sup>®</sup> /3DCeram, Colorado Springs; Bioplast HTR <sup>®</sup> /Sybron Kerr
<b>Polyether ether ketone (PEEK)</b>	Spinal surgery, craniofacial implants, osteosynthesis plates, screws, intramedullary nails, joint replacement	Zeniva <sup>®</sup> /Solvay Advanced Polymers, L.L.C.; PEEK-OPTIMA <sup>®</sup> /EPTAM Plastics, Ltd; OXPEKK <sup>®</sup> HA/Invibio Ltd; TecaPEEK <sup>®</sup> /Ensinger Ind; MediPEEK <sup>™</sup> -IM/Modern Plastics; ORTHOCORD <sup>®</sup> /DePuy
<b>Polyesters</b> <b>Poly(ethylene terephthalate) (PET)</b>	Vascular grafts; fixation of implants; nondegradable sutures; hernia repair; ligament reconstruction	Uni-Graft <sup>®</sup> W/B. Braun; AlboGraft <sup>®</sup> /LeMaitre Vascular, Inc; FLIXENE <sup>™</sup> /Atrium; Dakron <sup>™</sup> /Du Pont; Polydek <sup>®</sup> /Teleflex Medical OEM; LARST <sup>™</sup> - Ligament Augmentation & Reconstruction System/Corin Group PLC
<b>Polyamide</b>	Nonabsorbable surgical suture; wound dressing	Kevlar <sup>®</sup> /DuPont; ETHILON <sup>®</sup> /Ethicon Inc; BioBrane <sup>®</sup> /Bertek Pharmaceuticals Inc
<b>Polyurethanes (PU)</b>	Cardiovascular applications – vascular grafts, artificial heart bladders and valves; wound dressings; tracheal soft tissue and bone tissue engineering	PolySorb <sup>™</sup> /Covidien, Medtronic; DegraPol <sup>®</sup> /Ab Medica; AVflo <sup>™</sup> /Nicast; Tielle <sup>®</sup> , Bioclusive <sup>®</sup> /Johnson & Johnson; Allevyn <sup>®</sup> /Smith & Nephews; Lyofoam <sup>®</sup> /Seton; Spyrosorb <sup>®</sup> /PolyMedica; Omiderm <sup>®</sup> /Iatro Medica; Miraflex <sup>®</sup> /BritCare
<b>Silicone elastomers</b>	Finger joints; epidermal substitute; heart valves; breast implants; ear, chin, and nose reconstruction	Integra <sup>®</sup> /Integra LifeSciences Corp.
<b>Biodegradable synthetic polymers</b>		
<b>Poly(vinyl alcohol) (PVA)</b>	Cartilage replacement	Cartiva <sup>®</sup> SCI/Cartiva, Inc.

(continued)

**Table 1** (continued)

Polymer	Biomedical applications	Commercial product/ manufacturer
<b>Polyglycolide PGA</b>	Bone and cartilage repair; sutures	DEXON-Surgicryl <sup>®</sup> /Davis & Geck subsidiary of the American Cyanamid Corporation; Biofix <sup>®</sup> /Bioscience Ltd; PGA Yarn, Bondek <sup>®</sup> /Teleflex Medical OEM
<b>Poly lactide PLA</b>	Fracture fixation, interference screws; suture anchors; meniscus repair	Bio-Anchor <sup>®</sup> , Clearfix <sup>™</sup> /DePuy Mitek Division; Chondral Dart <sup>™</sup> , Meniscal Dart <sup>™</sup> /Arthrex; PLLA Resin/Teleflex Medical OEM
<b>Poly-lactic-co-glycolic PLGA</b>	Interference screws; suture, bone and cartilage repair artificial skin, wound healing	Vicryl <sup>®</sup> /Ethicon Inc; Immix Extenders <sup>®</sup> /Osteobiologics Inc; Resomer <sup>®</sup> /Boehringer Ingelheim Fine Chemicals Division; Polysorb <sup>®</sup> /Syneture; Purasorb <sup>®</sup> /Purac Biomaterials
<b>Poly(<math>\epsilon</math>-caprolactone) (PCL)</b>	Bone repair; sutures; dental orthopedic implants	MONACRYL <sup>®</sup> /Ethicon; SynBioSys <sup>™</sup> /InnoCore Technologies BV; Maxon <sup>®</sup> /Davis & Geck Inc; Acufex <sup>®</sup> /Smith & Nephew
<b>Polycarbonate (PC)</b>	Thin-wall applications	TECANAT <sup>®</sup> /Ensinger Inc; Zelux <sup>®</sup> GS/Westlake Plastics; Makrolon <sup>®</sup> /Bayer MaterialScience LLC

Protein-based composite biomaterials with tunable properties have been studied for different biomedical applications, including composite films, foams, gels, fibers, grafts, and particles. Typical fibrous natural protein-related biocomposites are designed as protein–synthetic polymer materials, protein–polysaccharide materials, protein–inorganic ceramic materials, or multicomponent materials. Protein composite-based medical devices such as sutures, plates, screws, and injectable gels can be envisioned for different tissue repair applications; protein composite-based new generation of medical devices with selectivity and tunable functions can be designed to control local drug delivery or as implantable diagnosis and medical treatment [26].

**Collagen** is the most abundant fibrous protein family in vertebrates which can be found in connective tissues such as the tendon, ligament, cartilage, bone, and skin. The most common glycine, proline, or hydroxyproline amino acid residues interactions allow collagen supramolecular organization in intertwined triple helix. Collagen contributes to mechanical properties, structural organization, and shape of tissues; moreover, it interacts with cells via several receptor families and regulates

their proliferation, migration, and differentiation. There are different types of collagen; mainly types I, II, and III have been used as biomaterials in various clinical applications. Gelatin is derived from collagen by irreversible hydrolyzation under thermal, acid, or alkaline conditions, resulting in charged polyelectrolytes of lower antigenicity compared to initial collagen that may interact with oppositely charged molecules to form polyionic complexes. Traditionally bovine and porcine sources have been used in the preparation and application of collagen biomaterials in medicine, eventually after removal of telopeptides for minimal antigenicity (atelocollagen), with maintaining cell recognition signals during processing and preserving biological and physicochemical features. However, in order to minimize potential pathogen contamination, extensive purification protocols are required. Recombinant collagen will be an alternative solution for large-scale production, the complementary DNA of interest being subcloned into an appropriate expression vector for the expression of the protein in a cultured system. Marine-derived collagens of marine invertebrate and vertebrate sources show much similarity to the human collagens and are gaining more importance as they are proved to be less immunogenic. Fish skin would be the richest source of collagens in terms of its production and application in various bioprocess and biomedical engineering. Collagen is easily biodegradable and bioresorbable and facilitates excellent attachment to cells with maintaining normal phenotype and guided growth along their fiber orientation. Collagen-based biomaterials such as very long and compact fibers, films, nano- and microparticles, or porous scaffolds have been obtained as components for biomimetic biocomposite for various biomedical applications. In order to improve relatively low mechanical properties of collagen, cross-linking and composite formulations are necessary, such as collagen–glycosaminoglycans for skin regeneration or collagen–hydroxyapatite for bone remodeling. The biocomposites of collagen with hydroxyapatite are bone biomimetic as collagen supports cell adhesion and proliferation, while hydroxyapatite acts as a seed for biomineralization, representing a natural choice for bone grafting. The advantage of collagen and hydroxyapatite composites is significantly inhibition of bacterial pathogen growth compared with the synthetic composites. Numerous innovations occurred in collagen-based biomaterials from injectable collagen formulations for tissue engineering applications. Clinical uses of collagen-derived composite include products that have been shown to be effective as porous sponges, gels, sheets, and prosthetic implants and for tissue engineering and drug delivery.

**Fibrin** is a protein matrix developed by polymerization of fibrinogen under the enzymatic action of thrombin, mediating the blood coagulation process. Fibrin glue (fibrinogen and thrombin) has been used widely as a tissue adhesive for surgical wound repair. Due to its biomimetic features, fibrin is utilized as a scaffold material for muscle and cartilage engineering degraded within days or weeks by cell-associated enzymatic activity during the physiological wound healing process.

**Elastin** proteins are essential in forming elastic fibers in most tissues, such as blood vessels and dermis. Different elastin protein networks can be isolated from animal tissues such as skin, while tropoelastin, the soluble precursor of elastin, is an alternative source. As a biomaterial, elastin can have various forms; the hydrophobic domains of elastin are rich in nonpolar amino acids, while hydrophilic domains

contain a high amount of lysine that are involved in elastin cross-linking necessary to stabilize the structure. Elastin-based nonwoven fabrics and fibers are produced by electrospinning with applications in biocomposites.

**Silks**, natural polypeptide composite materials commonly included in the group of fibrous proteins, are produced by certain species, most notably by spiders and by silk moths. While a spider may be able to produce up to seven different kinds of silk, a typical silkworm produces only one kind. The protein components of silkworm silks and spider silks are fibroins and spidroins, respectively. Among all these silks, dragline silk of orb-weaving spiders and the fibroin silk composite of the silkworm *Bombyx mori* are the most investigated as potential biomaterials. Silk fibroin is considered as the most promising natural fibrous protein replacement for collagen in tissue engineering due to their biocompatibility, controllable biodegradation, elasticity, and excellent mechanical properties. Silk fibroin exists in a water-soluble form in the salivary gland of *Bombyx mori* silkworms and is spun into fibers while being coated with glue-like sericin proteins. Being soluble in hot water or alkaline aqueous solutions, sericin can be easily removed and isolated as a pure product; sericin has been traditionally associated with the immune responses attributed to silk and due to biocompatibility concerns has been largely neglected as a potential biomaterial. While the amino acid compositions of spider silks and silkworm silks are characterized by the predominant contents of alanine and glycine, spider silk has higher contents of charge-carrying residues, such as glutamic acid and arginine. Silk fibroin of silkworms is a commonly available natural biopolymer with a long history of applications in the human body as sutures, currently silk sutures being used in lip, eye, and oral surgeries and in the treatment of skin wounds. The silk proteins (fibroins or spidroins) can be processed into many different types of materials including fibers, films, gels, and porous sponges, which can then be exposed to surface modifications to improve the cell interaction and the tissue development on the material or be used as template for biomineralization to make organic–inorganic composite materials [27–30].

## Polysaccharides

Polysaccharides, also known as glycans, consist of monosaccharides linked together by O-glycosidic linkages and can be classified as homopolysaccharides or heteropolysaccharides. Because glycosidic linkages can be generated to any of the hydroxyl groups of a monosaccharide, polysaccharides form linear and branched polymers. Monosaccharide composition, linkage types and patterns, chain shapes, and molecular weight, dictates physical properties, including solubility, gelling potential, and surface and interfacial properties of the corresponding polysaccharide [31].

**Glycosaminoglycans (GAGs)** represent a family of linear polysaccharides that can generally be described as an alternating repeating units of a hexamine unit (glucosamine or galactosamine), and a sugar (galactose, glucuronic acid, or iduronic acid) of molecular weights generally ranges from 5 to 5000 kDa. There are several specific GAGs used as biomaterials including heparin, heparan sulfate, keratan sulfate, dermatan sulfate, chondroitin sulfate, and hyaluronic acid. GAGs are naturally degraded by enzymes such as hyaluronidase, chondroitinase, and heparanase;

therefore, cross-linking techniques or the formation of hybrid composites is needed to produce stable biomaterials. In many connective tissues, GAGs are constituents of the native extracellular matrix. They modulate the function of various proteins, thus regulating cell adhesion, migration, proliferation, and differentiation.

**Hyaluronic acid (hyaluronan, HA)** is the only non-sulfated glycosaminoglycan, consisting of repeating disaccharide units of *N*-acetylglucosamine and glucuronic acid. It occurs primarily as the sodium salt under physiological conditions, and HA salts are referred as hyaluronan. HA exists in higher molecular weights (50–5000 kDa), unique among GAGs. In order to obtain a more stable design, it can also be covalently cross-linked or combined with other biomaterials. HA is an important glycosaminoglycan component of connective tissue (cartilage, tendon, skin, and blood vessel walls), synovial fluid, and the vitreous humor of the eye. It plays a significant role in wound healing. HA already has found its way into clinical application as a scaffold material for cartilage, bone skin, and other tissues.

**Chondroitin sulfate (CS)** is a sulfated glycosaminoglycan composed of repeating glucuronic acid and *N*-acetylgalactosamine units, also negatively charged. It is found covalently linked to a core protein forming proteoglycans, as a structural protein or on cell surfaces or basement membranes where it functions as a receptor. It represents a major component of cartilage tissue.

**Chitin** is the second most abundant natural polymer after cellulose, composed of *N*-acetylglucosamine and *N*-glucosamine units either randomly or block distributed throughout the biopolymer chain. Depending on the units ratio, the polymer is **chitin** when *N*-acetylglucosamine units represent majority or **chitosan** when *N*-glucosamine units [32]. Due to the strong hydrogen bonding that exists between its chains, chitin is insoluble in most typical processing solvents, which limits its accessibility and processability. The degree of deacetylation and the molecular weight of the polymer are both known to significantly affect the material properties and the resulting performance of the chitosan and chitosan derivatives. Initially used as a powder, chitosan and chitin are now being incorporated into a variety of biomaterials, including films and membranes, gels, and woven and nonwoven dressings. Primary sources are represented by marine crustacean shells and can usually be found in fungi, diatoms, nematodes, arthropods, crabs, shrimps, lobsters, coral, krill, squid, jellyfish, butterfly, ladybug, and mushrooms.

**Chitosan** is a linear polysaccharide formed by *N*-deacetylation of the natural polysaccharide chitin, enzymatically by the chitinase enzyme or chemically, and can also be isolated directly from the fungi cell wall; commercially available chitosans are usually prepared from chitin by chemical, fermentative method which is simple and convenient for large production. Chitosan is generally insoluble in neutral organic solvents; many derivatives have been developed to enhance its solubility and processability. The cationic nature of chitosan leads to an interaction with anionic molecules such as glycosaminoglycans and proteoglycans, which can make this polymer an effective carrier for growth factors or cytokines. Chitosan is known for its antibacterial and antifungal properties that can be enhanced by irradiation, partial hydrolyzation, chemical modifications, synergistic enhancement with antimicrobial agents, etc. Due to its biocompatibility, biodegradability, low toxicity, and nonantigenic properties, chitosan is a versatile material for various

biological and biomedical applications such as tissue engineering and drug delivery applications. While chitosan has many desirable properties, its mechanical strength is poor and for this reason it is often blended with other polymers and ceramics, such as hydroxyapatite. Chitosan forms colloidal particles and can entrap bioactive molecules through chemical and ionic cross-linking and ionic complex formation for the association of bioactive molecules to polymers and to control drug release. Chitosan can be used alone or in combination with other materials to form hydrogels, fibers, granules, or sponges and is an ideal biopolymer for developing antimicrobial films.

**Alginate** is a polysaccharide biopolymer composed of linear block copolymers of guluronic acid and mannuronic acid, considered to be biocompatible, nontoxic, nonimmunogenic, and biodegradable. It is found in seaweed and typically extracted from brown algae and can be produced from *Azotobacter* and *Pseudomonas*. Alginate can be ionically cross-linked by the addition of divalent cations in aqueous solution, and the gelation by cross-linking of the polymers is mainly achieved by the exchange of sodium ions from the guluronic acids with the divalent cations. During dissolution, alginate releases divalent cations into the surrounding tissue, making this process uncontrollable; therefore, various methods of cross-linking have been introduced to precisely control the degradation process and mechanical properties. Covalent cross-linking of alginate with poly(ethylene glycol)diamines of various molecular masses was first investigated in order to prepare gels. On the other hand, alginate is well known for forming strong complexes with polycations including synthetic polymers, proteins, and polypeptides or ceramic materials for obtaining alginate scaffolds able to mediate the regeneration of the bones, cartilage, and other tissues and organs, including skeletal muscles, nerves, pancreas, and liver. An attractive class of physically cross-linked gels is those that can be administered by injection as liquid formulation that jellify in situ when gel formation occurs at certain time after mixing the components or after a certain trigger (such as pH or temperature).

**Starch** is a polysaccharide composed of two polymers of D-glucose, amylose and amylopectin, being produced by higher plants and represents an attractive matrix due to its abundance in cereals and eases of extraction and its high biodegradability. Starch can be expanded into foam with open cell architecture, e.g., as matrix mixed with gelatin and bacterial polysaccharide for the manufacturing of 3D porous scaffolds by rapid prototyping with interesting mechanical properties.

**Cellulose** is a structural polysaccharide found in plants, formed by repeating glucose building blocks intimately associated with other polysaccharides and lignin, with abundant surface hydroxyl groups generating inter- and intramolecular hydrogen bonds, characterized by its hydrophilicity, chirality, biodegradability, and broad chemical-modifying capacity. A challenge associated with using cellulose nanofibers in composites is the lack of compatibility with hydrophobic polymers, and various chemical modification methods have been explored. The first biomedical applications of cellulose-derived materials were carboxymethyl cellulose in artificial saliva and cellophane in semipermeable hemodialysis membranes.

Cellulose fibers are also secreted extracellularly by certain bacteria, the most efficient being *Acetobacter xylinum* (or *Gluconacetobacter xylinus*) as a highly

hydrated and relatively pure cellulose membrane, and therefore no chemical treatments are needed to remove lignin and hemicelluloses. **Bacterial cellulose** has the same molecular formula as plant cellulose, but with unique and sophisticated three-dimensional porous network structures and series of distinguished structural features and properties such as high purity, high degree of polymerization, high crystallinity, high water content, and high mechanical stability, which is quite different from the natural cellulose. Bacterial cellulose unique properties including biocompatibility, biodegradability, moldability, and high tensile strength in the wet state generated an increased interest in its biomedical applications. However, lack of antibacterial and antioxidant properties has diminished its capabilities in biomedical applications. Bacterial cellulose-based composites have been obtained to overcome its limitations and increase its biomedical efficacy using bioactive polymers (e.g., collagen, gelatin, chitosan, polyethylene glycol) and different other materials, such as inorganic (e.g., montmorillonite, hydroxyapatite, silver) and polymeric nanoparticles, to confer also antibacterial, antiviral, antifungal, and antioxidant properties. Bacterial cellulose biomaterials have been studied for use as wound dressing materials, burn treatments, skin substitutes, blood vessel grafts, substrate for tissue engineering, and dental implants [33].

**Dextran** is a bacterial-derived polysaccharide, consisting essentially of glucopyranose residues with a few percentages of side chains. Dextran hydrogels can be designed by either physical or chemical cross-linking, taking advantage of the hydroxyl functional groups. Dextran particles have been widely used as separation matrices, as cell microcarriers, and as drug delivery vehicles. Considerable interest has been in dextran scaffolds for tissue engineering applications.

### **Polyhydroxyalkanoates**

Polyhydroxyalkanoates (PHA) represent a family of biodegradable and biocompatible polyhydroxyesters of 3-, 4-, 5- and 6-hydroxyalkanoic acids produced by bacterial fermentation in a nutrient-limiting conditions with excess carbon. Their physical properties are highly tailorable, and a range of desired properties can be achieved being of considerable interest in biomedical applications. Polymers of the PHA family are constantly increasing in number due to the continuous discovery of new homopolymers and copolymers resulting in the availability of a wide range of chemical structures and properties affecting the mode and rate of degradation biological environment. Commercial PHA products are available in the form of sutures, pins, films, screws, and other devices. Polyhydroxyalkanoate-based implants have different physiochemical properties and degrade at a tailored rate in biological media, retaining their mechanical strength for a given short or extended period of time. Recent reports on their application mention nonwoven fibrous materials, films, sutures, and other products used in surgery, transplantology, tissue engineering, and pharmacology. Various *in vitro* and *in vivo* tests have shown polymers from the polyhydroxyalkanoate family to be compatible with bone and cartilage tissue, blood, and various cell lines that allowed expanded applications in medicine to wound treatment (sutures, skin substitutes, nerve cuffs, surgical meshes, staples, swabs), vascular system devices (heart valves, cardiovascular fabrics,

pericardial patches, vascular grafts), orthopedics (scaffolds for cartilage engineering, spinal cages, bone graft substitutes, internal fixation devices), and drug delivery systems [34]. The current research is focusing on the development of a variety of dense and porous bioactive and biodegradable composite materials systems, with the bioactive inorganic phase incorporated as either filler or coating (or both) into the biodegradable polymer matrix. Composites resulting by addition of inorganic bioactive phases such as hydroxyapatite or bioactive glass, in the form of particles or fibers to biodegradable polymers, are considered for bone tissue engineering scaffolds. Various attempts have also been made to form polymer/ceramic composites using members of the PHA family and PCL, PLA, poly(vinyl acetate), and poly(ethylene oxide) [35].

## Synthetic Polymers

Synthetic polymers are highly useful in biomedical field since their properties (e.g., porosity, degradation time, and mechanical characteristics) can be tailored for specific applications. They are often cheaper than natural polymers, can be produced in large uniform quantities, and have a long shelf time. A limitation of synthetic polymers is the lack of biological cues that can promote cell adhesion, proliferation, and tissue recovery. In order to improve the bioproperties of synthetic polymers and to enhance their interactions with cells, composites combining synthetic polymers and natural polymers or natural polymer modified synthetic biodegradable polymers have been developed.

The medical use of **biostable** synthetic polymers has a long history and is used in a variety of biomedical applications such as nonabsorbable surgical sutures, tissue engineering scaffolds, films, foams, short-term medical devices (catheters, endotracheal tubes, cannulas), long-term implantable devices (vascular prostheses, intra-aortic balloons, infusion pumps, cardiac pacemakers), etc. Synthetic **biodegradable** polymers can be produced under designed structures and controlled conditions to exhibit predictable and reproducible mechanical and physical properties such as tensile strength, elastic modulus, and degradation rate.

Polymers are usually polydisperse, with limited control over functionality and architecture, and biomaterial selection for biomedical applications is focused on their inertness and on mimicking the physical properties of the damaged tissue. Advanced synthetic techniques like atom transfer radical polymerization (ATRP), reversible addition fragmentation chain transfer (RAFT) polymerization, ring-opening mediated radical polymerization (ROMP), and their creative combinations or synthetic chemistry pathways such as “click chemistry” have extended the array of available architectures, including the combination of synthetic polymers with natural polymers with formation of hybrid multifunctional and/or nanostructured materials for a variety of applications in biology and medicine.

Nowadays various materials based on smart stimuli-responsive polymers have attracted increased attention due to the ability to respond to small temperature, pH, photo, and electro variations, with applications in biomedical fields including tissue



engineering, drug delivery, bioseparation, and biosensor designing. Polymers with reversible bond, also called *supramolecular polymers*, *dynamers*, or *dynamic polymers*, include polymers with noncovalent interactions and/or dynamic reversible covalent bonds between polymeric entities that can change and tune their structures and constitutions in response to physical stimuli and chemical effectors, representing an interesting class of adaptive polymers, also termed *adaptamers* [36]. Dynamers are designed for developing self-healing, responsive, and adaptive biomaterials – *dynamats* – based on bond reformation through spontaneous but directed self-organization such as reversible covalent chemical bonds, for instance, the various imine-type bonds, disulfides, or reversible Diels–Alder reactions.

### **Synthetic Biostable Polymers**

The majority of synthetic polymers are inert under physiological conditions. Chemical bonds in these polymers are essentially nonbiodegradable, and elucidation of the biodegradation related to the chemical structure and composition has led to the development of partially biodegradable chemical derivatives with controlled degradation ratio.

### **Polyethylenes (PE), Polypropylenes (PP), and Polytetrafluoroethylene (PTFE)**

**Polyethylenes (PE)** represent linear polymers synthesized by radical or ionic polymerization of ethylene. PE are classified based on their density, branching, and molecular weight that significantly influence the crystallinity and mechanical properties of the polymer. The first shape memory effect in polymers was reported in the 1960s and consisted of a matrix of polyethylene. Based on the molecular weight, PE are classified as low-density PE, high-density polyethylene (HDPE), and ultrahigh molecular weight polyethylene (UHMWPE). HDPE and UHMWPE have gained much attention for the use of biomaterials due to chemical inertness, mechanical strength, limited tissue reaction, and biostability. HDPE characterized by a low degree of branching, strong intermolecular forces, and tensile strength has a long history as bone and cartilage substitutes and has been used clinically since its mechanical properties mimic the natural bones, e.g., HAPEX™ HAp/HDPE composite found to mimic minor load-bearing bones like the cheek and the middle ear bones. UHMWPE have chemical resistance and low coefficient of friction and are self-lubricating because of long linear structure. The fracture toughness, high impact strength, very high wearing resistance, and low density made UHMWPE a popular choice as the articulating surfaces of joint replacements, such as hip, knee, ankle, and shoulder. In an effort to improve wear resistance, highly cross-linked UHMWPE has been produced and used in joint replacement. PE is also used as polymer matrix for nanocomposites in HDPE or UHMWPE form. As HDPE is a ductile polymer, it allows the incorporation of large amounts of bioceramic particles, and the polymer can still be melt-processed even at high content of filler. Bioactive particulate ceramic-reinforced HDPE composites have been the first composites designed to mimic the structure of bone and used for production of middle ear implants. UHMWPE has recently attracted considerable attention as matrix for bioceramic composites. UHMWPE is generally biocompatible as in acetabular cup of a hip

prosthesis, whereas its fibrous form, as in a finely woven fabric, has been shown to produce a different, more adverse reaction. Furthermore, when the discontinuous phase is particles, whiskers, platelets, or microspheres with dimensions on a cellular scale, the inflammatory response can include their ingestion by immune cells and transport to other parts of the body.

**Polypropylenes (PP)** are biocompatible, biostable, excellent stiffness and strength compared to PE and widely used in clinical applications ranging from sutures to load-bearing implants. Superior mechanical performance in fatigue and temperature resistance offers mechanical property at body temperature for applications in orthopedic implants and in dentistry for root canal treatment. Due to their fiber-forming characteristics, PP has been used in the treatment of ventral incisional hernia.

**Poly(tetrafluoroethylene) (PTFE)** is a high molecular weight, highly crystalline perfluoropolymer also known as Teflon™ (DuPont). Replacing hydrogen in PE with fluorine results in dramatic changes to the physical and chemical properties; large size and mutual repulsion of adjacent fluorine atoms provide relatively weak intermolecular forces and cause PTFE macromolecule chains to exhibit a twisting helix. Tight helical packing and chain–chain slip make PTFE the most lubricious polymer available, with the lowest coefficient of friction among common polymers, this also making PTFE very susceptible to cold flow (creep) under stress. PTFE has excellent chemical resistance and is hemocompatible, making them important for biomedical tubing and central to advanced multi-lumen small-gauge medical-grade tubing required in many new minimally invasive catheters. Biomedical applications of PTFE (Teflon®) solids, fluorocarbon coatings, and perfluorinated fluids and gels include clinical interventional (catheters in many forms) and permanent implants (cardiovascular, dental, ocular, craniofacial, urological, and abdominal applications).

Expanded ePTFE is a fibrillated form of PTFE, produced by a series of extrusion, stretching, and heating processes to create a microporous material with pore size ranging from 30 to about 100 μm that provides increased strength-to-weight ratio and creep resistance compared to fully dense PTFE. Highly oriented filaments with high-crystallinity, hydrophobic, and strong ePTFE threads have been entirely overlooked as filler materials. ePTFE fiber meshes (Gore-Tex®) have become widely used in medical tubing, advanced catheters, vascular grafts, meshes, sutures, and other medical implants. Gore-Tex® is one of the two standard biomaterials of prosthetic vascular grafts used clinically, though the compliance of ePTFE grafts is still too high compared to natural arteries. ePTFE is also used as patches for soft tissue regeneration, such as hernia repair and surgical sutures. However, graft thrombosis is a general property of fluoropolymer meshes and weaves in blood, passivating surfaces rapidly for acute short-term use, but limiting long-term blood-contacting applications.

### **Poly(meth)acrylates and Polyacrylamides**

**Poly(meth)acrylates. Poly(methyl methacrylate) (PMMA)** is a nondegradable polymer with excellent bio- and hemocompatibility. Bioinertness, UV light resistance, transparency, and smooth surfaces made PMMA a standard implant material

for intraocular lens and for hard contact lenses. PMMA can be utilized as a dispersant for ceramic powders to stabilize colloidal suspensions in nonaqueous media. Initially an essential ingredient in denture restorations, PMMA became the most commonly applied nonmetallic implant material in orthopedics. Self-curing acrylic bone cements polymerized and cross-linked in situ have been widely used in orthopedics surgery for many decades, as filling agents and for fixation of joint prosthesis. The first dental composite resin was prepared by mixing the PMMA powder and a methyl methacrylate (MMA) monomer and clinically used; recently, photopolymerizable acrylic composite resins compounded with inorganic filler have been developed.

**Bone cements.** The PMMA self-curing bone cements consist of two primary components: a powder consisting of copolymers based on poly(methyl methacrylate) (PMMA) and methyl methacrylate (MMA) liquid monomer, mixed at an approximate ratio of 2:1 to form a poly(methyl methacrylate) cement. It also contains an initiator, an activator, a radiopaque filler such as barium sulfate or zirconium oxide, and a copolymer to influence the mixing and handling of the cement. In some cases, an antibiotic is included in the formulation to minimize infection during implantation. Common disadvantages are the considerable exothermic reaction and the toxicity of unreacted monomer resulting from incomplete polymerization that may leach into the surrounding tissues. Moreover, PMMA is a brittle material with low fracture toughness and poor fatigue life that could lead to fatigue fracture of the cement and may contribute to the mechanical failure. In order to improve to modulate curing kinetics and to enhance the mechanical, physical, and biological properties of acrylic bone cements, a successful strategy is to reinforce PMMA matrix with inorganic ceramics or bioactive glass which combines strength and elasticity with bioactivity. In orthopedic surgery, PMMA bone cements are used to affix implants and to remodel lost bone. The main functions of the bone cement are to transfer loads from prosthesis to bone and immediate immobilize of the prosthesis. The polymerization reaction results in a reduction in free volume, measurable as linear or volumetric polymerization shrinkage which results in polymerization contraction stresses and gap formation between cement and bone. Strategies to reduce the polymerization shrinkage comprise varying the monomer structure and composition and modifying type, size, size distribution, and amount of fillers added to the composite matrix.

**Dental restorative polymeric materials** are composed of two or more monomers that combine a relatively high viscosity dimethacrylate monomer (base) with a low viscosity dimethacrylate comonomer to obtain resins with suitable rheologies. The curing reaction in composite restorative materials involves light-initiated photopolymerization of dimethacrylate monomers to form a highly cross-linked material. These dental materials must be stable on the shelf and rapidly react to form a highly cross-linked composite with high modulus, high hardness, and high glass transition temperature while matching the thermal expansion of the tooth, minimizing moisture uptake, being chemically inert, and having minimal shrinkage and shrinkage stress. Currently, methacrylate resin formulations dominate the commercial market. The base monomers are usually Bis-GMA, EBPADMA, and

UDMA. To reduce viscosity and enable high filler content to be incorporated, base monomers are combined with various ratio of the diluent monomer such as TEGDMA, and the difference in their H-bonding potential results in compositions covering a broad range of viscosities and significantly different polymerization kinetics. While the addition of diluent monomers reduces the shrinkage, they are also needed to reduce the viscosity of the base monomers to enable maximum filler loading and to improve conversion and the physical and mechanical properties of the dental composite. The structures of the individual monomers, and the related viscosities of the comonomer mixtures, strongly influence both the rate and extent of conversion of the photopolymerization. At similar diluent concentrations, UDMA resins are significantly more reactive than Bis-GMA and EBPADMA resins, and EBPADMA resins provide the lowest polymerization reactivities. Optimum reactivities in the UDMA and EBPADMA resin systems are obtained with the addition of relatively small amounts of TEGDMA. The filler is important by its nature, type, size distribution, and surface modification and has several roles, including enhancing modulus and radiopacity, altering thermal expansion behavior, and reducing polymerization shrinkage by reducing the resin fraction. Each component of dental restorative materials represents an opportunity for improvements in the overall composite [37, 38].

**Poly(*N*-isopropylacrylamide) (PNIPAM)** is one of the most common thermosensitive polymers, undergoing a rapid coil-to-globule transition in an aqueous solution at 31–32 °C, LCST of physiological significance. Most temperature-responsive polymers contain both hydrophilic and hydrophobic moieties; when the temperature changes to an appropriate range, the balance between these moieties is broken, and reversible phase separation or precipitation occurs. This behavior is the consequence of strong hydrogen bonds between the thermoresponsive polymer and water molecules and the specific molecular orientations of these bonds. PNIPAM dissolves in water below the LCST; at and above the LCST, the polymer chains partially dissolve and undergo a coil-to-globule transition resulting in colloidal aggregation that may lead to gel formation or polymer precipitation. PNIPAM hydrogels formed at 32 °C are instable and collapse substantially as the temperature is increased above the LCST. The synthesis of PNIPAM copolymers and cross-linked networks, typically with hydrophilic building blocks, has resulted in reversible thermogelation materials and forms hydrogels without significant syneresis at physiological temperature. Smart hydrogels based on PNIPAM and its copolymers belong to the most intensively investigated thermoreversible systems and have gained great significance for injectable applications in drug and cell delivery using minimally invasive techniques. Injectable, *in situ* gelling temperature-responsive composites using functionalized PNIPAM suggest potential biological applications in tissue engineering and drug delivery.

### **Polyethers: Polyethylene Glycol (PEG) and Poly(ethylene oxide) (PEO)**

Commonly, PEG refers to the polymer with molecular weight of approximately 400–100,000 Da, while PEO is used for higher molecular weights greater than 100,000 Da. PEG and PEO are liquids or low-melting solids, also depending on

their molecular weights. PEG is nontoxic and nonimmunogenic, hydrophilic due to its polar and uncharged polyether structure, and highly flexible, properties that make it especially useful in various biological, chemical, and pharmaceutical applications, and approved by FDA for various medical applications. Studies demonstrate that 500–2000 Da PEG was sufficient in order to provide good protein repulsion surfaces, probably due to the resistance to unfolding of the polymer coil and the resistance of the PEG molecule to release both bound and free water from within the hydrated coil, non-fouling surfaces being of importance in medical devices where they may inhibit bacterial colonization and blood cell adhesion. PEG is one of the most widely used polymers for cross-linking with hydrogel formation in the biomedical field as it can provide a highly swollen elastic networks that mimics soft tissues and allows transport of nutrients or cellular waste, used for drug delivery and tissue engineering. Moreover, this polymer also restricts the protein adhesion, thereby reducing the immune response in the body, and can represent an excellent substrate for cell-based tissue engineering applications. PEG has also been immobilized on polymeric biomaterial surfaces to make them resistant to protein absorption and cell adhesion. This behavior is attributed to highly hydrated PEG chains that exhibit steric repulsion based on an osmotic or entropic mechanism. PEG and PEO are frequently used as hydrophilic polymeric building blocks in copolymers with more hydrophobic degradable or nondegradable polymers, with an emphasis on the chemistry of PEGylation and formulation of PEGylated biomaterials for drug delivery, gene delivery, tissue engineering scaffolds, medical devices, and implants. For artificial ECM networks, further improvements of hydrophilic PEG-based hydrogels can be achieved by incorporation of more sophisticated cross-linkers that mimic the natural components of ECM [39].

**Polyesters: Polyethylene terephthalate (PET)** is a semicrystalline thermoplastic engineered polyester. Despite the presence of hydrolytically cleavable ester linkage, PET is stable *in vivo*, largely due to the high crystallinity and hydrophobicity of aromatic groups. The properties such as hardness, stiffness, stability, and biocompatibility make PET a promising biomaterial for medical applications. Commercially known as Dacron<sup>®</sup>, PET is widely used as prosthetic vascular grafts, sutures, and wound dressings in either fiber or fabric form, representing one of the two standard biomaterials of prosthetic vascular grafts clinically used. However, Dacron<sup>®</sup> vascular grafts are strong and stiff, much less compliant than natural arteries. Moreover, major complication related to the PET graft is thrombus formation and inflammatory response. Various strategies have been designed to make the graft surface thrombo-resistant, including coating with fluoropolymer or with hydrophilic polymers, covalent or ionic binding of the anticoagulants or antithrombotic agents, etc.

**Polyamides** represent semicrystalline thermoplastic polymer, which contains amide groups as integral parts of the main polymer chain. Polyamides may be obtained by dicarboxylic acid and diamine dehydration or from an amino acid or its lactam that is able to undergo self-condensation. Nylon is the generic term for aliphatic polyamides, while Aramid is the generic name for fully aromatic polyamides – commercial Kevlar<sup>™</sup> and Nomex<sup>™</sup> (DuPont trademarks) or Twaron<sup>™</sup>

(Teijin/Twaron, Japan). Nylon 6,6 (PA-6,6), owing to its similarity to collagen protein in terms of chemical structure and active groups, is a common biomedical material with good biocompatibility and is used in surgical suture and biomedical applications. PA also exhibits excellent mechanical properties resulting from the strong hydrogen bonds between the amide groups in PA macromolecules. As a polar polymer with high polarity, PA absorb moisture and have a relatively high affinity to and may form chemical bonding with inorganic polar fillers such as bioceramics. Aramid fibers are relatively light, stiff, and strong and resist impact and abrasion damage. Aramid fiber composites are used commercially where high tensile strength and stiffness, resistance to impact damage, and resistance to fatigue and stress rupture are important. Main applications have been in dentistry, for ligament prostheses and bone fracture fixation plates.

**Polyether ether ketone (PEEK)** is a semicrystalline linear polycyclic aromatic thermoplastic, containing combinations of ketone and ether functional groups between the aryl rings. This special chemical structure makes PEEK exhibit stable chemical and physical properties that have been considered the gold standard in inter-body due to its modulus of elasticity and versatility as biomaterial. Moreover, PEEK exhibits good biocompatibility *in vitro* and *in vivo*, and the mechanical properties of PEEK are close to that of human cortical bone. These characteristics made PEEK an important high-performance candidate for replacing metal implant components, especially in orthopedic and traumatic applications. On the other hand, its stable chemical structure makes PEEK biologically inert, preventing effective bonding with surrounding bone tissue when it is implanted *in vivo*. Therefore, improving the bioactivity of PEEK is a significant challenge, including surface modification and composite preparation. Recent advances in processing have allowed shape memory behavior in PEEK with mechanical activation, technology that has expanded to applications in orthopedic surgery.

**Polyurethanes (PUs)** are composed of a chain of organic units joined by carbamate (urethane) links, typically produced through the reaction of a diisocyanate with a polyol (polyethers or polyesters). The resulting polymers are sequential block copolymers with the polyol soft segment and the diisocyanate component, often combined with a hydrocarbon chain extender, providing the hard segment. Because of the differences in polarity between the hard polar and soft nonpolar segments, segmented PU elastomers can undergo microphase separation. The exceptional mechanical properties and biocompatibility are due particularly to the chemical incompatibility between the soft and hard segments. The mechanical properties, including processability, as well as the biodegradation rate can be tuned by modifying the structure and the ratio of the hard and soft segments. Aliphatic diisocyanates are preferred over aromatic diisocyanates in the synthesis of biodegradable PUs, partly because of the putative carcinogenic nature of aromatic diisocyanates. PUs containing polyester soft segments have poor hydrolytic stability, while PUs with polyether soft segments are prone to oxidative degradation. Historically, PUs had been used in permanent medical devices such as pacemaker leads and ventricular assisting devices. More bioresistant PUs have been designed using polycarbonate or polyether macrodiols with larger hydrocarbon segments between ether groups and

siloxane-based macrodiols. Recent attempts have been made to enhance the biodegradability of PUs. Soft segments such as polylactide or polyglycolide, polycaprolactone, and polyethylene oxide are most commonly used for tissue engineering scaffolds, biodegradation being oriented to the hard segments. PUs are among the most commonly selected biomedical polymers for blood-contacting medical devices. Recently, a cardiology stent product has been released in the market which is placed inside the blocked coronary arteries after dilated with the help of a balloon made from smart shape memory polyurethane.

### **Synthetic Biodegradable Polymers**

Synthetic biodegradable polymers contain hydrolysable bonds like esters, anhydrides, carbonates, and amides that can be degraded inside the body as result of chemical, physical, and biological interactions. Biodegradation can occur by surface degradation or bulk degradation. Surface degradation appears in hydrophobic polymers while maintaining the inner structure, these polymers offering a better control of degradation rates. In the case of bulk degradation, water uptake by hydrophilic polymers is faster, causing the collapse of all the biomaterial since the degradation process occurs throughout their volume. When polymer biomaterials are exposed to the body fluids, in the first step, water contacts the water-labile bond into the polymer matrix; the biomaterial absorbs water and swells. Polymer interactions with water can be tailored by controlling the ratio of hydrophobic and hydrophilic monomers in a copolymer. Another way is to control the degree of crystallization of polymers, crystalline regions usually resisting infiltration of water molecules and affecting the swelling character. In polymer hydrogels, cross-linking density can reduce the swelling of these materials, providing another method of tailoring the interactions with water.

Hydrolytic degradation of polymers consists in the random cleavage of covalent bounds in the polymer backbone by the attack of water molecule and a decrease in the molecular weight, reactions catalyzed by acids, bases, salts, or enzymes known as hydrolases. The balance between water diffusion into the polymeric material and the kinetics of hydrolytic degradation determines whether a polymer degrades primarily from the surface (surface erosion mechanism) or by absorption of water and degradation in the polymer volume (bulk degradation mechanism).

### **Aliphatic Polyesters**

Linear aliphatic polyesters, most frequently used in tissue engineering, are biocompatible and degrade into nontoxic components with a controllable degradation rate in vivo, from several weeks to several years, by modifying chemical composition, crystallinity, molecular weight, and distribution. Upon degradation, the number of carboxylic end groups increases, which leads to a decrease in pH and an autocatalytic acceleration of the rate. Their related biodegradable materials have already demonstrated promising results in clinical applications as resorbable sutures and meshes, in tissue engineering or drug delivery. Modern bioactive polymers used as scaffolds for tissue engineering aim to mimic certain aspects of the native ECM while exhibiting controlled degradability [40].

**Poly(glycolic acid) PGA** is a highly crystalline linear polymer of hydroxyacetic acid – glycolic acid. Its high crystallinity is the main factor leading to its low solubility in water and organic solvents and relatively high strength. The *in vivo* degradation of PGA follows a bulk mechanism due to its low solubility in water. Due to its excellent fiber-forming ability and rapid degradation, PGA was used in the development of the first totally synthetic resorbable suture. DEXON<sup>®</sup> was the first biodegradable commercial suture approved by the FDA and later Biofix<sup>®</sup> a bone internal fixation device. Implants of PGA self-reinforced composite are stiffer than any other degradable polymeric system clinically and used in the treatment of fractures and osteotomies. Nonwoven PGA fabrics have been extensively used as scaffolding matrices for tissue regeneration due to its excellent degradability, good initial mechanical properties, and cell viability. Most recent research has focused on short-term tissue engineering scaffolds and the utilization of PGA as a filler material often fabricated into a mesh network and used as a scaffold for bone, tooth, cartilage, tendon, intestinal, lymphatic, and spinal regeneration. High degradation rates of PGA lead to significant local production of glycolic acid that, although bioresorbed, has been associated with a strong, undesired inflammatory response; because of this, PGA have been combined with other polymers, such as poly(lactide-co-glycolide) copolymers.

**Poly(lactic acid) (PLA).** Lactide is the cyclic dimer of lactic acid, which exists as two enantiomers; the polymerization of these monomers leads four optical active isomers of PLA, but only poly(L-lactic acid) PLLA and poly(D,L-lactic acid) PDLA have shown promise in biomedical applications. PLLA is a semicrystalline polymer with high tensile strength, low extension, and high modulus and a relatively slow-degrading rate, being considered an ideal biomaterial for load-bearing applications. Conversely, PDLA is an amorphous polymer with random distribution of both isomeric forms of lactic acid, which confers lower tensile strength and faster degradation rate. High molecular weight PLLA has been shown to take years to be completely resorbed *in vivo*; to reduce degradation time, blends or copolymer PLLA with other degradable polymers have been designed. Composites with desirable properties of PLLA and PDLA have been obtained by combining with other degradable polymers such as PLGA, PEG, or chitosan. PLLA-based biomaterials have been utilized in tissue engineering applications, from scaffolds and biocomposite for bone, cartilage, ligament, and tendon to neural and vascular regeneration. PLLA-based commercially available products are orthopedic fixation devices such Phantom Soft Thread Soft Tissue Fixation Screws<sup>®</sup>, Phantom Suture Anchors<sup>®</sup> (DePuy), Full Thread Bio Interference Screws<sup>®</sup> (Arthrex), BioScrews<sup>®</sup>, Orthopaedics Phusiline<sup>®</sup> and Sysorb interference screws, and BIOFIX<sup>®</sup> and PL-FIX<sup>®</sup> pins.

**Poly(lactide-co-glycolide) PLGA.** Random copolymerization of PLA (both PLLA and PDLA isomers) and PGA represents the most investigated biodegradable copolymer for biomedical applications such as sutures, medical devices, tissue engineering scaffolds, and drug delivery. PLA and PGA have significantly different properties, and modulation of copolymer composition allows the optimization of PLGA for intended applications. PLGA copolymers with lactide form amorphous



polymers which are very hydrolytically unstable compared with the more stable homopolymers. PLGA has been used in drug delivery applications, most often as microspheres, microcapsules, nanospheres, or nanofibers to facilitate controlled delivery of encapsulated or adsorbed drugs or proteins. The suture applications available on the market are Vicryls<sup>®</sup> and Vicryl Rapide<sup>®</sup> with an increased rate of degradation, Panacryl<sup>®</sup> with a decreased rate of degradation, and VicrylMesh<sup>®</sup> mesh utilized in Dermagraft<sup>®</sup> skin graft. PLGA proved cell adhesion and proliferation properties making it an excellent candidate for scaffold application in the engineering of bone, cartilage, tendon, skin, liver, and nerve tissues. Applications for tissue engineering include composites of PLGA fiber matrix scaffolds of varying fiber diameters for skin regeneration or composite microspheres of PLGA and ceramics for bone regeneration.

**Poly( $\epsilon$ -caprolactone) (PCL)** is a semicrystalline polyester with great organic solvent solubility. PCL exhibits several unusual properties not found among the other aliphatic polyesters, such as exceptionally low glass transition temperature, low melting temperature, and high thermal stability. The discovery that PCL can be degraded by a hydrolytic mechanism under physiological conditions even at a very low in vivo rate and high drug permeability made it a candidate for long-term implant delivery device. PCL has been used in composite formulations for tissue engineering and long-term drug delivery systems. Compared to limited drug delivery applications, tissue engineering implications of PCL are numerous. Good processability of PCL allows the formation of scaffolds made of adhered microspheres, electrospun fibers, or porous networks. PCL and PCL composites have been used as scaffolds for the regeneration of bone, ligament, cartilage, skin, nerve, and vascular tissues. As examples, PCL was polymerized in situ and reinforced with several different fibers such as knitted PLGA mesh and glass fibers as resorbable composite implants, aiming craniofacial repair. PCL and glass composite showed good potential as a dental root filling material, capable of releasing ionic species. PCL and collagen composites for skin tissue engineering demonstrated good cell attachment and proliferation. PCL and copolymers with PLA have been electrospun to create nanofibrous tissue-engineered scaffolds that show promise for vascular applications. Aligned PCL and collagen/PCL nanofibers are designed for axonal nerve regeneration. Nanocomposites are considered as one of the most highly researched areas in nanomaterials by the virtue of their improved mechanical properties, dimensional stability, thermal/chemical stability, and electrical conductivity. Nanocomposites usually comprise two or more phases of different chemical constituents or structures, with at least one of the chemical and/or structural phases having nanometric dimensions. These nanocomposites, due to their improved physical/chemical properties, establish applications ranging from energy, sensors, biotechnology, smart materials, filtration, and regenerative medicine [41].

**Poly(propylene fumarate) (PPF)** is a high-strength, biocompatible, osteoconductive, and biodegradable linear polyester with the degradation products biocompatible and readily removed from the body. The unsaturated fumarate double bond along the backbone of the polymer permits cross-linking in situ, which causes moldable material to harden within several min. PPF can be cross-linked via radical

polymerization by itself or with cross-linkers such as MMA, biodegradable macromers of PPF-diacrylate, PEG-diacrylate, etc. Injectable liquid PPF-based biomaterials which become solid during cross-linking allow the design of structures that may not be attainable from non-cross-linkable degradable polymers and represent potential for diverse orthopedic applications. The development of composite materials combining PPF and inorganic bioceramic or bioactive glasses particles has not been investigated to a large extent, compared with PLGA- and PLA-based composites, although it is attractive for use as a scaffold for guided tissue regeneration, often as part of an injectable bone replacement composite. PPF is often mixed with ceramics to create stronger, more bioactive scaffolds for osteogenic tissue engineering, with mechanical properties on the order of magnitude of human trabecular bone. Mechanical properties and degradation time of the composite may be tailored for specific applications by varying the PPF molecular weight, type of cross-linker, and cross-linking density. Recent applications have focused on the use of PPF to fill irregular-shaped bone defects such as ear ossicle or mandibular defects with minimal surgical intervention.

### **Polyanhydrides (PA)**

PA contain two carbonyl groups bound together by an ether bond and have been almost exclusively studied for biomedical applications due to their hydrolytic instability and excellent biocompatibility, eventually leading to their FDA approval as drug delivery vehicles. In vivo, PA degrades into nontoxic biocompatible diacid monomers that can be metabolized and eliminated from the body. Degradation rate can vary by over six orders of magnitude, depending on the hydrophobicity of monomers. Polyanhydrides are often fabricated into microparticles or nanoparticles for injectable, oral, or aerosol as short-term controlled delivery of bioactive compounds. To retard polymer degradation and extend time of delivery, aliphatic diacid monomers have been copolymerized with hydrophobic aromatic diacid monomers or aliphatic fatty acid dimers. So far, PA have only been approved by the FDA as a drug delivery system. PA due to their fast and uniform degradation has limited mechanical properties, and to increase their strength for tissue engineering applications, methacrylated polyanhydrides have been studied as injectable, cross-linkable biomaterials. Dimethacrylate monomers have been obtained by reacting diacids with methacryloyl chloride as liquids or soft solids that can be injected and cross-linked into solid scaffolds for tissue engineering applications. Cross-linked polyanhydrides have been studied for drug delivery and as structural support for bone tissue engineering.

### **Polycarbonates (PC)**

Polycarbonates are linear polymers that have two germinal ether bonds and a carbonyl bond. Although this bond is extremely hydrolytically stable, in vivo degradation occurs much more rapid. PC is one of the most widely used polymers due to its unusual combination of optical clarity, heat resistance, high impact strength, and dimensional stability. Biocompatibility, low water absorption, and ease of sterilization of PC have led to its use in a wide range of medical equipment,

including critical medical devices. The most extensively studied polycarbonate is poly(trimethylene carbonate) (PTMC), an aliphatic elastomer with a slow degradation profile, great flexibility, but poor mechanical strength. Its degradation into biocompatible 1,3-propanediol and carbonic acid makes it an ideal candidate for drug delivery applications. PTMC has been obtained into microparticles, discs, and gels for the delivery of angiogenic agents and antibiotics. It is often copolymerized with PLA, PCL, polyether, or poly(L-glutamic acid) to allow for the fabrication of sutures, micelles, and polymersomes. The continued exploration of new polycarbonates holds potential for the expansion of this class of degradable polymers for tissue engineering applications [42].

### Inorganic Polymers

Recent studies revealed that not only organic polymers but also inorganic polymers may possess biological activity. The study of inorganic polymers focuses on their application in the field of biomedicine, nanotechnology, or drug delivery. These polymers often exhibit multiple functions, for example, inorganic polyphosphates can be used as antimicrobial compounds, as a modulator of gene expression, or in mineralization of bone tissue and in blood coagulation and fibrinolysis and silica as skeletal element with unique property combinations for customized implants in surgery and dentistry.

**Silicon polymers.** Polymers based on a silicon and phosphorous backbone are typically characterized by a structure with wider angles, longer bonds among skeletal atoms, and bonds with considerable ionic character compared to their carbon-based counterparts. Such enhanced skeletal flexibility results in a high elasticity of inorganic polymers at low temperatures. A diversity of possible pendant side functionalities facilitates optimization of chemical, physical, and biological properties of the inorganic polymer to fit specific biomedical applications that have attracted attention. Inorganic polymers can be classified as fully inorganic, organic–inorganic hybrid, or organometallic elements. Currently, silicon-based materials, particularly polysiloxanes, are the best developed and widely utilized inorganic polymers. The mechanical properties of silicone elastomers, such as tensile strength or tear resistance, are somewhat lower than for other implantable elastomers such as PU. Like all hydrophobic implant materials, silicones are quickly coated with proteins when placed in tissue contact. Additionally, silicone elastomers are thermosetting materials, requiring different processing from conventional thermoplastics, which can on occasion be seen as a drawback. **Polysilanes** are composed of a linear backbone of continuous silicon atoms and organic substituent groups, and their solubility and crystallinity will be related to the abundance and functionality of pendant groups. Polysilane-based block copolymers show excellent potential for tissue engineering and other biomedical applications due to their biocompatibility and capacity to accomplish numerous bio-related functions, including topographical cell guidance, controlled drug delivery and release, mechanical stimulation, and electrical stimulation (for the regeneration of electrically responsive cells, such as nerves and muscles). Biomaterials based on organically modified silanes are flexible and bio-active and can find applications in soft and hard tissue engineering. **Polysiloxanes**

feature a backbone of repeating Si–O units, and depending on the functionality of the pendant groups, these inorganic polymers can exist as linear chains or cross-linked networks, and as such their viscosity can vary from fluids to gels to elastomers to resins. Biomedical applications of polysiloxanes build on their high hydrophilicity, excellent biocompatibility, permeability, stability, and inertness. Polysiloxane-based materials have been subject for soft contact lenses, artificial skin, organs, and tissues, as components of various prosthetic and cardiovascular devices, drug delivery systems and denture liners, etc. The most common silicone is polydimethylsiloxane, abbreviated as PDMS.

**Poly(phosphazene)s** are linear high molecular weight polymers with an inorganic backbone consisting of phosphorous and nitrogen atoms linked by alternating single and double bonds, with two organic side groups attached to each phosphorous atom. Common pendant functionalities include alkoxy, aryloxy, and amino acid groups as individual moieties or in combination with other functionalities. As with other Si-containing backbone polymers, the torsional and angular freedom within a phosphorus–nitrogen backbone facilitates both an enhanced elasticity and high molecular weight of the poly(phosphazene)s. This synthetic flexibility of poly(phosphazene)s makes them suitable for a wide range of applications, including artificial bone grafts, soft tissue prostheses, chemotherapeutic models, drug delivery systems, electrical and optical devices, and membranes. Several nondegradable fluorinated poly(organophosphazene)s were demonstrated to possess high levels of tissue compatibility. With regard to tissue engineering and controlled delivery and release systems applications, biodegradable poly(phosphazene)s are particularly attractive as they undergo hydrolytic degradation to nontoxic and pH neutral products, due to the buffering capacity of the phosphates and ammonia that are simultaneously released in the course of material degradation. Their physicochemical properties can be effectively controlled by the nature, composition, and abundance of functional groups. While amino acid esters and other hydrophilic functionalities contribute to the hydrolytic dissociation of poly(phosphazene) polymers, hydrophobic pendant chains, including p-methylphenoxy, p-phenylphenoxy, tyrosine, pyrrolidone, depsipeptide, and organic groups with –COOH functionalities, can be introduced to enhance polymer backbone rigidity and improve their mechanical properties. In order to achieve a balance between mechanical durability and timely degradation, different ratios of hydrophobic and hydrophilic moieties are introduced into the poly(phosphazene) structure. Special attention is also paid to the functional site on which the group is attached to the backbone.

---

## Fabrication of Polymer Biocomposites

Synthetic polymers can be classified according to their behavior on heating as elastomers that can be physically cross-linked (thermoplastic elastomers) or chemically cross-linked and thermosetting polymers [43].

**Thermoplastic polymers**, solid materials at room temperature turn viscous liquids when heated, consist of linear or branched chain molecules having strong

intramolecular bonds but weak intermolecular interactions as hydrogen bonds and dipolar forces, or crystalline regions, with tunable mechanical properties and degradation kinetics. Thermoplastic elastomers contain two separated microphases consisting of crystalline rigid segments that function as cross-linkers and provide mechanical strength and amorphous segments that provide flexibility. Examples include PUs, polyesters and copolyesters, polyolefins (PE, PP), polyhydroxyalkanoates, PCL, PC, PEEK, nylons, polycarbonates, etc. Most biomedical composites have thermoplastic matrices, dominated by thermoplastic polyesters such as PLA, PGA, PCL, and their blends or copolymers. Thermoplastic polymers present the advantage of easy fabrications by melting or solving processes, but they lack flexibility.

**Elastomers**, with viscoelasticity and high yield strain, are amorphous flexible polymers existing above their glass transition temperature. At ambient temperatures, they are relatively soft and deformable; their primary uses are for seals, adhesives, and molded flexible parts. **Chemically cross-linked elastomers** contain flexible polymer chains or segments linked together into a three-dimensional network structure by covalent bonds, introduced during curing process. Examples of chemically cross-linked elastomers are polyolefin and polydiene, cross-linked polycarbonates, silicone elastomers, etc. Cross-linked synthetic elastomers (especially polyester elastomers) are the most attractive for use as a substitute of collagen matrix in tissue engineering because they best match with the elasticity of biological tissue, are able to provide mechanical stability and structural integrity, allow closely control of structural and mechanical properties to suit various applications, and can safely degrade to natural metabolic products by simple hydrolysis with tailored degradation rates matching healing kinetics of injured tissue.

**Thermosetting polymers** have cross-linked or network structures and do not soften but decompose on heating. Once solidified by cross-linking process, they cannot be reshaped. Common examples are poly(meth)acrylates, polyepoxies, polyureas, silicones, polyimides. Thermosetting polymers have the disadvantage for biomedical applications as may be contaminated with unreacted monomer and cross-linking agents.

In both thermosetting and thermoplastic polymer composites, some residual monomers, solvents, or additives may leach from the matrix if they are not completely removed during processing, but these trace amounts may not be an issue if the application is external to the body, as in prosthetic limbs.

Composite biomaterials for **soft tissue applications** are used in primary or secondary wound dressings, dermal graft substitutes, composite meshes to prevent postsurgical adherence, vascular grafts, and composite neural guides and in applications related to heart valves, lower urinary tract, articular cartilage, tendons, and ligaments; the full potential of composite biomaterials in soft tissue repair applications has not yet been fully explored. **Hard tissue** applications relate mainly to bone replacement or augmentation, including head and neck applications (maxillofacial, aural, and dental) and axial skeleton applications (bone replacements, nails and screws, joint repair) where polymer composites can be tailored to fit the patient [44].

**Nanocomposite** fabrication requires the preprocessing of nanoparticles such as purification to eliminate the impurities, de-agglomeration for dispersing individual nanoparticles, and chemical functionalization to improve the nanoparticle–polymer interaction. Common processing techniques include in situ polymerization with improved dispersion and integration between the phases at a molecular scale, melt-mixing conventional processing techniques such as extrusion, internal mixing, injection molding, and solution-based methods facilitating mixing and dispersion.

## Conventional Fabrication Techniques

### Fabrication of Particle and Short-Fiber-Reinforced Composites

#### In Situ Manufacturing

Bone cements and dental restorative composites are manufactured in situ.

**Self-adhesive bone cements** are usually supplied as two-component systems that are made of liquid, mainly containing the monomers, and powder. Monomer free-radical polymerization begins at a rapid rate immediately after the components are mixed being initiated in the presence of free radicals generated by the initiator (benzoyl peroxide) and activator (usually dimethyl-*p*-toluidine). Self-curing occurs with changes of viscosity over time, finally turning into harden solid material. Due to the fast polymerization rate within minutes, an exponential increase in cement viscosity occurs, so the surgeon has a short handling time available to inject the bone cement. Cement polymerization is an exothermic reaction resulting in a temperature increase, temperature that may become superior to the critical level for the protein denaturation in the site. Porosity created by air inclusion during spatula mixing in the cement mixture results in lower volume shrinkage and weakness of bone cement; centrifugation may be an effective method for limiting porosity [45].

**Photopolymerizable dental composites** consist of four major components, organic polymer matrix (dimethacrylate monomers, mostly Bis-GMA), one or more inorganic filler particles (quartz or glass, ceramic and/or microfine silica or more recently nanoparticles), coupling agents (an organosilane, e.g., silorane), and the initiator–accelerator. The coupling agent is applied to the inorganic particles by the manufacturer to surface-treat the fillers before being mixed with the unreacted monomer mixture. The polymerization reaction of dimethacrylate monomers is a free-radical polyaddition that can be accomplished by light activation by visible light, self-curing (chemical initiation at room temperature with a peroxide initiator and an amine accelerator), or dual curing (chemical and light curing). Because the setting of light-cured composite is triggered by visible light, these materials are packaged in opaque, mostly black plastic syringes or unit dose capsules with advantage of lower risk of cross infection. Self-cured and dual-cured composites are supplied in two syringes, and the two pastes are mixed to initiate the chemical cure. Direct dental composites are placed by the dentist in a clinical setting, and polymerization is accomplished typically by a curing light with wavelengths specific

to the initiator and catalyst system. Light-cured composites provide denser restorations compared with self-cured resins because no mixing is required that might introduce air inclusion porosity. They can then be finally polished to achieve maximum aesthetic results. The incorporation of nanometer- and micrometer-sized particles (nanofillers and nanohybrids, respectively) provides the opportunity of creating high translucent nanocomposites as particle size is below that of visible length; moreover, it confers a high strength because of the large surface-to-area ratio and a long-term high polish quality.

**Glass-ionomer cements** used in dentistry are water-based self-adhesive restorative materials composed of copolymer of carboxylic acids matrix and fluoride-containing silicate glass as filler. The curing reaction involves an acid–base reaction between the components, when a variety of ionic constituents is released from the glass. There are two main types of glass ionomers, conventional glass ionomer and resin-modified glass ionomer. **Conventional glass ionomers** contain a matrix of polymeric carboxylic acids, finely ground fluoroaluminosilicate glass filler, water, and tartaric acid. The composites are supplied as two-part powder–liquid systems that require mixing for the acid–base curing reaction between the glass and the polycarboxylic acid to take place. **Resin-modified glass-ionomer** components are similar to those in conventional glass ionomers and in addition contain some conventional methacrylate components, either polycarboxylic acid polymer chain with pendant methacrylate group or the unmodified polycarboxylic acid with a mixture of hydrophilic methacrylate monomers. Visible light and/or self-cured redox initiators are added so the photo-initiated and/or redox curing reaction of the double bonds can occur, initially by light-activated polymerization which is followed by an acid–base reaction that arises from water uptake. Recently, resin-modified glass ionomers have been formulated in paste–liquid or two-paste systems, in a dual-barrel syringe type of construction; in the latest advancement, the two-paste systems are placed in side-by-side compartments of an auto-mixable single-unit direct delivery device. **Polyacid-modified composite resins or compomers**, another type of restorative composites used in dentistry, contain polyacid-modified monomers able to react with the pendant methacrylate groups of other monomers, as well as with the cations released by the fluoride silicate glass particles, formulated without water content. Compomers are packaged as single-paste formulations in syringes or unit dose capsules, cross-linking occurring primarily by light-cured polymerization and also by acid–base reaction as the compomer absorbs water after placement [46].

### **Closed: Mold Techniques**

The advantage of powder-filled and short-fiber-reinforced thermoplastic polymer materials, as a consequence of the filler geometry and relatively low volume fraction, is their ability to be mold processed using conventional polymer processing techniques. Melt molding methods have many advantages developed by modern optimization of processing techniques, such as reproducibility, ability to obtain desired shapes, filler homogeneous distribution, and low cost. Within a mold, the reinforcing and polymer matrix materials are combined compacted, and the polymer melted and

processed. The requirement is to avoid powder filler to agglomerate at any stage of the process and to achieve good dispersion, while the short fibers need to be of a specific format to achieve good mixing and a good fiber length distribution.

After the melting event, the part shape is essentially set. For a thermoset polymeric matrix material, the process is a curing reaction that is initiated by the application of additional heat or chemical reactivity such as an organic peroxide. Polymers used as composite matrix for biomedical applications fabricated by melt molding include PE, PEEK, PCL, etc.

**Injection molding** supposes a mold in which the thermoplastic polymer matrix mix is injected at elevated temperature and pressure, the finished part being removed after cooling. A screw-based extruder is used to melt and mix the molten resin with filler and pump the suspension into a mold to form the net shape. This is an extremely fast and inexpensive technique that offers the possibility of producing composite devices, such as bone plates and screws. The resin can also be injected in a closed mold that contains the filler already deposited in the desired geometrical sequence, the procedure being termed as **resin transfer molding**, and it was used for obtaining of stems for total hip joint replacement. It works with a large range of polymers, including polycarbonate, polypropylene, polyethylene, and thermoplastics.

**Compression molding** is a technique of molding in which the polymer precursor material is placed inside the two-piece mold. The mold is closed, and a top force is applied to squeeze the resin and the fibers to fill all regions and force the material into contact with all mold areas, while heat and pressure are maintained until the composite has cured. Although this process can be used with thermoplastics and thermoset matrix, mainly thermosets are used due to their ease in processing and low viscosity. This process is suitable for shell-like part geometry and can provide good finish, e.g., compression molding above melting of PEEK matrix with continuous carbon fibers resulted in composites for bone plates. Porous composites were obtained by melt-based compression molding followed by particulate leaching from a physically mixture of a polymer with defined amounts of leachable particles and loading this mixture onto a mold. In the next stage heat and compression were applied that resulted in the melting of the polymeric phase and packing of the mixture, promoting the formation of a continuous polymeric network structure. Finally, the molded polymer–porogen composite was immersed in a solvent that selectively dissolved the porogen agent. This technique has been successfully applied in the production of scaffolds based on PGA, PLLA, or PLGA–gelatin microspheres or chitosan and biodegradable synthetic aliphatic polyesters.

### **Fabrication of Fiber-Reinforced Composites**

Continuous fiber reinforcements usually provide the highest improvement in mechanical properties being introduced in various forms such as continuous fibers, woven or nonwoven fabric, and unidirectional or bidirectional fabric, imbedded in thermosets or thermoplastic polymer matrix. Continuous fiber materials cannot be manufactured using conventional polymer processing previously described because the viscosity of molten polymer is too high, leading to excessive pressure that may



disrupt the fibers and lead to significant fiber breakage. In essence, the polymer in the form of powder, film, or fibers is melted and pressed among the continuous fiber reinforcements that are either arranged axially in parallel or woven in a fabric form. An example is commercially available composite of PEEK fibers blended with carbon fibers in woven products. Fiber-reinforced biomedical composites are commercially produced by open molding techniques (hand lay-up and filament-winding processes) or by closed molding technique (continuous pultrusion).

**Hand lay-up** technique is one of the oldest, simplest, and the most commonly used methods for the preparation of thermosetting matrix such as epoxy resins and long-fiber composite, with relatively high fiber content and designed mechanical properties. Unidirectional or oriented fiber sheets are cut and deposited in the desired shape with preferred orientation and then impregnated with the suitable amount of resin. Successive layers of fibers may be added until the desired thickness is achieved. The system is usually enclosed in a plastic bag, vacuum is applied to extract air and compact the material, and finally the system undergoes a thermal curing to achieve resin cross-linking. For better-quality composites, cure is often accomplished under pressure, in an autoclave. This technique is potentially useful for the production of fracture fixation devices and total hip stems, hip prostheses or intervertebral discs, etc.

**Filament-winding process** is an open-mold process used to produce high-strength hollow cylinder composite structures. In this process, the fiber reinforcement is fed through a resin bath heated to above melting temperature and eventually under varying amounts of stress, and the wound is placed on a suitable mold or mandrel in an overlapping helical pattern for a number of times to create a layered cylinder with a preferred fiber lay-up. When the layers have been applied to the desired thickness, the fiber-polymer wound mandrel is cured, and when it is accomplished the mandrel is pulled out, leaving a composite tube. The high degree of fiber orientation and high fiber loading with this method creates a level of reinforcement that confers torsional strength and stiffness as well as preventing the bore from splitting. Biomedical applications for this process with thermoplastic polymers include intervertebral discs, ligament prostheses, artificial tendons, or vascular prostheses.

**Continuous pultrusion** is an automated process for manufacturing melted polymer materials into continuous, constant cross-sectional composite profiles, the product being pulled from the die rather than forced out by pressure. Cooling and solidification of the polymer material may be achieved by just air cooling or water cooling. A large number of profiles such as beams, channels, pipe, tubes, and various structural shapes can be produced using appropriate dies. The applications include intramedullary rodding or pin fixation of bone fragments.

## Solution-Based Techniques

The applications of porous composite include among others porous biomedical devices and prostheses, scaffold tissue regeneration, particulate foams for drug

delivery, diagnostic and sensing, etc. One approach to create porous composites with both biological activity and suitable properties is to combine natural and synthetic polymers by modifying the synthetic component to match the requirements for different tissues, such as mechanical properties, controlled degradation rate, easy processability, etc. Appropriate pore size, morphology, and interconnectivity are of great importance for applications as scaffolds and can be designed to support native tissue ingrowth, vascularization, oxygen and nutrient supply, and waste disposal, also small enough to disrupt fibrous tissue deposition. Consequently, a variety of solvent-based processing techniques have been developed to process the polymer components into a porous architecture appropriate for specific application [47].

**Solvent casting and particulate leaching** involve a polymer solution uniformly mixed with particles – porogens – of a specific diameter. This dispersion is further processed either by casting or freeze-drying. Next, the solvent is allowed to fully evaporate, and the composite structure is immersed in a bath of a suitable nontoxic solvent where the particles leach out to produce a porous structure. Such porogen can be an inorganic salt like sodium chloride, crystals of saccharose, gelatin spheres, etc. The size of the particles will affect the size of the pores, while the polymer-to-porogen ratio is directly related to the amount of porosity of the final structure. Highly porous materials with interconnected pores can be formed using this technique. A disadvantage is that it can only be used to produce thin membranes. This technique has been successively applied to different classes of biomaterials, such as synthetic (e.g., PLLA, PLGA, or PEG) and natural polymers for polymer membranes with applications in tissue engineering.

**Phase separation and freeze-drying.** Thermally induced phase separation and emulsification/freeze-drying techniques are based on thermodynamic phase separation of polymer emulsions rather than incorporation of a porogen. First, the polymer is dissolved into a suitable solvent, then water is added, and the two liquids are mixed in order to obtain an emulsion. The emulsion is brought into a thermodynamically unstable state by adding a non-solvent in the first case or by decreasing the temperature in the latter one. A multiphase system is formed, characterized by polymer-rich and polymer-poor phases, and the removal of the solvent from the system induces the crystallization of the polymer-rich phase and the formation of the porous network. Highly porous materials, with random or oriented pores, can be produced, depending on the polymer–solvent choice and phase separation conditions. The technique can also be applied to polymer–ceramic mixtures, although this complicates the fabrication process.

**Phase separation procedure** requires the use of a solvent with a low melting point that is easy to sublime. Following cooling below the solvent melting point and vacuum drying to sublime the solvent, a porous material is obtained. Using phase separation technique, nanoscale fibrous structure enables to be obtained that mimics natural extracellular matrix architecture.

In **freeze-drying technique**, before the two phases separate, the emulsion is cast into a mold and quickly frozen. In emulsification freezing stage, the polymer solution is cooled down to the temperature at which a solid–liquid phase separation is induced and the solvent forms ice crystals, forcing the polymer molecules to

aggregate into the interstitial spaces. In the subsequent phase, the solvent is removed by applying a vacuum to completely sublime the frozen solvent, generating a dry interconnected porous material. The porosity depends on the concentration of the polymer solution, while pore size distribution is affected by the freezing temperatures. As drawbacks, pore size is relatively small and porosity is often irregular. Matrices fabricated using the combination of natural polymers like alginate, agarose, gelatin, chitosan, etc., have shown encouraging results for their utility as matrices for cartilage and bone tissue engineering. Other tissue engineering applications that are being explored include neural tissue engineering, cardiac tissue engineering, skin tissue engineering, bioartificial liver devices, etc.

**Gas foaming.** In order to overcome the need to use organic solvents that can give toxic effects and generate inflammatory response *in vivo*, or solid porogens in the fabrication of porous polymer biomaterials, a new technique involving gas as a porogen has been developed. In the gas foaming process, a gas foaming agent such as CO<sub>2</sub> and nitrogen is dissolved inside the molded biodegradable polymers such as PLA, PLLA, or PLGA, at high pressure, followed by a controlled pressure drop to ambient pressure. This depressurization causes the nucleation and formation of pores with sizes ranging between 100 and 500 μm in the polymer matrix. Good control over porosity can be achieved by tuning the temperature and pressure values; the void's density and size decrease with increasing pressure and decreasing temperature. The main drawbacks of the method consist of the excessive heat used during compression molding that prohibits the incorporation of any temperature labile material into the polymer matrix and by generation of a structure with unconnected pores and a nonporous external surface. The porosity and pore interconnectivity can be significantly improved by combining the method with particulate leaching technique. For example, ammonium bicarbonate was mixed in highly viscous methylene chloride or chloroform polymer solution that can be shaped with a mold. The solvent is further evaporated, and the composite is either vacuum dried or immersed in warm water; vacuum drying causes the sublimation of ammonium bicarbonate, while immersion in water results in concurrent gas evolution and particle leaching. This combined method is preferred because it does not result in the creation of a nonporous outer skin and generates high porosity content with pore sizes from 200 to 500 μm. However, there are concerns about the use of organic solvents and the long-term effects of residues of ammonium bicarbonate.

**Electrospinning** is a simple, inexpensive, and highly versatile technique that can be used to produce continuous fibers under a large electric potential applied between two electrodes bearing electrical charges of opposite polarity, one electrode placed into the spinning polymer solution or melt and the other attached to a metal collector plate or rotating rod. In a typical electrospinning process, polymer solution flows through a small-gauge needle controlled by a syringe pump. The presence of electric potential causes charge to be induced within the polymer droplets, resulting in charge repulsion, opposing the surface tension. When the charge repulsion overcomes the surface tension, a jet of polymer is drawn toward the collector in a thin fibrous stream, and the solvent evaporates with deposition onto the target of a single and continuous fiber in a random nonwoven material with interconnected pore

structure. Modifying the variables such as polymer molecular weight and polydispersity, solution properties (viscosity, conductivity, and surface tension), magnitude of applied voltage, needle gauge, or distance to collector, the generated architecture can dramatically change. Solution viscosity has to be sufficiently high to allow polymer chain overlap to generate fibers; in the semi-dilute region, beading has been occasionally observed, with the diameter of the fibers increasing with increasing in polymer concentration. This technique has been used successfully to spin synthetic (PEO, PLGA, PLLA, PCL) and natural (collagen, silk, elastin, fibrinogen, chitosan) polymer solutions into fibers many kilometers in length and fiber diameters in the submicron range. Compared to synthetic polymers, electrospinning of natural polymers is less versatile because a suitable solvent that does not compromise its structural integrity has to be used. Porous or core-shell morphology can be generated depending on the type of polymers as well as the evaporation rates and miscibility for the solvents involved. The approach of using bioactive inorganic inclusions with degradable polymers is continuing to attract attention in finding suitable matrices for the regeneration of bone and its interfaced zone with cartilage. Combining degradable polymers with bioactive inorganic materials during the course of electrospinning generally cannot be intermixed well or homogenized, resulting in bead formation. In attempt to overcome inorganic nanoparticle agglomeration, different strategies have been developed, for example, by introducing a surfactant or by hybridization approach of using inorganic and organic phases in solution, such as the sol-gel process. Multiple electrospinning techniques open up the possibility of designing composite fibers which possess the ability to self-heal upon failure. Coaxial setup uses a multiple solution feed system which allows for the injection of one solution into another; if the solutions are immiscible, then a core shell structure is usually observed. A sequential multilayering electrospinning was performed on a rotating mandrel-type collector to design three-layered tubes for vascular grafts where the inner and outer layers of the tubular grafts were formed by collagen and chitosan and poly(L-lactide-co- $\epsilon$ -caprolactone) copolymer as a material for the middle layer. Applications are limited by difficulties in making substantial large-scale designed constructions. This technique can be used for obtaining either biomedical biocomposites for the production of wound dressing or scaffolds for tissue engineering, implant materials, and drug delivery. Electrospun fibers resembling the morphology of key ECM components, such as collagen fibers, in combination with a bulk or sprayed hydrogel system, resulted in electrospun fiber-hydrogel composite systems similar to the native microenvironment, e.g., cartilage analog [48].

**Textile technologies.** Major textile engineering techniques – knitting, braiding, weaving, and nonwoven – have been successfully employed for the preparation of woven and nonwoven meshes of different polymers for biomedical applications. Each of these fabric-forming processes produces geometries with unique properties that can be designed in order to facilitate a certain set of physical and mechanical properties required for the specific form and function, achieve desired porosity, control native tissue ingrowth, or act as a tissue barrier. Advanced textile engineering capabilities enable advanced medical device development such as simple or

bifurcated stent grafts, tapered tendon and ligament repair structures, heart valve solutions, etc. Different polymers are used for fabricating a variety of permanent – such as PE (Dyneema Purity<sup>®</sup>), UHMWPE, PP, PTFE, PET (Dacron<sup>®</sup>), nylon (Supramid<sup>™</sup>), PEEK, and absorbable fibers – such as PLA, PGA, PLGA, and PCL. One of the major applications is temporary barriers as thin film or meshes that can be placed between tissues in adhesion prevention after surgery. In particular, nonwoven PLGA structures have been tested for bioabsorbable nonwoven fabrics for pulmonary or abdominal surgery. Woven fabrics or resorbable meshes from natural polymers such as collagen, chitin, and PLLA are used as skin dressings. Materials such as nylon, PTFE, and PET in the form of fabrics or meshes are used to repair hernias. Neurovascular grafts can be prepared from either woven or knitted PET, which determines the porosity or mechanical property of the graft. Orthopedic biomaterial textile structures can be designed to accommodate static or dynamic loads while facilitating tissue ingrowth, as a critical component in knee, shoulder, and spinal implants and soft tissue repair (spinal disk, ligaments, tendons, extremities, etc.), or provide structural support for fractures.

## Advanced Fabrication Techniques

Rapid prototyping, also termed solid freeform fabrication, is a recent technology based on the advanced development computer-assisted design (CAD) and manufacturing (CAM), starting from a computer-generated model or prototype and manufacturing objects in layer-by-layer fashion. The potential to produce rapidly 3D products of complex geometries and intimately control the microstructure of porous channels with precision and reproducibility, better than those achievable by using traditional approaches, makes rapid prototyping an ideal process for fabricating implants and tissue engineering scaffolds. Furthermore, prosthesis may be fabricated with appropriate geometry, size, and weight for personalized treatment of a certain patient, for example, anatomical data obtained from computed tomography, magnetic resonance imaging, and other medical-imaging techniques may be used to guide CAD processes. These techniques initially focused on polymers and later extended to ceramics, metals, and composites. Polymer biocomposite processing should take into account that viscosity of conventional polymers decreases with the processing pressure, while biopolymers have an almost constant viscosity–pressure profile and a narrow temperature and pressure window available for processing. Moreover, when composites like pastes and hydrogels are used, the viscosity will greatly influence the processing parameters and composite characteristics such as pore structure and size.

Each technology has an almost same build strategy, the main feature representing the selective solidification or deposition of the material; hence, whereas for solidification, energy or a binder agent is added to a bed of material where the part needs to be built, for deposition techniques the material is dropped to build the part in a layer-wise fashion. Based on the way materials are deposited, there are three major groups of CAM commercially available systems: laser-based machines that

photo-polymerize liquid resin (stereolithography and two-photon polymerization), powdered based systems (selective laser sintering), and nozzle-based systems (fused deposition modeling and three-dimensional (3D) bioprinting). Each technique is suitable for a specific material or a specific form of the material and has its own advantages and drawbacks.

**Stereolithography** is based on the layer-by-layer spatially controlled photopolymerization of a liquid photosensitive monomer resin by using a computer-controlled laser beam of specific wavelength that moves across a specific area structure point by point and hardens the liquid resin. After removing the excess of resin, a post-curing polymerization of resulted material in order to complete the conversion of unreacted monomers may be necessary. Typical materials used are photosensitive liquid (e.g., acrylic or epoxy) resin composites. Stereolithography method was utilized to obtain porous scaffolds of PPF and ceramics for bone tissue engineering or PEO and PEG hydrogels–cell constructs for soft tissue engineering. Commercial machines to cure the liquid-based photopolymers are of two basic types: one uses a laser, while the other uses a masked illumination instead of a point-by-point method used by laser system. In an effort to improve the stereolithographic resolution down to few micrometers, microstereolithography method has been developed as a combination of small-spot laser curing photopolymerization and masked lamp technology to mimic the living microstructural organization. The resolution of the photopolymerization volume to nanometric scale was increased from tens of micrometers down to sub-100 nanometers by two-photon polymerization method based on multiphoton excitation of photoinitiator molecules that can occur with femtosecond pulse lasers, due to the nonlinear nature of two-photon absorption. Unlike conventional stereolithography, in which the photoinitiator is excited by single-photon absorption, two-photon polymerization excitation occurs via multiphoton absorption nearly simultaneous which creates an effect similar to single-photon absorption at significantly higher energies. ORganically MODified CERamics (Ormocer<sup>®</sup>s) organic–inorganic hybrids containing both polymer functional groups and ceramic functional groups are among of the most widely used classes of materials. Small prostheses of Ormocer<sup>®</sup>s such as for the middle ear bones, known as ossicular replacement prostheses, have been produced by two-photon polymerization method. Two-photon polymerization has been used to create 3D scaffolds for tissue engineering with complex geometries, containing pores of multiple sizes, which can ensure a selective transport of cells versus smaller molecules. Redox multiphoton polymerization of an organic–inorganic composite material employing a femtosecond laser operating system is a recent method able to self-generate radicals by photoinduced reduction of the metal species for the fabrication of fully 3D structures with nanometric resolution. Possibly, the most significant drawback is the time required for fabrication that increases cubically as resolution increases.

**Selective laser sintering** is the oldest rapid prototyping technology, being the first available commercial. The methods selectively sinter thin layers of powdered polymer-based mixtures, forming solid 3D composite objects with macro- and microscale features. The interaction of the laser beam, usually a CO<sub>2</sub> laser, with the powder raises the local surface temperature to the glass transition temperature of

the powder, just below the melting temperature. Heating the particles causes them to fuse or sinter together to create a solid thin slice; the solid layer is then covered by more powder and the next slice formed on top of it, until the object is completed. The powder that was not scanned by the laser beam is removed and recycled once fabrication of the object is completed. The method is highly capable of producing objects with irregular shapes and structures containing channels, overhanging features and gradient structures, being attractive for the fabrication of tissue engineered scaffolds with controlled porosity and customized scaffold architecture. Nondegradable or degradable biopolymers (e.g., PE, HDPE, PMMA, PEEK, PCL, PLLA, PLGA, etc.), ceramics, and composites can be processed into scaffolds for bone tissue repair or osteochondral tissue engineering. Due to their gradual modifications in chemical composition and structure, functionally graded scaffolds can mimic bone and cartilage properties and form the osteochondral interface. For bone tissue repair, bioceramics such as HAp have been dry-blended with a polymer, turned into a composite in an extruder, subsequently pelletized, and finally powdered for selective laser sintering. The disadvantages of the selective laser sintering technique for scaffold fabrication include inability to use hydrogels, impossibility to encapsulate cells in scaffolds, and limitation in forming sharp corners and clear boundaries, making it impossible to build small features.

**Fused deposition modeling** is a method using less complicated process and simple machines that are cheaper compared to other rapid prototyping techniques. This method can generate 3D models of heated thermoplastic material, extruded through a nozzle positioned over a computer-controlled platform in droplet or filament deposition until a single thin layer is formed. Unfilled areas may be filled with a soluble molten wax to the same thickness to act as the support material for next layer. The next layer is built on top, and molten droplets or filaments deposited on the working area will soften the material of the previous layer and then solidify, joining to the previous layer. When the object is completed, it is removed from the platform, and support materials are removed by dissolving using an appropriate technique. Biodegradable materials used for this method include PCL, PLGA, polycarbonate, polypropylene, and various polyesters. Furthermore, various polymer–ceramic composites such as PCL–HAp or PLLA–tricalcium phosphate formed custom-made implants to be investment cast for individual patients.

**Three-dimensional (3D) printing** is a process of reconstruction of a 3D physical model by the successive addition of material layers resulting in a 3D solid object based on CAD model design. The machine reads in data from a CAD drawing and lays down successive layers of liquid, powder, or the sheet material, and the process is repeated layer by layer until the part is complete. This technique is able to create almost any shape, or geometric feature allows defined internal architectures for implants. However, it is limited by the characteristics and chemistry of the particular narrow range of polymer-based inks designed for shape optimization rather than functionality. 4D printing concept recently introduced develops materials that self-assemble into 3D structures with configurations that change over time, hence adding the fourth dimension. It is based on traditional 3D printing technique and on shape

memory polymer fibers incorporated into the composites, resulting in composite materials that can morph into several different, complicated shapes based on different physical mechanisms. The shape memory effects like stretching, twisting, folding, or curling of the material are controlled by the orientation and location of the fibers within the composite.

**3D bioprinting** is the process of generating by layer-by-layer 3D printing of 3D tissue-like structures using viable cells, an encapsulation biomaterial, and growth and differentiation factors, into a next stage the bioprinted pre-tissue that is further transferred to an incubator when it matures into a tissue. Common biomaterials include natural and/or synthetic polymers and decellularized ECM [49]. 3D bioprinting is based on three central approaches: biomimicry, autonomous self-assembly, and mini-tissue building blocks. Considerations must be taken regarding material, cell type, and growth factor selection, from materials science, cell biology, engineering, and medicine approach. One major application area is in the tissue engineering field of regenerative medicine. Based on the methods used, 3D bioprinting systems are classified in three different categories with each own advantages and disadvantages: laser-based bioprinters using a laser direct write 2D precise patterns of viable cells suspended in a solution, thermal inkjet-based bioprinters of living cells that are printed in the form of droplets through cartridges, and microextrusion bioprinters using pneumatic or mechanical dispensing systems to extrude continuous beads of material and living cells. The easiest organs to generate are the flat structures with mostly one type of cell, such as human skin. Second, tubular structures with two major cell types, such as vascular grafts or tracheal splints, represent a greater challenge. A third level of complexity consists in making hollow organs such as the stomach or bladder, each with more complicated functions and interactions with other organs. Finally, the fourth level of complexity includes vascularized organs such as the liver, heart, and kidneys that could be suitable for surgical therapy and transplantation, which represents the ultimate goal for bioprinting evolution. The development of biomaterials for 3D bioprinting is still in its early stages, based on those developed for traditional tissue engineering polymer processing; for the future there is a need for new specially designed biomaterials for this method of fabrication.

---

## Summary

Polymers are important and attractive composite components due to the versatility of designing their chemical, physical, and biological properties for different biomedical applications. As multidisciplinary and interdisciplinary field science, polymeric biomaterials are about 50 years old, whose evolution is related to the new discoveries in the areas of physics, chemistry, materials science, biology, and medicine. The ultimate goal of polymer composite research is to design biomimetic composites with hierarchical structures from the macroscale, mesoscale, and microscale to the nanoscale, with dynamic and tunable properties mimicking the native microenvironment. The design of the interface in developing new composites plays an



important role in improving the performances, tuning desired properties, implementing fabrication process, and adapting to specific applications.

---

## References

1. Peppas NA, Langer R (1994) New challenges in biomaterials. *Science* 263:1715–1720
2. Hench LL, Polak JM (2002) Third-generation biomedical materials. *Science* 295:1014–1017
3. Holzapfel BM, Reichert JC, Schantz JT, Gbureck U, Rackwitz L, Nöth U, Jakob F, Rudert M, Groll J, Hutmacher DW (2013) How smart do biomaterials need to be? A translational science and clinical point of view. *Adv Drug Deliv Rev* 65:581–603
4. Studart AR (2012) Towards high-performance bioinspired composites. *Adv Mater* 24:5024–5044
5. Hench LL (1998) Biomaterials: a forecast for the future. *Biomaterials* 19:1419–1423
6. Narayan RJ (2010) The next generation of biomaterial development. *Philos Trans R Soc A* 368:1831–1837
7. Chen P-Y, McKittrick J, Meyers MA (2012) Biological materials: functional adaptations and bioinspired designs. *Prog Mater Sci* 57:1492–1704
8. Trask RS, Williams HR, Bond IP (2007) Self-healing polymer composites: mimicking nature to enhance performance. *Bioinspir Biomim* 2:1–9
9. Zhao Y, Sakai F, Su L, Liu Y, Wei K, Chen G, Jiang M (2013) Progressive macromolecular self-assembly: from biomimetic chemistry to bio-inspired materials. *Adv Mater* 25:5215–5256
10. Aida T, Meijer EW, Stupp SI (2012) Functional supramolecular polymers. *Science* 335:813–817
11. Fakirov S (2013) Nano-/microfibrillar polymer–polymer and single polymer composites: the converting instead of adding concept. *Compos Sci Technol* 89:211–225
12. Ramakrishna S, Mayer J, Wintermantel E, Leong KW (2001) Biomedical applications of polymer-composite materials. *Compos Sci Technol* 61:1189–1224
13. Pérez RA, Won J-E, Knowles JC, Kim H-W (2013) Naturally and synthetic smart composite biomaterials for tissue regeneration. *Adv Drug Deliv Rev* 65:471–496
14. Salerno A, Netti PA (2014) Introduction to biomedical foams. In: *Biomedical foams for tissue engineering applications*. Woodhead Publishing, Cambridge, pp 3–39
15. Ghanbari H, Marashi SM, Rafiei Y, Chaloupka K, Seifalian AM (2011) Biomedical application of polyhedral oligomeric silsesquioxane nanoparticles. In: *Applications of polyhedral oligomeric silsesquioxanes, vol 3, Advances in silicon science*. Springer, Netherlands, pp 363–399
16. Gaharwar AK, Peppas NA, Khademhosseini A (2014) Nanocomposite hydrogels for biomedical applications. *Biotechnol Bioeng* 111:441–453
17. Wang R, Zheng S, George Zheng Y (2011) Interface of polymer matrix composites. In: *Polymer matrix composites and technology*. Woodhead Publishing, Oxford, pp 169–209
18. Dry C (1996) Procedures developed for self-repair of polymeric matrix composite materials. *Comp Struct* 35:263–269
19. Blaiszik BJ, Kramer SLB, Olugebefola SC, Moore JS, Sottos NR, White SR (2010) Self-healing polymers and composites. *Annu Rev Mater Res* 40:179–211
20. Gomes ME, Reis RL (2004) Biodegradable polymers and composites in biomedical applications: from catgut to tissue engineering. *Int Mater Rev* 49:261–285
21. Williams DF (1992) Mechanisms of biodegradation of implantable polymers. *Clin Mater* 10:9–12
22. Lyu S, Untereker D (2009) Degradability of polymers for implantable biomedical devices. *Int J Mol Sci* 10:4033–4065
23. Yannas IV (2004) Classes of materials used in medicine: natural materials. In: *Biomaterials science-an introduction to materials in medicine*. Elsevier Academic Press, San Diego, pp 127–136

24. Halper J, Kjaer M (2014) Basic components of connective tissues and extracellular matrix: elastin, fibrillin, fibulins, fibrinogen, fibronectin, laminin, tenascins and thrombospondins. In: *Progress in heritable soft connective tissue diseases*. Springer, The Netherlands, pp 31–47
25. Silva TH, Alves A, Ferreira BM, Oliveira JM, Reys LL, Ferreira RJF, Sousa RA, Silva SS, Mano JF, Reis RL (2012) Materials of marine origin: a review on polymers and ceramics of biomedical interest. *Int Mater Rev* 57:276–306
26. Hu X, Cebe P, Weiss AS, Omenetto F, Kaplan DL (2012) Protein-based composite materials. *Mater Today* 15:208–215
27. Hardy JG, Scheibel TR (2010) Composite materials based on silk proteins. *Prog Polym Sci* 35:1093–1115
28. Kundu B, Rajkhowa R, Kundu SC, Wang X (2013) Silk fibroin biomaterials for tissue regenerations. *Adv Drug Deliv Rev* 65:457–470
29. Numata K, Kaplan DL (2010) Silk-based delivery systems of bioactive molecules. *Adv Drug Deliv Rev* 62:1497–1508
30. Harkin DG, George KA, Madden PW, Schwab IR, Hutmacher DW, Chirila TV (2011) Silk fibroin in ocular tissue reconstruction. *Biomaterials* 32:2445–2458
31. Aravamudhan A, Ramos DM, Nada AA, Kumbar SG (2014) Natural polymers: polysaccharides and their derivatives for biomedical applications. In: *Natural and synthetic biomedical polymers*, 1st edn. San Diego, CA, pp 67–89
32. Anitha A, Sowmya S, Sudheesh Kumar PT, Deepthi S, Chennazhi KP, Ehrlich H, Tsurkan M, Jayakumar R (2014) Chitin and chitosan in selected biomedical applications. *Prog Polym Sci* 39:1644–1667
33. Shah N, Ul-Islam M, Khattak WA, Park JK (2013) Overview of bacterial cellulose composites: a multipurpose advanced material. *Carbohydr Polym* 98:1585–1598
34. Williams SF, Martin DP, Horowitz DM, Peoples OP (1999) PHA applications: addressing the price performance issue: I. Tissue engineering. *Int J Biol Macromol* 25:111
35. Boccaccini AR, Blaker JJ (2005) Bioactive composite materials for tissue engineering scaffolds. *Expert Rev Med Devices* 2:303–317
36. Roy N, Bruchmann B, Lehn J-M (2015) DYNAMERS: dynamic polymers as self-healing materials. *Chem Soc Rev* 44:3786–3807
37. Kenny SM, Buggy M (2003) Bone cements and fillers: a review. *J Mater Sci Mater Med* 14:923–938
38. Cramer NB, Stansbury JW, Bowman CN (2011) Recent advances and developments in composite dental restorative materials. *J Dent Res* 90:402–416
39. Milton Harris J (1992) Introduction to biotechnical and biomedical applications of poly(ethylene glycol). In: *Poly(ethylene glycol) chemistry: biotechnical and biomedical applications*. Springer, New York, pp 1–14
40. Das R, Karumbaiah K (2015) Biodegradable polyester-based blends and composites: manufacturing, properties and applications. In: *Biodegradable polyesters*. Wiley, Weinheim, pp 321–340
41. Woodruff MA, Hutmacher DW (2010) The return of a forgotten polymer: polycaprolactone in the 21st century. *Prog Polym Sci* 35:1217–1256
42. Bendler JT (2000) *Handbook of polycarbonate science and technology*. Marcel Dekker, Basel, p 357
43. Chena Q, Liang S, Thouas GA (2013) Elastomeric biomaterials for tissue engineering. *Prog Polym Sci* 38:584–671
44. Cardon LK, Ragaert KJ, Koster RP (2009) Design and fabrication of biocomposites. In: *Biomedical Composites*. Elsevier © Woodhead Publishing, Cambridge, UK, pp 25–43
45. Deb S (2010) Acrylic bone cements for joint replacement. In: *Biomedical composites*. Woodhead Publishing/CRC Press, Cambridge, UK, pp 210–233
46. Sakaguchi RL, Powers JM (2012) Restorative materials-composites and polymers. In: *Craig's restorative dental materials*, 13th edn. Philadelphia, USA, pp 161–198

- 
47. Salerno A, Netti P (2014) Introduction to biomedical foams. In: Biomedical foams for tissue engineering applications. Elsevier © Woodhead Publishing, Cambridge, UK, pp 1–37
  48. Bhardwaj N, Kundu SC (2010) Electrospinning: a fascinating fiber fabrication technique. *Biotechnol Adv* 28:325–347
  49. Murphy SV, Atala A (2014) 3D bioprinting of tissues and organs. *Nat Biotechnol* 32:773–785

Toshiki Miyazaki, Masakazu Kawashita, and Chikara Ohtsuki

## Contents

Ceramic Biomaterials for Bone Tissue Repair .....	288
Organic–Inorganic Composites for Bone Repair .....	290
Coating of Calcium Phosphate on Organic Polymer Substrates .....	292
Composites for Cancer Diagnosis and Treatment .....	293
Conclusions .....	295
References .....	295

---

## Abstract

Several kinds of ceramics exhibit direct bone bonding through formation of biologically active hydroxyapatite layer after implantation in bony defects. They are called bioactive ceramics and play an important role in clinical applications. However, there are still some drawbacks on clinical applications because conventional bioactive ceramics essentially have lower fracture toughness and higher Young's modulus than natural bone. The bone takes an organic–inorganic composite where apatite nanocrystals are precipitated on collagen fibers. Therefore, problems on mechanical properties of the bioactive ceramics can be solved by designed composites composed of constituents driving bone-bonding capability. In this chapter, current research topics on development of the various

---

T. Miyazaki (✉)

Graduate School of Life Science and Systems Engineering, Kyushu Institute of Technology,  
Kitakyushu-shi, Fukuoka, Japan  
e-mail: [tmiya@life.kyutech.ac.jp](mailto:tmiya@life.kyutech.ac.jp)

M. Kawashita

Graduate School of Biomedical Engineering, Tohoku University, Sendai, Japan

C. Ohtsuki

Graduate School of Engineering, Nagoya University, Nagoya, Aichi Prefecture, Japan  
e-mail: [ohtsuki@apchem.nagoya-u.ac.jp](mailto:ohtsuki@apchem.nagoya-u.ac.jp)

organic–inorganic composites designed for biomedical application have been reviewed. Mechanical mixing of bioactive fillers in organic polymer matrix is a typical processing for fabrication of bioactive composites. In addition, coating in aqueous conditions is an important process for fabricating bioactive composites since their surface property and interaction with surrounding body fluid and tissues govern the biological activity of the materials. Functions of drug delivery, diagnosis, and treatment of cancer can be provided through material design based on organic–inorganic composites.

---

**Keywords**

Organic–inorganic composites • Hydroxyapatite • Calcium phosphate • Simulated body fluid (SBF) • Bone substitute • Drug delivery • Bone cement • Polymethyl methacrylate (PMMA) • Cancer diagnosis • Cancer treatment • Magnetite • Microsphere • Yttrium oxide • Imaging • Targeting

---

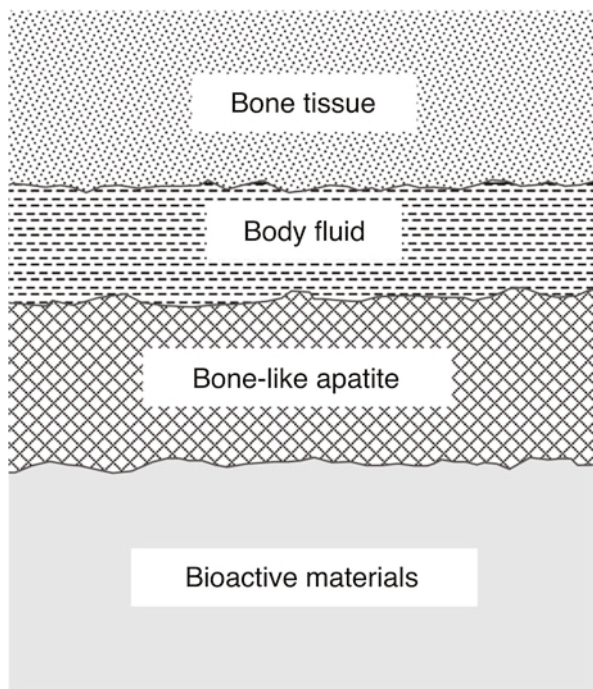
## Ceramic Biomaterials for Bone Tissue Repair

Ceramics are attractive for hard tissue reconstruction, since they are allowed to show high mechanical strength and hardness. However, those implanted in bony defects are generally encapsulated by fibrous tissues and consequently isolated from the surrounding bone [1]. This reaction is caused to protect our living body from foreign substances. On the contrary, several kinds of ceramics are known to directly contact to living bone without the encapsulation. They are called bioactive ceramics, meaning that they are capable of eliciting and modulating biological activity. Bioglass-type glasses [2, 3], sintered hydroxyapatite (HA,  $\text{Ca}_{10}(\text{PO}_4)_6(\text{OH})_2$ ) [4], and glass-ceramics A-W [5], where fluoroxyapatite and wollastonite are precipitated in glassy matrix, are known as the typical materials of bioactive ceramics, which show the property of direct bonding to bone tissues, namely, bone-bonding property.

Bioactive ceramics hitherto known cannot substitute load-bearing portions independently, because they essentially show more brittle and fragile than natural bone. Namely, their fracture toughness is lower and their Young's modulus is higher than those of human cortical bone. In addition, these ceramics are difficult to be formed into desired shapes during the operation for implantation. Not only bone-bonding property but also high flexibility and high machinability are required on the novel design of bioactive bone substitutes. Natural bone takes a kind of organic–inorganic composite where hydroxyapatite nanocrystals precipitate on collagen fibers at a typical constituent of hydroxyapatite: collagen = 70:30 in mass ratio [6]. Therefore, inspired design of organic–inorganic composites from the bone structure would give attractive materials having unique mechanical characteristics analogous to natural bone.

Alternative design of bioactive composites has been proposed from fundamental understanding on surface reaction of bioactive ceramics with body fluid. Typical findings have been reported on bioactive glasses and glass-ceramics showing bond-bonding property. Bioactive glasses and glass-ceramics achieve bone bonding

**Fig. 1** Schematic representation of bone-bonding mechanism of bioactive ceramics



through formation of hydroxyapatite layer, which consists of carbonate-containing hydroxyapatite of small crystallites and defective structure, on their surface after exposure to body fluid. The characteristics of the carbonate-containing hydroxyapatite are similar to those in natural bone mineral and the formed hydroxyapatite called “bone-like apatite.” It has been revealed that bioactive ceramics showed the bone-like apatite formation after exposure to body fluid and achieved direct bonding to living bone, as schematically shown in Fig. 1 [5, 7]. The bone-like apatite formation on bioactive ceramics has been identified as important events for ceramic biomaterials to achieve bone bonding in vivo. Therefore, the bioactive composites with bone-bonding property can be developed by the concept that designed materials are capable to form bone-like apatite after implantation in bone.

The formation of bone-like apatite is caused by chemical reaction of the implanted materials with surrounding body fluid. Capability of the bone-like apatite formation can be evaluated by using a type of simulated body fluid (SBF:  $\text{Na}^+$  142.0,  $\text{K}^+$  5.0,  $\text{Mg}^{2+}$  1.5,  $\text{Ca}^{2+}$  2.5,  $\text{Cl}^-$  147.8,  $\text{HCO}_3^-$  4.2,  $\text{HPO}_4^{2-}$  1.0, and  $\text{SO}_4^{2-}$  0.5 mol/m<sup>3</sup>) developed by Kokubo and his colleagues [8, 9]. This type of SBF is often called Kokubo solution named after the inventor. Kokubo solution is an acellular aqueous solution that has almost similar compositions of inorganic constituents to those in human blood plasma. pH of Kokubo solution is kept at around 7.2 ~ 7.4 by appropriate concentration of *tris*(hydroxymethyl)aminomethane and HCl (Tris buffer). Because Kokubo solution can evaluate the capability of the bone-like apatite formation, it has been used for in vitro assessment of the potential of bone-bonding

property of artificial materials. The drawback of Kokubo solution is that  $\text{HCO}_3^-$  concentration is lower and  $\text{Cl}^-$  concentration is higher than that of the human blood plasma. Some types of revisions of Kokubo solution were made to be completely the same ion concentrations as the body fluid [10].

The surface reaction on formation of the bone-like apatite layer in Kokubo solution was reported to obtain fundamental knowledge on novel design of bioactive materials with bone-bonding property. Kokubo solution is an aqueous solution that is supersaturated with respect to hydroxyapatite. On the formation of bone-like apatite, induction of heterogeneous nucleation on the substrate materials may determine the bone-like apatite layer. Once the nuclei of hydroxyapatite formed, they would grow spontaneously to construct a layer of bone-like apatite on the surface of materials. From the investigation of the bone-like apatite formation on metal oxide hydrogels and self-assembled monolayers (SAMs) in Kokubo solution and its related solution, heterogeneous nucleation of hydroxyapatite was enhanced by the existence of functional groups, such as Si-OH [8, 11], Ti-OH [11, 12], Zr-OH [13], Ta-OH [14, 15], Nb-OH [16], COOH [17],  $\text{PO}_3\text{H}_2$  [17], and  $\text{SO}_3\text{H}$  [18, 19]. Chemical and geometrical factors such as  $\text{Ca}^{2+}$  release [20] and spatial gap constructed on the material surfaces [21] can be also factors governing this phenomenon. Utilization of these functional groups is important for developing novel bioactive composites.

---

## Organic–Inorganic Composites for Bone Repair

The most popular preparation route of the organic–inorganic composites is mechanical mixing of ceramic powder and polymer followed by forming process. Mixing ratio of ceramics and polymer significantly governs mechanical and biological properties of the produced composites. Bioactivity implying bone-bonding property increases with increasing the amount of the bioactive ceramic filler, because bioactivity of the composites is caused by surface reaction with body fluid. Addition of too large amount of the ceramics leads to brittle character. Therefore, optimization of the composition is quite important.

Various kinds of organic–inorganic composites have been developed from poly-L-lactic acid (PLLA) [22], polyethylene (PE) [23], collagen [24, 25], carboxymethyl chitin [26], cellulose [27], and polyetheretherketone (PEEK) by the mixing methods with bioactive ceramic fillers. Bioabsorption behavior is significantly dependent on the kind of organic polymer. Namely, composites based on PLLA, collagen, and carboxymethyl chitin show bioabsorption but not that based on polyethylene.

PEEK has attracted much attention in orthopedic field because it shows excellent mechanical property as well as compatibility with X-ray, computed tomography (CT), and magnetic resonance imaging (MRI). Some orthopedic devices made of PEEK have been clinically used; still they cannot bond to living bone directly. Incorporation of hydroxyapatite in PEEK matrix has been conducted to produce PEEK-based bioactive composites for reconstruction of bone tissue [28]. Calcium silicate particles are also available for production of bioactive composites with high mechanical performances, because they allow reduction of amounts of bioactive

fillers, due to their capability of the bone-like apatite formation in body environment [29]. The PEEK-based composites reinforced with 20 vol.% of calcium silicate particles showed 123.5 MPa and 6.43 GPa in bending strength and Young's modulus, respectively. Coating of hydroxyapatite on carbon fiber reinforced PEEK also provided significantly increased interfacial shear strength between the bone and the composites. The achieved interfacial shear strength of the hydroxyapatite-coated carbon fiber reinforced PEEK implant was comparable to that of grit-blasted titanium alloy with hydroxyapatite coating [30].

Organic-inorganic composites are available for improvement of biological affinity of bone cements. They are injectable self-setting biomaterials suitable for repair of bone defects with complex shapes. So-called hydroxyapatite cements are composed of calcium phosphate powder and setting liquid. After implantation, they set as bone-like apatite by dissolution-precipitation reaction. Addition of organic polymers is attempted for improvement of morphological stability in body environment [31] and providing functions of drug delivery [32-34]. Various organic-inorganic composite particles have been also developed for drug delivery [35-38].

Hydroxyapatite-based composites are useful for reconstruction of not only hard tissues but also soft ones. Furuzono et al. developed composite scaffolds from poly (L-lactide-co- $\epsilon$ -caprolactone) microspheres coated with hydroxyapatite nanoparticles by a surfactant-free emulsion route [39]. Intramuscularly co-implantation of the microspheres with bone marrow mononuclear cells induced enhanced angiogenesis [40]. They are useful for an injectable scaffold for the treatment of severe ischemic disorders.

Modification of polymethyl methacrylate (PMMA) bone cements is an important approach for providing self-setting materials with bone-bonding property. PMMA-based bone cements are regarded as important biomaterials for fixation of artificial joints and reconstruction of spinal bone [41]. Setting of the cements is based on radical polymerization of methyl methacrylate monomer. Although they have high mechanical strength enough to be used *in vivo*, loosening is liable to occur after long implantation period due to their lack of bone-bonding property, i. e., bioactivity. Various bioactive ceramic fillers are incorporated into powder phase [42-44]. The present authors developed bioactive PMMA cements by chemical modification using alkoxysilane and water-soluble calcium salts [45, 46]. In this cement, apatite formation was observed in Kokubo solution by incorporation of the additives about 10-20 %, while addition of ceramic fillers described above would require about 40-70 % to make the composites bioactive. Enhanced compatibility of PMMA cements to bone by the chemical modification has been confirmed *in vivo*.

Organic-inorganic composites are also attractive for drug delivery carriers, since many kinds of drugs are hydrophobic and have compatibility with organic polymers. Bioactive organic-inorganic composites with bioabsorbability and appropriate pore structures provide biomaterials with attractive features as a scaffold for bone tissue regeneration. Scaffolds for bone regeneration with bioabsorbability would be gradually degraded to be replaced by the regenerated bone and continuous micropores with 100-300  $\mu\text{m}$  in size for cell migration into the scaffold. Moreover, novel



material design as a drug delivery carrier is available by appropriate control in their pore structure and hydrophilicity.

Kasuga et al. developed vaterite-poly(lactic acid) (PLA) composite for bone regeneration [47]. There are three polymorphisms of calcium carbonate, calcite, aragonite, and vaterite, but they used vaterite with higher solubility than calcite and aragonite so that vaterite releases calcium ions to enhance calcium phosphate deposition in body environment. In fact, the composite containing vaterite in 30 wt. % formed a bone-like apatite layer on its surface after soaking in Kokubo solution within 1 day [47]. Recently, it was confirmed that electrospun microfiber meshes of silicon-doped vaterite-PLA enhanced proliferation of osteoblast-like cells and new bone formed on the meshes when implanted into the calvaria of rabbits [48]. This mesh is expected to be useful for guided bone regeneration.

---

## Coating of Calcium Phosphate on Organic Polymer Substrates

Organic–inorganic composites can be designed by coating of the hydroxyapatite on polymer substrates under biomimetic condition. Kokubo solution can be used not only for the assessment of bone bonding but also for the coating of bone-like apatite on the polymers. The composites can be fabricated by simple soaking of the polymers with the functional groups able to induce the heterogeneous nucleation of hydroxyapatite in Kokubo solution. In this process, precise patterning of the apatite on substrates has been also reported by using a photoresist technique [49]. More concentrated solution than Kokubo solution is also used for the substrates with low apatite-forming ability [50, 51]. The polymer-hydroxyapatite composites have been prepared from various natural and synthetic polymers [52–54]. For example, the present authors prepared organic–inorganic composites from polyamide films containing COOH group in 1.5SBF, that is, an acellular aqueous solution with ion concentrations 1.5 times those of Kokubo solution [53]. Thin films were prepared by casting solution of synthetic polyamide containing COOH and  $\text{CaCl}_2$ . The films were then soaked in 1.5SBF for various periods. Not only density of the formed hydroxyapatite but also adhesion of the hydroxyapatite to the films was enhanced with increase in amount of the COOH group.

It should be noted that hydroxyapatite formation on polymer substrates is governed by ionic attraction between the functional groups and ion constituents of hydroxyapatite. Carboxy group on polymer substrates plays inductive roles on heterogeneous nucleation of hydroxyapatite in Kokubo solution. Observation of bone-like apatite deposition on pectin hydrogels cross-linked with  $\text{Ca}^{2+}$  containing different amount of COOH, after exposure to Kokubo solution, showed that pectic acid did not form the bone-like apatite, in spite that it has the largest amount of the COOH among the evaluated hydrogels [55, 56]. It is known that the carboxy group in the pectin constructs tight ionic bond to  $\text{Ca}^{2+}$  via so-called eggbox structure. The tightly bound  $\text{Ca}^{2+}$  hardly released from the hydrogels into Kokubo solution, although  $\text{Ca}^{2+}$  release enhance the hydroxyapatite nucleation. This phenomenon may cause poor hydroxyapatite formation on the pectic acid.

**Table 1** Mechanical properties of organic–inorganic composites developed for bone repair

Composite	Fracture mode	Strength/MPa	Young's modulus/GPa
HA–PLLA [22]	Bending	250–270	6.5–12
HA–collagen [24]	Bending	10–40	0.55–2.5
HA–PE [57]	Tensile	17–21	0.65–4.3
CaO–SiO <sub>2</sub> –PEEK [30]	Bending	0.12	6.4
CaO–SiO <sub>2</sub> –TiO <sub>2</sub> –poly(dimethylsiloxane) (PDMS) [58]	Bending	2.9–16	0.036–0.61
CaO–SiO <sub>2</sub> –starch [59]	Tensile	3.7–19	0.19–0.91
Cortical bone [1]	Tensile	50–150	7–30
Cancellous bone [1]	Tensile	10–20	0.05–0.5

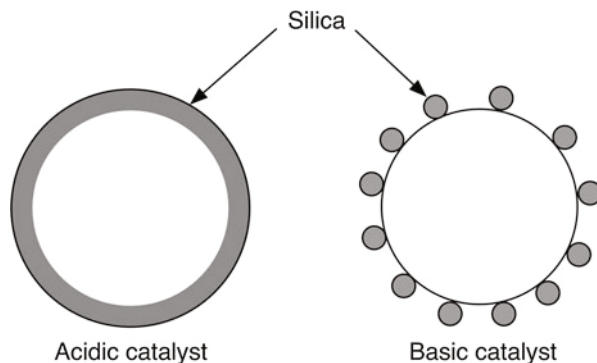
Table 1 summarizes mechanical properties of representative organic–inorganic composites developed for bone repair.

## Composites for Cancer Diagnosis and Treatment

Composite materials provide candidate biomaterials for cancer diagnosis and treatments. Iron oxide is a typical magnetic material and popularly used in the field of electronics. In addition, the iron oxide is also attracting much attention as various functional materials such as biomaterials and chemical catalysts, since the iron is naturally abundant and has low toxicity. This is also expected for cancer treatment in biomedical fields. Hyperthermia is the treatment where cancer cells in the tumors are killed by heat irradiation. It is regarded as a novel cancer treatment with low invasion and low side effects. Iron oxides with magnetite (Fe<sub>3</sub>O<sub>4</sub>) or  $\gamma$ -hematite ( $\gamma$ -Fe<sub>2</sub>O<sub>3</sub>) structure are attractive as thermoseeds for the hyperthermia in biomedical fields, since they achieve heat generation in alternative magnetic fields. In addition, Fe<sub>3</sub>O<sub>4</sub> microspheres have been also developed [60–62], since they exhibit an embolization effect by blocking the blood vessels near the tumors and consequently shutting off nutrition supply to the cancer cells.

Carboxymethyl dextran–Fe<sub>3</sub>O<sub>4</sub> composite has been developed for the thermoseed and contrast medium in MRI [63]. Microspheres composed of the composites have been also developed [64, 65]. The present authors prepared the microspheres of the carboxymethyl dextran–Fe<sub>3</sub>O<sub>4</sub> composite by an emulsion route. Sol was prepared by dispersion of the Fe<sub>3</sub>O<sub>4</sub> nanoparticles. Microspheres were obtained by dehydration of the sol in water-in-oil emulsion. Sol–gel silica coating was then attempted by using different catalysts for hydrolysis and polycondensation, since the microspheres released a lot of iron ions in aqueous condition. The silica coating using acidic catalyst was effective for the improvement of chemical durability in simulated body environment but not the coating using the basic one. Numerous spherical nanoparticles were observed on the microspheres prepared by the basic catalyst, as schematically shown in Fig. 2. Therefore, it is assumed that the formed silica

**Fig. 2** Schematic representation of sol–gel silica coating hydrolyzed by acidic and basic catalysts



nanoparticles on the carboxymethyl-dextran- $\text{Fe}_3\text{O}_4$  microspheres do not play a role as a continuous protective layer.

Matsumine et al. [66] proposed an  $\text{Fe}_3\text{O}_4$ -containing calcium phosphate-based cement for the hyperthermia of metastatic bone tumors in the femur, fibula, humerus, or tibia. They conducted clinical trials for hyperthermic treatment in 15 patients with metastatic bone lesions (HT group). The results were then compared with those for 8 patients treated by palliative operation (Op group) and 22 patients treated by operations as well as radiotherapy (Op + RT group). The patients in the HT group showed better radiographic outcomes than those in the Op group and no significant differences from those in the Op + RT group. The  $\text{Fe}_3\text{O}_4$ -containing calcium phosphate-based cement is useful for hyperthermic treatment for metastatic bone tumors, but the mechanical strength of calcium phosphate cement is generally lower than that of PMMA-based cement, and hence, the  $\text{Fe}_3\text{O}_4$ -containing calcium phosphate cement is not ideal for hyperthermic treatment of bone tumors subjected to high load. To overcome this disadvantage of the  $\text{Fe}_3\text{O}_4$ -containing calcium phosphate cement, PMMA cement containing  $\text{Fe}_3\text{O}_4$  nanoparticles has been proposed recently [67, 68].

$\text{Fe}_3\text{O}_4$  nanoparticles can be usually prepared by precipitation reaction in aqueous conditions. The present authors revealed effects of organic polymer coexistence on the crystalline structure of the prepared  $\text{Fe}_3\text{O}_4$  [69]. Cationic and neutral polymers hardly inhibit  $\text{Fe}_3\text{O}_4$  formation. On the other hand, anionic polymers significantly inhibited it. Especially,  $\text{Fe}_3\text{O}_4$  was not formed by the addition of polyacrylic acid. Anionic polymer easily constructs a complex with iron ions. The complex formation would retard the reaction with  $\text{OH}^-$  ions essential for conversion into  $\text{Fe}_3\text{O}_4$ . The results in this study provide a fundamental guideline for  $\text{Fe}_3\text{O}_4$ -based composite nanomaterials.

Biofunctionalization of  $\text{Fe}_3\text{O}_4$  nanoparticles for targeted hyperthermia is also attempted. Hayashi et al. prepared the  $\text{Fe}_3\text{O}_4$  nanoparticles modified with folic acid [70], based on the fact that tumor cells have folate receptors. They showed excellent monodispersiveness and heating ability.

$\text{Fe}_3\text{O}_4$  nanoparticles also manipulate cell movement. Shinkai et al. incorporated  $\text{Fe}_3\text{O}_4$  into various cells via cationic liposomes combined with  $\text{Fe}_3\text{O}_4$  nanoparticles [71]. The magnetized cell can be manipulated by a magnetic field. In addition, three

dimensional cell accumulation can be achieved, when synthetic RGD peptide was covalently bound to the magnetic liposome. Epidermis cell sheets have been developed by Ito et al. using this technique [72].

Local radiotherapy using  $\beta$ -emitting ceramics such as yttrium oxide ( $Y_2O_3$ ) is attractive as a treatment for various types of cancers. It is known that nonradioactive  $^{89}Y$  with a natural abundance of 100 % will convert into  $^{90}Y$  that can act in turn as  $\beta$ -emitters with a half-life of 64.1 h through neutron bombardment. Not only inorganic microspheres composed of  $Y_2O_3$ -containing glasses [73],  $Y_2O_3$  [74, 75], and yttrium phosphate ( $YPO_4$ ) [76, 77] but also  $Y_2O_3$ -based organic–inorganic composites [78] have been developed. Some of them are clinically utilized.

Development of not only cancer treatment but also diagnosis with high accuracy is needed. Quantum dots composed of inorganic fluorescent material are attractive for imaging with high accuracy. However, the problem is that ultraviolet light used for their excitation is liable to damage healthy body tissues. Soga et al. developed novel nanoparticles composed of  $Y_2O_3$  and  $YPO_4$  with well-controlled particle size able to be excited by near-infrared (NIR) light [79]. Cell-targeted fluorescent imaging is achieved by combination of the nanoparticles and various ligand molecules. In addition, Uo et al. incorporated these nanoparticles into dental composite resins for polymerization by NIR [80].

---

## Conclusions

Material design based on organic–inorganic composite facilitates improvement of mechanical properties and provides various biological functions such as drug delivery, tissue regeneration, and precise diagnosis of diseases. They are expected to be applied to various tissue reconstructions and contribute to high quality of life (QOL) of the patients.

---

## References

1. Hench LL, Wilson J (1993) Introduction. In: Hench LL, Wilson J (eds) An introduction to bioceramics. World Scientific, Singapore, pp 1–24
2. Hench LL, Splinger RJ, Allen WC, Greenlee TK (1972) Bonding mechanisms at the interface of ceramic prosthetic materials. *J Biomed Mater Res Symp* 2:117–141. doi:10.1002/jbm.820050611
3. Hench LL (1991) Bioceramics; from concept to clinic. *J Am Ceram Soc* 74:1487–1510. doi:10.1111/j.1151-2916.1991.tb07132.x
4. Jarcho M, Bolen CH, Thomas MB, Bobick J, Kay JF, Doremus RH (1976) Hydroxyapatite synthesis and characterization in dense polycrystalline forms. *J Mater Sci* 11:2027–2035. doi:10.1007/BF02403350
5. Kokubo T, Kim HM, Kawashita M (2003) Novel bioactive materials with different mechanical properties. *Biomaterials* 24:2161–2175. doi:10.1016/S0142-9612(03)00044-9
6. Park JB, Lakes RS (1992) *Biomaterials, an introduction*, 2nd edn. Plenum Press, New York
7. Neo M, Kotani S, Fujita Y, Nakamura T, Yamamuro T, Bando Y, Ohtsuki C, Kokubo T (1992) Differences in ceramic–bone interface between surface-active ceramics and resorbable ceramics:

- a study by scanning and transmission electron microscopy. *J Biomed Mater Res* 26:255–267. doi:10.1002/jbm.820260210
8. Cho SB, Nakanishi K, Kokubo T, Soga N, Ohtsuki C, Nakamura T, Kitsugi T, Yamamuro T (1995) Dependence of apatite formation on silica gel on its structure: effect of heat treatment. *J Am Ceram Soc* 78:1769–1774. doi:10.1111/j.1151-2916.1995.tb08887.x
  9. Kokubo T, Takadama H (2006) How useful is SBF in predicting *in vivo* bone bioactivity? *Biomaterials* 27:2907–2915. doi:10.1016/j.biomaterials.2006.01.017
  10. Oyane A, Kim HM, Furuya T, Kokubo T, Miyazaki T, Nakamura T (2003) Preparation and assessment of revised simulated body fluid. *J Biomed Mater Res* 65A:188–195. doi:10.1002/jbm.a.10482
  11. Li P, Ohtsuki C, Kokubo T, Nakanishi K, Soga N, de Groot K (1994) The role of hydrated silica, titania and alumina in inducing apatite on implants. *J Biomed Mater Res* 28:7–15. doi:10.1002/jbm.820280103
  12. Uchida M, Kim HM, Kokubo T, Fujibayashi S, Nakamura T (2003) Structural dependence of apatite formation on titania gels in a simulated body fluid. *J Biomed Mater Res A* 64:164–170. doi:10.1002/jbm.a.10414
  13. Uchida M, Kim HM, Kokubo T, Miyaji F, Nakamura T (2001) Bonelike apatite formation induced on zirconia gel in a simulated body fluid and its modified solutions. *J Am Ceram Soc* 84:2041–2044. doi:10.1111/j.1151-2916.2001.tb00955.x
  14. Miyazaki T, Kim HM, Miyaji F, Kokubo T, Nakamura T (2000) Bioactive tantalum metal prepared by NaOH treatment. *J Biomed Mater Res* 50:35–42. doi:10.1002/(SICI)1097-4636(200004)50:1<35::AID-JBM6>3.0.CO;2-8
  15. Miyazaki T, Kim HM, Kokubo T, Kato H, Nakamura T (2001) Induction and acceleration of bonelike apatite formation on tantalum oxide gel in simulated body fluid. *J Sol-Gel Sci Technol* 21:83–88. doi:10.1023/A:1011265701447
  16. Miyazaki T, Kim HM, Kokubo T, Ohtsuki C, Nakamura T (2001) Bonelike apatite formation induced on niobium oxide gels in simulated body fluid. *J Ceram Soc Jpn* 109:934–938. doi:10.2109/jcersj.109.1275\_929
  17. Tanahashi M, Matsuda T (1997) Surface functional group dependence on apatite formation on self-assembled monolayers in a simulated body fluid. *J Biomed Mater Res* 34:305–315. doi:10.1002/(SICI)1097-4636(19970305)34:33.0.CO;2-O
  18. Kawai T, Ohtsuki C, Kamitakahara M, Miyazaki T, Tanihara M, Sakaguchi Y, Konagaya S (2004) Coating of apatite layer on polyamide films containing sulfonic groups by biomimetic process. *Biomaterials* 25:4529–4534. doi:10.1016/j.biomaterials.2003.11.039
  19. Miyazaki T, Imamura M, Ishida E, Ashizuka M, Ohtsuki C (2009) Apatite formation abilities and mechanical properties of hydroxyethylmethacrylate-based organic-inorganic hybrids incorporated with sulfonic groups and calcium ions. *J Mater Sci Mater Med* 20:157–161. doi:10.1007/s10856-008-3556-5
  20. Ohtsuki C, Kokubo T, Yamamuro T (1992) Mechanism of apatite formation on CaO-SiO<sub>2</sub>-P<sub>2</sub>O<sub>5</sub> glasses in a simulated body fluid. *J Non-Cryst Solids* 143:84–92. doi:10.1016/S0022-3093(05)80556-3
  21. Sugino A, Tsuru K, Hayakawa S, Kikuta K, Kawachi G, Osaka A, Ohtsuki C (2009) Induced deposition of bone-like hydroxyapatite on thermally oxidized titanium substrates using a spatial gap in a solution that mimics a body fluid. *J Ceram Soc Jpn* 117:515–520. doi:10.2109/jcersj.117.515
  22. Shikunami Y, Okuno M (1999) Bioresorbable devices made of forged composites of hydroxyapatite and poly L-lactide (PLLA): part I. basic characteristics. *Biomaterials* 20:859–877. doi:10.1016/S0142-9612(98)00241-5
  23. Bonfield W (1993) Design of bioactive ceramic-polymer composites. In: Hench LL, Wilson J (eds) *An introduction to bioceramics*. World Scientific, Singapore, pp 299–303
  24. Kikuchi M, Itoh S, Ichinose S, Shinomiya K, Tanaka J (2001) Self-organization mechanism in a bone-like hydroxyapatite/collagen nanocomposite synthesized *in vitro* and its biological reaction *in vivo*. *Biomaterials* 22:1705–1711. doi:10.1016/S0142-9612(00)00305-7

25. Kawai T, Matsui K, Iibuchi S, Anada T, Honda Y, Sasaki K, Kamakura S, Suzuki O, Echigo S (2011) Reconstruction of critical-sized bone defect in dog skull by octacalcium phosphate combined with collagen. *Clin Oral Implants Res* 13:112–123. doi:10.1111/j.1708-8208.2009.00192.x
26. Muramatsu K, Oba K, Mukai D, Hasegawa K, Masuda S, Yoshihara Y (2007) Subacute systemic toxicity assessment of  $\beta$ -tricalcium phosphate/carboxymethyl-chitin composite implanted in rat femur. *J Mater Sci Mater Med* 18:513–522. doi:10.1007/s10856-007-2012-2
27. Yoshida A, Miyazaki T, Ishida E, Ashizuka M (2006) Bioactivity and mechanical properties of cellulose/carbonate hydroxyapatite composites prepared in situ through mechanochemical reaction. *J Biomater Appl* 21:179–194. doi:10.1177/0885328206059796
28. Ma R, Tang T (2014) Current strategies to improve the bioactivity of PEEK. *Int J Mol Sci* 15:5426–5445. doi:10.3390/ijms15045426
29. Kim IY, Sugino A, Kikuta K, Ohtsuki C, Cho SB (2009) Bioactive composites consisting of PEEK and calcium silicate powders. *J Biomater Appl* 24:105–118. doi:10.1177/0885328208094557
30. Nakahara I, Takao M, Goto T, Ohtsuki C, Hibino S, Sugano N (2012) Interfacial shear strength of bioactive-coated carbon fiber reinforced polyetheretherketone after in vivo implantation. *J Orthop Res* 30:1618–1625. doi:10.1002/jor.22115
31. Ishikawa K, Miyamoto Y, Kon M, Nagayama M, Asaoka K (1995) Non-decay type fast-setting calcium phosphate cement: composite with sodium alginate. *Biomaterials* 16:527–532. doi:10.1016/0142-9612(95)91125-1
32. Makinen TJ, Veiranto M, Lankinen P, Moritz N, Jalava J, Tormala P, Aro HT (2005) In vitro and in vivo release of ciprofloxacin from osteoconductive bone defect filler. *J Antimicrob Chemother* 56:1063–1068. doi:10.1093/jac/dki366
33. Schnieders J, Gbureck U, Thull R, Kissel T (2006) Controlled release of gentamicin from calcium phosphate-poly(lactic acid-co-glycolic acid) composite bone cement. *Biomaterials* 27:4239–4249. doi:10.1016/j.biomaterials.2006.03.032
34. Otsuka M, Nakagawa H, Ito A, Higuchi WI (2010) Effect of geometrical structure on drug release rate of a three-dimensionally perforated porous apatite/collagen composite cement. *J Pharm Sci* 99:286–292. doi:10.1002/jps.21835
35. Lee YM, Park YJ, Lee SJ, Ku Y, Han SB, Klokkevold PR, Chung CP (2000) The bone regenerative effect of platelet-derived growth factor-BB delivered with a chitosan/tricalcium phosphate sponge carrier. *J Periodontol* 71:418–424. doi:10.1902/jop.2000.71.3.418
36. Zhang Y, Zhang M (2002) Calcium phosphate/chitosan composite scaffolds for controlled in vitro antibiotic drug release. *J Biomed Mater Res* 62:378–386. doi:10.1002/jbm.10312
37. Takahashi Y, Yamamoto M, Tabata Y (2005) Enhanced osteoinduction by controlled release of bone morphogenetic protein-2 from biodegradable sponge composed of gelatin and  $\beta$ -tricalcium phosphate. *Biomaterials* 26:4856–4865. doi:10.1016/j.biomaterials.2005.01.012
38. Leeuwenburgh S, Jo J, Wang H, Yamamoto M, Jansen JA, Tabata Y (2010) Mineralization, biodegradation, and drug release behavior of gelatin/apatite composite microspheres for bone regeneration. *Biomacromolecules* 11:2653–2659. doi:10.1021/bm1006344
39. Liu X, Okada M, Maeda H, Fujii S, Furuzono T (2011) Hydroxyapatite/biodegradable poly-(L-lactide-co-caprolactone) composite microparticles as injectable scaffold by a Pickering emulsion route. *Acta Biomater* 7:821–828. doi:10.1016/j.actbio.2010.08.023
40. Mima Y, Fukumoto S, Koyama H, Okada M, Tanaka S, Shoji T, Emoto M, Furuzono T, Nishizawa Y, Inaba M (2012) Enhancement of cell-based therapeutic angiogenesis using a novel type of injectable scaffolds of hydroxyapatite-polymer nanocomposite microspheres. *PLoS One* 7:e35199. doi:10.1371/journal.pone.0035199
41. Kühn KD (2000) Bone cements. Springer, Berlin
42. Dalby MJ, Di Silvio L, Harper EJ, Bonfield W (1999) In vitro evaluation of a new polymethylmethacrylate cement reinforced with hydroxyapatite. *J Mater Sci Mater Med* 10:793–796. doi:10.1023/A:1008907218330

43. Shinzato S, Kobayashi M, Mousa WF, Kamimura M, Neo M, Kitamura Y, Kokubo T, Nakamura T (2000) Bioactive polymethyl methacrylate-based bone cement: comparison of glass beads, apatite- and wollastonite-containing glass-ceramic, and hydroxyapatite fillers on mechanical and biological properties. *J Biomed Mater Res* 51:258–272. doi:10.1002/(SICI)1097-4636(200008)51:2<258::AID-JBM15>3.0.CO;2-S
44. Goto K, Tamura J, Shinzato S, Fujibayashi S, Hashimoto M, Kawashita M, Kokubo T, Nakamura T (2005) Bioactive bone cements containing nano-sized titania particles for use as bone substitutes. *Biomaterials* 26:6496–6505. doi:10.1016/j.biomaterials.2005.04.044
45. Miyazaki T, Ohtsuki C, Kyomoto M, Tanihara M, Mori A, Kuramoto K (2003) Bioactive PMMA bone cement prepared by modification with methacryloxypropyltrimethoxysilane and calcium chloride. *J Biomed Mater Res* 67A:1417–1423. doi:10.1002/jbm.a.20042
46. Sugino A, Ohtsuki C, Miyazaki T (2008) In vivo response of bioactive PMMA-based bone cement modified with alkoxy silane and calcium acetate. *J Biomater Appl* 23:213–228. doi:10.1177/0885328207081694
47. Kasuga T, Maeda H, Kato K, Nogami M, Hata K, Ueda M (2003) Preparation of poly(lactic acid) composites containing calcium carbonate (vaterite). *Biomaterials* 24:3247–3253. doi:10.1016/S0142-9612(03)00190-X
48. Obata A, Hotta T, Wakita T, Ota Y, Kasuga T (2010) Electrospun microfiber meshes of silicon-doped vaterite/poly(lactic acid) hybrid for guided bone regeneration. *Acta Biomater* 6:1248–1257. doi:10.1016/j.actbio.2009.11.013
49. Ozawa N, Yao T (2002) Micropattern formation of apatite by combination of a biomimetic process and transcription of resist pattern. *J Biomed Mater Res* 62:579–586. doi:10.1002/jbm.10281
50. Hata K, Kokubo T, Nakamura T, Yamamuro T (1995) Growth of bonelike apatite layer on a substrate by a biomimetic process. *J Am Ceram Soc* 78:1049–1053. doi:10.1111/j.1151-2916.1995.tb08435.x
51. Habibovic P, Barrere F, van Blitterswijk CA, de Groot K, Layrolle P (2002) Biomimetic hydroxyapatite coating on metal implants. *J Am Ceram Soc* 517–522. doi:10.1111/j.1151-2916.2002.tb00126.x
52. Kawashita M, Nakao M, Minoda M, Kim HM, Beppu T, Miyamoto T, Kokubo T, Nakamura T (2003) Apatite-forming ability of carboxyl group-containing polymer gels in a simulated body fluid. *Biomaterials* 24:2477–2484. doi:10.1016/S0142-9612(03)00050-4
53. Miyazaki T, Ohtsuki C, Akioka Y, Tanihara M, Nakao J, Sakaguchi Y, Konagaya S (2003) Apatite deposition on polyamide films containing carboxyl group in a biomimetic solution. *J Mater Sci Mater Med* 569–574. doi:10.1023/A:1024000821368
54. Miyazaki T, Ishikawa K, Shirosaki Y, Ohtsuki C (2013) Organic-inorganic composites designed for biomedical applications. *Biol Pharm Bull* 36:1670–1675. doi:10.1248/bpb.b13-00424
55. Ichibouji T, Miyazaki T, Ishida E, Ashizuka M, Sugino A, Ohtsuki C, Kuramoto K (2008) Evaluation of apatite-forming ability and mechanical property of pectin hydrogels. *J Ceram Soc Jpn* 116:74–78. doi:10.2109/jcersj2.116.74
56. Ichibouji T, Miyazaki T, Ishida E, Sugino A, Ohtsuki C (2009) Apatite mineralization abilities and mechanical properties of covalently cross-linked pectin hydrogels. *Mater Sci Eng C* 29:1765–1769. doi:10.1016/j.msec.2009.01.027
57. Bonfield W (1996) Composite biomaterials. In: Kokubo T, Nakamura T, Miyaji F (eds) *Bioceramics*, vol 9. Elsevier, Oxford, pp 11–13
58. Chen Q, Miyata N, Kokubo T, Nakamura T (2000) Bioactivity and mechanical properties of PDMS-modified CaO–SiO<sub>2</sub>–TiO<sub>2</sub> hybrids prepared by sol-gel process. *J Biomed Mater Res* 51:605–611. doi:10.1002/1097-4636(20000915)51:4<605::AID-JBM8>3.0.CO;2-U
59. Miyazaki T, Yasunaga S, Ishida E, Ashizuka M, Ohtsuki C (2007) Effects of cross-linking agent on apatite-forming ability and mechanical property of organic-inorganic hybrids based on starch. *Mater Trans* 48:317–321. doi:10.2320/matertrans.48.317

60. Kawashita M, Tanaka M, Kokubo T, Inoue Y, Yao T, Hamada S, Shinjo T (2005) Preparation of ferrimagnetic magnetite microspheres for in situ hyperthermic treatment of cancer. *Biomaterials* 26:2231–2238. doi:10.1016/j.biomaterials.2004.07.014
61. Zhao J, Sekikawa H, Kawai T, Unuma H (2009) Ferrimagnetic magnetite hollow microspheres prepared via enzymatically precipitated iron hydroxide on a urease-bearing polymer template. *J Ceram Soc Jpn* 117:344–346. doi:10.2109/jcersj2.117.344
62. Miyazaki T, Miyaoka A, Ishida E, Li Z, Kawashita M, Hiraoka M (2012) Preparation of ferromagnetic microcapsules for hyperthermia using water/oil emulsion as a reaction field. *Mater Sci Eng C* 32:692–696. doi:10.1016/j.msec.2012.01.010
63. Mitsumori M, Hiraoka M, Shibata T, Okuno Y, Masunaga S, Koishi M, Okajima K, Nagata Y, Nishimura Y, Abe M, Ohura K, Hasegawa M, Nagae H, Ebisawa Y (1994) Development of intra-arterial hyperthermia using a dextran-magnetite complex. *Int J Hyperth* 10:785–793. doi:10.3109/02656739409012371
64. Minamimura T, Sato H, Kasaoka S, Saito T, Ishizawa S, Takemori S, Tazawa K, Tsukada K (2000) Tumor regression by inductive hyperthermia combined with hepatic embolization using dextran magnetite-incorporated microspheres in rats. *Int J Oncol* 16:1153–1158. doi:10.3892/ijo.16.6.1153
65. Miyazaki T, Anan S, Ishida E, Kawashita M (2013) Carboxymethyl-dextran/magnetite hybrid microspheres designed for hyperthermia. *J Mater Sci Mater Med* 24:1125–1129. doi:10.1007/s10856-013-4874-9
66. Matsumine A, Kusuzaki K, Matsubara T, Shintani K, Satonaka H, Wakabayashi T, Miyazaki S, Morita K, Takegami K, Uchida A (2007) Novel hyperthermia for metastatic bone tumors with magnetic materials by generating an alternating electromagnetic field. *Clin Exp Metastasis* 24:191–200. doi:10.1007/s10585-007-9068-8
67. Kawashita M, Kawamura K, Li Z (2010) PMMA-based bone cements containing magnetite particles for the hyperthermia of cancer. *Acta Biomater* 6:3187–3192. doi:10.1016/j.actbio.2010.02.047
68. Li Z, Kawamura K, Kawashita M, Kudo T, Kanetaka H, Hiraoka M (2012) In vitro heating capability, mechanical strength and biocompatibility assessment of PMMA-based bone cement containing magnetite nanoparticles for hyperthermia of cancer. *J Biomed Mater Res* 100A:2537–2545. doi:10.1002/jbm.a.34185
69. Kuwahara Y, Miyazaki T, Shirosaki Y, Kawashita M (2014) Effects of organic polymer addition in magnetite synthesis on its crystalline structure. *RSC Adv* 4:23359–23363. doi:10.1039/C4RA02073A
70. Hayashi K, Moriya M, Sakamoto W, Yogo T (2009) Chemoselective synthesis of folic acid – functionalized magnetite nanoparticles via click chemistry for magnetic hyperthermia. *Chem Mater* 21:1318–1325. doi:10.1021/cm803113e
71. Shinkai M, Yanase M, Honda H, Wakabayashi T, Yoshida J, Kobayashi T (1996) Intracellular hyperthermia for cancer using magnetite cationic liposomes: in vitro study. *Jpn J Cancer Res* 87:1179–1183. doi:10.1111/j.1349-7006.1996.tb03129.x
72. Ito A, Hibino E, Kobayashi C, Terasaki H, Kagami H, Ueda M, Kobayashi T, Honda H (2005) Construction and delivery of tissue-engineered human retinal pigment epithelial cell sheets, using magnetite nanoparticles and magnetic force. *Tissue Eng* 11:489–496. doi:10.1089/ten.2005.11.489
73. Erbe EM, Day DE (1987) Chemical durability of  $Y_2O_3$ - $Al_2O_3$ - $SiO_2$  glasses for the in vivo delivery of beta radiation. *J Biomed Mater Res* 27:1301–1308. doi:10.1002/jbm.820271010
74. Kawashita M, Takayama Y, Kokubo T, Takaoka GH, Araki N, Hiraoka M (2006) Enzymatic preparation of hollow yttrium oxide microspheres for in situ radiotherapy of deep-seated cancer. *J Am Ceram Soc* 89:1347–1351. doi:10.1111/j.1551-2916.2005.00867.x
75. Miyazaki T, Kai T, Ishida E, Kawashita M, Hiraoka M (2010) Fabrication of yttria microcapsules for radiotherapy from water/oil emulsion. *J Ceram Soc Jpn* 118:479–482. doi:10.2109/jcersj2.118.479



76. Kawashita M, Matsui N, Li Z, Miyazaki T, Kanetaka H (2011) Preparation, structure, and *in vitro* chemical durability of yttrium phosphate microspheres for intra-arterial radiotherapy. *J Biomed Mater Res B Appl Biomater* 99:45–50. doi:10.1002/jbm.b.31870
77. Miyazaki T, Suda T, Shirotsaki Y, Kawashita M (2014) Fabrication of yttrium phosphate microcapsules by an emulsion route for in situ cancer radiotherapy. *J Med Biol Eng* 34:14–17. doi:10.5405/jmbe.1451
78. Schubiger PA, Beer HF, Geiger L, Rösler H, Zimmermann A, Triller J, Mettler D, Schilt W (1991)  $^{90}\text{Y}$ -resin particles – animal experiments on pigs with regard to the introduction of superselective embolization therapy. *Int J Rad Appl Instrum B* 18:305–311. doi:10.1016/0883-2897(91)90126-6
79. Venkatachalam N, Saito Y, Soga K (2009) Synthesis of  $\text{Er}^{3+}$  doped  $\text{Y}_2\text{O}_3$  nanophosphors. *J Am Ceram Soc* 92:1006–1010. doi:10.1111/j.1551-2916.2009.02986.x
80. Uo M, Kudo E, Okada A, Soga K, Kogo Y (2009) Preparation and properties of dental composite resin cured under near infrared irradiation. *J Photopolym Sci Technol* 22:551–554. doi:10.2494/photopolymer.22.551

Iulian Vasile Antoniac, Madalina Georgiana Albu, Aurora Antoniac,  
Laura Cristina Rusu, and Mihaela Violeta Ghica

## Contents

Introduction .....	302
Biomaterials Used for Collagen–Bioceramic Composites .....	306
Bioceramics .....	306
Collagen .....	307
Processing and Characterization of the Collagen–Bioceramic Composites .....	311
Collagen–Bioceramic Composites Used as Drug Delivery Systems .....	312
Summary .....	318
References .....	318

---

I.V. Antoniac (✉)

University Politehnica of Bucharest, Bucharest, Romania

e-mail: [antoniac.iulian@gmail.com](mailto:antoniac.iulian@gmail.com)

M.G. Albu

INCDTP – Division of Leather and Footwear Research Institute, Bucharest, Romania

e-mail: [albu\\_mada@yahoo.com](mailto:albu_mada@yahoo.com)

A. Antoniac

Faculty of Materials Science and Engineering, University Politehnica of Bucharest, Bucharest,  
Romania

e-mail: [antoniac.aurora@gmail.com](mailto:antoniac.aurora@gmail.com)

L.C. Rusu

University of Medicine and Pharmacy “Victor Babes” Timisoara, Timisoara, Romania

e-mail: [laura.rusu@umft.ro](mailto:laura.rusu@umft.ro)

M.V. Ghica

Faculty of Pharmacy, University of Medicine and Pharmacy “Carol Davila” Bucharest, Bucharest,  
Romania

e-mail: [mihaelaghica@yahoo.com](mailto:mihaelaghica@yahoo.com)

---

**Abstract**

Bone regeneration remains one of the most challenging issues of today. 3D scaffolds that mimic native bone have been widely used in many implantable prostheses and play a critical role in improving human health. Inspired by the composition of the natural bone, a variety of collagen-based composites reinforced with different resorbable bioceramics have been developed. To mimic the natural bone, some requirements are imposed on the collagen–bioceramic composites. This chapter focuses on collagen-based composites, starting with the main biomaterials used to obtain the composites, and the methods used for obtaining the collagen–bioceramics-type composites. Different practical aspects related to the processing and characterization of some collagen-based composites that mimic bone tissue are revealed. Also, some characteristics that proved their properties and smart composite–drug delivery systems of the collagen–bioceramic-type composites are discussed.

---

**Keywords**

Composite • Biomaterial • Bioceramic • Collagen • Drug delivery system

---

**Introduction**

Bone tissue engineering in the field of orthopedic, dental, and craniofacial regeneration represents one of the most challenging issues of today [1, 2]. For the design and development of a new and superior 3D composite, which mimics bone, the composition knowledge and the understanding of structural and morpho-functional properties of natural bone is of paramount importance.

Bone is a connective tissue, strongly vascularized, made of different types of scattered cells [3, 4] in a porous tridimensional network, organized as an extracellular matrix (ECM) [5]. This matrix consists of an organic component named osteoid, which is the main scaffold of the anorganic or mineral component [4, 6–9].

The organic component (up to 30 %) is mostly represented by collagen (mainly type I and small amounts of type V), together with other organic materials: proteoglycans, glycosaminoglycans (the most important being hyaluronic acid and chondroitin sulfates), and lipids [4, 7, 10, 11].

The bone mineral (up to 70 %) is mostly made up of calcium salts, especially as phosphate in the form of hydroxyapatite (HA) with the chemical formula  $\text{Ca}_{10}(\text{PO}_4)_6(\text{OH})_2$ , along with other minerals such as sodium ions, magnesium, potassium, carbonate, fluoride, chloride, strontium, and zinc, in various proportions [4, 10, 12].

In addition to these two components, water (up to 20 %) is the third elementary ingredient, and the ratio between the main components is dependent on age [10, 11].

Nowadays, owing to the increased tendency of the population to age, accidents, increased incidence, and active life style, millions of people are suffering from different bone defects that markedly influence their quality of life [13–16]. Recent

studies show that a lot of costly osseous tissue procedures are performed annually in Europe and the USA [1, 14, 17, 18].

Generally, bone repair, reconstruction, and regeneration following trauma (severe fractures, teeth extraction), tumor resection, other pathological processes with different etiologies (osteoporosis, osteoarthritis, Paget's disease, etc.), and congenital deformities (imperfect osteogenesis) remain a clinical challenge in orthopedic, dental, and craniofacial surgery, a solution being needed to solve this issue [1, 2, 13, 19–21].

The conventional pathway approach to bone defects therapy is based on grafts, classified as autografts, allografts, and xenografts [7, 11, 13, 20, 22]. Recently, the modern strategy for treating bone insufficiency has included other promising alternatives such as the use of artificial graft materials, named alloplasts, which are the subject of tissue engineering [14].

The main biological properties (osteo-properties) to be replaced by the grafts are osteoconductivity, osteoinductivity, and osteogenicity. Osteoinductivity refers to the induction of osteoprogenitor cells and their differentiation into osteoblasts. Osteogenicity represents the property of the maturation of osteoblasts, which form the mineral part of the bone. Osteoconductivity is the process by which a bone graft promotes the attachment of the osteoblastic cells on its surface [2, 23–25].

*Autografts*, also known as autologous grafts, are considered “the gold standard” in bone transplantation. This procedure consists of removing a bone from the same patient and implanting it at the affected site [12, 13, 26, 27]. Because autografts originate from the same individual, their main advantages are osteoconductivity, osteoinductivity, and osteogenicity, and the lack of immunogenicity and disease transmission [13, 23–25, 28]. However, the use of autografts is restricted owing to post-operative donor site morbidity manifesting as necrosis, infection, inflammation, and chronic pain, which induce prolonged healing in addition to the one due to the affected osseous tissue [2, 7, 15, 20, 25, 27, 29], limited availability, and shape restriction [15, 18, 29].

*Allografts*, also known as homografts or allogeneic transplants, are bone obtained from human donors (alive or cadavers), specifically adjusted before transplantation [3, 23, 26]. Originating from other donors, the major advantage of these grafts resides in avoiding donor site morbidity [23]. The operations preceding the use of allografts in bone transplantation (such as sterilization, lyophilization, demineralization) have on the one hand benefits such as the reduction of disease transmission, immune response, and consequently the diminution of implant rejection risk, but on the other hand determine less osteoconductivity, osteoinductivity, and osteogenicity, and fewer mechanical properties [20, 22, 24, 25, 27, 30]. The costs of obtaining allografts and the donor shortage also remain a problem regarding their use [29].

Unlike allografts, *xenografts* are bones obtained from nonhuman species (e.g., from the pig) [12, 25, 26]. The advantages and limitations of their use in osseous procedures are the same as for allografts [20, 22].

Although the graft types previously mentioned have some advantages expressed as physico-chemical and biological properties similar to those of the affected osseous tissue [20], which also led to good clinical results, especially for autografts [23], to overcome their drawbacks the recent advances in tissue engineering have resulted in

an alternative approach to treating bone defects. These new artificial grafts, called *alloplasts*, represent an encouraging choice for successful, functional, tissue-engineered bone regeneration [1, 3, 12, 14, 15, 18, 27, 31].

Many biomaterials have been investigated as suitable scaffolds for bone regeneration to identify those that have the most suitable physical, chemical, and biological characteristics that favor *in vitro* bone production and healing.

Among them, scaffolds based on two distinct components have demonstrated potential in bone defect repair [1, 32]:

- Soft biopolymer of natural or synthetic origin,
- Mineralized inorganic materials that mimic the *in vivo* environment of mature bone.

Among natural polymers, which are generally biodegradable and have a high potential to interact with the osseous tissue, collagen, gelatin, silk fibroin, elastin, chitosan, alginate, cellulose, and glycosaminoglycans such as hyaluronic acid and chondroitin sulfate can be mentioned [1, 2, 6, 7, 13, 15, 33, 34]. A special interest is given to synthetic polymers, which have a higher predictability and reproducibility as poly(lactic acid) or polylactide, poly(glycolic) acid, poly(DL-lactic-co-glycolic acid), poly(caprolactone), poly(trimethylene carbonate), poly(dioxanone), polyurethane, poly(methylmethacrylate) [7, 18, 32, 33, 35–37]. Both categories have been considered to be adequate support for bone grafts and widely used in a variety of osseous tissue engineering applications [1, 13].

As inorganic materials, the most frequently used are bioactive ceramics with the common group of calcium phosphate (CaP) in the form of tricalcium phosphates, HA or a combination of the two (biphasic CaP), and bioactive glasses [1, 10, 13, 16, 19, 32, 38].

To improve the bioactivity (mainly the osteo-properties) and to overcome the mutual limitations of the physico-chemical properties, both of the biopolymers (poor mechanical stiffness and strength, fast degradability) [1, 7, 8, 10, 19, 20] and of the ceramics (poor fracture toughness and compressive strength, low biodegradability, nonresorbability) [1, 9, 39–41], the current trend in tissue engineering is to use a combination of the two in the form of 3D composites [9, 13, 33, 38, 39].

Composites are materials that incorporate at least two different components, such as biopolymers and bioceramics. This association has a synergistic effect on bioactivity and physico-chemical characteristics by combining the advantages of the properties of each element [13, 16, 24].

The composites can be processed in various forms [32, 42–45]:

- Porous matrices (sponges)
- Hydrogels
- Films
- Fibers
- Microspheres
- Nanoparticulate systems

For successful bone therapy, in addition to the aforementioned osteo-properties (osteoconductivity, osteoinductivity, and osteogenicity), composites have to fulfill some general performance criteria [2, 11–13, 15, 16, 19, 23, 25, 27, 28, 41]:

- Biocompatibility
- Biodegradability or resorbability
- Safety, nontoxicity and non-immunogenicity
- Predictability
- Reproducibility
- Mechanical strength
- Adequate 3D architecture
- High porosity and surface area,
- Osteo-cytological compatibility
- Low costs
- Defined bioactivity

The most frequently used strategy for regenerative bone therapy is to use a 3D composite that mimics bone composition, made by mineral CaP in the form of HA and collagen [46]. Thus, one of the most frequently used composites in bone defects repair is the combination of collagen and HA, which represents the closest compositional similarity to natural bone [7, 47–49]. Through different preparation techniques, detailed in following pages, the mechanical properties of collagen–HA composites can be enhanced [19].

Collagen is the natural ECM compound easy to purify and isolate from various animal species by chemical and enzymatic treatments. Collagen shows biodegradability, bioresorbability, high biocompatibility, hemostatic ability, no toxicity, low immunogenicity, a well-known structure, compliance with mechanical stability, reduced manufacturing costs, the possibility of being processed in various forms [42, 45, 50–52]. This natural soft polymer is one of the best candidates for being an organic part of the bone scaffold, proving the best results in tissue reconstruction research, and also its features recommend collagen as being a very attractive biomaterial for use in drug delivery systems (DDS) for the local treatment of the affected osseous tissues [36, 53, 54].

Hydroxyapatite is a major and essential component of natural bone [1]. For this reason, synthetic HA is one of the most widely used materials in bone defect repair and in oral and maxillofacial treatment because of the numerous advantages that make it suitable for use in composite scaffolds:

- (i) It can be combined with the existing osseous tissue through chemical bonds contributing to its regeneration.
- (ii) It has bioactivity, biocompatibility, stability, nontoxicity, non-immunogenicity, non-inflammatory properties, osteoconductivity, and controlled biodegradability.
- (iii) It is a good candidate for the delivery of a variety of pharmaceutical molecules [1, 9, 10, 15, 37, 39, 55–59].

A series of composite systems based on the association between collagen and HA with promising prospects for bone tissue regeneration were proposed [1, 3, 19, 60–62]. Moreover, to treat different osseous disorders, some drug or growth factors could be incorporated into the orthopedic and dental scaffolds. Collagen–bioceramic DDS are detailed in following paragraphs.

---

## **Biomaterials Used for Collagen–Bioceramic Composites**

### **Bioceramics**

Bioceramics are ceramic materials used to repair and replace the diseased or damaged parts of the skeletal tissue and to augment both hard and soft tissue [63]. Also, they are used in clinical practice as bone cements and bone graft substitutes. According to Mallick and Winnett [64] and Yamamuro [65] bioceramics can be divided into three categories:

- Inert (nonresorbable): alumina, silica, zirconia;
- Semi-inert (bioactive): calcium phosphate and glasses/glass ceramics;
- Bioresorbable: porous bioactive and new advanced ceramics.

### **Inert Bioceramics**

Alumina, zirconia, silica, and titania are the first-generation ceramics. They are widely used in medical applications because of their excellent mechanical properties for load-bearing.

### **Bioactive Bioceramics**

The class bioactive ceramics consists of several major groups: CaP and bioactive glasses/glass ceramics. Because of its compositional similarities to bone mineral, CaP is most widely used in orthopedics and dentistry [66]. Having excellent biocompatibility, bioactivity, biodegradability, and osteoconductive properties, CaP has been researched as the major component of scaffold material for bone tissue engineering [67–70]. The most common CaP-based ceramics are HA (Ca/P ratio = 1.67) and  $\beta$ -tricalcium phosphate ( $\beta$ -TCP; Ca/P ratio = 1.5). If the Ca/P is less than 1, the ceramics are very soluble and they cannot be used for biological implantation [63, 71].

Hydroxyapatite [Hap,  $\text{Ca}_{10}(\text{PO}_4)_6(\text{OH})_2$ ] is the main mineral constituent of the teeth and bone [66, 72]. HA is an osteoconductive material that exhibits a controlled degradation rate and combines with tissue by chemical bonding to form new bone tissue [63]. HA of natural origin is derived from corals or bovine bone [73, 74], but it is not pure, containing some trace elements such as Mg, Sr,  $\text{CO}_3$ , etc. Synthetic HA can be produced by classical methods including direct precipitation, hydrothermal techniques, hydrolysis of other CaP, or solid-state reaction [75].

Tricalcium phosphate [TCP,  $\text{Ca}_3(\text{PO}_4)_2$ ] is a biodegradable bioceramic that is soluble in media and can be used as degradable bone graft [63]. It has superior osteoconductivity, cellular adhesion, and mediation in accelerated differentiation

[76, 77]. B-TCP has higher solubility than HA, is gradually absorbed, and replaced with natural bone. It is processed using similar methods to HA and is used in obtaining completely biodegradable biomaterials [76, 77].

Bioactive glasses, amorphous silicates based on glass ceramics, were discovered by Larry Hench in 1969. According with Hench and Andersson [78], the first bioactive glass, BioGlass<sup>®</sup> consists of Na<sub>2</sub>O-CaO-SiO<sub>2</sub> glass with the addition of P<sub>2</sub>O<sub>5</sub>, B<sub>2</sub>O<sub>3</sub> and CaF<sub>2</sub>. The composition of glass can be adjusted and its degradation rate or solubility can be controlled. Glass ceramics are multiphase materials, manufactured from base glasses, using mechanisms of controlled nucleation and crystallization [79, 80]. A typical glass ceramic is apatite and wollastonite, while exhibiting bioactivity and fairly high mechanical strength [81]. Having a high level of bioactivity, the bioactive glasses are both osteoconductive and osteoinductive, favoring the formation of bone mineral-like phases [10].

### Bioresorbable Bioceramics

Bioresorbable ceramics are the third generation of bioceramics. They are gradually absorbed over time and allow newly formed bone tissue to grow [82].

### Collagen

Collagen is the main structural protein of most soft, loose, semi-rigid, and rigid connective tissues (skin, bone, tendon, basal membranes, etc.), mainly ensuring the structural integrity of the tissues [83]. Thirty percent of collagen is found in bone (reported to be dry matter) with glycoproteins, proteoglycans, and sialoproteins [12, 15, 84, 85].

Among the 29 types of collagen known and characterized to date, the most widely used as a biomaterial is type I collagen. Collagen is a natural, rod-type polymer consisting of 20 amino acids, arranged in a specific sequence, to form a unique conformational structure of a triple helix [86, 87]. Among the amino acids involved in the formation of the collagen molecule, the highest amount is glycine (Gly; 33 % of all amino acids), proline (Pro) and hydroxyproline (Hyp) (22 %), alanine (11 %), and glutamic acid and asparagine (12 %) [88]. The percentage composition of the amino acids of collagen is presented in Fig. 1.

Hydroxyproline is characteristic only of collagen and can be found in it at a relatively constant proportion of 9–10 %. The quantitative determination of hydroxyproline permits the collagen content in tissue to be calculated. Hydroxyproline provides stability to collagen, especially through intramolecular hydrogen bonds [89].

The sulfur-containing amino acids, cysteine and cysteine, are lacking in collagen and the aromatic amino acids (tryptophan and phenylalanine) are found in traces.

Collagen has a very complex structure, organized into four levels, called the primary, secondary, tertiary, and quaternary structures.

The primary structure is the linear sequence of amino acids bound covalently through peptide bonds to form the polypeptide chain. An  $\alpha$ -polypeptide chain



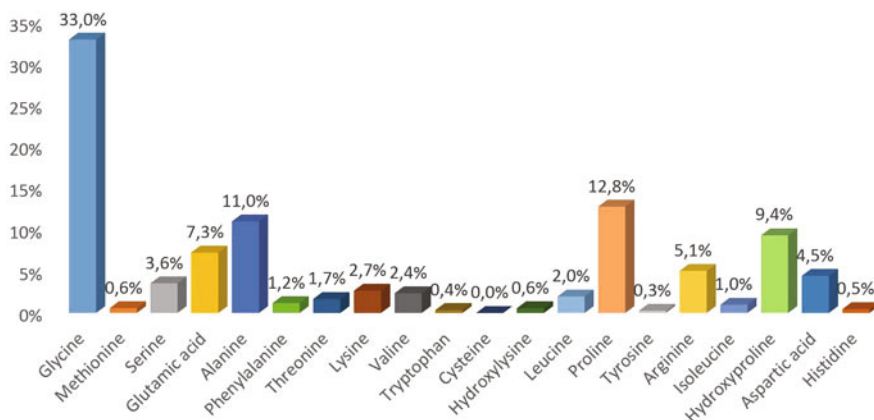


**Fig. 1** Composition of the amino acids in collagen [88]

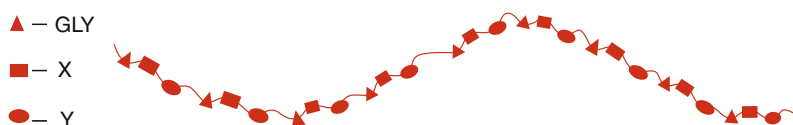


**Fig. 2** Model of the secondary structure of collagen

consists of about 1000–1100 amino acid residues arranged in a certain order (sequence).

The basic unit of collagen is the polypeptide consisting of a repeated sequence  $((\text{Gly}) - \text{X} - \text{Y})_n$ , where X is frequently Pro and Y hydroxyproline.

Research into the amino acids sequence from the  $\alpha$ -polypeptide chains that form collagen molecules showed that the chain contains two fundamentally different types of sequences:

- Helix-like, consisting of 1000–1050 amino acids, in which every third position is occupied by Gly, the smallest amino acid, allowing triple helix formation.
- Nonhelical, with the terminal regions NC1 or NC2, called telopeptides, which do not include Gly in every third position.

The tripeptide Gly – X – Y is found in one or more conformational blocks with different degrees of polymerization, depending on the type of collagen.

The secondary structure refers to the spatial arrangement of amino acids in a single  $\alpha$ -polypeptide chain. The sidechains of the main types of collagen have an  $\alpha$ -helix conformation (Fig. 2).

The structure of  $\alpha$ -helix is stabilized by hydrogen bonds involving a water molecule. There are many models that present the real conformation [90, 91].

The triple helix is specific to collagen molecules and represent the tertiary structure. The type I collagen molecule (tropocollagen) is an heterotrimer consisting

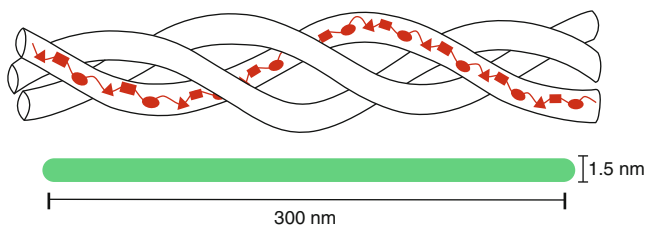


**Fig. 3** Model of the tertiary structure of collagen

of three polypeptide  $\alpha$  chains (two identical –  $\alpha 1$  and one different –  $\alpha 2$ ) twisted together from right to left around a common axis, forming a triple helix. The tropocollagen has a molecular weight of 285,000–300,000 Da, is 300 nm long, and 1.5 nm in diameter, as is schematically presented in Fig. 3.

The arrangement of the triple helix requires the presence of Gly in every third position of the chain, Gly being the only amino acid that can enter into the internal positions of the triple helix because of lower volumes caused by this single hydrogen atom. Also, triple helix formation is favored by the presence of Pro and Hyp in the X and Y positions because of rigid pyrrolidine rings that impose restrictions on rotation chains. Triple helix conformation is stabilized by hydrogen bonding between the constituent chains, involving water molecules and the hydroxyl groups of the Hyp, as well as other kinds of forces: Van der Waals, hydrophobic, and covalent [92, 93].

The quaternary structure represents the method of arrangement of the collagen molecule for fibrils, fibers, and finally conjunctive tissue formation.

Collagen molecules secreted by conjunctive tissues are assembled in cylindrical fibrils with uniform diameter, which vary at different stages of development between 5 and 200 nm.

Tropocollagen is assembled longitudinally and transversally by inter- and intramolecular bonds into microfibrils (4–8 collagen molecules) and then into fibrils. This periodic arrangement is characterized by the existence of gaps of 40 nm between successive molecules and by a periodicity of 67 nm (Fig. 4).

Type I collagen is the most abundant, representing about 80 % of all connective tissue. This is the type from which most of the information related to the collagen protein structure was obtained.

The stability of the quaternary structure is achieved, especially by intermolecular bonds, with hydrogen, with the participation of water molecules [94, 95], ionic, hydrophobic, and covalent. The last are established between collagen molecules aggregated in fibrils and fibrils and different constituents of connective tissue (noncollagenic protein, neutral carbohydrate, glycoproteins). Tissue maturation involves a considerable increase in the number of transversal bonds and the gradual formation of a tridimensional fibrous network [96].

Depending on the structural and functional characteristics, the types of collagen can be grouped into two classes: fibrillar and nonfibrillar. So far, 29 genetically distinct types of collagen have been identified [97, 98]. Types I, V, and XXIV fibrillar collagen and type XIII transmembrane collagen are found in bone tissue.

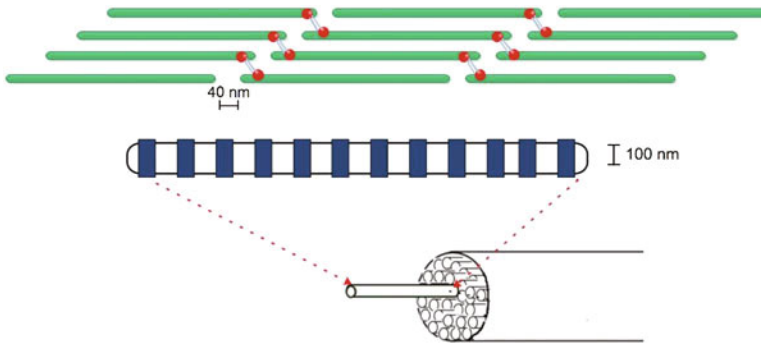


**Fig. 4** Supramolecular assembly of collagen molecules in quarter-staggered form

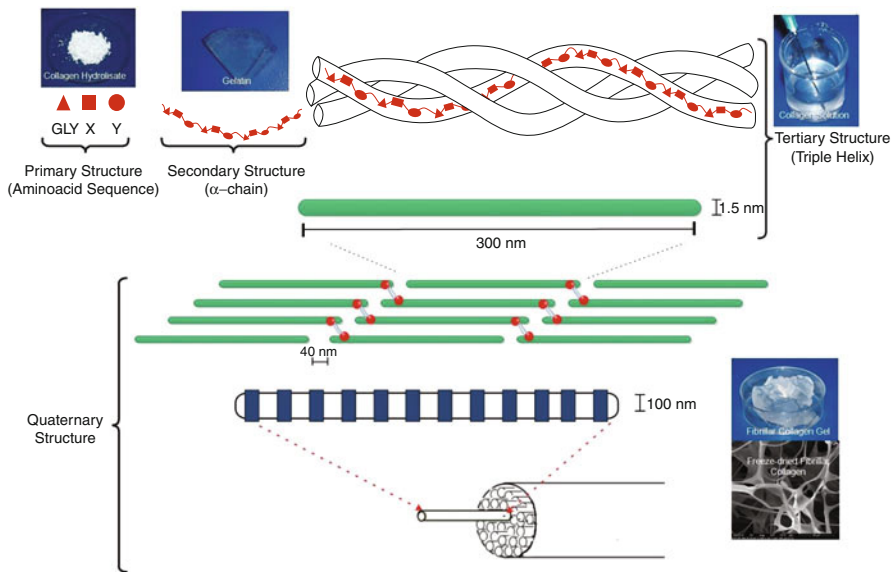


**Fig. 5** Collagen structures and the most common forms

Figure 5 presents the most common forms of type I collagen depending on the structural level. The basic form and their uses in composites are discussed in the next paragraph.

An important biological characteristic of collagen is biocompatibility, which is due to low toxicity and poor immunogenic responses. Also, collagen is weakly antigenic. Low antigenicity may be due to the presence of aromatic amino acids, particularly tyrosine. To reduce or eliminate the antigenicity of the collagen, the N-terminal regions of the polypeptide chains are removed during the extraction of collagen. As is shown in Fig. 5, collagen is often extracted as a gel or solution, the basic raw materials for obtaining a composite.

## Processing and Characterization of the Collagen–Bioceramic Composites

Collagen–bioceramic composites have some requirements to mimic the natural bone [99], such as:

- The chemical composition has to be as close to that of the natural bone as possible and to have well-defined pores and structure.
- The biodegradation has to be controllable, especially if the biomaterials are resorbable.
- The mechanical properties have to be strong enough for its function, without fragmentation of and damage to the surrounding tissues.
- Biocompatibility: nontoxic and non-immunological.
- A good response to the cells and tissues.
- Bioactivity and integration into the surrounding tissue.

Bone tissue, cortical or cancellous bone, was defined by Fernandez-Yague et al. [1] as “a nanocomposite 3D scaffold of nano-HA and type I collagen.” Starting from this hypothesis, collagen-based composites were developed with different compositions and formed to mimic the bone structure.

The living bone in the human skeletal system is composed of about 30 % collagen and 70 % bone minerals, by weight [10]. Trying to mimic bone composition, composites based on collagen and bone minerals were developed and characterized. Besides collagen (or gelatin) and HA/bioglass, other materials were added, such as glycosaminoglycan and growth factor (rhBMP-2) [100], phosphatidylserine [10], silk fibroin [7], chitosan and SiO<sub>2</sub> [29], carboxymethyl and chitosan [34], and to form a composite in the form of gels/hydrogels or the most frequent spongy form (matrices).

The most well-known methods for the preparation of HA–collagen composites are:

- In vitro collagen mineralization [101–106]
- Directly mixed to form composite gels
- Thermally triggered assembly of HA/collagen gels [38, 41]
- Drying of composite gel by free-drying or freeze-drying

One of the most frequently used methods of obtaining 3D composite matrices based on collagen and HA is the freeze-drying (lyophilization) process. An example of the freeze-drying process for obtaining composites based on collagen and minerals is presented in Fig. 6.

Suspension of HA/bioglass ceramic in collagen, cross-linked or uncross-linked, were freeze-dried for 48 h to obtain porous composites that mimic bone.

As Fig. 6 shows, the first step of freeze-drying is freezing. The suspension is frozen at  $-40\text{ }^{\circ}\text{C}$  for 8 h. The pore sizes can be modulated depending on the frozen temperature: the higher temperature, the larger the pore sizes. In the second step, the

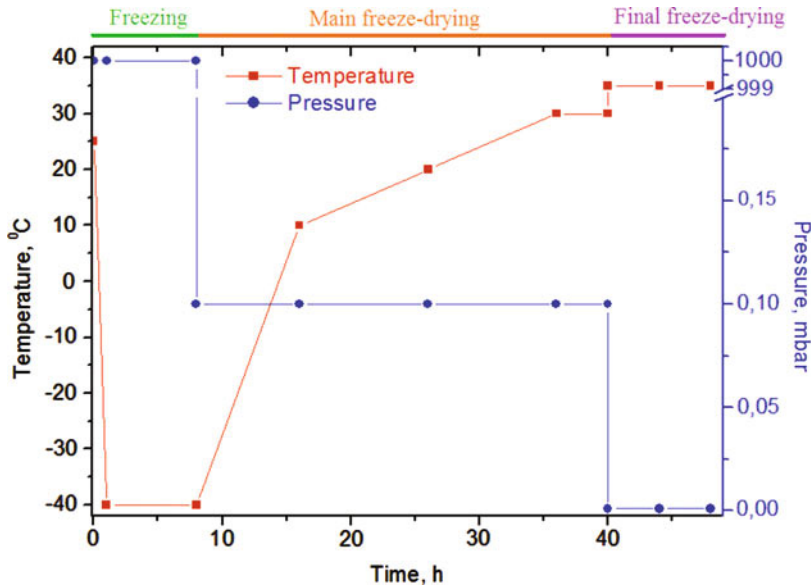


**Fig. 6** Diagram of freeze-drying collagen composites [107]

main freeze-drying process, the water is removed under pressure (0.12 mbar). The drying temperature is increased from  $-40\text{ }^{\circ}\text{C}$  to  $+10\text{ }^{\circ}\text{C}$  in the first 8 h, then to  $+20\text{ }^{\circ}\text{C}$  in the next 10 h, then to  $+30\text{ }^{\circ}\text{C}$  for the next 10 h, and maintained at  $30\text{ }^{\circ}\text{C}$  and 0.12 mbar for another 4 h until the water is removed.

In the last step, the final freeze-drying process, the sample is slightly warmed [19] at 0.001 mbar and  $35\text{ }^{\circ}\text{C}$  until dry.

Using this freeze-drying process on collagen:HA (25:75) cross-linked with glutaraldehyde, the porous composites presented in Fig. 7 were obtained.

The collagen/HA composites are then characterized by physical–chemical, mechanical, and biological properties.

The properties are dependent on the composition and structure of the composites. In Figs. 8 and 9 some scanning electron microscopy/energy dispersive X-ray analysis images of collagen/bioceramic composites are presented.

The pore size of the composites varies between 50 and  $200\text{ }\mu\text{m}$  and they decrease with increasing amounts of mineral materials in composites.

## Collagen–Bioceramic Composites Used as Drug Delivery Systems

A decisive step in the evolution of the field of bone and dental tissue engineering and a major advantage in HA/collagen 3D scaffold design implicitly consist of the fact that a biomimetic composite is considered both a structure that ensures optimal architecture for cell attachment, proliferation, migration, interaction,



**Fig. 7** Collagen/hydroxyapatite composites obtained by freeze-drying

differentiation, and organization, and a support that allows some drug release [9, 11, 14, 16, 108, 109].

Thus, in recent years the continuous development led to the attainment of some DDS that ensure drug release in a controlled manner for successful functional bone regeneration and restoration [9].

Drug delivery systems are defined as formulations able to deliver a drug safely and effectively by controlling the rate, the amount, the period, and the target location of drug release in the body to ensure the desired therapeutic effect [110–112]. The main purpose of a DDS is to maintain constant therapeutic levels, without reaching a toxic level, over a prolonged period, to favor bone healing [56, 57].

So far, different drugs have been incorporated into DDS to improve osseous therapy. Antibiotics and chemotherapeutic agents, analgesics, anti-inflammatories, and anticancer drugs are the most common in composites for bone disease treatment [9, 49, 56, 112, 113]. Among these drugs, special attention is given to antibiotics, as one of the most serious complications that can occur in the bone and periodontal regeneration process after different procedures is bacterial invasion and multiplication. This issue is even more serious for patients with immunosuppressive disorders, resulting in severely prolonged inflammatory disease, followed by poor bone healing, and, in severe cases, by bone destruction [1, 3, 36, 59, 113–118].

Infection of the bone (osteomyelitis) could have different causes: open fractures, open wound trauma after implantation or other sources of infection localized in various regions of the body [1, 13]. The treatment for the consequences of osseous and alveolar bone infection involves consistent financial costs and an increase in the duration of hospitalization, affecting the patient's quality of life [21, 23, 116]. Therefore, a first step in the improvement in osseous and dental tissue healing is the prevention and/or treatment of the infection from the affected site.

Bacterial contamination usually occurs within 48 h. The first 10 h are critical because bacteria at the lesion tissue level produce a biofilm that is resistant to antimicrobial agents. On the other hand, as the actual process of osseous and dental

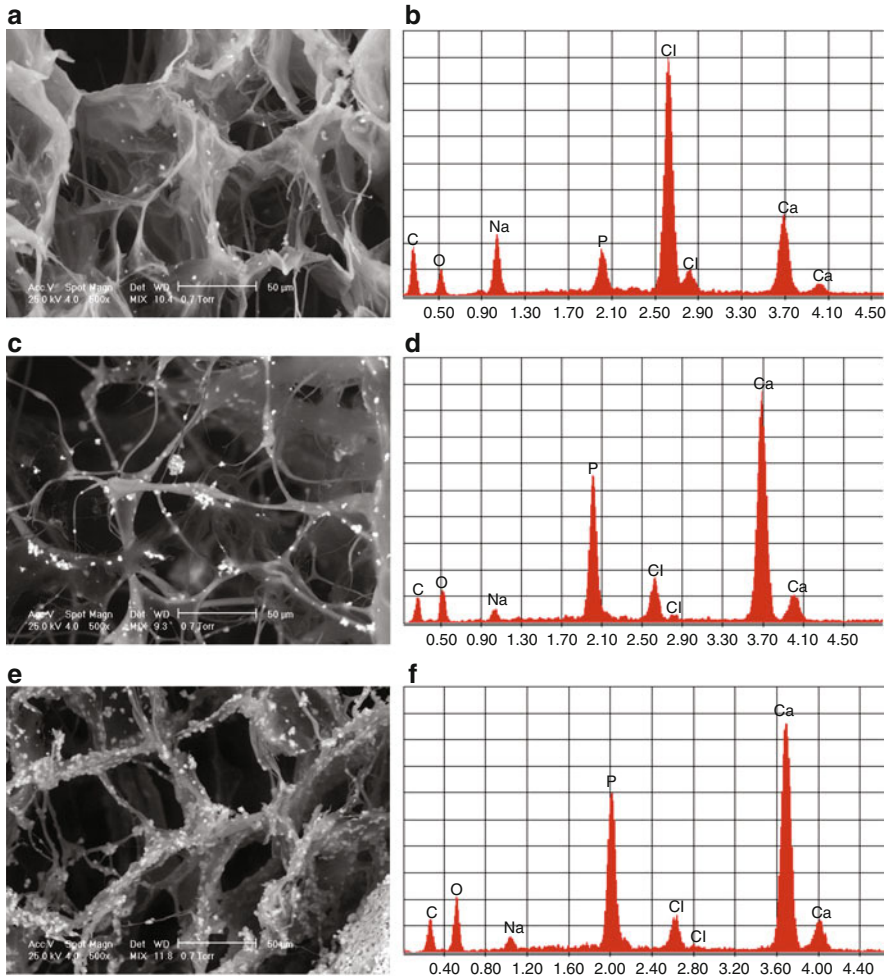


**Fig. 8** Scanning electron microscopy/energy dispersive X-ray analysis micrographs of collagen/HA (Coll/HA) composites: (a, b) Coll/HA – 75/25; (c, d) Coll/HA – 50/50; (e, f) Coll/HA – 25/75

tissue healing requires a long recovery period, longer-term protection against bacterial invasion is needed. The main means of the selective and effective elimination of pathogenic bacteria is the use of antimicrobial/antibiotic agents [13, 116, 119].

Topical antibiotic delivery systems for the prevention and/or treatment of infection at the osseous tissue level now constitute one of the most attractive and evolving topics of interest, offering several advantages compared with the conventional systemic route of administration (oral or intravenous): the avoidance of drug concentration fluctuations, overdose, systemic toxicity, and associated side effects, especially at the renal and liver levels, increased patient compliance, ensuring low bacterial resistance [36, 111, 112, 118]. Furthermore, local antibiotic release

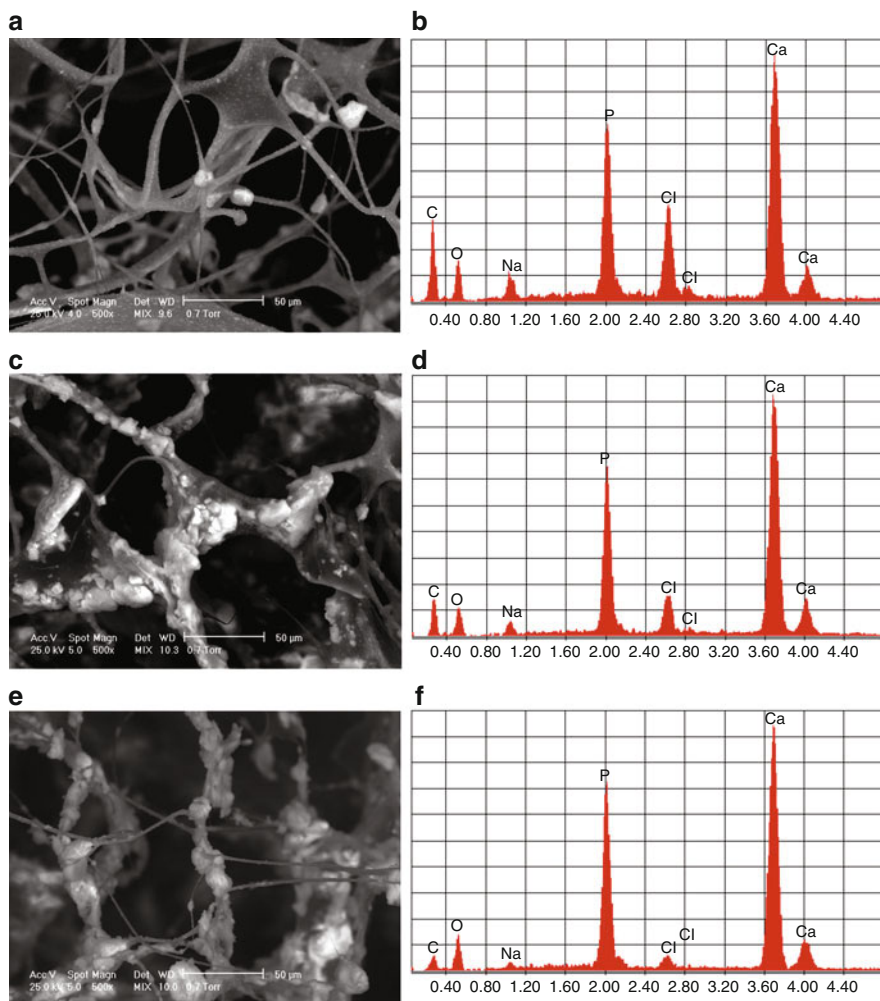


**Fig. 9** SEM/EDAX micrographs of collagen/beta tricalcium phosphate ( $\beta$ -TCP) composites: (a, b) Coll/ $\beta$ -TCP – 75/25; (c, d) Coll/ $\beta$ -TCP – 50/50; (e, f) Coll/ $\beta$ -TCP – 25/75

overcomes poor bone penetration of the drug administered systemically [40, 56, 120], the antibiotic delivery directly to the affected tissue, and in a controlled way, to maintain a sufficient and effective drug concentration at the infection site, being essential to controlling the proliferation rate of the pathogens [45, 111].

Common candidate antibiotics for local delivery systems in bone treatment are beta-lactams (cefalotin, cefazolin, cefuroxime), aminoglycosides (gentamicin, tobramycin), tetracyclines (tetracycline), lincosamide (clindamycin, lincomycin), macrolides (erythromycin), polymyxins (colistin), glycopeptides (vancomycin), quinolones (ciprofloxacin), used alone or combined [40, 113, 116, 121–124].



Among the antibiotics mentioned above, some of them, such as vancomycin [36, 125], were incorporated into collagen–HA composites, showing promising results for the treatment of an infection associated with bone defects.

Based on the clinical successes presented in the literature, an increasing number of orthopedic surgeons are using therapeutic agents for local antibiotic delivery [118, 126]. Limited clinical reports are available on collagen–gentamicin sponges and antibiotic-impregnated CaP [127].

Antibiotic release over time in a sustained and controlled manner is a very important prerequisite in the formulation of topical DDS [113, 119].

Nonetheless, challenges still exist in the release of therapeutic molecules at a clinical level. Thus, the importance of modeling and controlling the *in vitro* release kinetics of drugs from topical vehicles is highlighted by recent studies in this area [114, 128].

The release kinetics has to balance the advantage of reaching the therapeutical concentration with the disadvantage of the accumulation of toxic concentrations [43, 128]. In this way, the starting point in the biopharmaceutical evaluation of a drug incorporated in a topical form is the study of the *in vitro* drug release kinetics, which estimates the way it is released into the contact medium and the determination of the kinetic mechanism involved, in addition to the evaluation of some kinetic parameters that quantify the *in vitro* release from the designed systems [44, 56, 113].

Generally, for antibiotic topical composite forms, typical biphasic release profiles are recorded, with a marked effect of rapid drug release (the so-called burst release effect) followed by its slow, gradual release to ensure an adequate concentration at the administration site [57, 116, 119].

The burst release effect, a consequence of the rapid release of the drug from composite supports immediately after system contact with injured osseous tissue, ensures rapid bacteria diminution. On the other hand, a gradual release of the drug ensures the protection of osseous tissue against bacterial invasion that can occur during the longer period needed for healing [116].

Although such kinetics profiles are sought for the healing of infected bone when both an immediate and a long-term antimicrobial agent release are targeted, an issue of such formulations is that the rapid release effect is too pronounced during the first hours, with the risk of an significant amount of the drug being released before the infection is controlled [116, 119]. Thus, for the efficiency of infected bone defect healing, the modeling of drug release kinetics is followed, which can be accomplished in several ways:

- (i) Drug incorporation techniques
- (ii) The type of carrier used
- (iii) The way to obtain the carrier [56]

With regard to the drug incorporation technique, this can be retained on a composite support surface through physical adsorption [1, 14, 32], and in this case the burst release effect is significant [109], or through chemical immobilization [14, 109], inducing delayed drug release. Also, the vehicle in the delivery process

represents another important parameter that requires special attention in the design and development of topical formulations for the achievement of effective osteoactivity and controlled drug release [36, 57].

The manufacturing methods of topical composites modulate the drug release by the configuration of the carrier [14, 57] in different forms detailed in previous subchapters (injectable hydrogels, porous matrices, hydrogels, films, fibers).

To reduce the drug burst release effect and to ensure an extended and sustained drug release during the treatment to favor long-term bone healing, the improvements in topical delivery systems are focused on their formulation using various techniques that allow both gradual support degradation and slow drug release. In the particular case of antibiotic composites, one aspect that has to be considered is that antibiotic release that is too slow, at levels under the minimum inhibitory concentration, could determine bacterial resistance and, consequently, complicate the infection [116].

The latest development in the field of micro- and nanoparticulate systems offers the solution of drug incorporation in microcapsules or nanocarriers having the advantage of action on the affected area, avoiding the side effects on the non-affected cells. Thus, one of the most important current challenges for either the treatment or the prevention of difficult diseases is the design of various DDS that target different molecular mechanisms [32, 129, 130].

To ensure the gradual degradation of the composite support, different cross-linking techniques are used [19, 20], in addition to the design of complex structure vehicles in several layers having different physical–chemical and mechanical properties [14].

To investigate the drug release mechanism from different composites, including collagen–HA 3D scaffolds, one of the most frequently used kinetic models is the Power law model (Eq. 1):

$$\frac{m_t}{m_\infty} = k \cdot t^n \quad (1)$$

where  $m_t/m_\infty$  is the fraction of drug released at time  $t$ ,  $k$  is the kinetic constant reflecting the structural and geometrical properties of the polymeric system and the drug, and  $n$  the release exponent that can be related to the drug transport mechanism [43, 45, 113, 131, 132].

Two particular cases of the power law model are mentioned:

- (i)  $n = 1$  corresponding to the zero order model (the drug diffusion rate is much higher than the polymer relaxation rate, the amount of drug released being proportional to the release time)
- (ii)  $n = 0.5$ , corresponding to the Higuchi model (the drug diffusion rate is much lower than the polymer relaxation rate, the amount of drug released being proportional to the square root of the release time) [43]

Generally, owing to complex physico-chemical and biological processes that take place at the interaction between the composite support and the injured tissue, a

non-Fickian drug diffusion transport mechanism is recorded, drug release being simultaneously conducted through drug diffusion and composite support degradation [9, 122].

The local release principles and the aspects presented are also applicable to the other drug classes previously mentioned, which are incorporated into collagen–HA composites.

Currently, evolving attention is focused on the development of new topical DDS for the treatment and regeneration of different bone and alveolar defects, with many advantages compared with the conventional forms of dosage, such as enhanced bioavailability, lower toxicity, higher efficiency, and controlled and sustained release.

---

## Summary

In conclusion, 3D collagen–bioceramic composites obtained by freeze-drying mimic bone very well, being an alternative method to the hard tissue reconstruction of cortical and cancellous bone. An ideal bone composite needs to have a composition that is as close as possible to that of natural bone, well-defined pores and structure, good mechanical properties and biocompatibility, and the ability to degrade in a controllable way. Another trend in smart composite materials is to deliver active components (drug, growth factor) targeting an organ or tissue for a certain period of time. A successful strategy for hard tissue regeneration is bone tissue engineering, which requires a combination of appropriate scaffolding material, cell source, and culture environment to make scaffolds bioactive and to integrate them into the surrounding tissue.

---

## References

1. Fernandez-Yague MA, Abbah SA, McNamara L, Zeugolis DI, Pandit A, Biggs MJ (2015) Biomimetic approaches in bone tissue engineering: integrating biological and physico-mechanical strategies. *Adv Drug Deliv Rev* 84:1–29
2. Miranda SCCC, Silva GAB, Hell RCR, Martins MD, Alves JB, Goes AM (2011) Three-dimensional culture of rat BMMSCs in a porous chitosan-gelatin scaffold: a promising association for bone tissue engineering in oral reconstruction. *Arch Oral Biol* 56(1):1–15
3. Sowmya S, Bumgardener JD, Chennazhi KP, Nair SV, Jayakumar R (2013) Role of nano-structured biopolymers and bioceramics in enamel, dentin and periodontal tissue regeneration. *Prog Polym Sci* 38(s 10–11):1748–1772
4. Haulica I (1999) *Human physiology*, 2nd edn. Medical Publishing House, Bucharest
5. Pati F, Song TH, Rijal G, Jang J, Kim SW, Cho DW (2015) Ornamenting 3D printed scaffolds with cell-laid extracellular matrix for bone tissue regeneration. *Biomaterials* 37:230–241
6. Kundu B, Rajkhowa R, Kundu SC, Wang X (2013) Silk fibroin biomaterials for tissue regenerations. *Adv Drug Deliv Rev* 65(4):457–470
7. Chen L, Hu J, Ran J, Shen X, Tong H (2014) Preparation and evaluation of collagen-silk fibroin/hydroxyapatite nanocomposites for bone tissue engineering. *Int J Biol Macromol* 65:1–7

8. Pascu EI, Stokes J, McGuinness GB (2013) Electrospun composites of PHBV, silk fibroin and nano-hydroxyapatite for bone tissue engineering. *Mater Sci Eng C Mater Biol Appl* 33(8):4905–4916
9. Rogina A (2014) Electrospinning process: versatile preparation method for biodegradable and natural polymers and biocomposite systems applied in tissue engineering and drug delivery. *Appl Surf Sci* 296:221–230
10. Wu S, Liu X, Yeung KWK, Liu C, Yang X (2014) Biomimetic porous scaffolds for bone tissue engineering. *Mater Sci Eng* 80:1–36
11. Venkatesan J, Bhatnagar I, Manivasagan P, Kang KH, Kim SK (2015) Alginate composites for bone tissue engineering: a review. *Int J Biol Macromol* 72:269–281
12. Maas M, Hess U, Rezwan K (2014) The contribution of rheology for designing hydroxyapatite biomaterials. *Curr Opin Colloid Interface Sci* 19(6):585–593
13. Liu Y, Lim J, Teoh SH (2013) Review: development of clinically relevant scaffolds for vascularised bone tissue engineering. *Biotechnol Adv* 31(5):688–705
14. Lee SH, Shin H (2007) Matrices and scaffolds for delivery of bioactive molecules in bone and cartilage tissue engineering. *Adv Drug Deliv Rev* 59(4–5):339–359
15. Swetha M, Sahithi K, Moorthi A, Srinivasan N, Ramasamy K, Selvamurugan N (2010) Biocomposites containing natural polymers and hydroxyapatite for bone tissue engineering. *Int J Biol Macromol* 47(1):1–4
16. Bose S, Roy M, Bandyopadhyay A (2012) Recent advances in bone tissue engineering scaffolds. *Trends Biotechnol* 30(10):546–554
17. <http://www.reborne.org/>
18. Kim HJ, Kim UJ, Kim HS, Li C, Wada M, Leisk GG, Kaplan DL (2008) Bone tissue engineering with premineralized silk scaffolds. *Bone* 42(6):1226–1234
19. Puppi D, Chiellini F, Piras AM, Chiellini E (2010) Polymeric materials for bone and cartilage repair. *Prog Polym Sci* 35(4):403–440
20. Amruthwar SS, Janorkar AV (2013) In vitro evaluation of elastin-like polypeptide-collagen composite scaffold for bone tissue engineering. *Dent Mater* 29(2):211–220
21. Fu SZ, Ni P, Wang BY, Chu BY, Zheng L, Luo F, Luo JC, Qian ZY (2012) Injectable and thermo-sensitive PEG-PCL-PEG copolymer/collagen/n-HA hydrogel composite for guided bone regeneration. *Biomaterials* 33(19):4801–4809
22. Nadeem D, Kiamehr M, Yang X, Su B (2013) Fabrication and in vitro evaluation of a sponge-like bioactive-glass/gelatin composite scaffold for bone tissue engineering. *Mater Sci Eng C Mater Biol Appl* 33(5):2669–2678
23. Shrivats AR, McDermott MC, Hollinger JO (2014) Bone tissue engineering: state of the union. *Drug Discov Today* 19(6):781–786
24. Brown JL, Kumbhar SG, Laurencin CT (2013) Bone tissue engineering. In: Ratner BD, Hoffman AS, Schoen FJ, Lemons JE (eds) *Biomaterials science: an introduction to materials in medicine*, 3rd edn. Academic Press/Elsevier, Amsterdam, Nederland
25. Shrivats AR, Alvarez P, Schutte L, Hollinger JO (2014) Bone regeneration. In: Lanza R, Langer R, Vacanti J (eds) *Principles of tissue engineering*, 4th edn. Academic Press/Elsevier, London, UK
26. Bohner M (2010) Resorbable biomaterials as bone graft substitutes. *Mater Today* 13(1–2):24–30
27. You Z, Bi X, Fan X, Wang Y (2012) A functional polymer designed for bone tissue engineering. *Acta Biomater* 8(2):502–510
28. Venkatesan J, Pallela R, Bhatnagar I, Kim SK (2012) Chitosan-amylopectin/hydroxyapatite and chitosan-chondroitin sulphate/hydroxyapatite composite scaffolds for bone tissue engineering. *Int J Biol Macromol* 51(5):1033–1042
29. Kavya KC, Jayakumar R, Nair S, Chennazhi KP (2013) Fabrication and characterization of chitosan/gelatin/nSiO<sub>2</sub> composite scaffold for bone tissue engineering. *Int J Biol Macromol* 59:255–263

30. Oryan A, Alidadi S, Moshiri A, Maffulli N (2014) Bone regenerative medicine: classic options, novel strategies, and future directions. *J Orthop Surg Res* 9(1):18
31. Sajesh KM, Jayakumar R, Nair SV, Chennazhi KP (2013) Biocompatible conducting chitosan/poly pyrrole-alginate composite scaffold for bone tissue engineering. *Int J Biol Macromol* 62:465–471
32. Pérez RA, Won JE, Knowles JC, Kim HW (2013) Naturally and synthetic smart composite biomaterials for tissue regeneration. *Adv Drug Deliv Rev* 65(4):471–496
33. Fricain JC, Schlaubitz S, Le Visage C, Arnault I, Derkaoui SM, Siadous R, Catros S, Lalande C, Bareille R, Renard M, Fabre T, Cornet S, Durand M, Léonard A, Sahraoui N, Letourneur D, Amédée J (2013) A nano-hydroxyapatite – pullulan/dextran polysaccharide composite macroporous material for bone tissue engineering. *Biomaterials* 34(12):2947–2959
34. Mishra D, Bhunia B, Banerjee I, Datta P, Dhara S, Maiti TK (2011) Enzymatically crosslinked carboxymethyl–chitosan/gelatin/nano-hydroxyapatite injectable gels for in situ bone tissue engineering application. *Mater Sci Eng C* 31(7):1295–1304
35. Bliley JM, Marra KG (2015) Polymeric biomaterials as tissue scaffolds. In: Vishwakarma A, Sharpe P, Songtao S, Ramalingam M (eds) *Stem cell biology and tissue engineering in dental sciences*. Academic Press/Elsevier, London, UK
36. Lian X, Liu H, Wang X, Xu S, Cui F, Bai X (2013) Antibacterial and biocompatible properties of vancomycin-loaded nano-hydroxyapatite/collagen/poly(lactic acid) bone substitute. *Prog Nat Sci* 23(6):549–556
37. Simon D, Manuel S, Varma H (2013) Novel nanoporous bioceramic spheres for drug delivery application: a preliminary in vitro investigation. *Oral Surg Oral Med Oral Pathol Oral Radiol* 115(3):e7–e14
38. Kucharska M, Butruk B, Walenko K, Brynk T, Ciach T (2012) Fabrication of in-situ foamed chitosan/ $\beta$ -TCP scaffolds for bone tissue engineering application. *Mater Lett* 85:124–127
39. Bellucci D, Sola A, Gazzarri M, Chiellini F, Cannillo V (2013) A new hydroxyapatite-based biocomposite for bone replacement. *Mater Sci Eng C Mater Biol Appl* 33(3):1091–1101
40. Tian B, Tang S, Wang CD, Wang WG, Wu CL, Guo YJ, Guo YP, Zhu ZA (2014) Bactericidal properties and biocompatibility of a gentamicin-loaded  $\text{Fe}_3\text{O}_4$ /carbonated hydroxyapatite coating. *Colloid Surface B* 123:403–412
41. Wahl DA, Czernuszka JT (2006) Collagen-hydroxyapatite composites for hard tissue repair. *Eur Cell Mater* 11:43–56
42. Albu MG (2011) *Collagen gels and matrices for biomedical applications*. Lambert Academic Publishing, Saarbrücken
43. Albu MG, Titorencu I, Ghica MV (2011) Collagen-based drug delivery systems for tissue engineering. In: Pignatello R (ed) *Biomaterials applications for nanomedicine*. Intech Open Access Publisher, Rijeka
44. Ghica MV, Albu MG, Leca M, Popa L, Moisescu S (2011) Design and optimization of some collagen-minocycline based hydrogels potentially applicable for the treatment of cutaneous wounds infections. *Pharmazie* 66(11):853–861
45. Ghica MV, Albu MG, Popa L, Moisescu S (2013) Response surface methodology and Taguchi approach to assess the combined effect of formulation factors on minocycline delivery from collagen sponges. *Pharmazie* 68(5):340–348
46. Oliveira SM, Ringshia RA, Legeros RZ, Clark E, Yost MJ, Terracio L, Teixeira CC (2010) An improved collagen scaffold for skeletal regeneration. *J Biomed Mater Res Part A* 94(2):371–379
47. Zhou CC, Ye XJ, Fan YJ, Qing FZ, Chen HJ, Zhang XD (2014) Synthesis and characterization of CaP/Col composite scaffolds for load-bearing bone tissue engineering. *Composites* 62:242–248
48. Asran AS, Henning S, Michler GH (2010) Polyvinyl alcohol–collagen–hydroxyapatite biocomposite nanofibrous scaffold: mimicking the key features of natural bone at the nano-scale level. *Polymer* 51(4):868–876

49. Bose S, Tarafder S (2012) Calcium phosphate ceramic systems in growth factor and drug delivery for bone tissue engineering: a review. *Acta Biomater* 8(4):1401–1421
50. Coelho JF, Ferreira PC, Alves P, Cordeiro R, Fonseca AC, Gois JR, Gil MH (2010) Drug delivery systems: advanced technologies potentially applicable in personalized treatments. *EPMA J* 1(1):164–209
51. Liu C, Shen SZ, Han Z (2011) Surface wettability and chemistry of ozone perfusion processed porous collagen scaffold. *J Bionic Eng* 8(3):223–233
52. Zhang L, Li K, Xiao W, Zheng L, Xiao Y, Fan H, Zhang X (2011) Preparation of collagen–chondroitin sulfate–hyaluronic acid hybrid hydrogel scaffolds and cell compatibility in vitro. *Carbohydr Polym* 84(1):118–125
53. Glowacki J, Mizuno S (2008) Collagen scaffolds for tissue engineering. *Biopolymers* 89(5):338–344
54. Friess W (1998) Collagen-biomaterial for drug delivery. *Eur J Pharm Biopharm* 45(2):113–136
55. Wang W, Shi DL, Lian J, Guo Y, Liu G, Wang L, Ewing RC (2006) Luminescent hydroxylapatite nanoparticles by surface functionalization. *Appl Phys Lett* 89(18):183106
56. Ginebra MP, Traykova T, Planell JA (2006) Calcium phosphate cements as bone drug delivery systems: a review. *J Control Release* 113(2):102–110
57. Gu L, He X, Wu Z (2014) Mesoporous hydroxyapatite: preparation, drug adsorption, and release properties. *Mater Chem Phys* 148(s1–2):153–158
58. Cao T, Tang W, Zhao J, Qin L, Lan C (2014) A novel drug delivery carrier based on  $\alpha$ -eleostearic acid grafted hydroxyapatite composite. *J Bionic Eng* 11(1):125–133
59. Gentile P, Bellucci D, Sola A, Mattu C, Cannillo V, Ciardelli G (2015) Composite scaffolds for controlled drug release: role of the polyurethane nanoparticles on the physical properties and cell behaviour. *J Mech Behav Biomed Mater* 44:53–60
60. Vozzi G, Corallo C, Carta S, Fortina M, Gattazzo F, Galletti M, Giordano N (2014) Collagen-gelatin–genipin–hydroxyapatite composite scaffolds colonized by human primary osteoblasts are suitable for bone tissue engineering applications: in vitro evidences. *J Biomed Mater Res A* 102(5):1415–1421
61. Gleeson JP, Plunkett NA, O’Brien FJ (2010) Addition of hydroxyapatite improves stiffness, interconnectivity and osteogenic potential of a highly porous collagen-based scaffold for bone tissue regeneration. *Eur Cell Mater* 20:218–230
62. Liao S, Watari F, Zhu Y, Uo M, Akasaka T, Wang W, Xu G, Cui F (2007) The degradation of the three layered nano-carbonated hydroxyapatite/collagen/PLGA composite membrane in vitro. *Dent Mater* 23(9):1120–1128
63. Huang J, Best S (2014) Ceramic biomaterials for tissue engineering. In: Boccaccini AR, Ma PX (eds) *Tissue engineering using ceramics and polymers*, 2nd edn. Woodhead Publishing/Elsevier, Burlington, UK
64. Mallick KK, Winnett J (2014) 3D bioceramic foams for bone tissue engineering. In: Mallick K (ed) *Bone substitute biomaterials*. Woodhead Publishing/Elsevier, Cambridge, UK
65. Yamamuro T (2004) Bioceramics. In: Poitout DG (ed) *Biomechanics and biomaterials in orthopedics*. Springer, London, UK
66. Bose S, Tarafder S, Bandyopadhyay A (2015) Hydroxyapatite coatings for metallic implants. In: *Hydroxyapatite (Hap) for biomedical applications*. Woodhead Publishing/Elsevier, Cambridge, UK
67. Rezwani K, Chen QZ, Blaker JJ, Boccaccini AR (2006) Biodegradable and bioactive porous polymer/inorganic composite scaffolds for bone tissue engineering. *Biomaterials* 27(18):3413–3431
68. Zhou CC, Ye XJ, Fan YJ, Qing FZ, Chen HJ, Zhang XD (2014) Synthesis and characterization of CaP/Col composite scaffolds for load-bearing bone tissue engineering. *Compos B: Eng* 62:242–248
69. Hench LL, Polak JM (2002) Third-generation biomedical materials. *Science* 295(5557):1014–1017

70. Yu XZ, Cai S, Xu GH, Zhou W, Wang DM (2009) Low temperature fabrication of high strength porous calcium phosphate and the evaluation of the osteoconductivity. *J Mater Sci Mater Med* 20(10):2025–2034
71. Aoki H (1991) Science and medical applications of hydroxyapatite. JAAS, Tokyo
72. Bose S, Saha SK (2003) Synthesis and characterization of hydroxyapatite nanopowders by emulsion technique. *Chem Mater* 15:4464–4469
73. Rahaman MN (2014) Bioactive ceramics and glasses for tissue engineering. In: Boccaccini AR, Ma PX (eds) *Tissue engineering using ceramics and polymers*, 2nd edn. Woodhead Publishing/Elsevier, Burlington, UK
74. LeGeros RZ (2002) Properties of osteoconductive biomaterials: calcium phosphates. *Clin Orthop Relat Res* 395:81–98
75. Agrawal K, Singh G, Puri D, Prakash S (2011) Synthesis and characterization of hydroxyapatite powder by sol–gel method for biomedical application. *J Min Mater Charact Eng* 10(8):727–734
76. Arahira T, Matsuya S, Todo M (2015) Development and characterization of a novel porous  $\beta$ -TCP scaffold with a three-dimensional PLLA network structure for use in bone tissue engineering. *Mater Lett* 152:148–150
77. Algul D, Sipahi H, Aydin A, Kelleci F, Ozdatli S, Yener FG (2015) Biocompatibility of biomimetic multilayered alginate–chitosan/ $\beta$ -TCP scaffold for osteochondral tissue. *Int J Biol Macromol* 79:363–369
78. Hench LL, Andersson OH (1993) Bioactive glasses. In: Hench LL, Wilson J (eds) *An introduction to bioceramics*. World Scientific, Singapore
79. Kokubo T (1991) Bioactive glass ceramics: properties and applications. *Biomaterials* 12:155–163
80. Heikkilä JT, Aho AJ, Kangasniemi I, Yli-Urpo A (1996) Polymethylmethacrylate composites: disturbed bone formation at the surface of bioactive glass and hydroxyapatite. *Biomaterials* 17:1755–1760
81. Kokubo T, Ito S, Sakka S, Yamamuro T (1986) Formation of a high-strength bioactive glass-ceramic in the system MgO–CaO–SiO<sub>2</sub>–P<sub>2</sub>O<sub>5</sub>. *J Mater Sci* 21:536–540
82. Dorozhkin SV (2011) Medical application of calcium orthophosphate bioceramics. *BIO* 1:1–51
83. Ramachandran GN (1967) Structure of collagen at the molecular level. In: Ramachandran GN (ed) *Treatise on collagen*. Academic, London
84. Prockop DJ, Kivirikko KI (1995) Collagens: molecular biology, diseases, and potential for therapy. *Annu Rev Biochem* 64:403–434
85. Uitto J, Pulkkinen L, Chu ML (1999) Collagen. In: Freedberg IM (ed) *Dermatology in general medicine*. McGraw-Hill, New York
86. Trandafir V, Popescu G, Albu MG, Iovu H, Georgescu M (2007) Bioproduse pe bază de collagen. *Editura Ars Docendi*, Bucharest
87. Nair LS, Laurencin CT (2007) Biodegradable polymers as biomaterials. *Prog Polym Sci* 32:762–798
88. Albu MG (2009) Collagen gels and matrices with different degree of hydration and quasisolid structure for biomedical applications. Doctoral thesis, University of Bucharest, Bucharest
89. Bhat SV (2002) *Biomaterials*. Kluwer, Amsterdam
90. Fraser RDB, MacRae TP, Miller A, Suzuki E (1983) Molecular conformation and packing in collagen fibrils. *J Mol Biol* 167:497–521
91. Brodsky B, Tanaka S (1988) X-ray diffraction as a tool for studying collagen structure. In: Nimni M (ed) *Collagen*, vol 1. CRC Press, New York
92. Burjanadze TV (1992) Thermodynamic substantiation of water-bridged collagen structure. *Biopolymers* 32:941–949
93. Bella J, Brodsky B, Berman HN (1995) Hydration structure of a collagen peptide. *Structure* 3:893–906

94. Kang AH (1972) Studies on the location of intermolecular cross-links in collagen. Isolation of a CNBr peptide containing hydroxylysionorleucine. *Biochemistry* 11:1828–1835
95. Murphy G, Docherty AJP (1988) Molecular studies on the connective tissue metalloproteinases and their inhibitor. In: Glaucant AM (ed) *The control of tissue damage*. Elsevier, Amsterdam, Nederland
96. Von der Mark K (1999) Structure, biosynthesis and gene regulation of collagen in cartilage and bone. In: *Dynamics of bone and cartilage, metabolism*. Academic, Orlando
97. Myllyharju J, Kivirikko KI (2001) Collagen and collagen-related diseases. *Ann Med* 33:7–21
98. Sato K, Yomogida K, Wada T, Yoriyuzi T, Nishimune Y, Hosokawa N, Nagata K (2002) Type XXVI collagen, a new member of the collagen family, is specifically expressed in testis and ovary. *J Biol Chem* 277:37678–37684
99. Zhao X (2011) Bioactive materials in orthopaedics. In: Zhao X, Courtney JM, Qian H (eds) *Bioactive materials in medicine*. Woodhead publishing series in biomaterials. Elsevier, Edinburgh, UK
100. Lyons FG, Gleeson JP, Partap S, Coghlan K, O'Brien FJ (2014) Novel microhydroxyapatite particles in a collagen scaffold: a bioactive bone void filler? *Clin Orthop Relat Res* 472(4):1318–1328
101. Fikai A, Andronesu E, Voicu G, Ghitulica C, Fikai D (2010) The influence of collagen support and ionic species on the morphology of collagen/hydroxyapatite composite materials. *Mater Charact* 61(4):402–407
102. Fikai A, Andronesu E, Voicu G, Manzu D, Fikai M (2009) Layer by layer deposition of hydroxyapatite onto the collagen matrix. *Mater Sci Eng C* 29(7):2217–2220
103. Fikai A, Andronesu E, Voicu G, Ghitulica C, Vasile BS, Fikai D, Trandafir V (2010) Self-assembled collagen/hydroxyapatite composite materials. *Chem Eng J* 160(2):794–800
104. Fikai M, Andronesu E, Fikai D, Voicu G, Fikai A (2010) Synthesis and characterization of COLL–PVA/HA hybrid materials with stratified morphology. *Colloid Surf B: Biointerface* 81(2):614–619
105. Fikai A, Albu MG, Birsan M, Sonmez M, Fikai D, Trandafir V, Andronesu E (2013) Collagen hydrolysate based collagen/hydroxyapatite composite materials. *J Mol Struct* 1037:154–159
106. Fikai A, Andronesu E, Trandafir V, Ghitulica C, Voicu G (2010) Collagen/hydroxyapatite composite obtained by electric field orientation. *Mater Lett* 64(4):541–544
107. Marin S, Marin MM, Ene A-M, Türker IK, Chelaru K, Albu MG, Ghica MV (2014) Collagen-doxycycline spongy forms for infected tissues treatment. In: *Proceedings of ICAMS 2014 – 5th international conference advance material systems*, Bucharest, Romania, pp 249–254
108. Groeneveld EH, Van den Bergh JP, Holzmann P, ten Bruggenkate CM, Tuinzing DB, Burger EH (1999) Mineralization processes in demineralized bone matrix grafts in human maxillary sinus floor elevation. *J Biomed Mater Res* 48(4):393–402
109. Zhang Z, Hu J, Ma PX (2012) Nanofiber-based delivery of bioactive agents and stem cells to bone sites. *Adv Drug Deliv Rev* 64(12):1129–1141
110. Jain KK (2008) Drug delivery systems – an overview. *Methods Mol Biol* 437:1–50
111. Manzano M, Vallet-Regí M (2012) Revisiting bioceramics: bone regenerative and local drug delivery systems. *Prog Solid State Chem* 40(3):17–30
112. Arcos D, Vallet-Regí M (2013) Bioceramics for drug delivery. *Acta Mater* 61(3):890–911
113. Hesaraki S, Moztarzadeh F, Nezafati N (2009) Evaluation of a bioceramic-based nanocomposite material for controlled delivery of a non-steroidal anti-inflammatory drug. *Med Eng Phys* 31(10):1205–1213
114. Peel T, May D, Buising K, Thursky K, Slavin M, Choong P (2014) Infective complications following tumour endoprosthesis surgery for bone and soft tissue tumours. *Eur J Surg Oncol* 40(9):1087–1094
115. Ordikhani F, Simchi A (2014) Long-term antibiotic delivery by chitosan-based composite coatings with bone regenerative potential. *Appl Surf Sci* 317:56–66



116. Zilberman M, Elsner JJ (2008) Antibiotic-eluting medical devices for various applications. *J Control Release* 130(3):202–215
117. Zhang Y, Zhu J, Wang Z, Zhou Y, Zhang X (2015) Constructing a 3D-printable, bioceramic sheathed articular spacer assembly for infected hip arthroplasty. *J Med Hypotheses Ideas* 9(1):13–19
118. Soundrapandian C, Mahato A, Kundu B, Datta S, Sa B, Basu D (2014) Development and effect of different bioactive silicate glass scaffolds: in vitro evaluation for use as a bone drug delivery system. *J Mech Behav Biomed Mater* 40:1–12
119. Hickok NJ, Shapiro IM (2012) Immobilized antibiotics to prevent orthopaedic implant infections. *Adv Drug Deliv Rev* 64(12):1165–1176
120. Emanuel N, Rosenfeld Y, Cohen O, Applbaum YH, Segal D, Barenholz Y (2012) A lipid-and-polymer-based novel local drug delivery system – BonyPid™: from physicochemical aspects to therapy of bacterially infected bones. *J Control Release* 160(2):353–361
121. Campoccia D, Montanaro L, Speziale P, Arciola CR (2010) Antibiotic-loaded biomaterials and the risks for the spread of antibiotic resistance following their prophylactic and therapeutic clinical use. *Biomaterials* 31(25):6363–6377
122. Stewart S, Bryant SJ, Ahn J, Hankenson KD (2015) Bone regeneration. In: Atala A, Allickson J (eds) *Translational regenerative medicine*. Academic Press/Elsevier, Amsterdam, Nederland
123. Hake ME, Young H, Hak DJ, Stahel PF, Hammerberg EM, Mauffrey C (2015) Local antibiotic therapy strategies in orthopaedic trauma: practical tips and tricks and review of the literature. *Injury* 46(8):1447–1456
124. Nandi SK, Mukherjee P, Roy S, Kundu B, De DK, Basu D (2009) Local antibiotic delivery systems for the treatment of osteomyelitis – a review. *Mater Sci Eng C* 29(8):2478–2485
125. Lian X, Mao K, Liu X, Wang X, Cui F (2015) In vivo osteogenesis of vancomycin loaded nanohydroxyapatite/collagen/calcium sulfate composite for treating infectious bone defect induced by chronic osteomyelitis. *J Nanomater.* article ID 261492
126. Moojen DJ, Hentenaar B, Charles Vogely H, Verbout AJ, Castelein RM, Dhert WJ (2008) In vitro release of antibiotics from commercial PMMA beads and articulating hip spacers. *J Arthroplasty* 23(8):1152–1156
127. Tamilvanan S, Venkateshan N, Ludwig A (2008) The potential of lipid- and polymer-based drug delivery carriers for eradicating biofilm consortia on device-related nosocomial infections. *J Control Release* 128(1):2–22
128. Ghica MV (2010) Physico-chemical and biopharmaceutical elements of semisolid systems with topical action. Applications to indomethacin hydrogels. Printech Publishing House, Bucharest
129. Fischer KE, Alemán BJ, Tao SL, Hugh Daniels R, Li EM, Bünger MD, Nagaraj G, Singh P, Zettl A, Desai TA (2009) Biomimetic nanowire coatings for next generation adhesive drug delivery systems. *Nano Lett* 9(2):716–720
130. Vivero-Escoto JL, Slowing II, Wu CW, Lin VSY (2009) Photoinduced intracellular controlled release drug delivery in human cells by gold-capped mesoporous silica nanosphere. *J Am Chem Soc* 131(10):3462–3463
131. Phaechamud T, Charoentearaboon J (2008) Antibacterial activity and drug release of chitosan sponge containing doxycycline hyclate. *AAPS Pharm Sci Tech* 9(3):829–835
132. Sung JH, Hwang MR, Kim JO, Lee JH, Kim YI, Kim JH, Chang SW, Jin SG, Kim JA, Lyoo WS, Han SS, Ku SK, Yong CS, Choi HG (2010) Gel characterisation and in vivo evaluation of minocycline-loaded wound dressing with enhanced wound healing using polyvinyl alcohol and chitosan. *Int J Pharm* 392(1–2):232–240

Yaping Ding, Marina T. Souza, Wei Li, Dirk W. Schubert,  
Aldo R. Boccaccini, and Judith A. Roether

## Contents

Introduction .....	326
Composites as Useful Materials for Tissue Engineering .....	329
Development of Bioactive Glass–Biopolymer Composites .....	330
Biocomposite Microspheres .....	330
Composites from Solvent Casting-Particulate Leaching Process .....	333
Electrospun Composite Fibers .....	335
Composite Scaffolds by Freeze-Drying .....	341
Rapid Prototyping .....	343
Summary .....	350
References .....	351

---

## Abstract

Tissue engineering (TE) is a biomedical field in continuous expansion. However, there are still many challenges to be tackled. The further development of TE approaches requires interdisciplinary interaction and collaboration among various research areas with a notable contribution expected from biomaterials science. In the last couple of decades, significant advances in the development of biomaterial-based scaffolds for hard and soft tissue regeneration have been accomplished, including the manufacture of biocomposites that combine natural

---

Y. Ding • D.W. Schubert • J.A. Roether (✉)

Institute of Polymer Materials, University of Erlangen-Nuremberg, Erlangen, Germany  
e-mail: [yaping.ding@fau.de](mailto:yaping.ding@fau.de); [dirk.schubert@fau.de](mailto:dirk.schubert@fau.de); [judith.roether@ww.uni-erlangen.de](mailto:judith.roether@ww.uni-erlangen.de)

M.T. Souza

Department of Materials Engineering, Federal University of São Carlos, São Carlos, SP, Brazil  
e-mail: [marina\\_trevelin@hotmail.com](mailto:marina_trevelin@hotmail.com)

W. Li • A.R. Boccaccini

Institute of Biomaterials, University of Erlangen-Nuremberg, Erlangen, Germany  
e-mail: [wei.li@ww.uni-erlangen.de](mailto:wei.li@ww.uni-erlangen.de); [aldo.boccaccini@ww.uni-erlangen.de](mailto:aldo.boccaccini@ww.uni-erlangen.de)

or synthetic polymers with bioactive glasses or glass-ceramics. These novel biomaterials present the possibility of tailoring a variety of parameters and properties such as degradation kinetics, mechanical properties, and chemical composition according to the aimed application. This chapter presents a concise update of the field of biopolymer–bioactive glass composite scaffold development for TE covering several popular processing techniques for biocomposite fabrication, namely, microsphere processing, solvent casting-particulate leaching method, electrospinning, freeze-drying, and rapid prototyping techniques, which lead to scaffolds exhibiting a variety of 3D morphologies and different pore structures.

---

**Keywords**

Composite materials • Bioactive glass • Biodegradable polymers • Scaffolds • Bone tissue engineering • Soft tissue engineering • Porosity • Fabrication techniques • Degradation • Cell biocompatibility

---

**Introduction**

In the last decades enormous advances in the biomaterials field have been made especially considering the development of bioactive scaffold materials for tissue engineering (TE) applications. These materials fulfil two functions, i.e., they temporarily replace part of a damaged or diseased tissue and at the same time actively induce the regeneration of new tissue. Such bioactive materials in the form of “scaffolds” are essential for the advancement of the TE and regenerative medicine fields and numerous different types are being developed for the regeneration of practically every part of the human anatomy ranging from hard tissues such as the bone to soft tissues such as the skin, heart, and blood vessels [1–8]. In this interdisciplinary approach, cells and three-dimensional bioactive and bioresorbable structures, the “scaffolds,” are combined aiming to mimic the natural body structures and to accelerate tissue regeneration.

A large number of different materials are being investigated in this context. For many tissues, in particular for the bone, the combination of a bioresorbable polymer and a bioactive glass or glass-ceramic in a composite material is a promising approach as the unique properties of each material phase can be combined in one structure, while at the same time, the disadvantageous properties of the individual phases can be minimized [1].

Specific properties required for a successful scaffold material have been reported previously in the literature [9, 10]. These include properties such as biocompatibility, adequate pore sizes, a high degree of interconnected porosity of at least 60 %, mechanical properties closely matched to those of the tissue that needs to be regenerated, and adequately tailored biodegradability [11, 12]. Another relevant property for the regeneration of hard and soft tissues is bioactivity, that is, the biomaterials’ ability to interact with or bind to living tissues [13].

The combination of biopolymers and inorganic fillers to develop tissue engineering scaffolds has been investigated during the last 15 years with major efforts devoted to increase the bioactivity of otherwise bioinert polymers, including synthetic and natural polymers [1, 9, 10, 14]. A frequently considered inorganic filler or additive in biopolymer composites is bioactive glass in its many chemical compositions and morphologies, such as particles, granules or fibers [1]. The field of bioactive glasses started in the 1970s with the development of  $\text{Na}_2\text{O}-\text{CaO}-\text{SiO}_2-\text{P}_2\text{O}_5$  glasses [13]. In this system, one of the most bioactive glasses, currently known as 45S5 Bioglass<sup>®</sup>, was developed with the specific composition of 46.1  $\text{SiO}_2$ , 24.4  $\text{Na}_2\text{O}$ , 26.9  $\text{CaO}$ , and 2.6  $\text{P}_2\text{O}_5$  (mol.%) [13, 15]. 45S5 Bioglass<sup>®</sup> can induce a beneficial biological response to human host tissue, which is revealed by the formation of a surface hydroxyapatite (HA) layer when implanted, similar in composition to the mineral phase of the human bone. This HA-like layer is able to bond firmly to hard and soft tissues [9, 16]. Bioactive glasses have been applied in clinical treatments for many years in different product forms, such as granules and particulates, dense or porous implants. For example, bioactive glass granules or particulates have been widely used to fill spaces where bone grafting is needed and to enhance the natural repair process. Applications include general orthopedic, craniofacial, and maxillofacial prosthesis, chronic osteomyelitis treatment, soft tissue regeneration, and wound healing [8, 9, 13, 16].

In addition to the above mentioned oxides, varying amounts of other oxides can also be incorporated into glass compositions to impart specific properties; for example, SrO could improve bone healing [17] and  $\text{Ag}_2\text{O}$  leads to antibacterial features [10]. Furthermore, some trace elements when incorporated into bioactive glass compositions have been shown to provide additional properties that can be beneficial for tissue regeneration. For instance, zinc is responsible for vitamin A and E metabolism; magnesium can activate the phosphate-transferring enzyme; copper can help the formation of myelin sheaths for the neurological system, and vitamin B can enhance angiogenesis [18]. Therefore, numerous ion-doped bioactive glasses are being developed, which exhibit high biological activity and tissue regeneration capability [10, 33]. Table 1 summarizes relevant previous studies on metallic ion-doped bioactive glasses showing the different cell biology effects they provide. It is important to observe the fact that the excessive release of these elements in body fluids could harm healthy tissues; thus, the release of ions from bioactive glasses should be kept below the toxic level which may vary for different applications and conditions.

The traditional and first generation of bioactive glasses was mainly manufactured by the melt-quenching method at temperatures above  $1300\text{ }^\circ\text{C}$ , from which the silica content was limited within 60 % for effective bonding with the host tissue [37]. Melt-quenched glasses usually stay in the dense state and a stable oxide network occurs; hence, the bioactivity is strongly dependent on the silica content. The second generation of bioactive glasses was invented in the early 1990s through the sol-gel route, in which a gel structure is formed and self-assembled through hydrolysis and polycondensation of compositional precursors at room temperature followed by a

**Table 1** Summary of some of the most investigated ion-doped bioactive glasses

Elements	Expected effect	Ref.
Zinc	Antibacterial effect supports protein and DNA synthesis and cell proliferation	[19–21]
Magnesium	Directly stimulates osteoblast proliferation	[19, 20, 22]
Silver	Antimicrobial effect	[23, 24]
Iron	Drug delivery and hyperthermia treatment of cancer	[25, 26]
Fluoride	Positively influences bone density Forms fluorapatite (FAp), which is the main component of enamel and dentine and has higher acid resistance than HCA	[27, 28]
Copper	Enhances vascularization, osteostimulation, and bone-related gene expression Induces differentiation of stem cells and osteoblastic cells Antibacterial property	[29, 30]
Strontium	Accelerates bone healing process Increases bone mass and mechanical strength Enhances bone formation and decrease osteoporosis	[19, 31]
Cerium, gallium	Induce positive response to osteoblasts Increase bone calcium content Inhibit osteoclast activity	[32]
Cobalt	Mimics hypoxia and induces angiogenesis	[33, 34]
Boron	Helps new bone formation and maintenance Stimulates RNA synthesis in fibroblast cells	[10, 18, 33, 35]
Lithium	Enhances remyelination of peripheral nerves	[36]

drying or low-temperature sintering process [38]. The reacted silica network is abundant in Si–OH groups, therefore enabling much higher amount of silica (>90 %) for effective HCA formation [37]. In addition, incorporation of sodium is not necessary in sol–gel approaches since it basically reduces the melting point and enhances processability in melt-quenched glasses. Many ternary or binary sol–gel-derived bioactive glasses without sodium have been reported for excellent HCA-forming ability when immersed in simulated body fluid (SBF), such as 58S, 77S, or 70S30C [9]. Mesoporous bioactive glasses can be regarded the third generation of bioactive glasses. They are developed based on the sol–gel method but with involvement of a supermolecular surfactant as a template of ordered mesoporosity, typically in the 2–50 nm size range. Typical surfactants are triblock copolymers, such as P123 and F127 [38]. The mesopore size can be adjusted by altering the surfactant type and concentration, solvents, pH, and temperature. In comparison to dense bioactive glasses and sol–gel-derived glasses, highly ordered pore channels in mesoporous glasses enormously increase their surface area-to-volume ratio and porosity, which makes mesoporous bioactive glasses ideal carriers in sustained drug delivery combined with bioactivity [36]. Nevertheless, the low processing temperatures, wet-chemical reactions, and high porosity of sol–gel-induced bioactive glasses lead to a significant reduction of their mechanical properties. Thus, only small dimensional products can be produced, for example,

nanoparticles, microspheres, powders, thin films and coatings, or monoliths of size below 1 cm [37]. In addition, although bioactive glasses show impressive bioactivity for bone repair and tissue regeneration, their brittleness limits their clinical applications, especially when there is a significant stress and/or cycling load-bearing demand, in cases of some bone and joint grafts, or when flexible structures for soft tissue regeneration are required. Thus, the development of composites, with the incorporation of bioactive glass in biopolymer matrices, represents an interesting approach, not only to develop bioactive scaffolds with suitable mechanical properties but also to create a better environment for cell attachment and growth for TE applications.

Early reports on the combination of bioactive glasses and biodegradable polymers to produce tissue engineering scaffolds were published at the end of the twentieth century, as reviewed elsewhere [1], and tremendous research efforts have been devoted to these composite systems in the last 15 years. Indeed numerous different compositions of bioactive glasses are now available and suitable for combination with biopolymers for the design of composite scaffolds for tissue engineering.

In this chapter a concise update of the field of biopolymer–bioactive glass composite scaffolds for tissue engineering is presented, focusing on several established processing techniques, namely, microsphere processing, solvent casting-particulate leaching method, electrospinning, freeze-drying, and rapid prototyping methods. These processing techniques were chosen for the present discussion as they enable the fabrication of bioactive composites of different morphologies, including microspheres, fibers, foams, and architected scaffolds, illustrating the variety of systems currently available for TE.

---

## Composites as Useful Materials for Tissue Engineering

When a polymer and an inorganic phase are combined, it is possible to tailor the properties of the resulting composite for the intended applications. For a successful composite with desired mechanical properties, for example, it is necessary to control the interface between the polymer and the inorganic phase adequately, thus making it possible to fabricate composites which combine the favorable properties of each phase while at the same time minimizing the negative aspects of each phase. In addition, using the composite approach, it is possible to mimic the natural structure of the bone and other complex organs in the human body. In this framework, it is possible to balance the physical, mechanical, and biological properties of each of the individual phases and also to manufacture multilayer, gradient, and hierarchical structures. The addition of inorganic nanoparticles can also induce a nanoscale roughness on the surface of the scaffold that has been shown to stimulate the adhesion, proliferation, and maturation of different cell types [39–42]. Finally, the combination of polymeric and inorganic phases can also be conveniently used to control the overall degradation rate of the composite, which is of paramount importance to design scaffolds with tuned degradation kinetics.

## Development of Bioactive Glass–Biopolymer Composites

Dense or porous polymer–inorganic phase composite materials can be fabricated using different production methods such as solvent casting, thermally induced phase separation processes, freeze casting, electrospinning, freeze-drying, and rapid prototyping techniques, to mention a few. Several review papers and book chapters are available describing traditional methods employed to fabricate bioactive glass–biopolymer composites [1, 7, 8, 11, 14, 39, 42–46]. In some cases, both phases interact on a molecular level; thus strong bonds exist between the phases forming organic–inorganic hybrids [37]. Bilayer or multilayer structures are also being developed, which result from the combination of different composite parts on the macro-scale. These types of scaffolds can be used to regenerate defects where one or more tissue layers with different mechanical properties and biochemical composition need to be regenerated, such as osteochondral defects [47]. In this section several common processing methods with great potential to develop bioactive glass–biopolymer composite scaffolds are described, as they deliver different scaffold architectures useful in tissue engineering, namely, microspheres, (nano)fibers, and 3D porous structures.

### Biocomposite Microspheres

Polymer microspheres have been widely used as a delivery vehicle of drugs, proteins, and cells for the repair and regeneration of damaged tissue [48, 49]. These microspheres can encapsulate bioactive molecules and release them at controlled rates for relatively long periods of time, which makes this method preferable over traditional drug administration. Their spherical form enables them to easily fill defects of irregular and complex shapes and sizes; thus, they are promising as injectable and/or defective site-filling materials [49, 50].

A wide range of natural or synthetic polymers can be used to manufacture these structures. However, microspheres made from polymers alone are not the optimal material of choice for bone tissue engineering applications because of the absence of bioactivity. Therefore, bioactive glass particles can be dispersed or encapsulated in polymer microspheres, mainly to impart a bioactivity property, i.e., the microspheres will have the ability to develop a CaP layer on their surface enabling better integration with the bone tissue [50].

A variety of techniques are currently available for preparing microspheres. The most widely known is the emulsification–solvent evaporation process. Briefly, in this technique, a polymer solution is made with a volatile organic solvent, and during this process, it is possible to add drugs or other bioactive molecules such as proteins or growth factors. Then, the organic phase is emulsified to obtain an oil/water emulsion that can be stabilized as droplets. After that, the microspheres can be collected by filtration or centrifugation. Other available techniques for microsphere manufacture are coacervation (polymer phase separation), spray drying, milling, and supercritical fluid techniques [51]. The manufacturing process is selected depending on the nature of the polymer, the intended application, and the required degradation rate.

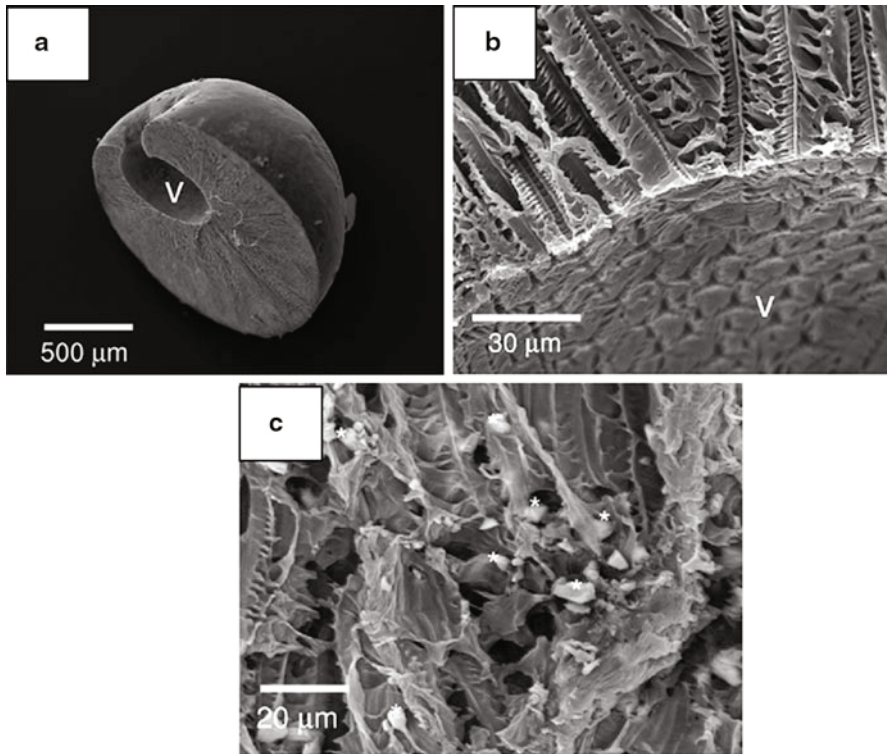


**Fig. 1** SEM images of highly porous PLGA/45S5 BG microspheres obtained by TIPS according to Kershaw et al. [53]: (a) macroview of microsphere, (b) higher magnification image, (c) higher resolution image showing the internal tubular structure with bioactive glass particles being distributed in the interconnected tubular structure (Reproduced from Ref. [53] with permission from Mary Ann Liebert, Inc. Publishers)

During these processes bioactive glass particles can be incorporated aiming a higher control of the polymer microsphere degradation, the increase of the reactivity of the microsphere, and acceleration of the healing process by enhancing the osteogenic and angiogenic potential.

In 2002, Qui et al. [52] incorporated colloidal hydroxyapatite (HA) or modified bioactive glass (mBG), of size under 20 μm, into degradable poly(lactic acid) (PLA) microspheres in different ratios (1:1, 1:3, and 1:9). After SEM, EDX, FTIR, and ion quantification characterizations, the obtained results indicated a significantly enhanced surface reactivity of the microspheres containing bioactive glass. Also, the mBG-containing microspheres showed greater bioactivity compared to microspheres containing HA as the filler material.

Keshaw et al. [53] prepared PLGA microporous spheres containing 10 % w/w 45S5 bioactive glass (BG) using a thermally induced phase separation (TIPS) method, and the typical microstructure of the microspheres is shown in Fig. 1. The



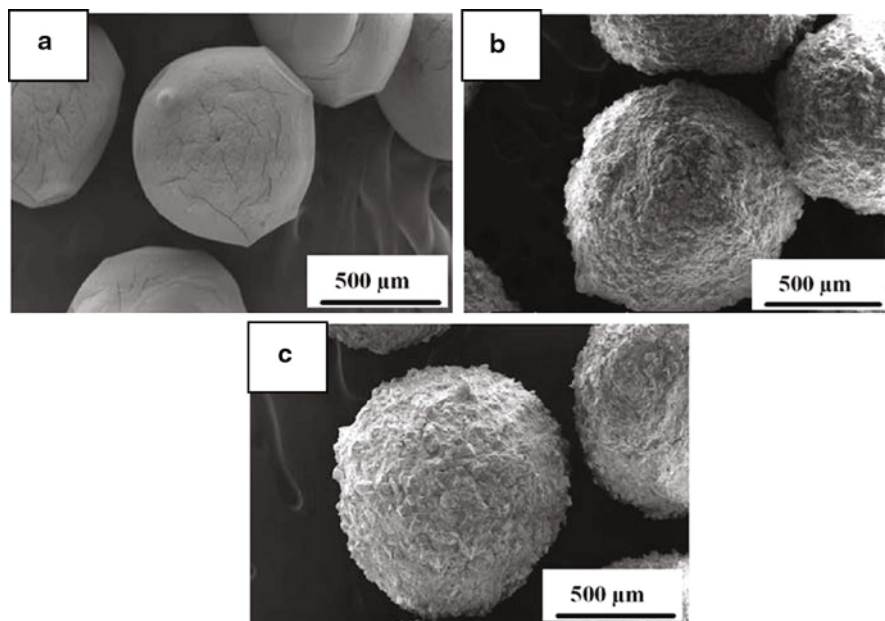


**Fig. 2** SEM images of alginate microspheres (a), alginate/mesoporous BG microspheres (b), and alginate/non-mesoporous BG microspheres (c) developed by Wu et al. [54] (Reproduced from Ref. [54] with permission from Wiley Periodicals)

produced composite spheres were 1.82 mm in diameter and had a porosity of 82.6%. Both the neat PLGA and PLGA/45S5 BG microporous spheres integrated rapidly with the host tissue in a subcutaneous wound model. Moreover, 45S5 BG-containing composite spheres showed a significant increase in vascular endothelial growth factor secretion from myofibroblasts.

In addition to the melt-derived bioactive glass, sol-gel-derived bioactive glasses including mesoporous glasses have also been incorporated into polymer microspheres [54, 55]. For example, Wu et al. [54] developed mesoporous glass/alginate composite microspheres, shown in Fig. 2, with controllable dexamethasone delivery ability. The obtained composite microspheres were shown to be bioactive, and the incorporation of mesoporous glass in the alginate microspheres enhanced the drug-loading capacity and altered the drug release profile. In order to treat osteoporosis-like bone defects, Mondal et al. [55] prepared poly(lactide-co-caprolactone) microspheres loaded with alendronate sodium and bioactive glass-ceramic using an oil-in-water emulsion solvent evaporation method, which are shown in Fig. 3. The composite microspheres were found to be bioactive, non-cytotoxic, and able to promote cell adhesion. The local delivery of alendronate sodium by microspheres represents a superior strategy to the oral administration, which is associated with oral discomfort and low bioavailability.

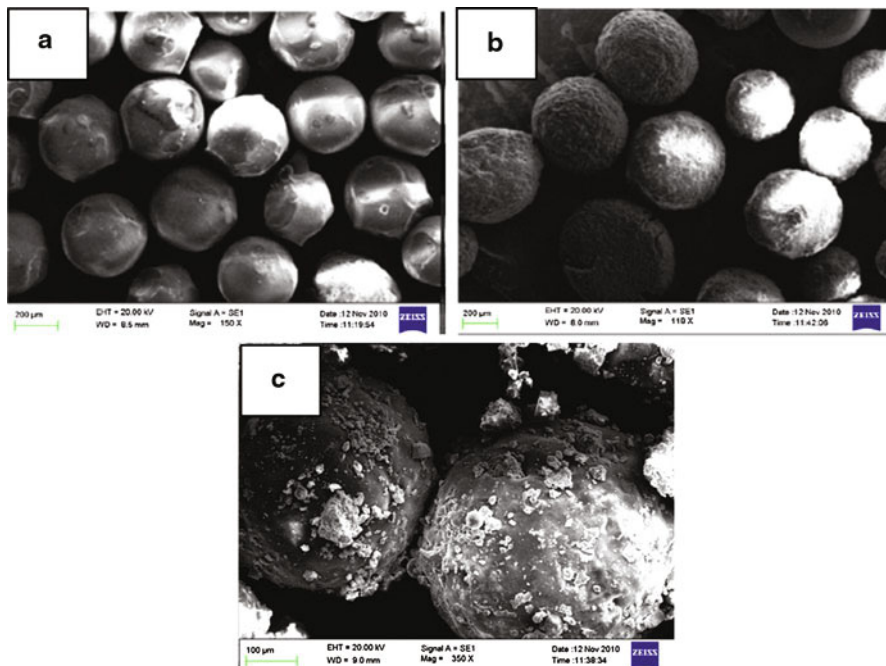


**Fig. 3** SEM images of P(LLA-co-CL) microspheres, scale of 200  $\mu\text{m}$  (a); P(LLA-co-CL) microspheres loaded with 50 wt% bioactive glass, scale of 200  $\mu\text{m}$  (b); and P(LLA-co-CL) microspheres loaded with 50 wt% bioactive glass and alendronate sodium, scale of 100  $\mu\text{m}$  (c); developed by Mondal et al. [55] (Reproduced from Ref. [55] with permission from Elsevier)

### Composites from Solvent Casting-Particulate Leaching Process

As a simple, straightforward and inexpensive method, solvent casting-particulate leaching (SCPL) process involves water-soluble porogens (sugar, salt, etc.) mixing into a polymer/monomer solution followed by mold casting into desired shape. Then, the solvent could be removed by evaporation or lyophilization and polymerization in the case of monomer mixtures. Afterwards, the porogens are leached away by water immersion and pores or pore channels are formed [56, 57]. Figure 4 schematically illustrates the process [58]. Porosity and pore sizes can be precisely adjusted by altering porogen amount and sizes. In this manner, scaffolds with porosity of up to 93 % and pore sizes of up to 500  $\mu\text{m}$  can be prepared. The simple operation and the adequate control of porosity confer the method wide applications and suitability for use with various polymers. However, pore shapes depend on the porogen morphology, which is usually cubic-like, equiaxed, or spherical. In addition full interconnectivity is difficult to achieve in these scaffolds, which limits the actual application fields.

As a conventional process for porous structure fabrication, diverse single polymers, blend polymers, and polymer/inorganic filler systems have been explored for

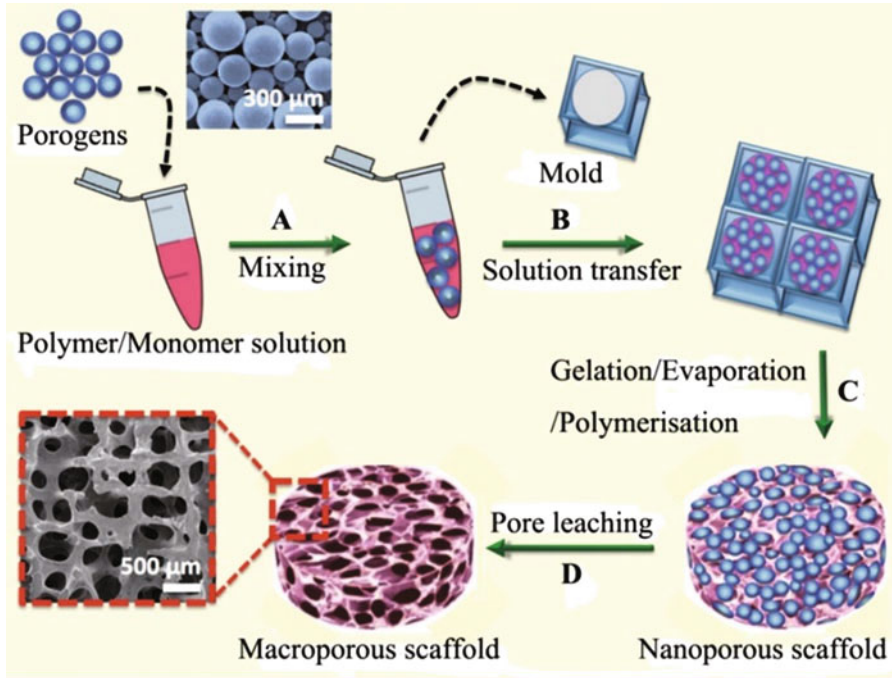


**Fig. 4** Illustration of the fabrication steps of macroporous scaffolds by solvent casting-particle leaching method (Reproduced from [58] with the permission of Korean Academy of Periodontology)

porous scaffold fabrication in tissue engineering [59]. Here, only specific examples relevant to bioactive glass containing composites will be introduced in the following paragraphs.

Li et al. [60] have incorporated both 40 wt% of normal sol-gel-derived bioactive glass (BG) and mesoporous bioactive glass (MBG) powders with a composition ratio of 80S15C into PCL matrix through SCPL method. Both PCL/BG and PCL/MBG scaffolds with porosity of around 90 % were successfully prepared. Wettability studies on the two scaffolds types implied that MBG not only greatly improved the hydrophilicity of the PCL matrix but also imparted better wettability than normal BG. The investigation involving ion release and SBF incubation for 3 weeks indicated that MBG released Si ions faster than BG, therefore leading to higher HCA formation ability. SEM images show that a dense and continuous apatite layer was formed on MBG-containing samples, but only scattered and discrete apatite appeared on BG-containing samples. The highly enhanced bioactivity of MBG-containing samples was attributed to the ordered channels and high surface to volume ratio of MBG particles, which accelerated the ion exchange during SBF incubation.

The ability to bond to bone tissue and promote bone regeneration is already well known for bioactive glasses, as discussed above. However, a recent study of

PHBV/Bioglass scaffolds by SCPL method demonstrated promising application in cartilage tissue engineering as well [61]. Wu et al. incorporated 20 wt% 45S5 Bioglass<sup>®</sup> powders into PHBV matrix for PHBV/BG porous scaffolds by the abovementioned SCPL method and conducted *in vitro* and *in vivo* tests by culturing chondrocytes and implanting into nude mice [61]. Results showed that not only the hydrophilicity and compressive strength were highly enhanced, but also the chondrocyte's penetration length, thickness of cartilage-like tissue of *in vivo* constructs, and the mechanical strength of the formed cartilage tissue were all promoted.

In a very recent study reported by Niu et al. [62], 30 wt% mesoporous bioactive glass particles were incorporated into PLLA scaffolds by the SCPL method using NaCl as the pore-forming agent. Figure 5 displays the typical porous microstructure of the obtained scaffolds with different MBG ratios: PLLA, PLLA with 15 wt% of MBG (15BPC), and PLLA with 30 wt% of MBG (30BPC). A detailed investigation on wettability, water absorption, degradability, *in vitro* culture of MC3T3-E1 cells, and *in vivo* implantation in rabbits was disclosed. Results demonstrated that hydrophilicity, water absorption, degradation rate, HCA formation ability, cell proliferation, and ALP activity were all significantly increased by MBG incorporation, which were both MBG content dependent and time dependent. In addition, bone growth in a femur defect in a rabbit model was fully developed and recovered when 30BPC was used within 12 weeks. Especially the histological analysis of *in vivo* implantation demonstrated that the PLLA scaffolds with 30 wt% MBG incorporation produced by SCPL have promising potential in clinical trials and further in bone tissue engineering.

## Electrospun Composite Fibers

Electrospinning has experienced a rapid and continuous development as a convenient process for micro- or nanofiber production for numerous applications including tissue engineering scaffolds [63, 64]. The method is based on the principle that under an electrostatic field, a continuous fiber jet is ejected from the tip of a charged solution when the electrostatic force exceeds the surface tension, and after solidification, the fibers will pile up on a grounded collector [63]. The diameter and morphology of the fibers are determined by the balance between electrostatic forces and surface tension. This technique makes possible the production of continuous fibers with diameters in the submicrometric scale by adjusting parameters regarding the solution, operation, and ambient conditions. Some other intrinsic parameters that can also affect the fiber manufacture are the polymer's molar mass, concentration, and solvent composition and concentration in the polymer solution. On the other hand, the applied voltage, collecting distance, and the feed rate are extrinsic operational variables also affecting the process outcomes. In addition, humidity and temperature can also alter the morphology of the product [63, 65]. Figure 6 shows a schematic representation of the electrospinning setup.

The simplicity of the electrospinning technique enables a broad applicability on various kinds of polymers. As the demand of biomaterial scaffolds for tissue

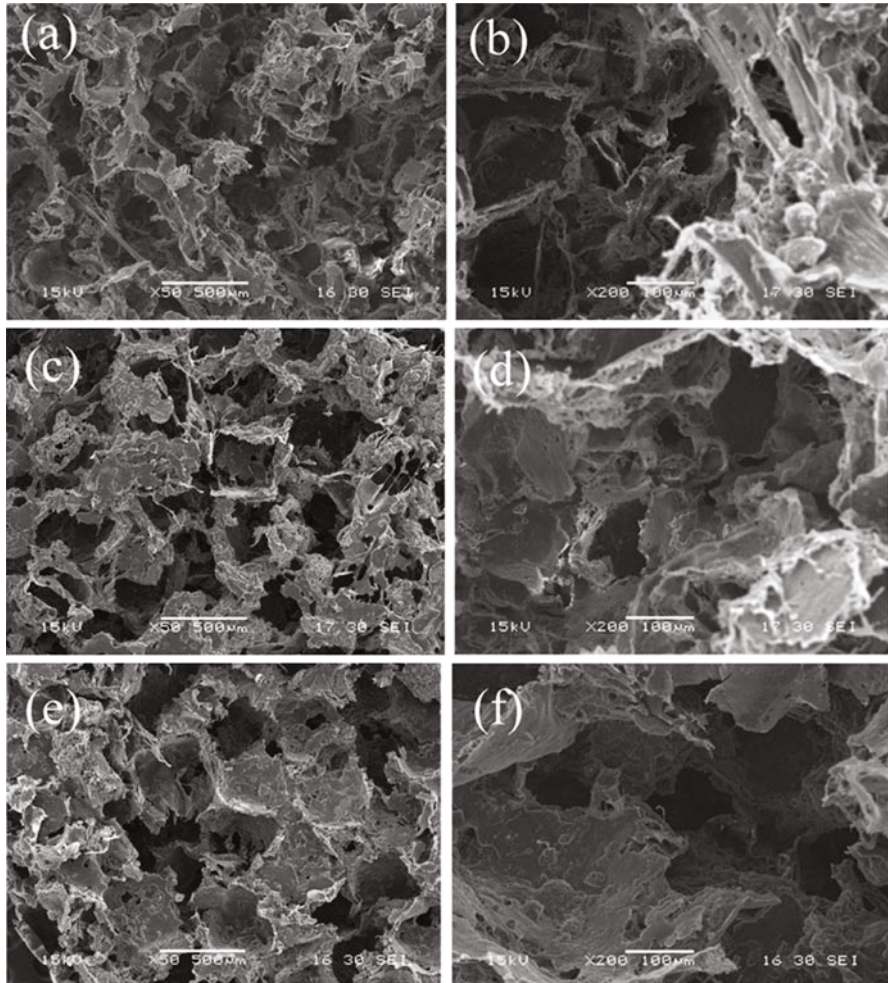
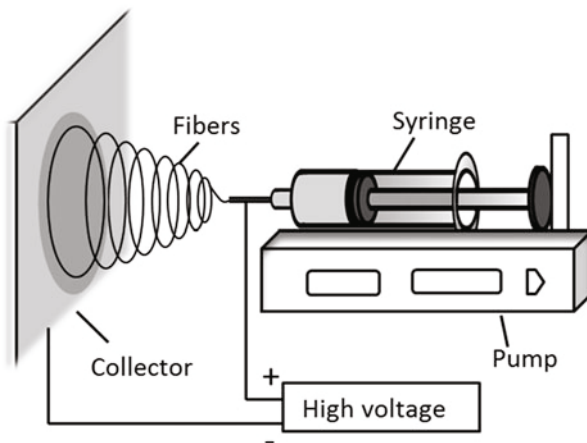


**Fig. 5** SEM images of the surface morphology of PLLA (a, b), 15BPC (c, d), and 30BPC (e, f) scaffolds at different magnifications [62] (Reproduced with permission from Royal Society of Chemistry (RSC) publishing)

engineering has dramatically increased in recent years, intense research on electrospinning of different biopolymers is being conducted, not only concerning natural polymers such as collagen, chitosan, gelatin, etc., but also synthetic biopolymers such as PLA, PLGA, PCL, PHB, PHBV [67]. To overcome the limitations of a single polymer or polymer blend, organic–inorganic composite and hybrid fibers are being also developed to combine and balance their physiochemical and biological properties [63, 68].

Many efforts have been devoted to the development and improvement of the electrospinning process of biopolymer–bioactive glass suspensions aiming a better

**Fig. 6** Schematic representation of the electrospinning setup [66] (Reproduced with the permission of Elsevier)



integration of the brittle and bioactive inorganic phase with the elastic and bioinert organic phase for hard and soft tissue regeneration. Basically, there are two strategies for bioactive glass particle incorporation; the first one is to associate melt or sol-gel-derived glass particles or fillers with the polymer solution with and without surfactants in an ultrasonic bath. Noh et al. [69], for example, fabricated bioactive glass nanofiller-reinforced PLA electrospun scaffolds, in which the nanofillers were chopped from fiber mats of electrospun sol-gel-derived bioactive glass. Results indicated a significant enhancement of the *in vitro* apatite formation on the composite nanofiber surface in SBF solution, and it was reported that osteoblastic cells could adhere and proliferate well on the composite nanofibers.

Kouhi et al. [70] and Lin et al. [71] both fabricated sol-gel-derived bioactive glass/PCL fibrous scaffolds through electrospinning from a solution of PCL and glass nanoparticles. The study of Kouhi et al. showed that bioactivity and cell differentiation activity were significantly improved due to the nanosized bioactive glass addition. Lin et al. fabricated a multifunctional bioactive scaffold (shown in Fig. 7) with controlled simvastatin-releasing property. Due to the suitable physical interactions between the polymer and inorganic particles, the BG loading up to 15 wt% led to the improvement of the tensile strength however simultaneously to a decrease in strain [71].

Ren et al. [72] obtained biocomposite scaffolds incorporating strontium-substituted bioactive glass (SrBG) particles in PCL (10 wt%) forming highly porous fibrous sheets. The scaffolds demonstrated to be non-cytotoxic *in vitro*, and, when compared to PCL-only scaffolds, they could enhance alkaline phosphatase activity and increased osteoblast differentiation through upregulation of gene expression (ALP and OCN) in MC3T3-E1 cells. The fibrous sheets also facilitated cellular attachment and proliferation and improved collagen deposition.

Another approach for inorganic phase incorporation in electrospun fibers is to combine the bioactive glass precursor with the polymer solution to prepare a hybrid solution for electrospinning. The obtained hybrid fibers have a uniform structure,

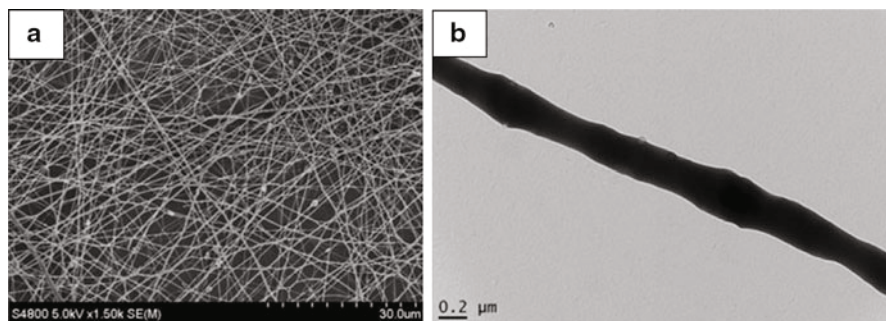


**Fig. 7** (a) SEM of electrospun PCL fiber mats with 10 wt% mesoporous BG powder fabricated by the direct mixing method, scale of 30  $\mu\text{m}$ , and (b) TEM image of a single fiber which shows that the mesoporous glass nanoparticles were attached to the fiber surfaces [71] (Reproduced with permission from Springer)

where the organic and inorganic phases interacted on a molecular level. Allo et al. [73] reported a single-phase electrospun  $70\text{SiO}_2\text{-}26\text{CaO-}4\text{P}_2\text{O}_5$  bioactive glass/PCL scaffold using electrospinning as well as the sol-gel method without using any coupling agent. The chemical characterization of the scaffolds revealed that natural polymers which possess multiple functional groups can easily be covalently bonded to sol-gel-derived bioactive glass; however, synthetic polyesters could only link to sol-gel-derived bioactive glass through hydrogen bonding, which is not helpful for the enhancement of all properties simultaneously.

Han et al. [74] developed a one-step solution, in which a mesoporous bioactive glass precursor ( $80\text{SiO}_2\text{-}15\text{CaO-}5\text{P}_2\text{O}_5$ ) was dissolved in PLA followed by the electrospinning process. The obtained scaffolds presented a hierarchical porous structure with macro- and mesoporous structure (10  $\mu\text{m}$  and 5 nm, respectively). The biocomposites demonstrated high bioactivity, wettability, and rapid hydroxyapatite (HAP)-inducing mineralization in SBF solution as well as good cell attachment (for HeLa cells in vitro tests) and controllable drug release (in this study ibuprofen was used).

In another relevant study, Gao et al. [75] successfully prepared  $70\text{SiO}_2\text{-}25\text{CaO-}5\text{P}_2\text{O}_5$  bioactive glass/gelatin hybrid fibrous scaffolds using the coupling agent 3-glycidoxypropyltrimethoxysilane (GPTMS) through a combination of the sol-gel method and electrospinning. GPTMS provided linkage for gelatin and hydrolyzed silanol groups and led to covalent bond formation, which enabled the manufacture of an organic-inorganic hybrid scaffold with dramatic enhancement of tensile strength and elongation at break (Fig. 8).

A different reported approach involving electrospinning is to reinforce electrospun-bioactive glass fiber mats with a polymer solution or the polymer melt. Kim et al. [76] prepared bioactive glass nanofiber-filled PLA composites, which proved to be highly bioactive and possessed a favorable osteoblastic response. Unlike the aforementioned strategies, in their study, the  $58\text{SiO}_2\text{-}38\text{CaO-}4\text{P}_2\text{O}_5$  bioactive glass nanosized fiber mats were first fabricated through the sol-gel

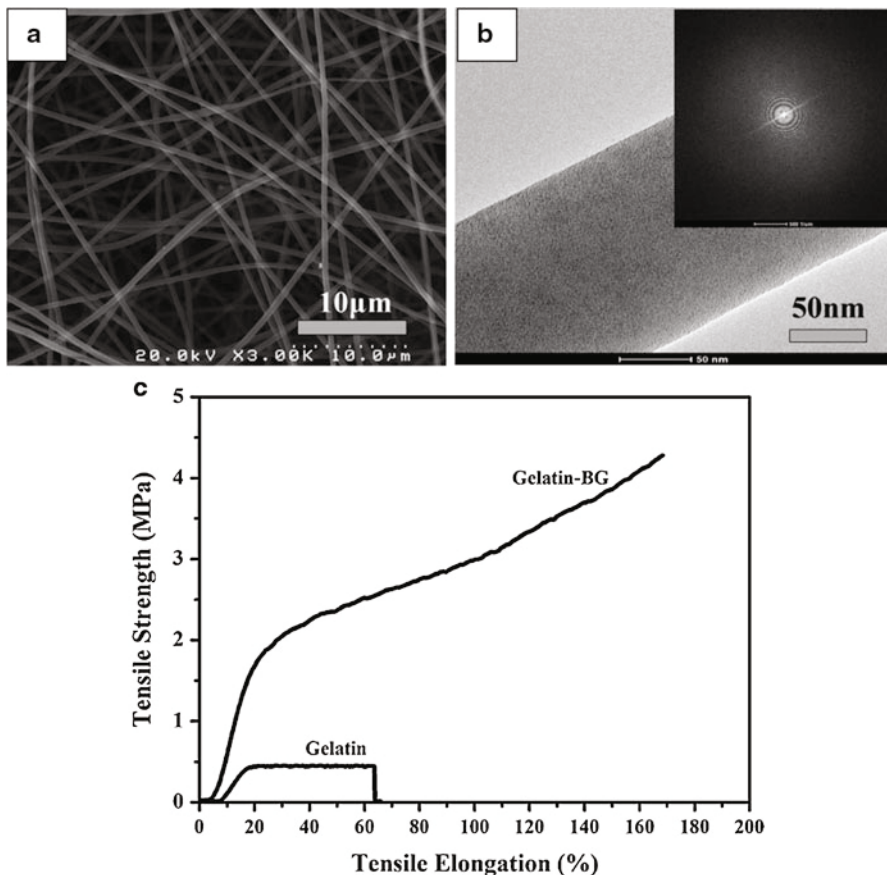


**Fig. 8** (a) SEM and (b) TEM of electrospun sol-gel-derived BG/gelatin hybrid fiber mats as prepared by Gao et al. [75] by associating the sol precursor and gelatin solution with the addition of a cross-linking agent; (c) the sol-gel fiber mats showed enhanced mechanical properties compared to gelatin alone (Reproduced from Ref. [75] with permission from Wiley Periodicals)

electrospinning method followed by sintering at 700 °C. Subsequently, different fractions of fiber mats were fully soaked and infiltrated with PLA/THF solutions and then dried. These procedures were followed by a thermal-compression process at 130 °C to obtain a homogeneous dense plate material. A schematic drawing of this process is shown in Fig. 9. The obtained nanocomposites had a higher in vitro bioactivity, and osteoblast cells attached and grew well on their surface as well as secreted collagen protein and improved the expression of ALP when compared to the pure PLA nanocomposites.

In another study using the same BG composition, Kim et al. [77] prepared a biocomposite for bone regeneration with this bioactive glass nanofiber (BGNF) and collagen. The BGNF and self-assembled collagen sol were combined in aqueous solution and cross-linked to produce a BGNF-collagen nanocomposite thin



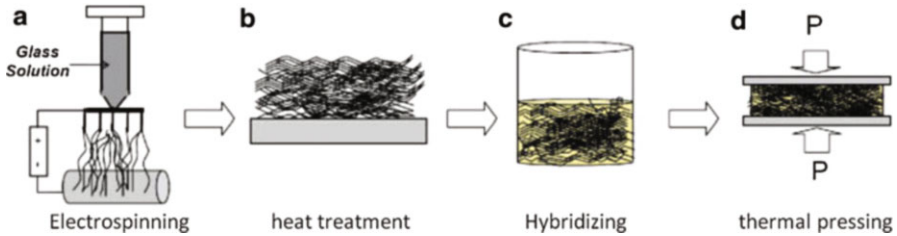


**Fig. 9** Process chart for the fabrication of PLA-reinforced bioactive glass fiber mats via electrospinning (Adapted from Ref. [76], reproduced with permission from Wiley Periodicals)

membrane or a macroporous scaffold. These biocomposites showed rapid formation of bone-like apatite minerals on their surfaces in SBF solution and exhibited good bioactivity *in vitro*. Cell viability test indicated that osteoblasts presented favorable growth, and the alkaline phosphatase activity was significantly higher for the cells exposed to the nanocomposite.

In a related study, Lee et al. [78] obtained membranes of nanofibrous bioactive glass and PCL. Sol–gel-derived bioactive glass (70SiO<sub>2</sub>–25CaO–5P<sub>2</sub>O<sub>5</sub>) nanofibers were added to a PCL solution at 20 wt%. The manufactured nanocomposite membranes induced rapid formation of apatite-like layer on the biomaterials' surface in SBF solution, and *in vitro* tests showed that murine-derived osteoblasts (MC3T3-E1) grew actively over the nanocomposite indicating a significant improvement on cell viability when compared to pure PCL membrane. Furthermore, the osteoblastic activity, as assessed by the expression of alkaline phosphatase, was significantly higher on the nanocomposite membrane than on the pure PCL membrane.

Jo et al. [79] also fabricated PCL/sol–gel-derived BG nanofiber (BGNF, 20 wt%) biocomposites and investigated their biocompatibility and mechanical properties in comparison with composites containing bioactive glass in the microparticulated form. The obtained microstructure, showed in Fig. 10, resulted in an improvement of the biological and mechanical properties, presenting a superior bioactivity and a higher elastic modulus. Moreover, *in vivo* animal experiments using Sprague–Dawley albino rats revealed that the PCL/BGNF biocomposites had a satisfactory biocompatibility and enhanced bone regeneration capability of calvarial bone defects.

In a recent study, Castaño et al. [80], using electrospinning as a suitable method to create fibers that mimic the extracellular matrix (ECM), produced hybrid fibrous mats with three different contents of Si (40 %, 52 %, and 70 % – compositions defined by the authors as ormoglass), using an ormoglass–polycaprolactone blend approach. These obtained mats showed a homogeneous structure, and the material and biological characterization suggested that the hybrid biomaterials with a Si content equivalent to 40 % released a fair quantity of calcium ions and were satisfactorily osteogenic, enhancing MC3T3-E1 cell differentiation (Fig. 11). These biocomposites also showed a greater ability to form blood vessels, since they could modulate the release of Ca<sup>2+</sup> in a rate suitable to activate the VEGF production cascade, thus demonstrating an angiogenic-promoting feature.

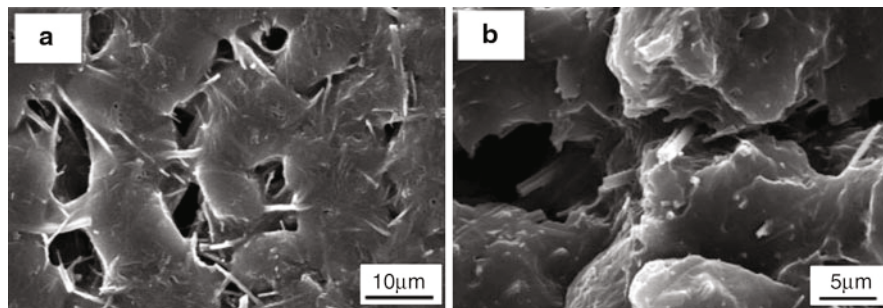
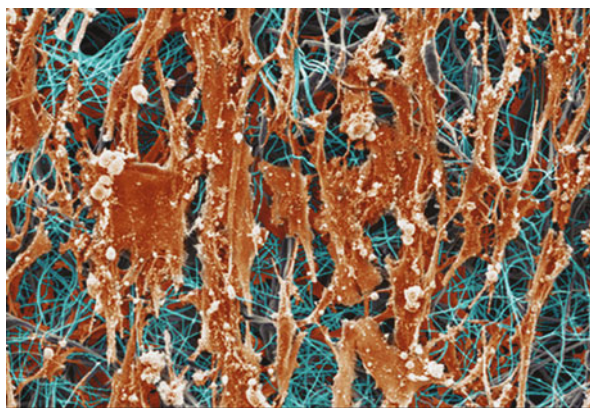


**Fig. 10** Surface (a) and cross-sectional (b) images of PCL/BGNF biocomposites containing 20 wt % of BGNF (Adapted from Ref. [79], reproduced with permission from Wiley Periodicals)

**Fig. 11** Cell adhesion to the fibrous scaffolds developed by Castaño et al. [80]. In this image cells and filopodia were artificially colored in order to calculate the biocomposites' surface occupation by MC3T3-E1 cells (Reproduced from Ref. [80] with permission from ACS Publications)



## Composite Scaffolds by Freeze-Drying

Freeze-drying, which sometimes is also termed cryodesiccation or lyophilization, belongs to the thermally induced phase separation techniques and was described by Ezekwo et al. in 1980 [81]. The technique has found increasing interest in the last years for fabrication of highly porous scaffolds with interconnected and tailored architecture [82–84]. This process has been investigated by a number of research groups pursuing the fabrication of polymer matrix composites with the incorporation of inorganic phases such as HA [82, 83], demineralized bone [85], calcium phosphates [86, 87], and bioactive glass particles [88–91].

In this technique, a solution, dispersion, or emulsion consisting of a solvent, the polymer, and the inorganic nanoparticles (and in some cases a cross-linking agent such as glutaraldehyde, genipin, or other) is subjected to rapid gelation, which causes the solids or the solute to be displaced by an advancing ice front into the interstitial spaces between ice crystals [88–90]. Once fully frozen, the freeze-drying process itself takes place, which typically employs temperatures of  $-20$  to  $-80$  °C for different periods of time. The suspension is then sublimated in vacuum for

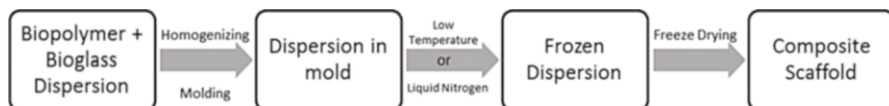


**Fig. 12** Schematic diagram of the freeze-drying process for the fabrication of composite scaffolds

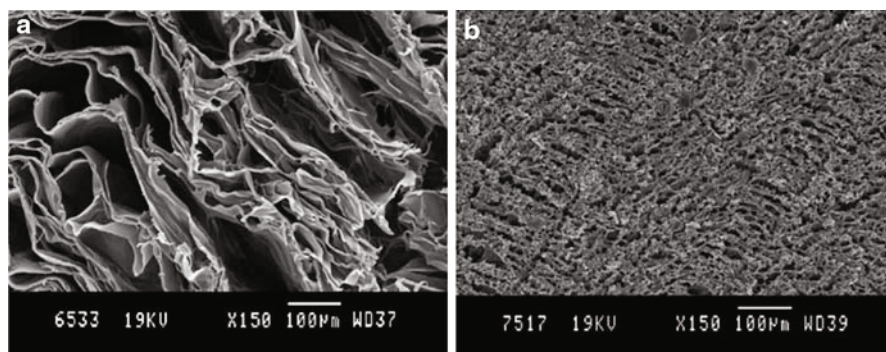


**Fig. 13** SEM images showing PLGA and PLGA/Bioglass<sup>®</sup> scaffolds by freeze-drying method (Reproduced from Ref. [93], with permission from Elsevier)

varying lengths of time at a temperature suitable for the sublimation of the solvent from the mixture.

The overall porosity, pore structure, and mechanical properties of the scaffolds can be tailored by adjusting processing parameters such as solvent concentration, concentration of solid component in the slurry, and processing time, among other parameters; hence, different scaffold morphologies can be attained [92]. This process can be simplified into four steps, as shown in Fig. 12, and typical microstructure of polymer/bioactive glass scaffolds made by freeze-drying are shown in Fig. 13 [93].

Therefore, just like in the case of electrospinning, freeze drying also allows the incorporation of bioactive glass particles for the obtainment of reinforced scaffolds. For example, fibrillar collagen/bioactive glass porous composites have been developed using a multistep sol–gel procedure, which were subsequently adsorbed from an acidic suspension using freeze-drying technology at different collagen/bioactive glass ratios (wt%): 20:80, 50:50, and 80:20 [94]. Mesoporous glasses in combination with silk have also been used as tissue engineering scaffolds [95]. These scaffolds showed higher mechanical strength, *in vitro* apatite mineralization, silicon (Si) ion release, and higher pH stability compared to scaffolds fabricated by the same technique but using melt-derived bioactive glass. *In vivo* studies of calvaria defects in SCID mice also showed that the new bone apposition was slightly higher for the scaffolds containing mesoporous glass [95].

Hunger et al. [96] investigated the structure–property–processing correlation in composite scaffolds fabricated by freeze-drying using a blend of chitosan and gelatin with 75 v.% of alumina particle reinforcement as a model system. They found that

the particle size of the inorganic reinforcing phase played a deciding role in determining the elastic modulus, compressive yield strength, and the failure mode of the composite scaffolds. Whereas small particles and bimodal particle size distribution led to thicker polymer walls and brittle failure, the incorporation of larger alumina particle sizes led to thinner pore walls with alignment of the particles in the polymer phase forming a structure type of “beads on a string.” The difference in failure modes was explained by the difference in the structure of the lamellar walls, which were more porous in the case of smaller and bimodal particle incorporation. The study also found that with increase of the rate of freezing the mechanical strength of the composites increased, while the lamellar spacing and the pore aspect ratio were reduced. Both the rate of freezing and the effect of particle size have also been investigated, and it was confirmed that these two factors must be considered to design scaffolds with compatible mechanical and morphological properties for a given application [88, 92, 96]. Compressive strength values as high as 11.5 MPa and elastic moduli as high as 215 MPa have been reported for freeze-dried BG-filled scaffolds [88].

Another important advantage of the freeze-drying technology is that bioactive molecules such as growth factors [97] or drugs [98] can be easily incorporated into the scaffolds since no high-temperature processing is required. Additionally, it is possible to make use of the ions leached from bioactive glasses to provide a favorable environment for the cells.

For novel materials and scaffold development, individual techniques can be combined leading to modifications of the microstructure and porosity of the final composite material. Qu et al. [99], for example, combined the sol–gel method, freeze-drying, and particulate leaching process to fabricate nanostructured gelatin/silicate bioactive glass (SBG) hybrid scaffolds. By utilizing the sol–gel technique, amorphous SBG was uniformly distributed into the gelatin matrix acting as a reinforcing phase. In comparison to directional pore arrangement by conventional freeze-drying process, the pores were round with sizes in the range of 250–420  $\mu\text{m}$ , which was determined by the leached particulates. Hierarchical pore structures with macropores of around several hundred micrometers and nanopores of around several hundred nanometers were generated from the particulate leaching and freeze-drying processes, respectively. The morphologies of gelatin/SBG with different SBG content are shown in Fig. 14 [99]. Dental pulp stem cell (DPSCs) cultures evidenced that the gelatin/SBG hybrid scaffolds were more favorable for cell adhesion, proliferation, and osteogenic differentiation than the gelatin-only scaffolds. Moreover, gene expression was highly promoted by SBG addition. The hybrid scaffolds showed a high potential for regeneration of decayed dentin/pulp structure.

## Rapid Prototyping

The advances of rapid prototyping (RP) (or solid freeform fabrication (SFF), additive manufacturing) techniques are bringing a wide range of possibilities to the biomedical field. These techniques permit the manufacture of customized

components conferring precise control of their architecture [12, 100]. These methods are based on computer-aided design to manufacture custom-made devices (scaffolds) directly from digital data. The most widely used RP technologies for manufacturing scaffolds for tissue engineering are stereolithography (SL or SLA), selective laser sintering (SLS), fused deposition modeling (FDM), 3D printing (3DP), multi-jet modeling (MJM), and laminated object manufacturing (LOM)

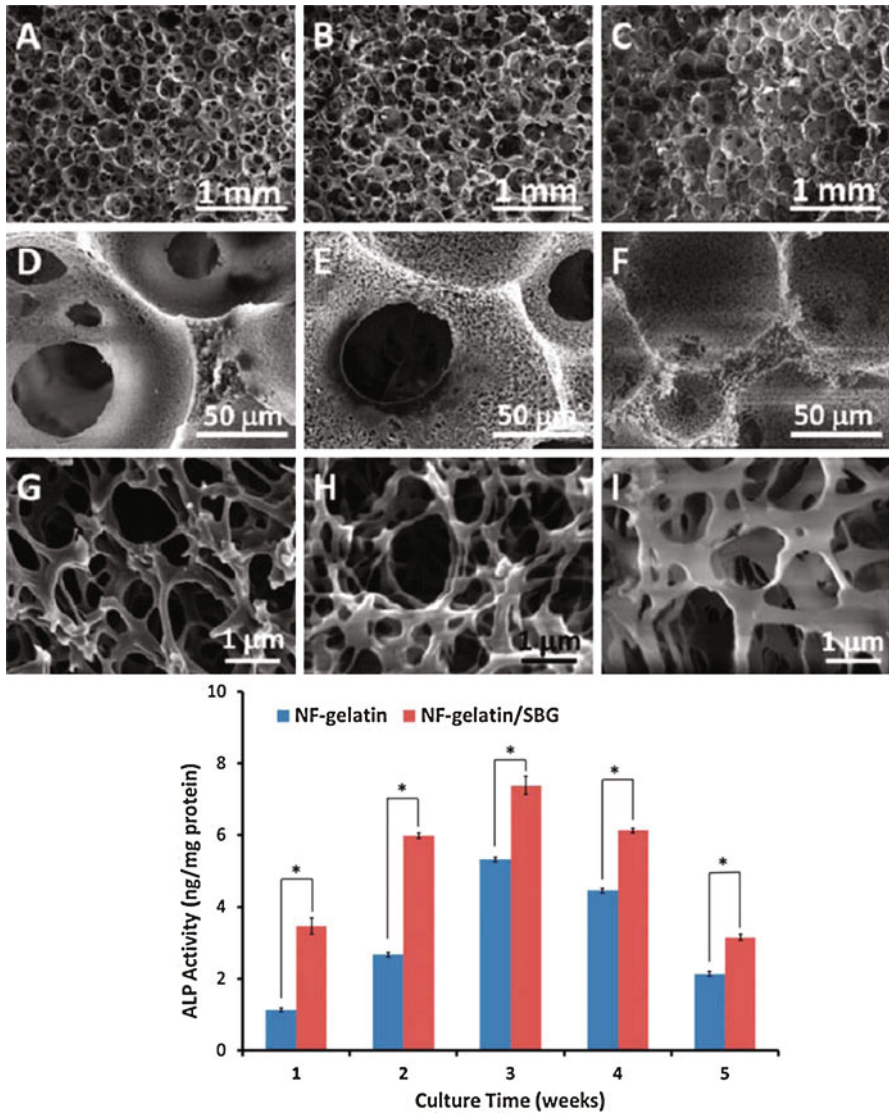
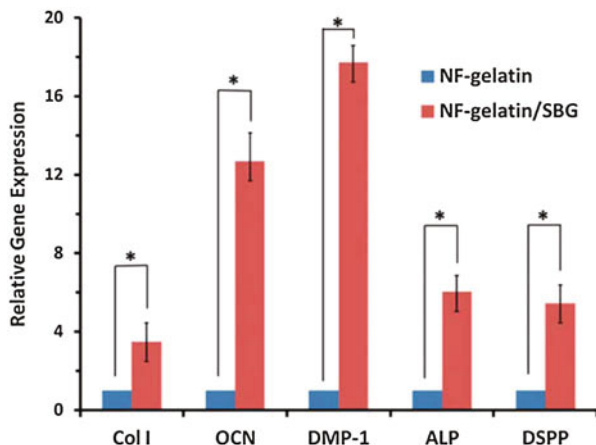


Fig. 14 (continued)



**Fig. 14** SEM micrographs of gelatin/SBG hybrid scaffolds with SBG ratios of 0 % (a, d, g), 5 % (b, e, h), and 10 % (c, f, i); ALP activity and gene expression of gelatin scaffolds and gelatin/SBG (5 %) scaffolds (Reproduced from Ref. [99] with permission from Royal Society of Chemistry (RSC) publishing)

[12]. Figure 15 shows representative schemes of different SFF methods reported in literature [100, 101].

The main advantages of SFF include reproducibility and precise control over the architecture of 3D scaffolds, mainly concerning the scaffold's internal structure, geometry, pore sizes and distribution. Scaffolds exhibiting high, controlled shape porosity and full interconnectivity can be obtained. SFF also allows the fabrication of scaffolds with high complexity, which can be based on patient-specific data and with anisotropic or graded microstructures. Generally, SFF techniques are versatile requiring a relatively low processing time, in comparison to conventional methods, generating scaffolds with enhanced mechanical and biological capabilities [12]. RP technologies are demonstrating a great potential in healthcare applications, and studies worldwide are starting to emerge which show the advantages of combining biopolymers and bioactive glasses through these modern techniques.

### Stereolithography (SLA)

SLA is a traditional RP technique based on the deposition of a photosensitive liquid resin in a movable platform, which is irradiated with an ultraviolet laser to cure and solidify the polymer. In this method, scaffolds are made through a layer-by-layer process, normally reaching a spatial resolution of approximately 50  $\mu\text{m}$  [12].

SLA can be used with a range of biopolymers and also to build bioceramic devices with a photosensitive polymer as a binder. The fabrication of polymer/ceramic composite scaffolds is more complicated due to the high viscosity of the final suspension and other limitations intrinsic to the technique. Some studies have shown the fabrication of Bioglass<sup>®</sup> scaffolds using a combination of SLA and casting techniques [102, 103]. In this indirect process, a polymer mold is obtained

by SLA, and after casting the bioceramic upon it, a thermal treatment is placed resulting in a ceramic scaffold. Also, Gmeiner et al. [104] successfully fabricated 3D dense bioactive glass-ceramic structures with increased mechanical properties and scaffolds with an accuracy of up to  $25 \times 25 \times 25 \mu\text{m}^3$  using ceramic and glass-ceramic slurries and the SLA technique. Tesavibul et al. [105] obtained a highly bioactive glass scaffold using lithography-based additive manufacturing. The technique allowed the tailoring of the scaffold's macroscopic and microstructural features, developing scaffolds with a pore size of  $500 \mu\text{m}$ .

Most recently, Elomaa et al. [106] developed a 3D scaffold with highly interconnected pores, combining photocrosslinkable PCL resin and S53P4 bioactive

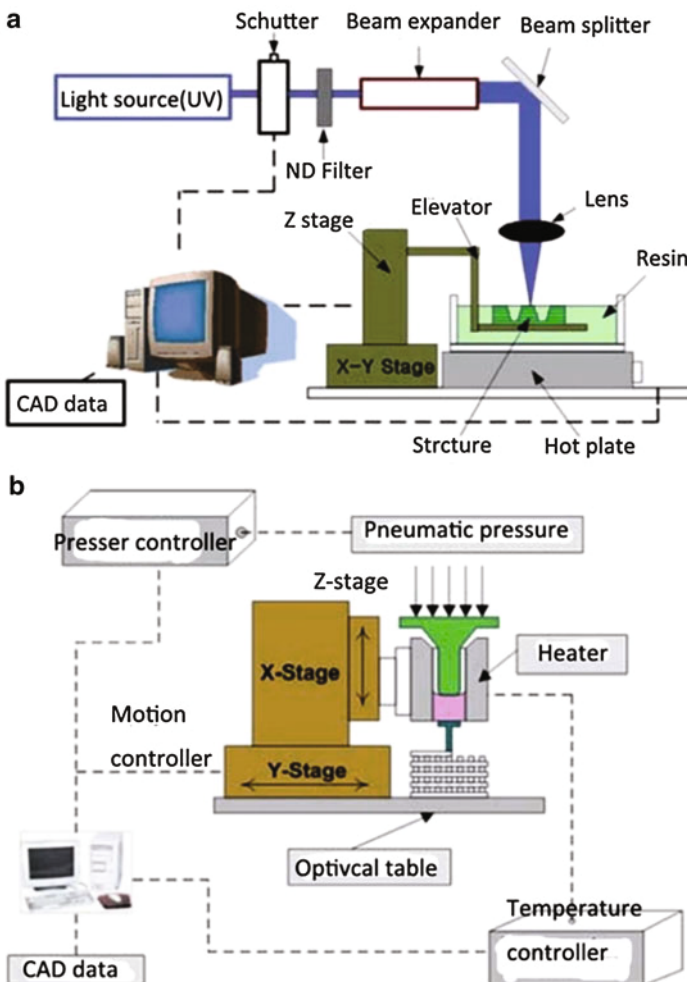


**Fig. 15** (continued)

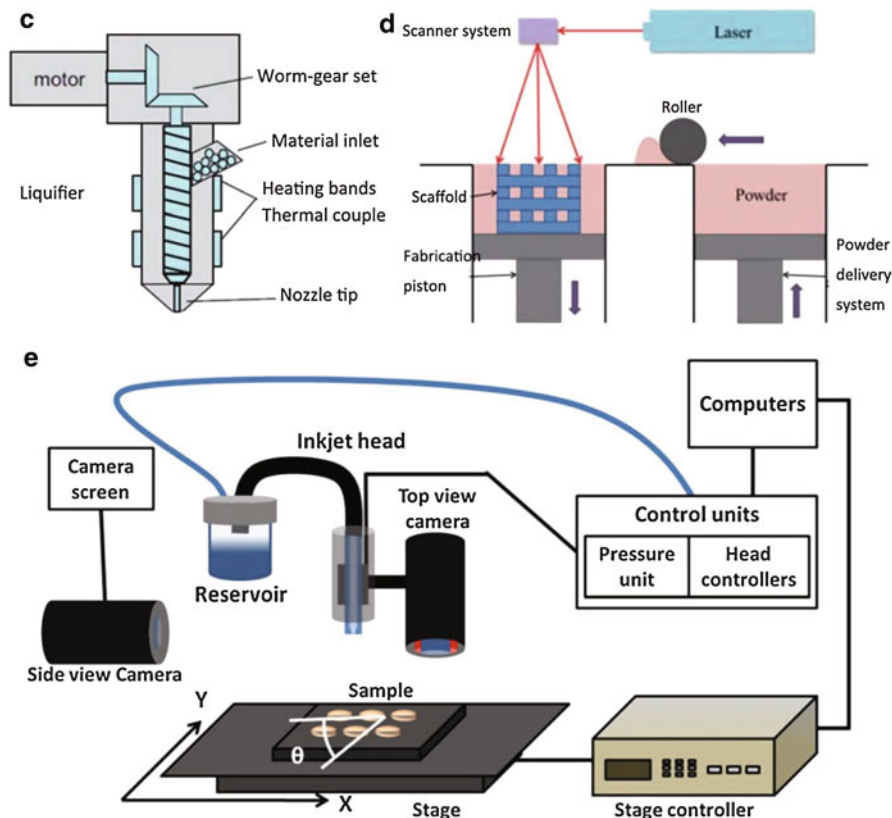


**Fig. 15** Schematic diagram of SFF technologies: (a) stereolithography, (b) fused deposition modeling, (c) mini-extruder in precision extrusion deposition, (d) selective laser sintering, (e) 3D printing (Reproduced from [100] and [101] with permissions from Royal Society of Chemistry (RSC) publishing and IOP publishing, respectively)

glass. The addition of the inorganic phase improved the compression modulus of the scaffolds and also their bioactivity, enhancing the attachment and the proliferation of human fibroblasts on the 3D structures.

### Selective Laser Sintering (SLS)

SLS uses a laser beam to selectively sinter or fuse some regions of a powder surface. This technique is used when high-complexity porous materials are desired. Due to limitations intrinsic to this technique such as optimal powder composition, particle size range, speed, and laser intensity, biopolymer–bioactive glass composites are still to be realized with this method [12]. However, some studies successfully obtained PLLA/HA [107] biocomposite scaffolds using this technique, thus opening the possibility for the fabrication of biopolymer–bioactive glass composites.



### 3D Printing (3DP)

3D printing has been widely used for the fabrication of scaffolds using different biopolymers and ceramics. This technique incorporates ink-jet technology to precisely place a liquid binder on a powder bed thus consolidating the powder and forming a cross-sectional layer. After this step, another powder layer is spread over the surface, and this process occurs until the pre-designed device is obtained. Following this procedure, the unfused excess powder is removed by compressed air or manually brushed.

Bergmann et al. [108] employed the 3D printing process to fabricate a composite of  $\beta$ -TCP and a bioactive glass (similar to 45S5 Bioglass<sup>®</sup>), using orthophosphoric acid ( $H_3PO_4$ ) and pyrophosphoric acid ( $H_7P_2O_7$ ) as binders. Results showed that the glass phase had no effect on the cement reaction and the maximum resolution obtained (a layer thickness) was approximately 50  $\mu m$ . The achieved bending strength was approximately 15 MPa and XRD analysis revealed the presence of two phases,  $CaNaPO_4$  and  $CaSiO_3$ , both biocompatible and feasible of biodegradation.

Zhao et al. [109] developed scaffolds with high osteogenic capability combining mesoporous bioactive glass (MBG) and poly(3-hydroxybutyrate-co-3-hydroxyhexanoate) (PHBHHx) via 3D printing. The biocomposite scaffolds had uniform interconnected macropores and high porosity, and their compressive strength was approximately 200 times higher than that of polyurethane foam templated MBG scaffolds. These scaffolds also presented high bioactivity tested by the proliferation and differentiation of human bone marrow-derived mesenchymal stem cells (hBMSC). In vivo tests revealed that MBG/PHBHHx biocomposite scaffolds had good osteogenic capability and stimulated bone regeneration in critical-size rat calvarial defects within 8 weeks. The morphologies of the 3D plotted scaffolds with varying weight ratio are shown in Fig. 16 [109].

Serra et al. [110] presented studies incorporating calcium phosphate glasses into PLA. In the first study, in 2013, they fabricated biodegradable 3D-printed PLA/CaP glass scaffolds via nozzle-based rapid prototyping. As reported, the addition of 5 % PEG to the PLA matrix allowed the fabrication of high-resolution scaffolds without affecting the polymer blending properties. The chosen technique also permitted the manufacture of highly porous scaffolds with satisfactory mechanical properties. The addition of the glass (and PEG) to the PLA matrix induced a more positive biological response, allowing cell (mesenchymal stem cells) adhesion and spreading on the biomaterial's surface [110]. The second study was aimed at identifying the optimal conditions for manufacturing PEG/PLA/CaP glass scaffolds via 3D printing [110]. Results showed that the incorporation of PEG in the PLA matrix could improve the matrix's wettability and elastic modulus. In vitro tests indicated that the inclusion of PEG significantly accelerated the degradation of the biomaterial rate and improved the processing features [111]. Almeida et al. [112] studied PLA/CaP glass and chitosan scaffolds. While all scaffolds supported monocyte/macrophage adhesion and stimulated cytokine production, PLA-based scaffolds induced higher production of interleukin (IL)-6, IL-12/23, and IL-10. This study also draws attention to the impact of scaffold geometry on macrophage morphology and cytokine

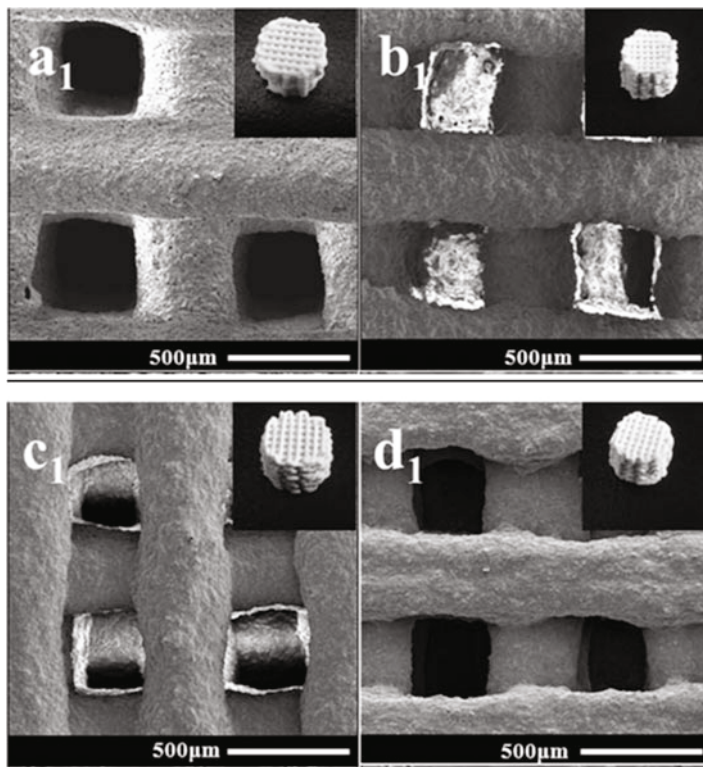


**Fig. 16** SEM images of 3D-printed MBG-based composite scaffolds: **a1** (MBG: PVA = 7:1 (w/w)); **b1**, **c1**, and **d1** represent the scaffolds with MBG: PHBHHx = 7:1, 5:1, and 3:1 (weight ratio) (Reproduced from Ref. [109] with permission from Royal Society of Chemistry (RSC) publishing)

secretion profile. Recently, Zhang et al. [113] fabricated strontium-containing mesoporous bioactive glass and PVA scaffolds by 3D printing. Results indicated that the scaffolds had uniform interconnected macropores and high porosity. Also, their compressive strength was approximately 170 times that of polyurethane foam templated MBG scaffolds. The manufactured scaffolds possessed good apatite-forming ability and stimulated osteoblast cell proliferation and differentiation. In this study, dexamethasone was also used as a model drug. The Sr-MBG/dexamethasone scaffolds exhibited sustained drug delivery capability for use in local drug delivery therapy.

### Fused Deposition Modeling (FDM)

This technique employs the concept of extruding a melt through a movable nozzle with a small orifice onto a substrate platform, depositing the material in parallel form, creating the layer. Normally, this process uses thermoplastic polymers, and the combination with bioceramics can produce highly porous 3D scaffolds. Korpela

et al. [114] have reported the manufacture of highly porous biocomposite scaffolds based on bioactive glass S53P4/poly( $\epsilon$ -caprolactone) via FDM process. SEM images showed that BG particles were present at the scaffold's surface. Also, the study indicated that this technique was suitable for developing mechanically durable and biocompatible biocomposites.

The studies discussed in this section can confirm that SFF offers a series of advantages when compared to conventional scaffold fabrication routes, and there are a range of processing techniques being explored in order to create highly complex polymer, ceramic, or composite scaffolds with precise control of pore size and spatial distribution, high reproducibility, and flexibility in shape and size. Currently, the SLA, SLS, 3DP, and FDM techniques are used for the fabrication of polymer/bioactive glass biocomposite scaffolds. The results obtained so far indicate that the newly developed biomaterials have achieved satisfactory mechanical properties and enhanced biological performance, making possible the manufacture of scaffolds with excellent accuracy and good surface quality. These relatively novel techniques thus bring new perspectives and opportunities for tissue engineering when combined with biopolymer–bioactive glass systems. They are expected to lead to improved scaffolds with tuned properties and pore structure for different applications.

---

## Summary

In the last 15 years, great advances in the development of tissue engineering scaffolds have been accomplished. A variety of combinations of natural or synthetic polymers with bioactive glasses or glass-ceramics have been explored. These composite structures have many advantages, including the possibility of tailoring the degradation kinetics, mechanical properties, and chemical composition according to the characteristics of the surrounding tissue where the scaffold will be applied.

The addition of biologically active ions to bioactive glass, such as strontium, boron, copper, etc. is an interesting approach being increasingly considered to provide enhanced functionalities to composite scaffolds. The fact that some bioactive glasses are able to bond to soft tissues offers great new pathways for the use of these types of composites in soft tissue engineering, especially for the regeneration of tissues with higher complexity, as recently reviewed [16].

However, some major challenges remain to achieve clinical applications of the different scaffolds developed over the years in particular considering the required balance between (time-dependent) physical, mechanical, and biological properties. The optimal scaffold needs to mimic the ECM as closely as possible. One of the most difficult challenges is to analyze the interaction between cells and scaffolds *in vitro* and *in vivo* (animal models) and to translate these findings successfully to the clinic, considering the time-dependent change of the scaffolds' structure and properties. In a composite biomaterial, this is particularly complex as the multiple phases are changing with time, in mechanical properties and composition, at different degradation rates.

As discussed in this chapter, biopolymer–BG composites, including mesoporous BG and nanoscale BG particles, represent promising materials for superior scaffolds for TE. With the expansion and improvement of processing techniques for such composites (some of which were discussed in this chapter in detail), new possibilities for the incorporation of the BG phase in different concentrations and in different geometrical arrangements become possible which should lead to tailored mechanical, biological and degradation behavior of the scaffolds. It is anticipated that further research in the field, likely involving combination of polymers, BGs (in different morphologies), and the smart addition of bioactive molecules [97], will lead to superior biomimetic composites for TE scaffolds with opportunities for clinical use.

---

## References

1. Rezwan K et al (2006) Biodegradable and bioactive porous polymer/inorganic composite scaffolds for bone tissue engineering. *Biomaterials* 27(18):3413–3431
2. Dahlin RL, Kasper FK, Mikos AG (2011) Polymeric nanofibers in tissue engineering. *Tissue Eng Part B Rev* 17(5):349–364
3. Place ES et al (2009) Synthetic polymer scaffolds for tissue engineering. *Chem Soc Rev* 38(4):1139–1151
4. Ferreira AM et al (2012) Collagen for bone tissue regeneration. *Acta Biomater* 8(9):3191–3200
5. Sabir MI, Xu X, Li L (2009) A review on biodegradable polymeric materials for bone tissue engineering applications. *J Mater Sci* 44(21):5713–5724
6. Sun J, Tan H (2013) Alginate-based biomaterials for regenerative medicine applications. *Materials* 6(4):1285–1309
7. Chu PK, Liu X (2008) *Biomaterials fabrication and processing handbook*. CRC press, Boca Raton
8. Ylänen HO (2011) *Bioactive glasses: materials, properties and applications*. Elsevier, Cambridge
9. Rahaman MN et al (2011) Bioactive glass in tissue engineering. *Acta Biomater* 7(6):2355–2373
10. Kaur G et al (2014) A review of bioactive glasses: their structure, properties, fabrication and apatite formation. *J Biomed Mater Res A* 102(1):254–274
11. Loh QL, Choong C (2013) Three-dimensional scaffolds for tissue engineering applications: role of porosity and pore size. *Tissue Eng Part B Rev* 19(6):485–502
12. Thavorniyutikarn B et al (2014) Bone tissue engineering scaffolding: computer-aided scaffolding techniques. *Prog Biomater* 3(2–4):61–102
13. Hench LL (2015) Opening paper 2015—Some comments on Bioglass: Four Eras of Discovery and Development. *Biomedical glasses* 1(1):1–11
14. Guarino V, Causa F, Ambrosio L (2007) Bioactive scaffolds for bone and ligament tissue. *Expert Rev Med Devices* 4(3):405–418
15. Hench LL (1998) Bioceramics. *J Am Ceram Soc* 81(7):1705–1728
16. Miguez-Pacheco V, Hench LL, Boccaccini AR (2015) Bioactive glasses beyond bone and teeth: emerging applications in contact with soft tissues. *Acta Biomater* 13:1–15
17. Gentleman E et al (2010) The effects of strontium-substituted bioactive glasses on osteoblasts and osteoclasts in vitro. *Biomaterials* 31(14):3949–3956
18. Durand LAH et al (2014) In vitro endothelial cell response to ionic dissolution products from boron-doped bioactive glass in the  $\text{SiO}_2\text{--CaO--P}_2\text{O}_5\text{--Na}_2\text{O}$  system. *J Mater Chem B* 2(43):7620–7630

19. Wang X et al (2011) Synthesis and characterization of hierarchically macroporous and mesoporous  $\text{CaO-MO-SiO}_2\text{-P}_2\text{O}_5$  ( $M = \text{Mg, Zn, Sr}$ ) bioactive glass scaffolds. *Acta Biomater* 7(10):3638–3644
20. Erol M, Özyuguran A, Çelebican Ö (2010) Synthesis, characterization, and in vitro bioactivity of sol-gel-derived Zn, Mg, and Zn-Mg Co-doped bioactive glasses. *Chem Eng Technol* 33(7):1066–1074
21. Varmette EA et al (2009) Abrogation of the inflammatory response in LPS-stimulated RAW 264.7 murine macrophages by Zn- and Cu-doped bioactive sol-gel glasses. *J Biomed Mater Res A* 90(2):317–325
22. Fooladi I et al (2013) Sol-gel-derived bioactive glass containing  $\text{SiO}_2\text{-MgO-CaO-P}_2\text{O}_5$  as an antibacterial scaffold. *J Biomed Mater Res A* 101(6):1582–1587
23. Blaker J, Nazhat S, Boccaccini A (2004) Development and characterisation of silver-doped bioactive glass-coated sutures for tissue engineering and wound healing applications. *Biomaterials* 25(7):1319–1329
24. Lohbauer U et al (2005) Antimicrobial treatment of dental osseous defects with silver doped bioglass: osteoblast cell response. *Key Eng Mater* 284:435–438
25. Zhu Y et al (2013) Magnetic mesoporous bioactive glass scaffolds: preparation, physicochemistry and biological properties. *J Mater Chem B* 1(9):1279–1288
26. Jayalekshmi A, Victor SP, Sharma CP (2013) Magnetic and degradable polymer/bioactive glass composite nanoparticles for biomedical applications. *Colloids Surf B Biointerfaces* 101:196–204
27. Brauer DS et al (2010) Fluoride-containing bioactive glasses: effect of glass design and structure on degradation, pH and apatite formation in simulated body fluid. *Acta Biomater* 6(8):3275–3282
28. Brauer DS et al (2008) Fluoride-containing bioactive glasses. *Adv Mater Res* 39:299–304
29. Erol M et al (2012) Copper-releasing, boron-containing bioactive glass-based scaffolds coated with alginate for bone tissue engineering. *Acta Biomater* 8(2):792–801
30. Wu C et al (2013) Copper-containing mesoporous bioactive glass scaffolds with multifunctional properties of angiogenesis capacity, osteostimulation and antibacterial activity. *Biomaterials* 34(2):422–433
31. Erol M et al (2012) 3D Composite scaffolds using strontium containing bioactive glasses. *J Eur Ceram Soc* 32(11):2747–2755
32. Shruti S et al (2013) Mesoporous bioactive scaffolds prepared with cerium-, gallium- and zinc-containing glasses. *Acta Biomater* 9(1):4836–4844
33. Hoppe A, Güldal NS, Boccaccini AR (2011) A review of the biological response to ionic dissolution products from bioactive glasses and glass-ceramics. *Biomaterials* 32(11):2757–2774
34. Azevedo M et al (2010) Synthesis and characterization of hypoxia-mimicking bioactive glasses for skeletal regeneration. *J Mater Chem* 20(40):8854–8864
35. Wu C et al (2011) Proliferation, differentiation and gene expression of osteoblasts in boron-containing associated with dexamethasone deliver from mesoporous bioactive glass scaffolds. *Biomaterials* 32(29):7068–7078
36. Wu C, Chang J (2014) Multifunctional mesoporous bioactive glasses for effective delivery of therapeutic ions and drug/growth factors. *J Control Release* 193:282–295
37. Jones JR (2013) Review of bioactive glass: from Hench to hybrids. *Acta Biomater* 9(1):4457–4486
38. Wu C, Chang J, Xiao Y (2011) Mesoporous bioactive glasses as drug delivery and bone tissue regeneration platforms. *Ther Deliv* 2(9):1189–1198
39. Boccaccini AR et al (2010) Polymer/bioactive glass nanocomposites for biomedical applications: a review. *Compos Sci Technol* 70(13):1764–1776
40. Luo C et al (2012) Modulating cellular behaviors through surface nanoroughness. *J Mater Chem* 22(31):15654–15664

41. Misra SK et al (2010) Characterization of carbon nanotube (MWCNT) containing P (3HB)/bioactive glass composites for tissue engineering applications. *Acta Biomater* 6(3):735–742
42. Boccaccini AR, Ma PX (Eds.) (2014) *Tissue engineering using ceramics and polymers*. Woodhead Publishing, Elsevier, Cambridge
43. Lu HH et al (2003) Three-dimensional, bioactive, biodegradable, polymer–bioactive glass composite scaffolds with improved mechanical properties support collagen synthesis and mineralization of human osteoblast-like cells in vitro. *J Biomed Mater Res A* 64(3):465–474
44. Roether J et al (2002) Novel bioresorbable and bioactive composites based on bioactive glass and polylactide foams for bone tissue engineering. *J Mater Sci Mater Med* 13(12):1207–1214
45. Liu W et al (2013) Application and performance of 3D printing in nanobiomaterials. *J Nanomater* 2013:13
46. Boccaccini AR, Maquet V (2003) Bioresorbable and bioactive polymer/Bioglass® composites with tailored pore structure for tissue engineering applications. *Compos Sci Technol* 63(16):2417–2429
47. Nooaeid P et al (2012) Osteochondral tissue engineering: scaffolds, stem cells and applications. *J Cell Mol Med* 16(10):2247–2270
48. Park J-H et al (2013) Microcarriers designed for cell culture and tissue engineering of bone. *Tissue Eng Part B Rev* 19(2):172–190
49. Freiberg S, Zhu X (2004) Polymer microspheres for controlled drug release. *Int J Pharm* 282(1):1–18
50. Yoon B-H, Kim H-E, Kim H-W (2008) Bioactive microspheres produced from gelatin–siloxane hybrids for bone regeneration. *J Mater Sci Mater Med* 19(6):2287–2292
51. Kulshreshtha AK, Singh ON, Wall GM (2010) *Pharmaceutical suspensions. From formulation development to manufacturing*. Springer, New York
52. Qiu QQ, Ducheyne P, Ayyaswamy PS (2002) Bioactive, degradable composite microspheres. *Ann N Y Acad Sci* 974(1):556–564
53. Keshaw H et al (2008) Assessment of polymer/bioactive glass-composite microporous spheres for tissue regeneration applications. *Tissue Eng Part A* 15(7):1451–1461
54. Wu C et al (2010) Bioactive inorganic-materials/alginate composite microspheres with controllable drug-delivery ability. *J Biomed Mater Res B Appl Biomater* 94(1):32–43
55. Mondal T et al (2012) Poly (l-lactide-co-ε-caprolactone) microspheres laden with bioactive glass-ceramic and alendronate sodium as bone regenerative scaffolds. *Mater Sci Eng C* 32(4):697–706
56. Subia B, Kundu J, Kundu S (2010) *Biomaterial scaffold fabrication techniques for potential tissue engineering applications*. INTECH Open Access Publisher, Rijeka
57. Lu T, Li Y, Chen T (2013) Techniques for fabrication and construction of three-dimensional scaffolds for tissue engineering. *Int J Nanomedicine* 8:337–350
58. Bencherif SA, Braschler TM, Renaud P (2013) Advances in the design of macroporous polymer scaffolds for potential applications in dentistry. *J Periodontal Implant Sci* 43(6):251–261
59. Liu X, Ma P (2004) Polymeric scaffolds for bone tissue engineering. *Ann Biomed Eng* 32(3):477–486
60. Li X et al (2008) A mesoporous bioactive glass/polycaprolactone composite scaffold and its bioactivity behavior. *J Biomed Mater Res A* 84A(1):84–91
61. Wu J et al (2013) Improvement of PHBV scaffolds with bioglass for cartilage tissue engineering. *PLoS One* 8(8):e71563
62. Niu Y et al (2015) Bioactive and degradable scaffolds of the mesoporous bioglass and poly (l-lactide) composite for bone tissue regeneration. *J Mater Chem B* 3:2962–2970
63. Huang Z-M et al (2003) A review on polymer nanofibers by electrospinning and their applications in nanocomposites. *Compos Sci Technol* 63(15):2223–2253
64. Bosworth L, Downes S (2011) *Electrospinning for tissue regeneration*. Woodhead Publishing, Elsevier, Cambridge

65. Li D, Xia Y (2004) Electrospinning of nanofibers: reinventing the wheel? *Adv Mater* 16(14):1151–1170
66. Ding Y et al (2014) Fabrication of electrospun poly (3-hydroxybutyrate)/poly ( $\epsilon$ -caprolactone)/silica hybrid fibermats with and without calcium addition. *Eur Polym J* 55:222–234
67. Bhardwaj N, Kundu SC (2010) Electrospinning: a fascinating fiber fabrication technique. *Biotechnol Adv* 28(3):325–347
68. Jang J-H, Castano O, Kim H-W (2009) Electrospun materials as potential platforms for bone tissue engineering. *Adv Drug Deliv Rev* 61(12):1065–1083
69. Noh K-T et al (2010) Composite nanofiber of bioactive glass nanofiller incorporated poly (lactic acid) for bone regeneration. *Mater Lett* 64(7):802–805
70. Kouhi M et al (2013) Poly ( $\epsilon$ -caprolactone) incorporated bioactive glass nanoparticles and simvastatin nanocomposite nanofibers: preparation, characterization and in vitro drug release for bone regeneration applications. *Chem Eng J* 228:1057–1065
71. Lin H-M, Lin Y-H, Hsu F-Y (2012) Preparation and characterization of mesoporous bioactive glass/polycaprolactone nanofibrous matrix for bone tissues engineering. *J Mater Sci Mater Med* 23(11):2619–2630
72. Ren J et al (2014) Melt-electrospun polycaprolactone strontium-substituted bioactive glass scaffolds for bone regeneration. *J Biomed Mater Res A* 102(9):3140–3153
73. Allo BA, Rizkalla AS, Mequanint K (2010) Synthesis and electrospinning of  $\epsilon$ -polycaprolactone-bioactive glass hybrid biomaterials via a sol – gel process. *Langmuir* 26(23):18340–18348
74. Han X et al (2014) One-pot synthesis of macro-mesoporous bioactive glasses/polylactic acid for bone tissue engineering. *Mater Sci Eng C* 43:367–374
75. Gao C et al (2013) In vitro evaluation of electrospun gelatin-bioactive glass hybrid scaffolds for bone regeneration. *J Appl Polym Sci* 127(4):2588–2599
76. Kim HW, Lee HH, Chun GS (2008) Bioactivity and osteoblast responses of novel biomedical nanocomposites of bioactive glass nanofiber filled poly (lactic acid). *J Biomed Mater Res A* 85(3):651–663
77. Kim HW, Song JH, Kim HE (2006) Bioactive glass nanofiber–collagen nanocomposite as a novel bone regeneration matrix. *J Biomed Mater Res A* 79(3):698–705
78. Lee H-H et al (2008) Bioactivity improvement of poly ( $\epsilon$ -caprolactone) membrane with the addition of nanofibrous bioactive glass. *Acta Biomater* 4(3):622–629
79. Jo JH et al (2009) In vitro/in vivo biocompatibility and mechanical properties of bioactive glass nanofiber and poly ( $\epsilon$ -caprolactone) composite materials. *J Biomed Mater Res B Appl Biomater* 91(1):213–220
80. Castaño O et al (2014) Angiogenesis in bone regeneration: tailored calcium release in hybrid fibrous scaffolds. *ACS Appl Mater Interfaces* 6(10):7512–7522
81. Ezekwo G, Tong H-M, Gryte CC (1980) On the mechanism of dewatering colloidal aqueous solutions by freeze-thaw processes. *Water Res* 14(8):1079–1088
82. Zhang R, Ma PX (1999) Poly ( $\alpha$ -hydroxyl acids)/hydroxyapatite porous composites for bone-tissue engineering. I. Preparation and morphology. *J Biomed Mater Res* 44(4):446–455
83. Sultana N, Wang M (2008) PHBV/PLLA-based composite scaffolds containing nano-sized hydroxyapatite particles for bone tissue engineering. *J Exp Nanosci* 3(2):121–132
84. O'Brien FJ et al (2004) Influence of freezing rate on pore structure in freeze-dried collagen-GAG scaffolds. *Biomaterials* 25(6):1077–1086
85. Thitiset T et al (2013) Development of collagen/demineralized bone powder scaffolds and periosteum-derived cells for bone tissue engineering application. *Int J Mol Sci* 14(1):2056–2071
86. Eslaminejad MB et al (2007) Bone differentiation of marrow-derived mesenchymal stem cells using  $\beta$ -tricalcium phosphate–alginate–gelatin hybrid scaffolds. *J Tissue Eng Regen Med* 1(6):417–424

87. Gelinsky M, Eckert M, Despang F (2007) Biphasic, but monolithic scaffolds for the therapy of osteochondral defects. *Int J Mater Res* 98(8):749–755
88. Pon-On W et al (2014) Mechanical properties, biological activity and protein controlled release by poly (vinyl alcohol)–bioglass/chitosan–collagen composite scaffolds: a bone tissue engineering applications. *Mater Sci Eng C* 38:63–72
89. Peter M et al (2010) Novel biodegradable chitosan–gelatin/nano-bioactive glass ceramic composite scaffolds for alveolar bone tissue engineering. *Chem Eng J* 158(2):353–361
90. Gentile P et al (2012) Bioactive glass/polymer composite scaffolds mimicking bone tissue. *J Biomed Mater Res A* 100(10):2654–2667
91. Voicu G et al (2014) Synthesis, characterization and bio-evaluation of bioactive composites scaffolds based on collagen and glass ceramic. *Dig J Nanomater Biostruct* 9(1):99
92. Wu J, Meredith JC (2014) Assembly of chitin nanofibers into porous biomimetic structures via freeze drying. *ACS Macro Lett* 3(2):185–190
93. Boccaccini AR et al (2005) Preparation and characterisation of poly (lactide-co-glycolide) (PLGA) and PLGA/Bioglass<sup>®</sup> composite tubular foam scaffolds for tissue engineering applications. *Mater Sci Eng C* 25(1):23–31
94. Abu MG, Radev LN, Titorenku ID, Vladkova TG (2014) Fibrillar collagen/bioactive calcium phosphate silicate glass-ceramic composites for bone tissue engineering. *Curr Tissue Eng* 2(2):14
95. Wu C et al (2011) A comparative study of mesoporous glass/silk and non-mesoporous glass/silk scaffolds: physicochemistry and in vivo osteogenesis. *Acta Biomater* 7(5):2229–2236
96. Hunger PM, Donius AE, Wegst UGK (2013) Structure–property–processing correlations in freeze-cast composite scaffolds. *Acta Biomater* 9(5):6338–6348
97. Guan J, Stankus JJ, Wagner WR (2007) Biodegradable elastomeric scaffolds with basic fibroblast growth factor release. *J Control Release* 120(1–2):70–78
98. Mouriño V et al (2013) Composite polymer-bioceramic scaffolds with drug delivery capability for bone tissue engineering. *Expert Opin Drug Deliv* 10(10):1353–1365
99. Qu T, Liu X (2013) Nano-structured gelatin/bioactive glass hybrid scaffolds for the enhancement of odontogenic differentiation of human dental pulp stem cells. *J Mater Chem B* 1(37):4764–4772
100. Seol Y-J, Kang T-Y, Cho D-W (2012) Solid freeform fabrication technology applied to tissue engineering with various biomaterials. *Soft Matter* 8(6):1730–1735
101. Jacot-Descombes L et al (2012) Fabrication of epoxy spherical microstructures by controlled drop-on-demand inkjet printing. *J Micromech Microeng* 22(7):074012
102. Padilla S, Sánchez-Salcedo S, Vallet-Regí M (2007) Bioactive glass as precursor of designed-architecture scaffolds for tissue engineering. *J Biomed Mater Res A* 81(1):224–232
103. Li Z et al (2013) Stiff macro-porous bioactive glass–ceramic scaffold: fabrication by rapid prototyping template, characterization and in vitro bioactivity. *Mater Chem Phys* 141(1):76–80
104. Gmeiner R et al (2015) Stereolithographic ceramic manufacturing of high strength bioactive glass. *Int J Appl Ceram Technol* 12(1):38–45
105. Tesavibul P et al (2012) Processing of 45S5 Bioglass<sup>®</sup> by lithography-based additive manufacturing. *Mater Lett* 74:81–84
106. Elomaa L et al (2013) Porous 3D modeled scaffolds of bioactive glass and photocrosslinkable poly ( $\epsilon$ -caprolactone) by stereolithography. *Compos Sci Technol* 74:99–106
107. Wiria F et al (2007) Poly- $\epsilon$ -caprolactone/hydroxyapatite for tissue engineering scaffold fabrication via selective laser sintering. *Acta Biomater* 3(1):1–12
108. Bergmann C et al (2010) 3D printing of bone substitute implants using calcium phosphate and bioactive glasses. *J Eur Ceram Soc* 30(12):2563–2567
109. Zhao S et al (2014) Three dimensionally printed mesoporous bioactive glass and poly (3-hydroxybutyrate-co-3-hydroxyhexanoate) composite scaffolds for bone regeneration. *J Mater Chem B* 2(36):6106–6118



110. Serra T, Planell JA, Navarro M (2013) High-resolution PLA-based composite scaffolds via 3-D printing technology. *Acta Biomater* 9(3):5521–5530
111. Serra T et al (2014) Relevance of PEG in PLA-based blends for tissue engineering 3D-printed scaffolds. *Mater Sci Eng C* 38:55–62
112. Almeida CR et al (2014) Impact of 3-D printed PLA-and chitosan-based scaffolds on human monocyte/macrophage responses: unraveling the effect of 3-D structures on inflammation. *Acta Biomater* 10(2):613–622
113. Zhang J et al (2014) Three-dimensional printing of strontium-containing mesoporous bioactive glass scaffolds for bone regeneration. *Acta Biomater* 10(5):2269–2281
114. Korpela J et al (2013) Biodegradable and bioactive porous scaffold structures prepared using fused deposition modeling. *J Biomed Mater Res B Appl Biomater* 101(4):610–619

Hanadi Y. Marghalani

## Contents

Introduction .....	358
Historical Background of RBDCs .....	359
Silicate Cement .....	359
Restorative Acrylic Resin .....	359
Polymethyl Methacrylate (PMMA) .....	360
Resin-Based Dental Composites (RBDC) .....	361
<i>Particulate Resin Composites</i> .....	362
Resin Matrix .....	362
Classification of Composites Based on Curing Method .....	365
The Setting Reaction (Polymerization) .....	368
Advancements in Resin Monomer .....	370
Degree of Conversion (DC) .....	377
Polymerization Shrinkage .....	379
Classification Based on Resin Matrix Type .....	383
Filler Particles .....	385
Historical Background and Classification of Fillers .....	386
Recent Advances in Filler Technology .....	389
Another Composite Classification Based on Viscosity and Clinical Application .....	395
Filler/Matrix-Coupling Agents .....	398
Historical Background and Classification of Coupling Agent .....	398
Other Properties of RBDCs .....	400
Mechanical Properties .....	400
Thermal Properties .....	400
Optical Properties .....	400
Shades and Coloring of Dental Composites .....	401
Water Sorption and Solubility .....	401
Biocompatibility .....	401
Summary: Future of RBDCs .....	402
References .....	403

---

H.Y. Marghalani (✉)

Operative Dentistry Department, King Abdulaziz University, Jeddah, Saudi arabia

e-mail: [hmarghalani@kau.edu.sa](mailto:hmarghalani@kau.edu.sa)

---

**Abstract**

Resin-based dental composite (RBDC) is among the most revolutionary development in restorative dental materials. This tooth-colored material was innovated mainly to restore the esthetic and function of the human dentition. The main objective of the chapter is to focus on reviewing the history of evolving of this material. Moreover, it gives highlights on the progress and advancement of their compositional formulations, physical and mechanical properties, as well as some related clinical perspective application. This chapter describes RBDCs according to their main composition components, namely; resin, filler, and silane coupling agent, and also the recent improvements in each of these components to fulfill higher standard prerequisites and properties as a dental restorative material. Additionally, classification of RBDCs was illustrated according to the basic way of: type, size of fillers and filler load, curing method, as well as viscosity of the resin. However, the recent classification was presented according to the clinical application as bulk-fill and also to different types of resin matrices innovated based on chemical structure other than dimethacrylate-based resin as silorane and ormocer. Nowadays, the focus of recent research is on bisphenol A (BPA)-free dental composites based on different chemistry of resin matrix in order to reduce human exposure to BPA derivative's side effects and to meet many properties for clinical application. Another important targeted aim of the RBDC's researches is concentrated on developing a resin chemistry of very low polymerization shrinkage and high general properties. Dental biomaterial researches are endeavored toward developing self-adhesive, self-repair, and bio-mimetic composites with antimicrobial release-on compounds.

---

**Keywords**

Resin dental composite • Silicate cement • Acrylic resin • Dimethacrylates • Nanocomposites • Bulk-fill composites • Chemical components • Classification • Filler particles • Inhibitors • Silane coupling agents • Resin monomer • Silorane • Dendrimers • Ormocers • POSS • Polymerization shrinkage • Polymerization stress • Degree of conversion • Mechanical properties

---

**Introduction**

The principal objectives of dental restorative treatment are the reconstruction and preservation of oral function, health, and esthetics. Several dental synthetic materials were developed in the field of restorative dentistry in order to replace decayed or lost tooth structure. Among these materials, resin-based dental composites (RBDC) were introduced to meet the patient's demand for esthetically pleasing appearance and to minimize the potential health hazards of mercury toxicity from dental amalgam. Nowadays, RBDCs are deliberated as worldwide tooth-colored material used in restorative dentistry. The development of resin composite as a dental restoration is considered as an important innovation in dental material science. Thus, they have

become the tooth-colored material of choice in the field of dentistry. During the last decade, research efforts have been focused on resin composites that evolved with each development of a new synthetic material and innovative restorative technique. Despite the rich history associated with the improvement of dental composites, their future is still even more promising in the dental field. This chapter in the book discusses mainly the historical background of the RBDCs as a tooth-colored material as well as their recent evolutions and future perspective advances.

---

## Historical Background of RBDCs

Dental materials were initially developed in the eighteenth century from cellulose nitrate (*Celluloid*), which was discovered by John Smith Hyatt [1]. It was discontinued because of its unpleasant taste, poor odor, and lack of stability [2]. In 1907, the first new organic and synthetic polymer material called phenol formaldehyde resin (*Bakelite*) was developed. It had main disadvantage of difficult handling and dimensional instability. In 1927–1932, cellulose acetate, polyvinyl chloride and polyvinyl acetate were utilized, but then they were withdrawn because of high residual stresses obtained [1].

### Silicate Cement

Silicate cement was developed by Thomas Fletcher in the late 1800s and became the only so-called esthetic direct dental filling material for anterior dentition. It was composed mainly of alumino-fluoro-silicate glass powder and phosphoric acid. Although it expressed an anticariogenic effect on the teeth by releasing fluoride, it was more prone to acidic degradation in the oral environment because of its high solubility, thus minimizing its shelf-life [3]. Moreover, it showed poor mechanical properties, pulpal damage, microleakage, and color instability.

### Restorative Acrylic Resin

In 1843, an acrylic acid was discovered, and by 1900, a methacrylic acid was synthesized along with several of its additives including methyl methacrylate, ethyl methacrylate, and *isopropyl* methacrylate (Fig. 1a, b). Later in 1937, auto-polymerizing acrylic resin was introduced to prosthetic dentistry as a denture base resin supplied in the form of powder (polymer) and liquid (monomer) systems. It was widely accepted because of its relatively good appearance, high dimensional stability, and ease of processing. For anterior direct restorations, silicate cements were replaced by acrylic resins [1]. Few years later, it was used as an indirect filling resin [4]. The first material used as a restoration was a heat-cured, unfilled, and low molecular weight acrylic resin. The restoration was made in a dental laboratory and then was cemented into the tooth. To improve the properties of unfilled acrylic resin,

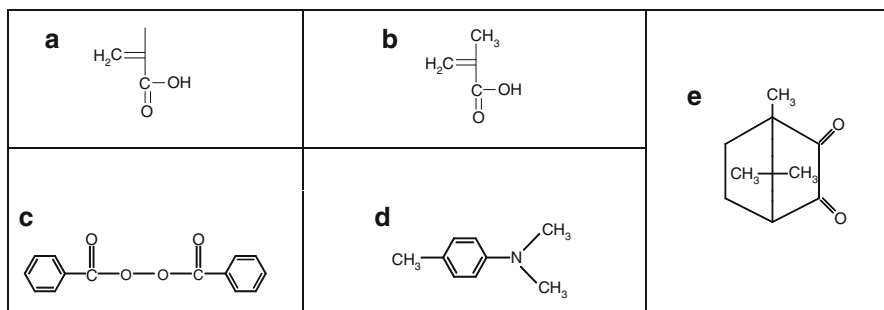


**Fig. 1** Structural formulae of the resin components and additives. (a) Acrylic acid, (b) methacrylic acid, (c) benzoyl peroxide, (d) *n,n*-dimethyl-*p*-toluidine, and (e) camphorquinone

attempts were made by adding suitable fillers to this resin. In the 1950s, acrylic filling materials with aluminosilicate glass fillers were formulated yielding some improvement of their physical and mechanical properties. In spite of such improved properties, they were still not good as filling materials because of some deficiencies in acrylic resin itself, such as high polymerization shrinkage resulting in increased liability for recurrent decay [4]. Buonocore in 1955 used orthophosphoric acid to facilitate the adhesion of acrylic resins to the enamel's surface.

## Polymethyl Methacrylate (PMMA)

A direct restoration made by cold-cured methyl methacrylate (MMA) resin was developed. This resin showed several negative properties, including high polymerization shrinkage, coefficient of thermal expansion, water absorption, microleakage, less adhesion to the tooth structure and relatively low strength, modulus of elasticity, and poor color stability, making them unacceptable as good filling materials [5]. Methyl methacrylate can be polymerized by an addition mechanism through the carbon-carbon double bonds to form polymethyl methacrylate (PMMA). After 1937, based on the experience with PMMA, a vast number of other resins, such as vinyl acrylic, polystyrene, epoxy, polycarbonate, nylon, vinyl styrene, and polyurethane, were developed. Nonetheless, PMMA became the most commonly used resinous material in restorative dentistry. The modified forms of acrylic resins were used as soft liners, direct restorations, denture repair materials, artificial teeth, and temporary crowns. A few years later in 1947, chemically cured resins were synthesized by German chemist LM Blumenthal, and subsequently, a chemically cured direct filling MMA resin, Sevriton™, was obtained. Until the 1950s, neither heat nor chemically cured resins were filled; then in 1959, the first glass-reinforced MMA composite was developed, but this did not exhibit acceptable clinical success as a filling material in stress-bearing areas.

Rafael L. Bowen, an American dentist, developed another synthetic resin called epoxy to overcome the inherent limitations of MMA resin as a restorative

material [6]. This resin hardened with minimal shrinkage yielding an insoluble polymer. Afterwards, few indirectly placed restorations of heat-cured epoxy resin composite showed good esthetics, whereas their use as a direct filling material was discontinued due to slow hardening. In 1951, the addition of mineral fillers to resins had been already proposed as a method of reinforcement. The major development was then occurred in discovering the photoinitiators to polymerize the composites by light-curing system.

## Resin-Based Dental Composites (RBDC)

Many materials used in dentistry, such as cements, wax, plaster, amalgam, impression, and porcelain, are composite in their component structure. Although a wide variety of different composite structures can be created, dental composites are classified into two main categories according to the shape of their reinforcing phase: *structural*, *particulate*, and *fiber-reinforced composites*. Literally, composite is defined as a material made of different phases yielding enhanced properties than these for each phase alone. The basic components of the dental composite is made mainly from (1) a cross-linked polymer resin matrix component which is usually dimethacrylate based, (2) initiator and inhibitor monomers depending on the mode of polymerization, (3) a diluent to control the viscosity of the resin to be flexible and less brittle, (4) dispersed components of filler particles and metallic tints, and (5) a silane coupling agent to adhere the resin to the fillers.

### Clinical Application

Primarily, RBDCs are used as a restorative material to restore decayed teeth either directly or indirectly. The direct composite restorations were used in small to moderately sized cavities subjected to mild amount of stresses. Hybrid composites were predominantly used to restore such cavities (This type of composite will be discussed later in the chapter). They were originally utilized to restore anterior dentition, and now they can be used for posterior restoration. However, indirect composite restorations that are fabricated in a laboratory can be used to restore a large cavity preparation that involves cusp coverage and high stress distribution area as permanent inlay, onlay, and crown restoration. This method utilizes heat under pressure in order to improve their general properties as good marginal adaptation, surface characteristic, and minimizing wear of opposing teeth. Proper treatment planning of choosing the proper type of dental composites will increase the longevity of these restorations. RBDCs are also used as pit and fissure sealant, liner, luting cement, root canal sealer, core buildup foundation, and provisional restoration. Moreover, because of the development of bonding agents, they are used to repair fractured ceramic prosthesis, for color characterization, and in manufacturing other types of restorative materials as resin-modified glass ionomers and resin cements. Versatile and different clinical applications of resin composite in dentistry are making the challenge of their development.

### **Advantages of Resin Composites**

Resin composite is the restorative material of choice in modern dentistry because its color mimics that of tooth substance. The cavity preparation for this material is conservative without the needs of extra means of retention other than that provided from the bonding agents. These restorations can be easily repaired, and also they are characterized by high fracture resistance. They are almost insoluble in oral fluid, less toxic to the pulp, and higher in mechanical and physical properties compared to the primarily fabricated materials.

### **Disadvantages of Resin Composites**

The main drawbacks of the resin composites are polymerization shrinkage, marginal leakage, staining, technique sensitivity, and inadequate bonding.

---

### **Particulate Resin Composites**

This term is used generally to refer to the resin-based restorative materials reinforced with a variety of inorganic fillers, which coupled to the resin by a silane agent. The mechanical and physical characteristics of the dental composites are dependent mainly on these three main components since each one of them is important for the success of the composite restoration. However, the significant developments in the evolution of commercial composites up-to-date have been directed toward modifications to these components. Dental composites were first introduced in the mid-1960s as a silicate and acrylic substitute.

### **Resin Matrix**

The resin is a chemically active component of the composite material made up of an organic polymeric matrix comprising a monomer system, a diluent monomer to adjust the viscosity of the material, an initiator monomer to trigger the free radical polymerization reaction, and a stabilizer to maximize the storage stability of uncured resin and the chemical stability of the cured resin composite.

### **Bis-GMA**

In 1962, Bowen commenced the first resin composite consisting of silane-treated silica and Bis-GMA (2,2-bis[4-(2-hydroxy-3-methacryloxypropyloxy)phenyl]propane) difunctional monomer, which was made of bisphenol A group and glycidyl methacrylate [7]. Since that date and till now, the Bis-GMA monomer became the most predominantly used resin matrix in restorative composites introduced into the field of dentistry (Fig. 2a). It has higher molecular weight than MMA yielding a very viscous resin that needs to be diluted with another flexible diluent monomer. In 1964, Adident™ was the first commercial anterior dental resin composite developed using Bis-GMA resin. The Bis-GMA-based resin composites used as restorative materials

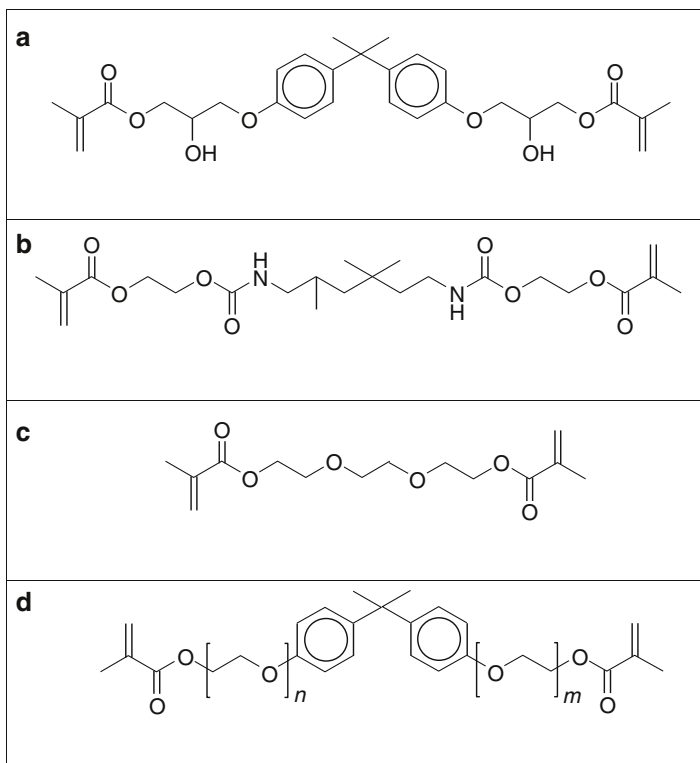


**Fig. 2** Chemical structure of basic monomers of dimethacrylate-based resin composites. (a) Bis-GMA, (b) UDMA, (c) TEGDMA, and (d) Bis-EMA

showed superior mechanical and physical properties, which could be due to their large molecular size and aromatic moiety.

### UDMA

In 1974, Foster and Walker introduced another dimethacrylate resin called urethane dimethacrylate (UDMA). It is characterized by a shorter-chain having the advantage of low viscosity, which facilitated increase filler loading without the need of adding a low molecular weight monomer (Fig. 2b). UDMA-based composites are more brittle and exhibit more polymerization shrinkage than Bis-GMA-based composites attributed to lower viscosity and shorter molecular length of this monomer [8]. However, some modified UDMA incorporated pendant hydrophobic substituent within the monomer backbone, which may result in reduction of water sorption and solubility of urethane-based dimethacrylate systems [9].

### TEGDMA

Bis-GMA has a very high viscosity because of the hydrogen bonding interactions that occur between the hydroxyl groups on the monomer molecules. Similarly,



UDMA is viscous due to its relatively high molecular weight. They must be diluted with a less viscous resin, such as triethylene glycol dimethacrylate (TEGDMA) to allow incorporation of more filler into the resin (Fig. 2c). Thus, this diluent increases the wetting ability of the resin by making it more flexible with good viscosity and copolymerization characteristics. It is characterized by smaller molecular size than Bis-GMA and higher amount of double bonds that facilitate polymerization reaction process resulting in more shrinkage, which adversely affects the material's properties, as increasing water uptake. Other diluents include MMA, benzyl methacrylate, ethylene glycol dimethacrylate (EGDMA), and hexamethylene glycol dimethacrylate (HMGDMA) added to enhance polymer chain elongation and polymerization reaction. These diluents can increase the degree of conversion (DC) but increase the polymerization shrinkage [10]. Other viscosity controllers are bisphenol-A-dimethacrylate (Bis-DMA), ethylene glycol dimethacrylate (EGDMA), and also UDMA. These formulations are functional and have resulted in significant advancements in the field of dentistry.

### **Bis-EMA**

Ethoxylated bisphenol-A-dimethacrylate (Bis-EMA) is a viscous monomer that structurally is analogous to Bis-GMA but without the two pendant hydroxyl groups (Fig. 2d). It can decrease water sorption of the resin, which subsequently permits its utilization to partially or completely substitute Bis-GMA in the recent formulation of dental composites. This chemical group participates in hydrogen bonding, thus accounting for the high viscosity of the resin. However, UDMA is more viscous than TEGDMA and Bis-EMA due to the hydrogen bonding between the  $-NH$  and  $C=O$  groups, but it is less viscous than Bis-GMA, since imino groups form weaker hydrogen bonds compared to hydroxyl groups [11].

### **Combined Resins**

In the past years, most of commercial dental composites used the Bis-GMA as a base monomer for their matrix-forming resin. A combination of different comonomers like TEGDMA or UDMA used with or without Bis-GMA was developed and contributed to diverse product profiles of the RBDCs. Both Bis-GMA and UDMA dimethacrylates became the main monomers for most dental composites that are widely used today. Other base monomers used in present commercial composites include bis(methacryloyloxymethyl) tricyclodecane (as Pertac Hybrid, ESPE-Premier products), urethane tetramethacrylate (UTMA) (as Clearfil Photoposterior, Kuraray products), and a linear polyurethane made from Bis-GMA and hexamethylene diisocyanate (HDI) (as Prisma APH and TPH, LD Caulk products). Because of the low viscosity of UDMA, some of UDMA-based composites were formulated with relatively low TEGDMA content. They are possibly still giving a high conversion and relatively lower shrinkage stress compared to Bis-GMA-based composites. Nevertheless, other properties are required to be considered to determine the actual chemical formulations suitable for clinical use.

The combination of these flexible monomers as UDMA and Bis-EMA is used to decrease the viscosity of the composite and to minimize the polymerization shrinkage. Another attempt is to create monomers with low viscosity, such as hydroxyl-free Bis-GMA, aliphatic urethane dimethacrylates, 1,6-bis[methacryloyloxy-2-ethoxycarbonylamino]-2,4,4-trimethylhexane, partially aromatic urethane dimethacrylate, or highly branched methacrylates.

All of these monomers have carbon-carbon double bonds as functional groups to react chemically by free radical addition polymerization. The dental composites can bond to the dentin by bonding agents which are made mainly from the same basic monomers used for the composite, and also these agents can be polymerized by the similar addition reaction.

### **Other Additive Ingredient Monomers**

Certain low molecular weight monomers are added to the resin to control the consistency and the polymerization reaction of the RBDC material. These components are identified as comonomers, initiators, accelerators, inhibitors, and UV stabilizers. The initiators are added to release the free radicals needed for the polymerization reaction. Therefore, the resin can be classified according to the mode of curing into heat-, cold-, and light-cured resins.

The chemical reaction during the polymerization occurs very rapidly and can be delayed by a component called an inhibitor, such as hydroquinone (HQ) and butylated hydroxytoluene (BHT). The polymerization of the surface layer of the composite is inhibited by atmospheric oxygen. Oxygen is considered as inhibitor that allows the placement of another new layer of composite on a recently cured one. This oxygen-inhibited layer is thicker and less wear-resistant in light-cured resin that makes the composite to wear faster. The inhibitors react with the free radicals and neutralizes them. Such a delay in the polymerization reaction is required to provide a working time during the clinical manipulation of the material, and also they prevent premature polymerization reaction.

The UV stabilizer is added to improve color stability by absorbing electromagnetic radiation, which can cause discoloration. The most commonly used absorber is 2-hydroxy-4-methoxy benzophenone. The use of additive novel comonomer systems with the addition of aldehyde and diketone functional groups would improve dental resin-composite properties [12].

## **Classification of Composites Based on Curing Method**

### **Heat-Activated Resins**

The polymerization reaction of these resins is initiated by benzoyl peroxide, which is activated and easily dissociated by heat above 65 °C to produce benzoyl free radicals (Fig. 1c). Well-controlled heat and pressure must be used to produce a higher concentration of free radicals suitable for proper polymerization. Most denture base resins use this system.

### Cold- or Chemically Activated Resins

These resins are supplied as two-paste or powder/liquid systems; one contains aromatic tertiary amines, such as *n,n*-dimethyl-*p*-toluidine, used as activators instead of heat application (Fig. 1d). The other one is benzoyl peroxide initiator, which reacts with activators to produce a (benzoyl) free radical. The resins polymerized by this mode are less rigid as the DC of cold-cured resins is lower than that of heat-cured resins. Chemically activated material as acrylic resin is used for provisional crowns, custom trays, and orthodontic retainers. Also, earlier types of dental composites have utilized this system of curing. In some of the new resin cements, this curing system permits higher DC of the material resulting in strong and durable cement once it sets. The curing of some of the buildup resin-based core materials is initiated by this system to ensure once thorough curing because they are placed in one increment. However, chemical type of curing leads to problems of mixing proportions and color instability. During mixing procedure, air may be incorporated in the form of voids into the resin which results in the weakening and sometimes staining of the set material because oxygen inhibits the polymerization.

### Light-Activated Resins

These types of resins are provided in a single paste that contained all the composite's constituents and several chemicals of initiators and activators. They have the advantage of a short setting time of the resinous material. Also, there is no need for mixing, thus minimizing the possibility of voids' inclusion in the set material. The chemical activator absorbs the light and then reacts with the initiator. Previously, *ultraviolet light (UV)* was used to split benzoin methyl ether into free radicals without tertiary amines. It can cause soft tissue injury, its light-producing lamp was expensive, and its penetration depth through the resin was limited. This light provides a shallow polymerization utilizing a wavelength of 365 nm.

The *visible blue light (VLC)* having a wavelength in the range of 460–480 nm (around 470 nm) becomes the most popular light to activate resin-based materials as dental composites. It is less tissue damaging, having a stable lamp for long periods, and it can be transmitted through the tooth and the resin obtaining better resin polymerization as well as color stability. Although the blue light is visible, it has a disadvantage of damaging the retina of the eyes when viewed directly. Therefore, light shield is needed for eye protection from this wavelength. The spectrum of light emission should cover the absorption range of the photoinitiator. This wavelength of the visible light is matching that of the chemical activator in the material. Therefore, the light can be absorbed mainly at this wavelength. The free radicals in this system are created by the application of this light in the presence of camphorquinone (CQ) (Fig. 1e). The latter is a commonly used  $\alpha$ -diketone photoinitiator (absorption peak  $\lambda = 468$  nm, which range from 360 to 520 nm) in dental composites. Optimum amount of CQ is required to obtain maximum polymerization, color stability, DC, and biocompatibility without compromising the overall properties of the composite [13]. Lucerin is a monoacylphosphine oxide (absorption peak  $\lambda = 380$  nm) that is mainly found in a light-shaded color of composites. A monoacylphosphine oxide

(MAPO) photoinitiator-based composite exhibited a significantly higher DC with increased strength and modulus compared with CQ-based material, without increasing polymerization stress, cuspal deflection, or microleakage [14].

Other photoinitiators are PPD (1-phenyl-1,2-propanedione) and Irgacure 819 (bisacylphosphine oxide) characterized by color stability and less yellowish effect. A novel CQ derivative possessing an acylphosphine oxide (APO) group yields a CQ-APO photoinitiator having maximum absorption wavelengths ( $\lambda_{max}$ ) at 372 nm from APO and 475 nm from CQ moieties. Resins comprising this combination of photoinitiators exhibited good polymerization reaction, color shading, higher DC, and mechanical strength. The colorless photoinitiator was innovated to minimize the yellowish effect of CQ, thus improving the potential of esthetic quality of dental composite restorations especially for bleach and translucent shades [15]. These photoinitiators can be iodonium salts, onium compounds, or acylphosphine oxides as TPO (2,4,6-trimethylbenzoyl-diphenylphosphine oxide). The latter showed a higher curing efficiency than that initiated by CQ. Lucirin TPO increased the speed of the reaction without increasing the shrinkage stress, cuspal deflection, or marginal leakage and improved the mechanical properties [15]. The photoinitiator allows a good time to manipulate the material before light curing, though it might be affected by the ambient light in the operator room.

The type of coinitiator present in the photoinitiator system plays a role in determining the physical and chemical properties of RBDCs. Different tertiary amines, such as DMPT (N, N-dimethyl p-toluidine), CEMA (N,N-cyanoethylmethylaniline), DEPT (N,N-diethanol p-toluidine), DMAEMA (2-dimethylaminoethyl methacrylate), and DABE (N,N-dimethyl-p-aminobenzoic acid ethylester) can be associated with the CQ component to allow light initiation of RBDCs. Resin comprising DMAEMA expressed higher DC, shrinkage, microhardness, and good optical properties [16].

Light polymerization is essential to stabilize the composite and to reduce the elution of unreacted monomers that may affect the biocompatibility of the material. Different light sources are available nowadays which include quartz halogen light, plasma arc, argon laser, and blue emitting diodes (LEDs). The halogen and LED lights are the most commonly used units in curing dental composites. The LED lamps are characterized by several advantages making them more effective over halogen ones. They have longer shelf-life, less heat production, do not require any filter, and can convert electricity to more efficient light. The wavelength of LEDs coincides with that absorption spectrum of the CQ. In order to enhance the polymerization of the dental composites, different curing modes as step, ramp, and pulse are built in the recent light-curing units. They attempted to control polymerization shrinkage by permitting better DC while reducing the contraction stresses.

### Dual-Activated Resins

The polymerization of these resins is initiated by a light-cured system and then continued by a chemical reaction. They comprised two separate components that required manual-mixing or auto-mixing with a slightly longer working time

of 6–8 min. This type of resin is utilized when light cannot reach the deepest area where polymerization is needed. Several dental materials such as resin cements have these both polymerization characteristics. They are utilized mainly in inaccessible areas to light as in core buildup foundation or during fiber post, indirect composite or ceramic restorations, and ortho-brackets' cementation.

## The Setting Reaction (Polymerization)

Polymerization is a chemical process of converting smaller molecule monomers into a large polymer. Accompanying this reaction, there is dimensional change and chemical contraction called polymerization shrinkage that is caused by exchanging interatomic spacing between molecules by which double bonds changed to single covalent ones. Such a conversion results in shortening of intermolecular distance between monomer units as they form polymer chains leading to shrinkage of the polymerized material. This reaction is exothermic and associated with thermal contraction creating internal stresses. During this chemical reaction, a vitrification process induces freezing of the radicals in the cross-linked structure, stopping further chemical reaction called post-contraction.

Composite monomers are polymerized by a free radical reaction to form glassy, cross-linked polymer networks that are relatively insoluble and somewhat brittle but reasonably strong. Part of the shrinkage occurs before the solidification, while the material is liable to flow called gel point. Rapid increase in stiffness of the composite that is becoming rigid enough to resist sufficient plastic flow to compensate for the original volume during the solidification process is referred as post-gelation. This can result in contraction stresses generated at the bonded surfaces yielding a gap formation. The polymerization of dental composites is one of the crucial deficiencies that complicates the use of this very versatile class of restorative materials and possibly limits service life expectations.

## Types of Polymerization

There are two major methods to form a polymer: addition and condensation polymerization. *Addition polymerization* is a reaction during which no by-product is formed as the chain grows and can be classified into free radical (common in Bis-GMA composites), ring-opening, and ionic reactions. *Condensation polymerization* is a reaction during which a smaller molecule is eliminated to produce a larger one without involving free radicals, and a by-product, mainly water, is formed as the chain grows.

## Free Radical Polymerization

This process is alternatively called addition polymerization because a molecule is added to the polymer chain as the reaction proceeds. Most of the setting reaction yielded by a resin-based material, such as composite, adhesive, cement, sealant, and acrylic involved this type of polymerization. It comprises three stages; the first step is *activation and initiation* which requires an external agency, such as heat, chemical,

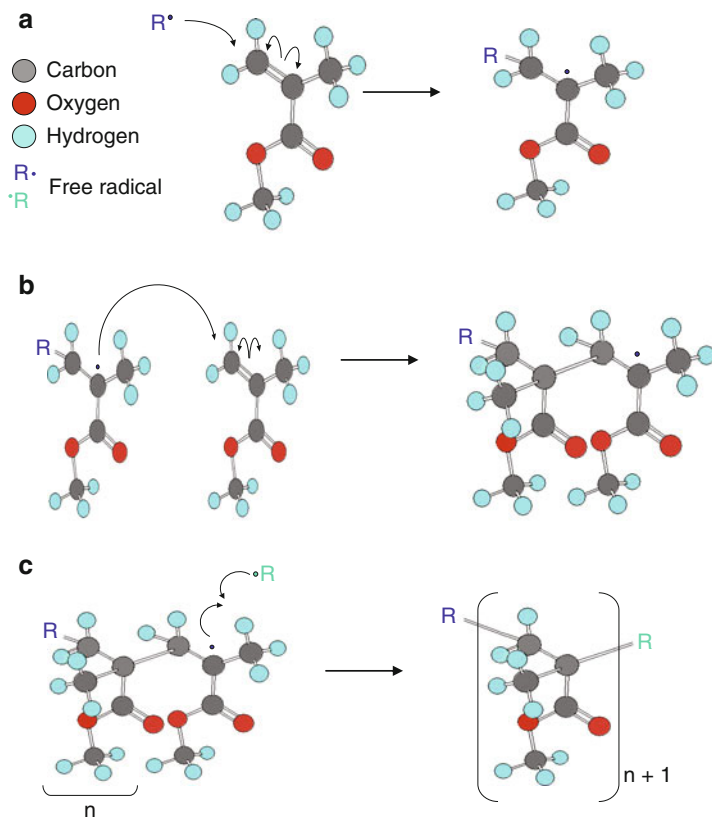


**Fig. 3** (a) Initiation of polymerization by a free radical ( $R\cdot$ ). (b) Chain propagation. (c) Chain termination results from the mutual reaction of two free radicals

or light to form a highly reactive single electron called free radical. A free radical attacks the functional or reactive group, which is a carbon–carbon double bond ( $\pi$ -bond) of the vinyl group in the monomer, resulting in the formation of a single bond ( $\sigma$ -bond) with another carbon and an unpaired electron (Fig. 3a). The monomer attached to a free radical becomes a new free radical. In the second step, *propagation*, the new free radical can attack another double bond which, in turn, attacks another double bond and so on, thus a chain lengthening is formed (Fig. 3b). The chain propagation continues until no free radicals are available to combine, resulting in the *termination* stage (Fig. 3c).

### Cationic Polymerization

Cationic reaction starts with the initiation process (*carbocation*) of an acidic cation, which opens the oxirane ring and generates a new acidic center. After the addition to an oxirane monomer, the epoxy ring is opened to form a chain, or in the case of two- or multi-functional monomers, a network is formed. The important difference in the

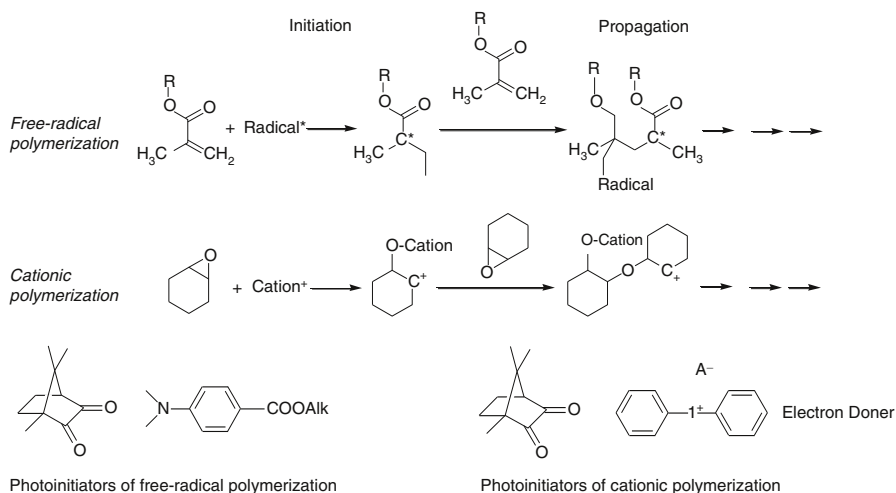


**Fig. 4** Free radical polymerization of dimethacrylates and cationic ring-opening polymerization of epoxy with their corresponding photoinitiators

cationic polymerization from the free radical polymerization reaction is that methacrylates are polymerized by radical intermediates, while oxiranes are polymerized via cationic intermediates (Fig. 4). Three initiating components comprising an electron donor (amine accelerator), an iodonium salt, and a CQ, provided in a constant ratio, yield the cationic reaction. In this reaction path, the electron donor acts as a redox agent and decomposes the iodonium salt to an acidic cation, which starts the ring-opening polymerization process, whereas CQ photoinitiator is utilized to match the emission spectra of the currently used curing lamps [17].

## Advancements in Resin Monomer

The major problem of present dental composites is polymerization contraction that results into shrinkage during curing. Therefore, it is highly desirable to develop a new or modified resin system that yields a minimum net shrinkage. Some new resins have been developed claiming to be less hydrophilic, less dimensional change, and tougher than the Bis-GMA. However, their clinical performance has been dramatically affected by differences in the resin composition. This is currently considered an area of intense research.

The vast majority of RBDC restoratives are comprised of dimethacrylate resins. Only during the last decades, the resin monomers for dental composites show a continuous development. Recent studies have explored the effects of incorporating different monomers as well as improving entirely new monomers for dental composites. The modern composites that started with Bowen's resin have been modified

differently regarding properties like viscosity, polarity, and functionality of their monomer resin backbones. The ultimate goal is to develop materials with minimal polymerization shrinkage, improved general properties, and biocompatibility.

Bis-GMA analogues and substitutes were synthesized to overcome the Bis-GMA resin deficiencies of high viscosity, water susceptibility, relatively low degree of double bond conversion, and their tendency to potential brittle fracture as well as wear. One of these analogues is *fluorinated monomer* which displayed a hydrophobic characteristic of the fluoride additive showing improved resistance to solubility (Fig. 5a). A resin composite synthesized from fluorinated monomers showed greater strength than conventional Bis-GMA-based materials after water storage as a result of reduced water sorption. Moreover, the potential resistance of these polymers to microbial attachment and their good biocompatibility makes them attractive for dental application. A composite containing an *antibacterial monomer* demonstrated adequate physical properties [18]. This attempt involves the inclusion, for example, of quaternary ammonium functionality or additives in the resin monomers reporting higher longevity of antibacterial activity [19]. Also, lesser wettability of the fillers by resin is advantageous in lowering surface free energy which resulted in less bacterial plaque adherence.

*Radiopaque monomers* were developed for posterior composite restorations in order to detect secondary caries, marginal defects, and overhangs. These are obtained by the incorporation of heavy metal or iodine–bromine residues in the monomer; however, they demonstrated reduced mechanical properties and low reactivity (Fig. 5b).

Some attempts were carried out to improve the properties of the dental composite by enhancing the polymerization and degree of monomer conversion. Likewise, improvement in flexural strength of experimental composite was observed by adding *benzaldehyde* due to increased DC by chain transfer reactions [20]. However, other trials aimed to increase the DC together with reduction of polymerization shrinkage. Adding cyclopolymerizable monomers termed as “oxy bismethacrylates” can give 90 % DC and 40 % reduction in contraction compared with TEGDMA resins of similar DC [21]. A series of difunctional oxy bismethacrylates, such as the *oligomer of ethoxylated bisphenol A diacrylate* (OEPBA), were synthesized and used to produce light-cured composites with properties similar to those of ethoxylated Bis-GMA composites. They expressed higher toughness and less shrinkage than conventional Bis-GMA-based composites. Similarly, *methylene-butyrolactone* (MBL), the cyclic analogue of MMA, was synthesized to increase the DC and improve the composite’s strength [22].

Another attempt to reduce the shrinkage is to enlarge the molecular size of reactive molecules in order to have more extensive cross-linking based on using multi-methacrylates and highly branched methacrylates. *Dendritic (dendrimers)* or *branched monomers* were produced for dental composites exhibiting low viscosity with reduced flexibility and low polymerization shrinkage of approximately 2.9 % (Fig. 5c) [23]. The resulting polymer network tends to be more flexible that may impair the mechanical properties as flexural strength and modulus of elasticity. However, the addition of hyperbranched multi-methacrylates to a mixture of



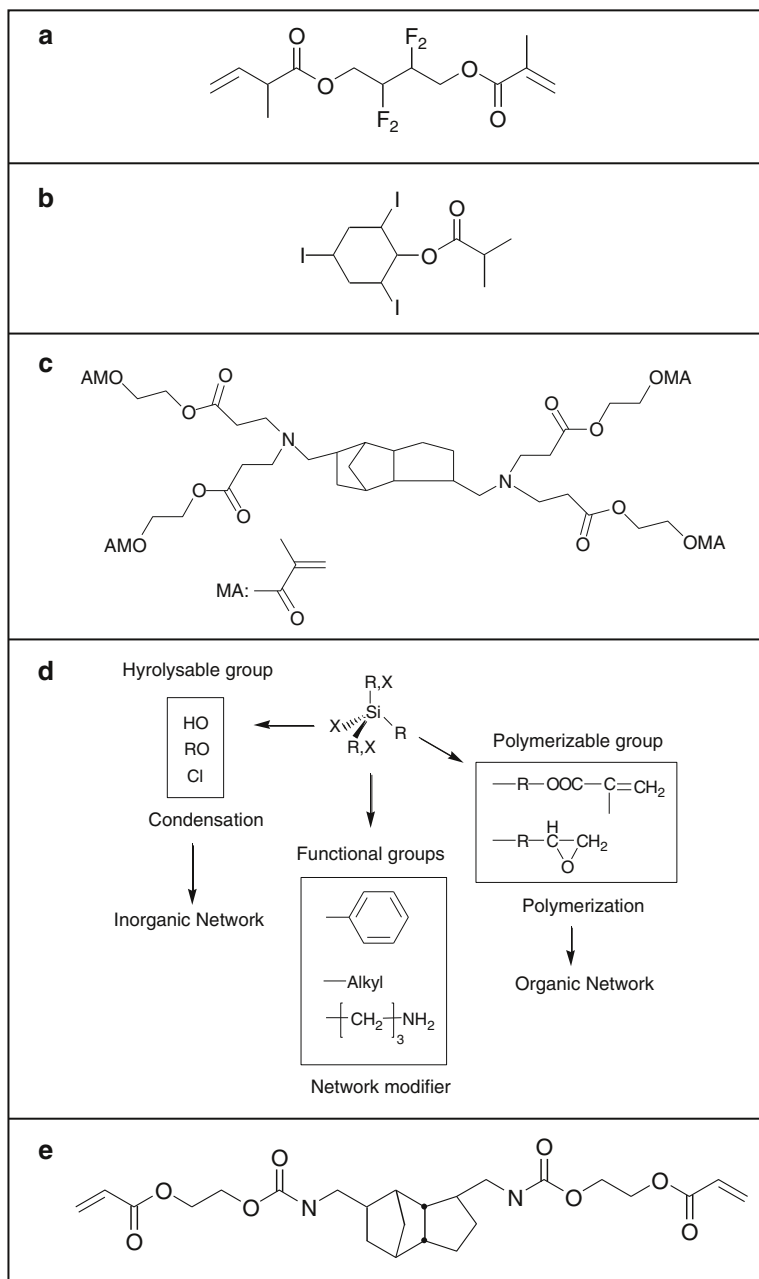


**Fig. 5** Different resin monomers used in RBDCs. **(a)** Fluoride-containing monomer, **(b)** radiopaque methacrylate monomer (tri-iodophenyl methacrylate), **(c)** branched monomer (tetramethacrylate), **(d)** ormocer synthesis, and **(e)** TCD-urethane monomer

Bis-GMA/TEGDMA resulted in enhancement of the mechanical properties and reduced the free monomer leachability [24].

Recently, several attempts have been made by scientific institutes and manufacturers to reduce shrinkage via changing the nature of the resin and the use of expanding monomer instead of the shrinking one [21]. In the 1970s, initial efforts aimed to obtain monomers that might expand upon polymerization. One approach involves the use of liquid *crystalline monomers* as a resin which potentially shrinks less upon curing (Fig. 6a). Another attempt involved the use of *vinylcyclopropane* derivatives, as low shrinkage and free radical-curing ring-opening monomers, that are also suitable to copolymerize with common methacrylate-based resins (Fig. 6b) [25]. Although the resultant cross-linking vinylcyclopropane showed a more stability in humidity and lower cytotoxicity, it expressed less reactivity than methacrylate [25].

Alternative approach to achieve less or no polymerization shrinkage was conveyed through the use of modified resins as spiro-orthocarbonates (SOC), cyclic silicon compounds, dioxiranes, and epoxides (Fig. 6c–e). The concept of the double ring-opening polymerization of expanding monomers (*polycyclic ring-opening monomers*, such as SOC, spiro-orthoesters, and bicyclic orthoesters) to produce shrinkage strain-free composites was patented [26]. It was based on yielding a sufficient double ring opening to produce enough expansion in order to counteract the free radical polymerization shrinkage of the dimethacrylates. The combination of SOC with dimethacrylate (Bis-GMA or TEGDMA) as additives demonstrated the highest conversion for both methacrylate and spiromethylene groups associated with mixed cationic/free radical initiator systems [27]. These monomers contain methylene groups capable of free radical polymerization, making them useful as additives to dimethacrylates. Then, methacrylates were substituted by spiro-orthocarbonate giving nearly complete ring opening of the SOC when polymerized in dilute solutions. Though the composite had about 1 % shrinkage, the resultant polymers were weak, and less ring opening was obtained when the resin was cured in bulk. It has main drawbacks of incomplete ring opening at room temperature, sensitivity against water and acidic compounds, as well as low UV stability leading to discoloration of the resultant composites.

New SOCs polymerized with epoxy resins via cationic UV photoinitiation were synthesized. These *alicyclic SOCs* contain four rings attached to a central spiro carbon, and expansion is also achieved by a double ring-opening polymerization (Fig. 6f). The cationic initiator used is (4-octyloxyphenyl) phenyliodonium hexafluoroantimonate, with chlorothioxanthone as a sensitizer. The mixing of 5 % of the SOC in an epoxy base produced a resin with substantial tensile strength and modulus, acceptable water sorption, solubility, and a slight expansion. Increased concentrations of the SOC produced greater expansion and slightly stronger polymers, but water sorption and solubility were high due to incomplete reaction of the SOC. The epoxy–polyol system combinations demonstrated 40–50 % less shrinkage than traditional ones [28]. However, another method involves the use of cationically polymerizable resin systems composed of dioxiranes and comonomers with their potential to expand upon polymerization. In the 1950s, *oxiranes (epoxy)*, evaluated

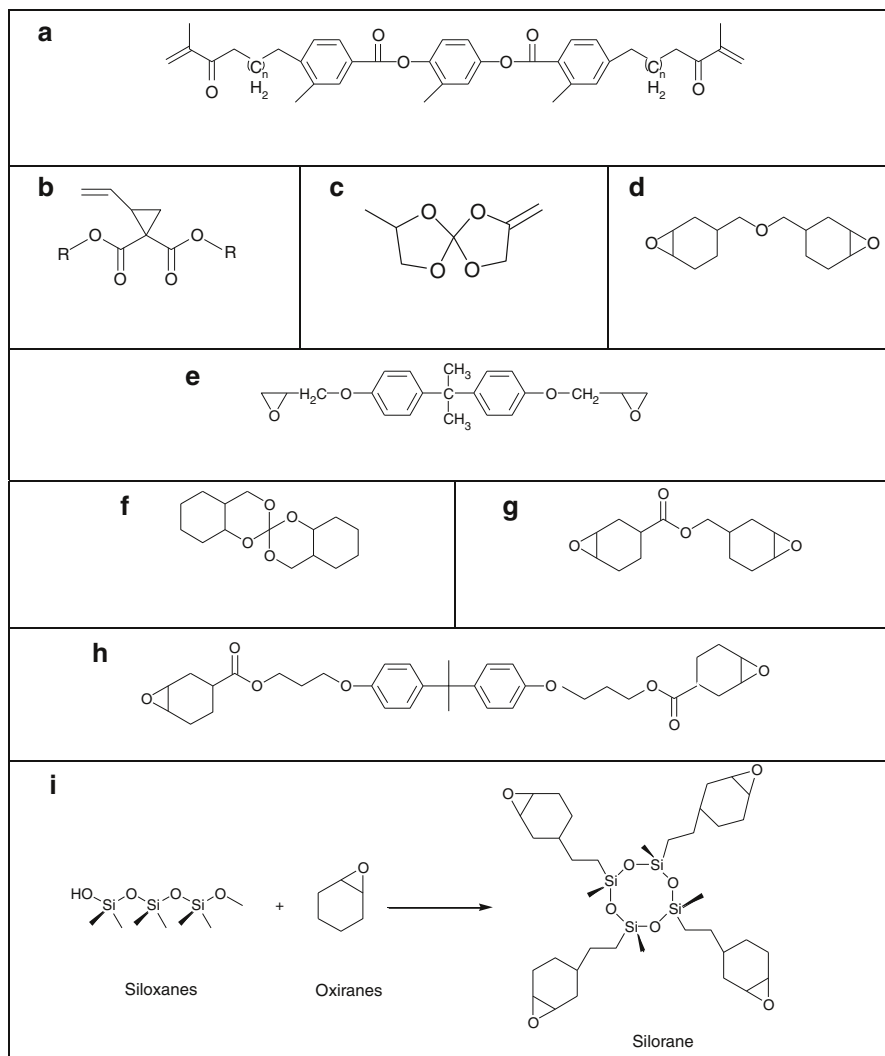


**Fig. 6** Chemical formulae of low shrinkage monomers. **(a)** Typical liquid crystalline monomer, **(b)** 2-vinylcyclopropane, **(c)** spiro-orthocarbonate, **(d)** oxirane, **(e)** epoxy resin of the diglycidyl ether of bisphenol A, **(f)** alicyclic spiro-orthocarbonate, **(g)** cycloaliphatic epoxy resin, **(h)** cycloaliphatic oxirane, **(i)** silorane: a merger of siloxanes and oxiranes

as dental resins, demonstrated higher reactivity and significantly lower shrinkage than methacrylate resins (Fig. 6g).

A different chemical approach was made by Eick and coworkers [29] focusing on the cationic ring-opening spiro-orthocarbonates, principally in combination with epoxy monomers (oxiranes). In recent years, a new cationic ring-opening monomer system evolved, with a target profile of low shrinkage and a highly reactive

biocompatible composite that withstands the oral environment. In order to achieve this, *siloranes* were developed that were derived from the combination of its chemical building backbones siloxanes and oxiranes (Fig. 6i). The polymerized network of siloranes is generated by the cationic ring-opening polymerization of the cycloaliphatic oxirane moieties (Fig. 6h), which stand for their low shrinkage and low polymerization stress (<1 %) and reduced cuspal deflection. The siloxane provided the hydrophobic component that minimized water sorption and solubility, lessened its sensitivity toward staining of the composite, and retained its gloss [17].

Filtek silorane (sometimes called Filtek P90, launched by altered names in different countries) was the only commercially available product in the dental market. It is accompanied by a specific adhesive system because of the hydrophobic nature of this composite. This composite is utilized mainly to restore posterior dentition due to its limited color shading and lower range of radiopacity and translucency. The hydrophobic characteristics of the silorane may not permit accumulation of *Streptococci* bacteria on this restoration. It has the ability to withstand storage in media of ethanol and artificial aging in food simulating liquids (FSL) as well as endure creep deformation under load. Also, the flexural strength and hardness of silorane are not affected by FSL as heptane and citric acid. It demonstrated superior mechanical properties with improved depth of cure and color stability after immersion in different staining solutions. An experimental silorane composite incorporated with nano-hydroxyapatite crystals demonstrated high mechanical properties, relatively as flexural strength and fracture toughness, but lower compressive strength and microhardness compared to dimethacrylate-based restorative composites [30].

The Bis-GMA-based dental composites showed some cytotoxicity in a number of cell culture systems due to its estrogenic effect. In an attempt to overcome these limitations associated with the conventional composites as elution of the monomers, a new restorative material was formulated called *ormocer or nanoceramic composite*. This class of dental composites was developed at Fraunhofer Institute for silicate research in Würzburg, Germany, in 1990 and contained inorganic–organic hybrid polymers. The use of these large siloxane molecules in dentistry was proposed by Wolter and others [31]. The ormocers have already been used in high-tech industrial fields, like optics coating, electronics, or medical technology. This innovative material has been utilized in dentistry as a substitute for Bis-GMA having a dual character that links glass-like components with polymer components via covalent bonds at the molecular level. They are nearly hard as glass with properties purposed to reduce polymerization shrinkage and improve strength, marginal adaptation, abrasion resistance, and biocompatibility. Laboratory testing suggests that ormocers displayed a significantly lower wear rate compared to traditional composites [32].

The acronym of this hybrid formulation stands for *organically modified ceramics*. It is based on organically modified silicon alkoxides and functionalized organic oligomers/polymers. Precursors are usually bifunctional organically modified Si-alkoxides. Structurally, it consists of a special pre-shaped copolymeric network having a large backbone functionalized with polymerizable organic units. It is not generated by the classic means of physically mixing a composite's constituents, but

it requires distinct processing based on molecular scale technology. It combines the organic and inorganic components at a nanoscale. The process of its formation started by a two-step process: hydrolysis and polycondensation reactions (sol-gel processing) of functionalized organosilane precursor (alkoxy silane) to form oligomeric Si-O-Si nanostructure (polymeric-inorganic condensate) (Fig. 5d). These inorganic-oxidic oligomers replace the conventional monomers in the composite by an organic cross-linking process resulting in a 3-D polymeric network formed during the polymerization of the functional group. This step is followed by an organic cross-linking process initiated by thermal energy, UV radiation, and redox initiation. Glass or ceramic filler particles (1–1.5  $\mu\text{m}$ ) are then incorporated into this cross-linked network matrix (up to 67 % vol.). Tailoring of multifunctional ormocer precursors is the basis for their use as matrices for dental composite. After incorporating different types of functionalized inorganic fillers, essential additives as photoinitiators, and dental monomers, a paste-like low shrinkage light curable ormocer composite is attained. The second step involves the radical-based polymerization of the connected methacrylate groups by the common visible light curing.

The resultant 3-D polymer structure varies with the type of the reactive functionalized organic group attached. Dependent on the functionality of each unit in the nonorganic-organic precursors, the material properties can be tuned to specific applications allowing a wide range of modification. New multifunctional urethane- and thioetheroligo(meth)acrylate alkoxy silanes as sol-gel precursors have been developed to alter the property of the formed ormocer. Two dental restorative ormocer-based composites, *Admira* (Voco) and *Definite* (Degussa), were first launched onto the dental market in 1998. Another example of ormocer nanocomposites is *Ceram-X* (Dentsply). Up to now, all commercially available composites have their common foundation in the free radical polymerization of methacrylates, and even the ormocers are polymerized by their methacrylate functionality. Pure experimental ormocer-based material, however, exhibited color stability and slight decrease in hardness [33].

A novel dental nanocomposite composed of polyhedral oligomeric silsesquioxane (POSS) developed with a low shrinkage characteristic. It is one of a typical kind of organic-inorganic hybrid nanocomposite and considered a new generation of high-performance materials, which were developed lately. They are characterized by improved mechanical properties because they combine the advantages of inorganic components, as rigidity and high stability, with those of organic polymers, as flexibility, and easy processing. Its nanostructural chemistry is based on a compact hybrid of 1.5 nm isotropic-inorganic cage or core made up of silicon (Si) and oxygen ( $\text{SiO}_{1.5}$ )<sub>n</sub>, where Si is attached to a methacrylate functional group. Both monofunctional and multifunctional POSS, with suitable reactive functional groups, have been used as modifiers and cross-linkers for polystyrene, epoxy, polycarbonate, and other polymer matrices. The POSS-MA is a multifunctional methacryl POSS molecule used to replace Bis-GMA. A dental nanocomposite based on 3 % wt. MA-POSS represents a good material for dental applications [34].

Recently, another novel polymer as thiol-ene oligomer is incorporated in the resin formulation of the dental composites as alternatives to dimethacrylate-based

RBDCs. It demonstrated a significant reduction in shrinkage stress and strain as well as rapid polymerization rates due to the delayed gelation, and most of the shrinkage occurs prior to gelation, thus reducing the shrinkage stress in the final set material. Also, this system expressed to some extent poor mechanical properties for dental applications as lower flexural strength compared to dimethacrylate-based composites due to the formation of flexible thioether linkages resulting in plastic deformation. The methacrylate–thiol–ene systems showed the advantages of both polymers exhibiting good mechanical properties, as fracture toughness and increased DC [35]. This system exhibits a combination of two reaction mechanisms: a radical chain-growth polymerization for methacrylate and a radical step-growth addition polymerization for thiol–ene. The later mechanism comprises the addition of a thiyl radical to an ene functional group, followed by chain transfer to a thiol, thus regenerating the thiyl radical.

The new development of resin chemistry should lead to remarkable improvements of the dental composites in terms of strength, wear resistance, durability, and stability in the oral environment. The greatest advances in resin technology were focused on the area of maximizing the DC and minimizing polymerization shrinkage and stress. Because the mechanical properties and clinical success of current composites appear to be dictated more by the filler component rather than by the resin matrix, it is debatable whether the newly developed monomers will have a remarkable effect on their clinical performance. Earlier efforts were not successful, but further investigations are needed to verify the acceptance of these dental composites with new monomers.

## Degree of Conversion (DC)

The commercially available dental composites are photo-curable pastes, which are hardened in situ by visible light-curing unit, undergoing mainly free radical polymerization. Hardening of dental composite is the result of a chemical reaction between dimethacrylate resin monomers producing rigid polymer network. The extent of this reaction, which is called the *degree of cure*, is necessary to dictate several physical and mechanical properties of resin-composite restoration. It, also, can predict the longevity of the restoration because under-curing of the resin may limit the efficiency of the composites clinically. The reported DC values of the resin-composite materials were in the range of 52–75 %. The optimum properties of light-cured composites depend on achieving an entire polymerization of the resin component. Inadequate curing of resin monomer due to limited irradiance levels or exposure times and any potential incompatibility between a photoinitiator system and the spectral output of the curing light is employed. This incomplete polymerization impairs the properties of the composite resulting in more leaching of residual monomers, loss of biocompatibility, color instability, retention, liability to fracture, and excessive wear.

Most of the current composites that possess 10–25 % of the monomers remain free unreacted molecules after polymerization capable of being released. The

unreacted methacrylate groups are present as pendant molecules at one end by linking with the polymer chain that is able to serve as internal plasticizer for the composite. Although the DC is maximized by the inclusion of a high percentage (40–50 %) of diluents in the resin, the cure of most composites is accompanied by significant polymerization shrinkage (1.5–3 % vol.). Conversely, if conversion is maximized to reduce these difficulties, then alternative problems of polymerization shrinkage and brittle fracture of the composite become more critical. Although optimal mechanical properties may be achieved with high DC, it must be considered that excessive cross-linking can lead to clinically unfavorable conditions. Under standard polymerization situations, a higher DC led to higher polymerization shrinkage values. However, the optimal goal of a material is to achieve a high degree of conversion with minimal polymerization shrinkage which is generally an antagonistic goal.

### **Factors Affecting Curing and Degree of Conversion**

The degree of cure or conversion is influenced by many factors that include the following:

#### **Polymerization Shrinkage and Amount of Photoinitiator**

Generally, the shrinkage depends on the type of organic resin or chemistry of the monomers, the concentration of polymerization initiators and inhibitors, and the diluent concentration. The shrinkage reduces with the increase of the monomer molecular weight and increases with increasing the DC. The photoinitiator (CQ) in many light-cured composites absorbs light near a wavelength of 470  $\mu\text{m}$ , and wavelengths outside this blue band have little effect on initiation of the polymerization reaction. Using less or more amount of photoinitiator than the optimum required tends to inhibit polymerization. The mode of activating the polymerization reaction whether chemical, heat, or light energy has also an effect on curing the dental composite. The DC decreased in composites having filler particles size that approached the output wavelength of the curing unit (470 nm) resulted from light-scattering effect of fillers during photoactivation [36].

#### **Power Density and Exposure Curing Time**

The power density (light intensity), which is the output irradiance of most light-curing units, is averaged to 400  $\text{mW}/\text{cm}^2$  and nowadays targeted to higher power densities that ranged from 600 to 1200  $\text{mW}/\text{cm}^2$ . Light intensity needed to polymerize direct composite restoration is  $\geq 400 \text{ mW}/\text{cm}^2$ , while that required for indirect restorations is  $\geq 800 \text{ mW}/\text{cm}^2$ . The total amount of energy given to a specific area for a period of time is referred to power density or irradiance (Joules per square centimeter). Diminished mechanical properties are associated with less light irradiance caused by aging of the curing lamp bulb, degradation of the filters, dropping of voltage, and damage to curing tips. The minimum curing time required for most conventional composites to initiate a chemical reaction to ensure an optimum polymerization by halogen tungsten light, under a continuous curing mode of

400 mW/cm<sup>2</sup> output, is 20–40 s. However, a much shorter period of time of about 10 s is required to cure the composite with LED light. Light curing of the dental composite depends on several factors as shade of the composite, power density, cavity depth, filler content, and thickness of the composite.

### **Distance and Angle Between Light Source and Resin Composite**

Optimum polymerization can be achieved if a proper distance between the light source and the composite surface is from 0 to 1 mm at 90° angle. The light irradiance reduced rapidly as that distance and the divergence from 90° increased. Therefore, the polymerization exposure time should be increased to compensate for the decreased irradiance.

### **Filler Type and Filler Content**

Macrofill composites containing larger quartz fillers polymerize more easily than the microfill composites. Heavily loaded composites associated with smaller fillers are difficult to polymerize because the increase in their opacity may require more duration for light exposure.

### **Material Thickness and Shade**

The optimum depth of polymerization occurs at 0.5–2 mm thickness of a lighter-shade resin composite. Additionally, as the thickness of the composite material increases, the degree of cure needed is accordingly increased. However, darker shades of the composite polymerized in slower and shallower rate require more exposure time than the lighter shades.

### **Temperature and Air Inhibition**

Resin composites cured at room temperature and their rapid polymerization is yielded as the temperature increases; furthermore, heat generated from lamps of the curing unit speeds the polymerization reaction. Oxygen in the air competes with polymerization and inhibits setting reaction of the resin, which can be minimized by using Mylar matrix during light curing of the restoration.

### **Polymerization Shrinkage**

Polymerization shrinkage is an inherent property of resin-based dental materials as it is subjected to many researches. Recently, shrinkage stress phenomenon was described as either concentrated internally, at filler particle–resin matrix interface, or externally, at the tooth–restoration interface. If the stress forces exceed the adhesive or cohesive strength between the substrates involved, separation will occur. This interest arises from the observed clinical problems, such as microleakage and recurrent caries, result from shrinkage of these materials in dental cavities. The magnitude of the shrinkage is dictated by the extent of the reaction and by the size of the monomer. Therefore, the goal of achieving maximum curing reaction with



enhanced properties of the resin matrix is at necessary to achieve good dental composite restoration.

Low molecular weight methyl methacrylate (MMA) produces polymerization shrinkage of 22.5 % vol. By increasing the molecular weight of MMA as in Bis-GMA in the unfilled resin, the shrinkage is reduced to 8 % vol. Low-filled flowable composites (45–67 % wt. filler load) exhibit typical shrinkage values of 4.0–5.5 % vol., while hybrid composites (74–79 % wt.) undergo a shrinkage reduction upon polymerization from 3.5 % to 1.9 %. Highly filled packable composites with optimized filler load of up to 82 % by addition of nanoparticles give shrinkage values down to 1.7 % vol.

The dimensional stability of composites is affected by the polymerization reaction of the resin phase. Initially, during the pre-gel phase, the resin-based composite is flexible, able to flow and relieve stresses within the developing polymer structure. Following the light irradiation, the free radical polymerization reaction of the dimethacrylate monomers is accompanied by closer packing of molecules transforming the material from a viscous–plastic phase into a rigid–elastic phase leading to bulk contraction. This produces a gel-stage in which the viscous flow of the curing monomer ceases and can no longer compensate for contraction stresses. The post-gel contraction stage is constricted by the strength of the adhesive bond at the tooth–restoration interface, and as a result, polymerization shrinkage of the composite is manifested as contraction stress. Many clinical problems of RBDCs arise primarily from polymerization shrinkage and stress, which are affected by several factors.

### **Factors Affecting Polymerization Shrinkage Strain and Stress**

Polymerization shrinkage is influenced by several variables; the *intrinsic* factors are concerned with the material's composition such as filler load, filler type, particle size, photoinitiator concentration, shade of the composite, and resin matrix formulation (amount, size, and type of monomer), which can influence shrinkage kinetic properties. The viscosity behavior of the material during the pre-gel phase and the duration of this phase greatly influence the shrinkage stress.

The *extrinsic* factors are related to the application techniques during the placement of the restoration, including the volume of polymerized material, mode and velocity of polymerization, direction of light application and exposure time of the light source, irradiance and wavelength of the light used, as well as the distance between the light beam and the composite. Longer light polymerization improves the rate of conversion (chain linking of the individual monomers), thus leading to less monomer release. The shrinkage stress developed in bonded composite restorations also depends on the geometric configuration of the cavity design, the C-factor, which is the ratio of the bonded surfaces to the unbonded ones. The shape of the prepared cavity, number of the opposing walls, and how they are opposed are main factors that monitor the behavior of the composite's shrinkage. This factor is high in Class I occlusal cavities, giving the greatest shrinkage stress effect. The higher number of C-factor is undesirable because it compromises the adhesion between the tooth and composite resulting sometimes to enamel crazing.

### **Procedures to Reduce the Polymerization Shrinkage Strain and Stress**

The polymerization shrinkage and the related stress of dental composites are the major parameters contributing to clinical challenges, such as reduced marginal integrity and postoperative sensitivity.

There are two main strategies to reduce polymerization shrinkage strain and stress:

#### **Exogenous Strategies (Clinical Approach)**

The reduction of shrinkage was previously achieved by minimizing the amount of a composite material placed in a cavity through the use of glass ionomer cement (sandwich technique) or a thick layer of the unfilled resin as a base or liner acting as elastic “stress-absorbing” linings. Moreover, various layering techniques for placement of dental composites such as oblique incremental insertion were introduced to fill the cavity. This way can improve the quality of the resin restoration, and therefore the shrinkage stress will be carefully controlled. Horizontal layering technique involves horizontal placement of almost 1.5–2 mm composite on top of each other to be polymerized individually and used mainly in small cavities. Generally, the maximum increment thickness is identified as 2 mm. The oblique technique was used instead of the ordinary horizontal one to orient the shrinkage stress in the direction of the bonding surface, thus reducing the C-factor. The incremental filling technique resulted in less shrinkage, which was antagonized by other analyses revealing that the bulk filling yielded lesser shrinkage. This contradicts the widely accepted belief that an incremental filling technique should be used to decrease polymerization stresses. Therefore, a bulk-fill composite is nowadays designed to allow one increment and quick application of the material with an efficient polymerization (it will be discussed later in this chapter).

The use of a light source designed to prolong the first phase of the material setting can minimize the shrinkage. Modification of the reaction dynamics by slowing down the polymerization rate during curing can reduce shrinkage stress, thus increasing the material flowability, which in turn yields stress relaxation and improve interfacial integrity. Different application and light irradiation regimes are advocated to reduce resin’s polymerization stress. Noncontinuous curing techniques that have been proposed to reduce the shrinkage stress are three-sited curing, soft-start curing, and pulse curing. In general, a rapid polymerization and a higher DC result in increased shrinkage stress, while reduced and slow initial irradiance as in soft-start technique leads to a slower development of stiffness of resin composite and prolongs the compensating flow during polymerization allowing stress relief.

Other attempts depend on the use of ceramic inserts to replace some of the volume of the shrinking composite or the use of indirect composite restorations allowing the majority of the shrinkage to occur before the restoration is bonded to the prepared cavity [37]. To enhance the marginal integrity of resin-composite restorations, strong bonding agents are used to withstand polymerization contraction forces, thus improving the bond strength property. Clinicians continually rely on an adhesive material to provide a durable marginal seal. In spite of improved bonding treatment

techniques, reliable adhesion without shrinkage stresses associated with restorative material has proved elusive. It is likely to develop a matrix polymer that undergoes zero or negligible curing contraction to be a major step toward solving the major difficulty involved in the use of dental composite and obviate the need for a very strong adhesive. Hence, the reduction of polymerization shrinkage is a real challenge in the dental restorative field.

### **Endogenous Strategies (Technological Approach)**

Technological approaches have focused on amounts and types of matrix monomer and filler, initiator level, and addition of nonbonding microparticles. Shrinkage stresses can be reduced, but not eliminated, by increasing filler load using multimodal filler particle size distributions. Another approach is to modify the composite by introducing elements that can provide sites for internal stress relief. For instance, the incorporation of porosity in composites has a stress relief mechanism. Nonbonded (40 nm colloidal silica) nanofillers might also act as stress-relieving sites by their local plastic deformation that enhanced when the resin phase was rich in diluent monomer. Composites with nanofiller particles treated with a nonfunctional silane developed 50 % less stress than composites with particles treated with a functional silane [38]. An alternative approach may include additives such as ultrahigh molecular weight polyethylene (UHMWPE) fibers that have the potential for plastic deformation during stress buildup from polymerization contraction. The addition of glass microspheres can reduce contraction stresses in filled and unfilled epoxy systems.

Alternative approaches to reduce shrinkage can be accomplished principally by using different types of resin or through reduction of reactive sites per volume unit. Primarily, the density of the reactive sites per volume unit can be reduced by increasing the molecular weight per reactive group or by increasing the filler load and limiting the number of polymerized methacrylate groups as well as the monomer conversion. Resin formulations that contain higher concentrations of low molecular weight monomers can reduce contraction stress by molecular relaxations and flow [39].

Increased filler load in the resin matrix also has its limitation at a certain level that cannot be further increased when the consequently reduced amount of resin cannot be provided any longer for wetting the increased filler particles surfaces. One method to counteract this problem is to use monomers of very large molecular weight, thus minimizing the contraction, but increases the viscosity. A high viscosity formulation had significantly lower stress than the medium or low viscosity resins. The investigation of a new monomer system with reduced polymerization shrinkage and stress has become a major focus in dental biomaterials.

In an attempt to decrease shrinkage, different monomer chemistry was developed, as the conventional ones: UDMA, Bis-EMA, to increase the cross-linking of polymer networks while the desirable mechanical properties were maintained, notwithstanding that a significant decrease in polymerization shrinkage has not been achieved. The development of a nonshrinking monomer capable of resisting the substantial force of polymerization contraction, thus minimizing the employment of

dimethacrylate matrices, would be challenging. A novel low-shrinking monomer system has identified the potential of cationic photoinitiated oxirane-based monomer chemistry as alternatives to dimethacrylates for dental composite application. The cationic ring-opening mechanism of silorane-based monomers may result in decreased polymerization shrinkage and the associated stresses [17]. The opening of oxirane ring during the polymerization reaction results in stress relaxation allowing the material to flow, thus compensating to some degree for the polymerization shrinkage.

Another method for introducing stress-relieving sites involves using multifunctional flexible monomers such as methacrylated cyclodextrin or diol dimethacrylate, branched methacrylates, and ormocers. Variations in the level of diluent monomer can alter the viscosity and the plasticity of the composite that will be reflected on the level of polymerization stress. The marginal gap formation resulting from polymerization shrinkage cannot be completely avoided clinically. The so-called smart materials are formulated to be based on the rationale that fluoride ions released under acidic conditions, presumably, limiting the amount of bacteria in marginal gaps or on restoration surfaces. Water sorption by the polymer network may contribute in reduction of the stress by hygroscopic expansion that takes place at a much slower rate.

### **The Adverse Effects of Polymerization Shrinkage**

The resultant stresses during polymerization of composite may compromise the synergy adhesive bond between the tooth and restoration, thus increasing the likelihood of mechanical failure. They may result in either postoperative sensitivity or gap formation at the resin–tooth interface with subsequent sequence of microleakage, marginal staining, bacterial infiltration, and eventually recurrent caries which may ultimately decrease the longevity of the restoration. When inherent shrinkage is opposed by insufficient interfacial adhesion between the resin and tooth substrate, stresses are conveyed to the substrate leading to cuspal deflection and even to crazing and cracking in tooth structure. Another consequence of the shrinkage stresses can be fatigue within the material resulting in marginal or bulk fracture of the restoration. The subsequent internal microcracks, debonding at the filler particle–resin interface, and imperfect margins may accelerate destructive effects, such as wear. Shrinkage stress represents one of the most important reasons for the replacement of existing composite restorations.

### **Classification Based on Resin Matrix Type**

The development of various resin matrix components necessitates a further classification of the composite's material. These resin matrices innovations lead to a new trend in classifying the dental composites that is based on the organic matrix components. The conventional organic matrix is founded on dimethacrylates chemistry mainly Bis-GMA and other monomers as TEGDMA including hybrids and nanocomposites. The inorganic matrix as ormocers is based mainly on inorganic

poly-condensates. The acid-modified methacrylates as compomers and resin-modified glass ionomers are established on polar groups and fluorosilicate glass. The ring-opening epoxide-based resin as silorane is founded on a cationic monomer system. The examples have already been described above.

Modifications in the polymer matrix composition of RBDCs may promise improvements of their mechanical properties, reduction of water uptake, polymerization shrinkage, and increasing DC. One of innovative kinds of matrix monomers is dimer acid dimethacrylates based on a patented resin system owned by the University of Colorado defined as multi-ethylene glycol dimethacrylate monomers [40]. These monomers are derived from a core structure of hydrogenated dimer acid of high molecular weight called cycloaliphatic carboxylic dibasic acids, a derivative of linoleic fatty acid. It is characterized by high molecular weight and low initial double bond concentration (low viscosity) that circumvent the incomplete polymerization shrinkage. The lower mobility of high molecular weight monomers can minimize the number of double bonds available to react per unit of matrix volume, thus reducing the shrinkage. Also, this material exhibits relatively high filler content (65 vol.%) that reduces shrinkage by decreasing the volume of organic resin matrix. Moreover, it represents another mean for reducing shrinkage by a polymerization-induced phase separation (PIPS) approach. It exhibited the lowest shrinkage values compared with conventional dimethacrylates, but not less than those presented by “low shrinkage” composites as silorane [41].

The resultant polymer is characterized by low modulus of elasticity and high flexibility due to low cross-linked density of dimethacrylates. A commercial product of this type of nanohybrid resin composite is N'Durance Septodont (France), which has reduced polymerization shrinkage from 2.4 % to 1.5 % and shrinkage stress from 2.5 % to 1.1 % associated with increased DC reaching 76 % and good mechanical properties [41]. The hydrophobic characteristic of this monomer together with the high DC can reduce sorption, solubility, and the leachability of the non-reacted monomers [42].

Another patented resin matrix monomer is urethane based called tricyclodecane (TCD)-urethane dimethacrylate incorporated in nanohybrid composites and promoted as alternatives to the conventional Bis-GMA monomers (Fig. 5e). It consists of special methacrylic acid derivatives of aliphatic structure including high reactive urethane groups of tricyclodecanes prepared by reaction of hydroxyalkyl (meth) acrylic acid esters with diisocyanates and subsequent reaction with polyols. The backbone structure of this resin is less viscous and rigid comparable to bisphenol-A yielding low shrinkage, contraction stress, and restricted chain mobility compared to the low-shrinking composites. It is incorporated in recent composite named Venus Diamond and Venus Diamond Flow (Heraeus Kulzer) as TCD-DI-HEA urethane monomer (Bis-(acryloyloxymethyl) tricycle [5.2.1.02,6] decane). This nanohybrid composite has lower modulus of elasticity due to the flexibility of the resin matrix that may attribute to large rings in its molecular structure centrally permitting slow curing. This resin matrix is characterized by lower water sorption due to hydrophobic nature of the monomer. It has low-shrinking strain and stress as well as high DC with reduced amount of free leachable monomer associated with improved

mechanical properties [43]. Both of these composites exhibited higher depth of cure in larger increments of the material.

Different kinds of modified urethane dimethacrylate resin have been developed in order to reduce the shrinkage. Another commercial product of this resin is Kalore (GC), which is a new universal composite innovated by monomer technology from DuPont. It has a higher molecular weight monomer, double than that of Bis-GMA and the conventional UDMA monomers. It implemented a novel methacrylate monomer (DX-511) of a long rigid stiff monomer core with flexible arms yielding lower shrinkage stress compared to conventional dimethacrylate composites but higher water sorption and expansion compared to the silorane. This can be attributed to its low concentration of initial reactive group and DC (48 %). Another contributing factor is the presence of pre-polymerized particles that increases the filler content (69 % vol.), reducing the polymerizable organic phase, which is responsible for shrinkage. It has good handling properties of the composite permitting easy spreading and sculpturing without slumping.

---

## Filler Particles

Hard filler particles were dispersed in the resin matrix to provide strengthening and reinforcement of dental composites. The first manufactured filler particles were made from quartz materials that were strong, hard, and chemically stable. Nowadays, the fillers are mainly made from glass, as fiberglass, or ceramic materials, and others can be prepared from natural minerals. The fillers are formed either by grinding process, which involves the change from bigger particles to finer ones, or by sol-gel precipitation technique, which alters the fillers from molecular size to particle size. The formulated glass has the similar good properties of quartz with better optical and coloring characteristics. Generally, the fillers can improve different properties of the material as increased stiffness, abrasion resistance, hardness and elastic modulus, reduced dimensional change, polymerization shrinkage, contraction setting, water sorption and thermal expansion, enhanced esthetics, gloss, radiopacity, and handling characteristics.

Usually, the physical and mechanical properties of the composite are enhanced in direct relation to the amount of filler added known as filler load. The filler load or content can be measured in percentage by weight (% wt.) or by volume (% vol.). There is a difference between these two measurements; the volume percentage is 10–15 % lower than the weight percentage. Although the manufacturer usually reports the percent by weight because it expresses the high filler content, the volume percentage is more accurate, and it is preferred by the researchers. As the filler content increases, the amount of resin matrix decreases, thus polymerization shrinkage decreases. Addition of fillers to polymer resin has a certain limit in order to achieve a proper wettability of the resin monomer to the fillers without formation of weak areas in between these two phases. Also, the size, shape, and distribution of the fillers play an important role in the composite's classification and properties. The spherical-shaped particles have smaller surface area and lower friction between them

than those of the irregular-shaped particles. The irregular-shaped fillers can achieve good mechanical retention within the resin matrix. Another shape may exist in the dental composites as porous spherical particles. Shrinkage stress and shrinkage stress kinetics are influenced by the variations in the fillers' size and shape. Composites with spherical filler particles demonstrated lower shrinkage stain and stress compared to those exhibited by irregular ones.

This chapter will discuss the different categories of dental composites based on their particle size as well as their clinical application. The dental composites can be classified into groups according to the filler particle size, content, resin matrix (as mentioned previously), and viscosity of the material.

## Historical Background and Classification of Fillers

Initially, the popularly used inorganic particulate for dental composites was fused or crystalline *quartz*, but nowadays the most commonly used fillers are *colloidal silica*-based glass fillers, such as amorphous or colloidal silica, fused silica, sol-gel zirconia-silica, lithium aluminosilicate glass, boron silicate, fluorosilicate, ytterbium trifluoride, and radiopaque silica glasses containing barium or strontium. The main particulate filler component that is commonly used in dental composites is silica and/or silicate, as silicon dioxide ( $\text{SiO}_2$ ). The crystalline form of silica, which is the quartz, is stronger and harder; and when it is used alone yield radiolucent composites that are difficult to finish and polish.

The significant changes in commercial dental composites have been made by altering the fillers' component. Such changes have prompted the periodic development of dental composite's classification systems based upon filler size, volume fraction, filler distribution, mode of curing, and handling property. In 1983, Lutz and Phillips categorized dental composites into *macrofilled*, *microfilled*, and *hybrid* based on the mean particle size (MPS). This system included conventional or macrofilled composites of an average particle size equal to 10–20  $\mu\text{m}$ , microfills of 0.01–0.04  $\mu\text{m}$ , and hybrids containing a mixture of ground glass and microfill particles of an average particle sizes of 5  $\mu\text{m}$  and 0.04  $\mu\text{m}$ , respectively. Most dental composites have the proportion of fillers in range between 30 % and 70 % vol. or between 50 % and 85 % wt.

The dental composites shifted from the strongest and highly abrasion-resistant fillers to the relatively softer and less abrasion-resistant fillers. The abrasion and wear rate in the former-based type composite are higher in the resin leaving a rough surface due to the strong fillers pulled out of the matrix. However, the softer fillers in the latter-based kind composite may wear out in a slower rate but stay embedded in the matrix yielding a good overall abrasion resistance. Resin composite containing leucite fillers expressed high wear resistance compared to hybrid composite [44].

### Macrofilled Composites

Macrofilled (conventional) composites are the first dental composite developed. The most common fillers of these composites introduced in the late 1950s are *glass* or

*quartz* types that were ground into particles of different sizes, ranging from 10 to 100  $\mu\text{m}$ . They were added to resin monomer at 70–80 % wt. (55–65 % vol.) filler content to make the dental composite material with a higher strength than that of unfilled resin. The quartz has an advantage of excellent optical match to the polymer resin; however, it has a disadvantage of difficult polishability, lacking the radiopacity and high coefficient of thermal expansion. These particles are large and very hard, characterized by high wear resistant in relation to the surrounding polymer matrix that may cause abrasion to the enamel. As the surface of this composite was abraded during function, the polymer matrix would wear away quickly, exposing the filler particles. They plucked out from the surrounding matrix and sometimes dislodged resulting in a rough and/or pitted surface of the restoration with compromised polishability and esthetics. The chance of plaque retention, discoloration, leakage, and recurrent decay is higher in these composites, thus their long-term clinical durability is adversely affected. The recent composites used macrofills of 1–10  $\mu\text{m}$  as foundations underneath the extra-coronal restorations because of their substantial higher strength.

### **Microfilled Composites**

In the late 1970s, microfills comprising amorphous silica of smaller filler size (0.03–0.5  $\mu\text{m}$ ) were developed to overcome the problems of roughening and low translucency associated with macrofilled composites. The typically very small submicroscopic particles are *silicon dioxide* or *pyrogenic silica* of 0.04  $\mu\text{m}$  average diameters. They are formed by firing and sintering the silicon in an oxygenated atmosphere to form chains of smaller  $\text{SiO}_2$  particles. The surfaces of silica particles are highly energetic that can form bonds with the monomer molecules yielding a thicker paste. These small particles have a large surface-area-to-volume ratio, thus requiring a considerable amount of resin monomer to wet their surface in order to produce a homogeneous, nonsticky composite paste. This characteristic impedes the filler loading to approximately 35 % wt., which in turn limits the strength and stiffness of the material. Also, the resultant higher amount of resin can increase the coefficient of thermal expansion of the composite. In order to circumvent these limitations, heavily filled polymer resin blocks were produced that can be milled into particles of 25  $\mu\text{m}$  in size known as pre-polymerized resin fillers (PPRF). When these fillers are added to the resin with additional microfill amorphous silica, the filler levels will reach 50–60 % wt. (35–45 % vol.), which is still considered low, and the viscosity is also minimum. Therefore, these fillers are incorporated into the resin alone, known as *homogeneous* microfilled composites, or they can be used as pre-polymerized resin fillers and agglomerates resulting in *heterogeneous* microfills. The latter can increase the volume of the filler particles in the composite.

The microfills are divided into three subclasses of pre-polymerized resin filler types that are incorporated into the resin of the whole composite giving splintered, spherical, or agglomerated microfiller complexes. The spherical particles can be incorporated in a higher amount than the irregular ones, thus increasing the fillers' load. However, strength and stiffness of these microfills are lower than those of quartz-filled or glass-filled composites containing larger particles. They undergo



greater marginal degradation and localized wear; therefore, they are contraindicated for stress-bearing area restorations as Classes I and II, or direct veneer in patient has parafunctional habit as bruxism. Also, they exhibit higher coefficients of thermal expansion, water sorption, solubility, and polymerization shrinkage due to their higher resin component and lower filler concentration. Microfill composites enhance high polish, lustrous, and esthetic appearance of anterior restorations maintained over time. They showed good optical properties and light transmission, thus achieving the anticipated enamel translucency. However, they demonstrated lower fracture resistance, toughness, stiffness, and fatigue strength than those of heavily filled composites with larger particles [45]. The flexibility or lower modulus of elasticity of these microfills makes them a good choice to restore Class V cavities where tooth flexion may occur. Such a characteristic allows better retention of these restorative materials rather than the other types of composites. The current trend toward minimizing filler size and maximizing filler load is an attempt to attain the requisites of dental composites.

The microfill fillers made from quartz are not radiopaque, which can be achieved by the addition of small concentrations of other fillers, such as ytterbium trifluoride (e.g., Heliomolar RO, Ivoclar Vivadent). Most currently available composites are filled with radiopaque silicate particles based on oxides of barium, strontium, zinc, aluminum, or zirconium. One of the classic examples of this composite is Renamel microfill (Cosmedent).

### Hybrid Composites

These composites were introduced in late 1980s to solve the shrinkage problem and the lack of good mechanical properties of microfills. They were obtained by combining the advantages of both macrofilled (strength and abrasion resistance) and microfilled (polishability) composites. They are the most commonly used composites to restore different classes of the cavity preparations on anterior and posterior dentitions to withstand masticatory forces. They have a wider range of filler particle sizes (0.1–5  $\mu\text{m}$ ). Microhybrids contain a blend of these small filler particles and submicron pyrogenic silica (0.04  $\mu\text{m}$ ). As they comprised dissimilar smaller filler particle sizes, they also contained different types of fillers: glass particles for enhanced properties and pyrogenic  $\text{SiO}_2$  for better polishability. Increasing the filler particle size of silica in resin composite resulted in a decrease in the transmitted amount of visible light, depth of cure, and Knoop hardness values.

Another classification system of dental composites was established by Willems and others in 1992 according to filler volume fraction. The hybrids are classified according to the filler content, distribution, and MPS. They are divided as midway filled (<60 % vol.) and compact filled (>60 % vol.), with subclassifications of ultrafine (MPS <3  $\mu\text{m}$ ) and fine (MPS >3  $\mu\text{m}$ ) within each category. These composites are usually called densified because they constitute high filler load reaching 85 % wt. (75 % vol.). The hybrid composites continued to be improved by increasing the filler content and varying the filler particle sizes and distributions. The modern hybrid composites involve reduction of filler particle size in nano-range associated with distribution of different sizes. This results in notable improvement in

the strength, polishability, and reduction of the polymerization shrinkage. An example for the commercially present hybrid composite is Tetric EvoCeram (Ivoclar Vivadent).

The modern microhybrid formulations have incorporated a blend of both submicron filler particles size ( $0.04\ \mu\text{m}$ ) and small particles ( $0.1\text{--}1\ \mu\text{m}$ ) with high filler content of more than 60 % by volume (87 % wt.) It demonstrated better overall properties by combining the strength and surface smoothness allowing their use in posterior stress-bearing areas and anterior esthetic areas. Contribution of different filler sizes allows the occupation of the smaller size particles to fill the spaces between the larger ones, thus increasing the filler volume content and achieving high density filler packing. This promotes a simpler classification system obtained by Bayne and others in 1994 by which the three types of composite are described by the size of their largest fillers as microfills (MPS =  $0.01\text{--}0.1\ \mu\text{m}$ ), minifills (MPS =  $0.1\text{--}1\ \mu\text{m}$ ), and midifills (MPS =  $1\text{--}10\ \mu\text{m}$ ). Some examples of these microhybrids are Z250 (3 M ESPE), Synergy (Coltene/Whaledent), and Vitalescence (Ultradent).

## Recent Advances in Filler Technology

Modification of the filler component remains the most important improvement in the evolution of resin composites, because filler particle size, amount, and distribution will affect the clinical success of the dental composites. Different approaches have been made to improve the quality of the filler component. One of them is the development of *bioactive* composites containing fillers that can release a substance having antibacterial effects or buffers the acids produced by bacteria. Bioactive glass containing resin composites exhibited superior mechanical properties over the commercial ones. This may attribute to high filler content and microstructure morphology, which promoted better toughening mechanism of crack deflection and bridging.

In order to enhance the cariostatic demineralization effect of the filling restoration, greater emphasis has been made on utilizing *fluoride*-containing inorganic fillers. Initially, in the 1970s, soluble free salts, such as NaF, KF,  $\text{SrF}_2$ , or  $\text{SnF}_2$ , were added to the composites. These salts can boost the initial high fluoride release leaving some micropores in the material resulting in lower mechanical properties and wear resistance. In the late 1980s up to the 1990s, some dental composite products have been manufactured containing sparingly soluble inorganic salts, such as ytterbium fluoride ( $\text{YbF}_3$ ) to provide substantial fluoride release. Other composites contain fluoride-releasing glass fillers, such as fluoro-aluminum-silicate glass. In spite the fact that these fluoridated composites release significant amounts of fluoride, their present ability to prevent secondary caries is questionable, and improvements in technology may be required to increase the fluoride release. A composite containing fluoro-aluminum-silicate fillers release fluoride continuously, which could be due to their greater solubility compared to ytterbium fluoride. Currently, nearly all commercially available composites are comprised of fluoride in their chemical components.

*Smart* composites are materials having therapeutic or diagnostic functionality, such as Ariston pHc, which were developed in 1998, in order to reduce secondary caries by providing remineralization. This type of composite is considered as a therapeutic composite having either antimicrobial or remineralizing effects. They are designed to release calcium, hydroxyl, and fluoride ions under acidic conditions (during caries formation) in areas immediately adjacent to the restorative material. However, they have a problem of absorbing water, which can affect their dimensional stability and overall properties. Others are containing and releasing bactericidal components, such as chlorhexidine, zinc oxide (ZnO) nanoparticles, quaternary ammonium polyethyleneimine nanoparticles, and 12-methacryloyloxydodecylpyridinium bromide (MDPB) monomer. Thereby, it limits bacterial biofilm formation and colonization on the surface of the restoration and bacterial growth inside marginal gap by buffering the acid produced by the cariogenic bacteria. Another approach includes the incorporation of metallic oxide particles/ions (silver, titanium, gold, and zinc) into the restorative materials as bactericidal and bacteriostatic agents. A trail resin composite containing ZnO nanoparticles has imparted antibacterial activity against *Streptococcus mutans* without compromising its mechanical properties except reduction in the depth of cure due to opacity of the particles [46]. Recently, incorporation of 2-dimethyl-2-dodecyl-1-methacryloxyethyl ammonium iodine (DDMAI) into resin has an inhibition effect on young *S. mutans* biofilm formation as well as providing radiopacity.

Another attempt to achieve dental remineralization similar to that obtained by saliva was suggested by the addition of *amorphous calcium phosphate* (ACP) as a nanofiller component of 100 nm in the composite material. Some resin composites contain ACP which is presently used in orthodontic adhesive and sealant. Pulp-capping composite was formulated with dentin repair simulated components, such as calcium phosphate, morphogenic proteins, biomimetic analogs noncollagenous proteins, and dentin simulating peptides. The concept of having a composite that can deposit secondary dentin associated with good strength and durability is desirable. These bioactive ACP-based fillers were formulated for potential utilization in sealants and liner/base materials in an attempt to remineralize existing or incipient lesions. Composites containing milled Zr-ACP fillers showed an improved mechanical stability that may beneficially extend their dental efficacy. Admixing of silanized silica nanofillers to the ACP-based composites can improve their mechanical properties, as flexural strength, and the kinetics of calcium and phosphate release by reinforcing the remineralizing effect.

Another main modification of fillers has involved the use of *radiopaque* glass fillers to obtain a sufficient radiopacity required to distinguish the composite from carious lesion and tooth substance on a radiograph. Radiopacity of composites can be achieved by the incorporation of heavy metals, such as barium, strontium, zirconium, aluminum, or zinc, which are radiopaque. The DC and shrinkage strain decrease linearly, but not significantly, with the increasing of opaque fillers contents. These two properties are affected mainly by monomer's concentration of the resin matrix. They decreased significantly with increasing Bis-GMA content in the matrix because of its higher molecular weight and viscosity. The incorporation of titanium

and silver–tin–copper fillers into composites can provide increased mechanical strength and radiopacity.

Alternative technologically advanced composite material called *Ceromer*<sup>TM</sup> (*ceramic optimized polymer*) was developed by Ivoclar Vivadent in Tetric composite. The *Ceromer* was designed to combine ceramic fillers (metal oxides) and 3-D loaded fillers in a polymer matrix, of which two are fluoride releasing without compromising delivery and handling characteristics. It has high wear resistance and esthetic properties as claimed by the manufacturer.

Modifications of the filler by adding small (1  $\mu\text{m}$ ) *hollow plastic spheres* can provide sites for stress relief during polymerization, thus minimizing the amount of contraction stresses. However, these hollow spheres would have a negative effect on the optical characteristics of the composite. Apparently, there has been no commercial application of this idea up-to-date. Moreover, when porous  $\text{SiO}_2$  glass particles of 0.5–50  $\mu\text{m}$  in size and of 20–120 nm in porosity size were added to the composite material, it showed an increase in abrasion resistance with a slight reduction in the polymerization shrinkage.

Alternatively, *megafilled* composite restorations were produced by bulk filling the prepared cavity with  $\beta$ -quartz glass inserts, which have been developed since the late 1980s (Lee Pharmaceuticals). The inserts are surrounded by light-cured composite, which bonds to the insert via a silane coupling agent. In 1991,  $\beta$ -quartz inserts were introduced onto the dental market in cylindrical or conical shape. SonicSys inserts (Vivadent, Schaan, Liechtenstein) are produced in a variety of shapes and sizes to fit different shapes of prepared cavities. When fitted into the cavity, they minimize the volume of shrinking composite, thus reducing the amount of contraction stress after polymerization. This can result in lower marginal gap, better adaptation of the restoration, and good proximal contact with improvement in fracture toughness and wear resistance.

Polymerization shrinkage and accompanied stresses are among the major problems opposing the use of composites. This can be antagonized by maximizing the amount of inert fillers, thus minimizing the quantity of the resin in composites resulting in less polymerization shrinkage while providing esthetics and strength. It can be achieved by manufacturing nanofillers (5–200 nm) below the wavelength of visible light, yielding *nanocomposites*. Therefore, they are unable to scatter or absorb this light, and usually the nanofillers are invisible, which enables to improve their optical properties. It combines the superior polish and gloss properties of microfills as well as good mechanical characteristics of hybrids, such as improved marginal seal and wear resistance. Most of the composite products utilized nowadays in the dental markets are nanofilled hybrid composites.

Nanofiller technology depends on molecular engineering that produced functional materials and structures in a nanoscale range of 0.1 to 100 by different physical or chemical methods. The new trend of microhybrids is to maximize filler load and minimize filler size. The latest version of microhybrids has used nanofiller technology to formulate what was referred to as nanohybrid composites. Therefore, nanocomposites can be classified into a true nanofilled composites, nanohybrids, and ormocers.

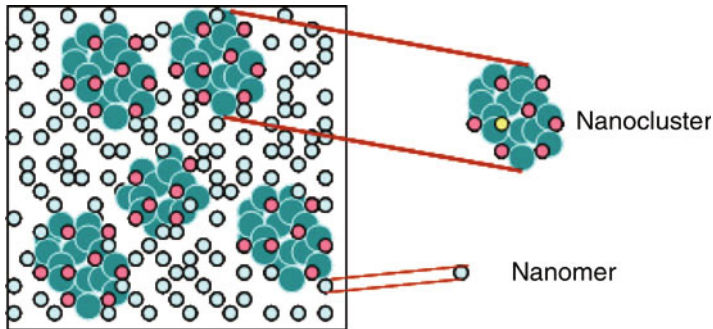


**Fig. 7** Nanofiller technology in nanocomposites

The true nanofilled composites can be formulated from nanomers, which are discrete (monodispersed) and non-agglomerated nanosphere particles of 20–75 nm in diameter. Also, they can be designed as nanoclusters, which are loosely bound agglomerates of nanosized particles making cluster particle size ranges from 0.6 to 1.4  $\mu\text{m}$  to be comparable to the particle size of hybrid composite (Fig. 7). Such very small filler particles will increase their surface areas, thereby limiting the total filler loading. The larger or smaller agglomerates made of zirconia–silica or silica only may act as a single unit, enabling high filler content (79 % wt.), thus giving the composite high strength. The nanocomposite system can reduce the polymerization shrinkage up to 1.4 or 1.6 % by vol. An example of this type of nanocomposite is Filtek Supreme (3 M ESPE).

The combination of nanomer-sized discrete silica particles (20 nm or range of 0.005–0.01  $\mu\text{m}$ ) and the nanocluster formulations or pre-polymerized fillers of 30–50  $\mu\text{m}$  as well as barium glass of 0.4  $\mu\text{m}$  can formulate nanohybrids. The discrete nanofillers reduce the interstitial spacing between the particles that reportedly provide increased filler loading up to 84 % by wt. The nanohybrids may be classified as universal resin composite with optimized features of better physical properties and longer retention of surface polish. They can be formulated as silica only or with other metal oxides to impart better coloration and shade property of the composites, thus obtaining superior esthetics. The huge surface free energy of nanoparticles permits a strong bond (agglomeration), either to each other or to other materials.

Hybrids showed a higher filler volume fraction (70 %) followed by microfills with a comparable value to nanofills (60 %). Similar to microhybrids, these nanofilled composites can be used either in anterior or posterior restorations. They expressed higher mechanical properties than the microhybrids and characterized by higher DC, good flexural strength, diametrical tensile strength, and low flexural modulus. One of the examples of nanohybrid composites is Premise (Kerr). However, microhybrids showed more color stability than nanocomposite and microfill composite.

The reinforcement of the composites, achieved by the incorporation of *fibers* or *whiskers*, resulted in a significant increase in the elastic modulus, flexural strength,

fracture toughness, and fatigue resistance with a decrease in the tensile strength. The strength and toughness of the composite can be increased twice by impregnating strong whiskers with silica nanobeads. Ceramic or bioactive composites such as hydroxyapatite whisker-reinforced composites are characterized by high toughness and reduced water uptake making them viable materials for load-bearing areas of dental restorations [47]. Most available fibers or whiskers, such as carbon, ceramic, glass, metal, and polymer, are bio-inert giving biocompatibility.

Other recent advances to improve the properties of the dental composites by modifying the fillers involve the addition of polymer nanofibers, titanium nanoparticles, and glass fibers. Incorporation of zirconia–silica or zirconia–yttria–silica ceramic nanofibers in dental composites can significantly improve their mechanical properties as stiffness, flexural strength, microhardness, fracture toughness, and fatigue resistance, thus extending their longevity. Fibrillar-based materials include organic polymer fibers, silica and glass fibers, ceramic whiskers, and carbon nanotubes. The inclusion and dispersion of hydroxylapatite nanofibers or nanofibrillar silicate can reinforce the resin and improve the mechanical property of dental resin composites. Hydroxyapatite nanorods may be used as an alternative to other fillers in the composite or in dental adhesive, taking the advantage of remineralizing decayed dentin at tooth–resin interface [48].

A smart nanocomposite material as nanoparticles of amorphous calcium phosphate (NACP) can release ions of Ca and  $\text{PO}_4$  at a cariogenic state of  $\text{pH} = 4$ . Nanocomposites containing  $\text{CaF}_2$  nanoparticles were also developed to release fluoride (F) ions with good mechanical properties. A concern now is to fabricate a composite with fused modified fillers as silica whiskers and dicalcium phosphate anhydrous (DCPA) or tetracalcium phosphate (TTCP) nanoparticles permitting remineralization by the release virtue of calcium and phosphate [49]. This kind of composite is strong and tough but with higher opacity that may limit its esthetic properties. These nano-DCPA–whisker composites have high strength that can be used in stress-bearing areas. The use of unsilanized nano DCPA together with whisker reinforcement provided the best microstructural tailoring method to produce a composite with high strength and ion release.

The *particulate* composites lack sufficient strength and toughness to be used for indirect restoration, such as crowns or bridges. Therefore, *fiber-reinforced composites* (FRC) were introduced to the dental field in the 1960s. It has been used for the construction of prosthetic devices by reinforcing fibers into polymethyl methacrylate (PMMA). Several kinds of fibers have been developed, such as carbon, ultrahigh modulus polyethylene (UHMPE), aramid, glass, and stick fibers. They are bonded to the resin via luting polymer and distributed in different directions and patterns in order to strengthen the resultant prosthesis. The physical and mechanical properties of FRCs depend upon many factors, such as type, diameter, length, volume fraction, distribution, orientation of the fibers, degree of resin impregnation, type of coupling agent used for wetting, bonding interface between fiber and resin matrix, and the presence of voids and microcracks. Fibers can be of different shapes or architectures: short, long unidirectional, bidirectional, woven, and braided. Whiskers are thin crystals with a larger length-to-diameter ratio, which can be distributed in different

directions in the matrix depending on the properties required. FRCs act as stress-bearing structure in which fibers can support force of occlusion as well as deflect crack propagation. FRC restorations can be done directly in the mouth or indirectly in the laboratory. The later technique can be done under heat and pressure to enhance strength and wear resistance. The first directly bonded FRC used in 1981 was Kevlar fibers. Different commercially available FRCs, such as Fibrespan, Adoro, and EverStick, are used to fabricate anterior bridge, mainly to replace missing central or lateral incisors demonstrating a higher flexural strength. The pre-impregnated reinforced glass fiber as EverStick expressed higher mechanical properties, such as stiffness.

Both ultrahigh molecular weight polyethylene fiber-based biaxial braided (Connect, Kerr) and leno weave (Ribbond) showed a deformation under flexural load without rupture, while a unidirectional E-glass prepreg (Splint-It, Jeneric/Petron) reinforced composite demonstrated a brittle mode failure. These fiber-reinforced composites are used clinically suitable for teeth-periodontal splints, orthodontic retainers, endodontic posts, anterior and posterior fixed partial dentures, and reinforcing for a single tooth restoration as in missing lateral incisor. Sometimes, it is used also for removable dentures and provisional restoration.

Indirect composite restorations (inlays and onlays) are used to restore large cavity preparation for posterior teeth with or without cuspal coverage as well as to fabricate, veneers, and resin-bonded bridges for missing anterior teeth. They are made and polymerized in dental laboratory to maximize the DC and minimize the main problems of the composite as polymerization shrinkage and subsequent microleakage resulted from the direct layering technique. This dilemma can result in different sequel of marginal discoloration, secondary decay, enamel cracks, and postoperative sensitivity. The large-sized part of the composite is heat-cured outside the prepared cavity, and only a thin layer of resin used for cementation is exposed to the shrinkage inside the cavity, thus producing a good marginal seal. These restorations showed preservation to tooth substance, acceptable reparability, improved overall properties, abrasion resistance, anatomical shape, and interproximal contact. Modification of the materials and the techniques of clinical application have been performed in attempts to counteract these problems and increase the longevity of the resin-based restorations. Microhybrid composites as commercially named Art-Glass (Jelenko), Solidex (Shofu), and BelleGlass (Kerr) are used to make these indirect restorations.

Direct restorative FRC, such as everX Posterior (GC), containing short glass resin showed improvements in physical properties compared with the commercial restorative composites. It contains randomly orientated E-glass fibers and inorganic particulate fillers as well as a combination of resin monomers, bis-GMA, TEGDMA, and PMMA. The latter form a matrix called semi-interpenetrating polymer network (SIPN) (*net*-poly(methyl methacrylate)-*inter-net*-poly(bis-glycidyl-A-dimethacrylate)), which gives good bonding properties and increases toughness and microhardness of the polymer matrix. Short E-glass fibers in nanohybrid composites can induce light transmission of resin composite permitting an acceptable depth of cure. The recent short glass microfiber-reinforced composite (XENIUS

base, GC) anticipated better performance in high stress-bearing dental areas especially in large cavities of vital and non-vital posterior teeth.

### **Another Composite Classification Based on Viscosity and Clinical Application**

Another approach to classify dental composites is according to their viscosity and intended clinical indication for application. The term universal composite has been obtained by dental manufacturers that competed to develop an optimum composite formulation for expanded use in anterior and posterior teeth. They provide the best blend of good material properties and clinical performance to restore both dentitions concurrently. They are made either from hybrid (MPS = 8–30  $\mu\text{m}$ ) or microhybrid (MPS = 0.7–3.6  $\mu\text{m}$ ) composites. They showed a varied flexural strength and modulus of elasticity compared to nanofilled composites. Moreover, dental composites can be classified according to their viscosity and handling properties into flowable, packable, and conventional hybrids. The latter was discussed previously.

*Flowable* composites introduced in the late 1990s are considered as a subclass of microfills. They were either with reduced filler loading of 20–25 % lower than the conventional composites (44–54 % by vol. or 40–60 % by wt.), retaining the small particle sizes (0.4–1  $\mu\text{m}$ ), or having a greater proportion of diluent monomers in their chemical formulation. Also, they can be obtained by adding some modifying agents (rheological modifiers) that enhance fluidity along with maintaining high filler contents.

The amount of flowability differs among the various products of this kind of dental composites. This may result in a material that is more prone to shrinkage upon polymerization, fatigues quickly, has less strength and wear abrasion resistance, and is more liable to staining. Therefore, it should be restricted to low stress-bearing areas associated with less wear property. Because of their lower viscosity, these composites possess high potential of flowability and wettability into undercut areas that can adapt easily and intimately to a cavity form preparation. It is difficult to control their handling properties due to their low viscosity; hence, they are suitable for small cavity preparation, as preventive resin restoration, sealer, pit and fissure sealants and luting agents for veneer cementation. They are characterized by low modulus of elasticity, so they can be used as liners in deep cavities then covered with a hybrid composite and also utilized in areas that need high flexibility (Class V carious and non-carious cavities, i.e., cervical wear) serving as stress absorbers. There were debates of using the flowable composite as an initial increment liner in the proximal box of a Class II cavity in order to reduce leakage. They may contribute to a reduction of microleakage and improvement in the marginal seal of the restoration, as well as repairing marginal defects. In an attempt to improve their mechanical properties, a new generation of flowable composites with higher filler load has been introduced and recommended to be used in large posterior restorations.

At the same time, *packable* composites (named condensable previously) were launched in the market pursuing to have handling characteristic similar to that of



dental amalgam in an attempt to facilitate placement of the material into the cavity. The resistance to sliding contacts among these particles causes the packable performance, which demonstrates the nonsticky stiff-thick tactility. It gives an improved ability of the dental composite to be scalped and shaped. This characteristic is derived from increasing the filler distribution and loading of more than 80 % wt. (48–65 % vol.) and/or modifying the resin matrix by having strong intermolecular attractions. Increasing the composite's viscosity can also be achieved by changing the shape of the filler particles to have interlock propensity. It can be accomplished by adding fiber-shaped fillers as in ALERT™, porous filler particles as in Solitaire®, or irregular filler particles as in SureFil™. These kinds of composites are usually referred to as a high density composite with larger particle sizes. Hence, they exhibit superior physical and mechanical properties with a slow wear rate. An easy bulk-fill technique is possible, although polymerization shrinkage and a relatively shallow depth of cure may still occur.

The packability of these materials makes them easier to be used by a condensing technique in posterior dentitions. Likewise, their packability, stiffness, high viscosity with lack of stickiness, and slumping can help to establish tight interproximal contacts better than other traditional composites, thus they are appropriate for large posterior restorations (Class II cavities). The higher filler loading can provide a tooth separating force as the material is packed into the prepared cavity. Sometimes, these heavily filled composites can be warmed to lower their viscosity, thus allowing enhanced handling and manipulation properties. The heavily filled packable composites exhibited higher fracture toughness, flexural strength, and modulus than conventional composites. In contrast, conventional composites lie in between these two extremes depending on their viscosities with different filler particles sizes between 1 and 50  $\mu\text{m}$ . Microfills are considered lightly viscous, hybrids and microhybrids are viscous, and some other microhybrids as well as nanofilled composites are highly viscous. Different types of hybrid composites contain some amorphous silica in order to improve the handling characteristics by minimizing stickiness.

Some pit and fissure sealants are based on lightly filled composites with a very small filler volume fraction. It is a kind of a flowable composite but with a very low viscosity in order to penetrate deeply into the pits and fissures of the tooth. Earlier sealants do not include fillers in their components, but the new products have small amounts of fillers to increase their functional durability and to control the viscosity. They have a higher level of initiator to allow quick curing of the material. Other sealants contain fluoride onto their resin chemistry having the advantage of anticariogenic effect.

Usually, incremental filling techniques are preferred over the bulk filling to attain an effective marginal seal. Although incremental technique has the advantages of reducing the polymerization shrinkage of the composite and ensure adequate DC, it has disadvantages of contamination from the oral fluid, voids entrapment, debonding between the increment layers, limited accessibility for placement in small cavities, and time-consuming in placing and curing each layer. Therefore, an innovative RBDC class referred as bulk-fill composite was developed to allow bulk filling

technique in large cavity especially in deep narrow ones. It is recently launched into the dental market following the trend of low-shrinking composite technology. It permits a one-step curing of up to 4 or 5 mm thickness of the material without a time-consuming layering technique. It can be presented as low or high viscosity according to filler volume fraction, particles size, and their surface area. Generally, bulk-fill RBDCs have a reduced filler load and increased filler size in order to enhance depth of cure.

The bulk-fill composites were designed to ease the clinical application by providing a bulk curing of the composite without compromising the obtained general properties. A recently introduced generation of flowable composites called bulk-fill flowable base composites (SureFil<sup>®</sup> SDR<sup>™</sup> Flow [Smart Dentin Replacement] and SDR<sup>™</sup> Posterior Bulk Fill Flowable; Dentsply) contains a monomer with incorporated photoactive group in a urethane methacrylate resin. They contain a high molecular weight modulator chemically embedded in the backbone of the polymerizable resin of the SDR<sup>™</sup> monomer allowing flexibility and network structure of the resin. They expressed a shrinkage stress reduction of 60–70 % compared to conventional flowable, nano- and microhybrid RBDCs, and even with silorane. This attributed to slow radical polymerization rate that characterized these resins, which are based on Stress Decreasing Resin or Smart Dentin Replacement (SDR) technology and also to their high reactivity to light curing. They showed higher plastic deformation (high creep) making a significant reduction of interfacial stress occurrence, cusp deflection and allowing better DC within the whole increment. Bulk-fill flowable composites of low elastic modulus can be used as a liner underlying the hybrid composite restoration with a good interfacial adhesion and adequate marginal adaptation. Because of their good mechanical properties, they are used for large posterior restorations.

Also, bulk-fill RBDCs are launched as posterior composite products of high filler loading that may decrease the creep strain. Most of these highly viscous bulk-fill composites exhibited a creep deformation within the range of regular RBDCs. They can fill a cavity in bulk up to 4 mm as in Tetric EvoCeram Bulk Fill (Ivoclar Vivadent) and to 5 mm as in SonicFill (Kerr). A direct restoration made from low viscosity bulk-fill composite by reducing the amount of fillers (SureFil<sup>®</sup> SDR<sup>®</sup>, Dentsply; Venus<sup>®</sup> Bulk Fill, Heraeus Kulzer; X-tra base<sup>®</sup>, VOCO; Filtek<sup>™</sup> Bulk Fill, 3M ESPE) should be surfaced with a regular composite as overlaying layer, while high viscosity type by increasing the filler size (SonicFill<sup>™</sup>, Kerr; Tetric EvoCeram<sup>®</sup> Bulk Fill, Ivoclar Vivadent; X-tra fil, VOCO) can be placed without this layer. Varied chemistry of resin formulations and filler characteristics (particle's size, type, volume fraction, density, and distribution) of these composites can contribute to significant differences in their properties. Most of bulk-fill composites, except SonicFill<sup>™</sup>, are more translucent for the visible light than the conventional composites to promote light-curing transmittance in order to achieve the high depth of cure. SonicFill<sup>™</sup> and Tetric EvoCeram Bulk Fill composites had the greatest depth of cure. Tetric EvoCeram Bulk Fill has a regular CQ/amine initiator system together with an Ivocerin initiator booster that enables the material to polymerize in depth.

## Filler/Matrix-Coupling Agents

During the initial development of dental composites, it was found that attaining and maintaining good properties of a composite material were dependent on formation of a strong bond at the interface between the filler particles and the polymer matrix. It is essential to achieve a desired strength at the area of phase separation between the organic (resin) and inorganic (filler), which is mainly silica ( $\text{SiO}_2$ ) components, especially in the oral environment, where water may penetrate along this interface. The filler surface is comprised of Si–OH group which is more sensitive to water, while the Bis-GMA monomer is hydrophobic that cannot wet the filler surface. Therefore, the synergy linking between these two phases can be achieved by coating the fillers with a coupling agent, usually an organosilane, which chemically bonds them, sharing the characteristics of both reinforcing filler and resin matrix.

Strong bonding at the interface allows the stress transfer from the weaker plastic polymer matrix to the relatively stiffer filler particles and its distribution throughout the material. It allows stable durable and long-lasting composite restoration with increased resistance to hydrolytic degradation. Therefore, it can reduce the risk of gradual loss of filler particles from the composite surface during wear or abrasion process. However, a poorly bonded interface may act as a crack initiation site resulting in fracture and subsequent degradation of the composite. Sufficient and effective amount of silane is required to wet the surface of the fillers in order to obtain optimum mechanical properties of the composite [50]. In the non-silanated filler-based composites, the filler particles may be pulled out from the resin matrix, which can be worn easily. This attributed mainly to the weak link between the filler particles and the resin matrix. Good bonding quality at filler–resin interface contributed significantly to the development of strong and wear-resistant composite material to be used for both anterior and posterior dentitions. The strength of a composite material is emphasized by silanization of the filler.

## Historical Background and Classification of Coupling Agent

The typical coupling agent for RBDCs has a long hydrolyzed molecular chain with two reactive ends; one links to the filler particle and the other one reacts to the polymer matrix. One end has a silanol (Si–OH) functioning group where silicon and oxygen atoms react with their correspondents on the surface of the filler particles. These bifunctional molecules are capable of forming siloxane ionic bonds (Si–O–Si) to the silicon–oxygen groups in the silica-based filler surface (inorganic phase) by a condensation reaction. The other end has methacrylate groups containing C=C double bonds conjugated with the polymer matrix (organic phase) forming strong covalent bonds via addition (free radical) polymerization reaction upon light activation of the resin (Fig. 8). Hence, the hydrophilic surface of the fillers becomes hydrophobic capable to bind to the matrix facilitating their wetting by resin. A workable viscosity of a composite can be attained by adding unbounded smaller filler particles in a range between 0.04 and 0.02  $\mu\text{m}$ .

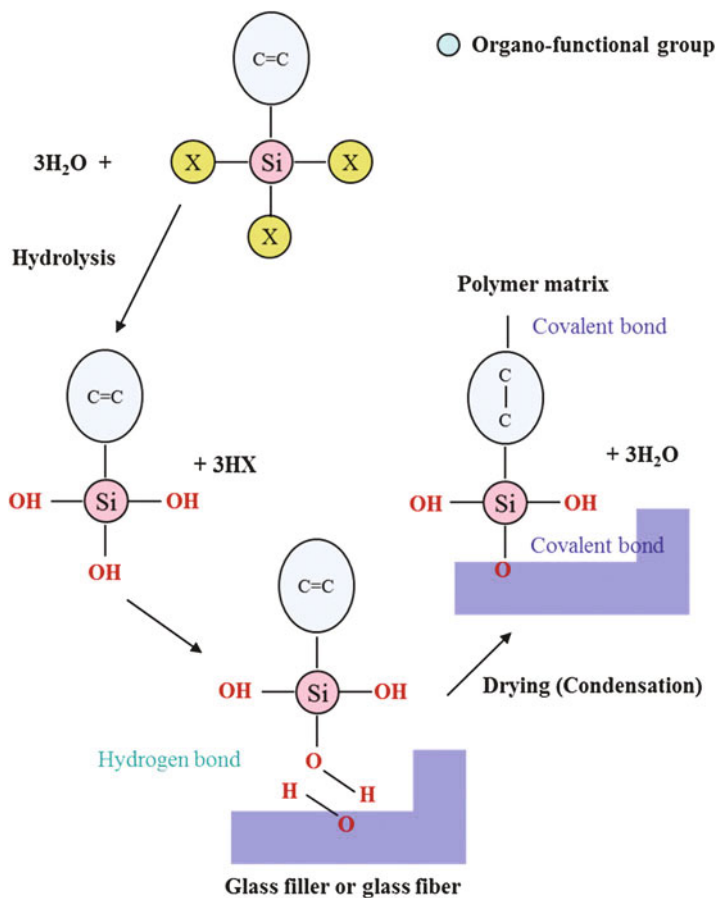


**Fig. 8** Silanization bonding between glass surface and polymer matrix

Majority of commercially available dental composites contain silica-based fillers and filler/matrix silane coupling agents associated with functional methacrylate groups. The most commonly used organosilane especially with glass-filled resin is  $\gamma$ -methacryloxypropyltrimethoxysilane ( $\gamma$ -MPS). It has a carbonyl group forming a hydrogen bond that is capable of breaking and reforming again. Another coupling agent known as 4-META has been tested with various titanates and zirconates, but none has been as successful as MPS. The MPS was compared with 3-acryloxypropyltrimethoxysilane (APS) and had shown to produce stronger and more stable composites with quartz or zirconia silicate fillers.

Studies have verified the crucial importance of the coupling agent in improving the mechanical properties and the clinical performance of the resultant composite to mediate a durable bonding between the dissimilar components. The addition of a fluoro-alkyl silane to MPS for Zr-silicate fillers results in composites having greater tensile strength and less water sorption compared to composites with MPS alone.

Further innovations of new fillers and resins for composites may necessitate the continued development of coupling agents or further refinements of the existing ones in terms of optimal amounts and modes of coverage.

---

## **Other Properties of RBDCs**

There are several requirements and characteristics for manufacturing a proper RBDC in modern dentistry. The principal functional, mechanical, and physical properties comprise high strength, fracture toughness, surface hardness, modulus of elasticity, radiopacity and low polymerization shrinkage, wear, water sorption and solubility, fatigue, and degradation. Additionally, biological considerations including biocompatibility, no postoperative pain or hypersensitivity, preservation of tooth structure from fractures or cracks, and caries are necessary. Moreover, esthetic properties, such as optimized color (shades, translucencies, and opacities) matching and stability, maximum polishability, long-term surface gloss, anatomical form, and absence of marginal or surface staining are also to be fulfilled in order to enhance the longevity of the restorations.

## **Mechanical Properties**

The strength of most available resin composites is close to that of the tooth substance. Several properties of dental composites are measured to achieve the ISO standards' testing in order to be applicable clinically. One of the most common properties is the flexural strength, which measures the amount of material's resistance to bend and flex before it breaks. Most of the dental composites expressed flexural strength of 100–150 MPa. Also, RBDC material should be tough enough to resist growth of cracks. Developing dental composite materials that can withstand high stress situations as in wear and parafunctional habit is still essential.

## **Thermal Properties**

Thermal expansion of dental composite is almost three times that of the tooth substance. Thus, the composite can expand and contract under hot and cold stimulus more than the tooth adding too much stresses at the bonding interface resulting in the loss of adhesion.

## **Optical Properties**

Dental composite can appear radiopaque or radiolucent on radiograph depending on the presence of some specific minerals in the fillers. Radiopaque heavy minerals are essential in dental composites to demarcate the area of the restoration and the tooth

structure as well as the detection of the recurrent caries, which occurs to be mainly radiolucent in the radiograph. Chemical components as pigments, opaquer, and UV light absorbers are added in the resin matrix to improve esthetic and optical properties of the composites. Metal oxide pigments are added to the composite to give different color shades and tints to contrast with the surrounding tooth structure. The fluorescent compounds are added to give a natural appearance of tooth substance. Heavy metal oxides as titanium oxides can be also added to obtain opaquer in order to mask the dark color of the tooth. The dental composites must contain fillers and matrix with refractive indices in a range of 1.45 and 1.56 similar to those for enamel and dentin, respectively. Mismatch of the refractive indices of filler and matrix can increase light scattering by the fillers, thus producing opaque materials. Utilization of filler particle size of  $\leq 400$  nm in the resin composite can result in superior esthetic properties with excellent translucency.

## **Shades and Coloring of Dental Composites**

Manufacturers provided dental composites in different coloring shades, opacities, and translucencies to obtain high esthetic quality of the restoration. Opaque composites are designed to obscure the undesired underlying color as stained, discolored dentin, and exposed metal in case of esthetic repair. The last shaded layer represented by translucency and coloring tints mimics the translucency of the enamel and its accompanying characterization such as white spot, fissures, and lines. Bleached color associated with different shades is also provided to gain more appealing look to keep up with modern esthetic dentistry.

## **Water Sorption and Solubility**

RBDC restorations are found in oral environment where they are exposed to water internally from saliva and externally from drinking fluids. Hydrolytic (hygroscopic) expansion of RBDCs may result from water sorption depending on composition of the composite and amount of resin matrix. Solubility of RBDCs may occur from external acids taken during eating or drinking or internal ones produced by oral bacteria in the plaque, if there is a similarity between solubility parameter of the fluid and that of the polymer resin.

## **Biocompatibility**

The local and systemic biocompatibility of RBDCs is essential to allow better longevity of the material. The release of leachable monomer components may induce series of biological responses to the human tissues. This can lead to allergic or toxic reactions manifested clinically as hypersensitivity, inflammation, or toxicity of the tissues.

## Summary: Future of RBDCs

Current changes meanwhile are further primarily focused on the polymeric resin matrix development in order to develop composite systems with less polymerization shrinkage and shrinkage stress and to formulate them to be self-adhesive, self-repairing, and smart motivating materials to the tooth substance. The evolution in dental resin composites should emphasize on enhancing their chemical formulations, esthetics, handling, and overall properties. Along the development of RBDCs, different changes have to be performed in filler content, size, shape, or surface treatment, alterations in monomer's chemistry, and/or structure, and modifications in dynamics of polymerization reaction have to be intended.

Several interesting developments and trends in the field of materials science and biomaterials may inspire future of dental composites to some extent. These developments include nanotechnology and nanostructuring resin-based materials that may actively combat oral microbes, stimuli-responsive materials, and tissue regeneration or self-repairing materials. For example, stimuli responsive for dental composites may allow release-on command of antimicrobial compounds. Self-repair attempts can develop synthetic materials that remodel and heal after tissue loss has occurred. The first self-repairing synthetic materials reported was an epoxy system found in resin-filled microcapsules. When they are destroyed near a crack line, they can release resin that can fill the crack resulting in its repair. Complex materials and sophisticated technology are needed to develop such engineering materials to regenerate dental tissues. Examples of these materials are bioactive glass and, more recently, polymer-ceramic biomimetic composite.

The focus of the nowadays research is attempting to impart the adhesive properties to dental composite by developing self-adhesive restorative composite. This approach was undertaken to facilitate a simple placement of the dental composite with minimal clinical technique sensitivity. For instance, flowable composite comprised of acidic adhesive monomer formulation along with traditional methacrylate systems provides adhesion by micromechanical and chemical interaction to the tooth substance. Commercial examples of these flowables containing adhesive monomer formulations are Vertise Flow (Kerr) and Fusio Liquid Dentin (Pentron Clinical). The former incorporates glycerol phosphate dimethacrylate (GPDM) acidic monomers, which may be able to generate adhesion to tooth structure. Such flowables can be utilized as a liner, base, or restoring a small cavity as a pit and fissure sealant. Some newly developed self-adhesive pulp-capping liners demonstrated fairly effective trial results. This may lead to evolution of similar composites that can restore larger cavities for both anterior and posterior dentitions. However, this kind of innovation is still challenging in order to design such a hydrophilic formulation to be self-adhesive and at the same time hydrophobic to minimize the risk of water sorption, which is most likely be in this resin.

Moreover, developing a dental composite that can release remineralizing ions or antimicrobial agents with good mechanical and physical properties is still a focal point of tremendous research. Increasing concern in recent studies for antibacterial activity of resin composites and adhesives has been taken to reduce risk of recurrent

decay around the restorations, thus minimizing the frequent reason for replacement of existing restorations. Novel experimental fluoride-releasing composite may combine the sustained release and recharge capabilities of the fluoride from the fillers and resin monomers with acceptable mechanical and physical properties. Also, modern efforts are oriented to deliver resin-composite materials with a potential therapeutic profit.

Bisphenol A (BPA) has already been detected to be released out of the dental composite materials causing endocrine abnormalities, as reproductive system, and some other toxic diseases. Therefore, BPA-free dental composites are the new era for dental composite researches aiming to reduce human exposure to BPA derivatives and to have a versatility to meet several properties and requirements for clinical application. A new dimethacrylate monomer SiMA without BPA structure potentially to replace Bis-GMA was synthesized and used as base resin for dental composite materials. It had no cytotoxic effect on human dental pulp cells *in vitro*; however, improvement of the mechanical properties is required.

This new innovation explores a novel reactive group and functionality of the dental polymers that is completely diverted from the traditional dimethacrylate resin. Very recent grant researches for BPA-free dental polymers have been started in the University of Colorado based on copper-catalyzed azide–alkyne cycloaddition reaction and thiol–vinyl sulfone reaction. Another research that focused on oxirane–acrylate systems has been started by the University of Health Science Center, San Antonio.

The targeted composite is directed not only to restore the tooth decay but to detect, prevent, and perhaps repair the damage. Biomimetic restorative materials are designed to mimic the structural components of the tooth which are enamel and dentin. They must be similar to tooth structures in their physical and mechanical properties, resist masticatory forces, and possess similar appearance to natural enamel and dentin. Restorative materials used in the oral environment must fulfill form, function, esthetics, and biocompatibility. The ideal material, however, still does not exist because many cannot fulfill all prerequisites.

---

## References

1. Peyton FA (1975) History of resins in dentistry. *Dent Clin North Am* 19:211–222
2. van Noort R (2002) A historical perspective. In: *Introduction to dental materials*, 2nd edn. Mosby-Elsevier, St. Louis, pp 6–10
3. Bowen RL, Paffenbarger GC, Millineaux AL (1968) A laboratory and clinical comparison of silicate cements and a direct-filling resin: a progress report. *J Prosthet Dent* 20:426–437
4. Tylman SC, Peyton FA (1946) *Acrylics and other synthetic resins used in dentistry*. JB Lippincott Co., Philadelphia
5. Coy HD (1953) Direct resin fillings. *J Am Dent Assoc* 47:532–537
6. Bowen RL (1956) Use of epoxy resins in restorative materials. *J Dent Res* 35:360–369
7. Bowen RL (1962) Dental filling material comprising vinyl silane treated fused silica and a binder consisting of a reaction product of bisphenol and glycidyl acrylate. US Patent 3066, p. 112



8. Floyd CJ, Dickens SH (2006) Network structure of Bis-GMA- and UDMA-based resin systems. *Dent Mater* 22:1143–1149
9. Kerby RE, Knobloch LA, Schricker S et al (2009) Synthesis and evaluation of modified urethane dimethacrylate resins with reduced water sorption and solubility. *Dent Mater* 25:302–313
10. Asmussen E (1982) Factors affecting the quantity of remaining double bonds in restorative resin polymers. *Scand J Dent Res* 90:490–496
11. Sideridou I, Tserki V, Papanastasiou G (2002) Effect of chemical structure on degree of conversion in light-cured dimethacrylate-based dental resins. *Biomaterials* 23:1819–1829
12. Prakki A, Tallury P, Mondelli RF et al (2007) Influence of additives on the properties of Bis-GMA/Bis-GMA analog comonomers and corresponding copolymers. *Dent Mater* 23:1199–1204
13. Musanje L, Ferracane JL, Sakaguchi RL (2009) Determination of the optimal photoinitiator concentration in dental composites based on essential material properties. *Dent Mater* 25:994–1000
14. Palin WM, Hadis MA, Leprince JG et al (2014) Reduced polymerization stress of MAPO-containing resin composites with increased curing speed, degree of conversion and mechanical properties. *Dent Mater* 30:507–516
15. Hadis MA, Shortall AC, Palin WM (2012) Competitive light absorbers in photoactive dental resin-based materials. *Dent Mater* 28:831–841
16. Furuse AY, Mondelli J, Watts DC (2011) Network structures of Bis-GMA/TEGDMA resins differ in DC, shrinkage-strain, hardness and optical properties as a function of reducing agent. *Dent Mater* 27:497–506
17. Guggenberger R, Weinmann W (2000) Exploring beyond methacrylates. *Am J Dent* 13(Spec No):82D–84D
18. Imazato S, McCabe JF (1994) Influence of incorporation of antibacterial monomer on curing behavior of a dental composite. *J Dent Res* 73:1641–1645
19. Beyth N, Yudovin-Farber I, Bahir R et al (2006) Antibacterial activity of dental composites containing quaternary ammonium polyethylenimine nanoparticles against *Streptococcus mutans*. *Biomaterials* 27:3995–4002
20. Antonucci JM, Stansbury JW, Keeny SM et al (1992) Effect of aldehydes on the mechanical strength of dental composites. *J Dent Res* 72:598
21. Stansbury JW (1990) Cyclopolymerizable monomers for use in dental resin composites. *J Dent Res* 69:844–848
22. Stansbury JW, Antonucci JM (1992) Evaluation of methylene lactone monomers in dental resins. *Dent Mater* 8:270–273
23. Ye S, Azarnoush S, Smith IR et al (2012) Using hyperbranched oligomer functionalized glass fillers to reduce shrinkage stress. *Dent Mater* 28:1004–1011
24. Viljanen EK, Skrifvars M, Vallittu PK (2007) Dendritic copolymers and particulate filler composites for dental applications: degree of conversion and thermal properties. *Dent Mater* 23:1420–1427
25. Moszner N, Völkel T, Fischer U et al (1999) Polymerization of cyclic monomers, 8. Synthesis and radical polymerization of hybrid 2-vinylcyclopropanes. *Macromol Rapid Commun* 20:33–35
26. Bailey WJ (1975) Cationic polymerization with expansion in volume. *J Macromol Sci-Chem* A9:849–865
27. Stansbury JW (1992) Spiro-orthocarbonate-substituted methacrylates: new monomers for ring-opening polymerization. *J Dent Res* 71:239
28. Tilbrook DA, Clarke RL, Howle NE et al (2000) Photocurable epoxy-polyol matrices for use in dental composites I. *Biomaterials* 21:1743–1753
29. Eick JD, Kotha SP, Chappelow CC et al (2007) Properties of silorane-based dental resins and composites containing a stress-reducing monomer. *Dent Mater* 23:1011–1017

30. Zakir M, Al Kheraif AA, Asif M et al (2013) A comparison of the mechanical properties of a modified silorane based dental composite with those of commercially available composite material. *Dent Mater* 29:e53–59
31. Wolter H, Storch W, Ott H (1994) New inorganic/organic copolymers (Ormocers) for dental applications. *Mater Res Soc Symp Proc* 346:143–149
32. Tagtekin DA, Yanikoglu FC, Bozkurt FO et al (2004) Selected characteristics of an Ormocer and a conventional hybrid resin composite. *Dent Mater* 20:487–497
33. Schneider LF, Cavalcante LM, Silikas N et al (2011) Degradation resistance of silorane, experimental ormocer and dimethacrylate resin-based dental composites. *J Oral Sci* 53:413–419
34. Wang W, Sun X, Huang L et al (2014) Structure–property relationships in hybrid dental nanocomposite resins containing monofunctional and multifunctional polyhedral oligomeric silsesquioxanes. *Int J Nanomedicine* 9:841–852
35. Beigi S, Yeganeh H, Atai M (2013) Evaluation of fracture toughness and mechanical properties of ternary thiol-ene-methacrylate systems as resin matrix for dental restorative composites. *Dent Mater* 29:777–787
36. Turssi CP, Ferracane JL, Vogel K (2005) Filler features and their effects on wear and degree of conversion of particulate dental resin composites. *Biomaterials* 26:4932–4937
37. Bowen RL, Eichmiller FC, Marjenhoff WA (1991) Glass-ceramic inserts anticipated for ‘megafilled’ composite restorations. Research moves into the office. *J Am Dent Assoc* 122:71, 73, 75
38. Condon JR, Ferracane JL (2002) Reduced polymerization stress through non-bonded nanofiller particles. *Biomaterials* 23:3807–3815
39. Meriwether LA, Blen BJ, Benson JH et al (2013) Shrinkage stress compensation in composite-restored teeth: relaxation or hygroscopic expansion? *Dent Mater* 29:573–579
40. Trujillo-Lemon M, Ge J, Lu H et al (2006) Dimethacrylate derivatives of dimer acid. *J Polym Sci* 44:3921–3929
41. Bracho-Troconis C, Trujillo-Lemon M, Boulden J et al (2010) Characterization of N’Durance: a nanohybrid composite based on new nano-dimer technology. *Compend Contin Educ Dent* 31(Spec No 2):5–9
42. Boaro LC, Goncalves F, Guimaraes TC et al (2013) Sorption, solubility, shrinkage and mechanical properties of “low-shrinkage” commercial resin composites. *Dent Mater* 29:398–404
43. Utterodt A, Ruppert K, Schaub M et al (2008) Dental composites with Tricyclo[5.2.0.2.6]decane derivatives. European Patent EP1935393 assignee: Heraeus Kulzer GmbH
44. Atai M, Yassini E, Amini M et al (2007) The effect of a leucite-containing ceramic filler on the abrasive wear of dental composites. *Dent Mater* 23:1181–1187
45. Braem MJ, Davidson CL, Lambrechts P et al (1994) In vitro flexural fatigue limits of dental composites. *J Biomed Mater Res* 28:1397–1402
46. Tavassoli Hojati S, Alaghemand H, Hamze F et al (2013) Antibacterial, physical and mechanical properties of flowable resin composites containing zinc oxide nanoparticles. *Dent Mater* 29:495–505
47. Zhang H, Darvell BW (2012) Mechanical properties of hydroxyapatite whisker-reinforced bis-GMA-based resin composites. *Dent Mater* 28:824–830
48. Sadat-Shojai M, Atai M, Nodehi A et al (2010) Hydroxyapatite nanorods as novel fillers for improving the properties of dental adhesives: synthesis and application. *Dent Mater* 26:471–482
49. Xu HH, Sun L, Weir MD et al (2006) Nano DCPA-whisker composites with high strength and Ca and PO(4) release. *J Dent Res* 85:722–727
50. Karmaker A, Prasad A, Sarkar NK (2007) Characterization of adsorbed silane on fillers used in dental composite restoratives and its effect on composite properties. *J Mater Sci Mater Med* 18:1157–1162

Stefan Ioan Voicu and Marius Sandru

## Contents

Introduction .....	408
Polymeric Membranes .....	408
Hybrid Membranes .....	413
Main Biomedical Applications of Membranes .....	413
Membranes for Artificial Organs .....	417
Artificial Kidney .....	417
Artificial Lungs .....	422
Artificial Liver .....	425
Artificial Pancreas .....	426
Conclusions .....	427
References .....	427

---

## Abstract

A special field of membrane separation technology consists in development of artificial organs. In the human body, with the exception of the heart and brain, all organs act as a membrane. Several solutions were investigated for various chronic diseases by replacing the function of the affected organ with a specific membrane process. This chapter describes the most important applications of polymeric and hybrid membranes for replacement or substitution of the kidney function, liver, pancreas, and lungs.

---

S.I. Voicu (✉)

Faculty of Applied Chemistry and Materials Sciences, University Politehnica of Bucharest,  
Bucharest, Romania

e-mail: [svoicu@gmail.com](mailto:svoicu@gmail.com)

M. Sandru

Department of Polymer Particles and Surface Chemistry, Sector Biotechnology and Nanomedicine,  
SINTEF Materials and Chemistry, Trondheim, Norway

e-mail: [marius.sandru@sintef.no](mailto:marius.sandru@sintef.no)

---

**Keywords**

Membranes • Polymer • Artificial organs • Kidney • Liver • Lungs • Pancreas • Biocompatibility • Extracorporeal treatment

---

## Introduction

### Polymeric Membranes

A membrane is a selective barrier made of functional materials that allows the passage of certain constituents such as ions, molecules, and particles and retains other constituents. Membranes are important because they are considered to be the first separation systems that have existed on Earth – the first single-celled organism membrane [1]. Membrane separation processes are low-cost and low energy consumption systems and are central to the development of environmental friendly separation technologies. Some of the main advantages of membrane processes are high separation selectivity and their ability to separate thermolabile compounds without their degradation, solving the problem of fractionation and concentration of biological products in medicine, biology, biotechnology, pharmacy, and organic chemistry. The development of membrane separation processes is based on both technological factors such as selective separation, technology reliability, productivity, and energy efficiency and economic factors such as the cost of facilities and equipment, operating and maintenance cost, and cost of raw materials. Membranes and membrane separation processes represent an interdisciplinary field whose explosive development was driven by the involvement of materials science, mathematics, physics, physical chemistry, biology, and engineering in all development steps, from theory to industrial process applications. Since the first synthetic membranes made by Bechhold in 1907 [2], the materials and processes have known a continuous development due to the multitude of practical applications. After a slow start due to lack of knowledge of polymer chemistry and physical chemistry of polymer solutions, membrane synthesis took off as a technological solution to filter and purify water after the end of World War II. The efforts of researchers to obtain filters for drinking water, sponsored by the US Army, were exploited later by Millipore Corporation, the first and still the largest manufacturer of microfiltration membranes in the USA.

Although as early as the beginning of the twentieth century was recognized the potential of synthetic membranes for the separation of species dissolved in a solvent, industrial applications of membranes remained limited until the development of the first asymmetric membranes by Loeb and Sourirajan in 1962 [3]. The importance of these membranes resides in the fact that for the first time, a very thin selective layer with a thickness of approximately 0.1–0.5  $\mu\text{m}$  was produced on the surface of the membrane. The selective layer is supported by the structure of the microporous layer (support) membrane with an average thickness between 0.1 and 0.2 mm, which gives mechanical stability of the membrane. These membranes were denominated

“asymmetric membranes” because the pores on one side of the membrane (active surface) have diameters in the order of nanometers or tens of nanometers, and the other membrane side has a more porous surface with larger pore size, having diameters in the order of microns or tens of microns. The pore size increases gradually from the active side to the bottom side (support side) of the membrane.

Synthetic polymer membranes can be obtained in several ways, by the phase inversion technique being the most versatile preparation method. Most commercial membranes are produced using various phase inversion techniques. The concept of phase inversion was introduced by KESTING [4] in the 1970s and can be summarized as follows: a homogeneous polymer solution in an appropriate solvent is converted into a two-phase system by evaporation and/or by solvent exchange using a non-solvent for the polymer. The resulting solid phase is the membrane, while the liquid phase (the solvent) is removed and will lead to the controlled formation of pores inside the solid phase, the membrane.

For the preparation of membranes by phase inversion, the polymer is first dissolved in a solvent or solvent mixture which is applied (cast) on a substrate such as glass, metal, Teflon, and textile and then treated under different conditions with a non-solvent to cause phase separation.

For the phase inversion of a polymer solution, there are four different techniques which can be used:

- (a) Precipitation in the vapor phase: the membrane formation being initiated by coagulant or non-solvent penetration from an atmosphere saturated with non-solvent vapor into the polymer solution film.
- (b) Precipitation by controlled evaporation: the polymer is dissolved usually in a mixture of two solvents, a volatile “good” solvent and a less volatile and relatively “bad” solvent for the polymer. By evaporation, the mixture changes gradually its composition ratio, enriching first in the poor solvent and finally by removing both solvents causing membrane formation.
- (c) Immersion precipitation technique, first used successfully by Loeb and Sourirajan for preparing reverse osmosis membranes, has been extensively exploited and developed to obtain membranes with filtration properties. The process consists basically on casting on a substrate of a film of polymer solution dissolved in a specific solvent, with a known concentration, followed by dipping the polymer film and the substrate in a non-solvent for the polymer. The non-solvent will replace the polymer solvent by solvent exchange resulting in the precipitation of the polymer film. The pores are generated by the molecules of solvent and non-solvent which are exchanged in the film during the precipitation process. The typical cone shape of the obtained pores can be explained by the fact that part of the polymer is entrained toward the surface of the film together with the solvent, in the direction of solvent removal. This produces a very thin and dense layer-the active surface of the membrane.
- (d) Thermal precipitation: by this technique, a polymer dissolved in a solvent mixture, close to the saturation point or precipitation, is precipitated by cooling.

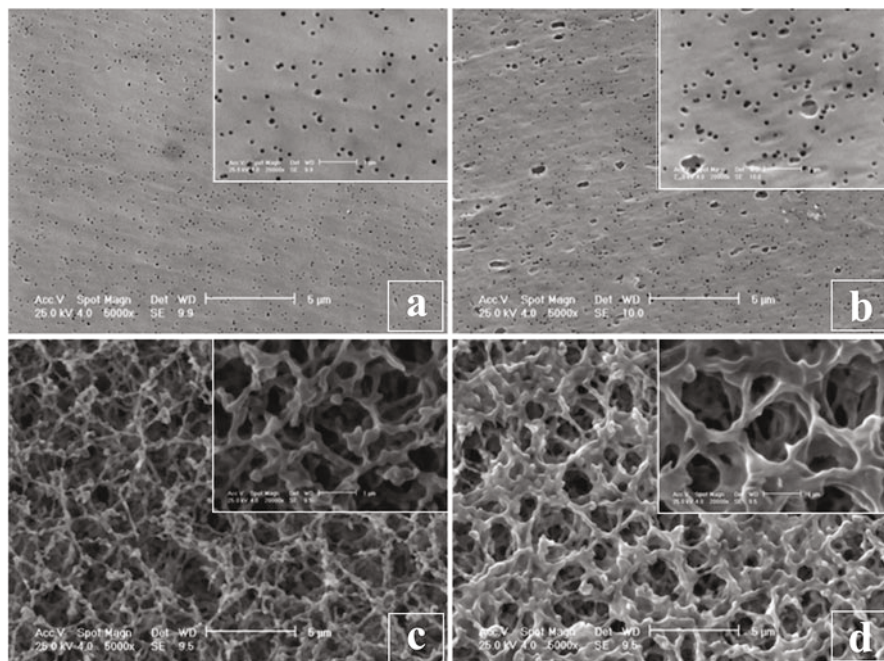


**Fig. 1** SEM images of nitrocellulose membrane active surface (a) and porous surface (b) and polysulfone membrane active surface (c) and porous surface (d)

Symmetric membranes are membranes with the same pore size on both sides having in general cylindrical pores. Due to the low selectivity in the absence of a dense-selective layer, the applications are quite limited and not widely used in separation processes [5].

From the abovementioned, it can be concluded that porosity, pore size distribution, and thus the separation properties and applications of polymeric membranes are strongly correlated with parameters used for membrane fabrication: the nature of the polymer, the concentration of the polymer solution, the thickness of the polymer solution film, and the nature of the non-solvent (coagulant) and temperature.

Figure 1 shows scanning electron microscopy pictures for two membranes, one of nitrocellulose and one of polysulfone, both precipitated from 10 wt% polymer solution dissolved in *N,N*-dimethylformamide and used as non-solvent water. Morphological differences can be easily observed between the two membranes, which are determined solely by the different nature of polymers and their different macro-molecular aggregate settlements during precipitation.

Another important parameter that determines the morphology and separation properties of membranes is the thickness of the polymer solution film from which the membrane is obtained. In Fig. 2, electron microscopy pictures are shown for membranes of cellulose acetate cast with different film thicknesses of the polymer solution: 100 µm, 200 µm, and 300 µm. The membranes were obtained from a

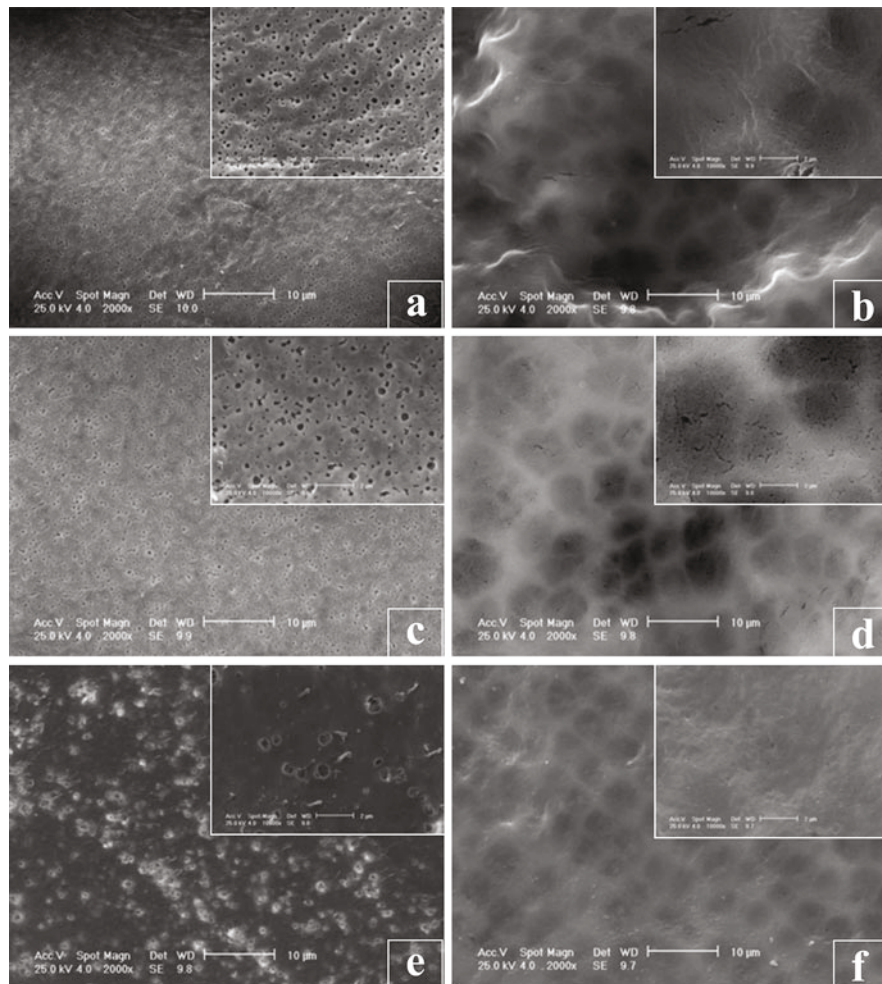


**Fig. 2** SEM images of cellulose triacetate membranes from different thicknesses of polymer solution film, 100  $\mu\text{m}$  (**a, b**), 200  $\mu\text{m}$  (**c, d**), and 300  $\mu\text{m}$  (**e, f**), active surface (**a, c, e**), and porous surface (**b, d, f**)

solution of cellulose acetate in dimethylformamide (DMF) 12 wt% precipitated in deionized water. It can be observed that the porosity of the obtained membrane is decreasing by increasing the film thickness of polymer solution. The shape and pore size distributions determine and influence the two essential properties of a membrane – the permeation flow and retention capacity of the membrane. The flow is the amount of a liquid or gas that can pass through the membrane per unit area in a given period of time. The retention capacity of the membrane represents the ability of the membrane to separate various species present in the permeating solution such as ions, molecules, molecular or macromolecular aggregates, and particles. Figure 3

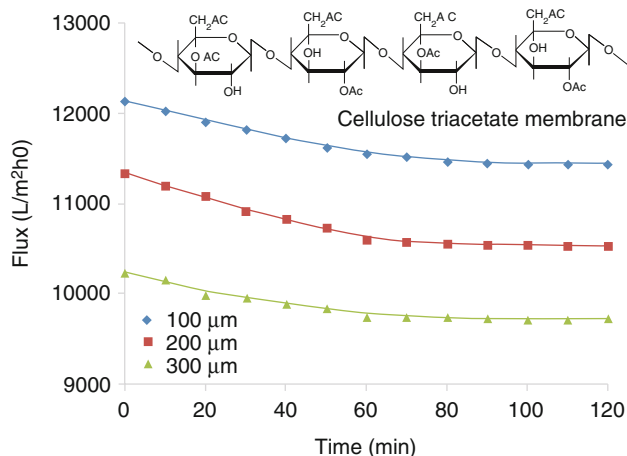


**Fig. 3** Water fluxes of cellulose triacetate membranes as function of the polymer solution film thickness

shows the flux through the synthesized membranes and the retention capacity for bovine serum albumin. The decrease of the flow and retention capacity by increasing the film thickness is due to an increased compactness of the active layer, the layer responsible for the separation properties of the membrane.

Depending on the diameter of the pores, pore size distribution, and separation mechanism, the membranes can separate certain species based on size discrimination leading to several main membrane processes: reverse osmosis, ultrafiltration, nanofiltration, microfiltration, ion exchange pervaporation, and gas separation. Reverse osmosis is a process used for the desalination of water using semipermeable membranes which are permeable to water but impermeable to salt. Pressurized water containing the salts dissolved on the feed side of the membrane permeates through the membrane, and the salt-depleted stream is removed at reduced pressure on the permeate side of the membrane. In 1931, the process was patented as a method for water desalination and was named “reverse osmosis.” Reid and Breton showed in 1959 that cellulose acetate films with a thickness of 5–20 μm could perform this type of separation at pressures up to 1000 psi, obtaining a 98 % removal of salt. The ultrafiltration employs porous membranes used to separate macromolecules and colloids in water. The average pore diameter of ultrafiltration membranes is in the range of 10–1000 Å.

The first synthetic ultrafiltration membranes were prepared by Bechhold from nitrocellulose (collodion), and he was the one who used first the term “ultrafiltration.” By the mid-1920s, collodion membranes for ultrafiltration and microfiltration were commercially available for laboratory use. Microfiltration refers to the filtration processes using porous membranes to separate suspended particles with diameters between 0.1 and 10 μm. The first large-scale application of microfiltration membranes was the removal of microbial cultures from drinking water; this remains a significant application also in our days. The first microfiltration tests were conducted



in Germany during World War II, as a quick way to decontaminate water supplies. Ion exchange membranes are used in a number of separation processes, of which the most important is the electrodialysis. In ion exchange membranes, electrically charged functional groups are attached to the polymer structure of the membrane material. These functional groups partially or completely exclude ions with the same charge that penetrate the membrane. This means that an anionic membrane with positively charged groups excludes positive ions, but is permeable to negative ions. Similarly, a membrane containing cationic groups with negative charges will exclude negative ions but will be permeable to positive ions. In electrodialysis system, anionic and cationic membranes are organized in a multicellular arrangement of up to 100 cells in a module. Cationic and anionic exchange membranes are stacked in an alternating pattern between the anode and the cathode. Each set of anionic and cationic membranes forms a pair of cells. The salt solution is pumped through cells while an electrical potential is maintained at the electrodes. Positively charged cations migrate through the solution toward the cathode, and negatively charged anions migrate toward the anode. Cations permeate easily through the membrane layer having cationic groups being detained (rejected) in layers of membrane having anionic groups. Similarly, anions are retained in membranes with cationic groups [6].

## Hybrid Membranes

The hybrid polymeric membranes represent bi- or multicomponent composite membranes, having at least one organic component and at least one inorganic component. Typically, the hybrid membranes are based on an organic polymer matrix containing inorganic particles (carbon nanotubes, fullerenes, graphene, magnetic particles, zeolites, etc.) involved in the separation process. Due to the membrane requirements of biocompatibility, it is preferred to use an organic polymer. Free movement of inorganic species in biological fluids is not always desired because of their toxic or carcinogenic potential effect. Often, the toxic potential of inorganic particles is very much dependent on the size of particles which may easily penetrate the cell wall and cause various mutageneses. This is the case of carbon nanotubes or graphenes which are not soluble in aqueous solution at physiological pH. The hybrid membranes are obtained by dispersing the inorganic fillers in the polymer solution by sonication followed by preparing the membrane using phase inversion, evaporation of the solvent, or extrusion [7–10].

## Main Biomedical Applications of Membranes

The first polymers used in biomedical applications are cellulose derivatives (natural polymers) and polysulfones (synthetic polymers). This is due to their biocompatibility and versatility for membrane fabrication. Polysulfones represent a class of amorphous thermoplastic polymers, characterized by high values of glass transition temperature, good mechanical strength and rigidity, outstanding thermal

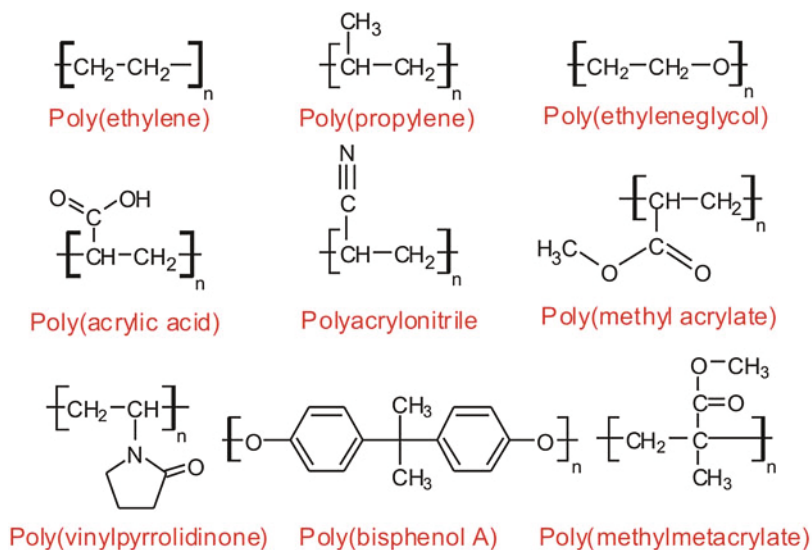


**Fig. 4** Molecular structures of main polymers for biomedical applications

characteristics, and resistance to oxidative environments. Due to their mechanical, thermal, and chemical properties, these polymers are increasingly used in various commercial applications. Basic repeating unit of any polysulfones contains a sulfonic group, one or more aryl-type units, an ether group, and other operating functional groups. Aromatic polysulfones have several key characteristics such as high glass transition point ( $T_g$ , generally less than  $170^\circ\text{C}$ ) and a high degree of thermal oxidative stability. Because of their nature, they present optical transparency, are resistant to hydrolysis in hot water or steam at medium temperatures, and are resistant to acids and bases for a wide range of concentrations and temperatures [11–15]. Other important polymers for biomedical applications are presented in Fig. 4.

Biomedical applications of membranes in the pharmaceutical industry are related to the production of medicaments based on enantiomers, separation and purification of reaction products, and encapsulation for the controlled release of active pharmaceutical ingredients. An ideal controlled release system will discharge the active substance in a specific area of the body in a constant and controlled manner over time. The main challenge of any controlled release system is the achievement of a constant release of the active substance in the blood in order to avoid multiple or high concentrated doses which can solicit additionally the liver [16]. Membranes for controlled release of drugs can be divided into two distinct systems:

Osmotic membrane systems consist of a reservoir made of a polymeric membrane which is permeable to water but not to the active ingredient (semipermeable membrane). When the water permeates through the membrane due to the osmotic

pressure of the solution, the pressure inside the reservoir will increase, and the active substance is released through an orifice valve. Using these devices can release various active substances at relatively high flows. If the system does not have an opening, it can be used for a single dose by breakage of the membrane when the osmotic pressure is high [17].

Diffusion-controlled membrane systems are systems where the drug release is controlled by the transport of the active substance across the membrane. The transport is dependent on the drug diffusivity through the membrane and the membrane thickness according to Fick's law. The membrane may be porous or nonporous and biodegradable or not. These systems are found in the form of pills, implants, or patches.

For the production of pills or tablets, the drug is pressed into tablets and coated with a hydrophilic nondigestible membrane. When the membrane is hydrated, this forms a viscous gel barrier through which the active ingredient diffuses slowly. Controlled release rate is determined by the type of the membrane used [18, 19].

The implants consist of a membrane reservoir containing the active substance in liquid or powder form. The drug diffuses slowly through the semipermeable membrane, and the diffusion rate is dependent upon both the characteristics of the active substance and the membrane. The thickness of the membrane is uniform to ensure constant release. If the membrane is degraded, the release is accompanied by membrane resorption into the body. If the membrane is made of a nonbiodegradable material, it must be surgically removed after use. The rupture of implant may lead to the sudden release of a large quantity of active substance [16].

The transdermal patch is an adhesive patch for drug delivery placed on the skin to administer drugs through the skin, being designed to achieve systemic absorption of the drug at a predetermined rate over a prolonged period of time [20]. The use of these devices is limited for the following reasons: drugs with hydrophilic structure have very low permeation rate through the skin, the adhesive or other excipients can cause local redness or swelling (erythema or edema), and the skin characteristics are different from person to person. Factors that must be considered when designing these devices are physicochemical (hydration level of the skin, the temperature and pH, the diffusion coefficient, drug concentration, and shape dimensions of the drug molecule) and biological (skin condition, age, blood flow, location of the body skin, skin metabolism). This makes the device to be difficult to design and produce being necessary to find a compromise between these parameters. The basic components of such a device are the reservoir containing the active substance, a semipermeable membrane, the adhesive for fastening on the skin, and the material encapsulating the entire device.

Recently, the so-called smart systems have been developed, which, unlike abovementioned systems, try to meet the needs of a particular patient and a particular disease. Controlled release systems (DDS) with feedback control should provide an effective therapeutic agent by detecting (e.g., identification of a marker) and quick response to a biological event even before symptoms are present. Such systems

would be an ideal therapeutic solution as will ensure timely release of the drug (when the concentration of the biomarker is at a high enough level) and at a concentration that is not toxic. The importance of these systems comes from the fact that increasingly more active substances are complex and potent, unable to be administered without a controlled dosing system in order to avoid adverse effects [21]. An elegant solution to this problem is the use of molecularly imprinted polymers as controlled release devices. Molecular imprinting is a method that allows obtaining molecular assemblies with desired structures and properties based on complementary immobilization via functional groups of a template molecule in a polymeric structure. This structure is derived either by polymerization of functional monomers in the presence of template molecule in the case of covalent imprinting or by incorporation into a block polymer template in the case of non-covalent imprinting. By removal of the template using specific reactions (for covalent imprinting) or a specific solvent (non-covalent imprinting), a snapshot of the system is taken, and the resulting molecular assembly provides specific binding to the template molecule and its analogs. The first research that exploited the ability of molecularly imprinted polymers for controlled release of active pharmaceutical substances was performed by Nichols et al. [22], which non-covalently molecularly imprinted polymethacrylic acid with theophylline, using the methacrylate monomer acid and ethylene glycol dimethacrylate as a cross-linking agent. Theophylline is a drug for asthma treatment with a narrow therapeutic window between 30 and 100  $\mu\text{M}$  and with a toxic effect at a concentration of 110  $\mu\text{M}$ . The polymer obtained was grinded in the form of a powder and placed in a column for the study of the active substance release depending on the pH of the extraction solution and on the loading of the assembly template (template 0.1–50 mg/g of dry polymer). The lowest release rate was obtained for a theophylline loading of 0.1 mg/g dry polymer at a pH value of 7. The molecular imprinted membranes are also used to achieve chiral separation of enantiomers present in pharmaceutically active substances. Chiral discrimination between the enantiomers is important for the pharmaceutical industry, being well known that many compounds of interest are racemic mixtures of enantiomers. One of the enantiomers present in the racemic mixture can influence favorably the physiological, pharmacological, pharmacokinetic, and pharmacodynamic properties, while others may have very different physiological interactions, sometimes presenting undesired physiological activities. Molecular recognition of enantiomers in an asymmetric center of a polymer unit is characterized by the presence of at least three points of interaction that may be attractive or repulsive. The interaction points may be represented by different receptors or functional groups such as crown ethers, cyclodextrins and derivatives, and polysaccharides [23].

A special field of application of the membrane is the artificial organs. In the human body, with the exception of the heart and brain, all organs act as a membrane. For these reasons, solutions were researched for various chronic diseases by replacing the function of the affected organ with a specific membrane process. This chapter will deal further with applications of polymeric and hybrid membranes for replacement or substitution of the kidney function, liver, pancreas, and lungs.

## Membranes for Artificial Organs

Different polymeric materials and polymeric membranes were used to design artificial organs such as the artificial heart (polyurethane), artificial kidneys (cellulose or polysulfone), or artificial lungs (polypropylene). The use of membranes for these applications requires, in addition to selectivity, the fulfillment of additional requirements such as fast biomolecular response and biocompatibility of the polymer material with the human tissue. When tissue or blood from a living organism comes into contact with a synthetic material, an immune response is generated. Because these immune reactions are generally catalyzed by adsorption of proteins on the membrane surface, adhesion of proteins should be minimized, especially of proteins in blood plasma. One of these proteins having an essential role is the fibrinogen. Biocompatibility of membranes used in artificial organ development must be closely correlated with a very low retention capacity of this protein. Biocompatibility of polymeric materials can be enhanced or induced by controlling the surface properties of the membrane (pore diameter and pore size distribution for porous membranes, hydrophilicity, or hydrophobicity) by surface modification using biomolecules or preparing membranes with biomimetic surface. The last technique is the most expensive, but offers the best results. Membrane surface properties can be tailored in the case of polydimethylsiloxane, polysulfone (hydrophobic surface), polyethylene oxide, polyvinyl alcohol (hydrophilic surface), or hybrid membranes by microphasic separation. Surface functionalization of membranes with biomolecules is performed using biological species that usually have some of the specific functions of an organ (e.g., heparin which inhibits internal coagulation or urokinase for kidney function) [24]. Other parameters to be taken into account refer to the proliferation of cells on the material, its mechanical strength, and chemical interaction with species dispersed or dissolved in biological fluids coming in contact with the material [25].

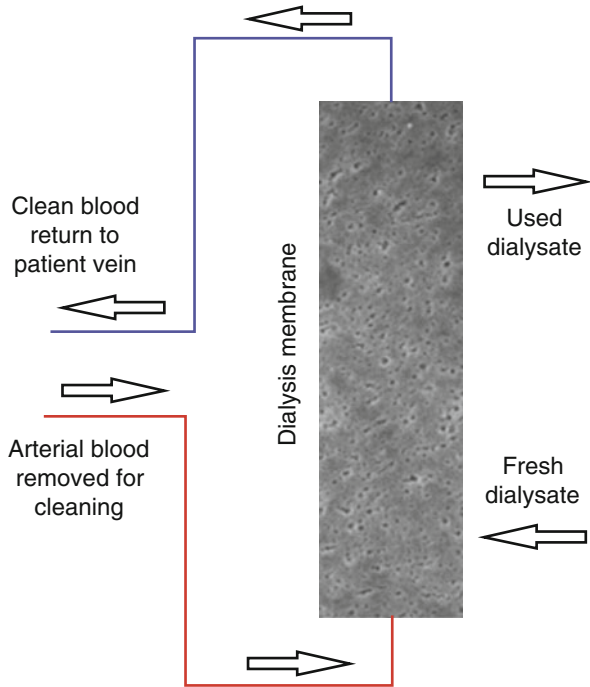
A more suitable definition of artificial organs based on membranes would be “therapeutic remedy by extracorporeal circulation of blood.” The extracorporeal blood circulation consists in removing blood from the body, its treatment or purification, and reinsertion inside the body. These procedures are carried out intermittently, partially or totally replacing a damaged organ. The most common therapeutic procedure for replacement of organ functions is represented by the artificial kidney and artificial lungs, these organs having mainly the role of a membrane: selective separation of various compounds [26].

---

## Artificial Kidney

Many diseases are associated with increased levels of endogenous or exogenous toxins in blood plasma, their presence being due to a malfunctioning of kidneys, the organs responsible to remove these toxins from the body. Effective treatment methods include blood purification outside the body, using filtration membranes

**Fig. 5** Principle of hemodialysis



with different structures and separation mechanisms such as hemodialysis, hemofiltration, hemodiafiltration, or hemoabsorption [27]. The principle of hemodialysis is presented in Fig. 5.

The kidneys are glandular pair organs (right and left) that constitute the bulk of urinary system and are localized inside the abdominal cavity, retroperitoneal in the lumbar region on both sides of the spine. They have a characteristic bean shape with a 10–12 cm length, 6.5 cm width, and 4.3 cm thickness, weighing 120–200 g and having a reddish brown color. They are composed of a fibrous capsule (envelope kidney) and renal parenchyma, kidney tissue which constitutes the main part of the kidney. Renal parenchyma consists of medulla and the cortex regions. Medullar area is divided into 8–15 triangular areas which correspond to renal or Malpighi pyramid configurations. The tip of each pyramid, called the papilla, has a variable number of 15–20 orifices through which urine flows into the small renal caliculus. The caliculus number corresponds to the number of pyramids. The cortical area is situated toward the exterior; it has a granular appearance and enters the medullar area between the renal pyramids.

Morphological and physiological unit of the kidney is the nephron, consisting of the glomerulus and the uriniferous tube. Glomerulus contains a bundle of capillary blood vessels, and the uriniferous tube consists of four segments (Bowman capsule, proximal convoluted, loop of Henle, and the distal convoluted tube), all involved in the formation and transport of urine.

**Table 1** Composition of urine

Constituents	In blood plasma (%)	In urine (%)	In urine from 24 h (g)
Water	90–93	93–95	930–1410
Protide, lipids, colloids	7–9	0	0
Glucose	0.1	0	0
Urea	0.03	2.5–3	20–35
Uric acid	0.004	0.05	0.5–1.25
Creatinine	0.001	0.07	1–15
Mineral salts	0.73	1.57	15–35

Within 24 h, approximately 1500 L of blood flows through kidneys, and about 1500 mL urine is excreted. Urine is formed in the uriniferous tubules during a three-phase process:

- Glomerular filtration (ultrafiltration) occurs in the Bowman capsule and is performed by permeating blood plasma components and retaining the proteins. The blood pressure reaches 75 mmHg in the glomerulus capillaries, much higher than the pressure inside the capsule cavity (5–10 mmHg), thereby realizing the blood filtration based on a pressure gradient. Glomerular capillary pressure is supplemented by the osmotic pressure created by plasma proteins and membrane, leading to the formation of the primitive urine into the capsule having the same composition as the blood plasma excepting proteins which cannot permeate through the capillary and capsule walls.
- Tubular reabsorption occurs in the other segments of the uriniferous tube and consists on water reabsorption (98–99 %) through microvilli of the uriniferous tube. Within 24 h, approx. 179 L of water is reabsorbed from 183 L of primitive urine, and only 1.4 L of urine is produced in the bladder. In addition to water, glucose is completely reabsorbed and some minerals to a lesser extent.
- Renal tubular secretion refers to the ability of uriniferous tube cells to secrete certain substances in the composition of the urine – ammonia, hippuric acid, renin, erythropoietin,  $H^+$ , and  $K^+$ . By renal reabsorption and renal secretion, the final urine is formed and is drained through the uriniferous collector tube.

The urine is an aqueous solution comprising of salts extracted from blood plasma, final products of metabolism in the body, and other introduced substances (drugs, food colorants). It has a slightly acidic pH (5–6), and chemical composition varies with diet and body condition. One liter of urine contains about 900 mL of water and 100 g of dissolved substances (approx. 40 g minerals and 60 g organic matter) [28]. The composition is summarized in Table 1 [28].

As the therapeutic process takes place outside the body, the first problem to be solved refers to the “vascular access,” meaning the choice of the veins to be used for removing the blood from the circulating blood inside the body through the membrane. During the first hemodialysis therapeutic procedure performed by G. Haas in 1924, glass needles were used; the blood was removed from the radial artery and

reintroduced into the body through the cubital vein. Since the 1960s, when it became a relatively common procedure, the Teflon arteriovenous shunt was introduced. This technique implies using two Teflon tubes, one inserted into the radial artery and the other in the adjacent cephalic vein. Initially, the two tubes were connected with Teflon tubing, which was later replaced with silicone rubber flexible tubes (polydimethylsiloxane). The importance of the tubing material lies in the influence it has on blood. The tubing material must be free of contaminants such as unreacted monomer residues or traces of catalyst from the polymerization reaction. The artery and the vein chosen for the removal or reintroduction of blood in the body must be part of the major pathways of blood flow, due to the fact that blood composition is not homogeneous in all the body parts: for capillaries or small vessels, usually blood has a variable composition depending on the role of tissue where the blood vessel is located [29].

Because blood is removed from the body during the hemodialysis process and recycled outside the body, the membranes should be treated with anticoagulants. Anticoagulants were immobilized in the polymer used for membrane preparation (e.g., immobilization of heparin on polysulfone). Modern research takes into account the use of natural substances to solve this problem. Anticoagulant activity was studied for a composite membrane having immobilized citric acid on polyurethane and blended with polyethersulfone [30]. Citric acid is one of the most known natural anticoagulants, and its immobilization is performed during polyurethane polymerization reaction of 4,4'-diphenylmethane diisocyanate with ethylene glycol or polyethylene glycol. The polymer support (polyethersulfone) was mixed in dimethylacetamide with polyurethane and citric acid to form membranes by phase inversion. In order to study the cytotoxicity of the membranes, the activity of human hepatocyte was monitored on the surface of the membrane, and a blood coagulation automatic system was used for measuring anticoagulant activity. Increasing the amount of functionalized copolymer resulted in a significant decrease of small platelet adhesion on the membrane surface. Anticoagulant activity was also more pronounced, whole blood clotting time (WBCT) increasing from a value of 53' 81'' for the polyethersulfone (standard) membrane to 255' 28'' for the composite membrane.

Vitamin E was used also as a direct additive on a polysulfone membrane, combining both its anticoagulant effect and its antioxidant effect [31]. It was found that hemodialysis as a medical procedure increases oxidative stress leading to complications such as atherosclerosis or amyloidosis. In recent years, approximately 40 % of patients on hemodialysis for long periods died of heart problems such as atherosclerosis. While initially it was thought that LDL cholesterol is responsible for atherosclerosis, it was recently found that its oxidized form is responsible for the disease. This is because the oxidized form of LDL is more susceptible to attack the vascular endothelium and to promote penetration of monocytes into it. As in the case of the polyurethane composite membrane, the polysulfone membrane with vitamin E showed a good cellular biocompatibility, beneficial effects on the immune system, antithrombotic effect, and enhanced antioxidant properties. The use of synthetic materials during dialysis favors the



appearance of free radicals of oxygen, but these are strongly inhibited when using vitamin E. In addition, the use of vitamin E provides additional stability conferred by an effect of membrane pseudo-crosslinking and inhibition of blood platelet aggregation, thus preventing some specific complications of this therapy.

One of the limitations of any membrane separation process is represented by the membrane pores clogging with the components to be separated. Because hemodialysis is performed in tubular membrane modules with hollow fiber membranes, there is a tendency to clog the membrane preferentially at the end of the module where the blood enters the membrane, which affects the process efficiency by decreasing the flow in time. To avoid this inconvenience, a larger number of hollow fibers with the small diameter can be used, which leads to uniform blood flow crossing the membrane [32].

The most used polymers for hemodialysis membranes are cellulose derivatives (nitrocellulose and cellulose triacetate) and polysulfone. Besides these, there is still widely used polyethersulfone, polymethylmethacrylate, or polyacrylonitrile. Membranes recently developed have a sandwich structure using three different types of polymer, arranged in layers, each with its own selectivity for a particular species of molecules and the last layer having also support (mechanical strength) role (e.g., composite membrane polysulfone/polyvinylpyrrolidone/polyamide). Since chemical species to be separated during hemodialysis have molecular weights covering a wide range of values, the membranes used must provide great versatility in the separation process. Among the chemical species to be separated are urea (MW = 60), creatinine (Mw = 113), insulin (Mw = 5200),  $\beta$ 2-microglobulin (Mw = 11,818), microglobulin (Mw = 17,000), and albumin (Mw = 66,000). Some of these polymers and their advantages for hemodialysis process are summarized below [33].

Cellulose triacetate membranes were among the first used in hemodialysis. They show excellent selectivity for  $\beta$ 2-microglobulin and albumin (which inhibits platelet adhesion to the surface, thus not leading to blood clotting problems and not requiring additional functionalization anticoagulants). The benefits also include antithrombogenicity and improving lipid metabolism. This is the only polymer from which symmetrical membranes for blood filtration were obtained, its natural origin eliminating many of the drawbacks and limitations for use [34].

Polymethylmethacrylate provides membranes with homogeneous cross section and high selectivity to separate species, acting essentially as a multilayer membrane. This membrane material does not interact with iron and therefore can be used successfully in patients with anemia [35].

Polyacrylonitrile membranes are hydrophilic during the filtration process leading to the formation of hydrogels which greatly increase the flow through the membrane. They showed high selectivity for proteins with average molecular weight and uremic toxins [36].

The polymers most frequently used as hemodialysis membranes are polysulfone and polyethersulfone. Both show great versatility methods of synthesis, being soluble in a wide range of solvents which provides multiple ways to achieve the desired porosity. By endotoxin retention, removal of uremic toxins, proteins with

average molecular weight, and biocompatibility properties, these membranes reach the most stringent standards required in hemodialysis. Their stability allows the use of several sterilization methods, and their chemical properties allow the preparation of composite membranes using other polymers or inorganic species in order to improve the selectivity or flow values [37].

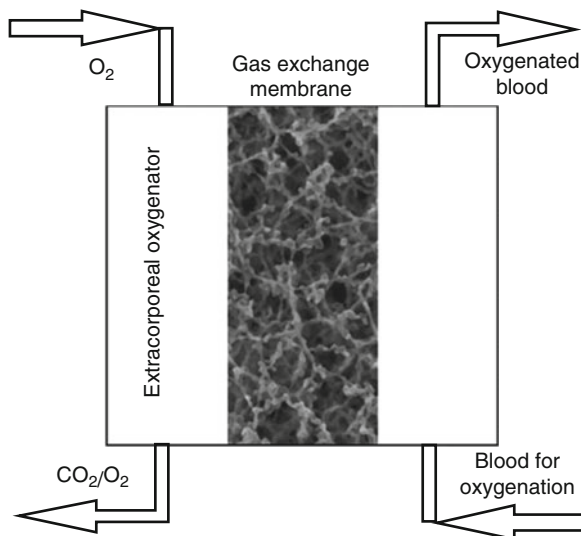
Recently, hybrid membranes based on carbon nanotubes were developed for hemodialysis. Irfan et al. [38] synthesized a composite polysulfone-polyvinylpyrrolidone-carbon nanotube membrane to filter urea, creatinine, and lysozyme. Carbon nanotubes have been treated with a mixture of sulfuric acid and nitric acid to generate -COOH and respective -OH groups on the surface and subsequently were bonded to polyvinylpyrrolidone (PVP). PVP-MWCNT nanocomposites were embedded in the membranes of polysulfone. Polysulfone solution had a concentration of 18 %, thereby achieving membranes with a water flow of 7.14 L/m<sup>2</sup>h. By adding nano-MWCNT PVP, due to polyvinylpyrrolidone hydrophilicity, the flow increased to values between 65.5 and 72.2 L/m<sup>2</sup>h for concentrations between 3 % and 5 % by weight of PVP-MWCNT. To assess membranes in hemodialysis processes, classical markers for uremic toxins, creatinine, and urea were evaluated. The highest value obtained for urea retention was 56.3 % and for creatinine the highest of 55.08 %, values very close to the standard parameters of commercial membranes used for hemodialysis. Bonding the nanotubes to the polymer structure is needed to prevent their leakage into biological fluids and their consequent cytotoxicity. Nechifor et al. reported the synthesis of membrane polysulfone-carbon nanotubes for the removal of heavy metals from the blood by hemodialysis [39]. The principle of retention is based on adsorption of heavy metals (ions of lead, mercury) from a solution of artificial blood on the surface of the nanotubes. In a first step, the polysulfone was functionalized in order to introduce into the polymer chain formyl or chloromethyl functional groups. Carbon nanotubes having amino groups on the surface were used for the covalent bonding to the polymer. Bonding of nanotubes with the polysulfone was achieved by functionalization reactions forming Schiff bases with the amino groups of the formyl or chloromethyl groups. Such covalent bonding provides additional stability to the material. The membranes showed high retention, up to 90 % of the heavy metals dissolved in synthetic plasma solution.

---

## Artificial Lungs

Membrane oxygenators (Fig. 6) have emerged as a necessity for the substitution of lung function during open heart surgery or heart transplant operations. The first oxygenator was built by G. H. A. Clowes, Jr., in 1956, based on a kidney dialysis device using a cellulose acetate membrane. Also in 1956, W. J. Kolff improved the device by using a spiral wound membrane made of polyethylene; the blood circulating through the membrane radially and oxygen are enriched in the center of the membrane module (eight such modules were needed for the efficient transfer of oxygen for a patient). In 1963, T. Kolobow also used a spiral wound membrane-based module, but

**Fig. 6** Principle of a membrane oxygenator



replaced the polyethylene with silicone rubber and nylon wrapped around a central core through which wet oxygen is flowing. Such a module could oxygenate venous blood at a rate of 1000 mL/m<sup>2</sup> membrane/min. In 1971, Kolobow used only a commercial membrane of silicone rubber produced by Fuji Systems, this being the first large-scale clinical use of the artificial lung for cardiopulmonary bypass during cardiac operations and, later, in assisted breathing devices [40].

The lungs are the organs that provide respiratory gas exchange and are placed in the chest cavity. Lung segment represents the morphological and functional clinic unit within a lung lobe. If at the lung surface the limits between lung segments are not observed, these limits exit inside the lungs in the form of intersegmental septa determined by the concentration of the conjunctive lung tissue. The right lung consists of three lobes (upper lobe which is composed of three segments, the middle lobe with two segments, and the lower with five segments), while the left lung is composed of only two lobes, each having five segments. Generally, the left lung is longer and narrower than the right one, due to the position of the heart and the fact that, in this part, the diaphragm is lower than in the right side. From a structural viewpoint, the lung is composed of intrapulmonary airways, lung parenchyma, blood-lymphatic network, and nerve network.

Pulmonary alveoli are the most characteristic formation of the lung structure, having a spherical shape with a diameter of about 150 μm. The existence of alveoli increases the surface of pulmonary acini, the number of alveolus being between 4 and 6 billion with a total area of over 160 m<sup>2</sup>. The pulmonary alveolar wall is a complex structure consisting of stromal tissue, epithelial cells, and blood capillaries. Epithelial cells form a discontinuous layer, made of alveolar cells placed on a thin membrane in contact with capillaries. The hematosis, the exchange of oxygen and carbon dioxide, takes place here, the alveolar air being in direct contact with the walls of the capillaries.

**Table 2** Chemical composition of the inspired and expired air

Elements	Inhaled air (%)	Exhaled air (%)
Nitrogen and rare gases	79.02	79.7
Oxygen	20.94	16.3
Carbon dioxide	0.04	4

Breathing consists in the function by which the body takes in the oxygen and releases carbon dioxide. This gas exchange has two steps:

- Pulmonary breathing (external) occurs in the pulmonary alveoli in which the gas exchanges between the external environment and the blood.
- Tissue breathing (internal), taking place in the tissues, consists of gas exchange between the cells and the body's internal environment.

For the subject of this chapter, pulmonary breathing presents interest and is explained briefly in the following lines. Introduction of oxygenated air into the lungs and elimination of air loaded with carbon dioxide are provided by the thoracic cage skeleton and respiratory muscles. Respiratory movements are changes in volume that occur in the respiratory mechanism and have as result the airflow through extrapulmonary airways and lungs, the lungs playing a passive role in this case. Following the occurrence of respiratory movements, two processes occur: inspiration (air entering the airways and lungs) and expiration (removing air from the lungs) [28]. The chemical composition of the inspired and expired air is shown in Table 2 [28].

The gas exchange in the alveoli is based on certain properties of the gas, physiological mechanisms, and the physical properties of the cell membrane. At this stage, the air is separated from the blood through the membrane walls of the alveoli and capillary wall. Permeation of the two gases is due to partial pressure difference. The oxygen diffuses from the air in the alveolar blood by diffusion, because the partial pressure of the alveolar air is 98 mmHg and 40 mmHg in the venous blood. Carbon dioxide diffuses from the blood into the alveolar air because its partial pressure in the blood is 47 mmHg, while the alveolar air partial pressure is 40 mmHg. This is possible also because carbon dioxide has a diffusion coefficient about 20 times bigger than oxygen. The passage of gases from one side to the other is facilitated by the fact that the blood flow rate is minimal at the capillary level and the contact between the capillaries and alveoli is very good [28].

Most common polymers used as extracorporeal membrane oxygenators are polymers forming dense membranes. These include polydimethylsiloxane, polystyrene, polybutadiene, polyethylene, polytetrafluoroethylene, and polyvinylidene chloride [26].

One of the most recently used polymers for artificial lungs is polymethylpentene. In contrast to polypropylene or polydimethylsiloxane, polymethylpentene provides some advantages in terms of lower adhesion of platelets, increased ability to exchange gases, and the ability to be used continuously for several weeks having a better wear resistance than traditional materials [41].

## Artificial Liver

The liver is the largest gland in the body and is placed into the abdominal cavity, supramesocolic floor at the top right. It consists of two lobes – right, consisting of two segments, anterior and posterior, and left, consisting of a lateral and a medial segment. Anatomical morphological and functional unit of the liver is the liver lobule in the shape of a pyramid with the base located at the liver surface and the tip inward. The lobe structure consists in vascular formations, liver cells (hepatocytes), bile ducts, and vegetative nerves [28]. The radical medical solution for liver failure is represented by liver transplant. This procedure raises several issues such as finding a donor and compatibility between the organ transplanted and host organism and problems that require time in which usually the patient's general condition is deteriorating. A temporary solution until transplantation is the replacement of liver function by extracorporeal blood treatment using composite membranes. In some countries, for ethical or religious reasons, this is the first line of problem solving, considering the improper introduction of a dead body in a living organism (e.g., Japan). Unlike kidneys and lungs where organ function was totally replaced by synthetic membranes, in the case of the liver, the solution consisted in immobilizing hepatocytes on synthetic membranes, the membrane serving only as a support material for functional cells [42]. The first attempts to replace liver functions using only hemodialysis polymeric membranes gave poor results. In 1958, five patients with cirrhosis caused by ammonia poisoning were treated by filtrating the blood using hemodialysis membranes to remove excess ammonia, four of them recovering completely [43]. In 1976, a polyacrylonitrile membrane is used for hemodialysis to treat severe hepatitis, blood being filtered through the membrane. The membranes retained most of the heavy molecules associated with encephalopathy, but there were no reported remarkable results on the survival of patients [44].

The liver is the organ with most of the metabolic functions (over 500) in the human organism, this complexity making it impossible to replace it with just one or a few functional units. Therefore, the source of cells for organ substitution is very important [45]. The main source of liver cells is represented by porcine hepatocytes. The largest clinical study involving 17 institutions from Europe and the USA for developing a bioartificial liver was the HepatAssist. Clinical solution consisted in getting immobilized porcine hepatocyte on hollow fiber membranes made of polytetrafluoroethylene or polysulfone, two charcoal columns, and an oxygenator membrane. First, blood cells are separated from plasma in a bioreactor, the porcine hepatocytes acting exactly as a healthy liver. After passing through the bioreactor, plasma is again enriched with blood cells and is reintroduced into the body [46]. Other systems include embedding hepatocyte between flat sheet membranes to ensure a better blood oxygenation. In such a system, porcine hepatocytes with non-parenchymal cells are trapped in a sandwich structure between collagen membranes, and the entire assembly is placed on an oxygen permeable membrane made of polytetrafluoroethylene [47]. Systems based on hepatocytes of human origin are difficult to obtain because of their low viability outside the body. However, it was obtained cultures of human hepatocytes on polyethersulfone membranes having a

surface modified with acrylic acid and covalently immobilized peptide (Arg-Gly-Asp) [48]. One factor to consider in the case of membrane systems for the artificial liver is the design of these systems, the immobilization procedure generating unused volumes in the material structure – large open spaces not actively participating to the treatment process. Therefore, the choice of membrane type (flat sheet or hollow fiber) is important. Flat sheet membranes provide smaller unused spaces, but do not provide large contact area between the separation system and the biological fluid. Hollow fiber membrane type provides a better flow, but has smaller efficacy. In both cases, these drawbacks can be overcome by using several successive treatment systems and by longer blood recirculation. In the case of treatment of blood for hepatic dysfunction, the blood circulation through a membrane can range between 4 and 6 h.

---

## Artificial Pancreas

The pancreas is an annex gland of the digestive tract but also an endocrine gland, being a gland with mixed secretion, placed in the abdominal cavity secondary retroperitoneal. The exocrine pancreas is a tubuloacinar gland that resembles as structure to the salivary glands. Pancreatic lobules are formed from glandular acini which have pancreatic cells in the structure that secrete pancreatic juice. Each acinus has an excretory caliculi which converge in open two large collector channels – Wirsung and Santorini. The endocrine pancreas is composed of glandular cells, located between glandular acini, which make up the islets of Langerhans [28].

Diabetes type 1 is caused by the loss of functionality of  $\beta$  cells in the pancreas, the cells responsible for insulin secretion. The clinical solution widely applied consists in daily insulin injections. This is not the optimal solution and requires a strict diet and often leads to large variations in blood glucose, one of the most serious consequences of noncompliance with this diet being diabetic coma. Because of this, various technical solutions were attempted to obtain for replacing this treatment, the pancreas having an essential role as a membrane reactor. As with the artificial liver, the artificial pancreas system development is based on immobilization of Langerhans islands in synthetic membranes. Most commonly used membranes are hollow fiber type due to the large contact surface provided. These systems can be extravascular where the cells are immobilized in a membrane and blood is circulated outside the body through the membrane, intravascular where the cells are integrated into the membrane which allows their passage in the blood, and microencapsulated where the cells are integrated in a semipermeable membrane of the biodegradable polymer which is introduced into the body. In this case, the membrane has more the role of preventing the body's aggressive immune response [16, 49]. The membranes used for these systems must ensure the permeability of both glucose and insulin simultaneously leading to the development of complex membrane systems, of sandwich-type membranes. Pancreatic cells were immobilized in a hollow fiber membrane type made of poly(amino urethane) which is permeable to glucose, and the fibers were coated with polytetrafluoroethylene which is permeable to insulin [16, 50].

Unlike other membrane systems for artificial organs, in the case of the pancreas, trials were conducted to obtain an implantable artificial pancreas. This consists either in a system composed of a glucose sensor, an insulin pump, and a processor running an algorithm to calculate the exact amount of glucose or a membrane containing Langerhans cells in contact with the bloodstream, in this case not being required the use of a glucose sensor. A major problem is represented by the viability in time of cells within the membrane system, the membrane synthetic nature not providing an optimum functionality of these cells over time [51].

---

## Conclusions

Currently, there are several technical solutions to replace or substitute the functions of each organ system in the human body except the brain. This chapter presents some of the applications of synthetic polymeric membranes for artificial organs replacing their functions: the kidneys, lungs, liver, and pancreas. The kidneys are the first organ which was replaced totally with polymer membranes in the case of failure leading to the hemodialysis process. Polysulfone or polyethersulfone membranes are currently successfully used, and most of the encountered difficulties of medical nature were already solved: coagulation, selective retention of certain proteins or blood species, and interaction with other solutes present in biological fluid. Lungs were the second organ investigated for replacement with a gas separation membrane process enriching blood with oxygen and eliminating carbon dioxide. The development of extracorporeal membrane oxygenation systems has made possible the development of cardiac surgery, the membrane process being essential during open heart surgery. Unlike the kidney and lungs, whose functions can be replaced completely with synthetic polymeric membranes, the artificial liver and artificial pancreas require immobilization of hepatic and respective Langerhans cells of natural origin (animal or human) in polymeric membranes in order to substitute the functions of these organs.

---

## References

1. Lehn J-M (1995) *Supramolecular chemistry*. VCH, Weinheim
2. Bechhold H (1907) Kolloid studien mit der Filtrations methode. *Z Phys Chem* 60:257
3. Loeb S, Sourirajan S (1963) Sea water demineralization by means of osmotic membrane in saline water conversion-II. vol 28. *Advances in chemistry series*. American Chemical Society, Washington DC, pp 117–132
4. Kesting RE (1972) *Synthetic polymer membranes*. McGraw Hill, New York
5. Mulder M (1984) *Evaporation. Separation of ethanol-water and of isomeric of xylenes*. PhD theses, Twente University
6. Baker RW (2004) *Membrane technology and applications*, 2nd edn. Wiley, Chichester
7. Lee HC, Park JY, Yoon DY (2009) Advanced water treatment of high turbid source by hybrid module of ceramic microfiltration and activated carbon adsorption: effect of organic/inorganic materials. *Korean J Chem Eng* 26:697–701

8. Seo GT, Suzuki Y, Ohgaki S (1996) Biological powdered activated carbon (BPAC) microfiltration for wastewater reclamation and reuse. *Desalination* 106:39–45
9. Stewart MH, Wolfe RL, Means EG (1990) Assessment of the bacteriological activity associated with antigranulocytes activated carbon treatment of drinking-water. *Appl Environ Microbiol* 56:3822–3829
10. Kim J-S, Lee S-J, Yoon S-H, Lee C-H (1996) Competitive adsorption of trace organics on membranes and powdered activated carbon in powdered activated carbon-ultrafiltration system. *J Water Supply Res Technol* 34:223–229
11. Voicu SI, Dobrica A, Sava S, Ivan A, Naftanaila L (2012) Cationic surfactants-controlled geometry and dimensions of polymeric membrane pores. *J Optoelectron Adv Mater* 14(11–12):923–928
12. Nechifor AC, Panait V, Naftanaila L, Batalu D, Voicu S (2013) Symmetrically polysulfone membranes obtained by solvent evaporation using carbon nanotubes as additives. Synthesis, characterization and applications. *Digest J Nanomater Biostruct* 8(2):875–884
13. Voicu SI, Nechifor AC, Serban B, Nechifor G, Miculescu M (2007) Formylated polysulphone membranes for cell immobilization. *J Optoelectron Adv Mater* 9(11):3423–3426
14. Voicu SI, Aldea F, Nechifor AC (2010) Polysulfone-carbon nanotubes composite membranes. Synthesis and characterization. *Rev Chim* 61(9):817–821
15. Voicu SI, Stanciu ND, Nechifor AC, Vaireanu DI, Nechifor G (2009) Synthesis and characterization of ionic conductive polysulfone composite membranes. *Rom J Inf Sci Technol* 12(3):410–422
16. Stamatiadis DF, Papenburg BJ, Girones M, Saiful S, Bettahalli SNM, Schmitmeier S, Wessling M (2008) Medical applications of membranes: drug delivery, artificial organs and tissue engineering. *J Membr Sci* 308:1–34
17. Kuethe DD, Augestein DC, Cresser JD, Wise DL (1992) Design of capsules that burst at predetermined times by dialysis. *J Control Release* 18:159–164
18. Baker RW (1987) Controlled release of biologically active agents. Wiley, New York
19. Chien YW (1985) Polymer controlled drug delivery systems. Plenum, New York/London
20. Kesarwani A, Yadav AK, Singh S, Gautam H, Singh HN, Sharma A, Yadav C (2013) Theoretical aspects of drug delivery system transdermal. *Bull Pharm Res* 3(2):78–89
21. Kryscio DR, Peppas NA (2009) Mimicking biological drug delivery through controlled release feedback systems based on molecular imprinting. *Bioeng Food Nat Prod* 55(6):1311–1324
22. Norell MC, Andersson HS, Nicholls IA (1998) Theophylline molecularly imprinted polymer dissociation kinetics: a novel sustained release drug dosage mechanism. *J Mol Recognit* 1:98–102
23. Izake EL (2007) Chiral discrimination and enantioselective analysis of drugs: an overview. *J Pharm Sci* 96(7):1659–1676
24. Kawakami H (2008) Polymer membrane materials for artificial organs. *J Artif Organs* 11:177–181
25. Kim B-S, Park I-K, Hoshiba T, Jiang H-L, Choi Y-J, Akaike T, Cho C-S (2011) Design of artificial extracellular matrices for tissue engineering. *Prog Polym Sci* 36:238–268
26. Ritchie AC (2013) Chapter II.5.5, Artificial organs. In: *Extracorporeal artificial organs*. Elsevier, Oxford
27. Thongboonkerd V (2010) Proteomics in extracorporeal blood purification and peritoneal dialysis. *J Proteomics* 73:521–526
28. Voiculescu IC, Petricu IC (1971) Anatomia si fiziologia omului. Editura Medicala, Bucuresti
29. Pantelias K, Grapsa E (2011) Chapter 4, Vascular access for hemodialysis. In: Penido MG (ed) *Technical problems in patients on hemodialysis*. Intech, Rijeka
30. Li L, Cheng C, Xiang T, Tang M, Zhao W, Sun S, Zhao C (2012) Modification of polyethersulfone hemodialysis membrane by blending citric acid grafted polyurethane and its anticoagulant activity. *J Membr Sci* 405–406:261–274
31. Sasaki M (2006) Development of vitamin E-modified membrane polysulfone dialyzers. *J Artif Organs* 9:50–60



32. Yamamoto K-I, Hiwatari M, Kohori F, Sakai K, Fukuda M, Hiyoshi T (2005) Membrane fouling and dialysate flow pattern in internal filtration-enhancing dialyzer year. *J Artif Organs* 8:198–205
33. A clinical update on dialyzer membranes, state-of-the-art considerations for optimal care in hemodialysis. Available online at [http://www.kidney.org/professionals/KLS/hddial\\_splash](http://www.kidney.org/professionals/KLS/hddial_splash). Accessed 15 Aug 2014, 16.20
34. Urbani A, Lupisella S, Sirolli V et al (2012) Proteomic analysis of protein adsorption capacity of different haemodialysis membranes. *Biosyst Mol* 8:1029–1039
35. Krummel T, Hannedouche T (2013) Clinical potentials of adsorptive dialysis membranes. *Blood Purif* 35:1–4
36. Thomas M, Moriyama K, Ledebro I (2011) AN 69: evolution of the world's first high permeability membrane. In: Saito A, Kawanishi H, Yamashita AC, Mineshima M (eds) High performance membrane dialyzers, vol 173, Contributions to nephrology. Karger, Basel, pp 119–129
37. Fujimori A (2013) Clinical comparison of super high-flux HD and online HDF. *Blood Purif* 35:81–84
38. Irfan M, Idris A, Yusof NM, Farahah KMN, Akhmim H (2014) Surface modification and performance enhancement of nano-hybrid f-MWCNT/PVP90/PES hemodialysis membranes. *J Membr Sci* 467:73–84
39. Nechifor G, Voicu SI, Nechifor AC, Garea S (2009) Nanostructured hybrid membrane polysulfone-carbon nanotubes for hemodialysis. *Desalination* 241:342–348
40. Iwahashi H, Yuri K, Nose Y (2004) Development of the oxygenator: past, present, and future. *J Artif Organs* 7:111–120
41. Cypel M, Keshavjee S (2014) Chapter 47, Artificial lung support in regenerative medicine applications in organ transplantation. Elsevier, Oxford
42. Onodera K, Sakata H, Yonekawa M, Kawamura A (2006) Artificial liver support at present and in the future. *J Artif Organs* 9:17–28
43. Kiley JE, Pender JC, Welch HF, Welch CS (1958) Ammonia intoxication treated by hemodialysis. *N Engl J Med* 259:1156–1161
44. Opolon P, Rapin JR, Hugué C, Granger A, Delorme ML, Bosch M, Sausse A (1976) Hepatic failure coma (HFC) treated by polyacrylonitrile membrane (PAN) hemodialysis (HD). *Trans Am Soc Artif Intern Organs* 22:701–710
45. Naruse K (2005) Artificial liver support: future aspects. *J Artif Organs* 8:71–76
46. Kobayashi N, Okitsu T, Nakaji S, Tanaka N (2003) Hybrid bioartificial liver: establishing a reversibly immortalized human hepatocyte line and developing a bioartificial liver for practical use. *J Artif Organs* 6:236–244
47. Bader A, Frühauf N, Tiedge M, Drinkgern M, De Bartolo L, Borlak JT, Steinhoff G, Haverich A (1999) Enhanced oxygen delivery reverses anaerobic metabolic states in prolonged sandwich rat hepatocyte culture. *Exp Cell Res* 246(1):221–232
48. De Bartolo L, Morelli S, Lopez LC, Giorno L, Campana C, Salerno S, Rende M, Favia P, DeTomaso L, Gristina R, d'Agostino R, Drioli E (2005) Biotransformation and liver-specific functions of human hepatocytes in culture on RGD-immobilized plasma-processed membranes. *Biomaterials* 26(21):4432–4441
49. Giorno L, De Bartolo L, Drioli E (2003) Polymer and biofunctional membranes. In: Bhattacharyya D, Butterfield DA (eds) New insights into the membrane science and technology, vol 8. Elsevier, Amsterdam, pp 187–217
50. Ikeda H, Kobayashi N, Tanaka Y, Nakaji Y, Yong Y, Okitsu T, Oshita M, Matsumoto S, Noguchi H, Narushima M, Tanaka K, Miki A, Rivas-Carrillo JD, Soto-Gutierrez A, Navarro-A'lvarez N, Tanaka K, Jun HS, Tanaka N, Yoon JW (2006) A newly developed bioartificial pancreas controls blood glucose successfully in totally pancreatectomized diabetic pigs. *Tissue Eng* 12(7):1799–1809
51. Ricotti L, Assaf T, Dario P, Menciaci A (2013) Wearable and implantable pancreas substitutes. *J Artif Organs* 16:9–22

Xingyi Xie and Marta Cerruti

**Contents**

Introduction .....	432
Composites Formed by Direct Deposition of Bioceramics on GFNs .....	433
GFN/HA Composites Obtained by Immersion in SBF .....	434
GFN/HA Composites Obtained by Separate Exposure to Calcium and Phosphate Precursor Solutions .....	437
Other Reports of GFN/Bioceramic Composites with the Ceramic Phase Produced In Situ .....	444
Composites Obtained by Mixing GFNs and Bioceramics .....	446
Dense Composites Sintered Under High Pressure .....	446
GFN/HA Coatings Obtained by Electrodeposition .....	450
Porous Composites Fabricated by 3D Printing .....	453
Summary .....	455
Self-Assembled Porous Graphene/HA Composites .....	456
Discussion and Prospective .....	457
Overall Result Comparison .....	457
Challenges .....	462
Prospective .....	464
References .....	465

**Abstract**

The Combination of graphene, graphene oxide or reduced graphene oxides with ceramic materials, especially hydroxyapatite, allows for the production of composites with better mechanical properties and often better biocompatibility and bioactivity than the individual components. This chapter reviews the work

---

X. Xie

College of Polymer Science and Engineering, Sichuan University, Chengdu, Sichuan, China

M. Cerruti (✉)

Department of Mining and Materials Engineering, McGill University, Montreal, QC, Canada

e-mail: [marta.cerruti@mcgill.ca](mailto:marta.cerruti@mcgill.ca)

published in this rapidly growing field, and discusses the challenges yet to be solved to allow graphene/bioceramic composites to fully meet their potential.

---

**Keywords**

Bioceramics • Biomimetics • Composites • Graphene • Hydroxyapatite

---

## Introduction

Graphene is a single layer of carbon atoms that are chemically bonded through  $sp^2$  hybridization, forming a 2D crystalline structure with a perfect hexagonal lattice. Since its discovery in 2004 [1], graphene has profoundly affected many aspects of material science and engineering due to its unique properties. The one-atom thickness confers graphene a specific surface area as high as  $2630 \text{ m}^2 \text{ g}^{-1}$  [2]. The  $\pi$ - $\pi$  conjugated delocalized electron cloud leads to a remarkable electron mobility within individual graphene sheets, with reported values of more than  $15,000 \text{ cm}^2 \text{ V}^{-1} \text{ s}^{-1}$  [3]. The corresponding electric resistivity of a graphene sheet ( $10^{-6} \Omega \cdot \text{cm}$ ) is the lowest known at room temperature [4]. The strong chemical bonds among the carbon atoms make single graphene sheet the strongest material ever tested, with tensile strength of 130 GPa and Young's modulus of 1100 GPa [5].

Graphene has been applied in a wide spectrum of fields, including energy technology (e.g., high-performance lithium ion batteries, fuel cells, solar cells) [6], electrochemical sensors [7], interfacial catalysis [8], and super-absorbents [9]. Not surprisingly, its unique structure and properties have motivated many researchers to explore biomedical applications of graphene, including bioimaging, drug delivery, neural regeneration, and bone tissue engineering [10, 11]. Graphene/bioceramic hybrid composites have recently started to be tested for the latter application.

Bioceramics are a class of biocompatible ceramic materials commonly used in dental and bone implants. They range from biologically inert ceramic oxides, like  $\text{Al}_2\text{O}_3$  and  $\text{Zr}_2\text{O}$ , to bioactive glasses, which can directly bond with living bones, or bioresorbable calcium phosphates, including nanosized hydroxyapatite (HA) and  $\beta$ -tricalcium phosphate ( $\beta$ -TCP), which are eventually replaced by the tissues they used to repair [12]. Among these materials, calcium phosphates are the most widely used because of their similar composition to the mineral found in bone, carbonated HA. For the same reason, most of the reported graphene/bioceramic composites are based on HA particles, as will be seen in the following sections.

The incorporation of graphene in bioceramics may improve their properties in several ways, making the resulting composites very attractive. The intrinsic brittleness of bioceramics still hinders their load-bearing applications, for example in cortical bone substitutions. By adding graphene nanosheets as fillers, bioceramics can be toughened. Also, since bones are piezoelectric nanocomposites [13], the interconnected, conductive graphene network in a graphene/bioceramic composite placed in a bone defect might transfer electrical signal from the surrounding natural bones, thus generating a beneficial microenvironment to help bone remodeling around the implant. Finally, recent studies show that graphene films can selectively

differentiate stem cells toward osteoblasts (i.e., bone-forming cells) [14, 15]. This implies that graphene/bioceramic composites may be even more bioactive than the bioceramic itself.

This review focuses on recent advances in graphene/bioceramic composites. The word “graphene” in the title of this review is used in the broad sense of materials belonging to what has been defined as the “graphene family nanomaterials” (GFN), which include not only single-layer graphene but also graphene oxide (GO), reduced graphene oxide (rGO), and their relatives such as graphene nanoplatelets (GNPs) [16]. Although the field is quite new, there are enough papers already published to allow us to provide a broad overview of what has been already attempted, thus showing the potential of these materials.

We divide the review in five sections. After this introduction, we discuss GFN/bioceramic composites synthesized by depositing the bioceramic material in situ on the GFN phase, starting from the ceramic precursor ions (section “[Composites Formed by Direct Deposition of Bioceramics on GFNs](#)”). Here, GFN loading can be very high and is used to improve both cell support and the mechanical properties of the composites. Next, we discuss GFN/bioceramic composites prepared by mixing GFN and bioceramics synthesized separately (section “[Composites Obtained by Mixing GFNs and Bioceramics](#)”). In this case, the GFN phase can be as low as 0.1 % and is mostly used to toughen the bioceramic. A homogeneous dispersion of one phase into the other is essential in this case. In section “[Self-Assembled Porous Graphene/HA Composites](#),” we introduce self-assembled graphene/bioceramic composites with 3D porous structure. This field is quite new, with only one paper published. Finally, we give a general discussion of the overall results achieved thus far, the challenges remaining to be solved, and a prospective on the future of this fast-developing area of research (section “[Discussion and Prospective](#)”).

---

## **Composites Formed by Direct Deposition of Bioceramics on GFNs**

In many reports of GFN/bioceramic composites, the ceramic phase is deposited on the GFN flakes in situ. This means that the GFN flakes are mixed in solutions that contain the ions of the mineral that is going to be deposited. Mineral deposition occurs spontaneously on the flakes or during a process that may at the same time lead to the reduction of GO to reduced graphene oxide (rGO), if GO was used as starting material. In this section we will review the papers that describe composites formed with any of these processes.

Most papers discuss the formation of composites between GFN and HA, thus our review will discuss these first. To produce GFN/HA composites, GFN flakes are often immersed in simulated body fluid (SBF). SBF is a solution that contains ions at a concentration similar to that of human serum, which is mildly supersaturated with respect to HA. Thus, HA deposits spontaneously on many substrates immersed in SBF. To facilitate or improve the deposition, GFN flakes are sometimes

functionalized with groups or molecules that can chelate the mineral precursor ions, thus locally increasing supersaturation even further.

In situ GFN mineralization often results in composites that have mineral content up to 60–70 %. These materials can be used as support for cell culture, and both the GFN and the mineral phase are important in determining cellular interactions and material structure. In a few cases, composites where the mineral phase is as high as 99 % or 99.5 % are produced. In these cases, the function of the GFN phase is to strengthen the ceramic; this is more similar to the materials produced by mixing the GFN and the ceramic phases discussed in the next section.

## GFN/HA Composites Obtained by Immersion in SBF

### Review of the Work

All the papers attempting to mineralize GFN in SBF start from GO, since the reduced forms (graphene, rGO) cannot be dispersed in an aqueous solution such as SBF. Although GO has several oxygenated functional groups, which may be able to attract  $\text{Ca}^{2+}$  ions, only a small amount of HA is deposited on GO immersed in SBF. Thus, most authors try to increase the mineralization of GO by modifying its surface with biomolecules.

A first example of this approach is the 2012 work by Liu et al. [17]. These authors started with GO and modified it with a layer of polydopamine obtained by in situ dopamine oxidation; this technique induced the simultaneous reduction of GO to rGO. After 2 weeks of immersion in a solution that contained 1.5 times the concentration of the ions present in SBF ( $1.5 \times \text{SBF}$ ), they formed a layer of spherical HA nanoparticles (NPs), with diameter of  $\sim 20$  nm, on the polydopamine-rGO substrate (Fig. 1a), corresponding to  $\sim 50$  % in weight of the composite. The resulting material was biocompatible, as shown by growing L929 fibroblasts on it.

A few years later, the same group modified GO with gelatin and then immersed the substrates in  $1.5 \times \text{SBF}$  for up to 2 weeks [18]. Gelatin was simply physisorbed on GO. After 3 weeks, a thick layer of HA precipitated on gelatin-GO forming micron-sized spherulites composed of nanoscale HA flakes, as often found when HA precipitates on surfaces (Fig. 1b). The authors did not quantify how much HA was deposited in this case. In contrast, they performed a number of cell culture studies to show the bioactivity of this substrate: they showed the MC3T3 cells were able to grow more on GO, and even more on gelatin-GO, than on glass substrates, and on both GO and gelatin-GO, the cells were more elongated than on glass, thus showing a better attachment to the GO-based substrates. Gelatin-GO induced more alkaline phosphatase (ALP) activity and more mineralization than unmodified GO, thus showing the importance of surface modification of the GO phase to synthesize composites for bone tissue engineering.

A larger amount of HA deposition was achieved by Fan et al. [19]. These authors covalently bound casein phosphopeptides (CPPs) to GO, since phosphonate groups are known to increase mineralization. To make CPP-GO, they first transformed GO into carboxylated GO (CGO) and then coupled CPPs to CGO via standard

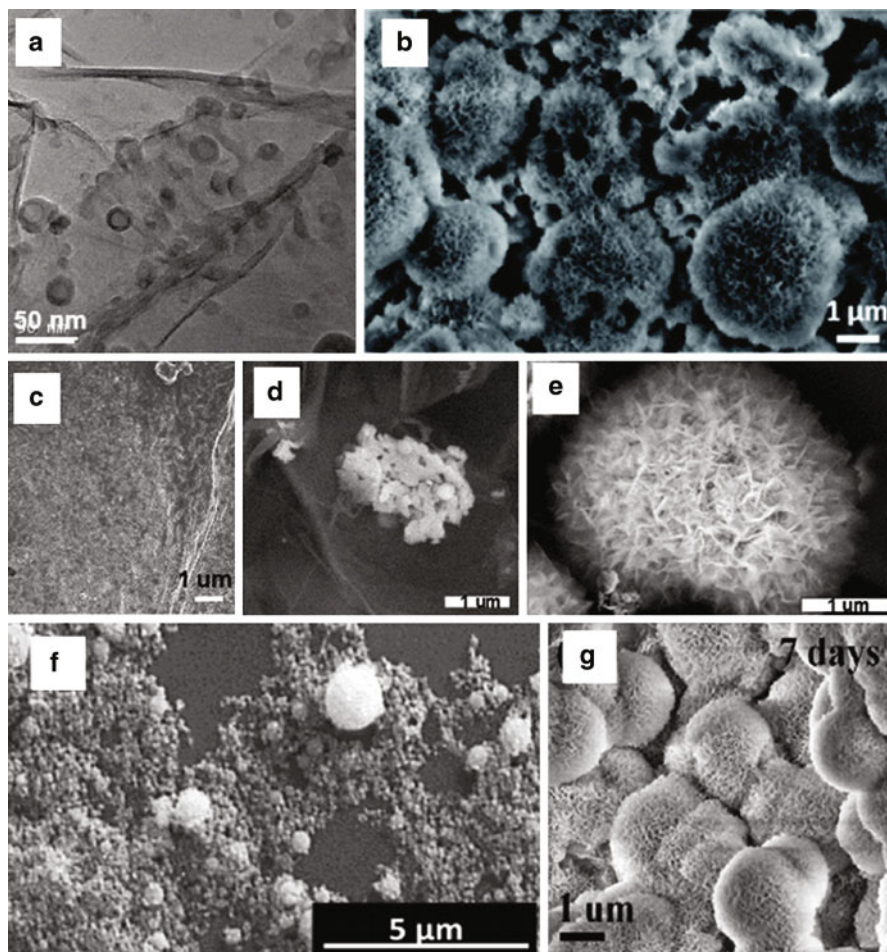


**Fig. 1** HA NPs deposited on GO in the presence of polydopamine (a), gelatin (b), CPPs (c), Glu (d), Arg (e), chitosan (f), or unmodified GO (g) after exposure to  $1.5 \times$  SBF (a–c and g),  $1 \times$  SBF (d, e), or  $5 \times$  SBF (f) for 3 (c), 7 (g), or 14 (b–e) days. Note that in (g) SBF was changed daily (Reproduced with permission from Liu et al. [17] (a) [18] (b), [19] (c), [20] (d, e), [21] (f), and [22] (g))

1-ethyl-3-(3-dimethylaminopropyl) carbodiimide hydrochloride (EDC) coupling (Fig. 2). A thick layer of HA was deposited on CPP-CGO immersed for 3 days in  $1.5 \times$  SBF, corresponding to approximately 80 wt% of the total material (Fig. 1c).

Very recently, Tavafoghi et al. [20] used a similar strategy to covalently bind a positive (arginine, Arg) and a negative (glutamic acid, Glu) amino acid on CGO. They immersed the substrates in SBF for up to 2 weeks and found that much more HA was deposited on Arg-CGO (Fig. 1e) than on Glu-CGO (Fig. 1d) (~65 % and 20 % of the composites were HA, respectively). This was a surprising result, since most previous work showed that negatively charged groups are more effective at

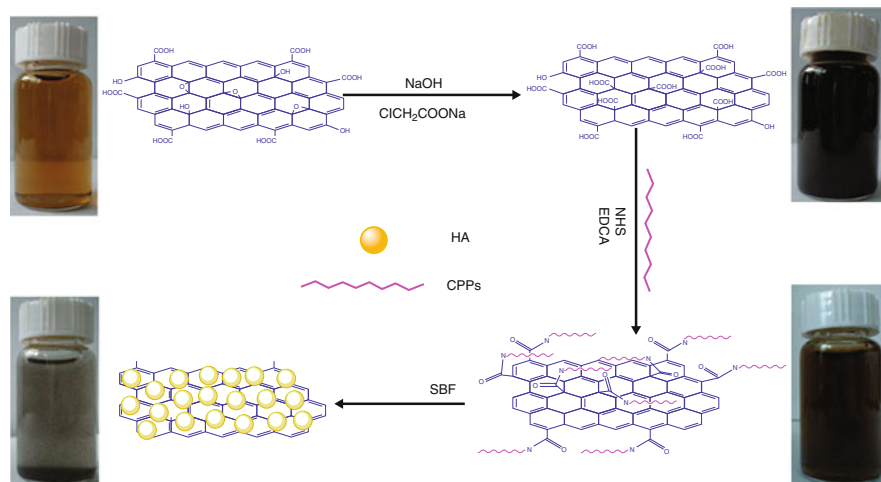


**Fig. 2** Schematic representation of the process adopted in Fan et al. [19] to covalently bind CPPs to GO. GO is first converted to CGO using  $\text{ClCH}_2\text{COONa}$  in a basic environment, and then CPPs are coupled to the carboxyl groups introduced using EDC chemistry. This substrate is used to induce mineralization of GO. A similar strategy is used in Tavafoghi et al. [20] to bind Arg and Glu to GO (Reprinted with permission from Fan et al. [19]. Copyright (2013) American Chemical Society)

nucleating HA than positively charged groups. The authors explained this result in terms of the larger affinity of Arg than Glu for the HA precursor ions and the electrostatic attraction of both calcium and phosphate ions on Arg-CGO, leading to an enhanced local supersaturation on this sample. The amount of HA deposited on Arg-CGO was comparable to that observed in the presence of large macromolecules such as gelatin or polydopamine on GO, thus showing the efficacy of a small, positively charged amino acid as GO mineralization enhancer.

Depan et al. [21] used EDC chemistry to covalently bind chitosan to GO; however, in contrast to the reports previously discussed, they did not increase the number of carboxylate groups prior to binding the biomolecules. The authors compare GO and chitosan-GO for their biomineralization properties using a very concentrated SBF solution ( $5 \times \text{SBF}$ ), in which the substrates are immersed for as long as 21 days. The results show that both GO and chitosan-GO (Fig. 1f) form a layer of HA on their surfaces after this time. Although the amount of HA is not quantified in either case, and the differences are hard to evaluate by the FTIR and SEM results provided, cell culture results show a clear advantage of the composite containing HA, chitosan, and GO compared to that containing only HA and GO: osteoblasts spread and mineralize more on the former substrate and are better attached to it, as evidenced by staining for fibronectin, actin, and vinculin.

Zhao et al. [23] chose a more complex route to mineralize GO: they first deposited Ag NPs in situ on GO, starting from  $\text{AgNO}_3$ . During the reduction of  $\text{Ag}^+$  to Ag and the deposition of the Ag NPs, GO was reduced to rGO. The resulting rGO/Ag composite was then modified with thioglycolic acid (TGA), to achieve the formation

of carboxyl groups on the Ag NPs. The carboxyl groups worked as nucleation points for HA, when the rGO/Ag/TGA substrate was immersed in SBF. In fact, after only 120 h of SBF immersion, an rGO/HA composite containing approximately 60 % HA was obtained. The authors suggested that the presence of Ag may induce an added antibacterial effect but did not perform any cell culture or antibacterial tests on the materials.

In one case, HA was deposited on GO without inducing any modifications on the GO surface. Wen et al. [22] immersed GO in  $1.5 \times$  SBF for a week and obtained a very compact coating made of HA spherulites (Fig. 1g) similar to those reported in [18] and [20]. In this work, though, the resulting GFN/HA composite was not used for bioapplications: the authors used the resulting GO/HA hybrids to separate Sr from aqueous solutions and showed that the composite was more efficient than either GO or HA alone. SEM images of the composite show a very dense coverage, but no quantification of the amount of HA deposited is given.

## Summary

Immersing GO in SBF is an effective strategy to synthesize GO/HA composites, especially if GO is covalently modified with molecules possessing functional groups that can act as HA nucleation sites. The resulting composites are biocompatible and seem to enhance mineral production when osteoblast cells are cultured on them.

The extent and morphology of HA deposition depends on the type and amount of functional groups added on GO, and on the time of immersion in SBF, its concentration, and how many times it is refreshed. A comparison of representative samples is shown in Fig. 1. The most effective HA nucleation agents explored thus far on GO are heavily phosphorylated compounds such as CPPs, covalently bound to GO. In this case, composites with as much as 80 % HA can be produced after immersion in  $1.5 \times$  SBF for only 3 days.

## GFN/HA Composites Obtained by Separate Exposure to Calcium and Phosphate Precursor Solutions

### Review of the Work

Similarly to what is discussed in section “[GFN/HA Composites Obtained by Immersion in SBF](#),” the composites are made mostly starting from GO, which is soluble in water; however, while in most papers discussed in section “[GFN/HA Composites Obtained by Immersion in SBF](#)” GO was modified with biomolecules prior to mineralization, here we will see that GO is almost always used unmodified. Thus, one of the main challenges in the works reported here is to prevent the formation of HA in solution and favor its heterogeneous nucleation on GO, in order to achieve a composite where the HA phase is strongly bound to the GFN phase.

To achieve heterogeneous nucleation on GO, the deposition always starts by mixing GO with solutions containing  $\text{Ca}^{2+}$  ions, obtained by dissolving either  $\text{CaNO}_3$  or  $\text{CaCl}_2$ . The phosphate ions are added later, in the form of  $\text{Na}_2\text{HPO}_4$  or  $(\text{NH}_4)_2\text{HPO}_4$ . Supposedly, this allows the  $\text{Ca}^{2+}$  ions to form a first layer on the GO



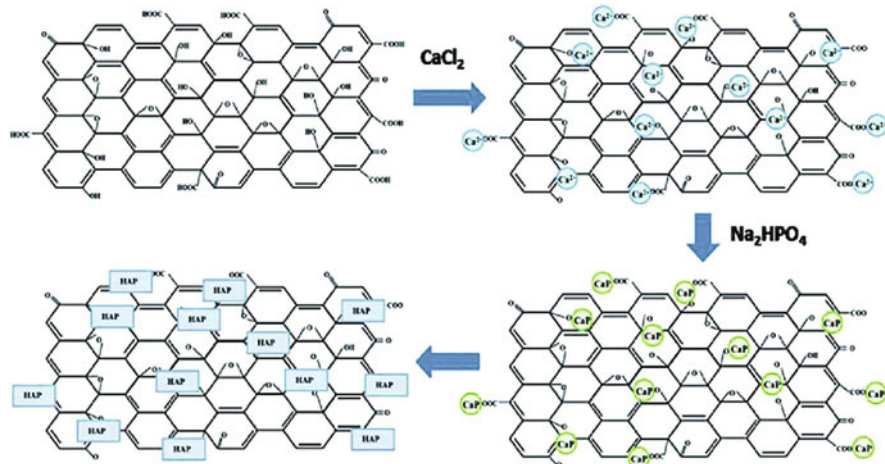


**Fig. 3** Proposed mechanism of GO mineralization in the presence of Ca and phosphate precursor solutions, highlighting that the Ca precursor solution is added first in order to form an electrostatically bound Ca layer on GO (Reprinted with permission from Li et al. [24]. Copyright (2014) American Chemical Society)

surface, which is negatively charged due to the presence of many oxygenated functionalities. The  $\text{Ca}^{2+}$  layer electrostatically attracts phosphate ions, thus favoring the formation of HA on GO rather than in solution (Fig. 3).

A few researchers further tried to favor heterogeneous nucleation by adding compounds that slow down the diffusion of  $\text{Ca}^{2+}$  and phosphate ions in solution. For example, Fan et al. [25] used citrate ions to chelate excess  $\text{Ca}^{2+}$  not physisorbed on GO, while both Li et al. [24] and Baradaran et al. [26] added ethylene glycol (EG) to increase the viscosity of the solution. We will start by discussing the latter strategy.

Both groups started by dispersing GO and  $\text{CaCl}_2$  in a mixture of EG and water. However, while Li et al. later added the phosphate precursor solution ( $\text{Na}_2\text{HPO}_4$ ) alone [24], Baradaran et al. mixed EG to the phosphate solution too ( $(\text{NH}_4)_2\text{HPO}_4$  in this case) [26]. Baradaran et al. also added dimethylformamide (DMF) to the resulting mixture [26].

In Li et al.'s work, the mineralization occurred at 85 °C over 12 h. In these conditions, EG allowed for the partial reduction of GO to rGO. A fine and uniform dispersion of HA NPs was achieved on the rGO sheets, resulting in composites containing approximately 68 % HA (Fig. 4a). These authors confirmed that the presence of EG led to the formation of strongly bound HA on the rGO/HA powders, by comparing the amount of HA on the samples before and after ultrasonication. In Baradaran et al.'s work, the mineralization occurred during a hydrothermal treatment in autoclave at 200 °C for 24 h. This led to a more complete reduction of GO to rGO and the formation of HA nanotubes instead of NPs (Fig. 4b). The authors hypothesized that this was due to the fact that while EG prevented homogeneous nucleation at room temperature, the viscosity of the solution drastically decreased in the

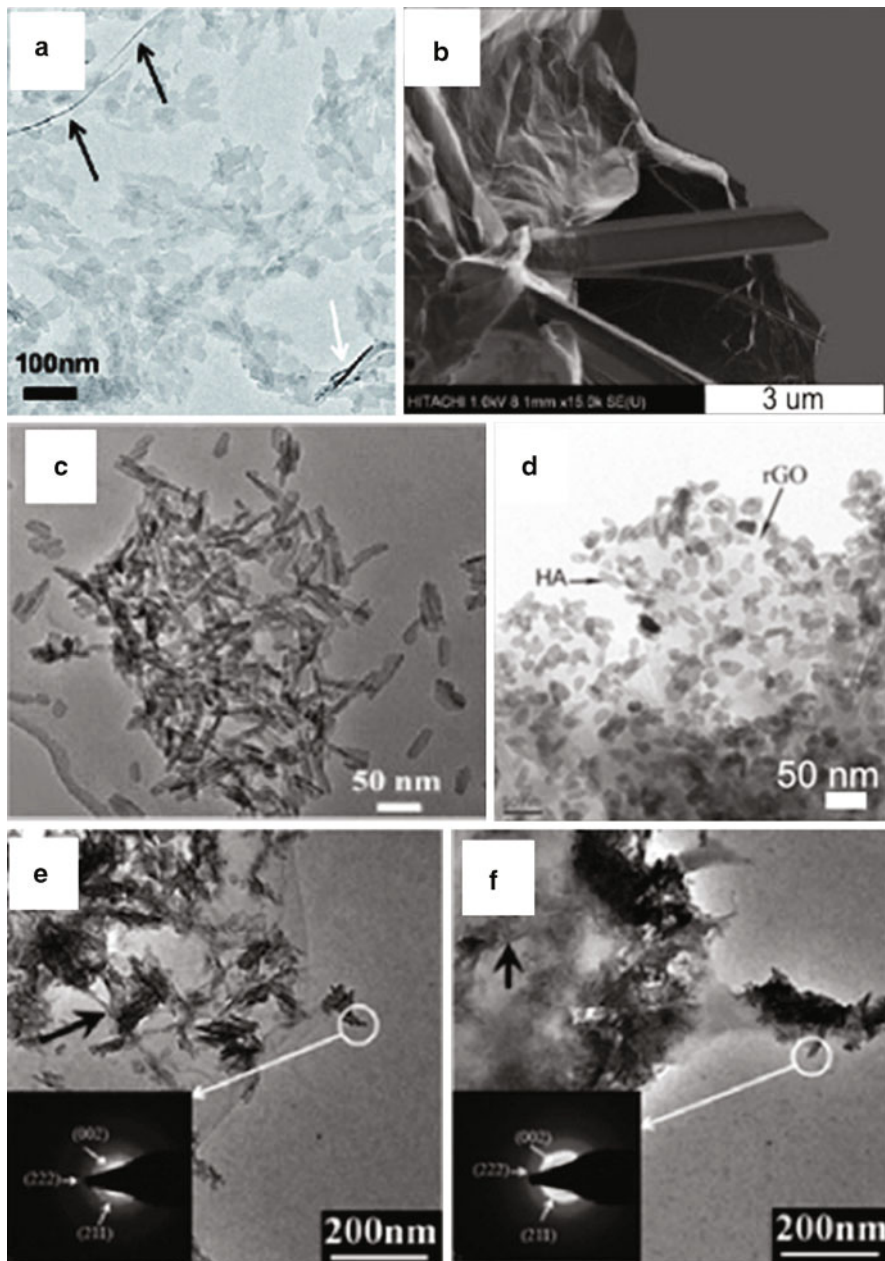


**Fig. 4** Different morphologies of HA deposited on GO in the presence of EG (a, b), without (a) or with (b) hydrothermal treatment, in the presence of citrate ions and CTAB and hydrothermal treatment (c), and without molecules aimed at slowing down homogeneous deposition (d–f). In (e), GO was modified with chitosan (Reprinted with permission from Li et al. [24] (a), Baradaran et al. [26] (b), Fan et al. [25] (c), Liu et al. [27] (d), Li et al. [28] (e, f). Copyright (2012, 2013, 2014) American Chemical Society)

hydrothermal conditions, giving rise to a slow dissolution and anisotropic reprecipitation process. Apparently DMF was important in this system to prevent aggregation of rGO during the treatment. The composites obtained were mostly made of HA, with rGO contents between 0.5 and 1.5 wt% rGO.

Both Li et al. and Baradaran et al. transformed the composite rGO/HA powders into bulk structures. Li et al. made rGO/HA sheets by vacuum filtering the rGO/HA powders. The sheets obtained were flexible, and XRD data evidenced that the HA NPs were packed in an ordered lamellar structure, with (100) planes parallel to the GO flakes. Such structure strongly improved the mechanical properties of the paper, which showed an elastic modulus as high as 16.9 GPa in the linear region and tensile strength of 75.6 MPa, both properties comparable to those of cortical bones. The rGO/HA sheets showed excellent biocompatibility, remarkably reducing the cytotoxicity observed for GO on human osteosarcoma cells (MG63), chosen as a representative of human osteoblasts.

Given the very high percentage of HA in the rGO/HA composites prepared in Baradaran et al. [26], bulk samples were obtained in this case using hot isostatic pressing (HIP) at 1150 °C in argon at 160 MPa for 1 h. Sintering caused the formation of extra defects in rGO but strongly increased the crystallinity of the HA phase. The high contact area and mechanical interlocking of the rGO and HA phase allowed for the production of composites with excellent mechanical properties. For example, the composite with 1.5 wt% of rGO had elastic modulus of 1.51 GPa and fracture toughness of 123 MPa. rGO increased the toughness of HA by deflecting cracks and creating bridges through the materials that slowed down crack propagation. The presence of rGO increased the attachment, proliferation, and growth of human osteoblasts compared to what was observed on discs made in pure HA.

Instead of EG, Fan et al. [25] used citrate as a means to prevent homogeneous nucleation. Specifically, they mixed trisodium citrate to the phosphate precursor solution ( $(\text{NH}_4)_2\text{HPO}_4$ ) and added a surfactant (CTAB, cetyltrimethylammonium bromide) to the solution containing GO and the Ca precursor ( $\text{Ca}(\text{NO}_3)_2$ ). Similar to Baradaran et al. [26], they achieved mineralization with a hydrothermal treatment (180 °C for 24 h), during which HA deposited on the surface of rGO in the form of nanorods, about 55 nm in length and 13 nm in diameter (Fig. 4c). The authors suggested that this morphology was achieved because of the presence of CTAB micelles and the slow growth allowed by the citrate ions, which supposedly prevented homogenous nucleation by chelating excess  $\text{Ca}^{2+}$  ions at room temperature and slowly released them during the hydrothermal treatment.

The mechanical properties of the rGO/HA composites with 40 % HA were measured by spin coating the powders on glass slides. The presence of rGO increased the resistance to indentation compared to pure HA coatings. An elastic modulus as high as ~6 GPa and hardness of ~242 MPa was achieved, both data being as twice as the values of pure HA coatings. Cell culture tests with osteoblasts were performed on sheets prepared by vacuum filtration, similarly to what was done by Li et al. [24]. Only the rGO/HA film with 40 % HA showed cell viability similar to that obtained on sheets made with pure rGO. The films made in pure HA or with HA contents of 20 % and 60 % showed lower osteoblast viability. Osteoblasts cultured

on rGO/HA composite with 40 % HA spread and adhered better than on pure rGO and HA. The authors hypothesized that the wrinkled structure of rGO improved cell adhesion compared to pure HA.

Liu et al. [27] also prepared rGO/HA composites with very little rGO. These authors, however, prerduced GO to rGO via a thermal vacuum treatment and then ultrasonicated rGO in water for 120 h at 300 W to create a dispersion. This process may very well have partially reoxidized rGO [29], thus allowing its aqueous dispersion, as shown by the presence of oxygenated groups in the FTIR spectra. After this, the authors added  $\text{Ca}(\text{NO}_3)_2$ , followed by  $(\text{NH}_4)_2\text{HPO}_4$ , adjusted the pH to 11, and reacted overnight after 2 h stirring. The composites contained between 0.1 and 1 wt% of rGO and showed rod-like HA NPs  $\sim 20\text{--}45$  nm in length and  $\sim 9$  nm in diameter (Fig. 4d). The authors suggest that HA and rGO are held together by van der Waals interactions and that the HA (300) and (100) planes are superimposed with the rGO surface, based on TEM data and some calculations of the spacing between Ca atoms from HA and C atoms on graphene.

To make discs out of the composites, Liu et al. used spark plasma sintering (SPS) instead of HIP. This caused a partial decomposition of HA to  $\beta$ -TCP, likely because of the high temperatures achieved due to the presence of electrically conductive rGO. The elastic modulus of the pellets reached values as high as  $\sim 150$  GPa in the presence of 1 wt% rGO and fracture toughness  $\sim 4$  MPa  $\text{m}^{1/2}$ , corresponding to a significant ( $\sim 200$  %) improvement over pure HA. Similar to Baradaran et al. [26], the authors suggest that rGO inhibits crack propagation and found enhanced proliferation and mineralization of human osteoblasts in the presence of 1 % rGO compared to pure HA pellets. A comparison of the fractured surfaces obtained in the composites found in Liu et al. [27] and Baradaran et al. [26] is shown in Fig. 5.

The same group [30] further sprayed the sintered rGO/HA powders onto metallic substrates as biocompatible layers. To do so, they adopted vacuum cold spraying: the rGO/HA fine powders and helium (carrier gas) were vigorously mixed to form a high-speed aerosol flow sprayed toward the substrates at room temperature. Shock loading solidified the deposited layers into dense structure with some plastic deformation of the HA NPs. Despite the small amounts (0.1 % and 1 %) added, rGO was the first layer that intimately contacted the substrate and created a layered structure parallel to it. The addition of rGO lowered the porosity, which ranged from 13.2 % for pure HA coating, to 12.9 % for HA-0.1 % rGO coating, and to 8.7 % for HA-1 % rGO coating. This suggested more interlocking among HA NPs due to the presence of rGO flakes. Fracture toughness was enhanced from  $0.109 \pm 0.012$  MPa  $\text{m}^{1/2}$  in pure HA coatings, to  $0.175 \pm 0.006$  MPa  $\text{m}^{1/2}$  at 0.1 % rGO, and further to  $0.421 \pm 0.011$  MPa  $\text{m}^{1/2}$  at 1 % rGO. The adhesion strength to the substrate was not affected by the rGO added. Human osteoblast cells adhered more and proliferated faster on the HA/rGO composites than on both HA coating and Ti substrates. Morphological observations revealed that filopodia extended from the cells and anchored onto the rGO flakes. This was explained by the preferred adsorption of fibronectin to rGO: apparently, fibronectin adsorbed on rGO unfolded into a stretched state (100–135 nm in length), exposing its cell binding site (arginine–glycine–aspartic acid peptide) and favoring cell adhesion.

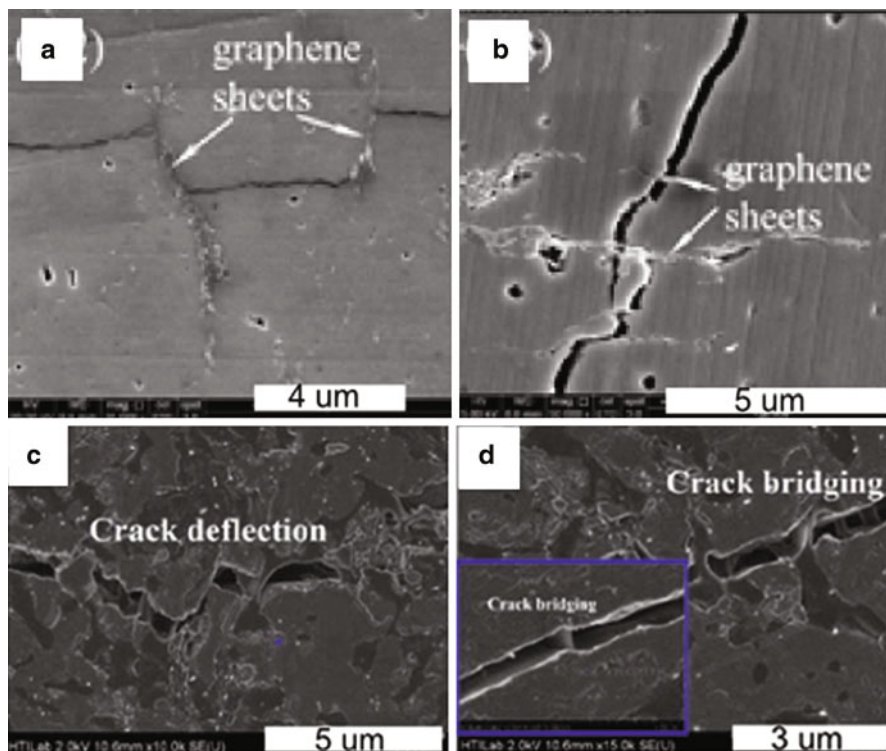


**Fig. 5** SEM images from the work of Liu et al. [27] (a, b) and Baradaran et al. [26] (c, d) showing crack deflection (a, c) and crack bridging (b, d) as reinforcement mechanisms related to the introduction of rGO in HA discs (Reprinted with permission from Liu et al. [27] (a, b) and Baradaran et al. [26] (c, d). Copyright (2013, 2014) American Chemical Society)

Like Liu et al. [27], Neelgund et al. [31] attempted depositing HA directly on rGO. They prerduced GO to rGO using ethylenediamine, possibly achieving only a mild reduction, since they were able to disperse the rGO powder in water [27]. Indeed, the FTIR spectra of rGO still showed evidence of many functional groups. After producing the suspension, the authors exposed it to  $\text{Ca}(\text{OH})_2$ , followed by addition of  $\text{H}_3\text{PO}_4$ . The paper lacks some important details, such as for how long the precipitation was allowed to take place. TEM images showed few HA particles deposited on rGO sheets. TGA data showed a large residue at 600 °C for rGO. The origin of this large residue was unexplained and made it impossible to determine how much HA was deposited on the composites.

Li et al. [28] and Zanin et al. [32] are the only authors who functionalized the GO or rGO substrate before exposing them to the calcium and phosphate precursor solutions. Li et al. physisorbed chitosan on GO by simply mixing GO and chitosan and then added  $\text{Ca}(\text{NO}_3)_2$  to the mix. After adjusting the pH to 10 and further

stirring, they added  $(\text{NH}_4)_2\text{HPO}_4$ , stirred for 1 h, and allowed to react for 24 h at  $37^\circ\text{C}$ . They filtered the resulting suspension to achieve pellets and produced similar composites in the absence of chitosan as control. HA was deposited on both GO and chitosan-GO in the form of spindles, with diameter of  $\sim 27$  nm and length of  $\sim 150$  nm (Fig. 4e and f). However, while the GO/HA composites contained  $\sim 90\%$  HA, the maximum amount of HA deposited on chitosan-modified GO (ch-GO) was  $\sim 60\%$ . GO/HA composites performed better mechanically than ch-GO/HA composites (19 GPa vs. 8.3 GPa as modulus and 624 vs. 465 MPa as hardness). However, ch-GO/HA composites were more cytocompatible toward both fibroblasts and osteoblasts and induced more osteoblast mineralization than the GO/HA composites.

Zanin et al. [32] started from a graphene layer obtained by chemical vapor deposition on titanium, which the authors (surprisingly) refer to as rGO. They functionalized this substrate by exposing it to oxygen plasma, thus making it superhydrophilic, and presumably converting it to a material similar to GO. Then, differently from all other reports discussed so far, they electrodeposited HA on this material: they immersed the films in a solution containing both  $\text{Ca}(\text{NO}_3)_2$  and  $(\text{NH}_4)_2\text{HPO}_4$ , and used them as working electrode, with a Pt coil as counter electrode. The HA films were deposited at a constant  $-2$  V potential, for 30 min, at  $70^\circ\text{C}$ , and were made of HA NPs preferentially exposing the (002) plane. Murine mesenchymal stem cells spread on the GO/HA films, although no comparison with films made in just GO or just HA was shown.

## Summary

While in the previous section the authors aimed at a “biomimetic” GO mineralization, using SBF at pH 7.4 and  $37^\circ\text{C}$ , and thus at most changed the overall SBF concentration, the authors of the papers discussed in this section explored a wide range of temperatures, pH, and concentration and achieved composites with HA contents ranging from 20 % to 99.9 %. Some representative examples of the morphology of the HA particles deposited in different conditions are shown in Fig. 4.

The inclusion of rGO always improved the mechanical properties compared to pure HA. Most reports showed that the composites had better cytocompatibility than pure HA [25–27], with the exception of [24].

The cytocompatibility with respect to pure GO was compared only in two cases [24, 25]; in one case the composites were found to behave better [24], while in the other worse [25] than pure GO. The differences in these results may be related to the different cell lines used, or to the different preparations of GO, since in Fan et al. [25] the original Hummers method was used, while in Li et al. [24] the authors used a modified version of it.

Many of the reports in this section showed the production of discs or sheets from the composite powders. This makes them closer to achieving the end goal of applying the composites in tissue engineering than the reports discussed in the previous section. Indeed, scaffolds, films, or discs are preferable to loose powders, since the cytocompatibility of GFN powders is questionable [16, 33].

## Other Reports of GFN/Bioceramic Composites with the Ceramic Phase Produced In Situ

While most papers discuss the formation of GFN/HA composites, we found two examples in the literature where the ceramic phase was different from HA.

Mehrali et al. [34] prepared rGO/calcium silicate composite powders with low rGO content (up to 1.5 wt%). The composite powders were obtained by exposing GO to a calcium precursor solution ( $\text{Ca}(\text{NO}_3)_2$ ) and adding a silicate precursor solution ( $\text{Na}_2\text{SiO}_3$ ) to it after adjusting the pH to 11.5. A hydrothermal treatment was then performed on the mixture (200 °C for 24 h), leading to the reduction of GO to rGO and the deposition of a very large amount of hydrated calcium silicate (xonotlite) nanowires on the rGO sheets (Fig. 6a and b). Like in Baradaran et al. [26], HIP was then used to transform the powders into discs. The best composite (1 wt% rGO) showed an elastic modulus of 115 GPa, microhardness of  $\sim 4.5$  GPa, and fracture toughness of  $\sim 2.7$   $\text{MPa m}^{1/2}$ , significantly higher than pellets made in pure calcium silicate. Crack bridging, deflection, and branching induced by rGO were again suggested as the reasons for the improved mechanical

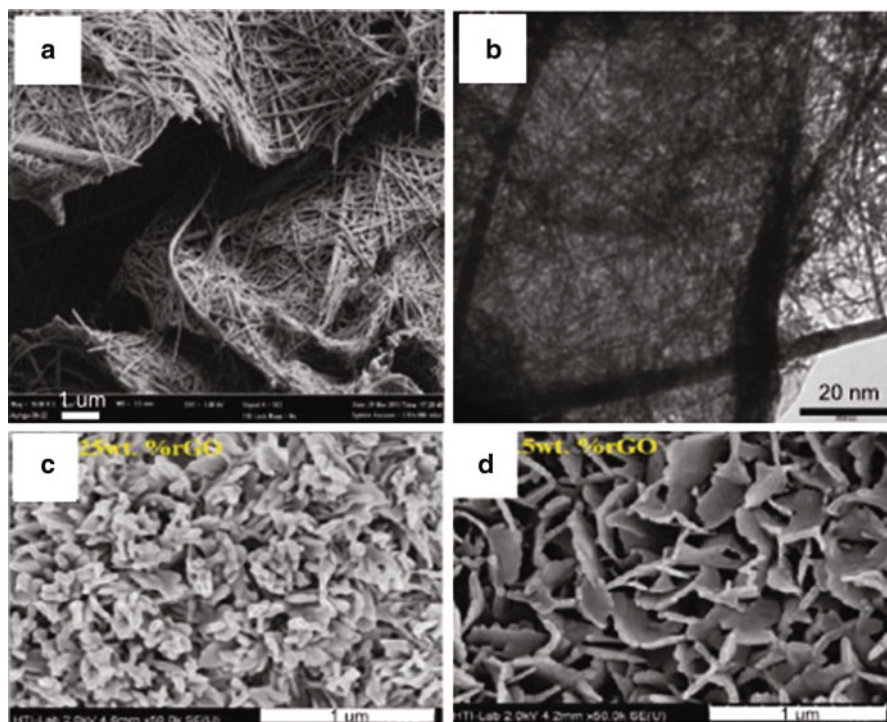


**Fig. 6** SEM (a) and TEM (b) images of the xonotlite nanowires deposited on GO upon hydrothermal treatment, and SEM images of the HA layer formed on GO/xonotlite composites containing 0.25 wt% (c) and 1.5 wt% (d) of GO (Reprinted with permission from Mehrali et al. [34]. Copyright (2014) American Chemical Society)

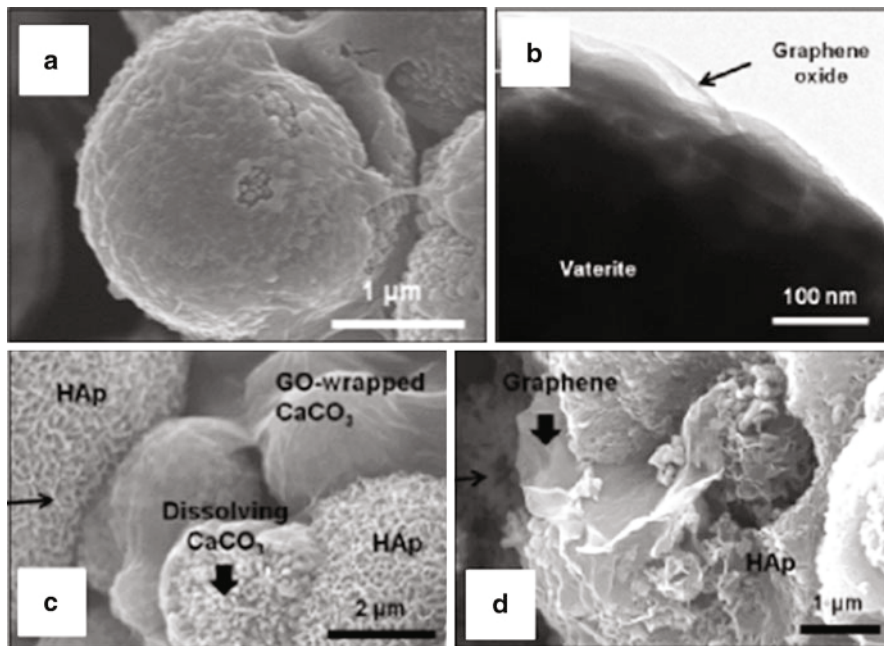


**Fig. 7** SEM (a) and TEM (b) images of GO/CaCO<sub>3</sub> composites, and SEM images of GO/CaCO<sub>3</sub> (c) and rGO/CaCO<sub>3</sub> (d) immersed in SBF for 4 days (Reprinted with permission from Kim et al. [35]. Copyright (2011) American Chemical Society)

properties. The presence of rGO in the composite pellets somewhat increased the amount of HA that got deposited in the pellets after exposure to SBF and changed its morphology (Fig. 6c and d). More osteoblasts were found on the composite pellets containing the larger amounts of rGO than on pure silicate pellets; similarly, larger ALP activity was found on these composites, indicating more mineralization.

Kim et al. [35] were among the first to show the formation of GFN/bioceramic composites. The authors prepared a GO/CaCO<sub>3</sub> composite film by bubbling CO<sub>2</sub> in a mix of GO and CaCl<sub>2</sub> and obtained a self-standing film composed by vaterite microspheres wrapped by an interconnected GO network (Fig. 7a and b). The GO/CaCO<sub>3</sub> films could be transformed to rGO/CaCO<sub>3</sub> films by reducing with hydrazine. Like in Mehrli et al. [34], the authors then tested the bioactivity of the films by immersing them in SBF. They found that HA was formed on both GO/CaCO<sub>3</sub> and rGO/CaCO<sub>3</sub>, but while in the former case CaCO<sub>3</sub> was still visible after immersion in SBF for 4 days, in the latter case all the CaCO<sub>3</sub> dissolved and HA reprecipitated in its place (Fig. 7c and d). This was attributed to a slower dissolution of CaCO<sub>3</sub> in the presence of GO because of interaction of vaterite with GO. No differences in cytocompatibility (using mouse osteoblasts) were found between films made of pure GO, pure rGO, and the GO/HA and rGO/HA composites. However, the cells were more elongated on the composite films than on the GO or rGO films



and showed fewer focal adhesion points. The authors commented that this was a positive result, since it indicated a three-dimensional interaction between the cells and the composite films.

---

## Composites Obtained by Mixing GFNs and Bioceramics

Despite the fact that most GFN/bioceramic composites are made by in situ deposition as described in section “[Composites Formed by Direct Deposition of Bioceramics on GFNs](#),” quite a few researchers tried to directly mix the two phases. In situ deposition methods usually result in highly homogenous composites with GFN content ranging from less than 1 % to above 80 % by weight. Contrary to this, most of the methods discussed in this section can only achieve GFN contents lower than 3 wt% because of the high tendency of GFN to aggregate. This limited graphene loading is usually sufficient to alleviate the brittleness of ceramics, thus extending the applications of the biocomposites.

An advantage of preparing the composite by mixing the two phases is that this method can be adapted to a variety of bioceramics. Powders of HA, biphasic calcium phosphate (BCP, with different ratios of HA to  $\beta$ -TCP), and bioglass have been used to prepare composites with GFN. Some ceramics that cannot be obtained by in situ deposition (like BCP, which is obtained by thermally sintering of calcium-deficient HA) can also be used to prepare these composites.

The key to prepare successful composites by mixing is to achieve a good dispersion of the GFN phase into the ceramic phase. This is generally achieved by solution blending of both phases under ultrasonication and then mechanical grinding, followed by thermal drying to obtain composite powders. The powders are then subjected to various consolidation processes like spark plasma sintering (SPS) or conventional thermal sintering, both suitable to manufacture bulky dense composites (section “[Dense Composites Sintered Under High Pressure](#)”).

More recent processing techniques include electrodeposition and 3D printing, to achieve anticorrosion coatings on metallic substrates or scaffolds with predefined geometries, respectively. These will be described in sections “[GFN/HA Coatings Obtained by Electrodeposition](#)” and “[Porous Composites Fabricated by 3D Printing](#).”

## Dense Composites Sintered Under High Pressure

Dense composites of GFN and bioceramics are achieved by applying high pressures during sintering. An attractive example of sintering technique is SPS; during SPS, high DC pulsed current is passed through the powder compacted under uniaxial mechanical pressure in vacuum, causing a very fast heating. Compared with conventional thermal sintering systems like hot pressing and hot isostatic pressing, SPS can achieve similar theoretical densities at lower sintering temperatures in a much shorter period of time (few minutes vs. several hours). This is essential to avoid GFN

decomposition and retain fine grain sizes in the resulting GFN/bioceramic nanocomposites.

Zhu et al. [36] first applied SPS to GFN/bioceramic synthesis in 2011. They started with commercial GO flakes (original mean size 350  $\mu\text{m}$ ) and HA particles with aspect ratio of 3 (diameter about 0.5–1  $\mu\text{m}$  by SEM). The GO flakes were treated at 700  $^{\circ}\text{C}$  for 10 s to obtain partially reduced GO, which was called graphene by the authors. Both the graphene flakes and HA particles were dispersed in water independently and then mixed to obtain composite solutions under ultrasonication, with graphene content varying from 0.5 to 2.0 wt%. The composite powders obtained after drying were consolidated by SPS at 900–1000  $^{\circ}\text{C}$  for 3 min under a pressure of 40 MPa. After sintering, the size of graphene flakes decreased to several microns in the composites. The sintered composites showed an increase of 12 % in bending strength at 0.5 % graphene loading compared with pure HA, reaching 96 MPa. Further increase of the filler content decreased the strength. Osteoblast cell morphology was similar on HA and on the composite at 2 % graphene, but the cell density on the composite was much lower than that on HA, as estimated by MTT assay.

Two years later, Zhang et al. [37] obtained more promising results in GFN/HA dense composites using a similar method with some modifications. SDS was used as a surfactant to aid the dispersion of both phases in solution. A higher final sintering temperature (1150  $^{\circ}\text{C}$  vs. 1000  $^{\circ}\text{C}$ ) was used by this group. Young's modulus, hardness, and toughness increased by 40 %, 30 %, and 80 % at a GNP (2–3 graphene monolayers; commercial) content of 1 %, respectively, compared to HA without graphene. Such improvements may be explained by the much finer raw materials used by this group (100 nm  $\times$  30 nm vs. several microns for HA and 0.8 nm vs. 20–60 nm in thickness of graphene flakes) besides the modifications of preparation method. As shown in Fig. 8, both phases were intimately contacting each other, as evidenced by the wrapping of graphene sheets around fine HA grains. This was absent when thicker GNP flakes and larger HA particles were used as in Zhu et al. [36]. The fine structure provided more grain boundaries for cracks to pass through, and the intimate interaction between two phases needed more energy to detach each other, both dissipating the fracture energy more effectively and improving the mechanical properties.

In addition to the mechanical improvement, the composites showed higher bioactivity than pure HA, as confirmed by the thicker HA layer deposited in SBF and the larger osteoblast cell density found on the composites. These results were explained based on the smaller grain size and the presence of defects, which could have helped HA dissolution and its reprecipitation in SBF, and on the rougher surface generated by the presence of graphene flakes that promoted cell adhesion.

Very recently, Klébert et al. [38] used eggshell-derived HA powder to prepare graphene/HA nanocomposites. The primary particle size of HA was 66 nm as calculated from the specific surface area (29  $\text{m}^2 \text{g}^{-1}$ ), and the original GNPs were 13.7 nm in thickness with lateral size less than 45  $\mu\text{m}$ . Both phases were mixed with 2 wt% HA in ethanol and milled using a highly efficient attritor mill at 4000 rpm for 2 h. The milled mixture was dried and consolidated by SPS. Thermodynamic calculations demonstrated that HA is chemically stable up to 1000  $^{\circ}\text{C}$  in the presence

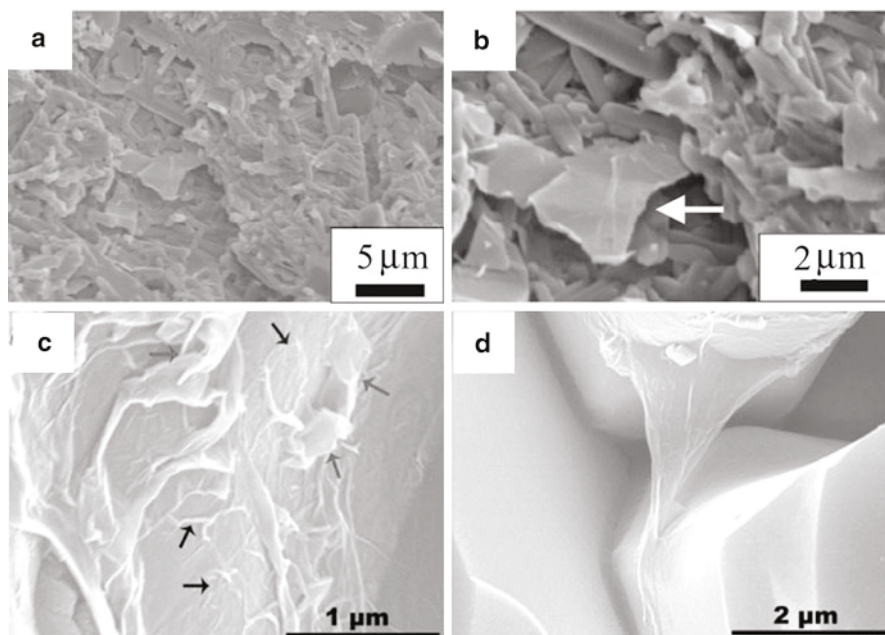


**Fig. 8** The effect of GNP thickness on the morphology of GNP/HA composites. (a, b) Stiff GNPs (white arrow, 1.5 wt%) cannot wrap the HA particles in the work of Zhu et al. [36]. (c, d) Flexible GNP sheets (0.5 wt%) wrap HA grains tightly [37]. Wrinkles are pointed out by black arrows and ridges by gray arrows. Bridging between neighboring HA grains is observed in (d) (Reproduced with permission from Zhu et al. [36] and Zhang et al. [37])

of carbon, while pure HA begins to decompose at around 1400 °C. Therefore lower sintering temperatures (700 °C and 900 °C) but longer holding times (5 min and 7 min) were used, compared with the previous two papers [36, 37]. The best mechanical properties (hardness  $4 \pm 0.5$  GPa and bending strength  $119 \pm 4.9$  MPa) were observed at 700 °C for 5 min. The authors claimed that an increase in mechanical strength was due to the incorporation of GNPs, by comparing with pure HA sintered at 600 °C (hardness  $3.9 \pm 0.2$  GPa and bending strength  $58 \pm 5$  MPa). However, no HA control sample sintered at the same temperature as the composites was produced. The decrease in mechanical properties at higher sintering temperature could have resulted from the partial decomposition of  $\text{CaCO}_3$  (decomposition temperature 860 °C) present at 6 wt% in the eggshell-derived HA. Therefore, any comparison between this and other works should be made with caution.

The work of Porwal et al. in 2014 [39] is the only paper using bioglass rather than HA to prepare GFN/bioceramic composites sintered by SPS. The size of GNPs exfoliated from graphite in *N*-methyl-2-pyrrolidone (NMP) was missing, but it can be estimated as approximately 3 μm based on the SEM reported for the composite. The thickness was likely to be several tens of nanometers, thus imparting a stiff graphite-like morphology. The original size of the bioglass particles (45S5, 45 wt%

SiO<sub>2</sub>, 24.5 wt% CaO, 24.5 wt% Na<sub>2</sub>O, and 6 wt% P<sub>2</sub>O<sub>5</sub>) was about 60 μm, which decreased to about 8–10 μm after ball milling (350 rpm and 4 h) in DMF (*N,N*-dimethylformamide) with GNP loadings of 1, 3, and 5 v%. The milled powder composites were densified by SPS at 600 °C and 70 MPa for 2 min, resulting in very dense composites with relative densities over 99 %. The incorporation of GNPs inhibited the devitrification of sodium calcium silicate (Na<sub>2</sub>CaSi<sub>3</sub>O<sub>8</sub>) from the glass during sintering (the crystallinity at GNP loadings of 0, 1, 3, and 5 v% was 89.3, 54.6, 62, and 54.8 %, respectively). This induced a higher bioactivity in the composites than in the bioglass control, since the amorphous phase dissolved faster and induced more HA formation in SBF. A sudden increase in electrical conductivity was observed between samples at 1 v% GNP ( $9.96 \times 10^{-8}$  S/m) and samples at 3 % and 5 v% GNP (3.22 S/m and 13 S/m, respectively). This 8–9 orders of magnitude increase revealed that percolating graphene network formed within the latter two composites. No mechanical data were provided in this paper.

Hot pressing (HP) is another technique to sinter and densify powder composites. This technique was used by Zhao and colleagues [40] to prepare GFN/BCP composites. To do so, commercial GNPs (0.5–20 μm × 1–5 nm) were ultrasonically dispersed in CTAB solution and mixed with BCP nanopowders (HA: β-TCP = 70:30, by weight; 50 nm) under ball milling for 8 h. The milled powders were treated at 500 °C for 1 h to remove CTAB and then sintered by HP at 1150 °C and 30 MPa for another 1 h. To avoid oxidative degradation of GNPs, all the thermal treatments were carried out in argon. The resulting composites were very dense with relative densities slightly decreasing from 98.54 % to 96.74 % at GNP content ranging from 0 % to 2.5 wt%. The main grain sizes of the composites were scattered in the range of 1.0–1.2 μm, irrelevant to the graphene loading. Similar to SPS, uniaxial pressure was applied during sintering. However, the holding time of 1 h was long enough to cause the GNPs to preferentially orient perpendicular to the HP direction (Fig. 9). The best mechanical properties were achieved at 1.5 wt% GNP loading, showing an increase of 55 % and 76 % in bending strength and toughness along HP direction, respectively. However, perpendicular to HP direction, the bending strength decreased by 30 %, and the toughness increased only by 39 %. This anisotropy in mechanical properties was due to the orientation of the GNP flakes. Such phenomenon cannot be observed when SPS is used, due to its much shorter treating time.

Unlike SPS and HP where the samples are sintered under uniaxial mechanical pressure, hot isostatic pressing (HIP) adopts high-pressure chemically inert gases as the heating and pressing medium to sinter the samples isostatically. Very recently, this technique was employed by Baradaran et al. [41] to explore GFN/Ni-doped BCP composites. The starting materials were commercial GNPs (1–50 μm × 1–20 nm) and as-synthesized Ni-doped (0, 3, and 6 wt%) HA NPs (Ni0-HA, Ni3-HA, and Ni6-HA) which were calcined at 900 °C for 1 h. Both GNP and Ni-HA were mixed in CTAB solutions, followed by ball milling and thermal drying, very similar to the method used by Zhao et al. [40]. These composite powders were pressed into discs at 250 MPa and then sintered by HIP at 1150 °C and 160 MPa for 1 h. The sintering pressure was much higher than the pressures commonly used in SPS and HP (30–70 MPa). All the sintered samples were similar in relative density (97 %) but varied in

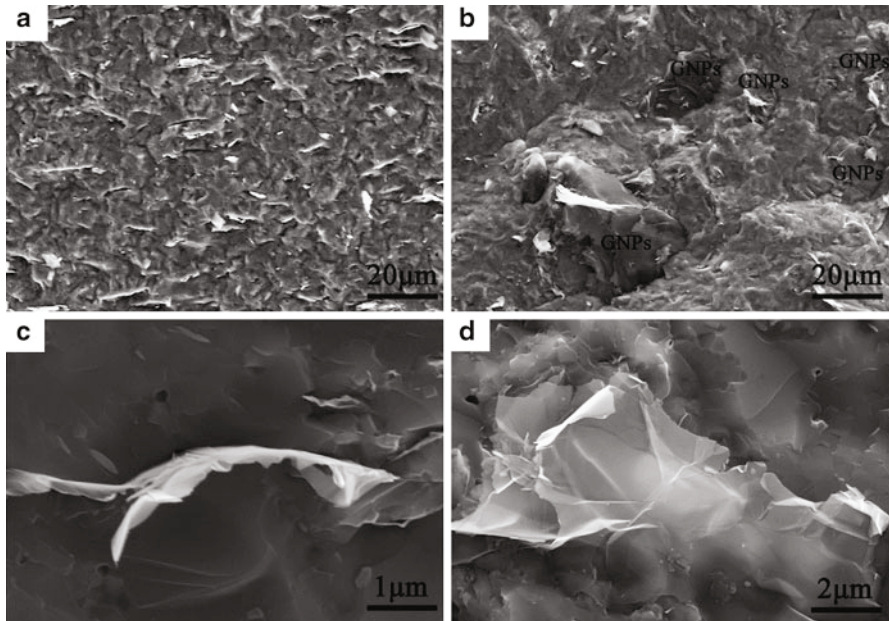


**Fig. 9** Anisotropic fracture surface morphology of GNP/BCP composites produced by HP. (a, c) Along the HP direction, GNPs can be seen sticking out, while GNPs look flat in the direction perpendicular to the HP (b, d). This shows that GNPs were oriented perpendicular to the HP direction (Reproduced with permission from Zhao et al. [40])

phase composition. Based on the XRD patterns (Fig. 10),  $\beta$ -TCP phase could not be detected in Ni0-HA, became visible in Ni6-HA, and dominated (86 %) in composites with 1.5 wt% GNPs (1.5-GNP/Ni6-HA). This was ascribed to the high thermal conductivity of GNP, which caused a fast and severe transition from HA to  $\beta$ -TCP. Ni doping increased all the tested mechanical properties, while the addition of GNPs further increased hardness and fracture toughness but decreased the elastic modulus. Compared to Ni0-HA, the three properties increased by 55 %, 59 %, and 120 % in Ni6-HA, respectively, and increased by 75 %, 163 %, and 85 % in 1.5-GNP/Ni6-HA. The high content of  $\beta$ -TCP in this composite was responsible for its relatively low modulus.

### GFN/HA Coatings Obtained by Electrodeposition

GFN/HA coatings can be regarded as dense composites, serving as biocompatible and corrosion-resistant layers for metals like Ti alloys used in artificial hips. One of the coating method is electrophoretic deposition of HA/GFN onto a Ti cathode, developed by two independent groups [42, 43].

Li et al. used a stainless steel plate as the anode [42]. They immersed both electrodes in a homogenous suspension made by ultrasonic mixing of commercial



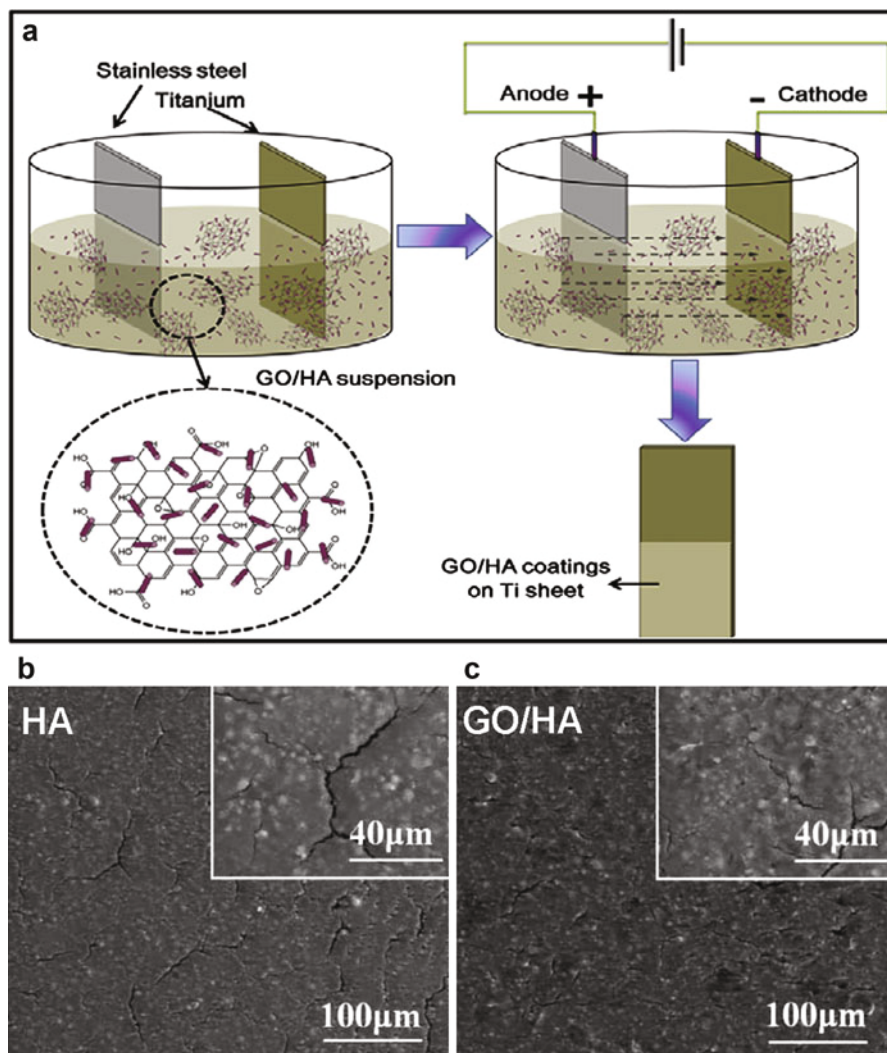


**Fig. 11** Schematic showing the electrodeposition process (a) and typical morphology of control HA coating (b) and 2 %-GO/HA composite coating (c) (Reproduced with permission from Li et al. [42])

HA NPs and GO flakes in ethanol (Fig. 11a). The addition of GO (2 % and 5 % by weight) helped the dispersion of HA NPs in the suspension since GO flakes are amphiphilic and can serve as a surfactant. An acidic environment (pH 3–4) was chosen because in this condition both the GO/HA hybrid particles and pure HA particles carry positive charges with corresponding zeta potentials over 30 mV. As a result, the hybrid particles deposited onto the Ti cathode using deposition voltages from 10 to 30 V. The thickness of the coated layer increased with increasing

deposition voltage and time. After air-drying for 24 h and sintering under vacuum at 600 °C for 1 h (thus achieving partial reduction of GO), the typical thicknesses (at 30 V for 1 min) were 52.8 μm, 42.1 μm, and 35.1 μm for pure HA, 2 %-GO/HA, and 5 %-GO/HA, respectively.

The drying stresses within the coatings, and the thermal expansion mismatch between the coating and the substrate caused severe surface cracks in pure HA coatings. However, surface cracking was hardly found in the composite coatings due to the toughening effect of the GO flakes (Fig. 11b and c). The adhesion strength was also significantly increased by GO ( $1.55 \pm 0.39$ ,  $2.75 \pm 0.38$ , and  $3.3 \pm 0.25$  MPa for HA, 2 %-GO/HA, and 5 %-GO/HA, respectively). The corrosion resistance of the Ti substrate in SBF was significantly improved by the composite coatings. The absence of surface cracks and the formation of GO stacks roughly parallel to Ti substrate likely hindered SBF diffusion and Ti corrosion. 2 %-GO/HA showed the best cell compatibility, while cell morphology and proliferation was similar on HA-5 % GO, HA, and Ti.

Janković et al. also used electrophoretic deposition [43], but with some modifications. They placed two platinum panels parallel to the working Ti cathode on opposite sides, to deposit a composite layer on both sides of the cathode. This layer was made of GNPs (30–50 monolayers; diameter 12 nm) and HA powders dispersed in ethanol by ultrasonication. Since the suspension was not stable, constant stirring was performed during the deposition. The resulting composite layers showed fewer surface cracks and better corrosion resistance than the HA control layer. The hardness was doubled and elastic modulus was enhanced by 50 %, compared with HA coatings. Slightly decreased cell viability was observed on the composite coatings with 1 % GNP (cell viability  $72.3 \pm 4.3$  % relative to the HA control), although these could be still regarded as nontoxic materials.

## Porous Composites Fabricated by 3D Printing

A suitable porous structure provides space for tissue ingrowth and thus is very important for scaffolds used in tissue engineering. Two research groups have shown the preparation of porous GFN/bioceramic composites [44, 45]. Both groups used 3D printing, a technique in which successive layers of composite powders were laid down onto previously consolidated layers under computer control.

Gao et al. [44] used bioglass 58S nanopowders ( $48.3 \pm 6.6$  nm, irregular in shape; the composition is 58 mol% SiO<sub>2</sub>, 33 mol% CaO, and 9 mol% P<sub>2</sub>O<sub>5</sub>) and commercial GNPs (0.8–3 μm × 0.7–1.2 nm) as the starting materials. Both phases were dispersed in *N*-methyl-2-pyrrolidone (NMP) under ultrasonication, followed by filtration, drying, and grinding to obtain composite powders with different GNP loadings (0 %, 0.1 %, 0.5 %, 1.0 %, and 1.5 % by weight). These powders were then printed out layer by layer to construct preset 3D porous scaffolds (Fig. 12a). Each layer was consolidated by selective laser sintering (SLS) immediately after its formation. The SLS was carried out in nitrogen atmosphere with laser power of 7.5 W, scan speed of 100 mm/min, and spot size of 1 mm, corresponding to 0.6 s



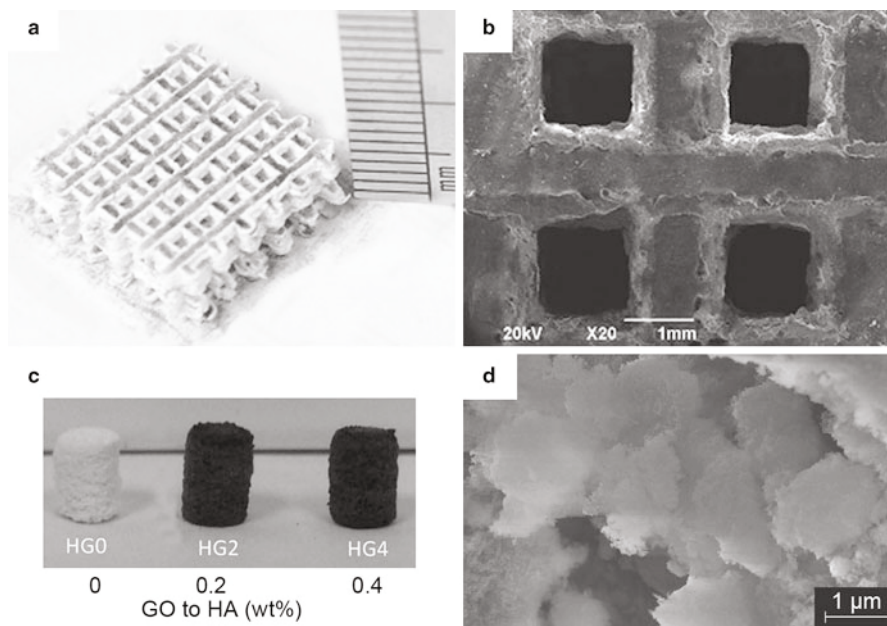


**Fig. 12** Porous GNP/HA composites made from 3D printing. (a, b) Regular interconnected pores were obtained in a composite with 0.5 % GNP [44], solidified by SLS. (c) Macroscopic structures (cylinders) made from 3D printing with aqueous binders [45]. Neither the porous morphology nor scale bar was provided. (d) The morphology of the composite powder (HG4, before 3D printing) with about 33 wt% maltodextrin as the dry binder (Reproduced with permission from Gao et al. [44] and Azhari et al. [45])

laser beam irradiation on individual particles. This very fast sintering process was expected to prevent thermal degradation of GNPs and to inhibit devitrification of 58S glass. Indeed, only weak diffraction peaks of wollastonite ( $\text{CaSiO}_3$ ) were observed in the sintered samples, independent from the graphene content. This result strikingly contrasted with what observed by Porwal et al. [39], who found over 50 % crystallinity ( $\text{Na}_2\text{CaSi}_3\text{O}_8$ ) in GNP/bioglass 45S5 composites sintered by SPS for 2 min.

The highest compressive strength ( $48.65 \pm 3.19$  MPa) and fracture toughness ( $1.94 \pm 0.10$  MPa  $\cdot$  m<sup>1/2</sup>) were achieved at a GNP content of 0.5 %, with an improvement of 105 % and 38 %, respectively, compared to the bioglass control. Bioactivity was confirmed by apatite formation in SBF. Osteoblast-like MG63 cells adhered and spread very well on the composites, showing good cell compatibility. Morphological observation by SEM showed a uniform 3D network with interconnected pores with 0.8 mm in size (Fig. 12b). The large pores and good mechanical properties of these composites suggest a high potential for these materials in bone tissue engineering.

Azhari et al. also prepared porous graphene/HA composites (Fig. 12c) [45]. They first treated GO aqueous dispersions with chloroacetic acid to obtain GO with

abundant carboxyl groups (GO-COOH); the carboxylic groups were then activated with EDC. Meanwhile, they dispersed HA particles in water using Darvan<sup>®</sup> C (commercial ammonium polymethacrylate) as the dispersant. Then they dripped the activated GO suspension in the HA suspension (0.2 and 0.4 wt% of GO), followed by addition of maltodextrin with a weight ratio of 1:2 to HA, which served as a binder in the later 3D composite preparation. The whole mixture was dried, ground, and sieved to be used as the raw material for 3D printing.

The authors suggested that flake-like HA particles (5  $\mu\text{m}$  in average) were decorated with spherical GO aggregates (50 nm), based on SEM observations (Fig. 12d). This is surprising, since GO usually displays flake-like morphology. It is possible that maltodextrin contributed to the morphology, since it was present in amounts as high as 33 % by weight in the composite powder. However, no SEM images were shown for any of the starting materials, making it difficult to discuss the morphology of the composite powder. The addition of GO improved flowability of the composite powder, compared with plain HA powder. This was advantageous to 3D printing.

The consolidation of each printed layer was achieved by injection of an aqueous binder. The composite powder spreading and the injection of the binder were iterated until the whole 3D structure was built up. The compressive strengths of the porous composites at 0.2 % and 0.4 % graphene loading were about 1 MPa and 7 MPa, respectively, i.e., 10 times and 70 times higher than those measured on HA control scaffolds. The authors reported porosities of over 50 % but did not show pore morphology. The mechanical strengths of the composites were comparable to those of cancellous bones (2–12 MPa), suggesting possible applications for bone tissue engineering. However, since the final composites contained considerable amounts of binders, the biocompatibility of the scaffolds should be tested before *in vivo* applications.

## Summary

To prepare the mixed composites reported in this section, most authors used water as a solvent to disperse both phases [36, 37, 40, 41, 45], sometimes with the aid of surfactants like SDS [37] and CTAB [40, 41]. The latter was favored because it imparted positive charges on the GFN flakes, which were able to attract negatively charged bioceramic particles, thus preventing GFN from agglomerating. Organic solvents including ethanol [38, 42, 43], DMF [39], and NMP [44] were also used. Among them, NMP was reported as a good dispersing agent for graphene because of H-bonding and surface energy matching between the two phases [44].

The methods used to consolidate the GFN/bioceramic powders were very diverse, depending on the final structure required for the composites. SPS, HP, and HIP were shown to be suitable to produce bulky dense materials. 3D printing was used to construct porous structures, which were then consolidated by SLS or by simply evaporating water and allowing binders to set. Electrodeposition allowed for the formation of GFN/HA composite coatings onto metallic substrates. It should be

noted that these methods could also be applied to any of the GFN/bioceramic powders prepared by in situ deposition described in section “Composites Formed by Direct Deposition of Bioceramics on GFNs.”

Similar to the results discussed in section “Composites Formed by Direct Deposition of Bioceramics on GFNs,” the incorporation of GFNs always improved the mechanical properties of the resulting composites. Only one exception was found, in the work of Baradaran et al. [41], where Ni-doped HA (6 wt% Ni) showed higher elastic modulus than the corresponding composite with 1.5 wt% GNPs. This was attributed to the high thermal conductivity of GNPs, which caused faster sintering by HIP and thus higher  $\beta$ -TCP content in the final composite than in the Ni-doped HA control. The presence of GNPs that form interconnected network can also significantly enhance the electrical conductivity of the composites [39].

---

## Self-Assembled Porous Graphene/HA Composites

Very recently, Xie et al. [46] developed a self-assembling method to prepare macroscopic porous rGO/HA composites. These authors employed stable HA hydrocolloids as the starting ceramic phase, rather than HA powders or in situ deposited HA NPs. The HA colloids were synthesized by mixing  $\text{Ca}(\text{OH})_2$  and  $\text{H}_3\text{PO}_4$  in the presence of trisodium citrate as the stabilizer. As shown in Fig. 13, an aqueous GO suspension was mixed with the HA colloids at a final GO concentration of  $4 \text{ mg mL}^{-1}$ , followed by a hydrothermal treatment at  $180^\circ\text{C}$  for 6 h. During this treatment, the GO flakes were gradually reduced to rGO sheets which stacked in situ due to the hydrophobic and  $\pi$ - $\pi$  interactions, forming 3D porous hydrogels. The HA NPs were trapped within the hydrogels and retained their colloidal state. The hydrothermal treatment only affected the morphology of HA NPs, which showed an increase in diameter from 2–3 nm to 4–5 nm while maintaining a length of 20–35 nm. The hydrogels possessed graphite-like shells which served as dialysis membranes to remove citrate ions. During the dialysis process, the trapped colloidal HA NPs gradually deposited onto the 3D porous graphene frames. Composite aerogels were obtained after freeze-drying, showing pore size of 1–4  $\mu\text{m}$  and porosity ranging from 94 % to 98 %. The final HA content in the aerogels changed between 27.6 % and 84.3 %, depending on the initial HA to GO weight ratio, which varied from 20:80 to 80:20.

The advantage of this method was the very homogeneous distribution of the HA NPs in the graphene scaffold. The final composite hydrogels were mechanically strong (comparable to cartilage tissues) and electron conductive. Mouse mesenchymal stem cells spread onto the composite hydrogel with 40 % HA, showing fine filamentous pseudopodia directly interacting with the material surface. The composite hydrogels might find applications in scaffolds for bone tissue engineering.

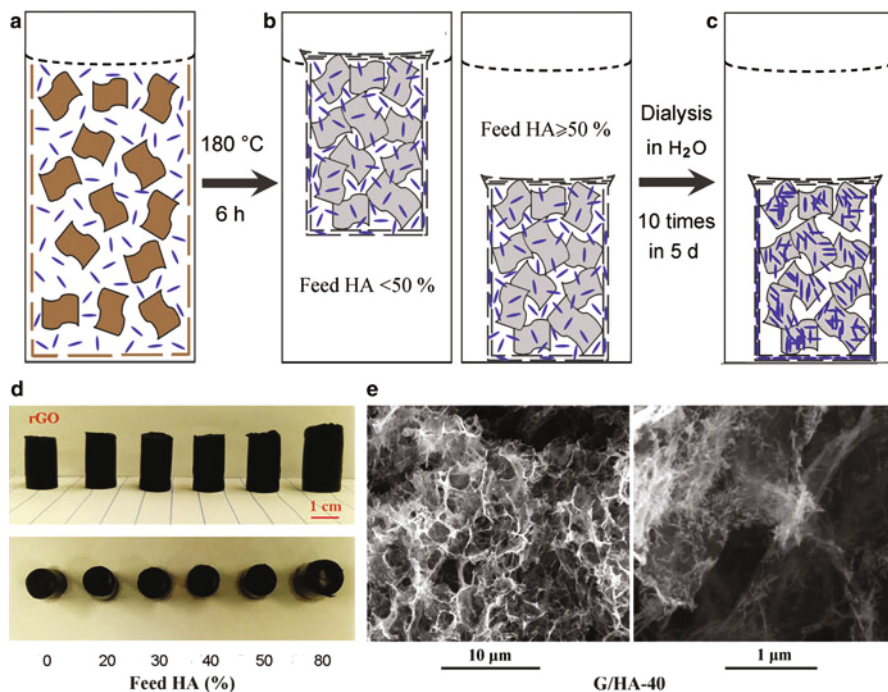


**Fig. 13** Self-assembling process to prepare 3D microporous rGO/HA composites. (a–c) The composite hydrogels were prepared by a three-step method including colloidal solution mixing, hydrothermal treatment, and dialysis. (d) The size of the macroscopic hydrogels varied with feed weight ratio of HA to rGO. (e) Typical SEM images of a representative sample prepared with 40 % HA show the microporous structure and uniform distribution of HA NPs on graphene walls (Reproduced with permission from Xie et al. [46])

## Discussion and Prospective

### Overall Result Comparison

Most of the papers reviewed here describe GFN/HA composites, so we focus our discussion on these materials. To compare the work of the various research groups, we summarize their results in Tables 1 and 2. Here, we have divided the papers based on the possible application of the hybrid material synthesized: in Table 1, we compare hybrids prepared to be used in bone tissue engineering applications, for example, as scaffolds, or to facilitate cell culture; in Table 2, we compare hybrids prepared as substitutes to conventional ceramics used as dense bone defect fillers or coatings for metallic artificial hip joints, where the main goal of the graphene phase is to toughen the ceramic phase. We have reported in the tables only the papers providing quantitative results concerning mechanical or cell culture characterization

**Table 1** Composites synthesized for tissue engineering applications. HA is frequently synthesized in situ on the GFN phase. E is the Young modulus and H is the hardness

GFN phase	HA origin	HA loading	Additives on GFN	Composite form	Mechanical properties	Cell culture results	Reference
GO	Separate Ca/P solutions	60 % with chitosan modification or 90 % without chitosan	Chitosan	Powders, pressed into tablets for mechanical tests	Without chitosan: E = 8.3 GPa; H = 465 MPa With chitosan: E = 19 GPa; H = 624 MPa	Cytocompatibility with fibroblasts and osteoblasts; increased mineralization with chitosan	[28]
GO, reduced during hydrothermal treatment	Separate Ca/P solutions	20–60 %	CTAB	Sheets, obtained by vacuum filtration of wet powders	At 40 % HA: E = 6 GPa; H = 242 MPa	Osteoblasts spread and proliferate better on composite	[25]
GO, mildly reduced by ethylenediamine	Separate Ca/P solutions	68 %	None; EG added during synthesis	Sheets, obtained by vacuum filtration of wet powders	On the sheets: E = 16.9 GPa; Tensile strength 75 MPa	Osteosarcoma cells have better viability on the composite than on pure GO	[24]
GO	5 × SBF for 21 days	Not quantified	Chitosan, covalently bound	Powders	Not provided	Preosteoblasts spread, mineralize, and bind better to composite with chitosan	[21]

GO	1.5 × SBF for 14 days	Not quantified	Gelatin, physisorbed	Powders	Not provided	Preosteoblasts proliferate, mineralize, and bind better on gelatin-GO	[18]
GO, reduced during deposition	1.5 × SBF for 7 days	50 %	Polydopamine	Powders	Not provided	Fibroblasts grow on the material	[17]
CVD graphene	Electrodeposition	Not quantified	Oxygen plasma	Coating	Not provided	Mesenchymal stem cells spread on the film	[32]
GO	Commercial HA particles dispersed in water by Darvan <sup>®</sup> C	99.6–99.8%, but with 1/3 of maltodextrin as binder	Treated with chloroacetic acid to obtain GO -COOH, then activated with EDC	3D printed macroscopic porous cylinder	Compressive strength 7 MPa with 0.4% GO, 70 times higher than without GO	Not provided	[45]
rGO (0.8–4.3 nm × 0.5–5 μm)	Citrate-stabilized HA hydrocolloid (Nanorods 25–35 nm × 4–5 nm)	20 %–80 %	Nothing	Self-assembled macroscopic porous hydrogel	At 40 wt% feed HA: Yield stress = 16 kPa; E = 200 kPa	Mesenchymal stem cells extend more filopodia on composites than on pure rGO	[46]

**Table 2** Composites synthesized to substitute traditional bioceramics, with GFN content less than 5%; E is the Young modulus,  $H_v$  and  $H_b$  are the hardness, values measured by a Vickers and Berkovich probe, respectively, and K is the fracture toughness

GFN phase	HA origin (size)	HA loading	How bulk samples prepared	Mechanical properties	Cell culture results	Reference
GO, reduced hydrothermally to rGO (lateral size: a few microns)	In situ, separate Ca/P solutions, EG added to form nanotubes (~300 nm × 5 μm)	98.5–99.5 %	HIP	At 1.5 % rGO: E = 123 GPa K = 1.51 MPa m <sup>1/2</sup>	Better osteoblast proliferation and attachment than on pure HA	[26]
rGO (2–6 layers)	In situ, separate Ca/P solutions, nanorods (9 nm × 20–45 nm)	99–99.9 %	SPS	At 1 % rGO: E = 150 GPa; K = 4 MPa m <sup>1/2</sup>	Better osteoblast proliferation and mineralization than on pure HA	[27]
GO, thermally reduced (20–60 nm × several μm)	Commercial nanorods (several μm)	98–99.5 %	Aqueous blending and drying, then SPS	At 0.5 % GO: maximum bending strength 98 MPa	Osteoblast cell morphology the same; but decreased cell viability by MTT on composites than on HA	[36]
GNP (0.8 nm × 0.5–2 μm)	Commercial nanorods (100 nm × 30 nm)	99–99.5 %	Blending in SDS solution; drying and SPS	At 1.0 % graphene: E = 141 GPa; $H_v$ = 7.22 Gpa K = 1.06 MPa m <sup>1/2</sup>	Graphene improved osteoblast density and bioactivity in SBF	[37]
GNP (13.7 nm; <45 μm)	From eggshell (66 nm NPs)	98 %	Milled; then SPS	Bending strength 119 MPa; $H_v$ = 4 GPa	Not provided	[38]
GO, 522 nm by dynamic light scattering	Commercial HA NPs (length: 75 nm; width: 22 nm)	95 %, 98 %	Electrodeposition on Ti in ethanol	At 5 % GO: Ti adhesion strength: 3.3 MPa	Fibroblast and osteoblast cell viability best at 2 wt% GO	[42]
GNP (12 nm × 4.5 μm)	As-prepared HA NPs (no dimensions provided)	99 %	Electrodeposition on Ti in ethanol	Surface cracks reduced; $H_b$ = 14.8 GPa; E = 190.9 GPa	Blood mononuclear cell viability decreased on composites (72 % compared to pure HA coatings)	[43]

of the resulting composites (i.e., mostly the papers described in sections “GFN/HA Composites Obtained by Immersion in SBF,” “Composites Obtained by Mixing GFNs and Bioceramics,” and “Self-Assembled Porous Graphene/HA Composites”). Many of the papers showing biomimetic deposition of HA on GFN (section “GFN/HA Composites Obtained by Immersion in SBF”) are more focused on the factors affecting HA formation on GFN than on the final properties of the materials synthesized; we will discuss these papers later, separately (section “Challenges”).

As shown in Tables 1 and 2, all the GFN/HA composites produced are compatible with a variety of cells, ranging from osteoblasts to fibroblasts or mesenchymal stem cells. In many cases, the presence of GFN improved some of the interactions with cells compared to pure HA, including cell adhesion [25, 26] and mineralization [27, 37]. The only exception is the work of Zhu et al. [36] where decreased cell viability was observed on composites compared with that of pure HA. This was largely due to the high thickness of GFN phase used (20–60 nm), which made it more similar to graphite. Previous work showed that graphene is much more cytocompatible than graphite [14]. Overall, the general improvement in cytocompatibility induced by GFN is consistent with the proven importance of nanoscale features in improving cell adhesion [47]. When GO was modified with a biomolecule, often the researchers found that the cell culture results were better on the composites including the biomolecules (e.g., chitosan [21, 28] and gelatin [18]).

The mechanical properties of the composites produced varied widely. When GFN was used in small amounts (usually  $\leq 2$  wt%) in the composites, improved mechanical properties like hardness, Young’s modulus, and fracture toughness were usually observed (Table 2). This is important for the application as coatings on Ti alloy hip joints, because such improvements mean better abrasive resistance, along with enhanced corrosion resistance [42, 43]. For other applications like bone cements and bone defect fillers, the improved fracture resistance is a great improvement over the brittleness of traditional bioceramics.

Since the resulting materials are intrinsically similar to bioceramics, they inherited their shortcomings as well. For example, HA has a Young’s modulus that is much larger than cortical bones (about 100 GPa vs. 10–20 GPa [24, 37]). This often causes load transfer onto the HA implants rather than on the neighboring bone tissues, which become weak due to the lack of mechanical stimulation. This is called “stress shielding effect” [48]. Such effect can be even more severe in graphene-reinforced HA because of the even higher modulus obtained in the composites (Table 2). Thus, the better mechanical properties are advantageous in the applications mentioned above but not to produce scaffolds for cortical bone replacement, for example.

When GO was used in larger proportions (Table 1), the mechanical properties of the resulting powders were tested by pressing them in the form of tablets [28] or by making them into films obtained by vacuum filtration [24, 25]. The strongest and hardest materials, in this case, were obtained on tablets prepared with ~60 % HA in the presence of chitosan [28]; however, almost similar elastic moduli were achieved if just a bit more HA (~68 %) was present in a composite prepared as a film by vacuum filtration. The film has the advantage of being a flexible support with



mechanical properties similar to cortical bones [24], possibly extending the applications of graphene/HA composites to bone substitutions. However, the lack of a porous structure may be a problem, since implant integration usually requires suitable pore size and porosity.

Very recently, porous graphene/HA composites (Table 1) have been produced by either 3D printing [45] or self-assembling [46]. These methods allowed to produce materials that had either mechanical properties similar to cancellous bones [45] or with high porosities [46] up to 98 %. The synthesis of a porous scaffold matching cortical bone properties still remains a big challenge in materials science.

## Challenges

Few researchers provide details on the nature of the GO or rGO flakes that they use in their composites. The flake size, degree of oxidation, and number of layers strongly influence many of the properties of GO and rGO, starting from something as obvious as the surface area, to the cytocompatibility [16], and the mechanical properties [36, 37]. These parameters in turn influence the properties of the resulting composite. For example, the surface area of the GFN phase strongly affects the interlocking with the ceramic phase, and the flake size will determine if the flakes can bridge between cracks or not. A systematic investigation of how parameters such as flake size, degree of oxidation, number of layers affect the cell culture and mechanical properties of a composite is still lacking.

Another issue that keeps coming up in this very young field is the lack of a detailed understanding of the mechanisms behind composite formation. For example, when HA is deposited in situ on GFN, authors take it for granted that the GFN surface needs to be negatively charged, in order to attract  $\text{Ca}^{2+}$  ions first and then phosphate ions, to be able to nucleate HA on it (Fig. 3). However, this hypothesis is never seriously put to test. A way to do this could be to attempt modifying GFN with positively charged groups, and then add the phosphate precursor solution first, and the Ca-containing solution in a second step. Would this lead to more or less HA deposition? Would the HA deposited be more or less strongly interacting with the GFN phase? These questions are important in order to determine the best conditions to prepare GFN/HA composites in situ.

In fact, a few papers proposed positively charged biomolecules to modify GO prior to mineralization: chitosan [21, 28] and arginine [20]. In the latter work, arginine (positively charged amino acid) and glutamic acid (negatively charged amino acid) were compared, in the same conditions, to test which was the strongest mineralizing agent on GO. Surprisingly, arginine was found to be more effective than glutamic acid, giving rise to faster, more abundant, and more crystalline HA precipitation. The authors of this study hypothesized that this was related to the presence of both negatively and positively charged groups on arginine-modified GO and to the fact that arginine is a stronger chelator for calcium and phosphate ions than glutamic acid. Thus, these authors conclude that the most effective inducers of mineralization on GO would be coatings that include both positively and negatively

charged groups and that are strong chelators of calcium and phosphate ions, such as amino and phosphonate groups.

Related to this, another aspect that still needs to be understood is the influence of surface modification or presence of additives in the mineralizing solution on the morphology of the HA particles deposited in situ on GFN. For example, Zanin et al. state that the surface modification of graphene grown via CVD was necessary in order to grow the HA film on the graphene substrate; they do not show results on samples produced in the absence of the plasma treatment [32]. Similarly, Fan et al. [25] used both citrate and CTAB in order to form nanorods of HA in situ on GO; however, they did not show control samples prepared in the absence of one or both additives. And the morphology obtained by this group and [24], who worked in the absence of both additives, was not very different (compare Fig. 4a and c). Vice versa, very similar conditions were used in [27] and in the control samples of [28] in the absence of chitosan; however, the morphology of the resulting HA is quite different (compare Fig. 4d and f).

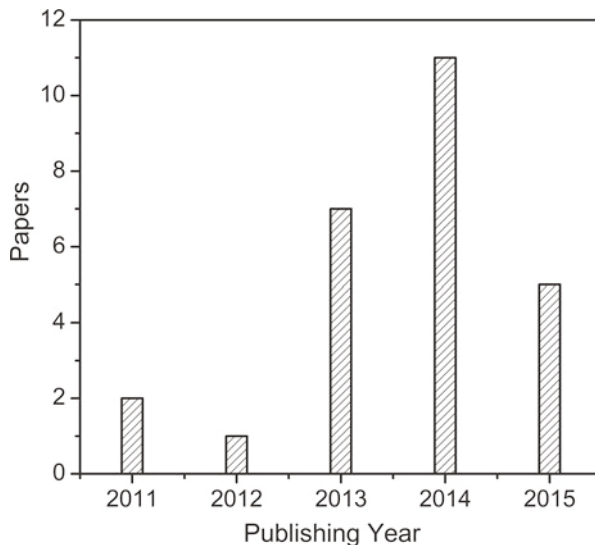
Another important aspect that still needs to be elucidated is how HA and GFN interact with each other. Liu et al., who grew HA in situ on GFN, hypothesized that van der Waals interactions are responsible for this [27]; however, this explanation was not solidly proven and seems to contradict the findings from many other groups showing that a very strong bond is achieved between HA and GFN when HA is grown in situ on GFN using conditions that allow for slow crystal growth [24, 25].

In the composites made by mixing the two phases (section “Composites Obtained by Mixing GFNs and Bioceramics”), frequently less than 2 wt% of graphene is present in the final composites. This is due to the fact that beyond this content, it is very difficult to homogeneously disperse graphene into the ceramic phase using methods like ultrasonication of the suspensions or ball milling of the mixed powder. This is quite different from the composites prepared by in situ deposition (section “Composites Formed by Direct Deposition of Bioceramics on GFNs”) or self-assembling (section “Self-Assembled Porous Graphene/HA Composites”), where homogeneous materials were obtained at any graphene content.

Last but not the least, the biocompatibility of graphene-based materials is still debated. Previous research has shown that nanosized graphene and GO suspended in water can cause cytotoxicity [33]. On the other hand, large graphene films (e.g., 1 cm × 1 cm) have shown good cytocompatibility, showing ability to support proliferation of mesenchymal stem cells and accelerate their specific differentiation toward bone cells [14].

This review shows that when micron-sized graphene flakes are incorporated into bioceramic composites, they usually display good cytocompatibility, even better than the ceramic matrix alone. These results suggest that immobilized graphene, either incorporated into a composite or attached on a surface, is more biocompatible than free graphene flakes in a suspension. This hypothesis needs to be tested in a more controlled manner and more extensively in vivo. So far, no in vivo data have been reported on GFN/bioceramic composites. Graphene hydrogels have been subcutaneously implanted into rats for up to 12 weeks, producing minimal fibrous capsule formation and mild host response [49]. This result is promising but

**Fig. 14** Histogram showing the quick growth of number of publications on the subject of graphene/bioceramic hybrids. Note that the papers in 2015 only include those published in January and February



long-term observation is still needed. Is graphene biodegradable in the long term? If not, is it possible to modify graphene to transform it into a biodegradable material? Also, how do cells react to graphene debris from a graphene-based implant? All these questions need to be answered before graphene/ceramic composites can be used in tissue engineering applications.

## Prospective

The field of GFN/bioceramic composites is very rapidly expanding: while the first two papers on the subject were published in 2011 [35, 36], 11 papers came out in 2014, and already five were published in 2015 by the end of February (Fig. 14). Most of these papers focused on the preparation methods, either by in situ deposition or by mixing the two phases. Only preliminary cell culture tests were reported to test the biocompatibility. We predict that the following years will see the optimization of the preparation methods of the composites and more detailed studies of their biological applications, especially in vivo performance.

Although the field is very new, this review has highlighted some encouraging results. All the composites proposed are biocompatible, at least in cell culture. Additionally, the papers show that the graphene content can be tailored to the desired application, ranging from very low (less than 1 %) to very high (80 %); just as an example, the structures achieved in [24, 25] show composites made with HA contents similar to that of cortical bone (60–70 wt%), making them particularly attractive for bone tissue engineering. Moreover, slow growth of HA particles in mixture of ethylene glycol and water (170:30 by v/v) which then in situ deposited onto rGO flakes resulted in very strong interactions of both phases [24]. The

nanocomposite papers prepared by filtration possessed mechanical properties similar to cortical bones. This highlights the importance of slow crystal growth to prepare bone-like composites. Indeed, biomineralization of natural bones is a process of in situ deposition of HA nanoplates onto collagen fibers which takes place very slowly as well [50]. We believe that insight into biomineralization in the future will help to design better graphene/HA composites for bone substitutions.

As we highlighted in the previous section, there are still many challenges, especially related to understanding the mechanisms beyond composite formation. Solving these challenges will allow researchers to better design the synthesis conditions for the next generation of GFN/bioceramic composites.

---

## References

1. Novoselov KS et al (2004) Electric field effect in atomically thin carbon films. *Science* 306(5696):666–669
2. Peigney A, Laurent C, Flahaut E, Bacsá RR, Rousset A (2001) Specific surface area of carbon nanotubes and bundles of carbon nanotubes. *Carbon* 39(4):507–514
3. Geim AK, Novoselov KS (2007) The rise of graphene. *Nat Mater* 6(3):183–191
4. Arndt A et al (2009) Electric carrier concentration in graphite: Dependence of electrical resistivity and magnetoresistance on defect concentration. *Phys Rev B* 80(19):195402
5. Lee C, Wei X, Kysar JW, Hone J (2008) Measurement of the elastic properties and intrinsic strength of monolayer graphene. *Science* 321(5887):385–388
6. Bonaccorso F et al (2015) Graphene, related two-dimensional crystals, and hybrid systems for energy conversion and storage. *Science* 347(6217):41
7. Lawal AT (2015) Synthesis and utilisation of graphene for fabrication of electrochemical sensors. *Talanta* 131:424–443
8. Kong X-K, Chen C-L, Chen Q-W (2014) Doped graphene for metal-free catalysis. *Chem Soc Rev* 43(8):2841–2857
9. Jihao L et al (2014) Ultra-light, compressible and fire-resistant graphene aerogel as a highly efficient and recyclable absorbent for organic liquids. *J Mater Chem A* 2(9):2934–2941
10. Yang Y, Asiri AM, Tang Z, Du D, Lin Y (2013) Graphene based materials for biomedical applications. *Mater Today* 16(10):365–373
11. Han ZJ et al (2013) Carbon nanostructures for hard tissue engineering. *RSC Adv* 3(28):11058–11072
12. Hench LL (1991) Bioceramics: from concept to clinic. *J Am Ceram Soc* 74(7):1487–1510
13. Marino AA, Becker RO (1970) Piezoelectric effect and growth control in bone. *Nature* 228:473–474
14. Nayak TR et al (2011) Graphene for controlled and accelerated osteogenic differentiation of human mesenchymal stem cells. *ACS Nano* 5(6):4670–4678
15. Crowder SW et al (2013) Three-dimensional graphene foams promote osteogenic differentiation of human mesenchymal stem cells. *Nanoscale* 5(10):4171–4176
16. Sanchez VC, Jachak A, Hurt RH, Kane AB (2012) Biological interactions of graphene-family nanomaterials: an interdisciplinary review. *Chem Res Toxicol* 25(1):15–34
17. Liu H et al (2012) Simultaneous reduction and surface functionalization of graphene oxide for hydroxyapatite mineralization. *J Phys Chem C* 116(5):3334–3341
18. Liu H et al (2014) Gelatin functionalized graphene oxide for mineralization of hydroxyapatite: biomimetic and in vitro evaluation. *Nanoscale* 6(10):5315–5322
19. Fan Z et al (2013) Casein phosphopeptide-biofunctionalized graphene biocomposite for hydroxyapatite biomimetic mineralization. *J Phys Chem C* 117(20):10375–10382

20. Tavafoghi M, Brodusch N, Gauvin C, Cerruti M (2015) Arginine and glutamic acid promote hydroxyapatite precipitation on graphene oxide (submitted)
21. Depan D, Pesacreta TC, Misra RDK (2014) The synergistic effect of a hybrid graphene oxide–chitosan system and biomimetic mineralization on osteoblast functions. *Biomater Sci* 2(2):264–274
22. Wen T et al (2014) Efficient capture of strontium from aqueous solutions using graphene oxide–hydroxyapatite nanocomposites. *Dalton Trans* 43(20):7464–7472
23. Zhao J et al (2014) Nucleation and characterization of hydroxyapatite on thioglycolic acid-capped reduced graphene oxide/silver nanoparticles in simplified simulated body fluid. *Appl Surf Sci* 289:89–96
24. Li Y et al (2014) Biomimetic graphene oxide–hydroxyapatite composites via in situ mineralization and hierarchical assembly. *RSC Adv* 4(48):25398
25. Fan Z et al (2014) One-pot synthesis of graphene/hydroxyapatite nanorod composite for tissue engineering. *Carbon* 66:407–416
26. Baradaran S et al (2014) Mechanical properties and biomedical applications of a nanotube hydroxyapatite-reduced graphene oxide composite. *Carbon* 69:32–45
27. Liu Y, Huang J, Li H (2013) Synthesis of hydroxyapatite–reduced graphite oxide nanocomposites for biomedical applications: oriented nucleation and epitaxial growth of hydroxyapatite. *J Mater Chem B* 1(13):1826
28. Li M et al (2013) In situ synthesis and biocompatibility of nano hydroxyapatite on pristine and chitosan functionalized graphene oxide. *J Mater Chem B* 1(4):475–484
29. Guittonneau F, Abdelouas A, Grambow B, Huclier S (2010) The effect of high power ultrasound on aqueous suspensions of graphite. *Ultrasonics Chem* 17:391–398
30. Liu Y, Dang Z, Wang Y, Huang J, Li H (2014) Hydroxyapatite/graphene-nanosheet composite coatings deposited by vacuum cold spraying for biomedical applications: inherited nanostructures and enhanced properties. *Carbon* 67:250–259
31. Neelgund GM, Oki A, Luo Z (2013) In situ deposition of hydroxyapatite on graphene nanosheets. *Mater Res Bull* 48(2):175–179
32. Zanin H et al (2013) Fast preparation of nano-hydroxyapatite/superhydrophilic reduced graphene oxide composites for bioactive applications. *J Mater Chem B* 1(38):4947
33. Pinto AM, Goncalves IC, Magalhães FD (2013) Graphene-based materials biocompatibility: a review. *Colloids Surf B Biointerfaces* 111:188–202
34. Mehrali M et al (2014) Synthesis, mechanical properties, and in vitro biocompatibility with osteoblasts of calcium silicate-reduced graphene oxide composites. *ACS Appl Mater Interfaces* 6(6):3947–3962
35. Kim S, Ku SH, Lim SY, Kim JH, Park CB (2011) Graphene-biomineral hybrid materials. *Adv Mater* 23(17):2009–2014
36. Zhu J, Wong HM, Yeung KWK, Tjong SC (2011) Spark plasma sintered hydroxyapatite/graphite nanosheet and hydroxyapatite/multiwalled carbon nanotube composites: mechanical and in vitro cellular properties. *Adv Eng Mater* 13(4):336–341
37. Zhang L et al (2013) A tough graphene nanosheet/hydroxyapatite composite with improved in vitro biocompatibility. *Carbon* 61:105–115
38. Klébert S et al (2015) Spark plasma sintering of graphene reinforced hydroxyapatite composites. *Ceram Int* 41:3647–3652
39. Porwal H et al (2014) Processing and bioactivity of 45S5 Bioglass<sup>®</sup>-graphene nanoplatelets composites. *J Mater Sci Mater Med* 25(6):1403–1413
40. Zhao Y et al (2013) Microstructure and anisotropic mechanical properties of graphene nanoplatelet toughened biphasic calcium phosphate composite. *Ceram Int* 39(7):7627–7634
41. Baradaran S et al (2015) Characterization of nickel-doped biphasic calcium phosphate/graphene nanoplatelet composites for biomedical application. *Mater Sci Eng C* 49:656–668
42. Li M et al (2014) Graphene oxide/hydroxyapatite composite coatings fabricated by electrophoretic nanotechnology for biological applications. *Carbon* 67:185–197

43. Jankovic A et al (2015) Bioactive hydroxyapatite/graphene composite coating and its corrosion stability in simulated body fluid. *J Alloys Compd* 624:148–157
44. Gao C, Liu T, Shuai C, Peng S (2014) Enhancement mechanisms of graphene in nano-58S bioactive glass scaffold: mechanical and biological performance. *Sci Rep* 4:4712
45. Azhari A, Toyserkani E, Villain C (2015) Additive manufacturing of graphene-hydroxyapatite nanocomposite structures. *Int J Appl Ceram Technol* 12(1):8–17
46. Xie X et al (2015) Graphene and hydroxyapatite self-assemble into homogenous, free standing nanocomposite hydrogels for bone tissue engineering. *Nanoscale* 7:7992–8002
47. Dalby MJ et al (2007) The control of human mesenchymal cell differentiation using nanoscale symmetry and disorder. *Nat Mater* 6(12):997–1003
48. Samiezadeh S, Avval PT, Fawaz Z, Bougherara H (2015) On optimization of a composite bone plate using the selective stress shielding approach. *J Mech Behav Biomed Mater* 42:138–153
49. Lu J et al (2013) Self-supporting graphene hydrogel film as an experimental platform to evaluate the potential of graphene for bone regeneration. *Adv Funct Mater* 23(28):3494–3502
50. Boskey AL (1998) Biomineralization: conflicts, challenges, and opportunities. *J Cell Biochem* 72(S30–31):83–91

---

## Part II

# Materials Engineering and Biological Interactions: Biomimetic Strategies

---

# Essential Requirements for Resorbable Bioceramic Development: Research, Manufacturing, and Preclinical Studies

# 16

Guy Daculsi, Eric Aguado, and Thomas Miramond

## Contents

Introduction .....	472
Definitions in Bioactive Calcium Phosphate Bioceramics .....	474
Specifications of a Smart Matrix .....	474
The Needs of the Surgeon .....	474
The Need for a Clinical Solution in Bone Regenerative Medicine .....	476
The Needs of the Manufacturer .....	480
Smart Matrix Basic Research and Optimization for Surgical Applications .....	481
Essential Requirements for Class III Medical Devices .....	483
Classification of Biomaterials .....	483
The Characterization and the <i>In Vitro</i> Evaluations .....	484
The Preclinical Studies and the <i>In Vivo</i> Evaluation .....	485
Regulatory Requirements: Legislation .....	485
Clinical Studies in Bone Regeneration .....	489
Example of a Smart Matrix Developed and Used in Bone Regeneration .....	490
Step 1: R&D Concept for a Specific Matrix to Support Tissue Engineering .....	491
Step 2: Physicochemical and Biological Evaluation of Medical Devices .....	491
Step 3: Specific Model to Support Efficiency and Performance .....	492
Step 4: Clinical Cases Selected for Orthopedic and Maxillofacial Defects .....	495
Conclusion .....	497
References .....	497

---

G. Daculsi (✉)

Dental Faculty, Laboratory for Osteoarticular and Dental Tissue Engineering, INSERM U791,  
Nantes University, Nantes, France

e-mail: [guy.daculsi@univ-nantes.fr](mailto:guy.daculsi@univ-nantes.fr)

E. Aguado

ONIRIS, National Veterinary School of Nantes, Nantes, France

e-mail: [eric.aguado@oniris-nantes.fr](mailto:eric.aguado@oniris-nantes.fr)

T. Miramond

Laboratory for Osteoarticular and Dental Tissue Engineering, INSERM U791, Nantes University,  
Nantes, France

e-mail: [thomasmiramond@biomatlante.com](mailto:thomasmiramond@biomatlante.com)



---

**Abstract**

There is a large variety of commercial bioceramic bone substitutes; however, the prerequisites for bone reconstruction and tissue engineering are often absent in research and clinical applications. The main criteria for the use of bioceramics are easily handled biomaterials that are solid, injectable, and/or shapeable. Furthermore, the material must have the appropriate osteoconductive and osteoinductive properties. New bone regeneration technologies, such as “smart matrices,” must be developed and optimized to increase their suitability for bone defects and to support suitable Ortho Biology. This contribution presents the basic smart bone substitutes used for bone regeneration, which will support the twenty-first-century challenge in osteoarticular pathology to replace autografts with more efficient synthetic materials. The paper is focused on the specifications required for the smart matrix (or osteo instructive matrix), the needs of the surgeon, the clinical indications, the regulatory constraints, and product development and marketing. Finally, an example was presented of a smart matrix medical device developed and used in bone regeneration and details the cascade of steps necessary to put it on the market: research and development, meeting the regulatory criteria, preclinical and clinical data, CE mark approval, and FDA (United States Federal Drug Administration).

---

**Keywords**

Bioceramics • Calcium Phosphate • Bone regeneration • Medical Device requirements • Osteoinduction • Tissue engineering

---

**Introduction**

Degenerative osteoarticular pathology in the aging population is a major societal issue of the twenty-first century. Autologous bone grafts are commonly used in dental, maxillofacial, orthopedic, trauma, and spinal surgeries. However, autologous grafts require a second surgical site on the patient, and the volume of graft is of limited and variable quality.

Bone regenerative medicine represents a new approach to this issue, where cell suspensions and/or osteoinductive agents are implanted, in association with a suitable advanced template, and trigger endogenous regenerative processes in bone, as well as the direct repair of injured tissues. There are several prerequisites that must be considered to successfully design a tissue repair strategy centered on activation of endogenous regenerative mechanisms for bone repair after injury or pathological disease. First, a three-dimensional microenvironment that enhances cell adhesion, proliferation, and osteogenic differentiation must be created. Second, an adequate template is needed to recruit diffusible growth factors and modulators of cell maturation and differentiation, which promote endogenous stem/progenitor cell recruitment. This facilitates bone tissue regeneration, including mineralization and bone architecture, vascularization, and bone physiology, such as bone turnover and

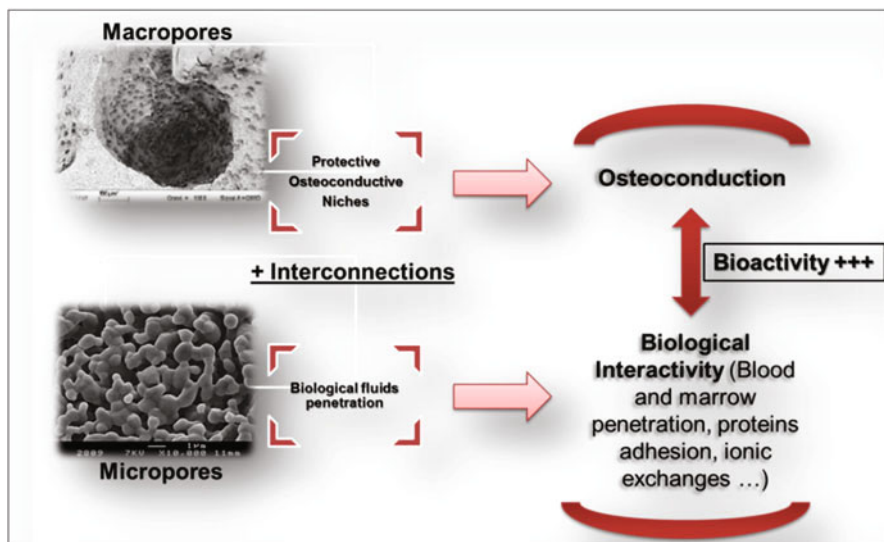


**Fig. 1** Smart bioceramic matrix using MBCP<sup>®</sup> Technology from the REBORNE European clinical trials

adaptation to mechanical loading. A 2009 review from Planell et al. [1] describes largely the challenges inherent in bone repair: specificity of bone, different biomaterials, and surgical technologies applied to bone reconstruction. A second review, recently published by Williams in 2014, details all of the prerequisites for health-care products and biomaterials in the twenty-first century [2].

In the field of biomaterials, bone substitutes require complex development to satisfy the requirement of efficient bone regeneration. This includes the complexity of the bone organ, physiopathology, and numerous functions performed by bone (skeleton, bone marrow, calcium phosphate (CaP) metabolism, mineral stock). In the last 30 years, there has been a large evolution in biomaterials and their related biotechnologies, which has resulted in the development of safe and efficient technologies for bone regeneration, that are equivalent to the gold standard (autograft).

The feasibility of bone tissue engineering was demonstrated with the production of a hybrid material made from autologous bone marrow associated with synthetic matrices [3]. All of the previous data indicated that the use of specific matrices to support these new and promising surgical technologies would be necessary. The main goal was to develop a synthetic bone substitute (“smart matrix”) that would promote both osteoconduction and osteopromotion, i.e., the ability to enhance osteoinduction. This property was confirmed with the use of a human mesenchymal stem cell (hMSC) suspension in combination with smart osteogenic matrix MBCP Technology in clinical trials (REBORNE 7th PCRD, [www.reborne.org](http://www.reborne.org)) (Fig. 1) [4].

The purpose of this chapter is to present the smart CaP bioceramic matrix, with details about the biotechnology and surgical applications and a description of the

development process, from research to manufacturing, and certification of the medical device for bone repair.

---

## Definitions in Bioactive Calcium Phosphate Bioceramics

Bone substitutes can produce newly formed bone when they are placed into the spaces between or around broken bone (fractures) or holes within bone (defects), sometimes in association with an osteosynthetic support to aid with the initial mechanical strength and ensure mechanical stability during healing [5]. Various processes and biological properties occur during this time, such as:

- Osteoconduction – ability of a matrix to support bone growth on its surface or down into its pores, channels, or pipes. Wilson-Hench [6] has suggested that osteoconduction is the process by which the bone is directed to conform to a material's surface
- Osteogenesis – natural bone growth, bone repair
- Osteoinduction – capacity to generate osteogenesis in an environment other than an osseous one, particularly under unfavorable conditions. This reflects stimulation of primitive, undifferentiated, and pluripotent cells to develop into a bone-forming cell lineage. One proposed definition focuses on the process by which osteogenesis is induced [6]. By contrast, osteoinduction can be also defined by active osteoinduction (i.e., growth factors and bone morphogenetic protein [BMP] activity) or passive osteoinduction (also known as osteostimulation) if the matrix is capable, through its nano- and microstructure, to induce/promote osteogenic cell differentiation as an “osteoinstructive” biomaterial.

---

## Specifications of a Smart Matrix

### The Needs of the Surgeon

The smart bioceramic matrix addresses the previously mentioned prerequisites for the repair and regeneration of the bone. However, this technology must also provide the surgeon with certain features:

- A resorbable medical device with versatile handling properties (either solid or injectable and moldable)
- Optimized presentation for combination with osteogenic suspensions
- A delivery system for growth factors or biomimetic peptides of bone morphogenetic proteins (BMPs)

Biomaterials are tools developed by scientists; however, their final use is governed by the needs of surgeons. The needs of these two groups are different, necessitating strong collaborations between medicine and engineering. Practicality

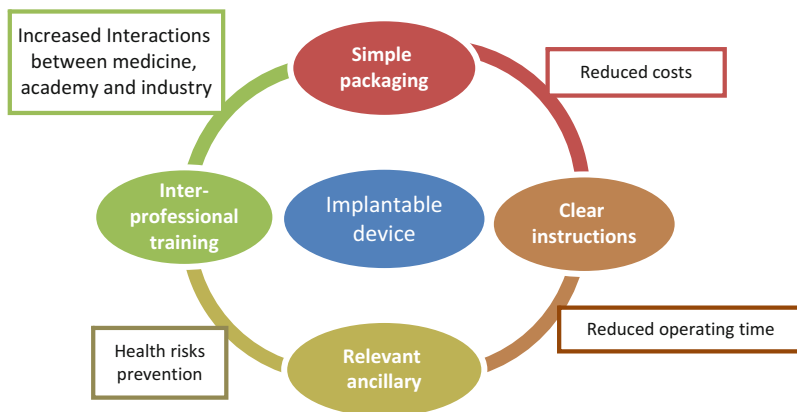


**Fig. 2** Basic key issues in the use and development of implantable medical devices

of the biomaterial is a key requirement, which allows the surgeon to focus on the patient and surgical procedure rather than the device itself. The device should not be a topic of concern during the surgery. The packaging must ensure the sterility of the device until its final implementation. However, the sterile packaging and preparation of the product must also be practical for the opening process, giving access to the device without cluttering the work or storage areas of the hospital, requiring an excessive number of staff or a huge amount of time specifically for this preoperative preparation. Materials used for the packaging and especially the ancillary parts, which are in direct contact with the patient, should be made of a material that avoids breakage of the components. During surgery, such incidents can harm the patient, surgeon, or nursing staff, which can be devastating for the patient's safety. Preventive tests are crucial to assess these scenarios. For example, opening of the package should be effortless and free of any snags, stress tests should demonstrate zero signs of weakness, and tribological testing of the ancillary surfaces should establish zero contamination by undesired particles at the implantation sites.

In some cases, marketing or commercial objectives have led to useless or even counterproductive elements, forcing the surgeon to adapt to the device rather than the reverse. A realistic balance must be achieved between the economic profitability for the investments in the technological advances and new expensive biological solutions and the reduction in costs for patients to ensure equal treatment and to allow advance purchases for hospitals, preventing any stock shortages. Although research and development scientists should be aware of these issues, it is essential to train surgeons through a combination of scientific literature, conferences, web seminars, and demonstrations. An intersection between the industrial engineers was required for developing implantable devices, academics who make the biological discoveries behind the devices, and surgeons who implant the devices and care for the patients. Interactions should be promoted between the various individuals in the private and public biomedical sectors on a regular basis to improve the standards of public health (Fig. 2).

## The Need for a Clinical Solution in Bone Regenerative Medicine

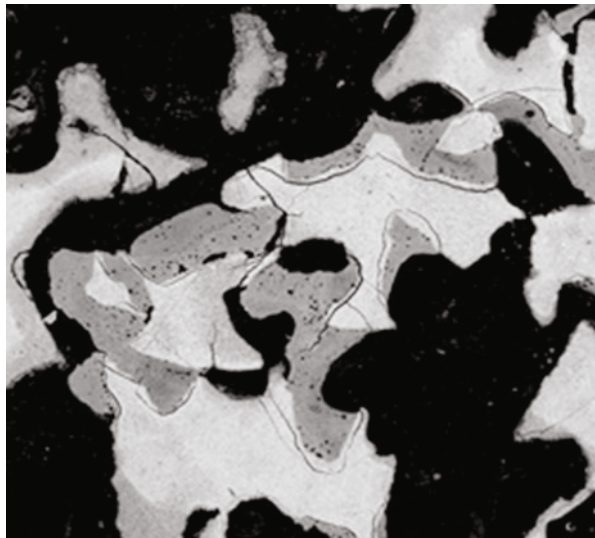
The smart matrix technology platform is considered by scientific experts and the clinical community to be part of the smart biomaterials “diamond concept” [7], which entails:

### Restore Volume, Stabilize, and Regenerate Bone

Several publications have recently demonstrated osteoinductive, osteostimulative, and other osteogenic properties for some micro- and macrostructured CaP bioceramics [8–12]. The key to their osteogenic properties lies at the nano- to microscale level. The micropores are involved in the early events of body fluid diffusion and the physicochemical interactions between the proteins, biological ions in the body fluids, and implant crystal surfaces. These interactions are thought to be either osteoinductive or a promoter of mineralization. This leads to the formation of carbonate apatite crystals after implantation [13]. This event appears both in bony site or ectopic implantation site. For example, the implantation of the osteoinductive scaffold in lumbar muscular area of goats involved ectopic bone formation with trabeculae bridging the MBCP granules but strictly limited to the implantation site, osteostimulation and osteoconduction combined effect (Fig. 3).

The bone defects that result from trauma or degenerative diseases, such as osteoporosis or cancer, require the appropriate clinical response in terms of surgery, immunological safety, and postoperative recovery for patients. The number of clinical cases involving the implantation of medical devices, including biomaterials, has continually increased because of the aging population and resulting rise in prevalence of these diseases. Bone diseases are the most prevalent disease in middle-aged individuals (25–60 years old) and the second most prevalent in people

**Fig. 3** Ectopic bone showed trabeculae bridging the MBCP granules



over 60 years old behind cardiovascular problems [14]. Thus the main clinical areas involved in the treatment of bone diseases are orthopedic; maxillofacial; ear, nose, and throat; and neurological surgery.

As long as autografts do not encounter any obstacles (available quantity, surgical feasibility, or morbidity related to their removal), they remain the standard method of treatment for bone defects [15]. Indeed, the osteogenic potential of autografts comes from their preservation of living cells and bioactive agents (enzymes, proteins, etc.) without the risk of reacting with the immune system [16]. Allografts and xenografts have some of the benefits of autografts, such as safeguarding the native structural properties (e.g., porous architecture, mechanical properties), but lack the biologically active characters (e.g., cells, growth factors) of autografts. They also have the major drawbacks of immune system activation and risk of viral transmission (prions, etc.) or bacterial contamination, which is inherent with these types of grafts [17]. However, the need to limit long and painful invasive surgery and avoid the risk of contamination or rejection now prevails, making alloplastic grafts from biomaterial engineering the preferred method to repair bone defects [15].

Since the 1980s, scientists and engineers have developed a new area of research at the intersection of materials science, biology, and medicine called regenerative medicine [18]. This research includes tissue engineering and cell and gene therapy. The field of biomaterials is booming; many synthesis routes are currently under development, and composites are increasingly being used because they combine the advantages of each type of material, creating innovative new properties that can be used with methods such as sol-gel, lithography, electrospinning, and rapid prototyping [19]. The concept of a synthetic matrix that is able to promote cell invasion, active adsorption, and bone tissue formation while simultaneously degrading itself without any adverse side effects is the cornerstone of alloplastic grafting.

The ideal biomaterial does not consist of a simple substitution but rather relies on biomimicry of the bone [20]. Living organs (including bone) are complex systems, and the biomimetic approach must take into account their multiple dimensions to develop intelligent synthetic matrices, or “smart matrices,” specifically tailored to their application. Materials science has to elucidate and approximate the chemical composition of the bone and its physical, surface, and mechanical properties. It must also understand the three-dimensional architecture of the bone, which is highly porous (e.g., the anastomosing spans in trabecular bone). These criteria fall within the domain of biomaterial engineering. Biology focuses on the interaction over time between the biomaterial and host environment, at both the local and systemic level. Finally, the ultimate goal of this research lies in the medical and surgical dimensions: to implement the biomaterial while reducing the risk to patients. Biomaterials that fulfill all of these requirements can then become a candidate smart matrix and play a role in regenerative medicine [21].

Since the late 1980s, tissue engineering has been commonly defined as an interdisciplinary field whose objective is to maintain, repair, or improve the properties of tissues or organs using synthetic matrices from biomaterial engineering and supplemented with bioactive agents derived from living matter. This area is at the

intersection of engineering and biology [22]. The main steps in tissue engineering are collection of living cells from the patient, addition of these cells to synthetic matrices in aqueous media suitable for their support and survival (such as cell culture medium), incubation of this hybrid system to enhance the invasion of the carriers, and implantation into the bone defect site [23].

The discovery in the 1950s of embryonic and MSCs in mice by L. Stevens and B. Pierce [24, 25] led to the first bone marrow transplant clinic by G. Mathe in 1958 [26]. This pioneering work paved the way for research on stem cells. The main interest in these cells relies both on their ability to differentiate into several types of cells and their ability to self-renew without limit, which does not occur with other types of differentiated cells [27]. In 1998, the first human embryonic stem cells were isolated, emphasizing the recent nature of this area of biology. Unlike embryonic stem cells whose use is prohibited in many countries (including France and the United States from 2003–2008 for bioethics), MSCs are easily accessible [28]. Researchers have been interested in MSCs from total bone marrow for tissue engineering for more than 50 years as they are precursors of osteoblasts [29].

Molecular biology has provided a better understanding of the growth factors involved in the differentiation of MSCs into pre-osteoblasts, osteoblasts, and osteocytes. The main growth factors identified involved in differentiation of MSCs into pre-osteoblasts are BMP-2 and BMP-7, which are part of TGF- $\beta$  family (transforming growth factor), IGF-1 (insulin-like growth factor), FGF-2 (fibroblast growth factor), and VEGF (vascular endothelial growth factor) [30, 31]. The BMPs are the best known growth factors because of their efficiency; however, they also have high costs and dramatic setbacks associated with their uncontrolled use. For example, the product Infuse<sup>®</sup> (Medtronic), which is made of recombinant human BMP-2, has produced severe and even lethal complications in patients. Parathyroid hormones also stimulate pre-osteoblasts and osteoblasts to synthesize growth factors in the extracellular matrix, causing proliferation of MSCs through mitosis. Bone tissue engineering endeavors to promote these interactive communications between pre-osteoblasts, osteoblasts, and MSCs [32].

The culture of concentrated isolated stem cells or stem cells diluted in bone marrow containing proteins and growth factors seeded on CaP matrices before implantation has been the subject of numerous studies [33]. These bioactive agents provide strong osteoinductive potential to the alloplastic grafts *in vivo* [34]. However, the osteoinductive properties of surface grafted isolated factors, without any cells, have also been shown to be effective [35]. Indeed, plasma-rich platelet and plasma-rich fibrin, obtained by the centrifugation of blood, also seem to have an osteoinductive role [36]. Finally, some studies have shown that even in the absence of these bioactive agents, some alloplastic grafts, using the latest in technology of biomimetic micro- and macroporous biphasic calcium phosphate (BCP), have the potential to differentiate MSCs into osteogenic cells. The concavities in the macropores act as cell niches [37, 38], and the interconnected micropores allow protein adsorption and a higher resorption rate [39]. The main advantage of osteoinductive potential is that it allows repair of bone defects of critical size or pathological sites that are impossible to repair solely by host bone remodeling [40].

Currently, the European Union's 7th Framework Programme REBORNE (FP7-HEALTH-2009-241879; <http://www.reborne.org/>) is testing the clinical concept of seeding hMSCs, previously expanded *in vitro* from a patient's own bone marrow onto BCP matrices (MBCP<sup>®</sup>, Biomatlante, Vigneux-de-Bretagne, France) in orthopedic and maxillofacial applications. The program is still in session (December 2014), but so far, the following results have been obtained:

- High *in vitro* cell adhesion and proliferation inside the macropores of BCP matrices [3]
- Potential proof of *in vivo* osteoinduction of BCP matrix with and without isolated hMSCs (hMSCs in ectopic preclinical model [nude mice]) [41]
- Clinical proof (feasibility and efficiency) that the spontaneous association of expanded hMSCs with BCP matrices (MBCP<sup>®</sup>) to form a hybrid implant, or cells only, can repair bone in orthopedic and maxillofacial surgery [42]

The limits of this bone tissue engineering are the expensive costs of cell extraction, transport, isolation, and expansion; the incubation of the cells with the smart matrices, which involves numerous individuals (scaffold manufacturer, transporter, biologists, surgeons); and the multi-step procedure. The challenge for future implementations of this strategy is the reduction of these costs. This can be achieved by upscaling the process at the industrial level, which is currently under development. For example, in Japan, high-tech factories that can manufacture sheet-based tissues with fully automated fabrication systems, called a “T-factory”, are under construction [43]. There is also an issue with the reproducibility of these systems because the extraction of stem cells from the bone marrow is highly dependent on the efficiency of the surgical technique and the quality of the marrow from the patient. However, all of these major issues with engineered osteogenic implants could be avoided with the development of a fully synthetic smart matrix, such as an enhanced biomimetic bioceramic [5].

The relevance of stem cells as a source of pluripotent cells has been challenged with the 2006 discovery of induced pluripotent stem cells (IPS). IPS are adult cells that have the same characteristics as embryonic stem cells after genetic reprogramming [44]. IPS avoid the existing bioethical issues associated with embryonic stem cells, and research in this area is thriving. However, more research is necessary to judge the benefits and risks of this new biotechnology.

Regenerative medicine has two complementary components: tissue engineering and gene therapy. As previously discussed, tissue engineering involves implantation of bioactive matrices supplemented with bioactive agents (cells, growth factors, etc.) to repair severe bone defects, making it a healing treatment “from the outside.” Gene therapy, by contrast, involves care “from within” through alteration of the gene pool, i.e., DNA. The cells of patients are then targeted by vectors containing synthetic plasmids that guide their genomic expression, depending on the specific clinical case that needs treatment. For bone and cartilage diseases, and in particular osteoarthritis, the European project GAMBA FP7-NMP3-SL-2010-245993 (“Gene Activated Matrices for Bone and Cartilage Regeneration in Arthritis”; [www.gamba-project.eu](http://www.gamba-project.eu))



directly induces stem cells to form osteoblasts by transfection with plasmids containing complementary DNA (cDNA) that encode proteins of interest, carried by cellular transfection vectors. The transfection vectors are contained within highly porous BCP granules made of hydroxyapatite/ $\beta$ -tricalcium phosphate (HA/ $\beta$ -TCP). Therefore, the GAMBA project is based on both tissue engineering, with its use of hybrid matrices of biomaterials and cells, and gene therapy to provide innovative solutions to treat osteoarthritis.

The first clinical application of gene therapy was conducted in the United States in 1990. Since then, over 1600 trials have been performed worldwide, although most trials have occurred in the United States (65 %) and Europe (30 %) [45]. Gene therapy is defined as the deliberate introduction of genetic material into human somatic cells to correct a genetic defect or overcome a missing protein by enhancing its gene expression [46]. There are several options to consider when setting up gene therapy. The type of transfection vector is the first variable to consider. Indeed, the genes of the cDNA must be placed into vectors that can penetrate the host cell without any harmful effects. The method of vector transfection can be either viral or non-viral. Transfection techniques using adenoviruses are recognized as efficient and safe [47]. However, liposomes and synthetic polymers, such as poly(ethylene imine), are also capable of encapsulating the cDNA. These non-viral vectors are now widely used because of the fear associated with viral vectors [48, 49].

All of these clinical strategies that have been tested for several years will soon be available to physicians and surgeons to use on a large scale, provided manufacturers and scientists succeed in reducing the costs and regulatory barriers associated with these procedures. It is crucial that ethical issues are addressed by scientists, doctors, and information campaigns for the general public.

## **The Needs of the Manufacturer**

The transition from the discovery of a biological interest of a device to its large-scale manufacturing, which should provide access to the general population, requires significant investments from manufacturers based on the industrial relevance of the innovation. The foundation for this upscaling strategy relies on the implementation of tools and production facilities that meet the highest health and safety standards. The initial risks taken are a function of the in-depth market research, which is offset by the belief in the feasibility of the development of these technologies at the regulatory level and in terms of intellectual property protection. Evaluation units that aid in the patenting and continuous protection of their innovations are a key feature. The margin of error is extremely limited in a highly competitive industry, where new products can hit the market after their development because of legislation and increasingly exacting norms.

To minimize the lag, which can take several years, between research and market placement, it is essential to devise upstream specifications drawn from a variety of considerations, including consultants who are experts in their field. Marketing tactics

and sales positioning, including the final price of the product, must be made intelligible to actors in the biomedical market and health insurance systems. Innovations must also be supported by the acquisition of technological and scientific monitoring tools. These tools should be made as simple as possible to coordinate with the centralized and accessible medical data from hospitals, clinics, liberal practitioners, and academic laboratories at both the country and supranational level. Biotech companies that develop innovative therapies are dependent on aid policies for research and agreements with public institutes that offer characterizations and assays that small and medium enterprises (SME) cannot afford.

The needs of industry must also lie within close proximity to professional training organizations, whose involvement is necessary to better target educational topics according to the current market demands. This interaction enables the recruitment of scientists and engineers whose sensitivities and skills are directly oriented to meet the industrial requirements. From a regulatory point of view, it is necessary to develop business evaluation and support units, including the compilation and administration of product marking files (CE, FDA, etc.). These records amalgamate the various normative tests, preclinical experiments, and lengthy and expensive clinical trials. The inclusion of these regulatory qualifications is often requested by SME in response to invitations to tender for major biomedical projects funded nationally or internationally. It is also necessary to highlight the need for continuous quality control management at all stages of production to meet the standards and audits of notified bodies and the financial burden of the manufacturers.

Systems of monitoring the biomaterial survey are also essential to promptly identify any potential health problems related to the product. Therefore, it is necessary to get systematic, bottom-up feedback on the clinical ease of use and medical potential of products, which requires a strong collaboration between the medical staff and the company. This should be considered as more of a partnership, rather than just suppliers, to set up a coherent whole around the patients. Finally, the implementation of a cultural policy on issues related to the industrial stakes involved in modern medicine and biology is necessary to dispel the fears and apprehension that can sometimes persist with concepts related to bioethics, potential hazards of technology, and approaches hitherto unknown.

---

## **Smart Matrix Basic Research and Optimization for Surgical Applications**

The smart matrix should have an original and unique nano- and microstructure that contacts biological fluids; a macrostructure for cells, bone marrow, and hMSCs interactions; a device that can participate in dynamic processes, including physico-chemical processes, crystal/protein interactions, cell and tissue colonization, and bone remodeling; and the ability for ingrowth at the expense of the bioceramic. The processes of CaP dissolution and biological precipitation into the micropores occur simultaneously with osteoid and bone formation after implantation in either bony or

non-bony sites. The specific interface formed by the biological precipitation allows the newly formed mineralized surface to act as an intelligent (or instructive) matrix for undifferentiated cells, promoting spreading and differentiation of osteogenic cells from the high environmental Ca and P ion content [50]. However, this process must be associated to the **niche concept** required for developing the best matrix.

The bioceramic granules can also be combined with a hydrogel to make an “injectable-moldable bioceramic.” For this review, the hydrogel will only be considered as a carrier, given the rheological properties of bioceramic granules [5].

**The main criteria** for the development of a biologically useful smart matrix are the physicochemical features that provide surgeons with an injectable and/or moldable biomaterial and the multi-scale bioactivity that leads to osteoconduction and osteoinductive properties. Therefore, to achieve the best suitability for the nature of the bone defect, the latest innovative synthetic processes and knowledge about the bone tissue engineering field should be incorporated with the following characteristics [51]:

- Multiple methods for biomaterial absorption by the surrounding host tissues:
  - Chemical dissolution processes [52]
  - Lacunar resorption by osteoclasts through the biomimetic mineral phase [53, 54]
  - Macrophage phagocytosis of bioceramic fragments [55]
- Multi-scale three-dimensional porosity:
  - Intragranular macropores acting as osteoconductive niches for cell adhesion, proliferation, and differentiation [56].
  - Intragranular micropores for interconnecting networks, improved specific surface area for bioactive molecule adsorption, and higher dissolution rates [57, 58].
  - Intergranular three-dimensional space available to circulating body fluids to create a bioactive environment that favors cell colonization, cell signaling, protein adsorption, and ionic exchanges [59]. The combination of this triple porosity requires a low-density bioceramic with high osteointegrative capability.
- Bioactive properties:
  - Ions released for bone metabolism (Ca, P) [60]
  - Apatitic re-precipitation and nucleation processes from bioceramic crystal dissolution [61, 62]
  - Interactions between body fluids and adsorbed biomolecules for cell adhesion, osteoinduction of growth factors, and integration in bone remodeling cycle [63, 64]
- Biomimetic properties:
  - Bone-like crystallography, microstructure, and chemistry [65]
- Osteoconduction and osteoinduction potential [66]
- Biocompatibility (non-immunogenic, noncytotoxic, etc.) [67, 68]

## Essential Requirements for Class III Medical Devices

Biomaterials were classified a long time ago; unfortunately, the classifications are unclear with regards to objective biomaterial sciences [2]. Indeed, there is a hierarchy in the classification scheme that is not directly associated with the biological properties. This classification system has also not been optimized for the new generation of bone substitutes used as matrices for drug delivery and tissue engineering, which should be classified at the border between drugs and medical devices (a combined product). Moreover, medical devices are classified differently for CE marks and FDA approval, demonstrating the need for a technical dossier.

The requirements for classification of medical devices are varied, and the classification rules are based on numerous criteria, such as the duration of contact with the patient, degree of invasiveness, intended purpose (the use for which the device was intended according to the data supplied by the manufacturer on the labeling, in the instructions, and/or in promotional materials), and the part of the body affected by the use of the device. The classification of biomaterials does not correspond to the classification of medical devices.

### Classification of Biomaterials

- Class 1: Metals
- Class 2: Ceramics
- Class 3: Polymers
- Class 3: Carbon-based materials
- Class 5: Composites
- Class 6: Engineered biological materials

According to this classification [2], bioceramics such as CaP matrices are classified in the second level of biomaterial ceramic systems (class 2.2 phosphates) or as bioglasses (class 2.4 silicates and silica-based glasses).

*Classification of medical devices for CE* (Medical devices guidance document, MEDDEV 2.4/1/Rev.9, June 2010, <http://ec.europa.eu/health/medicaldevices>)

Four classes have been defined for CE marks: class I, class IIa and IIb, and class III. Technical documentation is available for the products in class IIa, class IIb, and class III. For example, representative samples are available in Directive 93/42/EEC, in the context of Annexes II, V, and VI. According to this documentation on resorbable bone substitutes, smart matrices are classified as a class III medical device.

*Classification of medical devices according to the FDA* (Medical device classification, [www.fda.gov/MedicalDevices/DeviceRegulationandGuidance/Overview](http://www.fda.gov/MedicalDevices/DeviceRegulationandGuidance/Overview))

The process for FDA classification is different from obtaining a CE mark. The classification depends on the intended use (e.g., dental or orthopedic), resorption capacity, and process of approval. There are three classes. CaP matrices and

resorbable matrices for bone regeneration are in class II. Class III comprises drugs and some combined products. All devices must have premarket notification [510(k)]. For Class III devices, premarket approval is required.

For the approval process, a technical dossier must be made, making sure to include all of the essential realized, filling the entire requirements. The contents of the technical file or design dossier are described within the appropriately selected conformity assessment, which is partially contingent on the device's classification and the technical requirements needed to demonstrate the conformity of the device with the essential requirements. To some extent, the manufacturer determines and justifies the testing and documentation to assure that the device complies with the directive.

For smart matrices used in bone regeneration (CE class III, FDA class II), the minimum information that the technical file must include:

## The Characterization and the *In Vitro* Evaluations

Global standard – ISO 10993: “Biological evaluation of medical devices”

### Relative to Biological Interactions

- **Cytotoxicity**, ISO 10993-5 “Part 5: Tests for *in vitro* cytotoxicity”: determine the lysis of cells (cell death), the inhibition of cell growth, and other toxic effects on cells caused by materials and extracts from the materials using cell culture techniques.
- **Sensitization**, ISO 10993-10 “Part 10: Tests for irritation and sensitization”: estimate the potential for sensitization of a material using a test such as the guinea pig maximization test.
- **Systemic toxicity** (Acute), ISO 10993-11 “Part 11: Tests for systemic toxicity,” Thrombogenicity test: evaluate whether the blood-contacting materials will accelerate the processes of intravascular thrombosis. Describe test methodology and identify control materials.
- **Genotoxicity**, ISO 10993-3 “Part 3: Tests for genotoxicity, carcinogenicity and reproductive toxicity”: apply the mammalian and nonmammalian cell culture techniques to determine gene mutations, changes in chromosome structure and number, and other DNA or gene toxicities caused by materials and extracts from the materials. A battery of tests commonly accepted by the scientific community should be used.
- **Hemocompatibility**, ISO 10993-4 “Part 4: Selection of tests for interaction with blood”: determine the degree of red cell lysis and the separation of hemoglobin caused by materials *in vitro*. Describe test methodology and identify control materials.
- **Biodegradability**, ISO 10993-14 “Part 14: Identification and quantification of degradation products from ceramics”; ISO 10993-6 “Part 6: Tests for local effects after implantation”

- **Sterilization**, ISO 11137: “Sterilization of health care products – Requirements for validation and routine control – Radiation sterilization”
- **Packaging and Labeling**, ISO 11607-1 “Part 1: requirements for materials, sterile barrier systems and packaging systems”; ISO 15 223: “Medical devices – Symbols to be used with medical device labels, labelling and information to be supplied”
- **Quality Management**, ISO 13485: “Quality management systems – Requirements for regulatory purposes”

## The Preclinical Studies and the *In Vivo* Evaluation

Animal models are essential for understanding the various mechanisms that take place during modeling, bone remodeling, interactions with biomaterials. However, there are social movements to respect animal life that are at odds with these experiments, although this concept is not new. For example, in France, a law made in 1976 identified animals as sentient beings. In 1959 [69], the basis for an ethical approach to animal preclinical testing was the **3Rs (Replace, Reduce, Refine)** to save animal lives and respect the animal in Europe and North America. Replacement refers to alternative methods (*in vitro* models, mathematical models). Reduction is the identification of the need for experimental animals and the definition a priori of the minimum number of animals required to obtain valid results by estimating the variability and using properly advised statistical methods. Refinement is the reduction in suffering (use of anesthetics, analgesics) and the requirement to make every effort to improve the well-being of the animal (environmental conditions, food); the concept of end points must also be defined a priori in the study protocol. To enforce these rules, regulatory constraints have been implemented.

## Regulatory Requirements: Legislation

Animal testing is only possible under the regulatory framework fully defined by Directive 2010/63/EU, which completed, updated, and replaced Directive 86/609/EEC. The animal facility where the tests are conducted must be local and pet specific to the research activity. The animals must be housed separately to avoid stress. The animal cages must meet the species-specific standards, including the size of the enclosure, temperature range, relative humidity, air change, etc. If these constraints are subject to controls and penalties, they should not be regarded as a purely administrative obligation. The regulations incorporate the concept of well-being of the animal, and the ethical aspect is of paramount importance to the validity of the study results. The temperature is closely related to the relative humidity factor ( $55 \pm 10$ ). It influences the vitality of the viable colony and affects the respiratory system: a dry atmosphere promotes circulation of irritating dust, while extreme humidity increases the diffusion of ammonia. Light through its intensity, color, and

photoperiod influences animal behavior (e.g., aggression and cannibalism in rodents), body weight, reproduction, etc. [70]. Any changes to these environmental parameters can cause physiological disturbances in the animals that can alter the results of a study or increase the variability of the results, making them difficult or impossible to interpret. These concepts, which are often treated by the researcher or manufacturer as purely administrative constraints, can actually bias a study and are, therefore, of fundamental importance.

Another important parameter is the facility used for animal testing. The facility must have an appropriate enclosure for the species studied and size of the animals; this includes surgical equipment, operating theaters, etc. They must also meet the criteria for improvement to the welfare of the animals.

Staff working in these facilities must be trained in animal experiments and authorized by the institutions. The staff must be adequately educated and trained before they perform any of the following functions:

- Carrying out procedures on the animals
- Designing procedures and projects
- Taking care of the animals
- Animal euthanasia

In some countries in the European Union, those wishing to perform surgery on animals must undergo additional training for experimental surgery, with the exception of those who had prior surgical training (surgeon, veterinarian, etc.).

Traceability of all animal proceedings must be ensured by maintaining detailed records about the animals, holding rooms, drugs used, etc. The number of study samples needed should also be verified, not only for livestock issues but also for the interpretation of the results. Unexplained behavior can sometimes be the result of a defect in the setup of the experimental study. Moreover, this traceability is the only way to ensure the reproducibility of the study. These documents must be kept for 5 years from the end of the project, and they represent a key point for good laboratory practice (21 CFR 58 – Good Laboratory Practice for nonclinical laboratory studies).

To conduct an *in vivo* experiment, it is necessary to submit the project to an animal ethics committee. This usually entails submitting a comprehensive project for evaluation to the local ethics committee before starting. The evaluation takes into account the ethical considerations in the use of the animals, forms the core of the project authorization, and should ensure the implementation of the 3Rs in the project.

In the project report, it is necessary to justify the choice of the animal model. For example, when *in vitro* (cell culture) methods are used to test mechanisms of osteogenesis, osteoclasts, or to eliminate new biomaterials, they can fail to reveal all of the interactions within a living organism. Therefore, studies in a living body are required. It is important to understand the differences between experimental and clinical research. In experimental research, a random factor is varied as a function of controlled factors (species, breed, sex, diet, living environment, etc.), whereas in

clinical research, a random factor is studied that is dependent on other random factors. This difference explains how it is possible to make a conclusion on the outcome of an experiment with a few individuals (5–10 individuals per study group), while it takes a large cohort to draw conclusions from a clinical study. However, the use of animals as its own control increases the statistical power of the study by reducing the individual variability.

Animal models do not entirely mimic human conditions because no animal species has identical skeletal or biomechanical properties [71]. Therefore, the use of one small species (e.g., rodents or rabbits) and one large species (e.g., dog, pig, sheep, goat, and nonhuman primates) is recommended [71, 72]. The choice of the animal species in an experimental model depends on several factors [73–76]: specific features of the experiment, the state of knowledge about the species, anatomy, cost, objectives, etc. For instance, rodents have useful characteristics with regards to their handling, health status, and fertility, but their longevity is shorter than other species, making them unsuitable for long-term (>6 months) experiments.

The **state of knowledge** about the animal is also an important factor. Veterinary care is more developed in dogs than in goats and rabbits, and there is more knowledge about this species. Therefore, an experiment to test hip prostheses would be preferentially performed in dogs to allow the development of a model suitable for biomechanical constraints of the prosthesis, which are better characterized in this species. This choice reduces complications and limits the cost of animal lives.

Depending on the type of study, the **anatomical features** of the prosthesis may be detrimental to the use of certain species. To study dental biomaterial, animals with continual dental growth, such as lagomorphs (rabbits) or small ruminants, are often avoided, and swine or dogs are usually selected. It is essential to refer to the abundant anatomical literature in veterinary medicine during the development phase of the experimental protocol.

**Cost** is also a factor in the choice of animal model. For example, the cost of purchasing 1 dog corresponds to approximately 5 goats, 6 rabbits, or 40 rats. The cost of animal upkeep is also a parameter that needs consideration. The number of animals required for a study depends on the statistical power of the impact of the event, effect of treatment, and risk of error [77]. These can be summarized as follows:

- As the variability of the biological response increases, the number of animals needed increases.
- As the difference between the test and control biomaterial decreases, the number of animals needed to see differences between the two increases.

Rodents and lagomorphs from registered breeders are bred from animal lines that limit individual variability and thereby variability in the experimental results. These species are often selected first to test biocompatibility. The choice of an animal also depends on the biological parameters and purpose of the study [71, 75, 78]. To



investigate osteoinduction, an ectopic site should be used. However, animals vary in their anatomical makeup: the muscular or subcutaneous environment in sheep is higher in fat cells than rabbits and may show differing results for the same biomaterial. For tests looking at a specific bone disease such as osteoporosis, rodents and especially rats are often used because there are many models for this disease described in the literature with these animals [79–81]. For biocompatibility or biofunctionality, rabbits, dogs, sheep, goat, and pig are often used. Although rats are one of the most commonly used species in medical research, there are significant dissimilarities between rat and human bone, and their size limitations make rats unsuitable for simultaneously testing numerous implants [75]. While biocompatibility tests can verify the absence of adverse effects, they do not signify anything about the interest of the biomaterial within the animal, in terms of biology, biomechanics, and specific infectious indications. Therefore, biofunctionality testing is often carried out under identical conditions or conditions as close as possible to their ultimate use in humans.

Biocompatibility tests have been the subject of a large number of recommendations through the European standard ISO 10993-6 December 2009 (Biological evaluation of medical devices – Part 6: Tests for local effects after implantation). For experiments in bone, the recommendations are:

- One of four species should be used: rabbit, dog, sheep, or goat.
- Three experimental conditions should be tested: when degradation is minimal, when degradation occurs, and when degradation has stabilized or when the biomaterial is completely absorbed.
- Ten samples should be used per implantation period.
- Size of the specimens should be 2 mm diameter and 6 mm length for rabbits and 4 mm diameter and 12 mm length for the other animals.
- All bone sites are allowed, but the tibia and femur are recommended.
- The maximum number of specimens implanted in rabbits is six per animal (three tests, three controls); for other species, 12 is the maximum number (six tests, six controls).

The concept of a “critical size defect” (CSD) was developed in the 1980s as a parameter for bone biomaterials. The CSD may be defined as “the smallest size intraosseous wound in a particular bone and species of animal that will not heal spontaneously during the lifetime of the animal” [82, 83]. The idea behind the implementation of a biomaterial in a defect that would heal on its own is to evaluate the complete resorption of the biomaterial. However, apart from information about the toxicity of the resorption debris, these data do not provide a clinical answer to a major defect. Indeed, biomaterials do not accelerate the normal healing process; rather they avoid delays in healing that could occur under adverse conditions. Therefore, the use of a non-critical size defect (NCS) provides little information to the end user. Nevertheless, this is the recommendation of the ISO 10-993-6 standard. Some contradictions or ambiguities can occur with these recommendations:

- Researchers and industrial engineers may want to know if a new biomaterial would be useful for surgeons, which require the CSD parameter. CE accreditation of a biomaterial requires the biomaterial to follow NCSD standards. This could make it necessary to do both types of studies (CSD and NCSD). However, this would go against ethical recommendations (reducing the number of animal lives used in an experiment).
- Bone sites within the same individual are different, and the process of bone remodeling can differ [75, 84]. Therefore, it may be unwise to compare different biomaterials implanted in bone sites (ISO 10993-6).
- According to recommendations, two large animals per time of implantation (10 implants and 10 controls) are sufficient. This low sample number may introduce bias into the results.

It is admitted that the recommendations should be adapted for studies conducted by researchers, to reduce the number of animal lives used.

---

## Clinical Studies in Bone Regeneration

To determine the performance of the bone substitutes and satisfy the essential regulatory requirements, long-term clinical trials should be established. Indeed, clinical trials are an absolute requirement. Clinical trials are organized into four phases:

In phase I, a pilot study is conducted with a limited number of patients (generally <10). If this is the first time that the device is being used in humans, this pilot study can verify the safety of the medical device.

In phase II, the implant is tested in a larger group, generally 20–300 patients, to observe the efficiency of the device. Randomized studies are recommended, and the new technology is tested in comparison with the current standard procedure in a blind experiment. Equivalency or superiority of the device must be demonstrated in this phase.

In phase III, a larger group of 500–3000 patients is used. While this phase is generally required for drug testing, it is usually unnecessary for medical devices such as bone substitutes. The objective of phase III is to demonstrate the safety, side effects, and superiority of the device to other commonly used surgical technologies.

Phase IV encompasses the post-market studies, which entail a case analysis, additional information about the benefits/risks, and the optimal use of the product.

Medical devices used in bone regeneration must always go through phase I. Phase II is generally performed after approval of the device, and phase IV is absolutely necessary for renewal of the approval. In a lot of cases, the product has not undergone full phase I or II clinical trials. Indeed, because the studies may have been conducted with only a small number of subjects, the benefits and risks may not have been evaluated. In these cases, most regulatory authorities recommend a formal monitoring process in place, to record any adverse events or side effects and to provide well-informed decisions about the continued use of the medical device [2].

## Example of a Smart Matrix Developed and Used in Bone Regeneration

David Williams recently published a review on the “essentials in biomaterials science” [2]. The author presents the hugely topical field of biomaterials, including their background, relevance in biology and materials science, information about all of the existing clinical and experimental biomaterials, and the fundamental principles of biocompatibility. This review covers the past 40 years in the field of biomaterial compatibility. For any scientist or manufacturer involved in bone regeneration, it is important to understand each step in the evolution of biocompatibility for market approval (CE mark, FDA). In addition, it is also necessary to continually develop new tests for new technologies, new generations of biomaterials, and newly discovered bioactive and osteogenic properties. The following example of a smart matrix developed for tissue engineering and bone regeneration provides an example of a new generation bioactive ceramic and describes the processes of conception, evaluation, basic tests, clinical tests, and quality and regulatory management for CE mark and FDA approval.

The example is based on the concept of a micro-architected BCP bioceramic (MBCP™ technology, Biomatlante, SA, France) with CE 0123 (certificate n° G7 08 10 32283 021) and FDA (510 k) n°K051774 and selected for combination with hMSCs in orthopedic and maxillofacial clinical trials (REBORNE [4]) for biomimetic peptide drug delivery system in spine application [85–87]. This scaffold is fully resorbable (absorbable) as it was evidenced by human histological analysis in maxillofacial application. The kinetic of bone ingrowth at the expense of the bioceramic is demonstrated after immediate dental root fillings at 6 months, 2.5 years, and 5 years (Fig. 4).

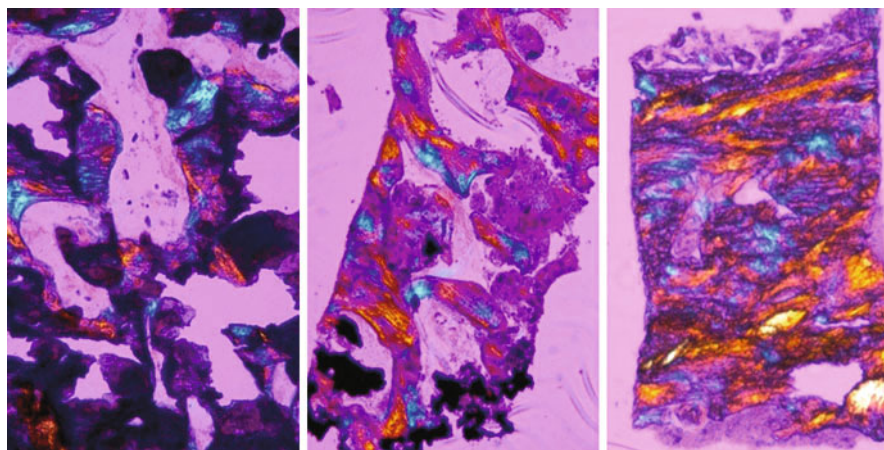


**Fig. 4** Maxillofacial application, bone regeneration after immediate dental root fillings at 6 months, 2.5 years, and 5 years

## Step 1: R&D Concept for a Specific Matrix to Support Tissue Engineering

Livingston Arinzeh et al. [88] reported a comparative study of BCP with different HA/ $\beta$ -TCP ratios as matrices for hMSCs to induce bone formation. Their study demonstrated that a BCP matrix with a lower HA/ $\beta$ -TCP ratio (20/80) loaded with hMSCs promoted the greatest amount of bone formation, and the new bone formed was uniformly distributed throughout the porous structure of the BCP matrix. Matrices made from 100 % HA, higher HA/ $\beta$ -TCP ratios, and 100 % TCP stimulated the least amount of bone formation at 6 weeks post-implantation. In their *in vitro* study of hMSC differentiation with 60/40 HA/ $\beta$ -TCP versus 20/80 HA/ $\beta$ -TCP, the hMSCs expressed osteocalcin, a bone specific marker, after 4 weeks only when grown in 20/80 HA/ $\beta$ -TCP without osteoinductive media. In their *in vivo* study, the enhanced bone formation in the hMSC-loaded 20/80 HA/ $\beta$ -TCP matrix and apparent differentiation into bone cells (characterized by osteocalcin expression *in vitro* under normal culture conditions) may be due in part to the rate of degradation. According to the literature on BCP [85], it was demonstrated that the kinetics of bone ingrowth by osteogenic cells relies on colonization inside the macropores. Without macro- and mesopores, the bioactive processes are unable to develop inside the implanted bioceramic. The association between dissolution at the crystal level, diffusion of the biological fluid at the micropore level, and resorption of the bioceramic by the macrophages and osteoclastic cells at the surface and macropore level involves a progressive substitution of the biomaterials by true bone. This process led to the development of a smart matrix to support new technologies in bone regeneration.

## Step 2: Physicochemical and Biological Evaluation of Medical Devices

1. Standard specifications for hydroxyapatite for surgical implants, ASTM F 1185-03, including assay of heavy metals
2. Standard specifications for  $\beta$ -tricalcium phosphate for surgical implants, ASTM F 1088A-04a, including assay of heavy metals
3. Implants for surgery – hydroxyapatite – Part 3: Chemical analysis and characterization of crystallinity and phase purity, ISO 13779-3
4. Pore size distribution and porosity of solid materials by mercury porosimetry and gas adsorption, ISO 15901-1 and ISO 15901-2
5. Implants for surgery, *in vitro* evaluation for apatite-forming ability of implant materials, ISO 23317
6. Fine ceramics (advanced ceramics, advanced technical ceramics). Test method for hardness of monolithic ceramics at room temperature, ISO 14705
7. Fine ceramics (advanced ceramics, advanced technical ceramics). Sample preparation for the determination of particle size distribution of ceramic powders, ISO 14703
8. Accelerated aging of sterile barrier systems for medical devices, ASTM F 1980-07

9. *In vitro* biological evaluation of medical devices – Part 5: Tests for *in vitro* cytotoxicity, ISO 10993-5
10. *In vivo* preclinical experimentation according to ISO 10 993-6 and 21 CFR Part 58

### Step 3: Specific Model to Support Efficiency and Performance

To support specific biological performance of the smart matrix, in terms of osteogenicity or an osteoinductive fundamental property, specific preclinical tests have been performed. The first test involved intramuscular implantation (non-bony site).

In this study [12], the osteoinductive potential of CaP ceramic particles was investigated through implantation into the dorsal muscles of eight adult female sheep for 6 months. The microporous biphasic calcium phosphate (MBCP) granules of 1–2 mm were composed of HA/ $\beta$ -TCP with macro- and micropores; the explants were hard and encapsulated with normal muscle tissue. Ectopic bone formation with Haversian structures was observed in close contact with the MBCP granules in the histological sections. Back-scattered electron microscopy and micro-computed tomography indicated that approximately 10 % of the mineralized bone and mature osteocytes had formed either between or upon the granules. The ectopic bone showed trabeculae bridging the MBCP granules (Fig. 3), and both the number and thickness of the trabeculae were comparable to those measured in spongy bone. Therefore, the overall results confirmed the presence of mature bone after intramuscular implantation of MBCP granules into sheep. Various hypotheses for the MBCP granule-induced ectopic bone formation are discussed; however, the authors believe that it was due to the micropore content, dissolution processes involving the release of Ca and P ions, and biological apatite precipitation, involving a specific interaction with the MSCs and mesenchymal stem cells, followed by osteogenic differentiation. The data demonstrated that synthetic bone substitutes with osteoinductive properties could be used in bone reconstructive surgery. Other papers have also reported similar ectopic bone formation with other CaP resorbable matrices, supporting the theory that the osteoinductivity of smart matrix plays a role in the differentiation of the mesenchymal stem cells (MSCs) [39, 89, 90].

However, the osteoinductive properties of a calcium phosphate bioceramics based on the crystal size, microporosity, Ca and P release, and biological precipitation must be associated to the macropore content. The association at the nanoscale physicochemical properties and the macroscale structure involved for the “smart scaffold” in tissue engineering the efficiency of the niche concept. The smart scaffold with the macropore structure acts as a niche able to support the pluripotency properties, quiescence, self-renewal/proliferation, and differentiation of hematopoietic stem cells. These different properties are finely regulated by structural intrinsic mechanisms but also by extrinsic mechanisms involving interactions with specialized microenvironments. The macropores act like stem cell niche for bone marrow

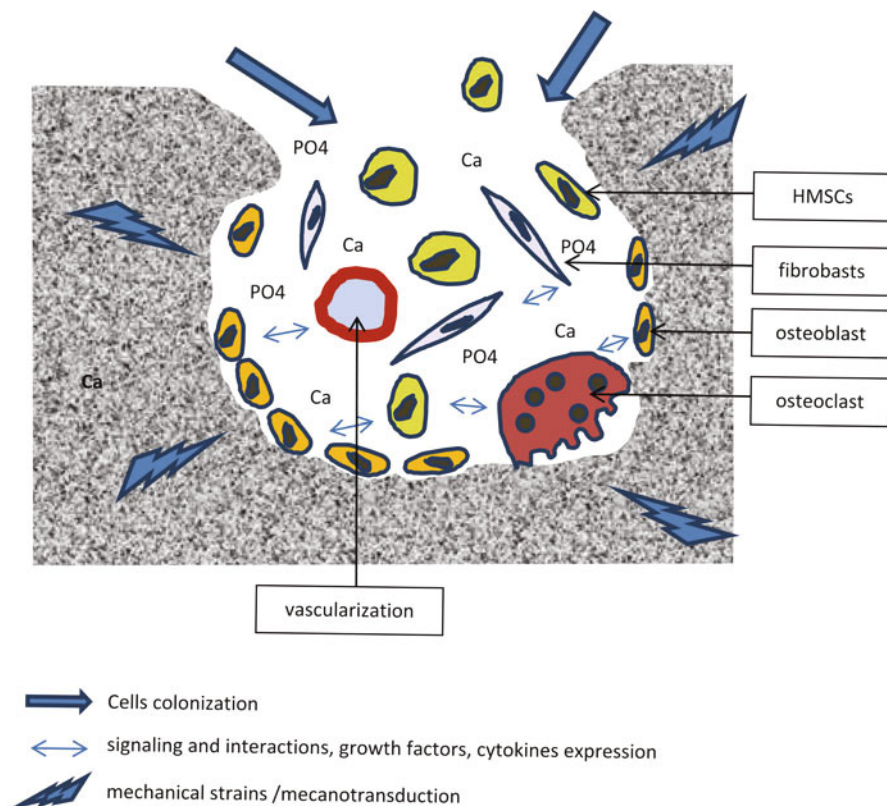


**Fig. 5** Niche concept: Macropore structure acts as a niche able to support quiescence, self-renewal/proliferation, and differentiation of hematopoietic stem cells. In this local environment, original mesenchymal osteoblasts and osteoclasts of hematopoietic origin participate to the cells quiescence and their phenotype expressions. The niches constituted by Ca and phosphate ionic environment, the angiogenesis, and the bone marrow represent a proliferation site/self-renewal and differentiation of hMSCs. In such niches, regulation of hMSCs involves interactions with different cell types (mesenchymal stromal cells, osteo-competent cells, adipocytes, endothelial cells, etc.), diffusible factors (cytokines, chemokines, etc.), molecules of the extracellular matrix (*ECM*), and environmental factors such as the concentration of calcium and phosphate contribute to extensive and functional bone regeneration at the expense on the bioactive CaP ceramic

and endosteal vascularization. In this local environment, original mesenchymal osteoblasts and osteoclasts of hematopoietic origin participate to the cell quiescence and their phenotype expressions. The niches constituted by Ca and phosphate ionic environment, the endothelial cells, and the bone marrow rather represent a proliferation site/self-renewal and differentiation of hMSCs. In such niches, regulation of hMSCs involves interactions with different cell types (mesenchymal stromal cells, osteo-competent cells, adipocytes, endothelial cells, etc.), diffusible factors

(cytokines, chemokines, etc.), molecules of the extracellular matrix (ECM), and environmental factors such as the concentration of oxygen, calcium and phosphate. Niches contribute to extensive and functional bone regeneration at the expense on the bioactive CaP ceramic.

Another model used for the evaluation of osteoinductivity was to test the smart matrix in a necrotic bone defect in rabbits [91]. The purpose of setting up a relevant model of artificially induced osteonecrosis was to reproduce the effects of bone diseases. Several techniques were developed to mimic these scenarios, such as induction of osteonecrosis by freezing or heating [92], surgical ischemia [93], or using an active moiety [94].

In this study, a thermocouple was used to induce local tissue necrosis in the femoral epiphysis of rabbits to reduce costs and simplify the implementation. Eighteen New Zealand rabbits had devices implanted into their femoral epiphysis, which had critical size defects of 5 mm in diameter and 8 mm in length. Animals were confined after implantation for 3, 6, and 12 weeks. MBCP+<sup>®</sup> granules (BCP with micro- and macropores) were used to fill the defects. The implants were recovered and analyzed with micro-tomography. After PMMA embedding, sections were prepared with a diamond saw microtome, for SEM, histology, and histomorphometry. The light microscopy demonstrated bone ingrowth in the defect filled with MBCP+ granules. Bone growth was induced after 3 weeks when in direct contact with the granules. Histological sections revealed that the bone content increased from 3 to 12 weeks and an absence of fibrous encapsulation or inflammatory tissues, which is consistent with previous results on MBCP+ matrix bioactivity [95]. Quantitative imaging showed statistically significant differences from 3 to 12 weeks between the osteonecrosed defect filled with MBCP+ and osteonecrosis control (without MBCP+), demonstrating that there was a much higher bone formation in osteonecrosed sites in the presence of bioactive MBCP+ implants. The absorption rate of the BCP matrices from 3 to 12 weeks was calculated from the three-dimensional volume of the micro-tomography images. The volume of the granules relative to the total volume of the defect decreased continuously, from 40 % at 3 weeks to 20 % at 12 weeks. This result is in agreement with the previous image analysis, demonstrating that the increasing amount of newly synthesized bone was made at the expense of biomaterial dissolution/resorption [85].

The development of a simple and effective preclinical model for osteonecrosis allowed simulation of the effects of bone degeneration pathologies without incurring additional costs. In this study, the osteoinductivity of the MBCP+<sup>®</sup> granules was statistically proven from 3 weeks of treatment. MBCP+<sup>®</sup> enhanced bone formation, which occurred in close contact with the BCP granules, further highlighting their osteoinductive and osteoconductive properties. Osteoinductivity has often been reported missing when using CaP granules without a specific micro- and macroporous structure [96]. The seminal roles played by the porosity and interface complement the chemical biomimetic composition of the BCP crystallographic phases HA:β-TCP and involve dissolution-precipitation processes [97].

## Step 4: Clinical Cases Selected for Orthopedic and Maxillofacial Defects

### Clinical Trial for Orthopedic Spine Defect

A clinical study (personal communication) concerned a prospective, comparative, monocentric, randomized clinical trial was performed for a bioceramic filling of an anterior cervical fusion of polyetheretherketone (PEEK) cages (personal communication). Vertebral pain affects approximately 70–95 % of the population at some point in life. However, in patients with degenerative disc disease, spinal canal stenosis, and/or spondylosis, nonsurgical therapies often fail, and spinal fusion must be considered. This study analyzed two groups of patients implanted with a Solis cage (Stryker; Mahwah, NJ, USA) for cervical interbody fusion either with or without a Tribone 80™ bioceramic (micro- and macroporous BCP) during the treatment of their spinal degenerative disorders, using clinical and radiological follow-ups. Group T (with Tribone 80 insert) had 51 patients, and group W (without bone substitute insert) had 48 patients. Fisher's exact tests, Mann–Whitney U-tests, and analyses of variance were used for the statistical analysis. X-rays were taken postoperatively at 1 and 6 months. The preoperative statistical analysis of the two groups indicated an equivalent distribution for their demographics, spinal degenerative diseases, and clinical preoperative criteria. No immediate postoperative complications were recorded, and no further complications were reported after 6 months in either group. The vertebral body bone fusion rate was significantly higher at 1 and 6 months for group T. Regeneration was also observed outside the cage implant into the interbody space for group T. There was no significant neck pain according to the EVA scoring, Neck Disability Index, and degree of lordosis and kyphosis at 6 months after surgery. Compared to the preoperative stage, there was a strong decrease in both neck and cervicobrachial pain for both groups. This study demonstrated the safety and efficiency of the association between the PEEK cage and osteogenic bone substitute (micro- and macroporous BCP) in a randomized clinical trial. They also reported a higher radiological bone fusion rate for the group using the insert. Radiographies confirmed the concurrent processes of biomaterial resorption and bone ingrowth. The bone fusion rate was also significant, 88.2 % versus 2.3 %, after 6 months (Fig. 6).

### Maxillofacial Clinical Trial

To avoid the use of autografts for dental implantations, it is important to prevent bone loss after tooth extraction or restore the alveolar bone level after pathological diseases [98]. While BCP with HA:β-TCP mixtures have been proven effective in orthopedics, few studies have been reported in dentistry. A clinical trial reported a 5-year clinical follow-up on bone regeneration after immediate dental root fillings. Micro- and macroporous BCP were used. The medical device was an intimate mixture of HA and β-TCP, with interconnected macro- and micropores. Forty cases were distributed into two groups for alveolar pocket filling. Seven cases



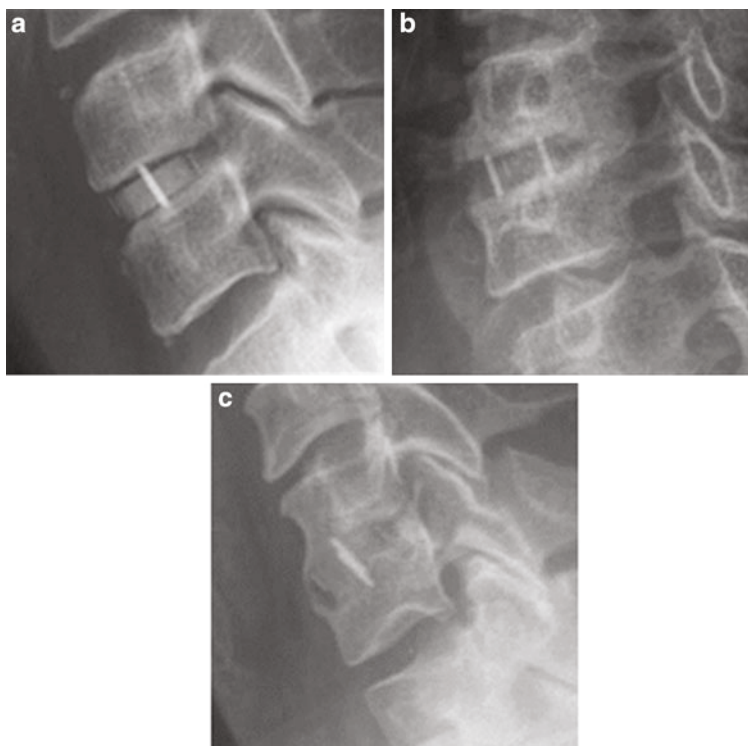


**Fig. 6** (a) Tribone appeared with higher radiopacity at 1 month, (*arrow*). (b) 6 months lateral view indicated a radiopacity decrease, the shape of the insert has changed, and no radiolucent area appeared at the *top* and the *bottom* of the implant. (c) At 20 months total bone regeneration was observed at the expense of the Tribone 80 insert

without filling were used as a control. X-rays were taken at zero, 3, 6, and 12 months and 5 years after the surgery. In all 40 cases, the radiopacity of the implantation area decreased over time, indicating the dual processes of bioceramic resorption and bone ingrowth (two ratios of HA: $\beta$ -TCP were used, 60:40 and 20:80). The X-rays did not reveal any differences in the resorption kinetics. After 1 year, the implantation area looked similar to physiological bone, and the appearance was maintained over time. Indeed, the newly formed bone was preserved 5 years after surgery. By contrast, the control cases (without filling) showed a decrease of 2–5 mm in the pocket. This study demonstrated that immediate filling of alveolar pockets after tooth extraction is an effective, preventive method for jaw bone resorption. Long-term (>1 year) resorption and bone ingrowth were demonstrated for both micro- and macroporous BCP at two different HA/ $\beta$ -TCP ratio.

These two clinical trials are part of the technical file supporting the CE0123 (certificate n° G7 08 10 32283 021) and FDA (510 k) n°K051774 illustrating some of the clinical data acquired during the development and approval of this product.

## Conclusion

For future research, smart matrices should support the synergistic role of micro- and macroporous architecture of CaP bioceramics in osteoinduction.

Studies have demonstrated that *de novo* bone regeneration can be achieved and potentially superior to autografts. Micropores and CaP absorption, in addition to the niche concept, appear to be key requisite features for efficient smart matrices during bone regeneration. Several programs from the European Union's 7th Framework Programme are representative examples of applications of the concept of "smart scaffolds" for tissue engineering or gene therapy.

A critical view of the tests required for market approval is needed, and the *in vivo* biocompatibility must be revisited to support new technologies. Smart matrices must be able to prove their fundamental properties of osteogenicity and osteoinductivity. However, the cascade of biological events leading to MSC differentiation and osteogenesis remains unclear and requires further research.

Large collaborations between manufacturers and both scientific and clinical laboratories are necessary to provide the foundation for innovation, evaluation, fulfillment of regulatory requirements, and development of an approved product for bone regeneration.

---

## References

1. Planell JA et al (2009) Bone repair biomaterials. Elsevier, CRC Press, Boca Raton, Woodhead Pub Limited Oxford
2. Williams D (2014) Essential biomaterials science. Cambridge University Press, Cambridge/New York
3. Daculsi G, Baroth S, Sensebe L, Rosset P, Durand M, Boisteau O, Layrolle P (2013) Association of cells and biomaterials for bone reconstruction. *IRBM* 32:76–79
4. Rosset P, Deschaseaux F, Layrolle P (2014) Cell therapy for bone repair. *Orthop Traumatol Surg Res* 100:S107–S112
5. Daculsi G et al (2013) Osteoconduction, osteogenicity, osteoinduction, what are the fundamental properties for a smart bone substitutes. *IRBM* 34:346–348
6. Wilson-Hench J (1987) Osteoinduction. *Prog Biomed Eng* 4:29
7. Giannoudis PV, Einhorn TA, Marsh D (2007) Fracture healing: the diamond concept. *Injury* 38: S3–S6
8. Fellah BH et al (2008) Osteogenicity of biphasic calcium phosphate ceramics and bone autograft in a goat model. *Biomaterials* 29:1177–1188
9. Yuan H et al (2006) Cross-species comparison of ectopic bone formation in biphasic calcium phosphate (BCP) and hydroxyapatite (HA) scaffolds. *Tissue Eng* 12:1607–1615
10. Habibovic P, de Groot K (2007) Osteoinductive biomaterials – properties and relevance in bone repair. *J Tissue Eng Regen Med* 1:25–32
11. Daculsi G, Layrolle P (2004) Osteoinductive properties of micro macroporous biphasic calcium phosphate bioceramics. *Key Eng Mater* 254:1005–1008
12. Le Nihouannen D et al (2005) Ectopic bone formation by microporous calcium phosphate ceramic particles in sheep muscles. *Bone* 36:1086–1093
13. Daculsi G et al (1990) Formation of carbonate-apatite crystals after implantation of calcium phosphate ceramics. *Calcif Tissue Int* 46:20–27

14. Danet S, Haury B (2011) L'état de santé de la population en France. In: Suivi des objectifs annexés à la loi de santé publique. Dress, Paris
15. Stevens B et al (2008) A review of materials, fabrication methods, and strategies used to enhance bone regeneration in engineered bone tissues. *J Biomed Mater Res B Appl Biomater* 85:573–582
16. Laurie SW et al (1984) Donor-site morbidity after harvesting rib and iliac bone. *Plast Reconstr Surg* 73:933–938
17. Burwell R (1985) The function of bone marrow in the incorporation of a bone graft. *Clin Orthop Relat Res* 200:125–141
18. Petit-Zeman S (2001) Regenerative medicine. *Nat Biotechnol* 19:201–206
19. Lam CXF et al (2002) Scaffold development using 3D printing with a starch-based polymer. *Mater Sci Eng C* 20:49–56
20. Pilliar R et al (2001) Porous calcium polyphosphate scaffolds for bone substitute applications – in vitro characterization. *Biomaterials* 22:963–972
21. Furth ME, Atala A, Van Dyke ME (2007) Smart biomaterials design for tissue engineering and regenerative medicine. *Biomaterials* 28:5068–5073
22. Langer R, Vacanti JP (1993) Tissue engineering. *Science* 260:920–6
23. Cancedda R et al (2003) Tissue engineering and cell therapy of cartilage and bone. *Matrix Biol* 22:81–91
24. Stevens L (1966) The biology of teratomas. *Adv Morphog* 6:1–31
25. Pierce GB (1967) Teratocarcinoma: model for a developmental concept of cancer. *Curr Top Dev Biol* 2:223–246
26. Thomas ED (2000) Landmarks in the development of hematopoietic cell transplantation. *World J Surg* 24:815–818
27. Pittenger MF et al (1999) Multilineage potential of adult human mesenchymal stem cells. *Science* 284:143–147
28. Halme DG, Kessler DA (2006) FDA regulation of stem-cell-based therapies. *N Engl J Med* 355:1730–1735
29. Harrison W (1962) The total cellularity of the bone marrow in man. *J Clin Pathol* 15:254–259
30. Whitfield JF (2003) How to grow bone to treat osteoporosis and mend fractures. *Curr Rheumatol Rep* 5:45–56
31. Mohan S, Baylink DJ (1991) Bone growth factors. *Clin Orthop Relat Res* 263:30–48
32. Caplan AI (1991) Mesenchymal stem cells. *J Orthop Res* 9:641–650
33. Augello A et al (2007) Cell therapy using allogeneic bone marrow mesenchymal stem cells prevents tissue damage in collagen-induced arthritis. *Arthritis Rheum* 56:1175–1186
34. Maitra B et al (2004) Human mesenchymal stem cells support unrelated donor hematopoietic stem cells and suppress T-cell activation. *Bone Marrow Transplant* 33:597–604
35. Burg KJ, Porter S, Kellam JF (2000) Biomaterial developments for bone tissue engineering. *Biomaterials* 21:2347–2359
36. Arpornmaeklong P et al (2004) Influence of platelet-rich plasma (PRP) on osteogenic differentiation of rat bone marrow stromal cells. An in vitro study. *Int J Oral Maxillofac Surg* 33:60–70
37. Ripamonti U, Roden L (2010) Biomimetics for the induction of bone formation. *Expert Rev Med Devices* 7:469–479
38. Miramond T et al (2014) Osteoinduction of biphasic calcium phosphate scaffolds in a nude mouse model. *J Biomater Appl* 29:595–604
39. Habibovic P et al (2005) 3D microenvironment as essential element for osteoinduction by biomaterials. *Biomaterials* 26:3565–3575
40. Assouline-Dayana Y et al (2002) Pathogenesis and natural history of osteonecrosis. In: *Seminars in arthritis and rheumatism*. Elsevier 32:94–124
41. Miramond T (2012) Développement de matrices céramiques et composites pour l'ingénierie tissulaire osseuse. In: *Nantes University PhD thesis*
42. Daculsi G, Baroth S, Sensebé L, Rosset P, Durand M, Boisteau O, Layrolle P (2011) Association cellules-matériaux pour Thérapies cellulaires Osseuses. *IRBM* 32:76–79

43. Kubo H et al (2013) Development of automated 3-dimensional tissue fabrication system tissue factory-automated cell isolation from tissue for regenerative medicine. In: Engineering in Medicine and Biology Society (EMBC), 2013 35th annual international conference of the IEEE, Osaka
44. Takahashi K, Yamanaka S (2006) Induction of pluripotent stem cells from mouse embryonic and adult fibroblast cultures by defined factors. *Cell* 126:663–676
45. Ginn SL et al (2013) Gene therapy clinical trials worldwide to 2012—an update. *J Gene Med* 15:65–77
46. Tolstoshey P (1993) Gene therapy, concepts, current trials and future directions. *Annu Rev Pharmacol Toxicol* 33:573–596
47. St George J (2003) Gene therapy progress and prospects: adenoviral vectors. *Gene Ther* 10:1135–1141
48. Lasic D, Templeton N (1996) Liposomes in gene therapy. *Adv Drug Deliv Rev* 20:221–266
49. Niidome T, Huang L (2002) Gene therapy progress and prospects: nonviral vectors. *Gene Ther* 9:1647–1652
50. Daculsi G et al (2013) Smart calcium phosphate bioceramic scaffold for bone tissue engineering. *Key Eng Mater* 529:19–23
51. Zhang Y et al (2013) Dissolution properties of different compositions of biphasic calcium phosphate bimodal porous ceramics following immersion in simulated body fluid solution. *Ceram Int* 39:6751–6762
52. Daculsi G et al (2010) Developments in injectable multiphasic biomaterials. The performance of microporous biphasic calcium phosphate granules and hydrogels. *J Mater Sci Mater Med* 21:855–861
53. Lan Levengood SK et al (2010) Multiscale osteointegration as a new paradigm for the design of calcium phosphate scaffolds for bone regeneration. *Biomaterials* 31:3552–3563
54. Yamada S et al (1997) Osteoclastic resorption of calcium phosphate ceramics with different hydroxyapatite/ $\beta$ -tricalcium phosphate ratios. *Biomaterials* 18:1037–1041
55. Jensen SS et al (2014) Osteoclast-like cells on deproteinized bovine bone mineral and biphasic calcium phosphate: light and transmission electron microscopical observations. *Clin Oral Implants Res* 26(8):859–64
56. Coathup MJ et al (2012) Effect of increased strut porosity of calcium phosphate bone graft substitute biomaterials on osteoinduction. *J Biomed Mater Res A* 100:1550–1555
57. Chan O et al (2012) The effects of microporosity on osteoinduction of calcium phosphate bone graft substitute biomaterials. *Acta Biomater* 8:2788–2794
58. Li X et al (2008) The effect of calcium phosphate microstructure on bone-related cells in vitro. *Biomaterials* 29:3306–3316
59. Hollister SJ (2005) Porous scaffold design for tissue engineering. *Nat Mater* 4:518–524
60. Sánchez-Salcedo S et al (2009) In vitro structural changes in porous HA/ $\beta$ -TCP scaffolds in simulated body fluid. *Acta Biomater* 5:2738–2751
61. LeGeros RZ, Ben-Nissan B (2014) Introduction to synthetic and biologic apatites. In: *Advances in calcium phosphate biomaterials*. Springer, Springer Verlag Berlin Heidelberg, pp 1–17
62. Campion CR et al (2013) Microstructure and chemistry affects apatite nucleation on calcium phosphate bone graft substitutes. *J Mater Sci Mater Med* 24:597–610
63. Cao W, Hench LL (1996) Bioactive materials. *Ceram Int* 22:493–507
64. Vasilescu E et al (2011) Interactions of some new scaffolds with simulated body fluids. *Rev Chim* 62:212–215
65. Chai YC et al (2012) Current views on calcium phosphate osteogenicity and the translation into effective bone regeneration strategies. *Acta Biomater* 8:3876–3887
66. LeGeros RZ (2002) Properties of osteoconductive biomaterials: calcium phosphates. *Clin Orthop Relat Res* 395:81–98
67. Legeros RZ (1993) Biodegradation and bioresorption of calcium phosphate ceramics. *Clin Mater* 14:65–88

68. Lu J et al (1998) Comparative study of tissue reactions to calcium phosphate ceramics among cancellous, cortical, and medullar bone sites in rabbits. *J Biomed Mater Res* 42:357–367
69. Russell WMS, Burch RL (1959) *The principles of humane experimental technique*. Methuen, London, p 238
70. Castelhana-Carlos MJ, Baumans V (2009) The impact of light, noise, cage cleaning and in-house transport on welfare and stress of laboratory rats. *Lab Anim* 43:311–327
71. Peric M et al (2014) The rational use of animal models in the evaluation of novel bone regenerative therapies. *Bone* 70:73–86
72. Hazzard DG et al (1992) Selection of an appropriate animal model to study aging processes with special emphasis on the use of rat strains. *J Gerontol* 47:B63–B64
73. Auer JA et al (2007) Refining animal models in fracture research: seeking consensus in optimising both animal welfare and scientific validity for appropriate biomedical use. *BMC Musculoskelet Disord* 8:72
74. Laroche MJ, Rousselet F (1997) *Les animaux de laboratoires – Ethique et bonnes pratiques*. Masson, Paris, p 393
75. Pearce AI et al (2007) Animal models for implant biomaterial research in bone: a review. *Eur Cell Mater* 13:1–10
76. Schimandle JH, Boden SD (1994) Spine update. The use of animal models to study spinal fusion. *Spine* 19:1998–2006
77. Laporte S, Mottier D (2007) Le nombre de sujets nécessaire. *Méd Thé* 13:262–69
78. Reichert JC et al (2009) The challenge of establishing preclinical models for segmental bone defect research. *Biomaterials* 30:2149–2163
79. Bonucci E, Ballanti P (2014) Osteoporosis – bone remodeling and animal models. *Toxicol Pathol* 42:957–969
80. Chappard D et al (2001) Texture analysis of X-ray radiographs is a more reliable descriptor of bone loss than mineral content in a rat model of localized disuse induced by the *Clostridium botulinum* toxin. *Bone* 28:72–79
81. Jee WS, Yao W (2001) Overview: animal models of osteopenia and osteoporosis. *J Musculoskelet Neuronal Interact* 1:193–207
82. Hollinger JO, Kleinschmidt JC (1990) The critical size defect as an experimental model to test bone repair methods. *J Craniofac Surg* 1:60–68
83. Schmitz JP, Hollinger JO (1986) The critical size defect as an experimental model for craniomandibulofacial nonunions. *Clin Orthop Relat Res* 205:299–308
84. Le Guehennec L et al (2005) Small-animal models for testing macroporous ceramic bone substitutes. *J Biomed Mater Res B Appl Biomater* 72:69–78
85. Daculsi G et al (2003) Current state of the art of biphasic calcium phosphate bioceramics. *J Mater Sci Mater Med* 14:195–200
86. Cunningham BW et al (2009) Ceramic granules enhanced with B2A peptide for lumbar interbody spine fusion: an experimental study using an instrumented model in sheep: laboratory investigation. *J Neurosurg Spine* 10:300–307
87. Smucker JD et al (2008) B2A peptide on ceramic granules enhance posterolateral spinal fusion in rabbits compared with autograft. *Spine* 33:1324–1329
88. Arinze TL et al (2005) A comparative study of biphasic calcium phosphate ceramics for human mesenchymal stem-cell-induced bone formation. *Biomaterials* 26:3631–3638
89. Yuan H et al (2001) Bone formation induced by calcium phosphate ceramics in soft tissue of dogs: a comparative study between porous  $\alpha$ -TCP and  $\beta$ -TCP. *J Mater Sci Mater Med* 12:7–13
90. Yuan H et al (2002) A comparison of the osteoinductive potential of two calcium phosphate ceramics implanted intramuscularly in goats. *J Mater Sci Mater Med* 13:1271–1275
91. Miramond T et al (2013) Osteopromotion of biphasic calcium phosphate granules in critical size defects after osteonecrosis induced by focal heating insults. *IRBM* 34:337–341
92. Fan M et al (2011) Emu model of full-range femoral head osteonecrosis induced focally by an alternating freezing and heating insult. *J Int Med Res* 39:187–198

93. Kim HK, Morgan-Bagley S, Kostenuik P (2006) RANKL inhibition: a novel strategy to decrease femoral head deformity after ischemic osteonecrosis. *J Bone Miner Res* 21:1946–1954
94. Yamamoto T et al (1995) Corticosteroid enhances the experimental induction of osteonecrosis in rabbits with Shwartzman reaction. *Clin Orthop Relat Res* 316:235–243
95. Jegoux F et al (2009) Reconstruction of irradiated bone segmental defects with a biomaterial associating MBCP<sup>®</sup>, microstructured collagen membrane and total bone marrow grafting: an experimental study in rabbits. *J Biomed Mater Res A* 91:1160–1169
96. Nakamura T (1996) Bioceramics in orthopaedic surgery. *Bioceramics* 9:31
97. LeGeros RZ (2008) Calcium phosphate-based osteoinductive materials. *Chem Rev* 108:4742–4753
98. Rodríguez C et al (2008) Five years clinical follow up bone regeneration with CaP bioceramics. *Key Eng Mater* 361:1339–1342

Sandra Pina, Joaquim Miguel Oliveira, and Rui L. Reis

## Contents

Introduction .....	504
Biomimetic Strategies for Bone Tissue Engineering .....	505
Scaffolds .....	505
Hydrogels .....	507
Fibers .....	509
Composites .....	510
Dynamic Systems .....	512
Current Processing Methodology in Biomimetic Engineering .....	513
Sponge Replica Method .....	513
Solvent Casting and Particulate-Leaching .....	513
Freeze-Drying .....	514
Gas Foaming .....	514
Phase Separation .....	515
Rapid Prototyping .....	515
Electrospinning .....	516
Summary .....	516
References .....	516

---

## Abstract

In the last few years, many reports have been describing promising biocompatible and biodegradable materials that can mimic in a certain extent the multidimensional hierarchical structure of the bone and can release bioactive agents or drugs in a controlled manner. Despite these great advances, new

---

S. Pina (✉) • J.M. Oliveira • R.L. Reis

3B's Research Group – Biomaterials, Biodegradables and Biomimetics, University of Minho, Headquarters of the European Institute of Excellence on Tissue Engineering and Regenerative Medicine, Taipas/Guimarães, Portugal

ICVS/3B's – PT Government Associate Laboratory, Braga/Guimarães, Portugal

e-mail: [sandra.pina@dep.uminho.pt](mailto:sandra.pina@dep.uminho.pt); [miguel.oliveira@dep.uminho.pt](mailto:miguel.oliveira@dep.uminho.pt); [rgreis@dep.uminho.pt](mailto:rgreis@dep.uminho.pt)

developments in the design and fabrication technologies are required to address the need to engineer suitable biomimetic materials to tune cell functions, i.e., enhance cell–biomaterial interactions and promote cell adhesion, proliferation, and differentiation abilities. Scaffolds, hydrogels, fibers, and composite materials are the most commonly used as biomimetics for bone tissue engineering. Dynamic systems such as bioreactors have also been attracting great deal of attention as it allows developing a wide range of novel *in vitro* strategies for the homogeneous coating of scaffolds and prosthesis with ceramics and production of biomimetic constructs, prior to its implantation in the body. Herein, the biomimetic strategies for bone tissue engineering, recent developments, and future trends are overviewed. Conventional and more recent processing methodologies are also described.

---

**Keywords**

Biomimetics • Bone tissue engineering • Porous scaffolds • Hydrogels • Fibers • Composites • Bioreactors • Dynamic systems • Sponge replica method • Solvent casting and particulate-leaching • Freeze-drying • Gas foaming • Phase separation • Rapid prototyping • Electrospinning

---

**Introduction**

Nowadays, the development of new biomaterials for bone tissue engineering has made important contribution to modern health care. Each biomaterial has specific chemical, physical, mechanical, and biological properties, important for the behavior and outcome of the implant.

Autografts and allografts have been used to repair bone fractures and other defects; however, concerns include risk of disease transfer, infection, potential immunogenicity, and insufficient supply [1].

Biomimetic materials have been attracting considerable attention, owing to their ability to mimic the structural, mechanical, and biological properties of natural tissues. The major difficulty in tissue engineering arises from the specificity of the tissue that it is proposed to treat, compliance of patients, and other related restrictions. A deeply progress has been made in designing and processing of new materials in order to properly address cell activity. This is an important issue to be considered as regeneration processes involve achieving the desired cell functioning, i.e., stimulate specific cellular responses and activate genes that stimulate cell differentiation and extracellular matrix (ECM) production for enhancing the regeneration of the damaged tissues. In the case of the bone, it is required three-dimensional constructs hierarchically structured that can comprise several levels of organization, i.e., from the macroscopic tissue arrangement down to the molecular arrangement of proteins [2]. These hierarchical structures also provide improved mechanical performance and allow a suitable transduction of the mechanical stimuli to the cellular level [3].



Different materials have been exploited for scaffolds fabrication, attending diverse need in bone tissue engineering, such as natural-based and synthetic polymers, inorganic/ceramic materials, and composites. Polymers have great design flexibility and mechanical strength. Polymers from natural origin offer the advantage of being similar to the extracellular matrix and do not cause chronic inflammation or immunological reactions and toxicity [4]. Ceramics such as hydroxyapatite ( $\text{Ca}_5(\text{PO}_4)_3\text{OH}$ , HA) and  $\beta$ -tricalcium phosphate ( $\text{Ca}_3(\text{PO}_4)_2$ ,  $\beta$ -TCP) are the most used in the clinics due to their good osteoconductivity, biocompatibility, and bioresorbability [5]. However, ceramic materials have low elasticity and high brittleness, resulting in poor mechanical strength, which can be solved by combining them with polymers as composite materials [6].

In the next sections, currently reported biomimetic strategies for bone tissue engineering are presented. A special focus is given on new developments for designing and processing of biomimetic materials.

---

## Biomimetic Strategies for Bone Tissue Engineering

Among the biomimetic materials that have been developed to engineer bone tissue scaffolds, hydrogels, fibers, and composites with controlled geometry and structures are the ones selected for discussion due to their important role in tissue engineering scaffolding. Each type of material offers its own advantages and disadvantages in mimicking the organization of native tissue structure. Considerations of scaffolds design include the shape of the original tissue, mechanical properties, ability to direct cell–matrix and cell–cell interactions, and porous structures for efficient mass transport. Materials used to engineer these tissues are of great importance because they also must be biocompatible and degrade at a rate matching that of the new tissue formation.

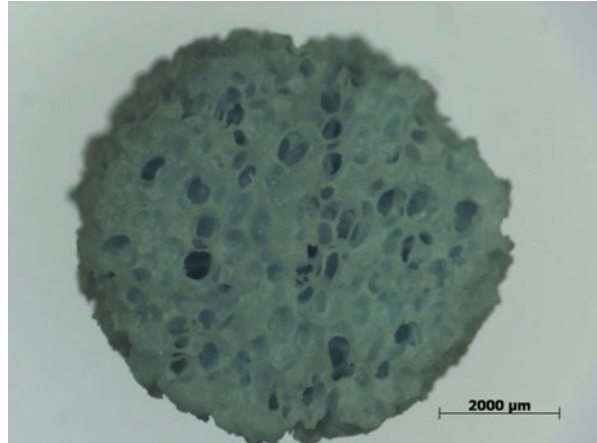
---

### Scaffolds

Scaffolds are defined as three-dimensional (3D) porous solid biomaterials designed to fulfill basic requirements, namely, (i) to promote cell–biomaterial interactions, cell adhesion, growth and migration, and ECM deposition; (ii) to permit sufficient transport of gases, nutrients, and regulatory factors to allow cell survival, proliferation, and differentiation; (iii) to degrade at a controllable rate that approximates the rate of tissue regeneration under the culture conditions of interest; (iv) to elicit a minimal degree of inflammation or toxicity *in vivo*; and (v) to possess adequate mechanical properties necessary to temporarily offer structural support until the formation of new tissue occurs [7].

Scaffolds targeted for bone tissue repair and regeneration can be produced from natural and synthetic polymers and bioactive ceramics and their combinations, with specific pore size, porosity, surface area-to-volume ratio, and crystallinity. Technologies applied for scaffolds fabrication include sponge replica method, solvent

**Fig. 1** Macroscopic appearance of the HA scaffolds after sintering at 1300 °C



casting and particulate-leaching, freeze-drying, phase separation, gas foaming, and rapid prototyping (RP).

Several studies have been reported concerning scaffolds design, characterization, and biological evaluation [6–9]. For example, Columbus et al. [10] have investigated the feasibility of varying the pore size of poly  $\epsilon$ -caprolactone (PCL) scaffolds by altering the molecular weight of the porogen and studied the effect of degradation on morphological characteristics and mechanical properties of scaffolds by correlating to the extent of degradation. The authors observed that degradation resulted in scaffolds with narrower pore size distribution that have better retention of morphological and mechanical characteristics as compared to scaffolds with broader distribution.

Our group has been developing porous structures for bone tissue engineering using diverse materials and techniques. Oliveira et al. [8] developed hydroxyapatite (HA) single scaffolds with a porosity of ~70 % and macropore diameter in the range of 50–600  $\mu\text{m}$  with high pore uniformity and interconnectivity across the scaffolds by means of sponge replica method (Fig. 1).

Oliveira et al. [11] developed semirigid 3D tubular porous structures consisting of starch/PCL, filled by a gellan gum hydrogel concentric core aimed at inducing the regeneration within spinal cord injury sites obtained through RP technology. It was demonstrated that bone-like apatite layers could be produced on the surface and interior of the constructs, and the mineralization process was controlled by the surface, which acted as a template for the nucleation and growing of the apatite layer. Lima et al. [12] developed a bottom-up approach that allows the construction of 3D biodegradable scaffolds from PCL and starch microfabricated membranes, by means of micro hot embossing. In addition, it was shown that the human bone marrow mesenchymal stem cells (hBMSCs) proliferated and maintained the expression of the stromal progenitor marker STRO-1 when cultured on both PCL and SPCL microfabricated membranes.

An important consideration for biomimetic materials engineering is their biocompatibility capacity. *In vitro* bioactivity and biocompatibility assays include mineralization tests in simulated body fluid (SBF) and the use of adequate cell cultures to induce cell adhesion, growth, proliferation, and differentiation [13, 14], respectively. For example, adipose derived stem cells (ASCs) with multi-lineage differentiation capacities have been demonstrated as an alternative cell candidate for bone regeneration [15]. It was reported that biomimetic constructions of undifferentiated rabbit ASCs with fully interconnected porous  $\beta$ -TCP scaffolds encapsulated by collagen hydrogel enhanced osteogenesis in a critical-sized defect of rabbit radii [14].

Scaffolds have also been developed with particular interest for bone and osteochondral tissue engineering applications, where both underlying bone and cartilage tissues are damaged. Therefore, a strategy for these applications is the construction of bilayered scaffolds consisting of both osteogenic and chondrogenic regions, which can be manufactured in a single integrated implant or fabricated independently and joined together with sutures or sealants. Thus, bilayered scaffolds are able to promote simultaneous regeneration of two tissues, bone and cartilage with different properties and biological requirements [9, 16]. For example, Oliveira et al. [16] fabricated a HA/chitosan bilayered scaffold by combining a sintering and a freeze-drying technique, aiming the regeneration of osteochondral defects. The bone region of the scaffold was composed of porous sintered HA and produced through sponge replica method. The cartilage region was composed of chitosan poured onto the top of the HA scaffold, previously prepared, followed by freeze-drying technique. In that work, it was demonstrated through *in vitro* cell studies that both HA and chitosan layers provided an adequate support for cell attachment, proliferation, and differentiation into osteoblasts and chondrocytes, respectively.

---

## Hydrogels

Hydrogels are water-swollen networks formed from hydrophilic polymer cross-linked to form insoluble polymer matrices, which are soft and elastic due to their thermodynamic compatibility with water [17]. Hydrogels can be classified into physical and chemical hydrogels according to their cross-linking mechanism [17, 18]. Physical cross-links keep the hydrogel from dissolving in water due to the entangled chains, hydrogen bonding, hydrophobic interaction, and crystallite formation. Chemical cross-links are permanent junctions formed by covalent bonds [19]. Hydrogels can also be classified by their ionic charge (neutral, cationic, anionic, and ampholytic), structure (amorphous, semicrystalline, and hydrogen bond), and preparation methods (homopolymer, copolymer, multipolymer, and interpenetrating polymer network) [17]. Hydrogel materials hold structural and compositional similarities with the ECM, making them attractive scaffolds owing to their swollen network structure, biocompatibility, efficient mass transfer, and ability to encapsulate cells and biomolecules. These properties are influenced by the nature of the polymer chains, the degree of cross-linking, the molecular arrangement, and the amount of water they absorb [20]. An innovative alternative to the

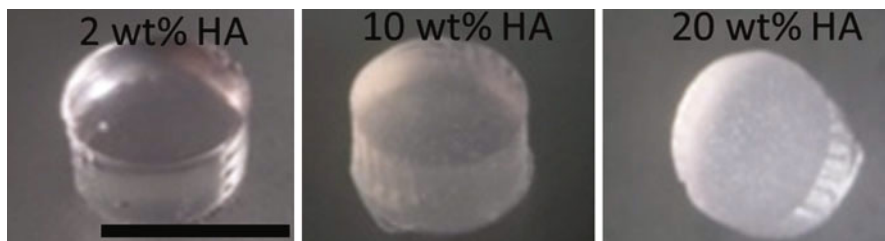


**Fig. 2** Macroscopic appearance of the methacrylated gellan gum hydrogels with different HA content, after ionic cross-linking (scale bar = 5 mm)

classical techniques to characterize cross-linked hydrogels has been reported. High-resolution magic angle spinning (HR-MAS) NMR spectroscopy enables to both characterize and quantify any unreacted cross-linkable moieties present in a chemically cross-linked, swollen hydrogel network [21]. Most hydrogels are injectable, allowing homogeneous seeding of cells throughout the scaffolds and formation of hydrogels in situ [22, 23].

There are three major classes of hydrogels, based on the polymer origin: natural, synthetic, or natural/synthetic hybrids. Natural hydrogels are derived from nature and have been used due to their biocompatibility, inherent biodegradability, and critical biological functions. Nevertheless, the use of natural hydrogels is often restricted because of purification, immunogenicity, pathogen transmission, and poor mechanical properties. On the other hand, synthetic hydrogels possess more reproducible chemical and physical properties, and it can be molecularly tailored with mechanical strength and biodegradability. Moreover, hydrogel porosity may be controlled by solvent casting/particulate-leaching, phase separation, gas foaming, solvent evaporation, freeze-drying, and blending with non-cross-linkable linear polymers. Excellent reviews regarding a depth description of natural and synthetic hydrogels are referred [24, 25].

Synthetic polymer-derived hydrogels are not always able to provide an alternative to natural-based polymers. Thus, hydrogels can be assembled through copolymerization or combined with additional synthetic or natural polymers to create semisynthetic materials with desired physical properties, reproducibility, and biological activity. To date, natural polymers, such as collagen, fibrinogen, hyaluronic acid, chitosan, and heparin, have been used to make hybrid hydrogels with synthetic polymers, such as polyethylene glycol (PEG), poly *N*-isopropylacrylamide, and polyvinyl alcohol (PVA) [26, 27]. The hybridization can occur at a molecular level depending on the size and nature of building blocks.

Our group is a pioneer in processing hydrogels based on a polysaccharide gellan gum, obtained from *Sphingomonas elodea*, for tissue engineering applications [28–30]. Methacrylated gellan gum hydrogels were produced through chemical modification by means of methacrylation of low-acyl gellan gum. Gellan gum-based hydrogels (Fig. 2) can be tunable to enhance the mechanical properties, allow controlling endothelial cells infiltration and blood vessel in growths, and can

be formed in situ in few minutes [29]. Recently, gellan gum-based hydrogels have also been proposed for bone and osteochondral applications by means of blending with hydroxyapatite particles [31, 32]. The composite showed superior mechanical properties as compared to the polymeric hydrogel, while the optimization of the HA content in the composite possibly tuning its bioactivity.

Hydrogels have been used as scaffolds to provide bulk and mechanical constitution to an engineered tissue, for cellular organization and morphogenic guidance. As aforementioned, it is desirable to synthesize scaffolds to mimic the structure and functions of ECM. Numerous bioactive peptide sequences derived from ECM proteins such as fibronectin, laminin, and collagen have been incorporated into synthetic hydrogels. In addition, cellular attachment, proliferation, and growth in hydrogels can be promoted with the inclusion of arginine–glycine–aspartic acid (RGD) peptide sequence [33]. This cellular adhesion and proliferation is assured by controlling the rate of biodegradation of the hydrogel scaffolds, which is achieved by clearing the implanted hydrogel based on a predetermined rate of hydrolytic breakdown of ester bonds in the polymer network.

Cells encapsulated in hydrogels during the cross-linking process have been produced and characterized for drug delivery and tissue engineering applications [34].

---

## Fibers

Fibrous scaffolds are a good option to mimic the fibrous structure present in native ECM, owing their high porosities, isotropic structures, and homogeneous fiber size and pore distribution. Porosity is interesting for various applications, namely, for the entrapment of bioactive molecules. The mechanical properties of fibrous scaffolds are dependent on their composition, fiber diameter, and orientation [35]. Fiber diameter can be reduced with synthetic polymers blended with proteins. Furthermore, nanoscale fibrous scaffolds with well-controlled patterned structures have received particular interest to enhance cell functions as cell adhesion, migration, proliferation, and differentiation. Nonwoven fibrous matrices with micro-sized fibers possess isotropic structure with a high porosity and mechanical strength and good chemical stability [36].

Fibrous scaffolds design comprises natural and synthetic polymers. Natural polymers recently used for bone tissue engineering include collagen, gelatin, silk fibroin, elastin, fibrinogen, hyaluronan, and chitosan due their high biological recognition [4]. For example, PCL is successfully processed with gelatin for obtaining a nanofiber network with random fiber distribution and good biocompatibility with mesenchymal stem cells in terms of adhesion and proliferation. Blends of starch-polycaprolactone (SPCL) have also been used to produce scaffolds by fiber meshing [37]. Interestingly, Oliveira et al. [38] showed that SPCL scaffolds (Fig. 3) supported BMSC osteogenic differentiation in vitro and de novo bone formation in vivo.

Fabrication techniques as molecular self-assembly, phase separation, and electrospinning have been used for fibrous scaffolds production. Molecular

**Fig. 3** Microscopic appearance of the SPCL scaffolds



self-assembly is able to produce highly ordered nanofibers, but it is limited to molecules for self-assembly. Phase separation method can only produce randomly distributed fibers in the submicron range. Electrospinning can generate fibers, from nano- to micro-size, with controllable pore size, fiber size and stiffness, and matrix turnover. Electrospun fiber scaffolds for bone tissue engineering have been recently reported [39]. Diverse cell types have been applied for electrospun fiber in vitro studies as neural stem cells, chondrocytes, cardiomyocytes, osteoblast-like cells, and mesenchymal stem cells.

The incorporation of bioactive agents to electrospun fibers can lead to enhanced biomimetic scaffolds. It has been demonstrated that cell–substrate interaction is strongly affected by the presence of chemical cues, able to support cell adhesion, proliferation, and differentiation [40].

The combination of electrospun fibers and hydrogels scaffolds can create synergistically superior structures to therapeutic use within the tissue engineering community.

---

## Composites

Composite materials appeared as a strategy to mimic the human bone, which is a 3D composite material, composed of organic, inorganic, and cellular phases, strictly assembled to form the natural tissue. Composites are considered as a combination of two or more materials, with different compositions and properties, resulting in a single structure with significantly improved mechanical and biological properties. Therefore, composites involving a polymeric matrix and bioactive inorganic fillers

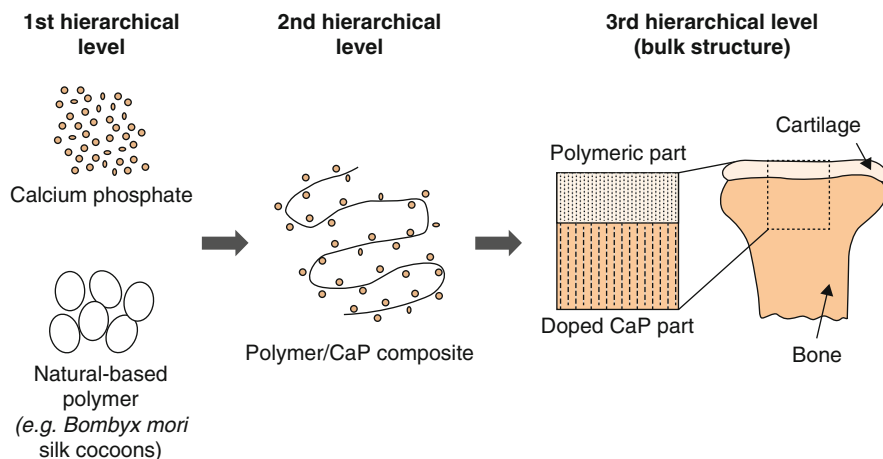


**Fig. 4** Schematic diagram of a hierarchical nanocomposite scaffold fabricated from polymer and calcium phosphates

(Fig. 2) have been developed as promising approach for bone tissue engineering applications.

Composites are most frequently manufactured from (i) natural origin, like polysaccharides (cellulose, chitin, glycosaminoglycans) and proteins (collagen, silk, fibrinogen, elastin), owing their similarities with the extracellular matrix, chemical versatility, and good biological performance; (ii) synthetic biodegradable polymers as polylactic acid (PLA), polyglycolic acid (PGA), its copolymer poly(lactic-co-glycolic acid) (PLGA), and PCL; and (iii) bioactive ceramic materials, such as HA,  $\beta$ -TCP, calcium silicate, and phosphate-based glasses, due to its biocompatibility, osteoconductivity, and degradation rate. There is a range of possible combinations capable of producing composites with enhanced properties. For example, the incorporation of HA in silk sponge matrices was shown to enhance the osteoconductivity and mechanical properties of the scaffolds [41]. Wang et al. [42] created biomimetic matrices using genetically engineered elastin-like polypeptides to construct mechanically robust elastin/HA composites.

Regarding the production of composite scaffolds, first of all, it is essential to achieve good compatibility between the phases while keeping a hierarchical and porous structure and the mechanical properties of the scaffolds (Fig. 4).

Our group synthesized calcium phosphates in silk fibroin by using an in situ synthesis method, where phosphate ions are added into the calcium chloride solution with dissolved silk fibroin, followed by salt-leaching/freeze-drying techniques to obtain the scaffolds [9]. Kim et al. [43] prepared aqueous-derived silk fibroin scaffolds with the addition of polyaspartic acid, followed by the controlled deposition of calcium phosphate by exposure to chloride and sodium phosphate monobasic solutions. In another study, HA microparticles were embedded in silk sponges to generate highly osteogenic composite scaffolds capable of inducing the formation of tissue-engineered bone [41].

In addition, the use of powder fillers from nano- to macro-size ranges with hierarchical structures has attracted special attention since it can easily mimic the structural and mechanical properties of natural tissues. The nanopowders often act as physical cross-links to the polymer chains, reinforcing the mechanical properties of the nanocomposites. Yan et al. [9] prepared a composite scaffold made from silk fibroin and nano-sized calcium phosphates, with size less than 200 nm and uniformly distributed in the scaffolds. Zhou et al. [44] fabricated electrospun fibrous bio-nanocomposite scaffolds reinforced with cellulose nanocrystals by using maleic anhydride grafted PLA as matrix, with improved thermal stability and mechanical properties.

A biocomposite of nano-sized calcium silicate and PCL was fabricated using nano-calcium sulfate slurry in a solvent-casting method [45]. It was shown that the hydrophilicity, compressive strength, and elastic modulus of n-CS/PCL composites were improved, as well as the *in vitro* bioactivity. The apatite layers that formed on the composite surfaces facilitated cell attachment and proliferation. Similar results were obtained by Kotela et al. [46].

Electrospun nanocomposite scaffolds containing a polymer matrix and nano-sized HA supported cell attachment, proliferation, and differentiation and are thus considered very promising tissue engineering.

---

## Dynamic Systems

For over two decades, *in vitro* mineralization assays have been used as a biomimetic route to evaluate the bioactivity and biocompatibility of biomaterials. The common *in vitro* studies are performed by immersing the materials in SBF at static conditions as proposed by Kokubo et al. [47]. However, the *in vitro* culture techniques have nutrient and mass transfer limitations that must be overcome to increase the feasibility of cell-based tissue engineering strategies. Thus, an *in vitro* biomimetic approach including dynamic studies using bioreactor systems has been used to relieve these limitations by continuously mixing media and by convectively transporting nutrients to cells, with appropriate mechanical stresses. A bioreactor is a culture system designed to support or expand a population of cells through dynamic culture and a controlled environment. Besides, when considering 3D porous architectures, dynamic mineralization environments can also be suitable to promote a homogeneous formation of an apatite layer inside the structure.

Several bioreactor systems for bone tissue engineering, such as spinner flasks, rotating wall vessels, and perfusion systems have been developed. Spinner flask and rotating wall systems create a homogenous media on the exterior of the scaffold, while on perfusion systems, the media is perfused through the pores of the scaffold, which enables local supply of nutrients, providing a better control of the cell microenvironment.

Some authors have studied the mineralization of apatite layers under dynamic conditions using bioreactor systems. Oliveira et al. [48] showed that bone-like apatite layers have been formed on the surface and inside of starch-polycaprolactone



scaffolds. Also, this process was accelerated under flow perfusion conditions when compared with static and agitated conditions.

Perfusion bioreactor systems have been also reported to improve human MSC proliferation and osteogenesis for bone tissue engineering. For example, hBMSCs cultured on nanofibrous electrospun poly(lactic-co-glycolic acid)/PCL scaffolds to implant into rat femoral condyle defects showed a more rapid bone regeneration in defects implanted with bioreactor-cultured scaffolds in comparison to defects implanted with statically cultured scaffolds [49].

---

## Current Processing Methodology in Biomimetic Engineering

A wide range of conventional techniques have commonly been used for bone scaffolding applications such as sponge replica method, solvent casting, particulate-leaching, freeze-drying, gas foaming, and phase separation. Rapid prototyping and electrospinning as more sophisticated techniques are also used for 3D structures and fibers, respectively. The conventional methods are often simple to design and inexpensive and flexible to optimize or modulate physicochemical properties. Despite being expensive and suffering from certain drawbacks of choice of materials and capital costs, rapid prototyping and electrospinning techniques are extremely attractive in their ability to mimic new tissue structures and possibility of incorporating pharmaceutical agents. A brief description of each technique is provided as follows.

---

### Sponge Replica Method

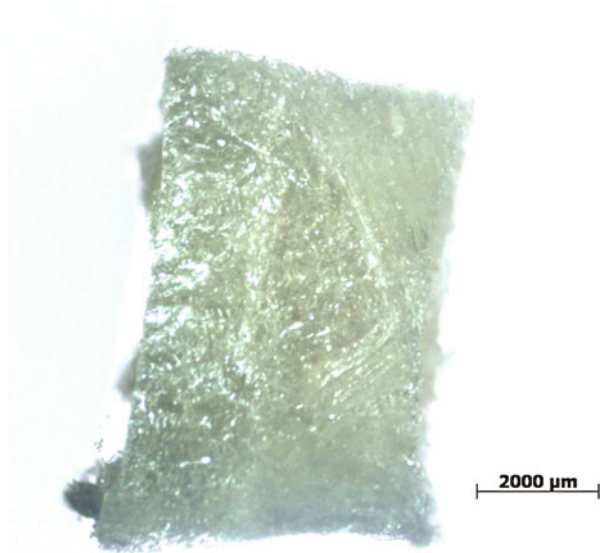
Sponge replica method is based in the impregnation of an aqueous suspension in porous synthetic polymeric (usually polyurethane) sponges until the total filling of the pores. The impregnated sponge is then passed through rollers or a centrifuge in order to remove the excess suspension and left to dry. After, the sponges are heated at temperatures between 400 °C and 900 °C for the diffusion of the polymeric template and a porous structure is obtained. Finally, the scaffolds are densified by sintering at high temperatures. This method can reach total open-porosity levels within the range of 40–95 % and is characterized by a reticulated structure of highly interconnected pores with sizes between 200 μm and 3 mm.

---

### Solvent Casting and Particulate-Leaching

Solvent casting and particulate-leaching is a technique widely used to successfully fabricate 3D porous scaffolds. This is a process based on the dispersion of a salt (e.g., sodium chloride, ammonium bicarbonate, and glucose) in a polymer dissolved in an organic solvent. The solvent is evaporated, resulting in the solidification of the polymer. Then, the salt crystals are leached away using water to form the pores of

**Fig. 5** Microscopic appearance of the chitosan freeze-dried scaffolds



the scaffold. The pore size can be controlled by the size of the salt crystals and the porosity by the salt/polymer ratio. This leaching process has been applied to the development of porous scaffolds for the growth of endothelial cells. However, certain critical variables such as pore shape and interconnectivity of the pores are not controlled with this method.

---

## Freeze-Drying

Freeze-drying is based on dissolution of a polymer into a solvent with addition of water, followed by quick freezing at different temperatures and rates. A porous polymeric structure is obtained after freeze-drying to remove the dispersed water and the solvent. The porosity level of the foams is controlled by varying the freezing time and the annealing stage. The main difficulty associated with this process is to ensure structural stability and adequate mechanical properties of the porous constructs after hydration. This limitation hinders its use when the application involves conditions with mechanical stress. Moreover, pore size is relatively small and porosity is often irregular.

Our group has used this method to develop porous single-layered (Fig. 5) and bilayered scaffolds [8, 9].

---

## Gas Foaming

Gas foaming technique utilizes high-pressure CO<sub>2</sub> gas dispersed throughout a polymer mixed with a porogen (e.g., sodium chloride) until saturation. The solubility of CO<sub>2</sub> is decreased rapidly until atmospheric level, resulting in nucleation and

growth of gas bubbles. After completion of foaming process, the porogen is removed and a highly interconnected pore structure is created. The porosity of the scaffolds depends on the amount of gas dissolved in the polymer. This technique does not require the use of organic solvents and high temperature as for the most fabrication techniques.

Porous polymeric foams prepared using gas foaming technique have emerged in recent years with application as scaffolds for bone tissue engineering. Results indicate that the micro-architecture of the pore structure of the scaffolds plays a crucial role in defining cell seeding efficiency, proliferation, and osteogenic differentiation.

---

## Phase Separation

Phase separation technique is based on the separation into more than one phase in order to lower the system free energy. Briefly, a polymer solution separates into two phases, a polymer-rich phase and a polymer-lean phase, and when the solvent is removed, the polymer-rich phase solidifies. This technique has been used to fabricate porous membranes for filtration and separation but has the disadvantage of forming pores with diameters on the order of a few to tens of microns and not uniformly distributed. However, controlled phase separation, as thermally induced phase separation, has been used for scaffolds fabrication. This process is based on the decrease in solubility associated with temperature increase. After demixing is induced, the solvent is removed by extraction, evaporation, or freeze-drying. For example, Mandoli et al. [50] prepared highly porous scaffolds made of poly L-lactide (PLLA) by thermally induced phase separation starting from 1,4-dioxane/PLLA solutions for applications in vascular nets and angiogenesis.

---

## Rapid Prototyping

Rapid prototyping (RP), also known as solid freeform fabrication or additive manufacturing, is an advanced technique used to design complex-shaped objects directly from computer data such as computer-aided design (CAD), computed tomography (CT), and magnetic resonance imaging (MRI) data. The fabrication process involves a 3D design of the scaffold, which is directly fabricated layer by layer. As a result, RP technique is considered the best alternative for achieving precise control of pore size, geometry, and interconnectivity, which enables cells to penetrate into the scaffold.

Robocasting is also an RP based process in which a colloidal suspension is extruded through a micron-sized nozzle in a defined trajectory to form a 3D structure. This technique has been used to fabricate porous  $\beta$ -TCP scaffolds with a controlled architecture, with enhanced compressive strength and toughness.

---

## Electrospinning

Electrospinning has received considerable interest for use in tissue engineering aimed at producing polymeric nanofiber non-woven membrane scaffolds to the order of nanometers with large surface areas and superior mechanical properties. This process is controlled by a high electric field applied between two electrodes, one being placed in the polymer solution and the other placed in the collector. During the electrospinning process, a polymer solution is held at a needle tip by surface tension. This electrostatic force opposes the surface tension, causing the initiation of a jet, producing the fibers. As this jet travels, the solvent evaporates and the nanofibers are deposited in the collector. The characteristics of the nanofibers depend on various properties of the solution and on the processing parameters. Electrospinning provides a simpler and more cost-effective means to produce scaffolds with an interconnected pore structure and fiber diameters in the submicron range when compared to other techniques like phase separation.

---

## Summary

Biomimetic strategies for bone tissue engineering are growing exponentially over time toward the development of novel materials capable of mimicking the structural, mechanical, and biological properties of native bone tissue. An ideal biomimetic material must also be biocompatible and degrade at a rate matching the ECM deposition rate. In addition, demanding for three-dimensional porous constructs hierarchically structured across a range of length scales arises from their unique structure-properties relationship. The use of dynamic systems, particularly perfusion bioreactors, to coat scaffolds with apatite layer is a key component for bone tissue engineering due to their ability of mass transfer and nutrients diffusion throughout the scaffolds.

Future developments of biomimetic materials for bone tissue engineering should be focused on the selection of materials, design, and fabrication of composite scaffolds hierarchically nanostructured, with appropriate mechanical properties and that can stimulate cell–biomaterial interactions and promote cell adhesion, proliferation, and differentiation.

---

## References

1. Finkemeier CG (2002) Bone-grafting and bone-graft substitutes. *J Bone Joint Surg-Am* 84:454–464
2. Aizenberg J, Weaver J, Thanawala MS, Sundar VC, Morse DE, Fratzl P (2005) Skeleton of *Euplectella* sp.: structural hierarchy from the nanoscale to the macroscale. *Science* 309:275–278
3. Sprio S, Ruffini A, Valentini F, D'Alessandro T, Sandri M, Panseri S, Tampieri A (2011) Biomimesis and biomorphic transformations: new concepts applied to bone regeneration. *J Biotechnol* 156(4):347–355

4. Mano JF, Silva GA, Azevedo HS, Malafaya PB, Sousa RA, Silva SS, Boesel LF, Oliveira JM, Santos TC, Marques AP, Neves NM, Reis RL (2007) Natural origin biodegradable systems in tissue engineering and regenerative medicine: present status and some moving trends. *J R Soc Interface* 4:999–1030
5. Bohner M (2000) Calcium orthophosphates in medicine: from ceramics to calcium phosphate cements. *Inj Int J Care Inj* 31:37–47
6. Oliveira JM, Costa SA, Leonor IB, Malafaya PB, Mano JF, Reis RL (2009) Novel hydroxyapatite/carboxymethylchitosan composite scaffolds prepared through an innovative “autocatalytic” electroless coprecipitation route. *J Biomed Mater Res A* 88(2):470–480
7. Langer R, Tirrell D (2004) Designing materials for biology and medicine. *Nature* 428:487–492
8. Oliveira J, Silva S, Malafaya P, Rodrigues M, Kotobuki N, Hirose M, Gomes M, Mano J, Ohgushi H, Reis R (2009) Macroporous hydroxyapatite scaffolds for bone tissue engineering applications: physicochemical characterization and assessment of rat bone marrow stromal cell viability. *J Biomed Mater Res A* 91:175–186
9. Yan L-P, Correia J, Correia C, Caridade S, Fernandes E, Sousa R, Mano JF, Oliveira J, Oliveira A, Reis RL (2013) Bioactive macro/micro porous silk fibroin/nano-sized calcium phosphate scaffolds with potential for bone-tissue-engineering applications. *Nanomedicine* 8:359–378
10. Columbus S, Krishnan L, Kalliyana K (2013) Relating pore size variation of poly ( $\epsilon$ -caprolactone) scaffolds to molecular weight of porogen and evaluation of scaffold properties after degradation. *J Biomed Mater Res B Appl Biomater* 102(4):789–796. doi:10.1002/jbm.b.33060
11. Oliveira A, Sousa E, Silva N, Sousa N, Salgado A, Reis R (2012) Peripheral mineralization of a 3D biodegradable tubular construct as a way to enhance guidance stabilization in spinal cord injury regeneration. *J Mater Sci Mater Med* 23:2821–2830
12. Lima M, Pirraco R, Sousa R, Neves N, Marques A, Bhattacharya M, Correlo V, Reis R (2013) Bottom-up approach to construct microfabricated multi-layer scaffolds for bone tissue engineering. *Biomed Microdevices* 16(1):69–78
13. Rumian L, Wojak I, Schamweber D, Pamula E (2013) Resorbable scaffolds modified with collagen type I or hydroxyapatite: in vitro studies on human mesenchymal stem cells. *Acta Bioeng Biomech* 15:61–67
14. Yang P, Huang X, Wang C, Dang X, Wang K (2013) Repair of bone defects using a new biomimetic construction fabricated by adipose-derived stem cells, collagen I, and porous beta-tricalcium phosphate scaffolds. *Exp Biol Med* 238(12):1331–1343. doi:10.1177/1535370213505827
15. Zreiqat H (2014) Mimicking bone microenvironment for directing adipose tissue-derived mesenchymal stem cells into osteogenic differentiation. *Methods Mol Biol* 1202:161–171
16. Oliveira JM, Rodrigues M, Silva SS, Malafaya PB, Gomes ME, Viegas CA, Dias IR, Azevedo JT, Mano JF, Reis RL (2006) Novel hydroxyapatite/chitosan bilayered scaffold for osteochondral tissue-engineering applications: scaffold design and its performance when seeded with goat bone marrow stromal cells. *Biomaterials* 27:6123–6137
17. Slaughter B, Khurshid S, Fisher O, Khademhosseini A, Peppas N (2009) Hydrogels in regenerative medicine. *Adv Mater* 21:3307–3329
18. Chung H, Park T (2009) Self-assembled and nanostructured hydrogels for drug delivery and tissue engineering. *Nano Today* 4:429–437
19. Liu S, Tay R, Khan M, Ee P, Hedrick J, Yang Y (2010) Synthetic hydrogels for controlled stem cell differentiation. *Soft Matter* 6:67–81
20. Hoffman A (2002) Hydrogels for biomedical applications. *Adv Drug Deliv Rev* 43:3–12
21. Van Vlierbergh S, Fritzing B, Martins J, Dubrue P (2010) Hydrogel network formation revisited: high-resolution magic angle spinning nuclear magnetic resonance as a powerful tool for measuring absolute hydrogel cross-link efficiencies. *Appl Spectrosc* 64:1176–1180
22. Tan H, Marra K (2010) Injectable, biodegradable hydrogels for tissue engineering applications. *Materials* 3:1746–1767

23. Kretlow J, Klouda L, Mikos A (2007) Injectable matrices and scaffolds for drug delivery in tissue engineering. *Adv Drug Deliv Rev* 59:263–273
24. Oliveira JT, Reis RL (2011) Polysaccharide-based materials for cartilage tissue engineering applications. *J Tissue Eng Regen Med* 5:421–436
25. Van Vlierberghe S, Dubrue P, Schacht E (2011) Biopolymer-based hydrogels as scaffolds for tissue engineering applications: a review. *Biomacromolecules* 12:1387–1408
26. Hiemstra C, van der Aa L, Zhong Z, Kijkstra P, Jan F (2007) Rapidly in situ-forming degradable hydrogels form dextran thiols through Michael addition. *Biomacromolecules* 8:1548–1556
27. Wang C, Stewart R, Kopecek J (1999) Hybrid hydrogels assembled from synthetic polymers and coiled-coil protein domains. *Nature* 397:417–420
28. Oliveira J, Martins L, Picciochi R, Malafaya P, Sousa R, Neves N, Mano J, Reis R (2010) Gellan gum: a new biomaterial for cartilage tissue engineering applications. *J Biomed Mater Res A* 93:852
29. Silva-Correia J, Oliveira J, Caridade S, Oliveira J, Sousa R, Mano J, Reis R (2011) Gellan gum-based hydrogels for intervertebral disc tissue-engineering applications. *J Tissue Eng Regen Med* 5:e97–e107
30. Silva-Correia J, Zavan B, Vindigni V, Silva T, Oliveira J, Abatangelo G, Reis R (2013) Biocompatibility evaluation of ionic- and photo-crosslinked methacrylated gellan gum hydrogels: in vitro and in vivo study. *Adv Healthcare Mater* 2:568–575
31. Manda-Guiba G, Oliveira M, Mano J, Marques A, Oliveira J, Correló V, Reis R (2012) Gellan gum – hydroxyapatite composite hydrogels for bone tissue engineering. *J Tissue Eng Reg Med* 6(2):15
32. Pereira D, Canadas R, Silva-Correia J, Marques A, Reis R, Oliveira J (2014) Gellan gum-based hydrogel bilayered scaffolds for osteochondral tissue engineering. *Key Eng Mater* 587:255–260
33. Shin H, Jo S, Mikos A (2003) Biomimetic materials for tissue engineering. *Biomaterials* 24:4353–4364
34. Rada T, Carvalho P, Santos T, Castro A, Reis R, Gomes M (2013) Chondrogenic potential of two hASCs subpopulations loaded onto gellan gum hydrogel evaluated in a nude mice model. *Curr Stem Cell Res Ther* 8:357–364
35. Vatankeh E, Semnani D, Prabhakaran MP, Tadayon M, Razavi S, Ramakrishna S (2014) Artificial neural network for modeling the elastic modulus of electrospun polycaprolactone/gelatin scaffolds. *Acta Biomater* 10:709–721. doi:10.1016/j.actbio.2013.09.015
36. Ng R, Zang R, Yang K, Liu N, Yang S (2012) Three-dimensional fibrous scaffolds with microstructures and nanotextures for tissue engineering. *RSC Adv* 2:10110–10124
37. Gomes M, Azevedo H, Moreira A, Ella V, Kellomaki M, Reis R (2008) Starch-poly(epsilon-caprolactone) and starch-poly(lactic acid) fibre-mesh scaffolds for bone tissue engineering applications: structure, mechanical properties and degradation behaviour. *J Tissue Eng Regen Med* 2(5):243–252
38. Oliveira J, Sousa R, Malafaya P, Silva S, Hirose M, Ohgushi H, Mano J, Reis R (2011) In vivo study of dendron-like nanoparticles for stem cells tune-up: from nano to tissues. *Nanomed Nanotechnol Biol Med* 7:914–924
39. Cheng Q, B. L-P L, Komvopoulos K, Li S (2013) Engineering the microstructure of electrospun fibrous scaffolds by microtopography. *Biomacromolecules* 14:1349–1360
40. Stankus J, Freytes D, Badylak S, Wagner W (2008) Hybrid nanofibrous scaffolds from electrospinning of a synthetic biodegradable elastomer and urinary bladder matrix. *J Biomater Sci Polym Ed* 19:635–652
41. Bhumiratana S, Grayson W, Castaneda A, Rockwood D, Gil E, Kaplan D, Vunjak-Novakovic G (2011) Nucleation and growth of mineralized bone matrix on silk-hydroxyapatite composite scaffolds. *Biomaterials* 32:2812–2820
42. Wang E, Lee SH, Lee SW (2011) Elastin-like polypeptide based hydroxyapatite bionanocomposites. *Biomacromolecules* 12(3):672–680
43. Kim HJ, Kim U-J, Kim HS, Li C, Wada M, Leisk GG, Kaplan DL (2008) Bone tissue engineering with premineralized silk scaffolds. *Bone* 42(6):1226–1234

44. Zhou C, Shi Q, Guo W, Terrell L, Qureshi AT, Hayes DJ, Wu Q (2013) Electrospun bio-nanocomposite scaffolds for bone tissue engineering by cellulose nanocrystals reinforcing maleic anhydride grafted PLA. *ACS Appl Mater Interfaces* 5(9):3847–3854
45. Wei J, Heo SJ, Liu C, Kim DH, Kim SE, Hyun YT, Shin JW, Shin JW (2009) Preparation and characterization of bioactive calcium silicate and poly(epsilon-caprolactone) nanocomposite for bone tissue regeneration. *J Biomed Mater Res A* 90(3):702–712
46. Kotela I, Podporska J, Soltysiak E, Konsztowicz J, Blazewicz M (2009) Polymer nanocomposites for bone tissue substitutes. *Ceram Int* 35:2475–2480
47. Kokubo T, Takadama H (2006) How useful is SBF in predicting in vivo bone bioactivity? *Biomaterials* 27:2907–2915
48. Oliveira A, Costa S, Sousa R, Reis R (2009) Nucleation and growth of biomimetic apatite layers on 3D plotted biodegradable polymeric scaffolds: Effect of static and dynamic coating conditions. *Acta Biomater* 5:1626–1638
49. Yeatts AB, Both SK, Yang W, Alghamdi HS, Yang F, Fisher JP, Jansen JA (2013) In vivo bone regeneration using tubular perfusion system bioreactor cultured nanofibrous scaffolds. *Tissue Eng Part A* 20(1–2):139–146. doi:10.1089/ten.TEA.2013.0168
50. Mandoli C, Mecheri B, Forte G, Pagliari F, Pagliari S, Carotenuto F, Fiaccavento R, Rinaldi A, Di Nardo P, Licoccia S, Traversa E (2010) Thick soft tissue reconstruction on highly perfusive biodegradable scaffolds. *Macromol Biosci* 10:127–138

Andy H. Choi, Sophie Cazalbou, and Besim Ben-Nissan

## Contents

Introduction .....	522
Biomimetics .....	524
Artificial Devices .....	524
Marine Materials and Synthetic Tissue Biology .....	527
Hard Tissue Scaffold Development .....	527
Marine Skeletons .....	528
Marine Sponges .....	528
Marine Shells .....	530
Sea Urchin .....	532
Marine Skeleton and Organic Matrices in Regenerative Medicine .....	534
Coral Skeletons in Tissue Engineering .....	535
Marine Structures in Drug Delivery Applications .....	536
Foraminifera .....	537
Marine Structures in the Regulation of Stem Cells .....	539
Concluding Remarks .....	541
References .....	542

---

## Abstract

During the last two decades, biomimetics has provided mankind new directions for the utilization of natural organic and inorganic skeletons for novel drug delivery systems and new medical treatment approaches with unique designs ranging from the macro- to the nanoscale. The use of ready-made organic and

---

A.H. Choi (✉) • B. Ben-Nissan  
School of Chemistry and Forensic Science, Faculty of Science, University of Technology Sydney,  
Ultimo, NSW, Australia  
e-mail: [ahchoi@hotmail.com](mailto:ahchoi@hotmail.com); [besim.ben-nissan@uts.edu.au](mailto:besim.ben-nissan@uts.edu.au)

S. Cazalbou  
CIRIMAT Carnot Institute, CNRS-INPT-UPS, Faculty of Pharmacie, University of Toulouse,  
Toulouse, France



inorganic marine skeletons has potentially created an opportunity of presenting one of the simplest cures to fundamental issues hampering the future development of regenerative medicine, dentistry, and orthopedics such as providing a richness of framework designs and devices and abundant and available sources of osteopromotive analogues and biomineralization proteins. Organic matrix and inorganic marine skeletons possess a habitat ideal for the proliferation of added mesenchymal stem cell populations and promoting clinically acceptable bone formation. It has been proven that self-sustaining musculoskeletal tissues can be supported by coral and marine sponge skeletons, and bone mineralization can be promoted by the extracts of spongin collagen and nacre seashell organic matrices. This idea is reinforced by the fact that bone morphogenetic protein molecules are produced by endodermal cells into the developing skeleton. Furthermore, the regenerative signaling proteins in bone therapeutics such as TGF and Wnt are also present in early marine sponge development and instrumental to the activation of stem cells in cnidarians. This chapter aims to give a brief background into the nature, morphology, and application of some of these structures in bone grafts, drug delivery, tissue engineering, and specific extracts such as proteins for regenerative medicine.

---

**Keywords**

Hydroxyapatite (HAp) • Calcium phosphate • Marine sponge • Marine shell • Foraminifera • Coral • Tissue scaffold • Urchin

---

## Introduction

Marine organisms are created and organized by materials containing a wide variety of characteristic and properties which might warrant their possible use within the biomedical arena. In addition, the pledge to exploit natural marine resources in a sustainable manner generates a highly interesting stage for the development of novel biomaterials together with both environmental and economic benefits. As a result, a growing number of compounds of different types are being isolated from aquatic organisms and converted into products for health applications including tissue engineering and controlled drug delivery devices.

The fabrication of highly capable scaffolds that can function at the macro-, micro-, and nanoscopic level will play a pivotal role in making regenerative medicine a clinical success in the future. These scaffolds will be able to arrange and organize cells into tissues and in a targeted manner releasing encapsulated chemical signals and conveying them into the body.

Abundant sources of materials and structures are currently available that can be utilized to perform different function than their original proposed one. A simple strategy is to use a predesigned and preformed structure such as unique marine structures and modify it in a specific manner to suit its new intended purpose [1]. Moreover, we can learn from nature and attempt to duplicate the essential

components and reinvent in a laboratory. Additionally, we strive to learn more from nature the principle of minimizing energy usage during the synthesis process, the importance of structural organization, and the execution of transformative self-assembly and nonequilibrium chemistry.

These materials as well as its designs have played an instrumental role in the introduction of one of the easiest resolutions to crucial problems in regenerative medicine and in providing frameworks and highly accessible avenues of osteopromotive analogues, nanofibers, micro- and microspheres, and mineralizing proteins. This is demonstrated by the biological efficiency of marine structures such as shells, corals, and sponge skeletons to accommodate self-sustaining musculoskeletal tissues and to promote bone formation through the use of nacre seashells and sponging extracts.

It has been discovered that molecules essential for regulating and guiding bone morphogenesis and in particular the actions accompanying mineral metabolism and deposition also exist in the earliest marine organisms. This is based on the fact that they symbolize the first molecular components recognized for calcification, morphogenesis, and wound healing. It has emerged that bone morphogenetic protein (BMP), the main cluster of bone growth factors for human bone morphogenesis, are secreted by endodermal cells into the developing skeleton. Furthermore, off-the-shelf organic and inorganic marine skeletons possess an ideal environment for the proliferation of added mesenchymal stem cell populations and promoting bone formation that is clinically acceptable.

The marine environment is distinctively rich in highly functional architectural structures with interconnected open pores. The chemical compositions and high mechanical strength of these structures make them ideal to be used for human implantation either in its original form or convert to materials more suitable for biomedical applications.

Areas such as new pharmaceutical drug delivery systems with enhanced properties and a more efficient design, hard and soft tissue engineering, and the discovery of a new generation of organic molecules have been the major emphases in the field of marine-based structures during the last two decades. More and more investigations on proteins and biopolymers produced by marine organisms have been carried out to examine its applications in the biomedical arena. At the moment, a growing number of compounds and materials are being identified from marine organisms such as calcium carbonates and proteins and applied to medical applications [2].

In tissue engineering applications, converted coralline apatites and coral skeletons are perfect examples [3]. They have demonstrated substantial clinical success as templates for tissue reconstruction. This has encouraged researchers to explore other skeletons with improved mechanical and/or biological properties. These unique three-dimensional marine structures are able to support the growth as well as an enhancement in differentiation of stem cell progenitors into bone cells. This is different to standard carbonate frameworks which do not induce stem cell differentiation.

## Biomimetics

In nature, biomaterials possess desirable properties such as complexity and sophistication, and we are gradually discovering ways to imitate nature to create similar levels of sophistication even though it is to a limited extent. Current 3-D printing methods are good examples; however, we are only able to recreate microscopic structures with some level of biomimetic detail. For the replication of bioinorganic structures, this has been particularly true. The utilization of biological microstructures as templates for the recreation of inorganic structures with identical features has emerged as a versatile approach. Through this technique, ordered silica microstructures have been produced using bacterial filaments and nanotubes produced from tobacco mosaic virus [4].

The main purpose in biomimetics is to synthetically duplicate the structures of selected inorganic biomatrices [4], and they play a clear part in the production of replacements for calcified tissues. This can be accomplished using techniques in biomineral-inspired materials chemistry. The idea is to make skeletons from molecules into macroscopic structures by utilizing the consecutive developmental pathway of systems that nature employs. The space of construction is defined by the foundations which are laid. Constant delivery of all the necessary building materials is provided and maintained throughout construction. In nature, the process begins with supramolecular pre-organization, interfacial recognition, and vectorial regulation leading to multi-level processing [1]. The continual multiplication of these assemblies accumulates into the emergence of morphology and macroscale biomimetic forms. In the fabrication of the simplest skeletons, researchers have realized the great benefits of using emulsion droplets to create porous hollow shells, foams, and bead templates in conjunction with using bio-continuous microemulsions to produce microskeletal networks [5].

Investigators have also examined another approach that uses the controlled mineralization of adapted organic matrices from natural skeletons [4] and has generated clinically relevant end results. These bio-imitation approaches and strategies are being examined with cellular and extracellular matrix inputs such as mineralizations of reverse microemulsions [6] and bi-liquid foams and bio-continuous microemulsions [7, 8] and template-mediated biomineralization of organic biomatrices [9]. Biomimetic microspheres synthesized within self-organizing microemulsions were routinely employed as highly functional constructs for the localized delivery of growth factors and genes to primary human cells. These unique particles were also capable of producing osteoid and neocartilage [10].

---

## Artificial Devices

A hundred years ago, artificial devices were produced from all sorts of materials such as gold and wood, and the development of these devices has reached a point where they could be used to replace different components of the human body. These

materials are capable of being in contact with bodily fluids and tissues for prolonged periods of time while demonstrating little or if any adverse reactions.

During the last two decades, acknowledging the importance of tissue-implant interactions on the nanoscale has led to the extensive development and application of nanotechnology in science and engineering. This is also based on the consideration that functional nanostructured materials are capable of being modified and incorporated into a range of biomedical devices. In addition, most biological systems such as viruses, protein complex, and membrane exhibit natural nanostructures. The synthesis method and the processing routes will govern the microstructure and properties of these new-generation nanostructured materials. Therefore, it is vital that the most appropriate technique is selected for the fabrication of materials with preferred design and property combinations.

Techniques such as solid-state, liquid-state, and gaseous ionic-state processing methods are frequently used for the synthesis of inorganic materials such as advanced ceramics. Additionally, wet chemical processing techniques such as sol-gel and coprecipitation have also been employed to obtain nanocoatings, nanoparticles, and nanostructured solid shapes and blocks. In modern ceramic technology, pressing is achieved by placing the powder into a die and compacting it through the exertion of pressure. For the production of bioceramics, the most commonly used methods are hot pressing and hot isostatic pressing. Compared to hot pressing, higher-density and smaller grain structure, essential for obtaining good mechanical properties, can be achieved through the use of hot isostatic pressure, whereby heat and pressure are applied simultaneously with the pressure being applied from all directions via a pressurized gas such as argon or helium. It is relatively easy to produce flat plates or blocks and nonuniform components using hot pressing or hot isostatic pressing.

Sol-gel processing is unique in that it can be utilized to synthesize various forms of the same composition such as coatings, fibers, powders, platelets, and monoliths simply by changing factors such as chemistry and viscosity of a given solution [11]. The sol-gel technique possesses a number of advantages, for instance, it is of the nanoscale and it results in a stoichiometric, homogeneous, and pure product as mixing takes place on the molecular scale. It also has the ability to produce uniform fine-grained structures and can be easily applied to complex shapes with a range of coating techniques.

Appropriate surface finish is required for most biomaterials intended to be utilized within the physiological environment to permit the attachment of soft or hard tissue without any adverse reaction. Furthermore, biomaterials with a similar chemical composition to bone are needed for hard tissue attachment. For the majority of the animals, the microstructure of bone is composed of interconnected pores micro- and nanoscopic in size. The hard tissues contain calcium and phosphate ions and their combined form as calcium phosphate compounds with a variety of minerals. With our currently available production techniques, it is of great difficulty or in some cases almost impossible to copy and produce synthetically these complicated designs as a consequence of the limitations in resolution. However, in the near future, this could be achieved through the use of the new-generation three-dimensional printing techniques.

Nature, on the other hand, has provided a solution to obtaining these intricately fine porous structures. As a product to their natural need, some marine structures contain excellent interconnected pores and architectures that can meet and answer the problems discussed previously. These marine structures have very fine interconnected pores from nanometer to a few hundred microns in range as well as excellent mechanical properties. More importantly, most of them are composed of or contain inorganic materials such as calcium phosphates and calcium carbonate with a range of minerals containing magnesium, strontium, and silicon which assist in improving the properties of hard tissues after implantation. Although small, the organic matter within the marine skeletons contains a variety of materials, for example, proteins with very promising possible medical applications [12, 13].

Mankind is facing the creation of new biomimetic material synthesis systems using living cells, and producing tailor-made biomaterials to our specifications and requirements accurately in a beaker or test tube can be considered to be one of the most fascinating bio-inspired approaches ever known [12]. This can be accomplished by careful adjustment in the growing environment. The convenient starting points are single and multicelled organisms such as Foraminifera, Diatoms, and coccolithophores as they are the most basic and elementary organisms to grow and support in artificial culture and provide enough utility for providing this approach as practically beneficial [2].

Of great interest for the advancement of new strategies in nanotechnology and molecular assembly are diatoms as they offer modes of construction at these scales that can potentially benefit the research and development of new-generation drug delivery devices as a result of their microscopic size and internal pore network structure [13]. Discovered throughout marine and freshwater environments, diatoms are photosynthetic secondary endosymbionts and are believed to be responsible for approximately one-fifth of the primary productivity on the planet. It was recently reported the genome sequence of the marine centric diatom *Thalassiosira pseudonana*, revealing a wealth of information about diatom biology.

Diatoms have also been labeled as “natural-born” lithographers [14] and inspired the fabrication of nanostructured templates for nano-imprint processes where large structural areas with nanometer precision are required. Sussman et al. [14] exploited the mechanisms of patterning by diatoms for applications in patterning microchips, while Belegreatis et al. [15] investigated the technical capabilities of the precise 3-D laser lithography based on two-photon polymerization of organic materials. This approach enabled the fabrication of arbitrary artificial diatom-inspired micro- and nanostructures and the design of an inverse structure. Therefore, only one replication step is required to obtain a template for nano-imprint processes.

There is also a vision to grow materials with living cells integrated during synthesis and construction in the field of biomimetic photonic materials. This represents an attractive proposition, and through this approach, the directed evolution may be conceivable with specific organisms that reproduce rapidly so that many thousands of generations are produced in short experimental time frames. At the moment, protocols are well established for the mass production of new proteins using site random mutagenesis combined with high-throughput screening [16].

## Marine Materials and Synthetic Tissue Biology

One of the most fundamental and effective way of resolving scientific and technological problems is the conversion of products from nature into technology. Natural history collections provide a unique and abundant source of practical ideas and answers aimed at the early stages of tissue reassembly in artificial culture. Gaining an understanding into the chemistry and evolution of tissues and organs as well as their design and function will create a new path in providing elements that can be utilized in the reconstruction of tissues in the most simple and practical manner feasible. Fossilized marine organisms can also be utilized as excellent templates for providing new materials. Despite the fact that nature cannot create the perfect designs, it can, however, produce the most optimized, ideal, and functional adaptive ones [1].

A relatively newly emerging discipline, synthetic tissue biology aims to engineer tissues and transform them into complex biological assemblies [17]. An approach being investigated is the reverse engineering of biological materials, tissues, organs, or systems and to interpret how they are constructed and how they function at the highest level of detail. It can be suggested that it can revolutionize the concept and approach for reengineering biological systems.

The formation of multicellular tissues via synthetic biology utilizes the most advanced techniques available to construct extracellular environments to direct morphogenesis of tissues and cells. From a different perspective, cells are designed and produced with innovative functions and combined into multicellular organizations. In the vast diversity of nature, there are numerous recognized blueprints into the production and arrangement of cells and tissues into organs. Through natural selection, the evolution of tissues has provided mankind with an insight into how different development strategies have been exploited by organisms according to function. For that reason, we should be able to develop simplified assembly strategies to recreate functional approximations of every human tissue.

## Hard Tissue Scaffold Development

Until now, naturally occurring biomatrices with wide-ranging chemical homologies and structural analogies to human extracellular matrices and whole tissues have been identified as a candidate in our quest of scaffolding materials. Examples of such biomatrices include marine shell and sponge skeletons, coral skeletons, and echinoderm skeletal elements. Certain species of these marine animals has been applied to the regeneration of human bone and cartilage as a result of their usefulness. On the other hand, the full effectiveness in these tissues and other marine animal and structure tissues has yet to be exploited and harnessed.

There are limitations when it comes to the regeneration potential of human bone especially in the case of repairing large bone defects. In general, autogenous and allogeneic bones are used as bone grafts. In spite of this, only a limited amount of autogenous bones can be used within the body, and there is a possibility of donor site morbidity. There is also the likelihood of transmission of infection from allografts if

they are based on demineralized bone. Consequently, synthetic bone-graft materials such as calcium phosphate ceramics, composites, and polymers have been widely developed [18].

The main inorganic mineral constituent close to human bone is hydroxyapatite (HAp), which is also an outstanding synthetic bone substitute because of its osteoconductive properties. HAp ceramics can be produced synthetically from its constituents using a variety of production techniques. In addition, demineralizing bovine or human hard tissues and natural marine structures such as corals and seashells and sea urchin to name just a few have also been used in the manufacture of HAp [1]. HAp powders are usually prepared using a range of methods such as hydrothermal conversion, wet chemical synthesis, calcination of bone, and solid-state reaction.

Synthetic bone-graft substitutes can be classified as inert, bioactive, and resorbable substitutes based on observed tissue response. For bone defect filling applications, resorbable bone-graft substitutes are preferred as they can be replaced after implantation by new natural bone. As a result of their fast dissolution characteristics,  $\beta$ -tri-calcium phosphate ( $\beta$ -TCP) and biphasic calcium phosphate mixture (with HAp) is one of the most commonly used bone substitute materials. It has also been suggested that the presence of magnesium stabilizes the  $\beta$ -TCP structure [19] and increases the transition temperature from  $\beta$ -TCP to  $\alpha$ -TCP and decreases the solubility of  $\beta$ -TCP [20].

## Marine Skeletons

The primary source of natural skeletons for bone tissue engineering has been natural and calcium phosphate-converted coral because of its morphology and crystallographic, chemical, and structural compatibility to native human bone [3]. As a result of the hydrothermal processing, natural skeletons can be used in a direct manner as a scaffold for growing cells into tissue and ultimately in the formation of new bone tissue [21]. Since then, invertebrate marine skeletons of hydrozoans and cuttlefish [22], marine sponges [6], nacre seashell, echinoderm spines [23], and others have been utilized. The basic reasoning to use these structures as clinical bone-graft materials is based on their macro and micro structures with appropriate ranges of pore sizes, its structural interconnected networks, which allow easy pathways for organizing and sustaining bone tissue growth. Whole natural skeletons have been used as templates for transporting biomolecules, and diatom skeletons have been tried with an antibody to be utilized in immunodiagnostics [24].

## Marine Sponges

Marine sponges share much in common with multicellular tissues. Similarities, from a biochemical and morphological perspective, exist between marine sponge and vertebrate extracellular matrix suggesting that the fundamental rules of organization

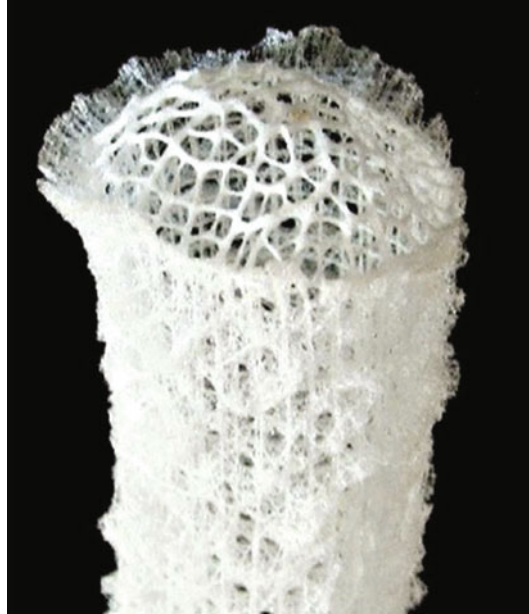
evolved initially by marine sponges. To date, three types of collagen have been identified from marine sponge. All sponges are comprised of collagen fibrils 22 nm thin with highly ordered periodic banding. These collagen fibrils are secreted in bundles in a similar fashion to vertebrates. The amino acid sequence and genome organization are similar even though the ultrastructure of collagen is relatively simple compared to vertebrate collagens. Correspondingly, collagen fibrils are closely associated with proteoglycans which, in mammalian tissue design, shape and form at long-range scale. Dermatopin, fibronectin, and tenascin polypeptides are also discovered in marine sponge collagen fibers and cross-react with antibodies raised against vertebrate analogies underlining their common origins. A number of sponge species possess an analogue of type IV collagen found in vertebrate basement membrane collagens [25]. The organization of collagen fibrils is analogous to collagen type XIII which sticks cells to surfaces [26]. It is with these properties (cell adherent collagens and fibronectin) that collagenous marine sponge represents a significant potential for future development as bioactive tissue engineering scaffolds.

Marine sponges are at the moment extensively exploited for novel biological compounds as potential treatments for leukemia, cancer tumors, and inflammation. They are also a source of collagen for cosmetics [27] and dermatological preparations [28]. Half of all marine-derived materials in total are sources from a wide spectrum of marine sponges. Collagenous marine sponge skeletons are extremely strong, soft, elastic, highly absorbent, and resistant to bacterial attack and high temperatures. They are very suitable for use in surgical procedures as a result of these properties. Investigations are being carried out by several researchers to examine feasibility and the exact conditions needed to commercially grow marine sponges on a large production scale. Some have established aquatic pilot forms for the cultivation of selected bath sponge species. An additional aim for cultivating marine sponges is the extraction of medically important secondary metabolites in much greater quantity than is possible compared to collections made by conventional bioprospecting.

It has been suggested that useful lessons in the construction of man-made frameworks with minimal starting materials for maximum strength have been provided by the superior optimized structural design of marine sponges [29, 30]. Consolidated silica spheres on the nanometer scale are arranged in well-defined microscopic concentric rings held together by organic matrix to form laminated spicules. Influenced by the laminated silica-based cement, the assembly of these spicules into bundles results in the formation of a macroscopic cylindrical lattice-like structure reinforced by diagonal ridges (Fig. 1). Hence, there is considerable mechanical benefit to specific arrangements of structural elements at many different hierarchies of scale.

The 3-D topology and specific surface features of hydrozoans have been suggested to initiate faster cell adhesion, proliferation, and differentiation [31]. Further work is needed to determine the exact mechanism of action between cell and material. The potential of a clinically relevant scaffold for a range of tissues such as the bone, cartilage, fat connective, liver, and kidney is accomplished by collagenous marine sponges. The fiber-bonded meshwork of sponges provides channels for cell



**Fig. 1** Glass sponge

guidance along with spaces for rapid tissue infiltration and infilling. The collagenous composition of the fibers has been found to promote attachment of all types of human cells. The unique layered ultrastructure may explain the high wettability and adsorption of growth factors onto the collagen fibers which infuse into attached cells and promote their activities. It has been shown that the formation of tissue *in vivo* within 4 weeks to be both extensive (completely filling the entire sponge implant) and well developed with the quality and structure of tissue being equivalent to immature bone and neocartilage [32].

## Marine Shells

The outer nacreous layer of a certain species of mollusk shell is an unlikely and unexpected source of biomaterial for engineering new bone. Mollusk shells (Fig. 2) are an interesting model for understanding the complexities of biomineralization such as controlling and regulating protein-mineral interactions. *Pinctada maxima*, nacre from the pearl oyster, are different from any other biomaterial that is able to stimulate osteogenesis and bone formation from latent osteoprogenitors along an endochondral pathway, consisting of a cartilage tissue intermediary phase [33].

Testing of nacre has been carried out on human, rabbit, and sheep models [34, 35]. In human patients, fresh woven bone bonded itself all the way through the nacre implant, augmented by the heightened activities of osteoblasts and osteoclasts. Its degradation and resorption are limited even though nacre is stably tolerated *in vivo*, and this could impede its use within calcified tissue requiring

**Fig. 2** Mollusk shell  
(*Nautilus pompilius*)



rapid self-renewal [34, 35]. While in some way controversial in definition, according to nacre researchers the “water-soluble matrix fraction” (WSM) of nacre directly induces bone formation [36]. Molecules from nacre matrix have been shown to reduce bone resorption by acting on osteoclast metabolism [37]. Evidence available suggests that mobile signal transmitters, involved in the biological control of mineralization (as an initiator and inhibitor of calcium carbonate crystallization at the mineralizing growing front), dissolve into solution-induced differentiation of surrounding latent osteoprogenitor cells [38]. The reason behind exactly how nacre encourages human cells to form new bone can be best explained by the idea that a “signaling” biomolecule is involved in the regulation of cell-mediated biomineralization which is common to both vertebrate bone tissue and nacre. Thus, these biomolecules must have been conserved by the burdens of evolutionary selection.

The supposed osteopromotive effect of nacre as determined by ALP expression is also proportionate with dexamethasone treatment, at least in fibroblasts. Size-exclusion HPLC of the water-soluble matrix has exposed protein fractions rich in alanine and glycine, with specific biochemical effects on human fibroblasts that modulate cell differentiation and proliferation [39]. In the nacre matrix, peptides are prevalent. Specific individual fractions have been revealed to give rise to certain responses from cultured osteoblast cells. The secretion of ALP is increased by protein fractions with low molecular weight (less than 1 kDa), while on the other hand protein fractions with high molecular weight leads to a reduction in ALP secretion. Detailed sequencing of water-soluble proteins using proteomics offers improved characterization of nacre matrix proteins. It has also been discovered that nacre WSM increases the secretion of cytoplasmic Bcl-2, a key inhibitor of apoptosis, as well as having an influence on rat calvarial osteoblast maintenance and survival. Low molecular weight fractions were recently found to increase expression of collagen type I and the osteogenic-associated mRNA expression of osteopontin and Runx-2 [40].

A further 110 molecules in the 100–70 Da range comprising of glycine-enriched peptides with structural similarities and high affinities for each other were discovered after detailed characterization of the bioactive low molecular weight molecules.

A highly defined matrix protein with a 10 kDa size called p10 has specifically demonstrated an increase in human fibroblast cell ALP expression [41] providing greater expectation that the osteogenic signal molecules can be isolated in their vital functional form. A soluble p60 protein conglomerate extracted from decalcified nacre possesses sufficient bioactivity on 3T3 and MSc to induce the secretion of mineral nodules. Some of the specific biomolecular mechanisms and associations between the signal molecules and cellular processes are being uncovered gradually [1].

Uncertainty arose among biomineralization researchers regarding the fact that nacre proteins are the primary cause of osteoinduction. A study revealed nacre failed to stimulate an *in vivo* osteogenic response even though bone-to-nacre apposition and bonding did occur directly [42]. The authors suggested that nacre provided a favorable surface chemistry to the recruitment of osteoclasts and osteoblasts. Surface-modified nacre was found not to be osteoinductive within demineralized bone matrix in an *in vivo* ectopic bone environment; however, its integration and fusion with bone were better than non-nacre controls. In another study, the relationship between interfacial properties and the biocompatibility of nacre and specifically its unique bone-bonding ability was investigated by Kim et al. [43]. They concluded that the organic matrix is the reason behind the excellent bonding that occurs between nacre and bone and is due to the creation of a favorable surface charge for optimal biological associations. The organic matrix of nacre is believed to create a new interfacial microenvironment when implanted that forms many functional associations with the surrounding tissue resulting in a better bone bonding than bioceramic implants without an organic matrix.

The osteogenic responses to nacre particles and pearl preceded much faster following soaking in a simulated body fluid (SBF) that generates a HAp-rich layer on the particles according to a study by Shen et al. [44]. The WSM was implicated in the formation of this HAp layer and the augmented cell responses [36, 40]. Combining all the facts, it can be concluded that nacre provides an appropriate tissue-compatible physical platform that shows unique peptides which initiate and drive bone formation.

Furthermore, due to its organic content and platelike design, nacre is mechanically tough with a fracture toughness equivalent to that of titanium, rapidly biodegradable, and non-immunogenic, without eliciting detrimental physiological effects. These characteristics of nacre offer us a unique substrate for the delivery of a functional and even possibly an osteopromotive agent to sites of bone loss in quantities that lead to rapid bone repair and regeneration.

## Sea Urchin

The skeleton of sea urchin spines consisted of large single crystals of magnesium-rich calcite which have smooth, continuously curved surfaces and form a three-dimensional fenestrated mineral network. Through hydrothermal reaction, spines of the echinoids *Heterocentrotus trigonarius* and *Heterocentrotus mammillatus* can be

converted to bioresorbable magnesium-substituted tricalcium phosphate ( $\beta$ -TCMP) at 180 °C. Conversion to  $\beta$ -TCMP occurs preferentially to hydroxyapatite formation due to the presence of magnesium in the calcite lattice. The three-dimensional interconnected porous morphology of the original spine is nonetheless maintained by the converted  $\beta$ -TCMP. It is believed that the primary conversion mechanism is the ion-exchange reaction, even though a dissolution-reprecipitation process taking place that creates some calcium phosphate precipitates on the surfaces of the spine network [1]. Using a rat model, the *in vivo* studies demonstrated new bone growth up to and around the  $\beta$ -TCMP implants after installation in femoral defects for 6 weeks. Some new bone was found to migrate through the spine structural pores indicating good bioactivity and osteoconductivity of the porous  $\beta$ -TCMP implants [1].

The skeletal plates of sea urchin are perforated by a very regular series of pores. Approximately three quarters of the pores are exits for tube feet (200  $\mu\text{m}$  pore diameters at the spine bases to 600  $\mu\text{m}$  pore diameters for the tube feet in *Centrostephanus nitidus*), and one quarter are channels connected to the alimentary and reproductive systems and to a great extent larger for the accommodation of more fluids (1000–2000  $\mu\text{m}$  per diameter). Echinoderm skeletons are made from a three-dimensional single crystalline meshwork that is both intricately shaped and unique with a topological structure in which every internal pore and channel is in direct contact with all others (periodic minimal surface). Mass transfer and tissue development are likely to be facilitated by this property [13]. Studies revealed that the replication of perforate echinoderm structural elements using the replamine form approach for hard tissue replacements to bone as well as candidate prostheses for the blood vessels and trachea is encouraging. In this context, the skeletal ossicles from the sea star (*Pisaster giganteus*) have been examined, and the results suggested they provide an ideal architecture along with chemical and physical properties beneficial to bone restoration [23].

Similar to bones and teeth, the sea urchin spicule is a composite of organic and inorganic materials that the animal produces using the most readily available elements in seawater. The fully formed spicule consisted of a single crystal with an unusual morphology in three dimensions (Fig. 3). It has no facets and forms a starlike shape. To achieve such unusual morphologies, sea urchin and other marine organisms initially deposit a disordered amorphous mineral phase and then allow it to transform slowly into a crystal aligned neatly into a lattice with a specific and regular orientation and at the same time maintaining their morphology. A unique transformation occurs from disordered amorphous to ordered crystalline structures. This amorphous-to-crystalline phase transformation from the liquid state can teach us to produce highly ordered and well-oriented synthetic nanomaterials and composites.

The sea urchin spicule is created inside a clump of specialized cells and begins as the animal sets down a single crystal of calcite, from which the rest of the spicule is generated. Three arms extend at 120° from each other starting from the crystalline center. The three radii are initially 40–100-nm-size amorphous calcium carbonate then gradually transform to well-organized and oriented calcite. The mechanism is

**Fig. 3** Sea urchin with spicules



unclear but may possibly be through dissolution and ordered precipitation mechanisms at known crystallographic orientations of aragonite or calcite.

---

### **Marine Skeleton and Organic Matrices in Regenerative Medicine**

It has previously been suggested that coral and marine sponge skeletons can support self-sustaining musculoskeletal tissues and that extracts of sponging collagen and nacre seashell organic matrices encourage bone mineralization. The use of ready-made organic and inorganic marine skeletons is one of the simplest possible answers to major problems hampering the future development of regenerative orthopedics such as providing a richness of framework designs and a potentially rich and accessible source of osteopromotive analogues and biomineralization proteins. This fact should not come as a surprise given that the crucial biomineralization proteins that orchestrate bone morphogenesis are also discovered in the earliest calcifying marine organisms. To further reinforce this concept, it has emerged that BMP molecules, the main cluster of bone growth factors for human bone morphogenesis, are secreted by endodermal cells into the developing skeleton. In addition, the regenerative signaling proteins are also present in early marine sponge development and instrumental to the activation of stem cells in cnidarians. Based on this partnership between the main developmental proteins of vertebrates and invertebrates, we have published the extent and nature of this evolutionary connection and used it to support the development of a new strategy which is to source certain marine-based organic matrices for novel metabolic signaling and structural proteins/peptides and protein analogues for applications in regenerative orthopedics, especially when using adult stem cells [13, 45]. Moreover, early-stage evidence based on our own findings revealed the presence of fibrinogen fragments and early osteopromotive effects of a coral organic matrix extract on stem cells [13].

In reality, the discovery of new osteopromotive and osteo-accelerant protein analogues will require the use of traditional chromatography techniques and osteoactivity assays to pinpoint potential protein of significance, while advanced proteomic tools will provide accurate sequencing and determine the mechanisms and molecular pathways involved in osteoactivation as well as the efficiency and effectiveness of marine skeleton-derived protein modulation of the stem cell proteome. Skeletal organic matrices may have ever-increasing function for regenerative orthopedics as more analogues are discovered using proteomic tools [13, 45].

## **Coral Skeletons in Tissue Engineering**

Natural coral exoskeletons have been extensively used in dental, craniofacial, neurosurgery, and orthopedic as a bone replacement due to their combination of good mechanical properties, open porosity, and its ability to form chemical bonds with bone and soft tissues *in vivo* [3]. Corals in general have the best mechanical properties of all the porous calcium-based ceramics. The organic composition has an important part to play in the excellent mechanical properties and biocompatibility of coral. The abundance, conformation, and composition of the organic matrices are responsible for the successful biological integration of coral with human host [3, 46].

The start of the coral life cycle begins with the polyps which absorb the carbonic acid and calcium ion available in the seawater to generate calcium carbonate in the form of aragonite crystals. The remaining composition composed of trace elements of magnesium, strontium, fluorine, and phosphorous in the phosphate form [47]. These elements play a critical role in the bone mineralization process once implanted in the human body as well as in the activation of key enzymes associated with bone remodeling cells. Strontium has been revealed to play a role in the mineralization process by stimulating osteoblasts while inhibiting osteoclasts [48]. In a similar fashion, bone formation is facilitated by fluorine through similar stimulatory effect on osteoblast proliferation. It is also a well-known fact that magnesium is also beneficial in bone remodeling by improving the mechanical properties of newly formed bone [49].

The use of coral skeletons for general routine orthopedic surgery and tissue engineering has until now been restricted to external fixation devices and unsuitable for strictly load-bearing applications due to their calcium carbonate structure with high dissolution rates. However, sol-gel coating technologies can be utilized to improve the strength of corals, and this will allow them to be used more frequently at different skeletal locations [11].

Either in their natural or hybridized synthetic forms, corals offer great opportunities to tissue engineering of the bone. When combined with *in vitro* expanded human bone marrow stromal cells (HBMSC), coral skeleton increased osteogenesis greater than those obtained with scaffold only or scaffold with fresh marrow [13]. Orthopedic and maxillofacial surgical studies showed *in vivo* large animal segmental defect that led to complete re-corticalization and formation of medullary

canal with mature lamellar cortical bone and onlay graft for contour augmentation of the face giving rise to clinical union in a large number of cases [50, 51].

Ehrlich et al. [52] emphasized that, as a result of the unique nanoscale organization of organic tissue and mineral, biomineralization and structural studies of coral can be used to enlighten the development of new advanced functional materials. The deep-sea bamboo coral exhibits at a macrostructural level bone-like biochemical and mechanical properties. A specialized collagen matrix (acidic fibrillar) acts as a model for future potential tissue engineering applications. Opportunities in tissue engineering using coral skeletons have yet to be fully realized and exploited. The matrix supported the growth of both osteoblast and osteoclast, and the exceptional bio-elastomeric properties of the collagen matrix (gorgonin) of this coral make it potentially ideal for use as blood vessel implants. Collagenous gorgonin proteins can be hardened and cross-linked using quinones, and the final product closely resembles human keratin. The mechanism by which gorgonin is synthesized and interacts with the process of mineralization may provide lessons for the production of a synthetic collagen-like material [52].

---

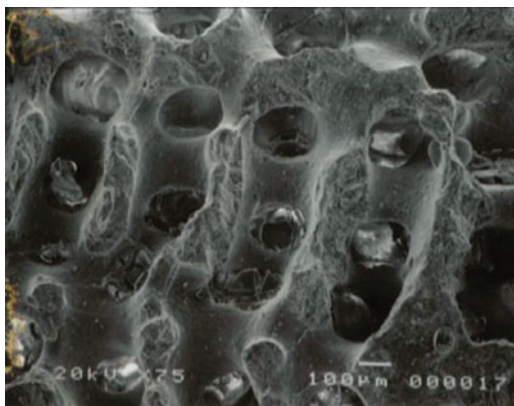
## Marine Structures in Drug Delivery Applications

Slow drug delivery system is a system which is capable of preloaded release of pharmaceutical agent to a site at a specific rate and most importantly at a therapeutically relevant concentration. The primary purpose of this kind of system compared with conventional drug intake such as injection or tablet is to enable the local and specific area delivery, dosage and duration control, and therefore appropriate active drug delivery at the same time causing minimal systemic side effects. The fundamental basis that defines the meaning of a drug delivery system remained unchanged even though technological advancement has produced innovative and refined drug delivery systems. The therapeutic advantages of these systems can be attributed to many underlining features such as the predictability of release rate and minimized drug concentration, thereby reducing any possible adverse systemic effect [53].

Prolonged duration of drug therapy such as the need for frequent re-dosing has been problematic in many global applications of drugs such as the treatment protocol in Africa for malaria. During the development of a drug delivery system, a number of factors are taken into consideration in accordance to the desired application. These include the administration route, the toxicity, the agent to be carried, the physical and chemical properties of the material, the rate of degradation, the loading efficiency, and the practicality for large-scale production, in addition to other parameters.

Various materials such as polymers, ceramics, polysaccharides, and alginate have shown potential advantages as drug delivery systems [54]. In spite of this, marine materials such as coral exoskeletons and marine shells show better potential due to their easy conversion to calcium phosphates, intricate interconnected pores, and their controllable dissolution rates. The interconnectivity and size of the coral pores are critical factors in the amount of coral used as a bone graft and slow drug delivery material (Fig. 4). Furthermore, the uniform porosity of the exoskeletons offers a

**Fig. 4** Coral structure showing micropores



more constant drug loading and therefore providing a more predictable drug release rate of which both are vital factors that directly influence the effectiveness of the drug delivery system.

## Foraminifera

Foraminifera are single-celled organisms with shells consisting of multilayer inner chambers commonly divided and added during its growth (Fig. 5). Depending on their environment, different species with different shapes can exist. The microstructure of Foraminifera includes meso- and micro-interconnected pores to assist filtration within marine environment. These observations created a novel idea in drug delivery, and Ben-Nissan and his coworkers applied these structures as slow drug delivery devices incorporating a range of mineral and therapeutic drugs including antibiotics [53]. Natural spheres loaded with drugs can spontaneously degrade and progressively release entrapped biological contents introduced during synthesis.

One significant and successful example of biomimetic materials chemistry applied to the delivery of drugs and/or genes utilizes template-mediated mineralization chemistry within a complex organized 3-D reaction field with patterning that mimics plankton shells. The design of this chemical system is to integrate processes of “self-organization” and “self-assembly” in space. In this manner, constructs that are created provide many clear advantages for tissue engineering as a physical template and a device for controlled release of a variety of drugs, proteins, genes, BMP, and growth factors. Biological molecules can be safely incorporated during synthesis as the chemistry consists of an aqueous phase and occurs at room temperature.

Another functional success has been the possibility for drug incorporation and delivery from nano-, micro-, and macrospheres. It was during an overseas summer break where a discovery was made by one of the authors of this chapter. After a close inspection, the sand on the beach appeared as perfect spheres and showed quite



**Fig. 5** Star Foraminifera structure from Australia



unique intricate structures. A small sample was taken back to our laboratory, and it was revealed the sand was in fact calcium carbonate marine shells instead of silica sand after scanning electron microscopy (SEM) and X-ray diffraction (XRD) analysis. After proper characterization, the marine structure was identified and it belongs to the Foraminifera family.

Spherical fossilized shells *Floresianus* (Foraminifera) from coral beach sand from the Great Barrier Reef in Australia were also collected. The samples were intact, lacked spines, and measured 0.5–1.5 mm in diameter. These “shells” or a more appropriate term “microspheres” possess unique fenestrated structures that have evolved to collect sunlight and circulate seawater for the mutual benefit of symbiotic algal cells that reside inside the shell. SEM and microcomputed tomography ( $\mu$ -CT) imaging confirmed that these shells were internally permeated by a 3-D network of microscopic interconnected channels measuring 1–10  $\mu\text{m}$  in diameter. A separate chapter in this book authored by Chou et al. will cover the details of some of the work on Foraminifera as drug delivery devices.

Before any marine material can be utilized as a graft or a drug delivery vehicle, they must first go through a laborious process to investigate the composition, morphology, purity, and suitability for drug loading and its slow dissolution without causing any adverse effect to the patient. Except in special cases, protein and organic matter are required to be extracted prior to the sterilization of calcium carbonate material. Any residual organic constituents are removed by immersing in sodium hypochlorite solution and then dried at a temperature of approximately 100 °C [13].

It is essential to hydrothermally convert these microsphere shells into  $\beta$ -TCP and/or HAp which is more stable and highly crystalline using the methods developed and published earlier [3]. In certain situations of drug delivery applications,  $\beta$ -TCP exhibits a more ideal composition compared with other calcium phosphates.

The original structure of the microspheres is not altered during the chemical conversion to calcium phosphate making the adsorption of selected drug compounds

possible as well as allowing new bone cells to penetrate into the micropores after bone-graft implantation. In the physiological environment, these microspheres can dissolve and supply calcium and phosphate ions in addition to the drugs incorporated to the immediate bone structure as a result of their pore architecture. The release profile shows relatively slow, local release of drugs such as bisphosphonate, gentamicin, and simvastatin from micro- and microspheres for extended periods [16, 53].

---

## Marine Structures in the Regulation of Stem Cells

Similarly, there is an increase in awareness that the composition of a scaffold material is critically important for the establishment of stem cell activities as they are dependent on the extracellular fabric for life support and to guide their subsequent evolution and development [2]. This can be accomplished through the use of natural structural biomaterials as well as their derivatives and reconstituted forms. Vital aspects of regenerative medicine are to improve stem cell processing, provide microenvironments that are better at regulating tissue formation and development, and manufacture less invasive transplantation modules with site-specific targeting properties. These can be demonstrated with the recreation of a mesenchymal stem/progenitor cell niche for regulating cell proliferation and outcome.

At the moment, an active area of research is the recreation of a native stem cell environment in which stem cells such as those of the bone marrow are protected, managed, and stabilized as self-renewing undifferentiated cells and instructions on how to regulate the rate of progenitor and replacement cells produced are provided. Nurcombe and Cool [55] suggested the glycosaminoglycan heparin sulfate is the master molecule controlling the dynamics of almost all stem cell functions.

Creating a unique and customized environment which is capable of regulating the differentiation and proliferation of stem cells is a fundamental goal intended at preserving their characteristics in artificial culture and for subsequent transplantation. Research groups from around the world have coordinated stem cell activities within microcapsules using a number of templates including polysaccharides. Cells are immobilized by the polysaccharide hydrogels in three-dimensional configurations lightly controlled by the substrate viscosity, additives used, and initial cell seeding density. Their broad applicability and versatility are significantly better compared to typical synthetic materials for most tissues within the human body. It has been reported that some of the most significant tissue responses have been observed when native extracellular matrix fragments of high molecular weight are embedded within polysaccharide frameworks. For instance, the addition of human aggrecan glycosaminoglycan to biomineral-coated chitosan/alginate microcapsules accelerated the endogenous production of cartilage matrix from embedded chondroprogenitors. However, it is important that proper modifications of chitosan and alginate are required to optimize their biological qualities as this will play a crucial role in the clinical outcomes. For example, it is now necessary to partially oxidize sodium alginate with sodium periodate to ensure a smooth and consistent

degradation which does not otherwise occur. The human body does not naturally produce enzymes that can promptly degrade alginate in its polymeric form.

Another significant aspect regarding the precise chemistry of alginate polymer chains is the composition and arrangement of the component sugar units. These properties have important effects on their relative bio-effectiveness. Due to their hydrophilic nature, protein deposition is more selective than on hydrophobic surfaces and more likely to recruit adhesion proteins. This can detrimentally reduce cell anchorage/attachment which has important consequences for cell survival as well as the regulation of migration, differentiation, and proliferation [56].

Therefore, it is important to increase cell attachment through blending candidate proteins with alginate or binding peptide sequences to the alginate biopolymer. The bio-responsiveness is characterized and directed by the sequential pattern of sugar residues along the alginate polymer chain. Higher mannuronic/gluconic ratios resulted in smaller pore sizes. Macrophages and lymphocytes are stimulated by mannuronic-rich alginates. However, high-gluconic alginates are preferred as they are more immune-suppressive in nature.

The sustained delivery of gene and protein therapeutics is a new and promising area of interest specifically in cancer research. It has been proven somewhat elusive when it comes to providing the correct dosage of regenerative factors in appropriate temporal sequence. Gene correction strategies have evolved to overcome this significant issue. Stem cell-mediated gene therapy using non-viral transduction agents is dependent on synthetic biomaterials, lipids, and physical disruption of the cell membrane to permit the entry of foreign genes. On the other hand, significant cell toxicity can be associated with these approaches. Alginate-chitosan matrices have been found to yield minimal cell toxicity of less than 5 % [13].

It is essential that the added bioactive factors are released in precise sequences at cell-instructive doses and at specific time frames in synchronization with the body's own biochemistry. Such actions will ensure that the added biological factors provide their maximum effect and potency. One of the primary issues is the release of individual factor in a slow and sustained manner for long periods of time to permanently restore tissue function. The release of encapsulates can be regulated in one of two ways. The first approach is to modify the composition and thickness of the capsule shell resulting in slow diffusion. This approach has been proven effective at delaying the release of plasmid deoxyribose nucleic acid.

On the other hand, it is also possible to create nested arrangements of bead within another bead. The host-guest arrangement of capsules can be an effective mechanism for temporal control of encapsulates. This idea was verified when the exogenous release of tyrosinase from embedded guest capsules was significantly delayed when compared to tyrosinase release from the surrounding host capsule. An additional mechanism for regulating encapsulates is to entrap them between shell layers or within one of a succession of layers such as entrapping BMP-2 at the interface between alginate and chitosan. Furthermore, it is also possible to coat successive alternating layers of positively and negatively charged polysaccharides around the original germinal core. The adaptability and versatility of this simple-to-construct delivery system are potentially suited to a wide range of applications. This can be

demonstrated by adding a series of bioactive proteins individually inside each, and later, as the layers peel away from the outer surface toward the core over time, the encapsulated protein is released in a sequential manner. Similarly, engineering an intricate series of protected domains within each shell is possible by laminating each applied shell layer with calcium phosphate. Then again, cells can be entrapped inside the individual layers. There is the capability with such assemblies of creating physiologically significant concentration gradients of genes, growth factors, and proteins within each capsule.

---

## Concluding Remarks

Marine structures have been widely explored during the past decade from the imitation of efficient designs of nature or biomimetics to soft and hard tissue engineering as well as from slow or controlled drug delivery to biosensors and bioreactor applications. The new approaches include the use of natural organic and inorganic skeletons, micro- and nanoscale slow drug delivery devices, new medical treatment protocols inspired by unique designs, and devices incorporating stem cells, proteins, and peptides.

In nature, structures possess desirable properties, and gradually we are discovering new ways of reproducing nature to create similar levels of sophistication even though only to a limited extent. One versatile approach is to use biological microstructures as templates for the reproduction of inorganic structures with identical features. They have a distinct consequence to the production of replacements for calcified tissues. This is achieved by using techniques in biomineral-inspired materials chemistry. The concept is to utilize the consecutive developmental pathway of systems that nature employs to make skeletons from molecules into micro- and macroscopic structures.

Additional studies of the manner of natural materials are constructed, and the condition they adapt to their environment will allow us to produce a breathtaking array of self-responsive structures and materials for regenerative medicine, structural applications, and applied engineering materials. In nature, biomaterials are composed of perfect resource and energy efficiency using common and readily available substrates through self-assembly into highly organized hierarchies. Examining the synthesis and design methods from these natural as well as marine structures will provide us with an opportunity to create structures with complex shapes and architectures that are customized to their functions and do not break down. Previously, science and engineering have shown us in what way biomimetic approaches can yield promising outcomes for application in tissue engineering of skeletal tissues. Current work is part of the continuing research toward the design of scaffolds that are clinically relevant for regenerative medicine using a unique set of self-organizing hierarchical structures invented and produced according to biological principles of design is very promising.

At present, there is a clear need for better tissue engineering scaffolds that possess more natural bio-responsive environments favorable to guiding the natural

procedures of regeneration which can be extremely intricate and dynamic in time and space. Therefore, intelligence must be incorporated into the scaffold designs to meet this biological challenge. We argue that there needs to be a transformation to scaffold environments that are responsive whereby the synthesized biomatrix evolves in real time to meet the demands and optimize for the adaptive growth and regeneration of human tissues. The environments of the scaffolds are adjusted as cells proliferate and differentiate.

Advanced biomimetic scaffolds in the future must be capable of adapting to these changes and undergo the ever-changing needs of developing tissues. It is anticipated the synthesis of biomaterial scaffolds with functional cross-links and pendant side groups that interact with surrounding cell population at three different levels: nano/meso (at the contact interface), micro (at the architectural level), and macro (at the bio-functional level). Nanofabrication utilizing biological principles of assembly and design is still in its infancy. The application of this bio-inspired nanofabrication for tissue engineering is a unique approach that has vast potential to improve scaffold design and shape physicochemical environments with the ability to micro-evolve. To learn from nature and grow materials with cells and promote the regulation of material synthesis with biogenics including antibodies, proteins and peptides are the most pertinent challenges.

---

## References

1. Ben-Nissan B, Green DW (2013) Marine materials in drug delivery and tissue engineering: from natural role models, to bone regeneration and repair and slow delivery of therapeutic drugs, proteins and genes. In: Kim S-K (ed) *Marine biomaterials*. Taylor and Francis/CSR Books, Boca Raton, pp 575–602
2. Green DW, Li G, Milthrope B, Ben-Nissan B (2012) Adult stem cell coatings using biomaterials for regenerative medicine. *Mater Today* 15:61–68
3. Ben-Nissan B (2003) Natural bioceramic: from coral to bone and beyond. *Curr Opin Solid State Mater Sci* 7:283–288
4. Mann S (1983) Mineralization in biological systems. *Struct Bond* 54:125
5. Gonzalez-McQuire R, Green D, Walsh D et al (2005) Fabrication of hydroxyapatite sponges by dextran sulfate/amino acid templating. *Biomaterials* 26:6652–6656
6. Green D, Walsh D, Yang X et al (2004) Stimulation of human bone marrow stromal cells using growth factor-encapsulated calcium carbonate porous microspheres. *J Mater Chem* 14:2206–2212
7. Walsh D, Mann S (1996) Feigning nature's sculptures. *Chem Br* 32:31–34
8. Walsh D, Boanini E, Tanaka J et al (2005) Synthesis of tri-calcium phosphate sponges by interfacial deposition and thermal transformation of self-supporting inorganic films. *J Mater Chem* 15:1043–1048
9. Hall SR, Swinerd VM, Newby FN et al (2006) Fabrication of porous titania (brookite) microparticles with complex morphology by sol-gel replication of pollen grains. *Chem Mater* 18:598–600
10. Green DW (2004) Bio-inspired ceramic structures: from invertebrate marine skeletons to biomimetic crystal engineering. *J Aust Ceram Soc* 40:1–7
11. Ben-Nissan B, Choi AH (2006) Sol-gel production of bioactive nanocoatings for medical applications. Part I: an introduction. *Nanomedicine* 1:311–319

12. Parker AR, Martini N (2006) Structural color in animals-simple to complex optics. *Opt Laser Technol* 38:315–322
13. Ben-Nissan B, Green DW (2014) Marine structures as templates for biomaterials. In: Ben-Nissan B (ed) *Advances in calcium phosphate biomaterials*, Springer series in biomaterials science and engineering (SSBSE). Springer, Berlin, pp 391–414
14. Mock T, Samanta MP, Iverson V et al (2008) Whole-genome expression profiling of the marine diatom *Thalassiosira pseudonana* identifies genes involved in silicon bioprocesses. *Proc Natl Acad Sci U S A* 105:1579–1584
15. Beleggratis MR, Schmidt V, Nees D et al (2014) Diatom-inspired templates for 3D replication: natural diatoms versus laser written artificial diatoms. *Bioinspir Biomim* 9:016004
16. Kim ES (2008) Directed evolution: a historical exploration into an evolutionary experimental system of nanobiotechnology, 1965–2006. *Minerva* 46:463–484
17. Sia SK, Gillette BM, Yang GJ (2007) Synthetic tissue biology: tissue engineering meets synthetic biology. *Birth Defects Res C Embryo Today* 81:354–361
18. LeGeros RZ (1993) Biodegradation and bioresorption of calcium phosphate ceramics. *Clin Mater* 4:65–88
19. LeGeros RZ, Gatti AM, Kijkowska R et al (2004) Magnesium tricalcium phosphate: formation and properties. *Key Eng Mater* 254–256:127–130
20. Ando J (1958) Tricalcium phosphate and its variation. *Bull Chem Soc Jpn* 31:196–201
21. Roy DM, Linnehan S (1974) Hydroxyapatite formed from coral skeleton carbonate by hydrothermal exchange. *Nature* 247:220–222
22. Rocha JHG, Lemos AF, Agathopoulos S et al (2005) Scaffolds for bone restoration from cuttlefish. *Bone* 37:850–857
23. Martina M, Subramanyam G, Weaver JC et al (2005) Developing macroporous bicontinuous materials as scaffolds for tissue engineering. *Biomaterials* 26:5609–5616
24. Townley HE, Parker AR, White-Cooper H (2008) Exploitation of diatom frustules for nanotechnology: tethering active biomolecules. *Adv Funct Mater* 18:369–374
25. Boute N, Exposito JY, Boury-Esnault N et al (1996) Type IV collagen in sponges, the missing link in basement membrane ubiquity. *Biol Cell* 88:37–44
26. Exposito JY, Cluzel C, Garrone R et al (2002) Evolution of collagens. *Anat Rec* 268:302–316
27. Swatschek D, Schatton W, Kellermann J et al (2002) Marine sponge collagen: isolation, characterization and effects on the skin parameters surface pH, moisture and sebum. *Eur J Pharm Biopharm* 53:107–113
28. Nicklas M, Schatton W, Heinemann S et al (2009) Preparation and characterization of marine sponge collagen nanoparticles and employment for the transdermal delivery of 17 $\beta$ -estradiol-hemihydrate. *Drug Dev Ind Pharm* 35:1035–1042
29. Aizenberg J, Weaver JC, Thanawala MS et al (2005) Skeleton of *Euplectella* sp structural hierarchy from the nanoscale to the macroscale. *Science* 309:275–278
30. Miserez A, Weaver JC, Thurner PJ et al (2008) Effects of laminate architecture on fracture resistance of sponge biosilica: lessons from nature. *Adv Funct Mater* 18:1241–1248
31. Abramovitch-Gottlieb L, Gersh S, Vago R (2006) Biofabricated marine hydrozoan: a bioactive crystalline material promoting ossification of mesenchymal stem cells. *Tissue Eng* 12:729–739
32. Vago R, Plotquin D, Bunin A et al (2002) Hard tissue remodeling using biofabricated coralline biomaterials. *J Biochem Biophys Methods* 50:253–259
33. Lopez E, Vidal B, Berland S et al (1992) Demonstration of the capacity of nacre to induce bone formation by human osteoblasts maintained in vitro. *Tissue Cell* 24:667–679
34. Lamghari M, Berland S, Laurent A et al (2001) Bone reactions to nacre injected percutaneously into the vertebrae of sheep. *Biomaterials* 22:555–562
35. Lamghari M, Antonietti P, Berland S et al (2001) Arthrodesis of lumbar spine transverse processes using nacre in rabbit. *J Bone Miner Res* 16:2232–2237
36. Rousseau M, Lucilia PM, Almeida MJ et al (2003) The water-soluble matrix fraction from the nacre of *Pinctada maxima* produces earlier mineralization of MC3T3-E1 mouse pre-osteoblasts. *Comp Biochem Physiol B* 135:1–7

37. Duplat D, Chabadel A, Gallet M et al (2007) The in vitro osteoclastic degradation of nacre. *Biomaterials* 28:2155–2162
38. Westbroek P, Marin F (1998) A marriage of bone and nacre. *Nature* 392:861–862
39. Almeida MJ, Pereira L, Milet C et al (2001) Comparative effects of nacre water-soluble matrix and dexamethasone on the alkaline phosphatase activity of MRC-5 fibroblasts. *J Biomed Mater Res* 57:306–312
40. Rousseau M, Boulzaguët H, Biagianti J et al (2007) Low molecular weight molecules of oyster nacre induce mineralization of the MC3T3-E1. *J Biomed Mater Res A* 85:487–497
41. Zhang C, Li S, Ma Z et al (2006) A novel matrix protein p10 from the nacre of pearl oyster (*Pinctada fucata*) and its effects on both CaCO<sub>3</sub> crystal formation and mineralogic cells. *Marine Biotechnol* 8:624–633
42. Liao H, Mutvei H, Hammarstrom L et al (2002) Tissue responses to nacreous implants in rat femur: an in situ hybridization and histochemical study. *Biomaterials* 23:2693–2701
43. Kim YM, Kim JJ, Kim YH et al (2000) Effects of organic matrix proteins on the interfacial structures at the bone-biocompatible nacre interface in vitro. *Biomaterials* 23:2089–2096
44. Shen Y, Zhu J, Zhang H et al (2006) In vitro osteogenic activity of pearl. *Biomaterials* 27:281–287
45. Green DW, Padula MP, Santos J et al (2013) A therapeutic potential for marine skeletal proteins in bone regeneration. *Mar Drugs* 11:1203–1220
46. Vago R (2008) Beyond the skeleton. Cnidarian biomaterials as bioactive extracellular micro-environments for tissue engineering. *Organogenesis* 4:18–22
47. Stanley G (2003) The evolution of modern corals and their early history. *Earth Sci Rev* 60:195–225
48. Bonnelye E, Chabadel A, Saltel F et al (2008) Dual effect of strontium ranelate: stimulation of osteoblast differentiation and inhibition of osteoclast formation and resorption in vitro. *Bone* 42:129–138
49. LeGeros R (1981) Apatites in biological systems. *Prog Cryst Growth Charact Mater* 41:1–45
50. Papacharalambous S, Anastasoff K (1993) Natural coral skeleton used as onlay graft for contour augmentation of the face. A preliminary report. *Int J Oral Maxillofac Surg* 22:260–264
51. Leupold J, Barfield W, An Y et al (2006) A comparison of ProOsteon, DBX, and collagraft in a rabbit model. *J Biomed Mater Res B Appl Biomater* 79:292–297
52. Ehrlich H, Etnoyer P, Litvinov SD et al (2006) Biomaterial structure in deep-sea bamboo coral (Anthozoa: Gorgonacea: Isididae): perspectives for the development of bone implants and templates for tissue engineering. *Mater Werkst* 37:552–557
53. Chou J, Valenzuela SM, Green DW et al (2014) Antibiotic delivery potential of nano and micro porous marine structures derived  $\beta$ -TCP spheres for medical applications. *Nanomedicine* 9:1131–1138
54. Bose S, Tarafder S (2012) Calcium phosphate ceramic systems in growth factor and drug delivery for bone tissue engineering: a review. *Acta Biomater* 8:1401–1421
55. Nurcombe V, Cool SM (2007) Heparan sulfate control of proliferation and differentiation in the stem cell niche. *Crit Rev Eukaryot Gene Expr* 17:159–171
56. Rowley JA, Madlambayan G, Mooney DJ (1999) Alginate hydrogels as synthetic extracellular matrix materials. *Biomaterials* 20:45–53

Y. L. Zhou, Z. G. Huan, and J. Chang

## Contents

Introduction .....	546
Silicate-Based Bioactive Inorganic–Organic Composites .....	548
Electrospun Fibers .....	549
Bioactive Composite Membranes and Coatings .....	549
Composite Scaffolds .....	552
Injectable Composite Hydrogels .....	557
Composite Bone Cements .....	560
Surface Modification of Silicate-Based Bioactive Inorganic Materials .....	561
Silicate-Based Bioactive Inorganic/Inorganic Composites .....	562
Silicate-Based Composite Ceramics .....	563
Silicate-Based Bone Cements .....	566
Other Types of Silicate-Based Bioactive Composites .....	571
Silicate/Metal Composites .....	572
Silicate-Based Bioactive Coatings on Nondegradable Metallic Substrates .....	573
Silicate Bioceramics Composite with Biodegradable Metallic Substrates .....	575
Summary .....	576
References .....	579

---

## Abstract

Silicon (Si) is an essential trace element in the human body, which has been confirmed to be necessary for bone development. Silicon participates in the biosynthesis of collagen, the basic component of connective tissue; has a beneficial effect on phosphorylation of proteins, saccharides, and nucleotides; and is also essential for the formation of cytoskeleton and other cellular structures of mechanical or supportive function. Considerable research has been focusing on

---

Y.L. Zhou • Z.G. Huan • J. Chang (✉)

State Key Laboratory of High Performance Ceramics and Superfine Microstructure, Shanghai

Institute of Ceramics, Chinese Academy of Sciences, Shanghai, China

e-mail: [jchang@mail.sic.ac.cn](mailto:jchang@mail.sic.ac.cn)



silicate-based materials, which have shown great potential in bone-related tissue engineering and tissue regeneration applications. Among them, silicate-based bioactive composites with proper composition and structure are promising bone regeneration materials owing to their enhanced and adjustable mechanical and biological properties. In this chapter, we reviewed the current status of silicate-based bioactive composites, including inorganic–organic, inorganic/inorganic, and inorganic/metallic systems, with the focus on fabrication methods and properties for bone tissue regeneration. Although it is evident that many advances have been achieved for silicate-based bioactive composites for the purpose of tissue regeneration, great efforts are still required in their development to fulfill the requirement of practical applications, which is an interdisciplinary and subjected to accumulation of materials science and engineering, chemistry, biology, and transplantation medicine. Therefore, the aim of this chapter is to provide hints for future development of silicate-based bioactive composites and design of bioactive materials for bone tissue regeneration.

---

**Keywords**

Silicate • Composites • Tissue regeneration • Scaffolds • 3D plotting • Electrospinning • Hydrogel • Membranes • Surface modification • Bioceramics • Bioactive glasses • Bone cements • Metal matrix composites • Metallic substrates

---

## Introduction

With the rapidly aging population and increased accidents, the need for bone regeneration with defects associated with poor healing caused by various reasons such as osteoporosis, fractures, trauma, or large-sized bone tissue injury is urgent. Autogenous bone grafting is the most effective treatment in clinical practice. However, the obvious restraint of this approach is insufficient amount of donor tissue. The immunological reaction in the host recipient is the main limitation for the use of allogeneic or xenogeneic bone grafts. Synthetic materials used for bone repair include metal materials, inorganic nonmetallic materials, organic materials, and composites, which have great potential in clinical applications. Inorganic nonmetallic materials, especially bioceramics, have received significant attention in hard tissue regeneration due to their ability to support new bone formation. Among the synthetic bone replacement materials available on the market, calcium phosphates such as hydroxyapatite (HA) and tricalcium phosphate (TCP) are important bioceramics which are widely used due to their excellent bioactivity, osteoconductivity, and similarities in the composition to the bone tissue.

Bioactivity and biodegradability are two critical aspects in the design of bioceramics for clinical application. Current efforts are devoted toward the synthesis of bioceramics with the degradation rate matching new bone formation process, which means the optimized maintenance of mechanical strength of the implants during the whole process after implantation. Bioinert ceramics such as  $\text{Al}_2\text{O}_3$  and

ZrO<sub>2</sub> could result in the formation of fibrous capsule along the surrounding bone after implantation which may lead to the failure of implantation. Previous studies have shown that sintered Ca–P bioceramics have poor biodegradability [1, 2]. In contrast, silicate-based bioactive inorganic materials with certain compositions have showed unique bioactivity to bond with living bone and soft tissue and adjustable biodegradability [3].

The main advantage of silicate-based inorganic materials over Ca–P-based bioceramics is dependent on the fact that silicon (Si) plays an essential role in mineralization and gene activation in bone regeneration process [4]. In the late 1960s, Hench et al. discovered that certain silicate-based glasses can induce formation of HA, the main mineral constitute of the bone, which forms a mechanically strong interfacial bond between the host tissue and the implants in physiological environment [5]. Based on these findings, subsequently a new concept of “bioactive” biomaterials was developed instead of inert biomaterials in terms of the implants [6]. Generally, bioactive materials are defined as a class of materials, which have the ability to induce specific biological activity [7], while narrowly, bioactive materials are defined as materials which can promote the interfacial bonding with tissues after implantation and enhance new tissue regeneration through a series of interfacial ion exchange reactions, and a silica-rich gel layer forms followed by the formation of the Ca–P layer on the material surface [8].

Preparation and evaluation of silicate-based biomaterials have attracted more attention in recent years. Silicate-based bioactive inorganic materials mainly fall into three categories: silica-based bioactive glasses, e.g., Bioglass<sup>®</sup>; crystalline silicate-based ceramics, including wollastonite ( $\beta$ -CaSiO<sub>3</sub>), pseudowollastonite ( $\alpha$ -CaSiO<sub>3</sub>), diopside (CaMgSi<sub>2</sub>O<sub>6</sub>), etc. [9]; and silicate-based glass–ceramics which were introduced as bone implant materials by Kokubo et al. in 1982 [10]. It has been well accepted that the Si and Ca ions released from silicate-based inorganic materials could stimulate proliferation, osteogenic differentiation of stem cells, and angiogenesis of endothelia cells [11, 12], which makes them hold the promise as a new class of bioactive materials for bone regeneration. However, the major disadvantages of silicate-based inorganic biomaterials, similar to their phosphate-based counterparts, remain their high brittleness, low mechanical strength, and poor machinability. One of the strategies to solve the problem of the poor mechanical properties of some ceramic materials is the preparation of composite materials with other materials such as other type of ceramics, polymers, and metals in order to combine the advantage of two different types of materials. Some recent studies have demonstrated that the combination of silicates with other materials has the advantages not only in the improvement of mechanical properties but also in the controllability of the degradation rate as compared to that of each single component, and the challenge of the approach is to maintain the bioactivity of the silicates with the change of the composition and structure, while the mechanical property is improved.

In recent years, many studies have demonstrated that combining silicates with other materials is an effective way to design bioactive biomaterials with improved properties for tissue regeneration, in particular as orthopedic and dental implants or

for bone tissue engineering applications. Therefore, in this chapter, a systematic review on the recent approaches in preparation and characterization of silicate-based composite biomaterials will be introduced. From the perspective of the material constituents in the composites, silicate-based bioactive composites can be generally classified into three categories: (1) silicate-based bioactive inorganic–organic composites, (2) silicate-based bioactive inorganic/inorganic composites, and (3) silicate-based bioactive inorganic/metallic composites. Therefore, this chapter will focus on these three parts with a short summary, and an outlook in future trends will be presented.

---

## **Silicate-Based Bioactive Inorganic–Organic Composites**

From materials perspective, the bone tissue is probably one of the most idealist composites in nature. It consists of the fundamental organic phase of proteins such as collagen and the reinforced inorganic nanocrystals of calcium carbonate hydroxyapatite (CHA), which is a typical model of functionally heterogeneous porous scaffolds designed for bone tissue engineering. The porosity and the interaction between the two phases play an important role in determining the mechanical properties of the bone. Inspired by the structure–strength mechanism of natural bone tissue, many researches have been focusing on the development of inorganic–organic composite biomaterials, aiming at combining the properties of traditional materials to some extent in order to achieve admirable improvement in their performance. In consequence, the actual performance of these composites depends on the nature and relative content of the constitutive inorganic and organic components, as well as the synthesis methods [13]. According to the preparation methods or the application purpose, silicate-based bioactive inorganic–organic composites mainly include electrospun fibers, membranes and coatings, scaffolds, hydrogels, and bone cements. Among the majority of these composites, the polymeric matrix would improve the mechanical properties, machinability, porosity, or other properties such as drug-loading ability, while the silicate-based bioactive inorganic particles would ensure the bone integration with the implant or as reinforcement phase to improve mechanical strength on the other hand. In some cases, silicate-based bioactive inorganic particles would serve as efficient drug reservoir if they are endowed with a mesoporous structure. In this session, these five categories of silicate-based bioactive inorganic–organic composites as mentioned above, mainly the fabrication process and properties of the hybrid materials, will be presented. As the interfacial interaction between inorganic silicate phase and polymer phase plays a critical role in determining the fabrication and the final properties of the composites, it is sometimes necessary to improve the compatibility of the two phases, such as the dispersion of one phase with the other. Therefore, in the last part of this section, the surface modification of silicate-based bioactive inorganic materials to enhance the dispersity of inorganic phase in polymer matrix is discussed.

## Electrospun Fibers

Electrospinning is a new emerging technique for fabrication of nanoscale continuous fibers with applications in many biomedical and industrial fields. Electrospun fibers display morphological similarities to the natural extracellular matrix (ECM) and have great potential in tissue engineering applications. Using electrospinning techniques, composite nanofibers of most soluble or fusible polymers and a large variety of additives can be fabricated in order to obtain high-performance materials with enhanced or novel properties. Studies have shown that electrospinning is a promising method to precisely control the arrangement of inorganic nanofillers within polymer matrices, which is commonly difficult to achieve using traditional techniques. Calcium silicate hydrate (CSH) nanowire/poly(L-lactide) (PLLA) nanocomposites with tailored CSH distribution, microstructures, and mechanical properties were successfully prepared through a combined method of electrospinning and hot pressing (Fig. 1). In this process, CSH nanowires in PLLA matrix could be controlled from completely randomly oriented to uniaxially aligned and then hierarchically organized with different interlayer angles, leading to corresponding nanocomposites with improved mechanical properties and varied anisotropies [14]. The addition of CSH nanowires greatly enhanced the bending strength, hydrophilicity, and apatite-forming ability of PLLA films, as well as the attachment and proliferation of bone marrow stromal cells (BMSCs).

Electrospinning is also proved to be a useful approach to prepare composite nanofibers consisting of degradable polymers and silicate-based inorganic bioactive particles with improved mechanical strength and biological functions [15]. Poly( $\epsilon$ -caprolactone) (PCL) nanofibers containing bioactive glass (BG) nanoparticles and simvastatin drug were produced by electrospinning. Incorporation of BG nanoparticles in a relatively low concentration (not more than 20 %) could strengthen the polymer matrix by increasing the crystallinity of PCL nanofibers due to the nucleating properties of BG nanoparticles. The chemical and structural characteristics of the polymer affected degradation kinetics of the composite, while incorporation of the BG phase could increase the water-adsorbing capacity of the material, leading to its increased hydrolytic degradation rate. Therefore, it is possible to modify the biodegradation and drug release behaviors of the composites by solely adjusting the BG concentration. The fibrous nanocomposite demonstrated excellent bioactivity such as inducing the precipitation of bone-like apatite minerals on its surface in simulated physiological medium [16]. In a word, the biomedical materials made of nanofibers with high porosity and interconnectivity would show promising potential in tissue regeneration by providing similar structure to that of ECM and controllable drug delivery function [17].

## Bioactive Composite Membranes and Coatings

### Bioactive Composite Membranes

Bioactive membranes for guided tissue regeneration in the area of wound dressing, nerve conduits, bone healing, and periodontal regeneration have received

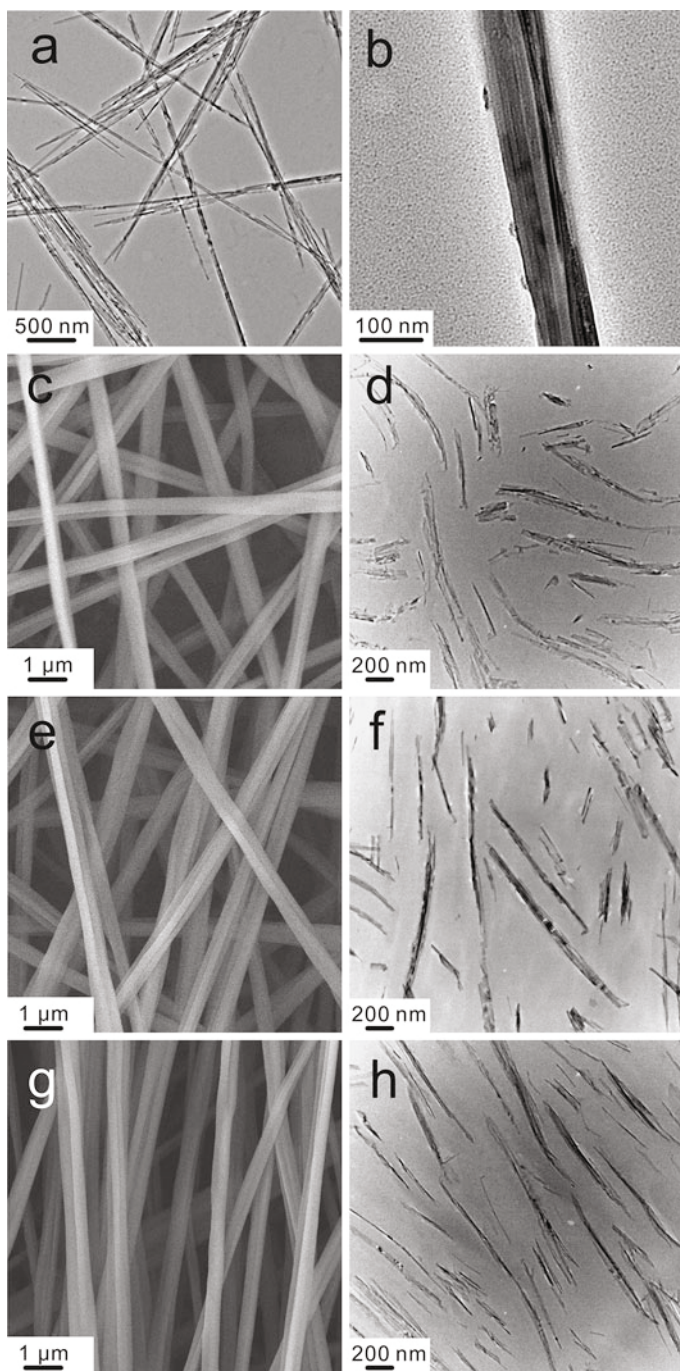


**Fig. 1** (continued)

increasing interests [18]. The matrix of these membranes mainly includes natural or synthetic biodegradable polymers. To achieve desirable bioactivity, silicate-based materials have been incorporated into different kinds of polymer membranes. The chitosan/tobermorite ( $\text{Ca}_5\text{Si}_6\text{O}_{16}(\text{OH})_2 \cdot 4\text{H}_2\text{O}$ ) composite membrane for periodontal regeneration was prepared by solvent casting method. The incorporation of tobermorite particles improved the bioactivity of the composite membranes by inducing formation of crystalline bone-like HA on the surface of the material in simulated body fluid (SBF). The growth of MG63 human osteosarcoma cells was enhanced by up to 30 % on the surface of the composite membranes compared to the blank control [19]. Additional incorporation of growth factors into silicate-containing membranes would further enhance tissue healing process, suggesting a potential approach in tissue engineering and regenerative medicine. A hybrid membrane of collagen and nanobioactive glasses (NBG) incorporated with basic fibroblast growth factor (FGF2) was developed for guiding bone regeneration. Three membrane groups, including pure collagen, collagen–NBG hybrid, and its combination with FGF2, were implanted in rat calvarium defects for 3 weeks. The results showed that the collagen–NBG–FGF2 membranes were most effective on the defect recover than collagen–NBG and pure collagen membranes [20].

In order to design biodegradable membranes with asymmetric bioactivity, the composite membranes with two distinct sides were produced by combining PDLA and Bioglass<sup>®</sup> particles in the process of solvent casting methodology that the Bioglass<sup>®</sup> particles were deposited by gravity to the bottom side. Only the inorganic-rich face promoted the deposition of bone-like apatite after immersing the composite membrane in SBF for 2 days. Interestingly, *in vitro* studies revealed that osteoblast-like cells seeded on both sides of the membranes present similar levels of metabolic activity and morphology after a period of 7 days [21].

Incorporation of silicate particles within membranes is an effective approach to achieve improved interaction between the material and surrounding tissues after implantation. It is obvious that the incorporation of biomolecules, embedment of physical signaling, and design of hierarchical macrostructures within the membrane would further endow the materials with further enhanced functionality, for which more investigations should be addressed.

### Silicate Coatings on Polymers

Biodegradable polymers are extensively used materials in the field of biomaterials owing to their tailorable degradation rates, biocompatibility, and formability. However, higher hydrophobicity and lack of surface bioactivity often result in



**Fig. 1** TEM images of (a) CSH nanowires and (b) PLLA/CSH composite nanofibers with 10 wt% nanowires. (c–h) SEM images of PLLA/CSH composite nanofibers with a 10 wt% nanowire content collected at different rotation speeds of (c) 100, (e) 1300, and (g) 2500 r.p.m. and (d, f, h) TEM images of the corresponding nanocomposites after hot pressing (c), (e), and (g), respectively [14]

poor tissue integration with the surrounding tissues after implantation. Coating the biodegradable polymers with hydrophilic silicate-based bioactive inorganic particles would enable improvement in the surface properties of the polymer substrate. For this purpose, BG coatings have been applied to modify the surface of polyethylene terephthalate (PET) artificial ligament grafts to enhance their osteointegration. In a rabbit extra-articular model, the BG-coated PET graft induced new bone formation between graft and host bone tissue after 12 weeks, and the average graft–bone interface width of the BG group became significantly lower than that of the control group. Furthermore, the BG coating on the ligament graft surface also stimulated expression of bone morphogenetic protein 2 (BMP-2) and vascular endothelial growth factor (VEGF) near the graft in vivo as compared to the control group after 3 weeks implantation ( $p < 0.05$ ). This study suggests that BG coatings on PET artificial ligaments have a positive effect on osteointegration of the implants by promoting bone regeneration at the interface between PET graft and bone tunnel [22]. To further explore the biofunctionality of the silicate-based coating on biodegradable polymers, internal structure and composition gradient along the thickness based on sophisticated design could be an interesting focus in the future [23].

## Composite Scaffolds

In contrast to conventional implants, bone tissue engineering (BTE) is an advanced biomedical technique that is considered as an effective approach for bone regeneration and reconstruction of lost bone tissue. In this approach, the scaffold with well-designed architecture, which performs as a temporary structural carrier for cells, and incorporated growth factors and living cells is one of the critical part of BTE. Currently, the paradigm for the development of BET is that bone substitute materials can promote the human body's own regenerative capacity in the repair process by stimulating expression of osteogenic genes, while appropriate degradability of the scaffolds is required to maintain the mechanical properties of the construct. In this regard, the scaffold should be designed as bone tissue “regeneration” rather than mere “replacement” [24].

Synthetic biodegradable polymers have been extensively investigated as scaffolds for tissue engineering applications because of good biocompatibility and processing convenience. However, poor mechanical property, lack of bioactivity, and the release of acidic degradation product limit their practical utilization. Some researches have shown that, coupled with preferable cellular response, the degradation of silicate-based bioactive inorganic materials would lead to an alkaline pH to the surroundings [25], which is in the very contrary to biodegradable polymers. Therefore, the development of composite scaffolds would enable the combination of individual advantages of polymers and silicate inorganic materials, which may increase the mechanical stability of the scaffolds and improve degradability and tissue interaction to meet the requirement of tissue engineering.

### Composites with Natural Biopolymers

Natural-derived polymers such as proteins including collagen and gelatin, and polysaccharides including chitosan, are usually used as chemical components for developing biomimetic bone regenerative materials which demonstrate good biocompatibility and biodegradability. The main disadvantages of natural-derived biopolymers are their poor mechanical strength and lack of bioactivity. It is assumed that both of these problems can be addressed by reinforcing biopolymers with silicate-based inorganic phase to improve mechanical strength and bioactivity of stimulating bone tissue formation [26].

As one of the most important natural polymers, proteins are the major structural components of many tissues. Incorporation of wollastonite into collagen matrix could improve the mechanical strength and *in vitro* bioactivity of the composite scaffold [27]. Further investigation also shows that wollastonite nanowires can reinforce collagen scaffolds and the hybrid scaffold with interconnected pores could promote osteogenic differentiation and angiogenic factor expression of mesenchymal stem cells (MSCs) [11/10]. In another study, porous bioglass/gelatin scaffolds were implanted on rabbit's ulna, and the results showed that the nanocomposite scaffold could significantly enhance bone growth and healing of the bone defect [3].

Derived from marine crustaceans, shrimp, and crab, chitosan and its derivatives have broad potential for applications as biomaterials due to their abundant source and good biocompatibility. However, porous chitosan scaffolds lack the required strength and thus may not provide sufficient mechanical support for tissue engineering. Incorporation of wollastonite particles into a macroporous chitosan scaffolds could enhance both the mechanical strength and bioactivity such as induction of HA formation [28]. The addition of NBG in chitosan/NBG scaffolds featured macro-/microdual pore structure and facilitated rapid induction of bone mineral-like apatite in SBF. The *in vitro* cellular responses demonstrated that the scaffolds provided 3D matrix environment to the cells, appropriate for bone cell anchorage, spreading, migration, and growth [29].

It is obvious that the incorporation of silicate-based bioactive materials into the biopolymers can endow the latter with superior bioactivity, and reasonable combination of biopolymers with bioactive silicate inorganic particles can render the development of novel composites with desirable microstructure, mechanical strength, and osteostimulation [30].

### Composites with Synthetic Polymers

Biodegradable synthetic polymers have been widely used for biomedical and pharmaceutical applications and have shown great potential in applications as tissue engineering scaffolds due to their adjustable and predictable degradation rates, mechanical strength, and machinability. Polyesters, including polylactide (PLA), polycaprolactone (PCL), poly(lactic-*co*-glycolic acid) (PLGA), polyhydroxybutyrate (PHB), etc. are currently the most promising polymers for biomedical applications. However, the release of acidic degradation by-products which lead to inflammatory responses has limited the use of these biodegradable



polyesters in tissue engineering applications. As silicate-based inorganic bioactive materials could release basic ions in aqueous solutions, it is assumed that its incorporation into the polyester matrix would counteract the acidification reaction caused by the release of the acidic degradation products of the polymers. Based on such assumption, some studies have been conducted and shown that the incorporation of silicate-based bioactive inorganic fillers, such as wollastonite and BG, could indeed effectively neutralized the pH value of the soaking media in a physiological range throughout the degradation process of PLGA. It was also found that the presence of these fillers reduced the degradation rate of the polymeric substrate to some extent [31]. In brief, incorporation of bioactive silicate particles is an effective way to compensate the pH decrease caused by the acidic degradation products of the polymer and to control the degradation behavior of scaffolds.

The addition of silicate-based inorganic particles in polymer matrix could improve the hydrophilicity and bioactivity of the composite surface. It has been found that incorporation of wollastonite into PDLGA scaffold could improve the hydrophilicity of the material and the bioactivity by inducing the formation of HA on the surface [32], and *in vitro* osteoblast culture experiment confirmed that the composite scaffolds could support the osteoblast proliferation [33]. Another study showed that the ionic products derived from the degradation of  $\beta$ -CaSiO<sub>3</sub>/PDLGA composite scaffolds could enhance cell viability, alkaline phosphatase (ALP) activity, calcium mineral deposition, and mRNA expression levels of osteoblast-related genes of rat bone marrow-derived mesenchymal stem cells (rBMSCs) without addition of extra osteogenic reagents, and it was further revealed *in vivo* that the composite scaffold dramatically stimulated new bone formation and angiogenesis as compared with TCP and PDLGA scaffolds (Fig. 2) [34]. The addition of wollastonite into PHBV scaffolds resulted in an increase of the water absorption and weight loss as compared to that of pure PHBV scaffolds, and the presence of wollastonite within the scaffolds benefited the adhesion, proliferation, and differentiation of human bone marrow-derived stromal cells (hBMSCs). A follow-up study confirmed that the ionic products (Ca and Si) released from wollastonite might contribute to this stimulatory effect [35].

Biocompatibility, porosity, mechanical properties, and degradability are most important factors that should be kept in mind during the design of scaffolds for tissue regeneration. It is clear that the incorporation of silicate-based bioactive inorganic particles into polymer matrix provides an effective approach to obtain composite scaffolds with improved properties in these aspects.

### **Silicate–Polymer Composite Scaffolds for Drug Delivery**

Beyond fulfilling the function of bone regeneration, BTE scaffolds have been incorporated with drugs or growth factors, aiming to achieve multifunctions such as inhibiting infections and accelerating angiogenesis. Compared to conventional drug delivery system, local drug release system into the implanting site has great advantages owing to the potential for dose reduction, controlled release pattern, and negligible side effect [36].

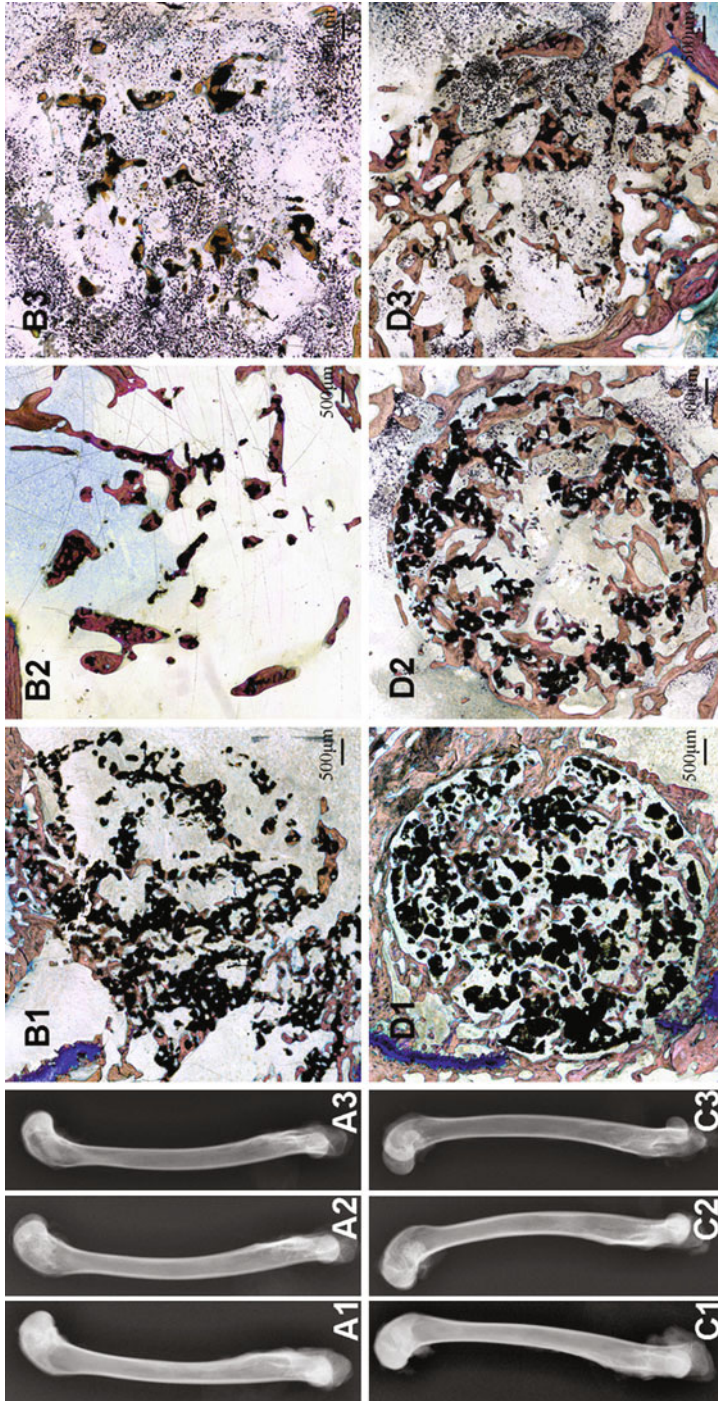


**Fig. 2** Radiographs of  $\beta$ -TCP (A1–A3) and PDLGA/ $\beta$ -CS (C1–C3) after 4 (1), 12 (2), and 20 (3) weeks postoperatively. New bone formation and material degradation in  $\beta$ -TCP (B1–B3) and PDLGA/ $\beta$ -CS (D1–D3) after implantation for 4 (1), 12 (2), and 20 (3) weeks (Van Gieson's picrofuchsin staining). Red, blue, and black represent the newly formed bone, fibrous tissue, and residual material, respectively. Scale bar, 500  $\mu$ m (For interpretation of the references to color in this figure legend, the reader is referred to the web version of this article) [34]

Silicate-based mesoporous bioactive glasses (MBG) have attracted much attention as drug delivery system owing to its highly ordered mesoporous channel structure, large surface area, and variable pore volume. It has been proved that MBG show great potential in drug delivery. Therefore, incorporation of drug-loaded MBG into a polymeric substrate appears to be an effective way to endow the scaffold with the ability of sustained and controlled drug eluting. Nanosized MBG/PLGA composite-coated  $\text{CaSiO}_3$  multifunctional scaffolds were used for delivering ibuprofen with a sustained release profile to prevent infections [37].

### **Fabrication Techniques for Composite Scaffolds**

Besides surface chemistry, factors including interconnectivity, volume, and size of the pores of scaffolds are also important parameters, which could affect functions of the scaffolds such as enhancement of tissue ingrowth in the early stage of tissue defect healing. It is generally accepted that open, interconnected, and suitable porous structure facilitates biological molecule and nutrient transportation to the inner part of the scaffolds, which is necessary to facilitate cell growth and vascularization, as well as excretion of waste products. Therefore, the development of fabrication techniques of composite scaffolds is essential for controlling the porous structure of the composites. Many conventional techniques are available for fabrication of various composite scaffolds based on the combination of biodegradable polymer and inorganic bioactive particles, including freeze-drying, solvent casting and particulate leaching, phase separation, and hot compression molding.

Freeze-drying is a common process suited to fabricate biopolymer such as collagen composite scaffolds which renders highly porous and interconnected homogenous biological constructs without damaging the structure of the biopolymer. Through the freeze-drying method, fabrication of biopolymer/silicate composite scaffolds with improved bioactivity and mechanical strength has been proved to be practical [11, 27]. In addition, freeze-drying method combined with other techniques, e.g., robocasting, was introduced to produce scaffolds with finely tuned structure of macroporous configuration, which contained well-developed micropores throughout the framework and thus have a prosperous prospect [29].

Solvent casting and particulate leaching methods mainly include three steps in sequence: mixing of polymer solution with silicate-based bioactive inorganic particles and salt particles as porogens, evaporation of the solvent, and leaching of the salt out in water. Such method allows for the fabrication of porous composite scaffold with high porosity (over 80 %), interconnected pores (300–450  $\mu\text{m}$ ), and compressive modulus (10–14 MP). However, the main shortcoming of this technique is that it could only prepare thin scaffolds (usually several millimeters in thickness) [33].

Phase separation is usually conducted at low temperature and generally covers two procedures, namely, quenching a solution with polymer and inorganic particles to form an inorganic particle-rich phase and a polymer-rich phase and solidifying the polymer-rich phase with the removal of the polymer-poor phase to form a porous polymer network. The composite scaffolds obtained by this technique have a wide range of pore size distribution (including micro- and macropore structure), which is

beneficial for scaffolds with the desire of tiny bioactive particles or biomolecule incorporation into the struts. Through this technique, wollastonite particles were dispersed uniformly on the pore walls of chitosan/wollastonite composite scaffolds with interconnected pores varied from 60 to 200  $\mu\text{m}$  [28].

Hot compression molding involves filling a mold with mixtures of polymer/inorganic particles and porogen powders and followed by heat treatment in high temperature together with intended pressure. The main virtue of this technique for preparation of biodegradable polymer/silicate bioceramics composite scaffolds is the relatively high mechanical properties of the scaffolds, whereas the disadvantages include the inefficient removing of the residual porogens and the high processing temperature that may be destructive to the chemical structure of some polymers [35].

Rapid prototyping (RP) methods are emerging techniques to design and fabricate scaffolds with complex and controlled pore size, shape, and interconnectivity directly from computer-aided design and manufacturing. Among RP techniques, 3D plotting has shown promising potential for direct fabrication of tissue engineering scaffolds with the advantage of mild processing conditions, which enables incorporation of drugs, biomolecules, and even cells during plotting. MBG/alginate hierarchical scaffolds with well-ordered nano-channels, micropores, and controllable macropores were fabricated by 3D plotting, and the structural architecture of the composite scaffolds could be optimized by control of the plotting parameters (Fig. 3). Furthermore, as a drug delivery system, the incorporation of MBG decreased the initial burst release and led to a more sustained release of dexamethasone from the composite scaffolds, and the release rate was a function of the MBG content [38]. Homogenous surface coating of MBG throughout the poly 3-hydroxybutyrate-co-3-hydroxyhexanoate (PHBHHx) scaffolds was prepared using combinational 3D printing and surface-doping protocol. These hierarchical scaffolds showed the bioactivity superior to that of scaffolds made of pure PHBHHx, and the MBG coating provided a more preferable environment for human mesenchymal stem cell (hMSC) attachment, proliferation, and osteogenic differentiation [12]. Therefore, 3D plotting could be a promising platform for the preparation of silicate/polymer composite scaffolds for BTE applications.

## **Injectable Composite Hydrogels**

Injectable hydrogels are cross-linked polymers with hydrophilic groups which can change structure in response to salt concentration, pH, temperature, etc. and have received much attention as they can provide hydrated 3D environment that is similar to the ECM of native tissues, thus holding a great promise in tissue engineering applications. Inspired by the advances in research on silicate-polymer composite scaffolds, intended incorporation of silicate-based bioactive inorganic particles into hydrogels has been investigated, aiming at combining the advantages of the hydrogel and silicate-based bioceramics. Up to now, several polymeric hydrogel/silicate bioceramics composite systems have been developed, and their performance for

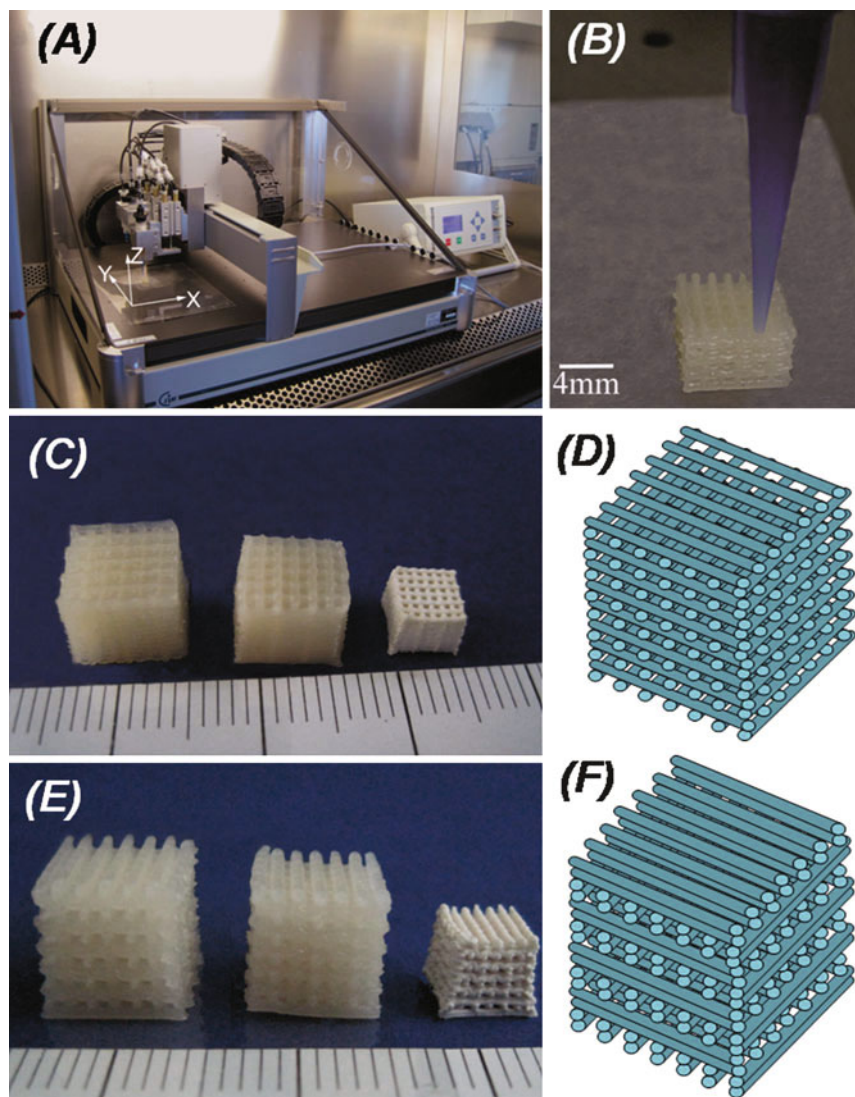


**Fig. 3** Photographs of the 3D plotting system (a) and a scaffold during plotting (b); CAD models (d, f) and scaffolds (30 % MBG/alginate) (c, e) with XY pattern (c, d) and XYYY pattern (e, f). (c) and (e), scaffolds are shown in wet state after plotting and after cross-linking in 500 mM  $\text{CaCl}_2$  solution and dry state, respectively (from *left to right*). In the design used for plotting, the cubic scaffolds had an edge length of 8 mm and a pore size of 850  $\mu\text{m}$  [38]

tissue engineering has been evaluated in details. Herein, the polymeric hydrogel substrate can be generally categorized based on their source, namely, natural hydrogels and synthetic hydrogel. Among the natural hydrogels, chitosan, alginate, and their derivatives have been studied extensively. Meanwhile, for the synthetic

group, poly(vinyl alcohol)- and poly(ethylene glycol)-based hydrogels have been investigated in recent years.

### **Silicate/Natural Polymer Composite Hydrogels**

Sodium alginate (SA) has the distinctive ability to form hydrogels via ionotropic cross-linking in the presence of divalent cations such as calcium ions ( $\text{Ca}^{2+}$ ) in the room temperature. Since  $\text{CaSiO}_3$  is degradable and could release  $\text{Ca}^{2+}$  in physiological environment during the degradation,  $\text{CaSiO}_3$ /SA composite hydrogel was prepared by self-cross-linking of alginate with  $\text{Ca}^{2+}$  in the presence of D-gluconic acid  $\delta$ -lactone (GDL) and the gelling time; compressive properties and swelling behavior could be controlled by varying the amounts of  $\text{CaSiO}_3$  and GDL. Here, GDL is functioning as a regulator to control the release of  $\text{Ca}^{2+}$ , which will control the injectability of the composite hydrogel. The CS/SA composite hydrogel showed bioactivity in stimulating osteogenic differentiation of rBMSCs and promotes angiogenesis of human umbilical vein endothelial cells as pure CS bioactive ceramics [39].

Alginate microspheres are considered as a promising material for drug delivery due to their excellent biocompatibility. However, their main disadvantage is the low drug loading efficiency and noncontrollable drug release. Incorporation of MBG into alginate was found to increase the loading amount of dexamethasone as compared to pure alginate microspheres, which was attributed to the large surface area and enrichment in hydroxyl groups of BG. Besides, it is interesting to note that the drug delivery ability of bioactive inorganic materials/alginate composite microspheres could be controlled by controlling the pH environment [40].

Maintenance of the pH value of the hydrogel is a vital issue for its clinical application, which allows for the incorporation of cells or bioactive agents. A novel chitosan/Bonelike<sup>®</sup> (glass based on the  $\text{P}_2\text{O}_5$ -CaO- $\text{Na}_2\text{O}$  system) hydrogel was synthesized by using  $\gamma$ -glycidoxypropyltrimethoxysilane (GPTMS) in a sol-gel process which was easy to inject. The time required for gelation and the degradability of the hydrogel could be controlled by controlling the concentration of chitosan and GPTMS. Most importantly, the pH changes caused by the chitosan/Bonelike<sup>®</sup> hydrogel were small which could not cause any deleterious effect in vivo [41].

The combination of silicate-based bioceramics and natural hydrogels retains the high water content network of the hydrogel and the bioactivity of silicate-based bioceramics which show great potentials in bone regeneration and tissue engineering applications.

### **Silicate/Synthetic Polymer Composite Hydrogels**

In comparison with natural hydrogels, the well-defined structure of synthetic hydrogels may lead to finely tunable degradation kinetic. However, the inherited low mechanical strength and lack of bioactivity of these synthetic hydrogels limit their applications. Recently, composite hydrogels with bioactive inorganic materials as reinforcement have received strong interests for biomedical applications. A series of polyvinyl alcohol (PVA)/bioglass composite hydrogels were synthesized through ultrasonic dispersion, heat high pressure, and freeze-thawed technique. Compared

with the pure PVA hydrogel, the elastic compression modulus of PVA/bioglass composite hydrogels was significantly improved by uniform distribution of bioglasses within the composites [42]. Another study has revealed that the incorporation of BG into PEG hydrogel could enhance the mechanical strength of the hydrogel, and the as formed PEGs/BG composite hydrogel possessed the ability to induce the deposition of apatite on the surface, making these hydrogel-based composites a suitable candidate as bioactive bone graft substitutes [43].

The development of advanced hydrogels with tunable physiochemical properties and desirable bioactivity remains a major challenge for tissue regeneration, for which silicate-containing hydrogels have provided promising solutions and are worthy of further investigations.

## Composite Bone Cements

Polymer bone cements, which mainly consist of polymethylmethacrylate (PMMA), have been used for fixation in joint replacement surgery, filling dental cavities, and augmentation of vertebrae. Despite the desirable mechanical strength and handability, the lack of bioactivity remains the major concern over clinical applications. Currently, researches have been focusing on the incorporation of silicate-based bioactive fillers into bone cements, such as BG and bioactive glass–ceramics, in order to improve the surface bioactivity as these inorganic materials can bond to the living bone inside the body through the formation of an apatite layer on the surface. In order to provide PMMA with bioactivity, granules of a BG  $50\text{CaO} \cdot 50\text{SiO}_2$  (mol %) were suspended into PMMA substrate through ultrasonic agitation in order to obtain bioactive cements. The addition of glass granules could soften the PMMA substrates. After 4 h soaking in SBF, aggregates of apatite particles appeared on the substrates. Apatite was precipitated on the whole substrate surface within 1 day. The silica gel islands on PMMA due to the silicate anions from the glass were considered to induce nucleation of the apatite particles [44]. The mechanical property and bioactivity of bioactive glass–ceramic particles (based on the  $\text{Na}_2\text{O}-\text{CaO}-\text{SiO}_2-\text{P}_2\text{O}_5$  glass system) and HA into commercial PMMA bone cement were compared. The PMMA/glass–ceramic sample showed a higher flexural strength and flexural modulus than those of PMMA/HA samples. Most importantly, apatite globules were formed on the surface of PMMA/glass–ceramic composite cements, verifying their improved surface bioactivity as compared with the original PMMA cements [45].

In recent years, calcium silicate-based cements (CSCs) with high bioactivity and enhanced osteogenesis, such as  $\text{Ca}_3\text{SiO}_5$  and  $\text{Ca}_2\text{SiO}_4$ , opened up new possibilities in the field of bone filling materials. However, the inappropriately long setting time and relatively low compressive strength of the cement made them difficult to deliver to bone defects with complex structures. One strategy to overcome these disadvantages is to combine CSCs with cohesion promoters such as chitosan. Wang et al. developed a novel rapid-setting root-canal filling and substitute materials consisting of chitosan oligosaccharide (COS) and  $\beta\text{-Ca}_2\text{SiO}_4$ . The incorporation of

5 wt% COS was obviously effective in shortening the setting time and enhancing the compressive strength of CSCs. In vitro experiments indicated that the hybrid cement containing 5% COS induced formation of HA in SBF after 1 day soaking [46]. Lin et al. prepared anti-washout carboxymethyl chitosan (CMCS)-Ca<sub>3</sub>SiO<sub>5</sub> (C<sub>3</sub>S) pastes. CMCS-C<sub>3</sub>S pastes were stable in the shaking SBF after immediately mixed. The addition of CMCS could significantly enhance the cohesion of particles and at the same time restrain the penetration of liquid and thus endow the anti-washout ability. The setting times of the composite pastes increased with the increase of CMCS concentrations in the hydration liquid [47]. In a word, calcium silicate-based inorganic cement composite with biopolymer could endow better performance, like shorter setting time and better mechanical properties as compared to pure CSCs.

## Surface Modification of Silicate-Based Bioactive Inorganic Materials

The interfacial interaction between bioactive inorganic particles and polymer matrix plays a significant role in determining the properties of the silicate inorganic materials/polymer hybrids. Similar to other hydrophilic inorganic particles, inorganic silicate powders tend to agglomerate in the hydrophobic polymer matrix due to their small dimensions and incompatible polarity with polymers, and the integral property of the composite would be influenced consequently. Therefore, it is critical to improve the compatibility between the silicate-based bioactive inorganic particles and the polymer components so as to obtain the uniform dispersion of silicate-based bioactive inorganic particles within the composites. For this purpose, surface modification of silicate-based bioactive inorganic materials is one of the most effective approaches to improve the compatibility of inorganic components in polymer substrates. The rationale is that the Si-OH on the surface of silicate-based bioactive particles could react with functional group of organic molecules, which would lead to a more compatible surface of the silicate particles to the polymeric substrate, which favors a more uniform dispersion and stronger interfacial strength.

## Silanization of Silicate-Based Bioactive Inorganic Materials

Coupling agents can enhance the adhesive bonds of dissimilar surfaces by developing a highly cross-linked interphase region. As a typical coupling agent, silanes as bifunctional compounds can bind the filler particles to the polymer matrix which may also provide protection for leaching, and thus the mechanical properties of the composite may be retained for a longer period [48]. The 3-aminopropyltrimethoxysilane (APS) is one of the most common nontoxic silane coupling agents which was used to modify the surface of BG in order to improve the phase compatibility between poly-L-lactide (PLLA) and BG. BG particles were uniformly dispersed without agglomeration in PLLA matrix after surface modification. Furthermore, the bending strength, bending modulus, and shearing strength of PLLA/BG-APS composites were all higher than those of unmodified composites [49]. Silane coupling agent (Z-6030,  $\gamma$ -methacryloxypropyltrimethoxy) has also been used as coupling agents to



eliminate the weak bonding between polymethylmethacrylate (PMMA) and  $\text{CaSiO}_3$  phases. The hydroxymethyl groups of Z-6030 could be substituted by hydroxyl groups that could chemically bond with  $-\text{OH}$  groups on the  $\text{CaSiO}_3$  particle surface forming  $\text{O}-\text{Si}-\text{O}$  chemical bonding. The results indicated that appropriate amount of  $\text{CaSiO}_3$  nanoparticles (0.6 %) modified by appropriate amount of Z-6030 (1.5 %) could improve the flexural strength and surface hardness of PMMA denture base materials [50].

Silane coupling agents improve the interfacial strength between silicate and polymer by developing a highly cross-linked interphase region, which is realized by the chemical bonding between the hydroxyalkyl groups of silane coupling agents and hydroxy groups on the surface of silicate-based bioactive inorganic particles. If the presence of silane coupling agent was inadequate, the combination between the agent and the silicate particles would not be sufficient to improve the mechanical strength or, even worse, may result in a decrease of the strength. Therefore, the proper ratio of the silane coupling agent to the silicate particles is essential for the effect and efficiency of surface modification [50].

### Surface Modification with Dodecyl Alcohol

Dodecyl alcohol was used to modify silicate-based bioactive inorganic particles through esterification reaction to improve the homogeneous dispersion of inorganic particles in polymeric matrix [51]. The hydroxyl groups of dodecyl alcohol condensed with the  $\text{Si}-\text{OH}$  groups on the surface of BG particles through esterification. The modified composite films can still induce the formation of HA on their surface after immersion in SBF, and the distribution of HA was more homogeneous on the composite films. However, the disadvantage of the modification with dodecyl alcohol was the decrease in hydrophilicity, which may affect the biocompatibility of the composite materials. Fortunately, this modification is reversible, and the dodecyl alcohol can be removed after the achievement of homogenous dispersion of silicate-based inorganic particles in composite materials by hydrolytic treatment in hot water. The properties (such as tensile strength) of the composite films after treatment will not be affected. Most importantly, cells on the composite films after hydrolysis showed a high proliferation rate [52] (Fig. 4).

In summary, it is a useful way to improve the dispersivity of inorganic particle in polymer matrix by modifying the surface of silicate-based bioactive inorganic particles with nontoxic organic molecules, especially biocompatible molecules.

---

## Silicate-Based Bioactive Inorganic/Inorganic Composites

The composite system is designated as inorganic composite systems if the components in the composites are mainly inorganic. Silicate-based bioactive inorganic composite materials are a kind of inorganic composite system which has attracted great attention in recent years owing to their enhanced properties if the constituents are optimally designed. The properties and functions of inorganic composites can be tuned by controlling the composition and fabrication methods. Basically, the silicate-based

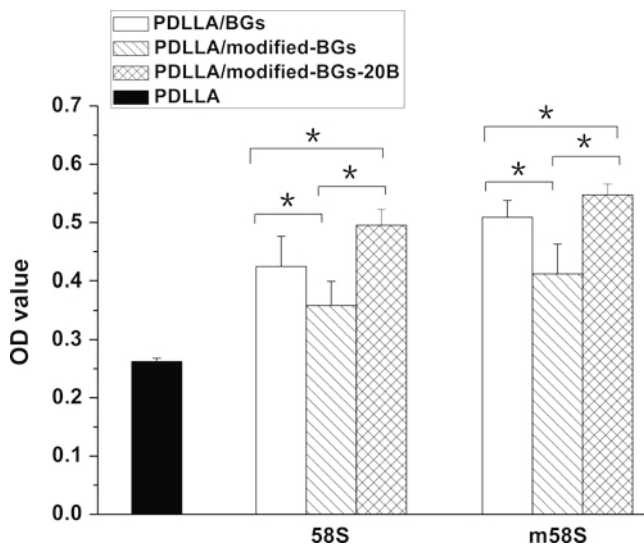


**Fig. 4** The dMSC proliferation on different composite films. OD value on y-axis represented the number of living cells. Asterisk indicates that the difference between the two data was significant ( $p < 0.05$ ) [52]

inorganic composite system could be generally classified into two categories, namely, the preformed silicate-based composite ceramics and the silicate-based bone cements with the ability of self-setting. At the end of this section, silicate-based bioceramic composites modified with graphene and SiC were also briefly reviewed.

## Silicate-Based Composite Ceramics

Compared to bioinert metal oxide ceramics (e.g.,  $\text{Al}_2\text{O}_3$  and  $\text{ZrO}_2$ ) and conventional calcium phosphate ceramics, silicate-based bioceramics with specific compositions possess distinct bioactive properties by enhancing the *in vitro* osteogenic and angiogenic differentiation of stem cells, which is also the main force for the development of the silicate-based bioceramics. However, the main shortcomings of silicate-based materials are intrinsic brittleness and mechanical weakness which restrict their intended medical applications. The design of composite materials thus offers an exceptional opportunity to allow well control of material properties. It is a common notion that the chemical composition is one of the most important factors that affect the properties of materials. The rational design of silicate-based composite ceramics is that their mechanical properties, degradation behavior, bone bonding, and regenerating ability could be regulated by tuning the components of the materials. Despite their successful applications, calcium phosphate ceramics and bioinert ceramics such as alumina and zirconia are still frequently investigated due to their poor biodegradability or lack of bioactivity [1, 2]. Previous studies have shown that

BG and glass–ceramic containing CaO and SiO<sub>2</sub> possessed good bioactivity and the CaO–SiO<sub>2</sub> system (like calcium silicate, CS) has been considered as the basis for the development of the third-generation tissue regeneration materials presently in development [6]. Meanwhile, silicate-based bioceramics in some certain composition show admirable biodegradability. Therefore, development of calcium phosphate–silicate and bioinert ceramic/silicate composite ceramics may offer a chance to produce novel bioceramics with improved bioactivity and biodegradability.

### Calcium Phosphate–Silicate Composite Ceramics

Calcium phosphate ceramics appear to be very prominent for hard tissue replacement due to their remarkable biocompatibility and their close chemical similarity to biological apatite in human hard tissues. Although some calcium phosphate bioceramics are osteoconductive, they lack the ability to stimulate cell differentiation and bone regeneration, which impede their wider clinical applications. Low degradability and mechanical strength also severely hinder their practical use [2]. The design of calcium phosphate–silicate composite materials is one of the primary approaches to enhance bioactivity of the materials.

Hydroxyapatite (Ca<sub>10</sub>(PO<sub>4</sub>)<sub>6</sub>(OH)<sub>2</sub>, HA) ceramic is one of the most frequently used calcium phosphate ceramics for hard tissue regeneration due to its remarkable biocompatibility, high osteoconductivity, and chemical similarity to biological apatite in human hard tissues. However, conventional HA bioceramics represent poor mechanical strength, and moreover their low degradability prevents complete bone replacement and bone remodeling. Therefore, there is urgent clinical demand for increasing the mechanical properties and degradability of the HA-based bioceramics, and one approach to solve these problems is to combine HA with a biodegradable and toughening phase. HA/CS composite bioceramics with different weight ratio were fabricated, and it was found that the mechanical properties, bioactivity, and the dissolution rate of the composites were upgraded with increasing CS content. Moreover, the proliferation rate of BMSCs on the composites was significantly higher than that of the pure HA ( $P < 0.05$ ). These results suggest that the mechanical properties, bioactivity, degradability, and cell activity of the HA/CS composite bioceramics could be tailored by adjusting the initial HA/CS ratio, and the HA/CS composites might be promising candidates for hard tissue repair [53].

Bioresorbable  $\beta$ -Ca<sub>3</sub>(PO<sub>4</sub>)<sub>2</sub> (TCP) is another widely used calcium phosphate bioceramics. However, relatively low bone formation ability of TCP may impede its further clinical applications. Calcium silicate (CaSiO<sub>3</sub>, CS) ceramics have been investigated as a new type of bioceramic for hard tissue regeneration owing to their excellent bone regeneration ability and biodegradability [54]. Liu et al. [55] investigated the in vivo effect of CS on the degradability, osteogenesis, and bioactivity of TCP by preparing porous TCP/CS composite bioceramics with different weight proportions. The results showed that the osteointegration and osteogenesis of porous TCP/CS composite bioceramics were significantly enhanced as compared with pure TCP ceramics, and the degradation rate of the composite was between those of pure TCP and CS. It was therefore assumed that a suitable combination of calcium

phosphate and calcium silicate ceramics may render greater functionality as compared to pure calcium silicate and calcium phosphate ceramics. Further experiment results proved that the TCP/CS composite scaffolds had excellent osteoconductivity and stimulated rapid bone formation compared with pure  $\beta$ -TCP and  $\beta$ -CS scaffolds in rabbit femur defects, and most importantly, they could degrade progressively at a rate matching the regeneration of new bone [56]. The introduction of CS into porous TCP bioceramics is thus an effective method to prepare bioactive bone grafting scaffolds for clinical applications.

### Calcium Silicate/Bioinert Metal Oxide Composite Ceramics

Although the silicate-based bioceramics possess good bioactivity, the insufficient mechanical properties hinder the silicate-based bioceramics in clinical application, especially in those where high mechanical strength is required. On the other side, some bioinert metallic oxide ceramics such as alumina and zirconia have high mechanical strength and toughness. Appropriate incorporation of tough metallic oxide ( $MO_x$ ) particles into silicate-based bioceramics is considered as a practical approach to improve mechanical properties of the materials.

Alumina ( $Al_2O_3$ ) and zirconia ( $ZrO_2$ ) as bioinert ceramics have been widely applied in the field of prosthodontics and orthopedics owing to their high mechanical properties, which makes them as ideal toughening fillers when improving the mechanical strength of silicate-based bioceramics is concerned. A uniform  $Al_2O_3$  and  $\alpha$ -calcium silicate ( $\alpha$ - $CaSiO_3$ ) composite ceramic were fabricated by mechanochemical method and then sintered at 1250 °C to produce composite ceramics with open porosity and high hardness and fracture toughness. A newly formed phase  $CaAl_2O_4$  from the reaction of CS and alumina mainly contributed to the improvement of mechanical properties of the composite ceramics [57]. Besides  $Al_2O_3$ , zirconia ( $ZrO_2$ ) ceramic is another bioinert ceramic that can be applied to reinforce silicate-based bioceramics.  $\beta$ - $CaSiO_3/ZrO_2$  nanocomposites were fabricated by spark plasma sintering (SPS) technique. The addition of  $ZrO_2$  could inhibit the phase transition of CS and increase its phase transition temperature. A nanocrystalline  $ZrO_2$  network structure was formed in the nanocomposites, by which the fracture toughness was significantly improved. The composites showed good in vitro bioactivity with HA layer formation on the surface of the nanocomposites in SBF [58].

Besides the  $MO_x$ -reinforced CS ceramics, different kinds of silicate-based ceramics hybrids have been developed. A series of  $\beta$ - $CaSiO_3/Mg_2SiO_4$  (CS/ $M_2S$ ) composites with different ratios were prepared by sintering the CS/ $M_2S$  composite powder compacts at different temperature. The heat treatment induced a reaction between the CS and  $M_2S$ , and the composites obtained were a mixture of CS,  $M_2S$ ,  $CaMg(SiO_3)_2$ , and  $Ca_2MgSi_2O_7$ . With the formation of these intermediate phases, the mechanical properties of CS/ $M_2S$  composites steadily increased with the increase of  $M_2S$  amount. It was also found that CS/ $M_2S$  composites retained the ability to induce apatite formation on the surface in SBF if the proportion of  $M_2S$  was reasonably selected. Furthermore, in vitro cell culture experiments indicate that the composites supported osteoblast-like cell proliferation effectively. The results

suggest that combination of CS and  $M_2S$  is a proper way to obtain Ca–Si–Mg composite ceramics with improved properties [59].

## Silicate-Based Bone Cements

In order to meet the need of minimal invasive surgery in clinical applications, the concept of self-setting bone cements has been introduced to be applied as injectable or moldable bone substitutes to augment human bone tissues [60]. Inorganic bone cements like calcium phosphate cements (CPC) and plaster ( $CaSO_4 \cdot 1/2H_2O$ , POP) have been steadily studied as self-setting bone filling materials. However, both CPC and POP have their own problems such as lack of osteogenic activity and unsatisfactory degradability. Recently, calcium silicate-based bone cements (CSCs) have attracted attention owing to their distinguished advantages such as apatite-inducing activity and osteostimulation ability. Similar to calcium silicate bioceramics, ionic products of calcium silicate-based cements during their degradation could significantly stimulate the proliferation and osteogenic differentiation of osteoblast-like cells and dental pulp cells [61]. It is therefore clear that the single-phase bone cements need to be modified to fully meet the clinical demand. Composite CSC with other inorganic phases may be an alternative way to obtain composite cements with adorable properties for practical application. In this section, the properties of CSC and their composites with other kind of inorganic bone cements are introduced, respectively.

### Calcium Phosphate–Silicate Composite Bone Cements

CPC have been extensively studied owing to their chemical similarity to the mineral phase of bone tissue and good osteoconductivity for bone reconstruction. In clinical applications, CPC can be used in the form of blocks or as a self-setting paste, which could rapidly set and provide supporting for bone regeneration. However, as soluble acidic phosphates are used as sources of phosphate ions, the setting process of some kinds of CPC (e.g., brushite cement) may cause a rapid decrease of pH in vivo immediately after implantation. This phenomenon can have an adverse impact on the biocompatibility of the material. Tricalcium silicate ( $Ca_3SiO_5$ ,  $C_3S$ ) is one of the main components of Portland cement. Once mixed with water,  $C_3S$  will react with water to create calcium–silicate–hydrate (C–S–H), and the polymerization and solidification of the C–S–H network contribute to the self-setting property of the material. However, this material could induce a significant increase in the surrounding pH ( $>10$ ), and the setting time of the cement paste is quite long, which may make it not suitable for clinical applications. Considering the characteristics of CPC and  $C_3S$  cements, composite cements were designed and prepared by hybridizing CPC, containing  $\beta$ -TCP and monocalcium phosphate monohydrate (MCPM), with bioactive  $C_3S$ . The results showed that the composite cements processed higher injectability by moderately prolonged setting time and mechanical strength as compared with their CPC counterparts. More importantly, the composite cements possessed an improved ability to promote osteoblastic differentiation of BMSCs,

indicating that the composites may possess a better support for bone regeneration [62].

Another calcium phosphate–silicate composite cement can be obtained by mixing  $\text{CaHPO}_4 \cdot 2\text{H}_2\text{O}$  (DCPD) and  $\text{C}_3\text{S}$  with 0.75 M sodium phosphate buffers ( $\text{pH} = 7.0$ ) as liquid phase. The setting times, injectability, degradability, and compressive strength are investigated and compared with that of DCPD/CaO cement system. With the weight ratio of  $\text{C}_3\text{S}$  varied from 20 % to 40 %, the workable DCPD/ $\text{C}_3\text{S}$  pastes set within 20 min, and the hydrated cement shows significantly higher compressive strength (around 34.0 MPa after 24 h) than that of the DCPD/CaO cements (approximately 10.0 MPa), and the degradability of DCPD/ $\text{C}_3\text{S}$  cement is improved. Additionally, the composite cement possesses better ability to support and stimulate cell proliferation than the DCPD/CaO cement [63].

These researches have demonstrated that the combination of bioactive calcium silicate with calcium phosphate cement is a possible approach to obtain bioactive self-setting composite cements with superior self-setting and biological properties for bone regeneration.

### Calcium–Silicate–Aluminate Composite Bone Cements

$\text{Ca}_3\text{Al}_2\text{O}_6$  has the fastest hydration rate among the main components of Portland cement. Although not suitable as single-phase bone cement due to its arguable cytocompatibility, it is assumed that the limited presence of  $\text{C}_3\text{A}$  in  $\text{C}_3\text{S}$ ,  $\text{C}_2\text{S}$ , or  $\text{C}_3\text{S}/\text{C}_2\text{S}$  (CSC) cements may accelerate the hydration process and improve the short-term compressive strength of the materials.  $\text{C}_3\text{S}/\text{C}_3\text{A}$  and  $\text{C}_2\text{S}/\text{C}_3\text{A}$  composite systems are able to form biphasic mixtures. Studies showed that the addition of  $\text{C}_3\text{A}$  into  $\text{C}_3\text{S}$  and  $\text{C}_2\text{S}$  indeed could reduce the setting time and improve the compressive strength of the substrates. Furthermore, both mixtures are bioactive and biocompatible and have a stimulatory effect on the L929 cell growth when the content of  $\text{C}_3\text{A}$  is below 10 % [64, 65]. Further study showed that the CSC/ $\text{C}_3\text{A}$  cement was notably more compatible with the human dental pulp cells compared with the commercially available Dycal<sup>®</sup> [66]. Therefore, silicate-based cements mixed with small amount of  $\text{C}_3\text{A}$  appear as a promising candidate as dental cement considering their relative short setting time, high compressive strength, good in vitro bioactivity, and biocompatibility.

### Calcium Silicate/Calcium Sulfate Cements

Plaster ( $\text{CaSO}_4 \cdot 1/2\text{H}_2\text{O}$ , POP) has been used as bone filling material for more than a hundred years. It can react with water promptly and transform into gypsum ( $\text{CaSO}_4 \cdot 2\text{H}_2\text{O}$ ), which is in the form of solid and hard lump. After 1 or 2 weeks of implantation, the gypsum degrades and tends to form many pores that allow the new bone tissues to grow in, and after 4–6 weeks, the gypsum degrades almost completely. An obviously too fast degradation rate and lack of bioactivity are the drawbacks of POP in its orthopedic applications. Some studies have found that the addition of POP into pure  $\text{C}_3\text{S}$  or  $\text{C}_2\text{S}$  cements could decrease the setting time and enhance the compressive strength and degradation rate [67, 68]. Most importantly, the composite paste showed activity in induction of apatite formation in SBF, and the

dissolution extracts of the paste had a stimulatory effect on cell growth in certain concentration range [69]. POP has also been composed with CSC to further improve the property, which showed that the addition of POP into CSC significantly decreased the initial and final setting time and enhanced the short-term compressive strength and degradation rate. The obtained composite cement with 30 % POP has been found to possess optimal setting time and short-term compressive strength. In addition, the prepared composite cements still maintain apatite-mineralization ability in SBF (Fig. 5), and their ionic extracts have no significant cytotoxicity to L929 cells [70].

Another study has shown that the addition of silicate bioceramics without hydration property such as calcium silicate (CS) into POP can also form bioactive bone cements. The POP/CS cements showed high surface bioactivity by introducing 23 % bioactive calcium silicate (CS) into POP, and these biphasic composites were favorable for decelerating the biodegradation rate by nearly 18.5% as compared to pure POP cements in 28 days *in vitro*. Further *in vivo* evaluation of the composite cements showed that the materials had a mild bioresorption rate of 39.6 % after 4 weeks, and enhanced new bone tissue regeneration was confirmed for the composite material as compared with pure gypsum in critical-sized femoral defects in rabbits [71].

### Calcium Silicate/Calcium Carbonate Cements

In cement industry, calcium carbonates are often used as hydration accelerator and filler component within cement pastes, which reduce the setting time and promote the mechanical strength of Portland pastes. In biomedical applications, calcium carbonates of biological origin (nacre and coral) and their derivatives have been used as biocompatible and resorbable bone substitutes in the form of powders, porous ceramics, and hydraulic cements. To combine the advantages of the silicate-based cements and  $\text{CaCO}_3$ ,  $\text{C}_3\text{S}/\text{CaCO}_3$  composite cements with the weight percent of  $\text{CaCO}_3$  in the range of 0, 10, 20, 30, and 40 % were synthesized. The results showed that the initial setting time was dramatically reduced from 90 to 45 min as the content of  $\text{CaCO}_3$  increased from 0 % to 40 %, and the workable paste with a liquid/powder (L/P) ratio of 0.8 ml/g could be injected within 20 min. The composite cement showed higher mechanical strength (24–27 MPa) than that of the pure  $\text{C}_3\text{S}$  paste (14–16 MPa). Furthermore, the composite cement could induce apatite formation and degrade in phosphate-buffered saline. This study indicates that the  $\text{C}_3\text{S}/\text{CaCO}_3$  composite paste has better hydraulic properties than pure  $\text{C}_3\text{S}$  paste and the composite cement is bioactive and degradable [72].

### Calcium Silicate–Fluoride Composite Bone Cements

Fluoride plays a significant role to protect enamel against demineralization and has already provided clinical benefits on tooth and skeleton repair. Incorporating fluoride into dental resins and glass ionomer cements has already been proved to be an effective method to increase the remineralization properties of filling materials. The mechanism of the protective effect of fluoride is that it can partially substitute –OH

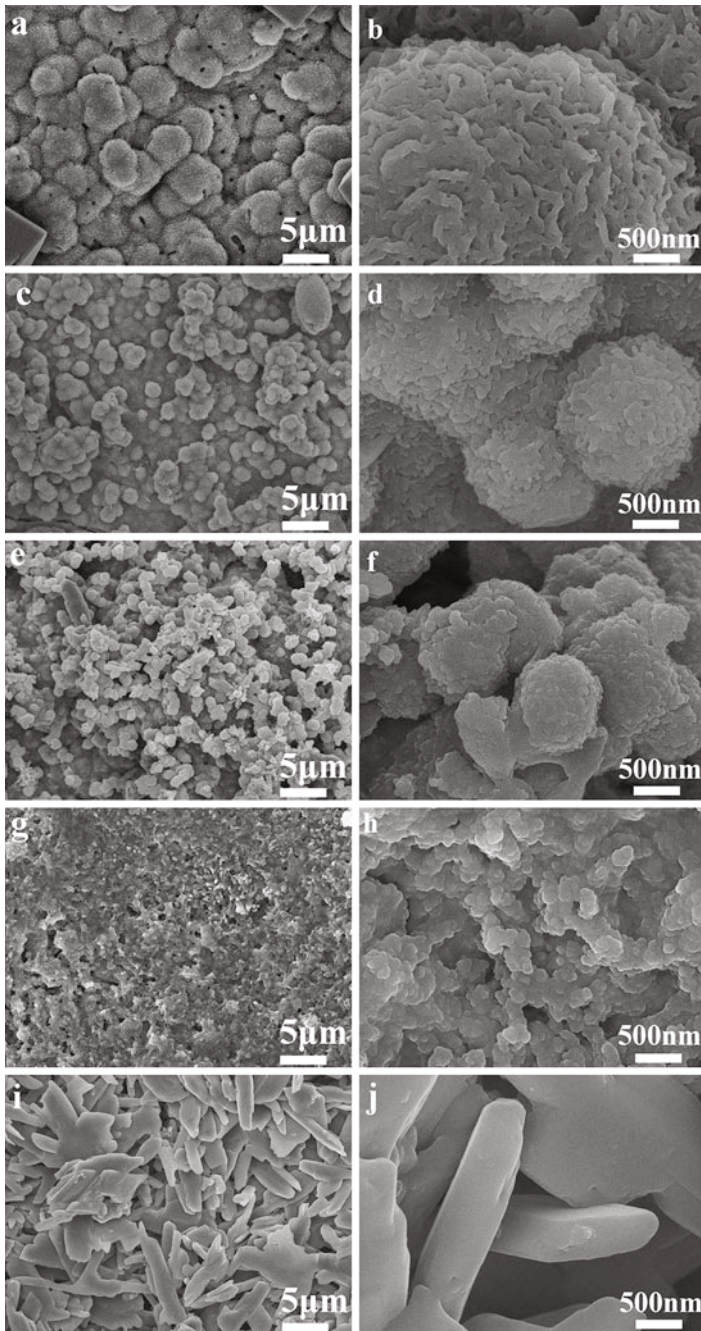


**Fig 5** SEM graphs of the different samples after soaking in the SBF solution for 7 days: (a, b) CSC, (c, d) CSC+30 % POP, (e, f) CSC+50 % POP, (g, h) CSC+70 % POP, and (i, j) POP [70]



**Table 1** Summary for the properties of silicate-based cements

Cements	Compressive strength after 1 day (MPa)	Compressive strength after 28 days (MPa)	Initial setting time (min)	Final setting time (min)	References
Ca <sub>2</sub> SiO <sub>4</sub>	0.6	~10	~300	~420	[64]
Ca <sub>2</sub> SiO <sub>4</sub> -C <sub>3</sub> A (10 %)	2.20	~18	~110	~160	[64]
Ca <sub>3</sub> SiO <sub>5</sub>	/	14–16	~90	~180	[72]
CSC Ca <sub>3</sub> SiO <sub>5</sub> -Ca <sub>2</sub> SiO <sub>4</sub> (20 %)	~26.4	~54.1	~100	~150	[70]
POP	~5	~10	~5	~15	[70]
CSC-POP (30 %)	~28	~35	~15	~25	[70]
Ca <sub>2</sub> SiO <sub>4</sub> -POP (40 %)	~5	~35	~15	~40	[67]
Ca <sub>3</sub> SiO <sub>5</sub> -POP (60 %)	/	~11.9 ± 0.6	~18	~35	[68]
CSC-C <sub>3</sub> A (5 %)	~33	~54	~30	~70	[66]
Ca <sub>3</sub> SiO <sub>5</sub> -MPM (20 %)	/	~18	~30	~90	[62]
Ca <sub>3</sub> SiO <sub>5</sub> -DCPD (60 %)	~22	~35	32 ± 1.6	60 ± 3.5	[63]
Ca <sub>3</sub> SiO <sub>5</sub> -CaCO <sub>3</sub> (30 %)	/	24–27	~45	~95	[72]

of HA and form fluoride-substituted HA which is more stable under acid conditions. Therefore, the addition of fluoride salts into silicate-based bone cements is an effective approach to increase the cement mineralization ability. Different amounts of CaF<sub>2</sub> (0, 1, 2, and 3 wt%) were incorporated into C<sub>3</sub>S cement to investigate the apatite formation ability of C<sub>3</sub>S pastes. The initial crystalline apatite formation time of the pastes with the addition of CaF<sub>2</sub> is 1 day, while the C<sub>3</sub>S pastes need 3 days to induce visible formation of the initial crystalline apatite. The thicknesses of apatite layers deposited on the surface of C<sub>3</sub>S doped with 0, 1, 2, and 3 wt% CaF<sub>2</sub> were about 88, 102, 168, and 136 μm, respectively, after soaking for 7 days. The high-level bioactivity of 2 wt% CaF<sub>2</sub>-doped C<sub>3</sub>S was attributed to F<sup>-</sup> released by the hydration product of C<sub>3</sub>S cements and the formation of F-substituted apatite with a formula of Ca<sub>8.94</sub>M<sub>1.06</sub>(PO<sub>4</sub>, HPO<sub>4</sub>)<sub>6</sub>(OH)<sub>1.95</sub>F<sub>0.05</sub> (M represents substituted ions such as Na, K, Mg) [73]. Therefore, the self-setting CaF<sub>2</sub>-doped C<sub>3</sub>S with excellent bioactivity and better mechanical properties might be more useful as bioactive materials for bone tissue repair.

The physicochemical properties such as setting time and mechanical strength of the cement play an important role in successful clinical applications. Therefore, a summary of the compressive strength and the initial and final setting time of the silicate-based composite cements after hydration for 1 day and 28 days is presented in Table 1.

It is clear to see that incorporation with CPC,  $C_3A$ ,  $CaF_2$ , POP, or  $CaCO_3$  will result in the improvement of some properties of CSC, such as shorter setting time, better mechanical properties, and admirable biodegradability as compared to pure CSC. And most importantly, the composite cements show high bioactivity which is important for bone filler materials. However, further *in vivo* studies are needed to prove the suitability of the composite cements as a filler material with adequate strength or reasonable setting rate for clinical applications.

## Other Types of Silicate-Based Bioactive Composites

One of the main challenges of implant technology is the development of new generation of light implant materials with enhanced mechanical properties, wear resistance, and better biological response. Graphene and silicon carbide (SiC) are two kinds of innovative materials which are very promising as base materials for medical implants.

### Silicate/Graphene Composites

Graphene possesses a flat monolayer of carbon atoms in a two-dimensional (2D) honeycomb lattice with high aspect ratio layer geometry and a very high specific surface area, which has received tremendous attention in recent years due to its exceptional thermal, mechanical, and electrical properties. Graphene is currently one of the most popular research areas and has been extensively studied for biotechnology applications due to its extremely large surface area, good biocompatibility, biostability, and ease of chemical functionalization. The addition of graphene into ceramics can improve the mechanical strength of the composites, while poor mechanical performance is the main drawback of silicate-based bioceramics which limits their applications under load-bearing conditions. Calcium silicate/reduced graphene oxide (CS-rGO) composites have been synthesized using a hydrothermal approach followed by hot isostatic pressing (HIP). CS – rGO composite with 1.0 wt% rGO shows improved hardness, elastic modulus, and fracture toughness as compared to pure CS. The addition of rGO does not affect the activity to induce apatite formation on CS ceramics in SBF. Interestingly, the introduction of rGO into the CS matrix stimulated human osteoblast cell proliferation and significantly increased ALP activity of the cells as compared with pure CS ceramics [74]. The graphene has also been incorporated into nano-58S bioactive glass scaffolds using a selective laser sintering system, which improved the mechanical properties of the composite scaffolds without affecting the bioactivity of bioactive glass component in SBF. The composite scaffold showed a good cell biocompatibility by *in vitro* cell culture tests, in which human osteoblast-like cells (MG-63 cells) colonized and grew favorably on the surface of composite scaffolds [75].

### Silicate/SiC Composites

Porous biomorphic SiC ceramics with hierarchical microcellular architecture and honeycomb-like microchannels have been considered as potential bone implants or

tissue engineering scaffolds for their sufficient biomechanical properties and intrinsic three-dimensional interconnected porous structure [76]. The combination of the excellent mechanical properties and low density of the biomorphic SiC ceramics with osteoconductive properties of the silicate-based materials opens new possibilities for the development of alternative dental and orthopedic implants with enhanced mechanical and biochemical properties that ensure optimum fixation to living tissue. Uniform and adherent BG film-coated biomorphic SiC by pulsed laser ablation using an excimer ArF laser possessed a dense apatite layer on the composite surface after 72 h immersion [77]. Moreover, *in vitro* cytotoxicity observation of BG-coated biomorphic SiC ceramics, using MG-63 human osteoblast-like cells, revealed that the biological response of the cells on the ceramics was similar to those on well-known implant materials like Ti<sub>6</sub>Al<sub>4</sub>V and bulk bioactive glass [78]. The BG-coated SiC ceramics which possess excellent bone-bonding ability are promising devices for dental and orthopedic applications.

---

## Silicate/Metal Composites

As “the first-generation biomaterials,” metallic biomaterials have been widely used in clinical applications as medical devices for replacement of hard tissues such as artificial hip joints, bone plates, and dental implants. Ti-based alloys, Co–Cr alloy, and stainless steel are the most commonly used metallic substrates in load-bearing orthopedic implants due to their reliable mechanical properties. However, for metallic substrates, there is always a concern about their corrosion resistance in physiological fluids and their bioactivity. The corrosion products of these conventional surgical alloys, e.g., toxic metallic ions and/or particles, may be potentially harmful to the human body. On the other side, metallic materials cannot bond directly with living bone tissues which means bioinert. After placed into the human body, metallic materials are frequently encapsulated by fibrous tissue, which cause loosening and premature failure [79]. Most importantly, conventional surgical alloys are nondegradable which often require second operations to remove after bone healing. Recently, degradable Mg alloys with good mechanical properties and biodegradability have attracted more attention as bone implant materials although some limitations like poor corrosion resistance, hydrogen elution during degradation, and lack of bioactivity need to be addressed before the clinical application [80]. Coatings with bioactive and osteoinductive properties have been made to improve the surface characteristics of metallic implants extensively [81]. As the silicate-based materials possess excellent bioactivity, it is not surprising that researchers have taken great efforts to combine metallic substrates and silicate bioactive materials to form composites with enhanced performance. In this part, the current status of silicate-based bioactive glass and ceramic coatings on the nondegradable and biodegradable metallic substrates are reviewed.

Despite the effectiveness of these coatings in prohibiting the corrosion and improving the surface bioactivity of the metallic substrate, the main concern remains over the interface between the coating and the substrate, which in some cases is

relatively weak in terms of bonding strength and thus susceptible to mechanical loading. Therefore, the development of metal matrix composites (MMCs) may represent an alternative method to achieve the desired improvements of silicate/metal composites biomaterials, thereby avoiding complications arising in coating processes [82]. Silicate-based BG and bioceramic composite with biodegradable Mg alloys are also addressed. Metal matrix composite with silicate particles as reinforcement has been proposed as a new concept to improve the bioactivity and moderate the degradability which will be presented in the last part.

## **Silicate-Based Bioactive Coatings on Nondegradable Metallic Substrates**

Metals normally cannot bond to living tissue in a natural manner; therefore, the rationale behind the deposition of ceramic coatings on bioinert metallic substrates is that the coating would endow the substrate with considerable surface bioactivity, thus leading to improved bone–implant integration [82]. Most of the previous studies have been focused on Ca–P ceramic coatings owing to their chemical similarity to the inorganic constitution of human bones. However, the interface between the Ca–P coating and the metallic substrate frequently suffers from inadequate bonding strength due to the mismatch between the thermal expansion coefficients of the two components [83]. In addition, the Ca–P coatings that have been developed in most of the currently available technologies present the characteristic of high crystallinity, which resulted in inferior bioactivity. In comparison, silicate-based ceramics possess similar thermal expansion coefficient to that of typical biomedical metals, e.g., titanium and its alloys, and superior bioactivity as compared with their Ca–P counterparts, which makes them an ideal bioactive coatings, and have attracted much attention in recent years [84]. In this part, the progresses in the development of bioactive coatings consisted of silicate-based bioceramics, such as wollastonite ( $\text{CaSiO}_3$ ), dicalcium silicate ( $\text{Ca}_2\text{SiO}_4$ ), bredigite ( $\text{Ca}_7\text{MgSi}_4\text{O}_{16}$ ), and akermanite ( $\text{Ca}_2\text{MgSi}_2\text{O}_7$ ), will be introduced, and the fabrication approaches will also be briefly reviewed.

### **CaO–SiO<sub>2</sub> Coatings**

Wollastonite coatings were prepared on Ti–6Al–4V substrate by plasma spraying technique, which exhibited high bonding strength as the thermal expansion coefficient of wollastonite is close to that of the Ti–6Al–4V substrates [85]. Biological evaluation revealed that, after 1 month of implantation in the muscle, a bone-like apatite layer was formed on the surface of the wollastonite coating. When implanted in the cortical bone, bone tissue could extend and grow along the wollastonite coating. The coating bonded directly to the bone without any gaps or fibrous tissue formation, indicating its good biocompatibility and bone–implant integration. The results suggest that deposition of wollastonite on the surface of Ti–6Al–4V is an effective way to enhance bioactivity of the metal substrates through the formation of bone-like apatite layer which was very important for implant bonding to the bone tissue.

C<sub>2</sub>S coating on titanium alloys has also been fabricated though plasma spraying, and a dense HAP layer could form on the surface after incubation in SBF solution for 2 days [86]. The results indicated that the plasma-sprayed C<sub>2</sub>S coatings possess excellent bioactivity. In order to expedite the bonding strength between the coating and the substrate, C<sub>2</sub>S-based composite coatings reinforced with titanium were fabricated via atmospheric plasma spraying on Ti-6Al-4V alloy substrates. The cross-sectional pictures of the coatings showed that the composite coatings had a typical lamellar structure with alternating C<sub>2</sub>S and Ti phases. The incorporation of Ti could effectively inhibit the propagation of the cracks in the coatings and increase the bonding strength of the composite coatings with an increase in Ti content, while the Ti-reinforced C<sub>2</sub>S coatings still showed good bioactivity [87].

### CaO-SiO<sub>2</sub>-MgO Coatings

It has been reported that Mg ions in certain concentration could stimulate adhesion and proliferation of osteoblastic cells, and CaO-SiO<sub>2</sub>-MgO ceramics have shown good bioactivity by stimulating bone regeneration [88]. On these bases, plasma spraying akermanite (Ca<sub>2</sub>MgSi<sub>2</sub>O<sub>7</sub>), diopside (CaMgSi<sub>2</sub>O<sub>6</sub>), and bredigite (Ca<sub>7</sub>MgSi<sub>4</sub>O<sub>16</sub>) as new silicate coatings on titanium alloys have been studied.

Akermanite possesses a relatively moderate degradability, and its ionic products could significantly stimulate proliferation and osteogenic differentiation of stem cells. Recently, akermanite coatings have been prepared on Ti-6Al-4V through plasma spraying technique. The bonding strength between the akermanite coatings and Ti-6Al-4V substrates is around 38.7–42.2 MPa, which is higher than that of plasma-sprayed HA coatings. The akermanite coatings revealed distinct apatite-mineralization ability in SBF and supported the attachment and proliferation of rabbit bone marrow mesenchymal stem cells (BMSCs). It is also noted that the proliferation rate of BMSCs on akermanite coatings is obviously higher than that on HA coatings [83]. The findings suggest that the akermanite coatings may be a promising candidate for orthopedic and dental applications.

Similar to akermanite, another two kinds of Mg-containing silicate ceramics, diopside (CaMgSi<sub>2</sub>O<sub>6</sub>) and bredigite (Ca<sub>7</sub>MgSi<sub>4</sub>O<sub>16</sub>), have also the ability to induce apatite formation and stimulate bone formation, while their degradation rates differ from that of the former [9, 89]. Diopside coatings were sprayed onto Ti-6Al-4V substrates using an atmospheric plasma spraying system [90]. The bonding strength of the diopside coating to the metallic substrate is approximately 32.5 MPa, which is higher than that of HA coatings. In addition, the diopside coating shows a Young's modulus of 38.56 GPa, which is close to the cortical bone. With similar fabrication method, the plasma-sprayed bredigite coating on Ti-6Al-4V substrate reveals an even higher bonding strength to titanium alloy substrate up to 49.8 MPa [91] and supports the attachment and proliferation of rabbit bone marrow stem cells. It is found that the proliferation rate of cells on bredigite ceramic coating is significantly higher than that on the HA coating. The released SiO<sub>4</sub><sup>4-</sup> and Mg<sup>2+</sup> ions from bredigite coating as well as the deposited nano-apatite layer on the coating surface might contribute to the improvement of cell proliferation. These results suggest that

diopside and bredigite coating may be potential candidates for modifying surface properties of metal orthopedic implants.

### **CaO–SiO<sub>2</sub>–MgO–SrO Coatings**

Concerning the importance of strontium (Sr) in stimulating the growth and mineralization of the bone, Sr<sub>2</sub>MgSi<sub>2</sub>O<sub>7</sub> (SMS) ceramics have been developed recently, which showed good activity in supporting BMSC growth and enhancing the ALP activity and bone-related gene expression of BMSCs as compared to β-TCP [92]. Coatings composed of Sr<sub>2</sub>MgSi<sub>2</sub>O<sub>7</sub> (SMS) ceramic have been prepared on Ti–6Al–4V by plasma spraying method [93]. The coatings have higher bonding strength (~37 MPa) than conventional hydroxyapatite (HA) coatings (mostly in the range of 15–25 MPa). Furthermore, a study has shown that the SMS coating could inhibit both the inflammatory reaction and the osteoclastic activities. Meanwhile, the coating depressed the expression of osteoclastogenesis-related genes (RANKL and MCSF) in BMSCs with the involvement of macrophages, while OPG expression was enhanced as compared to HA coatings, indicating its ability to downregulate osteoclastogenesis. All these results suggested that the SMS coating possesses multifunctional effects, including reduced inflammatory reaction, downregulated osteoclastic activities, and maintained osteogenesis.

Ideal coating materials for orthopedic implants should be able to induce osteointegration, which requires several important parameters, such as good bonding strength, limited inflammatory reaction, and balanced osteoclastogenesis and osteogenesis, to gain well-functioning coated implants with long-term life span after implantation. In some terms, silicate bioceramic coatings on nondegradable metallic substrates have shown great promise. However, more *in vitro* and in particular *in vivo* investigations are required to confirm the feasibility of this type of new coatings for clinical applications.

## **Silicate Bioceramics Composite with Biodegradable Metallic Substrates**

Degradability of magnesium alloys, which is unique from other metals used as biomedical implants, allows the gradual resorption of the implants and thus avoids the need for the second surgery to remove the implants after bone healing. However, its inappropriately too fast degradation rate and lack of bioactivity of the material have hindered its potential clinical applications. In order to improve the performance of Mg alloys, bearing of silicate-based coatings on the surface of Mg alloys and fabrication of Mg-based metal matrix composites containing silicates have been proved to be efficient. In this part, both the two approaches are introduced, respectively [94].

### **Silicate Bioactive Coatings on Biodegradable Mg Alloy Substrates**

Tailoring of the surface of Mg alloy substrates with suitable inorganic or organic coatings may reduce the corrosion rate. Coating biodegradable Mg alloy substrates with silicate-based bioactive coatings may provide the composite with biocompatibility and osteoconductivity. Silicate-based mesoporous bioactive glass (MBG) coatings have

been fabricated on pure Mg substrate uniformly using a sol–gel dip-coating method [95]. The MBG-coated Mg displays a significantly lower biodegradation rate in SBF in comparison with uncoated Mg samples, namely, the weight loss of the MBG-coated samples lost 10 % of its original weight, while the uncoated Mg showed a weight loss of 57 %. In another study, nanostructured diopside ( $\text{CaMgSi}_2\text{O}_6$ ) has been coated on AZ91 Mg alloy using a combined micro-arc oxidation (MAO) and electrophoretic deposition (EPD) method, aiming at decreasing the corrosion rate and improving the surface bioactivity and cytocompatibility of Mg alloys [96]. The results demonstrated that the diopside coating could not only slow down the corrosion rate but also improve the surface bioactivity and cytocompatibility of AZ91 Mg alloy.

### **Metal Matrix Composites**

Although coatings are efficient in improving surface properties of magnesium, it is always difficult to obtain a coating with high bonding strength to the substrate as the coating process has to be conducted in a relatively low temperature due to the high thermal reactivity of magnesium and its alloys. The delamination of coatings from the magnesium substrates has been frequently observed which may lead to a sudden increase in corrosion rate in the long term after implantation [97]. An alternative approach to improve the performance of Mg and its alloys might be the application of metal matrix composite (MMC) based on magnesium alloys, which could avoid complications arising from coating technologies. The advantage to use MMCs as biomaterials is the adjustable mechanical properties (Young's modulus, tensile strength) as well as the adjustable corrosion properties by choosing the appropriate composites [98].

Recently, biodegradable MMCs with ZK30 magnesium alloy (containing 3 wt% zinc and 0.5 wt% zirconium) as the matrix and 45S5 BG as the reinforcement component have developed the powder metallurgy (P/M) method [99]. BG particles were found to be homogeneously distributed in the composites with their chemical composition and morphology retained (Fig. 6). Immersion tests showed that the ZK30-BG composites possessed improved corrosion resistance and lower hydrogen evolution rates when compared with the ZK30 alloy, which was attributed to the accelerated Ca–P deposition on the surface of the composites, induced by the presence of BG within the composites. The cytotoxicity tests and ALP assay showed that the ZK30-BG composites not only were cytocompatible but also possessed superior abilities to stimulate cell proliferation and to promote osteoblastic differentiation of rBMSC as compared with the ZK30 alloy.

---

### **Summary**

Silicate bioactive glasses and ceramics have shown excellent bioactivity in tissue regeneration. However, common drawbacks of silicate-based bioactive materials are brittleness and uncontrollable degradability, while silicate-based biocomposites offer an optimal way for solving these problems from the materials science perspective. Silicate-based bioactive composites with proper composition and structure are one of the most promising bone regeneration materials owing to their bioactivity,

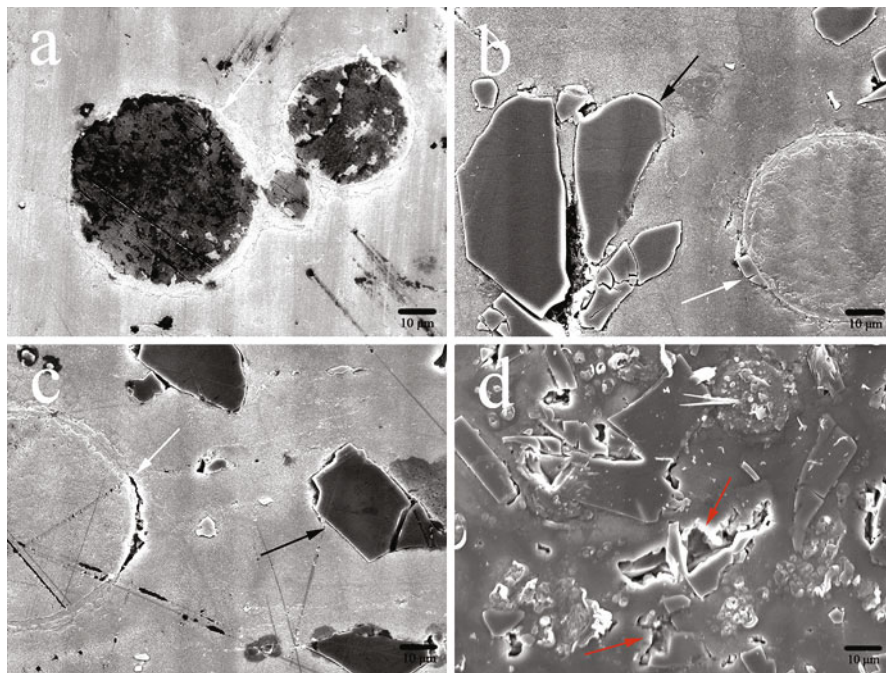


**Fig. 6** SEM micrographs of the extruded (a) ZK30, (b) ZK30-5 % BG, (c) ZK30-10 % BG, and (d) ZK30-15 % BG rods on the transverse section. The red arrows point to the micropores present in the ZK30-15 %BG composite. The white and black arrows point out ZK30 and BG particles, respectively [99]

degradability, and success in stimulating new bone growth by the action of their dissolution products on cells. The synthetic silicate-based composites reviewed in this chapter consist of silicate-based inorganic–organic composites, silicate-based inorganic/inorganic composites, and silicate-based inorganic/metallic composites.

Generally, the field of tissue regeneration has undergone tremendous progress in the last several decades. Worthy attempts have been made by applying hybrids of silicate-based inorganic materials with either natural or synthesized polymers to prepare tissue engineering scaffolds with proper pore structure, bioactivity, biodegradability, acceptable mechanical properties, and stimulation of new bone formation and angiogenesis. Compared to conventional composite processing methods, 3D plotting is more adoptable to obtain scaffolds with tailored porosity and pore structure which can accurately control the morphology of the scaffolds for predictable properties. Electrospinning is another simple technique to manipulate the microstructure of bioactive inorganic–organic nanocomposites for controllable mechanical strength and biological properties. Bioactive membranes, hydrogels, and bone cements made of silicate-based bioactive inorganic materials and natural polymers show favorable bioactivity, biocompatibility, and bioresorbability which have huge potential for guided tissue regeneration. The combination of efficient drug delivery



and bioactive silicate-based biocomposites to achieve large drug load and controlled drug delivery provides more options to treat tissue defects clinically. Due to their small dimensions and incompatible polarity with polymers, inorganic particles tend to agglomerate in the polymer matrix. Nontoxic organic molecules, especially biocompatible molecules, are useful to modify the surface of silicate-based inorganic particles for the improvement of the dispersivity in polymer matrix. As for silicate-based inorganic composites, the composite ceramic or cement systems are mainly designed to strengthen mechanical strength, regulate degradability, or improve self-setting properties. Silicate-based inorganic biomaterials could also composite with advanced materials, like graphene, to improve the mechanical strength. For metallic substrates, there is always a concern about their corrosion resistance in physiological fluids and their bioactivity. Coating silicate-based bioceramics on alloy substrates could endow the composites with favorable bioactivity. Metal matrix composites (Mg alloy/Bioglass<sup>®</sup>) showed corrosion resistance, bioactivity, and promotion of cell proliferation and differentiation which develop a new research area for silicate-based inorganic composites used in tissue regeneration.

Up to now, most of the materials assessments for silicate-based bioactive composites are conducted *in vitro* to evaluate the biomaterials' performance in the materials perspective, like the mechanical properties, the ability to form apatite *in vitro*, the self-setting properties, etc. While biomaterials are expected to perform in the body's internal environment in clinical perspective which is quite different from those exhibited in experimental condition. The internal environment is complicated and changeable, for example, bone tissue structure and mechanical strength vary by distinct and fluctuating loading conditions and different parts in the body. All of these requirements call for careful designing of biomaterials with composition, surface morphology, and physical and chemical properties. Perhaps one of the largest challenges for the application of biomaterials is the rational design of silicate-based bioactive composites based on the systematic evaluation of desired biological, chemical, and physical requirements [100].

Bone is the optimal composites and the hierarchical structure of the bone in macro-, micro-, and nanolength scale plays an important role in the mechanical properties of bone. Therefore, composites with finely tailored structure in various length scales are the main trend for the synthesized silicate-based biocomposites. 3D plotting has shown promising potential to overcome some of the limitations of the conventional methods and got some progress in the application of tissue engineering. New processing techniques, including 3D plotting, should be studied and developed for the development of scaffolds with improved mechanical properties without influencing the porosity and interconnectivity.

The general mechanism on the bioactivity of CaO–SiO<sub>2</sub>-based coatings on metallic substrates involved the dissolution of the coatings, which rendered the release of calcium ions and the formation of silica-rich layer that were necessary for the formation of an apatite layer. However, the dissolution process may result in the mechanical deterioration of the coatings. Fractures have thus been reported to occur within the coating and/or at the coating–substrate interface after implantation. Therefore, it is essential to improve the stability of the coatings, as well as its

bonding strength to the metallic substrate, for which coating techniques play an important role. Many techniques have been investigated to obtain silicate-based coatings, but none of them have been used in industrial practice and clinical application. More research works are needed to develop practical coating techniques to obtain silicate-based bioactive coatings with high stability and bonding strength.

---

## References

1. Kemal S, Sander CGL, Joop GCW, Li YB, John AJ (2012) Effect of calcium carbonate on hardening, physicochemical properties, and in vitro degradation of injectable calcium phosphate cements. *J Biomed Mater Res A* 100A:712–719. doi:10.1002/jbm.a.34009
2. Hu JZ, Zhou YC, Huang LH, Liu J, Lu HB (2014) Effect of nano-hydroxyapatite coating on the osteoinductivity of porous biphasic calcium phosphate ceramics. *BMC Musculoskeletal Disord* 15:114–124. doi:10.1186/1471-2474-15-114
3. Hafezi F, Hosseinejad F, Fooladi AIA, Mafi MS, Amiri A, Nourani RM (2012) Transplantation of nano-bioglass/gelatin scaffold in a non-autogenous setting for bone regeneration in a rabbit ulna. *J Mater Sci Mater Med* 23:2783–2792. doi:10.1007/s10856-012-4722-3
4. Hench LL (2009) Genetic design of bioactive glass. *J Eur Ceram Soc* 29:1257–1265. doi:10.1016/j.jeurceramsoc.2008.08.002
5. Hench LL, Paschall HA (1973) Direct chemical bond of bioactive glass-ceramic materials to bone and muscle. *J Biomed Mater Res* 7:25–42. doi:10.1002/jbm.820070304
6. Saravanapavan P, Jones JR, Verrier S, Beilby R, Shirliff VJ, Hench LL, Polak JM (2004) Binary CaO-SiO<sub>2</sub> gel glasses for biomedical applications. *Bio-Med Mater Eng* 14:467–486
7. Rahaman NM, Day ED, Bal SB, Fu Q, Jung BS, Bonewald FL, Tomsia PA (2011) Bioactive glass in tissue engineering. *Acta Biomater* 7:2355–2373. doi:10.1016/j.actbio.2011.03.016
8. Hench LL (1998) Bioceramics. *J Am Ceram Soc* 81:1705–1728. doi:10.1111/j.1151-2916.1998.tb02540.x
9. Wu CT, Chang J (2013) A review of bioactive silicate ceramics. *Biomed Mater* 8:032001–032012. doi:10.1088/1748-6041/8/3/032001
10. Kokubo T, Kushitani H, Sakka S, Kitsugi T, Yamamuro T (1990) Solutions able to reproduce *in vivo* surface-structure changes in bioactive glass-ceramic A-W3. *J Biomed Mater Res* 24:721–734. doi:10.1002/jbm.820240607
11. Zhang Q, Nakamoto T, Chen SW, Kawazoe NK, Lin KL, Chang J, Chen GP (2014) Collagen/wollastonite nanowire hybrid scaffolds promoting osteogenic differentiation and angiogenic factor expression of mesenchymal stem cells. *J Nanosci Nanotech* 14:3221–3227. doi:10.1166/jnn.2014.8607
12. Yang SB, Wang J, Tang LJ, Ao HA, Tan HL, Tang TT, Liu CS (2014) Mesoporous bioactive glass doped-poly (3-hydroxybutyrate-co-3-hydroxyhexanoate) composite scaffolds with 3-dimensionally hierarchical pore networks for bone regeneration. *Colloids Surf B Biointerfaces* 116:72–80. doi:10.1016/j.colsurfb.2013.12.052
13. Vallet-Regí M, Arcos D (2008) Nanostructured hybrid materials for bone implants fabrication. In: *Bio-inorganic hybrid nanomaterials*. Wiley, Weinheim, pp 367–399
14. Dou YD, Wu CT, Chang J (2012) Preparation, mechanical property and cytocompatibility of poly(L-lactic acid)/calcium silicate nanocomposites with controllable distribution of calcium silicate nanowires. *Acta Biomaterialia* 8:4139–4150. doi:10.1016/j.actbio.2012.07.009
15. Allo AB, Rizkalla SA, Mequanint K (2010) Synthesis and electrospinning of  $\epsilon$ -polycaprolactone-bioactive glass hybrid biomaterials via a sol-gel process. *Langmuir* 26:18340–18348. doi:10.1021/la102845k
16. Kouhi M, Morshed M, Varshosaz J, Fathi HM (2013) Poly( $\epsilon$ -caprolactone) incorporated bioactive glass nanoparticles and simvastatin nanocomposite nanofibers: preparation,

- characterization and in vitro drug release for bone regeneration applications. *Chem Eng J* 228:1057–1065. doi:10.1016/j.cej.2013.05.091
17. Shin SH, Purevdorj O, Castano O, Planell AJ, Kim HW (2012) A short review: recent advances in electrospinning for bone tissue regeneration. *J Tissue Eng* 3:1–12. doi:10.1177/2041731412443530
  18. Tirri T, Rich J, Wolke J, Seppa J, Yli-Urpo A, Narhi OT (2008) Bioactive glass induced in vitro apatite formation on composite GBR membranes. *J Mater Sci Mater Med* 19:2919–2923. doi:10.1007/s10856-007-3308-y
  19. Hurt AP, Getti G, Coleman NJ (2014) Bioactivity and biocompatibility of a chitosan-tobermorite composite membrane for guided tissue regeneration. *Int J Bio Macro* 64:11–16. doi:10.1016/j.ijbiomac.2013.11.020
  20. Hong KS, Kim EC, Bang SH, Chung CH, Lee YI, Hyun KJ, Lee HH, Jang JH, Kim TI, Kim HW (2009) Bone regeneration by bioactive hybrid membrane containing FGF2 within rat calvarium. *J Biomed Mater Res A* 94A:1187–1194. doi:10.1002/jbm.a.32799
  21. Caridade GS, Merino GE, Martins VG, Luz MG, Alves MN, Mano FJ (2012) Membranes of poly(DL-lactic acid)/Bioglass<sup>®</sup> with asymmetric bioactivity for biomedical applications. *J Bioact Compat Pol* 27:429–440. doi:10.1177/0883911512448753
  22. Li H, Chen SY, Wu Y, Jiang J, Ge YS, Gao K, Zhang PY, Wu LX (2012) Enhancement of the osteointegration of a polyethylene terephthalate artificial ligament graft in a bone tunnel using 58S bioglass. *Int Orthop (SICOT)* 36:191–197. doi:10.1007/s00264-011-1275-x
  23. Kim JJ, Won JE, Shin US, Kim HW (2011) Improvement of bioactive glass nanofiber by a capillary-driven infiltration coating with degradable polymers. *J Am Ceram Soc* 94:2812–2815. doi:10.1111/j.1551-2916.2011.04735.x
  24. Salinas AJ, Esbrit P, Vallet-Regi M (2013) A tissue engineering approach based on the use of bioceramics for bone repair. *Biomater Sci* 1:40–51. doi:10.1039/c2bm00071g
  25. Zhao L, Lin KL, Zhang ML, Xiong CD, Bao YH, Pang XB, Chang J (2011) The influences of poly(lactic-co-glycolic acid) (PLGA) coating on the biodegradability, bioactivity, and biocompatibility of calcium silicate bioceramics. *J Mater Sci* 46:4986–4993. doi:10.1007/s10853-011-5416-9
  26. Pielichowska K, Blazewicz S (2010) Bioactive polymer/hydroxyapatite (nano)composites for bone tissue regeneration. In: Abe A, Dusek K, Kobayashi S (eds) *Biopolymers: lignin, proteins, bioactive nanocomposites*. Springer, Berlin, pp 97–207
  27. Li XK, Chang J (2005) Preparation and characterization of bioactive collagen/wollastonite composite scaffolds. *J Mater Sci-Mater Med* 16:361–365. doi:10.1007/s10856-005-0636-7
  28. Zhao L, Chang J (2004) Preparation and characterization of macroporous chitosan/wollastonite composite scaffolds for tissue engineering. *J Mater Sci-Mater Med* 15:625–629. doi:10.1023/B:JMSM.0000026103.44687.d0
  29. Dorj B, Park JH, Kim HW (2012) Robocasting chitosan/nanobioactive glass dual-pore structured scaffolds for bone engineering. *Mater Lett* 73:119–122. doi:10.1016/j.matlet.2011.12.107
  30. Li JH, Baker AB, Mou XN, Ren N, Qiu JC, Boughton IR, Liu H (2014) Biopolymer/calcium phosphate scaffolds for bone tissue engineering. *Adv Healthcare Mater* 3:469–484. doi:10.1002/adhm.201300562
  31. Li HY, Chang J (2005) pH-compensation effect of bioactive inorganic fillers on the degradation of PLGA. *Comp Sci Technol* 65:2226–2232. doi:10.1016/j.compscitech.2005.04.051
  32. Li HY, Chang J (2004) Preparation and characterization of bioactive and biodegradable Wollastonite/poly(D, L-lactic acid) composite scaffolds. *J Mater Sci-Mater Med* 15:1089–1095. doi:10.1023/B:JMSM.0000046390.09540.c2
  33. Xu L, Xiong CZ, Yang DG, Zhang FL, Chang J, Xiong CD (2008) Preparation and in vitro degradation of novel bioactive polylactide/wollastonite scaffolds. *J Appl Polym Sci* 114:3396–3406. doi:10.1002/app.28475
  34. Wang C, Lin KL, Chang J, Sun J (2013) Osteogenesis and angiogenesis induced by porous beta-CaSiO<sub>3</sub>/PDLGA composite scaffold via activation of AMPK/ERK1/2 and PI3K/Akt pathways. *Biomaterials* 34:64–77. doi:10.1016/j.biomaterials.2012.09.021

35. Li HY, Chang J (2005) In vitro degradation of porous degradable and bioactive PHBV/wollastonite composite scaffolds. *Polym Degrad Stab* 87:301–307. doi:10.1016/j.polydegradstab.2004.09.001
36. Zhao L, Wu CT, Lin KL, Chang J (2012) The effect of poly(lactic-co-glycolic acid) (PLGA) coating on the mechanical, biodegradable, bioactive properties and drug release of porous calcium silicate scaffolds. *BioMed Mater Eng* 22:289–300. doi:10.3233/BME-2012-0719
37. Shi MC, Zhai D, Zhao L, Wu CT, Chang J (2014) Nanosized mesoporous bioactive glass/poly(lactic-co-glycolic acid) composite-coated  $\text{CaSiO}_3$  scaffolds with multifunctional properties for bone tissue engineering. *BioMed Res Int* 2014:323046–323057. doi:10.1155/2014/323046
38. Luo YX, Wu CT, Lode A, Gelinsky M (2013) Hierarchical mesoporous bioactive glass/alginate composite scaffolds fabricated by three-dimensional plotting for bone tissue engineering. *Biofabrication* 5:015005–015017. doi:10.1088/1758-5082/5/1/015005
39. Han Y, Zeng QY, Li HY, Chang J (2013) The calcium silicate/alginate composite: preparation and evaluation of its behavior as bioactive injectable hydrogels. *Acta Biomaterialia* 9:9107–9117. doi:10.1016/j.actbio.2013.06.022
40. Wu CT, Zhu YF, Chang J, Zhang YF, Xiao Y (2010) Bioactive inorganic-materials/alginate composite microspheres with controllable drug-delivery ability. *J Biomed Mater Res* 94B:32–43. doi:10.1002/jbm.b.31621
41. Shirotsaki Y, Botelho CM, Lopes MA, Santos JD (2009) Synthesis and characterization of chitosan-silicate hydrogel as resorbable vehicle for bonelike<sup>®</sup> bone graft. *J Nanosci Nanotechnol* 9:3714–3719. doi:10.1166/jnn.2009.NS56
42. Xu H, Wang YJ, Zheng YD, Chen XF, Ren L, Wu G, Huang XS (2007) Preparation and characterization of bioglass/polyvinyl alcohol composite hydrogel. *Biomed Mater* 2:62–66. doi:10.1088/1748-6041/2/2/002
43. Killion JA, Kehoe S, Geever LM, Devine DM, Sheehan E, Boyd D, Higginbotham CL (2013) Hydrogel/bioactive glass composites for bone regeneration applications: synthesis and characterization. *Mater Sci Eng C Mater Biol Appl* 33:4203–4212. doi:10.1016/j.msec.2013.06.013
44. Tsuru K, Hayakawa S, Ohtsuki C, Osaka A (1998) Ultrasonic implantation of calcium metasilicate glass particles into PMMA. *J Mater Sci Mater Med* 9:479–484. doi:10.1023/A:1008875502451
45. Hamzah AS, Mariatti M, Othman R, Kawashita M, Hayati ARN (2012) Mechanical and thermal properties of polymethylmethacrylate bone cement composites incorporated with hydroxyapatite and glass-ceramic fillers. *J Appl Polym Sci* 125:E661–E669. doi:10.1002/app.35295
46. Wang DG, Zhang Y, Hong GZ (2014) Novel fast-setting chitosan/ $\beta$ -dicalcium silicate bone cements with high compressive strength and bioactivity. *Ceram Int* 40:9799–9808. doi:10.1016/j.ceramint.2014.02.069
47. Lin Q, Lan XH, Li B, Yu YH, Ni YR, Lu CH, Xu ZZ (2010) Anti-washout carboxymethyl chitosan modified tricalcium silicate bone cement: preparation, mechanical properties and in vitro bioactivity. *J Mater Sci Mater Med* 21:3065–3076. doi:10.1007/s10856-010-4160-z
48. Oral O, Lassila LV, Kumbuloglu O, Vallittua PK (2014) Bioactive glass particulate filler composite: effect of coupling of fillers and filler loading on some physical properties. *Dent Mater* 30:570–577. doi:10.1016/j.dental.2014.02.017
49. Zhou ZH, Liu L, Liu QQ, Yi QF, Zeng WN, Zhao YM (2012) Effect of surface modification of bioactive glass on properties of poly-L-lactide composite materials. *J Macro Sci B Phys* 51:1637–1646. doi:10.1080/00222348.2012.672295
50. Qian C, Zhang XY, Zhu BS, Lin KL, Chang J, Zhang XJ (2010) The effect of  $\text{CaSiO}_3$  nanoparticles reinforced denture poly-methyl methacrylate. *Adv Comp Lett* 20:13–20
51. Gao Y, Chang J (2009) Surface modification of bioactive glasses and preparation of PDLLA/bioactive glass composite films. *J Biomater Appl* 24:119–138. doi:10.1177/0885328208094265
52. Zhou YL, Gao Y, Chang J (2010) Effects of hydrolysis on dodecyl alcohol-modified bioactive glasses and PDLLA/modified bioactive glass composite films. *J Mater Sci* 45:6411–6416. doi:10.1007/s10853-010-4724-9

53. Lin KL, Zhang ML, Zhai WY, Qu HY, Chang J (2011) Fabrication and characterization of hydroxyapatite/wollastonite composite bioceramics with controllable properties for hard tissue repair. *J Am Ceram Soc* 94:206–212. doi:10.1111/j.1551-2916.2010.04046.x
54. Xu S, Lin KL, Wang Z, Chang J, Wang L, Lu J, Ning CQ (2008) Reconstruction of calvarial defect of rabbits using porous calcium silicate bioactive ceramics. *Biomaterials* 29:2588–2596. doi:10.1016/j.biomaterials.2008.03.013
55. Liu S, Jin FC, Lin KL, Lu JX, Sun J, Chang J, Dai KR, Fan CY (2013) The effect of calcium silicate on in vitro physicochemical properties and in vivo osteogenesis, degradability and bioactivity of porous  $\beta$ -tricalcium phosphate bioceramics. *Biomed Mater* 8:025008. doi:10.1088/1748-6041/8/2/025008
56. Wang C, Xue Y, Lin KL, Lu JX, Chang J, Sun J (2012) The enhancement of bone regeneration by a combination of osteoconductivity and osteostimulation using  $\beta$ -CaSiO<sub>3</sub>/ $\beta$ -Ca<sub>3</sub>(PO<sub>4</sub>)<sub>2</sub> composite bioceramics. *Acta Biomater* 8:350–360. doi:10.1016/j.actbio.2011.08.019
57. Shirazi FS, Mehrali M, Oshkour AA, Metselaar HSC, Kadri NA, AbuOsman NA (2014) Mechanical and physical properties of calcium silicate/alumina composite for biomedical engineering applications. *J Mech Behav Biomed Mater* 30:168–175. doi:10.1016/j.jmbbm.2013.10.024
58. Long LH, Zhang FM, Chen L, Chen LD, Chang J (2008) Preparation and properties of  $\beta$ -CaSiO<sub>3</sub>/ZrO<sub>2</sub> (3Y) nanocomposites. *J Eur Ceram Soc* 28:2883–2887. doi:10.1016/j.jeurceramsoc.2008.05.006
59. Ni SY, Chang J, Chou L (2008) In vitro studies of novel CaO–SiO<sub>2</sub>–MgO system composite bioceramics. *J Mater Sci Mater Med* 19:359–367. doi:10.1007/s10856-007-3186-3
60. Dorozhkin SV (2009) Calcium orthophosphates in nature, biology and medicine. *Materials* 2:399–498. doi:10.3390/ma2020399
61. Zhao WY, Wang JY, Zhai WY, Wang Z, Chang J (2005) The self-setting properties and in vitro bioactivity of tricalcium silicate. *Biomaterials* 26:6113–6121. doi:10.1016/j.biomaterials.2005.04.025
62. Huan ZG, Chang J (2007) Novel tricalcium silicate/monocalcium phosphate monohydrate composite bone cement. *J Biomed Mater Res B Appl Biomater* 82B:352–359. doi:10.1002/jbm.b.30740
63. Huan ZG, Chang J (2009) Calcium–phosphate–silicate composite bone cement: self-setting properties and in vitro bioactivity. *J Mater Sci Mater Med* 20:833–841. doi:10.1007/s10856-008-3641-9
64. Liu WN, Chang J (2012) Setting properties and biocompatibility of dicalcium silicate with varying additions of tricalcium aluminate. *J Biomater Appl* 27:171–178. doi:10.1177/0885328211398507
65. Liu WN, Chang J, Zhu YQ, Zhang ML (2011) Effect of tricalcium aluminate on the properties of tricalcium silicate–tricalcium aluminate mixtures: setting time, mechanical strength and biocompatibility. *Int Endod J* 44:41–50. doi:10.1111/j.1365-2591.2010.01793.x
66. Liu WN, Peng WW, Zhu YQ, Chang J (2012) Physicochemical properties and in vitro biocompatibility of a hydraulic calcium silicate/tricalcium aluminate cement for endodontic use. *J Biomed Mater Res B Appl Biomater* 100B:1257–1263. doi:10.1002/jbm.b.32690
67. Huan ZG, Chang J, Huang XH (2008) Self-setting properties and in vitro bioactivity of Ca<sub>2</sub>SiO<sub>4</sub>/CaSO<sub>4</sub> dot 1/2H<sub>2</sub>O composite bone cement. *J Biomed Mater Res B* 87B:387–394. doi:10.1002/jbm.b.31116
68. Huan ZG, Chang J (2007) Self-setting properties and in vitro bioactivity of calcium sulfate hemihydrate–tricalcium silicate composite bone cements. *Acta Biomater* 3:952–960. doi:10.1016/j.actbio.2007.05.003
69. Zhao WY, Chang J, Zhai WY (2007) Self-setting properties and *in vitro* bioactivity of Ca<sub>3</sub>SiO<sub>5</sub>/CaSO<sub>4</sub> dot 1/2H<sub>2</sub>O composite cement. *J Biomed Mater Res A* 85A:336–344. doi:10.1002/jbm.a.31523
70. Liu WJ, Wu CT, Liu WN, Chang J (2013) The effect of plaster (CaSO<sub>4</sub> dot 1/2H<sub>2</sub>O) on the compressive strength, self-setting property, and in vitro bioactivity of silicate-based bone cement. *J Biomed Mater Res Part B* 101B:279–286. doi:10.1002/jbm.b.32837

71. Lin M, Zhang L, Wang JC, Chen XY, Yang XY, Cui WG, Zhang W, Yang GJ, Liu M, Zhao Y (2014) Novel highly bioactive and biodegradable gypsum/calcium silicate composite bone cements: from physicochemical characteristics to *in vivo* aspects. *J Mater Chem B* 2:2030–2038. doi:10.1039/c3tb21786h
72. Huan ZG, Chang J (2008) Study on physicochemical properties and *in vitro* bioactivity of tricalcium silicate–calcium carbonate composite bone cement. *J Mater Sci Mater Med* 19:2913–2918. doi:10.1007/s10856-008-3423-4
73. Lin Q, Li YB, Lan XH, Lu CH, Chen YX, Xu ZZ (2009) The apatite formation ability of CaF<sub>2</sub> doping tricalcium silicates in simulated body fluid. *Biomed Mater* 4:045005. doi:10.1088/1748-6041/4/4/045005
74. Mehrali M, Moghaddam E, Shirazi SFS, Baradaran S, Mehrali M, Latibari ST, Metselaar HSC, Kadri NA, Zandi K, Abu Osman NA (2014) Synthesis, mechanical properties, and *in vitro* biocompatibility with osteoblasts of calcium silicate-reduced graphene oxide composites. *ACS Appl Mater Interface* 6:3947–3962. doi:10.1021/am500845x
75. Gao CD, Liu TT, Shuai CJ, Peng SP (2014) Enhancement mechanisms of graphene in nano-58S bioactive glass scaffold: mechanical and biological performance. *Sci Rep* 4:4712. doi:10.1038/srep04712
76. Qian J, Kang YH, Wei ZL, Zhang W (2009) Fabrication and characterization of biomorphic 45S5 bioglass scaffold from sugarcane. *Mater Sci Eng C* 29:1361–1364. doi:10.1016/j.msec.2008.11.004
77. Gonzalez P, Serraa J, Listea S, Chiussia S, Leona B, Perez-Amora M, Martnez-Fernandezb J, Arellano-Lopezb RA, Varela-Feria MF (2009) New biomorphic SiC ceramics coated with bioactive glass for biomedical applications. *Biomaterials* 24:4827–4832. doi:10.1016/S0142-9612(03)00405-8
78. DeCarlos A, Borrajo JP, Serra J, Gonzalez P, Leon B (2006) Behaviour of MG-63 osteoblast-like cells on wood-based biomorphic SiC ceramics coated with bioactive glass. *J Mater Sci Mater Med* 17:523–529. doi:10.1007/s10856-006-8935-1
79. Mitsuo N (2008) Metallic biomaterials. *J Artif Organs* 11:105–110. doi:10.1007/s10047-008-0422-7
80. Staiger MP, Pietak AM, Huadmai J, Dias G (2006) Magnesium and its alloys as orthopedic biomaterials: a review. *Biomaterials* 27:1728–1734. doi:10.1016/j.biomaterials.2005.10.003
81. Razavi M, Fathi M, Savabi O, Beni BH, Vashae D, Tayebi L (2014) Surface microstructure and *in vitro* analysis of nanostructured akermanite (Ca<sub>2</sub>MgSi<sub>2</sub>O<sub>7</sub>) coating on biodegradable magnesium alloy for biomedical applications. *Colloid Surf B Biointerfaces* 117:432–440. doi:10.1016/j.colsurfb.2013.12.011
82. Sola A, Bellucci D, Cannillo V, Cattini A (2011) Bioactive glass coatings: a review. *Surf Eng* 27:560–572. doi:10.1179/1743294410Y.0000000008
83. Yi DL, Wu CT, Ma XB, Ji H, Zheng XB, Chang J (2012) Preparation and *in vitro* evaluation of plasma-sprayed bioactive akermanite coatings. *Biomed Mater* 7:065004. doi:10.1088/1748-6041/7/6/065004
84. Nihat CK, Aligul B, Ahmet YO, Muhammed HA (2009) Hydroxyapatite/bioactive glass films produced by a sol–gel method: *in vitro* behavior. *Adv Eng Mater* 11:B194–B199. doi:10.1002/adem.200900034
85. Xue WC, Liu XY, Zheng XB, Ding CX (2005) *In vivo* evaluation of plasma-sprayed wollastonite coating. *Biomaterials* 26:3455–3460. doi:10.1016/j.biomaterials.2004.09.027
86. Liu XY, Tao SY, Ding CX (2002) Bioactivity of plasma sprayed dicalcium silicate coatings. *Biomaterials* 23:963–968. doi:10.1016/S0142-9612(01)00210-1
87. Xie YT, Liu XY, Zheng XB, Ding CX (2005) Bioconductivity of plasma sprayed dicalcium silicate/titanium composite coatings on Ti–6Al–4V alloy. *Surf Coat Technol* 199:105–111. doi:10.1016/j.surfcoat.2004.11.034
88. Xia LG, Zhang ZY, Chen L, Zhang WJ, Zeng DL, Zhang XL, Chang J, Jiang XQ (2011) Proliferation and osteogenic differentiation of human periodontal ligament cells on akermanite and beta-TCP bioceramics. *Eur Cell Mater* 22:68–83

89. Wu CT, Ramaswamy Y, Zreiqat H (2010) Porous diopside ( $\text{CaMgSi}_2\text{O}_6$ ) scaffold: a promising bioactive material for bone tissue engineering. *Acta Biomaterialia* 6:2237–2245. doi:10.1016/j.actbio.2009.12.022
90. Xue WC, Liu XY, Zheng XB, Ding CX (2004) Plasma-sprayed diopside coatings for biomedical applications. *Surf Coat Technol* 185:340–345. doi:10.1016/j.surfcoat.2003.12.018
91. Yi DL, Wu CT, Ma XB, Ji H, Zheng XB, Chang J (2014) Bioactive bredigite coating with improved bonding strength, rapid apatite mineralization and excellent cytocompatibility. *J Biomater Appl* 28:1343–1353. doi:10.1177/0885328213508165
92. Zhang ML, Wu CT, Lin KL, Fan W, Chen L, Xiao Y, Chang J (2012) Biological responses of human bone marrow mesenchymal stem cells to Sr-M-Si (M = Zn, Mg) silicate bioceramics. *J Biomed Mater Res A* 100A:2979–2990. doi:10.1002/jbm.a.34246
93. Wu CT, Chen ZT, Yi DH, Chang J, Xiao Y (2014) Multidirectional effects of Sr-, Mg-, and Si-containing bioceramic coatings with high bonding strength on inflammation, osteoclastogenesis, and osteogenesis. *ACS Appl Mater Interfaces* 6:4264–4276. doi:10.1021/am4060035
94. Rojjaee R, Fathi M, Raeissi K, Taherian M (2013) Electrophoretic deposition of bioactive glass nanopowders on magnesium based alloy for biomedical applications. *Ceram Int* 40:7879–7888, 10.1016/j.ceramint.2013.12.135
95. Wang XJ, Wen C (2014) Corrosion protection of mesoporous bioactive glass coating on biodegradable magnesium. *Appl Surf Sci* 303:196–204. doi:10.1016/j.apsusc.2014.02.147
96. Razavi M, Fathi M, Savabi O, Vashaei D, Tayebi L (2014) *In vitro* study of nanostructured diopside coating on Mg alloy orthopedic implants. *Mater Sci Eng Mater Biolog Appl* 41:168–177. doi:10.1016/j.msec.2014.04.039
97. Hornberger H, Virtanen S, Boccacini RA (2012) Biomedical coatings on magnesium alloys – a review. *Acta Biomater* 8:2442–2455. doi:10.1016/j.actbio.2012.04.012
98. Foltz JV, Blackmon CM (1998) Matrix composites. *Adv Mater & Process* 154:19–23
99. Huan ZG, Leeftang S, Zhou J, Zhai WY, Chang J, Duszczek J (2012) *In vitro* degradation behavior and bioactivity of magnesium-Bioglass composites for orthopedic applications. *J Biomed Mater Res B Appl Biomater* 100B:437–446. doi:10.1002/jbm.b.31968
100. Dorozhkin SV (2013) Calcium orthophosphate-based bioceramics. *Materials* 6:3840–3942. doi:10.3390/ma6093840

---

# Biomimetic Customized Composite Scaffolds and Translational Models for the Bone Regenerative Medicine Using CAD-CAM Technology

# 20

Isidoro Giorgio Lesci, Leonardo Ciocca, and Norberto Roveri

## Contents

Introduction .....	586
Chemical–Physical Characteristics of Biogenic Nanohydroxyapatites .....	591
Synthetic Biomimetic Nanohydroxyapatite .....	592
Biomimetic Scaffold by Hydrothermal Synthesis from Natural Source .....	593
Organic/Inorganic Biomimetic Hybrid Composite Scaffolds .....	595
Clinical Application of Biomimetic Composite Scaffold .....	599
Conventional: Pre-plating .....	599
Intermediate Step: Surgical Guides and Bone Plates .....	600
Composite Scaffold Customization for Bone Regenerative Medicine .....	602
Determinant Factors for Composite Scaffolding in Bone Regenerative Medicine .....	605
Chemical–Physical Factors .....	605
Physical Factors .....	608
Summary .....	609
References .....	610

---

## Abstract

Nature produces soft and hard materials exhibiting remarkable functional properties by controlling the hierarchical assembly of simple molecular building blocks from the nano- to the macro-scale. Biogenic materials are nucleated in defined nano–micro-dimensioned sites inside the biological environments, in which chemistry can be spatially controlled, in order to monitor the size, shape, and structural organization of biomaterials. With the development of

---

I.G. Lesci (✉) • N. Roveri

Department of Chemistry “G. Ciamician”, University of Bologna, Bologna, Italy

e-mail: [isidorogiorgio.lesci@unibo.it](mailto:isidorogiorgio.lesci@unibo.it); [norberto.roveri@unibo.it](mailto:norberto.roveri@unibo.it)

L. Ciocca

Department of Biomedical and Neuromotor Sciences, University of Bologna, Bologna, Italy

e-mail: [leonardo.ciocca@unibo.it](mailto:leonardo.ciocca@unibo.it)

© Springer International Publishing Switzerland 2016

I.V. Antoniac (ed.), *Handbook of Bioceramics and Biocomposites*,

DOI 10.1007/978-3-319-12460-5\_28

585



nanotechnology, this strategy employing natural material genesis has attracted attention in designing bioinspired materials at the nanoscale dimensions.

In this contest, biomimetic nanostructured hydroxyapatite is a promising biomaterial for bone tissue engineering because this material exhibits excellent biological properties. However, hydroxyapatite is still limited as bone substitute due to the brittleness of the material. Hence, a widespread approach is the creation of hybrid materials with an inorganic or organic bioactive phase mimicking functional bony units and a polymeric phase of a consistency permitting the device to be manipulated to achieve an anatomically compatible shape and allowing surface adsorption of molecules that play active roles in the biological environment.

Recently, many studies were developed in order to prepare and test new bioengineered custom-made composite scaffold materials using a combination of CAD/CAM technology to restore full-thickness defects of the bone. Modern 3D printing techniques allow dimensioning of the external volume according to the surgical defect, thus simplifying the surgery and reducing biological morbidity. The use of CAD/CAM technology and the novel composite, biomimetic, and resorbable scaffolds are the promising way to interpret the need of bone regenerative medicine.

---

**Keywords**

Biom mineralization • Bone • Biomaterial • Composite biomaterial • Biomimetic hydroxyapatite • Synthetic nanohydroxyapatite • Mineralized collagen • Biomimetic scaffold • Hybrid biomimetic scaffold • Regenerative medicine • Surgery • Rapid prototype • Tissue engineering • CAD/CAM technology • Biodegradable polymers

---

**Introduction**

Human bone is a porous biohybrid composite, formed mainly by hydroxyapatite (HA) (70 wt%) and collagen (30 wt%) exhibiting an interesting complex hierarchy of anisotropic structures able to provide stability, under compression, tension, bending, and buckling stresses [1]. Their function is to move, support, and protect the various organs of the body, produce red and white blood cells, and store minerals. Bones appear in a variety of shapes and have a complex internal and external structure; they are lightweight yet strong and hard, in addition to satisfying their many other functions. One of the types of tissues that constitutes bone is the mineralized osseous tissue, also called bone tissue, that gives it rigidity and honeycomb-like three-dimensional structure. Other types of tissue found in bones include marrow, endosteum and periosteum, nerves, blood vessels, and cartilage. There are 206 bones in the adult body and about 300 bones in the infant body. Bone tissue consists of cells embedded in a fibrous, organic matrix, the osteoid, which is primarily constituted by type I collagen (90 %) and 10 % amorphous ground substance (primarily glycosaminoglycans and glycoproteins). Osteoid comprises approximately 50 % of bone by volume and 25 % by weight.

Osteoblasts are mononucleate cells responsible for the secretion of osteoid and subsequent bone formation through the mineralization of the osteoid matrix. They strongly produce alkaline phosphatase, an enzyme that has a role in the mineralization of bone, as well as many matrix proteins. When osteoblasts are trapped in the bone matrix, which they themselves produced, they become star-shaped cells named osteocytes, the most abundant cells found in bone. Osteocytes are mature bone cells, networked to each other via long processes that occupy tiny canals called canaliculi, which are used for exchange of nutrients and waste. They are actively involved in the maintenance of bony matrix, through various mechanosensory mechanisms regulating the bone's response to stress. Bone is a dynamic tissue constantly being reshaped by osteoblasts, cells which build bone, and osteoclasts, cells which resorb it. Osteoclasts are multinucleated cells responsible for the resorption of bone through the removal of the bone's mineralized matrix. The removal process begins with the attachment of the osteoclast to the osteon (predominant structures found in compact bone); the osteoclast then induces an infolding of its cell membrane and secretes collagenase and other enzymes important in the resorption process, such as tartrate-resistant acid phosphatase, secreted against the mineral substrate. During childhood, bone formation exceeds resorption, but, as the aging process occurs, resorption exceeds formation. The characteristic rigidity and strength of bone derives from the presence of mineral salts that permeate the organic matrix, formed by osteoid mineralization, due to the secretion of vesicles containing alkaline phosphatase, by the osteoblasts. The mineral phase comprises approximately 50 % of bone by volume and 75 % by weight. The principal constituents of bone mineral are calcium phosphate, mainly carbonated hydroxyapatite, amorphous calcium phosphate, and calcium carbonate, with lesser quantities of sodium, magnesium, silicon, and fluoride. The whole architecture of bone is very complex: starting from the smallest constituting elements to the largest scales, the bone is not only organized in an anisotropic manner, but the arrangement of its constituting elements is hierarchical; this means that its structural units are organized at increasing size levels, and this feature confers unique properties to the whole bone structure. In mammals, osteoblasts and odontoblasts fix ions of calcium and orthophosphate and then precipitate biological apatite onto an organic matrix. This is the process of physiological biomineralization that is restricted to the specific sites in skeletal tissues, including growth plate cartilage, bones, and teeth. Unfortunately, owing to aging, to various diseases, and under certain pathological conditions, blood vessels and some internal organs are calcified as well. This process is called pathological calcification or ectopic mineralization and leads to morbidity and mortality. In general, any type of abnormal accumulation of calcium phosphates in wrong places accounts for a disruption of systemic defense mechanism against calcification. Unwanted depositions always lead to various diseases, for instance, soft tissue calcification (in damaged joints, blood vessels, dysfunctional areas in the brain, diseased organs, scleroderma, prostate stones), kidney and urinary stones, dental pulp stones and dental calculus, salivary stones, gall stones, pineal gland calcification, atherosclerotic arteries and veins, coronary calcification, cardiac skeleton, damaged cardiac valves, calcification on artificial heart valves, carpal tunnel, cataracts, malacoplakia,

calcified menisci, dermatomyositis, and others. All these cases are examples of a calcinosis, which might be described as a formation of calcium phosphate deposits in any soft tissue. Contrary to the mineral phases of normal calcifications (bone, dentin, enamel, cementum, antlers), which consist of only one type of calcium phosphate (namely, biological apatite), the mineral phases of abnormal and/or pathological calcifications are found to occur as single or mixed phases of other types of calcium phosphates and/or other phosphatic and non-phosphatic compounds, in addition to or in place of biological apatite. This happens because the solution pH is often relatively low in places of pathological calcifications. However, in some cases, the chemical composition of an unwanted inorganic phase might depend on the age of pathological calcification and its location. It is interesting to note that the mineral phases of animal calculus (e.g., from dog) were found to consist of calcium carbonate and biological apatite, while human calculi do not contain calcium carbonate. Some findings suggested that the mechanisms and factors regulating the physiological biomineralization might be similar to those influencing the ectopic mineralization: both were initiated by various organics (i.e., membrane-enclosed particles released from the plasma membrane of mineralization competent cells) that were present [2].

Biomimeticism of synthetic materials for biomedical applications can be carried out at different levels according to the composition, structure, morphology, bulk, and surface chemical–physical properties. In this context, biomaterials can be turned biomimetic imprinting all these characteristics in order not only to optimize their interaction with biological tissues but even to mimic biogenic materials in their functionalities. Chemists, biologists, physicists, and engineers interested in material science are amazed at the high degree of sophistication, miniaturization, hierarchical organization, hybridizing, reliability, efficiency, resistance, and adaptability characterizing natural materials. These properties can be only partially obtained in man-made materials by present synthetic processes. For this reason, nature is a school for material science; in fact, biomimeticism and bioinspiration represent important tools for the design and the synthesis of innovative materials and devices. One of the most exciting and economically rewarding research areas of material science involves the applications of materials to health care, especially to reconstructive surgery. In the past, many implantations failed due to infections or a lack of knowledge about toxicity of the selected materials. In this case, the use of calcium phosphates, since they are the most important inorganic constituents of hard tissues in vertebrates, is valid due to their chemical similarity to the mineral component of mammalian bones and teeth. Thus, calcium phosphate-based biomaterials are now used in many different applications throughout the body, covering all areas of the skeleton. These applications include dental implants, percutaneous devices and use in periodontal treatment, treatment of bone defects, fracture treatment, total joint replacement (bone augmentation), orthopedics, cranio-maxillofacial reconstruction, otolaryngology, and spinal surgery.

During the last few decades, many synthetic inorganic, polymeric, and hybrid scaffolds mimicking the micro- and macroporosity of natural bone have been

developed and tested for biomedical applications like bone substitution, bone filler, bone tissue engineering, and bone-implanted drug delivery [2].

Bone regeneration within a large defect caused by tumor removal from the facial skeleton remains a major challenge to the maxillofacial surgeon seeking to restore normal anatomy. Also, oral rehabilitation of such patients remains problematic for the prosthodontist, who requires that the new osteomucosal anatomy should allow successful application of prosthetic therapy. The gold standard for bone restoration involves the use of a microvascular free flap harvested from the fibula or the iliac crest. Introduced by Hidalgo in 1989 [3], the fibula free-graft technique is routinely used to replace a missing mandible. However, rehabilitative problems remain in terms of reconstructive volumetric precision: the diameter of the fibula is only sufficient to restore the basal bone of the mandible and the maxilla but not the alveolar component of the native anatomy. This fibular anatomic feature determines an insufficient volume in the final bone restoration, making necessary over-contouring of the prosthesis to fill up the vacant anatomy. In such circumstances, implant-supported fixed restorations (Toronto bridge) may be used to fill the prosthetic space with a resin or ceramic prosthetic body, to create a false gingiva. Moreover, surgical complications may develop during the follow-up, often creating the need to treat the hyperplastic reactive gingival tissue that may grow around implants due to insufficient oral hygiene maintenance care.

For these reasons, recent advances in bone regenerative medicine have found ready application as substitutes of fibula free flaps. The reason why it is necessary to move toward a new CAD-/CAM-driven scaffold generation is related to the reconstruction of the native anatomy that involves both basal and alveolar bone. Many authors have sought to create new-generation bone substitutes mimicking the normal bony architecture and inducing bone regeneration, taking into account only the microanatomy of the trabeculae or the biological factors of the scaffold but not the potential use in customizing individual anatomies of the bone to reconstruct. Scaffolding has become a principal research focus of all orthopedic surgeons, and mesenchymal stem cells (MSCs) are highly promising to improve such therapies. Many materials have been investigated in terms of optimal osteointegration and complete resorption. The use of titanium, ceramic, and pure polymeric devices is problematic in terms of biodegradability, bioactivity (osteinduction, osteoconduction), and osteointegration [4]. Hydroxyapatite is a natural inorganic component of bone [5] and has been investigated in work on tissue engineering because the material exhibits excellent biological properties [6].

Biodegradable polymers and their copolymers are widely investigated for bone regeneration, dental repair, orthopedic fixation devices, as well as many other biomedical applications. Currently, no pure polymers can effectively bond to the host bone tissue *in vivo*, so organic/inorganic composites of biodegradable polymers with bioactive inorganic phases are still a promising approach in developing bioactive biomaterials for bone regeneration [7].

Many synthetic biodegradable polymers that have been recognized as biocompatible, polyglycolic acid (PGA), polylactic acid (PLA), poly(lactic-co-glycolic

acid) (PLGA), polycaprolactone (PCL), and polydioxanone PDO, which are all aliphatic polyesters, are the most commonly used for scaffolds in tissue engineering [8]. The degradation products of these polymers (glycolic acid and lactic acid) are metabolic products physiologically present in the human body and are removed by natural metabolic pathways. PGA has the simplest chemical structure among the aliphatic polyesters and has excellent fiber-forming ability by melt extrusion. It was the first synthetic biodegradable suture approved for human application by the Food and Drug Administration (FDA).

In the last decade, turning to the polymeric phase, many synthetic biodegradable polymers have been recognized as biocompatible. Of these, poly( $\epsilon$ -caprolactone) (PCL) exhibits optimal biocompatibility and good biodegradability [8]. Mineralized collagen fibers combined with PCL yield biomimetic constructs useful in bone tissue engineering, characterized not only by high-level biocompatibility and biodegradability but also by a hierarchical architecture (from the nanoscale to macroscopic dimensions) mimicking that of bone [7]. Apart from the chemical composition of the biomaterial, the structural architecture of the construct is of critical importance when biologically relevant integration and osteoinduction are required. In particular, the presence of pores and their dimensions, extent (as percentage of open porosity) of interconnection, and density are crucial determinants of all of cell adhesion, infiltration, proliferation, and differentiation [9]. Several techniques have been investigated in efforts to control construct architecture [10], with particular attention being directed to novel, direct or indirect, rapid prototyping methods. This promising group of techniques involves generation of a physical model of a construct using computer-aided design, yielding optimal morphological and architectural properties [11]. Although many polymer–inorganic phase mixtures have been tested, the main problem is related to the processing method, which offers little capability to control pore size, pore geometry, pore interconnectivity, spatial distribution of pores, and construction of internal channels within the scaffold.

Many fabrication methods have been tested [2], such as:

- *Solvent casting/particulate leaching*: solubilization of the polymer, addition of diameter-specific salt particles, evaporation of the solvent, and immersion in water for the salt particles to leach out.
- *Gas foaming*: carbon dioxide saturation of the polymer at high pressures and subsequent pressure lowering to allow nucleation and growth of gas cells.
- *Fiber bonding*: PLLA in solvent dissolution and casting over PGA meshes, evaporation of the solvent, and heating so as PGA melts. PLLA is then removed by solvent dissolution.
- *Phase separation*: solvent dissolution of the polymer and temperature lowering to produce a liquid–liquid phase separation and the subsequent two-phase solid, sublimation of the solvent.
- *Melt molding*: mold filling with PLGA and gelatin microspheres, mold heating to glass-transition temperature of PLGA, and water immersion for the gelatin microspheres to leach out. The melt-molding process was modified to incorporate short fibers of HA.

- *Emulsion freeze-drying*: ultrapure water addition to a solution of methylene chloride with PGA, homogenization, and subsequent freeze-drying.
- *Solution casting*: PLGA dissolution in chloroform, precipitation adding methanol. Demineralized freeze-dried bone can be combined with the PLGA, and the composite material is then pressed into a mold and heated to 45–48 °C for 24 h.
- *Freeze-drying*: polymer solvent dissolution to obtain porous matrices. Collagen scaffolds have been made by freezing a mixture of collagen so that the ice crystals interrupt the aggregation of collagen molecules. Modulating freezing rate and pH, the pore size can be controlled.

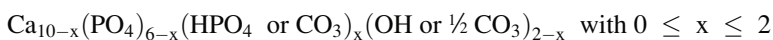
Rapid prototyping (RP) is a group of techniques that can generate a physical model directly from computer-aided design data, thus creating a custom-made scaffold based on patient's image datasets of the damaged area. In these processes, each part is added layer by layer, requiring minimal or no use of solvents and resulting in optimal mechanical properties, thanks to the control of structural parameters.

Recently, Ciocca et al. [7] published a pilot study to evaluate the feasibility of an experimental sheep model to test bioengineered custom-made composite scaffolds created to allow bone repair of a full-thickness defect of the mandible, without using microvascularized free flap. The conclusions of this study reported that the HA plate was acicular in shape, as in natural bone, and that the crystallinity level was sufficiently low to allow degradation under physiologic conditions. Moreover, the authors reported that biomimetic mineralized collagen fibrils were morphologically similar to natural fibers, with HA dispersed through the fibril depth. In this study, CAD/CAM technology used for metal prototyping of the bone plate and for customizing the scaffold allowed splitting the concepts of biomechanics from that of biomimesis: the bone plate gave the scaffold the necessary biomechanical support during function, maintaining the primary stability of the scaffold during healing and allowing the osteointegration and resorption of the scaffold material that does not need to possess itself the biomechanical structural resistance as a prosthetic device.

---

## Chemical–Physical Characteristics of Biogenic Nanohydroxyapatites

From a chemical point of view, the composition of nanocrystalline apatites also strongly differs from that of HA. Although it has been the object of much controversy during several decades in the middle of the twentieth century, the global chemical composition of biological apatites (or their synthetic analogues) can generally be described as:



(except maybe for very immature nanocrystals which may depart from this generic formula). In particular, this expression underlines the presence of vacancies in both

Ca and OH sites. For example, analyzing various cortical bone specimens, suggesting the following relatively homogeneous composition, and unveiling high-vacancy contents:



Minor substitutions are also found in biological apatites involving, for example, monovalent cations (especially  $\text{Na}^+$ ) in cationic sites. In this case, charge compensation mechanisms have to be taken into account.

It should however be kept in mind that such chemical formulas only enable to have a “global” insight on the nature and amount of ions present in the compound, but it does not reflect possible local variations that may be observed on the nanocrystals or in vivo within the osteons, linked to the local apatite crystal formation and, in vivo, to continuous bone remodeling.

The characterization of nanocrystalline apatites is a relatively arduous task due to their poor crystallinity and metastability. But despite the complexity of these systems, recent in-depth investigations have succeeded to reveal their particular surface features (and related reactivity in wet media) that may be exploited for the setup of new biomaterials or for a better understanding of natural or pathological biomineralization phenomena. Recent advances in the characterization of apatite nanocrystals were obtained, thanks to the use of spectroscopic techniques and, in particular, Fourier transform infrared (FT-IR) spectroscopy. FT-IR method is useful for drawing conclusions on the local chemical environment of phosphate, carbonate, and hydroxide ions as well as water molecules in such systems. Detailed analyses of the phosphate groups by FT-IR have enabled to distinguish in nanocrystalline apatites the presence of additional bands that cannot be attributed to phosphate groups in a regular apatitic environment. These chemical environments have been referred to by Rey as “non-apatitic” environments. Taking into account the data obtained from the literature, nanocrystalline apatites (whether biological or their synthetic analogues prepared under close-to-physiological conditions) may thus most probably be described as the association of an apatitic core (often nonstoichiometric). It is also structured by fragile surface hydrated layer containing water molecules and rather labile ions (e.g.,  $\text{Ca}^{2+}$ ,  $\text{HPO}_4^{2-}$ ,  $\text{CO}_3^{2-}$ , etc.) occupying non-apatitic crystallographic sites, even if in the case of biomimetic apatites, the layer is directly exposed on the surface and not included in a “sandwich-like” structure between two “apatitic” layers.

---

## Synthetic Biomimetic Nanohydroxyapatite

Calcium phosphate ceramics have been used in orthopedics for more than 30 years – thanks to their excellent biocompatibility – and are still, today, very popular implant materials for diverse orthopedic clinical applications [12]. Due to the rapid development of nanotechnology, the potential of nano-calcium phosphates has received considerable attention. Generally, nano-HA has been designed for use in not loaded

parts, due to its unsatisfactory mechanical properties. NanOssR bone<sup>®</sup> void filler from Angstrom Medica (Woburn, MA, USA) 90 is considered to be the first nanotechnologic medical device to receive clearance by the US Food and Drug Administration (FDA) in 2005. It is prepared by precipitating nanoparticles of calcium phosphate in an aqueous phase, and the resulting white powder is compressed and heated to form a dense, transparent, and nanocrystalline material. According to the company, NanOssR (Angstrom Medica) duplicates the microstructure, composition, and performance of human bone and possesses high osteoconductivity.

Synthetic nanohydroxyapatite exhibits good properties as a biomaterial, such as biocompatibility, bioactivity, osteoconductivity, direct bonding to bone, etc., exciting the applications of HA in the fields of bone tissue engineering and orthopedic therapies [2]. Many different methodologies have been proposed to prepare nanosized and/or nanocrystalline structures [13]. These are wet chemical precipitation [14], sol–gel synthesis [15], coprecipitation [16], hydrothermal synthesis [17, 18], mechanochemical synthesis [19], microwave processing [20], vapor diffusion [21], silica gel template [22], emulsion-based syntheses [23], and several other methods by which nanocrystals of various shapes and sizes can be obtained [24].

In general, the shape, size, and specific surface area of the apatite nanocrystals appear to be very sensitive to both the reaction temperature and the reactant addition rate. Hydroxyapatites with different stoichiometry and morphology have been prepared, and the effects of varying powder synthesis conditions on stoichiometry, crystallinity, and morphology have been analyzed. The effects of varying the concentration of the reagents, the reaction temperature and time, initial pH, aging time, and the atmosphere within the reaction vessel have also been studied [25]. In order to optimize their specific biomedical applications, especially drug delivery function, the physical and chemical features that should be tailored in synthetic biomimetic HA are dimensions, porosity, morphology, and surface properties [26]. It is well known that natural minerals in bone are homogeneous platelike HA crystals with widths of 15–30 nm and lengths of 30–50 nm and in enamel are rodlike HA crystals with diameters of 25–100 nm and lengths of 100 nm to microns. The study of higher-level biomineralization and biomimetic assembly involves the search for an advanced method so that the synthesis of HA nanocrystals can be accurately controlled [2]. Although each of the reported approaches to produce nanosized apatites has both scientific and practical relevance, very little attention has been paid to the physical and chemical details involved in the careful control of the particle size distribution and particle shape.

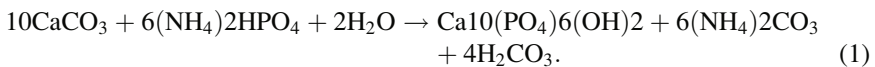
## **Biomimetic Scaffold by Hydrothermal Synthesis from Natural Source**

Nature is full of many interesting things to work with, but many natural resources are also protected. Finding the way to recycle natural-derived resources is a challenging task. In this view the recycling of aquaculture and fishery residues may lead to the

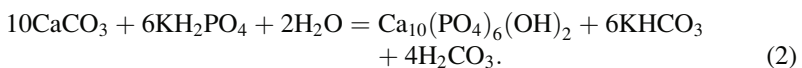


manufacture of new devices and the isolation of new molecules with potential application in medicine. The literature offers many examples of such an approach: chitins from crabs are used as drug deliveries and corals (Biocoral<sup>®</sup>) and nacres have been applied in orthopedic surgery as bone substitutes because of their unique porosity, interconnection, resorption properties, and mechanical characteristics. Hydrothermal transformations (HT) of aragonitic (CaCO<sub>3</sub>) corals from the Pacific Ocean to hydroxyapatite (HA) have gained interest since the 1970s, because of the resultant porous scaffolds featured, similar in composition and microstructure to the mineralized natural bone matrix. However, corals have a problem of environmental conservation. Cuttlefish bones (CBs) and corals have similar chemistry and crystallography. CBs often are used because of their organized hierarchic structures and their optimal and oriented porosities and interconnections.

The hydrothermal transformation (HT) of aragonitic (CaCO<sub>3</sub>) corals from the Pacific Ocean to hydroxyapatite (HA) is described by the following chemical equation (Eq. 1):



This transformation is similar to the inorganic mineralized structure of natural bones [17]. Partial or total transformations of the aragonite structures of corals into HA were considered for different clinical applications, depending on their remodeling and mechanical properties. Calcium carbonate is usually reabsorbed and remodeled faster than stoichiometric HA in bone but shows less mechanical resistance than HA. CB has a lamellar porous structure organized in an ordinate arrangement of hollow pillars, approximately 100 × 200 μm in diameter, connecting parallel lamellae, which appear to fulfill several requirements of scaffolds for bone tissue regeneration. In addition, its structure may be easily machined and shaped to create a custom-made device. However, up to now, there are few papers dealing with the conversion of the natural aragonite of CB into HA with the ultimate aim of obtaining a biomaterial. HA conversion was demonstrated by soaking CB in aqueous solution of NH<sub>4</sub>H<sub>2</sub>PO<sub>4</sub> at different concentrations and heated using different procedures, including sintering in a furnace at 1400 °C temperature or simply by boiling water for 48 h and drying at 110 °C. Battistella et al. [17] transformed CaCO<sub>3</sub> (aragonite) into hydroxyapatite (HA) by hydrothermal transformation (HT). The hydrothermal transformation (HT) of natural aragonite from CB templates into porous calcium phosphate-based scaffolds was performed inside an autoclave at 200 °C, ~ 15 atm using KH<sub>2</sub>PO<sub>4</sub> as a phosphate source, according to reaction (Eq. 2):



During conversion, the original architecture of CB is strictly preserved, and the process offers the further advantage of a careful modulation of the hydrothermal

conditions in order to opportunely tailor the biomaterial properties toward tissue engineering.

However, they are mostly used as templates, and they require chemical transformations from their original chemistry to the chemistry of calcium phosphate. For example, some woods have been transformed into scaffolds for bone surgery characterized by highly organized hierarchical structures [1]. These transformations involve the elimination or decomposition of organic materials. This can be performed using heat, which leaves a carbon template that can react with calcium and then with oxygen, creating a calcium carbonate. The latter is finally converted into HA using a phosphate donor [1]. The whole chemical conversion has been carried out through five chemical steps from native wood to porous hydroxyapatite: (1) pyrolysis of ligneous raw materials to produce carbon templates characterized by the natural complex anisotropic pore structure, (2) carburization process by vapor or liquid calcium permeation to yield calcium carbide, (3) oxidation process to transform calcium carbide into calcium oxide, (4) carbonation by hydrothermal process under CO<sub>2</sub> pressure for the further conversion into calcium carbonate, and (5) phosphatization process through hydrothermal treatment to achieve the final hydroxyapatite phase. The five steps of the phase transformation process have been set up in order to achieve total phase conversion and purity maintaining the original native microstructure. An innovative biomimetic apatite hierarchically structured in parallel fastened hollow microtubules has been synthesized, structurally characterized, and proposed as new inorganic biomorphic scaffold providing a biomimetic nanostructured surface for fascinating bone engineering applications.

---

## Organic/Inorganic Biomimetic Hybrid Composite Scaffolds

Different studies have shown that nanohydroxyapatite has excellent biological properties [27], but its application for tissue engineering is still limited due to its powdery and brittle nature. Another potential bioactive material is represented by mineralized collagen type I fibers; their self-assembly begins from nanosized building blocks simultaneously with crystallization of HA under specific reaction conditions, thus resulting in ordered mineralized collagen fibers very similar to natural ones.

Biomimetic mineralized collagen was synthesized using a near-stoichiometric bulk Ca/P molar ratio of ~1.6–1.7. The powder X-ray diffraction patterns of the material, compared to those of a natural material, exhibited the diffraction maxima characteristic of synthetic single-phase hydroxyapatite. The diffractogram of the mineralized collagen (Fig. 1B, a), as well as the biogenic bone (Fig. 1B, b), presents some distinct diffraction peaks, attributed to the mineral phase (by the characteristic Miller Plan showed in the figure), placed over on a broad band indicating an amorphous phase corresponding to the organic component of bone (type I collagen) [7]. TEM showed that the synthesized materials were very similar, in terms of both morphology (platelike) and dimensions (30–50 nm), to natural material. IR analysis

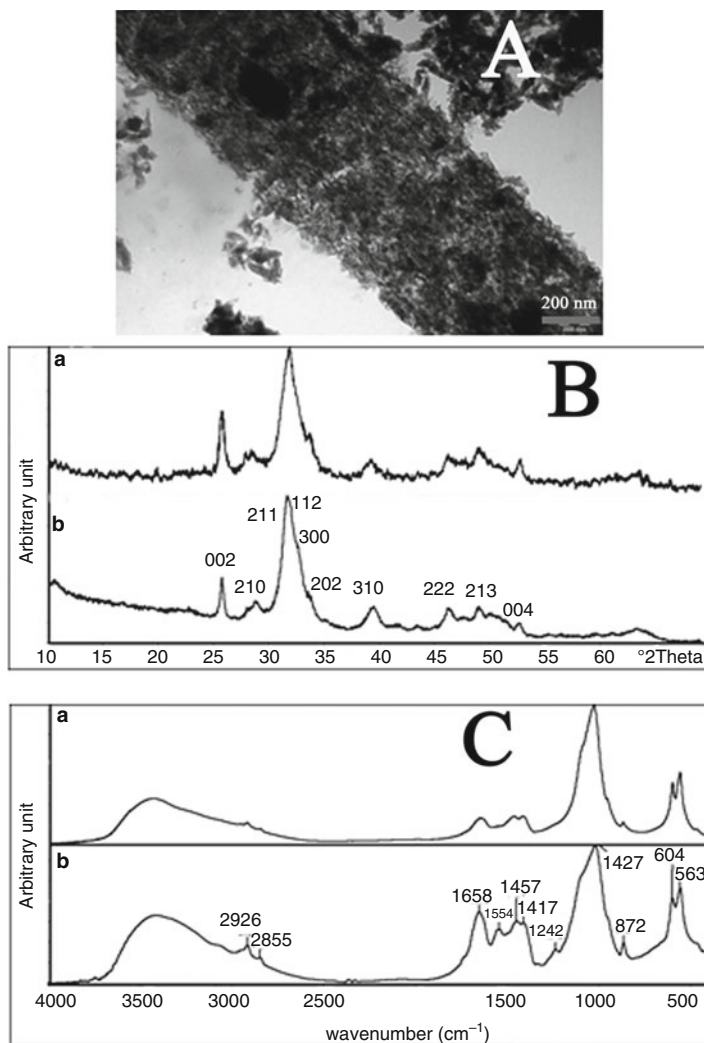


**Fig. 1** (a) TEM image of mineralized collagen showing the plate morphology of HA nanocrystals (scale bar 200 nm), (b) X-ray power diffraction data from (a) a synthetic biomimetic HA/collagen construct and (b) natural bone, and (c) IR spectra. (a) Synthetic biomimetic HA/collagen, (b) natural bone [7]

revealed that the spectrum of the HA/collagen material exhibited all of the most intense bands observed in the spectra of both hydroxyapatite (at 500–700  $\text{cm}^{-1}$  and 900–1,200  $\text{cm}^{-1}$ ) and collagen (at 1,200–1,700 and 2,800–3,700  $\text{cm}^{-1}$ ). Furthermore, some new bands (at  $\sim 870 \text{ cm}^{-1}$  and 1,400–1,450  $\text{cm}^{-1}$ ) were attributable to carbonate substitutions in both the crystal lattice of hydroxyapatite and biogenic bone (Fig. 1).

However, their inadequate biomechanical properties (i.e., high brittleness, low fatigue strength, and low flexibility) restricted the application in bone tissue engineering process. This imposes their combination with polymers to form composite systems in order to morphologically and functionally mimic the bone tissue [28]. Recently, different strategies including phase inversion/particulate leaching [29], rapid prototyping [7], phase separation, and freeze-drying [30] have been developed to realize hydroxyapatite-loaded polymer matrices with adverse success in tissue engineering application due to a lack of nonhomogeneous distribution of ceramic particles within the polymeric matrix which dramatically reduces the bioactive potential of the composite [28].

Biodegradable polymers and their copolymers are widely investigated for bone regeneration, dental repair, orthopedic fixation devices, as well as many other biomedical applications [2, 15]. Currently, no pure polymers can effectively bond to the host bone tissue *in vivo*, so organic/inorganic composites of biodegradable polymers with bioactive inorganic phases are still a promising approach in developing bioactive biomaterials for bone regeneration [7, 8]. Many synthetic biodegradable polymers that have been recognized as biocompatible, polyglycolic acid (PGA), polylactic acid (PLA), poly(lactic-co-glycolic acid) (PLGA), polycaprolactone (PCL), and polydioxanone PDO, which are all aliphatic polyesters, are the most commonly used for scaffolds in tissue engineering.

PCL shows a longer degradation rate than other biodegradable polyesters, requiring 3 years for complete removal from the body [31]. Recently, PCL was studied for meniscus and bone scaffolds in tissue engineering applications revealing not only good biocompatibility but also the possibility to use this polymer to deliver osteogenic cells and enhance bone formation *in vivo* [32]. Moreover, synthesized HA nanocrystals were mixed at room temperature with both PCL and PLLA polymer using both a “monophasic” and “biphasic” method to prepare by rapid prototyping technique two different hybrid bone-morphed scaffolds [8]. SEM analysis (Fig. 2) highlights some differences in the scaffold texture.

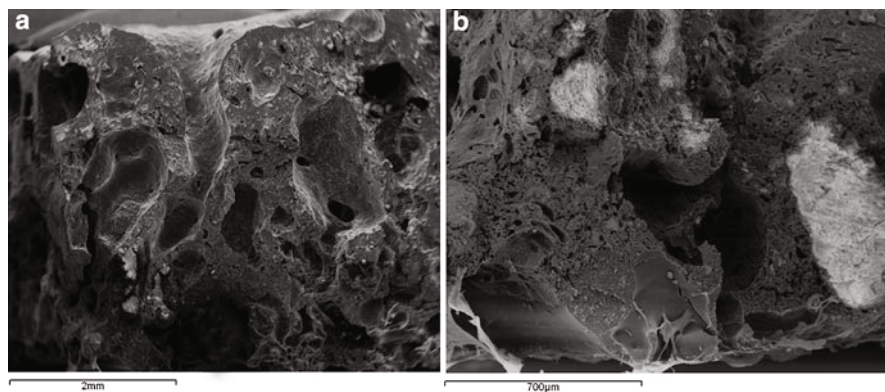


**Fig. 2** SEM image of the scaffold obtained by “monophasic” (a) and “biphasic” methods (b) [8]

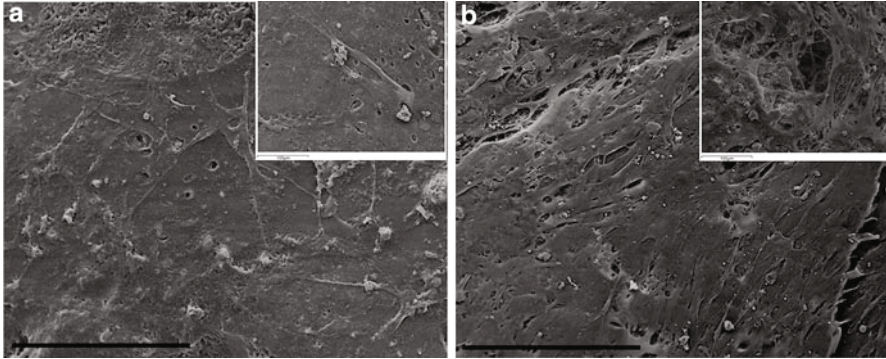


**Fig. 3** SEM images of scaffold surfaces with human mesenchymal stem cells after 7 days' incubation. **(a)** "Monophasic" scaffold, **(b)** "biphasic" scaffold. Networks of cells with well-spread morphology can be seen on both scaffold surfaces. Scale bar = 300  $\mu\text{m}$ . The images on the *top right corner* represented a higher magnification, scale bar = 100  $\mu\text{m}$  [8]

MSCs were cultured on the scaffolds for up to 7 days and observed by SEM (Fig. 3). MSC displayed a normal morphology, and cells formed a monolayer on most of the surface of the both scaffolds (Fig. 3a, b).

The bone-like morphology and the biocompatibility of the prepared hybrid scaffolds suggest that they are adequate for bone tissue engineering and will be useful for orthopedic and maxillofacial regenerative medicine. A fundamental point is that during the scientific history of the bone substitutes, the scientists split the problem: on one hand, they considered the bone substitute as a prosthesis, looking for a good biomechanical capacity of supporting the bone loadings and fixing screws; on the other hand, other scientists looked for a good resorbable material that might be completely resorbed and integrated by the native bone, often becoming brittle and not sufficiently resistant to mechanically support the screws connecting to the bone plate. But one problem cannot stay together with the other, because if you place the scaffold in a vacant area, you must be able to achieve primary stability for osteointegration. But, when you place a conventional bone plate, the only way to stabilize the scaffold is by connecting the bone plate with screws. Thus, you have to use a CAD-/CAM-driven custom-made bone plate that assumes all biomechanical duties, giving the scaffold by means of supportive circular arms only the primary stability without requiring screws into the scaffold that have to support all mechanical loading. This rationale is behind the new concept of integrated bone reconstruction that uses either custom-made bone plate with a specific and individual anatomy or scaffolds as bone substitutes.

Lately, Ciocca et al. [7] created a customizable biomaterial obtained by means of tissue engineering, for using in combination with custom-made bone plate, by combining mineralized collagen fibrils with PCL. The scaffold was obtained combining step-by-step an organic/inorganic materials using "building blocks" strategy.

## Clinical Application of Biomimetic Composite Scaffold

Bone pathologies can derive from an altered bone metabolism, tumors, or mechanical shocks (fractures). Some of these pathologic conditions need surgical reconstruction of the missing bone, such as:

- Benign and malignant tumors of the region: squamous carcinomas, salivary gland tumors (benign and malignant), and mesenchymal tumors (benign and malignant).
- Massive bone fractures: severe bone fractures or crushing may lead to lose a large part of long or short bone. This situation often needs the amputation of the limb or the involved part (foot or hand).

Tumors affecting the maxilla and the mandible need to be ablated, and the residual defect needs to be restored with reconstructive plastic surgery. In the last decades, the reconstruction is performed using the fibula free flap, a surgical technique introduced by Hidalgo in 1989 [3] that makes it possible to harvest from the fibula an osteo-myocutaneous microvascularized flap to be connected to the external carotid and to reconstruct the mandibular and (in selected cases) the maxillary missing bone after tumor ablation. But complications at the harvesting site such as pain, infection, and bleeding can lead to additional donor-site morbidity, over the one related to the final prosthetic rehabilitation of the oral functions (mastication and speech) and facial esthetics.

Nowadays, the surgical techniques involving the use of the fibula free flap are conventional pre-plating and CAD/CAM-driven mandibular reconstruction.

### Conventional: Pre-plating

The pre-plating technique involves the four following different modeling methods of the titanium bone plate, used in the reconstructive step of oncologic maxillofacial surgery of the mandible: buccal pre-plating, lingual pre-plating, double-plate technique, and Luhr technique.

#### Buccal Pre-plating

When the tumor does not involve the external cortical bone of the mandible, the bone plate may be modeled on the buccal surface of the mandible, immediately before the harvesting for the tumor removal. The bone plate is bended and positioned onto the cortical bone, and it is cut at least for leaving three screw holes free over the resection margins. Moreover, the bone plate is modeled on the lower border of the mandible, 1.5 cm up of the lower external contour of the mandible. This makes it possible that, during the inseting of the fibula free flap, the fibula units are aligned with the native anatomy of the inferior border of the mandible, for best conserving of the external face profile of the patient and its future correct occlusion after prosthetic rehabilitation. The fibula units of the free microvascularized flap are modeled by hand,

sectioning each unit as a wedge for the correct alignment in the arch form of the mandible and aiming at obtaining the best contact between the single units. High levels of skills are required to the surgeon for best reconstruction of the mandibular profile.

### **Lingual Pre-plating**

When the external, but not the inner, cortical surface is destroyed by tumor, lingual pre-plating may be considered. This technique is more difficult because the lingual access to the mandible requires more complex surgical techniques, for best preparing the surgical access and also for securing the fixation screws to the bone. This technique requires high skills for the surgeon.

### **Double-Plate Technique**

When both buccal and lingual cortical surfaces of the mandible are involved in the tumor, the double-plate technique allows the resection of the mandibular body maintaining the condyles and the rami in the correct occlusal position. Before ablation of the tumor, a bone plate is secured to the mandibular rami behind the sectioning line, in a way to maintain the spatial native orientation of the mandibular stumps and of the condyles in the fossae. After tumor resection, the second bone plate is modeled by hand to give support to the fibula units of the free microvascularized flap.

### **Luhr Technique**

One more chance when both buccal and lingual cortical surfaces of the mandible are involved in the tumor, is the Luhr technique. This option is usually used in orthognathic surgery and consists of two external bone plates that fix the mandibular rami to the maxilla, during tumor ablation, for best preserving the anatomical native relationship between the mandible and the skull.

## **Intermediate Step: Surgical Guides and Bone Plates**

With modern CAD/CAM technologies, it is nowadays possible to project the surgery straight onto the virtual environment using CT data and rapid prototyping technology for 3D printing of titanium or cobalt–chrome bone plate. The technique is also named prosthetically guided maxillofacial surgery (PGMS) due to its potential ability in projecting the final position of the fibula free flap in relation to the occlusal need of the final prosthetic rehabilitation [33–38]. PGMS computer-aided mandibular reconstruction involves three steps: (1) virtual planning of the surgical treatment, (2) CAD/CAM and RP procedures for the design and manufacture of the customized surgical devices, and (3) surgery.

### **Virtual Planning**

The planning begins with the acquisition of a high-resolution CT scan of the patient's craniofacial skeleton and soft tissue and with an angio-CT scan of the lower leg as a

donor site. CT imaging is performed using a multidetector CT scanner (HiSpeed CT scanning station; General Electric, Milan, Italy). Volumetric data are acquired (0.625-mm slice thickness, 0.312-mm slice spacing, 0° gantry tilt, 512 × 512-pixel resolution). DICOM-format data are processed by the surgeons using the CMF software, version 6.0 (Materialise, Leuven, Belgium). After a suitable threshold value is set, this software allowed the creation of 3D virtual models of the maxillofacial skeleton and the fibula and simulation of mandibular osteotomies. The planned surgery is used to design and manufacture the customized surgical devices (mandibular cutting guides, fibular cutting guides, and reconstructive plates).

### **CAD Procedure**

Customized mandible cutting guides are designed to precisely reproduce the site and orientation of the osteotomies for tumor ablation from the virtual plan into the surgical environment. The mandibular guides are designed with points of reference to allow only the planned positioning on the mandible: arms are included to allow the precise engagement of the device on the mandible. Four holes are created for fixation of the guides to the mandible with titanium screws.

A fibular osteotomy guide is also used for allowing the free flap to fit the defect perfectly, as planned preoperatively.

The third component of the device is the customized reconstructive bone plate that supported the fibula/ilial free flap. The bone plate is designed by thickening the outer surface of the healthy side of the mandible to obtain an ideal esthetic contour and avoid bone deformities on the side affected by the tumor, even if the buccal or the lingual cortical surface of the mandible is involved in the tumor. Positioning of the reconstructive plate could be guided using this method; the holes created to fix the guide are also used to position the reconstructive plates (“transferring principle”).

### **CAM and RP Procedures**

The STL files of the guide and plate are then manufactured by direct metal laser sintering (DMLS) using an EOSINT M270 system (Electro-Optical Systems, GmbH, Munich, Germany). DMLS is used to fuse the metal powder into a solid form and then melt it locally with a focused laser beam. Like with other additive manufacturing technologies, the components are built up additively in layers. The cutting guide, created using EOS Cobalt-Chrome MP1 (Electro-Optical Systems), is a multipurpose titanium or cobalt–chrome–molybdenum-based superalloy powder optimized for DMLS on EOSINT M systems. The bone plate is produced using EOS Titanium Ti64 (Electro-Optical Systems), a pre-alloyed Ti6AlV4 alloy in fine-powder form with excellent mechanical properties and corrosion resistance, low specific weight, and good biocompatibility, which makes it particularly suitable for the production of biomedical implants. To provide the surgeons “biomodels” of the mandible in the preoperative condition and after the planned osteotomy, the biomodels are manufactured directly using a 3D soluble support technology RP machine (Stratasys, Eden Prairie, MN, USA).



## **Surgery**

The mandible is accessed through a sub-transmandibular/cervicolateral incision, and the tumor is delineated. The cutting guide is introduced into the field and fixed to the mandibular bone, leaving the proposed surgical margins within safe tissues. The guide is stabilized in the correct position using the two arms (mesial and distal) on the lower margin of the mandible. These three points of reference allow the perfect engagement of the mandible in the planned position, with the boundaries of the resection located in safe tissues. The cutting guides are fixed with titanium screws, and a sagittal saw is then used to perform the osteotomy. The cutting guides are removed after resection of the tumor. The reconstructive bone plates are positioned and used to support the fibula/iliac free flaps to restore the original mandibular contour. The fibular surgical guide allows precise inseting of the perfectly refined fibular units into the custom-made bone plate. The fibular surgical guide is introduced and fixed to the mandible using the same holes with which the cutting guide has been fixed to assure the correct mutual positioning of the two components.

## **Composite Scaffold Customization for Bone Regenerative Medicine**

A forthcoming step is regenerative medicine by using scaffolds and customized bone plates.

Modern bone regenerative medicine aims to replace damaged tissues and/or stimulate the biological self-repair mechanisms. Nowadays, it is possible to guide the development of engineered tissues both in terms of micro- and macro-volume design. Most usual current strategies for repairing large bone defects involve bone grafting materials or prosthetic implants. However, limitations to these approaches, including the restricted availability of bone grafts, the possibility of disease transmission, poor biocompatibility, and failure at the bone–prosthesis interface, have increased the need for alternative strategies such as tissue engineering approaches. In the last decade, bone substitutes have been used in combination with osteogenic cells for the prefabrication of bioartificial bone grafts in several animal studies. The use of multipotent mesenchymal stem cells (MSCs) has opened up new therapeutic opportunities for bone substitution. The scaffold can be implanted into the patient to function as a replacement tissue after *in vitro* MSC colonization (tissue engineering), or it may be seeded with MSCs during surgery (regenerative medicine).

The success of tissue regeneration is related to the structure of the scaffold and its ability to allow invasion by cells and tissues. Blood vessels begin to grow around and into the construct; as the scaffold dissolves, newly formed tissues are eventually integrated into their surroundings and they finally replace the scaffold. The scaffolds are created from structural elements such as fibers and membranes with alternating voids and pores that can be ordered according to stochastic, fractal, or periodic principles and are thus reproducible using engineering approaches. These techniques may be used to construct 3D artificial tissues that allow the passage of fluids and cells.

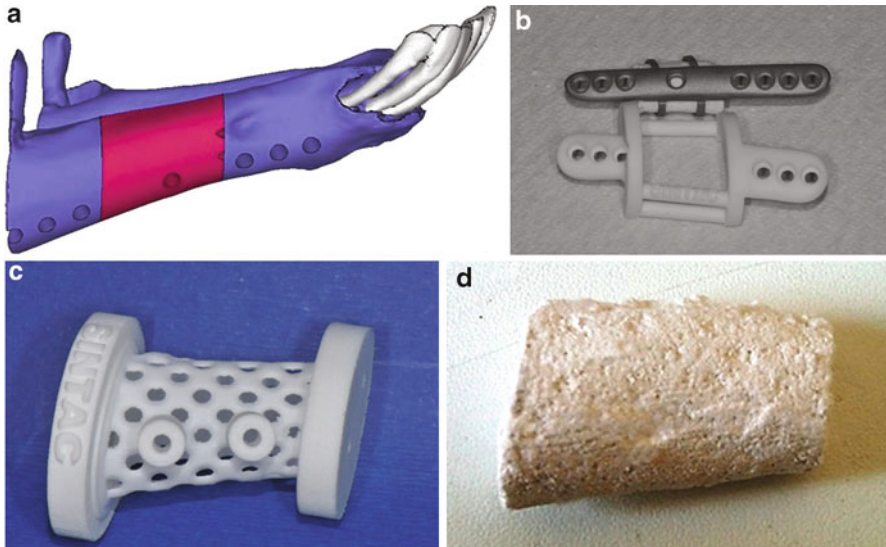


**Fig. 4** The CAD project of the bone plate and of the scaffold volume (a), the rapid prototyping of the surgical guide and the bone plate (b), the mold (c), and customized scaffold (d) [8]

Recent studies by Ciocca et al. [39–41] have described the complete workflow for the PGMS, using customized bone plates and surgical guides. However, this is only the intermediate step of the entire procedure for the bone regenerative medicine project. The aim of these studies is to substitute the fibula free flap and its morbidity for the patient: this may be obtained by manufacturing the scaffold for the bone regeneration, using CAD/CAM technology. Authors aimed to change the surgery because of the evident discrepancy between the anatomy of the mandible and the anatomy of the fibula: the bone volume of the fibula free flap is only sufficient to restore the basal bone of the mandible. Restoration of original anatomy with basal and alveolar bone was the main end point of their research.

Many studies have explored the potential of CAD/CAM and rapid prototyping (RP) procedures in the context of reconstructive surgery and scaffold synthesis [42–48]. Such techniques, using CT images derived from surgical hosts, effectively reproduce damaged areas, and custom-made scaffolds are perfect anatomical matches to wound sites. Moreover, as each bone defect is usually complex in terms of both architecture and shape, as might be expected from the ablative nature of cancer surgery, modern scaffolding techniques have been designed to effectively reproduce complex bone anatomy (Fig. 4).

- The principal hypothesis is that the use of a bone substitute (scaffold) supported by the bone plate is preferable over a bone substitute secured to that plate by bone screws. Only osteoconduction and no biomechanical properties is committed to the scaffold, because the scaffold primary stability is entirely entrusted to the bone plate. In terms of biomechanical loading, the principal problem is that if a scaffold

exhibits high resistance to biomechanical loads or retentive screw penetration, the microstructure becomes unfavorable in terms of resorption, complete bone substitution, and brittleness. A combination of a scaffold and a bone plate, with two distinct and important properties, was developed. First, the scaffold exhibits bone induction characteristics, in the absence of any consideration of the biomechanical resistance thereof to functional loads or retentive screws. Second, the bone plate supports and stabilizes the scaffold via a special form of ring retention. The primary stability of the scaffold described cannot be ascribed to the fixing screws as in conventional procedures (e.g., fibula free flap construction to restore mandibular continuity after demolishing cancer surgery), because the scaffold lacks the consistency necessary to support such screws. Thus, the bone plate is developed to provide support for and retain the scaffold, affording the necessary primary stability to the graft material. Thus, when the plate and scaffold are assembled before surgery, minimal pressure is required to insert the customized scaffold into the customized plate. Only a short titanium screw placed in the center of the plate is used just to immobilize the scaffold and to prevent scaffold movement during presurgical procedures (sterilization) and the surgical inset of bony reconstruction material.

- Scaffold customization. CAD/CAM and rapid modern prototyping allow biomaterials used in bone regeneration to be customized. The several techniques may be broadly grouped into two types; these are direct prototyping [49] and indirect molding. The first approach prints material using a 3D printer depositing incremental strata of dense material polymerizing upon ejection, with the desired anatomy. The second approach employs two methods: block reduction and molding. Block reduction commences with a pre-sintered block of material and reduces the volume to that desired. Molding features curing of material, at the desired volume, using rapid prototyped custom-made molds (see below). Specifically, the lateral wall of the mold is of mesh construction, to expose most material to the external vacuum, facilitating drying.
  1. Block reduction technique: as described by Ciocca et al. [48] in a preclinical study on sheep for the condyle substitution, a three-axis CNC subtractive automated milling machine (Cortini HS 644 P; Fidia S.p.A., Padova, Italy) is used to prepare the externally designed ceramic hydroxyapatite scaffold to replace the resected condyle. The 3D automated machining process starts from a block of porous HA of the required size ( $60 \times 30 \times 20$  mm). A machining tool with a 3-mm-diameter spherical milling bur is chosen, and the machining process is designed to build a scaffold with a depth of cut of 0.5 mm for the roughing step and 0.2 mm for the finishing step (Fig. 5).
  2. Molding technique: as recently described by Ciocca et al. [48] in a study describing the full-thickness harvesting of a mandibular segment in the sheep for bone substitution with a customized scaffold, commencing with a stack of CT slices, the mandibular corpus was virtually resected from the model, to artificially create a bony defect by reference to cutting lines running between the first molar and the incisors in the edentulous area of the sheep mandible. The ClayTools system (Freeform Modeling Plus software operating on the

**Fig. 5** The direct ceramic scaffold prototyping



Phantom Desktop haptic device; Sensable, Wilmington, MA) was used to this end. Surgical guides and the mold for the scaffold were made from EOS PA2200 polyamide powder and fixation plates from EOS Cobalt-Chrome SP2. The mold is designed for best opening after scaffold material processing, and it presents meshed walls for best exsiccation of the material (see Fig. 4).

3. Experimental and translational study model reveals the potential of CAD/CAM procedures in the surgical context. It:
  - (a) Easily transfers the virtual project into the surgical environment using the surgical guide
  - (b) Allows precise insertion of the scaffold into the site of a defect
  - (c) Achieves primary stability of the scaffold and secures mandibular stump repositioning

---

## Determinant Factors for Composite Scaffolding in Bone Regenerative Medicine

According to the ideal translational model described before, diverse options may exist to gain the final result of a perfect integration, material resorption, and new bone regeneration. The biocompatibility, bioactivity (osteinduction), reabsorption, osteoconduction, pore size dimension, external morphology, and surface functionalization represent the physical and chemical properties which should be tailored in synthetic HA crystals to optimize their specific biomedical applications. It is also to be considered the way by which the external volume of the scaffold may be obtained and the chemical characteristics that it has to possess for the best biocompatibility, cell seeding, and osteoinduction.

### Chemical-Physical Factors

- Hydrophilicity
- Resorbability
- Porosity: micro and total %

## Surface Hydrophobicity of Biomimetic Scaffold

The surface hydrophobicity is well known as a key factor to govern cell response. Previous studies showed that the more hydrophilic surface of material films increases the cell adhesion on the surface. For example, osteoblast adhesion was reported decreased when the contact angle of surface increased from  $0^\circ$  to  $106^\circ$ . Fibroblasts were found to have maximum adhesion when contact angles were between  $60^\circ$  and  $80^\circ$ . Interestingly, Vogler mentioned that the hydrophilic surface is suitable for the attachment of Madin-Darby canine kidney (MDCK) cells, but more hydrophilic surfaces (contact angle  $\theta < 65^\circ$ ) did not yield progressively high level of attachment efficiency. Furthermore, surface hydrophobicity is related to the rate of cell spreading and differentiation. On hydrophilic surfaces, cells generally showed good spreading, proliferation, and differentiation. Mouse osteoblast-like cell line MC3T3-E1 showed more fractal morphology on hydrophilic surface (contact angle  $\theta = 0^\circ$ ). 7 F2 mouse osteoblasts on hydrophilic surface (contact angle  $\theta = 24\text{--}31^\circ$ ) demonstrated accelerated metabolic activity and osteodifferentiation compared to their unmodified counterparts (contact angle  $\theta = 72^\circ$ ). The same phenomenon was observed in neuronal spreading and neurite outgrowth when the material surfaces reduced their hydrophobicity [50].

## Resorbability

Bone is a dynamic tissue constantly being reshaped by osteoblasts, cells which build bone, and osteoclasts, cells which resorb it. Osteoclasts are multinucleated cells responsible for the resorption of bone through the removal of the bone's mineralized matrix. The removal process begins with the attachment of the osteoclast to the osteon (predominant structures found in compact bone); the osteoclast then induces an infolding of its cell membrane and secretes collagenase and other enzymes important in the resorption process, such as tartrate-resistant acid phosphatase, secreted against the mineral substrate. During childhood, bone formation exceeds resorption, but, as the aging process occurs, resorption exceeds formation. The characteristic rigidity and strength of bone derives from the presence of mineral salts that permeate the organic matrix, formed by osteoid mineralization, due to the secretion of vesicles containing alkaline phosphatase, by the osteoblasts [15].

Porous HA biomimetic in simulating spongy bone morphology (porosity varying from a microporosity  $0.1\ \mu\text{m}$  to a macroporosity ranging from  $300$  to  $2000\ \mu\text{m}$ ) has been prepared using various technologies to control pore dimension, shape, distribution, and interconnections. However, HA ceramics processed by high-temperature treatment present a significant reduction of bioreactivity and growth kinetics of new bone due to the lack of resorbability [12]. The recent trend in biomaterials research is focused on overcoming the limitations of calcium phosphate and hydroxyapatite ceramics (low bioresorbability, surface area, and bioreactivity) and on improving their biological properties by exploring the unique advantages of nanotechnology. Using nanotechnology, it is possible to synthesize inorganic crystals with nanometric dimensions, characterized by a high bioresorbability, surface area, and surface structural disorder which increase crystal bioreactivity. The trend is shifting toward nanotechnology to improve the biological responses of HA, because nano-HA is a

constituent of bone [2]. For this purpose, investigation of novel biomaterial for bone engineering represents an essential area for planning tissue engineering approaches. Future biomaterials should combine bioactive and bioresorbable properties to activate in vivo mechanisms of tissue regeneration, stimulating the body to heal itself and facilitating replacement of the scaffold by the regenerating tissue. A variety of biomaterials, including synthetic polymers, ceramics, and natural polymers, are being used to fabricate synthetic scaffolds which act as guides and stimuli for three-dimensional tissue growth [28]. In this context, a promising biodegradable biomimetic nano-HA/polymer composite material has been successfully produced by rapid prototyping method [7, 28].

## Porosity

One of the most important parameters for bone scaffolding is porosity. Two variables concur to determine such biologically important parameter: the mean pore diameter and the total open porosity. The first one is defined as the diameter of the circumference area equivalent to the total porosity; the second is defined as the ratio between the total volume of the open porosities and the total volume of the material.

The mean pore diameter is essential for cell seeding: it has been extensively demonstrated that the ideal mean pore size for cell penetration is a diameter between 150 and 450  $\mu$ . Moreover, an ideal scaffold material should exhibit a total porosity (intended as the ratio between the total porosities volume and the total volume) up to 70 % of the total volume. The open porosity is intended as interconnected pores that allow penetrating of blood components in deeper part of the biomimetic scaffold. For this reason it is very important to distinguish between open and closed porosity, being the closed not useful for the biological process of cell seeding, osteoinduction, and resorption.

In the composite scaffold material presented in this chapter, the total open porosity percentage is different depending on the manufacturing technique. In the SM (subtractive manufacturing), the foaming process may lead to a maximum level of 58 % of total porosity, in which the interconnected pore percentage is 98 % (i.e., almost all pores are interconnected): even if the open porosity percentage is very high with respect to the total porosity, the total porosity itself does not reach acceptable level for cell seeding.

On the contrary, if the AM (additive manufacturing) is used, the 3D printing process straightly may produce (depending on the type of 3D printer used) an 80 % percentage of total porosity with a fully interconnected pores (100 % open porosity). This is one of the major reasons for choosing this kind of 3D printing instead of the subtractive manufacturing or the molding technique.

The micro-CT may help to measure the entire process of manufacturing and the post-op results in terms of cell seeding and material resorption. The methodology useful for this process may be resumed as follows: for the pre-op tests, specimens (2.2 cm  $\times$   $\varnothing$  1.4 cm) are scanned by means of high-resolution Skyscan 1172 (Bruker-MicroCT, Be) with 70-kV voltage, with 140- $\mu$ A amperage, and with a 0.5-mm-thickness aluminum filter at origin. All specimens are turned 180°, with a 0.5° progressive rotational angle. The slices with a pixel size of 0.5  $\mu$  (2096  $\times$  4000 pixel)

are elaborated using the software NRecon (version 1.6.8.0, Bruker, Be) to obtain micro-CT 4000 x 4000 pixel slices with a constant relative pixel size. As corrective factors, a correction of the beam hardening and a reduction of the ring artifacts are used, as well as the specific relative alignment of each single slice. For each specimen, a volume of interest (VOI) is defined (5-mm thickness), positioned in the center of the scaffold cylinder and with a perimeter coincident with the material perimeter.

## Physical Factors

Modern rapid prototyping techniques are available for giving to the scaffold the external anatomy necessary for restoring the bone defect: the identical volume to the native anatomy may be given to the scaffold for substituting the missing bone after cancer ablation. Two main modalities exist for customizing the volume: the subtractive and the additive manufacturing techniques, but an important difference should be considered when selecting one or the other. The main difference consists in the microporosity determination of the material: when using the subtractive technique, the material has to possess in itself the ideal microporosity, while, when using the additive technique, the microporosity of the material may be determined designing it by CAD. For the first option (subtractive manufacturing), a foaming process is necessary to determine the total microporosity, usually setting between 70 % and 80 %. For the second option, the total microporosity may be determined according to the potentiality of the 3D printing machine. In this specific option (additive manufacturing) moreover, not only the total porosity may be programmed but also the dimension of the pores: an ideal pore dimension should be between 150 and 450  $\mu$ , and the modern 3D printers may achieve these dimensions for printing.

A secondary modality to print a volume is the molding technique. It consists of an indirect method to give a volume to a material, leaving it harden at the inner of a customized mold that gives it the desired macroscopic volume.

The *subtractive manufacturing (SM) technique* considers the reduction of a given volume (usually a parallelepiped) to the desired form, by means of using a CAD/CAM process involving the use of a milling machine. A three-axis CNC subtractive automated milling machine may be used to prepare the externally designed scaffold to replace the resected bone. As previously described, the 3D automated machining process starts from a block of scaffold material of the standard size (usually 60  $\times$  30  $\times$  20 mm). A fixation support is projected to secure the scaffold parallelepiped to the milling machine. A machining tool with a 3-mm-diameter spherical milling bur is chosen, and the machining process is designed to build a scaffold with a depth of cut of 0.5 mm for the roughing step and 0.2 mm for the finishing step.

The *additive manufacturing (AM) technique* is the most promising method for customizing the scaffold, because it allows contemporary developing of the inner microstructure and the outer macrostructure of the material. This technique primarily depends on the 3D printer capacity of printing resolution, i.e., on the power of

printing system to produce microfilaments of scaffold material (minimum diameter no more than 100  $\mu$ ) and to assemble them in a grid with a box (pore) dimension no more than 450  $\mu$ . Moreover, this technique depends on the physical characteristics of the biomaterial, because there are two main modalities to harden the material after syringe extrusion: photo curing and heat curing. For photo-curing printing process, materials with photo-sensible molecules are necessary to allow curing after extrusion, by means of a light source applied at the external proximity of the extruding syringe. For heat-curing process, thermoplastic materials with temperature sensible components can be used, by heating them for the extrusion, in a computer-controlled pattern to construct scaffolds layer by layer. After extrusion, room temperature may be sufficient (depending on the material features) to harden the material. One more option is also available for 3D printing with the additive technique: the use of a solvent for giving fluent capacity to the material when flowing in the syringe and for immediate evaporation and consequent hardening at room temperature after extrusion. This option contributes to eliminate the temperature variable: if the scaffold composite material is a composite material, as the one presented in this chapter, by a collagen fibril composition, the temperature may become a problem if it is over 40 °C, because at this temperature some amino acid links alter their properties and compromise the conformation of the structure secondary of the collagen chains. However, at temperature lower than 40 °C, the printers sacrifice printing speed and become excessively time and cost consuming.

The *molding technique* consists of a process that produces a mold for the customization of the scaffold. According to the CAD design of the scaffold volume to restore the bone defect, a box (the mold) is designed to contain the scaffold composite material. For this application, the material is produced with a cream consistence, and the mold is constructed with more open pores as possible in its external surface, allowing the exsiccation of the material. Depending on the exsiccation process, this methodology may represent a further challenge for scaffolding, and for this reason it may be considered a second choice with respect to SM or AM.

---

## Summary

Advances in biotechnology have led to the new concept of personalized medicine. For tissue reconstruction cells can be harvested from the patient and after been cultured *in vitro* can be seeded on a scaffold produced by computer-aided design and machining (CAD/CAM) rapid prototyping to perfectly replace the missing tissue. A major challenge in bone replacement is the development of a scaffold that resembles bone's mechanical and physical properties while at the same time supports cells' adhesion and proliferation.

The study of nanocrystalline calcium phosphate physical–chemical characteristics and, thereafter, the possibility to imitate bone mineral for the development of new advanced biomaterials are constantly growing.

Biomimetic nanostructured hydroxyapatite, and in particular mineralized collagen, is a promising biomaterial for bone tissue engineering because this material



exhibits excellent biological properties. However, its application in the field of regenerative medicine needs to create hybrid materials with an organic bioactive phase in order to mimic functional bony units. The consistency of some biocompatible polymeric phase, such as PCL, permits the device to be manipulated to achieve an anatomically compatible shape and allow a surface adsorption of molecules that play active roles in the biological environment.

Many studies were developed in order to prepare and test new bioengineered custom-made composite scaffold materials using a combination of CAD/CAM technology to restore full-thickness defects of the bone. Modern 3D printing techniques allow dimensioning of the external volume according to the surgical defect, thus simplifying the surgery and reducing biological morbidity. Moreover, if a direct 3D printing is used, even the microporosity may be controlled by CAD, completing the morphologic workflow for 3D custom-made scaffolding. The use of CAD/CAM technology and the novel composite, biomimetic, and resorbable scaffolds are the promising way to interpret the need of bone regenerative medicine.

---

## References

1. Tampieri A, Sprio S, Ruffini A, Celotti G, Lesci IG, Roveri N (2009) From wood to bone: multi-step process to convert wood hierarchical structures into biomimetic hydroxyapatite scaffolds for bone tissue engineering. *J Mater Chem* 19(28):4973–4980
2. Roveri N, Palazzo B, Iafisco M (2008) *Expert Opin Drug Deliv* 5(8):861–877
3. Hidalgo DA (1989) Titanium miniplate fixation in free flap mandible reconstruction. *Ann Plast Surg* 23(6):498–507
4. Seyednejad H, Gawlitta D, Kuiper RV, de Bruin A, van Nostrum CF, Vermonden T, Dhert WJ, Hennink WE (2012) In vivo biocompatibility and biodegradation of 3D-printed porous scaffolds based on a hydroxyl-functionalized poly( $\epsilon$ -caprolactone). *Biomaterials* 33(17):4309–4431
5. Roveri N, Foresti E, Lelli M, Lesci IG (2009) Recent advancement in preventing teeth health hazard: the daily use of hydroxyapatite instead of fluoride. *Recent Pat Biomed Eng* 2:197–215
6. Moroni L, Hamann D, Paoluzzi L, Pieper J, de Wijn JR et al (2008) Regenerating articular tissue by converging technologies. *PLoS One* 3(8). doi:10.1371/journal.pone.0003032
7. Ciocca L, Donati D, Lesci IG, Dozza B, Duchi S, Mezini O, Spadari A, Romagnoli N, Scotti R, Roveri N (2014) Custom-made novel biomimetic composite scaffolds for the bone regenerative medicine. *Mater Lett*. doi:10.1016/j.matlet.2014.08.097
8. Lesci IG, Ciocca L, Dozza B, Lucarelli E, Squarzoni S, Donati D, Roveri N (2014) Innovative composite HA scaffold rapid prototyping for bone reconstruction: an in vitro pilot study. *Key Eng Mater* 583:56–63
9. Kim DH, Kim KL, Chun HH, Kim TW, Park HC, Yoon SY (2014) In vitro biodegradable and mechanical performance of biphasic calcium phosphate porous scaffolds with unidirectional macro-pore structure. *Ceram Int* 40:8293–8300
10. Sachlos E, Czernuszka JT (2003) Making tissue engineering scaffolds work. Review on the application of solid freeform fabrication technology to the production of tissue engineering scaffolds. *Eur Cells Mater* 5:29–40
11. Chua CK, Leong KF, An J (2014) Introduction to rapid prototyping of biomaterials. In: *Rapid prototyping of biomaterials*, Woodhead Publishing Limited, Oxford Cambridge, Philadelphia, New Delhi, 1–15

12. Ciocca L, Donati D, Fantini M, Landi E, Piattelli A, Iezzi G, Tampieri A, Spadari A, Romagnoli N, Scotti R (2013) CAD-CAM-generated hydroxyapatite scaffold to replace the mandibular condyle in sheep: preliminary results. *J Biomater* 28(2):207–218. doi:10.1177/0885328212443296
13. Mao Y, Park TJ, Zhang F, Zhou H, Wong SS (2007) Environmentally friendly methodologies of nanostructure synthesis. *Small* 3(7):1122–1139
14. Zhang Y, Lu J (2007) A simple method to tailor spherical nanocrystal hydroxyapatite at low temperature. *J Nanopart Res* 9(4):589–594
15. Roveri N, Palazzo B (2006) *Tissue, cell and organ engineering*. Wiley-VCH, Weinheim, pp 283–307
16. Rusu VM, Ng CH, Wilke M, Tiersch B, Fratzl P, Peter MG (2005) Size-controlled hydroxyapatite nanoparticles as self-organized organic–inorganic composite materials. *Biomaterials* 26(26):5414–5426
17. Battistella E, Mele S, Foltran I, Lesci IG, Roveri N, Sabatino P, Rimondini L (2012) Cuttlefish bone scaffold for tissue engineering: a novel hydrothermal transformation, chemical-physical, and biological characterization. *J Appl Biomater Funct Mater* 10(2):99–106
18. Chaudhry AA, Haque S, Kellici S et al (2006) Instant nano-hydroxyapatite: a continuous and rapid hydrothermal synthesis. *Chem Commun (Camb)* 21:2286–2288
19. Yeon KC, Wang J, Ng SC (2001) Mechanochemical synthesis of nanocrystalline hydroxyapatite from CaO and CaHPO<sub>4</sub>. *Biomaterials* 22(20):2705–2712
20. Liu J, Li K, Wang H, Zhu M, Xu H, Yan H (2005) Self-assembly of hydroxyapatite nanostructures by microwave irradiation. *Nanotechnology* 16(1):82–87
21. Iafisco M, Gomez Morales J, Hernandez-Hernandez MA, Garcia Ruiz JM, Roveri N (2010) Biomimetic carbonate-hydroxyapatite nanocrystals prepared by vapor diffusion. *Adv Eng Mater* 12(7):B218–B223
22. Iafisco M, Marchetti M, Gomez Morales J, Hernandez-Hernandez MA, Garcia Ruiz JM, Roveri N (2009) Silica gel template for calcium phosphates crystallization. *Cryst Growth Des* 9(11):4912–4921
23. Phillips MJ, Darr JA, Luklinska ZB, Rehman I (2010) Synthesis and characterization of nanobiomaterials with potential osteological applications. *J Mater Sci Mater Med* 14(10):875–882
24. Ye F, Guo H, Zhang H (2008) Biomimetic synthesis of oriented hydroxyapatite mediated by nonionic surfactants. *Nanotechnology* 19(24):245605. doi:10.1088/0957-4484/19/24/245605
25. Koutsopoulos S (2002) Synthesis and characterization of hydroxyapatite crystals: a review study on the analytical methods. *J Biomed Mater Res* 62(4):600–612
26. Cai Y, Tang R (2008) Calcium phosphate nanoparticles in biomineralization and biomaterials. *J Mater Chem* 18(32):3775–3787
27. Zhou H, Lee J (2011) Nanoscale hydroxyapatite particles for bone tissue engineering. *Acta Biomater* 7(7):2769–2781
28. Raucci MG, Guarino V, Ambrosio L (2010) Hybrid composite scaffolds prepared by sol–gel method for bone regeneration. *Compos Sci Technol* 70:1861–1868
29. Guarino V, Causa F, Netti PA, Ciapetti G, Pagani S, Martini D et al (2008) The role of hydroxyapatite as solid signal on performance of PCL porous scaffolds for bone tissue regeneration. *J Biomed Mater Res B Appl Biomater* 86B(2):548–557
30. Ma PX, Zhang R, Xiao G, Franceschi R (2001) Engineering new bone tissue in vitro on highly porous poly(a-hydroxyl acids)/hydroxyapatite composite scaffolds. *J Biomed Mater Res* 54(2):284–293
31. Sun H, Mei L, Song C, Cui X, Wang P (2006) The in vivo degradation, absorption and excretion of PCL-based implant. *Biomaterials* 7:1735–1740
32. Schantz JT, Hutmacher DW, Lam CXF, Brinkmann M, Wong KM, Lim TC (2003) Repair of calvarial defects with customized tissue-engineered bone grafts II. Evaluation of cellular efficiency and efficacy in vivo. *Tissue Eng* 9(Suppl 1):127–139

33. Marchetti C, Bianchi A, Mazzoni S, Cipriani R, Campobassi A (2006) Oromandibular reconstruction using a fibula osteocutaneous free flap: four different “preplating” techniques. *Plast Reconstr Surg* 118(3):643–651
34. Mazzoni S, Marchetti C, Sgarzani R, Cipriani R, Scotti R, Ciocca L (2013) Prosthetically guided maxillofacial surgery: evaluation of the accuracy of a surgical guide and custom-made bone plate in oncology patients after mandibular reconstruction. *Plast Reconstr Surg* 131(6):1376–1385. doi:10.1097/PRS.0b013e31828bd6b0
35. Tarsitano A, Mazzoni S, Cipriani R, Scotti R, Marchetti C, Ciocca L (2014) The CAD-CAM technique for mandibular reconstruction: an 18 patients oncological case-series. *J Craniomaxillofac Surg* pii: S1010–5182(14)00134-6. doi:10.1016/j.jcms.2014.04.011. [Epub ahead of print]
36. Ciocca L, Mazzoni S, Fantini M, Persiani F, Marchetti C, Scotti R (2012) CAD/CAM guided secondary mandibular reconstruction of a discontinuity defect after ablative cancer surgery. *J Craniomaxillofac Surg* 40(8):e511–e515. doi:10.1016/j.jcms.2012.03.015, Epub 2012 Apr 30
37. Ciocca L, Mazzoni S, Fantini M, Marchetti C, Scotti R (2012) The design and rapid prototyping of surgical guides and bone plates to support iliac free flaps for mandible reconstruction. *Plast Reconstr Surg* 129(5):859e–861e. doi:10.1097/PRS.0b013e31824a9f31
38. Ciocca L, Mazzoni S, Marchetti C, Scotti R (2014) Technical aspects of prosthetically guided maxillofacial surgery of the mandible. A pilot test study. *Acta Bioeng Biomech* 16(2):21–29
39. Ciocca L, Donati D, Ragazzini S, Dozza B, Rossi F, Fantini M, Spadari A, Romagnoli N, Landi E, Tampieri A, Piattelli A, Iezzi G, Scotti R (2013) Mesenchymal stem cells and platelet gel improve bone deposition within CAD-CAM custom-made ceramic HA scaffolds for condyle substitution. *Biomed Res Int* 2013:549762. doi:10.1155/2013/549762, Epub 2013 Sep 1. PubMed
40. Ciocca L, Mazzoni S, Fantini M, Persiani F, Baldissara P, Marchetti C, Scotti R (2012) A CAD/CAM-prototyped anatomical condylar prosthesis connected to a custom-made bone plate to support a fibula free flap. *Med Biol Eng Comput* 50(7):743–749. doi:10.1007/s11517-012-0898-4, Epub 2012 Mar 24
41. Ciocca L, De Crescenzo F, Fantini M, Scotti R (2009) CAD/CAM and rapid prototyped scaffold construction for bone regenerative medicine and surgical transfer of virtual planning: a pilot study. *Comput Med Imaging Graph* 33(1):58–62. doi:10.1016/j.compmedimag.2008.10.005, Epub 2008 Dec 2. PubMed
42. Kessler S, Mayr-Wohlfart U, Ignatius A, Puhl W, Claes L, Günther KP (2002) Histomorphological, histomorphometrical and biomechanical analysis of ceramic bone substitutes in a weight-bearing animal model. *J Mater Sci Mater Med* 13(2):191–195
43. Egli PS, Muller W, Schenk RK (1988) Porous hydroxyapatite and tricalcium phosphate cylinders with two different pore size ranges implanted in the cancellous bone of rabbits. A comparative histomorphometric and histologic study of bony ingrowth and implant substitution. *Clin Orthop Relat Res* 232:127–138
44. Mastrogiacomo M, Muraglia A, Komlev V, Peyrin F, Rustichelli F, Crovace A, Cancedda R (2005) Tissue engineering of bone: search for a better scaffold. *Ortho Craniofac Res* 8(4):277–284
45. Drury JL, Mooney DJ (2003) Hydrogels for tissue engineering: scaffold design variables and applications. *Biomaterials* 24:4337–4351
46. Thompson AY, Piez KA, Seyedin SM (1985) Chondrogenesis in agarose gel culture. A model for chondrogenic induction, proliferation and differentiation. *Exp Cell Res* 157:483–494
47. Diduch DR, Jordan LC, Mierisch CM, Balian G (2000) Marrow stromal cells embedded in alginate for repair of osteochondral defects. *Arthroscopy* 16: 571–7.x
48. Ciocca L, Donati D, Ragazzini S, Dozza B, Rossi F, Fantini M, Spadari A, Romagnoli N, Landi E, Tampieri A, Piattelli A, Iezzi G, Scotti R (2013) Mesenchymal stem cells and platelet gel improve bone deposition within CAD-CAM custom-made ceramic HA scaffolds for condyle substitution. *Biomed Res Int* 2013:549762. doi:10.1155/2013/549762, Epub 2013 Sep 1

- 
49. Moran JM, Pazzano D, Bonassar LJ (2003) Characterization of polylactic acid-polyglycolic acid composites for cartilage tissue engineering. *Tissue Eng* 9:63–70
  50. Chang H-I, Wang Y (2011) Cell responses to surface and architecture of tissue engineering scaffolds. In: Eberli D (ed) *Regenerative medicine and tissue engineering – cells and bio-materials*. InTech, Croatia, ISBN: 978-953-307-663-8

---

# In Vitro and In Vivo Evaluation of Composite Scaffolds for Bone Tissue Engineering

# 21

Svetlana Schussler, Khadidiatou Guiro, and  
Treena Livingston Arinzeh

## Contents

Introduction .....	616
Common Compositions Used in Composite Scaffolds .....	617
Bioceramics .....	617
Synthetic Polymers .....	617
Natural Polymers .....	617
Design and Fabrication of Composite Scaffolds .....	618
In Vitro Evaluation of Composite Scaffolds .....	620
Composite Scaffolds Alone and in Combination with Stem Cells or Other Cell Types ...	620
Growth Factor Release from Composite Scaffolds .....	620
In Vivo Evaluation of Composite Scaffolds .....	624
Composite Scaffolds in Combination with Stem Cells In Vivo .....	625
Growth Factor Release from Composite Scaffolds In Vivo .....	628
Summary .....	630
References .....	630

---

## Abstract

The repair of large bone defects resulting from trauma or disease remains a clinical challenge. Tissue engineering is a promising approach using scaffolds combined with cells and/or growth factors to simulate bone repair. Biocomposites, consisting of bioceramics and synthetic and/or natural polymers, have been sought for use as scaffolds because of their attractive properties in accelerating bone tissue formation. Bioceramics have proven osteoconductivity and can be combined with various types of polymers to

---

S. Schussler • K. Guiro • T.L. Arinzeh (✉)

Department of Biomedical Engineering, New Jersey Institute of Technology, Newark, NJ, USA  
e-mail: [sd36@njit.edu](mailto:sd36@njit.edu); [kg35@njit.edu](mailto:kg35@njit.edu); [arinzeh@njit.edu](mailto:arinzeh@njit.edu); [treena.arinzeh@njit.edu](mailto:treena.arinzeh@njit.edu)

© Springer International Publishing Switzerland 2016

I.V. Antoniac (ed.), *Handbook of Bioceramics and Biocomposites*,  
DOI 10.1007/978-3-319-12460-5\_39

615

create highly porous biocomposite scaffolds. This chapter will review bioceramic and polymer compositions used in composite scaffolds, their design, and their evaluation in *in vitro* and *in vivo* studies, demonstrating their potential for use in bone repair.

---

**Keywords**

Bioceramics • Biocomposites • Bone tissue engineering • Scaffolds

---

## Introduction

Autografts and allografts are commonly used to repair large bone defects resulting from trauma or disease [1]. However, these treatments have associated limitations such as donor site morbidity and a high risk of potential pathogen transfer [2]. In an attempt to overcome these issues, researchers in bone tissue engineering are focusing on the development of novel strategies that can promote bone repair [3, 4]. Biocomposites, consisting of bioceramics and synthetic and/or natural polymers, have been sought for use as scaffolds because of their attractive properties in accelerating bone tissue formation. Bioceramics, such as hydroxyapatite (HA),  $\beta$ -tricalcium phosphate ( $\beta$ -TCP), biphasic calcium phosphate (BCP) (which is a combination of HA and  $\beta$ -TCP), and bioactive glasses (BG), have been extensively investigated as synthetic bone graft substitutes for over 30 years [2, 5, 6]. Bioceramics demonstrate bone bioactivity, i.e., bond to bone tissue, proven biocompatibility, and excellent osteoconductivity. However, their brittle mechanical properties restrict their use to specific applications [7]. Therefore, bioceramics have been combined with various types of polymers to create highly porous biocomposite materials with improved mechanical properties for bone tissue engineering [8–18]. Ideal composite scaffolds should possess the following characteristics [19–21]:

- Low immunogenic and antigenic response
- Osteoconductive for bone ingrowth and scaffold incorporation
- Osteoinductive, enabling cell proliferation and differentiation, and support osteoprogenitor cells
- Biodegradability or bioresorbability that enables bone remodeling
- Porosity (macro- and nanoscale) that enables cell infiltration, growth, blood vessel formation, nutrient transfer, and metabolic waste transfer
- Mechanical stability
- Carrier for growth factors and cells
- Ease of use in clinical settings

This chapter describes commonly used bioceramic and polymer compositions used in composite scaffolds, their design and fabrication methods to improve properties, and their evaluation both in *in vitro* and *in vivo* studies, demonstrating their potential for use in bone repair.

## Common Compositions Used in Composite Scaffolds

### Bioceramics

Bioactive glasses and calcium phosphate ceramics, such as HA,  $\beta$ -TCP, and BCP, are widely investigated in composite scaffolds because they are bone bioactive and provide osteoconductive properties [20]. Bone bioactivity means an apatite forms on the ceramic's surface that facilitates bonding to the bone tissue [22]. Studies have shown cell proliferation, differentiation, and bone ingrowth on various compositions of calcium phosphate ceramics both in vivo and in vitro [20, 23–25]. Due to their charge, calcium phosphate ceramics are known to interact with proteins, growth factors [26], and cells making them a promising delivery vehicle [20, 27–29]. A potential drawback to using certain calcium phosphate ceramics is their low resorbability, especially in the case of HA [20]. Different preparation techniques can be applied to increase their rate of degradation [20].

Bioactive glass (BG), commercially available as Bioglass<sup>®</sup>, was discovered by Hench in 1964 and refers to glass compositions that have the ability to bond to the bone [20]. BG has a relatively fast rate of apatite layer formation when is immersed in simulated body fluid (SBF) in vitro or implanted in vivo in comparison to calcium phosphate ceramics, indicating its robust bioactivity [30]. BG can vary in composition to control rate of apatite formation and degradation; however, a major drawback of using BG is its brittle nature [30, 31]. Incorporating biodegradable polymers alters the mechanical and physical properties of ceramics [20, 24], providing a structure that can allow for higher porosity and can improve ceramic degradation rate.

### Synthetic Polymers

The poly- $\alpha$ -hydroxy esters – polylactic acid (PLA), poly(glycolic acid) (PGA), poly(lactic-co-glycolide acid) (PLGA), and poly- $\epsilon$ -caprolactone (PCL) – are the most investigated biodegradable synthetic polymers for bone tissue engineering [20, 23]. The PLA/PGA polymers are of interest due to their biocompatibility and degradation properties that can be tailored by changing different parameters, such as the molecular weight, tacticity, and L/G ratio in the case of PLGA [20, 23]. The main degradation mechanism is a hydrolysis reaction of the glycolic acid residue, which degrades faster than the polylactic acid. The overall degradation rate for the different polymers is as follows: PGA > PLGA > PLA > PCL [20, 23]. The different degradation profiles of the polymers allow for the formulation of composite scaffolds that will degrade as the new bone forms.

### Natural Polymers

Biocompatibility and degradability are important scaffold properties for bone tissue engineering [32]. Natural polymers offer this feature in addition to aspects of the

extracellular matrix (ECM) where cells or signaling molecules such as growth factors can attach. Natural- or biopolymer-based materials can be separated into two groups: (1) polysaccharides (starch, alginate, chitin/chitosan, hyaluronic acid derivatives) or (2) protein based (soy, collagen, fibrin gels, silk) [32].

Chitosan is a natural polysaccharide obtained from chitin that is a major component of the crustacean exoskeleton [33, 34]. Chitosan provides minimal foreign body reactions, an intrinsic antibacterial nature, biocompatibility, biodegradability, and the ability to be molded into various geometries to form porous structures, suitable for cell ingrowth and osteoconduction [33]. Chitosan can be readily processed into scaffolds using electrospinning [35–37], precipitation [38], lyophilization [39], and sintering [33, 34] techniques. The various preparation techniques allow for the formation of a composite with variable pore sizes and mechanical properties. Alginate is a polysaccharide obtained from seaweed and has been investigated for bone repair applications. Alginate like chitosan is considered biocompatible, biodegradable, and nontoxic [40].

Collagen type I is the major protein component of the bone extracellular matrix. Collagen is biocompatible, easily degraded and resorbed by the body by enzymatic action and allows for cellular attachment [41]. Incorporating HA, TCP, or BCP ceramics into collagen composites mimics the natural bone composition and can improve the mechanical properties of the scaffold [42].

Silk is the oldest naturally occurring polymer that has various applications. Silk is attractive for bone tissue engineering due to its biocompatibility, slow degradation, and mechanical properties [43]. Silk is easily processed allowing for controlled molecular structure and surface modifications [43].

---

## Design and Fabrication of Composite Scaffolds

Pore size and interconnected pores are a critical aspect in the fabrication of bone composite. Pore size and pore interconnectivity enhance infiltration, vascularization, degradation of the polymer/composite, as well as drug release. The optimal pore size for nutrient transport is 100  $\mu\text{m}$ , whereas pore sizes in the range of 150–500  $\mu\text{m}$  have been reported to be optimal for bone tissue ingrowth [25]. Electrospinning, three-dimensional (3-D) printing, solvent casting and particulate leaching, freeze-drying, and precision extrusion deposition (PED) are some examples of fabrication methods that produce porous scaffolds. These methods can produce scaffolds with varying morphological features, such as interconnected pores, nano- or micron-sized fiber dimensions, and mechanical properties. For example, electrospinning produces non-woven mats, where the fiber dimensions and interfiber spacing can be varied and controlled, whereas 3-D printing can be used to produce scaffolds with mechanical strength close to the trabecular bone [44]. Pore size and porosity can affect cellular response in vitro. Increased cell proliferation and osteogenic response were observed with increasing pore sizes for different scaffold compositions [45, 46]. Precision extrusion deposition (PED) process was used to fabricate PCL and composite scaffolds



containing PCL and HA with 60 % and 70 % porosity and 450 and 750 uL pore size [47]. Both PCL and PCL-HA scaffolds supported proliferation and differentiation of primary fetal bovine osteoblasts [47].

For growth factors incorporated within composites scaffolds, fabrication methods must maintain the bioactivity of the protein and provide the desired release or availability to the biological environment. Localized growth factor delivery can accelerate and enhance new bone formation during the bone healing process. Specific growth factors function at different stages of bone healing (Table 1). Therefore, the release of the appropriate growth factor during healing can augment bone formation [21, 28, 29, 48, 49]. Growth factors are incorporated in the composites by (1) physical attachment of the protein to the scaffold or (2) encapsulation in the scaffold [19–21, 48]. The use of organic solvents or harsh pH conditions is avoided because they can denature the protein [21] and potentially lead to undesired immunogenic response in vivo [50]. Additionally, the composite degradation products are considered because they should not inactivate the growth factor. Controlled delivery is another critical aspect when designing the composite scaffold for the release of growth factors. Scaffold formulations can show an initial burst release followed by a sustained release over a period of time. Recent work has been able to demonstrate improved sustained release by growth factor encapsulation into microparticles and incorporation into the composite [51].

**Table 1** Key signaling molecules involved in bone repair and their temporal expression [48]

Group	Growth Factor	Overall action	Source for growth factor	Temporal expression					
				0D	1D	3D	7D	14D	21D
Inflammation	IL-1 IL-6 TNF-α SDF1 GCSF MCSF OPG RANKL COX 2 HIF1α	Elicit inflammation and migration  Chemotactic factor	Macrophages Inflammatory cells Cells of mesenchymal origin	—	—	—	—	—	—
		Induces osteoclastogenesis Decoy receptor of RANKL Induces osteoclastogenesis  Angiogenic, hypoxic		—	—	—	—	—	
Growth and differentiation	TGF-β1 TGF-β2 TGF-β3 BMP-2 BMP-4 BMP-7 GDF 5 GDF 10 PDGF FGFs IGF-I	Differentiation of MSC to osteogenic cells Stimulate release of other growth  Osteogenic factor	Platelets, bone extracellular matrix, cartilage matrix Osteoprogenitor cells, osteoblasts, bone extracellular matrix  Platelets, osteoblasts, Macrophages, mesenchymal cells, Chondrocytes, osteoblasts	—	—	—	—	—	—
		Mitogenic and chemotactic factor Angiogenic Osteogenic factors		—	—	—	—	—	
Angiogenesis	VEGF-b,c Ang1 PTN	Neovascularization Angiogenesis	Osteogenic cells Platelet	—	—	—	—	—	—
Inhibitory	Noggin Chordin	BMP2, 4 and 7 specific inhibitor	Osteogenic cells	—	—	—	—	—	—
ECM	OPN Col2a1 Col10a1 CollA1 BSP		Osteogenic cells, fibroblasts	—	—	—	—	—	—

## In Vitro Evaluation of Composite Scaffolds

### Composite Scaffolds Alone and in Combination with Stem Cells or Other Cell Types

The osteogenic potential of the composites is evaluated for apatite formation by submerging the scaffolds in SBF and/or by evaluating the in vitro cellular response of cells seeded onto the composites. Electrospun composites consisting of (20/80) HA/TCP nanoceramics and PCL have been shown to support in vitro apatite formation when immersed in simulated body fluid and the osteogenic differentiation of human mesenchymal stem cells (hMSCs) [22]. Electrospun PLA/TCP scaffolds with increasing concentrations of TCP (0 %, 5 %, 10 %, and 20 %) promoted cell proliferation and osteogenic differentiation of human adipose-derived stem cells (hASCs) in the presence of osteogenic differentiating medium (Fig. 1) [52]. Increased cellular proliferation and alkaline phosphatase production was observed for 10 % and 20 % TCP [52]. PCL-TCP composites produced via a hybrid twin-screw extrusion/electrospinning process supported the proliferation and differentiation of mouse preosteoblast cells (MC3T3-E1) [53]. Highly porous BG-filled poly(DL-lactic acid) (PDLLA) composite foams with different concentrations of BG (5 and 40 wt%) showed cellular migration through the porous network and apatite layer formation when the composites were immersed in SBF, with more uniform apatite distribution with the higher bioactive glass concentration [27].

Composites made of natural polymers also show favorable cell response. Polysaccharide-containing composites (e.g., chitosan, alginate) support cell proliferation and differentiation [33–39, 54]. Collagen/calcium phosphate composites can provide an ideal microenvironment for bone regeneration since cells can attach directly to amino acid sequences in collagen. However, these composites lack mechanical strength. In vitro studies demonstrate the osteogenic activity of the composites comparable to collagen alone or ceramic alone [41, 42, 55, 56]. Silk-HA composites have shown to be osteoinductive in the absence of osteogenic differentiation stimuli [57]. The authors evaluated the osteogenic effect of silk sponges embedded with various concentrations of HA. The results showed increased bone-like structures (Fig. 2) and an increase in the equilibrium Young's modulus (up to fourfold or eightfold over 5 or 10 weeks of cultivation, respectively) as the concentration of HA increased in the silk sponge composite [57]. Other groups have shown that silk composites or premineralized silk composites show favorable osteogenic properties at various concentrations of HA [58, 59].

### Growth Factor Release from Composite Scaffolds

Table 2 lists growth factors commonly investigated for bone tissue engineering. Growth factors are intracellular signaling molecules that play a role in cellular recruitment, migration, growth, proliferation, and differentiation [21]. The biological activity of the growth factor is unique to the target cell, receptor type, and the

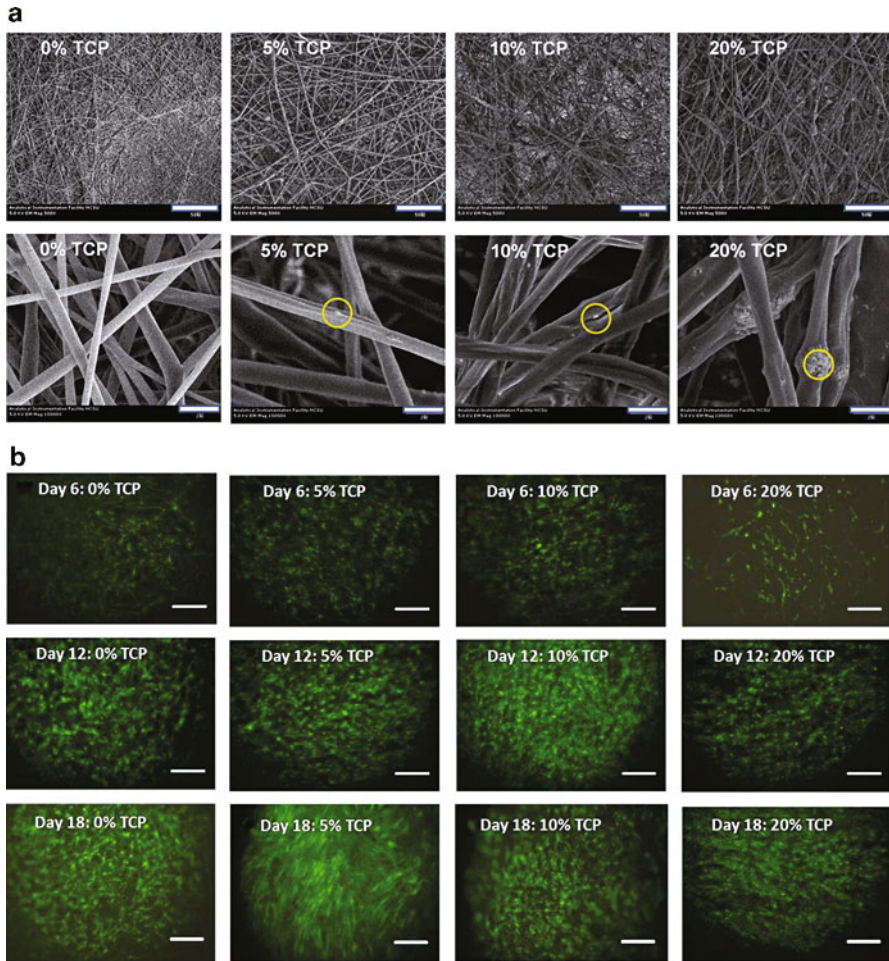


**Fig. 1** *Panel A:* scanning electron microscope (SEM) images of electrospun PCL/TCP composites with increasing TCP. *Yellow circles* indicate TCP crystals embedded within the fiber matrix. Scale bar in *top* row images =50  $\mu\text{m}$  and in *bottom* row images =2  $\mu\text{m}$ . *Panel B:* viability images of hASCs seeded on electrospun composites with increasing TCP content at days 6, 12, and 18. *Green* viable cell, *red* dead cell. hASCs were highly viable with minimal dead cells present on any scaffold. Scale bar=100  $\mu\text{m}$  [52]

biological environment or event (tissue growth, tissue healing) [19, 21]; however, a single growth factor can activate multiple cell types [48]. An orchestra of specific growth factors is responsible for the bone healing process [48]. The transforming growth factor (TGF)-beta growth factor superfamily is responsible for bone induction, MSC recruitment, proliferation, differentiation, and extracellular matrix (ECM) production. Within the TGF-beta family, the bone morphogenic proteins are most studied [19, 48]. Currently recombinant human bone morphogenic protein (rhBMP)-2 (Infuse<sup>TM</sup>, Medtronic Sofamor Danek, Inc., Minneapolis, MN) and BMP-7



**Table 2** Growth factors commonly used in bone regeneration (Adapted from Ref. [21, 48])

Growth factor	Abbreviation	Relevant known activities
Transforming growth factor- $\beta$	TGF- $\beta$	Proliferation and differentiation of bone
Bone morphogenetic protein-2	BMP-2	Differentiation of bone forming cells
Bone morphogenetic protein-7	BMP-7	
Insulin-like growth factor	IGF-1	Stimulates proliferation of osteoblasts and the synthesis of bone matrix
Fibroblast growth factor-2	FGF-2	Proliferation of osteoblasts
Platelet-derived growth factor	PDGF	Proliferation of osteoblasts
Vascular endothelial growth factor	VEGF	Angiogenesis, new blood vessel formation

(OP-1™, Stryker Biotech, Hopkinton, MA) are approved by the FDA for clinical treatment of nonunion defects, accelerated fracture healing, spinal fusion, alternate to Autogenous Iliac Crest Bone Grafting (AICBG) or co-therapy with AICBG for expanded bone graft [19, 28].

The most evaluated growth factor for bone tissue engineering is BMP-2. Recombinant BMP-2 (rhBMP-2) has been incorporated into various composite formulations, and the release and effect on cellular proliferation and differentiation have been evaluated. PCL-TCP-rhBMP-2 and PCL-TCP-fibrin-rhBMP-2 composites showed rhBMP-2 loading efficiency of 70 % and 40 %, respectively. rhBMP-2 was shown to be active as indicated by the alkaline phosphatase activity of human osteoblasts [60]. Silk-polyethylene oxide-nanoHA (nHA)-BMP-2 composites when cultured with hMSCs showed the highest calcium deposition as compared to the composite without nHA or BMP-2 [61]. Poly(DL-lactic-co-glycolic acid)/HA composite scaffolds loaded with BMP-2 were shown to induce in vitro osteogenic differentiation of human adipose-derived stromal cells [62]. Sustained release of BMP-2, over 21 days, has been shown for BMP-2 loaded into heparin/collagen type I coated TCP/HA composites [63].

Besides delivering growth factors, composite scaffolds can be used as delivery vehicles for genes and genetically modified cells to increase the production of the growth factors locally. PLGA/HA composite scaffolds with different HA contents (0 %, 5 %, and 10 %) were investigated for the delivery of BMP-2 plasmid DNA [64]. The plasmid DNA was incorporated using three different methods: naked DNA, encapsulated DNA/chitosan nanoparticles into scaffolds after fiber fabrication, and encapsulation of DNA/chitosan nanoparticles into scaffold by mixing with PLGA/HA solution before fiber fabrication [64]. The authors showed that the addition of HA enhanced the release of both naked and encapsulated DNA [64]. Incorporating HA in the scaffolds formulation enhanced the cell attachment, cell viability, as well as the DNA transfection efficiency [64]. PLGA-HA scaffold was used for the delivery of murine stromal cell line transfected with BMP-2 [65]. The authors were able to show that the composite supported cell attachment, growth, and BMP-2 production in vitro and served as a delivery vehicle for bioactive BMP-2 in vivo [65].

## In Vivo Evaluation of Composite Scaffolds

Bone tissue-engineering strategies using composites have been investigated in small and large animal models. In bone regeneration, animal models fall into two categories: (1) ectopic models are mainly used to differentiate between the proliferative and inductive ability of constructs, while (2) orthotopic models are used to test the efficacy and safety of the new constructs. Ectopic models are described to be usually simple, less costly, and less invasive [66, 67]. Mice, rats, and rabbits are the most commonly used species to study bone physiology and construct efficacy and safety comprising of approximately 80 % of all animals used to study bone repair. The remaining 20 % are composed of pigs, goats, sheep, dogs, and nonhuman primates [68].

In recent years, a large number of HA and polymer composite scaffolds have been developed and investigated for bone regeneration applications [69, 70]. For instance, to examine guided bone regeneration and in vivo biocompatibility and degradation of electrospun poly ( $\epsilon$ -caprolactone)-poly (ethylene glycol) – poly ( $\epsilon$ -caprolactone)/nano-hydroxyapatite (PCEC/nHA) fibrous scaffold, rectangular full-thickness defects with dimensions of 10 mm  $\times$  5 mm were made in the cranium of New Zealand white rabbits [71]. The scaffolds were biocompatible and showed new cortical bone fill within the scaffold after 20 weeks of implantation [71]. Similarly, in order to evaluate the healing of critical-size surgical defects after implantation of porous nanocrystalline hydroxyapatite/polyamide composite (nHAp/PA) blocks, Zhang and co-workers [72] studied a bilateral mandible model using adult New Zealand white rabbits for up to 24 weeks. Results showed the presence of active osteoblasts at week 4 within the pore structure, and the defects were completely occupied by the new bone with a density comparable to the host bone at 24 weeks (Figs. 3 and 4). Therefore, porous composites containing HA showed potential for bone tissue-engineering repair [72].

It is well known that scaffolds for bone tissue engineering should provide an osteoconductive surface to promote the ingrowth of the new bone after implantation into bone defects. This can be achieved by fabricating composites having distinct scaffold structures with HA. For instance, Laschke et al. examined the in vivo properties of a nano-hydroxyapatite (nHAp)/poly(ester-urethane) (PU) composite scaffold prepared by a salt leaching–phase inversion process [73]. In vivo analysis of the inflammatory and angiogenic response to implanted nHAp/PU scaffolds in the dorsal skinfold chamber of BALB/c mice model demonstrated that this composite was biocompatible and vascularization occurred. Therefore, nHAp/PU composite scaffolds represent a promising new type of scaffold for bone tissue engineering, combining the mechanically favorable properties of PU with the osteoconductive HA [73]. Moreover, porous bilayered scaffolds, fully integrating a silk fibroin (SF) layer and a silk-nano calcium phosphate (silk-nanoCaP) layer in a rabbit knee critical-size osteochondral defect (OCD) model, were investigated. The in vivo compatibility of the bilayered scaffolds also was assessed by subcutaneous implantation in the rabbit. The scaffolds firmly integrated into the host tissue after 4 weeks of implantation and subcutaneous implantation in rabbits demonstrated mild inflammation [74].

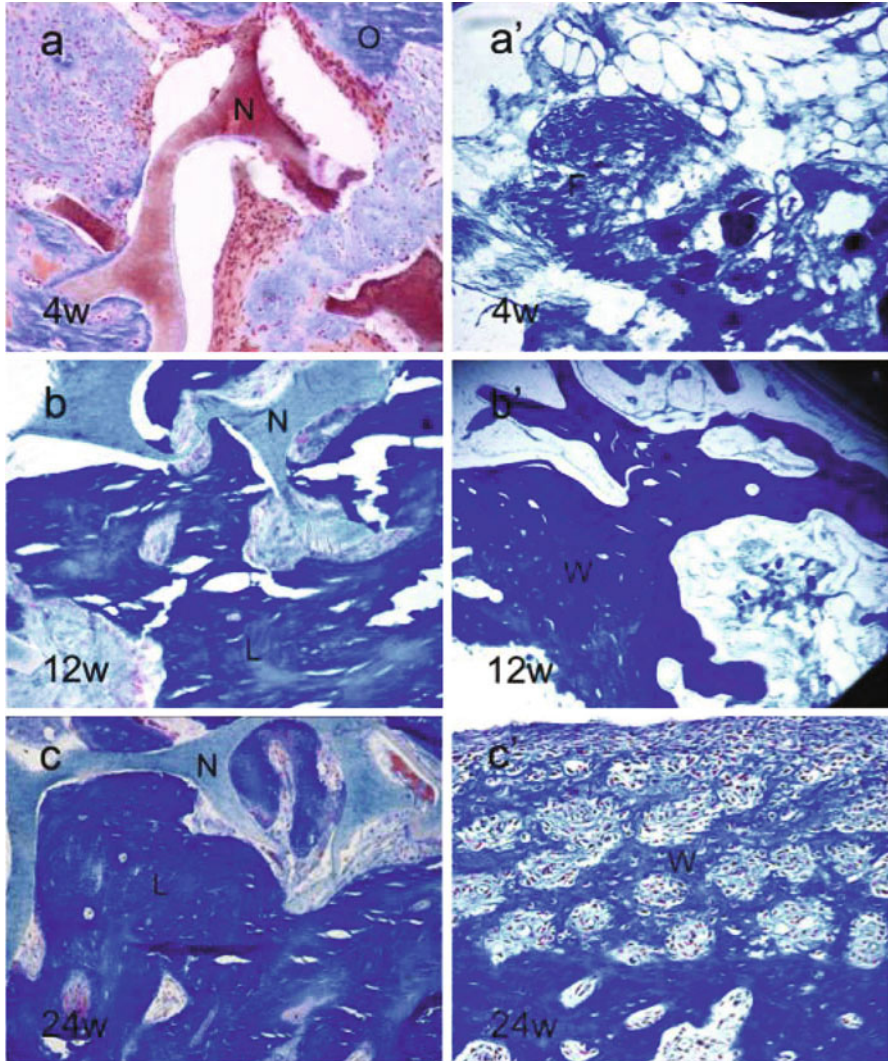


**Fig. 3** Histological cross sections of the newly formed bone 4, 12, and 24 weeks after nHA/PA implantation (**a–c**) and in blank controls (**a', b', c'**). The pore spaces of nHA/PA were filled with the bone marrow (**a–c**), showing that the interconnected pore structure could provide a channel for body fluid. Masson staining (magnification: 200 $\times$ ). *N* nHA/PA bone substitute, *O* osteoid, *L* lamellar bone, *F* fibrous and connective tissue, *W* woven bone [72]

### Composite Scaffolds in Combination with Stem Cells In Vivo

Tissue-engineering strategies utilize a combination of cells, biodegradable scaffolds, and growth factors to stimulate tissue regeneration [75–79]. The scaffold is used for its osteoconductive properties [80, 81], and the cells or growth factors are used for

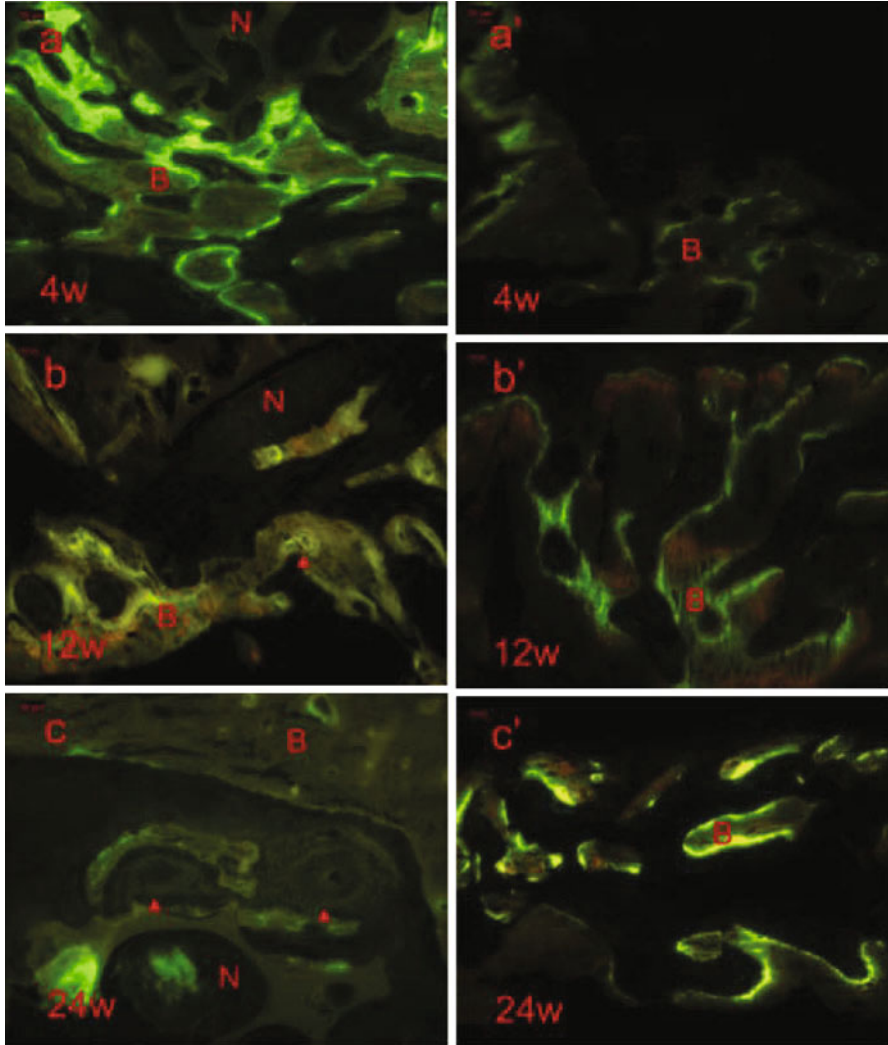


**Fig. 4** Characteristic distribution of the fluorescent dyes tetracycline (yellow) and calcein (green) in the central area of the defect 4, 12, and 24 weeks after nHA/PA implantation (a–c) and in blank controls (a', b', c'). (Magnification: 100 $\times$ ). N, the side of nHA/PA; B, new-formed bone; arrows denote the Haversian canals. (For interpretation of the references to color in this figure legend, the reader is referred to the web version of the article.) [72]

their osteoinductive or osteogenic properties [82, 83]. Bone tissue-engineering strategies utilizing stem cells have been investigated in small and large animal models to evaluate both safety and efficacy.

Mesenchymal stem cells (MSCs) are widely studied as the stem cell type in *in vivo* studies using composites [84–86]. MSCs are self-renewing, multipotent stem cells with the capability of differentiating into osteoblasts, chondrocytes,



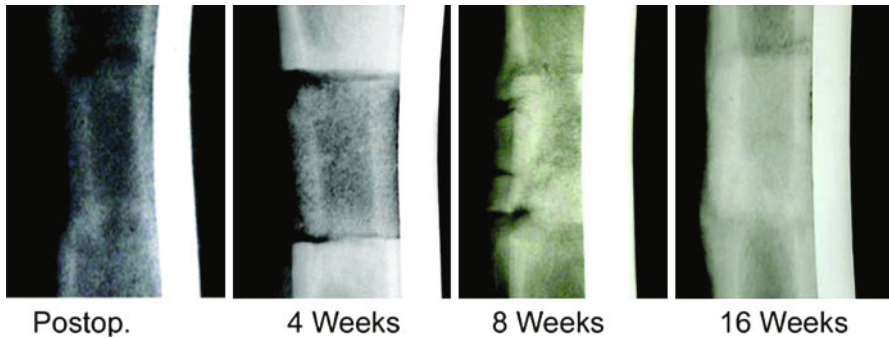


**Fig. 5** Radiographs of segmental defects treated with allogeneic mesenchymal stem cells loaded onto hydroxyapatite-tricalcium phosphate. Union at the host bone-implant interfaces was observed, and callus formed medially along the length of the implant by 8 weeks after implantation. The horizontal defects in the callus seen at 8 weeks were caused by the sutures holding the implant in place. At 16 weeks, the defect exhibited increased radiopacity and the medial callus was reduced [92]

adipocytes, tenocytes, myoblasts, and other cell types [87]. MSCs can be obtained from different sources such as the bone marrow (BM-MSCs), adipose tissue (AD-MSCs), umbilical cord, periosteum, and dental pulp [88, 89]. However, BM-MSCs have been the most investigated [88, 90]. Furthermore, studies have demonstrated that the use of allogeneic BM-MSCs can successfully repair the bone and other tissue types in various animal models without provoking an adverse immune response (Fig. 5) [91–93]. An allogeneic BM-MSC approach provides an off-the-shelf therapy, where allogeneic BM-MSCs are used as universal cells and, in turn, provide cells to a much larger clinical population. Allogeneic BM-MSCs also are currently in clinical trials for various disorders or conditions [94]. Consequently bone repair has been studied using BM-MSCs combined with composite scaffolds [90, 95, 96]. Composites consisting of natural or synthetic polymers with bioceramics using BM-MSCs have been investigated because they combine the toughness and compressive strengths of polymers with the bioactivity of ceramics in an attempt to achieve a similar structure to the bone [69]. These scaffolds have osteoconductive properties [95]. Recently, reports showed in vivo biocompatibility and osteogenesis of bioglass-collagen-phosphatidylserine (BG-COL-PS) scaffolds and rat mesenchymal stem cells/scaffold constructs [97]. A 3.5 by 4.5 mm diameter defect to bone marrow depth was created in the distal ends of rat femurs. The BG-COL-PS cell constructs were implanted in the femurs for 6 weeks. The results showed that BG-COL-PS cell composite scaffolds displayed good biocompatibility and osteoconductivity with the host bone and improved bone formation as compared to BG-COL-PS and BG-COL control groups. Similar findings were confirmed in scaffolds combining silicon-TCP scaffolds with BM-MSCs and implanted in mid-diaphysis tibial fractures in sheep [98]. After 3 months of implantation, new bone formation was present and corresponded with the scaffold resorption.

Embryonic stem cells (ESCs) also are being investigated for bone repair due to their pluripotent capabilities [99, 100]. However, safety concerns exist regarding their usage since ESCs can readily form tumors. Several attempts have been made to induce bone-forming cells from hESCs [101] for the treatment of large bone defects, since hESCs have great self-renewal abilities. A recent study demonstrated bone formation using osteogenic cells derived from human ESCs (OC-hESC) grown on porous PLGA/HA composite scaffold. Bone formation using OC-hESC-seeded scaffolds was significant in subcutaneous sites of immunodeficient mice at 4 and 8 weeks after implantation when compared to cell-free controls.

Other stem cell sources also are under investigation. Induced pluripotent stem cells (iPSCs) derived from adult somatic cells may be promising for autologous therapies. iPSCs share many characteristics with ESCs, including morphology, proliferation, surface antigens, gene expression, epigenetic status, and pluripotency [102, 103]. Results so far indicate that these cells may have potential as an unlimited source of therapeutically useful cells due to their self-renewal abilities. Therefore, the development of efficient and reproducible therapeutic methods using iPSCs is important for many regenerative medicine strategies. Dental pulp MSCs, human fetal MSCs, and amniotic fluid stem cells also are currently under investigation as a potential cell source for bone repair [104–106].

## Growth Factor Release from Composite Scaffolds In Vivo

In order to enhance osteogenic induction and bone formation, studies have used composite scaffolds to improve osseointegration and to deliver cytokines, growth factors, and specific genes [107–111]. BMPs have been extensively studied in inducing new bone formation in vivo and are in clinical use in bone defect repair [112–114]. The osteoinductive characteristics of BMPs have been widely studied with murine, bovine, and primate animal species [115, 116]. For instance, interconnected porous calcium hydroxyapatite (IP-CHA) mixed with poly(D,L-lactic acid)–polyethylene glycol (PDLLA–PEG) block copolymer composite was evaluated in a rabbit radii model for the bone-regenerating efficacy of recombinant human (rhBMP-2) (Fig. 6). At 8 weeks after implantation, PDLLA–PEG composite with rhBMP exhibited complete repair with sufficient strength and anatomical structure (Fig. 7) [117, 118]. Similarly studies by Sotome and co-workers [119] investigated hydroxyapatite/collagen–alginate (HAp/col–alginate) as a carrier for rhBMP-2 in the rat femur. Bone formation was observed throughout the implant 5 weeks after implantation. Studies have shown the combination of BMP-2 and BMP-7 significantly induces bone formation. Qing et al. used  $\beta$ -TCP scaffold combined with ADSCs co-transfected with BMP-2 and BMP-7 and implanted the constructs in rat femur defects for 6 weeks. Their results demonstrated that BMP-2 + BMP-7/ADSCs group had a significant increase in new bone formation as compared with BMP-2 group and BMP-7 group in vivo [120].

**Fig. 6** Soft X-ray photographs of the healing of a bone defect in a rabbit radius. (a) The IP-CHA-alone group at 8 weeks after implantation. Radiolucent lines are clearly visible between the IP-CHA and host bone, and the radiodensity of IP-CHA did not increase. (b) The recombinant human bone morphogenetic protein-2 (rhBMP-2, 5 mg)/IP-CHA group at 8 weeks after implantation. Bony unions were observed at the junction sites and the radiodensity of IP-CHA increased [117]

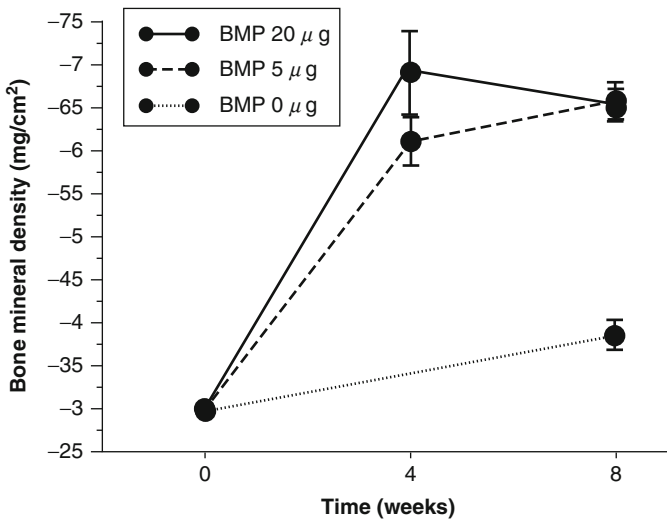
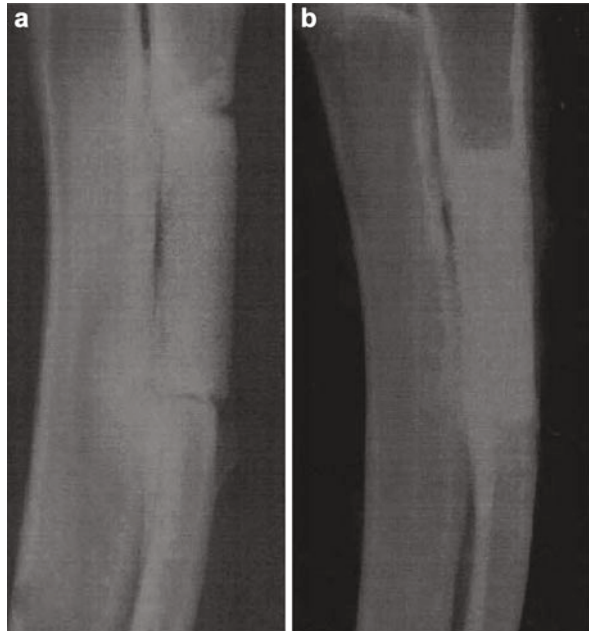


**Fig. 7** Bone mineral density of IP-CHA-alone group and BMP-5 and 20 µg groups was evaluated by dual-energy X-ray absorptiometry (DXA) using a PIXImus animal densitometer. Each data point represents an average and standard deviation ( $n = 5$ ) [118]

## Summary

Biocomposites containing bioceramics and polymers have shown promise as scaffolds for bone tissue-engineering applications. They support osteogenic activity, can effectively deliver growth factors, and are osteoconductive. Biocomposites provide the osteoconductive properties of bioceramics with the improved mechanical properties and degradation rate of polymers to support bone formation, integration, and remodeling. Future work will continue to use fabrication methods and polymer and ceramic chemistries to tailor micro- and nanostructures for promoting osteogenic activity. In vivo studies demonstrate that tissue-engineering strategies combining biocomposite scaffolds with stem cells and/or growth factors may be a viable approach to treating large bone defects.

---

## References

1. Petite H, Viateau V, Bensaid W, Meunier A, de Pollak C, Bourguignon M et al (2000) Tissue-engineered bone regeneration. *Nat Biotechnol* 18:959–963
2. Yaszemski MJ, Payne RG, Hayes WC, Langer R, Mikos AG (1996) Evolution of bone transplantation: molecular, cellular and tissue strategies to engineer human bone. *Biomaterials* 17:175–185
3. Langer R, Vacanti JP (1993) Tissue engineering. *Science* 260:920–926
4. Mistry AS, Mikos AG (2005) Tissue engineering strategies for bone regeneration. *Adv Biochem Eng Biotechnol* 94:1–22
5. Oki A, Qiu X, Alawode O, Foley B (2006) Synthesis of organic–inorganic hybrid composite and its thermal conversion to porous bioactive glass monolith. *Mater Lett* 60:2751–2755
6. Brodie J, Goldie E, Connel G, Merry J, Grant M (2005) Osteoblast interactions with calcium phosphate ceramics modified by coating with type I collagen. *J Biomed Mater Res A* 73:409–421
7. Yunos DM, Bretcanu O, Boccaccini AR (2008) Polymer-bioceramic composites for tissue engineering scaffolds. *J Mater Sci* 43:4433–4442
8. Habibovic P, van der Valk CM, van Blitterswijk CA, De Groot K, Meijer G (2004) Influence of octacalcium phosphate coating on osteoinductive properties of biomaterials. *J Mater Sci Mater Med* 15:373–380
9. Ripamonti U (1991) The induction of bone in osteogenic composites of bone matrix and porous hydroxyapatite replicas: an experimental study on the baboon (*Papio ursinus*). *J Oral Maxillofac Surg* 49:817–830
10. Ghanaati S, Udeabor SE, Barbeck M, Willershausen I, Kuenzel O, Sader RA, Ghanaati S, Udeabor SE, Barbeck M, Willershausen I, Kuenzel O, Sader RA et al (2013) Implantation of silicon dioxide-based nanocrystalline hydroxyapatite and pure phase beta-tricalciumphosphate bone substitute granules in caprine muscle tissue does not induce new bone formation. *Head Face Med* 9:1
11. Barrere F, van der Valk CM, Dalmeijer RA, Meijer G, van Blitterswijk CA, de Groot K et al (2003) Osteogenicity of octacalcium phosphate coatings applied on porous metal implants. *J Biomed Mater Res A* 66:779–788
12. Xin R, Leng Y, Chen J, Zhang Q (2005) A comparative study of calcium phosphate formation on bioceramics in vitro and in vivo. *Biomaterials* 26:6477–6486
13. Rucker M, Laschke MW, Junker D, Carvalho C, Tavassol F, Mülhaupt R et al (2008) Vascularization and biocompatibility of scaffolds consisting of different calcium phosphate compounds. *J Biomed Mater Res A* 86:1002–1011

14. Sinikovic B, Kramer FJ, Swennen G, Lubbers HT, Dempf R (2007) Reconstruction of orbital wall defects with calcium phosphate cement: clinical and histological findings in a sheep model. *Int J Oral Maxillofac Surg* 36:54–61
15. Chu TM, Warden SJ, Turner CH, Stewart RL (2007) Segmental bone regeneration using a load-bearing biodegradable carrier of bone morphogenetic protein-2. *Biomaterials* 28:459–467
16. Jegoux F, Goyenvalle E, Cognet R, Malard O, Moreau F, Daculsi G et al (2009) Reconstruction of irradiated bone segmental defects with a biomaterial associating MBCP +<sup>®</sup>, microstructured collagen membrane and total bone marrow grafting: an experimental study in rabbits. *J Biomed Mater Res A* 91:1160–1169
17. Davies JE, Matta R, Mendes VC, Perri de Carvalho PS (2010) Development, characterization and clinical use of a biodegradable composite scaffold for bone engineering in oro-maxillo-facial surgery. *Organogenesis* 6:161–166
18. Ignatius AA, Betz O, Augat P, Claes LE (2001) In vivo investigations on composites made of resorbable ceramics and poly (lactide) used as bone graft substitutes. *J Biomed Mater Res* 58:701–709
19. Vo TN, Kasper FK, Mikos AG (2012) Strategies for controlled delivery of growth factors and cells for bone regeneration. *Adv Drug Deliv Rev* 64:1292–1309
20. Habraken WJEM, Wolke JGC, Jansen JA (2007) Ceramic composites as matrices and scaffolds for drug delivery in tissue engineering. *Adv Drug Deliv Rev* 59:234–248
21. Blackwood KA, Bock N, Dargaville TR, AnnWoodruff M (2012) Scaffolds for growth factor delivery as applied to bone tissue engineering. *Int J Polym Sci* 2012:25. Article ID 174942. doi:10.1155/2012/174942
22. Patlolla A, Arinze TL (2014) Evaluating apatite formation and osteogenic activity of electrospun composites for bone tissue engineering. *Biotechnol Bioeng* 111:1000–1017
23. Rezwani K, Chen QZ, Blaker JJ, Boccaccini AR (2006) Biodegradable and bioactive porous polymer/inorganic composite scaffolds for bone tissue engineering. *Biomaterials* 27:3413–3431
24. Karageorgiou V, Kaplan D (2005) Porosity of 3D biomaterial scaffolds and osteogenesis. *Biomaterials* 26:5474–5491
25. Blokhuis TJ, Termaat MF, den Boer FC, Patka P, Bakker FC, Henk JTM (2000) Properties of calcium phosphate ceramics in relation to their in vivo behavior. *J Trauma-Injury Infect Crit Care* 48:179
26. Scopes RK (1994) Protein purification: principles and practice. Springer, New York
27. Blaker JJ, Gough JE, Maquet V, Notingher I, Boccaccini AR (2003) In vitro evaluation of novel bioactive composites based on Bioglass<sup>®</sup>-filled polylactide foams for bone tissue engineering scaffolds. *J Biomed Mater Res A* 67A:1401–1411
28. Nauth A, Ristevski B, Li R, Schemitsch EH (2011) Growth factors and bone regeneration: how much bone can we expect? *Injury* 42:574–579
29. Hudalla GA, Murphy WL (2011) Biomaterials that regulate growth factor activity via bioinspired interactions. *Adv Funct Mater* 21:1754–1768
30. Rahaman MN, Day DE, Bal BS, Fu Q, Jung SB, Bonewald LF et al (2011) Bioactive glass in tissue engineering. *Acta Biomater* 7:2355–2373
31. Maquet V, Boccaccini AR, Pravata L, Notingher I, Jérôme R (2004) Porous poly(alpha-hydroxyacid)/Bioglass composite scaffolds for bone tissue engineering. I: preparation and in vitro characterisation. *Biomaterials* 25:4185–4194
32. Swetha M, Sahithi K, Moorthi A, Srinivasan N, Ramasamy K, Selvamurugan N (2010) Biocomposites containing natural polymers and hydroxyapatite for bone tissue engineering. *Int J Biol Macromol* 47:1–4
33. Venkatesan J, Kim S-K (2010) Chitosan composites for bone tissue engineering – an overview. *Mar Drugs* 8:2252–2266
34. Di Martino A, Sittlinger M, Risbud MV (2005) Chitosan: a versatile biopolymer for orthopaedic tissue-engineering. *Biomaterials* 26:5983–5990

35. Zhang Y, Venugopal JR, El-Turki A, Ramakrishna S, Su B, Lim CT (2008) Electrospun biomimetic nanocomposite nanofibers of hydroxyapatite/chitosan for bone tissue engineering. *Biomaterials* 29:4314–4322
36. Bhattarai N, Edmondson D, Veiseh O, Matsen FA, Zhang M (2005) Electrospun chitosan-based nanofibers and their cellular compatibility. *Biomaterials* 26:6176–6184
37. Li L, Hsieh Y-L (2006) Chitosan bicomponent nanofibers and nanoporous fibers. *Carbohydr Res* 341:374–381
38. Chesnutt BM, Viano AM, Yuan Y, Yang Y, Guda T, Appleford MR et al (2009) Design and characterization of a novel chitosan/nanocrystalline calcium phosphate composite scaffold for bone regeneration. *J Biomed Mater Res A* 88:491–502
39. Thein-Han WW, Misra RDK, Thein-Han WW, Misra RDK (2009) Biomimetic chitosan–nanohydroxyapatite composite scaffolds for bone tissue engineering. *Acta Biomater* 5:1182–1197
40. Venkatesan J, Bhatnagar I, Manivasagan P, Kang K-H, Kim S-K (2015) Alginate composites for bone tissue engineering: a review. *Int J Biol Macromol* 72:269–281
41. Wahl D, Czernuszka J (2006) Collagen-hydroxyapatite composites for hard tissue repair. *Eur Cell Mater* 11:43–56
42. Catledge S, Clem W, Shrikishen N, Chowdhury S, Stanishevsky A, Koopman M et al (2007) An electrospun triphasic nanofibrous scaffold for bone tissue engineering. *Biomed Mater* 2:142
43. Wang Y, Kim H-J, Vunjak-Novakovic G, Kaplan DL (2006) Stem cell-based tissue engineering with silk biomaterials. *Biomaterials* 27:6064–6082
44. Bose S, Vahabzadeh S, Bandyopadhyay A (2013) Bone tissue engineering using 3D printing. *Mater Today* 16:496–504
45. Whited BM, Whitney JR, Hofmann MC, Xu Y, Rylander MN (2011) Pre-osteoblast infiltration and differentiation in highly porous apatite-coated PLLA electrospun scaffolds. *Biomaterials* 32:2294–2304
46. Phipps MC, Clem WC, Grunda JM, Clines GA, Bellis SL (2012) Increasing the pore sizes of bone-mimetic electrospun scaffolds comprised of polycaprolactone, collagen I and hydroxyapatite to enhance cell infiltration. *Biomaterials* 33:524–534
47. Shor L, Güçeri S, Wen X, Gandhi M, Sun W (2007) Fabrication of three-dimensional polycaprolactone/hydroxyapatite tissue scaffolds and osteoblast-scaffold interactions in vitro. *Biomaterials* 28:5291–5297
48. Mehta M, Schmidt-Bleek K, Duda GN, Mooney DJ (2012) Biomaterial delivery of morphogens to mimic the natural healing cascade in bone. *Adv Drug Deliv Rev* 64:1257–1276
49. Ginebra MP, Traykova T, Planell JA (2006) Calcium phosphate cements as bone drug delivery systems: a review. *J Control Release* 113:102–110
50. Bessa PC, Casal M, Reis RL (2008) Bone morphogenetic proteins in tissue engineering: the road from laboratory to clinic, part II (BMP delivery). *J Tissue Eng Regen Med* 2:81–96
51. Quinlan E, López-Noriega A, Thompson E, Kelly HM, Cryan SA, O'Brien FJ (2015) Development of collagen–hydroxyapatite scaffolds incorporating PLGA and alginate micro-particles for the controlled delivery of rhBMP-2 for bone tissue engineering. *J Control Release* 198:71–79
52. McCullen S, Zhu Y, Bernacki S, Narayan R, Pourdeyhimi B, Gorga R et al (2009) Electrospun composite poly (L-lactic acid)/tricalcium phosphate scaffolds induce proliferation and osteogenic differentiation of human adipose-derived stem cells. *Biomed Mater* 4:035002
53. Erisken C, Kalyon DM, Wang H (2008) Functionally graded electrospun polycaprolactone and beta-tricalcium phosphate nanocomposites for tissue engineering applications. *Biomaterials* 29:4065–4073
54. Lee YM, Park YJ, Lee SJ, Ku Y, Han SB, Choi SM et al (2000) Tissue engineered bone formation using chitosan/tricalcium phosphate sponges. *J Periodontol* 71:410–417
55. Rodrigues CVM, Serricella P, Linhares ABR, Guerdes RM, Borojevic R, Rossi MA et al (2003) Characterization of a bovine collagen–hydroxyapatite composite scaffold for bone tissue engineering. *Biomaterials* 24:4987–4997

56. Spalazzi JP, Doty SB, Moffat KL, Levine WN, Lu HH (2006) Development of controlled matrix heterogeneity on a triphasic scaffold for orthopedic interface tissue engineering. *Tissue Eng* 12:3497–3508
57. Bhumiratana S, Grayson WL, Castaneda A, Rockwood DN, Gil ES, Kaplan DL et al (2011) Nucleation and growth of mineralized bone matrix on silk-hydroxyapatite composite scaffolds. *Biomaterials* 32:2812–2820
58. Kim HJ, Kim U-J, Kim HS, Li C, Wada M, Leisk GG et al (2008) Bone tissue engineering with premineralized silk scaffolds. *Bone* 42:1226–1234
59. Rockwood DN, Gil ES, Park S-H, Kluge JA, Grayson W, Bhumiratana S et al (2011) Ingrowth of human mesenchymal stem cells into porous silk particle reinforced silk composite scaffolds: an in vitro study. *Acta Biomater* 7:144–151
60. Rai B, Teoh SH, Hutmacher DW, Cao T, Ho KH (2005) Novel PCL-based honeycomb scaffolds as drug delivery systems for rhBMP-2. *Biomaterials* 26:3739–3748
61. Li C, Vepari C, Jin H-J, Kim HJ, Kaplan DL (2006) Electrospun silk-BMP-2 scaffolds for bone tissue engineering. *Biomaterials* 27:3115–3124
62. Jeon O, Rhie JW, Kwon I-K, Kim J-H, Kim B-S, Lee S-H (2008) In vivo bone formation following transplantation of human adipose-derived stromal cells that are not differentiated osteogenically. *Tissue Eng Part A* 14:1285–1294
63. Hannink G, Geutjes P, Daamen W, Buma P (2013) Evaluation of collagen/heparin coated TCP/HA granules for long-term delivery of BMP-2. *J Mater Sci Mater Med* 24:325–332
64. Nie H, Wang C-H (2007) Fabrication and characterization of PLGA/HAP composite scaffolds for delivery of BMP-2 plasmid DNA. *J Control Release* 120:111–121
65. Laurencin CT, Attawia MA, Lu LQ, Borden MD, Lu HH, Gorum WJ et al (2001) Poly(lactide-co-glycolide)/hydroxyapatite delivery of BMP-2-producing cells: a regional gene therapy approach to bone regeneration. *Biomaterials* 22:1271–1277
66. Martini L, Fini M, Giavaresi G, Giardino R (2001) Sheep model in orthopedic research: a literature review. *Comp Med* 51:292–299
67. O’Loughlin PF, Morr S, Bogunovic L, Kim AD, Park B, Lane JM (2008) Selection and development of preclinical models in fracture-healing research. *J Bone Joint Surg Am* 90(Suppl 1):79–84
68. Pearce A, Richards R, Milz S, Schneider E, Pearce S (2007) Animal models for implant biomaterial research in bone: a review. *Eur Cell Mater* 13:1–10
69. Hutmacher DW, Schantz JT, Lam CXF, Tan KC, Lim TC (2007) State of the art and future directions of scaffold-based bone engineering from a biomaterials perspective. *J Tissue Eng Regen Med* 1:245–260
70. Kim HW, Song JH, Kim HE (2005) Nanofiber generation of gelatin–hydroxyapatite biomimetics for guided tissue regeneration. *Adv Funct Mater* 15:1988–1994
71. Fu S, Ni P, Wang B, Chu B, Peng J, Zheng L et al (2012) In vivo biocompatibility and osteogenesis of electrospun poly(*ε*-caprolactone)-poly(ethylene glycol)-poly(*ε*-caprolactone)/nano-hydroxyapatite composite scaffold. *Biomaterials* 33:8363–8371
72. Zhang JC, Lu HY, Lv GY, Mo AC, Yan YG, Huang C (2010) The repair of critical-size defects with porous hydroxyapatite/polyamide nanocomposite: an experimental study in rabbit mandibles. *Int J Oral Maxillofac Surg* 39:469–477
73. Laschke MW, Strohe A, Menger MD, Alini M, Eglin D (2010) In vitro and in vivo evaluation of a novel nanosize hydroxyapatite particles/poly(ester-urethane) composite scaffold for bone tissue engineering. *Acta Biomater* 6:2020–2027
74. Yan L-P, Silva-Correia J, Oliveira MB, Vilela C, Pereira H, Sousa RA et al (2014) Bilayered silk/silk-nanoCaP scaffolds for osteochondral tissue engineering: in vitro and in vivo assessment of biological performance. *Acta Biomater* 12:227–41
75. Richardson TP, Peters MC, Ennett AB, Mooney DJ (2001) Polymeric system for dual growth factor delivery. *Nat Biotechnol* 19:1029–1034
76. Street J, Bao M, deGuzman L, Bunting S, Jr Peale FV, Ferrara N et al (2002) Vascular endothelial growth factor stimulates bone repair by promoting angiogenesis and bone turnover. *Proc Natl Acad Sci U S A* 99:9656–9661

77. Salgado AJ, Coutinho OP, Reis RL (2004) Bone tissue engineering: state of the art and future trends. *Macromol Biosci* 4:743–765
78. Meinel L, Karageorgiou V, Fajardo R, Snyder B, Shinde-Patil V, Zichner L et al (2004) Bone tissue engineering using human mesenchymal stem cells: effects of scaffold material and medium flow. *Ann Biomed Eng* 32:112–122
79. Montjovent MO, Burri N, Mark S, Federici E, Scaletta C, Zambelli PY et al (2004) Fetal bone cells for tissue engineering. *Bone* 35:1323–1333
80. Kujala S, Ryhanen J, Danilov A, Tuukkanen J (2003) Effect of porosity on the osteointegration and bone ingrowth of a weight-bearing nickel-titanium bone graft substitute. *Biomaterials* 24:4691–4697
81. Hoshikawa A, Fukui N, Fukuda A, Sawamura T, Hattori M, Nakamura K et al (2003) Quantitative analysis of the resorption and osteoconduction process of a calcium phosphate cement and its mechanical effect for screw fixation. *Biomaterials* 24:4967–4975
82. Jukes JM, Both SK, Leusink A, Sterk LM, van Blitterswijk CA, de Boer J (2008) Endochondral bone tissue engineering using embryonic stem cells. *Proc Natl Acad Sci U S A* 105:6840–6845
83. Montjovent MO, Mark S, Mathieu L, Scaletta C, Scherberich A, Delabarde C et al (2008) Human fetal bone cells associated with ceramic reinforced PLA scaffolds for tissue engineering. *Bone* 42:554–564
84. Jaiswal N, Haynesworth SE, Caplan AI, Bruder SP (1997) Osteogenic differentiation of purified, culture-expanded human mesenchymal stem cells in vitro. *J Cell Biochem* 64:295–312
85. Caplan AI (1991) Mesenchymal stem cells. *J Orthop Res* 9:641–650
86. Beresford JN (1989) Osteogenic stem cells and the stromal system of bone and marrow. *Clin Orthop Relat Res* 240:270–280
87. Pittenger MF, Mackay AM, Beck SC, Jaiswal RK, Douglas R, Mosca JD et al (1999) Multilineage potential of adult human mesenchymal stem cells. *Science* 284:143–147
88. Strioga M, Viswanathan S, Darinskas A, Slaby O, Michalek J (2012) Same or not the same? Comparison of adipose tissue-derived versus bone marrow-derived mesenchymal stem and stromal cells. *Stem Cells Dev* 21(14):2724–52
89. Stockmann P, Park J, von Wilmowsky C, Nkenke E, Felszeghy E, Dehner J-F et al (2012) Guided bone regeneration in pig calvarial bone defects using autologous mesenchymal stem/progenitor cells – a comparison of different tissue sources. *J Cranio-Maxillofac Surg* 40:310–320
90. Arthur A, Zannettino A, Gronthos S (2009) The therapeutic applications of multipotential mesenchymal/stromal stem cells in skeletal tissue repair. *J Cell Physiol* 218:237–245
91. Chen L, Tredget EE, Liu C, Wu Y (2009) Analysis of allogenicity of mesenchymal stem cells in engraftment and wound healing in mice. *PLoS One* 4:e7119
92. Livingston Arinze T, Peter SJ, Archambault MP, Van Den Bos C, Gordon S, Krasus K et al (2003) Allogeneic mesenchymal stem cells regenerate bone in a critical-sized canine segmental defect. *J Bone Joint Surg Am* 85:1927–1935
93. Xie H, Yang F, Deng L, Luo J, Qin T, Li X et al (2007) The performance of a bone-derived scaffold material in the repair of critical bone defects in a rhesus monkey model. *Biomaterials* 28:3314–3324
94. Trounson A, Thakar RG, Lomax G, Gibbons D (2011) Clinical trials for stem cell therapies. *BMC Med* 9:52
95. Lobo SE, Livingston Arinze T (2010) Biphasic calcium phosphate ceramics for bone regeneration and tissue engineering applications. *Materials* 3:815–826
96. Szpalski C, Wetterau M, Barr J, Warren SM (2012) Bone tissue engineering: current strategies and techniques – part I: scaffolds. *Tissue Eng Part B Rev* 18:246–257
97. Xu C, Su P, Chen X, Meng Y, Yu W, Xiang AP et al (2011) Biocompatibility and osteogenesis of biomimetic Bioglass-Collagen-Phosphatidylserine composite scaffolds for bone tissue engineering. *Biomaterials* 32:1051–1058



98. Mastrogiacomo M, Papdimitropoulos A, Cedola A, Peyrin R, Giannoni P, Pearce SG et al (2007) Engineering of bone using bone marrow stromal cells and a silicon-stabilized tricalcium phosphate bioceramic: evidence for a coupling between bone formation and scaffold resorption. *Biomaterials* 28:1376–1384
99. Friedenstein A, Piatetzky-Shapiro I, Petrakova K (1966) Osteogenesis in transplants of bone marrow cells. *J Embryol Exp Morphol* 16:381–390
100. Hoffman LM, Carpenter MK (2005) Characterization and culture of human embryonic stem cells. *Nat Biotechnol* 23:699–708
101. Heng BC, Cao T, Stanton LW, Robson P, Olsen B (2004) Strategies for directing the differentiation of stem cells into the osteogenic lineage in vitro. *J Bone Miner Res* 19:1379–1394
102. Takahashi K, Tanabe K, Ohnuki M, Narita M, Ichisaka T, Tomoda K et al (2007) Induction of pluripotent stem cells from adult human fibroblasts by defined factors. *Cell* 131:861–872
103. Zhou H, Wu S, Joo JY, Zhu S, Han DW, Lin T et al (2009) Generation of induced pluripotent stem cells using recombinant proteins. *Cell Stem Cell* 4:381–384
104. Rodrigues MT, Lee B-K, Lee SJ, Gomes ME, Reis RL, Atala A et al (2012) The effect of differentiation stage of amniotic fluid stem cells on bone regeneration. *Biomaterials* 33:6069–6078
105. Zhang ZY, Teoh SH, Chong MSK, Lee ESM, Tan LG, Mattar CN et al (2010) Neo-vascularization and bone formation mediated by fetal mesenchymal stem cell tissue-engineered bone grafts in critical-size femoral defects. *Biomaterials* 31:608–620
106. Yamada Y, Ito K, Nakamura S, Ueda M, Nagasaka T (2011) Promising cell-based therapy for bone regeneration using stem cells from deciduous teeth, dental pulp, and bone marrow. *Cell Transplant* 20:1003–1013
107. Hofmann S, Hagenmüller H, Koch AM, Müller R, Vunjak-Novakovic G, Kaplan DL et al (2007) Control of in vitro tissue-engineered bone-like structures using human mesenchymal stem cells and porous silk scaffolds. *Biomaterials* 28:1152–1162
108. Uebersax L, Hagenmüller H, Hofmann S, Gruenblatt E, Müller R, Vunjaknovakovic G et al (2006) Effect of scaffold design on bone morphology in vitro. *Tissue Eng* 12:3417–3429
109. Kirker-Head C, Karageorgiou V, Hofmann S, Fajardo R, Betz O, Merkle H et al (2007) BMP-silk composite matrices heal critically sized femoral defects. *Bone* 41:247–255
110. Kofron MD, Laurencin CT (2006) Bone tissue engineering by gene delivery. *Adv Drug Deliv Rev* 58:555–576
111. Dimitriou R, Babis G (2007) Biomaterial osseointegration enhancement with biophysical stimulation. *J Musculoskelet Neuronal Interact* 7:253–265
112. Geiger M, Li RH, Friess W (2003) Collagen sponges for bone regeneration with rhBMP-2. *Adv Drug Deliv Rev* 55:1613–1629
113. Holland TA, Mikos AG (2006) Biodegradable polymeric scaffolds. Improvements in bone tissue engineering through controlled drug delivery. *Adv Biochem Eng Biotechnol* 102:161–185
114. Yoon BS, Lyons KM (2004) Multiple functions of BMPs in chondrogenesis. *J Cell Biochem* 93:93–103
115. Chen D, Zhao M, Mundy GR (2004) Bone morphogenetic proteins. *Growth Factors* 22:233–241
116. Kirker-Head CA (2000) Potential applications and delivery strategies for bone morphogenetic proteins. *Adv Drug Deliv Rev* 43:65–92
117. Yoshikawa H, Myoui A (2005) Bone tissue engineering with porous hydroxyapatite ceramics. *J Artif Organs* 8:131–136
118. Kaito T, Myoui A, Takaoka K, Saito N, Nishikawa M, Tamai N et al (2005) Potentiation of the activity of bone morphogenetic protein-2 in bone regeneration by a PLA-PEG/hydroxyapatite composite. *Biomaterials* 26:73–79

119. Sotome S, Uemura T, Kikuchi M, Chen J, Itoh S, Tanaka J et al (2004) Synthesis and in vivo evaluation of a novel hydroxyapatite/collagen–alginate as a bone filler and a drug delivery carrier of bone morphogenetic protein. *Mater Sci Eng C* 24:341–347
120. Qing W, Guang-Xing C, Lin G, Liu Y (2012) The osteogenic study of tissue engineering bone with BMP2 and BMP7 gene-modified rat adipose-derived stem cell. *J Biomed Biotechnol* 2012:410879

---

## **Part III**

# **Materials Engineering and Biological Interactions: Surface Engineering and Interactions with Living Cells**

Ipek Akin and Gultekin Goller

## Contents

Introduction .....	640
Types of Bioceramic Composites and Tissue Attachments .....	641
Processing Techniques for Bioceramics and Bioceramic-Based Composites .....	652
Powder Synthesis .....	652
Sintering .....	654
Pressureless Sintering .....	654
Pressure-Assisted Sintering .....	658
Sol–Gel .....	662
Summary .....	663
References .....	664

---

## Abstract

This chapter will provide a detailed overview of the processing techniques and properties of bioceramics, with special emphasis on nearly inert ceramics like alumina-based composites and bioactive ceramics like hydroxyapatite-based composites and machinable glass ceramics.

The chapter mainly covers the types of bioceramic implant–tissue attachments, powder synthesis, processing methods for porous and dense bulk bioceramics, and bioceramic-based composites production using conventional pressureless sintering and pressure-assisted sintering, mainly focusing on spark plasma sintering and glass and glass ceramic production with a controlled heat treatment of nucleation and crystallization. Further physical, microstructural, and mechanical characterization techniques are discussed including phase, surface, and differential thermal analyses. Biological behavior and bioactivity measurements

---

I. Akin • G. Goller (✉)  
Istanbul Technical University, Department of Metallurgical and Materials Engineering, Maslak,  
Istanbul, Turkey  
e-mail: [akinipe@itu.edu.tr](mailto:akinipe@itu.edu.tr); [goller@itu.edu.tr](mailto:goller@itu.edu.tr)

of bioactive hydroxyapatite-based composites, machinable glass ceramics, and zirconia toughened alumina composites in in vitro environments such as cell viability and alkaline phosphatase activity assays are also elucidated.

---

**Keywords**

Sintering • Microwave sintering • Spark plasma sintering • Hydroxyapatite • Alumina • Yttria-stabilized zirconia • Bioinert • Bioactivity • Composite • Processing • Ceramic • Sol–gel

---

**Introduction**

The most commonly accepted definition of ceramic is a refractory, inorganic, and nonmetallic material with essential components [1, 2]. Ceramics usually have combinations of covalent and ionic bondings. Advanced ceramics are utilized at specific applications that demand high performance [3]. Bioceramics, as a subgroup of advanced ceramics, are specifically designed for their use in medicine and dentistry and utilized for the repair or reconstruction of diseased or damaged parts of human bodies such as soft and hard tissues or organs for any periods of time [4]. They can be produced in crystalline (hydroxyapatite, glass ceramics, alumina, zirconia, etc.) or amorphous (Bioglass<sup>®</sup>) structures. In addition, bioceramics can be used as a coating material for metallic implants in order to enhance bonding abilities of implant materials.

Ceramic matrix composites involve ceramic matrices in which ceramic may form the reinforcement phase, the matrix, or both. Ceramic-based composites have been developed to overcome brittleness and lack of mechanical reliability of monolithic ceramics. One of the main reasons for producing ceramic matrix composites is to improve mechanical properties. For instance, bioceramic composites are produced to increase fracture toughness ( $K_{IC}$ ) and decrease modulus of elasticity ( $E$ ) to overcome complications associated with stress shielding which occurs when the implant has a much higher modulus of elasticity than the bone itself [5].

The reinforcing phase may also affect other properties of bioceramics such as biocompatibility, bone-bonding ability, biodegradation process, and cellular activity, tissue ingrowth, and physical, thermal, optical, or electrical in addition to the mechanical characteristics. There is a wide range of bioceramics and bioceramic composites that have been developed and investigated during the last 30–40 years, including hydroxyapatite (HA, dense or porous form), calcium phosphates, alumina and zirconia ceramics, zirconia toughened alumina (ZTA) composites, bioactive glasses (Bioglass<sup>®</sup>), and related composite materials combining bioactive inorganic materials with biodegradable polymers (peptides and proteins, polysaccharides, polyhydroxyalkanoates, polynucleotides), glass ceramics (apatite–wollastonite, apatite–devitrite), machinable glass ceramics (Bioverit<sup>®</sup> I, II, III, and Dicor<sup>®</sup>), and HA–polymer composites (HA–PEEK as an alternative material for load-bearing applications, HA–PMMA for bone cement applications, HA–PE composites commercialized with the name of HAPEX<sup>®</sup>) [2, 4].

These materials possess different properties and behavior which expand their use in different applications throughout the body. The following sections describe the types of bioceramics and bioceramic composites, tissue attachment and properties, powder synthesis, and various processing methods in more detail.

## Types of Bioceramic Composites and Tissue Attachments

Bioceramic composites can be divided into four groups based on bioceramic and tissue attachment mechanisms. In these groups, ceramic phase can be the matrix phase, or both matrix and reinforcing material. The type of bonding at the bioceramic–bone interface depends on the nature of the bioceramic implant. Table 1 summarizes the types of attachment of bioceramic composites and tissues.

Bioceramic implants do not form bonds or chemical reactions with bones in mechanical interlock-type attachment (Type 1). Instead there is a formation of fibrous tissue capsule around the implant material. Although nearly bioinert bioceramic composites maintain their physical and mechanical properties in the body, fracture and separation may occur at the interface of bone and implant materials.

Examples of nearly bioinert ceramic composites include alumina-based composites (e.g., reinforced with carbon nanotubes), zirconia toughened alumina composites (ZTA), and zirconia-based composites as in two basic types: yttria-stabilized tetragonal zirconia (TZP or YSZ) and magnesium oxide partially stabilized zirconia (Mg-PSZ).

Main applications of bioinert ceramics typically involve the replacement of the diseased balls in total hip prostheses, femoral component of total knee prostheses, and dental implants due to their high mechanical properties, high chemical and corrosion resistance, and good biocompatibility. Additionally, alumina ceramics are used in ear, nose, and throat (ENT) surgeries for full or partial ossicular bone replacements and tracheal support rings. Furthermore, a range of maxillofacial

**Table 1** Types of tissue attachment of bioceramic composites (Ref. [4])

Type number	Type of bioceramic composite	Type of attachment	Example
1	Bioinert	Mechanical interlock	Alumina ( $\text{Al}_2\text{O}_3$ )-based composites, zirconia ( $\text{ZrO}_2$ ), zirconia toughened alumina (ZTA) composites
2	Porous	Ingrowth of tissues into pores	Porous hydroxyapatite-based composites
3	Bioactive	Interfacial bonding	Hydroxyapatite (HA)-based composites, Bioglass-based composites
4	Biodegradable	Replacement with tissues	Tricalcium phosphate (TCP)-based composites

surgical and neurosurgical operations for repairing bone defects in the sub-occipital region, reconstruction of the orbital wall and sellar floor, orbital implants, and eye prostheses also involve the use of alumina implants [5].

Besides these applications, nanocrystalline yttria-stabilized zirconia (nc-YSZ) transparent prosthetic implants have recently been developed. This skull implant, which is referred to as the “window to the brain,” is a promising candidate material for various medical applications that include new treatments for life-threatening neurological disorders, such as traumatic brain injuries and brain cancers. A transparent material can be implanted in the skull for the long term and would permit for laser treatments or visual monitoring of the brain. In vivo studies are still being carried out [6].

Porous bioceramics that allow ingrowth of tissues into pores (Type 2 in Table 1) form an essential part of numerous components, which enable them to be utilized in many bioengineering applications.

The merging of the developing field of tissue engineering with biomaterial science in recent years will have a growing impact on biomedical research and its applications. This aims to improve biological functions by combining cells, biological signals, and bioceramics and regenerate or replace lost or damaged tissues by initiating the natural regeneration process. Tissue regeneration, in which bioceramics have an important role as a supporting scaffold for the growth of cellular components, is crucial in dental and orthopedic implants.

Tissue engineering deals with the production of new biological materials, improvement, and development of their properties as biological body parts. For this purpose, the most common procedure is to produce scaffold biomaterials which act as templates for tissue regeneration [7]. A scaffold (which can be either natural or synthetic material) is produced as a temporary support for the new tissue's growth and reorganization. Cells are seeded to the scaffold and lead them to colonize until they are compatible and viable within the environment. There are a number of key points to design a compatible scaffold. Firstly, the body part's physical and chemical properties, in which the scaffold will be placed, should be well known for choosing the suitable material and the shape of the scaffold [7].

The scaffold, which both physically and chemically mimics extracellular matrix (ECM), serves as a framework to support cell proliferation on its surface and makes the cells migrate to the damaged area from surrounding tissues [7].

There are four important features and related functions which need to be considered for the production of scaffolds: architecture, cyto-tissue compatibility, bioactivity, and mechanical properties [7].

Hydroxyapatite (calcium hydroxyapatite, HA) ceramics and HA-based composites are promising candidates as bone substitute materials. Natural bone is comprised of approximately 50 vol% hydroxyapatite.

Hydroxyapatite has long been investigated for bone regeneration due to its high bioactivity, high biocompatibility, good osteoconduction, and good cellular interactions for several types of cells such as osteoblasts, fibroblasts, osteoclasts, macrophages, and periodontal ligament cells. Additionally, HA ceramics allow the proliferation of osteoblasts, other bone cells, and fibroblasts with a remarkable similarity in their surface chemistry [5].

The tissue response to porous HA implants is completely different from dense HA implants because of the occurrence of ingrowth in the former type. Studies of bone ingrowth into porous HA have shown that the dimension and morphology of pores and size of inter-pore connections are important factors for an excellent osteointegration.

Adult human cortical bone, also known as compact bone, contains cylindrical lamellar structures called osteons or Haversian systems serving the fundamental functional unit of the bone. The average diameter of osteons varies in 190–230  $\mu\text{m}$ . In the case of trabecular bone, also known as cancellous or spongy bone, there is a three-dimensional structure of interconnected plates and rods named “trabeculae” which has a thickness of approximately 200  $\mu\text{m}$ . The trabecular bone is much more porous than the cortical bone, and porosity of cancellous bone is more than 75 %. The pores in cancellous bones are interconnected and filled with bone marrow [5].

For an idealized bone graft substitute and effective bone ingrowth, interconnected porous system of channels should have dimensions of minimum 150  $\mu\text{m}$  in diameter. Porosity and pore size are directly related to bone formation, since they provide the required surface and space for cell adhesions and bone ingrowths. Moreover, the interconnected pore structure allows tissue ingrowth and provide blood circulation and nutrition supply for the bone [8].

It should be noted that an optimum design in terms of pore size and structure of porous bioceramic composites must be achieved in order to balance sufficient fluid diffusivity, as well as adequate mechanical strength. In other words, the biomechanical properties of porous HA strongly depend on the degree of porosity.

Porous HA ceramics have found wide ranged use in biomedical applications. In recent years, a number of interconnected porous hydroxyapatite (IPHA) ceramics have been developed to utilize as graft material and scaffold for bone formation [8]. Porous implants can be placed in the maxilla, mandible, and midface in maxillofacial surgical operations, and porous bioceramics in the form of granules or bulk can be placed adjacent to the maxillary sinus. Traumatic defects of long bones can be reconstructed with porous hydroxyapatite and stabilized with several plates and screw fixations. In addition, porous hydroxyapatite implants can be directly coupled with an artificial eye to improve movement, which fits into a hole drilled through the conjunctiva and into the buried implant [5].

Neobone<sup>®</sup> hydroxyapatite is a functional synthetic bone filler, which has a porosity of about 75 %, with macropores of 100–200  $\mu\text{m}$  that are fully interconnected by openings of approximately 40  $\mu\text{m}$  in diameter. In 2006, ultra porous hydroxyapatite ceramics (Apaceram-AX<sup>®</sup>) with a well-controlled triple pore structure with 85 % porosity and a good osteointegration was developed. These commercially available products have been utilized as artificial bioceramics in bone replacement therapies [8].

The most widely used processing techniques to fabricate porous hydroxyapatite implants are isostatic compaction and sintering of calcium phosphate powders that contain volatile particles such as naphthalene. Processes are described in more detail in the following sections.



Bioactive implants form a bond with bones via chemical reactions at the interface (Type 3 in Table 1). A bioactive material causes a specific biological response at the interface of the bioceramic, which results in the formation of the bond between the tissue and the bioceramic. This type of interface requires the material to have a controlled rate of chemical reactivity.

The interfacial strength between bone and bioceramic implant is much greater for bioactive implant materials such as hydroxyapatite (HA), Bioglass<sup>®</sup>, and glass ceramics compared to nearly bioinert bioceramics like alumina, zirconia, or zirconia toughened alumina (ZTA) [5].

Bioactive glasses were first developed by Hench et al. in 1969. The bone can chemically bond to a certain glass composition. The base components for bioactive glasses involve SiO<sub>2</sub> as a glass network former and other oxides such as CaO, Na<sub>2</sub>O, and P<sub>2</sub>O<sub>5</sub>. For instance, the most known and well-studied composition termed as 45S5 Bioglass<sup>®</sup> contains 45 % SiO<sub>2</sub>, 24.5 % Na<sub>2</sub>O, 24.4 % CaO, and 6 % P<sub>2</sub>O<sub>5</sub>. The impact of P<sub>2</sub>O<sub>5</sub> has been controversial as it was assumed that P<sub>2</sub>O<sub>5</sub> was necessary for bioactivity. However, it is now known that phosphate-free glass compositions can possess bioactivity. The amount of aforementioned oxides should be in a specific range to induce bioactivity. The bioactive bonding boundary of compositions can be controlled by using the ternary SiO<sub>2</sub>–Na<sub>2</sub>O–CaO diagram. There have been many variations and modifications on the original composition, and they have been marketed as 58S, 70S30C, S53P4, etc. [5].

The main advantage of bioactive glasses is their rapid rate of surface reactions which result in fast tissue bonding. However, mechanical weakness with a bending strength of 40–60 MPa and low fracture toughness of bioactive glasses make them unsuitable for load-bearing applications [4].

As it is known, the bone-bonding characteristics of bioactive glasses are related to the chemical reactivity of glass in body fluids. The formation of hydroxycarbonate apatite (HCA) layer and bonding between bone and bioactive glass occur as a result of surface chemical reactions. Leaching, dissolution, and precipitation processes occur when a bioactive glass is immersed in a body fluid. The first step, leaching, is a release level where ion exchange of network modifiers (e.g., Na<sub>2</sub>O, CaO) takes place. The second process, dissolution, occurs by breaking of network formers (e.g., SiO<sub>2</sub>) and bridging oxygen bonds through the action of hydroxyl (OH) ions [4]. This network dissolution results in the release of silica into the body fluid in the form of silicic acid and the formation of hydrated silica (SiOH) on the glass surface. Polycondensation of neighboring silanols (SiOH) causes the production of silica-rich gel layer. Precipitation reactions occur in the final stage. Calcium and phosphate released from the glass composition combine with those from the solution in order to form a calcium-phosphate-rich (CaP) layer. The position of CaP layer differs depending on in vitro or in vivo conditions. It is primarily located on top and within the silica gel layer in the case of in vitro and in vivo, respectively. The calcium phosphate layer is initially amorphous and later crystallizes into a hydroxycarbonate apatite (HCA) structure by incorporating carbonate anions from the body fluid in both in vitro and in vivo conditions. For the formation of a bond between bioceramic and living tissue, it is important to note that a biologically active HCA layer must be

established. Reactions for the formation of HCA layer are time dependent and kinetics of reaction steps can be determined [5].

Basically, there are two methods to evaluate the *in vitro* bioactivity of bioceramics. One of the two analyzes bioceramics *in vitro* bone cell response using cell culture technique. Essentially the cell culture method is used to evaluate the biological compatibility of materials. In the cell culture method, cells (e.g., osteoblasts, fibroblasts, etc.) are grown under controlled *in vitro* conditions. Cells can be derived from living animals, but generally cell lines are purchased from biological suppliers or cell banks. Cell viability and proliferation rates are good indicators of cell health. For instance, osteoblasts are bone-forming stem cells and proliferate on the bone surface. Also, the osteoblast differentiation is an important step for bone formation and remodeling. Likewise, alkaline phosphatase (ALP) activity is an early sign of osteoblast differentiation and plays a crucial role in promoting mineralization of the bone. Thus, proliferation and cell viability (or cytotoxicity), metabolic activity, alkaline phosphatase activity, total protein content, mineralization, nitric oxide production level (especially important for stent applications), and other properties can be determined by using different cell lines and cell culture methods [9].

The other and most common *in vitro* bioactivity evaluation method is developed to examine the apatite formation ability of bioceramics in simulated body fluids (SBF). The research on the parameters that affect bone-like apatite formation is an effective approach to understand the mechanism of osteoinduction. In 1991, Kokubo and colleagues proposed the SBF method to examine the *in vitro* bone-like apatite formation on biomaterials. The method of simulated body fluid, which has inorganic ion concentrations nearly equal to those of human blood plasma, is useful for predicting the bone-bonding ability of a bioceramic. The bonding ability of different types of bioceramics having different structures (e.g., crystalline or amorphous) and compositions can be evaluated in a short period of time through the use of the SBF method [10].

SBF is a metastable solution containing calcium and phosphate ions and supersaturated with respect to apatite [10]. However, the revised SBF solution was proposed in 2003, to overcome problems associated with large amounts of calcium and magnesium concentrations binding to proteins and thus interfering apatite precipitation. The revised SBF solution contains calcium and magnesium ions that are 40 and 33 % lower concentrations than that of the original one, respectively [11].

Moreover, it is possible to prepare modified versions of SBF to accelerate the formation of bone-like apatite process, by increasing the concentrations (e.g.,  $1.5 \times$  SBF or  $3 \times$  SBF) of reagents or ions of the original SBF solution, using different compositions, changing chemicals, and applying variations in the experiment duration and operating conditions. However, the preparation of the SBF solution has to be carried out under well-controlled conditions to avoid coagulation and precipitation which could influence the *in vitro* test results. Typical *in vitro* bioactivity test steps using the SBF solution can be listed as follows: sterilization and cleaning, dissolution of chemicals, adjustment of pH, storage of solution at 5–10 °C, stability test in order to check occurrence of any precipitation, adjustment of test atmosphere

(e.g., air, nitrogen or carbon dioxide), temperature ( $\sim 36.5$  °C) and test conditions (e.g., dynamic or static), and characterization of the solution and samples. In vitro bioactivity tests by using the SBF solution can be performed up to 28 days or more, soaking time may vary from 1 h to several months. The formation of the reaction products begins at the end of first hour.

The number of animals sacrificed for in vivo tests for predicting bioactivity can be significantly reduced by using the SBF method. In addition, the SBF method contributes to a reduction of time and cost for evaluating the bone-bonding ability of bioceramics.

It should be noted that there are a few kinds of resorbable materials which bond to living bones without HCA formation on their surfaces. Therefore, the bone-bonding ability of a bioceramic must also be examined using animal models under in vivo conditions.

The composition, structure, and morphology of the bone-like apatite (calcium-deficient apatite or HCA) layer should be examined by detailed characterization techniques like thin film X-ray diffraction (TF-XRD), Fourier transform infrared (FTIR) spectroscopy, scanning electron microscopy (SEM), and transmission electron microscopy (TEM).

The Fourier transform infrared (FTIR) spectroscopy technique, which is nondestructive, requires no vacuum or special sample preparation and can be utilized as a quantitative quality assurance test method for molecular bond characterization. For instance, Si–O–Si bonds have different energy levels from Si–O–Ca bonds due to their unequal vibrational frequencies. A bioceramic can be analyzed before and after in vitro testing, and changes in vibrations can be evaluated when the surface composition and phases are altered by chemical reactions when immersed in SBF. The amorphous calcium phosphate layer has a single P–O mode, and when this is transformed into first crystalline apatite particles, two separate P–O modes appear, and finally three P–O modes are observed with the formation of well-developed apatite crystals [5].

The FTIR technique can be applied in either the specular reflection mode or the diffuse reflection mode if there is a significant scattering from surface reaction layers.

Phase analyses are performed by using thin film X-ray diffraction (TF-XRD) technique. X-ray diffraction is sensitive to thin films of atomic dimensions to thicknesses of many tens of micrometers. X-ray methods are used to obtain structural information (phase analysis, crystal structure) on thin films and layers, from crystalline to amorphous materials.

The microscopy technique is a rapid characterization method for SBF-immersed surfaces and interfaces. It is possible to determine the changes in surface morphology and composition after soaking the biomaterial in SBF. Additionally, the composition of the surface layer can be analyzed chemically with energy-dispersive X-ray spectroscopy (EDS).

Apart from these techniques, there are other detailed surface characterization methods, such as electron probe microanalyzer (EPMA), Auger electron spectroscopy (AES), X-ray photoelectron spectroscopy (XPS) also known as electron spectroscopy for chemical analysis (ESCA), secondary ion mass spectroscopy (SIMS), and surface charge analysis (SCA).

EPMA can be used to determine the thickness and compositional gradient of reaction layers formed on bioceramic implants. In this technique, compositional profiles are created, and the intensity of the X-ray signal for each element is plotted as a function of distance across the interface [5].

AES is one of the most accurate methods for determining the compositional gradients and detecting all elements in the periodic table (except hydrogen and helium) within the outermost layers of a bioceramics [5]. AES uses high-energy (2–10 keV) primary electron beams to examine the surface of a bioceramic with a resolution on the scale of 0.1 nm.

XPS is a surface-sensitive quantitative spectroscopic technique that measures the elemental composition of the parts per thousand range, empirical formula, chemical state, and electronic state of the elements that exist within a bioceramic.

SIMS is one of the most sensitive surface analysis techniques which also involves the removal of surface layers of bioceramics by sputtering with a focused primary ion beam, atom by atom, and the measurement of the concentration of the ejected secondary ions, with a mass spectrometer. The elemental, isotopic, or molecular composition of the surface can be detected to a depth of 1–2 nm.

SCA is required because the surface charge of a bioceramic may influence the protein absorption and affects the tissue response and other biological behaviors. Additionally, pH values of body fluids vary according to different conditions during wound healing or bone mineralization. For instance, body fluid is basic during bone mineralization. Consequently, it is important to determine whether the surface charges of bioceramics used for bone repair are compatible with pH values during the healing process or the reconstruction of the bone [5].

The conventional wet chemical methods, such as atomic emission or absorption spectroscopy, or inductively coupled plasma (ICP) can be used for chemical analysis for simulated body fluid (SBF).

Special group of glass ceramics, including apatite–wollastonite (A/W, commercially available as Cerabone<sup>®</sup>), apatite–devitrite (commercially available as Ceravital<sup>®</sup>), and machinable glass ceramics (commercially available as Bioverit I<sup>®</sup>), has the ability to bond with the living bones [12]. These bioactive glass ceramics have various applications in the repair and reconstruction of diseased and damaged hard tissues.

Glass ceramics are crystalline materials and offer the possibility of combining the special properties of ceramics and glasses in one material [12].

The processing of glass ceramics is carried out by applying a two-stage controlled heat treatment: nucleation (or nuclei formation) and crystallization (or crystal growth). The heat treatment converts the glass into uniformly distributed crystalline glass ceramics with superior properties compared to the parent glass. The development of fine and uniform or interlocking microstructure improves the strength [13]. Glasses are melted at high temperatures depending on their compositions, homogenization and refining processes should be applied, and thermally converted to a crystalline ceramic [12].

The nucleation and crystallization temperatures can be determined by the differential thermal analysis (DTA) technique. In order to achieve optimum nucleation,

heat treatment should be applied between the glass transition temperature ( $T_g$ ) and a temperature of 50–100 °C above  $T_g$ . In a DTA graph, glass transition temperature is not clearly defined. However, it is possible to determine this by taking the intersection of two tangents at the start and end points of the endothermic reaction.

The crystallization process initiates after nucleation with the application of secondary heat treatment, which is higher than the  $T_g$  and softening point ( $T_s$ ). Crystallization is an exothermic process. One or more phases can crystallize from the parent glass depending upon the number of crystalline phases. The nucleated glassy structure is heated above crystallization temperature. Generally end point of exothermic peak is a good indicator, for a sufficient time to achieve crystal growth.

In almost all cases, nucleation and crystallization temperatures are not constant for glasses. Moreover, dwell time for an efficient crystallization varies depending on the composition, solubility of components, viscosity of glass, existence of nucleating agents or crystallization catalysts, and conditions of heat treatment. For this reason, heat treatment should be applied over a wide range of temperatures obtained from DTA curves at different durations, and the best way for checking an effective nucleation and crystallization process is to apply successive heat treatments and phase analysis cycles.

Machinable glass ceramics, which are applied to orthopedic and dental applications, especially in the replacement of natural bone and dental restoration, are very important because of the development of controlled nucleation and crystallization of the glass ceramics. Mica-containing glass ceramics provide machinability. That is, they can be machined, cut, or drilled with normal metalworking tools. Their machinability results in an increased versatility of the products and numerous possibilities for industrial applications. The excellent machinability of mica glass ceramics results from the cleavage of interlocking layers of mica (phlogopite) crystals precipitated in the glass matrix. For an effective machinability, the precipitated mica phase must constitute more than two-thirds of the total volume.

For a material to be machinable and bioactive, it should contain both mica and apatite crystals. Apatite-containing glass ceramics are greatly important for surgical implantation due to high bioactivity and close crystallographic and chemical similarity to the human bone tissue. The crystalline phases occurring in these glass ceramics include essential apatite which provides the biocompatibility and bioactivity of glass ceramics and mica. Secondary crystalline phase is crystallized at higher temperature and provides the interesting mechanical properties such as machinability, high hardness, and high strength.

The *in vitro* bioactivity test results of machinable glass ceramics having a 3:7 weight ratio of fluorapatite to potassium mica have been reported [14]. Figure 1a shows the surface morphology of the glass ceramic that nucleated at 610 °C for 1 h and crystallized at 770 °C for 4 h, after immersion in SBF for 1 day. Additionally, Fig. 1b, c represent the surface and cross-sectional micrograph of the glass ceramic after immersion in SBF for 14 and 28 days, respectively. In view of this, the hydroxycarbonate apatite (HCA) layer precipitated from the SBF can be observed clearly as a continuous layer with a thickness ranging from 4 to 5  $\mu\text{m}$ .

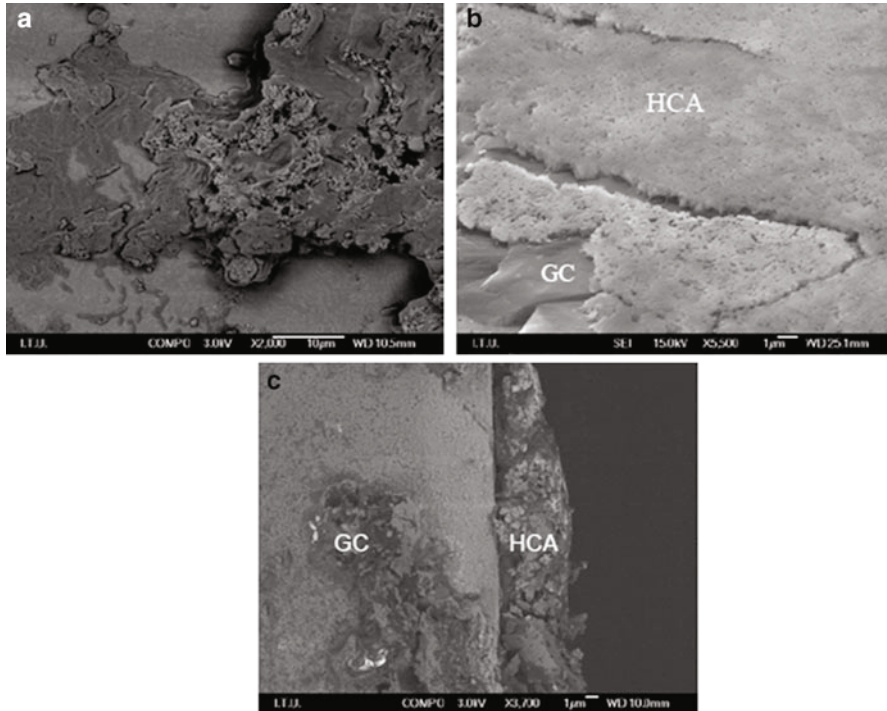


**Fig. 1** SEM micrographs of potassium mica–fluorapatite glass ceramic after 1 day (a), 14 days (b), and 28 days (c) of immersion in SBF (Ref. [14])

**Table 2** Comparison of mechanical properties of commercially available bioactive glass and glass ceramics (Ref. [5])

Property	Unit	Bioglass <sup>®</sup>	Ceravital <sup>®</sup>	A/W	BIOVERIT I
<b>Young's modulus</b>	GPa	35	100–159	118	70–88
<b>Compressive strength</b>	MPa	42	500	1080	500
<b>Bending strength</b>	MPa	160–190	130	215	140–180
<b>Hardness</b>	GPa	4.7	2.9	6.7	5.0
<b>Fracture toughness</b>	MPa · m <sup>1/2</sup>	2.0	4.6	2.0	1.2–2.1

Glass ceramics have a high crystal content, and in general they have higher mechanical properties than the parent glass. A significant improvement, especially in mechanical properties, can be achieved with the production of glass ceramics. In addition, precipitation of the desired phases can be obtained with controlled time–temperature-related heat processes. Mechanical properties of glass and glass ceramics are listed in Table 2.

In the production of glass ceramics, nucleating agents, such as ceria (CeO<sub>2</sub>), titania (TiO<sub>2</sub>), or zirconia (ZrO<sub>2</sub>), can be used in order to induce the bulk crystallization of the phases. Furthermore, the introduction of nucleating agents into the main

glass can decrease crystallization time and temperature. In a previous study, Goller et al. have investigated the role of  $\text{TiO}_2$  addition as a nucleating agent on the crystallization behavior of potassium mica and fluorapatite-based glass ceramics. According to the microstructural investigations and machinability test results, optimum  $\text{TiO}_2$  addition was determined as 1 wt% [15]. In another study, Leonelli et al. have investigated the *in vitro* bioactivity behavior of phosphosilicate glasses based on 45S5 Bioglass<sup>®</sup> doped with cerium oxide [16]. They have reported that the incorporation of  $\text{CeO}_2$  was related to its low toxicity and good bacteriostatic properties. In addition, cerium-doped bioactive glasses can be useful when the implant is surrounded by local infected areas.

The microstructural investigations of *in vitro* bioactivity of glass ceramics having 1 wt%  $\text{CeO}_2$ , nucleated at 610 °C for 1 h and crystallized at 750 °C for 3 h, are given in Fig. 2. The CaP precipitation was observed after 7 days immersion in SBF as indicated with white arrows in Fig. 2a. Precipitation started at individual particles and platelike crystals with size of 0.5–1  $\mu\text{m}$  formed. After 14 days, the morphology of platelike crystals changed and lath-like crystals (0.5  $\mu\text{m}$  in width and 1–1.5  $\mu\text{m}$  in length) started to form on the surface as shown in Fig. 2b. These lath-like crystals gradually grew in size (1–2  $\mu\text{m}$  in width and 6–8  $\mu\text{m}$  in length) and formed a dense layer on the glass ceramics surfaces at the end of the 21 days after immersion in SBF (Fig. 2c). After 28 days, dense and continuous biological apatite layer with a

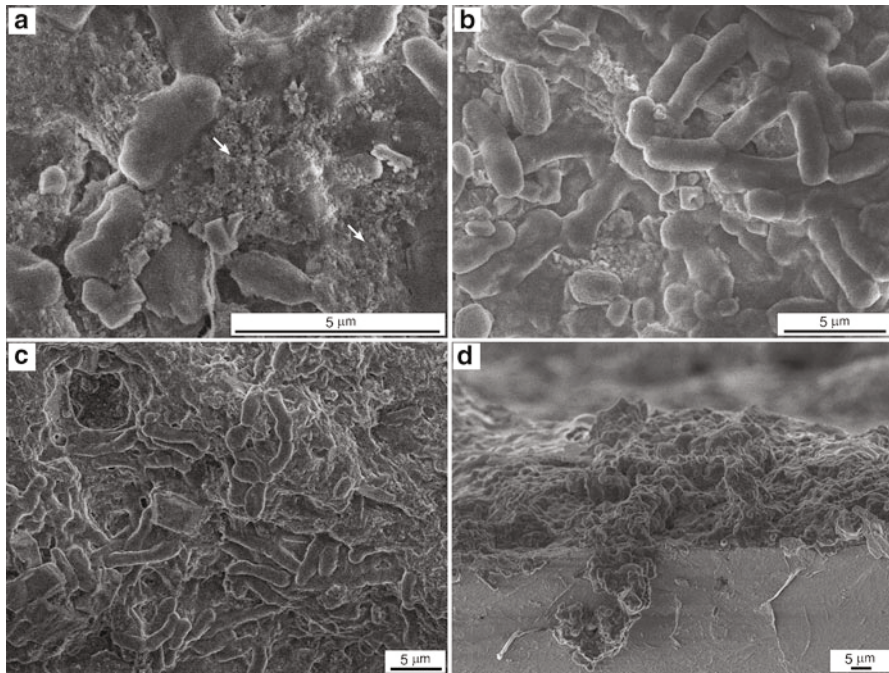


**Fig. 2** SEM micrographs of glass ceramics with 1 wt%  $\text{CeO}_2$  after 7 days (a), 14 days (b), 28 days (c) immersion in SBF, and cross-sectional micrograph at the end of the 28th day (d) (Ref. [9])

thickness of 5–8  $\mu\text{m}$  was observed, and this is illustrated in Fig. 2d as a cross-sectional micrograph image.

Thin-film XRD analysis revealed that after precipitation of initial crystals, crystallization proceeds and crystallization of precipitated hydroxycarbonate apatite peaks (HCA) appears after immersion for 28 days. In the same study [9], an osteoblast cell culture model system was utilized to investigate the effect of the addition of  $\text{CeO}_2$  on biocompatibility based on biological assays such as cell viability and metabolic and alkaline phosphate activities. It was observed that cell viability was not inhibited by the presence of the glass ceramics; in contrast, it was slightly enhanced. Thus, it is possible to conclude that glass ceramics stimulate osteoblast activity. Alkaline phosphatase production by the osteoblasts is an indication of biological activity of these cells, as growing bones require alkaline phosphatase production. These results indicate that biomaterials do not impede alkaline phosphatase function; instead they cause slight induction. This is another indication that the osteoblasts continue their physical characteristics normally in the presence of glass ceramics.

Nitric oxide (NO) production may be an indication of the homeostatic and development functions or immune response of the mammalian cells. There is usually no significant effect of materials on NO production. Andrade et al. have studied the *in vitro* bioactivity and biocompatibility of fiber and bulk bioactive glasses produced by the sol–gel method [17]. They have reported that osteoblast viability decreased 60 % in the presence of fiber glass and 20 % in the presence of bulk glass when compared to the control group. They have explained poor cell viability by the morphology of materials and fiber dimensions. Valerio et al. have investigated the behavior of osteoblast cells in the presence of a bioactive glass with 60 % of silica and a biphasic calcium phosphate produced by the sol–gel process [18]. They observed that osteoblast proliferation was 35 % higher in the presence of ionic products from the dissolution of bioactive glass with 60 wt% of silica, and they found that this type of bioactive glass acted as an NO donor. Silicic acid release also enhanced the collagen type I production. These results show that the morphology of the materials influences their physiological performance. The slight enhancement of osteoblast activity for glass ceramics containing 1 wt%  $\text{CeO}_2$  may be attributed to the release of silica. It may have caused by the addition of 1 wt%  $\text{CeO}_2$  contributing the network formation because the highest glass transition temperature was observed for this composition, and this change in the silica network caused higher amount of silica release. Wilson et al. have reported that bioglass implants have osteoproliferative qualities [19]. These kinds of materials do not simply serve as a scaffold for bone formation but also appear to improve osteoblast activity; the slow release of silicon produced from the consumption of graft particles may then promote an autocrine response leading to an enhancement of osteoblast activity.

The final group of implant–tissue attachment (Type 4) represents biodegradable bioceramics and/or bioceramic composites. When the bioactive interface reactions are rapid enough, the material dissolves or resorbs and is replaced by the surrounding living tissues. A resorbable bioceramic must have a composition that can be degraded chemically by body fluids or digested easily by macrophages [5].



Biodegradable ceramics such as tricalcium phosphate (TCP,  $\text{Ca}_3(\text{PO}_4)_2$ ) and composites are widely used as bone regeneration materials. Tricalcium phosphate has proved successful for resorbable hard tissue replacements when low loads are applied to the material. The stoichiometry of HA is highly significant where thermal processing (e.g., sintering) of the material is required. Slight variations from the standard molar ratio of 1.67 in the stoichiometric ratio of calcium and phosphorus in HA can lead to the appearance of either  $\alpha$ -TCP or  $\beta$ -TCP forms at the end of the heat treatment. Actually, TCP has four polymorphs:  $\alpha$ ,  $\beta$ ,  $\gamma$ , and super  $\alpha$ . The  $\gamma$  polymorph is a high-pressure phase, and the super  $\alpha$  polymorph can be obtained at temperatures above 1500 °C. Among these variants  $\beta$ -form has been more often used in the literature.

The calcium phosphate ceramic system has been the most intensely studied ceramic system, and numerous studies have shown that TCP is osteoconductive and supports bone healing in vivo. Various types of TCP ceramics are in commercial use and in development phases exhibiting different physical parameters such as shape, size, and porosity.

Hydroxyapatite (HA) ceramic and tricalcium phosphates (TCP) are used in orthopedics and dentistry alone or in combination with other substances, or also as a coating of metal implants (e.g., HA/TCP coating on titanium alloy). The reason for the use of bioceramics in combination with polymer matrix is in their ability to enhance the integration in bone while improving the device mechanical properties [20].

---

## Processing Techniques for Bioceramics and Bioceramic-Based Composites

Novel techniques for processing bioceramic composite materials are being developed which will provide improvements in the properties of materials. The production of bioceramics and ceramic matrix biocomposites comprises different steps ranging from raw materials, typically in the powder form, to the final ceramic product as follows: powder synthesis, drying, calcination, consolidation, binder-removal process, and sintering [21].

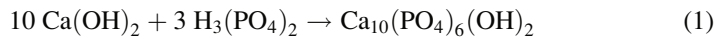
### Powder Synthesis

Powders are synthesized through dry and wet chemical methods. Dry powder synthesis is based on solid phase reactions, and there are three types of chemical reactions: oxidation or reduction, thermal decomposition, and solid-state reactions. On the other hand, different methods can be used for wet or liquid phase synthesis of ceramic powders such as precipitation, hydrothermal synthesis, sol-gel synthesis, and liquid drying [22, 23]. Wet chemical methods are widely used for the production of crystalline bioceramics because it is easier to achieve high compositional homogeneity at lower temperatures [23].

The preparation technique has a significant influence on powder morphology, surface characteristics, stoichiometry, and the degree of crystallinity [5].

Hydroxyapatite powders can also be prepared through solid-state reactions and wet chemical and hydrothermal treatment methods [5]. Actually, the wet chemical method is proven to be the best synthesis method for commercially available HA powders [23].

Wet chemical method involves hydroxyapatite precipitation via mixing aqueous solutions of compounds containing  $\text{Ca}^{2+}$  and ions at pH greater than 7, followed by holding the precipitate under appropriate conditions (Eq. 1). The most commonly used  $\text{Ca}^{2+}$  sources are  $\text{CaCl}_2$ ,  $\text{Ca}(\text{NO}_3)_2$ ,  $\text{Ca}(\text{OH})_2$ ,  $\text{CaCO}_3$ ,  $\text{CaSO}_4 \cdot 2\text{H}_2\text{O}$ , and  $(\text{CH}_3\text{COO})_2\text{Ca}$ , and typical phosphorus sources are phosphoric acid ( $\text{H}_3\text{PO}_4$ ),  $\text{NH}_4\text{H}_2\text{PO}_4$ ,  $(\text{NH}_4)_2\text{HPO}_4$ ,  $\text{Na}_3\text{PO}_4$ , and  $\text{K}_3\text{PO}_4$  [24]:



The precipitation and hydrolysis methods result in the formation of Ca-deficient apatite and cause the production of HA with  $\beta$ -TCP after sintering. Carrying out the reactions under basic conditions can induce the formation of stoichiometric conditions [5]. The obtained HA precursor can then go through Ostwald ripening to be changed to HA crystallites. During this process, pH should be greater than 10 in order to precipitate HA particles, and  $\text{CO}_2$  must be purged [23].

Thermal decomposition of the compounds can be used for preparation of powders  $\text{CaHPO}_4$  or  $\text{CaHPO}_4 \cdot 2\text{H}_2\text{O}$ . They are thermally decomposed to different pyrocalcium phosphates from amorphous structures to  $\alpha$ ,  $\beta$ , or  $\gamma$  forms. The type of the polymorph is controlled by the heating temperature [23].

The hydrothermal method is a kind of wet chemical process and promoted under high-pressure water above  $100^\circ\text{C}$ . In the case of HA powder synthesis, reactions are carried out hydrothermally at  $275^\circ\text{C}$ , under steam pressure of 85 MPa [5]. This method is effective in the crystallization of poorly soluble compounds. For instance, hydrothermal method enables the synthesis of HA whiskers and small-sized single crystals [23]. Tetracalcium phosphate,  $\beta$ -TCP,  $\text{Ca}_4\text{P}_2\text{O}_9$ , and  $\text{Ca}_4(\text{PO}_4)_2\text{O}$  can be converted to HA [5].

Drying technique should be applied in the wet chemical powder synthesis processes. Drying can be divided into two groups: heating (hot-gas drying, hot-plate drying, spray-drying, internal heating with microwave and electromagnetic wave) and non-heating (reduced-pressure drying, centrifugal drying, ultrasonic drying, freeze-drying, or lyophilization) [23]. The spray-drying technique is appropriate for large-scale and low-cost production of fine powders of granule characteristics for molding. Freeze-drying or lyophilization is a dehydration process. Two parameters are very important during the process: temperature and pressure. The freeze-drying process consists of three stages: pre-freezing, primary drying, and secondary drying. This technique allows the synthesis of fine powders [7, 23].

The lyophilization technique is also used to produce scaffolds in tissue engineering applications. During the lyophilization process, pores are formed as a result of water sublimation. Sublimated water moves to the surface and leaves the solution so

there would be pores instead of water molecules. The porous structure provides an advantage because of the increased interconnectivity producing a larger area and better nutrient flow which in turn causes an increase in cell adhesion and migration behavior [7].

The biological HA powders can be produced using biological materials including bovine bones, dentine, enamel, coral, seashell, eggshell, etc., and several methods of chemical synthesis have been developed for preparation of hydroxyapatite using different types of calcium (Ca) and phosphorus (P) sources. The synthesized hydroxyapatite is defined with its origin, like bovine hydroxyapatite or dentin hydroxyapatite.

For instance, hydroxyapatite can be derived from freshly extracted human teeth after sterilization, deproteinization cycles, and calcination heat treatment at 800–850 °C for several hours. As it is known, calcium-deficient hydroxyapatite is the main mineral of dental enamel and dentin. It was observed that at high temperatures, the dentin and enamel material can be separated easily and that approximately 60 vol% of the material was dentin.

## Sintering

Sintering is a heat treatment process to bond particles together of a pre-shaped green body or powder compact into a strong, coherent, predominantly solid structure [25, 26]. Sintering is carried out at temperatures about 55–70 % of the absolute melting temperature of the material. The main objective of sintering process is to achieve desired densification and fine and uniform microstructure.

The driving force for solid-state sintering is the reduction in surface energy. During sintering process, powder compacts try to decrease the surface energy and eliminate the pores by material transport mechanisms, i.e., surface transportation (diffusion, adhesion, or evaporation–condensation), grain boundaries, or bulk transportation (viscous flow, plastic flow, volume diffusion) [27]. The other possible driving forces can be listed as the curvature of the particle, chemical reaction, and applied pressure [25].

Depending on the application of external pressure during sintering, it is possible to classify these sintering processes into pressureless sintering and pressure-assisted sintering.

## Pressureless Sintering

The conventional pressureless sintering method which is carried out in a furnace under controlled atmosphere to bond particles of pre-consolidated powders is a relatively cheap and easy process.

Porous bioceramic implants can be fabricated by isostatic compaction and sintering of calcium phosphate which contain volatile particles like naphthalene. Vaporization of volatile particles leaves behind spherical voids and porosity. The size

**Table 3** Comparison of composition and mechanical properties of hydroxyapatite (HA), human enamel, and bone (Ref. [5])

Parameter	Hydroxyapatite (HA)	Human Enamel	Bone
Calcium (Ca, in wt%)	39.6	36.0	24.5
Phosphorus (P, in wt%)	18.5	17.7	11.5
Ca/P ratio (in molar)	1.67	1.62	1.65
Tensile strength (MPa)	100	70	150 (for cortical bone)
Elastic modulus (GPa)	0.010	0.014	0.020 (for cortical bone)

of these pores should be greater than 150  $\mu\text{m}$  for an effective bone ingrowth [5]. The porosity of HA is dependent on the numbers and dimensions of the volatilized or dissolved particles. Besides, the degree of compaction is necessary to determine the interconnectivity of porosity.

Biological apatite involves the mineral phases of calcified tissues, such as enamel, dentin, or bone. The biological apatite is different from pure hydroxyapatite (HA) in composition, stoichiometry, crystallography, and physical and mechanical properties (Table 3).

Pure hydroxyapatite (HA,  $\text{Ca}_{10}(\text{PO}_4)_6(\text{OH})_2$ ) has the theoretical composition as follows: 39.68 wt% Ca, 18.45 wt% P, and Ca/P molar ratio of 1.67. On the other hand, biological apatites are usually calcium deficient and carbonate substituted [5].

Apatite structure can be described as  $(\text{Ca},\text{M})_{10}(\text{PO}_4,\text{CO}_3,\text{Y})_6(\text{OH},\text{F},\text{Cl})_2$ , where M designates minor (e.g., Mg, Na, K, etc.) and trace (e.g., Sr, Pb, Ba) elements and Y represents acid phosphate, sulfates, borates, vanadates, etc. [5].

The biological apatites of enamel are different from dentin or bone in crystallinity and concentrations of minor elements. Enamel-based apatites contain least amount of carbonate (3.2 wt%) and magnesium (0.44 wt%) and have the largest crystal volume and size (1200–2000  $\text{\AA}$   $\times$  150–250  $\text{\AA}$ , length  $\times$  diameter), and their solubility product would be smaller compared to either dentin or bone apatites [5].

Sintering of biological apatites of human enamel, dentin, and bone above 800  $^\circ\text{C}$  engenders the formation of different phases. For instance, sintering of enamel and dentin apatites gives hydroxyapatite (HA) and small amounts of  $\beta$ -TCP as end products. If bone apatite is sintered above 800  $^\circ\text{C}$ , the final structure consists of mainly HA and small amounts of CaO [5]. In other words, if Ca/P molar ratio is equal to 1.67, only HA will be observed. If the Ca/P ratio is smaller than 1.67, in this case HA with other phases such as  $\beta$ -TCP, tetracalcium phosphate (TTCP),  $\text{Ca}_4\text{P}_2\text{O}_9$ , and  $\text{Ca}_4(\text{PO}_4)_2\text{O}$  will exist depending on the sintering temperature and conditions. If Ca/P ratio is greater than 1.67, HA and CaO phases will form [5].

The properties of starting powders of matrix and reinforcement phases and processing conditions strongly influence the physical (e.g., density, amount of porosity, etc.), mechanical (e.g., hardness, compressive, tensile, impact, bending or flexural strength, modulus of elasticity, shear modulus, fracture toughness, resistance to fatigue failure, etc.), microstructural (e.g., grain size, shape of grains and grain boundaries, etc.), and dissolution properties and crystallography of the final products.

The mechanical and dissolution properties of pure HA and biologically derived apatite have been analyzed in different studies. It is known that a homogeneous distribution of phases and absence of agglomeration, high density, and fine grain size are essential for enhanced mechanical properties. The studies showed that the presence of  $\beta$ -TCP caused a decrease in fracture toughness.

The effects of bioglass addition into the biologically derived apatite on mechanical properties were investigated for different sintering temperatures [28]. In this study, hydroxyapatite was derived from extracted deproteinized human teeth with calcination at 850 °C for 3 h. Easy separation of the dentine and enamel matter was observed after calcination at that temperature with a ratio of 60:40 (in wt%) of dentine and enamel.

The 45S5 Bioglass<sup>®</sup> was prepared from a mixture of high-purity SiO<sub>2</sub>, CaO, Na<sub>2</sub>CO<sub>3</sub>, and P<sub>2</sub>O<sub>5</sub> powders in the stoichiometric amounts to obtain the final Bioglass<sup>®</sup> composition. The calcined powder mixture was placed in a platinum crucible and heated to 1330 °C for 4 h. Subsequently they were poured into water in order to be in granular form of glass. Five and 10 wt% bioglass powders with an average particle size of 100–130  $\mu$ m were mixed with synthesized apatite. After pre-compaction, powder mixtures were subjected to sintering at 1200 and 1300 °C for 4 h.

In vitro dissolution of HA depends on several factors as follows: the type and concentration of the buffered and unbuffered solutions, pH of the solution, degree of saturation of the solution, solid/solution ratio, the length of suspensions in the solution, and the composition and crystallinity of HA. In the case of bulk HA, the degree of porosities, the amount and type of secondary phases, and the defect structure play an important role. If HA ceramic contains other calcium phosphate phases, dissolution behavior will be altered by the type and amount of phases. The extent of dissolution increases in the following order: HA <  $\beta$ -TCP <  $\alpha$ -TCP < TTCP [5].

### **Microwave Sintering**

The initial interest in microwave technology was originated by the military needs during the Second World War [29]. Later on, microwave technology has proven to be useful in a number of applications and is currently used for communication, chemistry, food processing, therapeutic medicine and diagnostic, plasma cutting, and drying and processing of various products [21]. Microwave sintering has been well employed in the field of sintering and joining of ceramics since the early 1970s. The advantages of microwave sintering over pressureless sintering include reduced sintering time, improved product uniformity, processing efficiencies, and achieving uniform microstructures [29].

The common frequencies for material processing are 0.91, 2.45, 5.80, and 24.12 GHz, and microwaves occupy the part of the electromagnetic spectrum from 300 MHz to 300 GHz. In microwave processing, heat is generated internally within the material first and then the entire volume is heated. Interactions of materials with microwave field and conductivity of materials play an important role for an efficient microwave processing. For instance, when an electric field is applied, electrons can

move freely and quite quickly in conductors; in this way electric current occurs and material is heated through resistive heating. However, metallic conductors and superconductors are not efficiently heated due to the reflection of microwaves. On the other hand, electronic distortions or reorientation of dipoles can induce heating for insulators. Hence, microwave processing might not be an appropriate technique for all materials [29], and it can be classified as material-dependent process [3]. The adsorption of microwave energy depends on the dielectric loss, magnetic properties, and microstructural properties [3].

Over the last few decades, considerable research has been conducted on microwave processing of bioceramics and bioceramic-based composites including hydroxyapatite, hydroxyapatite-biphasic HA–TCP composites, dense nanostructured bioceramics, YSZ–Al<sub>2</sub>O<sub>3</sub> composites, porous HA/β-TCP composites, and calcium phosphate-based functionally graded bioceramics.

### **Plasma Heating**

Similar to microwave sintering, plasma is created by microwave or induction fields using a low-pressure gas. Polyatomic gases such as N<sub>2</sub> or H<sub>2</sub> promote heating. A radiofrequency coil close to the powder compact is used to induce alternating currents which stimulate plasma sintering of the central powder compact. Concentration gradients are generated by the localized heating and initiate new transport mechanisms and result in improved densification. Plasma heating has been applied to yttria-stabilized zirconia ceramics and achieved a relative density of 93.5 % in 2.5 min [30].

### **Induction Heating**

Induction heating is a noncontact, rapid heating process. In this technique, the powder compact is surrounded by a conductive coil (usually water-cooled copper and operates at a frequency range of 50 Hz to several MHz) that carries alternating currents. For conductors, the current generates a magnetic field and induces eddy currents in the powder compact. With the reversal of the current direction in the coil, magnetic field alters polarity and reverses the eddy current direction. For insulating materials like bioceramics, a susceptor should be used to create heat via eddy currents. Although fast heating is possible with induction heating, low productivity associated with sintering a single compact at one time limits the application of this process [30]. For this reason, there are only a few studies where induction heating is applied to bioceramics. These are based upon the production of yttria-stabilized zirconia-reinforced hydroxyapatite composites and alumina–yttria-stabilized zirconia composites at high frequencies.

### **Laser Sintering**

Laser technology has been utilized for sintering due to high heat and power concentrations. Laser heating uses laser as the power source, but the energy decreases with an inverse-fifth-power dependence on the powder depth. For this reason, surface temperature of the powder bed is high, but depth of sintering is limited because of the poor heat transport through the powder compact. This effect

induces gradients in microstructure, densification, size, and dimension from the laser-heated surface to the interior of the powder compact. Selective laser sintering (SLS) technique was developed in the mid-1980s. High-power laser (e.g., carbon dioxide laser) is used to create a three-dimensional component. A powder bed is sintered to a shallow depth from one surface using a computer-aided scanning pattern. A fresh layer of powder is fed after each sintering scan. Ultimately, layers are coordinated to develop three-dimensional, complex-shaped products [30].

Different rapid prototyping and rapid tool generation techniques such as stereolithography (known as optical fabrication), three-dimensional printing, and selective laser sintering have been applied to produce implants and scaffold structures using composite materials consisting of polymers and bioactive ceramics like hydroxyapatite that are used for bone and tissue implantations in order to replace or repair bone defects due to damaged, traumatized, or lost bones.

## **Pressure-Assisted Sintering**

The development of high-performance bioceramics and biocomposites with controlled microstructure and greatly improved mechanical, optical, magnetic, thermal, and electrical properties by simultaneous application of temperature and pressure can be considered as the most important development in ceramic processing. The applied pressure during the sintering process enhances the sintering and contributes to sintering driving force. There are two principal methods to apply external pressure during sintering: isostatic pressure (e.g., hot isostatic pressing) and uniaxial pressure (e.g., hot pressing, spark plasma sintering) [3].

### **Hot Pressing (HP)**

Hot pressing has been successfully employed in the production of one-layer and/or multilayer bioceramics such as hydroxyapatite, alumina, and calcium phosphate ceramics with controlled microstructure, high density, and enhanced mechanical properties. Hot pressing is limited to simple solid shapes. Cylindrical, rectangular, or square cross sections can be produced. In this technique, powder is sintered under a uniaxial pressure between punches in a die. Graphite is preferred as die material due to its strength and creep resistance at high temperature, high thermal conductivity, relatively low thermal expansion, and low cost. However, atmosphere control is often necessary for hot pressing at high temperature. Above 2200 °C, an inert atmosphere should be used because of the vapor pressure of graphite [2, 3].

Sintering temperatures of up to 2400 °C are normally used. Mainly three different types of heating can be employed in hot pressing. The first one is conventional inductive heating where heat is generated within the die when it is subjected to a high-frequency electromagnetic field. Graphite or steel die is positioned within the induction coil. Heat is transferred into the die by thermal conductivity feature of the die material. Another heating method is indirect resistance heating. In this technique, die is placed in a heating chamber which is heated by graphite heating elements. Heat

is transferred into the die by convection. Electrical energy first heats the heating elements and then heats the die, so the process is called “indirect resistance heating”. This heating method is independent of the thermal conductivity of the die. Heating up the system and heat transfer from chamber atmosphere to the die take longer time when compared to conventional inductive heating technique. Heating rate is limited in both conventional inductive and indirect resistance heating techniques [3, 25].

The last heating method is direct heating or field-assisted sintering technique (FAST). In this heating method, die is directly connected to an electric power and heat is generated by unpulsed current. The resistivity of the die material and/or powder compact engender the heat directly inside the die. High heating rate, low sintering cycles, high sintering activity, and high-density products with a precise near-net shape are achieved with direct hot pressing technique [25].

### **Hot Isostatic Pressing (HIP)**

In this technique, pre-consolidated powder is enclosed in a container and sealed under a vacuum and then placed into a furnace that can be pressurized up to  $\sim 200$  MPa and sintered at a high temperature  $\sim 2000$  °C [3, 25]. During heating, the sample is collapsed by increased gas (Ar or He) pressure which has an isostatic effect. The main advantage of this method is the possibility of processing components with complex shapes due to homogeneous pressure distribution during sintering. The ability to produce products with irregular shapes provides several advantages over the uniaxial pressing technique, forging, and casting in terms of design flexibility and material properties [3, 25].

### **Spark Plasma Sintering (SPS)**

During the last decade, spark plasma sintering (SPS) or field-assisted sintering technique (FAST), pulsed electric current sintering (PECS), and current-activated pressure-assisted densification techniques have been developed as consolidation methods for producing high-density materials in a short period of time and at relatively low temperatures [31, 32]. Actually, the history of this technology dates back to the late 1930s with the introduction of sintering process using electrical energizing in the USA. In the 1960s, pulse current was applied for sintering in Japan, but the developments were limited up until the early 1990s. SPS is a third generation of the aforementioned technology with large pressures and DC pulse generators of 10–100 t and 1–30 kA, respectively [33].

SPS is a pressure-assisted, synthesis and processing technique which employs high current (pulsed direct current) and low voltage. SPS is similar to hot pressing (HP) but heating mechanism and heat transfer to the sample are different. In the SPS technique, direct heating of sample and graphite mold exists. A pulsed direct current (DC) passes through graphite punch rods and dies simultaneously with a uniaxial pressure. Heating is achieved through a pulsed (on/off) DC. Normally, external heating elements are not used. Application of on/off direct current results in the formation of arcs and spark discharges; thereby local high temperature states occur and cause vaporization and melting of the powder surfaces during process. This induces enhanced neck formation around contact area and improved densification



[31–33]. On the other hand, the appearance of plasma during SPS process is still a controversial issue.

The electrical conductivity of the material to be sintered has an important role in heat transfer during SPS process. If the pre-consolidated body is electrically conductive, the current mainly flows through the sample and a small part flows through the die. In the case of electrically insulating materials, all energy is dissipated through the die [33].

Spark plasma sintering technique is used to develop bioceramics and bioceramic composites. High-density sintered alumina ( $\text{Al}_2\text{O}_3$ ) ceramics are widely used for orthopedic implants such as total hip and knee replacement prostheses. Combination of good strength, high wear and chemical resistance, and good biocompatibility are main factors that led their widespread use [34, 35]. However, their slow crack-growth behavior resulted in a failure of the alumina ceramic component with time in service [36]. Many techniques have been investigated based on the addition of fibers, whiskers, and particulates such as zirconia ( $\text{ZrO}_2$ ) which is known to enhance the toughness of alumina [34]. A major drawback of zirconia ceramics is their strength reduction, because of an unfavorable tetragonal (t) to monoclinic (m) martensitic phase transformation with time when they are in contact with physiological fluids in the body. The  $t \rightarrow m$  transform is a reversible martensitic transformation, associated with a large temperature hysteresis (around 200 °C), a finite amount of volume change (4–5 %), and a large shear strain (14–15 %), which leads to the damage of the sintered part made of pure zirconia during cooling [37, 38]. It has been found that zirconia shows transformation toughening mechanism that exhibits resistance to crack propagation and the transformation toughening is influenced by the grain size, the grain size distribution, and the stabilizer content [39]. The tetragonal phase in zirconia ceramics can be obtained by using yttrium or cerium oxide stabilizers. Yttria is the most popular stabilizer used for zirconia ceramics for its excellent mechanical and wear properties and a good effect on tetragonal phase transformability. Advantages of combined high hardness of alumina with highly fracture-resistant yttria-stabilized zirconia (YSZ) make  $\text{Al}_2\text{O}_3$ –YSZ system as an alternative choice to alumina and zirconia monolithic ceramics for structural and functional applications [40, 41]. Similarly, hard particulates such as silicon carbide (SiC), titanium carbide (TiC), cerium oxide ( $\text{CeO}_2$ ) [40], or titania ( $\text{TiO}_2$ ) [41] have been incorporated into alumina.  $\text{Al}_2\text{O}_3$  and  $\text{Al}_2\text{O}_3$ –YSZ composites containing 3 and 5 mass%  $\text{CeO}_2$  and 3 and 5 mass%  $\text{TiO}_2$  were prepared at different compositions by using a spark plasma sintering method [40, 41].

The results of these studies showed that the relative density of approximately 99 % was achievable for monolithic  $\text{Al}_2\text{O}_3$ ,  $\text{Al}_2\text{O}_3$ –YSZ binary, and  $\text{Al}_2\text{O}_3$ –YSZ– $\text{CeO}_2$  and  $\text{Al}_2\text{O}_3$ –YSZ– $\text{TiO}_2$  ternary composites. The grain growth of alumina was suppressed by the addition of YSZ, and formation of elongated  $\text{CeAl}_{11}\text{O}_{18}$  grains with 5–10  $\mu\text{m}$  in length and 0.8–1.5  $\mu\text{m}$  in width was observed in the ceria-containing composites (Fig. 3).

Regarding mechanical properties,  $\text{Al}_2\text{O}_3$ –YSZ composites had higher hardness than monolithic  $\text{Al}_2\text{O}_3$  sintered body, and hardness of the composites was decreased with increasing YSZ content. Similarly, fracture toughness of  $\text{Al}_2\text{O}_3$  increased with

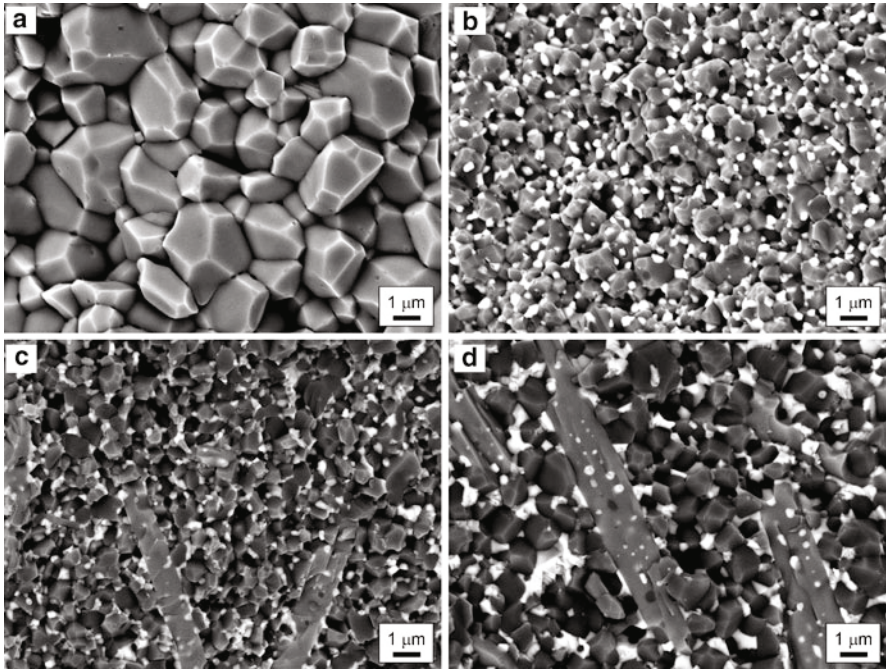
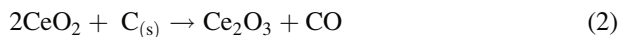


**Fig. 3** SEM micrographs of fracture surfaces of monolithic  $\text{Al}_2\text{O}_3$  sintered at  $1350\text{ }^\circ\text{C}$  (a),  $90\text{Al}_2\text{O}_3\text{-}10\text{YSZ}$  (vol%) (b),  $90\text{Al}_2\text{O}_3\text{-}10\text{YSZ}$  (vol%) with 3 wt%  $\text{CeO}_2$  (c), and  $90\text{Al}_2\text{O}_3\text{-}10\text{YSZ}$  (vol%) with 5 wt%  $\text{CeO}_2$  (d) composites sintered at  $1400\text{ }^\circ\text{C}$  for 5 min (Ref. [40])

the addition of YSZ, and the highest value of fracture toughness,  $6.2\text{ MPa} \cdot \text{m}^{1/2}$ , was achieved for the composite containing 30 vol% YSZ. Formation of elongated  $\text{CeAl}_{11}\text{O}_{18}$  grains resulted in lower Vickers hardness and fracture toughness values than that of the non-containing composites [40].

The formation of  $\text{CeAl}_{11}\text{O}_{18}$  grains could be related to the sensitivity of  $\text{CeO}_2$  on the sintering atmosphere.  $\text{CeO}_2$  can form nonstoichiometric oxides such as  $\text{Ce}_2\text{O}_3$  when sintering in a vacuum, in a reducing atmosphere, or at low oxygen pressure atmosphere [42]. During spark plasma sintering process, a reducing atmosphere was created due to high vacuum and close contact of the powder mixture with the graphite die/punch setup and the covered sheet (Eq. 2):



$\text{CeO}_2$  could be reduced to  $\text{Ce}_2\text{O}_3$ , and combination with  $\text{Al}_2\text{O}_3$  during sintering results in formation of  $\text{CeAl}_{11}\text{O}_{18}$  ( $\text{Ce}_2\text{O}_3 \cdot 11\text{Al}_2\text{O}_3$ ) grains during sintering. The reason for their elongated shape could be related to the presence of different ionic sizes of cerium. Cerium formally has the valance 4+ in  $\text{CeO}_2$ , and 3+ in  $\text{Ce}_2\text{O}_3$  [43]. The reduction of  $\text{CeO}_2$  to  $\text{Ce}_2\text{O}_3$  is associated with an increase in the ionic radius from 0.097 nm to 0.114 nm [44]. The crystal structure of  $\text{Ce}_2\text{O}_3 \cdot 11\text{Al}_2\text{O}_3$  has

a unit of four oxygen layers with hexagonal closed packing and one  $Ce_2O_3$  layer, while the  $Al_2O_3$  consists of the oxygen layers with hexagonal closed packing [45]. High cation size of ceria could cause a distortion between layers and an expanded lattice. Similar results were reported in the studies about ceria-stabilized zirconia or yttria and ceria-co-stabilized zirconia ceramics [46].

In the case of  $Al_2O_3$ -YSZ- $TiO_2$  composites, it was reported that  $TiO_2$  is an effective additive for  $Al_2O_3$ -YSZ composites, which resulted in lower sintering temperature and enhanced densification behavior.

Preliminary biocompatibility tests, in the rat model, indicated the presence of  $TiO_2$  in samples favored the osseointegration process. All implanted materials were well integrated in the bone defects and covered with a layer of soft tissue at 6 weeks after implantation. The specimen having 20 vol% YSZ and 5 wt%  $TiO_2$  showed the best integration. Histological analysis also confirmed the biocompatibility and osseointegration of the composites.

## Sol-Gel

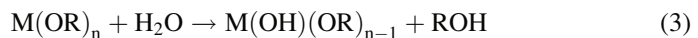
Experiments in sol-gel processing of inorganic materials began in the middle of the nineteenth century with Ebelman and Graham's studies on silica gels. It was reported that glass-like structure  $SiO_2$  was observed under acidic conditions by hydrolysis of tetraethyl orthosilicate (TEOS,  $Si(OC_2H_5)_4$ ). In the 1950s and 1960s, Roy et al. used the sol-gel method to synthesize high-purity ceramic oxide compositions, involving silicon, titanium, zirconium, etc. [47].

Sol-gel process is defined as a colloidal route used to synthesize ceramics with an intermediate stage including sol and/or gel states [48]. In this definition, sol represents the stable colloidal solution consisting of colloids with appropriate fluidity, and the term gel is the 3-dimensionally interconnected solid network obtained from sol, in which the solvent is retained by the framework consisted of polymerized colloids. If the solid network is composed of colloidal sol particles, the gel is designated as colloidal, or gel is polymeric if the network is comprised of sub-colloidal units [48, 49].

Sol-gel method is a wet chemical and low-temperature process. Therefore, the main advantage of sol-gel process is that homogeneous, high-purity powders or products can be prepared at lower temperatures in contrast to other conventional processes.

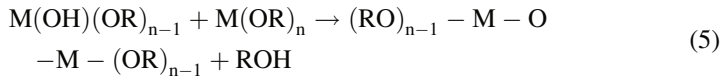
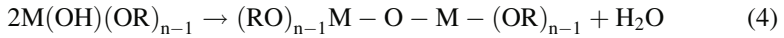
A typical sol-gel process starts with a solution consists of metal alkoxides ( $M(OR)_n$ , M is usually a metal, but in some cases it can be a nonmetallic material such as Si, and R is alkyl group such as  $CH_3$ ,  $C_2H_5$ , etc.). Chlorine and nitrate salts can also be used as precursor. The conversion of sol to a gel structure occurs by hydrolysis and condensation reactions and following drying and sintering processes to achieve oxide-based product.

During hydrolysis, metal alkoxides react with water easily and alcohol molecule is liberated as shown in Eq. 3:



Hydrolysis reaction can occur under acidic (defined as  $\text{pH} < 2.5$  for sol-gel processing based on point of zero charge) or basic ( $\text{pH} > 2.5$ ) conditions.

During condensation reactions two molecules are combined with the elimination of water or alcohol (Eqs. 4 and 5). This produces thermosetting polymers and phenolformaldehyde, nylon, and polycarbonates:



The sol-gel process has been utilized to produce bioceramic powders, coatings and substrates, fibers, glass, and glass ceramics. Sol-gel method has a strong molecular control over the incorporation and biological behavior of tissue, proteins, and cells and can be applied as implant and biosensor materials [49, 50].

Sol-gel process provides an alternative technique for processing a bioactive surface for improved bone attachment. Additionally, hybrid materials produced by the sol-gel technique possess ability to combine the advantages of both organic and inorganic properties. The sol-gel technique offers advantages such as the possibility of obtaining homogeneous hybrid materials at relatively lower processing temperatures, thereby allowing for the incorporation of different compounds [50].

Sol-gel processing is adaptable to fabricate bioceramics in a number of different forms as follows [47–50]:

- (i) Powder forms: bioactive glass powders, nanosized hydroxyapatite powders, bioactive nanocrystalline wollastonite powders, amorphous calcium phosphate powders, alumina powders
- (ii) Coating forms: yttria-stabilized zirconia-reinforced hydroxyapatite coatings on surgical-grade 316 L stainless steel, calcium titanate coatings on titanium, sol-gel-derived biphasic calcium phosphate ceramics on nitinol, hydroxyapatite coatings on titanium and titanium alloys, hydroxyapatite/titania double layer coatings on titanium
- (iii) Glass and glass ceramics: sol-gel-derived 45S5 Bioglass<sup>®</sup>, glass ceramic with a composition of  $\text{SiO}_2\text{-Al}_2\text{O}_3\text{-CaO-Na}_2\text{O-K}_2\text{O-P}_2\text{O}_5$  for dental applications, mica-based glass ceramics
- (iv) Fiber forms: Continuous or short silica and alumina fibers

---

## Summary

A variety of possibilities exist for the production of porous or dense bioceramics and bioceramic-based composites. The processing technique has a profound influence on structure, properties, and performance of the products, and accordingly, selecting the appropriate process is important to achieve the targeted properties.

**Acknowledgments** The authors wish to thank Simona Cavalu (in vivo tests), Viorica Simon (in vivo tests) and Huseyin Sezer (microstructural characterization). The financial support for the researches in this chapter by The State Planning Organization of Turkey (project number: 90150), The Scientific and Technological Research Council of Turkey (Turkey-Romania Bilateral Cooperation Project/111M455) and Istanbul Technical University Scientific Research Projects Division (project numbers: 32048 and 33667) are gratefully acknowledged.

---

## References

1. Kingery WD, Bowen HK, Uhlmann DR (1960) Introduction to ceramics. Wiley, Singapore
2. Carter CB, Norton MG (2007) Ceramic materials science and engineering. Springer, New York
3. Trunec M, Maca K (2014) Advanced ceramic processes. In: Shen JZ, Kosmač T (eds) Advanced ceramics for dentistry, 1st edn. Elsevier, Waltham, pp 142–147
4. Hench LL (1991) Bioceramics: from concept to clinic. *J Am Ceram Soc* 74:1487–1510
5. Hench LL, Wilson J (1993) An introduction to bioceramics. World Scientific, Singapore
6. Damestani Y, Reynolds CL, Szu J, Hsu MS, Kodera Y, Binder DK, Park BH, Garay JE, Rao MP, Aguilar G (2013) Transparent nanocrystalline yttria-stabilized-zirconia calvarium prosthesis. *Nanomed Nanotechnol* 9:1135–1138
7. Turkmen AK (2014) Production and characterization of chitosan-hydroxyapatite-fibrinogen 3D scaffolds by different techniques. MSc dissertation, Istanbul Technical University
8. Ren LM, Todo M, Arahira T, Yoshikawa H, Myoui A (2012) A comparative biomechanical study of bone ingrowth in two porous hydroxyapatite bioceramics. *Appl Surf Sci* 262:81–88
9. Akin I, Goller G (2009) Effect of CeO<sub>2</sub> addition on crystallization behavior, bioactivity and biocompatibility of potassium mica and fluorapatite based glass ceramics. *J Ceram Soc Jpn* 117:787–797
10. Kokubo T, Takadama H (2006) How useful is SBF in predicting in vivo bone bioactivity? *Biomaterials* 27:2907–2915
11. Bohner M, Lemaitre J (2009) Can bioactivity be tested in vitro with SBF solution? *Biomaterials* 30:2175–2179
12. Höland W, Beall GH (2002) Glass-ceramic technology. The American Ceramic Society, Westerville
13. El-Meliogy E, Noort R (2012) Glasses and glass ceramics for medical applications. Springer, New York
14. Goller G, Akin I (2008) Effect of CeO<sub>2</sub> addition on in-vitro bioactivity properties of K-mica-fluorapatite based glass ceramics. *Key Eng Mater* 361–363:261–264
15. Akin I, Goller G (2007) Effect of TiO<sub>2</sub> addition on crystallization and machinability of potassium mica and fluorapatite glass ceramics. *J Mater Sci* 42:883–888
16. Leonelli C, Lusvardi G, Malavasi G, Menabue L, Tonelli M (2003) Synthesis and characterization of cerium-doped glasses and in vitro evaluation of bioactivity. *J Non Cryst Solids* 316:198–216
17. Andrade AL, Valerio P, Goes AM, Leite MF, Domingues RZ (2006) Influence of morphology on in vitro compatibility of bioactive glasses. *J Non Cryst Solids* 352:3505–3511
18. Valerio P, Pereria MM, Goes AM, Leite MF (2004) The effect of ionic products from bioactive glass dissolution on osteoblast proliferation and collagen production. *Biomaterials* 25:2941–2948
19. Wilson J, Low S, Fetner A, Hench LL (1987) Bioactive materials for periodontal treatment: a comparative study. In: Pizzoferrato A, Marchetti PG, Ravaglioli A, Lee AJC (eds) *Biomaterials and clinical applications*, 1st edn. Elsevier, Amsterdam, pp 223–228
20. Ratner BD, Hoffman AS (2009) Biomedical engineering desk reference. Academic, Oxford
21. Agrawal D (2010) Microwave sintering of ceramics, composites and metal powders. In: Fang ZZ (ed) *Sintering of advanced materials: fundamentals and processes*, 1st edn. Woodhead Publishing, Oxford, pp 222–225

22. Ring TA (1996) Fundamentals of ceramic powder processing and synthesis. Academic, San Diego
23. Kokubo T (2008) Bioceramics and their clinical applications. Woodhead Publishing Limited and CRC Press, Cambridge
24. Orlovskii VP, Komlev VS, Barinov SM (2002) Hydroxyapatite and hydroxyapatite-based ceramics. *Inorg Mater* 38:973–984
25. Rahaman MN (2007) Sintering of ceramics. CRC Press/Taylor & Francis, Boca Raton
26. German RM (2010) Thermodynamics of sintering. In: Fang ZZ (ed) Sintering of advanced materials: fundamentals and processes, 1st edn. Woodhead Publishing, Oxford, pp 1–15
27. Angelo PC, Subramanian R (2009) Powder metallurgy: science, technology and applications. PHI Learning, New Delhi
28. Goller G, Demirkiran H, Oktar FN, Demirkesen E (2003) Processing and characterization of bioglass reinforced hydroxyapatite composites. *Ceram Int* 29:721–724
29. National Research Council Staff (1994) Microwave processing of materials. Academies Press, Washington, DC
30. German RM (1996) Sintering theory and practice. Wiley, New York
31. Olevsky EA, Bradbury WL, Haines CD, Martin DG, Kapoor D (2012) Fundamental aspects of spark plasma sintering: I. experimental analysis of scalability. *J Am Ceram Soc* 95:2406–2412
32. Munir ZA, Quach DV (2011) Electric current activation of sintering: a review of the pulsed electric current sintering process. *J Am Ceram Soc* 94:1–19
33. Tokita M (1997) Mechanism of spark plasma sintering. In: Miyake S, Samandi M (eds) Proceedings of the international symposium on microwave, plasma and thermochemical processing of advanced materials, 1st edn. JWRI, Osaka Universities, Osaka, pp 69–76
34. Balagopal N, Warriar K GK, Damodaran AD (1991) Alumina-ceria composite powders through a flash combustion technique. *J Mater Sci Lett* 10:1116–1118
35. De Aza AH, Chevalier J, Fantozzi G, Schehl M, Torrecillas R (2002) Crack growth resistance of alumina, zirconia and zirconia toughened alumina ceramics for joint prostheses. *Biomaterials* 23:937–945
36. Heros R, Willmann G (1998) Ceramics in total hip arthroplasty: history, mechanical properties, clinical results and current manufacturing state of the art. *Semin Arthroplast* 9:114–122
37. Szutkowska M (2004) Fracture resistance behavior of alumina-zirconia composites. *J Mater Process Technol* 153:868–874
38. Hannink RHJ, Swain MV (1994) Progress in transformation toughening of ceramics. *Annu Rev Mater Sci* 24:359–408
39. Chevalier J, Cales B, Drouin JM (1999) Low temperature aging of Y-TZP ceramics. *J Am Ceram Soc* 82:2150–2154
40. Akin I, Yilmaz E, Sahin F, Yucel O, Goller G (2011) Effect of CeO<sub>2</sub> addition on densification and microstructure of Al<sub>2</sub>O<sub>3</sub>-YSZ composites. *Ceram Int* 37:3273–3280
41. Ormanci O, Akin I, Sahin F, Yucel O, Simon V, Cavalu S, Goller G (2014) Spark plasma sintered Al<sub>2</sub>O<sub>3</sub>-YSZ-TiO<sub>2</sub> composites: processing, characterization and in vivo evaluation. *Mater Sci Eng C* 40:16–23
42. Shyu JZ, Weber WH, Gandhi HS (1988) Surface characterization of alumina-supported ceria. *J Phys Chem* 92:4964–4970
43. Skorodumova NV, Simak SI, Lundqvist BI, Abrikosov IA, Johansson B (2002) Quantum origin of the oxygen storage capability of ceria. *Phys Rev Lett* 89:166601-1-4
44. Huang TC, Moran E, Nazzal AI, Torrance JB, Wang PW (1989) Determination of the average ionic radius and effective valence of Ce in the Nd<sub>2-x</sub>Ce<sub>x</sub>CuO<sub>4</sub> electron superconductor system by X-ray diffraction. *Phys C: Supercond* 159:625–628
45. Tsukama K (2000) Conversion from β-Ce<sub>2</sub>O<sub>3</sub> · 11Al<sub>2</sub>O<sub>3</sub> to α-Al<sub>2</sub>O<sub>3</sub> in tetragonal ZrO<sub>2</sub> matrix. *J Am Ceram Soc* 83:3219–3221
46. Huang SG, Vanmeensel K, Van der Biest O, Vleugels J (2007) Influence of CeO<sub>2</sub> reduction on the microstructure and mechanical properties of pulsed electric current sintered Y<sub>2</sub>O<sub>3</sub>-CeO<sub>2</sub> co-stabilized ZrO<sub>2</sub> ceramics. *J Am Ceram Soc* 90:1420–1426

47. Hench LL, West JK (1990) The sol-gel process. *Chem Rev* 90:33–72
48. Pierre AC (1998) *Introduction to sol-gel processing*. Kluwer, Boston
49. Sakka S (2005) *Handbook of sol-gel science and technology, processing characterization and applications*. Kluwer, Boston
50. Nassar EJ, Katia J, Calefi PS, Rocha RA, De Faria EH, e Silva MLA, Luz PP, Banderia LC, Cestari A, Fernandes CN (2011) Biomaterials and sol-gel process: a methodology for the preparation of functional materials. In: Pignatello R (ed) *Biomaterials science and engineering*, 1st edn. InTech, Rijeka/Croatia, pp 1–12

Cristina Gruian, Emilia Vanea, Heinz-Jürgen Steinhoff, and  
Simion Simon

## Contents

Introduction .....	668
Proteins Structure .....	670
Factors That Influence Protein Interaction with Solid Surfaces .....	671
Methods Used for Studying Proteins Interaction with Solid Surfaces .....	672
Electron Paramagnetic Resonance Spectroscopy in Combination with Site-Directed Spin Labeling Technique .....	673
Fourier Transform Infrared Spectroscopy .....	674
X-Ray Photoelectron Spectroscopy .....	674
Protein Adsorption on Bioactive Glass Designed for Bone Tissue Engineering .....	675
Quantitative Adsorption Analysis Performed by cw EPR Spectroscopy .....	676
Conformational Changes Observed by cw and DEER EPR Spectroscopy .....	678
Secondary Structure Conformational Changes Investigated by FTIR Spectroscopy .....	682
Surface Coverage Explored by XPS .....	685
Protein Adsorption on Aluminosilicate Glass Ceramics Designed for Radiotherapy and Hyperthermia .....	688
Protein Loading on Si-Based Glass-Ceramics Designed for Drug Delivery .....	690
Loading Procedure: Adsorption .....	690
Loading Procedure: Encapsulation .....	695
Summary .....	698
References .....	699

---

C. Gruian • E. Vanea • S. Simon (✉)

Faculty of Physics and Institute of Interdisciplinary Research in Bio Nano-Sciences, Babes-Bolyai  
University, Cluj-Napoca, Romania

e-mail: [cristina.maier@phys.ubbcluj.ro](mailto:cristina.maier@phys.ubbcluj.ro); [emilia.vanea@phys.ubbcluj.ro](mailto:emilia.vanea@phys.ubbcluj.ro); [simons@phys.ubbcluj.ro](mailto:simons@phys.ubbcluj.ro);  
[simion.simon@phys.ubbcluj.ro](mailto:simion.simon@phys.ubbcluj.ro)

Heinz-Jürgen Steinhoff

Department of Physics, University of Osnabruk, Osnabruk, Germany

e-mail: [hsteinho@uos.de](mailto:hsteinho@uos.de)



---

**Abstract**

Understanding protein adsorption to solid surfaces represents a topic of general interest, this phenomenon being crucial for disciplines such as biochemical engineering, biotechnology, biomedicine, biology, and environment science. For instance, in the field of biomedicine, it is of great importance to assess the adsorption of blood proteins to implants. This complex process is driven by different protein–surface or protein–protein forces and is strongly influenced by parameters like pH, temperature, ionic strength, protein type, and by the chemical and physical characteristic of the surface. Despite an increased understanding of many peculiarities of protein adsorption achieved in recent years, there still are unanswered questions or contradictory opinions related to this research topic. The present chapter summarizes some basic characteristics of the protein adsorption process, with focus on glass-ceramic type materials. The examples of protein adsorption studies described in the present material aim to enlighten aspects related to conformational changes or structural rearrangements of the protein domains upon adsorption, influence of surface functionalization on proteins adsorption and to elucidate details concerning protein dynamics and the amount of the protein attached. Three types of glass-ceramic materials were considered as concrete examples: bioactive glasses designed for tissue engineering, aluminosilicate glass-ceramics intended for both hyperthermia and radiotherapy applications, and silica matrices aiming to be used for therapeutic proteins delivery. Among the many methods used to investigate adsorption of proteins on solid surfaces, three spectroscopic techniques are highlighted: the method of site-directed spin labeling combined with electron paramagnetic resonance, Fourier transform infrared, and X-ray photoelectron spectroscopy.

---

**Keywords**

Glass-ceramics • Protein adhesion • Albumin • Fibrinogen • Hemoglobin • MnME • Insulin • Silane/glutaraldehyde functionalization • SDSL-EPR • FTIR • XPS • SEM

---

**Introduction**

Protein–materials surface interaction was the subject of numerous studies for several decades, being considered one of the most important topics in the field of biomaterials and in the development of recent emerging areas such as biotechnology and biomedical science. Interaction of proteins with solid surfaces is not only a fundamental phenomenon but also a major component in the development of recent applications in the fields of drug delivery, biosensors, or tissue engineering. For example, electrical sensors or transdermal systems for controlled drug release should be designed to have optimum performance without causing skin irritation or hypersensitive responses. Protein–surface interactions are also critical for the assembly of protein interface constructs necessary to develop new analytical devices with biologically sensitive elements (biosensors). Pacemakers, arterial grafts, and dialysis

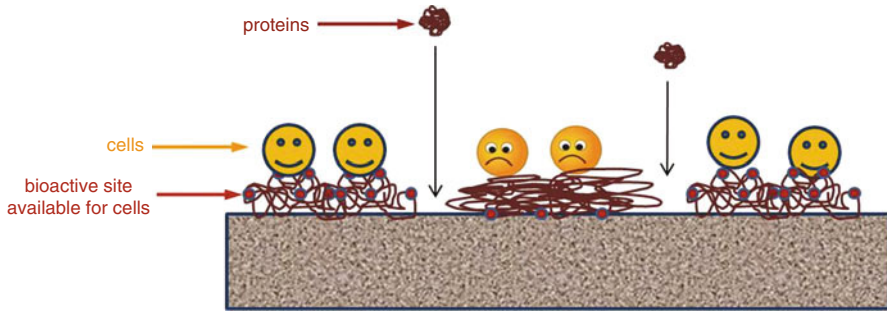


**Fig. 1** Schematic illustration of interaction between proteins (represented by the *purple random chain*) and a solid substrate; the type of bioactive sites that are presented by the adsorbed layer of proteins (*red circles*) can determine cell's response (*yellow faces*) (The protein/cell size is not represented in real proportion scale)

machines are devices which involve the interaction of artificial materials with tissues and/or body fluids (e.g., blood).

In the field of tissue engineering, protein–surface interactions are fundamentally responsible for the biocompatibility of medical devices, especially because they represent the first biochemical events that take place at the surface of a biomaterial, and are essential for further physicochemical interactions [1, 2]. All implant surfaces that come in contact with soft or hard tissues become rapidly coated with a 1–10 nm thick protein layer, most often with blood plasma. Such layers have different compositions, depending on the substrate chemistry and topography, and precede cell attachment, proliferation, and migration [3]. The types and the amount of proteins adsorbed, as well as their orientation, conformation, and packing density are determinants for material–cell interaction, as the protein–formed layer on the biomaterial surface provides the topographical and chemical cues to guide cells and increases the biomaterial ability to support and foster cells attachment [4]. When living cells approach the biomaterial surface, they bind to specific bioactive features presented by the adsorbed proteins, by means of their membrane receptors (Fig. 1). The understanding of protein adsorption process is, therefore, essential for controlling the cellular response [5].

Glass-ceramics have found wide applications in medicine as bone implants and attracted great interest in the field of biomaterials due to their excellent biocompatibility. Among the vast number of bioceramics developed during the last decades, considerable attention has been directed to Ca-P based systems used as bone graft substitutes, because of their ability to form *in vivo* a bone-like apatite layer capable of promoting the osteointegration [6]. Protein adsorption on osteoinductive bioceramic type surfaces plays a vital role during bone tissue regeneration [7] and helps in understanding the mechanisms of bioactivity [8]. Proteins are spontaneously adsorbed onto the surface, long before Ca-P precipitation, and can influence surface mineralization by affecting the nucleation and growth as well as the morphology, size, and orientation of Ca-P crystals [9, 10].

The aluminosilicate glass ceramics have also found several medical applications, in the field of biomaterials, as they are highly stable in the body. By adding radioactivable isotopes like yttrium, dysprosium, samarium, or rhenium, these materials can be used for in situ radiotherapy, while the addition of iron oxide makes them suitable for hyperthermia applications [11]. The simultaneous application of both radiotherapy and hyperthermia considerably enhances the therapeutic effects of these cancer treatment methods [12, 13]. In both therapy cases, the aluminosilicate particles have to be injected locally or intravenously at the tumor site, and they are rapidly coated by components of circulation, such as blood plasma proteins. A common failure in using this kind of systems is that they are recognized as foreign products by the body's major defence system (the reticulo-endothelial system) and are quickly removed from blood circulation. This inconvenient can be overcome by encapsulating the particles in a protein shell that avoids their detection by the reticuloendothelial system and ensures longer sustenance within the body [2]. In this respect, the preservation of the protein functionality and conformational structure upon interaction with particles surface is of great importance.

In the field of drug delivery, in order to improve the possibility of delivering therapeutic proteins (e.g., insulin, interferon) an effective method to increase the proteins stability and to preserve their functionality is to incorporate them into nanoparticulate systems [14]. It was shown that the nanostructured silica matrix can be effectively used to isolate the protein molecules, thus preventing their aggregation and denaturation. Recently reported studies have shown that insulin preserved in great extent its overall structure during encapsulation, storage, and release from such matrices [15, 16].

In the present approach, after introducing a few basic elements regarding the interaction between proteins and solid surfaces, attention will be focused on several examples representative for glass and glass-ceramic systems considered for the abovementioned applications.

---

## Proteins Structure

Before protein adsorption behavior can be understood, it is first important to understand the basic makeup of protein structure. Proteins are complex copolymers that are made up of four levels of structure, designated by the sequence of the 20 L-amino acids coded by the DNA of a cell. As part of a protein, a given amino acid is referred to as a peptide residue. Each amino acid consists of a common backbone part  $\{-\text{NH}-\text{CaHR}-\text{CO}-\}$  and a specific side group structure, unique for each type of residue, that gives the residue its specific functional characteristics (Fig. 2a). The amino acids are subcategorized into nonpolar (i.e., hydrophobic),  $\pm$  charged, and polar. Due to hydrogen bonds, the polypeptide chain formed by the primary sequence is organized into three basic types of secondary structure:  $\alpha$ -helices,  $\beta$ -sheets, and loops that connect helix and sheet elements (Fig. 2b). These secondary elements are folded into a tertiary structure (Fig. 2c). Finally, quaternary structure is

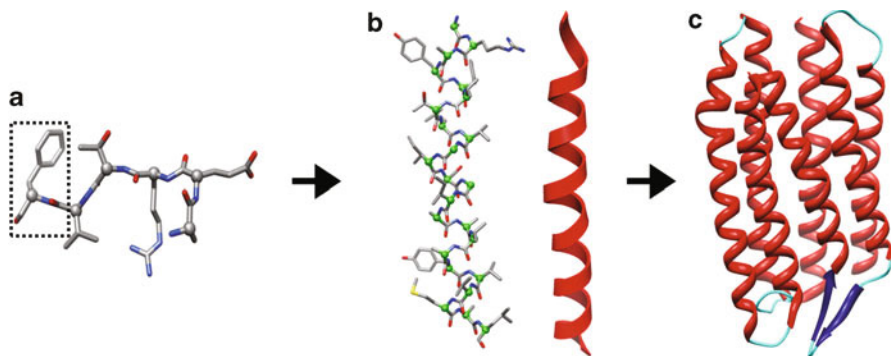


**Fig. 2** Protein structure: (a) primary structure showing example of residues (in the inserted area: phenylalanine; color code: *gray* = C, *blue* = N, *red* = O, H not shown). (b) Secondary structure ( $\alpha$  helix element): atom ball-stick view (*left*) and ribbon view (*right*). (c) Tertiary structure: Sensory rhodopsin II (PDB 1H68); Color code: *red* =  $\alpha$ -helix, *blue* =  $\beta$ -sheet, and *cyan* = connecting loops

formed by two or more individual polypeptide chains that are organized together, the result being a multisubunit complex.

Generally, proteins are structured so that their hydrophobic residues are buried within the protein core, while their hydrophilic residues are situated towards the protein solvent accessible surface. However, it is often encountered the situation where some hydrophobic residues are present on the surface while hydrophilic residues are buried within the protein core. The protein surface is thereby highly amphiphilic, namely it displays a multitude of different types of functional groups on its surface. This issue, together with the pKa value of each residue (defining the residue protonation state) has a major impact on protein behavior upon protein interaction with the solid surface [5].

## Factors That Influence Protein Interaction with Solid Surfaces

The organization of the protein layer at the biomaterial surface is influenced by both protein–surface as well as protein–protein interactions in the presence of the surrounding aqueous solution [5]. Therefore, all the participants to this phenomenon can influence the protein adsorption: *the protein* (by its chemical and physical structure), *the surface* of the substrate (by its texture, charge, and hydrophobic character) and *the aqueous solution* (in principal by its salt concentration and pH). For instance, it is known that a hydrophobic surface will adsorb more strongly proteins than a neutrally charged hydrophilic surface [5, 17], while higher pH results in higher adsorption of the protein [17]. Electrostatic interactions (which can be probed by studying ionic strength and pH effects on protein stability) are also of great importance, as contributing to macromolecular folding, conformational stability, and binding energies of biomolecules [17, 18]. Nevertheless, the protein

behavior during adsorption is highly dependent on the individual nature of the protein and the involved surface. In order to minimize structural changes of proteins, without weakening their effectiveness, one approach is to functionalize the surface with organic molecules (for e.g., protein coupling agents) that are able to provide accessible and chemical functional groups for protein immobilization [19] and to attach proteins without losing their conformational functionality [20].

Apart from the surface chemistry, the properties of the protein molecules have also great influence on the adsorption process. When protein molecules approach a solid surface, they do not behave like rigid symmetrical particles that are adsorbed or desorbed from the surface, like in the simple case of gas molecules. Proteins are complex biopolymers with complicated monomeric structures consisting of combinations of the 20 naturally occurring amino acids. Considering this unique diversity of the base elements, which results in a great complexity of the proteins structure and functionality, proteins behavior during the adsorption process cannot be treated in a simplistic manner. When treating with such subject, the ideal approach would be to take into account the unique personality of each individual type of protein molecule. Protein molecules exist in a great variety of size, shape, and structural properties. Due to the well-defined way in which they fold their secondary and tertiary structure, each protein presents a specific distribution of its hydrophobic, hydrophilic, positive or negatively charged side chains, an issue that has a major impact upon the adsorption process [21]. These properties may vary depending on the external environment such as pH, ionic strength, or temperature. Proteins behavior at the interface with a solid surface can thus be analyzed taking into account its size, structure, charge distribution, polarity, and structural stability.

---

## Methods Used for Studying Proteins Interaction with Solid Surfaces

When investigating proteins adsorption, four main issues have to be considered:

1. Is it possible to distinguish between the protein molecules and the substrate?
2. How much protein was attached (quantification)?
3. Which is the status of protein structure after adsorption (protein conformational changes)?
4. Which is the kinetics of protein adsorption onto the surface?

The fourth issue is no longer a problem if protein adsorption is monitored in solution. In this case, proteins can only be quantified or identified by using methods like colorimetric assay, ultraviolet-visible spectroscopy, sodium dodecyl sulfate-polyacrylamide gel electrophoresis, Western blotting, or enzyme linked immunosorbent assay – ELISA. However, this approach implies that the adsorbed protein must be detached from the surface or indirectly calculated by the difference between the protein amount in the solution before and after contact with the substrate. Quantification of protein attached is difficult to be done in this case, firstly because the

amount of adsorbed protein is usually below the detection limit of most of the techniques used, and secondly because the detachment of protein molecules from a surface is extremely dependent on the degree of protein–surface interaction [22].

There are, though, many and various techniques that can be used to study protein adsorption directly on the surface. Methods like Radiolabelling, Surface Plasmon Resonance (SPR), Ellipsometry, or Quartz Crystal Microbalance with dissipation (QCM-D) allow the determination of the protein amount adsorbed, while methods such as Fourier Transform Infrared spectroscopy (FTIR) and Atomic Force Microscopy (AFM) provide information concerning the conformation of the adsorbed protein layer. Some techniques are able to offer both quantification and structural information concerning the protein attached: Immuno-fluorescence/ELISA or Electron Paramagnetic Resonance (EPR) spectroscopy combined with the Site Directed Spin Labeling (SDSL). In addition, information regarding the surface coverage can be achieved by X-Ray Photoelectron Spectroscopy or AFM.

Among the high number and variety of techniques that can be used to study protein interaction with solid surfaces, three spectroscopic techniques were selected to be shortly described in the present paragraph, and further presented in various examples within this chapter: EPR-SDSL, FTIR, and XPS. The examples further presented in the present chapter are focused on quantitative analysis and details concerning structural and dynamic information for the adsorbed/encapsulated proteins.

## **Electron Paramagnetic Resonance Spectroscopy in Combination with Site-Directed Spin Labeling Technique**

SDSL combines site-directed mutagenesis with EPR spectroscopy: a paramagnetic nitroxide side is introduced via selective coupling to a cysteine inserted into the amino acid sequence by a substitution mutation. The nitroxide spin label is influenced by interactions with surrounding structures and by the protein motion, which is reflected in the EPR spectra of the spin label [23, 24]. Among the various spin labels available, the (1-oxyl-2,2,5,5-tetramethylpyrroline-3-methyl) methanethiosulfonate spin label (MTSSL) is the most often used in SDSL studies due to its sulfhydryl specificity and its small molecular volume [25]. In the several examples presented in the present chapter, MTSSL and the iodoacetamide-based (4-(2-Iodoacetamido)-2,2,6,6-tetramethyl-1-piperidinyloxy) spin label (IAASL) were used.

The method of SDSL was predominantly used for studying the structure and dynamics of soluble proteins in solution or membrane proteins reconstituted in their native membrane environment [25]. Only in the past decade it was shown that it can be extended to study proteins interaction with solid surfaces [26, 27]. Recently published studies demonstrated that this method can be applicable to proteins encapsulated [15] in or adsorbed on solid surfaces [28–32], thus permitting investigation of adsorption-induced conformational changes in conditions close to the proteins physiological environment (phosphate buffer solution at pH 7.4).

By following the EPR signal of the paramagnetic center attached, the following information can be achieved from the resulting EPR spectrum of a spin label in the adsorbed/encapsulated protein:

1. Spin label dynamics – can be observed in the cw-EPR line shape analysis and offers information about the putative immobilization of the protein on the BG surface and identifies conformational changes in the protein structure upon interaction with the substrate.
2. Spin label concentration – the second integral of the cw-EPR signals (first derivative absorption spectra) is directly proportional to the spin concentration in the sample and can be used to calculate the amount of protein attached onto the bioactive glass.
3. Inter-spin distances ranging from 2 up to approximately 8 nm – can be determined from pulse double electron electron resonance (DEER) spectroscopy and provides global information about changes in protein dynamics and tertiary structure upon adsorption.

## Fourier Transform Infrared Spectroscopy

Interaction of proteins with solid surfaces frequently results in conformation and/or orientation changes within the protein molecules. Because protein structures are relatively unstable, proteins tend to unfold, allowing internal regions to form additional contacts with a particular solid surface. Protein denaturation is often associated with a loss of secondary or tertiary structure and results in irreversible adsorption [33]. The Fourier Transform Infrared (FTIR) spectroscopy technique offers relevant information about changes in the adsorbed protein structure. The characteristic IR bands of proteins arise from the amide bonds that link the amino acids and include the amide I ( $1600\text{--}1700\text{ cm}^{-1}$ : 80 % C=O stretching mode), amide II ( $1500\text{--}1600\text{ cm}^{-1}$ : 60 % N-H bending and 40 % C-N stretching modes) and amide III ( $1200\text{--}1330\text{ cm}^{-1}$ : 40 % C-N stretching and 30 % N-H bending modes) absorption bands [34]. The locations of both the amide I and amide II absorption bands are sensitive to changes in protein secondary structure, however quantitative structural information is mostly obtained from the band position and relative band areas obtained by the deconvolution of amide I region of the protein FTIR spectra [33, 35, 36].

## X-Ray Photoelectron Spectroscopy

X-ray Photoelectron Spectroscopy (XPS) yields information concerning the atomic composition and chemical environment of the first 2–10 nm layer of a material surface and can accurately determine the surface coverage [37]. When an X-ray beam directs to the sample surface, the energy of the X-ray photon is adsorbed completely by the core electron of an atom. The emitted electron with the kinetic

energy  $E_k$  is referred to as the photoelectron. The binding energy of the photoelectron is characteristic of the orbital from which the photoelectron originates and depends on the final state configuration after photoemission, being thus very sensitive to the chemical environment of element. The same atom can be bonded to different chemical species, leading to changes in the binding energy of its core electron. The variation of binding energy results in the shift of the corresponding XPS peak, ranging from 0.1 eV to 10 eV. This effect is termed as “chemical shift”, which can be applied to studying the chemical status of element in the surface [38].

An XPS spectrum represents the photoelectron energy distribution. Because the core electrons of each element have characteristic binding energies, the peaks in the XPS spectra allow for identification of all elements, except H and He, which have a tiny cross-section for photoemission.

---

## Protein Adsorption on Bioactive Glass Designed for Bone Tissue Engineering

The first example reflects the use of SDSL-EPR, FTIR, and X-Ray Photoelectron spectroscopy to investigate the adsorption process of two proteins, regarded as model systems, (horse hemoglobin and the tRNA-modifying protein MnmE) on the solid surface of a sol–gel prepared bioactive glass identical in composition with the classical 45S5 Bioglass<sup>®</sup>: 45 % SiO<sub>2</sub>, 24.5 % Na<sub>2</sub>O, 24.5 % CaO, and 6 % P<sub>2</sub>O<sub>5</sub> (in molar%). In order to investigate the effect of a protein coupling agent on protein adsorption, the surface of the bioactive glass (BG) system was silanized with 3-aminopropyl-triethoxysilane (APTS) and subsequently modified with glutaraldehyde (GA) [28]. The influence of this chemical treatment on protein adsorption was determined by using the three spectroscopic techniques mentioned above. Pristine and GA functionalized powder samples were incubated for 4 h at room temperature in horse hemoglobin solution prepared with phosphate-buffered saline solution (pH 7.4), and in MnmE solution prepared with Tris-buffered solution (pH 7.4).

Hemoglobin is a globular metalloprotein found in blood cells that carry the oxygen from the lungs to the peripheral tissues. It consists of four polypeptide chains: two  $\alpha$  (141 amino acids each) and two  $\beta$  chains (146 amino acids each). The structure of horse hemoglobin displays a large similarity with human hemoglobin [39]. Each  $\beta$  chain contains one cysteine residue in position  $\beta$ -93, which was considered in the present example for spin labeling with IAASL (Fig. 3) [28].

MnmE is a GTP-hydrolyzing (G) protein conserved between bacteria and eukarya, belonging to the expanding class of G proteins activated by nucleotide-dependent dimerization (GADs). The protein is involved in the biosynthesis of a hypermodified nucleotide (nucleoside 5-methylaminomethyl- 2-thiouridine), which plays an important role in the structure and function of transfer ribonucleic acids. The crystal structure of MnmE dimer (pdb 1XZP, from *Thermotoga maritima*) reveals that each monomer consists of three domains: an N-terminal domain responsible for constitutive dimerization, a central helical domain, and the G domain [40]. In solution in the nucleotide-free state the G domains face each other with



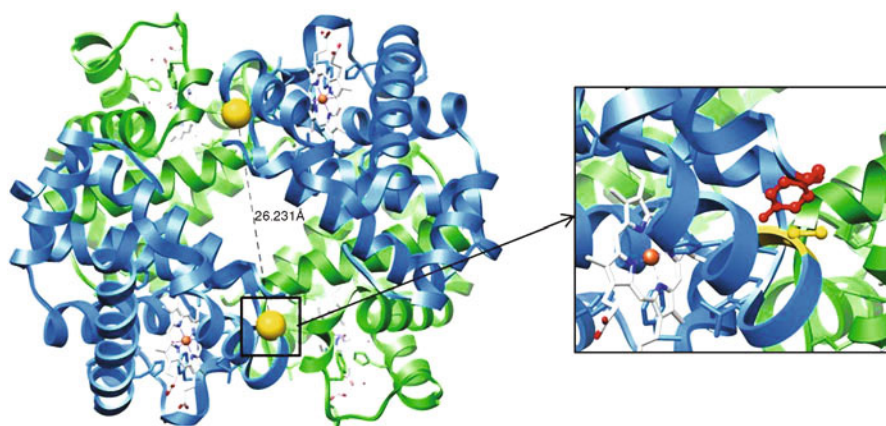


**Fig. 3** *Left:* Structure of horse hemoglobin obtained by X-ray crystallography (2ZLU from Protein Data Bank). The  $\alpha$ -chains are colored in green and the  $\beta$ -chains are colored in blue; heme groups are shown in stick representation. The  $C_{\beta}$  atoms of native cysteines from position  $\beta$ -93 are indicated as yellow spheres, with dashed lines showing the distance between the  $C_{\beta}$  atoms of both residues. *Right:* Detailed view onto the spin label binding site. The native amino acid at position  $\beta$ -93 (cysteine) is colored in yellow and the tyrosine situated in a pocket close to the C-terminus of the  $\beta$ -chain is colored in dark red (Taken from Klare [24])

their nucleotide binding sites (Fig. 1) without displaying any structural contacts between each other [41]. In the presence of  $\text{GDP}\cdot\text{AlF}_x$ , a transition state mimic for GTP hydrolysis, the G domains contact each other by overcoming a 20–30 Å distance gap (Fig. 4) [30]. The multidomain architecture and the observed large conformational change occurring upon activation renders this protein an ideal model system to study the influence of protein–BG interaction on functional conformational dynamics. The changes induced in the MnME structure by the adsorption process were investigated by SDSL-EPR spectroscopy in two steps of its GTPase cycle: the apo-state (nucleotide free) and the GTP hydrolysis transition ( $\text{GDP}\cdot\text{AlF}_x$  bound) state [30].

The amino acids at four positions within MnME were mutated to cysteine and subsequently spin labeled with the (1-oxyl-2,2,5,5-tetramethyl-3-pyrroline-3-methyl) methanethiosulfonate spin label (MTSSL) [30]: Ser278 and Glu287 (both located in the G-domain); Ile105 and Lys95 (both situated in the N terminal domain of the protein) (see Fig. 4).

### Quantitative Adsorption Analysis Performed by cw EPR Spectroscopy

The amount of the protein bound to the bioactive glass was estimated from the value of the spin concentration in the sample, which was calculated from the area of EPR absorption spectra.

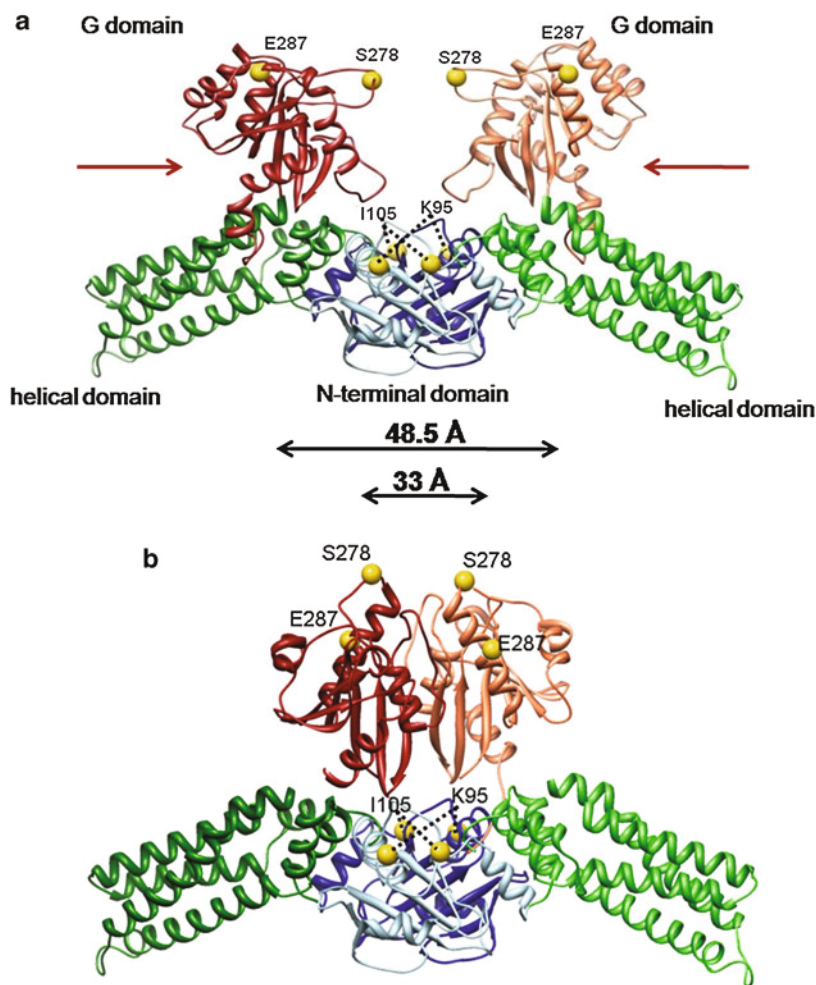


**Fig. 4** Crystal structure of the MnM homodimer in apo- (**a**, generated with pdb 1XZP) and GDP · AlF<sub>x</sub> bound state (**b**, pdb 2GJ8). Positions of native residues that were mutated to cysteines (E287, S278, I105 and K95) and spin labeled with MTSSL are indicated by *yellow spheres*. Upon GTP hydrolysis, the G domains move by approximately 15.5 Å, from 48.5 Å to 33 Å (Taken from Gruian et al. [28])

To verify the influence of the protein coupling agent on the efficiency of the adsorption process, samples containing protein attached to pristine and GA functionalized BG were ultrasonicated for 45 min at room temperature, then washed again with buffer solution to remove the protein that was detached from the surface. Afterwards, the samples were examined again by cw-EPR spectroscopy. Table 1 shows the amount of protein attached to the BG immediately after immersion and after ultrasonication. Although right after immersion both proteins show larger

**Table 1** Concentration of hemoglobin and MnmE protein adsorbed on pristine and GA functionalized bioactive glass, determined immediately after immersion and after ultrasonication. Errors are estimated to be  $\pm 10\%$ , due to experimental settings and uncertainties in baseline subtraction [28, 30]

Protein	MnmE ( $\mu\text{M}$ )		Horse hemoglobin ( $\mu\text{M}$ )		Protein removed from the substrate (%)	
	After immersion	After ultrasonication	After immersion	After ultrasonication	MnmE	Horse hemoglobin
<b>Pristine BG</b>	508	353	374	298	30	20
<b>GA functionalized BG</b>	491	408	319	313	16.9	0.02

affinity for BG nonfunctionalized with GA, the ultrasonication process removes more protein from the pristine BG, indicating stronger protein attachment on the GA functionalized surface. The data shown in Table 1 show that after employing the ultrasonication procedure, approximately 30 % of MnmE and 20 % of hemoglobin is removed from the pristine BG, while only 16.9 % (MnmE) and 0.02 % (hemoglobin) was removed from the GA-functionalized BG. This suggests that the presence of GA offers more stable and specific points for protein attachment on the BG substrate, so the binding and distribution of the protein might be more organized. If the BG substrate is not functionalized with GA, the protein covers every accessible place on the surface, with some protein molecules having only weak attachment points, so they can easily detach when the sample is ultrasonicated.

Hemoglobin represents a special case, since the amount removed after the ultrasonication process on the GA functionalized substrate is insignificant (0.02 %). It is known that glutaraldehyde induced polymerization of this protein in solution [42]. This protein has many lysine residues located on the surface, and interaction of these residues with GA leads to cross-linking of the protein, resulting in formation of macromolecules consisting of 8–10 proteins [42]. This heterogeneous mixture of hemoglobin products, with a variety of molecular weights and chemical modifications, makes the tetrameric structure of the molecule more rigid. Protein polymerization seems to be the cause for the very strong attachment of hemoglobin on the GA functionalized substrate. The Scanning Electron Microscopy (SEM) images presented in Fig. 5 [28] support this assumption, as a regular organization of the protein layer can be observed on this substrate. The chains that are observed on the surface have approximately 50 nm width, which would correspond to a cluster formed by 8–10 proteins.

## Conformational Changes Observed by cw and DEER EPR Spectroscopy

The free electron is situated in the nitroxyl radical ( $N-O$ ) of the spin label, and it has a strong anisotropic dipolar interaction with the nitrogen nucleus. Accordingly, the

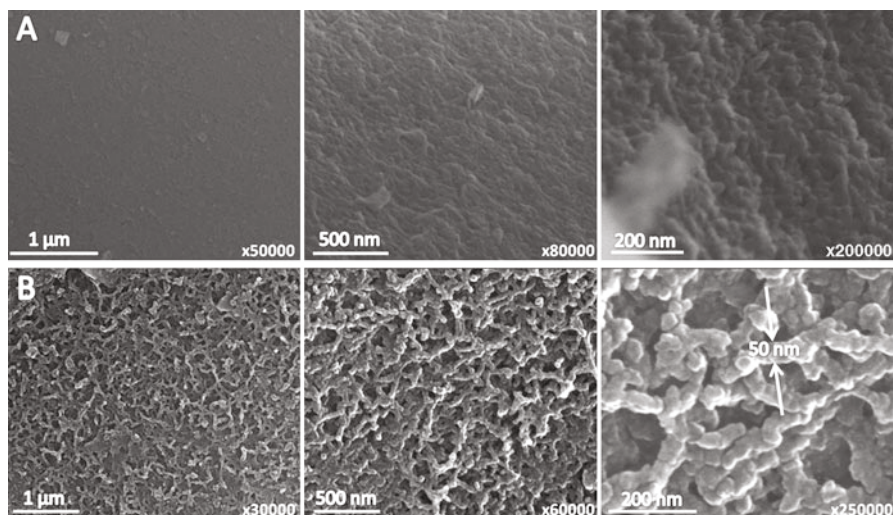


**Fig. 5** SEM images of the BG with GA, before (a) and after (b) immersion in protein solution (Taken from Gruian et al. [30])

EPR line shape will basically consist of a three-line pattern, each arising from one of the three quantum states of the nitrogen nucleus.

The EPR spectrum of spin-labeled proteins can generally be described by the coexistence of two spectral components, related to mobile (*M*) and immobile (*I*) fractions of the spin label side chain (Fig. 6) [28]. The immobile component arises from the EPR signal of a fraction of spin labels engaged in secondary and tertiary interactions which restrict their reorientational freedom (for e.g., having the N–O group hydrogen bonded to the protein). In particular, in horse hemoglobin the immobile component originates from spin labels entrapped in the so-called tyrosine pocket [28] (see Fig. 3). The mobile component corresponds to the signal provided by spin labels that have less constraints in their surroundings and that are exposed to aqueous environment [30].

Upon adsorption on the bioactive glass, for both spin-labeled proteins the equilibrium between the two states is significantly shifted towards component *I*, indicating a conformational change (Figs. 6 and 7). An additional notable feature is the increase of the line width observed for component *I* upon adsorption, observed for both hemoglobin and MnME protein. This line broadening can be explained by assuming that the movement of the entire protein molecule is restricted due to interaction with bioactive glass.

Regarding the influence of the protein coupling agent, in case of horse hemoglobin, the amplitude ratio of both components depends on the surface treatment, as GA reduces the *I/M* component amplitude ratio (cf. inset of Fig. 6). Thereby, when the BG substrate is functionalized with GA, restrictions in the overall spin label mobility are more pronounced, suggesting that the hemoglobin molecule becomes more rigid. This interpretation further fosters the hypothesis of

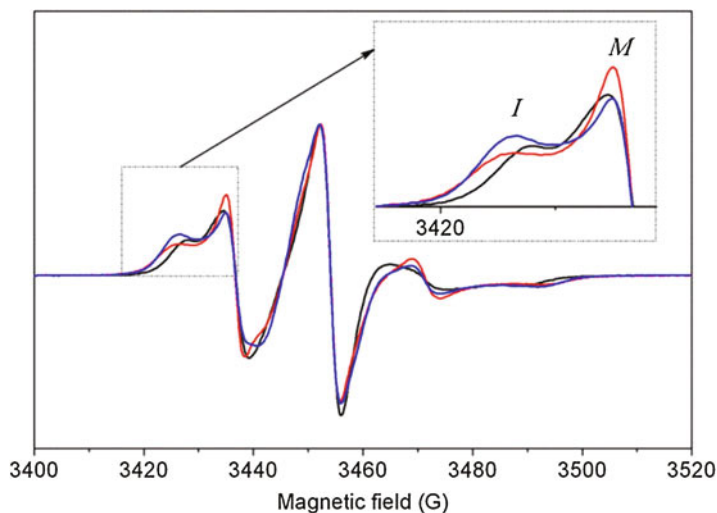


**Fig. 6** Room temperature cw-EPR spectra of horse methemoglobin spin-labeled in position  $\beta$ -93, recorded in solution (black) and in adsorbed state (red: on pristine BG; blue: on GA functionalized BG). *Inset*: The mobile and immobile components visible in the lower field spectral lines are depicted with *M* and *I*, respectively (Taken from Gruian et al. [28])

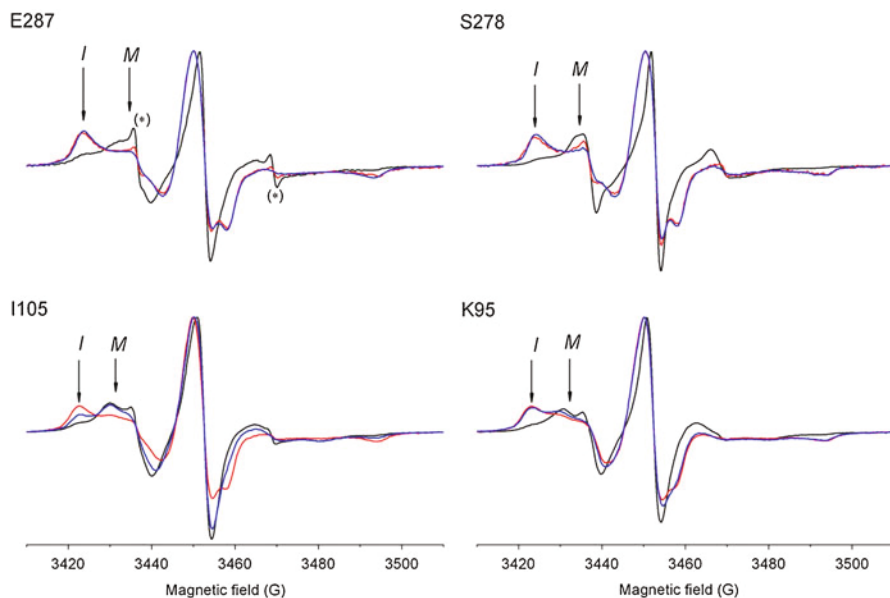


**Fig. 7** Room temperature cw-EPR spectra of the spin-labeled Mn mE mutants E287, S278, I105, and K95 in solution (black) and in adsorbed state (red: on pristine BG; blue: on GA functionalized BG). The mobile and immobile components are indicated by arrows and denoted with *M* and *I* respectively. The peak in the spectrum of E287R1 marked by an asterisk (\*) corresponds to remaining unbound spin label in solution (Taken from Gruian et al. [28])

hemoglobin polymerization on the GA functionalized substrate, which was confirmed also by SEM images (Fig. 5).

The extreme immobilization displayed by the spin labels attached at the two positions on the G domain of the MnmE protein (E287R1 and S278R1) is likely to appear due to direct interaction of this region with the BG surface, suggesting that these two positions may be located close to the contact points of the protein on the BG surface (Fig. 7) [30]. Further information needed to confirm this assumption was obtained from pulse EPR experiments (DEER). By this, it was possible to determine distance distributions between spin labels in native and adsorbed MnmE in order to compare protein dynamics by means of the observed distance distribution widths and to identify possible conformational changes induced in the protein structure upon attachment onto the BG substrate [30].

The DEER analyses of the samples containing MnmE adsorbed on BG revealed that only a very small number of spin label side chains exhibit dipolar interaction, indicating the dissociation of most of the protein dimers involved in the adsorption process. From DEER experiments it was possible to conclude that adsorption onto the pristine BG substrate induces not only dimer dissociation, but in addition domain motions, leading to a conformation where the G domain and the N-terminal domain of the monomers come into closer vicinity after adsorption. These results were schematically depicted in Fig. 8 [30]. The accepted hypothesis was that upon adsorption of MnmE onto the pristine BG (panel B) the dimers dissociate and the resulting monomers rearrange so that the G and N-terminal domains come in contact with the BG surface. These two regions display enhanced interaction with the substrate, since the hydrophobic domains of MnmE are mostly located in the inner parts of its three dimensional structure, which are mainly situated in the G domain and the N-terminal domain of the protein (Fig. 4). It remains questionable if the helical domain spreads onto the surface or if it dangles in solution. Based on the fact that this region displays a mainly hydrophilic surface, one plausible hypothesis would be that it does not interact strongly with the BG. However, the FTIR analysis presented in the following paragraph shows that MnmE loses approximately half of its  $\alpha$ -helical structure upon adsorption on this type of substrate, suggesting that part of the helical structure is also subjected to some interaction with the BG substrate.

Contrarily, a fraction of  $\sim 65\%$  of the protein keeps its dimeric form if the BG surface is functionalized with GA (Fig. 8c). This protein coupling agent seems to mediate the interaction between the protein molecules and the hydrophobic surface of the bioactive glass, leading to a less aggressive interaction between the protein domains and the BG substrates. Nevertheless, DEER results have also shown that the interaction of G domains with the substrate hampers G domain dimerization in the GTP hydrolysis transition state. The large conformational change observed for MnmE in solution upon GTP hydrolysis does not occur when the protein is attached to the functionalized BG substrate, suggesting that the protein is “locked” in the open state as consequence of strong immobilization of both G-domains onto the BG-GA surface.

The samples presented in this section were lyophilized and further analyzed by FTIR and XPS techniques.

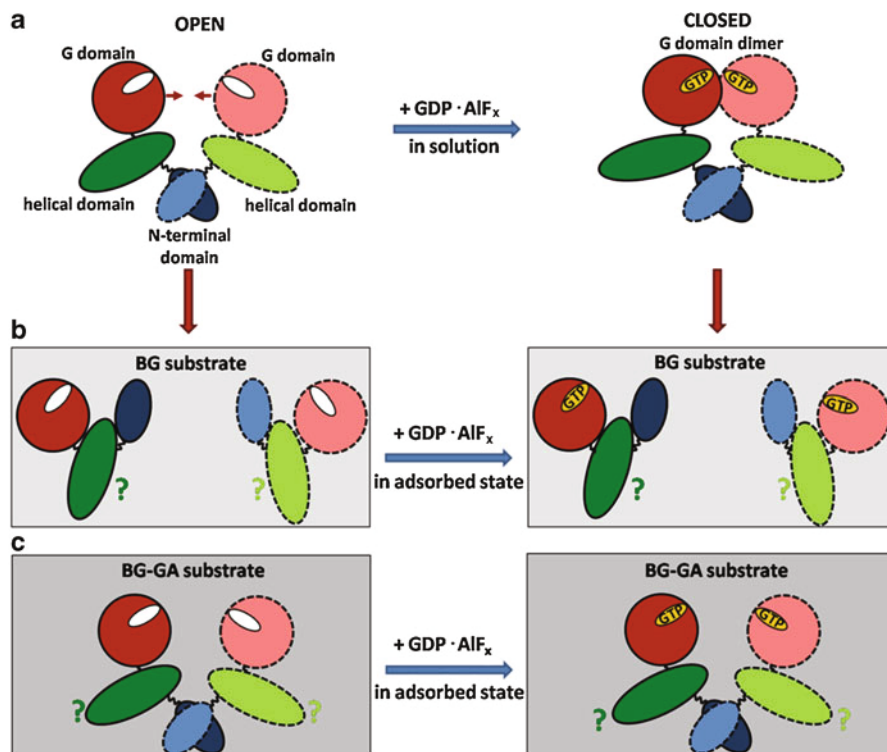


**Fig. 8** Schematic illustration of activation of MnME during GTP hydrolysis in solution and after adsorption on the bioactive glass (*top view*). (a) In solution, the G domains adopt an open conformation in the apo-state and a closed conformation in the GDP · AIF<sub>x</sub> bound-state; (b) Upon adsorption on the pristine BG, the strong interaction between the protein molecule and the BG substrate leads to dimer dissociation; the question marks emphasize that no information is available regarding the helical domain behavior, since no data were recorded for this region of the protein; (c) The protein coupling agent GA mediates the interaction between the protein molecules and the hydrophobic surface of the bioactive glass, so that a fraction of 65 % protein molecules keeps its dimeric form on the GA functionalized substrate. On both substrates, the G-domains are in contact with the BG substrate and, consequently, remain open after addition of GDP · AIF<sub>x</sub> (Taken from Gruian et al. [30])

## Secondary Structure Conformational Changes Investigated by FTIR Spectroscopy

Further information regarding the conformational changes induced in the secondary structure of horse hemoglobin and MnME protein upon adsorption on the BG substrate can be obtained by FTIR spectroscopy. The amide I absorption band is mostly used to extract information about the secondary structure of proteins; therefore we further focused on this region of the FTIR spectra. In the present example, quantitative structural information was obtained from the band position and relative band areas obtained by the deconvolution of amide I region of the protein FTIR

spectra. For this purpose, the baseline of the amide I region was adjusted from 1600 to 1710  $\text{cm}^{-1}$  and then smoothed with a 12-points Savitsky–Golay smooth function to remove the white noise. Finally, Gaussian peak analysis of the amide I band was performed to analyze the secondary structure of both proteins before and after adsorption on BG. Peak locations were determined by second derivative analysis and correlated with values found in previously published studies [33]. The area under each peak was considered to calculate the fraction of each component and the secondary structure composition.

For both proteins adsorbed on the nonfunctionalized BG substrate, the characteristic signal of the amide I band was found to be shifted from  $\sim 1655 \text{ cm}^{-1}$  to  $\sim 1649 \text{ cm}^{-1}$ , on the account of the water contained by BG substrate [34]. However, the main frequencies for each amide I subband obtained from Gaussian deconvolution are within the values found in the literature [33, 35]. As an example, the amide I deconvolution for MnmE protein is presented in Fig. 9 [33]. Briefly, in the amide I region, the components obtained in the 1640–1620  $\text{cm}^{-1}$  and 1700–1693  $\text{cm}^{-1}$  intervals are assigned to  $\beta$ -sheet, the ones between 1660 and 1650  $\text{cm}^{-1}$  to the  $\alpha$ -helix structure, and between 1690 and 1660  $\text{cm}^{-1}$  to  $\beta$ -turn structure (Fig. 9). The small component that appears around 1618  $\text{cm}^{-1}$  arises from primary amino acid side chain vibrations. These correlations have also been extended to adsorbed proteins [33]. Hemoglobin represents a special case, because it is an  $\alpha$ -helical protein (86 % helix, according to X-ray crystallography) and contains no  $\beta$ -sheets. The small peaks at about 1628, 1639, and 1694  $\text{cm}^{-1}$ , can therefore be assigned to the short loops connecting the helices [33, 43].

Upon adsorption to the nonfunctionalized BG surface, one additional peak centered at 1648  $\text{cm}^{-1}$  appears for both proteins, originating from random structure (Fig. 9). Also, the major bands at 1656 and 1654  $\text{cm}^{-1}$ , assigned to  $\alpha$ -helix structures in the native methemoglobin and MnmE, are shifted to higher wavenumbers. The higher band position corresponds to weaker hydrogen bonding [33], leading to more flexible helices, as a consequence of the interaction between the proteins and bioactive glass. Both proteins lose approximately half of the  $\alpha$ -helical structure after adsorption on this type of substrate (see Table 2). It was assumed that, during the adsorption process, a predominant fraction of  $\alpha$ -helical structure unfolds, and it is mainly transformed into loop and random structures, suggesting that the proteins are partly denatured. At the same time, for methemoglobin a concurrent increase in  $\beta$ -turns, loops, or random structure components can be observed (Table 2). In MnmE the fraction of  $\beta$ -sheet structure appears to be much higher after adsorption than in the native protein (Table 2), and for this increase two possible reasons have to be considered: (1) appearance of additional loops and turns that occur at similar wavenumbers [43] and (2) minor contributions originating from the BG substrate (at  $\sim 1636 \text{ cm}^{-1}$ ). In fact, adsorption on hydrophobic surfaces may lead to disruption of hydrogen bonding within  $\beta$ -sheets, so being transformed into more flexible structures. Thereby, the 1632–1634  $\text{cm}^{-1}$  region might be the result of  $\beta$ -sheet turn and loop structure overlapping [33, 43, 44]. This assumption is also supported by the low expression of MnmE amide II, which indicates a severe aggregation of the  $\beta$ -sheet type



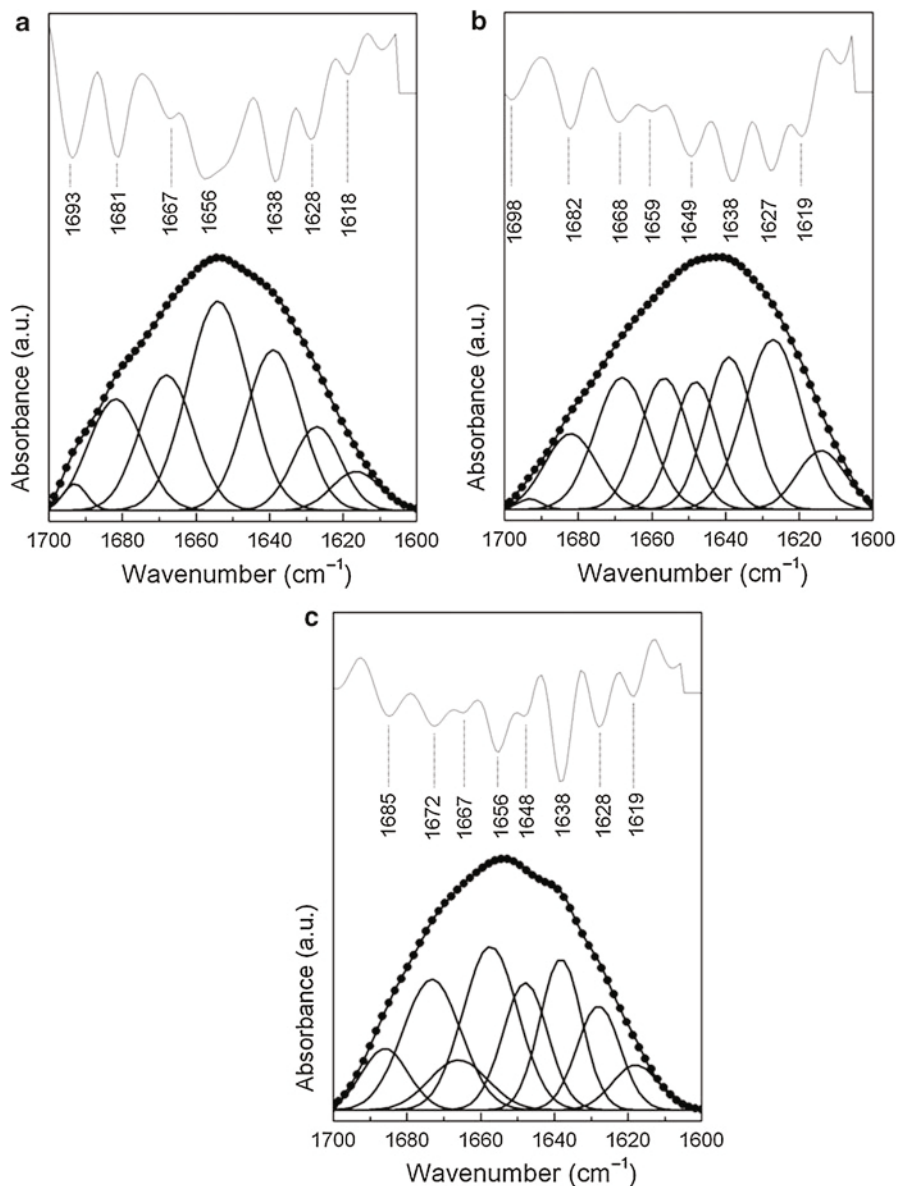


**Fig. 9** Separation of the amide I band into its component bands, for (a) lyophilized MnmE, (b) MnmE coated BG and (c) MnmE coated BG functionalized with GA. The *dots* represent the sum of the separated band components. The second derivative spectrum, denoting the positions of each peak, is shown above. The errors are estimated to  $\pm 1 \text{ cm}^{-1}$  for the band positions and  $\pm 5 \%$  for the peak areas (Taken from Gruian et al. [30])

**Table 2** Distribution of secondary structure elements in lyophilized proteins, protein-coated BG and protein-coated BG functionalized with GA for both horse hemoglobin and MnME. The uncertainty due to experimental and fitting procedure is within the limit of  $\pm 5\%$  [33]

	$\alpha$ -helix (%)	$\beta$ -sheet/loop/turn (%)	$\beta$ -turn (%)	Random (%)	Side-chain (%)
<b>Hgb</b>	77.1	11.1	9.6	0	2.2
<b>Hgb on BG</b>	36.7	34	15.1	10.4	3.8
<b>Hgb on BG-GA</b>	43.9	27.2	21.3	4.8	2.8
<b>MnME</b>	30.7	32.7	32	0	4.6
<b>MnME on BG</b>	14.9	39.5	25.8	13.3	6.5
<b>MnME on BG-GA</b>	21.9	26.4	32.7	5.2	13.8

structure. For both proteins, the change in conformation may arise from a strong interaction with the nonfunctionalized BG surface, a feature that has been previously reported for other proteins on this type of substrate [20, 45].

As a protein coupling agent, it is expected that GA maintains almost completely the native protein structure. The deconvolution of amide I band revealed that both proteins lose a smaller percentage of  $\alpha$ -helix structure when the BG is functionalized with GA (Table 2), confirming that the stability toward denaturation is higher on this substrate. However, the increase of the disordered structures ( $\beta$ -turn and random) toward more stable elements, like  $\alpha$ -helices or  $\beta$ -sheets, assumes a certain denaturation of both proteins even when the bioactive glass is functionalized with GA. This is another proof that protein adsorption implies strong interactions with the BG surface, which in turn can disrupt the hydrogen bonds involved in stabilization of  $\alpha$ -helices located at the outer parts of both proteins.

## Surface Coverage Explored by XPS

By XPS analysis it is possible to determine the elemental composition of the outermost layer (10 nm depth) in the presence and absence of horse hemoglobin and MnME. Usually the protein attachment on surfaces involves the evaluation of nitrogen and carbon, oxygen and nitrogen as key elements for protein identification [13].

In order to evaluate the uptake of proteins on bioactive glass surface, survey and C 1 s, N 1 s, and O 1 s high resolution spectra were examined. Table 3 shows the XPS elemental composition of the pristine and surface-modified bioactive glass. As expected, silica, calcium, phosphorus, sodium, oxygen, and carbon were detected on the surface of pristine bioactive glass. Carbon is ubiquitous and is detected on all samples exposed to the atmosphere. It is a common practice to use the carbon C 1 s peak at 284.6 eV as reference for charge compensation [13, 37, 45].

**Table 3** Elemental composition of bioactive glass before and after surface modification with methemoglobin [33]

Sample	Elemental composition (at %)							
	Si	Ca	P	Na	C	O	N	S
<b>MetHb</b>	–	–	–	–	64.8	18.4	16.7	0.1
<b>MnmE</b>	–	–	–	–	72	19	8.9	0.1
<b>BG</b>	32.6	5	2.3	1.4	5.6	53	–	–
<b>MetHb on BG</b>	16.9	3.8	3.7	0.6	28.2	42.4	4.3	–
<b>MnmE on BG</b>	15.3	8.5	6.7	1	19.1	47.1	2.2	–
<b>BG-GA</b>	18	2.9	1.5	–	40.5	33.6	3.4	–
<b>MetHb on BG-GA</b>	5.8	2.1	1	0.1	58.1	21.4	11.5	–
<b>MnmE on BG-GA</b>	11.08	1.72	0.6	–	52.6	26.9	7.1	–

Upon immersion in protein solutions, the nonfunctionalized bioactive glass surface became coated with proteins, as evidenced by the significant increase of carbon and nitrogen contents, which are considered indicators of protein adsorption (Table 3). The C 1 s high resolution spectra (Fig. 10) appear more intense, broadened, and asymmetric, indicating the presence of new types of carbon bonds [13, 37, 45]. The C 1 s photoelectron peaks were deconvoluted according to binding energies of carbon bonds in proteins (Fig. 10) [33]. For BG, the C 1 s photoelectron peak is well fitted with two lines centered at 284.6 eV and 289.4 eV, attributed mainly to the carbon from carbonate used as precursor for sample preparation (Fig. 7a). After protein attachment, the C 1 s peaks are well decomposed with one main component at 284.6 eV, corresponding to C–C and C–H bonds, and an additional component at 287.5 eV, containing contribution from both NH–CHR–CO and –C(=O)–NH<sub>2</sub> bonds [33]. The component at lower binding energies, around 281 eV, may appear due to inappropriate charge correction.

On APTS/GA functionalized surface, increases in carbon, silicon, and nitrogen were detected (Table 3), as expected, since APTS and GA include these three elements. Thus, the contribution of calcium, phosphorus, and sodium was less obvious, while the amount of carbon, nitrogen, and silica (40.5 % C, 3.4 % N and 18 %, respectively) is much higher, proof of surface functionalisation. After protein adsorption, the C 1 s peaks are well decomposed (Fig. 10) [33] with components at 284.6 eV, assigned to C–C and C–H bonds, at ~287 eV, corresponding to NH–CHR–CO bonds, and the component around 288 eV, corresponding to –C(=O)–NH<sub>2</sub> peptide carbons [33]. On the GA functionalized BG it was also observed a shift of O 1 s photoelectron peak from 532.5 eV to lower binding energies, 531 eV for methemoglobin and 531.6 eV for MnmE, on the account of the oxygen recorded for the two proteins. The results obtained from O 1 s photoelectron peaks suggest that the O 1 s photoelectrons correspond significantly to peptidic oxygen of proteins [13]. From the XPS survey data, it was also evidenced a significantly decrease of the silica, calcium, phosphorus, and sodium content, due to the denser layer of protein formed on the GA functionalized substrate (Table 3).

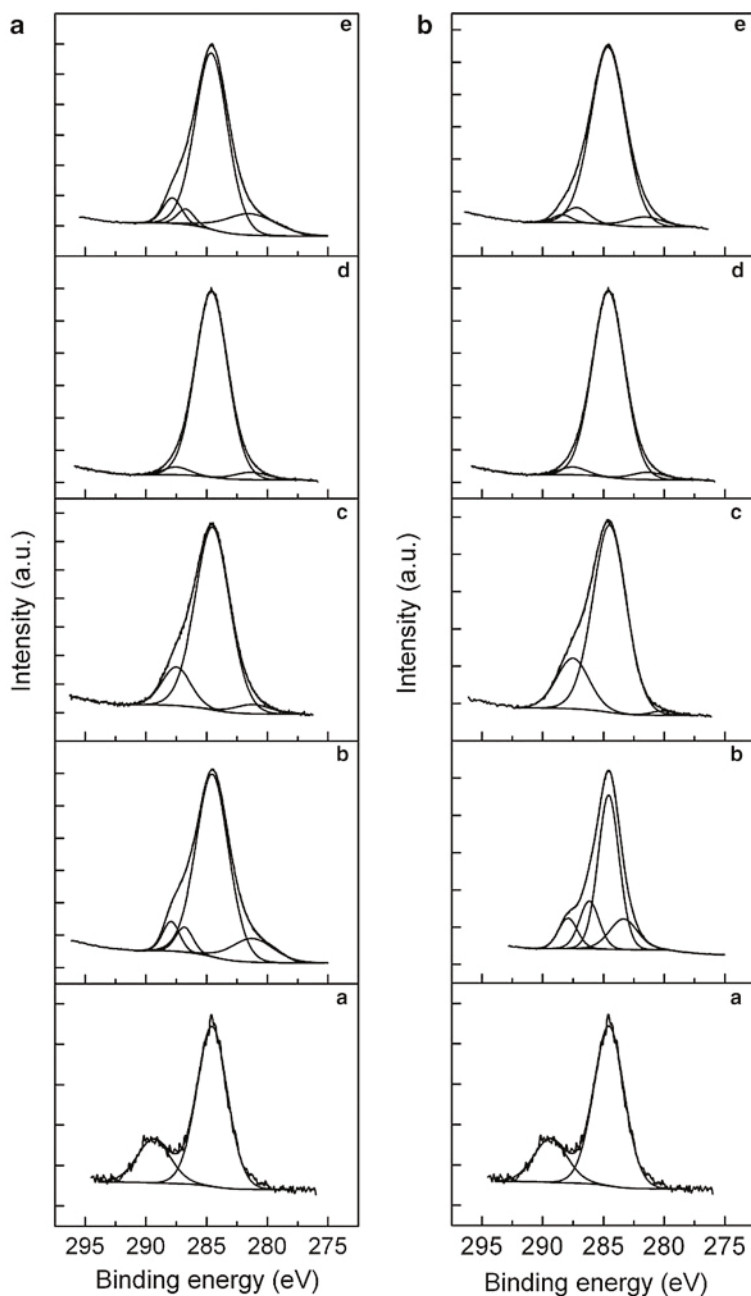


**Fig. 10** Deconvolution of XPS C 1s high resolution spectra of (a) BG, (b) lyophilized protein, (c) protein coated BG, (d) BG functionalized with GA, and (e) protein coated BG functionalized with GA. (a) Horse methemoglobin, (b) MnME (Taken from Gruian et al. [33])

## Protein Adsorption on Aluminosilicate Glass Ceramics Designed for Radiotherapy and Hyperthermia

The second example presented in this chapter describes the interaction between albumin/fibrinogen and biocompatible aluminosilicate systems containing yttrium, which could be used for hyperthermia and radiotherapy applications. For this purpose, The  $60\text{SiO}_2 \cdot 20\text{Al}_2\text{O}_3 \cdot 10\text{Y}_2\text{O}_3 \cdot 10\text{Fe}_2\text{O}_3$  (mol%) system was prepared by sol–gel method. After room temperature drying, it was heat treated at  $1200\text{ }^\circ\text{C}$  for 24 h, milled, and sieved to obtain particles  $<60\text{ }\mu\text{m}$  in size. Protein adsorption experiments were carried out by incubating the microspheres in simulated body fluid (SBF) prepared according to Kokubo composition [46] enriched with bovine serum albumin (BSA, 1 mg/ml), and in fibrinogen (FBR) solutions prepared in phosphate–buffered saline solution (PBS, pH 7.2, 2 mg/ml). After the desired adsorption time was reached, the samples were rinsed a few times with ultra pure water and then filtered, to ensure that any nonadsorbed protein molecules were removed. The samples were immersed in simulated biological media at  $37\text{ }^\circ\text{C}$  for different time intervals (5 min, 2 h and 24 h), under static conditions. The in vitro proteins adsorption was investigated by means of XPS analyses.

The X-ray diffraction patterns recorded for the investigated system indicated that the dried sol–gel sample is noncrystalline, but the  $1200\text{ }^\circ\text{C}$  heat treatment determines the development of  $\text{SiO}_2$  cristobalite and quartz [13],  $\text{Al}_6\text{Si}_2\text{O}_{13}$  mullite,  $\text{Fe}_2\text{O}_3$  hematite, and  $\text{Fe}_3\text{O}_4$  magnetite nanocrystals. Crystallite sizes estimated with the Scherrer equation according to the position and width of XRD peaks are up to 35 nm. The nanostructure is important because the protein adsorption is influenced by the crystallite size, in the sense that smaller crystallites are responsible for better protein absorption [13].

The XPS survey spectra recorded before and after immersion indicate that a decrease of silicon, aluminum, iron, and yttrium photoelectron peaks intensity occurred after immersion in protein solutions, that is due to the layer of protein adhered on the sample surface. The analysis of the survey spectra indicates N 1 s peaks occurring from the amino acids of the protein. The XPS results on nitrogen concentration (Table 4) can be interpreted as an indirect measure of the protein content [13]. The nitrogen concentration was practically null before the immersion of the sample in the protein solutions, so it can be used as a reliable marker for protein adsorption. At the same time, the N:C ratio is typically used as indicator of protein deposition. The N:C ratios of 0.2 and 0.25 established already after 5 min immersion time denote the quick attachment of BSA and FBR, respectively, on the microparticles surface (Table 4).

The XPS analysis indicates a sensible increase of nitrogen content by increasing the incubation time up to 24 h, with more nitrogen detected on the surface of the sample immersed in fibrinogen solution than on the surface of the sample immersed in BSA solution. The larger-sized fibrinogen protein (340 kDa), as compared with BSA (66.4 kDa), produces a higher nitrogen signal than the smaller-sized protein. This is because the larger protein molecule has more nitrogen atoms in XPS

**Table 4** Elemental composition on microparticles surface before and after immersion in SBF/BSA and PBS/FBR solutions [13]

Immersion time	Elemental composition (at %)													
	C		N		O		Al		Si		Fe		Y	
	SBF/ BSA	PBS/ FBR	SBF/ BSA	PBS/ FBR	SBF/ BSA	PBS/ FBR	SBF/ BSA	PBS/ FBR	SBF/ BSA	PBS/ FBR	SBF/ BSA	PBS/ FBR	SBF/ BSA	PBS/ FBR
<b>0</b>	6.9	43.1	–	10.7	53.1	2.3	36.8	0.2	0.2	0.7	–	–	–	–
<b>5 min</b>	28.4	51.8	5.7	11.5	37.7	2.2	25.4	0.1	15.9	0.1	0.1	0.1	0.5	0.2
<b>2 h</b>	28.9	48.6	6.4	13.5	37.2	1.7	25.2	0.1	13.0	0.1	0.1	0.1	0.5	–
<b>24 h</b>	33.2	–	6.7	–	35.2	1.5	23	–	10.0	–	–	–	0.4	–

sampling depth, thus the size of the protein needs to be taken into account for quantifying the number of adsorbed protein molecules [47].

According to previously published results on proteins adsorption, 14 at.% nitrogen in case of fibrinogen is an indicative that a full protein monolayer is formed [47]. With respect to fibrinogen adsorbed onto investigated aluminosilicate microparticles, the 13.5 at.% nitrogen content on the sample surface after 24 h of immersion in protein solution denotes the self-assembling of the protein in a monolayer. The N 1 s XPS signal can also be used to obtain quantitative information on the number of the attached protein molecules, based on normalized surface coverage, expressed as product of at% nitrogen and the normalising factor given by the ratio of compared proteins mass weight [13, 47]. In this approach, the number of the adsorbed protein molecules on a given substrate correlates with the size of the proteins. On the surface of the investigated microparticles, after 24 h, the number of BSA molecules is about 2.5 times higher than that of fibrinogen.

The deconvolution of the O 1 s core level spectra recorded before exposure to protein solutions shows a dominant component at 533.2 eV, and a second component at 531.5 eV, which are related to bridging oxygens (BO) and, respectively, nonbridging oxygens (NBO) occurring in the structural units of the aluminosilicate microparticles (Fig. 11) [13]. The connection type of oxygen atoms is important for biomaterials because the BO/NBO ratio influences their structure and stability in biological media [13]. Based on the preponderance of BO relative to NBO in the nanostructured aluminosilicate microparticles, they are expected to own a high stability in biological media.

After immersion in protein solutions, the O 1 s photoelectron peaks are evidently broader (Table 5) and shifted to lower binding energies, mainly on the account of the BSA component located at 530.3 eV, respectively of fibrinogen component located at 531.2 eV (Fig. 11). The results obtained by deconvolution of O 1 s photoelectron peaks suggest that the O 1 s photoelectrons correspond significantly to peptidic oxygen of proteins [13, 37]. At the same time, diminished oxygen content is detected on the microparticles surface for increasing immersion periods (Table 4), because after incubation in protein solutions the outmost layer consists in the attached BSA or FBR protein of lower oxygen content than that of the aluminosilicate bare sample.

In the particular case of peptides and small proteins attached on Si-based surfaces, the thickness of the protein layer can be estimated from the attenuation of the Si 2p signal [48]. This approach is not applicable for the BSA and FBR molecules, since these are large-size proteins, but it will be exemplified on the insulin molecule, in the following section.

---

## **Protein Loading on Si-Based Glass-Ceramics Designed for Drug Delivery**

### **Loading Procedure: Adsorption**

Porous silica particles are considered attractive drug carriers with properties enabling the control of drug release due to their high surface area, uniform pore diameter, and high chemical stability and adsorption capabilities. Increased or sustained release of

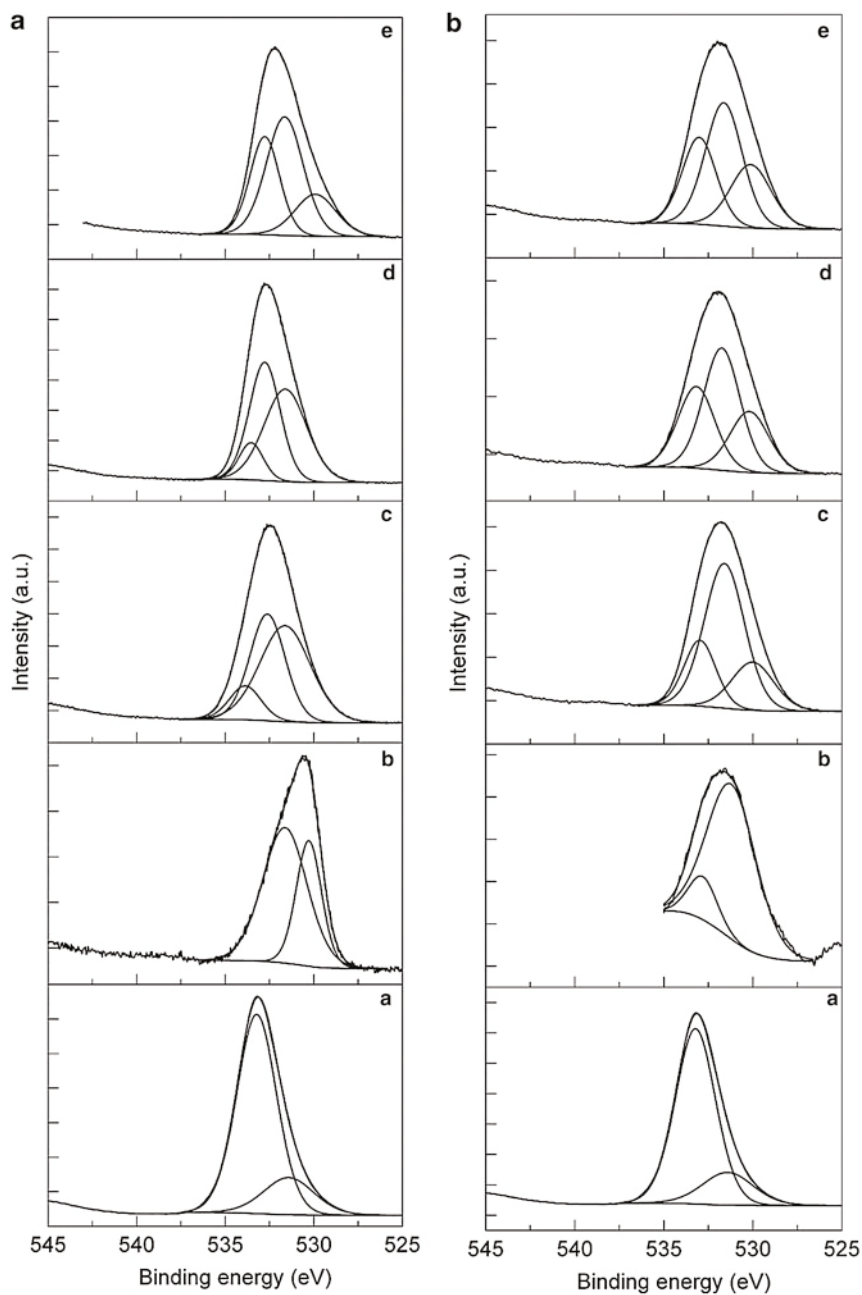


**Fig. 11** Deconvoluted O 1s high resolution XPS spectra of bare particles (a), lyophilised BSA and FBR (b), and of protein coated particles after 5 min (c), 2 h (d) and 24 h (e) immersion in solutions of SBF/BSA (column a) and PBS/FBR (column b) (Taken from Gruian et al. [33])



**Table 5** O 1 s full width at half maximum (FWHM) for different immersion periods in SBF/BSA and PBS/FBR solutions [13]

Immersion time	FWHM (eV)	
	BSA	FBR
<b>0</b>	2.9	2.9
<b>5 min</b>	3.3	3.6
<b>2 h</b>	3.0	3.8
<b>24 h</b>	3.2	3.8

the loaded drug can be regulated by the surface chemistry and the size of the pores [45]. As an example, the loading capacity of insulin in Si-Zn microparticles with different porosity of a zinc-containing silica matrix intended for insulin oral administration will be presented. The sol-gel synthesis was combined with freeze-drying and spray-drying methods to produce microparticles with different porosity. X-ray photoelectron spectroscopy (XPS) was employed to determine the changes induced on surface of the zinc-silica compounds by insulin embedment and to compare the amount of insulin adsorbed as a function of sample porosity.

The production of a drug delivery system to facilitate the oral administration of insulin is highly desirable and research to find new insulin formulations and new routes of administration continues. Amorphous silica (SiO<sub>2</sub>) is nontoxic and highly compatible with biological systems, and ZnO confers good stability to the systems at low pH values and preserves the insulin sensitive 3D structure by intermediating hexamer formation [45]. In the present example, amorphous Zn containing silica compounds with the composition of 80SiO<sub>2</sub> · 20ZnO (mol%) were synthesized by sol-gel method, and afterwards three different drying procedures were applied [45]:

- Part of it was spray dried with a Buchi Mini Spray Dryer B-290 – will be further named as SiZn-SD
- Part of it was left to gel undisturbed at room temperature – will be further named as SiZn-SG
- Part of it was poured in cryovials, designed to resist at temperatures as low as –196 °C, left also to gel at room temperature; afterwards, the cryovials were completely immersed for 30 min in liquid nitrogen, and then allowed to return to room temperature over night – will be further named as SiZn-FD.

Both solutions that were allowed to gel at room temperature appeared to be completely gelled into a homogeneous transparent matrix after 24 h. Both unfrozen and freeze dried gels were heated at 110 °C and then grounded to a fine powder. For the insulin loading procedure the samples were immersed for 4 h at 37 °C in sodium phosphate buffer solution (PBS) enriched with bovine insulin (10 mg/mL). After soaking, the filtered powders were rinsed a few times with ultra pure water to ensure that any nonadsorbed insulin molecules were removed. The samples were air-dried at 37 °C for 24 h before their investigation. The insulin loaded microparticles were correspondingly named: SiZn-SD-INS, SiZn-SG-INS, and SiZn-FD-INS.

The BET surface area and the mean pore volume were determined in order to evaluate the materials porosity features that will define further the loading

characteristics of the samples. Table 6 presents the BET specific surface area and mean pore volume values corresponding to zinc-silica microparticles before insulin loading. A significant difference in specific surface area and the mean pore volume can be observed for the three samples. The highest value was recorded for the freeze dried sample, as a consequence of the freezing procedure that involves favorable conditions to obtain a high porosity. The liquid nitrogen freezing procedure is believed to preserve the open polymeric structure of the gel leading to high surface area powders [45]. On the other hand, the BET measurements evidence for the microspheres very small values for both surface area and pore volume. The spray drying process parameters are found to produce spherical particles with smooth or nonporous surface.

The XPS survey spectra and the elemental percentages of the main elements occurring on samples surface before and after insulin loading (Table 7) are similar for SiZn-SG and SiZn-FD samples, while for the spray dried SiZn-SD sample a significant amount of zinc is recorded on its surface in detriment of silicon. The successful insulin loading was proven by changes in the measured atomic ratios of the insulin formulations as presented in Table 7.

Silicon was used as reference element, since its chemical environment should not be affected by the loading procedure (Fig. 12) [45]. A significant intensity decrease is observed in Si 2p high resolution spectra recorded from the insulin formulations that proves changes due to surface coverage by the protein. Both C:Si and N:Si ratios are higher than for the host samples, and highest value was determined for the freeze dried formulation, that was expected according to its higher surface area.

The high resolution spectra recorded for Zn 2p (Fig. 13) [45] show for the insulin formulations a slight decrease of intensities due to the surface coverage by insulin,

**Table 6** BET specific surface area and mean pore volume of zinc-silica particles [45]

Sample	BET surface area ( $\text{m}^2/\text{g}^{-1}$ )	Pore volume (ml/g)
<b>ZnSi-SG</b>	160	0.201
<b>ZnSi-FD</b>	235	0.246
<b>ZnSi-SD</b>	1.66	0.066

**Table 7** XPS data: elemental composition, atomic ratios, and insulin overlayer thickness [45]

Sample	Elemental composition (at %)								Insulin thickness (nm)
	Si	Zn	C	O	N	S	C:Si	N:Si	
<b>Native insulin</b>	–	–	70.8	15	12.7	1.5	–	–	–
<b>ZnSi-SG</b>	31.6	2.0	4.8	60.8	0.7	–	0.15	0.02	–
<b>ZnSi-SG-INS</b>	18.1	1.3	28.4	44.6	7.5	–	1.56	0.41	4.89
<b>ZnSi-FD</b>	32.2	2.4	2.7	60.6	2.0	–	0.08	0.06	–
<b>ZnSi-FD-INS</b>	12.0	1.3	39.9	37.3	9.4	–	3.32	0.78	5.9
<b>ZnSi-SD</b>	22.6	5.1	16.3	51.1	4.8	–	0.72	0.21	–
<b>ZnSi-SD-INS</b>	18.4	1.2	31.8	42.2	6.4	–	1.72	0.34	4.03

**Fig. 12** XPS Si2p high resolution spectra of zinc-silica microparticles before (*black lines*) and after (*gray lines*) insulin loading – SiZn-SG (*a*), SiZn-SG-INS (*b*), SiZn-FD (*c*), SiZn-FD-INS (*d*), SiZn-SD (*e*) and SiZn-SD-INS (*f*) (Taken from Vanea and Simon [13])

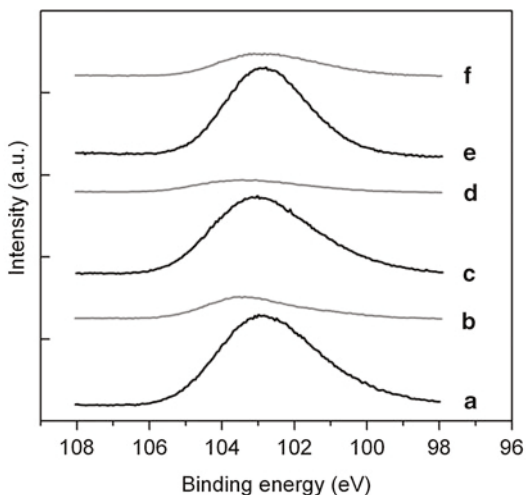
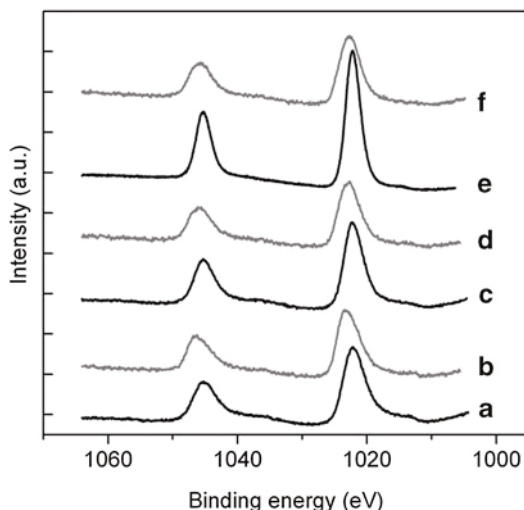


**Fig. 13** XPS Zn 2p high resolution spectra of zinc-silica microparticles before (*black lines*) and after (*gray lines*) insulin loading – SiZn-SG (*a*), SiZn-SG-INS (*b*), SiZn-FD (*c*), SiZn-FD-INS (*d*), SiZn-SD (*e*) and SiZn-SD-INS (*f*) (Taken from Vanea and Simon [45])



but at the same time a shift of the binding energy to higher values is noticed. This shift suggests the involvement of zinc in a new type of bond that may be attributed to the hexameric form of insulin developed with zinc ions released in solution during the loading procedure or later.

The thickness (*d*) of the immobilized insulin overlayer was estimated from the attenuation of the Si 2p signal [48]. Briefly, the calculations were performed considering the following equation:

$$A = A^0 \exp^{-\left(\frac{\lambda}{d}\right)}$$

where  $A^0$  represents the Si 2p under the peak area before insulin loading,  $A$  represents the Si 2p under the peak area after insulin loading, and  $\lambda$  represents the calculated mean free path correlated to the kinetic energy (KE) of the Si 2p following the equation:

$$\lambda = B(KE)^{\frac{1}{2}}$$

where  $B = 0.087$  nm for organic materials.

The thickness of insulin overlayer determined as mentioned above are displayed in Table 7. A layer of 5.9 nm was computed for the freeze dried sample, and of 4.89 nm for the unfrozen sample. Considering the low values determined for surface area and pore volumes of spray dried microspheres (Table 6), the insulin overlayer thickness of 4.03 nm is quite large. The XPS results point out a consistent amount of insulin on the surface of the microspheres. The insulin affinity towards this formulation can be explained by the presence of zinc in considerable amount on the surface of the microspheres that leads to an increased stability of the attached insulin.

### **Loading Procedure: Encapsulation**

In the field of drug delivery systems for therapeutic proteins, the encapsulation method enables the preservation of a native protein structure during preparation, storage, and release to ensure persistent functional integrity. The sol–gel polymerization procedures seem to be suitable for developing such drug delivery systems, since this technique enables the synthesis of nanostructured particles with homogeneous protein distribution and permits ambient temperature processing necessary for the manipulation of proteins [15]. As final example of interaction between proteins and solid surfaces, the encapsulation of spin-labeled insulin into silica matrix using the sol–gel procedure will be presented, aiming to monitor insulin dynamics and local structure during the sol to maturated-gel transition by SDSL-EPR and FTIR spectroscopies.

The silica matrix should isolate individual biomolecules preventing aggregation and protein denaturation caused by the restriction of the protein movement within the matrix [15]. During the gelation process, a hydrated porous silica matrix (pores size typically <10 nm in diameter) is formed around individual proteins, with inter-pore connections that allow the exchange of solvent while inhibiting the migration of large molecules such as proteins. The conventional sol–gel method is generally not suitable for the encapsulation of proteins due to a very low pH in the media and a high concentration of alcohol released as a hydrolysis reaction product. Both may lead to protein inactivation or denaturation. Insulin is a protein whose structure should not be affected by acid environment or by the presence of alcohol. However, in order to complete the condensation reaction, the gel has to be aged in the wet state. During this aging process, network shrinkage occurs that may lead to a loss of up to 20 % of protein activity. The gel can be kept in wet or dried state, but drying has to be performed in a conservative manner to avoid denaturation of

biomolecules. The vicinity of sol-gel encapsulated proteins is significantly different from the native environment, which requires monitoring possible changes of conformation and conformational dynamics [15].

Insulin is a small protein (5.808 kDa) composed of two polypeptide chains referred to as A and B chains. The native protein has six cysteines involved in three disulfide bridges: two of them cross-link chains A and B and the third one links two cysteine residues within the A chain. Two of the six cysteines are inaccessible for the spin labels, and the other four cysteines were spin labeled with IAASL [15].

Cw- and pulse-EPR methods were combined to monitor the spin labels mobility and to determine the distances between spin labels in native, denatured, and released insulin. By comparing the EPR spectra before and after encapsulation, small differences in spin label mobility could be observed (Fig. 14a) [15]. These changes can be interpreted as insulin structural modifications following the process of encapsulation. The insulin EPR spectrum recorded in PBS shows a high degree of mobility for all attached spin labels, whereas the spectrum of encapsulated insulin shows the superposition of at least two spectral components, indicating the presence of two distinct spin label species characterized by two different mobilities: one associated with fast motion (the mobile component) and the other one assigned to immobilized spin labels (the immobile component). The weight of the immobile component was estimated to increase from 5 % in PBS to 29 % in silica-gel. This increase was attributed to the constraints induced in insulin movement by the pore walls of the silica network.

Besides these changes associated with protein immobilization, the cw-EPR spectra of encapsulated INS-IA and INS-RX show only minor changes with respect to the native insulin, suggesting that unfolding and denaturation did not occur to a significant amount (Fig. 14a). This information is of utter importance for protein drug delivery carriers, since denaturation or aggregation can have negative effects on the protein activity. To test this hypothesis, the IA spin-labeled insulin was heat-denatured by incubation at 90 °C for 5 h, under continued stirring (250 rpm). As shown in Fig. 15b [15], significant changes in the mobility of spin labels can be observed upon protein denaturation.

Additional changes for INS-IA induced by the release process were studied using both cw-EPR and DEER spectroscopy. The increase in mobility observed in the cw-EPR spectrum and the additional small peak in the distance distribution curve of released insulin when compared to the native sample are both indicators of minor changes of the insulin conformation upon release (Fig. 14b). These changes are, however, insignificant in comparison to the temperature-denatured insulin [15].

The DEER traces also contain information concerning the protein distribution within the silica-gel. Based on the slope of the DEER traces, it was shown that intermolecular contributions are significantly reduced when insulin is encapsulated. This clearly indicates that insulin molecules are well separated within the matrix, being entrapped within the pores of the silica network. This assumption was sustained by the specific surface area ( $\sim 546 \text{ m}^2/\text{g}$ ) and the mean pore volume ( $\sim 1.13 \text{ cm}^3/\text{g}$ ) of lyophilized silica matrix entrapping insulin. The pore size distribution was found to be relatively narrow, with pore diameter as small as 2 nm and as

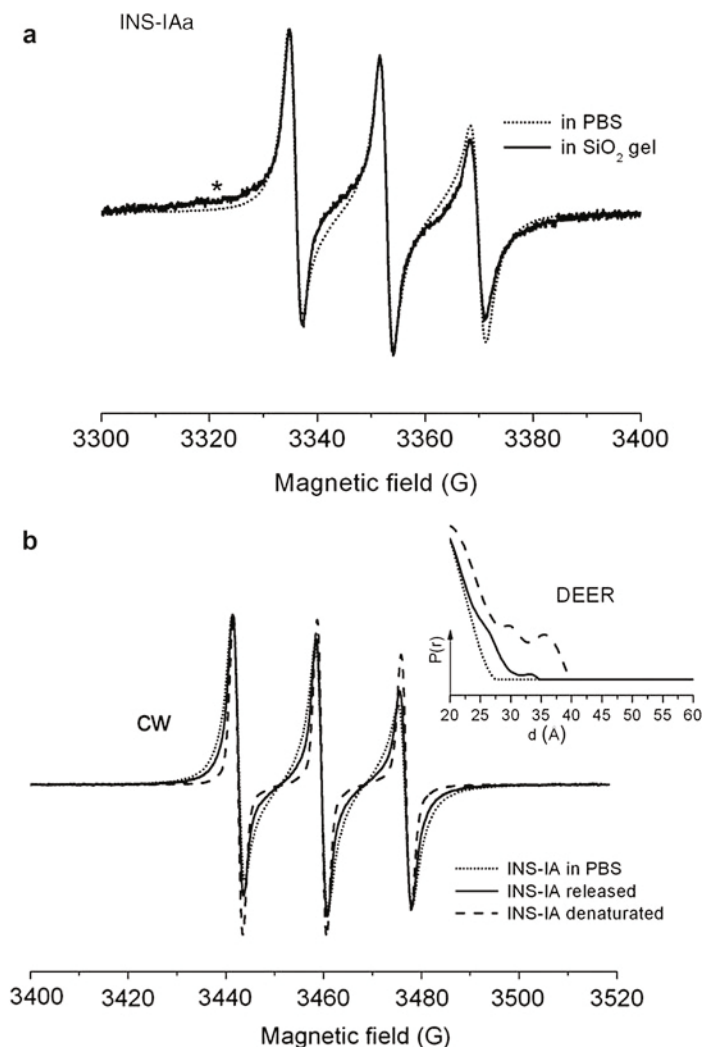


**Fig. 14** (a) Superposed cw-EPR spectra recorded at room temperature for the IA spin-labeled insulin in phosphate buffer pH 8.2 (*dotted line*) and encapsulated in silica-gel (*solid line*). The *star* indicates the immobile component of the EPR spectrum. (b) The room temperature cw-EPR spectra of IA spin-labeled insulin in PBS (*dotted line*), after release (*solid line*), and after denaturation (*dashed line*). The *inset* shows the distance distribution curves of the same samples obtained by analysis of the DEER data (Taken from Vanea and Simon [45])

large as 25 nm, which suggests that pores formed around the biomolecules. This proves that the silica gel was formed around protein with the protein acting as template (Fig. 15) [15].

The secondary structure of the insulin encapsulated silica particles was also evaluated by exploring the FTIR amide I band ( $1600\text{--}1700\text{ cm}^{-1}$ ). The content of

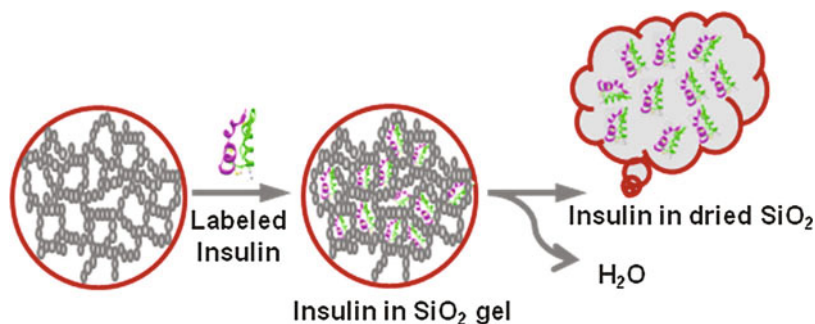


**Fig. 15** Schematic illustration of insulin entrapment within the silica gel matrix (Taken from Vanea et al. [15])

**Table 8** Distribution of secondary structure in native insulin and an insulin-encapsulated silica matrix in the dried state. The uncertainty due to experimental and fitting procedure is within the limit of  $\pm 1$  % [15]

	Secondary structure (%)		
	$\alpha$ -helix	$\beta$ -sheet	Random
<b>INS</b>	42	27	31
<b>INS in silica</b>	41	29	30

$\alpha$ -helices was considered for secondary structure examination, since this structure is invariable when the sample is lyophilized [15]. The results indicate that the insulin structure was only slightly altered after association with the silica matrix (Table 8). The two samples have almost the same  $\alpha$ -helix content ( $41 \pm 1$  %), which is consistent with previously published studies [15, 49, 50]. The increase in  $\beta$ -sheet content (from 27 % to 29 %) can be explained by the intermolecular  $\beta$ -sheet formation, in this case, representing the small amount of insulin spread on the surface of the silica particles [15].

The results presented proved that the silica matrix can be effectively used to isolate individual biomolecules, preventing aggregation and denaturation and that insulin preserves its global structure to a great extent during encapsulation, storage, and release.

## Summary

Interaction between proteins and solid surfaces represents a delicate and extremely important issue in the field of biomaterials, biosensors, or drug delivery systems. Although it was intensively studied in the past decades, there still are unanswered questions or contradictory opinions concerning details of the protein's structure, conformational changes, or aggregation once adsorbed onto solid surfaces. The present chapter presented a few of the latest studies published in this field, focused

on interaction between several proteins that may be regarded as model systems, with substrates designed for tissue engineering, radiotherapy, and hyperthermia applications and drug delivery systems. Among the various techniques used for investigating protein interaction with solid surfaces, the method of Site-Directed Spin Labeling combined with EPR spectroscopy was emphasized as newly introduced in this research field. These methods have the advantage of allowing both quantitative and structural analysis of the attached/encapsulated proteins. Moreover, the specificity of the labeling procedure can be further exploited for protein solutions consisting of different protein types (multicomponent solutions). The FTIR spectroscopy and XPS were also reflected in the examples presented, as they are powerful tools for secondary structure characterization and surface coverage analysis, respectively.

Nevertheless, it is generally accepted that more research into the mechanisms regarding the nature of the protein–surface interaction is needed, in order to develop new rational methods and devices or to improve the existing ones, for a more precise investigation of proteins adherence to biomaterials.

---

## References

1. Xie J, Riley C, Chittur K (2001) Effect of albumin on brushite transformation to hydroxyapatite. *J Biomed Mater Res* 57:357–365. doi:10.1002/1097-4636(20011205)57:3<357::AID-JBM1178>3.0.CO;2-1
2. Berry CC, Curtis AS (2003) Functionalisation of magnetic nanoparticles for applications in biomedicine. *J Phys D Appl Phys* 36:R198–R206. doi:10.1088/0022-3727/36/13/203
3. Tengvall P (2003) How surfaces interact with the biological environment. In: Ellingsen JE, Lyngstadaas SP (eds) *Bio-implant interface. Improving biomaterials and tissue reactions*. CRC Press, Boca Raton, pp 285–315
4. Koenig AL, Grainger DW (2002) *Method of tissue engineering*. Academic, San Diego
5. Latour RA (2008) Biomaterials: protein-surface interactions. In: Wnek GE, Bowlin GL (eds) *Encyclopedia of biomaterials and biomedical engineering*, 2nd edn. Informa Healthcare, New York, pp 270–284
6. Arcos D, Vallet-Regi M (2010) Sol–gel silica-based biomaterials and bone tissue regeneration. *Acta Biomater* 6:2874–2888. doi:10.1016/j.actbio.2010.02.012
7. Sawyer AA, Hennessy KM, Bellis SL (2005) Regulation of mesenchymal stem cell attachment and spreading on hydroxyapatite by RGD peptides and adsorbed serum proteins. *Biomaterials* 26:1467–1475. doi:10.1016/j.biomaterials.2004.05.008
8. Langstaff S, Sayer M, Smith TJN, Pugh SM (2001) Resorbable bioceramics based on stabilized calcium phosphates. Part II: evaluation of biological response. *Biomaterials* 22:135–150. doi:10.1016/S0142-9612(00)00139-3
9. Mavropoulos E, Costa AM, Costa LT, Achete CA, Mello A, Granjeiro JM, Rossi AM (2011) Adsorption and bioactivity studies of albumin onto hydroxyapatite surface. *Colloids Surf B* 83:1–9. doi:10.1016/j.colsurfb.2010.10.025
10. Wang K, Leng Y, Lu X, Ren F, Ge X, Ding Y (2012) Theoretical analysis of protein effects on calcium phosphate precipitation in simulated body fluid. *CrystEngComm* 14:5870–5878. doi:10.1039/c2ce25216c
11. Vujaskovic Z, Poulson JM, Gaskin AA, Thrall DE, Page RL, Charles HC, MacFall JR, Brizel DM, Meyer RE, Prescott DM, Samulski TV, Dewhirst MW (2000) Temperature-dependent changes in physiologic parameters of spontaneous canine soft tissue sarcomas after combined



- radiotherapy and hyperthermia treatment. *Int J Radiat Oncol* 46:179–185. doi:10.1016/S0360-3016(99)00362-4
12. Overgaard J, Gonzalez Gonzalez D, Hulshof MCCH, Arcangeli G, Dahl O, Mella O, Bentzen SM (2009) Hyperthermia as an adjuvant to radiation therapy of recurrent or metastatic malignant melanoma. A multicentre randomized trial by the European Society for Hyperthermic Oncology. *Int J Hyperthermia* 25:323–334. doi:10.1080/02656730903091986
  13. Vanea E, Simon V (2011) XPS study of protein adsorption onto nanocrystalline aluminosilicate microparticles. *Appl Surf Sci* 257:2346–2352. doi:10.1016/j.apsusc.2010.09.101
  14. des Rieux A, Fievez V, Garinot M, Schneider Y-J, Preat V (2006) Nanoparticles as potential oral delivery systems of proteins and vaccines: a mechanistic approach. *J Control Release* 116:1–27. doi:10.1016/j.jconrel.2006.08.013
  15. Vanea E, Gruian C, Rickert C, Steinhoff H-J, Simon V (2013) Structure and dynamics of spin-labeled insulin entrapped in a silica matrix by the sol–gel method. *Biomacromolecules* 14:2582–2592. doi:10.1021/bm4003893
  16. Silva CM, Ribeiro AJ, Ferreira D, Veiga F (2006) Insulin encapsulation in reinforced alginate microspheres prepared by internal gelation. *Eur J Pharm Sci* 29:148–159. doi:10.1016/j.ejps.2006.06.008
  17. Gray JJ (2004) The interaction of proteins with solid surfaces. *Curr Opin Struct Biol* 14:110–115. doi:10.1016/j.sbi.2003.12.001
  18. Sharp KA, Honig B (1990) Electrostatic interactions in macromolecules: theory and applications. *Annu Rev Biophys Chem* 19:301–332
  19. Jiao YP, Cui FZ (2007) Surface modification of polyester biomaterials for tissue engineering. *Biomed Mater* 2:R24–R37. doi:10.1088/1748-6041/2/4/R02
  20. Chen QZ, Rezwan K, Françon V, Armitage D, Nazhat SN, Jones FH, Boccaccini AR (2007) Surface functionalization of Bioglass<sup>®</sup>-derived porous scaffolds. *Acta Biomater* 3:551–562. doi:10.1016/j.actbio.2007.01.008
  21. Rabe M, Verdes D, Seeger S (2011) Understanding protein adsorption phenomena at solid surfaces. *Adv Colloid Interface Sci* 162:87–106. doi:10.1016/j.cis.2010.12.007
  22. Martins MCL, Sousa SR, Antunes JC, Barbosa MA (2012) Protein adsorption characterization. *Methods Mol Biol* 811:141–161. doi:10.1007/978-1-61779-388-2\_10
  23. Bordignon E, Steinhoff H-J (2007) Membrane protein structure and dynamics studied by site-directed spin labeling ESR. In: Hemminga MA, Berliner LJ (eds) *ESR spectroscopy in membrane biophysics*. Springer Science and Business Media, New York, pp 129–164
  24. Klare JP (2013) Site-directed spin labeling EPR spectroscopy in protein research. *Biol Chem* 394:1281–1300. doi:10.1515/hsz-2013-0155
  25. Klare JP, Steinhoff H-J (2009) Spin labeling EPR. *Photosynth Res* 102:377–390. doi:10.1007/s11120-009-9490-7
  26. Jacobsen K, Oga S, Hubbell WL, Risse T (2005) Determination of the orientation of T4 lysozyme vectorially bound to a planar-supported lipid bilayer using site-directed spin labeling. *Biophys J* 88:4351–4365. doi:10.1529/biophysj.105.059725
  27. Jacobsen K, Hubbell WL, Ernst OP, Risse T (2006) Details of the partial unfolding of T4 lysozyme on quartz using site-directed spin labeling. *Angew Chem Int Ed* 45:3874–3877. doi:10.1002/anie.200600008
  28. Gruian C, Vulpoi A, Steinhoff H-J, Simon S (2012) Structural changes of methemoglobin after adsorption on bioactive glass, as a function of surface functionalization and salt concentration. *J Mol Struct* 1015:20–26. doi:10.1016/j.molstruc.2012.01.045
  29. Gruian C, Vulpoi A, Vanea E, Oprea B, Steinhoff H-J, Simon S (2013) The attachment affinity of hemoglobin toward silver-containing bioactive glass functionalized with glutaraldehyde. *J Phys Chem B* 117:16558–16564. doi:10.1021/jp408830t
  30. Gruian C, Boehme S, Simon S, Steinhoff H-J, Klare JP (2014) Assembly and function of the tRNA-modifying GTPase MnmE adsorbed to surface functionalized bioactive glass. *ACS Appl Mater Interfaces* 6:7615–7625. doi:10.1021/am500933e

31. Vulpoi A, Gruian C, Vanea E, Baia L, Simon S, Steinhoff H-J, Goller G, Simon V (2012) Bioactivity and protein attachment onto bioactive glasses containing silver nanoparticles. *J Biomed Mater Res A* 100:1179–1186. doi:10.1002/jbm.a.34060
32. Magyari K, Gruian C, Varga B, Ciceo-Lucacel R, Radu T, Steinhoff H-J, Varo G, Simon V, Baia L (2014) Addressing the optimal silver content in bioactive glass systems in terms of BSA adsorption. *J Mater Chem B* 2:5799–5808. doi:10.1039/c4tb00733f
33. Gruian C, Vanea E, Simon S, Simon V (2012) FTIR and XPS studies of protein adsorption onto functionalized bioactive glass. *BBA-Proteins Proteomics* 1824:873–881. doi:10.1016/j.bbapap.2012.04.008
34. Chittur KK (1998) FTIR/ATR for protein adsorption to biomaterial surfaces. *Biomaterials* 19:357–369. doi:10.1016/S0142-9612(97)00223-8
35. Dong A, Randolph TW, Carpenter JF (2000) Entrapping intermediates of thermal aggregation in  $\alpha$ -helical proteins with low concentration of guanidine hydrochloride. *J Biol Chem* 275:27689–27693. doi:10.1074/jbc.M005374200
36. Kong J, Yu S (2007) Fourier transform infrared spectroscopic analysis of protein secondary structures. *Acta Biochim Biophys Sin* 39:549–559. doi:10.1111/j.1745-7270.2007.00320.x
37. Vanea E, Magyari K, Simon V (2010) Protein attachment on aluminosilicates surface studied by XPS and FTIR spectroscopy. *J Optoelectron Adv Mater* 12:1206–1212
38. Kibel MH (1992) X-ray photoelectron spectroscopy. In: O'Connor DJ, Sexton BA, Smart RSC (eds) *Surface analysis methods in materials science*, 2nd edn. Springer, Berlin/Heidelberg/New York, pp 175–202
39. Thomas JA, Poland B, Honzatko R (1995) Protein sulfhydryls and their role in the antioxidant function of protein S-thiolation. *Arch Biochem Biophys* 319:1–9. doi:10.1006/abbi.1995.1261
40. Scrima A, Vetter IR, Armengod ME, Wittinghofer A (2005) The structure of the TrmE GTP-binding protein and its implications for tRNA modification. *EMBO J* 24:23–33. doi:10.1038/sj.emboj.7600507
41. Meyer S, Böhme S, Krüger A, Steinhoff H-J, Klare JP, Wittinghofer A (2009) Kissing G domains of MnmE monitored by X-ray crystallography and pulse electron paramagnetic resonance spectroscopy. *PLoS Biol* 7:e1000212. doi:10.1371/journal.pbio.1000212
42. MacDonald SL, Pepper DS (1994) Hemoglobin polymerization. *Methods Enzymol* 231:287–308. doi:10.1016/0076-6879(94)31021-1
43. Severcan F, Haris PI (2003) Fourier transform infrared spectroscopy suggests unfolding of loop structures precedes complete unfolding of pig citrate synthase. *Biopolymers* 69:440–447. doi:10.1002/bip.10392
44. Buchanan LA, El-Ghannam A (2010) Effect of bioactive glass crystallization on the conformation and bioactivity of adsorbed proteins. *J Biomed Mater Res A* 93:537–546. doi:10.1002/jbm.a.32561
45. Vanea E, Simon V (2013) XPS and Raman study of zinc containing silica microparticles loaded with insulin. *Appl Surf Sci* 280:144–150. doi:10.1016/j.apsusc.2013.04.111
46. Kokubo T, Kushitani H, Sakka S, Kitsugi T, Yamamuro T (1990) Solutions able to reproduce in vivo surface-structure changes in bioactive glass-ceramic A-W3. *J Biomed Mater Res* 24:721–734. doi:10.1002/jbm.820240607
47. Michel R, Pasche S, Textor M, Castner DG (2005) Influence of PEG architecture on protein adsorption and conformation. *Langmuir* 21:12327–12332. doi:10.1021/la051726h
48. Iucci G, Battocchio C, Dettin M, Ghezzi F, Polzonetti G (2010) An XPS study on the covalent immobilization of adhesion peptides on a glass surface. *Solid State Sci* 12:1861–1865. doi:10.1016/j.solidstatesciences.2010.01.021
49. Han Y, Tian H, He P, Chen X, Jing X (2009) Insulin nanoparticle preparation and encapsulation into poly(lactic-co-glycolic acid) microspheres by using an anhydrous system. *Int J Pharm* 378:159–166. doi:10.1016/j.ijpharm.2009.05.021
50. Sarmento B, Ferreira DC, Jorgensen L, van de Weert M (2007) Probing insulin's secondary structure after entrapment into alginate/chitosan nanoparticles. *Eur J Pharm Biopharm* 65:10–17. doi:10.1016/j.ejpb.2006.09.005

Alina Vladescu, Maria A. Surmeneva, Cosmin M. Cotrut, Roman A. Surmenev, and Iulian Vasile Antoniac

## Contents

Introduction .....	704
Preparation and Characterization of the Bioceramic Coatings .....	707
Bioinert Coatings .....	710
Bioactive Coatings .....	711
Specific Aspects Related to the Bioceramic Coatings .....	712
Ultrathin HA Film Deposited on the Surfaces of Biodegradable Materials .....	712
Antimicrobial and Bioactive Coatings .....	716
Adhesion of the Bioceramic Coatings .....	721
Summary .....	725
References .....	726

## Abstract

The performance of present orthopedic implants and prostheses components made by metallic biomaterials is quite limited due to their corrosion in the human body. Therefore, it is important to develop methods for the biofunctionalization of the metallic surfaces by changes in the material's surface composition,

---

A. Vladescu  
National Institute for Optoelectronics, Magurele, Romania  
e-mail: [alinava@inoe.ro](mailto:alinava@inoe.ro)

M.A. Surmeneva • R.A. Surmenev  
Department of Experimental Physics, Tomsk Polytechnic University, Tomsk, Russia  
e-mail: [surmenevamarina@tpu.ru](mailto:surmenevamarina@tpu.ru); [surmenev@tpu.ru](mailto:surmenev@tpu.ru)

C.M. Cotrut  
Materials Science and Engineering Faculty, University Politehnica of Bucharest, Bucharest, Romania  
e-mail: [cosmin.cotrut@upb.ro](mailto:cosmin.cotrut@upb.ro)

I.V. Antoniac (✉)  
University Politehnica of Bucharest, Bucharest, Romania  
e-mail: [antoniac.iulian@gmail.com](mailto:antoniac.iulian@gmail.com)

structure, and morphology, which leave intact the mechanical properties of metallic biomaterials. Thus, the performance and service life of dental and orthopedic implants made by metallic biomaterials will be significantly increased. These requirements could be satisfied if biocompatible coatings with unique combinations of properties were produced. The best choice for the surface functionalization of the metallic implants or their parts that are in direct contact with bone is the bioceramic coatings which are classified in three main groups: bioinert, bioactive, and bioresorbable. Bioinert coatings are those which have a minimal interaction with its surrounding tissue after implantation in the human body, such as oxides, nitrides, oxynitrides, carbonitrides, or carbide, due to their valuable properties such as high hardness, better wear and corrosion resistance, and good biocompatibility. Bioactive coatings present after implantation a good interaction with the bone by enhancement adhesion between the bone and implants. In the case of bioresorbable coatings, these are dissolved in contact with the bone and form a new bone. The aim of this chapter is the discussion about different bioinert, bioactive, and bioresorbable coatings prepared by magnetron sputtering used in biomedical applications such as dental or orthopedic implants and medical instruments. Moreover, the possibility to enhance the osseointegration and the antibacterial properties of the metallic implants used in dentistry and orthopedic surgery is discussed in this chapter.

---

**Keywords**

Coatings • Hydroxyapatite • Nitride • Carbide • Carbonitride • Magnetron sputtering • Adhesion • Hardness • Friction coefficient • Corrosion resistance • Osseointegration

---

**Introduction**

The National Institutes of Health defined the biomaterials as “any substance or combination of substances, other than drugs, synthetic or natural in origin, which can be used for any period of time, which augments or replaces partially or totally any tissue, organ or function of the body, in order to maintain or improve the quality of life of the individual” [1]. At present, only three groups of metals and alloys are considered suitable to be used as hard tissue replacements, especially for the dental and orthopedic implants, namely, 316 L stainless steels, titanium, and cobalt-chromium alloys. Though these materials possess high strength, ductility, and good mechanical properties, their biocompatibility and wear and corrosion resistance are relatively low and have no biofunction (changing the surface of a medical device to improve its functionality) [2]. It has also been demonstrated that some metallic ions (Cr, Co, Ni, V) resulting during the *in vitro* corrosion of metallic alloys used as biomaterials cause alteration of the biocompatibility and inhibit the immune response as assessed by cell proliferation. For example, the survival of present orthopedic prostheses cannot be guaranteed beyond 10–12 years due to these complex problems. The increasing number of younger patients requiring replacements has emphasized the need for dental and orthopedic implants

with improved performance and longevity. Therefore, it is important to develop methods for functionalization of the metallic implant surfaces by changes in the material's surface composition, structure, and morphology, leaving intact the mechanical properties. Thus, the performance and service life of dental and orthopedic implants will be significantly increased. These requirements could be satisfied if biocompatible coatings with unique combinations of properties were produced. At this moment, the best choice for the functionalization of the implants or their parts that are in direct contact with bone appears to be the bioceramic coatings, due to their excellent osteoconductive properties and high chemical stability. Bioceramic coatings could be classified into three main groups: bioinert, bioactive, and bioresorbable. Bioinert coatings are those which have a minimal interaction with its surrounding tissue after the implantation in the human body. In this group, oxides, nitrides, oxynitrides, carbonitrides, and carbide were found. Many different transition metal nitride (TiN, TiAlN, ZrN, NbN [3, 4]), carbide (TiC [5]), oxide (ZrO<sub>2</sub> [6], TiO<sub>2</sub> [7]), or oxynitride (TiON [8]) coatings have a wide application as biomaterials, due to their valuable properties such as high hardness, better wear and corrosion resistance, and good biocompatibility. Bioactive coatings are those which, after the implantation, guarantee a good interaction with the bone by enhancement adhesion between the bone and implant. (Among different types of bioactive coatings (Table 1), hydroxyapatite (HA), with chemical formula Ca<sub>10</sub>(PO<sub>4</sub>)<sub>6</sub>(OH)<sub>2</sub>, is one of the most extensively used for implants used for repairing the hard tissues). Its common uses include bone repair and augmentation, as well as coating of implants, because of its chemical similarities to the component of bones and teeth. However, the low mechanical strength of plain HA ceramics and the relatively low bone-bonding rate restrict its use as biomaterials.

Some recent studies report that the *in vitro* and *in vivo* bioactivity of HA could be enhanced by the incorporation of Si in the HA lattice. Silicon-substituted HA is now successfully used as bone graft material in spinal fusion, but it is not a good alternative for the hard tissue, due to its low hydrophobicity, which decreases the

**Table 1** Different types of phosphate coatings

	Chemical formula	Ca/P ratio	References
Stoichiometric hydroxyapatite	Ca <sub>5</sub> (PO <sub>4</sub> ) <sub>3</sub> OH or Ca <sub>10</sub> (PO <sub>4</sub> ) <sub>6</sub> (OH) <sub>2</sub>	1.67	[12–19]
Calcium-deficient hydroxyapatite	Ca <sub>10-x</sub> (HPO <sub>4</sub> ) <sub>x</sub> (PO <sub>4</sub> ) <sub>6-x</sub> (OH) <sub>2-x</sub> , with 0 < x < 1	1.50 < Ca/P < 1.67	[20–24]
Carbonate hydroxyapatite	Ca <sub>5</sub> (PO <sub>4</sub> ) <sub>2.5</sub> (CO <sub>3</sub> ) <sub>0.5</sub> (OH) or Ca <sub>5</sub> (PO <sub>4</sub> ,CO <sub>3</sub> ) <sub>3</sub> (OH)	2.00	[25]
Fluorapatite	Ca <sub>5</sub> (PO <sub>4</sub> ) <sub>3</sub> F	1.67	[15, 26, 27]
Tricalcium phosphate	Ca <sub>3</sub> (PO <sub>4</sub> ) <sub>2</sub>	1.5	[28–30]
Tetracalcium phosphate	Ca <sub>4</sub> P <sub>2</sub> O <sub>9</sub>	2.00	[31, 32]
Octacalcium phosphate	Ca <sub>8</sub> H <sub>2</sub> (PO <sub>4</sub> ) <sub>6</sub> *5H <sub>2</sub> O	1.33	[17, 33–35]
Rhenanite	NaCaPO <sub>4</sub>	1.00	[36]
Oxyapatite	Ca <sub>10</sub> (PO <sub>4</sub> ) <sub>6</sub> O	1.67	[37]

adsorption of proteins onto a material's surfaces, and its mechanical and tribological characteristics. Some researchers have also proposed the incorporation of Mg in the HA lattice, in order to accelerate the osseointegration process of implants. However, a major drawback of the Si-HA or Mg-HA coatings is their high dissolution rate in physiological solutions, leading to a high pH value in the surrounding environment, which is detrimental to cell survival. The actual challenge in the field is to obtain metallic implants with bioactive and antibacterial surfaces, but still exist some major difficulties, as these surface characteristics present deterioration in time. A novel approach to obtain these surfaces is to modify the HA properties by doping with small amounts of beneficial elements for human bones like Mg and Si [9].

Bioresorbable coatings are those which are dissolved in contact with bone and form a new bone. The most common examples are tricalcium phosphate, tetracalcium phosphate, octacalcium phosphate, calcium oxide, calcium carbonate, and gypsum [10].

It is well known that the osseointegration of the implants used in dentistry or orthopedic surgery depends largely on the interface between the implant and the osteoblast cells forming the bone, a stable "implant surface-surrounding tissue" connection being an important prerequisite for the long-term success of such implants. But various phenomena may occur at the interface after implantation of a biomaterial into a living system. Initially, the proteins respond to the implant surface and form a thin layer of protein on the surface within few seconds. Since cells respond to the proteins, this protein film then controls the subsequent bioreaction. The cells then multiply and organize into various types of complex tissues. Therefore, the adsorption of proteins plays a vital role in the determination of the nature of the tissue-implant interface. Stimulation of the rapid cell growth for bone bonding is essential for the osseointegration of the dental or orthopedic implants. This can be done by depositing bioactive coatings on the implant surfaces, resulting in the increase of bonding rate. The research on the biocompatibility improvement by both bioactive and bioinert functionalization coatings deposited on metallic implant surfaces has become one of the hottest topics in biomaterials.

The new trend in medical application is to use the implants with antibacterial properties along with good mechanical and physical-chemical properties and high bond bonding. During the years, Cu and Ag were used for enhancement of the antibacterial properties of the materials [11]. Despite its abilities, those materials as coatings exhibited some drawbacks: Ag is expensive and Cu forms quickly CuO, due to its high affinity to the oxygen, and CuO is toxic for the human body. In medical applications, Cu is used to reduce environmental contamination and to control bacteria like *Legionella* and others that appear in hospital water distribution systems [11].

The main purpose of this chapter is the discussion about different bioinert, bioactive, and bioresorbable coatings prepared by magnetron sputtering used in order to improve the properties of metallic implants used in dentistry or orthopedic surgery. Moreover, the possibility to enhance the osseointegration and antibacterial properties of these implants is discussed.

## Preparation and Characterization of the Bioceramic Coatings

During the years, the bioceramic coatings used for biomedical applications were prepared by various deposition techniques, such as magnetron sputtering, ion beam-assisted deposition, plasma spraying process, sol-gel, thermal spraying, electrophoretic deposition, pulsed laser deposition, dynamic mixing, dip coating, biomimetic coating, and hot isostatic pressing [38–52].

*Arc ion plating* is another technique that has been extensively used for the deposition of the bioinert coatings with origins that can be traced back as far as 1877 [53]; due to the high deposition rates and highly ionized metal vapor, it allows for enhancing adhesion and also for the promotion of the deposition of dense films. Moreover, this one has the possibility to coat using metals with different melting points. The main disadvantage is the formation of macroparticles with size up to tens of microns, which have a negative effect on the properties of the coatings, especially on those of biological and tribological ones [54]. Up to date, no bioactive coatings were prepared by arc ion plating method.

*Plasma spraying* is a method with possibility to coat high- and low-melting materials with high thickness, due to high deposition rates. Compared to other techniques, this one has high efficiency and it is an economical method. By using this method, the bioinert and bioactive coatings, with suitable porosity for biomedical applications, can be performed. The bioinert coating produced using plasma spraying exhibited a high residual stress, with nonuniform distribution, and due to the rapid cooling process tends to form cracks which limit the application in the biomedical area [55]. The common limitations of the preparation of the bioactive coatings using plasma spraying are high temperatures which induce decomposition, poor thickness uniformity, insufficient crystallinity, and poor adhesion to the metallic surfaces and the poor control of chemical and physical properties [56].

*Sol-gel* method is a proper technique for the deposition of bioceramics in a wide variety of forms due to the low deposition temperatures, ease of compositional modifications by the control of the stoichiometry of precursor solutions, and the possibility to coat various types of substrates with complex shapes. Disadvantages of the sol-gel method are the limited repeatability of the thickness, the roughness and their biological properties, and poor adhesion to the metallic surfaces.

*Electrophoretic deposition* is a versatile method suitable for synthesis of the bioactive coatings due to high deposition rates and its cost-effectiveness, because it requires simple and cheap equipment. The coatings are uniform and they can be deposited on complex geometries. The coatings are prepared at high sintering temperatures, which produce the cracks, leading to the delamination of the coatings. This method is used for biomedical application because of its advantages of being cost-effective, its ability to form a film of uniform thickness, and its homogeneous properties irrespective of the surface shape of the implant [57, 58].

By *sputter ion plating* technique, a dense, uniform, and homogenous coating with excellent adhesion to metallic substrates can be prepared. This technique is suitable for the deposition of bioinert coatings, due to the high rate deposition and the possibility to obtain the multicomponent coatings. Regarding the bioinert coatings,

this technique facilitates the deposition of dense and well-adhered films with controlled elemental composition [52], by selecting appropriate values of the deposition parameters (discharge power, gas flow rate, working pressure, substrate temperature, deposition time, substrate bias voltage) [56]. The main drawback of this technique for preparation of bioinert coatings is that it produces coatings with low crystallinity, requiring post-deposition annealing treatment [59].

*Magnetron sputtering* is the most used technique of physical vapor deposition (PVD) methods. By using magnetron sputtering, the thickness of the coatings could be varied from a few nanometers to several micrometers. Various equipments for magnetron sputtering are available on the market, with one, two, or more magnetrons which can work independently or simultaneously, because they have different power supplies by each magnetron. Usually, the base pressure in the deposition chamber is ranged from  $10^{-4}$  to  $10^{-7}$  Torr. The working pressure is around 10–3 Torr, and by modifying this parameter, the film properties can be modified. The working pressure can be controlled by inserting a nonreactive gas such as Ar. By using the nonreactive gas, the coating compositions are the same as those of the targets. By using the reactive gases (e.g.,  $N_2$ ,  $O_2$ ,  $CH_4$ , and  $C_2H_2$ ), the coating obtained could be different (e.g., nitrides, oxide, oxynitrides, and carbides) in correlation with the gases that were used. Many authors suggest that the coatings for metallic implants can be successfully prepared by magnetron sputtering [52, 56, 59], because it permits the control of the coating properties by adjusting the deposition parameters. In the case of the calcium phosphate coatings, the main challenge is to obtain crystalline structures with Ca/P ratio of about 1.67. Until now, the calcium phosphate coatings were prepared by RF magnetron sputtering at substrate temperatures under 200 °C. At this temperature, only the amorphous structures were obtained, and in order to become crystalline structures, the coatings must be thermally treated, but during this treatment the coatings suffer delamination or lose their biological properties. In the last years, this disadvantage was eliminated by using a deposition system which permits that the substrate temperature be varied in the range 150–800 °C. Thus, the calcium phosphate coatings will be in the crystalline form after deposition, without the need of the supplementary treatment for crystallization. It is well known that the deposition after some thermal treatments could be delaminated, especially when the films are deposited on metallic substrates. The main reason for using the magnetron sputtering method is the possibility to control the deposition parameters in order to obtain uniform thin films without defects, with high adhesion to the substrates, low roughness, resistance to corrosion and wear and low internal stress, and essential properties of novel materials used for biomedical applications. Also, this method is efficient and productive, with high confidence in the reproducibility of the results obtained, and environmentally friendly. Another advantage of the magnetron sputtering method is the possibility to coat the samples with 3D geometry and not to induce the dimensional or structural modifications of the substrate, due to the low-energy ion flux. Also, this method is ideal for the preparation of biocompatible thin films, due to the possibility to control the stoichiometry of the compounds, and, as it was mentioned above, it permits the deposition at high substrate temperature, a good advantage in the case of deposition of calcium phosphate-based coatings. The



main drawback of deposition of calcium phosphate by magnetron sputtering remains the low deposition rate. The challenger is the optimization of the magnetron sputtering technology to achieve coatings with superior properties, facilitating their successful and reliable long-term exploitation in a wide range of biomedical applications.

The actual challenge in dental and orthopedic surgery is to use implants for the improvement of patient outcomes, minimization of incidence of complications, and reduction of hospital stays. For reaching these claims, it is important to offer the surgeon implants with good mechanical properties, high corrosion resistance in the human body, and high capability to be integrated with surrounding tissue. Up to date, the best solution was to coat the metallic implant surface with various types of coatings. By coatings of the metallic implant surfaces, an entire complex of implant properties were changed, especially the anticorrosive, tribological, and biological properties, due to the surface modifications in terms of composition, microstructure, and morphology. Comparing all the existent coatings, the bioceramic coatings appear to be the best choice for metallic implants. The advantages of various types of bioceramic coatings besides their applications are shown in Table 2. From all the bioceramics, the calcium phosphates were mostly used due to their higher apatite-inducing ability that, in turn, leads to rapid osseointegration. But it is important to mention the limitation of these coatings in the case of applications like load-bearing implants. For these implants, nitrides or carbide or carbon-based coatings could be

**Table 2** Bioceramic coatings with different coating materials used for medical applications in the human body

Coating material	Medical applications	Advantages
Nitrides (TiN, ZrN, NbN, TiAlN) Oxynitrides (TiON, ZrON, TiSiON)	Dental implants Fracture fixation devices Metal components of joint endoprostheses	High corrosion resistance High adhesion on the metallic surfaces Good friction coefficient
Carbon-based coatings (DLC, CN, a-C, carbides, carbonitrides)	Artificial heart valves Orthopedic fixation devices Artificial ligaments and tendons	Low friction coefficient and wear rate High biocompatibility with blood
Calcium phosphates, bioglass	Percutaneous devices Spinal implants Maxillofacial reconstruction Skull plates	High osseointegration capability
Oxides (TiO <sub>2</sub> , Al <sub>2</sub> O <sub>3</sub> , ZrO <sub>2</sub> )	Dental implants Devices for increasing alveolar area Maxillofacial reconstruction Ophthalmic implants	High corrosion resistance Good regenerative capability

the best solution, due to their high corrosion resistance. Thus, it is difficult for a single material to have all the required properties imposed in specific biomedical applications. In the last years, some scientists proposed the combination of two different alternating bioceramic layers, such as the synthesis of the multilayered structures composed of alternation of the nitride layer and carbon-based coatings or carbide and calcium phosphates. These combinations proved to be useful in many cases because it would combine the advantages of these categories: high hardness and excellent wear-corrosion behavior with bioactive abilities. Recently, some researchers proposed the substitution of the sputtered hydroxyapatite coatings with various metals of nitride or carbides in order to combine the mechanical and tribological properties of the first group with the ability to promote bone formation and reduce bone resorption of the hydroxyapatite.

## Bioinert Coatings

During the years, transition metal nitrides, carbides, or carbonitrides have been used as coatings to protect mechanical tools against wear and corrosion process and to offer thermal stability and decorative properties. In the last decades, these coatings were also proposed as biocompatible thin films to improve the wear and corrosion resistance of the dental or orthopedic implants and to prevent the toxic ion release from some metallic alloys used as implant materials like V from Ti6Al4V alloy, Cr from Co-Cr alloy, and Ni from Ni-Cr or Ti-Ni alloys. There are various types of nitrides prepared by magnetron sputtering, but TiN is mostly used in mono- or multilayered structures, due to its high adhesion to the metallic substrates which could be controlled by modifying the bias voltage applied to the substrates. Brama et al. reported that TiN has superior biological properties compared to other nitrides [5]. Another biocompatible nitride is TiAlN, which proved to be a good candidate for the biomedical applications despite its Al content [3]. Some researchers proved that the transition metal carbonitride coatings increased the service life of orthopedic implants, especially in terms of wear resistance in the biological environments [60–65]. In more recent papers, coatings based on quaternary carbonitrides, such as TiAlCN, TiNbCN, and TiCrCN, were found to possess improved mechanical, anticorrosive, and tribological properties, as compared to the commonly used TiCN or ZrCN coatings [65–68]. For example, carbonitride system deposited by magnetron sputtering showed the best behavior in terms of hardness and friction performance under wet/dry sliding conditions compared to carbides or nitride systems. Figure 1 illustrates this point better by categorizing various classes of bioinert coatings with respect to their hardness and friction coefficient, as deduced from the literature. The carbonitride class is hard but cannot provide what may be the lowest friction coefficient on known carbide and nitrides. However, DLC coatings are capable to provide not only high hardness and low friction coefficient but also good biological properties [69]. In the last decade, numerous papers have been devoted to the MeSiC, MeSiN, and MeSiCN hard coatings, where Me is a transition metal and Si is an alloying element. These coatings were found to have superior

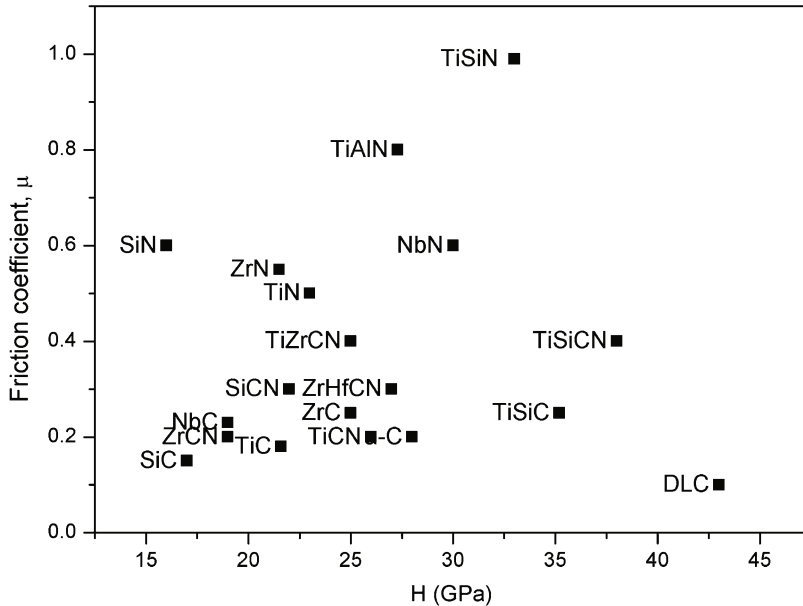


**Fig. 1** Comparative view on the hardness and the friction coefficient of various classes of bioinert coatings

mechanical properties (high hardness and strength), thermal stability, reduced friction, and enhanced wear-corrosion resistance [69, 70]. In particular, investigations on TiSi-based carbide or carbonitride coatings as a possible candidate for a variety of metallic implants have attached interest because they can combine the mechanical, anticorrosive, and tribological properties of the TiC or TiCN with the biological characteristics of the SiC or SiCN [71, 72]. Also, in the scientific literature it has been reported that SiC coatings prepared by magnetron sputtering are chemically inert and possess good biocompatibility and improve the corrosion resistance and the tribological performance of various steels [72–74]. In Fig. 1, we present a comparative view on the hardness and the friction coefficient of various classes of bioinert coatings after the compilation of different resources from the scientific literature.

## Bioactive Coatings

The bioactive coatings started to be investigated after the development of the bioinert coatings which proved that they were not useful to replace osseous tissues. Thus, the researchers were looking after ceramics, which can imitate the natural bone and its properties. Hydroxyapatite (HA) is an example of the most widely used bioinert coatings due to its high ability to form osseous tissue. However, the poor mechanical strength of plain HA coatings and the relatively high dissolution rate in the physiological environment within the body restrict its use as biomaterials in clinical

applications. A recent study reported that the *in vitro* and *in vivo* bioactivity of HA could be enhanced by the incorporation of Si in the HA lattice. Also, silicon-substituted HA is now successfully used as bone graft material in spinal fusion. However, it is not a good alternative for the hard tissue, due to its low hydrophobicity, that decreases the adsorption of proteins onto a material's surfaces, and its mediocre mechanical and tribological characteristics. Some researchers have also proposed the incorporation of Mg in the HA lattice, in order to accelerate the osseointegration process of dental or orthopedic implants [75]. However, a major drawback of the Si-HA or Mg-HA coatings remains their high dissolution rate in physiological solutions, leading to a high pH value in the surrounding environment, which is detrimental to cell survival.

Therefore, the actual challenge in the biomedical field is to obtain medical devices with bioactive and antibacterial surfaces, but the difficulties are redoubtable, as these surface characteristics have to present deterioration in time. A novel approach to obtain these surfaces is to modify HA properties by doping with small amounts of beneficial elements for human bones [9]. Azem et al. [76] and Vladescu et al. [77] reported that by SiC addition to the HA structure, their corrosion resistance and mechanical properties were enhanced, without deterioration of the bioactive abilities.

Figure 2 presents SEM micrographs of the HA coatings before and after 24 h of immersion in artificial saliva. The sputtered HA is a dense, uniform, and highly adherent coating and looks different to those immersed for 24 h in saliva, where the presence of individual crystallites is not evident. After 24 h of immersion, some crystalline leaflets which nucleated and grew on the substrate surface were formed.

Figure 3 shows the coefficient of friction as a function of sliding distance for a metallic alloy Ti6Al4V, usually used as implant material, in a different state. For the uncoated samples of alloy Ti6Al4V, the coefficient of friction  $\mu$  remained practically constant at a value of  $\sim 0.5$  during the test. For the sample with HA coatings on Ti6Al4V substrate, the friction coefficient is practically identical with the uncoated substrate. The HA coating with SiC addition on Ti6Al4V substrate presents a stable friction coefficient value until the distance of 480 m and then shows a dramatic increase, indicating the destruction of the coatings. Based on these results, we could consider that the SiC incorporation into the HA coating led to a notable reduction of the friction coefficients. This is valuable information for the case of dental implant, because the dental implants will be inserted in bone by screwing, and during this step the hydroxyapatite can be averted and the implant remained without the bioactive coating.

---

## Specific Aspects Related to the Bioceramic Coatings

### Ultrathin HA Film Deposited on the Surfaces of Biodegradable Materials

From the basic magnesium alloys and iron-based composites, the choice and technology for proposed biodegradable metals for medical applications have been progressed [78]. Some magnesium alloys, such as AZ31, AZ91, and Mg-Ca, enable

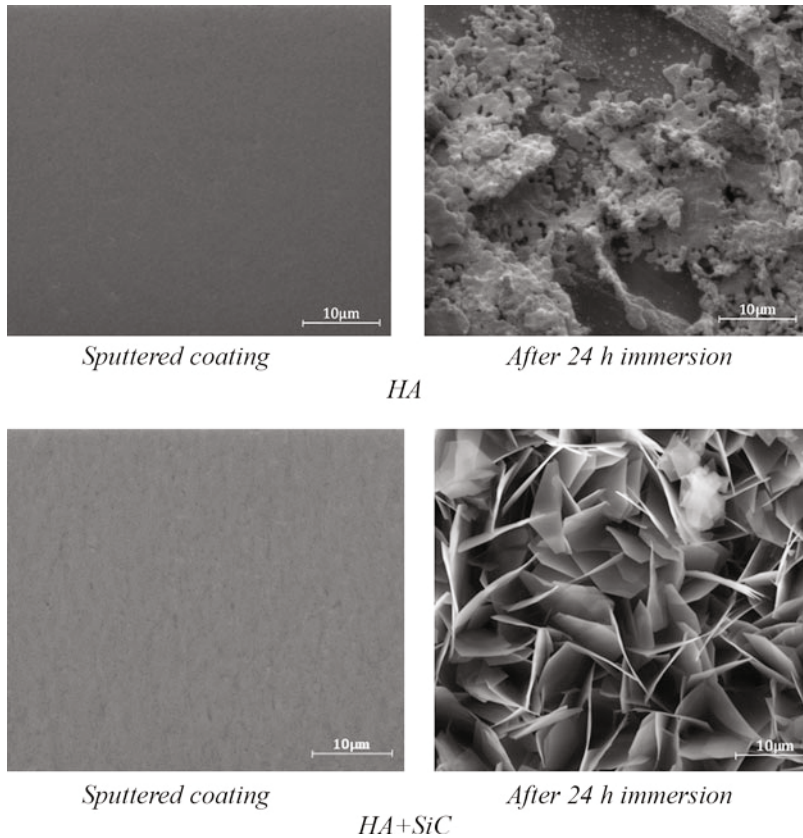


**Fig. 2** Scanning electron microscopy showing the morphology of the as-sputtered bioactive coating surfaces (HA, respectively HA+SiC, deposited on Ti6Al4V alloy) and after 24 h immersion in saliva

the decrease in the resorption rate of pure magnesium [79]. Such magnesium alloys have been prospected for the use in medical applications due to their excellent mechanical properties and controllable degradation behavior without inducing toxicological problems, but due to their low corrosion resistance, a wide application of these metallic materials is limited [78].

Over the past decade, various methods have been tested in order to improve the degradation performance of pure magnesium and its alloys. The deposition of biocompatible coatings such as polymers and ceramics is the most popular way that has been investigated [80]. In particular, biocompatible calcium phosphate (CaP) has gained great interest in recent years as a coating material on magnesium alloys [80]. Thick CaP coatings that were prepared by wet-chemical methods are well known [81]. Though, wet-chemical methods are suitable for CaP coating deposition on the surface of magnesium alloys, they often suffer from weak adhesive strength.

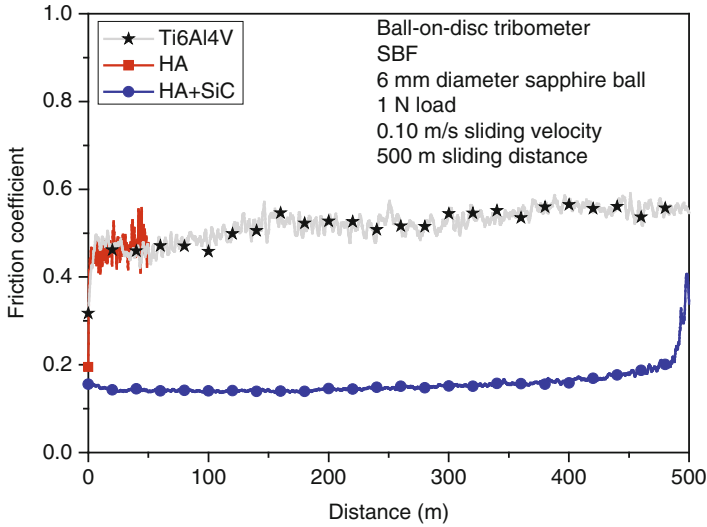


**Fig. 3** Friction coefficients versus sliding distance for the uncoated Ti6Al4V substrate, HA coatings, and HA coatings with SiC addition

Currently, the priority of researchers has shifted toward the formation of thin protective surface layers on the surface of alloys, which allows both preservation of the initial substrate topography and enhancement of the corrosion resistance [82]. Moreover, an HA coating, prepared using RF magnetron sputtering, is well adhered to the substrate [56]. Furthermore, in case of NiTi substrates, an average nickel release rate from the samples, with a dense crystalline ~600 nm thick HA coating deposited by RF magnetron sputtering, was reduced by 7–10 times compared to the uncoated substrates [83]. Therefore, the HA film deposited via RF magnetron sputtering onto the biodegradable materials was investigated as a potential candidate in order to be used as protective coatings against corrosion [84, 85].

The polarization tests in a 3.5 wt% NaCl solution were performed to examine the corrosion behavior of the HA-coated magnesium alloy AZ31 [84]. The potentiodynamic polarization test demonstrated that a 1500-nm thick nanocrystalline HA coating significantly improved the corrosion resistance of the AZ31 magnesium alloy (Fig. 4). It should be stressed that a much thinner RF magnetron sputter-deposited HA film could offer significant advantages over wet-chemical deposition techniques with respect to dense structure, crystallinity, and corrosion resistance.

Moreover, the magnesium alloy AZ31 coated with ultrathin HA film using RF magnetron sputtering has shown comparable mechanical and physical properties to those of uncoated alloys [86]. Thus, the nanoindentation tests demonstrated that the HA coatings increased the surface hardness on both the microscale and the nanoscale. The elastic strain to failure ( $H/E$ ) and the plastic deformation resistance ( $H^3/E^2$ ) for the HA coating were increased in comparison with the uncoated AZ31

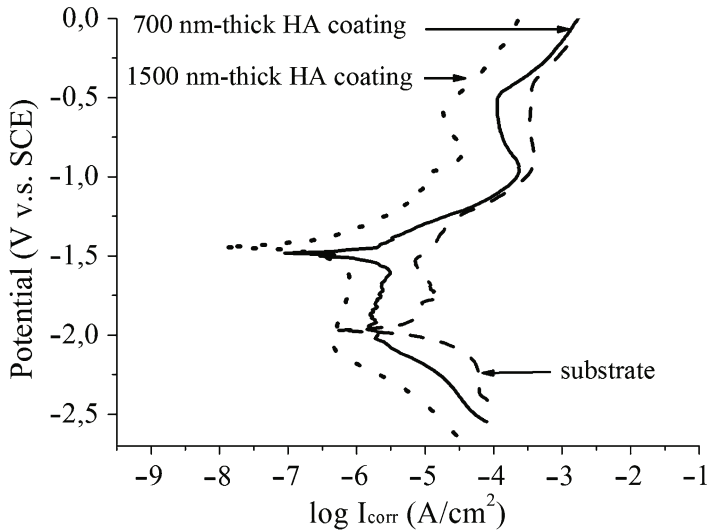


**Fig. 4** Potentiodynamic polarization curves of HA-coated and uncoated AZ31 substrates tested in a 3.5 wt% NaCl solution at 37 °C [84] (Reprinted from Vacuum, 117, Surmeneva MA, Surmenev RA, Microstructure characterization and corrosion behaviour of a nano-hydroxyapatite coating deposited on AZ31 magnesium alloy using radio frequency magnetron sputtering, 60–62, Copyright (2015), with permission from Elsevier)

magnesium alloy [86]. Therefore, the films deposited on the surface of the AZ31 magnesium alloy can significantly enhance the wear resistance of this alloy.

In addition, the polarization resistance ( $R_p$ ) of the magnesium-calcium alloy (1 wt% Ca) coated with HA films with the thickness ranging from 550 to 750 nm was found to be more than two orders of magnitude higher under in vitro conditions as compared to that of the bare alloy, i.e.,  $R_p = 63,346 \pm 13,422 \Omega \cdot \text{cm}^2$  for coated sample and  $R_p = 413 \pm 11 \Omega \cdot \text{cm}^2$  for bare alloy [85]. The cathodic current was significantly lower for the coated magnesium-calcium alloy, and as a result, the corrosion current density ( $i_{corr}$ ) for the coated alloy was ~98 % lower than that of the bare alloy (from  $90 \pm 14.1 \mu\text{A}/\text{cm}^2$  to  $1.8 \pm 1.8 \mu\text{A}/\text{cm}^2$ ) [85]. The degradation rate for the coated magnesium-calcium alloy was ~0.04 mm/year and ~2.07 mm/year for the bare alloy [85]. Thus, the decrease in the degradation rate due to the ultrathin coating is significantly high, which makes the coating technique very attractive for the magnesium-calcium alloy.

The degradation characteristics of the HA-coated metal-ceramic iron-tricalcium phosphate (Fe-TCP) composite and magnesium alloy AZ91D were investigated in vitro [88]. The nanostructured RF magnetron sputter-deposited coating with a thickness of 700 nm was demonstrated to promote a significantly better behavior of cells compared with the uncoated metallic substrates (Figs. 5 and 6). The nanostructured HA modification improves initial attachment of the human mesenchymal stem cell (hMSCs) on metallic substrate within the first 24 h. A higher ALP level has been observed on the HA-coated surface after 1 and

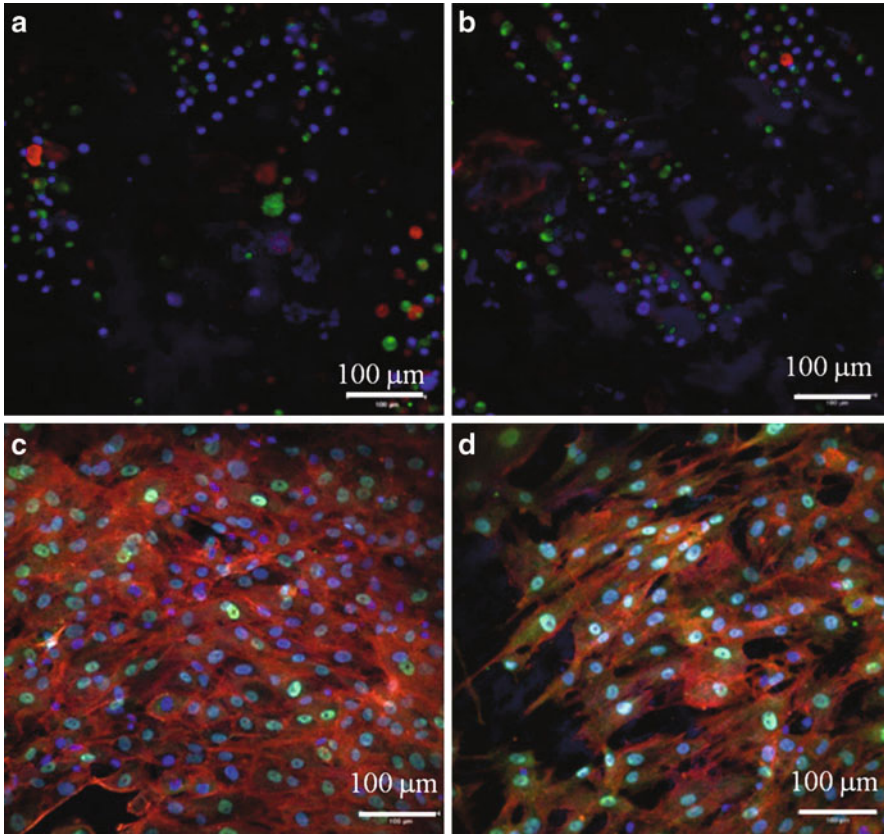


**Fig. 5** Cell adhesion on the uncoated (a, b) and HA-coated AZ91D (c, d) was evaluated at day 1 by fluorescence staining for actin (*red*) and vinculin (*green*) that are components of focal adhesions. Cells were either kept in proliferation medium (a, c) or in osteogenic medium (b, d) [87]

14 days. Therefore, HA-coated surfaces stimulated the expression of ALP activity. Consequently, the results demonstrated the potential of HA-coated magnesium- and Fe-TCP-based alloys to be developed as degradable composites for the biomedical applications.

### Antimicrobial and Bioactive Coatings

It was reported that the high stability and flexibility of the HA structure account for a variety of possible cationic and anionic substitutions (Ag, Cu, Mg, Zn, Si, etc.). Silicate-substituted HA,  $\text{Ca}_{10}(\text{PO}_4)_{6-x}(\text{SiO}_4)_x(\text{OH})_{2-x}$ , has received a great deal of interest recently as a potential bone substitute material [9, 89]. The silicate-containing HA-based (Si-HA) coatings have shown an improvement in biological performance over their undoped counterparts [90, 91].



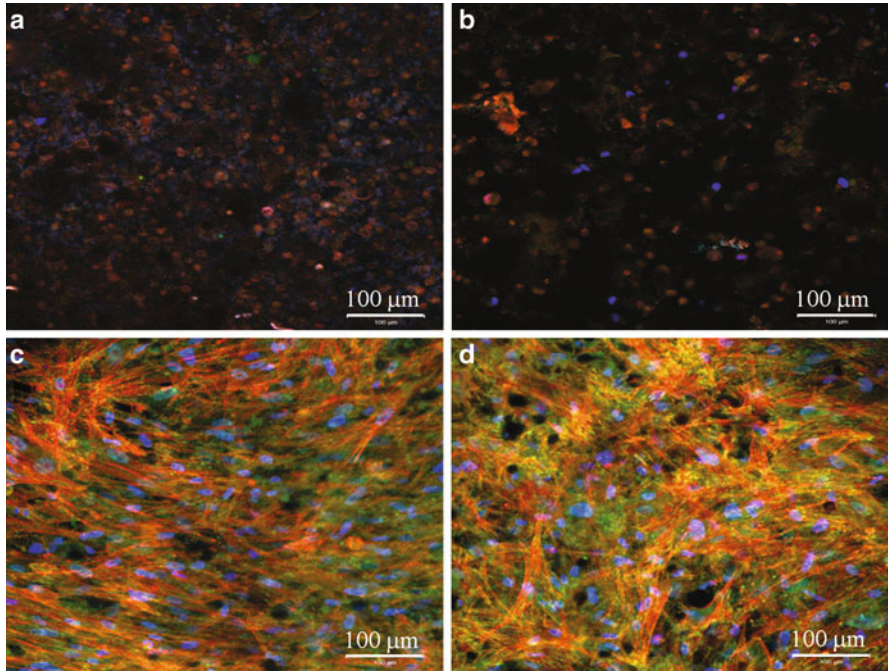


**Fig. 6** Cell adhesion on the uncoated (a, b) and HA-coated Fe-TCP (c, d) was evaluated at day 14 by fluorescence staining for actin (red) and vinculin (green) that are components of focal adhesions. Cells were either kept in proliferation medium (a, c) or in osteogenic medium (b, d) [88] (Reprinted from *Colloids Surf B Biointerfaces*, 135, Surmeneva MA, Kleinhans C, Vacun G, Kluger PJ, Mukhametkaliyev TM, Syromotina DS, Schönhaar V, M€uller M, Hein SB, Wittmar A, Ulbricht M, Prymak O, Oehr C, Surmenev RA, Nano-hydroxyapatite-coated metal-ceramic composite of iron-tricalcium phosphate: improving the surface wettability, adhesion and proliferation of mesenchymal stem cells in vitro, 386–393, Copyright (2015), with permission from Elsevier)

As a measure to achieve the dual aims of bacterial inhibition and enhancement of osteoblast functions of implant materials, silver-containing HA (Ag-HA) composite coatings are of special interest. For instance, successful results have been shown recently for silver-incorporated HA coatings developed by plasma electrolytic oxidation process on Ti6Al4V substrates [92]. Significant antibacterial properties and considerable biocompatibility as well as low toxicity of the Ag-HA thin films electrochemically deposited on TiO<sub>2</sub> nanotubes were shown elsewhere [93]. Similar results have been reported for silver-containing HA coating synthesized by sol-gel method [94], plasma spraying [95], and ion beam-assisted deposition [96, 97]. The coating was evaluated to be effective against *E. coli* and *S. aureus*. So, silver-doped HA coating seems to be very promising as a bone graft substitution material. The incorporation of the silver ions into the structure of HA coating revealed its homogenous distribution within the apatite structure and sustained release, which is the key factor to provide the long-term antibacterial effect after implantation. One-step coating technique refers to the technique that deposits the Ag- or Si-substituted

HA films with the simultaneous addition of Ag or Si and HA during the deposition process. Silver or silicate could be incorporated into HA prior to the deposition process, or Ag (or Si) and HA could be utilized as two separate coating targets. Based on the success of Si-substituted apatite bone grafts, the coatings prepared via RF magnetron co-sputtering of HA and Si targets were investigated by Thian et al. [90, 91, 98].

A novel Si-doped HA-based coating, in which the silicate ions are substituted by phosphorous ions, was fabricated [99–101]. Moreover, the precursor powder of Si-HA ( $\text{Ca}_{10}(\text{PO}_4)_{6-x}(\text{SiO}_4)_x(\text{OH})_{2-x}$ , where  $x = 0.5$  and  $1.72$ ) or Ag-HA ( $\text{Ca}_{10-x}\text{Ag}_x(\text{PO}_4)_6(\text{OH})_{2-x}$ , where  $x = 0.3$  and  $1.5$ ) was used for the deposition of the Si- or Ag-doped HA films [102]. To produce an RF magnetron sputter-deposited coating, first, a powder should be synthesized with the desired chemical and phase composition (e.g., by mechanochemical synthesis); second, a target for a further sputtering should be prepared (e.g., by ceramic technology, which involves the pressing of powder into pellets followed by annealing); and third, the coating is deposited. The scheme of HA coating fabrication process is presented in Fig. 7.

A powder of Si- and Ag-substituted HA was prepared via mechanochemical activation and was used then as a precursor powder to prepare a target for sputtering.

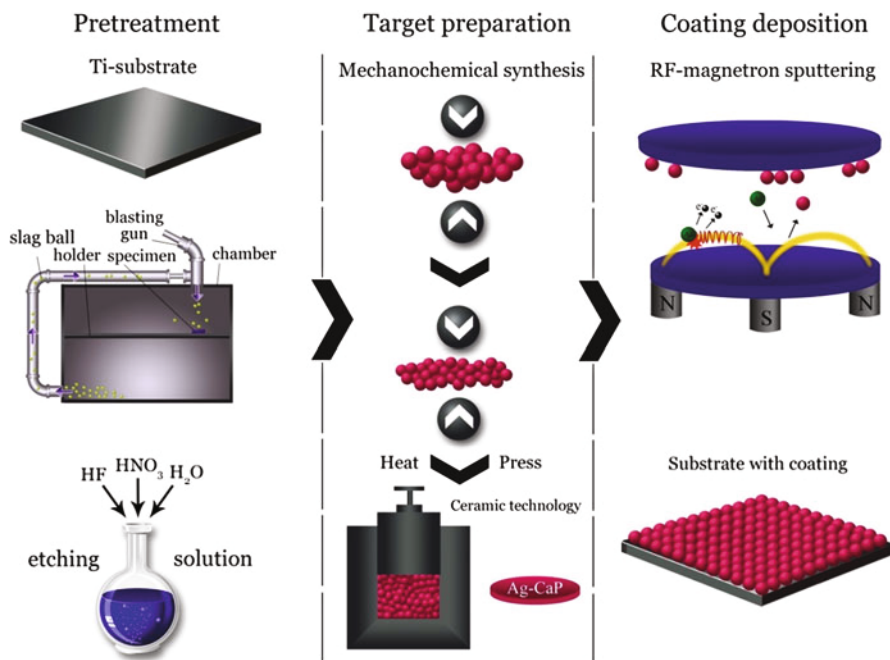


**Fig. 7** Schematic of the HA coating fabrication process [102] (Reprinted from Appl Surf Sci, 329, Ivanova AA, Surmenev RA, Surmeneva MA, Mukhametkaliyev T, Loza K, Prymak O, Epple M, Hybrid biocomposite with a tunable antibacterial activity and bioactivity based on RF magnetron sputter deposited coating and silver nanoparticles, 212–218, Copyright (2015), with permission from Elsevier)

The resulting HA, Ag-HA, and Si-HA powders exhibited an average particle size of ~70 nm [101, 103]. The investigations of the precursor powders and targets for sputtering were previously described [100, 101, 103]. It is very important to note that, in the case of Si-HA powder containing 1.22 and 4.9 at.% of Si, the preparation of the target resulted in the formation of the CaP phases HA and tricalcium phosphate (TCP), as determined by X-ray powder diffraction [100, 101]. Based on the obtained XRD, TEM, and HRTEM results, it can be concluded that the applied target preparation procedure in case of the Ag-doped HA nanostructured powder allows to obtain a precursor material with two uniformly distributed phases: HA and metallic silver [103].

RF magnetron sputtering of CaP thin films has been shown to offer significant advantages over other deposition techniques due to the fact that it can offer significant control over the processing conditions [104]. An extensive range of sputter deposition parameters have been investigated and shown to influence the properties of the resultant HA-based surfaces, including discharge power level [105], gas pressure [106], thermal processing conditions [107], and target stoichiometry [99, 100, 108]. For a given operational condition, the target composition and stoichiometry can directly influence the Ca/P ratio of the sputter-deposited surface [104]. The content of the silicon was 1.2 and 4.6 at.% for the coatings prepared using the Si-HA precursor powders with a chemical formula of  $\text{Ca}_{10}(\text{PO}_4)_{6-x}(\text{SiO}_4)_x(\text{OH})_{2-x}$ , where  $x = 0.5$  and  $1.72$ . It was evaluated that the content of Ag in the coating is lower than the initial Ag concentration in the sputtered target [102]. It is believed that the low silver amount in the coating is caused by a preferential sputtering phenomenon that takes place during RF magnetron sputtering. A similar observation was made in the case of Sr-containing HA coating sputter-deposited using a Sr-HA target [109].

The RF magnetron sputter-deposited HA films are characterized by their dense nanocomposite structure, smoothness, desired chemical composition, crystallinity, suitable nanohardness, elastic modulus, and good adherence [110, 111]. Moreover, the RF magnetron sputtering offers the possibility of tuning crystallographic orientations of HA coatings [112].

Ionic substitution of the HA structure of the films not only changes the chemical composition but also physicochemical and mechanical properties, such as morphology and crystallinity [102, 113]. The hardness and elastic modulus were found to decrease for the Si-HA thin films compared with the HA. The Si doping influenced the surface morphology and led to a smaller grain size. The tendency to form an amorphous structure increased with an increase in the Si content. The Si atoms could segregate on the HA crystallite surface and become incorporated into the HA structure and were found to be in the form of  $\text{SiO}_4^{4-}$  groups by being substituted in place of the phosphate groups of the HA structure. The segregation of Si atoms on the HA crystallite surface is responsible for the limitation of their growth. This segregation results in the formation of the amorphous phase in the HA films. The influence on the crystallinity and biological properties of the magnetron sputter-deposited films due to the silicate doping of the CaP coating was examined by the authors [91, 99]. The partial dissolution of the CaP ceramic initiates the re-precipitation of the biological apatite crystals and subsequent protein and cell

attachment to the implant surface [81]. Amorphous CaP coatings present faster bone formation and produced higher cell differentiation in *in vitro* studies [81]. However, crystalline HA-based films are preferred when long-term stability of the implant is desirable [82].

As-deposited sputtered Si-HA coatings with 4.6 at.% of Si are amorphous but can be annealed using an appropriate energy source to increase the presence of crystalline phases [104]. The annealed silicate-containing HA-based coatings have shown an improvement in biological performance over their undoped counterparts [90, 91].

It was found that the content of Ag in the coating is lower than the initial Ag concentration in the target being sputtered. Further studies were focused on the preparation of a multifunctional biocomposite based on an HA coating and silver nanoparticles (AgNPs) (Fig. 8) and the appropriate content of Ag needed to reach optimal antibacterial property without cytotoxicity [114]. AgNPs synthesized by a wet-chemical reduction method were deposited on Ti substrates using a dripping/drying method followed by deposition of CaP coating via RF magnetron sputtering.

The cumulative concentration of Ag ions released from the biocomposite after 7 days of immersion in phosphate and acetate buffers was estimated [114]. The obtained results revealed that the amount of silver in the solutions was  $0.27 \pm 0.02$

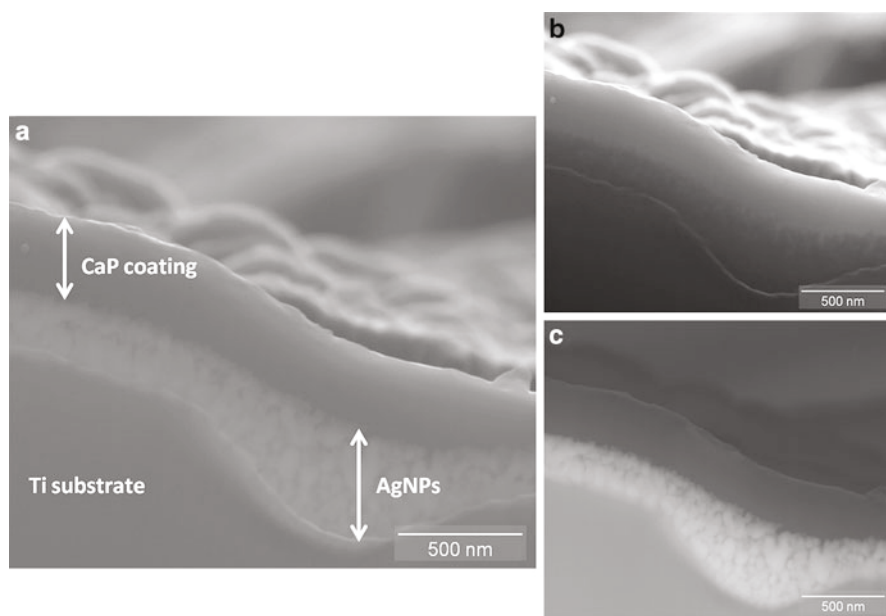


**Fig. 8** (a) SEM image of the biocomposite cross section, (b) image obtained from a secondary electron beam, and (c) backscattering reflections [114] (Reprinted from *Appl Surf Sci*, 329, Ivanova AA, Surmenev RA, Surmeneva MA, Mukhametkaliyev T, Loza K, Prymak O, Epple M, Hybrid biocomposite with a tunable antibacterial activity and bioactivity based on RF magnetron sputter deposited coating and silver nanoparticles, 212–218, Copyright (2015), with permission from Elsevier)

$\mu\text{g mL}^{-1}$  and  $0.54 \pm 0.02 \mu\text{g mL}^{-1}$  for the phosphate and acetate buffers, respectively, which is at the edge of the minimum inhibitory concentration range of silver ions reported in the literature. Thus, this study established a new route to prepare a biocompatible layer with the embedded AgNPs to achieve a local antibacterial effect.

The developed biocomposite will be investigated *in vitro* and *in vivo* to provide further evidence of their potential biomedical application. In the review paper [115], the authors discussed different applications of the combination of silver nanoparticles with HA and its use as bone graft biomaterials together with the addition of silicate. Therefore, it will be interesting to combine further the antibacterial effect of Ag nanoparticles and bioactivity of the Si-HA films.

The Ag-doped HA can be also prepared by magnetron sputtering using two targets in a confocal geometry made of HA (99.9 % purity) and Ag (99.9 % purity), respectively. By using this method, the Ag content in the HA coatings will be controlled. The XRD pattern of the as-deposited HA coatings with Ag addition (Ag = 3 at.%) prepared by magnetron co-sputtering is presented in Fig. 9. For the as-deposited Ag-HA films, the XRD revealed only the Ag and substrate peaks, indicating that the HA coatings were amorphous, as reported by almost all groups working with magnetron sputtering method [116–118]. For changing their crystallinity, the Ag-HA coatings were annealed at 600 °C for 30 and 120 min in a mixed atmosphere of  $\text{N}_2 + \text{H}_2\text{O}$  vapors with the heating rate of 12 °C/min. The XRD patterns of the Ag-HA coatings annealed at 600 °C for 30 and 120 min were illustrated in Fig. 9. After the thermal annealing, the location of the main peaks corresponding to HA was appeared. The Ag addition had no influence on the stoichiometry of HA. The SEM analysis showed that the surface of all coating is covered with some white spots, which represents local region with oxidation products, most probably phosphorous oxides. According to the AFM images shown in Fig. 9, as-deposited Ag-HA coatings were smooth, and after annealing treatment at 600 °C for 30 min, the coated surfaces are roughened, having some dome-rounded grains. Further increasing treatment time, enlarged boundary grains were seen.

The electrochemical results performed in artificial saliva confirm that HA coatings with Ag addition provide an efficient corrosion protection of Ti6Al4V substrate. Moreover, the corrosion behavior of the HA coatings with Ag addition was similar or better to the corrosion behavior of the HA coatings without Ag addition (Fig. 10). To sum up, it can be seen that the addition of small Ag content into the HA structures could be used for the improvement of the antibacterial properties of the HA-coated implants, because it does not influence the microstructure, morphology, or corrosion resistance of the HA coatings.

---

## Adhesion of the Bioceramic Coatings

In medical applications, the bonding between the coatings and metallic substrates plays an important role. The adhesion of coating/substrate system influences the mechanical, anticorrosive, tribological, and biological characteristics and the

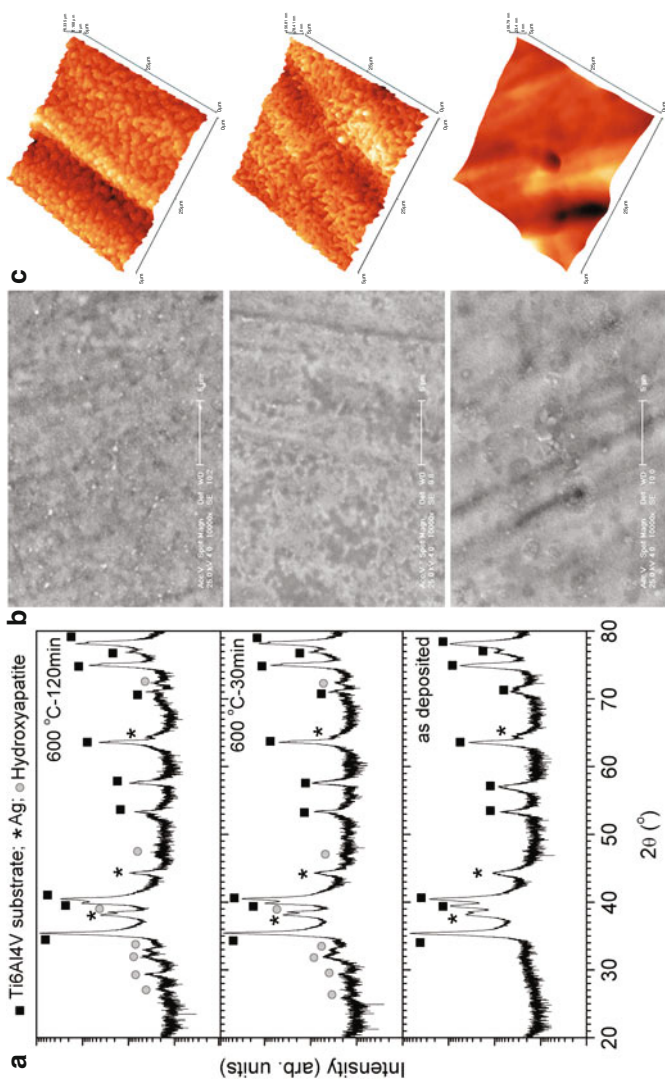


**Fig. 9** Surface characterization of the Ag-doped HA-deposited films before and after thermal treatment on Ti6Al4V alloy (Ag = 3 at.%): XRD patterns (a), SEM (b), and AFM images (c)

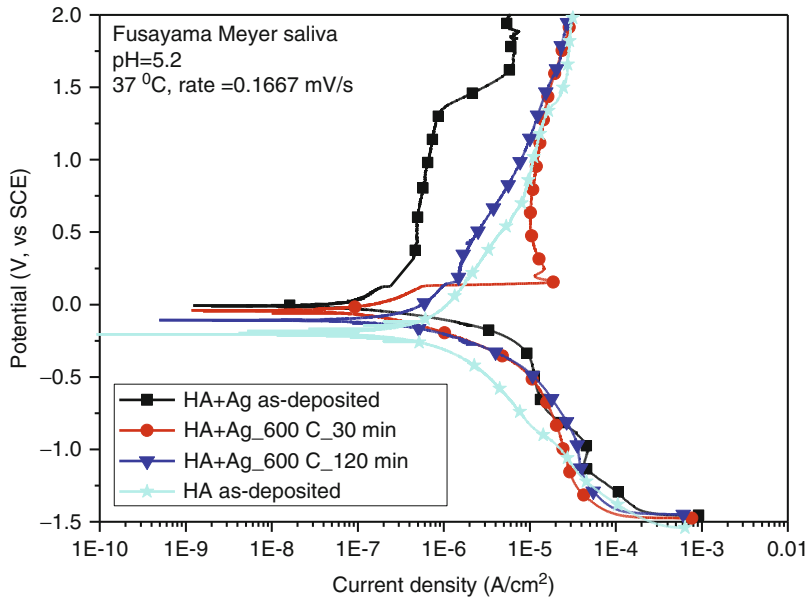


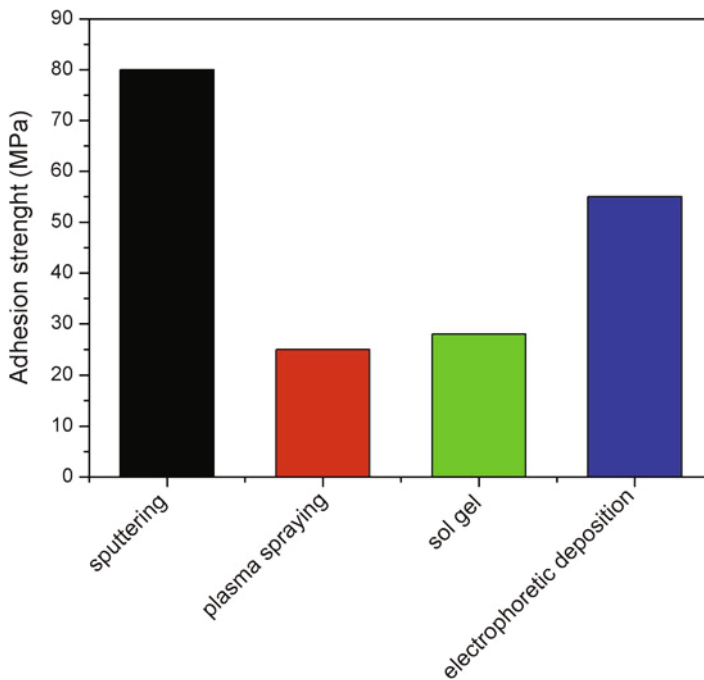
**Fig. 10** Potentiodynamic curves of the HA with 3 at. % Ag addition

integrity of the implant. The delamination of the coatings from the implant surface during the surgery or service in the human body could lead to the rejection of the implants to the adverse effects on the surrounding tissues after implantation. For the bioceramics, the adhesion can be measured by various techniques, depending on the type of bioceramics. Despite the constant improvements and developments in the techniques for determining the adhesion of the coating, several of these are limited for the bioceramic coatings. The choice for each test must be established considering the substrate and coating roughness, thickness, type of substrate, residual stress, and thermal expansion coefficients of coating/substrate system. Recommended adhesion tests for the bioceramic coatings used for biomedical applications are given in Table 3.

For the bioinert coatings, the scratch test is the most widely used technique, performed in concordance to the ISO 20502:2005. Many researchers reported that the adhesion of the carbonitrides/carbides/nitrides/oxynitrides to the metallic substrates could be improved by addition of thin interlayer between coatings and the substrate, with thickness of about 50 nm. For example, Ti [119–122] or SiC [123–125] or Ta [126] or AlN [127] interlayers were added between titanium-based alloy substrates and nitrides, oxynitrides, or carbon-based coatings. For the bioactive coatings, various types of interlayers were proposed such as SiC [128], SiO<sub>2</sub> [129], TiO<sub>2</sub> [130], Ti [131, 132], or TiAlVN [133]. It can be seen that there are a limited number of papers about the addition of interlayers between the metallic substrates and bioactive coatings prepared by RF magnetron sputtering. All researchers agreed that these interlayers improve the adhesion and reduce the

**Table 3** Adhesion tests appropriate for various bioceramic coatings

Adhesion test	Standard	Nitrides/ oxynitrides	Carbon-based coatings	Calcium phosphates, bioglass	Oxides
Scratch	ISO20502	√	√		
Pull-off	ISO 4624			√	√
Scribe-grid	ASTM B571	√	√		
Peel	ASTM B571	√			√
Shear strength	DIN 50,161	√	√	√	√
Tensile test	ASTM C633 ASTM F1147	√	√		√
Nanoindentation		√	√	√	√

**Fig. 11** Adhesion of the bioactive coatings prepared by various techniques

mismatch of thermal expansion coefficients between the ceramics and substrates, leading to the enhancement of the mechanical, tribological, and anticorrosive properties.

In Fig. 11, we present the adhesion of the bioactive coatings deposited on Ti6Al4V alloy by various techniques. The sputtered bioactive coatings exhibited the best adhesion, followed by coatings prepared by electrophoretic deposition.



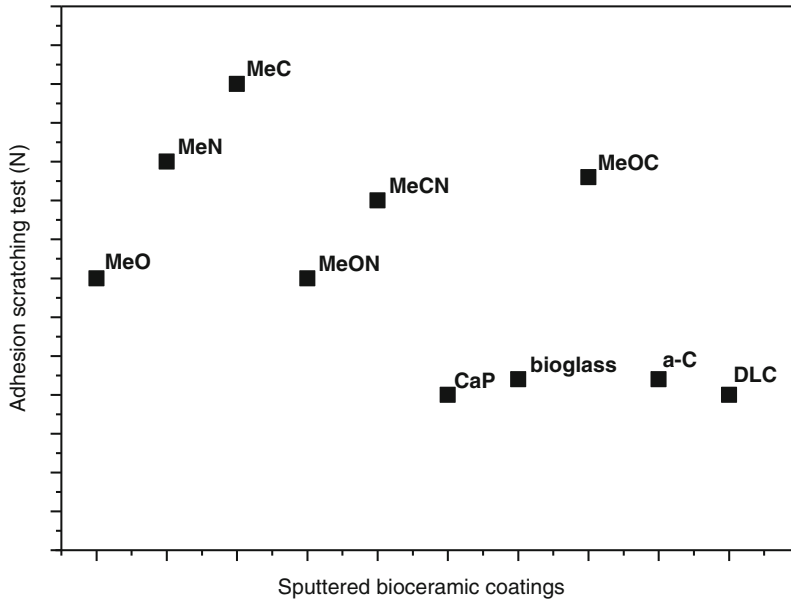


**Fig. 12** Adhesion by scratch test of the bioceramic coatings on metallic substrates

Also, the adhesion of different sputtered coatings is presented in Fig. 12. It can be seen that the high adhesion was found for the carbides. The oxynitrides or oxycarbides exhibited the adhesion between those of oxides and nitrides and carbides, respectively. Calcium phosphates, bioglass, and amorphous carbon proved to have a poor adhesion to metallic substrates, leading to the delamination of the films under fluid action and/or mechanical action. In this case, many researchers demonstrated that the addition of an adhesion layer, between coatings and substrate, is a well-known solution for the increasing adhesion of bioceramics to the metallic substrates [49, 132, 134].

## Summary

Mechanism of implant failure is recently the target of intensive research in order to increase their service life, since the bone fixation devices and artificial joints comprise 44 % of all medical devices. The demand on the improvement of implant's osseointegration, the bone bonding, and antibacterial properties call for the development of new coatings, with the improved properties related to wear and corrosion resistance and antibacterial and biocompatible character. This imposes strong requirements on the quality of the coatings, such as a high hardness combined with a high resistance against crack formation and adhesion to the substrate, superior corrosion and wear resistance, low friction coefficient,

absence of toxic reaction with the tissues surrounding implants, good protein adsorption, and cell adhesion.

It was demonstrated that the bioactive coatings are actively used to enhance biological fixation between the bone and the metallic implant, despite their poor mechanical and tribological properties and bioinert coatings for improving the service life of load-bearing implants due to their superior tribological properties in corrosive environment. All these will lead to better clinical success rates in the long term than uncoated metallic implants. On the other hand, the combination of excellent mechanical and tribological properties with antimicrobial properties, biocompatibility, and bioactivity is of great importance for the clinical application of the implants. This result could be obtained only by developing methods for biofunctionalization of the metallic surfaces by changes in material's surface composition, structure, and morphology, leaving intact the mechanical, anticorrosive, tribological, and biocompatible bulk properties. These requirements can be satisfied if coatings with unique combinations of properties could be produced. The bioceramic coatings could be a good solution, and their field is in progress, aiming at the developing of improved manufacturing processes, finding new or enhanced applications, and promoting the expansion of these materials on a global level.

**Acknowledgements** The authors thank Prof. M. Epple for fruitful discussions. This research was supported by different grants: FP7 Marie Curie (no.327701), Russian President's Stipend (no.SP-6664.2013.4, no.MK-485.2014.8), State order NAUKA (no.#11.1359.2014/K) and Romanian National Authority for Scientific Research (no.PN-II-PT-PCCA-2014-212). The authors are thankful to Mrs. A.A. Ivanova, Mrs. I.Y. Grubova, Mr. T.M. Mukhametkaliyev, Dr. O. Prymak, Mrs. G. Vacun, Dr. K. Kleinhans for help with the investigations.

---

## References

1. Giudice M, Colella G, Marra A (1982) Clinical applications of biomaterials. *NIH Consens Statement* 4(5):1–19
2. Hanawa T (2010) Biofunctionalization of titanium for dental implant. *Jpn Dent Sci Rev* 46:93–101
3. Chien CC, Liu KT, Duh JG, Chan KW, Chun KH (2008) Effect of nitride film coatings on cell compatibility. *Dent Mater* 24:986–993
4. Probst J, Gbureck U, Thull R (2001) Binary nitride and oxynitride PVD coatings on titanium for biomedical applications. *Surf Coat Technol* 148:226–233
5. Brama M, Rhodes N, Hunt J, Ricci A, Teghil R, Migliaccio S, Rocca CD, Leccisotti S, Lioi A, Scandurra M, Maria GD, Ferro D, Pu F, Panzini G, Politi L, Scandurra R (2007) Effect of titanium carbide coating on the osseointegration response in vitro and in vivo. *Biomaterials* 28:595–608
6. Denry I, Kelly JR (2008) State of the art of zirconia for dental applications. *Dent Mater* 24:299–307
7. Yang Y, Park S, Liu Y, Lee K, Kim HS, Koh JT, Meng X, Kim K, Ji H, Wang X, Ong JL (2008) Development of sputtered nanoscale titanium oxide coating on osseointegrated implant devices and their biological evaluation. *Vacuum* 83:569–574
8. Koerner RJ, Butterworth LA, Mayer IV, Dasbach R, Busscher HJ (2002) Bacterial adhesion to titanium-oxy-nitride (TiNOX) coatings with different resistivities: a novel approach for the development of biomaterials. *Biomaterials* 23:2835–2840

9. Thian ES, Huang J, Best SM, Barber ZH, Bonfield W (2007) Silicon-substituted hydroxyapatite: the next generation of bioactive coatings. *Mater Sci Eng C* 27:251–256
10. Heimann RB, Lehmann HD (2015) *Bioceramic coatings for medical implants: trends and techniques*. Wiley, Weinheim, p 496
11. O’Gorman J, Humphreys H (2012) Application of copper to prevent and control infection. Where are we now? *J Hosp Infect* 81:217–223
12. Liu Q, Matinlinna JP, Chen Z, Ning C, Ni G, Pan H, Darvell BW (2015) Effect of thermal treatment on carbonated hydroxyapatite: morphology, composition, crystal characteristics and solubility. *Ceram Int* 41:6149–6157
13. Suchanek K, Bartkowiak A, Gdowik A, Perzanowski M, Kac S, Szaraniec B, Suchanek M, Marszałek M (2015) Crystalline hydroxyapatite coatings synthesized under hydrothermal conditions on modified titanium substrates. *Mater Sci Eng C* 51:57–63
14. Hing KA, Best SM, Bonfield W (1999) Characterization of porous hydroxyapatite. *J Mater Sci* 10:135–145
15. Zhao J, Dong X, Bian M, Zhao J, Zhang Y, Sun Y, Chen JH, Wang XH (2014) Solution combustion method for synthesis of nanostructured hydroxyapatite, fluorapatite and chlorapatite. *Appl Surf Sci* 314:1026–1033
16. Ferraz MP, Monteiro FJ, Manuel CM (2004) Hydroxyapatite nanoparticles: a review of preparation methodologies. *J Appl Biomater Biomech* 2:74–80
17. Li C, Ge X, Li G, Gao Q, Ding R (2014) A facile hydrothermal method for synthesis of submillimeter-long octacalcium phosphate and hydroxyapatite as drug carriers with sustained release behaviors. *Adv Powder Technol* 25:1661–1666
18. Kondyurin A, Bilek M (2015) Biological and medical applications. In: *Ion beam treatment of polymers*, 2nd edn. Application aspects from medicine to space. Amsterdam, Netherlands; Oxford, UK; Waltham, MA: Elsevier, pp 185–216
19. Greish Y, Brown PW (2003) Phase evolution during the formation of stoichiometric hydroxyapatite at 37.4 degrees C. *J Biomed Mater Res B Appl Biomater* 67:632–637
20. Zhang H, Zhang M (2011) Characterization and thermal behavior of calcium deficient hydroxyapatite whiskers with various Ca/P ratios. *Mater Chem Phys* 126:642–648
21. Ren Y, Zhou H, Nabiyouni M, Bhaduri SB (2015) Rapid coating of AZ31 magnesium alloy with calcium deficient hydroxyapatite using microwave energy. *Mater Sci Eng* 49:364–372
22. Hurler K, Neubauer J, Bohner M, Doebelin N (2014) Friedlinde Goetz-Neunhoffer, effect of amorphous phases during the hydraulic conversion of  $\alpha$ -TCP into calcium-deficient hydroxyapatite. *Acta Biomater* 10:3931–3941
23. Bakhsheshi-Rad HR, Hamzah E, Daroonparvar M, Yajid MAM, Kasiri-Asgarani M, Abdul-Kadir MR, Medraj M (2014) In-vitro degradation behavior of Mg alloy coated by fluorine doped hydroxyapatite and calcium deficient hydroxyapatite. *Trans Nonferrous Metals Soc China* 24:2516–2528
24. Wang H, Zhu S, Wang L, Feng Y, Ma X, Guan S (2014) Formation mechanism of Ca-deficient hydroxyapatite coating on Mg–Zn–Ca alloy for orthopaedic implant. *Appl Surf Sci* 307:92–100
25. Acevedo-Dávila JL, López-Cuevas J, Vargas-Gutiérrez G, Rendón-Angeles JC, Méndez-Nonell J (2007) Chemical synthesis of bone-like carbonate hydroxyapatite from hen eggshells and its characterization. *Boletín de la Sociedad Española de Cerámica y Vidrio* 46:225–231
26. Stanić V, Radosavljević-Mihajlović AS, Živković-Radovanović V, Nastasijević B, Marinović-Cincović M, Marković JP, Budimir MD (2015) Synthesis, structural characterisation and antibacterial activity of Ag + -doped fluorapatite nanomaterials prepared by neutralization method. *Appl Surf Sci* 337:72–80
27. Shanmugam S, Gopal B (2014) Copper substituted hydroxyapatite and fluorapatite: synthesis, characterization and antimicrobial properties. *Ceram Int* 40:15655–15662
28. Bae J, Ida Y, Sekine K, Kawano F, Hamada K (2015) Effects of high-energy ball-milling on inject ability and strength of  $\beta$ -tricalcium-phosphate cement. *J Mech Behav Biomed Mater* 47:77–86

29. Alshemary AZ, Goh YF, Shakir I, Hussain R (2015) Synthesis, characterization and optical properties of chromium doped  $\beta$ -Tricalcium phosphate. *Ceram Int* 41:1663–1669
30. Singh SS, Roy A, Lee BE, Banerjee I, Kumta PN (2014) MC3T3-E1 proliferation and differentiation on biphasic mixtures of Mg substituted  $\beta$ -tricalcium phosphate and amorphous calcium phosphate. *Mater Sci Eng* 45:589–598
31. Ko CL, Chang YY, Liou CH, Chen WC (2015) Characterization of the aspects of osteoprogenitor cell interactions with physical tetracalcium phosphate anchorage on titanium implant surfaces. *Mater Sci Eng* 49:7–13
32. Moseke C, Gbureck U (2010) Tetracalcium phosphate: synthesis, properties and biomedical applications. *Acta Biomater* 6:3815–3823
33. Hiromoto S, Inoue M, Taguchi T, Yamane M, Ohtsu N (2015) In vitro and in vivo biocompatibility and corrosion behaviour of a bioabsorbable magnesium alloy coated with octacalcium phosphate and hydroxyapatite. *Acta Biomater* 11:520–530
34. Li C, Ge X, Li Y, Bai J, Li G, Su C, Yang Z (2015) Modulation of release behaviors of methylene blue from degradable silica-methylene blue@octacalcium phosphate powders with different shell structures. *Colloids Surf A Physicochem Eng Asp* 472:78–84
35. Itoigawa Y, Suzuki O, Sano H, Anada T, Handa T, Hatta T, Kuwahara Y, Takahashi A, Ezoe Y, Kaneko K, Itoi E (2015) The role of an octacalcium phosphate in the re-formation of infraspinatus tendon insertion. *J Shoulder Elbow Surg* 24:75–84
36. Jalota S, Bhaduri SB, Tas AC (2007) A new rhenanite ( $\beta$ -NaCaPO<sub>4</sub>) and hydroxyapatite biphasic biomaterial for skeletal repair. *J Biomed Mater Res B Appl Biomater* 80:304–316
37. Rey C, Fella BH, Miramond T (2014) Advances in calcium phosphate biomaterials. In: Ben-Nissan B (ed) Springer series in biomaterials science and engineering. Springer, Heidelberg. vol 2. Sydney
38. Stan GE (2009) Adherent functional graded hydroxylapatite coatings produced by sputtering deposition techniques. *J Optoelectron Adv Mater* 11:1132–1138
39. Ding SJ (2003) Properties and immersion behavior of magnetron-sputtered multi-layered hydroxyapatite/titanium composite coatings. *Biomaterials* 24:4233–4238
40. Choi JM, Kim HE, Lee IS (2000) Ion-beam-assisted deposition (IBAD) of hydroxyapatite coating layer on Ti-based metal substrate. *Biomaterials* 21:469–473
41. De Groot K, Geesink R, Klein C, Serekian P (2004) Plasma sprayed coatings of hydroxylapatite. *J Biomed Mater Res* 21:1375–1381
42. Li P, Kd G, Kokubo T (1996) Bioactive Ca<sub>10</sub>(PO<sub>4</sub>)<sub>6</sub>(OH)-TiO<sub>2</sub> composite coating prepared by sol-gel process. *J Sol-Gel Sci Technol* 7:27–34
43. Gross KA, Berndt CC (1998) Thermal processing of hydroxyapatite for coating production. *J Biomed Mater Res* 39:580–587
44. Han Y, Fu T, Lu J, Xu K (2000) Characterization and stability of hydroxyapatite coatings prepared by an electrodeposition and alkaline-treatment process. *J Biomed Mater Res* 54:96–101
45. Cleries L, Martinez E, Fernandez-Pradas J, Sardin G, Esteve J, Morenza J (2000) Mechanical properties of calcium phosphate coatings deposited by laser ablation. *Biomaterials* 21:967–971
46. Yoshinari M, Ohtsuka Y, Dérand T (1994) Thin hydroxyapatite coating produced by the ion beam dynamic mixing method. *Biomaterials* 15:529–535
47. Kaciulis S, Mattogno G, Napoli A, Bemporad E, Ferrari F, Montenero A, Gnappi G (1998) Surface analysis of biocompatible coatings on titanium. *J Electron Spectrosc Relat Phenom* 95:61–69
48. Habibovic P, Barrere F, Blitterswijk CA, Groot K, Layrolle P (2002) Biomimetic hydroxyapatite coating on metal implants. *J Am Ceram Soc* 85:517–522
49. Mohseni E, Zalnezhad E, Bushroa AR (2014) Comparative investigation on the adhesion of hydroxyapatite coating on Ti–6Al–4V implant: a review paper. *Int J Adhes Adhes* 48:238–257

50. Hallab NJ, Jacobs JJ, Gilbert JL (2006) Corrosion of Metallic Implants Nadim James Hallab. In: Shanbhag A, Rubash HE, Jacobs JJ (eds) Joint replacement and bone resorption. Taylor & Francis, New York, p 211
51. von Fraunhofer JA (1994) Protection by metallic coatings. In: Shrier LL, Jarman RA, Burstein GT (eds) Corrosion, 3rd edn. Butterworth Heinemann, Oxford, p 155
52. Shi JZ, Chen CZ, Yu HJ, Zhang SJ (2008) Application of magnetron sputtering for producing bioactive ceramic coatings on implant materials. *Bull Mater Sci* 31:877–884
53. Bendavid A, Martin PJ (2014) Review of thin film materials deposition by the filtered cathodic vacuum arc process at CSIRO. *J Australas Ceram Soc* 50:86–101
54. Anders A (2008) Cathodic arcs: from fractal spots to energetic condensation. Springer, New York, p 544
55. Arifin A, Sulong AB, Muhamad N, Syarif J, Ramli MI (2014) Material processing of hydroxyapatite and titanium alloy (HA/Ti) composite as implant materials using powder metallurgy: a review. *Mater Des* 55:165–175
56. Surmenev RA (2012) A review of plasma-assisted methods for calcium phosphate-based coatings fabrication. *Surf Coat Technol* 206:2035–2056
57. Park JE, Park IS, Bae TS, Lee MH (2014) Electrophoretic deposition of carbon nanotubes over TiO<sub>2</sub> nanotubes: evaluation of surface properties and biocompatibility. *Bioinorganic Chemistry and Applications*, 2014, Article ID 236521, p. 7
58. Rada AT, Hashjinc MS, Osmand NAA, Faghihia S (2014) Improved bio-physical performance of hydroxyapatite coatings obtained by electrophoretic deposition at dynamic voltage. *Ceram Int* 40:12681–12691
59. Yang Y, Kim KH, Ong JL (2005) A review on calcium phosphate coatings produced using a sputtering process-an alternative to plasma spraying. *Biomaterials* 26:327–337
60. Hollstein F, Kitta D, Louda P, Pacal F, Meinhardt J (2001) Investigation of low-reflective ZrCN–PVD-arc coatings for application on medical tools for minimally invasive surgery. *Surf Coat Technol* 1063:142–144
61. Serro AP, Completo C, Colaço R, Santos F, Silva CL, Cabral JMS, Araújo H, Pires E, Saramago B (2009) A comparative study of titanium nitrides, TiN, TiNbN and TiCN, as coatings for biomedical applications. *Surf Coat Technol* 203:3701–3707
62. Konca E, Cheng YT, Weiner AM, Dasch JM, Erdemir A, Alpas AT (2005) Transfer of 319 Al alloy to titanium diboride and titanium nitride based (TiAlN, TiCN, TiN) coatings: effects of sliding speed, temperature and environment. *Surf Coat Technol* 200:2260–2270
63. Balaceanu M, Petreus T, Braic V, Zoita CN, Vladescu A, Cotrut CM, Braic M (2010) Characterization of Zr-based hard coatings for medical implant applications. *Surf Coat Technol* 204:2046–2050
64. Cavaleiro A, Trindade B, Vieira MT (2003) Influence of Ti addition on the properties of W–Ti–C/N sputtered films. *Surf Coat Technol* 174–175:68–75
65. Zhang X, Jiang J, Yuqiao Z, Lin J, Wang F, Moore JJ (2008) Effect of carbon on TiAlCN coatings deposited by reactive magnetron sputtering. *Surf Coat Technol* 203:594–597
66. Caicedo JC, Amaya C, Yate L, Aperador W, Zambrano G, Gómez ME, Rivera JA, Saldaña JM, Prieto P (2010) TiCN/TiNbCN multilayer coatings with enhanced mechanical properties. *Appl Surf Sci* 256:5898–5904
67. Zhang S, Fu Y, Du H, Zeng XT, Liu YC (2003) Magnetron sputtering of nanocomposite (Ti, Cr)CN/DLC coatings. *Surf Coat Technol* 162:42–48
68. Shtansky DV, Kiryukhantsev-Korneev Ph V, Bashkova IA, Sheveiko AN, Levashov EA (2010) Multicomponent nanostructured films for various tribological applications. *Int J Refract Met Hard Mater* 28:32–39
69. Roy RK, Lee KR (2007) Biomedical applications of diamond-like carbon coatings: a review. *J Biomed Mater Res B Appl Biomater* 83:72–84
70. Zeng Y, Qiu Y, Xiangyang M, Shuyong T, Zhen T, Xuhai Z, Jian C, Jianqing J (2015) Superhard TiAlCN coatings prepared by radio frequency magnetron sputtering. *Thin Solid Films* 584:283–288

71. Caicedo JC, Amaya C, Yate L, Aperador W, Zambrano G, Gómez ME, Alvarado-Rivera J, Muñoz-Saldaña J, Prieto P (2010) Effect of applied bias voltage on corrosion-resistance for TiC1 – xNx and Ti1 – xNbxC1 – yNy coatings. *Appl Surf Sci* 256:2876–2883
72. Li D, Guruvankar S, Azzi M, Szpunar JA, Klemborg-Sapieha JE, Martinu L (2010) Corrosion and tribo-corrosion behavior of a-SiCx:H, a-SiNx:H and a-SiCxNy:H coatings on SS301 substrate. *Surf Coat Technol* 204:1616–1622
73. Ordine A, Achete CA, Mattos OR, Margarit ICP, Camargo SS Jr, Hirscht T (2000) Magnetron sputtered SiC coatings as corrosion protection barriers for steels. *Surf Coat Technol* 133–134:583–588
74. Li X, Wang X, Bondokov R, Morris J, An YH, Sudarshan Tangali S (2005) Micro/ nanoscale mechanical and tribological characterization of SiC for orthopedic applications. *J Biomed Mater Res B* 72:353–361
75. Suchanek WL, Byrappa K, Shuk P, Riman RE, Janas VF, TenHuisen KS (2004) Preparation of magnesium-substituted hydroxyapatite powders by the mechanochemical-hydrothermal method. *Biomaterials* 25:4647–4657
76. Azem F, Ak KA, Birlik I, Braic V, Luculescu C, Vladescu A (2014) The corrosion and bioactivity behaviour of SiC doped hydroxyapatite for dental applications. *Ceram Int* 40:15881–15887
77. Vladescu A, Birlik I, Braic V, Toparli M, Celik E, Ak Azem F (2014) Enhancement of the mechanical properties of hydroxyapatite by SiC addition. *J Mech Behav Biomed Mater* 40:362–368
78. Hermawan H (2012) Biodegradable metals: from concept to applications, S.-V.B.H.S., SpringerBriefs in materials Springer, Berlin/New York, 69 p
79. Kannan MB, Singh Raman RK (2008) In vitro degradation and mechanical integrity of calcium-containing magnesium alloys in modified-simulated body fluid. *Biomaterials* 29:2306–2314
80. Hornberger H, Virtanen S, Boccaccini AR (2012) Biomedical coatings on magnesium alloys – a review. *Acta Biomater* 8:2442–2455
81. Bosco R, Edreira ERU, Wolke JGC, Leeuwenburgh SCG, Beucken JJJP, Jansen JA (2013) Instructive coatings for biological guidance of bone implants. *Surf Coat Technol* 233:91–98
82. Surmenev RA, Surmeneva MA, Ivanova AA (2014) Significance of calcium phosphate coatings for the enhancement of new bone osteogenesis – a review. *Acta Biomater* 10:557–579
83. Surmenev RA, Ryabtseva MA, Shesterikov EV, Pichugin VF, Peitsch T, Epple M (2010) The release of nickel from nickel-titanium (NiTi) is strongly reduced by a sub-micrometer thin layer of calcium phosphate deposited by rf-magnetron sputtering. *J Mater Sci Mater Med* 21:1233–1239
84. Surmeneva MA, Surmenev RA (2015) Microstructure characterization and corrosion behaviour of a nano-hydroxyapatite coating deposited on AZ31 magnesium alloy using radio frequency magnetron sputtering. *Vacuum* 117:60–62
85. Surmeneva MA, Mukhametkaliyev TM, Khakbaz H, Surmenev RA, Kannan BM (2015) Ultrathin film coating of hydroxyapatite (HA) on a magnesium-calcium alloy using RF magnetron sputtering for bioimplant applications. *Mater Lett* 152:280–282
86. Surmeneva MA, Tyurin AI, Mukhametkaliyev TM, Pirozhkova TS, Shuvarin IA, Syrtanov MS, Surmenev RA (2015) Enhancement of the mechanical properties of AZ31 magnesium alloy via nanostructured hydroxyapatite thin films fabricated via radio-frequency magnetron sputtering. *J Mech Behav Biomed Mater* 46:127–136
87. Kleinhans C, Vacun G, Surmenev R, Surmeneva M, Kluger PJ (2014) Testing the in vitro performance of hydroxyapatite coated magnesium (AZ91D) and titanium concerning cell adhesion and osteogenic differentiation. *BioNanoMaterials* 16:41–50
88. Surmeneva MA, Kleinhans C, Vacun G, Kluger PJ, Mukhametkaliyev TM, Syromotina DS, Schönhaar V, Müller M, Hein SB, Wittmar A, Ulbricht M, Prymak O, Oehr C, Surmenev RA (2015) Nano-hydroxyapatite-coated metal-ceramic composite of iron-tricalcium phosphate:

- improving the surface wettability, adhesion and proliferation of mesenchymal stem cells in vitro. *Colloids Surf B Biointerfaces* 135:386–393
89. Best SM, Porter AE, Thian ES, Huang J (2008) Bioceramics: past, present and for the future. *J Eur Ceram Soc* 28:1319–1327
  90. Thian ES, Huang J, Best SM, Barber ZH, Bonfield W (2006) Novel silicon-doped hydroxyapatite (Si-HA) for biomedical coatings: an in vitro study using acellular simulated body fluid. *J Biomed Mater Res B* 76:326–333
  91. Thian ES, Huang J, Best SM, Barber ZH, Bonfield W (2005) Magnetron co-sputtered silicon-containing hydroxyapatite thin films – an in vitro study. *Biomaterials* 26:2947–2956
  92. Zhou L, Lü GH, Mao FF, Yang SZ (2014) Preparation of biomedical Ag incorporated hydroxyapatite/titania coatings on Ti6Al4V alloy by plasma electrolytic oxidation. *Chin Phys B* 23:035205
  93. Yan YJ, Zhang X, Huang Y, Ding Q, Panga X (2014) Antibacterial and bioactivity of silver substituted hydroxyapatite/TiO<sub>2</sub> nanotube composite coatings on titanium. *Appl Surf Sci* 314:348–357
  94. Iconaru SL, Chapon P, Coustumer P Le, Predoi D (2014) Antimicrobial activity of thin solid films of silver doped hydroxyapatite prepared by sol-gel method. *Sci World J* 2014:8 pp
  95. Podporska-Carroll J, Quilty B, Devery R (2013) Non-cytotoxic and antimicrobial plasma sprayed coatings for orthopaedic application. *Mater Lett* 112:54–57
  96. Bai X, More K, Rouleau CM, Rabiei A (2010) Functionally graded hydroxyapatite coatings doped with antibacterial components. *Acta Biomater* 6:2264–2273
  97. Bai X, Sandukas S, Appleford M, Ong JL, Rabiei A (2012) Antibacterial effect and cytotoxicity of Ag-doped functionally graded hydroxyapatite coatings. *J Biomed Mater Res B Appl Biomater* 100:553–561
  98. Thian ES, Huang J, Vickers ME, Best SM, Barber ZH, Bonfield W (2006) Silicon-substituted hydroxyapatite (SiHA): a novel calcium phosphate coating for biomedical applications. *J Mater Sci* 41:709–717
  99. Surmeneva MA, Kovtun A, Peetsch A, Goroja SN, Sharonova A, Pichugin VF, Teresov AD, Koval NN, Buck V, Wittmar A, Ulbricht M, Prymak O, Epple M, Surmenev RA (2013) Preparation of a silicate-containing hydroxyapatite based coating by magnetron sputtering: structure and osteoblast-like MG63 cells in vitro study. *RSC Adv* 3:11240–11246
  100. Surmeneva MA, Surmenev RA, Chaikina MV, Kachaev AA, Pichugin VF, Epple M (2013) Phase and elemental composition of silicon-containing hydroxyapatite-based coatings fabricated by RF-magnetron sputtering for medical implants. *Inorg Mater Appl Res* 4:227–235
  101. Surmeneva MA, Chaikina MV, Zaikovskiy VI, Pichugin VF, Prymak O, Epple M, Surmenev RA (2013) The structure of an RF-magnetron sputter-deposited silicate-containing hydroxyapatite-based coating investigated by high-resolution techniques. *Surf Coat Technol* 218:39–46
  102. Grubova IY, Surmeneva MA, Ivanova AA, Kravchuk K, Prymak O, Epple M, Buck V, Surmenev RA (2015) The effect of patterned titanium substrates on the properties of silver-doped hydroxyapatite coatings. *Surf Coat Technol* 276:595–601
  103. Ivanova AA, Surmeneva MA, Grubova IY, Sharonova AA, Pichugin VF, Chaikina MV, Buck V, Prymak O, Epple M, Surmenev RA (2013) Influence of the substrate bias on the stoichiometry and structure of RF-magnetron sputter-deposited silver-containing calcium phosphate coatings. *Mater Werkst* 44:218–225
  104. Boyd AR, O’Kane C, Meenan BJ (2013) Control of calcium phosphate thin film stoichiometry using multi-target sputter deposition. *Surf Coat Technol* 233:131–139
  105. van Dijk K, Schaeken HG, Wolke JGC, Maree CHM, Habraken FHPM, Verhoeven J, Jansen JA (1995) Influence of discharge power level on the properties of hydroxyapatite films deposited on Ti6Al4V with RF magnetron sputtering. *J Biomed Mater Res* 29:269–276
  106. Boyd AR, Burke GA, Duffy H, Cairns ML, Meenan BJ (2008) Characterisation of calcium phosphate/titanium dioxide hybrid coatings. *J Mater Sci Mater Med* 19:485–498

107. Boyd AR, Duffy H, McCann R, Meenan BJ (2008) Sputter deposition of calcium phosphate/titanium dioxide hybrid thin films. *Mater Sci Eng C* 28:228–236
108. O’Kane C, Duffy H, Meenan BJ, Boyd AR (2008) The influence of target stoichiometry on the surface properties of sputter deposited calcium phosphate thin films. *Surf Coat Technol* 203:121–128
109. Boyd AR, Rutledgea L, Randolph LD, Meenan BJ (2015) Strontium-substituted hydroxyapatite coatings deposited via a co-deposition sputter technique. *Mater Sci Eng C Mater Biol Appl* 46:290–300
110. Surmeneva M, Surmenev R, Nikonova Y, Selezneva I, Ivanova A, Putlyayev V, Prymak O, Epple M (2014) Fabrication, ultra-structure characterization and in vitro studies of RF magnetron sputter deposited nano-hydroxyapatite thin films for biomedical applications. *Appl Surf Sci* 317:172–180
111. Surmeneva MA, Surmenev RA, Tyurin AI, Mukhametkaliyev TM, Teresov AD, Koval NN, Pirozhkova TS, Shuvarin IA, Oehr C (2014) Comparative study of the radio-frequency magnetron sputter deposited CaP films fabricated onto acid-etched or pulsed electron beam-treated titanium. *Thin Solid Films* 571:218–224
112. Ivanova AA, Surmeneva MA, Surmenev RA, Depla D (2015) Influence of deposition conditions on the composition, texture and microstructure of RF-magnetron sputter-deposited hydroxyapatite thin films. *Thin Solid Films* 591:368–374
113. Surmeneva MA, Mukhametkaliyev TM, Tyurin AI, Teresov AD, Koval NN, Pirozhkova TS, Shuvarin IA, Shuklinov AV, Zhigachev AO, Oehr C, Surmenev RA (2015) Effect of silicate doping on the structure and mechanical properties of thin nanostructured RF magnetron sputter-deposited hydroxyapatite films. *Surf Coat Technol* 275:176–184
114. Ivanova AA, Surmenev RA, Surmeneva MA, Mukhametkaliyev T, Loza K, Prymak O, Epple M (2015) Hybrid biocomposite with a tunable antibacterial activity and bioactivity based on RF magnetron sputter deposited coating and silver nanoparticles. *Appl Surf Sci* 329:212–218
115. Lim PN, Chang L, Thian ES (2015) Development of nanosized silver-substituted apatite for biomedical applications: a review. *Nanomed Nanotechnol Biol Med* 11:1331–1344
116. van Dijk K, Schaeken HG, Wolke JGC, Jansen JA (1996) Influence of annealing temperature on RF magnetron sputtered calcium phosphate coatings. *Biomaterials* 17:405–410
117. Ong JL, Lucas LC (1994) Post-deposition heat treatments for ion beam sputter deposited calcium phosphate coatings. *Biomaterials* 15:337–341
118. Yang Y, Kim K, Agrawal CM, Ong JL (2003) Effect of post-deposition heating temperature and the presence of water vapor during heat treatment on crystallinity of calcium phosphate coatings. *Biomaterials* 24:5131–5137
119. Liu J, Li C, Chen L, Zhang YY, Hei LF, Lv FX (2011) Preparation and characterization of diamond-TiC-Ti-Ag/Cu gradient metallization system. In: *Functional and electronic materials*. Book series: Materials science forum, vol 687. pp 722–728
120. Polcar T, Vitu T, Cvreck L, Novake R, Vyskocild J, Cavaleiro A (2009) Tribological behaviour of nanostructured Ti-C:H coatings for biomedical applications. *Solid State Sci* 11:1757–1761
121. Escudeiro A, Polcar T, Cavaleiro A (2013) a-C(:H) and a-C(:H)-Zr coatings deposited on biomedical Ti-based substrates: tribological properties. *Thin Solid Films* 538:89–96
122. Vitu T, Polcar T, Cvreck L, Novak R, Macak J, Vyskocil J, Cavaleiro A (2008) Structure and tribology of biocompatible Ti-C:H coatings. *Surf Coat Technol* 202:5790–5793
123. Xu X, Chen D, Xin X, Tian K, Yu CH, Sheng XL (2011) Friction/wear properties of magnetron sputtered TiB<sub>2</sub>-TiN composite films on biomedical metallic titanium alloy. *Adv Mater Res* 284–286:2505–2508
124. Xu XJ, Wang H, Cheng XN (2009) Improvement of tribological behaviour of biomedical nanocrystalline titanium by magnetron sputtered DLC/SiC double layer films. *Mater Res* 610–613:1026–1033
125. Hu Z, Li H, Wen X et al (2006) Research on carbon film doped with chromium on the carbon-carbon composites with SiC interlayer. *Rare Met Mater Eng* 35:1204–1207



126. Thorwarth K, Thorwarth G, Figi R, Weisse B, Stiefel M, Hauert R (2014) On interlayer stability and high-cycle simulator performance of diamond-like carbon layers for articulating joint replacements. *Int J Mol Sci* 15:10527–10540
127. Cai X, Liu YM, Li L, Chen QL, Hu YW (2005) The mechanical property of TiN film deposited on N + –implanted aluminum by magnetron sputtering. *Key Eng Mater* 297–300:1713–1717
128. Azem F, Ak BI, Braic V, Toparli M, Celik E, Parau A, Kiss A, Titorencu I, Vladescu A (2015) Effect of SiC interlayer between Ti6Al4V alloy and hydroxyapatite films. *Proc Inst Mech Eng H J Eng Med* 229:307–318
129. Mediaswanti K, Wen C, Ivanova EP, Berndt CC, Wang J (2013) Titanium alloys: advances in properties control. In: Sieniawski J, Ziaja W (eds) Chapter 2 Sputtered hydroxyapatite nanocoatings on novel titanium alloys for biomedical applications. InTech. doi:10.5772/54263
130. Berezhnaya AY, Mittova VO, Kukueva EV, Mittova IY (2010) Effect of high-temperature annealing on solid-state reactions in hydroxyapatite/TiO<sub>2</sub> films on titanium substrates. *Inorg Mater* 46:971–977
131. Mamayeva AA, Panichkin AV, Aubakirova RK (2014) Investigation of surface characteristics of hydroxyapatite/titanium composite layer obtained by HF magnetron sputtering. *Adv Mater Res* 970:60–63
132. Feddes B, Wolke JGC, Weinhold WP, Vredenber AM, Jansen JA (2004) Adhesion of calcium phosphate coatings on polyethylene (PE), polystyrene (PS), poly(tetrafluoroethylene) (PTFE), poly(dimethylsiloxane) (PDMS) and poly-L-lactic acid (PLLA). *J Adhes Sci Technol* 18:655–672
133. Lo WJ, Grant DM (1999) Hydroxyapatite thin films deposited onto uncoated and (Ti, Al, V)N-coated Ti alloys. *J Biomed Mater Res* 46:408–417
134. Toque JA, Herliansyah MK, Hamdi M, IdeEktessabi A, Sopyan I (2010) Adhesion failure behavior of sputtered calcium phosphate thin film coatings evaluated using microscratch testing. *J Mech Behav Biomed Mater* 3:324–330

B. Ben-Nissan, A. H. Choi, I. J. Macha, and S. Cazalbou

## Contents

Introduction .....	736
Sol-gel Developed Bioglasses and Glass Ceramics .....	738
Synthesis of Bioactive Glass .....	739
Sol-gel Processing .....	741
Advantages and Disadvantages of the Sol-gel Process .....	743
Sol-gel Coating Techniques .....	744
Dip-Coating .....	744
Spin Coating .....	746
Other Coating Techniques .....	746
Drying .....	747
Hydrolysis .....	747
Firing .....	748
Biomedical Applications of Hydroxyapatite Nanocoatings .....	749
Bone Graft Applications .....	750
Other Biomedical Applications of Nanocoatings .....	751
Concluding Remarks .....	752
References .....	753

## Abstract

The ability to produce homogeneous high-purity materials is of great interest to industrial and medical applications. In addition, the chemical and physical changes observed at the nanoscale and their influence on properties have been

---

B. Ben-Nissan (✉) • A.H. Choi • I.J. Macha  
School of Chemistry and Forensic Science, Faculty of Science, University of Technology Sydney,  
Ultimo, NSW, Australia  
e-mail: [besim.ben-nissan@uts.edu.au](mailto:besim.ben-nissan@uts.edu.au); [ahchoi@hotmail.com](mailto:ahchoi@hotmail.com)

S. Cazalbou  
CIRIMAT Carnot Institute, CNRS-INPT-UPS, Faculty of Pharmacie, University of Toulouse,  
Toulouse, France

an important academic interest. The gel-structure transition plays a critical role in the formation as well as the current production of various types of sol-gel-derived materials such as nanopowders, nanofibers, nanocoatings, nanocomposites, and solid monoliths. It is the area of thin film coatings produced by sol-gel technology that this chapter covers. In particular, this chapter focuses on the basic synthesis and application methods to produce nanocoatings for biomedical applications. This chapter also attempts to answer some of the pertinent questions related to sol-gel processing and production methods and issues related to the fundamental understanding of the sol-gel process.

---

**Keywords**

Alkoxide • Bioceramics • Calcium phosphates • Coral • Hydroxyapatite • Nanocoatings • Sol-gel • Synthesis

---

## Introduction

By definition, a sol is a suspension of colloidal particles in a liquid [1]. A sol differs from a solution in that a solution is a single-phase system, whereas a sol is a two-phase, solid-liquid system. Colloidal particles are in the approximate size range 1–1000 nm, hence gravitational forces on these particles are negligible and interactions are dominated by short-range forces such as van der Waals forces and surface charges. Diffusion of the colloids by Brownian motion leads to a low-energy arrangement, thus imparting stability to the system [2].

The stability of the sol particles can be improved through a reduction in the surface charge. If the surface charge is reduced sufficiently, gelation is induced and the resultant product is able to maintain its shape without the assistance of a mold. Gels are regarded as composites as they consist of a solid skeleton or network, which encloses a liquid phase or excess of solvent. They are usually soft and have a low elastic modulus and can be obtained through controlled polymerization of the hydrolyzed starting compound. In this case, a three-dimensional network forms, resulting ultimately in a high molecular weight polymeric gel. The resultant gel can be considered as a macroscopic molecule that extends throughout the solution. The gelation point is the time taken for the last bond in this network to form.

The sol-gel process was initially identified in 1846, when Ebelmen observed the hydrolysis and polycondensation of tetraethylorthosilicate (TEOS) [3]. From the late 1800s through to the 1920s, the phenomenon of Liesegang rings formed from gels became the topic of intense investigation [4, 5]. The first sol-gel patent was published in 1939, covering the preparation of SiO<sub>2</sub> and TiO<sub>2</sub> coatings [6]. In 1955, Roy and Roy [7] recognized the potential for producing high-purity glasses using methods not possible with common ceramic processing techniques. It is from this time onward that serious scientific interest in sol-gel processing as a commercially viable technique began. Their work in the 1950s and 1960s and the extension of this by Iler [8] in the 1960s have resulted in the development of Du Pont's "Ludox" colloidal silica spheres.

Parallel to the expansion of sol-gel processing on powders and fibers were a range of new commercial incentives initiated to produce thin-layer coatings and films, particularly for the treatment of glass. The work was pioneered by Geffcken and Berger [6] in 1939 for single oxide coatings on behalf of Jenaer Glaswerk. Together with Dislich and Hinz [9], they pioneered the development of multicomponent oxide coatings including glass, glass-ceramics, and other crystalline materials. Shortly after, Schroeder [10] reported the first investigation carried out by Schott Glass involving sol-gel synthesized coatings. While they were mainly interested in single-oxide optical coatings of  $\text{SiO}_2$  and  $\text{TiO}_2$ , mixed oxide coatings were also developed.

In 1968, Stober et al. [11] extended Iler's work [8] to detail the effects of reaction conditions and catalysts on the hydrolysis process. The result of this work was to show how the morphology and the particle size of powders produced by the sol-gel process could be controlled. From their pioneering work another commercial product, "Stober's spherical silica powder," resulted. Antireflective coatings and solar reflective coatings went into production in 1964 and 1969 respectively.

During the late 1960s through to the early 1970s, Hench and Wilson [12] developed sol-gel-based bioglasses (Bioglass<sup>®</sup>), which bond to living tissue and open a new phase in their biomedical applications.

The next major advance in sol-gel processing came in the early 1980s with Matijevic et al. [13] producing a wide range of powders with controlled size and morphology. These products included oxides, hydroxides, carbonates, sulfides, metals, composites, and coated particles.

In the 1980s, emphasis shifted from purely inorganic systems to hybrid organic-inorganic systems. Hybrid organic-inorganic materials consist of regions containing organic elements such as carbon, hydrogen, nitrogen, and oxygen mixed with areas comprising of inorganic compounds such as silica, titania, and alumina.

Around that time the importance of reactions of several metal alkoxides in solution was signified. Thence, the production of defined multicomponent oxide glasses, glass-ceramics, and crystalline thin films were formed in molding presses, which consequently led to the production of transparent granulates. Following this, a number of developments came forth such as fibers and unsupported films [14] in addition to preforms for fiber optics and other monolithic structures were examined implementing a supercritical drying step.

The applications of sol-gel process include coatings, catalysts, lenses, high-strength ceramics, superconductors, insulating materials, and nuclear waste encapsulation and as biomaterial synthesis methods [15]. Silicon alkoxides are the most widely used precursors, and other alkoxides such as those of titanium, aluminum, zirconium, and boron are also used.

The sol-gel process is a colloidal route used to synthesize inorganic and hybrid organic-inorganic materials. Typically, chemical precursors are hydrolyzed through a solution state (colloidal suspension/nanosol) and then a gel state (solid network in a continuous liquid phase) before being dehydrated to give the final material. From a chemical perspective for aqueous-based routes, the process is one of hydrolysis and polycondensation to form a predominately covalently bonded network [15–19].

In the past decade many of these oxide coatings have also been deposited by the sol-gel process using alkoxides as precursors.

In biomedical applications, sol-gel developed bioactive glasses are a unique compositional range of dense, amorphous calcium, sodium phosphosilicate (CSPS) materials that develop strong chemical bonds with the collagen of living tissues [20–26]. The composition labeled 45S5 Bioglass<sup>®</sup> [20] is used widely for dental and orthopedic applications under the trademarks of Novabone<sup>®</sup>, Perioglas<sup>®</sup>, and Novamin<sup>®</sup>, an ingredient in consumer oral care products [27–33]. The history of the development of bioactive glasses and their widespread clinical applications has been documented elsewhere [27].

This chapter describes the sol-gel process and the changes that take place during the processing of ceramics from sols. It also provides a brief background into sol-gel production techniques as well as addressing the reasons behind choosing the sol-gel route over conventional processing techniques. Applications where sol-gel technologies have been used are also given.

---

## Sol-gel Developed Bioglasses and Glass Ceramics

Since the discovery by Hench and Wilson [12] various types of bioactive glasses and glass-ceramics with different functions such as high machinability and mechanical strength and fast-setting ability have been developed.

Glasses that are primarily based on silica ( $\text{SiO}_2$ ) which may also contain small amounts of other crystalline phases have been investigated for implantation purposes. The most successful and prominent application is Bioglass<sup>®</sup>, which is described in detail in various comprehensive reviews [34–36].

The first-generation bioactive glass compositions lie in the  $\text{Na}_2\text{O}$ - $\text{CaO}$ - $\text{P}_2\text{O}_5$ - $\text{SiO}_2$  system. In 1971, the first development of such a bioglass began when 45S5 Bioglass<sup>®</sup> with a composition of 45 %  $\text{SiO}_2$ , 24.5 %  $\text{CaO}$ , 24.5 %  $\text{Na}_2\text{O}$ , and 6 %  $\text{P}_2\text{O}_5$  by weight was proposed [20].

It was suggested by Hench [34] and Vrouwenvelder et al. [37] that when compared to hydroxyapatite (HAp), Bioglass<sup>®</sup> 45S5 has greater osteoblastic activity which is accredited to a rapid exchange of alkali ions with hydronium ions at the surface. This in turn led to the formation of a silica-rich layer over a period of time. The migration of  $\text{Ca}^{2+}$  and  $\text{PO}_4^{3-}$  is permitted on this layer to the silica-rich surface where they combine with soluble calcium and phosphate ions from the solution and the formation of an amorphous  $\text{CaO}$ - $\text{P}_2\text{O}_5$  layer takes place. Upon the interaction with  $\text{OH}$ ,  $\text{CO}_3^{2-}$ , and  $\text{F}$  from solution, this layer will then undergo crystallization. Andersson and Kangasniemi [38] have also observed a similar phenomenon in bioglass with slightly modified compositions.

Glass-ceramics from a similar composition with various degrees of crystallinity was prepared by Li et al. [39]. They discovered the formation of an apatite layer which was directly influenced by the amount of glassy phase still remains, with total inhibition when the glassy phase constitutes less than about 5 weight percent (wt%). These specific glasses (for instance, Bioglass<sup>®</sup>) have been accepted as bioactive

biomaterials as a result of their surface activity and utilized for non-load-bearing applications.

Sol-gel developed Bioglasses<sup>®</sup> have been used successfully in clinical applications as artificial middle-ear bone implants and alveolar ridge maintenance implants [12] and recently as toothpaste additives.

A bioactive glass with precipitated crystalline apatite and reduced alkaline oxide content can be produced by using a specific heat treatment method. The resultant glass ceramic is referred as Ceravitals and has been shown to have a higher mechanical strength but lower bioactivity compared to Bioglass<sup>®</sup>.

Kokubo et al. [40] produced a glass-ceramic named A-W glass ceramic (Cerabones A-W) that contains oxyfluorapatite and wollastonite ( $\text{CaO} \cdot \text{SiO}_2$ ) in an  $\text{MgO-CaO-SiO}_2$  glassy matrix. It was reported in the early 1990s that the A-W glass-ceramic spontaneously bonded to living bone without the formation of fibrous tissue around the glass. They have also developed a bioactive and machinable glass-ceramic containing apatite and phlogopite ( $(\text{Na,K})\text{Mg}_3(\text{Al-Si}_3\text{O}_{10})(\text{F})_2$ ) called Bioverits utilized in the past in clinical applications such as the artificial vertebra. Currently the production and application of A-W glass is only restricted to research and commercial production has been discontinued.

## Synthesis of Bioactive Glass

Nanoparticles and nanofibers of bioactive glass have been made available several years ago and used either as a stand-alone product or combined with polymers in the form of a nanocomposite in the biomedical field.

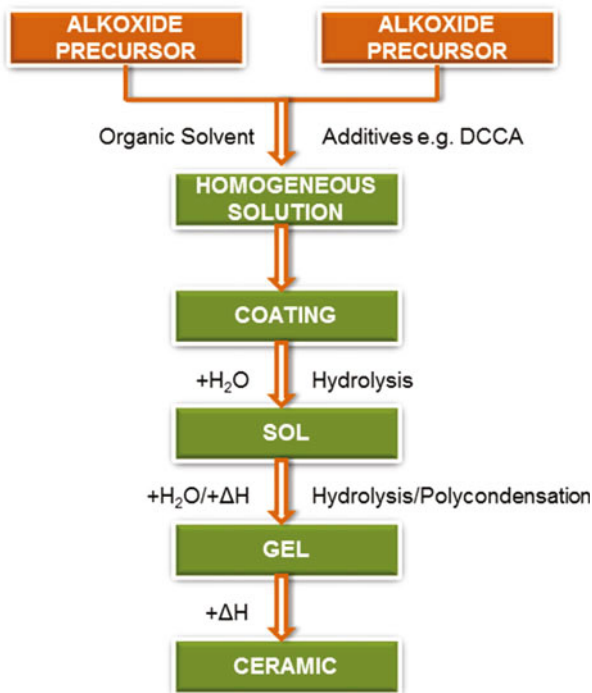
From the early days of the sol-gel research studies indicated that under acidic conditions, the hydrolysis of  $\text{Si}(\text{OC}_2\text{H}_5)_4$ , tetraethyl orthosilicate (TEOS) resulted in  $\text{SiO}_2$  in the form of a glass-like material [41]. To obtain crack-free solid material, the silica gels in the early days were dried for more than a year in order to avoid the gel fracturing into a fine powder, and as a result of this, the whole process was lost to technological interest.

Compared with traditional glass melting or ceramic powder methods, the motivation for sol-gel processing is first and foremost the potentially higher homogeneity and purity and the lower processing temperatures associated with the process [42].

On the other hand the sol-gel process involves the synthesis of an inorganic network by mixing the metal alkoxides in solution, followed by hydrolysis, gelation, and low-temperature firing to produce a dense and stable glass powder (Fig. 1). The network structure of the gel can be modified by controlling hydrolysis and polycondensation reactions during productions. Hence, structural variation from highly porous to monolithic solids can be produced without compositional changes (Fig. 2).

Using gels, bioactive glasses can be prepared by sintering at temperatures between 600 and 700 °C which reduces most of the disadvantages of high-temperature processing with much higher control over purity. Furthermore, by either modifying the microstructure or composition through processing parameters, a broader range as well as better control of bioactivity can be achieved [43].

**Fig. 1** Flow diagram representing the process taking place during the production of a ceramic coating via sol-gel synthesis



Li et al. [44] reported that  $\text{SiO}_2\text{-CaO-P}_2\text{O}_5$  powders produced by sol-gel are more bioactive than the melt-derived glasses of the same composition. In addition, Sepulveda et al. [45] examined the rates of dissolution and formations of surface layer on sol-gel and melt-derived bioglass and noticed the 45S5 melt-derived bioglass exhibited lower rates than the 58S sol-gel bioglass powder. The high bioactivity of the sol-gel-derived materials is related to the microstructural features of the gels, i.e., pore size and pore volume associated with the large surface area, higher rate of dissolution, and the negative surface charge [46]. Furthermore, sol-gel-derived bioactive glasses have been proposed as alternative to glasses produced by melt and quenching methods, as they exhibit in addition to excellent degradation/resorption properties more rapid bone bonding, improved homogeneity and purity, and higher rates of apatite-layer formation.

A certain compositional range of bioactive glasses containing  $\text{SiO}_2$ ,  $\text{Na}_2\text{O}$ ,  $\text{CaO}$ , and  $\text{P}_2\text{O}_5$  in specific proportions has been demonstrated to show bonding of glass to bone. As mentioned earlier, three compositional changes separate them from soda-lime-silica glasses: high  $\text{Na}_2\text{O}$  and  $\text{CaO}$  content, less than 60 %  $\text{SiO}_2$ , and a high  $\text{CaO/P}_2\text{O}_5$  ratio. Highly reactive surfaces are created from these compositional features when exposed to an aqueous medium. On the other hand, the amount of  $\text{SiO}_2$  in bioactive glasses ranging between 45 and 60 % and as a result of repeated hot working can easily lead to problems in the form of phase separation and crystallization of the glassy material [20, 47]. Crystallization of the material can cause a

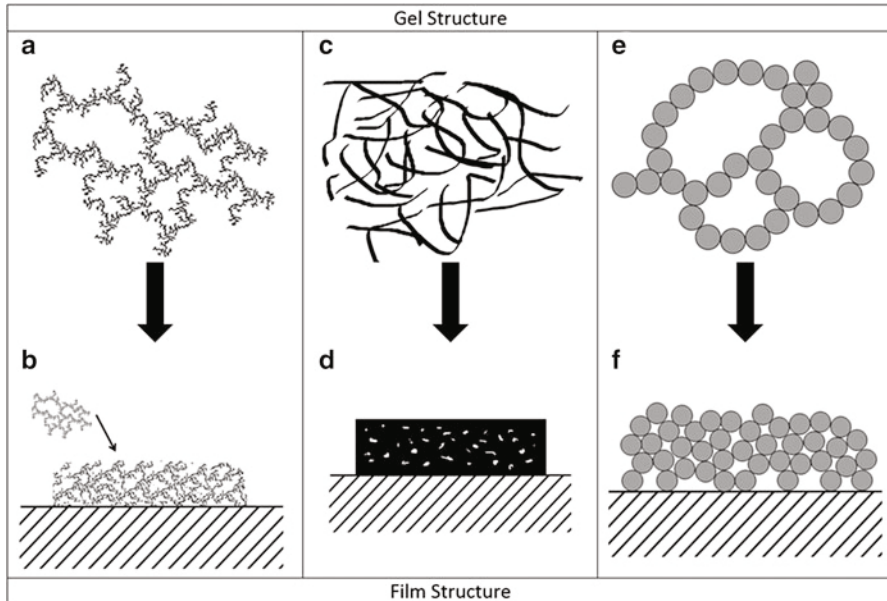


**Fig. 2** Structural variations from the sol-gel process. (a) network of random aggregates; (b) highly porous coatings; (c) entangled linear polymers; (d) dense coating; (e) network of random particles; (f) controlled, fine porosity coating

reduction in the rate of bioactivity of the glass [48], and a glassy phase of uncontrollable composition is the result of partial crystallization. Crystallization of a sol-gel-derived bioactive glass can be controlled by its chemical composition [49, 50].

It has been reported that a new generation of bioactive glasses in the  $\text{Na}_2\text{O-K}_2\text{O-MgO-CaO-B}_2\text{O}_3\text{-P}_2\text{O}_5\text{-SiO}_2$  system can be repeatedly heated without the risk of devitrification [51]. Hence, microspheres can be produced and sintered into porous implants of different shapes and sizes [52]. The porosity of a bioactive glass body does not only noticeably increase the total reacting surface of the glass but also allows a three-dimensional formation of the healing bone tissue. The mechanical strength and porosity of the bioactive glass implants can be controlled with different sintering times and temperatures [53]. To achieve the best mechanical strength of the sintered implant, the glass must retain its amorphous structure during the heat treatment.

## Sol-gel Processing

Sol-gel processing can be categorized into either an aqueous- or an alcohol-based system. As the name suggests, aqueous-based systems generally are carried out in the presence of water, whereas alcohol-based systems exclude water build-up until the hydrolysis stage. On the other hand, there are also nonhydrolytic sol-gel processes which do not require the presence of solvents at all.



Correspondingly, sol-gel precursors can also be generally categorized as either alkoxides or nonalkoxides. While alkoxides are the preferred precursors for sol-gel production due to their faster volatility, other compounds, such as metal salts, can also be used. This is often the case for Group I and II elements whose alkoxides are solid, nonvolatile, and in many cases have a low solubility [54].

Metal alkoxides are probably the best starting materials in sol-gel preparations [55]. All metals are capable of forming metal alkoxides in the form of  $M(OR)_x$ , where  $M$  is a metal,  $R$  is an alkyl group, and  $x$  is the valence state of the metal. Another type of alkoxide that exists is the double alkoxide, which has the general formula of  $Mx'My(OR)_z$ , where  $M'$  and  $M$  are metals,  $R$  is an alkyl group, and  $x$ ,  $y$ , and  $z$  are the valence states of the metals. Double alkoxides have the added advantage of retaining their stoichiometry [56].

While alkoxides are the most favorable sol-gel precursors, there are two exceptions to this rule. These are the alkoxides of silicon and phosphorus. Silicon alkoxides require an acid or base catalyst for hydrolysis, and even with such an addition, hydrolysis is very slow. In the same way, trialkylphosphates are very stable and difficult to hydrolyze, and as a result they are generally not used widely as phosphorus precursors in sol-gel production [56].

An alternative to alkoxides is provided by the use of metal salts. This only applies if the metal salts can be changed readily into their respective oxides by thermal or oxidative decomposition. It is also preferable for such salts to be soluble in organic solvents. Examples are salts produced from organic acids such as acetates, citrates, and formates. The most ideal inorganic salts are nitrates as chlorides and sulfates are thermally more stable and their removal may prove to be difficult [57, 58]. The use of nitrates in amounts greater than a few hundred grams on the other hand should be avoided, as nitrates are very strong oxidizing agents and can lead to uncontrollable exothermic reactions and even explosions during drying [56]. Acetates are a suitable alternative to nitrates, reducing the possibility of explosions. However, they do not thermally degrade as readily as nitrates, often leaving behind organic residues [59–61].

Modification of sols through the use of organic compounds such as drying control chemical additives (DCCA) can reduce these problems by controlling the evaporation rates of volatile species, which in turn control hydrolysis rates. They also influence properties such as micro- and nanoporosity [62, 63]. Examples of drying control chemical additives include acetylacetone,  $\beta$ -diketones, carboxylic acids, or glycol.

It is essential to avoid precipitation when it comes to the production of homogeneous gels from a liquid. This is also a pertinent requirement in the fabrication of homogeneous coatings. Precipitation can be induced by physical agglomeration or by chemical reaction in alkoxide systems [64]. Chemical precipitation from sol-gel solutions is a result of the alkoxide reacting with water or a chelating agent to form an insoluble product such as a hydroxide or organic salt. Factors affecting precipitation include alkoxide precursor chemistry, temperature of the environment, and water concentration. Modified synthesis and production methods can solve the problems.

The precipitation reaction is controlled by the reactivity and quantity of the modifying group. The coordination number, hygroscopicity, and reactivity of the alkoxide are factors that determine the quantity of the additive required to stabilize the alkoxide. Adding such modifying agents can also increase the time to gelation, and therefore can increase the stability or useful lifetime of a sol-gel-derived product [65]. The formation of precipitates can often be affected by the amount of water available and the manner in which the water is absorbed. For example, when water is adsorbed (or absorbed) from the atmosphere, the hydrolysis is gradual and uniform. However, if water is added dropwise, a heterogeneous reaction takes place, with the resultant hydroxide precipitating out instantaneously [64].

Cracking during the production stages can be a problem due to the large amounts of organic material needed in the processing of sol-gel-derived forms. In the case of monoliths, shrinkage during drying is common. Phenomena such as inhomogeneities as a result of phase separation, thermal mismatch with the substrate used, or a number of other factors related to the drying process are often the causes of cracking in thicker coatings (>400 nm).

---

## Advantages and Disadvantages of the Sol-gel Process

Sol-gel processing is unique in that it can be used to produce different forms such as powders (including monodispersed spherical powders), coatings, fibers, and monoliths of the same composition merely by varying the viscosity of a given solution [62]. Furthermore, the range of different compositions that can be produced includes single oxides, mixed oxides, and nonoxides such as nitrides, borides, and chlorides.

Processing by sol-gel of powders, spheres or coatings have a number of advantages over conventional ceramic processing routes [66] such as:

- Increased chemical homogeneity (down to molecular scale for alkoxide solutions if liquids have a similar rate of hydrolysis and condensation, or atomic scale for aqueous systems where a sol is formed).
- Powders have a high surface-to-volume ratio (therefore they require a lower sintering temperature to form near theoretical density bodies with uniform fine-grained structures).
- High purity can be maintained as grinding can be avoided.
- Fibers, powders, coatings, and spheres can be prepared easily from simple solutions.

However, in the processing of monoliths using this method, there are a number of problems [67]:

- Relatively high cost of precursors.
- Problems associated with drying stresses and large shrinkages in monolithic solid formation.
- Effective removal of volatiles.

The problems do not apply to coatings due to their relatively low thickness and the small amount of material used. Furthermore, nanoscale coatings have the added advantages:

- Precursor cost is relatively unimportant.
- They can dry rapidly without cracking.
- Shrinkage is fairly uniform, perpendicular to the substrate.
- Elimination of volatiles is relatively easy.
- Different coating techniques can be used to coat substrates of nearly any shape or size.

Sol-gel film deposition also offers an advantage over other film deposition techniques such as physical vapor deposition (PVD), chemical vapor deposition (CVD) and sputtering, in that properties such as pore volume, size, and surface area can be controlled, which is of particular importance in the field of antireflective coatings [68]. Other advantages over these processes include the ability to coat complex shapes, because processes such as dip-coating are not line-of-sight methods, more flexible processing conditions, as operations do not have to be carried out in a vacuum, as well as increased production rates [2].

---

## Sol-gel Coating Techniques

In all coating techniques, an important factor that will affect the quality, in particular the uniformity of the coating, is “how well” the solution wets the substrate. Ethanol is the preferred solvent, although other organic solvents can also be employed. Reactions can be controlled by the way in which the aliphatic radicals split off during the formation of the final oxide, hence it is preferable for the reaction to take place by hydrolysis rather than pyrolysis.

The versatile nature of the sol-gel process allows coatings to be applied via numerous techniques. These include dip-coating, spin coating, premetered coating techniques, and spray coating.

### Dip-Coating

The dip-coating process is mainly used for the production of coatings on items such as flat glass plates but can also be used for coating objects such as tubes, rods, pipes, and fibers (Fig. 3). This deposition method has the advantage that it can produce single-layered coatings around 100 nm thick or multilayered coatings with a high degree of uniformity up to 1  $\mu\text{m}$  thick. Dependent on the chemistry, viscosity, and pullout rate, a single layer can be in the range of 50–120 nm. It can also be used to coat large samples, and the process is often economized in this manner. In addition, multiple-layered coatings can be produced with specific optical characteristics and used commercially in the coating of window glass. Dip-coating is usually a batch

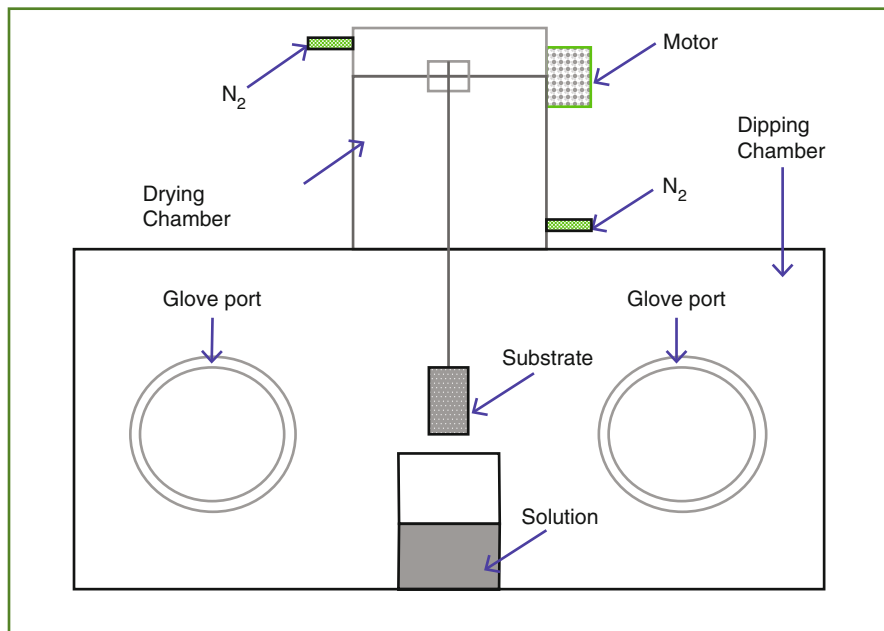


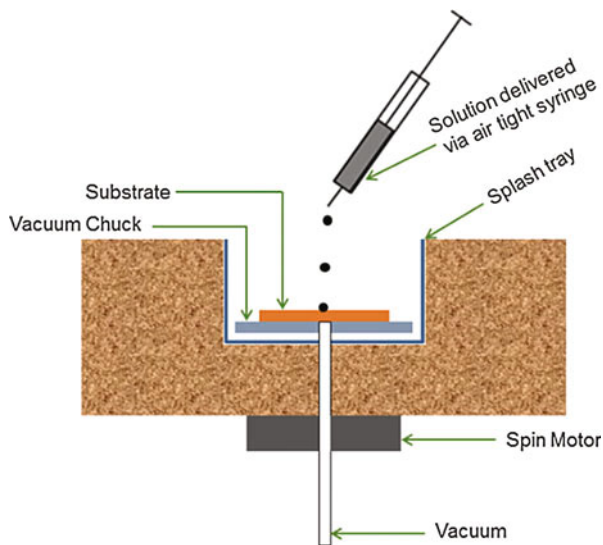
**Fig. 3** Schematic diagram of the dip-coating process carried out in a controlled environment (dry box)

process but can be adapted to coat long flexible sheets and wires. The overall process can be broken up into five stages: immersion, start-up, deposition, drainage, and evaporation. The first three stages are always sequential, the third and fourth concomitant, and the fifth may take place throughout the entire process unless the necessary precautions are taken [69].

The thickness of the deposited layer theoretically is dependent on factors such as viscous drag which is proportional to liquid viscosity ( $\mu$ ) and substrate speed ( $U$ ) as well as gravity ( $g$ ) which is proportional to liquid density ( $\rho$ ) and surface tension ( $\gamma$ ). Other forces such as inertia and surface tension gradient exist but are usually insignificant. Surface tension can be neglected as liquid viscosity and substrate speed are sufficient to keep meniscus curvature to a minimum, then the film thickness “ $h$ ” can be determined when viscous drag and gravity are balanced. Thus, for a given solution, film thickness of a single layer thus is governed by withdrawal speed. However, thickness can also be modified by changing the physical properties of the solution such as the viscosity and density in addition to the number of layers deposited.

When substrates are dip-coated using batch process, the thickness of the film will be thinnest at the edges. At the leading edge, coating thickness is lower as there is a delay in development of drag forces. Thickness at the sides is also lower because surface tension beneath the convex meniscus raises the pressure in the liquid causing it to drain away. Characteristically, thickness is extremely thin at the edges but increases in a linear manner to a constant value. The constant-thickness region forms similarly to coatings produced using the continuous process.

**Fig. 4** Schematic diagram of the spin coating process



## Spin Coating

Spin coating is a batch process suited to flat shapes such as disks, plates, lenses, and bowls. The process can be separated into four stages: deposition, spin up, spin off, and evaporation (Fig. 4). While the first and second stages may overlap, the first three stages are always sequential. As with dip-coating, evaporation can take place throughout the entire coating process.

The first stage involves delivering excess liquid to the substrate while it is stationary or spinning. During the second stage, rotation causes the liquid to move radially outward due to centrifugal forces. This may happen while the substrate is being accelerated to maximum speed. Excess liquid flows to the perimeter and detaches in the form of droplets in stage three. If the substrate has a central hole, drainage takes place in the same manner as in the batch dip-coating process, otherwise the film thins down to a fairly uniform thickness, except for the edge which thins due to the surface tension-derived edge effect. As the film thins, flow decreases as drag forces increase, and thinner films are affected more by evaporation, which raises the solution viscosity by concentrating nonvolatiles. Evaporation becomes the dominant process once spin-off has ceased.

Neglecting edge effects, film thickness is mainly determined by spin-off. Film thickness will reach uniformity provided that its viscosity is insensitive to shear. Uniformity will occur when centrifugal forces are balanced by viscous forces.

## Other Coating Techniques

Spray coating as the name suggests involves spraying a solution onto the substrate material. However, hydrolysis during spraying can induce problems. This particular

method also does not lend itself to the production of uniformly thin films and is typically used only to deposit thick films.

Premetered coatings are an alternative to dip-coating, and the process involves delivering the liquid to the substrate across its width or around its perimeter at a controlled rate. The thickness of the deposited film is the feed rate per unit width divided by substrate speed. A number of variations of this method are available. While the range of substrates that can be coated is more limited, premetered coatings offer advantages over dip-coating including the ability to produce coatings more quickly, production of thinner coatings at the same speed, as well as offering greater control.

## Drying

In the coating procedure specifically by dipping method, once the coated substrate had been returned to the upper chamber of the coating box (Fig. 3), the film is allowed to remain in contact with the protective atmosphere for a period of time. This was determined in a previous work using a number of oxides, mixed oxides, and phosphate coatings by Fourier transform infrared (FTIR) studies of the respective solutions. The time required for the film to reach equilibrium in the inert atmosphere is called the drying time and, for most solutions, is 10 min or less.

For 100 nm thick thin films, the majority of the solution weight is lost during the first 10 min. The weight loss in this stage can be as much as 90 % of the weight of solution deposited. For thicker films, i.e., with a thickness of 500 nm, it is during this stage that the film is most likely to crack as a result of tensile stresses building up during the solvent loss. As the film is “locked” at the edges (as it completely coats both sides of the substrate), the only avenue open to the film to relieve stress during this evaporation step is by reduction in film thickness. There is a critical film dipping speed of approximately 20 mm/min for most solutions which gave crack-free films but films cracked or crazed if dipped faster.

In our sol-gel developed thin film studies the greater part of the drying process occurred during the firing procedure. Gels were allowed to remain in contact with the atmosphere, during which time hydrolysis took place. So, when the films were put into the furnace, they were essentially in stage one drying, the gel pores predominantly filled with alcohol and water. DTA/TGA analyses (heating rate 10 °C/min in flowing air) were used to determine both the temperatures at which the major transitions in “gel structure” took place and also the critical temperatures for processing each gel.

## Hydrolysis

The hydrolysis of the deposited alkoxides can be carried out by exposing the coatings to ambient atmosphere. The time required for achieving complete hydrolysis can be determined experimentally for each solution by FTIR analysis and can be standardized to 60 min.

In our FTIR trials, a thin film of dried alkoxide was exposed to the atmosphere and scans taken at 30 s intervals. The time taken for the film to reach a steady state was recorded and used as the guideline for the hydrolysis time required for films made from that solution. The FTIR scans also allowed examination of the reaction products for the presence of contaminant reaction products, such as carbonates, which would reduce the effectiveness of films.

It was found with some films, especially the stabilized aluminum isopropoxide films, that atmospheric hydrolysis was ineffective. The reaction rate of the stabilized alkoxide was so slow as to be outside the viable range for a commercial product. Based on previously published work [15], a procedure was followed whereby the films were hydrolyzed by dipping them into boiling water for 1 min. Not only the hydrolysis rate could be controlled by this method but also the hydroxide form produced. The hydroxide created determines the oxide content of the gel developed. The oxide content of the gel controls the weight loss of the gel during the firing stage. The higher the oxide content of the gel, the lower the weight loss required by the gel to form a fully dense ceramic film. The lower the mass loss required from the gel during firing, the lower the chance that defects such as stress cracking will occur. For alumina, hydrolysis at temperatures lower than 80 °C resulted in the formation of  $\text{Al}(\text{OH})_3$  which has an equivalent oxide content of 65 %. At temperatures higher than 500 °C the hydroxide formed was  $\text{AlOOH}$  where the equivalent oxide content was 85 %. The resulting films were found to be significantly different from those where hydrolysis by atmospheric moisture was attempted.

## Firing

The firing of a film is required to achieve the following aims: the removal of free and physically bound water; the removal of reaction-generated and residual solvent; the dehydroxylation of the gel to form a ceramic material; the removal of residual carbon formed during organics “burn-out”; the closure of small pores and crystallization of required phases or avoidance of crystallization, as required.

The firing schedules used were determined by DTA/TGA analyses. The temperatures and weight loss which were considered critical for the formation of a defect-free film were noted for each gel. Firing schedules were primarily determined by these results, although the limitations of substrate materials had to be considered.

Firing rates had to be controlled to allow for stress relief and weight loss within the gel to be accommodated. During the firing cycle, a gel lost approximately 70 % of its weight. This loss was primarily water and solvent, both physically and chemically bound. A smaller percentage of the weight loss can be accounted for through the “burnout” of trapped organic residues or degradation of unreacted alkoxide.

Firing in an argon atmosphere was required to avoid oxidation of susceptible substrate materials such as titanium alloys, zirconium metal, graphite, or stainless steel. The use of an argon atmosphere did not show any adverse effect on the final densified ceramic film itself. DTA/TGA results show that the only result of using an

inert atmosphere for firing was the delayed removal of organic by-products. The uses of titanium and zirconium alloys were mainly for biomedical applications.

---

## Biomedical Applications of Hydroxyapatite Nanocoatings

For orthopedic and maxillofacial applications, four conventional industrial coating procedures have been proposed for the manufacture of bioactive HAp coatings during the past 40 years. The first technique, spray or plasma coating, utilizes a method that employs relatively thick calcium phosphate coatings with thickness ranging from 100  $\mu\text{m}$  to 2 mm for bone ingrowth [70]. The second technique was developed by Hench and colleagues [42] for the fabrication of thick bioglass coatings for increased surface bioactivity. During the early 1990s, a third technique was developed by Kokubo and coworkers [71], and the method was based on self-assembly by precipitation in a SBF solution. Currently, this method is only applied and utilized to investigate the biocompatibility in a range of newly developed biomaterials.

The first “nanocoating techniques” using calcium phosphate was developed by Ben-Nissan and coworkers in 1989 [72]. The method involves dipping in sol-gel-derived HAp solutions to produce strong 70–100 nm thick single or multilayered nanocoatings [73]. The original chemistry is used to produce a range of calcium phosphate coatings and nanopowders by using alkoxide-based system containing calcium diethoxide, triethyl phosphite, ethanediol, and ethanol [72].

Achieving ideal bioactivity and biocompatibility is essential when it comes to the production of implant materials, and nanocoatings can provide an efficient and cost-effective way to alter the interactions of the implant material with its destined “host” environment [74–78]. Lewis et al. [79] and Zreiqat et al. [80, 81] examined the changes in the activity of osteoblast-like cells seeded on top of nanocoatings of carbonated HAp and zirconia. The surfaces were characterized by FTIR spectroscopy and light microscopy. Cell adhesion, proliferation and viability, as well as expression of alkaline phosphatase, which is used to identify signs of bone formation, were assessed as indicators of biocompatibility. Their results revealed sol-gel-derived nanocrystalline HAp was an ideal surface for implant coatings.

In 2011, Roest et al. [82] investigated the mechanical properties and adhesion behavior of HAp nanocoatings on commercially pure titanium and Ti-6Al-4 V alloy in relation to their anodizing treatment. They observed the substrate and the anodized layer thickness have the most influence on the interfacial adhesion of HAp, with nanocoatings on Ti-6Al-4 V exhibiting significantly better interfacial bonding in comparison to commercially pure titanium.

Normally, the alkoxide method employed involves the formulation of a homogeneous solution containing all of the component metals in the correct stoichiometry. Mixtures of metal alkoxides and/or metal alkanoates in organic solvents that have been stabilized against precipitation by chemical additives (amines, glycols, acetylacetone, etc.) have been proven to be the most successful (Fig. 5). A dry



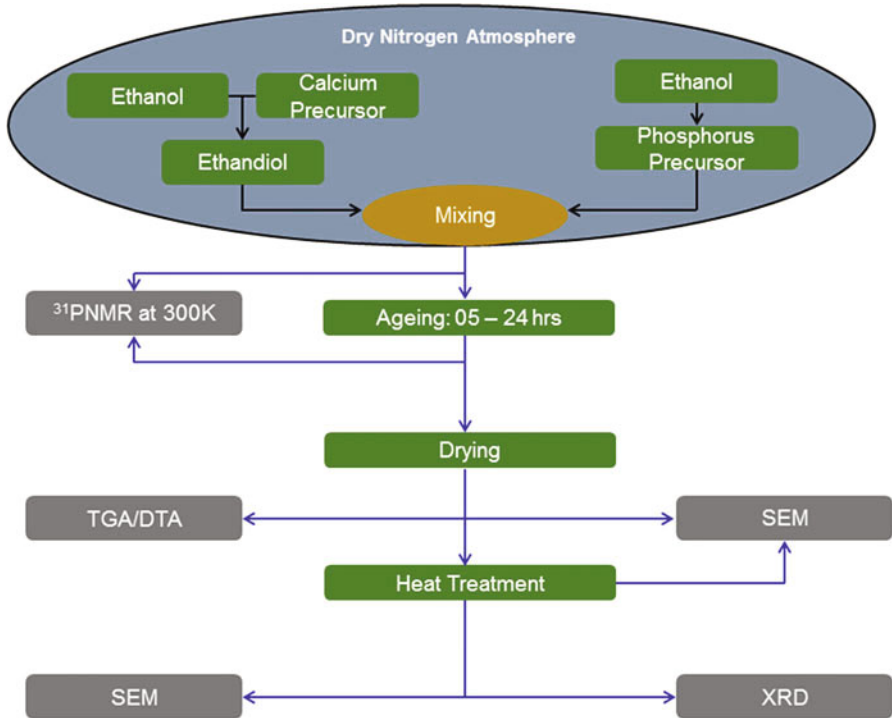


**Fig. 5** Flow schematic diagram outlining sample preparation, analysis techniques, and their stages of implementation over the course of production of hydroxyapatite

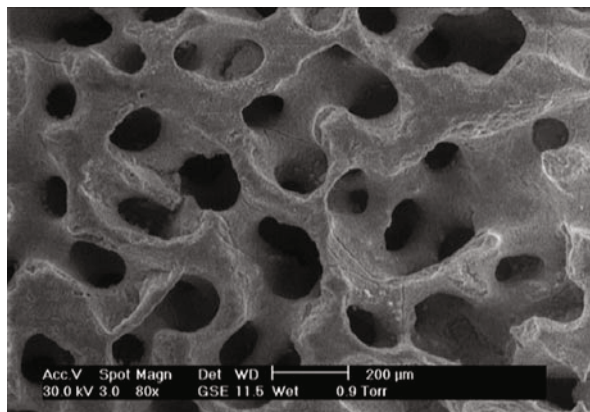
nitrogen atmosphere was used for the preparation of sols due to the hygroscopic nature of the starting calcium and phosphate alkoxide precursors.

## Bone Graft Applications

Use of coral skeletons for general routine orthopedic surgery and tissue engineering has so far been limited to external fixation devices as they are inappropriate for strictly load-bearing applications.

There has been a considerable amount of success in the use of coral mineral as a bone graft material because of its interconnected porous structure ranging from 150 to 500  $\mu\text{m}$ . It is similar to the human cancellous bone in morphology and is one of a limited number of materials that will form chemical bonds with bone and soft tissue in vivo. Conversely, without the modification via chemical means, coral as calcium carbonate is not completely ideal for load-bearing bone graft applications because of its high dissolution rate. Sol-gel coating technologies can be used to enhance the strength of corals, and this enables them to be used at more skeletal locations [77, 78]. The conversion of the calcium carbonate to HAp and the use of further carbonate

**Fig. 6** Coral structure showing macropores



hydroxyapatite nanocoating improves a range of properties. Nanocoated coralline HAp has been reported to have enhanced bioactivity and strength [74–76].

Commercially used bone graft materials using hydrothermal conversion only reach partial conversion of coralline calcium carbonate to HAp. However, being limited to the outer surface, the inner core remains as unconverted calcium carbonate of the original coral [83]. To overcome this problem the coral can be converted and coated to improve its mechanical properties. The method involves a unique patented two-step conversion-coating procedure. Corals possessing a suitable macropore structure are converted to pure HAp in the first step, with complete replacement of calcium carbonate by phosphatic material throughout the specimen by the hydrothermal process. The reaction can be carried out at 250 °C with an ammonium monohydrogen phosphate solution [74]. Additional stage involves the use of sol-gel-derived carbonate HAp over to the converted coralline apatite [75]. It was reported that application of this nanocoating increased the compression strength of a commercial product from 3 MPa to 33 MPa.

In addition to the macropores, coral is known to possess meso- and nanopores ranging between 5 and 50 nm within a fibrous platelike structure that constitutes the interpore area between the large macropores (Fig. 6), which increases the surface area and hence the bioactivity. As a result of the application of the HAp nanocoatings two major effects were achieved: firstly, an improvement in the mechanical properties compared to traditional coral materials; secondly, the bioactivity of the material was enhanced. Mechanical testing indicated that all properties have increased including compression, biaxial, flexural strengths, and the elastic modulus [75, 76].

---

## Other Biomedical Applications of Nanocoatings

Considerable effort has been devoted to modifying the surface characteristics of biomaterials in an attempt to improve the initial implant/tissue interlocking and improve bioactivity. The effect of surface chemistry modification of titanium alloy

(Ti-6Al-4 V) with alkoxide-derived “carbonate HAp coating” on human bone-derived cell behavior has been further investigated by various research groups [80, 81, 84]. Western blotting demonstrated that sol-gel coating of Ti-6Al-4 V with carbonate HAp upregulated the expression of key signaling protein. Furthermore, MAP kinase pathway was also upregulated suggesting its role in mediating osteoblastic cell interactions with coating.

Possible use of a coating material modified from calcium silicate known as sphene ( $\text{CaTiSiO}_5$ ) for orthopedic and dental implants also has been investigated [85, 86]. In another study HAp derived from triethyl phosphite and calcium nitrate as precursors was coated on the surface of a titanium-niobium (Ti-Nb) alloy and the in vitro bioactivity assessed using cell culture of SaOS-2 osteoblast-like cells [86]. Furthermore, they have also examined the bone-like apatite-forming ability of HAp/ $\text{TiO}_2$  coatings derived from tetrabutylorthotitanate, triethyl phosphite, and calcium nitrate on titanium-zirconium alloy (TiZr) [87].

In a study conducted by Standard et al. [88], the phase transformation of  $\gamma\text{-Al}_2\text{O}_3$  to  $\alpha\text{-Al}_2\text{O}_3$  in alumina coatings on CoCr alloy as function of heat treatment temperature and time was investigated. The CoCr disks were coated with either pure boehmite ( $\gamma\text{-AlOOH}$ ) sol or boehmite sol seeded with  $\alpha\text{-Al}_2\text{O}_3$  nanoparticles. The coated samples were then dried, calcined, and heat treated. They observed the initial deposited phase of boehmite transformed to  $\gamma\text{-Al}_2\text{O}_3$  and then to  $\alpha\text{-Al}_2\text{O}_3$  with increasing temperature.

Zirconia coatings on implant materials are well known. It has been stated that some reaction between sol-gel zirconia coatings and stainless steel has been observed and for this reason, the effect of this thickness-dependent phase change phenomenon on the properties of sol-gel zirconia coatings on stainless steel is important to assess if these materials are to be applied as biomedical coatings [89]. In 1996, Paterson et al. examined the structural, mechanical, and thermal barrier properties of sol-gel-derived multilayer zirconia coatings on 316 stainless steel [90–92]. Measurements taken using ultramicroindentation revealed the hardness increased with film thickness. The highest hardness value was 6.12 GPa for a 900 nm thick film.

---

## Concluding Remarks

During the last 50 years, sol-gel technology has revolutionized from traditional materials science such as the synthesis of ceramic powders to advanced applications such as biomedical nanocoatings and optoelectronic applications. The term *sol-gel* is currently used to describe any chemical procedure or process capable of producing ceramic oxides, nonoxides, and mixed oxides from solutions.

Sol-gel processing is a versatile and attractive technique since it can be used to fabricate ceramic powders, fibers, or coatings from solutions by chemical means. The sol-gel process is relatively easy to perform and complex shapes can be coated, and it has also been demonstrated that the nanocrystalline grain structure of sol-gel coatings produced results in improved physical and mechanical properties.

The future of sol-gel powder and coating production methods is far from over. The option of varying both the selection of precursors and synthesis parameters is limitless in both industrial and biomedical applications.

---

## References

1. Floch HG, Belleville PF, Priotton JJ et al (1995) Sol-gel optical coatings for lasers. *Int Am Ceram Soc Bull* 74:60–63
2. Brinker CJ, Scherer GW (1990) Sol-gel science: the physics and chemistry of sol-gel processing, 1st edn. Academic, San Diego
3. Ebelmen J (1846) Untersuchungen über die Verbindung der Borsäure und Kieselsäure mit Aether. *Ann Chim Phys Ser* 57:319–355
4. Liesegang RE (1896) Über einige Eigenschaften von Gallerten. *Natur Wochschr* 11:353–362
5. Rayleigh L (1919) Periodic precipitates. *Philos Mag* 38:738
6. Geffcken W, Berger E (1939) Änderung des Reflexionsvermögens Optischer Glaser. German Patent 736411
7. Roy DM, Roy R (1955) An experimental study of the formation and properties of synthetic spintines and related layer silicates. *Am Mineral* 39:957–975
8. Iler RK (1955) The chemistry of silica. Wiley, New York
9. Dislich H, Hinz P (1982) History and principles of the sol-gel process, and some new multicomponent oxide coatings. *J Non-Cryst Solids* 48:11–16
10. Schroeder H (1965) Water-dispersed industrial and architectural coatings. *Paint Varnish Prod* 55:31–46
11. Stöber W, Fink A, Bohn E (1968) Controlled growth of monodispersed spheres in the micron size range. *J Colloid Interface Sci* 26:62–69
12. Hench LL, Wilson J (1984) Surface active materials. *Science* 226:630–636
13. Matijevic E (1984) Monodispersed colloidal metal oxides, sulfides, and phosphates. New materials for research and applications. In: Hench LL, Ulrich DR (eds) *Ultrastructure processing of ceramics, glasses, and composites*. Wiley, New York, pp 334–352
14. Klein LC (1988) Sol-gel technology for thin films, fibers, preforms, electronics and specialty shapes. Noyes, Park Ridge
15. Roy R (1987) Ceramics by the solution-sol-gel route. *Science* 238:1664–1669
16. Kirk P, Pilliar R (1999) The deformation response of sol-gel-derived thin films on 316L stainless steel using a substrate straining test. *J Mater Sci* 34:3967–3975
17. Wongcharee K, Brungs MP, Chaplin R et al (2004) Influence of surfactant and humidity on sol-gel macroporous organosilicate coatings. *J Sol-gel. Sci Technol* 29:115–124
18. Gan WY, Chiang K, Brungs M et al (2007) Dense TiO<sub>2</sub> thin film: photoelectrochemical and photocatalytic properties. *Int J Nanotechnol* 4:574–587
19. Rodgers LE, Holden PJ, Knott RB et al (2005) Effect of sol-gel encapsulation on lipase structure and function: a small angle neutron scattering study. *J Sol-gel Sci Technol* 33:65–69
20. Hench LL, Splinter RJ, Greenlee TK et al (1971) Bonding mechanisms at the interface of ceramic prosthetic materials. *J Biomed Mater Res* 2:117–141
21. Beckham CA, Greenl TK, Crebo AR (1971) Bone formation at a ceramic implant interface. *Calcif Tissue Res* 8:165
22. Greenlee TK, Beckham CA, Crebo AR et al (1972) Glass ceramic bone implant. *J Biomed Mater Res* 6:235–244
23. Hench LL, Paschall HA (1973) Direct chemical bonding of bioactive glass-ceramic materials and bone. *J Biomed Mater Res Symp* 4:25–42
24. Hench LL, Paschall HA (1974) Histo-chemical responses at a biomaterials interface. *J Biomed Mater Res* 5:49–64

25. Piotrowski G, Hench LL, Allen WC et al (1975) Mechanical studies of the bone bioglass interfacial bond. *J Biomed Mater Res Symp* 9:47–61
26. Hench LL, Paschall HA, Allen WC et al (1975) Interfacial behavior of ceramics implants. *Nat Bureau Standards Special Pub* 415:19–35
27. Hench LL, Hench JW, Greenspan DC (2004) Bioglass: a short history and bibliography. *J Aust Ceram Soc* 40:1–43
28. Hench LL (1991) Bioceramics: from concept to clinic. *J Am Ceram Soc* 74:1487–1510
29. Hench LL, West JK (1996) Biological applications of bioactive glasses. *Life Chem Rep* 13:187–241
30. Hench LL (1990) Bioactive glasses and glass-ceramics: a perspective. In: Yamamuro T, Hench LL, Wilson J (eds) *Handbook of bioactive ceramics*. CRC Press, Boca Raton, pp 7–23
31. Hench LL, Wilson J (1993) *Introduction to bioceramics*. World Scientific Press, Singapore
32. Hench LL (2013) *Introduction to bioceramics*, 2nd edn. Imperial College Press/World Scientific Press, London/Singapore
33. Hench LL (1998) Bioceramics. *J Am Ceram Soc* 81:1705–1728
34. Hench LL (1988) Bioactive ceramics. In: Ducheyne P, Lemons JE (eds) *Bioceramics: material characteristics vs. in vivo behavior*. New York Academy of Science, New York, p 54
35. Kokubo T (1990) Novel biomaterials derived from glasses. In: Soga W, Kato A (eds) *Ceramics: towards the 21st century*. Japan Ceramic Society, Tokyo, pp 500–518
36. Kokubo T (1991) Recent progress in glass-based materials for biomedical applications. *J Ceram Soc Jpn* 99:965–973
37. Vrouwenvelder WCA, Groot CG, de Groot K (1993) Histological and biochemical evaluation of osteoblasts cultured on bioactive glass, hydroxylapatite, titanium alloy, and stainless steel. *J Biomed Mater Res* 27:465–475
38. Andersson OH, Kangasniemi I (1991) Calcium phosphate formation at the surface of bioactive glass in vitro. *J Biomed Mater Res* 25:1019–1030
39. Li P, Yang Q, Zhang F et al (1992) The effect of residual glassy phase in a bioactive glass-ceramic on the formation of its surface apatite layer in vitro. *J Mater Sci Mater Med* 3:452–456
40. Kokubo T, Shigematsu M, Nagashima Y et al (1982) Apatite-wollastonite containing glass-ceramic for prosthetic application. *Bull Inst Chem Res* 60:260–268
41. Eblemen M (1846) On the synthesis of silica gels from alkoxides. *Ann Chim Phys* 16:129
42. Hench LL, West JK (1990) The sol-gel process. *Chem Rev* 90:33–72
43. Sakka S (1985) Glasses and glass-ceramics from gels. *J Non-Cryst Solids* 73:651
44. Li R, Clark AE, Hench LL (1991) An investigation of bioactive glass powders by sol-gel processing. *J Appl Biomater* 2:231–239
45. Sepulveda P, Jones JR, Hench LL (2001) Characterization of melt-derived 45S5 and sol-gel-derived 58S bioactive glasses. *J Biomed Mater Res* 58:734–740
46. Pereira MM, Hench LL (1996) Mechanisms of hydroxyapatite formation on gel-silica substrates. *J Sol-gel Sci Technol* 7:59–68
47. Andersson ÖH (1992) Glass transition temperature of glasses in the  $\text{SiO}_2\text{-Na}_2\text{O-CaO-P}_2\text{O}_5\text{-Al}_2\text{O}_3\text{-B}_2\text{O}_3$  system. *J Mater Sci Mater Med* 3:326–328
48. Peitl Filho O, LaTorre GP, Hench LL (1996) Effect of crystallization on apatite-layer formation of bioactive glass 45S5. *J Biomed Mater Res* 30:509–514
49. Brink M (1997) Bioactive glasses with a large working range. Dissertation, Åbo Akademi University
50. Hayakawa S, Tsuru K, Ohtsuki C (1999) Mechanism of apatite formation on a sodium silicate glass in a simulated body fluid. *J Am Ceram Soc* 82:2155–2160
51. Arstila HE, Vedel L, Hupa L et al (2004) Measuring the devitrification of bioactive glasses. *Key Eng Mater* 254–256:67–70
52. Ylänen HO, Helminen T, Helminen A et al (1999) Porous bioactive glass matrix in reconstruction of articular osteochondral defects. *Ann Chir Gyn* 83:237–245
53. Fröberg L, Hupa L, Hupa M (2004) Porous bioactive glasses with controlled mechanical strength. *Key Eng Mater* 254–256:973–976

54. Percy MJ, Bartlett JR, Spiccia L et al (2000) The influence of b-diketones on hydrolysis and particle growth from zirconium (IV) N-propoxide in n-propanol. *J Sol-gel Sci Technol* 19:315–319
55. Schroder H (1966) New sun-shielding glasses for architectural purposes. *Vetro Silicati* 10:10–14
56. Thomas IM (1988) Multicomponent glasses from the sol-gel process. In: Kelen LC (ed) *Sol-gel technology for thin films, fibers, preforms, electronics and specialty shapes*. Noyes, Park Ridge, pp 2–15
57. Wallace S, Hench LL (1984) Metal organic-derived 20L gel monoliths. *Ceram Eng Sci Proc* 5:568–573
58. Schwart I, Anderson P, de Lambilly H et al (1986) Stability of lithium silicate gels. *J Non-Cryst Solids* 83:391–399
59. Cassidy DJ, Woolfrey JL, Bartlett JR et al (1997) The effect of precursor chemistry on the crystallization and densification of sol-gel derived mullite gels and powders. *J Sol-gel Sci Technol* 10:19–30
60. Southon PD, Bartlett JR, Finnie KS et al (1999) The formation of zirconium hydroxide nanoparticles from aqueous nitrate solutions. *J Aust Ceram Soc* 35:7–13
61. Southon PD, Bartlett JR, Woolfrey JL et al (2002) Formation and characterization of an aqueous zirconium hydroxide colloid. *Chem Mater* 14:4313–4319
62. Orel G, Hench LL (1986) Effect of formamide additive on the chemistry of silica sol-gels: part I. NMR of silica hydrolysis. *J Non-Cryst Solids* 79:177–194
63. Schmidt H, Rinn G, Nab R et al (1988) Film preparation by inorganic–organic sol-gel synthesis. *Mater Res Soc Symp Proc* 32:743–754
64. Zheng H, Colby MW, Mackenzie JD (1988) The control of precipitation in sol-gel solutions. In: Brinker CJ, Clark DE, Ulrich DR (eds) *Better ceramics through chemistry*, 3rd edn. Materials Research Society, Pittsburgh, pp 537–540
65. Melpolder SM, Coltrain BK (1988) Optimization of sol-gel film properties. In: Brinker CJ, Clark DE, Ulrich DR (eds) *Better ceramics through chemistry*, 3rd edn. Materials Research Society, Pittsburgh, pp 811–816
66. Turner CW (1991) Sol-gel process-principles and applications. *Ceram Bull* 70:1487–1490
67. Uhlmann DR, Rajendran GP (1988) Coatings: the land of opportunity for sol-gel technology. In: Mackenzie JD, Ulrich DR (eds) *Ultrastructure processing of advanced ceramics*. Wiley, New York, p 241
68. Pettit RB, Ashley CS, Reed ST et al (1988) Antireflective films from the sol-gel process. In: Kelen LC (ed) *Sol-gel technology for thin films, fibers, preforms, electronics, and specialty shapes*. Noyes, Park Ridge, pp 80–109
69. Ben-Nissan B, Choi AH (2006) Sol-gel production of bioactive nanocoatings for medical applications: Part I: an introduction. *Nanomedicine* 1:311–319
70. Ducheyne P, Radin S, Heughebaert M et al (1990) Effect of calcium phosphate ceramic coatings on porous titanium: effect of structure and composition on electrophoretic deposition, vacuum sintering and in vitro dissolution. *Biomaterials* 11:244–254
71. Kokubo T, Kim HM, Kawashita M et al (2000) Novel ceramics for biomedical applications. *J Aust Ceram Soc* 36:37–46
72. Choi AH, Ben-Nissan B (2014) Advancement of sol-gel technology and nanocoatings in Australia. *J Aust Ceram Soc* 50:121–136
73. Ben-Nissan B, Choi AH, Green DW et al (2011) Synthesis and characterization of hydroxyapatite nanocoatings by sol-gel method for clinical applications. In: Zhang S (ed) *Biological and biomedical coatings handbook*, vol 1. CRC Press, Boca Raton, pp 37–70
74. Hu J, Russell JJ, Ben-Nissan B et al (2001) Production and analysis of hydroxyapatite from Australian corals via hydrothermal process. *J Mater Sci Lett* 20:85–87
75. Ben-Nissan B, Milev A, Vago R et al (2004) Sol-gel derived nano-coated coralline hydroxyapatite for load bearing applications. *Key Eng Mater* 254–256:301–304
76. Ben-Nissan B, Russell JJ, Hu J et al (2000) Comparison of surface morphology in sol-gel treated coralline hydroxyapatite structures for implant purposes. *Key Eng Mater* 192–195:959–962

77. Ben-Nissan B (2003) Natural bioceramics: from coral to bone and beyond. *Curr Opin Solid State Mater Sci* 7:283–288
78. Ben-Nissan B, Milev A, Vago R (2004) Morphology of sol-gel derived nano-coated coralline hydroxyapatite. *Biomaterials* 25:4971–4976
79. Lewis K, Valenzuela SM, Ben-Nissan B (2008) Changes in the activity of osteoblast like cells with sol-gel derived hydroxyapatite and zirconia nanocoatings. *Key Eng Mater* 361–363:633–636
80. Zreiqat H, Roest R, Valenzuela S et al (2005) Human bone derived cell (HBDC) behavior of sol-gel derived carbonate hydroxyapatite coatings on titanium alloy substrates. *Key Eng Mater* 284–286:541–544
81. Zreiqat H, Valenzuela SM, Ben-Nissan B et al (2005) The effect of surface chemistry modification of titanium alloy on signaling pathways in human osteoblasts. *Biomaterials* 26:7579–7586
82. Roest R, Latella BA, Heness G et al (2011) Adhesion of sol-gel derived hydroxyapatite nanocoatings on anodized pure titanium and titanium (Ti6Al4V) alloy substrates. *Surf Coat Technol* 205:3520–3529
83. Shors EC (1999) Porous ceramics and bone growth factors for bone grafting: now and into the millennium. In: 12th international symposium on ceramics in medicine, bioceramics 12, Japan
84. Ramaswamy Y, Ben-Nissan B, Roest R et al (2006) Human osteoclasts behavior on sol-gel derived carbonate hydroxyapatite coatings on anodized titanium alloy substrates. *Key Eng Mater* 309–311:709–712
85. Wu CT, Ramaswamy Y, Gale D et al (2008) Novel sphenic coatings on Ti-6Al-4V for orthopedic implants using sol-gel method. *Acta Biomater* 4:569–576
86. Xiong JY, Li YC, Hodgson P et al (2009) Bioactive hydroxyapatite coating on titanium-niobium alloy through a sol-gel process. *Mater Sci Forum* 618–619:325–328
87. Wen C, Xu W, Hu WY et al (2007) Hydroxyapatite/titania sol-gel coatings on titanium-zirconium alloy for biomedical applications. *Acta Biomater* 3:403–410
88. Bae IJ, Standard OC, Roger GJ et al (2004) Phase and microstructural development in alumina sol-gel coatings on CoCr alloy. *J Mater Sci Mater Med* 15:959–966
89. Shane M, McCartney ML (1990) Sol-gel synthesis of zirconia barrier coatings. *J Mater Sci* 25:1537–1544
90. Paterson MJ, Ben-Nissan B (1996) Multilayer sol-gel zirconia coatings on 316 stainless steel. *Surf Coat Technol* 86–87:156–158
91. Paterson MJ, McCulloch DG, Paterson PJK et al (1997) The morphology and structure of sol-gel derived zirconia films on stainless steel. *Thin Solid Films* 311:196–206
92. Paterson MJ, Paterson PJK, Ben-Nissan B (1998) The dependence of structural and mechanical properties on film thickness in sol-gel zirconia films. *J Mater Res* 13:388–395

---

# Biomaterial Functionalized Surfaces for Reducing Bacterial Adhesion and Infection

# 26

Maria G. Katsikogianni, David J. Wood, and Yannis F. Missirlis

## Contents

Introduction .....	758
Nonfouling Surfaces .....	759
Plasma-Assisted Surface Treatment .....	759
Surface Charge .....	761
Surface Topography Modification .....	761
Antimicrobial Surfaces .....	763
Contact-Killing Antimicrobial Surfaces .....	763
Surfaces that Release Antimicrobial Agents .....	766
Dual-Function Antimicrobial Surfaces .....	768
Dual-Contact and Release-Based Antimicrobial Surfaces .....	768
Dual-Contact Killing and Nonfouling Surfaces .....	768
Dual-Function Contact-Killing and Bacterial Released Surfaces .....	770
Bacterial Interference .....	770
Biofilm Dispersal Agents .....	771
Bacteriophage Releasing Materials .....	771
Tissue Integration .....	771

---

M.G. Katsikogianni (✉)

Laboratory of Biomechanics and Biomedical Engineering, Department of Mechanical Engineering and Aeronautics, University of Patras, Rion, Patras, Greece

Biomaterials and Tissue Engineering Group, School of Dentistry, University of Leeds, Leeds, UK

Advanced Materials Engineering, Faculty of Engineering and Informatics, University of Bradford, Bradford, UK

e-mail: [Maria.g.katsikogianni@gmail.com](mailto:Maria.g.katsikogianni@gmail.com)

D.J. Wood

Biomaterials and Tissue Engineering Group, School of Dentistry, University of Leeds, Leeds, UK

e-mail: [D.J.Wood@leeds.ac.uk](mailto:D.J.Wood@leeds.ac.uk)

Y.F. Missirlis

Laboratory of Biomechanics and Biomedical Engineering, Department of Mechanical Engineering and Aeronautics, University of Patras, Rion, Patras, Greece

e-mail: [misirlis@mech.upatras.gr](mailto:misirlis@mech.upatras.gr)



Examples of Orthopedic and Dental Implants Used at Present .....	772
Bone Graft-Based Delivery Vehicles .....	774
Synthetic/Protein-Based Delivery Vehicles .....	774
Concluding Remarks and Future Perspectives .....	775
General Healthcare Market and Medical Devices .....	775
Antimicrobial Strategies .....	776
Parameters to be Taken Into Consideration .....	777
References .....	779

### Abstract

This chapter describes the current approaches to reduce bacterial adhesion to various biomaterial surfaces, focusing on nonfouling surfaces through patterning and hydrophobicity plasma-assisted surface treatment and deposition; incorporation of antimicrobials, antibiotics, antibiofilms, and natural extracts that are either immobilized or released; dual function antimicrobial surfaces; incorporation of nonpathogenic bacteria, bacteriophages, and biofilm dispersal agents but also reduced bacterial adhesion through tissue integration. To facilitate the design of new materials, the role of physical, chemical, and biological surface properties on bacterial adhesion is reviewed in each case, as an insight into the chemical and physical cues that affect bacterial adhesion and biofilm formation can provide ideas for creating successful antifouling or antimicrobial surfaces. The application of these surfaces is explored based on the clinical needs and the market gaps. How multidisciplinary research on surface design and engineering may have an impact on both fundamental understanding of bacterial adhesion to biomaterials and applied biomaterial science and technology is finally discussed.

### Keywords

Bacterial adhesion • Biomaterials • Surface chemistry • Surface energy • Surface charge • Surface topography • Self-assembly • Plasma treatment • Plasma deposition • Antifouling • Antimicrobials • Antibiotics • Natural extracts • Surface analysis • Adhesion mechanism • Fluid shear

## Introduction

Nowadays, irreparable damage to the human body does not necessarily imply functional loss or reduced quality of life. Millions of patients worldwide benefit from permanent implants such as prosthetic joints, dental implants, stents, vascular grafts, and pacemakers, or from temporary inserted devices such as intravascular and urinary catheters. Biomaterial implant and device applications, versatility, and performance represent in many cases a success story [1].

However, a non-negligible fraction of devices fail in practice due to device-associated infections (DAI), which are always connected with microbial contamination of an implant or device, either inferred during surgery or at a later stage [1–4]. Once microorganisms adhere to the biomaterial, they start proliferating

rapidly as biofilms, in which they are protected against both antibiotics and immune clearance [5]. Bacterial species living in a biofilm have great viability advantages requiring 500–5000 times higher doses of antibiotics to get eradicated compared to planktonic organisms [5]. DAI are therefore often resistant to many of the currently available antibiotics and have a substantial and largely unchanged clinical incidence, increased chances for revision surgeries, associated morbidity, and mortality [2–7].

Biomaterial compositions and applications may differ widely, but all attract microorganisms, representing niches for medical device-related infections in vivo. Continued microbial presence interferes with the intended function of an implant or device and adds risks to human use. DAI therefore constitutes one of the key reasons for clinical failure, impaired functionality, and reduced lifetime of medical devices, resulting in high distress for the patients and huge socioeconomic costs [6, 7].

In most cases antimicrobial strategies rely on the systemic administration of antibiotics. However, the extensive use of antibiotics worldwide during the last decades has led to a threatening situation where a large number of bacteria have developed resistance against conventional antibiotics [6–8]. This has therefore resulted in a number of infectious diseases, for which limited treatment exists.

Over the last few years there has been heightened international concern about the growing resistance of bacteria to antibiotics. An example is the methicillin-resistant *Staphylococcus aureus* (MRSA), which is one of the most widespread causes of hospital infections [6]. About a third of people carry some form of *S. aureus* on their skin, where the bacteria do no harm. However, if they enter the bloodstream, they can cause disease. And if the resulting illness cannot be treated because the bacteria are drug resistant, the infection can prove fatal.

Antimicrobial strategies supplemental to systemically administered antibiotics therefore often focus on modifying implant or device surfaces. Nowadays, three surface strategies are mostly employed toward the preparation of antimicrobial surfaces and these are surfaces that hinder bacterial adhesion and biofilm formation (nonfouling), antimicrobial surfaces that kill bacteria either by contact or release of antimicrobial agents and those that have dual function and both kill bacteria and resist bacterial adhesion or kill and release the attached bacteria (Fig. 1).

In this chapter, these strategies for designing antibacterial surfaces with single or dual functionality are introduced, while their inherent advantages and disadvantages are discussed.

The chapter is concluded with a presentation of future research directions for developing antimicrobial surfaces based on clinical needs and market gaps.

---

## Nonfouling Surfaces

### Plasma-Assisted Surface Treatment

A wide range of surface treatments have been used to prevent bacterial adhesion to polymers (Fig. 1a). Amongst these plasma processing of the material surface presents many advantages and some of these are (a) its ability to change the substrate

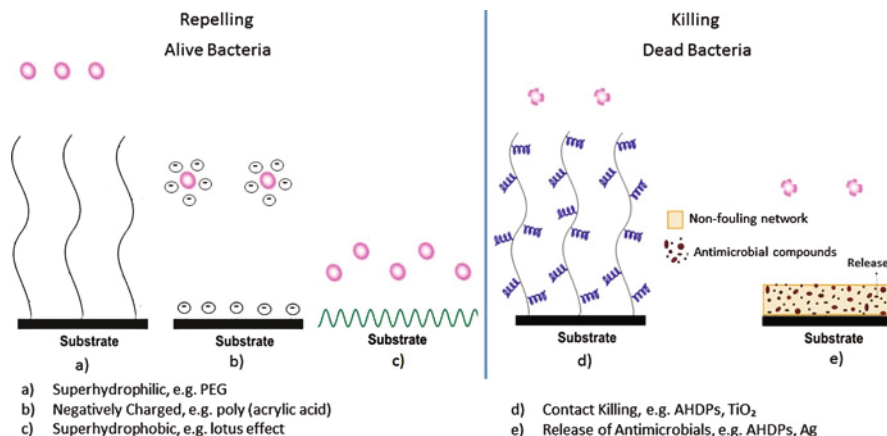


**Fig. 1** Types of antimicrobial coatings

surface chemistry without altering its bulk properties; (b) the sterilizing effect of the plasma; (c) ease of process scale-up to industrial scale and shapes. For example, companies such as PlasmaTreat system currently have commercially available atmospheric plasma systems for the activation and coating of surfaces at processing speeds of 25 m/min. Therefore, not only the vacuum but mostly the atmospheric plasma surface modification technologies are readily scalable and raw material costs are relatively low compared with the potential added value that can be obtained using these surface treatments.

Increased material surface energy has been suggested as one way to reduce bacterial adhesion to material substrates and in this direction Katsikogianni et al. examined the effect of He and He/O<sub>2</sub> treatment of PET on the adhesion of *S. epidermidis* and the results showed that the adhesion was reduced on the treated materials in comparison to PET, whereas the aging effect and the consequent decrease in the surface free energy and polar component favored bacterial adhesion [9]. Therefore, the plasma parameters should be chosen in such a way so that the aging effect and the subsequent hydrophobic recovery are minimized. Similarly, Balazs et al. observed that O<sub>2</sub> plasma-treated PVC reduced *Pseudomonas aeruginosa* adhesion as much as 70 % [10]. However, in a recent study Rochford et al. showed that there are controversies concerning the effect of the material surface free energy on bacterial adhesion and this should be taken into account [11]. These controversies may be due to differences in the bacterial strains used or in the experimental conditions, and lead to questions about the applicability of this method for the preparation of antimicrobial substrates.

In the same direction the plasma deposition of PEO-like coatings has been proposed as an effective method for the preparation of surfaces resistant to bacterial adhesion [12, 13]. The long-term stability and performance of protective antifouling layers is, however, questionable. Kingshott et al. showed that physisorbed PEO polymers did not provide lasting reduction in bacterial adhesion, whereas PEO

chains covalently attached to a bulk material showed stable effectiveness [14]. An explanation is that bacteria can displace physisorbed polymer chains from the bulk material surface, whereas covalently surface-grafted polymer chains resist such displacement presenting longer-lasting effectiveness. Toward enhanced coating stability, a number of studies have used plasma polymer coatings as interlayers for the covalent grafting of fouling-resistant polymers or for the deposition of the antifouling polymers [12, 13, 15].

Moreover, plasma deposition of diamond-like carbon [16] and superhydrophobic coatings [17] has been proven to significantly reduce bacterial adhesion in comparison to untreated surfaces.

## Surface Charge

The surface charge of the substratum surfaces is another parameter that significantly influences bacterial adhesion and toward material strategies that reduce bacterial adhesion negatively charged substrates may be a way forward (Fig. 1b). Katsikogianni and Missirlis observed that bacterial adhesion was lowest onto the OH-terminated glass which was negatively charged and this because the two tested bacterial strains appeared negatively charged, when bacteria were suspended in 0.01 and 0.1 M PBS [18].

Moreover, Kiremitci and Pesmen showed that bacterial adhesion was reduced on the negatively charged PMMA/AA (acrylic acid), while it was increased on the positively charged PMMA/DMAEMA (dimethylamino ethyl methacrylate) [19]. In the same direction, Tang et al. showed the bacterial antiadhesive properties of polysulfone (PSU) microfiltration membranes modified with poly(allylaminehydrochloride) (PAH)/poly(acrylic acid) (PAA) polyelectrolytemultilayers (PEMs) and this was partially attributed to their negative charge [20].

## Surface Topography Modification

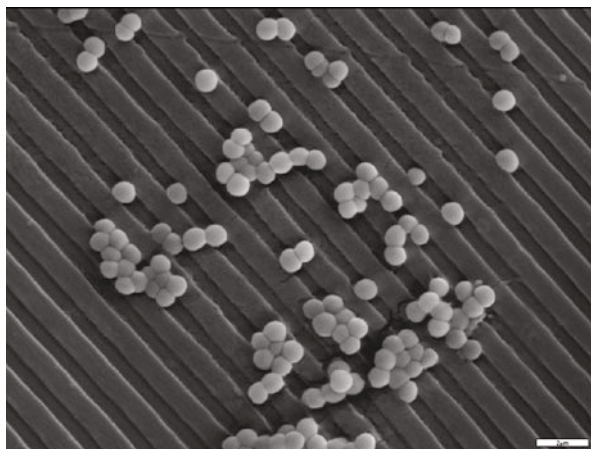
In addition to surface chemistry and charge, another factor influencing microbial adhesion is surface roughness and configuration. Surface modifications usually introduce numerous functional groups and chemical cross-links changing not only the surface energy but the roughness and the configuration as well [16, 21, 22]. While the effect of roughness on bacterial adhesion has not been systematically studied, amongst the results that have been reported is that plasma roughened LDPE exhibited higher initial microbial deposition rate than the smooth surface, whereas an inverse effect was found after long-term adhesion [21]. Katsikogianni et al. showed that surface modification by means of plasma for the deposition of CF<sub>4</sub>, silver, amorphous carbon, hydrogenated and not, and combination of the latest with silver, changed not only the water contact angle and therefore the surface free energy of the substrates but the configuration and roughness as well [16]. In particular, it was observed that the amorphous carbon coating, which was the material with the highest

surface roughness, prevented bacterial detachment due to enhanced shear rate [16]. Moreover, Katsikogianni et al. showed plasma activation of PET substrate by He plasma changed not only the surface free energy  $\gamma_S^{tot}$  and its dispersive ( $\gamma_S^d$ ) and polar components ( $\gamma_S^p$ ) but significantly increased the roughness as well, by enhancing the already existing granular structures of PET [21]. It can be concluded therefore that surfaces with similar surface free energy but higher average surface roughness (Ra) values, as these were measured by means of AFM, favored bacterial adhesion in comparison to the ones with lower Ra values [16, 21, 22]. Furthermore, according to Truong et al., roughness variation of titanium substrates at the nano-scale, as this was observed by AFM but not by profilometry, influenced bacterial adhesion, with more bacteria adhering to the rougher substrate (Ra of  $1.12 \pm 0.30$  nm, in comparison to  $0.59 \pm 0.27$  nm) [23]. It has been therefore shown that the irregularities of a surface promote bacterial adhesion and biofilm deposition. This may happen since a rough surface has a greater surface area and the crevices in the roughened surfaces provide more favorable sites for colonization [16].

Moreover, the presence of grooves alters bacterial adhesion patterns, depending on the groove size. The synthetic shark skin pattern, for example, has been shown to reduce *E. coli* biofilm formation over a number of days in comparison to flat substrates [24]. The widths of the grooves ranging between 10 and 40  $\mu\text{m}$  displayed no effect on bacterial adhesion in some other studies, meaning possibly that bacteria preferentially adhere to irregularities that conform to their size (Fig. 2) since this maximizes the bacteria-surface contact area [25, 26]. Grooves or scratches too small, for the bacterium to fit them, reduce the contact area of the bacterium and hence binding [27].

Toward the preparation of nonfouling surfaces nature represents a source of inspiration particularly in the field of biomimetics, where biological systems are fundamentally studied for their biotechnological applications. Some of the low-adhesive, superhydrophobic, and self-cleaning surfaces found in nature have been investigated for their potentially antibiofouling characteristics [24, 28]. Indeed,

**Fig. 2** Scanning electron microscopy image of *Staphylococcus epidermidis* adhering to grooved PCL (Katsikogianni MG and Missirlis YF, Unpublished data)



natural and biomimicked surfaces of insect wings [28], gecko skin [29], and shark skin [24] exhibit antibiofouling through their nanotopology – e.g., nanopillars or grooves – and chemical properties by preventing contaminating particles, algal spores, and bacterial cells from attaching to their surface.

Toward the use of nanotopology for the preparation of antifouling surfaces, a range of different nanofabrication techniques have been used to control surface roughness and configuration at the nm level. The main approaches are based on nanoimprint lithography [30], orientation of thin phase separated block copolymer films, which could subsequently be used as polymer masks/templates for nanolithography [31], self-organization of well-defined, nanosized gold islands onto a substrate [32], and microinjection molding [33]. Although these concepts generally lead to well-ordered surface nanostructures, up to date a high degree of patterning can only be obtained through proper manipulation of thin polymer layers. Moreover, uniform surface patterning is often only observed over a relatively small surface area as the costs associated with using these nanofabrication techniques preclude broader commercial applications outside the semiconductor industries.

Furthermore, it should be taken into consideration that bacterial strains – even within the same species – can vary significantly in size and shape. For a given material surface, different bacterial species and strains adhere differently since different species and strains have different physicochemical characteristics. Therefore, the relationship between roughness/configuration and attachment can be quite complicated and generalization should be avoided.

Additionally, to the best of our knowledge, no material has been developed so far that completely resists bacteria adhesion and the nonfouling surfaces do not actively kill bacteria. Therefore, these surfaces may eventually become contaminated especially due to their deterioration under physiological conditions. For these reasons, surfaces that kill bacteria have been suggested and are introduced in the following section.

---

## **Antimicrobial Surfaces**

### **Contact-Killing Antimicrobial Surfaces**

#### **Surface Polymerization and Functionalization Toward the Incorporation of Antimicrobial Compounds**

In order to kill adherent bacteria, contact-based bactericidal surfaces are coated with antimicrobial agents by either covalent conjugation or physical adsorption. The antimicrobials used in this respect range from synthetic chemicals such as quaternary ammonium compounds (QACs), polycations, and various antibiotics to natural biomolecules such as chitosan and antimicrobial peptides (AMPs).

Toward the immobilization of the antimicrobial compounds a number of methods have been developed and are briefly described below.

Surface polymerization takes place by the polymerization of an antimicrobial compound on the surface via different means such as covalent bonding or atom

radical transfer [34–37]. Surfaces possessing chemically bonded hydrophobic polycations of quaternary ammonium salts have been found to possess bactericidal properties [34]. Lee et al. have used an atom transfer radical polymerization (ATRP) approach to modify surfaces with quaternized ammonium groups or host (antimicrobial) defence peptides [35, 36]. This method shows a permanent antibacterial effect because the surfaces can be reused without loss of activity [35, 37]. Nevertheless, the commercial applications of this manufacturing method are still in development and require more investigation before they can be applied to wide-scale industrial implementation as it is time consuming and requires a number of steps.

Plasma polymerization is well suited toward the deposition of adhesive interlayers for the covalent surface immobilization of antimicrobial organic molecules. In contrast to ATRP, plasma polymerization is easy to be used and scaled up toward the deposition of coatings with good adherence on most substrate materials it provides reactive chemical surface groups, for covalent grafting, that are not available on the underlying bulk material/device [38]. Toward surface functionalization, surface treatments that involve the use and immobilization of antimicrobial compounds such as antibiotics, cationic compounds, and natural antimicrobials have been used effectively to prevent bacterial adhesion. In this direction, antimicrobial molecules that contain chemically reactive groups such as hydroxyl, carboxyl, amino, etc. can be covalently immobilized onto plasma polymer surfaces or ATRP, using well-known facile chemical interfacial reactions as described below.

### **Antibiotics**

The application of commercial antibiotics onto the material surface is one way against bacterial adhesion. In order though to enhance the long-term stability and the effectiveness of the products, it has been suggested that the antibiotics should be covalently grafted on the surface and in this direction plasma pretreatment of the substrate has been used in order to enable the grafting of commercially available antibiotics [38]. Although effective, the ongoing presence of antibiotics promotes the development of resistant microbial strains [39].

The issue of selecting resistant bacterial strains through an excessive use of antibiotics is one of the main driving forces behind research into new antibacterial substances such as cationic compounds, synthetic and natural, but also natural antimicrobials.

### **Cationic Compounds**

A number of cationic surfaces have been found to possess antibacterial activity *in vitro*. While the mechanism of action is not fully understood, the leading hypothesis is that the cationic chains attract the negatively charged bacterial cells, as described in the section about the effect of the surface charge on bacterial adhesion, and penetrate the cell membrane causing loss of the membrane integrity.

For the covalent grafting of various cationic compounds such as quaternary ammonium compounds (QACs) [34], cationic peptides such as melittin [40], host defence (antimicrobial) peptides (HDPs) [41] or chitosan [42], and cationic proteins

such as lysozyme [43] a number of studies have used plasma polymer coatings as interlayers or the ATRP method.

The difficulty, however, is to develop a readily scalable process to apply these chemical functionalities, as adherent coatings, while the main concern remains the cytotoxicity of many of these compounds, especially of QACs, or the effectiveness of others such as chitosan. For this reason the use of natural antimicrobials is further explored.

### **Natural Antimicrobials**

Antimicrobial peptides (AMPs) and HDPs represent natural alternatives to traditional synthetic biocidal compounds. In particular, HDPs not only deactivate bacteria in biofilms at low concentrations [44] but also modulate the innate and adaptive immune responses, promote wound healing, inhibit proinflammatory responses to bacterial lipopolysaccharide, prevent biofilm formation through multiple mechanisms, or specifically kill bacteria within a biofilm [41].

These biomolecules can be immobilized on supporting surfaces either physically [45] or chemically [41] to fabricate bactericidal coatings with a broad spectrum of antimicrobial activity, high efficacy even at low concentrations, and a lack of susceptibility to bacterial resistance.

Apart from the AMPs and HDPs, the use of extracts from plants and herbs as well as of honey as a traditional remedy for bacterial infections has been known since ancient times. The antimicrobial compounds in plant materials are commonly found in the essential oil fraction of leaves, flowers or buds, seeds, and fruits [46]. The bioactive compounds found in plant extracts can be divided into several categories. Various phenols and phenolic acids, quinones, flavonoids, flavones, flavonols, tannins, coumarins, terpenoids, alkanoids, lectins, and polypeptides have been found to exert a broad spectrum of biological activities, including antimicrobial properties [47]. The mechanism of the antibacterial action of these substances remains largely unknown. However, recent studies suggested that inhibition of nucleic acid synthesis, binding to cell wall, disruption of the microbial membrane, interference with the two bacterial cell communication strategies of quorum sensing, and swarming or inactivation of bacterial adhesins, enzyme, and cell envelope transport proteins may be the primary causes of the antibacterial character of at least some of these compounds [47].

However, most of the active compounds found in the natural antimicrobials, such as furanones, do not possess convenient chemical groups for interfacial covalent bonding and they should therefore be linked using less common chemical strategies.

In agreement with the results observed using the self-assembled monolayers (SAMs) [18], hydroxyl groups are essential for the antimicrobial function. Therefore the furanone ring structure and the phenolic hydroxyl group in the case of serrulatanes should remain away from the substrate and undisturbed when covalent immobilization is attempted. For this reason copious pathways have been suggested that are slow and the antibacterial activity is less upon functionalization [48].



The difficulty therefore for the preparation of contact-active antimicrobial surfaces is to develop a readily scalable process to apply these chemical functionalities in a continuous process onto a wide range of materials. The surfaces that release antimicrobial agents appear as an alternative and are briefly described below.

## Surfaces that Release Antimicrobial Agents

### Incorporation of Antimicrobial Compounds

As in the case of contact-killing antimicrobial surfaces, these surfaces incorporate antimicrobial compounds such as antibiotics, natural antimicrobials, and metal ions, which are progressively released as described below.

#### Antibiotics

There are several types of release-based bactericidal surfaces that use antibiotics such as tobramycin incorporated into biomimetic hydroxyapatite coatings on titanium [49], gentamicin-loaded bone cements, and gentamicin sandwiched between titanium and PLGA overcoat [50]. Although effective, the release of antibiotics is quite difficult to be controlled over time and the ongoing release of antibiotics promotes the development of resistant microbial strains, which is one of the most important problems facing modern medicine [39]. The issue of selecting resistant bacterial strains through an excessive use of antibiotics is perhaps the main driving force behind research into new antibacterial substances.

#### Natural Antimicrobials

As described in the contact-killing antimicrobial surfaces section, there are a number of natural antimicrobial compounds such as AMPs, HDPs, and compounds found in plant extracts that can be released from various surfaces providing antimicrobial properties [45].

As observed in our recent study the release of HDPs such as the IDR-1018 or E6 at low concentrations (16  $\mu\text{g/ml}$ ) was sufficient to kill *Staphylococcus epidermidis* in an overnight formed biofilm (Fig. 3a, b), while nisin, a commercially available AMP, was not as effective (Fig. 3c) [44].

In addition to plant extracts, honey has been widely reported to exhibit antibacterial activity and a honey-infused bandage called Medihoney was granted FDA approval. Several studies have shown that certain honey types possess an antibacterial activity which persists even after removal of hydrogen peroxide by catalase. In particular it has been reported that Manuka honey, derived from the Manuka tree, has a very high level of antibacterial activity based on the 1,2-dicarbonyl compound Methylglyoxal, and its antibacterial action is due to its effect on the DNA, RNA, and protein synthesis in bacterial cells, while the common bacterial strains *Escherichia coli* and *Staphylococcus aureus* do not develop noticeable resistance against these surfaces [51].

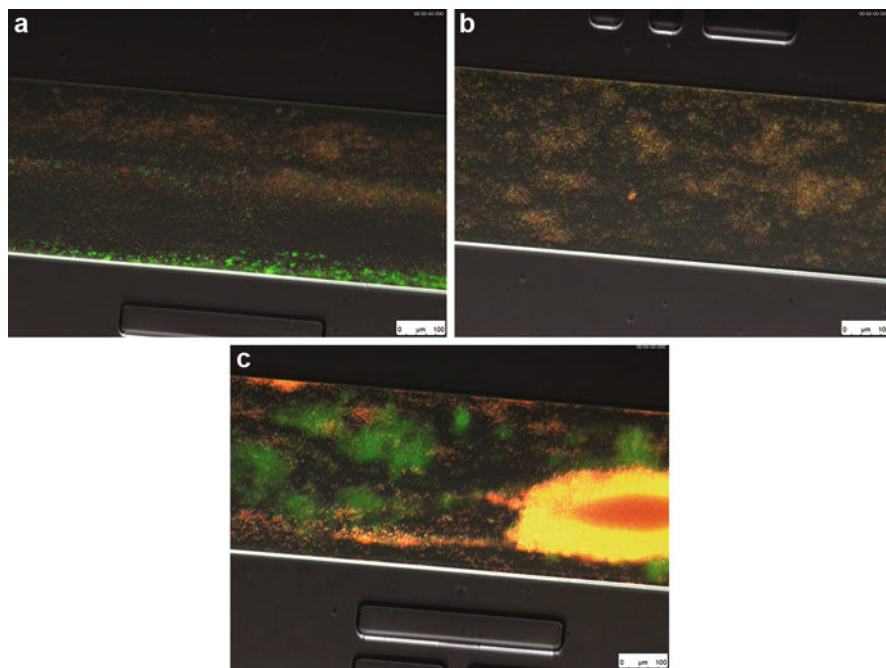


**Fig. 3** Effect of 16  $\mu\text{g/ml}$  of (a) E6, (b) IDR-1018, (c) Nisin on *S. epidermidis* overnight formed biofilms, after 3 h of exposure to the antimicrobials at  $50 \text{ s}^{-1}$  (Katsikogianni MG, Hancock REW, Devine DD, Wood DJ, presented in [44] and unpublished data)

However, honey has not been applied as a thin coating, reducing the cost and enhancing the mechanical properties and the stability of the coating, while, as in the case of antibiotics, the difficulty is the controlled release over a period of time and the fact that the surfaces lose their antimicrobial capacity after the completion of the antimicrobial compound release.

### Metal Ions

Due to its antimicrobial properties silver has been widely applied on a number of commercially available products ranging from wound dressings to clothing, vascular and urinary catheters, and other medical devices. The problem, however, is the toxicity of the released silver into the environment and there have therefore been calls to severely limit its application [52]. Moreover, silver is an expensive element that compromises the optical properties of the final material.

A number of other metal ions are also known to possess antibacterial activity and their release from polymeric coatings can analogously be used to achieve short-term prevention of bacterial adhesion to materials. Copper [53] and ZnO [54] have been deposited by sputtering, ion implantation, plasma-enhanced chemical vapor deposition, or through microwave-plasma synthesis. As in the case of silver though, toxicity effects need to be considered.

## Dual-Function Antimicrobial Surfaces

### Dual-Contact and Release-Based Antimicrobial Surfaces

Nowadays, antimicrobial surfaces that rely on the usage of two different antimicrobial compounds incorporated into one system have been designed so that they operate through both contact-based and release-based mechanisms. These surfaces are of particular interest because they can provide long-term antimicrobial efficiency by killing both planktonic and attached bacteria. Such an example is the development of a coating that is composed of two layered functional regions; a polyelectrolyte multilayer reservoir for the loading and release of bactericidal silver nanoparticles (AgNPs) and a silica surface with immobilized QACs [55]. Dual-function coatings of this type show high initial bacteria-killing efficiency due to the release of silver ions while they retain significant antimicrobial activity after the depletion of the embedded AgNPs due to the immobilized QACs.

As in the case of surfaces that release the associated active ingredients (silver, chlorohexidine, etc.) this results in environmental contamination and a growing microbial resistance.

### Dual-Contact Killing and Nonfouling Surfaces

This type of dual-function antibacterial surfaces is based on the combination of antimicrobial and nonfouling properties. These surfaces can be divided into four categories based on the method used to incorporate the antimicrobials into nonfouling materials. The antimicrobials can be tethered to nonfouling hydrophilic polymers, embedded in a superhydrophobic coating, deposited as layers in between nonfouling layers, or stored in a nonfouling matrixes and progressively released.

### Tethering of Antimicrobial Compounds to Nonfouling Hydrophilic Polymers

Hydrophilic polymers are widely used as spacers for the immobilization of bioactive molecules such as antimicrobial compounds, to create biofunctional surfaces because they are capable of resisting nonspecific protein adsorption as well as bacteria and cell adhesion, reducing unwanted biological responses, they can maintain the bioactivity of the antimicrobial compounds, and they can enhance the accessibility of the antimicrobial compounds to targets through their long chains [56]. In recent years, several hydrophilic polymers have been used for the attachment of antibiotic molecules to create antibacterial surfaces with both bactericidal and nonfouling properties. PEG is such a polymer and several antibiotics, including penicillin and gentamicin, can be immobilized on this, along with two different antibiotics such as penicillin and gentamicin simultaneously, using two different types of conjugation chemistry and aiming at simultaneously resisting the growth of their target bacteria strains, Gram-positive and Gram-negative [57]. One main drawback of antimicrobial surfaces based on PEG is that the concentration of

antimicrobial molecules that can be attached is quite limited as each PEG chain has only one functional group at its free end. To increase the density of binding sites for active antimicrobials, such as peptides, more attention has been paid to the application of comb-like polymers with side chains and the ATRP method (as shown in Fig. 1d) [36].

### **Layer-by-Layer Deposition of Nonfouling Layer and Antimicrobial Layer**

The layer-by-layer (LbL) deposition of polyelectrolytes on charged surfaces offers another approach to simultaneously reducing bacterial adhesion and killing adhered bacteria onto a surface. In this method, antimicrobial compounds and nonfouling agents with opposite charges are physically adsorbed onto substrates alternately to form a multilayer film. This method presents advantages such as simplicity, low operating costs, and control over film thickness. A typical dual-function antibacterial surface prepared by the LBL method is based on chitosan, a cationic antibacterial molecule, and heparin, an anionic antiadhesive molecule. The results showed that the chitosan/heparin multilayer modified surface significantly reduced bacterial *E. coli* adhesion and killed the adherent bacteria [58].

### **Combination of Super Hydrophobic Surface and Antimicrobial Compounds**

Super hydrophobic surfaces provide a biomimetic approach to significantly reducing bacterial attachment [17, 28, 29]. Although super hydrophobic films or coatings are effective in inhibiting short-term bacterial adhesion, it should be noted that their nonfouling properties may gradually deteriorate after exposure to complex environments. The combination of a super hydrophobic surface as a protection layer and the presence of antimicrobial compounds may provide a solution to this drawback. The combination therefore of super hydrophobic surfaces and antimicrobial compounds is an effective strategy toward antimicrobial surfaces that both resist and kill bacteria. Such an example is a novel lotus-leaf-like antimicrobial film which was produced by loading mesoporous silica microcapsule-supported AgNPs on a fluorosilicone resin film, followed by hydrophobic surface modification [59]. The combination of the hierarchical micro-/nanoscale structure of the mesoporous silica microcapsules and a surface coating with low surface energy reduced bacterial adhesion, while the silver ions reduced bacterial viability for both planktonic and attached bacteria [59].

### **Nonfouling Polymers that Release Antimicrobial Compounds**

Most antimicrobial surfaces based on the contact-killing mechanism can effectively kill bacteria attached to surfaces, but they have limited antimicrobial activity against planktonic bacteria. On the other hand, the controlled release of antimicrobial agents from surfaces can be used to reduce microbial colonization on surfaces and inhibit the proliferation of planktonic bacteria. To achieve both bulk antimicrobial and surface nonfouling properties, we recently examined the incorporation of silver in organic coatings that were plasma deposited (as shown in Fig. 1e) and the results showed that such a system can significantly decrease the bacterial adhesion but also viability with time, in comparison to the organic coating alone [60].

## Dual-Function Contact-Killing and Bacterial Released Surfaces

The third type of dual-function antimicrobial surface is based on the combination of antimicrobial compounds and bacteria-release properties into one system. Common contact-killing antimicrobial surfaces suffer a serious problem associated with the accumulation of dead bacteria and other debris, which not only degrades the antimicrobial activity but also provides nutrients and sites for other bacteria to attach. Toward maintaining the surface antimicrobial properties over long periods of time, it would be beneficial to be able to remove or release the killed bacteria from surfaces.

In this direction, Yu et al. developed a new platform exhibiting switchable bioactivity based on nanopatterned PNIPAAm brushes. The temperature-induced conformational changes of the nanopatterned PNIPAAm brushes provide the capacity to spatially control the conformation of biomolecules between brushes, leading to an ON/OFF switch for surface bioactivity [61–63]. Two antimicrobial compounds, QACs [61] and lysozyme [63], have been immobilized in the polymer-free regions between nanopatterned PNIPAAm brushes. Above the lower critical solution temperature (LCST) collapsed PNIPAAm chains facilitated the attachment of bacteria and exposed the antimicrobial compounds that kill adhered bacteria. Upon decreasing the temperature below the LCST, swollen PNIPAAm chains promote the release of dead bacteria.

---

## Bacterial Interference

Improving materials antimicrobial performance and cost-effectiveness, while meeting environmental and toxicity requirements, is nowadays also being explored through alternative approaches to traditional antimicrobial agents and in particular through “bacterial interference.” The concept that bacteria can actively inhibit one another while competing for resources in the same environment could be explored toward the preparation of materials that either kill or resist the attachment of pathogenic bacteria. This approach may be explored to prevent infections related to the use of devices implanted in areas normally occupied with microflora, such as urinary catheters or dental implants.

Trautner et al. employed the concept of “bacterial interference” to prevent catheter-associated infection, using a strain of *Escherichia (E.) coli* that lacks the virulence factors for infection but colonize the catheter material [64]. This *E. coli* strain, which was grown in a biofilm on catheters before implantation, prevented the adherence of pathogenic gram-positive, gram-negative, and fungal organisms in vitro, and was successful in patient studies [64].

In the same direction, *Lactobacillus acidophilus* was encapsulated into nanofibers of various polymers, toward the development of biohybrid nanowebs that could potentially treat bacterial vaginosis, through the delivery of the probiotics, however its effectiveness against pathogens has not been tested [65].

An oral probiotic organism *Streptococcus (S.) salivarius* may be used toward the prevention of pathogenic colonization of dental implants, as it has been shown to

inhibit the growth of oral pathogens such as *Streptococcus mutans* [66]. Its potential though has not been as yet explored for the purpose of precoating dental implants to prevent pathogenic colonization, while the effect of probiotics on tissue integration is unknown. Utilizing therefore probiotic bacteria and bacterial interference appears as a new and exciting approach for protecting biomaterials from pathogenic infection, for at least some particular applications that the biomaterial does not need to integrate, e.g., catheters.

---

## Biofilm Dispersal Agents

Biofilm dispersal agents are molecules that either prevent the formation of biofilms by inhibiting their growth or inducing biofilm bacteria to detach and return to the planktonic state. A number of studies have shown that bacteria naturally produce biofilm dispersal agents when their quorum sense signals biofilm bacteria to detach toward colonizing new sites, and these agents include D-amino acids and naturally occurring peptides and enzymes amongst others [67, 68]. D-Amino acids, particularly D-tyrosine, D-tryptophan, D-leucine, and D-alanine, are particularly attractive as dispersal agents, as they are inexpensive and potent in combination [67]. Apart from dispersal agents' immobilization, current research aims at developing vehicles, such as polymer sponges and biodegradable microspheres, for their controlled and sustained release.

---

## Bacteriophage Releasing Materials

Bacteriophages, and especially the ones that have been engineered, are viruses that can directly lyse bacteria as well as penetrate and destruct a biofilm, by cleaving the polysaccharide components, while maintaining their efficacy [69]. Materials science approaches have been employed toward the delivery of bacteriophages to destruct biofilms. Bacteriophages have successfully been immobilized on modified silicon surfaces [70] and once incorporated or delivered, the ability of bacteriophages to lyse both bacteria and biofilm components can be used to treat or prevent biofilm formation. Bacteriophages could therefore have great potential in preventing or treating infections, but due to their specificity, it may be difficult to use them as broad-range antimicrobials and translate this technology for biomedical applications.

---

## Tissue Integration

Another approach that appears promising against medical device-associated infections is that of tissue integration. Clinically, oral wounds heal faster in comparison to epidermal ones [71, 72] with saliva promoting healing by containing an abundance of growth factors such as epidermal, fibroblast, nerve, and transforming growth factor (TGF)- $\alpha$ , maintaining host cell viability and proliferation [73]. The fast

healing of oral tissue in the continuous presence of commensal bacteria and opportunistic pathogens enables the formation of a soft tissue seal around the implant and this seems to offer protection of the osseointegrated part against invasion by periodontopathogens [74]. In particular, the presence of *Streptococcus mutans* seems to increase  $\beta 1$  integrin expression in periodontal ligament fibroblasts [75], leading to thoughts that bacterial presence and stimulation, without the development of infection, may improve healing that reduces infection risk and associated failure over time.

In this direction, surfaces with multiple functionalities that reliably select host cells and therefore tissue integration over microbes have been suggested and an example is the simultaneous incorporation of RGD, that enhances cell adhesion, and a HDP that reduces bacterial adhesion and viability [44]. Our preliminary results show promising signs for the use of RGD in combination with HDPs toward the preparation of antimicrobial materials that allow tissue integration [44]. Orthopedic and dental implants would therefore be a great application for this kind of combined HDPs/RGD systems, as the soft tissue seal represents an important barrier that provides implant with protection from pathogens and therefore its restoration seems to prevent infection.

---

## Examples of Orthopedic and Dental Implants Used at Present

Clinically available orthopedic implants encompass a variety of materials: titanium, stainless steel, and poly(methyl methacrylate) (PMMA), and are used for a range of applications, such as fixation devices and osseointegrated implants, bone cements for arthroplasty, and antibiotic carriers [76]. In the past their properties were varied, toward enhanced osseointegration, by mainly varying the size, shape, topography, roughness and configuration, or the material itself.

While these materials have been successful in many cases and meet important medical needs, infection remains a major impediment to their long-term use. A recent study showed that PMMA is the most susceptible to bacterial colonization, followed by stainless steel, then titanium [76]. Moreover, there are studies that show that PMMA and antibiotic-loaded PMMA beads, a common clinical method for local antibiotic delivery that treats or prevents infections after orthopedic implantation, can host bacteria that cause acute, chronic, and delayed-onset infections [77, 78]. Furthermore, there are studies suggesting that bioactive substances such as hydroxyapatite may be more prone to bacterial adhesion than bioinert metals, such as titanium alloys and stainless steel [79]. Therefore, the choice of biomaterial in the case of orthopedic implants is not an easy-made decision and nowadays there are other vehicles for the controlled local delivery of antibiotics as described below.

In parallel, dental implants are one of the most common types of implanted devices that restore both function and aesthetics. These implants have three basic components: the implant screw, the abutment, and the crown. The implant screw interfaces with the craniofacial bone, the abutment is at the junction of the bone and

soft tissue, and the crown is eventually placed over the abutment. In the two-piece implantation system, the abutment is connected to the implant screw after some months, whereas the one-piece system has the abutment and screw fused together and implanted during the first procedure. While there are studies showing no histological differences in lesions between two-piece and one-piece systems in canine, there are other studies showing more inflammation and greater bone loss in the two-piece system [80].

The fact that dental implants are in contact with the oral flora, a microbiome consisting of more than 700 different bacterial species, makes them more vulnerable to infection [81]. Chronic bacterial infection associated to the use of dental implants is known as peri-implantitis, which is defined as an inflammatory reaction in the oral cavity with loss of supporting bone in the tissues surrounding an implant. Dental implant failures therefore refer to the disruption between mineralized bone and an implant, and recent data show that peri-implantitis affects 20 % of patients and 10 % of implant sites, making it a serious challenge in long-term implant dentistry [82]. Following peri-implantitis, bone resorption, and soft tissue damage at the implant site makes the replacement of the implant a real challenge, while the replacement has low survival rates. Designing therefore implants that are less prone to infection is a clinical need.

Over the last two decades, as in the case of orthopedic implants, the properties of dental implants that mainly varied was the roughness and configuration, along with the shape and size. As discussed in the “[Surface Topography Modification](#)” section, the studies that investigate the effect of roughness on bacterial adhesion present results that in some cases appear controversial [23]. In particular, it was observed that supragingival biofilm accumulation was increased on the rougher surface, but no difference was observed subgingivally [83]. In a canine model, surface roughness had no effect on plaque formation, inflammatory lesions, soft tissue, or microbial attachment and species [84]. However, in another canine model that peri-implantitis is allowed to continue spontaneously developing after ligature-induced inflammation [85], greater plaque formation, and bone loss was observed in the case of a rough porous titanium oxide surface [86].

Apart from metals, bioceramics have been of particular interest to researchers. Hydroxapatite (HA) has long been investigated and as a result is the most widely used bioceramic in medicine and dentistry due to the strong affinity to bone tissue. This property improves the implant-bone interface and thus favors early osseointegration [87]. HA though does not present antimicrobial properties and its use has declined due to reports of HA coating delamination from oral implants, resulting in poor performance and uncertain long-term success [88]. Likewise, comparing materials of different surface coatings, such as hydroxyapatite, sprayed titanium, and titanium alloy, has shown little difference on bacterial load [89].

The literature therefore suggests that more complex strategies and highly controlled studies are necessary for the prevention of peri-implantitis and orthopedic implants associated infections. In this direction, the following antibiotic delivery systems have been suggested and are currently used in the clinics.



## Bone Graft-Based Delivery Vehicles

Bone graft materials have been suggested as antibiotic carriers. Autologous bone graft, demineralized bone matrix (DBM), but also Calcium sulfate can be mixed with antibiotics during surgery as an easy and efficient way to deliver antibiotics locally [90]. Incorporation of antibiotics into autologous bone graft is convenient, but release is not sustained. Approximately 70 % of incorporated antibiotic is released after 24 h with negligible release after 7 days [95]. Similarly, DBM releases approximately 45 % of its drug load after 24 h with negligible release after 7 days [91]. Calcium sulfate appears as a better option since it is resorbable and osteoconductive [90]. In particular, it has been shown that bactericidal levels of tobramycin elute from calcium sulfate over 14 days, but levels are sub-bactericidal by day 28, pointing this as a drawback due to the increased chances of antibiotic resistance development [90]. While therefore mixing bone graft materials with antibiotics is a simple process that takes place during the surgery, the release kinetics from these materials point the need for more sophisticated systems. In this direction, the use of synthetic and protein-based systems is suggested and discussed below.

## Synthetic/Protein-Based Delivery Vehicles

As discussed earlier, nondegradable PMMA has been a popular carrier of antibiotics due to the ease of antibiotic incorporation, and the FDA has approved products that use PMMA as an antibiotic carrier. However, release of antibiotic from PMMA occurs in a non-desirable early “burst” followed by negligible release after the first few days [92]. To overcome the issue of “burst” release, degradable polymer matrices have been suggested as antibiotic carriers due to their ability to provide controlled release, preserve the bioactivity of the drug, and release almost all the incorporated drug. Some examples of biodegradable polymer carriers include poly(lactic-co-glycolic acid) (PLGA), poly( $\epsilon$ -caprolactone) (PCL), poly(DL-lactic acid) (PLA), and combinations of the above. These polymers are most commonly used to entrap antibiotics in microcapsules, microspheres, or electrospun fibers [93]. In contrast to antibiotic-loaded PMMA, antibiotic release from these constructs is on the timescale of weeks; a coelectrospun collagen and PLA carrier for gentamicin was capable of releasing antibiotics over at least 2 weeks [94], while PLGA microspheres have been able to maintain antibiotic release up to 35 days [95]. However, degradable polymers for antibiotic delivery are still in the investigational stage, and have been mostly used for the delivery of other types of drugs.

Protein-based materials for antibiotic delivery include collagen, gelatin, and fibrin glue [96, 97]. For the purposes of orthopedic drug delivery, collagen sponges are the most commonly used vehicle clinically, as they are flexible, can cover infected areas, and have excellent biocompatibility [98]. In a rat osteomyelitis model, gentamicin-loaded collagen sponges performed better than gentamicin-loaded PMMA [96]. However, even these sponges typically release most of the drug load within the first few hours, resulting in a large amount of drug initially with very little

sustained release after 7 days [99], requiring the design of systems that will release the antibiotic in a more controlled way.

---

## Concluding Remarks and Future Perspectives

### General Healthcare Market and Medical Devices

An overwhelming need to reduce the hospital-acquired infection rates is a serious concern in the health care industry which suggests the use of antimicrobial coatings. In most of the cases the hospital-acquired infections are associated to the use of medical devices and in the USA 40 % of all hospital-acquired infections are related to urinary catheters, while about 3 % of those ultimately result in mortality. According to the CDC report, urinary catheter infections affect 10–50 % of patients undergoing short-term catheterization (7 days) and virtually all undergoing long-term catheterization (28 days) [100].

According to the BCC Report (2012) the global medical device coating market reached \$4.8 billion in 2010 and \$5.4 billion in 2011 and is expected to grow to nearly \$8 billion in 2017, a 5-year compound annual growth rate (CAGR) of 6.7 %, with North America and the European Union accounting for the vast majority of this market [101].

In particular the United States market for medical device coatings reached \$2.7 billion in 2011, \$3 billion in 2012, and should total nearly \$4.4 billion by 2017, a 5-year CAGR of 8.1 %. The European Union market for medical device coatings reached \$1.3 billion in 2011, \$1.4 billion in 2012, and should surpass \$2 billion in 2017, a 5-year CAGR of 7.0 %.

Therefore, the antimicrobial coating market is expected to grow with the increasing need to address microbial growth in end-application markets like the health care facilities. In this direction the antimicrobial coating suppliers, such as Smith and Nephew, SurModics Inc., Nanophase Technologies, and AcryMed Inc., are expected to focus on research and development activities to create competitive products, and offer extended product lines that provide a broad-spectrum application reach in health care facilities.

Regarding the medical devices, their compositions and applications may therefore differ widely, but all attract microorganisms. The antibacterial surface modification technologies could therefore have potential application for a wide range of implantable and non-implantable medical devices. The implantable devices include catheters (intravenous, urethral), stents (ureteral, prostatic, biliary, coronary), shunts, endotracheal tubes, lenses (intraocular), and the like. The nonimplantable devices category includes syringes, forceps, clamps, dressings, device packaging, etc. In addition to antibacterial applications of the surface modification technology the adhesion of cells or proteins onto biomaterials could also be enhanced or reduced by tailoring surface structure and chemistry.

Selecting some applications to help demonstrate the scale of the medical device market, the case of catheter-associated urinary-tract infections is highlighted

[102]. In 2002 there were 424,060 urinary-tract infections in the USA alone and it is reported that the costs associated with this type of infection are between \$589 and \$758 per infection [103]. In the case of permanent, totally internal devices, these face two challenges with respect to their extended use *in vivo*: medical device-associated infections and lack of native tissue integration.

In the case of antimicrobial wound dressings, Frost & Sullivan predict that the market will continue to grow at a rate in the USA of over 15 % annually up to 2017. The total Advanced Wound Care Market is expected to reach \$3650 M in 2017 with a CAGR of 9.6 % [104].

In the case of bone and dental implants the infection incidence has been reported as 1–10 %, depending on the application. Although hip and knee joint replacements have a relatively low infection rate (2–4 %), the open fractures and especially those of the tibia that are more common than in any other long bone can be infected at a rate of up to 55 % [105]. Rate of tibial diaphysis fractures reported from 2 per 1000 population to 2 per 10,000 and of these approximately one fourth are open tibia fractures [106]. Health economic studies showed that in the UK £4.3 billion was spent on orthopedic and dental disease and trauma between 2011 and 2012 [107]. Nowadays, 230,000 fractures are recorded per year in the UK, many of these related to osteoporosis, and by 2016 are expected to be over 384,000 fractures per year. As our life expectations are increasing [108], these numbers are expected to further increase. If we also take into consideration the fact that the average costs of combined medical and surgical treatment of bony infections are as high as \$25,000 per case [109], it becomes obvious that there is a great clinical need, commercial potential, and market gap that demands antimicrobial strategies.

## Antimicrobial Strategies

Toward the fabrication of antimicrobial surfaces a large amount of research work has been done utilizing various materials such as polymers, metals, ceramics, glass, and composites, various bacterial strains-species and concentrations, but also experimental procedures; static and dynamic conditions amount of time and environmental parameters such as temperature and humidity.

From the results obtained using a number of surfaces it seemed that bacteria preferentially colonize surfaces that have lower surface energy and polar character. Taking the topography into consideration, it appears that increased roughness at the nano and microscale and especially irregularities that conform bacterial shape increase bacterial adhesion.

Therefore, surfaces that present OH- groups appear more resistant to colonization and therefore surface modification in this direction using either chemical or natural extracts seems a promising way to prevent biofilm formation. The use of natural extracts is not based on a single pharmaceutical agent or biocidal activity and therefore common bacterial strains have not developed noticeable resistance against these surfaces.

In the case of antimicrobial surfaces, an increase in roughness and positive charge would possibly enhance the antibacterial properties of the surface, by killing the more attached bacteria to their increased surface area.

Apart from the surfaces that present one function against bacteria either nonfouling or bactericidal, over the past few years, a significant number of dual-function antimicrobial surfaces have been suggested for the prevention of initial bacterial attachment and biofilm formation. These surfaces combine the antimicrobial activity through the presence of one or more antimicrobial compounds and the bacteria-resistant or bacteria-release capability accompanied by the use of certain materials, usually functional polymers. The dual-function surfaces present advanced properties compared with conventional antimicrobial surfaces with a single functionality.

Although a large amount of work has been done and considerable progress has been made in this area with promising experimental results, many challenges in both fundamental science and applied technology remain, and further efforts are required toward the optimization of the design and the fabrication process.

Regarding the dual-function antimicrobial surface multifunctionality, kill and resist, or kill and release, is achieved by two or more functional components. However, antimicrobial activity, through the use of various compounds, and bacteria-resistance/bacteria-release properties usually compromise each other. Therefore, the composition of the surfaces must be optimized to obtain the highest performance.

Apart from the surface chemistry, the integration of surface micro- and nanotopography has been suggested and it was briefly described above. Mimicking nature to provide engineering solutions offers a model for the development of functional surfaces with special antimicrobial properties. For example, bio-inspired structures that mimic shark skin and lotus leaves endow synthetic surfaces with effective nonfouling – bacteria-resistance properties. It will be interesting therefore to explore whether the integration of surface topography, especially on the nano-scale, into existing multifunctional antibacterial surfaces yields novel properties and the impact it has on other biological responses [110].

Depending on the application, apart from the antimicrobial properties, addition of other functionalities may be required so that synthetic surfaces exhibit specific properties. To date, a few research groups have incorporated additional functional groups into antibacterial surfaces to improve other specific properties and achieve better performance. For blood-contacting devices, hemocompatibility is a property that has to be present [111]. For orthopedic and dental implants, surfaces should inhibit bacterial colonization but promote osteoblast adhesion and this may be realized by the addition of both host defence (antimicrobial) peptides and RGD [44].

## Parameters to be Taken Into Consideration

As mentioned earlier, many challenges in both fundamental science and applied technology remain, and further efforts are required toward the optimization of the

design and the fabrication process of antimicrobial surfaces especially if these need to present additional functionalities.

Since bacterial adhesion is a very complicated process affected by many factors, such as bacterial-material properties and environment, more investigations are still needed to advance our understanding of the mechanisms of bacterial adhesion and to attain appropriate methods to prevent them from happening.

To complicate matters even more, it needs to be mentioned that many bacteria are able to sense and respond to surfaces and environmental signals using mechanisms that remain poorly understood. Most of the research so far has been conducted to investigate bacterial responses to soluble biochemical factors, such as growth factors and bacterial density [112], salts, ethanol, iron, nutrient-limited factors and heat [113, 114], and to low-energy pulsed ultrasonic simulation [115]. The results have shown that there is an increase in biofilm formation when bacteria are under stress due to various environmental factors that were altered in order to examine how bacteria-material interactions are influenced by their surroundings.

In our recent studies it was observed that not only bacterial adhesion but PIA, slime production, and biofilm formation were much higher on the CH<sub>3</sub>-terminated glass than on the OH-terminated one, for four *Staphylococcus epidermidis* strains, and this was in agreement with the *icaA* and *icaD* gene expression results that showed increased expression for the bacteria adhering to the CH<sub>3</sub>-terminated substrate, especially under the higher shear rate [116]. In addition, it was observed that *Staphylococcus epidermidis* strains *icaA* and *icaD* gene expression and slime production were enhanced by silver ions that were released at sub-bactericidal concentrations, under high shear rate conditions [60]. This shows that the release of the antimicrobial compound has to be designed very carefully so that it kills remaining bacteria and it prevents this kind of bacterial responses.

Moreover, surface chemical modifications often lead to surface heterogeneity and increased surface roughness. Trace impurities in many of the polymers used and coating defects result in uncertainties.

In the area of applied technology, the main difficulty in applying these antimicrobial strategies along with other functionalities, depending on the application, is to develop a readily scalable process to apply these functionalities, as adherent coatings, in a continuous process onto a wide range of polymers. Moreover, the main concern remains the toxicity of many of these compounds. It should be noted that, for in vivo biomedical applications, the toxicological effects of antibacterial surfaces should be determined first and that the biocompatibility of these surfaces must be improved. The fabrication of these surfaces should be low cost and reproducible.

Therefore, a rigorous study of the effects of surface chemistry/topography on bacterial adhesion and protein adsorption under conditions relevant in vivo remains a prerequisite for the understanding of the bacterial adhesion mechanism and toward the design of both nonfouling and antimicrobial materials, pointing the importance of the detailed surface analysis to ensure reliable interpretation of biointerfacial interactions.

**Acknowledgement** MGK work for this chapter was partially funded by WELMEC, Centre of Excellence in Medical Engineering funded by the Wellcome Trust and EPSRC, under grant number WT 088908/Z/09/Z. Professor REW Hancock is acknowledged for providing the peptides used in Fig. 3 and Ref. [44] and Professor DD Devine for valuable discussions on peptides antimicrobial properties. Dr. S Patel (Fluxion Ltd.) is acknowledged for his help with the BioFlux, a microfluidic system used for the biofilm formation presented in Fig. 3.

---

## References

1. Ratner BD (2012) A history of biomaterials. In: Ratner BD, Hoffman AS, Schoen FJ, Lemons JE (eds) Biomaterials science, 3rd edn. Elsevier, Amsterdam, p xli
2. von Eiff C, Jansen B, Kohnen W, Becker K (2005) Infections associated with medical devices. Pathogenesis, management and prophylaxis. *Drugs* 65(2):179–214
3. Von Eiff C, Peters G, Heilmann C (2002) Pathogenesis of infections due to coagulase-negative staphylococci. *Lancet Infect Dis* 2:677–685
4. Maki DG, Stolz SM, Wheeler S, Mermel LA (1997) Prevention of central venous catheter-related bloodstream infection by use of an antiseptic-impregnated catheter: a randomised, controlled trial. *Ann Intern Med* 127:257–266
5. Costerton JW, Stewart PS, Greenberg EP (1999) EP Bacterial biofilms: a common cause of persistent infections. *Science* 284:1318–1322
6. Klevens RM, Morrison MA, Nadle J, Petit S, Gershman K, Ray S, Harrison LH, Lynfield R, Dumyati G, Townes JM, Craig AS, Zell ER, Fosheim GE, McDougal LK, Carey RB, Fridkin SK (2007) Invasive methicillin-resistant *Staphylococcus aureus* infections in the United States. *JAMA* 298(15):1763–1771
7. UK, Office for National Statistics. MRSA deaths decrease for second year running (2009) Available at <http://www.statistics.gov.uk/CCI/nugget.asp?ID=1067>
8. Kumarasamy KK, Toleman MA, Walsh TR, Bagaria J, Butt F, Balakrishnan R, Chaudhary U, Doumith M, Giske CG, Irfan S, Krishnan P, Kumar AV, Maharjan S, Mushtaq S, Noorie T, Paterson DL, Pearson A, Perry C, Pike R, Rao B, Ray U, Sarma JB, Sharma M, Sheridan E, Thirunarayan MA, Turton J, Upadhyay S, Warner M, Welfare W, Livermore DM, Woodford N (2010) Emergence of a new antibiotic resistance mechanism in India, Pakistan, and the UK: a molecular, biological, and epidemiological study. *Lancet Infect Dis* 10:597–602
9. Katsikogianni M, Amanatides E, Mataras DS, Missirlis YF (2008) *Staphylococcus epidermidis* adhesion to He, He/O<sub>2</sub> plasma treated PET films and aged materials: contributions of surface free energy and shear rate. *Colloids Surf B: Biointerfaces* 65(2):257–268
10. Balazs DJ, Triandafillu K, Chevolut Y et al (2003) Surface modification of PVC endotracheal tubes by oxygen glow discharge to reduce bacterial adhesion. *Surf Interface Anal* 35:301–309
11. Rochford ETJ, Poulsson AHC, Salavarieta Varelaa J, Lezuo P, Richards RG, Moriarty TF (2014) Bacterial adhesion to orthopaedic implant materials and a novel oxygen plasma modified PEEK surface. *Colloids Surf B: Biointerfaces* 113:213–222
12. Da Ponte G, Sardella E, Fanelli F, d'Agostino R, Gristina R, Favia P (2012) Plasma deposition of PEO-like coatings with aerosol-assisted dielectric barrier discharges. *Plasma Process Polym.* doi:10.1002/ppap.201100201
13. Stallard CP, Solar P, Biederman H, Dowling DP (2015) Deposition of non-fouling PEO-like coatings using a low temperature atmospheric pressure plasma jet. *Plasma Process Polym.* doi:10.1002/ppap.201500034
14. Kingshott P, McArthur S, Thissen H, Castner DG, Griesser HJ (2002) Ultrasensitive probing of the protein resistance of PEG surfaces by secondary ion mass spectrometry. *Biomaterials* 23:4775–4785

15. Kingshott P, Wei J, Bagge-Ravn D, Gadegaard N, Gram L (2003) Covalent attachment of poly(ethylene glycol) to surfaces, critical for reducing bacterial adhesion. *Langmuir* 19:6912–6921
16. Katsikogianni M, Spiliopoulou I, Dowling DP, Missirlis YF (2006) Adhesion of slime producing *Staphylococcus epidermidis* strains to PVC and diamond-like carbon/silver/fluorinated coatings. *J Mater Sci Mater Med* 17:679–689
17. Stallard CP, McDonnell KA, Onayemi OD, O’Gara JP, Dowling DP (2012) Evaluation of protein adsorption on atmospheric plasma deposited coatings exhibiting superhydrophilic to superhydrophobic properties. *Biointerphases* 7(1–4):1–12
18. Katsikogianni MG, Missirlis YF (2010) Interactions of bacteria with specific biomaterial surface chemistries under flow conditions. *Acta Biomater* 6:1107–1118
19. Kiremitci-Gumustederelioglu M, Pesmen A (1996) Microbial adhesion to ionogenic PHEMA, PU and PP implants. *Biomaterials* 17:443–449
20. Tang L, Gu W, Yi P, Bitter JL, Hong JY, Fairbrother DH, Chen KL (2013) Bacterial anti-adhesive properties of polysulfone membranes modified with polyelectrolyte multilayers. *J Membr Sci* 446:201–211
21. Olde Riekerink MB, Engbers GHM, Van der Mei HC, Busscher HJ, Feijen J (2001) Microbial adhesion onto superhydrophobic fluorinated low density poly(ethylene) films. In: Olde Riekerink MB (ed) Thesis: structural and chemical modification of polymer surfaces by gas plasma etching. Printpartners Ipskamp, Enschede, p 65
22. Katsikogianni MG, Syndrevelis C, Amanatides EK, Mataras DS, Missirlis YF (2007) Plasma treated and a-C:H coated PET performance in inhibiting bacterial adhesion. *Plasma Process Polym* 4:S1046–S1051
23. Truong VK, Lapovok R, Estrin YS et al (2010) The influence of nano-scale surface roughness on bacterial adhesion to ultrafine-grained titanium. *Biomaterials* 31:3674–3683
24. Chung KK, Schumacher JF, Sampson EM, Burne RA, Antonelli PJ, Brennan AB (2007) Impact of engineered surface microtopography on biofilm formation of *Staphylococcus aureus*. *Biointerphases* 2(2):89–94
25. Scheuerman TR, Camper AK, Hamilton MA (1998) Effects of substratum topography on bacterial adhesion. *J Colloid Interface Sci* 208:23–33
26. Wang L, Chen W, Terentjev E (2015) Effect of micro-patterning on bacterial adhesion on polyethylene terephthalate surface. *J Biomater Appl* 29(10):1351–1362
27. Edwards KJ, Rutenberg AD (2001) Microbial response to surface microtopography: the role of metabolism in localized mineral dissolution. *Chem Geol* 180:19–32
28. Pogodin S, Hasan J, Baulin VA et al (2013) Biophysical model of bacterial cell interactions with nano-patterned cicada wing surfaces. *Biophys J* 104:835–840
29. Watson GS, Green DW, Schwarzkopf L, Li X, Cribb BW, Myhra S, Watson JA (2015) A gecko skin micro/nano structure – a low adhesion, superhydrophobic, anti-wetting, self-cleaning, biocompatible, antibacterial surface. *Acta Biomater* 21:109–122
30. Cui B, Cortot Y, Veres T (2006) Polyimide nanostructures fabricated by nanoimprint lithography and its applications. *Microelectron Eng* 83(4):906–909
31. Hamley IW (2003) Nanostructure fabrication using block copolymers. *Nanotechnology* 14(10):R39
32. Baia M, Baia L, Astilean S (2005) Gold nanostructured films deposited on polystyrene colloidal crystal templates for surface-enhanced Raman spectroscopy. *Chem Phys Lett* 404(1–3):3–8
33. Rodgers JW, Casey ME, Jedlicka SS, Coulter JP (2013) Micro injection molded microtopographic polymer plates used to mechanically direct stem cell activity. In: Proceedings of the 8th international conference on MicroManufacturing, University of Victoria, Victoria, 25–28 Mar
34. Tiller JC, Liao CJ, Lewis K, Klibanov AM (2001) Designing surfaces that kill bacteria on contact. *Proc Natl Acad Sci U S A* 98:5981–5985

35. Lee SB, Koepsel RR, Morley SW, Matyjaszewski K, Sun Y, Russell AJ (2004) Permanent, nonleaching antibacterial surfaces. 1. Synthesis by atom transfer radical polymerization. *Biomacromolecules* 5:877–882
36. Guangzheng G, Lange D, Hilpert K, Kindrachuk J, Zou Y et al (2011) The biocompatibility and biofilm resistance of implant coatings based on hydrophilic polymer brushes conjugated with antimicrobial peptides. *Biomaterials* 32:3899–3909
37. Yang WJ, Cai T, Neoh K-G, Kang E-T (2011) Biomimetic anchors for antifouling and antibacterial polymer brushes on stainless steel. *Langmuir* 27:7065–7076
38. Aumsuwan N, Heinhorst S, Urban MW (2007) The effectiveness of antibiotic activity of penicillin attached to expanded poly(tetrafluoroethylene) (ePTFE) Surfaces: a quantitative assessment. *Biomacromolecules* 8:3525–3530
39. Campoccia D, Montanaro L, Spezialec P, Arciola CR (2010) Antibiotic-loaded biomaterials and the risks for the spread of antibiotic resistance following their prophylactic and therapeutic clinical use. *Biomaterials* 31(25):6363–6377
40. Thierry B, Jasieniak M, De Smet L, Vasilev K, Griesser HJ (2008) Reactive epoxide thin film by pulsed-plasma polymerization. *Langmuir* 24(18):10187–10195
41. Hilchie AL, Wuerth K, Hancock REW (2013) Immune modulation by multifaceted cationic host defense (antimicrobial) peptides. *Nat Chem Biol* 9:761–768
42. Joerger RD, Sabesan S, Visioli D, Urian D, Joerger MC (2009) Antimicrobial activity of chitosan attached to ethylene copolymer films. *Packag Technol Sci* 22:125–138
43. Conte A, Buonocore GG, Sinigaglia M et al (2008) Antimicrobial activity of immobilized lysozyme on plasma-treated polyethylene films. *J Food Prot* 71:119–125
44. Katsikogianni MG, Hancock REW, Devine DD, Wood DJ (2015) Cell vs. bacterial viability in the presence of host defence peptides and RGD. *Eur Cell Mater* 30(2):55
45. Kazemzadeh-Narbat M, Kindrachuk J, Duan K, Jenssen H, Hancock REW, Wang R (2010) Antimicrobial peptides on calcium phosphate-coated titanium for the prevention of implant-associated infections. *Biomaterials* 31:9519–9526
46. Joerger RD (2007) Antimicrobial films for food applications: a quantitative analysis of their effectiveness. *Packag Technol Sci* 20:231–273
47. Cowan MM (1999) Plant products as antimicrobial agents. *Clin Microbiol Rev* 12(4):564–582
48. Vasilev K, Griesser SS, Griesser H (2011) Antibacterial surfaces and coatings produced by plasma techniques. *Plasma Process Polym* 8:1010–1023
49. Stigter M, de Groot K, Layrolle P (2002) Incorporation of tobramycin into biomimetic hydroxyapatite coating on titanium. *Biomaterials* 23:4143–4153
50. Danielle N, Dijkstra RJB, Thompson JI, van der Mei HC, Busscher HJ (2011) Antibacterial efficacy of a new gentamicin-coating for cementless prostheses compared to gentamicin-loaded bone cement. *J Orthop Res* 29:1654–1661
51. Mavric E, Wittmann S, Barth G, Henle T (2008) Identification and quantification of methylglyoxal as the dominant antibacterial constituent of Manuka (*Leptospermum scoparium*) honeys from New Zealand. *Mol Nutr Food Res* 52(4):483–489
52. Chopra I (2007) The increasing use of silver-based products as antimicrobial agents: a useful development or a cause for concern? *J Antimicrob Chemother* 59:587–590
53. Daniel A, Le Pen C, Archambeau C, Reniers F (2009) Use of a PECVD–PVD process for the deposition of copper containing organosilicon thin films on steel. *Appl Surf Sci* 256: S82–S85
54. Perelshtein I, Apperlot G, Perkas N et al (2009) Antibacterial properties of an in situ generated and simultaneously deposited nanocrystalline ZnO on fabrics. *ACS Appl Mater Interfaces* 1(2):361–366
55. Li Z, Lee D, Sheng X, Cohen RE, Rubner MF (2006) Two-level antibacterial coating with both release-killing and contact-killing capabilities. *Langmuir* 22:9820–9823
56. Yu Q, Zhang Y, Wang H, Brash JL, Chen H (2011) Anti-fouling bioactive surfaces. *Acta Biomater* 7:1550–1557



57. Aumsuwan N, McConnell MS, Urban MW (2009) Tunable antimicrobial polypropylene surfaces: simultaneous attachment of penicillin (Gram+) and gentamicin (Gram-). *Biomacromolecules* 10:623–629
58. Follmann HD, Martins AF, Gerola AP, Burgo TA, Nakamura CV, Rubira AF et al (2012) Antiadhesive and antibacterial multilayer films via layer-by-layer assembly of TMC/heparin complexes. *Biomacromolecules* 13:3711–3722
59. Yang H, You W, Shen Q, Wang X, Sheng J, Cheng D et al (2014) Preparation of lotus-leaf-like antibacterial film based on mesoporous silica microcapsule-supported Ag nanoparticles. *RSC Adv* 4:2793–2796
60. Katsikogianni MG, Foka A, Sardella E, Ingrosso C, Favia P, Mangone A, Spiliopoulou I, Missirlis YF (2013) Fluid flow and sub-bactericidal release of silver from organic nanocomposite coatings enhance *ica* operon expression in *Staphylococcus epidermidis*. *J Biomater Nanobiotechnol* 4(4A):30–40
61. Yu Q, Cho J, Shivapooja P, Ista LK, Lopez GP (2013) Nanopatterned smart polymer surfaces for controlled attachment, killing, and release of bacteria. *ACS Appl Mater Interfaces* 5:9295–9304
62. Yu Q, Johnson LM, Lopez GP (2014) Nanopatterned polymer brushes for triggered detachment of anchorage-dependent cells. *Adv Funct Mater* 24:3751–3759
63. Yu Q, Ista LK, Lopez GP (2014) Nanopatterned antimicrobial enzymatic surfaces combining biocidal and fouling release properties. *Nanoscale* 6:4750–4757
64. Trautner BW, Hull RA, Thornby JI, Darouiche R (2007) Coating urinary catheters with an avirulent strain of *escherichia coli* as a means to establish asymptomatic colonization. *Infect Control Hosp Epidemiol* 28(1):92–94
65. Nagy ZS, Wagner I, Suhajda A, Tobak T, Haraszto AH, Vigh T, Soti PL, Pataki H, Molnar K, Marosi G (2014) Nanofibrous solid dosage form of living bacteria prepared by electrospinning. *Exp Polym Lett* 8(5):352–361
66. Tamura S, Yonezawa H, Moteg M, Nakao R, Yoneda S, Watanabe H, Yamazaki T, Senpuku H (2009) Inhibiting effects of *Streptococcus salivarius* on competence-stimulating peptide-dependent biofilm formation by *Streptococcus mutans*. *Oral Microbiol Immunol* 24(2):152–161
67. Kolodkin-Gal I, Romero D, Cao S, Clardy J, Kolter R, Losick R (2010) D-amino acids trigger biofilm disassembly. *Science* 328(5978):627–629
68. Pavlukhina SV, Kaplan JB, Xu L, Chang W, Yu X, Madhyastha S, Yakandawala N, Mentbayeva A, Khan B, Sukhishvili SA (2012) Noneluting enzymatic antibiofilm coatings. *ACS Appl Mater Interfaces* 4(9):4708–4716
69. Lu TK, Collins JJ (2007) Dispersing biofilms with engineered enzymatic bacteriophage. *Proc Natl Acad Sci U S A* 104:11197–11202
70. Cademartiri R, Anany H, Gross I, Bhayani R, Griffiths M, Brook MA (2010) Immobilization of bacteriophages on modified silica particles. *Biomaterials* 31(7):1904–1910
71. Schrementi ME, Ferreira AM, Zender C, DiPietro LA (2008) Site-specific production of TGF-beta in oral mucosal and cutaneous wounds. *Wound Repair Regen* 16:80–86
72. McKeown ST, Barnes JJ, Hyland PL, Lundy FT, Fray MJ, Irwin CR (2007) Matrix metalloproteinase-3 differences in oral and skin fibroblasts. *J Dent Res* 86:457–462
73. Zelles T, Purushotham K, Macauley S, Oxford G, Humphreys-Beher M (1995) Concise review: saliva and growth factors: the fountain of youth resides in us all. *J Dent Res* 74:1826–1832
74. Chai WL, Brook IM, Palmquist A, Van Noort R, Moharamzadeh K (2012) The biological seal of the implant soft tissue interface evaluated in a tissue-engineered oral mucosal model. *J R Soc Interface* 9:3528–3538
75. Engels-Deutsch M, Rizk S, Haïkel Y (2011) *Streptococcus mutans* antigen I/II binds to  $\alpha 5 \beta 1$  integrins via its A-domain and increases  $\beta 1$  integrins expression on periodontal ligament fibroblast cells. *Arch Oral Biol* 56:22–28

76. Gad GFM, Aziz AAA, Ibrahim RA (2012) In-vitro adhesion of *Staphylococcus* spp. to certain orthopedic biomaterials and expression of adhesion genes. *J Appl Pharm Sci* 2:145–149
77. Trampuz A, Zimmerli W (2006) Diagnosis and treatment of infections associated with fracture-fixation devices. *Injury* 37:S59–S66
78. Anagnostakos K, Schröder K (2012) Antibiotic-impregnated bone grafts in orthopaedic and trauma surgery: a systematic review of the literature. *Int J Biomater.* vol. 2012, Article ID 538061:9
79. Oga M, Arizono T, Sugioka Y (1993) Bacterial adherence to bioinert and bioactive materials studied in vitro. *Acta Orthop Scand* 64(3):273–276
80. Broggini N, McManus LM, Hermann JS, Medina RU, Oates TW, Schenk RK, Buser D, Mellonig JT, Cochran DL (2003) Persistent acute inflammation at the implant-abutment. *J Dent Res* 82(3):232–237
81. Aas JA, Paster BJ, Stokes LN, Olsen I, Dewhirst FE (2005) Defining the normal bacterial flora of the oral cavity. *J Clin Microbiol* 43(11):5721–5732
82. Klinge B, Meyle J, Working G (2012) Peri-implant tissue destruction. The third EAO consensus conference 2012. *Clin Oral Implants Res* 23(S6):108–110
83. Elter C, Heuer W, Demling A, Hannig M, Heidenblut T, Bach FW et al (2008) Supra- and subgingival biofilm formation on implant abutments with different surface characteristics. *Int J Oral Maxillofac Implants* 23(2):327–334
84. Zitzmann NU, Abrahamsson I, Berglundh T, Lindhe J (2002) Soft tissue reactions to plaque formation at implant abutments with different surface topography. *J Clin Periodontol* 29(5):456–461
85. Berglundh T, Gotfredsen K, Zitzmann NU, Lang NP, Lindhe J (2007) Spontaneous progression of ligature induced peri-implantitis at implants with different surface roughness: an experimental study in dogs. *Clin Oral Implants Res* 18:655–661
86. Albouy J-P, Abrahamsson I, Berglundh T (2012) Spontaneous progression of experimental peri-implantitis at implants with different surface characteristics: an experimental study in dogs. *J Clin Periodontol* 39:182–187
87. Alsabeeha NH, Ma S, Atieh MA (2012) Hydroxyapatite-coated oral implants: a systematic review and meta-analysis. *Int J Oral Maxillofac Implants* 27(5):1123–1130
88. Cheng K, Weng W, Wang H, Zhang S (2005) In vitro behavior of osteoblast-like cells on fluoridated hydroxyapatite coatings. *Biomaterials* 26(32):6288–6295
89. Tillmanns HWS, Hermann JS, Tiffée JC, Burgess AV, Meffert RM (1998) Evaluation of three different dental implants in ligature-induced peri-implantitis in the beagle dog. Part II. Histology and microbiology. *Int J Oral Maxillofac Implants* 13:59–68
90. Turner TM, Urban RM, Hall DJ, Chye PC, Segreti J, Gitelis S (2005) Local and systemic levels of tobramycin delivered from calcium sulfate bone graft substitute pellets. *Clin Orthop Relat Res* 437:97–104
91. Miclau T, Dahners LE, Lindsey RW (1993) In Vitro pharmacokinetics of antibiotic release from locally implantable materials. *J Orthop Res* 11:627–632
92. Kent ME, Rapp RP, Smith KM (2006) Antibiotic beads and osteomyelitis: here today, what's coming tomorrow? *Orthopedics* 29:599–603
93. Huang Z-M, He C-L, Yang A, Zhang Y, Han X-J, Yin J, Wu Q (2006) Encapsulating drugs in biodegradable ultrafine fibers through co-axial electrospinning. *J Biomed Mater Res A* 77:169–179
94. Torres-Giner S, Martinez-Abad A, Gimeno-Alcaniz JV, Ocio MJ, Lagaron JM (2012) Controlled delivery of gentamicin antibiotic from bioactive electrospun polylactide-based ultrathin fibers. *Adv Biomater* 14:B112–B122
95. Shi M, Kretlow JD, Nguyen A, Young S, Baggett LS, Wong ME, Kasper FK, Mikos AG (2010) Antibiotic-releasing porous polymethylmethacrylate constructs for osseous space maintenance and infection control. *Biomaterials* 31:4146–4156

96. Mendel V, Simanowski H-J, Scholz HC, Heymann H (2005) Therapy with gentamicin-PMMA beads, gentamicin-collagen sponge, and cefazolin for experimental osteomyelitis due to *Staphylococcus aureus* in rats. *Arch Orthop Trauma Surg* 125:363–368
97. Tofuku K, Koga H, Yanase M, Komiya S (2012) The use of antibiotic-impregnated fibrin sealant for the prevention of surgical site infection associated with spinal instrumentation. *Eur Spine J* 21:2027–2033
98. Bennett-Guerrero E, Ferguson TB, Lin M, Garg J, Mark DB et al (2010) Effect of an implantable gentamicin-collagen sponge on sternal wound infections following cardiac surgery. A randomized trial. *JAMA* 304:755–762
99. Becker PL, Smith RA, Williams RS, Dutkowsky JP (1994) Comparison of antibiotic release from polymethylmethacrylate beads and sponge collagen. *J Orthop Res* 12:737–741
100. CDC (2013) Report online at [http://www.cdc.gov/nhsn/pdfs/validation/2013/pscmanual\\_july2013.pdf](http://www.cdc.gov/nhsn/pdfs/validation/2013/pscmanual_july2013.pdf)
101. BCC Research (2012) HLC049C medical device coatings. Available online at <http://www.bccresearch.com/market-research/healthcare/medical-device-coatings-market-hlc049c.html>
102. Klevens RM, Edwards JR, Richards CL, Horan TC, Gaynes RP, Pollock DA, Cardo DM (2007) Estimating health care-associated infections and deaths in U.S. Hospitals 122:160–166
103. Scott RD (2009) The direct medical costs of healthcare-associated infections in U.S. hospitals and the benefits of prevention. Available online at [http://www.cdc.gov/hai/pdfs/hai/scott\\_costpaper.pdf](http://www.cdc.gov/hai/pdfs/hai/scott_costpaper.pdf)
104. Frost and Sullivan (2010) N71A-54 U.S. Advanced wound care market. Available online at <http://www.frost.com/sublib/display-report.do?id=N71A-01-00-00-00&bdata=bnVsSBEB%2BQJEJhY2tAfkAxMzk0NzA3NzZmZDU4>
105. Sorger JI, Kirk PG, Ruhnke CJ, Bjornson SH, Levy MS, Cockrin J, Tang PAB (1999) Once daily, high dose versus divided, low dose gentamicin for open fractures. *Clin Orthop Relat Res* 1(366):197–204
106. Court-Brown CM, McBirnie J (1995) The epidemiology of tibial fractures. *J Bone Joint Surg (Br)* 77(3):417–421
107. Department of Health (2012) National schedule of reference costs 2011–2012. Available online at [https://www.gov.uk/government/uploads/system/uploads/attachment\\_data/file/213060/2011-12-reference-costs-publication.pdf](https://www.gov.uk/government/uploads/system/uploads/attachment_data/file/213060/2011-12-reference-costs-publication.pdf)
108. Life expectancy (UK): Period expectations of Life (Years), (2013) Government Actuary Department
109. Darouiche RO (2004) Treatment of infections associated with surgical implants. *N Engl J Med* 350(14):1422–1429
110. Li D, Zheng Q, Wang Y, Chen H (2013) Combining surface topography with polymer chemistry: exploring new interfacial biological phenomena. *Polym Chem* 5:14–24
111. Zhao J, Song L, Shi Q, Luan S, Yin J (2013) Antibacterial and hemocompatibility switchable polypropylene nonwoven fabric membrane surface. *ACS Appl Mater Interfaces* 5:5260–5268
112. Baca-Delancey RR, South MMT, Ding X, Rather PN (1999) *Escherichia coli* genes regulated by cell-to-cell signalling. *Proc Natl Acad Sci U S A* 96:4610–4614
113. Fitzpatrick F, Humphreys H, Smyth E, Kennedy CA, O’Gara JP (2002) Environmental regulation of biofilm formation in intensive care unit isolates of *Staphylococcus epidermidis*. *J Hosp Infect* 42:212–218
114. O’Gara JP (2007) *Ica* and beyond: biofilm mechanisms and regulation in *Staphylococcus epidermidis* and *Staphylococcus aureus*. *FEMS Microbiol Lett* 270:179–188
115. Ishibashi K, Shimada K, Kawato T, Kaji S, Maeno M, Sato S, Ito K (2010) Inhibitory effects of low-energy pulsed ultrasonic stimulation on cell surface protein antigen C through heat shock proteins GroEL and DnaK in *Streptococcus mutans*. *Appl Environ Microbiol* 76(3):751–756
116. Foka A, Katsikogianni MG, Anastassiou ED, Spiliopoulou I, Missirlis YF (2012) The combined effect of surface chemistry and flow conditions on *Staphylococcus epidermidis* adhesion and *ica* operon expression. *Eur Cell Mater* 24:386–402

---

# Biocomposites used in Orthopedic Applications: Trends in Biocompatibility Assays

# 27

Martin J. Stoddart and Mauro Alini

## Contents

Introduction .....	786
Biocompatibility Definitions .....	788
Regulatory Aspects .....	791
Efficacy Aspects of Biocompatibility .....	793
Osteoconduction .....	793
Osteoinduction .....	793
Osteogenesis .....	794
Osseointegration .....	794
Classical Biomaterials Testing Algorithms .....	797
Material Property Tests .....	797
Degradation Characteristics .....	799
Controlled Release of Compounds Using Biocomposites .....	799
In Vitro Tests .....	800
In Vivo Tests .....	803
3R Principles .....	803
Large Animal .....	809
Practical Examples of Biomaterials Testing .....	810
Species Differences .....	814
Future Directions .....	815
Organ on a Chip .....	816
Summary .....	818
References .....	818

---

## Abstract

Biocompatibility assays have undergone a revolution from the early tests designed to investigate inertness of materials that were intended to remain within the patient indefinitely. With the increasing use of biodegradable materials and

---

M.J. Stoddart (✉) • M. Alini  
AO Research Institute Davos, Davos Platz, Switzerland  
e-mail: [martin.stoddart@aofoundation.org](mailto:martin.stoddart@aofoundation.org); [mauro.alini@aofoundation.org](mailto:mauro.alini@aofoundation.org)

functional materials that actively play a role in the repair process, the complexity of the assays required to analyze their biocompatibility has also increased. This has led to a change in the definition of biocompatibility, with increasing emphasis being placed on tests designed to ensure a material generates the most beneficial tissue response, without any unwanted local or systemic effects. In essence this leads to more assays associated with function. Within this chapter, we aim to highlight the changing definition of biocompatibility and explain the biocompatibility testing process while providing some examples. Various *in vivo* assays will be described and their benefits and limits will be discussed. Aspects of regulation and standards will be discussed, and differences between the various assays will be explained.

---

**Keywords**

Autologous bone graft • Bioreactor systems • Induced pluripotent stem cell lines (iPS cells) • Lab on a Chip • Organ cultures • Osteoconduction • Osteogenesis • Osteoinduction • Species Differences

---

**Introduction**

The word orthopedics derives from the Greek words *orthos* (“correct,” “straight”) and *paidion* (“child”), and it was initially coined by Nicholas Andry in 1791 while discussing the correction of skeletal deformities in children. Since then, the correction of deformities and repair of injuries in adults, and children, has become standard practice. As such, replacing large quantities of bone is required daily in clinical practice, with over two million bone grafting procedures being performed annually. High-impact trauma, tumor resection, and avascular necrosis or infection, among others, can all lead to the requirement to remove and subsequently replace large volumes of bone. The current gold standard is autologous bone graft, which is normally obtained from the patient’s own iliac crest. The bone is harvested in an open procedure, broken into smaller pieces, and then reimplanted at the defect site to aid the healing response. While highly effective, this technique has some significant disadvantages. Pain at the donor site in the hip is a frequent side effect, with incidences of over 40 % reported, and in some cases the pain at the harvest site persists beyond the pain at the site of injury. Various other side effects, such as nerve damage and infection, have also been reported, further increasing the complication rate. In addition, the volume of bone graft which can be harvested is limited; once the defect volume exceeds the available bone graft, an artificial material is also required as a void filler. Due to the unwanted side effects at the harvest site, and the limited quantity of autologous bone graft available, biomaterials are increasingly being used as an alternative or an additive. Biomaterials also offer the potential to be multifunctional. They can be used as a void filler, e.g., ceramic granules that are present to fill space rather than having an overt stimulatory response. Alternatively, they can also have a biologically active effect, e.g., demineralized bone matrix (DBM), which contains a biologically active stimulation. DBM is derived from

native bone by a series of treatments that remove cellular material and the mineralized matrix, making it a natural scaffold. Remaining is the proteinaceous material, including a number of growth factors which are contained within the native bone matrix. These growth factors can then be released after implantation and upon interaction with cells lead to an enhanced response. Other scaffolds in the class of natural materials include materials such as collagen, hyaluronic acid, and fibrin. Alternatively, materials can be synthetic, such as polyurethane or polyetheretherketone (PEEK). Synthetic materials offer greater flexibility in their properties but often have a higher potential risk of eliciting an unwanted response as they are not native to the body. In cases where the device is designed to be implanted indefinitely, the material used is a nonbiodegradable synthetic material which is frequently intended to be as inert as possible.

A normally inert implanted biomaterial can also be combined with bone graft or bone marrow aspirate within the surgical operating room in order to provide an intermediate that has the physical inert properties of the original material, with the added benefit of an enhanced biological healing response. Alternatively they can be combined with other scaffolds or biologics. This multicomponent, multifunctional aspect has greatly increased the potential complexity of the implanted materials. This has in turn led to lengthier, more complex testing algorithms, which often need to be specifically tailored to the biocomposite under investigation.

In addition, orthopedics frequently involves the implantation of nondegradable implants made of metal. A fractured bone leads to inherent instability that if left untreated can impair or prevent healing. While a simple splint or plaster cast may be sufficient to provide the required stability, in some cases the broken bony ends are held in place using metallic plates, screws, or nails using a method called internal fixation. These materials will not only be completely enveloped within the host but will often have direct interaction with blood due to the surgery involved during implantation. Artificial joints, such as knees and hips, also have metal parts that need to directly integrate with the bone. In addition, the articulating surfaces are frequently made of a second material in order to allow for the reduced friction articulation that is required during movement. Ideally, artificial, or prosthetic, implants should remain within the patient for as long as possible as this reduces the number of required surgeries. It also limits the complications associated with removal of an old artificial joint and replacing it with a new one.

This poses extra challenges from a biocompatibility point of view due to the length of time the material will remain in the patient, with some implants intended to be left indefinitely within the host. To investigate the potential ill effects of materials that are contained within the harsh, moist, biological environment of a human being for decades is difficult, particularly when one considers that ideally the tests should be capable of being performed within a realistic time frame. Investigating degradation or oxidation products continually over 20 years is not an analysis that can realistically be performed prior to the introduction of a new implant material or device. This has led to a series of standardized tests that can be performed in a timely

manner in order to estimate the biocompatibility. Once successful, products are generally monitored during their use in patients to establish whether an unexpected side effect develops at a later date. However, it should be considered that current standards do not demand that an implanted device survives the lifetime of the patient. Frequently an expected lifetime is provided. For example, it is accepted that while a hip replacement may last 30–40 years, generally it will need to be replaced after 15–20 years. This then takes into account the potential benefits of the implant and the risks of implant failure versus the consequences of leaving the patient untreated. If the benefits outweigh the risks, the devices can then be used. In the case of the hip replacements, they function quite well until the final failure point, and the alternatives to maintain mobility in patients with severe hip arthritis are vastly inferior to joint replacement.

### **Biocompatibility Definitions**

As with many definitions, the definition of biocompatibility can mean different things to different people. The word biocompatibility is frequently used, yet there is also increasing confusion as to what it actually means, which obviously leads to questions on how it is possible to test for it and which tests need to be done. One thing that is clear is that it encompasses many varying aspects, and over the last few years, it increasingly includes aspects more traditionally associated with efficacy. Originally it was the concept that the implanted material does not lead to harm of the recipient. The material must not be toxic or injurious or cause immunological rejection within the host, and both local and systemic effects should be evaluated. Other potential risks such as tumorigenicity (causing cancer) and teratogenic effects (a teratogenic agent is one that can disturb the development of the embryo or fetus) must be excluded. This is a large list of potential unwanted side effects and information must be obtained not only on the device itself, but in the case of degradable materials, the degradation products (and their intermediates) must also be tested and any residuals remaining from the manufacturing process. Furthermore, certain devices may require additional tests. In the case of total hip or knee replacements, the devices have articulating surfaces that rub together. Depending on the materials, this can result in small wear particles that may elicit a cellular response. In such cases, the generation and any potential biological response of the wear particles must also be investigated to ensure no unwanted side effects develop over time. This has led to a drive to develop more predictive, high-throughput in vitro testing protocols that can quickly screen multiple composites.

Various definitions for biocompatibility exist. The Merriam-Webster dictionary alone has two, albeit similar ones.

- ▶ **Definition 1** “Compatibility with living tissue or a living system by not being toxic, injurious, or physiologically reactive and not causing immunological rejection.”

The Merriam-Webster dictionary also has a medical definition of biocompatibility.

► **Definition 2** “The condition of being compatible with living tissue or a living system by not being toxic or injurious and not causing immunological rejection.”

These definitions derive from the initial view of biocompatibility that a material can achieve biocompatibility through chemical and biological inertness. In effect, if the material does nothing, it can do no harm. For the metal implants discussed above, or for implants intended to reside within the patient for many years, this definition was entirely satisfactory, as in many cases their primary function was to provide mechanical stability. In the case of internal fracture fixation plates, the metal implant would be placed on, or against, the bone in order to hold the broken ends in proximity, thus allowing healing to take place. The healing of the bone is then distant to the actual location of the medical implant, and the healing itself was only reliant on the mechanical stability the implant provided, not any intrinsic property of the material itself. The physical distance between the implant and the defect then reduces the potential for the implanted material to negatively influence the healing response.

As materials have evolved, so has the function, or functions, that they are required to perform. Increasingly materials provide a biodegradable scaffold, which is degraded, remodeled, and replaced with functional tissue over time. The time taken to degrade can vary from weeks to years, and this needs to be taken into account when devising a testing protocol. Biodegradable materials lead to an initially implanted device and multiple intermediate breakdown products which form as the material degrades. For new materials this poses particular challenges, as their characteristics are essentially unknown.

Not all biocomposites are completely new materials. Classical established materials may be mixed with growth factors or other materials in order to enhance their performance by producing biocomposites. For example, beta-tricalcium phosphate ( $\beta$ -TCP) is a well-characterized material that has been used for many years as a scaffold material and void filler for bone regeneration. GEM 21S<sup>®</sup> Growth-factor Enhanced Matrix from *Osteohealth* is a combined product, where classical  $\beta$ -TCP is combined with highly purified recombinant human platelet-derived growth factor (rhPDGF-BB). This produces a more complex multifunctional biocomposite. Increasingly, biocomposites are being developed with the aim of being a cell carrier for tissue engineering or regenerative medicine approaches. Tissue engineering was originally conceived as a combination of scaffolds, cells, and stimuli in order to provide a de novo replacement for damaged tissues. Originally coined by Langer and Vacanti in the early 1990s, tissue engineering has become a field in its own right [1] while still having significant biocompatibility testing requirements. As a further advance, biocomposites that are able to provide a controlled release of growth factors or antibiotics are increasingly becoming available. While the release is often a passive process, in some cases the release is triggered by enzymic reactions



induced by the invading cells, deliberately making the materials responsive to their environment. By definition these advanced materials modify their properties over time and have an inherent functionality that may or may not be triggered by interactions with viable cells. This leaves the classical biocompatibility concept of inertness as dated and incompatible with modern materials, raising complex questions on how and what should be analyzed.

The International Union of Pure and Applied Chemistry (IUPAC) have a more recent biocompatibility definition which defines biocompatibility for a biomedical therapy.

► **Definition 3** “Ability of a material to perform with an appropriate host response in a specific application.”

Due to the mention of appropriate host response, this includes function and efficacy, as well as safety and immunological responses. The function and efficacy of the implanted material is critical in a successful repair in situations where the material is present in the area undergoing repair. For example, an unsuitable material may lead to fibrous encapsulation as the body attempts to “seal off” the foreign body. This then results in an avascular sequestration that in a best-case scenario prevents the ingrowth of new tissue. However, more frequently, such a reaction can lead to multiple complications that can have a detrimental effect on the host. The material can trigger an immune response, leading to acute or chronic inflammation. Sequestrations containing a bacterial contamination can lead to a severe infection; this is made worse by the lack of blood supply preventing the infiltration of immune cells. As such complications encompass aspects such as complement activation, immunological responses, foreign body response, vascularization, and functional tissue development, this cannot be investigated *in vitro*.

As function increasingly becomes an aspect of biocompatibility, the performance of materials is increasingly investigated. In a seminal opinion piece in 2008, Williams proposed an overarching definition of biocompatibility [2]. It was proposed that biocompatibility should be redefined as follows:

► **Definition 4** “Biocompatibility refers to the ability of a biomaterial to perform its desired function with respect to a medical therapy, without eliciting any undesirable local or systemic effects in the recipient or beneficiary of that therapy, but generating the most appropriate beneficial cellular or tissue response in that specific situation, and optimizing the clinically relevant performance of that therapy.”

This takes into account the multiple new roles biomaterials must perform and provides a more detailed definition along similar lines to that proposed by the IUPAC. Investigating the “clinically relevant performance” has opened new areas of biocompatibility testing. This chapter is written with the Williams definition in mind and so will encompass aspects of function, as well as safety.

## Regulatory Aspects

Currently, biocompatibility tests are a prerequisite for the preclinical testing of any novel material, including biocomposites, that aims to eventually be used in humans. ISO-10993 “Biological Evaluation of Medical Devices” is a 20-part series of standards for evaluating the biocompatibility of a medical device prior to its use in clinical trials (Table 1). A detailed description of each of these standards is beyond the scope of this chapter, but investigators should be aware of their existence and, if needed for their application, devise protocols for their implementation. The ISO-10993 standards are intended as a guide towards which assays should be applied and in which conditions. They are not a rigid set of tests with pass/fail criteria, as the range of potential devices to be investigated, and their potential for negative side effects, is much too broad and could not be adequately encompassed within a single text. In keeping with reducing the numbers of animals used for safety testing, preference where possible is given to *in vitro* tests, with the stated aim of minimizing the number and exposure of test animals. This became more evident in the 2009 revision, where much more guidance was presented on when biocompatibility tests were needed as opposed to how to perform them. This change in emphasis highlighted the potential that existing historical data could be presented to regulatory agencies as the basis of the safety assessment for novel devices, thus

**Table 1** Detailed list of the ISO-10993 series “Biological Evaluation of Medical Devices.” Each part is self-contained, and all parts may not be required for all devices

Part 1	Evaluation and testing in the risk management process
Part 2	Animal welfare requirements
Part 3	Tests for genotoxicity, carcinogenicity, and reproductive toxicity
Part 4	Selection of tests for interactions with blood
Part 5	Tests for <i>in vitro</i> cytotoxicity
Part 6	Tests for local effects after implantation
Part 7	Ethylene oxide sterilization residuals
Part 8	Selection of reference materials (withdrawn)
Part 9	Framework for identification and quantification of potential degradation products
Part 10	Tests for irritation and delayed-type hypersensitivity
Part 11	Tests for systemic toxicity
Part 12	Sample preparation and reference materials (available in English only)
Part 13	Identification and quantification of degradation products from polymeric medical devices
Part 14	Identification and quantification of degradation products from ceramics
Part 15	Identification and quantification of degradation products from metals and alloys
Part 16	Toxicokinetic study design for degradation products and leachables
Part 17	Establishment of allowable limits for leachable substances
Part 18	Chemical characterization of materials
Part 19	Physicochemical, morphological, and topographical characterization of materials
Part 20	Principles and methods for immunotoxicology testing of medical devices

reducing the number of tests required. The US Food and Drug Administration (FDA) is not always in total alignment with ISO-10993 as to which tests are required for which devices, and therefore, investigators need to be aware of where differences apply. To assist with this, the FDA has issued a guideline document entitled “Use of International Standard ISO-10993, “Biological Evaluation of Medical Devices Part 1: Evaluation and Testing”” with the specific aim of providing guidance relating to the implementation of the ISO-10993 within their regulatory framework. While specific for ISO-10993, the information contained within is also relevant to other standards, such as those distributed by ASTM international (formerly known as the American Society for Testing and Materials (ASTM)). The FDA guideline document highlights that the biocompatibility tests should be performed on the final finished device. This is because the biocompatibility of a final device depends not only on the materials but also on the processing of the materials, the manufacturing methods (including the sterilization process), and the manufacturing residuals that may be present on the final device. In cases where it can be demonstrated that the new device is comparable in intended use, composition, production, and storage to currently available products, it is possible that no biocompatibility testing will be required.

In addition, the FDA guidelines provide three attachments that aim to assist laboratories in choosing which tests are required and how they should be performed. All tests may not be required for all devices, but a scientifically based rationale for omission of any recommended test should be included with the application, and the emphasis is on the investigating laboratory to provide this rationale.

The chemical characteristics of device materials and the nature, degree, frequency, and duration of exposure to the body are critical when selecting the appropriate tests for the biological evaluation of a medical device. Taken together, this requires a level of understanding on the part of the investigator as to how to adequately interpret the guidelines and therefore arrive at the appropriate testing regime. Due to the variability and increasing complexity of the materials, this is not a simple task and for investigators new to the field significant training would be required.

Biocompatibility protocols need to be performed in a reliable and reproducible manner. Any *in vitro* or *in vivo* biocompatibility tests involving toxicity or injurious behavior should be conducted in accordance with recognized good laboratory practice (GLP), which requires an established testing protocol that is reproducible and can offer thorough traceability. It employs standard operating procedures (SOPs), which when followed results in consistency between experiments and between investigators. Each step is rigorously documented, and the records must be kept for at least 10 years, although this requirement varies from country to country. Generally, for medical products, it is desirable that records should be retained as long as the device is in use. GLP and record keeping are particularly critical in cases where regulatory approval will be applied, as agencies such as the FDA require full access to all relevant data and the mechanism by which it was obtained. The archiving of paper-based medium is relatively straightforward; however, managing electronic documents can require certified software, or alternatively a well-validated work flow process. GLP archiving requirements regarding raw

electronic data were modified in 1997. Prior to that date, laboratories could elect to print and sign electronic-based data and then keep only the printed version. Since 1997 all electronic data becomes the raw data immediately upon being stored on a durable storage device such as a computer hard disk and must be archived for the duration as required by GLP requirements.

## **Efficacy Aspects of Biocompatibility**

While traditional biocompatibility has been mainly related to the potential toxic or immunological aspects, whether a material plays a negative or inhibitory role on the healing or repair response is increasingly being considered within the definition of biocompatibility. This is highlighted by the inclusion of the “appropriate host response” clause contained within the IUPAC definition. Particularly when considering tissue reconstruction or repair, the implanted material must also be able to allow for the natural healing response to proceed unhindered. In the case of bone, for example, this requires the implanted material to allow for the penetration of blood vessels and the deposition and remodeling of new bone tissue, which then integrates into the host bone. While toxicity and immunological reaction tests are standardized for differing materials to be used in different applications, efficacy tests are much more specific for the application for which the materials will be used.

A critical aspect of all functional biocomposites is their mechanism of action, of which in materials for bone repair, there are generally considered to be three main mechanisms: osteoconduction, osteoinduction, and osteogenesis.

### **Osteoconduction**

Osteoconduction is when the bone graft material serves as a permissive scaffold for new bone growth. Osteoblasts, or their progenitors, invade from the edges of the defect and utilize the bone graft material as a framework upon which to spread and generate new bone. A minimum requirement of any bone graft material is that it should be osteoconductive. In most cases, the scaffold material is degraded and over time remodeled into bone. Depending on the material, this can take from weeks (collagen-based scaffolds) to years (ceramics). Titanium meshes can also be used as a structural base, and in this example the mesh would not degrade and would remain for the lifetime of the patient.

### **Osteoinduction**

Osteoinduction involves the differentiation of osteoprogenitor cells into osteoblasts, which are then involved in new bone formation. This most commonly involves an incorporated growth factor, such as a bone morphogenetic protein. As these growth factors are naturally present in DBM, osteoinduction is one of the main mechanisms

involved when using DBM. Synthetic biomaterials have also been designed with the strategy of growth factor release. The clinically available products, such as Infuse from Medtronic (a collagen scaffold releasing recombinant BMP-2) tend not to have a controlled release. The scaffold material has a limited retention effect and the biologic is released relatively rapidly. Newer-generation materials currently in pre-clinical studies have begun to more finely regulate the release characteristics of the materials.

## **Osteogenesis**

Osteogenesis requires the presence of vital osteoblasts within the bone graft material. These cells will then contribute to new bone formation in addition to bone generated via osteoconduction and osteoinduction. Few synthetic scaffolds fulfill this criterion as the regulatory requirements are much greater and an off-the-shelf product is unfeasible. Harvested bone marrow graft is one example of an osteogenic scaffold material containing viable osteoblasts. Osteogenesis relating to material properties should not be confused with in vitro assays designed to differentiate mesenchymal stem cells into osteoblasts. This is also referred to as osteogenic differentiation (or osteogenesis) but is not the same osteogenesis being discussed here.

Currently, there are an increasing number of artificial biocomposites available for clinical use to replace and repair bone. Each of them varies in their properties and claimed mechanism of action. There is an online resource listing clinically available products with a description of their mechanism of action [3]. This can be a useful overview of a number of approved clinical products.

## **Osseointegration**

In addition, for nondegradable implants, such as hip prosthetics, osseointegration is a critical aspect. Osseointegration is the formation of a direct interface between an implant and bone, without intervening soft tissue, and is required to allow for a stable integration of the implant with the host bone. This is a major requirement of implant materials that are intended to remain in place over a long period of time. Stable initial osseointegration leads to less motion and therefore less microdamage to the surrounding bone. This then leads to fewer complications and a more durable device.

While it is desirable to increase the life span of implants such as hip and knee prosthetics by enhancing osseointegration, there are cases where osseointegration is less desirable. During fracture fixation, a metal implant is initially applied in order to provide initial stability, thus allowing for more rapid patient mobility and quicker healing. However, once the healing is complete, plate removal may be required. This is particularly required in; pediatrics, high-risk areas such as the skull where the plate can migrate towards the brain and in cases where complications may occur, such as tendon attachment in the hand. While implant materials may conform to traditional safety testing, if an implant allows for tendon attachment instead of tendon gliding,

this would prevent it being functionally compatible with use in areas such as the wrist. Modifying the surface topography by polishing has been shown to reduce the potential for osseointegration. This then allows for improved tendon gliding and a more functionally compatible implant design.

One of the greatest current challenges in orthopedic biomaterials testing is that of standardization, particularly when considering functional compatibility. Routine tests performed within laboratories often have a wide range of seemingly minor differences, which when added together can lead to vastly different results. This then makes studies difficult to compare between groups, especially when there is a lack of appreciation as to how the differences modify the outcomes. In addition, studies are often interpreted in similar ways, even though the conditions applied were significantly different enough that the differences should be taken into account when analyzing the data. This is more of an issue when investigating efficacy, where the established tests are less standardized than those for toxicity.

Increasingly there is the initiative to attempt to standardize methods. ASTM International has an ever-growing number of standards relating to the testing of orthopedic materials, ranging from calcium quantification methods, to guidelines on how the cellular aspect of *in vitro* studies should be performed. It is hoped with time these standards, or ones similar, will be adopted, if only to provide a point of reference between studies to allow a more accurate comparison of materials tested in different laboratories. Two main types of study into bone-related function can be performed *in vitro*, osteoinductive and osteoconductive. The osteoinductive properties of a material can be investigated by using mesenchymal stem cells (MSCs), such as bone marrow-derived stem cells (BMSCs). MSCs are often harvested by density separation of the bone marrow aspirate, resulting in an enriched mononuclear fraction. This fraction is then placed in culture flasks and the adherent cellular fraction is allowed to attach. After a period of time, commonly 24–96 h the non-adherent cells are removed and medium replaced with proliferation medium. Cells are grown to a certain passage to produce enough cell numbers to perform the required assays. The osteoinductive properties of materials are then investigated using monolayer expanded cells obtained in this manner. Although increasing cell number on tissue culture plastic is referred to as monolayer expansion, in the case of a mixed population of primary cells, such as those found in the bone marrow, it is also a form of artificial cell selection. Thus, when using cells derived in such a manner, the cells being used to investigate the material of interest are not likely to be the same as the population of cells that will initially interact with the material upon implantation. Their growth has been optimized for *in vitro* culture, and the population lacks the interactions between different cell types that would be present during the host response. This raises the question of relevance to the *in vivo* situation where the invading naive cells have not been subjected to monolayer expansion.

It is also of interest to note that when using primary animal-derived cells, the age and species of the animal must be considered. Cells from an immature animal will by definition have an increased potential for proliferation and general metabolic activity, as they would normally perform the act of growth within the young animal. For

example, results obtained from cells derived from young, healthy rats will likely be much more dramatic than that seen using cells from adult human donors.

Functional compatibility assays for osteogenic cells often investigate the osteoconductivity and osteoinductivity of the new material. The ability of cells to undergo osteogenic differentiation can then be compared to an established standard that can be used as a baseline. In this instance, tissue culture plastic and dexamethasone-containing medium is the most commonly used comparison group.

For osteoconductivity assays, an established osteoblast cell line or primary isolated osteoblasts are used (Table 2). In these studies it is not the development or induction of an osteogenic phenotype which is under investigation. The primary aim

**Table 2** Advantages and disadvantages of primary osteoblast cells and osteoblastic cell lines models (Modified with permission from Ref. [4])

Cell type	Advantages	Disadvantages
<b>Primary human cells</b>	No interspecies differences Relevant for clinical studies	Heterogeneous phenotype Long isolation procedure Limited accessibility Cell phenotype sensitive to donor-related factors
<b>Primary mouse/rat cells</b>	Easily available Possibility to control the selection of donor animals Cell extraction from all bones in the skeleton	Interspecies differences Genomic differences Cell phenotype sensitive to age and site of isolation factors
<b>Primary bovine/ovine/rabbit cells</b>	Potential for wider evaluation of bone remodeling and healing process Potential formation of trabecular structures (bovine osteoblasts)	Inconsistent results regarding cell mineralization Need for optimizing culture conditions Lack of extensive characterization of cells Limitations for molecular biology methods
<b>SaOs-2</b>	No interspecies differences Unlimited number of cells Homogenous Similar to primary human osteoblast cells cytokine and growth factor expression profile Sensitive to hormonal administration Matrix mineralization	Do not mirror the whole range of osteoblast phenotypic changes Sensitive to Pi substrates
<b>MG-63</b>	No interspecies differences Unlimited number of cells Hormonal administration response similar to human Ob cells Similar to human integrin subunits profile	Arrested in preosteoblast state Inconsistent regarding cell mineralization
<b>MC3T3-E1</b>	Unlimited number of cells Homogenous character Phenotypic differentiation from preosteoblasts to mature osteoblasts	Interspecies differences Some signs of cellular replicative senescence

is to establish whether the material is permissive to the normal osteoblastic phenotype and function.

---

## Classical Biomaterials Testing Algorithms

Novel biomaterials for bone often undergo a fairly standard series of tests to determine their safety and compatibility. Initial tests on material properties are followed by *in vitro* cytotoxicity testing and *in vitro* efficacy testing. If the materials appear promising at this stage, they can be further tested *in vivo* for biocompatibility and efficacy. There is a clear difference between cytotoxicity, which is investigated *in vitro* and biocompatibility, which must be investigated *in vivo*. Cytotoxicity occurs when the material, or its degradation products, produces an acute toxic response leading directly to cell death by either necrosis or apoptosis. Necrosis is an uncontrolled mechanism of cell death caused by a severe insult, whereas apoptosis is a series of events that are coordinated by the cell, resulting in a controlled cell death [5]. It evolved in multicellular organisms as a way to protect the organism as a whole from various insults which may eventually lead to a carcinogenic cell mass.

Sample preparation is crucial when performing biocompatibility assays. The material being tested, and any residuals from its processing, should be indistinguishable from the final product. There are obvious reasons as to why this is the case. For example, the materials within the developing product may be quite stable during their production and processing. However, the sterilization process may then modify the material in such a way that toxic by-products leach into the surrounding tissue upon implantation.

## Material Property Tests

The inherent material properties can play a role on the biocompatibility of the material. The mechanical properties of the implanted material also determine its suitability to allow the development of a *de novo* functional tissue.

One of the main properties that have an influence on biocompatibility is hydrophobicity/hydrophilicity. This can be investigated by contact angle measurements where a drop of water is placed on the material and the angle of the droplet in relation to the material is measured using a contact angle goniometer. The larger the angle, the more hydrophobic a material is (Fig. 1).

Mechanical properties of implanted materials are very important. This is even more so when the material will be used within the musculoskeletal system, which is subjected to daily cyclical load. During motion these loads can be significant; for a 70 kg person, a load of 700 N through a single standing leg is not uncommon. For some applications, such as within a bone fracture, the load bearing may be performed by one device, while a healing response is instigated by a second material. For example, a biocomposite may be used as a void filler and to aid the healing response, but the load itself is then transmitted across a metallic fracture fixation plate. Under



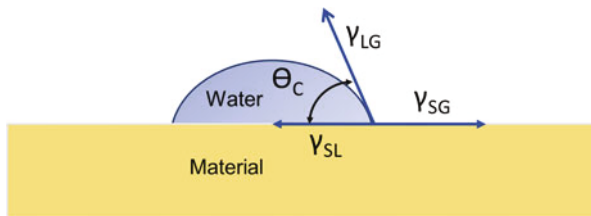


**Fig. 1** Schematic of a material contact angle measurement. The theoretical description of contact arises from the thermodynamic equilibrium between three phases: the liquid phase ( $L$ ), the solid phase ( $S$ ), and the gas phase ( $G$ ). If the solid–vapor interfacial energy is denoted by  $\gamma_{SG}$ , the solid–liquid interfacial energy by  $\gamma_{SL}$ , and the surface tension by  $\gamma_{LG}$ , then the equilibrium contact angle  $\theta_C$  is determined from these quantities by Young’s equation  $O = \gamma_{SG} - \gamma_{SL} - \gamma_{LG} \cos \theta_C$

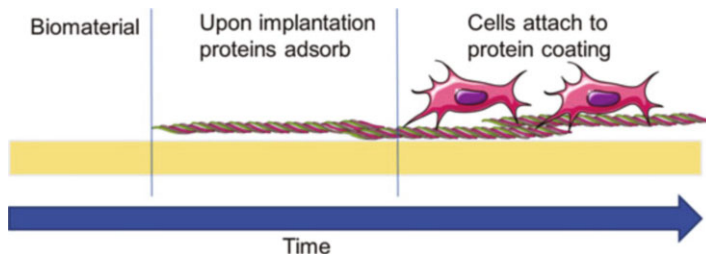


**Fig. 2** Upon implantation, proteins from the local milieu attach to the biomaterials surface. This often occurs within seconds of contact. Over time this protein coat acts as anchorage sites for invading cells. The cells attach, spread, and over time remodel the cell matrix interaction by secreting their own matrix products to form a basement membrane (Produced under the creative commons license from Servier Medical Slides)

these conditions, the biocomposite itself does not need to fully support the load applied; it would, however, need to be able to withstand a degree of compression and torsion. These forces are required across the defect to allow for natural healing to occur.

The initial response of any biomaterial is the deposition of protein onto its surface in a process known as protein adsorption, and this is heavily influenced by the surface properties such as charge, chemistry, hydrophobicity/hydrophilicity, and topography. Cell adhesion to any material is dependent of the presence of a superficial protein coat, and it is the composition of the protein coat that directs the following cellular responses. The proteins that coat the material derive from the local milieu, and the surface property of the material is critical in the type of protein that can be deposited and the speed at which deposition occurs. The protein from the local environment rapidly attaches to the surface of the implanted material. These proteins then provide anchorage, or binding sites, for the invading cells (Fig. 2).

Various proteins provide differing epitopes for the cell surface adhesion molecules called integrins. In humans there are  $18\alpha$  and  $8\beta$  integrin subunits that can combine to produce at least 24 different heterodimers, each of which can bind to a various cell surface ligands, ECM, or soluble protein ligands. Integrins are transmembrane proteins mostly known for their adhesion function but they are also able to potentiate signals. The cellular focal adhesions that form around integrins form the basis of signal transmission by external soluble signal molecules, and they associate with various transmembrane receptors. Thus, modifying the surface properties can modify which proteins adsorb, which can change which integrins are then used to bind the cell to the underlying material. This feature can be used to modify the downstream cellular response as various responses have been shown to be related to specific integrins. An example would be  $\alpha 5\beta 1$  which due to the presence of the  $\alpha 5$  element has been associated with osteogenesis. This can greatly modify the functional aspects of biocompatibility.

### **Degradation Characteristics**

Material degradation rate is also initially investigated *in vitro*. The material is incubated in isotonic solution and the supernatant is harvested at regular intervals for testing. The incubation fluid can be simple, such as a phosphate buffered saline, or can be more complex. In the early 1990s simulated body fluids (SBFs) were developed to more accurately mimic the *in vivo* environment. SBF is a solution with an ion concentration close to that of human blood plasma, maintained with a physiological pH and temperature. The medium is conditioned by exposure to the material of interest and is then tested for the presence and concentration of the compound. In the case of biocomposites containing bioactive factors, the release of the factor over time and its biological potency can also be investigated. Ideally, this assay then should be performed in the presence of cells, either on the surface of the material or embedded with the material. This then provides data on how the release is modified by the presence of viable cells, which may actively be involved in the breakdown of the carrier material.

### **Controlled Release of Compounds Using Biocomposites**

Increasingly, biocomposites are being used to provide a physical scaffold into which the *de novo* tissue can develop, while at the same time incorporating the controlled release of an incorporated soluble mediator. This increases the complexity of the material and therefore the required biocompatibility tests. The release characteristics may be independent or dependent on the material degradation. Due to its simplicity, current scaffolds that release soluble mediators rely on simple diffusion. The factor is mixed in the soluble phase and is released quite quickly into the surrounding tissue. Alternatively, the factor can be physically linked in some way to the scaffold material, only being released as the material degrades. This then leads to a longer

duration of release, but the linkage mechanism might affect the bioactivity of the molecule.

## **In Vitro Tests**

A vast majority of investigations into novel biomaterials are performed *in vitro*. This is in part explained by their simplicity, cheap cost, and the ability to perform the tests in cell culture laboratories with a relatively basic level of equipment. By their nature, *in vitro* tests are also amenable to testing multiple materials in parallel, and improved assay sensitivity has increased this aspect. High-throughput assays are increasingly becoming the norm, and to assist with this, there are an increasing number automated plate reader systems and automated live assay microplate microscope systems to allow rapid, automated assays to be performed. *In vitro* tests have many potential variables: primary cells v cell lines (of which there are large numbers to choose from), mesenchymal stem cells v osteoblasts, medium composition, and the effect of various serum batches to name but a few. In addition, the analyses done, and the time point on which they are performed, can also vary widely from study to study. This makes comparing various studies extremely difficult, in particular when considering topics such as function and osseointegration. Primary osteoblasts, or osteoblast cell lines, can be used to establish the osteoconductive potential of the material under investigation, whereas progenitor cells can be used to investigate the ability of the material to induce an osteoblast phenotype.

It should be noted that from a regulatory standpoint, ISO-10993-5:2009 states: “Established cell lines are preferred and where used shall be obtained from recognized repositories. Where specific sensitivity is required, primary cell cultures, cell lines and organotypic cultures obtained directly from living tissues shall only be used if reproducibility and accuracy of the response can be demonstrated.” This to an extent simplifies the tests as cell lines are easier to maintain and lead to more reproducible results. It is interesting to note from a scientific standpoint that cell lines are generally considered inferior as they often do not entirely represent the native primary cell type. While cell lines enhance reproducibility within and between laboratories, it does raise the question as to whether their use reduces the accuracy with which they can predict *in vivo* functional outcomes. This is an area where academic outcomes and regulatory outcomes diverge to an extent.

Cytotoxicity tests are required to ensure the materials are not toxic. In addition, if the material is biodegradable, the toxicity of any breakdown products must also be investigated. Cytotoxicity tests are straightforward to perform, and there are a number of assays available to assess viability [6]. A fixed number of cells are seeded 1 or 2 days before the assay is performed. The cells are allowed to attach and the medium is changed to medium that contains the compound of interest. After a fixed period of time, the viability or metabolic activity is assessed and compared to an untreated control. For materials which aim to result in cell attachment and differentiation, the cells can be seeded directly onto the material. This allows attachment and proliferation to be assessed in parallel. Viability and attachment, or proliferation,

cannot be assessed in the same sample as cell numbers need to be directly compatible between samples to allow for an accurate viability assessment. Differing attachment profiles will lead to different numbers of cells being present. The most accurate measurement of cell number is to quantify DNA content. As this requires a number of steps, it is difficult to implement DNA measurement in a high-throughput protocol. For this reason metabolic assays are often used as a surrogate measurement. This is routinely performed by culturing cells on, or in the presence of, the material and investigating metabolic activity using assays such as 3-(4,5-dimethylthiazol-2-yl)-2,5-diphenyltetrazolium bromide (MTT) or alamarBlue. In such assays a metabolic dye is added to the live cells and penetrates the cell membrane. The dyes are then metabolized within live cells, mainly in the mitochondria, producing a derivative that can be measured colorimetrically or fluorescently using a micro plate reader. MTT produces an intracellular product, which requires the cell to be lysed and the metabolite to be dissolved. Dyes such as alamarBlue offer the advantage that the metabolite is released by the live cells into the culture medium; therefore, the sample does not need to be destroyed to obtain the measurement. This means multiple viability measurements can be made at different time points or secondary assays can be performed on the same sample. This is a great advantage when developing new materials that may only be available in small quantities. Alternatively, adenosine triphosphate (ATP) measurements can be performed as a more sensitive assay. This allows a smaller number of cells to be used in the assay and is again amenable to high-throughput assays.

The time at which the assay is performed can also have an influence on the results obtained. Extreme necrotic inducing reactions can be observed very quickly. However, the material may induce a stress response, which then leads to a later apoptotic response. This can take longer to develop and may be missed if only early time points are investigated. Therefore, investigating viability at multiple time points provides a more accurate assessment of cytotoxic effects.

In keeping with the drive towards more functional outcomes of biocompatibility, in addition to toxic effects leading to a change in viability, changes in cellular function are also being increasingly performed using *in vitro* assays. This is due to the fact that a material may not be cytotoxic but might lead to a sublethal stress response within the cell population. Stressed cells can have a reduced function, ranging from decreased activity to no activity at all in certain functions, and this would lead to delayed, or possibly an inhibition of the healing response when the biomaterial is intended to be placed within the defect site. This requires a number of device- or tissue-specific tests that determine any functional changes in cell behavior due to the influence of the material or its degradation products. In particular, anabolic activity should be investigated to confirm cells are still able to build functional tissue.

### **Ex Vivo and Bioreactors**

Due to the constraints of 2D culture, more and more studies are employing three-dimensional culture models in an attempt to more accurately mimic the natural *in vivo* environment. These may consist of true *ex vivo* organ cultures, where the tissue is explanted and cultured whole or as parts. This allows for complex, 3D

multicellular interactions to be maintained. Classic examples of this would be the chicken embryo chorioallantoic membrane assay (CAM assay) and chick limb organ culture. The CAM assay has been used to investigate angiogenesis since the 1970s. It involves using an early-stage fertilized chick egg, opening the shell to expose the air pocket above the developing embryo, and then placing a material or compound of interest directly on the chorioallantoic membrane. The egg can then be resealed with sellotape to allow for a viewing window through which the vascular bed can be monitored. This has the advantage that it is a fully functioning natural environment; it does, however, require a large number of fertilized eggs.

A more orthopedic related example is the chick limb organ culture model [7]. Freshly isolated chick femora, typically embryonic day 11, are placed on a Transwell insert where they can be cultured for up to 18 days. This system can then be used to establish toxic effects and the influence of test materials on bone development and formation. The lack of vasculature is still an issue in this system, but this can partially be overcome by combining it with the chorioallantoic membrane, which then provides some limited vascularization. Such systems while providing an environment closer to *in vivo* than classical 2D culture models often have the disadvantage that they are limited by size and duration due to a lack of functioning vasculature and hence improper nutrition and removal of waste products.

Attempts are being made to overcome this issue by the development of more sophisticated bioreactor systems that are able to better regulate the environment of 3D tissues. When combined with perfusion systems, adequate nutrition exchange can also be maintained. Bioreactor systems capable of applying mechanical load are common, while controlled perfusion systems, which automatically regulate flow based on pH or oxygen levels, are increasingly being seen. These bioreactor systems can then be used either to maintain tissue explants for a longer period of time or can be used to culture tissue-engineered constructs under more physiological conditions.

### **Infection Resistance**

Increasingly the interaction of a material with bacterial isolates is being investigated both *in vitro* and *in vivo*. The initial response of an implanted material is the protein adsorption that provides adhesion sites for both bacteria and host cells. Properties, such as topography, have been shown to influence the rate at which mammalian cells and bacteria are able to attach, and they compete for binding sites in what has been coined “the race for the surface.” Any modification that enhances the attachment of mammalian cells will reduce the potential risk of infection, in particular if it concurrently reduces bacterial adhesion. Infection susceptibility is a biocompatibility aspect that has been largely overlooked for a number of years, and yet all implanted devices have an inherent risk of infection. However, in areas where infection is a particular risk, such as open tibia fractures, the inherent infection risk of a novel material is increasingly being investigated. Nondegradable implants with solid surfaces have an increased risk of infection than biodegradable gels, which over time have no surfaces which can be colonized. Materials particularly favorable for bacterial growth can lead to a highly resistant biofilm formation. A biofilm is an

aggregate of individual bacteria which are embedded within a self-produced matrix of extracellular polymeric substance (EPS). When a bacteria switches to a biofilm mode of growth, it undergoes a phenotypic shift in behavior and differentially regulates a large number of genes. Once formed, a biofilm provides a relatively impenetrable layer, which can provide protection for the underlying bacteria even in the presence of antibiotics or host immune cells. Thus, prevention of biofilm development is an important aspect of material biocompatibility. In establishing susceptibility to bacterial infection, materials are grown *in vitro* in liquid cultures. Cell growth and biofilm formation are then determined for the native material. Surface modifications can then be investigated for their ability to reduce the adhesion and growth of bacteria. Initial tests *in vitro* can be used to establish bacterial adhesion and proliferation in the presence of SBF.

---

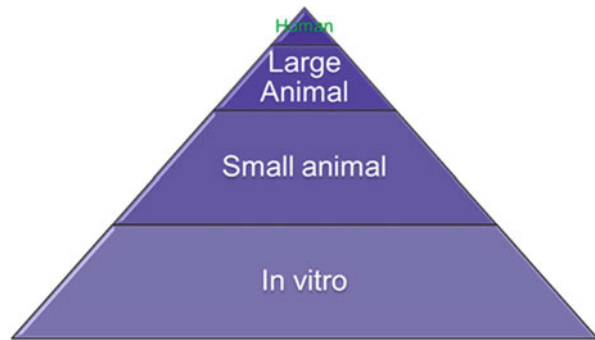
## In Vivo Tests

Once sufficient *in vitro* tests have been performed to confirm a lack of cytotoxicity and imply a degree of efficacy, the materials then typically undergo *in vivo* testing. While simple cytotoxicity can be evaluated *in vitro*, more complex responses, such as immune activation or liver toxicity caused by degradation products, require more extensive *in vivo* tests. Such *in vivo* tests are normally longer, more expensive, and ethically questionable due to issues surrounding animal welfare. Due to the increased concerns surrounding animal testing, extensive efforts are being made to reduce animal biocompatibility testing. Despite this, large numbers of animal studies are still performed as current *in vitro* or *ex vivo* tests are unable to fully replace *in vivo* studies.

## 3R Principles

Reducing the number of animals required for research is a very important issue as animal welfare is increasingly relevant in experimental design, particularly in the context of 3R principles (replace, reduce, refine). Since they were first described in 1959 by W. M. S. Russell and R. L. Burch [8], these principles have become widespread in order to minimize the number of animal tests required to confirm the safety and efficacy of new therapies. Replacement of animal tests mainly consists of developing new *in vitro* or *ex vivo* tests, and in this regard high-throughput screens and bioreactors are playing an increasing role. Reduction can be achieved by careful experimental planning, use of historical controls, and more modern imaging techniques, such as *in vivo* Ct, that allow for repeated measures in the same animal. While investigating bone defects, repeated Ct images on live small animal models (*in vivo* Ct) allow for fewer animals to be monitored in more detail. Healing within the same animal can be repeatedly imaged allowing for a more accurate assessment of healing progression and time to bridging. Refinement focuses more on improving the environment in which the animals are maintained and improving training for the

**Fig. 3** A schematic emphasizing the number of studies performed. Building up from the base of the pyramid, the number of studies reduces as they progress through the different stages



researchers performing the work. A major element is improved and optimized pain control to ensure the animals do not suffer. These advances have drastically improved the standard of animal care, and efforts are ongoing to make further improvements. Most major grant agencies increasingly highlight animal welfare and the 3R principles when making funding decisions. In addition, reducing animals reduces costs and potentially allows for more materials to be investigated.

A typical progression of the tests applied to new materials can be seen in Fig. 3. When considering the number of studies performed at each stage, the largest numbers of studies performed are done *in vitro* or *ex vivo*. The *ex vivo* are studies being performed using explant cultures or increasingly using bioreactor systems. A large proportion of materials are taken further to carry out small animal *in vivo* tests. However, much fewer materials are then investigated in large animals; in some cases the reason is not a lack of function or compatibility, but a lack of facilities or sufficient funds. This is one area of biomaterials development that is often overlooked and leads to a large number of potentially promising materials not being fully investigated. Once in large animal studies, a number of materials that looked promising in small animal models then go on to fail functionally in the larger, more clinically relevant defect. Of the materials that are successful in the large animal proof of principle studies, there is still a major hurdle to overcome. Any material that wishes to be approved for clinical use must receive regulatory approval. For complex biocomposites, this could demand numerous safety tests, which may need to be performed under GLP conditions depending on their composition and functionality. As most research laboratories do not have such facilities, this entails contracting the testing to an external laboratory at significant cost.

As the complexity of the device increases, so does the required safety testing and the number of assays required. This aspect needs to be considered when developing new materials for translational use, as without the funds to perform the relevant regulatory tests required, any material will remain as a preclinical proof of concept. The development of new materials as an academic endeavor is of great value, but without access to significant funds for the safety and efficacy trials, the new material often remains within the laboratory. This has led to a trend of forming spin-off companies based on material platforms, in order to try and raise the required funds. This results in a tiny minority of the initial materials developed finally making it to

human trials. In part this is explained by the poor correlation of *in vitro* efficacy data to *in vivo* results. In the case of bioactive composites, this discrepancy can be even larger as the biological effect of a molecule on rodent cells may not be the same as that seen in larger animals or humans. The drop in efficacy between small animal and large animal studies is often attributed to the increase in defect volume being more difficult to overcome; however, the differences in biology should not be overlooked.

When using biocomposite materials that polymerize *in situ*, it is recommended that not only the potential toxicity of the final material is tested but also intermediate time points should be investigated as the material gels. For biodegradable devices, additional time point toxicity tests are also recommended during the degradation process to ensure the safety of the final degradation product(s) and all its intermediates. Initially, degradation is often investigated *in vitro*, in order to obtain some baseline data; however, *in vivo* tests allow for more accurate data on degradation rate to be obtained and can more accurately determine toxicity over time of the degradation products. This is particularly relevant in cases where the material can be actively degraded by the cells in the local environment. Toxicity may be local or may be distant from the site of implantation. Therefore, toxicity tests should not only focus on local toxicity, but also systemic effects should be determined by investigating distant tissues including, but not limited to, the lung, kidney, liver, spleen, lymph node, and heart.

### **Small Animal**

Various small animals are used during the initial stages of biocompatibility testing. Ectopic implantation is where the material is implanted into a site where it will not eventually be used. Orthotopic implantation is when the material is placed in the location where it is intended to function. Subcutaneous, or intramuscular, implantation of materials into rodents is a commonly used approach to determine biocompatibility in an ectopic site. Differences are seen between the two sites, most likely due to differences in the vascularization. Multiple test materials can be implanted per animal, with rats frequently having more implants due to their increased size. Acute and chronic responses can then be investigated using these soft tissue models. Implanted samples are excised at a later time point to allow for histological evaluation, in particular regarding unwanted immunological reactions and angiogenesis. On occasion, efficacy data can be obtained if there is a particularly robust osteogenic signal present, e.g., bone morphogenetic protein 2 (BMP-2). However, due to the ectopic nature of the implantation site, it is not generally advisable to use ectopic implantation to investigate efficacy of biomaterials. In particular the locally produced niche signals may actively inhibit new bone or cartilage formation giving a false-negative result.

Orthotopic implantation provides much more robust efficacy data. Orthotopic studies need to take into account the type of defect to be treated and the mechanism by which the target site naturally heals. Bones can form and heal by way of two different mechanisms, and the cellular transition and timing of the two mechanisms are different. Direct healing, or intramembranous ossification, is when the progenitor cells differentiate directly into osteoblasts. This type of healing is for flat bones and is



quite slow, with a few micrometers of new bone being deposited per day. It is also the most relevant mechanism for osseointegration of implant materials. For intramembranous healing, the calvaria is the site of choice. Endochondral ossification occurs when the cells initially differentiate into chondrocytes and produce a glycosaminoglycan-rich extracellular matrix or callus. Over time blood vessels penetrate and the cartilage is calcified. The calcified cartilage is invaded by osteoblasts and remodeled into bone. This is the most common form of fracture healing in long bones. Endochondral healing is most commonly investigated in a femoral defect.

Mice are often used for ectopic studies, whereas rats are more frequently used for orthotopic sites due to their increased size. For larger orthotopic defects rabbits can also be used. Small animal models have the advantage that studies are less expensive than large animal studies and as such can be used to screen multiple materials with the aim of selecting the most promising candidates. Small animal studies also tend to be shorter in duration, which allows for more rapid progress.

### **Biocompatibility**

A suitable use of ectopic implantation studies is to investigate potential immunological reactions against the material being implanted. As an extreme response, necrosis can occur due to toxic materials or degradation products. In reality, such events are not common, as toxic materials are normally identified during the *in vitro* toxicology tests. A more unpredictable risk is whether the material activates the immune system. Activation of the immune system can be acute or chronic, and due to the complexity of the immune system, a number of various responses can be observed.

Implantation of a material or device by its very nature leads to injury and a sequence of events involved in repair. The timing and extent of the response is dependent on the biocompatibility of the material.

#### **Sequence of host reactions following the initial injury after material implantation:**

- Blood–material interactions
- Clotting cascade
- Acute inflammation
- Chronic inflammation
- Granulation tissue
- Foreign body reaction
- Fibrosis/fibrous capsule development

The initial response to any implanted material is largely acellular. Blood comes into contact with collagen, leading to activation and aggregation of platelets. Fibrin and fibronectin are cross-linked, forming a mesh that prevents further bleeding and provides a framework on which cells can migrate. The platelets release cytokines that act as an attractant for invading cells, which digest the fibrin clot and replace it with a granuloma tissue. The invading macrophages clear the damaged tissue and

dead cells, and in a normal healing response, the inflammatory phase is resolved. In cases where a nonbiodegradable or slowly resorbed material maintains the immune response, the inflammatory phase can become chronic, leading to long-term complications. Macrophages and multinuclear giant cells in the granuloma are activated and attempt to clear all the material within the wound. In cases where this is not possible, they then attempt to “seal off” persistent material as part of a foreign body response (or foreign body reaction) (FBR). A foreign body response is an observable response of biological tissue to any foreign material present in the tissue, which can result in tissue encapsulation. The presence of an implant can change the healing response, normally delaying or perhaps even inhibiting healing. A granuloma forms containing macrophages, multinucleated foreign body giant cells, and fibroblasts. This also reduces the space being filled by tissue-specific cells that can enhance the repair. For some biodegradable materials, this can be a short-lived acute response, which may not actually hinder the healing process. As the material degrades, macrophages and giant cells remove the material by phagocytosis. It is the speed at which this process occurs that determines whether a more permanent fibrous capsule forms.

In some cases, implanted materials are also able to activate elements of the complement cascade. The complement cascade is protein-based part of the innate immune system, normally assisting phagocytic cells and antibodies in clearing pathogens from the body. The multiple proteins, and their cleavage products, enhance phagocytosis of antigens (opsonization), lead to cell rupture by creating pores in the cell membrane (cell lysis), and can assist by clustering pathogens (agglutination). A further role of the complement system is chemotaxis, where it attracts macrophages and neutrophils. If activated by a biomaterial, this cell attraction can prolong the inflammatory phase where no pathogens are present. Complement activation by biomaterials is a frequently overlooked aspect of biocompatibility.

### **Angiogenesis Models**

One aspect of biocompatibility is the angiogenic potential of the implanted material. With the exception of cartilage, tissues require the development of a new vascular bed to bring cells and nutrients to the developing tissue while removing waste products to maintain a physiological environment and pH. A healthy vascular system also reduces the potential for a bacterial infection to take hold as it provides a means to replenish immunological cells. Avascular areas are immunocompromised as there is a lack of supply of immune cells, leading to impaired healing due to a necrotic, hypoxic environment. Implant materials that aim to provide a scaffold on which a new tissue is formed have an absolute requirement to allow the ingrowth of new blood vessels, and this is dependent on the pore size of the material. In addition to assays for inflammation and foreign body response, angiogenesis can also be investigated by use of a skin fold chamber model. The dorsal skin fold chamber consists of two symmetrical frames with a cover glass observation window. One layer of skin and subcutis with the panniculus carnosus muscle, as well as the two layers of the retractor muscle, are completely removed from the back of the mouse.

The frame is attached with the material of interest implanted between the skin and a glass observation window, with a size typically being  $3 \times 3 \times 1$  mm. With the use of intravital fluorescence microscopy, both angiogenesis and inflammatory host tissue response to implanted biomaterials can be observed directly and monitored over time. In principle this model could be used for long-term analysis; in reality the elasticity of the skin fold weakens after 2–3 weeks limiting its use to this time frame. Therefore, this model is not suitable for long-term studies investigating the chronic foreign body reaction, but it can be used to investigate the early inflammatory and angiogenic host tissue response to the implanted material. In many cases it is this early response which is critical in determining the biocompatibility of the material.

A visualization of the angiogenic potential of materials can be performed in the skin fold chamber. Alternatively, histological sections can be prepared and the vascular density established by counting lumen stained with antibodies selective for endothelial cells, such as platelet endothelial cell adhesion molecule (PECAM-1, or cluster of differentiation 31 [CD31]) or vascular endothelial growth factor receptor 1 (VEGFR1). Indian ink can be injected into live animals prior to euthanasia, and this can be used to determine whether the vessels were functional by investigating the presence of the dye within the de novo vessels. More recently, functional analysis of angiogenesis using computed tomography imaging (Ct) has become increasingly common. Ct angiography requires the injection of a contrast agent into the bloodstream, which then allows the functional vessels to be visualized *in vivo* in a live animal. Due to the cost of the contrast agent, this method is mostly limited to small animals, but it can be readily applied to larger animals once cost-effective contrast agents are available.

### **In Vivo Infection Models**

The rise in the numbers of infection studies has also led to a development in animal models that more accurately mimic the clinical situation. An example of this would be the development of more clinically relevant infection models for internal fracture fixation. Previously, a fracture fixation plate would be applied to an intact bone and the bacterial inoculate added locally. Under these conditions there is limited soft tissue damage, limited impairment of the vasculature, and critically no bony defect whose healing could be negatively affected by the presence of bacteria. To overcome this, more recent studies have included an osteotomy (a cut into the bone) after application of the internal fixation plate or intramedullary nail. Bacterial inoculate is then applied locally as a trigger for an acute infection. The healing of this osteotomy defect can then be monitored, and the role of the biomaterial on the progression of the infection can be assessed. The ability of novel anti-infection biomaterials can then be investigated in a clinically relevant bone healing environment.

### **Efficacy**

The final aspect of *in vivo* biocompatibility testing is the ability of the material to allow the formation of a functional replacement tissue. This is also the ultimate test of any material as it needs to fulfill the desired function, and in the case of translation into the clinic, the new material needs to outperform the currently available products.

Efficacy studies are occasionally performed ectopically. This is not ideal, as even a failed result does not necessarily mean the material will fail in its purpose when placed in the target tissue. Studies into efficacy have only recently been considered part of the biocompatibility spectrum, but this aspect is becoming increasingly important as the complexity and functionality of materials increases. While efficacy studies are performed in small animals, regulatory requirements mean it must also be demonstrated in non-rodent mammals. This then leads to orthotopic studies in large animals, such as sheep, goat, and minipig.

---

## Large Animal

The final stage of biomaterials testing is normally the upscaling from small to large animals. This is in part to investigate the final full-sized device for its safety, but also its functionality can be better tested in an orthotopic defect of a similar size to that found in a patient. This produces increased challenges both from the infrastructure of the facilities required and from the actual technological challenge of healing a larger defect. The choice of large animal should reflect the actual question being asked by the study being performed. Traditionally the dog was a common large animal model, particularly for devices such as prosthetic hips, where it is still favored today. Being a companion animal raises many ethical questions, and for this reasons its use has dramatically reduced over the last two decades. In its place, goats and sheep have become increasingly popular. While both have reduced ethical concerns as they are farm animals, the use of sheep in particular has increased due to their docile nature, which makes them easy to handle. Sheep also has an advantage in orthopedics as their long bones are a similar size to human and they are of a similar weight. This allows implants that have been designed for humans to be directly tested in sheep without a need to be modified. For simple, or inert, implants requiring the more basic set of tests, biomechanical considerations such as these can be the principal driver when choosing the animal model. However, once the device has a more complex biological element, the choice of animal model must be made more critically. For this reason, the domesticated pig and minipig breeds such as Göttingen and Yucatan are becoming increasingly popular. The pig is regarded as a suitable animal model because of its hematological and cardiovascular similarities to humans. There is also a close DNA sequence homology between pigs and humans suggesting it would provide a more comparable genetic background when investigating response to pharmacologic or soluble mediators, such as growth factors. It is well characterized and bred to high-quality standards, and there is the potential for transgenics to be generated. It is also an accepted model from a regulatory standpoint. An EU FP6 Specific Support Action (SSA) called RETHINK was established with the objective to report on the impact of toxicity testing in the minipig as an alternative approach in regulatory toxicity testing. In 2010, its findings were published as a series of papers in the *Journal of Pharmacological and Toxicological Methods*, and they can be obtained from the RETHINK website [9]. The group concluded that the minipig is an advantageous model for investigating complex biotechnology products.

There are cases where nonhuman primates are still used for biocompatibility and toxicology studies. However, for cost and ethical reasons, their use is declining and they are increasingly being replaced by the minipig.

---

## Practical Examples of Biomaterials Testing

The implantation of various materials can lead to different outcomes histologically. Within this section some examples of biocompatibility assays will be illustrated.

The rabbit offers an intermediate-sized animal within which materials can be tested. It is large enough that bigger implants can be investigated and small enough to be easy to house and handle. This makes it ideally suited for orthotopic testing of materials intended for cartilage repair. The joint of a rabbit is of sufficient size that defects can be reproducibly created while also allowing the implanted material to be large enough to provide potential functional data. When considering immunological responses alone, younger animals can be used. For functional aspects, skeletally mature animals should be used, as there is a tendency for spontaneous healing in young rabbits. Within this example, materials were tested in New Zealand white rabbits, in an osteochondral defect measuring 2.7 mm diameter and 4 mm in depth. An osteochondral defect is one which penetrates the cartilage into the underlying bone, resulting in a defect that encompasses two different tissues. The cartilage is avascular, while the bone is highly vascularized. This allows interaction of the material with the bone marrow-derived cells and provides information regarding functional outcomes for both cartilage and bone. After 12 weeks of implantation, samples were decalcified and paraffin embedded and 6  $\mu\text{m}$  sections prepared. The sections were then stained with hematoxylin and eosin (H&E) in order to provide an overview. Initially, the appearance of the native host tissue should be assessed as a control (Fig. 4a). In the case of osteochondral defects, a reaction within the underlying subchondral bone should also be looked for. Normal osteochondral tissue has a thin layer of lightly stained cartilage over a layer of dense subchondral bone (Fig. 4a). The underlying marrow shows a more fatty marrow, in part due to the age of the animals. When a hyaluronic acid-based hydrogel is implanted into the defect, a healing response can be seen (Fig. 4b). A thicker layer of cartilage can be found in the defect area, with a dense layer of subchondral bone underneath. The subchondral bone is highly vascularized. On either side of the defect, the marrow appearance is similar to normal bone. Directly under the defect pockets of the biomaterial can be seen, which is slowly being replaced by marrow.

However, upon implantation of a polyurethane-based macroporous scaffold, a totally different response can be observed (Fig. 4c). While a cartilage layer, which is thicker than the native cartilage, has developed in the upper area of the scaffold, little underlying bone can be seen. The macroporous scaffold is still visible and there is significant reaction around the material.

At higher magnifications, it can be seen that with the hydrogel, the area is mostly acellular, and the marrow is starting to fill the bony structures around the edge of the residual gel (Fig. 5a). Within the PU group, the space is largely filled, large

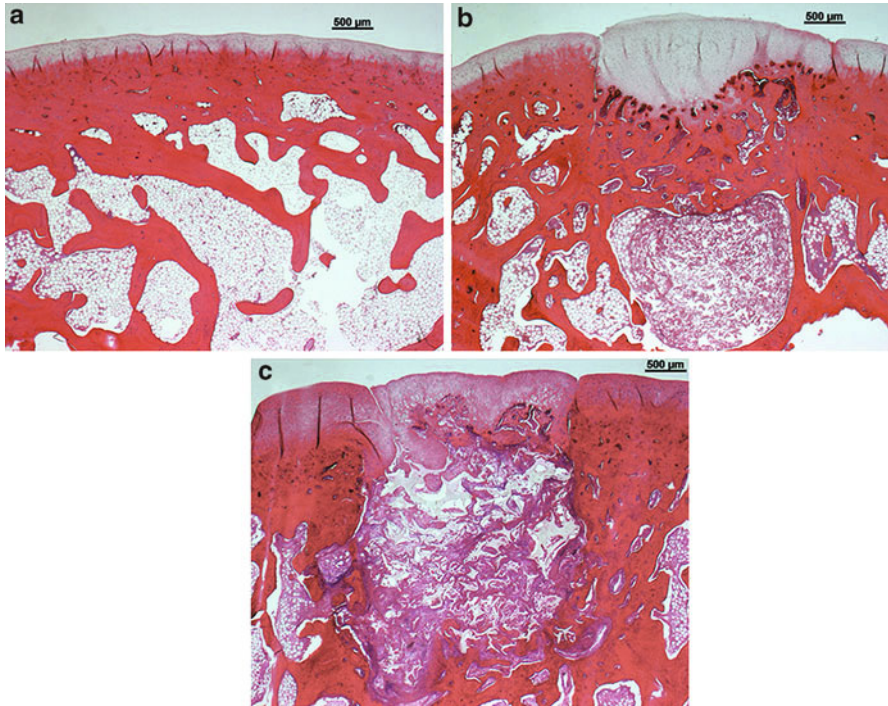


**Fig. 4** Low-magnification images of rabbit joints. (a) Normal joint, (b) osteochondral defect filled with a hyaluronic-based hydrogel and (c) osteochondral defect filled with a polyurethane macroporous scaffold. While healing is progressing in the hydrogel-filled defect, the macroporous polyurethane has induced unwanted immunological reactions and prevented the formation of a subchondral bone plate

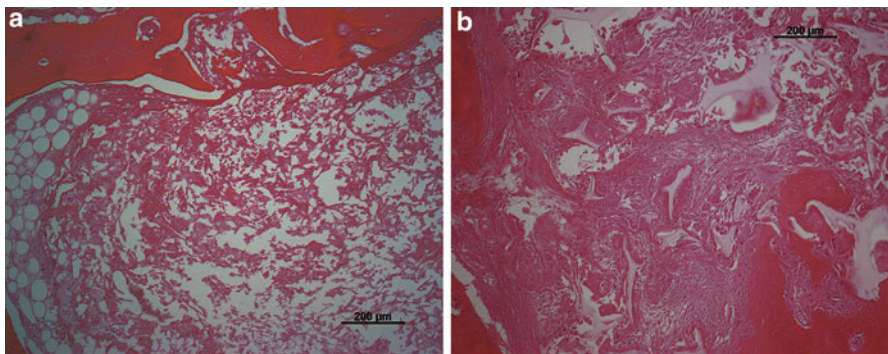


**Fig. 5** Higher-magnification images of (a) implanted hyaluronic acid-based hydrogel and (b) macroporous polyurethane scaffold. Remnants of the hydrogel can still be seen, with the marrow cavity edges being gradually replaced by marrow. A multicellular granuloma has formed between the pores of the polyurethane, which has shown little degradation

multinucleated macrophages can be seen, and an inflammatory granuloma has developed (Fig. 5b). The reaction has led to a complete inhibition of bone formation even after 12 weeks. This raises questions about its level of biocompatibility from both an inflammatory response and a functional aspect.

In cases where an increased number of samples within a bony environment are required, a larger animal model, such as the sheep, can be used. Due to the complexity of *in vivo* testing, it is to be expected that different animals will generate slightly different responses. Inbred animals will result in smaller variation, while outbred animals can result in significant heterogeneity. One way to encompass the heterogeneity is to increase the number of animals being used to test the materials, thus increasing the statistical power of the study and producing data with a greater confidence. This solution, however, is not ideal as the increased number of animals leads to increased cost and greater animal ethic concerns. An alternative solution is to implant a number of different materials into the same animal. This offers the advantage that within one animal, the response to the different materials will be standardized, as only one host response will be present; thus, any differences can be directly related to the material itself. Using an internal control within the same animal dramatically reduces the number of animals required to produce data with the same statistical power as that obtained from using one material per animal group.

One example of such a model is the determination of biocompatibility and osseointegration of materials with different surface properties. Polyetheretherketone (PEEK) is an inert material increasingly being used in orthopedic applications. One of the most common areas is the construction of spine cages, which are designed to be infiltrated by newly growing bone during spinal fusion. While PEEK has many attributes that are highly suited to orthopedic applications, such as being inert, possessing a high strength per weight, and being radiotranslucent, it is limited in its osseointegration due to its hydrophobicity. This can be modified by treating its surface to modify its hydrophobic properties, thus allowing for greater protein deposition and cell attachment. Once the surface has been subjected to various treatments, it is imperative to establish the safety of the new surface and its functionality, in this case to allow direct osseointegration. In order to do this, 4 mm cylinders of surface treated PEEK were placed in multiple circular defects in a sheep tibia. This orthotopic model also allows for load to be applied, as would naturally occur in a weight-bearing bone. Samples were left in place for 12 weeks before being harvested and being prepared for histological analysis. The calcified tissue was embedded in poly(methyl methacrylate) (PMMA) polymer resin to allow for hard tissue histology. Sections measuring 120  $\mu\text{m}$  in thickness were prepared and stained with Giemsa eosin as a general stain. With standard PEEK the expected lack of integration can be seen (Fig. 6a). A thin film of fibrous tissue (stained blue) can be seen to surround the material. At higher magnification (Fig. 6b), the nuclei within the fibrous tissue can also be distinguished. The bone itself (pink) looks healthy with the osteocyte lacunae predominately occupied and a normal looking marrow cavity. No local immunological response can be seen. Looking at the surface treatment

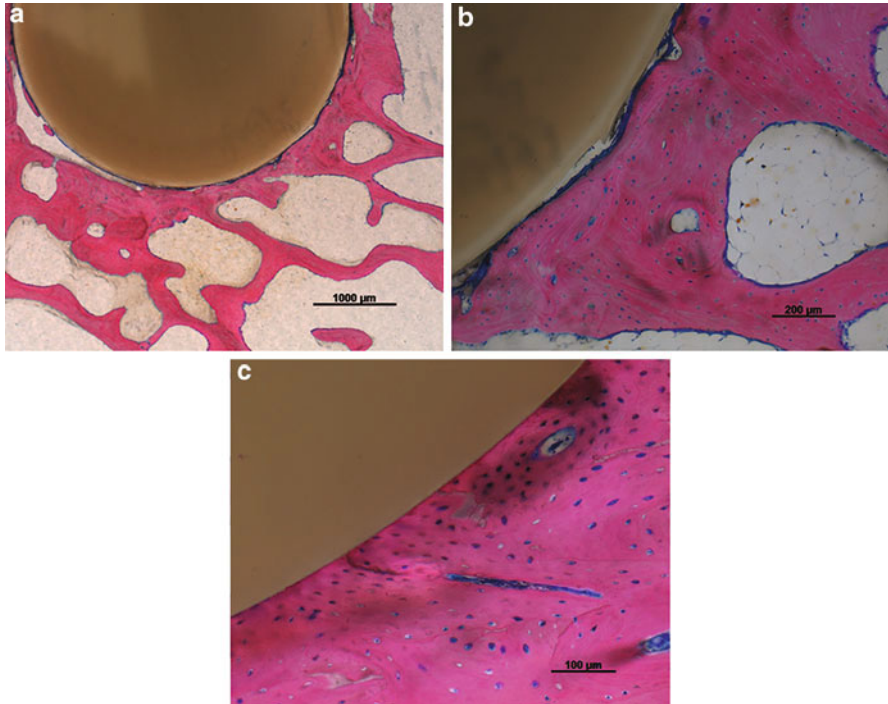


**Fig. 6** PEEK cylinders implanted into sheep tibias. The standard PEEK material (a, b) has a thin fibrous layer (stained blue) surrounding the material. All other aspects of the bone look normal. Treated PEEK (c) demonstrates an intimate contact between the new bone (pink) and the material surface

group at high magnification (Fig. 6c), the same healthy bone with numerous osteocytes can still be seen, with no indication of a negative immunological response. However, in this case, there is a tight integration of the bone directly with the material, with no fibrous capsule (blue stained material) surrounding the PEEK cylinder.

Within the two examples described above, different animal models were used for different applications, and the animal model used was dependent on the number of samples and the type of investigation. Neither the inert PEEK nor the surface-modified PEEK resulted in a localized immunological reaction in sheep, yet the difference in function was clearly observed. However, the macroporous polyurethane did lead to an unwanted immunological response, and this then led to an inhibition of bone remodeling within an osteochondral defect model in rabbits. The lack of an immune response, and the robust bone formation in the same type of defect using a hyaluronic acid-based material, demonstrates that the effects seen with the polyurethane scaffolds were a material-directed response and not a general lack of healing associated with the particular defect site. In both cases, the use of correct controls assisted with interpreting the data obtained.



## Species Differences

The choice of species used for *in vivo* studies does not only include a consideration of the size and weight-bearing potential of the animal. The macro- and microanatomy of the bone, as well as the general physiology of the animal, should also be taken into account.

As biocomposites become more complex and include aspects such as biological stimulation and the incorporation of growth factors, species differences when looking at the response of the material need to be considered more closely. These differences can initially be investigated *in vitro* by comparing the cell behavior of cells obtained from the animal of interest to cells obtained from humans. To accurately predict the human response to a particular dose of released growth factor or soluble mediator, it is critical that the biology of the animal model is comparable to the biology of humans. While this cannot always be achieved, at a minimum an understanding of the differences must be present in order to correctly interpret the data while realizing its limitations. A number of differences have been observed, especially between rodent and human cells. Some of these differences will be due to age-related factors such as young animals being used for studies while adult humans are often the actual therapeutic target. However, a number of these differences are species specific and therefore will change the outcome of the *in vitro* and *in vivo* tests. A common problem is to focus entirely on rodents, building a large body of data. If these data are species specific, this can then result in a failure when changing to humans or even to other small animals such as rabbit. Indeed, functional and efficacy differences have even been observed between rats and mice. For example, the effects of expanded polytetrafluoroethylene (ePTFE) were compared between Sprague–Dawley rats and 129-SVJ mice. Angiogenesis around the implant, neovascularization of new vessels penetrating into the pores of the material implants, inflammation, and fibrous encapsulation were assessed. While no differences were observed in angiogenesis or neovascularization, significant differences were seen in the number of activated macrophages and giant cells between the two species. It was concluded that due to the rat's more extensive inflammatory response, it may provide a more appropriate model of inflammatory cell recruitment and differentiation than the mouse. It has also been shown that the foreign body reaction to biodegradable materials is different not only between the rat and mouse species but also between different strains of each species. The foreign body reaction is different to a much greater extent between the mouse and the rat while only slightly differing between strains of the same species. When scaling up to larger animals, further differences can be seen. This is part of the reason why small animal studies alone are insufficient and regulatory agencies require studies be performed in non-rodent mammals.

These differences can become more apparent when investigating the influence of biologics. Over time, a better understanding of the differences in the general immune response of various strains and species is developing. This then requires a constant monitoring of the literature to allow for more informed choices to be made when selecting the correct animal for the study at hand.

## Future Directions

Increasing consistency between biocompatibility studies performed at different research institutes is still a major challenge. This would require changes at multiple levels of the process. For complex biocomposite materials, the individual nature of the material must be taken into account to select the most relevant biocompatibility tests, and this in itself will lead to an inherent variability between testing sites. To a degree this cannot easily be overcome; however, more detailed publications, with a greater justification of the models employed, would at least increase the general understanding. For increased translation to the clinic, ultimately a small number of test materials, each tested in groups with large samples sizes and in multiple species, will be required to ensure biocompatibility and functionality. For this to become a reality, more predictive *in vitro* and small animal screens will be required to accurately assess potential and limit the number of candidate materials that are moved through the pipeline. A number of modifications to current testing protocols could potentially improve this situation. Adoption of a set of *in vitro* standards would lead to improved consistency between laboratories, in particular the addition of a comparison group that would be performed at all institutions. These standards would need to be more explicit and would need to describe methods that can be reliably repeated in multiple laboratories in multiple countries. This could be achieved by choosing a cell line, such as SaOS-2, which is then seeded at a specific density into a specific culture vessel. Defined assays could then be performed at clearly defined time points. This would lead to a dataset that should be fairly comparable between different laboratories, providing a baseline to which other data can be compared. For this to become a practical reality, it would also be necessary to develop a standardized, defined, serum-free medium for *in vitro* studies. The natural variation present in serum is not compatible with a testing regime that will be consistent over time, and as one serum batch is limited in volume, it is not possible to supply too many different laboratories with the same serum. Some groups attempt to overcome this by buying sufficient quantities to last a number of years, but this is limited by expiry date and still will require stocks to be eventually replenished with a different batch.

One of the greatest challenges to the implementation of novel orthopedic materials is how to screen huge numbers of various materials in order to reliably select a small number of promising candidates for further investigation. Large animal studies to investigate material biocompatibility and efficacy are costly and lengthy. To an extent this is unavoidable, and thus, more predictive screens earlier in the process, which are able to eliminate less promising materials, are desperately required. The development of more predictive *in vitro* screens for efficacy would reduce the number of materials taken to the later *in vivo* testing stage. This would lead to more focused studies with larger number of samples per group that allows for greater statistical power. It is not uncommon that due to the desire to investigate as many compositions as possible in the same study and produce a scientific publication of greater interest due to a broader range of data, experiments can be flawed at the design stage by having too many groups and too few samples per group. This results in inconclusive studies, making it more difficult to make decisions on suitability with

any degree of confidence. The downstream effect of this is that potentially interesting materials are discarded at an early stage due to a seemingly lack of statistical significance.

Where materials are determined to have a statistical difference, repeating studies at more than one site would also lead to a greater confidence in the results obtained, as the robustness and reproducibility of the data would also be established. This, however, is difficult to achieve due to the costs associated with performing the studies, and in the current “publish or perish” scientific environment, it is often difficult for investigators to establish an academic career when performing the required confirmation studies. This is a hurdle for translational studies in general; mechanisms and metrics to adequately assess translational research still have not been developed, creating a challenge for such studies. For clinical use, implants must be easy to handle and robust and have a degree of tolerance to improper use. These features can also be more easily assessed by multiple sites testing a single material. All too often, what appear to be highly promising materials are actually too impractical to use in a general uncontrolled setting.

More improved and better regulated bioreactor systems are currently being developed; these will help bridge the gap between classical *in vitro* tests and *in vivo* studies. In particular the standardization of perfused tissues from multiple cell types will yield standardized 3D systems where the influence of materials on toxicity and tissue development can be better assessed.

## **Organ on a Chip**

One of the most exciting recent developments has been in the field of microfluidics and the aim to produce various organ mimics within a “lab on a chip.” While still in its relative infancy, there is a concerted drive towards producing organ, or organ system, mimetics at the microscale, which can be produced from just a few cells. These platforms still have a significant development to undergo before they can be routinely used but they have shown initial promise, and they are potentially extremely powerful *in vitro* tools. With sufficient development, they have the potential to replace large numbers of animal tests while at the same time resulting in more reliable data as they would be performed using human cells. This would effectively produce a more *ex vivo* approach to materials testing that would lead to much greater accuracy.

Tissues such as heart, lung, liver and pancreatic islands are being developed and incorporated into microfluidic platforms. The aim is to produce the tissues in a reproducible manner with multiple samples allowing for replicates. The low cell number and small volumes lead to dense microarrays which are extremely cost-efficient while still producing data from a large sample size. Multiple assays can then be performed with microliter volumes, allowing for a large prescreen of molecule libraries rapidly and at low cost. One attempt to standardize the assays has been the utilization of cells derived from induced pluripotent stem cell lines (iPS cells), which results in an unlimited supply of well-defined cells from human origin. Induced

pluripotent stem cells are generated by taking a somatic cell, such as a fibroblast from skin, and reprogramming it using a cocktail of factors to a more primitive, embryonic-like state. These cells then contain all the pluripotent benefits of embryonic stem cells, allowing multiple cell types to be generated, without any of the inherent ethical concerns. This technology can then be expanded to cell lines derived from multiple donors to establish the extent of variation derived from host heterogeneity. In addition, donors containing a genetic predisposition to various diseases can be produced, leading to a disease-specific cell line. This can also be critical in determining relatively simple questions regarding donor variability and could be used to detect potentially fatal effects that would normally only be observed in a small subset of patients. It is known that material properties alone are not entirely predictive of the biocompatibility response. All implanted materials interact with the host tissue and the host response can also be variable. Age, sex, comorbidities and the required medications taken by the patient, lifestyle, and the patient's general health can all influence the final reaction to the implanted material. This is particularly pertinent when considering biologically active biocomposites. Lab on a chip would provide the ability to screen materials against a number of cells derived from multiple donors, providing a more detailed characterization of the material properties. Materials can then be investigated in more detail than ever before as different genetic backgrounds can be compared to ensure a wide range of tolerability in differing hosts.

For this to become a reality, controlled differentiation and preparation of the cells and microtissues is required, and this is the main area which still needs to be established. While iPS cell lines can be generated relatively easily, there can be a drastic variation in their underlying phenotype and no established criteria to clarify these differences exist. At a superficial level, such as investigating some functional outcomes, the differing cell lines can appear remarkably similar. Yet more detailed sequencing of the DNA can reveal a number of differences, at both the genetic and epigenetic levels. Furthermore, it is difficult to differentiate cells *in vitro* into stable, mature, tissue-specific cell types. This is still a challenge irrespective of the initial source of cellular material. Reliable differentiation protocols will be required to generate a reproducible, homogenous cell source from the various donors. In addition, unless the generated cell behaves in an identical manner to primary cells obtained from a patient, the responses obtained cannot be considered physiological, weakening their reliability.

Once a source of phenotypically stable, tissue-specific cells can be identified, a further development is the need to produce structurally relevant tissue that behaves in a functionally comparable manner to the natural organ. A collection of liver cells is not necessarily the same, and may not function in the same way, as a small piece of liver tissue. This will be more challenging for tissues made of different cell types that actively collaborate to produce the desired function. For a lab on a chip system to become a reality within a biocompatibility screening algorithm, the microorgans produced must reliably mimic the function and the physiological interaction between various organs within a human host. Otherwise, the observed response will not be comparable to that seen *in vivo*.

Nevertheless, these new platforms have the potential to revolutionize biomaterials testing, and significant advances have already been made. Producing microorgans within a microfluidic platform would also allow for different organs to be combined either parallel or sequentially. Using these multiple organ platforms, the effect of cross talk between organs and the metabolism of the materials and their derivatives can be analyzed to a level only currently possible in live animals.

---

## Summary

The concept of biocompatibility has evolved over the last decade from one of developing and testing inert materials which do no harm, to a highly complex algorithm used to investigate safety and functionality of combinatorial material devices. Materials, their intermediates, and the compounds they release all need to be characterized for their safety and tolerance by the host. Their effects may be local or distant and, due to the increasing complexity of the materials, may also play a role in directing the healing response. This has led to an increase in high-throughput screens and miniaturization to allow for more assays with reduced reagents. As materials science has progressed, and the applications of the devices has expanded, the incorporation of functional aspects into the biocompatibility testing protocols has increased. In addition, the choice of animal model is increasingly incorporating biology in addition to the more classical biomechanical environment.

**Acknowledgments** The authors thank Dr. David Eglin, AO Research Institute Davos, for providing the histological example sections. Both authors are supported by the AO Foundation and are part of the EU-FP7-LARGE-Biodesign program to develop novel biomaterials testing algorithms.

---

## References

1. Vacanti J, Vacanti CA (2007) Chapter one – the history and scope of tissue engineering. In: Vacanti RLL (ed) Principles of tissue engineering, 3rd edn. Academic, Burlington, pp 3–6
2. Williams DF (2008) On the mechanisms of biocompatibility. *Biomaterials* 29:2941–2953
3. Summary of typical bone-graft substitutes that are commercially available (2010) <http://www.aatb.org/aatb/files/ccLibraryFiles/Filename/000000000323/BoneGraftSubstituteTable2010.pdf>
4. Czekanska EM, Stoddart MJ, Richards RG et al (2012) In search of an osteoblast cell model for in vitro research. *Eur Cell Mater* 24:1–17
5. Alberts B, Johnson A, Lewis J et al (2007) Molecular biology of the cell. Science, Garland
6. Stoddart MJ (2011) Cell viability assays: introduction. *Methods Mol Biol* 740:1–6
7. Smith EL, Kanczler JM, Oreffo RO (2013) A new take on an old story: chick limb organ culture for skeletal niche development and regenerative medicine evaluation. *Eur Cell Mater* 26:91–106; discussion 106
8. Russell WMS, Burch RL (1959) The principles of humane experimental technique. Methuen, London
9. RETHINK <http://www.rethink-eu.dk/index.php?page=seven&id=16>

---

## **Part IV**

# **Clinical Performance in Bioresorbable and Load-Bearing Applications: Orthopedics**

Corrado Piconi and Giulio Maccauro

## Contents

Introduction .....	822
Design of Ceramic Components for Joint Replacements .....	826
Bioinert Ceramics in Joint Replacements .....	832
Alumina in Joint Replacements .....	832
Zirconia in Joint Replacements .....	835
Alumina-Zirconia Composites in Joint Replacements .....	837
Non-oxide Ceramics in Joint Replacements .....	841
Clinical Results .....	842
Clinical Results of Bioinert Ceramics in Hip Replacements .....	842
Clinical Results of Alumina and Zirconia in TKR .....	847
Clinical Results of Zirconia in Other Joints .....	849
Clinical Results of Bioinert Ceramic Composites in Joint Replacements .....	849
Ceramic-Related Complication in Joint Replacements .....	851
Trends and Perspectives of Bioinert Ceramics in Joint Replacements .....	853
Summary .....	854
References .....	854

---

## Abstract

Ceramics have a wide field of application in joint replacements. This chapter is focused on the application of oxide ceramics in joint replacement bearings. The development of alumina, zirconia, and alumina-zirconia composites for this application is traced since the early 1970s. The criticalities in the design of ceramic components for joint replacements are described, as well as their main causes of failures in clinical use. The clinical results of the different bearing

---

C. Piconi (✉) • G. Maccauro

Medicine and Surgery Department, Clinical Orthopedics and Traumatology Institute, Catholic University, Rome, Italy

e-mail: [corpico@libero.it](mailto:corpico@libero.it)

couples making use of ceramic components are reported, and the future tendencies in this field of application are summarized.

---

**Keywords**

Alumina • Alumina matrix composite • Alumina-toughened zirconia • Ceramic on ceramic • Ceramic on polyethylene • Clinical results • Magnesia-partially stabilized zirconia • Silicon nitride • Total hip • Replacement • Total knee replacement • Yttria-stabilized tetragonal zirconia polycrystal • Wear • Zirconia • Zirconia-toughened alumina • Zirconia platelet-toughened alumina

---

**Introduction**

The use of bioceramics in joint replacements is a well-established technology in arthroplasty. Ceramics, especially alumina ( $\alpha\text{-Al}_2\text{O}_3$ ) and zirconia (Y-TZP, Mg-PSZ), are used as components of hip and knee replacement bearings, while either calcium phosphate ceramics or bioactive glasses are used as osteoconductive coatings on surfaces of the implants in contact with the bone. Ceramics (especially monoclinic zirconia but also non-oxide ceramics, e.g., titanium nitride (TiN)) are also used as coatings on the articulating surface of metallic ball heads to improve the wear behavior of metal-on-polyethylene bearings.

Other chapters of this handbook deal with calcium phosphate ceramics and coatings in detail, and then this chapter will deal with the applications of ceramics in the bearings of joint replacement.

Ceramic components are in use in a number of joint replacements. Besides ball heads and inlays for hip replacement that represent their best-known application, modern ceramics are used also in condyles and tibial plateau for knee replacements, glenoid head for shoulder replacements, finger joints, and disk replacement in the spine (Figs. 1 and 2).

The ideal material to be used in a joint replacement would have an optimum equilibrium among several characteristics:

- Long-term stability in the physiological environment
- Biological safety of bulk materials and of its wear debris
- High-quality surface finish achievable
- Suitable mechanical properties both static (tensile and compressive strength, elastic modulus) and dynamic (fatigue strength, fatigue limit)
- Hardness (prerequisite for low wear and for stability of the surface finish)
- Surface wettability by body fluids
- Suitability for component design and manufacturing technology

In the case of ceramics, these tough specifications limit the selection to a few ceramic biomaterials: only oxide ceramics (alumina and zirconia) have been used clinically so far in this challenging application, although other ceramic materials



**Fig. 1** Ceramic ball heads and inserts for hip replacement bearings (Courtesy of CeramTec GmbH, Medical Products Division, Plochingen, Germany)



**Fig. 2** Ceramic knee replacement (Author's photo)

(e.g., silicon nitride ( $\text{Si}_3\text{N}_4$ )) are presently investigated in view of their use in joint replacement bearings.

The rationale for the use of oxide ceramic in joint replacements is in the need of minimizing wear of the joint. The wear of the bearing surfaces is still prominent among the complications that limit the long-term survival of arthroplasties. Namely, the host reaction to wear debris from the artificial joint – many of them less than  $1\ \mu\text{m}$  in size – starts a cascade of cellular reactions leading to osteolysis and

eventually to the aseptic loosening of the implant, making mandatory a revision surgery. The Swedish Hip Arthroplasty Register data show that more than one-half of the revision surgeries of total hip replacements (THRs) are due to aseptic loosening. Then, it is not surprising that surgeons and engineers devoted their efforts to the development of suitable wear couples for hip replacements since the very beginning of arthroplasty, because of the economic and social relevance of this problem, as revision arthroplasty is a surgery more difficult to perform and costly and has poorer outcomes than primary surgery.

The success of arthroplasty has increased the importance of wear performance of the bearings, because today patients – in comparison to the ones that underwent arthroplasty in the past – have higher expectations and intend to improve their activity upon returning to an active lifestyle. Moreover, many of them undergo primary surgery at a relatively young age and with a long life expectancy. This implies more stress and more motion on their THR and the need of an extended service life. CoC THR bearings are especially suited for these patients, because they demonstrate in randomized prospective clinical studies the absence of joint-related complications and a significant reduction in wear and related revision rates (see section “[Clinical Results](#),” this chapter).

Moreover, oxide ceramic wear debris elicit lower biological reactions than metallic or polyethylene ones. This was evident since the early ceramic implants [1] and confirmed in cell cultures performed on wear debris retrieved after hip simulator studies. The combination of a small volume of wear with the low biological activity of the debris gives the “functional biological activity of the debris,” as defined by Fisher and coworkers [2]. They reported a functional biological activity of the alumina debris 20 times lower than cross-linked polyethylene and 80 times lower than the conventional UHMWPE. The complications specific to metallic debris (e.g., metallosis, lymphocytic reactions, or pseudotumors [3]) are avoided. The high biological acceptance of ceramic wear debris allows avoiding the risk of systemic adverse reactions, an aspect which is especially relevant for patients with an active lifestyle and/or long life expectancy (Fig. 3).

So far, it is widely accepted that ceramic-on-ceramic (CoC) bearings have the lowest wear among the bearings currently available and that the ceramic particles generated have the lowest biological reactivity in comparison with the debris coming from the other bearing couples commonly used in joint arthroplasty.

This is the reason why the use of ceramic heads in hip replacement bearings is spreading: in some European countries (Austria, France, Germany, Italy, and Switzerland), more than 50 % of the hip implants are making use of ceramic ball heads, and in Asian countries, e.g., Korea, 72 % of THRs have an alumina ball head. Also in countries where the introduction of ceramic bearing components took place later (the USA, China, India, Eastern European countries), the number of ceramic components used in clinics is increasing.

Several companies are today manufacturing ceramic ball heads for THRs (Table 1). Some of them are also making inserts for the acetabular component of the implant, while a few of them are offering components made of alumina-zirconia composites for use in joint replacements (zirconia-toughened alumina (ZTA),

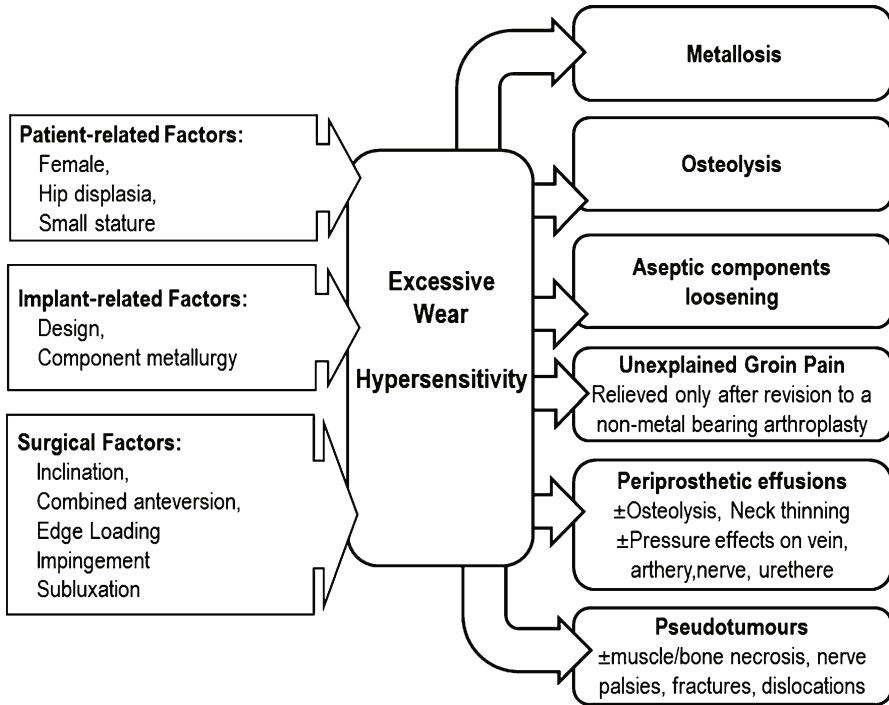


**Fig. 3** Adverse reactions to metallic debris (Adapted from Ref. [3])

**Table 1** Manufacturers of ceramic components for joint replacements

Company	Country	Materials
Ceraver Osteal	France	Alumina
CeramTec GmbH	Germany	Alumina, ZPTA
Mathys Ltd. Bettlach	Germany	Alumina, ZTA, ATZ
C5 Medical Werks	USA	Alumina, ZPTA
IFGL Refractories	India	Alumina
Metoxit	Switzerland	ATZ
Kyocera Medical Corporation (formerly JMM)	Japan	Alumina, ZTA
Morgan Technical Ceramics	UK	Alumina, ZTA

alumina-toughened zirconia (ATZ), zirconia platelet-toughened alumina (ZPTA)). Presently, CeramTec GmbH (Plochingen, Germany) is the market leader with more than 10 million BIOLOX<sup>®</sup> components sold and more than one million pieces per year delivered to the hip implant manufacturers. On the other hand, ceramic knee replacements are still a niche market in orthopedics. KYOCERA Medical Corporation (Kyoto, Japan) which was a pioneer in this field is manufacturing a device made of zirconia (Y-TZP) which was implanted in Japan since 2001 and is now in clinical trial in the USA, while CeramTec GmbH is manufacturing two TKR designs made of the alumina matrix composite (BIOLOX<sup>®</sup>delta).

In summary, the development of ceramics for joint replacement undertaken during the early 1970s by pioneers in arthroplasty from France, Germany, and Japan has proven its effectiveness in more than 40 years of clinical use [4]. The introduction of new alumina qualities combined with substantial technological improvements resulted in the marked enhancement of the properties of the material, e.g., the bending strength of BIOLOX<sup>®</sup> ceramics has been increased more than threefold since their introduction into the market.

Currently, the most commonly used representative of the fourth-generation alumina ceramics for hip arthroplasty – BIOLOX<sup>®</sup> *delta* – thanks to the synergistic toughening effect of zirconia and of platelets homogeneously dispersed in the alumina matrix, incorporates significant improvements in toughness and strength in comparison to its predecessor BIOLOX<sup>®</sup> *forte*, resulting in remarkable advantages in terms of wear reduction even under worst-case conditions (joint separation, edge loading, etc.) and a tenfold decrease in failure rates.

## Design of Ceramic Components for Joint Replacements

The processing of ceramic components for joint replacements has been outlined in Chap. 4, “► [Bioinert Ceramics: Zirconia and Alumina](#)” of this handbook.

### Ceramic Heads for Total Hip Replacements

The introduction of ceramic heads in arthroplasty put in evidence the problem of the connection between the ceramic head and the metallic stem. The attempts made using epoxy resins or solders to stabilize the ceramic head onto a metallic trunnion on the stem led to a series of failures in the early years of use of alumina in THRs. The introduction of the taper fitting was a brilliant solution to the problem, due to researchers of the companies Sulzer (Winterthur, Switzerland) and Feldmühle (now CeramTec GmbH, Plochingen, Germany). The taper fitting, used in clinics since 1974, offers several specific features:

- Connecting the head to the stem is easy and quick to perform, easing the handling of the head in the surgical theater.
- The connection is stable for the long time, and ball-to-stem movement is eliminated.
- No adhesives or solders are necessary that may pose problems of stability in the long term.

Moreover, taper fitting offers the advantage of modularity. Thanks to the taper fitting, a stem may host metallic or ceramic heads that can be coupled to an acetabular component made up of a metallic shell hosting ceramic, metal, or polyethylene inserts (see Fig. 4).

Implant modularity encompasses necks with different offsets and stems with several neck angles, giving rise to a family of implants. It provides the surgeon a

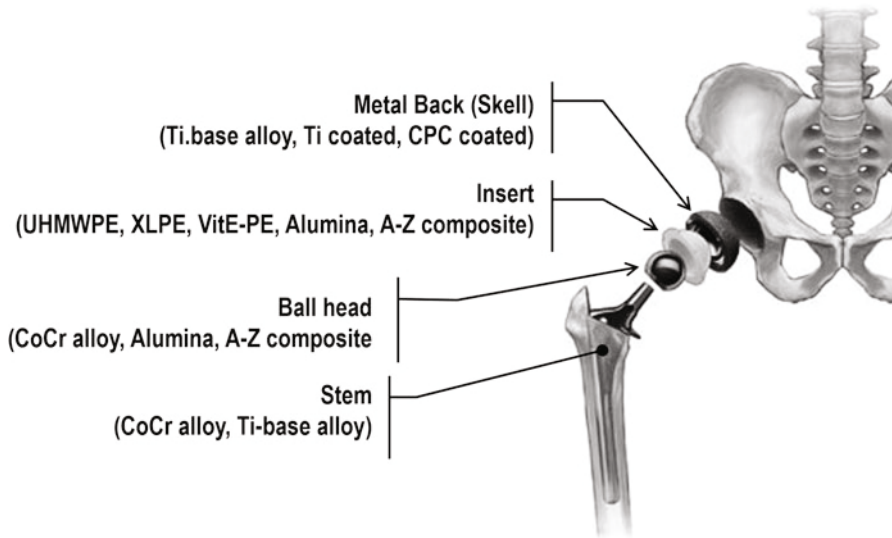


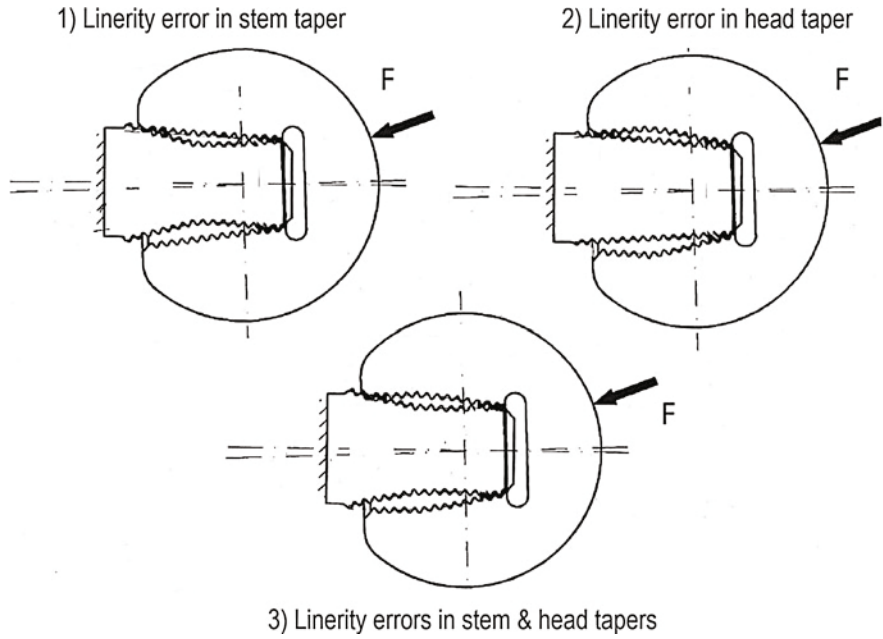
**Fig. 4** Total hip replacement, schematic

way to select the size of implant that better suits the biomechanics of the patient's hip and the wear couple that suits better the age range and activity level of patients.

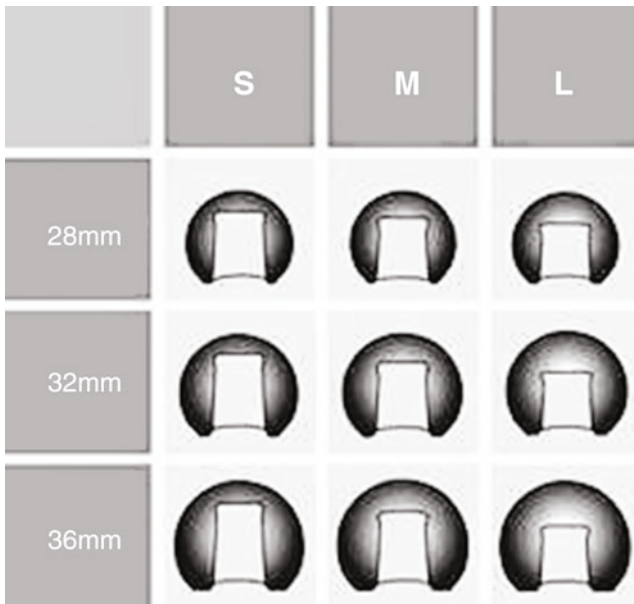
Besides the coupling between ceramic surfaces in ceramic bearings also the interface of the ceramic components with the stem and the metal back is playing a major role. The loads applied to the joint due to patient activity generate two main tensile stresses in the ceramic head, e.g., in the head dome due to bending, and homoradial (hoop) stresses close to the taper surface. The stress distribution and intensity within the ceramic head is then depending on the friction between the taper surfaces and on characteristics, e.g., extent of the contact, cone angle, surface roughness, roundness, and straightness.

It is noted that perfect matching of the metal taper and of the ceramic cone is an ideal representation of the connection: in real life there are unavoidable dimensional tolerances during machining of the metallic and ceramic surfaces through which the loads are transferred between the two components (Fig. 5). To compensate for the machining tolerances, manufacturers make use of the ductility of metals, the effects of which are enhanced by providing grooves to the taper surface ("structured" taper). Provided that the angle of the bore into the head is slightly wider than the trunnion one, when the head is positioned onto the trunnion and loaded, the tip of the grooves will be deformed progressively. In this way, the contact area is increased smoothly and stress concentrations are avoided. Also the friction torque is increased, improving the rotational stability of the coupling. A real diffusion joint is obtained, as it is evident observing in the taper of retrieved ceramic heads the marks of transferred metal.

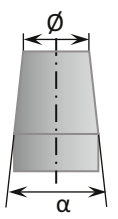
A critical point in the design of the taper fitting is the extension of the contact surface. In THRs the taper fitting offers the advantage of the control of the protrusion



**Fig. 5** Schematic of the effect of shape errors after taper machining



**Fig. 6** Taper fitting and neck length in ceramic THR ball heads

**Table 2** Different tapers designated “12/14” by the manufacturers (after Schreuber LF et al., 2014 [6])


Taper #	1	2	3	4	5	6
Ø (mm)	12.41	12.53	11.0	12.57	12.41	12.51
α	5°40'0"	5°40'0"	5°40'0"	5°37'46"	5°2'0"	5°40'30"

of the ball head from the stem neck using heads of different sizes as outlined previously. There are commonly three selections for the neck length, namely, +3.5 mm (L, long), 0 mm (M, medium), and -3.5 mm (S, short) (Fig. 6), for the same stem.

A consequence is that the areas of the contact surface for L-type are smaller than M-type and much smaller than the S-type. On the other hand, for a given head diameter, the S-type has a smaller section in the apical part of the dome in comparison to heads with other neck lengths. This implies that the design of long neck (L-type) and short neck (S-type) heads is more challenging from the viewpoint of mechanical design, especially in diameters 28 mm or less.

A conclusive remark concerns the errors that may happen in coupling heads and tapers from different manufacturers: many taper angles in the range from 5° to 6° are used by implant manufacturers of hip replacements. Besides angles, taper connections may differ in length and in surface roughness, because each manufacturer owns design and machining tolerances. That is, notwithstanding the efforts made to standardize the taper fitting establishing its geometry and finish (the so-called EuroCone), so far there is no standard taper for use in arthroplasty. Although most of the orthopedic companies are using 12/14 tapers in their products, significant differences in design can be observed, as depicted in Table 2. Calés et al. [5] demonstrated that the stress distribution in the ceramic ball head could have critical variations depending on the design of the coupling to the metallic taper.

Care should be taken when using ceramic heads and stems from different manufacturers or from different implant models of the same manufacturer. The use of bearing components identified by the manufacturer as part of the same implant system is recommended, as well as to avoid the use of wear coples not authorized by the manufacturer of the device. That is, besides the nominal diameter, manufacturing tolerances are unavoidable and are different for each THR manufacturer. Randomized coupling may lead to catastrophic wear and to the failure of the implant: “never mix and match” is the golden rule.

### Ceramic Inserts for Total Joint Replacements

Today, THR ceramic ball heads can be coupled either to a ceramic or to a polyethylene (UHMWPE, XLPE, Evit-XLPE) acetabular component. This component

(socket) consists of a metallic shell (metal back) containing a ceramic liner. The socket may be preassembled (in the so-called monoblock cups) or may have a modular design: a ceramic liner (or inlay) is fixed into the metallic shell by a taper connection. Some designs allow hosting of inserts made of either polyethylene or CoCr alloy as an alternative to ceramic. The shell taper must be self-locking, but it must also be possible to remove the liner intraoperatively, e.g., in case of mispositioning within the metal back, or during revision surgery, if necessary. The shell taper should provide torsional stability and large enough interfacial surface to avoid stress concentrations. As described for ball heads in 1.1.1, the initial stress distribution within the ceramic liner depends on the difference between the angle of the insert and the angle of the taper in the metal back. Many of the considerations made in the previous paragraph about the taper connection of the ceramic head to the stem apply also to the taper connection in the socket. Loads are transferred from the metal back to the liner through the taper interface, and then errors in coupling may determine disastrous stress concentrations. The high safety of modular sockets hosting ceramic liners depends on the roundness, straightness, and roughness of the metal-ceramic interface. Moreover, the design of the mechanical interlock between the liner and the metal back has to assure the stability of the inlay, e.g., when seated into the metal back, the liner has to resist pullout, torsion moments, and/or lever-out moment due to the forces exerted on it when implanted.

Besides the taper angle, the point of early ceramic-to-metal contact in metal-backed ceramic inserts is different from the ones used in the design of ceramic ball heads. The inner angle of the metal back has to be slightly narrower than that of the ceramic inlay in such a way that the ceramic-to-metal contact after insert installation takes place in the region near the metal back rim. Care has to be taken that when the liner is completely seated into the metal back, the contact will be limited to the tapered part only, avoiding contact in the dome region of the metal back to avoid the pushout of the inlay. Opposite considerations may be applied when using polyethylene inserts in the same metal back: due to the difference in elastic properties between ceramic and polyethylene, the initial contact of PE inserts has to take place in the inner part of the taper and has to be extended to the dome region to achieve the maximum load transmission with minimum deformation, avoiding in such a way the “brake” effect on the ball head.

### **Ceramic Knee Replacements**

The rationale for the use of ceramics in knee replacements is in the advantages in terms of wear and biocompatibility that ceramics have in comparison with metals. Using ceramic condyles, the wear of the polyethylene tibial surface is reduced in comparison with metal condyles of the same design because of the scratch hardness of ceramics higher than the metals one, implying better resistance to damage that will save the polished surface of the articulating condyles, combined with the degree of finish achievable in ceramic surfaces which is far beyond the one achievable in metals. Moreover, ceramics will allow better lubrication of the articulating surface due to their high wettability by the synovial liquid and then a lower wear rate of the PE liner of the tibial component. A further reason for the selection of ceramics is



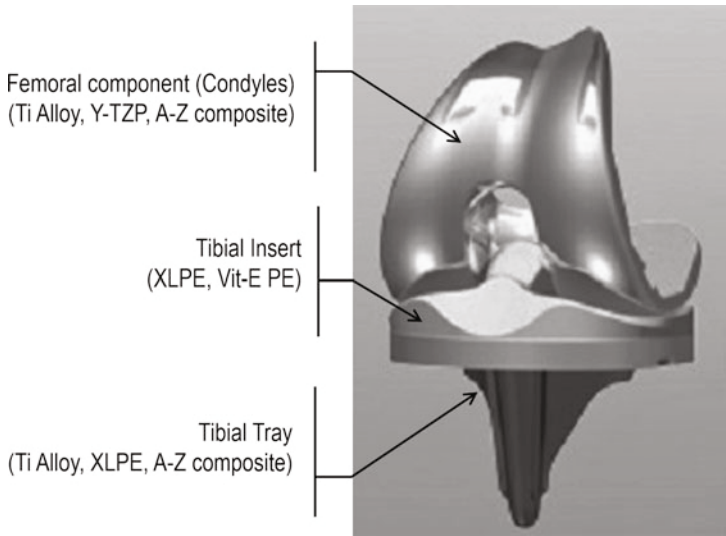


**Fig. 7** Total knee replacement, schematic

linked to the growing incidence of allergic reaction to metal ions. Today patients may be bearer of several metallic implants within their body. The introduction of ceramic devices will limit the extent of metallic surfaces, decreasing the extent of the sources of potentially sensitizing ions.

Total knee replacements (TKRs) are made up of three main components: the femoral component, the tibial component that is composed of an insert and a tray, and a patellar component. The femoral component and the tibial tray are usually made of metal alloys (CoCr, Ti-based alloys, stainless steel). Polyethylene (UHMWPE or XLPE) is used for the tibial insert and the patellar component (see Fig. 7).

Aseptic loosening of each one of the main components of the implant may occur, due to high wear of the articulating surfaces or due to mobilization of the components following bone resorption for stress shielding.

Total knee replacements modify the load transfer to the host bone, and according to Wolff's law, bone remodeling occurs in the zones "shielded" by the implant, especially in the parts behind the anterior flange of the femoral component. The wear debris due to the mobilization of the components can damage the surface of the femoral component (third body wear), increasing the wear of the tibial insert leading eventually to aseptic loosening.

The use of XLPE increases the resistance of the insert to delamination, but it cannot withstand the abrasive wear due to a damaged metallic counterface, scratched and ridged by hard third bodies. In addition, the ions released by the metallic debris could elicit reactions of the immune system in allergic patients.

Ceramics may constitute a valid solution both to wear of polyethylene and to potential allergy to metal ions in total knee replacements. First, thanks to their

hardness, which is much higher than that of the metal alloys, ceramics have a much higher resistance to scratching. Second, should scratching occur, it is not associated to ridges for the lack of plastic flow [7]. Third, the better wettability of oxide ceramics in comparison with metals is a further factor contributing to wear reduction of polyethylene, as the clinical record of ceramic-polyethylene bearings in total hip replacements shows.

As described earlier in this chapter, ceramics have tensile strength much lower than compressive and shear strength and are sensitive to stress concentrations that can stimulate the inherent defects to grow. This behavior is relevant in the design of ball heads and inserts for hip replacement bearings notwithstanding their simple geometry. It becomes of paramount importance in knee replacements for the complex geometry of the implant, especially of the femoral component. The design of alumina replacement resulted then in rather being bulky, consequently requiring massive bone resections. The use of toughened ceramics solved the problem, the thickness of ceramic components being the same for metal and ceramic femoral components but different in some specific design features.

The femoral component experiences two opposite loading conditions [8, 9]. The first one termed “regular loading” takes place on leg extension, as the posterior condyles are loaded against the tibial plate, while the patellar component loads the anterior condyles due to the quadricep tension. In this situation, the femoral component tends to “close” on itself (the posterior condyle and the patellar region tend to be nearer) thus putting the articulating surfaces in tension. The opposite situation occurs during “wedge loading,” a situation that occurs during the insertion of the femoral component onto the resected femur when the posterior condyle and the patellar region tend to increase their distance. The wedge loading could be especially critical if the design of the device neglects the stress concentration that takes place on the back face at the discontinuities between the implant surfaces corresponding to the resection planes.

---

## Bioinert Ceramics in Joint Replacements

The chemical, physical, mechanical, and biological behavior of alumina and zirconia are discussed in detail in Chap. 4, “► [Bioinert Ceramics: Zirconia and Alumina](#)” of this handbook. In the following these aspects are briefly mentioned, if necessary for clarity of the text.

### Alumina in Joint Replacements

#### Alumina in Hip Replacements

The alumina ceramic selected for biomedical application is alpha-alumina, a close-packed hexagonal arrangement of aluminum and oxygen ions which is very highly thermodynamically stable. The alumina in clinical use today for the construction of ball heads and inlays for joint replacements is the result of more than 50 years of

**Table 3** Selected characteristics of the different generations of alumina bioceramics

Property	Units	Alumina (1970s)	BIOLOX <sup>®</sup> (>1974)	BIOLOX <sup>®</sup> forte (>1995)
Al <sub>2</sub> O <sub>3</sub> content	Vol %	99.1–99.6	99.7	>99.8
Density	g/cm <sup>3</sup>	3.90–3.95	3.95	3.97
Av. grain size	µm	≤4.5	4	1.75
Flexural strength	MPa	>300	400	630
Young's modulus	GPa	380	410	407
Hardness	HV	1,800	1,900	2,000

- Setup of a “proof test” and its introduction in the testing protocol. The use of this nondestructive test allowed avoiding the release to the market of ball heads and inlays containing a critical size flaw that may shorten their expected lifetime.

### Alumina in Knee Replacements

The first use of alumina in the knee is by Langer, who performed the cementless implant of unicondylar ceramic tibial components in 73 cases from 1972 to 1980 in the Orthopedic Clinic of the University of Jena [12]. The devices were manufactured by the company Keramed (Hermsdorf, Germany) in the former German Democratic Republic.

The development of total ceramic knee replacements was carried out since 1980 by Japanese researchers. The first total knee replacement using alumina component is by Oonishi and Hasegawa [13]. The femoral component in these TKRs that was manufactured by KYOCERA Medical Corporation, Kyoto, Japan (the so-called KOM1), followed the shape of native condyles with a grooved surface for stability in the inner part in contact with bone. The tibial component, also made of alumina, was cementless stabilized into the bone by a rather huge stud with a rectangular cross section perpendicular to the tibial plateau, hosting a polyethylene platform. The KOM1 knee replacement was implanted cementless in 134 patients. The implant evolved with time: the kinematics was improved, a titanium alloy tibial tray was introduced, and design was modified for cemented fixation of both the tibial and the femoral components. These improved versions have been implanted in 534 joints until 2006.

Other types of alumina TKRs that we mention for completeness are the TSD alumina ceramic total knee replacements (made of ceramic and femoral components with polyethylene interlay), the NCU ceramic total knee replacement (introduced and used from 1989 to 1993 in 89 knees in 60 patients), the low-friction arthroplasty (LFA) and the Yokohama Medical Ceramic Knee (YMCK) both made by KYOCERA Medical Corporation (Kyoto, Japan), the Kyoto total knee cementless prosthesis KC-1, and the Bisurface<sup>®</sup> total knee replacement now made also out of Y-TZP in its latest version. Besides the knee replacements designed for routine applications, alumina was used also for custom-made knee replacements, used in case of tumor ablation. Heimke and coworkers [14] report that rods of single-crystal alumina were used to extend the tibial and femoral components of the KC-1.

**Table 4** Comparison of selected properties of alumina and zirconia

Property	Unit	Alumina	Y-TZP	Mg-PSZ
Bending strength	MPa	500–630	900–1,200	400–650
Fracture toughness	MPa m <sup>1/2</sup>	3.5	7–9	8–11
Density	g/cm <sup>3</sup>	3.97	6	5.5
Hardness	GPa	20	12.5	12.5
Thermal conductivity (298 K)	W/mK	30	3	3.1

## Zirconia in Joint Replacements

### Zirconia in Hip Replacements

The rationale for the use of zirconia in place of alumina is in the mechanical properties of this ceramic biomaterial, consequent to toughening by phase transformation that enhances the resistance of the material to crack propagation. The phase transformation under the matrix constraint (see Chap. 4, “► Bioinert Ceramics: Zirconia and Alumina”) of the metastable tetragonal grains at the crack tip to monoclinic phase is the dissipative mechanism for the elastic energy driving the advancing crack (Table 4).

This mechanism, operating at microscopic scale, results in the increase of toughness at macroscopic level and in a bending strength more than double that of the 1980s alumina. Table 4 summarizes some properties of zirconia, in comparison with those of the second-generation alumina. Zirconia (yttria-stabilized tetragonal zirconia polycrystal (Y-TZP)) was introduced in joint replacements in the second half of the 1980s [15] thanks to the work of the team led by two French scientists, Bernard Calés and Pascal Christel. In 2000 about 600,000 ball heads were implanted worldwide, most of them manufactured by St. Gobain Advanced Ceramics Desmarquest (SGAC Desmarquest, Evreux, France) under the trade name Prozyr<sup>®</sup>. The promising career of zirconia as a biomaterial was stopped in 2001, when a worldwide product withdrawal took place, due to an unexpectedly high rate of fracture that affected two batches of Prozyr<sup>®</sup> ball heads.

Although Y-TZP was the material used in the large majority of hip replacements, also heads made of magnesia-partially stabilized zirconia (Mg-PSZ) were in clinical use. Hip replacements with zirconia ball heads had a relatively large diffusion in the USA and in Europe, especially in France. A list of ceramic manufacturers who contributed to the development of zirconia ball heads is given in Table 5.

The metastability of tetragonal zirconia is the root of its unique mechanical properties. It is also the origin of its main drawback, consisting in the spontaneous transformation of the metastable tetragonal phase into monoclinic. This behavior is known as aging or low-temperature degradation (LTD). Readers may refer to Chap. 4, “► Bioinert Ceramics: Zirconia and Alumina” for a detailed description of LTD mechanisms in zirconia.

Wet environment and heat increase enhance LTD; then zirconia ball heads cannot be steam-sterilized. Moreover, zirconia is not suitable for hard-on-hard bearings because of its low thermal conductivity (about 1/10 of the alumina). That is, should

**Table 5** Manufacturers of zirconia THR ball heads

Manufacturer	Country	Material	Trade name
St. Gobain Advanced Ceramics Desmarquest	France	Y-TZP	Prozyr
Ceraver	France	Y-TZP	
HTI Technologies	France	Y-TZP	Biozyr
Cerasiv	Germany	Y-TZP	Ziolox
Morgan Matroc	UK	Y-TZP	Zyranox
Metoxit	Switzerland	Y-TZP	TZP Bio-HIP
Kyocera Medical Corporation	Japan	Y-TZP	Bioceram
Astro Met	USA	Y-TZP	
Xylon	USA	Mg-PSZ	

dry contact occur, the local temperature increase will trigger LTD. For this reason zirconia ball heads in THRs were coupled with polyethylene cups only.

The progress of the phase transformation leads to the increase of stresses in the material surface, to the increase of surface roughness, and eventually to the pullout of surface grains. The consequent increase of the wear of polyethylene inserts that are the counterface of zirconia heads in THRs leads eventually to osteolysis and failure of the implant. Ceramic manufacturers claimed that doping Y-TZP with, e.g., either alumina or ceria ( $\text{CeO}_2$ ) can limit LTD for the lifetime of THR joint, but it is noted that the clinical outcomes of zirconia ball heads reported in the literature are giving mixed results [16]. This is likely due to the fact that papers are spread for about ten years, and during this time lapse, many changes were underwent in ceramic processing, e.g., the introduction of hot isostatic pressing for final densification. In addition, each zirconia manufacturer was continuously improving its product using proprietary unpublished process parameters: therefore, the year of production is also a relevant variable. The consequence of this situation is that a number of materials named “zirconia” with pretty much different characteristics have been used (e.g., black zirconia, HIP-treated zirconia, etc.) and that different microstructural parameters are known to affect LTD. Moreover, the characteristics of the polyethylene cups that were coupled to zirconia ball heads may differ from one study to another because of the evolution in processing, e.g., some papers are making reference to devices using UHMWPE gamma sterilization in air, a technology soon abandoned because of the free radicals generated and the consequent oxidative degradation of the material [16].

### Zirconia in Knee Replacements

Ytria-stabilized zirconia ceramic total knee replacements (TKRs) are used especially in Japan, and a clinical trial is in progress in the USA. It must be remarked that in Japan total knee replacements have to face a particular biomechanical problem due to the floor-sitting posture that is customary in several Far Eastern countries.

This position implies a flexion of the knee joint of more than  $140^\circ$ , and notwithstanding a special design of total knee replacements accounting for this requirement, the fixation of the implants concerned and the stresses on the femoral component of

the implant may be more critical. The development of zirconia condyle component of TKRs made in Japan could be linked then to its improved mechanical properties in comparison with alumina.

KYOCERA Medical Corporation (Kyoto, Japan) manufactured the KU-type TKR which is in clinical use since 2001 [17]. In this device the zirconia condyles were coupled to a polyethylene insert placed on a titanium alloy tibial tray. A similar configuration characterizes the Bisurface<sup>®</sup> TKR that in its latest version has zirconia femoral component, also made by KYOCERA Medical Corporation [18]. The tibial component is made up of a UHMWPE insert placed on a titanium alloy tray. The Bisurface<sup>®</sup> TKR, also made by KYOCERA Medical Corporation, comes in five sizes as extra small, small, standard, large, and extra large that can host UHMWPE insert of thickness from 9 mm to 18 mm. The implants are fixed with bone cement and cruciate ligaments are sacrificed.

Also the Gem<sup>™</sup> Total Knee System is a knee replacement with zirconia femoral component, articulating on a polyethylene insert hosted onto a metallic tibial tray. This device is made by Kinamed, Inc. (Camarillo, CA, the USA), in the framework of a partnership with KYOCERA Medical Corporation (Kyoto, Japan), which is actually the manufacturer of the ceramic component for this further implant. The Gem<sup>™</sup> Total Knee System is approved in the USA for investigation purposes only. According to Kinamed, Inc., press release, the company developed on the basis of its prior experience an articular topography aimed to optimize the load transfer across the wear couple, carefully controlling the contact area throughout range of motion to minimize peak stress loading on the polyethylene insert and the resulting potential for polyethylene wear debris generation.

A further knee replacement with femoral component made of zirconia was manufactured by SGAC Desmarquest (Evreux, France) in the framework of an agreement with Encore Orthopedics, Inc. (Austin, TX, the USA) [19]. The zirconia condyles were coupled to a polyethylene insert placed on a CoCr alloy tibial base plate. Also in this implant all components were fixed by bone cement. Due to the abandon of the medical devices marketed by SGAC Desmarquest following the Prozyr<sup>®</sup> recall, the development of this device is likely to have been stopped.

## **Alumina-Zirconia Composites in Joint Replacements**

The practical abandon of zirconia in hip arthroplasty in 2001 opened a technological gap. That is, at that time, the orthopedic market was demanding new ceramic components for joint arthroplasty, some of them with challenging designs (e.g., thinner inserts, knee replacement, ball heads for revision surgery). This aspect became evident about the turn of the century, when surgeons were demanding components for hip replacements more challenging in design, e.g., ball heads with extra-long neck length (XL, XXL), small-diameter ceramic ball heads ( $7/8'' = 22.22$  mm), ceramic heads for revision surgery, thin-walled inlays, knee implants, and spinal implants. The design of these devices put in evidence the need of a ceramic material with mechanical behavior higher than the ones achievable by alumina. This

**Table 6** Manufacturers of commercial alumina-zirconia composites and their nominal compositions

Manufacturer	Country	Material composition (nominal)	Trade name
CeramTec GmbH	Plochingen, Germany	Al <sub>2</sub> O <sub>3</sub> 74 wt% Y-TZP 24 wt% Other oxides 2 wt%	BIOLOX <sup>®</sup> <i>delta</i>
CoorsTek Medical	Grand Junction, Co, USA	ZTA	CeraSurf
Kyocera Medical Corporation	Kyoto, Japan	Al <sub>2</sub> O <sub>3</sub> 79 wt% ZrO <sub>2</sub> 19 wt% Other oxides 2 wt%	JMM-ZTA
Metoxit	Thayngen, Switzerland	Al <sub>2</sub> O <sub>3</sub> 20 wt% ZrO <sub>2</sub> 76 wt% Other oxides 4 wt%	ATZ Bio-Hip
Matsushita Electric Works	Osaka, Japan	Al <sub>2</sub> O <sub>3</sub> 30 wt% (Ce-Ti) TZP 70 wt%	NANOZR
Mathys Ltd. Bettlach	Bettlach, Switzerland	Al <sub>2</sub> O <sub>3</sub> 20 wt% Y-TZP 68 wt% ZrO <sub>2</sub> 12 wt%	CERAMYS

fostered the development of alumina-zirconia composites for joint replacements that so far are the state-of-the-art ceramics in this class of products.

The first alumina-zirconia composite was introduced into the orthopedic market by CeramTec GmbH in 2002. This ceramic biomaterial, which is known under the trade name BIOLOX<sup>®</sup> *delta*, is today the most used ceramic in hip arthroplasty. Since 2002, more than 3 million BIOLOX<sup>®</sup> *delta* ball heads and inserts have been released to market. Besides CeramTec GmbH, which is the largest provider of ceramic composites for the worldwide orthopedic market, several ceramic manufacturers are proposing alumina-zirconia composites components for joint replacements (see Table 6).

These materials are identified as either zirconia-toughened alumina (ZTA) when alumina is the major component of the ceramic or alumina-toughened zirconia (ATZ) when the main component of the ceramic is zirconia. The microstructural behavior of these composites has been described in Chap. 4, “► Bioinert Ceramics: Zirconia and Alumina” of this handbook. Briefly, mechanical properties of alumina-zirconia composites are enhanced by the increase in stiffness of the matrix due to the presence of alumina (in ZTA) and of alumina joined to cubic zirconia (in ATZ). In this way energy threshold that has to be overcome in the phase transformation of zirconia is increased, and the contribution of transformation toughening to the mechanical properties of the composite is increased too.

A peculiar feature of BIOLOX<sup>®</sup> *delta* is in its microstructure. That is, the alumina matrix contains both finely and homogeneously dispersed zirconia grains, both platelets of strontium hexa-aluminate nucleated in situ during processing. Then, the material is toughened and reinforced by two concurrent mechanisms: the constrained t-m phase transformation of the zirconia grains that dissipates the energy

**Table 7** Selected properties of alumina-zirconia composite (BIOLOX<sup>®</sup> delta) in comparison with pure alumina (BIOLOX<sup>®</sup> forte) and Y-TZP (Prozyr<sup>®</sup>)

Property	Units	BIOLOX <sup>®</sup> delta	BIOLOX <sup>®</sup> forte	Prozyr <sup>®</sup>
Nominal composition	wt%	Al <sub>2</sub> O <sub>3</sub> : 74 Y-TZP: 24 Other oxides: 2	Al <sub>2</sub> O <sub>3</sub> > 99.8	Y-TZP
Density	g/cm <sup>3</sup>	4.37	3.97	>6
Av. grain size	µm	0.54	1.75	<0.5
Flexural strength	MPa	1,390	630	>1,300
Young's modulus	GPa	358	407	210
Hardness	HV	1,760	2,000	1,250

of an advancing crack and the need of the crack to contour the platelets, increasing the length of its path thus dissipating further energy (Table 7).

The improvement in mechanical properties of composites with respect to either alumina or zirconia ceramics is remarkable (see Table 7): there is an increase not only in bending strength but also in fracture toughness with remarkable consequences on wear properties and in reliability of the components of joint replacements.

### Alumina-Zirconia Composites in Hip Replacements

One of the main consequences of the improvement in mechanical properties is the increase in reliability of ceramic ball heads and inserts. The overall in vivo fracture rate of pure alumina BIOLOX<sup>®</sup> forte heads was 21/100,000, while the fracture rate of the composite BIOLOX<sup>®</sup> delta heads is one-tenth of it (0.002 %). It is noted (see Fig. 2) that most of the BIOLOX<sup>®</sup> forte fractures occurred in 28 mm heads, mostly in long and short neck designs.

Also, the wear rate of the BIOLOX<sup>®</sup> delta bearings significantly improved in comparison with the former BIOLOX<sup>®</sup> forte, due to the better mechanical properties of the composite. This aspect is especially relevant in the successful outcomes of the arthroplasty of the hip, taking into account the role of wear debris in the cascade of biological events leading to osteolysis.

The wear tests performed in hip simulators under standard laboratory conditions on third-generation BIOLOX<sup>®</sup> forte CoC bearings show wear rates two orders of magnitude lower than metal/PE. The results of these tests demonstrated the absence of any difference in wear depending on the clearance of the CoC bearings (20 µm and 30 µm), nor variations in wear after tilting the cup angle from 45° to 60°.

Nevertheless, it has to be put in evidence that with the spreading of ceramics in joint replacements, a significant number of them are operating in suboptimal conditions. The composite ceramic BIOLOX<sup>®</sup> delta – that can be taken as the latest development in alumina technology – thanks to its outstanding bending strength and toughness, shows excellent wear behavior also in unfavorable conditions representative of a hip joint with high laxity. This type of wear test, the so-called microseparation mode, simulates a joint where at heel strike during gait the head will sublux and impinge on the superior rim of the insert producing a local stress



concentration (edge loading). Even under these severe conditions, the wear of BIOLOX<sup>®</sup> *delta* bearings was about one-half that of the BIOLOX<sup>®</sup> *forte* bearings tested under the same conditions. Also, the wear stripes onto components were different between the two ceramics tested. These stripes on BIOLOX<sup>®</sup> *delta* were shallower than the ones observed on BIOLOX<sup>®</sup> *forte* alumina heads, resulting from the improved mechanical properties of the BIOLOX<sup>®</sup> *delta* composite ceramic.

### **Alumina-Zirconia Composite in Knee Replacements**

The development of the alumina-zirconia composite knee replacement has been exhaustively traced by Heimke et al. [14]. Briefly, the introduction of alumina ceramics in knee arthroplasty during the late 1970s was aimed to obtain a stable, reliable, cement-free anchorage and the reduction of polyethylene wear thanks to the alumina-UHMWPE wear couple. While the follow-up studies confirmed the marked reduction in wear, they put in evidence the lack of improvements regarding the cementless fixation. Consequently, the alumina ceramic femoral components were cemented and supplied with polyethylene tibial components hosted on metal tibial tray that in most designs were intended for cement fixation.

A further approach to the reduction of polyethylene wear in total knee arthroplasty was the introduction of a separate meniscus component allowing to overcome the incongruity of the femoral condyle and tibia plateau replacements. Tests performed with this design demonstrated that the alumina available would not offer acceptable safety margins in clinical use. The introduction of the ceramic composite BIOLOX<sup>®</sup> *delta* has changed this situation, and a prototype of TKR with mobile meniscal components was developed and tested, as well as a unicondylar knee replacement with metal-backed ceramic BIOLOX<sup>®</sup> *delta* wear couple.

Two different models of total knee replacement made of alumina-zirconia composite are available so far, both made by CeramTec GmbH (Plochingen, Germany) using BIOLOX<sup>®</sup> *delta*: the Multigen Plus Total Knee Replacement made by Lima Corporate (San Daniele del Friuli, Italy) and the BPK-S made by PETER BREHM (Weisendorf, Germany), as shown in Fig. 8. The ceramic components are designed to be fixed to bone by cement in both devices.

The Multigen Plus TKR is already available for clinical use, while the tests on BPK-S are still in progress. Both the femoral and the tibial plates of the BPK-S are made up of BIOLOX<sup>®</sup> *delta*. The tibial plate hosts a semi-constrained XLPE insert free to rotate on the tibial plateau. A stump in the inferior part of the insert controls its mobility, leaving it free to rotate. The Multigen Plus TKR was designed initially with a metallic tibial tray, while in its more recent version, the ceramic femoral component articulates with a monoblock tibial component made of XLPE.

### **Alumina-Zirconia Composite in Shoulder Arthroplasty**

Episodically attempts to use ceramics in shoulder replacements can be traced in the literature. The first ceramic replacement in shoulder arthroplasty was a complete humerus which had been affected by a destructive bone tumor. The outcomes of this device made by Rosenthal were reported by Sim et al. in 1980 [20]. Rare reports related to shoulder prostheses with ceramic couplings were reported later also [21],

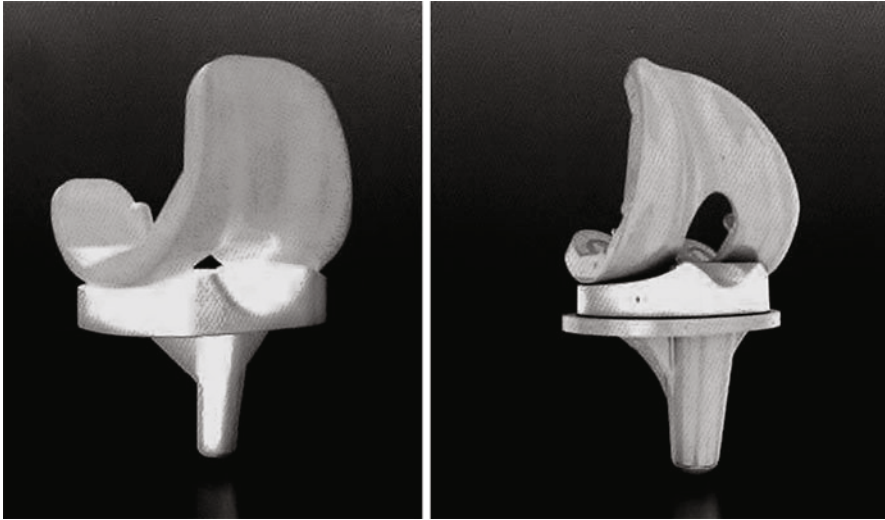


**Fig. 8** BIOLOX<sup>®</sup> *delta* knee replacements. *Left side:* Multigen Plus Total Knee Replacement (Lima Corporate, San Daniele del Friuli, Italy). *Right side:* BPK-S (PETER BREHM, Weisendorf, Germany) (Courtesy of CeramTec GmbH, Plochingen, Germany)

but at the turn of last century, the use of ceramics in shoulder arthroplasty looks abandoned.

Reverse total shoulder arthroplasty (RTSA) is a powerful new procedure in the treatment of patients with previously not reconstructable shoulder problems and/or failed arthroplasty. Semi-constrained RTSA involves replacement of the humeral articulating surface with a humeral component containing a polyethylene socket and replacement of the glenoid with a ball, known as a glenosphere, which generally is made from highly polished metal. In spite of the promising results obtained by the new designs and the inversion of bearing components in reverse total shoulder arthroplasty, both the patient's age and the increasing number of allergic reactions to metals are of concern. Caution should be taken in indicating reverse total shoulder arthroplasty in young and active patients as well as in allergic ones, taking into account the implant options now at disposal. These considerations were basically for the design of a ceramic liner for the glenosphere in the SMR Reverse Shoulder System (Lima Corporate, San Daniele del Friuli, Italy). The use of composite ceramics may give a new momentum to ceramic components in shoulder arthroplasty bearings.

### **Non-oxide Ceramics in Joint Replacements**

Several non-oxide ceramics (titanium nitride (TiN), chromium nitride (CrN), diamond-like carbon (DLC)) have been proposed or are already in clinical use as wear-protective coatings in THR bearings.

Silicon nitride makes an exception among non-oxides as its mechanical properties allow its use as a bulk ceramic biomaterial. Toughness of up to  $K_{IC} = 10 \text{ MPa m}^{1/2}$  and bending strength of up to 1,100 MPa had been reported [22]. However, the mechanical properties of silicon nitrides depend on processing conditions, e.g., an important variability of mechanical properties has been reported depending on the sintering additives used. Silicon nitride for medical devices has been investigated for almost 30 years, and it is established as a biomaterial in a number of applications implying different requirements and material behavior. This ceramic is used today clinically in cervical spacers and in spinal cages with encouraging short-term outcomes, while other applications ranging from dental implants, miniplates and screws for osteosynthesis in maxillofacial surgery, aneurism clips, and component of hip replacement bearings are still under development.

Although the biocompatibility, mechanical properties, and stability of silicon nitride especially doped with alumina and/or yttria satisfy the requirements of bioceramics for use in joint replacements [23], it is noted that the devices currently in clinical use do not imply wear-resistant surface as do the bearings of joint replacement. The results of hip simulator tests reported so far have been run to one million cycles only [24], performed in the so-called standard mode. Especially the long-term wear behavior both in normal and in off-normal conditions is a relevant characteristic for the materials to be used in THR bearings. Within the limits of predictability of laboratory tests, data on the long-term wear behavior also in off-normal conditions (e.g., edge loading, joint laxity, etc.) and on the biological safety of silicon nitride wear debris and of their degradation products are still demanded.

---

## Clinical Results

### Clinical Results of Bioinert Ceramics in Hip Replacements

In the second-generation alumina-on-alumina bearings, there were significant improvements of reliability of components in comparison with the first generation [1, 25, 26]. In addition, in order to improve cup stability, since the early 1990s, the predominant design has been a rough or porous-coated titanium shell with a ceramic liner. Thanks to the improvement of acetabular fixation in manufacturing process, long-term results of ceramic-on-ceramic (CoC) THRs confirmed excellent survivorship that in modern implants reaches up to 97 % at 10 years [1]. In addition, ceramic bearings are relatively inert, and they have excellent wear properties so periprosthetic loosening is rare, and in the literature, they have been only reported in isolated case reports of osteolysis around CoC bearings. Because of the preserved bone stock, the revision surgery of hip replacements with CoC bearings is easier to perform and with better outcomes [25–27].

Alumina-on-alumina bearings are offering the advantage of a very low wear, but the risk of chipping of the acetabular insert and the need of an accurate positioning to avoid edge loading and damage of the bearing surface can be felt as a heavy

limitation by users. Kim et al. [28] carried out a study on the outcomes of alumina-on-alumina ceramic and alumina-on-highly cross-linked polyethylene bearings in the same patient. The aim of this study was to assess the prevalence of osteolysis in a cohort of 100 young active patients (66 male and 34 female, mean age 45.3 years at the time of surgery – range 21–49 years) who have undergone bilateral cementless total hip arthroplasty with an alumina-on-alumina ceramic-on-ceramic (CoC) bearing in one hip and an alumina-on-highly cross-linked polyethylene (CoP) in the other. The mean follow-up was 12.4 years (range 11–13 years) with annual control for all the 200 implants. At the final follow-up, radiographic findings of the component were not significantly different between the two groups. The mean polyethylene linear penetration was  $0.03 \pm 0.004$  mm per year. No hips in either group displayed osteolysis. In both groups survivorship at 12.4 years with revision as the end point was 100 % for the femoral component and 99 % for the acetabular component.

As a general conclusion, the debate on the best choice of bearing surfaces in total hip arthroplasty in the younger and more active patient is still open, as remarked by Cash and Khanduia [29]. The improvements obtained in both polyethylene and ceramics thanks to the introduction of the new composites offer the opportunity for long-lasting bearings, because ceramic femoral heads have consistently been shown to produce less in vivo polyethylene wear than metal heads of the same size. Ceramic-on-polyethylene bearing – following these authors – could potentially become the preferred bearing for a young adult hip replacement. Similar conclusion was made by Epinette and Manley [30] who carried out the comparison between a cohort of 412 patients (447 hips) with alumina-on-alumina CoC bearings and a cohort of 216 patients (228 hips) with alumina-on-highly cross-linked polyethylene (HXLPE) bearings. With bearing-related complications as end point, they did not observe any significant difference in survivorship between cohorts 10 years after surgery.

In addition, they found no significant differences in clinical and radiographic findings between cohorts leading to the conclusion that, taking into account the difference in pricing, alumina-on-HXLPE bearings could be a reasonable alternative to alumina-on-alumina ceramic-on-ceramic bearings in total hip arthroplasty.

The studies as a whole are putting in evidence a new aspect in the selection of the bearing for hip arthroplasty: taking into account the reduction in wear while long-term results were significantly better in the case of alumina-on-UHMWPE bearings in comparison with metal-on-UHMWPE bearings, the introduction of the newly cross-linked polyethylenes can offer a substitute to alumina-on-alumina. Nevertheless, while this solution offers the advantage of reduction in risk of noises and of intraoperative acetabular rim chipping, it implies the drawback that the wear debris made by UHMWPE are more aggressive than the ceramic ones.

It is worthwhile to underline that today arthroplasty alpha-alumina components have been replaced almost completely by the new alumina-zirconia composites. Data released in 2013 by the main manufacturer of bioinert ceramics for hip replacement bearings (CeramTec GmbH, Plochingen, Germany) show that alumina components (BIOLOX<sup>®</sup> forte) are only about 10 % of its production, the composite AMC BIOLOX<sup>®</sup> delta being the balance.

### Clinical Results of Alumina-on-Polyethylene Total Hip Replacements

In the last 30 years, the relevance of the wear of THRs' joints has become more and more high because the advance in material science and in technology related to arthroprostheses allowed orthopedic surgeons to perform total hip replacements in younger patients. This resulted in the improvement of functional outcomes but also in the increase of the risk of complications related to polyethylene wear. There is a different approach among countries in the choice of friction couple. In the USA, there is a prevalence of cross-linked polyethylene inserts coupled to CoCr alloy heads, while in European countries (Austria, France, Germany, Italy, Switzerland), there is for a long time a prevalence of ceramic heads coupled to ceramic liners either to standard or cross-linked PE.

Large cohorts with long-term clinical follow-up or smaller studies with high-precision measurements are necessary to evaluate the wear performance of different implants. In the case of ceramic-on-polyethylene (CoP) THR bearings, the main parameters for wear were summarized by Kabo [31] as follows:

- PE thickness
- Head diameter
- The patient's activity and age (>3 m cycles per year in an active subject)
- Metal back and acetabulum modularity
- Extent of head articulating surface

Due to the number of parameters to be taken into account, to establish the effect of ball head material on polyethylene wear of total hip replacement appears a challenging task. In addition, there are significant differences among the clinical studies, namely, various head sizes, different modes of implant fixation, different polyethylene materials, and a number of methods for the measure of wear, all of which are factors making comparisons of different trials difficult, if not impossible.

A few papers, like e.g., in Sychterz et al. [32], reported that the rate of wear of the ceramic-polyethylene group is slightly greater (0.09 mm/year, SD 0.07) than the one measured in cobalt-chrome-polyethylene group (0.07 mm/year, SD 0.04). However, there is general consensus on the advantages offered in terms of polyethylene wear reduction by using ceramic ball heads instead of metal ones. The survival rate of CoP bearings is excellent. Delaunay [33] reported 86 % survival rate after 15 years in patients under 50 years of age and 13 % revision at 20 years in subjects under 40 years of age. A matched-pair analysis of the wear of ceramic and metal femoral heads on conventional polyethylene in uncemented total hip replacements was carried out by Meftha and Ranawat [34] at a minimum of 15 years of follow-up. Thirty-one pairs of young and active patients (age at surgery was between 23 and 65 years, mean 55) were matched on the basis of age, sex, body weight, diagnosis, and activity level. All surgeries were made by the same surgeon using 28 mm heads coupled to argon-sterilized GUR 4150 UHMWPE. The follow-up duration was 15–20 years (mean 17). The mean wear rates for the ceramic group and the metal group were  $0.086 \pm 0.05$  mm/year and  $0.137 \pm 0.05$  mm/year, respectively ( $p = 0.0015$ ), confirming that ceramic femoral heads produced significantly less wear on

conventional polyethylene liners. Moreover, there was only one reoperation in the ceramic group because of distal femoral osteolysis while three failures took place in the metal group, requiring isolated liner exchange in two hips and revision of the acetabular component in one hip because of wear-induced osteolysis and/or loosening.

While long-term results were significantly better in the case of 28 mm diameter CoP bearings (alumina heads coupled with conventional polyethylene) than in the case of similar diameter metal-on-polyethylene up to 10 years postoperatively [35, 36], in the case of 22 mm diameter, clinical results are controversial. Wroblewski [37] reported an initial bedding-in of up to 0.41 mm in the first two years after 22 mm alumina ball head was coupled with cross-linked polyethylene on a flanged Charnley stem. After the initial bedding-in, no further progression was observed in this series, and neither clinical nor radiographic signs of failure were seen. These values should be compared with the ones reported by Caton [38] who reported a wear rate of 0.1 mm/year in metal polyethylene Charnley LFA bearings with a follow-up of up to 25 years.

### **Clinical Results of Alumina-on-Alumina Total Hip Replacements**

Ceramic-on-ceramic bearings are characterized by an extremely low wear, making this articular couple especially suitable for young and active patients, who have very high expectations after surgery. Unfortunately, the risk of revision rates has been traditionally higher in this class of patients than in older patients, due to their higher activity levels and increased demands. The increased reliability of modern ceramics has made available ceramic bearing couples suitable for CoC bearings with a remarkable survivorship. With reference to high-feared risk of fracture, the already cited survey performed by Tateiwa T et al. [26] remarks only 24 fractures of ceramic components on more than 35,000 cases followed for 3–25 years. There were 24 reported fractures. The incidence of intraoperative chipping of the rim of ceramic insert, which is also a much feared complication, was reported between 2 % and 3 %.

D'Antonio et al. [39] using revision for any reason as endpoint, observed 97 % survivorship at 10 years postoperatively in a cohort of 209 THRs implanted in 194 patients by six surgeons in six different institutions. The survivorship taking as end point bearing surface failure or aseptic loosening was 99 % in this cohort. No evidence of osteolysis was observed at the latest follow-up on routine radiographs. Imbuldeniya et al. [40] reported survivorship of 96.5 % at 10 years with revision for any reason as an end point in a series of 120 primary cementless alumina-on-alumina consecutive total hip arthroplasties performed between June 1997 and February 1999 in 110 patients under the age of 55 years at time of surgery. At the latest follow-up clinical information was available for 106 hips in 96 surviving patients. All femoral stems had stable bone ingrowth, with no migration. Osteolysis was not observed nor signs of radiological wear. There were no cases of ceramic fracture in this younger, active cohort of patients nor any signs of adverse reaction to wear debris who could practice sports or heavy occupational work once they have recovered from surgery.

Similar results were reported by Lee et al. [41] who followed for a minimum of ten years a cohort of 89 hybrid alumina-on-alumina hip replacements implanted in 46 men and 43 women with an average age of 51 years. At a mean radiographic follow-up of 123 months, no osteolysis was observed in this cohort. Revision surgery was performed in one patient for bilateral femoral component loosening at 11.2 years and 11.9 years, respectively. Survivorship at 13.5 years with implant revision for any reason as the end point was 96.2 %.

While most of the clinical studies are focused on the wear of the bearing and on the osteolysis induced by the cellular reactions to the wear debris, Hernigou et al. [42] addressed their attention on the risk of dislocation associated with the different bearing couples. They observed that ceramic-on-ceramic bearings decreased the cumulative risk of dislocation in hip arthroplasty as compared with ceramic-on-polyethylene bearing couples. Their study was aimed to assess the factors affecting dislocations: that is, it is unclear if dislocations are related either to mechanical impingement of the implant components or to a biological mechanism that decreases the stability provided by the capsule (e.g., inflammation secondary to osteolysis). They investigated the influence of several factors: (i) bearing type (CoP vs. CoC), (ii) patient factors (age, sex, and diseases), (iii) mechanical factors (component malposition, penetration resulting from creep and wear), or (iv) biological hip factors at revision (thickness of the capsule, volume of joint fluid removed at surgery, histology). The study was carried out on 252 bilateral implants and the cumulative risk of dislocation (first-time and recurrent dislocation) was calculated at a minimum of 27 years. While 31 dislocations took place in the CoP group, only four took place in the CoC group. The lower incidence of late dislocation in CoC implants was correlated with increased capsular thickness (mean 4.5 mm, range 3–7 mm) compared with the thinnest (mean 1.2 mm, range 0.2–2 mm) capsule of CoP hips. Taking into account that dislocations are the second cause of hip replacement revision (first is aseptic loosening and then osteolysis), this result shows the significant advantage springing out from the use of ceramics in hip arthroplasty bearings.

### **Clinical Results of Zirconia in Total Hip Replacements**

The literature reports controversial outcomes of Y-TZP-polyethylene bearings. Nevertheless, revision rates are very low in most of the series despite the variable penetration rates reported, the differences in implant design and in patient-related factors, and the relatively short duration of the follow-ups, as reported formerly by the authors [16].

The complications reported in zirconia-UHMWPE bearings are related either to the accelerated wear of the UHMWPE or to fractures of the ceramic heads. Zirconia ball heads (Y-TZP) in hip replacements were coupled with UHMWPE inserts, because the characteristics of this ceramic (relatively low hardness, very low thermal conductivity) do not allow its use in hard-on-hard bearings.

The accelerated wear of the joint was either due to LTD in the metastable ceramic or due to the quality of the UHMWPE. That is, the reports on the outcomes of THR with zirconia-UHMWPE bearings deal with a number of different implants using

ball heads made by different manufacturers and then using different precursors and process additives. In addition, most of the studies were carried out on ball heads belonging to the first generations of Y-TZP ceramics, e.g., sintered without final hot isostatic pressing and without introduction of additives to control the kinetics of LTD. The polyethylene cups also underwent different processing routes, e.g., standard or cross-linked, gamma sterilization in air, or by other methods: many studies had been performed on implants making use of Hylamer<sup>®</sup> inserts, a UHMWPE gamma cross-linked in air that was withdrawn from the market due to its poor outcomes in the clinical setting.

It has been remarked that zirconia heads from different manufacturers show different LTD behavior [16, 43]. Although the increase in monoclinic phase is generally ascribed to environmentally induced degradation, the production process – and especially the surface finishing by grinding – also has a strong influence on this behavior. In addition, steam sterilization prior to surgery of zirconia heads cannot be excluded, especially in the first years of clinical use of the new material, and this would have started the LTD of the ball head articulating surface.

A further set of complications is due to fracture of ceramic heads. There were only a small number of fracture reports of zirconia heads before 2000, associated with trauma, critical metal-ceramic couplings, or implant of new zirconia heads onto revised stems [44]. These fractures are not related to specific characteristics of zirconia. On the other hand, it is noted that a high number of fractures of Prozyr<sup>®</sup> heads reported after 2001 – that led to the recall of the product from the market – took place in two batches marked “TH.” This logo indicates that these ceramic heads have been sintered in a tunnel furnace, an innovation introduced to increase the production capability of Prozyr<sup>®</sup> that formerly was made in batch kilns (BH batches), as highlighted by the authors in a former paper [44].

The Prozyr<sup>®</sup> recall ruined the confidence in zirconia, which was already under scrutiny for the poor performance records described above. Its inability to articulate in hard-on-hard bearings limited its versatility in device design, and joined to the LTD risks due to its intrinsic metastable nature led to the practical abandon of its use in orthopedic surgery.

## Clinical Results of Alumina and Zirconia in TKR

There are only a few reports on mid- and long-term follow-up outcomes of first-generation ceramic total knee replacements. The results achieved by the different authors are putting in evidence the relevance of cemented fixation to achieve a good implant stability in the long term and the reduction in wear of the polyethylene tibial inserts obtained by the use of ceramic femoral components in place of CoCr alloy.

In 2002 Heimke et al. presented an excellent retrospective review on the development and clinical outcomes of alumina total knee replacements [14]. They observed that there was a high frequency of loose implants and of sinking in the implants belonging to the first generation after 14–16 years follow-up. These findings were not correlated to the fixation of the implant (cemented or cementless).



These results were confirmed in a 3–18-year report by Oonishi et al. [45] who, in reviewing their experience with KOM-type implants of the second and third generations, did not report neither loosening nor sinking in of any components while observing some radiolucent lines around implants. In a successive report, they analyzed retrospectively 26 years of experience [46]. The implants were performed from 1990 to 2005 (534 implants, all cemented). Radiolucency was observable in the tibial medial part in about 4 % of the implants, while in lateral areas, it was about 2 % only. The absence of osteolysis and of implant loosening was observed in the cases available at follow-up. These authors remarked that the surface of ceramic femoral components retrieved after long-term clinical service maintained the original surface finish. In comparison with CoCr femoral components, the alumina ones produced less UHMWPE wear, reducing in this way the risk of osteolysis.

Akagi et al. [47] reviewed the clinical results of the first procedures performed with the Bisurface<sup>®</sup> Knee System from December 1989 to May 1994 in order to assess the outcomes of this new implant. One hundred and sixty-six patients treated with a total of 223 consecutive primary total knee arthroplasties were enrolled in the study, and 182 knees were followed for 3.9 to 9.0 years (mean 5.8 years). They observed an increase in HSS score and in range of flexion. No prosthesis had loosened aseptically, and no ceramic femoral component was broken by the time of the latest follow-up, although 20 % of the knees sometimes felt loose in daily living activities. This led to improved intrinsic stability of the prosthesis by improving the congruity of the ball-and-socket joint. The rate of survival of the implant was 94 % (95 % confidence interval, 90–98 %) at 6 years.

Although the outcomes of total hip replacements with alumina femoral components were good and the absence of osteolysis around the implant components, the mechanical properties of alumina make it necessary to use thick femoral components. Moreover, some cases of fractures due to accidents were reported but especially during impaction (5/2000 based on manufacturer's data) [18]. All this led to the development of Y-TZP of zirconia femoral components for total knee replacements, exploiting the better mechanical behavior of zirconia over alumina.

Bal et al. [19] reported the clinical results of 35 total knee implants with zirconia femoral component, the Foundation Knee System<sup>®</sup> (Encore Orthopedics, Inc., Austin, TX, USA). The mean duration of the follow-up was 31 months (range 24–40 months). The implant components included a cobalt-chrome alloy tibial base plate and a polyethylene patella, while the femoral component was made of yttria-stabilized tetragonal zirconia polycrystal (Y-TZP) manufactured by SGCA Desmarquest (Evreux, France). All components were fixed by cement. The clinical result was excellent for 34 knees and good for one knee only. No change in implant position either radiolucent lines or osteolysis around any component of the implants was put in evidence in radiographs taken during follow-up. The results of this short-term clinical study show the absence of complications related to the ceramic, while the outcomes observed are comparable to those seen with traditional total knee replacements using cobalt-chromium alloy and UHMWPE articulating surfaces.

Nakamura et al. [18] presented the results achieved in 33 implants of the zirconia (Y-TZP) version of the Bisurface<sup>®</sup> total knee replacement at an average follow-up of

3.1 years (2–4.1 years) postoperatively. This version was developed to overcome the risk of intraoperative fractures that were observed while implanting the femoral components of the previous versions. They started to use the Bisurface<sup>®</sup> knees with zirconia ceramic since 1999. At final follow-up, there was a general improvement in implant score (Japan Orthopaedic Association) and in knee flexion, while the radiological examination revealed no loosening and no implant failure. All the patients were satisfied with their knee replacements. No fracture occurred intraoperatively nor within the final follow-up.

## Clinical Results of Zirconia in Other Joints

The use of Y-TZP has not been limited to hip and knee joints. This ceramic material has been used for spheres to be used in interpositional arthroplasty in carpometacarpal joints [48]. The early outcomes of these devices have not been encouraging, and its use appears abandoned: Athwal and coworkers [49] reported that at a mean of 33 months postoperatively, not one of the patients was satisfied of the outcomes. Six out of seven implants subsided into the trapezium resulting in pain, weakness, and stiffness, and five of them required revision.

## Clinical Results of Bioinert Ceramic Composites in Joint Replacements

### Clinical Results of Alumina-Zirconia Composites in Hip Replacements

The first clinical use of BIOLOX<sup>®</sup> *delta* AMC ball heads in the USA took place in June 2000, after the approval of the US Food and Drug Administration (FDA) of the bearing couple BIOLOX<sup>®</sup> *delta* heads – polyethylene inserts. In 2009 Masson [50] reported that after 6 years of clinical use of BIOLOX<sup>®</sup> *delta*, more than 65,000 ball heads and 40,000 inserts of this material have been implanted all over the world and that during this period no reports of complications were sent to the manufacturer. So far (December 2014), BIOLOX<sup>®</sup> *delta* THA components are clinically used in over 3.5 million cases. This material is today the ceramic golden standard in THA.

Hamilton et al. [51] reported the early outcomes and complications of a prospective, randomized, multicenter trial of 263 patients (264 hips) at eight centers, comparing 177 BIOLOX<sup>®</sup> *delta* AMC ceramic-on-ceramic (CoC) articulation with 87 BIOLOX<sup>®</sup> *delta* AMC ceramic head-cross-linked polyethylene bearing combination (CoP). Clinical and radiographic results were provided for the 233 patients with minimum 2-year follow-up (average, 31.2 months; range, 21–49 months). Survivorship was similar in both groups. There were four (2 %) revisions in the CoC group and two (2 %) in the CoP group. The main concerns were related to liner fractures due to chipping.

In the short term, the BIOLOX<sup>®</sup> *delta* CoC articulation provided similar functional scores and survivorship and complication rates with the ceramic head combined with cross-linked polyethylene. Different results were reported by White

et al. [52] in the critical review of the results obtained in the Ranawat Orthopaedic Center. They found that BIOLOX<sup>®</sup> *delta* ceramic-on-polyethylene has consistently shown lower in vivo wear rates compared to metal-on-polyethylene. The latest generation of ceramic-on-polyethylene, BIOLOX<sup>®</sup> *delta* on highly cross-linked polyethylene has shown an excellent linear wear rate (0.006 mm/year), much lower than the one of cobalt chrome-on-highly cross-linked polyethylene (0.011 mm/year), thus increasing the long-term survivorship of the implants, and became the new gold standard bearing in total hip arthroplasty. Also Kim et al. [53] reported a 100 % survival rate – in agreement with White et al. – in a cohort of 263 THR at a mean 7.45 years after surgery.

This result was obtained using 36 mm CoC BIOLOX<sup>®</sup> *delta* (delta-on-delta) bearings with an ultrashort metaphyseal fitting anatomic cementless stem. The implants were made in 138 hips in obese patients and 125 hips in non-obese patients. Both groups of patients were highly active. Mean age in the obese group was 50.7 years and 48.2 years in the non-obese group. Osteolysis was observed in any patient. Clinical outcomes were similar in both groups with one dislocation in each group. Survivorship at follow-up was 100 % in both groups; no hip in either group had thigh pain or a revision or ceramic fracture.

### **Clinical Results of Alumina-Zirconia Composites in Knee Replacements**

There are no clinical data available so far concerning the BPK-S TKR (PETER BREHM, Weisendorf, Germany), while Bergschmidt et al. [54] presented the preliminary results (24-month follow-up) of a multicentric, prospective noncomparative study on the Multigen Plus Total Knee Replacement (Lima Corporate, San Daniele del Friuli, Italy). The study was aimed to evaluate the clinical and radiological outcomes of the BIOLOX<sup>®</sup> *delta* ceramic femoral component and was classified as evidence-based medicine (EBM) level 4.

Seven clinical centers participated in the study (three in Germany, three in Italy, and one in Spain) after ethics committee approval and enrolled 108 patients who gave informed written consent. The study group included 81 (73.6 %) TKAs in female and 29 (26.4 %) TKAs in male patients with BMI, and ages were  $28.7 \pm 3.5$  (19.1–33.6) and  $67.7 \pm 6.0$  (48–75), respectively. Surgery was performed on 48 (43.6 %) left and 62 (56.4 %) right knees.

Of 110 total knee arthroplasties enrolled in the study, only 96 knees were available for evaluation at 24 months. HSS, WOMAC, and SF-36 scores improved significantly (WI test  $p < 0.001$ ) from the preoperative to the postoperative evaluations. Improvements in all scores were seen especially up to 12 months, whereas differences in all scores between 12 and 24 months were small, while range of motion as a functional aspect improved the most between 3 and 12 months.

The radiological evaluation revealed radiolucent lines around the femoral ceramic component in four cases. In contrast, we observed radiolucent lines on the tibial side in up to 16 %. This may be due to a stress-shielding phenomenon and is described in up to 17 % in the literature. In the absence of component misalignment, progression cannot usually be expected, but subsequent follow-up investigations would clarify if

the progression of radiolucent lines influences clinical results and implant survival rates.

In this study all the Multigen Plus TKRs were implanted with a PMMA cement layer about 2 mm thick. Nevertheless, taking into account that some patients can be sensitive to bone cement components, the development in progress includes the modification of the ceramic surfaces in order to achieve cementless fixation by bone ingrowth.

## Ceramic-Related Complication in Joint Replacements

The most feared complications associated with the use of ceramic in hip joint replacements are the fracture of the ball head or the insert. These fears are not justified by facts. High rates of fracture of ball heads were characteristics of some products in the 1970s and 1980s [55]. The materials in production today are very different in terms of density, grain size, and mechanical properties, as described above, resulting from four decades of continuous development. The present generation of composite alumina-zirconia ceramics has strength and toughness nearly double that of the alumina of the former generation. CeramTec GmbH declared in 2012 that the rate of fracture of the composite BIOLOX<sup>®</sup>delta was 0.001 % (1/100,000) calculated on 1.61 million ball heads sold, while the fracture rate of the former generation alumina BIOLOX<sup>®</sup>forte was 0.021 % (21/100,000, on 2.97 million ball heads sold). It should be taken into account however that “high-performance material” does not mean “unlimited performances,” and then care should be made in avoiding the most common technical errors that could lead to the failure of the prosthetic components.

As espoused in section “[Design of Ceramic Components for Joint Replacements](#),” this chapter, the features of the taper connection determine the stresses in the ceramic component (head and insert). Many taper designs are in clinical use, then care is to be made in avoiding random coupling of ceramic ball heads and metallic tapers. A further caveat in clinical practice concerns the cleanliness of the taper: blood clots, bone or cement chips, wires, etc. trapped at the metal-ceramic interface will act as local stress concentrators, leading eventually to ceramic failure [56] (Fig. 9).

The fractures of ceramic inserts on the other hand are much more frequent, most of them happening as intraoperative chipping of the ceramic rim during insertion into the metal shell. This is a consequence of poor insertion of the insert in the shell prior to impaction. A further cause of liner fracture is its dissociation from the metal back, due to poor impaction during surgery or to incorrect seating of the liner into the shell. The introduction into the market of monoblock (preassembled) sockets was aimed to overcome these problems. In these devices, the insert is installed into the metallic cup in the implant factory. A further approach was the development of special instruments that assure the proper seating of the insert before impaction. In addition, some implant manufacturers developed proprietary insert design of the ceramic inserts aimed to obtain the correct positioning.

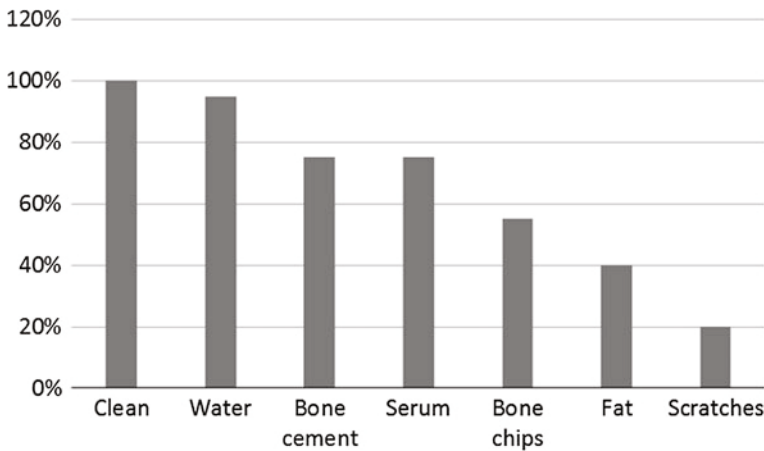


**Fig. 9** Percent variation of ceramic ball head burst load due to taper contamination or damage (Adapted from Ref. [56])

Edge loading is a complication of hip replacements occurring when the ball head runs on the edge of the acetabular insert. In this way, the loads are concentrated on small surfaces of the ball head and of the insert, leading to a typical damage known as “stripe wear,” for the shape of the wear track can be observed on retrieved bearings that were operating under edge load. The roughness of the surfaces undergoing stripe wear is increased, in the most severe cases in association with ceramic grain pullout. Severe edge loading is a consequence of poor positioning of the acetabular component [1] although subluxations, microseparation due to laxity in the joint, can also likely lead to this complication. However, the small volume of the ceramic debris due to edge loading and the biological safety inherent in oxide ceramics [2] do not lead to osteolytic reactions, a significant advantage of ceramic-on-ceramic bearings over metal-on-metal ones. It is noted that should edge loading occur in bearings with polyethylene insert, the concentrated loads may lead to the increase in wear of the PE and in most severe cases to the fracture of the insert rim.

Noises, especially squeaking, were object of high attention during the last years. This is too a hip replacement-related complication that was evident especially in some countries, likely due to the prevalence of some device designs in these markets. Acoustic vibrations (noise) due to stick-slip friction [57] can be generated in a number of conditions, e.g., ceramic debris in the bearing interface, starved lubrication, and metal transfer onto the bearing surfaces. The results of clinical studies show that there are significant correlations among noises and implant position, edge loading, implant design, patient body mass and activity level. However, noises do not appear as a major complication in hip replacement, being in most cases a transient condition only.

The reports of complications related to ceramic knee implants are a few, due to limited diffusion in the clinical practice of these devices. The Japanese experience shows that the complications observed in the early series are mainly the lack of

stability of cementless implants, a problem overcome by the optimization of the cementing technique, and the sinking of the tibial plateaus. Other complications were related to the bulky design of these experimental devices.

Intraoperative fractures of alumina femoral components were reported by Nakamura et al. [18]. Four intraoperative fractures of BIOLOX<sup>®</sup> *delta* ceramic femoral component have been also reported that took place during the first implantation procedures, with no consequences for the patients [54]. Fractures during impaction of femoral components may be due to high tension stress for excessive wedge loading. In intraoperatively fractured BIOLOX<sup>®</sup> *delta* ceramic femoral components, the fracture lines were located in the corners of the femoral resection showing the relevance of precise intraoperative preparation of the bone stock. The problem was overcome both by the optimized design of the device and by the optimization of the instrumentation that allowed the precise preparation of the bone avoiding inadequate anterior and posterior bone resection. However, no fractures of the implanted components were observed during the 24-month follow-up.

---

## Trends and Perspectives of Bioinert Ceramics in Joint Replacements

So far, it can be calculated that more than six million alumina ball heads have been implanted worldwide since the introduction of alumina in arthroplasty. Notwithstanding, the excellent clinical results of alumina in THR bearings, especially in ceramic-on-ceramic bearings, and the intrinsic brittleness of alumina limit the flexibility in design of ceramic components. The development of third-generation, fine-grained, HIP-treated alumina increased the bending strength of the material, but the limits in toughness remain. On the other hand, the unexpected *in vivo* fracture of about 400 heads in 2000 [58] and the worldwide recall of Prozyr<sup>®</sup> that was the leader of zirconia orthopedic market created a lack of confidence in this material. Consequence of this situation was the sudden decrease of the sales of zirconia ball heads, a situation not fully justified, because as a matter of fact Prozyr<sup>®</sup> fractures were limited to two well-identified batches. So far only one hip resurfacing device is making use of Mg-PSZ shell, while a knee replacement with Y-TZP femoral component is under clinical investigation in the USA. Y-TZP is presently used mainly in dentistry [10] for bridges, crowns, dental implants, and endodontic posts.

The abandon of zirconia opened a technological gap in orthopedics that stimulated the development of alumina-zirconia composites (ZTA and ATZ). The mechanical behavior of ceramic composites allows flexibility in device design and a reliability of ceramic components which was not previously achievable with pure alumina. In fact, these high-performances, tough composite ceramic biomaterials for joint replacements are today the standard ceramic for arthroprosthesis bearings, leaving pure alumina components only a niche role in today's orthopedic market.

The new composites made possible the development of a series of innovative ceramic devices that will contribute to satisfy the needs of today's patients and to even further increase the positive outcomes of hip and knee arthroplasty. Further

developments can be expected by the application of ceramic components in shoulder arthroplasty, where there is growing relevance of the treatment of patients with metal hypersensitivity and young and active ones, providing high biocompatibility and reduced wear.

---

## Summary

The use of alumina and zirconia bioceramics in arthroprostheses is a consolidate technology, especially in the bearings of total hip replacements. The use alumina for the ball head and socket of hip implant started about 1970 in Europe, and today several millions of these components have been implanted worldwide. On the other hand, Zirconia ball heads (tetragonal zirconia polycrystal) were used coupled to polyethylene cups from 1995 to 2001 only. So far, zirconia is used almost exclusively in ceramic composites with alumina, which are the state-of-the-art of bioceramics in joint replacement bearings. The rationale of the use of ceramics in the bearings of prosthetic joints is the minimization of the volume of wear debris released during patient activity, which are the triggers of a chain of cellular reactions leading to osteolysis and mobilization of the implant.

The chapter gives an historical overview of the development of alumina, zirconia and of their composites as biomaterials for the construction of ball heads and inserts for hip replacement sockets, as well as of their use in shoulder and in knee replacements. Ceramic knee are presently under clinical trials in the EU and in the USA, and are the latest and more challenging application of oxide bioceramics. The literature reporting the outcomes of bioceramics in the clinical setting is extensively discussed, as well as the specific complications of this technology.

---

## References

1. Jeffers JRT, Walter WL (2012) Ceramic-on-ceramic bearings in hip arthroplasty. *J Bone Joint Surg Br* 94-B:735–745
2. Fisher J, Jin Z, Tipper J, Stone M, Ingham E (2006) Tribology of alternative bearings. *Clin Orthop* 453:25–34
3. Daniel J, Holland J, Quigley L, Sprague S, Bandhari M (2012) Pseudotumors associated with total hip arthroplasty – current concepts review. *J Bone Joint Surg Am* 94:86–93
4. Piconi C, Streicher R (2013) Forty years of ceramic-on-ceramic THR bearings. *Sem Arthrop* 24:188–192
5. Calés B, Stefani Y (1998) Risks and advantages in standardization of bores and cones for heads in modular hip prostheses. *J Biomed Mater Res* 43:62–68
6. Schreuber LF, Usbeck S, Petkow F (2011) The taper in hip arthroplasty: what does the surgeon have to pay attention for? *Ceranews* 1:17–19
7. Piconi C, Porporati AA, Streicher RM (2015) Ceramics in THR bearings: behavior under off-normal conditions. *Key Eng Mater* 631:3–7
8. Dalla Pria P, Giorgini L, Kuntz M, Pandorf T (2006) Ceramic knee design. In: Benazzo F, Falez F, Dietrich M (eds) *Bioceramics and alternative bearings in joint arthroplasty*. Steinkopff, Darmstadt, pp 115–123

9. Kluess D, Bergshmidt P, Mueller I, Mittelmeier W, Bader R (2012) Influence of the distal femoral resection angle on the principal stress in ceramic total knee components. *Knee* 19:846–850
10. Piconi C, Condò SG, Kosmac T (2014) Alumina- and zirconia-based ceramics for load bearing applications. In: Shen JZ, Kosmac T (eds) *Advanced ceramics for dentistry*, 1st edn. Butterworth-Heinemann, Waltham, pp 220–225
11. Piconi C (2011) Alumina. In: Ducheyne P, Healey KE, Huttmacher DW, Grainger DW, Kirkpatrick CJ (eds) *Comprehensive biomaterials*, vol 1, 1st edn. Elsevier, Amsterdam, pp 73–94
12. Langer G (2002) Ceramic tibial plateau of the 70s. In: Garino JP, Willmann G (eds) *Bioceramics in joint arthroplasty*. Thieme, Stuttgart, pp 128–130
13. Oonishi H, Hasegawa T (1981) Cementless alumina ceramic total knee prostheses. *Orthop Ceram Implants* 1:157–160
14. Heimke G, Leyen S, Willmann G (2002) Knee arthroplasty – recently developed ceramics offer new solutions. *Biomaterials* 23:1539–1551
15. Piconi C, Maccauro G (1999) Zirconia as a ceramic biomaterial. *Biomaterials* 20:1–25
16. Piconi C, Maccauro G, Angeloni M, Rossi B, Learmonth ID (2007) Zirconia heads in perspective: a survey of zirconia outcomes in total hip replacement. *Hip Int* 17:119–130
17. Oonishi H, Kim SC, Oonishi H, Kyomoto M, Iwamoto M, Ueno M (2007) Comparison of in-vivo wear between polyethylene inserts articulating against ceramic and cobalt chrome femoral components in total knee prostheses. In: Chang J-D, Billau K (eds) *Bioceramics and alternative bearings in joint arthroplasty*. Steinkopff, Darmstadt, pp 149–159
18. Nakamura T, Oonishi E, Yasuda T (2004) New knee prosthesis with bisurface femoral component made of zirconia-ceramic. *Key Eng Mater* 254–256:607–610
19. Bal BS, Greenberg DD, Aleto TJ (2005) Primary total knee replacement with a zirconia femoral component. In: D'Antonio J, Dietrich M (eds) *Bioceramics and alternative bearings in joint arthroplasty*. Steinkopff, Darmstadt, pp 183–190
20. Sim FH, Chao EY, Pritchard DJ, Salzer M (1980) Replacement of the proximal humerus with a ceramic prosthesis: a preliminary report. *Clin Orthop* 146:161–174
21. Huckstep RL, Sherry E (1996) Replacement of the proximal humerus in primary bone tumours. *Aust NZJ Surg* 66:97–100
22. Piconi C (2010) Non-oxide ceramics. Status quo in THR and future options. In: Cobb JP (ed) *Modern trends in THA bearings*. Springer, Berlin, pp 37–44
23. Bal BS, Rahaman M (2011) The rationale for silicon nitride bearings in orthopaedic applications. In: Sikalidis C (ed) *Advances in ceramics – electric and magnetic ceramics, bioceramics, ceramics and environment*. InTech Europe, Rijeka, pp 421–432
24. Bal BS, Khandkar A, Lakshminarayan R, Clarke I, Hofman AA, Rahaman M (2008) Testing of silicon nitride ceramic bearings for total hip arthroplasty. *J Biomed Mater Res Appl Biomater* 87B:447–454
25. Sedel L (2000) Evolution of alumina-on-alumina implants: a review. *Clin Orthop Relat Res* 379:48–54
26. Tateiwa T, Clarke IC, Williams PA et al (2008) Ceramic total hip arthroplasty in the United States: safety and risk issues revisited. *Am J Orthop* 37:E26–E31
27. Hannouche D, Zaoui A, Zadegan F, Sedel L, Nizard R (2011) Thirty years of experience with alumina-on-alumina bearings in total hip arthroplasty. *Int Orthop* 35:207–213
28. Kim YH, Park JW, Kulkarni SS, Kim YH (2013) A randomised prospective evaluation of ceramic-on-ceramic and ceramic-on-highly cross-linked polyethylene bearings in the same patients with primary cementless total hip arthroplasty. *Int Orthop* 37:2131–2137
29. Cash DJ, Khanduja V (2014) The case for ceramic-on-polyethylene as the preferred bearing for a young adult hip replacement. *Hip Int* 24:421–427
30. Epinette JA, Manley MT (2014) No differences found in bearing related hip survivorship at 10–12 years follow-up between patients with ceramic on highly cross-linked polyethylene bearings compared to patients with ceramic on ceramic bearings. *J Arthroplasty* 29:1369–1372



31. Kabo JM, Gebhard JS, Loren G, Amstutz HC (1993) In vivo wear of polyethylene acetabular components. *J Bone Joint Surg Br* 75:254–258
32. Sychterz CJ, Engh CA Jr, Young AM, Hopper RH Jr, Engh CA (2000) Comparison of in vivo wear between polyethylene liners articulating with ceramic and cobalt-chrome femoral heads. *J Bone Joint Surg Br* 82:948–951
33. Delaunay C (2001) Couple de frottement des prothèses totales de hanche. Ce qu'un chirurgien orthopédiste devrait savoir. *Cahiers SOFCOT* 78:63–96
34. Meftah M, Klingenstein GG, Yun RJ, Ranawat AS, Ranawat CS (2013) Long-term performance of ceramic and metal femoral heads on conventional polyethylene in young and active patients: a matched-pair analysis. *J Bone Joint Surg Am* 95:1193–1197
35. Wang S, Zhang S, Zhao Y (2013) A comparison of polyethylene wear between cobalt-chrome ball heads and alumina ball heads after total hip arthroplasty: a 10-year follow-up. *J Orthop Surg Res* 8:20
36. Dahl J, Söderlund P, Nivbrant B, Nordsletten L, Röhrli SM (2012) Less wear with aluminium-oxide heads than cobalt-chrome heads with ultra high molecular weight cemented polyethylene cups: a ten-year follow-up with radiostereometry. *Int Orthop* 36:485–490
37. Wroblewski BM, Siney PD, Fleming PA (2005) Low-friction arthroplasty of the hip using alumina ceramic and cross-linked polyethylene. A 17-year follow-up report. *J Bone Joint Surg Br* 87:1220–1221
38. Caton J, Prudhon JL (2011) Over 25 years survival after Charnley's total hip arthroplasty. *Int Orthop* 35:185–188
39. D'Antonio JA, Capello WN, Naughton M (2014) High survivorship with a titanium-encased alumina ceramic bearing for total hip arthroplasty. *Clin Orthop Relat Res* 472:611–616
40. Imbuldeniya A, Chana R, Walter W, Zicat B, Walter W (2013) Long-term results of third generation alumina-on-alumina ceramic bearings in patients under the age of 55: a ten year minimum follow-up. *Bone Joint J Orthop Proc Suppl* 95-B:198
41. Lee GC, Knox DE, Garino JP (2013) Long-term results of hybrid alumina-on-alumina total hip arthroplasty: 10-14-year results. *Semin Arthrop* 24:202–205
42. Hernigou P, Homma Y, Pidet O, Guissou I, Hernigou J (2013) Ceramic-on-ceramic bearing decreases the cumulative long-term risk of dislocation. *Clin Orthop* 471:3875–3882
43. Chevalier J, Gremillard L, Deville S (2007) Low temperature degradation of zirconia an implication for biomedical implants. *Annu Rev Mater Res* 37:1–32
44. Piconi C, Maccauro G, Burger W, Muratori F, Richter HG (2006) On the fracture of a zirconia ball head. *J Mater Sci Mater Med* 17:289–300
45. Oonishi H, Murata N, Saito M et al (2001) Three to 18 year clinical results of total knee replacements with ceramic components. *Key Eng Mater* 192–195:881–884
46. Oonishi H, Oonishi H, Kim SC, Kyomoto M, Iwamoto M, Masuda S, Ueno M (2006) Ceramic total knee arthroplasty: advanced clinical experiences of 26 years. *Sem Arthrop* 17:134–140
47. Akagi M, Nakamura T, Matsue T, Ueo T, Nishijio K, Ohnishi E (2000) The bisurface total knee replacement: a unique design for flexion. *J Bone Joint Surg Am* 82-A:1626–1633
48. Calandruccio JH, Jobe MT (1997) Arthroplasty of the thumb carpometacarpal joint. *Sem Arthrop* 82:135–147
49. Athwal GS, Chenkin J, King GJ et al (2004) Early failures with a spheric interposition arthroplasty of the thumb basal joint. *J Hand Surg (Am)* 29:1080–1084
50. Masson B (2009) Emergence of the alumina matrix composite in total hip arthroplasty. *Int Orthop* 33:359–363
51. Hamilton WG, McAuley JP, Dennis DA, Murphy JA, Blumenfeld TJ, Politi J (2010) THA with Delta ceramic on ceramic: results of a multicenter investigational device exemption trial. *Clin Orthop* 468:358–366
52. White PB, Ranawat AS, Ranawat CS (2013) Ceramic-on-polyethylene: the experience of the Ranawat orthopaedic center. *Sem Arthrop* 24:206–210
53. Kim YH, Park JW, Kim JS (2014) Outcome of an ultrashort metaphyseal-fitting anatomic cementless stem in highly active obese and non-obese patients. *Int Orthop* 39(3):403–409

continuous development. Although the idea of using alumina as a biomaterial can be traced back to the 1930s and that several alumina dental implants were used clinically during the 1960s [10], it is widely acknowledged that the use of alumina in orthopedics is due to Dr. Pierre Boutin who developed, with the assistance of Pierre Blancquaert, the first ceramic-on-ceramic (CoC) THR bearing in the early 1970s made by Ceraver (Roissy, France) [11]. In Boutin's implants both the stem and the cup were cemented into the host bone, while in its first series, the ball head is fixed to the stem by epoxy glue.

In the same year, the German government launched a comprehensive research program on alumina for medical implants. This program led to two main achievements: the development of BIOLOX<sup>®</sup> alumina and the setup of the taper connection between the head and femoral stem. While BIOLOX<sup>®</sup> alumina is “the ceramic” in orthopedics, it is acknowledged that the development of taper connection opened the way to the modularity in THR which is today used worldwide by implant manufacturers.

Several ceramic manufacturers worldwide entered into the business of manufacturing alumina ball heads for THR. This led to an array of different alumina biomaterials depending on the precursors used, the process additives, the sintering, and finished products.

However, it is acknowledged that – depending of the process used – one can identify three consecutive “generations” of alumina ceramic biomaterials.

The “first-generation alumina” corresponds to the pioneering stage. Several of the products of this period were obtained by a suboptimal sintering cycle and were characterized by coarse grains, pores, and calcium impurities. Many failures occurred, and several manufacturers withdrew from the medical market. The production of this first-generation alumina ended about 1980. During this year, the International Standards Organization established the ISO 6474 that specifies the minimum requirements of chemical purity, density, grain size, and strength that are mandatory for the alumina ceramics intended for use as implant for surgery. This led to the production of the so-called second-generation alumina based on high-purity precursors, optimized batch and sintering cycle combined with the improvements in overall quality of the manufacturing process. There were also improvements in machining, which allowed the release of CoC bearings to the market without selecting “matched pairs” of ball heads and sockets.

The “third-generation alumina” was introduced into the market by the different manufacturers around 1995 (Table 3). It was the result of a number of process developments:

- Laser marking for component identification that resulted in an increase in reliability of alumina ceramic components. This technology replaced the marks made by diamond engraving before firing, an operation that was raising concerns about local stress concentrations leading to fracture.
- Final densification by hot isostatic pressing (HIP). This thermal treatment – performed slightly below the sintering temperature under extremely high pressures (100–200 MPa) – allows obtaining high density limiting the development of the grain size.

54. Bergschmidt P, Bader R, Ganzer D et al (2012) Ceramic femoral components in total knee arthroplasty – two year follow-up results of an international prospective multicenter study. *Open Orthop J* 6:172–178
55. Piconi C, Labanti M, Magnani G, Caporale M, Maccauro G, Magliocchetti G (1999) Analysis of a failed alumina THR ball head. *Biomaterials* 20:1637–1646
56. Pandorf T (2010) The importance of clean taper conditions using ceramic hip implants. In: Cobb JP (ed) *Modern trends in THA bearings*. Springer, Berlin, pp 97–102
57. Sciberras N, Sexton SS, Walter WL (2011) A review of squeaking in total hip arthroplasty. *Sem Arthrop* 22:276–279
58. Maccauro G, Piconi C, Burger W, Pilloni L, De Santis E, Muratori F, Learmonth ID (2004) Fracture of a Y-TZP ceramic femoral head. *J Bone Joint Surg (Br)* 86-B:1192–1196

Marius Niculescu, Bogdan Lucian Solomon, George Viscopoleanu,  
and Iulian Vasile Antoniac

## Contents

Introduction .....	860
Bone Cements Used in Cementing Techniques .....	862
Composition of Bone Cement .....	863
Properties of Bone Cement .....	864
Clinical Processing and Handling of Bone Cement .....	870
New Trends in Bone Cements Available for Clinical Use .....	871
Clinical Aspects About Cementing Techniques .....	873
Methods and Materials Used in Cementing Techniques .....	873
Surgical Technique and Operative Steps of a Cemented Hip Arthroplasty .....	884
New Concepts in Cemented Total Hip Arthroplasty .....	890
Aspiration of the Iliac Wing .....	890
Modification of the Metallic Stem Surface .....	891

---

M. Niculescu (✉)

Department of Orthopaedics and Trauma I, Colentina Clinical Hospital, Bucharest, Romania

Faculty of Medicine, Titu Maiorescu University, Bucharest, Romania

e-mail: [mariusniculescu@yahoo.com](mailto:mariusniculescu@yahoo.com)

B.L. Solomon

Royal Adelaide Hospital, Department of Orthopaedics and Trauma, Centre for Orthopaedic and Trauma Research and Discipline of Orthopaedics and Trauma, The University of Adelaide, Adelaide, SA, Australia

e-mail: [bogdansolomon@me.com](mailto:bogdansolomon@me.com)

G. Viscopoleanu

Department of Orthopaedic Surgery, “Foisor” Orthopaedic Hospital, Bucharest, Romania

e-mail: [ge0\\_visc0@yahoo.com](mailto:ge0_visc0@yahoo.com)

I.V. Antoniac

University Politehnica of Bucharest, Bucharest, Romania

e-mail: [antoniac.iulian@gmail.com](mailto:antoniac.iulian@gmail.com)

Preheating of the Metallic Stem .....	894
Special Cementing Techniques .....	894
Summary .....	896
References .....	897

## Abstract

Cementing techniques have evolved considerably since cemented hip arthroplasty was first introduced by Sir John Charnley in the 1970s. Much has been learned about the properties of bone cement, and with this understanding, techniques associated with its use have evolved. Substantial improvements have been made during its evolution from the first to third generation of cementing techniques. The main developments have been in the areas of bone preparation, cement preparation, and cement delivery. First-generation cementing techniques were quite rudimentary, and long-term results for cemented implants were not impressive by today's standards. These techniques have evolved significantly over time, in line with the increased knowledge regarding cement properties and behavior and the impact of bone preparation on the bone-cement interface. Since the beginnings of cemented arthroplasty, many important factors which can affect the quality of fixation have been improved. The mean survival of a cemented hip implant in the early years was approximately 10 years. With the evolution of cementing techniques, this value has increased significantly with some hip implants now surviving over 25 years. The survivorship is greatly influenced by the quality of the fixation, which is dependent on a solid bone-cement interface. This interface is created by interdigitation of cement particles in the cancellous bone of the femur. The bone bed must be cleaned of debris and blood in order for the cement to penetrate the cancellous bone as deeply as possible. Penetration is dependent on pressurization of the cement in the femoral canal and acetabulum and is achieved by the use of specialized tools. The cementing techniques and materials used in modern orthopedic practice and possible future developments will be discussed. In order to give more practical information related to the cementation in orthopedic surgery, authors will present the surgical technique and operative steps of a cemented hip arthroplasty, well illustrated with images during surgical intervention. Also, different concept recently introduced in the field of cemented total hip arthroplasty will be presented.

## Keywords

Cementation technique • Bone cements • Hip arthroplasty • Stem • Bone • Interface • Mixing • Cement mantle

## Introduction

Cementing techniques have evolved considerably since cemented hip arthroplasty was first introduced by Sir John Charnley in the 1970s. Much has been learned about the properties of bone cement, and with this understanding, techniques associated

**Table 1** Evolution of cementing techniques

Generation	Type of mixing	Bone preparation	Insertion of cement	Centralization
<b>First</b>	Hand mix	Rasp only	Manual insertion, finger packing	None
<b>Second</b>	Hand mix	Aggressive rasping, pulsatile lavage	Cement gun, canal plug	Early distal centralizers
<b>Third</b>	Hand mix, vacuum mix/centrifugation	Aggressive rasping, pulsatile lavage	Cement gun with pressurization, distal canal plug	Proximal and distal centralizers

with its use have evolved. Substantial improvements have been made during its evolution from the first to third generation of cementing techniques. The main developments have been in the areas of bone preparation, cement preparation, and cement delivery [1–3].

First-generation cementing techniques were quite rudimentary, and long-term results for cemented implants were not impressive by today's standards. These techniques have evolved significantly over time, in line with the increased knowledge regarding cement properties and behavior and the impact of bone preparation on the bone-cement interface.

Since the beginnings of cemented arthroplasty, many important factors which can affect the quality of fixation have been improved. The mean survival of a cemented hip implant in the early years was approximately 10 years. With the evolution of cementing techniques, this value has increased significantly with some hip implants now surviving over 25 years. The survivorship is greatly influenced by the quality of the fixation, which is dependent on a solid bone-cement interface. This interface is created by interdigitation of cement particles in the cancellous bone of the femur. The bone bed must be cleaned of debris and blood in order for the cement to penetrate the cancellous bone as deeply as possible. Penetration is dependent on pressurization of the cement in the femoral canal and acetabulum and is achieved by the use of specialized tools [3] (Table 1).

Polymethyl methacrylate (PMMA) bone cement has a very important role in modern orthopedics. It is widely used in joint replacement procedures, but especially in hip, knee, and shoulder arthroplasty, for the reconstruction of bone defects in fractures and tumor surgery, and in spinal surgery for percutaneous vertebroplasty and kyphoplasty. Bone cement was first introduced and used over 60 years ago, and it now has a key role in modern practice. The understanding of its properties has improved over time, and along with progress in orthopedic practice tissue science and biomechanics, this has led to important changes in implant designs and cementing techniques.

The use of acrylic bone cement will continue, and as the knowledge of its properties and applications improves, better clinical results can be expected [1]. Polymethyl methacrylate was first revealed by the chemical industry in 1843 and was first synthesized by Otto Röhm, a German chemist. In 1936, the Kulzer

company discovered that mixing a powdered polymer with a liquid monomer and an initiating agent resulted in a dough which could be molded, making it one of the first biomaterials. Its first applications were in dentistry and later in orthopedic surgery where it was mainly used for the fixation of implants. During the Second World War, it was discovered that this dough could be polymerized at room temperature, and it was used in cranioplasties and also, by Jean and Robert Judet, for securing femoral head prostheses.

The most important breakthrough in the use of PMMA in total hip arthroplasty (THA) was made by Sir John Charnley in the 1970s, who pioneered its use for fixation of the acetabular and femoral components to the bone. Charnley was looking for a viscous material with resistance to body fluids, low toxicity, which could be easily manipulated, and had a reasonable setting time. Charnley experimented with various materials before settling on PMMA, a material which had all the desired properties. He found that acrylic cement could easily fill the medullary canal and blended with the bone morphology, providing an increase in mechanical stability and decreasing the stress on the implant [2].

Although many improvements have been made since Charnley first described cemented THA, and implant survivorship has significantly improved in both hip and knee arthroplasty, the orthopedic and scientific communities are still searching for ways to improve the techniques and materials used, in order to further increase the survival rate of implants to the extent that revision surgery will be needed in as few cases as possible.

The cementing techniques and materials used in modern orthopedic practice and possible future developments will be discussed. In order to give more practical information related to the cementation in orthopedic surgery, authors will present the surgical technique and operative steps of a cemented hip arthroplasty, well illustrated with images during surgical intervention. Also, different concept recently introduced in the field of cemented total hip arthroplasty will be presented.

---

## **Bone Cements Used in Cementing Techniques**

Otto Röhm is considered the developer of PMMA in 1901. Industrial synthesis of methyl methacrylate was achieved in the 1920s, and the first clinical use of bone cement was in the field of dentistry. In 1936 it was discovered that mixing the methyl methacrylate monomer with polymer and a peroxide initiator resulted in a doughy material which could be shaped to its desired form, and then it would harden to become a very resistant material. Since its introduction into clinical practice, bone cement properties have been studied closely and improved in order to achieve mixtures that serve the needs of modern medical practice [1, 4, 5].

In the last decades, PMMA bone cement (acrylic cement) has been successfully used for the fixation of total joint replacement prostheses to adjacent bone, for augmentation of bone defects, and in spinal surgery for vertebroplasty. The acrylic bone cement used in modern orthopedic practice consists of two components, a

**Table 2** Constituents of commercial bone cement

Constituent	Role
<i>Powder components</i>	
<b>Polymer</b>	Polymethyl methacrylate
<b>Copolymer (e.g., MA-MMA)</b>	Alter physical properties of the cement
<b>Barium sulfate or zirconium dioxide</b>	Radio-opacifiers
<b>Antibiotics</b>	Antimicrobial prophylaxis
<b>Dye (e.g., chlorophyll)</b>	Distinguish cement from bone
<i>Liquid components</i>	
<b>Monomer</b>	Methyl methacrylate monomer
<b>N,N-Dimethyl-p-toluidine (DMPT)</b>	Initiates cold curing of polymer
<b>Benzoyl peroxide</b>	Reacts with DMPT to catalyze polymerization
<b>Hydroquinone</b>	Stabilizer preventing premature polymerization
<b>Dye (e.g., chlorophyll)</b>	Distinguish cement from bone

**Table 3** Mechanical properties and values for different bone cements

Property	Value range (MPa)
<b>Ultimate tensile strength</b>	36–47
<b>Ultimate compressive strength</b>	80–94
<b>Bending strength (four-point configuration)</b>	67–72
<b>Shear strength</b>	50–69
<b>Mean fracture toughness</b>	1.52–2.02 (MPa√m)

liquid and a powder, that are mixed in the operating room to form a doughy material that is applied to the bone before the insertion of the desired implant (Tables 2 and 3).

The main function of bone cements in joint replacement is to provide stable and durable fixation of the components to the bone. In 1958, Sir John Charnley was the first to use acrylic cement for fixation of the femoral component in the medullary canal in a similar fashion to how it is done in modern arthroplasty. The early cemented hip replacements had high failure rates which were not caused by the cement itself but by the use of polytetrafluoroethylene acetabular cups. The first packages of sterilized bone cement, for use in arthroplasty, were manufactured in 1966 [1, 6].

There are many factors that influence the properties and behavior of bone cement. Chemical composition, porosity, viscosity, addition of antibiotics and opacifiers, mixing techniques, sterilization, and surrounding temperature all affect the clinical performance of bone cement.

## Composition of Bone Cement

Commercial acrylic bone cement packs are comprised of two components: a powder component, usually in a 40-g package, and a liquid component, in a 20-mL bottle. There are several reasons behind using two components instead of polymerizing



pure methyl methacrylate monomer. The polymerization of the methyl methacrylate monomer is very slow and can take hours to days. Additionally, the pure methyl methacrylate monomer is very slow and can take hours to days. Additionally, the pure methyl methacrylate monomer has very low viscosity and can easily diffuse into the blood stream, leading to severe cardiorespiratory complications.

The heat generated during polymerization can increase to over 100 °C and could lead to boiling of the volatile methyl methacrylate monomer. Thus, the use of less monomer along with the presence of prepolymerized PMMA beads in the powder decreases the number of polymerization reactions and so reduces the amount of released heat, decreasing the overall temperature.

Another important consideration is that of cement shrinkage. After polymerization of pure methyl methacrylate into PMMA, the overall volume reduction would be of about 21 %, because of differences in density between the two materials. This would be unacceptably high as it would lead to large gaps at the cement-bone and cement-prosthesis interfaces, severely compromising the quality of fixation [1, 7].

The powder is usually the variable part of bone cements, contributing to the differences in properties between different commercial brands. The powder is composed mainly of prepolymerized PMMA beads which constitute 83–99 % of the powder. These prepolymerized beads include copolymers of methyl methacrylate with styrene, methyl acrylate, or butyl methacrylate comonomers. The other components of the powder are radio-opacifiers (barium sulfate, zirconium dioxide), initiator molecules (benzoyl peroxide), dye, and, increasingly common, antibiotics. It is known that the methyl methacrylate monomer can polymerize under exposure to heat and light, but this process is very slow. So, a reaction initiator must be included in the powder component. Apart from dibenzoyl peroxide (BPO), other initiators used are tri-*N*-butylborane and the accelerator 2,5-dimethylhexane-2,5-hydroperoxide [8].

The liquid monomer is a colorless liquid with a distinct odor and is packed in specially designed ampules. Its components are consistent among different commercially available cements. It consists of 99 % methyl methacrylate. *N,N*-Dimethyl-*p*-toluidine (DMPT) represents up to 2.8 % of the mixture, by weight, and its role is as an accelerator which speeds up the polymerization and setting of the bone cement.

Because the methyl methacrylate can spontaneously polymerize, it requires addition of a stabilizer (usually hydroquinone), which prevents premature polymerization [9].

Methyl methacrylate polymerization takes place by the mechanism of free radical polymerization. This reaction consists of three steps: initiation, propagation, and termination.

## Properties of Bone Cement

### Heat Production During Polymerization

The polymerization of PMMA is an exothermic reaction. The temperatures measured in vitro reach as high as 120 °C, with in vivo temperatures as high as 40–56 °C.

The methyl methacrylate monomer contains carbon-carbon double bonds, which react with free radicals produced by the initiators. The free radicals from the monomer interact with other monomer molecules and create a growing polymer chain. During polymerization, the powder transforms to a moldable dough [8]. This reaction releases 52 kJ/mol of monomer, this being equivalent to a heat production of  $1.4 - 1.7 \times 10^8 \text{ J/m}^3$ . In vitro studies have shown that thicker cement mantles and a greater ratio of monomer to polymer lead to higher ambient temperatures and greater heat production. Recorded temperatures range between 70 °C and 120 °C. Knowing that collagen denaturates at temperatures in excess of 56 °C, many authors have emphasized the risk of thermal necrosis of the surrounding tissues.

Despite these concerns, in vivo studies have recorded lower peak temperatures. There are several reasons for the lower in vivo temperatures: blood circulation, large surface area of the interface, heat dissipation to the prosthesis and the surrounding tissue, thin layer of bone cement, and poor thermal conductivity of the cement.

Reckling and Dillon measured the temperature at the bone-cement interface in 20 patients undergoing total hip replacement, and the maximum recorded temperature was 48 °C. However, Harving, Soballe, and Bunger recorded temperatures higher than 56 °C but only for short periods of time (2–3 min). So, it can be speculated that the bone temperature during cementation might not surpass the coagulation temperature of proteins [1, 10].

### **Curing of Bone Cement**

When the powder and liquid are mixed, two processes are started. The polymer powder mixes with the monomer liquid and forms a viscous fluid or dough. This is explained by the swelling and dissolution process of the monomer and polymer powder. Also, a chemical process is initiated, which is responsible for the hardening of the bone cement.

The initiator (BPO) and the activator (DMPT) interact and produce free radicals in the initiation reaction. The resultant radicals start the polymerization of methyl methacrylate. This results in a growing chain of polymers that builds up macromolecules. Because of the high number of free radicals that are generated, many growing polymer chains are quickly formed, and this results in a fast conversion of the methyl methacrylate to PMMA. When two polymer chains meet, they unite and are terminated, resulting in an unreactive polymer molecule.

Polymerization is an exothermic reaction and is influenced by the chemical composition of the cement, the powder to liquid ratio and the presence of a radio-opacifier [8].

### **Polymerization Shrinkage**

Polymerization essentially means a conversion of a large number of monomer molecules to a smaller number of polymer molecules. This explains the shrinkage of bone cement during the curing phase. The phenomenon can be explained by the fact that the molecular distance between free monomer molecules is greatly reduced when they are bonded in the polymer chains. The volume shrinkage has been measured at approximately 21 %.

Commercially available bone cements use a variable quantity of prepolymerized powder, and the content of methyl methacrylate is reduced to approximately a third of the mass. Therefore, the shrinkage of commercial bone cements is about 6–7 %. The real shrinkage is even lower, because of the air inclusions in the cement dough.

Considering these facts, the real volume shrinkage of hand-mixed cement should be lower than that of the vacuum-mixed ones because these have very few air inclusions. Acrylic bone cement absorbs water, meaning that the actual shrinkage is compensated for by the expansion caused by fluid absorption [9].

### Viscosity of Bone Cements

The dynamic viscosity ( $\eta$ ) of fluids is denoted by shear stress (F)/shear rate (S). A fluid is considered as Newtonian as shear stress is related linearly to shear rate. Bone cement behaves as a non-Newtonian fluid in its liquid phase, having high viscosity which decreases as shear rate is increased. This is called pseudoplastic or shear-thinning behavior. However, the viscosity of all cements increases during polymerization, with the lengthening of the polymer chains. The viscosity can be altered by the manufacturer, by changing the molecular weight, by adding copolymers, and by varying the methods of sterilization. Also, the curing process can be controlled by modifying the proportions of initiator and monomer and thus changing the working properties [11].

Once the cement components are mixed, they turn into a viscous liquid, which then turns into a viscoelastic material and finally hardens into an elastic solid. It is important to monitor the dynamic viscosity and the viscoelastic parameters such as the storage modulus (G) and loss modulus ( $G''$ ). A high storage modulus indicates a more solid-like material, whereas a high loss modulus means that the material is more viscous [8].

The viscosity of bone cements in their dough stage is determined mainly by their chemical composition and the powder to monomer ratio. These parameters should never be modified in the operating room in order to change the viscosity. Methods for modifying cement viscosity without altering its properties actually exist. One such method is prechilling of the cement. It is a known fact that the velocity of the polymerization reaction and hence the viscosity of the cement is temperature dependent.

Another method of changing viscosity is the preheating of the cement in order to accelerate the polymerization. Studies have shown that heating of the cement powder leads to an alteration of its properties and structure. This is dependent on the characteristics of the main constituent of the powder, which differs between brands, and it can have a low or high resistance to degradation by the preheat temperature. Cement viscosity can also be changed by modifying the molecular weight using copolymers [9].

Bone cement must be liquid enough during the working phase such that it can be forced through a delivery device and then flow under the pressures applied in order to penetrate the trabeculae of the cancellous bone, achieving microinterlock.

There are three types of bone cement, depending on viscosity: low, medium, and high viscosity cements.

- (a) *Low viscosity cements*: these types have a long waiting phase of up to 3 min which is known as the sticky phase. The viscosity then rapidly increases during the working phase, and the final hardening phase takes 1–2 min.
- (b) *Medium viscosity cements*: these types have a long waiting phase of 3 min, a working phase during which the viscosity increases slowly and a hardening phase of 1.5–2.5 min.
- (c) *High viscosity cements*: these types have a short waiting/sticky phase which is followed by a long working phase. The viscosity remains fairly constant until the end of the working phase. The hardening phase is about 1.5–2-min long. It is obvious that high viscosity cements are more forgiving with the surgeon and are the most frequently used type in modern orthopedics [1].

The rate of curing of cement is very sensitive to environmental factors. Low ambient temperatures during storing and mixing, and high humidity, lead to a prolonged setting time.

Examples of low viscosity cements are as follows: Palacos LV (Schering-Plough; Heraeus Kulzer), Versabond (Smith & Nephew; Memphis/USA), Cemfix 3 (Teknimed), CMW 3 (DePuy), Sulcem 3 (Zimmer; Baar/Switzerland), Osteopal (Biomet Merck; Heraeus Kulzer), and Osteobond (Zimmer; Warsaw/USA).

Examples of high viscosity cements: Palacos R (Biomet Inc; Warsaw/USA; Schering-Plough; Heist-op-den-Berg/Belgium; Heraeus Kulzer; Wehrheim/Germany), Palamed (Biomet Merck; Ried/Switzerland; Heraeus Kulzer), Simplex P (Stryker; Limerick/Ireland), Cemfix 1 (Teknimed; Vic en Bigorre/France), and CMW 1 (DePuy; Blackpool/England).

High viscosity during mixing can lead to entrapment of air which can lead to a reduction of the overall shear strength of the cement [8].

### **Residual Monomer**

A radical polymerization of all monomer molecules does not take place because the mobility of the remaining monomer molecules is inhibited at high conversion rates.

Thus, some residual monomer molecules will remain unpolymerized. Right after the curing process is completed, the content of any residual monomer is approximately 2–6 %. This percentage is reduced to about 0.5 % in the next 3 weeks. The main part of the remaining monomer is polymerized slowly after curing of the cement. A small part of it is released from the cement and metabolized to carbon dioxide and water in the citric acid cycle.

In past years it was believed that the main reason for cardiorespiratory side effects of cementing was the remaining monomer particles. However, it is now known that these problems are a result of increased intramedullary pressure and fat embolism [8].

### **Cement Morphology**

Hardened bone cement consists of prepolymerized beads of PMMA or copolymers fused with polymerized methyl methacrylate monomer, radio-opacifiers, and additives such as antibiotic powder, plus pores and voids and residual initiator particles.

These parts of a cement composition can lead to flaws in the final structure. When a critical flaw size is achieved, it acts as a site of stress concentration, which weakens the overall strength of the cement.

The Griffith crack criterion assumes that there is a critical flaw size unique to each material, above which its fracture strength is compromised. The critical flaw size for PMMA is approximately 70  $\mu\text{m}$ . Thus, if the pore size is smaller than the critical flaw size for PMMA, the porosity will not compromise the fracture strength of the cement.

It is known that hardened bone cement contains both macropores and micropores. Considering the Griffith theory, it is very important to eliminate the macropores which are bigger than 70  $\mu\text{m}$  in diameter. Elimination of macropores from the cement is achieved with the use of centrifugation and vacuum mixing methods.

Another source of flaws which can create stress concentration is radio-opacifier powder particles. The substances usually used are barium sulfate or zirconium oxide, and the particle sizes reach 0.2–2  $\mu\text{m}$  in diameter. Zirconium oxide is harder than barium sulfate. Poor spreading of the radio-opacifier particles between the prepolymerized cement beads can influence crack initiation and propagation if the generated flaws are larger than the critical size for PMMA. The radio-opacifier particles do not bond with the PMMA; they reside instead within the pores [9, 12].

### **Mechanical Properties of Bone Cement**

The most important function of bone cement is to provide stable and durable fixation of the implant to the bone. After surgery and over subsequent years, the cement mantle must endure considerable stresses at the two interfaces, and so an adequate strength of the cement column is of utmost importance for the long-term stability and survival of the fixation.

The cement mantle has the effect of acting like an elastic buffer between the prosthesis and the bone. The transfer of load from the prosthesis to the bone via the two interfaces, as efficiently as possible, is a decisive factor for the long-term stability of the implant. The total load which is transferred to the cement mantle is a mixture of compressive loading combined with bending, tension, shear, and torsion. It is very hard to reproduce this kind of force in a laboratory setting.

There are two fundamental measuring principles for determining the mechanical properties of bone cements: applying static stresses and dynamic stresses. Static tests imply uniaxial loading, increasing until failure, and dynamic tests involve some form of cyclic loading. Bone cement has a high compressive strength, but it is susceptible to fracture after tensile loading. The tensile strength of most bone cements is in the region of 50–60 MPa. Addition of antibiotics seems to reduce the tensile strength, but the differences in strength between plain and antibiotic cement are not statistically significant.

The compressive strength of bone cement is greater than its flexural strength which in turn is higher than tensile strength. This descending order is characteristic of all polymer materials. This means that tensile loading is the highest risk factor for failure. However, pure tensile forces are not really found in vivo, with complex loading type combinations being more relevant to functional situations.

Shear strength is very important to the survival of the implant. Debonding at the stem-cement interface plays a very important role in the failure of cemented femoral stems. The shear strength of the interface is influenced by the type of cement, the porosity of the cement, and the roughness of the implant surface. The increase of roughness over a certain level seems to have no beneficial effect. Cement type and its porosity have a minor influence on the static interface strength [11, 13, 14].

### **Water Uptake and Glass Transition**

Most of the tests performed on bone cement are executed with dry specimens, at room temperature. In the human body, the cement must perform at a temperature of 37 °C and in contact with body fluids. It is known that the mechanical properties of polymers vary significantly in relation to temperature and water uptake. Absorption of water by the material leads to a lower modulus of elasticity and a less stiff material. This, however, is not always a negative consequence. A decrease in stiffness may be good for fracture resistance and long-term stability.

The water uptake for commercial bone cements is about 1–2 % for plain types and slightly higher for antibiotic-loaded cements. The water uptake is higher during the first days *in vivo*, and the cement is completely saturated by 4–8 weeks after implantation.

The glass transition temperature is a physical parameter which defines the softening range of a material. This refers to a transition from a hard and rigid glassy state to a soft rubbery state with a low modulus of hardness, by heating the polymer. If the material used for fixation of an implant was soft and rubbery, it would not provide adequate fixation.

Bone cements can be used for the fixation of implants at temperatures which are less than their glass transition temperature and in the glassy state. The glass transition temperatures of acrylic bone cements in a dry state are in the region of 80–100 °C. These high temperatures are not achieved in the human body. The water absorption of the cement leads to a reduction of the glass transition temperatures of 20–30 °C 8 weeks after implantation. Therefore, the glass transition temperatures of water-saturated bone cement are approximately 60–70 °C.

Considering the fact that there is still a big difference between this parameter and the temperature of the human body, it is safe to say that the risk of loosening of the implant because of creep is very low [13].

### **Creep Behavior of Bone Cement**

PMMA bone cement presents a combination of elastic and viscous properties making it a viscoelastic material. If a polymer material is under constant load, its resulting deformation can be divided into immediate elastic deformation and time-dependent continuous deformation. Elastic deformation is the immediate result of the force applied to the material. It is a recoverable deformation. After this, a delayed continuous deformation takes place as a result of stress. A part of this deformation is recoverable over time after the load is removed. This aspect is called delayed elastic deformation or primary creep. The permanent deformation is called secondary creep.

Creep is dependent on the composition of the material, load, load duration, and temperature. If the bone cement is injected late, it will have an increased creep. We can conclude that creep not only depends on material properties but also on the handling of the cement by the surgeon. Cement creep leads to a relaxation of cement stress and generates a more uniform distribution of stress in the cement mantle [1, 13, 15].

### **Factors Which Influence Fatigue Behavior of Bone Cement**

In order for the implant to survive and remain fixed to the bone, the cement mantle must resist the various loads it is subjected to during gait. Fatigue behavior of bone cement is very important, and it can determine whether a fixation will survive for a long time or fail early.

The cement mantle in hip arthroplasty is subjected to numerous repeated cycles of loading during its lifetime. It seems that the sterilization process and the polymer powder influence the fatigue behavior of bone cements.  $\gamma$  and  $\beta$  irradiation significantly lowers the molecular weight of the polymer powder, whereas sterilization with ethylene oxide does not influence the polymer whatsoever. It has been demonstrated that a high molecular weight bone cement has a better fatigue performance than a low molecular weight cement.

Porosity of the cement also has a major influence on its fatigue life. Pores and other voids in the structure act as stress concentrators that initiate cracks and can lead to failure of the construct. The sources of porosity are considered to be the air surrounding the powder, air entrapment in the cement during mixing, and during transfer from the mixing container to the delivery device.

The number of pores in the cement mixture has been greatly reduced with the introduction of third-generation cementing techniques (vacuum mixing and centrifugation). Lower porosity means greater strength of the cement mantle [13, 14, 16].

### **Clinical Processing and Handling of Bone Cement**

Handling of bone cement and its behavior and properties during the setting phases are of utmost importance for orthopedic surgeons. Only by understanding these aspects and following the instructions recommended by the manufacturer can the cementation of the implant be successful and solid.

The handling and setting of bone cement has four different phases:

*Phase 1 – The mixing phase:* takes up to 1 min, and during this period the monomer powder and the liquid are homogenized by hand in a bowl or in specific containers (mixing systems) depending on the generation of cementing technique used.

*Phase 2 – The waiting phase:* takes several minutes, depending on the type of cement and handling temperature. In this phase the cement is sticky.

*Phase 3 – The working phase:* is approximately 2–4 min long, and during this period the surgeon must apply the cement and insert the prosthesis. The viscosity of the

cement must be appropriate in order to penetrate the bone trabeculae and withstand the bleeding pressure. If the viscosity is too high, the two interfaces between the bone, the implant, and the cement will not be satisfactory, and this can lead to early failure of the fixation.

*Phase 4 – The hardening phase:* is about 1–2 min long, and it is represented by the final setting process with production of polymerization heat.

During the waiting phase, swelling of the beads occurs, and this allows the polymerization to begin, causing an increase in viscosity. The cement becomes a sticky dough.

The working phase begins after the cement is not sticky any more, but it has a low enough viscosity which allows the surgeon to handle it and apply it to the desired place. During this phase, the polymerization of the chains continues, and there is an increase in viscosity.

When the cement is inserted, it must have a high enough viscosity to withstand the bleeding pressure of the blood flowing from the bone. If blood flow did occur, laminations would be formed, and the cement mantle would weaken.

The heat which is produced in this phase generates thermal expansion of the cement. Shrinkage of the cement also takes place as the monomer converts into polymer chains. In the final hardening phase, the polymerization ends, and the hardened cement is generated. The cement temperature initially rises and then decreases to body temperature. In this phase, as the cooling takes place, volumetric and thermal shrinkage occurs.

Variables such as the type of cement, its viscosity, the type of mixing system used, the surrounding temperature, the preheating of the powder, or the prosthesis components can significantly influence the handling phases [8, 9].

## **New Trends in Bone Cements Available for Clinical Use**

### **Antibiotic-Loaded Cement**

In the 1970s Buchholz and Engelbrecht were the first to incorporate the antibiotic gentamicin in PMMA bone cement. At first, the antibiotic powder was added by hand, and later it was incorporated during the manufacturing process. This has made antibiotic-loaded cement widely available for use in modern orthopedics for prophylaxis in primary arthroplasty and for the treatment of prosthetic joint infection. Over time it has been shown that oxacillin, cefazolin, vancomycin, clindamycin, tobramycin, and gentamicin are all stable in PMMA bone cement and are released into the surrounding tissues to produce their desired effect. The highest amounts of antibiotics are released in the first 24 h after implantation, but it has been demonstrated that bactericidal concentrations persist in the periprosthetic bone for up to 21 days after implantation. Small traces of antibiotics have even been found more than 5 years from the time of surgery.

The use of antibiotic-loaded cement only provides short- to medium-term protection against infection and should be accompanied by intravenous antibiotic



prophylaxis. In order to achieve the desired protection, the antibiotic must be released from the cement in concentrations which exceed the minimum inhibitory concentration of the colonizing bacteria [1, 17].

Bone cement acts as a matrix for the local application of antibiotics. With the use of antibiotic-loaded cement, a high concentration of antibiotic is established in the surrounding tissue. It is known that artificial implants are very sensitive to bacterial contamination because bacteria can proliferate on their surface without being disturbed by the immune system. The rapidly proliferating bacteria create a protective mucous layer, and they become resistant to antibiotics from the blood flow. So, generating a high concentration of antibiotic locally is very important to fight infection. The antibiotic concentration should be much higher than the minimum inhibitory concentration of the microorganism. To avoid the selection of resistant strains, a very high initial level of active substance must be generated with subsequent release in the following days or weeks [8].

Any antibiotic used in addition to PMMA bone cement should have a series of physical and chemical properties which make it suitable for use: low incidence of primary resistant bacteria, low rate of developing resistances, low allergenic potential, a good antibacterial effect at low concentrations, low protein bonding, chemical and thermal stability, good water solubility, adequate release from bone cement, and it should not influence the bone cement biomechanics [8]. After close study of the elution behavior of bone cement, gentamicin was shown to be one of the most suitable antibiotic additives for bone cement. It has a good antibacterial spectrum, a good concentration-dependent bactericidal activity, water solubility, and thermal stability.

Antibiotics are added to the bone cement in powdered form which means that it is almost impossible for the antibiotic to diffuse through a hard polymer. Thus, the mechanism of elution from the polymer is closely related to the water-absorbing properties of the cement. The diffusion rate is dependent on several factors such as the chemical composition of the cement, the surface area of the cement-bone interface, and also the handling of the cement. It has been demonstrated that the use of vacuum mixing decreases the rate of elution by as much as 50 %. Some authors investigated the release of two antibiotics, such as vancomycin and tobramycin, combined in the same mixture. They observed that the combination of two antibiotics led to an increased rate of elution. Because powdered gentamicin is an expensive material, its liquid form, which is much cheaper, has been tested for efficiency in bone cement.

Hsieh et al. investigated the use of liquid gentamicin alone or in combination with powdered vancomycin for the treatment of serious bone infections. They demonstrated that the vancomycin elution was increased by 45 % and the gentamicin by 146 %. The addition of liquid gentamicin, however, led to an increase in cement porosity and a decrease in compressive strength of the cement. Though it may not be indicated to use double antibiotic-loaded cement (vancomycin and gentamicin) for primary arthroplasty, it may be a solution for temporary spacers which are used for the treatment of complex bone infections [18–20].

Considering the fact that the manual addition of powdered antibiotics to the cement mixture can lead to a decrease in overall strength of the cement, the accepted

method is that of premixing the antibiotics in the cement powder by the manufacturer. It has been demonstrated that adding liquid antibiotics to the cement mixture increases porosity and decreases mechanical strength by as much as 45 %, due to the interference with the early stages of polymerization of the methyl methacrylate monomer. The recommended amount of antibiotic which should be added to a 40-g pack of PMMA varies between 0.5 and 3 g. However, even the addition of powdered antibiotics has been shown to lower the flexural strength of the cement but not as much as the addition of liquid antibiotics. The explanation would be that excessive amounts of added powder may create undissolved aggregates which generate flaws in the cement structure. The addition of 2 g of powdered antibiotics has no significant adverse effect on the properties of the cement [21, 22].

There is clearly a need for more research into the effects of single and multiple antibiotic additives on the properties of PMMA bone cement, in order for the materials to evolve and approach the ideal standard.

### **Chemotherapeutic Drugs in Acrylic Bone Cement**

PMMA can be used as a skeletal drug delivery system. As described above, acrylic bone cement is routinely used for local delivery of antibiotics with very good results in prophylaxis for arthroplasty and the treatment of osteomyelitis. Curettage of a tumor and packing of the bone defect with PMMA bone cement are currently a routine practice for many types of bone tumors.

A few studies have investigated the effect of methotrexate, doxorubicin, and cisplatin loaded in acrylic bone cement for the treatment of recurrence of bone tumors. It has been shown that these substances remain active against different tumors; they resist heat polymerization and do not significantly alter the mechanical properties of the cement. Methotrexate is slowly released from bone cement for a few months, and it remains biologically active during this period. A few studies have tested the local effect of chemotherapeutic drug-loaded acrylic cement, and the results have been promising. The fact that sample sizes were small and patients with different pathologies were included makes the results inconclusive. Nevertheless, such approaches are full of potential, and further investigation is necessary [23].

---

## **Clinical Aspects About Cementing Techniques**

### **Methods and Materials Used in Cementing Techniques**

The implementation of modern cementing techniques, well known as third-generation cementing techniques, has led to better results of hip arthroplasty, with better long-term function and clinical outcomes and longer survivorship of the implant.

The main factor for long-term success of a hip arthroplasty is establishing good interlock at the cement-bone interface.

This can be seen on a regular anteroposterior and lateral radiograph as the absence of radiolucent lines between the cement mantle and the acetabular or femoral bone. A radiographical example is shown in Fig. 1.

**Fig. 1** Radiological image of one well-cemented hip arthroplasty with no radiolucent lines at the bone-cement interface and even distribution of cement

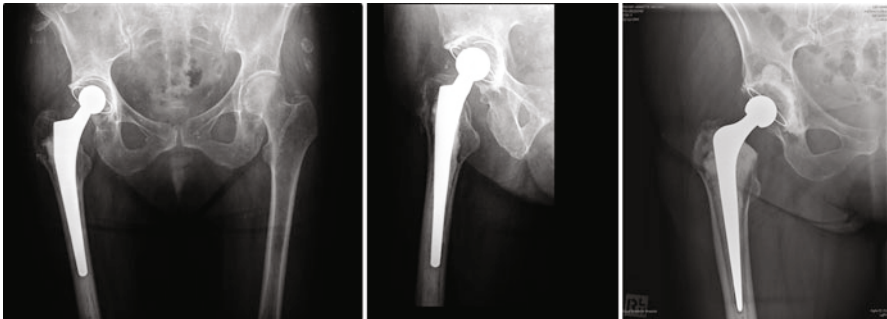


**Fig. 2** Radiological images of different clinical cases with deficiencies in cementation of a hip prosthesis – the presence of radiolucent zones at the cement-bone interface on AP and lateral X-rays

The presence of radiolucent zones at the cement-bone interface is unwanted as it represents a high risk of aseptic loosening of the implant in the years to come [24]. Figure 2 shows some radiological images of different clinical cases with deficiencies in cementation of the hip prosthesis.

Modern cementing techniques aim to obtain a solid and durable cement mantle, with a strong bone-cement interface which has a high shear strength that can resist axial loading, and thus provide a long-lasting fixation of the femoral stem and acetabular cup.

Third-generation cementing techniques refer to the following methods and materials:

- Thorough bone-bed preparation with pulsatile lavage
- Use of a distal cement restrictor

**Fig. 3** Pulsatile lavage system (intraoperative image)



- Retrograde cement application via a cement gun
- Femoral and acetabular pressurization
- The use of femoral stem centralizers
- Vacuum mixing (centrifugation) of bone cement

### **Pulsatile Lavage**

Bone preparation is critical for establishing a good cement-bone interface at the level of the cup and the femoral stem. The goal is to provide a clean and thin bed of cancellous bone for cement interdigitation. The operating team should use a pulsatile lavage system to remove all blood and debris from the bone surface which was obtained after reaming and broaching. A clean bone bed leads to better interdigitation of cement in the bone trabeculae, facilitating a more solid fixation and thus greater shear strength (Figs. 3 and 4).

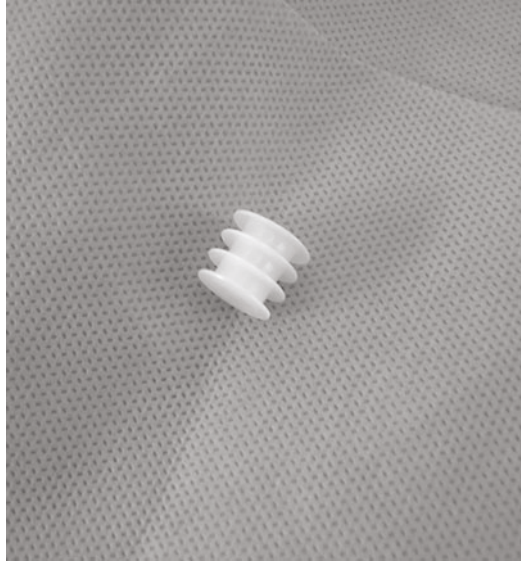
Pulsatile lavage consists of the application of saline solution under high pressure and immediate aspiration of the washing fluid. Pulsatile lavage, along with cement pressurization, is considered the most important and decisive step of modern cementing techniques, and with their introduction, the quality of fixation has significantly improved. Some authors argue that pulsatile lavage should be considered as a second- or third-generation technique, but irrespective of this debate, the fact remains that it is of utmost importance in modern hip arthroplasty.

This method of cleaning the bone bed is utilized for the acetabulum as well as the femur. It is also useful in many other situations in modern orthopedic practice [25].

### **The Distal Cement Restrictor**

The distal cement restrictor is a very important component of modern cementing techniques as without it cement pressurization would not be possible. As noted previously, pressurization is vital for obtaining good cement interdigitation, making the distal restrictor a vital component of the entire concept of cemented hip arthroplasty.

**Fig. 4** Example of a distal cement restrictor used in clinical practice



Even in early times, surgeons acknowledged the benefit of pressurization and prevention of distal migration of cement. Decades ago, bone grafts and cement were used to craft distal restrictors. However, the sealing and stability they provided was not good enough to prevent distal migration of the restrictor or leakage of cement. The presence of effective distal sealing also contributes to the uniformity of the cement mantle. A longer cement column that extends distal to the tip of the femoral stem is of no benefit as it does not increase stability in any way. Taking into consideration that the number of revision arthroplasties is rising, the presence of a bone or cement restrictor, or a longer cement column, is likely to cause problems if long stems need to be implanted. Bearing this in mind, the intramedullary plug should be positioned approximately 2 cm distal to the tip of the prosthesis, and it should be able to withstand the forces generated during pressurization of the femoral canal, which are approximately 0.21–0.42 MPa [24, 26, 27].

Modern distal cement restrictors are manufactured from polyethylene or other bioresorbable materials like gelatine. Their most important roles are to provide stability, not migrate distally, and to prevent leakage of the cement.

There are different ways to achieve these roles. Some flexible models, being larger than the canal, rely on a press-fit fixation. Others are rigid and lock proximal to the femoral isthmus. The third type of fixation is based on the expansion of the restrictor after it is implanted in the femoral canal. This kind of mechanism allows it to be positioned distal to the femoral isthmus in the setting of stovepipe femurs. All these types of restrictors have different instruments which are used for measuring the diameter of the canal and implantation.

After the canal is occluded with the plug, the bone must be thoroughly cleaned using pulsatile lavage and then dried. Although the canal is most commonly dried using a hydrogen-peroxide-soaked vaginal pack, this is controversial (as hydrogen

peroxide has been reported to cause emboli as it can enter venous system), and some surgeons use dry pack only. The prepared surface of the bone should appear white and without any blood. The surgeon can now apply the cement.

### **Femoral Cement Application via a Cement Gun**

First-generation cementing techniques applied cement in the femur in an antegrade fashion with the surgeon using the thumb for packing. Needless to say this method had many shortcomings: it did not generate enough pressure for adequate cement interdigitation to occur, air and blood were trapped in the cement mantle, and the cement was not uniformly distributed. These problems were risk factors for early loosening of the implant and subsequent implant failure.

In modern practice, a cement gun is used to deliver the doughy material in a retrograde fashion. A small tube is placed inside the canal when applying the cement in order for the air to be eliminated from the cavity. It is pulled out alongside the barrel of the cement gun.

The tip of the barrel should be placed directly above the distal plug in order for the cement column to begin in the correct place. The gun should be slowly pushed outside of the canal by the cement column itself [24, 27].

There are different types of cement guns on the market, belonging to different manufacturers. As could be seen in Fig. 5, the cement guns could be with and without cement recipient. In this last case, the bone cement is mixed in the recipient which is later attached to the cement gun.

The best timing for introduction of the cement depends on the type of cement used. Fast-setting cements should be applied very early after mixing because they polymerize very quickly. They sometimes cannot be introduced via a cement gun because the resistance generated by the dough is very high. Lower viscosity cement must be applied after a setting cycle in order to avoid delivery of a very fluid material that can protrude out of the femoral canal and into the joint or surrounding soft tissue. If the cement is not at the appropriate consistency, it can also mix with blood and increase the chance of pulmonary embolism. The ideal time for delivery is when the cement is doughy but not sticky [24, 27].

Studies comparing the effectiveness of different types of cement guns have been inconclusive. The performance of each system is dependent on the operator and the type of cement used. Low viscosity cement has a faster delivery time. In our opinion, there is no ideal system on the market, and further research is needed to compare the effectiveness of cement delivery systems [24].

### **Pressurization of Bone Cement in the Femur and Acetabulum**

Pressurization of bone cement and the use of pulsatile lavage have proven to be the most decisive and important parts of modern cementing techniques. Cement must enter the bone trabeculae as deeply as possible, and a clean bone bed is critical to achieve good interdigitation and microinterlock (Figs. 6, 7, and 8).

After the cement column has been applied via a cement gun, pressurization must begin. This can be accomplished either by the surgeon pressing with the thumb at the top of the canal or by using special tools (e.g., a cone) applied to the barrel of the

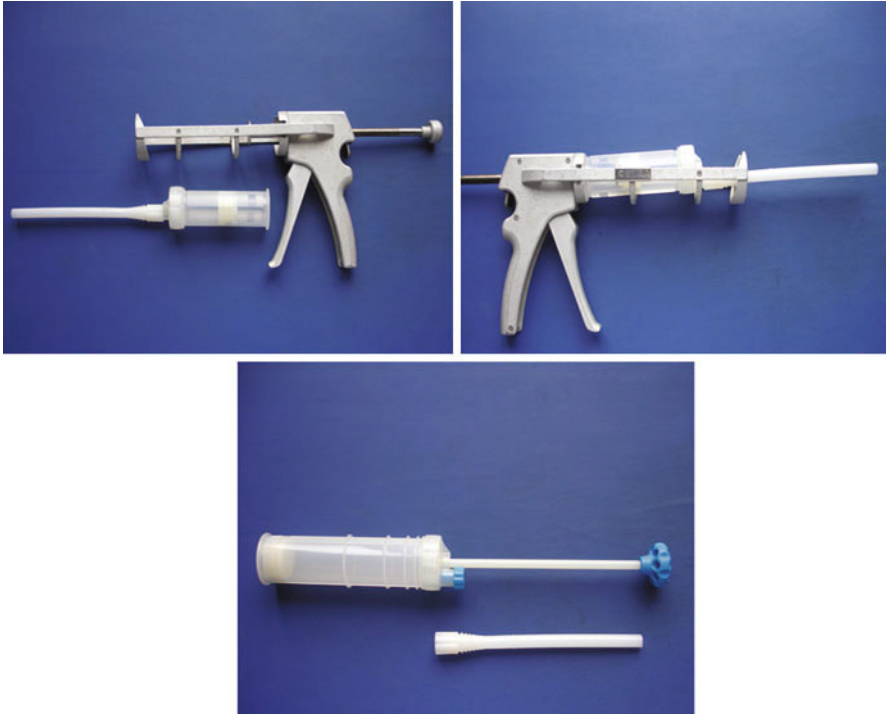


**Fig. 5** Cement guns with and without cement recipient used in clinical practice

cement gun. Special pressurization cones achieve better sealing of the proximal femur and thus greater pressurization.

The pressurization of the cement must exceed blood pressure which brings blood to the cement-bone interface. In order to achieve interdigitation, the pressure generated in the cement column must surpass blood pressure.

These methods have been shown to generate pressures of over 30 mmHg in the proximal cement mantle. Studies have shown that shear strength is higher if greater pressure levels are generated [28, 29].

Another important step in cementing techniques used in cemented hip arthroplasty is the introduction of the femoral stem. Introduction of the femoral stem has been shown to generate high pressure in the cement mantle surrounding it.

Some studies have shown that the highest pressures are achieved during insertion. It has also been shown that the later the stem is inserted, the higher the pressure levels. However, it is important not to wait too long because the cement might get too hard, making insertion of the femoral component impossible. It is clear that the cement should be applied via a cement gun in a more fluid state, and the stem must be inserted with the cement in a more doughy state [28, 29].

For application of cement to the acetabulum, the principles applied are very similar to those of femoral application, with the main difference being that the cement is usually manually applied. The acetabular cavity is prepared with reamers

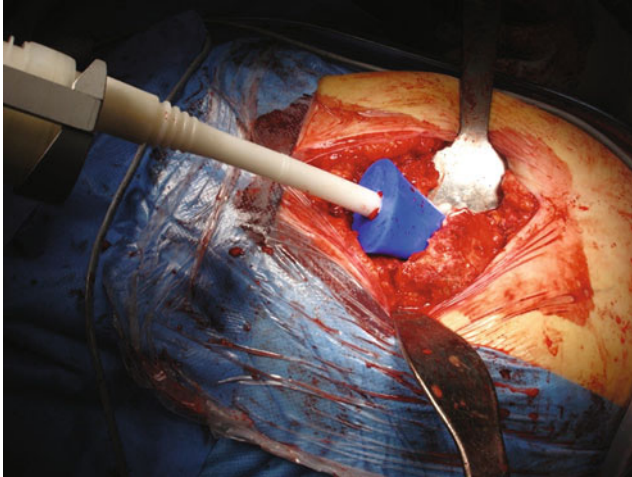


**Fig. 6** Surgical aspects related to the application of bone cement using a cement gun and a proximal restrictor

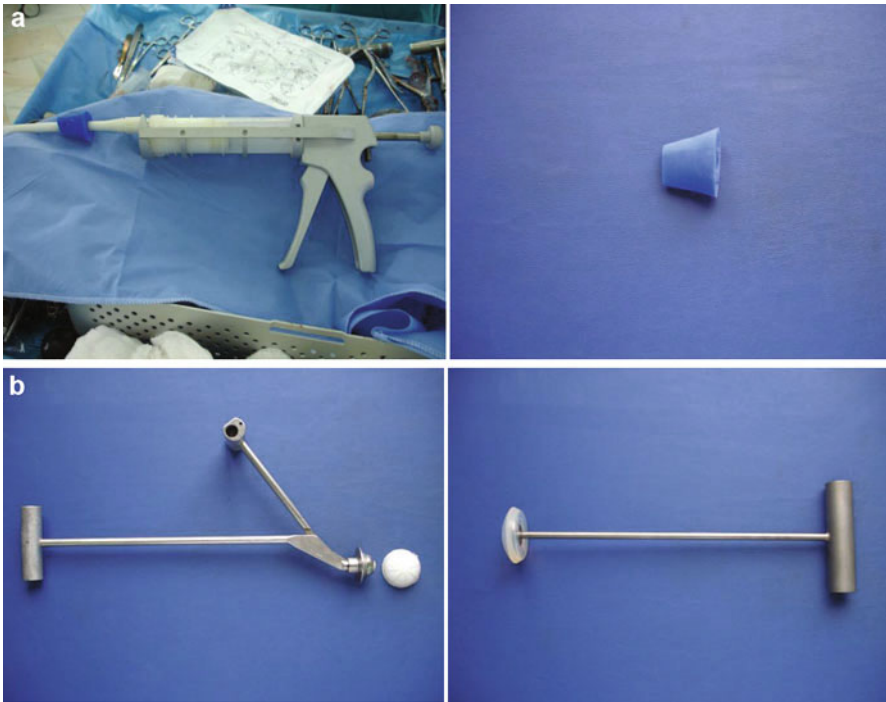


**Fig. 7** Different pressurizers used in cemented hip arthroplasty: (a) proximal femoral pressurizer; (b) acetabular pressurizer and polyethylene cup introducer



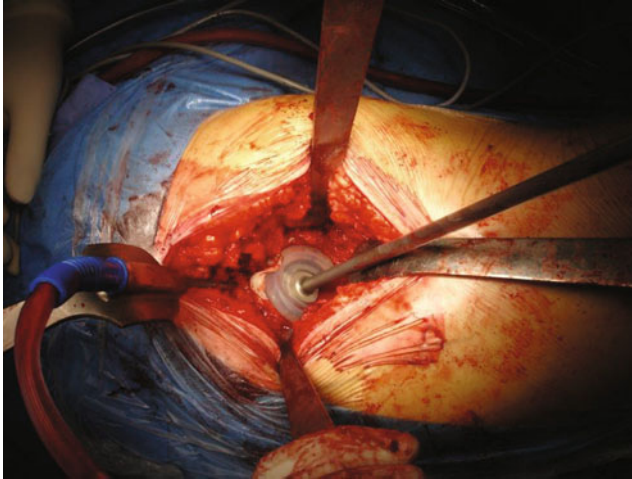


**Fig. 8** Acetabular pressurizer being used during surgery

in order to visualize cancellous bone and give the cavity its final form. Pulsatile lavage is very important in order to have a bone bed without blood and debris. Anchor holes should be drilled in the superior quadrants of the acetabulum to improve long-term fixation. After thorough lavage and drying of the bone surface, the cement is applied by hand or with a cement gun.

The cement must be in a doughy state, to prevent leakage outside of the cavity. Pressurization is mandatory and can be done with special instruments or with a sponge covered by a surgical glove. After pressurization, the cup is applied with an introducer that helps the surgeon maintain correct orientation during polymerization of the cement. The excess cement that has been pushed out should be removed, to prevent impingement or formation of loose particles [24].

### **Vacuum Mixing of Bone Cement**

First- and second-generation cementing techniques used hand mixing for the preparation of bone cement. This technique had many shortcomings. The cement dough obtained was not always of the highest quality, there were often powder particles which were not mixed with the monomer, there was a high exposure to fumes evaporating from the mixture, and the cement had a high porosity level. Studies have shown that the presence of pores in the cement mantle has a negative impact on the overall mechanical strength of the two interfaces that appear in the case of cemented hip prosthesis: metallic stem-bone cement and bone cement-bone interface. A detailed representation of these interfaces is shown in Fig. 9.

These pores in the cement are caused by trapped air bubbles that result in weak points in the solid structure of the cement mantle (an example is shown in Fig. 10).

Different problems that appear due the mixing process of the bone cements, like the presence of some gaps at the stem-cement interface or agglomeration of the powder phase of the bone cement, have a major influence on the stability of hip

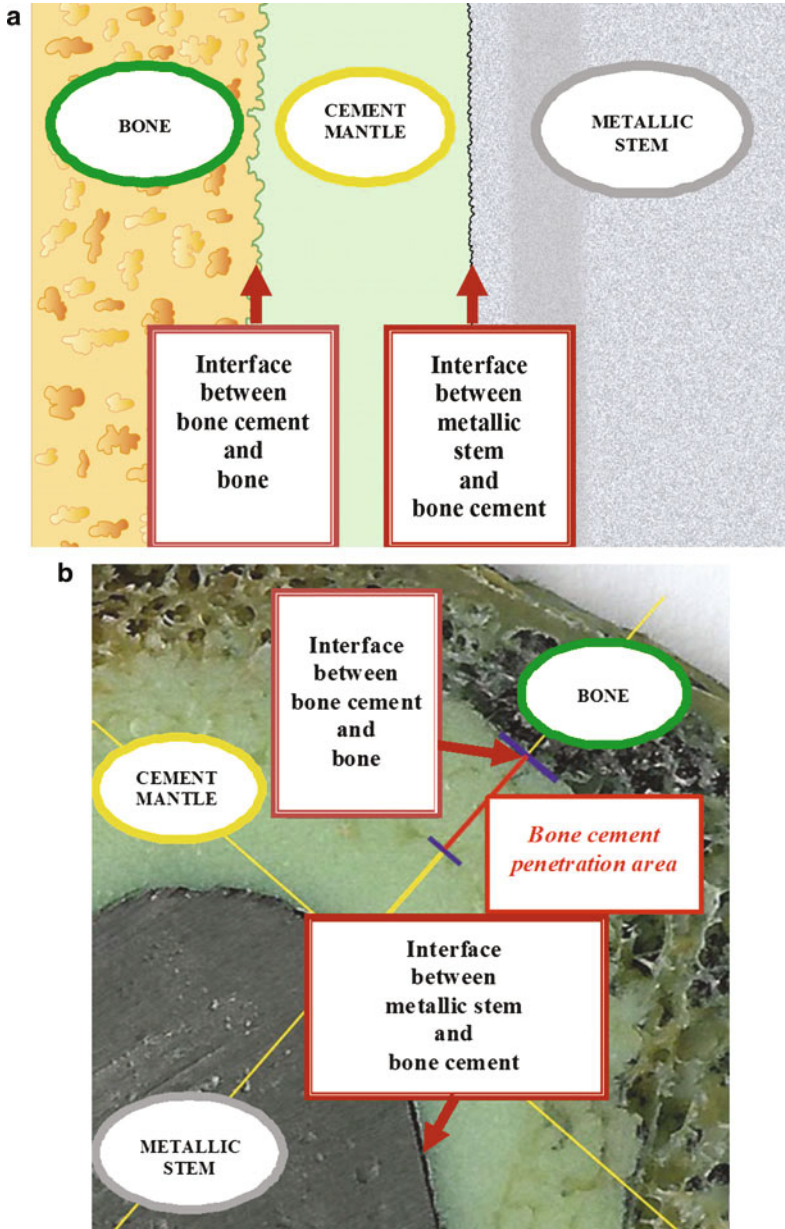


**Fig. 9** The interfaces that appear in the case of cemented hip prosthesis: metallic stem-bone cement and bone cement-bone interface (schematic view, *top*; interfaces on a retrieved prosthesis, *bottom*)

prosthesis. Unfortunately, these kinds of problems could be observed just using advanced microscopic techniques like scanning electron microscopy on the retrieved specimens (Fig. 11).

**Fig. 10** Macroscopic view of a failed hip prosthesis, showing the trapped air bubble into the cement mantle



The removal of these pores has been shown to lead to an increased overall strength of the cement. The current method for mixing cement in orthopedic practice is vacuum mixing/centrifugation [30, 31].

Different studies have demonstrated that vacuum mixing reduces macro- and microporosity in the cement. However, some authors claim that centrifugation eliminates only the macropores from the mixture. Other studies have shown that there isn't a great deal of difference in mechanical strength between hand- and vacuum-mixed cement. Mau et al. showed that although there was a significant difference in porosity between hand- and vacuum-mixed cement, this did not translate into a difference in the mechanical strength of the two interfaces [31].

Although there is still some debate on the subject, the general opinion is that vacuum mixing and centrifugation reduce the overall porosity of bone cement, and this should translate into an increased resistance of the two interfaces. Another benefit of vacuum mixing and centrifugation is that of reducing exposure to toxic methyl methacrylate fumes, as the concentration of toxic fumes in the surrounding air is ten times greater when hand mixing is used.

There are many vacuum mixing systems on the market (some of these are shown in Fig. 12), and the results vary depending on the type of system, the cement used, and the operator.

It has been demonstrated that the ratio between the quantity of the cement and the volume of the system's recipient has a direct impact on the porosity of the cement. Small packs of cement mixed in large recipients generate a higher level of porosity due to the higher volume of air trapped inside. It is also known that the vacuum pump doesn't always create a perfect void. Thus, while it would seem obvious that manufacturers should adapt the size of the mixing cartridge to the quantity of the cement used, this is not the case, with most manufacturing companies having only one or two sizes of cartridges [31].

**Fig. 11** Scanning electron microscopy images showing some problems that could appear due to mixing process of the bone cements: (a) presence of the gap at the stem-cement interface; (b) agglomeration of the powder phase of the bone cement

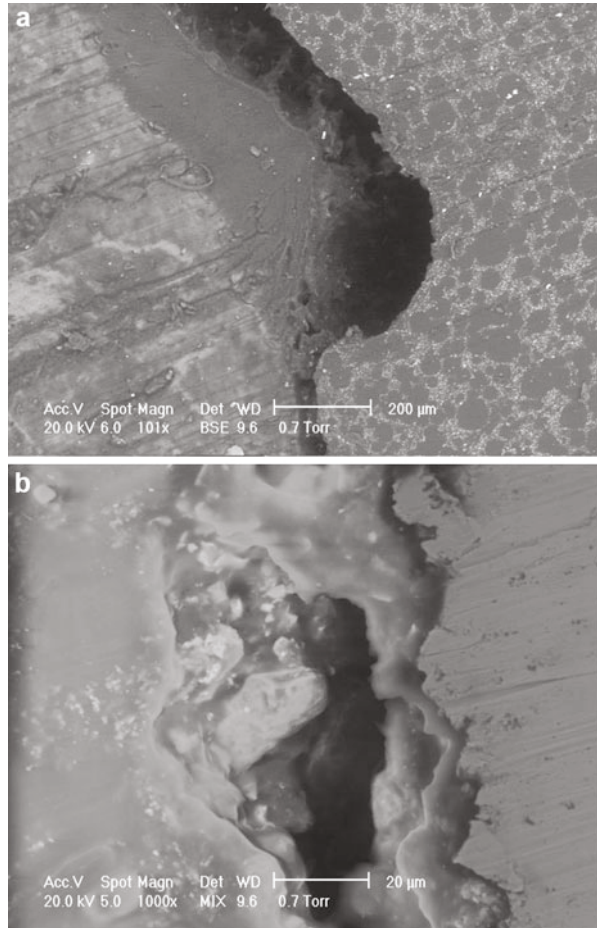


**Fig. 12** Different mixing systems used for bone cement



**Fig. 13** Example of the femoral stem centralizer: Exeter stem with distal plug centralizer

### Femoral Stem Centralizers

Achieving an adequate and even cement mantle around the femoral stem is very important for the long-term survival of the fixation. The stem must be well aligned, and its tip must not touch the bone walls of the medullary canal. While the entry point in the proximal femur is crucial, stem centralizers have proved to have a very important role in helping the surgeon insert the stem in a central position, avoiding varus or valgus positioning. If the prosthesis is positioned correctly, a uniform cement mantle will result, and the shear forces will be evenly distributed along the interfaces ensuring a higher survival rate of the implant [32].

An example of the femoral stem centralizer is shown in Fig. 13.

The use of distal centralizers in isolation helps the surgeon avoid direct contact between the tip of the prosthesis and the bone. However, they do not prevent cement mantle deficiencies in the proximal femur. Proximal stem centralizers have also been used and are considered an important part of modern cementing techniques.

The concomitant use of proximal and distal centralizers has proved very useful and has led to better results regarding stem positioning and cement mantle uniformity. Some studies have also demonstrated increased intramedullary pressures with their use [33, 34].

## Surgical Technique and Operative Steps of a Cemented Hip Arthroplasty

The surgical technique and the operative steps are very important for achieving a successful, well-fixed total hip arthroplasty. There are many variations of techniques which are used depending on the surgeon's preference, experience, and necessity for the case. We will describe in the following paragraphs the basic principles and the steps of a cemented hip arthroplasty (Figs. 14 and 15).

### Step 1. Positioning of the Patient on the Operating Table

The patient who is undergoing surgery is placed in either a supine or lateral decubitus position, depending on the surgeon's personal preference or depending on the type of approach that is going to be used.



**Fig. 14** Patient placed in lateral decubitus on the operating table before undergoing hip arthroplasty



**Fig. 15** Location of skin incision for surgical approach to the hip joint

The surgical approach can be defined as the way the surgeon dissects the anatomical planes in order to reach the desired structures.

After positioning on the operating table, the patient is draped, and the surgical site is cleaned with antiseptic solution. After the surgeons are dressed in sterile gowns and wear sterile gloves, the surgery can start.



**Fig. 16** Specialized reamers used for preparation of the acetabulum

### **Step 2. The Surgical Approach**

There are many approaches that can be used for hip surgery, depending on the surgeon's preference, the type of pathology addressed, or the type of surgical instruments available.

The most common used approaches are anterior, direct lateral, posterior, and anterolateral, all of them with variations used for minimally invasive surgery.

After the surgeon makes the skin incision, he starts dissecting the underlying muscular planes in order to reach the hip joint. Several specific instruments are used in order to facilitate exposure and achieve good visualization of the desired anatomical structures.

### **Step 3. Preparation of the Acetabulum**

After the hip joint is exposed, the femoral head must be dislocated from the acetabular cavity and resected in order to properly assess the local situation of the surface on which the polyethylene cup will be fixed with cement.

In the majority of cases in which an arthroplasty is required, the surface of the acetabulum is abnormal. The cartilage is destroyed, the cavity itself is deformed, and there is aberrant bone growth or there are bone defects which must be addressed.

In order for the surgeon to be able to fix the acetabular component with or without cement, the surface of the acetabular cavity must be clean, round shaped, and must have bleeding healthy cancellous bone on all its walls. So, when we say "preparation of the acetabulum," we refer to the actions the surgeon must undertake in order to achieve a cavity suitable for implantation of a cemented or uncemented cup.

This is achieved with a variety of specialized tools. The most important of those tools are the reamers which are round and have different diameters (Fig. 16).

Using reamers, the acetabulum is rounded, and bone and cartilage are resected until the desired diameter is reached, and the surface is adequate for implantation.

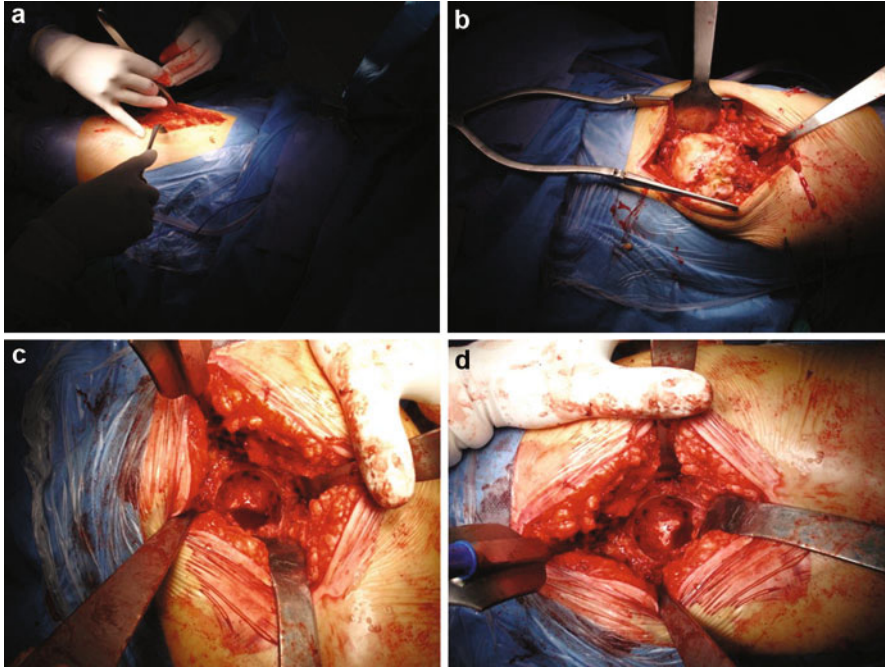


**Fig. 17** Surgical steps for preparation of the acetabulum: (a) dissection of muscles in a direct lateral approach to the hip joint; (b) dislocated femoral head; (c) exposure of acetabular cavity using specialized retractors; (d) aspect of acetabulum prepared for cup implantation

#### **Step 4. Implantation of a Cemented Cup**

After the bone of the acetabular cavity is prepared, it is thoroughly washed using a pulsatile lavage system in order to clean the cancellous bone trabeculae of blood and debris, and then it is dried using gauze swabs (Fig. 17).

After this, the cement, which has been mixed by the assistant on the instrument table, is inserted into the cavity, and pressurization is started immediately using either a glove packed with gauze swabs or a specialized pressurizer.

After the cement has been pressurized in the cavity for a few minutes, the polyethylene cup is inserted with a specialized instrument or by hand, and it is further compressed, until the cement has hardened. The inclination of the cup must be at about 45° (30–50°). The excess cement is removed.

The surgical steps for implantation of a cemented cup are shown in Fig. 18.

#### **Step 5. Preparation of the Femur**

The femoral stem is inserted and fixed in the medullary canal. As in the case of the acetabulum, the femur must be prepared in order to accommodate the stem and achieve a good fixation.



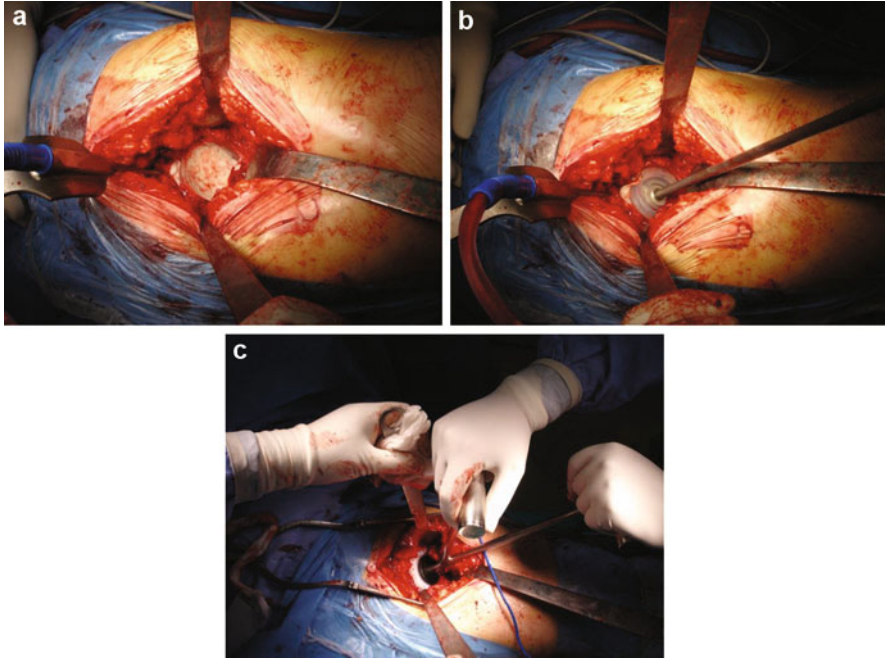


**Fig. 18** Surgical steps for implantation of a cemented cup: (a) acetabulum filled with bone cement; (b) bone cement pressurization; (c) polyethylene cup cemented in acetabulum

The femoral head is resected before the acetabulum is prepared. The resection line is at 1.5–2 cm above the lesser trochanter at an angle of approximately  $35^\circ$  to the femoral shaft axis. At the resection level, the entry point in the femoral canal is made with a specialized instrument, at the piriformis fossa, and then the canal is entered with a T-handle canal finder. Cancellous bone should be preserved medially and anteriorly (Figs. 19, 20, and 21).

After the direction of the canal is established, preparation can begin using specialized instruments called broaches. They are of different sizes and have the same shape as the femoral stem.

After the last broach is inserted in the femoral canal (as measured on the preoperative planning), the canal is washed of debris and blood multiple times using a pulsatile lavage system.

After this step, the distal cement restrictor is inserted in the canal at the appropriate depth (usually 2 cm distal to the expected tip of the hip prostheses). The assistant starts preparing the cement using a vacuum mixing system. During this step, the canal is packed with gauze swabs in order to thoroughly dry the bone. Usually 80 g (two packs) of cement is used. After it has reached the desired viscosity, the mixed cement is loaded in a cement gun and is delivered in the femur in a retrograde fashion. The nozzle of the gun should not be pulled back; it should be allowed to be pushed back by the cement pressure.



**Fig. 19** Surgical instruments used for preparation of the femoral canal

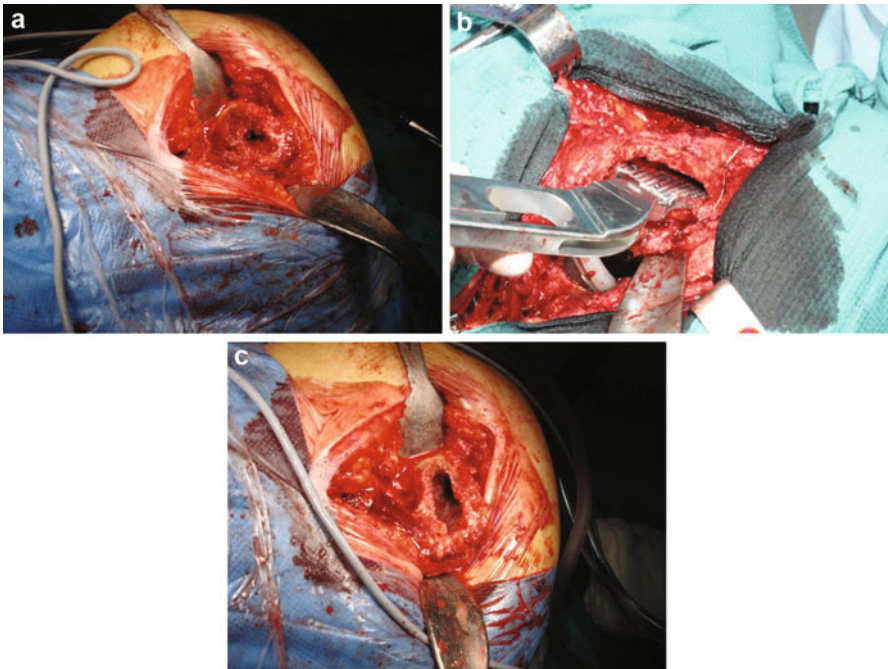


**Fig. 20** Surgical steps of femoral canal preparation: (a) entry point in the medullary canal of the femur; (b) preparation of the femoral canal using specialized instruments; (c) femoral canal prepared and ready for next step

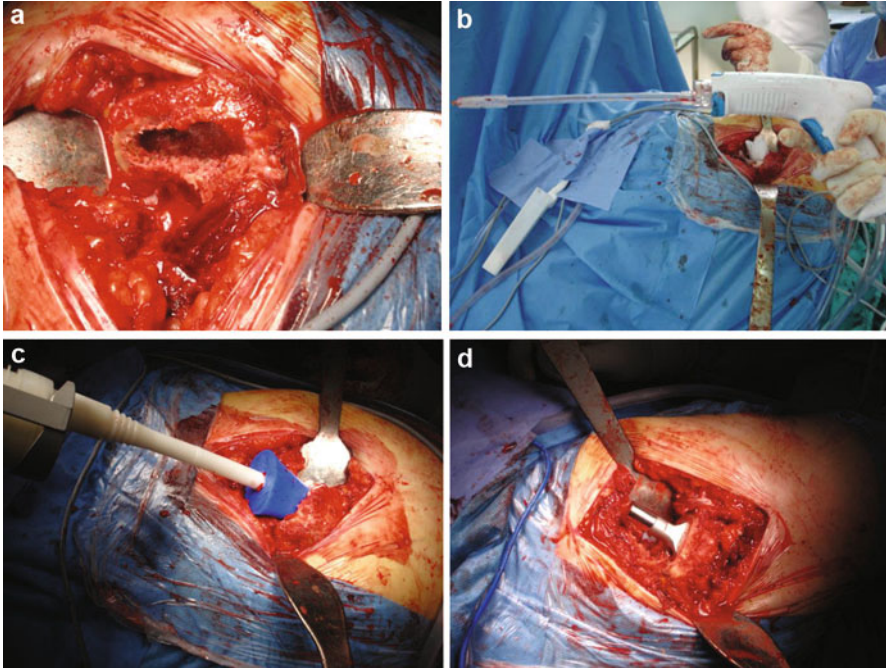


**Fig. 21** Surgical steps of the cementation after femoral canal preparation: (a) femur cleaned with pulsatile lavage; (b) pulsatile lavage system for femur preparation; (c) cementation of the femur; (d) final aspect of a cemented femoral stem

After the femur has been filled with cement, the surgeon should seal the proximal femur in order to generate pressure. After a few seconds the proximal seal is mounted. With the proximal seal in place, more cement pressure, with the gun, is applied for 2–3 min. After this step, the definitive femoral stem is inserted with gentle pressure applied by the surgeon's hand or using a stem introducer. It should go in easily. It is not necessary to hammer it.

After the cement has hardened, a trial reduction with a trial head is made and stability is assessed. The definitive head is mounted, and the prostheses are reduced into the acetabulum. The wound is then closed in anatomical layers over drain tubes.

## New Concepts in Cemented Total Hip Arthroplasty

### Aspiration of the Iliac Wing

It has been demonstrated that the most important risk factor for aseptic loosening of cemented acetabular and femoral components is failure to achieve a good initial fixation at the bone-cement interface. The strength and durability of the bone-cement

interface is dependent on the depth of penetration of the cement in the bone trabeculae.

The most important factor that influences the bone-cement interlock is cement pressurization. The higher the pressures, the better the cement interdigitation and interlock achieved. The pressures generated must be higher than blood pressure which acts to push blood out of the bone and thus interferes with the cement penetration.

In order to minimize bleeding at the interface, hypotensive epidural anesthesia is currently part of standard practice for cemented total hip arthroplasty. Cleaning of the bone bed with pulsatile lavage and thrombin or hydrogen-peroxide-soaked swabs has become standard practice. These methods minimize bleeding and provide a clean bone bed ready for the cement to be applied [35].

A modern technique for minimizing bleeding at the bone-cement interface in the acetabulum that has been employed in some orthopedic surgical centers around the world is aspiration of the iliac wing.

Aspiration of the iliac wing during cement pressurization and cup insertion has proved to be very effective at achieving a better bone-cement interface, with better cement penetration in the bone of the acetabulum. The iliac wing aspirator (Fig. 22) is introduced with the aid of a trocar at a depth of 2 cm in the ilium, superior to the acetabulum.

Suction is connected to the aspirator before cement insertion and maintained during cement pressurization and cup insertion until the cement has hardened or until cement is sucked into the aspiration device (Fig. 23).

The good clinical results of the use of iliac wing aspiration system [35], materialized by better cement penetration and strong interface between bone and bone cement, can be observed after surgery on standard pelvic anteroposterior radiographs. In the radiological comparison made in Fig. 24 a much better cement penetration in the superior area of the acetabulum can be achieved if the iliac wing aspiration system is used during cementation.

## **Modification of the Metallic Stem Surface**

It is well established in modern orthopedics and especially in hip arthroplasty that third-generation cementing techniques are the current gold standard and should be used by every surgeon when performing a cemented hip arthroplasty. The use of these techniques has led to a significant increase in survivorship of cemented femoral and acetabular components. However, although this aspect is not a subject of debate, the type of femoral stem which should be used is still controversial. In America the vast majority of implanted stems are cementless, while in Europe, the majority is cemented. This trend has emerged from the early times of hip arthroplasty in the United States, when the use of badly designed stems along with first-generation cementing techniques led to poor results. However, the experience in Europe was different, and as a result cemented stems are preferred [36, 37].



**Fig. 22** Picture of the iliac wing aspiration system

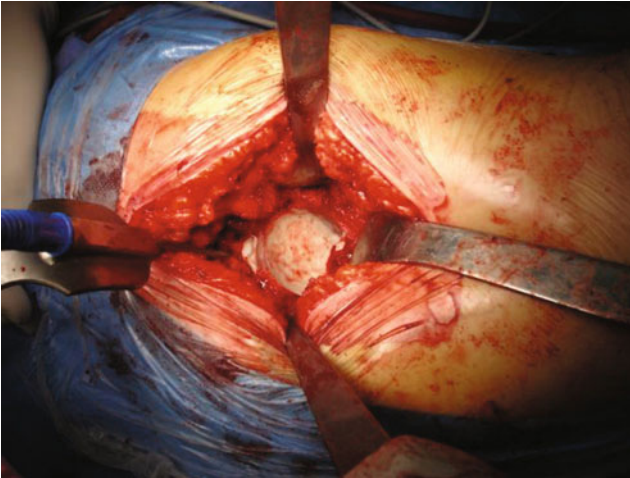


**Fig. 23** The iliac wing aspiration system used during hip arthroplasty

It has been observed that aseptic loosening of the femoral stem has been greatly associated with marked subsidence of the stem within the cement mantle. As a result of these observations, it has been thought that creating a stronger bond between the surface of the implant and the cement would prevent subsidence.

Many types of new stems were developed, which had matte surfaces, collars, and PMMA precoating. The results were not those expected and even higher failure rates

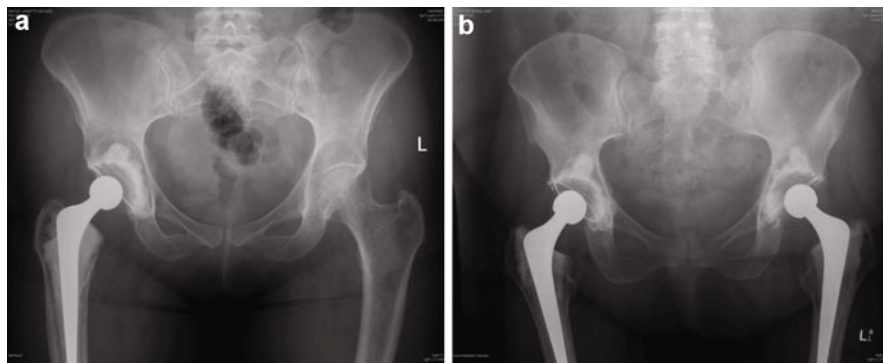


**Fig. 24** Radiographic comparison of cemented acetabular components without (a) and with (b) use of an iliac wing aspiration system

were recorded. The reason for this was the fact that all stems, regardless of their surface, debond from the cement, and so movement at the stem-cement interface appears. If the stem used has a matte or rough surface, movement at the stem-cement interface will wear away the coating, and the cement and loose debris will be generated and subsequent loosening will occur.

In Europe, however, the majority of stems used were polished (Exeter, Charnley). Survival rates of 20–30 years were common, and this led to an increase in implantation and further development of these types of implants. In case of a polished femoral stem, the inevitable subsidence leads to better fixation of the stem and is considered part of its functioning mechanism. Radiostereometric analysis has shown that an Exeter stem subsides within the cement mantle, but there is no movement at the bone-cement interface. It seems that in case of a polished stem, there is approximately 0.9–1.4 mm of migration in the first year and very little afterwards [38, 39]. After the first year, these stems tend to stabilize. The migration takes place regardless of the type of cement, its viscosity, and the thickness of the surrounding mantle. Because these stems are polished, the surrounding cement is not damaged and no debris is generated. The subsidence of the stem generates radial compression forces on the adjacent cement which are transferred to the bone-cement interface, leading to better survival of the implant. The cement column does not fracture if it is put under pressure [39].

Another aspect which is in favor of polished stem designs is that they are forgiving for the surgeon. It is easier to achieve optimal orientation, offset, and leg length than it is in case of a cementless stem. In some studies the failure rate of these implants was found to be independent of alignment and quality of cementing. A cemented implant can be used in case of good or bad bone quality, in case of deformity of the femur, and in case of difficult revisions (cement-in-cement revision has very good results). Cement can be also used to deliver local antibiotics [39].

Although polished stems seem to be preferred by surgeons when performing a cemented hip arthroplasty, results from literature are subject to much debate. Dennis K. Collis and Craig G. Mohler reported better results with a polished stem, compared

to a rough design, in a study on 244 patients undergoing THR with similar geometry stems. Vaughn et al. compared a satin-finished stem to a precoated one and reported better results with the polished stem at minimum 2-year follow-up. Paul F. Lachiewicz et al. found no significant differences in 219 cemented hip arthroplasties when comparing two similar designed; polished and precoated components. In conclusion, the subject remains controversial, and it is obvious that further research is necessary in order find the best design and surface finish for cemented stems.

## **Preheating of the Metallic Stem**

The metallic stem-bone cement interface is the region of the cement mantle with the highest recorded peak stresses. The presence of pores in this region may predispose to fatigue fractures in the cement which can lead in turn to early aseptic loosening and failure of fixation. Vacuum mixing has greatly reduced the overall porosity of the cement used for fixation of components in cemented total hip arthroplasty. However, this method does not eliminate micropores in the mixture, and researchers are still looking for methods to further decrease the porosity.

One method recently employed to further reduce porosity is preheating of the femoral component before its insertion. Studies have demonstrated that preheating of the femoral stem, associated with vacuum mixing of cement, further reduces the overall porosity of the acrylic bone cement used for hip arthroplasty.

Reduction of the porosity at the stem-cement interface translates in an overall increase of the shear strength of the interface. A higher implant temperature seems to restrict the expansion of the voids at the interface. This could be explained by the fact that higher temperatures lead to early polymerization of the cement, and so the voids cannot expand in the hardened cement. The bone temperature recorded just before cement insertion was at 32.3 °C.

Heating of the implant reduces the porosity depending on the temperature achieved. A significant effect has been observed at a minimum difference of 3 °C between the implant and the bone. However, higher stem temperatures may increase the risk of thermal osteonecrosis, although some authors did not record an increase of temperature at the actual cement-bone interface. It has been discovered that the temperature difference that produces optimal results regarding porosity reduction is 7 °C, as it provides a balance between the desired effects and the subsequent risk of necrosis associated with increased temperature. Considering the fact that the bone surface is not at body temperature, but at 32.3 °C, the recommended heating temperature for the components has been established as 40 °C [40, 41].

## **Special Cementing Techniques**

Cementing techniques have been continuously evolving in the last 30–40 years, and this has led to a significant increase in implant survivorship since cemented hip

arthroplasty was first introduced by Sir John Charnley in the 1960s. Although much progress has been made in this field, the end point of most cemented hip arthroplasties is aseptic loosening that leads to a revision surgery, and this can happen either after a few years from the initial surgery or after 30 years. Taking into account that there are lots of young people who undergo hip arthroplasty, this is a major problem, and the ideal situation would be that in which a cemented hip implant would last longer and would not require a revision. Cementless implants have not solved this problem, the survival of these types of implants being similar to cemented ones. Surgeons have found that in case of a cemented hip, the most predictive factor for early aseptic loosening is the presence of radiolucent zones (spaces seen on an X-ray between the interfaces) at the bone-cement interface. So, the aim would be to obtain a perfectly cemented hip implant, with no radiolucent zones, which can last for at least 30 years before revision surgery is required.

Many surgeons have tried different cementing techniques and materials in order to have better results and longer survival of their implants. It is a known fact that acrylic cement used in orthopedic surgery is not osteoconductive and does not integrate with the surrounding bone. This is considered to be the main cause for aseptic loosening of the implant, under sustained stresses from the patient's gait.

Taking this aspect into consideration, Oonishi et al. tested a new method for cementing hip implants. They tried to create a physicochemical bond between cement and bone by interposing crystal hydroxyapatite granules at the bone-cement interface. This technique was called *interface bioactive bone cement*, and it manages to create bioactivity at the cement surface, for better implant fixation.

For their study, Oonishi et al. smeared hydroxyapatite granules on the bone surface of the acetabulum and femur, before cementing with the contemporary techniques. They used large (300–500  $\mu\text{m}$ ) and small (100–300  $\mu\text{m}$ ) crystals for two groups (192 and 209 patients). The minimum follow-up was 15 years. The result was similar, with 91.7 % survival at 15 and 17 years in the first generation (1986–1988) and 91.2 % survival at 15 and 17 years in the second generation (1989–1991). Although the survival rate was similar, better results regarding the presence of radiolucent zones, osteolysis, and loosening were recorded in the first generation in which large granules of hydroxyapatite were used.

In that time period, in the Finnish Arthroplasty Register, the mean survival interval for a cemented hip was at 88 % at 10 years. Modern cementless implants are also covered with a layer of HA (hydroxyapatite), but it is amorphous, and it is absorbed in the following years. In contrast, the crystals of HA used in the technique described above are not absorbed, and their osteoconductivity properties are exercised for a longer period of time. In studied models, it has been found that the HA granules are incorporated in remodeled bone trabeculae making the HA-bone interface a more complex and strong structure than the simple bone-cement interface. The larger granules of HA (300–500  $\mu\text{m}$ ) have had better results regarding the presence of radiolucent zones at the cement-bone interface because they seem to bond more effectively with the cement and the bone, whereas the smaller granules tend to sink into circulating blood and interposed blood between the bone and cement leads to radiolucent zones. Because the HA granules fill the bone trabeculae,



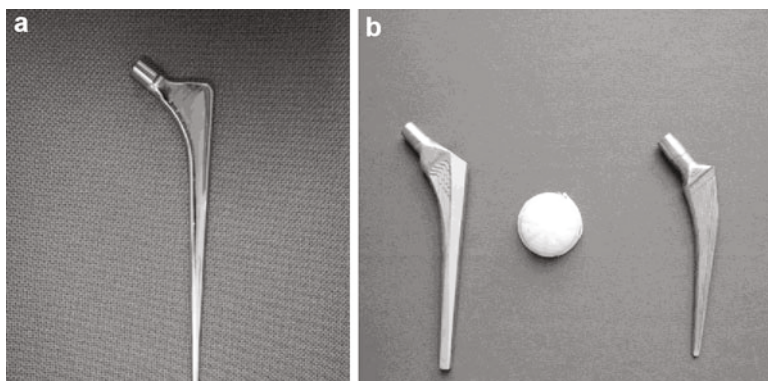


**Fig. 25** Cemented femoral stems with different surfaces: (a) polished and (b) matte

cement interdigitation is slightly reduced, and so the surgeon should make more small anchor holes to ensure a better initial fixation of the construct [42–44].

Oonishi et.al were the first to study the long-term effects of this technique. The follow-up for their patients was over a long period of time, and the results could be compared to the survival of cemented hips using conventional cemented techniques from that period. Other authors have used this technique in association with more modern third-generation cementing techniques, but the long-term results are still to be evaluated. This type of research can certainly lead to new methods for cementing orthopedic implants which may lead to greater survival rates of the implants and may eliminate the need for revision surgery (Fig. 25).

---

## Summary

Cementing techniques have evolved considerably since cemented hip arthroplasty was first introduced, due to the developments related to the bone cements and the new surgical techniques associated with its use. The main developments have been in the areas of bone preparation, cement preparation, and cement delivery.

From a surgical point of view, new procedures for preparation could be introduced in the future, in order to obtain a proper cancellous bone surface and improve the bonding between bone and cement. New developments related to the bone cements could assure in the future the delivery of antiseptic agents or alternative antibiotic. Also, the bone cement properties could be improved by the addition of some new filler into the chemical composition of these. On the other hand, new surgical techniques could be developed in order to overcome the fact that bone cement is in contact with two parts (human bone and metallic stem) with different surface properties.

The surgical technique and operative steps of the cementation is very important for a successful cemented hip arthroplasty. The survivorship of the cemented hip prosthesis is greatly influenced by the quality of the fixation, which is dependent on a

solid interface. Education and training of the surgeons will remain the fundamental aspect for optimizing cement handling and application during surgery, although more technical assistance to guide the surgeon during the cementation procedure is expected to appear in the years to come. Another conclusion is that the cementation techniques are very important for a surgeon because the bone cements are manufactured in the operating room.

---

## References

1. Webb JCJ, Spencer RF (2007) The role of polymethylmethacrylate bone cement in modern orthopaedic surgery. *J Bone Joint Surg [Br]* 89-B:851–857
2. Paul Fenton MRCS (2009) Ashok Rampurada MRCS Ed, Ford Qureshi FRCS Bone cement, its history, its properties and developments in its use. <http://usmorthopaedic.wordpress.com/2009/08/24/bone-cement-its-history-its-properties-and-developments-in-its-use>
3. Dalury DF (2005) The technique of cemented total hip replacement. *Orthopedics* 28(8 Suppl): s853–s856
4. Dennis C et al (2005) The genesis and evolution of acrylic bone cement. *Orthop Clin North Am* 36(2005):1–10
5. Todd J et al (2010) DO polymethylmethacrylate: properties and contemporary uses in orthopaedics. *J Am Acad Orthop Surg* 18:297–305
6. Charnley J et al (1964) The bonding of prostheses to bone by cement. *J Bone Joint Surg Br* 46:518–529
7. Klaus-Dieter K et al (2005) Acrylic bone cements: composition and properties. *Orthop Clin North Am* 36:17–28
8. Bellare A et al (2007) Orthopaedic bone cement, *The Adult Hip*, 2nd edn. Lippincott Williams & Wilkins, pp 144–155, ISBN/ISSN:9780781750929
9. Reckling FW et al (1977) The bone- cement interface temperature during total joint replacement. *J Bone Joint Surg* 59A:80–82
10. Lewis G et al (1997) Properties of acrylic bone cement: state of the art review. *J Biomed Mater Res* 38:155–182
11. Bridgens J et al (2008) Stockley orthopaedic bone cement do we know what we are using? *J Bone Joint Surg [Br]* 90-B:643–7
12. Kuehn K-D et al (2005) Acrylic bone cements: mechanical and physical properties. *Orthop Clin North Am* 36:29–39
13. Demian HW et al (1998) Regulatory perspective on characterization and testing of orthopedic bone cements. *Biomaterials* 19:1607–1618
14. Verdonschot N et al (2000) Creep properties of three low temperature-curing bone cements: a preclinical assessment. *J Biomed Mater Res* 53:498–504
15. Lewis G et al (1999) Effect of two variables on the fatigue performance of acrylic bone cement: mixing method and viscosity. *Biomed Mater Eng* 9:197–207
16. Armstrong M et al (2002) Antibiotic elution from bone cement: a study of common cement-antibiotic combinations. *Hip Int* 12:23–27
17. Perry AC et al (2002) Antimicrobial release kinetics from polymethylmethacrylate in a novel continuous flow chamber. *Clin Orthop Relat Res* 403:49–53
18. Baleani M et al (2008) Biological and biomechanical effects of vancomycin and meropenem in acrylic bone cement. *J Arthroplasty* 14.23(8):1232–1238
19. Hsieh PH et al (2009) Liquid gentamicin and vancomycin in bone cement: a potentially more cost-effective regimen. *J Arthroplasty* 24(1):125–130
20. Anguita-Alonso P et al (2006) Comparative study of antimicrobial release kinetics from polymethylmethacrylate. *Clin Orthop Relat Res* 445:239–244

21. Goss B et al (2007) Elution and mechanical properties of antifungal bone cement. *J Arthroplasty* 22(6):902–908
22. Gouran Savadkoohi D, Sadeghipour P, Attarian H, Sardari S, Eslamifar A, Shokrgozar MA (2008) Cytotoxic effect of drugs eluted from polymethylmethacrylate on stromal giant-cell tumour cells an in vitro study. *J Bone Joint Surg [Br]* 90:973–979
23. Breusch SJ, Malchau H. *The Well Cemented Hip Arthroplasty. Theory and Practice*. Springer 2005 ISBN: 978-3-540-24197-3 (Print) 978-3-540-28924-1 (Online)
24. Breusch SJ, Norman TL, Schneider U, Reitzel T, Blaha JD, Lukoschek M (2000) Lavage technique in total hip arthroplasty: jet lavage produces better cement penetration than syringe lavage in the proximal Femur. *J Arthroplasty* 15(7):921–927
25. Heisel C, Norman T, Rupp R, Pritsch M, Ewerbeck V, Breusch SJ (2003) In vitro performance of intramedullary cement restrictors in total hip arthroplasty. *J Biomech* 36(6):835–843
26. Heisel C, Schelling K, Thomsen M, Schneider U, Breusch SJ (2003) Cement delivery depends on cement gun performance and cement viscosity. *Z Orthop Ihre Grenzgeb* 141(1):99–104
27. Dozier JK, Harrigan T, Kurtz WH, Hawkins C, Hill R (2000) Does increased cement pressure produce superior femoral component fixation? *J Arthroplasty* 15(4):488–495
28. Breusch SJ, Schneider U, Kreutzer J, Ewerbeck V, Lukoschek M (2000) Effects of the cementing technique on cementing results concerning the coxal end of the femur. *Orthopade* 29(3):260–270
29. Dunne NJ, Orr JF (2001) Influence of mixing techniques on the physical properties of acrylic bone cement. *Biomaterials* 22(13):1819–1826
30. Mau H, Schelling K, Heisel C, Wang JS, Breusch SJ (2004) Comparison of various vacuum mixing systems and bone cements as regards reliability, porosity and bending strength. *Acta Orthop Scand* 75(2):160–172
31. Egund N, Lidgren L, Onnerfält R (1990) Improved positioning of the femoral stem with a centralizing device. *Acta Orthop Scand* 61(3):236–239
32. Goldberg BA, al-Habbal G, Noble PC, Paravic M, Liebs TR, Tullos HS (1998) Proximal and distal femoral centralizers in modern cemented hip arthroplasty. *Clin Orthop Relat Res* 349:163–173
33. Aydin N, Bezer M, Akgulle AH, Saygi B, Kocaoğlu B, Guven O (2009) Comparison of distal and proximal centralising devices in hip arthroplasty. *Int Orthop* 33(4):945–948. doi:10.1007/s00264-008-0610-3, Epub 2008 Aug 19
34. Hogan N, Azhar A, Brady O (2005) An improved acetabular cementing technique in total hip arthroplasty. Aspiration of the iliac wing. *J Bone Joint Surg Br* 87(9):1216–1219
35. Garellick G, Karrholm J, Rogmark C, Rolfson O, Herberts P. *The Swedish Hip Arthroplasty Register. Annual report (2011)* [http://www.shpr.se/Libraries/Documents/%C3%85rsrapport\\_2011\\_eng\\_webb.sflb.ashx](http://www.shpr.se/Libraries/Documents/%C3%85rsrapport_2011_eng_webb.sflb.ashx)
36. National Joint Registry for England and Wales 9th annual report (2012). <http://www.njrcentre.org.uk>
37. Lachiewicz PF, Kelley SS, Soileau ES (2008) Survival of polished compared with precoated roughened cemented femoral components a prospective, randomized study. *J Bone Joint Surg* 90-A(7):1457–1463
38. Scheerlinck T, Casteleyn P-P (2006) The design features of cemented femoral hip implants. *J Bone Joint Surg [Br]* 88-B:1409–1418
39. Murray DW (2013) Cemented femoral fixation the North Atlantic divide. *Bone Joint J* 95-B (Suppl A):51–52
40. Jaffri AA, Green SM, Partington PF, McCaskie AW, Muller SD (2004) Pre-heating of components in cemented total hip arthroplasty. *J Bone Joint Surg [Br]* 86-B:1214–1219
41. Madrala A, Nuño N, Bureau MN (2010) Does stem preheating have a beneficial effect on PMMA bulk porosity in cemented THA? *J Biomed Mater Res B Appl Biomater* 95(1):1–8. doi:10.1002/jbm.b.31673
42. Oonishi H, Ohashi H, Oonishi H Jr, Kim SC (2008) THA with hydroxyapatite granules at cement–bone interface 15- to 20-year results. *Clin Orthop Relat Res* 466:373–379

- 
43. Otsuka H (2013) High survival of cemented acetabular component in total hip arthroplasty using a novel cementing technique with hydroxyapatite granules at bone-cement interface. *Bone Joint J* 95–B(Suppl 15):295
  44. John Timperley A, Nusem I, Wilson K, Whitehouse SL, Buma P, Crawford RW (2010) A modified cementing technique using BoneSource to augment fixation of the acetabulum in a sheep model. *Acta Orthop* 81(4):503–507

Iulian Vasile Antoniac, Florin Miculescu, Dan Laptoiu,  
Aurora Antoniac, Marius Niculescu, and Dan Grecu

## Contents

Introduction .....	902
Research Methodology for Retrieval Analysis .....	905
Failure Analysis of Hip Implants .....	908
Failure Analysis of Hip Prosthesis Type Metal–Polyethylene .....	911
Failure Analysis of Hip Prosthesis Type Metal–Metal Used in Resurfacing Arthroplasty .....	916
Failure Analysis of Hip Prosthesis Type Ceramic–Ceramic .....	924
Summary .....	929
References .....	930

---

I.V. Antoniac (✉)  
University Politehnica of Bucharest, Bucharest, Romania  
e-mail: [antoniac.iulian@gmail.com](mailto:antoniac.iulian@gmail.com)

F. Miculescu • A. Antoniac  
Faculty Materials Science and Engineering, University Politehnica of Bucharest, Bucharest,  
Romania  
e-mail: [f\\_miculescu@yahoo.com](mailto:f_miculescu@yahoo.com); [antoniac.aurora@gmail.com](mailto:antoniac.aurora@gmail.com)

D. Laptoiu  
Department of Orthopaedics and Trauma I, Colentina Clinical Hospital, Bucharest, Romania  
e-mail: [danlaptoiu@yahoo.com](mailto:danlaptoiu@yahoo.com)

M. Niculescu  
Department of Orthopaedics and Trauma I, Colentina Clinical Hospital, Bucharest, Romania  
Faculty of Medicine, Titu Maiorescu University, Bucharest, Romania  
e-mail: [mariusniculescu@yahoo.com](mailto:mariusniculescu@yahoo.com)

D. Grecu  
Department of Orthopaedics, University of Medicine and Pharmacy Craiova, Craiova, Romania  
e-mail: [grecudan@ortopezi.ro](mailto:grecudan@ortopezi.ro)

---

**Abstract**

The investigation of retrieved orthopedic devices and adjacent tissues can be of value in the assessment of clinical complications associated with the use of a specific implant design. Adequate orthopedic implant retrieval and evaluation require the quantitative assessment of host and implant responses using specific analytical protocols and nondestructive and destructive testing procedures. Techniques used for implant and tissue evaluation should be both device designed and material specific, in order to assure the collection of quantitative data that can provide correlations and cause-and-effect relationships between biomaterial, implant design, and different variables (mechanical, manufacturing, clinical, and biological). Tools for failure analysis of orthopedic implant range in size, cost, complexity, and utility. The most valuable tool is a large database and a systematic method to characterize and store data related to orthopedic device characteristics. Continued investigation of retrieved devices is recommended to deepen our knowledge of implant failure mechanisms and to evaluate the impact of newer biomaterials and design on the performance of orthopedic implants and prostheses.

---

**Keywords**

Retrieval analysis • Biomaterials • Ceramic–ceramic • Wear • Microscopy

---

**Introduction**

Orthopedic implants remain a major percentage of the devices being used in the current medical practice. With a success rate of more than 90 % reported in the literature, they represent a major change in the outcome of orthopedic reconstructive surgery. With the increase in traumatic events, with ever-aging population, and with more and more sports injuries, orthopedic implants are more utilized than ever. However, their longevity can be compromised by fatigue, wear, corrosion, and other degradation mechanisms [1–3].

As mentioned, medical practice used different types of orthopedic implants and endoprosthesis, starting with the first generation of bioinert implants, followed by a second generation named bioactive devices with some special inductive properties. Now, a modern generation of biomimetic (adaptative) materials and novel designs are in development. Adverse biologic responses to these biomaterials as well as the products from degradation can lead to significant local and general reactions and may complicate following surgeries. This is why it is important to fully understand what mechanisms are in action and carefully evaluate the strategies needed to modify and eliminate complications linked to resorption, wear, and degradation processes [3, 4].

Devices retrieved during revision surgery provide with important information regarding the performance of orthopedic implants. Surface characterization of the implant, biomechanical and failure analysis, and histological sampling of tissues surrounding the implant provide many important elements of information for improvement of long-term survival of these devices.

All these orthopedic implants have an established role to relieve pain and restore function. The longevity of implants is related to a large number of factors, beginning with the material and device design and concluding with the surgical technique. Orthopedic implants vary from simple pins for fracture fixation to complex devices for total joint and limb replacements. For device improvement and better clinical results, biomaterial and engineering scientists, together with orthopedic surgeons, complete studies from characterization of implant's resistance to fatigue and wear to biological responses to degradation particles of bioresorbable materials.

One important conclusion of these retrieval studies was that there still is an important difference between *in vitro* and *in vivo* conditions. The specific behavior of a certain implant due to the different biological and mechanical constraints of the different human bodies is very difficult to predict unless products retrieved at revision or during normal ablation of osteosynthesis implants are methodically analyzed [5–7].

Metallic implants have been the mainstay for the fixation of fractures, osteotomies, and arthrodeses in the past because of their high mechanical strength, low reactivity reactions, and relatively low price, even if these implants are considerably stiffer than the bone. Another disadvantage is that metallic implants are radiopaque, and the iron content can make computed tomography and magnetic resonance imaging (MRI) studies less efficacious and impair the imaging of that body part [8]. A second surgery may be required for removal of the implant, which exposes the patient to further surgical risks. Due to biomechanic stresses inside the human body, their design is still under amelioration, a lot of information being from implants retrieved due to mechanical failure or related to other complications. Implant failures will cause new complications for patients, lengthen the healing process, and increase treatment costs. An implant failure often leads to a refracture, thus complicating the functional status of the patient; more strain is induced by the current rehabilitation protocols that require faster return to work or sports activities. On occasion there is the need for additional, often more complicated repeated surgeries. These complications show the importance of exploring the causes of this problem [7].

Also, implant failures can result from an intrinsic device fault or external factors such as mishandling during the surgical process, patient noncompliance with implant instructions, and the severity of the musculoskeletal injury. Most common reason for failure was related to a trauma before complete healing of the fracture. Internal fixation is useful until trabeculation has crossed the fracture site and bony union is formed, typically taking more than 8 weeks in the ideal clinical situation. If more stable the faster the rehabilitation can be. Therefore, the presence of internal fixation implants is most important through the healing phase, after which time, there is no longer a need for internal fixation. This leads to one of the strongest reasons to use absorbable fixation.

Absorbable implants seek to overcome some disadvantages of metallic implants. Bioabsorbable implants theoretically prevent stress shielding because the implants will slowly be hydrolyzed and weakened gradually, thus transferring the load to the healing bone, which can lead to normal bone remodeling and normal bone density [9]. Bioabsorbable implants eliminate the need of a second surgery for hardware removal and are radiolucent, which will improve the imaging ability to assess bone healing. Unfortunately, bioabsorbable implants have any other problems like a

decreased risk of infection, which may be due to the hydrolysis of the implants because they degrade, which creates an environment where bacteria cannot proliferate and thus make infection unlikely to occur. Also, the mechanical resistance of bioabsorbable implants is inferior to metallic implants and as such is not indicated for fixation of fractures, which requires a high degree of interfragmentary compression and primary stability. Bioabsorbable implants that are placed under greater loads tend to degrade faster and are therefore not indicated in the bridging of bony deficits or in severely comminuted fractures.

Bioabsorbable implants are typically more expensive than metallic implants. However, there is a cost saving when used in applications whereby hardware removal is frequently performed because the need for a second surgery would be eliminated. Inflammatory reactions and osteolysis have been reported in the literature for bioabsorbable implants [9]. These adverse reactions are thought to be due to the rapid rate of degradation of the implant with local accumulation of breakdown products outperforming the local tissue's ability to clear them.

Retrieval analysis provides a unique set of samples that can be studied to evaluate the effect of the implant on the human body and also the effect of the host environment on the implant. If is made a systematic analysis of retrieved components, in combination with histology, medical images, and clinical data, it is possible to provide valuable comprehension into the mechanisms of failure of the biomaterials used in orthopedic implants. Continued investigation of retrieved devices is recommended to deepen our knowledge of implant failure mechanisms and to evaluate the impact of newer biomaterials and design on the performance of orthopedic implants and prostheses.

Retrieval studies of failed implants in orthopedic surgery have given surgeons and manufacturers insight into many implant problems in the past, like bearing surfaces (titanium as a bearing, carbon fiber-reinforced polyethylene), implant design (taper junctions for modularity and corrosion), and manufacturing (cast versus forged alloys and sterilization issues). Most recently, concerns relating to hip prosthesis type metal-on-metal bearings have led to an emphasis on retrieval analysis techniques, which can aid in our understanding of why devices fail in patient and furthermore why standard in vitro studies using different animals may not always correlate to ensure all issues pertaining to a device's design and biomaterial structure are improved and accepted.

Because many failures would not happen in the absence of mechanical input from the user, patient history is an important factor in failure analysis. As such, compliance with ethical principles of human subject research is very important.

Evaluation of a retrieved orthopedic implant requires a review of the patient's medical history and radiographs and other studies (e.g., EKG, MRI) where pertinent. Some anatomic and physiologic conditions that may influence the failure or success of orthopedic and cardiovascular implants are osteoarthritis, trauma, infection, polyarthritis, connective-tissue disorders, tumor, primary joint disease, osteonecrosis, and metabolic and endocrine disease.

The general objectives of retrieval analysis in the case of orthopedic devices are [8]:

- Identify the rates, patterns, and mechanisms of implant failure.
- Determine effects of patient and implant factors on performance.



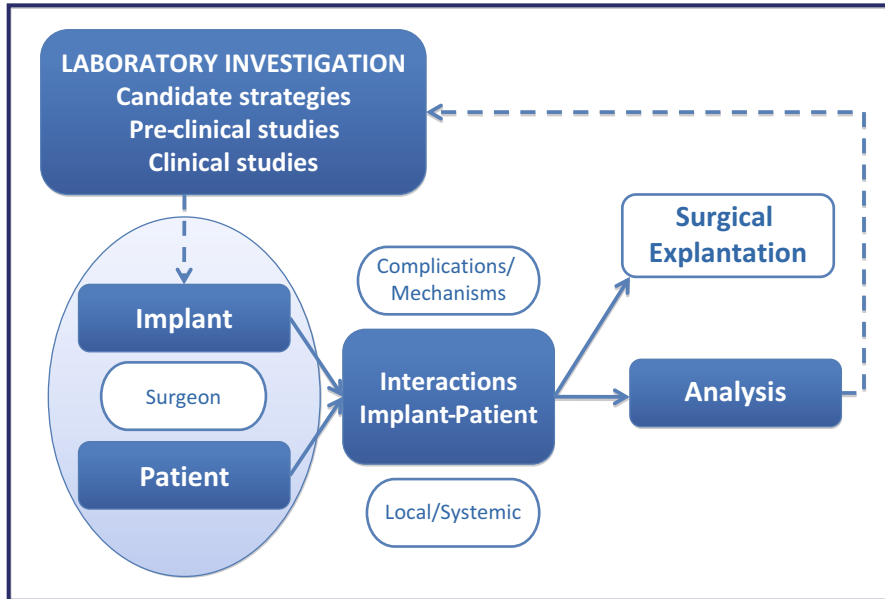


**Fig. 1** Role of orthopedic implant retrieval and their evaluation

- Determine mechanisms of tissue–material and blood–material interactions.
- Determine adequacy of animal models.
- Develop design criteria for future implants.

Implant failures can be characterized as implant or material dependent or clinically or biologically dependent, but in general many modes and mechanisms of failure are dependent on both implant and clinical factors.

The role of implant retrieval and evaluation, briefly represented in the Fig. 1, is very important not just for manufacturers but also for orthopedic surgeons.

In the future, as in the past, retrieval studies and analysis of failed and well-functioning implants will be important in the field of orthopedic biomaterials and medical devices as long as we continue to design and implant into the human body different medical devices in order to replace or repair bones and joints damaged by trauma and diseases.

Also, the importance of retrieval analysis was recognized by international standard organizations because they publish standards like ASTM F561-97 (1997) [8].

## Research Methodology for Retrieval Analysis

The investigation of retrieved orthopedic devices and adjacent tissues can be of value in the assessment of clinical complications associated with the use of a specific implant design.

Adequate orthopedic implant retrieval and evaluation require the quantitative assessment of host and implant responses using specific analytical protocols and nondestructive and destructive testing procedures. Techniques used for implant and tissue evaluation should be both device designed and material specific, in order to assure the collection of quantitative data that can provide correlations and cause-and-effect relationships between biomaterial, implant design, and different variables (mechanical, manufacturing, clinical, and biological).

Tools for failure analysis of orthopedic implant range in size, cost, complexity, and utility. The most valuable tool is a large database and a systematic method to characterize and store data related to orthopedic device characteristics.

The evaluation techniques appropriate for a particular case may be mutually exclusive, and the choice of a subset of techniques for evaluation could be influenced by the key clinical questions and the availability of the retrieved implant and tissue specimens. While a multilevel strategy is necessary for evaluation, analytical protocols and techniques are only used following a thorough understanding of the patient's medical history and associated information [8, 9].

In order to make an accurate analysis, it is essential that the orthopedic device and associated tissues be removed without alteration of their form and structure. Also, it is essential that the tissues be handled in such a way as to avoid microbial contamination of the investigator or the workplace. For a better interpretation of experimental results, it is essential to capture a minimum data set regarding the clinical findings, any other studies about the performances of the analyzed orthopedic device, and clinical reasons for orthopedic device removal.

In general, analytical techniques for assessing host and implant responses can be divided into two categories: nondestructive and destructive testing procedures. It should be noted that the techniques for implant evaluation are commonly destructive techniques, that is, the implant or portions of the implant and the surrounding tissues must be altered to obtain the desired information on the properties of the implant or biomaterial. Of course, the availability of the implant and tissue specimens will dictate the choice of technique [10, 11].

In these investigations, detailed studies of the device–tissue interface are significant. Appropriate methods are provided to facilitate a study of the particles in the tissues, and chemical analysis for the by-products of degradation of the implant, and histologic evaluation of the cellular response to the implant. Detailed analysis of the implant–tissue interface often necessitates that both a piece of tissue and a piece of the implant which it contacts be sectioned and examined as one unit, that necessitate special procedures which generally precludes any other analysis of that specimen. Also, chemical analysis of a piece of tissue for metal ion concentration requires acid digestion and thus precludes morphological analysis. Thus, consideration must be given to either selection of multiple specimens or division of a specimen before processing, just to permit part to be used for morphological and part for chemical analyses. Each of these portions needs to be further subdivided to be processed according to the specific requirements of each test.

Since many of the procedures include cutting or sectioning a portion of the retrieved implant, the permission for use of destructive methods may be necessary.

Techniques for evaluation		
Implant/Biomaterial	Implant-tissue	Tissue
EDAX ESCA ATR-FTIR X-ray diffraction Porosity analysis Gel permeation chromatography Hardness studies Fatigue studies Fracture analysis Contact angle measurements		Biochemical analysis Immunocytochemistry Immunofluorescence Immunohistochemistry Immunoperoxidase Enzyme histochemistry  Gel electrophoresis Histology Microbiologic cultures Molecular analysis for cellular gene expression
	Radiography Macrophotography Stereomicroscopy Light microscopy Scanning electron microscopy Transmission electron microscopy Atomic force microscopy Atomic absorption spectrophotometry	

**Fig. 2** Different techniques used for evaluation of the retrieved orthopedic devices; grouped according to the specimen who could be investigated (Adapted after Recum [11])

Also, for clinical and pathological correlation studies that involve utilization of both patient data and pathological findings, approval of the ethical commission from the hospital is required to ensure that the confidentiality and other interests of the patients from whom the implants were removed will be maintained [11].

Just simply evaluation of the retrieved implant without attention to the tissue will produce an incomplete evaluation. In Fig. 2 is mentioned a partial list of techniques for evaluating orthopedic implants and tissues, even we consider that new bio-materials and implants will dictate further techniques to be used in evaluating tissue–biomaterial interactions, and new specific analytical techniques will likely be developed [8, 11]. Also, it’s important to mention that even some techniques could be used for analyzing all the specimens’ type (implant/biomaterials, tissue, and implant–tissue); each of these specimens need specific techniques for sample preparation and specific methodology for analyzing the specimens (e.g., transmission electron microscopy).

Also, analysis techniques can be grouped according to purpose in four main categories: surface characterization, metallurgical characterization, mechanical characterization, and chemical characterization. Starting from very simple techniques, like macrophotography, to advanced techniques, like scanning electron microscopy

or atomic force microscopy, these techniques have proven useful information in identifying the root cause of orthopedic failures.

Surface measurements can range in scale from using macro indicators for dimensional analysis (useful to identify wear, creep or deformation, changes in orthopedic device geometry) to micro and nano indicators (for changes in surface roughness, scratches, or microscopic features).

In order to perform a metallurgical characterization of the metallic biomaterials, the destructive testing is necessary to obtain details about the microstructure of these biomaterials. The necessity of the metallurgical analysis is also justified by many previous cases when the poor choice of metallic biomaterials was the main cause for implant failure due to some microstructural defects or microstructural modifications that appear during the manufacturing process. Light microscopy and sometimes scanning electron microscopy are most used techniques to put in evidence the microstructural aspects of the metallic biomaterials [12–14].

Beyond visual analysis, chemical techniques have also been used for failure analysis of orthopedic devices. One of the most valuable techniques is Fourier transform infrared spectroscopy (FTIR) which allows a variety of features to be determined from analysis of polymeric components (like the effect of sterilization procedures or the estimation of the crystallinity of the polymers). Other chemical techniques can be used to identify chemical changes in a failed orthopedic device, like differential scanning calorimetry (useful for determination of crystallinity and crystal size distribution), gel permeation chromatography (for molecular distribution), and mass spectrometry (for detection of chemical species present in a biomaterial or tissue) [11].

Mechanical characterization techniques are very important because the properties of biomaterials have the potential to change with time and the result can be increasing the wear, accelerated fatigue failure, or gross mechanical failure of the orthopedic device. A series of standard techniques could be used, like hardness testing, dynamic mechanical analysis, small punch testing, and peel or tensile testing, but in some cases could be necessary to design some specific conditions for testing, in order to simulate the functionality of the orthopedic devices.

Also, the use of different methods (like finite element analysis) for simulation and modeling the mechanical functionality of specific orthopedic devices could be very useful to identify the failure causes and the failure mechanism for orthopedic devices.

---

## **Failure Analysis of Hip Implants**

Hip prosthesis is one of the most analyzed orthopedic implant from the point of retrieval studies.

The total hip prosthesis is a mechanical assembly which is intended to take the natural biomechanical function of the hip joint, in conditions of a serious illness of the latter, which results in significant limitations on its physiological function [15].

It is to be noted the great diversity of hip prostheses, each producer trying to impose their own design, but using the same basic principles. From a constructive point of view, the total hip prosthesis is made of three parts: the femoral component, the femoral head, and the acetabular component, the latter having a high molecular density polyethylene insert (UHMWPE). The femoral component has a cervical (neck) and a rod (tail) and can be a single piece (monobloc type) or can be made up of two parts, in case of modular head components. The femoral head is the component of the total hip prosthesis that is fixed in the upper part of the femoral component by different techniques. It is generally made of metallic biomaterials (usually type Co–Cr alloys), but some models also use ceramic biomaterials like alumina or zirconia. Hip prostheses can be classified in terms of the interface between components, as follows: metal–plastic, metal–metal, and ceramic–ceramic. All devices used in total hip endoprosthesis prosthetic arthroplasty involve two primary components (femoral and acetabular) each with three elements. Regarding the attachment element, it can be said that all hip prostheses are fixed with the help of a femoral component (also called stem) that is inserted into the femoral medullar canal. The attachment of prosthesis of the hip bone is one of the parameters determining its stability, which is a limiting factor for the viability of a hip prosthesis and the most common long-term complication [5, 14].

The classification of the femoral component of the total hip prosthesis according to the attachment to the bone is made in cemented and uncemented. The cemented femoral components are fixed in the bone tissue by means of polymer-based cement, which takes some of the shock and evenly diffuses loading forces. The improvement of the fixation through modifications of the bone–implant properties was done by giving up the attachment with cement and by using the capacity on bone tissue to form a stable bond with the implant, which lasts in time. This prosthesis was designed with porous surfaces that are fixed without cement, allowing extra bone growth by simulating a “familiar” environment to the bone tissue. These femoral components with porous surfaces, although they have the advantage of greater stability, they have the disadvantage that they can only be used in case of a relatively healthy bone which can grow through the pores on the surface of the prosthesis and lead to its fixation [15, 16].

The cementation without fixation of the femoral components can be achieved in the following ways [17]:

- Using the textured surface of components; the fixing is achieved by increasing the textured surface of the bone prosthetic component (“ongrowth tissue”) when the fixing morphology is obtained.
- Using components porously coated with different materials; the fixing is achieved by the penetration and development of the bone tissue into the pores of the coating (“ingrowth tissue”), obtaining a biological fixation.
- Using bioactive materials on the surface; the fixing is due to chemical reactions on the interface of the implant/bone tissue, reactions through which on the surface of the prosthetic components form a biologically active layer.

**Table 1** Common failure mechanisms for total hip replacement prosthesis [18, 19]

Failure mode		Causes
Loosening		Tissue reaction to implant High elastic modulus of the implant materials Excessive micromotion at implant–tissue interface Improper attachment of hip prosthesis components Improper surgical technique Mismatching between implant selection and bone quality of the patient
Wear	Three body wear	Generation of wear particles (UHMWPE) Generation of metallic particles at nonarticulation surfaces Coating failure due to particle generation
	Excessive ball-socket wear	Polymeric degradation Poor material selection for friction couple
Biological reaction		Allergic reaction (e.g., Ni allergy) Infection
Corrosion		Moderately corrosive environment Improper use of different metallic biomaterials (e.g., Co–Cr ball and Ti stem) Degradation of passive film from the metallic biomaterials surface
Macroscopic failure		Improper metallic biomaterials structure Improper implant design for mechanical load Improper processing technique which generates stress concentration

An improvement of fixing can be achieved by a combination of ways, such as using a bioactive ceramic coating over a porous surface in order to achieve a direct relationship between the bone tissue and the surface inside the pores of the porous material. Development of the bone–implant interface is dependent on various factors such as:

- Volume and surface properties of the implant material
- Geometric shape of the implant
- Implant surface topography
- Relative motion at the interface

There are many modes of failure that depend upon which hip prosthesis is considered and these are summarized in Table 1.

Some failure modes can present themselves independently of other problems, whereas modes such as loosening of the stem often occur in conjunction with a different mechanism (like excessive polyethylene wear).

The most catastrophic mode of failure is macroscopic fracture of the stem itself. Due to the high potential for localized corrosive attack in the area of stress, alternating stresses can fatigue crack an implant well within the “safe” fatigue fracture stress ranges determined under noncorrosive conditions. A subset of the observed implant fatigue failure modes is known as corrosion fatigue.

Corrosion fatigue is a common failure mechanism for stainless steel implants, but has been observed in other alloy systems as well. It initiates predominantly in areas that have been subjected to design or surface stresses such as notches, machined grooves, or regions of sharp radii of curvature [20, 21].

Failure can also occur when the stem becomes loose. It may even protrude through the outer wall of the femur if it places too much stress on the inner surface of the cortical bone of the femur. The first few weeks after the implantation of the hip replacement are critical. If the stem is loaded too soon, any bone–stem bonding that may have formed can be lost. Further loading will only serve to cause more extensive loosening and tissue damage [22].

Loosening can also be caused by biological reaction (most likely to polyethylene or metallic particles surrounding the implant) where a “capsule” of fibrous tissue made up of proteins and inflammatory cells develops around the implant and isolates it from the bone. This capsule can encourage osteolysis or osteonecrosis (bone loss or bone death) which further enlarges the cavity intended to snugly support the implant, leading to even further loosening. The stem can also loosen when the surrounding bone atrophies (commonly referred to as demineralization) from disuse. Often, this demineralization can be caused by a stress shielding mechanism, which can occur when the metallic stem bears more of the patient’s weight than that which is ideal for bone health and maintenance. Indeed, stress is essential for minerals to deposit and remain deposited upon the precursor protein fibers that serve as bone’s scaffolding structure.

Polyethylene debris released from the articulating surface has also been implicated in the loosening process owing to its tendency to stimulate bone-dissolving cells (osteoclasts) into action [23–25].

## **Failure Analysis of Hip Prosthesis Type Metal–Polyethylene**

The most common mechanism in total hip arthroplasties has been shown to be surface wear. Hydroxyapatite (HA) forms biological bonds between host bone and implant, being used as a surface coating for total hip arthroplasties since the 1980s [15]. Important questions still remain regarding the use of HA-coated acetabular components in total hip arthroplasty. Osteolysis due to bearing surface wear is the greatest unsolved problem that limits the durability of joint replacement. Retrieval studies of clinically well-functioning acetabular components should help to answer some of these questions.

We examined four clinically successful HA-coated cementless acetabular components retrieved at revision between 6 and 15 years after implantation. All components were of the same design (smooth-surfaced HA-coated acetabular shell with two to three screws).

The radiological images of one clinical case that was investigated in detail are shown in Fig. 3.

The prosthesis component was analyzed using different microscopical techniques, but firstly was made a macroscopic analysis (Fig. 4).

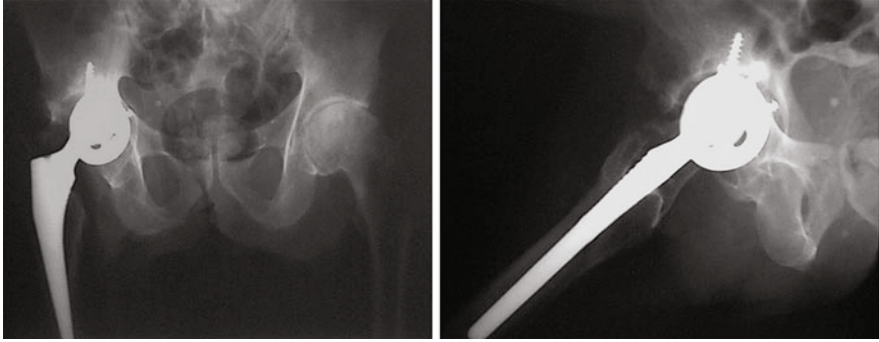


**Fig. 3** X-ray images of the clinical case investigated for failure of a hip prosthesis type Landos (Patient details: M.T., 72 years)



**Fig. 4** Macroscopy view of the primary implant components that were analyzed: acetabular cup, polyethylene liner, screws

The surrounding bone was prepared for qualitative histological and quantitative histomorphometric analysis [26]. The percentage of bone growth onto the implant, the relative bone area around the implant, the extent of residual HA coating, and the coating thickness were measured. Retrieved metallic shells were initially visually analyzed, then digital pictures were taken, areas of HA demarked, and extent of bone ingrowth and HA absorption was analyzed. ESEM analysis was the next step, using



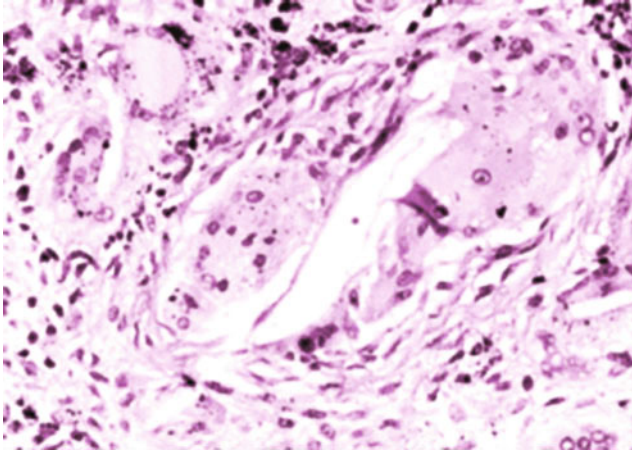


**Fig. 5** Histological analysis of the tissue surrounding the implant (optical microscopy image). 1, foreign bodies; 2, foreign body inside giant cell; 3, giant cell and fibrin exudation (hematoxylin eosin, coloration of sample tissues; x 200)

two types of electron detectors: LFD and BED – composition images on shell surface and retrieved broken screws.

The primary implants – cementless HA-coated smooth surface (Landos, France) – had an HA coating of 60  $\mu\text{m}$  thick and five screw holes on the surface. Tissues samples retrieved at the time of revision surgery for a migrated cementless acetabular implant associated with important osteolysis have demonstrated a consistent histological pattern. All intraoperative bacteriological cultures were negative. The most common finding was extensive chronic inflammation with a predominance of plasma cells and lymphocytes. Other anatomic-pathologic features included granulomas, foreign-body giant cells, necrosis, and fibrin exudation (Fig. 5). Each acetabular cup was removed with as much care as possible with regard of the bone stock and surrounding tissues. Gross inspection at the retrieved acetabular liners revealed a group of changes.

The results of stereomicroscopy analysis performed on the prosthesis component are shown in Fig. 6.

On the UHMWPE component, it was observed backside deformity with loss of machining lines and advanced wear along the peripheral rim where impingement occurred. Also, the surface of acetabular cup presents some remnant areas covered with hydroxyapatite on the base metallic biomaterial.

The digital analysis of the implants showed the degree of bone ingrowth at an average of 10–15 %, and the HA resorption extent averaged from 60 % to 85 % of the surface. ESEM analysis showed two patterns. The Ti6Al4V alloy type screws present unhomogenous material. Surface morphology analysis indicates a fatigue screw breakage type of failure, probably because of the presence of the polyhedral compounds with a different composition compared with base metal (Fig. 7).

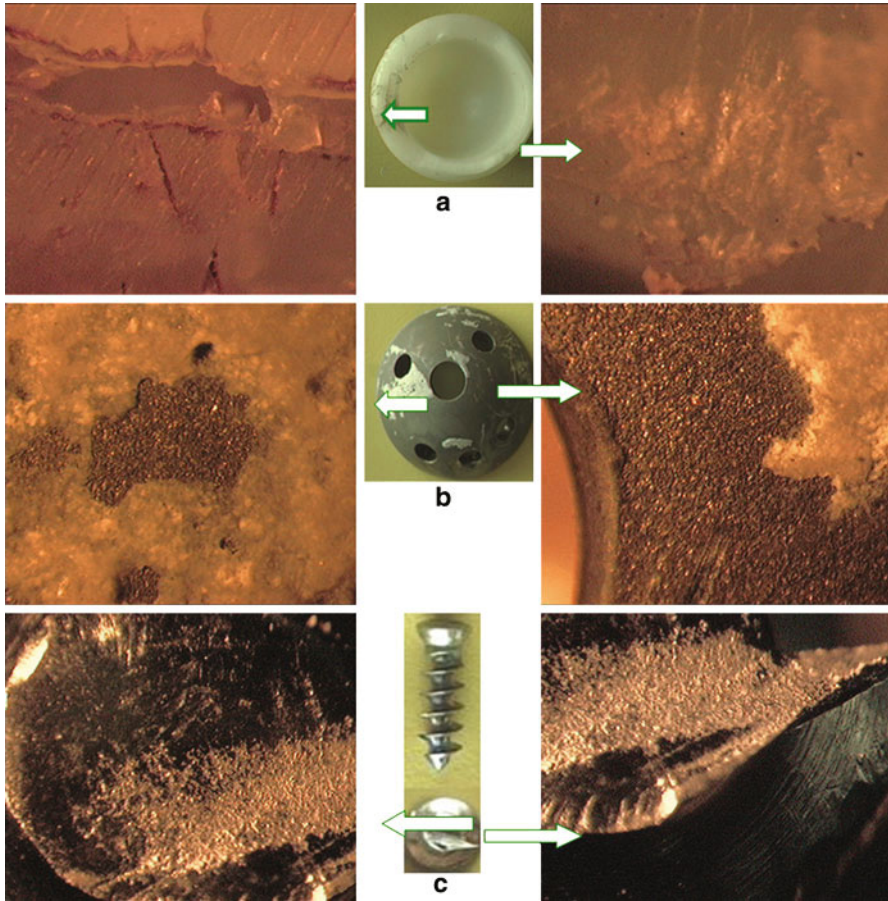


**Fig. 6** Stereomicroscopy analysis on the retrieved component of the prosthesis type Landos: (a) polyethylene component; (b) acetabular component; (c) metallic screw used for acetabular component fixation

The up surface of acetabular cup presents three different zones: base material porous type titanium, remnant areas covered with hydroxyapatite, and areas polished by fretting (Fig. 8).

Regarding the fixation failure, poor biological fixation may be related to surgical errors at primary implantation; the best option is to have a porous surface HA sprayed. Because of biocompatibility and osteoconductivity, HA-coated implants become stabilized by strong bone; whether macro- or microtextured surface of the implant is better for bone ingrowth and prosthesis longevity is still a subject of debate [3, 16, 17, 21]. The screws in acetabular fixation, usually not needed for press-fit primary fixation, prevent rotation and tilt (good for revisions) but provide access for debris and development of “cold flow” mechanism.

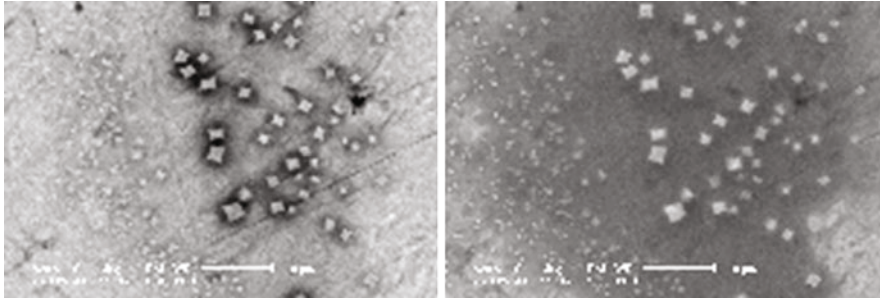


**Fig. 7** Scanning electron microscopy (SEM) of the screw breakage area: *left* BSE, *right* LFD (x2931); note the polyhedric compounds with a visible different composition than surrounding metal basis, a possible source for weakness and failure

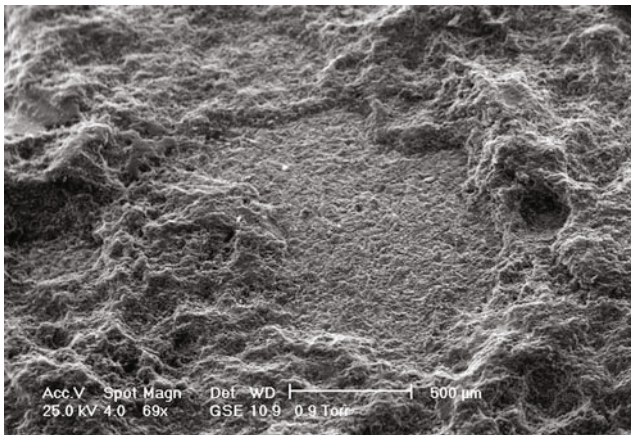


**Fig. 8** Scanning electron microscopy (SEM) of the external surface of the acetabular shell (x69); could be seeing the difference in porosity between HA-coated area and TiAlV smooth metal surface

In our cases we think that the failure of the smooth-surfaced HA-coated implant occurred over time. It is not reasonable to expect soft tissue interlocking of such an implant, and with no osteointegration, the cup will be instable and fail. The screws not sufficiently well implanted at primary intervention became mobile and an initial source of debris. The screw holes reduced the potential area for bone ingrowth and became the entry for polyethylene debris in the acetabular bone testimony being brought by the important screw hole markings on the backside of the polyethylene liner (according to Fig. 4). The small particles are well known to produce a strong notch effect; in the gap created, oxygen content is consumed with a decrease in the local pH value of the body fluid and an increase of the corrosion rate. The added cell-mediated HA resorption seems to be the main reason for loss of HA coating.

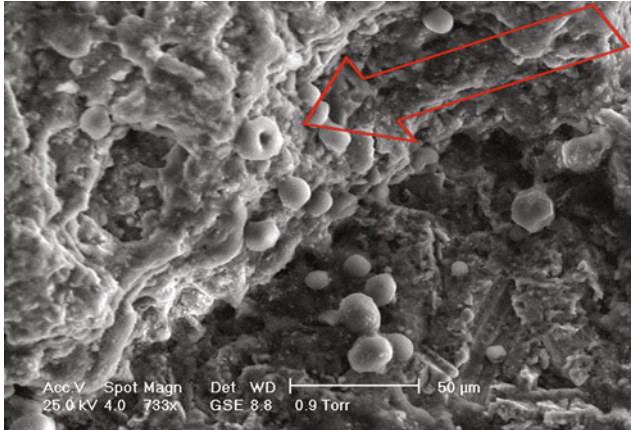


**Fig. 9** Scanning electron microscopy (SEM) of the same area of the acetabular shell at the interface HA metal (733X); note the important cell adhesions (bone and erythrocytes) related to the remnant HA in contrast with the smooth surface

The area of bone ongrowth was within a certain range (15–40 %) of the measured surfaces, and it was independent of the amount of HA residue.

The excessive wear generated important debris, and the inflammatory answers of the organism lead to osteolysis, excessive HA restoration, and failure of the acetabular cup.

The analyzed failure cases may be caused by the inaccurate insertion of the cup with inefficient screws that led to a combination of metal and polyethylene debris disease. After an initially normal clinical evolution, the local biological and mechanical factors led to failure of the initially good but insufficient lamellar bone and eventually bony bridges.

### **Failure Analysis of Hip Prosthesis Type Metal–Metal Used in Resurfacing Arthroplasty**

Hip resurfacing arthroplasty (HRA) represents a modern treatment for osteoarthritic hips in young patients. In a conventional total hip replacement, orthopedic surgeons remove the head of the femur, or the ball of the hip joint, and replace it with a metal stem inserted into the thigh bone. They fit the socket of the joint with a metal shell that typically includes a plastic liner. In hip resurfacing, the femoral head is preserved but its surface is reshaped to accept a rounded cap with a short stem that sits in the femoral neck. A thin metal cup is pressed into the hip socket. Both components are made entirely of cobalt chrome alloy. The resurfacing was first introduced in 1967 using the “press-fit” method to fix the 43 mm-diameter prosthetic components, but this method was quickly abandoned in favor of total hip arthroplasty which was using the polyacrylic cement as a method of fixing the prosthetic components. Furthermore, the studies of Charnley from 1969 introduced the concept of “low

friction.” He postulated that a metal-on-polyethylene (ultra high molecular weight polyethylene (UHMWPE)) friction torque with diameters as small as it could be for the artificial femoral head (22.25 mm) should be used [27].

The hip resurfacing results were very disappointing in the 1970s–1980s, and the procedure was abandoned except for a limited number of orthopedic centers. For current knowledge, the first generation of resurfacing is a great example of arthroplasty with massive attrition. The attempts to increase the diameter of the femoral head in order to achieve implant stability resulted in high rates of failure for the hip resurfacing arthroplasty using metal–polyethylene friction torque. The large diameters of the artificial femoral head and polyethylene components caused excessive wear and a massive production of biologically active particles, resulting in osteolysis and loosening of the components.

Renaissance of metal–metal friction torque in hip replacement started in the 1980s, when Weber began using a Co–Cr alloy with high carbon content with excellent characteristics [28]. The availability of a metal-on-metal (MoM) low wear surfaces that could be used in joint implants with large diameters led Wagner in Germany and McMinn in the United Kingdom to introduce the second generation of resurfacing beginning with 1991 [29, 30]. At the end of 2004, most of the leading manufacturers of implants for hip arthroplasty have already introduced systems for the metal-on-metal hip resurfacing. All these types have a number of common elements: the material is a Co–Cr alloy, the acetabular component is cementless, and the femoral one is cemented. The second generation of implants with metal–metal friction torque have further improved geometry, in the sense of sphericity and high-diameter joint clearances. The materials used were proven to be efficient both in terms of tribological characteristics and the resistance, corrosion, and biological effects.

The most controversial issue on the materials used is related to the manufacturing technology. Co–Cr alloys containing higher or lower carbon can be wrought or cast. The cast ones can then undergo heat treatment (hot isostatic pressure-HIP or solution heat treatment-SHT). These treatments result in a decrease in distribution of the carbide on the surface (which confer resistance) but in vitro results on simulators show that differences are not noteworthy.

Even if differences in metallurgical technology may be important, the control of the geometry is critical for the behavior of the surface in large-diameter metal-on-metal prosthesis: the radial clearance, the sphericity, and the roughness, all dependent on the manufacturing process, are decisive in influencing the tribological characteristics such as wear in the initial period (running-in wear) or in the steady-state wear period. Metal–metal joint systems require a diameter of 38 mm minimum to produce a type of lubrication to minimize wear between the steady-state wear, after an initial period, and the radial clearance should be small enough (but does not fall below a value when meshing of surfaces appears) [31, 32]. It is difficult, however, to appreciate the value in vivo because there are many variable factors that influence physical deformation: body weight, activity level, bone quality, implant position, design components, etc. Although metal–metal artificial bearings are used in orthopedic surgery for over 40 years, there is no conclusive study to

suggest potential harm (e.g., carcinogenic) for short or long term. Metal–metal friction torque in the human body produces serum levels of cobalt and chromium greater than metal-on-polyethylene joints. Numerous articles also show increasing concentration of metal ions in metal–metal artificial joints compared to other joints [7, 20, 33–35]. It is difficult, however, to compare these studies because they use different combinations of biological parameters (serum, blood, urine, erythrocytes, etc.) and different measurement techniques [36]. The importance of generation of wear particles resides in the possibility of appearance of periprosthetic effects. Although it is still unclear how metal particles or ions can cause periprosthetic problems, clinical cases of periprosthetic soft-tissue masses and osteolysis have recently been reported. Lymphocyte infiltrations in periprosthetic tissue, described as ALVAL (aseptic lymphocytic vasculitis-associated lesions), were observed in the first- and second-generation MoM total hip arthroplasty [37–39] as well as in MoM hip resurfacing arthroplasty [40, 41]. Analyzing the periprosthetic tissues from 19 MoM implants that were revised for pain and swelling, Willert observed intense perivascular lymphocytic cuffing and suggested that a T lymphocyte-mediated hypersensitivity reaction of type IV (delayed-type hypersensitivity) resulted from the metal-wear debris from the MoM bearing couple [38].

In the absence of osteolysis secondary to wear particles, displacement of the femoral component is the result of fracture or osteonecrosis. The ways by which acetabular component is displaced are different. McMinn compared different ways of fixing the resurfacing arthroplasty, and the results have shown that cementless acetabular components covered with hydroxyapatite (HA) give the best results in terms of survival (on a series of 446 HRA no aseptic loosening cup) [29], and Amstutz on a sample of 600 cases of cementless cups reported a single review of acetabular cup [28]. Atasei perform a review on failure causes in hip resurfacing arthroplasty and present the advantages versus disadvantages of resurfacing arthroplasty of the hip (Table 2) [19].

The long-term results are also good for the conventional total hip arthroplasties if cementless acetabular cups are used. The aseptic loosening of this prosthesis is caused by the osteolysis secondary to the large volume of polyethylene wear particles; this theoretical problem is no longer a complication of the resurfacing arthroplasty because of the lack of polyethylene between implant components.

The first detailed analysis of a type of hybrid metal–metal arthroplasty implant Conserve Plus showed that the main cause of failure was loosening of the femoral component, as in the resurfacing site of the first generation (metal–polyethylene) [28]. However, secondary osteolysis wear particles found were not the cause of the radiolucent and loosening areas, as in metal–polyethylene friction torque (measuring the wear rate, it was found that it was very low, and virtually none of the particles generated could trigger biological response that could lead to osteolysis).

The main factors for femoral failure identified by some authors are [28, 42]:

- Presence of bone cysts with diameter more than 1 cm in the femoral head
- Small area for fixing the femoral component
- Varus positioning of the femoral component

**Table 2** Advantages versus disadvantages of resurfacing arthroplasty of the hip [19]

Advantages of hip resurfacing	Disadvantages of hip resurfacing
Preserves the femoral head and neck	Difficult surgical technique, longer learning curve Risk of femoral neck fracture Elevated levels of metallic ions in blood and tissues
Preserves the femoral diaphysis	
Minimal risk of dislocation	
Low level of osteolysis, “stress shielding” absent	
Minimal or absent leg-length discrepancy preserves the proprioception of the hip	
No thigh pain	

Amstutz demonstrates in a prospective multicenter study that by improving surgical techniques through rigorous training to prepare the neck receiver (by adding drill holes in the dome and chamfer region, the removal of the bone cysts, lavage and adequate drying of the neck stump), one can ensure good bone–cement interface at femoral level [43]. In addition, for patients with high risk (greater than 1 cm cysts, components smaller than 46 mm), he recommends cementing centromedular stem femoral component.

Although the preparation of the acetabulum for resurfacing arthroplasty is similar to conventional total arthroplasty, there are particular issues in case of resurfacing, concerning the relationship between diameter of the acetabulum bone, thickness of the acetabular component of the implant, surgical technique, and acetabular bone density: a large-diameter acetabular cup (and thin) can be deformed if implanted in a press fit too “tight” if there is an increased bone density in the anterior and posterior walls of acetabulum. This could have negative consequences on radial clearance and on the type of contact and lubrication [44]. Therefore the surgeons must be aware of this and adapt their surgical technique accordingly: a press fit too “tight” in the dense bone may be undesirable in the case of a thin acetabular component, with large diameter and small radial clearance of the implant. Correct positioning of the acetabular cup respects the same criteria as for the total arthroplasty (abduction 40–50°, anteversion 15–20°). Recent studies have shown that malpositioning of the acetabular component in excessive abduction or anteversion could cause increased edge loading and excessive wear, leading to a greater amount of metal debris consecutively.

Preserving the femoral neck in resurfacing arthroplasty exposes the patient at risk of fracture at this level in the immediate postoperative period or later, with advancing age. Factors that increase the risk of femoral neck fracture in patients with resurfacing arthroplasty were also identified. They were classified into three categories: risk factors related to patient status, surgical risk factors, and risk factors in the postoperative period. Risk factors related to patient status include gender and proximal femoral bone quality. A conclusion regarding the age limit could not be drawn but notes that reduced bone mineral density in postmenopausal women is a risk factor [45].

Surgical risk factors associated to femoral neck fracture were the destruction of the upper femoral neck cortex (notching) or the placement in varus of the femoral component. The positioning of the femoral component in varus position increases

the compressive forces that occur medially and generates distractive forces at the lateral femoral cortex resulting in appearance of a shear torque at the base of the implant. De Smet points out issues that may lead to intraoperative malposition of the femoral component: destruction of the upper femoral neck cortex, incorrect positioning of the guide pin, excessive removing of soft tissue around the femoral neck (the vascular source for the femoral head and neck), the prepared bone not entirely covered by the prosthesis, implantation with excessive force (cement too viscous or too much quantitatively) or on the wrong direction, and excessive bone resection [46].

Risk factors in the postoperative period are tied to the immediate postoperative recovery. Allowing immediately partial or full weight bearing (elements present in most postoperative protocols) in conjunction with changes at the femoral neck caused by surgery (intramedullary instrumentation, cylindrical and chamfer reaming) that can affect bone strength may constitute as a risk category. Therefore, a period of assisted weight bearing can be beneficial, especially if there are associated risk factors from other categories. Another issue related to the postoperative period is that of bone remodeling at the femoral neck. Theoretically, preparation for resurfacing may cause femoral head avascular necrosis and, consequently, failure by loosening or periprosthetic fracture. The femoral head vascularization in osteoarthritic hips is disrupted, and new vascularization is developed within the bone at the expense of the subsynovial one [47]. Recent studies that show a low incidence of avascular necrosis rate of failure come to confirm to some extent this, especially as the traditional surgical approach path is posterior (an approach that sacrifices the ascending branch of the medial circumflex artery, which is a major supplier of blood for subsynovial vascularization) [48]. However, preexisting osteonecrosis can lead to femoral failures after hip resurfacing; therefore indications for hip resurfacing in AVN (avascular necrosis) of the femoral head are limited nowadays.

Due to large diameter of the artificial joint and due to the fact that biomechanical conditions are closer to normal, the rate of dislocation in resurfacing is significantly lower compared with that of classic total hip arthroplasty. Most studies do not report cases of dislocation and among those who do, the incidence is small [46, 49].

Possible causes of this complication are those that we can find also in total hip arthroplasty (malposition of the components, particularly for acetabular cup, incorrect offset, deficiencies in restoring the anatomical structures, etc.). While for malpositioning of the resurfacing components the surgeon must make more errors than for total hip arthroplasties, the situation is reversed for the recovery of the femoral offset: an excessive bone resection at the femoral neck is more difficult to be compensated in resurfacing than for total hip arthroplasty, where the modular femoral implant allows easier adjustment.

Risk factors which could lead to failure in HRA are described in Fig. 10.

Our group analyzes a large series of HRA explants (more than 50) obtained from different orthopedic clinics between March 2005 and July 2014. From the surgical intervention point of view, most of the hips were operated for primary osteoarthritis, but also were mentioned AVN of femoral head, inflammatory arthritis, and post-traumatic arthritis. Follow-up period was 10 months–5 years post-op. Short- and



<b>Risk factors related to implant</b>	<ul style="list-style-type: none"> <li>• a brittle friction torque or one producing large quantities of biologically active wear products</li> <li>• an inappropriate tribology (roughness, radial clearance)</li> <li>• shape and size of implant</li> </ul>	
<b>Risk factors related to surgery</b>	- <b>pre-op</b>	<ul style="list-style-type: none"> <li>• wrong indication</li> <li>• poor preoperative planning</li> </ul>
	- <b>intra-op</b>	<ul style="list-style-type: none"> <li>• malpositioning of components</li> <li>• destruction of the upper femoral neck cortex (notching)</li> <li>• excessive bone resection</li> <li>• wrong methods of inserting the components</li> </ul>
	- <b>post-op</b>	<ul style="list-style-type: none"> <li>• immediate weight-bearing associated with other risk factors for femoral neck fracture</li> </ul>
<b>Risk factors related to patient status</b>	<ul style="list-style-type: none"> <li>- poor proximal femoral bone stock</li> <li>-metal hypersensitivity/ALVAL</li> </ul>	<ul style="list-style-type: none"> <li>• primary / secondary – osteoporosis</li> <li>• bone remodeling</li> </ul>

**Fig. 10** Risk factors for failure in hip resurfacing arthroplasty (HRA) [19]

medium-term evaluation was done clinically by means of Harris hip score values and radiologically (positioning and migration of prosthetic components and bone remodeling on standard digital X-rays).

In Fig. 11 are shown the relevant radiological images on the failed BHR hip resurfacing prosthesis. In the radiological images, we could see dislocation of the prosthetic components first day postoperative which was treated nonoperatively by closed reduction with good result (Fig. 11a), femoral neck fractures (Fig. 11b), and dislocation due to improper cementing technique (Fig. 11c).

They necessitated a conversion to total hip arthroplasty with big femoral head, keeping in place the acetabular cup.

Periprosthetic tissues from hip during revision were subjected to histologic analysis. Retrieved implants were longitudinally cut (Fig. 12), and a thorough analysis of all interfaces was performed by scanning electron microscopy.

The results obtained after the analysis of failed specimen using scanning electron microscopy (SEM) are presented in Fig. 13.

Both the fractures of the femoral neck and the dislocation were caused by intraoperative errors; the fractures were due to notching of the upper femoral cortex during reaming and vicious cementing of the femoral component. Despite a 3-month non-weight-bearing postoperative period, the neck eventually fractured. The re-intervention procedure consisted in implanting a classical femoral stem with a matching big femoral head on the in situ acetabular cup. This procedure is equivalent to the femoral timing in the total hip replacement so it has the theoretical advantage of being easier than a classical revision of femur. The dislocation was caused by excessive bone resection on the femoral head which lead to instability. The closed

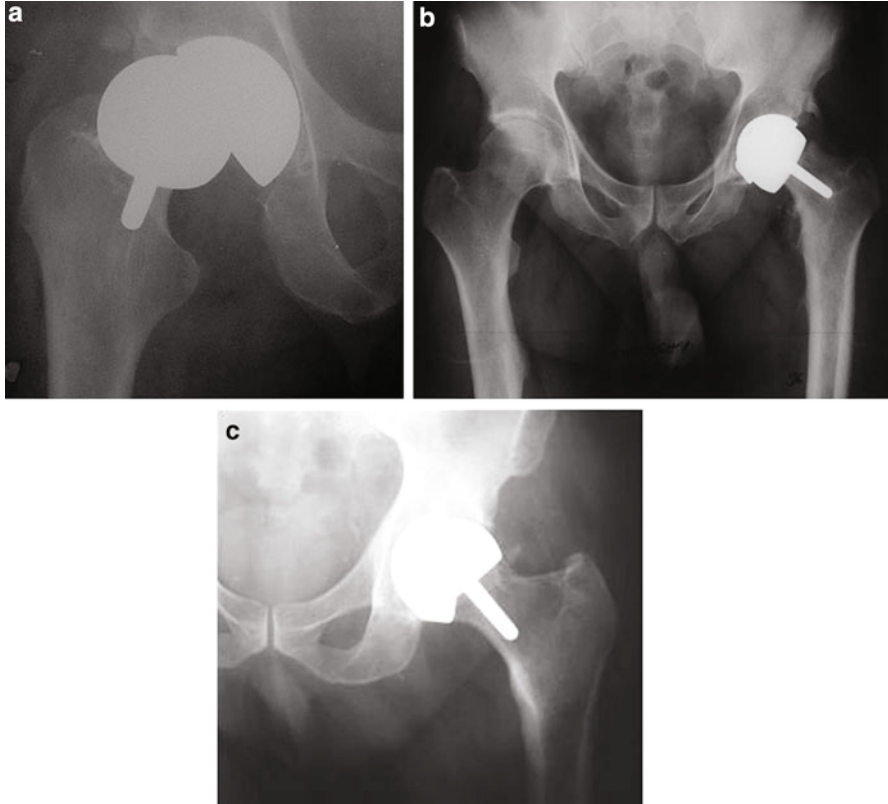


**Fig. 11** Relevant radiological aspects on the failed Birmingham hip resurfacing prosthesis (Smith & Nephew, UK): (a) dislocation of components; (b) femoral neck fracture due to intraoperative notching; (c) femoral neck fracture due to improper cementing technique

reduction followed by an abduction orthosis for 4 weeks succeeded in gaining enough stability.

Some issues can be discussed after the experimental analysis:

- Notching of the femoral cortex leads to low resistance of the femoral neck.
- Inadequate cementation technique (a too thick pressurized cement mantle with poor impaction of the femoral component); the retrieval analysis demonstrates problems with cement penetration and possible fracture lines.
- The bone quality of the patient is very important.

In conclusion, we could consider that the hip resurfacing arthroplasty is still an area of development in orthopedic surgery. Early or late failures are the result of one or some combination of causes. The advantage of the method is that if the treatment fails, then the surgeon is facing a total primary arthroplasty, at least in terms of femoral bone stock. Surgical factors that determine the failures are undoubtedly very

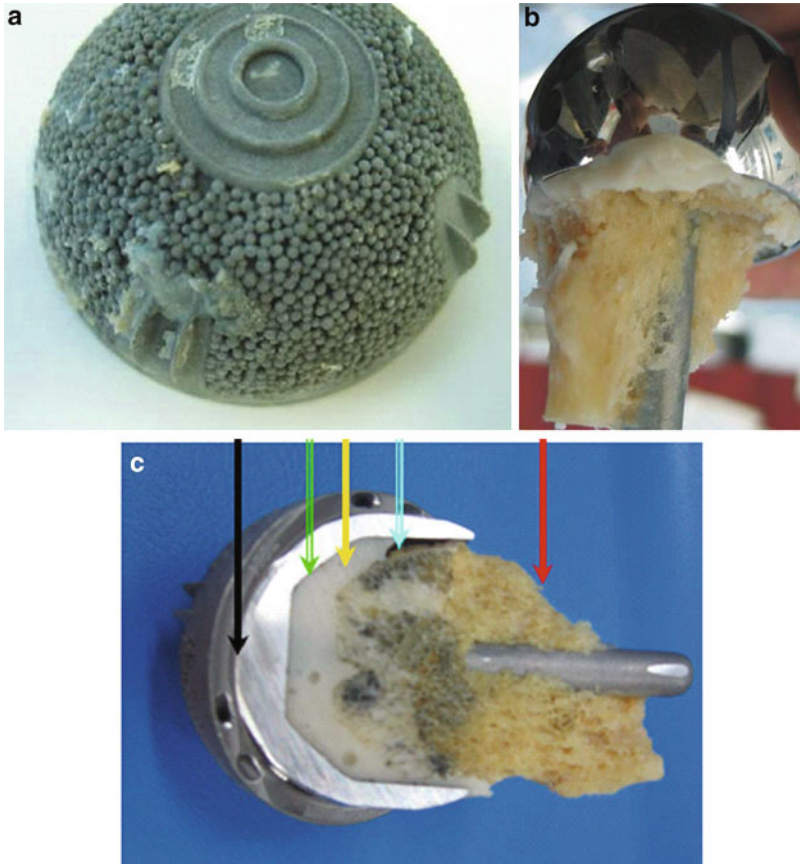


**Fig. 12** Macroscopic view of one failed BHR prosthesis component, with visible interfaces between bone, cement, and metallic components: (a) acetabular component; (b) femoral component; (c) acetabular and femoral components sectioned for analysis

important. Clinical and biomechanical studies have allowed an improvement of surgical technique. Besides the ability of the surgeon to perform intraoperative certain requirements, he needs to correctly assess (pre- or intraoperatively) the cases in which failure is predictable. It is therefore mandatory to inform patients prior to surgery on these risks and opportunities. With the passage to the second generation of resurfacing, most of the problems created by the implant itself seem to be resolved (much better properties for the used biomaterials and designs which give them a significantly increased lifetime).

The causes of failure related to patient's status can be removed by establishing a correct surgical indication. Thus, patients with a high risk of failure for total hip arthroplasty with a favorable femoral anatomy are candidates for resurfacing. In this category generally enter arthritic male patients younger than 60 years, with good quality femoral bone stock. It is preferable that surgical intervention should take

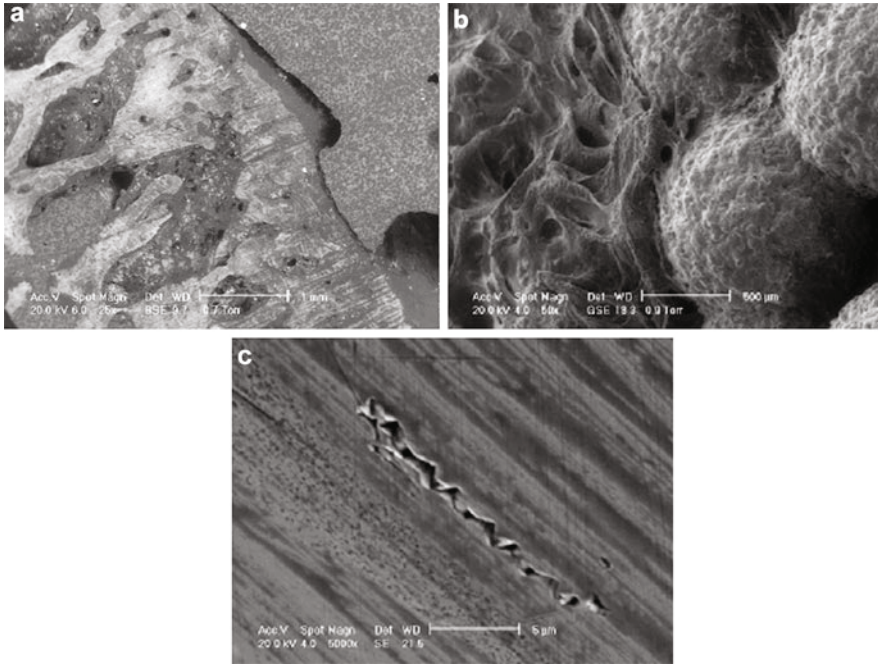


**Fig. 13** Scanning electron microscopy images obtained after the analysis of failed BHR prosthesis components: (a) bone–cement interface, improper bonding probably due to too fast polymerization (25x); (b) external surface of the implant with details of the sintered beads with good attached bone tissue (50X); (c) retrieved metallic component surfaces (5000x) with wear pattern of the classic polar loaded areas (micro-pits of 1 to 2 μm in diameter)

place before appearance of important arthritic secondary phenomena (bone cysts, osteopenia). Modular head for conversion to a total hip and salvage of the metal-on-metal interface should exist in every center that performs resurfacing arthroplasty.

The first question raised is about femoral periprosthetic bone undergoing a remodeling process in its proximal regions that may compromise the long-term outcome of resurfacing arthroplasty.

The importance of bone density should not be overlooked and a case may be made for DEXA scans before operation. Also, the cementation technique should be carefully selected, and the recommendation is to use high-viscosity cement for cementation.

### Failure Analysis of Hip Prosthesis Type Ceramic–Ceramic

Due to the clinical complications associated with osteolysis from hip prosthesis type metal–metal or metal–polyethylene, increased attention has been paid to utilizing

ceramic–ceramic bearings, especially in the case of younger patients, in order to minimize the risk of revision [50, 51]. Many orthopedic surgeons consider that hip prosthesis with main bearing components made by inert ceramic materials is now to be the best alternative for hip prosthesis type metal–polyethylene or metal–metal due to their superior tribological performance associated with excellent biocompatibility [52–54].

Alumina and phase-stabilized zirconia are bioinert ceramics used for manufacturing hip prosthesis components due their low reactivity associated with good mechanical features like low wear and high stability [51].

Also, during the last years, there were many research in order to develop composite material like ATZ, alumina-toughened zirconia (a phase-stabilized zirconia matrix reinforced with alumina particles), or ZTA, zirconia-toughened alumina (an alumina matrix reinforced with zirconia particles), with superior properties to the currently used bioinert ceramics [53].

First generation of alumina components, previously made for industrial applications, had a poor microstructure with low density, large grain size, and impurities in their composition. Different reports of alumina femoral head failures have appeared in the orthopedic literature since alumina bearings were introduced in total hip arthroplasty [55–59].

In general, early failures of alumina bearings were related to a combination of suboptimal material quality, taper design, prosthesis fixation, and clinical aspects related to the patient selection criteria [50, 52, 53]. Apart of the material and manufacturing variables, it's important to know that the safety of alumina bearings in total hip arthroplasty depends on the design of the taper, because a properly design for Morse taper can optimally transfer loads and avoid stress at the interface between some components of the hip prosthesis (metallic stem and alumina femoral head) [50, 52]. Different papers reveal that a suboptimal taper will contribute to the risk of failure for alumina femoral head in total hip arthroplasty [55, 56].

The characterization of retrieved components from hip prosthesis type ceramic–ceramic during revision surgery is very helpful in obtaining future improvements in biomaterials and hip prosthesis design. Affatato examined the surfaces of different retrieved ceramic components in order to compare the damage caused by in vivo wear with the results obtained in vitro [57].

Even if the ceramic–ceramic bearing couple showed excellent wear properties, some complication appears. An important problem is the “squeaking noise” which has gained recent attention [60–65].

After these results, multiple potential causes have been implicated [62]:

- Metallic particle transfer
- Stripe wear
- Impingement
- Poor offset
- Vibration of metallic stem

Anyway, due to the small number of retrieved hip prosthesis that was revised for squeaking, it is difficult to present a clear conclusion, in the absence of many data available.

Our group has the possibility to analyze some retrieved components of hip prosthesis type ceramic–ceramic after different periods of time in function, made by alumina. Also, in our study was introduced an alumina femoral which was broken during intraoperative. The implants came from different orthopedic clinics. According with other authors, we consider that the surface analysis of retrieved ceramic implants would present interesting damages and it's important to be evaluated [53, 63, 67].

We evaluate the surface characteristics of the explanted ceramic heads with the use of two different methods: macroscopic and microscopic surface analysis with a scanning electron microscope type Philips ESEM-40. Based on the macroscopic analysis, the femoral head was considered to be non-damaged if no modification was visible on the ceramic head. Presences of metal particles, stripe wear, or other macroscopic visible damage on the ceramic head surface were noted.

According to the images shown in Fig. 14, we consider that all alumina femoral heads were slightly damaged because the damaged region was less than 10 % of the total head surface. Also, macroscopic analysis reveals presence of the metal transfer on all alumina femoral heads and visible stripe wear. Also, the visible traces of impingement were observed inside the femoral heads. All mentioned aspects were more clearly revealed after the surface analysis made by scanning electron microscopy (Fig. 14). Using SEM analysis, it was observed the same wear pattern at the surface of all retrieved alumina femoral head.

The EDS results after the analysis performed on the surfaces of explanted alumina femoral head are shown in Fig. 15. These confirm without any doubts the presence of metallic particle (titanium) at the alumina surface.

Our experimental results are in accordance with other scientific reports. Restrepo et al. noticed, after the analysis of four retrieved alumina hip prosthesis components revised due to squeaking, the presence of stripe wear and signs of femoral neck–acetabular rim impingement for all specimen analyzed and presence of metal transfer for some of them [61]. Other studies mention that all their retrieved implants showed evidence of edge loading and impingement [60, 62]. Even some authors like Dorlot [63] didn't observe problems of squeaking; the presence of stripe wear on retrieved ceramic heads is clearly noticed.

Some of previously mentioned studies reveal that during surgery for revision was found subsynovial fibrous tissue that contain abundant metallic debris associated with a mild mononuclear inflammatory infiltrate [60, 61, 63]. Those experimental results tend to demonstrate that third body wear plays an important role with squeaking.

The prosthesis design and interface between metallic stem and ceramic head appear to be an essential factor to avoid or to generate impingement, which produce metal transfer leading to squeaking.

According to Chevillotte et al., the squeaking with ceramic-on-ceramic bearings seems to be a multifactorial problem [64]. Not just the design of prosthesis

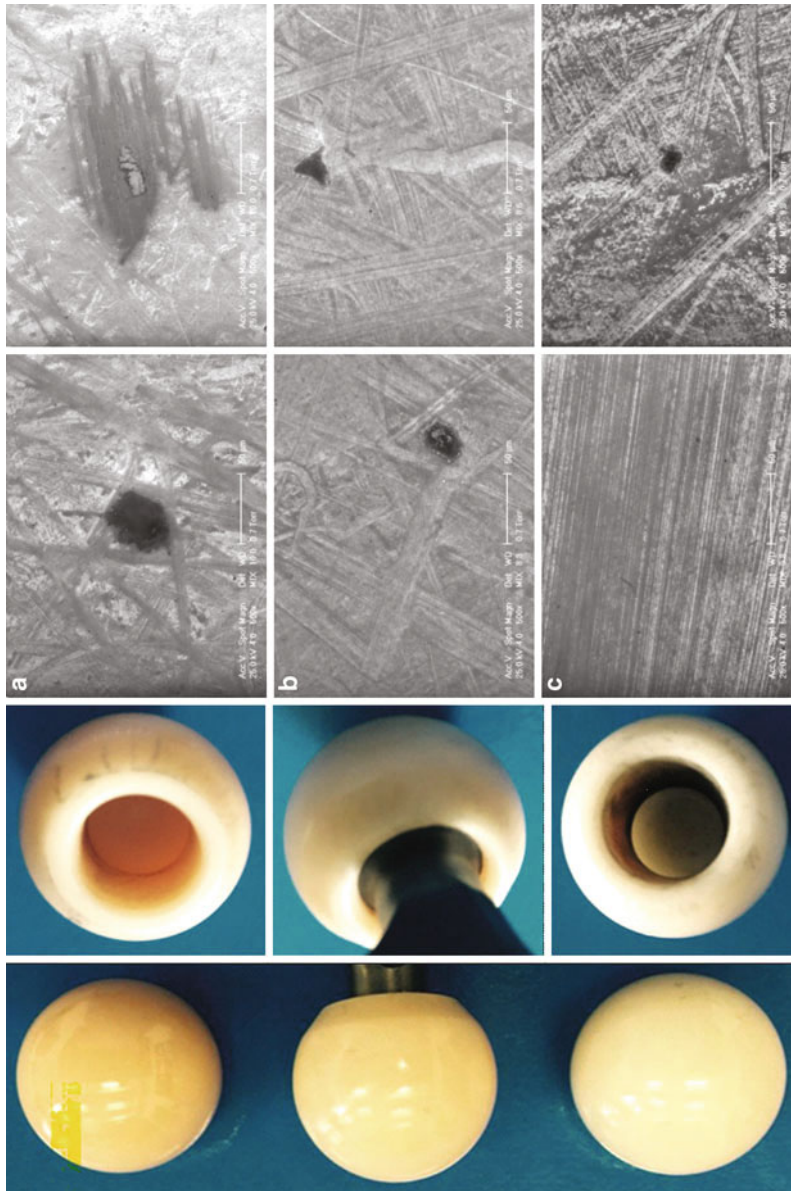


**Fig. 14** Macroscopic aspects of the explanted alumina component – femoral head of the hip prosthesis type ceramic–ceramic, from different clinical cases: *right* macroscopic aspects; *left* surface analysis made by scanning electron microscopy

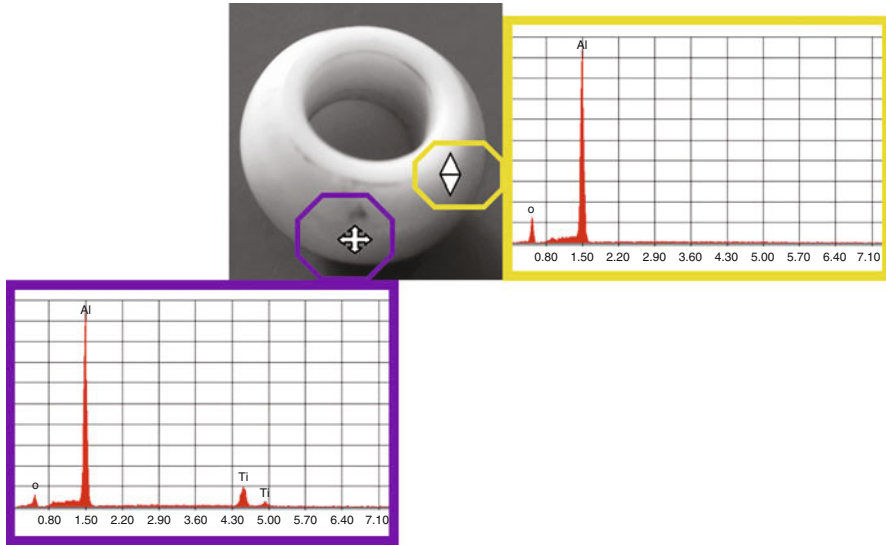


**Fig. 15** Results of the EDS analysis performed on the surfaces of explanted alumina component – femoral head of the hip prosthesis type ceramic–ceramic

components or surface properties are important factors in generating squeaking but also the prosthesis positioning. All of these factors may play a role in the disruption of film fluid lubrication, secondary to an abnormal roughness of the ceramic head, leading to squeaking.

According to Garino et al., an important aspect is that fractures of ceramic components occur as a result of some event, with the difficulty being the limited information available for analysis. These kinds of adverse events include severe trauma, autoclaving of the component that affects their structure, mismatch between the femoral head diameter and the acetabular insert, gross malpositioning of the acetabular component, recurrent hip dislocations, and others [66].

Based on our experimental analysis, we noticed that the autoclaving of the ceramic components has immediate consequences because the ceramic head failed during first hip arthroplasty surgery. In Fig. 16, we present the macroscopic aspects of the broken ceramic head, and SEM analysis of different parts from the broken alumina femoral head reveals the microstructural modifications that appear due to the wrong autoclaving.

Implant tapers optimized for ceramic femoral heads have been designed so that the taper bores concentrate loads proximally near the strongest portion of the alumina component. The metal tapers also often have a microscopic pattern of peaks and valleys on the surface, which flatten when the alumina ball is impacted on the taper in order to increase the contact friction and evenly distribute the loads.

Thus, stem or cup material, contact area, taper angle, trunnion–bore distance, and the chamfer design at the base of the alumina head are important engineering variables that contribute to the safety of alumina femoral heads [66–70].



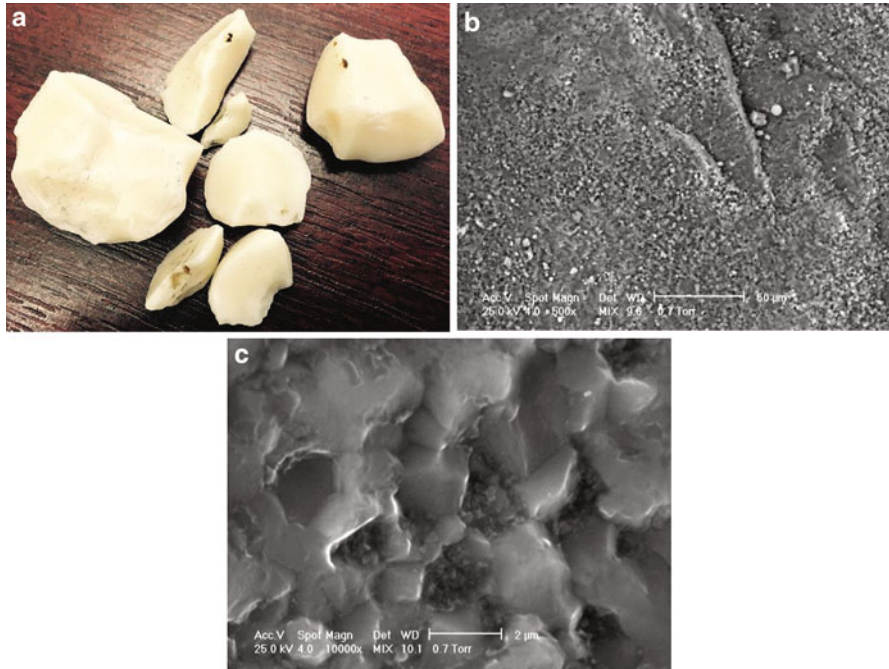


**Fig. 16** Failed alumina component – femoral head of the hip prosthesis type ceramic–ceramic: (a) macroscopic view; (b, c) SEM analysis of the surface for different broken parts of this component

The microstructural aspects of inert ceramics like alumina and zirconia directly influence the wear rate. Modern manufacturing of alumina components included tightly controlled material processing environments to minimize inclusions and impurities and to optimize material homogeneity. Also, highly specialized sintering and hot isostatic pressing techniques have resulted in reduced grain size of the alumina and improved material density. The improvement related to the fine microstructure of the alumina offers amelioration in wear properties.

The third generation of inert ceramic components of hip prosthesis represents a significant improvement in ceramic density, purity, and grain size. They are better in terms of wear than their predecessors under *in vitro* edge-loading conditions and demonstrate improved resistance to stress upon retrieval analysis [69, 70].

Anyway, based on our experience, we could consider that the risk of a ceramic bearing fracture is very low after primary surgery.

---

## Summary

The utility of orthopedic implant retrieval and evaluation was demonstrated many times until now. Early studies were focused primarily on the metallic implants used for osteosynthesis and reveal problems related to the poor metallurgy or weak areas

due to poor design. Other studies describe other aspects, like the pitfall of stamping the manufacturer's name in the middle of the plate where stresses are high. The low-friction total hip arthroplasty concept developed by Charnley is a classical example of how implant retrieval can yield important clinical information which impacts biomaterials and implant design. Now, attention of many researchers is focused on the clinical and retrieval studies which describe the performance of total hip bearing couples.

Orthopedic implant retrieval has provided critical information toward understanding the anchoring of implants in bone. For example, porous coatings may be applied to different prosthetic components to facilitate bony ingrowth but are not recommended for osteosynthesis implants. Also, the relationships between pore size and bony ingrowth have come from retrieval studies.

Implant retrieval studies have demonstrated that the success of a biomaterial in one application may not necessarily translate to another. For example, titanium works very well as a bone–implant interface, but it may be subject to severe wear as a bearing surface. An alternative approach in the hip was to use titanium alloy stems with modular press-fit heads made of a more wear-resistant cobalt alloy.

Even the focus of this chapter has been on the retrieval analysis of orthopedic implants used in humans, the approaches, techniques, and methods may also be applied to the evaluation of new biomaterials, preclinical testing for implant biofunctionality, and premarket clinical evaluation. Each type of analysis reveals the unicity of clinical situation and the implant–host interactions and therefore requires the development of a unique strategy for retrieval and evaluation.

Indeed, for investigation of bioresorbable materials and bioresorbable orthopedic implants, in which interactions between the implant and the surrounding tissue are complex, novel and innovative approaches must be used in the investigation of *in vivo* tissue compatibility.

---

## References

1. Ratner B, Hoffman AS, Schoen FJ, Lemons JE (1996) *Biomaterials science: an introduction to materials in medicine*. Academic, New York. ISBN 0125824610
2. Bunea D, Nocivin A (1998) *Materiale biocompatibile*. BREN, Bucharest. ISBN 973-98447-2-3
3. Burke M, Goodman S (2008) Failure mechanisms in joint replacement. In: Revell P (ed) *Joint replacement technology*. Woodhead, Cambridge, UK, pp 264–285
4. Cook SD, Renz EA, Barrack RL, Thomas KA, Harding AF (1985) Clinical and metallurgical analysis of retrieved internal fixation devices. *Clin Orthop* 184:236–247
5. Antoniac V, Neculescu A, Cosmeleata G (2009) Chapter 25. Biocompatible materials and shape memory alloys. In: *Materials science and engineering handbook, vol 3*. AGIR, Bucharest, pp 1463–1495. ISBN 978-973-720-261-1/978-973-720-064-0
6. Silva M., Heisel C., Schmalzried T.P. (2005) Metal-on-metal total hip replacement. *Clin Orthop Relat Res* (430):53–61
7. Howlett CR, Zreiqat H, Wu Y, McFall DW, McKenzie DR (1999) Effect of ion modification of commonly used orthopedic materials on the attachment of human bone-derived cells. *J Biomed Mater Res* 45:345–354

8. ASTM F561-97, Practice for retrieval and analysis of implanted medical devices, and associated tissues, ASTM International, West Conshohocken, PA, 1997, [www.astm.org](http://www.astm.org)
9. Antoniac I (2013) Biologically responsive biomaterials for tissue engineering, Springer Series in Biomaterials Science and Engineering 1, Springer Science+Business Media New York, ISBN 978-1-4614-4327-8
10. Bruck S (1980) Properties of biomaterials in the physiological environment. CRC Press, Boca Raton
11. Von Recum AF (1999) Handbook of Biomaterials Evaluation: Scientific, Technical, and Clinical Testing of Implant Material, Second Edition, Taylor & Francis, Philadelphia, ISBN 1-56032-479-1
12. Bronzino J (1992) Handbook of bioengineering. CRC Press, New York. ISBN 0-471-96935-4
13. Purghel F, Badea R, Antoniac I (2001) Medicina pentru ingineri. Printech, Bucharest. ISBN 973-652-358-6
14. Antoniac I, Laptoiu D, Blajan AI, Cotrut C (2011) Instrumentar chirurgical si dispozitive medicale. Printech, Bucharest. ISBN 978-606-521-665-5
15. Furlong RJ, Osborn JF (1991) Fixation of hip prosthesis by hydroxyapatite ceramic coatings. *J Bone Joint Surg* 73:741–745
16. Cristofolini L, Teutonico AS, Monti L, Cappello A, Toni A (2003) Comparative in vitro study on the long term performance of cemented hip stems: validation of a protocol to discriminate between “good” and “bad” designs. *J Biomech* 36:1603–1615
17. Ramaniraka NA, Rakotomanana LR, Leyvraz PF (2000) The fixation of the cemented femoral component: effects of stem stiffness, cement thickness and roughness of the cement-bone interface. *J Bone Joint Surg Br* 82(2):297–303
18. Antoniac I (2007) Biomateriale metalice utilizate la executia componentelor endoprotezelor totale de sold. Printech, Bucharest. ISBN 978-973-718-881-6
19. Atasiei T, Antoniac I, Laptoiu D (2011) Failure causes in hip resurfacing arthroplasty – retrieval analysis. *Int J Nano Biomater* 3(4):367–381
20. Agins HJ, Alcock NW, Bansal M, Salvati EA, Wilson PD (1998) Metallic wear in failed titanium-alloy hip replacements. *J Bone Joint Surg Am* 70(3):347–356
21. Ebramzadeh E, Campbell PA, Takamura KM, Lu Z, Sangiorgio SN (2011) Failure modes of 433 metal-on metal hip implants: how, why, and wear. *Orthop Clin N Am* 42:241–250
22. Jacobs JJ, Patterson LM, Skipor AK, Urban RM, Black J (1999) Postmortem retrieval of total joint replacement components. *J Biomed Mater Res (Appl Biomater)* 48:385–391
23. Kurtz SM, Hozack WJ, Purtill JJ, Marcolongo M, Kraay MJ (2006) Significance of in vivo degradation for polyethylene in total hip arthroplasty. *Clin Orthop Relat Res* 453:47–57
24. Revell PA (2008) The combined role of wear particles, macrophages, and lymphocytes in the loosening of total joint prostheses. *J R Soc Interface* 5:1263–1278
25. Schmalzied TP, Campbell P, Schmitt AK, Brown IC, Amstutz HC (1997) Shapes and dimensional characteristics of polyethylene wear particles generated in vivo by total knee replacements compared to total hip replacements. *J Biomed Mater Res (Appl Biomater)* 38:203–210
26. Frayssinet P, Hardy D, Conte P, Delince P, Guilhem A, Bonel G (1993) Histological analysis of the bone-prosthesis interface after implantation in humans of prostheses coated with hydroxyapatite. *J Orthop Surg* 7:246–253
27. Charnley J, Kamangar A, Longfield MD (1969) The optimum size of prosthetic heads in relation to the wear of plastic sockets in total replacement of the hip. *Med Biol Eng* 7:31–39
28. Amstutz HC, Grigoris P (1996) Metal-on-metal bearings in hip arthroplasty. *Clin Orthop Relat Res* 329:S11–S34
29. McMinn DJW, Tracy R, Lyn K, Pynsent P (1996) Metal on metal surface replacement of the hip: experience of the McMinn prosthesis. *Clin Orthop Relat Res* 329:S89–S98
30. Wagner M, Wagner H (1996) Preliminary results of uncemented metal on metal stemmed and resurfacing hip arthroplasty. *Clin Orthop Relat Res* 329:S78–S88

31. Rieker CB, Schon R, Roberts P, Grigoris P (2005) Influence of the clearance on in-vitro large diameter metal-on-metal articulations pertaining to resurfacing hip implants. *Orthop Clin N Am* 36:135–142
32. Udofia II, Jin ZM (2003) Elastohydrodynamic lubrication analysis of metal-on-metal hip resurfacing prostheses. *J Biomech* 36:537–544
33. Back DL, Young DA, Shimmin AJ (2005) Serum metal ion levels following a hip resurfacing. *Clin Orthop* 36:187–193
34. Brodner W, Bitzan P, Meisinger V (1997) Elevated serum cobalt with metal on metal articulating surfaces. *J Bone Joint Surg Br* 79(2):316–321
35. Skipior AK, Campbell PA, Patterson LM (2002) Serum and urine metal ion levels in patient with metal on metal surface arthroplasty. *J Mater Sci Mater Med* 13(12):1227–1234
36. Mabilileau G, Kwon YM, Pandit H, Murray DW, Sabokbar A (2008) Metal-on-metal hip resurfacing arthroplasty. A review of periprosthetic biological reactions. *Acta Orthop* 79(6):734–747
37. Davies AP (2005) An unusual lymphocytic perivascular infiltration in tissues around contemporary metal-on-metal joint replacements. *J Bone Joint Surg Am* 87(1):18–27
38. Willert HG (2005) Metal-on-metal bearings and hypersensitivity in patients with artificial hip joints. A clinical and histomorphological study. *J Bone Joint Surg Am* 87(1):28–36
39. Witzleb WC (2007) Neo-capsule tissue reactions in metal-on-metal hip arthroplasty. *Acta Orthop* 78:211–220
40. Pandit H (2008) Pseudotumours associated with metal-on-metal hip resurfacings. *J Bone Joint Surg Br* 90:847–851
41. Toms AP (2008) MRI of early symptomatic metal-on-metal total hip arthroplasty: a retrospective review of radiological findings in 20 hips. *Clin Radiol* 63:49–58
42. Beaulieu P, Dorey F, Le Duff M (2004) Risk factors affecting early outcome of metal-on-metal surface arthroplasty of the hip in patients 49 years old and younger. *Clin Orthop* 418:87
43. Amstutz H, Le Duff M, Campbell PA, Dorey F (2007) The effects of technique changes on aseptic loosening of the femoral component in hip resurfacing. Results of 600 Conserve Plus with a 3 to 9 year follow up. *J Arthroplasty* 22:481–489
44. Schmalzried TP, Fowble VA, Bitsch RG, Choi ES (2007) Total resurfacing hip. In: Callaghan JJ, Rosenberg AG, Rubash HE (eds) *The adult hip*, vol. 2, Philadelphia, Lippincott, Williams & Wilkins, pp 969–979
45. Beaulieu P, Lee J, Le Duff M (2004) Orientation of the femoral component in surface arthroplasty of the hip: a biomechanical and clinical analysis. *J Bone Joint Surg* 86-A:2015–2021
46. De Smet KA (2005) Belgium experience with metal-on-metal surface arthroplasty. *Orthop Clin N Am* 36:203–213
47. Freeman MAR (1978) Some anatomical and mechanical considerations relevant to the surface replacement of the femoral head. *Clin Orthop* 134:19–24
48. Revell MP, McBryde CW, Bhatnagar S, Pynsent PB, Treacy RBC (2006) Metal-on-metal hip resurfacing in osteonecrosis of the femoral head. *J Bone Joint Surg Am* 88:98–103
49. Siebel T, Maubach S, Morlock MM (2006) Lessons learned from early clinical experience and results of 300 ASR hip resurfacing implantations. *Proc Inst Mech Eng H* 220(2):345–353
50. Semlitsch M, Dawihl W (1994) Basic requirements of alumina ceramic in artificial hip joint balls in articulation with polyethylene cups: technical principles, Design and safety of joint implants. Hogrefe & Huber, Seattle, pp 99–101
51. Chana R, Facek M, Tilley S et al (2013) Ceramic-on-ceramic bearings in young patients. *Bone Joint J* 95-B:1603–1609
52. Bal BS, Garino J, Ries M, Rahaman MN (2007) A review of ceramic bearing materials in total joint arthroplasty. *Hip Int* 17:21–30
53. Piconi C, Streicher RM (2014) Forty years of ceramic-on-ceramic THR bearings. *Semin Arthroplasty* 24(4):188–192
54. D'Antonio JA, Sutton K (2009) Ceramic materials as bearing surfaces for total hip arthroplasty. *J Am Acad Orthop Surg* 17:63–68

55. Hannouche D, Nich C, Bizot P et al (2003) Fractures of ceramic bearings: history and present status. *Clin Orthop Relat Res* 417:19–26
56. Hohman WD, Affonso J, Anders M (2011) Ceramic-on-ceramic failure secondary to head–neck taper mismatch. *Am J Orthop* 40(11):571–573
57. Affatato S, Traina F, De Fine M, Carmignato S, Toni A (2012) Alumina-on-alumina hip implants. A wear study of retrieved components. *J Bone Joint Surg Br* 94-B:1–6
58. Piconi C, Labanti M, Magnani G, Caporale M, Maccauro G, Magliocchetti G (1999) Analysis of a failed alumina THR ball head. *Biomaterials* 20(18):1637–1646
59. Maccauro G, Piconi C, Burger W (2004) Fracture of a Y-TZP ceramic femoral head. Analysis of a fault. *J Bone Joint Surg Br* 86:1192–1196
60. Murali R, Bonar SF, Kirsh G, Walter WK, Walter WL (2008) Osteolysis in third-generation alumina ceramic-on-ceramic hip bearings with severe impingement and titanium metallosis. *J Arthroplasty* 23:1240e13–1240e19
61. Restrepo C, Parvizi J, Kurtz SM, Sharkey PF, Hozack WJ, Rothman RH (2008) The noisy ceramic hip: is component malpositioning the cause? *J Arthroplasty* 23:643–649
62. Walter WL, Waters TS, Gillies M et al (2008) Squeaking hips. *J Bone Joint Surg Am* 90(Suppl 4):102–111
63. Dorlot JM (1992) Long-term effects of alumina components in total hip prostheses. *Clin Orthop Relat Res* 282:47–52
64. Chevillotte C, Trousdale RT, Chen Q, Guyen O, An KN (2009) Hip Squeaking: a biomechanical study of ceramic-on-ceramic bearing surfaces. *Clin Orthop Relat Res* 468:345–350
65. Abdel MP, Heyse TJ, Elpers ME et al (2014) Ceramic liner fractures presenting as squeaking after primary total hip arthroplasty. *J Bone Joint Surg Am* Vol 96:27–31
66. Garino J, Rahaman MN, Bal BS (2006) The reliability of modern alumina bearings in total hip arthroplasty. *Semin Arthroplasty* 17(3):113–119
67. Affatato S, Modena E, Toni A et al (2012) Retrieval analysis of three generations of Biolox femoral heads: spectroscopic and SEM characterization. *J Mech Behav Biomed Mater* 13:118–128
68. Pfaff H, Ing D (2000) Ceramic component failure and the role of proof testing. *Clin Orthop Relat Res* 379:29–33
69. Al-Hajjar M, Fisher J, Tipper JL et al (2013) Wear of 36mm BIOLOXs delta ceramic-on-ceramic bearing in total hip replacements under edge loading conditions. *Proc Inst Mech Eng Part H J Eng Med* 227:535–542
70. Piconi C, Porporati AA, Streicher RM (2015) Ceramics in THR bearings: behavior under off-normal conditions. *Key Eng Mater* 631:3–7

Rodica Marinescu and Iulian Vasile Antoniac

## Contents

Introduction .....	936
General Considerations About Arthroscopy .....	936
Biodegradable Implants Used in Knee Arthroscopy .....	937
Biodegradable Implants Used in ACL Reconstruction .....	937
Biodegradable Implants Used in Meniscus Surgery .....	943
Biomaterials Used In Cartilage Repair .....	949
Biodegradable Implants Used in Shoulder Arthroscopy .....	954
Biodegradable Implants Used in Shoulder Instability .....	955
Biodegradable Implants Used in Rotator Cuff Repair .....	958
Biomaterial Implants Future .....	961
Summary .....	961
References .....	962

---

## Abstract

Arthroscopy is considered a revolution in joint surgery, and it had an explosive development during the last years. Biodegradable implants were developed in the effort to avoid the complications related to classic metallic implants used during intra-articular procedures. Limitations and complications related to these implants are documented.

Most frequently performed arthroscopic procedures are in the knee joint: meniscus suture, meniscal replacement and transplantation, anterior cruciate ligament reconstruction, cartilage repair, etc. Every one of these procedures had

---

R. Marinescu (✉)  
Carol Davila University of Medicine, Bucharest, Romania  
e-mail: [rodicamarinescu@ymail.com](mailto:rodicamarinescu@ymail.com)

I.V. Antoniac  
University Politehnica of Bucharest, Bucharest, Romania  
e-mail: [antoniac.iulian@gmail.com](mailto:antoniac.iulian@gmail.com)

gone thru a long improvement process of the surgical technique and of the implants used during each of them. That is why we talk today about several generations of biodegradable implants in this area. Selecting the best devices and having in mind all complications related to their use, we may find a way to improve our clinical practice and to develop better implants.

The shoulder is the second joint where the arthroscopy is most used. Shoulder instabilities and rotator cuff pathology are addressed arthroscopically, and that is why for these two procedures a lot of biodegradable implants were developed and used during the last 20 years. Reviewing their history and long-term results is helpful in making the best choice during surgery and continues the improvements in developing the implants.

---

**Keywords**

Anterior cruciate ligament (ACL) • Articular cartilage (AC) • Extracellular matrix (ECM) • Collagen meniscus implant (CMI) • Magnetic resonance imaging (MRI) • Biocompatibility • Osteoconductive • Osteoinductive • Hydroxyapatite (HA) • Tricalcium phosphate (TCH) • Osteolysis • Arthropathy • Mesenchymal stem cells • Polyetheretherketone (PEEK) • Polylactic acid (PLA) • Poly-L-lactic acid (PLLA) • Polyglycolic acid (PGA) • Poly-L-glycolic acid (PLGA)

---

**Introduction**

Orthopedic surgery has changed a lot after arthroscopy development during the last 30 years. What started as a challenge to see the inside of a joint evolved to continuous improvement in minimal invasive surgical techniques. In time, as the surgeons' skills grew, the field in which arthroscopy has been used expanded tremendously up to the point where so-called extraarticular arthroscopy showed up. There is place today for arthroscopy not only in sports medicine but in degenerative pathology, in articular fracture treatment, and in foot and ankle pathology. New minimal invasive techniques were developed as a result of the above-mentioned fields, and all of them necessitated a completely new generation of implants. As a particularity, the size and design of these new implants are different from the classical ones. As the surgeons' and patients' preferences moved toward arthroscopically assisted techniques, several generations of implants were developed. The purpose of this chapter is to analyze the most frequent complications related to their use.

---

**General Considerations About Arthroscopy**

Arthroscopy was a revolution in joint surgery and treatment; it is considered one of the three greatest improvements in orthopedic care. It dramatically changed the understanding of knee joint, and it allows concomitant treatment for associated

injuries. It also allows the surgeon to switch from an open surgery to a minimally invasive surgery with all the related benefits. It became in less than 30 years the most performed orthopedic procedure.

Arthroscopy is a procedure which uses a video camera to view the inside of the joint; all the images are projected on a monitor. For the articular space is a virtual space, the joint is distended with sterile saline solution. The distension allows the surgical instruments used during procedure to be inserted without being harmful to the articular structures. Incisions – usually two, one for the arthroscope and one for the instruments used during intervention – are as small as 4 mm each and are called “portals.” Since its first use, the area of arthroscopic treatment has continuously grown. It started with diagnostic arthroscopy and progressed to high-performance procedures done entirely arthroscopically (meniscus sutures, meniscal transplantation) or arthroscopically assisted (multiple ligament injury reconstructions, articular cartilage procedures).

The knee was the first joint approach arthroscopically; now, arthroscopy can be performed in many joints – the shoulder, hip, ankle, foot, elbow, and wrist – as well as in extra-articular spaces in a procedure called “extra-articular arthroscopy”, e.g., for peroneal tendons and Achilles tendon pathology.

Among the great benefits arthroscopy creates is a severe reduction in postoperative infection rate; in arthroscopic procedures, reported rate is as low as 0.01 %. It also turns several procedures in outpatient procedures or in one-day surgery procedures. A tremendous benefit was noted in the decrease of postoperative pain that, together with minimally invasive procedure, less harmful to connective articular structures, led to improving rehabilitation time and physical performances after surgery.

Since a lot of procedures switch from open to arthroscopically assisted procedures, it becomes obvious that some specific instruments and devices for use during such procedures must be developed. First, because the size of these instruments needs to be dramatically cut down, second because specific implants are needed during particular procedures. This is a field of continuous development in which new techniques and implants are promoted every day. As an orthopedic surgeon, you should be aware of this progress and able to make the best choice for your patients. From this point of view, a summary of the most used, up-to-date, biodegradable implants in arthroscopic surgery and their longtime clinical behavior is always required.

---

## **Biodegradable Implants Used in Knee Arthroscopy**

### **Biodegradable Implants Used in ACL Reconstruction**

Anterior cruciate ligament (ACL) is very frequently involved in knee sports and sports-related trauma. The accuracy of diagnosis in torn ACL has improved a lot in the last 30 years as well as the surgical techniques for its reconstruction. From extra-articular procedures to anatomical arthroscopic procedure is a long way, a long path



of improvements in understanding of normal anatomy of ACL and continuous efforts in developing a technique secure, reproducible, and feasible to restore its function. Being one of the most frequently performed arthroscopic procedures is an increased interest in evaluating the results and selecting the best approach when dealing with a torn ACL.

Reconstruction is necessary because ACL never heals (except cases in which the entire tibial eminence is avulsed with ACL insertion); if unaddressed, the torn ACL induces a knee laxity with anterior displacement of tibia toward the femur. This laxity, experienced by the patient as instability or “giving way,” reduces the patient’s ability to perform physical or sports activity. As great majority of patients with torn ACL are young and very young, they will not accept these limitations and will demand a complete restoration of knee function. The number of ACL reconstructions has continuously increased in the last 30 years; it is presumed that about 175,000 of these procedures are done every year in the USA [1].

ACL reconstruction is done using a graft placed – in bone-drilled tunnels – on femoral and tibial sites; in the tunnel, the graft is secured with various implants. It is critical that the primary fixation of the graft be strong; in this way the patient may start the rehabilitation protocol very soon. On long terms, the stability of the graft is achieved by its integration inside the bone tunnel.

Same details are critical for the success of the reconstruction:

- An adequate graft should be chosen to replace the native ACL. The chosen graft should have a tensile strength at least as that of native ACL.
- Primary graft fixation should have enough strength to provide proper fixation until the bone/bone or tendon/bone fixation is achieved and to allow the beginning of rehabilitation protocol the very next day following surgery.
- The placement of the graft should be as accurate as possible – in order to reproduce anatomically the ACL and to be able to restore its biomechanical properties.
- The return to strenuous physical or sports activities should be delayed until graft is healed and muscular function is completely restored.

The surgeon’s preference regarding graft used in ACL reconstruction has changed in the last 30 years. Before 1990 patellar graft was considered “golden standard” and was used in more than 65 % of cases; since that time the interest for so-called soft tissue graft has tremendously increased, so in 2014 hamstring graft took the first place with 53 % of case prevalence. The soft tissue grafts are grafts integrally formed by tendon tissue; this group includes semitendinosus autograft, quadriceps autograft, Achilles tendon allograft, etc. There is not a consensus among orthopedic surgeons regarding the ideal graft, and this is still an issue in debate.

When we talk about healing after ACL reconstruction, this implied both the healing of the graft inside tunnels and the intra-articular graft “ligamentization” process. It was proven that the graft incorporation inside the tunnels occurs faster when a graft with bone blocks is used, while the incorporation of tendon inside bone tunnel is slower and inhomogeneous. The patellar tendon, which has bone-to-bone

features at tunnel site integration about 4–6–8 weeks, as fast as in fracture healing, was documented. Also the patellar tendon has the advantage of natural tendon insertion to the bone. Comparing to the healing in hamstring graft, which is a tendon to bone, healing is much slower, as about 6–15 weeks [2].

The part of the graft placed inside the joint also sustains some biological process after implantation; in the first phase, the graft cells die and are gradually replaced by host cells. These new cells start producing collagen fibers, and this collagen is – at the beginning – in an amorphous state; later it starts to develop fibers – organized in fascicules and oriented toward force moments. This process might take 6–12 months, and during it, the graft is fragile and might be easily torn. It was demonstrated that later than 12 months, same mechanoreceptors develop inside graft; these are important in knee coordination and graft protection during unexpected movements [3].

The tensile strength of the graft used has been well documented. All grafts used in ACL surgery have tensile strength much higher than native ACL. For patellar tendon this strength is between 2,300 N and 2,977 N, according to different investigators [4, 5]; for quadrupled hamstring graft, the tensile strength is evaluated as high as 4108 N [6] or 954 N/mm, and for quadriceps tendon, it is about 2,352+/- 495 N which is around patellar tendon strength [4].

It seems that the biggest problem related to these grafts is the so-called pullout strength which is quantified as the ability of the fixed graft to resist to forces applied on it. It mainly depends upon the fixation device used, and this is the area where most of the research is currently focused.

After the 1990s, it became obvious that something needs to be done in order to reduce the complications related to metallic fixation devices, especially those related to possible graft laceration during insertion or removal, about the imaging artifacts during MRI investigation, or difficulties encountered at device removal. This was the moment when biodegradable implants seemed to be a good idea. Since the most used device in graft fixation that time was the metallic screw for interference fixation, a similar device was developed from a biodegradable material. Interference is defined as the amount by which the diameter of the screw exceeds the gap between the graft and osseous tunnel.

Interference screw achieves the graft fixation close to the joint line and close to the active part of the new ACL in the so-called aperture fixation. This fixation type reduces most of the movements of the graft inside the tunnel during healing process [6]. Also, the screw compresses the graft against the tunnel wall allowing direct graft-to-tunnel healing. Various factors affect the primary stability of the fixation when a biodegradable interference screw is used, among them: length and diameter of the screw, screw geometry, screw divergence, the correct match between graft and tunnel, bone marrow density, screw design, and insertion torque [7–9]. Secondary stability is related to the integration of the graft and the degradation process of the implant.

First materials used for biodegradable interference screw were polylactic and polyglycolic acids derived as PLLA or PLGA. There were inquiries about the rate of material degradation and bone replacement. Studies have shown some complications

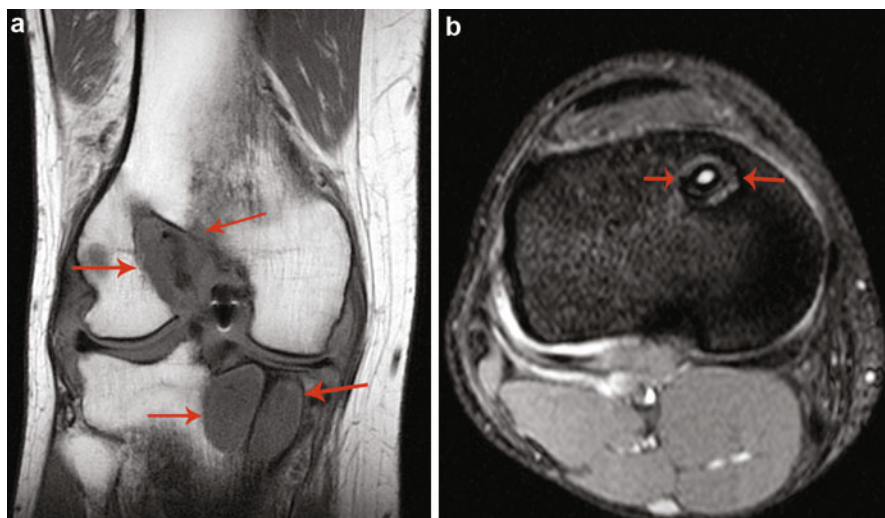


**Fig. 1** Magnetic resonance imaging (MRI) remains an important tool for bioresorbable implant follow-up. *Left* image shows important osteolysis with cyst formation (*red arrows*) at 2 years after crystalline interference screw fixation. *Right* image shows tunnel enlargement around the tibial screw

related to their use: tunnel enlargement, cystic formation, and osteolysis [10]. It seems that these were mainly caused by the products released during resorption time and the acidic environment created as a result of it. So, the development of a new material able to induce and promote bone replacement seems reasonable. The biocomposite materials tried to resolve this issue. Biocomposites add to a biodegradable material the advantages of an osteoinductive/osteoconductive supplement. This supplement is usually tricalcium phosphate (TCF) or hydroxyapatite (HA) (Fig. 1).

After more than 20 years from the time of first use, studies could analyze implant behavior in long time. It appears that the *in vivo* implant degradation is not uniform and might be slower than the expected time from *in vitro* studies. Clinical studies have reported screw persistence longer than 2 years and no evidence for bone in growth at the time of examination [1].

Also, reports of broken screws – with a long time interval after their implantation – start to be published [11, 12]. Breakage of biocomposite screws at 8 months and 2–4 years postoperative time was published. In the reported cases, the breakage was not related to a trauma event. Usually the patients reported acute pain, episodes of catching or “giving way,” and – consequently – a decrease of physical activity. The breakage of the screw was revealed on MRI or arthro-CT examination. The tip of the screw was usually located in the intercondylar fossa. Depending on the time passed from the breakage to the diagnosis, some lesions on articular cartilage were noted. A mismatch between the length of the tunnel and that of the screw may be the first cause on the tibial site failure; this is why it is mandatory that the length of the tibial

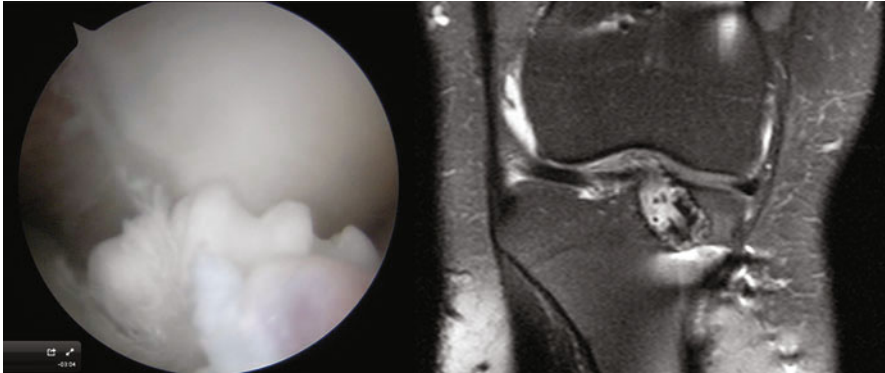


**Fig. 2** On the *left*, image from arthroscopic retrieval of broken screw fragment inside the knee joint. On the *right*, MRI of the same patient shows important reaction around the biocomposite screw during resorption, probably due to insufficient stable fixation

tunnel be securely measured and the length of the screw be correlated with it [11]. Also, at the end of procedure, a final look might reveal the tip of a protruded screw, and the issue may be solved intraoperatively. There are reports that measured the importance of screw length in graft fixation (it appears that – for hamstring grafts – it is mandatory to achieve a length of the screw of at least 23 mm to have a proper pullout strength) [13] (Fig. 2).

If the interference fixation type is almost the rule on the tibial side, on the femoral side, there are in use a lot of different fixation modalities:

1. Interference fixation type: the same fixation idea like in tibia except that bone mass density is much stronger than in tibial metaphysis, and, consequently, the fixation is much stronger. As a matter of fact, the interference fixation type for patellar tendon was the golden standard for several decades.
2. Suspensory fixation type: Endobutton (Smith & Nephew), Tightrope (Arthrex), Toggleloc (Biomet). They may be of adjustable-length or fixed-length loop that secure the graft inside tunnel; it has been proven that fixed-length suspensory fixation devices have fewer occurrences for tunnel enlargement or loosening after ACL reconstruction [14]. As they are not in the group of resorbable implants, we will not focus on them in this chapter.
3. Transfemoral fixation type: Cross pin (Mytek), Transfix (Arthrex), and Biosteon (Stryker) available as metallic device or biodegradable, biocomposite device. The fixation is achieved by means of a single or double implant that penetrates the tunnel, the graft, and the tunnel again and fixes them all together. The primary fixation is stronger and it is presumed that the occurrence of micromotions inside the tunnel is reduced [15]. Using a bioresorbable component in these systems of fixation reduces the stress shielding effect produced by the strong rigid fixation of the similar technique using metallic implants [15]. Further research was incorporated in some designs to retain strength for an adequate interval – as combining the PLLA with hydroxyapatite in Biosteon Stryker implants [16]. The effect

observed was of direct biological fixation in the bone through osteoconduction – in MRI studies, there were no fibrotic reactions or local reactions during follow-up [17]. Agrawal described since 1996 the pH-buffering effect of HA which reduces sterile cyst formation related to lactic acid degradation, creating a more controlled resorption process.

At their apparition it was presumed that some problems related to bone-tendon healing process will be solved. We are talking about:

- No device left in the tunnel to affect the healing process inside the tunnel
- Strong primary fixation, with good pullout strength
- Restriction of the micromotion of the graft inside tunnel to preventing the developing of tunnel enlargement

As a result of all the above, it was presumed that graft integration is facilitated when using this type of devices. Clinical studies documented good results [15–18].

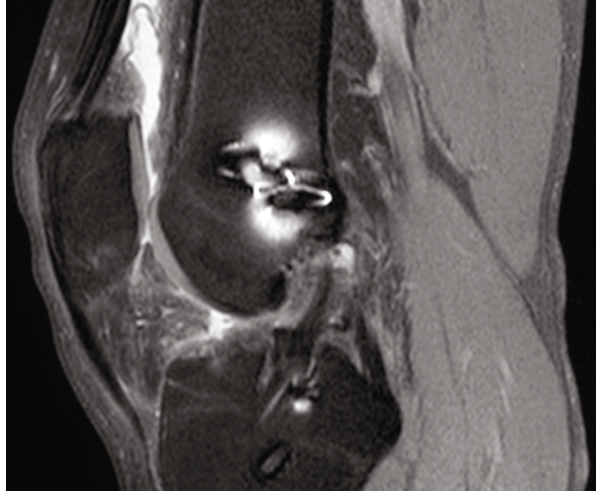
Two technical problems are related with the use of these implants: the procedure is a very demanding one, and it was developed for transtibial approach. As the preference of surgeons moves toward anatomical ACL reconstruction, a transfemoral device for approaching the drilling of femoral tunnel from the anteromedial portal was developed for cross-pin implants (Biomet Sports).

Not all presumptions made at the time these implants were developed were confirmed in practice, and papers reporting their behavior in clinical practice show up.

The complications related to use of these devices are of two categories:

- (A) Related to difficulties encountered during surgery:
- (a) A breakage of cartilage may appear due to an inappropriate drilling of the tunnel.
  - (b) Bending and – eventually – breakage of the implant during implantation due to incorrect positioning.
  - (c) An implant that remained “extruded,” not completely flatten on the femoral condyle; from this position, it may cause friction on the iliotibial band and cause pain during flexion/extension movements. Also – on long terms – it may get broken and loose inside the knee.
- (B) Complications developed at long time after the surgery. There are papers reporting the breakage of such implants long time after implantation – like 4–7–11 years. Despite their presumed biodegradable qualities at such long time, the degradation rate seems to be low and the material is still causing abrasion on articular cartilage. The implants can migrate either in femoropatellar compartment or posterior, to the back of femoral condyle. If the implant was too proud and impinge on iliotibial band, it may get break and lose in the medial gutter of the knee.

**Fig. 3** MRI FatSat imaging of broken cross-pin fixation inside the femoral tunnel at 2 years' follow-up. Even if important artifacts due to metallic debris related to drilling instruments are present, reaction around the crystalline pins can be observed. At examination time, the graft was healed without signs of clinical instability



In a study published in 2006, Cossey et al. reported a 16 % complication rate in cases using BioTransFix for femoral ACL fixation; complications consists in fracture or deformed implants, which mainly developed during period of graft incorporation [19].

The reports about cross-pin devices are even more worrisome. In 2010 Studler et al. analyzed the MRI findings and reported the following complications: fractured pins in 17 % of cases, breach of posterior cortex in 28 % of cases, and migration of fractured pin in 6 % of cases [17]. Interestingly, most of the cases were asymptomatic or have nonspecific symptoms, and the complications do not correlate with detrimental knee laxity (Fig. 3).

In contrast with the two abovementioned papers, Choi et al. in an MRI study published in 2007 reported a 38.7 % fracture rate for RigidFix implants at a medium follow-up of 6 months and found a high correlation with knee instability [20]. To prevent further complications, to develop a careful insertion during operation room is required; as the patient symptoms may be nonspecific whenever a complications related to the implant is suspected, an MRI investigation is required in order to assess the graft status and the implant mode of failure.

This is why it is recommended that the patient with biodegradable fixation devices should be on a longtime surveillance, and the surgeon should be alert and well informed about possible complications.

## Biodegradable Implants Used in Meniscus Surgery

Menisci are natural constituents of the knee joint with great impact on knee biomechanics and health joint preservation. Their function in the knee joint is well

documented; they facilitate load dispersion into the joint, act like shock absorbers, promote joint lubrication, interfere with joint stability (especially medial meniscus), and improve the relative incongruence between tibia and femur [21]. All together they are considered natural joint protectors against cartilage degeneration. This is why during the last three to four decades all efforts were done in order to repair the meniscus and its functions.

Meniscus tear is a frequent pathology; in the USA every year, about one million people sustained a knee injury involving the menisci. The tearing mechanism usually associates falling on a twisted knee or pivoting on the knee with leg fixed on the ground. Usually a severe knee spring occurred and meniscus is not the only one of knee components involved. Usually there are associated lesions; among them are ACL tear and articular cartilage injury. The patient may experience pain along joint line, effusion, blocking knee, or giving way. All symptoms are increased during physical activities and that finally direct the patient to reduction of the level of physical or sport activities. The correct and only solution is to surgically address this pathology.

After an early period, in which the total meniscectomy was considered the best approach to every meniscal tear, it appears very clear that meniscectomy is detrimental to knee biomechanics. Starting with arthroscopy age, all efforts were done in order to preserve as much as possible from meniscal tissue. First step was the conversion from total or subtotal meniscectomy to partial meniscectomy, either sectorial or circumferential. There are still a number of young patients sustaining a type of tear which necessitates a large meniscectomy, in order to be cured. For these tears, the meniscus suture gradually became the optimal approach.

Meniscus suture is the best tactic for meniscal tears; it ensures meniscal preservation and restores meniscus function. Repaired or healed meniscus restores its function that transfers the axial compressive force to the circumferential tensile strain in the knee joint [22]. A lot of papers confirm that meniscal healing actually takes place, and the repaired meniscus preserves its beneficiary function for the knee [21, 22]. MRI examination, which assesses the gradual reduction in size of gap tear or arthro-CT, may be helpful in considering a tear healed. Clinical assessments are used to evaluate the healing of sutured meniscus, but only a second-look arthroscopy can actually demonstrate the healing. The healing of sutured meniscus is evaluated according to Henning's criteria but that involves a second look – during an arthroscopy – to be done. It may be difficult and unsuccessful to persuade a patient to accept a second arthroscopical examination while he has no symptoms. This is why clinical criteria became more popular and more used.

During time, three major techniques were developed for meniscus suture, named about the way the repairing device approaching the knee: outside-in, inside-out, and all-inside. The purpose of meniscus suture is to bring together the two edges of the tear and recreate a strong fixation to the peripheral capsular margin – the point of best anchorage. In this manner the anatomical shape of meniscus is recreated and its function is well preserved. The meniscal repair is a biological process and necessitates time to occur. The meniscus healing process involves two cell populations: meniscocytes and synoviocytes. Since they are adult cells with restricted healing

potential, it is mandatory to get activated. There are some technical procedures to do that: synovial abrasion, trepanation, and vascular access channel. After activation, the cells start to repopulate the repair area and to restore the normal meniscal anatomy. During this time, it is important that the devices used for suture have the strength and resistance to pull out forces applied to them.

If in outside-in and in inside-out type of suture different fibers (resorbable or nonresorbable) are used to bring the two edges of the rupture together, in all-inside type, various implants are used to do that. The variants of fibers used for suture are Dexon (polyglycolic acid, PGA), later Vicryl (a copolymer of PGA and polylactic acid, PLA), and PDS (polydioxanone), similar to all resorbable sutures.

In the outside-in technique, the suturing fibers are approaching the tear from the outside part of the joint to the inside part of it. From the outside the needles are approaching the peripheral capsule then the tear from the peripheral part of it, followed by the central one; in this manner the two parts of the tear are connected altogether to the capsular strength point [23]. Needles with different shapes are used as suture “carriers.” Resorbable, slowly resorbable, or nonresorbable fibers were used during time for this procedure. Small additional incisions (4 mm each) are needed to place the knot supracapsular and subcutaneous; these small incisions interest only the skin and a blunt dissection is done in the subcutaneous tissue to slide the knot. The results of the technique are good and the devices used are inexpensive [23]. The technique addressed best the body of the meniscus, but it may be difficult in the posterior horn where special curved needles may be needed. In long tears – like in bucket handle type – the need for more suture points may increase the surgical time (Fig. 4).

For many years the inside-out technique was the golden standard for meniscal repair. In inside-out technique, the suturing fibers are directed from inside the joint outward; special needles to direct the fibers are used for this purpose, and a small posteromedial portal is necessary to – safely – direct the needles out. It is a technique which is suitable for the body and posterior horn of meniscus and has the advantages that may allow the placement of several suture points; consequently the suture is more stable as the fixation points are increased. Other advantages are that it is a versatile technique and inexpensive. The technique has some possible complications: risk of increased morbidity as a result of posteromedial portal needed, risk of neurovascular injury, and risk of stiffness or flexion contracture. As it was shown in a cadaveric study [24], the structures around the knee are not punctured by the needle but usually been entrapped in the suture knot. That is the case for the lateral side too where the common peroneal nerve may be at risk [25]. That is why a small accessory incision in the “safe zone” is recommended. Cyst formation around the suture point is not encountered very often; it may be related to soft tissue irritation caused by nonabsorbable suture material [26]. Looking to overcome these complications, the all-inside technique was developed.

In all-inside techniques, bioresorbable implants are used to enhance meniscus fixation to meniscal peripheral rim; different shapes and materials were used: anchors, pins, and staple form devices. As the interest for meniscus suture continuously grows, new generations of all-inside meniscus techniques were developed.



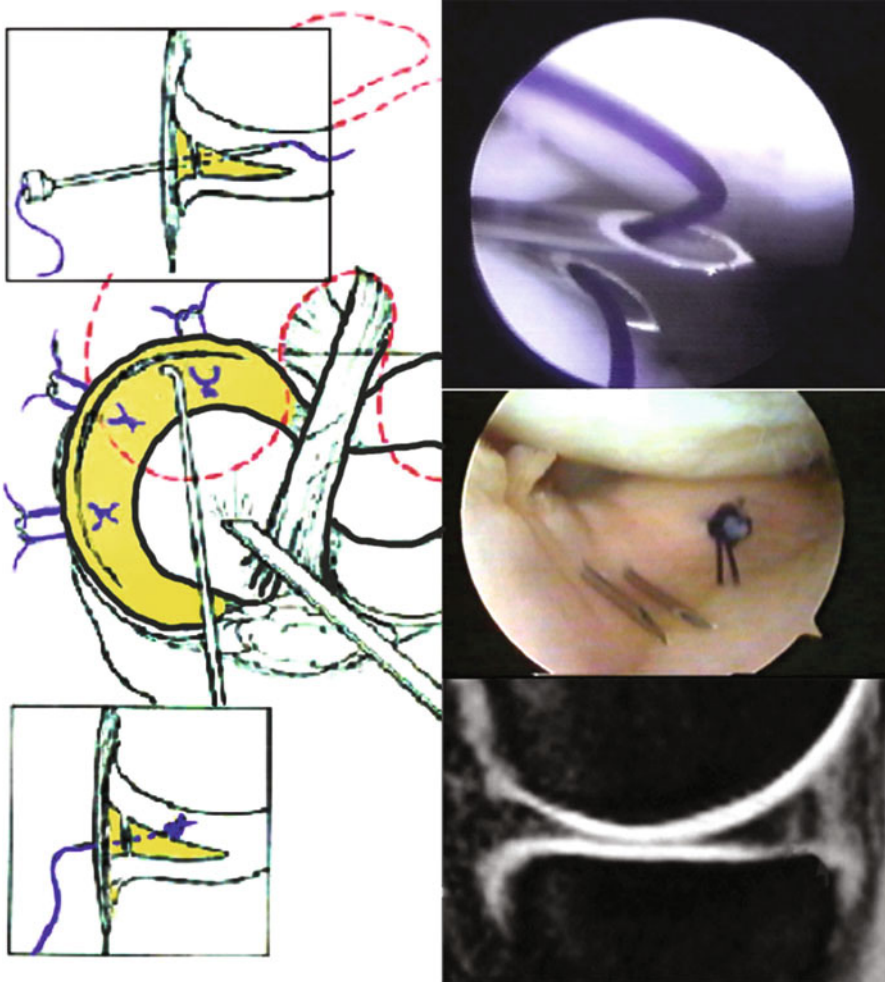


**Fig. 4** Schema of the meniscal suturing technique. On the *right side*: *top* arthroscopic image with the needles used as carriers, *middle* image with the final arthroscopic image of the sutured meniscus inside the knee, and *bottom* image with MRI follow-up of the sutured area which remains stable after 1 year

First-generation all-inside technique was described by Morgan in 1991 and used curved hooks through accessory portals to pass sutures across the tear; the knots were retrieved and tied arthroscopically. The technique was demanding and continues to put neurovascular structure at risk.

Second-generation all-inside technique used specific devices placed across the tear and anchored peripherally. The prototype of this generation was T-Fix, a polyethylene bar with an attached braided polyester suture, deployed through a needle or cannula to capture the meniscus or capsule. Adjacent knots were then

arthroscopically done and pushed toward meniscal surface. Risk for neurovascular damage was diminished and was no need for accessory portal. The main drawbacks of this technique were the inability to proper tension the suture after placement and possible chondral damage related to nonresorbable knot placements [27].

Third-generation all-inside technique used various devices to complete the suture: arrows, screws, darts, and staples. Most of them were composed of rigid poly-L-lactic acid (PLLA) which retains its strength for up to 12 months and need about 2–3 years to completely resorb. The most used is the meniscal arrow, for its ease insertion and good postoperative healing rate. However, complication related to their use was reported: transient synovitis, cyst formation, device failure, and chondral damage [28]. Chondral damage is related to an implant placed too prominent or to a device that loosens or migrates before resorption. As the chondral damage was a serious complication, third-generation devices were gradually abandoned. Despite technical improvement, the complication rate for these devices is high in some papers; Jones in 2002 reported a complication rate as 31.6 % resulting from device migration, device prominence with consequent chondral damage, and soft tissue inflammatory reaction [29].

Fourth-generation all-inside devices are flexible and suture based, have lower profile, and allow for variable compression and tensioning across the meniscal tear. In current use these prototype devices are Fast-Fix (Smiths & Nephew, USA) and RapidLoc (Mitek Surgical Products, MA). Fast-Fix device consists of two small anchors, 5 mm, made from PLLA, connected together with a No 20 polyester suture with a pre-tied sliding knot. RapidLoc consists of smaller absorbable backstop anchor connected to a top hat by a No 20 absorbable suture. High-incidence failure rate is reported when using Fast-Fix; they are related, according to authors, to the anchorage slippage to the capsule during tightening or by complete failure of anchor deployment [28]. Anchor deployment failure may be attributed to design flaw (sometimes anchors do not fully deploy and are not able to lock behind the capsule) or to the meniscal tissue quality (poor meniscal quality may cause dislocation of anchor because of a lack of grip).

Overall, the current clinical reports are in agreement about good results concerning fixation resistance of all these devices. There still are clinical cases describing anchors and pin breakage, both at moment of implantation or at a longtime follow-up. One limitation of these implants is related to their size and the difficulties to accommodate them – in a minimally invasive, arthroscopic approach – either in meniscal tissue or in the capsule, behind the meniscal rim. The proper placement is the element offering a good point to which the entire meniscus is then fixed. Despite the resorbable properties of the implants, there are studies that documented their persistence in the knee long after the resorption estimated time.

In a study published in 2006, Hantes et al. stated that there are no major differences – in terms of complications – between the three meniscus suture techniques [30]. Having in mind the statement of Stein in 2010 that any meniscectomy increases the arthritis risk with 20–60 %, any effort should be done in order to preserve the meniscus and its functions. It is the surgeon's duty to make the choice for what he considers the best choice for a specific case and to keep himself updated

with new and demanding techniques. Unfortunately, only one in ten meniscus tears has a pattern which is appropriate for meniscus suture. That is especially true in the case of old, neglected tears where new tears are added during time to a simple, longitudinal tear. For these cases, in order to prevent the knee damage caused by meniscal absence, a collagen meniscus implant was developed. Its role is to compensate the meniscal deficiency chronically.

Usually the meniscus collagen implant (CMI) is a porous collagen contained in a glycosaminoglycan matrix; the matrix is one of defined geometry, density, thermal stability, and mechanical strength. The collagen consisted of 97 % type I collagen and the matrix consisted in a combination of chondroitin sulfate and hyaluronic acid [31]. The collagen implant is a temporary template and serves as a scaffold for tissue segmental regrowth. Typically, CMI is made of bovine collagen; it is biocompatible and absorbable and it may be arthroscopically stitched to the area where meniscal tissue is missing. The suture may be similar to that used for meniscal suture and might be augmented with platelet-enriched plasma products. Once in place, CMI provides a scaffold onto which recipient meniscus cells start to migrate and build a new meniscal tissue. Over time, as regeneration takes place, the body resorbs the CMI leaving free the new meniscal tissue. During the last 20 years since its discovery, the CMI proved to be a functional alternative to removal and permanent loss of meniscus.

In 1997, Stone demonstrated a regenerated tissue similar of fibrous composition to that one of meniscal cartilage at 6 months' follow-up after CMI implantation. Not only the regeneration inside the matrix was proven; in 2008, Rodkey demonstrated an inhibition in osteoarthritis progression at 24 months' follow-up after CMI implantation. It is presumed that the matrix is progressively resorbed; however, remnants of the implants are still visible on MRI examination at 3 years' follow-up [32].

Recent papers show that for better results, it is mandatory that cases selected to CMI should fulfill same criteria at the time of implantation:

1. The meniscal loss should be at least 25 % of meniscus body.
2. The anterior and posterior meniscal horn should be intact.
3. The ACL deficiency should be corrected within 12 months' time.
4. The patient must be willing to cooperate during rehabilitation protocol.
5. The patient must be able to understand and follow the procedure.

Also, Rodkey demonstrated in 2008 that using the CMI in acute cases is not followed by better results, so – for the moment – this technique is reserved to chronic cases of meniscal deficiency [33]. Concerning the results, Harstan published in 2011 a study that shows good results in 70 % of the cases. For better evaluation Rodkey compared the results of medial CMI with results after medial meniscectomy at 5 years' follow-up. Its study confirms better results in cases that used CMI [33]. In 2014 Zaffagnini studies indicated better results after using CMI in terms of osteoarthritis evolution and clinical scores at 10 years' follow-up [34]. Same good results were reported in 2011 by different authors [35].

As promising as the studies are so far in using of CMI, there are still cases in which the technique is not suitable, and some other solution should be found in order to compensate to meniscal deficiency. As difficulties were reported in handling and suturing the meniscus implant during surgery, a second generation of meniscal implants was developed.

The second-generation polyurethane porous scaffold is robust and flexible when being handled, and it has been reported to decompose into nontoxic products as well as supporting the ingrowth of the new tissue [31]. This class started with Actifit (Smith & Nephew, USA) which is composed of two constituents: polyester (the soft segment) and polyurethane (the hard segment). The soft segment consists of poly-epsilon-caprolactone which provides the flexibility and determines the degradation rate. The hard component is a semicrystalline polyurethane which provides mechanical strength. Recent clinical reports after their use documented good results at 2 years' follow-up, especially on the pain and function scores of the knees [36]. These results suggest that second generation of porous scaffolds for meniscal deficiency replacement remains a good option for a patient group for whom currently only restricted treatment options are available [21].

To improve the ingrowth of the new tissue, scaffolds may be used in combination with cells, resulting in a bioactive composite. Meniscal fibrochondrocytes from the injured meniscal tissue are mostly used. As only a small amount of these cells may be harvested, alternative sources are still searched: dermal fibroblast, synovial cells, and chondrocytes may be the answer. In order to preserve cells' ability to growth and replication, various growth factors (bioactive agents) may be added to sustain the technique. Also the mesenchymal stem cells contained in bone marrow aspirate may be utilized due to their well-documented qualities: great proliferative capacity and aptitude to differentiate to specific cells, including cartilage cells. This is already the beginning of a new era: engineering of the meniscal tissue. As defined by Langer and Vacanti in a book published in 2013, tissue engineering is an innovation in regenerative medicine and consists of three elements: cells, scaffolds, and growth factors [37]. For the new complex construct, it is presumed that cells adhesion and proliferation is improved and is under better healing conditions.

## **Biomaterials Used In Cartilage Repair**

Hyaline cartilage is a special cartilage type, which covers bony articular surface. Its name comes from its clinical appearance – hyaline meaning transparent. Articular cartilage is composed of specialized cells called chondrocytes that produce a large amount of extracellular matrix composed of collagen fibers (more than 90 % of type II) and an abundant substance rich in proteoglycan and elastin fibers. There are no blood vessels or nerves in cartilage, nor lymphatic vessels; instead, nutrients diffuse through the matrix. Despite the fact that it is considered connective tissue, hyaline cartilage has a low growth rate and no regenerative capabilities. This is why it is so difficult to repair an articular cartilage. The main function of articular hyaline cartilage is to absorb the shocks acting like a load-bearing element that protects

the bony surfaces and maintain a smooth sliding during motion. Whenever its surface is damaged, the proper, friction-free motion inside the joint is compromised, and highly friction movements are generated. This abnormal movement is a cause of further deterioration of the cartilage; in this manner a vicious circle is closed and the deterioration of cartilage continuously progress. This is why it is critical to diagnose and treat the cartilage damage as soon as possible. Sometimes, the damage of articular cartilage may remain unknown and may lead to progressive joint deterioration.

A lot of technical procedures were used to promote hyaline cartilage repair. The problem is they do not succeed to restore hyaline cartilage, only fibrocartilage. Fibrocartilage has no ability to absorb shocks or to uniformly disperse the stress through the joint. Even its appearance barely resembles hyaline cartilage. Among the techniques mostly used in cartilage repair, there are microfractures, Pridie drilling, osteochondral autograft transplantation, autologous chondrocytes transplantation, and bioactive matrices.

The reason for microfracture treatment is based on the idea that by drilling into the subchondral bone, channels for vascular access are created, and through these channels, the already mentioned, pluripotent mesenchymal cells came into the affected area and may induce hyaline cartilage formation. The number of cells accessing the area – which may be about several milliliters in volume – is around 100 cells, while in healthy cartilage the number is around 10 million. As a result, a fibrocartilage is obtained during this procedure; the fibrocartilage has no appropriate qualities for being a long-term load-bearing element into the joint. What was kept from this technique is the subchondral drilling which facilitates the vascular access and the anchorage for the new tissue – being an important step in all implantations of modern bioactive materials.

The autologous osteochondral transplantation – known as mosaicplasty – is a technique in which plugs of healthy cartilage and adjacent bone are harvested from nonbearing area of the joint and implanted in the affected area [39]. It is a technique that may need an extensive approach to the joint; also in case of large defects, the amount of the graft needed may be insufficient to cover the defect. Also allograft may be used in these cases, but the allograft is expensive and hard to find, and its use may be related to infectious disease transmission. The results of autologous osteochondral transplantation are good in terms of restoring hyaline-like cartilage improving pain and function of the knee. However MRI studies suggest that the high and shape of the original cartilage cannot be fully restored in contrast with fully integration of the osseous part of the graft; relief in knee pain and improving functional outcome were noticed [38]. This contradicts Hangody paper from 2003 who reported an even articular surface, with congruency and similar appearance with healthy cartilage at 6 years' follow-up [39]. No matter auto- or allografts used their availability is far beyond the necessity, and an alternative procedure should be developed.

In order to replicate the tridimensional structure of the osteochondral plugs, some biphasic, bioresorbable devices were developed: one is Biomatrix CRD (Arthrex). The implant mimics the subchondral bone by means of a beta-tricalciumphosphate

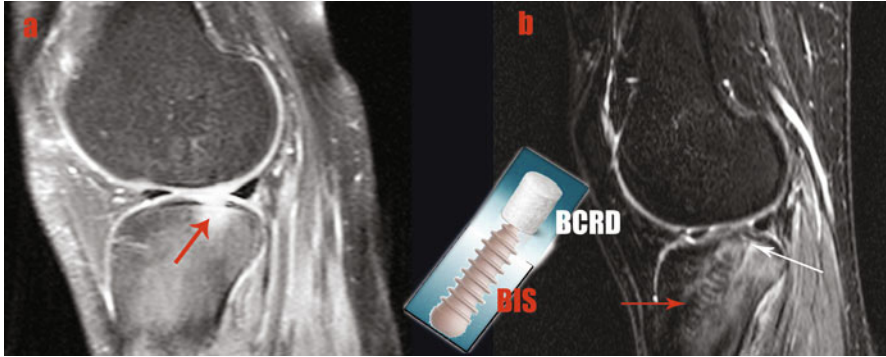


**Fig. 5** (a) Shows preoperative MRI with tibial cyst related to chondrolysis after left meniscus arthroscopy. Repair was performed using an anterograde reconstruction with Biomatrix CRD (BCRD) and an interference biocomposite screw (BIS). One-year follow-up MRI shows (b) incorporation of the graft and the screw with remodeling of the articular surface; the patient is able to perform sport activities free of pain

(beta-TCP) suspended with polylactic acid (PLA) and has a cover of bovine collagen scaffold for the chondral area. It functions as a porous architecture that is cultivated with platelet-rich plasma and promotes matrix ingrowth (Fig. 5).

For all the complexity necessitated by cartilage repair, new techniques were developed in order to improve surgeon's ability to sustain cartilage regeneration. For being able to sustain and promote the repair of hyaline cartilage, the biomaterials used as scaffolds should be biodegradable, biocompatible, noncytotoxic, biomechanically stable, permeable and with high porosity, and able to regulate cellular activities; should possess an appropriate surface chemistry; and should have the capability to be shaped in various forms and sizes. They should have the capability to serve as temporary support for chondrocyte and be able to avoid induction of adverse reaction induction. Before being applied onto the defect, the defect area is regularized and an even bed is created to receive the material. Sometimes, the ability of joint to promote the repairing process is stimulated either through adjuvant techniques (microfracture), through mesenchymal stem cells, or through platelet-enriched plasma products added in situ. The results are promising, especially in cases of focal, unique traumatic defect, with no adjacent cartilage degeneration and healthy environment for the healing process.

Since their first use till now, three generations of scaffolds have been developed.

Autologous chondrocyte implantation (ACI) is a technique already in use for some time (first implantation in 1987) with results documented and which succeeded to restore hyaline cartilage. As the research in the area of cartilage regeneration continues to develop, in the last 20 years, new techniques were established starting from this one [40]; that is why, now, when we are talking about ACI, we refer to this technique as the first-generation approach to cartilage regeneration. Despite the fact that it restores hyaline-like cartilage, there are disadvantages related to the use of this technique:

1. A two-step procedure is required – first, the cartilage is harvested from a healthy area and is cultured in the lab, and, in the second stage, the cultured cells are implanted into the defect area.
2. It is a technique which associates periosteal coverage of the graft, for sealing the cells inside. In 10–25 % of the cases, there is necessary a revision surgery; main reason is the hypertrophy of the periosteal flap, which may cause pain and increase risk for complications [41]. The average time for the third surgery is from 3 to 8 months.
3. An extensive approach to the joint may be needed to permit the ACI implantation and that increases the risk for complications as stiffness and arthrofibrosis.

The whole procedure of ACI is expensive and needs a long waiting time for patient – from 4 to 6 weeks. An important observation of Brittberg et al. was related to the cultured cells that, in order to maintain their active properties, had to insert in a three-dimensional, multilayered matrix – because monolayers of cells had the tendency to loose their chondrocyte profile and degenerate.

The second generation of scaffolds was developed starting from these documented problems; it covers the cells with a collagen type I/III membrane in order to avoid the use of periosteal flap. Gooding et al. compare the results of ACI and periosteal coverage with ACI and collagen I/III membrane in a randomized study of 68 patients. At 2 years' follow-up, the functional results were similar, but in periosteal group, there were complications related to periosteal symptomatic hypertrophy [41].

For further improvement, the third generation was developed. The third generation of scaffolds used for cartilage regeneration consists of a three-dimensional scaffold in which the cells are seeded; the assembly is inserted in the prepared place and fixed with a glue. Usually, prior to implantation, the affected area is debrided and drilling into the subchondral bone is done. The generic name for this procedure is matrix-induced autologous chondrocyte implantation (MACI). Regarding the results, patients report improvement in pain, functional score, and activity level as early as 3 months, but – more often – benefits occur during the first year.

As the impact of hyaline cartilage damage in joint biomechanics is huge, a lot of efforts were done in order to develop new techniques feasible, reproducible, and minimally invasive to restore it. An untreated damage on articular cartilage naturally evolves toward joint degeneration. There is an increased number every year of patients suffering from degenerative joint disease, among 600,000 each year in the USA. That is why the research in area of biodegradable scaffolds explodes.

The aim of using biodegradable scaffolds is to obtain a more biological treatment and to restore the damaged surface with hyaline cartilage. The scaffolds are used since 2000; it's a new and promising approach to cartilage problem. Since their first use, a lot of materials and various techniques to prepare materials for cartilage treatment were developed.

Based on their predominant architecture, scaffolds can be divided in two categories: membranes and hydrogels. Based on their composition, current scaffold materials used in cartilage tissue engineering are classified into natural and synthetic scaffolds.

The natural scaffolds are:

1. Protein-based polymers: fibrin, gelatin, and collagen
2. Carbohydrate-based polymers: hyaluronic acid, alginate, chitosan, agarose, and polyethylene glycol

The key advantage of natural scaffolds is that they have the natural ability to interact with cells and cellular enzymes and to be degraded or remodeled when space for growing tissue is necessary. There are still issues related to their purifications and mechanical properties.

As for the hyaluronic acid, it is a natural component of ECM (extracellular matrix) in all connective tissue and interacts with chondrocytes and collagen fibrils. Also, it is able to integrate chitosan, alginate, and fibrin gel products creating a surrounding comparable to ECM in which the new cartilage may grow. It improves adhesion between cells and ECM and plays a role in cartilage nutrition, maintaining cartilage characteristics and natural joint lubrication. It is in medical use for the treatment of osteoarthritis for – at least – 4 decades and has fewer complications and documented good results. Combining hyaluronic acid with cells – hyaluronic acid hydrogel containing chondrocytes – further enhances and promotes the healing of articular cartilage, as proven by the study of Zhao in 2014 [42]. Another major advantage is that it may be delivered at the repair site via injection or minimally invasive approach which further increases its performance (it is well known the susceptibility of articular cartilage to its exposure during surgery). For all these reasons, hyaluronic acid-based polysaccharide gel biocomposites are considered one of the best choices in articular cartilage repair.

The synthetic scaffolds used in cartilage repair techniques are:

1. Simple: polylactic acid (PLA), polyglycolic acid (PGA), polycaprolactone, polylactic-co-glycolic acid, polybutyric acid, carbon fiber, Dacron, and Teflon
2. Ceramic type: tricalcium phosphate, hydroxyapatite, and bioactive gels.

The synthetic polymers provide a better control on physical and chemical properties.

There are some disadvantages related to use of synthetic scaffolds:

1. Acidic by-products are created and accumulated during their use.
2. They have poor biocompatibility.
3. The by-products resulted in course of material degradation have toxicity and may rise to an inflammatory reaction.

The already proven role of subchondral bone in the development of articular cartilage pathology brought the idea that a better scaffold should address both cartilage and subchondral bone at the same time. The idea of biphasic scaffold shows up. At this moment, only two products of this kind are available, and the follow-up for them is contradictory. The first one is a bilayer PLGA – calcium



phosphate polymer (TruFit CB Smith & Nephew, USA). It is made of 75:25 PLGA-PGA calcium sulfate biopolymer shaped into form by different size cylinders. The design provided a complete resorption and was first used to replace the tunnels left after harvesting the autografts used in mosaicplasty. Barber and al demonstrated in a CT study the absence of ingrowth inside the tunnel and the formation of a cyst [43].

The second one is nanostructured 3-layer biomimetic scaffold (MaioRegen, Finceramica, Italy); a pilot study shows good clinical and MRI results at 2 years' follow-up. However, the results look poorer for old patients of the patellar location of cartilage defect.

The final design of this new scaffold mimics the natural aspect of cartilage and subchondral bone:

1. The first upper layer is smooth on the surface and made of equine type I collagen fibrils.
2. The intermediate one is made of 60 % collagen and 40 % magnesium ions mixed into hydroxyapatite.
3. The lower one consists of 70 % magnesium ions with hydroxyapatite and 30 % of collagen fibrils.

This scaffold, in animal studies, demonstrated an organized regeneration tissue; this good preclinical studies conduct to a cell-free technique using it in humans. Several reports were done after 2010 based on their use. The scaffold was used alone [44] or in addition with other techniques, such as tibial wedge osteotomies and meniscal allograft transplantation in a complex treatment for unicompartmental osteoarthritis in young people [34], and good results were reported. Regarding the fixation type of this scaffold, a study from 2014 [45] found a significant difference – in terms of results – between press fit and glue fixation; in the press-fit technique, there were reported cases with deformation, delamination, and dislodgement that affect the final outcome. The study suggested that whenever this material is used, a glue fixation type is needed for better initial fixation and faster recovery.

New approach came from combining biomaterials with nanoparticles. Small amount of nanoparticles can dramatically change the physical properties of the scaffolds, a manner in which synergetic property combination is achieved, with properties unable to be reproduced by any individual component [44].

---

## **Biodegradable Implants Used in Shoulder Arthroscopy**

Shoulder is probably the second most frequent joint address with arthroscopic surgery. It's a history of about 20 years of shoulder arthroscopy, which started with diagnostic arthroscopy and evolved toward shoulder instability surgery and rotator cuff repair.

## Biodegradable Implants Used in Shoulder Instability

A shoulder is considered “unstable” when it dislocates frequently or slips partially out of the joint. This is a painful condition and causes restriction of the motion because of anxiety and worries that a dislocation may occur. It may be an acute or chronic (recurrent) condition. In recurrent dislocation a new dislocation is produced by smaller trauma or movements in the shoulder joint. It will severely impair the shoulder function, especially in the case of athletes or hard workers, as well as workers above the head. In these cases the surgical shoulder stabilization is indicated. The shoulder stabilization procedure restores shoulder stability by addressing the involved structure; usually the articular labrum is avulsed, the anterior glenohumeral ligaments are torn, and tendons around shoulder may be torn. The avulsion of the anterior-inferior labrum is the main cause for shoulder instability and is described as Bankart lesion; it is causing the loosing of the stabilizing function of labrum by abolition of socket-deepening effect. The restoration of shoulder stability usually implicates the labrum repair. Surgery of shoulder instability is a challenging one, with a lot of surgical procedures described and a lot of place remained for further improvement.

Shoulder instability consists of two clinical entities: recurrent luxation and subluxation.

Surgery involving stabilization for shoulder instability is one of the most frequently performed arthroscopically. Before arthroscopy development, the shoulder procedure was done in an open fashion; most of surgical techniques used transosseous tunnel to secure the soft tissue to the bone. For there were technical difficulties related with drilling and positioning these tunnels, the anchor devices were developed. It was proved that anchors provide the same pullout strength like transosseous tunnels. They have small dimensions – 1 cm long and 2, 7–5, 6 mm wide – which are appropriate to be used during arthroscopic procedures. Anchors’ low-profile design is a factor considered to reduce the damage on articular cartilage while offering an anatomical reconstruction of the glenoid labrum and glenohumeral ligament complex [47]. Knots are placed on the capsular side of Bankart lesion, recreating the socket-deepening bumper effect of the labrum and hence restoring the concavity-compression mechanism of the glenoid labrum on the humeral head (Fig. 6).

There are certain advantages related to the arthroscopic technique; among them are preservation of motion, improvement in function, cosmetic benefits, and post-operative pain reduction. Despite these benefits still a higher recurrence rate comparing to open repair is still reported, even at 30 % comparing to less than 10 % reported for open procedures. Besides that there are complications related to surgical technique itself; complications related to devices used during stabilization were reported: articular cartilage damage, stiffness, implant migration or loosening, and soft tissue reaction to implants.

The main purpose in shoulder stabilization is to recover complete function of the joint while maintaining the stability. For this reason the avulse structures – articular



**Fig. 6** MRI follow-up imaging at a patient with resorbable anchors used for a Bankart lesion repair. Arrows show the low-profile implants with partial resorption at 1 year after surgery

labrum, tendons, ligaments – are positioned onto the bone with proper tensioning . For achieving this goal, devices that attached these soft tissues to bone are used. Anchors are mostly used. Anchors are buried into the bone while reattaching the soft tissue structure in charge for shoulder stability. Suture anchor consists of:

1. Anchor, which is inserted into the bone.
2. Eyelet is a hole or a loop in the anchor used for suture passage through.
3. The suture, which may be nonresorbable or resorbable one.

The anchor is inserted into the bone and the suture attached the soft tissue (labrum, tendon, and ligament) to the bone and fixed it here. Healing of soft tissue to the bone requires a stable biomechanical construct to up to 12 weeks, independent from material in which anchor consists. If these requirements are not fulfilled, the healing may not occur and repair may fail.

First anchors used in shoulder instability were metallic. Due to MRI artifacts, difficulties encountered in revision cases, damage of articular cartilage, loosening, implant migration, incarceration in glenohumeral joint, and bioresorbable anchors were developed. When we are talking about bioresorbable anchor, we are referring at the anchor and the eyelet, not considering the suture material [46].

Speer et al. identified four criteria to be fulfilled by materials used for bioabsorbable anchors:

1. Material should have the initial fixation strength to co-opt material soft tissue to the bone.
2. Material qualities and resorption time should be in accordance with the estimated healing time, 12–16 weeks.

3. The implant should not degrade too slowly.
4. The material should not cause antigenicity, pyrogenicity, toxicity, or carcinogenicity.

The first bioabsorbable tack used in shoulder surgery was made from PGA polymers (Suretac – Acufex Microsurgical, MA). The reported degradation time for PGA is 3 to 4 months. Early reports documented a high rate of failure due to rapid loss of fixation strength with consequent loose bodies, synovitis, and osteolysis [47].

Because of early resorption of PGA, next generation of anchors were made from PLLA, which disintegrate slower. Degradation rate for PLLA is reported to 10–30 months [48]. In contrast, as the PLLA degradation takes longer, there are inquiries about osseous replacement as well as papers reporting anchor persistence years after their implantation.

In order to improve inquiries related to plain bioresorbable anchors, next step was to ameliorate polymer properties by adding osteoconductive bioceramics as TCP or HA; the resulted material is called biocomposite. Reports documented an osseous ingrowth and minimal tissue reaction with their use. These calcium ceramic materials along with polymers further improve anchors' behavior in human body. They have proven good fixation strength and resorption with bone ingrowth. In Milewski report for 2012, the CT analysis proven that at 12 and 24 months' follow-up, the amount of anchor material resorption was about 68–98 %, while MRI analysis proven that 9–20 % of the total anchor material was replaced by bone [49]. Tunnel widening was seen in 55 % of cases but decrease after 12–24 months, consistent with bone ingrowth.

A new material propose to be used in anchor manufacturing is Regenesorb, a biocomposite consisting in PLGA polymer and two osteoconductive components: beta-TCP and calcium sulfate. The reason for mixing two osteoconductive substances came from their different resorption time: TCP act in early phase as a scaffold and sustained bone formation after 18 months, while calcium sulfate has been proven to work in early stages like 4–12 weeks. The material sounds promising and the experimental studies are encouraging.

The next material used was polyetheretherketone (PEEK), already used in trauma and spine surgery. PEEK-based implants are strong, radiolucent, and relatively inert and can be drilled out during revision cases. Next direction for improvement is to develop a composite made with PEEK base [50].

For refining the outcomes, knotless anchors were developed for labrum restoration. One of them was made from the poly-L-lactide polymer, for it demonstrated reliable fixation and good pullout strength [51]. In a 2012 paper, Boden suggested that the use of knotless anchor may induce earlier severe arthropathy and compare its behavior with that documented for the first used polyglycolic-used implants. Further studies are needed to validate this fixation type device.

Not only the material is different in various anchors; the anchor design itself is different. Screw-in anchors have the design similar to screw except that instead of the head there is an eyelet to accommodate the suture anchor strands.

The push-in anchors have a small profile and a high pullout strength. New design with open architecture was imagined for further improvements in anchor qualities. The Healicoil (Smith & Nephews) anchor differs from core-solid implants by eliminating the material between the anchor threads. The open architecture is presumed to allow for bone ingrowth to take place in fenestration between the threads and in central channel as soon as 12 weeks, as proved in preclinical studies.

Clinical limitations of anchors used in shoulder arthroscopy are related to their complications. Freehill et al. reported a 19 % rate of complication with the use of PLLA tacks; complications consist of synovitis, material debris, and chondral injury. Small multiple lytic areas were reported at insertion anchor sites. In a more recent study (2014), there were still reported complications associated with the use of lactide-containing suture anchors [48].

Osteolysis and arthropathy after the use of PLLA anchor were also reported by Athwal et al.; it was not clear if the mechanism inducing them was purely mechanic or there was a contribution from resorption by-products and acidic environment related to it [52].

Glenoid rim fracture after capsulolabral repair with anchors was reported lately, related to the usage of both resorbable and nonresorbable anchors [47]. Many factors were involved in generating these complications. Among them are the stress risers from pilot drill holes, anchor size and configuration, and material composition. In addition to these, cyst formation and osteolysis around a resorbable implant were implied [49].

The proper placement of the anchor during surgery seems to be the key to a successful repair. A prospective study of Ejerhed et al. reports no difference in outcome and complications when using resorbable or metallic anchors [53]. Furthermore they demonstrated cystic changes in both groups. The most frequent modalities of failure for anchors were reported by Barber: not burying the anchor enough to cover the eyelet in the bone, anchor migration after insertion, anchor loosening due to overaggressive rehabilitation, and anchor breakage during insertion [50]. In the same area, Strauss discussed attention that should be paid at the angle insertion in order to prevent anchor protrusion and consequently cartilage laceration. Meticulous surgical technique may obviate many potential complications [54].

## **Biodegradable Implants Used in Rotator Cuff Repair**

The rotator cuff is a name given to four tendons and muscles that adhere to the capsule of the shoulder and stabilize and externally rotate the humerus. Their insertion site at humeral tuberosity is usually referred as rotator cuff footprint. The rotator cuff tear is a painful condition, which restricted shoulder function and its external rotation. It may be an acute or a chronic tear depending on the mechanism involved. The diagnosis is clinical and MRI.

When the surgical treatment is indicated, there are three modalities to do it: in an open fashion, mini-open, or arthroscopic procedure. As the tendon should be put in place to recreate the original footprint and to restore their function, a few factors are

involved in technique success: suture material qualities, tendon release for allowing a correct replacement, a good grasping technique, and tendon-to-bone secure fixation.

No matter what approach is used, the rotator cuff repair is the next area for the use of suture anchor. The number of anchors used during this procedure is dictated by the rotator cuff size and varies between 2 and 6. Two techniques were developed: single row and double row, in the effort to recreate the original footprint of rotator cuff insertion to the humeral head. Single-row repairs are performed placing the anchors in a linear fashion; a double-row repair consists of a row of anchors placed medially at the articular cartilage margin of the anatomic neck of humerus and a second one placed laterally, along the tuberosity [55]. Double-row repair succeeds to cover about 90 % of the original footprint insertion, while single row restored about 45 % of it [56]. The biological coverage is not followed by biomechanical improvement; the potential advantage of a larger footprint should be balanced with added surgical time, adding implants and costs, increasing complexity of the procedure [57].

For a proper fixation of the anchor – and subsequently of the tendon – a good bone quality is required. In a 2003 experimental study, Tingart et al. demonstrated that the better bone qualities rest in proximal part of tuberosity and on its anterior part [58]. As a result, the pullout strength of the anchor placed in this area increases with an average of 53 %. Their paper proposes the proximal location for anchor positioning for better outcoming results. For adequate results the insertion of the anchor should not be too deep because that adjustment does not improve biomechanical stability.

The healing of the tendon to the bone is a complex issue and includes several biological processes. To sustain and enhance the healing process, a decortication in the bone area is done to receive the tendon; a bleeding zone is created in this manner and consequently an environment friendly to repair is created.

In a paper from 2009, DeFranco et al. put a warning about decortication procedure at the site of anchor insertion on humeral head [59]. They suggested that, for a proper fixation, the anchor should rest on a cortical margin, and, therefore, a careful attention should be paid to bone preparation during rotator cuff repair. As the bone preparation is mandatory for its biological support during repair process, an adequate balance should be maintained during surgery between too less and too much.

The tendon quality is another issue affecting the strength of fixation. The older is the tear, the more degenerative modifications are noted inside the tendon, and its strength may jeopardize the procedure success.

The angle at which the anchors must be inserted for better results has also been under debates. In a cadaveric study from 2008, Strauss et al. demonstrated that placing the anchors under a 90° angle – comparing to the 45° propose before and known under the name of deadman angle – a better soft tissue fixation stability was achieved [54]. For anchors inserted at an acute angle, windshield wiper-type motion can develop at bone-anchor interface. As a result the amount of motion is increased in overall fixation complex during each load, causing the suture loop to mechanically saw through the tendon with cycling. The tendon strength, tissue quality, and its

properties are also very important in failure mechanism. A poor tendon may introduce an additional risk for failure in the tendon-suture interface, usually along the tendon fibers rather than through it [54].

As the rotator cuff procedures gradually increase, the clinical complications related to it were reported.

Magee in 2003 reported a 30 % rate of anchor dislocation after rotator cuff repair associated with supraspinatus tendon re-tear in 10 % of cases [61]. The anchors get loose in the shoulder joint, and patients complain of pain, effusion, and locking episodes. The plain radiography was unable to detect the anchors, so either a MRI or an arthro-CT was done in order to detect the anchor placement. The retrieved implants were in different phases of resorption according to time since first surgery. At 1 year, there were still anchors resembling the initial form, and signs of bone ingrowth were hardly seen.

In a report from 2014, Medina et al. described an unusual location of a migrated anchor: it was located into the acromioclavicular joint, far away from the place where it was implanted [62]. At 2 years' follow-up, the anchor was found and retrieved; the second anchor used during rotator cuff procedure was also avulsed from humeral head but remained attached to tendon stump. The rotator cuff tear was unhealed and necessitates a revision surgery.

Nho in 2003 put a warning on the fact that resorbable anchor in cuff repair is frequently complicated with osteolysis and cyst formation [47]. As the adequate resorption of the anchor and the preservation of bone stock were the reasons for their use, the author suggested that their use should be reconsidered for it may interfere with revision.

In cases of partial rotator cuff tear, the surgical procedure may vary; it may consist of retaining the healthy part and transtendinous repair of the affected part. Concerns were raised related to the transtendinous passage of the anchor during procedure. In a cadaveric study published in 2013, Zang et al. demonstrated that the tendon damaged area increases gradually with the size of anchor used; it was suggested that – particularly for these cases – smaller diameter anchor should be used [63].

In cases of big rotator cuff tear, the failure rate may range between 20 % and 90 %. A lot of patient-related factors are linked to that big failure rate: bad tendon quality as a result of degenerative changes and fatty degeneration, lack of tissue elasticity and big tissue retraction, irregular shape of the tear, and poor bone quality. Additional procedures may be needed for these cases to sustain the healing [60]. The use of a patch may be necessary to enhance the tendon biology and enhance its strength.

Patch augmentation in rotator cuff repair was recommended in case of: bad tissue qualities, rupture of two or more tendons, and failed primary or revision of rotator cuff [64]. The patch may be resorbable or nonresorbable in terms of behavior; also they may be synthetic or natural, based on source used for their fabrication.

Despite the fact that natural patch is considered acellular, small amounts of DNA were found inside them; these remnants are related with inflammatory reactions reported after their use [65]. One of these class representatives is made from chemically cross-linked, acellular collagen/elastin material, derived from porcine

dermis (Zimmer Collagen Patch). Results with the use of a nonresorbable patch made from polycarbonate polyurethane-urea (Biomerix) were published in 2011 by Diaz et al.; they reported reduce with 10 % in retear rate and no local inflammatory or adverse reaction related to its use [66].

One of the resorbable patches is X-Repair, made from poly-L-lactic acid. Because of its slow rate of resorption, it is retaining about 90 % of its mechanical properties at 12 months' follow-up; it also has a tensile modulus of 500 MPa which makes it appropriate for sustaining the repair of tendons. The preclinical studies are encouraging, but further testing should be done to prove the safeness of the device. In 2014 Proctor reported 83 % success rate at 12 months and 78 % success rate at 42 months' follow-up [64].

No matter resorbable or nonresorbable, the use of patches in large rotator cuff improved the rate of good results. Longer follow-up studies are necessary to document their efficiency and safeness.

---

## Biomaterial Implants Future

Many further improvements may happen in this area of continuous and rapid change. The role of nanoparticles and nanoscience is still not fully understood or used, new and unexpected biocomposite materials are waiting to appear each day, switching from one to three dimension approach in materials used for tissue restoration has only begun, and the mesenchymal stem cells still retain unexploited qualities. The continuous reporting of the clinical behavior of biomaterials will further enhance our ability to develop proper and safe devices for our patients.

Being a surgeon may be frustrating sometime; we apply a new device in good hope that it will solve the problems related to a certain procedure and – at least in the beginning – things seem great. We convince our patients of its usefulness. After a while unexpected complications related to the use of that product appear, and we convince – again – our patients that we are able to do something better for them. Sometimes, this proven to be hazardous. Our results are highly related to the products and techniques we use, and we should be more cautious when deciding to make a change.

---

## Summary

In chapter “Clinical Limitations of the Biodegradable Implants Used in Arthroscopy,” the author – Rodica Marinescu – is approaching several complications related to the use of biodegradable implants in arthroscopic surgery. Implants used in knee and shoulder arthroscopy are described and their clinical complications are outlined, based on the author's personal experience as well as on current literature. The evolution of these implants is also presented and possible directions for further improvement are included. The chapter is completed with pictures illustrating some complications and a vast bibliography is supporting the text.



## References

1. Kim HS, Seon YK, Jo AR (2013) Current trends in anterior cruciate ligament reconstruction. *Knee Surg Relat Res* 25(4):165–173
2. Pinczewski LA, Clingeleffer AJ, Otto DD, Bonar SF, Corry S (1997) Integration of hamstring tendon graft with bone in reconstruction of the anterior cruciate ligament. *Arthroscopy* 13 (5):641–643
3. Shimizu T, Takahashi T, Wada Y, Tanaka M, Morisawa Y, Yamamoto H (1999) Regeneration process of mechanoreceptors in the reconstructed anterior cruciate ligament. *Arch Orthop Trauma Surg* 119(7–8):405–409
4. Schatzmann L, Brunner P, Stäubli HU (1998) Effect of cyclic preconditioning on the tensile properties of human quadriceps tendons and patellar ligaments. *Knee Surg Sports Traumatol Arthrosc* 6(Suppl 1):S56–S61
5. Cooper DE, Deng XH, Burstein AL, Warren RF (1993) The strength of the central third patellar tendon graft. A biomechanical study. *Am J Sports Med* 21(6):818–823
6. Brown CH Jr, Hecker AT, Hipp JA, Myers ER, Hayes WC (1993) The biomechanics of interference screw fixation of patellar tendon anterior cruciate ligament grafts. *Am J Sports Med* 21(6):880–886
7. Weiller A, Hofmann RP, Siepe CJ (2000) The influence of screw geometry on hamstring tendon interference fixation. *Am J Sports Med* 28:356–359
8. Kohn JC, Pienkowski D, Sterage E (2000) Interference screw fixation strength of a quadrupled hamstring tendon graft is directly related to bone mineral density and insertion torque. *Am J Sports Med* 28:705–710
9. Kohn D, Rose C (1994) Primary stability of interference screw fixation: influence of screw diameter and insertion torque. *Am J Sports Med* 22:334–338
10. Konan S, Haddad FS (2009) A clinical review of bioabsorbable interference screws and their adverse effects in anterior cruciate ligament reconstruction surgery. *Knee* 16:6–13
11. Appelt A, Baier M (2007) Recurrent locking of the knee joint caused by intraarticular migration of bioabsorbable tibial interference screw after arthroscopic ACL reconstruction. *Knee Surg Sports Traumatol Arthrosc* 15(4):378–380
12. Sharma V, Curtis C, Mitcheli C (2008) Extraarticular extraosseous migration of a bioabsorbable femoral screw after ACL reconstruction. *Orthopedics* 31(10):pii
13. Herrera A, Martínez F, Iglesias D, Cegoñino J, Ibarz E, Gracia L (2010) Fixation strength of biocomposite wedge interference screw in ACL reconstruction: effect of screw length and tunnel/screw ratio. A controlled laboratory study. *BMC Musculoskelet Disord* 11:139. doi:10.1186/1471-2474-11-139
14. Eguchi A, Ochi M, Adachi N, Deie M, Nakamae A, Usman MA (2014) Mechanical properties of suspensory fixation devices for anterior cruciate ligament reconstruction: comparison of the fixed-length loop device versus the adjustable-length loop device. *Knee* 21(3):743–748
15. Harilainen A, Sanden J, Janssen KA (2005) Cross-pin femoral fixation versus metal interference screw fixation in ACL reconstruction with hamstring tendon: results of a controlled prospective study with 2-years follow-up. *Arthroscopy* 21:25–33
16. John AH, Jill T (2008) Callaghan: polymer-HA versus polymer interference screw in ACL reconstruction in large animal model. *Knee Surg Sports Traumatol Arthrosc* 16:655–660
17. Studler U, White LM, Naraghu AM (2010) ACL reconstruction using bioabsorbable cross-pin: MR-imaging at follow-up, comparison with clinical findings. *Radiology* 255(1):108–116
18. Hapa O, Barber FA (2009) ACL fixation devices. *Sports Med Arthrosc* 17(4):217–223
19. Cossey AJ, Kalairajah J, Morcom R, Springgins AJ (2006) MRI evaluation of biodegradable interference fixation used in ACL reconstruction. *Arthroscopy* 22(2):199–204
20. Choi NH, Lu JH, Victoroff BN (2007) Do broken cross-pin compromise stability after ACL reconstruction with hamstring tendons? *Arthroscopy* 23(12):1334–1340
21. Verdonk P, Espregueira J, Monllau JC (2013) Meniscal transplantation. ISAKOS, Toronto

22. Becker R, Wirz D, Wolf C, Göpfert B, Nebelung W, Friederich N (2005) Measurement of meniscofemoral contact pressure after repair of bucket-handle tears with biodegradable implants. *Arch Orthop Trauma Surg* 125(4):254–260
23. Marinescu R, Laptioiu D, Negrusoiu O (2003) Outside-in meniscus suture technique-5 year's follow-up. *Knee Surg Sports Traumatol Arthrosc* 11(3):167–172
24. Espejo-Baena A, Golano P, Meschian S, Garcia-Herrera JM, Serrano Jiménez JM (2007) Complications in medial meniscus suture: a cadaveric study. *Knee Surg Sports Traumatol Arthrosc* 15(6):811–816
25. Liao CP, Lee H-M, Shih J-T, Hung S-T (2013) Common peroneal nerve palsy as a postoperative complication in lateral meniscus repair. *Form J Musculoskeletal Disord* 4(2):48–50
26. Kang HJ, Chun CH, Kim SH, Kim KM (2012) A ganglion cyst generated by non-absorbable meniscal repair suture material. *Orthop Traumatol Surg Res* 98(5):608–612
27. Gwathmey FW Jr, Golish SR, Diduch DR (2012) Complications in brief: meniscus repair. *Clin Orthop Relat Res* 470(7):2059–2066
28. Walgrave S, Claus S, Bellemans J (2013) High incidence of intraoperative anchorage failure in Fast-Fix all inside meniscal suturing device. *Acta Orthop Belg* 79:689–695
29. Jones HP, Lemos MJ, Wilk RM, Smiley PM, Gutierrez R, Schepsis AA (2002) Two-year follow-up of meniscal repair using a bioabsorbable arrow. *Arthroscopy* 18(1):64–69
30. Hantes ME, Zachos VC, Varitimidis SE, Dailiana ZH, Karachalios T, Malizos KN (2006) Arthroscopic meniscal repair: a comparative study between three different surgical techniques. *Knee Surg Sports Traumatol Arthrosc* 14(12):1232–1237
31. Tienen TG, Heijkants RG, Buma P, De Groot JH, Pennings AJ, Veth RP (2003) A porous polymer scaffold for meniscal lesion repair - a study in dogs. *Biomaterials* 24(14):2541–2548
32. Bulgheroni P, Murena L, Ratti C, Bulgheroni E, Ronga M, Cherubino P (2010) Follow-up of collagen meniscus implant patients: clinical, radiological, and magnetic resonance imaging results at 5 years. *Knee* 17(3):224–229
33. Rodkey WG, DeHaven KE, Montgomery WH 3rd, Baker CL Jr, Beck CL Jr, Hornel SE, Steadman JR, Cole BJ, Briggs KK (2008) Comparison of the collagen meniscus implant with partial meniscectomy. A prospective randomized trial. *J Bone Joint Surg Am* 90(7):1413–1426
34. Grassi A, Zaffagnini S, Marcheggiani Muccioli GM, Benzi A, Marcacci M (2014) Clinical outcomes and complications of a collagen meniscus implant: a systematic review. *Int Orthop* 38(9):1945–1953
35. Monllau JC, Gelber PE, Abat F, Pelfort X, Abad R, Hinarejos P, Tey M (2011) Outcome after partial medial meniscus substitution with the collagen meniscal implant at a minimum of 10 years' follow-up. *Arthroscopy* 27(7):933–943
36. Bouyarmane H, Beaufile P, Pujol N, Bellemans J, Roberts S, Spalding T, Zaffagnini S, Marcacci M, Verdonk P, Womack M, Verdonk R (2014) Polyurethane scaffold in lateral meniscus segmental defects: clinical outcomes at 24 months follow-up. *Orthop Traumatol Surg Res* 100(1):153–157
37. Lanza R, Langer R, Vacant J (2013) Principles of tissue engineering, 4th edn. Academic
38. Kokkinakis M, Kafchitsas K, Rajeev A, Mortier J (2008) Is MRI useful in the early follow-up after autologous osteochondral transplantation? *Acta Orthop Belg* 74(5):636–642
39. Hangody L, Ráthonyi GK, Duska Z, Vásárhelyi G, Füles P, Módis L (2004) Autologous osteochondral mosaicplasty. Surgical technique. *J Bone Joint Surg Am* 86-A(Suppl 1):65–72
40. Ochi M, Adachi N, Nobuto H, Yanada S, Ito Y, Agung M (2004) Articular cartilage repair using tissue engineering technique—novel approach with minimally invasive procedure. *Artif Organs* 28(1):28–32
41. Gooding CR, Bartlett W, Bentley G, Skinner JA, Carrington R, Flanagan A (2006) A prospective, randomised study comparing two techniques of autologous chondrocyte implantation for osteochondral defects in the knee: Periosteum covered versus type I/III collagen covered. *Knee* 13(3):203–210
42. Feng Zhao, Wei He, Yueling Yan et al (2014) The application of polysaccharide biocomposites to repair cartilage defects. *Int J Polym Sci* 2014:9 p. Article ID 654597

43. Barber FA, Herbert MA, McGarry JE, Barber CA (2008) Insertion force of articular cartilage transplantation systems. *J Knee Surg* 21(3):200–204
44. Kon E, Delcogliano M, Filardo G, Busacca M, Di Martino A, Marcacci M (2011) Novel nanocomposite multilayered biomaterial for osteochondral regeneration: a pilot clinical trial. *Am J Sports Med* 39(6):1180–1190
45. Filardo G, Drobnic M, Perdisa F, Kon E, Hribernik M, Marcacci M (2014) Fibrin glue improves osteochondral scaffold fixation: study on the human cadaveric knee exposed to continuous passive motion. *Osteoarthritis Cartilage* 22(4):557–565
46. Speer KP, Warren RF (1993) Arthroscopic shoulder stabilization. A role for biodegradable materials. *Clin Orthop Relat Res* 291:67–74
47. Nho SJ, Provencher MT, Seroyer ST, Romeo AA (2009) Bioabsorbable anchors in glenohumeral shoulder surgery. *Arthroscopy* 25(7):788–793
48. Cobaleda Aristizabal AF, Sanders EJ, Barber FA (2014) Adverse events associated with biodegradable lactide-containing suture anchors. *Arthroscopy* 30(5):555–556
49. Milewski MD, Diduch DR, Hart JM, Tompkins M, Ma SY, Gaskin CM (2012) Bone replacement of fast absorbing biocomposite anchors in arthroscopic shoulder labral repair. *Am J Sports Med* 40(6):1392–1401
50. Barber FA, Herbert MA, Beavis RC, Barrera Oro F (2008) Suture anchor materials, eyelets, and designs: update 2008. *Arthroscopy* 24:859–867
51. Boden RA, Burgess E, Enion D, Srinivasan MS (2009) Use of bioabsorbable knotless suture anchors and associated accelerated shoulder arthropathy: report of 3 cases. *Am J Sports Med* 37(7):1429–1433
52. Athwal GS, Shridharani SM, O'Driscoll SW (2006) Osteolysis and arthropathy of the shoulder after use of bioabsorbable knotless suture anchors. A report of four cases. *J Bone Joint Surg Am* 88(8):1840–1845
53. Ejerhed L, Kartus J, Funck E, Köhler K, Sernert N, Karlsson J (2000) A clinical and radiographic comparison of absorbable and non-absorbable suture anchors in open shoulder stabilisation. *Knee Surg Sports Traumatol Arthrosc* 8(6):349–355
54. Strauss E, Frank D, Kubiak E, Kummer F, Rokito A (2009) The effect of the angle of suture anchor insertion on fixation failure at the tendon-suture interface after rotator cuff repair: deadman's angle revisited. *Arthroscopy* 25(6):597–602
55. Cole BJ, ElAttrache NS, Anbari A (2007) Arthroscopic rotator cuff repairs: an anatomic and biomechanical rationale for different suture-anchor repair configurations. *Arthroscopy* 23(6):662–669
56. Costic RS, Brucker PU, Smolinski PJ, Gilbertson LG, Rodosky MW (2006) Arthroscopic double row anchor repair of full thickness rotator cuff tear: Footprint restoration and biomechanical properties. Presented at the annual meeting of the Orthopaedic Research Society, Chicago, 19–22 Mar 2006
57. Mahar A, Tamborlane J, Oka R, Esch J, Pedowitz RA (2007) Single-row suture anchor repair of the rotator cuff is biomechanically equivalent to double-row repair in a bovine model. *Arthroscopy* 23(12):1265–1270
58. Tingart MJ, Apreleva M, Zurakowski D, Warner JJ (2003) Pullout strength of suture anchors used in rotator cuff repair. *J Bone Joint Surg Am* 85-A(11):2190–2198
59. DeFranco MJ, Cole BJ (2009) Current perspectives on rotator cuff anatomy. *Arthroscopy* 25(3):305–320
60. Bravman JT, Guttman D, Rokito AS, Kummer FJ, Jazrawi LM (2006) A biodegradable button to augment suture attachment in rotator cuff repair. *Bull Hosp Jt Dis* 63(3–4):126–128
61. Magee T, Shapiro M, Hewell G, Williams D (2003) Complications of rotator cuff surgery in which bioabsorbable anchors are used. *AJR Am J Roentgenol* 181(5):1227–1231
62. Medina G, Garofo G, D'Elia CO, Bitar AC, Castropil W, Schor B (2014) Bioabsorbable suture anchor migration to the acromioclavicular joint: how far can these implants go? *Case Rep Orthop* 834–896

63. Zhang QS, Liu S, Zhang Q, Xue Y, Ge D, O'Brien MJ, Savoie FH, You Z (2012) Comparison of the tendon damage caused by four different anchor systems used in transtendon rotator cuff repair. *Adv Orthop* 798521
64. Proctor CS (2011) Long term successful arthroscopic repair of large and massive rotator cuff repair with a functional and degradable reinforcement device. *J Shoulder Elbow Surg* 120:1508–1513
65. Malcarney HL, Bonar F, Murrell GA (2005) Early inflammatory reaction after rotator cuff repair with a porcine small intestine submucosal implant: a report of 4 cases. *Am J Sports Med* 33 (6):907–911
66. Enclada-Díaz I, Cole BJ, MacGilivray J (2011) Rotator cuff augmentation using a novel polycarbonate polyurethane patch :preliminary results at 12 months follow-up. *J Shoulder Elbow Surg* 20:788–794

Gianluca Vadalà, Fabrizio Russo, Luca Ambrosio, and Vincenzo Denaro

## Contents

Introduction .....	968
Spinal Fusion: Basic Principles .....	969
Grafts .....	970
Iliac Crest Bone Graft .....	970
Local Bone Graft .....	971
Allograft .....	972
Xenograft .....	973
Demineralized Bone Matrix .....	974
Ceramics .....	975
Bone Morphogenetic Proteins .....	978
Platelet-Rich Plasma .....	980
Bone Marrow Aspirate .....	981
Vertebral Augmentation .....	982
Summary .....	983
References .....	985

## Abstract

Spinal arthrodesis is an essential procedure in spine surgery which is performed to fuse two or more vertebrae. Success rates and outcomes strictly depend on substrates used to achieve a solid bony fusion of the vertebral segments. Autologous bone graft, usually harvested from the iliac crest or even locally, is traditionally considered the gold standard for its potential to lead to bone formation and integrate within surrounding tissues, although donor-site morbidity cannot be disregarded. This has led to develop alternative strategies for spinal arthrodesis, such as allogenic bone graft (both human and animal, also known as

---

G. Vadalà (✉) • F. Russo • L. Ambrosio • V. Denaro  
Department of Orthopaedic and Trauma Surgery, Campus Bio-Medico University of Rome, Rome, Italy  
e-mail: [g.vadala@unicampus.it](mailto:g.vadala@unicampus.it); [g.vadala@gmail.com](mailto:g.vadala@gmail.com)

xenograft), demineralized bone matrix (DMB), synthetic and biodegradable bioceramics, local administration of bone morphogenetic proteins (BMPs), and products derived from peripheral blood (platelet-rich plasma, PRP) and bone marrow (bone marrow aspirate, BMA). While autograft exhibits ideal osteoconductive, osteoinductive, and osteogenic properties, other options must be combined to obtain constructs that own all the features.

The design of an ideal bioscaffold that emulates the natural bone structure and function is still challenging. New biofabrication technologies of hybrid organic/inorganic materials with controlled architecture associated with osteoinductive growth factors can overcome the limitations of the current alternates.

---

**Keywords**

Spine surgery • Spinal fusion • Arthrodesis • Intervertebral disk • Bone substitutes • Biocomposites • Bone • Tissue engineering • Bone marrow • Platelet-rich plasma

---

**Introduction**

Over the last few decades, the total number of spine surgical procedures, as consequences of trauma, degeneration, tumor, infection, and inflammation, has raised significantly. Spinal fusion is a fundamental technique, whose success is essentially related to highly specialized instrumentation and substrates that are electively selected, according to both the affected spinal segment and the surgical approach being performed.

Autologous bone graft harvested from the iliac crest has been used for many years and still represents the gold standard for spinal fusion. Indeed, autograft has three key properties that are essential to promote bone neoformation [1]:

- Osteogenesis: capacity to lead bone formation by the presence of cells that produce the organic bone matrix
- Osteoinduction: process by which growth factors stimulate differentiation of mesenchymal stem cells (MSCs) into osteoblasts, thus leading osteogenesis
- Osteoconduction: mechanism by which the bone grows on a surface and adapts to its tridimensional structure, thus granting neovascularization and osteoprogenitor cell migration

However, high donor-site morbidity, blood loss, increased operative time, and postoperative pain are still relevant issues that have fueled research in order to develop alternative strategies to autograft.

Currently, bone graft substitutes that are used in spine surgery include bone allograft, demineralized bone matrix (DMB), synthetic bioceramics, bone morphogenetic proteins (BMPs), platelet-rich plasma (PRP), and bone marrow aspirate (BMA). Application of biomaterials and biotechnologies in spine surgery is rising

as well in the treatment of vertebral compression fractures and degenerative disk disease. Polymethacrylate cement is currently injected during vertebroplasty and kyphoplasty procedures to treat vertebral burst fractures. Research is mainly oriented toward nucleus pulposus regeneration, annulus fibrosus repair, and biomaterials and tissue engineering which are fields of growing interest among both surgeons and manufacturing companies, with a major involvement in spine surgery.

---

## **Spinal Fusion: Basic Principles**

After an adequate spinal decompression, arthrodesis is an essential surgical procedure performed to achieve stability of the spine in order to treat traumatic, infective, neoplastic, degenerative, inflammatory, or iatrogenic diseases affecting facet joints and intervertebral disks.

Spinal fusion is required when conservative treatment has proven to be ineffective: aforementioned clinical scenarios are primarily associated with back pain, which is often caused by instability of involved spinal segments. This surgical technique aims to establish a structural and functional unity between affected segments, thus relieving pain despite loss of local flexibility. Each affected spinal segment needs a highly specific surgical approach, which may depend on several factors. To achieve spinal fusion, the graft should be placed in the intervertebral disk space after discectomy (interbody fusion), between the transversal processes or near facet joints after decompression (posterolateral fusion). The surgical approach differs according to the location and the indication to surgery. After graft placement, spinal segments are fixed with specialized instrumentation, in order to obtain a long-lasting spinal fusion.

Spinal fusion healing and consequent bone neoformation are complex processes, difficult to be staged. Graft incorporation triggers a prompt inflammatory response that lasts up to 14 days: decortication and vascular injury lead to hematoma formation, which is rapidly surrounded by inflammatory cells (macrophages, lymphocytes, polymorphonuclear cells) and fibroblast-like cells. The latter are responsible for the synthesis of a fibrovascular matrix that supports the whole tissue regeneration process. The cruciality of this phase is demonstrated by significant decreases in fusion rates after the administration of anti-inflammatory drugs (especially NSAIDs) in the perioperative period.

Thereupon, vascular buds sprout within the granulation tissue stroma and branch out forming anastomoses, thus driving neoangiogenesis of primary membranous bone that grows besieging the decorticated bone.

Vascularity of host bone tissues is thusly considered a major factor for successful spinal fusion healing. Cervical vertebrae are vascularized by several vertical arteries, whose segmental branches are highly anastomosed, especially in the anterior spinal plexus region: for this reason, increased blood flow density accounts for expeditious healing and recovery. Conversely, thoracolumbar segments are supplied by segmental arteries which origin directly from the descending aorta, while post-laminar

branches are deprived of blood by large vessels that vascularize the erector spine. Lower blood flow density and significantly fewer anastomoses cause lumbar fusion healing to be definitely slower [2].

As vascularity increases, osteoinductive factors released within the graft induce chemotaxis and differentiation of MSCs into chondrocytes, which lead to cartilage synthesis. Then, vascular invasion highlights the transformation of an intermediate phase of hypertrophic chondrocytes into neofomed bone tissue through endochondral ossification. The entire process spreads from the central region of the fusion mass toward the peripheral portion of the graft and is specifically marked by the differentiation of MSCs into osteoblasts.

Bone matrix synthesis, characterized by secretion of type I collagen, bone-specific proteoglycans, and  $\text{Ca}^{2+}$  incorporation, occurs simultaneously with necrotic tissue and immature bone resorption, mediated by osteoclasts. This process is denominated “creeping substitution” and leads to the formation of vascular channels belonging to new haversian systems, thus laying the groundwork for mature cortical bone development. Osteoconduction is then followed by tissue remodeling and cortical rim thickening; in the meanwhile, bone marrow activity increases resulting in the formation of secondary spongiosa. Complete healing is typically accomplished in 1 year’s time [3].

Pseudarthrosis rate subsequent to spinal fusion varies from 5 % to 35 % depending on several factors, such as affected spinal segment (cervical or lumbar), number of involved levels (single or multiple), fusion site (interbody or posterolateral), instrumentation, and patient-related factors (including age, tobacco use, and concurrent metabolic disorders) [4]. Pseudarthrosis actually leads to a leaky joint between bone surfaces, causing pain, mechanical instability, and disability [2]. Therefore, it is fundamental to select an appropriate graft defined as any implanted material that, solely or combined with other substrates, mediates spinal fusion through bone tissue neoformation.

To achieve a stable arthrodesis, a graft must show osteogenic, osteoinductive, and osteoconductive activity; in addition, it should be able to support loading forces that act on the spine during the fusion process.

Indeed, from a biomechanical point of view, transmission of feeble physical stresses is thought to promote spinal fusion; on the contrary, excessive motion may impair spinal fusion healing. For this reason, spinal arthrodesis should be achieved establishing such a solid stabilization of vertebral segments that still allows physiological mechanical loads to contribute to the healing process [5].

---

## Grafts

### Iliac Crest Bone Graft

Autologous bone graft harvested from the iliac crest has been, and still is, considered to be the gold standard in bone grafting. It provides an osteoconductive matrix composed of collagen and hydroxyapatite, with a stromal component which is



populated by cells having osteogenic potentials. Several growth factors, such as BMPs, can be found among non-collagenous proteins within the graft mineralized bone matrix. Furthermore, the corticocancellous structure of autologous bone graft has adequate biomechanical properties to support loading forces. In addition, autograft is fully histocompatible, non-rejectable, and not associated with risks of disease transmission.

In order to harvest the bone graft, the ilium can be approached via either the anterior or posterior accesses. Posterior iliac crest generally provides such an amount of cancellous bone that is sufficient for a multiple-level spinal fusion, although lacking of structural integrity. Anterior iliac crest is more conveniently accessed during anterior spinal procedures; notably, anterior superior iliac crest is constituted by a tricortical structure with consistent compressive strength that can be easily harvested [6].

A systematic review reported an average arthrodesis rate of 77 % using autograft, with lower values for multiple-level fusion and higher percentages for single-level approaches [7]. However, donor-site morbidity represents an important issue: complications occur in 4–49 % of patients and include long-lasting postoperative pain, hematoma, infection, bruising, peritoneal perforation, pelvic fracture, hernia, gait, ureteral injury, neurological and vascular injury, cosmetic defects, increased operative time, and blood loss, thus resulting in prolonged rehabilitation time. A retrospective study on single-level anterior cervical discectomy and fusion (ACDF) has shown that 26.1 % of patients complained of persistent pain, while 15.7 % suffered from numbness at the donor site. Low quality and exiguous supply of autologous bone graft are also notable issues in patients undergoing reoperation or requiring high graft volumes. Moreover, autograft shows poor handling characteristics, as it is often morselized during harvest and not retained within the implantation site. This has led to the development of graft extenders (such as platelet concentrates, DMB, or BMA) to both improve autograft handling features and enrich its osteoinductive properties.

Certain studies have reported the use of cortical autografts derived from uncommon sites, such as the fibula, the clavicle, the manubrium, and the ribs. Indeed, the fibular diaphysis can be partially remodeled in order to obtain a substrate that has a cortical/cancellous ratio and vascular features that closely resemble those of grafts used in cervical fusion. Autograft from the rib can be obtained during thoracotomy, which is usually performed to expose the thoracic and upper lumbar spine; rib grafts show ideal vascularization but lack significant structural and biomechanical properties [7].

On the other hand, cancellous bone grafts can be harvested from Gerdy's tubercle, the distal portion of the radius, and the distal portion of the tibia [5].

## **Local Bone Graft**

In order to overcome postoperative issues related to iliac crest bone grafting, autologous bone substrate might be obtained locally, from laminectomy and

facetectomy sites during spinal decompression. This local graft then undergoes removal of soft tissues and morselization, in order to provide a substrate that may be suitable for a single-level posterolateral spinal fusion. Different studies have reported that local bone graft shows inferior performances in spinal arthrodesis compared to autologous bone harvested from the iliac crest, due to the high cortical/cancellous rate and soft tissue content [6].

In a retrospective and comparative study, Sengupta et al. have reported clinical and radiologic outcome of instrumented posterolateral lumbar spinal arthrodesis comparing local bone and iliac crest bone grafts; all the patients underwent decompression and fusion with pedicle screw instrumentation. Fusion rates were comparable between the two groups in single-level spinal fusion but significantly lower in multiple-level fusion within the group treated with local bone graft [8].

## **Allograft**

Allograft, defined as a bone graft harvested from cadavers, is most often used as a substitute for autologous bone graft in spine surgery. While it significantly shortens operating time, lowers blood loss, and avoids morbidity associated with the harvesting site, this procedure shows notable disadvantages. However, even though undergoing extensive processing, meticulous donor serologic screening, and advances in bone collection, cadaveric grafts still suffer from concerns of immunogenicity and disease transmission. Mainly involved pathogens are hepatitis B virus (HBV), hepatitis C virus (HCV), and human immunodeficiency virus (HIV). To date, risk of disease transmission in musculoskeletal allografts seems to be significant only when using unfrozen and unprocessed autologous bone grafts. Moreover, allograft substrates are troublesome to standardize due to heterogeneity of donor population; bone banks may be required to obtain a bone graft, thus increasing the cost of the entire process.

Allograft adopted for orthopedic applications can be mineralized (fresh-frozen or freeze-dried) or demineralized. Fresh-frozen allografts are harvested aseptically in order to lower the risk of bacterial contamination and are then processed to remove residual tissues, such as fat, bone marrow, internal blood, and surface material. They are highly osteoconductive with slight osteoinductive capacity but lack osteogenic properties, because graft cells do not sustain processing and transplantation. In addition, fresh-frozen grafts tend to maintain their initial biomechanical strength. Once harvested from the donor and undergone similar procedures, freeze-dried grafts are obtained through lyophilization and vacuum packing; sterilization may also be performed during the preparation process [7]. Freeze-dried bone is osteoconductive, while it shows poor osteoinductive properties; nonetheless, lyophilization might lower original strength up to 50 %, especially against torsional and bending forces [5]. Additionally, donor age is inversely correlated with freeze-dried substrates osteoinductive properties, due to a loss of bioactive growth factors. Freeze-dried grafts are available in a wide assortment of preparations, which are

mainly classified into three groups, according to their composition: cortical, cancellous, and particulate grafts. Cortical bone supplies significant mechanical and structural support, while it is slowly revascularized and only partially resorbed; its incorporation occurs through the formation of an external fibrocartilage callus surrounding the allograft as a consequence of periosteal osteogenesis initiated by the host bone. On the contrary, cancellous and particulate bones do not provide structural support, while they undergo prompt revascularization and resorption; incorporation takes place with new bone tissue developing on the surfaces of the trabeculae, thus increasing the area for bone formation. These differences in mechanical and biological properties among graft types should orientate toward different choices and approaches depending on the clinical situation, in order to achieve intended outcomes [9].

As reviewed by Buttermann et al., allograft use in spine surgery can be contemplated taking into account the type of allograft preparation, the patient's age, and the anatomical fusion site [10]. Cortical allografts are recommended for an anterior single-level lumbar and cervical interbody fusion, with a fusion rate comparable to that achieved through autograft implantation. Jagannathan et al. reported a 94 % fusion rate after a single-level ACDF, even without the use of a postoperative collar [11]. A meta-analysis of four studies involving 310 patients who were treated with single-level and two-level ACDF demonstrated that allograft has a lower fusion rate than autograft evaluated by radiography, as well as increased rates of graft subsidence [12]. Moreover, several studies have showed allograft to be associated with increased pseudarthrosis and collapse rates [13], higher number of fused levels, kyphotic deformity, and delayed union when compared to autograft [14]. The use of anterior cervical plating has been suggested to increase fusion rates and diminish subsidence, thus effectively making allograft a valid alternative to autograft: Schlosser et al. reported a 94.5 % arthrodesis rate in patients who underwent from one- to four-level plated unions [15]; long-term follow-ups of patients transplanted with allografts in association with plating showed clinical and radiological success [16].

Cortical allografts harvested from fibulae have showed enhanced biomechanical properties, however, with a lower osteoconductive capacity compared to iliac crest substrates [17]; Martin et al. reported fusion rates of 90 % and 72 % at one- and two-level ACDF, respectively, while Suchomel et al. have not found any statistically significant difference for nonunion or collapse between using fibula allograft and iliac crest autograft [18]. Cancellous and particulate grafts can be also added as autograft extenders in posterior spinal fusion, especially to treat thoracolumbar deformities [9].

## **Xenograft**

Animal allografts (xenografts) were firstly adopted by Maatz and Bauermeister [19], who harvested bovine bone substrates, now commercially available under the names of Kiel bone and Surgibone.

Xenograft implantation leads to bone healing with a major fibrotic component; inflammation, low biocompatibility, possible viral transmission, and increased reoperation rates are fundamental issues to be considered.

High immunogenicity, insufficient biological activity, thorough sterilization processing, and structural incompatibility between nonhuman mammals and human anatomical specimens have significantly limited the effective use of animal grafts in spine surgery.

However, several studies showed favorable results, and Savolainen et al. have reported no significant differences in fusion rates or angulation deformity comparing xenograft with autograft in 250 ACDF [20].

## **Demineralized Bone Matrix**

Demineralized bone matrix (DBM) is an allograft substrate devoid of its mineral phase, which is mainly composed of crystalline calcium hydroxyapatite [ $\text{Ca}_{10}(\text{PO}_4)_6(\text{OH})_2$ ]. The mineralized component is entirely removed by acid extraction processing: once harvested, allograft is crushed to fine particles and then demineralized in 0.5 N HCl mEq/g for 3 h. Residual acid is then removed by washing the substrate in a solution with sterile water, ethanol, and ethyl ether [5]. This process actually retains type I collagen, non-collagenous proteins, and growth factors (especially BMPs, albeit in low concentrations); moreover, it significantly reduces the risk of disease transmission and inactivates HIV.

Therefore, DBM shows osteoinductive and osteoconductive properties, but it lacks of structural support due to its amorphous nature [21]. In situ DBM osteoinductive potential strictly depends on the biological features of the transplantation environment, such as stability of the substrate, contact with the host bone, and vascularity of the graft bed [9].

DMB is, to date, available in different forms such as putty, gel, and flexible sheets or combined with cortical chips. Commercial preparations are commonly associated with fillers, fibers, or carrier materials including glycerol, hyaluronic acid, gelatin, and calcium sulfate powder, in order to improve their handling characteristics [22].

However, these carriers can significantly influence DMB osteoinductive activity: glycerol, for example, might lower host cells response due to its acidic pH, while hyaluronic acid, having a neutral pH, does not impair host environment.

Furthermore lack of both standardization in preparation processes and quantification of growth factors, whose concentrations may vary consistently among manufacturing companies (and even within different batches from the same manufacturer), makes DBM actual efficacy arduous to be assessed. Moreover, good quality of donor graft is also essential to achieve an acceptable performance in vivo [22].

DMB contribution to spinal fusion has been intensely studied in animal models. DMB used alone or combined with autograft resulted in successful posterolateral lumbar spinal fusion in rabbits and nonhuman primates. However, other clinical studies have demonstrated that the sole DMB is not capable of driving spinal fusion

but may be used to extend a small autograft, in order to achieve a more solid spinal arthrodesis [23].

The need for graft extenders is fundamental while performing multi-level spinal fusion surgery, such as for the treatment of scoliosis. On the other hand, the combination of DMB with a structural carrier (e.g., allograft, titanium mesh cages, bioceramics) has shown adequate fusion rates, albeit associated with higher rates of graft collapse and pseudarthrosis in anterior cervical arthrodesis, if compared to autograft [24].

Indeed, a multicenter prospective study has evaluated graft incorporation comparing both allograft with DMB and autograft. Graft collapse and pseudarthrosis rates were significantly higher in the first group, thus demonstrating that preparations currently available do not possess adequate osteoinductive properties to drive solid arthrodesis [9].

## Ceramics

Ceramics represent a wide array of biomaterials with metallic and nonmetallic components, characterized by biocompatibility, biodegradability, and inorganic, nontoxic, nonimmunogenic, and osteotropic properties. Regarding to their structure, they can be classified as either crystalline (with regular and periodic tridimensional molecular arrangement) or amorphous (lacking long-range atomic order).

Calcium phosphate ( $\text{CaPO}_4$ ) ceramics have been the most thoroughly used composites in spine surgery: they are synthesized by fusion of individual crystals through a thermal reaction called sintering, which occurs at approximately 1000 °C and leads to formation of polycrystalline structures. Calcium phosphate bioceramic scaffolds are mainly composed of synthetic  $\beta$ -tricalcium phosphate ( $\beta$ -TCP) and hydroxyapatite, which may be synthesized or coral derived as well. In the latter case, calcium carbonate coralline skeleton is heated in an aqueous phosphate solution in order to lead hydrothermal exchange of calcium carbonate within the coral with calcium phosphate diluted into the aforementioned solution. The coral species *Porites astreoides* has been elected as an ideal substrate, because its porosity showed to favor bone ingrowth significantly [5].

Different processing methods allow to craft products with variable chemical, biomechanical, and structural properties, in order to mimic the mineral phase of the bone. Moreover, the possibility to mold substrates into different shapes and size accounts for their peculiar versatile features.

Calcium phosphate ceramics show an intrinsic porosity which avoid aggregation of crystals during the precipitation process. Such micrometer-sized pores are essential to enhance material resorbability, molecular diffusion, MSC attachment, differentiation, and, consequently, bone tissue regeneration. Porosity architecture is fundamental to promote cell infiltration and angiogenesis: analytic studies have reported that ceramics polycrystalline lattices should have an average macropore size of 300  $\mu\text{m}$  in order to resemble cancellous bone structure, thus maximizing graft osteoconductive performances [25].

However, as porosity and ergo osteoconductivity increase, bioceramics mechanical properties critically worsen. Given that the organic phase of the bone is responsible for its structural integrity, the inorganic nature of these composites accounts for their stiffness, brittleness, low fracture resistance, high elasticity, insufficient tensile, and shear strength. Even if synthetic (as well as geologic) hydroxyapatite and bone apatite share approximately the same crystalline structure and chemical composition, the latter is characterized by different crystal size, short-range order, and peculiar arrangements of carbonate ( $\text{CO}_3^{-2}$ ) and phosphate ( $\text{PO}_4^{-2}$ ) groups. These differences may explain why synthetic hydroxyapatite resorbs so slowly that prevents new bone tissue from remodeling under physiological loads; in addition, its radiopacity makes eventual arthrodesis difficult to be assessed.

Tricalcium phosphate substrates often show inadequate resorbability features as well:  $\beta$ -TCP undergoes rapid degradation, thus lacking of mechanical support within the implantation site.

In general, higher crystallinity degrees provide more biomechanical strength, while amorphous preparations yield inadequate resorption rates.

Graft incorporation occurs in association with hemorrhage, inflammation, revascularization, and local integration of the substrate within the host bone tissue. This process might be inhibited by histocompatibility mismatch and decreased biological activity due to graft processing.

Bone neoformation is characterized by a creeping substitution process in which calcium phosphate cements are replaced with organic and mineral phases ordinarily found in bone tissue [9].

The first cells to interact with the ceramic graft are erythrocytes, osteoblasts, and notably macrophages that are the major infiltrating cells after TCP and hydroxyapatite implantation. The presence of the ceramic substrate triggers the secretion of  $\text{H}^+$  by macrophages, thus initiating the resorption process, and the synthesis of inflammatory cytokines (such as IL-1, IL-6, and  $\text{TNF-}\alpha$ ) and gelatinases by fibroblasts.

Graft mineralization occurs directly on the surface of macropores and micropores: once collagen is secreted, mineralized fiber deposition leads to mature lamellar bone formation [26].

Calcium phosphate-based bioceramic grafts are available in many different preparations, such as putty, pellets, powders, and injectable cements (used in vertebroplasty).

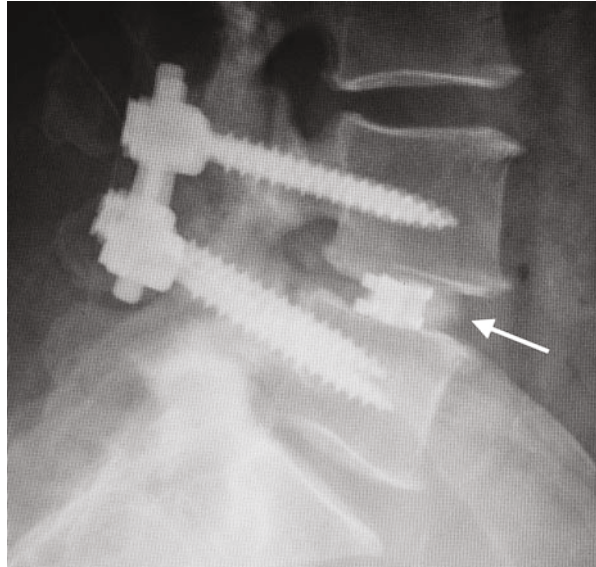
$\beta$ -TCP [ $\text{Ca}_3(\text{PO}_4)_2$ ] has been widely incorporated as a bone void filler: it shows high biocompatibility and bio-resorbability but lacks structural and impact resistance.

To overcome the load-bearing deficiency, interbody fusion is performed using titanium cages filled with TCP pellets or powder applied in the intradiscal space (Fig. 1).

Porous TCP (micropores size: 3–5 nm) almost resembles cancellous bone in compressive and tensile strength features and tends to dissolve more promptly than hydroxyapatite in an acidic media.

To date, the majority of bioceramic grafts used in spinal surgery are composed of  $\beta$ -TCP and hydroxyapatite with or without bovine type I collagen. This combination

**Fig. 1** X-ray image of L4-L5 interbody fusion with instrumentation using a titanium cage and  $\beta$ -TCP in pellets (arrow)



allows to diversify resorption properties and scaffold shape and bind osteoinductive agents such as rhBMP-2; preclinical data support the use of these composites [4].

Healos (DePuy Spine) is a synthetic injectable substrate which is primarily composed of bovine type I collagen (80 %) and hydroxyapatite (20 %) fixed into a tridimensional matrix. The efficacy of this graft has been evaluated in a rabbit model of bilateral intertransverse lumbar arthrodesis: different groups underwent spinal fusion through the implantation of iliac crest autograft, Healos matrix alone, and Healos matrix mixed with autologous bone marrow. At 8-week follow-up, radiographically determined fusion rate was 100 % for the group treated with Healos soaked in bone marrow aspirate, 75 % for the autograft group, and only 18 % for the group injected with Healos alone. Indeed, bioceramics are neither osteogenic nor osteoinductive and therefore need to be associated with osteogenic agents, such as BMA, to offer a valid alternative to autologous bone graft in spinal arthrodesis [27].

A study conducted on primates investigated the comparison between  $\beta$ -TCP, with or without BMA or autograft in a model of posterolateral arthrodesis. Authors reported an 87 % fusion rate in animals treated with  $\beta$ -TCP and bone marrow progenitor cells and a 67 % rate in the group transplanted with autologous bone graft; no fusion evidence was shown by implantation of  $\beta$ -TCP alone [28].

Several clinical studies support the use of ceramic bioscaffold associated with BMA when used in spinal arthrodesis. Epstein et al. assessed the performance of a porous synthetic scaffold composed of  $\beta$ -TCP (80 %) and bovine type I collagen (20 %) combined with BMA and local bone graft, in order to achieve a one-level or two-level instrumented posterolateral lumbar arthrodesis. At 6 months after surgery, computed tomography (CT) examination showed a solid spinal fusion rate in 96 % and 85 %, respectively [29]. Dai and Jiang, in a randomized prospective study, compared  $\beta$ -TCP coupled with local autograft versus iliac crest autograft in a

single-level instrumented posterolateral lumbar arthrodesis: no differences were noted between the two groups [30]. Neen et al. published a prospective case controlled study to compare the effectiveness of Healos combined with BMA to iliac crest autograft in lumbar arthrodesis. The same posterolateral spinal fusion rate was shown between the two groups, while a significantly lower intersomatic arthrodesis rate was recorded within the group treated with the Healos biocomposite [31].

The variability among achieved fusion rates and eventual outcomes depends upon different factors, such as bioceramic grafts, biological features, and design (including porosity, resorbability, osteophilicity, and biomechanical properties).

However, the most relevant issues regard host environment conditions: exposed bone status, stability of segments involved (both directly related to the technique performed), and individual tissue response determine kinetics of graft incorporation, biocompatibility, and interactions between scaffold and osteoprogenitor cells.

---

## Bone Morphogenetic Proteins

Bone morphogenetic proteins (BMPs) are cytokines that belong to the wide TGF- $\beta$  superfamily and are mainly involved in tissue development, most notably in bone homeostasis. Bone remodeling is a continuous process that persists throughout life and is coordinated by the balance established between bone resorption and bone formation, respectively, achieved through the activity of osteoclasts (OCs) and osteoblasts (OBs). BMPs are essential to regulate bone formation: once released, they induce osteogenesis by recruiting mesenchymal OB precursors, which result from the differentiation of cells residing both in the bone marrow as MSCs and in surrounding capillaries as pericytes. Active OBs synthesize the organic bone matrix, which is completed by the inclusion of inorganic components, thus leading osteogenesis. BMPs have been divided into four subfamilies, considering functions and sequence analogies:

1. BMP-2 and BMP-4
2. BMP-5, BMP-6, BMP-7, BMP-8a, and BMP-8b
3. BMP-9 and BMP-10
4. BMP-3, BMP-3b, BMP-11, BMP-12, BMP-13, BMP-14, BMP-15, and BMP-16

Surprisingly, BMPs in the fourth group do not exhibit osteogenic properties, while they can even antagonize BMP function; otherwise, BMP-2 and BMP-7 have been recognized for their osteoinductive activity [32]. BMPs are primarily secreted by OBs, endothelial cells, and chondrocytes as dimers including a secretion signal peptide at the N-terminus (known as prodomain) and a cystine knot motif at the C-terminus [33]. Once they are cleaved by serine endoproteases residing within the cell, BMPs turn into their active form by dimerization before being released. BMP receptors are serine/threonine kinase complexes located at the cell surface; they are classified as type I receptors (which contain a GS domain, rich in glycine and serine)



and type II receptors [34]. As a BMP ligand binds to a receptor, this latter undergoes hetero-oligomerization, thus initiating the signaling cascade. Additionally, BMP binding can be modulated on multiple levels, e.g., by binding BMP co-receptors, by cross talk to other pathways (both across the membrane and in the cytosol), and by competition with pseudoreceptors [32]. Furthermore, BMP bioavailability is strictly influenced by binding to ECM proteins (mainly collagen and fibrillin): during osteogenesis, these interactions establish BMP gradients, thus guiding the entire process of bone formation. BMP receptor activation leads to phosphorylation of a group of transcription factors (called R-SMAD) that translocate to the nucleus and modulate BMP-responsive gene expression. SMAD signaling can be also altered by interfering with other pathways, most notably those led by inflammation [35]. In addition, it was also observed that bone progenitor cells undergoing prominent mechanical loading show higher SMAD signaling activity and lower expression of BMP antagonists.

Due to their osteoinductive properties, BMPs have been extensively studied, and synthesized recombinant BMP-2 and BMP-7, which were firstly isolated by Urist in 1965 [36], are now available and clinically approved by the FDA. In addition, BMPs can also be extracted and purified from demineralized bone matrix, although in very low amounts (order of nanograms), which are insufficient to drive significant bone formation.

Another preparation that is currently produced, but not approved by the FDA and consequently not available in the United States, is bovine BMP extract (bBMPx). Once bovine bone is harvested, fat and mineralized matrix are removed so that BMPs can be extracted and purified by chromatography. This substrate is rich in growth factors, such as BMPs, TGF- $\beta$ 1, TGF- $\beta$ 2, TGF- $\beta$ 3, FGF-1, and non-collagenous proteins, which may enhance aforementioned factor activity. On the other hand, bBMPx occasionally shows immunogenicity, as well as the presence of contaminants that might lower or inhibit the osteoinductive potential of the preparation itself [5]. As osteoinductive agents, BMPs can be successfully combined with osteoconductive biocomposites, thus leading to bone regeneration. These scaffolds should be characterized by reversible affinity to ECM glycoproteins; structural features such as biomechanical rigidity, porosity, and malleability; and restricted immunogenicity and be completely resorbable being replaced by the bone [9]. Porous hydroxyapatite-based ceramics grafts containing recombinant human BMP-2 (rhBMP-2) have showed significant results in anterior cervical spine interbody fusion, as well as higher stiffness values in flexion, extension, and lateral bending tests, both in goats' and in rhesus monkeys' spine models [37]. Within these grafts, BMPs are often combined with a carrier matrix which resembles ECM environment: assessing BMPs-collagen-binding affinity allows to modulate release kinetics and prevent BMPs from diffusing away, thus retaining the release and concentration over time [24].

Nonetheless, BMPs have shown to counteract the inhibitory effect of systemic nicotine, which downregulates osteoblast activity and decreases bone nourishment through microvasculature impairment [38]. On the other hand, using BMPs often results in serious side effects, such as heterotopic bone formation, pseudarthrosis,

and local inflammation. Moreover, the use of appropriate amount of BMPs to induce osteogenesis results in a very expensive procedure, thus causing unbearable costs [39].

Gene therapy may represent another approach to induce BMP expression. Genes encoding osteogenic and osteoinductive factors can be targeted in order to increase their expression and, as a consequence, synthesis of the corresponding protein.

After the human BMP DNA sequence is linked to the vector genome, the virus is transfected into a mammalian host cell in order to amplify BMP-coding gene expression. The cell line is then expanded and frozen, so it can be thawed upon requirement and cultured in extensive media, from which BMPs can be easily purified [5].

Gene therapy shows many advantages, such as cost-effectiveness, no need for autologous cell culture, and simple techniques to evaluate transduction which can be, however, arduously assessed *in vivo* [3]. Gene therapy has shown promising results in *in vivo* models of spinal fusion: Alden et al. injected BMP-2 gene into the paraspinal region of rats and reported endochondral bone growth at 12 weeks after injection [40]. In addition, autologous target cells (most often MSCs) can be harvested, expanded, transduced, and then implanted back into the patient using an *ex vivo* approach.

---

## Platelet-Rich Plasma

Platelets are an optimal source of autologous growth factors, such as transforming growth factor- $\beta$ 1 (TGF- $\beta$ 1), insulin-like growth factor-1 (IGF-1), vascular endothelial growth factor (VEGF), and platelet-derived growth factor (PDGF), which all reside within  $\alpha$ -granules. Once released upon platelet activation by  $\text{Ca}^{2+}$  and thrombin, these cytokines induce chemotaxis, mitosis, anabolic activity, and differentiation of osteoprogenitor cells, thus driving bone regeneration, acting as osteoinductive agents, and favoring spinal fusion [4].

Platelet concentrates are products enriched in platelets that can be derived from platelet-rich plasma (PRP), which is obtained just before or during surgery. Peripheral venous blood is taken from the patient and then centrifuged in order to concentrate platelets from whole blood and then form a buffy coat that is suspended in plasma [41]. Variable amounts of thrombin and/or calcium/chloride are added to achieve a gel-like consistency. The effect of platelet concentrates has been assessed *in vitro* on human MSCs and on cultures of bone cells derived from the trabecular ends of human fetal long bones. PRP has shown to favor chemotaxis of MSCs toward the site of inoculation in a dose-dependent manner; furthermore, stem cell mitosis increased leading to a significant increment in the synthesis of organic bone matrix [42].

Apart from enhancing bone-healing environment by the presence of concentrated growth factors, PRP induces the formation of a fibrin clot capable of both improving grafts handling characteristics and providing a fully biocompatible scaffold for bone repair.

In vivo studies have reported promising results in animal models: Walsh et al. analyzed the effect of PRP using a resorbable hydroxyapatite calcium carbonate bone graft substitute or autograft in a sheep model of posterolateral lumbar spinal fusion. A plasma concentrate termed autologous growth factor (AGF) loaded in autograft resulted in showing the best outcomes and spinal fusion rate among all the combinations [43]. Siebrecht et al. studied PRP osteoinductive properties examining a subcutaneous bone chamber in a rat model; plasma concentrate was loaded into a porous coralline hydroxyapatite graft and demonstrated significant increase in bone ingrowth compared to other models [44].

However, discrepant results in other studies on human models make the osteoinductive properties of PRP difficult to be evaluated. A retrospective study from Carreon et al. evaluated the effect of adding PRP to autograft in order to obtain a solid multiple-level spinal fusion. After a 2-year follow-up, it was shown that pseudarthrosis occurred in 25 % of the group treated with PRP and only in 17 % of the group treated with the sole autograft. Therefore, authors concluded that PRP did not improve autograft osteoinductive properties [45]. In a similar study, Weiner and Walker assessed posterolateral fusion rate using iliac crest bone grafts with or without adding PRP: arthrodesis percentages were 91 % and 62 %, respectively [46]. Castro et al. obtained comparable results evaluating intersomatic arthrodesis fusion rate that turned out to be 19 % lower using PRP [47]. Inconsistency between results in animal and human studies can be attributable to different reasons: diffusion of growth factors away from loading site due to fibrinolysis and consequential resorption of the gel, insufficient concentration of platelets, the presence of growth factors that can inhibit bone formation, and variability in processing methods (e.g., different classification, terminology, platelet counting methods). Further studies should be oriented toward the understanding of the actual role and concentration of growth factors contained in PRP, as well as of the defined concentration needed to lead osteoinduction significantly.

---

## **Bone Marrow Aspirate**

Autologous bone marrow aspirate (BMA) harvested from the iliac crest through percutaneous needle aspiration has been adopted in orthopedic surgery and in spine surgery as an adjuvant during bone transplants; it provides a wide population of growth factors and osteoprogenitor cells. Bone marrow contains two species of stem cells: hematopoietic stem cells (HSCs) and MSCs. The former give rise to all blood cell types, while the latter can differentiate into osteoblasts, chondrocytes, adipocytes, and myocytes; both undergo self-renewal. MSCs represent less than 1 % of the bone marrow cells, while they can be found in higher amounts in adipose tissue. The aspirate can be centrifuged in order to obtain higher MSCs concentrations: through this procedure, which can be performed in the operating room by using a disposable kit, it is possible to gather a 6–10 ml concentrate of MSCs from a 60 ml aspirate sample. This concentrate can be combined with a PRP gel, thus forming a compact preparation that prevents MSCs from diffusing away from the arthrodesis site.

Given that low concentration of osteoprogenitor cells obtainable from bone marrow is a relevant issue that might decrease BMA osteogenic potential, various methods have been developed to overcome this limitation.

MSCs can be harvested from the donor through bone marrow aspiration and expanded *ex vivo*: cells are then isolated and seeded in culture plates whose specific environment favors mitogenesis. As cultured cells reach a significant amount, they can be reimplanted back into the patient.

Another methodology consists in retaining MSCs directly harvested from bone marrow onto implantable grafts. During this process, BMA is flowed through a bone graft matrix which is placed into a concentrator: the graft material is characterized by specific features (e.g., porosity, chemical composition, electrostatic charge) that are selectively designed to achieve osteoprogenitor cell retention. Additional parameters that can be set to further improve the efficiency of this technology regard rheological aspects of the process, such as flow rate of the aspirate through the graft, flow direction, number of flow cycles, and turbulent/steady flow [42]. Since BMA alone lacks structural support, it is often loaded into a scaffold, such as a ceramic [22]. Moreover, the addition of BMA to osteoconductive bioceramic grafts has shown a slightly lower effectiveness compared to autograft in achieving arthrodesis during spine surgery [4]. The effect of autologous bone marrow cell concentrate has been analyzed in promoting spinal fusion in association with a PRP gel on corticocancellous bone allograft, both in cervical and lumbar fusion. In this preliminary study, such combination of MSCs, growth factors, and allograft scaffold was implanted unilaterally during posterolateral lumbar fusion, while allograft alone was introduced in the contralateral side. Radiographic follow-up showed higher bone formation at the side treated with the cells/growth factors/scaffold graft. Indeed, bone marrow cell concentrates, despite minimal cellular manipulations, can effectively enhance osteoinductive scaffolds with osteogenic properties, thus designing a substrate that strictly resembles autograft features.

---

## Vertebral Augmentation

Vertebroplasty represents the percutaneous application of acrylic bone cement, polymethylmethacrylate (PMMA), for the treatment of vertebral body injuries that cause pain due to vertebral compression fractures. The procedure consists of the injection of cement into vertebral defects in order to harden the vertebra increasing its strength and stability and avoiding collapse and pain. It was first pioneered in 1987 by Galibert et al. to treat an aggressive and painful hemangioma which resulted in good pain relief [48]. Since then, it has been extensively used, and several studies have demonstrated the magnificent results obtained through this technique, with an optimal pain management in more than 80 % of patients. To produce PMMA-based cements, the liquid monomer is added to the powder and mixed leading to a polymerization exotherm. Temperature in vertebrae undergoing vertebroplasty has been measured reaching maximum temperature of  $75.8 \pm 1.5$  °C. However, reducing the temperature can reduce the degree of polymerization since it is a chemical

process. Moreover, attention should be paid when PMMA-based cements are injected in the spine since increasing opacifier content is being used in such applications. Indeed, mechanical properties are reduced by the presence of the opacifier, which decrease the tensile and compressive strength. Indeed, maintaining a similar Young's modulus close to that of the bone is fundamental in order to have an optimal load transfer between the cement and the trabeculae. PMMA, representing a stiffer reinforcing material within the vertebra, may lead to stress concentrations on adjacent vertebrae or intervertebral disks. It is also associated to potential late complications. Indeed, cement augmentation reduces fragment motion at the fracture site and produces an exothermic reaction that may hinder bone healing.

Due to the various disadvantages linked to PMMA usage in vertebroplasty, other filler materials such as bioactive cements, which may allow bone healing, have been investigated. Biocements, composed of calcium phosphate, can be injected in liquid form and then harden at body temperature. Being totally reabsorbable and capable of strengthening the bone in the same way as PMMA cements, they represent a suitable alternative. However, their clinical application must still be defined. Different composites have been developed and tested. A bioactive cement made of glass-ceramic-reinforced composite material (Orthocomp, Orthovita, Malvern, PA) is biocompatible and able to better restore bone properties having a lower exotherm than PMMA. Another material to be used in vertebroplasty is an experimental brushite cement (EBC). It is biocompatible and has a shear-thinning behavior, which is favorable for injection.

While being an effective technique for pain relief, vertebroplasty does not enable fracture reduction and is associated with a high rate of cement extrusion. Kyphoplasty responds to these pitfalls. Indeed, it is a procedure, which aims to treat the pain caused by an osteoporotic vertebral fracture by recovering the vertebral body height and the sagittal plane lost. The technique consists of the placement of an inflatable bone tamp into the vertebral body that is inflated at high pressure, restoring vertebral body height and creating a void which can be filled with cement. The results of this procedure are comparable to vertebroplasty in terms of pain relief, with a 50–90 % restoration of vertebral height if patients are threaten within 3 months of injury [49] (Fig. 2).

---

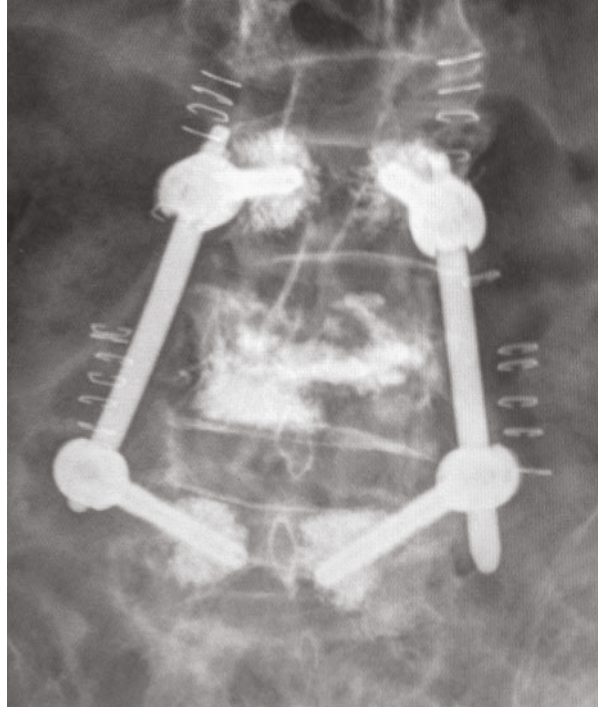
## Summary

A solid arthrodesis in spine surgery can be achieved through different approaches, in order to promote bone neof ormation between two adjacent vertebrae. Even though several efforts and advances have been accomplished in the field of biocomposites and biotechnology, autologous bone graft remains the most advantageous option.

To summarize it is possible to conclude that:

1. Autograft is still considered to be the gold standard in spinal fusion, even though donor-site morbidity persists as a major issue.

**Fig. 2** X-ray image of L3-L5 percutaneous instrumentation with augmented screws using PMMA cement and L4 vertebroplasty for the treatment of an L4 osteoporotic burst fracture



2. Allograft shows satisfactory osteogenic and osteoinductive properties, albeit inferior to autograft bone neoformation capacity and thus is still contemplated as a valid alternative.
3. Bioceramics allow to achieve spinal fusion in association with acceptable success rates and affordable costs, therefore being an alternative option to autograft.
4. Bone marrow cells and platelet concentrates (PRP) definitely enhance biomaterials with osteogenic and osteoinductive potentials, enriching their effectiveness.
5. BMPs demonstrate notable osteoinductive properties, but high preparation cost is a limiting disadvantage.

Designing an ideal bioscaffold, which may emulate natural structure and functions of autologous human bone, is still an open challenge. New fabrication biotechnologies of hybrid organic/inorganic materials, characterized by controlled architecture coupled with gradual osteoinductive growth factor release, may ideally overcome the limitations of current alternatives.

In this regard, adult stem cells, once expanded *ex vivo* and associated with bioscaffolds, have shown the capacity to generate tissue-engineering constructs that could equal autograft properties. Costs and safety issues surrounding these new strategies should be meticulously considered, as autologous bone graft is, to date, the most indicated alternative to obtain a complete and solid arthrodesis.

## References

1. Albrektsson T, Johansson C (2001) Osteoinduction, osteoconduction and osseointegration. *Eur Spine J* 10:S96–S101
2. Reid JJ, Johnson JS, Wang JC (2011) Challenges to bone formation in spinal fusion. *J Biomech* 44:213–220
3. Gupta A, Kukkar N, Sharif K, Main BJ, Albers CE, El-Amin Iii SF (2015) Bone graft substitutes for spine fusion: a brief review. *World J Orthop* 6:449–456
4. Vadala G, Papapietro N, Di Martino A, Denaro V (2011) Bioscaffold and biotechnologies in spine surgery. *GIOT* 37:S191–S198
5. Lupporelli S et al (2004) Advances in technology and spinal fusion: a clinician's perspective. In: Lewandrowski K-U, Wise DL, Trantolo DJ, Yaszemski MJ, White AA III (eds) *Advances in spinal fusion: molecular science, biomechanics and clinical management*. Marcel Dekker, New York, pp 497–530
6. Sherwood P et al (2004) The morbidity of autogenous bone graft donation. In: Lewandrowski K-U, Wise DL, Trantolo DJ, Yaszemski MJ, White AA III (eds) *Advances in spinal fusion: molecular science, biomechanics and clinical management*. Marcel Dekker, New York, pp 665–679
7. Chau AM, Mobbs RJ (2009) Bone graft substitutes in anterior cervical discectomy and fusion. *Eur Spine J* 18:449–464. doi:10.1007/s00586-008-0878-4
8. Sengupta DK, Truumees E, Patel CK, Kazmierczak C, Hughes B, Elders G, Herkowitz HN (2006) Outcome of local bone versus autogenous iliac crest bone graft in the instrumented posterolateral fusion of the lumbar spine. *Spine* 31:985–991
9. Berven S, Tay BK, Kleinstueck FS, Bradford DS (2001) Clinical applications of bone graft substitutes in spine surgery: consideration of mineralized and demineralized preparations and growth factor supplementation. *Eur Spine J* 10:S169–S177. doi:10.1007/s005860100270
10. Buttermann GR, Glazer PA, Bradford DS (1996) The use of bone allografts in the spine. *Clin Orthop Relat Res* 324:74–85
11. Jagannathan J, Shaffrey CI, Oskouian RJ, Dumont AS, Herrold C, Sansur CA, Jane JA (2008) Radiographic and clinical outcomes following single-level anterior cervical discectomy and allograft fusion without plate placement or cervical collar. *J Neurosurg Spine* 8:420–428. doi:10.3171/SPI/2008/8/5/420
12. Floyd T, Ohnmeiss D (2000) A meta-analysis of autograft versus allograft. *Eur Spine J* 9:398–403. doi:10.1007/s005860000160
13. Zdeblick TA, Ducker TB (1991) The use of freeze-dried allograft bone for anterior cervical fusions. *Spine* 16:726–729. doi:10.1097/00007632-199107000-00006
14. Bishop RC, Moore KA, Hadley MN (1996) Anterior cervical interbody fusion using autogeneic and allogeneic bone graft substrate: a prospective comparative analysis. *J Neurosurg Spine* 85:206–210
15. Schlosser MJ, Schwarz JP, Awad JN, Antezana DF, Poetscher AW, Yingling J, Long DM, Davis RF (2006) Anterior cervical discectomy and fusion with allograft and anterior plating: a report on 219 patients/469 levels with a minimum of 2-year follow-up. *Neurosurg Q* 16:183–186. doi:10.1097/01.wnq.0000214028.77731.f2
16. Yue WM, Brodner W, Highland TR (2005) Long-term results after anterior cervical discectomy and fusion with allograft and plating: a 5- to 11-year radiologic and clinical follow-up study. *Spine* 30:2138–2144. doi:10.1097/01.brs.0000180479.63092.17
17. Deutsch H, Haid R, Rodts G Jr, Mummaneni PV (2007) The decision-making process: allograft versus autograft. *Neurosurgery* 60:S98–S102. doi:10.1227/01.NEU.0000249221.50085.AD
18. Suchomel P, Barsa P, Buchvald P, Svobodnik A, Vanickova E (2004) Autologous versus allogenic bone grafts in instrumented anterior cervical discectomy and fusion: a prospective study with respect to bone union pattern. *Eur Spine J* 13:510–515. doi:10.1007/s00586-003-0667-z

19. Bauermeister A, Maatz R (1957) A method of bone maceration. Results of animal experiments. *J Bone Joint Surg Am* 39:153–166
20. Savolainen S, Usenius JP, Hernesniemi J (1994) Iliac crest versus artificial bone grafts in 250 cervical fusions. *Acta Neurochir (Wien)* 129:54–57. doi:10.1007/BF01400873
21. Finkemeier CG (2002) Bone-grafting and bone-graft substitutes. *J Bone Joint Surg Am* 84-A:454–464
22. Hsu WK, Nickoli MS, Wang JC, Lieberman JR, An HS, Yoon ST, Youssef JA, Brodke DS, McCullough CM (2012) Improving the clinical evidence of bone graft substitute technology in lumbar spine surgery. *Global Spine J* 2:239–248
23. Cammisa FP Jr, Lowery G, Garfin SR, Geisler FH, Klara PM, McGuire RA, Sassard WR, Stubbs H, Block JE (2004) Two-year fusion rate equivalency between Grafton DBM gel and autograft in posterolateral spine fusion: a prospective controlled trial employing a side-by-side comparison in the same patient. *Spine* 29:660–666. doi:10.1097/01.BRS.0000116588.17129.B9
24. Miyazaki M, Tsumura H, Wang JC, Alanay A (2009) An update on bone substitutes for spinal fusion. *Eur Spine J* 18:783–799. doi:10.1007/s00586-009-0924-x
25. Cama G (2014) Calcium phosphate cements for bone regeneration. In: Dubruel P, Van Vlierberghe S (eds) *Biomaterials for bone regeneration novel techniques and applications*. Woodhead/Elsevier, Cambridge, UK
26. Korkusuz P, Korkusuz F (2004) Hard tissue-biomaterial interactions. In: Yaszemski MJ, Trantolo DJ, Lewandrowski K-U, Hasirci V, Altobelli DE, Wise DL (eds) *Biomaterials in orthopedics*. Marcel Dekker, New York
27. Tay BK, Le AX, Heilman M, Lotz J, Bradford DS (1998) Use of a collagen-hydroxyapatite matrix in spinal fusion. A rabbit model. *Spine* 23:2276–2281
28. Orii H, Sotome S, Chen J, Wang J, Shinomiya K (2005) Beta-tricalcium phosphate (beta-TCP) graft combined with bone marrow stromal cells (MSCs) for posterolateral spine fusion. *J Med Dent Sci* 52:51–57
29. Epstein NE (2006) A preliminary study of the efficacy of beta tricalcium phosphate as a bone expander for instrumented posterolateral lumbar fusions. *J Spinal Disord Tech* 19:424–429
30. Dai LY, Jiang LS (2008) Single-level instrumented posterolateral fusion of lumbar spine with beta-tricalcium phosphate versus autograft: a prospective, randomized study with 3-year follow-up. *Spine* 33:1299–1304
31. Neen D, Noyes D, Shaw M, Gwilym S, Fairlie N, Birch N (2006) Healos and bone marrow aspirate used for lumbar spine fusion: a case controlled study comparing healos with autograft. *Spine* 31:E636–E640
32. Sánchez-Duffhues G, Hiepen C, Knaus P, Ten Dijke P (2015) Bone morphogenetic protein signaling in bone homeostasis. *Bone*. doi:10.1016/j.bone.2015.05.025
33. Mueller TD, Nickel J (2012) Promiscuity and specificity in BMP receptor activation. *FEBS Lett* 586:1846–1859
34. Wrana JL, Tran H, Attisano L, Arora K, Childs SR, Massagué J, O'Connor MB (1994) Two distinct transmembrane serine/threonine kinases from *Drosophila melanogaster* form an activin receptor complex. *Mol Cell Biol* 14:944–950
35. Guo X, Wang XF (2009) Signaling cross-talk between TGF- $\beta$ /BMP and other pathways. *Cell Res* 19:71–88
36. Urist MR (1965) Bone: formation by autoinduction. *Science* 150:893–899
37. Spivak JM, Hasharoni A (2001) Use of hydroxyapatite in spine surgery. *Eur Spine J* 10: S197–S204. doi:10.1007/s005860100286
38. Claytor B, Theiss S (2004) Overcoming chemical inhibition of spine fusion. In: Lewandrowski K-U, Wise DL, Trantolo DJ, Yaszemski MJ, White AA III (eds) *Advances in spinal fusion: molecular science, biomechanics and clinical management*. Marcel Dekker, New York, pp 90–97
39. Vadalà G, Di Martino A, Tirindelli MC, Denaro L, Denaro V (2008) Use of autologous bone marrow cells concentrate enriched with platelet-rich fibrin on corticocancellous bone allograft for posterolateral multilevel cervical fusion. *J Tissue Eng Regen Med* 2:515–520



40. Alden TD, Pittman DD, Beres EJ, Hankins GR, Kallmes DF, Wisotsky BM, Kerns KM, Helm GA (1999) Percutaneous spinal fusion using bone morphogenetic protein-2 gene therapy. *J Neurosurg* 90:109–114. doi:10.3171/spi.1999.90.1.0109
41. Tarantino R, Donnarumma P, Mancarella C, Rullo M, Ferrazza G, Barrella G, Martini S, Delfini R (2004) Posterolateral arthrodesis in lumbar spine surgery using autologous platelet-rich plasma and cancellous bone substitute: an osteoinductive and osteoconductive effect. *Global Spine J* 4:137–142
42. Kapur TA, Kadiyala S, Urbahns DJ, Bruder SP (2004) Autologous growth factors and progenitor cells as effective components in bone grafting products for spine. In: Lewandrowski K-U, Wise DL, Trantolo DJ, Yaszemski MJ, White AA III (eds) *Advances in spinal fusion: molecular science, biomechanics and clinical management*. Marcel Dekker, New York, pp 375–389
43. Walsh WR, Loeffler A, Nicklin S, Arm D, Stanford RE, Yu Y, Harris R, Gillies RM (2004) Spinal fusion using an autologous growth factor gel and a porous resorbable ceramic. *Eur Spine J* 13:359–366
44. Siebrecht MA, De Rooij PP, Arm DM, Olsson ML, Aspenberg P (2002) Platelet concentrates increases bone ingrowth into porous hydroxyapatite. *Orthopedics* 25:169–172
45. Carreon LY, Glassman SD, Anekstein Y, Puno RM (2005) Platelet gel (AGF) fails to increase fusion rates in instrumented posterolateral fusions. *Spine* 30:E243–E247
46. Weiner BK, Patel NM, Walker MA (2007) Outcomes of decompression for lumbar spinal canal stenosis based upon preoperative radiographic severity. *J Orthop Surg Res* 2:3
47. Castro FP Jr (2004) Role of activated growth factors in lumbar spinal fusions. *J Spinal Disord Tech* 17:380–384
48. Galibert P (1987) Preliminary note on the treatment of vertebral angioma by percutaneous acrylic verte- broplasty. *Neurochirurgie* 33:166–168
49. Lieberman IH, Dudeney S, Reinhardt M (2001) Initial outcome and efficacy of kyphoplasty in the treatment of painful osteoporotic vertebral compression fractures. *Spine* 26:1631–1638

---

## Part V

# Clinical Performance in Bioresorbable and Load-Bearing Applications: Dentistry

Lia Rimondini, Andrea Cochis, Elena Varoni, Barbara Azzimonti,  
and Antonio Carrassi

## Contents

Introduction .....	992
Innovative Methods for Oral Microbiome Analyses .....	995
The Normal Oral Microbiome .....	998
The Oral Microbiome in Oral Diseases: A Focus on Implant and Prosthetic Dental Materials .....	1002
Definition, Structure, and Composition of the Biofilm .....	1006
Biofilm Metabolism .....	1007
Biofilm-Related Medical Device Infections .....	1008
Biofilm Formation and Propagation .....	1008
Biofilm/Substratum/Environment Interaction .....	1011
The Substrate Effect: Surface Energy and Hydrophilic/Hydrophobic Properties .....	1012
The Environment Effect .....	1013
The Effect of Surface Roughness at Micro- and Nanoscales .....	1015
The Effect of Protein Absorption .....	1016
Biofilm Formation on Dental Implants and Prosthetic Dental Materials .....	1017
Biofilm Formation on Dental Implants .....	1017
Biofilm Formation on Restorative and Prosthetic Materials .....	1019

---

L. Rimondini (✉) • B. Azzimonti

Dipartimento di Scienze della Salute, Università del Piemonte Orientale, Novara, Italy

e-mail: [lia.rimondini@uniupo.it](mailto:lia.rimondini@uniupo.it); [barbara.azzimonti@uniupo.it](mailto:barbara.azzimonti@uniupo.it)

A. Cochis

Dipartimento di Scienze della Salute, Università del Piemonte Orientale, Novara, Italy

Dipartimento di Scienze Biomediche, Chirurgiche ed Odontoiatriche, Università degli Studi di  
Milano, Milan, Italy

e-mail: [andrea.cochis@uniupo.it](mailto:andrea.cochis@uniupo.it)

E. Varoni • A. Carrassi

Dipartimento di Scienze Biomediche, Chirurgiche ed Odontoiatriche, Università degli Studi di  
Milano, Milan, Italy

e-mail: [elena.varoni@unimi.it](mailto:elena.varoni@unimi.it); [antonio.carrassi@unimi.it](mailto:antonio.carrassi@unimi.it)

---

The Role of Chemistry in Dental Biofilm Limitation .....	1020
Current Strategies .....	1020
Further Strategies .....	1023
Summary .....	1024
References .....	1024

---

**Abstract**

The human body is subdivided into niches containing a wide variety of commensal microorganisms with essential functions for the host's health. When the balance of the resident microflora changes, pathological conditions may occur. Based on this premise, this chapter first describes the composition of one of these niches, the oral cavity: its oral microbiome and the most frequent biofilm-related medical device infections promoted by multidrug-resistant strains, the so-called super bacteria or super bugs. In this context, the discussion focuses on the key events that unbalance the microbiome homeostasis and induce commensal bacteria to biofilm formation and describes how metabolites can influence the prevalence of bacterial species within the microbial community, thus promoting the onset of infectious diseases. As implantable devices are increasingly being used in dentistry, as in other medical fields, there is a pressing need for control strategies, able to counteract the events involved in biofilm formation, especially the adhesion phase, in order to reduce the occurrence of infection-associated implant failures. In this connection, the second part of this chapter briefly examines currently available strategies and the role of chemistry in biofilm prevention: the development of materials with intrinsic antibacterial properties, bioactive coatings with bactericide agents or materials delivering antibiotics, and nanostructured anti-adhesion surfaces or anti-biofilm bioactive molecules. Emerging and future approaches to fight biomaterial-associated infections are still to be clarified.

---

**Keywords**

Dental materials • Dental plaque • Oral biofilm • Oral diseases • Oral implants • Oral microbiome

---

**Introduction**

The human body contains numerous different tissues and cell types, as well as a huge variety of different microorganisms. The commensal human microbiome is now estimated to outnumber human cells ( $\sim 10^{13}$ ) about tenfold ( $\sim 10^{14}$ ); they include viruses, protozoa, fungi, archaea, and bacteria. Members of this complex microbial community are normal residents of the skin, the oral cavity, and the vaginal and intestinal mucosa and exercise a broad range of functions indispensable for the host's well-being; these include providing energy for our metabolism, making essential vitamins, and acting as first-line defense against potential pathogens. In only a few

cases are they harmful and a potential source of disease; this occurs when, for any reason, the balance between microbiota and host is lost: weakened host defense mechanism, increased bacterial proliferation, and prevalence of some species over others.

The oral cavity is a very interesting example of the interaction between the human body and commensal microbiome; the latter has now been studied minutely, and phylogenetic data on all oral bacteria have been collected into a huge database, known as the human oral microbiome database (HOMD). As an example, studies on the salivary microbiome report that this biological fluid can hold about  $10^8$  colony-forming units (CFU)/ml of bacteria, an enormous number of microorganisms. The oral cavity appears to possess one of the most complex microbiomes of the organism, second only to the colon, and of the various biological niches, such as the gastroenteric tract or the skin; it has the largest core of commonly shared microorganisms among unrelated individuals. The HOMD is thus a comprehensive repository of oral bacteria taxa, obtained using 16 rRNA identification tools, and of oral bacterial genome sequences, and it may also play a pivotal role in understanding oral health and diseases.

Moreover, intriguingly and unlike other sites of the human body, an imbalance between host and normal oral microbiome underlies the development of most oral diseases, including caries, prosthetic stomatitis, periodontal disease, peri-implant mucositis, and peri-implantitis. However, this microbiome-related etiopathogenesis does not correlate with the concept of “infection”: it distinctively indicates an impaired balance among commensal microbiota, host susceptibility, and environmental factors, such as dietary and smoking habits. Among others, one crucial element that can contribute in disturbing this equilibrium is the presence of dental biomaterials within the oral cavity. Microorganisms, adhering to and proliferating on these “exogenous” substrates, show a range of capacities to form their peculiar biofilm structure, known as “dental plaque.” Particularly in the presence of dental biomaterials, such as titanium implants, or the ceramics, composites, and metals used in restorative and prosthetic dentistry, dental plaque can acquire a distinctive composition, producing local inflammation and promoting the in situ adhesion of cariogenic, periodontal, and peri-implant pathogens. Nonetheless, evidence shows that the oral biofilm forming on the resin surfaces of removable dentures chiefly comprises fungal species, such as *Candida albicans*, which can produce mucosal inflammation under the prosthetic resin base, for the most part on the palate; this condition is called prosthetic stomatitis and is one of the most common diseases of the elderly.

Mechanical oral hygiene comprises tooth brushing, with the adjunctive use of toothpaste and, in selected cases, of antiseptic mouthwashes, is able to remove dental biofilm and maintain a healthy dental status. Disruption of the biofilm is pivotal for preserving the correct balance of the oral microbiome, which, in turn, is directly related to oral health. Oral hygiene procedures enable local plaque accumulation to be controlled and successfully counteract the preponderance of one or more pathogen species over the others. In particular, they limit both their overgrowth and the increase of sugars on dental surfaces, which are their major sources of energy.

**Table 1** Genera and species of bacteria frequently found in the oral cavity

Genus	Species	Genus	Species
<i>Actinomyces</i>	<i>israelii</i>	<i>Haemophilus</i>	<i>influenzae</i>
<i>Aggregatibacter</i>	<i>naeslundii</i>	<i>Lactobacillus</i>	<i>haemolyticus</i>
<i>Arachnia</i>	<i>viscosus</i>	<i>Leptotrichia</i>	<i>acidophilus</i>
<i>Bacteroides</i>	<i>odontolyticus</i>	<i>Neisseria</i>	<i>casei</i>
<i>Campylobacter</i>	<i>actinomycetemcomitans</i>	<i>Rothia</i>	<i>salivarium</i>
<i>Capnocytophaga</i>	<i>propionica</i>	<i>Selenomonas</i>	<i>buccalis</i>
<i>Clostridium</i>	<i>gingivalis</i>	<i>Staphylococcus</i>	<i>dentium</i>
<i>Eikenella</i>	<i>intermedius</i>	<i>Streptococcus</i>	<i>pharyngis</i>
<i>Fusobacterium</i>	<i>melaninogenicus</i>	<i>Treponema</i>	<i>catarrhalis</i>
	<i>loescheii</i>	<i>Veillonella</i>	<i>meningitidis</i>
	<i>denticola</i>	<i>Wolinella</i>	<i>dentocariosa</i>
	<i>sputorum</i>		<i>sputigena</i>
	<i>ochracea</i>		<i>aureus</i>
	<i>sputigena</i>		<i>epidermidis</i>
	<i>gingivalis</i>		<i>mutans</i>
	<i>tetani</i>		<i>sanguinis</i>
	<i>botulinum</i>		<i>salivarius</i>
	<i>corrodens</i>		<i>mitis</i>
	<i>nucleatum</i>		<i>denticola</i>
	<i>polymorphum</i>		<i>oralis</i>
			<i>vincentii</i>
			<i>parvula</i>
			<i>recta</i>

For these reasons, a full understanding of the mechanisms regulating the oral microbiome in health and in disease, as well as its interaction with oral tissues and dental materials, is a key factor in the diagnosis, prevention, and successful treatment of these multifactorial, biofilm-related dental diseases.

The oral cavity has from the early days of microbiology provided an extraordinary opportunity for microbiological investigation. The description of bacteria as “living animalcules” was first given by van Leeuwenhoek (1632–1723), who observed materials taken from his gums, using his primitive microscopes. The microbes sketched in his notebook are graphical representations of some of the most abundant bacteria in the oral cavity, including cocci, fusiform bacteria, and spirochetes. W. D. Miller was the next important scientist to make a significant contribution to our understanding of oral microbiology. In 1890, he published a book entitled *Microorganisms of the Human Mouth* in which he postulated a correlation among dental caries, microorganisms, and fermentable carbohydrates. He hypothesized that the microorganisms found in “dental plaque” were responsible for carbohydrate fermentation, which led to acid production and the dissolution of mineralized dental tissues. “Dental plaque,” the three-dimensional biofilm growing on oral surfaces, is still the term commonly used to identify the oral microbiome. It is now known that dental plaque comprises a multitude of microorganisms, mostly identified (Table 1) by culture-based methods. It is highly probable that even more microbes will be found, since the number of classified species is increasing, more or

less in parallel with the development of new technologies becoming available for their taxonomic classification, as discussed in the following paragraphs.

## **Innovative Methods for Oral Microbiome Analyses**

The innovative methods that have recently been made available by molecular biology include the use of culture-independent methods to identify the composition of the oral microbiome, along with the new molecular techniques for DNA sequencing. The latter have greatly increased the resolution of detection and can be applied both to identify the genetic heterogeneity of bacterial species and to investigate the effect of the environment on each microbial phenotype. Thus, over time, the number of sequences obtained per sample has risen very markedly, with a corresponding significant reduction in both time and economic costs of the determination.

Typically, analyses on microbiota include three main fields: (i) the composition of microorganisms; (ii) the environmental conditions in which the microbial communities grow, basically consisting of host nutritional status, salivary pH variations, and reduction-oxidation potential; and (iii) functions and metabolic activities of the microbiota, in turn pivotal outputs for pathogenesis. Investigations in each of these fields may entail several steps, ranging from genetics to metabolomics, following a closely interconnected biological hierarchy. Briefly, the multistage path from gene to metabolite analyses can be described as follows. The genome comprehends the whole set of genes belonging to the human body, thus the genetic information that explains which gene is used for what function or activity; the same group of genes can then be transcribed to the corresponding ensemble of mRNAs, namely, the transcriptome. Subsequently, the transcriptome is translated into its corresponding set of proteins, known as the proteome, comprising the potential effectors of a specific function. When these concepts are related specifically to the oral microbiome, the groups of expressed genes and proteins produced by the dental plaque are called metatranscriptome and metaproteome, respectively. The final step of this biological hierarchy corresponds in determining the resulting assortment of metabolites, the so-called metabolome, which, in the case of the oral biofilm, intuitively involves the metabolism of the microbial community [1].

*Genetics* – Through the operational taxonomic unit (OTU), the operational definition of a species or group of species can be defined; OTUs identify a specific genus or family and correspond to 16S rRNA gene variable v3–v5 region sequences, clustered at 97 % similarity. Indeed, 16S rRNA genes, via the pyrosequencing of 16S rRNA polymerase chain reaction (PCR), have been used to define the identity or closest relatives of the species in the oral microbiome, in order to obtain a comprehensive description of the oral microbiota. However, the PCR method may lead to some bias: although accurate identification of the taxonomic composition of oral samples is of great importance in terms of scientific knowledge, it only provides scant information about the specific functional activity of each microbial community within the oral cavity.

*Metagenomics* – Moving beyond genetics, metagenomics provides a new tool to understand the genetic information relating to the oral microbiome and ideally to obtain details on the function of each member of this structure. Without the need for traditional culturing and/or PCR techniques, metagenomics consists of the direct analysis of the total DNA content belonging to bacterial communities. This is achieved using the DNA extracted from oral samples and then analyzed by the following two methods:

- (i) *Direct DNA sequencing* of the total DNA belonging to a bacterial community. This group of methods has been widely used to investigate dental plaque from donors. Interestingly, functional assignment via currently available databases indicated the putative function in about half of the sequences. This finding confirms that a large portion of oral bacteria genes remains functionally unknown. A wide interindividual difference among samples has also emerged, and subjects who have never experienced carious lesions during their lives displayed an overexpression of genes encoding antimicrobial peptides and quorum-sensing genes, compared to the oral specimens from subjects having experienced caries. The latter specimens also showed an increased frequency of genes deputized to iron scavenging and oxidative and osmotic stress [1].
- (ii) *DNA cloning methods*, which include a first step of DNA fragmentation, a second stage of fragment cloning into a vector within a “bacterial host,” and a third phase in which the cloning process is repeated, leading to a “metagenomic library” with multiple clones. This library can be defined as the ensemble of all different fragments of DNA coming from the bacterial community under investigation. Metagenomic vectors, which in most cases correspond to the bacteria *Escherichia coli*, are microorganisms able to accommodate large DNA inserts; these artificial bacterial chromosomes possess the advantage of cloning the entire operons and enhancing the probability of detecting their functions. In addition, the possibility of freezing libraries for future experiments makes it possible to further sequence the inserted DNA by traditional methods and to revise the genetic information in consequence. Regarding the oral microbiome, four metagenomic libraries have been produced by the DNA cloning technique and then screened for antibiotic resistance: all libraries contained clones resistant to tetracycline and amoxicillin, while only three of them included clones resistant to gentamicin [1].

*Metatranscriptomics* – Although the above metagenomics approach reveals the total genetic potential of a microbial community, it should be taken into account that the “functionally active” bacterial pool may be modified under the pressure of several environmental conditions. As an example, changes in the salivary flow rate, which varies with the time of day or since the last meal, can significantly influence bacterial activities.

Environmental effects can, at different stages, alter the oral microbiome composition and also biofilm formation. In the light of these alterations, metatranscriptomics aims to determine which microorganisms are active and which genes



are expressed under particular conditions, by analyzing the RNA extracted from the samples. First applied to human gut specimens and in vitro oral biofilm models, metatranscriptomics entails extracting total RNA and then reversely transcribing it to cDNA and sequencing by ad hoc technologies. A recent metatranscriptomics study on oral microbiota showed that each combination of disease plus its associated bacterial community displayed a distinct metabolic profile and that this did not differ among patients [2]. The most important limitation of this approach is the high percentage of rRNA in bacterial samples, which normally accounts for over 90 % of total RNA and can confuse findings.

Metagenomic and metatranscriptomic methods are to a great extent complementary, successfully contributing in investigating the taxonomic composition of oral microorganisms, their functional outputs, and the actively expressed genes.

*Metabolomics* – The term “metabolome” was first used in the 1960s to identify and quantify metabolites in certain biological systems. A Human Metabolome Database is now available. It was initially used to recognize the intermediates of the Embden-Meyerhof-Parnas (EMP) pathway in human red blood cells, after which it was successfully customized and implemented for detecting oral bacteria metabolites, among others *Streptococcus* spp. and *Actinomyces* spp. In the last two decades, metabolomics has rapidly grown on the wave of technological advances in molecular biology and chemical analyses. It has now become a highly reliable tool, able to accurately identify biological molecules. In terms of the instruments employed, capillary electrophoresis (CE) associated to mass spectrometry (CE-MS) has been proposed as one of the most reliable approaches to separate and compute metabolites from the different metabolic pathways, i.e., the central carbon metabolism, the pentose-phosphate pathway, and the tricarboxylic acid (TCA) cycle. The results appear to be reliable even using the very small samples coming from supragingival plaque. Using these techniques, the human metabolome profiles of supragingival plaque have been obtained, before and after a glucose rinse; the changes in these profiles mirrored those occurring individual bacterial strains of *Streptococcus sanguinis*, *Streptococcus mutans*, *Actinomyces oris*, and *Actinomyces naeslundii*. These findings support the recent idea of a unique “bacterial superorganism,” since a microbial community consists of an enormously large number of different bacteria but expresses its functions, from the metabolomics perspective, as one single organism, i.e., the “superorganism” [1].

Considering that the presence of dental plaque is not univocally related to dental diseases, the oral biofilm can be associated to either a healthy or a pathological status and is affected by wide intra- and interindividual variability, mainly due to specific environmental conditions. Metabolome analyses could contribute in investigating the composition of the microbiome, possibly helping to explain the fundamental concept of “dental plaque homeostasis.” The supragingival plaque contains bacteria that utilize endogenous energy sources, mainly from the salivary substrate. Saliva contains a plethora of proteins, glycoproteins, and urea which can, respectively, be degraded by bacterial enzymes to peptides and amino acids, to sugars, or to ammonia and carbon dioxide. Supragingival bacteria thus appear able to produce alkalis as well as acids, ensuring the stability of the supragingival plaque pH. The pH is also

associated to the correct balance between demineralization and remineralization processes at the tooth surface, ensuring the healthy condition of enamel and dentine. When sugars are supplied to the oral cavity, bacterial acid production rapidly decreases the plaque pH; the pH then slowly returns to the original level, mainly through the salivary buffer effect and bacterial alkali production. In the case of carious lesions, acid production exceeds alkali production, leading to tooth decay. In this connection, complete analyses of the metabolic pathways involved in alkali/acid production are likely to add new information about oral microbiome homeostasis during health and disease [1].

*Metaproteomics* – Metaproteomics lies between metagenomics/metatranscriptomics and metabolomics. The application of proteomics to the oral biofilm, generally using differential proteomic analysis such as 2D electrophoresis, may provide pivotal information on the synthesis of proteins and on their posttranslational modifications. The main limitation of this approach is the difficulty of recognizing microbial proteins among the wealth of host proteins: the former are highly variable and cannot be identified univocally. Future research will focus on overcoming this drawback, also considering that preliminary proteomic findings already enable the appropriate protocols for sample treatment and data analysis to be set up successfully.

Taken together, the above *-omics* techniques will contribute in clarifying changes occurring to the oral microbiota during pathogenesis and in response to therapies, acquiring even more importance in the presence of dental biomaterials.

## The Normal Oral Microbiome

The human oral cavity is heavily colonized by a wide range of microorganisms which, including bacteria, fungi, archaea, viruses, and protozoa, form the oral microbiome. Currently, most studies investigating the “normal” microbiome limit their findings to the so-called bacteriome, often generically named “microbiome,” and only a small number of reports specifically refer to the mycobiome (fungal-related microbiota).

Recently, the American organization “National Institute of Health” (NIH) conducted the “Human Microbiome Project” (HMP), one of the most important scientific missions of the twentieth century. The HMP discovered that (i) the oral microbiome is highly defined at the species level, with certain geographical differences, and (ii) it faces daily mechanical and chemical modifications, due to the intake of nutritional substances and personal oral hygiene practices (for instance, the number of tooth brushings or the number of meals during the day). A number of external agents and mechanical forces can change the temperature and pH of the oral cavity and influence the composition of its microbiota; these include the use of antiseptic compounds, diet, smoking, as well as oral hygiene procedures.

Besides viruses, the most frequent and important species detectable within the oral cavity are bacteria, fungi, and mycoplasmas. Briefly, the features of these three classes will be described:

- (i) *Bacteria*. The HMP initially analyzed the bacterial composition of oral microbiome, from 200 subjects of both genders, and identified 185–355 genera, belonging to 13–19 bacterial phyla. Nine intraoral sites were considered: buccal mucosa, hard palate, keratinized gingiva, palatine tonsils, saliva, sub- and supragingival plaque, throat, and tongue dorsum. Although depending upon the specific oral site considered, the high-abundance core genera (defined as genera present at >10 % abundance and at >75 % ubiquity) can be summarized in two groups: *Streptococcus* (OTU, 2, 6) and unclassified *Pasteurellaceae* (OTU, 19, –, 16). Further major core genera (>1 % abundance at >80 % ubiquity) include *Gemella* (OTU, 11), *Veillonella* (OTU, 4), *Prevotella* (OTU, 10), *Fusobacterium* (OTU, 9), *Porphyromonas* (OTU, 7), *Neisseria* (OTU, –, 8), *Capnocytophaga* (OTU, –), *Corynebacterium* (OTU, –, 15), unclassified *Neisseriaceae* (OTU, 21), *Actinomyces* (OTU, 14), and unclassified *Lactobacillales* (OTU, 13) [3]. A single OTU dominated nearly all oral mucosal sites of this large cohort: *Streptococcus* (OTU, 2).

Thus, about half of the total cultivable flora comprises oral streptococci, which can be detected on almost all surfaces of the oral cavity; these are dominated by *S. mutans*, i.e., the pathogen primarily responsible for dental caries. Other Gram-positive cocci, such as enterococci and staphylococci, are usually in less abundance, as are *Actinomyces* and lactobacilli, in turn the most frequently detectable Gram-positive rods. The Gram-negative cocci species *Neisseria*, seldom implicated in dental diseases, are also a common finding, with an abundance equal to that of *Actinomyces* spp. The most frequent Gram-negative oral rods are *Haemophilus* spp. and *Aggregatibacter* spp. Of note, *Aggregatibacter actinomycetemcomitans* has been associated with aggressive forms of periodontal diseases, and the relative abundance in the oral microbiome of healthy subjects appears negligible. Considering other bacteria involved in the pathogenesis of periodontal diseases, i.e., *Porphyromonas* species, *Treponema denticola*, and *Fusobacterium nucleatum*, evidence exists to support their drastic increase in dental plaque when the appropriate mechanical oral hygiene procedures are not performed.

- (ii) *Fungi*. *Candida* is the main fungal component of the oral environment, also being found in healthy people because of its commensal feature, together with further genera, such as *Aspergillus* and *Saccharomyces*, detectable as a minor component. *Candida albicans* is the most commonly isolated yeast species, followed by other clinically relevant “non-*Candida albicans* species,” which include *Candida tropicalis*, *Candida krusei*, and *Candida glabrata*. *Candida* is a usual component of the oral biofilm, and its relative abundance in dental plaque is particularly high in patients with oral candidiasis: as mentioned above, one of the most common clinical pictures is prosthetic stomatitis, occurring in areas beneath the resin base of removable dentures.
- (iii) *Mycoplasmas*. These pleomorphic microorganisms differ from other oral bacteria in that they lack an outer membrane. They have been isolated from the oral cavity, the most typical species being *Mycoplasma pneumoniae*, considered a surface parasite; it may be an etiological factor in infections of the upper respiratory tract, mainly in immune-compromised patients.

*Development of the oral microbiome* – The oral microbiome as it exists today can be seen as the product of microorganisms' long adaptation in cohabiting within the human body. From this fascinating perspective, microorganisms have been tailored to live in human organisms under a mutually beneficial symbiosis between microorganisms and human tissues [3]. This coevolution of the oral microbiome with the human host has resulted in a process known as “colonization resistance”: this term describes the ensemble of host-associated microbial communities, fully equipped with mechanisms enabling them to prevent colonization by and establishment of foreign microbes. Five principal types of interactions among oral bacteria have been identified, namely, competition for nutrients, synergy, antagonism, neutralization of virulence factors, and interference in signaling mechanisms. Bacterial interspecies communication is a cornerstone of colonization resistance, together with a broader inter-kingdom communication, both processes being crucial in oral microbial ecosystem homeostasis. For instance, biofilm formation by *C. albicans* appears to be partially regulated by certain bacteria that produce a range of selective signaling molecules; *C. albicans*'s metabolites are, in turn, compounds known to be able to influence bacterial growth.

The acquisition of a normal, beneficial oral microbiome, including the process of colonization resistance, is an essential step in the growth of newborns. The oral microbiome in infants is closely connected to that of the gastroenteric tract, but after 2 weeks of life, it already differs as the oral cavity is rapidly colonized by bacteria originating from the environment where the newborn lives. Bacterial transfer from the mother, or from other external sources, including other people sharing the same environment, greatly affects dental biofilm morphogenesis.

As recently reviewed by Zaura et al. [3], the key aspects pivotal for the physiological acquisition of a normal microbiota during development are:

- (i) *Vertical transmission of the microbiome* from mother to child starts with delivery, whether vaginal or through Caesarian section, which to a large extent determines which microorganisms initially colonize the infant's oral cavity (vagina- or skin-derived). Infants born by Caesarian section acquire *Streptococcus mutans* earlier than vaginally born infants, while vaginal birth enables newborns to acquire a greater bacterial taxonomic diversity by the third month of life. Similarly, breast-feeding versus infant formula feeding appears to influence acquisition of the oral microbiome; breastfeeding gives the infant “beneficial” oral lactobacilli that are not detectable in formula-fed infants.
- (ii) *Preservation of the oral microbiome*, after acquisition during the first stage of life, involves bidirectional interactions between the microbiome and the host; thus, the human immune system develops in a continuing dialogue with the commensal populations of microbiota. This communication exploits the following three main ways: the first includes the host pattern recognition receptors (PRRs), especially the toll-like receptor (TLR) family, expressed by oral mucosa cells, i.e., keratinocytes, macrophages, mucosal dendritic cells (DCs, which belong to the Langerhans cell subtype), polymorphonuclear leukocytes, and natural killer cells. Altered expression patterns of TLRs have been found in

several dental and oral diseases, suggesting their specific role in pathogenesis, while it has been suggested that mucosal DCs are peculiar intermediaries able to avoid infectivity of the oral cavity by commensal microbiota. A second tool to stimulate antigenic tolerance, and thus avoid the risk of local infectious disease, is the expression of lipopolysaccharide (LPS) receptors CD14, TLR2, and TLR4 by DCs, at the level of the non-inflamed oral epithelium. Finally, chemical sensing is the third pivotal tool that the host can exploit to monitor microbial activity. In recent decades, studies have suggested there may be a direct link between secreted bacterial products and chemosensory activation mechanisms for mucosal clearance.

The fundamental role of the immune system in preserving oral health becomes increasingly evident when examining the impaired situation due to the patient's pathological status; typical examples are those of patients receiving hematopoietic stem cell transplant and who require immunosuppressive therapy or of patients affected by head and neck carcinoma and treated with local radiotherapy. One of the most severe and painful adverse effects is the mucosal damage known as "severe mucositis," which is potentially associated to life-threatening viral and fungal supra-infections.

- (iii) *The secretory immunoglobulin A (S-IgA)*, usually delivered via the saliva and gingival crevicular fluid, limits and controls microbial adhesion and colonization. Conversely, bacterial ability to evade S-IgA guarantees their survival within the oral cavity, again highlighting their ongoing symbiotic coevolution with the human body host. S-IgA elusion is mainly achieved through bacterial IgA proteases, which neutralize the immunoglobulin. These proteases are known virulence factors of several human pathogens, such as *Neisseria meningitidis* and *Streptococcus pneumoniae*, and of other commensal streptococci (*Streptococcus mitis*, *Streptococcus oralis*, and *Streptococcus sanguinis*). The latter have been defined as "primary colonizers" and are also the foremost species in infants.
- (iv) *Salivary flow rate and saliva composition* also play key roles in maintaining the healthy oral microbiome. Focusing on protein composition of the saliva, microbial homeostasis is strongly affected by the presence of salivary glycoproteins, because they contain glycans that may act as traps to prevent pathogens from adhering to epithelial cells. Other salivary proteins that influence the oral microbiome include lysozyme, peroxidase, mucins, lactoferrin, defensins, and agglutinins.

*The oral cavity as a biological niche* – From the topographical standpoint, two main subniches are described in the oral cavity: the supragingival niche and the subgingival niche. The supragingival niche includes the teeth or implants and the mucosal tissue outside the gingival sulcus. The plaque recovered from this area in healthy subjects generally comprises aerobic Gram-positive bacteria, mostly *Streptococcus* spp. (*Streptococcus sanguinis*, *Streptococcus mutans*, *Streptococcus mitis*, *Streptococcus salivarius*) and lactobacilli. In contrast, the subgingival niche (i.e., the gingival sulcus) is characterized by the presence of some Gram-negative microaerophilic bacteria, in addition to Gram-positive and aerobic species. Many

**Table 2** Bacterial species recoverable subgingivally in healthy subjects

Gram-positive	Morphotypes	Gram-negative	Morphotypes
<i>Actinomyces</i>	Rod	<i>Bacteroides</i>	Rod
<i>Clostridium</i>	Rod	<i>Fusobacterium</i>	Rod
<i>Lactobacillus</i>	Rod	<i>Neisseria</i>	Coccus
<i>Staphylococcus</i>	Coccus	<i>Prevotella</i>	Rod
<i>Streptococcus</i>	Coccus	<i>Treponema</i>	Motile rod
		<i>Veillonella</i>	Coccus
		<i>Wolinella</i>	Rod
		<i>Eikenella</i>	Coccus
		<i>Aggregatibacter</i>	Coccus
		<i>Porphyromonas</i>	Rod/coccus
		<i>Tannerella</i>	Rod
		<i>Campylobacter</i>	Long rod
		<i>Capnocytophaga</i>	Rod

of these are rods, with some motile bacteria and facultative intracellular bacteria (e.g., *Porphyromonas gingivalis*) [4].

Table 2 lists the most frequent genera and species recoverable from the sulci of healthy subjects.

These microorganisms are natural commensals of the oral cavity, where they are found either in their planktonic form or within structured and complex 3D biofilm communities. The formation of the biofilm community is a key factor in the transition of bacteria from commensals to putative pathogens. When bacteria grow in the biofilm, they may accumulate high concentrations of bacterial metabolites (e.g., fatty acid end products, ammonia, hydrogen peroxide, oxidants, and carbon dioxide) in their local environment, which influence the prevalence of species both within the microbial community and in the host. For instance, as already mentioned, carious lesions are closely related to certain biofilm-forming bacteria, mainly *Streptococcus mutans*, which is able to adhere to the teeth, proliferate, and produce lactic acid, which in turn can dissolve the mineralized components of enamel and dentine. In the presence of sugar, *S. mutans* overwhelms the other non-acid-producing *Streptococcus* spp. that make up the supragingival plaque. *Actinomyces* spp. are among the dominant taxa in both the supra- and the subgingival plaque, from both healthy subjects and periodontitis patients. *Porphyromonas gingivalis*, *Bacteroides forsythus*, and *Treponema denticola* have been detected in supragingival and subgingival plaque samples of both healthy subjects and individuals affected by periodontitis, although they are significantly more prevalent in both supra- and subgingival plaque samples from the latter.

## The Oral Microbiome in Oral Diseases: A Focus on Implant and Prosthetic Dental Materials

In the light of the concepts described above, biological properties that confer stability to the microbiome are important for the prevention of disease-related

“dysbiosis,” producing the microbial shift toward periodontitis or carious lesions. Although the processes underlying the healthy equilibrium of a normal microbiome remain poorly understood, the mechanisms that underlie oral diseases have been investigated in depth; in particular, research has focused on oral microbiome changes that occur on the surface of implants and prosthetic dental materials. In addition, the surface adhesion of microbes, such as bacteria and fungi, and the subsequent formation of biofilms contribute to multidrug-resistant infections in humans and, consequently, to the failure of medical devices.

*Peri-implant microbiome* – Having been the object of numerous high-quality studies, osseointegrated dental implants are today a therapeutically successful option in prosthetic dentistry, for the rehabilitation of complete, partial, and single edentulism. Oral implantology is based on technologically advanced devices, highly customized to replace missing teeth, satisfying both functional and esthetic requirements.

Implant rehabilitation may be considered one of the foremost discoveries of the twentieth century; however, from the oral microbiome perspective, dental implants also represent new artificial surfaces within the oral cavity, which appear more prone than natural tooth surfaces to form bacterial biofilms. Dental plaque, similar to what occurs on natural teeth, can easily accumulate. Biofilm formation on the implant surface is a trigger factor for the further inflammatory process of peri-implant tissues, namely, peri-implant mucositis (when the inflammation only involves the peri-implant mucosa) or peri-implantitis (when the inflammation progresses toward the surrounding alveolar bone).

The oral microbiome in peri-implant infections has been studied by conventional, molecular, and metagenomic analyses. Using the 16S rRNA-based PCR detection method on crevicular fluid samples, the biofilm adhering to abutments showed the presence of both *A. actinomycetemcomitans* and *P. gingivalis* [5]. Moreover, the oral microbiota growing on dental and implant surfaces has recently been investigated in partially edentulous patients, in a large, 10-year retrospective clinical trial, on 504 implants and 493 adjacent teeth [6]. The microbiota analyses of dental plaque specimens, collected after the placement of sandblasted and acid-etched implants, revealed the presence of some bacterial species associated with periodontitis, such as aerobic Gram-negative rods and staphylococci, although abundances were very wide ranging (from 6.2 % to 78.4 % of implants). The study authors reported a higher abundance of *Tannerella forsythia*, *Parvimonas micra*, *Fusobacterium nucleatum/necrophorum*, and *Campylobacter rectus* at implant sites than on dental surfaces. Based on these data, the prevalence of *Prevotella intermedia*, *Treponema denticola*, *Campylobacter rectus*, and *Staphylococcus warneri* has been suggested to be associated with peri-implantitis. In addition, comparing smokers versus nonsmokers, the latter showed higher counts of periodontopathogenic species; similar to the comparison between periodontal versus non-periodontal patients. These latter findings again support the role of the two major risk factors, i.e., smoking and periodontal disease, in the pathogenesis of peri-implant inflammation.

Considering the composition of the oral microbiome, although some evidence suggests that the miscellaneous microbial flora of peri-implant infections may bear a

resemblance to that of periodontal infections, some recent studies suggest there may be certain differences. It is likely that future breakthroughs will occur with the increasing application of metagenomics and metatranscriptomics. These innovative technologies have recently been applied to evaluate the microbiota associated with osseointegrated implants and to investigate peri-implant disease pathogenesis. The current state of the art was reviewed by Charalampakis and colleagues, who analyzed the existing knowledge on peri-implant microbiology and the diversity of the microbial communities associated with peri-implantitis [7].

The peri-implant microbiome in healthy individuals includes a preponderance of Gram-positive cocci and nonmotile bacilli, with a small number Gram-negative anaerobic species, similar to what occurs in the normal gingival tissue. The switch to the first step of inflammation around implants, i.e., peri-implant mucositis, correlates with the increased presence of cocci, motile bacilli, and spirochetes, to an extent equivalent to that of gingivitis. Conversely, the further shift to peri-implantitis is mainly related to the appearance of Gram-negative, motile, and anaerobic species, which are frequently detected in periodontitis. Through molecular biology, *A. actinomycetemcomitans*, *Porphyromonas gingivalis*, *Prevotella intermedia*, and several *Fusobacterium* spp. have been detected in dental implant plaque specimens.

It has been suggested that, in general, the bacterial profile of peri-implantitis derives from periodontitis, since most peri-implant lesions shares common features with periodontal disease. In particular, the so-called “red complex” group of periodontopathogens (*Porphyromonas gingivalis*, *Tannerella forsythia*, and *Treponema denticola*) was found to be more abundant at sites affected by peri-implant disease than at healthy ones. Conversely, the count of *S. aureus*, markedly higher at implant sites than at others, supports the possibility of detecting unique and distinctive microbiological features related to peri-implantitis. Indeed, although the metagenomics approach has yet to provide robust data, owing to the paucity of investigations, emerging data support the view that the peri-implant microbiome is a specific entity, different from the periodontal microbiome. Interestingly, further evidence suggests that implant sites and adjacent teeth appear to share similar microbiota, probably because they are spatially close and comparable ecological niches. Indeed, in the case of fully edentulous patients, healthy implants displayed similar bacterial colonizers as do healthy periodontal sites. However, in the case of partially edentulous patients, the implant surface was colonized by the same species as the adjacent teeth and oral mucosa. In addition, *A. actinomycetemcomitans* and *P. gingivalis*, usually detectable only in the presence of teeth, were detected in peri-implantitis in fully edentulous patients, indicating that the bacterial species might originate from niches in the oral cavity other than the subgingival sites, such as the soft tissues or saliva; alternatively, these bacteria might remain in place after tooth extraction and subsequently colonize the oral surfaces, including dental implants [8].

*Dental caries and the oral microbiome* – Dental caries have been investigated microbiologically, at the molecular level, in a number of studies, and the principal findings have been summarized in a recent review by Nyvad and colleagues [1]. In order to extend scientific knowledge of this common disease, cariology



progressively exploits the new and complementary approaches, including metagenomics, metatranscriptomics, metaproteomics, and metabolomics analyses of dental biofilms, along with refined microbial sampling techniques. One of the priorities for caries microbiologists in the near future will be to verify the performance, and not just the composition, of the entire microbial community. In particular, the metabolism resulting from the activities of oral microbiota greatly affects the dynamic processes of caries. Chiefly for this reason, metabolomics is expected to acquire a decisive role in this field, to facilitate research in assessing bacterial functions. Integrated approaches will make it possible to assess which genes are expressed and which phenotypic characteristics of the biofilms are detectable at specific dental sites, since caries is a localized disease. Taking into account that one of the major difficulties is sample collection, it is essential that biofilm specimens be taken from specific and specified tooth sites. Indeed, the use of pooled samples has been found not to be appropriate, since the bacterial inoculum collected from salivary samples of patients with different caries experiences would be unable to provide insight into the cariogenic potential of site-specific biofilms. Unfortunately, most molecular studies on caries have used saliva samples or pooled plaque samples.

In a recent study, the 16S rRNA gene was cloned and sequenced, in order to characterize the microbial composition of the oral biofilm in the presence of carious lesions. Custom-made arrays, specifically targeted to individual patient groups, detected a microbial diversity in patients' subgingival plaque. The main methodological limitation of this technique is that only those microorganisms specifically targeted by the probes can be detected. Samples collected from healthy and carious root surfaces of older patients were analyzed for their taxonomic microarray, showing that great bacterial diversity and the presence of *Actinomyces* spp. were more frequent at healthy sites, whereas several species of lactobacilli and *Pseudoramibacter alactolyticus* were associated with root caries [1]. A further study on the transcriptome determined a functional core microbiota, consisting of about 60 species; it identified numerous functional networks and provided support for the hypothesis that interindividual environmental differences affect the selection of microbial groups. Dominant functions of bacteria, such as the capacity of dental plaque microbes to metabolize diverse sugars and to handle the acid production and oxidative stress that result from sugar fermentation, were expressed by the oral microbiota [9].

Metagenomics and metatranscriptomics, via pyrosequencing analyses, can retrieve millions of partial 16S rRNA gene sequences in one sequencing run; they have been used in a cross-sectional study to analyze the oral microbiota of Chinese children with and without dental caries. The findings supported the hypothesis that the presence in the plaque of the genera *Streptococcus*, *Veillonella*, and *Actinomyces* is significantly associated with dental caries. Focusing on adulthood, the comparison between "healthy" and "cariogenic" salivary microbiome revealed that the latter was significantly more variable in terms of community structure. This outstanding result, i.e., that "healthy" microbiomes are more preserved than caries microbiomes, was consistent with other evidence from a study applying microarrays to analyze the microbial composition of saliva in children in relation to their caries status [1].

*Removable denture oral microbiome* – Changes of the oral microbiota before and after wearing removable dentures (RD) appear possibly related to a local imbalance of the microbial community, leading to oral candidiasis; however, there is as yet no certainty. Possible variations in the human oral bacterial community related to wearing partial RD have been analyzed in the four main kinds of biological oral specimens: saliva, supra- and subgingival plaque, and oral mucosal surfaces. A recent study collected these four types of plaque samples from RD wearers ( $n = 10$ ) at three different times, i.e., before and after 1 and 6 months of wearing RD; a further ten healthy adults were selected as control group [10]. After cloning and sequencing, the health-associated genera, such as *Streptococcus*, *Neisseria*, *Corynebacterium*, *Gemella*, *Veillonella*, *Selenomonas*, and *Actinomyces*, showed a decreasing trend in RD wearers, while species associated to disease, mainly *Streptococcus mutans*, appeared to increase.

Considering that *Candida*-related prosthetic stomatitis is correlated to a marked elevation in the number of *Candida* species cells present on the acrylic base of dentures, an interesting recent trial investigated the relationship between the *Candida* load and the bacterial diversity, in the saliva of older patients [11]. Patients were partially edentulous, with or without partial RD, or edentulous, with total upper and lower RD: almost all subjects were positive for *Candida*, with a negative correlation between *Candida* load and bacterial profiles of the saliva. When the *Candida* load increased, the diversity of the salivary microbiome decreased, and its composition shifted toward dominance by streptococci and lactobacilli, while genera within the *Fusobacteria* and *Bacteroidia* classes disappeared. Decreased bacterial variety was associated with a lack of equilibrium among the microbiome communities.

---

## Definition, Structure, and Composition of the Biofilm

The oral microbiome, adhering to hard substrates, can assemble into three-dimensional structures, called “dental biofilm” or “dental plaque”: the soft white material that may be observed on the surfaces of both teeth and dental materials.

The term “biofilm” indicates a community of microorganisms adhering to a surface, glued into an extracellular polymer matrix, also known as “slime,” within which there are water channels. These channels generally consist of glycoproteins, proteins, and polysaccharides, which are secreted by the microorganisms themselves. Thanks to this complex and dynamic structure, the microorganisms acquire multiple properties, including improved protection against host defenses and against new invading microbes. Salivary proteins, adhering onto tooth surfaces and forming the dental pellicle, help microorganisms to bind to the surface, which is the first step of biofilm arrangement. Biofilms can form on both body tissues and material surfaces. Although mixed-species biofilms predominate in most environments, including the oral cavity, single-species biofilms exist in a variety of infections and on the surface of implantable medical implants such as orthopedic implants or

catheters [12]. Indeed, the dental biofilm (corresponding to the oral microbiome) is composed of all the components of the oral microbiota and may thus comprise a single or multiple microbial species, mainly bacteria, fungi, and mycoplasmas. The saliva can also contain certain types of protozoa, such as *Trichomonas* species, but mainly in immunocompromised subjects.

In the process of biofilm development, Gram-positive bacteria, such as *Streptococcus* spp. and *Actinomyces* spp., are called “pioneer species,” since they are usually the first to adsorb onto the dental pellicle and start to proliferate. They play an important role in producing conditions suitable for other microbes to further colonize the substrate; indeed, their respiration process reduces the oxygen tension and increases the level of carbon dioxide, resulting in hypoxic conditions that are suitable for anaerobic species. A number of oral microorganisms easily proliferate in this environmental setting: they are facultative anaerobes and account for most oral cavity bacteria, for example, oral streptococci, which survive deep within the dental biofilm.

## Biofilm Metabolism

Bacterial biofilm metabolism chiefly relies upon carbohydrates as principal source of energy, in order to produce ATP. In particular, glucose is converted to pyruvate via the glycolysis metabolic pathway; pyruvate then follows diverse pathways depending on the oxygen tension and the type of microorganism. For example, glucose is degraded to pyruvate via the central carbon metabolism, following the classic glycolysis reaction; however, under anaerobic conditions, it is further degraded into lactate and acetate, by bacteria including *Streptococcus*, *Actinomyces*, and *Lactobacillus* spp. Conversely, in the presence of oxygen, pyruvate is converted to acetate by *Streptococcus* and *Lactobacillus*, and lactate is converted to acetate by *Actinomyces*. When bicarbonate is also present, as often occurs in the saliva, phosphoenolpyruvate is converted to succinate with bicarbonate assimilation; for instance, *Actinomyces* follows this metabolic pathway. Lastly, in *C. albicans* pyruvate is directly metabolized into acetyl CoA by the pyruvate dehydrogenase complex in aerobic conditions, but under hypoxia the anaerobic route is activated, and small amounts of acetaldehyde may be produced. Since ethanol is toxic to microorganisms at high concentrations, the preferential metabolism is aerophilic and avoids ethanol accumulation.

As has been said, biofilm metabolism is crucial for several dental diseases, and microorganisms' metabolic pathways have been elucidated, using single bacterial strains in preclinical studies; they have not yet been confirmed by in vivo analyses on supragingival plaque. The main limitation on these studies is that the amount of supragingival plaque that can be sampled from the oral cavity is insufficient for a conventional metabolic study: metabolome analysis could be an excellent alternative to overcome this difficulty.

## Biofilm-Related Medical Device Infections

The most common biofilm-related medical device infections are due to the Gram-negative *Pseudomonas aeruginosa*, *Pseudomonas fluorescens*, or *Escherichia coli* or to the Gram-positive *Staphylococcus epidermidis*, *Staphylococcus aureus*, or enterococci.

Hospital and health-care facilities are peculiar environments in which dangerous antibiotic-resistant pathogens can live and evolve. Hospital-based pathogens show continuous dynamic change, and this influences their distribution through the body over time and their pathogenicity [13]. To fight the multidrug resistance (MDR) of several bacteria is still the major global challenge. Table 3 summarizes the strains correlated to hospital-based infections; to date, the MDR strains identified are the species *Enterococcus faecium*, *Staphylococcus aureus*, *Klebsiella pneumoniae*, *Acinetobacter baumannii*, *Pseudomonas aeruginosa*, and *Enterobacter* spp., collectively known under the acronym of “ESKAPE.” Hospital-based pathogens may infect the oral cavity and intraoral devices.

At the beginning of the antibiotic era, hospital-acquired infections were mainly due to *Staphylococcus* spp., initially kept under close control by penicillin. Then, as *Staphylococci* started producing beta-lactamase, beta-lactamase-resistant compounds were synthesized in order to counteract these pathogens. Subsequently, methicillin-resistant *S. aureus* (MRSA) and Gram-negative bacilli emerged and became the chief bacteria responsible for hospital-acquired infections (HI); however, the use-abuse of antibiotics has favored the selection of bacteria with methicillin resistance combined with resistance to other types of antibiotics. In the late 1960s, *Enterobacteriaceae*, such as *Escherichia* spp., became increasingly involved in hospital-based infections, finally leading to the emergence of multidrug-resistant (MDR) Gram-negative *Pseudomonas aeruginosa* and *Acinetobacter* spp., causing very difficult therapeutic problems and a frustrating and never-ending search for a solution.

The World Health Organization (WHO) has now recognized MDR as one of the three most important problems facing human health [14]. MDR is often due to the presence of specific resistance gene “islands” that, under the pressure of antibacterial agents, can be rapidly switched, developing a dynamic and always novel mechanism of antibiotic counteraction. In most cases, MDR strains attain these “islands” from bacteria of unrelated genera, as confirmed by sequence similarity and phylogenetic analyses [15]. This gives rise to the so-called super bacteria or super bugs, resistant to most, if not all, antibiotic regimes. However, the mechanisms underlying MDR vary in different pathogens, often reflecting the cellular structure of the bacterium.

## Biofilm Formation and Propagation

Oral biofilm formation is part of a biological cycle that includes four main stages: initiation, maturation, maintenance, and dissolution (Fig. 1).

**Table 3** Principal hospital-based infections, microorganisms, and human body sites involve

Hospital-based infection (HI)	Infective agents at different body sites Microorganism
Surgical skin (SSI) and soft tissue infections (SSTI)	<i>Staphylococcus (S.) aureus and epidermidis; Acinetobacter (A.) baumannii; Escherichia (E.) coli; Pseudomonas (P.) aeruginosa; Enterococcus (E.) faecalis</i> ; coagulase-negative <i>Staphylococci; Candida (C.) albicans</i>
Bloodstream infections (BSI)	<i>S. aureus; E. coli; Enterococcus spp.; Streptococcus (S.) spp.; Proteus spp.; Staphylococcus (S.) spp.; P. aeruginosa; Candida (C.) spp.</i> ; hepatitis B and C virus; <i>Cytomegalovirus</i>
Meningitis (MI)	<i>Enterovirus</i> ; herpes simplex type II; varicella-zoster virus; <i>Adenovirus</i> ; parotitis virus; HIV; <i>Flavivirus, Arbovirus; Neisseria (N.) meningitidis; Streptococcus (S.) pneumoniae; Haemophilus (H.) influenzae; S. aureus; P. aeruginosa; E. coli; Listeria monocytogenes; Cryptococcus neoformans; Histoplasma capsulatum; Coccidioides immitis; Blastomyces dermatitidis; Candida spp.</i>
Respiratory infections (RI) in intensive care units (ICU)	<i>Streptococcus (S.) pneumoniae; Haemophilus (H.) influenzae; Moraxella (M.) catarrhalis; S. aureus; P. aeruginosa; A. baumannii; E. coli; Legionella; Aspergillus (A.) fumigatus; Pneumocystis (P.) jirovecii; Mycobacterium (M.) tuberculosis, Klebsiella (K.) pneumoniae; Serratia (S.) marcescens</i>
Endocarditis (EC)	<i>S. aureus; Streptococcus (S) pyogenes and pneumoniae; E. faecalis; P. aeruginosa; Candida (C.) albicans</i>
Gastroenteritis (GI)	<i>Rotavirus; Campylobacter; S. aureus; Pseudomonas (P.) aeruginosa; E. coli O157:H7; Salmonella spp.; Giardia (G.) lamblia and intestinalis; E. faecalis and faecium</i> ; Norwalk virus, <i>Adenovirus, Astrovirus; Calicivirus; Cryptosporidium parvum</i>
Urinary infections (UI)	<i>E. coli; Pseudomonas (P.) aeruginosa; Klebsiella spp.</i> ; coagulase-negative <i>Staphylococci; E. faecalis and faecium; S. aureus; Proteus (P.) spp.; S. marcescens; Citrobacter (C.) spp.</i>
Genital/pelvic infections (GI)	Human papillomavirus; <i>Trichomonas vaginalis; E. faecalis and faecium; C. albicans; Proteus (P.) spp.; Klebsiella spp.; E. coli</i> ; group B hemolytic <i>Streptococcus; Gonococci; Chlamydia; Herpes Simplex Virus; Mycoplasma</i>

Bacteria appear to initiate biofilm development in response to specific environmental cues, such as nutrient availability: microorganisms undergo a transition from free-living, planktonic cells to sessile, surface-attached cells in response to a nutrient-rich medium. Biofilms continue to develop as long as fresh nutrients are provided, but when bacteria are nutrient deprived, they detach from the surface and return to a planktonic mode of growth. This starvation response is thought to allow the cells to search for a fresh source of nutrients and is driven by well-known adaptations that bacteria actuate when nutrients become scarce.

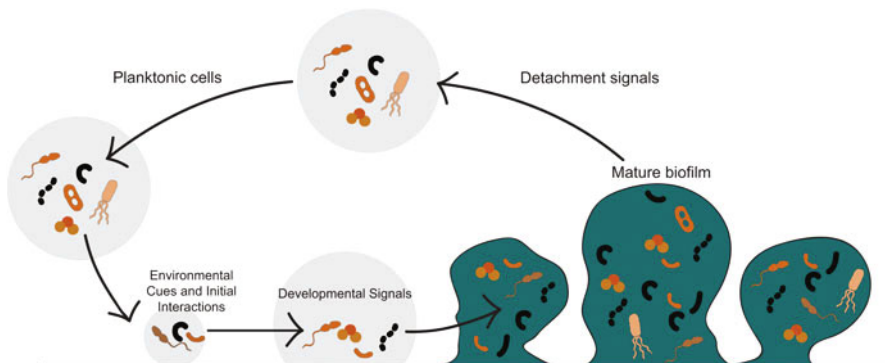


**Fig. 1** Biological cycle of bacteria, including initiation, maturation, maintenance, and dissolution of the biofilm (Artgraph by Eng. Ettore Varoni and Dr. Silvia Bovo)

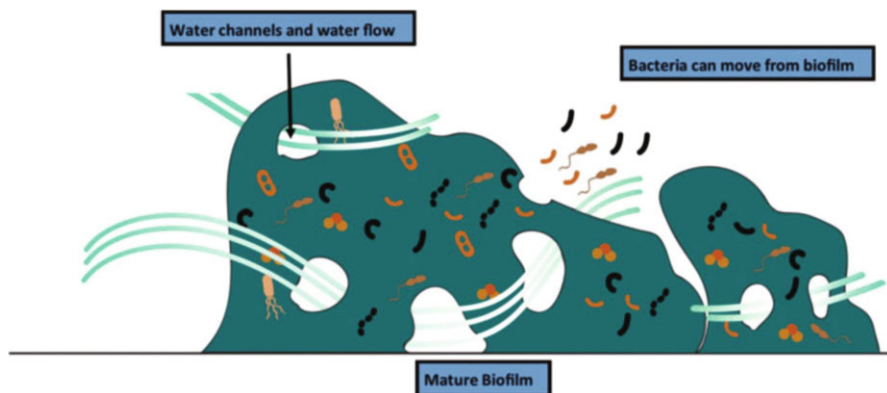


**Fig. 2** Mature biofilm water channels. Channels can be used for microbial network signaling and to dilute drugs (Artgraph by Eng. Ettore Varoni and Dr. Silvia Bovo)

Conversely, the biofilm is also a complex protected arrangement, self-developed by the bacteria to enable them to survive in a hostile environment more easily than when they are in planktonic form. In particular, it enables them to optimize nutrient uptake, shelters them from removal forces, and protects them from desiccation, from host defense mechanisms, and from potential toxic or harmful agents, including antimicrobial agents. Interestingly, it is easy for the biofilm to develop antibiotic resistance, and it very frequently occurs, because the microbial community can regulate the opening and closing of the water channels biochemically (Fig. 2) and can consequently control the concentration of metabolites within the structure and/or stop the entrance of drugs.

Bacteria cells in the biofilm community coordinate efforts with their neighbors, to accomplish cooperative activities such as bioluminescence production, biofilm

development, and exoenzyme secretion. Coordination occurs through a mechanism of cell-to-cell communication called quorum sensing. This mechanism gives bacteria the capacity to recognize the population density by measuring the accumulation of a specific signaling molecule secreted by members of the community. When this density reaches a certain level, accumulation of the signal in the extracellular environment is sufficient to promptly activate the biofilm response to maintain its correct balance [16]. Moreover, “quiescent cells” have been also found inside the biofilm. These cells cannot be killed by antibiotics because they are at a low metabolic stage, assuring the protection of the structure and sustaining the drug’s ineffectiveness [17–19].

*Biofilm formation stages* – It is crucial to clarify and understand in depth the events involved in biofilm formation on material surfaces, in order to develop effective control strategies. Adhesion is the first step in colonization and is a cornerstone for starting biofilm formation, since it allows bacteria to grow on certain surfaces and then invade host tissues. The sequence of the interaction, between floating bacteria and a surface, may be summarized as follows [20]:

1. Convective transport of fluids and active bacterial chemotaxis.
2. Van der Waals attractive forces, which operate at separation distances greater than 50 nm.
3. At distances of 10–20 nm, the interaction of van der Waals attractive forces and electrostatic repulsion produces a weak area of attraction, which maintains reversible adhesion.
4. At the same distance and even closer, adhesion between bacterial adhesin and ligands adsorbed onto the biomaterial surface from biological fluids, when the material was installed, begins to operate.

After surface colonization by pioneer bacteria, co-aggregation of other bacteria to cells that are already attached can occur. Multiplication of the attached organisms produces confluent growth of microorganisms, and a biofilm starts to form.

Figure 3 shows the sequential steps of supragingival biofilm formation on a root cementum surface, through scanning electronic microscope (SEM) images.

---

## **Biofilm/Substratum/Environment Interaction**

Materials science and tissue engineering offer a unique opportunity to investigate biofilm formation. The availability of a stable surface is a prerequisite for the bacteria cells to attach and for consequent biofilm formation, and the properties of the surface can affect the outcome and bacteria/surface interactions.

Several aspects can affect biofilm formation and growth; the most important effects related to substrate and environment will be described in the next sections.

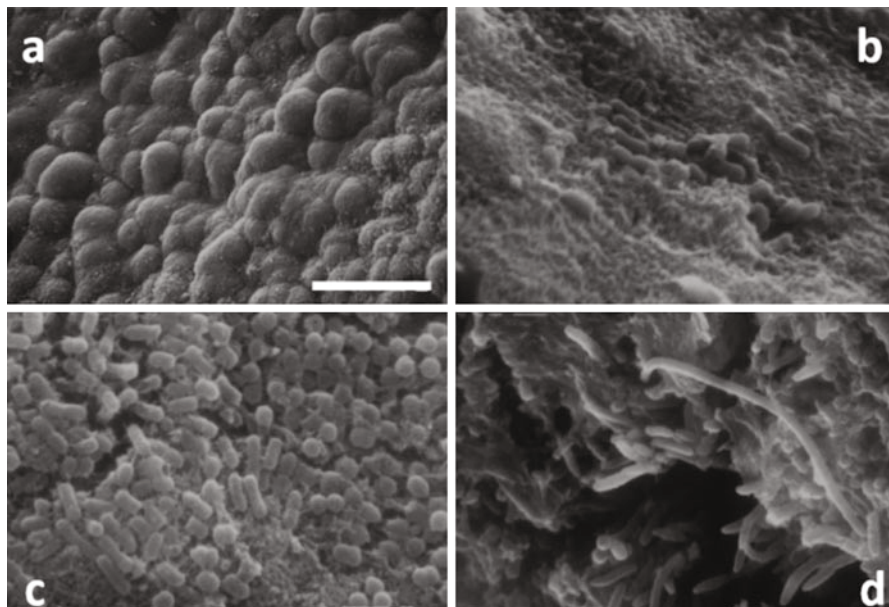


**Fig. 3** Sequential steps of bacterial colonization in the oral cavity (SEM images). Clean and sterile cementum of the dental root surface, which is suddenly covered by a salivary pellicle (Adapted from Carrassi [21]): after 2 h, the cementum surface is colonized by a few cocci; after 12 h, the surface is completely covered by cocci and short rods; after 24 h, the biofilm has developed. Many bacteria, cocci, and short and long rods can be observed on the root surface, adhering to the slime layer

### The Substrate Effect: Surface Energy and Hydrophilic/Hydrophobic Properties

The initial interactions between the bacterial cell wall and a surface (including those of other cell walls) are primarily influenced by interfacial electrostatic forces (repulsion or attraction) and van der Waals forces. However, many different nonspecific interactions and interfacial forces also influence cell attachment, including hydration forces, hydrophobic interactions, and steric forces [22]. Hydrophobic (low surface energy) and electrostatic (charge) interactions are the most widely investigated phenomena.

In general, bacteria may be modeled as colloidal particles approaching surfaces with a Brownian motion [48]. The interaction may be described by the Derjaguin-Landau-Verwey-Overbeek (DLVO) theory focused on long-range interactions between particles and substrate. This interaction includes the Lifshitz-van der Waals interaction and the interaction resulting from the overlapping of two layers of interactions. The forces are additive, and the energy of adhesion is a function of the distance between the particle and the substrate. In the case of bacteria, the DLVO



is not fully descriptive, and short-range Lewis acid-base interaction and hydration must also be taken into account (XDLVO).

The charge upon the bacteria wall is generally measured as electrophoretic mobility. It is usually electronegative, especially in the case of Gram-negative bacteria, as is that of many material surfaces. Thus, from the theoretical standpoint, bacteria do not adhere closely except to strongly electropositive surfaces. However, in practice they may show paradoxical behavior, because of the ability of the cell wall to dynamically alter its charge in response to environmental conditions, such as pH or ionic strength in the medium. In addition, fibrils, fimbriae, and flagella may expose different charges at their tips. The walls may also be penetrated by solvents, causing dynamic rearrangement of the wall polymers and consequently altering surface charge. These phenomena explain why the bacteria/substrate interaction is not fully described by the DLVO or XDLVO theories, and bacterial behavior in regard to the electrostatic properties of the substrate is not fully predictable (Table 4) [23].

In addition to electrostatic attraction, chemotaxis and possibly haptotaxis also contribute to the initial attachment [24]; this occurs in response to chemoattractants in the environment or adsorbed onto the surfaces, such as amino acids, peptides, and glucides.

The interactions between bacteria and surface, as described above, are generally reversible, but they evolve rapidly toward irreversible bonds characterized by molecular-specific reactions between bacterial surface structures and the substratum. The interactions are mediated by bacterial surface polymeric structures, called adhesins, included in the capsules, fimbriae, or pili and in the slime. For instance, *S. aureus* binds fibronectin, while *S. epidermidis* has several polysaccharide adhesins that mediate the adhesion of this bacterium to various material surfaces and protein tissues. Of the adhesins, the most important are (i) capsular polysaccharide/adhesion (PS/A), (ii) a biosurfactant known as “surface-active agent” (SAA), (iii) polysaccharide intracellular adhesion (PIA), (iv) a polysaccharide composed of  $\beta$ -1,6-linked *N*-acetylglucosamines with partly deacetylated residues, and (v) peptidoglycan, an accumulation-associated protein (AAP). PS/A and SAA take part in bacteria-material interactions, whereas PIA and AAP are implicated in cell-cell interactions [25] (Fig. 4).

## The Environment Effect

Temperature, exposure time, bacterial concentration, and the presence of antibiotics or other antibacterial molecules affect bacteria adhesion and biofilm development. In addition, physical stresses, including flow, scraping, or epithelial detachment, have a great influence on biofilm formation. In general, high mechanical stresses inhibit biofilm formation and its maturation.

All these phenomena are evident in the oral cavity, where environmental conditions change frequently. It is a common observation that, in subjects who

**Table 4** Representative examples of deviations from the DLVO or XDLVO theory observed in bacterial adhesion studies (Adapted from Poortinga et al. [23])

Strain	Experiment	Findings
<i>Arthrobacter</i> , <i>Corynebacterium</i> , <i>Rhodococcus</i> , <i>Pseudomonas</i> , <i>Gordona</i>	Adhesion to glass and Teflon	Experimentally obtained energy barriers against adhesion are some orders of magnitude smaller than DLVO predictions at low ionic strength
<i>E. coli</i>	Adhesion to sludge flocs	Adhesion does not correlate with bacterial zeta potential but with a fraction of the positive charge present on the bacterial cell surface
<i>Vibrio alginolyticus</i>	Adhesion to hydroxyapatite	Bacterial adhesion increases at increasing ionic strength, in accordance with the DLVO theory, but decreases when ionic strength exceeds 0.1 M
<i>Corynebacterium</i>	Accumulation of bacteria at air-water interface	In contrast to DLVO predictions, under repulsive conditions, accumulation decreases for increasing ionic strength
<i>S. salivarius</i>	Adhesion to glass	Despite small differences in DLVO interaction energies, adhesion rates of a fibrillated and non-fibrillated strain differ greatly
Marine strains	Adhesion to hydrophobic and hydrophilic polystyrene	No correlation found between adhesion and ionic strength
<i>Sphingomonas paucimobilis</i>	Adhesion to bare glass and EPS-coated glass	The XDLVO theory can explain adhesion to glass but cannot explain adhesion to glass coated with bacterial EPS
<i>Pseudomonas</i>	Adhesion to sand	A fraction of the bacteria adheres faster than the rest, while DLVO calculations predict no difference
<i>E. coli</i>	Direct measurement of bacterial interaction force with glass, mica, and hydrophobic polymers	Force measurements do not correlate with XDLVO calculations for a lipopolysaccharide covered strain but do correlate for a strain with truncated lipopolysaccharide chain
<i>Pseudomonas</i> and <i>Burkholderia</i>	Measurement of bacterial interaction with silicon nitride AFM tip	A repulsive force extending over longer distances (>100 nm) than predicted by the DLVO theory is measured

do not brush their teeth efficiently, plaque accumulation is abundant. In xerostomic patients, who are deficient in saliva amount and flow, plaque accumulates very

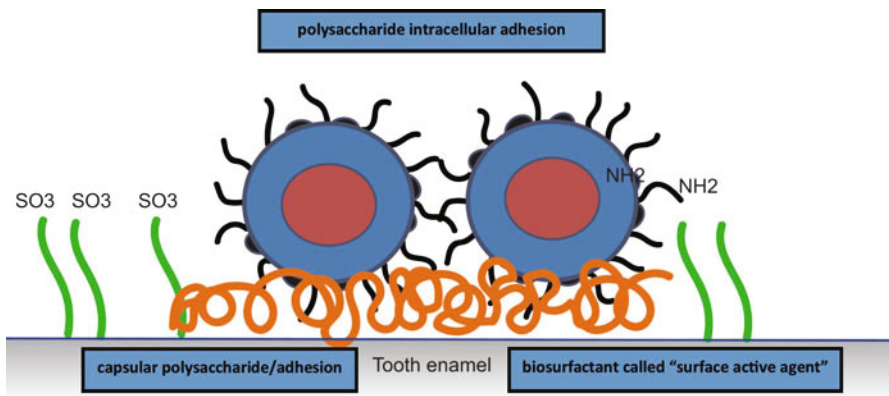


**Fig. 4** Molecular interaction between bacteria and substrate (Adapted from Katsikogianni and Missirlis [25])

rapidly, and the clinical consequences consist of a prevalence of caries and periodontal disease.

### The Effect of Surface Roughness at Micro- and Nanoscales

Certain physical parameters, such as surface roughness and morphology, are thought to closely affect biofilm formation. It is well known that rough restorative materials accumulate more plaque and expose patients to the risk of developing caries and gum diseases at neighboring sites. This is a key aspect in implantology, because most implants available on the market are designed to be rough and grooved, in order to improve primary stability, healing of mineralized and soft tissues, and maintenance of tissue integration around the implants over time, whether in healthy or diseased subjects. However, when rough surfaces are exposed to the oral environment, biofilm formation is swift, mainly because of the roughness and grooving shelter bacteria from physical removal, hindering cleaning procedures. Biofilm formation around implants is an etiological factor for peri-implantitis and implant failure or loss [26].

It has been observed that, although roughness and wettability are related, the roughness parameter is often predominant [22]. The clinical roughness threshold for biofilm formation in the oral cavity has been shown to be  $R_a = 0.2 \mu\text{m}$ : below this threshold, for  $R_a$  values within the microscale, there is no significant improvement in inhibiting bacterial adhesion [21, 27]. In contrast, at the nanoscale, rough and geometrically determined surface morphology has been shown to produce antifouling properties. At this scale, interaction of the bacteria with the surface remains limited to the surface of physical protrusions, like drops of dew on the leaves of a lotus flower (*Nelumbo* spp.), and bacteria are repulsed [28].

## The Effect of Protein Adsorption

As described earlier in this chapter, the first step in the pathogenesis of foreign body-related infections is bacterial adhesion. The mechanisms involved in adhesion lead to passive adsorption of the bacterial cells on the solid material, through physico-chemical surface interactions with bacterial structures termed bacterial adhesins. Thus, bacterial behavior varies as a function of material hydrophobicity and electrostatic charge. Chemo-physical properties and functional groups exhibited by the biomaterial surface interact with those of the bacterial cells, determining the kinetics of microbial adhesion.

However, in many cases of implanted or invasive medical devices, materials first come into contact with body fluids. This is particularly true in the oral cavity, where installed materials are immediately wetted by the saliva, crevicular fluid, or blood, depending on the anatomic site of application.

The components of body fluids, mainly proteins, are rapidly adsorbed onto the material surface. The protein film that quickly forms on the biomaterial surface during the initial exposure to physiologic fluids may thus be considered as the true interface with the bacteria. Nonspecific effects have been described, such as those derived from albumin surface adsorption, thought to alter the physicochemical characteristics of the surface and to increase the degree of hydrophobicity, while competing for the surface with other pro-adhesive host proteins. In addition, various host proteins mediate bacterial adhesion by interacting with bacterial adhesins; these are frequently receptor proteins known as “microbial surface components recognizing adhesive matrix molecules” (MSCRAMMs). The bacteria-binding host proteins include collagen, fibrinogen, fibronectin, laminin, vitronectin, clumping factors A and B, bone sialoprotein, elastin, and IgG. Charged surfaces can also interact electrostatically with other extracellular polymeric components. In addition to polysaccharides, other extracellular polymeric substances are produced by biofilm-forming bacteria; these include extracellular DNA, teichoic acids, and amphiphilic molecules, whose production or proportion may depend on the specific growth phase. Effective low-adhesion surfaces are thus hydrophilic, highly hydrated, and non-charged. These types of surface appear to prevent or limit contact between a bacterium and the potential attachment points of the material surface [28].

The adsorption of proteins on a surface can be reduced, either by altering the interaction potential or by slowing down the rate of adsorption through high-potential barriers to interaction. This latter method of controlling the kinetics of adsorption can be achieved by polymer grafting, resulting in the introduction of long-range repulsive forces. Other strategies to achieve lower bacterial adhesion to biomaterials exposed to protein solutions rely on conditioning the surface by pre-adsorption of molecules claimed to increase apolar hydrophilicity and hydrophobicity or to compete with host adhesion adsorption [29]. In addition, the possibility of controlling tissue integration while contrasting bacterial adhesion, simply by acting on the topographical features of the biomaterial surface, is certainly very

attractive. Specifically patterned surfaces can direct the alignment and spatial distribution of bacterial cells. At the same time, customized superficial nanostructures can reduce the areas of contact where eukaryotic and bacterial cells can anchor. Topographies can achieve a degree of complexity that confers entirely new properties on the material surface [30].

---

## Biofilm Formation on Dental Implants and Prosthetic Dental Materials

### Biofilm Formation on Dental Implants

Biofilm formation on dental implants is the crucial step toward the inflammation of peri-implant tissues, jeopardizing the long-term success of osseointegrated implants. In general, the assessment of the microbiological and immunopathological aspects of peri-implant diseases has shown a microbiological diversity of peri-implantitis biofilms and a specific local immune response of the host [8].

Bacterial colonization and adhesion at the implant surface starts already 30 min after placing the device and lasts for several months. For instance, the presence of *S. aureus* has been confirmed as long as 1 year later. As pointed out in the paragraph “Peri-implant microbiome,” the bacterial composition of the newly formed implant biofilm closely resembles that of the nearest teeth, suggesting that the microbial flora on dental substrates can act as a “reservoir” for the bacteria that compose the biofilm around implants. Importantly, bacteria of subgingival biofilms, collected from peri-implantitis patients, displayed multiple antibiotic resistances in vitro, for example, in the case of *Prevotella intermedia*, *Prevotella nigrescens*, or *Streptococcus constellatus*.

Although the qualitative composition of the biofilm in peri-implantitis shows similarities to that of periodontitis, supporting the hypothesis that patients with active periodontal disease are at higher risk for developing peri-implantitis, several further microorganisms, very uncommon in periodontitis, have been recognized in peri-implantitis; these include *Staphylococcus aureus*, *Staphylococcus epidermidis*, *Escherichia coli*, *Peptostreptococcus micros*, and *Pseudomonas* spp. [8]. A further peculiar element in peri-implant mucositis, and subsequently in peri-implantitis, is that inflammation acquires typical features defined as the “specialized innate response.” Peri-implantitis displays larger numbers of immune cells, mainly interstitial dendritic cells and related inflammatory mediators. The progression from mucositis to peri-implantitis is characterized by a drastic increase in neutrophils, osteoclasts, macrophages, and lymphocytes, in findings supported by transcriptome analyses. Compared to the inflammatory tissue from periodontitis sites, the peri-implant granulation tissue displayed a specific innate response, with greater mRNA expression of pro-inflammatory cytokines, such as interleukin (IL)-1, IL-6, and IL-8. Moreover, resident primary fibroblasts showed increased production of

vascularization factors, matrix metalloproteases, and complement receptor C1q, with decreased production of metalloprotease inhibitors and growth factors for collagen synthesis [8].

Recent studies have analyzed samples of crevicular fluid collected from the sulcus around abutments and report a significant difference between supra- and subgingival plaque: these findings supported the hypothesis that the cellular adherence of peri-implant tissue to titanium implant, via hemidesmosome, actin filaments, and microvilli, greatly reduces the risk of formation of anaerobic subgingival pockets. Indeed, the biofilm coating observable on supragingival abutment surfaces appeared significantly thicker than that on subgingival sites.

Together with surface localization (supra- and subgingival) of oral biofilm, surface modification of biomaterial also appeared to significantly affect the health status of tissues around implant abutments. Two main aspects are particularly involved, i.e., the local immune response to biomaterial and the biofilm adhesion and proliferation on it. With regard to the former, particularly in the case of mucositis, the physicochemical treatment of the implant surface during manufacturing appears to affect the inflammatory response of the adjacent mucosal tissue, in terms of different microvessel density and amount of inflammatory infiltrate. Regarding biofilm adhesion and growth, the surface chemistry and the design features of the implant-abutment configuration can affect biofilm formation. As mentioned, increased surface roughness and surface free energy appear to promote dental plaque formation on implant and abutment surfaces, although this conclusion derives chiefly from descriptive literature, rather than from high-quality meta-analyses. A considerable debate still surrounds the issue, and in particular the precise role played by physicochemical and textural properties of the implant surface on microbial composition is still unknown. It is hypothesized that greater roughness and higher free energy at the implant surface might promote biofilm formation, so that peri-implantitis might occur and progress more quickly. However, and conversely, some evidence also supports the hypothesis that abutments with different surface characteristics do not greatly influence either biofilm formation on the implant surface or the extent and composition of the inflammatory response. No implant system or surface type has been found superior over any other in terms of marginal bone preservation, the main reason for this probably being related to the presence of salivary proteins at the interface between the host tissue and biomaterial. The latter adheres first at the implant surface and can mediate bacterial adhesion: any differences in bacterial adhesion due to surface microstructures may partially be “counteracted” or masked by this salivary pellicle, which mediates the mucosa-implant interconnection [8].

Taken together, the results of these studies suggest that the diversity of the microbial community and the subsequent immunity response of peri-implantitis versus periodontitis might not be as close as has been believed: further investigations targeting the multiplicity of peri-implant-specific microbiota will be needed to identify the best approach for peri-implantitis management, still an important clinical challenge.

## Biofilm Formation on Restorative and Prosthetic Materials

As was said in the paragraph “Dental caries and the oral microbiome,” dental caries is chiefly the result of an imbalance in metabolic activity within the oral biofilm, which becomes skewed toward a strong acidification of the milieu at the tooth surface, leading to the dissolution of hard dental tissues (enamel and dentine). From a metabolomics perspective, the cariogenic potential of the microbial community must be described in terms of activities relevant to acid production. Recent studies have shown that metabolomics may explain caries pathogenesis better than a focus solely on microbiome composition; unsurprisingly, sound evidence exists to confirm that carbohydrate metabolism is a cornerstone in caries development, because of its capacity to acidify the environment and dissolve dental tissues, leading to tooth decay.

For dental applications, antimicrobial coatings killing bacteria upon contact are more promising than antimicrobial-releasing coatings. Moreover, certain natural polymers, used as biomaterials with intrinsic antibacterial properties, such as chitosan or pectins, could be useful tools, in that they would contextually exert antimicrobial activity during tissue regeneration [31, 49].

Biofilms appear to form in different ways, depending on the different types of biomaterials used in restorative and prosthetic dentistry. On gold and amalgam, the *in vivo* growth of dental plaque appears thick and can almost completely coat the substrate, but it is also barely viable. Conversely, on ceramics oral biofilms are thin but highly viable. Dental plaque on composites and glass ionomer cements has been reported to produce surface decay, which appears to further enhance biofilm proliferation. In particular, residual monomers released from composites affect plaque development *in vitro*, but the corresponding *in vivo* effects are less striking, probably due to the greater dilution of these compounds, which become dissolved in a huge volume of saliva, which is continuously replaced by the flow rate.

Dental plaque grows readily on the acrylic bases of dentures, mainly because of their porous structure. The composition of oral biofilms on the mucosal and prosthetic surfaces has been investigated, to determine any differences. A recent study analyzed 61 edentulous subjects with complete maxillary and mandibular dentures [32]: “supragingival” plaque samples were collected from the acrylic base; from the dorsal, lateral, and ventral surfaces of the tongue; from the floor of the mouth, the buccal mucosa, the hard palate, the vestibule/lip, and the attached gingiva; and from the saliva. The microbial profiles of plaque from the soft tissues differed with the site considered, but the main periodontal pathogens, *i.e.*, *Aggregatibacter actinomycetemcomitans* and *Porphyromonas gingivalis*, were detectable in all specimens. In particular, samples from the dorsum of the tongue showed the highest bacterial counts, followed by the adherent gingiva and the lingual margins; the lowest counts were recorded for samples from the buccal mucosa and the labial vestibular mucosa. The patterns of microbial colonization versus harvesting site showed three clusters: the first cluster included the saliva, the supragingival plaque, and the lateral and dorsal surfaces of the tongue; the second cluster comprised the six remaining soft tissues; and the third cluster comprised all species on the denture palate.

## The Role of Chemistry in Dental Biofilm Limitation

### Current Strategies

Numerous strategies are currently available to hinder the formation of “pathogenic” oral biofilm on dental biomaterials and the development of related dental disease. These include strategies relating to the materials themselves, substances used to dope materials, and different types of surface coating including bioactive coatings, micro- and nano-particles, etc.

*Materials with intrinsic antibacterial properties* – Bulk materials that exert antibacterial action without requiring any modification are generally described as intrinsically antibacterial. Numerous metals, such as silver, zinc, and copper, are known to be intrinsically bactericidal. However, their activity is not usually highly specific and is not solely oriented against prokaryotic cells: there is generally a certain degree of cytotoxicity against host cells in peri-prosthetic tissues, reducing their viability. This is often due to the metals becoming corroded in the physiological environment or to its inexorable leaching that leads to the release of high concentrations of active ions, causing local toxicity and, in some cases, accumulation in distant target organs. Silver is certainly the most widely used for biomedical applications; its bactericidal activity is related to the inactivation of critical enzymes of the respiratory chain (e.g., succinate dehydrogenase) by binding to thiol groups and induction of hydroxyl radicals. Recently, the utilization of silver as thin nano coatings, in doped solid or hydrogel materials, in the formulation of bioactive alloys and glasses and its use in the form of micro- or nanoparticles, has progressively advanced, although the possible inactivation of silver-mediated antibacterial activity in physiological fluids and the low biocompatibility index are still debated.

Gallium-based treatments provide promising titanium anti-biofilm coatings to develop new bone-implantable devices for oral, maxillofacial, and orthopedic applications [33]. Recent evidence shows that the biological functions of  $\text{Fe}^{3+}$  are impaired by replacing iron with gallium; gallium inhibits  $\text{Fe}^{3+}$  biological functions by what is known as a “Trojan horse” strategy [33].

Chitosan is another substance known to possess intrinsic antibacterial and anti-fungal activities [34]. However, chitosan is a polycationic polymer derived from chitin, and it only has bland bactericidal activity, usually enhanced at low pH.

*Bioactive coatings with bactericidal agents* – Bioactive antibacterial coatings have been developed with the purpose of achieving desirable new anti-infective properties at the biomaterial-tissue interface, without compromising the characteristics of the bulk material. In the so-called contact biocides, anti-infective surfaces involve the use of non-leachable substances, such as some antimicrobial peptides, quaternary amines, and *N*-halamines. These bioactive surfaces only kill bacteria on contact, as the bactericidal substances are not released, and are activated following direct interaction with the bacterial cells. Direct contact-killing is based on extremely high electrostatic forces on the surface that can disrupt bacterial cell membranes by removing anionic lipids [35]. The limit of this strategy is that surfaces can potentially



be masked and inactivated when filmed by the host proteins present in protein-rich physiologic fluids.

Nitrogen monoxide (NO), a natural molecule with pleiotropic functions, usually produced by leukocytes as host defense against microbial pathogens, plays an important role as a bioactive bactericide [36]. However, NO can interact with superoxide in the tissues, in conditions of oxidative stress, generating the highly cytotoxic peroxynitrite ( $\text{ONOO}^-$ ); this makes it very important to fine-tune the beneficial and toxic effects of NO, by carefully controlling the release kinetics.

Great interest is directed toward substrates that become antimicrobial following a process of photoactivation; these include titanium oxide ( $\text{TiO}_2$ ).  $\text{TiO}_2$  surfaces undergo photoactivation upon irradiation, with an adsorption wavelength of 385 nm; this irradiation excites the anatase allomorph, which is one of the three main  $\text{TiO}_2$  polymorphs. The bactericidal action of irradiated titanium surfaces is due to reactions of photooxidation, which involve  $\text{O}_2$  and  $\text{H}_2\text{O}$ , with the formation of hydroxyl radicals ( $\text{HOO}\cdot$ ) and the direct and indirect oxidation of organic substances. These radicals are highly effective at disrupting bacterial membranes. In particular,  $\text{AgTiO}_2$  appears to be a very promising coating, combining the known oligodynamic bactericidal properties of silver ions with an enhanced photocatalytic activity, conferred by facilitating electron-hole separation and/or increasing the surface area for adsorption [24].

*Materials delivering antibiotics* – An obvious step to produce biomaterials with anti-infective properties is to incorporate antibiotics within the biomaterials. Antibiotics can be incorporated variously into the bulk or coating of a biomaterial, and the incorporation can be either in molecular or in particle form. The release can consequently occur by different modalities, including diffusion to the aqueous phase, erosion/degradation of resorbable loaded matrices, and hydrolysis of covalent bonds. Thus, delivery kinetics depends on the stability of the molecular bonds or on the rate of biodegradation/bioerosion of the matrices entrapping the antimicrobial agent. However, these delivery mechanisms have been widely debated, especially regarding their efficacy over the long term (>3 weeks) [37].

Urinary and central venous catheters provide a significant example of the use of materials delivering antibiotics: a study comparing different types of antibiotic- and metal/antibiotic-doped urinary catheters found no difference in bacteria reduction at 3 weeks between doped and non-doped catheters; however, during the first week, the bactericidal efficacy of the doped catheters was clearly superior to that of their non-doped counterparts. A study examining the bactericidal efficacy of central venous catheters found efficacy to be closely related to the implant site: the infection rate was reduced in the femoral and jugular veins but remained unchanged in the subclavian vein [50].

There is general concern that the routine use of antibiotic-loaded biomaterials will increase the spread of antibiotic resistance: after an initial burst, antibiotic release diminishes and becomes subinhibitory. A number of studies have reported that subinhibitory concentrations of certain antibiotics enhance, rather than inhibit, biofilm formation by bacteria. This leads to the need for new therapeutic agents.

Antimicrobial peptides (AMPs) are a very interesting emerging class of molecules that occur naturally in the mechanisms of innate immune defenses in multicellular organisms. AMPs show broad-spectrum activity against a large class of pathogens, and their microbicidal action is related to their ability to determine transmembrane pores. Thus, AMPs are considered to be a very promising class of bactericidal agents, and they have been studied in depth and tested in several clinical trials in order to clarify their biocompatibility.

*Nanostructured anti-adhesion surfaces* – Certain nanostructural features of material surfaces have been shown capable of altering the 3D conformation of adsorbed proteins, and this might have an effect on host adhesins that film the biomaterial surfaces [38]. In this connection, one of the most rapidly expanding strategies in the field of nanotechnologies is the exploitation of the antibacterial properties of nanoparticles (NPs). The bactericidal activity clearly depends on the NPs' characteristics in terms of material, charge, and size. In the case of gold NPs, the bactericidal action has been found to be determined by inhibition of ATP synthase activity associated to the change in membrane potential and by inhibition of the subunit of ribosome for tRNA binding. Silver NPs (AgNPs) appear to interact with the bacterial cell wall, disturbing its permeability, inactivating essential proteins such as thiol-containing enzymes, causing DNA condensation, and leading to Reactive Oxygen Species (ROS) generation [39]. However, together with these positive bactericidal effects, it must be stressed that NPs can sometimes have toxic effects: the induction of apoptosis and genotoxic effects related to NPs' translocation to distant tissues/organs have been reported [40]. Thus, the chemical composition, size, shape, concentration, rate of dissolution/degradation, and surface properties of nanoparticles must be clearly understood and fine-tuned to achieve the best performance in terms of the benefits/drawbacks ratio.

*Anti-biofilm bioactive molecules* – Recent progress in understanding the molecular mechanisms implicated in the physiology of biofilm formation has opened new vistas concerning how to contrast the colonization of bacteria on biomaterial surfaces [41, 42]. This has led to the development of numerous different active substances, including molecules with different mechanisms of action: enzymes capable of selectively degrading extracellular polymeric substances of the biofilm (e.g., dispersin B, rhDNase I), bactericidal molecules capable of killing metabolically quiescent bacterial cells (e.g., lysostaphin, certain AMPs), molecules and other microorganisms interfering with the quorum sensing system and inducing biofilm dispersion (e.g., furanones), and molecules downregulating the expression of biofilm extracellular polymeric substances (e.g., *N*-acetylcysteine) [43]. All these molecules have a serious defect in common: their efficacy is limited to a single species or at best to a small number of species; this greatly restricts their effectiveness against bacterial communities. Exceptions are the proteolytic enzymes, such as trypsin and proteinase K, which can degrade even host extracellular matrix proteins, and whose internal use in an *in vivo* physiological environment could obviously have adverse effects on the wound healing process. The most promising therapies now being studied comprise combinations of anti-biofilm molecules and conventional wide-spectrum antibiotics, as, for example, was shown in a study [44] combining

dispersin B and cefamandole for the treatment of staphylococcal biofilm growth on polyurethanes.

## Further Strategies

With regard to pathogenesis, the combination of the different “-omics” and related innovative technologies will provide an increasingly comprehensive view of the role that the oral microbiota can play in health and biomaterial-related dental diseases, from peri-implantitis to prosthetic candidiasis. Among others, metabolome analysis is probably the most promising method to monitor these dynamic metabolic activities, helping to clarify pathogenesis. Nonetheless, it may also be applied in examining the effectiveness of both conventional drug therapies and novel compounds and might even provide useful insights for the identification of pioneering biomarkers relevant for the development and progression of biomaterial-related diseases.

While ongoing preclinical and clinical studies hope to accumulate more data on the disease pathogenesis, as well as on the efficacy of current anti-infective strategies, new possibilities to counteract biomaterial-associated infections are advancing. Pre-inoculating urinary catheters with nonpathogenic *E. coli* were found to significantly impede catheter colonization by *E. faecalis*. However, some practical difficulties surround the introduction of this approach into clinical trials, as it would entail applying non-sterile catheters.

The use of phages as “biological weapons” has been attempted, with controversial results: whereas a high inhibition ratio  $>4$  log has been shown in *in vitro* experiments, no significant result emerged from *in vivo* studies [45]. Moreover, the use of phages as therapeutic agents is severely limited by (i) their high specificity, (ii) bacterial resistance, (iii) pre-inactivation by the immune system, (iv) poor resistance in the surface immobilization step, and (v) high risk of unpredicted virus expansion using phages as vector.

A possible future approach to combating biomaterial-associated infections, while avoiding the use of today’s antibiotics, might be provided by antisense peptide nucleic acids (PNAs). These can interfere with the expression of critical bacterial genes that are involved in antibiotic resistance, biofilm formation, and bacterial reproduction/survival. Gram-positive bacteria are less susceptible to cell-penetrating peptides conjugated with PNAs; however, studies have shown positive results on Gram-negative bacteria by targeting the *rpoD* gene, which encodes an RNA polymerase primary  $\sigma$  (70) that is essential for bacterial growth [46]. However, a number of critical concerns surrounding the safety of PNAs must be addressed before this technology will be able to enter clinical trials on human patients; in particular, these concern possible mutagenic effects deriving from the complexation of PNAs and their degradation products, which might match DNA and knockdown, or even knockoff, sequences of the human genome.

An alternative strategy has been presented, which is based on contrasting bacterial infections by modulating the host’s local immune response, rather than by

counteracting bacterial colonization directly [47]. Two active cytokines, namely, monocyte chemoattractant protein-1 (MPC-1) and interleukin 12 p70 (IL-12), were tested. The former is a powerful macrophage-recruiting cytokine, while the latter, IL-12, can induce T-helper cells to secrete Th1 cytokines, such as interferon-g (IFN-g), which in turn stimulate the bactericidal activity of macrophages. The results are promising, but no synergic activity between the cytokines was observed.

Finally, autologous platelet-rich plasma (PRP) was also found to be bactericidal when used as surface coating: *in vitro* experiments have shown that PRP can cause a reduction in colony-forming units of two logs.

The increasing use, in dentistry as well as in other medical fields, of implantable devices and the apparently unstoppable advance of drug-resistant bacteria are combining to make it imperative that we understand and combat the development of bacterial biofilm on non-biological surfaces. Several interesting approaches are being developed, in the hope that further research will lead to eradicating infection-associated implant failures.

---

## Summary

- The human body contains complex microbial communities with essential functions for the host's health.
- The oral cavity is an example of a dynamic microbial niche.
- The increasing use of implantable devices has led to the emergence of biofilm-related device infections on the part of apparently unstoppable multidrug-resistant bacteria.
- New prevention strategies are being developed in order to reduce the frequency of infection-related implant failures.
- Emerging approaches are still a matter of debate.

---

## References

1. Nyvad B, Crielaard W, Mira A et al (2013) Dental caries from a molecular microbiological perspective. *Caries Res* 47:89–102. doi:10.1159/000345367
2. Jorth P, Turner KH, Gumus P et al (2014) Metatranscriptomics of the human oral microbiome during health and disease. *MBio* 5:e01012–e01014. doi:10.1128/mBio.01012-14
3. Zaura E, Nicu EA, Krom BP, Keijsers B (2014) Acquiring and maintaining a normal oral microbiome: current perspective. *Front Cell Infect Microbiol* 4:85. doi:10.3389/fcimb.2014.00085
4. Takeuchi H, Furuta N, Amano A (2011) Cell entry and exit by periodontal pathogen via recycling pathway. *Commun Integr Biol* 4:587–589. doi:10.4161/cib.4.5.16549
5. Heuer W, Elter C, Demling A et al (2007) Analysis of early biofilm formation on oral implants in man. *J Oral Rehabil* 34:377–382. doi:10.1111/j.1365-2842.2007.01725.x
6. Eick S, Ramseier CA, Rothenberger K et al (2015) Microbiota at teeth and implants in partially edentulous patients. A 10-year retrospective study. *Clin Oral Implants Res*. doi:10.1111/clr.12588

7. Charalampakis G, Belibasakis GN (2015) Microbiome of peri-implant infections: lessons from conventional, molecular and metagenomic analyses. *Virulence* 6:183–187. doi:10.4161/21505594.2014.980661
8. Belibasakis GN (2014) Microbiological and immuno-pathological aspects of peri-implant diseases. *Arch Oral Biol* 59:66–72. doi:10.1016/j.archoralbio.2013.09.013
9. Peterson SN, Meissner T, Su AI et al (2014) Functional expression of dental plaque microbiota. *Front Cell Infect Microbiol* 4:108. doi:10.3389/fcimb.2014.00108
10. Zhu X, Wang S, Gu Y et al (2012) Possible variation of the human oral bacterial community after wearing removable partial dentures by DGGE. *World J Microbiol Biotechnol* 28:2229–2236. doi:10.1007/s11274-012-1030-5
11. Kraneveld EA, Buijs MJ, Bonder MJ et al (2012) The relation between oral *Candida* load and bacterial microbiome profiles in Dutch older adults. *PLoS One* 7:e42770. doi:10.1371/journal.pone.0042770
12. Shah SR, Tatara AM, D’Souza RN et al (2013) Evolving strategies for preventing biofilm on implantable materials. *Mater Today* 16:177–182. doi:10.1016/j.mattod.2013.05.003
13. Bereket W, Hemalatha K, Getenet B et al (2012) Update on bacterial nosocomial infections. *Eur Rev Med Pharmacol Sci* 16:1039–1044
14. Bassetti M, Ginocchio F, Mikulska M (2011) New treatment options against Gram-negative organisms. *Crit Care* 15:215. doi:10.1186/cc9997
15. Perez F, Hujer AM, Hujer KM et al (2007) Global challenge of multidrug-resistant *acinetobacter baumannii*. *Antimicrob Agents Chemother* 51:3471–3484. doi:10.1128/AAC.01464-06
16. Solano C, Echeverez M, Lasa I (2014) Biofilm dispersion and quorum sensing. *Curr Opin Microbiol* 18:96–104. doi:10.1016/j.mib.2014.02.008
17. Gilbert P, Maira-Litran T, McBain AJ et al (2002) The physiology and collective recalcitrance of microbial biofilm communities. *Adv Microb Physiol* 46:202–256
18. Kamruzzaman M, Udden SMN, Cameron DE et al (2010) Quorum-regulated biofilms enhance the development of conditionally viable, environmental *vibrio cholerae*. *Proc Natl Acad Sci U S A* 107:1588–1593. doi:10.1073/pnas.0913404107
19. Wu M-Y, Sendamangalam V, Xue Z, Seo Y (2012) The influence of biofilm structure and total interaction energy on *Escherichia coli* retention by *Pseudomonas aeruginosa* biofilm. *Biofouling* 28:1119–1128. doi:10.1080/08927014.2012.732070
20. Yang L, Liu Y, Wu H et al (2011) Current understanding of multi-species biofilms. *Int J Oral Sci* 3:74–81. doi:10.4248/IJOS11027
21. Rimondini L, Farè S, Brambilla E et al (1997) The effect of surface roughness on early in vivo plaque colonization on titanium. *J Periodontol* 68:556–562. doi:10.1902/jop.1997.68.6.556
22. Cochis A, Fini M, Carrassi A et al (2013) Effect of air polishing with glycine powder on titanium abutment surfaces. *Clin Oral Implants Res* 24:904–909. doi:10.1111/j.1600-0501.2012.02490.x
23. Poortinga AT, Bos R, Norde W, Busscher HJ (2002) Electric double layer interactions in bacterial adhesion to surfaces. *Surf Sci Rep* 47:1–32. doi:10.1016/S0167-5729(02)00032-8
24. Foster HA, Ditta IB, Varghese S, Steele A (2011) Photocatalytic disinfection using titanium dioxide: spectrum and mechanism of antimicrobial activity. *Appl Microbiol Biotechnol* 90:1847–1868. doi:10.1007/s00253-011-3213-7
25. Katsikogianni M, Missirlis YF (2004) Concise review of mechanisms of bacterial adhesion to biomaterials and of techniques used in estimating bacteria-material interactions. *Eur Cell Mater* 8:37–57
26. Lang NP, Berglundh T, Working Group 4 of Seventh European Workshop on Periodontology (2011) Periimplant diseases: where are we now? – consensus of the seventh European workshop on periodontology. *J Clin Periodontol* 38(Suppl 11):178–181. doi:10.1111/j.1600-051X.2010.01674.x

27. Teughels W, Van Assche N, Sliepen I, Quirynen M (2006) Effect of material characteristics and/or surface topography on biofilm development. *Clin Oral Implants Res* 17(Suppl 2):68–81. doi:10.1111/j.1600-0501.2006.01353.x
28. Crick CR, Ismail S, Pratten J, Parkin IP (2011) An investigation into bacterial attachment to an elastomeric superhydrophobic surface prepared via aerosol assisted deposition. *Thin Solid Films* 519:3722–3727. doi:10.1016/j.tsf.2011.01.282
29. Ruggieri MR, Hanno PM, Levin RM (1987) Reduction of bacterial adherence to catheter surface with heparin. *J Urol* 138:423–426
30. Mitik-Dineva N, Wang J, Truong VK et al (2008) *Escherichia coli*, *Pseudomonas aeruginosa*, and *Staphylococcus aureus* attachment patterns on glass surfaces with nanoscale roughness. *Curr Microbiol* 58:268–273. doi:10.1007/s00284-008-9320-8
31. Varoni EM, Iriti M, Rimondini L (2012) Plant products for innovative biomaterials in dentistry. *Coatings* 2:179–194. doi:10.3390/coatings2030179
32. Sachdeo A, Haffajee AD, Socransky SS (2008) Biofilms in the edentulous oral cavity. *J Prosthodont* 17:348–356. doi:10.1111/j.1532-849X.2008.00301.x
33. Cochis A, Azzimonti B, Della Valle C et al (2015) Biofilm formation on titanium implants counteracted by grafting gallium and silver ions. *J Biomed Mater Res A* 103:1176–1187. doi:10.1002/jbm.a.35270
34. Muzzarelli R, Tarsi R, Filippini O et al (1990) Antimicrobial properties of *N*-carboxybutyl chitosan. *Antimicrob Agents Chemother* 34:2019–2023
35. Bieser AM, Tiller JC (2011) Mechanistic considerations on contact-active antimicrobial surfaces with controlled functional group densities. *Macromol Biosci* 11:526–534. doi:10.1002/mabi.201000398
36. Friedman A, Friedman J (2009) New biomaterials for the sustained release of nitric oxide: past, present and future. *Expert Opin Drug Deliv* 6:1113–1122. doi:10.1517/17425240903196743
37. Brambilla E, Ionescu A, Gagliani M et al (2012) Biofilm formation on composite resins for dental restorations: an in situ study on the effect of chlorhexidine mouthrinses. *Int J Artif Organs* 35:792–799. doi:10.5301/ijao.5000165
38. Ferraris S, Venturello A, Miola M et al (2014) Antibacterial and bioactive nanostructured titanium surfaces for bone integration. *Appl Surf Sci* 311:279–291. doi:10.1016/j.apsusc.2014.05.056
39. Hajipour MJ, Fromm KM, Ashkarran AA et al (2012) Antibacterial properties of nanoparticles. *Trends Biotechnol* 30:499–511. doi:10.1016/j.tibtech.2012.06.004
40. Albers CE, Hofstetter W, Siebenrock KA et al (2013) In vitro cytotoxicity of silver nanoparticles on osteoblasts and osteoclasts at antibacterial concentrations. *Nanotoxicology* 7:30–36. doi:10.3109/17435390.2011.626538
41. Sungurtekin-Ekci E, Ozdemir-Ozenen D, Duman S et al (2014) Antibacterial surface properties of various fluoride-releasing restorative materials in vitro. *J Appl Biomater Funct Mater*. doi:10.5301/jabfm.5000212
42. Van Staden AD, Dicks LMT (2012) Calcium orthophosphate-based bone cements (CPCs): applications, antibiotic release and alternatives to antibiotics. *J Appl Biomater Funct Mater* 10:2–11. doi:10.5301/JABFM.2012.9279
43. Artini M, Papa R, Scoarughi GL et al (2013) Comparison of the action of different proteases on virulence properties related to the staphylococcal surface. *J Appl Microbiol* 114:266–277. doi:10.1111/jam.12038
44. Donelli G, Francolini I, Romoli D et al (2007) Synergistic activity of dispersin B and cefamandole nafate in inhibition of staphylococcal biofilm growth on polyurethanes. *Antimicrob Agents Chemother* 51:2733–2740. doi:10.1128/AAC.01249-06
45. Phee A, Bondy-Denomy J, Kishen A et al (2013) Efficacy of bacteriophage treatment on *Pseudomonas aeruginosa* biofilms. *J Endod* 39:364–369. doi:10.1016/j.joen.2012.10.023
46. Bai H, You Y, Yan H et al (2012) Antisense inhibition of gene expression and growth in gram-negative bacteria by cell-penetrating peptide conjugates of peptide nucleic acids targeted to rpoD gene. *Biomaterials* 33:659–667. doi:10.1016/j.biomaterials.2011.09.075

47. Li B, Jiang B, Boyce BM, Lindsey BA (2009) Multilayer polypeptide nanoscale coatings incorporating IL-12 for the prevention of biomedical device-associated infections. *Biomaterials* 30:2552–2558. doi:10.1016/j.biomaterials.2009.01.042
48. Israelachvili JN (2011) Intermolecular and surface forces, rev 3rd edn. Academic Press, Elsevier, Waltham, Massachusetts, United States
49. Cochis A, Fracchia L, Martinotti MG, Rimondini L (2012) Biosurfactants prevent in vitro *Candida albicans* biofilm formation on resins and silicon materials for prosthetic devices. *Oral Surg Oral Med Oral Pathol Oral Radiol* 113:755–761. doi:10.1016/j.oooo.2011.11.004
50. Jahn P, Beutner K, Langer G (2012) Types of indwelling urinary catheters for long-term bladder drainage in adults. *Cochrane Database Syst Rev* 10:CD004997. doi:10.1002/14651858.CD004997.pub3

Mishel Weshler and Iulian Vasile Antoniac

## Contents

Introduction .....	1030
Biomaterials Available for Dental Bone Graft Substitutes .....	1033
Autogenous Bone Graft .....	1034
Osteoinductive Agents .....	1036
Osteoconductive Materials .....	1042
Collagen .....	1045
Future Directions .....	1048
Principle of Guided Bone Regeneration .....	1049
Biological Principles of Guided Bone Regeneration .....	1051
Biological Factors Influencing the Reconstruction of the Alveolar Bone .....	1053
Tissue Integration .....	1053
Membrane Design Criteria and Material Selection .....	1054
Biocompatibility .....	1055
Non-resorbable Membranes .....	1055
Biodegradable Barrier Membranes .....	1056
Resorption Patterns of the Alveolar Ridge .....	1056
Surgical Techniques .....	1057
Post-extraction Sites .....	1057
Immediate Technique .....	1057
Delayed Technique .....	1058
Horizontal Defects .....	1058
Dehiscences and Fenestrations .....	1058
Autogenous Intraoral or Extraoral Blocks .....	1059
Vertical Defects .....	1059
Vertical GBR with Membrane .....	1059

---

M. Weshler (✉)  
Laniado Hospital, Netanya, Israel  
e-mail: [mishel@veshler.com](mailto:mishel@veshler.com)

I.V. Antoniac  
University Politehnica of Bucharest, Bucharest, Romania  
e-mail: [antoniac.iulian@gmail.com](mailto:antoniac.iulian@gmail.com)



Sinus Elevation .....	1061
Preoperative Antibiotics .....	1062
Flap Design .....	1063
Site Preparation .....	1063
Graft Material Positioning .....	1064
Membrane Selection and Positioning .....	1065
Biodegradable Membranes .....	1065
Non-resorbable Membranes .....	1065
Suturing .....	1066
Follow-Up .....	1066
Temporary Dentures .....	1067
Membrane Removal .....	1068
Summary .....	1069
References .....	1069

---

### Abstract

Guided bone regeneration (GBR) membranes were originally developed to promote new tissue growth within a protected volumetric defect for periodontal regeneration. The desire to promote new bone growth without resorting to grafting procedures led to the widespread use of this technique in implant surgery. The main aim is to allow ingress of bone cells to promote bone formation within the defect.

Over the last two decades, the development of the technique of guided bone regeneration (GBR) has had a significant impact on esthetic reconstruction in conjunction with implant therapy. This technique involves the use of physical barrier membranes during the healing phase in order to avoid ingrowths of undesired tissue types into a wound area.

Different practical aspects related to the use of bone graft and guided bone regeneration for dental implants will be revealed.

---

### Keywords

Guided bone regeneration • Dental bone graft • Biomaterial • Bioceramics • Collagen • Membrane • Design • Surgical technique

---

## Introduction

Bone grafts are necessary to provide support, fill voids, and enhance biologic repair of skeletal defects. They are used by orthopedic surgeons, neurosurgeons, craniofacial surgeons, and periodontists. Bone harvested from donor sites is the gold standard for this procedure. It is well documented that there are limitations and complications from the use of autograft, including the limited quantity and associated chronic donor site pain. Despite the increase in the number of procedures that require bone grafts, there has not been a single ideal bone graft substitute. Scientists, surgeons, and medical companies, thus, have a tremendous responsibility to develop

biologic alternatives that will enhance the functional capabilities of the bone graft substitute and potentially reduce or eliminate the need for autograft.

The overriding requirement for successful implant placement is to have enough bone volume of sufficient density to enable an implant of the appropriate size and requirements to be placed in a desirable position and orientation. Many of the grafting materials and procedures described in this chapter have been developed as localized procedures to overcome small anatomical limitations. There is also a need occasionally to employ more complex techniques to change the entire alveolar ridge form that may additionally involve an associated change in the skeletal base.

Aside from the obvious osseous component to this problem, there are also many situations where the soft tissue in the area of the proposed implant placement is deficient. The soft tissues play a vital role in maintaining the peri-implant environment and long-term health and also contribute greatly to the resulting esthetics, particularly in the anterior region. The peri-implant soft tissues must be able to maintain their structural integrity during normal function and oral hygiene procedures.

Bone grafts therefore may be employed to:

- Enable a better implant placement or implant placement at all
- Restore any jaw defects caused by large or small infection
- Enhance esthetics and improve soft tissues
- Change the preexisting jaw relationship

We must remember that the purpose for all of this is dental restoration, thus the initial planning stages take on even greater levels of importance in potential graft cases. By their very nature, they are more difficult to plan and execute, and the end result may fall short of both the clinician's and patient's expectations. It is important that all the alternatives are considered and presented to the patient so that they can make an informed decision with regard to their treatment. In particular, it is important to consider whether a compromise solution using prosthetic techniques may be more desirable and achievable as well as more predictable in the long term.

Another alternative is to consider whether the utilization of the various implant designs may overcome the problem.

The bone is a highly dynamic tissue comprising a mineralized extracellular matrix embedded with bone cells, blood vessels, and nerves. Bone contains three main bone-specific cell types: the *osteocyte* is a mature cell that sits in the bone lacunae, communicates with other osteocytes through long cellular processes, senses mechanical stress in the bone, and sends signals for bone remodeling as a result of mechanical stress. The responding cells are *osteoblasts*, cells specialized to secrete the unique collagen-rich extracellular matrix in the bone that enables mineralization, and *osteoclasts*, macrophage-like cells that degrade the bone structure through a combination of localized acidification (removes the minerals) and protease secretion (breaks down matrix). Osteoclasts tunnel through the bone and are usually followed close behind by osteoblasts. The bone is in a constant state of remodeling in healthy individuals.

The bone is formed developmentally, and during wound healing, by either *endochondral ossification* or by *intramembranous ossification*. In the endochondral ossification process, mesenchymal progenitor cells first form the cartilage. The chondrocytes then hypertrophy and the extracellular matrix mineralizes. Blood vessels invade the site, bringing cells that break down the existing matrix. Osteoprogenitor cells go on to form the bone. Long bones are formed by this process during normal development. Intramembranous bone formation is a more direct process, in which *osteoprogenitor cells* form the bone directly. Cranial bones are formed by this process during development. Wound healing in the bone may proceed by either process, depending on local environmental factors that include how much the ends of the bone can move relative to each other, with motion favoring the endochondral process. *Osteoprogenitor cells* are cells that have the potential to become bone cells and reside in the periosteum and the marrow. Osteoprogenitor cells are derived from connective tissue progenitor cells that reside also in the surrounding tissue (muscle) [1].

“Osteogenic cells”: – details of osteogenic (bone-forming) cells. A summary is as follows:

*Stem cell > osteoprogenitor cell > preosteoblast > osteoblast resting > proliferation > matrix deposition > mineralization*

In some applications (e.g., dental reconstruction), there are enough progenitor cells in the local area that stimulation of these cells will induce local bone formation. In a compromised site, such as where a tumor was removed and the local tissue irradiated, there may not be many local progenitor cells, and further, it may not be a good idea to release growth factors in a site where a tumor was removed, so alternative approaches must be considered. In addition to the local conditions at the wound site, the patient’s age and lifestyle habits (such as smoking) may influence the wound healing [2].

The use of barrier membranes for the regeneration of bone defects has significantly changed implant dentistry in the past 20 years. This principle, often called guided bone regeneration (GBR or GBR technique), was first described in 1959 by Hurley and colleagues for experimental spinal fusion treatment. In the 1960s, the research teams of Bassett and Boyne tested microporous cellulose acetate laboratory filters (Millipore) for the healing of cortical defects in long bones and for osseous facial reconstruction, respectively. The authors used these filters to establish a suitable environment for osteogenesis by excluding fibrous connective tissue cells from bone defects. However, these pioneering studies did not immediately lead to a broad clinical application of barrier membranes in patients. The clinical potential of the membrane technique was not recognized until the early 1980s, when the research team of Karring and Nyman systematically examined barrier membranes in various experimental and clinical studies for periodontal regeneration. A few years later, barrier membrane techniques were tested in experimental studies on bone regeneration.

Based on promising results in these studies, clinical testing of membranes began in implant patients in the late 1980s. Since that time, the GBR technique has

continued to evolve, necessitating an updated analysis of its scientific basis and clinical applications.

The biological principles and indications for the use of guided bone regeneration (GBR) are described with specific focus on the esthetic zones in the upper and lower jaws. The efficacy of barrier membranes in conjunction with bone healing and reconstructive therapy is the result of mechanical, cellular, and molecular mechanisms. Basic studies on guided bone regeneration have shown the same sequence of healing occurring as in regular fracture repair. Different kinds of biological membranes, resorbable as well as non-resorbable, are described in the chapter.

Clinical results are presented and a section on complications is also included. The author concludes that the underlying bone structure of the alveolar process plays a key role in the overall esthetic appearance.

---

## **Biomaterials Available for Dental Bone Graft Substitutes**

The term biomaterial generally indicates any substance used to create a medical device destined for diagnosis, prevention, control, mitigation, or therapy of a human disease, on condition that it persists in the body for at least 30 days after implantation. First of all, cytotoxicity, genotoxicity, and hemocompatibility of a biomaterial have to be evaluated. After that, attention has to be paid to its macrostructure and microstructure, by evaluating the isotropy. Finally, its mechanical, physical, and chemical properties should be taken into consideration. Which characteristics should a biomaterial have to be considered for implantation in the human body? They can be summarized as follows:

- Noncarcinogenic
- Nonantigenic
- Hydrophilic
- Radiopaque
- Versatile (usable in several clinical fields)
- Sterile
- Osteoconductive or osteoinductive
- Favorable clinical handling
- Resorption and replacement by host bone
- Available in sufficient quantities
- Low in cost

Biomaterials can be obtained from the patient (autogenous), from beings belonging to the same species (homologous), from beings belonging to different species (xenogeneic), or from minerals (alloplasts). Apart from autogenous bone, which has osteoconductive, osteoinductive, and osteoproliferative properties, and homologous bone, whose properties are mainly osteoconductive and slightly inductive, all the biomaterials used for bone regeneration are only osteoconductive scaffolds. Bone substitutes were created in order to promote bone regeneration, avoiding the

necessity of harvesting the bone from the patient. The first materials on the market were represented by ceramic hydroxyapatite of different macrostructures (coral, bioglass, ceramic hydroxyapatite), and the osteoconductive potential and the resorbability were not excellent with regard to the implant field. A few years later, demineralized freeze-dried bone allograft (DFDBA) from human donors was introduced in the USA; osteoinductive properties were claimed for this, because the demineralization process was able to expose bone morphogenetic proteins (BMP). In addition, some publications confirmed an osteoconductive property for this material [3–5]. Unfortunately, the properties of DFDBA were not confirmed by later histologic and clinical studies in sinus elevation and guided bone regeneration (GBR) procedures.

At the same time, xenogeneic anorganic bone was obtained from the cattle [6–8], followed by similar materials from equine or porcine sources. These mineral scaffolds, resulting from a treatment to eliminate any trace of organic material, promote colonization of the bone tissue via osteoconduction. They are slowly replaced by newly formed bone; both the quality and the quantity of lamellar bone are well documented, and at the moment, they are considered a first-choice material in bony defect repair in implantology, with the exception of classes V and VI atrophies (Cawood and Howell1), where the use of autogenous bone, alone or in association with xenogeneic materials, is mandatory to rebuild the bony architecture prior to implant placement.

The degree of bone grafting required for implant placement varies from localized deficiencies to cases where there is a need to change the entire arch form and/or jaw relationship. There exist, therefore, a great many techniques and materials to facilitate such grafting procedures, many of which may be used in combination. The interaction between the graft and the surrounding host bone is very important and is the subject of much research.

Although some grafts will act merely as space fillers, the ideal graft will be osseoconductive and osseoinductive. Osseoconduction is the property of promoting bone growth from the surrounding host bone onto the surface of the graft material, using the graft as a framework.

The graft material in such cases may be resorbed or remain virtually intact, depending on the material used. Osseoinduction is the ability to promote reformation of remote bone from the host bone even within noncalcified tissues. Bone morphogenetic proteins and other bone-promoting factors have this latter property.

## **Autogenous Bone Graft**

Autogenous bone graft is considered the very best jaw bone transplant, since it is originally from the same person to be implanted to. There is complete identity between the object to which it should connect, and thus the chances of success of this very type of transplant are the best. The ready availability of autogenous bone has always meant that it is the first choice of bone grafting material for many clinicians. However, patient's acceptance of autogenous bone harvesting may be low, given the potential morbidity associated with such techniques. Although a great



**Fig. 1** Bone chips from the drilling site

amount of research and clinical time has been spent over many years to develop substitutes for autogenous bone, it remains the gold standard by which all other materials are judged and is the material of choice for the present authors. Its main advantages are:

- Availability
- Sterility
- Biocompatibility
- Osseoinductive potential
- Osseoconductive potential
- Ease of use

The graft acts as a scaffold for the ingrowth of blood vessels and as a source of osteoprogenitor cells and bone-inducing molecules. The graft is eventually resorbed as part of the normal turnover of the bone. Principal autogenous bone graft sources are ascending mandibular ramus, symphysis mentis, occipital bone, tibia, iliac crest, and rib bone.

However there is one more autogenous bone graft source, very handy and simple to obtain but only in small portions, mainly on account of the fact that it is obtained from the drilling site chosen for the implant placement (Fig. 1).

Autogenous bone graft has a documented 2–4-month period from integration to regeneration, but with a low capacity of preserving its initial volume at time of integration. Although the gold standard for bone grafting remains the patient's own bone, the limitations on the amounts available (particularly from sites other than the iliac crest) mean that there remains a great demand for alternative graft materials. **Xenografts** is a graft of tissue taken from a donor of one species and grafted into a recipient of another species; **allogeneic grafts (allografts)** are taken from different individuals of the same species; **herbal-based bone filler** is an alternative biomaterial, with excellent bone regeneration potential generated from soybean; **porous titanium granules** are a regenerative material treating a local osseous defect around titanium dental implant; and **alloplasts** are synthetic materials. The macrostructure

and microstructure of these grafts have an enormous influence on their efficacy. The pore diameter and volume are therefore of great importance.

Bone grafts and their substitutes can be divided according to their properties of osteoinduction, osteoconduction, and osteogenesis.

## **Osteoinductive Agents**

Osteoinductive agents are bone graft substitutes, generally proteins, which induce differentiation of undifferentiated stem cells to osteogenic cells or induce stem cells to proliferate. Several osteoinductive agents have been identified. Among these compounds are transforming growth factor (TGF) [9] bone morphogenetic proteins (BMPs), [9–12] fibroblast growth factors (FGFs) [13, 14], insulin-like growth factors (IGFs) [15], and platelet-derived growth factors (PDGFs) [16].

## **Demineralized Bone Matrix**

Since the initial studies performed by Urist [3], the osteoinductive capacity of DBM has been well established [17]. DBM is produced by the acid extraction of human cortical bone, and the components of the bone that remain behind include the non-collagenous proteins; bone osteoinductive growth factors, the most significant of which is BMP; and type I collagen. DBM provides no structural strength, and its primary use is in a structurally stable environment. Hydroxyapatite, autograft, allograft, or bone marrow cells may be added to DBM. A carrier may be added to DBM to improve its handling characteristics and mechanical properties. DBM obtained from allogeneic human cortical bone shows variable efficacy and osteoinductive index. A reproducible and rapid bioassay, using human cells of osteoblastic lineage, SAOS-2 cells, has been developed to correlate the activity of DBM [18]. Relevant images obtained by scanning electron microscopy of relevant products are shown in Fig. 2.

## **Bone Morphogenetic Proteins**

The BMPs (BMP 1-7) are low-molecular-weight non-collagenous glycoproteins that belong to an expanding TGF superfamily of at least 15 growth and differentiation factors. They make up only 0.1 % by weight of all bone proteins. Unlike DBM, which is a mixture of BMPs and immunogenic, noninductive proteins, the pure form of BMPs is non-immunogenic and non-species specific. Currently single BMPs are available through recombinant gene technology, and mixtures of BMPs are available as purified bone extracts for clinical studies.

The recombinant human BMPs extensively studied are rh-OP-1 (osteogenic protein 1), rh-BMP-2 (Genetics Institute, Cambridge, MA), and rh-BMP-7 (Creative Biomolecules, Hopkinton, MA).

In October 2001, approval was granted by the FDA for recombinant OP-1 implant, for use as an alternative to autograft in recalcitrant long bone nonunions. This is the first BMP approved for clinical use in the USA. The approved product, OP-1 implant, is a combination of rh-OP-1 and a bovine collagen carrier.

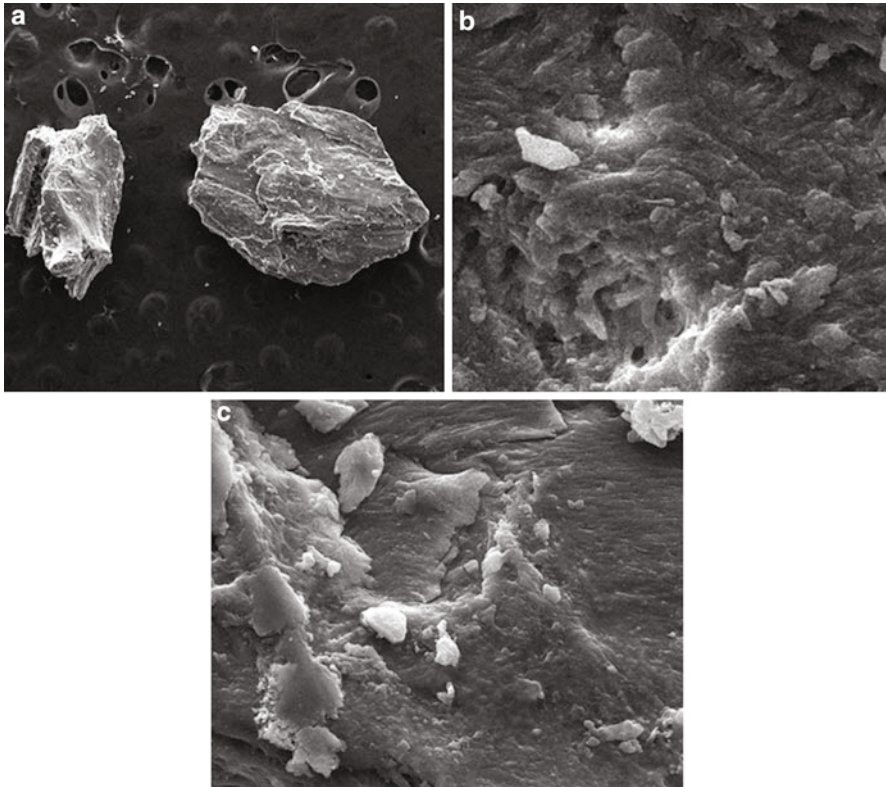


**Fig. 2** Relevant images obtained by scanning electron microscopy of relevant demineralized bone matrix: (a) Puros cortical; (b) Puros cancellous; (c) Puros cortical-cancellous mix

The rh-OP-1 is derived from a recombinant Chinese hamster ovary cell line, and the bovine collagen is derived from the diaphyseal bone and is primarily type I. It is a white lyophilized powder, which has to be reconstituted with two to three ml of saline, prior to use. It forms a paste which is then surgically implanted at the fracture site.

The osteogenic activity of OP-1 has been proven in a validated critically sized fibular defect in human subjects [19]. In November 2001, the first two-year results of a clinical study of rh-BMP-2 were presented at the North American Spine Society meeting.

### **Other Growth Factors**

Besides the growth factors expressed from the extracellular matrix of the bone (DBM, BMP), there are other factors in the circulating blood, which play a role in bone healing. TGF is the most extensively studied growth factor in the field of bone biology. It comprises an entire family of molecules that includes the BMPs. In 1994, Genentech, Inc. (San Francisco, CA) was issued the patent for developing TGF through recombinant technology. This covered the nucleic acids, vectors, and host cells used for production of recombinant TGF. In an animal study, it was found that BMP, and not TGF, enhanced bone formation [20]. PDGF is another factor whose



effect was studied on the bone healing of unilateral tibial osteotomies in rabbits. It was concluded that PDGF had a stimulatory effect on fracture healing [16].

Autologous growth factors (AGF) is an innovative concept. AGF gel is obtained from the buffy coat of the blood collected in the cell saver during surgery, through the process of centrifugation. It is rich in growth factors, especially TGF and PDGF. Approximately 20 ml of AGF is derived from 500 ml of blood in ten minutes and it is placed at the operating site. Bovine-derived bone morphogenetic protein extract is a cocktail of growth factors and is currently being evaluated for its role in human spine fusion and periodontal repair. It can be combined with either DBM or a coralline calcium carbonate carrier.

Basic fibroblast growth factor (bFGF) is produced locally in the bone during the initial phase of fracture healing and is known to stimulate the cartilage and bone-forming cells [13].

A combined product is a formulation of bFGF and hyaluronic acid (Hy). It is delivered as a single minimally invasive injection into the fracture site. Hy is a viscoelastic polymer found throughout the body that cushions and protects soft tissues. The synergistic combination of bFGF and Hy appears to accelerate the operating site healing process and underscores the importance of using an appropriate carrier not only for bFGF but also possibly for other growth factors.

### **Allogeneic Bone Graft**

The dry weight of the bone comprises 70 % inorganic materials and 30 % organics; 90 % of the organic material is type I collagen, while the other 10 % comprises proteins that induce mineralization and signal for regeneration. It was demonstrated in the 1960s that demineralized bone (bone exposed to acid to dissolve the inorganic component, leaving the organic matrix = demineralized bone matrix) could induce ectopic bone formation via the endochondral process (ectopic = any site that is not the normal physiological site). It was hypothesized that a diffusible factor was present in demineralized bone matrix.

Characterization of the properties of demineralized bone matrix led to identification and cloning of a molecule (now called BMP-2) that could induce ectopic bone formation on its own. The BMP family has grown substantially and it is now recognized that these molecules also play important and essential roles in development.

BMPs induce cell migration, proliferation, and differentiation, and it is not entirely clear yet which of these processes dominate *in vivo*. In order for BMPs to be effective, progenitor cells that can be induced to form bone must be present in the local area. This means that BMPs will not likely be effective in very large defects or defects which have been compromised by irradiation or large infection.

Allogeneic bone graft has a documented 3–4-month period from integration to regeneration, but with a low capacity of preserving its initial volume at time of integration (Figs. 3 and 4).

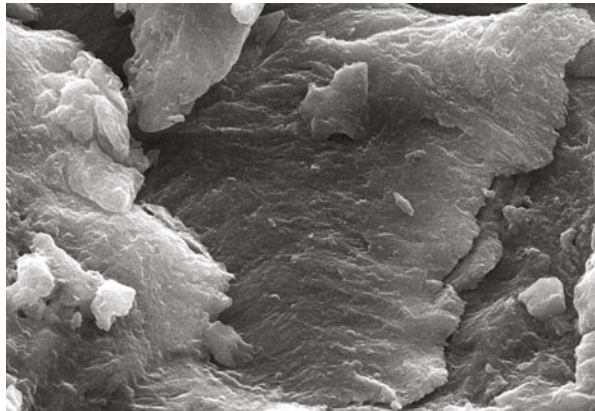
### **Xenogeneic Bone Graft**

Xenografts derived from natural bone sources have been extensively investigated in multiple experimental and clinical studies. In particular, cancellous bovine bone

**Fig. 3** Allogeneic bone chips of 0.5–1.00 mm mixed with sterile sodium chloride 0.9 % solution



**Fig. 4** SEM image of the allogeneic bone chips of 500–1000  $\mu\text{m}$  ( $\times 5000$ )



has been used as a source for these bone substitute materials because of its close similarity to cancellous human bone. The organic component is removed by heat treatment, by a chemical extraction method, or by a combination of the two to eliminate the risk of immunologic reactions and disease transmission. Since the first reports of bovine spongiform encephalopathy, there has been a particular focus on the ability of these extraction methods to completely eliminate all protein from the bovine bone source. However, despite the hypothetical risk of organic remnants in bovine bone substitutes, there have been no reports of disease transmission from these materials. In contrast, a few cases of transmission of human immunodeficiency virus and hepatitis related to allogeneic materials have been reported.

Deproteinized bovine bone minerals (DBBMs) are in general known to be biocompatible and osteoconductive, although the production methods have a strong impact on their biologic behavior. Two bovine bone substitutes derived from bovine cancellous bone, one deproteinized by high temperatures and the other mainly by chemical means.

This is an osteoconductive and slow-resorbing material composed of an anorganic mineral matrix deprived of the organic scaffold in order to leave intercrystalline microtunnels and microcapillaries between the bovine apatite crystals. The high osteoconductivity is due to the natural microstructure of the material, which demonstrates a large inner surface area and a system of intracrystalline spaces and microtunnels available for ingrowth of blood vessels and osteoblast migration. Long-term stability has been proved by many clinical studies. There must be no direct contact of the material with the implant surface for good implant osseointegration. The only early contact is between the clot and the matrix particles, and the angiogenesis and osteoblasts deposition occur from there. Integration is due to replacement of the bone substitute with newly formed bone.

Histomorphometric analysis demonstrated that anorganic bovine bone increases the mineral portion in regenerated areas as compared to host bone areas [9–12]. Some of the material remains in the bone tissue and is slowly embedded in lamellar bone, resulting in denser bone, and this could explain the high survival rate of implants placed in areas augmented with it.

Xenogenic bone graft has a documented 6–9 month period from integration to regeneration, but has a high capacity of preserving its initial volume at time of integration (Figs. 5 and 6).

### **Herbal Based Bone Filler**

Soybean is a natural material made of protein and carbohydrate fractions (approximately 40 % by weight for each fraction), of an oil fraction (approximately 18 %), and of minerals (approximately 2 %). Soybean also contains isoflavones, phytoestrogens with an ascertained action on eukaryotic cells. Isoflavones inhibit tumor cell proliferation and immunocompetent cell activation and seem to reduce scar formation in wound healing. Recently, a new class of biomaterials has been developed from defatted soybean curd and flour. The processing of these components by either thermo-setting or extraction allows the preparation of materials with different physico-chemical properties; by these processes membranes, films, granules and gels can be obtained. The bone regeneration potential of these biomaterials has been demonstrated by *in vitro* studies highlighting their inhibitory effect on monocytes/macro-phages and osteoclasts as well as their ability to induce osteoblast differentiation and bone nodule mineralization [21].

Soybean-based biomaterials clearly promote bone repair through a mechanism of action that is likely to involve both the scaffolding role of the biomaterial for osteoblasts and the induction of cell differentiation. Therefore, these biomaterials have a potential to become fillers alternative to osteoconductive products such as those based on either autologous bone or ceramics or PLA/PGA hydrogels. Indeed, in addition to their bone repair potential, the ductility of Soybean bone filler biomaterials brings advantages in the surgical practice when compared to the brittle and not malleable ceramics or to the relatively loose consistency of hydrogels.

Soybean-based bone filler has a documented 4–6-month period from integration to regeneration, but has a high capacity of preserving its initial volume at the time of integration (Fig. 7).

**Fig. 5** Xenogeneic bone chips mixed with sterile sodium chloride 0.9 % solution

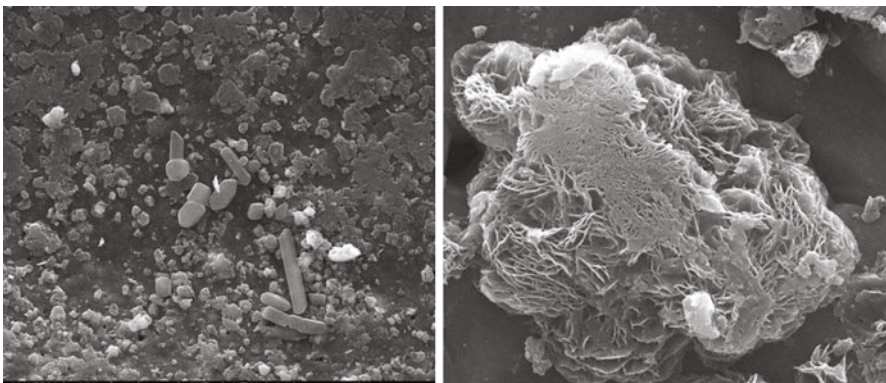


**Fig. 6** SEM images of the xenogeneic bone chips at different magnification

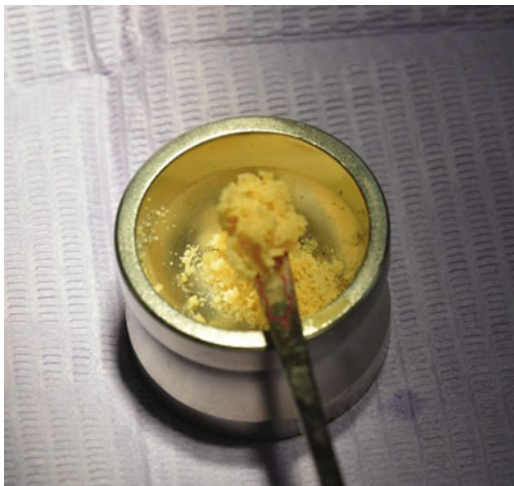
### **Porous Titanium Granules**

The search for osteoinductive as well as osteoconductive materials has led to the novel idea of using titanium in bone augmentations of the alveolar crest. The indications for the use of porous titanium granules material in this area have so far been limited to recently reported sinus augmentations and for defects around dental implants, even though the idea was first tried in a pilot case in 1995 [22, 23].

The material has also been evaluated in a clinical study of sinus augmentations where the main part of the included study subjects (12 patients) had implants simultaneously installed and porous titanium granules material placed around them in the sinus floor in a one-stage procedure. Four patients had a delayed placement of implants due to insufficient primary stability at the time of augmentation.

Three implant losses after an observation period of 12–36 months were seen and two of these were in the staged group. In the simultaneous placement group, one implant was lost after one year of loading (after a history of postoperative sinus

**Fig. 7** Soybean chips of 0.1–0.2 mm mixed with sterile sodium chloride 0.9 % solution



infection). The authors raised questions regarding the usage of the material in staged sinus lifts as well as further explore the risk of displacement of granules into the sinus during augmentation [23].

Porous titanium granules are not being replaced, but have a high capacity of preserving its initial volume at the time of integration (Figs. 8 and 9).

## Osteoconductive Materials

Osteoconduction is a three-dimensional process that is observed when porous structures are implanted into or adjacent to the bone. Porosity alone, however, is not adequate for bone ingrowth. Porosity with interconnectivity is the most essential prerequisite. This is based on the three-dimensional interconnections between the lacunae in the bone that provide intercellular communication. Although there are alternative views, the consensus of research indicates that the requisite pore size for bone ingrowth into porous implants is 100–500  $\mu\text{m}$ , and the interconnections must be larger than 100  $\mu\text{m}$  [24].

Synthetically produced bioceramics have the advantage of having no risk of cross infection but may still give rise to an antigenic response. Their physical properties can be manipulated to a great degree, and they may be used also in combination with bone-promoting molecules to enhance their effectiveness. They act as a framework for bone formation on their surface and are therefore osseoconductive.

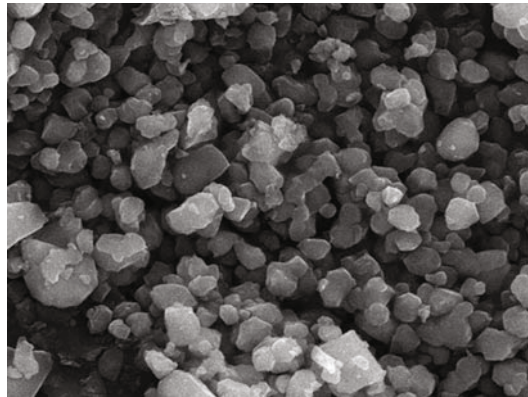
They include:

- Calcium sulfate
- Calcium phosphate
- Bioactive glasses
- Calcium carbonate

**Fig. 8** Porous titanium granules of 0.5–1.00 mm mixed with sterile sodium chloride 0.9 % solution



**Fig. 9** SEM images of porous titanium granules of 500–1000  $\mu\text{m}$  ( $\times 20,000$ )



### Calcium Sulfate

Gypsum, also referred to as plaster of Paris, owes its name to a village just north of Paris. Although its external use for creation of hard setting bandages dates back to the seventeenth century, the first internal use to fill bony defects was reported in 1892 by Dressmann [19]. The application of plaster of Paris as a bone void filler, and the use of antibiotic-laden plaster in the treatment of infected bony defects, has been supported by various studies [20–23]. Calcium sulfate ( $\text{CaSO}_4$ ) has long been used in its partially hydrated form. Medical-grade calcium sulfate is crystallized in highly controlled environments producing regularly shaped crystals of similar size and shape. It possesses a slower, more predictable solubility and reabsorption. This material typically dissolves *in vivo* within 30–60 days depending on the volume and location. The chief advantages are that it can be used in the presence of infection and it is comparatively cheaper. Since it is bioabsorbable, it has inherent advantages over other antibiotic carriers, such as polymethyl methacrylate, which become a nidus for further infection after elution of the antibiotics, thus requiring a separate operation for removal from the surgical site. When this is combined with the eradication of dead

space and the acidic environment created during its resorption, the compound can be an extremely effective treatment for acute bony infections with bone loss.

### Calcium Phosphate

The earliest application of calcium phosphate salts was in the form of powders [25]. The most commonly used calcium phosphate ceramics are hydroxyapatite (coral based or synthetic) and tricalcium phosphate, used in the form of implant coatings and defect fillers. These materials require high temperature and high pressure processing to produce dense, highly crystalline, bioinert ceramics, which are not moldable intraoperatively and also have poor fatigue characteristics.

### Porous Coralline Ceramics

Chiroff et al. [26] first recognized that corals made by marine invertebrates have skeletons with a structure similar to both the cortical and cancellous bone, with interconnecting porosity. There are two processes for manufacturing coralline implants. One approach is to use coral directly in calcium carbonate form. These materials are called natural corals. The trade name for natural coral is biocoral. The other process is replamineform process that converts calcium carbonate to hydroxyapatite [24]. Although there are hundreds of genera of stony corals, *Porites* and *Goniopora* are the only two genera meeting the required standards of pore diameter and interconnectivity [24]. The exoskeleton of the genus *Porites* is similar to the cortical bone, and the exoskeleton of the genus *Goniopora* has a microstructure similar to the cancellous bone. The products are trade named either Pro Osteon or InterPore porous hydroxyapatite. A version of hybrid, coralline product has also been developed. It is a composite of calcium carbonate and calcium phosphate. A calcium phosphate layer, largely hydroxyapatite, is formed on the calcium carbonate pores. The thickness of the hydroxyapatite layer is adjusted to alter the resorption rates. In December 2001, a synthetic porous-coated hydroxyapatite (PCH) bone substitute has been launched in Europe. It is a porous calcium phosphate scaffold with a biomimetic coating – first-generation tissue-engineered product. Its surface structure resembles that of the natural bone, which makes it osteoconductive.

### Tricalcium Phosphate

Tricalcium phosphate (TCP) is a bioceramic with bioabsorbable and biocompatible character, but its inadequate porosity, comparatively small grain size and its rapid dissolution (six weeks), makes it a poor bone graft substitute. Biocompatible and resorbable calcium phosphate cement has been introduced for augmentation of fracture repair. The chemical composition and crystallinity of the material are similar to those of the mineral phase of the bone. It undergoes the same in vivo remodeling as normal bone to reestablish the bone morphology and strength.

BSM – bone substitute material is a poor crystalline calcium phosphate cement with favorable absorption characteristics and easy intraoperative handling characteristics [27]. It is hydrated with saline to form a workable paste, which remains formable for hours at room temperature but hardens within 20 minutes at physiologic body temperature (Fig. 10).

**Fig. 10** Tricalcium phosphate of 0.2–0.5 mm powder granules



## Collagen

Type I collagen is the most abundant protein in the extracellular matrix of the bone. It has a structure that is conducive to promoting mineral deposition, and it binds the non-collagenous matrix proteins, which initiate and control mineralization by itself. Collagen functions poorly as a graft material, but when coupled with bone morphogenetic proteins, osteoprogenitor precursors, or hydroxyapatite, it enhances incorporation of grafts significantly. The fibrillar collagen is highly purified collagen obtained from bovine dermis.

Autologous bone marrow aspirate can be added to these materials or it can be mixed with autologous bone as a bone graft extender. It does not offer structural support by itself and its movement may be difficult to control [28, 29]. A mineralized collagen sponge, launched in Europe for clinical use in 2000, is shown in Fig. 11.

Each microscopic type I collagen fiber is coated with hydroxyapatite; these fibers are then fabricated and cross-linked into a three-dimensional, continuously porous, and stable final format (Fig. 12).

It can be mixed with bone marrow aspirate to provide osteogenic and osteoinductive potential. Another novel bone-inducing protein, MP52, is integrated with mineralized collagen sponge bone graft substitute, to induce bone formation. MP52 is a member of the bone morphogenetic protein (BMP) family.

Collagen, the major constituent of connective tissues and the major structural protein of each organ, is of particular interest as a natural polymer for obtaining drug delivery systems. It acts as a hemostatic and promotes the new tissue granulation and wound epithelialization, functioning as a dressing for different types of wounds. However, collagen itself cannot produce the healing of an infected wound because it is a protein in nature, and bacteria can use it as a substrate. But combined with suitable antibiotics highly efficient drug delivery systems for wound treatment can be obtained, due to a potential synergistic effect. An ideal drug delivery system must show a low allergization quota, stability at body temperature, tissue compatibility, bactericidal activity, high bacterial resistance, broad activity spectrum, and low resorption rate.



**Fig. 11** Collagen sponge  
20 × 20 mm 19,2 mg from  
porcine origin and 12,8 mg  
disodium hydrogen phosphate

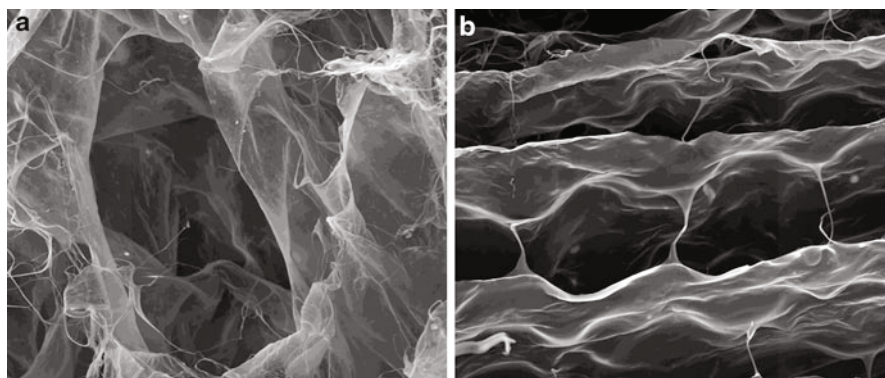


**Fig. 12** SEM images of the collagen sponge obtained by lyophilization: (a) without conductive layer; (b) with conductive layer ( $\times 1000$ )

Antibiotics' local delivery has been studied successfully in clinics for aminoglycosides like gentamicin and tobramycin as well as for minocycline, tetracycline, teicoplanin, or sulbactam-cefoperazone. Although doxycycline is a bactericide for a broad spectrum of bacteria and inhibits the action of collagenase, so far it is found in very few drug delivery systems.

In order to improve the biochemical and mechanical properties of support and control the release of drugs, the collagen has to be cross-linked, the usual cross-linking agent being glutaraldehyde [30] (Figs. 13 and 14).

Tissue engineering is a rapidly evolving multidisciplinary field that applies the principles of biology and engineering in order to develop tissue substitutes to restore, repair, or improve the function of diseased or damaged human tissues. Cell-based therapies might therefore offer hope for a number of diseases, in particular those in which single pharmacological agents are not sufficient. The success of numerous therapies in regenerative medicine requires the ability to control the formation of stable vascular networks within tissues. The formation of new blood vessels, or neovascularization, is mediated, in part, by the interaction between endothelial cells

**Fig. 13** Collagen membrane  
20 × 20 mm 5 mg of collagen  
bovine origin with 1 mg  
doxycycline and 0.001 mg  
glutaraldehyde

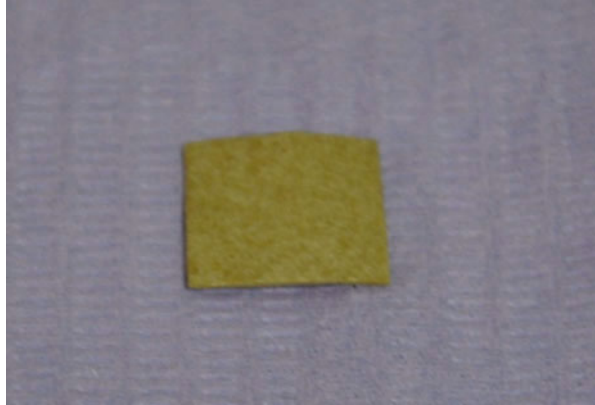
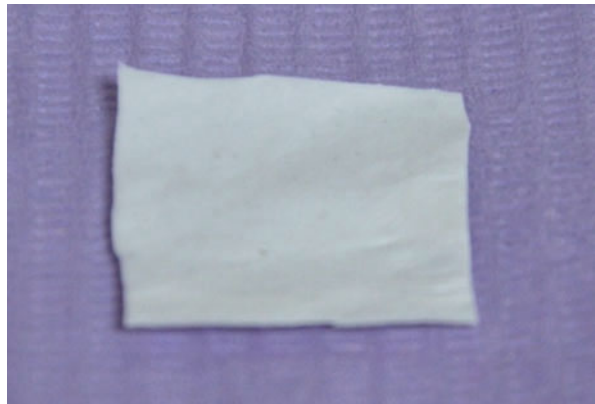


**Fig. 14** Collagen membrane  
20 × 30 mm from bovine  
origin



and insoluble factors of the extracellular microenvironment. These interactions are determined by the chemical, physical, and mechanical properties of the matrix.

In tissue engineering, the role of the scaffold is comparable to the role of the extracellular matrix and consists in supporting the development of cells and tissue. Collagen is a significant constituent of the natural extracellular matrix (ECM) and plays an important role in the formation of tissues and organs, being involved in the functional expressions of cells.

Collagen scaffolds have been used in a variety of applications due to a number of valuable characteristics like low antigenicity, high biocompatibility, and hemostatic and cell-binding properties. It is now evident that collagen and collagen-derived fragments control many cellular functions, including cell shape and differentiation, migration, and synthesis of numerous proteins.

Several *in vitro* studies of cell-scaffold interactions and tissue synthesis as well as *in vivo* studies on induced tissue and organ revealed the excellent biological performances of collagen. To promote cell adhesion and growth, a biologically active scaffold must satisfy a number of features. The scaffold biomaterial has to

be biocompatible and degrade in the body at a controlled rate; the average pore diameter must be large enough for cells to migrate through the pores and small enough to provide a critical total surface area for appropriate cell binding and has to preclude the risk of infection during applications.

An essential element in graft procedure is the blood supply. The prevention of implant failure caused by hypoxia and following infection is still a challenge. However, in general, cell-based tissue engineering provides a successful treatment in wound healing disorders. It is known that endothelial cells that form the inner lining of blood vessels participate in important physiological processes including exchanges of molecules, coagulation, and wound healing. Also these cells are essential for vascularization of the new tissue during the wound healing and tissue formation processes. A requirement for promoting faster vascularization is the presence of large pore sizes into the scaffolds. The scaffolds made up of porous collagen matrices provide a three-dimensional (3D) structure which has a significant effect on cellular activity.

Three-dimensional cell culture systems offer a milieu to study biosecretory, migratory, and proliferative functionality. Embedding of endothelial cells in three-dimensional collagen-based matrices allows them to grow and attain confluence in a controlled environment. Such constructs permit endothelial cells to retain a quiescent state, the secretion of essential regulatory factors, and the associated potential for vaso-regulatory control, within matrices (vehicles) that can be stored, manipulated, functionally validated, and implanted at sites protected from environmental forces [31].

## Future Directions

Considerable interest has developed in creating osteoconductive matrices using nonbiologic materials. Degradable polymers, bioactive glasses, and various metals have been studied. The advantage of nonbiologic materials includes the ability to control all aspects of the matrix, avoidance of immunologic reaction, and excellent biocompatibility. Polylactic and polyglycolic acid polymers have been used extensively as suture materials and biodegradable fracture fixation implants. These materials have the advantage of being assembled in various forms and can be integrated with growth factors, drugs, and other compounds to create multiphase delivery systems. A synthetic bone graft scaffold, tissue engineered from amorphous D, L-poly(lactide-co-glycolide) (PLG), is designed to resorb within 12–20 weeks following implantation. They provide a porous architecture for the ingrowth of new bone and then fully degrade. Hydroxyapatite coating of metal surfaces enhances ingrowth and direct bonding of the bone to porous surface [32, 33]. Essentially, these coatings can be used on implants with relatively simple surface geometry and use excessive high temperatures. This means that it is difficult to coat implants with complex surface geometry (e.g., porous surface) and that no biologically active agents can be added to the coating during the spraying process. A technology has been developed that allows the growth of a thin layer of bone-like ceramic over medical devices [34].

The calcium phosphate coating is grown from an aqueous fluid at ambient temperatures. In contrast to conventional technologies, these “biomimetic” coatings can be applied on to surfaces with complex geometry, and active agents such as growth factors or antibiotics can be coprecipitated. This creates the possibility of using these coatings as slow release systems [35]. Alloplastic bone substitute has a documented 4–6-month period from integration to regeneration, but with a very low capacity of preserving its initial volume at the time of integration.

Advances in tissue engineering and the integration of the biological, physical, and engineering sciences will create new carrier constructs that regenerate and restore functional state. These constructs are likely to encompass additional families of growth factors, evolving biological scaffolds, and incorporation of mesenchymal stem cells. Ultimately, the development of *ex vivo* bioreactors capable of bone manufacture with the appropriate biomechanical cues will provide tissue-engineered constructs for direct use in the skeletal system. There are some new bone tissue engineering products developed for application in dental implants, revision surgery, and spinal fusion. The bone marrow cells are harvested from the patient, then multiplied in culture, shaped in appropriate structure on a scaffold, and implanted into the patient. The process takes 4 weeks. Once considered a fantasy, there is a compelling evidence to support the utility of gene therapy for bone induction in humans [28]. Studies have successfully demonstrated several safe, effective strategies to form new bone via gene therapy in animals. Gene therapy involves the transfer of genetic information to cells. When a gene is transferred to a target cell, the cell synthesizes the protein encoded by the gene. The duration of protein production that is required and the anatomic location where the protein must be delivered determine the strategy employed. The gene therapy used for bone induction is short-term, regional therapy. The gene can be introduced directly to a specific anatomic site (*in vivo* technique), or specific cells can be harvested from the patient, expanded, and genetically manipulated in the tissue culture and then reimplanted (*ex vivo* technique). The vehicle for gene delivery can be either viral (adenovirus, retrovirus) or non-viral (liposomes, DNA-ligand complexes). The gene can be selectively transferred to a targeted cell (osteoblast, fibroblasts) at the bone induction site.

---

## Principle of Guided Bone Regeneration

Guided bone regeneration (GBR) membranes were originally developed to promote new tissue growth within a protected volumetric defect for periodontal regeneration. The desire to promote new bone growth without resorting to grafting procedures led to the widespread use of this technique in implant surgery. The main aim is to allow ingress of bone cells to promote bone formation within the defect. The original membranes were expanded polytetrafluoroethylene (PTFE, Gore-Tex™). It is a non-resorbable material that requires removal at second-stage surgery.

The need for removal led to the development of resorbable membranes made of synthetic polymers such as polylactate and polyglycolic acid, as well as collagen

membranes. Resorbable materials should be functional between 3 and 6 months after insertion. However, they may be resorbed or lose their shape too quickly and limit the amount of bone regeneration achieved. The creation and maintenance of a volumetric defect are critical, and this may be improved by reinforcing PTFE membranes with titanium strips.

Further enhancement of the space-maintaining properties is achieved by the use of fixation pins and screws that serve to “tent” the membrane. This can be achieved also by placing small bone chips within the defect, which will also act as osseoconductive/osseoinductive grafts. The cortical bone within the defect is perforated with surgical burs to promote osteogenic cells to occupy the space created.

Guided bone regeneration is also commonly used at the time of implant placement to repair small fenestrations and dehiscences around implants. It should be remembered that any such bone created will not function to stabilize the implant at the time of placement and that initial implant stability remains the overriding priority. The amount of new bone created can be quite substantial but the degree to which it becomes osseointegrated is variable. The amount of the bone to implant contact of the newly generated bone is thought to change with time and loading. Guided bone regeneration is most predictable when attempting to increase the buccolingual dimension, but increasing the vertical dimension using this technique is very difficult and unpredictable.

Although membranes are designed to allow the passage of nutrients, they nonetheless tend to compromise the blood supply to the overlying soft tissues. This can result in breakdown of the soft tissues, exposure of the membrane, and infection. This may result in a net loss of the bone in the surgical area or failure of implants to osseointegrate. It is important that all incisions are kept as remote from the grafted area as possible and that the wound is sutured hermetically and without undue tension. Supporting the tissues with sutures that take large bites and “sling,” the flaps can reduce tension at the wound edges.

A variety of techniques and materials has been used to establish the structural base of osseous tissue for supporting dental implants. GBR is a surgical concept which has been in clinical use for well over two decades. It has undergone several developments and improvements and is nowadays considered a predictable treatment modality, once the previously described issues have been taken fully into account. Doubts have previously been raised regarding the quality and lasting capability of membrane-regenerated bone when being put into clinical function.

Previous experimental studies have clearly shown the positive dynamics of this type of bone over time. Recently this has also been confirmed in several clinical studies. In a recent review study by Aghaloo and Moy [36], the GBR technique was compared to different types of grafting procedures such as autogenous onlay, veneer (OVG), interpositional inlay grafting (COG), distraction osteogenesis (DO), and ridge splitting (RS). The data originated from a database search which identified 526 articles. Finally 335 articles met the criteria. Implant survival rate was 95.5 % for GBR technique, 90.4 % for OVG, 94.7 % for DO, and 83.8 % for COG. Hence GBR technique performed better or equal to more advanced bone grafting procedures using autogenous bone. Another interesting clinical finding is that it seems slightly

easier to augment the bone in the maxilla compared to the mandible. The use of provisional restoration during the healing period seems to improve the result. Early implant placement also seems to be preferable if possible, due to alveolar ridge preservation, more favorable defect morphologies, and probably a higher regenerative capacity of the adjacent bone [37]. Bone augmentation of the atrophic jaw bone and, particularly, in the esthetic zone in the maxilla is a delicate and technique-sensitive procedure. The principle of GBR offers an alternative that is less resource demanding and also results in less morbidity for the patients. Predictable results can be obtained if a thorough understanding of the biological principles is applied in the clinical setting.

When bone reconstruction of the posterior atrophic maxilla is needed, different surgical procedures can be used. Following the loss of teeth, alveolar ridge resorption leads to a combined vertical and horizontal reduction of the bony support, at the same time increasing maxillary sinus pneumatization. Such a condition makes implant placement impossible, either because of insufficient vertical bone volume or an alteration of the intermaxillary relationship which is not compatible with prosthetically guided implantology. As for other areas, bone augmentation procedures can be performed prior to placement of the implant, concurrent with implant placement, or subsequent to it.

Up to 10 years ago, autogenous bone was considered to be the gold standard in the reconstruction of atrophic areas of the jaws, due to its osteoconductive, osteoinductive, and regenerative properties; it should still be chosen as the most suitable material in severe atrophies (classes V and VI according to Cawood and Howell [38]).

In the treatment of smaller defects (classes III and IV), bone substitutes of synthetic and xenogeneic origin have been playing an important role in implant surgery. All those materials, generally called “biomaterials,” are able to favor the adherence of cells and tissue regeneration, thanks to a variable degree of osteoconductive activity; after being tested for several years through randomized prospective or retrospective studies, they can be considered as a reliable way to rebuild the bone.

Something fundamental is to remember that the difficulty in rebuilding a bone defect is more related to its extent than its depth. In other words, a very deep but localized defect is easier to treat than a superficial but extensive one. Careful preoperative analysis of the site to be regenerated is important instead of deciding at the time of surgery.

## **Biological Principles of Guided Bone Regeneration**

Over the last two decades, the development of the technique of guided bone regeneration (GBR) has had a significant impact on esthetic reconstruction in conjunction with implant therapy. This technique involves the use of physical barrier membranes during the healing phase in order to avoid ingrowth of undesired tissue types into a wound area [39–43]. During the 1980s the principle of guided tissue regeneration (GTR) was developed for regenerating periodontal tissues lost as a

result of inflammatory periodontal disease. A series of studies documented the possibility of excluding undesirable cells from populating the wound area by means of membrane barriers. This favors the proliferation of defined tissue cells to produce a desired type of tissue.

The principle of physical sealing of an anatomic site for improved healing of certain tissue types is by no means new. During the mid-1950s attempts were made for neural regeneration by the use of cellulose acetate filters [44]. GBR refers more precisely to the goal of the membrane application than guided tissue regeneration.

This concept promotes bone formation by protection against an invasion of competing, non-osteogenic tissues. To this end, bone defects are tightly covered by a barrier membrane of defined permeability and excellent biocompatibility. Experimental studies have proven that certain tissues within the body possess the biologic potential for regeneration if the proper environment is provided during healing.

The ultimate goal of GBR is to use a temporary device to provide the necessary environment so the body can use its natural healing potential and regenerate lost and absent tissues.

The efficacy of barrier membranes in conjunction with bone healing and reconstructive therapy is probably the result of a combination of different mechanisms – mechanical, cellular, and molecular.

Examples of these are:

- Prevention of fibroblast mass action
- Prevention of contact inhibition by heterotopic cell interaction
- Exclusion of cell-derived soluble inhibitory factors
- Local concentration of growth stimulatory factors
- Stimulatory properties of the membrane itself

The basic studies on GBR have shown that the sequence of healing occurring in regular fracture repair follows the same basic pattern that is found in osseous lesions during GBR therapy. Based on the scientific evidence available, it can be stated that certain conditions must be met for new bone formation to be predictably accomplished by GBR:

1. There must be a source of osteogenic cells. Viable bone must be present adjacent to the defect where regeneration is desired.
2. An adequate source of vascularity is essential. This supply originates mostly from the adjacent bone surface (Volkman's canals and marrow compartment).
3. The wound site must remain mechanically stable during healing.
4. An appropriate space must be created and maintained between the membrane and the parent bone surface.
5. Soft connective tissue cells must be excluded from the space created by the membrane barrier. The structure of the material used must be able to accomplish this.

The general function of a membrane used for GBR therapy is to create an environment that will allow the normal healing process to form the bone in a defined

region. Hence, the host tissue-biomaterial interaction should not interfere with bone formation and maintenance to a clinically significant degree. Biomaterial chemistry and structure should result in minimal foreign body response. Optimal bone-biomaterial interaction characteristics are also desirable.

A GBR membrane that allows close adaptation of bone tissue will allow more complete fill of the space defined by the membrane and stabilization of the membrane within the overall system.

## **Biological Factors Influencing the Reconstruction of the Alveolar Bone**

An absolute prerequisite for implant treatment is the availability of sufficient alveolar bone to support and retain the endosseous implant [45].

Factors such as infection, cystic lesions, tooth-alveolar trauma, or congenital tooth agenesis cause a reduction of the alveolar ridge dimensions to a varying degree. With the increasing drive for optimal esthetic outcome of implant treatment, restoring both the hard and soft tissue levels is essential [46].

Tooth replacement in the anterior maxilla is a demanding treatment, since the absence of, or poor, preoperative planning or the choice of an inappropriate treatment approach can lead to everything from esthetic shortcomings to real disasters. Esthetic complications can be related to malpositioned implants and the choice of inappropriate prosthetic components. The most critical factors, however, are the anatomic causes that include bone deficiencies in the horizontal or vertical dimensions and often a combination of the two. This is not infrequently associated with soft tissue defects of the alveolar ridge. Alveolar atrophy and anatomic alterations will have a negative influence on the proper buccal-palatal position of the implant [46, 47]. Malposition of the implant may have effects on the shape, emergence profile, and interproximal contour.

It is important for the clinician to understand that the anatomic contour of the ridge comprises the soft tissue and the underlying supporting bone tissue in all directions. Hence, the soft tissue contour is heavily influenced by the bone anatomy present. The concept of the so-called biological width has increased the knowledge and understanding of the interaction between the different tissue types and different biomaterial surfaces [48]. In brief, the soft tissue demonstrates relatively constant dimensions in thickness; the peri-implant soft tissue thickness is about 3–4 mm. It is slightly thinner on the buccal aspect and more pronounced at the interproximal areas. The soft tissue is also slightly thicker in the anterior maxillary area in contrast to the posterior region of the mandible, which demonstrates the thinnest portion in the oral cavity.

## **Tissue Integration**

The phenomena of ingrowth and surface bonding of tissue to a biomaterial are termed integration. Surface and microstructural characteristics are usually responsible



for these events. The clinical benefits of GBR membranes that have the capacity to integrate with surrounding tissues are a result of a more mechanically stable (and therefore predictable) wound healing environment. While tissue integration appears to be necessary for optimal performance of a GBR membrane, chemical and structural properties that encourage tissue integration must be balanced with the overall functional needs for alveolar ridge augmentation.

---

## Membrane Design Criteria and Material Selection

The acceptance of membrane-assisted regeneration of osseous lesions in the oral cavity has introduced reconstructive dentistry to new therapeutic procedures and biomaterials. Clinicians are being exposed to an increasing number of membrane materials used, or proposed for use, in GBR. In order to select the best material for a specific clinical indication, it is imperative to understand the functional requirements demanded of membrane barriers for GBR procedures.

If the only requirement of a membrane material used in GBR was to provide a barrier to the proliferation of fibrous connective tissue, any suitable biocompatible material in the form of a cell-occlusive film could be used in clinical practice. However, a membrane that is used for alveolar ridge augmentation must meet a number of requirements in addition to acting as a passive physical barrier:

1. The membrane must be constructed of acceptable biocompatible material. The interaction between the material and the tissue should not adversely affect the surrounding tissue, the intended healing result, or the overall safety of the patient.
2. The membrane should exhibit suitable occlusive properties to prevent fibrous connective tissue (scar) invasion of the space adjacent to the bone and provide some degree of protection from bacterial invasion should the membrane become exposed to the oral environment.
3. The membrane must be able to provide a suitable space into which osseous regeneration can occur. Space making provides necessary volume with specific geometry for functional reconstruction.
4. The membrane should be capable of integrating with or attaching to the surrounding tissue. Tissue integration helps to stabilize the healing wound. It helps to create a "seal" between the bone and the material and prevent fibrous connective tissue leakage into the defect and retards the migration of epithelium around the material should it become exposed.
5. The membrane must be clinically manageable.

Two different types of membrane are the most commonly used on the market. Non-resorbable, e-PTFE (expanded polytetrafluoroethylene) membrane was the first material to be successfully applied for GBR. The use of this material requires a

removal procedure once the healing is completed. Although this material demonstrates superior biological response, the extra steps in clinical handling led to the development of biodegradable membranes such as collagen or synthetic polymers. Furthermore, attempts have also been made using other types of barrier membranes such as lyophilized dura, calvarial bone, and peritoneal tissue. However, the results regarding these latter materials are still somewhat limited in applications related to implant treatment.

## **Biocompatibility**

When discussing the clinical outcome of membrane materials, biocompatibility is a fundamental requirement for acceptable function of any implantable medical device. Although this requirement is often taken for granted, tissue interactions involve many application-specific factors that are governed by complex mechanisms.

A classical definition of biocompatibility by Williams [49] is “the state of affairs when a biomaterial exists within a physiological environment, without the material adversely and significantly affecting the body.” This should be interpreted with regard to biomaterial used, the indication, and the environment in which the material is placed and maintained. For example, degradable materials are clearly affected by the environment of the body; however, safe degradation is one of the primary intended functions of this class of biomaterials. Biocompatibility is a relative term. All implanted materials interact with the host tissue to some extent. Biomaterials with dissimilar chemical composition or biomaterials with the same chemical composition but with different macro- and microstructure will demonstrate different cellular or systemic responses.

## **Non-resorbable Membranes**

As previously described, non-resorbable membranes were the first materials successfully used in GBR. The best documented material is e-PTFE (expanded polytetrafluoroethylene) (Gore-Tex Augmentation Material, W.L. Gore & Ass. Inc., Flagstaff, AZ, USA).

Originally used in medical applications such as synthetic vascular graft and heart patches, the material has an extensive documentation with regard to tissue response and safety. In the 1990s, barrier membranes with special characteristics for GBR were developed and became commercially available. Substantial experimental and clinical data are available for this type of membrane. The biological response is near to ideal, and the e-PTFE membrane is still considered the “gold standard” in membrane technology [50]. The material is made up of carbon and fluorine chains strongly bonded to each other. This creates a highly chemically stable and hydrophobic material which is ideal for biocompatible tissue interaction.

The material has an open outer structure for early tissue integration and stabilization and an inner portion which is responsible for the occlusive properties of the device.

## Biodegradable Barrier Membranes

Collagen membranes are resorbed by enzymatic degradation, while synthetic polymers are resorbed via degradation into lactic acid and water. Bio-Gide<sup>™</sup> was the first collagen barrier membrane designed for GBR and is by far the best documented product in the literature. It is made from native, noncross-linked collagen types I and III and consists of two functional layers. The compact layer is cell occlusive and fulfills barrier function, while the porous layer allows tissue integration. The membrane has hydrophilic properties, which enable self-adherence to the bone surface, thus providing easy clinical handling. Due to the lack of stiffness, collagen membranes are usually used in combination with bone chips or bone substitutes.

Pure synthetic biodegradable membranes are also available on the market. These materials usually consist of a combination of PLA/PGA (polylactide and polyglycolide). An example of such membranes is RESOLUT (W.L. Gore & Ass. Inc., Flagstaff, AZ, USA) [51]. Although this demonstrates excellent biological behavior in experimental studies, the amount of clinical data is still somewhat limited.

## Resorption Patterns of the Alveolar Ridge

As the alveolar crest is wider in the premolar and molar area than in the anterior region, vertical resorption is slower in the posterior parts. On the other hand, molars and premolars are usually lost earlier than incisors.

Thus when patients seek implant placement, the posterior regions are usually equally or more resorbed than the anterior. In the posterior molar area, resorption usually results in a wider arch and a wider crest as resorption reaches the oblique and mylohyoid lines. In the first molar and especially in the premolar area, two different resorption patterns are seen, although combinations of the two are common. Whether the resorption mode is due to the angulation of the alveolar crest or genetically determined is not known. The usual pattern is vertical resorption. This results in a flat and rather wide crest. If the resorption is moderate, leaving more than 10 mm height of bone superior to the mandibular canal, implant placement is usually uncomplicated. However, as resorption continues, the height above the mandibular canal is reduced, and in advanced cases, where resorption reaches the level of the mandibular canal, the foramen is found on the top of and even slightly lingual to the top of the crest with part of the alveolar nerve positioned under a thin layer of the bone or even directly under the alveolar mucosa. The other, less frequent, resorption pattern is lateral resorption. This results in a narrow crest, in advanced cases in a very high, thin ridge made up of cortical bone which is totally unsuitable for implant placement.

## Surgical Techniques

The choice of procedure for reconstructing the posterior areas of the maxilla depends both on the depth and the extent of the defect. Starting from the post-extraction defects up to the most severe atrophies, the classification according to Cawood and Howell [36] clarifies, in a simple way, what kind of surgical technique is the most suitable for each specific bony defect. In accordance with that classification, the defects can be listed as follows:

- Post-extraction sites
- Horizontal defects (including dehiscences and fenestrations around implants)
- Vertical defects
- Combined (vertical and horizontal defects)
- Sinus elevation

## Post-extraction Sites

An alveolar bone loss of 23 % in the first 6 months after tooth extraction and of 11 % during the following 5 years was demonstrated by Carlsson [52]. Alveolar bone loss not only reduces the amount of bone available for adequate support of the prosthetic load but can also adversely affect the implant position, the peri-implant hard and soft tissue anatomy, and, consequently, the final esthetic and functional outcome.

The immediate insertion of an implant in a post-extraction site would therefore preserve a greater amount of alveolar bone and also reduce the treatment time. Whenever an immediate implant placement cannot be carried out due to the impossibility of obtaining primary stability for the fixture, physiological resorption due to the remodeling processes must be avoided. This goal can be easily achieved by filling the alveolus with bone substitutes and a free gingival graft, and implant placement surgery can be carried out about 6 months later [53]. Where there is an infection in the extraction area, immediate implant insertion should be avoided and the surgery postponed until 40–60 days after the extraction.

## Immediate Technique

When the gap between implant and alveolus is less than 1 mm, tissue regeneration is entrusted to the clot. For larger gaps, bone substitutes can be used to fill the defect, and the area is covered with a collagen membrane and a free gingival graft, which improves the quantity and the quality of the soft tissues around the implant at the time of connection of the healing abutment (Fig. 15). The soft tissue graft is obviously useless in cases of immediate temporary crown placement.

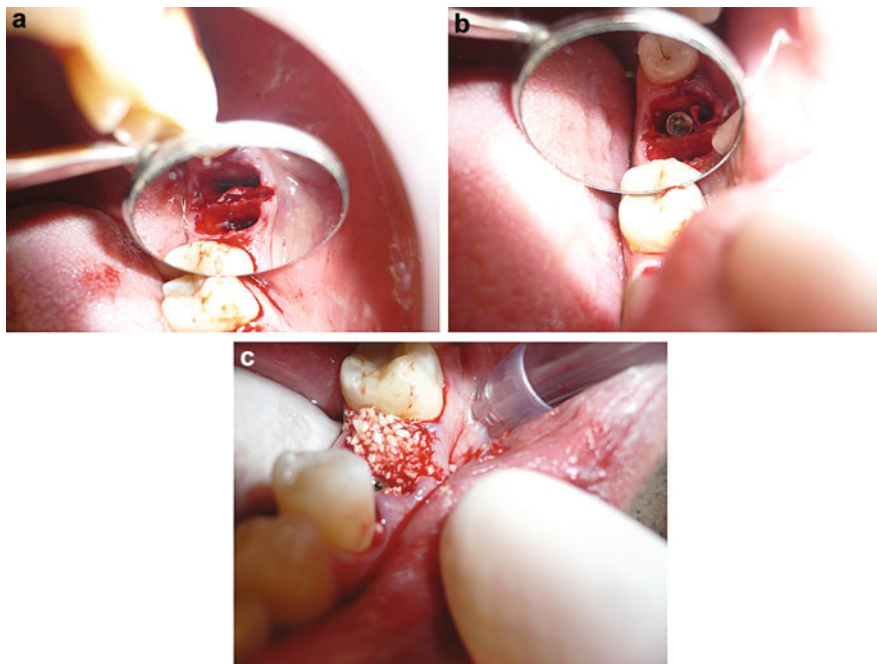


**Fig. 15** Representative clinical case for immediate technique: (a) post-extraction site; (b) immediate implantation; (c) immediate augmentation

### Delayed Technique

In this situation, 6–8 weeks are needed to rebuild the gingival tissue after extraction, and implant placement is performed by means of a standard procedure.

### Horizontal Defects

These defects occur where there is adequate height but insufficient width of the ridge. They include implant dehiscences and fenestrations and can be treated with GBR procedures associated with autogenous bone chips and bone substitutes as well as ridge expansion techniques (at implant placement time) or autogenous bone blocks (prior to the implant placement).

### Dehiscences and Fenestrations

Dehiscences are exposures of the implant at the level of its head, occurring when the thickness of the ridge is insufficient in the most coronal area. Fenestrations are exposures of the middle third or the apical portion of the implant with or without involvement of the implant head.

A bone regeneration technique using autogenous chips, bone substitutes, and resorbable or non-resorbable membranes is a possible treatment. Most dehiscences and fenestrations can easily be treated with a resorbable membrane acting as a stabilizer of the underlying material (granules or chips). When the exposed surface of the implant exceeds 1 mm outside the bone envelope and a large volume of bone has to be regenerated, non-resorbable e-PTFE membranes are indicated. In both cases, membranes have to be stabilized with pins or mini-screws, and periosteal releasing incisions of the buccal flap are mandatory to avoid tension at suturing. Vertical mattress and single sutures are required in all the techniques.

### **Autogenous Intraoral or Extraoral Blocks**

Harvesting bone blocks from inside the mouth (chin, mandibular body, or ramus) is indicated in the correction of a class IV atrophic ridge, particularly in the case of an extended narrow ridge. When a larger amount of bone is necessary (such as a resorbed maxillary ridge in edentulous patients), blocks can be harvested from the hip or the calvaria. In all these situations, attention must be paid to the block's resorption during the 4 months' healing. An average resorption of 20–30 % can be observed [54, 55] at implant placement time, in blocks harvested from the chin or the hip, due to their cancellous component, and 15 % resorption occurs in blocks harvested from the mandibular body and the ramus, which are basically made of cortical bone. An original technique to reduce the resorption of autogenous blocks was presented in 2005 [56], involving a layer of anorganic bovine bone placed on the top of the block and covered by a collagen membrane. Using this procedure it is possible to maintain the original size of the block; it can be successfully used for either intraoral or extraoral grafts [57].

### **Vertical Defects**

If the bone height is insufficient to guarantee long-term implant stability or the prosthetic rehabilitation would result in too long crowns, vertical ridge augmentation is mandatory. Vertical augmentation can be achieved by means of corticocancellous blocks harvested from the chin or the ramus or, alternatively, with cancellous bone chips, bone substitutes (Figs. 16 and 17), and a titanium-reinforced e-PTFE membrane [58, 59].

### **Vertical GBR with Membrane**

This procedure is very predictable, but it has to be carried out strictly according to the surgical protocol, in order to limit the risks of the membrane exposure.

The most common flap design comprises a full-thickness mid-crestal incision within the keratinized mucosa of the edentulous ridge, extended mesially and

**Fig. 16** Vertical defect caused by an apical infection of the two upper central incisors

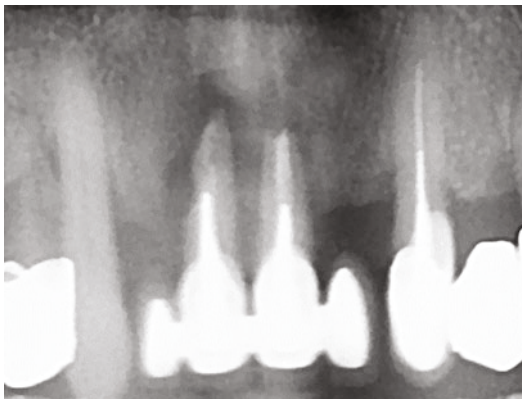
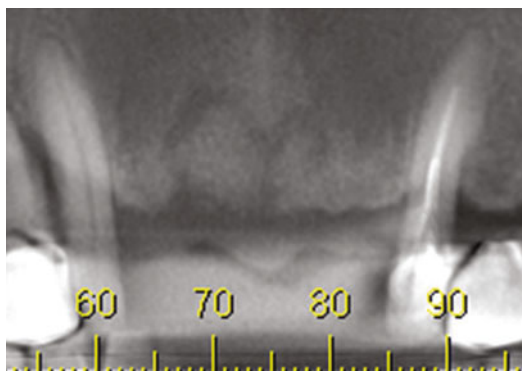


**Fig. 17** Same vertical defect after 3 months treated with allogeneic and xenograft bone chips mixed in a ratio of 1:1



distally to at least one adjacent tooth. Vertical releasing cuts are performed at the mesial and distal line angles of the incision. A proper preparation of the recipient site is crucial for new bone formation.

The buccal and palatal flaps are reflected and gently managed to avoid any perforation of the flap. Stainless steel mini-screws are used as “tent poles” to prevent collapse of the membrane and to predetermine either the width or the height of the future alveolar ridge.

The mini-screws are placed and left to protrude out from the bone level to the expected height. The cortical plate is then drilled with a round bur to expose the cancellous bone and to provoke some bleeding. The titanium structure of the e-PTFE membrane is bent with pliers to adapt it to the ridge anatomy, and it is trimmed with scissors to extend at least 4–5 mm beyond the margins of the defect. Once placed over the surgical recipient site, the membrane is secured to the lingual and palatal aspect of the bone crest with fixation mini-screws or pins. The cancellous autogenous chips mixed with the bone substitute are placed to reconstruct the defect, and the buccal portion of the membrane is adapted to the vestibular bone plate and also secured with screws or pins. A releasing horizontal incision of the periosteum is now performed to give elasticity to the flap and obtain tension-free adaptation at closure.

The two margins of the flap can be considered sufficiently released when they overlap by at least 7–10 mm. Closure is done with horizontal mattress sutures first and with interrupted sutures later. The membrane is usually removed 6 months after surgery, at implant placement time.

## Sinus Elevation

When atrophy of the posterior maxilla reduces the amount of bone suitable for implant placement and a bone augmentation procedure is required, first of all one needs to evaluate if the sinus really has migrated from apical to coronal toward the margin of the alveolar ridge or if the sinus is in its previous position and the vertical height loss is due to vertical resorption.

In the first case, a sinus elevation procedure is indicated, while in the second situation, vertical ridge augmentation should be performed without any sinus involvement.

Once the necessity of performing a sinus elevation has been decided upon, the second step is the choice between a one- and a two-stage procedure. According to the recent literature [60], a residual alveolar ridge of 2 mm is the absolute minimum height for bone augmentation and simultaneous implant placement, and a two-stage technique must be done where there is a residual height of 0–2 mm (Fig. 18).

The surgical procedure is the well-known Boyne and James technique [61], and autogenous bone or bone substitutes have been used for a long time to fill up the subantral cavity. At present, long-term prospective and retrospective studies confirm that bone substitutes are able to regenerate new bone without harvesting autogenous bone and that the implant survival rate in augmented sinuses with biomaterials is significantly higher than that obtained using autogenous bone chips [62–64].

In Cawood and Howell I class VI defects, only autogenous bone is recommended, since the severe atrophy needs all the power of an osteoproliferative material [65]. This means that at least 80 % of sinus elevation procedures can be done by using biomaterials alone (Fig. 19).

What kind of bone substitute should be chosen to get the best result? All the bone substitutes currently used in the sinus elevation procedures, either xenogenic or alloplasts, offer osteoconductive properties only. The decision should be taken after considering the human hydroxyapatite structure: the more a granule of a biomaterial is similar to a human hydroxyapatite crystal, the more it is possible to get an osteoconductive effect.

Another parameter to be taken into consideration is the biomaterial's resorption time. A material which is resorbed too quickly does not allow the osteoblasts and the new vessels to promote formation of woven bone. A material which is resorbed too slowly, by delaying its total substitution with newly formed bone, inhibits bone–implant contact which is essential for osseointegration. A resorption time of 6–10 months can be considered reasonably ideal. In the author's experience, anorganic bovine bone has given excellent results in over 15 years of sinus elevation surgeries, giving a new bone quality close to a class 2 native bone, [66] and a very good osteoconductive property, as verified from many histomorphometric studies [67–69].



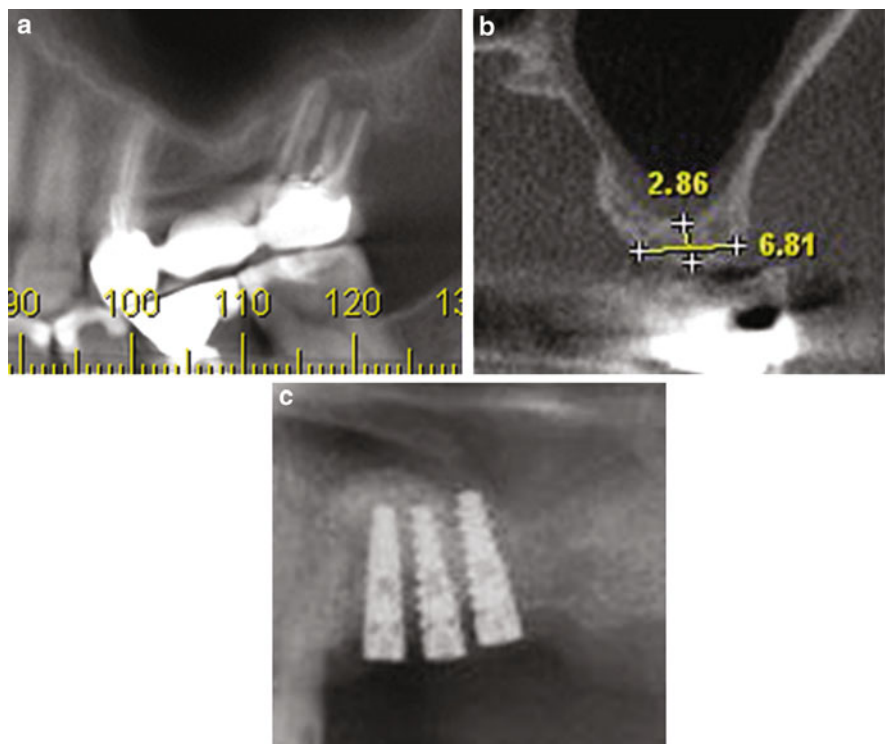


**Fig. 18** Representative radiological images for sinus elevation: (a) before sinus elevation; (b) sinus floor dimension before sinus elevation; (c) the same site after 8 months

Nevertheless, the author has been using other bone substitutes, such as beta TCP, calcium sulfate, and DFDBA, whose clinical efficacy has been demonstrated in some studies, although with a lower predictability in terms of bone quality and implant survival rate.

When the height of the residual ridge is 6–7 mm, the surgeon can decide whether to use short implants or elevate the sinus floor 2–3 mm with the Summer’s osteotome technique. The procedure, wrongly named “minor sinus elevation,” is a blind procedure and should be considered with care. In order to elevate the sinus membrane with this procedure, any of the biomaterials can be equally used, since the primary stability of the implant is guaranteed by the residual ridge [70].

### Preoperative Antibiotics

The same antibiotic prophylaxis is recommended as in conjunction with implant placement [71–76]. According to standard protocol, usually a 1-day regimen including 2 g of penicillin per day is enough. For advanced GBR cases, 1 week’s antibiotic coverage postoperatively is recommended.

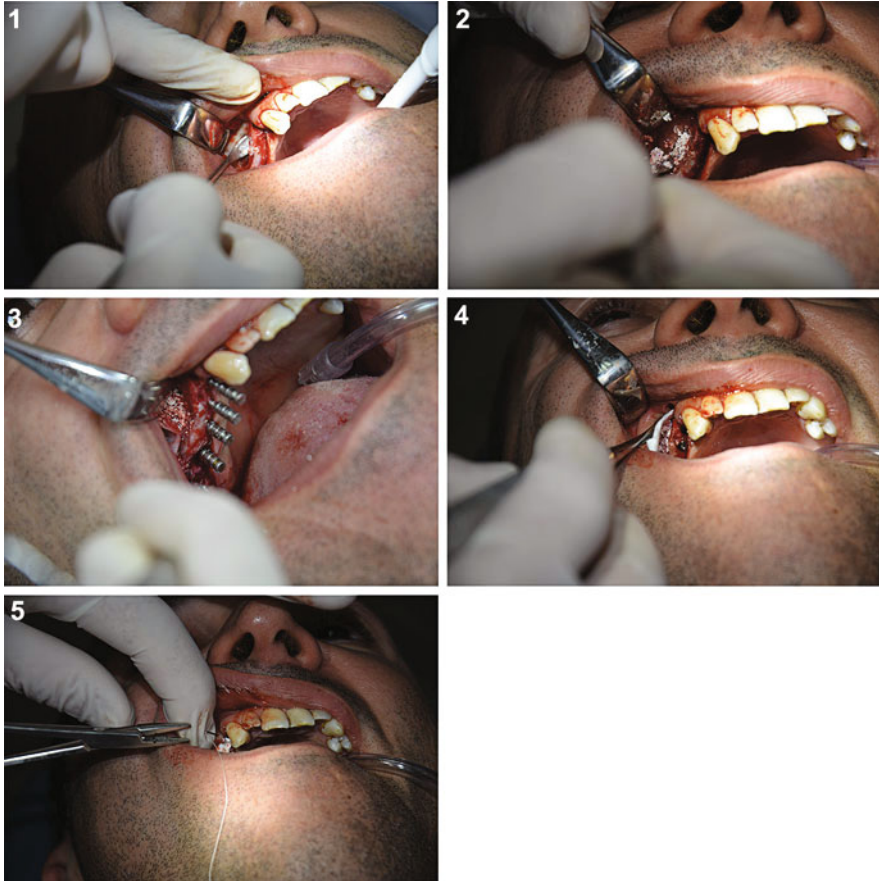


**Fig. 19** Representative clinical case for sinus elevation. (1) Elevating the Schneider membrane; (2) filling the created space with xenograft 1.2 ~ 1.7 mm of bovine origin; (3) implant direction positioning; (4) collagen membrane placing; (5) tight stitching for good sealing

## Flap Design

A full-thickness crestal incision, slightly buccal but still within attached mucosa, is performed and extended mesially and distally to the adjacent teeth. Diverging releasing incisions are then performed buccally. Full-thickness mucoperiosteal flaps are elevated (Fig. 20).

## Site Preparation

Based on the available amount of host bone present, simultaneous implant placement can be performed. If optimal position and direction and satisfactory primary stability cannot be obtained, a two-stage procedure should be considered. The bone surface in

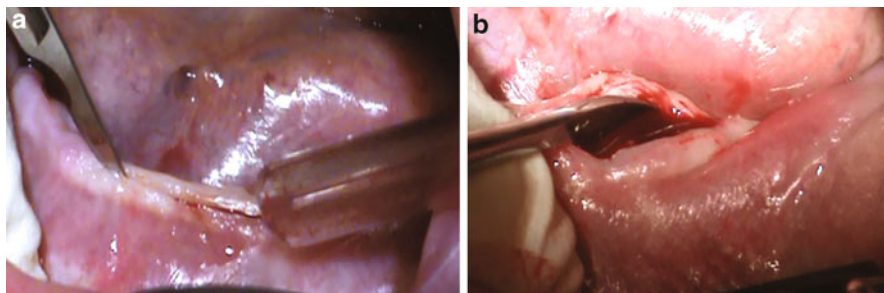


**Fig. 20** Relevant clinical images for flap design: (a) releasing incisions performed buccally; (b) full-thickness mucoperiosteal flaps

**Fig. 21** Implant placement for a removable prosthesis



the augmentation area should be carefully debrided in order to remove all remnants of the soft tissue. If implant placement is performed, it should be performed according to the protocol of the implant system used, aiming at a prosthetic-driven position (Fig. 21).

Prior to placement of graft material and the barrier membrane, the buccal bone plate in the defect area must be perforated to create access for multipotent cells and blood vessels emanating from the marrow cavity. This can be performed either with a spiral or a round bur with a dimension of approximately 1 mm. This surgical procedure is believed to stimulate osteogenesis by activating a cascade effect of growth factors. Furthermore it allows the formation of an appropriate coagulum which will act as a matrix for the initial bone formation.

### Graft Material Positioning

The use of spacemaking materials underneath the membrane has been proven to provide a more predictable regenerative result and is today considered state of the art. Many different materials, including autogenous bone chips, freeze-dried-demineralized, deproteinized bovine bone, and synthetic graft materials such as

**Fig. 22** An allogeneic and xenograft bone chips mixed in a ratio of 1:1



TCPs, have been tested with varying results. The best documented filling material with predictable outcome is a combination of deproteinized bovine bone (Bio-Oss, Geistlich, Switzerland) and autogenous bone chips mixed in a ratio of 1:1. The addition of xenograft has been shown to minimize resorption of the newly regenerated bone (Fig. 22).

## Membrane Selection and Positioning

The anatomic shape of the defect to be regenerated dictates the choice of membrane material. The following protocols can be recommended.

### Biodegradable Membranes

Most defects can be treated with resorbable membranes together with autogenous bone chips alone or in combination with bone substitutes. Usually the autogenous bone chips are placed in contact with either the bone surface or the exposed parts of the implant and then covered with a layer of xenograft chips. Alternatively the two filling materials are mixed together in a ratio of approximately 1:1.

The membrane must be cut and trimmed to adapt to the anatomy of the ridge and applied over the defect in order to cover the bone graft. Due to the hydrophilic properties of the collagen membrane, it will “stick” to the bone surface once wetted either with saline or blood (Fig. 23). Hence no fixation screws or tacks are needed for stabilization in most cases.

### Non-resorbable Membranes

When a large volume of bone (outside the bone envelope) must be regenerated, the use of non-resorbable e-PTFE membrane is indicated. The preparation of the augmentation site is identical to that described above. However, extra attention

**Fig. 23** Collagen membrane placing to cover a bone implant site



must be paid to the membrane adaptation and fixation. The membrane must be cut to extend at least 4–5 mm beyond the filling material to avoid interference with the surrounding soft tissue. It is important to avoid creating sharp edges since they can increase the risk for membrane perforation during healing. A critical note is to trim the membrane so a distance of 1–2 mm is maintained from the root surface of the neighboring teeth. This is to avoid contamination due to bacterial downgrowth along the root and also to enhance periodontal reattachment.

Finally, the membrane should be fixated using either micro-screws or specially designed tacks. It is practical to start this procedure on the palatal side prior to the placement of the bone graft material. A critical technique is the adjustment of the flaps prior to suturing. A completely tension-free environment must be created by performing periosteal releasing incisions at the base of the buccal flap.

## Suturing

Suturing is recommended using non-resorbable sutures in a biocompatible material. A double suture layer should be created with a combination of horizontal mattress sutures (4/0) (on top of the crest) followed by single interrupted sutures (5/0 or 6/0) for mucosal closure.

## Follow-Up

Due to the compromised wound, the recommendation is to maintain the sutures in place for at least 14 days. The patient should receive systemic antibiotics (amoxicillin) for 5–10 days when they have undergone a more advanced GBR procedure. In addition, the patient should rinse with chlorhexidine solution for 3 weeks after placement of the GBR barrier. This could thereafter be switched to a 1 % chlorhexidine gel which is gently applied in the wound area only once daily.

**Fig. 24** Radiological image of a big defect of the maxilla

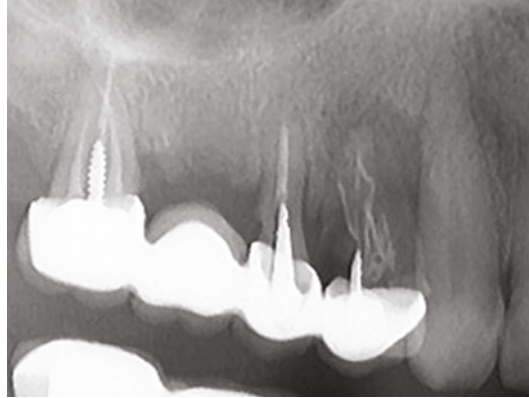
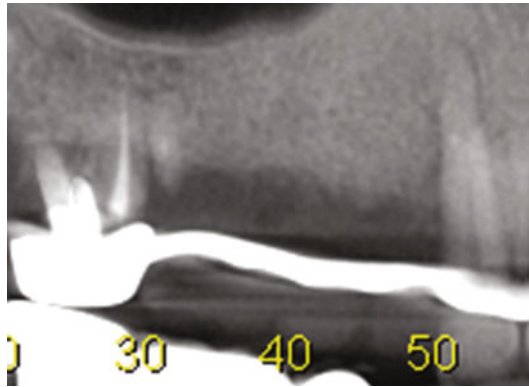


**Fig. 25** Radiological image of the same area than Fig. 24 after 8 months from augmentation



The e-PTFE membranes are removed after 6–8 months (either at the time of fixture installation or abutment connection). During this healing period, the patients are checked once a month for plaque removal and any complications.

## Temporary Dentures

Implant treatment and related bone augmentative procedures are usually associated with a situation where the patient needs a temporary solution during the respective healing phases. Clinical studies have demonstrated a clear correlation between membrane exposure and pressure from temporary dentures in the wound area. Hence, strict rules apply for the design of the temporary solution in conjunction with GBR. Ideally, fixed solutions such as Maryland bridges or conventional temporary bridges are the first choices if possible. If a temporary removable denture is necessary, it should be designed in such a way that no contact is present between

**Fig. 26** Radiological image of a clinical case before extraction of infected alveolars

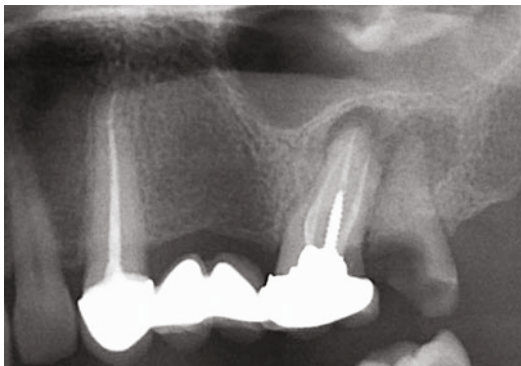
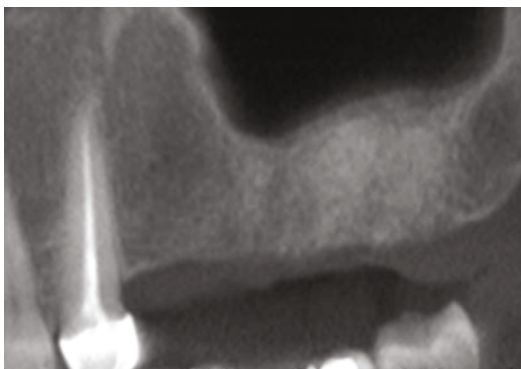


**Fig. 27** Radiological image of the same area than Fig. 26 after 4 months from augmentation for bone preservation



the base of the denture and the soft tissue covering the GBR membrane. Furthermore, occlusal support of the denture is mandatory in order to prevent a pumping pressure when chewing.

## Membrane Removal

A non-resorbable barrier membrane is removed under local anesthesia. Technically the easiest way to approach the membrane is from the lateral aspect and to dissect it free from the covering soft tissue layer. Following this procedure, it is usually easy to remove the barrier from the underlying bone tissue. Great care should be taken to remove the entire membrane material. This is usually performed in conjunction with either implant placement or abutment connection.

Biodegradable barrier membranes do not usually require this procedure. Most biodegradable membranes on the market are designed with a resorption pattern of less than 6 months.

## Summary

A variety of techniques and materials has been used to establish the structural base of osseous tissue for supporting dental implants. GBR is a surgical concept which has been in clinical use for well over two decades. It has undergone several developments and improvements and is nowadays considered a predictable treatment modality, once the previously described issues have been taken fully into account. Doubts have previously been raised regarding the quality and lasting capability of membrane-regenerated bone when being put into clinical function. Previous experimental studies have clearly shown the positive dynamics of this type of bone over time (Figs. 24 and 25)

Another interesting clinical finding is that it seems slightly easier to augment the bone in the maxilla compared to the mandible. The use of provisional restoration during the healing period seems to improve the result.

Early implant placement also seems to be preferable if possible, due to alveolar ridge preservation, more favorable defect morphologies, and probably a higher regenerative capacity of the adjacent bone. Bone augmentation of the atrophic jaw bone and, particularly, in the esthetic zone in the maxilla is a delicate and technique-sensitive procedure.

The principle of GBR offers an alternative that is less resource demanding and also results in less morbidity for the patients. Predictable results can be obtained if a thorough understanding of the biological principles is applied in the clinical setting (Figs. 26 and 27).

Complications may arise due to inadequate coverage of the graft or flaps which are stretched too much, with compromised vascular circulation. Exposure of the graft may result in loss of part or all of the graft.

---

## References

1. Fleming JE, Cornell CN, Muschler CF (2000) Bone cells and matrices in orthopedic tissue engineering. *Orthop Clin North Am* 31:357–374
2. Bauer TW, Muschler GF (2000) Bone graft materials. An overview of the basic science. *Clin Orthop Relat Res* 371:10–27
3. Urist MR (1965) Bone formation by auto-induction. *Science* 150:893–899
4. Schwartz Z, Mellonig JT, Carnes DL Jr et al (1996) Ability of commercial demineralized freeze-dried bone allograft to induce new bone formation. *J Periodontol* 67:918–926
5. Shigeyama A, D'Errico JA, Stone R et al (1995) Commercially prepared allograft material has biological activity in vitro. *J Periodontol* 66:478–487
6. Hammerle CH, Karring T (1998) Guided bone regeneration at oral implant sites. *Periodontol* 2000 17:151–175
7. Valentini P, Abensur D (1998) Histological evaluation of Bio-Oss in a two stage sinus floor elevation and implantation procedure. *Clin Oral Implants Res* 9:59–64
8. Wenz B (2003) Characteristics of Bio-Oss and Bio-Gide. In: Simion M (ed) *Advanced Techniques for Bone Regeneration with Bio-Oss and Bio-Gide* (Maiorana C. RC Books, Milano, pp 73–81
9. Joyce ME, Jingushi S, Bolander ME (1990) Transforming growth factor- $\beta$  in the regulation of fracture repair. *Orthop Clin North Am* 21:199–209



10. Bostrom MP, Lane JM, Berberian WS, Missri AA, Tomin E, Weiland A et al (1995) Immunolocalization and expression of bone morphogenetic protein 2 and 4 in fracture healing. *J Orthop Res* 13:357–367
11. Onishi T, Ishidou Y, Nagamine T, Yone K, Imamaru T, Kato M et al (1998) Distinct and overlapping patterns of localization of bone morphogenetic protein (BMP) family members and a BMP type II receptor during fracture healing in rats. *Bone* 22:605–612
12. Sakou T (1998) Bone morphogenetic proteins: from basic studies to clinical approaches. *Bone* 22:591–603
13. Bourque WT, Gross M, Hall BK (1993) Expression of four growth factors during fracture repair. *Int J Dev Biol* 37:573–579
14. Nakamura T, Hara Y, Tagawa M, Tamura M, Yuge T, Fukuda H et al (1998) Recombinant human basic fibroblast growth factor accelerates fracture healing by enhancing callus remodeling in experimental dog tibial fracture. *J Bone Miner Res* 13:942–949
15. Trippel SB (1998) Potential role of insulinlike growth factors in fracture healing. *Clin Orthop* 355S:301–313
16. Nash TJ, Howlett CR, Martin C, Steele J, Johnson KA, Kicklin DJ (1994) Effect of platelet-derived growth factor on tibial osteotomies in rabbits. *Bone* 15:203–208
17. Tuli SM, Singh AD (1978) The osteoinductive property of decalcified bone matrix: an experimental study. *J Bone Joint Surg Br* 60:116–123
18. Adkisson HD, Strauss-Schoenberger J, Gillis M, Wilkins R, Jackson M, Hruska KA (2000) A rapid quantitative bioassay of osteoinduction. *J Orthop Res* 18:503–511
19. Geesink RGT, Hoefnagels NHM, Bulstra SK (1999) Osteogenic activity of OP-1 bone morphogenetic protein (BMP-7) in a human fibular defect. *J Bone Joint Surg Br* 81:710–718
20. Heckman JD, Ehler W, Brooks BP, Aufdemorte TB, Lohmann CH, Morgan T et al (1999) Bone morphogenetic protein but not transforming growth factor- $\beta$  enhances bone formation in canine diaphyseal nonunions implanted with a biodegradable composite polymer. *J Bone Joint Surg Am* 81:1717–1739
21. Giavaresi G, Fini M, Salvage J, Nicoli Aldini N, Giardino R, Ambrosio L, Nicolais L, Santin M (2010) Bone regeneration potential of a soybean-based filler: experimental study in a rabbit cancellous bone defects. *J Mater Sci: Mater Med* (2010) 21:615–626
22. Holmberg L, Forsgren L, Kristerson L (2008) Porous titanium granules for implant stability and bone regeneration—a case followed for 12 years. *Ups J Med Sci* 113(2):217–220
23. Bystedt H, Rasmusson L (2009) Porous titanium granules used as osteoconductive material for sinus floor augmentation: a clinical pilot study. *Clin Implant Dent Relat Res* 11(2):101–105
24. White E, Shors EC (1986) Biomaterial aspects of Interpore-200 porous hydroxyapatite. *Dent Clin North Am* 30:49–67
25. Ferraro JW (1979) Experimental evaluation of ceramic calcium phosphate as a substitute for bone grafts. *Plast Reconstr Surg* 63:634–640
26. Chiroff RT, White EW, Weber KN, Roy DM (1975) Tissue ingrowth of replamineform implants. *J Biomed Mater Res* 6:29–45
27. Knaack D, Goad ME, Aiolova M, Rey C, Tofighi A, Chakravarthy P et al (1998) Resorbable calcium phosphate bone substitute. *J Biomed Mater Res* 43:399–409
28. Cornell CN, Lane JM, Chapman M, Merkow R, Seligson D, Henry S et al (1991) Multicenter trial of Collagraft as bone graft substitute. *J Orthop Trauma* 5:1–8
29. Chapman MW, Bucholz R, Cornell CN (1997) Treatment of acute fractures with a collagen-calcium phosphate graft material: A randomized clinical trial. *J Bone Joint Surg Am* 79:495–502
30. Albu MG, Ghica MV, Leca M, Popa L, Borlescu C, Cremenescu E, Giurginca M, Trandafir V (2010) Doxycycline delivery from collagen matrices crosslinked with tannic acid. *Mol Cryst Liq Cryst* 523:97 = [669]–105 = [677]
31. Titorencu I, Albu MG, Giurginca M, Jinga V, Antoniac I, Trandafir V, Cotrut C, Miculescu F, Simionescu ANDM (2010) In vitro biocompatibility of human endothelial cells with collagen-doxycycline matrices. *Mol Cryst Liq Cryst* 523:97 = [669]–105 = [677]

32. Soballe K, Hansen ES, Brockstedt-Rasmussen H, Bunger C (1993) Hydroxyapatite coating converts fibrous tissue to bone around loaded implants. *J Bone Joint Surg Br* 75:270–278
33. Tisdell CL, Goldberg VM, Parr JA, Bensusan JS, Staikoff LS, Stevenson S (1994) The influence of a hydroxyapatite and tricalcium phosphate coating on bone growth into titanium fiber-metal implants. *J Bone Joint Surg Am* 76:159–171
34. Leeuwenburgh S, Layrolle P, Barrere F, de Bruijn J, Schoonman J, van Blitterswijk CA et al (2001) Osteoclastic resorption of biomimetic calcium phosphate coatings in vitro. *J Biomed Mater Res* 56:208–215
35. Liu Y, Layrolle P, de Bruijn J, van Blitterswijk C, de Groot K (2001) Biomimetic coprecipitation of calcium phosphate and bovine serum on titanium alloy. *J Biomed Mater Res* 57:327–335
36. Aghaloo TL, Moy PK (2007) Which hard tissue augmentation techniques are the most successful in furnishing bony support for implant placement? *Int J Oral Maxillofac Implants* 22:49–70
37. Zitzmann NU, Scharer P, Marinello CP (1999) Factors influencing the success of GBR. Smoking, timing of implant placement, implant location, bone quality and provisional restoration. *J Clin Periodontol* 26:673–682
38. Cawood JL, Howell RE (1988) A classification of the edentulous jaws. *Int J Oral Maxillofac Surg* 17:232–236
39. Dahlin C, Linde A, Gottlow J, Nyman S (1988) Healing of bone defects by guided tissue regeneration. *Plast Reconstr Surg* 81:672–676
40. Dahlin C, Sennerby L, Lekholm U, Linde A, Nyman S (1989) Generation of new bone around titanium implants using a membrane technique: an experimental study in rabbits. *Int J Oral Maxillofac Implants* 4:19–25
41. Schenk RK, Buser D, Hardwick WR, Dahlin C (1994) Healing pattern of bone regeneration in membrane-protected defects: a histologic and histomorphometric study in the mandible of dogs. *Int J Oral Maxillofac Implants* 9:13–29
42. Buser D, Ruskin J, Higginbottom F, Hardwick R, Dahlin C, Schenk R (1995) Osseointegration of titanium implants in bone regenerated in membrane-protected defects. A histologic study in the canine mandible. *Int J Oral Maxillofac Implants* 10:666–681
43. Esposito M, Grusovin MG, Worthington HV, Coulthard P (2006) Interventions for replacing missing teeth: bone augmentation techniques for dental implant treatment. *Cochrane Database Syst Rev* (1):CD003607
44. Campbell JB, Bassett CAL (1956) The surgical application of monomolecular filters (Millipore) to bridge gaps in peripheral nerves and to prevent neuroma formation. *Surg Forum* 7:570–574
45. Lekholm U, Zarb G (1985) Patient selection and preparation. In: *Tissue-integrated prostheses: osseointegration in clinical dentistry*. Quintessence, Chicago, p 199
46. Buser D, Martin W, Belser C (2004) Optimizing esthetics for implant restorations in the anterior maxilla: anatomic and surgical considerations. *Int J Oral Maxillofac Implants* 19(Suppl):43–61
47. Tarnow DP, Magner AW, Fletcher P (1992) The effect of distance from the contact point to the crest of bone on the presence of the interproximal dental papilla. *J Periodontol* 63:995–996
48. Lindhe J, Karring T (1997) Anatomy of the periodontium. In: Lindhe J, Karring T, Lang N (eds) *Clinical periodontology and implant dentistry*. Munksgaard, Copenhagen, pp 21–25
49. Williams DF (1981) Biomaterials and biocompatibility: an introduction. In: Williams DF (ed) *Fundamental aspects of biocompatibility*, vol 1. CRC Press, Boca Raton, p 1
50. Hardwick R, Scantlebury T, Sanchez R, Whitley N, Ambruster J (1994) Membrane design criteria for guided bone regeneration of the alveolar ridge. In: Buser D, Dahlin C, Schenk R (eds) *Guided bone regeneration in implant dentistry*. Quintessence, Chicago, pp 101–136
51. Stavropoulos F, Dahlin C, Ruskin JD, Johansson C (2004) A comparative study of barrier membranes as graft protectors in the treatment of localized bone defects. An experimental study in a canine model. *Clin Oral Implants Res* 15:435–442
52. Carlsson GA (1967) Changes in the contour of maxillary alveolar process under immediate dentures. *Acta Odontol Scand* 25:45–75

53. Nevins M, Camelo M, De Paoli S et al (2006) A study of the fate of the buccal wall of extraction sockets of teeth with prominent roots. *Int J Periodontics Restorative Dent* 26:19–29
54. Nystrom E, Ahlqvist J, Gunne J et al (2004) Ten year follow-up of onlay bone grafts and implants in severely resorbed maxillae. *Int J Oral Maxillofac Surg* 33:258–262
55. Nystrom E, Ahlqvist J, Legrell PE (2002) Bone graft remodeling and implant success rate in the treatment of the severely resorbed maxilla: a 5 year longitudinal study. *Int J Oral Maxillofac Surg* 31:158–164
56. Maiorana C, Beretta M, Salina S et al (2005) Reduction of autogenous bone graft resorption by means of Bio-Oss coverage: a prospective study. *Int J Periodontics Restorative Dent* 1:19–24
57. Maiorana C, Sommariva L, Brivio P, Sigurta D, Santoro F (2003) Maxillary sinus augmentation with anorganic bovine bone (Bio-Oss) and autologous platelet-rich plasma: preliminary clinical and histologic evaluations. *Int J Periodontics Restorative Dent* 23:227–235
58. Simion M, Trisi P, Piattelli A (1994) Vertical ridge augmentation using a membrane technique associated with osseointegrated implants. *Int J Periodontics Restorative Dent* 14:496–511
59. Simion M, Jovanovic S, Tinti C et al (2001) Long term evaluation of osseointegrated implants inserted at the time or after vertical ridge augmentation. A retrospective study on 123 implants with 1–5 year follow-up. *Clin Oral Implants Res* 12:35–45
60. Maiorana C, Simion M (2003) Chapter 3. In: *Advanced techniques for bone regeneration with Bio-Oss and Bio-Gide*. RC Books, Milano, pp 41–50
61. Boyne PJ, James R (1980) Grafting of the maxillary sinus floor with autogenous bone marrow and bone. *J Oral Surg* 38:613–618
62. Valentini P, Abensur D, Wenz B et al (2000) Sinus grafting with porous bone mineral (Bio-Oss): a study on 15 patients. *Int J Periodontics Restorative Dent* 20:245–252
63. Valentini P, Abensur D (2003) Maxillary sinus grafting with anorganic bovine bone: a clinical report of long-term results. *Int J Oral Maxillofac Implants* 18:556–560
64. Maiorana C, Sigurta D, Mirandola A et al (2005) Bone resorption around implants placed in grafted sinuses: a clinical and radiologic follow-up after up to four years. *Int J Oral Maxillofac Implants* 2:261–265
65. Geurs NC, Wang JC, Schulman LB et al (2001) Retrospective radiographic analysis of sinus graft and implant placement procedures from the Academy of Osseointegration Consensus Conference on sinus graft. *Int J Periodontics Restorative Dent* 21:517–524
66. Haas R, Mailath G, Dortbudak O et al (1998) Bovine hydroxyapatite for maxillary sinus augmentation: analysis of interfacial bond strength of dental implants using pull-out tests. *Clin Oral Implants Res* 17:151–175
67. Maiorana C, Redemagni M, Rabagliati M et al (2000) Treatment of maxillary ridge resorption by sinus augmentation with iliac cancellous bone, anorganic bovine bone and implants: a clinical and histologic report. *Int J Oral Maxillofac Implants* 15:873–878
68. Wallace SS, Froum SJ, Cho SC et al (2005) Sinus augmentation utilizing anorganic bovine bone (Bio-Oss) with absorbable and non absorbable membranes placed over the lateral window: histomorphometric and clinical analyses. *Int J Periodontics Restorative Dent* 25:551–559
69. Hallman M, Sennerby L, Lundgren S (2002) A clinical and histologic evaluation of implant integration in the posterior maxilla after sinus floor augmentation with autogenous bone, bovine hydroxyapatite, or a 20:80 mixture. *Int J Oral Maxillofac Implants* 17:635–643
70. Santoro F, Maiorana C (2005) Chapter 5. In: *Advanced osseointegration*. RC Books, Milano, pp 117–124
71. Dressmann H (1892) Ueber Knochenplombierung bei Hohlenformigen Defekten des Knochens. *Beitr Klin Chir* 9:804–810
72. Mousset B, Benoit MA, Bouillet R, Gillard J (1993) Plaster of Paris: a carrier for antibiotics in treatment of bone infections. *Acta Orthop Belg* 59:239–248
73. Mousset B, Benoit MA, Delloye C, Bouillet R, Gillard J (1995) Biodegradable implants for potential use in bone infection: an in-vitro study of antibiotic - loaded calcium sulphate. *Int Orthop* 19:157–161
74. Peltier LF (1959) The use of plaster of Paris to fill large defects in bone. *Am J Surg* 97:311–315

- 
75. Sidqui M, Collin P, Vitte C, Forest N (1995) Osteoblast adherence and resorption activity of isolated osteoclasts on calcium sulphate hemihydrate. *Biomaterials* 16:1327–1332
  76. Scaduto AA, Lieberman JR (1999) Gene therapy for osteoinduction. *Orthop Clin North Am* 30:625–633

Diana Dudea, Camelia Alb, Bogdan Culic, and Florin Alb

## Contents

Introduction .....	1076
Composition .....	1077
The Organic Matrix .....	1077
The Inorganic Fillers .....	1078
The Coupling Agent .....	1078
The Initiator-Accelerator .....	1078
Optical Modifiers .....	1079
Indications .....	1079
Classification .....	1079
Flowable Composites .....	1080
Condensable Composite .....	1080
Conventional Composites .....	1080
Microfilled Composites .....	1081
Hybrid Composite Resins .....	1081
Nanofilled Composites .....	1082
Direct Composite Resins Restorations .....	1082
Anterior Direct Composites .....	1083
Posterior Composite Restorations .....	1090
Clinical Consideration Regarding the Composite Properties .....	1095
Clinical Problems Generated by Direct Composites .....	1098
Indirect Composite Restorations in Dentistry .....	1100
Advantages and Disadvantages of Laboratory Processed Inlays .....	1101
Technological Alternatives for Indirectly Processed Composite Restorations .....	1103
References .....	1111

---

D. Dudea (✉) • C. Alb • B. Culic

Department of Prosthetic Dentistry and Dental Materials, University of Medicine and Pharmacy  
“Iuliu Hatieganu”, Cluj–Napoca, Romania

e-mail: [ddudea@umfcluj.ro](mailto:ddudea@umfcluj.ro); [cameliaalb@yahoo.com](mailto:cameliaalb@yahoo.com); [bogdanculic@yahoo.com](mailto:bogdanculic@yahoo.com)

F. Alb

Department of Periodontology, University of Medicine and Pharmacy “Iuliu Hatieganu”,  
Cluj–Napoca, Romania

e-mail: [albflorin@yahoo.com](mailto:albflorin@yahoo.com)

---

**Abstract**

Resin composites, also named resin-based composites, composite resins, or composites, contain four major components: an organic polymer, inorganic fillers, a coupling agent, and an initiator-accelerator system. Classification of the composite resins takes into account the consistency of the material (correlated with the filler/organic matrix ratio) and, further, the size of the fillers' particles. The area of indications of the composite materials in dentistry covers a large range of domains: from direct and indirect restorative materials, veneers, provisional restorations, inlays, onlays, crowns, sealants, cements used in adhesive cementation of the composite or ceramic crowns and bridges, inlays, root canal posts, and composite teeth for dentures.

The present chapter emphasizes the characteristics of composite resins such as direct and indirect restorations, advantages and disadvantages, clinical indications and clinical protocols used to process them, clinical considerations regarding the composites properties, and practical problems that can be encountered when used.

Direct composites offer rapid, minimally invasive, single-session methods of treatment. Due to the large range of materials available on the market, the esthetic results may be excellent. The clinical choice of a direct composite is based on the priority that should be given to mechanical or esthetic characteristics: if the mechanical parameters are mostly important, the material showing the highest percentage of filler is selected; in the case of special esthetic needs, the particle size is the factor that influences the selection.

The indirect processed composite resins are alternatives for large restorations, on several teeth in a quadrant, when used to replace functional cusps, in patients with bruxism or parafunctional habits. Their advantages over the ceramic restorations include: repair capabilities, resilience for comfort and shock absorption, adjustable in the mouth, and no wear of opposing structures in functional contact.

---

**Keywords**

Direct composites • Indirect composites • Composite resins • Anterior composites • Posterior composites • Composite inlays • CAD-CAM processed composites • Optical properties • Color • Translucency • Inorganic fillers • Coupling agents • Initiator-accelerator system • Conventional composites • Hybrid composites • Microfilled composites • Nanofilled composites

---

**Introduction**

Esthetic dentistry is a continuous developing area of dental treatments, due to the patients' increased demands in respect to the appearance of the dental arches and, consequently, of their restorations.

The materials currently available for the esthetic restoration of dentition are composite resins and dental ceramics; in contrast to the ceramics that can be processed only in the dental laboratory or by using in-office CAD-CAM technology,

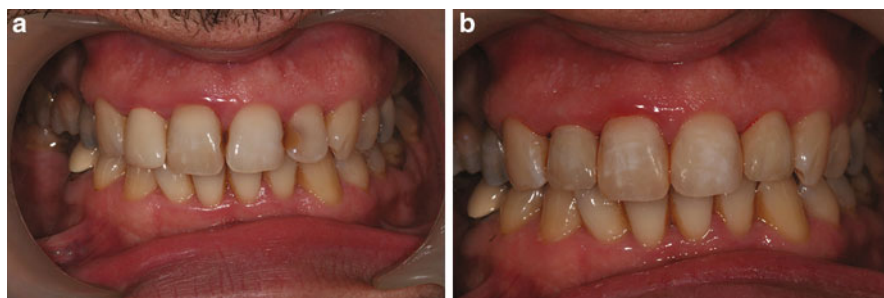


**Fig. 1** Direct composite resins. (a) Initial situation. Old discolored restoration on the upper incisors. (b) Clinical appearance of the restored teeth with direct composites (Clinical case Dr. Bogdan Culic)

composite resins are materials that can be used either in direct reconstruction of the dental structure (dentist-processed filling materials) or as laboratory-made fixed appliances (inlays, onlays, crowns, posts, and cores). The introduction of composite resins in dentistry is closely related to the initiation of enamel acid etching (aimed to improve the adhesion to the dental substrate, and to bis-GMA monomer development [1] (Fig. 1a, b).

---

## Composition

Resin composites, also named resin-based composites, composite resins, or composites [2], contain four major components: an organic polymer, inorganic fillers, a coupling agent, and an initiator-accelerator system [3].

## The Organic Matrix

The organic matrix is represented most often by a mixture of aromatic and/or aliphatic dimethacrylate monomers – most often bisphenol glycidyl methacrylate (bis-GMA or the Bowen's resin), urethane dimethacrylate (UDMA), or a combination between the two [4]. Bis-GMA constitutes around 20 % v/v of standard composite resins [5]. However, it is a high-viscosity material that explains the addition of a low-viscosity monomer, like TEGDMA – triethylene glycol dimethacrylate [4].

Another shortcoming of bis-GMA is the contraction – its proportion in the composite mass is inversely correlated with the shrinkage [1]. One of the most important directions to improve the organic matrix is oriented toward decreasing the contraction. In this respect, the epoxy-based silorane system (Filtek Silorane LS) 3M Espe provides verified lower shrinkage than typical dimethacrylate-based resins, due to the epoxide curing reaction that involves the opening of an oxirane ring [6, 7].

## The Inorganic Fillers

The inorganic fillers can be represented by fine particles of radiopaque glass or quartz, microfine particles of zirconium oxide, aluminum oxide or colloidal silica, glass fibers, nanoparticles of silicon dioxide, and silica-zirconia nanoclusters. The dimension of the inorganic fillers is the bases for the composite classification.

Filler is the portion of the composite responsible for the hardness, compressive and tensile strength, and abrasion resistance; for the reduction in polymerization shrinkage; and for the volumetric stability; it is also the component that stands for the reduction in water sorption and staining and for a viscous consistency that is easier to handle during insertion into cavity [4].

The inorganic particles such as strontium, barium, glass, and zirconium are also responsible for the radiopacity.

The glass fillers are more sensitive to acidic attack, and as a consequence, the glass-based composites are more susceptible to abrasive wear than silica filler-based resins.

The content of filler ranges between 30 and 70 % vol or 50 and 85 wt% of a composite [4].

Addition of new formulas of fillers is experimented; the remineralizing potential of the material by adding dicalcium or tetracalcium phosphate nanoparticles is a promising direction, even if the opacity of such composites limits their esthetic appearance [6, 8, 9]. In the same idea, other formulas, based on calcium fluoride, have been developed [6, 10]. In this case, remineralization may be promoted by the slow release of calcium and phosphate ions followed by the precipitation of new calcium phosphate mineral [6, 9, 10].

## The Coupling Agent

The coupling agent covers the inorganic particles and creates the bond between the previous two phases. This agent is a molecule with silane groups at one end (ion bond to  $\text{Si}_2\text{O}$ ) and methacrylates at the other end (providing covalent bond with the resin) [1]. A properly coupling agent prevents the water penetration at the resin-filler interface, preventing leaching [4].

## The Initiator-Accelerator

The initiator-accelerator system allows for the curing process, either by chemical reaction (self-curing, chemically activated composites), light activated (light curing), or dual activated (chemically and light activated).

The light activation is enabled by a photoactivator (camphorquinone) which absorbs the 470 nm wavelength light, responsible for the curing process; the reaction is further activated by a tertiary organic amine containing a carbon ring double bond [3].

The light-curable composites are maintained in light-proof syringes. The two components of the activation system – the photosensitizer and the amine



initiator – contained in the paste do not interact as long as they are not exposed to light [4].

In order to reduce the yellowish effect generated by the camphorquinone, other photoinitiators have been introduced lately (PPD-1-phenyl-1,2-propanedione) [7], Lucirin TPO (monoacylphosphine oxide), and Irgacure 819 (bisacylphosphine oxide) [6, 11].

Chemical curing is enabled by the reaction of an organic amine (contained in the catalyst paste) with an organic peroxide (catalyst paste) [3].

## Optical Modifiers

Optical modifiers are responsible for the translucency and color. They are represented by metallic oxides that act in terms of colorants or opacifiers (titanium dioxides, aluminum oxides).

---

## Indications

The area of indications of the composite materials in dentistry covers a large range of domains:

- Direct restorative materials of the anterior and posterior teeth, when the dental structure is lost due to dental decay, fractures, erosions, and attritions;
- Direct composite veneers when the change of the dental shape, position, and dimension is aimed or is needed to mask a discromic tooth or to close diastemas;
- Indirect (laboratory processed) veneers, inlays, onlays, and crowns;
- Direct or indirect provisional restorations, during the intermediate stages of fixed prosthetic treatments;
- Cavity liners in deep cavities;
- Fissures and pit sealants of the recently erupted teeth, in preventive dentistry;
- Resin-based cements used in adhesive cementation of the composite or ceramic crowns and bridges, inlays, onlays, and veneers;
- Root canal posts;
- Composite teeth for dentures [1–6]

---

## Classification

Classification of the composite resins takes into account the consistency of the material (correlated with the filler/organic matrix ratio) and, further, the size of the fillers' particles.

The **viscosity-based** classification of composites includes: the **conventional (universal)** restorative materials indicated for restorations of anterior and posterior teeth, **flowable materials**, and **packable condensable** composites. Conventional composites are used for the restoration of the anterior and posterior teeth.

Flowable composites are used as sealants, liners, or layers aimed to enhance the adaptation of the conventional composite to the cavity walls; the resin-based cements are, also, flowable composites.

Packable composites are more viscous materials used only on the posterior teeth, due to their enhanced mechanical resistance and their ability to reproduce tight contact areas [6].

## **Flowable Composites**

Flowable composites have the advantage of a highly wettability of the dental surface that ensures their penetration into narrow spaces and their ability to form thin layers; these properties made them the materials of choice for preventive methods and minimally invasive techniques of dental decays. In the first instance, dental sealants are used to block the fissures and pits on the dental surface, in order to prevent the dental plaque accumulation; the infiltration with newer flowable composite resins of demineralized enamel, in the earliest stages of dental decay, is the philosophy of the minimally invasive treatment approach.

Another characteristic, the high flexibility, explains the indication in the treatment of cervical lesions (dental decays or wear cervical lesion) so they are less likely to be displaced under an increased stress. The most frequent area of indication is, still, their application as liners under high- or medium-viscosity composites; they provide a thin-layer material that fills the irregularities of the prepared dental surface and favor a better application of the restorative material.

In order to enhance the adhesion and to reduce the clinical steps, flowable composites with acidic adhesive monomers, typically found in dentin bonding agents, have been developed. These self-adhesive flowable composite resins recommended as liners, sealants, or restorative materials for small lesions are controversial in respect to their longevity [1, 2, 4, 6].

## **Condensable Composite**

Condensable composites are used as alternatives to amalgam fillings or indirect restorations (composite or ceramic inlays) for the posterior teeth. Due to the characteristics of the filler portion, either modified in respect to the size distributions of the particles or by addition of fibers, they are designed to resist the occlusal forces in this segment of dentition [6, 12]. In addition, due to their higher consistency, they allow for a good contact area between adjacent teeth; in this respect, the main indication area are the restorations that involve the proximal surfaces (class II) [1].

## **Conventional Composites**

Conventional composites are classified, further, according to the dimensions of the filler particles in traditional (macrofilled), hybrid, microfilled, and nanofilled composite resins.

The first traditional dental composites had large particle fillers, 1–50  $\mu\text{m}$ . Sometimes, the term conventional is used in order to refer to this class. Even if these materials had increased strength, they were difficult to polish, since the large particles that were loosen in the process generated rough surfaces. In addition, in time, the organic matrix develops abrasion faster than the filler that results in protruding particles from the surface. This uneven surface is also susceptible to staining [1, 4, 6].

## Microfilled Composites

Microfilled composites have inorganic particles, more often amorphous spherical silica (colloidal silica), of 0.04  $\mu\text{m}$  (one-tenth of the wavelength of visible light) and the loading rate low that explains the mechanical weakness of this group of materials. Their indication in the posterior zone is limited due to the fractures that occur mostly in class II cavities.

The high percentage of resin (40–80 vol%) is responsible for the water sorption and of their increased staining resistance; however, the microfilled composites are the materials of choice for the anterior zone, in the exposed dental areas, due to their highly polishable surfaces. Their filler particles are smaller than the abrasive particles of the instruments used for finishing; in the process of polishing, the fillers are removed in addition to the resin matrix that leave a smooth surface. However, even in this area, they are not indicated in class IV cavities, when the incisal margins or angles are involved, due to the limited resistance to incisal forces; in this case, a combination with a palatal hybrid composite portion is indicated.

The addition into the organic matrix to prepolymerized resin fillers (PPRF) increases the filler content that results in reduced shrinkage.

The preparation of the PPRF involves adding 50 % vol of silane-treated colloidal silica to the monomer; the composite paste is further heat cured and ground into particles. These fillers are often referred to as organic filler; however, the term composite filler is preferred, since a high level of silica is contained, to lower the viscosity. When a more extended restoration in the anterior area is required, it is indicated to combine the microfilled composite with a hybrid composite; the latter, used for the reconstruction of the palatal portion, is responsible to stand the occlusal stress, while the microfilled resin provides a polished labial surface of the restoration [2–4].

## Hybrid Composite Resins

In order to increase the rate of loading, a combination of inorganic particles ranging 0.04–4 is used that enables increased resistance to stress but reduces the esthetic appearance of the labial surfaces. The composition consists mainly of colloidal silica and ground particles of glasses containing heavy metals, the latest with 0.4–1,0  $\mu\text{m}$ .

They are the material of choice for anterior (even for class IV restorations) and posterior restoration, in the case of less-demanding esthetic needs. They were obtained by further grinding of the particles that formed the macrofilled composites and by the addition of submicron-sized silica.

Microhybrid and nanohybrid composites are hybrid resins with the average of the particle size less than 1  $\mu\text{m}$  (0.4–1  $\mu\text{m}$ ). They are nowadays considered the universal composites, since they combine the mechanical and esthetic characteristics, so they are used in both anterior and posterior zone, with good results. They are also recognized to have better handling and lustering properties [1–4, 6].

## Nanofilled Composites

Nanofilled composites are the materials with nano-sized fillers, dispersed in the organic matrix either as 5–100 nm isolate particles or as fused aggregates of primary nanoparticles, with the cluster size significantly exceeding 100 nm. They were introduced in order to improve their mechanical and esthetic characteristics (Filtek Supreme XT, 3 M Espe).

Currently, nanofill and nanohybrid composites are considered the state of the art in the domain of filler formulation [2, 6, 13–15].

Studies aimed to increase the clinically relevant properties of the composite resins were conducted lately toward reducing the filler size to provide more effectively polished and with greater resistance materials and toward improving the polymeric matrix, in order to reduce polymerization shrinkage and to develop self-adhesive composites [6].

---

## Direct Composite Resins Restorations

Direct restorations represent the most commonly used restorative method, in case of dental decays, erosions, fractures, and abrasions, when reconstruction of the original dental configuration is usually aimed. It is also indicated for direct recontouring, in situations of dental shape or dimension anomalies or to close diastemas.

The composite resins are frequently used materials, when direct restoration of either anterior or posterior teeth is aimed. They offer rapid, minimally invasive methods of treatment with satisfactory esthetic results [15, 16, 17]. The reasons to indicate these methods originate in their ease of use, the reduced number of treatment sessions, the increased adhesion to dental structure, and the large range of materials available on the market. In order to satisfy the requirements of a proper restoration, the composite resin should have adequate mechanical, biological, and esthetic properties, according to the position of the tooth in the dental arch.

The clinical choice of a composite is based on the priority that should be given to mechanical or esthetic characteristics – if the mechanical parameters are mostly important, the material showing the highest percentage of filler is selected; in the

case of special esthetic needs, the particle size is the factor that influences the selection [1].

## **Anterior Direct Composites**

For the restorations placed in the esthetic zone, the importance of the optical properties is predominant, since a natural aspect of the restored tooth is aimed. From an optical point of view, the goal of an esthetic restoration is to match as closely as possible the color and translucency of the natural dentition.

### **Dental Optical Characteristics**

Dental optical characteristics should be thoroughly understood, in order to be able to replicate them correctly by using dental composites. In terms of dental anatomy, young teeth, recently erupted, have a convex surface and are well contoured, with lobes, grooves, and fossae that produce a diffuse reflection of incidental light, which accounts for the “textured” aspect. Both the convexity of the surface and the texture diminish with the attrition, due to aging [18, 19].

The enamel, the dentin, and the pulp, which form the tooth crown, are different from the point of view of their structure, composition, and optical properties: dental pulp influences less the overall optical aspect; in contrast, the dentin and enamel, through their properties and thickness in each tooth area, are responsible for the optical dental characters.

It is considered that, due to its dominant volume, saturation, and opacity, the dentin generates the global color of the tooth. This is more easily assessed in the cervical area, where the enamel is thin and dentin is seen through the transparency. The dentin, in shades of yellow-orange-brown, has different degrees of saturation, which increases with age and may be reduced by “whitening” procedures that induce, in fact, a “desaturation.”

The chromaticity of the enamel is less important; however, it varies in shade (white-gray, white-bluish). The optical behavior of the enamel is dominated by translucency; the thicker the enamel (as in young teeth), the lighter will be the general appearance. A thinner enamel layer, as in elderly persons, reveals the dentin, which accounts for the reduced lightness. Crystallographic studies indicate the possibility of correlating the dimensions of the hydroxyapatite crystals in the enamel with its lightness [18–21]. The dentin and enamel are differently distributed in the tooth configuration; therefore, the gradient in the optical properties – color and translucency – varies along the dental crown.

In conclusion, the dentin presents a chromatic translucency, with increasingly stronger saturation, with age, due to extrinsic pigmentation; the enamel is either achromatic translucent or chromatic translucent, with a grayish-white or yellowish-white aspect [22]. Due to the unlimited possibilities regarding the available shades and opacities used to reproduce the optical properties of the dental structures, the initial aspect of the direct composite restorations may be excellent [23–29].

## Indications of the Anterior Composite Resins

Indications of the composite restoration on the anterior teeth are represented by:

- **Loss of dental structure**, from various causes (dental decays, fractures, erosion, abrasion, or attrition) that affect different portions of the tooth. The dental decays are initiated mainly on the proximal surfaces, and according to the invasion into the dental structure, either a cavity class III (without the involvement of the corresponding incisal angle) or a class IV (when the angle is to be restored) is prepared (Figs. 2a, b and 3a, b).

Fractures can affect only the incisal portion, or the entire crown, when a more extensive restoration is needed; however, it is aimed, often, to maintain a minimally invasive treatment method, and the buildup of a composite is the method of choice (Fig. 4a, b).

Erosion can be located either on the palatal surface, when the acidic cause has an intrinsic origin, or on the labial surface – in the case of acidic food intake.

Abrasion affects the incisal edge but, in the case of parafunctional traumatic forces, cervical noncarious lesions are to be treated, as well.

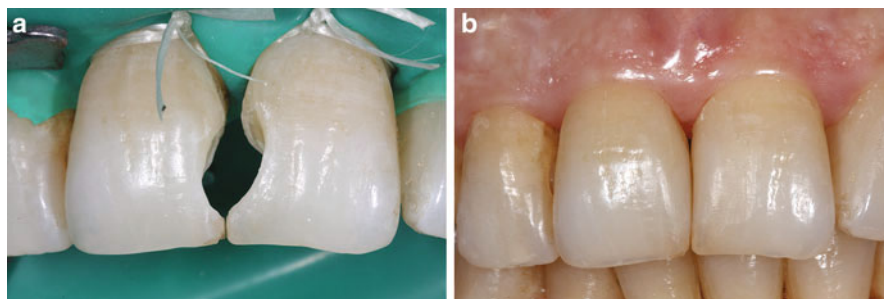


**Fig. 2** Proximal decays. (a) Preparations without incisal angle involvement. (b) Restorations with direct composite resins (Courtesy Dr. Mihai Varvara)

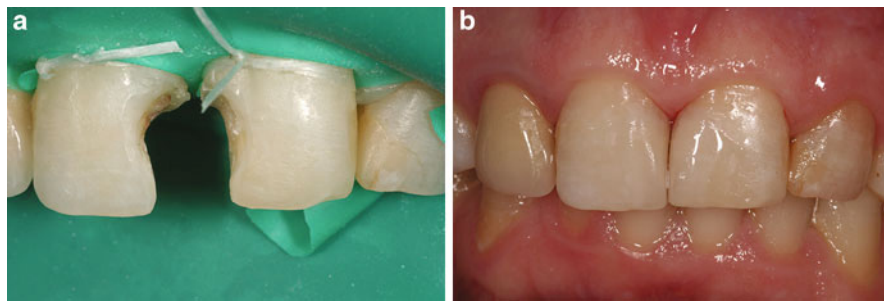


**Fig. 3** Proximal dental decays. (a) Preparations with the incisal angle involvement. (b) Restorations with direct composite resins (Clinical case Dr. Bogdan Culic)

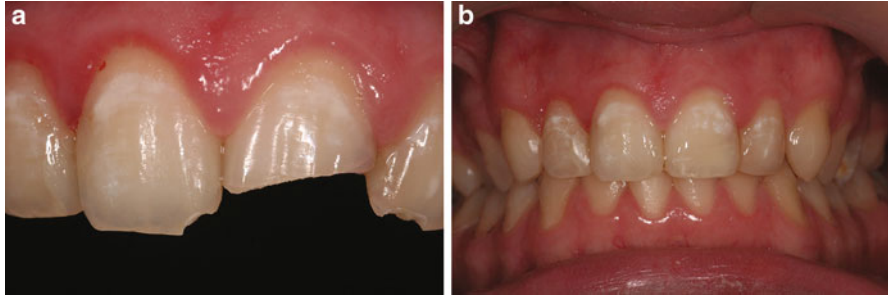


**Fig. 4** Fractures of the incisal margin. (a) Initial situation. (b) Restoration in composite resins (Clinical case Dr. Bogdan Culic)

- **Spaces** (diastema) between adjacent teeth;
- Peg shaped or other abnormality in the anatomy of the frontal teeth; more often the maxillary lateral incisor is subjected to these malformations;
- Discoloration of one or more anterior teeth, due to an intrinsic cause (pulp necrosis, tetracycline-induced discoloration).

In these cases, a veneering is indicated, and, when needed, an individualized reshaping of the respective tooth.

As in the case of posterior restorations, the only absolute contraindications are the allergic history to constituents of the composite materials. However, caution should be taken to situations of abnormal occlusal forces (bruxism), when crown lengthening is indicated for esthetic reasons.

Other relative contraindications are poor oral hygiene and increased receptivity for caries, gingival inflammation, and other conditions that limit the isolation of the operatory field.

### **Clinical Protocol for Direct Anterior Composites**

The materials of choice for anterior composites are micro- and nanocomposites and hybrid composites with micronic and submicronic fillers. However, in the case of reconstruction of the incisal margin or edge, when the fracture resistance is challenging, a combination between hybrid composite (for palatal surface) and microfilled composite (for labial surface) is recommended.

For cervical lesions, flowable resins are indicated, with an elasticity module comparable with that of the dentin.

In order to restore the dental structure in composite resins, tooth preparation follows the protocols indicated for class III–IV or class V cavities, modified in the respect of minimal invasive tendencies. A good isolation is required, either with the rubber dam or with retraction cord inserted into the gingival sulcus.

One of the most challenging missions regarding anterior composites is to restore the optical characteristics of the dentition to mimic the adjacent dental structures. In this respect, two steps are followed: color matching and reproducing the optical

properties of the dentition by selection and stratification of the most appropriate combination of composite resins.

A. **Color matching** is a clinical step that can be initiated either by visual or instrumental observation. When the global shade is taken with a measurement system, the visual observation is still mandatory, in order to specify the individualization of the tooth (translucency, opaque spots or pigmentation, fissures).

Instrumental assessment of the dental color can be done either with a spectrophotometer (e.g., Spectrophotometer Vita Easyshade<sup>®</sup> in global mode or tooth area mode, depending on the extension of the future restoration); the results of the recordings, expressed in Vita Classic coding system, are used as a “starting point” that is further completed by the visual observation. Another option is a spectrophotometric device that enables the color map of the tooth (SpectroShade) or a colorimetric system.

Visual selection aims to match the tabs of a shade guide with the dental area. Vita classical shade guide or the shade guides available in the composite kits (if applicable) are used. It was stated that a common mistake in color selection step is to use ceramic shade guides, since they are fabricated from materials that differ completely from composite resins and, in addition, it is difficult to find a similarity between the ceramic shade guide and the correspondent composite resin. The custom-made shade guides are the best option, with different material thickness and separation for enamel and dentin [23].

Color selection involves the analysis of each tooth area; further, these segments are assembled in order to design the color and translucency map for each tooth. The most evident instrumental errors are generated in the incisal zone, in the case of translucent areas; the spectrophotometer interprets these areas as dark-colored portions. The corrections are done by visual observation of the tooth (Fig. 5a–d).

Most composite kits have their own shade guides, either universal or differentiated in terms of dentin and enamel shades. There are composite kits that have stratified shade guides, to suggest the perceived color when increasing thicknesses of composite. Some shade guides have “recipes” of combinations of the available composites, necessary to get the selected shade.

When the shade is analyzed, several rules should be respected:

- The lighting should be uniform; either indirect natural lighting or illuminants with color-corrected spectrum should be used. The selection is then verified in several color sources, to avoid differences in color perception, due to metamorphism; the nature of incidental light plays a major role in determining the amount of light transmission or reflection. The nature of the light source influences, by this, the way in which a restoration is perceived [30].
- The color matching should be planned at the beginning of the clinical session, before the rubber dam is fixed; however, all the intense colors from the adjacent area of operatory field should be removed.
- The observation of the matching pairs is done at a distance of 25–35 cm, keeping the shade tab in the proximity of the reference tooth; this can be either the tooth to be restored or adjacent or contralateral teeth.



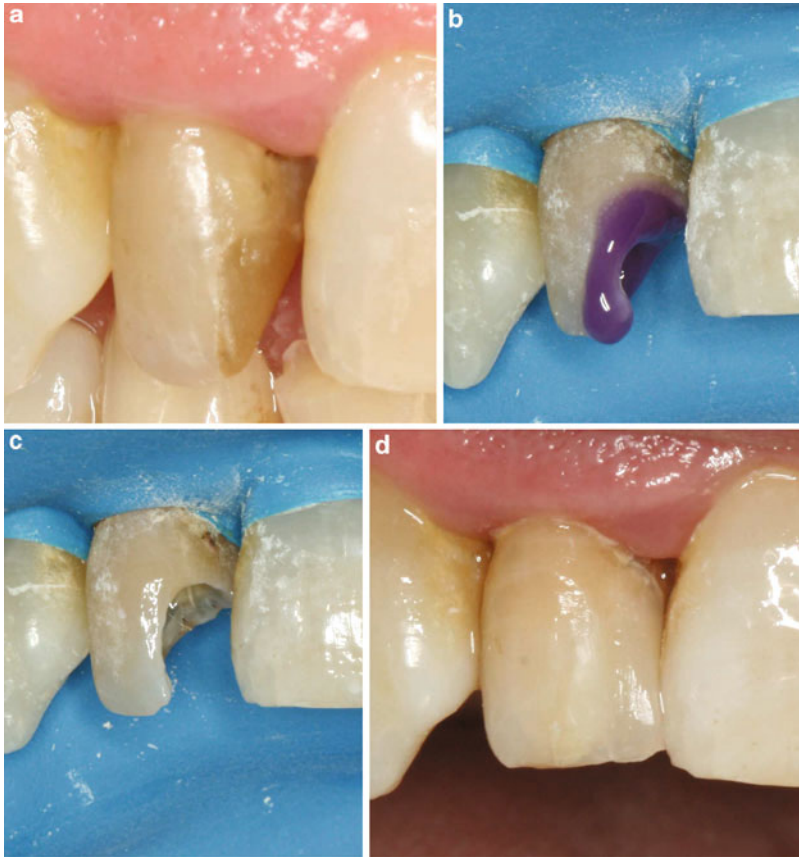


**Fig. 5** Non-vital, discolored tooth. It was decided to preserve the remaining dental structure and to provide a direct composite, for a short term; however, the color matching is difficult in this situation. **(a)** Defective restoration. Selected spectrophotometric shades C4, C4, A4; **(b)** acid etching. Visual correction of the shade: A4, A3, A3. **(c)** Adhesive (Adper Single Bond 2™ – 3M Espe). **(d)** Final result. Opacities used: A4D, A3.5B, A3E, TY (Filtek Ultimate- 3M Espe) (Clinical case Dr. Diana Ducea)

**B. Composite selection and buildup**, in order to generate a restoration in concordance with the natural adjacent teeth. In these cases, the replacement of dental tissues with materials having optical properties similar to the enamel and dentin is aimed. In order to effectively mimic the dental structures, the restorative materials must have a refraction index as close as possible to the dental tissues [19, 20]. Moreover, within the layering techniques, it is therefore important not only to choose materials with optical properties similar to natural structures but also to build them in order to gain effects of chromatic “depth” that characterize natural dentition [19].

When the composite material is selected, from the optical point of view, two factors should be considered:

- The color parameters that are selected usually by using the Vita Classic color coding (A, B, C, or D – most often A shades are recommended)
- The translucency/opacity that is influenced by the composition of the composite material, mainly by the differences in the refractive index between filler and organic matrix, the amount of filler, and the filler size [16, 31]

Translucency is intermediary between transparency and opacity – in nature, the translucency of the enamel varies among teeth and is subjective perceived; however, four factors should be considered when the translucency of the composite resin is decided: presence or absence of color, thickness of the enamel, degree of translucency, and surface texture [22].

The terminology used to indicate various classes of opacities is sometimes confusing, since there are different systems used by the producers of composite materials; in general, four categories can be differentiated:

- Opaque composite material (opaque dentin, opaque) is the most opaque group of materials – they have an increased opacity in comparison with the human dentin [31] that is used to block the passage of the incidental light; they are used to mask discromic substrate or to avoid the effect generated by the darkness of the oral cavity in the restorations which involve both the lingual and the labial surface (labial-lingual class III or class IV); with no dentinal opacity, even if the composite's color is a perfect match with the remaining dental structure, the restoration will appear too dark, because a relative translucent material is not able to mask the dark background of the oral cavity [31].
- Intermediate opacity (body dentin, body) that mimics the dentin used to provide the “basic” hue and saturation of the tooth. It is the opacity of choice when a single material is used for the restoration; “body” is also used to design composites used to substitute both the dentin and enamel [33], but there are also authors who design “artificial enamel” or “body” with the meaning of a material to replace the natural enamel [32].
- Translucent material (enamel) responsible for the translucent layer that covers the dental surface enables the diffraction of the light and controls the lightness.
- Transparent material (incisal, transparent) aims to create a natural, opalescent zone in the incisal area.

More recently, value-changing composite resins were developed to alter the luminosity of a restoration [34].

For the small-sized restorations, when the teeth are not discolored, the blending or the chameleonic effect is considered; this effect was defined as the composite adaptability, in terms of its color, to the surrounding area. It was, however, demonstrated that the blending effect is generated by the relative translucency of the composites, which enable the influence of the optical properties of the underlying and surrounding dentin and/or the enamel on the perceived aspect of the restored tooth [35, 36].

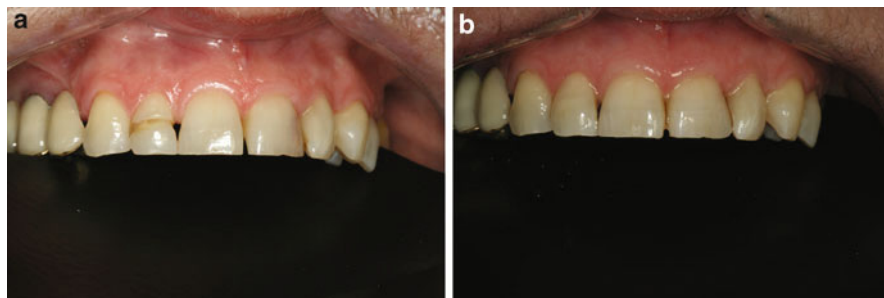


**Fig. 6** 1.2. Labial lack of substance – dysplastic condition 2.1. Dental decay – (a) initial situation. (b) 1.2. Labial filling, 2.1. distal filling. Filtek Ultimate (3M Espe). Spectrophotometric color selection: 1.2. A2, A2, A1. 2.1. A2, A2, A1. Shade used – 1.2: A2B, A1E, 2.1. A3D, A3B, A2E (Clinical case Dr. Diana Ducea)

For the intermediate-sized restorations, two layers of composite are most frequently applied: body dentin/enamel – the former aimed to replace the dentin (several colors are occasionally used, the cervical more saturated than the incisal layers) and the last added for the value and translucency control (Fig. 6a, b).

In larger defects, when an increased amount of dental structure should be restored, several opacities are needed. In these cases, the histological stratification or layering technique should be used: the more opaque materials (dentin shades) are required for masking the discolored dental structure and to generate a background in the larger class III and IV restorations, in order to prevent the grayish effect due to the darkness of the oral cavity. The more translucent materials, body and enamel, are layered superficially, in order to create the natural depth from within the restoration [27, 31].

When the stratification technique is used, a good understanding of the dental morphology and structure is required, since the complexity of the optical aspect of teeth is related to their particularities of shape and structure.

In these cases of advanced tooth structure loss, a direct mock-up of wax-up, followed by indirect mock-up, should be performed, in order to provide a silicon index aimed to sustaining the composite material during the buildup process (Fig. 7a–d).

For the stratification technique, several opacities should be used:

- Palatal layer, incisal margin, and proximal walls are built in enamel shades.
- Dentin and body dentin shades replace the dentinal tissue; during buildup, it is aimed to reconstruct the configuration of the dentinal lobes, in one or several chromatic tonalities.
- In case of young dentition, in the incisal third, in close proximity to the incisal edge, small increments of transparent should be added, in order to mimic the natural opalescence.
- The spaces between the dentinal lobes should be filled with body dentin and, incisally, with enamel.
- The final outer layer is reconstructed in enamel shades.

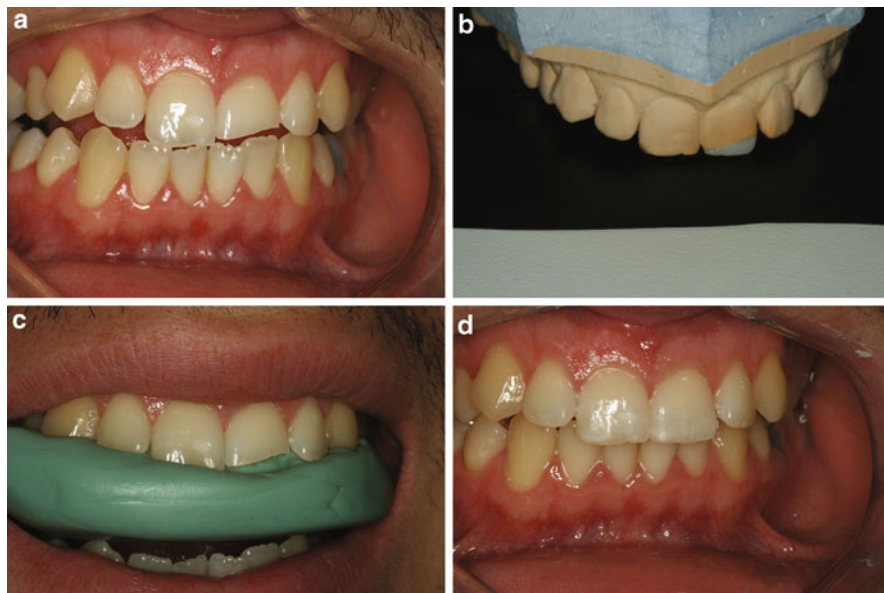


**Fig. 7** (a) 2.1. Fracture of the incisal third – initial case. (b) Wax-up on the model necessary for the silicon index. (c) Silicon index in position used for stratification. (d) Direct composite resin restoration – stratification (Clinical case Dr. Diana Dudea)

When a discromic dental substrate is to be masked, it is recommended to start with an opaque composite (opaque dentin), or an opaque layer, that is used to cover the dark surface; however, these layers remove the natural dental translucency that is further reproduced artificially with a dentin shade of hybrid composite and, superficially, fine veneer of microfine composite in enamel shades [1]. Translucent shades are used to mimic the natural opalescence of the incisal margin.

Finally, the texture is modeled during the grinding and polishing, depending on the clinical situation, more or less pronounced, according to the adjacent teeth.

## Posterior Composite Restorations

When a posterior restoration is envisioned, several treatment options should be taken into account: direct restoration, using amalgam or a tooth-colored material, or indirect restorations that require teamwork – dentist-dental technician (inlays, onlays, crowns) (Fig. 8).

### Indications of Direct Composite Restorations in the Posterior Area

In the last decades, the amalgam fillings are, more and more, replaced by direct or by indirect composite restorations, in laboratory processed inlays, onlays, or crowns.

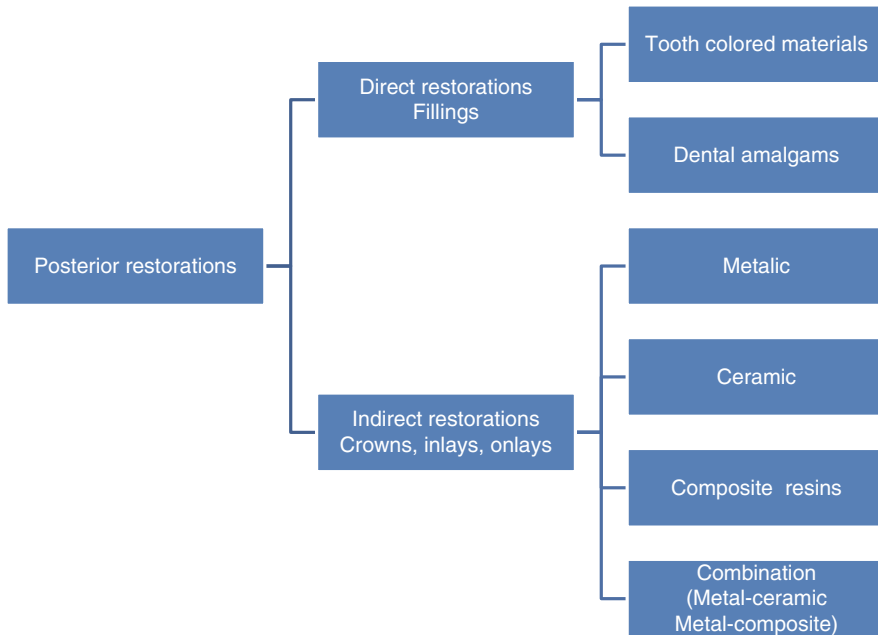


**Fig. 8** Restorations of the posterior teeth – technical possibilities and materials used

The larger use of composite resins in the posterior area is due to increasingly demands for a natural appearance and to the large range of available composite colors and translucencies that allows for a natural reconstruction of the teeth, in most of the cases.

Secondly, concerns regarding the toxicity of the amalgam fillings, due to their content in mercury, are reasons that explains the preferences for composites, in comparison to the amalgam restorations. However, it is stated that the concerns regarding the biocompatibility of the amalgam restorations are not based on scientific evidences [37].

The design of the required cavity is also beneficial, in respect to the conservation of the dental structure: in the case of the composites, due to the chemical bonding, the undercuts are not needed, so the preparation minimally invades the sound dental structure. Currently, the design of preparation is limited to the removal of the tooth structure that involves carious dentin and fragile [38, 39].

The preparation is narrower; by this, in addition to the minimally invasive principle, the area of restorative material exposed to occlusal forces is reduced. A limited quantity of composite is desirable also in order to prevent the polymerization contraction and to limit the marginal leakage at the dentin-restoration interface.

The composite materials are clinical solutions for patients experiencing thermal sensitivity generated by amalgam fillings.

**In comparison with the indirect restorations**, posterior direct composites are provided by a limited number of sessions – the treatment requires a single, in-office session; the costs are reduced since the dental laboratory is not involved.

The benefits of the adhesive restorations over the classical-cemented crowns, inlays, or onlays should be mentioned – not only the quality of the cementation but also the reinforcement of the remaining weakened dental structure is demonstrated in the case of chemical-bonded material.

However, in spite of their excellent imitation of the dental structures, both from an optical and from mechanical point of view, their **technique sensitivity** during the insertion, modeling, and polymerization is recognized. A durable composite filling requires a good isolation of the operatory field; moreover, the clinical protocol, starting with etching, bonding, insertion into the cavity, modeling, curing, and polishing – all technical steps – should be followed according to the respective instructions.

In practice, the posterior direct composite restorations are indicated as sealants and reconstruction materials of premolars and molars, with loss of substance in dental decays, fractures, abrasions or attritions, and erosions. Due to the performance of the currently available composites, there are no absolute contraindications of the direct composite restorations, with the exception of allergic history to materials' components.

However, several clinical situations should be regarded as relative contraindications and the treatment plan decided after a careful assessment of the general and local conditions:

- Lack of oral hygiene and limitations in the patients' ability to improve the status of the dental cleaning;
- Gingival bleeding – considering the importance of a clean operatory field and of a good isolation, the composite filling placement should be planned after a rigorous professional cleaning, to avoid gingival inflammation due to bacterial deposits;
- Difficult clinical accessibility, when the possibility of isolation is limited (distal cavities, malpositioned teeth, reduced opening of the oral cavity, difficult communication with the patient);
- Large defects with extended enamel loss due to the reduced surface responsible for a durable bonding;
- Defects extended below the gingival margin, unless a gingivectomy is performed, in order to place the gingival limit of the restoration above the free gingiva. If the cervical limit is located on the cementum or in the next proximity of the gingival margin, an open-sandwich restoration, with the gingival portion represented by an increment of resin-modified glass ionomer, could be the treatment of choice;
- In the case of teeth subjected to traumatic forces – premature contacts and bruxism – the failures, in these cases, involve not only the composite resins (fracture, attrition, or debonding) but also the remaining dental structure that can be subjected to cracks or fractures;
- Lack of substance of the occlusal surface that involves the reconstruction of one or more cusps (mainly supportive cusps), due to the large amount of force that is transmitted in this area.

### **Clinical Steps for Direct Posterior Composite Restorations**

In the posterior area, depending on the extension of the substance loss, various clinical protocols of preparation and application could be followed:

**Dental sealants** – basically, the procedure consists in the blocking of the shallow depressions on the dental surface with composite resins, in order to prevent the dental plaque accumulation and the consecutive demineralization of the dental structures; it is indicated on both primary and permanent posterior teeth, at a moment that follows closely the eruptive stage.

Among the composites, the materials of choice are flowable composite resins, but also other groups of materials could be used: glass ionomers and resin-modified glass ionomers. The clinical protocol is initiated by the dental surface cleaning and, according to the type of resin, is followed by the conditioning of the area (acid etching and bonding). In the case of self-adhesive composites, the preliminary etching and bonding step is not required.

The most important clinical limit of this procedure is the sealants' debonding due to lack of retention; patients should be included in preventive programs and followed on a regular basis.

**Preventive restorations** consist in minimally invasive cavities that with a limited extension, at the carious fissures and pits. The preparation is in contradiction with the classical principles of preventive extension and retention of cavities, and it is recommended due to the development of adhesive dentistry (dental surface etching, composite bonding).

According to the cavity extension, either flowable composite resin (when only shallow fissures or pits are involved) or a combination is used – conventional composite to restore the occlusal morphology and flowable to fill the fissures and pits and to cover the entire restoration (when a more extended cavity is needed).

**Conventional restorations** extended on one or more of the dental surfaces:

Class I cavities, for the occlusal surface, is limited more often to preventive restorations. In the case of deep decay, a pulpal protection, with a liner (glass ionomer), is indicated, followed by the bonding procedures; the restoration involves the placement and model of the occlusal morphology using the incremental technique.

Class II cavities are extended on a single or both proximal surfaces and on the occlusal surface; as in class I, the use of a liner is limited to the cases with close proximity of the dental pulp. In these cases, the restoration of the proximal walls requires a matrix band; this should be placed in close contact with the adjacent tooth, in order to obtain the contact area. The matrix is blocked with a wedge that allows to create proper space for the dental papilla.

In the light of preventive dentistry, a minimally invasive approach is indicated in this location, as well: each proximal and occlusal cavity should be prepared and restored separately [38] (Fig. 9a–f).

In deep cavities, or when the exposure of the dental pulp is suspected, a calcium hydroxide-based liner is indicated. Another option is the glass ionomer liners that have the benefit of bonding by the subjacent dental tissue and by the overlying composite.



**Fig. 9** 3.6, 3.7. Occlusal direct restorations. (a) Defective restorations. (b) Occlusal boxes, protective liner on the cavity floor. (c) Acid etching. (d) Application of the adhesive system. (e) Buildup of dental morphology, by using incremental technique. (f) Composite restorations. Occlusal contacts are verified with articulating paper (Clinical case Dr. Florin Alb)

Various formulas and corresponding protocols could be followed further in order to apply the bonding system: self-etching, total etching, in one, two, or three steps.

Traditionally, the composites indicated for the posterior area are highly viscous materials that allow for a better condensation and modeling of the occlusal details and of the proximal contours. An option was the packable and condensable composites, based on elongated, fibrous fillers, with a textured surface [4], that resist flow and enable a better condensation that mimics the insertion of the amalgam fillings.

However, viscous materials are difficult to adapt to the cavity walls – thicker consistency has significantly more voids than the medium or thinner consistency [38, 40]. It is recommended to inject the material by using composite capsules or placemen tips that allow a better adaptation and a more homogenous composite mass in comparison to the classical method of insertion with conventional spatulas; another method of decreasing the viscosity is to use heated composite to 60–68 °C. This method facilitates the insertion of the composite into the cavity, improves the adaptation to the cavity walls, and reduces the voids into the composite mass [38, 40].



In order to improve the marginal adaptation, a first increment of flowable resin could be used on the gingival and pulpal floor and for the proximal cavity. This improves the marginal adaptation, since the flowable consistency allows for the penetration in all the cavity details and also reduces total polymerization shrinkage. Another advantage is the easier handling of the next increments of viscous material that adheres easier to the cured flowable.

The conventional hybrid composites are most often the materials of choice for posterior area.

The insertion of the composite into the cavity is, more often, based on the incremental or layering technique. According to this technique, the composites are inserted into the cavity in layers that do not exceed 2 mm in thickness, in order to both ensure a complete cure of the material by the curing light and control polymerization shrinkage [6]. The layers are positioned in an oblique pattern that means to avoid the connection of two opposite walls by the same increment. This prevents cuspal flexure due to composite shrinkage and subsequent fissures or fractures that are more frequent in the horizontal layering technique.

The incremental technique influences the ratio of bonded to unbonded restoration areas – the “C-factor” – that should be decreased, in order to lower the total bond strength of the composite filling [38].

The bulk placement technique is advocated lately, due to the newer class of composites with reduced polymerization shrinkage.

Whatever the technique used, the final increments are placed according to the occlusal morphology. The objective of this procedure is not only to fill the cavity and to ensure a good marginal adaptation but also to rebuild the occlusal morphology: cusps, ridges, grooves, and fossae. At this point, the occlusal contacts are verified – it is intended to keep them outside the enamel-composite interface.

For good occlusal adjustment, contacts are verified in maximum intercuspation and protrusive and laterotrusive movements; finishing and polishing are required to prevent plaque accumulation and abrasion of the opposite occlusal surface.

## **Clinical Consideration Regarding the Composite Properties**

When a composite restoration is envisioned, two main objectives should be considered:

- To provide a long-term resistant substitute for the dental structure, by using a material that is comparable, in terms of the mechanical properties, with the tooth itself;
- To enable a natural look of the restored tooth, in other words, to use a material or a combination of composite resins that mimic the optical properties of the tooth;

The decision regarding the composite used in a certain clinical situation is based on the location of the tooth to be restored (anterior vs. posterior) and the dimension of the future restoration [1].

In the case of large restoration, in the posterior area, either an indirect composite or a direct restoration with a radiopaque composite, with a high inorganic load is needed [1, 41].

The anterior composites should provide the highest polished surface, fluorescence, and the proper level of translucency; microfilled or nanofilled resins will be indicated in this case, either by themselves or in combination with a stronger, more flexural, and fracture-resistant composite, for the palatal surface, as was described previously [1]. In these cases, the stratification will take into account not only the optical characteristics but also the mechanical resistance.

The properties of the direct composite resins are influenced by their composition and the polymerization process. Among the constituents, the inorganic filler and the coupling agents are responsible for the composite's hardness, flexural resistance, translucency, and coefficient of thermal expansion, while the chromatic stability and the shrinkage are influenced by the organic matrix [16, 23, 24].

The factors that are directly correlated with the properties and, consequently, with the clinical applications are the average size of the filler, filler volume level, size distribution, index of refraction, radiopacity, and hardness of the filler [4].

### Handling Characteristics

Handling characteristics are regarded in respect to the composite viscosity and the tendency to stick to the instrument.

Flowable material provides the easiest adaptation to the cavity walls. However, there is the risk of air trapping and the void formation, within these materials.

Conventional softer materials adhere well to the margins and to the cavity walls; however, they could stick to the instruments and are difficult modeled.

More viscous materials are less sticky, but they are more difficult to be inserted into the cavity and have to be modeled with special designed instruments.

### Optical Properties

**The optical properties** of the composite resins are represented by the composite **color** (shade) and **translucency/opacity**; they should mimic the respective optical properties of the dental structures, in order to gain a natural appearance. **Opalescence** and **fluorescence** are characteristics that influence, in addition, the optical appearance of a restoration.

### Color

The available commercially composites are manufactured in a wide range of opacities and shades. They are designated most often according to the Vita Classic shade guide codification system. Among the four shades (A, B, C, and D), the most used are the A groups, since it is recognized that the majority of human teeth have A shades. For this reason, there are composite sets that include only A shades, in various saturations. According to the position into the dental arch, one or more shades can be used in order to reproduce the natural aspect of the tooth, and the map of the tooth is built.

## Translucency

Translucency is the ability of a material to allow light to pass through and thus to allow the appearance of the underlying background to show through [16, 42, 43]. Translucency is influenced by the composition of the material, mainly by the differences in the refractive index between the filler and organic matrix, the amount of filler, and the filler size [16, 42]. For acceptable esthetics, the translucency of a composite restoration needs to be similar with the optical properties of the dental structure. The index of refraction of the filler needs to closely match that of the resin (around 1.50) [4].

A multitude of translucencies are provided in the composite kits, in order to offer support to mimic the natural aspect of the dentition. The corresponding terminology was discussed previously. However, when similar colors and translucencies of composite resins originating from different brands were evaluated, poor color compatibility of pairs of identical shade designation was observed. The best color match was recorded for A2 shade pairs, followed by C2 pairs, B2 pairs, and opaque A2 shade pairs [44].

In order to characterize the composite translucency, different parameters are in use: translucency parameter (TP), contrast ratio (CR), and relative translucency (T).

The translucency parameter of a material refers to the difference in color between a uniform thickness of the material over a white background and the same thickness of the material over a black background and provides a value corresponding to the common visual perception of translucency [42]. Another method used to measure translucency is by calculating contrast ratio, as the ratio of illuminance (Y) of a certain material over a black background (Y<sub>b</sub>) to the illuminance of that material over a white background.

Another important optical measure is the refractive index (the relationship between the speed of the light in vacuum and in a certain material); the refractive index of a composite material should be as close as possible to the refractive index of the dental structures (e.g., enamel) [22].

The specific factors that should be considered when a certain composite material is selected in respect to the translucency are the translucency of the material, itself, the thickness of the dental layer to be replaced, the chromaticity that should be imitated, and the surface texture of the labial surface.

The thickness of composites is also important in the perception of the final esthetic outcome. When the thickness of translucent chromatic composite increases, the chroma increases and value decreases. The level of polish influences the perception of a shade. The more polished a surface, the more light is transmitted and less reflected – the value decreases as a consequence [22, 45].

Light curing creates changes of the translucency/opacity of a composite. Saturation, value, and translucency may decrease or increase after light-curing, and the variation is related to the nature of the composite. In microfilled composites, the translucency and chroma decrease after polymerization, while in hybrid composite resins, the same parameters increase as a result of curing [22].

Composite resins should have **fluorescence** similar to the natural teeth that emit blue fluorescence when exposed to ultraviolet light. Fluorescence, although

minimally perceptible under normal light, becomes important when the tooth is viewed under UV illumination; due to fluorescence, the teeth and corresponding restorations are brighter in the natural daylight; however, external staining and sealant application on the composites' surfaces decrease the fluorescence [46].

### **Radiopacity**

Radiopacity is required mostly in the case of posterior fillings, since here the secondary caries are more difficultly detected by clinical means; it is believed that the optimal radiopacity of a dental composite should be comparable to that of the enamel; an increased radiopacity can act as a barrier that masks the radiotranslucency of a marginal gap [4].

### **Polymerization Contraction**

Polymerization contraction ranges between 1.5 % and 5 % – as a result, gap formation, marginal leakage, cusp reflection, and corresponding fissures of the cavity walls are among the most undesirable events that affect the composite longevity. The polymerization contraction occurs toward the cavity wall that proves to be more bonding resistant; this is generally represented by enamel surfaces. Current research is oriented both to find new formulas of monomers with a lower contraction rate and to adopt technologies that provide less contraction. In order to reduce polymerization shrinkage, incremental technique, with the addition and polymerization of reduced portions of material at a time, is recommended. In addition, two-step polymerization, with increasing irradiance of the curing regimens, decreases the contraction rate [38, 47].

## **Clinical Problems Generated by Direct Composites**

### **Marginal Leakage**

Marginal leakage is due to polymerization shrinkage and to the quality of bonding between the composite and the dental substrate (enamel or dentin). A common situation is that of the proximal or cervical fillings, where the gingival wall is represented by dentin or cement and the other walls of the cavity by enamel; in this case, the material tends to pull away from the dentin or cement during curing, due to polymerization shrinkage, with gap formation [4]. The formation of the marginal gap is followed by the progression of the cariogenic bacteria inside the space and, consequently, by the development of **secondary caries**.

### **Postoperative Sensitivity**

Postoperative sensitivity is correlated with the flexure of opposing cavity walls, due to polymerization shrinkage, or with the application of the composites in deep cavities, without pulpal protection; in order to prevent the second shortcoming, a glass ionomer, resin-modified or flowable composite liner is used, in addition to the composite restoration, in such clinical situations [7]. Cuspal flexure is avoided by using oblique increments during stratification, so that every layer contacts directly a

single wall. Another explanation for the postoperative sensitive is gap formation between the filling and the cavity wall; either as a result of thermal, chemical, or bacterial stimuli, the fluid within the dental tubules migrates and stimulates the odontoblastic processes that result in pain sensation [38, 48]. It is shown that postoperative sensitivity increases for larger restorations [38, 49].

### **Marginal Staining**

Marginal staining occurs as a result of microleakage, due to composite contraction, but also as a result of inappropriate bonding – when the excessive layers of adhesive will change color and form a dark zone around the restoration.

### **Fracture Due to Inadequate Mechanical Properties**

Fracture may be due to inadequate mechanical properties of the composite, incorrect indication of the particular area of placement (anterior or posterior), but also as a result of poor design and preparation of the cavity, with limitations in the quantity and quality of the adjacent remaining dental tissues [6]. In order to prevent adhesive or cohesive fractures, large restorations should be avoided, cusp coverage is also indicated. For patients with bruxism, other methods of treatment are suggested.

### **Microcracks**

Microcracks at the surface or in the volume of restoration can be correlated with the water sorption – water sorption is a function of the resin content of the material and the strength of the resin-filler interface. Extreme water sorption causes the expansion and plasticizing of the resin, which leads to reduced longevity of the composite resin and hydrolysis of saline, which in turn creates microcracks [16, 27, 50, 51, 52].

### **Wear of the Composite Surface**

Wear of the composite surface is dependent on the intrinsic mechanic composites but also on the occlusal contact with adjacent teeth, the material of the opposite restorations, and the position of the tooth in the dental arch. Posterior teeth, being subject of increased occlusal forces, are more exposed to attrition.

It is considered that the resin composite wear occurs as a result of the combination between the chemical and the mechanical degradation of the restorative material.

The mechanical loading is due to either the attrition or abrasive factors. In the first instance, the cause is the contact with the opposite dental surface [38]. In this respect, the quality of the occlusal surface of the opposite teeth or restoration is paramount. Ceramic materials, particularly when inappropriate glazed, induce the most important wear; loss of occlusal morphology, due to cracks followed by fracture and loss of composite mass, is experienced. The consecutive egression of the opposite teeth is expected in these clinical situations.

In the case of abrasion, the food particles in mastication are responsible for the organic matrix wearing and for the exposure, as a result, of the inorganic filling.

The average rates for posterior composite resin are between 7–12  $\mu\text{m}/\text{year}$  and 0.1–0.2 mm more than enamel over 10 years [4, 37].

The differences in the origin of the traumatic forces may explain the behavior of the composite resins. Among the groups of composites, the microfilled have the most critical rate, due to the lowest filler concentration (30–50 %) to the attrition, but they are more resistant to abrasion since they have finer particles and reduced interparticle spaces [38, 39].

Unfortunately, the occlusal wear occurs under normal loading, when the composite restoration is in contact with intact enamel (0.1–0.2 mm/10 years, more than the enamel) [4]. The indication of direct posterior composites is questionable for the clinical situation of bruxism, due to the higher occlusal stress.

### **Water Sorption**

Water sorption is due to the organic matrix of the composite; it is responsible for the composite restorations' increase in volume. The internal structure may be compromised, due to reduction of bond strength [2].

### **Staining**

One of the most important shortcomings of the composite resins is their discoloration over time; the color changing can be caused by internal or external factors. Internally induced discolorations are permanent and are related to polymer quality, type, and amount of the inorganic filler, as well as the synergist added to the photo initiator system. Components like unconverted camphorquinone and tertiary aromatic or aliphatic amines are responsible for a yellowish or brownish discoloration [16, 43, 53–55]. The intrinsic discoloration can be assessed by artificial accelerated aging tests. It was demonstrated that these methods are suggestive when the characteristics of the composition that interfere the optical properties are assessed.

The extrinsic discoloration is due to exposure to food colorants, UV radiation, temperature change, and water absorption [16, 23–29]. In order to assess the extrinsic discoloration, various accelerated staining protocols have been developed. Staining solutions and immersion time are significant factors that affect color stability of composite resins. The samples of composite materials are immersed in various natural colorants (tea, coffee, red wine, fruit extracts or beverages, chocolate) and artificial staining solutions [16].

There are studies that show that, in spite of their excellent esthetic appearance, nanocomposites undergo a greater color change than microhybrid composites after staining [16, 53, 56].

---

## **Indirect Composite Restorations in Dentistry**

Our patients require today highly esthetic solutions also in the posterior teeth, that are at the same time functional and long-lasting. While direct composite restorations have adequate properties to be used in most areas of the mouth, concern still exists when these materials are placed in large preparations, on several teeth in a quadrant, and mostly when used to replace functional cusps, in patients with bruxism or parafunctional habits [6]. The concerns are related to the fracture of the restoration,

its wear – and also the ability to restore a correct contact area in class II direct restorations. Microleakage at the interface composite filling – tooth structure with the risk for secondary caries – represents today the most frequent cause for direct composite replacement. If the gingival floor of the proximal box is placed subgingivally, the glass ionomer (GI) cements or resin-modified glass ionomer (RMGI) cements used to cement an inlay will provide better adhesion than a direct composite [57].

Esthetic inlays and onlays – made in composite and ceramics – offer a viable alternative for patients who desire a more esthetic option than gold, but a more functional alternative than direct composite fillings. While ceramic inlays/onlays provide the patients with a lot of benefits – high esthetics and stability over time – composite resins present some major advantages, including repair capabilities, resilience for comfort and shock absorption, adjustability in the mouth, less chance for differential wear at the luting agent-restoration interface, and no wear of opposing structures in functional contact [58] (Fig. 10a–d).

### Advantages and Disadvantages of Laboratory Processed Inlays

The **advantages** of laboratory-fabricated composite restorations over the direct composite restorations are:

- Restoration of the contact area at the right position and shape with the use of removable dyes, giving the technician the ability to reproduce the complex convex-concave morphology of proximal surfaces.
- Better reproduction of the occlusal morphology in the lab with the use of an articulator – while direct techniques the patient is under rubber dam isolation so the dentist cannot use the opposing teeth to check occlusal contact only when the restoration is finished;

Both proximal and occlusal details can be achieved especially with the use of CAD-CAM technology in composite inlays (Vita Enamic, Vita or Lava Ultimate, 3M).

- Excellent esthetic results that can be achieved with shade matching, a better color stability over time because of superior polymerization obtained in the laboratory;
- Excellent mechanical properties similar to those of the natural tooth (the flexural strength and the elasticity modulus are close to those of the dentin);
- Improved resistance to wear, because of the composition and structure of these materials that have a higher filler content than the in office composites;
- Ability to restore the vertical dimension of occlusion (VDO);
- Less marginal leakage than the direct techniques. With the lab composite, polymerization shrinkage took place in the lab stage and any marginal gap of the inlay will be filled with a film layer of dual-cure composite or GI cements;
- Ability to be finished and polished in the laboratory easier and better than in the mouth;

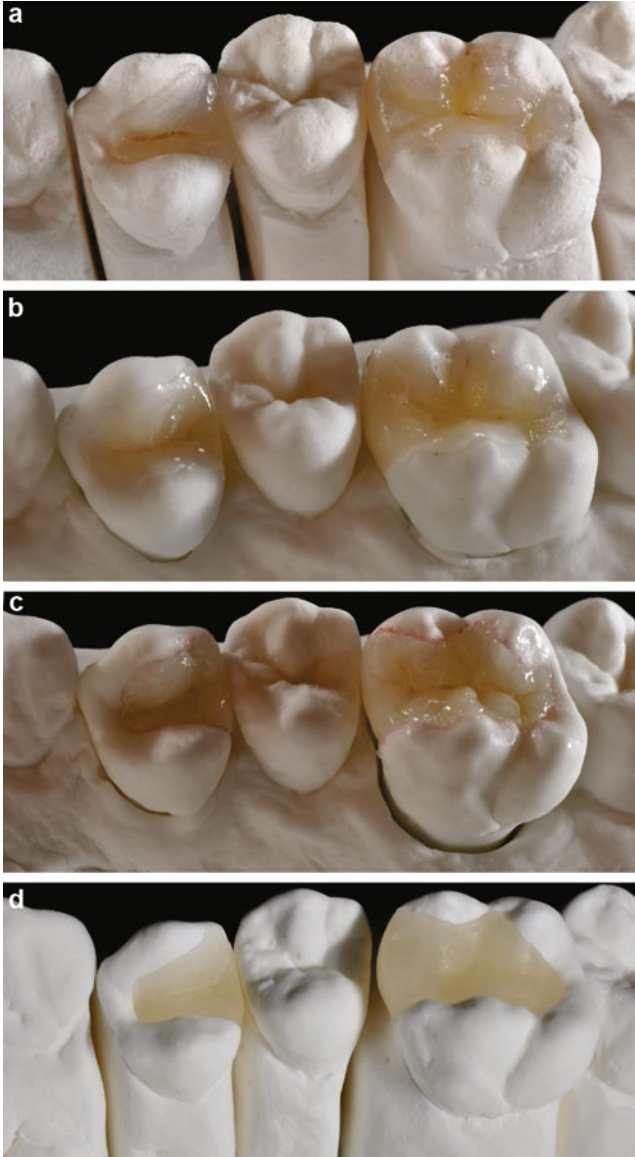


**Fig. 10** (a–d) Four types of esthetic inlays: (a) composite inlays; (b) feldspathic inlays; (c) pressed ceramic eMax inlays; (d) CAD-CAM-produced ceramic inlays

- The triple polymerization performed in the lab, under light, heat, and pressure, will generate less unreacted monomers so better mechanical, biological, and esthetic properties overall;
- Reduced chair time in cases with more inlays on the same quadrant; the preparation and impression are faster than the direct technique [18, 59].



**Disadvantages** would include:

- Inlay preparation and cementation is a sensitive technique that is very much dependent on the skills of the dentist, but this is also true for direct composites;
- Longer processing time and additional costs.

## Technological Alternatives for Indirectly Processed Composite Restorations

There are two methods available for the fabrication of indirectly processed restorations: conventional and CAD-CAM methods.

### Conventional Technique

The conventional technique includes additional laboratory cost and a second appointment needed for inlay cementation as compared to the direct restorations. These can be successfully eliminated by the use of CAD-CAM in-office technology that is able to produce both ceramic and composite inlays, onlays, and crowns, using systems such as CEREC (Sirona), E4D Dentist (E4D Technologies), and Lava system (3M). Results are impressive, because certain clinical steps are eliminated, including the conventional impression, long-distance transportation to the dental lab, and additional clinical appointments. As the inlay can be completed in several hours, the patient no longer needs to be recalled a second time in the office; the cementation can be performed 3–4 h later, which means a lot of time saved for the dentist and the patient. The precision of these inlays is extremely high, and the materials from which they are milled, have optimal properties [60, 61] (Fig. 11a–d).

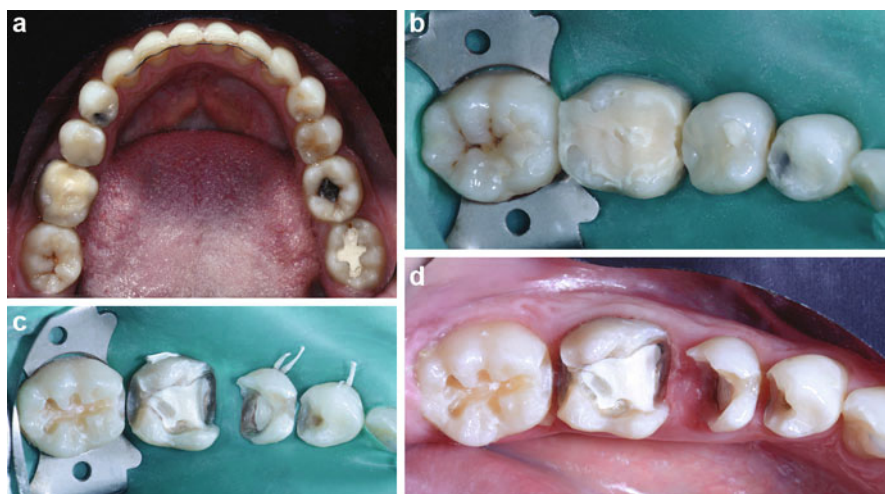


**Fig. 11** (a–d) Clinical case (a) initial aspect of teeth; (b) rubber dam in place before preparation; (c) preparation; (d) ready for PVS impression (Clinical case Dr. Florin Alb)

The clinical case of a 28-year-old patient TC who presented after orthodontic treatment to replace old restorations with secondary caries on teeth 4.4, 4.5, 4.6, 4.7 clearly illustrates the technique and pro's and con's for these indirect restorations. Teeth 4.5 and 4.6 are non-vital teeth endodontically treated and restored with fiber post and core (4.6). Due to subgingival extension of the cavities, all four being on one quadrant, the decision was made to apply four composite inlays in one single arch impression. Preparation was performed under the rubber dam isolation.

After the preparation was finished, the rubber dam was removed for the impression (polivinylsiloxane impression material in a double-mix impression technique) The inlay was fabricated in the lab using Vita LC composite (Vita), following the Vita 3D-Master shade guide, which allows the dental technician to use a logical approach in layering the desired shades.

Shade matching was done before the rubber dam was placed and also after the impression was taken for the core color of the inlay using the Vita Dentin shade guide. A cast is created in the lab and it is mounted in an articulator. Next, any slight undercuts were filled with wax (Classic Opaque Sculpting Wax, Renfert) on the model. The first layer of indirect composite (Vita LC, Vita) base dentin shade was placed and cured. Then, the tooth was built up incrementally with dentin and enamel shades layered to create a more lifelike appearance. The inlays and onlays were placed in the Ivoclar curing unit (under light and heat) for the recommended time limit. Once the restorations were cured, they were finished and polished, then protected with a layer of wax before micro-sandblasting the inner surfaces. Some practitioners also apply on the inner surface a composite-activating primer in order to reactivate the surface of the heavily polymerized composite (over 95 % degree of monomer conversion).

Before cementation, the rubber dam was applied. The internal surfaces of the preparations were cleaned with orthophosphoric acid 37.5 % for 10 s, rinsed, and dried. The composite inlays/onlays were tried in for fit – this being a major advantage for the composite restorations as compared to the ceramic ones, they can be easily fitted and adjusted and then refinished at the chair side. The RMGI cement (G-Cem, GC) was applied in the cavity and on the inner surface of the inlay. The composite restorations are applied using low pressure and ultrasounds with a silicone insert. Pre-curing for 1 s, about 1 cm away from the margins, is very beneficial as it allows for easy removal of the excess. Other materials frequently used for inlay cementation are the self-adhesive dual-cure composite cements like Panavia, Kuraray, and Rely-X, 3M. Composite inlays on teeth 4.5 and 4.7 show very good fit after cementation (Fig. 12).

There is also a very conservative “trend” in dentistry nowadays, so dentists are also looking for an alternative to crowns and bridge retainers, frequently favoring an inlay or an onlay over a full-crown preparation. During the last 5 years, in the United States alone, over 200 million crowns were placed and many of those crowned teeth could have benefited from a more conservative treatment [62]. Recent literature studies indicate a 10-year success rate of composite and ceramic inlays above 90 %, which is close to the gold standard – the noble alloy inlays that are among the most successful and long-lasting indirect restorations [63, 64].

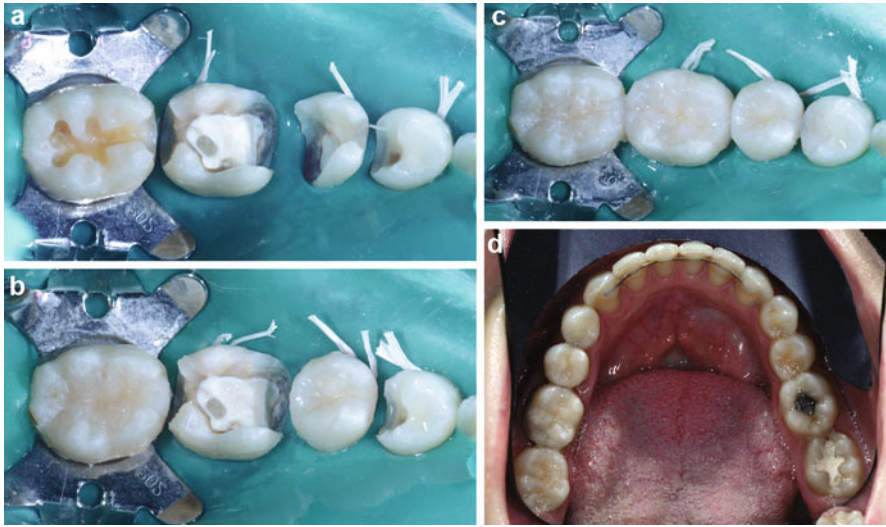


**Fig. 12** (a–d) Cementation of the composite inlays. (a) Rubber dam in place for adhesively luting the indirect composite restorations; (b) inlays cemented on teeth 4.7 and 4.5; (c) inlays cemented on all teeth; (d) final aspect of composite inlays in the mouth (Clinical case Dr. Florin Alb)

An important step in the use of indirect composites for larger restorations than inlays and onlays was the discovery and applications of reinforcing fibers – dating back to the 1960s, it was first proposed for reinforcing denture base acrylic and is now most commonly used in prefabricated endodontic fiber posts. With the fiber-reinforced composite (FRC), we are now able to fabricate orthodontic retainers, periodontal splints, and fiber-reinforced bridges as short- to medium-term provisional and temporization during the healing phase of implant treatment [65]. They offer some advantages over PFM technology: no preparation or limited preparation required, lower cost, less chairside time, and good medium-term survival (75 % at 4 years) [66, 67].

The fiber-reinforced composite bridges (FRCB) can be fabricated directly in the patient's mouth or by indirect technique (Fig. 13).

Composite resins used in indirect techniques have a wide variety of applications in dentistry today: from inlays, onlays, overlays, and table tops, to provisional crowns and bridges, adhesive bridges, to extended splinting systems fabricated in the lab for patients with periodontal disease, to orthodontic devices used for short period of time, and to long-term resin crowns and bridges. The applications of composite resins – in direct and indirect procedures, both in the dental office and in the dental laboratory – have increased exponentially during the last 60 years since their introduction in the 1950s, and it is most likely that their uses will continue to grow both in frequency and application due to their versatility [65].



**Fig. 13** (a, b) Fiber-reinforced composite bridges (FRCB). (a) Initial case, missing lateral incisors. (b) FRCB was fabricated in the lab using Construct fibers (Kerr) and Vita VM LC composite (Vita) (provisional treatment for esthetic rehabilitation during the osteointegration phase) (Clinical case Dr. Florin Alb)

## CAD/CAM Processed Composites

### CAD/CAM Systems

In the last years, CAD/CAM technologies (computer-aided design/computer-aided manufacturing) became an important component of dental medicine. The technique is orientated to the future and focused on high efficiency and standardization of prosthodontics treatment [68].

The advantages in CAD/CAM technologies consist in the quality of the materials, industrial processing, reproducibility, and low cost/unit. CAD/CAM systems available are “in-office” systems, or laboratory systems.

All CAD/CAM systems have three main components (Fig. 14):

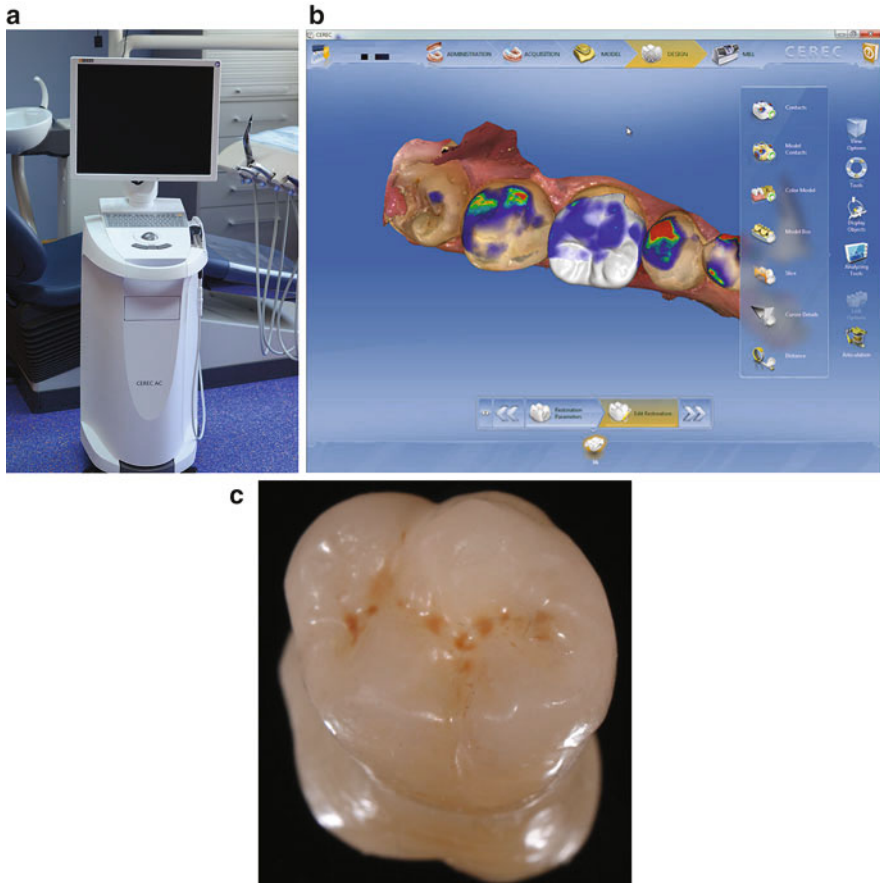


**Fig. 14** (a) CEREC Omnicam (Sirona, Germany). (b) Restoration design. (c) Final restoration (Vita Enamic)

- A scanner – for image acquisition, transforming images into data
- An image software – for data processing, restoration 3D design
- A milling unit – for transforming the virtual design into a finite product (inlays, onlays, crowns, bridges)

For direct clinical application, intraoral scanners were developed (Fig. 14a).

Acquiring optical images of the prepared teeth directly with the intraoral camera eliminates the need for conventional impression procedures and improves patient comfort [69, 70]. With the aid of the chairside software, the restoration is designed (Fig. 14b) and then milled in the office, within a single-visit restoration (Fig. 14c). Single-visit restoration eliminates the need for provisional restorations, increases durability of adhesion to dental tissues, and also reduces postoperative sensitivity.

**Advantages** of in-office CAD/CAM systems:

- The possibility to obtaining tooth crowns, inlays, onlays, veneers, or bridges in a single visit;
- Eliminates the temporary restorations;
- Esthetic restorations are obtained;
- When inlays or onlays are fabricated, the longevity of the restorations is higher, when compared to direct composites.

**Disadvantages**

- For a ceramic restoration glazing has to be performed; for composite, external staining is necessary in order to obtain esthetic restorations;
- CAD/CAM system cost [71].

The major concerns about chairside CAD-CAM restorations are the accuracy of intraoral digital impressions and the resulting internal and marginal fit discrepancies. However, recent studies demonstrated that digital impression systems allow the fabrication of fixed prosthetic restorations with similar accuracy as conventional impression methods. According to the results of previous studies, marginal gap of the feldspathic crowns fabricated with CEREC Omnicam (Sirona, Germany) system ranged from 18 to 40  $\mu\text{m}$  and is in clinically acceptable limits [72].

**Composite Materials for CAD/CAM Technology**

Innovative materials were developed in order to fulfill researchers, clinicians, and patient demands. A great variety of dental ceramics and a large selection of composite resin materials are nowadays on the market.

Advantages of ceramics are a high flexural strength and great color stability, while disadvantages are high antagonistic tooth wear and loss of tooth structure due to a minimum thickness of 1.5–2.0 mm. These two parameters are better for composite resins, but the wear of the material itself is higher. While ceramics are stiffer and harder than natural tooth structure, composite resins show lower values [73].

For many years, composites were used for provisional crowns and bridges (Vita CAD-TEMP, Vita, Germany; Telio CAD, Ivoclar Vivadent, Lichtenstein) (Figs. 15 and 16) with a maximum use of 12 months. VITA CAD-Temp composite blocks consist of a fiber-free, homogeneous, high-molecular, and cross-linked acrylate polymer with microfiller. CAD-Temp is used for the fabrication of multi-unit, temporary bridge restorations with up to two pontics and temporary crowns. Telio CAD consists of acrylate polymer (PMMA) blocks for the fabrication of long-term temporaries using CAD/CAM technology.

Recent materials like Lava Ultimate (3M Espe, USA) (Fig. 16) and Vita Enamic (Vita, Germany) represent high improvements in CAD/CAM dentistry material science. Material indications are for permanent restorations in the anterior and posterior areas, veneers, inlay, and onlays. The options for



Fig. 15 Vita CAD-TEMP



Fig. 16 Telio CAD

Fig. 17 Lava Ultimate



composite block color are large, in order to cover different clinically situations, monochromatic and polychromatic blocks (with three different shades in one block) being available [74].

**Lava Ultimate** is a resin nanoceramic material which blends approximately 80 % nanoceramic particles with a highly cured resin matrix. With a flexural strength of 200 MPa, the material is less brittle than glass ceramic; it resists chipping and cracking when milled (Fig. 17). It enables a simple, efficient, no-firing process for making CAD/CAM restorations. Staining and manual polishing is required.

**Vita Enamic** combines the properties of ceramic and polymer. It consists of a hybrid structure with two interpenetrating networks of ceramic and polymer, a so-called double-network hybrid.

Due to the fine structure of feldspar ceramic and the acrylate polymer network, this material has a similar abrasion, high flexural strength, and elasticity close to dentin. The Vickers hardness was evaluated with values between those for dentin and enamel. Indications are inlays, onlays, veneers, and crowns on the posterior area. No-firing process is required [75]. Using light-cured staining materials, external characterizations can be made for maximum esthetics (Fig. 18a–f).

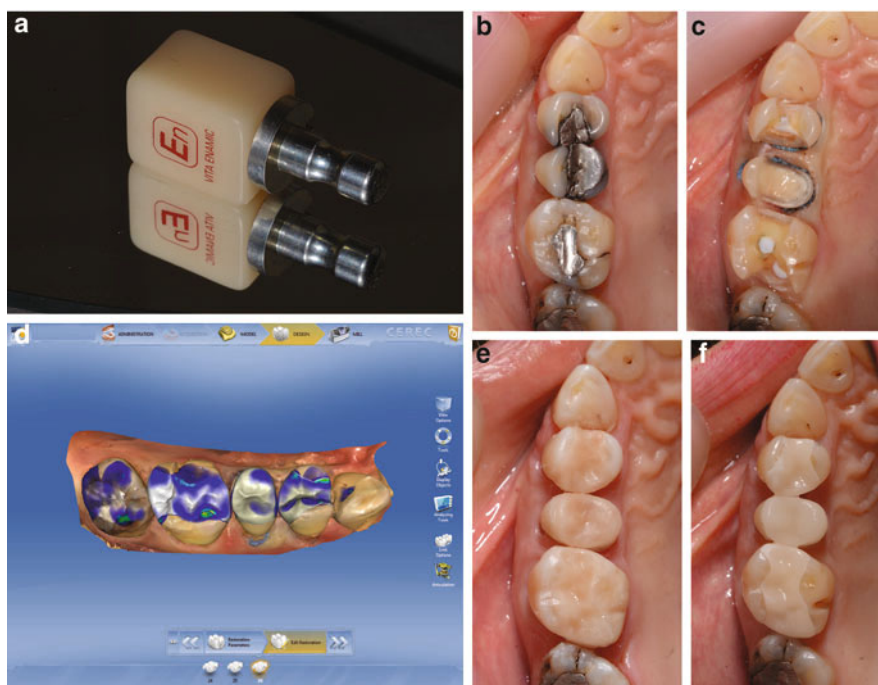


**Fig. 18** (a) Vita Enamic Block. (b) Initial situation. (c) Tooth preparation inlays on 26, 24, and onlay 25. (d) Virtual model and restoration design. (e) Milled restorations on site. (f) Stained and polished restorations – final result (Clinical case dr Bogdan Culic)



## References

1. García AH, Martínez Lozano MA, Cabanes Vila J, Barjau Escribano A, Fos Galve P (2006) Composite resins. A review of the materials and clinical indications. *Med Oral Patol Oral Cir Bucal* 11(E):215–220
2. Marcos VA, Bergeron C, Murchison DF, Roeters J, Chan DCN (2013) Direct anterior restorations. In: Hilton TJ, Ferracane JL, Broome JC (eds) *Summitt's fundamentals of operative dentistry. A contemporary approach*, 4th edn. Quintessence, Chicago
3. Powers JM, Sakaguchi RL (2006) Chapter 9: Resin composite restorative materials. In: *Craig's restorative dental materials*, 12th edn. Mosby Elsevier, Philadelphia
4. Rawls HR, Esquivel-Upshaw JF (2003) Restorative resins. In: Anusavice KJ (ed) *Phillips' science of dental materials*, 11th edn. Saunders, St Louis
5. Holter D, Frey H, Mulhaupt R (1997) Branched bismethacrylates based on Bis-GMA. A systematic route to low shrinkage composites. *Polym Prepr* 38:84–85
6. Ferracane JL (2011) Resin composite – state of the art. *Dent Mater* 27:29–38
7. Weinmann W, Thalacker C, Guggenberger R (2005) Siloranes in dental composites. *Dent Mater* 21:68–74
8. Xu HHK, Sun L, Weir MD, Antonucci JM, Takagi S, Chow LC et al (2006) Nano DCPA-whisker composites with high strength and Ca and PO(4) release. *J Dent Res* 85:722–727
9. Xu HHK, Weir MD, Sun L, Moreau JL, Takagi S, Chow LC et al (2010) Strong nanocomposites with Ca, PO<sub>4</sub>, and F release for caries inhibition. *J Dent Res* 89:19–28
10. Xu HHK, Moreau JL, Sun L, Chow LC (2010) Novel CaF<sub>2</sub> nanocomposite with high strength and fluoride release. *J Dent Res* 89:739–745
11. Neumann MG, Miranda WG Jr, Schmitt CC, Rueggeberg FA, Correa IC (2005) Molar extinction coefficients and the photon absorption efficiency of dental photoinitiators and light curing units. *J Dent* 33:525–532
12. Choi KK, Ferracane JL, Hilton TJ, Charlton D (2000) Properties of packable dental composites. *J Esthet Dent* 12:216–226
13. Cramer NB, Stansbury JW, Bowman CN (2011) Recent advances and developments in composite dental restorative materials. *J Dent Res* 90(4):402–416
14. Klapdohr S, Moszner N (2005) New inorganic components for dental filling composites. *Monatsh Chem* 136:21–45
15. Chen M-H (2010) Update on dental nanocomposites. *J Dent Res* 89:549–560
16. Prodan DA, Gasparik C, Mada DC, Miclăuş V, Băciuţ M, Ducea D (2014) Influence of opacity on the color stability of a nanocomposite. *Clin Oral Invest*. doi:10.1007/s00784-014-1315-1
17. Queiroz RS, Lima JPM, Malta DAMP, Rastelli ANS, Cuin A, Porto Neto ST (2009) Changes on transmittance mode of different composite resins. *Mater Res* 2:127–132
18. Touati B, Miara P, Nathanson D (2000) *Esthetic dentistry and ceramic restoration*. Martin Dunitz, London
19. Ducea D, Varlan C (2013) Principii generale in estetica dentara si dento-faciala [General principles in dental and dent-facial esthetics]. In: Lazarescu F (ed) *Incursiuni in Estetica dentara*. SSER, Bucharest
20. Vanini L (2010) Conservative composite restorations that mimic nature. A step-by-step anatomical stratification technique. *J Cosmet Dent* 26(3):80–98
21. Eimar H, Marelli B, Nazhat SN, AbiNader S, Amir WM, Torres J, Albuquerque RF Jr, Tamimi F (2011) The role of enamel crystallography on tooth shade. *J Dent* 39(Suppl 3):e3–e10
22. Villarreal M, Fall N, De Sousa AM, De Oliveira OB (2011) Direct esthetic restorations based on translucency and opacity of composite resins. *J Esthet Restor Dent* 23:73–88
23. Dietschi D, Campanile G, Holz J, Meyer JM (1994) Comparison of the color stability of ten new-generation composites: an in vitro study. *Dent Mater* 10:353–362
24. Van Landuyt KL, Snauwaert J, De Munck J, Peumans M, Yoshida Y, Poitevin A, Coutinho E, Suzuki K, Lambrechts P, Van Meerbeek B (2007) Systematic review of the chemical composition of contemporary dental adhesives. *Biomaterials* 28:3757–3785

25. Hosoya Y (1999) Five-year color changes of light-cured resin composites: influence of light-curing times. *Dent Mater* 15:268–274
26. Kolbeck C, Rosentritt M, Lang R, Handel G (2006) Discoloration of facing and restorative composites by UV-irradiation and staining food. *Dent Mater* 22:63–68
27. Vichi A, Ferrari M, Davidson CL (2004) Color and opacity variations in three different resin-based composite products after water aging. *Dent Mater* 20:530–534
28. Sabatini C, Campillo M, Aref J (2012) Color stability of ten resin-based restorative materials. *J Esthet Restor Dent* 24:185–199
29. Jain V, Platt JA, Moore K, Spohr AM, Borges GA (2013) Color stability, gloss, and surface roughness of indirect composite resins. *J Oral Sci* 55(1):9–15
30. Nahsan FPS, Mondelli RFL, Franco EB, Naufel FS, Ueda JK, Schmitt VL, Baseggio W (2012) Clinical strategies for esthetic excellence in anterior tooth restorations: understanding color and composite resin selection. *J Appl Oral Sci* 20(2):151–156
31. Ryan E-A, Tam LE, McComb D (2010) Comparative translucency of esthetic composite resin restorative materials. *J Can Dent Assoc* 76:a84
32. Araújo EM, Baratieri LN, Monteiro S et al (2003) Direct adhesive restoration of anterior teeth: part 3 (procedural consideration). *Pract Proced Aesthet Dent* 15:433–437
33. Fahl N, Denehy GE, Jackson RD (1995) Protocol for predictable restoration of anterior teeth with composite resins. *Pract Period Aesthet Dent* 7(8):13–22
34. Fahl N (2006) A polychromatic composite layering approach for solving a complex class IV/direct veneer-diestema combination: part I. *Pract Proced Aesthet Dent* 18(10):641–645
35. Paravina RD, Westland S, Kimura M, Powers JM, Imai FH (2006) Color interaction of dental materials: blending effect of layered composites. *Dent Mater* 22(10):903–908
36. Paravina RD, Westland S, Imai FH, Kimura M, Powers JM (2006) Evaluation of blending effect of composite related to restoration size. *Dent Mater* 22(4):299–307
37. Sadowsky SJ (2006) An overview of treatment considerations for esthetic restorations: a review of the literature. *J Prosthet Dent* 96:433–442
38. Hilton TJ, Broome JC (2013) Direct posterior esthetic restorations. In: Hilton TJ, Ferracane JL, Broome JC (eds) *Summitt's fundamentals of operative dentistry. A contemporary approach*, 4th edn. Quintessence, Chicago
39. Hinoura K, Setcos JC, Phillips RW (1988) Cavity design and placement techniques for class 2 composites. *Oper Dent* 13:12–19
40. Opdam NJ, Roeters JJ, Peters TC, Burgersdijk RC, Kuijs RH (1996) Consistency of resin composites for posterior use. *Dent Mater* 12:350–354
41. Lyons K (2003) Direct placement restorative materials for use in posterior teeth: the current options. *N Z Dent J* 99:10–15
42. Johnston WM, Ma T, Kienle BH (1995) Translucency parameter of colorants for maxillofacial prostheses. *Int J Prosthodont* 8:79–86
43. Ghinea R, Perez MM, Herrera LJ, Rivas MJ, Yebra A, Paravina RD (2010) Color difference thresholds in dental ceramics. *J Dent* 38(Suppl 2):e57–e64
44. Paravina RD, Kimura M, Powers JM (2006) Color compatibility of resin composites of identical shade designation. *Quintessence Int* 37:713–719
45. Peyton JH (2004) Finishing and polishing techniques: direct composite resin restorations. *Pract Proced Aesthet Dent* 16(4):293–298
46. Lee YK, Lub H, Powers JM (2006) Changes in opalescence and fluorescence properties of resin composites after accelerated aging. *Dent Mater* 22:653–660
47. Feilzer AJ, de Gee AJ, Davidson CL (1988) Curing contraction of composites and glass-ionomer cements. *J Prosthet Dent* 59:297–300
48. Bryant RW, Mahler DB (1986) Modulus of elasticity in bending of composites and amalgams. *J Prosthet Dent* 56:243–248
49. Van Dijken JW (2000) Direct resin composite inlays/onlays: an 11 year follow-up. *J Dent* 28:299–306

50. Imazato S, Tarumi H, Kobayashi K, Hiraguri H, Oda K, Tsuchitani Y (1995) Relationship between the degree of conversion and internal discoloration of light-activated composites. *Dent Mater* 14(1):23–30
51. Ferracane JL, Berge XH, Condor JR (1998) In vitro aging of dental composites in water effect the degree of conversion, filler volume and filler/matrix coupling. *J Biomed Mater Res* 42:465–472
52. Bayne SC, Taylor DF, Heymann HO (1992) Protection hypothesis for composite wear. *Dent Mater* 8:305–309
53. Al Kheraif AA, Qasim SS, Ramakrishnaiah R, Rehman I (2013) Effect of different beverages on the color stability and degree of conversion of nano and microhybrid composites. *Dent Mater J* 32(2):326–331
54. Ren YF, Feng L, Serban D, Malmstrom HS (2012) Effects of common beverage colorants on color stability of dental composite resins: the utility of thermocycling stain challenge model in vitro. *J Dent* 40(Suppl 1):e48–e56
55. Lee BS, Huang SH, Chiang YC, Chien YS, Mou CY, Lin CP (2008) Development of in vitro tooth staining model and usage of catalysts to elevate the effectiveness of tooth bleaching. *Dent Mater* 24:57–66
56. Yazici AR, Celik C, Dayangac B, Ozgunaltay G (2007) The effect of curing units and staining solutions on the color stability of resin composites. *Oper Dent* 32:616–622
57. One-visit biomimetic composite resin inlays/onlays. [www.dentistrytoday.com](http://www.dentistrytoday.com). June 2010
58. Kois JC (1996) The restorative periodontal interface: biological parameters. *Periodontology* 2000(11):29–38
59. Roberson TM, Heymann HO, Swift EJ (2002) *Sturdevant's art and science of operative dentistry*, 4th edn. Mosby, St Louis
60. Schlichting LH, Maia HP, Baratieri LN, Magne P (2011) Novel-design ultra-thin CAD/CAM composite resin and ceramic occlusal veneers for the treatment of severe dental erosion. *J Prosthet Dent* 105:217–226
61. Rekow ED (2006) Dental CAD/CAM systems – a 20-year success story. *J Am Dent Assoc* 137:5s–6s
62. Christensen GJ (2008) Considering tooth-colored inlays and onlays versus crowns. *J Am Dent Assoc* 139:617–620
63. Thordrup M, Isidor F, Hörsted-Bindslev P (2006) A prospective clinical study of indirect and direct composite and ceramic inlays: ten-year results. *Quintessence Int* 37(2):139–144
64. Peumans M, Voet M, De Munck J, Van Landuyt K, Van Ende A, Van Meerbeek B (2013) Four-year clinical evaluation of a self-adhesive luting agent for ceramic inlays. *Clin Oral Invest* 17:739–750
65. Belvedere P, Turner WE (2002) Direct fiber-reinforcement composite bridge. *Dent Today* 21:88–94
66. Van Heumen CM, van Dijken WV, Tanner J, Pikaar R, Lassila VJ (2009) 5 year survival of 3 unit fiber-reinforced composite fixed partial denture in the anterior area. *Dent Mater* 25:820–827
67. Khatavkar RA, Hegde VS (2010) A conservative treatment option for a single missing premolar using a partial veneered restoration with the SR Adoro system. *J Conserv Dent* 13(2):102–105. doi:10.4103/0972-0707.66722
68. Beuer F, Schweiger J, Edelhoff D (2008) Digital dentistry: an overview of recent developments for CAD/CAM generated restorations. *Br Dent J* 204(9):505–511
69. Birnbaum NS, Aaronson HB (2008) Dental impressions using 3D digital scanners: virtual becomes reality. *Compendium* 29(8):494–505
70. Feuerstein P, Puri S (2009) An overview of CAD/CAM and digital impressions. *Oral Health* 99(9):65–71
71. Davidowitz G, Kotick PG (2011) The use of CAD/CAM in dentistry. *Dent Clin N Am* 55(3):559–570

72. Armetzl GV, Armetzl G (2013) Reliability of nonretentive all-ceramic CAD/CAM overlays. *Int J Comput Dent* 15(3):185–197
73. Ruse ND, Sadoun MJ (2014) Resin-composite blocks for dental CAD/CAM applications. *J Dent Res* 93:1232–1235. doi:10.1122/0022034514553967
74. Coldea A, Swain MV, Thiel N (2013) Mechanical properties of polymer-infiltrated-ceramic-network materials. *Dent Mater* 29:419–426
75. He LH, Swain M (2011) A novel polymer infiltrated ceramic dental material. *Dent Mater* 27(6):527–534

Domenico Baldi, Jacopo Colombo, and Uli Hauschild

## Contents

Introduction .....	1116
Zirconium .....	1117
Criteria .....	1118
Laboratory Techniques .....	1119
Kinds of Operations .....	1121
Crowns and Bridges .....	1121
Abutments .....	1121
Complex Direct Screwing Cases .....	1122
Lithium Disilicate .....	1122
Crowns and Inlays in Lithium Disilicate .....	1124
Cases with Mixed Use Between the Two Materials .....	1124
Clinical Case .....	1124
References .....	1127

---

## Abstract

In recent years there has been a huge leap forward in the prosthetic field, primarily linked to the ability of the clinician to exploit new technologies and new materials.

In fact, the application of CAD/CAM techniques which are already well known, for example, in engineering, has allowed us to spread the use of new ceramic materials, making the spread much easier.

Principally two materials have greatly changed dental practice: the zirconium and lithium disilicate.

---

D. Baldi (✉) • J. Colombo • U. Hauschild  
Department of Fixed Prosthodontics, University of Genova, Genova, Italy  
e-mail: [baldi.domenico@unige.it](mailto:baldi.domenico@unige.it); [jacopocolo@tiscali.it](mailto:jacopocolo@tiscali.it)

The purpose of this publication will be to investigate the characteristics of these two materials and their clinical applications, trying to rationalize the selection criteria and operational protocols.

In fact, if, on one hand, therapeutic results that were unthinkable until a few years ago are possible, on the other hand, these materials require a thorough understanding of their characteristics in order not to run into avoidable failures.

---

**Keywords**

Prosthodontics • Dental materials • CAD/CAM • Metal-free • Prosthetic protocols • Dental ceramic

---

## Introduction

In recent years, the changing socioeconomic conditions of the population and the increased attention to everything that concerns the sphere of personal image and aesthetics have had a profound effect on society.

Furthermore, relatively new concepts in medicine have been established. These concepts include minor invasion and biological saving, that is, the tendency to choose therapeutic approaches that are minimally invasive and more respectful of the anatomical structures of the patient, where this is obviously possible [1].

For this reason, over the years dental research has been decisively oriented toward the development of new materials, especially in the prosthetics and restorative field, that would provide an improvement in aesthetic performance and a less invasive approach concerning dental structures.

In conservative dentistry, one merely has to think about the current predictability of dental enamel adhesives and composite resins that consent infinitely more aesthetic and more conservative approaches than the use of traditionally reliable materials, such as silver amalgam.

In the prosthetics field, innovations have been even more overwhelming. Simply think that up to not more than 15 years ago, the state of the art of complete tooth restoration was represented by gold artifacts and ceramics or, in situations limited to frontal areas, by integral ceramic articles.

At present two major revolutions have been made. The first is represented by the introduction of a range of new materials which, in a relatively short period of time, are proving to be able to ensure functional performance comparable to those of materials with a much more experienced background. I am particularly thinking about the zirconium, in a monolithic form or layered with ceramic, and lithium disilicate [2].

The other big novelty has been the development and the perfecting of CAD-CAM systems for the processing of these materials, which have ensured their accessibility for most dentists.

Indeed materials such as zirconium and lithium disilicate were introduced because the simultaneous development of CAD-CAM systems allowed to obtain

products by milling blocks of material which were previously prepared in industrial form.

This system consents the manufacturing of articles starting from a digital print of a preparation or of a stone model. The CAD (Computer-Aided Design) part allows to project the scanned image on a computer where, by means of a software, the operator can establish the parameters of the artifact.

At this point, the file is sent to the CAM (Computer-Aided Manufacturing) system to realize the reconstruction with a micro milling machine. A block of the selected material, which has been industrially produced, is milled to the exact dimensions established by the operator. This is very important because the process of the realization of industrial and standardized blocks ensures a controlled production that compensates the elevated contraction of highly resistant ceramic materials during the sintering process [3].

In a very short lapse of time, all this has led to a range of innovations that require time and application in order to be included in the daily routine of a dental practice, as well as thorough knowledge, which can frequently be distorted by an abundance of often scientifically invalid information from companies.

The purpose of this chapter is to provide a key to be able to understand the fundamental features of these new materials and their applications, in order to introduce them to daily practice without the risk of having to handle unexpected complications.

This discussion will specifically examine two materials in particular, zirconium and lithium disilicate, which were introduced to dental practice in relatively recent times. There will be a brief analysis of their characteristics and above all of their clinical use.

---

## Zirconium

Zirconium commonly refers to zirconium oxide, which is a metal frequently found in nature combined with silica oxide.

Zirconium is an extremely interesting material that has been valued in dentistry for some outstanding features, namely, its mechanical strength, its dimensional stability, and an elastic form similar to that of steel.

From the chemical point of view, zirconium can take on three forms that vary in function of the temperature: the cubic phase over 2370 °C, the tetragonal phase between 2370 and 1170 °C, and the monoclinic phase below 1170 °C. These three phases obviously correspond to different mechanical behaviors of the material. Without going into detail, what happens is that with decreasing temperature and thus in the transition from the cubic phase to the monoclinic, there is a worsening of the mechanical properties and a decrease in the density of the material that virtually translates into a reduction in the dimensions.

For this reason, to stabilize the zirconium at room temperature and to control the transformations, metal oxides such as yttrium or ceria are added to the crystal structure. This leads to the formation of multiphase materials known as partially stabilized zirconium [4-7].

An extremely important mechanical characteristic in dentistry use is the ability of the zirconium to stop the propagation of fracture lines. This characteristic, which is unique of zirconium oxide, is explained by the fact that the area immediately preceding the fracture is in a state of compression. This is due to the fact that when a fracture starts to propagate, it develops a state of stress at high energy that determines the transformation of the zirconium crystal from tetragonal to monoclinic. This determines a difference of volume between the area of the fracture and the following one, which leads to a compression that stops the fracture line.

This extremely important feature does not obviously exclude the possibility that the material will fracture. It has however been highlighted how failures of this type are always attributable to either design errors of the article or clinical errors [8–10].

From the clinical point of view, zirconium can be used in two different forms: pure in the form of tetragonal zirconium polycrystals stabilized with yttrium or infiltrated in the interior of glass ceramics [11].

In the first case, we are dealing with a material, which has all the main characteristics of zirconium, thus mostly resistant to fracture and flexions combined with high biocompatibility.

The main drawback is the lack of translucency that makes this material less efficient in areas with high aesthetic value compared to integral ceramic systems.

This material can be machined with CAD-CAM technology and used in a wide range of clinical situations.

The main uses are related to a fixed prosthesis, in particular as a substructure for anterior and posterior crowns and bridges of limited extensions, or to realize abutments for dental implants.

This material can also have other less frequent but still viable uses, such as for example, the realization of endodontic posts, onlays and overlays, and Maryland bridges [12–17].

---

## Criteria

What mainly interests the clinician are the criteria for the choice of this material that we are going to analyze.

1. **Aesthetics**– Substructures in zirconium have a great aesthetic advantage linked to the fact that, especially in the presence of periodontal phenotypes of type II, they allow to minimize the so-called umbrella effect and consequently the gray halo that shines below the portion of the free gum, which is fairly common in traditional metal-ceramic prosthesis. However, in general, the use of a white substructure in any case allows to minimize the effects of failures due to gum recession even in a medium-long term [18].
2. **Preparations** – From the design point of view of the abutment, the choice of zirconium-ceramic does not determine upheaval in preparation techniques. Substantially the same types of preparation and the same space required for the



modeling of a manufactured metal ceramic are anticipated, which is about 2 mm occlusal and 1, 5 mm circumferential.

There are situations, especially in posterior occlusal or anterior palatal areas, in which one may decide not to coat the zirconium with ceramic, leaving the zirconium itself in occlusion, thus earning between 0.5 and 1 mm. This choice must be carefully weighed considering the occlusion and the type of antagonist, because zirconium has an elevated hardness and a different abrasion form from a natural tooth [19].

3. **Impressions** – The impression technique and the material decided to be use do not vary when choosing artifacts in zirconium ceramic, metal ceramic. What may vary can be the retraction technique of periodontal tissues. In fact, the high aesthetic qualities of zirconium can, in certain situations, favor a juxtagingival positioning of the margin.
4. **Luting** – The luting of zirconium is always of traditional type. The systems are the same as those of the metal ceramic, and the choice mainly falls on glass ionomeric or zinc oxyphosphate cement. In fact, because zirconium is not a silica-based material, it does not turn out to be etchable, and thus an adhesive-type luting is not practicable.

The only possibility of taking this path is to use silica-coating techniques of the substrate by means of high-speed silica powder jets [20].

This technique is recommended whenever one wants to realize articles, such as Maryland Bridge or overlays, in which the adhesive luting technique plays a key role.

---

## Laboratory Techniques

Zirconium is delivered to the laboratory in blocks of different shapes and colors ready to be milled.

There are essentially two types of production of the blocks: uniaxial cold pressing and isostatic cold pressing.

Uniaxial pressing provides for the application of a uniaxial pressure to zirconium powder contained in a mould. This determines a high resistance of the material due to the deformation and interlocking of the particles, but at the same time determines different degrees of density within the block due to friction between the particles and between the particles and the mould, which can compromise the integrity of the structure, even after the milling.

Isostatic pressing involves the insertion of zirconium powder in a deformable container subjected to external isostatic pressure that is uniform in all directions.

Regardless of the method used to obtain these zirconium blocks, they are referred to as unrefined. At this point they are stabilized and thickened by a sintering process in a furnace at zero pressure.

In dental systems, materials are normally used in an unrefined phase because zirconium is easier to work and wears less on the milling machines, even if at this

stage the blocks should be milled to an enlarged size of 20–25 % to compensate for the shrinkage during sintering. With regard to this fact, the unrefined zirconium blocks have a label that identifies the density, so that the technician can exactly calibrate the milling machine to obtain a correctly oversized article [10].

Alternatively the mechanical properties of zirconium can be further improved through a process called hot isostatic post-compaction (HIP) that eliminates all porosity and increases the hardness and density of the material, making it unnecessary to compensate for the sinter shrinkage [21, 22].

At this point, the dental technician, regardless of whether he/she chooses unrefined zirconium blocks or HIP, has two techniques for the construction of the building available: CAD-CAM or MAD-MAM. In both cases, the work is subdivided into three phases: scan, design, and milling.

The CAD-CAM, which we have already mentioned earlier, involves the scanning of the abutment, either in the mouth or on the model, and the creation of an image on the computer, on which a user can draw the artifact and send data to a milling machine that realizes it, via software.

Milling is a subtractive process starting from a block and is the most widely used method. However, in CAD-CAM systems, there are also alternative methods to obtain the artifact. The additive method and the selective fusion mainly also exist.

The additive method involves the construction of the article by adding material to an abutment. For an article in zirconium, an oversized metallic abutment must be realized to compensate for the sintering shrinkage. Compact zirconium powder will be added under isostatic pressure and then sintering will be carried out.

On the other hand, selective melting is an experimental method for zirconium, but widely used for metals, which involves the creation of the article-collecting CAD data and then proceeding to melt thin layers of powder, which is susceptible to the heat of a laser beam.

CAD-CAM systems, which are currently the most widely used, can be closed or open. That is, the dental laboratory can realize the design on a type of file that may or may not be read by machines of different brands from the one that scanned the file. Closed systems were the first to be introduced to the market and have a major setback of forcing the technician, after having made a significant financial investment, to work only with that particular manufacturer. The advantage is linked to the fact that these large milling centers use much more expensive machines that guarantee the milling also of HIP blocks.

In open systems instead, which are becoming increasingly more popular, there is the opportunity of interacting with different CAD and CAM systems using universal file formats. The advantage is related to greater versatility and of the laboratory being able to work with different milling centers [23, 24].

The MAD-MAM system also consists of two phases: the first MAD (Manual-Aided Design) consists of transferring information. Generally a wax copy of the artifact to be obtained is made and it is then positioned in a pantograph. At this point the MAM (Manual-Aided Manufacturing) system component comes into action. The “tactile arm” of pantograph reads the wax model and transfers the information to the milling machine arm, where a system of drills grinds the zirconium block.

Also in this case, if unrefined zirconium is being used, the final dimensions of the article after milling have to be oversized by 20–25 % to compensate for sinter shrinkage.

These systems exploit pantograph technology, which has been known for hundreds of years, and their diffusion has been supplanted by the adoption of CAD-CAM systems. However, manual systems, with respect to softwares, have the great advantage of being able to intervene and correct any errors while making the wax model [24, 25].

---

## **Kinds of Operations**

### **Crowns and Bridges**

Zirconium gives the structure stability and supports the layered ceramic. This consents an increase in the transparency of the color and the uniqueness of the color with stratification by hand. The product combines all advantages to give aesthetic, functional, and mechanical yields. It is very suitable in cases where there are missing teeth to construct bridges between natural teeth and over gaps created by extracted teeth.

Zirconium exists in different qualities, depending on the sintering of more or less transparent materials.

The more opaque zirconium consents the covering of devitalized dental parts or metal posts.

The semitranslucent zirconium, as the name suggests, lets more light in and however gives the same stability and increases the aesthetics due to the play of light.

The monolithic zirconium is also known as “Prettau,” which is a name that comes from the country of its first user, Enrico Steger, who has made it a strong point of his company as well as marketing it worldwide.

Until a short time ago, only one type existed. It had to be colored before sintering to render the raw element more natural and aesthetic. Through this technique, the technician could choose a color according to the needs of the case. The monolithic zirconium, against a less aesthetic yield, allows to obtain greater stability and resistance to chewing forces, eliminating the possibility of any “chipping.”

Then there is a third relatively new variant of zirconium, commercially known as is zirconium anterior, which is created via a different pressure and temperature of sintering. A greater transparency that however maintains a higher mechanical strength of lithium disilicate is able to be reached, thanks to this variant.

It is not suitable for structures that are too long.

### **Abutments**

Besides using zirconium for the construction of crowns and bridges, it best demonstrates its properties even in the manufacturing of abutments for implants.

The exceptional hardness of this material allows the direct screwing on of the platform, which is a progress that is not however particularly suitable because of the different resistance between zirconium and titanium. The latter is less hard and therefore subject to wear over time if in contact with the first.

The state of the art in oral implantology suggests a bonding connection between a titanium abutment and an individualized body in zirconium. This allows to take advantage of a perfect connection between titanium and titanium, a proper support to the soft tissues, in addition to a more pleasant aesthetics and a maximum biocompatibility, thanks to the characteristics of zirconium.

## **Complex Direct Screwing Cases**

In complex cases it may be necessary to use a body in translucent or monolithic zirconium, which has to be layered successively. The latter has a less aesthetic yield but guarantees greater resistance to fracture and chipping.

If we work on implants, it is possible to screw them directly to the structure after a well-calculated study of size and morphology.

Nowadays, thanks to the expansion that guided computer surgery is having, it is possible to have definite implant positions with the positive result of an access to the screw through the central axis of the manufactured teeth. This can be achieved, thanks to a positive implant design following prosthetic rules.

In this type of structure, it is however advisable to cement titan base abutments, only after having finalized and polished the artifact.

Only after a final inspection, we can proceed with bonding just like with individual abutments.

As we can see, the zirconium has excellent translucency, which the value may vary depending on the choice of the specific material, needs, and abilities of the technician.

---

## **Lithium Disilicate**

Lithium disilicate (LIS2) is a material that belongs to the glass-ceramics family.

The main component is, as in most of the ceramics, silicon oxide, which is supplemented with materials so-called smelters that serve to lower the melting temperature and others so-called “stabilizers” which give the glassy component greater stability and better chemical-physical characteristics.

These materials are produced by compacting powders that are then heated to such temperatures, which bind the particles together. They differ from traditional ceramics because they also contain a glassy phase which is able to interact with the remaining solid refractory material and while cooling it may solidify and bind the particles that have not yet merged together.

The glassy phase gives the ceramics some peculiar properties including a good hardness and mechanical strength and excellent corrosion resistance.

Lithium disilicate has been developed to improve the mechanical properties of glass ceramics and expand the use of integral ceramic in posterior sectors. It presents a flexural resistance of up to 450 MPa, and the fracture toughness is three times more in comparison, for example, to leucite.

In fact, in this material, the main glass phase, which is precisely a lithium disilicate, covers approximately 70 % of the total volume and forms an unusual microstructure. This microstructure consists of many small crystalline plates, which are connected to each other and oriented in a confused way. These plates seem to play a very important role in increasing the resistance of the material. This arrangement also appears to have the capacity to restrain fractures, causing them to branch and deviate.

Lithium orthophosphate is a secondary vitreous part, which is also present in this material, but it is much less important in relation to the total volume.

Lithium disilicate is obtained by a hot-pressing system at 920 °C [26–28].

From the clinical point of view, lithium disilicate can be treated as an integral ceramic, so the choice to perform a restoration with this material is mainly due to aesthetic reasons.

Disilicate guarantees an excellent aesthetic appeal combined with excellent mechanical properties, definitely higher than those of feldspathic ceramics.

The mechanical capacity of the material makes it possible to work with reduced thickness of material. In particular, especially in the anterior, we can reach thicknesses of restoration of less than 1 mm.

Obviously being a highly translucent material that provides a great passage of light, it is very important to be careful, especially in the front areas of the substrate on which the restoration is carried out. The latter can greatly influence the aesthetic characteristics of the material.

Moreover, the other great advantage of the disilicate is the ability to perform adhesive luting, thereby increasing the mechanical characteristics of the material.

If this direction is chosen, the adhesive approach must be the same as that used with ceramic materials. Thus protocol anticipates well-defined steps on both the substrate and on the restoration.

With regard to the substrate, the use of the rubber dam is recommended, followed by etching with 37 % phosphoric acid for 20 s and rinsing with water, and then the application of a primer. If there are areas of exposed dentin, air should be gently blown and thus the application of a bonding without polymerize.

Instead with regard to restoration, acid etching with hydrofluoric acid at 9 % is recommended, followed by rinsing with water, silane application and then drying with preferably hot air. At this point a bonding without polymerize is applied.

After the completion of the surface treatment the choice of the color of the photo or autopolymerizing resin cement, depending on whether you want to saturate or desaturate the final color. Then, the work is heated using special ovens and the color is applied inside the restoration with a spatula, proceeding to inserting the latter in the mouth.

At this point excesses are removed and any necessary occlusal retouches are made [29, 30].

---

## Crowns and Inlays in Lithium Disilicate

When we are faced with cases of single teeth, particularly the anterior or we have to complete a portion of the teeth even if partially filed, the best choice is an element in lithium disilicate, so as to mimic nature as much as possible.

These elements can be modeled manually and pressed with appropriate ovens or milled by a CAD-CAM system.

We can manufacture the anatomical shape or a “core” by later layering with ceramic, so as to add a touch of individuality and to increase reflection of the light.

Disilicate inlays are more delicate and must be prepared by the clinic according to their mechanical properties. When luting it is necessary that the thicknesses are uniform and have a homogeneous support.

It is recommended to use a microscope in order to have a better-sealed circumferential closure.

## Cases with Mixed Use Between the Two Materials

The clinician is free to choose the most suitable materials according to the complexity of the case and the requests of the patient.

The processes and materials can be mixed with each other, but for what concerns the majority of our cases, the appearance of the frontal implants is obtained by using lithium disilicate, while in the area of the molars is layered with the zirconium ceramic, always taking into detailed account the criteria of protecting the zirconium where it is necessary to avoid any future cracks in the ceramic due to the chewing load.

---

## Clinical Case

The case presented is that of a young patient who has a fracture of the element 1.1 (Figs. 1 and 2).

It is decided to remove the element and immediately insert a fixture in the post-extraction position. A connective tissue graft taken from a part of the palate is simultaneously performed (Fig. 3).

So, a transfer imprint with open tray technique is performed after a temporary period of about 3 months with a two tab Maryland Bridge (Fig. 4) and the realization of a customized abutment in zirconium, on which a second provisional structure is positioned to guide the maturation of tissues (Figs. 5 and 6).

After other 3 months, the case is finalized with a lithium disilicate crown (Figs. 7 and 8).

This case is an example of how the combined and aware use of these materials can guarantee excellent results.

**Fig. 1** Baseline of the patient: frontal view



**Fig. 2** Baseline of the patient: palatal view



**Fig. 3** Implant inserted and connective tissue graft

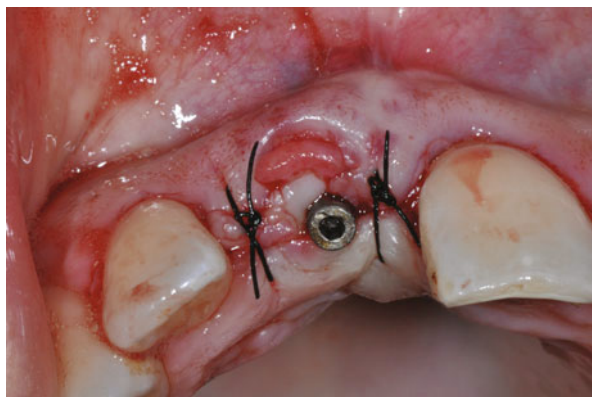


**Fig. 4** Provisional Maryland bridge after the surgery



**Fig. 5** Zirconium abutment in situ after 3 months from the surgery



**Fig. 6** Second provisional structure is positioned to guide the maturation of tissues

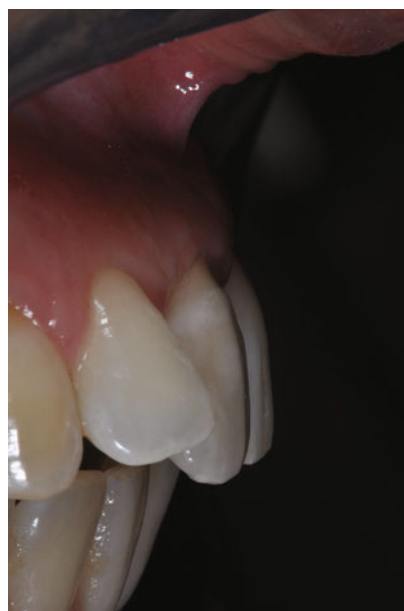




**Fig. 7** Final PFZ restoration:  
frontal view



**Fig. 8** Final PFZ restoration:  
lateral view



## References

1. Touati B, Miara P, Nathanson D (1999) Esthetic dentistry and ceramic restorations. Martin Dunitz, London
2. Zillio A (2013) Zirconia-The power of light. Teamwork Media, Brescia
3. Sturdevant JR, Bayne SC, Heymann HO (1999) Margin gap size of ceramic inlays using second generation CAD/CAM equipment. *J Esthet Dent* 11(4):206–214
4. Piconi C, Maccauro G (1999) Zirconia as a ceramic biomaterial. *Biomaterials* 20:1–25
5. Von Clausburch C (2003) Zirkon and zirkonium. *Dent Lab* 51:1137–1142

6. Frieman S (1991) Introduction to ceramics and glasses. In: ASM engineering materials handbook, vol 4. ASM International, Philadelphia, pp 1–40
7. Duran P, Moure C (1984) Sintering at near theoretical density and properties of PZT ceramics chemically prepared. *J Mater Sci* 20(3):827–833
8. McLaren EA, Giordano RA (2005) Zirconia based ceramics: material properties, esthetic and layering techniques of new veneering porcelain. *Quintessence Dent Technol* 28:100
9. Helvey GA (2006) Press to zirconia: a case study utilizing cad/cam technology and the wax injection method. *Pract Proced Aesthet Dent* 18(9):547–553
10. Raidgrodski AJ (2004) Contemporary all ceramic fixed partial dentures: a review. *Dent Clin N Am* 48:531–544
11. Christel P, Meunier A, Heller M, Torre JP (1989) Mechanical properties and short term in vivo evaluation of yttrium oxide partially stabilized zirconia. *J Biomed Res* 23(1):45–61
12. Meyenberg KH, Luthy H, Scharer P (1995) Zirconia posts: a new all-ceramic concept for nonvital abutment teeth. *J Esthet Dent* 7(2):73–80
13. Luthardt RG, Sandkhul O, Reitz B (1999) Zirconia-TZP and alumina-advanced technologies for the manufacturing single crowns. *Eur J Prosthodont Restor Dent* 7(4):113–119
14. Glauser R, Sailer I, Wohlwend A, Studer S (2004) Experimental zirconia abutments for implant supported single tooth restorations in esthetically demanded regions: 4-years results of a prospective clinical study. *Int J Prosthodont* 17(3):285–290
15. Blatz MB (2002) Long term clinical success of all ceramic posterior restorations. *Quintessence Int* 33(6):415–426
16. Hayashi M, Tsuchitani Y, Miura M, Takhsige F (1998) 6-years evaluation of fired ceramic inlays. *Operat Dent* 23(6):318–326
17. Sailer I, Feher A, Filser F, Luthy H (2006) Prospective clinical study of zirconia posterior fixed partial dentures: 3-years follow up. *Quintessence Int* 37:685–693
18. Gamborena I, Blatz MB (2006) A clinical guide to predictable esthetics with zirconium oxide ceramic restorations. *Quintessence Dent Technol* 29:11–23
19. Robertson T, Heymann H, Swift E (2002) Sturdevant's art and science of operative dentistry, 4th edn. Mosby, St. Louis
20. Blatz MB, Sadan A, Blatz U (2003) The effect of silica coating on the resin bond to the intaglio surface of Procera AllCeram restorations. *Quintessence Int* 34(7):548–555
21. Rogers J, Weber W (2007) Ceramic materials are not all the same. *Spect Dialogue* 6:76–80
22. Li J, Liao H, Hermansson L (1996) Sintering of partially stabilized zirconia hydroxyapatite composites by hot isostatic pressing and pressureless sintering. *Biomaterials* 17(18):1787–1790
23. Reichert A, Herkommer D, Muller W (2007) Copy milling of zirconia. *Spect Dialogue* 6:40–56
24. Tinschert J, Natt G, Hassenpflug S, Spiekermann H (2004) Status of current CAD/CAM technology in dental medicine. *Int J Comput Dent* 7(1):25–45
25. Liu PR (2005) A panorama of dental CAD/CAM restorative dentistry. *Compend Contin Educ Dent* 26(7):507–512
26. Blatz MB, Sadan A, Kern M (2004) Ceramic restorations. *Compend Contin Educ Dent* 25(6):412–416
27. Tinschert J, Natt G, Mautsch W, Aughtun M (2001) Fracture resistance of lithium disilicate, alumina and zirconia based three unit fixed partial dentures: a laboratory study. *Int J Prosthodont* 14(3):231–238
28. Margeas RC (2007) Material and clinical considerations for full coverage all ceramic restorations. *Funct Esthet Restor Dent* 1(3):20–24
29. Blatz MB, Oppes S, Chiche G, Holst S (2008) Influence of cementation technique on fracture strength and leakage of alumina all ceramic crowns after cycling loading. *Quintessence Int* 39(1):23–32
30. Blatz MB, Sadan A, Kern M (2003) Resin ceramic bonding: a review of the literature. *J Prosthet Dent* 89(3):268–274

Dan Pătroi, Teodor Trăistaru, and Sergiu-Alexandru Rădulescu

## Contents

Introduction .....	1130
Aesthetic Criteria .....	1131
Lips .....	1131
Attached Gingiva Area .....	1132
Teeth .....	1133
Perception of Shape Depending on the Position of the Teeth .....	1134
Materials Used for Veneering .....	1135
Acrylic Materials .....	1136
Composite Materials .....	1137
Ceramic Materials .....	1139
Indications of Full-Ceramic Veneers .....	1143
Contraindications of Full-Ceramic Veneers .....	1144
Full-Ceramic Veneers Advantages .....	1145
Disadvantages of Full-Ceramic Veneers .....	1146
Longevity .....	1147
Therapeutic Protocol .....	1148
The First Treatment Session .....	1148
Second Treatment Session .....	1150
Third Treatment Session .....	1151
Fourth Treatment Session .....	1152
Summary .....	1155
References .....	1156

---

## Abstract

Aesthetic treatment of the anterior teeth has always been a challenge in clinical practice. Along with the evolution of dental materials, the number of therapeutic options increased: in addition to aesthetic fillings or direct composite resin

---

D. Pătroi (✉) • T. Trăistaru • S.-A. Rădulescu  
UMF Carol Davila, Department of Fixed prosthodontics and Occlusology, Bucharest, Romania  
e-mail: [dan.patroi@gmail.com](mailto:dan.patroi@gmail.com); [proteticafixa@gmail.com](mailto:proteticafixa@gmail.com); [sergiualexandru@yahoo.com](mailto:sergiualexandru@yahoo.com)

veneering and all-ceramic crowns, ceramic veneers and inlays are now available. In these circumstances, dentists and their patients can choose the best therapeutic option from a range of possibilities outnumbered 15–20 years ago.

This choice is based both on the study of aesthetic criteria and the patient desires in accordance with therapeutic needs that he has.

The commonly used material for aesthetic restorations is dental ceramics, due to its color stability, biocompatibility, mechanical properties, and excellent aesthetic results. Minimally invasive dental restoration idea is gaining more ground in current dental practice, and thus full-ceramic veneers are increasingly used.

There are three types of ceramics used for manufacturing these veneers: feldspathic ceramics, leucite-reinforced glass ceramics, and lithium disilicate-reinforced glass ceramics. All these have special optical and aesthetic properties, miming natural tooth appearance, but the mechanical properties are different. As full-ceramic veneers are single-tooth restorations with very low thicknesses, mechanical resistance of the material is important both for their handling during manufacturing phases or intraoral cementation and especially for preserving the integrity of the restoration in the oral cavity.

Teeth preparation techniques for full-ceramic veneers differ depending on the aesthetic needs of the patient, the type of veneers to be made, and their indications and contraindications. Operator protocol includes four treatment sessions at the end of which the patient has the veneers cemented on the natural teeth. There are many advantages of natural teeth veneering and some disadvantages, which are small compared to the benefits.

The survival rate of full-ceramic veneers is very high, with some authors communicating a percentage of  $96 \% \pm 2 \%$  at 21 years and others of  $95.6 \%$  at 10 years.

---

### Keywords

Full-ceramic veneers • Preparation techniques • Advantages • Disadvantages • Survival rate • Success rate • Veneers longevity • Veneers indications • Veneers contraindications • Aesthetic criteria • Ceramic materials • Composite materials • Acrylic materials • Feldspathic ceramics • Leucite-reinforced glass ceramic • Lithium disilicate-reinforced glass ceramic • CAD/CAM technology • Therapeutic protocol

---

## Introduction

The success of an aesthetic restoration can be cumulated under the concept: “Beauty lies in the eyes of a concerned”; thus the dentist becomes an artist, and his work of art is the patient himself, both being involved equally, emotionally, and subjectively during treatment plan.

Beautiful art always catches the attention of those who look, and smile itself being the first contact with the speaker exerts a powerful influence on first impression. It is

said that “a smile is worth a thousand words.” Smile is given more importance in modern society, so with an attractive and healthy smile the patient can integrate more easily into society.

Dentistry involves a synergistic combination of biofunctional-aesthetic-mechanical principles and constantly changing in a direction always influenced by social, economic, and cultural factors. Thus emerged in recent decades an increase in concerns for dental aesthetics and sometimes cosmetic dentistry. The main purpose of this domain is the analysis, design, and implementation of the “perfect smile,” based on rules, located on the border between art on the one hand and science on the other. In the designing and implementation of a treatment plan, compliance with these aesthetic criteria plays an important role in getting the best and lasting therapeutic outcome, at whose touch contribute, at least to the same extent other principles mentioned requirements.

Aesthetic treatment of anterior teeth has always been a challenge in current clinical practice. With the development of dental materials, the number of treatment options increased; now available, in addition to aesthetic restorations or direct composite resin veneers and all-ceramic crowns, veneers, and ceramic inlays. In these circumstances, dentists and their patients can choose the best therapeutic solution from a range of possibilities, wider than 15–20 years ago.

---

## Aesthetic Criteria

Aesthetic rehabilitation of the anterior region must take into account the general criteria of beauty, which specialists in cosmetic dentistry have standardized as features of “perfect smile” with all components: lips, fixed gum area, and teeth. In turn, each of the three main elements has several variables that must be considered:

**Lips** – shape, color, texture, symmetry, tonicity, and smile line

**Attached gingiva area** – color and texture, shape and volume, symmetry, contour and gingival zenith, and gingival papillae

**Teeth** – shape, dimensions, central incisor ratio and golden proportion, mark (decreasing vertical dimension of lateral teeth), midlines, axial tilt and location of contact points, the free incisal edge, lower lip line and buccal corridor, arch shape, teeth texture, and teeth color

### Lips

Overall artistic impression created by a picture can be enhanced or diminished by the frame. Lips can have the same effect on smile appearance. It is analyzed by:

- Size
- Symmetry
- Shape
- Color

- Tonicity
- Texture
- Corners line (parallel to the pupillary line)
- Positioning ratio compared to the teeth

Average length of the upper lip, measured at rest from the center bottom of the nose to its inferior margin, has the following average values: 20–22 mm in young women and 22–24 mm in young men [1]. Shorter lips allow visibility of teeth at rest, and hyperactive lips reveal a great amount of attached gingiva during smiling, the so-called gummy smile.

The analysis of these parameters is made clinically by asking the patient to pronounce phonemes “M” and “E.” Through repeated pronunciation of the letter “M” on average, a portion 2–4 mm from the free lateral incisor is visible, and the pronunciation of the letter “E” determines the maximum extension of the lips highlighting the smile line which can’t exceed more than 2–3 mm to the central incisor gingival margin [1].

The amplitude of vertical movement of the upper lip from the rest position to the highest position in laughter is typically 6–8 mm; in the case of hyperactive lip, movement is about two times larger [1].

Lip appearance varies from person to person and obviously changes with age. Position and volume of frontal dentures can significantly alter the appearance of the lips. For this reason, some descriptive parts (smile line, midline, canine line) can be sent to the dental laboratory in the idea that the denture must be performed in harmony with the surrounding elements.

## Attached Gingiva Area

Pleasant appearance of smile can be affected by some deviation from the normal attached gingiva area.

**Shape and volume** – the volume is physiologically variable. In the literature three gingival patterns have been described, normal, thin, and thick, and these three types are differentiated by different thicknesses of alveolar bone margin, the appearance of the gingival free margin, and gingival contour. Thin and thick gingival types evolve differently if periodontal damage is present: thin type evolves toward bone resorption and gingival retraction, whereas in patients with thick type, it is associated with true or false gingival pockets and gingival hypertrophy [2]. In gingival hypertrophies, constitutional or pathological, the visible teeth shape changes; they become small and wide.

**Symmetry, contour, and gingival zenith** – gingival contour follows the free gingival margin so that the free gingival margin of lateral incisors must be above the central incisors and canine line. A detailed analysis of gingival contour introduces a third element, namely, gingival zenith: the highest point of the gingival curvature of each tooth. Due to the mesial tilt of dental vertical axis, this point is not always located midway mesial-distal but slightly distal [3].

**Gingival papillae** – another element that influences the aspect during smiling is the gingival embrasures: triangular shape spaces delimited by proximal faces and edges of the teeth, from the free gingival margin to the contact point. These spaces are occupied, normally, by the gingival papillae. When great gingival loss is present, the papilla volume is smaller than the newly created space, and black triangles appear, which are unaesthetic.

## Teeth

**Teeth shape** – the natural look of teeth varies according to age, sex, constitutional type, and patient personality; moreover, some theories argue that the shape of upper central incisor corresponds to the inverted contour of the face. The shape is determined by the ratio between the height and width of the tooth, the free edges, proximal faces, and free gingival margin. Visual perception of teeth is influenced by their inclination to the reference axes in the three plans.

**Teeth dimension and “golden proportion”** are closely related to the shape and size of the teeth. The size will vary from patient to patient, and it is considered normal if they are proportional to each other and at the same time as the size of the face, the proportionality in which we find “the golden proportion.” “The golden proportion” or “the golden ratio,” related to  $1/1,618$ , is a permanent retrieved constant in all shapes considered beautiful or proportionate. Starting from the elements of nature and to analyze the human body, this “golden rule” itself defines beauty as perceived by the human eye. This ratio can be found in people deemed “beautiful” [4].

Restricting the theory of divine proportion to the perfect smile, it is considered that assigning a unit value to the mesial-distal width of the lateral incisor visible from the standard frontal view and then the mesial-distal length of the central incisor will be 1,618 times greater and the canine 0.618 times less. As well, the actual average size of the frontal teeth group varies according to the sex.

Speaking of shape and size, it must be specified the role of visual illusion in the perception of an image. The optical illusion is the phenomenon by which the eye perceives a different image of reality. By understanding this phenomenon, it can become a useful tool in practice.

When creating an optical illusion, an important role is played by the light and the white/black alternation [5]. Based on this idea and analyzing the degree of convexity of the facial surface, which changes depending on the amount of light reflected, the notion of “apparent surface” of a tooth appeared. This is represented by the flat area of the facial surface, which may be closer or further as size from the contour of the tooth. Basically, tooth size perceived by the human eye is given by this “apparent surface” that reflects light toward the observer, while the curved areas, which continue to the edges of the tooth, reflect the light sideways, appearing darker and narrower than in reality. Thus, when the size of the two areas is approaching the values, the tooth is flat and “seems” wider, and vice versa.

## Perception of Shape Depending on the Position of the Teeth

**Midlines** – symmetry is an essential element of the concept of “beauty.” Numerous studies have shown, however, that in reality there is not absolute symmetry. Human faces, even the most perfect, have small asymmetries compared to the median or to the horizontal plane. One of the most used techniques for the analysis of facial symmetry is using the midline as landmark. Face image is divided into two halves which are then replicated and placed in the mirror. The two resulting images are similar to each other and to the original. As the differences are smaller, the more elements respect the symmetry. Thus, midline becomes an important milestone in facial and dental aesthetics. The normal situation implies that the two incisive lines should correspond one to another, and both should correspond to the facial midline.

Another element that is analyzed is the **buccal corridor**. It is the term used to describe the space between vestibular surfaces of posterior teeth and corners of the mouth or the inner wall of the cheek. A narrow arch will allow a very large buccal corridor, with dark look and, conversely, a wide arch will narrow the buccal corridor, creating a feeling of “mouth full of teeth.”

**Axial inclination and location of contact points** – another criterion used in the analysis of aesthetic smile is slight inclination of the vertical axes of teeth toward mesial. This tilt causes, along with tooth shape, the position of contact points on a vertical axis ranging from central incisors to canine and further premolars. In turn, the position of the contact point determines the shape and size of the gingival and incisal embrasures. The lack of embrasures or excessive size causes deviations from normal that give a bad look.

**Incisal edge, lower labial line, and buccal corridor** – the free edge of upper frontal teeth is a critical element of the perfect smile. Due to the different sizes of teeth in this area, incisal edges lie on a line with two curves: concave at the level of central incisors, continuing convex toward the lateral incisors and returning to its original shape toward canines. As against the lower lip line, central incisors and canines have to be in slight contact and the lateral incisors at a distance of approximately 0.5–1 mm. Also, the symmetry of these landmarks as against the midline is analyzed. In the overall smile analysis, it is considered that the incisal line is a continuous curve, concave upper, and must be parallel with the lower lip line.

Due to the normal curvature of the dental arch and remoteness of the point of observation, the apparent vertical and mesiodistal dimensions of teeth, from canine to second molar, should be decreasing distally. The ratio between these apparent sizes, the width of the entire arch visible when smiling, the wideness of the frontal group, and the width of central incisor respect, ideally, the gold proportion. Dr. Levin created, in 1975, a teeth proportionality analysis grille for wide smile. The set designed by Dr. Levin consists of 20 different sizes of grids that follow the same pattern, made of transparent material, so that they can be used in the dental office by direct overlap [6].

**Arch form** – in all three normal forms of arches, parabola, ellipse, and “U” frontal teeth are aligned on a curved segment. In practice, the analysis of arch form is drawing a line through the central canines, which must pass through the retroincisive papilla.



A line located anteriorly shows a stretched arch, and the line situated posterior from the incisive papilla occurs with narrow arches. Generally, these abnormalities of dental arch form are associated by default with dentoalveolar spacing or crowding, modifying obvious negative aesthetic.

**Dental surface texture** – differs according to person. Facial surfaces can have small concavities, convexities, fissures, grooves, and striations. Dental surface geography has a very important role in light reflection and color perception; that is why special attention is required when restoring these surfaces with dental remodeling techniques, partial or total, with direct or indirect methods.

**Teeth color** – color is the property of a substance to reflect or absorb some of the visible white light and perceptual ability of the human eye. The color cannot exist without light, object, and observer. Its perception is directly influenced by the characteristics of these three elements.

All these characteristics vary in the population from one race to another. The criteria presented above are generally available in the Caucasian racial group. Thus, for example, African or Asian population, dental characteristics differ from the Caucasian population.

Although dental aesthetics can be considered a form of art, there are principles of dental aesthetics, defined in literature, that can be used as a guide for real therapeutic success.

---

## Materials Used for Veneering

Dental veneers (sometimes called porcelain veneers or laminated porcelain veneers) are very thin-fixed partial dentures, covering the front of the teeth (facial) in order to improve the patient's appearance. They can be molded into any shape, size, length, and color and be bonded (cemented) adhesive to the surface of teeth.

Veneers were invented in 1928 by dentist Charles Pincus from California to be used in order to temporarily change the appearance of actors' teeth for various movies made there [7]. Later, in 1937 this dentist fabricated acrylic veneers that were cemented temporarily because adherence of dental cements available at that time to dental tissue was very poor. Buonocore, in 1959, introduced etching in order to adhesively cement porcelain veneers to the etched enamel. Simonsen and Calamia [8] in 1982 showed that even porcelain can be etched with hydrofluoric acid and thus obtain a bond strength between composite resin and porcelain, supposed to be able to maintain veneers on a permanent tooth surface. This was confirmed by Calamia [9] in an article describing a technique for fabrication and cementation of acid etched all-ceramic veneers using the refractory die, and Horn [10] describes the method of manufacture of veneers on platinum foil.

Dental veneers can be made of ceramic, composite resin, or acrylic material. Thus, the final aesthetic degree of veneer depends directly on the aesthetic possibilities of the material used. Ceramic veneers have the highest degree of aesthetic, which basically mimic the appearance of natural teeth due to the optical properties of ceramic materials: translucency, fluorescent, transparency or opalescent, and color

**Table 1** Proprieties of the materials used for veneers

	Acrylic	Composite	Ceramic
Optical proprieties	Low	Good	Excellent
Aesthetic proprieties	Low	Medium-good	Excellent
Biologic proprieties	Gingival irritation	Good	Biologically inert
Mechanical proprieties	Poor	Medium	High
Survival rate	Low	Medium-high	High
Success rate	Low	Medium-high	High
Cost	Low	Medium	High
Cementation	Provisional or absent	Adhesive	Adhesive
Treatment session	1	1–3	3–5

stability in time. Composite veneers have a lower degree of aesthetics due to the lack of translucency of the material and color stability in time. In a clinical trial, Gresnigt, Kalk, and Ozcan discuss the emergence of a porous surface with composite veneers and marginal discoloration [11] which leads to decreased aesthetic properties of these types of veneers. Acrylic veneers have the lowest aesthetic degree due to limitations imposed by the material, which are generally used for temporary veneers made in the dental office.

A comparison between the three types of materials used in veneering is shown in Table 1.

## Acrylic Materials

Although the aesthetic qualities of this class of materials are low, they are commonly used to obtain the provisional veneers during dental treatments or for temporarily changing the appearance of teeth (e.g., Snap-On Smile™, DenMat Laboratories, USA).

When it comes to dental treatment through veneering, after tooth preparation, the patient should recover both physiognomy and jaw functionality. Thus, through direct methods of provisional prosthesis, temporary veneers are made to be worn by the patient until the final restorations will be done. The materials used are entirely provisional prosthetic materials: Telio CS C & B (Ivoclar Vivadent), Access Crown (Centrix), Protemp (3 M ESPE), Luxatemp (DMG), etc. In current dental practice, these restorations are made directly in the dental office, by copying natural teeth before preparing them or by coping a wax-up model. Later, after the preparation of the teeth, a temporary prosthetic material is applied in this impression, and the impression is inserted in the oral cavity. After material setting the impression is removed from the oral cavity, the temporary veneer is removed from the impression, and it is finished and then temporarily cemented to the dental preparation. The patient wears it until the end of the treatment.

Snap-On Smile™ (DenMat Laboratories, USA) is a reversible treatment procedure, completely noninvasive. The manufactured restoration can be easily removed

and reapplied by the patient, because it is not cemented to the natural teeth. This therapeutic procedure involves a noninvasive approach, fully reversible and easily accessible regarding the price of a restorative and cosmetic dentistry procedure. Clinical protocol is quite simple. The first step is to determine whether the patient is a suitable candidate and if he/she can understand both the advantages and limitations of this therapeutic option. Then, the shape and position of teeth that are intended to be corrected are analyzed and recorded. No preparation of the natural teeth is necessary. Full-arch impression using silicone material are made and an occlusal record is necessary. It is important that dental impressions to be accurate and precise to record all the convexities and the full contour of natural teeth, and at the free gingival margin, the impression should not be torn or modified.

The impressions are then sent to the dental laboratory with a form detailing the changes, and there the provisional will be made following aesthetic and functional criteria.

Patients can wear these restorations whenever they want and how long they are comfortable. They can apply and remove them from the oral cavity without the need for a dentist intervention.

---

## Composite Materials

Composite materials have better optical and aesthetic properties than acrylic materials but lower comparing with ceramic materials. Facial veneering concept became possible after the discovery of adhesive cementing techniques that provide aesthetic and functional needs of maintaining adequate bond. Meanwhile, originally used acrylic veneers have become aesthetically unacceptable due to early loss of color and low resistance in the oral environment. These disadvantages are offset to a large extent when using composites for veneering and are absent in ceramic materials [12]. Porcelain veneers have the highest rate of survival time, followed by composite veneers, and then the acrylic ones due to both physical and biological properties of these materials and methods of manufacturing the veneers (Table 1). If we refer only to methods of producing indirect composite veneers, then their survival rate is comparable to ceramic veneers [13]. To achieve composite veneers, it can be used both direct and indirect methods. Direct techniques aimed at achieving veneers in the dental office, by the dentist, using composites for crown restorations. The indirect techniques involve the dental laboratory, manufactured by a dental technician and then cemented in the mouth by the dentist.

When direct technique is used, the dentist starts with ultrasonic scaler, airflow, and brushing in order to clean the teeth for both color composite materials election and prepare their surface for an adhesive technique if teeth preparation is not necessary. When the preparation is necessary, this should be achieved with tapered diamonds with smooth tip, especially for creating a feather edge margin, with continuous water cooling, removing between 0.5 and 1 mm of the enamel, taking care to keep the preparation solely at the enamel level. Incisal edges will be prepared with embrasures according to dentine mamelons. At the proximal surfaces the

contact point will be removed only where caries will require or when we want to close the interdental spaces.

Before starting the actual direct veneering process, whether or not the tooth has been prepared, it is necessary to isolate the teeth involved. This can be done with the OptraGate (Ivoclar Vivadent) device to avoid the change of clinician perception of hue and translucency of teeth generated by the rubber dam isolation. When using this device, gingival eviction is needed to achieve isolation in the gingival sulcus. It will use one or two nonimpregnated braided cords, depending on the depth of the gingival sulcus.

Depending on clinician experience and indications of the composite material total etch, no etch or self etch adhesive systems will be used. Of these, the total etch systems involving etching of the enamel with 37.5 % phosphoric acid provide the best adhesive bond of the composite to the tooth [14].

Composite resin will be added in layers, using shades of the dentin and enamel for final color-rendering effects for the veneer and shades (clear, transparent, opalescent) for achieving transparencies from the incisal edge or proximal surface, according to final aesthetic needs. Final stratification will be about 2 mm, and the application of composite resin will start from the center of the tooth extending to the proximal and facial areas. For application and modeling layers of the composite, it can be used as dental spatulas and special tools for modeling, and to restore the contact point and the proximal areas, celluloid matrix fixed with wood wedges with triangular profile are used.

Composite layer polymerization is made with a LED lamp using a light intensity and curing time according to the manufacturer.

Finishing will be done with diamond or carbide burs along with abrasive discs and tapes, and the final polish will be achieved with rubber cups, which incorporate particles of aluminum oxide or diamond, and brushes with polishing paste.

Direct veneering technique versus indirect technique has the main advantages of short working time, one session of treatment required, and low-cost price.

Composite veneers, as well as the ceramic ones, can be achieved through indirect techniques involving dental laboratory. In this case they will be made by the dental technician, and the dentist in advance must polish the tooth/teeth involved, make an impression of the prepared teeth, and send the impression to the laboratory with a lab sheet that contains data about the color and the final shape of the teeth. Dental technician is the one who will manufacture the veneers with composites for dental laboratory use: Sinfony (3 M ESPE), SR Nexco (Ivoclar Vivadent), etc. Later they will be cemented by adhesive intraoral dental composite cements: Variolink II (Ivoclar Vivadent), Nexus NX3 (Kerr), Duo-Link (Bisco), etc.

As a result of development of composite materials, prefabricated composite veneers were recently introduced in the dental practice. These prefabricated veneers were designed as an alternative to full-ceramic veneers, to be more accessible for patients in need of an aesthetic solution regarding the price compared with that of a full-ceramic veneer. They are available in different shapes, colors, and sizes, in kits which include a flowable composite material for intraoral cementation. Such a system is Componeer (Colthene). These prefabricated veneers will be customized

directly intraoral by the dentist depending on the patient's needs and then be adhesively cemented to the frontal teeth of the patient in order to restore the patient's aesthetic appearance. The necessity of prior preparation of the teeth is minimal or absent even in case of using these veneers and is necessary only one appointment at the dentist for their application, as in the case of direct veneering. This new technique has the potential to be used routinely to lengthen the anterior teeth, to correct the teeth with minor malpositions, to mask some dental stains, and to close the treme or diasteme. The technique can also be used to restore extended caries and dental fractures, especially when other treatment options are refused by the patient for financial reasons. However, it is extremely important to perform controlled clinical trials with this restoration technique, before recommending it without restriction in general practice [15].

---

## Ceramic Materials

Since the introduction of indirect veneering technique more than two decades ago, restoration of teeth with the acid-etched ceramic veneers has proved to be a sustainable and aesthetic treatment. Clinical success of this technique can be attributed to higher attention on the details of a set of procedures:

- Case planning with accurate indications
- Conservative tooth preparation
- Correct selection of the ceramic used
- Appropriate selection of materials and methods of adhesive cementation
- Proper planning for continued maintenance of these restorations

This treatment method is used because of color stability of ceramic, biocompatibility, mechanical properties, and excellent aesthetic results. The idea of minimally invasive dental restorations is gaining more and more ground in current dental practice, and so, ceramic veneers are increasingly used.

There are three types of ceramics used for manufacturing these veneers:

- Feldspathic ceramics
- Glass-based ceramic reinforced with leucite crystals
- Lithium disilicate glass ceramic

All of these have special optical and aesthetic proprieties, miming natural tooth appearance, but the mechanical properties are different. As ceramic veneers have very low thicknesses for single-tooth restorations, mechanical resistance of the material is important both for their handling during manufacture and intraoral cementation especially to preserve the integrity of the restoration in the oral cavity.

**Feldspathic veneers** are made by firing ceramic powder on metal foils (e.g., platinum) or directly on the refractory die. Mechanical strength of these veneers has low values of 30–40 MPa, which requires their handling very carefully. After the

adhesive cementation on dental hard tissues, their strength reaches proper functionality; in the literature there are studies that communicate a success rate of about 95 % at 10 years [16].

**Glass-ceramic veneers** have a higher resistance compared to the feldspathic ones, reaching values of 170–180 MPa for glass-ceramic reinforced with leucite crystals and 400 MPa for the lithium disilicate one. Glass-ceramic material has a polycrystalline structure produced by controlled crystallization of glass. This class of materials has many common properties such as glass and ceramics. They have an amorphous phase and one or more crystalline phases produced by a “controlled crystallization” as opposed to spontaneous crystallization, which usually is not desirable in the manufacture of glass. Properties resulting from the process of “controlled crystallization” include the absence of porosity, high strength, hardness, translucency or opacity, color, opalescent, very low thermal expansion, or even absent, high-temperature stability, fluorescence, biocompatibility, and thermal and electrical insulation capacity. These properties can be adjusted as needed by controlling the composition of the base glass and the type of crystals (leucite or lithium disilicate) introduced into the ceramic structure.

To obtain full-ceramic veneers, these materials are either hot injected into a pattern that is shaped like the future veneer or CAD/CAM milled from ceramic bars. Hot injection is performed at high temperatures of 1100 °C for system IPS Empress (Ivoclar Vivadent) containing ceramic reinforced with leucite or at 920 °C for system IPS e.max Press (Ivoclar Vivadent) containing ceramic reinforced with lithium disilicate, either at low temperatures of 160 °C for Cerestore system. The pattern is made in the dental laboratory from refractory materials using wax elimination technique. Veneers thus obtained are then processed and individualized by the dental technician for obtaining final restoration which will be adhesively cemented on the prepared teeth.

CAD/CAM technology is the newest method introduced in prosthodontics, and its target is automated manufacturing of dental restorations. The design of the restoration is made using a computer program after prior intraoral scanning of the prepared tooth (optical impression) or of the working cast in the dental laboratory, and the finite prosthetic veneer is obtained by a milling machine from a ceramic block. This technology produces dental restorations that have superior marginal adaptation to the preparation [17] compared with conventional techniques. Theoretically, it would result in a better survival rate for these restorations, but studies published in the literature communicate survival rates similar to hot-pressing technique, when evaluating prosthetic restorations[18].

Regardless of the technology used, the preparation of teeth that are about to be veneered is the same. The techniques of preparation are divided into the following categories:

- Classic preparation technique
- Minimum preparation
- Partial preparation
- No preparation

The classic preparation technique involves facial surface reduction, proximal surfaces reduction within the contact point, and the reduction of the incisal edge. Facial reduction needed is about 0.5–0.7 mm for maxillary teeth and about 0.3 mm for smaller teeth such as mandibular incisors. Sometimes it is necessary to reduce small portions of dentin, with the amendment that dentin reduction should be up to 50 %, but the terminal limit must be situated in the enamel. Average tooth tissue reduction is 0.5 mm, but the preparation is reduced toward cervical (0.3 mm) and more pronounced toward incisal (0.75 mm), the reason being the cervical enamel is thinner, and when possible the entire preparation must be located in the enamel. Preparation must respect the anatomy of the tooth, so it is performed in the different planes as the primary morphology of the tooth. Depth orientation grooves are placed in the facial surface between 0.5 and 0.7 mm with a cylindrical diamond bur. Orientation grooves are connected to achieve a uniform reduction. Chamfer margin is used and placed closely to the gingival crest in the enamel.

Proximal preparation must be performed with care not to damage adjacent teeth and also should not neutralize the contact point, the preparation margins being placed at this level. There are some clinical situations involving reduction of proximal surface entirely: proximal cavities or fillings, diastema, or interdental space closure which involve changing of the gingival emergence profile of the tooth concerned. Usually it is necessary that the enamel on the margins of the preparation has to be removed using a chisel to avoid sharp edges that often result when using the bur. Contact area will be precisely reproduced on the definitive cast, which will facilitate its separation in mobile abutments without affecting the preparation.

Incisal edge preparation can be done in four different ways (Fig. 1):

- Window – the preparation finishes at 0.75 mm before the incisal edge; this preparation has the advantage that preserves natural enamel in the incisal edge but at the expense of a thin enamel at this level. This type of preparation is indicated for teeth with thicker incisal edge. Loosening or fracturing risks when biting or in end-to-end relationship are zero. The veneer edge will become visible if the incisal edge will wear off.
- Feather – preparation is extended to the incisal edge but it is not reduced. This type of preparation is recommended for incisors with thin or narrow incisal edges, but there is a risk of fracturing or loosening in protrusion movements or in end-to-end relationship.
- Bevel – the inclination is facial palatal preparing the entire width of the incisal edge. The technique offers a very good control of incisal edge aesthetics, and it is indicated especially when there are small fractured incisal angles or edges. The type II occlusal contacts must be considered because they are not allowed to interfere with the junction between the tooth and veneer but must be placed at least 0.5 mm from the junction.
- Overlap – involves preparation of the incisal edge, and then it is extended on the palatal surface and sometimes can extend all the way to the cingulum.

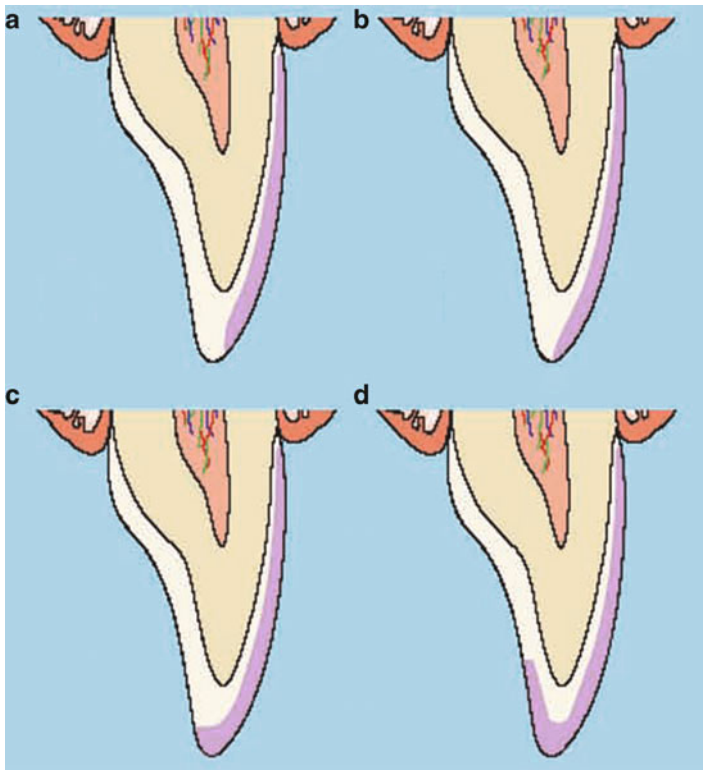


**Fig. 1** Incisal edge preparation techniques: (a) window, (b) feather, (c) bevel, and (d) overlap [39]

Of these, the latter two provide the greatest resistance to fracture under occlusal forces [19]. Window-type preparation is rarely used in indirect veneering, being most common in the direct methods of preparation.

**Minimal preparation and partial preparation** targeting removal of trace amounts of dental tissue. In this case, before the clinician starts preparing the tooth, along with the dental technician, they must perform a diagnostic wax-up of the final outcome. Wax-up cast has to be in office before preparing the teeth. Through it's impression, a silicone index is obtained which will then be used during preparation. A second index, of transparent silicone, is used to transfer the diagnostic wax-up to the oral cavity (mock-up). First the transparent index is used to create the mock-up on which one can analyze the position of future veneers, integrated in the dental arch. The transparent silicone index is filled with fluid composite and then positioned on the arch; after curing it is removed carefully and the mock-up is ready. Remove excess from gingival mucosa. To obtain the mock-up two techniques are used:

1. We can fill the index of transparent silicone with fluid material and then apply in the mouth and light cure it. This technique does not require a long time to yield good results.



2. Fill one third of the transparent silicone index with fluid composite, apply it to the prosthetic field, then light cure it. Carefully remove the index and then the rest of the surface is filled with composite material; by this technique the clinician has more control over the final result but requires more time.

Dr. Galip Gurel [20] calls this mock-up APT (aesthetic pre-evaluative temporaries), but it results from the impression of the wax-up, to provide a silicone key that will be used intraorally to the patient. It evaluates functional movements and static occlusion in order to see if any occlusal obstacles are present or premature contacts. It also analyzes the phonetics to exclude such problem in the future, related to pronunciation of certain words or phonemes.

The technique consists in preparing the teeth with the mock-up so that the result is similar to natural teeth. It starts with a guide bur for creating guiding grooves both the facial surface and the incisal edge. Facial surface is prepared according to morphological anatomy of that tooth with a diamond bur with rounded tip, taking into account the fact that the preparation should not exceed the enamel-dentin junction. For incisal edge one of the classical preparation techniques can be used. In the end, finishing burs are used to smooth the preparation margins and remove sharp edges and also to finish the gingival and proximal margins. Once the preparation is ended, the depth is verified with the silicone index. Depending on how much the tooth surface was prepared, one can define if the preparation is minimal or partial.

No-prep technique does not imply preparation of natural teeth. Decision for making veneers without preparation must be well instrumented by the clinician, both in accordance with the indications and contraindications of no-prep veneers and depending on the patient's expectations. In general, the thickness of this type of restoration is very low, which makes solving dental discoloration or major change in tooth color not possible.

---

## Indications of Full-Ceramic Veneers

Full-ceramic veneers offer conservative solutions from biological point of view and a high degree of aesthetics for the following clinical situations:

- Dental discoloration: tetracycline-discolored teeth, dental fluorosis, or discoloration due to age.
- Defects of the enamel: different types of enamel hypoplasia and dysplasia, with birth defects, can be masked or corrected.
- Diastema and interproximal spaces: closes interdental spaces, to achieve an aesthetically pleasing appearance.
- Teeth with malpositions: it should be noted here that severe dental malposition is a contraindication for veneers, but minor malpositions such as dental rotations and mild crowding or spacing may be resolved by veneers, if orthodontic treatment is not desired by the patient. Otherwise, the orthodontic treatment is

the best choice in these situations. In these situations, veneers can create an “optical illusion” of shape changing, tooth position modification, dimension, and tooth surface alteration.

- Malocclusion: configuration of palatal surface of the upper front teeth can be modified by veneering this surface to restore lost anterior guidance and type II occlusal contacts, for example, if a patient is periodontally compromised. Veneering will be used but after solving periodontal problems and if orthodontic treatment is not desired by the patient.
- Direct restorations failure: frontal teeth with multiple or repeated superficial fillings which are no longer suitable from aesthetic point of view.
- Incisal edge wear: different patients due to professional vicious habits (carpenter, tailor) or developed independently (pen or nails chewing) that produce incisal edge changes.
- Fractured teeth: they can be restored to normal morphology with partial or full-ceramic veneers.
- Small teeth: frequently, veneering of small lateral incisors is the solution of choice for rendering patient’s smile; often in these cases veneering the entire frontal teeth group is necessary to preserve their relative size.
- Lateral incisor agenesis: often when lateral incisor is absent, the canine erupts in its place and thus creates an unpleasant aspect of smile. Remodeling the canine into a lateral incisor using a veneer reduces the ugly smile, but often in these cases intervention on central incisors and first premolars is necessary in order to obtain a high aesthetic result.

“Permanent” dental whitening: full-ceramic veneers are a good alternative when conventional teeth whitening procedures are contraindicated or when the patient wants a permanent change of tooth color.

Masking gingival retraction: if some minimal tooth root is exposed, this defect can be masked by veneers.

---

## **Contraindications of Full-Ceramic Veneers**

Full-ceramic veneers are not indicated in following situations:

- Massive crown loss: when a great amount of dental crown tissue is lost either by caries or trauma.
- Diastema or interproximal space with mesial-distal enlarged space: when intraoral or on diagnostic cast measurements are suggesting that the space is too big.
- Severe dental malpositions: ectopic teeth that needs orthodontic treatment.
- Endodontically treated teeth: represents a relative contraindication for veneers from the dental tissue resistance point of view and because of the low color stability in time. In this case, a full-ceramic crown is the best solution.
- Poor dental hygiene: patients who do not take care of their natural teeth and end up having a high caries level are not candidates for treatment with all-ceramic

veneers in order to restore the aesthetics of natural teeth, because on the uncovered tooth surfaces, after veneering new caries may appear and compromise the veneer.

- **Bruxism:** is a relative contraindication. Patients with bruxism, if they do not wear the mouth guard, destroy their natural teeth, the same thing happening with any kind of dental restoration, but in terms of a compliant patient (wearing mouth guard and respects the dentist indications) veneering is possible.

---

## Full-Ceramic Veneers Advantages

Compared with the composites or acrylics, ceramic materials through their proprieties are the optimal material for dental hard tissue replacement for the following reasons:

- **Color stability:** ceramic materials offer a double advantage – on the one hand ability to reproduce any color or transparency of the natural teeth and on the other hand ability to maintain color in time.
- **Chemical adhesion to the enamel:** after adhesive cementation by both veneer etching and dental tissue, by applying silanization agents on ceramic material and bonding agents on dental tissue, and, finally, by interposing between the two conditioned components a composite cement, a stable chemical bond of the veneer to tooth surface is obtained.
- **Periodontal health:** the ceramic surface, after glazing, is very glossy and thus prevents the accumulation of dental plaque. Also, due to special ceramic aesthetics, the preparation margin can be placed above the free gingival margin (can be placed at 0.5 mm above the gum), and thus artificial cleaning and auto-pruning are possible. In case of no-prep veneers, however, the cervical margin will be finished until thickness becomes sometimes 0.1 mm, and in this case there is a potential risk of dental plaque retention at that level.
- **Abrasion resistance:** resistance to wear and abrasion of ceramic materials is extremely high compared with composite resins and acrylic materials. Regarding opposing natural tooth abrasion, new ceramic materials, reinforced with lithium disilicate (IPS e.max – Ivoclar Vivadent) has a comparable hardness to that of the enamel and thus does not cause excessive wear of opposing teeth [21].
- **Tear resistance:** full-ceramic veneer itself is quite fragile, but once it is adhesively cemented to the enamel, the restoration develops a high resistance to tensile and shear forces. For example, ceramic materials reinforced with lithium disilicate have a fracture resistance of 400 MPa and after adhesive cementation may reach values of 1000 MPa [22].
- **Resistance to fluid absorption:** after glazing ceramic materials are inert to fluid absorption compared to composite resin or acrylic materials, where fluid absorption in the oral environment is a well-documented disadvantage.
- **Aesthetics:** regarding ceramic materials, dental technician has much greater possibilities of obtaining the desired color and texture of the restoration surface

compared with other materials. Porcelain can be colored both internally and externally (superficial), resulting in a restoration that mimics natural tooth appearance. Both texture and microtexture can be made on the veneer surface in order to simulate the appearance of adjacent teeth and can be maintained indefinitely after intraoral cementation.

- Light transmission: dental ceramic is the only translucent, fluorescent, and opalescent material that is able to mimic all the optical properties of natural teeth.
- Preservation of dental hard tissue: most of the time the preparation for full-ceramic veneers is made exclusively in the enamel, with a reduction varied between 0.3 and 0.7 mm, with/without involving incisal edge. Thus dental veneers are a more biological method for restoring dental stain or dental fractures compared to crowns.
- Local anesthesia: if the preparation is strictly limited to the enamel, local anesthesia is not required, although there are more emotive patients requiring administration of anesthesia.
- Interim restoration: not required for no-prep veneers.

---

## Disadvantages of Full-Ceramic Veneers

- Time: indirect veneering is a sensible technique and, hence, time consuming. Any kind of negligence in the manufacture protocol, either in dental laboratory or in the office, can have a disastrous effect on the final restoration.
- Fracture repair: after adhesive cementation, any kind of veneer repair actually means replacing it.
- Color: it is both an advantage and a disadvantage. After adhesive cementation in the oral cavity, any color change is impossible. Considering that while natural teeth change color and ceramic materials not, practically patients with such restorations become addicted to whitening treatments if not all of the teeth in aesthetic area are restored. But this is true for any fixed or removable prosthetic restoration.
- Fragility: veneers are difficult to handle due to their resistance to tear, especially those made of feldspathic ceramics.
- The price: the price of a full-ceramic veneer can be equal to or even higher than that for a crown.

In general, full-ceramic veneers failure is associated with one of the following factors: inobservance of this type of restoration by the dentist, poor preparation of the involved teeth, interim restoration, inobservance of manufacturing process by the dental technician, veneer handling, choice of cement and cementing technique, and patient communication.

Full-ceramic veneer remains the prosthetic restoration that best completes mechanical, biological, and aesthetic proprieties today. This type of restoration avoids the use of metal structures or zirconium oxide and thus achieves excellent aesthetic qualities. It is also the most conservative type, capable of preserving

significant amount of the natural tooth enamel. The high rate of treatment success by veneering indicates this technique as the solution of choice in dental aesthetics.

---

## Longevity

In a recent study (year 2012), Layton and Walton [23] watched for 21 years a number of 499 full-ceramic veneers manufactured with feldspathic ceramic, adhesively cemented to a total number of 155 patients. For case selection, endodontically treated teeth, molars, and teeth with periodontal problems were excluded. Before the adhesive cementation, all veneers were etched with hydrofluoric acid and then silanized. Teeth were prepared so that a minimum of 80 % of their surface would be covered with enamel. After an observation period of 21 years, they announce a survival rate of 96 %  $\pm$  2 %. Also, they noted that the loss of veneers is not random, but the same patient has lost more veneers, which implies the patient's compliance both during treatment and especially after treatment, in the follow-up period.

A literature review on survival rate of feldspathic veneers, published in 2013 by Walt and Conway [24], shows high survival rates of 95.7 % at 5 years and 95.6 % at 10 years. They have considered 11 published studies, both prospective and retrospective, and have concluded that feldspathic veneers have a high survival rate when they are adhesively cemented to the enamel.

Taking into account the necessity of redoing all kind of full-ceramic restorations (inlay/onlay, veneers, and crowns), both before cementation and after intraoral cementation, Hekland, Riise, and Berg [25] published in 2003 a study which included 2069 feldspathic ceramic restorations (ColorLogic) and 1136 leucite-reinforced ceramic restorations (IPS Empress 1 and 2). A 4.4 % percentage of the total restorations included in this study needed adjustments before cementation, and full-ceramic veneers were the most frequently adjusted restorations. After 2 years from cementation, the reconstruction rate was 1 % which indicates a general survival rate of the full-ceramic restorations of 99 %. The highest survival rate within the group was acquired by inlay/onlay restorations (99.8 %) and the lowest one by the full-ceramic crowns (98.4 %). Full-ceramic veneers had a survival rate of about 99 % at 2 years.

Full-ceramic veneers can be used as a treatment method for patients with parafunctions (bruxism). Regarding this, Beier, Kapferer, Burtscher, and Dumfahrt published in 2012 a study realized on 84 patients, half of which (42 patients) had bruxism. The authors realized a total number of 318 full-ceramic veneers on maxillary and mandibular frontal teeth. The survival rate of the veneers from this group was 94.4 % at 5 years, 93.5 % at 10 years, and 82.93 % at 20 years. The authors' conclusion was that full-ceramic veneers are an aesthetic, predictable, and successful treatment option for restoring frontal teeth. The fact that half of the patients had bruxism produced only a minor decrease of survival rate at 10 years comparable with the other studies published in the literature [26].

Using leucite-reinforced ceramic material for manufacture of full-ceramic veneers, namely, IPS Empress system (Ivoclar Vivadent), Fradeani presents a

survival rate of 98.8 % at 6 years [27]. Same author together with Redemagni and Corrado finds a survival rate of 94.4 % at 12 years on a research group of 46 patients which received 182 cemented full-ceramic veneers. This survival rate is reached only when full-ceramic veneers are correctly adhesive cemented [28].

Lithium disilicate-reinforced ceramics have the highest fracture resistance (400 MPa). This is why the indications of this ceramic type include besides single-tooth restorations (inlay/onlay, veneers, frontal, and lateral coverage crowns) even three-unit bridge in the frontal or bicuspid area, as well as implant restorations. Once lithium disilicate ceramic material appeared (IPS e.max Press – Ivoclar Vivadent) in 2002, realizing high aesthetic restorations becomes possible, which mimic natural teeth both in lateral area and on implants. A recent clinical study, published this year (April 2014), consists of a total number of 860 restorations like inlay/onlay, veneers, crowns, and implant restorations adhesively cemented in frontal and lateral area and reports a success rate between 95.39 % and 100 %, along with a survival rate between 95.46 % and 100 %. Restorations from this study were checked for a 3–6-year period. This study included a total of 312 patients, among whom were patients with parafunctions (bruxism), but periodontally compromised patients were excluded. Of the 860 full-ceramic restorations, a total of 26 have developed complications after cementation: 17 partial fractures of the ceramic, five total fractures, and four unluted restorations. Conclusion of this study: all-ceramic restorations made of lithium disilicate-reinforced ceramic prove to be efficient and reliable both on short and medium term [29].

---

## Therapeutic Protocol

Dental aesthetic philosophy comprises a therapeutic algorithm to be covered by any dentist with the patient or when aesthetics is the main reason why the patient comes to the doctor. Depending on the expectations of the patient, the dentist may suggest different clinical procedures that have indications of choice in the case as follows:

- Changes in color: the first option is the external coronal tooth whitening and/or internal.
- Dental malpositions: the option of choice is the orthodontic treatment.
- Shape/contour tooth modification: if there are small shape changes, they should be evaluated if they cannot be made by selective preparation followed by fluoridation.

Only when the above options are excluded, the dentist will consider restoring teeth with aesthetic veneers or crowns.

---

## The First Treatment Session

Treatment plan for veneering, as in other prosthetic treatments, will start by checking indications and contraindications for the type of restoration, e.g., full-ceramic veneers. It is also very important to check patient's bucco-maxillary system's



**Fig. 2** (a) Initial view of frontal maxillary teeth. (b) Initial view of dental arches

functionality: static occlusion, especially the anterior occlusal contacts, and protrusive and laterotrusive movements. Subsequently key elements in dental aesthetics must be evaluated: contour, position, and color of teeth. All these things will be examined and discussed in the first treatment session, along with patient's examination.

Following clinical examination, if the treatment solution is veneering the teeth, then, in the first appointment, impressions for study casts will be taken, along with occlusal relationship recordings which are necessary for mounting the casts in the articulator. All these records are sent to the dental technician for mounting casts in the articulator, programming it to reproduce mandibular movements of the patient, and producing a diagnostic modeling (wax-up). In addition, the dental technician receives a communication sheet from the dentist which contains all necessary changes that were established after discussion with the patient and eventually photos of dental arches (Fig. 2a, b) and the patient's face and profile. Thus, the dental technician can achieve by wax addition on the cast of the final design of patient smile.

Diagnostic wax-up comprises several design phases and encompasses different anatomic shapes of teeth according to facial aesthetic details but with patient wishes regarding personal appearance, without which diagnostic wax-up is doomed to failure [30]. Stages of wax-up for teeth in frontal area are:

1. Diagnostic wax-up should start with maxillary central incisors modeling. The process begins by creating a flat surface up to the new incisal edge and to the new length determined by the clinician. From the two maxillary incisors, a single tooth so-called unitooth is created, by adding wax to the facial area. This step is very important because once created, the new incisal edges parallel to a flat surface; thus the perpendicular interincisive line can be easily positioned. Positioning of the interincisive line can be checked by placing both maxillary

and mandibular casts in the articulator, such that the maxillary interincisive line to correspond with the mandibular one.

2. Once the interincisive line was placed, it should create an angle of  $90^\circ$  with the incisive edge. Subsequently check if interincisive line coincides with the center line of the face. Registration of the center line is realized in the first treatment session, and then it is transferred to the study casts and reported to the technician (T – reference).
3. The next step includes central incisors anatomical modeling taking into account previous measurements. It is important that the shape of the central incisors be identical as a mirror image of each. Keeping mesial edge and the mesio-vestibular angle of the facial area of central incisors slightly rounded, the overall look of central incisors will be a square, but if we round these limits, teeth will get a round look. In this stage dental technician can help himself with special measuring tools, such as special rulers.
4. During the diagnostic wax-up process, it is very important that the technician evaluates the progress after each step. For a successful diagnostic wax-up, the dental technician must follow the rule “apply wax-stop-look-check-modify.”
5. After the anatomical shape of central incisors is established, the technician goes to create the maxillary lateral incisors. The key point is that the technician determines the correct width of the lateral incisor in relation to central incisor. Unlike central incisors, lateral incisors should not be perfectly identical. Anatomical variations of lateral incisors occur frequently and are easily tolerated by those who observe.
6. The technician must define the final shape of lateral incisors such that they are approximately symmetric.
7. Wax is added to the canine to establish anterior guidance, lateral guidance, and aesthetics. Canines are generally symmetrical and light asymmetries at this level can be seen easily.
8. If the technician places on a flat surface the wax-up, he can observe the incisal edges level and frontal teeth symmetry. At this point it is good for the technician to let aside the cast, and when he returns, the technician can see things that he could miss.
9. Next steps include future occlusal relations, such as new guidance surfaces, which the technician can check by mounting the casts in articulator.
10. Finishing details to the canine’s form; making the canine’s facial surface with a rounded shape unlike flat facial surfaces of incisors [31].

Once completed, diagnostic wax-up is sent to the dentist office (Fig. 3), where with a silicone key it is transferred to the patient’s mouth.

---

## Second Treatment Session

This operation is called mock-up and it is realized during the second appointment. So you get a preview of the final result and also the patient’s consent on the final shape of the teeth (Fig. 4a, b). Without any preparation of the patient’s teeth, the silicon index is filled with composite material used for provisional prosthesis and is applied intraorally. After setting of the provisional prosthetic material, the silicone index is





**Fig. 3** Diagnostic wax-up: final aspect



**Fig. 4** (a) Mock-up dental arches view. (b) Maxillary mock-up view

removed, and both patient and physician can examine the final shape of future veneers. Transferring the diagnostic wax-up into the patient's mouth implies growth of the predictability of final aesthetic result because it offers a preview of it. Any change desired by the patient or dictated by functionality of the stomatognathic system are possible to realize directly on the mock-up through finishing by the dentist. During this second treatment session, both functionality of stomatognathic system and aesthetic facial landmarks related with smile line, inferior lip line and superior lip line are examined, along with the patient comfort and speech with new teeth shape. Once all these conditions are met and the patient agrees to the final aesthetics of future restorations, the third treatment session is scheduled.

---

### Third Treatment Session

The objective of the third patient scheduling is to achieve the preparations needed for future veneers (Fig. 5a, b). The preparation type is selected according to clinical and aesthetic needs of each tooth. In general the dentist will remove 0.5–0.8 mm from the



**Fig. 5** (a) Prepared teeth facial view. (b) Prepared teeth occlusal view

enamel's thickness in order to create space for the full-ceramic veneer and to obtain a good adhesion of the veneer to the tooth after adhesive cementation [32]. Care must be taken not to cut more than 0.5–0.8 mm especially from the proximal and cervical areas where enamel thickness is less, so the preparation should be done exclusively in the enamel as possible. Extending the preparation into dentine leads to a decrease of adhesion of the veneer to the tooth in the area, although dentine adhesives have experienced a significant evolution in the last period of time [33].

After completing the preparation, in the same treatment session, the dentist will make an impression of the preparations, followed by manufacture of composite or acrylic temporary veneers. The easiest method to make temporary veneers is direct technique of copying and transfer the wax-up to the prepared teeth, as in the case of mock-up. For a superior aesthetic result of provisional restorations, prefabricated polycarbonate veneers can be used along with composite or acrylic provisional material [34].

---

## Fourth Treatment Session

Next, the dental technician is the one who manufactures the full-ceramic veneers, in the laboratory. They will arrive in the dental office and so the fourth treatment session begins. This is the last session, when the adhesive cementation of all-ceramic veneers is realized. To obtain a predictable and sustainable result over time, special attention must be paid to the cementation session, because it involves both processing dental surface and the internal surface of the veneer in order to obtain an adhesive bond between ceramic and dental tissue.

Adhesive cementation is responsible for the success or failure of the entire treatment, and thus the latter is more important in clinical stage. Depending on the number of veneers to be cemented, the best would be to start out cementation from the midline to distal, preferably the two central incisors should be simultaneously cemented.

Once the veneers arrive in the dental office, they should be checked in the mouth. For this maneuver, glycerine gel can be used in order to maintain the veneers on the tooth. Some manufacturers of adhesive cements provide a glycerin gel, color coded as the final cement, which gives you a preview of the final cementation (e.g., Variolink Veneer – Ivoclar Vivadent). The final color of ceramic restorations is influenced by underlying dental tissue color and by default of the cement's color, as ceramic materials are translucent. Thus, this glycerine test gel (try-in gel) becomes mandatory to use before cementation when you wish to obtain a maximum aesthetics of the final result. Their application on the dental tissue surface before adhesive cementation brings no harm to the final veneer adhesion if their removal protocol is followed, namely, water wash and drying the tooth because the gels are water soluble [35]. Test phase should include phonetic and functional tests and patient's views on the aesthetic outcome of the result.

After the try-in phase has ended and glycerin gel was cleaned, cementation of veneers is realized. It starts with conditioning the internal surface of the ceramic veneer using hydrofluoric acid. Time and concentration of hydrofluoric acid vary depending on the type of ceramic used (e.g., hydrofluoric acid used for IPS e.max Press ceramic has a concentration of 4.9 % and the recommended action time is 20 s). Hydrofluoric acid is known to selectively dissolve the crystals and the glass component causing an uneven and porous surface. The microporosity of the ceramic surface increases the adhesion area and offers a micromechanic adhesion to the resin component of the adhesive cement system. Density of leucite crystals found on the surface influences the formation of microporosity in the etching stage with hydrofluoric acid. Leucite crystals are better dissolved unlike the glass component, in hydrofluoric acid. Microporosity formed after acid application increases the adhesion surface and thus increases the success rate of the adhesive bond [36].

After etching the internal surface of the ceramic veneer, a hydrofluoric acid neutralizing agent can be used, which will be removed from the veneer together with the acid by washing in running water or in an ultrasonic bath using a mixture of alcohol and water. Ultrasonic cleaning is the most effective method of removing debris, resulting in the internal surface of veneer after etching [37]. After etching the ceramic material will be silanized. The silanization process has the ability to decrease the superficial tension of the internal surface of the veneer. Silane is a coupling agent that links inorganic particles on the surface of ceramic and organic matrix from the adhesive cementation system. After the silanization agent was applied, wait one minute while evaporating ethanol/alcohol used as a solvent in silane agent, and optionally one can apply a bonding – Heliobond (Ivoclar Vivadent). This adhesive protocol is completed for the ceramic restoration.

Adhesive protocol for dental surfaces begins with their wash. For this stage, use solution containing chlorhexidine and/or benzene, followed by washing under

running water and drying to remove debris from the surface of the tooth. Full adhesive protocol for dental surfaces runs under isolation. Isolation can be done with a rubber dam or special devices (OpraGate) whose purpose is to prevent the saliva to reach the tooth surface. Once isolation is done by these methods, soft parts such as lips and cheeks are automatically removed, facilitating intraoral handling of the veneer. If a good control of gingival crevice fluid is desired, we can use gingival displacement cord placed before the application of the rubber dam, positioned carefully in order to avoid the gingival sulcus bleeding.

Before cementing veneers, interdental celluloid strip are positioned between teeth, for a better control over the excess of the adhesive system and cement that can suppress the neighboring teeth. The next stage is the demineralization. Orthophosphoric acid of 37.5 % is applied for 40 s onto the enamel and 5–15 s onto dentin. Remove with a water jet and air followed by air drying, avoiding desiccating dental tissue. After etching adhesive system of the cement is applied, used according to the manufacturer. Often it is the successive application of a primer and bonding with dual cure. In the gingival third of the tooth surface, there is a risk that the preparation would penetrate the dentin. In this case it is recommended to apply a sealer to the exposed dentin area, which protects the dentin area and decrease sensitivity after cementation. According to the literature, areas of exposed dentin onto preparations surface cause a decrease in adhesive bond strength between ceramic and dental tissues, which leads to a decrease in the success rate of veneers in such cases [38].

Silane agent is applied, both the tooth surface and the internal surface of the veneer, using an applicator or brush for adhesives, and the excess is removed with the airflow. Next apply cement on both the tooth surface and the veneer, taking care not to form bubbles in the cement mass. Then position the veneer onto preparation and insert it with moderate pressure so as to avoid accidents like fracture. The most important factor in this situation is the cement viscosity: as the viscosity is lower (cement is fluid), the lower the risk of fracture. After the veneer is positioned on the tooth, it is light cured for 5 s, and then the excess cement is removed. Final light curing is about 20 s from each side of the tooth; thus the veneer is finally fixed on the tooth (Fig. 6a–c).

If there is excess cement after light curing especially in the gingival area, it can be removed with: dental floss, hand instruments, or ultrasonic instruments.

Following the steps described above, in just four sessions at the dentist, a high aesthetic result of teeth can be achieved, with high predictability. After final cementation the patient is enrolled in a program of dispensarization, with regular checkups.

With the advent of newer conservative treatments such as vital and unvital teeth whitening, with orthodontic treatments that provide a high degree of dental aesthetic during treatment (In Visa Line), indication for veneering could be reduced. Porcelain veneers are still commonly used as a way to make cosmetic changes for teeth that are discolored, worn out, or fractured or to align teeth. With the advent of new ceramic materials and developing adhesive techniques, porcelain veneers are considered to be a reliable option, with high aesthetics and a good long-term prognosis.

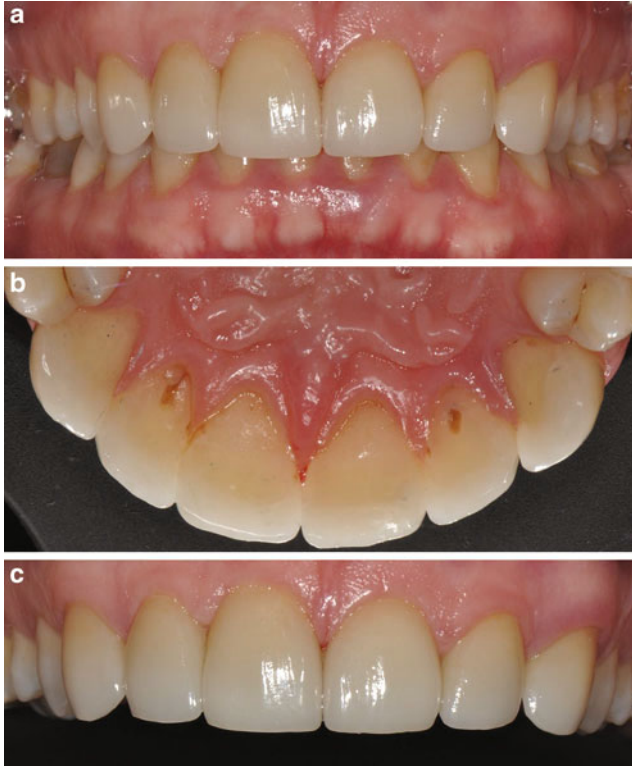


**Fig. 6** (a) Intraoral view of the full-ceramic veneers. (b) Full-ceramic veneers occlusal view. (c) Final view of the veneered teeth

---

## Summary

With the development of dental materials, treatment options are wide: in addition to aesthetic fillings or direct composite resin veneers, now are available full-ceramic crowns, ceramic veneers, and ceramic inlays.

The commonly used material for aesthetic restorations is dental ceramics, due to its color stability, biocompatibility, mechanical properties, and excellent aesthetic results. There are three types of ceramics used for manufacturing these veneers: feldspathic ceramic, leucite reinforced ceramic, and glass ceramic reinforced with lithium disilicate. These materials have particular aesthetic properties, mimicking natural tooth look, but their mechanical properties are different. Because full-ceramic veneers have very low thickness, mechanical strength of the material is important for their handling during manufacturing or cementation process and especially for preserving the integrity of the restoration.

Teeth preparation techniques for ceramic veneers varies, depending on the aesthetic needs of the patient, type of veneers to be made, and their indications or

contraindications. The operative protocol includes four treatment sessions at the end of which the patient has the veneers cemented over his teeth. There are many advantages for veneering natural teeth and disadvantages are low compared to their benefits.

---

## References

1. Al-Hababbeh R, Al-Shammout R, Al-Jabrah O, Al-Omari F (2009) The effect of gender on tooth and gingival display in the anterior region at rest and during smiling. *Eur J Esthet Dent* 4 (4):382–395
2. Kebschull M, Demmer RT, Grün B, Guarnieri P, Pavlidis P, Papananou PN (2014) Gingival tissue transcriptomes identify distinct periodontitis phenotypes. *J Dent Res* 93(5):459–468
3. Chu SJ, Tan JH, Stappert CF, Tarnow DP (2009) Gingival zenith positions and levels of the maxillary anterior dentition. *J Esthet Restor Dent* 21(2):113–120
4. Rosenstiel SF, Ward DH, Rashid RG (2000) Dentists' preferences of anterior tooth proportion – a web-based study. *J Prosthodont* 9(3):123–136
5. Mayekar SM (2001) Shades of a color. Illusion or reality? *Dent Clin N Am* 45(1):155–172
6. Levin EI (1978) Dental esthetics and the golden proportion. *J Prosthet Dent* 40(3):244–252
7. Pincus CL (1937) “Building mouth personality” A paper presented at: California State Dental Association. San Jose, California
8. Simonsen RJ, Calamia JR (1983) Tensile bond strengths of etched porcelain. *J Dent Res* 62: Abstract #1099
9. Calamia JR (1983) Etched porcelain facial veneers: a new treatment modality based on scientific and clinical evidence. *N Y J Dent* 53(6):255–259
10. Horn HR (1983) A new lamination, porcelain bonded to enamel. *N Y State Dent J* 49 (6):401–403
11. Gresnigt MM, Kalk W, Ozcan M (2012) Randomized controlled split-mouth clinical trial of direct laminate veneers with two micro-hybrid resin composites. *J Dent* 40(9):766–775. doi:10.1016/j.jdent.2012.05.010, Epub 2012 Jun 2
12. Kreulen CM, Creugers NH, Meijering AC (1998) Meta-analysis of anterior veneer restorations in clinical studies. *J Dent* 26(4):345–353
13. Gresnigt MM, Kalk W, Ozcan M (2013) Randomized clinical trial of indirect resin composite and ceramic veneers: up to 3-year follow-up. *J Adhes Dent* 15(2):181–190. doi:10.3290/j.jad.a28883
14. Reis A, Loguercio AD, Manso AP, Grande RH, Schiltz-Taing M, Suh B, Chen L, Carvalho RM (2013) Microtensile bond strengths for six 2-step and two 1-step self-etch adhesive systems to enamel and dentin. *Am J Dent* 26(1):44–50
15. Gomes G, Perdigão J (2014) Prefabricated composite resin veneers – a clinical review. *J Esthet Restor Dent*. doi:10.1111/jerd.12114
16. Layton DM, Clarke M, Walton TR (2012) A systematic review and meta-analysis of the survival of feldspathic porcelain veneers over 5 and 10 years. *Int J Prosthodont* 25(6):590–603
17. Ng J, Ruse D, Wyatt C (2014) A comparison of the marginal fit of crowns fabricated with digital and conventional methods. *J Prosthet Dent*. doi:10.1016/2013.12.002, pii: S0022-3913(14) 00035-3
18. Wittneben JG, Wright RF, Weber HP, Gallucci GO (2009) A systematic review of the clinical performance of CAD/CAM single-tooth restorations. *Int J Prosthodont* 22(5):466–471
19. Jankar AS, Kale Y, Kangane S, Ambekar A, Sinha M, Chaware S (2014) Comparative evaluation of fracture resistance of Ceramic Veneer with three different incisal design preparations – an in-vitro study. *J Int Oral Health* 6(1):48–54, Epub 2014 Feb 26
20. Galip Gürel DDS (2008) Predictable and precise tooth preparation techniques for PLVs in complex cases. *Aust Dent Pract* 19:140–150

21. Esquivel-Upshaw JF, Rose WF Jr, Barrett AA, Oliveira ER, Yang MC, Clark AE, Anusavice KJ (2012) Three years in vivo wear: core-ceramic, veneers, and enamel antagonists. *Dent Mater* 28 (6):615–621. doi:10.1016/j.dental.2012.02.001, Epub 2012 Mar 10
22. Stappert CF, Att W, Gerds T, Strub JR (2006) Fracture resistance of different partial-coverage ceramic molar restorations: an in vitro investigation. *J Am Dent Assoc* 137:514–522
23. Layton DM, Walton TR (2012) The up to 21-year clinical outcome and survival of feldspathic porcelain veneers: accounting for clustering. *Int J Prosthodont* 25(6):604–612
24. Watt E, Conway DI (2013) Review suggests high survival rates for veneers at five and ten years. *Evid Based Dent* 14(1):15–16. doi:10.1038/sj.ebd.6400914
25. Hekland H, Riise T, Berg E (2003) Remakes of Colorlogic and IPS Empress ceramic restorations in general practice. *Int J Prosthodont* 16(6):621–625
26. Beier US, Kapferer I, Burtscher D, Dumfahrt H (2012) Clinical performance of porcelain laminate veneers for up to 20 years. *Int J Prosthodont* 25(1):79–85
27. Fradeani M (1998) Six-year follow-up with Empress veneers. *Int J Periodontics Restorative Dent* 18(3):216–225
28. Fradeani M, Redemagni M, Corrado M (2005) Porcelain laminate veneers: 6- to 12-year clinical evaluation – a retrospective study. *Int J Periodontics Restorative Dent* 25(1):9–17
29. Fabbri G, Zarone F, Dellificorelli G, Cannistraro G, De Lorenzi M, Mosca A, Sorrentino R (2014) Clinical evaluation of 860 anterior and posterior lithium disilicate restorations: retrospective study with a mean follow-up of 3 years and a maximum observational period of 6 years. *Int J Periodontics Restorative Dent* 34(2):165–177. doi:10.11607/prd.1769
30. Simon H, Magne P (2008) Clinically based diagnostic wax-up for optimal esthetics: the diagnostic mock-up. *J Calif Dent Assoc* 36(5):355–362
31. Geissberger M (ed) (2010) *Esthetic dentistry in clinical practice*. Blackwell Publishing, Ames, pp 61–66
32. Van Meerbeek B, Perdigão J, Lambrechts P, Vanherle G (1998) The clinical performance of adhesives. *J Dent* 26(1):1–20
33. Tirlot G, Crescenzo H, Crescenzo D, Bazos P (2014) Ceramic adhesive restorations and biomimetic dentistry: tissue preservation and adhesion. *Int J Esthet Dent* 9(3):354–369
34. Bidra AS, Manzotti A (2012) A direct technique for fabricating esthetic anterior fixed provisional restorations using polycarbonate veneers. *Compend Contin Educ Dent* 33(6):452–454, 456
35. Prata RA, de Oliveira VP, de Menezes FC, Borges GA, de Andrade OS, Gonçalves LS (2011) Effect of ‘Try-in’ paste removal method on bond strength to lithium disilicate ceramic. *J Dent* 39(12):863–870. doi:10.1016/j.jdent.2011.09.011, Epub 2011 Oct 6
36. Zoghbeib LV, Bona AD, Kimpara ET, McCabe JF (2011) Effect of hydrofluoric acid etching duration on the roughness and flexural strength of a lithium disilicate-based glass ceramic. *Braz Dent J* 22(1):45–50
37. Belli R, Guimarães JC, Filho AM, Vieira LC (2010) Post-etching cleaning and resin/ceramic bonding: microtensile bond strength and EDX analysis. *J Adhes Dent* 12(4):295–303. doi:10.3290/j.jad.a17709
38. Gresnigt M, Ozcan M, Kalk W (2011) Esthetic rehabilitation of worn anterior teeth with thin porcelain laminate veneers. *Eur J Esthet Dent* 6:298–313
39. Walls AWG, Steele JG, Wassell RW (2002) Crowns and other extra-coronal restorations: porcelain laminate veneers. *Br Dent J* 193:73–82. doi:10.1038/sj.bdj.4801489

Cena Dimova, Biljana Evrosimovska, Katerina Zlatanovska,  
and Julija Zarkova

## Contents

Introduction .....	1161
Aim of Alveolar Augmentation .....	1163
Bone Quality and Quantity .....	1164
Bone Quality After Tooth Extraction .....	1165
Techniques to Preserve the Bone After Tooth Extraction .....	1166
Bone Grafts and Donor Location .....	1167
Autogenous Bone Graft (Autografts) .....	1169
Types of Autogenous Bone Graft .....	1169
Allogenic Bone Grafts (Allografts) .....	1170
Xenogenic Bone Grafts (Xenografts) .....	1171
Donor Location (Site) .....	1171
Bone Augmentation Techniques and Material (Horizontal, Vertical) .....	1174
Clinical and Radiological Assessments .....	1174
Bone Augmentation Procedures .....	1176
Bone Substitutes .....	1181
Calcium Phosphates .....	1182
Beta Tricalcium Phosphate ( $\beta$ TCP) .....	1183
Nanosized HAP .....	1183
Synthetic Hydroxyapatite (HA) .....	1184
Coralline Hydroxyapatite .....	1184

---

C. Dimova (✉) • K. Zlatanovska • J. Zarkova  
Faculty of Medical Sciences, Dental Medicine, Macedonia FYR, University “Goce Delcev” – Stip,  
Stip, FYR Macedonia  
e-mail: [cena.dimova@ugd.edu.mk](mailto:cena.dimova@ugd.edu.mk); [cedimova@gmail.com](mailto:cedimova@gmail.com); [katerina.zlatanovska@ugd.edu.mk](mailto:katerina.zlatanovska@ugd.edu.mk);  
[julija.zarkova@ugd.edu.mk](mailto:julija.zarkova@ugd.edu.mk)

B. Evrosimovska  
Faculty of Dentistry, Macedonia, FYR, University “Sts. Cyril and Methody” Skopje, Skopje, FYR  
Macedonia  
e-mail: [bevrosimovska@gmail.com](mailto:bevrosimovska@gmail.com)



Calcium Sulfate .....	1185
Bioactive Glasses .....	1185
Glass Ionomers .....	1186
Combined Synthetic Materials .....	1186
Mechanism of Bone Regeneration After Ridge Augmentation .....	1187
The Terms “Guided Bone Regeneration” (GBR) and “Guided Tissue Regeneration” (GTR) .....	1187
Guided Tissue Regeneration .....	1188
Guided Bone Regeneration .....	1189
Membrane .....	1190
Nonresorbible Membranes .....	1191
Resorbible Membranes .....	1192
Collagen Membranes .....	1193
Sinus Floor Augmentation, Bone Splitting, Distraction Osteogenesis .....	1193
Maxillary Sinus Floor Elevation – Lateral Window Technique .....	1194
Transalveolar Sinus Floor Elevation .....	1194
Bone Splitting/Expansion and Immediate Implant Placement and Split-Ridge Techniques with Interpositional Bone Grafts and Delayed Implant Placement .....	1195
Distraction Osteogenesis .....	1195
Summary .....	1196
References .....	1197

## Abstract

Bone retention, bone augmentation, and bone regeneration are central topics in oral surgery, implantology, and periodontology. Bones and teeth are the only structure within the body where calcium and phosphate participate as functional pillars. Despite their mineral nature, both organs are vital and dynamic. The major sequel from human tooth loss is the loss of alveolar bone. After tooth extraction, the residual alveolar ridge generally provides limited bone volume because of ongoing, progressive bone resorption. The process of healing on bone defect in the region of alveolar ridge passes through several stages from the coagulum formation to the mature lamellar bone. The healing process within postextraction sites reduces the dimension of the socket over time.

Bone grafts and bone graft substitutes support regeneration in bone defects and can be used for bone augmentation. Bone graft substitutes are classified by their origin as autogenous bone grafts, bone graft substitutes (allogenic from human origin and xenogenic materials from animal origin), and synthetic (alloplastic) bone graft substitutes, manufactured from mineral raw materials, whose composition is precisely defined and whose availability is unlimited. Alveolar ridge augmentations are classified according to their morphology and severity. Bone augmentation techniques can be used for the application of socket defect grafting, horizontal ridge augmentation, vertical ridge augmentation, and sinus augmentation.

Ridge augmentation methods are therefore very important developments and have so far been promising especially in view of the fact that life is increasingly prolonged especially in economically well-developed countries and the incidence of the disease is expected to further increase in the future.

**Keywords**

Tooth extraction • Socket • Augmentation • Alveolar ridge • Bone regeneration • Grafting • Bone grafting techniques • Bone graft substitutes • Ridge preservation • Autogenous • Alloplastic • Horizontal ridge augmentation • Vertical ridge augmentation • Guided bone regeneration • Guided tissue regeneration

**Introduction**

Immediately after tooth extraction the bony walls of the alveolus present significant resorption, the central part of the socket is partly filled up with woven bone, and the extraction site becomes markedly reduced in size. Edentulous site diminishes in all dimensions, i.e., buccal-lingual, buccopalatal, and apical-coronal. At the same time, the soft tissues in the extraction site undergo adaptive changes that clinically may appear as deformations of the jaw. In health, the different structures of the alveolar process, the cortical and cancellous bone, are constantly undergoing remodeling in response to functional forces acting on the teeth. Once when teeth are lost, the attachment apparatus is destroyed, and the alveolar process, mainly the alveolar ridge, undergoes significant structural changes; these are referred to as *disuse atrophy* [1].

Alveolar ridge atrophy after loss of teeth occurs secondary to advancing age, to deterioration of general health, to systemic or metabolic diseases, and due to occlusion defects or to denture pressure. The condition causes serious problems for both the dentists and the patients. The toothless mandibular resorption or the high muscular attachments caused by senile atrophy produce unsuitable conditions for total denture.

Resorption of the edentulous or partially edentulous alveolar ridge or bone loss due to periodontitis or trauma frequently compromises dental implant placement in a prosthetically ideal position. Therefore, augmentation of an insufficient bone volume is often indicated prior to or in conjunction with implant placement to attain predictable long-term functioning and an aesthetic treatment outcome [2].

The basic knowledge of alveolar augmentation included the use of bone grafting material with respect to the principles of biological mechanism. To optimize therapeutic approaches to bone augmentation and regeneration principles of osteogenesis, osteoconduction, osteoinduction, osteointegration, osteoperception, and osteopromotion can be used [3].

*Osteogenesis* – this term means that primitive, undifferentiated, and pluripotent cells are somehow stimulated to develop into the bone-forming cell lineage. One proposed definition is the process by which osteogenesis is induced. Osteogenesis has been described as the direct transfer of vital cells to the area that will regenerate new bone.

*Osteoconduction* – includes the principle of providing the space and a substratum for the cellular and biochemical events progressing to bone formation. The term means that bone grows on a surface. An osteoconductive surface is one that permits bone growth on its surface or down into pores, channels, or pipes. Osteoconduction

is a process by which bone is directed to conform to a material's surface. The space maintenance requirement for many of the intraoral bone augmentation procedures allows the correct cells to populate the regenerated zone.

*Osteoinduction* – embodies the principle of converting primitive, undifferentiated, and pluripotential mesenchymal-derived cells along an osteoblast pathway with the subsequent formation of bone. This term means that pluripotent cells are somehow stimulated to develop into the bone-forming cell lineage. This concept was established in 1965, with heterotopic ossicle formation induced by the glycoprotein family of morphogenesis known as the bone morphogenetic proteins (BMPs). A bone graft material that is osteoconductive and osteoinductive will not only serve as a scaffold for currently existing osteoblasts but also can trigger the formation of new osteoblasts, theoretically promoting faster integration of the graft. The most widely studied type of osteoinductive cell mediators are bone morphogenetic proteins (BMPs) [4].

*Osteoperception* – is the term used to describe the ability by patients with osseointegrated fixtures to identify tactile thresholds transmitted through their prostheses. It is a phenomenon of importance in both dental and orthopedic applications of osseointegration. The identification of osteoperception as a phenomenon of osseointegration was the result of work carried out in the dental sciences by Torgny Haraldson.

*Osteopromotion* – involves the enhancement of osteoinduction without the possession of osteoinductive properties. For example, enamel matrix derivative has been shown to enhance the osteoinductive effect of demineralized freeze dried bone allograft (DFDBA) but will not stimulate from the new bone growth alone [5].

*Osseointegration* – Brånemark [6] introduced the term “osseo integration” to describe this modality for stable fixation of titanium to bone tissue. Osseointegration was originally defined as a direct structural and functional connection between ordered living bone and the surface of a load-carrying implant. It is now said that an implant is regarded as osseointegrated when there is no progressive relative movement between the implant and the bone with which it has direct contact. In practice, this means that in osseointegration there is an anchorage mechanism where no vital components can be reliably and predictably incorporated into living bone and that this anchorage can persist under all normal conditions of loading.

Osseointegration provides an attachment mechanism for incorporation into living bone of nonvital components made of titanium. As a biological phenomenon it has been amply demonstrated and clinically tested, and it is now widely accepted. The present range of clinical applications is

- In the field of oral surgery worldwide, more than 800,000 patients have been treated since 1965 until now with osseointegration dental reconstructions, according to Brånemark. The results indicate superiority over conventional prosthodontics, with respect to long-term success rates.
- Facial prosthesis (extraoral applications of osseointegration include anchorage for craniofacial prostheses including ear, eye, and nose) finger prosthesis, etc.

## Aim of Alveolar Augmentation

Atrophy of the alveolar ridge may cause aesthetic and surgical problems in prosthetic dentistry, especially when implant treatment is planned. After the loss of teeth atrophy of the alveolar processes occurs in a vertical as well as a horizontal plane. The term *atrophy* is defined in the dictionary as "a wasting away; a diminution in the size of a cell, tissue, organ, or part" [7]. This process is starting and continuous throughout life because of the lack of stimuli seen on alveolar process of the jaws. The importance of teeth for jaw bone health is extensively exploited in the contemporary scientific literature. When one or more teeth are missing, it can lead to jawbone loss at the site of the gap. This loss of jawbone can develop into additional problems, both with the patient's appearance and overall health. Natural teeth are embedded in the jawbone and stimulate the jawbone through activities such as chewing and biting.

Immediate alveolar ridge prophyllaxis after tooth extraction includes

- Preservation of the alveolar process by retention of endodontically treated roots (physiologically most accepted)
- Immediate implant placement
- Guided bone regeneration
- The use of root analogues [8]

Etiopathogenesis of atrophy of alveolar ridge is teeth loss followed by loss of supporting alveolar bone which leads to alveolar defects, usually starts along the labial surface of the alveolar crest which results with loss of alveolar width, 40–60 % of bone loss within first 36 months with decrease to 0.25–0.5 % annually after 3 years, pneumatization of sinus, as well as periodontal disease associated with increased postextraction bone loss.

When teeth are missing, the alveolar bone, or the portion of the jawbone that anchors the teeth in the mouth, no longer receives the necessary stimulation and begins to break down, or resorb. The body no longer uses or "needs" the jawbone, so it deteriorates.

Without intervention (natural healing), the results of all nine studies showed a significant loss of ridge width (–2.6 to –4.6 mm), and the results of five studies showed a statistically significant loss of bony ridge height (–0.55 to –3.3 mm).

The aims of alveolar ridge augmentation are to

1. Restore the function of the jaw in anterior, posterior, vertical, and lateral dimensions
2. Increase the bone tissue in cases where the lower jaw has been atrophied
3. Create an optimal support for dentures and better distribution of the jaw's functional forces
4. Fulfill the biomechanical requirement of the prosthesis
5. Restore the intermaxillary ridge relationship
6. Rehabilitate the dentures for efficient functioning and to produce better facial aesthetics

7. Ensure good aesthetic results
8. Re-establish adequate amount of bone volume for implant placement
9. Provide biological acceptance of implants or transplants
10. Obtain healthy bone to ensure osseointegration and survival of the implant

There seems to be no uniformity of opinion about which of the available methods provide the best anatomical and functional results. Among the produces proposed to restore the alveolar ridge, bone grafts were the first to be popularized. Kruger who favored this method recommended iliac grafts. Although costal grafts can perhaps better be adjusted to the mandibular arch, there can occur 50 % loss due to contraction. These results are akin to those of Steinhouser and Obwegeser who concluded that significant amount of atrophy and defects are observed of the mandibular or on the maxilla after bone grafting. Other studies have reported satisfactory results in general for treatment of atrophic ridge using hydroxyapatite with lesser percentage of neural injuries. Postoperative ridge resorption is observed only in 4–10 % of cases, a figure which compares favorably with other procedures aiming to correct alveolar ridge atrophy.

---

## Bone Quality and Quantity

Dental implants have become the most popular and reliable treatment option for restoring missing teeth. Since early times of implantation era preoperative studies include incision of gingiva in order to get a view of the bone surface. Preoperative studies are required because a jawbone must offer *proper quality and adequate quantity of the bone*. The overall dental implant success rate is considered to be influenced by both the volume (quantity) and density (quality) of available bone for implant placement (a great extent on the volume and quality of the surrounding bone). Therefore, it is important to measure the alveolar process precisely so that the proper system may be chosen. There are number of classifications suggested for assessment of the degree of atrophy of partially or fully edentulous jaws.

Lekholm and Zarb [9] classify quality of residual alveolar bones into four types:

- Type 1 = large homogenous cortical bone
- Type 2 = thick cortical layer surrounding a dense medullar bone
- Type 3 = thin cortical layer surrounding a dense medullar bone
- Type 4 = thin cortical layer surrounding a sparse medullar bone

Classification of quality of residual alveolar bones indicates a good correlation with bone mineral content. The system for bone quality assessment with three classes, dense, normal, and soft bone, is proposed. Bone quality is classified into four groups according to the proportion and structure of compact and trabecular bone tissue: groups 1–4 or type I to IV (Fig. 1 Bone Quality Index-BQI) [10].

Also, it is important to know the bone quantity and quality of the jaws when planning implant treatment. Bone quantity of jawbone is classified into five groups

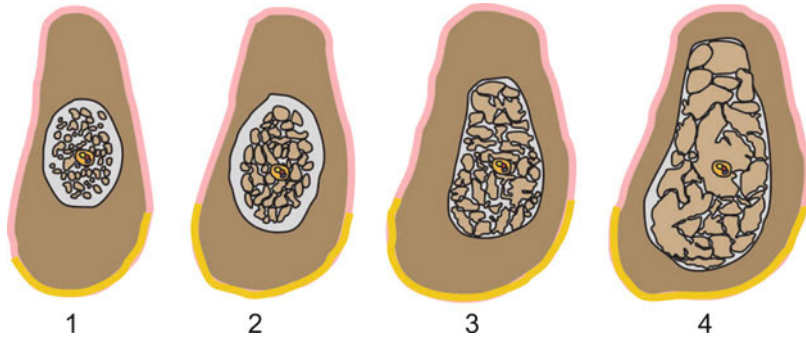


**Fig. 1** Bone quality index. 1- Type I: homogeneous cortical bone; 2. Type II: thick cortical bone with marrow cavity; 3. Type III: thin cortical bone with dense trabecular bone of good strength; 4. Type IV: very thin cortical bone with low-density trabecular bone of poor strength

(from minimal to severe, A–E), based on residual jaw shape and different rates of bone resorption following tooth extraction.

During all stages of atrophy of the alveolar ridge, characteristic shapes result from the resorptive process. It is difficult to obtain implant anchorage in bone that is not very dense. Sufficient bone density and volume are therefore crucial factors for ensuring implant success [9, 10].

However, this classification, like many others, described changes only of jaw shapes in general and failed to indicate precise measurements. Alveolar ridge deformities are classified according to their morphology and severity. This classification has been done to standardize communication among clinicians in the selection of reconstructive procedures designed to eliminate these defects.

- A class I defect has buccal-lingual loss of tissue with normal ridge height in an apicocoronal direction.
- A class II defect has apical-coronal loss of tissue with normal ridge width in a buccal-lingual direction.
- A class III defect has a combination of buccal-lingual and apical-coronal loss of tissue resulting in loss of height and width.

Critical-sized alveolar ridge defects in the horizontal and vertical dimensions may occur following tooth loss, fractures, or different pathological processes. Such defects may compromise the ideal implant placement as prescribed prosthetically with an unfavorable outcome.

## Bone Quality After Tooth Extraction

Since the beginning of the twentieth century, the concept of osteoconduction in bony changes in the oral cavity showed a wide range of biomaterials and their osteoinductive potential that emerged gradually and has to a large extent improved

the quality of the bone prior to the placement of an implant. Alveolar bone loss is a major concern after tooth extraction in patients, and therefore atraumatic extraction procedures should be followed to avoid further bone loss. To overcome the alveolar bone loss and to augment support for placing dental implants, many bone regenerative substitutes are available such as allografts, autografts, xenografts, synthetic biomaterials, and osteoactive agents [11].

Tooth extraction is one of the most widely performed procedures in dentistry today, and it has been historically well documented that this procedure may induce significant dimensional changes of the alveolar ridge. The dilemma that clinicians face is how to manage tooth extractions to provide for the future placement of a dental implant or to maximize ridge dimensions for the fabrication of a fixed or removable prosthesis. If performed inadequately, the resulting deformity can be a considerable obstacle to the aesthetic, phonetic, and functional results that both our patients and we clinicians expect at this current time [12].

Severe resorption of the maxillary alveolar crest presents a more demanding situation for the restorative team. Thus, it would be valuable to assess outcomes for this immediate loading treatment protocol in subjects with marked maxillary alveolar crest atrophy. Immediate loading of implants in the edentulous maxilla has previously been successfully performed and reported [13].

While the ability of various grafting materials to preserve extraction socket morphology has been adequately reviewed, the quality of the grafted bone in the socket is not as well understood. Based on a limited number of prospective comparative studies, the use of grafting materials for socket augmentation might change the proportion of vital bone in comparison to sockets allowed to heal without grafting. Whether these changes in bone quality will influence implant success and peri-implant tissue stability remains unknown.

In light of the steady progress in bone grafting techniques and graft materials, it has become possible to improve the volume, width, and height of bone in deficient areas of the oral cavity. These advances in regenerative dentistry thus facilitate an easy and convenient placement of an implant in an ideal position and angulations resulting in superior aesthetics and function. Bone grafting materials and their substitutes are the alternative filler materials, which facilitate to reduce additional surgical procedures, risks, or chances of cross-infection involved in placing autografts and allografts into the bony structures. This review literature highlights various biomaterials that are helpful in bone healing and thus creates an anatomically favorable base for ideal implant placement [11].

## **Techniques to Preserve the Bone After Tooth Extraction**

Several techniques can be used to preserve the bone and minimize bone loss after the tooth extraction. Immediate alveolar ridge prophylaxis after tooth extraction includes preservation of the alveolar process by

- Retention of endodontically treated roots (physiologically most accepted)
- Guided bone regeneration

- Immediate implant placement
- Use of root analogues

In one common method, the tooth is removed and the socket filled with bone or bone substitute. It is then covered with gum, artificial membrane, or tissue stimulating proteins to encourage the body's natural ability to repair the socket. With this method, the socket heals eliminating shrinkage and collapse of surrounding gum and facial tissues. The newly formed bone in the socket also provides a foundation for an implant to replace the tooth using autografts, allografts, xenografts, guided bone regeneration (GBR), and growth factors which are used with varying degrees of success in an effort to maintain the anatomical dimensions of the alveolus before implantation. There is suggestion for strategy of immediate implant placement into an extraction socket and simultaneous GBR. Guided bone regeneration techniques and the use of bone replacement materials have been shown to enhance socket healing and potentially modify the resorption process.

Also, there are various recommendations regarding timing of implant placement after tooth extraction. The implant can be placed immediately following the extraction during the same surgical procedure (immediate implant placement), following a delay of 2–6 weeks (late implant placement), or following a delay of 3–6 months (delayed implant placement). Today, the combination of anatomically oriented implant designs, new biomaterials such as zirconia ceramics, and surface technologies has resulted in dental implants that are specially designed to replace each individual tooth.

The use of root analogues as preimplant therapy can provide adequate quantity of bone and soft tissue for implant placement. Many authors showed that different bone substitute materials had been used as root analogues, some of them being dense hydroxyapatite, polyglycolic acid, polylactic acid, bioabsorbable polylactic polyglycolic acid (PLGA), deproteinized bovine bone mineral integrated in a 10 % collagen matrix,  $\beta$ -tricalcium phosphate ( $\beta$ -TCP) combined with type I collagen and  $\beta$ -TCP/PLGA [14], and  $\beta$ -TCP coated with PLGA root analogue [8].

The development of new medical technologies enables use of achievements in material science, biochemistry, molecular biology, and genetic engineering while creating new combined synthetic materials for bone grafting (osteoplasty). Modification of their bulk structure, which brings their structure closer to natural bone tissue, including cytokine growth factors and morphogens into their composition, enables to provide synthetic materials with not only osteoconductive but also osteoinductive properties. This also enables control of the speed of biodegradation, bringing it closer to the kinetics of osteogenesis.

---

## Bone Grafts and Donor Location

Grafting refers to a surgical procedure when transplanting a tissue from one site to another on the body, or from another person, without bringing its own vascularization with it. Instead, a new blood supply grows in after it is placed. A graft also can



be an artificially manufactured substance that has similar chemical composition with the tissue that replaces it.

The main indications for *bone grafting* are

- Socket preservation
- Ridge augmentation
- Defects following cyst removal/apicoectomies and periodontal defects
- Sinus lifts
- Distraction osteogenesis
- Implants placing

Bone grafting can be used for a localized or more generalized alveolar ridge augmentation like correction of intermaxillary relationships. This procedure is done by adding the patient's own bone from a secondary location, or utilizing an organic or inorganic material like a bone substituent from another patient, species or artificially made.

According to their origin there are four different types of bone grafts:

- Autografts
- Allografts
- Xenografts
- Alloplasts – synthetic bone substitutes

Bone grafts in general can be made like bone blocks or particulates, in order to be able to adapt it better to a defect, and can be applied with inlay technique. Ideal bone graft material should have all properties like osseointegration, osteoconduction, osteoinduction, and osteogenesis.

Osseointegration is the ability to chemically bond to the bone surface without scar; Osteoconduction means which provides matrix for bone growth, and support growth of bone over its surface.

Osteoinduction is the characteristic when the graft can induce differentiations of pluripotential stem cells from surrounding tissue to an osteoblastic phenotype.

Osteogenesis means directly producing new bone by osteoblastic cells present within the graft material.

The ideal characteristics of a bone graft material have been described by Hammerle 1999 [15] as follows:

1. Sterile
2. Nontoxic
3. Nonimmunogenic
4. Osteoconductive or osteoinductive
5. Favorable clinical handling
6. Resorption and replacement by host bone
7. Synthetic

8. Available in sufficient quantities
9. Low in cost.

### **Autogenous Bone Graft (Autografts)**

Many clinicians as a first choice for alveolar augmentation use autogenous bone graft. It is considered as a “gold standard” by which all other graft materials are judged because of its osteogenic, osteoconductive, and osteoinductive properties [15]. According to the potency of their best features various types of autografts exist like cancellous, vascularized cortical, free vascular transfers (nonvascularized cortical), cortical-cancellous bone grafts, and bone marrow aspirates. The advantages that make this graft great are avoided rejection reactions and the possibility of antigenicity. But there are also some disadvantages like low patient acceptance of autogenous bone harvesting given the potential morbidity associated with such techniques, chronic postoperative pain, hypersensitivity, infection, etc. There are also other limitations as to how much bone tissue can be harvested, and harvesting requires an additional surgery at the donor site.

For this kind of grafts bone development is occurring in two phases. The first one lasts almost 4 weeks. During this phase the living cells from the graft contribute to bone formation, and during the second, host cells are taking the main role. The endosteal lining cells and marrow stromal produce more than half of the new bone, whereas osteocytes make a small (10 %) contribution. Free hematopoietic cells of the marrow make a minimal contribution in this process.

### **Types of Autogenous Bone Graft**

*Cancellous bone* is the most commonly used source of autogenous bone graft. Due to the porous trabeculae lined with functional osteoblasts, good space filler can be easily revascularized; in other words it is a very effective osteogenic and osteoconductive material. A small quantity of growth factors in this bone graft can result in high osteoinductive power. Even though the initial support is not so strong, after some time the graft material is rapidly incorporating and ultimately achieves strength equivalent to that of a cortical graft after 6–12 months.

When the implantation is finished there are still life donor osteocytes, and combined with graft porosity and local cytokines they promote angiogenesis and host mesenchymal stem cell recruitment. These recruited mesenchymal stem cells have the potential to differentiate into osteoblasts; thus, the graft may be fully vascularized within 2 days. New bone formation is observed within a few weeks and typically is remodeled by 8 weeks, with complete graft turnover by 1 year. This turnover occurs by the process of creeping substitution, defined as concomitant osteoblast deposition of new osteoid and osteoclast resorption of necrotic donor trabeculae.

*Cortical bone grafts* are less biologically active compared to cancellous bone, less porous, with less cellular matrix, prolonged time to revascularization, but are more compact and can be used to provide better initial structural support when needed. Cortical grafts serve as highly osteoconductive material with minimal osteoinductive and osteogenic properties. The dense cortical matrix results with relatively slow revascularization and incorporation, as resorption must occur before deposition of new bone, and limited perfusion and donor osteocytes make this option poorly osteogenic. Although no vascularized cortical grafts provide immediate structural support, they become weaker than vascularized cortical grafts during the initial 6 weeks after transplantation, as a result of resorption and revascularization.

### **Vascularized Cortical Bone Grafts**

In order to improve graft incorporation and healing, cortical and corticocancellous grafts can be harvested with a vascular pedicle

### **Corticocancellous Bone Graft**

This type of bone grafts offers the advantages of both cortical and cancellous bone: an osteoconductive medium and immediate structural stability from cortical bone and the osteoinductive and osteogenic capabilities of cancellous bone.

### **Bone Marrow**

Bone marrow grafts are highly osteoblastic materials due to stem cells found in bone marrow. Injections of autologous bone marrow provide a graft that is osteogenic and potentially osteoinductive through cytokines and growth factors secreted by the transplanted cells.

### **Allogenic Bone Grafts (Allografts)**

Allogenic bone is a nonvital osseous tissue taken from one individual and is transferred to another individual of the same species. Bone derived from cadavers has been widely used in implant dentistry as well as periodontology. These types of grafts are harvested from donors with good documented medical history, tested for safety from all common infectious diseases.

Usually we use three forms of allogenic bone: fresh frozen, freeze dried bone allograft (FDBA), and demineralized freeze dried bone allograft (DFDBA) [11].

The type of autografts can be used as demineralized bone matrix, morselized and cancellous chips, corticocancellous and cortical grafts, and osteochondral and whole-bone segments.

Demineralized bone matrix acts as an osteoconductive material providing a matrix for new bone formation and growth, and should be resorbed as part of the normal turnover of bone, but some particles appear to remain intact for some time after the graft has been placed and possibly as an osteoinductive material.

The grafts are produced as particulates with a reasonably uniform grain size or as sheets and large blocks. Demineralized bone matrix revascularizes quickly. It also is a

suitable carrier for autologous bone marrow. Demineralized bone matrix is prepared by a standardized process in which allogeneic bone is crushed or pulverized to a consistent particle size (74–420  $\mu\text{m}$ ) followed by demineralization in 0.5 N HCL mEq/g for 3 h.

Current methods of processing demineralized bone matrix follow the same basic steps, but refinements of the technique, many of which have been patented, have been developed by several companies and tissue banks. The biological activity of demineralized bone matrix is presumably attributable to proteins and various growth factors present in the extracellular matrix and made available to the host environment by the demineralization process. Fresh bone allografts are highly antigenic and have limited time to test for immunogenicity or diseases.

### **Xenogenic Bone Grafts (Xenografts)**

These grafts are harvested from animals, usually cows. That is why this is processed to make it sterile and totally biocompatible.

Advantages of xenografts:

- Only one procedure is needed as the bone is not being harvested from the patient.
- Natural bone growth is encouraged.

Disadvantage of xenografts is the minimal risk of bovine spongiform encephalopathy due to the fact that all organic components of the bone are extracted.

The most widely used xenograft bone is deproteinized bovine bone mineral like Bio-Oss (Geistlich Pharma, Wolhusen, Switzerland). Bio-Oss has similar properties to human cancellous bone, in its macrostructure and its crystalline content; it also has similar physical properties to the human bone. This is a purely mineral graft and is osteoconductive but also can go through some resorption, so its use also has limitation. When used in a particulate form it is mixed with the patient's blood and packed into the defect. Some authors [11, 15] have described improved results when combining this with a membrane to protect the blood clot. Bio-Oss Collagen is the latest version of this material combining bone mineral and collagen to produce a block of material that can be carved to shape or used as a particulate graft.

### **Donor Location (Site)**

Autogenous bone grafts have been used for many years for ridge augmentation and are still considered the gold standard for jaw reconstruction. The use of autogenous bone grafts with osseointegrated implants originally was discussed by Brånemark and colleagues, who often used the iliac crest as the donor site. Other external donor sites include calvarium, rib, and tibia. For repair of most localized alveolar defects, however, block bone grafts from the symphysis and ramus buccal shelf offer advantages over iliac crest grafts, including close proximity of donor and recipient sites, convenient surgical access, decreased donor site morbidity, and decreased cost.

There are several donor sites that are available for autogenous bone harvesting. Grafts can be taken from intraoral and extraoral sites, depending of the indications and the volume of defect for augmenting, as well as advantages and disadvantages of the grafts. Therefore the selection of this location requires careful preoperative planning to obtain adequate block size.

**Extraoral harvesting** requires hospitalization of the donor and general anesthesia, two surgery sites, and more cost. On the contrary intraoral harvesting can be performed with local anesthesia, intravenous sedation, or premedication. The most valuable advantages of intraoral harvesting are that local donor sites have convenient access and the bone is very short time ischemic. Also there is no morbidity due to second operation field since the same person is donor and recipient.

**The most utilized location for extraoral harvesting is** the ilium, ribs, calvarium, tibia, and sometimes distal part of radius. Extraoral harvesting of the iliac crest is most often used for major jaw reconstruction. Both marrow and cortical iliac bone autografts are known as the most sure for bone growth of all. Bone can be taken from anterior and posterior iliac crest. Considerable large amounts of bone supply can be provided especially from the posterior iliac crest. Complications associated with the use of fresh iliac bone and marrow included root resorption and ankylosis, in regard to bone grafting around teeth. Later, these complications were minimized by either freezing the bone graft in a storage medium or adding autologous intraoral bone to the harvested iliac crest bone graft mixture.

**Intraoral autogenous bone grafts** have been harvested from various intraoral sites including mandibular symphysis, mandibular ramus and retromolar area, maxillary tuberosity, coronoid process, mandibular and palatal tori, and zygomatic bone. Augmentation of local alveolar defect when implanting can be done using bone harvested from maxillary tuberosity. Main sources of cortical bone suitable for onlay grafting are the mandibular and retromolar ramus. Mandibular symphyseal bone can be used for secondary alveolar cleft bone grafting maxillary sinus and rafting alveolar defects before implants placement.

### **Autogenous Bone Graft Harvested Form: Mandibular Symphysis**

From all intraoral donor sites mandibular symphysis produces biggest amount of graft bone. Maximum average bone block size is approximately  $21 \times 10 \times 7$  mm or 4.7 ml bone. But in clinical study conducted by Misch the approximate volume for the symphysis graft was 1.74 ml. This donor location is indicated when the surgeon needs cortical bone, but if he needs more cancellous bone an alternative donor site is preferred. In some cases bicortical bone blocks can be harvested, but there are some complications afterward. Usually monocortical block bone is harvested and cancellous bone taken with use of curettes for scooping [16]. Access to the mandibular symphysis area can be achieved by one of three different incision designs: (1) sulcular, (2) attached gingiva, or (3) vestibular [17].

**Block bone grafts harvested from the symphysis** can be used for predictable bone augmentation up to 6 mm in horizontal and vertical dimensions. The range of this cortical cancellous graft thickness is 3–11 mm, with most sites providing 5–8 mm. The density of the grafts is D-1 or D-2, and up to a three-tooth edentulous

site can be grafted. In contrast, the ramus buccal shelf provides only cortical bone with a range of 2–4.5 mm (with most sites providing 3–4 mm). This site is used for horizontal or vertical augmentation of 3–4 mm.

Symphysis block graft – indications:

- Horizontal augmentation 4–7 mm (up to three-tooth defect)
- Vertical augmentation 4–6 mm (up to three-tooth defect)

### **Autogenic Bone Graft Harvested Form: Mandibular Retromolar Area and Ramus**

This donor location for autogenic bone graft is relatively easy for producing a cortical bone harvest. The usually used area is the buccal site at the second and third molar area distal to the molar. The average amount of bone that can be taken from site is in volume 0.9 ml and in dimensions  $35 \times 10 \times 4$ . Harvesting of bone from this area requires knowledge of the mandibular canal anatomy to prevent nerve injury. There is less postoperative complication compared to symphysis site, and depending on the amount of harvested bone these complications can become more severe. The deficiency of the block taken from the mandibular ramus harvest site will regrow and may be reharvested at a later date.

### **Autogenic Bone Graft Harvested Form: Maxillary Tuberosity**

This donor site is usually used for producing cancellous bone grafts, and the volume of the graft is very limited. This procedure of harvesting can be done when additional bone is needed for extending the bone volume with other intraoral harvest.

### **Other Intraoral Bone Donor Sites**

Other locations which can be used for bone harvesting are mandibular and palatal tori, zygomatic bone, and bone from coronoid process. If there is a palatal or mandibular torus alveolar augmentation on edentulous ridges can be mainly done with cortical bone harvested with burs or suction traps. Zygomatic bone as donor site is a technique with very mild complications and can be done with local anesthesia. It can be used as donor site for alveolar bone reconstructions, and the amount harvested is 0.5–1.5 ml in volume. A new method for the reconstruction of small anterior maxillary alveolar bone defects was described using donor bone from the zygomatic buttress region.

**One ramus buccal shelf** can provide adequate bone volume for up to a three- and even four-tooth segment. Bone density is D-1 with minimal, if any, marrow available. Some sites require extensive bone graft volume, which necessitates simultaneous bilateral ramus buccal shelf and symphysis graft harvest. For graft volume of more than 6–7 mm thickness, a secondary block graft can be used after appropriate healing of the initial graft.

Ramus buccal shelf block graft – indications:

- Horizontal augmentation 3–4 mm (up to four-tooth defect)
- Vertical augmentation 3–4 mm (up to four-tooth defect)

Despite the many advantages block grafts offer for alveolar ridge augmentation, complications can occur when mandibular block autografts are used for horizontal and vertical augmentation. Morbidity with this grafting protocol is associated with donor and recipient sites. Symphysis donor site morbidity includes intraoperative complications, such as bleeding; mental nerve injury; soft tissue injury of cheeks, lips, and tongue; block graft fracture; infection; and potential bicortical harvest. Pain, swelling, and bruising occur as normal postoperative sequel and are not excessive in nature.

Complications associated with the recipient site include trismus, bleeding, pain, swelling, infection, neurosensory deficits, bone resorption, dehiscence, and graft failure. Trismus is expected if the recipient site is the posterior mandible, which affects the muscles of mastication.

---

## **Bone Augmentation Techniques and Material (Horizontal, Vertical)**

Dentistry has entered an era in which patients no longer need to accept an edentulous or partially edentulous condition or any other situation when their chance for dental implants can be dismissed because of insufficient alveolar bone volume, height, or width. A significant dimensional change in the alveolar bone appears as a result of tooth extraction, fractures, or pathological processes. These events eventually conduct to reduction in ridge height and width, with notable changes in both bone crests, whereupon buccal crest resorbs more quickly than the lingual one.

This loss of alveolar bone volume has negative effect of the final result to restore the lost dentition. The consequences of lost bone height and ridge width can make it difficult to get an ideal placement of an implant and can result in compromised aesthetics of the prosthetic restoration.

Therefore, augmentation of an insufficient bone volume is often indicated prior to or in combination with implant placement to achieve predictable long-term functioning and an aesthetic treatment outcome [2].

## **Clinical and Radiological Assessments**

Jaw dental segment (JDS) is defined as a vertically cut jaw segment with tooth, alveolar bone, and all or part of the basal bone. The location of bone suitable for implantation is identical with the former location of a tooth in the jaw. The number of the JDS describing the position of a planned implant in the jaw can be shown. If the JDS is edentulous, the term *edentulous jaw dental segment (eJDS)* is used (Fig. 2).

To obtain clinical and radiological assessments of the eJDS, evaluation was begun at the widest point of each segment. Because the crest of the alveolar process was often thin, it was necessary to save it and thus produce a plane surface for the planned implant installation. In such cases, the heights of eJDS would have been

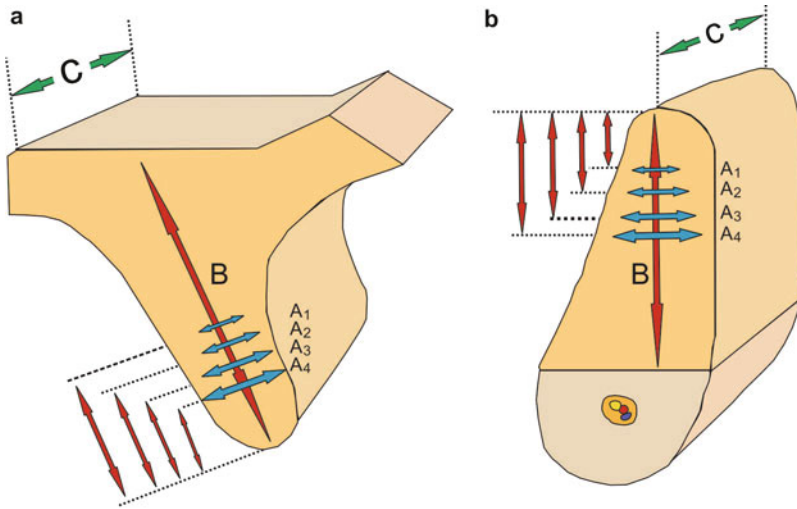


**Fig. 2** Edentulous jaw segments: (a) upper jaw, (b) lower jaw (A1, A2, A3, A4: width; B: height; C: length)

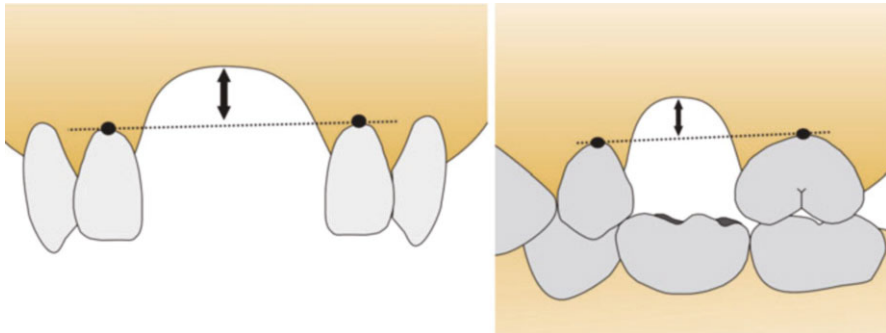


**Fig. 3** Alveolar ridge vertical position (RVP). The vertical component of the alveolar bone defect is measured from the lowest point of the defect to an imaginary tangent running through the necks of the adjacent teeth (A – in aesthetic zone; B – in no aesthetic zone). A distance of 3 mm constitutes a significant cosmetic defect

shortened by 1–3 mm; this change had to be considered when performing dental segment height evaluation. The height of the alveolar process (H) is the distance between the crest of the alveolar process and the important vital structures of the jaws (nasal sinus floor, mental foramen, anterior loop of mental nerve).

*Alveolar ridge vertical position (RVP)* is the distance from the lowest points of alveolar ridge crest to the cervicoenamel line of the adjacent teeth. This parameter is important for achieving of implant-supported restoration length equality to contralateral tooth (Fig. 3).



The main goals of radiological jawbone examination are to determine the quantity, quality, and angulations of bone; select of the potential implant sites; and verify absence of pathology. Clinicians should choose proper radiographic method which provides sufficient diagnostic information with the least possible radiation dose.

## Bone Augmentation Procedures

Bone augmentation procedures can be done some time before implant placement (two-stage procedure) or at the same time as implant placement (one-stage procedure), using various materials and techniques [18]. A two-stage augmentation procedure is usually indicated to place an implant with the desired dimensions in an alveolar ridge with insufficient height or width. The first outcome parameter of interest in a two-stage bone augmentation procedure is the possibility of implant placement in an ideal position for the later prosthetic restoration.

The long-term goal, for both one-stage and two-stage augmentation procedures, is the stability of the augmented bone volume, allowing unhindered masticatory function and optimal aesthetics, as expressed by implant survival, bone stability, and soft tissue stability [2].

There are different indications, numerous alternative techniques, and various *biologically active* agents and biomaterials currently used to augment bone. Therefore, which bone augmentation technique will be used to reconstruct different ridge defects depends on the horizontal and vertical extent of the defect. The predictability of the corrective reconstructive procedures is influenced by the span of the edentulous ridge and the amount of attachment on the neighboring teeth; typically, reconstructive procedures are less favorable in defects that exhibit horizontal and vertical components [3].

Thus, the choice of augmentation technique will depend on the size of defect, horizontal or vertical, anatomical structures, and size of area to be augmented. Some surgical techniques used to augment bone volume include

1. Onlay bone grafting
2. Interpositional bone graft
3. Ridge split technique
4. Guided bone regeneration
5. Distraction osteogenesis
6. Sinus augmentation

*Horizontal bone augmentation procedures:* any technique aimed at making the recipient bone wider or thicker in order to receive dental implants of adequate diameter (usually of a 3.5 mm diameter or wider). For horizontal defects mostly used is onlay bone graft, ridge split, and guided bone regeneration.

*Vertical bone augmentation procedures:* any technique aimed at making the recipient bone higher in a vertical dimension in order to receive dental implants of

adequate length (usually 9 mm or longer). In many instances a combination of horizontal and vertical bone augmentation is needed, and these procedures were included in the vertical augmentation group. Techniques used for vertical defects are onlay bone graft, distraction osteogenesis, interpositional bone grafting, sinus lift, and guided bone regeneration.

### **Onlay Bone Grafting**

The graft material is laid over the defective area to increase insufficient alveolar bone volume, height or width, or both of them. The host bed is usually perforated with a small bur to encourage the formation of a blood clot between the graft and recipient bed. The graft is immobilized with screws and plates or with dental implants. Onlay bone grafting can be made by block onlay grafts or particulate bone grafts.

### **Block Grafting Technique**

When using autogenous block graft approaches for bone augmentation, a considerable amount of horizontal augmentation can be added predictably to the defect area [4]. Intramembranous bones (calvarias, mandible) have reduced rates of resorption compared to endochondral bone (iliac crest) due to a more dense cortical structure and architecture, have more structural integrity than particulate bone, and show less absorption. The graft should be 3–4 mm larger than recipient site to allow contouring, adaptation, and resorption of graft. The thickness of the bone graft should be slightly larger than the planned width or thickness. The stabilization and intimate contact of these block grafts to the recipient bed has been considered crucial to a successful outcome [19]. This can be achieved with the use of bone fixation screws [4] or the simultaneous placement of dental implants. Aggressive recipient bed preparation with decortication, intramarrow penetration, and inlay shaping also has been supported, because of increases in the rate of revascularization, the availability of osteoprogenitor cells, and the increased rate of remodeling [4, 19]. Vertical onlay graft has two major concerns:

- Increased risk of graft exposure due to overexpansion of the soft tissue. Covering of membrane with PRP gel reduces chance of graft exposure.
- Adequate adaptation of the bone graft.

In cases where cortical bone grafts are too thin, a stack technique can be used. All spaces should be filled with particulate bone and covered with a membrane. All grafts must be rigidly fixated with a screw to prevent movement of the graft. Movement will disrupt blood clot adhesion and will compromise vascularity.

### **Particulate Bone Grafting Technique**

This augmentation technique has advantages of rapid vascularization, higher rate of resorption, and must be covered with membrane. Today allogenic and xenogenic particulate grafts are growing in popularity. Particulate onlay grafts must be used with a membrane. When a rigid membrane is used, the choice of material is less

important as the membrane will maintain space and protect the graft. The particulate graft must have the strength to resist deformation when a nonrigid membrane is used.

As any other technique, onlay bone grafting has advantages and disadvantages. This technique is less invasive compared to the other augmentation techniques and can be used for both horizontal and vertical augmentation. There is no injury to inferior alveolar nerve. A disadvantage is their high incidence of bone resorption (41.5 % during first 6 months (Cordaro et al.); 17.4 % during first 6 months (Proussaefs et al.); 20 % during first 5 months (Pikos)). Bone resorption is higher in vertical grafts. It can be reduced with use of membranes or metallic mesh and must be kept in position for entire healing period. Block graft is a better option although both can be used.

### **Interpositional Bone Graft**

This is an augmentation technique where a section of jawbone is surgically separated and graft material sandwiched between two sections. It is based on theory that bone placed between two pieces of pellicled bone with internal cancellous bone will undergo rapid and complete healing and graft incorporation. Grafts heal with rapid vascularization and bone remodeling in the bone gap. There is minimal bone resorption, and these grafts are almost indistinguishable from the surrounding tissue at 12 weeks post op.

Interpositional bone grafting technique is useful in reconstruction of atrophic alveolar ridges. Apart from the ridge split technique, interpositional bone grafts are mainly used for vertical defects. It can however also be used in conjunction with horizontal onlay grafts. Its use is however restricted and abandoned due to the risk of nerve damage and lack of bone retention after grafting.

### **Ridge Split Technique**

Ridge splitting is an alternative to the various techniques described for horizontal ridge augmentation where the alveolar ridge is split longitudinally and parted to widen it and allow placement of an implant or graft material or both in the void. The longitudinal split can be limited by placing transverse cuts in the bone.

This technique is used for horizontal defects to widen the alveolar ridge. There must be at least 2 mm of crestal bone width and minimal reflection of surrounding soft tissue in order to maintain blood supply. Bone is forced buccal with interpositional bone grafts to keep segments separated. It is important to keep ridge relationship between mandible and maxilla in mind. The segments must be stable to prevent disruption of vascularization of new bone.

### **Guided Bone Regeneration (Bone Augmentation with Barrier Membrane Technique)**

The concept of GBR was described first in 1959 when cell-occlusive membranes were employed for spinal fusions. The terms “guided bone regeneration” and “guided tissue regeneration” (GTR) often are used synonymously and rather inappropriately. GTR deals with the regeneration of the supporting periodontal apparatus, including cementum, periodontal ligament, and alveolar bone, whereas GBR

refers to the promotion of bone formation alone. GBR and GTR are based on the same principles that use barrier membranes for space maintenance over a defect, promoting the ingrowth of osteogenic cells and preventing migration of undesired cells from the overlying soft tissues into the wound. Protection of a blood clot in the defect and exclusion of gingival connective tissue and provision of a secluded space into which osteogenic cell from the bone can migrate are essential for a successful outcome. The sequence of bone healing is not only affected by invasion of nonosteogenic tissue but more so by the defect size and morphology [4].

Grafting materials can be categorized in one of the following groups [2]:

- No graft (coagulum)
- Autograft block (extraoral or intraoral donor site)
- Autograft particulate
- Autograft from bone trap
- Membrane alone (nonresorbable or resorbable)
- Allograft (freeze-dried bone allograft [FDBA] or demineralized freeze-dried bone allograft [DFDBA])
- Xenograft (demineralized bovine bone mineral [DBBM], algae-derived, or coral-derived)
- Alloplast (hydroxyapatite [HA], – tricalciumphosphate [TCP], bioglass, or calcium sulfate or allograft + alloplast).

### Autogenous Bone Grafts

Autogenous bone corresponds to bone graft obtained from the same individual and used to build up the deficient area. It is considered to be the material of choice (Palmer 2000), i.e., it is the *gold standard* [18]. Autogenous grafts are biologically compatible as they are from the same patient and provide a scaffold into which new bone may grow. They are not immunogenic and contain osteoblasts and osteoprogenitor stem cells, which are capable of proliferating. These grafts, therefore, are osteoinductive.

Autogenous grafts are presented as blocks or particles and can be used isolated or associated with allogenic or alloplastic grafts.

Autogenous grafting may include cortical, cancellous, or cortical-cancellous bone. The donor area can be from intraoral sites (mentonian region, retromolar area, maxillary tuberosity) and extraoral sites (iliac crest, rib, cranium, tibia, and fibula) [20]. Because the survival of osteocytes depends on the presence of a vascular supply within a distance of 0.1 mm, cortical bone grafts lacking vascular and cellular pools on endosteal and periosteal surfaces may not be able to sustain cellular viability. Cancellous bone grafts may have a greater likelihood of supporting cell survival because of the possibility of diffusion of nutrients and revascularization from the recipient bed [21].

Nevertheless, this type of graft may cause morbidity in the donor area, hematoma, edema, infection, chronic pain, and vascular and nerve lesions. In addition, this technique spends more time for surgical procedure and is limited for large

reconstructions. So, biomaterials have been suggested as an alternative to solve those limitations and reduce the gap between bone and implant [20, 22].

### **Allografts**

Allografts are bone grafts that are harvested from cadavers. Allograft material is freeze dried, demineralized, irradiated, and treated with ethylene oxide to prevent the transmission of disease. They contain no viable cells. Allografts are resorbable and supplied by specially licensed tissue banks in several convenient ways such as bone particles or large blocks [9]. Examples of allografts are fresh-frozen bone, freeze-dried bone, and demineralized freeze-dried bone. Freeze-dried bone and demineralized freeze-dried bone allografts are reported to be less immunogenic than fresh-frozen bone allografts. These materials are frequently used in mixtures with osteoinductive autogenous bone or bone substitutes [21].

The advantages of using allografts are that the material is available in large quantities and there is no donor site within the patient. The disadvantages are that the process for preparing the graft (i.e., freeze-drying and irradiating) decreases the material's integrity and osteogenic potential, and the immunological response to it may diminish its incorporation into the recipient bone.

### **Xenografts**

Xenografts are made of naturally derived deproteinized cancellous bone from animals such as cow or bone-like minerals (calcium carbonate) derived from corals or algae [18]. Deproteinized bovine bone is the most researched grafting material and is widely used in dentistry because of its similarity to human bone. Proteins in deproteinized bovine bone have been extracted to avoid immunological rejection after implantation; however, as the deproteinizing procedure eliminates the osteoinductive capacity, deproteinized bovine bones act solely as an osteoconductive scaffold [21].

The risk of transmission of diseases such as bovine spongiform encephalopathy is negligible because the bone's organic component is extracted. The advantages and disadvantages of using xenografts are similar to those of using allografts.

### **Alloplasts**

Alloplasts are synthetic bone substitutes. They are made of biocompatible, inorganic materials including synthetic hydroxyapatite, tricalcium phosphate, calcium carbonate, and bioactive glass. Whether synthetic hydroxyapatite is resorbable or nonresorbable depends on the temperature at which it is prepared. High-temperature preparation of hydroxyapatite results in a nonresorbable, nonporous, dense material, which is used as a filler. Tricalcium phosphate acts as a filler and is partially resorbable. Calcium carbonate, which is derived from coral, is biocompatible and resorbable so that it acts as a filler, which eventually may be replaced by new bone. Bioactive glass is a silicone-based, osteoconductive material that bonds to bone through the formation of carbonated hydroxyapatite.

Some surgeons use these materials in combination with autogenous bone grafts or allografts [18]. The advantage of alloplasts is that they have no potential for disease transmission.

### **Barrier Membranes for Guided Bone Regeneration (GBR)**

This technique uses special barrier membranes to protect defects from the ingrowth of soft tissue cells so that bone progenitor cells may develop bone uninhibited. Ingrowth of soft tissue may disturb or totally prevent osteogenesis in a defect or wound. Examples of membranes are expanded polytetrafluoroethylene, porcine collagen, and polyglactin. Membranes can be resorbable or nonresorbable [18].

### **Bone Morphogenetic Proteins (BMPs) and Platelet-Rich Plasma (PRP)**

BMPs are a family of proteins naturally present in bone and responsible for activation of bone development (Valentin-Opran 2002). BMPs may encourage bone formation. They may be incorporated into any of the above graft types. Growth factors and PRP are used to promote bone formation [18]. Many techniques exist for effective bone augmentation. The approach largely is dependent on the extent of the defect and specific procedures to be performed for the implant reconstruction. It is most appropriate to use an evidence-based approach when a treatment plan is being developed for bone augmentation cases [4]. Furthermore, every type of augmentation material can be used combined with a variety of different surgical techniques. There is possibility of many treatment combinations, and the situation is rather complicated.

In addition, new techniques and “active agents” are continuously introduced in clinical practice [18]. Future bone augmentation approaches likely will use molecular, cellular, and genetic tissue engineering technologies.

---

## **Bone Substitutes**

The need for bone substitution materials has been increased due to tooth loss, trauma, and tumor and bone reconstructive surgery. A variety of grafting materials are used for bone augmentation in modern dentistry. All osteoplastic materials can be divided into four groups by origin: autogenic (the donor is the patient), allogenic (the donor is another person), xenogenic (the donor is an animal), and synthetic (on the basis of calcium salts) [14]. Although the autogenous bone is still considered as first option for bone reconstruction in implantology some limitations, such as donor site morbidity availability and unpredictable graft resorption, have stimulated the search for suitable synthetic grafting material [23]. However, the perfect grafting material has yet to be identified.

There are four characteristics that an ideal bone graft material should demonstrate which include *osseointegration*, *osteoconduction*, *osteoinduction*, and *osteogenesis*. Only autogenous bone graft satisfies all of these requirements. Synthetic bone grafts at most possess only two of these four characteristics (osseointegration, osteoconduction).

The ideal bone graft substitute is biocompatible, bioresorbable, osteoconductive, osteoinductive, structurally similar to bone, has no risk to disease transmission, appropriate lifetime, easy manipulation, able to form a suitable shape easily, and accessible cost [20].

From a mechanical point of view synthetic bone graft substitutes should have a similar strength to that of the cortical/cancellous bone being replaced. This needs to be matched with a similar modulus of elasticity to that of bone in an attempt to prevent stress shielding as well as maintaining adequate toughness to prevent fatigue fracture under cyclic loading. Synthetic materials that demonstrate some of these properties are composed of calcium, silicon, or aluminum.

Alloplastic bone substitutes represent a large group of chemically diverse synthetic calcium-based biomaterials. They vary in chemical composition, structure, and mechanical and biological properties. Some of them are nonresorbable, while others are chemically resorbable with a concomitant release of bioactive ions. Their pore size is a very important determinant of the ability to form bone. Alloplastic graft materials with pore sizes  $<100\ \mu\text{m}$  may not permit cell and capillary invasion and therefore may not induce bone formation. Pore sizes  $>300\ \mu\text{m}$  show enhanced formation of new capillaries and bone. Most of the current commercial materials do not exhibit any pores [21].

Synthetic resorbable materials were intended as an inexpensive substitute for natural bone. Synthetic graft materials include various types of ceramics:

- Tricalcium phosphate (CP)
- Bioglass
- Hydroxyapatite (HAP) and its compositions with collagen, sulfated glycosaminoglycans such as keratin and chondroitin sulfate, as well as sulfate and
- Calcium phosphate.

Now, many various forms of porous nanostructured calcium phosphate ceramics, bone cements, biohybrids, and biocomposite compounds have been created [24, 25].

## Calcium Phosphates

The calcium phosphate family of alloplastic graft materials has both osteoconductive and osseointegrative characteristics. Osseointegration results from the formation of a layer of hydroxyapatite (HA) shortly after implantation. The  $\text{Ca}^{2+}$  and  $\text{PO}_4^{2-}$  ions required to establish this layer are derived from the implant and surrounding bone. The pathways of both  $\text{Ca}^{2+}$  and  $\text{PO}_4^{2-}$  ions have been traced in serum and urine without any significant elevation in serum levels from which it can be concluded they are handled as part of the normal body ion pool. They have an excellent record of biocompatibility with no reports of systemic toxicity or foreign body reactions.

Calcium phosphate materials such as tricalcium phosphate (TCP) and hydroxyapatite (HA) for the first time were established for clinical use in the 1980s. They can be found in a variety of forms (e.g., pastes, putties, solid matrices, granules). Based

upon their chemical composition, calcium phosphates can be separated into hydroxyapatite (HA), tricalcium phosphate (TCP), and composite grafts [26].

### **Beta Tricalcium Phosphate ( $\beta$ TCP)**

Beta tricalcium phosphate ( $\beta$ -TCP) was one of the earliest calcium phosphate materials used for a bone augmentation. In 1920 Albee and Morrison reported that the rate of bone union was increased when  $\beta$ -TCP was injected into the gap of a segmental bone defect.

The  $\beta$ -tricalcium phosphate is one of the most frequently used alloplasts in implant dentistry and has been regarded as a material of choice because it is osteoconductive, absorbable, and nonosteoinductive [20].  $\beta$ -TCP may be a suitable bone substitute that will biodegrade and be replaced by newly mineralizing bone tissue without fibrous tissue proliferation [23]. These biomaterials facilitate attaching, proliferation, migration, and phenotypic expression of the bone cells, which leads to apposition growth of the bone on the graft surface [14]. When particles of  $\beta$ -TCP are mixed with the blood clot and surrounded by the bony walls of the alveolar socket, osteogenic cells, including undifferentiated mesenchymal stem cells, start migrating from the existing bone surface between and over the surface of the particles, stimulated mostly by an adhesive glycoprotein, called fibronectin, a component of the forming blood clot [23]. Because of their capability of adsorbing proteins, function of osteoclasts and osteoblasts is stimulated, wherefore the function of competing cells is inhibited [23].

Despite the aforementioned positive biological properties, the drawback of most CP materials is poor mechanical durability and slow resorption in the body tissues, which limits its use in bone augmentation procedures performed for aesthetic purposes [21].

It has been found to be brittle and weak under tension and shear but resistant to compressive loads. Beta tricalcium phosphate undergoes reabsorption via dissolution and fragmentation over a 6–18-month period. Unfortunately the replacement of  $\beta$ TCP by bone does not occur in an equitable way. That is, there is always less bone volume produced than the volume of  $\beta$ TCP reabsorbed. Beta tricalcium phosphate is available in porous or solid form as either granules or blocks. Structurally porous  $\beta$ TCP has a compressive strength and tensile strength similar to cancellous bone.

### **Nanosized HAP**

HAP also could be found in the form of nanosized crystals. This material has two elements which are most important for the physiology of bone tissue: they are in a dynamic equilibrium with their biological environment in the remodeling cycle (resorption/mineralization) and manifest a high level of mechanical properties. Nanocrystalline HAP possesses an enhanced capability to adsorb proteins required



for the vital activity of the cells, as well as discrimination regarding the function of the cells which form osseous and fibrous tissues.

Earlier preclinical studies have shown that nanostructural HAP obtained at temperatures below 60 °C possesses a significantly larger capability to stimulate reparative osteogenesis compared with its polycrystalline (high-temperature) analogue. Nanocrystals of biological HAP make the bone harder and stiffer, whereas collagen fibers ensure elasticity and high cracking resistance as well as an adequate resorption and bone regeneration rate [14, 27].

## **Synthetic Hydroxyapatite (HA)**

Hydroxyapatite  $C_{10}(PO_4)_6(OH)_2$  forms the principal mineral component of bone. Synthetic HA comes in ceramic or nonceramic form as porous or solid, blocks or granules. Ceramic refers to the fact that the HA crystals have been heated (sintered) at between 700 °C and 1300 °C to form a highly crystalline structure. Ceramic HA preparations are resistant to reabsorption *in vivo*, while nonceramic HA is more readily reabsorbed. Synthetic HA have good compressive strengths but are weak in tension and shear. Synthetic HA in solid block form is difficult to shape, does not permit fibro-osseous ingrowth, and has a much higher modulus of elasticity than bone. Synthetic HA has been successfully used to coat metal implants to enhance their osseointegration [28].

Synthetic HAP is used in the form of nonporous (nonresorbable) and porous (resorbable) ceramics. With nonporous ceramics no osteogenesis is taking place directly in the area occupied by the bone and porous HAP ceramics is an osteoconductor.

One of the forms of porous ceramics used is its granulate form after implantation of high-temperature ceramic granulates into bone defects, with extension growth of the connective tissue and the osteogenic cells present within it. This served as the base for using this material as a surface coating for endoprostheses, osteosynthesis constructions, and dental implants. The process is most intensive primarily near the surface of HAP particle conglomerates close to the source of osteogenic cells (bone defect walls) [14]. Porous granular form has been used alone or with bone graft to fill voids.

## **Coralline Hydroxyapatite**

Another form of alloplast graft material developed in 1971 with a purpose to create a HA implant with a consistent pore size and improved interconnectivity is Coralline HA. Coralline HA utilizes the genetically determined highly regular and permeable structure of marine coral, which closely resembles that of cancellous bone. The replamineform process involves processing of the calcium carbonate coral to remove the bulk of its organic matter. It is then subject to both extreme pressure and heat in an aqueous phosphate solution. This converts the calcium carbonate coral skeleton

entirely to calcium phosphate (HA) as well as sterilizing it at the same time. Mechanically coralline HA is only slightly greater in compressive strength than cancellous bone. Like the other HA preparations it is weak in tension, brittle, and difficult to shape. Its main advantage is that its interporous structure allows complete ingrowth of fibro-osseous tissue. Fifty to eighty per cent of the void is filled within 3 months. Coralline HA initially does not possess the strength of trabecular bone nor the plastic properties because it lacks a collagen matrix; but with completion of fibro-osseous ingrowth the coralline HA becomes stronger but is less stiff than cancellous bone. Coralline HA has been successfully used in nonweightbearing applications such as maxillofacial, periodontal augmentation, and also for distal radial fractures, spinal fusions, and orbital restorations.

### Calcium Sulfate

Calcium sulfate (plaster of Paris) has been used in craniofacial surgery for more than 100 years, although its use is documented for fracture treatment by the Arabs even in the tenth century. In 1892 a German by the name of Dreesman successfully used plaster of Paris medicated with a 5 % phenol solution to fill skeletal defects, and De Leonardis and Pecora have used the material for sinus floor augmentation in implant dentistry [21].

Calcium sulfate is thought to act as an osteoconductive matrix for the ingrowth of blood vessels and associated fibrogenic and osteogenic cells. For this to occur it is critically important that the implanted calcium sulfate is adjacent to viable periosteum or endosteum. Over a period of 5–7 weeks the calcium sulfate is reabsorbed by a process of dissolution. Calcium sulfate resorbs quickly and is substituted by new bone. The rapid resorption rate can pose a potential problem because the volume of the graft may not be maintained for a sufficiently long period of time to yield reliable grafting results in the aesthetic zone [21].

Its compressive strength is greater than the cancellous bone and has slightly less tensile strength. However, calcium sulfate needs a dry environment to set, and if it is re-exposed to moisture it tends to become soft and fragment. Because of this, it has no reliable mechanical properties *in vivo*, and its application should be limited to a contained area.

### Bioactive Glasses

Two families of silicon-based compounds have the ability to bond directly to bone. These are the bioactive glasses and the glass ionomers. Bioactive glasses are hard, solid (nonporous), materials consisting of four components: sodium oxide, calcium oxide, silicon dioxide (silicate, which is the main component), and phosphorous pentoxide [25]. By varying the proportions of sodium oxide, calcium oxide, and silicon dioxide, forms can be produced that are soluble *in vivo* (solubility being proportional to the sodium oxide content) right through to those that are essentially nonresorbable.

Bone substitute materials within the group of bioactive glass display osteoinductive and osteoconductive properties. They are bioactive, as they interact with the body. Bioactivity depends upon the SiO<sub>2</sub> content; the bonding between bone and glass is best if the bioactive glass contains 45–52 % SiO<sub>2</sub> [26].

A mechanically strong bond between bioactive glass and bone forms as a result of a silica-rich gel layer that forms on the surface of the bioactive glass when exposed to physiological aqueous solutions. Within this gel Ca<sup>2+</sup> and PO<sub>4</sub><sup>2-</sup> ions combine to form crystals of hydroxyapatite (HA) similar to that of bone, hence a strong chemical bond.

The extracellular proteins attract macrophages, mesenchymal stem cells, and osteoprogenitor cells. Subsequently, the osteoprogenitor cells proliferate into matrix-producing osteoblasts [26].

Bioglass is slowly resorbed, so it takes 12–16 months before the graft is replaced by newly formed bone, and that is a factor that should be considered when planning the graft healing time. The studies by Tadjoein et al. and Turunen et al. suggest that bioglass can be used in a mixture with autogenous bone at the floor of the maxillary sinus, thus decreasing the amount of autogenous bone required [21].

## Glass Ionomers

Glass ionomer cements were first introduced in 1971 for dental use where cement was required to bind tooth enamel in a moist environment. Ionomeric cement consists of calcium/aluminum/ fluorosilicate glass powder (0.001–0.1 mm diameter) which is mixed with polycarboxylic acid. This results in an exothermic reaction ( $\leq 56$  °C) with CO<sub>2</sub> evolution to produce a porous cement paste. The paste sets hard in approximately 5 min after which it is water insoluble. Prior to this it must be protected from wound fluids which will dissolve it. After 24 h it has a compressive strength (180–220 MPa) and modulus of elasticity comparable to cortical bone. It is biocompatible and osseointegrates in a manner similar to bioactive glasses. Its porous structure aids osteoconduction and subsequent bone ingrowth. It is non-reabsorbable and therefore is not replaced by bone. Except in dentistry, it is also used in nose, ear, and throat surgery and in maxillofacial reconstructive surgery, but its use in contact with neural tissue or cerebrospinal fluid (CSF) is contraindicated because the release of aluminum ions and polyacid in its unset form is neurotoxic.

## Combined Synthetic Materials

Combined synthetic materials for bone augmentation are a polymeric matrix (polylactide, polyglycolic acid, polyoxybutyrate, and their combinations) and nano-HAP as a filler. Development of composites made of synthetic HAP in different forms (powders, granules, gels) in combination with other preparations (protein collagen, alginate, polysaccharides chitosan, hyaluronic acid, peptides, embryonic stem cells) expanded the opportunities of bone reconstruction [14].

## **Mechanism of Bone Regeneration After Ridge Augmentation**

Following tooth removal, the normal healing process takes place over approximately 40 days, starting with clot formation and culminating in a socket filled with bone covered by connective tissue and epithelium. Complete preservation and restoration of the original ridge volume after tissue remodeling would be ideal for future implant placement. Unfortunately, this is usually not the case. In fact, without further treatment, crestal bone resorption is common and unavoidable which can lead to significant ridge dimensional changes. These changes range from an average vertical bone loss of 1.5–2 mm and an average horizontal ridge width loss of 40–50 % over 6–12 months healing. Most of the dimensional changes occur during the first 3 months and can continue over time, with as much as an additional 11 % of volumetric bone loss during the following 5 years [28–31]. Tooth extraction resulted in approximately 40–60 % loss of bone height and width respectively within 2–3 years. More often, greater bone resorption occurs in the horizontal plane than in the vertical plane, leading to more severe loss of alveolar width. The presence of bone dehiscences or fenestrations during extraction may increase postextraction alveolar remodeling, leading to an even more severe buccal concavity after healing.

## **The Terms “Guided Bone Regeneration” (GBR) and “Guided Tissue Regeneration” (GTR)**

One technique of ridge augmentation is guided bone regeneration (GBR). GBR is a surgical procedure that uses barrier membranes with or without particulate bone grafts or/and bone substitutes.

Guided bone regeneration (GBR) and guided tissue regeneration (GTR) are surgical techniques that utilize barriers made by different membranes to provide navigation of the growth of new bone or gingival tissue. These techniques were first described by Melcher (1976) and are used in everyday practice for more than three decades.

These two terms, guided bone regeneration and guided tissue regeneration, often are used synonymously, but that is inadequate. GTR primarily is linked with regeneration of the supporting periodontal apparatus, including periodontal ligament, cementum, as well as alveolar bone. GBR is oriented only to the promotion of bone tissue formation.

GBR and GTR are based on the same biological and surgical principles. In both barrier membranes are used to make space maintenance over a defect, promoting the pluripotential of osteogenic cells and preventing migration of undesired cells from the overlying soft tissues into the wound. So, guided bone regeneration is similar to guided tissue regeneration but is focused on development of bone tissues in addition to the soft tissues of the periodontal attachment.

GTR and GBR are used at sites that are having insufficient quantity or quality of bone or gingiva. Nowadays, guided bone regeneration is predominantly applied in dentistry to get support for new bone tissue growth on an alveolar ridge to make

adequate placement of dental implants. In fact guided bone regeneration originate from guided tissue regeneration, but these techniques are directed to regenerating tissue in osseous defects adjacent to natural teeth.

For adequate and successful results from these procedures, protection of a blood clot in the wound and exclusion of gingival connective tissue is necessary. Also provision of a secluded space into which osteogenic cell from the bone can migrate is essential for adequate outcome. The sequence of bone healing is not only affected by invasion of nonosteogenic tissue but more by the size of the defect and its morphology.

The patterns of bone regeneration are very complex and include various pathological and pathophysiological changes. This process primarily involves angiogenesis (of new blood vessels) and ingress of osteogenic cells from the defect periphery toward the center. In this way is created new well-vascularized granulation tissue in the surgical defect. This provides a scaffold for woven bone proliferation and bone apposition within the defect.

A very important factor for GTR and GBR is the size of the defect. The dimensions of the defect have influence on the bone healing capacity. In circumstances where the wound is too large to generate a biomechanically stable central scaffold, bone formation is limited to the marginal stable zone with a central zone of disorganized loose connective tissue. Thus, combined use of bone grafts or bone replacement substitutes with barrier membranes are the best for bone regeneration of larger defects.

Biologically, no matter if it is GBR or GTR, these three factors have the main role:

1. Progenitor cells that can produce appropriate tissue and supporting structures also
2. Growth factors for coordinating these activities
3. Scaffolds to provide space and a structure framework for deposition of extracellular matrix

Except the differences between GTR and GBR, these two different surgical techniques share some common prognostic factors. For adequate GTR or GBR there is a need of stable blood clot, to achieved wound healing *per primam intentionem*, isolation of the primary defect from the gingival tissue, and space provision. Also, GBR and GTR today have benefits from contemporary advances in different fields of regenerative medicine including gene therapy, cell therapy, or usage of growth factors.

## **Guided Tissue Regeneration**

Guided tissue regeneration consists of positioning barriers to cover the bone and periodontal ligament, thus separating them from the gingival epithelium temporarily. With this surgical technique the gingival epithelium and connective tissue are excluded from the bone surface in the postsurgical phase. In this way is made

prevention of epithelial migration into the surgical wound and favors repopulation of different mesenchymal cells from the periodontal ligament and alveolar bone [32].

Guided tissue regeneration is primary periodontal occupation and is theoretically based on the potential that only periodontal cells possessed for regeneration of the attachment apparatus of the tooth. This procedure prevents epithelial migration along the dental cement of the pocket with help of biomembrane. The final result from this surgical procedure should be reconstruction of the attachment and coverage of the cementum.

GTR is induced when there is loss of periodontal tissue and infrabony defects. The aim of this technique is recontouring of the periodontal ligament which have adequate organized and oriented collagen fibers in newly formed cementum and alveolar bone.

Today, contemporary GTR surgical techniques have minimally invasive approach with minimal patient morbidity and reduced need for membranes. In periodontology are used particulated grafts from autogenous, xenogenic, allogenic, and rarely synthetic origin.

In the GTR different types of membranes have high importance. Applying membranes between the gingival epithelium and connective tissue and the periodontal ligament and alveolar bone prevents migration of the gingival epithelium and gingival connective tissue cells into the defect along the root surface. Progenitorial cells form the periodontal ligament and from the alveolar bone colonize the blood clot, and periodontal regeneration is induced [33].

Three different outcomes can be noticed after the GTR. If mesenchymal cells from the periodontal ligament or from the perivascular region proliferate into the defects, regeneration occurs. If bone cells migrate and make adherent on the root surface resorption or ankyloses occurs. If gingival epithelial cells proliferate along the root surface, the result will be long functional epithelial attachment. But, if gingival connective tissue migrates along the root surface, a connective tissue attachment can be the result. Also, this can result with root resorption.

## Guided Bone Regeneration

Guided bone regeneration is defined as a surgical procedure in which barrier membranes with or without particulate bone grafts or/and bone substitutes are used. Biologically, as is noticed, this type of regeneration by GBR depends on the migration of pluripotential and osteogenic cells (osteoblasts derived from the periosteum and/or adjacent bone and/or bone marrow) to the bone defect site and exclusion of cells impeding bone formation (epithelial cells and fibroblasts). This is the biggest difference from the guided tissue regeneration.

Guided bone regeneration is indicated for

1. Filling bone defects after tooth extraction
2. Preparation of the bone for successful implantation
3. Building up of new bone tissue around dental implants in immediate implantation

4. Filling bone defects after cystectomy
5. Filling bone defects after impacted tooth replacement

The main goals of GBR are preservation of the postextraction alveolar ridge quantity and quality (normally it is spontaneously reduced), reconstruction of the alveolar bone after extraction for realizing implantation procedure, correction of peri-implant dehiscence and fenestrations, and reconstruction of the lost bone after peri-implantitis [34].

For GBR particulate or block grafts from autogenous, xenogenic, allogenic, and rarely synthetic origin can be used. These two scaffolds can be used to fill the defect and provide support and space for regeneration. Membranes used in GBR have a specific purpose – to prevent gingival epithelial cells or fibroblasts access into the wound, which results with fibrous connective tissue forming. The membrane must be carefully positioned, so a space must be created beneath the membrane, but it must isolate the defect from the overlying oral soft tissue. This space primarily is filled with fibrin clot, which is scaffold for settlement of progenitor cells. This cell originates from adjacent bone or bone marrow.

Today, development of new improved osteoplastic bone grafting materials and growth and differentiation factors and tissue engineering made this surgical method very simple for realization. GBR today becomes a predictable surgical method to enhance new bone formation in peri-implant bone deficiencies and alveolar ridge augmentation, requiring excellent surgical skills [33].

After the surgical procedure is done, series of sequences in the wound take place. In the first 24 h the space which was made is filling with blood clot. It releases different substantives such as growth factors (mainly platelet-derived growth factor) and cytokines (IL-8). They attract two types of cells: neutrophils and macrophages. The blood clot is absorbed and replaced with young granulation tissue rich with new blood vessels that result from an enormous angiogenesis in this tissue. Through these vessels except nutrition, stem cells capable for osteogenesis can be transported. They are responsible for osteoid formation. This osteoid is a template for apposition of mineral and forming a lamellar bone. All of this at the end results with newly formed bone with compact and reticular bone tissue and mature bone marrow. This occurs 3–4 months after the surgery [35].

---

## Membrane

Membranes are used in periodontal and oral surgery to disable migration of cells, primarily epithelial, into the defects. The main role of the membranes is to prohibit epithelial cells, which have bigger regeneration capacity, into areas with tissue that has slower regeneration capacity, like bone tissue. These membranes are dominantly used for guided tissue regeneration (GTR) and guided bone regeneration (GBR) [36].

Membranes used in oral and periodontal surgery should fulfill some basic requirements as

1. Biocompatibility (the interaction between membranes and host tissue should not induce negative effect on these tissues)
2. Space-making (the membrane should have ability to maintain a space for cells from surrounding bone tissue to migrate for stable time duration)
3. Cell occlusiveness (the membrane should prevent fibrous tissue that delays bone formation to invade into the defect site)
4. Mechanical strength (the membrane should have proper physical properties to allow and protect the healing process, including protection of the underlying blood clot)
5. Degradability (this characteristic is typical for resorbable membranes and means adequate degradation time matching the regeneration rate of bone tissue to avoid a secondary surgical procedure to remove the membrane), nonimmunogenicity (membranes should not provoke immune response of the host), nontoxicity (membranes should not act toxic on the organism) [33, 36]

In history, the first membranes developed and fabricated were nonresorbable. The biggest disadvantage of these types of membranes is necessarily of second surgical intervention, after the healing process is finished. This disadvantage of the nonresorbable membranes is exceeded with development of the resorbable membranes. Thus the need of second surgical intervention is surpassed.

Membranes used in dentistry can have natural or synthetic origin. Based on their capability of resorption, membranes are subdivided in three big groups:

- (a) Resorbable
- (b) Synthetic nonresorbable
- (c) Natural biodegradable

Using of nonresorbable membranes has one more disadvantage – bigger risk of loss of some of the regenerated bone further to flap reflection. That's why these types of membranes in contemporary dentistry are replaced with bioresorbable membranes.

## **Nonresorbable Membranes**

As it is mentioned nonresorbable membranes require second surgical intervention to be displaced, because they retain their primary form and structure in the tissue. In this way additional trauma and resorption of the alveolar bone may occur; additional patient discomfort also can be caused, and it has social meaning; this intervention costs more.

### **Polytetrafluoroethylene**

Nonresorbable membranes made from polytetrafluoroethylene (PTFE) can be divided into expanded polytetrafluoroethylene (e-PTFE) and high-density polytetrafluoroethylene (d-PTFE). This classification is made according to the structure.



PTFE has unique chemical structure, it is a simple polymer because it is built up from two chemical elements: carbon and fluorine. This chemical structure has a long, straight carbon backbone to which the fluorine atoms are connected. Both the C–C and C–F connections are extremely strong. In addition, the electron cloud of the fluorine atoms forms a uniform helical sheath that protects the carbon backbone. The even distribution of fluorine atoms makes it nonpolar and nonreactive. The combination of strong bonds, a protective sheath, and no polarity makes PTFE extremely inert as well as thermally stable. Biologically PTFE is chemically identical, causes minimal inflammatory reaction in different tissues, and allows tissue ingrowth [36].

The e-PTFE has micropores, which allows nutrients to be supplied through multiple pores although it can allow the invasion of bacteria when the membrane is exposed to the oral cavity. The d-PTFE completely blocks the penetration of food and bacteria, and thus even if it is exposed to the oral cavity, the d-PTFE membranes exert good guided tissue regeneration (GTR) effects [37].

In contrast, other polymeric membrane materials have some or all of the fluorine atoms replaced with hydrogen or other elements. This results in weaker bonds and a more polar, reactive molecule. The substitution also increases the surface free energy. Therefore, these polymers are less hydrophobic, less thermally stable, and more reactive than PTFE.

### **Titanium Mesh**

Titanium mesh is another nonresorbable membrane which can be used as an option in GBR. Titanium mesh has mechanical strength and rigidity, so it can be used in large bone or tissue defects. Titanium mesh has low density and elasticity and rigidity corresponding with low weight. It also has high resistance of corrosion, although this is a metal. As metal titanium is highly reactive, but soon after its exposure is covered by layer of titanium oxide it becomes unreactive and corrosion stable.

Titanium mesh is good alternative for e-PTFE, because it makes good bone graft stabilization, provides extensive space for GBR and GB, and prevents contour collapse. Its stability prevents graft displacement and its plasticity enabling adequate adaptation of any type of defect. Its elasticity prevents mucosal compression. Its smooth surface makes smaller chance for bacterial colonization. But titanium mesh has its own disadvantages as irritation of the mucosal flap and its sharp edges may cause cutting of the surrounding tissue [38].

The most important characteristic of this mesh is presence of macroporosity, which maintained good blood supply and diffusion of extracellular matrix through the membrane. These make difficulties in removing the membrane in the second surgical intervention and also with it excellent pathway for microorganisms can be done. That is the reason for increased presence of infections after using of titanium mesh.

### **Resorbable Membranes**

Resorbable membranes are widely used in oral and periodontal surgery. They are subdivided in two groups: polymers of lactic or glycolic acid. These types of

membranes have a lot of advantages in comparison with the nonresorbable membranes like

- (a) There is no need of secondary surgical intervention for removal of the membrane.
- (b) Eliminate the need of follow-ups; reducing the possibility of secondary infection during the secondary intervention.
- (c) Patients' discomfort is minimized or totally reduced.
- (d) Eliminate potential surgical complications and in this way.
- (e) The cost is reduced [39].

As indicated by their name they disintegrate in the tissue. Disintegration of the resorbable membranes starts soon after placement in the tissue. A specific characteristic of these membranes is different speed of disintegration. Persistence of these types of membrane is between 4 weeks and several months. Resorbable membranes release free acid that can cause inflammation and compromise the wound healing and regeneration outcome.

## Collagen Membranes

Collagen membranes are used for GTR, GBR, and root coverage. A variety of collagen materials are available including soluble collagen, collagen fibers, sponges, membranes, and bone implants allowing diverse usage of this material, for example, collagen fibers and sponges for hemostatic, collagen membranes for wound covering or implantation, and injections of soluble collagen in plastic surgery. They come from collagen type I and II from pigs or cows. With their biocompatibility and capacity of prompting wound healing they are widely used in oral and periodontal surgery, as well as in dental implantology, bone defect, and ridge augmentation nowadays [40].

Collagen membranes are resorbable membranes, and duration of their disintegration is between 4 and 40 weeks. They have a lot of advantages because they are used in dentistry to inhibit epithelial migration and promote attachment of new connective tissue. Also collagen membranes prevent blood clot by platelet aggregation in early stage of clot formation and wound healing [41].

The use of autogenous periosteum taken from the hard palate as a membrane is described in the literature. In this way there is a possibility of this periosteum to be used for GTR and GBR [42, 43].

---

## Sinus Floor Augmentation, Bone Splitting, Distraction Osteogenesis

Soft and hard tissue defects result from a variety of causes, such as infection, trauma, and tooth loss. These create an anatomically less favorable foundation for ideal implant placement [44].

Survey of various literatures using Internet sources, manual searches, and common textbooks on dental implants shows that a thorough knowledge of conventional augmentation procedures such as bone augmentation techniques, guided bone regeneration, alveolar distraction, maxillary sinus elevation techniques with or without grafting, and contemporary techniques of implant placement provides effective long-term solutions in the management of the atrophic maxilla [45].

Autogenous bone grafting is the best and the gold-standard technique for bone augmentation procedures prior to implant placement. If the amount of available intraoral donor bone is insufficient, it is necessary to harvest bone graft from extraoral sites, such as calvarias. Although this technique is well established, only a few case reports show the histological analysis of the grafted bone at the moment of implant placement [46].

### **Maxillary Sinus Floor Elevation – Lateral Window Technique**

It is a surgical technique using a window into the lateral wall of the maxillary sinus to gain access to the maxillary sinus membrane. Following mobilization and elevation of the sinus membrane, bone augmentation materials (i.e., autografts, allografts, alloplasts, xenografts, or combination mixtures) are used to elevate the sinus floor and allow the placement of dental implants. If the original bone height permits sufficient primary implant stability, then a simultaneous procedure can be used.

Sinus floor elevation is commonly used in cases where alveolar bone resorption has led to insufficient bone height for the placement of dental implants. Lateral wall sinus elevation is carried out when the bone is severely deficient. Although this procedure has a high rate of success, it may present surgical problems. A description of the anatomy of the maxillary sinus and lateral wall augmentation techniques leads to a discussion of the various challenges and complications that may arise and their management [47].

### **Transalveolar Sinus Floor Elevation**

A transalveolar approach for sinus floor elevation with subsequent placement of dental implants was first suggested by Tatum in 1986. In 1994, Summers described a different transalveolar approach using a set of tapered osteotomies with increasing diameters. The transalveolar approach of sinus floor elevation, also referred to as “osteotomy sinus floor elevation,” the “Summers technique,” or the “Crestal approach,” may be considered as being more conservative and less invasive than the conventional lateral window approach.

The surgical technique uses a transalveolar approach to elevate the sinus floor by using osteotomy instruments. Anatomic aspects, such as an oblique sinus floor or insufficient bone height, can limit the use of this delicate surgical technique in daily practice. This is reflected by the fact that more than 9 out of 10 patients who experienced the surgical procedure are willing to undergo it again.

The main indication for transalveolar sinus floor elevation is reduced residual bone height, which does not allow standard implant placement. Contraindications for transalveolar sinus floor elevation may be intraoral, local, or medical. The surgical approach utilized over the last two decades is the technique described by Summers, with or without minor modifications. The surgical care after implant placement using the osteotomy technique is similar to the surgical care after standard implant placement.

The patients are usually advised to take antibiotic prophylaxis and to utilize antiseptic rinses. The main complications reported after performing a transalveolar sinus floor elevation were perforation of the Schneiderian membrane in 3.8 % of patients and postoperative infections in 0.8 % of patients [48].

The scientific literature demonstrated that maxillary sinus grafting is a reliable surgical technique which permits implants to be placed in the atrophic posterior maxilla with an excellent long-term prognosis. Similar results have been obtained with different grafting materials, such as autogenous bone, allografts, xenografts, alloplastic materials, and mixtures of these materials. Survival rates of implants placed in grafted sinuses are consistent with those of implants placed in no grafted edentulous maxillae.

### **Bone Splitting/Expansion and Immediate Implant Placement and Split-Ridge Techniques with Interpositional Bone Grafts and Delayed Implant Placement**

Bone splitting/expansion seems to be a reliable and relatively noninvasive technique to correct narrow edentulous ridges. Survival and success rates of implants placed in the expanded ridges are consistent with those of implants placed in native, nonreconstructed bone. The gap created by sagittal osteotomy/expansion undergoes spontaneous ossification, following a mechanism similar to that occurring in fractures. New bone formation permits a consolidation between the oral and buccal bone plates of the alveolus, and implants placed in expanded ridges seem to withstand the biomechanical demands of loading.

However, some considerations have to be made. Bone splitting/expansion can be applied only when the buccal and palatal/lingual plates are separated by spongy bone. Therefore, the indications are more limited as compared to onlay grafts and GBR, which can be also applied in cases presenting with severe horizontal atrophy. Another limitation is represented by unfavorable inclination of implants placed in expanded areas. This procedure may lead to excessive buccal inclination of implants, which may create problems from a functional and aesthetic viewpoint. In the case of unfavorable bone angularity, GBR or bone grafting techniques seem to represent more adequate surgical procedures [48].

### **Distraction Osteogenesis**

Despite the limited number of patients and implants placed in the retrieved articles, the following conclusions can be drawn:

- Distraction osteogenesis provides an opportunity to obtain a natural formation of bone between the distracted segment and basal bone in a relatively short time span, thus avoiding the necessity of autogenous bone harvesting. This leads to a reduction of morbidity and a shortening of operating times. Soft tissues can follow the elongation of the underlying bone (neohistogenesis), and there is a lower risk of infection of the surgical site (0 % in this case series). Both limited and extended (fully edentulous patients) defects can be treated.

Some disadvantages of vertical distraction osteogenesis must be emphasized:

- Frequent lingual/palatal inclination of the distracted segment has been reported by some authors, with an incidence varying from 13 % to 35.4 %, probably due to local muscle pull, inappropriate device positioning, and/or poor device trajectory. To solve this complication, different solutions have been suggested, including the use of fixed or removable prosthodontic and orthodontic devices to guide the distracted segment to its proper final position. Ideally, a multidirectional alveolar distraction device would allow the vector to be modified and guided in several planes of space [49].

---

## Summary

Recently there has been significant improvement in understanding bone repair. This has notable implications for the future management of bone loss. Currently autogenous and allograft bone are the main sources for bone grafting procedures. Concerns related to the use of both autograft and allograft has led to the search for alternatives. The synthetic bone graft substitutes as yet offer only a part solution to the treatment of localized bone loss.

They have some of the desired mechanical qualities of bone as well as osseointegrative/conductive properties but are largely reliant on viable periosteum/bone for their success. Ideally a synthetic bone graft substitute should mimic the native bone in both mechanical and osteogenic properties.

The identification of osteoinductive proteins and other factors involved in the promotion of osteoblastic proliferation, differentiation, and function has enhanced the potential for manipulating local repair in a beneficial manner. The restoration of an adequate blood supply and the ability to maintain stability and controlled loading during the repair process are also important in achieving a satisfactory outcome. In order to obtain optimum results it is likely that manipulation of this process will require a combination of strategies depending on the clinical situation.

A large but heterogeneous body of literature was available regarding augmentation of localized bone defects in the alveolar ridges after including all levels of clinical evidence except expert opinions. The major development in aesthetic dentistry, and more so the introduction of implant dentistry, led to significant developments aimed to regenerate or restore bony defects and bone loss in the edentulous ridge. Most clinical efforts in the developments in bone augmentation

procedures are related to either simplifying clinical handling or influencing of biological processes. Many techniques exist for effective bone augmentation. The approach largely is dependent on the extent of the defect and specific procedures to be performed for the implant reconstruction. It is most appropriate to use an evidence-based approach when a treatment plan is being developed for bone augmentation cases.

---

## References

1. Tal H, Artzi Z, Kolerman R, Beitlitum I, Goshen G (2012) Augmentation and preservation of the alveolar process and alveolar ridge of bone, bone regeneration. In: Prof. Haim Tal (ed) ISBN: 978-953-51- 0487-2. InTech, Available from: <http://www.intechopen.com/books/bone-regeneration/augmentation-and-preservation-of-the-alveolar-process-and-alveolar-ridge-of-bone>
2. Jensen SS, Terheyden H (2009) Bone augmentation procedures in localized defects in the alveolar ridge: clinical results with different bone grafts and bone-substitute materials. *Int J Oral Maxillofac Implants* 24(Suppl):218–236
3. Dimova C, Papakoca K, Papakoca V (2014) Alveolar bone augmentation. *Key Eng Mater* 614: 89–94. © Trans Tech Publications, Switzerland. doi:10.4028/www.scientific.net/KEM.614.89
4. McAllister BS, Kamran H (2007) AAP-commissioned review bone augmentation techniques. *J Periodontol* 78(3):337–396
5. Nguyen Ngoc Hung (2012) Basic knowledge of bone grafting, bone grafting. In: Dr Alessandro Zorzi (ed) ISBN: 978-953-51-0324-0. InTech, Available from: <http://www.intechopen.com/books/bone-grafting/basicknowledge-of-bone-grafting>
6. Brånemark R, Brånemark P-I, Rydevik B, Myers RR (2001) Osseointegration in skeletal reconstruction and rehabilitation. *J Rehabil Res Dev* 38(2):175–181
7. The Academy of Prosthodontics. The glossary of prosthodontic terms (2005) *J Prosthet Dent* 94 (1): 10–92
8. Koković V, Lj T (2011) Preimplantation filling of tooth socket with  $\beta$ -tricalcium phosphate/polylactic polyglycolic acid ( $\beta$ -TCP/PLGA) root analogue: clinical and histological analysis in a patient. *Vojnosanit Pregl* 68(4):366–371
9. Lekholm U, Zarb GA (1985) Patient selection and preparation. In: Branemark PI, Zarb GA, Albrektsson T (eds) *Tissue integrated prostheses: osseointegration in clinical dentistry*. Quintessence Publishing, Chicago, pp 199–209
10. Gulsahi Ayse (2011) Bone quality assessment for dental implants, implant dentistry – the most promising discipline of dentistry. In: Ilser Turkyilmaz (ed) pp 437–452. ISBN 978-953-307-481-8. InTech, Available from: <http://www.intechopen.com/books/implant-dentistry-the-most-promising-discipline-of-dentistry/bone-qualityassessment-for-dental-impl>
11. Nazirkar G, Singh S, Dole V, Nikam A (2014) Effortless effort in bone regeneration: a review. *J Int Oral Health* 6(3):120–124
12. Horowitz R, Holtzclaw D, Rosen PS (2012) A review on alveolar ridge preservation following tooth extraction. *J Evid Based Dent Pract* 12(Suppl 3):149–160. doi:10.1016/S1532-3382(12)70029-5
13. Thor A, Ekstrand K, Baer RA, Toljanic JA (2014) Three-year follow-up of immediately loaded implants in the edentulous atrophic maxilla: a study in patients with poor bone quantity and quality. *Int J Oral Maxillofac Implants* 29(3):642–649. doi:10.11607/jomi.3163
14. Ivanov SY, Mukhametshin RF, Muraev AA, Solodkaya DV (2013) Synthetic materials used for the substitution of bone defects. Critical review. *Ann Oral Maxillofac Surg* 1(1):4
15. Palmer RM, Howe LC, Paul J (2012) *Implants in clinical dentistry*, 2nd edn. Informa Healthcare, 37–41 Mortimer Street, London
16. Brener D (2006) The mandibular ramus donor site. *Aust Dent J* 51(2):187–190

17. Toscano N, Shumaker N, Holtzclaw D (2010) The art of block grafting. A review of the surgical protocol for reconstruction of alveolar ridge deficiency. *J Implant Adv Clin Dent* 2(2):45–66
18. Esposito M, Grusovin MG, Felice P, Karatzopoulos G, Worthington HV, Coulthard P (2009) Interventions for replacing missing teeth: horizontal and vertical bone augmentation techniques for dental implant treatment. *Cochrane Database Syst Rev Issue 4*. Art. No.: CD003607. doi:10.1002/14651858.CD003607.pub4
19. De Carvalho PS, Vasconcellos LW, Pi J (2000) Influence of bed preparation on the incorporation of autogenous bone grafts: a study in dogs. *Int J Oral Maxillofac Implants* 15:565–570
20. Santos PL, Gulinelli JL, Telles CS, Betoni WJ, Okamoto R, Buchignani VC, Queiroz TP (2013) Review article bone substitutes for peri-implant defects of postextraction implants. *Int J Biomater* Article ID 307136, 7 pages
21. Hallman M, Thor A (2000) Bone substitutes and growth factors as an alternative/complement to autogenous bone for grafting in implant dentistry. *Periodontology* 47(2008):172–192
22. Trejo PM, Weltman R, Caffesse R (2000) Treatment of intraosseous defects with bioabsorbable barriers alone or in combination with decalcified freeze-dried bone allograft: a randomized clinical trial. *J Periodontol* 71(12):1852–1861
23. Brkovic B, Prasad HS, Konandreas G, Radulovic M, Antunovic D, Sándor GKB, Rohrer MD (2008) Simple preservation of a maxillary extraction socket using beta-tricalcium phosphate with type I collagen: preliminary clinical and histomorphometric observations. *J Can Dent Assoc* 74(6):523–528
24. Dimova Cena (2014) Socket preservation procedure after tooth extraction. *Key Eng Mater* 587: 325–330. © (2014) Trans Tech Publications, Switzerland. doi:10.4028/www.scientific.net/KEM.587.325
25. Byrne G (2011) Socket preservation of implant sites. A critical summary of Ten Heggeler JMAG, lot DE, Van der Weijden GA., Effect of socket preservation therapies following tooth extraction in non-molar regions in humans: a systematic review (published online ahead of print Nov. 22, 2010). *Clin Oral Implants Res* 22(8):779–788
26. Van der Stok J, Van Lieshout EMM, El-Massoudi Y, Van Kralingen GH, Patka P (2011) Bone substitutes in the Netherlands – a systematic literature review. *Acta Biomater* 7:739–750
27. Dorozhkin SV (2009) Nanodimensional and nanocrystalline apatites and other calcium rthophosphates in biomedical engineering, biology and medicine. *Materials* 2 (4):1975–2045
28. Strnad Z, Strnad J, Povysil C, Urban K (2000) Effect of plasma sprayed hydroxyapatite coating on the osteoconductivity of commercially pure titanium implants. *Int J Oral Maxillofac Implants* 15:483–490
29. Pikos MA (2005) Mandibular block autografts for alveolar ridge augmentation. *Atlas Oral Maxillofac Surg Clin N Am* 13:91–107
30. Gellrich NC, Held U, Schoen R, Pailing T, Schramm A, Bormann KH (2007) Alveolar zygomatic buttress: a new donor site for limited preimplant augmentation procedures. *J Oral Maxillofac Surg* 65(2):275–280
31. Liu J, Kerns David G (2014) Mechanisms of guided bone regeneration: a review. *Open Dent J* 8:56–65
32. Giardino R, Aldini NN, Fini M, Giavaresi G, Torricelli P (2002) Guided tissue regeneration in dentistry. *J Trauma* 52(5):933–937
33. Bottino MC, Thomas V, Schmidt G, Vohra YK, Chu TM, Kowolik MJ, Janowski GM (2012) Recent advances in the development of GTR/GBR membranes for periodontal regeneration—a materials perspective. *Dent Mater* 28(7):703–721
34. Nyman S (1991) Bone regeneration using the principle of guided tissue regeneration. *J Clin Periodontol* 18:494–498
35. Farzad M, Mohammadi M (2012) Guided bone regeneration: a literature review. *J Oral Health Oral Epidemiol* 1(1):3–18
36. Zhang Y, Zhang X, Shi B, Miron RJ (2013) Membranes for guided tissue and bone regeneration. *Ann Oral Maxillofac Surg* 1(1):10

37. Sculean A, Nikolidakis D, Schwarz F (2008) Regeneration of periodontal tissues: combinations of barrier membranes and grafting materials – biological foundation and preclinical evidence: a systematic review. *J Clin Periodontol* 35(Suppl 8):106–116
38. Rakhmatia YD, Ayukawa Y, Furuhashi A, Koyano K (2013) Current barrier membranes: titanium mesh and other membranes for guided bone regeneration in dental applications. *J Prosthodont Res* 57(1):3–14
39. Duskova M, Leamerova E, Sosna B, Gojic O (2006) Guided tissue regeneration, barrier membranes and reconstruction of the cleft maxillary alveolus. *J Craniofac Surg* 17(6):1153–1160
40. Bunyaratavej P, Wang HL (2001) Collagen membranes: a review. *J Periodontol* 72(2):215–229
41. Patino MG, Neiders ME, Andreana S, Noble B, Cohen RE (2002) Collagen as an implantable material in medicine and dentistry. *J Oral Implantol* 28(5):220–225
42. McCabe J, Yan Z, Al Naimi O, Mahmoud G, Rolland S (2011) Smart materials in dentistry. *Aust Dent J* 56:3–10. doi:10.1111/j.1834-7819.2010.01291
43. Dori F, Huszar T, Nikolidakis D, Arweiler NB, Gera I, Sculean A (2007) Effect of platelet-rich plasma on the healing of intra-bony defects treated with a natural bone mineral and a collagen membrane. *J Clin Periodontol* 34(3):254–261
44. McAllister BS, Haghghat K (2007) Bone augmentation techniques. *J Periodontol*. doi:10.1902/jop.2007.060048, 377
45. Ali SA, Karthigeyan S, Deivanai M, Kumar A (2014) Implant rehabilitation for atrophic maxilla: a review. *J Indian Prosthodont Soc* 14(3):196–207. doi:10.1007/s13191-014-0360-4, Epub 2014 Apr 22
46. Bastos AS, Spin-Neto R, Conte-Neto N, Galina K, Boeck-Neto RJ, Marcantonio C, Marcantonio E, Marcantonio E Jr (2014) Calvarial autogenous bone graft for maxillary ridge and sinus reconstruction for rehabilitation with dental implants. *J Oral Implantol* 40(4):469–478. doi:10.1563/AAID-JOI-D-11-00090
47. Caudry S, Landzberg M (2013) Lateral window sinus elevation technique: managing challenges and complications. *J Can Dent Assoc* 79:d101
48. Mazor Z, Peleg M, Garg AK, Chaushu G (2000) The use of hydroxyapatite bone cement for sinus floor augmentation with simultaneous implant placement in the atrophic maxilla. A report of 10 cases. *J Periodontol* 71:1187–1194
49. Chiapasco M, Casentini P, Zaniboni M (2009) Bone augmentation procedures in implant dentistry. *Int J Oral Maxillofac Implants* 24(Suppl):237–259



Alexandru Eugen Petre

## Contents

Introduction .....	1202
Dental Ceramics .....	1202
Overview of All-Ceramic Materials .....	1202
Clinical Success of Prosthetic Restorations .....	1207
Dental CAD/CAM Systems .....	1208
Clinical Characteristics of All-Ceramic CAD-CAM Restorations .....	1213
References .....	1214

---

### Abstract

High-strength ceramic materials such as polycrystalline alumina and zirconia-based ceramics can be used for the fabrication of various implant- or teeth-supported prostheses. Zirconia based ceramics can be successfully used for multiple unit – long span bridges or allow for the thickness reduction of the restorations in non-critical bio-mechanical situations. These materials have been introduced in dental practice, along with new technologies like the computer-assisted design/computer-assisted manufacturing (CAD/CAM) of dental restorations.

---

### Keywords

Dental ceramics • High-strength ceramics • Computer-assisted design/computer-assisted manufacturing (CAD/CAM) of dental restorations

---

A.E. Petre (✉)

Department of Prosthodontics, Discipline of Fixed Prosthodontics and Dental Occlusion,  
University of Medicine and Pharmacy “Carol Davila”, Bucharest, Romania  
e-mail: [petre.alex@gmail.com](mailto:petre.alex@gmail.com)

## Introduction

Fixed and removable dental prostheses can be produced using a plethora of dental materials and laboratory technologies. Classically, the longevity of dental prostheses has been accomplished mainly by the use of metallic alloys and precision casting technologies. However, due to the past decades' public demand for aesthetics and improved biocompatibility, an active search for metal-free prostheses has been pursued. Traditionally, the best aesthetic results for dental prostheses are obtained with glass-ceramics like the feldspathic porcelain, but their use for metal-free restorations is limited by their limited strength especially for support (premolar and molar) area crowns and fixed partial dentures (dental bridges). In this process many high-strength ceramic materials such as polycrystalline alumina and zirconia-based ceramics can be traced back in the late 1960s. Consequently, several types of zirconia were used for the fabrication of dental implants and various restorations and parts for implant- or teeth-supported prostheses. Zirconia based ceramics can be successfully used for multiple unit – long span bridges or allow for the thickness reduction of the restorations in non-critical bio-mechanical situations. These materials have been introduced in dental practice, along with new technologies like the computer-assisted design/computer-assisted manufacturing (CAD/CAM) of dental restorations.

In this chapter we present (1) dental ceramics, (2) dental CAD/CAM systems, (3) clinical characteristics of all-ceramic CAD-CAM restorations, and (4) further developments for all-ceramic restorations and manufacturing technologies.

---

## Dental Ceramics

Ceramic materials are used in dentistry for over 200 years. On May 11, 1791, following the ideas of the pharmacist Alexis Duchâteau, Nicolas Dubois de Chémant (1753–1824), a French dentist, patents in England the “teeth of mineral paste.” In 1889 Charles H. Land patented the all-porcelain jacket crown. Since then, mechanical strength, aesthetics, and stability were proven as the main advantages of dental ceramics, but the fragility caused by their brittle nature made these materials rarely used without a metal substructure – first developed by Abraham Weinstein in the late 1950s. Metal-ceramic restorations are until today the first choice for fixed dental prostheses as they blend in a convenient and durable way – marginal adaptation, mechanical strength, biocompatibility, and aesthetics [11, 15].

## Overview of All-Ceramic Materials

In 1965, MacLean and Hughes developed metal-free crowns from an alumina reinforced porcelain core with a flexural strength of 120–150 MPa [16], and after that several classes of high-strength ceramics have been fabricated.

An overview of these materials is presented in Table 1 as opposed to the ISO specifications for ceramics used for fixed prosthetic restorations (Table 2).

**Table 1** Types of dental ceramics vs. dental enamel and dentine – modified after [22]

Material	Commercial products	Crystalline phase	Processing method	Physical properties: $\sigma$ , flexural strength; $K_{Ic}$ , fracture toughness; $H$ , hardness; $E$ , Young's modulus; CTE, coefficient of thermal expansion	Clinical indication
Feldspathic porcelain		Amorphous glass	Powder slurries for the layering and firing technique	$\sigma$ , 60–70 MPa; $K_{Ic}$ , 0.92–1.26 MPa.m <sup>1/2</sup> ; $E$ , 70 GPa; $H$ , 6 GPa; CTE, varying depending on application	Resin-bonded laminate veneers and veneering of metallic and ceramic cores
Reinforced feldspathic porcelain (aluminous, leucite, fibers)	Vitadur <sup>®</sup> (Vita), Vitablocs <sup>®</sup> Mark II (Vita), Optec <sup>®</sup> HSP (Jeneric/Pentron), Mirage <sup>™</sup> (Chameleon Dental Products)	Alumina, leucite, fibers	Powder slurries for the layering and firing technique hot press	$\sigma$ , 120–150 MPa; $K_{Ic}$ , 1.5 MPa.m <sup>1/2</sup> ; CTE, 16.0–17.3 $\times 10^{-6}$ K <sup>-1</sup> (multi-indication alloys); CTE, 13.8–15.2 $\times 10^{-6}$ K <sup>-1</sup> (high gold content, reduced precious metal content, palladium-based and non-precious metal alloys); CTE, 16.0–17.5 $\times 10^{-6}$ K <sup>-1</sup> (gold-palladium-silver alloys); CTE, 7.2–7.9 $\times 10^{-6}$ K <sup>-1</sup> (alumina, spinell, and zirconia glass-infiltrated ceramics); CTE, 9.0–10.5 $\times 10^{-6}$ K <sup>-1</sup> (zirconia)	Resin-bonded laminate veneers and crowns, veneering of multunit bridges

*(continued)*

**Table 1** (continued)

Material	Commercial products	Crystalline phase	Processing method	Physical properties: $\sigma$ , flexural strength; K <sub>Ic</sub> , fracture toughness; H, hardness; E, Young's modulus; CTE, coefficient of thermal expansion	Clinical indication
Glass-ceramics (fluor mica tetrasilicic mica, apatite glass-ceramic)	Dicor <sup>®</sup> (Corning Inc.) (Dentsply), Cera Pearl <sup>®</sup> (Kyocera Corp)	K <sub>2</sub> Mg <sub>5</sub> Si <sub>8</sub> O <sub>20</sub> F <sub>4</sub>	Castable CAD/CAM	$\sigma$ , 150 MPa; K <sub>Ic</sub> , 1.4–1.5 MPa.m <sup>1/2</sup> ; H, 362 MPa (Knoop); E, 70.3 GPa; CTE, $7.2 \times 10^{-6} \text{ K}^{-1}$ ; S, 127/147 MPa; K <sub>Ic</sub> , 1.4–1.5 MPa.m <sup>1/2</sup> ; H, 3.3–3.5 GPa (Knoop); E, 68 GPa; CTE, $6.4 \times 10^{-6} \text{ K}^{-1}$	Resin-bonded laminate veneers, anterior crowns, posterior inlays
Leucite glass-ceramic	IPS Empress <sup>®</sup> , IPS Empress <sup>®</sup> CAD (Ivoclar), Optimum Pressable Ceramic OPC <sup>®</sup> (Jeneric/Pentron), Finesse <sup>®</sup> (Dentsply), Authentic <sup>®</sup> (Iensen Dental), PMTM (Vita)	KAlSi <sub>3</sub> O <sub>6</sub> (tetragonal phase)	Hot press CAD/CAM	$\sigma$ , 160 MPa; K <sub>Ic</sub> , 1.3 MPa.m <sup>1/2</sup> ; H, 6.2 GPa (Vickers); E, 65 GPa; CTE, $16.6 \times 10^{-6} \text{ K}^{-1}$ (100–400 °C); CTE, $17.5 \times 10^{-6} \text{ K}^{-1}$ (100–500 °C)	Resin-bonded laminate veneers, inlays, onlays, and crowns
Lithium disilicate glass-ceramic	IPS Empress II <sup>®</sup> , now IPS e.max <sup>®</sup> (Ivoclar)	Li <sub>2</sub> Si <sub>2</sub> O <sub>5</sub>	Hot press CAD/CAM	$\sigma$ , 360/400 MPa; K <sub>Ic</sub> , 2.25/2.75 MPa.m <sup>1/2</sup> ; H, 5.8 GPa (Vickers); E, 95 GPa; CTE, $10.2 \times 10^{-6} \text{ K}^{-1}$ (100–400 °C). CTE, $10.5 \times 10^{-6} \text{ K}^{-1}$ (100–500 °C)	Resin-bonded laminate veneers, inlays and onlays, crowns, bridges in the anterior region up to premolars

Fluorapatite glass-ceramic	IPS e.max <sup>®</sup> Ceram (Ivoclar)	Ca <sub>5</sub> (PO <sub>4</sub> ) <sub>3</sub> F		Powder slurries for the layering and firing technique	Slightly higher strength and fracture toughness of the pressable vs. CAD/CAM ceramic	Resin-bonded laminate veneers, veneering of lithium disilicate glass-ceramic and zirconia frameworks
Glass-infiltrated spinell	Vita In-Ceram <sup>®</sup> Spinell	MgAl <sub>2</sub> O <sub>4</sub>		Slip casting CAD/CAM	$\sigma$ , 90 MPa; H, 5.4 GPa (Vickers); CTE, $9.5 \times 10^{-6} \text{ K}^{-1}$ (100–400 °C)	Inlays and anterior crowns
Glass-infiltrated alumina	Vita In-Ceram <sup>®</sup> Alumina	Al <sub>2</sub> O <sub>3</sub> (hexagonal phase)		Slip casting CAD/CAM	$\sigma$ , 400 MPa; K <sub>Ic</sub> , 2.7 MPa.m <sup>1/2</sup> ; E, 185 GPa; CTE, $7.7 \times 10^{-6} \text{ K}^{-1}$	Laminate cores, crowns, abutments, anterior bridges
Glass-infiltrated zirconia	Vita In-Ceram <sup>®</sup> Zirconia	ZrO <sub>2</sub> (yttria-stabilized tetragonal phase)		Slip casting CAD/CAM	$\sigma$ , 500 MPa; K <sub>Ic</sub> , 3.9 MPa.m <sup>1/2</sup> ; E, 280 GPa; CTE, $7.4 \times 10^{-6} \text{ K}^{-1}$	Anterior and posterior crowns and bridges
Pure alumina (corundum)	Procera <sup>®</sup> (Nobel Biocare)	Al <sub>2</sub> O <sub>3</sub> (hexagonal phase)		CAD/CAM	$\sigma$ , 600 MPa; K <sub>Ic</sub> , 4.4 MPa.m <sup>1/2</sup> ; E, 258 GPa; CTE, $7.8 \times 10^{-6} \text{ K}^{-1}$	Laminate cores, crowns, 4-unit bridges
Ytria-stabilized tetragonal zirconia polycrystals (3Y-TZP)		ZrO <sub>2</sub> (yttria-stabilized tetragonal phase)		CAD/CAM	$\sigma$ , 500–700 MPa; K <sub>Ic</sub> , 4.5 MPa.m <sup>1/2</sup> ; E, 270–380 GPa; H, 12 GPa; CTE, $7.10^{-6} \text{ K}^{-1}$	Laminate cores, anterior and posterior crowns and bridges
Enamel		Ca <sub>5</sub> (PO <sub>4</sub> ) <sub>3</sub> OH (hydroxyapatite)			$\sigma$ , 900–1400 MPa; K <sub>Ic</sub> , 6–10 MPa.m <sup>1/2</sup> ; E, 205–210 GPa; H, 13.9 GPa; CTE, $10.5 \times 10^{-6} \text{ K}^{-1}$	
					$\sigma$ , 261–288 MPa (10 MPa if not supported by dentin); K <sub>Ic</sub> , 0.6–1.5 MPa.m <sup>1/2</sup> ; E, 70–100 GPa; H, 3–5 GPa	

(continued)

**Table 1** (continued)

Material	Commercial products	Crystalline phase	Processing method	Physical properties: $\sigma$ , flexural strength; K <sub>1c</sub> , fracture toughness; H, hardness; E, Young's modulus; CTE, coefficient of thermal expansion	Clinical indication
Dentin		<p>≈70 %  <math>\text{Ca}_5(\text{PO}_4)_3\text{OH}</math>            (hydroxyapatite)</p>		<p><math>\sigma</math>, 232–305 MPa; K<sub>1c</sub>, 3.1 MPa.m<sup>1/2</sup>; E, 15–30 GPa; H, 0.6 GPa</p>	

**Table 2** Classification of ceramics for fixed prostheses by intended clinical use (ISO 6872:2008)

Class	Recommended clinical indications	Mechanical and chemical properties	
		Flexural strength minimum (mean), MPa	Chemical solubility maximum, mg cm <sup>-2</sup>
1	(a) Aesthetic ceramic for coverage of a metal or a ceramic substructure (b) Aesthetic ceramic: single-unit anterior prostheses, veneers, inlays, or onlays	50	100
2	(a) Aesthetic ceramic: adhesively cemented, single-unit, anterior or posterior prostheses (b) Adhesively cemented, substructure ceramic for single-unit anterior or posterior prostheses	100 100	100 2000
3	Aesthetic ceramic: nonadhesively cemented, single-unit, anterior or posterior prostheses	300	100
4	(a) Substructure ceramic for nonadhesively cemented, single-unit, anterior or posterior prostheses (b) Substructure ceramic for three-unit prostheses not involving molar restoration	300	2000
5	Substructure ceramic for three-unit prostheses involving molar restoration	500	2000
6	Substructure ceramic for prostheses involving four or more units	800	100

## Clinical Success of Prosthetic Restorations

It has been proposed a quantitative rating scale for which may be used for evaluating clinical success for new types of restorations [2]:

1. Superior performance: Survival of all FDPs (100 %) for at least 5 years and a success rate of 95–100 %
2. Excellent performance: Survival of 95–100 % of all FDPs for at least 5 years and a success rate of 90–95 %
3. Good performance: Survival of 90–95 % of restorations for at least 5 years and a success rate of 90–95 %
4. Poor performance: Survival of less than 90 % of restorations or a success rate of less than 90 %

## Survival of Metal-Ceramic Restorations

There are several reports about survival rates of metal-ceramic restorations: at 5-year 95.6 % for metal-ceramic single crowns [20] 94.4 % for metal-ceramic fixed partial dentures (FPD) [21]; 10-year survival rates of 92 % and 74 % 15-year survival for FPD [24] 18-year survival rates of 75 % for crowns on vital teeth and 79 % on nonvital teeth were found in a retrospective evaluation [8] or 78 % for FPDs [18].

### Survival of All-Ceramic Restorations

For anterior teeth, it is accepted that clinicians may select from any all-ceramic system for any restoration type. For example, the survival of lithium disilicate restorations shows a cumulative survival rate over a 10-year period of 96.7 % [19]. For molar restorations there are few all-ceramic systems that provide predictable long-term success. Clinical complications of all-ceramic multiunit fixed dental prostheses are frequent, even for those with enlarged connectors [14]. The medium-term survival of lithium disilicate restorations for fixed partial dentures is only 70.9 % with the lateral areas being the most affected by failure [19]. Kaplan-Meier survival rates were reported for 3-unit fixed partial dentures for end points ranging from 1 to 10 years, with a mean end point of approximately 5.6 years [14].

Hydrothermal aging of zirconia can cause significant transformation from tetragonal to monoclinic crystal structure, which results in a decrease in mechanical properties [10].

### Dental CAD/CAM Systems

In 1972, François Duret filed in France a patent application and in 1973 completed a doctoral thesis on the theme “le rayon laser en dentisterie et prothèse.” Duret invented optical impression in dental prosthetics and thereby created the possibility of computer aided designing and fabrication of dental prostheses [9]. Werner Mörmann (Switzerland) and Marco Brandestini (Italy) developed the first commercial system – the CEREC, acronym for Chairside Economical Restoration of Esthetic Ceramics [17]. The system allows dentists to chairside fabricate single ceramic restorations in one appointment, and it has been upgraded several times in the past decades. In the 1980s Diane Rekow developed a CAD-CAM system in the United States. In 1983 Matts Andersson from Sweden developed the Procera method of manufacturing high-precision dental crowns which was acquired in 1989 by Nobelpharma, later Nobel Biocare (<http://corporate.nobelbiocare.com/en/our-company/history-and-innovations/> at 13.11.2014).

Since the early 1980s, the CAD-CAM systems continued to develop, but in the last years, the growth was exponential (Table 3).

**Table 3** PubMed search result in number of publications in the past two decades with CAD-CAM keyword and DENTISTRY as major topic

Year	No. of references
2012–2013	467
2010–2011	375
2008–2009	307
2006–2007	211
2004–2005	161
2002–2003	140
2000–2001	109
1998–1999	85
1996–1997	47
1994–1995	48



Currently, commercial CAD-CAM systems allow for the fabrication of practically all types of fixed restorations: anatomical copings and bridge frameworks, full anatomical crown and bridges, inlays, onlays, inlay bridges, veneers, multi-layer crowns and bridges [7], wax-up, digital temporaries, post and cores, telescopes, customized implant abutments, bars and bridges, full dentures, removable partial dentures, custom trays and models for classic technology, occlusal splints, orthodontic analysis and appliances, and surgical guides for dental implants (<http://www.3shapedental.com/restoration/dental-lab/digital-lab/next-step-for-cadcam-dentistry/> at 13.11.2014). Comparing virtual models can also compare and measure teeth movements during different dental treatments [4].

The main advantages of the CAD-CAM technology are the speed and the predictable quality of the final restorations at increasingly competitive costs due to the time-saving procedures and increased commercial offer [25].

There are three ways in which CAD-CAM technology can be used:

#### ALL LAB

1. Classical impression (analogue, with impression materials)
2. Model fabrication with removable dies and articulation
3. Model digitization and virtual model creation

In this variant, clinical work is completely separate from CAD-CAM technology, used exclusively in the dental lab. The virtual model and the resulting dental prosthesis are likely to include all the errors from the impression and model-pouring steps.

On the other hand, the existence of a physical model makes possible the try-in and potential adjustments as well as subsequent phases such as the traditional aesthetic ceramic veneering of metal or zirconia frameworks. Due to the versatility in accommodating both fabrication methods, the all-lab CAD-CAM technology is for the moment the most commonly used.

#### IMPRESSION SCANNING

1. Classical impression
2. Digitization of the impression and transformation into a virtual model without pouring a model

Impression scanning can be done either in the dental office or in the laboratory and has the advantage that it avoids casting and preparing the model and therefore the possible errors of this phase. Impression scanners can be dedicated devices for in-office or in-lab use or classic laboratory scanners with an impression scanning add-in. Any impression scanner can digitize also models, but the dedicated lab scanners with the impression scanning option are usually more expensive than their model-only counterparts.

Scanning mainly negative reliefs is sometimes difficult and often requires shortening impression borders or the use of antireflective powder before digitization, which might pose problems with custom or universal metal trays with high borders that cannot be shortened without risking deformation of the impression.

Pouring models in the scanned impression is of limited utility for the subsequent lab phases. The prostheses fabricated after digitized impressions present an uncertain fit on these models mainly because of the soft tissue areas.

Whenever the CAD-CAM process does not start from a poured model but there is the need for further steps like the aesthetic veneering, there are two options:

- Producing a physical model from the virtual one through a model designing software.
- Doing an intraoral try-in and making a position impression of the framework; further stages are then continued in the traditional dental lab.

Dedicated impression scanners could be an economic solution for digitalization in prosthetic dentistry as they allow for an in-office creation of the virtual model and a faster clinical feedback regarding the quality of the preparations. Besides, there are cases in which intraoral scanning is not feasible because of large edentulous spans, highly mobile mucosa or other mobile anatomical structures in the close vicinity of the preparations, or deep and narrow interdental spaces. As a consequence of the need, in some cases, for traditional impression, it is likely that further developments of intraoral scanners could include the option for impression scanning.

## INTRAORAL SCANNING

1. Intraoral scanners enable the work in an entirely virtual environment which brings numerous advantages:
  - Impression accuracy and fit of prosthetic structures produced in this technology are considered within clinically acceptable limits as the flaws in the classical impressions are notoriously frequent [5]. In one study, the mean marginal (internal) discrepancies for restorations produced after several intraoral scanners were significant but clinically acceptable: iTero 90 (92)  $\mu\text{m}$ , TRIOS 128 (106)  $\mu\text{m}$ , CEREC AC with Bluecam 146 (84)  $\mu\text{m}$ , and Lava COS 109 (93)  $\mu\text{m}$  [23].
  - The control of the preparations on the scanner desktop, at an important magnification, enables the clinician to validate the preparations in real time (Fig. 1).
  - Corrected preparations or inaccurate reproduced areas from the digital model can be selectively removed and re-added to the digital impression, which makes complete retaking of the impression never necessary, as in the classical counterparts (Fig. 2).
  - In the cases in which one takes the conformational approach of the occlusion, intraoral scanning allows immediate validation of the reference mandibulo-maxillary position – by real-time observation of the coincidence of intraoral occlusal contacts with the virtual models (Fig. 3).
  - The incorporation in the virtual model of the pre-preparation geometry is very simple; it can also be scanned and used in the design process of the provisional restorations or mock-up's geometry (Figs. 3 and 4).
  - Transport and storage do not change the virtual model as in the case of classical impressions.

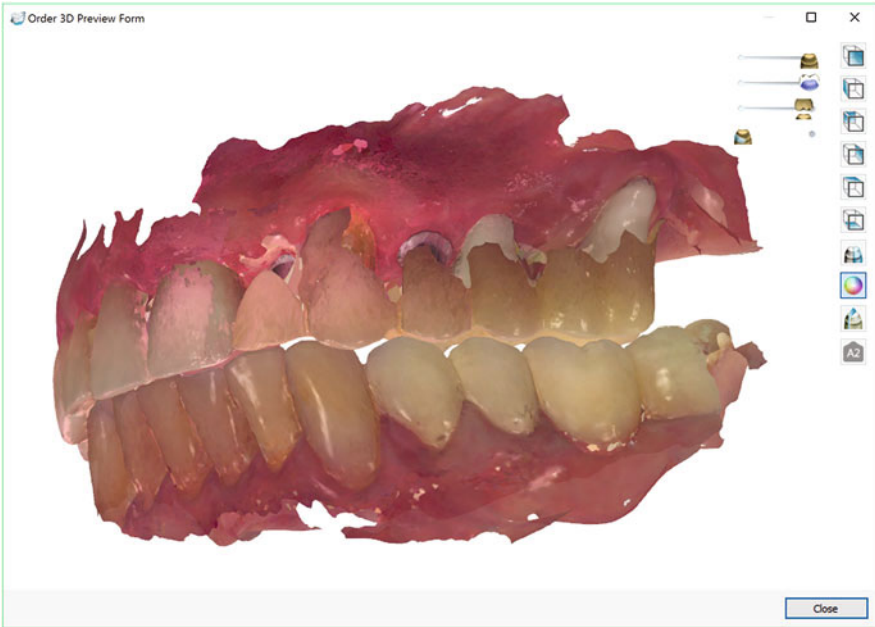


**Fig. 1** Intraoral direct scanning of a pre-preparation situation for the prosthetic restoration of teeth 22 23 24

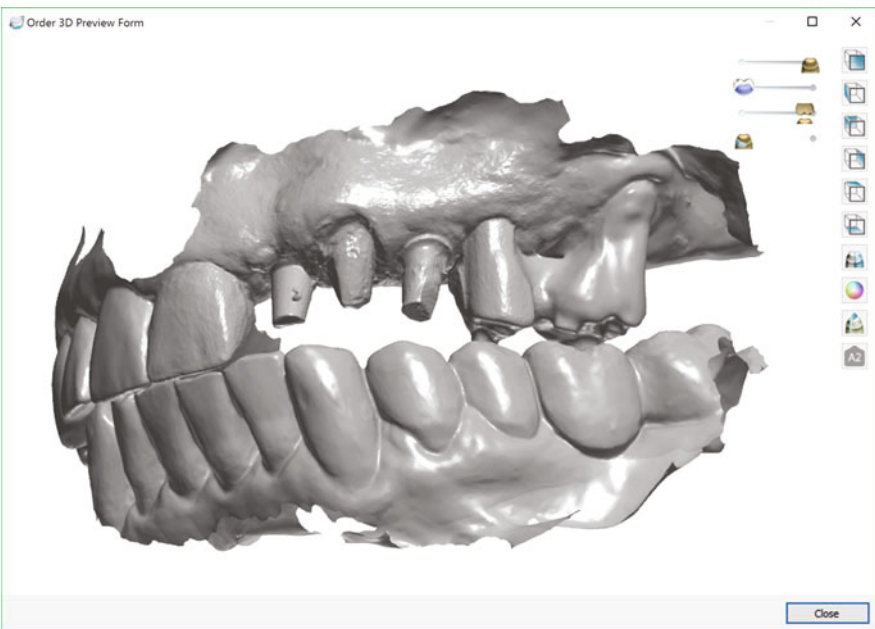


**Fig. 2** Intraoral direct scanning of the preparations for the prosthetic restoration of teeth 22 23 24

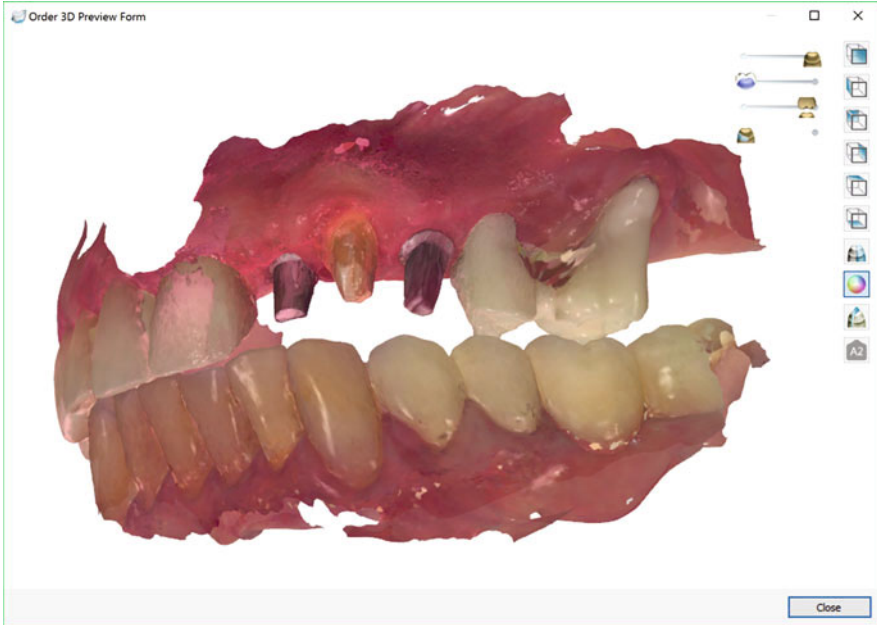


**Fig. 3** Scanning can be visualised either in true color display for the correct tissue identification or color evaluation or monochromatic for a better evaluation of the scanning process

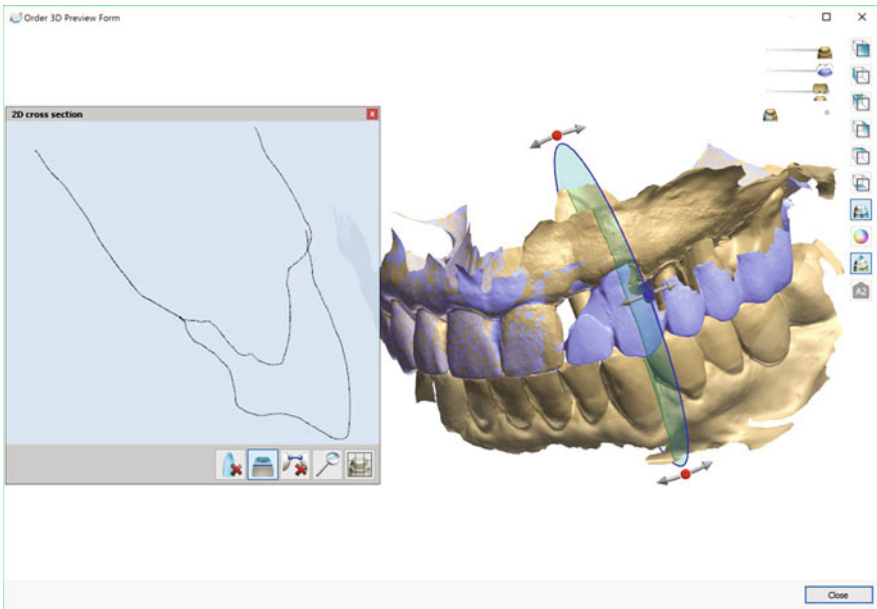


**Fig. 4** On the digital models one can make several measurements and sectional views for better clinical evaluation

- The oldest commercial CAD-CAM system includes a milling machine that provides immediate, ceramic or composite blocks of single prosthetic elements and other milling machines small enough for an in-office use which have been developed very recently and are now commercially available (<https://www.amanngirrbach.com/products/milling-cam/ceramill-mikro/> at 13.11.2014).
- Some commercial intraoral scanners are able to make color measuring (<http://www.3shapedental.com/news/using-shade-measurement/> at 13.11.2014).
- The online or direct connection communication with the dental lab is largely facilitated by the built-in modules of the scanner and design software.

Disadvantages of CAD-CAM technology:

- The high initial investment and periodic license/support /upgrade fees.
- The need for some computer literacy and specific training for scanning, designing, and machining applications even though the software is often quite intuitive.
- Compatibility and interconnection problems when using a mixed environment, e.g., different types of intraoral scanner, design software, and cam software and hardware.
- The need of producing high-precision physical models from the digital data by printing or milling which add to the restoration cost; alternatively the model can be produced in a traditional manner, after a position impression of the milled framework.
- Few available high aesthetic solutions for multiple restorations.
- Lack of a true virtual articulator: the current systems require mounting the working models in a real articulator and then transferring the parameters in the virtual environment which excludes impression and/or intraoral scanning from their use without producing a physical model; there are several reports of experimental methods of transferring the location of the maxillary dental arch from the patient directly to a virtual articulator (virtual facebow) [26–28].

---

## Clinical Characteristics of All-Ceramic CAD-CAM Restorations

It has been demonstrated that milling titanium and zirconia frameworks produces some peri-implant strain. There are reports in which the zirconia frameworks produced significantly less strain than titanium. Combining the qualitative and quantitative information indicates that the implants were under vertical displacement rather than horizontal. The vertical fit was similar for zirconia (3.7  $\mu\text{m}$ ) and titanium (3.6  $\mu\text{m}$ ) frameworks; however, the zirconia frameworks exhibited a significantly finer passive fit (5.5  $\mu\text{m}$ ) than titanium frameworks (13.6  $\mu\text{m}$ ) [1].

Dental zirconia specimens sintered at 1450 °C for 1 h combined good mechanical properties with the best resistance to low-temperature degradation independent of the commercial brand. Larger temperatures and times were detrimental for the structures [12].

**Table 4** Surface average roughness values after different zirconia surface treatments – modified after [3]

Surface treatment	Surface average roughness (S.D.) nm
Airborne-particle abrasion 125 $\mu\text{m}$ $\text{Al}_2\text{O}_3$ particles applied for 10 s at 60–100 psi	7.11 (1.1)
9.5 % hydrofluoric acid etching for 90 s	5.23 (0.9)
Selective infiltration etching (SIE)	26.02 (8.8)
Experimental etching (10 min, 30 min, 60 min) methanol (800 ml), 37 % HCl (200 ml), and ferric chloride (2 g)	54.22 (29.0), 81.79 (8.0), 103.02 (31.2)
Non-treated	6.94 (1.3)

A marginal preparation angle smaller than  $60^\circ$  may increase the risk of cervical chipping when using some milling systems [29].

The surface of zirconia ceramic is damaged during grinding which may affect the mechanical properties of the material. The micromotor produced a significantly higher temperature ( $127^\circ\text{C}$ ) than a high-speed handpiece ( $63^\circ\text{C}$ ) [13].

Ceramic surface polishing can be obtained by airborne-particle abrasion, polishing kits with or without polishing paste, or autoglaze at  $621^\circ\text{C}$  for 3 increase of  $83^\circ\text{C}/\text{min}$  up to  $918^\circ\text{C}$  for 30 s. For all ceramic types, the smoothest surfaces are obtained after autoglazing [6].

Among different cement types proposed for cementing zirconia restorations, those containing 10-MDP-based resin luting agents seem to have the best adhesive properties, but the bonds may be more effective and durable if associated with micromechanical retentions. Several surface treatments have been investigated (Table 4).

## References

1. Abduo J, Lyons K, Waddell N, Bennani V, Swain M (2012) A comparison of fit of CNC-milled titanium and zirconia frameworks to implants. *Clin Implant Dent Relat Res* 14(Suppl 1): e20–e29
2. Anusavice KJ (2012) Standardizing failure, success, and survival decisions in clinical studies of ceramic and metal–ceramic fixed dental prostheses. *Dent Mater* 28(1):102–111
3. Casucci A, Osorio E, Osorio R, Monticelli F, Toledano M, Mazzitelli C, Ferrari M (2009) Influence of different surface treatments on surface zirconia frameworks. *J Dent* 37 (11):891–897
4. Chen H, Lowe AA, de Almeida FR, Wong M, Fleetham JA, Wang B (2008) Three-dimensional computer-assisted study model analysis of long-term oral-appliance wear. Part 1: Methodology. *Am J Orthod Dentofacial Orthop* 134(3):393–407
5. Christensen GJ (2005) The state of fixed prosthodontic impressions: room for improvement. *J Am Dent Assoc* 136(3):343–346
6. Coşkun Akar G, Pekkan G, Çal E, Eskitaşçıoğlu G, Özcan M (2014) Effects of surface-finishing protocols on the roughness, color change, and translucency of different ceramic systems. *J Prosthet Dent* 112(2):314–321
7. Davidowitz G, Kotick PG (2011) The use of CAD/CAM in dentistry. *Dent Clin N Am* 55 (3):559–570

8. De Backer H, Van Maele G, Decock V, Van den Berghe L (2007) Long-term survival of complete crowns, fixed dental prostheses, and cantilever fixed dental prostheses with posts and cores on root canal-treated teeth. *Int J Prosthodont* 20(3):229–234
9. Duret F, Preston JD (1991) CAD/CAM imaging in dentistry. *Curr Opin Dent* 1(2):150–154
10. Flinn BD, deGroot DA, Mancl LA, Raigrodski AJ (2012) Accelerated aging characteristics of three yttria-stabilized tetragonal zirconia polycrystalline dental materials. *J Prosthet Dent* 108(4):223–230
11. Goodacre CJ, Bernal G, Rungcharassaeng K, Kan JYK (2003) Clinical complications in fixed prosthodontics. *J Prosthet Dent* 90(1):31–41
12. Inokoshi M, Zhang F, De Munck J, Minakuchi S, Naert I, Vleugels J, Van Meerbeek B, Vanmeensel K (2014) Influence of sintering conditions on low-temperature degradation of dental zirconia. *Dent Mater* 30(6):669–678
13. İşeri U, Özkurt Z, Yalnız A, Kazazoğlu E (2012) Comparison of different grinding procedures on the flexural strength of zirconia. *J Prosthet Dent* 107(5):309–315
14. Land MF, Hopp CD (2010) Survival rates of all-ceramic systems differ by clinical indication and fabrication method. *J Evid Based Dent Pract* 10(1):37–38
15. Libby G, Arcuri MR, LaVelle WE, Hebl L (1997) Longevity of fixed partial dentures. *J Prosthet Dent* 78(2):127–131
16. McLean JW, Hughes TH (1965) The reinforcement of dental porcelain with ceramic oxides. *Br Dent J* 119(6):251–267
17. Mormann WH (2006) The evolution of the CEREC system. *J Am Dent Assoc* 137(Suppl):7s–13s
18. Napankangas R, Raustia A (2011) An 18-year retrospective analysis of treatment outcomes with metal-ceramic fixed partial dentures. *Int J Prosthodont* 24(4):314–319
19. Pieger S, Salman A, Bidra AS (2014) Clinical outcomes of lithium disilicate single crowns and partial fixed dental prostheses: A systematic review. *J Prosthet Dent* 112(1):22–30
20. Pjetursson BE, Brägger U, Lang NP, Zwahlen M (2007) Comparison of survival and complication rates of tooth-supported fixed dental prostheses (FDPs) and implant-supported FDPs and single crowns (SCs). *Clin Oral Implants Res* 18:97–113
21. Sailer I, Pjetursson BE, Zwahlen M, Hämmerle CHF (2007) A systematic review of the survival and complication rates of all-ceramic and metal–ceramic reconstructions after an observation period of at least 3 years. Part II: fixed dental prostheses. *Clin Oral Implants Res* 18:86–96
22. Saint-Jean SJ (2014) Chapter 12 – Dental glasses and glass-ceramics. In: Shen JZ, Kosmač T (eds) *Advanced ceramics for dentistry*. Butterworth-Heinemann, Oxford, pp 255–277
23. Schaefer O, Decker M, Wittstock F, Kuepper H, Guentsch A (2014) Impact of digital impression techniques on the adaption of ceramic partial crowns in vitro. *J Dent* 42(6):677–683
24. Scurria MS, Bader JD, Shugars DA (1998) Meta-analysis of fixed partial denture survival: Prostheses and abutments. *J Prosthet Dent* 79(4):459–464
25. Service, U. D. E. C. (2011). *Synopsis of CAD/CAM systems*
26. Solaberrieta E, Mínguez R, Barrenetxea L, Etxaniz O (2013) Direct transfer of the position of digitized casts to a virtual articulator. *J Prosthet Dent* 109(6):411–414
27. Solaberrieta E, Mínguez R, Barrenetxea L, Sierra E, Etxaniz O (2013) Novel methodology to transfer digitized casts onto a virtual dental articulator. *CIRP J Manuf Sci Technol* 6(2):149–155
28. Solaberrieta E, Otegi JR, Mínguez R, Etxaniz O (2014) Improved digital transfer of the maxillary cast to a virtual articulator. *J Prosthet Dent* 112(4):921–924
29. Giannetopoulos S, van Noort R, Tsitrou E (2010) Evaluation of the marginal integrity of ceramic copings with different marginal angles using two different CAD/CAM systems. *J Dent* 38(12):980–986

Florin Miculescu, Lucian Toma Ciocan, Marian Miculescu,  
Andrei Berbecaru, Josep Oliva, and Raluca Monica Comăneanu

## Contents

Introduction .....	1218
Overview of Dental Prostheses .....	1219
All-Ceramic Dental Prostheses .....	1220
Metal-Ceramic Dental Prostheses .....	1224
Dental Prostheses Failure Analysis .....	1227
Causes of Failure for Ceramic Dental Materials .....	1232
Causes of Failure for Metal-Ceramic Dental Materials .....	1237
Conclusions .....	1243
References .....	1244

## Abstract

To accurately assess the real causes of failure of dental prostheses, the assemblies, the materials, and their surfaces should be analyzed to highlight the exact morphological and compositional aspects, which is also the aim of this chapter.

F. Miculescu (✉) • M. Miculescu • A. Berbecaru

Faculty of Materials Science and Engineering, University Politehnica of Bucharest, Bucharest, Romania

e-mail: [f\\_miculescu@yahoo.com](mailto:f_miculescu@yahoo.com); [marian.miculescu@upb.ro](mailto:marian.miculescu@upb.ro); [andrei\\_berbecaru@yahoo.com](mailto:andrei_berbecaru@yahoo.com)

L.T. Ciocan

Dental Medicine Faculty, “Carol Davila” University of Medicine and Pharmacy from Bucharest, Bucharest, Romania

e-mail: [tciocan@yahoo.com](mailto:tciocan@yahoo.com)

J. Oliva

Clinica Oliva Dental, Barcelona, Spain

e-mail: [dr.josep.oliva@gmail.com](mailto:dr.josep.oliva@gmail.com)

R.M. Comăneanu

Faculty of Dental Medicine, Titu Maiorescu University, Bucharest, Romania

e-mail: [monica\\_tarcolea@yahoo.co.uk](mailto:monica_tarcolea@yahoo.co.uk)



The experimental demonstration of the main causes and types of failure of dental prostheses consists of analysis of removed dental implants, fixed, single, and multitooth prostheses. These were collected from dental laboratories after their failure.

Within the presented analyses prospects related to the cross-section sample microstructure or prosthetic surface (where the failure appeared due to surface defects) were targeted.

Restorative dental materials include representatives of the main classes of metallic materials, polymers, ceramics, and composites. Most of the restorations are described by their physical, chemical, and mechanical parameters resulted from laboratory tests. Improvements of these characteristics may seem attractive for laboratory studies, but the real test of the materials' performance is done in the mouth cavity environment.

Although, at this point, the dental materials became of high performance, many types of dental prostheses fail fast or after a certain period of time, smaller than the estimated one.

---

### Keywords

Failure analysis • Dental prostheses • Dental ceramics • All-ceramic dental prostheses • Metal-ceramic • SEM • Surface analysis • Morphology • Interface • Fracture analysis

---

## Introduction

During the last century, dentistry has significantly transformed, becoming a very complex subject area. With this transformation, materials obtained a crucial role in every stage of dental treatment. Dental materials are in a continuous development as the technology progresses. Also, an increasingly important requirement of the patients is the natural appearance of the teeth, which leads to a higher focus on the aesthetic component [1–4]. Developments in the field of materials science and engineering have dramatically changed the way we look on the human anatomy replacing components, and thus, the dental restoration materials represent the foundation on the tooth structure replacement.

The form and function of the dental prostheses contribute enormously to the quality of life. Proper functioning of the mouth elements – teeth and soft tissue – is essential for speech, chewing, swallowing, and breathing. Dental restorative materials allow the reconstruction of hard dental tissues. Due to their success in long-term use, patients often expect dental restoration to have more quality than the natural teeth. The use of material science in the dental field is unique because the mouth has a high complexity. One can find bacteria presence, high stresses, variable pH, and a warm, fluid environment. The oral cavity is considered to be as one of the harshest environments for a material in the body [2, 4].

Restorative dental materials include representatives of the main classes of metallic materials, polymers, ceramics, and composites. Most of the restorations are

described by their physical, chemical, and mechanical parameters resulted from laboratory tests. Improvements of these characteristics may seem attractive for laboratory studies, but the real test of the materials' performance is done in the mouth cavity environment.

Although, at this point, the dental materials became of high performance, many types of dental prostheses fail fast or after a certain period of time, smaller than the estimated one. Therefore, to accurately assess the real causes of failure of dental prostheses, the assemblies, the materials, and their surfaces should be analyzed to highlight the exact morphological and compositional aspects, which is also the aim of this chapter [5–8]. In this respect, within this chapter the experimental demonstration of the main causes and types of failure of dental prostheses consists of analysis of removed dental implants, fixed, single, and multitooth prostheses. These were collected from dental laboratories after their failure.

Within the presented analyses prospects related to the cross-section sample microstructure or prosthetic surface (where the failure appeared due to surface defects) were targeted. Prosthesis surface characterization was performed without the special preparation of the samples. For the cross-section analysis, the samples were kept cool (the temperature during the polymerization and preparation of the samples did not exceed 45 °C) in a two-component polymeric resin, then were sectioned to reveal the sagittal and transverse planes, grounded and polished until ogling surfaces were obtained. Sample preparation was made using a Buehler metallographic sample preparation system. Electron microscopic analyses of the prosthesis were performed with scanning electron microscope Philips XL 30 ESEM TMP, equipped with an EDS EDAX Sapphire spectrometer, at University Politehnica of Bucharest, Department of Metallic Materials Science and Physical Metallurgy. The chemical compositions were analyzed on each component and each material constituent component.

---

## Overview of Dental Prostheses

Dental prostheses are natural bodies made of special materials in order to restore morphofunctional dent alveolar tissues. Generally, dentistry involves the use of two such categories: dental prostheses, which replace the missing tissue morphology and restore the functions of the affected maxillary and also the use of prosthetic device, to prevent, correct, or maintain certain ratios of the dentodental, dental-alveolar, or interarch [4].

Depending on the nature of fixity or mobility to the remaining teeth in the mouth, the dental prostheses can be fixed (aggregated to dental tissues intimately and cemented for long periods of time), movable (partially edentulous prosthetic field maintained by anchoring or use of special sliding), and mobile (total edentulous prosthetic field maintained by the phenomenon of suction, adhesion, muscle tonicity, anatomical retention) [3, 4] (Fig. 1).

The fixed prostheses can be microprostheses (single-tooth implants with small dimensions – Jacket Crown) or bridges (two or more teeth) and can be metallic (high

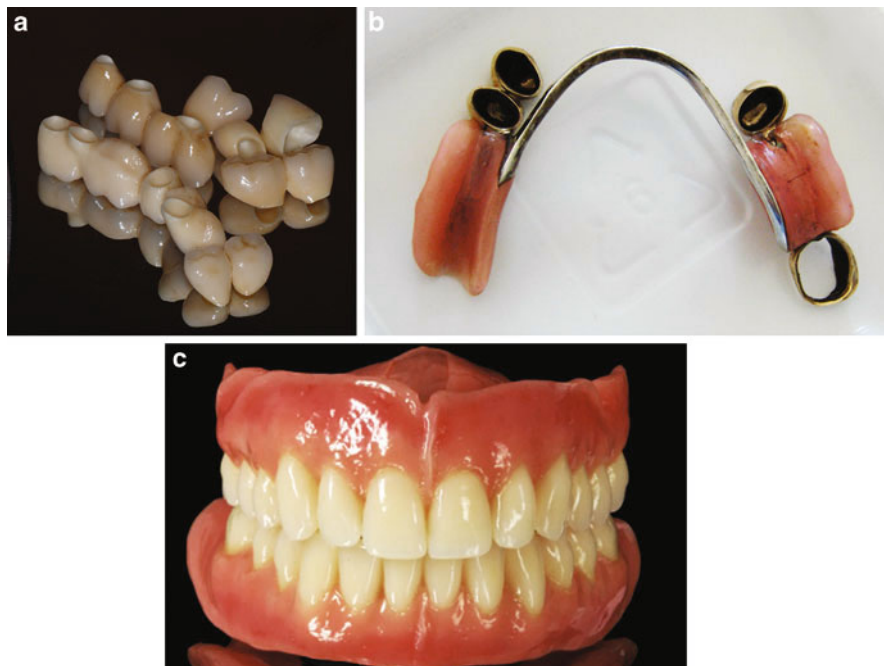


**Fig. 1** The main types of dental prostheses: (a) fixed; (b) movable; (c) mobile

noble alloys, noble alloys and common – steel, bronze), nonmetallic, acrylic resins, and dental ceramics or metal-acrylic metal-ceramic and composites [4].

Depending on production technology, the small prostheses can be molded, stamped, embossed (stamped), and soldered (crown from two pieces), polymerized, obtained by synthesis or obtained by combined techniques, cast synthesized, cast polymerized, or cast photopolymerized. Regardless of the type of the prosthetic restoration, all sides must be polished without micropores [6, 9]. In this chapter we consider some of the most common ceramic-ceramic and metal-ceramic technology-based dental prosthesis failure possibilities.

### All-Ceramic Dental Prostheses

In the vast field of dentistry, ceramic materials have become among the most used materials. Ceramics are one of the oldest known materials and are represented by compounds of one or more metals with a nonmetallic element (typically oxygen). They are made of chemical and biochemical substances that are stable, resistant, hard, brittle, inert, and that do not conduct heat and electricity [9–11].

Dental practice has proved that dental ceramics are dental restorative materials that can realistically duplicate hard dental structures. Although composite resins have a similar aesthetic potential, the major difference is that dental ceramics are way

more durable, wear resistant, and virtually indestructible in the oral environment. They are immune to the oral fluids and absolutely biocompatible. Due to their huge potential, there are many ways of research and development in dental ceramics. Ceramic applications include inlays and onlays, dental veneers, natural teeth, ceramic crowns, fixed partial dentures in the short- and long-term aesthetic component to metal crowns and bridges (metal-ceramic), artificial teeth (dentures – total or partial), columns, ceramic cores, and ceramic orthodontic appliances [1, 12].

Getting an aesthetic and durable material that can accurately reproduce missing teeth or tooth structure has always been a priority. Prior to using porcelain, dental crowns were made entirely of gold and other alloys. As the aesthetic appreciation grew, so has the use of colored resin tooth shades as a layer on the metal surface. Porcelain crowns were introduced in dentistry in the early 1900s, but back then they had many shortcomings: difficulty of manufacture, not being set well, and an easy tendency to fracture (half moon type). In the early 1960s, McLean developed a ceramic that could be deposited on metal. This led to the possibility of obtaining metal-ceramic prosthesis, which is now a significant proportion of the dental restorations [12, 13].

However, research on all-ceramic crowns continued. Although metal-ceramic restorations were a big success, they were not the final solution. The metal component, unlike the natural teeth, prevented light from reflecting and passing through, and in certain conditions, these crowns appear dense, dark, and opaque. The ideal aesthetic in this perspective would have involved the opportunity to reflect accurately the color of the dentin. Also, restoration edges appear dark, even when hidden under the gums, as they develop a bluish tint [4].

The first major breakthrough in full ceramic restoration was done in 1965, when McLean and Hughes proposed an alumina-reinforced core material, which increased the strength of porcelain. Even so, resistance was not strong enough for later use, and there is also the problem of marginal adaptation. The 1990s were the years in which all-ceramic crowns and fixed partial dentures have made major improvements. Restoration resistance increased alongside the rise of technology and with new types of porcelain. The new generation of ceramics included pourable glasses, uncompressed cores, cores that are modeled by injection, infiltrated alumina cores with high-strength glasses, CAD-CAM ceramics, etc. [13–15]. Modern all-ceramic dental restoration has partially solved one of the biggest problems of the first ceramics: low mechanical strength. However, there is still place for improvement as ceramic systems are complicated; they involve expensive manufacturing processes and equipment and dentist and dental technician extensive experience [6].

For the presentation and for fully understanding the types and causes of failure in prosthetic restorations with ceramics, we will present briefly the types of materials and possibilities of obtaining dental prostheses. Based on the sintering temperature, dental ceramics can be fused at high temperature (above 1300 °C), fused at medium temperatures (1100–1300 °C), fused at low temperature (850–1100 °C), or fused at ultralow temperature (below 850 °C). From the perspective of the manufacturing process, ceramic materials can be condensed, glass infiltrated, hot pressed, pourable, mechanically processed, or various combinations of the above processes [4, 12, 15, 16].

Ceramic materials with possible use in dental prosthetic technologies are feldspathic porcelain, leucite-reinforced glasses, glasses based on tetrasilicon fluoride, ceramics based on lithium disilicate, alumina-reinforced ceramics, zirconia-reinforced ceramics, and ceramics reinforced with spinel. The structure of these can be vitreous, crystalline, or vitrocrySTALLINE. The biggest disadvantage of the porcelain is that it is brittle. This liability drastically limits its use. For fixing this problem there have been developed numerous systems that prevent the formation and propagation of the cracks in the inner layer of the porcelain restoration. A possible approach involves the use of a pure alumina core on which the porcelain crown can be built. Alumina is a really hard material, opaque, which is less susceptible to cracks than porcelain. Another possible approach is the use of alumina inserts. These are small plates of alumina that are usually placed in the back of the crown to not affect the aesthetics [4].

The alumina powder may be added to the porcelain composition to achieve a significant increase in resistance. These improvements are obtained not only as a result of the superior mechanical properties of alumina but also because of the good compatibility between alumina and porcelain. The two materials have very close values of the coefficients of thermal expansion and elastic modulus. Therefore the interface region between the porcelain and the alumina is substantially free of tension and does not encourage propagation of cracks around the particles of alumina [11, 17].

Porcelain that contains alumina is called aluminous porcelain, and the designated alumina content is typically 40 %. Although aluminous porcelain has clear advantages in terms of mechanical properties, it is opaque; therefore it can only be used to achieve the inner dental restoration. It is an accepted fact, since the internal area is the one in which cracks appear, so that has to be reinforced [17–19].

Using additions of alumina for porcelain reinforcement was taken a step further by introducing sintered alumina core. For such a system, the first stage for the restoration manufacturing involves the formation of duplicated plaster dies from a special plaster. A strip of alumina is then created from aluminum powder and water on the matrix. The moist from the strip is then absorbed by the plaster, leaving behind a layer of alumina powder with the ideal thickness of 0.5 mm. This is later sintered using frittation at 1120 °C for 2 h. Sintering makes the matrix's material to compress, making it easy to remove the sintered alumina core. The external surface of the core is then coated with a suspension of glass powder; after that another frittation once at 1100 °C is done in order to liquefy the glass that will flow and fill the spaces between sintered alumina particles. In this case the type of glass named lanthanum aluminosilicate is used. Lanthanum reduces viscosity and assists infiltration. It also increases the refractive index of the glass and improves the translucency of the ceramic. The excess glass is then removed by sablation and fritted at 960 °C to ensure a good infiltration of the glass into the alumina [16].

A more advanced development of this method is making a sintered alumina core that contains a significant amount of zirconium oxide to gain better mechanical strength and bending resistance of approximately 800 MPa. A limitation of this method is given by the quite high opaqueness of the resulted core that can be hard to



**Fig. 2** Lithium disilicate all-ceramic crown with no defects

hide with glass infiltrations, thus limiting the aesthetic qualities of the final restoration [20, 21] (Fig. 2).

The ones obtained by injection and by compression represent another class of ceramic materials. These materials have been introduced in the early 1980s for manufacturing full-ceramic anterior and posterior crowns. The first commercial method that was based on this principle involved the production of a core for crown by injection, eliminating the need to use a platinum foil and improving the marginal adaptation of the crown. Noncompression properties are obtained by incorporating a substantial amount of magnesium oxide in the ceramic material. During fritation, it reacts with the alumina and forms a mixed metallic oxide named spinel. Spinel is less dense than the original mixture, and its making leads to an expansion that compensates compression during fritation. The latest pressing approach is based on disilicate lithium ceramics. The resulted piece can reach values of flexural strength similar to ceramics with sintered alumina core (300–400 MPa). This type of material is suitable for the manufacturing of three-unit bridges (fixed partial dentures) used to replace anterior or premolar teeth [4, 11].

Currently, the methods that are part of the polycrystalline ceramics and the poured glass materials category are only used for the manufacturing of unitary crowns and are substituted for other mentioned methods. The melted ceramic is centrifugally poured in the matrix at approximately 1350 °C. The result is a transparent glass crown that is afterward thermally treated in an oven at 1075 °C for 10 h. This thermal treatment induces a partial crystallization, creating crystals that contain K, Mg, Si oxides and significant quantities of fluorine, which have dual effect; they slowly reduce translucency and increase strength [7].

Color matching is achieved by applying to the surface a series of porcelains with different shades and refritting. The development of new materials in which the shade can be incorporated in the crown will undermine this method. Glazes used at the surface for establishing the color can cause a really realistic effect. Unfortunately, if any adjustment is needed for the shape of the crown, then these are removed and the crown needs to be reglazed. The pouring technique gives the ability to create

all-ceramic crowns that can be accurately adjusted and that can be strong enough to be used in the posterior region without the use of a metal substructure.

Another material that is introduced in dentistry is based on yttrium – tetragonal zirconia polycrystals (Y-TZP). Yttrium oxide is mixed with zirconia oxide to create a multiphase material known by the name of partially stabilized zirconia. This form of restoration can be processed using pouring methods or can be molded from monolithic blocks of partially of fully sintered material. For these kinds of Y-TZP ceramics there have been reported really high resistance values, both at flexural (900–1200 MPa) and yield point. The transformations from the crystalline lattice resulted in the volume growth that leads to the appearance of compression tensions around the beginning of the crack points. This minimizes the possibility of crack propagation [12].

One of the most modern technologies involves the use of ceramic restorations with CAD-CAM. The short name CAD-CAM comes from Computer-Aided-Design – Computer-Aided Manufacturing. This is a powerful approach that provides patients with sustainable restoration in natural colors. The method involves the recording of an optical impression, and afterward a restoration can be made with the help of a computer. The image details will be used to build the restoration with the help of a high-precision drill that will cut a block of ceramics under computer control. This technique is quite flexible from the point of view of the restorations that can be made. Restorations with three or four complex surfaces and ceramic facets can be achieved. The optical impression is recorded with a miniature video camera that scans the tooth for approximately 10 s. The surface of the tooth needs to be clean, dry, and covered with a reflecting powder in order to maximize the quality of the image. This layer of powder needs to be flat and as thin as possible. It can capture also an optical image of the antagonist teeth in order to determine the normal pattern of teeth, thus achieving a proper restoration surface anatomy [4, 7, 9].

## **Metal-Ceramic Dental Prostheses**

The mixed metal-ceramic crown is a modern form of treatment in the field of prosthetic coronary restoration and reduced edentation solving from their indicated perspective as dental bridge aggregation elements. Metal-ceramic dental prostheses are a part of the mixed dentures category, made out of a metal structure intimal contacted to the dental blunt and an aesthetic component. The aesthetic component partly or fully covers the metal structure, and in a mixed restoration it can be represented by thermal polymerizable acrylic resins, preparing ceramic masses and composites. Metal-ceramic restorations have been developed in 1965. The molded metal core has significantly increased the strength of porcelain restorations and, shortly after, it became the most used method of ceramic restoration. A study in the 1990s showed that approximately 90 % of dental restorations are metal-ceramic based [4].

Metal-ceramic restoration methods can be classified into poured metal-ceramic restorations (feldspathic porcelain cast and noble alloys, master alloys and titanium

castings and feldspathic porcelain cast porcelain fusion and ultralow temperature) and forged metal-ceramic restorations (gold sheet covering, platinum sheet covering).

The description of a metal-ceramic restoration can be realized from more points of view: from the aesthetic point of view, from the masticator point of view, and from the biological point of view. The aesthetic point of view is ideal because of the chromatic stability, the shades of color, translucency, and permanent gloss. These features are determined by the presence of inorganic dyes (mineral oxides), by the inertia of the compositional elements, and by the compact and waterproof structure of the ceramic mass. The aesthetic aspect is durable in time, being superior as against the aesthetic aspect of the mixed metal-acrylic crowns that modifies their color shades. Because of the existence of the metallic component on which the ceramic mass is sintered and because of the physicochemical phenomenon of oxidation that causes the bonding between the two materials, it is not possible to obtain the same optical effect as the Jacket porcelain crown or of natural teeth. For the correction of the aesthetic aspect, ceramic masses are being created and applied on the surface of the metallic cap instead of the primer. This has the advantage that it can be used way more easily than the primer. They are burnt two times in a row to fully opacify the metal component. These substances are deposited on a 0.2 mm width layer [4, 7] (Fig. 3).

From the masticatory point of view and from the functional occlusion stability point of view, the palatine faces for the frontal group and the occlusal faces for the

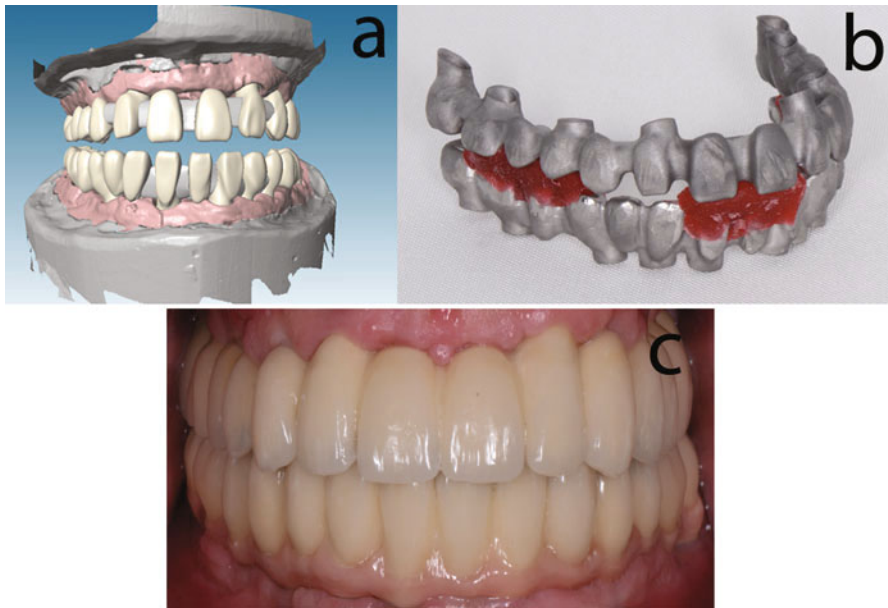


**Fig. 3** Porcelain fused to metal prostheses (a) CAD-CAM design, (b) metal framework, (c) PFM restorations “in situ”)



side group that are made out of ceramic mass or from a metallic alloy with morphofunctional individualized pattern that can efficiently participate in the food crushing process and maintain stable dentodental contacts. The ceramic mass, because of the glazed layer, is more resistant to wear than the ones without the layer, but the resistance at compression is the same. From the clinical point of view, to obtain multiple simultaneous and stable contacts, the required grinding can't be made after the cementing. Areas with no glazing, after a period of use, favor the appearance of wear facets participating in this way to the maxillary self-balancing [21].

From the biological point of view, it is not possible for a statement to be made to exhibit preference for this type of crown instead of the metal-acrylic one, because for both types of crowns, it is necessary to reduce the vestibular side to create the necessary space for the metallic and nonmetallic (aesthetic) component. Metallic component wall thickness is 0.3–0.5 mm. The thickness of the ceramic mass burned in the vestibular face is 1 mm. At the edges of the incision and occlusal sides, the layer thickness is larger than 1.5–2 mm. This space is obtained by grinding the natural tooth crown tissues. The ceramic masses' biological tolerability is far superior to the acrylic resins. Ceramics are well supported by the tissue, being inert [22].

Inflammatory reactions of the marginal periodontal that can be observed after the cementation of the metal-ceramic restoration are determined by the existence of a cervical margin of an oversized mixed crown. The ceramic mass layer and the cap wall overpass the dental abutment threshold, compressing the marginal periodontium including interdental papilla. The edge oversizing has two causes: tooth abutment preparation with an insufficiently sized threshold or the desire to obtain a particular aesthetic by applying a thick ceramic mass.

Indications and contraindications of the mixed metal-ceramic crown are required to be discussed in terms of what characteristics define the qualities, adding the comparative analysis with two other microprostheses that the specialists possess in the treatment options and may prefer in a given clinical situation, represented by mixed metal-acrylic crown and replacement crown. Metal-ceramic crown indications are ideal aggregation element in terms of physiognomy, biology, masticatory, and functional occlusion of dental bridges in all types of edentulism; restores coronary morphology of anterior and lateral teeth showing the shape and volume changes due to the lack of substance decay products, dysplasia, fractures, and abrasions; restores the color appearance of devital teeth; morphologically restoring a tooth group to provide functional occlusion conditions [7].

The mixed metal-ceramic crown contraindications are represented by the natural tooth crown morphology. All low-volume crowns particularly determined by the cervical incisal or occlusal very low size (primary or secondary) cannot get a mixed crown cover as the side surfaces are not effective to achieve the microprostheses retention on the dental abutment.

Casted metal-ceramic prostheses are very popular. Due to the metal frame being really resistant, it makes possible the completion of some long-term fixed dental restorations. They can also be used in difficult cases where the all-ceramic restorations can't be used due to the existence of really large tensions. Feldspathic porcelain

is used for fixation on metal. The ceramic composition used for metal-ceramic restorations is different than the composition of the porcelain used for full-ceramic restorations, being richer in potassium oxide and sodium oxide. High content of alkaline was necessary to increase the coefficient of thermal expansion. Unfortunately, this increased the tendency of the ceramic material to devitrify and gave it a cloudy aspect [4].

The ceramic masses made for the use of being burnt on metallic alloys have in their composition 10 % potassium oxides, 15 % aluminum oxides, and 55 % silicon oxides, to which sodium and calcium oxides are added. For some special ceramic materials, titanium and cesium are added. The main physicochemical characteristics of ceramic masses burned on metal alloys are summarized below.

Usually, these materials are impenetrable to the oral environment, property conferred by the inorganic compact structure.

Technologically speaking, it is possible to obtain the required colors after sintering, due to the selection of the material from the vials with the help of the color key. These ceramic masses have good plasticity, and so after the preparation of the paste, a mass will result that can be put on and molded into those surfaces. Due to evaporation of the slurry preparation liquid during the firing they have a low contraction coefficient. The fact that it does not change its volume, which would favor the production of cracks, is really important, and so it has thermal stability at temperature variations and are unfavorable in the firing cycle.

The links between the metallic material and the ceramic material can be the chemical bond type at the porcelain-metal interface or the mechanical adhesion of porcelain to metal type. The chemical bonding is considered to be the main linking mechanism. An adherent oxide layer is essential for a good bonding. In the case of base alloys, the chromium oxide is responsible for the bond, but in the case of noble alloys this role is played by the tin alloy, indium oxide, and possibly iridium oxide. Inappropriate oxide formation and oxide excess may lead to poor bond formation and result in the delamination of the porcelain layer. The main advantages are better resistance to tearing due to the metallic reinforcement and better marginal fixing because of the metal frame. Significant disadvantages involve lower aesthetics in comparison to total-ceramic restorations, because the metal layer and the opaque reduce the general translucency of the tooth, and also the fact that this metallic frame is sometimes visible at the edge of the tooth, resulting in dark edges. Regardless of the type of prosthesis, ceramic-ceramic or metal-ceramic, it needs to be mounted inside oral environment [22–26]. The final cementation is done for longer periods of time expressed in more or less years. The final cementation is realized if a cement that was manufactured and marketed for this purpose is used.

---

## Dental Prostheses Failure Analysis

Dental restoration materials are subjected to a hostile environment, in which the PH, the saliva quantities, and the mechanical charge are fluctuating constantly and often quickly. These challenges have resulted in substantial research and development in

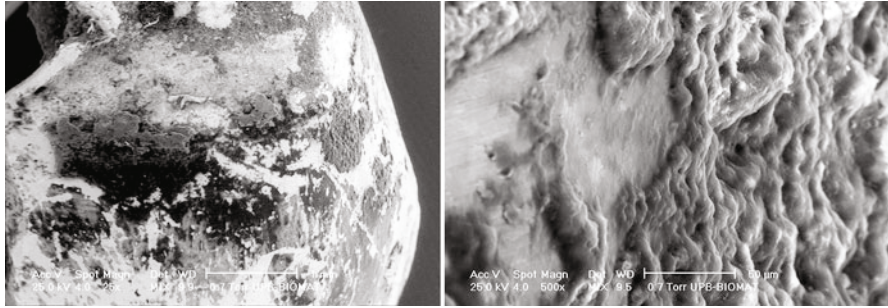


**Fig. 4** Deposits of biological material on the surface of a dental prosthesis-emergence of degradation phenomena

order to provide the dentists with functional products. These things are possible due to the application of some fundamental concepts of material science. Understanding the polymers, ceramics, and metal properties is crucial in order to select and achieve the dental restoration plan. No material property can define its quality by itself. To describe the quality of the material, usually more properties taken from standardized laboratory and clinical tests need to be appreciated. Standardization of laboratory tests is essential to quality control and to allow the comparison of results between different researchers [27–29]. While it is important to know the comparative values of restorative material properties, it is also essential to analyze the hard and soft tissues that support the prosthetic restoration (Fig. 4).

Many dental restorations fail clinically due to fracture or deformation. This is an issue of material property. Also, some restorations flawlessly realized become useless after the failure of the supportive tissue. This is an interface or substrate failure. Therefore, when designing a restoration and when interpreting laboratory tests, it is important to note that the success of dental restorations depends not only on the physical and mechanical properties of the used materials but also on the biophysical and physiological features of the support tissues. According to a study on the causes of failure of dental prosthetics, 30 % are due to oral diseases and 70 % for mechanical reasons [23].

And so, the failure of dental materials can be the result of different factors such as biological (saliva, plaque deposition), mechanical (wear, fractures), technological (voids, inclusions, incorrect overlaps), or the patient (occlusive tension size, pH value in the mouth). Also, in the mouth, restorative materials are exposed to changes in the chemical, thermal, and mechanical nature. These may cause deformation of the material. The performance of the material in the oral environment depends on concepts such as elastic, plastic, and viscoelastic deformations and mechanical quantities such as force, stress, strength, hardness, and toughness [23, 30] (Fig. 5).

Occlusal forces that are formed between the teeth of adults are higher in the posterior region and descend from molars to incisors. The maximum occlusive forces range from 200 to 3500 N. Forces on the first and second molars range from 400 to 800 N, and the average load on the bicuspid, cuspid, and incisors is

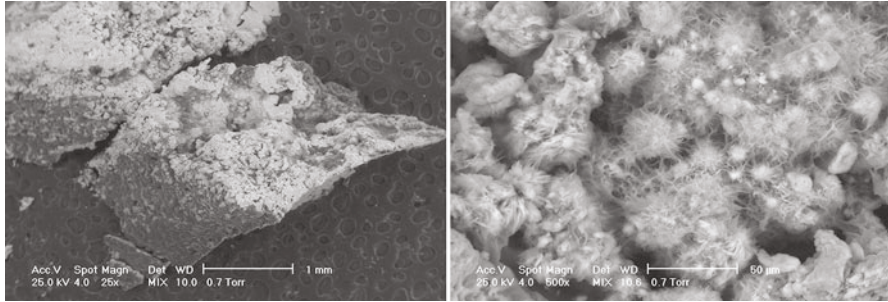


**Fig. 5** Peeled tartar deposition on the surface of fully ceramic dentures

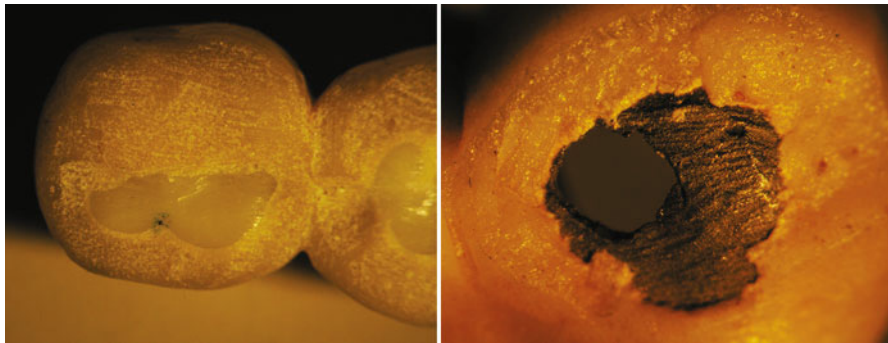


**Fig. 6** Metal-ceramic and all-ceramic prosthesis degraded by abrasion in the mouth

300, 200, and 150 N. In the case of dentures, occlusal forces are generally smaller than the natural dentition forces. For patients with movable partial dentures generate occlusive forces in the range of 65–235 N. For patients with complete artificial teeth, the molars and bicuspid medium force is about 100 N and for incisors 40 N. Variations in the age and sex of population contributes to the large variation in forces. In general, the occlusive force produced by women is 90 N less than that those produced by men. The shape and the define degree of facial muscles are also factors that determine the magnitude of the occlusive force [7, 31].

The maximum occlusal force and the response of surrounding tissue change with anatomical location, age, with the occlusal scheme and placement of dental implants. When designing a restoration and when the materials are selected, it is important to take into account the location, the opposing teeth, and the patient's ability to generate force. These factors can often be estimated by the success or failure of other restorations in the mouth. A material or a model of restoration may be suitable for occlusive forces of the anterior segment but not strong enough for posterior segment [4, 7] (Fig. 6).

Tensions are crucial. When a constraint force is acting on a body, this resists to the initial force. This internal reaction is equal in size and opposite in direction with the

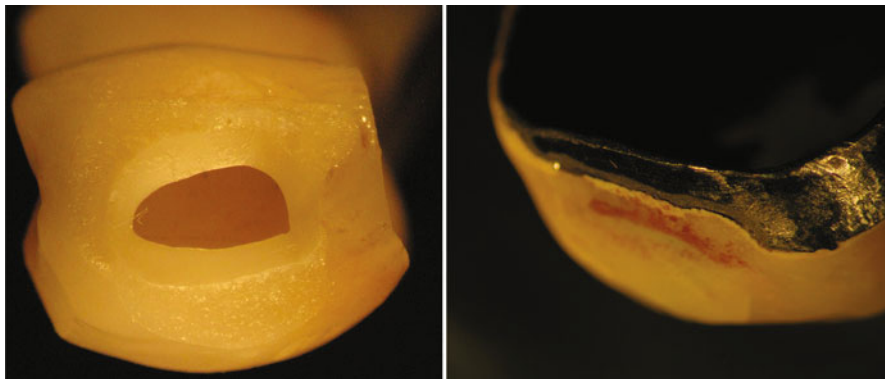


**Fig. 7** The failure of prostheses due to ceramic layer mechanical exfoliation (*left*) and a full-ceramic restoration cracking following tensions and forces applied (*right*)

applied force and it's called stress, denoted by  $\sigma$ . As the tension in a structure varies proportionally with the force and inversely proportionally with the area, that area on which force is applied is very important to consider. This is even more important for dental restorations, where the areas over which large forces are acting are often very small [4, 32]. For example, at the corner of a tooth, the contact surface may have a section area of only 0.15–0.015 cm<sup>2</sup> (Fig. 7).

The stress is always normalized on an area of 1 m<sup>2</sup>, but dental restoration in the form of a small occlusive cavity may have a surface area of up to 4 mm<sup>2</sup>, if the side of the restoration is 2 mm. If an occlusive force of over 400 N is concentrated in this area, the developed stress will be around 100 MPa. So, tensions equivalent to several hundreds of MPa are often encountered in dental restorations. Therefore, when an occlusion is balanced, multiple simultaneous occlusive connections are required. Distribution of occlusal forces on larger surfaces reduces local occlusive stress. Very rarely do forces and stresses happen to be isolated on a single axis. The forces applied individually may be defined as axial, of shear, of torsion, and of bending [4, 33, 34].

Each type of tension is capable of producing a deformation corresponding to that body. Deformation from a stretching tension is an elongation of the material, while the one from the compressive tensions is a compression of the material. The deformation,  $\varepsilon$ , is described as being the change in length ( $\Delta L = L - L_0$ ) on the original length ( $L_0$ ) of the body that is subjected to a mechanical load. Deformation is often reported as a percentage. This will be different depending on the type of material and the applied force magnitude. Deformation is an important factor in the analysis of dental restorative materials, such as orthodontic wires or implant screws, which deforms extensively before failure. The wires can be bent and adjusted without fracture [7].

Determining the yield limit of the dental material is important for several reasons. Any dental restoration that is permanently deformed due to masticatory forces may be considered to a certain extent a functional failure. For example, a fixed partial

denture, which is permanently deformed by excessive occlusive forces, will present altered occlusal contacts. Restoration is permanently deformed because a tension equal to or greater than the yield limit was generated. It is important to note that a distorted restoration is possibly subjected to higher stresses than the original because of the occlusion, which was previously spread over a larger number of contacts, it is now carried out on a much smaller number of contacts. Under these conditions, fracture does not occur if the material is capable of plastic deformation. And so the permanent deformation of the restoration resulted, which is an example of destructive deformation [11].

Permanent deformation of dental materials and the application of tensions higher than the elasticity limit are desired when seeking the shaping of an orthodontic arch wire or when you adjust the bracket of a removable partial denture. In these examples, stresses need to exceed the flow limit in order to bend permanently the element. Elastic deformation occurs when the wire or fastener attaches and detaches from the cervical area of the tooth. The retention is achieved by elastic deformation on a smaller scale.

The tension at which a brittle material is fractured is called ultimate strength. This is very important for ceramic materials. It should be noted that the material does not necessarily break at the point in which the largest stress occurs. After a maximum stretching force is applied to the ductile materials, the sample begins to elongate excessively, which leads to the bottleneck phenomenon, or the considerable decrease in the sectional area. However, this does not occur with brittle materials. The tension calculated with the force and cross-sectional area may decrease prior to the final fracture. In specific cases of many dental alloys and ceramics subjected to stresses, ultimate strength and braking strength values are similar [35].

The elasticity of a material is described by the term *tensile modulus*, or *Young's modulus*. Other materials such as elastomers and other polymers have low elastic module values, while different metals and ceramics have higher values. The modulus of elasticity is the stiffness of a material in the elastic interval. It can be determined from a stress–strain curve with the equation: modulus of elasticity ( $E$ ) = Stress ( $\sigma$ )/strain ( $\epsilon$ ). For ceramics, this curve has a specific form.

Strength is the maximum stress a material can withstand before its failure. Depending on the applied tension, the resistance can be compressive or tensile. Basic strength of an alloy used in dentistry specifies both maximum supported load and minimum sectional area when developing a restoration. An alloy that was loaded up to the breaking limit will remain permanently deformed, so a restoration receiving that amount of tension during operation becomes unnecessary. An error range needs to be incorporated into restoration achievement plan and the material selection to ensure that the breaking limit is not reached in the normal operation of the device. Yield point is often of greater importance than the breaking point for the selection of the material as it is an approximation of the moment in which the material will begin to deform permanently. Most dental materials have those values clearly determined and recorded in the product data [4, 36].

The resilience of a material is the resistance to breaking and indicates the energy required to cause a fracture. The area under the elastic and plastic portions of the

curve of stress/strain is the toughness of the material. In the case of ceramics for dental use, the resilience may be superior to that of dentin but usually is less than or close to the enamel's value. Tenacity is the energy necessary to strain the material to the point where it fractures. Brittle materials tend to have low toughness because small plastic deformations occur before failure, so the area near the elastic and plastic zones of the curve is not that much different from the area just beside the elastic zone. From this perspective, dental ceramics have low values of toughness [4].

Recently, the concept of fracture mechanism has been applied to a number of problems in dental materials. The fracture mechanism characterizes the behavior of materials with cracks and other defects and can usually be identified by means of microscopy (stereo or scanning electron). Defects and cracks may occur naturally in a material after it has been in use for a while. Any defect weakens the material, and as a result, fracture occurs at lower stress than the flow limit. Catastrophic fractures often occur in the case of brittle materials, which don't have the ability to be plastically deformed and to redistribute tensions. The field of breaking mechanisms analyzes the behavior of materials during this type of failures. For brittle materials such as glass, the absence of local plastic deformation is associated with fractures, while for a ductile material, a plastic deformation such as the ability to bend happens with no fracture [37–39]. The ability of a material to be plastically deformed without breaking is called fracture toughness.

Generally, when a defect is larger, the stress required to cause fracture is smaller. This thing occurs because tensions, which are normally supported by the material, now concentrate on the starting point of the defect. Fracture toughness was measured for various important restorative materials such as acrylic ones for the denture base, composite, corrective ceramic braces, cements, alloys, natural enamel, and dentin. Typically, the binder addition in polymers can significantly increase the fracture toughness. Strengthening mechanisms are believed to be binder-matrix interactions, but this is still not clear. Similarly, the addition of up to 50 % of the weight of zirconia in ceramics increases fracture toughness [40].

---

## **Causes of Failure for Ceramic Dental Materials**

Alumina (aluminum oxide) is the only solid oxide of aluminum ( $Al_2O_3$ ). Alumina was firstly used in the 1970s, but clinical applications from this period showed a fracture rate of 13 %. Failure in this first generation of ceramic is due to the fact that they could not be processed to a high final density. A second improved generation presented a higher density and smaller grains. Fracture rates associated with the second generation decreased with 5 %. Today, a third generation of ceramic components is available, characterized by high purity, maximum density, and fine microstructure [15].

However, despite the best properties and the potential possibility of use as a structural material it has been greatly limited by typical fracture strength of ceramic material. The cracks rapidly propagate in the ceramic, and so they unexpectedly fail during use, and in many cases catastrophically, even when the impact force is below

the resistance of the ceramic material. The resistance to crack propagation is the ability to activate a mechanism of increasing resistance, such as the deflection [16, 17].

A current study indicates that certain ceramic crowns have a good wear resistance, similar to metal-ceramic crowns. The role of ceramic surface treatments that may be responsible for changing the wear rate is still determined by clinical trials. Tooth structure wear is a natural process that cannot be avoided and occurs when two teeth or a tooth and a dental restoration are in contact and they slide. This natural process can be accelerated by the introduction of a restoration whose wear properties differ from those of the tooth structure of which it is in contact. It can be shown that enamel can be loaded to high levels of wear when in contact with a ceramic material. So far, restoration materials with a wear behavior similar to natural enamel is aimed, because excessive wear can lead to serious clinical problems such as loss of vertical dimension of occlusion, reduced masticatory function associated with temporomandibular joint remodeling, dentin hypersensitivity, etc. [41].

In the mouth there are many factors that contribute to the wear of enamel and dentine, such as the nature of occlusal contacts with opposing teeth (attrition), chewing, tooth brushing, dust breathing (abrasion), acid attack due to consumption of certain fruits or drinks, inhaling industrial acid, or gastric regurgitation when suffering of bulimia and anorexia (corrosion). To observe and quantify the wear it is necessary to know the teeth wear mechanism and how it can be measured and evaluated, both clinically and in the laboratory. The attrition, abrasion, and corrosion terms are often used to identify the various mechanisms that lead to wear or dental restoration failure. Tooth-to-tooth contact causes a wear type called attrition, this taking place without the presence of food or other foreign substances during swallowing and clenching; it is typically characterized by the sides of tooth on an opposite tooth. It gets worse during bruxism [7].

Abrasion is the wear caused by friction between a tooth and an exogenous element. Masticatory abrasion occurs usually when friction is given by the food presence, while abrasion is the result of harmful habits such as nails, pencils, and other hard object biting, opening hair clips with the teeth, etc. Occupational abrasion can occur when repeating a harmful gesture is related to the individual restoration (such as musicians). Ceramic has a high hardness, which can be defined as nonbiological. Even normal cleaning process may cause abrasion of the used tooth restoration material, over time. In developed countries, the main factor that leads to abrasion is the toothpaste that affects to a greater extent the enamel dentine. Brushing without toothpaste has absolutely no effect on the enamel and negligible clinical effects on dentin [42].

The **degradation** is the loss of material from the tooth surface caused by chemical dissolution. Depending on the acid source that produces dissolution, there are two types of degradation: intrinsic and extrinsic. Tooth degradation (corrosion) caused by intrinsic sources such as bulimia and gastroesophageal reflux gives a translucent and thin enamel surface. In addition, consumption of food and drinks with a pH value of less than 5.5 can cause degradation and demineralization of teeth (Fig. 8).



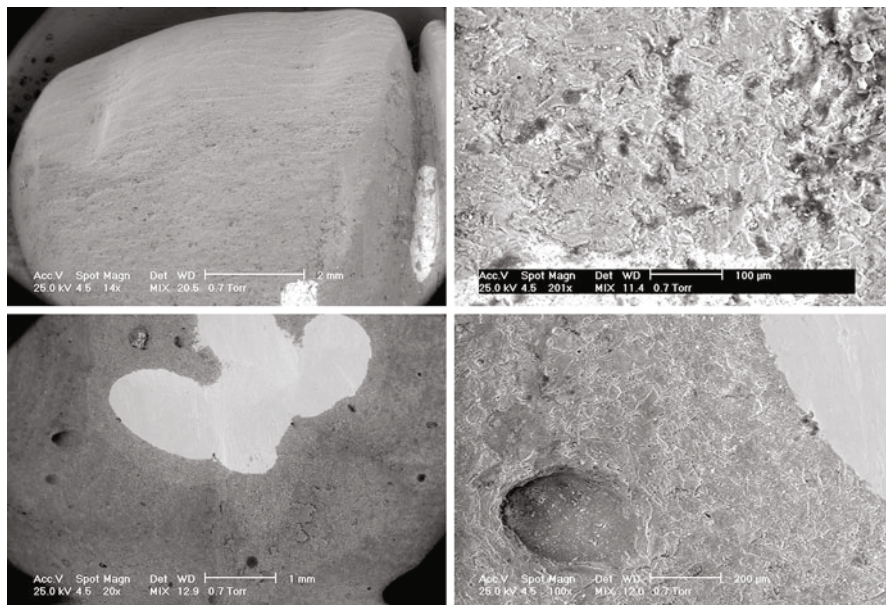


**Fig. 8** Ceramic prostheses degradation by abrasion phenomena (left-macroscopic analysis and right-detailed images of the same area)

Weakened enamel that is exposed to saliva for an appropriate period can regain minerals, thus increasing its mechanical strength. On the other hand, it was proven that fluoridated toothpaste has a protective effect on enamel corrosion progress. In vivo and in vitro studies indicate that the wear mechanisms rarely act alone, but instead they interact with each other so that teeth wear is the result of three processes: abrasion, corrosion, and attrition [23].

**Gaseous inclusion** appearance is one of the most important issues that may arise during the obtaining of ceramic bodies. All the ceramic masses that are burned at atmospheric pressure have interwoven structure, with more or less air microcavities. In dental ceramic masses burned in vacuum, most of the air is absorbed from the substance particles, allowing the melted feldspar to flow in the gaps. Gas inclusions in the structure of dental ceramic have negative influence to their physical properties. The bigger the number and the volume of gas inclusions the greatly diminished transparency (Fig. 9).

The pores in the ceramic structure create unfavorable conditions for polishing the Jacket crown's surfaces. Open pores are retentive microspaces that cause debris deposition and promote discoloration. The worst is that gas inclusions decrease the resistance of the walls making it possible to fracture more easily [6].

The main causes of gas inclusions are described below. Powder dental ceramic masses are prepared by mixing it in distilled water or alcohol. The amount of liquid is minimized by vibration and drying (buffering), and after the evaporation of the

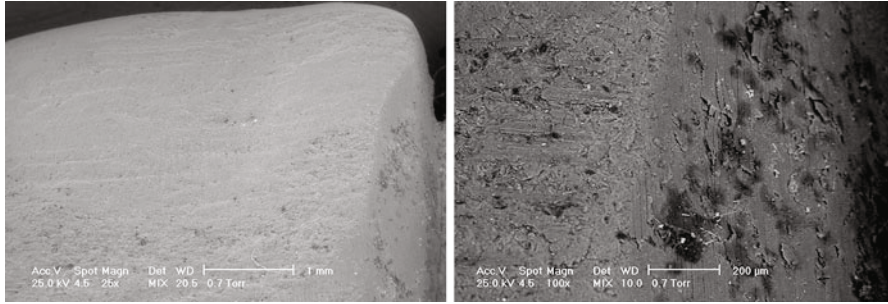


**Fig. 9** All-ceramic restoration surface degradation through chemical dissolution phenomena

liquid (drying and firing) gaps remain. They are more and bigger when not built up conscientiously (vibration and buffering).

Also, dental-ceramic masses have nonplastic material composition (feldspar and quartz). Organic matter is added after drying in order not to crumble (dextrin, sugar, starch). These ingredients burn without leaving a trace, though creating blanks after burning. An additional reason is due to the fact that during the preparation of the paste and deposition of the ceramic mass, there is the possibility of air incorporation, which remains between particles of different substances. At the same time, the molten silicates incorporate gases at high temperatures, which are not released when decreasing temperature [43].

Another possibility of the pore occurrence is due to the fact that during agglutination, small mineral powder gaps occur at the particles' boundary. They form a small part of the total pore volume. It is known that in the ceramic mass containing particles of a single size case, keeping as closely as possible is the most effective means of condensation, the space between them representing 45 % of the total volume. If the particles present two dimensions, the space may be reduced to a minimum of 25 %; when three or more dimensions are used then it can be reduced to 22 %. Different powder particle size of ceramic masses favors the approach between them, creating, after burning, more compact and resistant bodies (Figs. 10 and 11).

By using a high-vacuum oven, it is possible obtain the removal of gas from the unburned structure. The burning conducted exclusively in vacuum creates a surface with crater-like depressions. The bursting of bubbles close to the surface forms them. It has been proven that only by combining vacuum combustion and atmospheric pressure, a smooth surface can be obtained. \*The vacuum is maintained until the end point of the agglutination is done; after that it stops in order to obtain a smooth surface [44, 45].

Although dental restorations must meet strict aesthetic criteria, the most important aspect remains the functional need. Recent research and development of new technologies have led to the introduction of new ceramic materials for dental prosthetics, with its aim of obtaining an optimal combination between strength and aesthetics. Numerous clinical studies have shown that the rate of fracture of

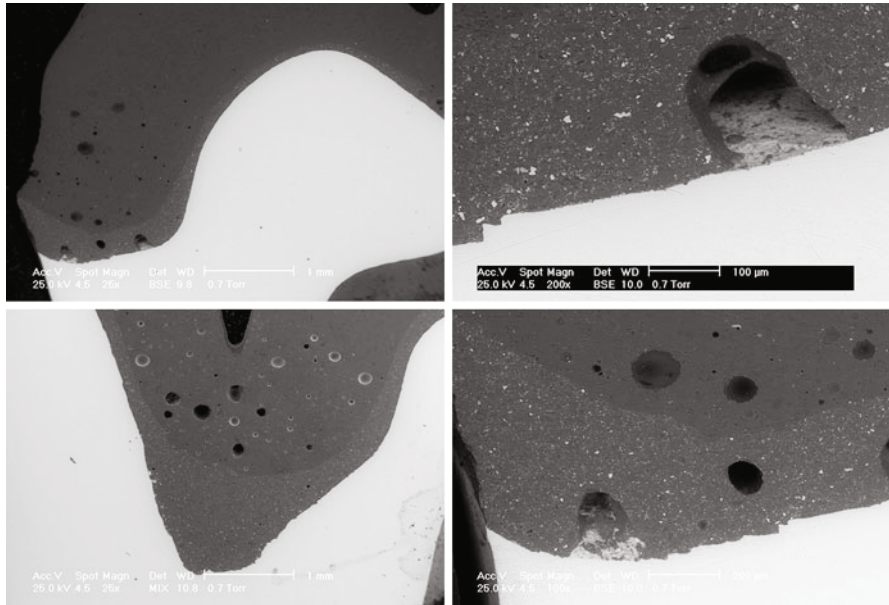


**Fig. 10** Pores – gaseous inclusions in the ceramic layers of coverage media for zirconia-ceramic prostheses

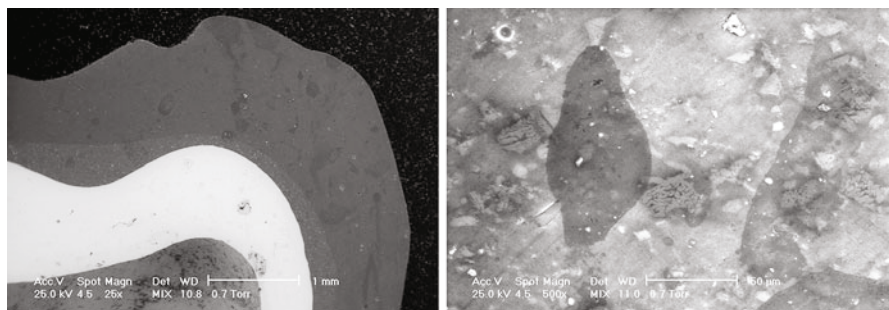


**Fig. 11** Microstructural inhomogeneity in all the layers of all-ceramic prostheses

porcelain faces mounted on zirconium core varies between 6 % and 15 % over a period of 3–5 years, while it is only 4 % for conventional metal-ceramic restorations. The types of fractures that can occur with these types of dental restorations are

- Cohesive: the fracture is located in the internal structure of the porcelain coating (cutting).
- Adhesive: porcelain – zirconium interface.
- Complete: complete rupture of the crown.

As a result of laboratory research, it can be said that porcelain restoration on zirconia core has a higher proportion of cohesive fracture (72 %), as compared with the metal-ceramic ones (8 %); However, metal-ceramic restorations show a much higher rate of adhesive breakage (92 %), as compared with porcelain-zirconium (25 %). Both crowns are susceptible to deformation of the outer layer in the occlusal zone, with fracture projecting from the central point of the force application area to the periphery, where the porcelain delamination occurs. To date, few studies are made on the resistance of dental restorations with zirconia core covered with porcelain in comparison with the abundance of information on metal-ceramic crowns. The zirconia-based dental crown fractures are found most frequently within the porcelain layer, which are more than in the case of metal-ceramics, the top product failure being the chipping. Until this moment, there have not been identified any chemical bonds between zirconium and the porcelain layer. The two substances are fixed by mechanical interposition and by the forming of compressive stress resulting from thermal contraction during cooling after sintering. Therefore, we can say that the most common fractures occur in the layer of porcelain and at the zirconia-porcelain interface [46].

---

## Causes of Failure for Metal-Ceramic Dental Materials

Factors that may lead to the failure of dental metal-ceramic prosthetic restorations include technical factors, factors owed to the dentist, material properties, direction, size and frequency of the applied force, environmental factors, etc. Because ceramic materials are a very important component of metal-ceramic prostheses, some of the causes of failure of these prostheses are similar to those that can occur in all-ceramic prostheses. Currently, a significant part of the metallic materials used in dentistry is titanium (titanium alloys), Co-Cr alloys, and Ni-Cr alloys. Good physical-mechanical properties of these materials, relatively low Young's modulus, fatigue strength, and good corrosion and biocompatibility are all very important. Choosing a metallic material type in metal-ceramic technology holds several technical, medical, and economical considerations [47] (Fig. 12).

Regardless of the particular alloy and the technology and materials used, inherently, there may be different types of defects that lead to failure of dental prosthetic restoration [4, 11]. The main causes of defect occurrence in these cases are

- The mass and alloys have not been compatible.
- Bonding or oxidation have been misused.
- Cape made with deformable walls.
- Stress insertion on the blunt.
- The cement with high viscosity, the insert was obtained under high pressure.
- Reduced size of the ceramic layer.
- Adhesion oxides were thick.
- Sintering was performed with incorrect technical regimes.

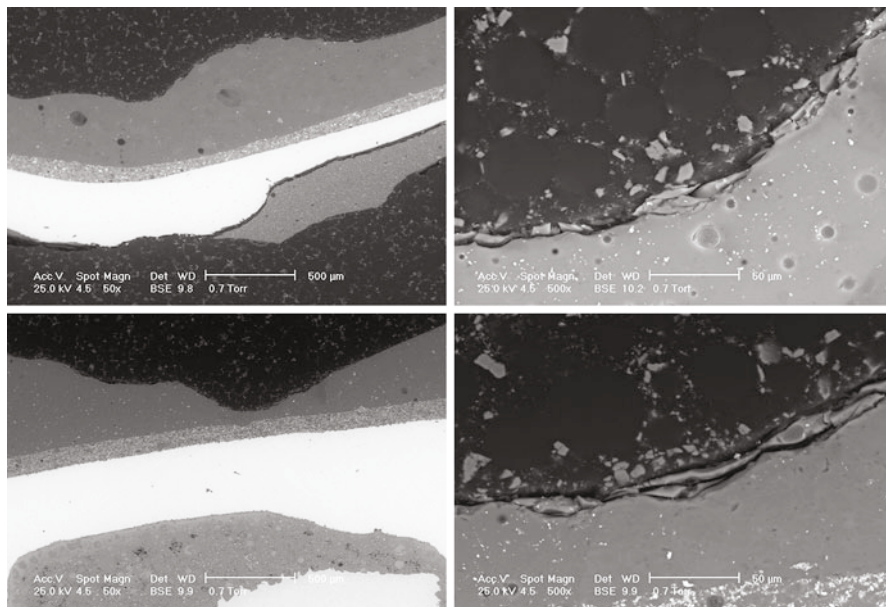


**Fig. 12** Identification of wear and delamination phenomena by abrasion of ceramic layer on a metal-ceramic restoration

- Restoration carried out in adverse conditions, many impurities in the working space [11].

Metal-ceramic prostheses are durable, but most often the failure is due to premature fracture of the ceramic coating. It has been proven that there is a direct relationship between the fracture of the porcelain and the durability of fixed partial dentures. Compared to uncoated ceramic prosthesis, the metal-ceramic show, after 10 years, a much higher risk of failure [6]. It is well known that the fracture resistance is severely reduced when the ceramic material is deposited on an oxidized metal substrate. At the same time, the risk of fracture of the ceramic component of the prosthesis increases with the increasing thickness of the oxide layer above a certain limit [11] (Fig. 13).

A very important factor of the compatibility of metal-ceramic prosthesis components is the expansion coefficient of metal and ceramic material. The stress concentration at the metal-ceramic interface is due to the major difference between the expansion coefficients of the two components. To reduce the possibility of failure for this reason, the coefficient of thermal expansion of the ceramic material should be slightly smaller than that of the metal parts of the dental prosthesis [11]. It is also known that the mechanical strength of the prosthesis decreases with the increase of the ceramic layer thickness. The ceramic component at the interface with the metal substrate is usually tensioned, as the metal shrinks more than the ceramic. In this sense, to minimize the possibility of fracturing the ceramic layer

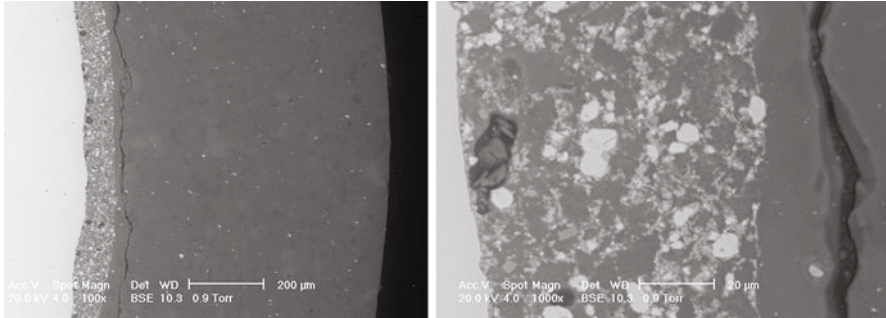


**Fig. 13** The appearance of cracks in the ceramic layer longitudinally in the opaque layer of metal-ceramic restorations

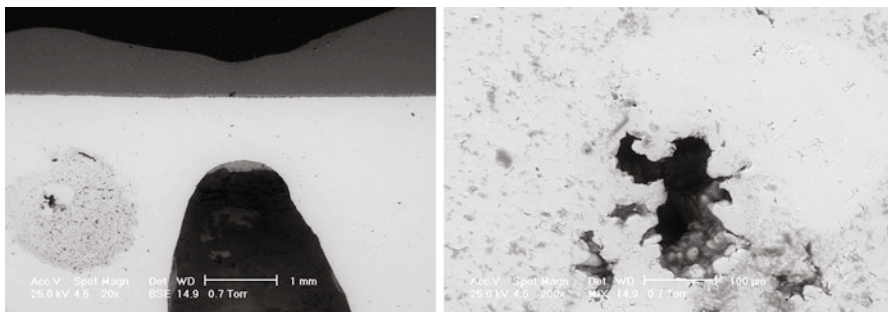


**Fig. 14** Metal mass casting pore defect type

deposited on the metal, it is recommended to obtain a uniform thickness of the ceramic deposit (Fig. 14).

The identified defects (pores and cracks) in the ceramic masses deposited on metal frames appear due to technical problems during the application of ceramic materials. Cracks may occur due to the incomplete densification that induces the appearance of angular residual pores. This type of failure may occur, however, when the metal substrate doesn't have a modulus of elasticity big enough to withstand mechanical loads of the dentomasticatory device. An important aspect that should be followed during the obtaining of metal-ceramic restoration, in order to avoid cracks, is the heating and cooling rates. From this perspective, repeated thermal cycling and overheating the sintering furnace can induce the appearance of superficial or deep imperfections in the ceramic material [7, 11].

Poor clinical interventions are always followed by other problems in the lab. When probing, the axial and transversal inadequacy in the cervical zone may be noted. When one finds axial inadequacy, the short cape requires rebuilding after a new mask or on the same model if the defect appears on the model. Transversally inappropriate cape (large) is recovering after another masking and model manufacturing. The long caps are retouched step by step. At the same time, the

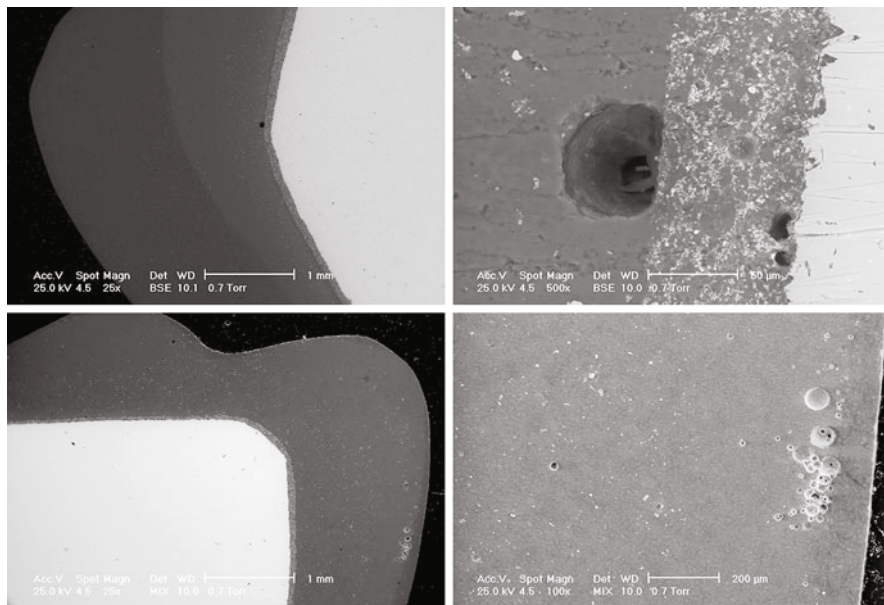


**Fig. 15** Pore type defect in the opaque layer and first ceramic layer of metal-ceramic restorations

occurrence of some casting defects represented by pores is possible. Defects in the form of pores determine the restoration of the cape. Isolated pluses that are well contoured are polished [6]. Additionally, the sizes and cross-sectional outlines of all components have important effects on the stability and strength of the entire metal-ceramic prosthesis structure [4]. The connector must be thick enough to support the occlusal loads, but gingival and occlusal embrasures must be obtained so as to be aesthetic (Fig. 15).

Failure factors correlated to the dentist are different. Within them, the most important are related to the fact that metal anterioposterior substructures are curving when loaded complexly or excessively, which leads to the fracture of the ceramic coating of the prosthesis. Also, a major risk of failure presents the prosthetic replacement restorations of three posterior teeth. For the risk avoidance associated with uneven distribution of forces and possible mechanical failures in these cases it is recommended to use implant supported prosthetics or partially mobilized teeth [11]. One factor that can lead to failure of the prosthesis because of the dentist is the inappropriate preparation of the teeth (resulting interocclusal space insufficient for the metal structure and overlapping the ceramic deposits). Therefore, cracks may occur during the technological process or shortly after starting. That's why the experience of the dentist is very important in order to obtain a correct design, this inherently leading to achieving a long-lasting prosthetic restoration (Figs. 16 and 17).

Detailed analysis of denture fractures is rare in the literature and dental biomechanics. In most cases, the fracture surface of the prosthesis, which is essential for fracture analysis, is destroyed or severely damaged over the point where

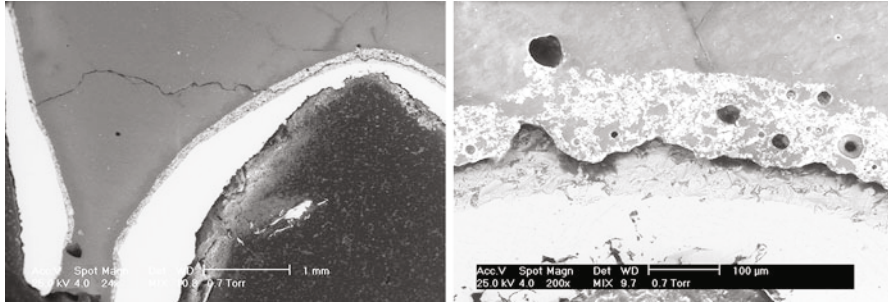


**Fig. 16** Opaque layer peeling from the metal substrate and the appearance of pore type defects in the ceramic coating

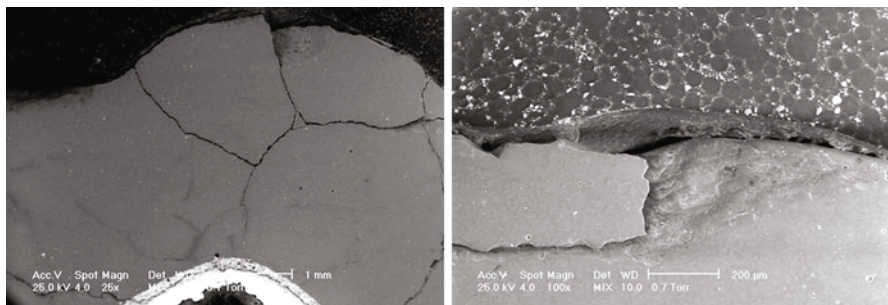


**Fig. 17** Fully fractured outer ceramic layer and opaque coverage; identification of pores in the ceramic layer

fractographic analysis can be performed [6]. In addition to the incomplete oxidation, the presence of fractures and cracks that cause separation is determined by the presence of impurities, by the fact that the ceramic slurry drying wasn't made progressively, by the physical and chemical incompatibility between the alloy and the ceramic mass, by the metal's unsuitable size, by the ceramic layer's nonuniform size, by sudden changes in the thermal values, or by the forced insertion of the model abutment or dental abutment if it has flaws [46–49]. Since the 1950s it was proved that water could act chemically on the crack edges, reducing the strength of ceramics. This phenomenon is called crack propagation chemically assisted or static fatigue. Inside wet environments the metal-ceramic bond strength is reduced by about one-fourth, which leads to crack propagation along the microcracks and the final prosthetic restoration failure. In addition, low pH beverages induce cracks generating in the vitreous materials for dental restorations [11].

Detaching the ceramic from the metal parts after cementing is the most serious fault that is remedied only after removal of the coping, generally by sectioning. Intervention is difficult, accompanied by unfavorable repercussions for that dental cabinet. After removal shall also mark the prosthetic field to resume all technological stages [6] (Figs. 18 and 19).



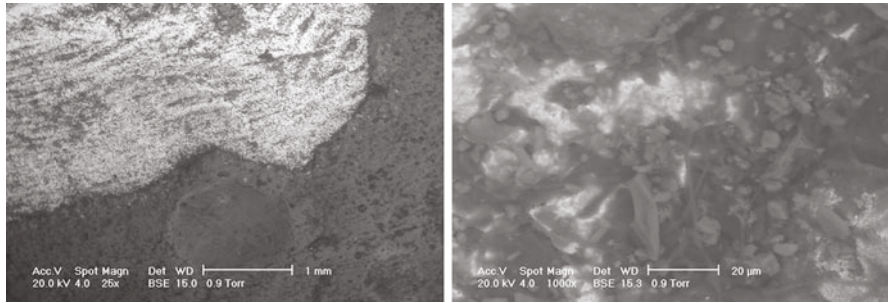


**Fig. 18** Degradation of metal-ceramic restorations by partially peeling the layer ceramic

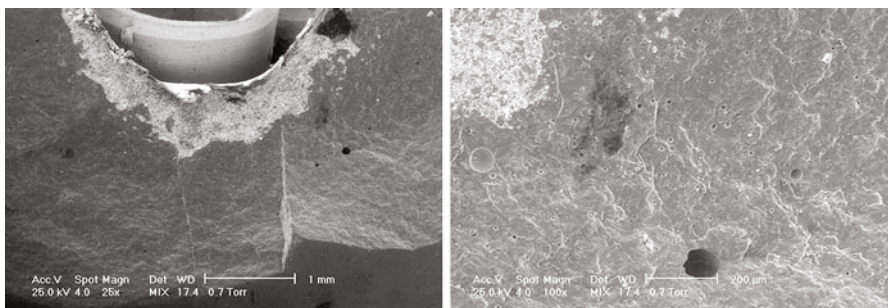


**Fig. 19** Fracture of metal-ceramic restorations mounted on a Ti implant

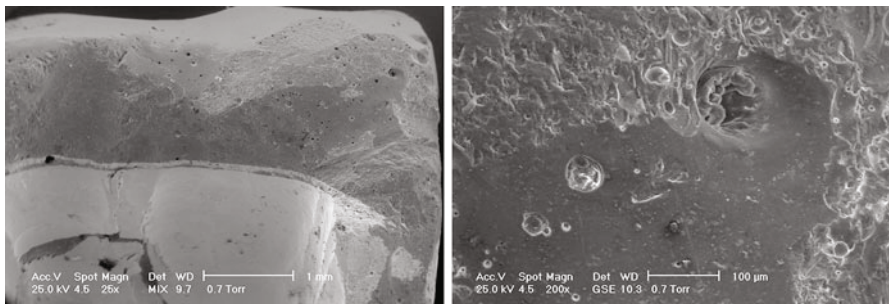


**Fig. 20** Abrasion on the surface of metal-ceramic restorations and identification of pores in the outer ceramic layer

Implant-supported prostheses are susceptible to failure compared to fixed natural teeth. In these cases, failure is generally due to fracture of ceramics (especially in patients with bruxism habits) [38]. The most likely explanation is that in these cases the natural tooth (along with periodontal) provides a sensitive detection of the occlusal loads, while implants are not receiving this mechanism and cannot absorb shocks. These effects can be limited by the use of nonrigid connectors for decreasing the forces applied to the superstructure [41] (Fig. 20).

If the fracture surface shows ductile fracture and fatigue ribs, the main cause of fracture is most likely the presence of transgranular stress that determines corrosion and cracking. Corrosion can be the main factor that has caused the failure of the prosthesis, in which case one searches for products of corrosion or corrosion points. Also, the deposition of calcium and phosphorus on the surface of the prosthesis may be an integral part of the mechanism that leads to failure [11].

---

## Conclusions

The result of the studies and research carried out in this work confirms the theoretical data on metal-ceramic dental restorations and full-ceramic single and multitooth. Of all dental restorative materials analyzed in this study, the material showing the best features is the yttrium-doped zirconia ceramics type. In this case major defects that could lead to failure dentures were not found. However, a major disadvantage of this type of dental restoration is the high cost of both the material itself and the processing technology and labor in the dental cabinets.

In the case of metal-ceramic prostheses, there are many factors that can lead to failure, especially because of the ceramic fracture. These factors may be associated to technician, dentist, environment, prosthesis design, or inherent metal or ceramic material structure and microstructure. Regardless the type of the used prosthesis, possible factors leading to the failure of the dental restoration prosthesis are abrasion, peeling, delamination, the presence of material defects that become sources of crack propagation, occlusive stress, etc. Common types of ceramic like porcelain and alumina ceramics have many internal defects such as pores, voids, and gas inclusions. Also their surface is susceptible to flaking, abrasion, and corrosion.

Although all-ceramic restorations with superior mechanical properties are an ideal of the aesthetics, their strength is far below the metal-ceramic. Dental metal-ceramic prostheses are more accessible in terms of manufacturing technology and cost of materials, but their main disadvantage is aesthetically (often the metal component may change the prosthesis color or become visible in contact with the gum tissue). There is also the risk of adhesive cracking at metal-ceramic interface, the risk that does not appear in all-ceramic restorations. To eliminate the main causes of failure, highest strength characteristics of the materials must be exploited, and the weakest should be removed. Making the future of all-ceramic restorations with mechanical properties better than metal-ceramic ones is a priority in modern dentistry.

**Acknowledgments** This work was supported by a grant of the Romanian National Authority for Scientific Research and Innovation, CNCS – UEFISCDI, project number PN-II-RU-TE-2014-4-0590.

## References

1. Raigrodski AJ (2004) Contemporary materials and technologies for all-ceramic fixed partial dentures: a review of the literature. *J Prosthet Dent* 92(6):557–562
2. Chadwick B, Treasure E, Dummer P et al (2001) Challenges with studies investigating longevity of dental restorations – a critique of a systematic, review. *J Dent* 29:155–161
3. Darvell BW (2009) *Materials science for dentistry*, 9th edn. Oxford: Boca Raton: Woodhead Pub.; CRC Press, pp 546–563
4. Bratu D, Gosescu D, Romănu M (1998) *Materiale dentare*, 2nd edn. Helicom, Timișoara: Brumar, pp 237–293
5. de Backer H, van Maele G, de Moor N, van den Berghe L, de Boever J (2006) A 20-year retrospective survival study of fixed partial dentures. *Int J Prosthodont* 19:143–153
6. Bechir A, Comaneanu RM, Smatrea O, Ghergic DL, Tarcoela M, Miculescu F (2011) Microscopic studies regarding the causes of micro-fractures in an aesthetic dental bridge. *Int J Nano Biomater* 3(4):382–391
7. Manappallil JJ (2008) *Basic dental materials*, 2nd edn. Jaypee Brothers Medical, New Delhi, pp 346–350
8. Stan GE, Pina S, Tulyaganov DU et al (2010) Biomineralization capability of adherent bioglass films prepared by magnetron sputtering. *J Mater Sci Mater Med* 21:1047–1055
9. McCabe JF, Walls A (eds) (2008) *Applied dental materials*, 9th edn. Oxford; Ames, Iowa: Blackwell Pub., pp 97–108
10. Voicu SI, Nechifor AC, Serban B, Nechifor G, Miculescu M (2007) Formylated polysulphone membranes for cell immobilization. *J Optoelectron Adv Mater* 9:3423–3426
11. Sakaguchi RL, Powers JM (2011) *Craig's restorative dental materials (Dental materials: properties & manipulation (Craig))*, 13th edn. Philadelphia, PA: Elsevier/Mosby, c2012, pp 255–272
12. Mohammed Sagir VM, Babu BP, Chirayath KJ, Mathias J, Babu R (2011) Zirconia in restorative dentistry: a review. *Int J Clin Dent Sci* 2(3):1–6
13. Bateli M, Kern M, Wolkewitz M, Strub JR, Att W (2014) A retrospective evaluation of teeth restored with zirconia ceramic posts: 10-year results. *Clin Oral Investig* 18:1181–1187
14. Stan GE, Pasuk I, Husanu MA et al (2012) Highly adherent bioactive glass thin films synthesized by magnetron sputtering at low temperature. *J Mater Sci Mater Med* 22(12):2693–2710
15. Al-Sanabani FA, Madfa AA (2014) Alumina ceramic for dental applications: a review article. *Am J Mater Res* 1(1):26–34
16. Walter MH, Wolf BH, Wolf AE, Boening KW (2006) Six-year clinical performance of all ceramic crowns with alumina cores. *Int J Prosthodont* 19(2):162–173
17. Anusavice KJ (1992) Degradability of dental ceramics. *Adv Dent Res* 6:82–89
18. Voicu SI, Dobrica A, Sava S, Ivan A, Naftanaila L (2012) Cationic surfactants-controlled geometry and dimensions of polymeric membrane pores. *J Optoelectron Adv Mater* 14(11–12):923–928
19. Borba M, de Araújo MD, Fukushima KA, Yoshimura HN, Cesar PF, Griggs JA, Della Bona Á (2011) Effect of the microstructure on the lifetime of dental ceramics. *Dent Mater* 27(7):710–721
20. Gernhardt CR, Bekes K, Schaller HG (2005) Short-term retentive values of zirconium oxide posts cemented with glass ionomer and resin cement: an in vitro study and a case report. *Quintessence Int* 36:593–601
21. Sharma A, Rahul GR, Shetty K (2012) Removal of failed crown and bridge. *J Clin Exp Dent* 4(3):167–172
22. Shadid RM, Sadaqah NR, Abu-Naba'a L, Al-Omari WM (2013) Porcelain fracture of metal-ceramic tooth-supported and implant-supported restorations: a review. *Open J Stomatol* 3:411–418

23. Bragger U, Karoussis I, Persson R et al (2005) Technical and biological complications/failures with single crowns and fixed partial dentures on implants: a 10-year prospective cohort study. *Clin Oral Implants Res* 16:326–334
24. Taskonak B, Mecholsky JJ Jr, Anusavice KJ (2006) Fracture surface analysis of clinically failed fixed partial dentures. *J Dent Res* 85(3):277–281
25. Ozcan M (2003) Fracture reasons in ceramic fused to metal restorations. *J Oral Rehabil* 30:265–269
26. Tan K, Pjetursson BE, Lang NP, Chan ES (2004) A systematic review of the survival and complication rates of fixed partial dentures (FPDs) after an observation period of at least 5 years – III. Conventional FPDs. *Clin Oral Implants Res* 15:654–665
27. Anusavice KJ (2012) Standardizing failure, success, and survival decisions in clinical studies of ceramic and metal–ceramic fixed dental prostheses. *Dent Mater* 28(1):102–111
28. Stan GE, Popa AC, Galca AC et al (2013) Strong bonding between sputtered bioglass-ceramic films and Ti-substrate implants induced by atomic inter-diffusion post-deposition heat treatments. *Appl Surf Sci* 280:530–538
29. Wilson NA, Whitehead SA (2003) Reasons for the placement and replacement of crowns in general dental practice. *Prim Dent Care* 10(2):53–59
30. Briggs P, Ray-Chaudhuri A, Shah K (2012) Avoiding and managing the failure of conventional crowns and bridges. *Dent Update* 39(2):78–80
31. Anusavice KJ, Kakar K, Ferree N (2007) Which mechanical and physical testing methods are relevant for predicting the clinical performance of ceramic-based dental prostheses? *Clin Oral Implants Res* 18(3):218–231. doi:10.1111/j.1600-0501.2007.01460.x
32. Kosmac T, Oblak C, Jevnikar P, Funduk N, Marion L (1999) The effect of surface grinding and sandblasting on flexural strength and reliability of Y-TZP zirconia ceramic. *Dent Mater* 15(6):426–433. doi:10.1016/S0109-5641(99)00070-6
33. Cesar PF, Yoshimura HN, Miranda WG Jr et al (2006) Relationship between fracture toughness and flexural strength in dental porcelains. *J Biomed Mater Res B Appl Biomater* 78:265–273. doi:10.1002/jbm.b.30482
34. Bona AD, Anusavice KJ, DeHoff PH (2003) Weibull analysis and flexural strength of hot-pressed core and veneered ceramic structures. *Dent Mater* 19:662–669. doi:10.1016/S0109-5641(03)00010-1
35. Yilmaz H, Aydin C, Gul BE (2007) Flexural strength and fracture toughness of dental core ceramics. *J Prosthet Dent* 98(2):120–128
36. Bottino MA, Salazar-Marochó SM, Leite FP, Vasquez VC, Valandro LF (2009) Flexural strength of glass-infiltrated zirconia/alumina-based ceramics and feldspathic veneering porcelains. *J Prosthodont* 18(5):417–420
37. Napankangas R, Salonen-Kemppi MA, Raustia AM (2002) Longevity of fixed metal ceramic bridge prostheses: a clinical follow-up study. *J Oral Rehabil* 29:140–145
38. McLaren E, Giodano IIR, Pober R, Abozenada B (2003) Material testing and layering techniques of a new two-phase allglass veneering porcelain for bonded porcelain and high-alumina frameworks. *Quintessence Dent Technol* 26:69–81
39. Miculescu F, Ciocan LT, Meghea D, Miculescu M (2014) Morphologic characterization of ceramic-ceramic dental systems failure. *Key Eng Mater* 614:140–143
40. Shemtov-Yona K, Rittel D (2014) Identification of failure mechanisms in retrieved fractured dental implants. *Eng Fail Anal* 38:58–65
41. Hmaidouch R, Weigl P (2013) Tooth wear against ceramic crowns in posterior region: a systematic literature review. *Int J Oral Sci* 5(4):183–190
42. Schuh C, Kinast EJ, Mezzomo E, Kapczynski MP (2005) Effect of glazed and polished surface finishes on the friction coefficient of two low-fusing ceramics. *J Prosthet Dent* 93:245–52
43. De Souza F, Francci C, Bombana AC, Kenshima S, Barroso LP, D’Agostino LZ, Loguercio AD (2012) Qualitative SEM/EDS analysis of microleakage and apical cap formation of adhesive root-filling materials. *J Appl Oral Sci* 20(3):329–334

44. Farga-Ninoles I, Agustin-Pandero R (2013) Fractographic study of the behavior of different ceramic veneers on full coverage crowns in relation to supporting core materials. *J Clin Exp Dent* 5(5):260–266
45. Quinn JB, Quinn GD, Kelly JR, Scherrer SS (2005) Fractographic analyses of three ceramic whole crown restoration failures. *Dent Mater* 21(10):920–929
46. Guazzato M, Albakry M, Ringer SP, Swain MV (2004) Strength, fracture toughness and microstructure of a selection of all ceramic materials. Part I: pressable and alumina glass infiltrated, ceramics. *Dent Mater* 20:441–448
47. Aboushelib MN, Kleverlaan CJ, Feilzer AJ (2008) Evaluation of a high fracture toughness composite ceramic for dental applications. *J Prosthodont* 17:538–544
48. Gonzaga CC, Yoshimura HN, Cesar PF, Miranda WG Jr (2009) Subcritical crack growth in porcelains, glass-ceramics, and glass-infiltrated alumina composite for dental restorations. *J Mater Sci Mater Med* 20(5):1017–1024
49. Etman MK, Woolford M, Dunne S (2008) Quantitative measurement of tooth and ceramic wear: in vivo study. *Int J Prosthodont* 21(3):245–252

---

## Part VI

# Clinical Performance in Bioresorbable and Load-Bearing Applications: Other Applications

---

# Bioceramics and Composites for Orbital Implants: Current Trends and Clinical Performance

# 41

Francesco Baino

## Contents

Introduction .....	1250
Essential Medical Background .....	1252
Historical Overview: A Century of Evolution (From the Late Nineteenth Century to 1980s) .....	1255
Currently Used Ceramic Porous Implants .....	1257
HA .....	1257
Alumina .....	1262
Bioactive Glasses and Glass Ceramics .....	1263
Composites and Coatings .....	1264
HA/Silicone Composite Implant .....	1264
Bioactive Glass/PE Composite Porous Implant .....	1264
HA-Coated Alumina Implants .....	1266
HA Implants Coated with Mesoporous Bioactive Glass .....	1266
Summary and Outlook .....	1267
References .....	1270

---

## Abstract

The applications of ceramics in the medical field are mainly related to the repair of hard tissues, like the bone and teeth, whereas their potential for the repair of other tissues has been often underestimated. A clinical area where porous ceramics are playing a key role is anophthalmic surgery, which deals with the removal of diseased eyes and their substitution by a (usually) spherical orbital implant replacing the ocular volume. Over the years, many bioceramics have been proposed for such an application, including glass, hydroxyapatite, and alumina.

---

F. Baino (✉)

Institute of Materials Physics and Engineering, Applied Science and Technology Department,  
Politecnico di Torino, Torino, Italy  
e-mail: [francesco.baino@polito.it](mailto:francesco.baino@polito.it)

Recently, polymer/bioceramic composites have been also experimented in order to reduce the stiffness mismatch between the ceramic constituent of the orbital implant and the surrounding soft tissues. This chapter provides an overview of the currently used ceramic-based orbital implants, also exploring new research directions and highlighting the promises for the future disclosed by the recent advances in bioceramics science.

### Keywords

Hydroxyapatite • Alumina • Bioactive glass • Ceramic/polymer composites • Porosity • Fibrovascularization • Tissue ingrowth • Angiogenesis • Antibacterial properties • Eye orbit • Enucleation • Ocular surgery

## Introduction

The removal of an eye (enucleation) is one of the most serious and difficult decisions that a surgeon must consider in case of severe ocular trauma or potentially life-threatening diseases to the patient [1]. This approach, however, leaves a partially or totally empty socket and creates significant cosmetic issues for the patient. Therefore, an orbital implant is then permanently placed in the orbit in order to restore the volume previously occupied by the ocular globe as well as to ensure adequate support to surrounding tissues (Fig. 1). Aesthetic outcome has been improved by

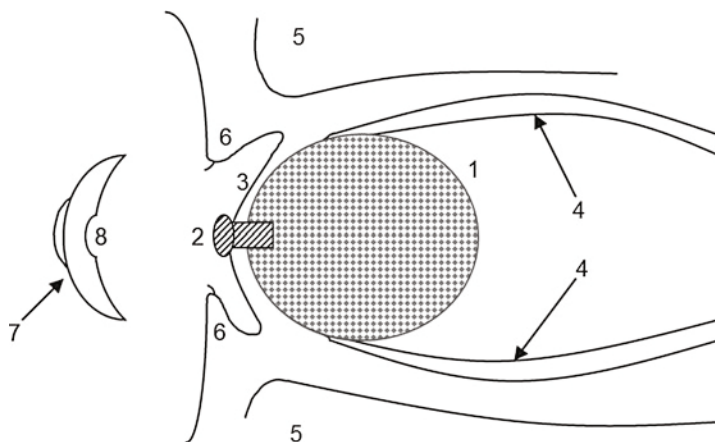


**Fig. 1** Placement of an orbital implant in the anophthalmic socket following enucleation surgery: 1 orbital implant (a porous sphere is schematically depicted; wrapping of the ceramic implant within a sheet of soft and smooth material, such as a polymer, is recommended to facilitate its insertion into the anophthalmic socket and to avoid erosion of surrounding tissues by the outer irregular surface); 2 frontal peg (it is optional, and extra-surgery is needed for its placement after at least 6 weeks from primary surgery); 3 patient's conjunctiva; 4 extraocular muscles attached to the implant; 5 orbital bone; 6 preserved eyelids; 7 ocular prosthesis; 8 seat to host the implant peg, in order to transmit a life-like motility to the artificial eye



the development of ocular prostheses, also known as “artificial eyes,” that are typically polymeric inserts which the patient places behind the eyelids and in front of the conjunctiva. The outer surface of the ocular prosthesis is painted to almost exactly match the appearance of the contralateral eye; it can be temporarily removed for cleaning and when the patient goes to sleep. If the extraocular muscles are attached to the orbital implant, some movement may be consequently transmitted to the overlying ocular prosthesis, which is a highly desirable characteristic known as motility.

Over the years, orbital implant design evolved from simple solid sphere (glass, silicone, poly(methyl methacrylate) (PMMA)) to more complex devices having specific sites for extraocular muscle attachment (the class of the so-called Allen implants made of PMMA) to porous spheres (hydroxyapatite (HA), polyethylene (PE), alumina) allowing better biointegration [2–4]. In this regard, bioceramics has been mainly employed to produce porous orbital implants, alone (as single-phase materials) or in the form of composites [5]. These implants incite minimal host response, characterized by the formation of a pseudocapsule around the implanted material. However, the success of these devices was hampered by the development of long-term complications, such as late migration and extrusion.

An ideal orbital implant should display a number of characteristics, including biocompatibility (which should be a sort of precondition), adequate socket volume replacement, good motility transmitted to the ocular prosthesis, adequate support for the ocular prosthesis, low cost, easiness of implantation, non-degradability, and overall very low rate of complications.

Many evidences seem to demonstrate that porous orbital implants lead to better performances and outcomes with respect to the other existing solutions. These implants are typically characterized by a 3-D network of interconnected pores, resembling – at least to some extent – the trabecular structure of human cancellous bone [6]. Fibrovascularization, defined as the ingrowth of viable vascular connective tissue, typically occurs within 4 weeks from implantation, and tissue reaction is often minimal (Fig. 2). Wrapping within a sheet of soft, smooth material of biological or synthetic origin (e.g., autologous sclera, polymeric mesh) at the time of surgery can be useful to reduce the risk of abrasion of the conjunctiva – and associated implant exposure – due to the irregular surface of ceramic porous implants.

From a general viewpoint, the growth of tissue into a porous orbital implant offers several key advantages that can be summarized as follows [2, 4]:

- Extrusion is generally very rare.
- With sufficient time for fibrovascularization to occur, any exposures (due to the abrasion of the conjunctiva by the implant) might be able to heal spontaneously due to the good blood supply within the implant.
- The presence of adequate blood supply within the implant can significantly reduce the risk of implant infection.
- Porous implants can be pegged, thereby improving the motility and the life-like appearance of the ocular prosthesis that can more closely follow the movement of the contralateral eye.

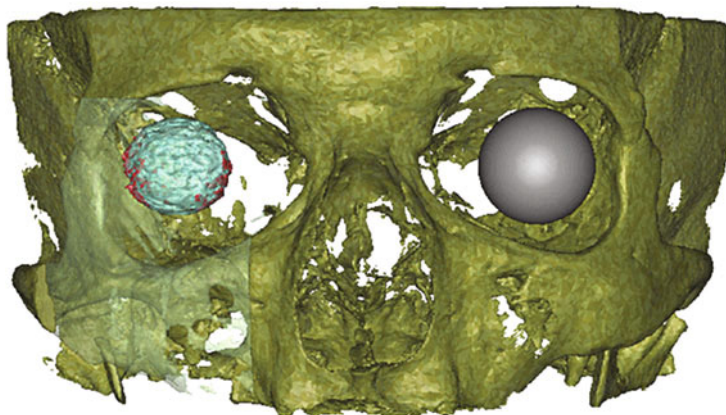


**Fig. 2** Reconstruction by cone beam computed tomography (CBCT) of an orbital implant (synthetic HA porous sphere) implanted in the right orbit of a human patient where the red zones represent the areas of fibrovascularization that starts at the implant periphery; the vitreous body of the contralateral eye is represented as a gray sphere (Courtesy of Lukats et al. [6])

The last advantage deserves a short discussion for better understanding. Looking at the historical evolution of orbital implants, previous attempts to establish a direct mechanical connection between nonporous orbital implants (e.g., a simple polymeric sphere) and the ocular prosthesis had been invariably met with the development of infections (due to bacterial colonization of the implant region to be connected with the prosthesis), exposure, and other complications. Thanks to the fibrovascularization of porous implants, it is possible to drill a hole in the implant and to insert a peg between implant and ocular prosthesis (Fig. 1). The presence of a good blood supply allows the drilled area to re-epithelialize with conjunctiva; thus, the implant remains separated from the external environment by the living conjunctival layer but retains a direct connection to the prosthesis, thereby providing enhanced motility without exposure of the implant and the associated complications.

This chapter provides an overview of ceramic-based orbital implants, including both the devices currently adopted in the clinical practice and those fallen in disuse; some indications for prospective research and future challenges are also given in the light of the recent advances in bioactive ceramic science. Table 1 provides a short glossary of the medical terms that are not explained directly in the text and which may be unclear or unknown to nonspecialist readers.

---

## Essential Medical Background

A short overview of the reasons why the removal of an eye can be necessary, as well as the related surgical procedures, is given in this section for the reader's benefit. At present, the removal of a diseased eye can be carried out by one of three different

**Table 1** Medical glossary (terms listed alphabetically)

Term	Explanation
Conjunctiva	Clear mucous membrane constituted by stratified columnar epithelium that covers the sclera and lines the inside of the eyelids. It contributes to eye lubrication by producing mucus and tears, although in a smaller amount with respect to lachrymal glands. In addition it prevents the entrance of pathogenic agents and foreign bodies into the eye
Ectropion	Turning out of the eyelid (usually the lower eyelid) so that its inner surface is exposed
Endophthalmitis	Inflammatory condition of the intraocular cavities containing the aqueous/vitreous humor usually caused by infection. Panophthalmitis is the inflammation of all coats of the eye including intraocular structures; endogenous endophthalmitis results from the hematogenous spread of organisms from a distant source of infection; exogenous endophthalmitis are due to direct inoculation of bacteria/fungi from the outside as a complication of ocular surgery, foreign bodies, or penetrating ocular trauma
Enophthalmos	Recession of the eyeball or orbital implant inserted in the anophthalmic socket within the orbit; it may be a congenital anomaly or be acquired as a result of trauma (e.g., blowout fracture of the orbit) or else be related to postoperative complications of oculo-orbital surgery
Exposure	Break in the tissue overlying the orbital implant, which in severe cases may lead to extrusion of the entire implant. Poor surgical technique, excessively large implant size, and infection may all contribute to this postoperative complication
Extraocular muscles	Group of six muscles, attaching to the sclera/orbital implant, that control the movements of the eye/implant
Migration	Change in position of the implant following placement within the anophthalmic socket
Pegging	Surgical procedure that can be optionally performed after some months from orbital implant placement in the anophthalmic socket (primary surgery). In this procedure, a hole is drilled into the front surface of the implant, and a polymeric or metal peg is inserted into this hole. The peg articulates with a cavity in the back surface of the prosthetic eye, thereby providing improved motility. Pegging is usually adopted only for porous implants, as fibrovascularization allows to decrease the risk of infections that might follow the pegging procedure
Pyogenic granuloma	Overgrowth of tissue due to irritation or physical trauma. Its appearance is usually a color ranging from red/pink to purple and can be smooth or lobulated. Younger lesions are more likely to be red because of the high number of blood vessels, whereas older lesions begin to change into a pink color. It can be painful, grow rapidly, and often bleed profusely with little or no trauma
Retinoblastoma	Rare type of eye cancer that affects the retina and usually develops in early childhood, typically before the age of 5 (it is typically diagnosed in children aged 1–2 years). Retinoblastoma is due to the mutation of RB1 gene, which can be inherited (in this case the tumor typically develops in both eyes) or occur in the early stages of fetal development
Sclera	Opaque, fibrous, protective, outer layer of the eye. Primarily constituted by collagen, it maintains the shape of the globe, offers resistance to internal and external forces, and provides an attachment for the extraocular muscle insertions. The thickness of the sclera varies from 1 mm at the posterior pole

*(continued)*

**Table 1** (continued)

Term	Explanation
	to 0.3 mm just behind the rectus muscle insertions. It is commonly referred to as the “white of the eye”
Sympathetic ophthalmia	Bilateral diffuse granulomatous uveitis (a kind of inflammation) of both eyes following ocular trauma. It is quite rare but can leave the patient completely blind; early symptoms (e.g., pain, photophobia) may develop from days to several years after a penetrating eye injury
Tenon’s capsule	Sheet of connective tissue that lines the eyeball and aims to provide a smooth socket for allowing the free movement of the ocular globe
Wrapping	Preoperative strategy involving the wrapping of an orbital implant within a sheet of a smooth material with the aim of facilitating its placement within the soft tissue of the eye socket, diminishing tissue drag, and helping precise fixation of the rectus muscles to the implant surface. Wrapping is particularly recommended for porous implants in order to provide a physical barrier over their slightly irregular porous surface. Suitable wrapping materials include scleral autografts and allografts, bovine pericardium, and synthetic polymer sheets

surgical approaches, i.e., evisceration, enucleation, and exenteration, according to the particular pathology and the medical history of each patient [1].

Evisceration involves the removal of the intraocular contents of the eye, while the sclera, Tenon’s capsule, conjunctiva, extraocular muscles, and optic nerve are left intact [7]. Enucleation is another option involving the removal of the globe from the orbital socket, together with the scleral envelope and a portion of the optic nerve, while, as with evisceration, the conjunctiva, Tenon’s capsule, and extraocular muscles are spared [1, 7]. In the final stage of surgery, an orbital implant is placed within the scleral envelope after evisceration or within the Tenon’s capsule after enucleation; an ocular prosthesis will be then worn by the patient to restore an appropriate aesthetic appearance, including life-like motility (Fig. 1).

Removal of an eye can be necessary in the cases of intraocular malignancy (e.g., retinoblastoma, which can develop especially in children), blind painful eye, prevention of sympathetic ophthalmia in a blind eye, severe trauma, and infections not responsive to pharmaceutical therapy. From a general viewpoint, evisceration is less invasive and less surgically complex than enucleation, but in some cases the complication rate for evisceration, specifically implant extrusion, may be significantly higher [7]. Evisceration is indicated in the treatment of active, uncontrolled endophthalmitis and in all cases when there may be a danger of intraocular infection spreading back along a cut optic nerve sheath; enucleation may be indicated if the infection has spread to the sclera. Evisceration is also recommended in patients who have bleeding disorders since it is a faster, easier procedure and damages fewer blood vessels than enucleation. Evisceration is absolutely contraindicated in the presence of intraocular malignancy as it does not allow for eradication of tumor cells that have spread to the sclera.

Enucleation is generally indicated for tumors that are confined to the ocular globe; if the malignancy has spread to the extraocular structures (i.e., the conjunctiva and

eyelids, adjacent sinuses, cranial bones, face muscles, and skin), a radical procedure of exenteration, which involves the removal of the entire orbit and surrounding tissues, is recommended [8]. In this case, silicone or acrylic custom-made large prosthetic devices are attached to the orbit and the skin with various types of adhesives to provide good cosmetic results [9].

---

## Historical Overview: A Century of Evolution (From the Late Nineteenth Century to 1980s)

Since the ancient Roman age, a wide variety of materials, including wool, clay, gold, and silver, has been used to manufacture more or less rudimental orbital fillers, often painted or enameled to mimic the natural iris, with the aim of replacing the anophthalmic socket volume and restoring an acceptable aesthetic appearance to the patient's face. The first clear description of a production process to make orbital implants dates back to the end of sixteenth century, when Venetian glassmakers began to fabricate prosthetic eyes of blown glass that however were brittle and had poor fit and little comfort [3].

The modern era of anophthalmic surgery started in 1885, when Mules first described in detail the surgical placement of a hollow glass sphere into an eviscerated globe [10]. Since the early 1900s, the use of orbital implants coupled with glass ocular prostheses began to be adopted in order to restore a better aesthetic appearance to the patient's face; the prosthesis was a glass shell placed between the closed conjunctival surface covering the orbital implant (bulbar conjunctiva) and the eyelids (palpebral conjunctiva) (see also Fig. 2). Glass eyes had to be worn with caution as they were brittle and prone to implosion with acute changes in temperature; furthermore, they became etched from exposure to body secretions.

It was not until the First World War that glass eyes were used by the general population; from 1920 to 1940, Germany became the main supplier of glass orbital implants due to the superior glass-blowing techniques as well as the improvements adopted in implant design (thicker glass shell to reduce the risk of fracture, the so-called Snellen implant) [11]. In a study involving 52 patients, Burch estimated failures in less than 10 % of cases using the Snellen implant in the mid 1940s [12].

The battle casualties of the Second World War caused a large demand of artificial eyes, but the wartime shortage of glass eyes imported from Germany led to the development of PMMA orbital devices. PMMA implants allowed to overcome the problems of glass implants (brittleness and chemical etching by body secretion), permitted custom fitting at a relatively low cost, and allowed better motility of the prosthesis due to a new design for improved muscle attachment [13–15]. In the last decades, the use of glass spheres as orbital implants has been almost totally abandoned, and only occasionally they were still implanted in selected cases [16, 17].

As an alternative to brittle glass implants, small spheres of natural ivory from elephant's tusks, a biocomposite constituted by nano-sized HA-like crystals (about

70 wt%) and organic matter (a complex network of type I collagen fibers) that is eliminated after the death of the animal, were experimented as orbital implants in the first half of the twentieth century [18]; after the Second World War, no other application of such type of biological apatite has been reported in the ophthalmic field.

Animal-derived HA implants were also prepared by heating spheres of bovine cancellous bone to destroy all organic matter, leaving only the calcium phosphate mineral framework [19–21]. Interestingly, these porous HA implants derived from charred bone were widely used before the Second World War and recommended as “the most satisfactory of all orbital implants” [18].

Since the late 1940s, biologically inert nonporous polymeric spheres (silicone and PMMA) progressively displaced these early types of porous implants due to the easier material processing and low cost. However, the concept of a bone-derived HA orbital implant was resurrected by Molteno and coworkers in the 1980s and led to the development of the “M-Sphere,” which is still currently used in the clinical practice (see the section “[Bone-derived HA](#)”).

In the late 1970s, a ceramic/polymer felt-like composite, called Proplast I, gained a certain popularity as an orbital implant material. Proplast I was constituted of polytetrafluoroethylene (PTFE) and carbon fibers and, when implanted, could be invaded by fibrous tissue, thereby overcoming the problem of extrusion and rejection [22]. Studies in human patients who received Proplast I hemispherical orbital implants were promising, with no cases of migration or extrusion after a 2-year follow-up [23]. In recent years, however, the popularity of Proplast I has declined because of long-term postoperative complications, primarily late infections, associated with its use in other medical applications [24].

One decade later, the implantation of porous enucleation implants made of Proplast II, an evolution of Proplast I, was reported. This new device was different from its predecessor in the composition (Proplast II was an alumina/PTFE composite) and in having a siliconized nonporous posterior surface to allow smoother movements, together with a porous anterior portion to ideally facilitate fibrovascular ingrowth [25, 26]. Proplast implant II had a nipple on its anterior surface (lined by the patient’s conjunctiva) that could integrate with a depression on the posterior surface of the ocular prosthesis. Several Proplast implants II required subsequent removal because of poor motility and, over histopathological examination, were found to be completely avascular and surrounded by a thick pseudocapsule [27]; therefore, since then the use of Proplast II to fabricate orbital implants was abandoned. However, in the mid-1990s, Proplast II was successfully adopted to manufacture subperiosteal implants for the correction of anophthalmic enophthalmos in 34 patients having poor orbital volume replacement despite the prior insertion of an adequately sized spherical implant within the orbital socket [28].

At present, all the ceramic-based orbital implants mentioned above are fallen in disuse; they are also collected in Table 2. Maybe their use might be reconsidered in the future, in the light of new advances of biomedical materials research.

**Table 2** Currently abandoned ceramic-based orbital implants

Material	Type of implant	Recipient	Remarks	References
Glass (noncrystalline ceramic)	Hollow sphere (blown glass)	Human	It was the standard orbital implant from the late 1800s to the Second World War. In recent years it has been almost totally abandoned	[10–12, 16, 17]
Tusk-derived HA (ivory)	Solid sphere	Human	It was used till the Second World War	[18]
HA derived from heat-treated bovine bone	Porous sphere of charred cancellous bone	Human	It was used till the Second World War and considered an excellent alternative to glass orbital implants	[18–21]
Carbon/PTFE composite (Proplast I)	Hemispherical implants	Human	Despite the fibrovascular ingrowth and generally good outcomes, it was abandoned in the 1980s due to the risk of late infections	[22–24]
Alumina/PTFE composite (Proplast II)	Porous implant having a siliconized nonporous posterior surface to allow smoother movements	Human	It was abandoned due to poor motility and absence of fibrovascular ingrowth	[25–28]

## Currently Used Ceramic Porous Implants

This section mainly focuses on HA-derived and alumina orbital implants that are commonly used in the current clinical practice; their main characteristics are summarized in Tables 3 and 4. Furthermore, the results of recent studies involving the experimental use of bioactive glass orbital implants in humans are also mentioned.

### HA

HA formally belongs to the class of calcium orthophosphates and, especially in the form of coralline and synthetic HA, has been widely used since more than 50 years in orthopedics and dentistry, thanks to its chemical and compositional similarity to biological apatite of hard tissues [29]. Porous HA is widely used as an orbital implant material due to its biocompatibility, non-absorbability, and as it allows biointegration through fibrovascular ingrowth.

**Table 3** Currently used ceramic porous orbital implants and comparison with porous PE devices

Material	Type of implant	Recipient	Remarks <sup>a</sup>	References
Bovine bone-derived HA	Porous sphere	Human	Commercial product, M-Sphere; cost, around 500€. Problems of brittleness can occur	[30–35]
Coralline HA	Porous sphere, egg-shaped porous implants	Human	Commercial product, Bio-Eye <sup>®</sup> , cost, around 600 €	[36, 37, 44–54]
Synthetic HA	Porous sphere, egg-shaped porous implants	Human	Mostly used commercial products, FCI3; cost, around 450 €. Other less expensive implants are available (with problems associated with low purity)	[38–43]
Alumina	Porous sphere	Human	Commercial product, bioceramic implant; cost, around 450€	[56–65]
Porous PE	Porous sphere, egg-shaped and conical porous implants, other variations with gradients of porosity	Human	Commercial product, Medpor <sup>®</sup> ; cost, around 150€	[58, 76]

<sup>a</sup>Prices are indicative only and refer to unwrapped implants; they may vary depending on country, hospital, and number of implants ordered

**Table 4** Microstructural characteristics of the ceramic porous orbital implants that are in common use and comparison with porous PE devices

Material	Marketed product	Porosity (vol.%)	Pore size (µm)	Surface structure
Bovine bone-derived HA	M-Sphere	Around 80	above 300	Ultramicroscopic crystals typical of bone HA
Coralline HA	Bio-Eye <sup>®</sup>	Around 65	300–700	Irregular microcrystals of HA with size around 2 µm
Synthetic HA	FCI3	Around 50	300–500	Hexagonal microcrystals of HA with size within 1–5 µm
Alumina	Bioceramic implant	Around 75	500	Cobblestone pattern of microcrystals with size within 0.4–1.1 µm
PE	Medpor <sup>®</sup> spherical implants	30–70	100–1000	Woven texture; presence of surface irregularities



### **Bone-Derived HA**

In the 1970s, the research group coordinated by Dr. Molteno carefully reviewed the available literature on orbital implants and noted that the postoperative exposures of bone-derived HA spheres used till the Second World War were generally rare, small, and frequently tended to heal spontaneously [18]. This behavior, which was quite unlike that observed with smooth-surfaced polymeric orbital implants, suggested that the biodegradable nanocrystalline HA matrix of the bone would constitute a superior orbital implant since, once organized by host connective tissue, it would not migrate through the tissues, while any small exposures would heal spontaneously. Furthermore, the mass of host connective tissue incorporating the bone mineral implant would likely persist unchanged for the patient's whole life. The early trials of this type of implant (the so-called M-Sphere) involved the use of deproteinized (antigen free) bone of calf fibulae and confirmed that the mineral matrix of cancellous bone was readily incorporated into the tissues and that small exposures were followed by spontaneous crumbling of the exposed bone with healing of the overlying conjunctiva [30, 31]. Other 52 cases with up to 10-year follow-up were reported in 1991 [32], and the long-term successful outcomes of 120 M-Sphere orbital implants inserted after enucleation between 1977 and 2000 were more recently documented [33]. This implant is significantly more porous (around 80 vol.%) than other available HA orbital implants (50–65 vol.%); the use of a lighter device is an advantage leading to decreased stress on the lower lid and associated ectropion formation. However, due to the high porosity, the M-Sphere orbital implant is fragile and may be unable to support a peg [34, 35]. This drawback associated to its relatively high cost (around 500€, lower than coralline HA but significantly higher than porous PE implants, see Table 3) may have contributed to its limited diffusion.

### **Coralline HA**

Porous orbital implants spread worldwide since the 1990s after the introduction of modern HA orbital implants that are not based on treated bone deriving from animal sources. Perry first experimentally introduced the coralline porous HA sphere (Bio-Eye<sup>®</sup>) in anophthalmic surgery with excellent postoperative outcomes [36]. The interconnected porous structure of the HA implant allowed host fibrovascular ingrowth, which potentially reduces the risk of migration, extrusion, and infection [37]. Apart from discouraging bacterial colonization of implant surface, vascularization also allows the treatment of ocular infection by antibiotic therapy. After some months from primary surgery, the frontal region of the HA implant can be drilled to place a peg that can be subsequently coupled to the posterior surface of the ocular prosthesis (Fig. 1), so that a wide range of artificial eye movements (especially along the horizontal axis) as well as fine darting eye movements (commonly seen during close conversational speech) can be achieved, thereby imparting a more life-like quality to the prosthetic eye.

However, the use of coralline porous HA implants is associated to two peculiar drawbacks [2, 4]. The first problem is ecological, as the manufacture of such implants involves damage to marine ecosystems due to the harvesting of natural

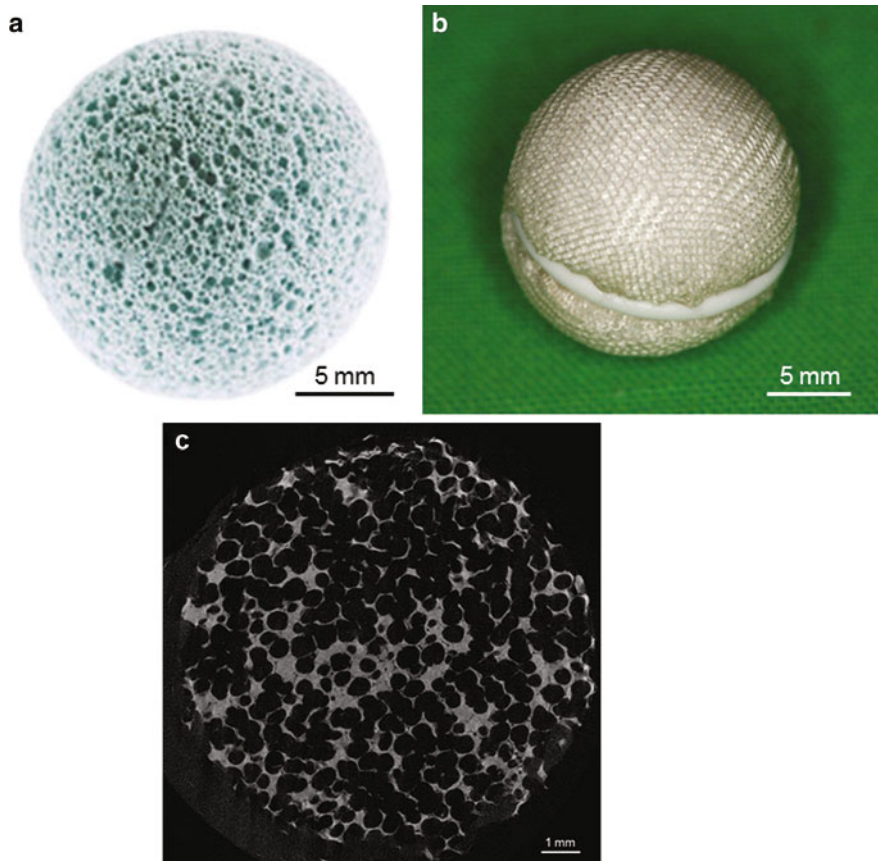


**Fig. 3** Synthetic HA orbital implant: (a) appearance of the porous sphere; (b) sphere wrapped in a smooth, soft mesh of polyglactin 910 prior to implantation; (c) microstructure of the HA implant (planar reconstruction by micro-CT) (Courtesy of Lukats et al. [6])

corals; the second issue is related to the high cost (around 600€) compared to other options (e.g., porous PE; see Table 3, or nonporous silicone, and PMMA spheres whose price is around 50€). Primarily in order to reduce the cost of the device, other forms of HA have been proposed as potentially suitable and less expensive materials for orbital implant fabrication.

### Synthetic HA

Chemically synthesized HA implants (the reference implant is the so-called FCI3 sphere) (Fig. 3) have an identical chemical composition to that of the Bio-Eye® [38], although scanning electron microscopy (SEM) investigations revealed some architectural differences (lower porosity: 50 vs. 65 vol.%; decreased pore size uniformity; presence of blind pouches and closed pores) [39]. Implant interconnectivity (Fig. 3c)

is still sufficient to allow central implant fibrovascularization [40]. FCI3 implant has gained increasing popularity over the past 10 years especially as it is significantly less expensive than the Bio-Eye<sup>®</sup> (see Table 3) and easier to drill for peg placement.

Low-cost versions of synthetic HA orbital implants have been developed and are currently in use especially in some emerging countries; however, they exhibit a number of drawbacks that strongly limit their economic advantage over the other available options. Some of these implants have been reported to contain CaO impurities that, after hydration in host tissues, may form  $\text{Ca(OH)}_2$ , which is caustic [41]. Other implants have higher weight, lower porosity (below 50 vol.%), and lower pore interconnectivity than FCI3 devices, with consequent limited fibrovascularization and enhanced risk of implant migration [42]. A new type of synthetic HA orbital implants (75 vol.% porosity, pore sizes ranging from 100 to 300  $\mu\text{m}$ ) was recently experimented by Kundu et al. [43] with apparently good outcomes, but their study is still too limited (25 patients, 2.5 years of follow-up) to draw definite conclusions on their long-term safety and efficacy.

### Shortcomings of HA Orbital Implants

Among porous orbital implants, coralline and synthetic HA devices are still the preferred choice by the majority of ophthalmic surgeons worldwide. However, despite the relatively good overall biocompatibility profile, HA generally exhibits certain drawbacks for use in orbital implants. Being a porous ceramic, its brittle nature precludes suturing the extraocular muscles directly to the implant [1, 7]; thus, preoperative placement of the HA implant within a sheet of soft material is necessary for muscles attachment. Furthermore, there are convincing evidences that the rough surface of HA implants may contribute to the development of late exposure due to the abrasion of the relatively thin conjunctiva and Tenon's capsule as the implant moves. Therefore, also for this reason it is generally recommended that HA implants are placed within a sheet of wrapping material (Fig. 3b) before introduction into the orbit [44, 45]. It was also shown that the majority of exposed HA implants can be successfully treated by using patch grafts of different origin (e.g., scleral graft, dermis graft, oral mucosa graft) without the need for implant removal [46–48]. In case of orbital implant infections associated to exposures, administration of systemic antibiotics and topical eye drops can solve the problem, but if no symptoms improvement is noticed, implant removal should be considered [49]. Other reported complications include conjunctival thinning (followed or not by exposure), socket discharge, pyogenic granuloma formation, midterm to chronic infection of the implant, persistent pain or discomfort, and peg extrusion from drilled HA implants [50–54].

In the search for an “ideal” porous orbital implants with a reduced complication profile and diminished surgical and postoperative costs, alternative materials such as porous PE (not treated in the present chapter; the interested reader is addressed to some recently published articles [2, 4]) and alumina have been investigated over the last two decades.

## Alumina

Aluminum oxide ( $\text{Al}_2\text{O}_3$ ), commonly termed alumina, has been used for decades in orthopedics, thanks to its attractive mechanical properties (high hardness and compressive strength, excellent resistance to wear), biocompatibility, and bio-inertness. For instance, the introduction of alumina and, later, alumina-based ceramic composites for manufacturing prosthetic femur heads had a significant impact in the field of hip joint replacement, leading to an improvement of prosthesis duration and performance as well as of patient's life quality [55]. Since the late 1990s, alumina began to be introduced as an alternative to HA for the fabrication of porous orbital implants; this type of device was then approved by Food and Drug Administration in 2000 and is currently marketed under the commercial name of "bioceramic implant." There are convincing evidences showing that alumina implants are a reliable and even more effective alternative to the available porous HA devices under many viewpoints, including cost (these implants are significantly less expensive than Bio-Eye<sup>®</sup>; see Table 3), low tendency to exposure/extrusion (smoother surface compared to HA implants; see Table 4), and overall postoperative performances.

The first in vivo study was reported in 1998 by Morel et al. [56], who evaluated the clinical tolerance of porous alumina implants in 16 eviscerated rabbits: only one infection was observed without conjunctival breakdown, and fibrovascular ingrowth started 15 days postoperatively and was complete after 1 month. These promising results were confirmed 2 years later by Jordan et al. [57], who compared the performance of alumina and HA implants in rabbits and highlighted that the new alumina implant was as biocompatible as HA and less expensive, and its manufacturing did not involve any damage to marine life ecosystems as may occur in the harvesting of coral for coralline HA devices.

An accurate comparison about the proliferation of orbital fibroblasts in vitro after exposure to bioceramic implant and other three implants made of different materials (coralline HA, synthetic HA, porous PE) was reported by Mawn et al. [58]. The proliferation of fibroblasts differed on the various studied implants and, specifically, was maximum on the bioceramic implant; furthermore, the fibroblasts growing on the Bio-Eye<sup>®</sup>, synthetic HA, and PE implants all had debris associated with them, whereas the alumina implant was free of these debris, which was mainly attributed to its finely crystalline microstructure (see also Table 4).

Promising results were also published in 2002 by Akichica et al. [59], who implanted pieces of alumina with 75 vol.% porosity in the eye sockets of albino rabbits. There were no signs of implant rejection or prolapse of the implanted material over an 8-week follow-up; at 4 weeks after implantation, fibroblast proliferation and vascular invasion were noted, followed by tissue ingrowth by the 8th week.

The first outcomes of bioceramic implant in humans (107 patients over a 3-year follow-up) were reported by Jordan et al. in 2003 [60]. Postoperative problems encountered with its use were substantially similar to those observed with coralline HA orbital implants (Bio-Eye<sup>®</sup>) but appeared to occur rarely; the incidence of exposure associated with the bioceramic implant was significantly less than that

reported for the HA ones, and infection did not occur in any patient. In a following study, Jordan and coworkers further confirmed that alumina implant infections are rare [61] and, after reviewing a clinical case series of 419 patients who received a bioceramic orbital implant, estimated an implant exposure rate of 9.1 % with the majority of the exposures occurring after a 3-month follow-up period [62]. Wang et al. [63] reported that exposures of bioceramic implants occurred only after long-term follow-up and were preferentially associated with evisceration, pegging, and prior ocular surgeries, whereas no late side effects were found in enucleated eyes.

Implant wrapping was demonstrated to be an excellent strategy to avoid exposure and related complications [64]. In case of exposure, successful treatment (without the need for implant removal) can be performed by covering the exposed area with appropriate patches of biological origin (e.g., retroauricular myoperiosteal graft containing myofibrovascularized tissue) [65].

## Bioactive Glasses and Glass Ceramics

Glasses are noncrystalline ceramics that, due to their attractive optical properties, have been used for centuries to correct visual deficiencies, like myopia or other refractive diseases. As first demonstrated by Hench and coworkers in the early 1970s [66], a special subset of biocompatible glasses, referred to as bioactive glasses, exhibit the unique property to bond to host bone stimulating the growth of new tissue. Therefore, bioactive glasses are recognized as ideal materials for bone substitution and have been widely investigated over the years in the form of dense implants, fine particulates, coatings on metal prostheses, and 3-D porous scaffolds mainly for orthopedic and dental applications [67, 68]. Few bioactive silicate glass and glass-ceramic formulations have been occasionally proposed in ophthalmology for the manufacture of porous orbital implants in the form of single-phase materials or as a second phase added to a polymeric matrix (composites; see the section “[HA-Coated Alumina Implants](#)”). There is a general paucity of scientific literature on this topic, although it has been recently highlighted that bioactive glass can have a great potential for application in ocular surgery [5].

In the late 1990s, Xu and coworkers [69] implanted bioactive glass-ceramic porous orbital implants in enucleated rabbits and observed no rejection during a 6-month postoperative follow-up; ultrasound examination revealed a venous-flow-like spectra in the implants after 3 months, and histological analysis showed that around 90 % of the implant pores were filled by fibrovascular tissue after 6 months from operation. Encouraged by these promising results, the same authors implanted glass-ceramic orbital devices in 102 human patients, declaring a success rate of 96.1 % (98 cases) [70]. In four cases the conjunctiva was torn partly when suture stitches were taken out of the wound, and one patient needed the implant removal. There were no reported complications after a follow-up of 6 months to 2 years, and all patients were satisfied with their cosmetic appearance, although implant drilling and placement of the motility peg to connect the implant to the ocular prosthesis were never performed as a secondary procedure.

The use of bioactive glass to fabricate orbital implants was also claimed in a recent patent by Richter et al. [71], but no manufacturing or clinical studies have been reported yet in the literature on this type of implant.

Another interesting application involves the use of bioactive glass as a “contingency plan” to fill old peg tracts and to permit repegging in porous HA orbital implants, if the initial drilled tunnel was not perpendicular and central to the implant surface [72]. This approach has been reported in a study on three patients who had persistent problems with their pegged HA orbital implants and no longer responded to conservative treatment. After removal of the old peg, the hole was partially filled with bioactive glass, and after 2 months, two patients also underwent successful redrilling of the implant followed by insertion of a new titanium peg, with satisfactory connection to the ocular prosthesis and absence of complications over a 3-year follow-up.

---

## Composites and Coatings

This section provides an overview of the polymer/ceramic composites and bioceramic coatings that have been proposed in recent years for the manufacture of orbital implants; their main characteristics are summarized in Table 5.

### HA/Silicone Composite Implant

In the early 1990s, Guthoff and coworkers [73] developed a composite orbital implant comprising a hemispherical anterior part made of synthetic porous HA to guarantee tissue integration and joined to a posterior part that was manufactured using silicone rubber; the horizontal and vertical eye muscles were sutured crosswise in front of the implant to ensure better stability and motility. Overall implant biocompatibility was excellent, and the transmission of the motility to the ocular prosthesis was generally acceptable [74, 75]. At present this implant is mainly employed in Europe; its diffusion is limited due to the high cost and complex surgical procedures needed for its implantation compared to “standard” spherical porous implants made of HA, alumina, or PE.

### Bioactive Glass/PE Composite Porous Implant

A couple of studies reported by two different groups of Chinese researchers are currently available on this type of implant. In 2006, the effects of the incorporation of bioactive glass powder on the fibrovascular ingrowth occurring in porous PE orbital implants were investigated in rabbits [76]. Forty-eight rabbits were divided into four equally sized groups, according to the different surgical techniques and implanted materials used: groups 1 and 2 received porous PE after enucleation or evisceration, respectively (reference groups), whereas groups 3 and 4 were implanted with

**Table 5** Ceramic-based composites and coatings used in the fabrication of orbital implants

Type of composite or coating	Type of implant	Recipient	Remarks	References
HA/silicone	Implant comprising a hemispherical anterior part made of synthetic porous HA and a posterior part made of silicone rubber	Human	It is commonly known as “Guthoff implant.” It exhibits good postoperative outcomes but has high cost and requires complex surgical procedures of implantation	[73–75]
Bioactive glass/PE	Porous sphere	Human	Absence of a clear improvement in implant fibrovascularization with respect to porous PE. Studies involving a higher number of patients would be necessary for a more exhaustive assessment	[76, 77]
HA-coated alumina	Porous sphere	Rabbit	Absence of a clear advantage over bare alumina orbital implants	[78–81]
HA coated with Cu-containing mesoporous bioactive glass	Porous sphere	In vitro tests	Encouraging antibacterial results against <i>S. Aureus</i> and <i>E. Coli</i>	[82]

bioactive glass/PE composite porous implants after enucleation or evisceration, respectively. Histological examinations revealed that there was no statistically significant difference with regard to fibrovascular ingrowth among the four groups up to 8 weeks of postoperative follow-up. Apparently, the inclusion of bioactive glass particulate did not significantly promote the rate of fibrovascular ingrowth into porous PE orbital implants.

In 2011, the clinical outcomes of 170 enucleated patients receiving bioactive glass/PE composite porous orbital implants were reviewed by Ma and coworkers [77]. The majority of patients experienced no complications (161 cases) and had comfortable socket characterized by good implant motility, without conjunctival thinning or inflammation; excessive discharge and implant exposure occurred in two and seven cases, respectively. All exposures were successfully treated with antibiotics or additional surgery; secondary surgeries were required by some patients but were not due to implant-related complications (ectropion repair in five patients and volume augmentation in three patients). These early results suggest that bioactive glass/PE composite implants may be an interesting option for orbital reconstruction,

but comparative studies are necessary to definitely estimate their performance with respect to the other available – and routinely used – implants.

## HA-Coated Alumina Implants

The clinical effects of a synthetic HA coating on the struts of a porous alumina implant were first investigated by a group of Korean researchers in the early 2000s. This experimental implant was fabricated by the polymer sponge replication method: the porous alumina skeleton acted as load-bearing structure, whereas a 20- $\mu\text{m}$ -thick HA layer deposited on it was advocated to provide superior biocompatibility and better long-term stability in the eye [78]. Animal studies in eviscerated rabbits receiving 12-mm-sized HA-coated alumina spheres with different pore sizes (300, 500, and 800  $\mu\text{m}$ ) revealed peripheral fibrovascularization of the implant in all groups after 15 postoperative days and also at the center of the implant after 28 days; fibrovascularization was more predominant in the group of implants having 500- $\mu\text{m}$  pores compared to the other two types [79].

In 2002 Jordan et al. [80] reported a comparative study on the implantation of experimental alumina implants coated with HA or calcium metaphosphate in rabbits. Both types of implant had multiple interconnected pores and, in comparison to the uncoated device, the coatings increased the size of the trabeculae from 150 to 300  $\mu\text{m}$ ; therefore, the pores appeared smaller but still ranged in the 300–750- $\mu\text{m}$  range. There was no clinical difference in the socket response between coated and uncoated implants, and fibrovascularization occurred uniformly throughout each implant at 4, 8, and 12 weeks after implantation.

A few years later, Chung et al. [81] investigated the fibrovascular ingrowth and fibrovascular tissue maturation of HA-coated porous alumina implants in comparison with commercial HA spheres in enucleated rabbits over a 24-month follow-up and found no significant difference between the two groups.

No other studies about HA-coated implants have been published; probably, the absence of a clear advantage from a clinical viewpoint (HA coatings did not appear to facilitate or inhibit fibrovascular ingrowth with respect to uncoated implants) and the presence of significant amounts of CaO as a contaminant (related to the coating manufacturing) [80] discouraged the researchers from performing further investigations in this direction.

## HA Implants Coated with Mesoporous Bioactive Glass

Very recently, Ye et al. [82] coated macroporous HA orbital implants with a thin layer of CuO-containing mesoporous bioactive glass (Cu-MBG): the aim of this research was to combine the antibacterial effect (copper shows potent antibacterial activity in suppressing a range of bacterial pathogens involved in hospital-acquired infections [83]) and drug delivery capacity (drug molecules can be hosted within the glass mesopores [84]) of the Cu-MBG coating to improve the final outcomes of



anophthalmic socket surgery. Cu-MBG coatings with 0, 2, or 5 mol% of CuO were prepared by dipping the porous HA implants into the sol precursor of the mesoporous glass, followed by evaporation, aging, and calcination. With the peculiarity of releasing antibacterial ions as the Cu-MBG degrades (viability of *S. Aureus* and *E. Coli* was inhibited) and good drug uptake/delivery ability (in this study ofloxacin), Cu-MBG coating could be a promising, multifunctional tool in the prevention of implant-related infections.

---

## Summary and Outlook

The available literature seems to demonstrate that the performances of porous orbital implants, including the commercial ceramic ones (porous HA and alumina), are superior to those of nonporous devices, such as solid polymeric spheres (silicone or PMMA) and Allen implants (PMMA); the interested reader is addressed to some recent publications for further details [2, 4]. In summary, there is convincing evidence that the exposures occurring in porous implants are more amenable to conservative management without a second operative procedure; in contrast, exposures in nonporous implants, unless very limited, almost always require implant removal [2]. This peculiarity is possible due to the fibrovascularization of the porous implant in vivo, as vascular ingrowth not only helps to anchor the implant in situ but also discourages bacterial colonization of the surface. In the case of ceramic orbital implants, wrapping is useful to decrease the risk of exposure, since the smooth wrapping material acts as a barrier between the overlying soft tissue and the micro-/macro-rough surface of the implant [44, 85]. Furthermore, a frontal peg can be inserted in porous orbital implants to improve the motility transmitted to the ocular prosthesis.

The use of porous devices is discouraged in children as a subsequent implant exchange will be necessary later since the patient is growing, but implant removal is difficult due to fibrovascularization [86]; at present, nonporous polymeric implants (e.g., solid silicone and PMMA spheres) remain the preferred choice by surgeons for the pediatric population [87].

It is instructive to report part of the results of a recent questionnaire addressed to UK ophthalmologists to evaluate current clinical practice in the management of the anophthalmic socket [88]. The surgeons' responses indicated that 56 % used porous orbital implants (HA, alumina, or PE) as their first choice, and HA (coralline or synthetic) was the preferred option; most porous implants were spherical (diameter 18–20 mm), with only a minority being egg shaped or conical; the majority of surgeons wrapped the implant after enucleation using salvaged autogenous sclera (20 %), donor sclera (28 %), or synthetic polymeric mesh (42 %); only 7 % placed motility pegs in selected cases, usually as a secondary procedure; postoperative exposure occurred in 14 % of cases, and extrusion was reported by 4 % after enucleation and 3 % after evisceration. In summary, this survey highlights that most UK surgeons use porous orbital implants with a synthetic wrap after enucleation, but only a few perform motility pegging. The validity of these results may be

reasonably extended to the whole European area; however, in other areas of the world, different options may be preferred.

From a general viewpoint, the choice of an “optimal” orbital implant is deeply influenced by many “extra-material” factors, including the overall cost and economic viability of the patient, the specific characteristics of the injury/disease, the experience/opinion of the surgeon, and the patient’s clinical history and age. The clinical performance, however, is strictly related to the physicochemical, mechanical, and biological properties of the implanted material; in this regard, it is useful to summarize few key concepts and to provide some highlights for material improvement and future research directions. Looking at the microstructural characteristics of ceramic orbital implants, there is a paucity of relevant studies in the literature since the majority of reports focused on the *in vivo* biological compatibility and postoperative performances, giving less importance to the assessment and understanding of the basic properties of the materials. From a general viewpoint, it is known that cell-substrate interactions at the micro- and nanoscale can be regarded as one of the major factors ultimately determining the long-term performance of a biomaterial/implant *in situ* [89]. Mawn et al. in the late 1990s [39] and more recently Choi et al. [90] investigated by SEM the microstructural and architectural features of coralline HA, synthetic HA, and alumina porous orbital implants, also providing a comparison with other polymeric devices available on the marketplace. As shown in Table 4, there were marked variations of crystal size/shape and surface topography among the analyzed orbital implants. The authors of these studies suggested that surface roughness could influence the inflammatory response after implantation, and crystal size could determine the material-induced phagocytic response: in fact, bioceramics with crystal size around 2–3  $\mu\text{m}$  (coralline and synthetic HA) showed greater tissue reaction in comparison to implants with finer grain (alumina), which was probably due to increased phagocytic activation by crystals of larger size. In this regard, Nagase et al. [91] showed that smooth HA crystals have been associated with less inflammation than sharp-edged crystals.

From these results it is still impossible to unequivocally claim that one porous material is clearly superior to the others, even though alumina, exhibiting excellent biocompatibility and favorable microstructural features, seems a promising candidate.

An additional issue to be considered is the effect of micro- and nanoscale topography on bacteria, since cells may have to compete with pathogens in the ocular environment. In a fascinating scenario, the surface topography of ceramic orbital implants could be purposely designed (e.g., by micro- and nano-fabrication techniques or by the optimization of the sintering temperature and time to develop crystals with a specific size thus creating a customized surface roughness) to encourage cells to colonize while limiting bacterial adhesion and risk of infection [89].

Pore size, interconnectivity, and overall macroscale architecture also influence the success of an orbital implant. The presence of an interconnected porous network is of crucial importance to promote fibrovascularization, as blood vessel access favors immune surveillance and permits treatment of infections (often following implant

exposure) via systemic antibiotics. Rubin et al. [92] studied the vascularization in porous HA orbital implants with various pore size and suggested that the optimal pore diameter to encourage fibrovascular tissue ingrowth should be around 400  $\mu\text{m}$ .

Other issues deserving careful attention concern the material surface chemistry and response to biological fluids. It has been demonstrated that the presence of an interconnected 3-D network of macropores is a sufficient condition per se to encourage fibrovascularization in orbital implants (like in the case of porous HA and alumina); the use of bioactive glasses in implant manufacturing could carry the significant added value of eliciting specific, desired responses via the release of appropriate ions [93]. In this regard, it is instructive to underline the importance of the study by Ye et al. [82], who coated a porous HA orbital implant with a layer of Cu-containing MBG: although these authors focused on the antibacterial effect of released  $\text{Cu}^{2+}$ , it was also demonstrated that  $\text{Cu}^{2+}$  induces migration and proliferation of endothelial cells during in vitro culture, which could lead to an improved fibrovascularization of the orbital implant in vivo. Looking at the future, appropriate design of bioactive glass composition could impart angiogenetic properties to the material for enhancing the fibrovascular ingrowth, with consequent improvement of clinical performances. Indeed, these smart bioactive glasses should be characterized by high stability once implanted in the ocular environment, as orbital implants are intended as permanent devices, i.e., they must remain in situ indefinitely during the patient's whole life without undergoing degradation to ensure an adequate socket volume replacement.

The incorporation of zirconia ( $\text{ZrO}_2$ ) in a bioactive silicate glass has been recently proposed, intended to act as a radiopaque phase in composite bone cements for better visualization under radiographic imaging [94]; a similar approach could be useful also in the field of orbital implants for better assessment of implant position and to detect problems of undesired postoperative migration.

Bioactive glasses also have other two important advantages with respect to HA and alumina, i.e., they can be processed at lower sintering temperatures and have a lower density. The latter could be an important added value to reduce the risk of migration downward with possible ectropion and incorrect replacement of orbital socket volume.

In order to limit the issues related to bacterial colonization of the implant, deposition of an antiseptic Ag nanoclusters/silica composite layer on the surface of ceramic orbital implants could be a valuable strategy, as recently suggested by Bairo et al. [95]. This coating, whose thickness can be properly modulated in the 1–1000-nm range, is produced by co-sputtering from silver and silica targets, exhibits a good adhesion on a wide range of substrates (glasses, crystalline ceramics, polymers), and has a good durability in biological environment [96, 97].

A final interesting issue is related to the mechanical properties of orbital implants that, especially if made of ceramic materials (HA, alumina), are remarkably stiffer than the ocular globe as well as the surrounding tissues like orbital fat. Indeed, the use of stiff biomaterials has a number of advantages from an operative viewpoint – e.g., the surgeon can easily handle and place the implant within the orbit with a great control over its position – but compliance mismatch between implant and overlying

conjunctiva/soft tissues, in combination with repetitive movement of the implant by the extraocular muscles, might contribute to inflammation and soft tissue necrosis, leading to implant exposure. Therefore, future research directions toward an ideal orbital implant might consider the use of novel polymer/ceramic composites to obtain more compliant biomaterials; potential options for the polymeric phase might be adapted, for instance, from the field of experimental vitreous substitutes, such as hydrogels that are biocompatible, porous, and able to absorb water and thus have similar physico-mechanical properties to living ocular tissues [98–100].

---

## References

1. Moshfeghi DM, Moshfeghi AA, Finger PT (2000) Enucleation. *Surv Ophthalmol* 244:277–301
2. Chalasani R, Poole-Warren L, Conway RM, Ben-Nissan B (2007) Porous orbital implants in enucleation: a systematic review. *Surv Ophthalmol* 252:145–155
3. Sami D, Young S, Petersen R (2007) Perspective on orbital enucleation implants. *Surv Ophthalmol* 52:244–265
4. Baino F, Perero S, Ferraris S, Miola M, Balagna C, Verné E et al (2014) Biomaterials for orbital implants and ocular prostheses: overview and future prospects. *Acta Biomater* 10:1064–1087
5. Baino F, Vitale-Brovarone C (2014) Bioceramics in ophthalmology. *Acta Biomater* 10:3372–3397
6. Lukats O, Buijtar P, Sandor GK, Barabas J (2012) Porous hydroxyapatite and aluminium oxide ceramic orbital implant evaluation using CBCT scanning: a method for in vivo porous structure evaluation and monitoring. *Int J Biomater* 749–764
7. Custer PL (2000) Enucleation: past, present, and future. *Ophthal Plast Reconstr Surg* 16:316–321
8. Levin PS, Dutton JA (1991) A 20-year series of orbital exenteration. *Am J Ophthalmol* 112:496–501
9. Bartley GB, Garrity JA, Waller RR, Henderson JW, Ilstrup DM (1989) Orbital exenteration at the Mayo Clinic 1967–1986. *Ophthalmology* 96:468–473
10. Mules PH (1885) Evisceration of the globe, with artificial vitreous. *Trans Ophthalmol Soc UK* 5:200–206
11. Kelley JJ (1970) History of ocular prostheses. *Int Ophthalmol Clin* 10:713–719
12. Guyton JS (1948) Enucleation and allied procedures: a review and description of a new operation. *Trans Am Ophthalmol Soc* 46:472–527
13. Allen L (1950) A buried muscle cone implant – development of a tunneled hemispherical type. *Arch Ophthalmol* 43:879–890
14. Spivey BE, Allen L, Burns CA (1969) The Iowa enucleation implant – a 10-year evaluation of technique and results. *Am J Ophthalmol* 67:171–188
15. Fan JT, Robertson DM (1995) Long-term follow-up of the Allen implant: 1967 to 1991. *Ophthalmology* 102:510–516
16. Helms HA, Zeiger HE Jr, Callahan A (1987) Complications following enucleation and implantation of multiple glass spheres in the orbit. *Ophthal Plast Reconstr Surg* 3:87–89
17. Christmas NJ, Gordon CD, Murray TG, Tse D, Johnson T, Garonzik S et al (1998) Intraorbital implants after enucleation and their complications: a 10-year review. *Arch Ophthalmol* 116:1199–1203
18. Spaeth EB (1941) *The principles and practice of ophthalmic surgery*, 2nd edn. Lea & Febiger, Philadelphia
19. Schmidt H (1906) Zur lösung des problems der kugeleinheilung. *Z Augenheilk* 16:63–80

20. Schmidt H (1910) Zur Lösung des Problems der Kugeleinheilung. Nachtrag 1909. *Z Augenheilk* 23:321–339
21. Klement R, Trömel G (1932) Hydroxylapatit, der Hauptbestandteil der anorganischen Knochen und Zahnschmelze. *Hoppe Seyler's Z Physiol Chem* 230:263–269
22. Lyall MG (1976) Proplast implant in Tenon's capsule after excision of the eye. *Trans Ophthalmol Soc UK* 96:79–81
23. Neuhaus RW, Greider B, Baylis HI (1984) Enucleation with implantation of a proplast sphere. *Ophthalmology* 91:494–496
24. Whear NM, Cousley RR, Liew C, Henderson D (1993) Post-operative infection of proplast facial implants. *Br J Oral Maxillofac Surg* 31:292–295
25. Girard LJ, Esnaola N, Sagahon E (1990) Evisceration implant of Proplast II – a preliminary report. *Ophthal Plast Reconstr Surg* 6:139–140
26. Girard LJ, Eguez I, Soper JW, Soper M, Esnaola N, Homsy CA (1990) Buried quasi-integrated enucleation implant of Proplast II: a preliminary report. *Ophthalmic Plast Reconstr Surg* 6:141–143
27. Christenbury JD (1991) Use of Proplast II. *Ophthalmic Plast Reconstr Surg* 7:223
28. Shah S, Rhatigan M, Sampath R, Yeoman C, Sunderland S, Brammer R et al (1995) Use of Proplast II as a subperiosteal implant for the correction of anophthalmic enophthalmos. *Br J Ophthalmol* 79:830–833
29. Dorozhkin SV (2007) Calcium orthophosphates. *J Mater Sci* 42:1061–1095
30. Molteno ACB, Van Rensberg JHJ, Van Rooyen B, Ancker E (1973) Physiological orbital implant. *Br J Ophthalmol* 57:615–621
31. Molteno ACB (1980) Antigen-free cancellous bone implants after removal of an eye. *Trans Ophthalmol Soc NZ* 32:36–39
32. Molteno ACB, Elder MJ (1991) Bone implants after enucleation. *Aust NZ J Ophthalmol* 19:129–136
33. Suter AJ, Molteno ACB, Bevin TH, Fulton JD, Herbison P (2002) Long term follow up of bone derived hydroxyapatite orbital implants. *Br J Ophthalmol* 86:1287–1292
34. Jordan DR, Hwang I, Brownstein S, McEachren T, Gilberg S, Grahovac S et al (2000) The Molteno M-Sphere. *Ophthal Plast Reconstr Surg* 16:356–362
35. Perry JD, Goldberg RA, McCann JD, Shorr N, Engstrom R, Tong J (2002) Bovine hydroxyapatite orbital implant: a preliminary report. *Ophthal Plast Reconstr Surg* 18:268–274
36. Perry AC (1991) Advances in enucleation. *Ophthal Clin North Am* 4:173–182
37. Dutton JJ (1991) Coralline hydroxyapatite as an ocular implant. *Ophthalmology* 98:370–377
38. Jordan DR, Munro SM, Brownstein S, Gilberg S, Grahovac S (1998) A synthetic hydroxyapatite implant: the so-called counterfeit implant. *Ophthal Plast Reconstr Surg* 14:244–249
39. Mawn LA, Jordan DR, Gilberg S (1998) Scanning electron microscopic examination of porous orbital implants. *Can J Ophthalmol* 33:203–209
40. Jordan DR, Bawazeer A (2001) Experience with 120 synthetic hydroxyapatite implants (FCI3). *Ophthal Plast Reconstr Surg* 17:184–190
41. Jordan DR, Pelletier C, Gilberg SM, Brownstein S, Grahovac SZ (1999) A new variety of hydroxyapatite: the Chinese implant. *Ophthal Plast Reconstr Surg* 15:420–424
42. Jordan DR, Hwang I, Gilberg S, Brownstein S, McEachren T, Grahovac S et al (2000) Brazilian hydroxyapatite implant. *Ophthal Plast Reconstr Surg* 16:363–369
43. Kundu B, Sinha MK, Mitra S, Basu D (2005) Synthetic hydroxyapatite-based integrated orbital implants: a human pilot trial. *Indian J Ophthalmol* 53:235–241
44. Gayre GS, Lipham W, Dutton JJ (2002) A comparison of rates of fibrovascular ingrowth in wrapped versus unwrapped hydroxyapatite spheres in a rabbit model. *Ophthal Plast Reconstr Surg* 18:275–280
45. Owji N, Mosallaei M, Taylor J (2012) The use of mersilene mesh for wrapping of hydroxyapatite orbital implants: mid-term result. *Orbit* 31:155–158
46. Jeong JH, Jeong SK, Park YG (1996) Clinical report of hydroxyapatite orbital implant. *J Korean Ophthalmol Soc* 37:1775–1783

47. You SJ, Yang HW, Lee HC, Kim SJ (2002) Five cases of infected hydroxyapatite orbital implant. *J Korean Ophthalmol Soc* 43:1553–1557
48. Mourgues T, Adenis JP (2001) Repair of hydroxyapatite orbital implant exposure with a conjunctival Muller muscle flap. *Oper Tech Oculoplast Orbital Reconstr Surg* 4:36–38
49. You JR, Seo JH, Kim YH, Choi WC (2003) Six cases of bacterial infection in porous orbital implants. *Jpn J Ophthalmol* 47:512–518
50. Remulla HD, Rubin PA, Shore JW, Sutula FC, Townsend DJ, Wooq JJ et al (1995) Complications of porous spherical orbital implants. *Ophthalmology* 102:586–593
51. Jordan DR, Brownstein S, Jolly SS (1996) Abscessed hydroxyapatite orbital implants – a report of two cases. *Ophthalmology* 103:1784–1787
52. Oestreicher JH, Liu E, Berkowitz M (1997) Complications of hydroxyapatite orbital implants – a review of 100 consecutive cases and a comparison of Dexon mesh (polyglycolic acid) with scleral wrapping. *Ophthalmology* 104:324–329
53. Jin SM, Kim JH, Kim IC (2000) Complications of hydroxyapatite orbital implants (a review of 110 consecutive cases). *J Korean Ophthalmol Soc* 41:2144–2156
54. Chee E, Kim YD, Woo KI, Lee JH, Kim JH, Suh YL (2013) Inflammatory mass formation secondary to hydroxyapatite orbital implant leakage. *Ophthal Plast Reconstr Surg* 29:40–42
55. Rahaman MN, Yao A, Sonny Bal B, Garino JP, Ries MD (2007) Ceramics for prosthetic hip and knee joint replacement. *J Am Ceram Soc* 90:1965–1988
56. Morel X, Rias A, Briat B, El Aouni A, D’Hermies F, Adenis JP et al (1998) Biocompatibility of a porous alumina orbital implant: preliminary results of an animal experiment. *J Fr Ophthalmol* 21:163–169
57. Jordan DR, Mawn LA, Brownstein S, McEachren TM, Gilberg SM, Hill V et al (2000) The bioceramic orbital implant: a new generation of porous implants. *Ophthal Plast Reconstr Surg* 16:347–355
58. Mawn LA, Jordan DR, Gilberg S (2001) Proliferation of human fibroblasts in vitro after exposure to orbital implants. *Can J Ophthalmol* 36:245–251
59. Akichika N, Futoshi H, Hitoshi M, Kosuke S, Shinichiro K, Katsuhito K (2002) Biocompatibility of a mobile alumina-ceramic orbital implant. *Folia Ophthalmol Japon* 53:476–480
60. Jordan DR, Gilberg S, Mawn LA (2003) The bioceramic orbital implant: experience with 107 implants. *Ophthal Plast Reconstr Surg* 19:128–135
61. Jordan DR, Brownstein S, Robinson J (2006) Infected aluminum oxide orbital implant ophthalmic. *Plast Reconstr Surg* 22:66–67
62. Jordan DR, Klapper SR, Gilberg SM, Dutton JJ, Wong A, Mawn L (2010) The bioceramic implant: evaluation of implant exposures in 419 implants. *Ophthal Plast Reconstr Surg* 26:80–82
63. Wang JK, Lai PC, Liao SL (2009) Late exposure of the bioceramic orbital implant. *Am J Ophthalmol* 147:162–170
64. Zigiotti GL, Cavaretta S, Morara M, Nam SM, Ranno S, Pichi F et al (2012) Standard enucleation with aluminium oxide implant (bioceramic) covered with patient’s sclera. *Sci World J*. Article ID 481584
65. Wang JK, Lai PC (2008) Bioceramic orbital implant exposure repaired by a retroauricular myoperiosteal graft. *Ophthalmic Surg Lasers Imaging* 39:399–403
66. Hench LL, Splinter RJ, Allen WC, Greenlee TK (1971) Bonding mechanisms at the interface of ceramic prosthetic materials. *J Biomed Mater Res* 5:117–141
67. Rahaman MN, Day DE, Bal BS, Fu Q, Jung SB, Bonewald LF et al (2011) Bioactive glass in tissue engineering. *Acta Biomater* 7:2355–2373
68. Baino F, Vitale-Brovarene C (2011) Three-dimensional glass-derived scaffolds for bone tissue engineering: current trends and forecasts for the future. *J Biomed Mater Res A* 97:514–535
69. Xu X, Wang C, Huang T, Ding L, Huang Z, Zhang X (1997) An experimental study of bioactive glass ceramics as orbital implants. *Bull Hunan Med Univ* 22:25–28
70. Xu X, Huang T, Wang C (1997) Clinical study of bioactive glass-ceramics as orbital implants. *Bull Hunan Med Univ* 22:440–442

71. Richter PW, Talma J, Gous PNJ, Roux P, Minnaar M, Levitz LM et al (2009) Orbital implant. US Patent no. 2009/0309274A1
72. Heringer DM, Ng JD (2006) A novel approach to re-pegging hydroxyapatite implants using bioactive glass. *Ophthal Plast Reconstr Surg* 22:45–47
73. Guthoff R, Vick HP, Schaudig U (1995) Prevention of postenucleation syndrome: the hydroxylapatite silicone implant – preliminary experimental studies and initial clinical experiences. *Ophthalmologie* 92:198–205
74. Klett A, Guthoff R (2003) How can artificial eye motility be improved? The influence of fornix configuration and tissue thickness in front of hydroxyapatite-silicone implants in 66 patients. *Ophthalmologie* 100:445–448
75. Klett A, Guthoff R (2003) Muscle pedunculated scleral flaps – a microsurgical modification to improve prosthesis motility. *Ophthalmologie* 100:449–452
76. Choi HY, Lee JE, Park HJ, Oum BS (2006) Effect of synthetic bone glass particulate on the fibrovascularization of porous polyethylene orbital implants. *Ophthal Plast Reconstr Surg* 22:121–125
77. Ma X, Schou KR, Maloney-Schou M, Harwin FM, Ng JD (2011) The porous polyethylene/bioglass spherical orbital implant: a retrospective study of 170 cases. *Ophthal Plast Reconstr Surg* 27:21–27
78. You CK, Oh SH, Kim JW, Choi TH, Lee SY, Kim SY (2003) Hydroxyapatite coated porous alumina as a new orbital implant. *Key Eng Mater* 240–242:563–566
79. Seong YS, Lee SY, Kim SJ (2001) Morphological study of a new orbital implant: hydroxyapatite-coated porous alumina in rabbit. *J Korean Ophthalmol Soc* 42:1354–1361
80. Jordan DR, Brownstein S, Gilberg S, Coupal D, Kim S, Mawn L (2002) Hydroxyapatite and calcium phosphate coatings on aluminium oxide orbital implants. *Can J Ophthalmol* 37:7–13
81. Chung WS, Song SJ, Lee SH, Kim EA (2005) Fibrovascularization of intraorbital hydroxyapatite-coated alumina sphere in rabbits. *Korean J Ophthalmol* 19:9–17
82. Ye J, He J, Wang C, Yao K, Gou Z (2014) Copper-containing mesoporous bioactive glass coatings on orbital implants for improving drug delivery capacity and antibacterial activity. *Biotechnol Lett* 36:961–968
83. Ruparelia JP, Chatterjee AK, Duttgupta SP, Mukherji S (2008) Strain specificity in antimicrobial activity of silver and copper nanoparticles. *Acta Biomater* 4:707–716
84. Baino F, Fiorilli S, Mortera R, Onida B, Saino E, Visai L et al (2012) Mesoporous bioactive glass as a multifunctional system for bone regeneration and controlled drug release. *J Appl Biomater Funct Mater* 10:12–21
85. Nunnery WR, Heinz GW, Bonnin JM, Martin RT, Cepela MA (1993) Exposure rate of hydroxyapatite spheres in the anophthalmic socket: histopathologic correlation and comparison with silicone sphere implants. *Ophthal Plast Reconstr Surg* 9:96–104
86. Moon JW, Yoon JS, Lee SY (2006) Hydroxyapatite orbital implant in pediatric patients with retinoblastoma. *J Korean Ophthalmol Soc* 47:1225–1232
87. Jordan DR, Klapper SR (2010) Controversies in enucleation technique and implant selection: whether to wrap, attach muscles and peg? In: Guthoff RF, Katowitz JA (eds) *Oculoplastics and orbit*. Springer, Berlin, pp 195–211
88. Viswanathan P, Sagoo MS, Olver JM (2007) UK national survey of enucleation, evisceration and orbital implant trends. *Br J Ophthalmol* 91:616–619
89. Anselme K, Davidson P, Popa A, Giazson M, Liley M, Ploux L (2010) The interaction of cells and bacteria with surfaces structured at the nanometer scale. *Acta Biomater* 6:3824–3846
90. Choi S, Lee SJ, Shin JH, Cheong Y, Lee HJ, Paek JH et al (2011) Ultrastructural investigation of intact orbital implant surfaces using atomic force microscopy. *Scanning* 33:211–221
91. Nagase M, Nishiya H, Abe Y (1993) The effect of crystallinity on hydroxyapatite induced production of reactive oxygen metabolites by polymorphonuclear leukocytes. *FEBS Lett* 325:247–250

92. Rubin PA, Popham JK, Bilyk JR, Shore JW (1994) Comparison of fibrovascular ingrowth into hydroxyapatite and porous polyethylene orbital implants. *Ophthal Plast Reconstr Surg* 10:96–103
93. Mourino V, Cattalini JP, Boccaccini AR (2012) Metallic ions as therapeutic agents in tissue engineering scaffolds: an overview of their biological applications and strategies for new developments. *J R Soc Interface* 9:401–419
94. Tallia F, Gallo M, Pontiroli L, Baino F, Fiorilli S, Onida B et al (2014) Zirconia-containing radiopaque mesoporous bioactive glasses. *Mater Lett* 130:281–284
95. Baino F, Perero S, Miola M, Ferraris S, Verne E, Ferraris M (2012) Rivestimenti e trattamenti superficiali per impartire proprietà antibatteriche a dispositivi per oftalmoplastica. IT Patent No. TO2012A00051
96. Ferraris M, Balagna C, Perero S, Miola M, Ferraris S, Baino F et al (2012) Silver nanocluster/silica composite coatings obtained by sputtering for antibacterial applications. *IOP Conf Ser Mater Sci Eng* 40:012037
97. Balagna C, Ferraris S, Perero S, Miola M, Baino F, Coggiola A et al (2013) Silver nanocluster/silica composite coatings obtained by sputtering for antibacterial applications. In: Njuguna J (ed) *Structural nanocomposites – perspectives for future applications*. Springer, Berlin, pp 225–247
98. Baino F (2010) The use of polymers in the treatment of retinal detachment: current trends and future perspectives. *Polymers* 2:286–322
99. Baino F (2011) Towards an ideal biomaterial for vitreous replacement: historical overview and future trends. *Acta Biomater* 7:921–935
100. Kleinberg TT, Tzekov RT, Stein L, Ravi N, Kaushal S (2011) Vitreous substitutes: a comprehensive review. *Surv Ophthalmol* 56:300–323



Dumitru Mohan, Aurel Mohan, Iulian Vasile Antoniac, and  
Alexandru Vlad Ciurea

## Contents

Introduction .....	1276
Applications of Biomaterials in Cranioplasty .....	1278
General Aspects About Neurosurgery .....	1278
Specific Aspects About Cranioplasty .....	1279
Available Biomaterials for Cranioplasty .....	1281
Clinical Requirements for Biomaterials Selection .....	1281
Metals .....	1283
Bioceramics .....	1284
Biopolymers .....	1291
Biocomposites .....	1294
Recent Developments and Future Approaches .....	1296
Tissue Engineering .....	1296
Modern Manufacturing Techniques for Personalized Implants .....	1297
Case Report: Cranioplasty with PEEK Personalized Implant .....	1298
Introduction .....	1298
Clinical Case Details .....	1299
Clinical Case Follow-Up .....	1302
Summary .....	1302
References .....	1303

---

D. Mohan (✉) • A. Mohan  
University of Oradea, Oradea, Romania  
e-mail: [mohan\\_dumitru@yahoo.com](mailto:mohan_dumitru@yahoo.com); [mohanaurel@yahoo.com](mailto:mohanaurel@yahoo.com)

I.V. Antoniac  
University Politehnica of Bucharest, Bucharest, Romania  
e-mail: [antoniac.iulian@gmail.com](mailto:antoniac.iulian@gmail.com)

A.V. Ciurea  
University of Medicine and Pharmacy “Carol Davila” Bucharest, Bucharest, Romania  
e-mail: [prof.avciurea@gmail.com](mailto:prof.avciurea@gmail.com)

---

**Abstract**

The loss of cranial bone integrity due to a trauma, a surgical intervention, or the natural aging process is a contemporary example of tissue failure, which usually requires the permanent or temporary implantation of a bone substituent and may become challenging in case of large defects. Additionally, the neurosurgical procedures developed for restoring cranium defects require an optimum aesthetic outcome and avoidance of artifacts during imagistic investigations. The current research includes both polymeric materials and ceramics, due to the need for different material delivery forms. Small-sized cranial reconstructions are usually performed with cements, for which the calcium phosphates and other ceramics seem to be a reliable solution, as well as polymethyl methacrylate (PMMA). However, the larger-sized bone defects are the more challenging applications in cranioplasty. Nowadays, the polyether ether ketone (PEEK) seems to be a reasonably material for large-sized implants, especially for its physical and mechanical characteristics, as well as for its suitability for tridimensional printing techniques, which may allow for better aesthetic outcomes. In the next step, the use of biocomposite materials will also improve a wide set of biomedical applications, due to the large number of properties that may be acquired through proper manufacturing control. Both the structure and the biological behavior may be improved through phases' variation and filler distribution.

---

**Keywords**

Cranioplasty • Neurosurgery • Injury • Personalized implants • PEEK • Case report • Clinical follow-up

---

**Introduction**

The loss of cranial bone integrity due to a trauma, a surgical intervention, or the natural aging process is a contemporary example of tissue failure, which usually requires the permanent or temporary implantation of a bone substituent and may become challenging in case of large defects. Additionally, the neurosurgical procedures developed for restoring cranium defects require an optimum aesthetic outcome and avoidance of artifacts during imagistic investigations.

The main objective of a bone graft is the osseointegration, which strongly depends on factors like extracellular processes, resorption of the implanted material, tissue vascularization, mechanical support, sterilization procedures, or inflammation-related mechanisms. Until now, the autologous bone is the standard material used in cranioplasties due to its biocompatibility, osteoinductive and osteoconductive properties, and chemical composition. However, autologous bone's main disadvantage is the limited supply (because only a few body parts can provide an optimal bone graft), as well as the multiple surgical procedures, which will lead to anesthetic scars and will increase the healing time [1–3].

The use of xenografts (e.g., bovine bone tissue fragments) as bone replacement may increase the risk of biological contamination, infections, and faster resorption (before the complete bone regeneration). Other solutions, like allografts (human bone grafts, sampled from another individual), are associated with difficult harvesting and storage procedures, as well as high risks of tumoral cell transmission or pathogenic agents, and sometimes with host incompatibility [1].

Since each of the previously mentioned solutions has its own limitation and the requirements for bone substitution materials are rapidly increasing, the research and development of alloplastic materials became an important objective of biomaterials science. The synthetic materials have an increased availability and may easily fulfill the various requirements imposed by their use in a large series of medical devices. Furthermore, these materials have a lower risk of biological contamination or immunological incompatibility [1, 4].

Various alloplastic materials may be currently used as bone tissue replacements. An ideal bone substitute will have to mimic the structure and function of the original tissue; to be osteoinductive, osteoconductive, and biodegradable; and to have an appropriate chemical composition and porosity which will allow for tissue vascularization and new bone formation. Also, the ideal bone substitute should ensure the mechanical support for the newly formed bone, until its complete regeneration is fulfilled. Finally, sterilization resistance, ease of storage, and economical processing methods are strongly needed [4–8].

The first materials used in primitive cranial bone reconstructions were the precious metals, along with gourds and coconuts crusts. Cranioplasty was not mentioned until the sixteenth century, when the material of choice was gold, and became efficient only after the beginning of antiseptic practices. In the beginning of the twentieth century, silver was introduced as a cranial bone reconstruction material and as a more economical and easier to shape alternative to gold, but the new material could not provide the adequate mechanical strength nor the biocompatibility required by this type of surgical procedure. The research for an optimum cranioplasty material continued with platinum, lead, and aluminum, and soon after this step, the alloys were also considered viable solutions. Vitallium and multiple classes of steel were tested, but currently only titanium is used in cranial reconstruction.

An important development in cranioplasty materials began with the introduction of bone substitutes in the current practice. Celluloid was first used because it does not interact with the dura, and later, acrylic resins and tantalum were considered better solutions. Both are still used, especially acrylics (polymethyl methacrylate is still the first option as a material for cranioplasty).

The current research includes both polymeric materials and ceramics, due to the need for different material delivery forms. Small-sized cranial reconstructions are usually performed with cements, for which the calcium phosphates and other ceramics seem to be a reliable solution, as well as polymethyl methacrylate (PMMA). However, the larger-sized bone defects are the more challenging applications in cranioplasty. Nowadays, the polyether ether ketone (PEEK) seems to be a reasonably material for large-sized implants, especially for its physical and

mechanical characteristics, as well as for its suitability for tridimensional printing techniques, which may allow for better aesthetic outcomes. However, PEEK implants are still expensive, and their lack of bioactive properties may lead to displacement and infection-related complications.

The current step in cranioplasty materials development is testing of composite materials, especially as biodegradable implants. Many composite formulas, constantly improved due to tissue engineering contribution, have already been tested with good results, both *in vitro* and *in vivo*. Alloplastic materials will continue to be upgraded for providing optimal solutions when autologous bone is not available for cranioplasty [9].

This chapter describes various alloplastic materials that are currently used or tested as a cranioplasty material as well as some of the future approaches from this area.

---

## Applications of Biomaterials in Cranioplasty

### General Aspects About Neurosurgery

Neurosurgery is defined as “an area of medicine that includes diagnosis and treatment of tumours, infections, hematomas, degenerative disorders or others legally treatable entities by surgical point of view, identified in the central, peripheral or autonomic nervous system” [10].

The main divisions of neurosurgery are

- (a) *The vascular and endovascular neurosurgery*, which deals with the diagnosis and treatment of various diseases of the central nervous system by using catheters and radiological techniques
- (b) *Stereotactic, functional, and epileptic neurosurgery*, a branch targeting patients with neuromotor disorders, epilepsy, and obsessive-compulsive disorder and uses nerve stimulation techniques mainly guided by microelectrodes
- (c) *Oncologic neurosurgery* responsible for treating tumors located in the brain and spinal cord
- (d) *The spine neurosurgery* which refers to treating spine conditions located in the meninges or spinal cord
- (e) *The cranial neurosurgery* that diagnoses and treats various lesions of the skull, located both at bone tissue level as well as at the level of the central nervous system components
- (f) *Peripheral nerve neurosurgery* that deals with restoring the peripheral nervous system components

A field of neurosurgery that is being treated separately is *pediatric neurosurgery*, which requires multidisciplinary approaches and uses methods specific to each area of neurosurgery, where the use of biomaterials has been documented separately [11–13].

Both spine surgery and cranial surgery intensively use biomaterials. For spine surgery, the use of biomaterials began with the use of metallic biomaterials for improving the mechanical properties of medical devices like stabilization systems which use screws and pins. Currently, the surgical interventions for spine bone reconstruction are applicable both in the case of degenerative diseases as well as traumatic pathologies. Most medical devices designed for such applications use autologous bone, but its limitations may affect the performance of the intervention. Biocomposite or bioceramic materials are used mainly for the healing of bone defects caused by osteoporotic spinal fractures and bone infections caused by osteomyelitis, as well as for replacing bone tissue fragments that are removed to facilitate the extirpation of cysts or tumors [14].

In cranial neurosurgery, a wide variety of biomaterials are used either as [15]:

- Carriers of drugs for treating neurological disorders
- In the form of neuron electrodes for the recovery of neurological function
- Grafts, to restore the nervous and bone tissues' integrity

The nervous tissue is superior to bone tissue both structural and physiologically. It needs to receive, decode, and transmit information throughout the entire body, and its functional unit, the neuron, has lost its ability to divide. The neuron is however capable of cellular division and may be involved in tissue regeneration. The use of biomaterials that support the nervous tissue restoration often involves the use of additional growth factors or cells.

By having a much more limited regeneration capacity, the central nervous system challenged tissue engineering to provide an optimum substrate which allows for the neuronal infiltration and proliferation without compromising tissue vascularization or generating a host response. Some hydrogels based on hyaluronic acid and laminine already proved their capacity to support the nerve tissue restoration, while the biocompatible single-walled carbon nanotubes are intensively tested for the same reason [15].

Finally, regarding cranial bone defects, it is well known that spontaneous skull ossification occurs only until the age of two, so after this age the use of bone substitutes becomes necessary.

Different surgical techniques may be used with a common purpose of craniofacial reconstruction. However, each method and material has limitations and may lead to poor resorption, release of toxic products generated by the material's biodegradation, aesthetic irregularities, biological contamination, or infection development.

## **Specific Aspects About Cranioplasty**

Cranioplasty is a surgical procedure performed in order to treat the cranial deformations or defects [4, 16, 17] and aims to restore the tissue subjected to injury, trauma, or tumor removal. Also, the infections and congenital defects could be mentioned. The main indications for cranioplasty are decompressive craniectomies, but a cranial

reconstruction may also be recommended after tumor removal, to restore a posttraumatic cranial defect, or in case of an infectious osteitis [4, 18].

Indications generally accepted for cranioplasty are brain protection to the underlying bone defect produced by direct mechanical trauma and aesthetic purposes, especially when bone defect is situated in frontal region.

Cranioplasty is also indicated with less sustainable arguments for:

- Combating posttraumatic epilepsy
- Brain protection against direct atmospheric pressure
- Preventing structures deviation of median line
- Combating “Burr syndrome” (symptomatic spectrum that occurs in patients with bone defects: headache, dizziness, fatigue, insomnia, and depression)
- Neurological improvement by improving cerebral blood flow underlying bone defect
- Normalization of the intracranial pressure

The favorable outcome of this procedure mostly depends on the technical skills of the neurosurgeon but also on the adjacent soft tissues’ condition and, obviously, on the type and size of the bone defect [16, 19], which may be congenital or gained [20]. In pediatric neurosurgery, the cranioplasty also supports the development of the nervous system [16]. Bone defects smaller than 2–3 cm, when they are located in regions covered by hair or on temporal region, where the temporal muscle disguises and protects aesthetic, do not require cranioplasty. Optimal time for practicing a cranioplasty is between 6 months and 1 year after surgery that caused the defect.

Post-surgery replacement of the bone tissue with a new material has both protective and aesthetic roles. Furthermore, the cranioplasty may reduce some neurological symptoms like depression or headache [4, 18, 19, 21]. However, excessive inflammation, infection, displacement, bone resorption, seizures, intracranial hematoma or hemorrhage, and wound breakdown are sometimes identified as complications of cranioplasty [17, 22, 23]. Still, many of these complications are strongly related to the defect’s dimension and location rather than the material used for reconstruction.

For most of the neurosurgeons, autologous bone is the recommended option as a cranioplasty biomaterial. However, bone resorption is one of the major disadvantages of most autologous bone cranioplasties, but this strongly depends on the cranial defect dimensions and neither on its cause nor location. Hence, the number of associated secondary surgical interventions may be twice as high in comparison with some alloplastic materials like hydroxyapatite or polymethyl methacrylate. The results are yet contradictory and require further research [19].

On the other hand, infection may be induced by the low blood supply at the implantation site, which is influenced by radiation treatment or repeated surgical procedures. The risk of infection is also associated with the reconstruction location [19]. The infection derived from cranioplasty or vertebral reconstruction affects both the patient and the implanted material: the patient will suffer severe pain while the implanted material will degrade and eventually fail.

Clinically, two forms of infection are significant and easy to distinguish: the first one is the overt infection (which is revealed through an increase of body's temperature) and the second one is the inflammatory response (characterized by localized warmth, pain, and sometimes redness and swelling). Some less severe forms of infection located near the implanted area may be difficult to detect because the same bacteria characteristic to biomaterial-related infections may produce specific substances that allows them to avoid the host's immune system.

The first steps in infection's treatment are the removal of the implant and the elimination of the infectious agent through proper medication. Currently, the cements doped with antibiotics (gentamicin) are an efficient solution for diminishing the infection-related risk. However, a possible disadvantage arises from the fact that almost 80 % of the antibiotic will be fixed in the cement's internal structure, and it may be released after months from implantation through microcracks [24].

---

## Available Biomaterials for Cranioplasty

### Clinical Requirements for Biomaterials Selection

The diagnostic and treatment methods for cranial defects or deformations are considerably developed in the last years, and many of these developments have been influenced by [3]:

- **The use of modern imagistic techniques** like CT or MRT, for tridimensional localization of bone and soft tissues. These techniques have a superior accuracy (only a few millimeters) and are also used, along with modeling software, to localize or to stimulate bone defects.
- **The use of modeling techniques** for the simulated defect restoration and pre-shaped implant manufacture, based on a virtual model (generated by a computer).
- **The biomaterials** used for hard tissue reconstruction. Since the cranial reconstruction has vital, functional, and cosmetic outcomes, the choice of biomaterials must be preliminary to the surgical intervention.

Among these, the biomaterial choice for cranial reconstruction is a very important step for performing a successful surgical intervention. Besides material characteristics, other aspects may be considered [3, 19]:

- **Indication for the procedure** (if a tumor disease is involved or not) – if the hard tissue reconstruction is necessary after a tumor removal, it is very important for the material to allow for future imagistic investigations.
- **Location and size of the implant** – some locations (frontal sinuses, ear, etc.) might be subjected to failure due to anatomical factors, reduced soft tissue coverage, or the presence of bacteria flora [19]. In this case, an inflammatory

response is expected both intraoperatively and long time after the surgery, so the antibiotic prophylaxis is recommended [3].

Large-sized implants have to be covered by the adjacent tissues and a sized implant will affect the local vascularization, which may lead to complications. Currently, large-sized implants have perforations to allow for tissue vascularization, but long-term stabilization may become an issue for these applications [25]. For the larger cranial defects, material's aesthetic outcome and mechanical support are the main requirements.

- **The complexity of the procedure** – the complexity of the procedure will increase if both dura and cranial bone must be replaced. The material used for the hard tissue reconstruction should favor the alloplastic dura integration or at least to induce a minimal influence.

The easiest method for performing a cranioplasty is the reattachment of the initial bone flap, because it will ensure a perfect fit, a good biocompatibility, and will support bone regeneration [16, 19]. The bone flaps' storage methods influence biomaterial's future behavior. Autologous bone may be stored inside patient's body with the advantage of maintaining the bone cells viability while providing a reduced infection risk but may be uncomfortable for the patient and will induce additional scars. When the storage is performed outside patient's body, the deproteination of bone tissue is usually required, and this will affect the cellular regeneration while increasing the risk of bone resorption [16, 18, 26].

Besides the disadvantages induced by the storage methods, autologous bone is associated with a high risk of infection, resorption, poor mechanical behavior, and difficult intraoperative modeling which will affect the aesthetic appearance, particularly in case of large defects [4, 19, 27, 28]. All these downsides led to the development of alloplastic biomaterials, but the choice between them must be evaluated for each individual [19]. Nowadays, the second option for cranioplasty materials, after the autologous bone, is the polymethyl methacrylate, used especially as cement. Although current cranioplasty alloplastic materials are parts of all material classes (metals, polymers, ceramics, and composites), neither one of them represents the optimal solution for human skull reconstruction [17].

When an alloplastic material is chosen for cranial reconstruction, its manufacture technique becomes one of the aspects that need to be considered, besides the one mentioned earlier in this chapter. A novel domain, called "biomanufacturing" and defined as "the use of additive technologies, biodegradable and biocompatible materials, cells and growth factors to produce biological structures for tissue engineering" aims to deliver high-quality devices for medical applications.

The final products used as medical devices are available in multiple delivery forms. Among these, implants (biodegradable or nondegradable) and cements have significant importance in cranioplasty. Implants are medical devices designed for replacing, assisting, or enhancing the functionality of bone tissue. Besides the ones replacing the biological structures, many other types of implants are available for



drug transportation or body function observation [29]. In the specific case of cranioplasty, the implants are conventionally manufactured with respect to the location and size of the cranial defect, by using a plaster impression achieved through the overlying skin, so the general accuracy of the impression will be poor. Furthermore, the presence of edema, hemorrhage, swelling, and overlying muscles will induce further dimensional errors; therefore, additional steps may be required for improving implant's shape [17]. Currently CAD/CAM and solid free-form fabrication techniques may be used with imagistic investigation methods for developing personalized implants. In cranioplasty these techniques are intensively used for titanium plates, hydroxyapatite, or polymethyl methacrylate pre-shaped implants [17, 30, 31].

Biodegradable implants or scaffolds are porous structures which are implanted for enhancing bone regeneration. These devices also ensure the support required for cell attachment, differentiation, and proliferation [29]. The scaffolds used for cranioplasties must fulfill the same mechanical requirements as the natural bone and should take in the mechanical loads of the newly formed tissue until the bone regeneration is complete. The composites with polymeric matrix and ceramic fillers are the appropriate choice for cranioplasty scaffolds due to their similarity with the bone tissue, both chemically and structurally. Nowadays, the development of this research area led to the use of nanotechnology for improving material performance [17].

## Metals

Metallic biomaterials are used intensively as load-bearing implants, due to their superior mechanical properties. The most popular applications are the hip and knee prosthesis, as well as a series of wires, screws, or rods used for fixation. The metallic biomaterials are regarded as "bioinerts" because they induce minimal response when they interact with a living body. The main risk associated with these materials is their corrosion in the physiological environment which may lead to the release of potentially harmful ions and to the mechanical damage of the implant.

Some metals are widely known for their use in medicine: titanium and its alloys, the austenitic stainless steels, cobalt-chromium alloys, and the precious metals' alloys. Among these, titanium is mostly used in neurosurgery due to its excellent biocompatibility (the material forms a protective oxide layer at its surface) and to the influence upon the osseointegration process, which allows for a structural and functional connection with the surrounding bone tissue [29]. Titanium is often used with other synthetic materials in neurosurgery [4], mostly because its biocompatibility may be improved by applying a bioceramic coating on the outer surfaces that come in direct contact with the host tissue [1].

Although the use of titanium is associated with high complication rates, a recent study on titanium cranioplasties revealed that the main associated complications are infection and plate removal, which are mostly influenced by the size of defect, the timing of cranioplasty, and location of the implant [32]. The overall complication

rate may be improved if prefabricated implants are used in the procedure [33]. Also, very recently, titanium meshes were used with bioceramic cements (brushite, hydroxyapatite, and monetite) for large cranial defects' treatment with very promising results [34].

## **Bioceramics**

A bioceramic material is defined as “any ceramic, glass or glass-ceramic that is used as a biomaterial” [35]. These materials are used especially for repairing the locomotive system's components and have direct contact with both the bone and with the surrounding tissues [36].

Bioceramics are currently used for a wide area of medical applications like lenses, thermometers, or other glass-derived products, optical fibers for endoscopy, and drug delivery agents, as restoration materials used in stomatology or as coatings for a biocompatibility improvement of metallic biomaterials [14, 15, 37–39]. The bioceramics are used for reducing the pain or restoring the impaired, lost functions of the calcified tissues (bones and teeth) existent in human or animal organisms, and their final goal is replacing a tissue that is either aged or degraded, with a material that may ensure the functionality of the initial component for an adequate amount of time (the patient's whole life or until the complete tissue regeneration), in a non-friendly environment: biological environment (saline and corrosive), at approximate 37 ° C, under the influence of mechanical loads with different intensities and distributions [39]. In neurosurgery, the bioceramics are mostly used as implants for tissue reconstruction subsequent to trauma or other medical interventions performed on the neural components.

The clinical applications exploit the bioceramics in different forms: films, powders, or solid blocks (which are either dense or porous). The bone substituents are generally prepared from porous calcium phosphates. The same materials may be chosen for repairing large bone defects which are not subdued to significant mechanical loads. The dense bioceramics, like alumina or zirconia, are used as components of hip prostheses, while the thin hydroxyapatite films are used as coatings for artificial teeth or metallic components of hip prostheses. All these forms of bioceramics are prepared through application-specific methods and manufacture processes. In the special case of hard bioceramics with a fine microstructure, the strict limitation of the impurities concentration is essential due to the catastrophic effects which they may have regarding the mechanical behavior after the implantation [40].

The use of bioceramics as scaffolds (degradable implants) provides the mechanical support needed during bone regeneration [38, 39] but requires the understanding of the interactions which take place at the bioceramics–tissue interface after implantation. In this case the bioceramics reactivity is an important material feature which allows for their classification and a thorough control of their applications. After implantation, some chemical reactions occur at the material–host tissue interface. After implantation, these reactions will modify the biomaterial surface characteristics and the behavior of the host tissue [39].

According to Hench et al. [36, 37], four types of implant tissue interactions may be described: toxic, inert, bioactive, and bioresorbable. This information led to the following classification of bioceramics [7, 36–38, 41]:

- Inert bioceramics (dense): are those nonporous bioceramics with superior mechanical properties, like alumina or zirconia. For the field of medical applications, the term “inert” is unspecific [35] and should be understood as “a material which will induce a minimal response from the host tissue and will lead to the formation of a thin, fibrous and non-adherent layer on the surface of the medical device” [7], because any material which is implanted will generate a body reaction. The attachment of these materials to the host tissue is accomplished through pressing or cementation and is called “morphological fixation.”
- Inert bioceramics (porous): although these materials induce the same type of reaction at the material–tissue interface, they constitute separate category due to their increased porosity which allows a mechanical attachment to the tissue, which is called “biological fixation.”
- Active bioceramics: are nonporous materials enabling the chemical bonding with the surrounding tissue (“bioactive fixation”). The most popular materials from this category are the bioglasses, the glass-ceramics, and the hydroxyapatite.
- Resorbable bioceramics: these materials have different porosity levels and are slowly replaced by the osseous tissue, while becoming directly involved in the metabolic processes of the body. Calcium sulfate and tricalcium phosphate are illustrative for this class of materials.

Another bioceramic classification may be performed based on the regeneration processes (“osteogenesis”) which begin after implantation. Therefore, the first group of materials (*class A materials*) increase both the osteoconduction (“process of passively allowing bone to grow and remodel over a surface” [35]) and the osteoinduction (“act or process of stimulating osteogenesis” [35]), while the second group (*class B materials*) will only encourage the osteoconduction [7, 37, 42, 43].

Finally, the bioceramics may be categorized by their chemical composition [40]. This classification is presented in detail in the following pages, including their properties, their specific applications, and the presentation of some composite materials prepared by matching each bioceramic class with other suitable material types.

Alumina or aluminum oxide ( $\text{Al}_2\text{O}_3$ ) is one of the most popular ceramics in engineering and medicine. Among its most known uses are the ones of abrasive material, for the manufacture of cutting instruments for laboratories, in the textile industry and paper industry. In the medical field, alumina and zirconia bioceramics are mostly used in dental and orthopedic applications.

Aluminum oxide with a purity of 99.99 % was designed as an alternative to metal biomaterials, due to its roughness (the ionic and covalent bonds in the material block the movement of dislocation in the crystal lattice), its reduced friction number, and its good resistance to corrosion and fatigue, properties that recommend its use in medical applications specific to orthopedics. In order to maintain its stability in time,

alumina needs a reduced porosity, a reduced quantity of additives, and a fine and homogenous microstructure. Decreasing the additives content is necessary to avoid their concentration at the grain boundary, because this will also decrease the fatigue resistance, especially in corrosive environments, while a fine and homogenous microstructure inhibits static stress that interferes with the loaded material [37, 40].

A major drawback of alumina bioceramics is given by their high modulus of elasticity (it is 10–50 times higher than the one of the bone tissue), which can additionally load the bone tissue during its regeneration process. Therefore, the use of aluminum oxide in these applications should be performed with respect to the age of the patient, the type of disease, and the biomechanics specific to the application [37].

However, the aluminum oxide has proven its non-cytotoxicity after being tested in cell cultures. After being tested through the implantation of some biomaterial samples in rabbits orbit, alumina samples have proven good acceptance of the material from the host tissue, cellular and vascular proliferation, and bone growth [41].

In biomedical applications, the aluminum oxide is used especially in orthopedics and dental applications: in knee prosthesis, maxillofacial reconstruction, or as a substitute for bone or in dental implants. In neurosurgery, the use of alumina has drawn the specialists' attention due to its mechanical resistance and the aesthetic benefits which resemble the acrylic materials. The experimental studies conducted on dogs have shown that the bone tissue can regenerate in the presence of multiple ceramic implants, but the aluminum oxide had a superior behavior compared to the titanium, with respect to mechanical properties and the compatibility with the bone tissue [44]. Furthermore, the addition of yttrium to the aluminum oxide offers radio-opaque properties [4]. Its usage in cranioplasty is documented in an article from 1987 [45, 46].

The zirconium oxide ( $ZrO_2$ ) is another material with an enormous potential as a bioceramic material due to its excellent mechanical properties. Nowadays, it is used in hip prostheses and in dentures, but its development as a biomaterial is possible in other medical devices as well.

Until now, the cytotoxicity tests performed on polycrystalline zirconia have proven the nontoxic character of the material. On the other hand, a possible risk agent in the case of using the zirconium oxide is given by the other radioactive elements presents in the chemical composition as residues. The effects of the concentration of radioelements on the tissues and organs have already been characterized through measuring the activity of femoral implants [41].

The glass and the bioactive glass-ceramics are made of high-purity materials through a series of standardized production techniques which ensure high biocompatibility and good osteoconduction properties so the material allows the formation of direct bonds with the bone without the formation of a fibrous capsule [1].

In time, various chemical compositions of glass and bioactive glass-ceramics have proven their functionality in medical applications, especially in orthopedics, thanks to appropriate mechanical properties [37]. By changing the chemical composition of the bioactive glass, one can enhance significantly the behavior of this

material: new series of bioactive glasses, based on boron oxide and phosphorus oxide, have proven their biocompatibility and their ability to promote the bone tissue regeneration. Porous glasses based on boron oxide are both biodegradable and can be designed with a degradation matched with the regenerating speed of the bone tissue [47].

Their biological properties have been intensely studied and documented, both in *in vitro* and *in vivo* [37, 41]. Briefly, the studies made to evaluate the biocompatibility of these materials have proven the absence of toxicity. Moreover, the class A bioactive glass-ceramics have interfered in tissue regeneration by creating chemical bonds with specific actions on the cells and tissues. These phenomena are directly dependent on the resorption speed and the ion quantities released after implantation [48, 49]. Special attention was pointed toward the study of the adherent layer formed on the bioglass–tissue interface, whose chemical composition was estimated as being rich in calcium and phosphorus [41], which are the main chemical elements in bone tissue, after carbon and oxygen [50, 51].

The development of the adherent layer of ceramic glasses is activated in saline or sanguine environments. The chemical bonds between silicon and oxygen are broken with release of salicylic acid, whose condensed form is a negatively charged gel situated on the biomaterial surface. The gel later crystallizes in a calcium phosphate and produces a new layer of apatite at the tissue–implant interface. The initiation of the bioactivity takes place when the apatite layer interacts with bone’s collagen, polysaccharides, and glycoproteins, which incorporate the apatite layers in their structure. These chemical bonds represent the beginning of tissue regeneration [52].

Although glass and bioactive glass-ceramics are characterized by the good biocompatibility, the large-sized bone substitutions made with these materials are long time implanted in the body and affect bone vascularization [5]. Besides this, the major disadvantage of glasses is their poor mechanical behavior: they have low-impact resistance due to their bidimensional amorphous lattices and high risk of crevicing at implantation, due to their fragile character [53].

The applications of bioglasses and bioactive glass-ceramics in orthopedics and dentistry have been documented since the end of the 1980s [6, 40, 45, 54–57]. A series of bioglasses or bioactive glass-ceramics products have been developed to replace bones in the middle ear, to repair dental defects, or to cover the implants used in different biomedical applications [37].

Until now, the ceramic glasses fulfilled all neurosurgical requirements regarding biological behavior, but the classical manufacturing process could not meet the necessary aesthetic appearance characteristic to personalized implants. Currently, the modern tridimensional printing techniques are able to produce personalized implants made of ceramic glass with minimal chemical composition changes, without altering the bioactive properties of the material. In addition, some bioactive glass composites were already used for craniomaxillofacial reconstruction. Thus, a biocomposite made of bioactive glass and bone sampled from the iliac crest had an improved healing time when compared with autografts, and a similar composite, with bone particles sampled upon a trephination, was used for skull reconstruction without side effects or further surgical interventions [52].

Another development aims for reducing their disadvantages by the addition of new ingredients, for preparing composite materials. An example is the glass-ceramic and titanium oxide composite which has been examined after implantation in patients' spinal cords. The material presents a good biocompatibility and long-term stability without forming a fibrous capsule on the interface with the body and without artifacts in the MRT investigations [33]. An apatite-wollastonite bioactive glass-ceramic has also been used in spine surgery [58, 59].

Calcium sulfate known as "gypsum" has been used since ancient times as a construction material. Products made of gypsum can be found in a great variety of shapes and purities, and their hydration degree can be adjusted through controlled heating. To obtain the hemihydrated form of calcium sulfate ( $\text{Ca}(\text{SO}_4)_2 \cdot \frac{1}{2} \text{H}_2\text{O}$ ) mostly used in biomedical applications, various hydrated forms are being processed and chemically treated in controlled conditions.

The calcium sulfate acts as an osteoconduction material and allows the vascularization of the bone tissue and the migration of the osteoblast if it is implanted in direct contact with the periosteum. Its usage increases the adhesion of bone cells with reduced or no inflammation at the implant site. The most important feature of the calcium sulfate is its high absorption speed in a physiologic environment (from several weeks to several months) [20, 40].

Although the material has been documented in literature, its usage is still limited. Applications in the pharmaceutical field have established a precedent in its usage as a biomaterial for orthopedics, and in the last decades calcium sulfate has been used as a bone substitute material, a binder for hydroxyapatite ceramic particles, or in different formulas for composite cements [40].

To avoid the fast absorption of calcium sulfate, the hydroxyapatite was introduced in a composite material designed to ensure the presence of non-resorbable hydroxyapatite particles at implantation site for enhancing bone regeneration. Two mixtures of this kind have been successfully tested on cats with frontal and parietal cranial defects. The study has proven that the material allows the regeneration of the bone tissue, is easily molded, and does not produce infections in the frontal sinus area [43]. Other composites, based on calcium sulfate and calcium carbonate, were tested on rats, through the implantation of some cylindrical samples in the femoral condyle, along with *in vitro* testing. The study showed that calcium carbonate incorporation in calcium sulfate decreases the biomaterial's degradation rate while enhancing the bone regeneration [60].

Besides the testing of biocomposites based on calcium sulfate, some studies are being developed to evaluate its use as drugs or growth factor delivery agents or if it has hemostatic or angiogenic properties [40]. A porous material formed of almost equal percentages of hydroxyapatite and calcium sulfate has already been approved to be used as antibiotic delivery system in osteomyelitis [4].

Calcium phosphates are ceramic materials with an excellent biocompatibility, a fact proven by their presence in the human body (bones, teeth, and tendons) [61]. Currently, the calcium phosphates are being used as bone substituents due to their chemical similarity with the inorganic component of bone. These materials have the ability to stimulate the regeneration of the bone tissue, by actively

interfering in the bone remodeling processes. However, calcium orthophosphates are difficult to use as implant materials or for large-size applications, due to their mechanical properties.

Calcium phosphates are currently used in orthopedics and neurosurgery in the treatment of bone defects and fractures [6], in spinal cord surgery [62–67], and in cranio-maxillo-facial reconstruction [54, 68–73]. Nevertheless, just a limited variety of calcium phosphates can be used in biomedical applications. For example, the compounds with a Ca/P report smaller than one are acids and are extremely soluble, while others, like tetracalcium phosphate (TTCP), are too basic for the needs of the living body. These materials can be used in medicine just combined with other calcium phosphates or other chemical substances [39], like the bone cement obtained from mixing tetracalcium phosphate (TTCP) and dicalcic phosphate (DCP), in the presence of water. Their reaction is isothermal and leads to the formation of a resorbable dense paste. If a buffer solution based on calcium phosphates is used during preparation, the reaction may be accelerated. Various studies conducted on cats have shown that the calcium phosphate bone cement is easy to shape, and its postsurgical aesthetic appearance was evaluated as “excellent” [32, 16].

Authors also draw attention on bone cement complications, especially on infection and the displacement of large defects restorations. Moreover, cases of mechanical failure have appeared even after trauma with reduced intensity. Apparently, a secondary restoration also accentuates the reabsorption of the material, which may eventually lead to infection. This drawback can be avoided if supplementary stabilization techniques are used [33].

Chemically, most bioceramics based on calcium phosphates are either in hydroxyapatite's (HA) or tricalcium phosphate's (TCP) class. Recently, some biphasic compounds HA +  $\beta$ -TCP or HA +  $\alpha$ -TCP have risen interest in the scientific literature, and their preparation and biological behavior are being intensively tested [74]. In comparison, the hydroxyapatite has a better stability in a physiological environment and it is reabsorbed in an increased amount of time than tricalcium phosphate. Hence, the success of a type BCP product will be determined by the report between the stable phase (HA) and the resorbable phase (TCP) [39].

BCP scaffolds' healing properties have been tested with good results in canine mandibular defects [20]. The *in vivo* behavior of a BCP formula was also recently tested in rat cranial defects with bone formation similar to  $\beta$ -TCP [75, 76].

Hydroxyapatite (HA) is a calcium phosphate very stable in aqueous environments, with the chemical formula  $\text{Ca}_{10}(\text{PO}_4)_6(\text{OH})_2$ . HA contains approximately 40 % calcium and 18.5 % phosphorus (in mass percentages) and has a hexagonal crystal lattice. The Ca/P report of the stoichiometric hydroxyapatite is 1.667 and is one of the most important indicators used to evaluate the different processes of obtaining this kind of material [6, 39, 54, 77].

Since approximately 70 % of the human bone is made of a nonstoichiometric form of hydroxyapatite, this material may be described as an ideal bone substitute. Different forms of porous hydroxyapatite lattices are available nowadays to repair bone defects or to support the tissue regeneration in almost the entire body. However, the geometry, porosity, and lattice substitutions are important characteristics which

affect the material's capacity to heal bone defects. These properties have already been tested in animal models [8, 20, 78].

The results from the cell cultures conducted to evaluate the biological properties of the nonstoichiometric form of hydroxyapatite have been evaluated with respect to their chemical composition [40]. The study revealed that hydroxyapatite with a higher content of carbonate groups increased the activity of the osteoclasts, and this result suggests that bone reabsorption (the phenomenon underlined by the activity of the osteoclasts) is directly influenced by the functional groups incorporated in hydroxyapatite crystal lattice. Another conclusion targets the fluoride ions substitutions, which stimulate the cell proliferation.

Still, a major drawback of hydroxyapatite is its brittle character (specific to bioceramics), the reduced tensile stress, and a high risk of infection after implantation. The larger bone defects may be difficult to repair with hydroxyapatite due to the reduced osseointegration and the structural transformation in contact with cerebrospinal fluid [4].

Various hydroxyapatite implants were evaluated in 2013 in a study that analyzed the clinical data for 1549 cases of patients who have had cranioplasty with personalized devices [63]. The results shown the material's compliance with the requirements assessed by this kind of surgical intervention and how well it is tolerated by both children and adults. Its brittle character may be balanced by increasing medical devices' depth and also by permanently improving the surgical technique. In comparison with the polymethyl methacrylate (PMMA), which does not allow for the expansion of the cranium in the growing, developing, or regenerating processes, the hydroxyapatite may be successfully used in pediatric neurosurgery applications. Also, the hydroxyapatite does not induce rejection reactions coming from the organism and ensures a relatively good attachment on the bone tissue [4].

Due to its various delivery forms, hydroxyapatite's bioresorbable character was evaluated in a comparative study of ceramic blocks and cements, conducted on sheep. The results have shown that differences between the reabsorption of the materials are not significant even after a year from the implantation, but tissue regeneration has been accelerated only for hydroxyapatite blocks, and not for the cement, as it has been expected [32, 16]. Hence, hydroxyapatite cement can be used in cranioplasty, because it does not induce bone growth and is not reabsorbed in the human body.

Since hydroxyapatite is also available as cement, this form is used in cranioplasty because it can be easily shaped [6]. A series of porous ceramic blocks or titanium may be added to enhance the mechanical properties of hydroxyapatite-based cement. This may avoid the thermal shock induced by the exothermal polymerization of polymethyl methacrylate. Moreover, the hydroxyapatite-based cement is quickly fixed, after approx. 5 min [33].

Some frequent side effects of cranioplasties made with bone cements based on hydroxyapatite are the accumulation of serum [32] and the infections, especially in the frontal sinus area [62]. The complications rate varies between 0 % and 20 % in the retrospective studies reviewed by Neovius and Engstrand [19]. Excellent results, without significant side effects, have been obtained in the case of using grains of



hydroxyapatite previously mixed with blood to form a paste with adhesive consistency [32].

Tricalcium phosphate (TCP) is rapidly diluted in physiological environment, which allows for bone tissue development after implantation. The TCP is found in four states, among which the most known are the  $\alpha$  and  $\beta$  [6].

The  $\beta$ -TCP ( $\beta$ -tricalcium phosphate,  $\beta$ -Ca<sub>3</sub>(PO<sub>4</sub>)<sub>2</sub>) can be prepared through thermal decomposition of the calcium-deficient hydroxyapatite, at temperatures over 800 °C, and through bone calcination. Pure  $\beta$ -TCP is not normally found in calcified tissue in human or animal bodies, but a magnesium substituted form, named whitlockite, may be found in renal calculus or arthritic cartilages [51]. This biomaterial has proven its biocompatibility with some results comparable with autografts' behavior [78].

The  $\alpha$ -TCP ( $\alpha$ -tricalcium phosphate,  $\alpha$ -Ca<sub>3</sub>(PO<sub>4</sub>)<sub>2</sub>) is a state of the tricalcium phosphate obtained by heat treating at approx. 1100 °C, but the addition of silicates in its structure has allowed the stabilization at temperatures lower than 1000 °C. The  $\alpha$ -TCP and the  $\beta$ -TCP have the same chemical composition but are fundamentally different in regard with the crystalline structure and the dissolution behavior:  $\alpha$ -TCP has an emphasized reactivity in aqueous environments and is able to be hydrolyzed along with other calcium-based phosphates. Nowadays, the  $\alpha$ -TCP is used in bone cements [51].

Both known states of the tricalcium phosphates have a superior solubility in comparison with the hydroxyapatite, and they are reabsorbed faster after implantation in the biological environment. This is why the  $\alpha$ -TCP and the  $\beta$ -TCP are used to obtain degradable biocomposite materials. Among these, a composite based on gelatin and  $\beta$ -TCP showed good results in the *in vivo* testing. The material is biocompatible, osteoconductive, and biodegradable and does not require a new surgical intervention to remove the device [1, 24].

Although the clinical applications of  $\beta$ -TCP are still limited, a bone substitute prepared from beta-tricalcium phosphate was already used in pediatric surgery to evaluate the healing rate of cranial bone defects in 23 patients. The healing was most effective for defects smaller than 40 cm, without graft-associated side effects [79].

## Biopolymers

The polymers are organic materials which incorporate large molecules in their entities called "monomers." The monomers' chemical bounds contribute to a giant chain formation and produce high ductile materials. The polymeric materials are similar to lipids, proteins, and polysaccharides from the biological environment, and the variations among them refer to chemical composition, molecular mass, crystallinity, solubility, and thermal properties. All these characteristics may be "programmed" by choosing the polymer type, its chain length, or by combining two polymers through copolymerization.

The polymers can be easily dispersed in complex forms (like gels, sponges, and materials with complex porosity systems) and are nonmagnetic and transparent to

X-rays, hence compatible with the modern medical imagistic methods. However, most of the polymers do not react favorably in the biological environment because they can generate either an inflammatory chronic response or a series of toxic degradation products. Polymers which however fulfill these biocompatibility requirements (named “biopolymers”) lack the necessary rigidity, ductility, or mechanical properties to resist to major loads or may be influenced by sterilization procedures.

The polymers may fulfill the matrix role in biocomposite materials with different properties, including biodegradation, and polymeric materials involved in preparation may be either natural or synthetic, the natural biopolymers being a better choice for biocomposites used in bone substitution due to their excellent biocompatibility and degradation properties [1, 80]. Natural organic materials were studied in order to identify their role in bone tissue functionality, in the same manner in which calcium phosphates were studied for their similarity with bone mineral component [81]. Polysaccharides, proteins, and biofibers were found to be appropriate biopolymers for composite materials because they possess a material structure able to guide the cells for biasing the time- and space-dependent local growth, simultaneously with stimulation of an immune response. In general, a biopolymer can be designed with a certain degradation rate which will allow for a gradual transfer of the mechanical load from the implanted material to the newly formed bone. The requirements for these materials include mechanical strength and lack of toxic degradation products, along with degradation and absorption rates comparable with the bone tissue healing rate.

Nowadays, the polymeric materials are especially used for soft tissue replacements or as matrixes for biocomposites. Different types of polymers, like polymethyl methacrylate (PMMA), polyether ether ketone (PEEK), or porous ethylene, are however used in neurosurgical applications [4, 24, 26, 52, 82, 83].

One of the most popular natural biopolymer is the collagen, which joins under this name several types of proteins that have an abundant contribution for the human body. These are indexed with Roman figures, considering the discovery date, and constitute structural unities that are capable to fulfill several connective tissue functions. Different types of collagen can be found in bone tissue, cartilages, or just partially in highly specialized tissues. The type I collagen is present in both soft and hard tissues, the type II collagen is found in bone epiphyses, and osteoblasts secrete a collagen type III fiber matrix along the periosteal surface. The collagen matrixes used in composite materials can suffer some improvements by adding cross-linking agents or by physical treatments like heating, irradiation, or copolymerization [81]. Another biopolymer which may be successfully used as a biocomposite matrix is chitosan, because of its ability to degrade simultaneously with bone tissue regeneration, without any toxic product release or other major inflammatory responses. The use of hydroxyapatite as a dispersed phase enhances the biocompatibility of the newly designed material, especially when HA is incorporated as nanometric particles. Fibrin also presents mechanical properties close to those of the bone tissue. Besides this, its incorporation in a hydroxyapatite composite

material was tested on rat cranial defects and proved to stimulate bone regeneration [1, 80].

PMMA is the polymerized form of methyl methacrylate, which is a liquid material. During polymerization, the material solidifies over a known amount of time, which makes it suitable for the use in surgical procedures. In chemical applications, the monomer is mixed with PMMA powder. The powder will dissolve and will initiate a polymerization reaction defined by viscosity increase followed by solidification [24]. Additionally, zirconium dioxide may be incorporated in the material for improving the results of X-ray analyses or CT [53]. The main advantages of PMMA are the transparency, the ease of preparation, the mechanical properties, and the low price [53]. Also, PMMA is well tolerated by the body. After implantation a fibrous tissue will evolve at the interface between the material and the surrounding tissue, and the osseointegration will begin with a host reaction. The immune response expresses both locally and systemic and is distinguished by the macrophage activation.

The PMMA is used in neurosurgery in vertebra stabilizations and replacements, as well as in cranioplasties, either as cement or as a pre-shaped solid implant. For small-sized defects in vertebrae or in the skull, the cement is prepared intraoperatively and then shaped and fixed by the surgeon, while the pre-shaped, solid implant is rigorously dimensioned and designed using patient's imaging results, for restoration of larger defects [24].

The use of PMMA cement is limited by its temperature rise during polymerization, the toxicity of the liquid monomer, and by the reduced bone vascularization after implantation. In spine surgery all these factors may lead to bone resorption followed by mechanical failure, while in the cranial neurosurgery the increased temperature may affect the surrounding tissues and lead to disfiguration or may damage the nervous system [24]. Also, loosening of the implant (with both mechanical and biological origins) is one of the high-risk disadvantages in spine surgery because PMMA implants are fixed with metallic rods and screws. This risk has been overcome in cranioplasty which allowed for the development of better fixation systems [24, 53], but the complications rate still varies between 0 % and 23 %, most of them due to the location and size of the cranial defect and to postoperative radiation treatment [19, 84].

Polyether ether ketone (PEEK) is a polymeric semicrystalline material with mechanical properties similar with those of the autologous bone [4, 25, 85, 86] and good resistance to sterilization techniques, without inducing CT or MRI artifacts [4]. PEEK implants are superior to metallic implants in terms of thermal and biological properties. Also, they may be easily shaped and can be manufactured through 3D printing techniques [4, 53].

Until recently, PEEK has been intensively used in spinal surgery [53, 87, 88], but the appropriate properties lead to its usage for the reconstruction of cranial bone defects caused by tumors, traumatic injuries, or infectious lesions [85]. PEEK cranioplasty leads to good aesthetic outcomes and is more comfortable because the material is light and is resistant to thermal modifications [86].

The main disadvantages of PEEK implants are their expensive prices and the lack of bioactive properties. The last one may lead to further complications like infections, foreign body reactions, and high risk of dislocations [4, 25, 86]. Unfortunately, very few data is available in the literature and the long-term follow-up of PEEK cranioplasty has not been thoroughly documented.

The porous polyethylene is a strongly biocompatible material with pore dimensions that allow for cellular migration. Moreover, this material is slightly malleable and does not induce resorption phenomena. When placed in a biological environment, the porous ethylene forms a connective tissue layer which contributes to the stabilization of the implant, along with the titanium screws which are usually used with this biomaterial.

However, the porous ethylene has some limitations regarding the malleability and impact resistance, which make it useful just for the small-sized defects. Furthermore, some adverse reactions were observed at the implantation near mucosa. The material is not recognized by X-ray analysis, is poorly detected by CT, and does not induce major artifacts in MRT [3].

## **Biocomposites**

Composite materials are manufactured from at least two components which possess different chemical and physical properties. The components will remain macroscopically separate within the new material structure, so composites are heterogeneous materials where in each of the phase conserves its characteristics and main properties and their interaction is intermediated by an interface. The manufacture of this type of material allows the procurement of new, enhanced characteristics which cannot be defined separately for each of the components. Similar with the other types of materials (metals, ceramics, or polymers), a composite material which is biocompatible is termed "biocomposite" [1, 17, 37, 48, 89, 90].

The components or phases of a composite material are defined in two groups: the first component is the matrix (continuous phase), which integrates the material's volume and constantly supports and maintains the position of the second phase type – the reinforcing material (the dispersed phase). The reinforcing material enhances the matrix's properties (especially the mechanical properties but some other features like density, biocompatibility, or X-ray transparency as well). Additionally, the composite materials may be designed to fulfill a wide range of preset conditions, by severely controlling the volume fractions and the local or global distribution of the phases. A higher volume of dispersed phase will considerably enhance the mechanical properties, while the long and aligned fibers will prevent crack propagation and will ensure the anisotropic behavior of the composite [1, 90].

The development of a composite material should consider a range of factors like components selection, the choice of proper preparation and processing methods, and aspects of internal and external appearance of the final medical device. During manufacture, the composites are mounted in a preset shape, while the sequence of

**Table 1** Classification of composites based on phases' dispersion in the material [1, 80, 81]

Composite type	Number of dispersed phases	Distribution of dispersed phases in the matrix	Observations
Simple	Single	Homogenous	–
Complex	Multiple	Homogenous	–
Graded	Single/multiple	Heterogeneous	–
Hierarchical	Single/multiple	Homogenous/heterogeneous	A primary composite is dispersed in a second matrix

phase's addition in the shape depends on the required material and on the previously selected preparation method.

Composites preparation requires, of course, the combination of at least two different materials. Therefore, phases' miscibility, adhesion, and polarity are important factors which interfere in this process. The lack of adhesion between the phases will lead to a failure at the interface, followed by a decrease of mechanical properties. From the chemical point of view, the interaction between the components of a composite material may be strong (ionic, covalent, or coordinative bonds) or weak (van der Waals forces, hydrogen bonds), while a third type of interaction does not imply any chemical bonding between the phases.

Composite materials may be categorized based on multiple criteria. Hence, based on phases' dispersion in the material, one could distinguish between the materials presented in the following Table 1 [1, 80, 81].

Finally, a different classification system for the composite materials depends on the matrix type (polymer, ceramic or metal) or on each component's type (polymer-ceramic, metal-ceramic, etc.). Among these different types of biocomposites, the ceramic-polymer ones release the highest concentration of toxic products and are limited by their organization in a preset shape. The metals bring multiple complications due to the corrosion processes while the ceramics coated on metallic implants degrade as the implantation time increases. The ceramic-ceramic composites possess some biological superiority, due to their similarity with the mineral component of bones and calcified tissues, and have an additional advantage as they may be shaped in different forms. Conclusively, the biological response of any material type is strongly influenced by the mechanical load from the body, so an insight into the local biomechanics is imperative for a proper selection of an optimum biomaterial [41].

Polymer-ceramic composite materials have been intensively tested on cell cultures and on animal models: the use of a composite material based on coralline hydroxyapatite and polyglycolic acid has been tested in the rabbit's skull, and the results confirm the lack of side effects and the ease of fixation on the adjacent bone tissue [91]. The gelatin was also used in another composite material, which has been evaluated in vivo after the introduction of particles of tricalcium phosphate to establish its potential as a substitution material for the cranial bone. The material has proven to be easy to shape, biocompatible, osteoconductive, and biodegradable, with a progressive replacement of the material with the regenerated tissue

[92]. Another biocomposite material based on gelatin and octacalcium phosphate (OCP/Gel) was tested on rats for different filler concentrations. The results have shown that the material has excellent biodegradable properties and stimulates cell migration [93]. The polymer- $\beta$ -TCP composites, manufactured using modern tridimensional printing techniques, have also been analyzed from a mechanical perspective. The tests have shown that the resistance to bending of the new material is 5–22 times higher, depending on the used polymer (PCL, respectively, PLA) [94]. A multiple composite material with notable results both in vitro and in animal testing is manufactured from layers of polylactide polymers, amorphous calcium phosphate, and calcium carbonate. The inner layers are porous and biodegradable and are involved in bone regeneration, while the outer layers are more stable for ensuring protection [3].

Currently, one of the most popular biomaterials for cranial reconstruction is based on a polymer matrix (epoxy resin) filled with carbon fibers. This material may be easily shaped during surgical intervention for improving the aesthetic outcome, is resistant to sterilization techniques, does not induce artifacts in imagistic results, is lighter than metals but with superior mechanical properties, and is biocompatible (is able to form a connective tissue layer at the implant–host interface) [3, 17].

---

## Recent Developments and Future Approaches

### Tissue Engineering

The simultaneous evolution of the complementary areas which collaborate for achieving a better functionality of medical applications allows, in our days, for the use of innovative strategies which aim to achieve biomimicry for bone substitute materials. The use of biomaterials with a degradation rate adapted to the tissue regeneration rate requires substantial development in various aspects of a relatively new field, called “tissue engineering.” Tissue engineering is a multidisciplinary domain which harmonizes the principles of engineering and life sciences in order to develop biological replacements for restoring, maintaining, or enhancing tissue functions, and its approaches recommend the use of porous scaffolds impregnated with cells and growth factors which will enhance the bone regeneration.

The development of composite biomaterials which will mimic the bone tissue architecture requires a proper identification and characterization of its tridimensional architecture, followed by the replication of an environment which will promote the cellular communication through cells and extracellular matrix's components and also through highly specialized proteins. All these components enhance the cellular proliferation, differentiation, and migration.

Latest approaches regarding biomaterials used for substitution of osseous tissue are related to:

- The use of biocomposite materials with nanoparticles: tissue engineering can use specialized techniques for simulating tissue properties at a macroscopic and microscopic scale, but they are still unable to replicate the microscopic aspects

which are key factors of bone regeneration. Additionally, the inflammatory reaction generated by the cellular activity and by the formation of the fibrous tissue will affect the regeneration process. “Nanobiomaterials” and especially the composites with nanoparticles are considered “promising platforms” which will provide the structural support required by the cells. Furthermore, the biomaterial design aims to introduce components which will guide the cellular behavior [17, 95].

- Involving cellular therapy in biomaterials development: the cellular regeneration may be simulated by incorporating bone growth factors in a polymeric matrix. This may enhance the protection while improving the implant’s aesthetic outcome [19]. Some bone morphogenetic proteins or polypeptide growth factors are already being prepared for further distribution in porous matrixes that will the osteoinduction and bone growth [16]
- Ensuring a proper vascularization from the implanted material: the vascularization may be achieved by developing materials with controlled porosity which will provide permeability and proper conditions for oxygen and nutrients diffusion through their structure. Also, the development of some microsurgical techniques may allow the shaping of “axially vascularized tissues” and reduce the contemporary limitations regarding tissue vascularization [96].
- Using modern manufacture techniques (“solid free-form fabrication”) in correlation with high-resolution imagistic techniques for developing personalized biomedical applications. All these tissue engineering aspects require the preparation of scaffolds that resemble the natural bone tissue, but the methods used by classical engineering involve the use of solid, simple, and large materials which will be shaped in smaller and complex forms without the possibility of controlling the geometric parameters (like the ones regarding porosity). This is one of the reasons why the structures required by tissue engineering are incompatible with the current manufacture techniques. In contrast, a modern series of manufacturing techniques named “solid free-form techniques” starts with small-sized units (powders) and organizes them in a preset shape. The solid free-form techniques are described in more detail in the following pages.

## Modern Manufacturing Techniques for Personalized Implants

Solid free-form fabrication techniques rapidly gained interest for potential uses in tissue engineering but are not extensively used yet due to some disadvantages of their final products like high costs, lack of geometry’s accuracy, low mechanical properties, or lack of adequate raw materials. Within the solid free-form fabrication techniques, tridimensional (3D) printing creates a solid material after the interaction between a layer of powder and a liquid which is atomized above it. The liquid may act as a binder or may generate a chemical reaction which will bond the solid particles. After solidification a new layer will form over the previous one which will also act as a support for the manufacturing of the entire material.

The common advantage of all solid free-form fabrication techniques is the possibility of acquiring a diversity of materials. Natural polymers, like polysaccharides,

may be used with water-based binders without any solvents. From this point of view, a minor disadvantage related to the solid free-form preparation of polymers is the need for organic solvents which may compromise the biocompatibility of the final product. On the other hand, ceramic materials may be used with polymeric binders, which will lead to the manufacture of composite materials, or with specialized cements which dissolve the particles and form new crystals in a ceramic structure [97].

In the medical devices industry, all these techniques have already been implemented in integrated systems, along with digital imagistic techniques (computerized tomography or magnetic resonance) for the manufacture of large models which mimic anatomical characteristics. In neurosurgery, as we mentioned at the beginning of this chapter, the fabrication of personalized titanium and PMMA implants is already available. These implants have a high anatomical accuracy and are prepared through tridimensional printing, followed by surface abrasion and sterilization [26, 30, 98, 99]. Another technique, called “laser cladding,” allowed for the construction of functional products for low-bearing applications, prepared from bioactive glasses. Implant technique did not induce any significant variation in terms of chemical composition while the structural modifications were minimal. Moreover, the bioactive glasses processed this way were tested in simulated body fluid for evaluating their biological behavior, and the results were similar to those of their precursors [100].

Achieving the best results in terms of accuracy and precision of solid free-form fabrication techniques requires advanced imagistic methods and a proper statistical evaluation of precision and reproducibility. High-resolution computerized tomography allows for the scaffolds’ quantitative analysis simultaneous with the investigation of the mineralization process. Beyond any doubt, the understanding of mechanical properties remains an area with large research opportunities, which will be able to offer significant information regarding devices’ behavior after implantation [30].

Finally, the improvement of cranial defects treatment by applying the principles of tissue engineering and modern manufacturing techniques is a complex concept, whose success depends on various interdisciplinary collaborations. Szpalski et al. identified a number of stages of research and development needed to improve neurosurgical techniques: the *in vivo* animal model testing for evaluating reparation of defects, optimal biomaterials choice, and developing strategies of vascularization and cell proliferation [20]. So it is possible in the future that biodegradable biomaterials manufactured through tissue engineering techniques will cover bone defects for an appropriate amount of time while releasing bioactive molecules which transform the personalized implant into a functional tissue [16].

---

## Case Report: Cranioplasty with PEEK Personalized Implant

### Introduction

Bone lesions caused by traumatic injuries often require the tissue reconstruction through cranioplasty, and the choice of a proper biomaterial is a challenge for neurosurgeons. PEEK implants have already showed good results in cranioplasties,



although their applications are still limited. The following pages describe a successful cranioplasty performed with a custom-made PEEK implant.

## Clinical Case Details

### History

A male patient, aged 21, suffered a craniocerebral traumatic injury due to a car accident. The subsequent evaluation showed that the patient suffered a comminuted cranial bone fracture with osseous fragments blockage, along with a sub-adjacent cerebral hemorrhagic contusion. The first surgical procedure, performed in a local hospital, allowed for the removal of temporal osseous fragments with favorable postsurgical outcomes. The patient regained its consciousness after approximately 2 days, and his neurological status was completely restored.

### Case Examination and Operation

After approx. 8 months from the initial surgical intervention, the patient came at “Sanador Clinic” in Bucharest for a general and craniocerebral evaluation. The initial CT examination revealed a cranial bone defect in the right temporoparietal area, of approximately 23 mm length, near an adjacent right porencephalic cavity in the parieto-occipital area (24/66 mm maximum axial diameters and 27 mm longitudinal diameter). No other unusual aspects were identified by this initial CT scan, as one may observe in Fig. 1.

Since a consequent MRI investigation was contraindicated due to a foreign body with metallic density identified in the pelvic region during the CT examination, an EEG investigation was performed without any further observation of pathological aspects. Also, an ENT checkup was carried out with normal clinical outcomes.

The second CT investigation confirmed the presence of a sequellar cerebral lesion in the right posterior temporal area and bone loss with 3.5/2.7 mm diameters in the right retroauricular field. Based on these results, a tridimensional cranial bone reconstruction was simulated using dedicated software (Fig. 2).

The previously acquired data, the imagistic aspect, and the proper amount of time since the first surgical intervention allowed for performing a cranioplasty. The alloplastic implant was designed based on the CT results, in order to achieve an accurate anatomical shape of the implant. The material of choice was polyether ether ketone (PEEK), recommended by its advantages in this field previously described: PEEK is a light material which ensures mechanical support, is compatible with the personalized implants’ manufacturing techniques, and does not induce artifacts in the imagistic analyses. The personalized PEEK implant was surgically implanted and subsequently mounted using two “CranoFix 2” devices (11 mm diameter), and a keloid scar located near the reconstruction site was removed. The intraoperative aspect of the implanted material is presented in Fig. 3.

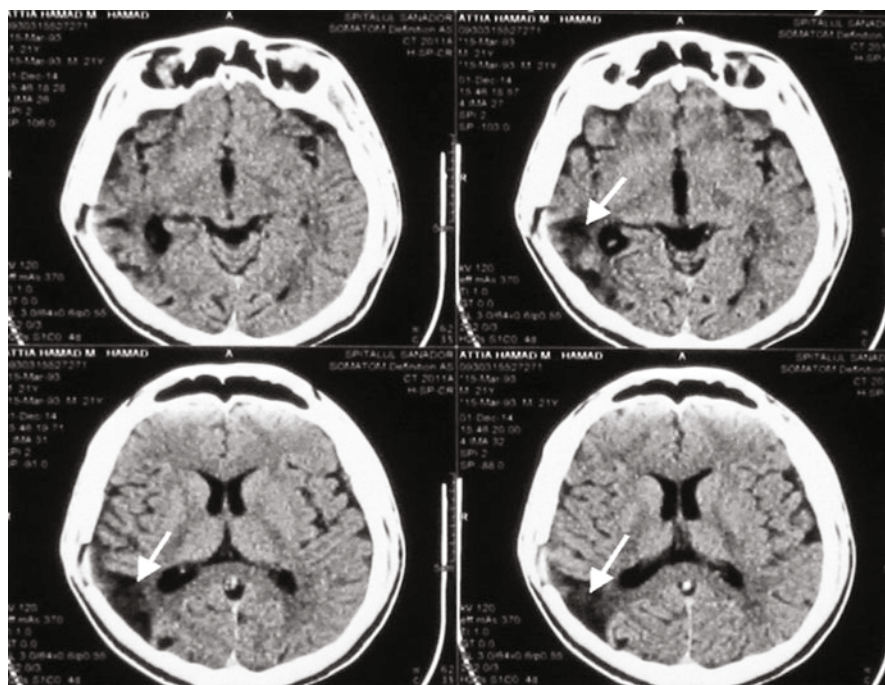


**Fig. 1** The initial CT examination (8 months after the traumatic injury)

**Fig. 2** Cranial 3D reconstruction. The bone defect is emphasized

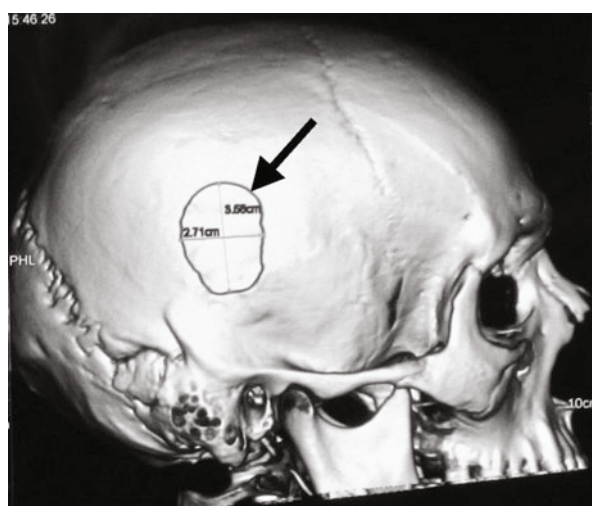


**Fig. 3** Intraoperative aspect of the cranioplasty material after implantation and mounting

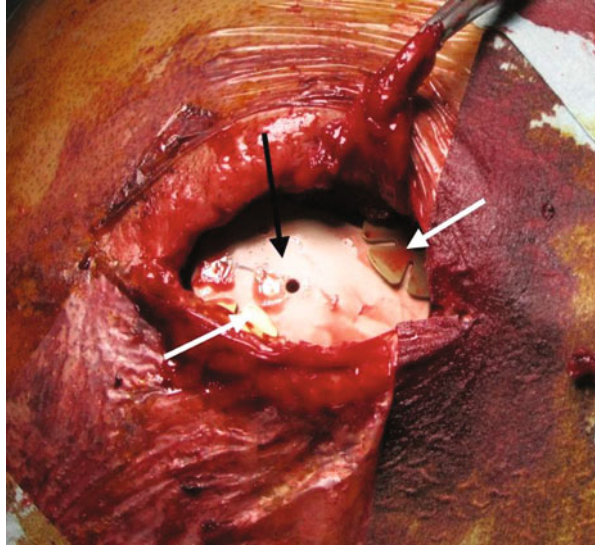
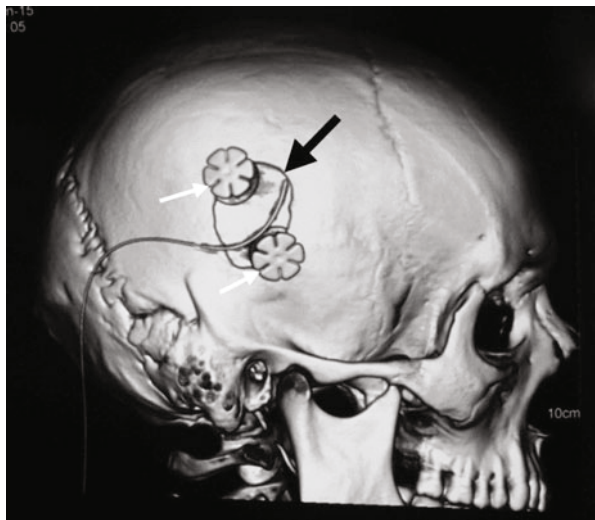


**Fig. 4** 3D CT examination at 24 h after the surgery. The cranioplasty, the fixation devices, and the drainage tube are revealed



### Postoperative Care

The surgical intervention was performed without any complications, and the post-surgical outcome was favorable for both short and long time after implantation. A postsurgical CT result is displayed in Fig. 4.

The suture was removed 10 days after the cranioplasty, and the general wound aspect was evaluated (Fig. 5). No other neurological deficits or complications were further identified.



**Fig. 5** Wound aspect and general evaluation (10 days after the surgery)

### **Clinical Case Follow-Up**

This clinical experience comprises the use of a relatively new material used in cranioplasty. PEEK already proved in usage in spine surgery, as a bone replacement which does not interfere with the components of the nervous system components. Moreover, this material is already used as a material for cranial bone repair with good outcomes which were also observed in this case. Long-term follow-up will be performed for evaluating material's degradation and permanently evaluate the patient's general condition.

---

### **Summary**

This chapter began with some general information regarding the use of biomaterials in neurosurgery and cranioplasty. Currently, a wide variety of biomaterials, especially biopolymers and bioceramics, are used or tested for the restoration of cranial bone defects or deformations, and the choice between them depends on multiple factors, like the size and location of the defect or if a tumor is involved in the pathology or not. Although the biomaterials involved in cranial bone restoration does not induce major influences upon the overall complications rate, the biomaterials choice represents one of the key factors that will lead to a successful surgical intervention.

The current use of biomaterials for cranioplasty is divided based in the size of the bone defect: if a small-sized defect needs to be restored, cement may be used for this application so PMMA, hydroxyapatite, or other bioceramics may be used as a biomaterial. On the other hand, if a larger defect needs to be restored, an implant will be required at the implantation site so its manufacture will begin before the

surgical intervention. Titanium is still used as an implant, along with PEEK, hydroxyapatite, or PMMA. However, each application has its specific requirements and the selected biomaterial must fulfill all of them, or at least the majority.

The current research for an optimum biomaterial aims for developing a new materials generation, which will enable bone regeneration by stimulating specific host tissue response, and the porous bioceramics may be considered their precursors. Furthermore, the use of modern techniques for the biomaterial design and manufacturing will lead to a faster development, especially since their current use significantly improve the functionality and the aesthetic aspects of the implants designed for cranial reconstruction [39].

In the next step, the use of biocomposite materials will also improve a wide set of biomedical applications, due to the large number of properties that may be acquired through proper manufacturing control. Both the structure and the biological behavior may be improved through phases' variation and filler distribution. However, the current use of composite materials is limited due to some limitations [89] regarding the lack of clinical and experimental results about the long-term materials' behavior, the complex preparation techniques, and the limited specific standard test methods. If these critical aspects will be thoroughly addressed, a new step to composite commercialization may be made, because the perspectives regarding composite materials are optimistic and depend solely on the good collaboration between engineering medicine, chemistry, biology, and biomaterial science specialists [39].

---

## References

1. Dorozhkin SV (2011) Biocomposites and hybrid biomaterials based on calcium orthophosphates. *Biomater* 1(1):3–56
2. Dorozhkin SV (2010) Bioceramics of calcium orthophosphates. *Biomaterials* 31(7):1465–1485
3. Maier W (2009) Biomaterials in skull base surgery. *GMS Curr Top Otorhinolaryngol Head Neck Surg* 8:Doc07
4. Shah AM, Jung H, Skirboll S (2014) Materials used in cranioplasty: a history and analysis. *Neurosurg Focus* 36(4), E19
5. Neumann A, Kevenhoerster K (2009) Biomaterials for craniofacial reconstruction. *GMS Curr Top Otorhinolaryngol Head Neck Surg* 8:Doc08
6. Aydin S et al (2011) Cranioplasty: review of materials and techniques. *J Neurosci Rural Pract* 2(2):162–167
7. Best SM et al (2008) Bioceramics: past, present and for the future. *J Eur Ceram Soc* 28(7):1319–1327
8. Frassanito P et al (2013) The fate of a macroporous hydroxyapatite cranioplasty four years after implantation: macroscopical and microscopical findings in a case of recurrent atypical meningioma. *Clin Neurol Neurosurg* 115(8):1496–1498
9. Harris DA et al (2014) History of synthetic materials in alloplastic cranioplasty. *Neurosurg Focus* 36(4), E20
10. Kehr P, Kaech D, Lumenta CB, Di Rocco C, Haase J, Mooij JJA (2013) Neurosurgery (European manual of medicine). *Eur J Orthop Surg Traumatol* 23(2):243–243
11. Ciurea AV, Davidescu HB (2007) Cranio-cerebral traumatology. “Carol Davila” University Publishing House, Bucharest, pp 257–260
12. Hockley A et al (1990) Skull repair in children. *Pediatr Neurosurg* 16(4–5):271–275

13. Blair G, Gordon D, Simpson D (1980) Cranioplasty in children. *Pediatr Neurosurg* 6(2):82–91
14. Barbanera A et al (2013) Potential applications of synthetic bioceramic bone graft substitute in spinal surgery. *Prog Neurosci* 1(1-4):97–104
15. Zhong Y, Bellamkonda RV (2008) Biomaterials for the central nervous system. *J R Soc Interface* 5(26):957–975
16. Redfern RM, Pühlhorn H (2007) Cranioplasty. *Adv Clin Neurosci Rehabil* 7(5):32–34
17. De Santis R, Gloria A, Ambrosio L (2010) Materials and technologies for craniofacial tissue repair and regeneration. *Top Med* 16(1-4):1–16
18. Lemée J-M et al (2013) Autologous bone flap versus hydroxyapatite prosthesis in first intention in secondary cranioplasty after decompressive craniectomy: a French medico-economical study. *Neurochirurgie* 59(2):60–63
19. Neovius E, Engstrand T (2010) Craniofacial reconstruction with bone and biomaterials: review over the last 11 years. *J Plast Reconstr Aesthet Surg* 63(10):1615–1623
20. Szpalski C et al (2010) Cranial bone defects: current and future strategies. *Neurosurg Focus* 29(6), E8
21. Rotaru H et al (2006) Silicone rubber mould cast polyethylmethacrylate-hydroxyapatite plate used for repairing a large skull defect. *J Cranio-Maxillofac Surg* 34(4):242–246
22. Gooch MR et al (2009) Complications of cranioplasty following decompressive craniectomy: analysis of 62 cases. *Neurosurg Focus* 26(6), E9
23. Rubin PJ, Yaremchuk MJ (1997) Complications and toxicities of implantable biomaterials used in facial reconstructive and aesthetic surgery: a comprehensive review of the literature. *Plast Reconstr Surg* 100(5):1336–1353
24. Baxter D, Yeh J (2012) 10 – the use of polymethyl methacrylate (PMMA) in neurosurgery. In: Ambrosio L, Tanner E (eds) *Biomaterials for spinal surgery*. Woodhead Publishing, Philadelphia, pp 365–384
25. Lethaus B et al (2014) Interval cranioplasty with patient-specific implants and autogenous bone grafts—success and cost analysis. *J Cranio-Maxillofac Surg* 42(8):1948–1951
26. Lee S-C et al (2009) Cranioplasty using polymethyl methacrylate prostheses. *J Clin Neurosci* 16(1):56–63
27. Bhaskar IP, Inglis TJ, Lee GY (2014) Clinical, radiological, and microbiological profile of patients with autogenous cranioplasty infections. *World Neurosurg* 82(3):e531–e534
28. Schoekler B, Trummer M (2014) Prediction parameters of bone flap resorption following cranioplasty with autologous bone. *Clin Neurol Neurosurg* 120:64–67
29. Bartolo P et al (2012) Biomedical production of implants by additive electro-chemical and physical processes. *CIRP Ann Manuf Technol* 61(2):635–655
30. Jardini AL et al (2014) Cranial reconstruction: 3D biomodel and custom-built implant created using additive manufacturing. *J Cranio-Maxillofac Surg* 42(8):1877–1884
31. Staffa G et al (2007) Custom made cranioplasty prostheses in porous hydroxy-apatite using 3D design techniques: 7 years experience in 25 patients. *Acta Neurochir* 149(2):161–170
32. Mukherjee S et al (2014) Complications of titanium cranioplasty – a retrospective analysis of 174 patients. *Acta Neurochir (Wien)* 156(5):989–998; discussion 998
33. Williams L, Fan K, Bentley R (2015) Custom-made titanium cranioplasty: early and late complications of 151 cranioplasties and review of the literature. *Int J Oral Maxillofac Surg*, 44(5):599–608
34. Engstrand T et al (2014) Development of a bioactive implant for repair and potential healing of cranial defects: technical note. *J Neurosurg* 120(1):273–277
35. Williams DF (1999) *The Williams dictionary of biomaterials*. Liverpool University Press: Liverpool, UK
36. Hench LL (1992) Bioceramics: research and development opportunities. *Braz J Phys* 22(2):70–76
37. Hench LL (1991) Bioceramics: from concept to clinic. *J Am Ceram Soc* 74(7):1487–1510
38. Ratner BD (2004) *Biomaterials science: an introduction to materials in medicine*. Academic Press, 2nd edn 2004; Elsevier, Canada

39. Dorozhkin SV (2010) Calcium orthophosphates as bioceramics: state of the art. *J Funct Biomater* 1(1):22–107
40. Kokubo T (2008) *Bioceramics and their clinical applications*. Woodhead Publishing, ISBN: 9781835692049
41. Thamaraiselvi T, Rajeswari S (2004) Biological evaluation of bioceramic materials—a review. *Carbon* 24(31):172
42. Oonishi H et al (1999) Comparative bone growth behavior in granules of bioceramic materials of various sizes. *J Biomed Mater Res* 44(1):31–43
43. Wilson J, Low SB (1992) Bioactive ceramics for periodontal treatment: comparative studies in the Patas monkey. *J Appl Biomater* 3(2):123–129
44. Okumura T et al (1984) Alumina ceramic (Bioceram) as the cranioplastic material – experimental study and application in cranioplasty. *No Shinkei Geka* 12(3 Suppl):246–252
45. Hench LL, Best SM (2013) Chapter I.2.4 – Ceramics, glasses, and glass-ceramics: basic principles. In: Ratner BD, Hoffman AS, Schoen FJ, Lemons JE (eds) *Biomaterials science: an introduction to materials in medicine*, 3rd edn. Academic, San Diego, pp 128–151
46. Kobayashi S et al (1987) Usefulness of ceramic implants in neurosurgery. *Neurosurgery* 21(5):751–755
47. Rahaman MN et al (2011) Bioactive glass in tissue engineering. *Acta Biomater* 7(6):2355–2373
48. Davis H, Leach J (2008) Hybrid and composite biomaterials in tissue engineering, chapter 10. In: Ashammakhi N (ed) *Topics in multifunctional biomaterials and devices*, vol 1. pp 1–26
49. Hench L et al (2000) Bioactive materials to control cell cycle. *Mater Res Innov* 3(6):313–323
50. Bahrololoom M et al (2009) Characterisation of natural hydroxyapatite extracted from bovine cortical bone ash. *J Ceram Process Res* 10:129–138
51. Dorozhkin S (2009) Calcium orthophosphates in nature, biology and medicine. *Materials* 2(2):399–498
52. Cho YR, Gosain AK (2004) Biomaterials in craniofacial reconstruction. *Clin Plast Surg* 31(3):377–385, v
53. Spetzger U, Vougioukas V, Schipper J (2010) Materials and techniques for osseous skull reconstruction. *Minim Invasive Ther Allied Technol* 19(2):110–121
54. Kokubo T (1991) Bioactive glass ceramics: properties and applications. *Biomaterials* 12(2):155–163
55. Vats A et al (2003) Scaffolds and biomaterials for tissue engineering: a review of clinical applications. *Clin Otolaryngol Allied Sci* 28(3):165–172
56. Hench LL (1998) Bioactive glasses and glass-ceramics. In: *Materials science forum*, vol 293 Trans Tech Publication, Switzerland
57. Gabbi C et al (1995) Bioactive glass coating: physicochemical aspects and biological findings. *Biomaterials* 16(7):515–520
58. Yamamuro T, Shimizu K (1994) Clinical application of AW glass ceramic prosthesis in spinal surgery. *Nihon Seikeigeka Gakkai zasshi* 68(7):505–515
59. Yamamuro T et al (1990) Replacement of the lumbar vertebrae of sheep with ceramic prostheses. *J Bone Joint Surg Br Vol* 72(5):889–893
60. Dewi AH et al (2013) Behavior of plaster of Paris-calcium carbonate composite as bone substitute. A study in rats. *J Biomed Mater Res A* 101A(8):2143–2150
61. Dorozhkin SV, Epple M (2002) Biological and medical significance of calcium phosphates. *Angew Chem Int Ed* 41(17):3130–3146
62. Spivak JM, Hasharoni A (2001) Use of hydroxyapatite in spine surgery. *Eur Spine J* 10(2):S197–S204
63. Boden SD et al (1999) The use of coralline hydroxyapatite with bone marrow, autogenous bone graft, or osteoinductive bone protein extract for posterolateral lumbar spine fusion. *Spine* 24(4):320–327
64. Bohner M (2001) Physical and chemical aspects of calcium phosphates used in spinal surgery. *Eur Spine J* 10(2):S114–S121

65. Passuti N et al (1989) Macroporous calcium phosphate ceramic performance in human spine fusion. *Clin Orthop Relat Res* 248:169–176
66. Cavagna R, Daculsi G, Jean-Michel B (1999) Macroporous calcium phosphate ceramic: a prospective study of 106 cases in lumbar spinal fusion. *J Long-Term Eff Med Implants* 9(4):403–412
67. Steffen T et al (2001) Porous tricalcium phosphate and transforming growth factor used for anterior spine surgery. *Eur Spine J* 10(2):S132–S140
68. Klammert U et al (2010) 3D powder printed calcium phosphate implants for reconstruction of cranial and maxillofacial defects. *J Cranio-Maxillofac Surg* 38(8):565–570
69. Saijo H et al (2009) Maxillofacial reconstruction using custom-made artificial bones fabricated by inkjet printing technology. *J Artif Organs* 12(3):200–205
70. Chen TM et al (2004) Reconstruction of post-traumatic frontal-bone depression using hydroxyapatite cement. *Ann Plast Surg* 52(3):303–308
71. Burstein FD et al (1997) The use of porous granular hydroxyapatite in secondary orbitocranial reconstruction. *Plast Reconstr Surg* 100(4):869–874
72. Tada H et al (2002) Preshaped hydroxyapatite tricalcium-phosphate implant using three-dimensional computed tomography in the reconstruction of bone deformities of craniomaxillofacial region. *J Craniofac Surg* 13(2):287–292
73. Reddi S et al (1998) Hydroxyapatite cement in craniofacial trauma surgery: indications and early experience. *J Craniomaxillofac Trauma* 5(1):7–12
74. Dorozhkin SV (2012) Biphasic, triphasic and multiphasic calcium orthophosphates. *Acta Biomater* 8(3):963–977
75. Kunert-Keil C et al (2015) Comparative study of biphasic calcium phosphate with beta-tricalcium phosphate in rat cranial defects-A molecular-biological and histological study. *Ann Anat.* 199:79–84
76. Lee JH et al (2013) Fabrication and evaluation of porous beta-tricalcium phosphate/hydroxyapatite (60/40) composite as a bone graft extender using rat calvarial bone defect model. *Scientific World Journal* 2013:9
77. Dorozhkin S (2009) Calcium orthophosphate-based biocomposites and hybrid biomaterials. *J Mater Sci* 44(9):2343–2387
78. Ohyama T et al (2002) Beta-tricalcium phosphate as a substitute for autograft in interbody fusion cages in the canine lumbar spine. *J Neurosurg* 97(3 Suppl):350–354
79. Biskup NI et al (2010) Pediatric cranial vault defects: early experience with beta-tricalcium phosphate bone graft substitute. *J Craniofac Surg* 21(2):358–362
80. Swetha M et al (2010) Biocomposites containing natural polymers and hydroxyapatite for bone tissue engineering. *Int J Biol Macromol* 47(1):1–4
81. Meyer U, Meyer T, Wiesmann HP (2006) Bone and cartilage engineering. Springer, Berlin
82. Suwanprateeb J, Chumnanklang R (2006) Three-dimensional printing of porous polyethylene structure using water-based binders. *J Biomed Mater Res B Appl Biomater* 78(1):138–145
83. Suwanprateeb J et al (2012) Development of porous powder printed high density polyethylene for personalized bone implants. *J Porous Mater* 19(5):623–632
84. Bobinski L, Koskinen L-OD, Lindvall P (2013) Complications following cranioplasty using autologous bone or polymethylmethacrylate – retrospective experience from a single center. *Clin Neurol Neurosurg* 115(9):1788–1791
85. Merola J et al (2012) Case report: destructive neuroendocrine cranial tumour and the role of pre-fashioned polyetheretherketone (PEEK) cranioplasty. *Open Cancer J* 5:7–10
86. Thien A et al (2015) Comparison of polyetheretherketone and titanium cranioplasty after decompressive craniectomy. *World Neurosurg.* 83(2):176–180
87. Kurtz SM (2012) Applications of polyaryletheretherketone in spinal implants: fusion and motion preservation. In: Kurtz SM (ed) *The PEEK biomaterials handbook*. Elsevier: William Andrew, pp 201–220
88. Kurtz SM, Devine JN (2007) PEEK biomaterials in trauma, orthopedic, and spinal implants. *Biomaterials* 28(32):4845–4869



89. Salernitano E, Migliaresi C (2003) Composite materials for biomedical applications: a review. *J Appl Biomater Biomech* 1(1):3–18
90. Lakes RS (1995) Composite biomaterials, In: Bronzino JD, (ed). *The Biomedical Engineering Handbook*. CRC Press, Boca Raton, pp 598–610
91. Antikainen T et al (1992) Polylactide and polyglycolic acid-reinforced coralline hydroxyapatite for the reconstruction of cranial bone defects in the rabbit. *Acta Neurochir* 117 (1–2):59–62
92. Yao C-H et al (2005) Calvarial bone response to a tricalcium phosphate-genipin crosslinked gelatin composite. *Biomaterials* 26(16):3065–3074
93. Handa T et al (2012) The effect of an octacalcium phosphate co-precipitated gelatin composite on the repair of critical-sized rat calvarial defects. *Acta Biomater* 8(3):1190–1200
94. Martínez-Vázquez F et al (2014) Effect of polymer infiltration on the flexural behavior of  $\beta$ -tricalcium phosphate robocast scaffolds. *Materials* 7(5):4001–4018
95. Fernandez-Yague MA et al (2015) Biomimetic approaches in bone tissue engineering: integrating biological and physicommechanical strategies. *Adv Drug Deliv Rev* 84:1–29
96. Stevens MM (2008) Biomaterials for bone tissue engineering. *Mater Today* 11(5):18–25
97. Butscher A et al (2012) Printability of calcium phosphate powders for three-dimensional printing of tissue engineering scaffolds. *Acta Biomater* 8(1):373–385
98. Dean D, Min K-J, Bond A (2003) Computer aided design of large-format prefabricated cranial plates. *J Craniofac Surg* 14(6):819–832
99. Lee M-Y et al (2002) Custom implant design for patients with cranial defects. *IEEE Eng Med Biol Mag* 21(2):38–44
100. Lusquiños F et al (2014) Bioceramic 3D implants produced by laser assisted additive manufacturing. *Phys Procedia* 56:309–316

---

# Marine Biomaterials as Drug Delivery System for Osteoporosis and Bone Tissue Regeneration

# 43

Joshua Chou and Jia Hao

## Contents

Introduction .....	1310
Coral Exoskeletons .....	1311
Synthesizing Calcium Phosphates from Coral Exoskeletons .....	1312
Biomimetic Calcium Phosphate Drug Delivery Systems .....	1313
Drug Loading, Coatings, and Characterization .....	1313
Biomimetic Drug Delivery Systems for Pharmaceuticals .....	1315
Biochemical Modifications of Biomimetic Scaffolds .....	1317
Biomimetic Scaffold Effect on Bone Mesenchymal Stem Cells .....	1319
Stem Cell Coating of Biomimetic Scaffold .....	1320
Applications of Marine Biomimetic Scaffolds .....	1322
Localized Treatment of Osteoporosis .....	1322
Long-Term Systemic Treatment of Osteoporosis .....	1324
Marine Biomimetic Scaffolds for Maxillofacial Bone Repairs .....	1327
Future Prospect and Developments .....	1330
Summary .....	1330
References .....	1331

---

## Abstract

There is currently an urgent need to develop sustainable and therapeutically relevant advanced drug delivery systems to treat the prevalence of ongoing human diseases and ailments. The effectiveness of such system will depend

---

J. Chou (✉)

Advanced Tissue Regeneration and Drug Delivery Group, University of Technology Sydney, Sydney, NSW, Australia

e-mail: [joshua.chou@uts.edu.au](mailto:joshua.chou@uts.edu.au)

J. Hao

Oral Implantology and Regenerative Dental Medicine, Tokyo Medical and Dental University, Tokyo, Japan

e-mail: [haoirm@tmd.ac.jp](mailto:haoirm@tmd.ac.jp)

primarily on the properties and characteristics of the carrier material. In this chapter, marine materials are investigated as potential drug delivery carriers for bone tissue engineering and in the treatment of osteoporosis. This chapter will explore the unique structures of marine materials that set it apart from its synthetic counterparts and the conversion to biocompatible calcium phosphates combined with synthetic modifications, and case studies will demonstrate the potential clinical applications.

---

**Keywords**

Bioceramic • Biomimetic • Calcium phosphates • Bone tissue engineering

---

## Introduction

The twenty-first century is regarded as the era of tissue engineering and regenerative medicine. The notion that human soft and hard tissues can both be regenerated or expedited was once a figment of imagination and science fiction. Advances in science and the merging of interdisciplinary fields have catapulted innovation and novel technologies with the goal of increasing human longevity. To achieve this, developments in novel material design with complex structures are required to mimic as closely to the human tissues.

Moreover, the synthesis process must adhere to strict regulatory guidelines and economic implementation. The main driving force behind the push in regenerative medicine research is the diverse clinical applications of tissue engineering strategies and the specificity of these treatments. A key area of research in tissue regeneration is the development of both organic and inorganic scaffolds. These provide the basis to the fundamental development of direct and/or indirect stimulation of tissue regeneration. There is a continuous need to explore new avenues in which materials, cells, and biologically active molecules can be combined to deliver therapeutic responses. This is critical, as cells and growth factors are key elements for an effective regeneration process. Currently there exist clinically a vast range of biomaterials that have been extensively studied and shown to be capable of accommodating clinical needs. However, with a global rise in an aging population, more ailments and sickness are going to prevalent. Taking into account the rise in society's middle class with the option of accessing better healthcare, there is a natural demand calling for improvements to current practices and the shortening of medical treatments which has both patient and socioeconomic implications. With global rise in healthcare costs, governments and institutions are keen on developing and supporting tissue engineering and regenerative medicine research.

Current researches have been focused on improving existing scaffold materials by making it more bioactive, meaning increasing the material's ability to stimulate a specific response. This approach has shown to be quite effective and it is a trend that continues to be followed. Among the diverse range of biomaterials available, calcium phosphates are one of the most attractive and extensively studied and

clinically used bioceramic material. Calcium phosphates are generally used as a bone substitute material due to the compositional similarity to the original human bone, essentially allowing the material to be biocompatible within the body without inducing any inflammatory or host responses. As such, the majority of research using calcium phosphates center on its use in bone tissue regeneration. It should be noted that this is a general misconception, as biocompatible calcium phosphates can be adapted for treatments of other diseases and not just limited to bone tissue engineering. One of the key disadvantages of bioceramics is the brittle nature of the material which only allows its use for non-load-bearing applications.

This adds another dimension to the challenge in synthesizing calcium phosphate material with complex and integrated architectural structures which is necessary to allow cells and key nutrients to infiltrate the material to promote and sustain a strong bond between the scaffold and its surrounding. This is particularly crucial for bone substitutes as irregular structures and pore sizes have shown to cause inflammatory response and scaffold rejection [1]. With the increase in knowledge and understanding between bioceramics and bone, it has become apparently clear that scaffolds need to possess structural characteristics similar to natural bone to initiate the required cellular response to promote bone remodeling. Ideally, scaffold materials should favor cellular attachment, growth, and differentiation by providing a highly porous, open-pored, and fully interconnected geometry for the cells. Microporosity with pores less than 10  $\mu\text{m}$  is needed for capillary ingrowth and cell-matrix interactions. At the same time, macropores allows for nutrient supply and waste removal of cells. In addition, scaffolds should be resorbable so as to allow replacement by newly formed bone in the long term. It is also preferable that the external shape of the scaffold material can easily adapt to the defect size. While there are a number of bioceramic materials that address all these criteria and requirements, often their therapeutic effectiveness has limits. To explore an alternative approach and strategy, this chapter will examine a new class of calcium phosphate material derived from marine biomimetics.

This chapter will describe in detail the rationale and interests in the use of natural marine-sourced materials as precursors for development of scaffolds for drug delivery systems (DDS).

---

## **Coral Exoskeletons**

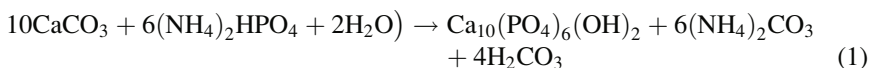
The earth's surface is covered by &70 % water and contains 80 % of all life found on the planet [2]. It is no wonder then that the ocean has been and still is a source of food, let alone a vast source of therapeutic molecules. The marine habitat houses a tremendous amount of varying living organisms of which many are still yet to be discovered due to technological limitations of exploring the ocean depth. However, with integrated advancement of submersible and the realization of exotic organisms containing therapeutic compounds, more species are being uncovered and studied. Nature in many ways can inform us on how to build structures, architectural designs, and the fabrication of new materials with exemplary performance using the most

energy-efficient process with maximum optimization. To study natural materials can provide fresh and new approach for generating unique scaffolds for use in regenerative medicine with the potential to outperform conventional man-made advances. Most synthetic materials require some form of modification to meet the essential requirements of an adequate bone scaffold. This is however not the case for natural materials, in particularly corals.

The coral life cycle begins with the polyps which absorbs the calcium ions and carbonic acid present in the seawater to produce the calcium carbonate in the form of aragonite crystals representing 97–99 % of the coral exoskeleton [3]. The remaining composition is made up of various elements and is dependent on the environment but mainly consists of trace elements of magnesium (0.05–0.2 %), strontium, fluorine, and phosphorous in the phosphate form (0.02–0.03 %) [4]. Coral polyps edify a centripetal exoskeleton upon which they reside, a process reminiscent of bone formation. During human bone remodeling, bone-building osteoblasts secrete collagen, which forms the framework of bone. Similarly, the outer layer of coral consists of calicoblast cells that secrete aragonite which calcifies to form the coral scaffold with an architecture characteristic to each species.

## Synthesizing Calcium Phosphates from Coral Exoskeletons

The initial testing of coral material displayed unsatisfactory results due to the structural instability once exposed to physiological environment. To address this, a new synthesis process was developed by Roy and Linnehan [5] in which hydrothermal conversion was capable of replacing the carbonate component with phosphate to produce calcium phosphate bioceramics base on the following chemical reaction (Eq. 1.):



The general process generally involves placing the coral precursor material in phosphatic solution under 15000psi for 24–48 h at 220–250 °C. The calcium/phosphate (Ca/P) ratio can be altered to synthesize different forms of calcium phosphates including the more stable hydroxyapatite to the more degradable alpha tricalcium phosphate. The key benefit of the hydrothermal treatment is the simplicity of chemically modifying the compositional component of the material but, more importantly, the process is a replacement process in which the physical structures are not affected. This preservation of the unique porous characteristic of coral species is what makes this process attractive. The sintering temperature at ~220 °C is a lot lower compared with conventional synthesis of tricalcium phosphates (800–1100 °C). This enables biomaterial scientist the option and flexibility to synthesize natural bioceramics depending on the clinical application.

Calcium phosphate solubility is dependent on the Ca/P ratio and as such for drug delivery applications; one can predict the degradation rate for the intended purpose.

For more fast-acting delivery systems, one might not necessarily need to convert the coral scaffold but as a calcium carbonate may be appropriate. However, for bone tissue engineering, beta-tricalcium phosphate ( $\text{Ca/P} = 1.5$ ) has remained one of the most attractive material as a scaffold and as a drug delivery vehicle. Different drug delivery systems using coral exoskeletons as a precursor material have been developed and studied [6–8].

---

## **Biomimetic Calcium Phosphate Drug Delivery Systems**

The development of biomimetic calcium phosphate-based drug delivery systems have gained significant momentum in recent years as scientists are realizing the potentials in harvesting and utilizing natural products especially from the marine environment. Natural polymers such as chitin and chitosan are shown to be versatile functional materials that possess excellent biocompatibility, biodegradability, non-toxicity, and adsorption properties [9, 10]. While marine calcareous exoskeletons have been extensively shown and applied as a bone substitute material, little has been done on using it as a scaffold for drug delivery applications.

A successful drug delivery system is characterized by the drug loading efficiency and, more importantly, the release rate of the drug. These are defining parameters that significantly impact on the therapeutic outcome. As previously discussed, the structural properties of foraminifera materials possess interconnected uniform porous chambers consisting of both macro- and micropores, which make them ideal candidate as drug carriers. The consistency in these structural properties allows for predictable and constant drug loading and release compared with nonuniform structural drug carriers. In addition, the hydrothermal treatment allows these materials to be biocompatible, and the degradation rate of different types of calcium phosphates can therefore be controlled and predicted.

This section will discuss drug loading strategies and the applications of using foraminifera as a precursor material for drug delivery systems in bone tissue engineering.

## **Drug Loading, Coatings, and Characterization**

Biodegradable drug delivery systems have always being an attractive alternative to nondegradable materials or direct injection as they do not require removal after serving its purpose. Therefore calcium phosphate-based drug carriers are ideal for delivery pharmaceuticals. The therapeutic efficiency of a drug delivery system will depend on the loading efficiency and that correlates with how the drugs are loaded initially. The most common and straightforward approach is by directly immersing the biomimetic material into a concentrated solution containing the desired pharmaceutical which will over time adsorb onto the scaffold. Depending on the type of pharmaceutical, this may be sufficient to load the drugs. Surface charges, chemical composition, and structural properties are all crucial defining factors. To

increase the loading efficiency, in a previous study, the converted scaffolds were immersed in the concentrated drug solution in a rotary evaporator which allowed for deeper drug penetration into the material due to the vacuum pressure [7].

For a more long-term and sustainable drug release, coatings are required. Strategies and coating methods are extensively studied for calcium phosphate materials and can be adapted for these biomimetic scaffolds. It was shown in a previous study that apatite coating around the scaffold was able to achieve controlled release of the drug simvastatin, thereby generating improvement in the therapeutic efficacy of the overall drug delivery system [7]. Similarly, liposome coatings have also been demonstrated to be achievable with these biomimetic scaffolds [8].

Upon optimizing the drug loading efficiency, the release rate of the drug from the material is the next essential element. Generally once these biomimetic drug delivery systems are inserted into its targeted environment, drugs will start to elude initially through the surface, then through the pores as physiological fluids infiltrate, and, finally, through the degradation of the material itself. Different types of buffer solution are commonly used to “simulate” the likely physiological environments that the material will be exposed to gain an understanding and overview on how the carrier material will interact and behave. These biomimetic scaffolds have been evaluated in simulated body fluids (SBF), in phosphate buffer saline (PBS), and in acetate buffer solutions [6–8, 11, 12]. It was found that in the initial stages between 0 and 24 h, burst release of the drugs from the surface and the pores are observed. This generally accounts for a very small percentage of the total incorporated drugs.

To characterize these properties and determine the drug-eluting mechanism, a drug release plot based on the Higuchi equation can be made. The Higuchi equation is described in (Eq. 2):

$$M_t = A \sqrt{C_s \frac{D_t \varepsilon}{\tau} (2C_d - \varepsilon C_s) t} \quad (2)$$

where  $M_t$  is the amount of drug release after time  $t$ ,  $A$  is the matrix surface area,  $D$  is the diffusion coefficient of the drug,  $C_s$  is the solubility,  $C_d$  is the concentration of the drug in the matrix,  $\tau$  is the tortuosity, and  $\varepsilon$  is the porosity of the matrix. The release mechanism was demonstrated using a model drug incorporated with the biomimetic calcium phosphate material and plotting a subsequent drug release profile based on the Higuchi plot shown in Fig. 1. The Higuchi plot shows two phases of drug release: a surface release slope (a) and drug diffusion release from the matrix material slope (b). The initial burst release was due to conventional release of drug from the surface of the carrier material as illustrated by slope (a). The second-order release profile shows a linear slope (b) in the Higuchi plot suggesting that the release of the drug from the matrix material is based on a drug diffusion process through the macro- and micropores of carrier. This provides an overview on the release mechanism profile from using these carrier materials and can allow further optimization by controlling these release profiles.

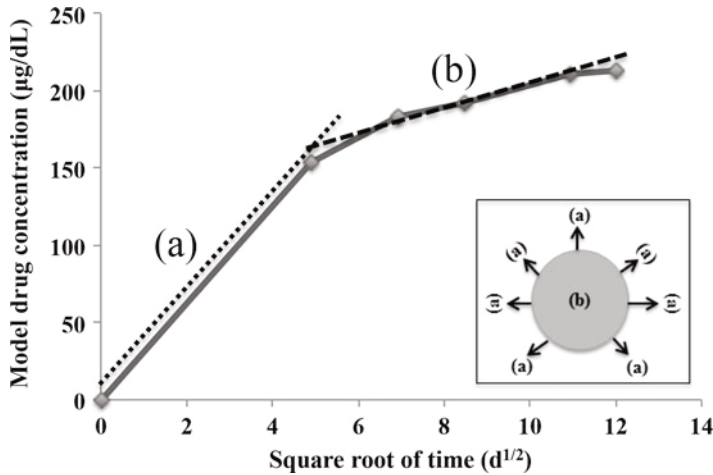


**Fig. 1** Higuchi plot showing the initial burst release is through (a) the surface of the material followed by (b) diffusion mechanism through the matrix material

## Biomimetic Drug Delivery Systems for Pharmaceuticals

Calcareous precursor materials are ideal candidates not only as scaffolds but also as carriers for pharmaceuticals. These natural materials can be easily translated into clinically applicable drug delivery systems. As discussed in the previous section, biomimetic scaffolds can adsorb drugs and release them based on a two-stage process including an initial burst release followed by diffusion through the material by the actions of macro- and micropores. As a proof of principle, two types of drug delivery systems for bone tissue engineering will be discussed in this section.

### Antibacterial and Bone-Stimulating Drug Delivery System

Despite increase in surgical precautions and sterilization, today's orthopedic surgeries still face the looming challenge of bacterial infection during bone repair. With reports of increase in bacterial resistance to antibiotics, clinicians are evermore cautious about the use of antibiotics. The reason for concern is during bone fracture repair procedures; the most common infection is from *Staphylococcus aureus* (*S. aureus*). Symptoms from *S. aureus* infection do not present itself till weeks after the surgery which by then would require a revision surgery to remove the infected implant. This directly impacts the patient's recovery ability and adds to the already-overburdened healthcare system. This has motivated biomaterial scientists to develop scaffolds with antibiotics incorporated to prevent the initial colonization of *S. aureus*. Precaution must be taken to ensure that the antibiotic concentration released must be at a therapeutic level where the bacteria would not develop resistance to the antibiotic or reoccur. As such, efforts into the development of controlled release antibiotic drug delivery systems have gained significant traction.



Biocompatible and biodegradable tricalcium phosphates derived from marine calcareous precursors were incorporated with gentamicin antibiotics (TCP-Gen) and tested against methicillin-resistant *Staphylococcus aureus* (MRSA) removal and prevention in vitro. TCP-Gen were introduced into MRSA culture during the exponential growth phase, and it was determined that within 20 mins the bacteria were completely eliminated and reoccurrence did not occur during the 48 h experimental observation. This suggests that the amount of gentamicin released during the initial burst release was sufficient to eliminate the actions of MRSA growth and more importantly prevent the bacteria from regrowth. It was calculated that the amount of gentamicin released only accounted for 20 % incorporated, and it is predicted that the remaining antibiotics will continue to be released as the material degrades with calcium phosphate ions. Further tests to examine the attachment of MRSA to the biomimetic scaffold also proved the effectiveness of the incorporated gentamicin. Adhered MRSA were completely removed and dysfunctional within 15 mins and reoccurrence were not observed during the 48 h experimental period. These results shows promising potential for the use of these biomimetic tricalcium phosphate scaffolds as controlled release delivery systems capable of sustaining therapeutic level release of gentamicin to combat MRSA. In addition to the incorporated antibiotics, bisphosphonate, which is commonly prescribed to stimulate bone regeneration, was also incorporated together with the gentamicin as a dual drug delivery system. In vitro studies showed that this type of dual system was able to stimulate osteoblast cell proliferation and do not induce any cell toxicity while preserving the underlying antibacterial properties [13]. The results obtained have encouraged further evaluation in in vivo rodent models to determine the biological efficacy of this dual drug delivery system. It is envisioned that this type of biomimetic delivery system could one day be clinically applied as a bone substitute material that can stimulate bone regeneration while preventing the occurrence of bacterial infections.

### **Controlled Drug Delivery System for Osteoporosis**

Osteoporosis treatment is at the center of research focus globally with the rise of the middle class population and the significant increase in aging populace. While currently there does not exist any pharmaceuticals to completely reverse the osteoporotic condition, drug treatments are able to manage and improve the conditions of patients with a good degree of recovery. As a systemic-wide disease within the body, a therapeutic approach would require a sustained long-term infusion of pharmaceuticals within the body to effectively restore the balance of bone remodeling. Most of the drugs shown therapeutic effectiveness all possesses some form of stimulation to osteoblasts and inhibition of osteoclasts. The family of bisphosphonate and its many derivatives have reached a peak in its therapeutic treatments, and signs of side effects associated with long-term use of bisphosphonates are surfacing with mixed response from clinicians. In the past few years, simvastatin has shown in studies to be a strong contender as an alternative medication to treat osteoporotic patients. Developed initially as a cholesterol-lowering agent, the drug was later found to affect positively on bone remodeling cells. This has generated various forms of calcium phosphate-based materials

incorporated with simvastatin to be applied for bone tissue engineering [14]. One of the key challenges with the use of simvastatin clinically is the effect of high dosage concentration inducing severe side effects including muscle inflammation and deterioration. Therefore any formulae involving simvastatin would require therapeutic optimization to ensure the concentration does not exceed the therapeutic range. This requires a high degree of control and release mechanism to be effective.

Biomimetic tricalcium phosphates were incorporated with simvastatin at a concentration described in literature to be therapeutically effective. To control the release of simvastatin and to ensure a sustained and long-term release of the drug, an additional apatite layer was coated around the scaffold material to preserve the release of the drug and limit the initial burst release. This system was tested *in vitro* by implanting the samples intramuscularly near the femur bone of osteoporotic mice. The bone mineral content (BMC) and bone mineral density (BMD) of the femur bones on both sides examined by CT analysis showed a much higher statistical increase in the bone BMC and BMD from the apatite-coated scaffolds compared with no coating and with direct injection of simvastatin. It was also observed by direct injection that the mice suffered from severe muscle deterioration and inflammation as a result of having high localized concentration of the drug [7]. This again signifies the importance of controlled release of pharmaceuticals to limit the immunological host response. This demonstrates that controlled release can be achieved with the use of biomimetic scaffolds, and further optimizations can increase the therapeutic efficacy of such systems to become clinically applicable.

---

## Biochemical Modifications of Biomimetic Scaffolds

Among many strategies into the development of more bioactive scaffolds, significant interest has been vested on the incorporation of inorganic dopants such as magnesium and strontium. These dopants have shown to possess unique properties in stimulating osteoblast proliferation, inhibiting the actions of osteoclast resorption and increasing the mechanical properties of newly formed bone [15–18]. While many studies have shown the potentials for the use of these inorganic compounds combined with scaffolds for different bone tissue applications, an alternative key biological element has been vastly overlooked in comparison. Zinc, an essential element responsible for the regulation and metabolism of cells, has shown in studies to also possess the ability to stimulate osteoblast bone formation when synthesized with tricalcium phosphates [19–23]. Different types and formulations of zinc tricalcium phosphate (Zn-TCP) have been developed in the form of injectable powders in osteoporotic rats [21, 24] and injectable nanoparticles in jawbone [25] and in rabbit femora with over 50 % newly formed bone [26]. Adding on to this, more recent studies have established a relationship between zinc deficiencies in osteoporotic patients in particularly in the elderlies [27].

As tricalcium phosphate bioceramics are resorbable with a higher solubility rate compared with hydroxyapatite, the degree of degradation of Zn-TCP materials becomes crucial. If the Zn-TCP degrades too rapidly, this may result in high levels

of zinc concentration that lead to severe cytotoxic effects [20–22]. As such, the concentration levels and the release of zinc ions are the two main factors in developing therapeutically effective Zn-TCPs. To date, studies conducted have shown that the optimal zinc concentration level is around 5 % [28] and most studies have based their formulation around this concentration. Another key challenge with the synthesis of Zn-TCP ceramics is the high temperature sintering required which is generally between 800 °C and 1100 °C.

One of the key attracting factors of using marine exoskeletons as precursor materials for synthesizing bioceramics is that they naturally possess inorganic compounds within their chemistry as part of their natural calcification process. Interestingly, both strontium and magnesium are naturally part of the material, and *in vitro* studies have shown to stimulate osteoblasts and the inhibition of macrophages [12]. Natural materials are designed over time to become more efficient and optimal and are open to scientific discoveries and modifications to be adapted or further improve for human applications. With this in mind, the synthesized biomimetic TCP material was further modified by incorporating zinc within the crystallographic structure of the material.

Just as phosphate replaced the carbonate component of the original precursor material by hydrothermal exchange, the synthesized TCP underwent another hydrothermal process in which the solution contained zinc. These zinc ions would replace the calcium ions within the material but only to a small degree. Initial findings showed that 0.5 % zinc incorporation was achieved [6]. The concentration of zinc incorporated is dependent on the zinc solution concentration and the time of the hydrothermal treatment. Micro-CT cross-sectional images shown in Fig. 2 reveal the intricate internal porous architectural structure of the foraminifera material and the preservation of the integrity after conversion to Zn-TCP. One can start to appreciate the elegance of natural scaffold materials with its elaborate structures combined with macro- and micropores.

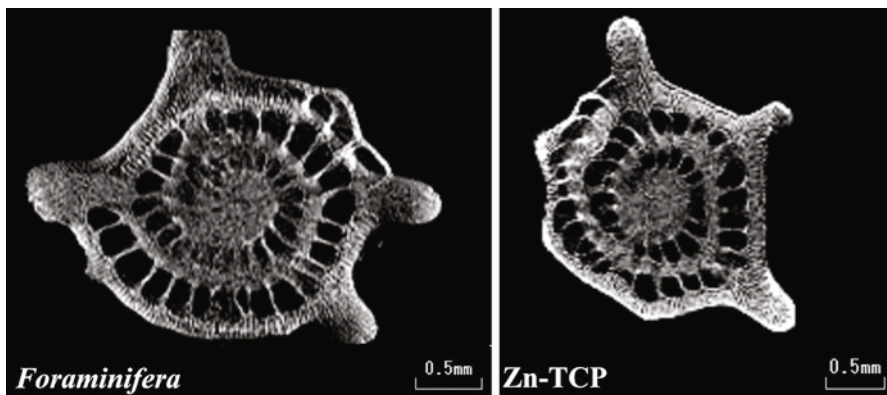


**Fig. 2** Micro-CT images showing the internal porous network of foraminifera precursor material and the preservation of the integrity of the scaffold after hydrothermal conversion to Zn-TCP

Zinc release studies from the Zn-TCP showed no release in physiological buffer solutions over 7 days. This is indicative on the stability of the zinc within the material. When exposed to an acidic buffer environment (pH 4.5), zinc release was observed, but over 7 days this only accounted for 0.2 % of the total zinc incorporated.

These results demonstrate the ability to synthetically modify biomimetic scaffolds by incorporating inorganic ions to change the overall properties of the material. This strategy to combine natural materials with scientific alterations for specific applications can be potentially applied to a vast range of materials with real-life clinical implications.

---

## **Biomimetic Scaffold Effect on Bone Mesenchymal Stem Cells**

The effect of biomaterial scaffolds on cellular response in the initial stages of characterization provides a fundamental understanding and insight into “how” the material will behave in a more complex biological environment. For stem cell-based bone tissue engineering, the material substrate should guide the initial anchorage of cells and their proliferation and assist in stimulating the cells’ differentiation into osteoblasts. The commitment of BMSCs to differentiate into an osteogenic lineage is highly dependent on the physicochemical properties of the surrounding environment and the scaffold on which they are cultured. Surface composition, roughness, and topography all contribute to the osteogenic process. The general focus is to promote an increase in osteoblast cell to stimulate a higher rate of bone regeneration. Other key cells including osteoclasts, osteoblasts, macrophages, etc. are all readily available and are commonly used in *in vitro* characterization.

In a previous study, the osteogenic differentiation of primary BMSC when grown in the presence of biomimetic  $\beta$ -TCP and Zn-TCP was investigated [11]. The first in a series of tests is the biocompatibility of the material. The results from this study showed that both materials were able to sustain a good cell viability of &95 % during the 14-day period. This is reflective of the biocompatibility nature of calcium phosphate materials that is nontoxic to the cells. Examining the cell number, it was found that by 10 day, Zn-TCP exhibits a statistical number in cell growth compared with its counterpart and control. This was also observed at 14 day. Considering that zinc plays a crucial role in cell metabolism and proliferation [29], these results would suggest that the action of the zinc ions being released is having an impact on the proliferation of the BMSC. This would be potentially advantageous in an *in vivo* environment where the Zn-TCP could essentially stimulate more BMSC growth, thereby increasing the amount of differentiated osteoblasts.

Stein and Lian [30], in their osteoblastic differentiation model, reported that MSCs generally proliferate for up to 7–14 days before secreting extracellular matrix proteins that produce early differentiation markers, such as alkaline phosphatase (ALP), which can be observed as early as 7 day. Osteogenic differentiation of osteoblast-like cells is one of the key steps in determining the success of bone and material integration. Among these, ALP activity is one of the widely recognized

biomarkers in determining osteogenic differentiation, which is regulated by phosphate metabolism [31]. ALP is associated with osteoblast differentiation, and, as such, the level of ALP gives an indication of the stage of osteoblast differentiation. Interestingly at 10 day, ALP levels in Zn-TCP were statistically higher compared with the cell control and  $\beta$ -TCP. By 14 day, ALP level dropped which is an indication that differentiation has completed or near completion. The rate at which osteogenic differentiation occurs is crucial to increase the integration between the scaffold material and newly formed bone.

Thirdly, observation of calcium mineralization, which is reflective of the maturation of osteoblasts after differentiation, distinctly shows significantly higher levels of mineralized nodules compared with  $\beta$ -TCP and control group. This again supports the crucial role and effect of zinc on BMSC differentiation which would impact the bone-material integration in an *in vivo* environment. While synthetic derivatives of Zn-TCP have also shown similar biological response from human bone marrow-derived mesenchymal stem cells [29, 32], it should be emphasis the unique structural characteristic of the biomimetic material that is currently being characterized and, more importantly, the release of zinc ions are at a rate capable of sustaining BMSC differentiation into osteoblasts.

## Stem Cell Coating of Biomimetic Scaffold

One of the key contributing factors that have excited research in tissue engineering is the versatility of stem cells and their ability to differentiate to different cell types. In the context of developing more bioactive scaffolds/biomaterials, the incorporation of stem cells with these materials have therefore being extensively studied and applied [33, 34]. Many strategies and protocols developed are generally centered on isolating host patient cells and either expanded *ex vivo* than seeded directly onto the scaffold construct before placing the material back into the patient. The success of such construct is highly dependent on the efficiency of the seeding, the rate of cell adhesion to the scaffold, the viability of the cells once seeded, and the distribution of cells on the material [35]. Cell-material interaction is a key factor in the initial stages of cell attachment, and the morphology and architectural structure of the scaffold play a crucial role in determining the cell attachment rate and viability. Studies have shown, for example, that smaller scaffold pore diameters ( $\sim 30 \mu\text{m}$ ) enhance cell-seeding efficiency compared with larger pore sizes ( $\sim 70 \mu\text{m}$ ) [35, 36]. Since stem cells are anchorage dependent, the faster the cells are able to attach to the scaffold, the likelihood of the cells to remain viable is much higher.

One of the simplest approaches for cell seeding onto scaffold/biomaterials is by directly seeding the cells on the construct and allowing the cells to grow and spread throughout the construct over time in an undisturbed environment [37]. A more dynamic approach would include a setup similar to bioreactors in which the seeded scaffold is exposed to a constant flow of media allowing the oscillatory pressure to spread the cells through the material [38]. While these methods have produced satisfactory results, they are however time consuming and often require a high cell

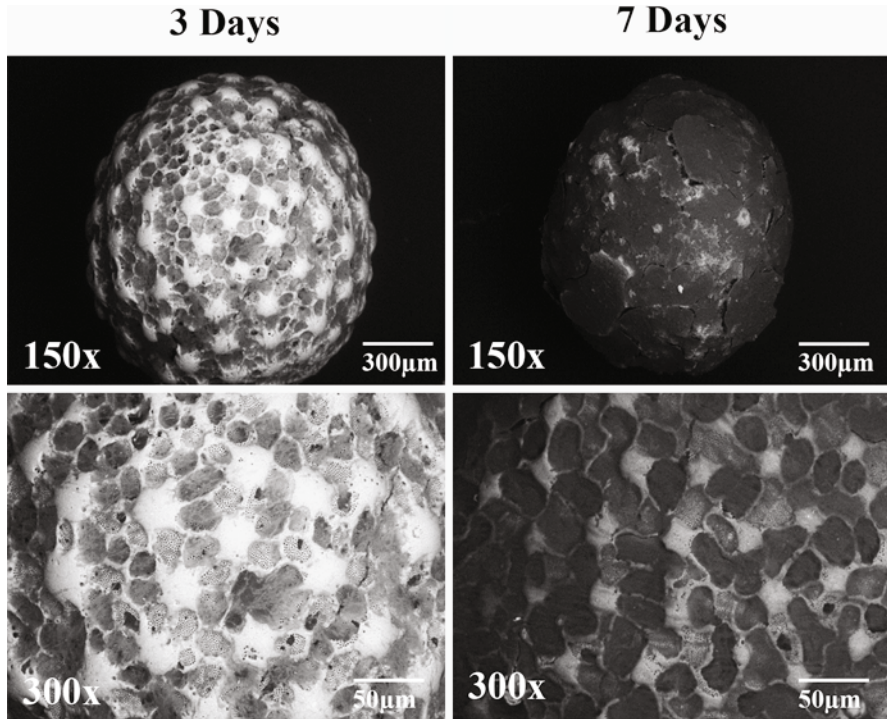


**Fig. 3** Examination of the stem cells distribution throughout the biomimetic scaffold, after different days post-seeding.

concentration for seeding as only a percentage of the cells completely adhere to the material and some loss in cell viability. Therefore there exists a need for an alternative seeding process and to determine if biomimetic scaffolds can provide the framework for stem cell attachment.

In this study, a general laboratory centrifuge was used to “spin coat” the stem cells onto the biomimetic scaffold. This approach would provide a quick and easy method for coating other biomaterials and can be easily accessible in laboratories. During the optimization process, it was found that 1-min centrifugation seeded higher numbers of cells onto the scaffold compared with 2- and 3-min centrifugation, which resulted in significantly lower numbers of adhered cells. It is believed that by increasing the centrifugation time, the cells are being pushed off the scaffold. It was also found that the rotational speed of the centrifuge set at 700 g gave the most optimal amount of cell adherence. It was found that the cells seeded were 95 % viable at 7 days post-seeding.

Figure 3 shows that at 3 days post-seeding, the stem cells were well distributed throughout the material and spreading of the cells could be observed. One can say that the seeded cells were uniformly distributed on the surface of the scaffold. At 7-day post-seeding, it is apparent that the stem cells have spread and covered the vast

majority of the scaffold material. From these observations one can easily control the level of confluency of cell spreading on the scaffold material depending on the intended application. It can therefore be said that the biomimetic scaffold material not only can sustain cell adherence but at the same time it is capable of allowing and possibly promote cell spreading on the material. This is encouraging and possesses obvious advantages in bone tissue engineering. Future studies will examine the *in vivo* response of these stem cell-coated biomimetic scaffolds to determine the optimal cell concentration.

---

## Applications of Marine Biomimetic Scaffolds

### Localized Treatment of Osteoporosis

Osteoporosis is a serious and silent musculoskeletal condition in which the normal bone remodeling process is disrupted with bone-destroying osteoclasts taking dominance over osteoblasts, thereby decreasing significantly the mechanical strength of the bone. Intense international research into the development of osteoporosis treatment has so far remained limited and focuses primarily on the management of the condition rather than having a “cure.” It is generally agreed that any kind of treatment for osteoporosis would require a multi-targeted systemic approach, likely in the form of multifunctional drug delivery systems.

As previously discussed, foraminifera exoskeletons can be hydrothermally converted to contain the addition of bioactive zinc ions on top of the already-present strontium and magnesium. The aim of this study was to demonstrate the use of these converted marine scaffold templates with multi-stimulatory ion doped as a drug delivery system [6]. As the material degrades in the local environment, the key dopants would be released into the host’s blood stream to provide a systemic-wide distribution to target the osteoporosis condition. The *in vivo* study was examined in an osteoporotic mice model by ovariectomy. The Zn-TCP samples were implanted intramuscularly just above the femur bone (Fig. 4) which possess abundant systemic blood flow to the local femur bone and throughout the host.

It should be noted this is an *in vivo* experimental model to observe the local and systemic effect of drug delivery systems and does not reflect on the actual clinical application. It is envisioned that Zn-TCP would be clinically applied by inserting the material into the medulla cavity where there is minimal obstruction. In addition, the osteoporotic condition affects the overall health condition and survivability of the mice, and as such this model was only used to observe the short-term (4 weeks) localized effect of the treatment.

Micro-CT images (Fig. 5) also displayed a higher amount of cancellous bone in the + Zn group compared with the other experimental group and closely match those in the normal group. These results are an indication that Zn-TCPs have the potential of reversing the osteoporotic condition on the localized bone within a 4-week period compared with -Zn and the other control groups.

**Fig. 4** Radiological image of the Zn-TCP samples implanted intramuscularly just above the femur bone

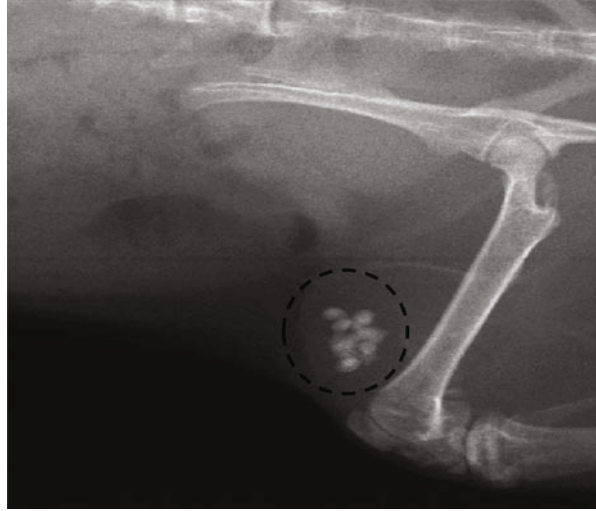


**Fig. 5** Examination of the bone mineral content growth after 4 weeks using Micro-CT show cortical bone to be significantly increased by the presence of Zn-TCP compared with the other experimental group

The results showed that at 4 weeks, the cortical bone of the localized femur bone (Fig. 6) was significantly higher in both the + Zn and -Zn experimental group and the density remained at similar levels. Interestingly, the cancellous bone content in the + Zn group showed tremendous growth (22 %) compared with negative growth in the other experimental groups consistent with bone loss due to the osteoporosis condition.



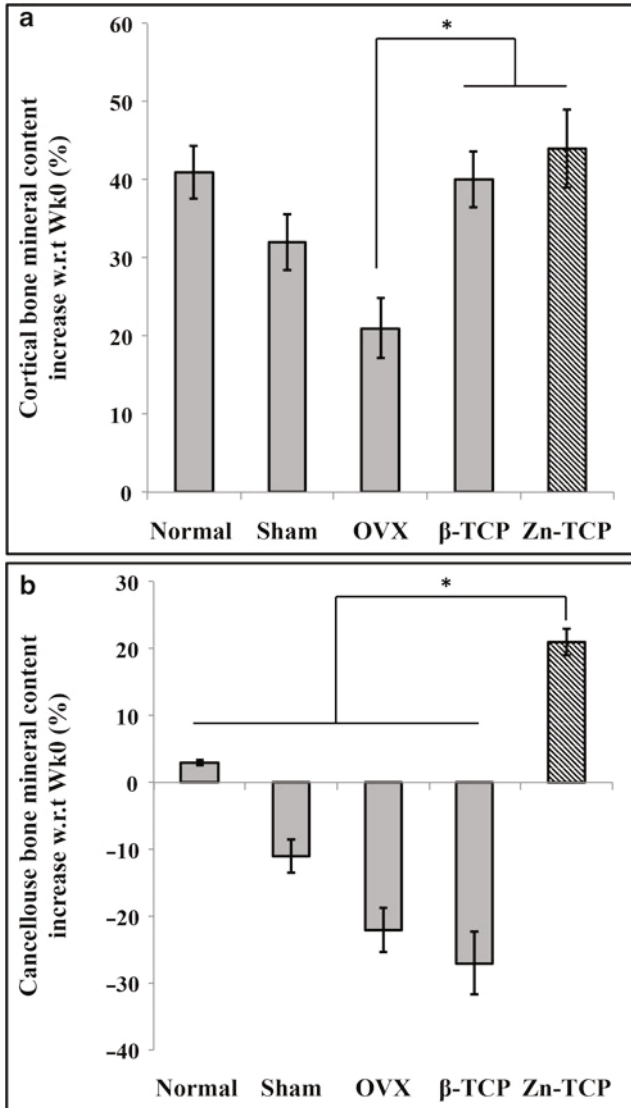


**Fig. 6** Examination of the bone mineral content growth after 4 weeks show (a) cortical bone to be significantly increased by the presence of Zn-TCP compared with OVX (ctrl), and (b) cancellous bone was also significantly stimulated by Zn-TCP compared with negative growth by OVX (ctrl). Asterisk sign represents  $p < 0.05$ , which was considered statistically significant

### Long-Term Systemic Treatment of Osteoporosis

As previously discussed, osteoporosis is a long-term and body-wide skeletal disease that requires a continual and systemic treatment, and current stand-alone

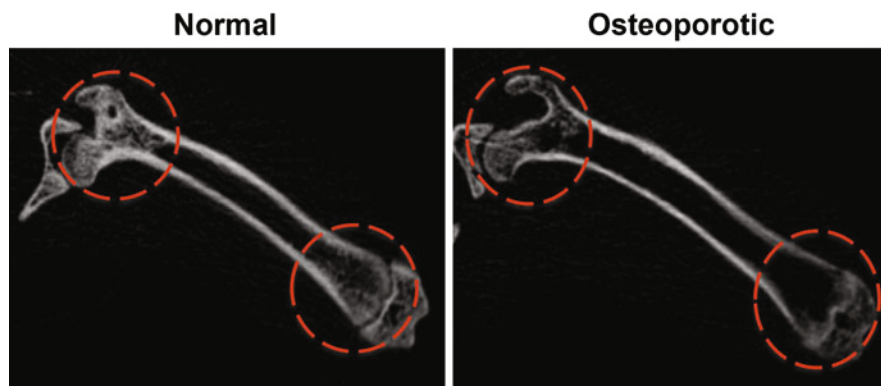


**Fig. 7** Micro-CT imaging showing the loss of cancellous bone in normal healthy rats and the absence of cancellous bone in osteoporotic rats after 3 month conditioning

pharmaceutical therapy is limited in its effectiveness. The development of advanced drug delivery systems is ideally suited for treatment of osteoporosis as it will allow for sustained release of compounds to suppress and hopefully reverse the conditions. The use of calcareous foraminifera to synthesize bioactive Zn-TCP has shown to be effective in a localized manner over short-term treatment (1 month). This section will discuss the long-term (3 months) treatment of osteoporosis using biomimetic Zn-TCP in ovariectomized rats. After ovariectomy, the rats were maintained for 3 months on a calcium-, magnesium-, and zinc-deficient diet. This is an established model and induces the systemic-wide bone loss associated with osteoporosis as illustrated in Fig. 7.

Zn-TCP was implanted intramuscularly near the left femur bone to again allow for the systemic-wide distribution of bioactive ions released from the Zn-TCP into the blood stream. In Fig. 8 the quantitative assessment of both the left and right femur bone mineral content over 12 weeks is displayed. First, let us look at the left femur bone which is the bone closest to the implanted Zn-TCP. It can be seen that the +Zn group displayed a statistically higher bone mineral growth at 4 weeks and maintained higher bone growth until 12 weeks compared with the other experimental control groups.

This is in agreement with previous findings that calcium and phosphate supplements alone are not sufficient enough to treat and reverse the osteoporotic condition [6, 7]. What is of particular interest is the right femur bone mineral content which will determine if the release of zinc ions were able to induce a systemic-wide effect. From the results it is encouraging to see that the bone mineral content of the right femur, which is the opposite bone to the implanted side, also showed statistically higher bone growth at 12 weeks compared with the other groups. This indicates that our hypothesis was confirmed and the zinc released from the Zn-TCP material was able to be delivered through the host's blood stream to targeted sites where it is required over an extended period of time. While these results are indeed promising, however, the aim of achieving complete reversal of the osteoporotic condition has

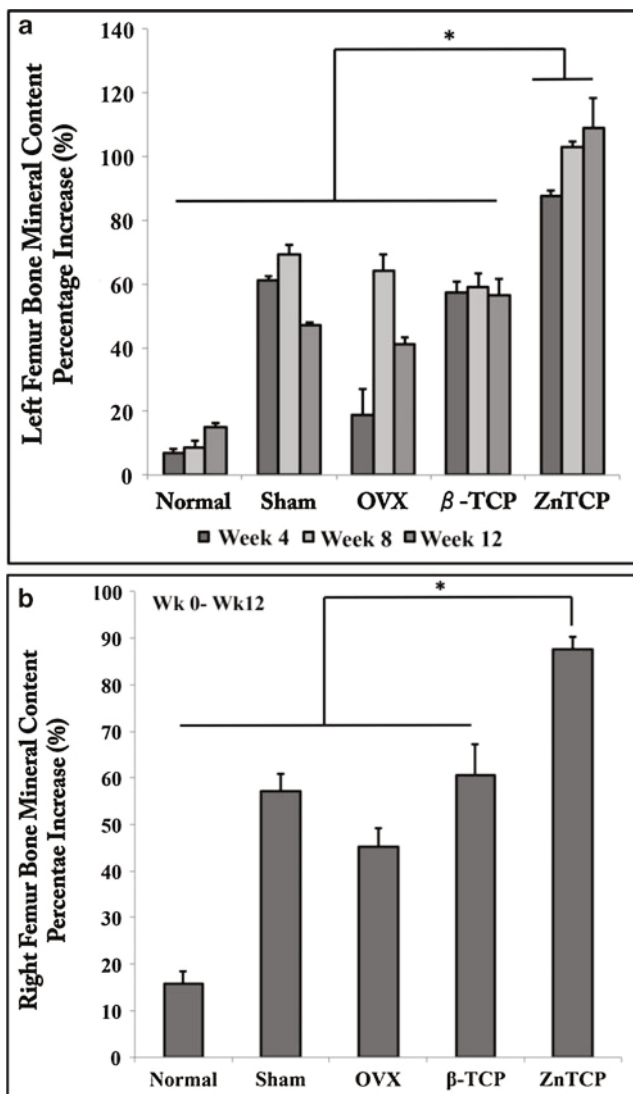


**Fig. 8** Examination of the bone mineral content growth after 4 weeks show (a) cortical bone to be significantly increased by the presence of Zn-TCP compared with OVX (ctrl), and (b) cancellous bone was also significantly stimulated by Zn-TCP compared with negative growth by OVX (ctrl). Asterisk sign represents  $p < 0.05$ , which was considered statistically significant

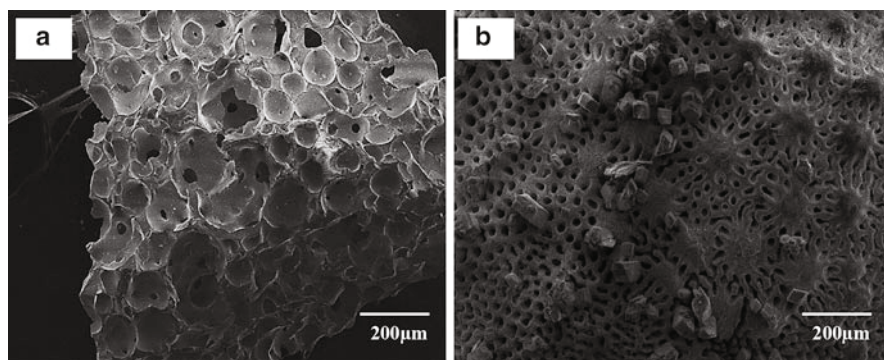
yet to be achieved. This study presents a demonstration of what can be achieved using a biomimetic material which chemically contains key ions relevant to bone restoration. Combining this material with synthetic modifications by hydrothermally converting the material to biocompatible calcium phosphate and adding zinc dopants, bone formation was stimulated in osteoporotic rats. However, there remains a

gap between the bone of the healthy rats and the diseased rats. Osteoporosis is a complex condition and will likely require a multi-targeted approach by using a combination of therapeutics. It should be noted that the incorporation of zinc into the biomimetic material is achieved by chemical insertion into the crystallographic lattice structure. The unique interconnected porous structure of the material that distinguishes this material apart from synthetic counterparts remains available for incorporation of pharmaceuticals.

Synthetically modified marine bioceramics can offer an alternative solution and/or strategy as a therapeutically effective drug delivery system that can or may surpass synthetic materials. The vast marine environment holds an abundance of uncategorized materials that can potentially be adapted to treat an array of human medical conditions that is not limited to only bone tissue regeneration.

### Marine Biomimetic Scaffolds for Maxillofacial Bone Repairs

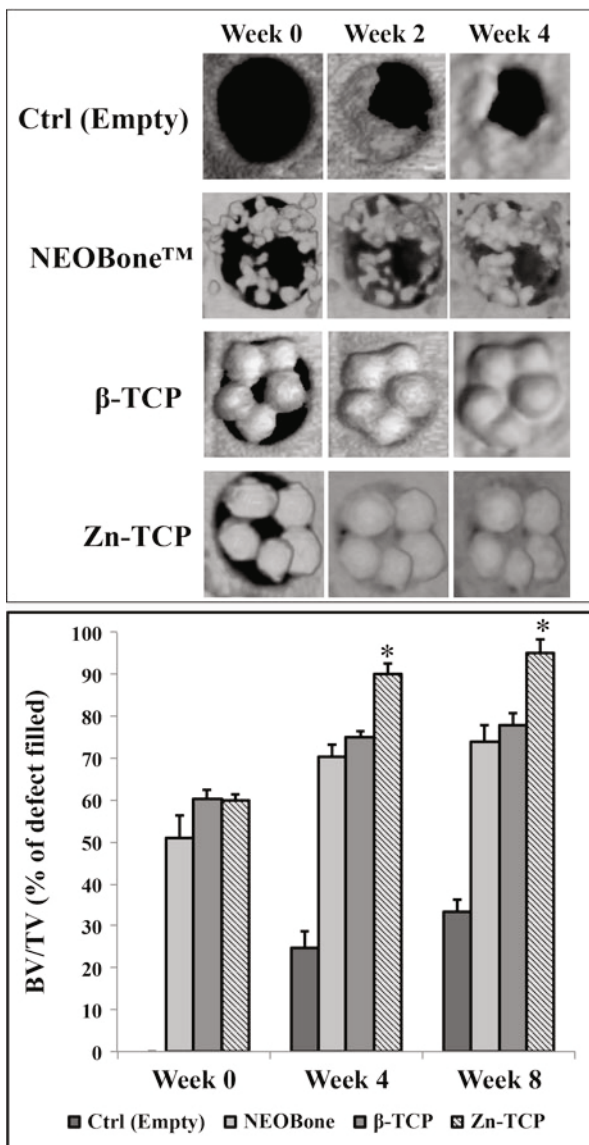
A crucial aspect of bone tissue engineering is the repair and regeneration of bone especially in bone fractures. It is common practice, under certain conditions, to apply calcium phosphate bone substitutes/fillers as a scaffold for promoting new bone growth and integration. The development of bioceramic materials has been extensively studied, and focus has shifted to making scaffolds more bioactive by incorporation of bioactive dopants or pharmaceuticals. In some way, this concept/strategy is very similar to the characteristics of a drug delivery system. Based on this concept, zinc incorporated in TCP was evaluated to determine if this biomimetic material can be therapeutically effective as a scaffold to promote bone regeneration in fractures. The first model examined was a rat calvarial defect which is commonly used to evaluate scaffold materials for maxillofacial and cranial applications. Zn-TCP samples were implanted for 4 weeks in a 5-mm defect and compared with clinically used Neobone™ (beta-tricalcium phosphate) substitutes and empty control (Fig. 9).



**Fig. 9** Scanning electron micrographs showing (a) Neobone™ samples with irregular macropore distribution compared with (b) Zn-TCP samples which have both macro- and micropores

The empty control group was unable to completely regenerate new bone formation at the defect. All the defects with scaffolds inserted all displayed a higher degree of bone regeneration compared with the empty control group (Fig. 10). However, Zn-TCP on the other hand stimulated statistically higher bone formation (&95 % bone filled) within the defect compared with  $\beta$ -TCP (&80 %) and Neobone™ (85 %) groups. The purpose of a scaffold is to provide the “space” for infiltration of bone remodeling cells and vital nutrients to induce the bone formation at the defect site.

**Fig. 10** Micro-CT images showing an overview of new bone regenerated in the defect site in the presence of the scaffold materials. It can be seen that Zn-TCP induced a higher degree of bone recovery amount and rate compared with the other experimental groups. Quantitative analysis also supports the findings from the micro-CT images. Asterisk sign represents  $p < 0.05$ , which was considered statistically significant



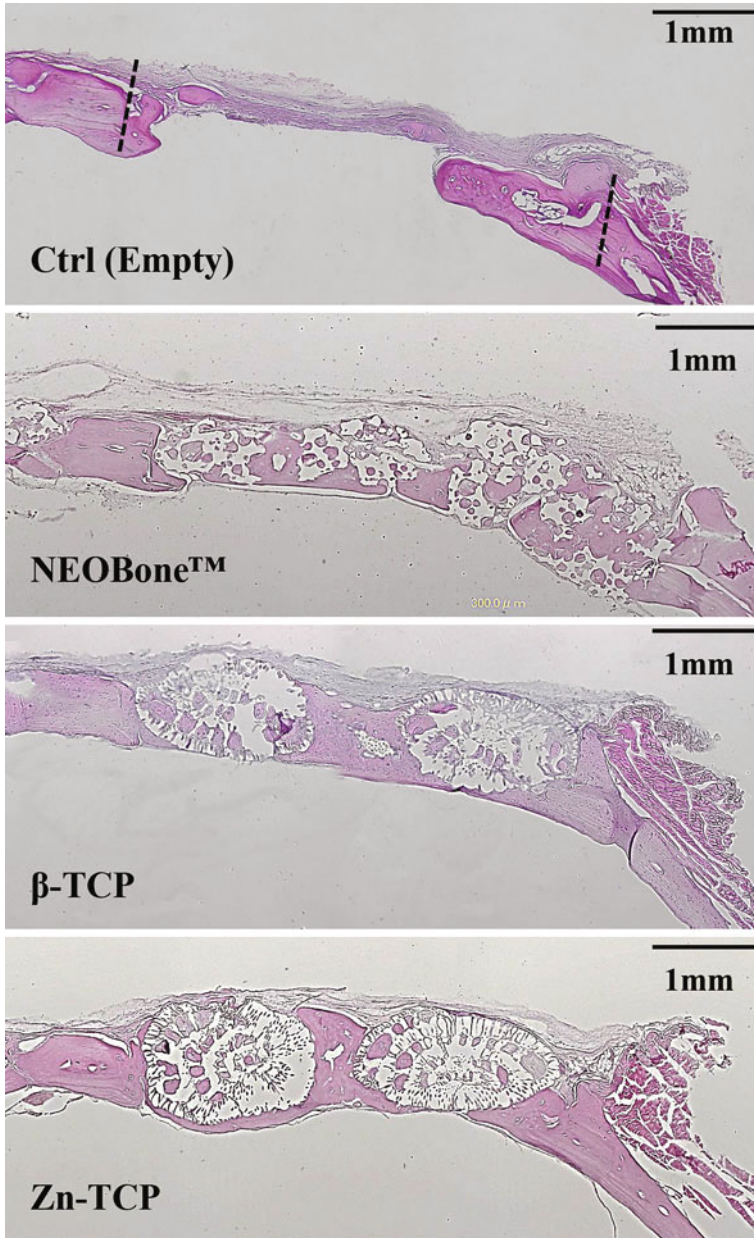


**Fig. 11** H&E stained images showing new bone were able to infiltrate the porous structures of all the scaffold material and integrate with the new bone. It can be seen that new bone formed in the biomimetic scaffolds was mature and the thickness was near the same as the original bone

Without the presence of scaffolds, even though the host body will replenish new bone to a certain extent, it will be a much slower process, and the regenerated bone will unlikely to be fully mature. The histological images shown in Fig. 11 unveil in more detail the new bone integration with the scaffold materials. It can be seen that in all the scaffold samples, new bone growth were integrated well within the material itself. One can see the uniformity of the internal porous structure from the biomimetic scaffold compared with Neobone™. Both  $\beta$ -TCP and Zn-TCP scaffolds show mature bone regenerated within the defect, and the thickness of the replaced bone is at the same level as the original bone.

The fact that  $\beta$ -TCP by itself can reach similar levels of bone regeneration in the defect compared with Neobone™ is encouraging. These results support the need for further development in optimizing the formulation of zinc and/or other dopants that can be incorporated into these biomimetic materials. To achieve a faster rate of bone regeneration will allow prospective patients quicker recovery, thereby minimizing socioeconomic and healthcare costs.

---

## Future Prospect and Developments

Going forward, the development of biomimetic drug delivery systems will require further studies into the underlying mechanisms of cell-material interaction and the optimization of drug loading efficiency and release. It is likely that to raise the therapeutic effectiveness of the system especially for osteoporosis, other combination of drugs will need to be screen.

The discovery and use of marine materials as a precursor for synthesizing biocompatible calcium phosphates for drug delivery applications is justifiable and deserves future developments in this area. As demonstrated in this chapter, the versatility of these materials is vast and can be easily adapted for applications well beyond bone tissue engineering. With the ocean still vastly uncharted, many novel materials with unique structures and properties are still awaiting to be discovered. Just as interest has turned to drug development from marine organisms, similarly, marine materials can aid scientific advancements. The use of natural materials combined with synthetic modifications and optimizations can potentially be a strong contender to synthetic materials and provides scientist with an alternative material to explore.

---

## Summary

Basically the chapter details the use of marine-sourced materials as biomaterial scaffolds for treatment of osteoporosis and in bone tissue regeneration. It details the general concept of using marine biomaterials and how it can be utilized and processed as a successful bioceramic, and case study detailing the specific applications for treating osteoporosis and different type of bone defects is described.

## References

1. Karageorgiou V, Kaplan D (2005) Porosity of 3D biomaterial scaffolds and osteogenesis. *Biomaterials* 26(27):5474–5491
2. Bruckner A (2002) Life-saving products from coral reefs. *Issues Sci Technol* 18(3):35
3. Demers C, Hamdy CR, Corsi K, Chellat F, Tabrizian M, Yahia L (2002) Natural coral exoskeleton as a bone graft substitute: a review. *Biomed Mater Eng* 12(1):15–35
4. Patat JL, Guillemin G (1989) Natural coral used as a replacement biomaterial in bone grafts. *Ann Chir Plast Esthet* 34(3):221–225
5. Roy DM, Linnehan SK (1974) Hydroxyapatite formed from coral skeletal carbonate by hydrothermal exchange. *Nature* 247(5438):220–222
6. Chou J, Hao J, Hatoyama H, Ben-Nissan B, Milthorpe B, Otsuka M (2013) The therapeutic effect on bone mineral formation from biomimetic zinc containing tricalcium phosphate (ZnTCP) in zinc-deficient osteoporotic mice. *PLoS One* 8(8):e71821
7. Chou J, Ito T, Bishop D, Otsuka M, Ben-Nissan B, Milthorpe B (2013) Controlled release of simvastatin from biomimetic beta-TCP drug delivery system. *PLoS One* 8(1):e54676
8. Chou J, Ben-Nissan B, Green DW, Valenzuela SM, Kohan L (2011) Targeting and dissolution characteristics of bone forming and antibacterial drugs by harnessing the structure of microspherical shells from coral beach sand. *Adv Eng Mater* 13(1–2):93–99
9. Sashiwa H, Saimoto H, Shigemasa Y, Ogawa R, Tokura S (1990) Lysozyme susceptibility of partially deacetylated chitin. *Int J Biol Macromol* 12(5):295–296
10. Shigemasa Y, Saito K, Sashiwa H, Saimoto H (1994) Enzymatic degradation of chitins and partially deacetylated chitins. *Int J Biol Macromol* 16(1):43–49
11. Chou J, Hao J, Hatoyama H, Ben-Nissan B, Milthorpe B, Otsuka M (2015) Effect of biomimetic zinc-containing tricalcium phosphate (Zn-TCP) on the growth and osteogenic differentiation of mesenchymal stem cells. *J Tissue Eng Regen Med* 9(7):852–858
12. Chou J, Valenzuela SM, Santos J, Bishop D, Milthorpe B, Green DW, Otsuka M, Ben-Nissan B (2014) Strontium- and magnesium-enriched biomimetic beta-TCP microspheres with potential for bone tissue morphogenesis. *J Tissue Eng Regen Med* 8(10):771–778
13. Chou J, Valenzuela S, Green DW, Kohan L, Milthorpe B, Otsuka M et al (2014) Antibiotic delivery potential of nano- and micro-porous marine structure-derived beta-tricalcium phosphate spheres for medical applications. *Nanomedicine (Lond)* 9(8):1131–1139
14. Nyan M, Sato D, Oda M, Machida T, Kobayashi H, Nakamura T et al (2007) Bone formation with the combination of simvastatin and calcium sulfate in critical-sized rat calvarial defect. *J Pharmacol Sci* 104(4):384–386
15. Kishi S, Yamaguchi M (1994) Inhibitory effect of zinc compounds on osteoclast-like cell formation in mouse marrow cultures. *Biochem Pharmacol* 48(6):1225–1230
16. Yamaguchi M, Oishi H, Suketa Y (1987) Stimulatory effect of zinc on bone formation in tissue culture. *Biochem Pharmacol* 36(22):4007–4012
17. Ishikawa K, Miyamoto Y, Yuasa T, Ito A, Nagayama M, Suzuki K (2002) Fabrication of Zn containing apatite cement and its initial evaluation using human osteoblastic cells. *Biomaterials* 23(2):423–428
18. Yamada Y, Ito A, Kojima H, Sakane M, Miyakawa S, Uemura T et al (2008) Inhibitory effect of Zn<sup>2+</sup> in zinc-containing beta-tricalcium phosphate on resorbing activity of mature osteoclasts. *J Biomed Mater Res A* 84(2):344–352
19. Luo X, Barbieri D, Davison N, Yan Y, de Bruijn JD, Yuan H (2014) Zinc in calcium phosphate mediates bone induction: in vitro and in vivo model. *Acta Biomater* 10(1):477–485
20. Otsuka M, Marunaka S, Matsuda Y, Ito A, Naito H, Ichinose N et al (2003) Effect of particle size on zinc release from zinc containing tricalcium phosphate (ZnTCP) in Zn-deficient osteoporosis rats. *Biomed Mater Eng* 13(2):103–113
21. Otsuka M, Ohshita Y, Marunaka S, Matsuda Y, Ito A, Ichinose N et al (2004) Effect of controlled zinc release on bone mineral density from injectable Zn-containing beta-tricalcium phosphate suspension in zinc-deficient diseased rats. *J Biomed Mater Res A* 69(3):552–560



22. Otsuka M, Oshinbe A, Legeros RZ, Tokudome Y, Ito A, Otsuka K et al (2008) Efficacy of the injectable calcium phosphate ceramics suspensions containing magnesium, zinc and fluoride on the bone mineral deficiency in ovariectomized rats. *J Pharm Sci* 97(1):421–432
23. Kannan S, Goetz-Neunhoeffler F, Neubauer J, Ferreira JMF (2011) Cosubstitution of zinc and strontium in  $\beta$ -tricalcium phosphate: synthesis and characterization. *J Am Chem Soc* 94(1):230–235
24. Sogo Y, Sakurai T, Onuma K, Ito A (2002) The most appropriate (Ca + Zn)/P molar ratio to minimize the zinc content of ZnTCP/HAP ceramic used in the promotion of bone formation. *J Biomed Mater Res* 62(3):457–463
25. Tokudome Y, Ito A, Otsuka M (2011) Effect of zinc-containing beta-tricalcium phosphate nano particles injection on jawbone mineral density and mechanical strength of osteoporosis model rats. *Biol Pharm Bull* 34(8):1215–1218
26. Kawamura H, Ito A, Miyakawa S, Layrolle P, Ojima K, Ichinose N et al (2000) Stimulatory effect of zinc-releasing calcium phosphate implant on bone formation in rabbit femora. *J Biomed Mater Res* 50(2):184–190
27. Yamaguchi M (2010) Role of nutritional zinc in the prevention of osteoporosis. *Mol Cell Biochem* 338(1–2):241–254
28. Ito A, Kawamura H, Miyakawa S, Layrolle P, Kanzaki N, Treboux G et al (2002) Resorbability and solubility of zinc-containing tricalcium phosphate. *J Biomed Mater Res* 60(2):224–231
29. Lu H, Kawazoe N, Tateishi T, Chen G, Jin X, Chang J (2010) In vitro proliferation and osteogenic differentiation of human bone marrow-derived mesenchymal stem cells cultured with hardystonite (Ca<sub>2</sub>ZnSi<sub>2</sub>O<sub>7</sub>) and  $\beta$ -TCP ceramics. *J Biomater Appl* 25(1):39–56
30. Stein GS, Lian JB (1993) Molecular mechanisms mediating proliferation/differentiation interrelationships during progressive development of the osteoblast phenotype. *Endocr Rev* 14(4):424–442
31. Marom R, Shur I, Solomon R, Benayahu D (2005) Characterization of adhesion and differentiation markers of osteogenic marrow stromal cells. *J Cell Physiol* 202(1):41–48
32. Pina S, Vieira SI, Rego P, Torres PM, da Cruz e Silva OA, da Cruz e Silva EF et al (2010) Biological responses of brushite-forming Zn- and ZnSr- substituted beta-tricalcium phosphate bone cements. *Eur Cell Mater* 20:162–177
33. Dan H, Vaquette C, Fisher AG, Hamlet SM, Xiao Y, Huttmacher DW et al (2014) The influence of cellular source on periodontal regeneration using calcium phosphate coated polycaprolactone scaffold supported cell sheets. *Biomaterials* 35(1):113–122
34. Vaquette C, Fan W, Xiao Y, Hamlet S, Huttmacher DW, Ivanovski S (2012) A biphasic scaffold design combined with cell sheet technology for simultaneous regeneration of alveolar bone/periodontal ligament complex. *Biomaterials* 33(22):5560–5573
35. Li Y, Ma T, Kniss DA, Lasky LC, Yang ST (2001) Effects of filtration seeding on cell density, spatial distribution, and proliferation in nonwoven fibrous matrices. *Biotechnol Prog* 17(5):935–944
36. Kitagawa T, Yamaoka T, Iwase R, Murakami A (2006) Three-dimensional cell seeding and growth in radial-flow perfusion bioreactor for in vitro tissue reconstruction. *Biotechnol Bioeng* 93(5):947–954
37. van den Dolder J, Bancroft GN, Sikavitsas VI, Spauwen PH, Jansen JA, Mikos AG (2003) Flow perfusion culture of marrow stromal osteoblasts in titanium fiber mesh. *J Biomed Mater Res A* 64(2):235–241
38. Dunkelmann NS, Zimmer MP, Lebaron RG, Pavelec R, Kwan M, Purchio AF (1995) Cartilage production by rabbit articular chondrocytes on polyglycolic acid scaffolds in a closed bioreactor system. *Biotechnol Bioeng* 46(4):299–305

---

# Antibacterial Potential of Nanobioceramics Used as Drug Carriers

# 44

T.S. Sampath Kumar and K. Madhumathi

## Contents

Introduction .....	1334
Bone and Joint Infections .....	1334
Statistics .....	1337
Antimicrobial Therapy in Orthopedic Surgery .....	1338
Drawbacks of Systemic Delivery .....	1338
Local Drug Delivery .....	1338
Combination Devices as Local Drug Delivery Systems .....	1340
Requirements of Ideal Local Drug Delivery System .....	1340
Selection of Antibiotics .....	1342
Selection of Drug Carriers .....	1342
Bioceramics for Local Drug Delivery .....	1343
Nanobioceramics for Efficient Antibiotic Delivery .....	1344
Methodology .....	1347
Drug–Carrier Interactions .....	1349
Surface Functionalization .....	1351
Characterization Studies .....	1352
Drug Delivery from Various Types of Nanobioceramics .....	1354
Overcoming Antimicrobial Resistance: Ion Substitutions as Mode of Antibacterial Action .....	1363
Titania Nanoparticles .....	1365
Alumina Nanoparticles .....	1365
Bioactive Glass .....	1366
Iron Oxide (Fe <sub>3</sub> O <sub>4</sub> ) Nanoparticles .....	1366
Ion-Substituted Bioceramics .....	1366
Nitric oxide (NO)-Releasing Silica Nanoparticles .....	1369
Drug Delivery Using Ion-Substituted Nanobioceramics .....	1369
Summary .....	1370
References .....	1371

---

T.S. Sampath Kumar (✉) • K. Madhumathi  
Department of Metallurgical and Materials Engineering, Indian Institute of Technology Madras,  
Chennai, Tamil Nadu, India  
e-mail: [tssk@iitm.ac.in](mailto:tssk@iitm.ac.in); [madhumathi1984@gmail.com](mailto:madhumathi1984@gmail.com)

---

**Abstract**

Infectious diseases continue to be one of the major challenges faced by the medical community despite many advancements in the field of health care and research. Alarming infections, which were the leading cause of death worldwide a hundred years ago, have made a dramatic resurgence. This comeback is mainly attributed to the resistance shown by the bacteria to major antimicrobial drugs that are currently used. Attempts have been made to overcome this crisis by discovering newer antibiotics and developing efficient modes of drug delivery. In this regard, the role of nanotechnology in infection control has evinced tremendous interest especially with the development of nanocarriers for antibiotics delivery and antibacterial nanoparticles. Bioceramics, a class of inorganic biomaterials, are widely used as bone substitutes for bone reconstruction. Using bioceramics as local drug delivery agents in such instances offers a safer, efficient mode of antibiotic delivery at the surgical site either to treat an incumbent infection or provide prophylactic benefit. Antibacterial bioceramics have also been developed by incorporating antibacterial ions, which have great potential to overcome antibiotic resistance. Both the approaches have been widely researched using *in vitro* and *in vivo* models. This chapter discusses the antibacterial potential of bioceramic nanoparticles with emphasis on combating bone infections.

---

**Keywords**

Bioceramics • Nanoparticles • Nanocoatings • Antibiotics • Calcium phosphate • Bioglass • Mesoporous silica • Drug release • Ion substitutions • Silver • Copper • Strontium • Zinc • Dissolution • Modeling • Local drug delivery • Controlled release • Titania • Alumina • Functionalization • Antibiotic resistance • Bone infections • Device-associated infections • Antimicrobial resistance • Hydroxyapatite • Tricalcium phosphate • Silica • Nanocarriers • Nanotherapeutics • Surface functionalization

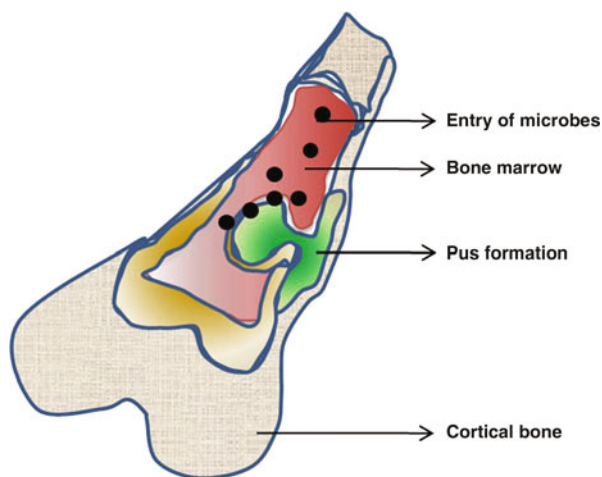
---

**Introduction****Bone and Joint Infections**

Infection is defined as a homeostatic imbalance between the host tissue and the presence of microorganisms at a concentration that exceeds  $10^5$  organisms per gram of tissue or the presence of beta-hemolytic streptococci [1]. Despite infrequent occurrence, infections affecting the bones and joint are usually debilitating and potentially life-threatening. Common bone and joint infections include osteomyelitis (infection of bones), septic arthritis (infection of joints), and prosthetic joint infections. They are usually caused by gram-positive bacteria like *Staphylococcus aureus* but can also be of polymicrobial or mixed nature sometimes. Table 1 lists the bacteria associated with bone infections (see Figs. 1, 2, and 3).

**Table 1** List of bone infections and their causative organisms [2, 3]

S. no.	Disease	Causative organisms	Pictorial representation
1.	Osteomyelitis	Gram-positive <i>Staphylococcus aureus</i> (methicillin sensitive and resistant), <i>Haemophilus influenzae</i> , <i>Streptococcus pneumoniae</i> , group A and B $\beta$ -hemolytic <i>Streptococcus</i> Gram-negative bacilli ( <i>Escherichia coli</i> , <i>Enterobacteriaceae</i> )	See Fig. 1
2.	Septic arthritis	<i>Staphylococcus aureus</i> (methicillin sensitive and resistant), $\beta$ -hemolytic streptococci, <i>Streptococcus pneumoniae</i> , coagulase-negative staphylococci	See Fig. 2
3.	Prosthetic joint infection	<i>Staphylococcus aureus</i> (methicillin sensitive and resistant), $\beta$ -hemolytic <i>Streptococci</i> and <i>Enterococci</i> , coagulase-negative <i>Staphylococci</i> , <i>Propionibacterium acnes</i> , <i>Streptococcus pneumoniae</i> Gram-negative bacilli ( <i>Pseudomonas aeruginosa</i> , <i>Escherichia coli</i> )	See Fig. 3

**Fig. 1** Schematic diagram of osteomyelitis

**Bone infection (osteomyelitis)** is a local or generalized infection of the bone and bone marrow typically caused by bacteria introduced by trauma, surgery, and implant use, by direct colonization from a proximal infection, or through systemic circulation [1, 3]. Presentation is with pain, swelling, lack of mobility, and systemic symptoms such as fever. While acute conditions need only antibiotics, chronic infections contain necrosed bone needing surgical excision. Most often, these surgeries leave behind bone defects or in severe cases result in amputation. Bone defects due to disease, trauma, surgical intervention, or congenital deficiencies represent a substantial clinical challenge for orthopedic surgeons.

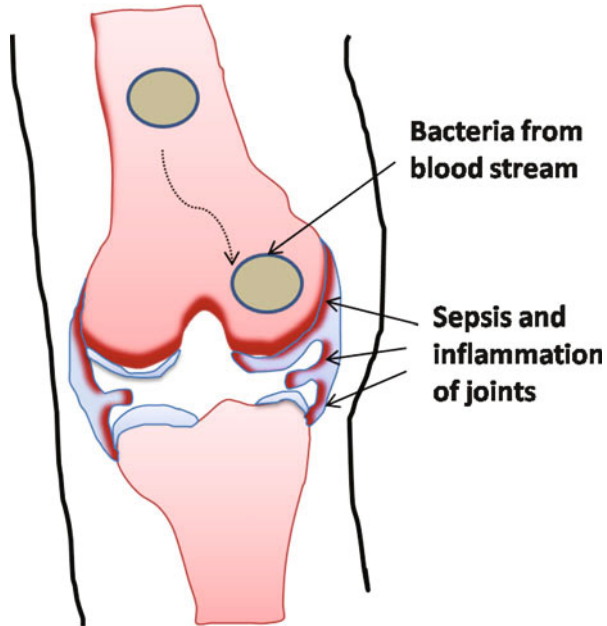


**Fig. 2** Schematic diagram of septic arthritis

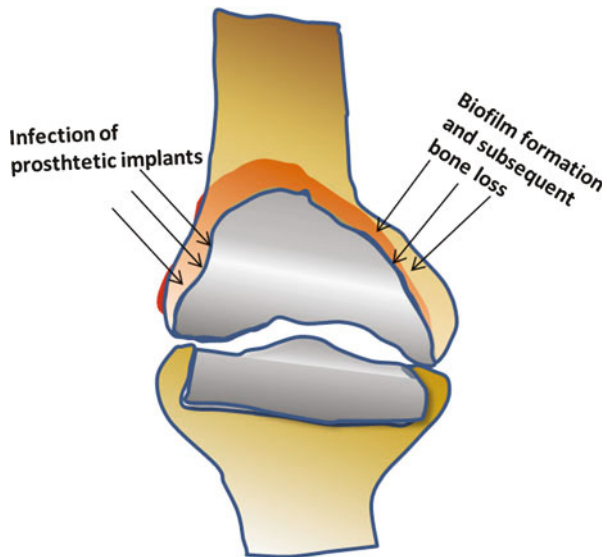


**Fig. 3** Schematic diagram of prosthetic joint infection

Another class of infections is **nosocomial or hospital acquired**. The sources of contamination are the air of the operating room and resident bacteria on the patient's skin and body [1]. More importantly, most of the drug-resistant infections are hospital acquired, and the medical costs associated with such infections are extremely high due to prolonged hospitalization. In a 2009 report by the US Centers for Disease Control (CDC), the annual direct medical costs of these infections to US hospitals were estimated to be \$28.4 to \$33.8 billion increasing up to \$45 billion for inpatient services. **Device-associated infections** are the result of biofilm formation following bacterial adhesion at the implantation site. All implanted medical devices like cardiac valves, prosthetic joints, pacemakers, and coronary stents suffer from device-associated infection. Higher infection incidence and associated morbidity are observed with increasing clinical use of medical implants. Such device-associated infections are difficult to treat, as the biofilm formation renders bacteria resistant to most antibiotics and affects the life of medical implants. Upon implantation, there is a competition between the material integration with surrounding tissue and bacterial adhesion on the implant surface, described as "a race for the surface." Implantation will be successful only if tissue integration occurs ahead of bacterial adhesion, thus preventing bacterial colonization and biofilm formation on the implant [4].

Bacteria that can adhere on implants occur through following pathways:

- (a) Exogenous – bacteria from patient's skin or unsterile surgical environment gaining direct access to the implant site (nosocomial)
- (b) Endogenous – opportunistic bacteria circulating in the body that turn pathogenic and colonize the implant site

In both the pathways, bacterial infection occurs through the following steps:

1. Bacterial adhesion to device surfaces (through extension of fibrils, expression of new surface receptors, and secretion of polysaccharide adhesins)
2. Rapid bacterial proliferation forming resident colonies
3. Formation of a protective, complex mucopolysaccharide "biofilm" barrier

Once a biofilm is formed, bacteria forms satellite colonies that migrate and attach to non-colonized surfaces. It is well known that it is difficult to eliminate bacteria within a mature adherent biofilm by both antibiotics and host immune mechanisms.

## Statistics

Every year, more than 2.2 million persons are treated surgically for musculoskeletal disorders (trauma and tumor extirpation). Bone infections occur in approximately 5 % of surgeries for fracture fixation devices, 2 % of primary joint replacements, and 1.4–4 % of total hip and knee replacements [5]. Nosocomial infections occur in more than two million hospitalizations in the USA each year, with the average hospital cost near US \$15,000 per patient [3].

## Antimicrobial Therapy in Orthopedic Surgery

Antibiotics are used both in the treatment of existing bone infections and prevention of nosocomial and implant-associated infections. Antibiotics regimen is included in all orthopedic and reconstructive surgeries both for prophylactic and therapeutic purposes. Drugs are administered through various routes including systemic (oral, intravenous, intramuscular, subcutaneous, sublingual), topical (nasal, cutaneous, ocular, aural), and other local administration routes as listed in Table 2. Though a course of systemic antibiotic therapy is considered necessary in such situations, it is often associated with side effects and toxicity.

### Drawbacks of Systemic Delivery

A systemic antibiotic regimen is expensive, prone to complications, and influenced by factors like the dose to be administered, the dosage interval, and the dosage duration. Antibiotics administered systemically exhibit a sinusoidal or pulsatile plasma concentration with time as they undergo processes like biotransformation and elimination before reaching the target tissue or organ [6] (Fig. 4). In addition, systemic therapy provides inadequate local concentration for bone infections associated with poorly vascularized or necrotic areas and for destroying the bacterial biofilm. In order to overcome this limitation and achieve therapeutic drug concentration in the affected area, higher systemic doses are generally required, which may cause serious side effects such as anaphylactic shock, damage to hearing (ototoxicity), damage to kidneys (nephrotoxicity), and reduction of platelets [7].

### Local Drug Delivery

New routes such as local delivery of antibiotics have been developed to overcome the drawbacks associated with systemic delivery and to improve the prognosis of patients with musculoskeletal infections. The local delivery of antibiotics for the prevention and treatment of musculoskeletal infection is becoming increasingly popular with several studies confirming the benefits of local antibiotics delivery. It is always desirable for antibiotics to maintain therapeutic plasma concentration throughout the treatment regimen. With local delivery, therapeutic concentrations are maintained at the affected site throughout the treatment period (greater bioavailability), with reduced side effects and toxicity in addition to being patient friendly [6]. High local concentration of antibiotics facilitates diffusion to poorly vascularized areas and increases the vulnerability of biofilms [5]. Due to these advantages, local antibiotic therapy is often desired in treating osteomyelitis, periodontitis, and implant-associated infections.

The advantages of local drug delivery are as follows:

- (a) Lowered antibiotic dose
- (b) Greater control over toxicity and bioavailability of dose (Fig. 4)

**Table 2** Popular routes of drug delivery, their advantages and disadvantages [7]

Routes of administration	Advantages	Disadvantages
<b>Oral</b> (administering a drug through mouth)	Convenient, portable, safe, painless, self-administered, economical, low risk of infections	Poor bioavailability due to first-pass effect, drugs affected by food and low stomach pH, not possible for unconscious patients, multiple doses need patient compliance
<b>Sublingual</b> (placement of drug under the tongue)	Rapid absorption, high bioavailability, convenient placement, low infection risk, avoidance of first-pass metabolism	Large dose is difficult to place, drug taste needs to be masked
<b>Intravenous (IV)</b> (injection of drug through veins)	Fast acting, precise control over plasma concentration, complete bioavailability, useful for drugs not absorbed orally	Fluctuating concentration at target site, chance of infections, possible toxicity, expensive, painful, requires trained personnel, risk of hemolysis, thrombosis, and local tissue damage
<b>Subcutaneous (SC)</b> (injecting drugs directly into subcutaneous tissue below the skin)	Self-administered, complete absorption via diffusion, constant, slow and sustained effect	Painful, local tissue damage, small doses only, slower than IV
<b>Rectal</b> (administration via rectum)	Reduced first-pass effect, protection from gastric acid, useful for young children, unconscious patients, and in vomiting condition	Erratic absorption, suitable for very few drugs
<b>Intramuscular (IM)</b> (injecting drugs into muscle)	Depot or sustained release, larger volume than SC, easy administration than IV	Variable absorption, painful, needs trained personnel, local tissue damage
<b>Inhalation</b> (administration through nose or mouth)	Used for both local and systemic effect, rapid absorption bypassing the liver, ideal for gaseous drugs, effective for treatment of respiratory problems	Inefficient absorption of solids and liquids, particle size-dependent absorption, difficulty in regulating dose
<b>Transdermal</b> (application of drugs to the subcutaneous tissue via skin-adhering patch)	Used for both local and systemic effect, sustained release	Absorption is quite slow, skin irritation, varying rate of absorption depending on skin condition, and lipophilicity of drug

- (c) Less susceptibility to promoting antibiotic resistance
- (d) Extended duration of release
- (e) Possibilities to combine local and systemic drugs with different kinetics
- (f) Controlled release from surfaces of combination devices directly to site
- (g) Avoidance of systemic drug exposure
- (h) Direct mitigation of device-centered infection using combination device release [3]



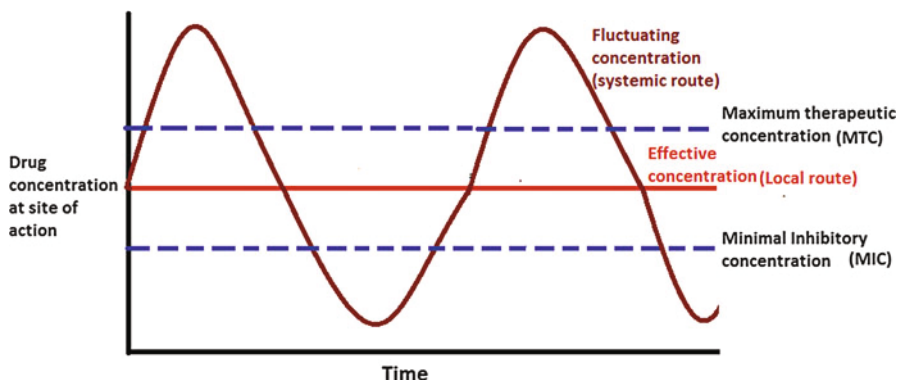


**Fig. 4** Drug concentration in plasma in conventional therapy vs. local drug delivery systems

However, the challenges of local antibiotic therapy are avoiding antibiotic resistance, due to infection with methicillin-resistant *Staphylococcus aureus* (MRSA), and achieving antimicrobial activity without impairing osseointegration [5].

### Combination Devices as Local Drug Delivery Systems

The two components of a local antibiotic delivery system are the antibiotic drug and drug carrier/delivery vehicle. New technologies that are designed to facilitate the delivery of local antibiotics in novel ways such as impregnating drugs onto carrier systems to develop combination devices are being explored. These combination devices are used in various fields like cardiovascular disease, orthopedics, and cancer therapy. The FDA (Food and Drug Administration) defines a combination device as, “comprising two or more regulated components, i.e., drug/device, biologic/device, or drug/device/biologic, that are physically, chemically, or otherwise combined or mixed and produced as a single entity; or two or more separate products packaged together in a single package or as a unit and comprised of drug and device products, device and biological products, or biological and drug products” [3].

In case of musculoskeletal infection, vehicles such as drug-impregnated cement beads, spacers, premolded implants, drug-impregnated bone cements, and antibiotic-eluting bioceramics and polymers are used. Currently, the gold standard in local delivery of antibiotics in bone infection is the drug-loaded polymethyl methacrylate (PMMA) cement approved by FDA and PMMA beads used in Europe. Since the treatment of most bone infections usually includes bone regeneration, the osteoinductive and osteoconductive biomaterials are preferred as delivery vehicles of antibiotics.

### Requirements of Ideal Local Drug Delivery System

The extensive use of medical devices invariably accompanied by serious infection problems makes it imperative to focus on the development and design of robust local

drug delivery system (DDS) for controlled release of antibiotics. An ideal local drug delivery system should ensure (a) provision of therapeutically effective drug dosage to target site; (b) provision for prolonged therapeutic drug release, if needed [3]; (c) safe drug levels in the systemic circulation; (d) easy application, handling, and removal; (e) patient friendliness; and (f) inexpensiveness.

Developing a DDS for bone infections should therefore be based on the following aspects:

- (a) Delivery technique – Whether delivered from coatings, particles, or scaffolds, whether antibiotic is mixed physically or incorporated within the carrier, etc.
- (b) Selection of clinically effective antibiotic – While penicillin derivatives and aminoglycosides are used for *S. aureus* and enterococcal bone infections, MRSA infections require vancomycin or daptomycin. Cephalosporins are widely used for *Pseudomonas aeruginosa* infections. Multidrug-resistant infections can also benefit from a combination of these antibiotics.
- (c) Pharmacokinetics (bioavailability, toxicity, and clearance).
- (d) Effective dosage, duration, and release kinetics at site – A controlled release of antibiotics with concentration above the minimal inhibitory concentration throughout the treatment period is preferred. The duration of drug release varies widely between 1 week for periodontal infections to 8 weeks for MRSA infections. The dosage and duration can be increased in cases of prosthetic implants associated with biofilms.
- (e) Used as prophylaxis and/or therapy – The drug dose and duration of treatment vary between prophylactic dosage regimen to prevent implant-associated bone infections and the therapeutic regimen to treat existing bone infections.
- (f) Possibility of combination with osteoconductive and osteoinductive factors – This is a major factor when considered for bone repair and regenerative applications. Since bacterial infection affects complete osseointegration of implants as well as causes bone destruction, coupling both applications are highly preferred.
- (g) Device design – Depending on the site of delivery and regenerative requirements, the device design may vary. In case of a prophylaxis for prosthetic implant infections, coatings are the ideal way to incorporate antibiotics. In case of large defects associated with infections, 3D scaffolds are more suitable. Similarly, in case of periodontal infections associated with bone loss, an injectable or moldable cement that can be packed within the cavity are suitable.
- (h) Site of delivery – The site of delivery such as long bones, jaw bones with asymmetric defects and cranial defects influences the device design greatly.
- (i) Not impair the device performance – Uncontrolled antibiotic release beyond the toxic limit can affect surrounding mammalian cells like osteoblasts and osteoprogenitor cells thereby counteracting the effect of bone substitute materials used as carriers.
- (j) Simple efficient processes for biomaterial synthesis, conjugation, and sterilization – Ensures industrial production of large quantities of targeted drug delivery systems [3, 8].

For effective local delivery, the antibiotic must bind and be released adequately above MIC (minimum inhibitory concentration) from the delivery vehicle. The release of subtherapeutic drug concentrations can worsen the existing infection by inducing antibiotic resistance. In case of preexisting infections, an initial high release rate is necessary followed by a sustained release to combat those bacteria possibly introduced during surgical procedure or circulating systemically [1]. In such cases, an initial high MIC release pattern of antibiotics (first 1–2 days) followed by a prolonged release of a lower MIC for another four weeks is desired. The antibiotic agent should diffuse at least 1 cm into the surrounding tissues [8]. In the case of implant-based infections, factors such as compromised healing and fertile environment for microbial colonization and anticipated primary and secondary pathogens must be considered in drug selection, dosing, and release mechanisms.

### **Selection of Antibiotics**

Antibiotics are selected based on the causative organisms, their sensitivity and pathogenicity, the acuteness of the infection, and the presence of foreign body. Since the most prevalent microbes associated with bone infections are *Staphylococcus aureus*,  $\beta$ -hemolytic *Streptococcus*, and gram-negative bacteria (Table 1), the most common antibiotics used are aminoglycosides (gentamicin, tobramycin), various  $\beta$ -lactam antibiotics (penicillin derivatives, cephalosporins), vancomycin, clindamycin, and fluoroquinolones like ciprofloxacin [9]. Traditionally, antibiotics target five main aspects of cellular machinery: (1) cell wall synthesis (e.g., penicillin), (2) folic acid production (e.g., sulfonamides), (3) ribosomal function (e.g., tetracyclines and macrolides), (4) DNA replication (e.g., fluoroquinolones), and (5) cell membrane damage (e.g., daptomycin, vancomycin, and other peptide antibiotics) [7]. Based on whether they kill, these antibiotics are classified into bactericidal (kills the bacteria) and bacteriostatic (inhibit growth) drugs. The drugs which cause disruption of the cell wall or cell membrane or damage the DNA are bactericidal. Bacteriostatic agents inhibiting bacterial replication such as sulfonamides, tetracyclines, and macrolides act by inhibiting protein synthesis. However, this distinction is not absolute and is insignificant in most in vivo cases. Bactericidal agents are generally preferred in the case of serious, acute infections. Certain antibiotics like aminoglycosides are less active in an oxygen-deprived, low-pH, high-protein environment of abscesses which are sometimes observed in osteomyelitis. A combination therapy of antibiotics is useful to reduce the toxicity of individual agents, to prevent the emergence of resistance, and to treat mixed infections [7].

### **Selection of Drug Carriers**

The biophysicochemical properties of drug carriers or delivery vehicles can have a profound effect on the activity and kinetics of antibiotics at target site. The properties

required of a biomaterial to be effective for the delivery of drugs specifically for bone therapeutics include critical features like biocompatibility and osteoconductivity. The drug adsorption depends largely on the specific surface area, charge, porosity, roughness, hydrophilicity, nature of surface ligands, and particle size of the carrier. In addition, the composition, size, and chemical structure of a carrier affect its resorption rate, which can influence the drug release profile. Finally, the degradation of the carrier and the sterilization process should not produce toxic metabolites or degrade the loaded drug.

Drug delivery carriers developed for local delivery of antibiotics are of two types, nonbiodegradable and biodegradable carriers. Among nonbiodegradable carriers, PMMA-based preloaded beads and cements are used in Europe and the USA, respectively. However, PMMA being nonbiodegradable has to be removed surgically after completion of antibiotic release, which is a major drawback. Hence, various biodegradable systems have been developed for local delivery of antibiotics in the treatment of bone infections. The biodegradable antibiotic delivery materials have been classified into four categories: bone graft and bone substitutes, protein-based materials (natural polymers), synthetic polymers, and miscellaneous biodegradable materials [10]. The benefits of biodegradable systems are the avoidance of secondary surgical procedures to remove the carrier, the possibility to match the rate of implant biodegradability according to bone regeneration and the type of infection treated, and the ability to function as a guide for bone repair and tailor the magnitude and duration of antibiotic delivery. Furthermore, secondary release of the antibiotic may occur during the degradation phase of the carrier, which could increase antibacterial efficacy compared to nonbiodegradable carriers [11].

## **Bioceramics for Local Drug Delivery**

Ceramics used for the purpose of repair and reconstruction of diseased or damaged parts of the body are termed bioceramics. In addition to being classified by their macroscopic surface characteristics (smooth, fully dense, roughened, or porous), bioceramics are specifically classified into bioinert (alumina, zirconia), bioactive (hydroxyapatite, bioactive glasses, and glass ceramics), and resorbable (tricalcium phosphate, calcium sulfate, and modified bioactive glasses) according to the tissue response and mode of attachment [12]. The development of controlled drug delivery systems based on bioceramics, which are designed for bone repair and regeneration, in order to treat infections is on the rise. Bioactive and degradable bioceramics are promising candidates for such applications. The reactivity of these materials leads to formation of a surface calcium phosphate layer that promotes proteins and cell adhesion resulting in a strong bond between the bone and the substitute. Traditionally, polymers and polymer composites dominate the field of drug delivery. Certain issues such as local inflammatory response to polymers and its degradation products, lack of bioactivity and uneven degradation of polymer scaffolds, etc., shifted the attention to ceramic materials. Compared to polymers, the bioceramics show bioactivity, low immunogenicity, and low toxicity in addition to their degradation

products being ions commonly found in human blood and tissues. It is technologically possible to include pharmaceuticals into these ceramics without compromising its function of bone regeneration. Delivery of pharmaceuticals from these bioceramics can be controlled with various parameters such as size, degradation rate, composition, surface chemistry, surface area, surface topography, and functionalization. Wide variety of techniques available for drug incorporation is also an added bonus. Since the repair of bone defects is expensive anyways, it is more cost-effective to include antibiotics into bioceramics compared to a separate systemic antibiotic regimen. Bioceramics find applications in the fields of dental, periodontal, middle ear, cranial, maxillofacial, otolaryngology, and spinal surgery and can thus serve as drug carriers to combat infections in the abovementioned areas.

---

### **Nanobioceramics for Efficient Antibiotic Delivery**

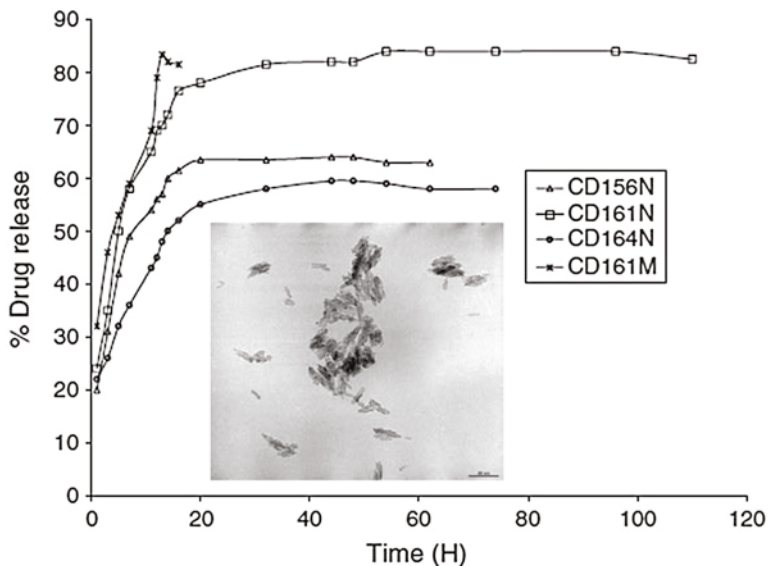
Novel efficient local drug delivery systems for medical applications have been developed with the help of nanotechnology. Nanotechnology is defined as the use of materials and systems whose structures and components exhibit novel and significantly changed properties when control is gained at the nanoscale (specifically,  $<100$  nm or  $<10^{-7}$  m) [13]. Nanotechnology has the potential to revolutionize the field of pharmacology by enabling targeted delivery of drugs to specific tissues, improving delivery of hydrophobic drugs, aiding in membranal transport of drugs across tight junctions and barriers, delivering drugs within cells, permitting multiple drug delivery, providing theragnostic applications (allowing visualization of sites of drug delivery) by combining therapeutic agents with imaging modalities, and in vivo real-time monitoring of the pharmacodynamics of the therapeutic agent. Nanomaterial-based platforms are being considered for the delivery of drugs, vaccines, proteins, peptides, and nucleotides as they help in modifying the bioavailability, pharmacokinetics, and distribution of a drug. Furthermore, the physical structure and chemistry of the nanostructure directly influence the behavior of the cell in contact with the surface. The cellular interactions of nanomaterials via the molecular building blocks of life such as proteins, carbohydrates, nucleic acids, and lipids, which are all nanosized structures, are crucial for controlling cell functions and the production of the extracellular matrix. Bioceramics, specifically in nanoscale, are gaining popularity, especially for bone therapeutics due to their bioactivity, material and surface chemistry, size, composition, ease of modification, and biodegradability. Table 3 lists the various bioceramic nanoparticles used for local drug delivery to hard tissues. The advantage of nanosized over micron-sized nanoparticles has been well documented. In a study by SP Victor et al., nanosized calcium-deficient hydroxyapatite (CDHA) carriers have shown controlled release profile of an antibiotic doxycycline compared to the burst release observed from microspheres of CDHA (Fig. 5) for the treatment of periodontitis [14]. CDHA nanoparticles of different Ca/P ratios (1.5, 1.61, and 1.64) were synthesized, and an antibiotic doxycycline was loaded on them through electrostatic interactions. While the drug loading was directly dependent on the surface area, the drug release was not so. It was found that the release

**Table 3** List of various nanobioceramic carriers for antibiotic delivery

S. no.	Carrier	Type	Antibiotics	Application
1.	<b>Calcium phosphates</b>	Hydroxyapatite nanoparticles Calcium-deficient hydroxyapatite nanoparticles Nanoporous calcium phosphate rods Calcium phosphate nanocoating	Ciprofloxacin Tetracycline, doxycycline Norfloxacin Nafcillin, levofloxacin Tobramycin	Osteomyelitis [17] Periodontitis [14, 18] Antibiotic carriers [19] Osteomyelitis [20]
2.	<b>Silica</b>	Nanoparticles Mesoporous phosphosilicate nanospheres Nanowire arrays Nanoporous coatings	Gentamicin Tetracycline Penicillin and streptomycin Ciprofloxacin	Sustained drug release [21] Controlled release [12] Controlled release [22] Coating on middle ear prosthesis to prevent otitis media [23]
3.	<b>Titania</b>	Nanoscaffolds, nanocoatings Nanotubes	Gentamicin, penicillin, streptomycin Cefuroxime	Controlled drug delivery [24–26]
4.	<b>Alumina</b>	Nanotubular coating	Amoxycillin	Controlled drug delivery [27]
6.	<b>Bioactive glass</b>	Amino-functionalized mesoporous nanoparticles	Sodium ampicillin	Delivery of therapeutic molecules [28]

profile had a strong dependence on Ca/P ratio with CDHA of Ca/P showing the highest release. These advantages have encouraged research in developing nanobioceramic-based drug delivery platforms chiefly for hard tissue applications. Common formulations of nanobioceramics are in the form of particles, coatings, and scaffolds for antibiotic delivery.

**Nanoparticles:** Particulate drug carriers are probably the most common bioceramic drug delivery platforms. Particulate carriers can easily transport drug entities through blood vessels, the digestive tract, and across cell membranes to reach the targeted site. Nanoparticles, in particular, have unique physicochemical properties like small and controllable size, tailorable morphology and porosity, large surface area to mass ratio, and functional flexibility, which enable greater interactions with drugs, microorganisms, and host cells. Nanoparticle-based DDS delivers larger quantity of drug (high payload), prolongs drug half-life, improves drug solubility, and has the ability to provide sustained, stimuli-responsive, targeted drug release [15]. Highly pure particulate materials are easier and inexpensive to fabricate as well. Nanosized drug-carrying particles also facilitate endocytosis of drugs by target cells and enhance their cellular uptake. Bioceramic nanoparticles can be synthesized by various methods, namely, precipitation, hydrothermal, sol-gel, multiple emulsion, electrodeposition, biomimetic deposition, etc.



Size, cell parameters, surface area and loading efficiencies of CDHA nanocarriers.			
Sample\properties	CD156	CD161	CD164
Ca/P ratio	1.56	1.61	1.64
Drug loading amount (mg/mg)	66/100	82/100	72/100
Surface area (m <sup>2</sup> /g)	62	94	80
Loading efficiency (%)	66	82	72
Cell parameters: <i>a</i> , <i>c</i> (nm)	0.943, 0.688	0.943, 0.686	0.942, 0.686
Size (TEM) length and breadth (nm)	20×30	25×28	26×29

**Fig. 5** Comparison of release profile of doxycycline from nano- and microcarriers of CDHA (Reproduced with permission from Ref. [14]). The TEM image of nanosized CDHA is shown in the inset (Reprinted with permission from Ref. [14], Fig. 3, 8 and Table I from Tailoring Calcium-Deficient Hydroxyapatite Nanocarriers for Enhanced Release of Antibiotics. *Journal of Biomedical Nanotechnology*, 4, 203–209 (2008). Copyright©American Scientific Publishers)

**Nanocoatings:** Surface modification of biomaterials using bioceramic nanocoatings is an effective method to improve their surface bioactivity for orthopedic applications. Generally, bioceramics are coated on metallic and polymeric materials that lack bioactivity with the help of techniques such as plasma spraying, electrophoretic deposition, pulsed laser deposition, ion beam deposition, biomimetic precipitation from SBF, and electron and magnetron sputtering. Nanocoatings of

bioceramics can not only influence the cell attachment, proliferation, migration, and differentiation but also regulate osteogenic factors. Nanoporous coatings with pore sizes less than approximately 100 nm and large surface area have attracted considerable attention as modern techniques allow for precise control on pore size, distribution, and pore density [16].

**Nanoscaffolds:** Nanoscaffolds serve as depots for controlled drug delivery beside their primary purpose of serving as a biomimetic construct aiming at bone regeneration and repair. Bioceramic scaffolds, in particular, actively assist with the proliferation and differentiation of bone cells. 3D nanobioceramic scaffolds with high porosity, high surface area, high structural stability, and long degradation times are ideally suited for the storage and controlled release of drugs like antibiotics. Various methods like electrospinning and anodization are employed for fabrication of nanoscaffolds.

## Methodology

**Drug loading:** Drug loading is the process by which the drug is incorporated or associated with the carrier. Nanoparticles are loaded with antibiotics via two routes, the in situ method where the drug is incorporated during the synthesis of nanoparticles and the ex situ method where the prepared nanoparticles are immersed for specified duration in the drug solution facilitating their adsorption. Both methods have certain advantages and disadvantages. While the in situ method enables a controlled release profile of the drug, the synthesis conditions can adversely affect the drug activity. On the other hand, the drugs incorporated through “immersion” method or ex situ method, a typical biphasic fashion is observed with an initial burst release followed by a controlled and importantly, largely incomplete release that continues for days to months. However, for most part, the drugs are unaffected retaining their activity. The duration of drug loading should be adequate to reach the equilibrium for maximum loading. For example, in a study by Ahmed El-Fiqi et al., when an antibiotic, sodium ampicillin was loaded onto the amine-functionalized bioglass, the loaded amount increased with increasing time of loading with saturation at approximately 120 min [28]. Drug loading for the nanocoatings generally is performed through capillary action by either immersing the templates in the concentrated drug solution or dropping the solution slowly on the template surfaces. Different techniques like sonication or stirring are used to increase the intake of the drug. The maximum drug loading capacity is usually determined by adsorption isotherms. Adsorption isotherms are plotted by varying the initial concentrations of drug and measuring the corresponding loaded amounts.

**Drug release:** The in vitro release studies are performed by mimicking the in vivo conditions using various buffers, usually with phosphate buffer solution (PBS) and simulated body fluid (SBF). In most cases, drug-loaded nanomaterials are soaked in a container (beaker/bottle/sampling tube) with or without controlled agitation [29]. The volume of dissolution media depends on drug solubility and the detection limit of the analysis technique. The sampling methods also vary, either withdrawing



and replacing a specific volume or replacing the entire volume with fresh media after taking a sample. The tests are sometimes performed under sink conditions (availability of sufficient buffer volume to dissolve the total drug) or using continuous flow-through chambers. The drug release must be adapted according to the necessary therapeutic dosage. In addition, the loading and drug release must guarantee the integrity of the chemical structure of the loaded drug.

Various techniques of drug release evaluation include membrane diffusion method (dialysis, reverse dialysis, and diffusion cell) and “sample and separate” method (centrifugation and/or filtration) [29]. The membrane diffusion method employs a dialysis membrane to physically separate the drug-loaded nanoparticles from the release media which is permeable for the drug but not for the carrier system. In dialysis technique, the drug-loaded particles are loaded in a dialysis bag, and samples are withdrawn from the outer release media. In reverse dialysis, the drug-loaded carriers are placed in the outer release medium, and samples are taken from inside the dialysis bags. This technique minimizes membrane clogging. Diffusion cell contains two chambers separated by dialysis membrane. The disadvantage of all these techniques is that true release rate cannot be measured, as the diffusion through membrane is a rate-limiting step. In the “sample and separate” method, the drug-loaded nanoparticles are incubated in the release media under controlled agitation. At specific intervals, sample media is withdrawn after separating the nanoparticles from release media containing dissolved drug by centrifuging or filtering. The disadvantage of this method is the high sampling frequency and time-consuming separation procedures. In order to characterize the drug release, a drug release profile should be generated, in which release (dissolution) values are determined as a function of time. This “multipoint” sampling is required to characterize release from the drug product, to test for possible alterations during storage, and to confirm batch-to-batch consistency.

Traditional dissolution techniques are in fact found to be unreliable when nanoparticles are concerned, and new novel in vitro techniques are being suggested [8]. Nanoparticulate systems present a challenge in developing suitable drug release methods due to the difficulty in separating the nanoparticles from the medium in a rapid, efficient way, poor understanding of drug release mechanism from these systems and the complexity of certain nanoparticulate systems which are designed not to release drug until uptake by the target cells in vivo. Currently, there is no standard protocol or technique available, though several in vitro tests have been performed to explore the suitability of nanomaterials as drug carriers. The flow-through cell and paddle-type dissolution apparatus have been found to be satisfactory for the drug release study from nanoparticles.

The main mechanism of drug release applicable for nanobioceramic-based DDS is dissolution and/or diffusion (Fig. 2). Dissolution is a diffusion-controlled process, and the dissolution rate is defined as the mass of drug dissolved at a given time. The dissolution rate is given by:

$$\frac{dM}{dt} = \frac{[DA (C_s - C)]}{h} \quad (1)$$

where  $\frac{dM}{dt}$  is the dissolution rate,  $D$  is the diffusion coefficient of the drug in solution,  $A$  is the surface area of the solid in contact with the medium,  $C_s$  is the drug solubility in medium,  $C$  is the concentration of the drug at time  $t$ , and  $h$  is the thickness of the diffusion boundary layer at solid's surface. The drug dissolution rate is directly proportional to the surface area of the particle and the drug solubility and inversely related to the particle size and the thickness of the diffusion boundary layer. These parameters are altered when a system changes from micro- to nanosized particles and affect the dissolution rate of drugs. The specific surface area is increased by decreased particle size, yielding a higher dissolution rate. In case of drug release through dissolution from nonbiodegradable matrices, the total drug loaded in the matrix, the drug solubility in the matrix, and the diffusion coefficient of drug in matrix (depends on drug-carrier interaction) also affect the dissolution rate. In case of degradable matrix, the drug release is more complex due to the effect of the degradation rate of the matrix, which in turn depends on its size. In most degradable carrier systems, the drug release occurs by both diffusion and dissolution mechanisms. There are several types of drug release models such as the first-order kinetics and zero-order kinetics. The first-order kinetics is associated with antibiotics attached by surface adsorption where the release rate is concentration dependent, i.e., dependence on the concentration gradient between the static liquid layer next to the solid surface and the bulk liquid. The log cumulative drug remaining in percentage is plotted against time. The zero-order kinetics describes the systems where the drug release rate is independent of its concentration. Here, the cumulative drug release in percentage is plotted against time. Higuchi, Hixson-Crowell, and Korsmeyer-Peppas models are other popular models studied for drug release. The Hixson-Crowell cube root law describes drug release from systems where there is a change in surface area and diameter of particles. The cube root of remaining drug percentage is plotted against time. Higuchi model describes release of a drug from an insoluble matrix as the square root of a time-dependent process based on Fickian diffusion. Hence, the plot made is cumulative drug release in percentage vs. square root of time. Korsmeyer-Peppas model described drug release mechanism as Fickian, non-Fickian, case II transport, and super case II transport by fitting the first 60 % of drug release data. The plot made is the log percentage of drug release vs. log time [30]. The main method for selecting the right type of model employs the coefficient of determination,  $R^2$ , to assess the fit of the model. Since it is difficult to choose a single model, usually multiple models are fitted, and comparative studies are made. The various kinetic models are shown in Fig. 6.

## Drug-Carrier Interactions

Drugs interact with their carriers through physical processes, chemical interaction, or both. Hydrogen bonding, ionic interaction, dipole interaction, physical entrapment, precipitation, covalent bonding, and adsorption are few processes by which drugs bind to their carrier [29]. Since ceramics present a specific surface area, conditioned

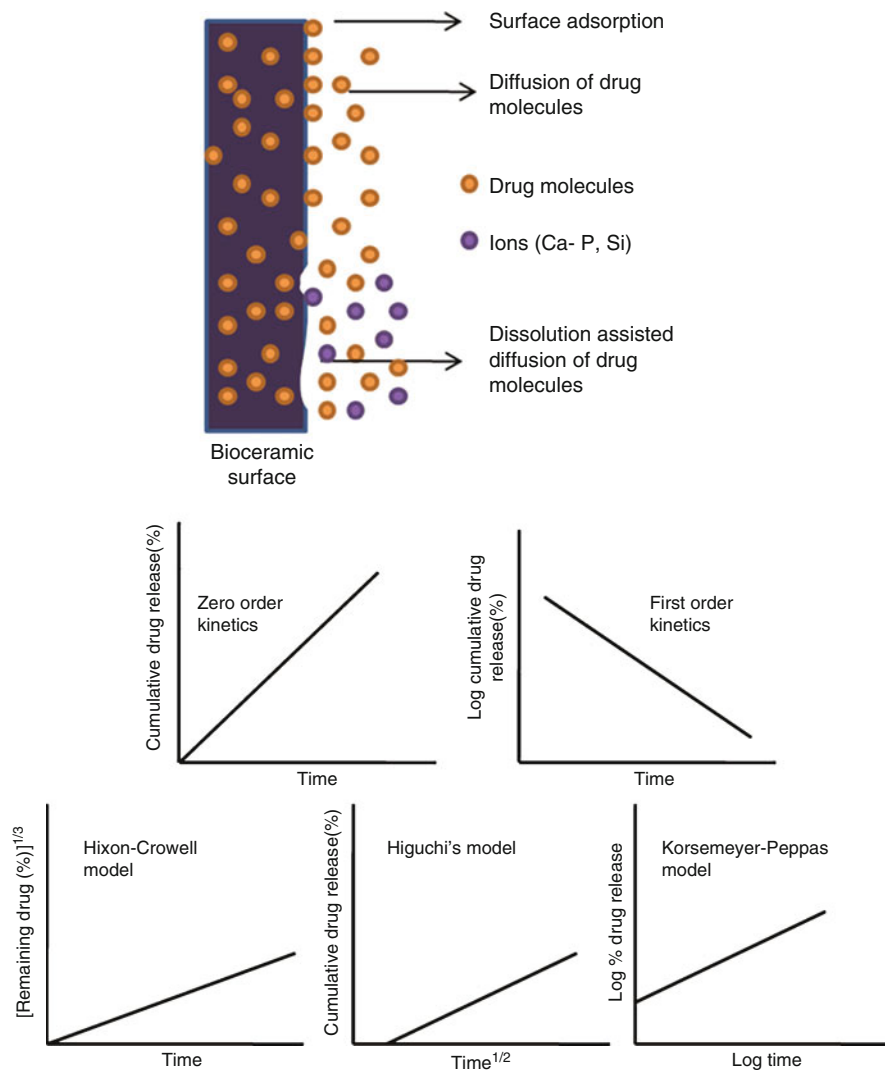


**Fig. 6** Schematic representation of drug release from bioceramic carriers and typical plots of various kinetic drug release models

by their composition and subsequent thermal treatment, they have a variable capacity to adsorb molecules onto their surface. In case of nanoporous coatings, the drug loading and release can be altered by varying the pore size, distribution, and density as well as surface modification. Surface charges of these pores can be modified to hydrophobic or hydrophilic to accommodate variety of drug molecules. The pore size of the membrane is extremely important especially when it becomes comparable with the size of the drug molecule since the diffusion rate becomes pore size dependent, a phenomenon referred to as hindered or restricted diffusion [16].

## Surface Functionalization

Surface functionalization of bioceramics has been carried out in order to improve colloidal stability, promote cell adhesion, ensure controlled antibiotic release, and prevent bacterial adhesion. Hydroxyapatite, for example, has been grafted with polymers like  $\gamma$ -benzyl-L-glutamate-*N*-carboxyanhydride, chitosan, dodecyl alcohol, vinyl phosphonic acid, and amino acids such as glycine, alanine, serine, lysine, and arginine to enhance colloidal stability [31] and also with silica to improve bioactivity.

Mesoporous bioglass nanoparticles have been surface functionalized with aminopropyl groups through a post-synthesis procedure so that their surface was modified with amine groups, which can impart a positive charge [28] in order to enhance drug binding.

Silica nanoparticles are widely modified to enhance antibiotic binding [32]. The various methods of surface functionalization on silica nanoparticles are summarized. Polypeptide polymer-grafted silica nanoparticles have been synthesized from covalently attaching poly-L-lysine, and their efficacy as antimicrobial agents was proved on both gram-negative *E. coli* and gram-positive *B. subtilis*. The grafting of an antibacterial polymer, poly(vinylbenzyltributylphosphonium chloride), onto silica surface by a radical graft polymerization endowed strong antibacterial activity that was shown to be retained even after boiling in water for 24 h. Quaternary ammonium compounds were also applied for the surface modification of silica nanoparticles, providing antibacterial properties against bacteria (*S. aureus*) and fungi (*C. albicans*), due to the hydrophobicity of the modified surface, showing lower minimal inhibitory concentrations (MIC) against bacteria and fungi than soluble surfactant. Reverse enhancement of antibacterial activity of certain molecules by linking with silica is also possible. Hybrid-silica nanoparticles containing the FDA-approved antimicrobial triclosan were found to be superior in killing bacteria, as compared with the free triclosan. Lysozyme-coated mesoporous silica nanoparticles were reported as antibacterial agents that exhibit efficient antibacterial activity both in vitro and in vivo with low cytotoxicity and negligible hemolytic side effect. Lysozyme is a natural enzyme abundant in body secretions and provides immunity against microbes by damaging the bacterial cell walls. This type of nanoparticle included the lower risk of development of resistance compared to antibiotics, selective damage of the bacterial walls, and enhanced stability of lysozyme (positively charged) by immobilizing it on the negatively charged silica via electrostatic interactions. Good antibacterial efficacy of lysozyme nanoparticles was observed when evaluated in vivo by using an infected mouse model, as their minimal inhibition concentration (MIC) was fivefold lower than that of the free enzyme in vitro.

Nanotubular titanium oxide (TiO<sub>2</sub>) has been explored in recent years as a new biomaterial for implants, drug delivery systems, cell growth, biosensors, immunoisolations, bioartificial organs, and tissue engineering. Since chemical inertness is the main weakness of this material, functionalization or surface modification has been carried out in order to promote controlled drug delivery. For example,

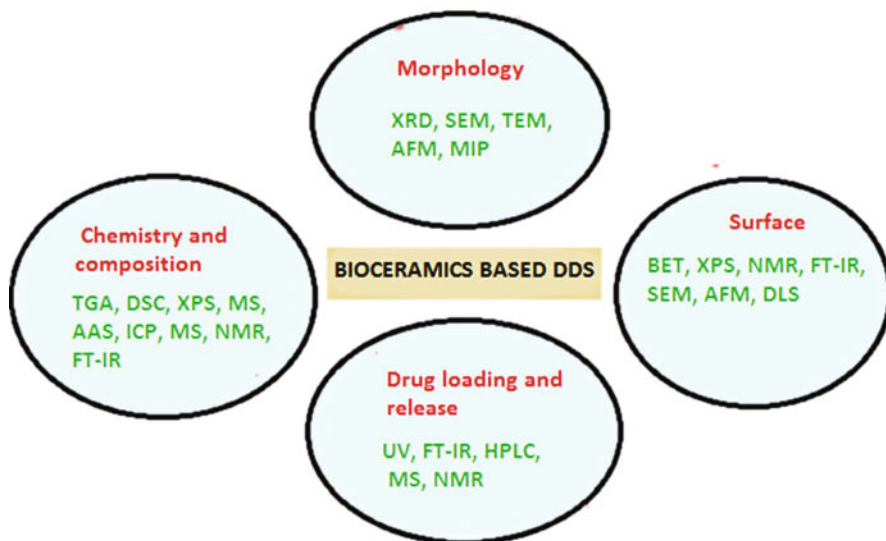


**Fig. 7** Characterization techniques required for nanobioceramic DDS

plasma surface modification using allylamine (AAPP) has been applied to generate a chemically reactive polymer film rich in amine groups on top of the TiO<sub>2</sub> nanotube surface. This initial hydrophobic polymer film was used for further surface functionalization with polyethylene glycol (PEG) or poly(sodium styrenesulfonate) (PSS) [33].

## Characterization Studies

Nanobioceramic-based DDS can be characterized for material properties, drug loading, and drug release. These techniques include X-ray diffraction (XRD), Fourier transform infrared spectroscopy (FT-IR), scanning electron microscopy (SEM), atomic force microscopy (AFM), transmission electron microscopy (TEM), mercury intrusion porosimetry (MIP), X-ray photon spectroscopy (XPS), nuclear magnetic resonance (NMR) spectroscopy, dynamic laser scattering (DLS), mass spectrometry (MS), inductively coupled plasma (ICP), thermogravimetric analysis (TGA), and differential scanning calorimetry (DSC). Drug loading and release are characterized using techniques such as UV–vis spectroscopy, FT-IR spectroscopy, high-performance liquid chromatography (HPLC), etc. Figure 7 shows the various characterization techniques for analyzing the surface and bulk features of the nanobioceramic DDS. Some important drug release characterization techniques are explained below.

**Ultraviolet–visible light (UV–vis) spectroscopy:** UV–vis spectroscopy is the study of how a sample responds to ultraviolet and visible light. When a beam of

light passes through a substance or a solution, some of it may be absorbed, and the remainder is transmitted through the sample. The UV–vis range of the electromagnetic spectrum covers the range 190–700 nm. Most assays using UV are concerned with quantification of chemical compounds. The most important principle in absorption analysis is the Beer–Lambert law. This law states that, for a given ideal solution, there is a linear relationship between concentration and absorbance ( $A$ ) if the path length is kept constant as;

$A = \epsilon cl$  where  $\epsilon$  = the absorptivity of the substance,  $c$  = concentration, and  $l$  = path length; the absorptivity is a constant for each molecule for each wavelength.

Most of the drug molecules have sufficient UV absorbance, and quantitative estimation by UV is easy to perform. Usually, a calibration curve is prepared by plotting the absorbance of a series of standard samples of drugs as a function of their concentration. If the absorbance of an unknown sample containing the drug is then measured, the concentration of the absorbing component can be assessed from this graph.

**Fourier transform infrared (FT-IR) spectroscopy:** FT-IR technique is used to characterize compounds based on the vibrational frequencies of their chemical groups. FT-IR technique makes use of infrared rays of wavelength 7000–500  $\mu\text{m}$ , which can excite molecular vibrations. If infrared energy absorption causes a vibrational excitation in a material, its FT-IR spectra contain absorption peaks which correspond to the frequencies of vibrations between the bonds of atoms present in the material. The FT-IR spectrum can be plotted in either transmission or absorption mode. The percent transmittance or absorbance is plotted against frequency (wave number between 4000 and 400  $\text{cm}^{-1}$ ). FT-IR technique is useful in assessing the type drug–carrier interaction (physical or chemical) as well as the structural and functional alterations of the drug due to these interactions.

**High-performance liquid chromatography (HPLC):** High-performance liquid chromatography is one of the most powerful tools in pharmaceutical analysis. It has the ability to separate, identify, and quantify the compounds that are present in any sample that can be dissolved in a liquid. Compounds in trace concentrations as low as parts per trillion [ppt] can be identified. The mechanism behind HPLC-based characterization is based upon the difference in the sample flow rate and retention when eluted through a “stationary” adsorbent column. The samples can be any chemical or drug compound dissolved in a solvent which react with the adsorbent chemically or physicochemically. These interactions affect the flow rate and the drug compounds are separated. The presence and quantity of drugs can be calculated from chromatograms showing specific peaks of the compound similar to UV spectroscopy. HPLC is more suited than UV spectroscopy in cases of multidrug formulations where more than one drug share the same absorbance maxima. It is more sensitive, accurate, and error free compared to UV spectroscopy. For drugs that do not show UV absorbance or when their absorbance is affected by their degradation products, HPLC is the method of quantification. However, UV–vis spectroscopy is faster, cheaper, and simpler compared to HPLC. Often, HPLC and UV–vis spectroscopy are combined such that the drugs separated by HPLC are quantified using the UV detector.

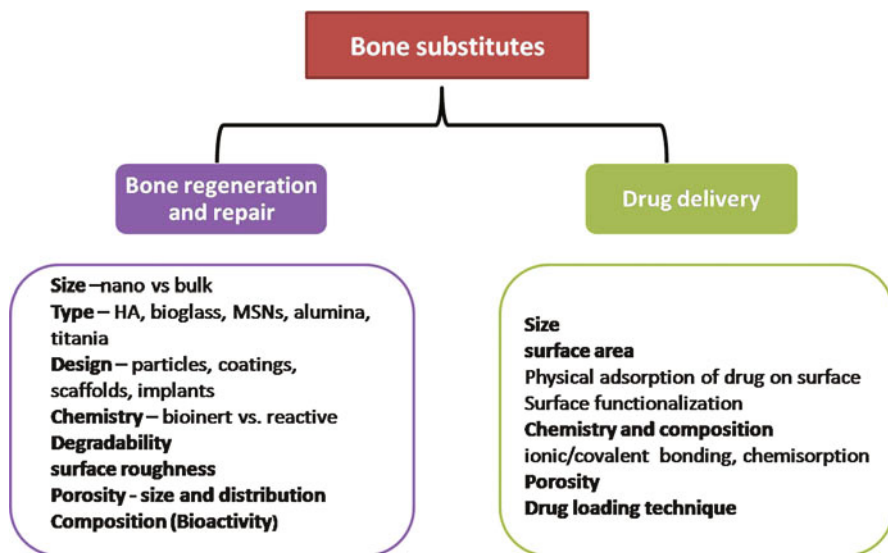


**Fig. 8** Parameters deciding the efficiency of a bone substitute-based DDS

## Drug Delivery from Various Types of Nanobioceramics

Although a great variety of polymeric nanoparticles are available, such as liposomes, dendrimers, core–shells, etc., inorganic nanoparticles for drug delivery technology have evinced a significant interest due to the advances in the control over the synthesis of nanoscale inorganic materials and improved techniques for functionalized nanomaterial surface. Thus, it is possible to produce nanoparticles with controlled size, shape, morphology, charge, surface chemistry, and physico-chemical properties. Ceramic nanoparticles possess several unique properties compared with polymeric or metallic nanoparticles for bone therapeutics. Firstly, ceramic nanoparticles usually have longer biodegradation times that can retain drugs for longer times after administration. Secondly, unlike polymers, ceramic nanoparticles exhibit high stability at varied pH or temperature in aqueous conditions, without swelling or changes in porosity. Thirdly, ceramic nanoparticles can be properly fabricated to possess the same chemistry and crystalline structure like the bone. The various parameters affecting the application of ceramic nanoparticles as drug delivery systems and regenerative materials are shown in Fig. 8. Nanophase bioceramics have been synthesized by both top-down and bottom-up approaches. The top-down approaches where nanoparticles are disaggregated from bulk materials include ball milling, ultrasound, hydrolysis, radio frequency thermal plasma method, etc. The bottom-up approach where controlled nucleation and crystal growth are observed includes solution-mediated synthesis methods like precipitation, sol–gel synthesis, ultrasonic or microwave irradiation, emulsion, solvothermal, hydrothermal, and mechanochemical processing.

## Calcium Phosphates

Calcium phosphates (CaP) are widely used in tissue engineering of hard tissues such as teeth or bone replacement, repair, and regeneration due to their bioactivity, biocompatibility, biodegradability, and compositional similarities to bone mineral. Our bone tissue can be considered as a composite material composed of collagen biopolymer (~20 %) and reinforced with inorganic carbonated nonstoichiometric apatite (~70 %). The natural minerals in the bone are homogeneous platelike crystals with widths of 15–30 nm and lengths of 30–50 nm, and in enamel are rodlike crystals with diameters of 25–100 nm and lengths of 100 nm to microns. In situ drug delivery from compositionally similar CaPs in bone therapeutics can provide specific tissue response and assured drug bioavailability. Degradation products of CaPs such as  $\text{Ca}^{2+}$  and  $\text{PO}_4^{3-}$  ions are already present in the body with their concentration in blood stream being 1–5 mM [34]. Thus, among the many inorganic drug delivery systems, special importance is given to CaP nanomaterials. CaP is used in mostly non-load-bearing clinical situations, including reconstructive orthopedics, dental, ear, nose, and ophthalmic surgeries. Current research on expanding the biological function of CaPs is focused on optimizing its osteogenic potential and extending its biofunctionality in pathological conditions.

CaPs are available in different forms and phases. The common types of CaPs evaluated for bone therapeutics are hydroxyapatite (HA), calcium-deficient hydroxyapatite (CDHA),  $\beta$ -tricalcium phosphate ( $\beta$ -TCP), and biphasic calcium phosphate (BCP). CaPs differ in their bioactivity and degradation behavior, both of which depend on the Ca/P ratio, crystallinity, and phase purity. HA [ $\text{Ca}_{10}(\text{PO}_4)_6(\text{OH})_2$ ; Ca/P = 1.67] is the most stable and least soluble of all CPCs as it resists hydrolytic degradation. On the other hand,  $\beta$ -TCP [ $\text{Ca}_3(\text{PO}_4)_2$ ; Ca/P = 1.5] is considered to be a rapidly degrading CPC which forms HA in vivo. CDHAs [ $\text{Ca}_{10-x}(\text{HPO}_4)_x(\text{PO}_4)_{6-x}(\text{OH})_{2-x}$ ; Ca/P = 1.33–1.66] with tailorable Ca/P ratio and degradability are fast becoming the first choice for antibiotic delivery. CDHA is structurally similar to stoichiometric HA and compositionally similar to TCP [14]. BCPs are composed of two phases, the low soluble, osteoconductive HA and the soluble, osteoinductive  $\beta$ -TCP at different ratios.

CaP nanoparticles can be synthesized through various routes such as wet precipitation, solid-state reaction, sol–gel, flame spray pyrolysis, hydrothermal, spray-drying, micelle-mediated, reverse micelle-mediated, and double emulsion-mediated synthesis [34]. The shape, size, crystallinity, stoichiometry, and specific surface area of the CaPs are very sensitive to the concentration of the reagents, reactant addition rate, reaction temperature and time, initial pH, and aging time. In order to optimize their specific biomedical applications, especially drug delivery, features such as porosity, morphology, and surface properties should be tailored. Precipitation techniques have been used to prepare nanoparticles from precursor solution containing related ions. Various parameters like initial composition, molarity, Ca/P ratio, pH, temperature, reactant addition rate, and stirring time decide the purity, size, and shape of resulting products. It is a very inexpensive and versatile method. It has been shown that microwave-assisted wet chemical synthesis method produces highly pure calcium phosphate nanoparticles of narrow particle size distribution within a very



short time by homogenous nucleation [35]. In this method, rapid synthesis of CDHA was achieved by precipitation using calcium nitrate tetrahydrate and phosphoric acid and subsequently subjecting to microwave irradiation in a domestic microwave oven for 15 min. Needle or platelet-like CDHA nanoparticles having length less than 40 nm and width less than 20 nm were obtained by this method. CDHA nanoparticles prepared by this method have been used for delivery of tetracycline group of antibiotics [14, 18]. Similarly, wet precipitation synthesis was also used in conjunction with hydrothermal method to obtain apatitic nanoparticles [20]. It was observed that CaP nanoparticles with Ca/P closer to HA were obtained with an increase in hydrothermal pressure or temperature.

Biomimetic method of precipitation from simulated body fluids (SBF) is a method to synthesize HA nanoparticles at physiological pH and temperature. SBF prepared with ion concentrations similar to that of human blood plasma were first used by Kokubo to prove the similarity between in vitro and in vivo behavior of certain glass ceramics. Biomimetic, nanosized, carbonated, “bone-like” HA powder can be obtained from calcium nitrate tetrahydrate and diammonium hydrogen phosphate salts dissolved in SBF at 37 °C and at pH of 7.4 by chemical precipitation [25]. The antibiotics can be coprecipitated during HA precipitation.

Bone cements based on self-setting nano-calcium phosphates are very popular due to improved sinterability, enhanced densification, and better bioactivity than coarser crystals. Cement properties, such as setting time, degradation speed, porosity, or mechanical behavior, can be controlled by changing the type or amount of calcium phosphate and additives. An example of approved nano CaP for clinical treatments such as fractures, osteotomies, acetabulum reconstruction, and filling cages in spinal column surgery is the OstimR<sup>®</sup>. Cements based on calcium phosphate can be used as convenient drug carriers for antibiotics since the drugs can be incorporated into the whole cement volume releasing drugs for more prolonged duration, unlike other carriers where drugs are usually adsorbed on the surface. Thus, dental cements have great potential for controlled drug delivery. Porous blocks and cements composed of nanoparticulate CaPs and incorporated with antibiotics like gentamicin have been developed [34]. The inorganic phase of calcium phosphate cement systems consists of dicalcium phosphate (DCP), dicalcium phosphate dihydrate (DCPD), tetracalcium phosphate (TTCP), amorphous calcium phosphate (ACP), calcium-deficient HA, carbonate HA,  $\alpha$ -TCP,  $\beta$ -TCP, or octacalcium phosphate (OCP). The moldable or injectable cement usually hardens in situ without significant heat development. These cements have been employed in vertebral augmentation of biomechanically stable vertebral fractures in children.

Nanophase CaP coatings on implants are important methods to enhance the bioactivity of inert metallic implants thereby accelerating bone growth and fixation. Nanostructured hydroxyapatite coatings on implant surfaces have shown to improve the osteoblast adhesion and differentiation [13]. The problems of coagulation and thrombus formation on CaP-coated implant surface can be avoided by surface functionalizing the coating with an appropriate anticoagulant like heparin. CaP nanocoatings are deposited on implant surfaces using techniques such as plasma spray deposition, ion beam-assisted deposition, electrophoretic deposition, chemical

vapor deposition, microarc oxidation, magnetron sputtering apart from sol-gel route, and biomineralization. It is also possible to coat implants with nanosized carbonated HA and other Ca/P compounds biomimetically, by immersing implants in SBF to influence the bioactivity of the implant. In this method, biologically active agents like antibiotics can be added to the supersaturated solutions and be coprecipitated with the CaP coating on the metal implant.

Electrospinning has emerged as a very promising strategy for fabricating bone-mimetic nanofiber scaffolds. The popularity of electrospinning is likely due to the simplicity of the experimental setup, the ability to incorporate bioactive molecules, and the versatility it provides. Fiber diameter and porosity can be fine-tuned through simple changes made in the spinning setup. In electrospinning, the bulk material of interest is dissolved in an organic solvent and subsequently pulled under the influence of an electric field through a needle and finally deposited in a nonwoven pattern on a collector plate. Both *in vitro* and *in vivo* studies have demonstrated that osteoprogenitor cells differentiate, proliferate, and adhere much better in nanofibrous matrices. Nanocomposites of hydroxyapatite and other CaPs along with polymers like collagen, chitosan, gelatin, alginate, polycaprolactone, etc., are widely used to develop 3D scaffolds. This is an ideal technique to develop controlled release formulations as drugs can be incorporated into the scaffold *in situ* by mixing it with the precursor solution and spinning.

CaPs have been used as delivery carriers for antibiotics (gentamicin sulfate, flomoxef sodium, tetracycline, doxycycline, etc.), anti-inflammatory agents (ibuprofen, salicylic acid, indomethacin), anticancer drugs (mercaptapurine), growth factors (bone morphogenic proteins, transforming growth factor- $\beta$  (TGF- $\beta$ ), etc.), proteins (e.g., collagen, osteocalcin), and DNA. Nanosized calcium phosphates are shown to maintain a sustained and steady drug release over time [17]. Drugs are mainly associated with CPCs by physical adsorption, chemisorption, chemical binding, complex formation, chelation, etc. These processes of association affect the release profile of the loaded drug. The drug release kinetics can be modified by tailoring calcium phosphate nanoparticle grain size, surface area, and calcium-to-phosphorus ratios.

Apart from traditional nanophase CaPs, modified ion-substituted CaPs like carbonated apatites, silica-substituted apatites, and fluorinated apatites are also used for drug delivery. CaPs derived from eggshells and marine sources are also becoming popular. Novel drug carriers based on CaP such as nanoceramic scaffolds and smart systems using ultrasonically triggered nanoceramic particles have also been developed. In one method, hollow, well-dispersed, and stable CaP nanospheres were synthesized in a modified wet chemical reaction in the presence of a surfactant [36]. Amylose was preloaded into these nanospheres of approximately 145 nm diameter with inner hollow cavity of 60 nm diameter. When ultrasonic treatment (40 kHz, 150 W) was applied, the hollow structures were deconstructed to form pin-like nanocrystallites, and amylose was released. 3D porous CaP-based ceramic nanoscaffolds have also been developed which can provide initial structural integrity for bone cells, direct their proliferation and differentiation, and assist in the ultimate assembly of new tissue. They mimic the *in vivo* environment of cells more

completely than nanoparticles. The structural advantages of ceramic nanoscaffolds include high porosity, high volume-to-area ratios, high surface area, high structural stability, and long degradation times. These properties make them potent systems for the storage and controlled release of drugs for in situ delivery [15]. The template method has also been used to synthesize nanoshell form of calcium phosphate, as reported by Schmidt and Ostafin [37]. The nanoshells were produced with a liposome as a template. The lipid was the phosphatidic acid 1, 2-dioleoyl-*SN*-glycero-3-phosphate (DOPA). Nanoshells with a shell thickness of 2–10 nm and a liposome/water core of 45–100 nm in diameter were obtained. Nanoshells, unlike nanospheres where the drug is dispersed, are vesicular systems where the drug can be stored and protected from a premature inactivation. As a result, calcium phosphate nanoshells have potential as sustained drug delivery vehicles. In this technique, calcium and phosphate solutions are added alternatively to maintain liposome stability leading to the precipitation of a calcium phosphate layer on the surface of this liposomal template.

### Bioactive Glass

Bioactive glasses are amorphous solids classified as ceramic materials. They exhibit high bioactivity and biocompatibility. Bioactive glass usually consists of formers like silicon dioxide and phosphorus pentoxide, with oxides of calcium and sodium as modifiers. Other oxides of potassium, magnesium, iron, aluminum, and calcium fluorides are also present. *45S5 Bioglass*<sup>®</sup>, a bioactive glass approved by FDA, was developed by Hench et al., through melt quenching, and is composed of 46.1 mol% SiO<sub>2</sub>, 26.1 mol% CaO, 24.4 mol% Na<sub>2</sub>O, and 2.5 mol% P<sub>2</sub>O<sub>5</sub> [12]. When placed in a physiological medium, bioactive glasses leach Na<sup>+</sup> ions first followed by K<sup>+</sup>, Ca<sup>2+</sup>, P<sup>5+</sup>, Si<sup>4+</sup>, and SiOH ions. These are replaced with H<sub>3</sub>O<sup>+</sup> ions from the medium through an ion-exchange reaction that produces a silica-rich gel surface layer. This depletion of H<sup>+</sup>/H<sub>3</sub>O<sup>+</sup> ions in solution causes a pH increase further enhancing dissolution. These amorphous ceramics form apatite-like crystals out of the initially formed silica hydrogel layer on contact with body fluids. Bioactive glasses are widely used in tissue engineering as fillers, scaffolds, and coatings because of their unique properties such as rapid surface reaction and easy designing of the required composition.

Generally, bioactive glasses are prepared using methods such as sol-gel, melt quenching, and sonication. The bioactivity of a bioactive glass is influenced by factors such as composition, texture, density, and porosity. Nanobioactive glasses have been used as scaffolds, nanocomposites, and coatings. Bioactive glasses developed at the nanoscale possess better surface properties, accelerating the interactions with other materials/molecules due to which they have been used with biopolymers to form nanocomposites or delivery systems. Bioactive glass nanoparticles are also of potential interest in dentistry because of their antibacterial properties and the ability to remineralize dentine [28]. Bioactive glasses of the SiO<sub>2</sub>-Na<sub>2</sub>O-CaO-P<sub>2</sub>O<sub>5</sub> composition have antimicrobial activity in aqueous solutions due to the release of their ionic compounds over time. The release of the dissolution

products result in a high pH environment, which is not well tolerated by bacteria. In addition, the release of silica has been also linked to the antibacterial bioactive glass effect [32]. The antibacterial efficiency of bioactive 45S5 Bioglass<sup>®</sup> derived glass–ceramic substrates against common gram-positive and gram-negative bacteria, and yeast has been reported. Moreover, the shift from micro- to nanosized bioglass materials afforded a tenfold increase in silica release and solution pH elevation by more than three units. As a result, the killing efficacy was substantially higher for the nanomaterial against all strains of *E. faecalis*. However, their antibacterial efficacy is still inferior to that of other materials so that attempts have been made to spike bioactive glass with antimicrobial agents to increase its antimicrobial efficacy [32].

Sol–gel method is a very popular route to synthesize nanosized bioceramics in a simple and rapid manner at low processing temperature. The name refers to a low-temperature method using chemical precursors that can produce homogenous and pure ceramics and glasses. Recently, applications in biotechnology, where biomolecules are incorporated into sol–gel matrix, have been extensively studied. To synthesize high-purity bioglass nanoparticles, the precursors are homogeneously mixed at molecular level. Usually, a modified Stober method (MSM) is used for synthesis of nanobioceramics. In this two-step procedure, tetraethyl orthosilicate (TEOS) is first hydrolyzed under acidic conditions. The precursors are added and afterwards condensed to gel particles in alkaline solution. The factors such as pH, volume of solvents, or ratio of reagents influence the chemical process of hydrolysis and polycondensation, determining the final size of the sol–gel-derived particles. Bioactive molecules can be easily encapsulated within silica particles by combining sol–gel polymerization with either spray drying or colloidal chemistry. Antibiotic-loaded silica nanoparticles have also been developed by this route by adding gentamicin to the hydrolyzed TEOS sol. Silica rods incorporated with gentamicin were obtained through this route, and a biphasic release of the drug was observed [21]. Sol–gel method is also used to develop nanoporous coatings. Sol–gel-derived nanostructured titania and titania–silica ceramic with high porosity have been developed. The sol–gel method can produce materials with controlled surface properties and high homogeneity and purity with pore sizes between 1 and 500 nm [16].

Sol–gel-derived coatings are usually produced using the spin coating or dip coating techniques. The spin-coating process consists of four stages, namely, deposition, spin-up, spin-off, and evaporation. For complex-shaped substrates, the commonly used sol–gel technique is dip coating. The dip coating consists of three steps: dipping, withdrawal, and heating. In dip coating, the substrate is dipped in a homogeneous sol solution containing various metal compounds which finally form the desired simple or complex oxides. A liquid film on the substrate becomes a gel film due to gelation, upon withdrawal of substrate from the solution. Finally, the substrate with a gel film is heated to a certain temperature to produce chemical bonding between the film and substrate. The resulting micronanostructure in the sol–gel coating depends on the precursors as well as relative rates of condensation and evaporation during film deposition.

## Mesoporous Silica

Nanoporous silica materials possessing pores on the lower nanoscale (3–10 nm) are designated as mesoporous materials. Mesoporous silica nanoparticles (MSNs) are also defined as solid materials comprising of a honeycomb-like porous structure with empty channels (pores) of nanosized dimensions. Their pore diameters are sufficiently large for the adsorption of larger drug molecules. The biomedical application research on MSNs has received great attention in the last few years. MSNs have been suggested for use in controlled drug/gene release and as delivery carriers, biosensors, biomarkers, etc. MSNs have attracted attention as promising drug delivery systems due to their simple synthesis methods, tunable size, morphology and porosity, thermal and chemical stability, easy functionalization, low toxicity, and capacity to carry different payloads (drugs, peptides, proteins, or even other nanoparticles) within the mesoporous cavities [6]. Their textural parameters, large pore volumes, high surface areas, and high and ordered porosity allow them to load a large amount of active drugs within their pores, thus providing sufficient concentrations for local treatment. The surface of silica materials is reactive due to the presence of silanol groups. This allows for surface modification by silanization reactions and thus opens possibilities for enhancing the drug loading and controlling the drug release. Their internal and external surfaces can be functionalized independently, thereby conjugation with different groups is made possible, without affecting the drug loading and release capabilities. In addition to this, it protects the bioactivity of drugs, together with the appropriate release pharmacokinetics and zero premature release. MSNs have the significant advantage of being free from various biochemical attacks and bioerosions. The possibility of tissue specificity and site directing ability represents an added value for these nanocarriers. The bone-forming bioactivity of mesoporous bioceramics together with their high specific surface area, well-ordered pores, and large pore volume has postulated these materials for the treatment of bone infection. The research in the biomedical application of this material as DDS has focused on nanoporous silica nanoparticles and coatings on prosthesis.

MSNs are generally prepared under basic, acidic, or neutral conditions. Under basic conditions, both the morphology and nanoscaled particle size of MSNs are easily controllable. However, tuning the pore size is difficult. In case of drug delivery, MSNs possessing a nanoscaled particle size and large pore diameter are highly desired. Under acidic conditions, in contrast, the pore size is controllable in a wide range, but its particle size can be controlled only in the micrometer scale. Under neutral conditions, addition of surfactants can produce monodispersed MSNs with regular spherical morphology, and controllable size in nanoscale range has been successfully synthesized. Hollow MSNs (HMSNs) with a large cavity in the core have become popular because of their low density, large specific surface areas, high loading capacities, and the potentially reduced amount of carriers used. The general synthetic strategy for these special HMSNs is the typical soft-/hard-templating method, which includes the formation of uniform soft/hard templates, their surface functionalization, followed by the deposition of the desired shell. The soft templates could be emulsion drops, Polyvinylpyrrolidone, or micellar aggregates, while the hard templates could be iron oxide nanocrystals, silver nanoparticles, polystyrene, or

carbon spheres. Studies have shown that hollow silica nanospheres are capable of entrapping an eightfold increased quantity of drug species compared with solid silica nanospheres. Another study revealed that hollow silica nanospheres had a time-delayed multiple-stage release profile (including an initial burst release for 20 min, a prolonged steady release up to 10 h, and a final fast release for another 2 h). Hollow silica nanospheres have been fabricated into well-controlled shapes and sizes by using templates or self-templating molecules. Ordered MSNs are synthesized using a surfactant-templating method named liquid crystal templating wherein the dimensions of pore channels can be tailored through the choice of surfactants, additives, and synthesis conditions [38]. In this method, an increasing amount of surfactant molecules is dissolved in an aqueous solution, and when surfactant concentration reaches the critical micellar concentration (CMC), “micelles” are formed with the hydrophobic tails of the surfactant congregating on the inside while their hydrophilic heads are facing outside toward the water. These micellar liquid crystals act as templates for the formation of the mesoporous materials. These liquid crystal structures depend on the surfactant type, surfactant concentration, pH, temperature, presence of additives, etc. In the final, once the silica source has condensed around the micelles, the surfactant is removed by thermal degradation or solvent extraction. This surfactant removal gives rise to a network of cavities within the silica framework. A recent exciting work on pH-mediated drug release from MSNs by capping them with zinc oxide (ZnO) quantum dots merits mention. Luminescent ZnO quantum dots that were acid soluble were used to cap the MSNs loaded with doxorubicin. After cellular internalization, these ZnO dissolve in acidic environments thereby releasing the drug. Such pH-mediated applications can also be useful for antibiotic delivery [39].

## **Titania**

Titania or titanium oxide ( $\text{TiO}_2$ ) is inarguably one to most widely researched nanomaterial due to its exceptionally efficient photoactivity and high chemical stability. Titanium dioxide exists in three phases, namely, anatase, brookite, and rutile. While rutile is the most thermodynamically stable form in bulk state, anatase crystal structure is dominant in the nanocrystalline regime. Until the photocatalytic applications in biomedical aspect were evaluated, titania was solely used as a bioinert implant capable of osseointegration. Initial studies on the nanocrystalline titania were focused on its photocatalytic property for the cancer treatment. However, interest in other biomedical applications of titania especially as protein and drug delivery was kindled due to its excellent binding of various chemicals and molecules attributed to uncoordinated surface sites of high energy.

Surface modification of titanium implants by depositing a layer of titanium oxide nanotubes in a controlled fashion to facilitate localized drug delivery has also been carried out. For example, vertically oriented titania nanotube arrays with tube diameter between 20 and 150  $\mu\text{m}$  and tube length up to 200  $\mu\text{m}$  have been fabricated [16]. In case of  $\text{TiO}_2$  nanotubes, different electrolytes such as hydrofluoric acid, fluoride ion-containing baths, or chlorine-based electrolytes are used. The tube size and aspect ratio of titania template can be controlled by the type and pH of the

electrolyte as well as the applied voltage similar to fabrication of alumina. Arrays of TiO<sub>2</sub> nanotubes can be formed by this method. The diameter of nanotube, nanotube wall thickness, and overall film thickness can be controlled through experimental parameters. The synthesized TiO<sub>2</sub> nanotube arrays can be annealed at high temperature to convert from anatase to rutile phase as well as to improve the mechanical properties. Also, drugs like gentamicin, penicillin, and streptomycin have been incorporated into the titania nanotubes to combat bone infections [24–26]. These coatings mimic the surface chemistry of the natural oxide layer of commercial titanium implants. Popat et al. studied the effects of titania nanotube templates as sustained antibiotic release platforms. Their studies showed that there is approximately 70 % reduction in the bacterial population with drug-releasing nanotemplate compared with those without any antibiotic after 4 h of incubation [24]. Another in vitro study has shown improved properties of titanium by anodizing and subsequently coating the titanium with antibacterial and anti-inflammatory drugs. The drugs were loaded by two different methods: simple physical adsorption which consists of soaking the templates in the drug solution and simulated body fluid (SBF) in which templates soaked in the combination of drug and SBF solutions. The release measurements showed improved prolonged release of both types of drugs in case of SBF assisting loading comparing with simple adsorption. Other fabrication methods of TiO<sub>2</sub> nanoporous surfaces include the use of a block copolymer in combination with a precursor TiCl<sub>4</sub>. This method could be used for fabricating templates with about 5.5 nm diameter nanoholes of titania [16].

## Alumina

Alumina or aluminum (III) oxide (Al<sub>2</sub>O<sub>3</sub>) is the stable oxide of the highly reactive, soft, durable, lightweight aluminum metal. It exists in two forms,  $\alpha$ -Al<sub>2</sub>O<sub>3</sub> and  $\gamma$ -Al<sub>2</sub>O<sub>3</sub>. Both forms vary by different dissolution behaviors.  $\gamma$ -Al<sub>2</sub>O<sub>3</sub> is soluble in strong acid and base, while  $\alpha$ -Al<sub>2</sub>O<sub>3</sub> is insoluble and inert. Above 800 °C  $\gamma$ -Al<sub>2</sub>O<sub>3</sub> converts into  $\alpha$ -Al<sub>2</sub>O<sub>3</sub> form. Traditionally, alumina has been used in dentistry and orthopedics as implants. In nanophase, alumina exhibits bioactivity. Nanophase alumina, such as nanoporous and nanotubular forms, shows higher protein adsorption and osteoblast adhesion. Alumina coatings on implants have been incorporated with various drugs and studied. Regarding nanocoatings, anodization has been the most preferred technique for fabrication of both titania and alumina. In case of nanoporous alumina coating, the fabrication method starts with the aluminum film being exposed to an acidic medium due to which an oxide layer forms over the metal. During the anodization, the applied voltage leads to pore formation and the growth of the oxide layer. While the type and pH of the acid determine the inter-pore distances, the applied voltage during the anodization determines the pore diameter of the templates. Generally, the longer the anodization, the thicker the resulting porous template is. However, the acidic medium also causes the dissolution of the oxide layer, and eventually the growth and dissolution rates become equal. This determines the ultimate thickness of the oxide layer. Nanoporous anodic alumina is a chemically stable, bioinert, and biocompatible material used widely as coating on dental and orthopedic implants. Ordered nanoarchitected alumina templates with broad size

range can be directly grown on metal implant surface because of the well-refined anodization techniques. Unlike nanopore configuration, the nanotube configuration has a unique feature in that spacing between neighboring nanotubes allows a continuous supply of body fluids, nutrients, and proteins underneath adhered and growing cells. In contrast, simple nanopored configuration gets covered with adhered cells thus blocking the supply of body fluid. These nanotubes can be utilized as “nanodepots” for advanced drug delivery therapeutics. The nanotube geometry, as compared to the nanopore geometry with similar pore diameter, provides twice the surface area, which can provide more binding locations for increased adsorption of drug molecules. The use of nanotubes toward drug release for longer periods of time was evaluated with an antibiotic, amoxicillin. Controlled, sustained antibiotic release was achieved for over 5 weeks, with a possibility of extending the drug release to much longer periods [27]. This alumina nanotube system presented a diffusion-controlled release, where the entrapped drug diffuses out of a matrix at a defined rate.

---

### **Overcoming Antimicrobial Resistance: Ion Substitutions as Mode of Antibacterial Action**

The phenomenon of antimicrobial resistance (AMR) is an extremely serious problem capable of undermining the progress achieved by medical scientists in the field of medicine and surgery. AMR results in reduced efficacy of antibacterial, antiparasitic, antiviral, and antifungal drugs, making the treatment of patients difficult, costly, or even impossible. The impact on particularly vulnerable patients is most obvious, resulting in prolonged illness and increased mortality. Most international, national, and local agencies have issued warnings, declarations, and resolutions on this problem with limited success. The 2014 WHO global report on surveillance of AMR warns of the possibility of a “post-antibiotic era,” in which common infections and minor injuries can kill humans, becoming a very real possibility for the twenty-first century [40]. According to WHO, AMR is frequently observed to be associated with common infectious bacteria like *S. aureus*, *E. coli*, and *K. pneumoniae* which are implicated in bone infections as well.

All microorganisms including bacteria are capable of developing resistance against any type of drug compound as a part of evolutionary process. However, it has been accelerated by the widespread use of antibacterial drugs. Resistant strains are able to propagate and spread through a wide range of biochemical and physiological mechanisms when preventive and control measures are not adhered to. Various ways of dealing with this worldwide threat of microbial resistance include developing newer, more potent antibiotics, preventive vaccines and preserving the efficacy of existing drugs through measures to minimize the spread of resistance. Unfortunately, the discovery of new antibiotics is not up to the speed with the microbial pathogen’s fast and frequent development of resistance. Drug research and development is expensive and time-consuming with the average cost per each new drug developed to be US\$ 800 million to 1.7 billion. A report from the European Centre for Disease Prevention and Control and European Medicines



Agency in 2009 showed that only two new antimicrobials were under development, both in the early stages when the failure rates are high. There is also a decrease in diversity of new antibiotics with most of them being modifications of existing molecules. There is a decrease in discovery research efforts and in antibacterial trials, reflecting a diminishing industry focus on antibacterial drug research and development. This challenge posed by the emergence of bacterial strains resistant to many currently used antibiotics demand for longer-term solutions. A fresh outlook on tackling this challenge of antibiotic resistance lies in the world of next-generation antimicrobial nanomaterials, to which microbial pathogens are unable to develop resistance.

Nanomaterials that either show antimicrobial activity by themselves or elevate the effectiveness and safety of antibiotics administration are called “nanoantibiotics” [41], and their capability of controlling infections *in vitro* and *in vivo* has been explored. Unlike many conventional antibiotics, antimicrobial nanoparticles may not pose any known direct and acute adverse effects. Antimicrobial nanoparticles offer many advantages in reducing adverse effects, overcoming resistance, and lowering cost, when compared to conventional antibiotics. Recently, a study found that despite of antibiotic release from PMMA cement beads, the bacteria continued to grow and potentially develop antibiotic resistance. Implant surfaces are favorable to the growth of bacteria, despite the presence of antibiotics. In the presence of antibiotics, the bacterial population evolved by modifying itself as an adaptive response. By considerably limiting the penetration of antibiotics and reducing the growth rate of bacteria biofilms facilitate the formation of more persistent cells. These modifications could participate in the emergence of resistant bacterial strains [5]. Most importantly, antimicrobial nanoparticles tackle multiple biological pathways found in broad species of microbes and therefore necessitate many concurrent mutations in order to develop resistance against these nanoantibiotics. Compared to antibiotics synthesis, preparation of antimicrobial NPs can be cost-effective, and they are stable enough for long-term storage with a prolonged shelf life. In addition, some nanoantibiotics can withstand harsh conditions, such as high-temperature sterilization, under which conventional antibiotics are inactivated [41]. In addition, these antimicrobial nanoparticles can be used as DDS for antibiotics offering multiple advantages such as increased potency of drugs, rapid and sustained antibacterial effect, and broad spectrum activity.

Several nanomaterials are already used as antimicrobial agents in consumer products and medical field like silver nanoparticle-impregnated garments, wound dressings, etc. Nanomaterials exhibiting antibacterial activity include inorganic nanoparticles of metals or metal oxides, fullerenes, nanotubes, bioglasses, and ion-substituted nanobioceramics. Metal oxide nanoparticles can be composed of variety of materials, including titanium, zinc, cerium, aluminum, and iron oxides. Though the antibacterial activity of these metallic or oxide nanoparticles is potent, they are also toxic to mammalian cells. The mechanism of action of various antibacterial nanoparticles is given in Fig. 3. Among bioceramics, bioglasses and  $\text{TiO}_2$  are inherently antibacterial, while others like calcium phosphates can be made antibacterial by substituting metal ions such as silver ( $\text{Ag}^+$ ), zinc ( $\text{Zn}^+$ ), copper

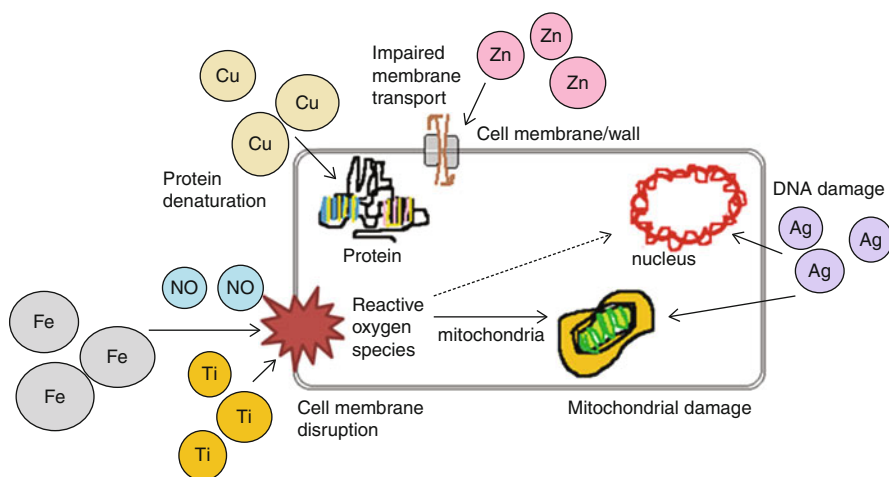


**Fig. 9** Schematic diagram of antimicrobial mechanisms of bioceramics via ion release

( $\text{Cu}^+$ ), and strontium ( $\text{Sr}^+$ ). The various types of antibacterial bioceramic nanoparticles are detailed in this section (Fig. 9).

## Titania Nanoparticles

The antimicrobial behavior of titania nanoparticles have been extensively studied over the years. Titania was observed to have the maximum activity against *E. coli* and minimum activity against the fungi *Candida albicans* which was related to the complexity of the cell membrane. Titania, a semiconductor photocatalyst, exhibits bactericidal activity in the presence of UV rays. The photocatalytic antimicrobial activity depended on the membrane thickness and was studied to be highest in virus when compared to bacteria and bacterial spores. Reactive oxygen species (ROS) production has been observed to be the attributing factor for the antimicrobial activity of titania nanoparticles for which the microbial cell surface is the primary target. Microorganisms resistant to UV radiation and desiccation have been studied to be inactivated by titania nanoparticles [42]. The antibacterial activity of  $\text{TiO}_2$  is ascribed to the production of reactive oxygen species, cell membrane, and wall damage.

## Alumina Nanoparticles

A study on the antibacterial effect of alumina revealed a mild inhibitory effect toward *E. coli* at high concentrations of 1000  $\mu\text{g}/\text{ml}$ . A decrease in the extracellular protein content after nanoparticle exposure was also observed as indicated by protein assays and FT-IR studies. Few studies have compared the difference in toxicity

between nano and bulk alumina. The activity of nanoscale alumina against *B. subtilis*, *E. coli*, and *P. fluorescens* was examined and compared with its bulk counterpart. The nanoparticle had higher toxicity than bulk at the concentration studied, and it was observed that *P. fluorescens* was the most sensitive. Similar results were also observed with *Salmonella* species showing more mutagenicity toward alumina nanoparticles when compared to the bulk [42].

## Bioactive Glass

Bioactive glasses are known to exhibit antimicrobial activity in aqueous solutions due to the release of their ionic compounds such as silica. For example, ions released from a bioactive glass of composition  $\text{SiO}_2\text{-Na}_2\text{O-CaO-P}_2\text{O}_5$  increased pH of immediate environment discouraging bacterial growth. Antibacterial and antifungal activity of bioactive 45S5 Bioglass<sup>®</sup>-derived glass-ceramic substrates has also been reported. Particle size also appear to play a role as a shift from micro- to nanosized bioglass materials resulted in a tenfold increase in silica release and high pH elevation by more than three units thereby exhibiting bactericidal action against *E. faecalis* bacteria.

## Iron Oxide ( $\text{Fe}_3\text{O}_4$ ) Nanoparticles

Iron oxide has been widely researched in the field of medical imaging due to their magnetic properties. Iron oxide nanoparticles are known to generate reactive oxygen species that can damage cell membrane. The antibacterial activity of these nanoparticles was tested against *S. aureus*. These particles of approximately 10 nm diameter were delivered from a polyvinyl alcohol matrix. It was found that they exhibited strong bactericidal activity against *S. aureus* [43].

## Ion-Substituted Bioceramics

Metallic ion-substituted bioceramics represent an effective strategy to combat antimicrobial resistance while ensuring biocompatibility through controlled ion release and can also be multi-functionalized with antibiotics. The most common ions substituted in nanobioceramics are silver, zinc, and copper for providing antibacterial activity.

**Silver substitutions:** Silver ions are well known for their antibacterial activity. The antibacterial action of silver is attributed mainly to deactivation of mitochondrial enzymes involved in electron transport and Adenosine triphosphate synthesis, by binding to their thiol groups. Another mode of action would be to bind to DNA, leading to its condensation and denaturation and preventing their replication. Silver has been the most substituted ion in bioceramics such as calcium phosphates and bioglasses to impart antibacterial activity. The antibacterial activity and

biocompatibility of silver-substituted HAs have been studied by Rameshbabu et al. [44]. The silver (0.5–3 at. %) substituted nanosize HAs (AgHAs) were synthesized by a rapid microwave-accelerated wet chemical method. AgHAs showed larger lattice parameters due to the substitution of larger  $\text{Ag}^+$  ions (1.28 Å) for  $\text{Ca}^{2+}$  ions (0.99 Å) preferentially in the Ca(1) site of HA. At an optimum substitution of 0.5 % silver, the AgHAs exhibited antibacterial activity against *E. coli* and *S. aureus*, while osteoblast attachment on these AgHAs remained unaffected. Although at higher concentrations (>0.5 % substitution) the antibacterial activity was enhanced, the osteoblast cell adhesion was compromised. Silver has also been incorporated into bioglass (AgBG;  $\text{SiO}_2\text{-CaO-P}_2\text{O}_5\text{-Ag}_2\text{O}$ ) synthesized through a sol-gel route [34]. 3 wt%  $\text{Ag}_2\text{O}$  was incorporated into this system, and the antibacterial activity was compared with 45S5 Bioglass<sup>®</sup> against *E. coli*, *P. aeruginosa*, and *S. aureus*. While bacterial growth was inhibited at concentrations of AgBG in the range of 0.05–0.20 mg/ml of culture medium, complete bactericidal effect was observed at 10 mg/ml. These studies illustrate that the bioceramic particle size, amount of substitution of silver ions, and degradation rate can be used to control the release rates of ions like silver thereby inflicting minimal damage on mammalian cells. Cell culture experiments of Ag-doped  $\text{CaO-SiO}_2$  glasses using human fibroblasts, osteoblasts, and keratinocytes also established the safety limits of silver release. Biofilm formation that causes biomaterial-centered infection and poor tissue integration is a problem faced by many medical devices. Inhibiting bacterial adhesion is often regarded as the most critical step in preventing such infections. This can be achieved by coating the medical device with antibacterial ion-substituted bioceramics. A borate bioactive glass coating on titanium implants containing 0.75–1.0 wt%  $\text{Ag}_2\text{O}$  significantly improved the antibacterial properties of against methicillin-resistant *S. aureus* in an in vivo study after 6 weeks of implantation. Similarly, an in vivo study on silver-containing calcium phosphate coating on titanium implants was tested for antibacterial activity against *S. aureus*. Silver-coated titanium implants simulating knee prostheses were inserted into rabbit's knees. Prior to implantation, *Staphylococcus aureus* was inoculated into the femoral canal. The site was evaluated by radiologically (periosteal reaction, osteolysis, or sequestrum formation), microbiologically (implant colonization/positive cultures), and histologically (leukocyte infiltration, necrosis, foreign body granuloma, devitalized bone). The results revealed a lower proportion of positive culture and lower rate of colonization in silver-coated implants than in uncoated implants. No cellular inflammation or foreign body granuloma was observed around the silver-coated prostheses suggesting their safe clinical usage [45].

Silica nanoparticles immobilized with Ag ions, such as Ag-SiO<sub>2</sub> hollow composite nanospheres and nanotubes, were studied for the antibacterial activity against *E. coli* and *S. aureus* [46]. It was observed that although both showed antibacterial activity, nanotubular Ag-SiO<sub>2</sub> showed a stronger antibacterial ability than spherical structures due to higher silver retention. A core-shell structure with a silver core and amorphous silica shell was fabricated using TEOS as silica precursor and reducing silver nitrate with ascorbic acid. These nanoparticles had excellent antibacterial effects against *E. coli* and *S. aureus*. Silver has also been successfully incorporated

within zeolites or aluminosilicate ceramics that can electrostatically bind with the  $\text{Ag}^+$  ions. Silver zeolite with 2.5 wt% exhibited contact inhibition of the periodontal pathogens such as *A. actinomycetemcomitans*, *P. gingivalis*, and *P. intermedia* implicated in chronic periodontitis and peri-implantitis [47]. They also exhibited fungicidal action against common oral fungi, *C. albicans*. The formation of dental biofilm or plaque was also disrupted on using a silver zeolite mouth rinse.

**Zinc substitutions:** Zinc is an important trace element in our body. Zinc has a direct effect on the proliferation of osteoblastic cells while inhibiting osteoclastic bone resorption. It also has anti-inflammatory and antioxidant properties. Zinc ions also show an inhibitory effect on bacteria, by binding to the bacterial membranes impairing calcium uptake and changing the fluidity of the membrane. It also prolongs the lag phase of the growth cycle. Gram-positive bacteria are more susceptible to zinc ions than gram-negative bacteria due to the difference in the protein constituents of their cell walls. In a study by Venkatasubbu et al., zinc ions were substituted in HA by a wet chemical synthesis at concentrations of 2–5 wt% and found to be effective against *S. aureus* and *P. aeruginosa*. The  $\text{Zn}^{2+}$ -substituted HAs showed a reduction in the crystallinity and crystal size of HA with increasing zinc content due to the smaller ionic radius for  $\text{Zn}^{2+}$  (0.74 Å) than that of  $\text{Ca}^{2+}$ . It is believed that the antibacterial mechanism of  $\text{Zn}^{2+}$  may be due to binding of the ions on the crystal surface with thiol, imidazole, and amino and carboxyl groups of bacterial membrane proteins, causing structural changes resulting in increased permeability leading to cell death [48].

**Copper substitutions:** Copper is a heavy metal, which has antimicrobial property with relatively low toxicity toward mammalian cells. Copper exerts its antibacterial activity by inactivating bacterial enzymes and proteins. Spherical Cu-SiO<sub>2</sub> nanocomposite particles have been synthesized by depositing Cu ions on the surface of spherical silica nanoparticles. Excellent antibacterial activity was observed on testing with disk diffusion studies. A core-shell copper-silica nanoparticle was prepared by first preparing silica seed particles by the base-catalyzed Stober process, followed by an acid-catalyzed growth of the copper-silica shell layer around the core [32]. The seed particle size was 380 nm and the shell thickness was 35 nm. Antibacterial efficacy of these copper-silica core-shells showed them to be more effective than insoluble copper hydroxide particles against *E. coli* and *B. subtilis*, most likely due to improved Cu bioavailability due to the particle structure.

**Strontium substitutions:** Strontium is one of the trace minerals present in the calcified hard tissues. Strontium is known to promote osteoblast proliferation and downregulate osteoclast formation in both normal and osteopenic cells, with an increase in the alkaline phosphatase activity. Therefore, strontium-substituted hydroxyapatite has provoked increased interest in treatment of osteoporosis. In addition to these bone-strengthening properties, strontium ions also possess antibacterial action. The  $\text{Sr}^{2+}$  ion can be substituted for  $\text{Ca}^{2+}$  at the Ca(II) cation site in the HA structure for the whole range of composition with a linear increase in the lattice parameters. The antibacterial properties of 50–100 % strontium-substituted HA nanoparticles on *E. coli*, *S. aureus*, and *Lactobacillus* have been

reported. In a study by Narmada Ravi et al., [49] strontium was substituted into CDHA at 5 and 10 at.% substitutions and evaluated for antibacterial activity and biocompatibility. It was found that the antibacterial activity of these samples tested against *S. aureus* and *E. coli* showed positive antibacterial results with a quantitative reduction of the colony count with increasing strontium substitution. Higher antibacterial activity was observed with the *E. coli* over *S. aureus* with 10 % substituted CDHA showing a microbial reduction of ~56 % for *E. coli* and 35 % for *S. aureus*. The higher antimicrobial activity was attributed to the alteration of the zeta potential on partial substitution of strontium for calcium.

**Multi-ion substitutions:** Multi-ion-substituted bioceramic nanoparticles have also been synthesized. For example, HA nanoparticles substituted with zinc (0.2 wt%), silver (0.25 wt%), and gold (0.025 wt%) were synthesized through a wet chemical method coupled with a reduction process for silver and gold [50]. These HA nanoparticles were mixed with Ag<sub>2</sub>O nanoparticles and incorporated into an organic matrix of methacrylate monomers which were subsequently polymerized. Antibacterial activities of these composites were investigated against several pathogens like *S. aureus*, *E. coli*, *B. cereus*, *C. albicans*, and *Staphylococcus* species. It was found that the antibacterial activity was enhanced on increasing of silver content within these composites. Similar studies on Cu–Zn-substituted and Zn–Ag-substituted HA have also shown potent antibacterial activity.

## Nitric oxide (NO)-Releasing Silica Nanoparticles

The antibacterial activity of nitric oxide, a reactive-free radical produced by inflammatory cells, is a host mechanism well known to inhibit or kill broad spectrum of microbes. NO-releasing silica nanoparticles have been used to control the biofilm formation of *P. aeruginosa* and *E. coli*. NO-releasing silica nanoparticles were synthesized using *N*-methyl aminopropyl trimethoxysilane (MAP3), tetraalkoxysilanes, or TEOS as the precursors. Co-condensation with diazeniumdiolate NO donors or by exposure to 5 atm. of NO results in NO-releasing silica nanoparticles' formation [32]. The MAP3 silica nanoparticles were highly active against *P. aeruginosa* biofilms due to the smaller size of MAP3 nanoparticles that allow them to penetrate biofilm matrix. The electrostatic and/or hydrophobic interactions between the Si nanoparticles and bacterial cell membranes result in high local concentrations of NO and more efficient delivery of NO to the bacterial cells.

## Drug Delivery Using Ion-Substituted Nanobioceramics

Combining antibiotics with antimicrobial nanobioceramics is also a promising approach to improve antimicrobial activity and potentially overcome resistance to the current antibiotics. Certain metal ions are known to enhance the effect of antibiotics. For example, antibacterial activities of chloramphenicol, kanamycin, erythromycin, and ampicillin against gram-positive and gram-negative bacteria

were increased in the presence of silver nanoparticles. It was also reported that the antibacterial activity of cefoperazone against MRSA was enhanced when it was used with colloidal silver. Venkatasubbu et al. [48] used zinc-substituted hydroxyapatite as a carrier for ciprofloxacin release. It was observed that the zinc substitution in HA increased the percentage of drug release linearly between 2 % and 4 % substitution although the mechanism is unknown. All the ciprofloxacin-loaded zinc-doped hydroxyapatite nanoparticles have greater antibacterial activity against *S. aureus* and *P. aeruginosa* compared to the ciprofloxacin-loaded pure hydroxyapatite. It is highly probable that the use of such antibacterial nanobioceramic will be at the forefront treating bacterial infections, especially by MRSA, vancomycin-resistant *Staphylococcus aureus* (VRSA), and multidrug-resistant *P. aeruginosa*.

---

## Summary

Bone infections have long since been treated with conventional systemic drug delivery. It cannot be doubted that the appropriate use of antimicrobial agents has decreased morbidity and mortality from orthopedic-related infections. However, with the increasing problems of drug resistance and higher incidence of device-associated infections, newer methods of counteracting infection need to be probed. Appropriate local drug delivery can achieve increased antibiotic dose at site, decreased toxicity, and greater efficacy. There is considerable interest in finding methods of delivering effective doses of antimicrobial drugs locally, not only in orthopedics but also across a range of medical specialities. With the recently proven clinical success and successive FDA approval of local drug release systems and recognition of the therapeutic value of locally released antimicrobials in several clinical device classes including catheters, bone cements, and wound dressings, local drug delivery/device combination therapy has increased. For many reasons, the surface of any implanted medical device provides an excellent platform for the formation of bacterial colonies or biofilms, producing life-threatening infections. In the case of antimicrobial strategies, many different biomaterial approaches with different antibiotics have been studied and can exhibit unique opportunities to help treat bone- and device-related infections. These medical devices provide drug reservoirs to infection sites and exhibit capabilities for multiple drug release and site-sensitive stimulated release control mechanisms. Despite significant efforts in this direction, several challenges are yet to be resolved. These include understanding the link between the parameters such as processing conditions and the physicochemical properties of the nanomaterial-based delivery systems as well as the stability of the incorporated drug. The choice of the optimal bone substitutes for treatment of infection is not straightforward and largely depends on the clinical application and associated biological and mechanical needs. Other challenges also include achieving accurate spatiotemporal control of drug release, ensuring specific quantities of drug for determined applications, and engineering the release patterns, which, in turn, are related to the interaction between the drug and the carrier, drug solubility, and amount of drug loaded. Further, only limited work has been reported on how

processing parameters and sterilization can affect the stability and the release kinetics of the drug incorporated. The *in vitro* drug release studies also need an overhaul in order to more closely mimic the *in vivo* release and be more suitable for nanoparticles. This lack of suitable trials comparing them *in vivo* makes their evaluation difficult. On the other hand, the development of antimicrobial materials such as metal ions and metal oxide nanoparticles looks promising due to their high potency, especially in overcoming antibacterial resistance. The major concern associated with these materials is toxicity to mammalian cells. However, this problem can be solved with a rational approach aimed at controlling the ion release. The incorporation of ions into bioceramics is a safe alternative in this regard. It is to be expected that such combinations of antibacterial and regenerative techniques necessary for treatment of bone infections will take time to achieve clinical results. It is therefore expected that this field presents an exciting frontier for research and has the potential to transform the medical solution to bone infections.

---

## References

1. Zilberman M, Elsner JJ (2008) Antibiotic-eluting medical devices for various applications. *J Control Rel* 130:202–215. doi:10.1016/j.jconrel.2008.05.020
2. Bejon P, Robinson E (2013) Bone and joint infection. *Medicine* 41:719–722. doi:10.1016/j.mpmed.2013.09.008
3. Wu P, Grainger DW (2006) Drug/device combinations for local drug therapies and infection prophylaxis. *Biomaterials* 27:2450–2467. doi:10.1016/j.biomaterials.2005.11.031
4. Gristina AG (1987) Biomaterial-centered infection: microbial adhesion versus tissue integration. *Science* 237:1588–1595
5. Verron E, Bouler JM, Guicheux J (2012) Controlling the biological function of calcium phosphate bone substitutes with drugs. *Acta Biomater* 8:3541–3551. doi:10.1016/j.actbio.2012.06.022
6. Arcos D, Vallet-Regi M (2013) Bioceramics for drug delivery. *Acta Mater* 61:890–911. doi:10.1016/j.actamat.2012.10.039
7. Harvey RA, Clark MA, Finkel R, Rey JA, Whalen K (2011) Lippincott's illustrated review: pharmacology. Wolters Kluwer, Philadelphia
8. Mourino V, Boccaccini AR (2010) Bone tissue engineering therapeutics: controlled drug delivery in three-dimensional scaffolds. *J R Soc Interface* 7:209–227. doi:10.1098/rsif.2009.0379
9. Lima ALL, Oliveira PR, Carvalho VC, Cimerman S, Savioc E (2014) Recommendations for the treatment of osteomyelitis. *Braz J Infect Dis* 18:526–534. doi:10.1016/j.bjid.2013.12.005
10. McLaren A (2004) Alternative materials to acrylic bone cement for delivery of depot antibiotics in orthopaedic infections. *Clin Orthop Relat Res* 427:101–106. doi:10.1097/01.blo.0000143554.56897.26
11. Nandi S, Mukherjee P, Roy S et al (2009) Local antibiotic delivery systems for the treatment of osteomyelitis – a review. *Mater Sci Eng C* 29:2478–2485. doi:10.1016/j.msec.2009.07.014
12. Hench LL, Thompson I (2010) Twenty-first century challenges for biomaterials. *J R Soc Interface* 7:S379–S391. doi:10.1098/rsif.2010.0151.focus
13. Webster T (2003) Nanophase ceramics as improved bone tissue engineering materials. *Am Ceram Soc Bull* 82:23–28
14. Victor SP, Sampath Kumar TS (2008) Tailoring calcium-deficient hydroxyapatite nanocarriers for enhanced release of antibiotics. *J Biomed Nanotech* 4:1–7. doi:10.1166/jbn.2008.019



15. Yang L, Sheldon BW, Webster TJ (2010) Nanophase ceramics for improved drug delivery: current opportunities and challenges. *Am Ceram Soc Bull* 89:24–31
16. Gultepe E, Nagesha D, Sridhar S, Amiji M (2010) Nanoporous inorganic membranes or coatings for sustained drug delivery in implantable devices. *Adv Drug Deliv Rev* 62:305–315. doi:10.1016/j.addr.2009.11.003
17. Kumar GS, Govindan R, Girija EK (2014) In situ synthesis, characterization and in vitro studies of ciprofloxacin loaded hydroxyapatite nanoparticles for the treatment of osteomyelitis. *J Mater Chem B* 2:5052–5060. doi:10.1039/c4tb00339j
18. Madhumathi K, Sampath Kumar TS (2014) Regenerative potential and anti-bacterial activity of tetracycline loaded apatitic nanocarriers for the treatment of periodontitis. *Biomed Mater* 9:035002. doi:10.1016/j.colsurfb.2014.09.052
19. Fan J, Lei J, Yu C, Tu B, Zhao D (2007) Hard-templating synthesis of a novel rod-like nanoporous calcium phosphate bioceramics and their capacity as antibiotic carriers. *Mater Chem Phys* 103:489–493. doi:10.1016/j.matchemphys.2007.02.069
20. Ferraz M, Monteiro F, Manual C (2004) Hydroxyapatite nanoparticles: a review of preparation methodologies. *J App Biomater Biomech* 2:74–80
21. Nampi PP, Mohan VS, Sinha AK, Varma H (2012) High surface area sol–gel nano silica as a novel drug carrier substrate for sustained drug release. *Mater Res Bull* 47:1379–1384. doi:10.1016/j.materresbull.2012.03.003
22. Brammer KS, Choi C, Oh S et al (2009) Antibiofouling, sustained antibiotic release by Si nanowire templates. *Nano Lett* 9:3570–3574. doi:10.1021/nl901769m
23. Lensing R, Bleich A, Smokzek A et al (2013) Efficacy of nanoporous silica coatings on middle ear prostheses as a delivery system for antibiotics: an animal study in rabbits. *Acta Biomater* 9:4815–4825. doi:10.1016/j.actbio.2012.08.016
24. Popat KC, Eltgroth M, LaTempa TJ, Grimes CA, Desai TA (2007) Decreased staphylococcus epidermis adhesion and increased osteoblast functionality on antibiotic-loaded titania nanotubes. *Biomaterials* 28:4880–4888. doi:10.1016/j.biomaterials.2007.07.037
25. Chennell P, Feschet-Chassot E, Devers T et al (2013) In vitro evaluation of TiO<sub>2</sub> nanotubes as cefuroxime carriers on orthopaedic implants for the prevention of periprosthetic joint infections. *Int J Pharm* 455:298–305. doi:10.1016/j.ijpharm.2013.07.014
26. Yao C, Webster TJ (2009) Prolonged antibiotic delivery from anodized nanotubular titanium using a co-precipitation drug loading method. *J Biomed Mater Res Part B Appl Biomater* 91B:587–595. doi:10.1002/jbm.b.31433
27. Noh K, Brammer KS, Choi C, Kim SH, Frandsen CJ, Jin S (2011) A new nano-platform for drug release via nanotubular aluminum oxide. *J Biomater Nanobiotech* 2:226–233. doi:10.4236/jbnb.2011.23028
28. El-Fiqi A, Kim TH, Kim M, Eltohamy M, Won JE, Lee EJ (2012) Capacity of mesoporous bioactive glass nanoparticles to deliver therapeutic molecules. *Nanoscale* 4:7475–7488. doi:10.1039/c2nr31775c
29. Judefeind A, Villiers MM (2009) Drug loading into and in vitro release from nanosized drug delivery systems. In: de Villiers MM (ed) *Nanotechnology in drug delivery*. Springer, New York, pp 129–162
30. Singhvi G, Singh M (2011) Review: in-vitro drug release characterization models. *Int J Pharm Studies Res* 2:77–84
31. Gonzalez-McQuire R, Chane-Ching JY, Vignaud E, Lebugle A, Mann S (2004) Synthesis and characterization of amino acid-functionalized hydroxyapatite nanorods. *J Mater Chem* 14:2277–2281. doi:10.1039/B400317A
32. Camporotondi DE, Foglia ML, Alvarez GS et al (2013) Antimicrobial properties of silica modified nanoparticles. In: Mendez-Vilas A (ed) *Microbial pathogens and strategies for combating them: science, technology and education*. Formatex Research Center, Spain, pp 283–290
33. Vasilev K, Poh Z, Kant K, Chan J, Michelmore A, Losic D (2010) Tailoring the surface functionalities of titania nanotube arrays. *Biomaterials* 31:532–540. doi:10.1016/j.biomaterials.2009.09.074

34. Bose S, Tarafder S (2012) Calcium phosphate ceramic systems in growth factor and drug delivery. *Acta Biomater* 8:1401–1421. doi:10.1016/j.actbio.2011.11.017
35. Siddharthan A, Seshadhri SK, Sampath Kumar TS (2004) Microwave accelerated synthesis of nanosized calcium deficient hydroxyapatite. *J Mater Sci: Mater Med* 15:1279–1284
36. Cai Y, Pan H, Xu X, Hu Q, Li L, Tang R (2007) Ultrasonic controlled morphology transformation of hollow calcium phosphate nanospheres. *Chem Mater* 19:3081–3083. doi:10.1021/cm070298t
37. Schmidt H, Ostafin AE (2002) Liposome directed growth of calcium phosphate nanoshells. *Adv Mater* 14:532–535
38. Colilla M, Manzano M, Vallet-Regí M (2008) Ceramic implants as drug delivery systems. *Int J Nanomed* 3:403–414
39. Muhammad F, Guo M, Qi W et al (2011) pH-triggered controlled drug release from mesoporous silica nanoparticles via intracellular dissolution of ZnO nanolids. *J Am Chem Soc* 133:8778–8781. doi:10.1021/ja200328s
40. World Health Organization (2014) Antimicrobial resistance global report on surveillance. World Health Organization, Geneva
41. Huh AJ, Kwon YJ (2011) Nanoantibiotics: a new paradigm for treating infectious diseases using nanomaterials in the antibiotics resistant era. *J Control Rel* 156:128–145. doi:10.1016/j.jconrel.2011.07.002
42. Mukherjee A, Sadiq M, Prathna TC, Chandrasekaran N (2011) Antimicrobial activity of aluminium oxide nanoparticles for potential clinical applications. In: Mendez-Vilas A (ed) *Science against microbial pathogens: communicating current research and technological advances*. Formatex Research Center, Spain, pp 245–251
43. Tran N, Mir A, Mallik D, Sinha A, Nayar S, Webster TJ (2010) Bactericidal effect of iron oxide nanoparticles on *Staphylococcus aureus*. *Int J Nanomed* 5:277–283
44. Rameshbabu N, Sampath Kumar TS, Prabhakar T, Sastry V, Murty K, Rao KP (2007) Antibacterial nanosized silver substituted hydroxyapatite: synthesis and characterization. *J Biomed Mater Res A* 80:581–591. doi:10.1002/jbm.a.30958
45. Kose N, Otuzbir A, Peksen C, Kiremitci A, Dogan A (2013) A silver ion-doped calcium phosphate-based ceramic nanopowder-coated prosthesis increased infection resistance. *Clin Orthop Relat Res* 471:2532–2539. doi:10.1007/s11999-013-2894-x
46. Wang JX, Wen LX, Wang ZH, Chen JF (2006) Ag–SiO<sub>2</sub> hollow composite nanospheres and nanotubes and their antibacterial effects. *Mater Chem Phys* 96:90–97. doi:10.1016/j.matchemphys.2005.06.045
47. Kawahara K, Tsuruda K, Morishita M, Uchida M (2000) Antibacterial effect of silver-zeolite on oral bacteria under anaerobic conditions. *Dent Mater* 16:452–455. doi:10.1016/S0109-5641(00)00050-6
48. Venkatasubbu GD, Ramasamy S, Ramakrishnan V, Kumar J (2011) Nanocrystalline hydroxyapatite and zinc-doped hydroxyapatite as carrier material for controlled delivery of ciprofloxacin. *3 Biotech* 1:173–186. doi:10.1007/s13205-011-0021-9
49. Ravi ND, Balu R, Sampath Kumar TS (2012) Strontium-substituted calcium deficient hydroxyapatite nanoparticles: synthesis, characterization, and antibacterial properties. *J Am Ceram Soc* 95:2700–2708. doi:10.1111/j.1551-2916.2012.05262.x
50. Mocanu A, Furtos G, Rapuntean S et al (2014) Synthesis; characterization and antimicrobial effects of composites based on multi-substituted hydroxyapatite and silver nanoparticles. *App Surf Sci* 298:225–235. doi:10.1016/j.apsusc.2014.01.166

# Index

## A

- Acrylic materials, 1136–1137
- Acrylic Resin, 359–360, 366
- Adhesion, 705, 707, 710, 717, 721–725
- Adhesion mechanism, 778
- Aesthetic rehabilitation, 1131
  - gingival area, 1132
  - lips, 1131
  - teeth, 1133–1134
- Albumin, 688
- Alkaline phosphatase (ALP) activity, 434
- All-ceramic dental prostheses, 1220–1224
- Allografts, 477, 616
- Alloplastic grafts, 1179, 1182, 1195
- Alumina, 1262–1263, 1362–1363, 1365–1366
  - alumina-zirconia composites, 837–841, 849–851
  - ceramics, 641
  - clinical results of, 844–846
  - grain growth, 660
  - hardness, 660
  - in hip replacements, 832–834
  - in knee replacements, 834
  - matrix composite, 825
  - mechanical properties, 63–66
  - physical properties, 62–63
  - properties of, 835
  - stability of, 66
- Alumina-toughened material (ATZ), 838
  - mechanical properties of, 79
  - stability of, 80
  - structure of, 79
- Alveolar ridge, 1161, 1163–1166, 1168, 1174–1175, 1178, 1190
- Angiogenesis, 1269
- Anionic ions
  - carbonate substitution, 174–177
  - chloride substitution, 179–180
  - fluoride substitution, 177–179
  - selenium oxyanions substitution, 181–182
  - silicate substitution, 182–185
  - sulfate substitution, 180–181
- Anterior composite, 1085–1090
  - resins, 1084–1085
- Anterior cruciate ligament (ACL), 937–943
- Antibacterial properties, 1266, 1269
- Anti-biofilm bioactive molecules, 1022
- Antibiotic resistance, 1340, 1342, 1364
- Antibiotics, 764, 766, 768, 774
  - CaPs, 1357
  - local delivery of, 1338
  - materials delivering, 1021
  - nanobioceramics for, 1344–1363
  - selection of, 1342
- Antifouling, 760, 763
- Antimicrobial properties, 163
- Antimicrobial resistance (AMR)
  - alumina nanoparticles, 1365–1366
  - bioactive glasses, 1366
  - copper substitutions, 1368
  - ion substituted nanobioceramics, 1369–1370
  - iron oxide nanoparticles, 1366
  - multi-ion substitutions, 1369
  - NO releasing silica nanoparticles, 1369
  - silver substitutions, 1366–1368
  - strontium substitutions, 1368–1369
  - titania nanoparticles, 1365
  - WHO global report, 1363
  - zinc substitutions, 1368
- Antimicrobials, 760, 763–770, 772, 775–777
- Applications
  - amorphous calcium phosphates, 108
  - $\beta$ -tricalcium phosphate, 105
  - calcium-deficient hydroxyapatite, 110
  - dicalcium phosphate anhydrous, 103
  - dicalcium phosphate dihydrate, 102

- Applications (*cont.*)  
 fluorapatite, 112  
 hydroxyapatite, 111
- Arthrodesis, 970–972, 977, 981, 983
- Arthropathy, 957–958
- Articular cartilage (AC), 940, 944, 949,  
 952–953, 955, 959
- Artificial organs, 417
- Augmentation, 1161, 1172  
 alveolar, 1163–1164  
 bone, 1174–1181
- Autogenous  
 bone graft (autografts), 1169  
 types, 1169–1170
- Autografts, 616
- Autologous bone graft, 786
- B**
- Bacterial adhesion, 759–762, 765, 769, 772
- Bacteria, recoverable species, 1002
- $\beta$ -tri-calcium phosphate ( $\beta$ -TCP), 528
- Bioactive coatings with bactericidal agents, 1020
- Bioactive glass bone grafts  
 clinical applications, 28–32  
 history, 24–26  
 tissue regeneration, 26–28
- Bioactive glasses, 547, 549, 551, 560, 571–572,  
 576, 617  
 biocomposite microspheres, 330–333  
 electrospun composites fibers, 335–341  
 first generation of, 327  
 freeze drying process, 341–344  
 in clinic treatments, 327  
 mesoporous bioactive glasses, 328  
 rapid prototyping, 345–350  
 45S5 Bioglass<sup>®</sup>, 327–328, 1263–1264  
 second generation of, 327  
 solvent casting-particulate leaching process,  
 333–335
- Bioactivity, 40–41, 46, 53, 644, 646, 648
- Bioceramics, 306–307, 546, 557, 559,  
 563–566, 568, 571, 573, 575–576,  
 617, 1042, 1044, 1310–1311, 1317  
 biological properties, 43–45  
 CaP (*see* Calcium phosphate (CaP)  
 bioceramics)  
 description, 37–38  
 for efficient antibiotic delivery, 1344–1363  
 for local drug delivery, 1343–1344  
 mechanical properties, 45  
 physico-chemical properties, 38–41  
 porosity, 41–43
- Biocompatibility, 37, 53, 417, 948, 951, 953
- Biocomposite materials, 239, 244  
 fabrication, 271–283  
 medical applications, 239–249  
 natural polymers, 250–259  
 synthetic polymers, 259–271
- Biocomposites  
 biological and mechanical properties, 52–53  
 biomolecule incorporation, 53–54  
 description, 46–47  
 reinforcements, 49–51  
 sol–gel method, 47–49  
 spine surgery (*see* Spine surgery)
- Biodegradability, 484
- Biodegradable polymers, 329, 589, 597
- Biodegradable synthetic polymers,  
 259, 266–271
- Bio-Eye<sup>®</sup>, 1259–1260, 1262
- Biofilm  
 definition, 1006  
 environment interaction, 1011–1017  
 formation and propagation, 1008–1011  
 formation, dental implants, 1017–1018  
 formation, restorative and prosthetic  
 materials, 1019  
 formation stages, 1011  
 medical-device infections, 1008  
 metabolism, 1007
- Bioglass<sup>®</sup>, 737–738, 1358–1359, 1366
- Bioinert, 641
- Bioinert ceramics  
 alumina (*see* Alumina)  
 batch preparation, 85  
 carcinogenicity, 81–83  
 ceramic wear debris, 83–84  
 compaction, 85–86  
 consolidation, 86  
*in-vitro* tests, 81  
*in-vivo* tests, 81  
 machining and finishing, 86–87  
 zirconia (*see* Zirconia)
- Bioinspired materials, 239
- Biological apatite, 148–149
- Biological properties, 10, 14–15
- Biological role, 153, 155, 158, 160, 164–168,  
 171–174, 177, 179–182
- Biomacromolecules, 239
- Biomaterials, 588, 606, 758, 772, 775, 904,  
 907–908, 925  
 collagen-bioceramics composites, 306–318  
 dental bone graft (*see* Dental bone graft)
- Biomedical polymers, 238, 249–250  
 natural polymers, 250–259

- synthetic polymers, 259–271
  - Biomimesis, 138
  - Biomimetics
    - biochemical modifications, 1317–1319
    - biomaterials, 237
    - bone mesenchymal stem cells, 1319–1322
    - calcium phosphate drug delivery systems (see Calcium phosphates)
    - composites, 510–512
    - dynamic studies, 512
    - electrospinning, 516
    - fabrication, 524
    - fibres, 509–510
    - freeze-drying, 514
    - gas foaming, 514
    - hydroxyapatite, 592–593
    - materials, 52, 239
    - maxillofacial bone repairs, 1327–1330
    - mineralization, 524
    - osteoporosis treatment, 1322–1327
    - phase separation, 515
    - rapid prototyping, 515
    - scaffolds, 505–507, 593–595
    - solvent casting and particulate-leaching, 513
    - sponge replica method, 513
    - 3-D printing methods, 524
  - Biom mineralization, 587, 593
  - Biomorphic transformation, 137–140
  - Bioreactors, 512
    - systems, 802
  - Biostable synthetic polymers, 259–266
  - Bioverits, 739
  - Biphasic calcium phosphate (BCP), 446
  - Bone
    - bone morphogenetic proteins, 978–980
    - bone marrow aspirate, 981–982
    - constituents, 587
    - demineralized bone matrix, 974–975
    - fractures, 599
    - iliac crest bone graft, 970–971
    - local bone graft, 971–972
    - pathologies, 599
    - plate, 600
    - regeneration, 589 (see also Regenerative medicine)
    - tissue, 586
  - Bone apatite. See Carbonate apatite
  - Bone cell response, 167, 177
  - Bone cements, 291, 548, 560–561, 566–571
    - acrylic bone cement, 873
    - antibiotic-loaded cement, 871–873
    - clinical processing and handling, 870–871
    - composition, 863–864
    - interface, 861, 864–865, 869, 872–875, 878, 890–891, 893–895
    - properties, 864–870
  - Bone grafting technique, 1177–1178
  - Bone graft substitutes, 1182, 1196
  - Bone infections, 1335, 1337–1338, 1370
    - causative organisms, 1335
    - DDS for, 1341
  - Bone marrow, 981–982, 984
  - Bone mineral density, 629
  - Bone morphogenetic protein (BMP), 523
  - Bone regeneration, 130, 134, 138, 140, 1163, 1166–1167, 1176
    - clinical studies in, 489
    - guided, 1178–1179, 1181, 1189
    - ridge augmentation, 1187
    - smart matrix (see Smart matrix)
  - Bone remodeling, 216, 226–227
  - Bone replacement, carbonate apatite. See Carbonate apatite
  - Bone scaffold, 130, 132–133, 135, 138, 140
  - Bone substitutes, 288, 968, 972, 981
  - Bone tissue
    - engineering, 46, 52, 54, 330, 335, 505, 1313, 1315–1317, 1322
    - neo-formation, 42
    - regeneration, 52
  - Brownian motion, 736
  - Bulk-fill composite, 396–397
- C**
- CAD/CAM systems. See Computer-aided design/computer-aided manufacturing (CAD/CAM) systems
  - Calcium carbonate ( $\text{CaCO}_3$ ) 221–222
  - Calcium orthophosphates
    - $\alpha$ -tricalcium phosphate, 105–106
    - amorphous calcium phosphates, 106–108
    - anhydrous phase diagram, 96
    - $\beta$ -tricalcium phosphate, 104–105
    - biphasic calcium phosphate, 114
    - calcium-deficient hydroxyapatite, 108–110
    - crystallographic data, 99
    - dicalcium phosphate anhydrous, 103
    - dicalcium phosphate dihydrate, 102–103
    - fluorapatite, 111–112
    - geological and biological occurrence, 93–96
    - hydroxyapatite, 110–111
    - ion-substituted, 115
    - monocalcium phosphate anhydrous, 101–102
    - monocalcium phosphate monohydrate, 99
    - multiphasic formulation, 114

- Calcium orthophosphates (*cont.*)
  - octacalcium phosphate, 103
  - oxyapatite, 112
  - tetracalcium phosphate, 113
  - triphasic formulations, 115
- Calcium phosphates (CaP), 292–293, 1311, 1343, 1345, 1355–1358
  - antibacterial and bone stimulating drug delivery system, 1315–1316
  - coral exoskeletons, 1312–1313
  - drug loading, coatings and characterization, 1313–1314
  - osteoporosis, 1316–1317
- Calcium phosphate (CaP) bioceramics
  - bioactivity and osteogenic properties, 14–15
  - challenge of, 16
  - commercial products, 8–9
  - composites, 16–17
  - definition, 474
  - development of, 6
  - feature of, 6
  - mechanical properties, 14
  - physicochemical properties, 12–13
- Calcium sulfate, 219, 225–226
- Cancer diagnosis and treatment, 293–295
- Carbide, 705, 709
- Carbonate, 174–177
- Carbonate apatite
  - and hydroxyapatite, 216–219
  - cells' response, 226–227
  - dissolution-precipitation reaction, 219–226
  - tissue response, 229–231
  - type A carbonate apatite, 215
  - type B carbonate apatite, 215
- Carbonitrides, 705, 710–711
- Case report, PEEK personalised implant
  - case examination and operation, 1299
  - clinical case follow-up, 1302
  - history, 1299
  - postoperative care, 1301
- Casein phosphopeptides (CPPs), 434
- Cationic ions
  - cobalt substitution, 173
  - copper substitution, 171–172
  - gallium substitution, 171
  - iron substitution, 167–168
  - lanthanide substitution, 168–170
  - magnesium substitution, 153–155
  - manganese substitution, 166–167
  - potassium and sodium substitution, 164–165
  - silver substitution, 160–164
  - strontium substitution, 155–160
  - titanium substitution, 165–166
- Cell biocompatibility, 340
- Cementing techniques
  - bone cements (*see* Bone cements)
  - clinical aspects, 873–890
  - first generation, 861
  - hip arthroplasty, 889–896
- Cement mantle, 865, 868, 870–871, 873, 876–878, 880, 882, 884, 892–894
- Ceramic-ceramic, 924–929
- Ceramic-on-ceramic (CoC), 824, 827, 833, 842, 845–846, 852–853
- Ceramic-on-polyethylene (CoP), 844
- Ceramic/polymer composites, 1256, 1264–1267
- Ceramics
  - based composites, 640
  - bioceramic composite types, 641, 652
  - definition, 640
  - processing, bioceramics (*see* Processing techniques)
- Ceramic veneers
  - advantages, 1145–1146
  - contraindications, 1144–1145
  - disadvantages, 1146
  - feldspathic veneers, 1139
  - glass-ceramic veneers, 1140
  - indications, 1143–1144
  - intraoral view, 1155
  - longevity, 1147
  - preparation technique, 1141–1142
  - treatment method, 1139
- Ceravitals, 739
- Chemical components, RBDC, 361–362, 365, 367, 370, 375, 377, 383, 386, 388–390, 396, 398–399, 401
- Chitosan, 618
- Chloride (Cl<sup>-</sup>) 179–180
- Classification, RBDC
  - composites, curing method, 365–368
  - coupling agent, 398–400
  - fillers, 386–389
  - Resin Matrix Type, 383–385
  - viscosity and clinical application, 395–397
- Clinical follow-up, 1302
- Clinical results, 842–853
- Coatings, 705–706
  - antimicrobial, 716–721
  - bioactive, 711–712
  - bioceramic, 707–710
  - bioinert, 710–711
  - bioresorbable, 706
  - phosphate, 705
- Cold isostatic pressing method, 86

- Collagen, 305, 307–310, 1036, 1038, 1045–1048  
  bioceramics composites, 306–318  
Collagen meniscus implant (CMI), 948  
Collagen type I, 618  
Colonization resistance, 1000  
Color, 1086  
Composite, 302, 304–305, 510–512  
Composite biomaterial  
  clinical application, 599–605  
  organic/inorganic scaffolds, 595–598  
Composite inlays, 1105  
Composite materials, 326, 330, 343, 1137–1139  
Composite resins  
  direct restorations, 1082–1100  
  optical properties, 1096  
Composite scaffolds  
  common compositions used in, 617–618  
  design and fabrication of, 618–619  
  growth factor release, 620–623  
  *in vitro* evaluation of, 620–623  
  *in vivo* evaluation of, 624–628  
  vs. stem cells *in vivo*, 625–628  
Collagen bioceramics, 306–318  
  biodegradable bioceramics, 651  
  bioinert ceramics, 641  
  ceramic matrix, 640  
  hydroxyapatite-based, 642  
  porous ceramics, 642 (*see also* Silicate-based bioactive composites)  
Computer-aided design/computer-aided manufacturing (CAD/CAM) systems, 1116, 1120  
  processed composites, 1108–1110  
  technology, 603–604  
Computer-assisted design/computer-assisted manufacturing (CAD/CAM) of dental restorations, 1208  
  advantages of, 1209  
  clinical characteristics of, 1213–1214  
  dental lab, 1209  
  disadvantages of, 1213  
  impression scanning, 1209–1210  
  intraoral scanning, 1210–1213  
Controlled release, 1339, 1341, 1347, 1358  
Copper, 1368  
Coral skeletons, 535–536  
Corrosion resistance, 704, 709–714, 721, 725  
Coupling agent, 1078  
Cranioplasty  
  aspects of, 1279–1281  
  bioceramics, 1284–1291  
  biocomposites, 1294–1296  
  biomaterials selection, clinical requirements for, 1281–1283  
  biopolymers, 1291–1294  
  case report, PEEK personalised implant (*see* Case report, PEEK personalised implant)  
  metals, 1283–1284  
  personalised implants, 1297–1298  
  tissue engineering, 1296–1297  
Critical size defect (CSD), 488  
Cytotoxicity, 155, 164, 182, 484
- D**  
Degradation, 330–331, 349  
Degree of conversion (DC), 364  
  RBDC, 377–379  
Dendrimers, 371  
Dental biofilm, 1006  
  limitation, role of chemistry, 1020–1024  
Dental bone graft  
  autogenously bone graft, 1034–1036  
  collagen, 1045–1048  
  osteoconductive materials, 1042–1044  
  osteoinductive agents, 1036–1042  
Dental ceramics, 1119, 1121–1122, 1124, 1220–1221, 1232, 1234  
  classification of, 1207  
  vs. dental enamel and dentine, 1203–1206  
  prosthetic restorations, clinical success of, 1207–1208  
Dental caries, and oral microbiome, 1004–1005  
Dental materials, 1116  
  lithium disilicate, 1122–1124  
  zirconium, 1117–1122  
Dental plaque, 993–994, 1006  
Dental prostheses  
  all-ceramic, 1220–1224  
  description, 1219  
  metal-ceramic, 1224  
  types, 1220  
Dental veneers, 1135  
Dermapotin, 529  
Design, membrane. *See* Membrane  
Device associated infections, 1337, 1370  
Dimethacrylates, 364, 373, 383–384  
Dip coating, 744–745  
Dipping method, 747  
Direct composites, 1077  
  anterior, 1084–1085  
  clinical problems, 1098  
Direct DNA sequencing, 996  
Dissolution, 1347–1349, 1362

- Dissolution-precipitation reaction, 219–226  
 DNA cloning methods, 996  
 Drug delivery, 291–292  
   systems, 312–318  
 Drug release, 1341, 1347–1349, 1371  
 Drying control chemical additives (DCCA), 742  
 Dynamic systems, 512  
 Dysbiosis, 1002
- E**
- Electrodeposition, 446, 450–453  
 Electrospinning, 516, 549, 577, 618  
 Embryonic stem cells (ESCs), 628  
 Enucleation, 1254, 1256, 1264, 1267  
 Ethylene glycol (EG), 438  
 Extracellular matrix (ECM), 953  
 Extracorporeal treatment, 425  
 Eye orbit, 1255
- F**
- Fabrication techniques  
   electrospinning, 335–341  
   freeze drying, 341–344  
   microsphere processing, 330–333  
   rapid prototyping, 345–350  
   solvent casting-particulate leaching process, 333–335  
 Failure analysis, dental prostheses, 1227–1232  
 Feldspathic veneers, 1139  
 Fibres, 509–510  
 Fibrinogen, 688  
 Fibronectin, 529  
 Fibrovascularization, 1251–1252, 1261, 1266, 1268–1269  
 Filler particles, 361, 376, 378, 382, 385–395  
 Firing, 748–749  
 Fluid shear, 762  
 Fluorapatite, 111–112  
 Fluoride, 177–179  
 Foraminifera, 537–539  
 Fourier transform infrared (FTIR)  
   spectroscopy, 682–686  
   trials, 748  
 Fracture analysis, 1240  
 Freeze-drying, 514  
 Friction coefficient, 710–712, 714, 725  
 Full ceramic veneers, 1155  
 Functionalization, 1351–1352  
 Fungi, 999
- G**
- Gas foaming, 514  
 Gelatin, 434  
 Gene therapy, 480  
 Genotoxicity, 484  
 Glass-ceramics, applications, 669  
 Glass-ceramics, drug delivery  
   adsorption, 690–695  
   encapsulation, 690–695  
 Glass-ceramic veneers, 1140  
 Glass sponge, 530  
 Grafting, 1164, 1166–1168, 1172, 1174, 1177–1178, 1194–1195  
 Graphene family nanomaterials (GFN), 458–460  
   bioceramic composites, ceramic phase, 444–446  
   challenges, 462–464  
   definition of, 433  
   dense composites, 446–450  
   electrodeposition, 450–453  
   HA composites (*see* Hydroxyapatite (HA))  
   morphology of, 448  
   3D printing, 453–455  
 Graphene oxide (GO), 434, 437  
 Graphene/bioceramic composites. *SBF*, 434–437. *See also* Graphene family nanomaterials (GFN)  
 Growth factors, in bone regeneration, 623  
 Guided bone regeneration (GBR), 1178–1179, 1181, 1187–1189  
   alveolar bone, reconstruction of, 1053  
   biological principles, 1051–1053  
   dental bone graft, biomaterials (*see* Dental bone graft)  
   membrane design criteria and material selection, 1054–1056  
   surgical techniques, guided bone regeneration)  
   tissue integration, 1053–1054  
 Guided tissue regeneration (GTR), 1178, 1187–1189
- H**
- Haemocompatibility, 484  
 Hardness, 710–711, 714, 719, 725  
 Hemoglobin, 675  
   amplitude ratio, 679  
   concentration, 678  
   structure, 675–676  
   XPS, 685  
 High strength ceramics, 1202



- Higuchi Model, 1349
- Hip arthroplasty
  - iliac wing aspiration, 890–892
  - metallic stem preheating, 894
  - metallic stem surface modification, 891–894
  - special cementing techniques, 894–896
  - surgical technique and operative steps, 884
- Horizontal ridge augmentation, 1165, 1172–1181
- Hot isostatic pressing (HIP), 440, 449, 451, 525 treatment, 86
- Hot pressing, 525
- Human bone marrow stromal cells (HBMSC), 535
- Human Microbiome Project (HMP), 998
- Human oral microbiome database (HOMD), 993
- Hybrid biomimetic scaffold, 595–598
- Hybrid composites, 1081
- Hybrid nano-composite, 132–137
- Hydrogels, 507–509, 548
  - silicate/natural polymer composite, 559
  - silicate/synthetic polymer composite, 559
- Hydrolysis, 747–748
- Hydroxyapatite (HAp), 39, 110–111, 458–460, 464, 528, 642, 644, 654–655, 705, 710–712, 941, 953–954, 1257, 1344, 1351, 1355–1357, 1368
  - alumina implants, 1266
  - biological systems, 121–123
  - bone-derived HA, 1259
  - calcium and phosphate precursor solutions, 437–443
  - cements, 291
  - coralline HA, 1259–1260
  - electrodeposition, 450–453
  - formation, 289
  - heterogeneous nucleation, 290
  - hybrid nano-composite, 132–137
  - ionic substituted biomimetic, 127–130
  - mesoporous bioactive glass, 1266–1267
  - morphology of, 448
  - nanocoatings, 749–751
  - nanoparticles, 435
  - orbital implants, 1261
  - in polyetheretherketone, 291
  - on polymer substrate, 292–293
  - rGO, 440
  - SBF, 434–437
  - self-assembled porous graphene, 456
  - silicone composite implant, 1264
  - superparamagnetic phase, 130–132
  - synthesis, 123–125
  - synthetic HA, 1260–1261
  - 3D hierarchically organized ceramics, 137–140
  - 3D printing, 453–455
- I**
- Imaging, 290, 295
- Implant and prosthetic dental materials, 1002–1006
- In vitro* bioactivity, 147, 152, 155, 164
- Incisal edge preparation techniques, 1142
- Indirect composite, 1100–1110
- Induced pluripotent stem cells (iPSCs), 479, 628
- Infuse<sup>®</sup>, 478
- Inhibitors, 365, 378
- Initiator-accelerator system, 1078
- Injury, 1279, 1299
- Inorganic fillers, 1078
- Insulin
  - entrapment, 698
  - formulation, 693
  - loading capacity, 692
  - thickness, 695
- Interface, 1222, 1227–1228, 1236, 1238
- Intervertebral disc, 969, 983
- Intrinsic anti-bacterial properties, 1020
- Ionic substituted biomimetic hydroxyapatite, 127–130
- Ion substitutions, 1363–1370
- K**
- Kidney, 417–422
- L**
- Laminated porcelain veneers, 1135
- Liver, 425–426
- Local drug delivery
  - advantages of, 1338–1339
  - bioceramics for, 1343–1344
  - components of, 1340
  - requirements of, 1340–1342
- Lungs, 422–424
- M**
- Magnesia-partially stabilized zirconia (Mg-PSZ), 835, 853
- Magnesium, 153–155
- Magnetic resonance imaging (MRI), 939–940, 942–944, 950, 956–958

- Magnetite, 293  
 Magnetron sputtering, 706, 708–711, 714, 719, 721  
 Marine materials, synthetic tissue biology  
   hard tissue scaffold development, 527–528  
   marine shells, 530–532  
   marine skeletons, 528  
   marine sponges, 528–530  
   sea urchin, 532–534  
 Marine skeleton and organic matrices,  
   regenerative medicine, 534–536  
 Marine structures  
   in drug delivery applications, 536–539  
   stem cells, regulation of, 539–541  
 Maxillary mock-up, 1151  
 Mechanical properties, 45, 154, 169, 176, 178–179  
   RBDC, 400  
 Membrane, 548–551, 577  
   alveolar ridge, resorption patterns of, 1056  
   biocompatibility, 1055  
   biodegradable barrier membranes, 1056  
   non-resorbable membranes, 1055–1056  
   artificial organs, 417  
   biomedical applications, 413–416  
   hybrid polymeric, 413  
   kidneys, 417–422  
   liver, 425–426  
   lungs, 422–424  
   pancreas, 426–427  
   polymeric, 408–413  
 Mesenchymal stem cells (MSCs), 478, 626, 949  
 Mesoporous silica, 1351, 1360–1361  
 Metabolomics, 997  
 Metal-ceramic dental prostheses, 1224  
 Metal free, 1118  
 Metallic substrates, 572–576  
 Metal matrix composites (MMCs), 573, 575–576  
 Metaproteomics, 998  
 Metatranscriptomics, 996–997  
 Microbial surface components recognizing  
   adhesive matrix molecules  
   (MSCRAMMs), 1016  
 Microfilled composites, 1081  
 Microporous biphasic calcium phosphate  
   (MBCP), 492  
 Microscopy, 908, 924  
 Microsphere, 293  
 Microstructure, 168, 184–185  
 Microwave sintering, 656–657  
 Mineralized collagen, 590, 595  
 Mixing, 862, 867, 870–872, 875, 877, 880–883, 894  
 Mn<sub>2</sub>E, 675  
   activation of, 682  
   concentration, 678  
   crystal structure, 675, 677  
   DEER analyses, 681  
   EPR spectra, 680  
 Mock-up dental arches, 1151  
 Mollusk shells, 530  
 Morphology, 1226  
 Mycoplasmas, 999  
  
**N**  
 Nanocarriers, 1360  
 Nanocoatings, 1346–1347  
 Nanocomposites, 376, 383, 391–393  
 Nanofilled composites, 1082  
 Nano-imprint processes, 526  
 Nanoparticles, 1345, 1351, 1354–1355, 1364–1365  
   alumina, 1365–1366  
   iron oxide, 1366  
   NO releasing silica, 1369  
   titania, 1365  
 Nano-structured anti-adhesion surfaces, 1022  
 Nanotherapeutics, 1354  
 Natural extracts, 765–766, 776  
 Natural polymers, 241, 250, 279, 617–618  
   polyhydroxyalkanoates, 258–259  
   polysaccharides, 255–258  
   proteins, 250–255  
 Neurosurgery  
   cranial, 1278–1279  
   definition, 1278  
   oncologic, 1278  
   paediatric, 1278, 1280  
   peripheral nerve, 1278  
   PMMA, 1293  
   spine, 1278  
   stereotactic, functional and epileptic, 1278  
   vascular and endovascular, 1278  
 Nitride, 710  
 Nitrogen monoxide (NO), 1021  
 n-methyl-2-pyrrolidone (NMP), 453  
 Non-critical size defect (NCSD), 488  
 Novabone<sup>®</sup>, 738  
 Novamin<sup>®</sup>, 738  
  
**O**  
 Occurrence, 93–96  
 Ocular surgery, 1263  
 Operational taxonomic unit (OTU), 995

- Optical properties, 1096–1098
- Oral cavity, biological niche, 1001–1002
- Oral microbiome  
 analyses, 995–998  
 dental caries and, 1004–1005  
 development, 999–1001  
 oral diseases, 1002–1006  
 preservation, 1000–1001  
 removable denture, 1005–1006  
 vertical transmission, 1000
- Organ cultures, 801
- Organic–inorganic composites  
 bone repair, 290–293  
 cancer diagnosis and treatment, 293–295  
 hydroxyapatite coating, 292–293
- Ormocers, 375–376, 383, 391
- Osseointegration, 706, 709, 712, 725
- Osteoblasts, 216, 226, 231
- Osteochondral scaffold, 134
- Osteoclasts, 216–218, 226–227, 231
- Osteoconduction, 474, 793
- Osteoconductive bioceramics, 957
- Osteoconductive property, 54
- Osteoconductive supplement, 940
- Osteogenesis, 474, 794
- Osteoinduction, 474, 793
- Osteoinductive supplement, 940
- Osteolysis, 940, 957–958, 960
- P**
- Packaging and labeling, 485
- Pancreas, 426–427
- Particulate-leaching, 513
- Peri-implant microbiome, 1003
- Perioglas<sup>®</sup>, 738
- Personalized implants  
 case report, 1298–1302  
 modern manufacturing techniques for, 1297–1298
- Phase separation, 515
- Physicochemical properties, 12–13
- Plasma deposition, 760–761, 769
- Plasma treatment, 759–761, 764
- Platelet-rich plasma (PRP), 980–981
- Poly L glicolic acid (PLGA), 939, 953, 957
- Poly L lactic acid (PLLA), 939, 941, 947, 957–958
- Polyether ether ketone (PEEK), 957, 1277, 1293  
 disadvantages of, 1294  
 personalised implant, case report, 1298–1302
- Polyglycolic acid (PGA), 953, 957
- Polyhedral oligomeric silsesquioxane (POSS), 376
- Polylactic acid (PLA), 951, 953
- Polymerization  
 shrinkage, 360, 362–365, 367–368, 371, 373, 375, 377–383  
 stress, 367, 375, 377, 380–383
- Polymers  
 natural, 617–618  
 synthetic, 617
- Polymethylmethacrylate (PMMA), 291
- Porcelain veneers, 1135
- Pore size, 618
- Porosity, 41–43, 328, 332–334, 342, 350, 618, 1259, 1261–1262
- Porous scaffolds, 513
- Posterior composites, 1090–1095
- Precision extrusion deposition (PED), 618
- Precursor, 219–226
- Premetered coatings, 747
- Processing techniques  
 hot isostatic pressing, 659  
 hot pressing, 658  
 induction heating, 657  
 laser sintering, 657–658  
 microwave sintering, 656–657  
 plasma heating, 657  
 powder synthesis, 652, 654  
 sintering, 654  
 sol–gel processing, 662–663  
 spark plasma sintering, 659, 662
- Properties  
 biomedical, 115  
 hydroscopic, 102  
*in vitro*, 115  
 mechanical, 109
- Prosthetic dental materials, 1002–1006
- Prosthetic protocols, 1122
- Prosthodontics, 1116, 1122
- Protein absorption, 1016–1017
- Q**
- Quality management, 485
- R**
- Rapid prototype, 604, 515
- RBDC. *See* Resin-based dental composites (RBDC)
- Reduced graphene oxide (rGO), 438
- Regenerative medicine, 27, 477

- Regenerative medicine (*cont.*)  
 composite scaffold customization, 602–605  
 physical factors, 608–609  
 porosity, 607–608  
 resorbability, 606–607  
 surface hydrophobicity, 606
- Removable denture oral microbiome, 1005
- Replace, reduce, refine (3Rs), 485
- Resin-based dental composites (RBDC), 358  
 Clinical Application, 361  
 Historical Background, 359–362
- Resin Monomer, 370–377
- Retrieval analysis, hip prostheses, 904  
 ceramic-ceramic, 924–929  
 chemical techniques, 908  
 clinical and pathological correlation studies, 907  
 hip resurfacing arthroplasty, 916–924  
 implant and tissue evaluation, 906  
 mechanical characterization techniques, 908  
 metallurgical characterization, 908  
 metal-polyethylene, 911–916  
 nondestructive and destructive testing  
 procedures, 906  
 objectives of, 904  
 quantitative assessment, 906  
 role of, 905  
 surface measurements, 908
- Ridge preservation, 1187, 1190
- S**
- Salivary flow rate and saliva composition, 1001
- Scaffolds, 41–43, 52–54, 326, 330, 333, 337, 341–344, 346, 348, 351  
 Fabrication Techniques, 556–557  
 Natural Biopolymers, 553  
 Silicate-Polymer Composite, 554–556  
 synthetic polymers, 553–554
- Scanning electron microscopy (SEM), 538, 678–679, 1219
- SDSL-EPR, 675–676
- Sea urchin, 532–534
- Secretory immunoglobulin A (S-IgA), 1001
- Self-assembly, 765
- Self-healing polymeric composites, 248
- SEM. *See* Scanning electron microscopy (SEM)
- Sensitization, 484
- Silane coupling agents, 361, 391, 399
- Silane/glutaraldehyde functionalization, 675
- Silicate ( $\text{SiO}_4^{4-}$ ), 182–185
- Silicate based bioactive composites  
 advantages, 547  
 biodegradable metallic substrates, 575–576  
 bone cements, 560–561  
 calcium phosphate/silicate composite ceramics, 564–565  
 calcium silicate/bioinert metal oxide composite ceramics, 565–566  
 electrospun fibers, 549  
 fabrication techniques, 556–557  
 injectable hydrogels, 557–560  
 membranes, 549–551  
 natural biopolymers, 553  
 non-degradable metallic substrates, 573–575  
 preparation and evaluation, 547  
 silanization, 561–562  
 silicate based bone cements, 566–571  
 silicate coatings, 551  
 silicate/graphene composites, 571  
 silicate-polymer composite scaffolds, 554–556  
 silicate/SiC composites, 571–572  
 surface modification, 562  
 synthetic polymers, 553–554
- Silicate cement, 359
- Silicon nitride, 842
- Silk, 618
- Silorane, 375, 383–385, 397
- Silver (Ag), 160–164, 1366–1368
- Simulated body fluid (SBF), 289, 433, 532
- Sintering, 86, 654  
 laser, 657–658  
 microwave, 656–657  
 spark plasma, 659, 662
- Slime, 1006
- Small and medium enterprises (SME), 481
- Smart matrix  
 characterization and in vitro evaluations, 484–485  
 clinical solution, 476–480  
 efficiency and performance, 492–494  
 maxillofacial clinical trial, 495–496  
 need of manufacturers, 480–481  
 need of surgeons, 474–475  
 orthopedic spine defect, 495  
 physico-chemical and biological evaluation, 491–492  
 preclinical studies and in vivo evaluation, 485  
 regulatory requirements, 485–489  
 surgical applications, research and optimization for, 481–482  
 tissue engineering, R&D, 491
- Socket, 1161, 1166–1168, 1187
- Soft tissue engineering, 326–327, 329, 337, 350

- Sol-gel processing, 525, 662–663  
 advantages and disadvantages of, 743–744  
 aqueous-bases systems, 741  
 bioglasses and glass ceramics, 738–741  
 chemical precipitation, 742  
 dip coating process, 744–745  
 drying, 747  
 firing, 748–749  
 hydrolysis, 747–748  
 metal alkoxides, 742  
 non-hydrolytic sol-gel processes, 741  
 premetered coatings, 747  
 spin coating process, 746  
 spray coating, 746
- Solvent casting, 513
- Spark plasma sintering (SPS), 441, 659, 662
- Species differences, 814
- Sphene, 752
- Spinal fusion, 969–970, 974
- Spin coating, 746
- Spine surgery  
 allograft, 972–973  
 bone marrow aspirate, 981–982  
 bone morphogenetic proteins, 978–980  
 ceramics, 975–978  
 demineralized bone matrix, 974–975  
 iliac crest bone graft, 970–971  
 local bone graft, 971–972  
 platelet rich plasma, 980–981  
 principles, 969–970  
 vertebral augmentation, 982–983  
 xenograft, 973–974
- Sponge replica method, 513
- Spray coating, 746
- Stem, 884, 891–894
- Sterilization, 485
- Stress shielding effect, 461
- Strontium, 155–157, 1368–1369
- Subcritical crack growth (SCG), 66
- Substituted hydroxyapatite, 151–152
- Superparamagnetism, 130–132, 141
- Supramolecular polymers, 239, 248, 260
- Surface analysis, 778, 1219
- Surface charge, 761, 764
- Surface chemistry, 760, 763–764, 778
- Surface energy, 760–761, 769, 776
- Surface functionalization, 1351–1352
- Surface modification, 561–562
- Surface topography, 761–763, 777
- Surgery, 602
- Surgical techniques, guided bone regeneration  
 autogenous intraoral/extraoral blocks, 1059  
 biodegradable membranes, 1065  
 dehiscences and fenestrations, 1058–1059  
 delayed technique, 1058  
 flap design, 1063  
 follow-up, 1066–1067  
 graft material positioning, 1064–1065  
 horizontal defects, 1058  
 immediate technique, 1057  
 membrane removal, 1068  
 membrane selection and positioning, 1065  
 non-resorbable membranes, 1065–1066  
 postextraction sites, 1057  
 preoperative antibiotics, 1062  
 sinus elevation, 1061–1062  
 site preparation, 1063–1064  
 suturing, 1066  
 temporary dentures, 1067–1068  
 vertical defects, 1059  
 vertical GBR, membrane, 1059–1061
- Synthetic nanohydroxyapatite, 592–593
- Synthetic polymers, 617
- Systemic toxicity, 484
- T**
- Targeting, 294
- Tenascin polypeptides, 529
- T-factory, 479
- Thermoplastic polymers, 264, 271–272, 274–275
- Thermosetting polymers, 272
- Thioglycolic acid (TGA), 436
- 3-D laser lithography, 526
- 3D plotting, 557–558, 577, 578
- 3D printing, 446, 453–455  
 methods, 524
- 3-D topology, 529
- Tissue engineering, 477, 479, 491, 597, 969, 984
- Tissue ingrowth, 1262, 1269
- Tissue regeneration, 237, 261, 267, 269, 276.  
*See* Silicate based bioactive composites
- Tissue replacement, 236–237
- Titania, 1361–1362, 1365
- Titanium alloy, 751
- Titanium-niobium (Ti-Nb) alloy, 752
- Titanium-zirconium (TiZr) alloy, 752
- Tooth extraction, 1161, 1163, 1165–1166, 1187, 1189
- Total hip replacement (THR), 824  
 ceramic heads for, 826–829  
 clinical results, 844–847
- Total knee replacement (TKR), 831, 836  
 clinical results, 847–849

- Total knee replacement (TKR) (*cont.*)  
  component of, 837  
  prototype of, 840  
Translucency, 1097–1098  
Tricalcium phosphate, 223, 1343  
Tricalcium phosphate (TCH), 940, 953
- V**  
Veneers, properties, 1136  
Vertical ridge augmentation, 1165, 1174–1181
- W**  
Water soluble matrix fraction (WSM), 531–532  
Wear, 823–824, 830–831, 839, 841, 844, 903, 910–911, 916–918  
Wet chemical processing techniques, 525
- X**  
Xenografts, 477  
X-ray photoelectron spectroscopy (XPS), 674  
  deconvolution, 687, 691  
  surface coverage, 685–686  
  zinc–silica microparticles, 694
- Y**  
Yttria stabilized zirconia, 657, 660–661  
Yttria-stabilized tetragonal zirconia polycrystal (Y-TZP), 69, 825, 834–836, 846, 848  
Yttrium oxide, 295
- Z**  
Zinc, 158–160, 1368  
Zirconia  
  alumina-zirconia composites, 837–841  
  clinical results of, 846–849  
  coatings, 752  
  development of, 67  
  in hip replacements, 835–836  
  in knee replacement, 836–837  
  mechanical properties, 70–71  
  physical properties, 68–70  
  radioactivity of, 72–73  
  stability of, 71–72  
Zirconia platelet toughened alumina (ZPTA), 825  
Zirconia toughened alumina (ZTA), 838, 853  
  mechanical properties of, 76–78  
  structure of, 74–76